PERGAMON

Phytochemistry 58 (2001) 1–7

PHYTOCHEMISTRY

www.elsevier.com/locate/phytochem

Molecules of Interest

Taxol biosynthetic genes

Kevin Walker*, Rodney Croteau

Institute of Biological Chemistry, Washington State University, Pullman, WA 99164-6340, USA

Received 23 January 2001

Abstract

The function and properties of heterologously expressed full-length cDNA clones, isolated from a *Taxus* cDNA library and specific to Taxol biosynthesis, are summarized. Recombinant enzymes are described that catalyze early steps of the pathway, including taxadiene synthase, taxadien-5α-ol-*O*-acetyltransferase and taxadien-5α-yl acetate 10β-hydroxylase, and that catalyze late steps, including 10-deacetylbaccatin III-10β-*O*-acetyltransferase and taxane 2α-*O*-benzoyltransferase. The properties of *Taxus* geranylgeranyl diphosphate synthase are also described; although this synthase does not mediate a committed step of Taxol biosynthesis, it does provide the universal plastidial diterpenoid precursor, geranylgeranyl diphosphate, for initiating Taxol biosynthesis. © 2001 Elsevier Science Ltd. All rights reserved.

Keywords: *Taxus*; Taxol biosynthesis; Taxadiene synthase; Taxadien-5α-ol-*O*-acetyltransferase; Taxadien-5α-yl acetate 10β-hydroxylase; 10-Deacetylbaccatin III-10β-*O*-acetyltransferase; Taxane 2α-*O*-benzoyltransferase

1. Introduction

The projected increase in the use of Taxol (paclitaxel) for basic research and cancer chemotherapy (Herdeg et al., 2000; Miyake et al., 2000; Reinecke et al., 2000) warrants effort to improve existing production processes for this important plant natural product. The total synthesis of the drug (Holton et al., 1995b; Nicolaou et al., 1995), while a major accomplishment, is costly and low yielding, and thus is an unrealistic alternative for commercial supply. Semisynthesis is currently the major route for the production of Taxol and related taxoids (Guénard et al., 1993; Kingston et al., 1993; Georg et al., 1994; Commerçon et al., 1995; Holton et al., 1995a); this process involves a limited number of synthetic steps (e.g. C13-side chain attachment) to convert abundant, advanced Taxol pathway intermediates (e.g. baccatin III isolated from *Taxus* needles) to the target compound. Although semisynthesis procedures are efficient, the purification of semisynthesis precursors from plant tissue requires substantial effort in the separation of the desired intermediate(s) from abundant phenolics, lipids, and other contaminants occurring in planta. The isolation of Taxol and other useful taxoids from *Taxus* cell cultures requires fewer steps than purification from intact tissue because the quantities of interfering substances are lower; however, the production yields of taxoids in cell culture are too low at present for this to be commercially viable (Ketchum and Croteau, 1998).

For the foreseeable future, Taxol and its precursors for semisynthesis will continue to be produced by biological means. The few organisms that produce Taxol include a diverse group of endophytic fungi of *Taxus* species (*Taxomyces andreanae*, *Pestalotiopsis*, *Fusarium*, and *Alternaria*) but these microbial systems have not yet achieved sustainable production of the drug (Stierle et al., 1993; Strobel et al., 1996; Kim et al., 1999; Mu et al., 1999). A most promising biological production system is *Taxus* cell cultures which respond to methyl jasmonate elicitation with increased synthesis of Taxol (Ketchum et al., 1999; Furmanowa and Syklowska-Baranek, 2000; Shin et al., 2000; Yukimune et al., 2000). Taxoid production levels in cell culture are substantially higher than that of microbial systems, but, as indicated, not sufficiently high or reliable as yet to serve as a commercial source.

Induced *Taxus* suspension cultures also provide an excellent experimental tool for in vivo and in vitro elucidation of the complex biosynthetic pathway leading to Taxol by affording elevated titers of the relevant enzymes (and nucleic acids) and intermediates for structural

* Corresponding author. Tel.: +1-509-335-1790; fax: +1-509-335-7643.

E-mail address: toyota@mail.wsu.edu (K. Walker), croteau@mail.wsu.edu (R. Croteau).

0031-9422/01/$ - see front matter © 2001 Elsevier Science Ltd. All rights reserved.
PII: S0031-9422(01)00160-1

analysis. Additionally, novel taxane metabolites and derivatives can potentially be generated in culture by genetic manipulation (Han et al., 1994) and/or by altering growth conditions (Ketchum et al., 1999; Ma et al., 1994).

As biological methods comprise the only viable means of taxoid production, it is increasingly important to understand the pathway and enzymatic reactions involved in Taxol biosynthesis, since manipulation of the slow steps can provide the means for improved production of taxoids. The biosynthesis of Taxol, following diversion of primary plant metabolism, requires a dozen steps; the improved flux through slow steps by overexpression of the corresponding genes in transgenic cells would be expected to raise the production titers of these medicinally useful taxane diterpenoids to commercially significant levels. Genetic manipulation of transcription factors for the global up-regulation of the pathway, and improved efficiency of the intracellular metabolite trafficking and extracellular secretion machinery, can also be anticipated to improve production yields and the ease of drug isolation from the medium.

Over the past 5 years, major advances have been made in the identification of genes responsible for Taxol biosynthesis, a process requiring an estimated dozen enzymatic reactions involving the construction of the tetracyclic skeleton and the addition of the various oxygen and acyl functional groupings (Fig. 1). Presently, five cDNAs encoding pathway enzymes have been isolated from a *Taxus* cDNA library and functionally expressed from an appropriate vector in bacteria or yeast as host. The properties of the cDNA clones and the catalytic function of the corresponding recombinant enzymes are summarized; these include the first committed pathway enzyme, taxadiene synthase, which constructs the taxane skeleton, a cytochrome P450 taxane hydroxylase and three taxoid *O*-acyltransferases. Also, since the provision of geranylgeranyl diphosphate as the taxoid precursor is necessary, the *Taxus* geranylgeranyl diphosphate synthase is described, as are several important enzymatic steps for which the corresponding genes have not yet been isolated.

2. Geranylgeranyl diphosphate synthase: provision of the essential precursor

The tricyclic carbon skeleton of Taxol is derived by cyclizaton of the universal diterpenoid precursor (*E*,*E*,*E*)-geranylgeranyl diphosphate (GGPP; Fig. 1); the heterocyclic oxetane ring (D-ring) is formed later by a separate

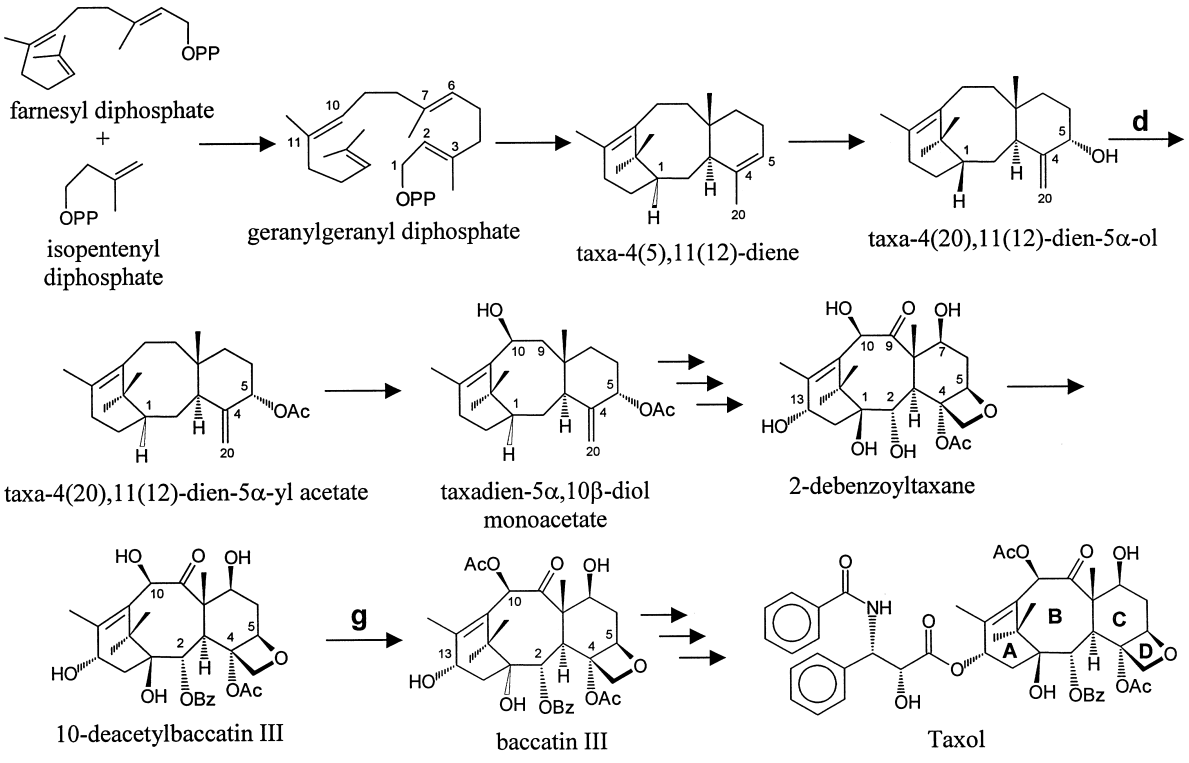

Fig. 1. Outline of early steps of the Taxol biosynthetic pathway. (a) The coupling of isopentenyl diphosphate and farnesyl diphosphate to geranylgeranyl diphosphate by geranylgeranyl diphosphate synthase, (b) the cyclization of geranylgeranyl diphosphate to taxadiene by taxadiene synthase, (c) the hydroxylation to taxadien-5α-ol by cytochrome P450 taxadiene 5α-hydroxylase, (d) the acetylation of taxadien-5α-ol by taxa-4(20),11(12)-dien-5α-ol-*O*-acetyltransferase, (e) the hydroxylation of taxadien-5α-yl acetate by cytochrome P450 taxane 10β-hydroxylase, (f) the benzoylation of a 2-*O*-debenzoyl taxane by a taxane 2α-*O*-benzoyltransferase, (g) and the acetylation of 10-deacetyl baccatin III to baccatin III by a 10-deacetyl baccatin III-10-*O*-acetyltransferase are illustrated. Multiple arrows indicate several as yet undefined steps.

and distinct reaction sequence (Fig. 2). The acyclic precursor is biosynthesized by GGPP synthase, a prenyltransferase that catalyzes the electrophilic coupling of farnesyl diphosphate (FPP) and isopentenyl diphosphate (IPP) as the terminal step (Fig. 1). Genes encoding this prenyltransferase are of considerable interest because the enzyme produces the branch-point progenitor of a variety of diterpenoids and tetraterpenoids (Schultz et al., 1985; Kleinig, 1989; Rilling et al., 1989; Clarke, 1992), several of which are relevant to the process of photosynthesis.

Since Taxol biosynthesis occurs in non-photosynthetic, terminally differentiated stem tissue *in planta*, or in non-photosynthetic, undifferentiated cells in culture, the molecular regulation of GGPP synthase is of interest, particularly in the context of flux control in the formation of this branch point precursor in an instance where high level production to drive essential primary metabolic processes is absent.

Isolation of the gene coding for this prenyltransferase has been achieved and the sequence determined (Hefner et al., 1998). A hybridization probe with significant homology to an angiosperm GGPP synthase yielded a cDNA encoding the GGPP synthase from a *Taxus canadensis* library, and the clone was confirmed by functional expression in yeast. The cDNA has an open reading frame of 1179 nucleotides and encodes a deduced protein of 393 residues (42.6 kDa) containing a presumptive N-terminal transit peptide (Hefner et al., 1998) that likely directs this nuclear gene product to the plastids for proteolytic processing to the mature form (Russell et al., 1993). The presence of a plastid-specific targeting sequence in GGPP synthase (and taxadiene synthase as described later) is consistent with the observation that diterpenes, monoterpenes and tetraterpenes, as well as their corresponding precursor prenyl diphosphates, are biosynthesized in plastids (McCaskill and Croteau, 1999a,b; Turner et al., 1999). The encoded GGPP synthase protein shares significant amino acid identity (62–75%) with other GGPP synthases of plant origin and with the large subunit of the heterodimeric geranyl diphosphate synthase from mint (Burke et al., 1999). RNA blot analysis showed that the steady state mRNA levels for GGPP synthase in methyl jasmonate-induced *Taxus* cells were discernibly higher than in non-induced control cells (Hefner et al., 1998) suggesting that methyl jasmonate modulates the production of this synthase at least at the level of transcription.

3. Taxadiene synthase: the first committed enzyme of Taxol biosynthesis

Taxadiene synthase, another plastidial enzyme, catalyzes the cyclization of geranylgeranyl diphosphate to taxa-4(5),11(12)-diene (Koepp et al., 1995), and, in constructing the unique taxane skeleton, constitutes the committed step in the biosynthesis of Taxol and related taxoids (Fig. 1). Taxadiene synthase activity was first observed in cell-free extracts of *Taxus brevifolia* stems, and the enzyme was purified by a series of traditional chromatographic steps (Hezari et al., 1995). The native, operationally soluble enzyme is monomeric (~79 kDa), exhibits a pH optimum at 8.5, a requirement for a divalent metal ion (Mg^{2+} preferred), and a K_m value of 3 μM for the prenyl substrate (Hezari et al., 1995). A homology-based PCR cloning strategy, based on conserved sequence elements of terpenoid synthases from angiosperms, was applied to acquire a hybridization probe for this gymnosperm cyclase. The subsequent screen of a cDNA library from *T. brevifolia* stems (initially employed as the PCR template) yielded a full-length clone that was functionally expressed in *E. coli* (Wildung and Croteau, 1996). The cDNA sequence specifies an open reading frame of 2586 nucleotides, and the deduced full-length preprotein (862 residues, ~98.3 kDa) includes a long N-terminal targeting sequence for localization to and processing in the plastids, and the typical terpene synthase DDXXD divalent metal ion-substrate complex binding motif (Wildung and Croteau, 1996; Davis and Croteau, 2000). Comparison of the translated taxadiene synthase sequence to other terpene synthase sequences shows significant homology to abietadiene synthase (46% identity, 67% similarity) from grand fir (Wildung and Croteau, 1996).

The protein has been heterologously overexpressed as a thioredoxin fusion which resembles the native enzyme in general properties (Huang et al., 1998); however, a pseudomature form of taxadiene synthase having 60 amino acids deleted from the N-terminus of the preprotein was found to be superior with respect to the level of expression, ease of purification, solubility, sta-

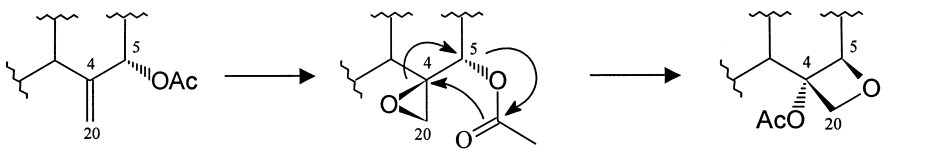

Fig. 2. Postulated biosynthetic scheme for the formation of the oxetane D-ring of Taxol and related late-stage taxoids, in which the 5α-acetoxy-4(20)-ene functional grouping is converted by epoxidation to the 5α-acetoxy-4β(20)-oxirane followed by intramolecular rearrangement to the 4α-acetoxy oxetane moiety.

bility, and catalytic efficiency with kinetics comparable to the native enzyme (Williams et al., 2000b). During the course of the N-terminal truncation studies, it was found that, in addition to the major product, taxa-4(5),11(12)-diene (94%), this synthase (both native and recombinant) produces a small amount of taxadiene isomers (~6%; Williams et al., 2000b). The stereochemistry of the taxadiene synthase reaction has been defined, and the enzyme shown to mediate a unique intramolecular hydrogen migration in the B/C-ring closure step of the catalytic cycle (Williams et al., 2000a).

4. Hydroxylation of the taxadiene nucleus by cytochrome P450 oxygenases

The oxygenation patterns of the various taxoid intermediates found in *Taxus* are established by hydroxylations of the taxane skeleton which have been shown directly to be mediated by cytochrome P450 monooxygenases (Hezari and Croteau, 1997). This conclusion is independently supported by $^{18}O_2$-feeding studies and NMR-based survey of oxygen labeling in taxayunnanine C (a taxadien-2α,5α,10β,14β-tetraol derivative) isolated from *Taxus yunnanesis* cell cultures (Eisenreich et al., 1998).

4.1. Taxadiene 5α-hydroxylase

Taxol biosynthesis from taxa-4(5),11(12)-diene continues with the oxidative modifications of this progenitor olefin. The first of these oxygenations constitutes the second specific step of Taxol biosynthesis and leads to the formation of taxa-4(20),11(12)-dien-5α-ol, which has been identified as a metabolite in *Taxus* cell cultures and confirmed as a pathway intermediate (Hefner et al., 1996). The responsible enzyme has been established as a *Taxus* microsomal cytochrome P450 mixed-function monooxygenase (Hefner et al., 1996); however, a cDNA encoding this regiospecific heme-thiolate protein has not yet been isolated. This unusual P450 catalyzes not only the regio- and stereospecific insertion of oxygen at C5α of the taxane nucleus but also the migration of the 4(5)-double bond to the 4(20)-position, a characteristic structural feature of many intermediate taxoids.

The order of subsequent oxygenations can be formulated based on consideration of the relative abundances of oxygen functional groupings present at the various carbons of the taxane ring of the now over 350 identified naturally occurring taxoids (Baloglu and Kingston, 1999). Based on such frequency of occurrence in defined taxane metabolites, the suggested order of oxygenation (after C5) is C10, followed by C2 and C9 (sequence uncertain), then C13, while oxygenations at C1 and C7 are considered to occur late in the biosynthetic pathway (Floss and Mocek, 1995; Walker and Croteau, 1999).

4.2. Taxane 10β-hydroxylase

By comparing transcripts from elicited (methyl jasmonate) and nonelicited *Taxus* cells, a set of related full-length cytochrome P450 cDNA clones was obtained by a differential display of mRNA-reverse transcription-PCR method, followed by traditional library screening. Selected clones, based on homology to other plant cytochrome P450s, were used to individually transform yeast (*Saccharomyces cerevisiae*) and the transformants were screened for oxygenase function with a series of taxoid substrates. One such clone yielded a functional enzyme that catalyzed the conversion of taxadien-5α-yl acetate to a single product which was subsequently identified as 10β-hydroxy taxadien-5α-yl acetate by combined radio-HPLC, GC-MS and 2D-NMR methods. The cDNA encoding the taxane 10β-hydroxylase has an open reading frame of 1494 base pairs corresponding to a deduced protein of 498 residues with a calculated molecular weight of 56,690, and the sequence bears all of the structural motifs anticipated for a cytochrome P450 monooxygenase (Schoendorf et al., 2001). The recombinant protein produces the same taxadien-5α,10β-diol monoacetate as the native, microsomal cytochrome P450 from *Taxus* cells (Lovy-Wheeler et al., 2001). Preliminary specificity studies with the recombinant enzyme (such experiments are not possible with the native microsomal enzyme because of the presence of competing cytochrome P450s) indicate this hydroxylase to be highly regio- and stereospecific.

5. Acylation of the taxane nucleus by CoA-dependent acyltransferases

When compared to taxadienol, taxadienyl acetate is a more efficient substrate for subsequent cytochrome P450-mediated hydroxylations by *Taxus* microsomes from cell cultures (Hezari and Croteau, 1997), and the acetate ester yields more highly functionalized products (Lovy-Wheeler et al., 2001). Therefore, taxa-4(5),11(12)-dien-5α-yl acetate likely represents the third specific intermediate in the Taxol biosynthetic pathway (Fig. 1). Taxanes bearing this 5α-acetoxy-4(20)-ene functional grouping are also considered to be the immediate precursors (via the 5α-acetoxy-4(20)-epoxy intermediate) of the late-stage 4α-acetoxy-4β,5β-oxetane compounds, including Taxol (Fig. 2).

5.1. Taxadien-5α-ol-*O*-acetyltransferase

Acetyl CoA:taxadien-5α-ol-*O*-acetyltransferase activity was readily demonstrated in soluble enzyme extracts of induced *Taxus* cells (Walker et al., 1999). Purification of this enzyme and internal microsequencing led to a reverse genetic approach for isolating a full-length cDNA

encoding taxa-4(20),11(12)-dien-5α-ol-*O*-acetyltransferase from an induced *Taxus* cell cDNA library (Walker et al., 2000). Expression of this clone in *E. coli* yielded a functional enzyme as determined by radiochemical assay and combined gas chromatographic-mass spectrometric verification of the acetylated product derived from taxadienol and acetyl coenzyme A as co-substrates. The open reading frame of 1317 nucleotides corresponds to a deduced amino acid sequence of 439 residues (Walker et al., 2000). Consistent with the size of the operationally soluble native enzyme (Walker et al., 1999), the DNA appears to encode a monomeric protein of molecular weight 49,079 that bears no N-terminal organellar targeting information (Walker et al., 2000). The recombinant and native enzymes exhibit a pH optimum at 9.0 and K_m values for co-substrates of 4.2 μM and 5.5 μM for taxadienol and acetyl CoA, respectively (Walker et al., 1999; Walker et al., 2000), and both enzymes were incapable of *O*-acetylating the advanced Taxol precursor 10-deacetylbaccatin III (possessing free hydroxyls at C1, C7, C10 and C13), suggesting that the 5α-acetyltransferase is highly specific towards the C5 hydroxyl position (Walker et al., 1999).

5.2. 10-Deacetylbaccatin III-10β-O-acetyltransferase

In addition to the first acetylation at the C5 hydroxyl of the taxane nucleus, the Taxol pathway involves another transacetylation reaction at the C10 hydroxyl of 10-deacetylbaccatin III (a late-stage Taxol pathway intermediate). A full-length cDNA clone for 10-deacetylbaccatin III-10β-*O*-acetyltransferase, which catalyzes formation of the last diterpene intermediate, baccatin III, on the Taxol biosynthetic pathway (Fig. 1), has been isolated from *Taxus cuspidata* (Walker and Croteau, 2000a). Thus, a homology-based PCR cloning strategy was employed to amplify a probe that ultimately identified a full-length putative 10-deacetylbaccatin III-10β-*O*-acetyltransferase by library screening. The gene was expressed in *E. coli* to afford the functional enzyme, as determined by ^{1}H NMR and MS verification of the product, baccatin III, derived from 10-deacetylbaccatin III and acetyl coenzyme-A as co-substrates. The full-length cDNA has an open reading frame of 1320 base pairs corresponding to a deduced protein of 440 residues with a calculated molecular weight of 49,052, consistent with the size of the operationally soluble, monomeric native acetyltransferase demonstrated in *Taxus* cell extracts (Walker and Croteau, 2000a). The recombinant acetyltransferase has a pH optimum at 7.5, K_m values of 10 and 8 μM for 10-deacetylbaccatin III and acetyl coenzyme A, respectively, and is seemingly regiospecific towards the 10β-hydroxyl group of the taxane ring (Walker and Croteau, 2000a).

5.3. Taxane 2α-O-benzoyltransferase

The homology-based PCR cloning strategy employed to isolate the 10-deacetylbaccatin III-10β-*O*-acetyltransferase gene from the methyl jasmonate-induced *Taxus* cell library provided a set of related full-length cDNA clones, one of which encoded a taxane 2α-*O*-benzoyltransferase (Walker and Croteau, 2000b). Expression of this aroyltransferase in *E. coli* yielded a recombinant enzyme that catalyzed the conversion of 2-debenzoyl-7,13-diacetylbaccatin III, a semisynthetic substrate, to 7,13-diacetylbaccatin III. Thus, this transferase appears to function at a late-stage acylation step of the Taxol biosynthetic pathway. The functionally expressed benzoyltransferase was confirmed by radio-HPLC, ^{1}H-NMR and combined HPLC-MS verification of the product, 7,13-diacetylbaccatin III, derived from 2-debenzoyl-7,13-diacetylbaccatin III and benzoyl CoA as cosubstrates in the corresponding cell-free extract of the transformed bacteria. The full-length cDNA has an open reading frame of 1320 base pairs and encodes a deduced protein of 440 residues with a calculated molecular weight of 50,089. The recombinant benzoyltransferase has a pH optimum of 8.0, K_m values of 0.64 and 0.30 mM for 2-debenzoyl-7,13-diacetylbaccatin III and benzoyl coenzyme A, respectively, and is apparently regiospecific for acylation of the 2α-hydroxyl group of the functionalized taxane nucleus. Kinetic evaluation of the selectivity of the aroyltransferase revealed that acetyl-CoA is a significantly less efficient donor than benzoyl-CoA at saturation (Walker and Croteau, 2000b).

The three acyltransferases described contain a highly conserved HXXXDG sequence motif found in other transacylases. Site-directed mutagenesis and chemical modification studies have shown that the histidine residue of this element is essential for catalytic activity of these enzymes, and it has been suggested that the histidine may function as a general base in catalyzing the transfer of the acyl group from acyl/aroyl-CoA to the alcohol substrate (Carbini and Hersh, 1993; Brown et al., 1994).

6. Conclusion

Of the dozen genes involved specifically in Taxol biosynthesis, those encoding taxadiene synthase, taxadien-5α-ol-*O*-acetyltransferase, cytochrome P450 taxadienyl acetate 10β-hydroxylase, 10-deacetylbaccatin III-10β-*O*-acetyltransferase, and taxane 2α-*O*-benzoyltransferase have been isolated, expressed, and characterized. The remaining pathway genes include at least seven additional hydroxylases for oxygenation of the taxane ring (at C1, C2, C5, C7, C9 and C13) and of the phenylpropanoid side chain, an oxidase for the formation of the C9 carbonyl function, the C13-*O*-phenylisoserinyl acyl-

transferase, and the side chain *N*-benzoyltransferase, as well as those genes responsible for the catalysts that construct the oxetane D-ring of Taxol. With the corresponding enzymes demonstrated and assays developed, the contribution of each step to pathway flux can be assessed by in vivo and in vitro studies, the slow steps identified, and suitable strategies devised to isolate and overexpress the corresponding genes in bioengineered *Taxus* cell cultures for improved production titers of Taxol. With the pathway(s) to Taxol defined and the corresponding genes made available, it should also be possible to suppress, by sense or antisense technologies, undesirable side-routes and metabolic dead-ends, or to direct the pathway toward other intermediates or, potentially, new taxoid derivatives.

Acknowledgements

We thank Joyce Tamura for preparation of the manuscript. The work by the authors was supported by Grant CA-55254 from the National Institutes of Health, Cytoclonal Pharmaceutics, and McIntire-Stennis Project 0967 from the Washington State University Agricultural Research Center.

References

Baloglu, E., Kingston, D.G.I., 1999. The taxane diterpenoids. J. Nat. Prod. 62, 1448–1472.

Brown, N.F., Anderson, R.C., Caplan, S.L., Foster, D.W., McGarry, J.D., 1994. Catalytically important domains of rat carnitine palmitoyltransferase II as determined by site-directed mutagenesis and chemical modification. Evidence for a critical histidine residue. J. Biol. Chem. 269, 19157–19162.

Burke, C.C., Wildung, M.R., Croteau, R., 1999. Geranyl diphosphate synthase: cloning, expression, and characterization of this prenyltransferase as a heterodimer. Proc. Natl. Acad. Sci., USA 96, 13062–13067.

Carbini, L.A., Hersh, L.B., 1993. Functional analysis of conserved histidines in choline acetyltransferase by site-directed mutagenesis. J. Neurochem. 61, 247–253.

Clarke, S., 1992. Protein isoprenylation and methylation at carboxyl-terminal cysteine residues. Ann. Rev. Biochem. 61, 355–386.

Commerçon, A., Bourzat, J.D., Didier, E., Lavelle, F., 1995. Practical semisynthesis and antimitotic activity of docetaxel and side-chain analogs. ACS Symp. Ser. 583, 233–246.

Davis, E.M., Croteau, R., 2000. Cyclization enzymes in the biosynthesis of monoterpenes, sequiterpenes, and diterpenes. In: Vederas, J.C., Leeper, F.J. (Eds.), Biosynthesis: Aromatic Polyketides, Isoprenoids, Alkaloids, Vol. 209. Springer-Verlag, Berlin, pp. 53–95.

Eisenreich, W., Menhard, B., Lee, M.S., Zenk, M.H., Bacher, A., 1998. Multiple oxygenase reactions in the biosynthesis of taxoids. J. Am. Chem. Soc. 120, 9694–9695.

Floss, H.G., Mocek, U., 1995. Biosynthesis of Taxol. In: Suffness, M. (Ed.), Taxol: Science and Applications. CRC Press, Boca Raton, FL, pp. 191–208.

Furmanowa, M., Syklowska-Baranek, K., 2000. Hairy root cultures of *Taxus*×*media* var. Hicksii Rehd. as a new source of paclitaxel and 10-deacetylbaccatin III. Biotechnol. Lett. 22, 683–686.

Georg, G.I., Ali, S., Zygmut, J., Jayasinghe, L.R., 1994. Taxol: a novel antitumor agent. Exp. Opin. Ther. Patents 4, 109–120.

Guénard, D., Guéritte-Voegelein, F., Potier, P., 1993. Taxol and Taxotere: discovery, chemistry, and structure–activity relationships. Acc. Chem. Res. 26, 160–167.

Han, K.-H., Fleming, P., Walker, K., Loper, M., Chilton, W.S., Mocek, U., Gordon, M.P., Floss, H.G., 1994. Genetic transformation of mature *Taxus*: an approach to genetically control the in vitro production of the anticancer drug, Taxol. Plant Science 95, 187–196.

Hefner, J., Ketchum, R.E.B., Croteau, R., 1998. Cloning and functional expression of a cDNA encoding geranylgeranyl diphosphate synthase from *Taxus canadensis* and assessment of the role of this prenyltransferase in cells induced for Taxol production. Arch. Biochem. Biophys. 360, 62–74.

Hefner, J., Rubenstein, S.M., Ketchum, R.E.B., Gibson, D.M., Williams, R.M., Croteau, R., 1996. Cytochrome P450-catalyzed hydroxylation of taxa-4(5),11(12)-diene to taxa-4(20),11(12)-dien-5α-ol: the first oxygenation step in Taxol biosynthesis. Chem. Biol. 3, 479–489.

Herdeg, C., Oberhoff, M., Baumbach, A., Blattner, A., Axel, D., Schroder, S., Heinle, H., Karsch, K., 1969. Local paclitaxel delivery for the prevention of restenosis: biological effects and efficacy in vivo. J. Am. Coll. Cardiol. 35–1976, 2000.

Hezari, M., Croteau, R., 1997. Taxol biosynthesis: an update. Planta Med. 63, 291–295.

Hezari, M., Lewis, N.G., Croteau, R., 1995. Purification and characterization of taxa-4(5),11(12)-diene synthase from Pacific yew (*Taxus brevifolia*) that catalyzes the first committed step of Taxol biosynthesis. Arch. Biochem. Biophys. 322, 437–444.

Holton, R.A., Biediger, R.J., Boatman, P.D., 1995a. Semisynthesis of Taxol and Taxotere. In: Suffness, M. (Ed.), Taxol: Science and Applications. CRC Press, Boca Raton, FL, pp. 97–121.

Holton, R.A., Somoza, C., Kim, H.-B., Liang, F., Biediger, R.J., Boatman, P.D., Shindo, M., Smith, C.C., Kim, S., et al., 1995b. The total synthesis of paclitaxel starting with camphor. ACS Symp. Ser. 583, 288–301.

Huang, K.-X., Huang, Q.-L., Wildung, M.R., Croteau, R., Scott, A.I., 1998. Overproduction, in *Escherichia coli*, of soluble taxadiene synthase, a key enzyme in the Taxol biosynthetic pathway. Protein Express. Purif. 13, 90–96.

Ketchum, R.E.B., Croteau, R., 1998. Recent progress toward an understanding of Taxol biosynthesis in plant cell cultures. In: Ageta, H., Aimi, N., Ebizuka, Y., Fujita, T., Honda, G. (Eds.), Towards Natural Medicine Research in the 21st Century (Proceeding of the International Symposium on Natural Medicines). Elsevier Science, Amsterdam, pp. 339–348.

Ketchum, R.E.B., Gibson, D.M., Croteau, R.B., Shuler, M.L., 1999. The kinetics of taxoid accumulation in cell suspension cultures of *Taxus* following elicitation with methyl jasmonate. Biotechnol. Bioeng. 62, 97–105.

Kim, S.-U., Strobel, G., Ford, E., 1999. Screening of Taxol-producing endophytic fungi from *Ginkgo biloba* and *Taxus cuspidata* in Korea. Agric. Chem. Biotechnol. 42, 97–99.

Kingston, D.G.I., Molinero, A.A., Rimoldi, J.M., 1993. The Taxane Diterpenoids. Springer-Verlag, New York.

Kleinig, H., 1989. The role of plastids in isoprenoid biosynthesis. Annu. Rev. Plant Physiol. Plant Mol. Biol. 40, 39–59.

Koepp, A.E., Hezari, M., Zajicek, J., Vogel, B.S., LaFever, R.E., Lewis, N.G., Croteau, R., 1995. Cyclization of geranylgeranyl diphosphate to taxa-4(5),11(12)-diene is the committed step of Taxol biosynthesis in Pacific yew. J. Biol. Chem. 270, 8686.

Lovy-Wheeler, A., Long, R.M., Ketchum, R.E.B., Rithner, C., Williams, R.M., Croteau, R., 2001. Taxol biosynthesis: differential transformations of taxadien-5α-ol and its acetate ester by cytochrome P450 hydroxylases from *Taxus* suspension cells. Arch. Biochem. Biophys. (in press).

Ma, W., Park, G.L., Gomez, G.A., Nieder, M.H., Adams, T.L., Aynsley, J.S., Sahai, O.P., Smith, R.J., Stahlhut, R.W., Hylands,

P.J., 1994. New bioactive taxoids from cell cultures of *Taxus baccata*. J. Nat. Prod. 57, 116–122.

McCaskill, D., Croteau, R., 1999a. Isopentenyl diphosphate is the terminal product of the deoxyxylulose-5-phosphate pathway for terpenoid biosynthesis in plants. Tetrahedron Lett. 40, 653–656.

McCaskill, D., Croteau, R., 1999b. Strategies for bioengineering the development and metabolism of glandular tissues in plants. Nature Biotechnol 17, 31–36.

Miyake, H., Monia, B., Gleave, M., 2000. Inhibition of progression to androgen-independence by combined adjuvant treatment with antisense bcl-xL and antisense Bcl-2 oligonucleotides plus Taxol after castration in the Shionogi tumor model. Int. J. Cancer 86, 855–862.

Mu, J.H., Bollon, A.P., Sidhu, R.S., 1999. Analysis of β-tubulin cDNAs from Taxol-resistant *Pestalotiopsis microspora* and Taxol-sensitive *Pythium ultimum* and comparison of the Taxol-binding properties of their products. Mol. Gen. Genet. 262, 857–868.

Nicolaou, K.C., Ueno, H., Liu, J.J., Nantermet, P.G., Yang, Z., Renaud, J., Paulvannan, K., Chadha, R., 1995. Total synthesis of Taxol. 4. The final stages and completion of the synthesis. J. Am. Chem. Soc. 117, 653–659.

Reinecke, P., Knopf, C., Schmitz, M., Schneider, E., Gabbert, H., Gerharz, C., 2000. Growth inhibitory effects of paclitaxel on human epithelioid sarcoma *in vitro* — Heterogeneity of response and the multidrug resistance phenotype. Cancer 88, 1614–1622.

Rilling, H.C., Breunger, E., Epstein, W.W., Crain, P.F., 1989. Prenylated proteins: demonstration of a thioether linkage to cysteine of proteins. Science 247, 318–320.

Russell, D.A., DeBoer, D.L., Stark, D.M., Preiss, J., Fromm, M.E., 1993. Plastid targeting of *E. coli* β-glucuronidase and ADP-glucose pyrophosphorylase in maize (*Zea mays* L.) cells. Plant Cell Rep. 13, 24–27.

Schoendorf, A., Rithner, C., Williams, R., Croteau, R., 2001. Molecular cloning of a cytochrome 450 taxane 10b-hydroxylase cDNA from *Taxus* and functional expression in yeast. Proc. Natl. Acad. Sci. USA 97, 1501–1506.

Schultz, G., Soll, J., Fiedler, E., Schulze-Siebert, D., 1985. Synthesis of prenylquinones in chloroplasts. Plant Physiol. 64, 123–129.

Shin, S.-W., Kim, Y.S., Lim, S., 2000. Elicitors for the regulation of baccatin III biosynthesis in plant cell culture system. Yakhak Hoechi 44, 60–65.

Stierle, A., Strobel, G., Stierle, D., 1993. Taxol and taxane production by *Taxomyces andreanae*, an endophytic fungus of Pacific yew. Science 260, 214–216.

Strobel, G.A., Hess, W.M., Ford, E., Sidhu, R.S., Yang, X., 1996. Taxol from fungal endophytes and the issue of biodiversity. J. Ind. Microbiol. Biotechnol. 17, 417–423.

Turner, G., Gershenzon, J., Nielson, E.E., 1999. Limonene synthase, the enzyme responsible for monoterpene biosynthesis in peppermint, is localized to leucoplasts of oil gland secretory cells. Plant Physiol. 120, 879–886.

Walker, K., Croteau, R., 1999. Taxol Biosynthesis: a review of some determinant steps. Recent Adv. Phytochem. 33, 31–50.

Walker, K., Croteau, R., 2000a. Molecular cloning of a 10-deacetylbaccatin III-10-*O*-acetyl transferase cDNA from *Taxus* and functional expression in *Escherichia coli*. Proc. Natl. Acad. Sci. USA 97, 583–587.

Walker, K., Croteau, R., 2000b. Taxol biosynthesis: molecular cloning of a benzoyl-CoA:taxane 2α-*O*-benzoyltransferase cDNA from *Taxus* and functional expression in *Escherichia coli*. Proc. Natl. Acad. Sci. USA 97, 13591–13596.

Walker, K., Ketchum, R.E.B., Hezari, M., Gatfield, D., Golenowski, M., Barthol, A., Croteau, R., 1999. Partial purification and characterization of acetyl coenzyme A:taxa-4(20),11(12)-dien-5α-ol-*O*-acetyl transferase that catalyzes the first acylation step of Taxol biosynthesis. Arch. Biochem. Biophys. 364, 273–279.

Walker, K., Schoendorf, A., Croteau, R., 2000. Molecular cloning of a taxa-4(20),11(12)-dien-5α-ol-*O*-acetyl transferase cDNA from *Taxus* and functional expression in *Escherichia coli*. Arch. Biochem. Biophys. 374, 371–380.

Wildung, M.R., Croteau, R., 1996. A cDNA clone for taxadiene synthase, the diterpene cyclase that catalyzes the committed step of Taxol biosynthesis. J. Biol. Chem. 271, 9201–9204.

Williams, D.C., Carroll, B.J., Jin, Q., Rithner, C.D., Lenger, S.R., Floss, H.G., Coates, R.M., Williams, R.M., Croteau, R., 2000a. Intramolecular proton transfer in the cyclization of geranylgeranyl diphosphate to the taxadiene precursor of Taxol catalyzed by recombinant taxadiene synthase. Chem. Biol. 7, 969–977.

Williams, D.C., Wildung, M.R., Jin, A.Q., Dalal, D., Oliver, J.S., Coates, R.M., Croteau, R., 2000b. Heterologous expression and characterization of a "pseudomature" form of taxadiene synthase involved in paclitaxel (Taxol) biosynthesis and evaluation of a potential intermediate and inhibitors of the multistep diterpene cyclization reaction. Arch. Biochem. Biophys. 379, 137–146.

Yukimune, Y., Hara, Y., Nomura, E., Seto, H., Yoshida, S., 2000. The configuration of methyl jasmonate affects paclitaxel and baccatin III production in *Taxus* cells. Phytochemistry 54, 13–17.

PERGAMON

Phytochemistry 58 (2001) 9–32

PHYTOCHEMISTRY

www.elsevier.com/locate/phytochem

Review

^{18}O Pattern and biosynthesis of natural plant products

Hanns-Ludwig Schmidt *, Roland A. Werner [1], Andreas Roßmann

Technische Universität München, Lehrstuhl für Biologische Chemie, Vöttinger Str. 40, D-85350 Freising-Weihenstephan, Germany

Received 22 September 2000; received in revised form 20 December 2000

Abstract

Oxygen atoms in plant products originate from CO_2, H_2O and O_2, precursors with quite different $\delta^{18}O$ values. Furthermore their incorporation by different reactions implies isotope effects. On this base the resulting non-statistical ^{18}O distributions in natural compounds are discussed. The $\delta^{18}O$ value of cellulose is correlated to that of the leaf water, and the observed ^{18}O enrichment ($\sim +27‰$) is generally attributed to an equilibrium isotope effect between carbonyl groups and water. However, as soluble and heterotrophically synthezised carbohydrates show other correlations, a non-statistical ^{18}O distribution — originating from individual biosynthetic reactions — is postulated for carbohydrates. Similarly, the $\delta^{18}O$ values of organic acids, carbonyl compounds, alcohols and esters indicate water-correlated, but individual ^{18}O abundances (e.g. O from acyl groups $\sim +19\%$ above water), depending upon origin and biosyntheses. Alcoholic groups introduced by monooxygenase reactions, e.g. in sterols and phenols, show $\delta^{18}O$ values near $+5‰$, in agreement with an assumed isotope fractionation factor of $\sim$1.02 on the reaction with atmospheric oxygen ($\delta^{18}O = +23.5‰$). Correspondingly, a "thermodynamically ordered isotope distribution" is only observed for oxygen in some functional groups correlated to an origin from CO_2 and H_2O, not from O_2. The individual isotopic increments of functional groups permit the prediction of global $\delta^{18}O$ values of natural compounds on the basis of their biosynthesis. © 2001 Published by Elsevier Science Ltd.

Keywords: $\delta^{18}O$ Value; ^{18}O Abundance; ^{18}O Pattern; Kinetic isotope effect; Equilibrium isotope effect; Biosynthesis; Mechanism of enzyme catalysed reactions; Natural compounds; Carbohydrates; Phenylpropanes; Isoprenoids; Alkaloids; Acids; Alcohols; Esters; Carbonyl compounds

Contents

1. Introduction 10

2. Results and discussion 11
   2.1. Carbohydrates and related compounds — oxygen atoms from carbon dioxide and/or water 11
   2.2. Aliphatic acids, esters, carbonyl compounds and alcohols — oxygen from water by addition or equilibration 15
   2.3. Aromatic compounds — oxygen functions from O_2 18

3. Concluding remarks 24

4. Experimental 25
   4.1. General experimental procedures 25
   4.2. Origin of purchased natural compounds 26
   4.3. Isolation of natural compounds from various sources 26
      4.3.1. Cellulose from beet leaves and roots 26
      4.3.2. Sugars from fruit juices 27

* Corresponding author. Tel./fax: +49-871-44497.

E-mail address: hlschmidt@nikocity.de (H.-L. Schmidt).

[1] Present address: Max-Planck-Institut für Biogeochemie, Postfach 10 01 64, D-07701 Jena, Germany.

0031-9422/01/$ - see front matter © 2001 Published by Elsevier Science Ltd.
PII: S0031-9422(01)00017-6

4.3.3. Glycerol from milk and wine 27
4.3.4. Lactose from cattle milk 27
4.3.5. Pretreatment of alkaloids 27
4.4. Hydrolysis of aliphatic esters 27
4.5. Estimation of the kinetic ^{18}O isotope effects on the H^+-catalyzed esterification of *n*-hexanol and butyric acid 27
4.5.1. Esterification with excess of n-hexanol 27
4.5.2. Esterification with excess of butyric acid 27
4.5.3. Ester hydrolysis 27
4.5.4. Isotope abundance measurements and calculations 28

Acknowledgements 28

Note added in proof 28

References 29

1. Introduction

Oxygen is a very important bioelement, providing functional groups for most organic compounds, thus essentially contributing to their physical and chemical properties. The element is found in nature as a mixture of three stable isotopes (mean relative natural abundance for ^{16}O: 99.7587 atom%, ^{17}O: 0.0374 atom% and ^{18}O: 0.2039 atom%); ^{17}O is the only oxygen isotope with a nuclear magnetic moment. The biosphere is in permanent contact and oxygen exchange with three virtually infinite inorganic oxygen reservoirs: Atmospheric carbon dioxide ($\delta^{18}O$:[2] +40.3 to +42.5‰, depending on geographical latitude and altitude; Francey and Tans, 1987), ground-water ($\delta^{18}O$: −10 to +2‰, leading to leaf water with −5 to +10‰) and atmospheric oxygen gas ($\delta^{18}O$ = +23.5 to +23.8‰; Kroopnick and Craig, 1972; Horibe et al., 1973). These are the primary sources for the oxygen atoms in any organic material.

Most organic compounds contain only one or a few oxygen atoms with the exception of carbohydrates. The $^{18}O/^{16}O$ ratio of cellulose has been the target of many investigations, in particular since the observation of Libby and Pandolfi (1974) that the $\delta^{18}O$ value of tree rings is correlated to the $\delta^{18}O$ value of the leaf water and thus can be used as a climate indicator (tree ring thermometer). Corresponding measurements unequivocally prove a defined correlation between the $\delta^{18}O$ values of cellulose and leaf water (Epstein et al., 1977; Sternberg et al., 1986; Yakir and DeNiro, 1990); they are compiled and discussed in a recent review by Farquhar et al. (1998) (see also Sternberg, 1989).

The generally accepted ^{18}O enrichment in cellulose of trees relative to the water present during its biosynthesis is +27±4‰ (Sternberg, 1989). As this corresponds numerically to an equilibrium oxygen isotope effect between a carbonyl group and water as measured for acetone (1.027; Sternberg and DeNiro, 1983), it is generally assumed that the $\delta^{18}O$ value of cellulose is an expression of the oxygen isotope equilibration between water and carbonyl groups (DeNiro and Epstein, 1979), which can occur in any position of the molecule during the biosynthesis of carbohydrates. However, because there are examples for cellulose from other plants than trees and also for carbohydrates from animal origin (see later), which do not show this "equilibrium" enrichment, and because the slopes of the most correlation lines for tree cellulose and water do never attain the value 1.0 (Yakir and DeNiro, 1990), we believe that the numerical coincidence of the 27‰ enrichment and the equilibrium isotope effect may be at least partially accidental. Saurer et al. (1997) for instance found evidence that there is a dependence of the cellulose $\delta^{18}O$ value upon plant species and actual metabolic status. Therefore, as already outlined in former contributions (Schmidt et al., 1995; Schmidt and Gleixner, 1998a,b) we think that several effects contribute to the $\delta^{18}O$ value of cellulose, that for example after the first step of the photosynthetic carboxylation reaction, the $\delta^{18}O$ value of carbon dioxide (...+41‰...) is primarily contributing to the $\delta^{18}O$ value of carbohydrates, that the thus attained

[2] $\delta^{18}O[‰]_{V\text{-}SMOW} = \left[\frac{(^{18}O/^{16}O)_{sample}}{(^{18}O/^{16}O)_{V\text{-}SMOW}} - 1\right] \times 1000$

Stable isotope abundances of bioelements are generally expressed as the relative difference of the isotope ratio of a compound to that of an international standard in ‰. This standard for oxygen isotope ratio measurements is: V-SMOW = Vienna Standard Mean Ocean Water with an $^{18}O/^{16}O$ ratio of $(2005.20 \pm 0.45) \times 10^{-6}$, according to international agreement (Gonfiantini et al., 1995). $\delta^{18}O$ values measured by us are normalized according to Coplen (1988). Procedure and problems with oxygen isotope standardization are reported elsewhere (Kornexl et al., 1999a). $\delta^{13}C$ and $\delta^{2}H$ represent the corresponding stable carbon and stable hydrogen isotope ratios with the respective international isotope ratio standards V-PDB and V-SMOW.

primary high enrichment is partially lost later by oxygen isotope exchanges from carbonyl groups. On the other side, reactions implying kinetic isotope effects directly introduce oxygen atoms from H_2O into organic intermediates. From here, we suppose that in carbohydrates a distinct non-statistical ^{18}O pattern like that found in glucose for ^{13}C (Rossmann et al., 1991) and ^{2}H (Zhang et al., 1994a) must exist, with individual relative ^{18}O enrichments and ^{18}O depletions, and that the summation of these individual positional ^{18}O abundances will finally lead to the reported global mean ^{18}O enrichment of $+27\pm4$‰ of the carbohydrate relative to the water from the same source.

While this global $\delta^{18}O$ value of carbohydrates is in line with predictions and theoretical considerations for "thermodynamically ordered positional isotope abundances" (Galimov, 1985), this is not the case with $\delta^{18}O$ values of lignin and other aromatic compounds. Oxygen in these products must originate from O_2, introduced by monooxygenase reactions. Furthermore, the $\delta^{18}O$ value of lignin around $+13.5\pm1.5$‰ (Gray and Thompson, 1977), suggests a kinetic isotope effect on these oxygenase reactions.

Except for carbohydrates, no systematic investigation aiming on the explanation of global and positional $\delta^{18}O$ values of organic, mainly natural compounds has been performed so far. $\delta^{18}O$ Values from various secondary products are available from the literature, however, not always in connection with those of their precursors, mainly water from the same source. We have therefore systematically analysed representatives of the main biosynthetic pathways in higher plants in order to fill the gaps of experimental data not available in the literature for the demonstration of the global correlations of ^{18}O abundances and biosynthetic pathways. Probably due to experimental difficulties and the danger of artifacts implied in degradations methods, so far very few oxygen isotope patterns in organic molecules were available (see, for example, Fronza et al., 1999). We have recently succeeded in measuring ^{17}O patterns of esters by semi-quantitative ^{17}O NMR (Schramm et al., 1998); the data correspond to the ^{18}O pattern obtained by degradation (Werner, 1998; Schmidt et al., 1999).

In the present contribution, we have compiled $\delta^{18}O$ values (and partial ^{18}O patterns) of many types of natural products and of their synthetic counterparts, if available, and we correlate them to the corresponding primary oxygen sources, to (bio)synthetic reactions and possible oxygen isotope exchanges, and to the equilibrium and kinetic isotope effects accompanying these processes. We aim at a general view and explanation of the origin of intermolecular oxygen isotope distributions and intramolecular isotope patterns, and at their prediction as a contribution to the elucidation of biosyntheses and to the discrimination between natural and synthetic organic compounds.

2. Results and discussion

2.1. Carbohydrates and related compounds — oxygen atoms from carbon dioxide and/or water

As already pointed out, the mean global $\delta^{18}O$ value of autotrophically synthesized cellulose is obviously correlated in a defined manner to that of the leaf water present during its biosynthesis (Sternberg et al., 1986; Yakir and DeNiro, 1990). This defined correlation is a

Table 1
$\delta^{18}O$ Values or related indications characterizing isotope abundances of carbohydrates and immediate descendents

Compound and source	$\delta^{18}O[‰]_{V\text{-}SMOW}$ or α[a]	Reference
Cellulose, different trees	$\alpha = 1.027 \pm 0.003$	Sternberg and DeNiro (1983)
Cellulose, beet (*Beta vulgaris*) leaves and roots	$\delta^{18}O = +21.6\pm2$	This work
Soluble sugars, orange (*Citrus sinensis*)	$\delta^{18}O = +34.9\pm3$	Doner et al. (1987)
Soluble sugars, beet (*Beta vulgaris*)	$\delta^{18}O = +27.8\pm3$	Doner et al. (1987)
Soluble sugars, beet (*Beta vulgaris*)	$\delta^{18}O = +24$ to $+25$	Hillaire-Marcel (1986)
Soluble sugars, cane (*Saccharum officinarum*)	$\delta^{18}O = +28$ to $+34$	Hillaire-Marcel (1986)
Soluble sugars, maple (*Acer saccharum*)	$\delta^{18}O = +19$ to $+24$	Hillaire-Marcel (1986)
Soluble sugars, grape (*Vitis vinifera*), apple (*Malus*)	$\alpha = 1.030 \pm 0.015$	After Bricout (1978)
Soluble sugars, water plants	$\alpha = 1.024 \pm 0.028$	After Bricout (1978)
Soluble sugars, orange (*Citrus sinensis*)	$\delta^{18}O = +32\pm1.5$	This work
Soluble sugars, apple (*Malus*)	$\delta^{18}O = +29\pm1.5$	This work
Glycerol (see also Table 3)	$\delta^{18}O = +22$ to $+27$	This work
Glycerol from olive (*Olea europeae*) oil	$\delta^{18}O = +21\pm1.5$	Reniero (pers. commun.)
Quinic acid (*Cinchona ledgeriana*)	$\delta^{18}O = +25.4$[b]	This work
"Furaneol®" from strawberry (*Fragraria*)[c]	$\delta^{18}O = +31\pm1.5$	Hilkert (pers. commun., this work)
"Furaneol®", synthetic[c]	$\delta^{18}O = +8$ to $+12$	Hilkert (pers. commun., this work)

[a] $\alpha = \left(\delta^{18}O_{compound} + 1000\right)/\left(\delta^{18}O_{water} + 1000\right)$.
[b] $\delta^{18}O$ Value predicted from biosynthesis $+25.6$‰; see Section 2.3.
[c] "Furaneol®" = 2,5-dimethyl-4-hydroxy-3(2H)-furanone.

well known fact, irrespective of the question if this is really the expression of a complete intramolecular oxygen isotope randomization, or the result of an overlap of many reactions and isotope effects in the course of the biosynthesis, leading to a non-statistical intramolecular oxygen isotope distribution. According to Table 1 soluble carbohydrates reflect the physiological characteristics of the plant in question and the climate and precipitation of their origin as does cellulose (Table 2), and this is meanwhile routinely used, e.g. for fruit juice geographical origin assignment and/or the proof of its adulteration with sugar from other sources (Houerou et al., 1999). It is furthermore quite obvious that the $\delta^{18}O$ value of immediate descendants of carbohydrates, e.g. glycerol, is dominated by that of the precursor; as outlined later, even for glycerol from fermentations the $\delta^{18}O$ value is more influenced by that of the precursor carbohydrate than by that of the water in contact during the fermentation.

Also very convincing in this context is the $\delta^{18}O$ value of quinic acid, a reduction product of dehydroquinic acid, an early intermediate of the shikimic acid pathway (see Section 2.3). Assuming a mean $\delta^{18}O$ value of +30‰ for three oxygen atoms originating from erythrose-4-phosphate as one of the precursors and the same for one from the phosphoenolpyruvate moiety, and . . . + 19‰. . . for the two from the carboxyl group (see Section 2.2), a mean $\delta^{18}O$ value of +25.6‰ is to be expected, which will, like the $\delta^{18}O$ value of the precursors, individually depend on the $^{18}O/^{16}O$ ratio of the leaf water in question. The $\delta^{18}O$ value found for the sample investigated (Table 1) confirms exactly this expectation.

Another immediate descendant from carbohydrates is "furaneol®". This natural product is a flavour compound from strawberry (*Fragraria*) and pineapple (*Ananas sativus*). Roscher et al. (1997) and Schwab (1998) have shown that it is derived from fructose-1,6-biphosphate by a kind of "Natural Maillard Reaction". In accordance with this

Table 2
Correlation of $\delta^{18}O$ values of carbohydrates to water from the same source under autotroph and heterotroph synthesis conditions

Compound and source	$\delta^{18}O[‰]_{V\text{-}SMOW}$	Reference
Cellulose, germs *Ricinus comm.*	$\delta^{18}O = 0.76\times\delta^{18}O_{H_2O} + 29.0$	Sternberg et al. (1986)
Cellulose, *Daucus car.*, on sucrose	$\delta^{18}O = 0.47\times\delta^{18}O_{H_2O} + 24.6$	Sternberg et al. (1986)
Cellulose, *Lemna gibba*, autotroph	$\delta^{18}O = 0.77\times\delta^{18}O_{H_2O} + 29.3$	Yakir and DeNiro (1990)
Cellulose, *Lemna gibba*, on sucrose	$\delta^{18}O = 0.38\times\delta^{18}O_{H_2O} + 30.4$	Yakir and DeNiro (1990)
Cellulose, potato shoots[a]	$\delta^{18}O = 1.02\times\delta^{18}O_{H_2O} + 30.5$	DeNiro and Cooper (1989)
Starch, potato tubers[a]	$\delta^{18}O = 0.88\times\delta^{18}O_{H_2O} + 33.0$	DeNiro and Cooper (1989)
Soluble sugars, orange	$\delta^{18}O = 0.79\times\delta^{18}O_{H_2O} + 30.7$	Houerou et al. (1999)
Lactose from milk	$\delta^{18}O = 0.59\times\delta^{18}O_{H_2O} + 20.6$	This work

[a] The water in these measurements is the water in the potato tubers; correlation $\delta^{18}O_{Cellulose} = 1.15\times\delta^{18}O_{Starch} - 7.5$.

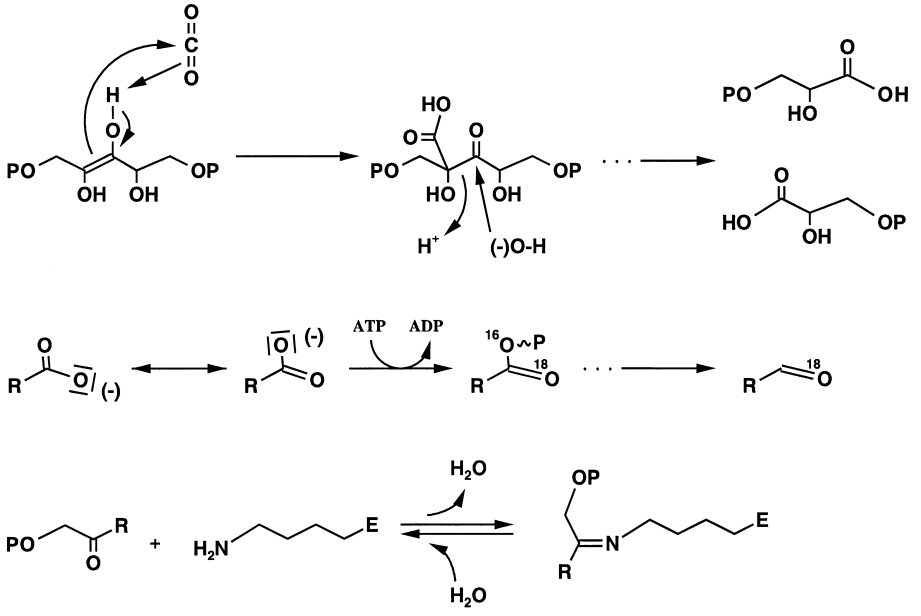

Fig. 1. Mechanisms of some reactions in the Calvin cycle and/or glycolysis involving introduction or elimination of O atoms: oxygen isotope exchange or equilibration of carbonyl groups is not indicated. First row: ribulosebiphosphate-carboxylase reaction; second row: biochemical activation of an acid; third row: binding of fructose-1,6-biphosphate and dihydroxiacetone-phosphate to aldolase (E).

biosynthesis, the $\delta^{18}O$ value found for the natural compound was $+31 \pm 1.5$‰, while that of synthetic counterparts, synthesized from different other precursors (for chemical synthesis reactions see, e.g. Bauer et al., 1990), was near $+10$‰, as expected from their corresponding synthesis reactions (Werner, 1998).

The $\delta^{18}O$ value of these compounds is thus indirectly correlated, probably via their precursors, to that of the water present during their biosynthesis. Systematically, this correlation has been investigated for carbohydrates, mainly cellulose. The numerical correlations reported for the $\delta^{18}O$ value of these compounds to that of the water in contact during their biosynthesis are compiled in Table 2. In most cases the ^{18}O enrichments for autotrophically synthezised cellulose are by $+30$‰ as compared to the water, however, the slopes of the correlation lines are quite different and practically never attain the value 1.0. Very recently, Roden and Ehleringer (1999) even proved that, although the correlation between cellulose and water exists, the oxygen isotope exchange between them can be incomplete. In the case of heterotrophic carbohydrate synthesis, the correlation seems to be even more complex. Therefore, one can assume that, as postulated, the equilibration of carbonyl groups with an isotopic shift of $+27$‰ is not exclusively responsible for the ^{18}O enrichment of the carbohydrates, even though this fits numerically very well with the corresponding isotope effect. A definite proof will only be possible on the base of carbohydrate isotope pattern elucidations and on the study of individual reactions of the carbohydrate metabolism, their mechanisms of oxygen incorporation and the possible isotope effects accompanying these reactions.

One can start from the premise that in plants a real isotope equilibrium certainly exists between water and CO_2. The equilibrium isotope effect for the system CO_2/H_2O provides carbon dioxide enriched in ^{18}O by about 41‰ against the water [O'Neil et al. (1975); see also Brenninkmeijer et al. (1983) and literature cited therein], and this equilibrium is rapidly attained in living systems under the influence of carbonic anhydrase (Silverman, 1982; Farquhar et al., 1998), although recent results indicate that in C_4 monocotyl plants this equilibrium may not always be complete (Gillon and Yakir, 2000). On the other hand, the possible isotopic equilibration of carbonyl groups with water under non-catalyzed conditions and at surrounding temperatures is relatively slow (order of hours; Rittenberg and Graff, 1958; Samuel and Silver, 1965), but can be very fast in the presence of enzymes (Hamilton and Westheimer, 1959; Model et al., 1968; Sternberg et al., 1986). In non enzyme-catalyzed reactions, oxygen isotope exchange occurs most rapidly with aldehydes, followed by ketones and acids, depending on their substituents and reaction conditions applied (Byrn and Calvin, 1966; Wedeking and Hayes, 1983). It is therefore unlikely that a non-catalyzed isotope exchange under the conditions of metabolism (pH 7–8, moderate temperatures, rapid turnover of intermediates) will always lead to a complete isotopic equilibration of any carbonyl group of short-lived intermediates with water. On the other hand, it is very likely that enzymes do not only catalyze such equilibrations but also introduce oxygen atoms directly from water with individual ^{18}O enrichments or depletions, depending on the mechanism and the degree of reversibility of the reaction. This will be discussed for the following reactions involved in the biosynthesis of carbohydrates (Fig. 1): The ribulosebiphosphate–carboxylase reaction proceeds by binding "equilibrated" CO_2 (as explained above) to the enediol intermediate, while a kinetic oxygen isotope effect will accompany the OH^--binding to position C-3. Two molecules of 3-PGA (3-phosphoglyceric acid) will arise, one with high ^{18}O enrichment in both O-atoms of the carboxyl group, the other with a relative ^{18}O depletion on at least one of these two oxygen atoms. The next step is an activation of the carboxyl group.

The oxygen atoms in a dissociated carboxyl group are equivalent, due to a mesomeric dissipation of the negative charge. Therefore, one can assume that a substitution of one of them implies an intramolecular IE (isotope effect); the phosphoglycerate-kinase will probably prefer the "light" oxygen of the carboxylate for the substitution with phosphate (intramolecular IE), and the subsequent reduction of the 1,3-bisphosphoglycerate will eliminate this oxygen atom with the phosphate. Hence the product glyceralphosphate [glycerol aldehyde phosphate (GAP)] will be highly enriched in ^{18}O, independent from the fact that the compound itself implies the possibility of a secondary oxygen isotope exchange with water, depending on its lifetime. In the next step of the Calvin cycle, the triosephosphate–isomerase reaction, there will probably be no oxygen isotope exchange from the diol intermediate, however, both trioses themselves will certainly be submitted to an oxygen isotope exchange in their carbonyl groups, even though probably not attaining an equilibrium under the condition of metabolism.

More dramatic is the oxygen isotope exchange in the subsequent step, the aldolase reaction. Aldolase type I enzymes completely replace the oxygen atom of the keto groups in both directions, because the enzyme–substrate complex is a Schiff base, which is hydrolyzed with water from the medium; it is not known whether this is accompanied by a kinetic isotope effect. However, it is well-known that aldolase catalyzes the oxygen isotope exchange of the substrates with water (Model et al., 1968), and hence the final state of the oxygen isotope introduction by aldolase will depend on the velocities of substrate binding and turnover.

On the base of these processes and other reactions of the Calvin cycle, an oxygen isotope pattern will result in hexoses which will probably be different from ^{18}O equilibrium concentrations for some positions. There is even one oxygen atom which will virtually never be touched by

exchange reactions after its very primary incorporation (either from CO_2 or H_2O), namely that in position C-6 (hexoses) or C-5 (pentoses), because it remains phosphorylated from the beginning. We have already pointed out in our interpretation of the ^{13}C pattern of glucose (Rossmann et al., 1991) that this position is probably the only "isotopically normal" and constant one.

The following observations may serve as an indirect proof for the individual history of the oxygen atoms in certain positions of carbohydrates. As indicated (Fig. 2, Table 2) lactose from cattle milk has a $\delta^{18}O$ value between +15 and +20‰, while that of the water of the milk is −10 to −2‰; slope and enrichment in the corresponding correlation line (0.59 and 20.6‰) are different from that for plant sugars and better corresponding to that for cellulose synthezised under heterotrophic conditions (Table 2). In parallel we found that the ethanol from a yeast fermentation of this lactose is relatively enriched in ^{13}C by 1.4‰ (Versini and Roßmann, unpublished), in contrast to a ^{13}C depletion by 1.7‰ generally observed for ethanol from plant carbohydrates (Roßmann et al., 1996). This finding is in complete agreement with data from Vallet et al. (1998) and from Masud et al. (1999), who found the same ^{13}C enrichment especially for ethanol from animal, mainly ruminant lactose, and in addition a ^{2}H pattern in galactose from animal origin different from that of plant origin, especially for the hydrogen atoms bound to position C-6 (Zhang et al., 1994b). All these results suggest an unusual isotopic pattern for all three elements in lactose (galactose and glucose moiety), different from that of plant carbohydrates, at least in position C-6.

The observations have to be discussed on the base of the biosynthesis of carbohydrates in ruminants (Fig. 3): In these animals glucose and galactose, hence also lactose, are synthesized from propionate, leading via methylmalonate, succinate, fumarate, malate and oxaloacetate to phosphoenolpyruvate and finally to 3-phosphoglycerate (3-PGA). In this sequence, which is probably unidirectional, hence irreversible, two molecules of H_2O are introduced by lyase reactions, namely by the fumarase and by the enolase reaction, respectively. The reverse of both reactions is accompanied by large kinetic ^{18}O isotope effects (Anderson, 1991) and one can postulate the same for the water addition (equilibrium ^{18}O isotope effect at pH 5.5 for the fumarase reaction: 1.033; Blanchard and Cleland, 1980). As the oxygen atom introduced by the enolase reaction is immediately protected from oxygen isotope exchange with water by phosphorylation (phosphoglyceromutase reaction), it remains the same until the final product lactose.

Starting from the observed mean $\delta^{18}O$ value of the water in milk (−6‰) and assuming an in vivo kinetic isotope effect of 1.02 for the enolase reaction, a $\delta^{18}O$ value of −25.5‰ will result in the position C-6 of lactose. If we use the correlation formula for orange sugars as a base for the calculation of the ^{18}O enrichment in the other positions (Table 2: $\delta^{18}O = 0.79 \times -6 + 30.7 = +25.96$), a $\delta^{18}O$ value of +26‰ has to be assumed for these (beginning from 3-phosphoglycerate any other reaction is identical to those in plants), and a global $\delta^{18}O$ value for lactose can be calculated according to $(9 \times 26 - 2 \times 25.5)/11 = +16.6$‰, which is very close to the observed mean one (+17.5‰). This has to be verified by the degradation of lactose.

The reactions in Fig. 3 will probably also be a base for a satisfactory explanation of the unusual deuterium enrichment at the hydrogen atom bound in position C-6 observed as mentioned above, and even for the unusual ^{13}C pattern postulated from the ^{13}C enrichment in the ethanol from lactose fermentation: In the course of the carbohydrate resynthesis from propionate, and probably already during the propionic acid fermentation, symmetrical intermediates (succinic and fumaric acid)

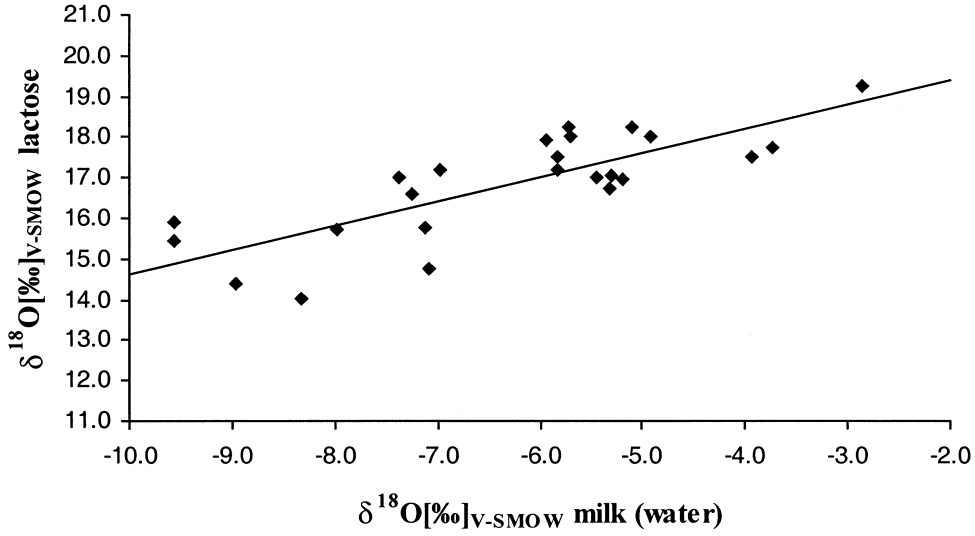

Fig. 2. Correlation between $\delta^{18}O$ values of water and lactose from cattle milk. $\delta^{18}O = 0.59 \times \delta^{18}O_{H_2O} + 20.6$‰, correlation coefficient $r = 0.80$.

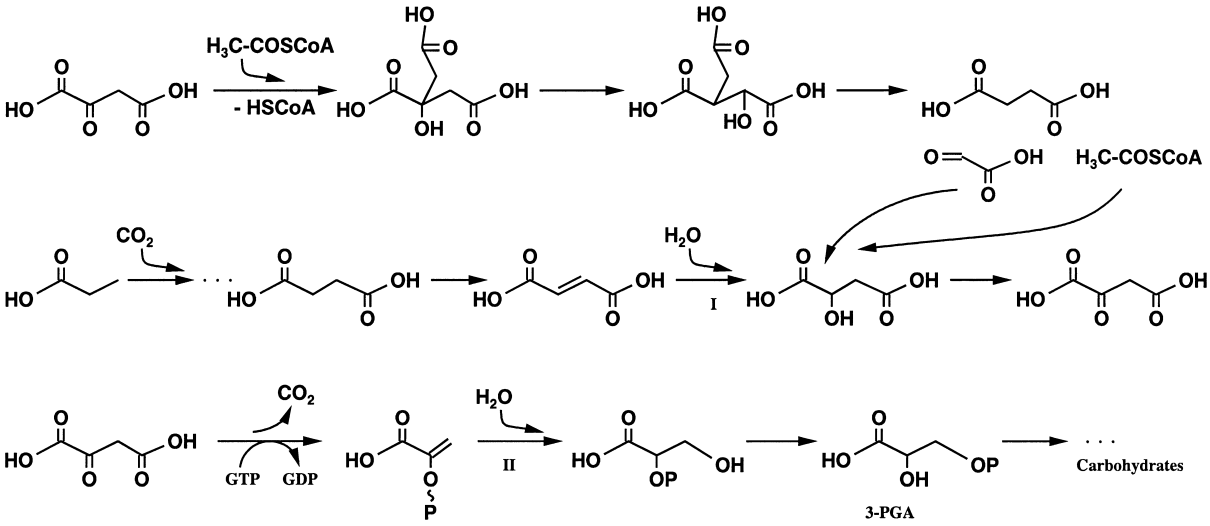

Fig. 3. Synthesis of 3-PGA in ruminants (second and third row) and in germinating oil seeds (first and third row). The O-atom introduced by the fumarase reaction (I) may exchange with water in oxaloacetate, however, the one introduced by the enolase reaction (II) will be preserved until the carbohydrates. The fumarase reaction prefers OH^- binding to ^{13}C.

occur, in which the original positions C-2 and C-3 of pyruvate from the fermented carbohydrates (here positions C-2/C-5 and C-1/C-6) are scrambled; we know from the ^{13}C pattern of malic acid synthezised from fumaric acid under the influence of fumarase that the water addition implies an intramolecular ^{13}C isotope effect leading to a relative ^{13}C enrichment on the C atom with the OH group (Schmidt et al., 2000), the same one which becomes C-1 in ethanol.

One would expect similar results for cellulose from *Ricinus communis* germs grown in the dark (Sternberg et al., 1986), because this cellulose should originate from fats via the glyoxylate pathway and meet that described for propionic acid (Fig. 3); however, its $^{18}O/^{16}O$ ratio was correlated to that of the surrounding water like in photosynthesizing plants (Table 2). Nevertheless, heterotrophic cellulose synthesis (Luo and Sternberg, 1992; Terwilliger and DeNiro, 1995) generally ends in products, which definitely indicate the influence of gluconeogenesis on their $^2H/^1H$ and $^{18}O/^{16}O$ ratio. Investigations on ^{18}O patterns of carbohydrates will allow a deeper insight into this matter.

2.2. Aliphatic acids, esters, carbonyl compounds and alcohols — oxygen from water by addition or equilibration

Carbonyl compounds and organic acids can exchange oxygen atoms with water; the velocity of this reaction is dependent on pH (O'Neal et al., 1983) and temperature. So, Wedeking and Hayes (1983) found for the equilibration of benzoic acid with water a rate constant 1.4×10^{-3} min^{-1} at 80°C and pH 1.0; the equilibration factor was $1.0172 + 0.0009$. Other equilibration factors reported (Rishavy and Cleland, 1999) range from 1.016 (acetaldehyde) to 1.035 (formic acid), indicating an important influence of the substituents of the CO group (cf. also 1.027 for acetone; Sternberg and DeNiro, 1983).

The facts given above suggest that under the conditions prevailing in biological systems, a complete equilibration will not always be attained, especially not with short-lived intermediates. However, this must be completely different, when the CO group is implied in the mechanism of an enzyme catalyzed reaction. So, for example, asparaginase catalysed the rapid oxygen isotope exchange of the carbonamide group in position C-4 of its substrate, while that of the carboxyl group in position C-1 remained completely unaffected (Röhm and Van Etten, 1986). For practical reasons in the present context we will use a mean empirical equilibration factor 1.019 for carboxyl and some carbonyl groups, corresponding to a relative enrichment of these groups to the water in contact of $\geqslant 19‰$ in case of complete equilibration.

In cases where water is an immediate reactant or a participant of the reaction in question, the introduction or elimination of an oxygen atom may be accompanied by a kinetic isotope effect. As outlined before (phosphoglycerate-kinase reaction), the activation of carboxyl groups by ATP/CoASH (coenzyme A) may even lead to a higher ^{18}O enrichment, independent whether or not aldehydes produced from these activated acids may partially exchange oxygen atoms with H_2O molecules before their further reduction to alcohols, depending on their chemical structure and the relative velocity of these competing reactions.

As already pointed out, the $\delta^{18}O$ value of glycerol is correlated to that of water, but on a "higher" level, in that it preserves the oxygen atoms from sugars (Table 3), and this is even true for fermentations; correspondingly, the correlation factor for $\delta^{18}O$ values of glycerol and

Table 3
$\delta^{18}O$ Values of natural and nature identical aliphatic alcohols, carbonyl compounds and (fatty) acids; indication of $\delta^{18}O_{H2O}$ [‰]$_{V\text{-}SMOW}$ when available

Compound and origin	$\delta^{18}O$[‰]$_{V\text{-}SMOW}$	Reference
Glycerol, wine (water 0±2‰) (Central Europe)	+25±2	Roßmann et al. (1998)
Glycerol, plant fats (Central Europe)	+27±2	Roßmann et al. (1998)
Glycerol, animal fats (Central Europe)	+22±4	Roßmann et al. (1998)
Glycerol, hydrolysate olive oil (*Olea europeae*)	+21.5±1.5	Reniero (pers. commun.)
Aliphatic alcohols, olive oil ($n=55$)[a]	+12.9 (+9 to +16)	Reniero (pers. commun.)
Ethanol, yeast ferm. (sucrose +24.8, water +9.1‰)	+16.4	Bricout (1978)
Ethanol, fruit and beet sugar	+18±2	Misselhorn et al. (1983)
Ethanol, flour and cellulose	+20±2	Misselhorn and Grafahrend (1990)
Ethanol, synthetic	+8.1	Dunbar (1982)
Ethanol, synthetic	+3±2	Misselhorn et al. (1983, this work)
Sterols (mainly sitosterol), olive oil ($n=55$)[b]	+5.5±2.4	Reniero (pers. commun.)
Ergosterol, probably yeast	0[c]	This work
L-Menthol, natural	+5.9	Bricout (1978)
Menthone a. isomenthone, unknown	+9.6	Bricout (1978)
Pulegone, natural, unknown	+4.7	Bricout (1978)
Citral, plants	+13.4 to +19.7	Kornexl and Werner (unpublished)
Citral, nature identical	+7 to +16.8	Kornexl and Werner (unpublished)
Citric acid, orange juice, (water −2.1 to +7.8‰)	+18.9 to +25.4	Houerou et al. (1999)
Fatty acids, water plants (water −5.9‰)	+11.7±1.4	Bricout (1978); Bricout (1979)
Fatty acids, water plants (water 0.8‰)	+16.7	Bricout (1978); Bricout (1979)
i-Butanol, natural	+4.5	Schmidt et al. (1998)
i-Butanol, nature-identical	+14.5	Schmidt et al. (1998)

[a] These alcohols were by-products in olive oil indicated in Table 4; they showed local differences in ^{18}O, which were, however not so obviously correlated to the local precipitation water as the whole oil.
[b] As expected for O from O_2 (see Section 2.3), the $\delta^{18}O$ values were absolutely independent from the harvest area and its water characteristics.
[c] Contained approximately 20 mol% (crystal?) water.

water in wine is quite low ($\sigma = 0.68$), and a fermentation in ^{18}O enriched water is accompanied by only 15% oxygen isotope exchange between water and glycerol. The $\delta^{18}O$ value of glycerol from animal fat is lower as compared to that from plant fat. Like already outlined for lactose, the biosynthesis of glycerol in ruminants may be different from that in plants, and this may be responsible for the relatively smaller ^{18}O enrichment of glycerol, at least from ruminant fats. In parallel to the situation with lactose, we have to expect that the relative ^{18}O depletion is probably concentrated to position C-3, however, the experimental proof of this will be a task of future work.

It is in line with the fast irreversible conversion of glucose to ethanol by yeast that also for this product only a partial oxygen isotope equilibration of the intermediates with water takes place, and that ethanol thus preserves a quite high ^{18}O enrichment from the precursor; correspondingly, fermentations in ^{18}O enriched water indicate an only partial oxygen isotope exchange. One can assume that the rate of isotope exchange is the lower the larger is the reduction velocity of acetaldehyde. This is confirmed by the observation that also the $\delta^{2}H$ value of the –CH_2OH–group of ethanol is depending on the fermentation conditions (Vallet et al., 1996). On the other hand the low $\delta^{18}O$ value of synthetic ethanol results from the addition of water to ethylene. Water is also the source of oxygen functions in open chained isoprenoids (citral), introduced by the addition of OH^- to the intermediate carbenium ion.

The primary oxygen source for certain positions of cyclic isoprenoids (menthol, pulegone) is O_2, from where one oxygen atom is introduced into the substrate by hydroxylation (e.g. by limonene-3-hydroxylase; Richter, 1996; see also Fuchs et al., 1999). The resulting $\delta^{18}O$ value is quite low (+5 to +6‰), but may raise because of (partial) secondary oxygen exchange with water at the stage of biosynthetic intermediates with carbonyl groups. This is not possible for the 3-position of sterols, and therefore here the primary, not water-correlated ^{18}O abundance is preserved. The $\delta^{18}O$ value of oxygen atoms introduced by hydroxylations will extensively be discussed in Section 2.3 of this paper in context with aromatic compounds.

A slight ^{18}O enrichment is found in alcohols from olive oil. As they are probably reduction products of fatty acids, their $\delta^{18}O$ values are primarily going back to these precursors, which may be submitted to partial secondary oxygen isotope exchange with water. Citric acid from orange juice is ^{18}O enriched relative to the water between +17.6 and +21‰ in excellent agreement with the expected mean $\delta^{18}O$ value ~+19‰ (see first paragraph of this section). In conclusion, there is an oxygen isotopic correlation between carboxyl/carbonyl groups and water, but it is not as distinctly expressed as between carbohydrates and water, probably due to partially incomplete equilibrations.

The situation must be more complicated with higher fermentation alcohols, some of which are originating from amino acids or intermediates of their biosynthesis (e.g. *i*-butanol and *i*-pentanol; Fig. 4). Their precursors, α-keto acids, can be products of transamination reactions, and their keto group must therefore contain oxygen atoms from water introduced by the hydrolysis of a Schiff-base with pyridoxalphosphate (PLP). As discussed for the aldolase, the corresponding introduction of oxygen atoms from H_2O may imply a kinetic isotope effect (KIE), and the enzyme may even catalyze an oxygen isotope exchange; thus the final degree of equilibration will depend on the relative velocity of substrate binding and transformation. The subsequent oxidative decarboxylation of the α-keto carbonic acid will probably not alter this situation, and therefore the $\delta^{18}O$ value of the aldehydes and alcohols should be close to the level of the surrounding water. Corresponding experiments are in progress in our laboratory.

The logic continues with natural esters (Table 4). Once synthezised, they do no longer exchange oxygen atoms with water under the conditions in biological systems, hence preserve the $\delta^{18}O$ values of their precursors and the isotope fractionations implied by the isotope effects in the course of their formation.

The alcohols from natural esters show $\delta^{18}O$ values as already found and discussed for the corresponding (non equilibrated) free alcohols (+4 to +8‰, Table 3), while the acid moieties, obtained from difference calculations, show very high ^{18}O enrichments. These are probably due to an intramolecular ^{18}O isotope effect on their activation during esterification, as already outlined before (Fig. 4). This may not be the case with fatty acids, because they are directly transfered to CoASH from the

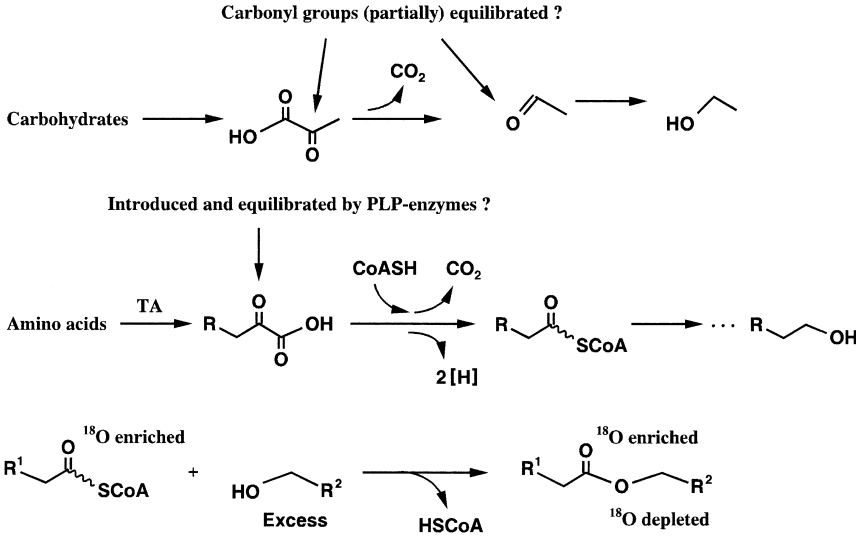

Fig. 4. Oxygen origin in alcohols and esters. In the course of the fast alcoholic fermentation to ethanol, the oxygen atoms from positions C-2 and C-5 may partially be preserved. Oxygen in higher alcohols originating from amino acids, may originate from water. The formation of esters is accompanied by isotope effects. TA = transamination, PLP = pyridoxalphosphate.

Table 4
Global and positional $\delta^{18}O$ values of natural and nature identical esters[a,b]

	$\delta^{18}O$[‰]$_{V\text{-}SMOW}$ Natural			$\delta^{18}O$[‰]$_{V\text{-}SMOW}$ Nature identical			Reference
Compound	Ester	Alcohol	Acid	Ester	Alcohol	Acid	
Isoamylbutyrate	+22.9	+7.7	+38.1	+21.1	+1.9	+41.5	Werner (1998)
Isobutylacetate	+30.5	+6.5	+54.5	+16.3	+5.9	+26.7	Werner (1998)
cis-Hexenylacetate	+34.7	+4.0	+65.4	+0.4	-15.1	+16.1	Werner (1998)
Linalylacetate	+19.5	+8.0	+31.6	+15.6	+9.6	+21.6	Werner (1998)
Triglycerides, apple (water −3.2‰)	+11.3						Bricout (1978)
Triglycerides, citrus (water +4.7‰)	+22.0						Bricout (1978)
Triglycerides (peanut, corn, cotton, cambra, soya)	+10.0 to +16.6						Hillaire-Marcel (1986)
Olive oil (Italy)	+29.4						Hillaire-Marcel (1986)
Olive oil (Mediterranean)	+20.7 to +28.5 [+22 to +28] [+16 to +22]						Angerosa et al. (1999)

[a] After hydrolysis only the $\delta^{18}O$ value of the alcohol has been determined, that of the acid is calculated from the difference to the ester.
[b] Values in parentheses are calculated from mean $\delta^{18}O$ values of glycerol (Table 3).

multienzyme complex of fatty acid biosynthesis. In this context it has to be mentioned that the incorporation of ^{18}O from labelled acetate into fatty acids is less than the 50%, which are to be expected from the loss of one O atom by the activation reaction (Pollard and Ohlrogge, 1999). As a possible reason the authors discuss a kinetic isotope effect on this reaction, although they admit that they are "unaware of its magnitude and direction". We believe that such an isotope effect would more probably lead even to ^{18}O enriched acetyl-CoA and that therefore the observed ^{18}O depletion must be due to an overlap of a partial oxygen isotope exchange of the precursor with water before its activation.

Anyway, the $\delta^{18}O$ values of triglycerides from various plants suggest their ^{18}O enrichment of approximately +17‰ above the plant water. A more reliable indirect calculation can be made for (the triglycerides from) olive oil (Angerosa et al., 1999): Independent of the extreme abundance range of their $\delta^{18}O$ values (+19 to +31‰), the mean $\delta^{18}O$ values for olive oils from the same region are more constant (e.g. Italy $+20.7\pm1.5$‰, Morocco $+28.5\pm1.2$‰) and they correspond to the $\delta^{18}O$ values of the precipitation in these areas (−8.8 to 0‰; Förstel et al., 1975). If we assume from here that the mean $\delta^{18}O$ values of the leaf water are in the range of −2 to +7‰, an ^{18}O enrichment of the triglycerides relative to water of approximately +22‰ results. As the enrichment observed for glycerol is approximately +25‰ (Table 3), the enrichment for the fatty acid moiety must be near +19‰. Again this $\delta^{18}O$ value is as observed for free fatty acids (Table 3) and is as expected (Wedeking and Hayes, 1983). On the base of a $\delta^{18}O$ value range for water in plants between −5 and +8‰ (different organs), a range of +14 to +26‰ has to be assumed for equilibrated fatty acids and their descendants; carbonyl compounds may be more enriched in ^{18}O.

The ^{18}O pattern of synthetic esters (sometimes produced from natural precursors) is similar to that of natural ones. This is in line with the mechanisms and isotope effects on the corresponding synthesis reactions (Fig. 5). For example, the acid-catalyzed esterification of *n*-butyric acid with *n*-hexanol was accompanied by a large intramolecular isotope effect on the oxygen elimination from the carboxyl moiety [$k_{16}/k_{18} = 1.058$] leading to a high ^{18}O enrichment in this moiety, and a kinetic isotope effect on the oxygen atom of the alcohol moiety [$k_{16}/k_{18} = 1.014$] which has for consequence a ^{18}O depletion in the corresponding position (Werner, 1998). The actual $\delta^{18}O$ values were depending on the individual conditions of the esterification, especially on the relative ratio of the reactants used for esterification. Furthermore, it has to be pointed out, that the use of carbonic acid anhydrides for esterification implies additionally a large intramolecular carbon isotope effect, because the preferred transfer of the "light" acyl group results in a remarkable ^{13}C depletion at the CO position of the acyl moiety (Werner, 1998; Schmidt et al., 1999).

Like the enolase and the fumarase reaction, other lyase reactions, isomerisations (e.g. by aconitase) and epimerisations (glucose/galactose) as well as any hydrolase reaction will introduce OH^- from water into their products (Mayer and Larner, 1959), and all of them probably imply kinetic isotope effects. Finally, one has to keep in mind that also most synthase reactions basing on phosphorylations with ATP deal in some way with participation of OH groups of the reactants and water.

2.3. Aromatic compounds — oxygen functions from O_2

It has been known for a long time (Gray and Thompson, 1977) that the $\delta^{18}O$ value of aromatic compounds, mainly lignin, shows an ^{18}O depletion in comparison to primary compounds, such as cellulose, attaining $\delta^{18}O$ values around +12‰. The fundamental structural element of these compounds is the phenylpropane unit, synthesized via the shikimic acid pathway (Haslam, 1993a) from erythrose-4-phosphate and phosphoenolpyruvate (PEP; Fig. 6). Some aromatic compounds are thought to

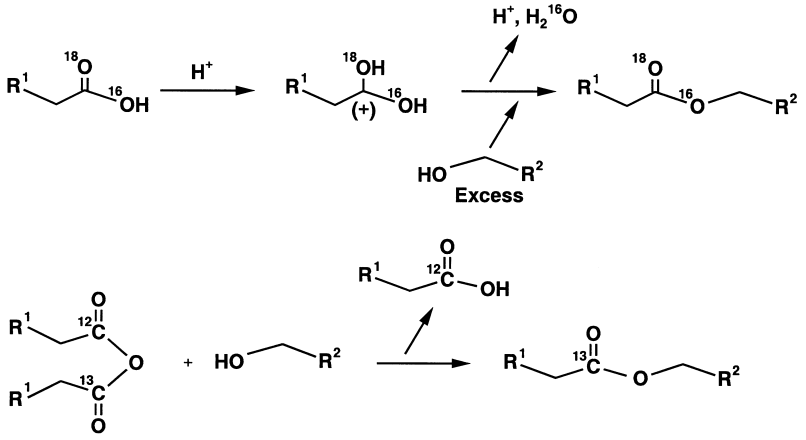

Fig. 5. Intramolecular ^{13}C- and ^{18}O-isotope effects on the acid moiety, and kinetic ^{18}O-isotope effects on the alcoholic component in the course of an acid catalyzed esterification.

be synthezised directly from shikimic acid, which would imply the origin of their phenolic hydroxyl group from this precursor, and therefore a high ^{18}O abundance (corresponding to quinic acid; Table 1). In the synthesis of phenylpropanes by plants the last non-aromatic intermediate is arogenic acid, yielding tyrosine by dehydrogenation, phenylalanine by dehydratation. As plants cannot hydroxylate phenylalanine, here any tyrosine and its descendants, like some alkaloids, preserve the highly ^{18}O enriched oxygen function from erythrose in the *p*-position. Tyrosine can also be converted to *p*-coumaric acid, however, a remarkable tyrosine-ammonia-lyase activity has so far only been observed in *Gramineae* (or *Poacea*, grasses, cereals; Kindl, 1991; Richter, 1996). The predominant pathway in plants to *p*-coumaric acid is the hydroxylation of cinnamic acid, hence by introduction of oxygen from O_2. Correspondingly, most further oxygen bound to the aromatic ring originates from O_2, and is introduced through hydroxylations by monooxygenases, mainly of the P-450-type (Haslam, 1993b; Bolwell et al., 1994; Richter, 1996). Plant dioxygenases (Prescott and John, 1996) introduce both oxygen atoms from O_2 into their substrates; however, very often one of the primarily bound O atoms is rapidly lost as H_2O or transferred to an acceptor, the other one can, after a secondary conversion of the oxygen function to an sp^2 structure, be exchanged with the surrounding water (synthesis of jasmonic acid, initiated by a lipoxygenase). This is also the case for the oxygen atoms introduced in the course of photorespiration (Berry et al., 1978; Cooper and DeNiro, 1989). Dioxygenases are for example involved in the biosynthesis of tropolones and some alkaloids; here they may lead to non-exchangeable oxygen functions, which should, however, in the present context, not much differ from those introduced by P-450-type monooxygenases.

It is very probable that all these reactions imply (kinetic) isotope effects. However, as no corresponding data are available for the oxygenated products, we have to deduce them from measured isotope effects on O_2, obtained in context with the production, reduction and activation of this molecule by biological systems: Molecular oxygen in the atmosphere has a constant $\delta^{18}O$ value of about +23.5‰ and is thus largely enriched relative to sea water [''Dole effect''; Dole (1935); Morita (1935); for a recent review see, e.g. Keeling (1995)]. Already Lane and Dole (1956) showed that an important contribution to this enrichment is due to isotope discriminations by respiration (see also, e.g. Wagener, 1974). While oxygen from the photosynthetic water fission is not ^{18}O enriched, dissolved oxygen in the ocean can be enriched in ^{18}O up to 14‰, and this enrichment is inversely correlated with the O_2 content of the water; this effect is attributed to bacterial respiration processes (Kroopnick and Craig, 1976). It has generally been observed that the photosynthetically evolved O_2 originates from the water in the chloroplasts (Guy et al., 1993; Keeling, 1995). Climate and transpiration may indirectly contribute to a small variation of the absolute $\delta^{18}O$ value via the enrichment of the leaf water (Dongman et al., 1972; Wagener, 1974); so Schleser (1979) observed the formation of O_2 with +4.5‰ from land plants. Stevens et al. (1975)

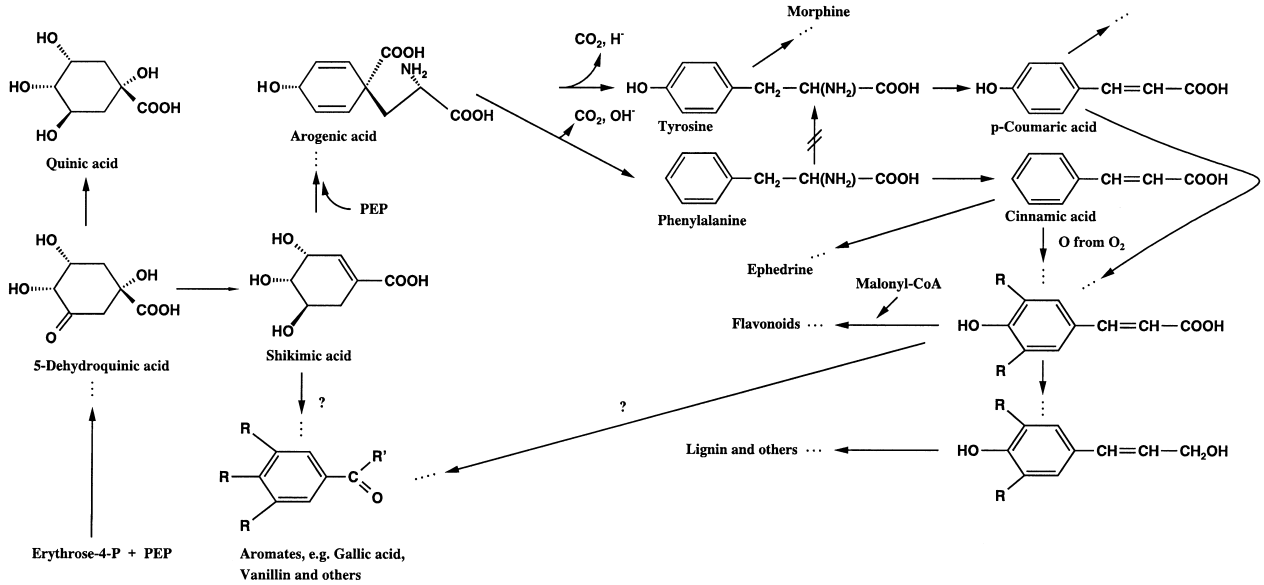

Fig. 6. Oxygen sources in aromatic compounds originating from the shikimic acid pathway. Indication of the different origin of the oxygen atom in *p*-position depending on the dehydrogenation or dehydratation of arogenate, respectively. Correspondingly, the alternative possibilities of the biosynthesis of vanillin are shown. In case of the direct origin of oxygen from shikimic acid the phenolic oxygen in *p*-position would be highly ^{18}O enriched. The synthesis via cinnamic acid implies hydroxylation, hence a $\delta^{18}O$ value near +6‰. The latter pathway is confirmed by the $\delta^{18}O$ values of vanillin (Table 6). PEP = phosphoenolpyruvate, R = –H,–OH or –O–CH_3; R′ = –H or –OH.

showed that photosynthetically produced O_2 by blue-green and green algae has nearly the same $\delta^{18}O$-value as the surrounding water ($\Delta\delta^{18}O$: −0.5‰). A certain contribution to the ^{18}O enrichment of atmospheric O_2 can also be due to photorespiration (Berry et al., 1978; Guy et al., 1987), the kinetic oxygen isotope effect on the ribulosebiphosphate–oxygenase reaction itself being near 1.03 (Kreckl et al., 1989). A further small contribution may also originate from the ''Mehler reaction'', the production of H_2O_2 by O_2 reduction in the case of a lack of another electron acceptor (Kreckl, 1988). However, in total the Dole effect is due to isotope effects on oxidation reactions.

Any electron transfer to O_2 by proteins is preceded by a (reversible?) binding of O_2, which by itself could already imply an equilibrium isotope effect. In Table 5, observed equilibrium and kinetic constants for oxygen binding, reduction and activation are compiled. The following conclusions can be derived from this table: Isotope discriminations are implied in O_2 binding, reduction and activation; the discrimination connected to a hydroxylation seems to depend on the enzyme system involved. So, for example, the isotope effects on the cytochrome oxidase and on spinach mitochondria reactions correspond to that between the binding isotope effect by a porphyrin and a copper protein, respectively, while, on the other hand, the discrimination observed for the Mehler reaction (probably flavoprotein catalyzed) exceeds that calculated for the H_2O_2 formation. In total, all oxygenase and oxidase reactions obviously imply oxygen isotope fractionations; these seem to be partially due to equilibrium isotope effects on the binding of O_2, however, may be overlapped by isotope effects on oxygen activation and transfer. In addition, in living plants, isotope effects on oxygen diffusion processes may contribute to the in-vivo oxygen isotope discrimination (Zanconato et al., 1992; Aggarwal and Dillon, 1998).

Any data reported in Table 5 deal with the ^{18}O enrichment of the non-converted dioxygen. The stoichiometry of a monooxygenase reaction ($R–H + O_2 + NADPH + H^+ \rightarrow R–O–H + H_2O + NADP^+$; Sono et al., 1996) and the isotope balance demand a corresponding ^{18}O depletion in both products, R–O–H and H_2O, independent on the relative influence or contribution of the above mentioned oxygen isotope effects. Assuming in an first approach a statistical transfer of the two oxygen atoms from O_2 to R–O–H and H_2O, respectively, one can postulate, on the base of the data in Table 5, as a mean value of a discrimination factor for the hydroxylation reaction $\alpha = 1.02 \pm 0.003$, where $\alpha = 1023.5/\left(\delta^{18}O_{Prod.} + 1000\right)$. Starting from the infinite O_2 pool with $\delta^{18}O = +23.5‰$, one has to expect $\delta^{18}O$ values for R–O–H between 0 and +7‰; the $\delta^{18}O$ values found for sterols ($+5.5 \pm 2.4‰$, Table 3) confirm very well this expectation. Deviations

Table 5
Oxygen isotope fractionations and discriminations implied in O_2 binding, activation, transfer procedures, and on oxygen reductions by oxidases

Process/reaction with oxygen isotope fractionation	Fractionation indications			References
	α[a]	$^{18}(V/K)$	$^{18}(K)$[b]	
Cytochrome oxidase	1.013			Feldman et al. (1959)
Respiration yeast	1.019			Schleser (1979)
Respiration spinach leaves	1.025			Lane and Dole (1956)
Respiration spinach mitochondria		1.013		Kreckl (1988)
O_2 binding hemerythrine			1.0113 (m)	Tian and Klinman (1993)
O_2 binding hemoglobine			1.0039 (m)	Tian and Klinman (1993)
$O_2 + 4e^- + 4H^+ \Longleftrightarrow 2H_2O$			1.02275 (c)	Tian and Klinman (1993)
Cytochrome oxidase, soybean[c]	1.020			Ribas-Carbo et al. (1997)
$O_2 + 2e^- + 2H^+ \Longleftrightarrow H_2O_2$			1.0089 (c)	Tian and Klinman (1993)
Mehler reaction (H_2O_2 format.)[d]		1.016		Kreckl (1988)
Mitochondrial alternative oxidase[e]	1.025			Sluse and Jarmuszkiewicz (1998)
Mitochondrial alternative oxidase[e]	$\geqslant$1.027			Ribas-Carbo et al. (2000)
RuBP–oxygenase reaction[f]		1.033		Kreckl et al. (1989)
RuBP–oxygenase	1.020			Guy et al. (1987)
Cytochrome P-450 oxygenase, rat		~1.02		Klinman (pers. commun.)
Dopamine-β-monooxyg. reaction		1.02		Klinman et al. (1993)
				Tian et al. (1994)
Bov. ser. amine oxidase reaction		1.0097		Su and Klinman (1998)
Glucose oxidase reaction		1.028		Su and Klinman (1999)

[a] Definitions of fractionation factors α are different in individual papers. The values can therefore not be absolutely compared among each other, but are nevertheless quite valuable for orientation.

[b] Equilibrium constants $^{18}(K)$ from Tian and Klinman (1993) as measured (m) or calculated (c).

[c] Part of discrimination attributed to cytochrome oxidase; α for total mitochondrial discrimination: 1.025–1.030.

[d] Mehler reaction = transfer of photosynthetic reduction equivalents to O_2. For isotope effects on O_2-binding see Rakowski and Paneth (1996).

[e] Discrimination by alternative oxidation of mitochondria without cytochrome oxidase.

[f] The active site of this enzyme is different from those of any other oxygen transferring proteins.

Table 6
$\delta^{18}O$ Values of natural and some (semi)synthetic aromates in dependence on their origin and precursors[a,b]

Compound and origin	Precursors and (bio)synthesis	Source of oxygen atom(s)	$\delta^{18}O[‰]_{V\text{-}SMOW}$		Reference
			Expected	Found	
H_5C_3–C_6H_4–O–CH_3	n.; shikimic acid, cinnamic acid	O_2, enzym. hydroxylation	...+6...	+6 to +8	Bricout (1978);
Anethol, estragol; anis				+11.4	Kornexl and Werner (unpublished)
(*Pimpinella anisum*)	n.i.; synthetic phenol, anisol	diverse	?	+13.4 to +18.5	Kornexl and Werner (unpublished)
H_5C_3–C_6H_3(OH)–O–CH_3	n.; shikimic acid; cinnamic acid	O_2, enzym. hydroxylation	...+6...	+5.0	Bricout (1978)
Eugenol, isoeugenol; (unknown)					
H_5C_3–C_6H_3–(O,O)=CH_2	n.; shikimic acid, cinnamic acid	O_2, enzym. hydroxylation	...+6...	+6.9	This work
Safrole; (unknown)					
C_6H_5–CHO	n.; shikimic acid, phenylalanine	O_2, enzym. hydroxylation	...>+19...	+19.3	Schmidt et al. (1998)
Benzaldehyde; almonds	n.i.; benzalchloride	tap H_2O-exchange	?	+6.8	Schmidt et al. (1998)
(*Prunus amygdalus*)	n.i.; toluene, cat. oxidation	O_2, catalytic activated	?	+14.1	Schmidt et al. (1998)
		all sec. H_2O-exchange			Schmidt et al. (1998)
C_6H_5–CH=CH–CHO	n.; shikimic acid	H_2O-exchange	...>+19...	+14.9	Schmidt et al. (1998)
Cinnamic aldehyde; cinnamon	n.i.; unknown		?	+20.2	Schmidt et al. (1998)
(*Cinnamonum aromaticum*)					
HO–C_6H_4–$(CH_2)_2$–CO–CH_3	n.; shikimic acid, cinnamic acid	O_2, enzym. hydroxyl. and	...+14...	+13.3	Fronza et al. (1999)
Raspberry ketone, *Taxus bacc.*	+ malonyl–CoA	H_2O-exchange	...+14...	+12.4	Fuganti, personal communication
Aeonium lindleyi (Crassulaceae)	n.i.; variable	?	?	+29.9; +9.1	Fronza et al. (1999)
HO–C_6H_4–$(CH_2)_2$–CH(OH)–CH_3	n.; shikimic acid, cinnamic acid	O_2, enzym. hydrolysis and	...+14...	+9.2	Fronza et al. (1999)
Betuligenol; *Taxus bacc.*	+ malonyl-CoA	H_2O-exchange	...+12...	+10 to +12.5	Brenninkmeijer and Mook (1982)
OCH–C_6H_3–(OH)–O–CH_3	n.; shikimic acid, cinnamic acid,	O_2, enzym. hydroxyl. and			
Vanillin; *Vanilla planif.*	side chain degradation	H_2O-exchange		+11.2; +14.7	Dennis et al. (1998)
	n.i.; oxidative degradation	O_2, enzym. hydroxylation,	<+12	+8.2 to +12.5	Koziet (1997); Werner (1998)
	of curcumin, lignin, ferulic acid,	H_2O-exchange		+11.5	Fronza et al. (2001)
	eugenol	oxidant, H_2O		+7.5 to +14.5	Koziet (1997); Werner (1998)
				+9.0 to +15	This work
				+15.9	Schmidt et al. (1999)
				+9.9	Fronza et al. (2001)
	n.i.; *nat.* and *synth.* guajacol	H_2O of diverse $\delta^{18}O$	...0...	−2.8±0.3	Koziet (1997)
	+ glyoxyl. acid			−0.2±1.9	Dennis et al. (1998)
				−2.1 to +8.3[c]	Hilkert (pers. commun.)
				+9.9[c]	Fronza et al. (2001)
Lignin; (unknown)	n.; shikimic acid, cinnamic acid	O_2, enzym. hydroxyl. and	...+10...	+13.5±1.5	Gray and Thompson (1977)
		H_2O (partial) exchange		+7.3	Dunbar and Wilson (1983)
Emodin; *Frangula* roots	acetate (polyketid pathway)	H_2O, via carboxyl group	...+19...	+18.0	This work
Hesperetin (flavonoid); citrus	cumaric acid + 3 acetate	O_2(2) + 4 carboxyl groups	...+19.3...	+21.1	This work
Hesperidin (glycoside); citrus	cumaric acid + 3 acetate + sugar	O_2, carboxyl group, sugar	...+29.3...	+32.7	This work
(hesperetin rutenoside)					

(*continued on next page*)

Table 6 (*continued*)

Compound and origin	Precursors and (bio)synthesis	Source of oxygen atom(s)	$\delta^{18}O$[‰]$_{V\text{-}SMOW}$		Reference
			Expected	Found	
Chlorogenic acid; (unknown)	ester quinic acid + caffeic acid	O_2, carboxyl group, sugar descendant	…+21.7…	+22.5	This work
L-(−)-Ephedrine; *Ephedra spp.*	benzaldeh. from Phe, acetaldeh.	H_2O via carbonyl group	> +26	+33.1	Zimmer (1999)
(−)-Cocaine; *Erythrox. coca*	ornithine, acetoac., benzoic acid	H_2O via carboxyl group	+14…+19	+13.9±0.7	Zimmer (1999)
Papaverine; *Papaver somnif.* (?)	shikimic acid, tyrosine	erythrose, O_2,	+16	+14.7±0.3	This work
Morphine; *Papaver somnif.*	shikimic acid, tyrosine	erythrose, O_2, H_2O	+17	−2.2±1	This work
Caffeine; *Caffea arabica, Camellia sinensis*	glycine, formiate, HCO_3^-	H_2O, HCO_3^-	…0…	−4.3 to +9.9	Dunbar and Wilson (1982)

[a] n. = natural; n.i. = nature identical.
[b] Calculation of most expected $\delta^{18}O$ values are based on the mean $\delta^{18}O$ values for molecule parts or functional groups: phenolic OH = +6‰; carbonyl and carboxyl O = +19‰ above water.
[c] Probably guajacol of natural origin as precursor.

from this $\delta^{18}O$ range may occur from partial incorporation of intrinsic oxygen from photosynthesis with a very low $\delta^{18}O$ value, and from differences in the ^{18}O discrimination by individual enzymes.

In order to arrive at a uniform discussion of the available experimental results, we have assumed a mean $\delta^{18}O$ value of +6‰ for the non-exchanging oxygen functions in aromates originating from O_2. By inclusion of the former outlined $\delta^{18}O$ values of other oxygen containing functional groups, mean $\delta^{18}O$ values of natural compounds can be deduced from the increments (Table 6).

Thus the $\delta^{18}O$ values of anethol, eugenol and safrole, respectively, as representatives for aromatic compounds containing only phenolic oxygen from O_2, fit very well with those expected from the preceding considerations. The same is true for the $\delta^{18}O$ values of natural benzaldehyde and cinnamic aldehyde, representing aromatic compounds with a carbonyl group as oxygen function, provided this is not caused by an artifact in the course of the isolation procedure. The calculated $\delta^{18}O$ value of raspberry ketone as a representative for both groups is identical to that found experimentally by Fronza et al. (1999), while the $\delta^{18}O$ value found for the corresponding alcohol from the same source, betuligenol, is only +9.2‰ (expected $\delta^{18}O$ value +14.0‰). The reductive elimination of the phenolic hydroxyl group leads to 4-phenyl-butanol-(2) with a $\delta^{18}O$ value of +19.2‰ (correct carbonyl $\delta^{18}O$ value !), from where a $\delta^{18}O$ value for the phenolic group of −0.8‰ results. The oxygen isotope pattern of raspberry ketone from lindleyin, a glycoside from a succulent, is quite similar (total $\delta^{18}O$ value +12.4‰, phenolic OH group +0.6‰, from where a $\delta^{18}O$ of +24.2‰ results for the carbonyl group. (Fuganti, personal communication). Thus, the $\delta^{18}O$ value of the OH group of this compound is at the lower edge of the $\delta^{18}O$ range assumed for products of monooxygenase reactions (0 to +7‰). This is not the case with the $\delta^{18}O$ value of the *p*-hydroxyl group of the phenylpropane unit of naringenin, a flavonoid from citrus fruits, which was found to be +12‰ (Fuganti, personal communication); a tentative explanation for this unexpected finding could be that the molecule moiety in question is *partially* originating from tyrosine, thus preserving in part the oxygen atom from shikimic acid (Fig. 6).

Investigations so far available on the biosynthesis of natural vanillin did not permit a decision between two alternative pathways (Funk and Brodelius, 1994; Schmidt and Gleixner, 1998b; Werner, 1998; Fig. 6); the ^{18}O data could help to solve this problem. One of them, the immediate origin from shikimic acid, would imply the preservation of one of the oxygen functions of this precursor in the aromatic nucleus ($\delta^{18}O$ value expected +30‰; see quinic acid, Table 1). This would have for consequence a mean $\delta^{18}O$ value of vanillin of (+30‰ +6‰ +24‰)/3 = +20‰. The experimentally found $\delta^{18}O$ value of approximately +12‰ confirms that the

aldehyde is synthezised via β-oxidation of ferulic acid, which demands a $\delta^{18}O$ value $(2\times6‰ + 24‰)/3 = +12‰$. Recent experimental data of the ^{18}O pattern of natural vanillin (Fronza et al., 2001) showed $\delta^{18}O$ values of $+5.8‰$ for the phenolic oxygen, $+2.7‰$ for the methoxyl oxygen (probably due to the introduction of the second oxygen atom by a copper containing monooxygenase with slightly higher isotope discrimination), and $+26.2‰$ for the carbonyl oxygen (corresponding to an enrichment $> +19‰$), and a mean global $\delta^{18}O$ value $+11.5‰$.

If we apply our theoretical increments to the oxygen atoms from the different functional groups of other aromates (Fig. 7), in most cases a perfect agreement results with their experimental $\delta^{18}O$ values. The somewhat too low $\delta^{18}O$ values as calculated for hesperidin and hesperetin may result from a wrong $\delta^{18}O$ value assumed for citrus water (however, compare discussion above on naringin). In the case of lignin a prediction is quite difficult: The monomers contain 1, 2 or 3 phenolic O–R groups, and one oxygen from the alcoholic function in the side chain, for which at least the mean $\delta^{18}O$ value of $+19‰$ may be assumed. Furthermore, we have to take into account that in the course of the oxidative polymerisation some additional oxygen functions from O_2 are introduced into the polymer. Hence, approximately 2–3 phenolic oxygen atoms will come on one alcoholic one; the resulting $\delta^{18}O$ value $(2.5\times6‰ + 19‰)/3.5 = +9.7‰$ fits quite satisfactorily into the scheme.

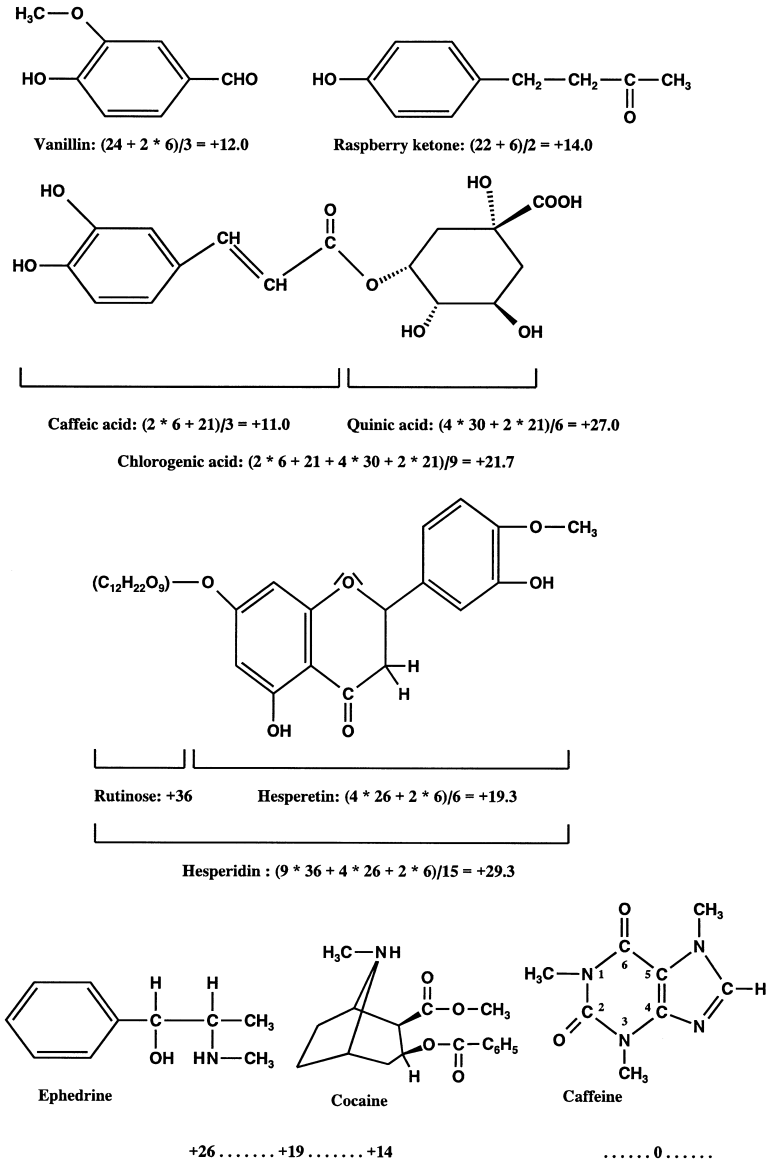

Fig. 7. Structures and calculated global mean $\delta^{18}O$ values of some natural aromatic compounds. The following $\delta^{18}O$ increments are used for calculation of $\delta^{18}O$ values of the different molecule parts (functional groups): Sugars: $+30$ to $+36‰$ (Tables 1 and 2); immediate carbohydrate descendents: $\ldots+30\ldots$ (Table 1); carbonyl and carboxyl groups: $\ldots+19\ldots$, lower limit $+13$, upper limit $+26‰$ above water; phenolic hydroxyl groups from O_2: $\ldots+6\ldots$ (corresponding limits 0 and 7‰).

The $\delta^{18}O$ values of some alkaloids with well-known origin and biosynthesis are included in Table 6. Ephedrine is a sympathicomimetic drug from *Ephedra vulgaris* or *Ephedra distachys*, shrubs growing in dry areas of Asia and America and around the Mediterranean Sea. The main precursor of the alkaloid is phenylalanine (Grue-Sørensen and Spenser, 1988); this is degraded to benzaldehyde, which is then condensed with "active acetaldehyde" to phenylacetylcarbinol. The alcoholic oxygen atom remaining in the side chain at the end of the biosynthesis is originating from the intermediate benzaldehyde; it is obvious that the $\delta^{18}O$ value (+33‰) is due to a large ^{18}O-enrichment of the plant water in an aride climate, simultaneously, it is the expression of an exceptional equilibrium isotope effect. The source of (−)-cocaine is *Erythroxylon coca*, a bush growing originally in the higher areas of Peru and Bolivia. The precursors of the alkaloid are ornithine, acetoacetate and benzoate. The oxygen carriers are therefore exclusively carbonyl/carboxyl groups, and the $\delta^{18}O$ value is — with regard to the altitude of the growth area — to be placed at the lower edge of the abundance limits, namely near +14‰ (recent tracer studies on the biosynthesis of tropane alkaloids with ^{18}O labelled precursors proved a complete oxygen isotope exchange with water; Duran-Patron et al., 2000). Again the $\delta^{18}O$ value found ($+13.9 \pm 1$‰, $n=7$) is in absolute agreement with this prediction. The precursors of natural papaverine and morphine are two moles of tyrosine in both cases, hence introducing oxygen from erythrose. In papaverine these are supplemented by two oxygen atoms from O_2; the expected $\delta^{18}O$ value is therefore $(2\times 26‰ + 2\times 6‰)/4 = +16‰$. The quite satisfactory agreement of the experimental $\delta^{18}O$ value ($+14.7 \pm 0.3$‰) may nevertheless be by chance, because most commercially available papaverine samples are said to be synthetic. In the case of the biosynthesis of morphine from tyrosine (Amann and Zenk, 1996), the primary introduced oxygen atoms are partially equilibrated with those from water. Even if one takes this into account, the experimental global $\delta^{18}O$ value (-2.2 ± 1‰) is far away from that as expected (+17.0‰). Easier to know and understand is the origin of the oxygen atoms in caffeine. One of them is introduced in the course of the incorporation of HCO_3^- into position 6 of the purine nucleus, the other by the addition of H_2O to the double bond between positions 2 and 3. One has to assume that the first oxygen function is probably heavily enriched towards water (for HCO_3^-/H_2O, $K=1.033$ at 0°C), while the second one is probably depleted due to a kinetic isotope effect on the addition reaction. Furthermore, both positions should be submitted to a secondary partial oxygen isotope exchange with water. This complicated situation implies a correlation of the $\delta^{18}O$ value of caffeine to the leaf water, however, in a way very sensitive to the individual conditions of plant cultivation and climate. This is exactly what has been found by Dunbar and Wilson (1982); the $\delta^{18}O$ value of caffeine varies between large limits, and it depends from the plant and the individual climate conditions of its cultivation.

Therefore, the systematic determination and observation of $\delta^{18}O$ values of natural compounds does not only help with the confirmation and explanation of biosynthetic pathways; the results also underline the general importance of the present considerations for the authenticity assignments e.g. of flavour, aroma compounds and drugs.

3. Concluding remarks

Our first successful systematic attempt to correlate $\delta^{18}O$ values of a compound to its precursors and (bio)-synthesis dealt with nitrate; on the basis of this result it became possible to assign the origin of this important ion to bacterial nitrification, chemical synthesis and atmospheric events (Amberger and Schmidt, 1987; Voerkelius and Schmidt, 1990). The present compilation of ^{18}O abundances of natural compounds and their interpretation on the base of biosynthetic reactions and their mechanisms confirms our earlier postulation (Schmidt et al., 1995; Schmidt and Gleixner, 1998a,b) that oxygen atoms in these molecules are originating from three different primary sources, namely H_2O, CO_2 and O_2, and that they are introduced by different mechanisms with different isotope effects and are submitted to different degrees of equilibration with water.

As summarized in Fig. 8, leaf water in plants is the most important oxygen source, either directly (addition or exchange) or indirectly via CO_2 or as the source of photosynthetic O_2. So far, it has generally been assumed that carbohydrates in photosynthesizing plants are in isotopic equilibrium with the surrounding water in any position. This is obviously not always the case (Roden and Ehleringer, 1999), and therefore we believe that carbohydrates have a distinct ^{18}O pattern, and that their global $\delta^{18}O$ value, which is correlated to that of the water, is only a mean of this pattern. Our opinion is supported by the fact that the expected correlation slope near unity has been reported only once (DeNiro and Cooper, 1989). Furthermore, differences between the $\delta^{18}O$ values of cellulose and reserve carbohydrates from the same source are observed: The latter are explained on the base of the partial degradation of these precursors to trioses before resynthesis of hexoses (Hill et al., 1995). Correspondingly, variations observed in the $\delta^{18}O$ values of monosaccharides and glycerol from different species are discussed on the base of physiological differences and variations of time for oxygen isotope equilibration (Fogel and Cifuentes, 1993). Finally, there is evidence that the postulated oxygen isotope equilibrium is not attained in the case of heterotrophically synthesized carbohydrates.

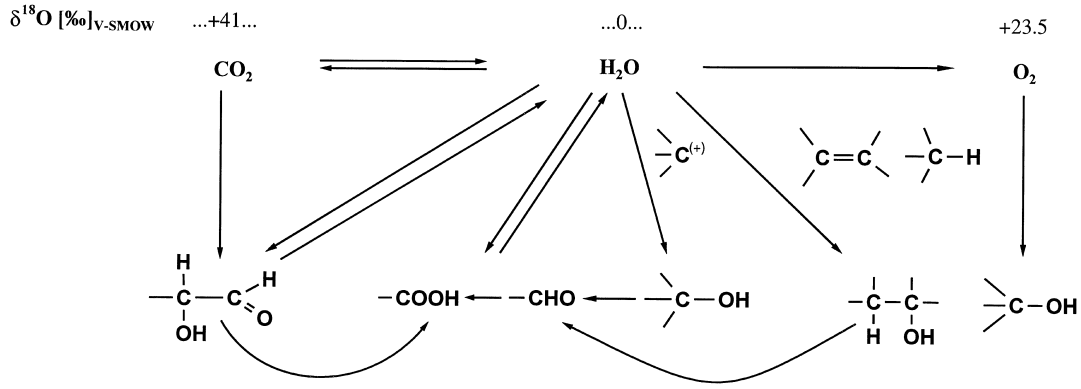

	carbohydrates and [direct descendants]	carboxyl-, carbonyl-functions and alcohols from there	open chained isoprenoids	OH-functions by H_2O-addition	sterols, phenols cycl. isoprenoids	
Correlation to H_2O	$0.8 * \delta_{H_2O} + 30$	$x * \delta_{H_2O} + 19$ [1]	$y * \delta_{H_2O} + 2$	$z * \delta_{H_2O} - 5$	none	secondary
$\delta^{18}O$-Range	+36 ... +28; [+30 ... +25]	+26 ... +13	+20 ... +5	+10 ... 0	+7 ... 0	> 7

Fig. 8. Correlations between the $\delta^{18}O$ values of organic compounds or functional groups and that of the primary oxygen sources in plant metabolism (modified after Schmidt and Gleixner, 1998b; Werner, 1998). [1]O from acyl groups; O from carbonyl groups may exceed this value by 7‰.

Our data prove that also carbonyl and carboxyl groups from other compounds exchange oxygen atoms with water, however, the equilibrium may not always be attained and the enrichment is not as high as in carbohydrates. Distinct $\delta^{18}O$ values are observed for alcohols, depending on wether they are synthezised by addition of OH^- or H_2O, by reduction of carbonyl compounds or by hydroxylation. The latter is the case for sterols and aromatic compounds; and the monooxygenase reactions imply an isotope fractionation factor near 1.02. In total, on the base of these explanations the $\delta^{18}O$ value of a corresponding position and the global $\delta^{18}O$ value of a given compound can be predicted, and this is not only of fundamental importance for the understanding and elucidation of biochemical pathways but also for the origin and authenticity assignment of flavour and fragrance compounds.

If we apply Galimov's theory of the "thermodynamically ordered isotope distribution" to oxygen isotope abundances, a good correlation between $\delta^{18}O$ values and β_Σ-factors (Galimov, 1985) is found for H_2O, CO_2, and some plant products like carbohydrates (by chance?) and related compounds (Fig. 9); in these cases, small deviations from the thermodynamic equilibrium line may indicate that the equilibration with water has not completely been attained. Larger shifts, as observed for aliphatic acids and esters, may be due to the fact that only "basic" β_i increments have been available. They are expressions of binding enthalpies, and for a given bond, they are modulated by the type of other substituents of the same carbon atom (Galimov, 1985). This must also be true for oxygen–carbon bonds found in different functional groups, as unequivocally demonstrated by the substituent influence on oxygen equilibrium isotope effects on acids, esters and carbonyl compounds (Rishavy and Cleland, 1999). Thus, in the present case the applied β_i increments do have only preliminary character. The reason for the large deviation from the equilibrium line for all compounds, to which oxygen had been introduced by hydroxylation reactions (sterols, phenols) must be quite different. These substances are products of an irreversible unidirectional process, hence far away from equilibration with water. Therefore, their $\delta^{18}O$ value is kinetically determined, while the prerequisite for a thermodynamically dominated introduction of oxygen is that the biological system in question is close to steady-state conditions. A global view and critical general discussion of this aspect is the topic of a forthcoming paper by H.-L. Schmidt and E.M. Galimov.

4. Experimental

4.1. General experimental procedures

For the determination of the $\delta^{18}O$ value of soluble sugars, cellulose, glycerol, lactose and furaneol the coupled elemental analyser–IRMS system described elsewhere (Werner et al., 1996; Werner, 1998) was used. A sample amount corresponding to 80 μmol O was wrapped into silver capsules, put into the autosampler and pyrolysed at 1080°C over an inert glassy carbon grit. The pyrolysis gases were swept by the He carrier gas (He 5.0, 60 ml min^{-1}) through ascarite, magnesium perchlorate and active charcoal traps to remove residual traces of CO_2 and H_2O and to adsorb other unwanted

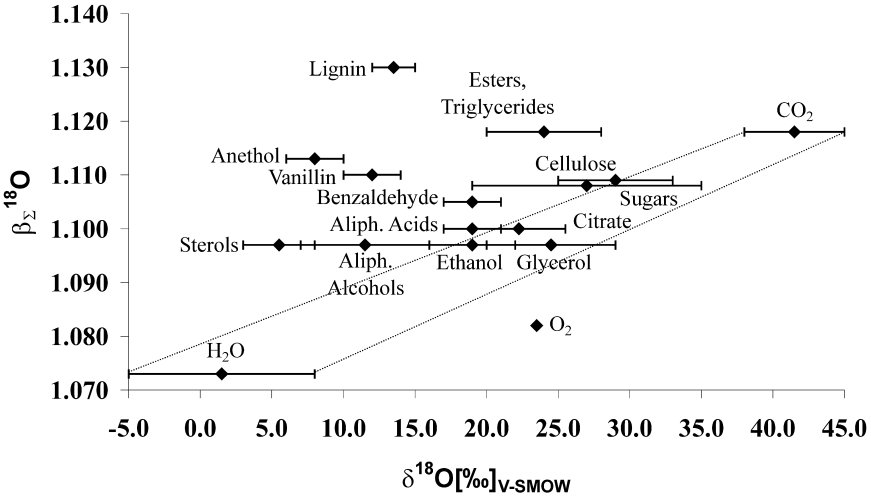

Fig. 9. $\delta^{18}O$ Values of H_2O, CO_2 and O_2 in mean natural abundance and $\delta^{18}O$ of natural products as compared with β_Σ ^{18}O factors calculated after Galimov (1985): The β_Σ factors are theoretical relative ^{18}O enrichments of the molecules in the state of "thermodynamical order". They are for H_2O: 1.0734, O_2: 1.0818 and for CO_2: 1.1086. The β_i increments for atoms in given positions are for ≡C–O–H: 1.097, =C=O: 1.105 and for ≡C–O–C≡: 1.130; from these results $\beta_\Sigma = 1/n\sum_i^n \beta_i$.

pyrolysis by-products. The pyrolysis gases then passed through a GC column packed with a molecular sieve 5 Å to separate the isobaric decomposition products N_2 (in case N-containing samples were pyrolyzed) and CO. Ergosterol, (–)-quinic acid, citral, anethol, emodin, hesperetin, hesperidin and chlorogenic acid were pyrolysed with the apparatus and method described by Kornexl et al. (1999b). At 1400°C, the samples (also wrapped in Ag capsules) were quantitatively converted to CO, H_2 and C (with traces of CH_4). The gases passed an ascarite trap and were separated on a GC column as described above. The minimum sample amount was 50 μmol O. Esters, corresponding alcohols and vanillin were pyrolysed using a "carbon reduction" irm–GCMS system (for details, see Werner, 1998). This carbon reduction coupling is analogous to that of the conventional GC combustion (and reduction) technique (Brand et al., 1994) with some modifications (Werner, 1998). The reduction furnace of the irm–GCMS system (freshly prepared, no CuO) was inactivated (120°C in order to avoid condensing and other unwanted reactions of water and other less volatile substances on/with the copper and to avoid possible isotope exchange reaction between copper oxide and CO). The alumina tube (320×1.0 mm i.d.) of the pyrolysis reactor contained a Ni tube (0.8 mm, ending in the heated area of the furnace). The transfer capillary to the reactor was adjusted into the Ni tube; additionally, a make-up or reaction gas flow enters the alumina tube in the GC furnace (outside the Ni tube). This "tube in tube" system was operated at 1250–1300°C. At this temperature the yield of CO from the conversion of H_2O and CO_2 with excess carbon was higher than 99.9%. The analyte mixture was separated on a GC column preceeding the pyrolysis reactor.

4.2. Origin of purchased natural compounds

Hesperidin from citrus, hesperetin (4-methoxy-3′, 5, 7-trihydroxy-flavanone), origin unknown, and emodin from *Frangula* roots were from Lancaster, 63155 Mülheim, Germany; chlorogenic acid and ergosterol, both of unknown origin, were purchased from Sigma-Aldrich Chemie GmbH, Deisenhofen, Germany; and (−)-quinic acid from *Cinchona ledgeriana* was from Roth, Karlsruhe, Germany. (L)-Ephedrine was a kind gift from Professor W. Steglich, München, Germany; (−)-cocaine and papaverine were kindly provided by Dr. R. Dahlenburg, Bundeskriminalamt, Wiesbaden, Germany. Natural and nature-identical furaneol® (2,5-dimethyl-4-hydroxy-3(2H)-furanone) was a gift from Dr. K. Kempe, Silesia, Neuss, Germany, and Professor A. Mosandl, Frankfurt, Germany. Most natural and nature-identical flavour and aroma compounds (anethol, benzaldehyde, cinnamic aldehyde, citral, various esters, vanillin from several sources) were also kindly provided by Dr. K. Kempe.

4.3. Isolation of natural compounds from various sources

4.3.1. Cellulose from beet leaves and roots

Sugar beet plants were separated in leaves and tubers, which were frozen in liquid N_2; the plant material was ground, freeze-dried and stored at −18°C.

Methods described by Brugnoli et al. (1988) and by Garnier-Dardart et al. (1976) were adapted for the isolation of different fractions from the plant material. 5 g ground leaf or tuber material were extracted three times with 150 ml boiling water. After centrifugation at 1200 *g* for 20 min the supernatant was collected for the isolation of soluble compounds. Dowex-50 (H^+) and Dowex 1X8 (Cl^-) resins were used to separate the ionic fractions

from the non-ionic soluble sugar fraction. This fraction was freeze-dried and stored in dry form at −18°C. The insoluble pellet was suspended several times in a boiling mixture of 80% ethanol/aceton (80:20), until after centrifugation both supernatant and pellet were colourless. Transitory starch was twice extracted with 20% HCl (w/w), and the solution was discarded. The residual plant material (1 g) was rinsed with water and then heated to 90°C for 1 h in 300 ml water containing 10 g $NaClO_2$ and 3 ml acetic acid (Green, 1963). Another 10 g sodium chlorite and 3 ml of acetic acid were added and heating was continued; this procedure was repeated twice. The solution was discarded and the residual fraction was washed with hot and several times with cold water. The residual holocellulose fraction was treated with 17% NaOH under continous stirring for 40 min. The cellulose was washed with 17% NaOH followed by several washings with 10% acetic acid and then distillated water. The product was dried after solvent exchange with acetone. A further drying for 72 h in vacuo followed. The isolated α-cellulose was stored in dry form at −18°C. The $\delta^{18}O$ value of the soluble sugar fraction and the cellulose was determined with EA–pyrolysis–IRMS as described above.

4.3.2. Sugars from fruit juices

The isolation was as described by Houerou et al. (1999).

4.3.3. Glycerol from milk and wine

The procedure was adapted from Kornexl et al. (1997) and Weber et al. (1997), respectively. The lipids from 1 l raw milk were separated by centrifugation at 3000 *g* for 10 min. The lipid phase obtained was dried in vacuo. 12.5 g of the dry lipids were heated with 100 ml 2 N NaOH for 1 h to 60°C under continuous stirring. After that the solution was acidified by 100 ml 2 N HCl, and the fatty acids were extracted with 100 ml diethylether/petroleum ether (1:1) in three portions. The aqueous phase was concentrated under reduced pressure, and the remainder was extracted with ethanol (1×20 ml, 3×10 ml). The combined extracts were filtered, the solvent was removed under reduced pressure, and the glycerol was purified by vacuum distillation (0.1 torr, 200°C). About 800 mg product were thus obtained. Animal fats were treated correspondingly. The isolation of glycerol from wine was performed as described by Roßmann et al. (1998).

4.3.4. Lactose from cattle milk

0.1 N HCl was added to 100 ml skim milk (Section 4.3.3) until the pH was 4.3. The casein was separated by centrifugation (1000 *g*, 10 min) and the precipitate washed twice with water. The first two supernatants were combined, filtered and then evaporated to dryness by lyophylisation. 1.1 g of the residue were redissolved in 30 ml water, the solution was heated for 10 min to 80°C. The precipitated whey proteins were separated by filtration. The filtrate and the first washing were lyophilized to yield approx. 1 g lactose.

4.3.5. Pretreatment of alkaloids

L-(−)ephedrine and papaverine were analyzed as received, (−)-cocaine was precipitated from an aqueous solution of the hydrochloride by 3.5% solution of NH_3, isolated by filtration and dehydrated over night at 65°C.

4.4. Hydrolysis of aliphatic esters

The hydrolysis of the esters and the separation of the products for isotope ratio analysis was as described under Section 4.5.3.

4.5. Estimation of the kinetic ^{18}O isotope effects on the H^+-catalyzed esterification of n-hexanol and butyric acid

4.5.1. Esterification with excess of n-hexanol

In order to obtain a 20% turnover of the alcohol and a complete consumption of the acid, 1 g (11.4 mmol) butyric acid, 5.8 g (56.9 mmol) *n*-hexanol and 0.23 g H_2SO_4 were heated for 5 h to 150°C (reflux). The excess *n*-hexanol was then eliminated by distillation. The remainder was treated with a 5-fold amount of ice water, and the ester was twice extracted with diethylether. The combined organic phases were neutralized by washing with Na_2CO_3 solution, then dried over Na_2SO_4 and concentrated in vacuo. The crude *n*-hexylbutyrate was purified by MPLC on kieselgel 60, using as eluent 10 ml *n*-pentane/methanol (99:1), then dichloromethane as solvent. The ester was detected via its absorption at 255 nm, its purity was controlled by GC. The ester containing fractions were combined, the solvent eliminated in vacuo.

4.5.2. Esterification with excess of butyric acid

The complete consumption of *n*-hexanol and a 20% turnover of butyric acid was attained by reacting 5 g (56.9 mmol) butyric acid, 1.16 g (11.4 mmol) *n*-hexanol and 0.23 g H_2SO_4. Reaction conditions and product isolation were as described before.

4.5.3. Ester hydrolysis

0.1 ml ester, 1.0 ml 0.1 N methanolic KOH and 0.25 ml 15% aqueous KOH were heated to the boiling point in a tightly closed test tube for 10 min. After cooling 1 ml diethyl ether and 0.5 ml saturated NaCl-solution were added, and the solution was acidified by dropwise addition of conc. HCl. After separation of the phases by centrifugation, the organic phase was washed with 0.5 ml saturated NaCl solution, and adjusted to pH 5.0 by the addition of a few drops of a 10% Na_2CO_3 solution. Then the organic phase was dried over Na_2SO_4.

4.5.4. Isotope abundance measurements and calculations

The $\delta^{13}C$ and the $\delta^{18}O$ values of the reactants and products were measured simultaneously by irm–GCMS as described under 4.1; the $\delta^{18}O$ value of acids from ester hydrolyses had to be calculated from the difference ester/alcohol.

The calculation of the intramolecular ^{18}O isotope effect on the acid during the esterification after O'Leary (1980) based on the δ value shift between acid and ester under the conditions of total alcohol consumption; it was $k_{16}/k_{18} = 1.058$ [k_{16}/k_{18} kinetic ^{18}O isotope effect]. Using this value and determining the $\delta^{18}O$ shift between starting materials and ester and/or conditions of partial alcohol but total acid turnover, the intermolecular oxygen isotope effect on the alcohol could be calculated $k_{16}/k_{18} = 1.014$ (for details see Werner, 1998).

Acknowledgements

The authors thank: Fabiano Reniero (JRC, Ispra, Italy) for valuable discussions and the provision of unpublished data on sterols, Claudio Fuganti (Centro CNR, Milano, Italy) and Fabiano Reniero and their colleagues for the permission to use data from their unpublished manuscripts on raspberry ketone and naringin, and on vanillin, respectively, Claude Hillaire-Marcel (Montreal, Quebec, Canada) for providing valuable references, Judith P. Klinman (Berkeley, CA, USA) for discussion on oxygen isotope effects and providing unpublished data, M.H. Zenk (LMU, München, Germany) for discussions on the tyrosine metabolism in plants, Willi A. Brand (MPI für Biogeochemie, Jena, Germany) for helpful discussions, Andreas Hilkert (Finnigan MAT, Bremen, Germany) for providing unpublished data, Barbara E. Kornexl (UFZ GmbH, Leipzig, Germany) for making available unpublished data and for the performance of some $\delta^{18}O$ value measurements, Harigh Avak (Finnigan MAT, Bremen, Germany) as well as Elke Sada (JRC, Ispra, Italy) for the performance of some $\delta^{18}O$ value measurements. Klaus Kempe (Silesia, Neuss, Germany) for supply of flavourings and performance of esterification and ester hydrolysis, A. Mosandl (Johann Wolfgang Goethe Universität, Frankfurt, Germany) for supply of strawberry flavourings and R. Dahlenburg, BKA Wiesbaden for providing some alkaloids.

Note added in proof

While this paper was in press, some additional data on polyketids and on flavonoids, natural products with oxygen functions from acyl groups, became available, which permitted to confirm and generalise the empirically assumed ^{18}O-enrichment of these oxygen atoms by $\sim +19$‰ above plant water. According to Burk and Stuiver (1981) the $\delta^{18}O$-value of precipitation water ($\delta^{18}O_{prec}$) in the northern hemisphere is correlated to the latitude ($\delta^{18}O_{prec} = -0.31^{*\circ}N + 5.76$), from where the oxygen isotope abundance of this precipitation water can be calculated in cases, where the $\delta^{18}O$-value of the plant water is not known. For corresponding calculations in the present context the following mean geographical latitudes have been assumed: Israel, Morocco, Tunisia 31°N; Cyprus, Spain, Turkey 35°N; Greece 38°N; (Central-)Italy 41°N; Central Germany 50°N.

Plant water is always enriched in the heavy isotopes ^{18}O and ^{2}H relative to the precipitation or ground water, and this enrichment depends on plant transpiration as a function of assimilation type (C_3-, C_4- or CAM-plant), plant species and organ, and on local conditions of climate (microenvironment and water availability). Thus, it can be assumed that the plant water ^{18}O-enrichment relative to precipitation water decreases with increasing northern latitude. So Houerou et al. (1999) give $\delta^{18}O$-values of the water from orange juices from Israel and Morocco +5.65‰, from Cyprus and Turkey +1.85‰; the calculated $\delta^{18}O$-values for the precipitate water of these areas (−3.85 and −5.09‰, respectively) indicate an ^{18}O-enrichment of +9.50 and +6.94‰ by the plant. The ^{18}O-enrichment of the citric acid from these juices relative to plant water is $+19 \pm 0.5$‰.

On the base of this knowledge it is now possible to exploit other data for a systematic correlation of oxygen from acyl groups to plant water: the mean $\delta^{18}O$-values given by Angerosa et al. (1999) for olive oil from Morocco/Tunisia are +27.30‰, from Spain/Turkey +25.04‰, from Greece +23.15‰ and from Italy +20.70‰. If one assumes for the plant water in these areas an ^{18}O-enrichment of +8.0, +6.5, +5.5, and +4.5‰ relative to the corresponding precipitation water, as calculated from the above equation ($\delta^{18}O$: −3.85, −5.09, −6.02 and −6.95‰), an identical ^{18}O-enrichment of $+23.5 \pm 0.5$ ‰ above plant water results for the triglycerides from all areas. Taking into account that half of the oxygen atoms in these triglycerides is originating from glycerol, which is enriched by +28‰ ($+27 \pm 2$‰, see Table 3 of review), a coresponding enrichment for the acyl moiety of $\sim +19$‰ results, identical to the experimental $\delta^{18}O$-value for citric acid mentioned before (Houerou et al., 1999).

The application of these results now permits to compare measured bulk global $\delta^{18}O$-values of natural compounds with those of their estimated patterns (Fig. 10). Assuming that hesperidine (Table 6 and Fig. 7 of review) is originating from oranges from Israel, the $\delta^{18}O$-values of its carbohydrate and its polyketid moieties can be calculated from the corresponding mean $\delta^{18}O$-value of orange juice water (+5.65‰); for the latter results +24.65‰, in case of the highest $\delta^{18}O$-value for this orange juice water (+6.50‰) +25.40‰, more

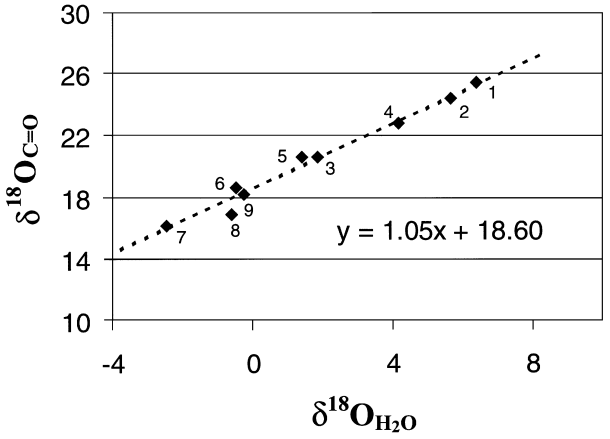

Fig. 10. Correlation between the $\delta^{18}O$ values of oxygen atoms in natural compounds originating from acyl groups ($\delta^{18}O_{C=O}$) and those of plant water ($\delta^{18}O_{H_2O}$). In cases where the latter was not directly available, it was estimated from the precipitate water as calculated after Burk and Stuiver (1981). Samples 2 and 3, citric acid from orange juice; samples 4 to 7 acid moiety of olive oil from Morocco/Tunisia, Spain/Turkey, Greece, and Italy, respectively; samples 1, 8 and 9 polyketid moieties from hesperidine (Israel?) and malvidine glucosides from Germany, respectively.

or less identical to the empirically assumed $\delta^{18}O$-value (+26.0‰). The reverse calculation for two malvidine glucosides from Palatine wines (Degenhardt et al., 2000) with global $\delta^{18}O$-values +18.10±0.45 and +18.56±0.24‰ for the organic compound and −0.62 and −0.25 ‰ for the corresponding water yields (on the base of an ^{18}O-enrichment of the oxygen atoms in the sugar moiety by 0.8* $\delta^{18}O_{H_2O}$ +29‰ and the $\delta^{18}O$-value +6‰ for the oxygen atoms introduced by hydroxylation) a $\delta^{18}O$-value +16.89 and +18.24 ‰ for the polyketid originating oxygen atoms, corresponding to their ^{18}O-enrichment of +17.51 and +18.49‰ above the water of the wines.

A calculation of the $\delta^{18}O$-values of the acyl originating oxygen atoms of two polyketids from the fungus *Cortinarius sanguineus Fr*. (Steglich and Austel, 1966: emodine, 4 acyl oxygen atoms, 1 from O_2, $\delta^{18}O = +17.8 \pm 0.2$‰ and dermocybine, 4 acyl oxygen atoms, 3 from O_2, $\delta^{18}O = +14.7 \pm 0.2$‰) yielded the identical $\delta^{18}O$-values +21.0±0.2‰ for the acyl oxygen atoms. This would correspond to a fungus cell water of +2‰, hence a quite high ^{18}O-enrichment of this water above the ground water from the origin area near München $\delta^{18}O$: ∼−10‰). Although it is known that these fungi are capable of remarkably enriching ^{2}H in their cell water relative to that of the host (H. Ziegler, private communication), a total ^{18}O-enrichment of +12‰ is quite improbable, and therefore an explanation of the result must be left to future discussions.

This is not the case with a contribution to the elucidation of an open question from the biosynthesis of gallic acid (Wolfgang Eisenreich and Adelbert Bacher, Technische Universität München, Germany, we are grateful for the permission to use these data), where the origin of the phenolic hydroxyl groups had to be elucidated. A product obtained by acid hydrolysis of a gallotannine from *Rhus* sp. in water ($\delta^{18}O = -10.7$‰) had a $\delta^{18}O$-value +21.2±0.7‰. The calculation [2*(19–10.7) +3*X]/5 = +21.2‰ yielded +29.8‰ for all phenolic OH-groups, hence their unequivocal immediate origin from shikimic acid; the alternative with one oxygen atom originating from O_2 would have demanded a global $\delta^{18}O$-value of +16.5‰.

We are highly obliged to Wolfgang Steglich (LMU München, Germany) for kindly providing the polyketid and to Peter Winterhalter (Technische Universität Braunschweig, Germany) for the malvidine glucoside samples. We thank Heike Geilmann (MPI für Biogeochemie Jena, Germany) for the $\delta^{18}O$ measurements.

References

Aggarwal, P.K., Dillon, M.A., 1998. Stable isotope composition of molecular oxygen in soil gas and groundwater: a potentially robust tracer for diffusion and oxygen consumption processes. Geochimica et Cosmochimica Acta 62, 577–584.

Amann, T., Zenk, M.H., 1996. Endogenes Morphin, Schmerzmittelsynthese in Mensch und Tier. Deutsche Apotheker Zeitung 136, 519–527.

Amberger, A., Schmidt, H.-L., 1987. Natürliche Isotopengehalte von Nitrat als Indikatoren für dessen Herkunft. Geochimica et Cosmochimica Acta 51, 2699–2705.

Anderson, V.E., 1991. Isotope effects on enzyme-catalyzed β-eliminations. In: Cook, P.F. (Ed.), Enzyme Mechanism from Isotope Effects. CRC Press, Boca Raton, pp. 389–430.

Angerosa, F., Bréas, O., Contento, S., Guillou, C., Reniero, F., Sada, E., 1999. Application of stable isotope ratio analysis to the characterisation of the geographical origin of olive oils. Journal of Agricultural and Food Chemistry 47, 1013–1017.

Bauer, K., Garbe, D., Surburg, H., 1990. Common fragrance and flavour materials. VCH, Weinheim, pp. 114–115.

Berry, J.A., Osmond, C.B., Lorimer, G.H., 1978. Fixation of $^{18}O_2$ during photorespiration. Plant Physiology 62, 954–967.

Blanchard, J.S., Cleland, W.W., 1980. Use of isotope effects to deduce the chemical mechanism of fumarase. Biochemistry 19, 4506–4513.

Bolwell, G.P., Bozak, K., Zimmerlin, A., 1994. Plant cytochrome P450. Phytochemistry 37, 1491–1506.

Brand, W.A., Tegtmeyer, A.R., Hilkert, A., 1994. Compound-specific isotope analysis: Extending towards $^{15}N/^{14}N$ and $^{18}O/^{16}O$. Organic Geochemistry 21, 585–594.

Brenninkmeijer, C.A.M., Mook, W.G., 1982. A new method for the determination of the $^{18}O/^{16}O$ ratio in organic compounds. In: Schmidt, H.-L., Förstel, H., Heinzinger, K. (Eds.), Stable Isotopes, Proceedings of the 4th International Conference. Elsevier Scientific, Amsterdam, pp. 661–666.

Brenninkmeijer, C.A.M., Kraft, P., Mook, W.G., 1983. Oxygen isotope fractionation between CO_2 and H_2O. Isotope Geoscience 1, 181–190.

Bricout, J., 1978. Recherches sur le fractionnement des isotopes stables de l'hydrogène et de l'oxygène dans quelques végétaux. Revue de Cytologie et de Biologie Végétales — Le Botaniste 1, 133–209.

Bricout, J., 1979. Natural abundance levels of ^{2}H and ^{18}O in plant organic matter. In: Klein, E.R., Klein, P.D. (Eds.), Stable Isotopes, Proceedings of the 3rd International Conference. Academic Press, New York, pp. 215–222.

Brugnoli, E., Hubick, K.T., von Caemmerer, S., Wong, S.C., Farquhar, G.D., 1988. Correlation between the carbon isotope discrimination in leaf starch and sugars of C_3 plants and the ratio of intercellular and atmospheric partial pressures of carbon dioxide. Plant Physiology 88, 1418–1424.

Burk, R.L., Stuiver, M., 1981. Oxygen isotope ratios in trees reflect mean annual temperature and humidity. Science 211, 1417–1419.

Byrn, M., Calvin, M., 1966. Oxygen-18 exchange reactions of aldehydes and ketones. Journal of the American Chemical Society 88, 1916–1922.

Cooper, L.W., DeNiro, M.J., 1989. Oxygen-18 content of atmospheric oxygen does not affect the oxygen isotope relationship between environmental water and cellulose in a submerged aquatic plant, *Egeria densa* Planch. Plant Physiology 91, 536–541.

Coplen, T.B., 1988. Normalization of oxygen and hydrogen isotope data. Chemical Geology (Isotope Geoscience Section) 72, 293–297.

Degenhardt, A., Hofmann, S., Knapp, H., Winterhalter, P., 2000. Preparative isolation of anthocyanins by high-speed countercurrent chromatography and application of the color activity concept to red wine. Journal of Agricutural and Food Chemistry 48, 5812–5818.

DeNiro, M.J., Epstein, S., 1979. Relationship between the oxygen isotope ratios of terrestrial plant cellulose, carbon dioxide, and water. Science 204, 51–53.

DeNiro, M.J., Cooper, L.W., 1989. Post-photosynthetic modification of oxygen isotope ratios of carbohydrates in the potato: Implications for paleoclimatic reconstruction based upon isotopic analysis of wood cellulose. Geochimica et Cosmochimica Acta 53, 2573–2580.

Dennis, M.J., Wilson, P., Kelly, S., Parker, I., 1998. The use of pyrolytic techniques to estimate site specific isotope data of vanillin. Journal of Analytical and Applied Pyrolysis 47, 95–103.

Dole, M., 1935. The relative atomic weight of oxygen in water and in air. Journal of the American Chemical Society 57, 2731.

Doner, L.W., Ajie, H.O., Sternberg, L.d.S.L., Milburn, J.M., DeNiro, M.J., Hicks, K.B., 1987. Detecting sugar beet syrups in orange juice by D/H and $^{18}O/^{16}O$ analysis of sucrose. Journal of Agricultural and Food Chemistry 35, 610–612.

Dongmann, G., Förstel, H., Wagener, K., 1972. ^{18}O rich oxygen from land photosynthesis. Nature New Biology 240, 127–128.

Dunbar, J., 1982. The non-exchangeability of oxygen between ethanol and water in a simulated wine. Zeitschrift für physikalische Chemie Neue Folge 130, 247–250.

Dunbar, J., Wilson, A.T., 1982. Determination of geographic origin of caffeine by stable isotope analysis. Analytical Chemistry 54, 590–592.

Dunbar, J., Wilson, A.T., 1983. The origin of oxygen in soil humic substances. Journal of Soil Science 34, 99–103.

Duran-Patron, R., O'Hagan, D., Hamilton, J.T.G., Wong, C.W., 2000. Biosynthetic studies on the tropane ring system of the tropane alkaloids from *Datura stramonium*. Phytochemistry 53, 777–784.

Epstein, S., Thompson, P., Yapp, C.J., 1977. Oxygen and hydrogen isotopic ratios in plant cellulose. Science 198, 1209–1215.

Farquhar, G.D., Barbour, M.M., Henry, B.K., 1998. Interpretation of oxygen isotope composition of leaf material. In: Griffiths, H. (Ed.), Stable Isotopes. Integration of Biological, Ecological and Geochemical Processes. BIOS Scientific Publishers Ltd, Oxford, pp. 27–62.

Feldman, D.E., Yost, H.T., Benson, B.B., 1959. Oxygen isotope fractionation in reactions catalyzed by enzymes. Science 129, 146–147.

Förstel, H., Putral, A., Schleser, G., Lieth, H., 1975. The world pattern of oxygen-18 in rainwater and its importance in understanding the biogeochemical oxygen cycle. In: IAEA Symposium: Isotope Ratios as Pollutant Source and Behaviour Indicators. IAEA, Vienna, pp. 3–20.

Fogel, M.L., Cifuentes, L.A., 1993. Isotope fractionation during primary production. In: Engel, M.H., Macko, S.A. (Eds.), Organic Geochemistry. Principles and Applications. Plenum Press, New York and London, pp. 73–98.

Francey, R.J., Tans, P.P., 1987. Latitudinal variation in oxygen-18 of atmospheric CO_2. Nature 327, 495–497.

Fronza, G., Fuganti, C., Pedrocchi-Fantoni, G., Serra, S., Zucchi, G., Fauhl, C., Guillou, C., Reniero, F., 1999. Stable isotope characterization of raspberry ketone extracted from *Taxus baccata* and obtained by oxidation of the accompanying alcohol (betuligenol). Journal of Agricultural and Food Chemistry 47, 1150–1155.

Fronza, G., Fuganti, C., Serra, S., Guillou, C., Reniero, F. 2001 The positional $\delta^{18}O$-value of extracted and synthetic vanillin. Helvet. Chim. Acta 84, 351–359.

Fuchs, S., Zinn, S., Beck, T., Mosandl, A., 1999. Biosynthesis of menthofuran in *Mentha x piperita*: Stereoselective and mechanistic studies. Journal of Agricultural and Food Chemistry 47, 4100-4105.

Funk, C., Brodelius, P.E., 1994. *Vanilla planifolia* Andrews: In vitro biosynthesis of vanillin and other phenylpropanoid derivatives. In: Bajaj, Y.P.S. (Ed.), Biotechnology in Agriculture and Forestry, Vol. 26, Medicinal and Aromatic Plants VI. Springer Verlag, Berlin, pp. 377–402.

Galimov, E.M., 1985. The biological fractionation of isotopes. Academic Press, London, pp. 204–205.

Garnier-Dardart, J., Deleéns, E., Lerman, J.C., 1976. Carbon isotope composition of biochemical fractions isolated from a plant with crassulacean acid metabolism (CAM): methodology. In: Klein, E.R., Klein, P.D., (Eds.), Proceedings of the 2nd International Conference on Stable Isotopes, 20–23 October 1975, Oak Brook, IL, pp. 645–654.

Gillon, J.S., Yakir, D., 2000. Naturally low carbonic anhydrase activity in C_4 and C_3 plants limits discrimination against $C^{18}OO$ during photosynthesis. Plant, Cell and Environment 23, 903–915.

Gonfiantini, R., Stichler, W., Rozanski, K., 1995. Standards and intercomparison materials distributed by the International Atomic Energy Agency for stable isotope measurements. In: IAEA, Reference and Intercomparison Materials for Stable Isotopes of Light Elements. Proceedings of a Consultants Meeting held in Vienna, 1–3 December 1993, IAEA-Tecdoc-825. IAEA, Vienna, pp. 13–29.

Gray, J., Thompson, P., 1977. Climatic information from $^{18}O/^{16}O$ analysis of cellulose, lignin and whole wood from tree rings. Nature 270, 708–709.

Green, J.W., 1963. Wood cellulose. In: Whistler, R.L., (Ed.), Methods of Carbohydrate Chemistry. Academic Press, New York, pp. 9–21.

Grue-Sørensen, G., Spenser, I.D., 1988. Biosynthesis of ephedrine. Journal of the American Chemical Society 110, 3714–3715.

Guy, R.D., Fogel, M.F., Berry, J.A., Hoering, T.C., 1987. Isotope fractionation during oxygen production and consumption by plants. In: Biggins, J. (Ed.), Progress in Photosynthesis Research, Vol. 3. Martinus Nijhoff Publishers, Dordrecht, pp. 597–600.

Guy, R.D., Fogel, M.L., Berry, J.A., 1993. Photosynthetic fractionation of the stable isotopes of oxygen and carbon. Plant Physiology 101, 37–47.

Hamilton, G.A., Westheimer, F.H., 1959. On the mechanism of the enzymatic decarboxylation of acetoacetate. Journal of the American Chemical Society 81, 6332–6333.

Haslam, E., 1993a. Shikimic Acid, Metabolism and Metabolites. John Wiley & Sons Ltd, Chichester, pp. 1–16 and 156–184.

Haslam, E., 1993b. Shikimic Acid, Metabolism and Metabolites. John Wiley & Sons Ltd, Chichester, pp. 234–238.

Hill, S.A., Waterhouse, J.S., Field, E.M., Switsur, V.R., ap Rees, T., 1995. Rapid recycling of triose phosphates in oak stem tissue. Plant, Cell and Environment 18, 931–936.

Hillaire-Marcel, G., 1986. Isotopes and food. In: Fritz, P., Fontes, J.C. (Eds.), Handbook of Environmental Isotope Geochemistry, Vol. 2: The Terrestrial Environment B. Elsevier, Amsterdam, pp. 507–547.

Horibe, Y., Shigehara, K., Takakuwa, Y., 1973. Isotope separation factor of carbon dioxide-water system and isotopic composition of atmospheric oxygen. Journal of Geophysical Research 78, 2625–2629.

Houerou, G., Kelly, S.D., Dennis, M.J., 1999. Determination of the oxygen-18/oxygen-16 isotope ratios of sugar, citric acid and water

from single strength orange juice. Rapid Communications in Mass Spectrometry 13, 1257–1262.

Keeling, R.F., 1995. The atmospheric oxygen cycle: the oxygen isotopes of atmospheric CO_2 and O_2 and the O_2/N_2 ratio. Reviews of Geophysics, Supplement, US National Report to International Union of Geodesy and Geophysics, 1991–1994, pp. 1253–1262.

Kindl, H., 1991. Biochemie der Pflanzen, 3rd Edition. Springer Verlag, Berlin, p. 239.

Klinman, J.P., Berry, J.A., Tian, G., 1993. New probes of oxygen binding and activation: applications to dopamine β-monooxygenase. In: Karlin, K.D., Tyeklár, Z. (Eds.), Bioinorganic Chemistry of Copper. Chapman & Hall, New York, pp. 151–163.

Kornexl, B.E., Werner, T., Roßmann, A., Schmidt, H.-L., 1997. Measurement of stable isotope abundances in milk and milk ingredients — a possible tool for origin assignment and quality control. Zeitschrift für Lebensmittel-Untersuchung und - Forschung A Food Research and Technology 205, 19–24.

Kornexl, B.E., Werner, R.A., Gehre, M., 1999a. Standardization for oxygen isotope ratio measurement — still an unsolved problem. Rapid Communications in Mass Spectrometry 13, 1248–1251.

Kornexl, B.E., Gehre, M., Höfling, R., Werner, R.A., 1999b. On-line $\delta^{18}O$ measurement of organic and inorganic substances. Rapid Communications in Mass Spectrometry 13, 1685–1693.

Koziet, J., 1997. Isotope ratio mass spectrometric method for the on-line determination of oxygen-18 in organic matter. Journal of Mass Spectrometry 32, 103–108.

Kreckl, W., 1988. Isotopendiskriminierungen in der Photorespiration. Ein Beitrag zum Mechanismus der RuBP-Carboxylase/Oxygenase-Reaktion und zur Erklärung des Dole-Effekts. PhD Thesis, Technische Universität München, D-85350 Freising, Germany.

Kreckl, W., Kexel, H., Melzer, E., Schmidt, H.-L., 1989. Oxygen isotope effects on the ribulosebisphosphate oxygenase reaction. Journal of Biological Chemistry 264, 10982–10986.

Kroopnick, P., Craig, H., 1972. Atmospheric oxygen: isotopic composition and solubility fractionation. Science 175, 54–55.

Kroopnick, P., Craig, H., 1976. Oxygen isotope fractionation in dissolved oxygen in the deep sea. Earth and Planetary Science Letters 32, 375–388.

Lane, G.A., Dole, M., 1956. Fractionation of oxygen isotopes during respiration. Science 123, 574–576.

Libby, L.M., Pandolfi, L.J., 1974. Temperature dependence of isotope ratios in tree rings. Proceedings of the National Academy of Sciences of the United States of America 71, 2482–2486.

Luo, Y.-H., Sternberg, L.d.S.L., 1992. Hydrogen and oxygen isotopic fractionation during heterotrophic cellulose synthesis. Journal of Experimental Botany 43, 47–50.

Masud, Z., Vallet, C., Martin, G.J., 1999. Stable isotope characterization of milk components and whey ethanol. Journal of Agricultural and Food Chemistry 47, 4693–4699.

Mayer, F.C., Larner, J., 1999. Substrate cleavage point of the α- and β-amylases. Journal of the American Chemical Society 81, 188–193.

Misselhorn, K., Brückner, H., Müßig-Zufika, M., Grafahrend, W., 1983. Nachweis des Rohstoffs bei hochrektifiziertem Alkohol. Die Branntweinwirtschaft 123, 162–170.

Misselhorn, K., Grafahrend, W., 1990. Rohstoffnachweis bei hochgereinigtem Alkohol. Die Branntweinwirtschaft 130, 70–73.

Model, P., Ponticorvo, L., Rittenberg, D., 1968. Catalysis of an oxygen-exchange reaction of fructose 1,6-diphosphate and fructose 1-phosphate with water by rabbit muscle aldolase. Biochemistry 7, 1339–1347.

Morita, N., 1935. The increased density of air oxygen relative to water oxygen. Journal of the Chemical Society of Japan 56, 1291.

O'Leary, M.H., 1980. Determination of heavy-atom isotope effects on enzyme-catalyzed reactions. In: Purich, D.L., (Ed.), Enzyme Kinetics and Mechanisms, Part B. In: Colowick, S.P., Kaplan, N.O., (Eds.), Methods in Enzymology, Vol. 64. Academic Press, New York, pp. 83–104.

O'Neal, C.C., Bild, G.S., Tombras Smith, L., 1983. Facile oxygen exchanges of phosphoenolpyruvate and preparation of [^{18}O]phosphoenolpyruvate. Biochemistry 22, 611–617.

O'Neil, J.R., Adami, L.H., Epstein, S., 1975. Revised value for ^{18}O fractionation between CO_2 and H_2O at 25°C. Journal of Research of the US Geological Survey 3, 623–624.

Pollard, M., Ohlrogge, J., 1999. Testing models of fatty acid transfer and lipid synthesis in spinach leaf using in vivo oxygen-18 labeling. Plant Physiology 121, 1217–1226.

Prescott, A.G., John, P., 1996. Dioxygenases: Molecular structure and role in plant metabolism. Annual Review of Plant Physiology and Plant Molecular Biology 47, 245–271.

Rakowski, K., Paneth, P., 1996. Isotope effects on binding. Journal of Molecular Structure 378, 35–43.

Ribas-Carbo, M., Lennon, A.M., Robinson, S.A., Giles, L., Berry, J.A., Siedow, J.N., 1997. The regulation of the electron partitioning between the cytochrome and alternative pathways in soybean cotyledon and root mitochondria. Plant Physiology 113, 903–911.

Ribas-Carbo, M., Robinson, S.A., Gonzàles-Meler, M.A., Lennon, A.M., Giles, L., Siedow, J.N., Berry, J.A., 2000. Effects of light and respiration on oxygen isotope fractionation in soybean cotyledons. Plant, Cell and Environment 23, 983–989.

Richter, G., 1996. Biochemie der Pflanzen. Georg Thieme Verlag, Stuttgart, pp. 161–162, p. 397, p. 418.

Rishavy, M.A., Cleland, W.W., 1999. ^{13}C, ^{15}N, and ^{18}O equilibrium isotope effects and fractionation factors. Canadian Journal of Chemistry 77, 967–977.

Rittenberg, D., Graff, C., 1958. A comparison of the rate of mutarotation and O^{18} exchange of glucose. Journal of the American Chemical Society 80, 3370–3372.

Roden, J.S., Ehleringer, J.R., 1999. Hydrogen and oxygen isotope ratios of tree-ring cellulose for riparian trees grown long-term under hydroponically controlled environments. Oecologia 121, 467–477.

Röhm, K.H., Van Etten, R.L., 1986. The ^{18}O isotope effect in ^{13}C nuclear magnetic resonance spectroscopy: mechanistic studies on asparaginase from *Escherichia coli*. Archives of Biochemistry & Biophysics 244, 128–136.

Roscher, R., Schreier, P., Schwab, W., 1977. Metabolism of 2,5-dimethyl-4-hydroxy-3(2H)-furanone in detached ripening strawberry fruits. Journal of Agricultural and Food Chemistry 45, 3202–3205.

Rossmann, A., Butzenlechner, M., Schmidt, H.-L., 1991. Evidence for a nonstatistical carbon isotope distribution in natural glucose. Plant Physiology 96, 609–614.

Roßmann, A., Schmidt, H.-L., Reniero, F., Versini, G., Moussa, I., Merle, M.H., 1996. Stable carbon isotope content in ethanol of EC data bank wines from Italy, France and Germany. Zeitschrift für Lebensmittel-Untersuchung und - Forschung 203, 293–301.

Roßmann, A., Schmidt, H.-L., Hermann, A., Ristow, R., 1998. Multielement stable isotope ratio analysis of glycerol to determine its origin in wine. Zeitschrift für Lebensmittel-Untersuchung und Forschung, A Food Research and Technology 207, 237–243.

Samuel, D., Silver, B.L., 1965. Oxygen isotope exchange reactions of organic compounds. Advances in Physical Organic Chemistry 3, 123–186.

Saurer, M., Aellen, K., Siegwolf, R., 1997. Correlating $\delta^{13}C$ and $\delta^{18}O$ in cellulose of trees. Plant, Cell and Environment 20, 1543–1550.

Schleser, G.H., 1979. Contribution of the respiratory oxygen isotope fractionation to the ^{18}O budget of the atmosphere. In: Krumbein, W.E. (Ed.), Environmental biogeochemistry and geomicrobiology, Vol. 3, methods, metals and assessment. Ann Arbor Science, Ann Arbor, MI, pp. 825–836.

Schmidt, H.-L., Kexel, H., Butzenlechner, M., Schwarz, S., Gleixner, G., Thimet, S., Werner, R.A., Gensler, M., 1995. Non-statistical isotope distributions in natural compounds: mirror of their biosynthesis and key for their origin assignment. In: Wada, E., Yoneyama, T., Minagawa, M., Ando, T., Fry, B.D. (Eds.), Stable Isotopes in the Biosphere. Kyoto University Press, Kyoto, pp. 17–35.

Schmidt, H.-L., Gleixner, G., 1998a. Carbon isotope effects on key reactions in plant metabolism and ^{13}C-patterns in natural compounds. In: Griffiths, H. (Ed.), Stable Isotopes. Integration of Biological, Ecological and Geochemical Processes. BIOS Scientific Publishers, Oxford, pp. 13–25.

Schmidt, H.-L., Gleixner, G., 1998b. Isotopic patterns in natural compounds origin and importance in authenticity analysis. In: Schreier, P., Herderich, M., Humpf, H.-U., Schwab, W. (Eds.), Natural Product Analysis, Chromatography — Spectroscopy — Biological Testing. Friedrich Vieweg & Sohn Verlagsgesellschaft mbH, Braunschweig, Wiesbaden, pp. 271–280.

Schmidt, H.-L., Roßmann, A., Werner, R.A., 1998. Stable isotope ratio analysis in quality control of flavourings. In: Ziegler, E., Ziegler, H. (Eds.), Flavourings — Production, Composition, Applications, Regulations. Wiley-VCH GmbH, Weinheim, pp. 539–594.

Schmidt, H.-L., Weber, D., Rossmann, A., Werner, R.A., 1999. The potential of intermolecular and intramolecular isotopic correlations for authenticity control. In: Teranishi, R., Wick, E.L., Hornstein, I. (Eds.), Flavor Chemistry. Thirty Years of Progress. Kluwer Academic/Plenum Publishers, New York, pp. 55–61.

Schmidt, H.-L., Gensler, M., Weber, D., 2000. Nachweis eines unerlaubten Zusatzes von naturidentischen Säuren zu Obstsäften mit Hilfe von Isotopenverhältnismessungen. Flüssiges Obst 67, 131–136.

Schramm, S., Hertkorn, N., Bengsch, E., Kettrup, A., Schmidt, H.-L., 1998. On the way to semi-quantitative ^{13}C- and ^{17}O-NMR analysis in the natural abundance level for site-specific isotope ratio determination. Isotopes in Environmental and Health Studies 34, 223, (abstract).

Schwab, W., 1998. Application of stable isotope ratio analysis explaining the bioformation of 2,5-dimethyl-4-hydroxy-3(2H)-furanone in plants by a biological Maillard reaction. Journal of Agricultural and Food Chemistry 46, 2266–2269.

Silverman, D.N., 1982. Carbonic anhydrase: Oxygen-18 exchange catalyzed by an enzyme with rate-contributing proton-transfer steps. In: Purich, D.L., (Ed.), Enzyme Kinetics and Mechanism, Part C. In: Colowick, S.P., Kaplan, N.O., (Eds.), Methods in Enzymology, Vol. 87. Academic Press, New York, pp. 732–752.

Sluse, F.E., Jarmuszkiewicz, W., 1998. Alternative oxidase in the branched mitochondrial respiratory network: an overview on structure, function, regulation and role. Brazilian Journal of Medical & Biological Research 31, 733–747.

Sono, M., Roach, M.P., Coulter, E.D., Dawson, J.H., 1996. Heme-containing oxygenases. Chemical Reviews 96, 2841–2887.

Steglich, W., Austel, V., 1966. Die Strukter des Dermocybins und Dermoglaucins. Tetrahedron Letters 26, 3077–3079.

Sternberg, L.d.S.L., 1989. Oxygen and hydrogen isotope ratios in plant cellulose: Mechanisms and applications. In: Rundel, P.W., Ehleringer, J.R., Nagy, K.A. (Eds.), Stable Isotopes in Ecological Research, Ecological Studies 68. Springer Verlag, New York, pp. 124–141.

Sternberg, L.d.S.L.O'R., DeNiro, M.J.D., 1983. Biogeochemical implications of the isotopic equilibrium fractionation factor between the oxygen atoms of acetone and water. Geochimica et Cosmochimica Acta 47, 2271–2274.

Sternberg, L.d.S.L., DeNiro, M.J., Savidge, R.A., 1986. Oxygen isotope exchange between metabolites and water during biochemical reactions leading to cellulose synthesis. Plant Physiology 82, 423–427.

Stevens, C.L.R., Schultz, D., Van Baalen, C., Parker, P.L., 1975. Oxygen isotope fractionation during photosynthesis in a blue-green and a green alga. Plant Physiology 56, 126–129.

Su, Q., Klinman, J.P., 1998. Probing the mechanism of proton coupled electron transfer to dioxygen: the oxidative half-reaction of bovine serum amine oxidase. Biochemistry 37, 12513–12525.

Su, Q., Klinman, J.P., 1999. Nature of oxygen activation in glucose oxidase from *Aspergillus niger*: the importance of electrostatic stabilization in superoxide formation. Biochemistry 38, 8572–8581.

Terwilliger, V.J., DeNiro, M.J., 1995. Hydrogen isotope fractionation in wood-producing avocado seedlings: biological constraints to paleoclimatic interpretations of δD values in tree ring cellulose nitrate. Geochimica et Cosmochimica Acta 59, 5199–5207.

Tian, G., Klinman, J.P., 1993. Discrimination in oxygen binding to the reversible oxygen carriers hemoglobin, myoglobin, hemerythrin, and hemocyanin: a new probe for oxygen binding and reductive activation by proteins. Journal of the American Chemical Society 115, 8891–8897.

Tian, G.C., Berry, J.A., Klinman, J.P., 1994. Oxygen-18 kinetic isotope effects in the dopamine-β-monooxygenase reaction: Evidence for a new chemical mechanism in non-heme metallomonooxygenases. Biochemistry 33, 226–234, (Correction: Tian, G.C., Berry, J.A., Klinman, J.P., 1994. Oxygen-18 kinetic isotope effects in the dopamine-beta-monooxygenase reaction. Evidence for a new chemical mechanism in metallomonooxygenases. Biochemistry 33, 14650).

Vallet, C., Saïd, R., Rabiller, C., Martin, M.L., 1996. Natural abundance isotopic fractionation in the fermentation reaction: influence of the nature of the yeast. Bioorganic Chemistry 24, 319–330.

Vallet, C., Masud, Z., Martin, M.L., 1998. Isotopic characterization of the bioconversion of lactose into ethanol. Food Chemistry 63, 115–123.

Voerkelius, S., Schmidt, H.-L., 1990. Natural oxygen and nitrogen isotope abundances of compounds involved in denitrification. Mitteilungen der Deutschen Bodenkundlichen Gesellschaft 60, 361–366.

Wagener, K., 1974. Isotopenfraktionierungen im Sauerstoffzyklus der Erde. Zeitschrift für Naturforschung 29a, 245–250.

Weber, D., Kexel, H., Schmidt, H.-L., 1997. ^{13}C-Pattern of natural glycerol: origin and practical importance. Journal of Agricultural and Food Chemistry 45, 2042–2046.

Wedeking, K.W., Hayes, J.M., 1983. Exchange of oxygen isotopes between water and organic material. Isotope Geoscience 1, 357–370.

Werner, R.A., 1998. Entwicklung neuer Verfahren für die on-line $^{18}O/^{16}O$- und $^{2}H/^{1}H$-Isotopenverhältnismessung und ihre Anwendung zur Authentizitäts- und Herkunftsbestimmung bei Naturstoffen. PhD Thesis Technische Universität München, Hieronymus Buchreproduktions GmbH, München.

Werner, R.A., Kornexl, B.E., Roßmann, A., Schmidt, H.-L., 1996. On-line determination of $\delta^{18}O$ values of organic substances. Analytica Chimica Acta 319, 159–164.

Yakir, D., DeNiro, M.J., 1990. Oxygen and hydrogen isotope fractionation during cellulose metabolism in *Lemna gibba* L. Plant Physiology 93, 325–332.

Zanconato, S., Cooper, D.M., Armon, Y., Epstein, S., 1992. Effect of increased metabolic rate on oxygen isotopic fractionation. Respiration Physiology 89, 319–327.

Zhang, B.-L., Quemerais, B., Martin, M.L., Martin, G.J., Williams, J.M., 1994a. Determination of the natural deuterium distribution in glucose from plants having different photosynthetic pathways. Phytochemical Analysis 5, 105–110.

Zhang, B.-L., Vallet, C., Blanchard, F., Martin, G.J., Combaut, G., 1994b. Characterization of galactose from carrageenans by natural abundance site-specific isotope parameters. Phytochemical Analysis 5, 291–296.

Zimmer, E., 1999. Anwendung der Isotopenverhältnismessung zu vergleichenden Herkunftsuntersuchungen bei Arzneistoffen und illegalen Drogen. PhD Thesis Technische Universität München, D-85350 Freising, Germany.

PERGAMON

Phytochemistry 58 (2001) 33–41

PHYTOCHEMISTRY

www.elsevier.com/locate/phytochem

Review

Mechanisms of survival of necrotrophic fungal plant pathogens in hosts expressing the hypersensitive response

Alfred M. Mayer[a,*], Richard C. Staples[b], Nir L. Gil-ad[a]

[a]*Department of Botany, The Alexander Silberman Institute of Life Sciences, The Hebrew University of Jerusalem, Givat Ram Campus, Jerusalem 91904, Israel*

[b]*Boyce Thompson Institute, Cornell University, Ithaca, NY 14853, USA*

Received 13 September 2000; received in revised form 15 January 2001; accepted 6 April 2001

Abstract

The hypersensitive response (HR), elicited when resistant hosts are infected by incompatible races of biotrophic fungi, has been researched extensively. New studies on host responses to necrotrophic fungi are beginning to show that when the HR occurs in hosts colonized by necrotrophs, fungal growth is accelerated rather than retarded. We review current knowledge about how necrotrophs survive in host plants in which the HR is expressed. We discuss how necrotrophs cope with the environmental factors formed as a result of the HR. Necrotrophs contain an array of enzymes, which can help in exploiting the hostile environment in order to colonize the host and to remove or inactivate active oxygen species (AOS). Among this array of enzymes are superoxide dismutase (SOD), peroxidases, catalase, and perhaps laccases and polyphenol oxidases. Of these, only SOD and catalase have been studied in any detail. The precise significance of SOD and catalase in host invasion and fungal resistance is still not adequately known. The importance of different peroxidases is also still far from clear. We speculate that AOS species may trigger the response of necrotrophs to the host environment. © 2001 Elsevier Science Ltd. All rights reserved.

Keywords: Fungi; Active oxygen species; Superoxide dismutase (SOD); Peroxidase; Catalase; Phenoloxidases

Contents

1. Introduction 34

2. The host environment 34
   2.1. The hypersensitive response 34
   2.2. Sources of active oxygen species (AOS) 35
      2.2.1. Reactions leading to AOS production in plants 35
      2.2.2. Reactions leading to AOS production in fungi 35

3. Survival of necrotrophic fungi in the host environment 35
   3.1. Effects of AOS on fungi 35
   3.2. Necrotrophs in the HR environment 36
   3.3. Fungal enzymes capable of inactivating AOS 36
      3.3.1. Superoxide dismutases (SOD) 36
      3.3.2. Activities of SOD in fungal pathogens 37

Abbreviations: AOS, active oxygen species; SOD, superoxide dismutase; O_2^-, superoxide ion; •OH, hydroxyl radical; NO, nitrogen oxidel; NO, nitric oxide

* Corresponding author. Tel.: +972-2-658-5232; fax: +972-2-658-4425.
E-mail address: eitanamm@vms.huji.ac.il (A.M. Mayer).

0031-9422/01/$ - see front matter © 2001 Elsevier Science Ltd. All rights reserved.
PII: S0031-9422(01)00187-X

3.4. Destruction of hydrogen peroxide 37
3.4.1. Catalase 37
3.4.2. Peroxidases 38
3.4.3. Host-produced oxidases 39
3.4.4. Laccases and polyphenol oxidases 39
3.4.5. Alternative oxidase 39

4. Discussion and perspectives 39

Acknowledgements 40

References 40

1. Introduction

It is has been shown that various species of active oxygen (AOS), which are produced from dioxygen, i.e. the superoxide ion, O_2^-, the hydroxyl radical, $^{\bullet}OH$, and hydrogen peroxide, H_2O_2, are deleterious to cellular growth and development of many, if not all, living organisms (Halliwell and Gutteridge, 1998). Such active oxygen species, also termed "ROI, reactive oxygen intermediates" (Govrin and Levine, 2000), "ROS, reactive oxygen species" (Emri et al., 1999), or "active oxygen" (Greenberg, 1997), can disrupt cellular membranes, induce oxidative changes in DNA, and disrupt cellular metabolism (Halliwell and Gutteridge, 1998).

Nitrogen oxide (nitric oxide, $NO^{\bullet}$) is also involved in the host-pathogen interaction, and can modify the HR reaction. Nitric oxide is known to be formed readily by plants (Leshem, 1996; Leshem et al., 1998), and its production is induced as part of the host response to pathogens (Delledonne et al., 1998; Durner et al., 1998).

Lamb and Dixon (1997) describe the chemistry of active oxygen and give details of the reactions leading to their formation: the so-called "oxidative burst" i.e. the generation of active oxygen species in response to pathogens. Their review discusses the importance of this oxidative burst to disease resistance in higher plants. We also employ their terminology for the superoxide ion, O_2^-, and the hydroxyl radical, $^{\bullet}OH$.

Two classes of fungal plant pathogens are relevant to the discussion in this review:*necrotrophic fungi,* which kill host tissue and *biotrophic fungi,* which grow on living hosts. In this review we will stress aspects of the behaviour of necrotrophic fungi, e.g. *Botrytis cinerea*.

Necrotrophic fungi are able to exploit the host defense mechanism, enlarge the infection court and colonise the host (Govrin and Levine, 2000). Necrotrophic fungi are apparently not deterred by the hypersensitive reaction of the host, and stimulation of the HR facilitates host infection by *Botrytis cinerea*. In their work, Govrin and Levine do not discuss the enzymatic mechanisms by which the fungus protects itself from the host response and the formation of AOS. We suggest that in order to inactivate or remove the AOS species formed and to exploit the environment created by the hypersensitive reaction, necroptrophic fungi utilise an array of enzymes.

In this review, we pose the question: how does a necrotrophic fungal pathogen survive on a host expressing the HR, while a biotrophic pathogen does not? We analyse current knowledge of this aspect of the behaviour of necrotrophic fungal pathogens of plants (and probably all fungal pathogens). We also discuss how such pathogens protect themselves from the toxic or destructive effects of AOS during colonization of a host's tissue, and stress the importance of the enzyme systems, which may be involved. Disease resistance mechanisms other than the HR also have a role in defense against fungal pathogens (Yu et al., 1998), but we focus here on the HR of the host and the fungal response to it.

2. The host environment

In order to define the conditions that a necrotroph encounters when it colonizes a host plant, the HR environment is briefly described below.

2.1. The hypersensitive response

Fungal infection of a host resistant to a fungal plant pathogen leads to the "hypersensitive reaction", a term coined by Stakman (1915). The hypersensitive reaction includes a localized tissue collapse and cell death at the infection site. This is an active process triggered by fungal elicitors and orchestrated by an oxidative burst, which occurs rapidly, often within hours of the attack by avirulent pathogens (Levine et al., 1994; Lamb and Dixon, 1997).

The oxidative burst is one of the earliest responses of plants to an attack either by a non-pathogen, an avirulent race of a biotrophic pathogen (Lapinskas et al.,

1993; Lu and Higgins 1999), or by a necrotroph (Govrin and Levine, 2000). There is visible necrosis of the host tissue, and the necrotic region, which arises as a result of very complex events in the host, constitutes a defensive barrier. While this barrier prevents the spread of biotrophic fungi (Lamb and Dixon, 1997; Lu and Higgins, 1999), it does not prevent the subsequent spread of necrotrophic fungi. However, AOS alone may not always be sufficient to cause programmed cell death in the HR response, and additional factors such as iron availability or production of nitric oxide may be required.

In plants, the effects of the AOS can apparently be reversed or inhibited by NO, and it may act as a scavenger of AOS (Beligni and Lamattina, 1999). Yeast strains deficient in catalase or SOD showed increased sensitivity to peroxynitrite and nitric oxide (Jakubowski et al., 1999). These authors suggest that secondary AOS species are involved in the peroxynitrite induced cell death. Free radical scavengers were able to protect against the cytotoxicity of peroxynitrite. A regulatory role of NO in the interaction of plants and microorganisms has been discussed by Wojtaszek (2000) and by Bollwell (1999). Thus, NO formation by the host is part of the signalling process during the oxidative burst. Whether *Botrytis* or other necrotrophs are capable of removing NO or whether they can interfere in its formation remains to be determined.

Toxins produced by the pathogen may also contribute to host cell death (Duran-Patron et al., 1999).

2.2. Sources of active oxygen species (AOS)

AOS can be formed both by the host plant and by the invading fungal pathogen, and it is often difficult to distinguish experimentally between the actual sources of the AOS.

2.2.1. Reactions leading to AOS production in plants

The chief source of AOS in plants is the NADPH-oxidase catalyzed reaction between NADPH and O_2 leading to O_2^- formation, followed by a number of additional reactions including dismutation, which in turn lead to H_2O_2 production. There is some evidence for additional sources of AOS in plants, including their formation by oxalate oxidase and lipoxygenase, although these have not yet been described adequately (Lamb and Dixon, 1997). Hutcheson (1998) has extensively reviewed the oxidative burst in plant defense.

2.2.2. Reactions leading to AOS production in fungi

Fungi are themselves able to produce AOS using a number of mechanisms (Deighton et al., 1999; Von Goenner et al., 1993; Von Tiedemann, 1997). The precise mechanism that is operating in any given set of conditions probably depends to a large extent on the nutritional status of the fungus. The level of different enzymes that can breakdown or utilize hydrogen peroxide is also clearly affected by the conditions of growth of the fungus (Gil-ad and Mayer, 1999). Some of the possible reactions leading to AOS formation by fungi are briefly discussed below.

NAD(P)H-oxidases are enzymes that catalyze a widely described reaction that forms AOS as a by-product of mitochondrial electron transport and flavin dehydrogenase reactions. The O_2^- produced can be converted into other active oxygen species of which $^{\bullet}OH$ is the most reactive. The NAD(P)H-oxidases have been shown to produce superoxide in animals, higher plants, and fungi (Luttik et al., 1998). Apparently, they have not been studied in fungal pathogens, but they may be important in all aspects of host–parasite relations.

Sugar oxidases are a group of flavin, iron, and/or copper-containing proteins that oxidize their substrates while reducing dioxygen to hydrogen peroxide. For example, one of the major sugar oxidases is glucose oxidase, which is present in many fungal species. This enzyme is a FAD-containing protein that catalyzes the conversion of glucose to delta-gluconolactone and hydrogen peroxide. A glucose oxidase from *Botrytis cinerea* was characterized as a non-glycosylated tetrameric protein with a native molecular weight of about 160 kDa (Liu et al., 1998). The expression of glucose oxidase in *B. cinerea* and *Phanerochaete chrysosporium* was induced by low glucose concentrations in the culture medium (Kelly and Reddy, 1986; Liu et al., 1998).

Fungi usually contain a wide variety of sugar oxidases. Their many forms, whose activities result in formation of H_2O_2, suggest their potential importance in fungal metabolism and the infection process. However, since sugars are easily inter-convertible in fungi it would probably be difficult to show by gene-deletion analysis that a specific sugar is essential for the pathogenicity process

Xanthine oxidase catalyzes the formation of O_2^-, and often is used to generate free-radicals in assay protocols (Jocelyn, 1970; Zeng et al., 1997). Lipoxygenase activity, at least in plants, can also result in the formation of free radicals (Brash, 1999). Xanthine oxidase and lipoxygenase have been studied far less in plant and fungal systems than the sugar oxidases. Thus the list of enzymatic reactions, which are the basis for the HR is probably still incomplete.

3. Survival of necrotrophic fungi in the host environment

3.1. Effects of AOS on fungi

Studies on the yeast, *Saccharomyces cerevisiae*, provide an instructive view of the deleterious effects of AOS on fungal growth. Mutants of *Saccharomyces cerevisiae*,

null for both *SOD1* and *SOD2*, are defective in sporulation, have a high rate of mutation, and are unable to biosynthesize lysine and methionine (Liu et al., 1992). Yeast suppressors, which have bypassed the SOD defect ("bsd" strains), e.g. cells which lack SOD but which are resistant to oxygen toxicity, suppress a variety of biological defects associated with *sod1* and *sod2* null mutants. Thus, a single gene mutation can alleviate the requirement for SOD in cell growth. Both "bsd" complementation groups isolated by Liu et al. (1992) were unable to utilize many non-fermentable carbon sources, suggesting a possible suppressor-linked defect in electron transport.

3.2. Necrotrophs in the HR environment

How might necrotrophs protect themselves in the HR environment? Fungal parasites do have the ability to secrete enzymes in order to protect themselves from a hostile chemical in the environment. For example, *Botrytis cinerea* can protect itself against fungicides using some of the enzymes present in the fungus. Changed enzyme activities have been shown to occur in fungicide-resistant strains of *B. cinerea*. Choi et al. (1997) reported that Vinclozolin-resistant strains of *B. cinerea* had enhanced activities of both catalase and Cu,Zn-SOD. They suggested that both enzymes appear to be involved in protecting strains of *B. cinerea* resistant to the dicarboximide fungicide, Vinclozolin. In addition, catalase and SOD activities were considerably enhanced one hour after fungicide treatment in Vinclozolin-resistant isolates compared with the susceptible isolate.

Do necrotrophs secrete enzymes that would protect them against AOS in the environment of a host expressing the HR? There is an interesting correlation between AOS, resistance to fungicides, and infection that suggests how necrotrophs can survive in an AOS-rich host environment. It has been shown that AOS might be instrumental in killing host tissue during the initial stages of infection (Levine et al., 1994; Lamb and Dixon, 1997). In fact, Govrin and Levine (2000) have shown from detailed studies that the HR response by plants to pathogens facilitated the rapid growth and spread of *Botrytis cinerea* and probably also *Sclerotium sclerotiorum*. The hypersensitive response induced by other pathogens or elicited by fungi themselves restricted the spread of biotrophic pathogens, but accelerated the growth of necrotrophs. Their evidence has also suggested that the bulk of the hydrogen peroxide produced during an attack by *B. cinerea* originates from host metabolism.

3.3. Fungal enzymes capable of inactivating AOS

What enzymes, then, might fungal pathogens employ to protect themselves in an AOS-rich environment? Staples and Mayer (1995) considered the enzymes present in fungi that are able to breakdown cell walls and complex phenolics, as part of the attack mechanism. Here, we focus on fungal enzymes that may be active in protecting the fungus against the adverse environment created by the elicitation of the HR (Fig. 1).

3.3.1. Superoxide dismutases (SOD)

Superoxide dismutases (SODs) rapidly convert O_2^- and $^{\bullet}OH$ to O_2 and H_2O_2. SODs are metalloproteins found in all aerobic organisms. The enzymes prevent damage to cellular membranes caused by oxygen toxicity and photo-oxidation, and they are the primary

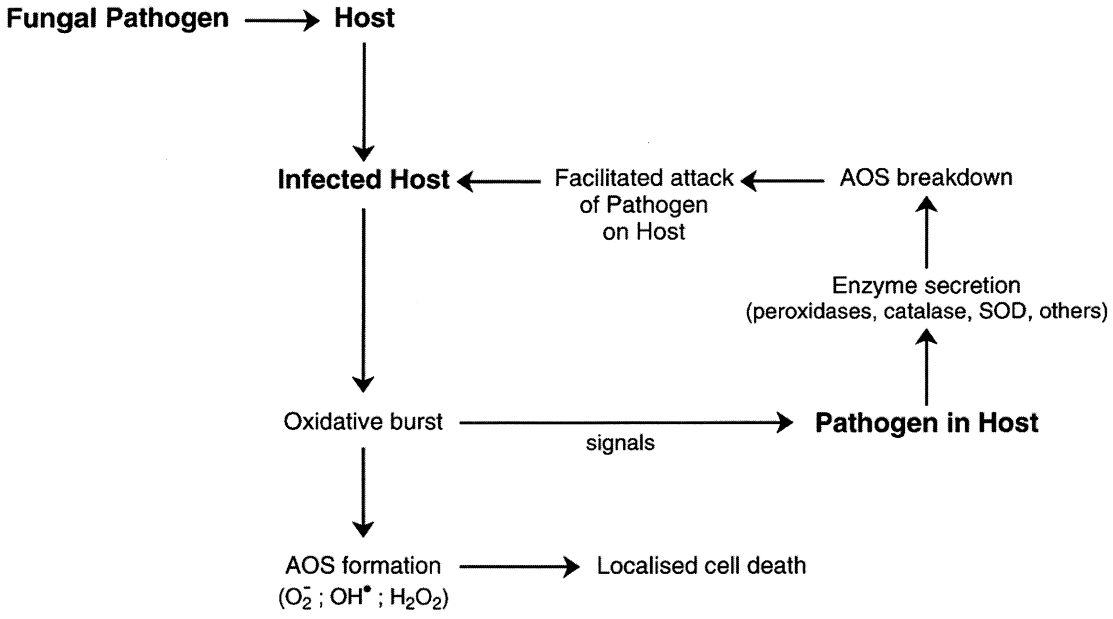

Fig. 1. Schematic presentation of some of the interactions between a plant host and a necrotrophic pathogenic fungus.

defense against the cellular damage that can be caused by the superoxide ion O_2^- (Fridovich, 1997). Fungal tissues, which lack the enzyme or in which it has been inactivated, exhibit a variety of defects.

There are at least three forms of SOD in eukaryotes: a cytosolic Cu,Zn-SOD, a mitochondrial Mn-SOD, and an extracellular Cu,Zn-SOD (Fridovich, 1997; Halliwell and Gutteridge, 1998). In addition, there is perhaps an iron-containing SOD. A wide variety of fungi have been shown to contain at least two of the three forms of SOD. Besides the earlier demonstration of SODs in yeast and *Neurospora*, the Cu,Zn-form of SODs have been found in various fungi that are pathogenic on plants and animals, including *Botrytis cinerea* (Choi et al., 1997), *Candida albicans* (Hwang et al.,1999; Rhie et al., 1999), *Cryptococcus neoformans* (Chaturvedi et al., 1999), and *Aspergillus japonicus* (Lin et al., 1994).

Fungal Cu,Zn-SODs appear to be rather closely related in terms of both structure and function. For example, the native Cu,Zn-SOD from *Candida albicans* (Hwang et al., 1999) has a mass of 39.4 kDa and is composed of two identical subunits with a molecular mass of 19.6 kDa. The gene *SOD1*, predicted a protein with 154 amino acids and a molecular mass of 16,143 Da, was found to be 79 and 69% similar to SOD genes from *Neurospora crassa* and *Saccharomyces cerevisiae*, respectively. The cloned *SOD1* contained an intron of 245 nucleotides. The gene for a cell-wall associated/excreted SOD was cloned recently from *Botrytis cinerea* (*BCSOD1*) by T. Quidde, K.-M. Weltring, and B. Tudzynski (pers. comm.). The gene has high homology to *CPSOD1* from *Claviceps purpurea* and to *SOD1* from *N. crassa*. A 21-kDa monomer of a tetrameric 85-kDa Cu,Zn-SOD was also isolated from *Uromyces appendiculatus* (Lamboy et al., 1995). A cell-wall associated, excreted Cu,Zn-SOD, which was cloned recently from *C. purpurea* (Moore and Tudzynski, pers. comm.) might be of the EC-SOD type; if proved, it would be new for pathogenic fungi.

A manganese-containing SOD from *Candida albicans* (Rhie et al., 1999) was a 106-kDa-protein composed of identical subunits with molecular masses of 26 kDa each. The gene *SOD2*, predicted a manganese-containing SOD, which contained 234 amino acid residues with a molecular mass of 26,173 Da, displayed 57% sequence identity to the homologue of *Saccharomyces cerevisiae*.

3.3.2. Activities of SOD in fungal pathogens

Vegetative hyphae of the phytopathogen *Fusarium oxysporum* differentiate into chlamydospores when triggered by growth on low-carbon media (Kono et al., 1995). In vegetative hyphae, three isozymes of SOD were present, none of which were inhibited by hydrogen peroxide and cyanide, whereas in chlamydospores, an isozyme was present and was inhibited by hydrogen peroxide but not by cyanide. Kono et al. (1995) concluded that as differentiation proceeded the Mn-type of SOD disappeared while an Fe-type of SOD appeared, and suggested that the Fe-type SOD is specifically expressed during chlamydospore formation. Direct evidence confirming the presence of an Fe-type SOD in *F. oxysporum*, which would be unusual for a fungus, was not provided.

3.4. Destruction of hydrogen peroxide

3.4.1. Catalase

This iron-containing enzyme catalyzes the rapid conversion of hydrogen peroxide to dioxygen and water. However, the enzyme appears to degrade hydrogen peroxide external to the fungal mycelia rather than the hydrogen peroxide produced internally by metabolism. Catalase is itself vulnerable to hydrogen peroxide as demonstrated by DeLuca et al. (1995).

Catalase is thought to play a key role as an antioxidant, protecting aerobic organisms from the toxic effects of hydrogen peroxide. For example, the filamentous penicillin-producing fungus, *Penicillium chrysogenum*, is especially resistant to the oxidative stress caused by high concentrations of H_2O_2 (Emri et al., 1997). Emri et al. (1997) claimed that the majority of the exogenous peroxide was likely removed by the high levels of catalase in the fungus, but that peroxide generated endogenously was removed by glutathione-pathway related enzymes. This could be taken as a hint that glutathione peroxidase also functions to reduce endogenous levels of peroxide in fungi. Thus, catalase appears to be involved only in protecting the fungus from exogenous hydrogen peroxide. However, the results reported by Gil-ad and Mayer (1999) do not support this conclusion as being general. Gil-ad and Mayer suggested that the involvement of catalase in breakdown of hydrogen peroxide seemed to be ruled out because the very specific inhibitor of catalase, 3-aminotriazole, had no effect on hydrogen peroxide breakdown. This is supported by the fact that SOD (but not catalase activities) responded when *P. chrysogenum* was treated with menadione, a drug that caused significant increases in the intracellular peroxide concentration of the fungus (Emri et al., 1999).

Wysong et al. (1998) cloned the *CAT-1* gene from the animal pathogen *Candida alibcans,* which coded for a protein of 487 amino acid residues and developed *CAT-1*-deficient mutants. These mutants exhibited normal morphology and comparable growth rates of both yeast and mycelial forms of the fungus. Enzymatic analyses revealed an abundance of catalase in the wild-type strain, decreasing catalase activity in heterologous mutants, and no detectable catalase in a homozygous null mutant. Mutant strains were more sensitive to damage by concentrations of exogenous peroxide that were sublethal for the parental strain, and the homozygous null mutant was far less virulent for mice. The authors suggested that catalase may be a pathogenicity

factor of *C. albicans* by protecting the fungus from the deleterious effects of hydrogen peroxide during host colonization.

Van der Vlugt-Bergmans et al. (1997) have proposed that the release of hydrogen peroxide by fungal oxidase activity served to facilitate host penetration by *Botrytis cinerea*, and they proposed that catalase activity might play a role in protecting the fungus against the damaging effects of hydrogen peroxide. They were able to show that *B. cinerea* contains a single-copy intracellular catalase gene, *CAT-A*, that codes for a 480-amino acid protein that most closely resembles the peroxisomal catalases. However, when *B. cinerea* colonized broad bean, *Vicia faba*, no *CAT-A* expression was detected by RNA blot analyses. From studies using tomato as the host plant, van der Vlugt-Bergmans et al. (1997) were able to confirm that there was no expression of *CAT-A* during host colonization by *Botrytis cinerea*, although hydrogen peroxide induced gene expression in an in vitro system of the fungus. It is known that hydrogen peroxide is produced during fungal colonization of the host plant, tomato, from the time of fungal penetration onwards. This hydrogen peroxide production therefore induced the tomato *cat1* gene, but not the fungal *CAT-A* gene. It is possible either that *B. cinerea* does not experience oxidative stress to the same extent as the plant host does, or that the fungitoxic effects of plant defense compounds accumulated around the necrotic lesion abolish *de novo* gene expression (Van der Vlugt-Bergmans et al., 1997). It is also possible that additional catalases other than *CAT-A* are present in *B. cinerea*, which may serve as pathogenicity factors.

More recent studies strongly suggest that indeed there are additional genes coding for catalase in *Botrytis* besides *CAT-A*. Evidence for at least one gene encoding an extracellular catalase in *B. cinerea* has now been obtained (Schouten and van Kan, pers. comm.), and the activities of these genes may account for the residual catalase activity demonstrated by Gil-ad and Mayer (unpublished data). Knowledge of the role of catalase in protecting fungal necrotrophs during host colonization awaits cloning and analysis of the additional genes.

Two catalase genes, *CPCAT1* and *CPCAT2* have been cloned from the fungal plant pathogen *Claviceps purpurea* (S. Moore and P. Tudzynski, pers. comm.). The role of these enzymes in the virulence of the pathogen is not known yet.

Two very divergent catalase genes, *CAT1* and *CAT2* have been described *in Cladosporium fulvum* (Bussink and Oliver, 2001). *CAT1* codes for a catalase subunit corresponding to peroxisome-localised catalases of yeasts and animal tissues. However, *CAT2* codes for a subunit of catalase similar to those found in filamentous fungi and bacteria. These two genes were differentially expressed, the product of expression of *CAT1* appearing in spores, while the *CAT2* gene was expressed in the mycelium. Neither of these catalases had an obvious secretory signal, nor could an extracellular catalase be detected. The catalase system of *Cladosporium fulvum* is clearly very complex and differs from that of yeast and of *Claviceps* and*Botrytis*.

Hydrogen peroxide diffuses readily into tissues, and it would therefore be difficult to determine whether an intracellular catalase or a secreted, extracellular catalase is acting on the substrate. The existence of a concentration gradient of peroxide between the medium and the mycelium would result in the disappearance of extracellular hydrogen peroxide by the action of either of these enzymes (Gil-ad et al., 2000; Gil-ad and Mayer, 1999). It has recently been shown that horseradish peroxidase can act as a scavenger of H_2O_2. (Baker et al., 2000). Thus, it is not impossible that some of the anomalous results on the function of catalase are due to a similar activity of fungal peroxidases.

3.4.2. Peroxidases

These are haem-containing proteins that catalyze the reduction of hydroperoxides, especially hydrogen peroxide to water. In addition, vanadium-dependent peroxidases are known (Van Schijndel al., 1993), and a haem-less peroxidase was reported as occurring in *Streptomyces* (Picard et al., 1997). A large number of peroxidases have been reported from fungi (Nakayama and Amachi, 1999), and elevated levels of peroxidase activity in host tissue have been repeatedly reported (Eshdat et al., 1997). But the origin of the increased activity is by no means clear, and may arise either from the host or from the pathogen.

Peroxidases have been found in almost all fungi studied. Among the fungal plant pathogens, *Botrytis cinerea* stands out as being very resistant to hydrogen peroxide (Gil-ad and Mayer. 1999). Spores of *B. cinerea* can germinate in the presence of up to 180 mM hydrogen peroxide, and mycelia are even more resistant (Gil-ad and Mayer, 1999). The breakdown is not inhibited by inhibitors of catalase, but is considerably reduced by inhibitors of peroxidase. The peroxidases in *Botrytis* and other pathogens have not been adequately characterized. Assay of a general peroxidase activity (guaiacol peroxidase) may not be an adequate measure of the ability of pathogens to remove hydrogen peroxide. Additional peroxidases, such as glutathione peroxidase and ascorbic peroxidase may well have a central function. Thus, while the level of guaiacol peroxidase activity showed great fluctuation depending on conditions of culture, ascorbic peroxidase and glutathione peroxidase levels were far more steady (Gil-ad et al., 2000).

There has not yet been a convincing demonstration that peroxidase protects a fungal pathogen from AOS encountered during colonization of its host plant. However, Gil-ad and Mayer (1999) concluded on the

basis of studies with inhibitors that the necrotrophic fungus *Botrytis cinerea* could protect itself from harmful peroxides by breaking them down with peroxidase. This conclusion is supported by the finding that *B. cinerea* forms intra- and extracellular peroxidases, including ascorbate peroxidase (Gil-ad et al., 2000).

Other peroxidases include the haloperoxidases, which have been described in the pathogenic fungi *Curvularia inaequalis* (Van Schijndel et al., 1993) and *Caldariomyces fumago* (Hager et al., 1966; Morris and Hager, 1966) and *Botrytis cinerea* (Bar-Nun and Mayer, unpublished). While the function of glutathione peroxidase, which inactivates hydrogen peroxide in animal tissues (Halliwell and Gutteridge, 1998), has not yet been investigated in fungi, its presence in plants has recently been demonstrated (Eshdat et al., 1997; Gil-ad et al., 2000).

3.4.3. Host-produced oxidases

While host-produced peroxidases might also serve as scavengers of AOS in the infection court (Gil-ad and Mayer, 1999; Von Tiedemann 1997), a direct demonstration has not been possible yet. However, consider, for example, that a versatile peroxidase able to oxidise Mn^{+2} as well as phenolic and non-phenolic aromatic compounds was isolated from *Pleurotus eryngii*, as well as the gene, *mmp1*, coding for it (Ruiz-Dueñas et al., 1999). Strong induction of *MMP1* expression was caused when the fungus was exposed to exogenous hydrogen peroxide, probably by a stress-response mechanism.

3.4.4. Laccases and polyphenol oxidases

An additional group of enzymes universally present in fungi (Mayer, 1987) include the polyphenol oxidases and laccases. An intermediary reaction product of the activity of laccases is a free radical, which could then easily interact with a variety of other radicals (Ferrari et al., 1997). While such reactions could lead to the initiation of complex reactions, including those with hydrogen peroxide or with other free radicals, little is known yet about the actual participation of these enzymes in protecting fungi in plant hosts expressing the hypersensitive response.

3.4.5. Alternative oxidase

Recently, a number of reports have indicated that plants deficient in the cyanide-sensitive alternative oxidase (AOX) had increased levels of AOS (Maxwell et al., 1999), while plants with reduced ability to detoxify AOS were hypersensitive to pathogen infection (Mittler et al., 1999). These results raise the possibility that fungal parasites could induce an increase in the level or activity of AOX in the host, for example by activating it, thereby reducing the levels of AOS. The activity of AOX is normally very tightly regulated. In either case, the hypersensitive reaction of the host would be reduced, thus facilitating pathogen development. At present, there is no evidence that fungal plant pathogens modify the levels of AOX in their hosts. However, it is also worth noting that fungi, including *Botrytis cinerea* contain an AOX, whose regulation differs from that of the plant enzyme (Tamura et al., 1999; Umbach and Siedow, 2000). The fungal AOX activity is not regulated by dimerisation. It is conceivable that such AOX could divert electrons from a host pool of ubiquinol following damage to the host cells.

4. Discussion and perspectives

When fungal plant pathogens colonize their hosts, they usually encounter a host resistance response, the generation of an environment around the pathogen rich in AOS, and death of host cells surrounding the infection site (Fig. 2). The dead host cells become a defensive layer that deprives the biotroph of a food supply. This layer also acts as a mechanical barrier, which the pathogen finds difficult to breach (Lamb and Dixon, 1997; Gilchrist, 1998). However, necrotrophs can exploit this host defense mechanism and enlarge the infection court to colonize the host (Govrin and Levine, 2000). In order to protect themselves and exploit this hostile environment, necrotrophic fungi contain an array of enzymes useful for infection of hosts, i.e. an assortment of enzymes capable of removing or inactivating toxic AOS. The mechanisms by which the production of some of these enzymes are controlled, either

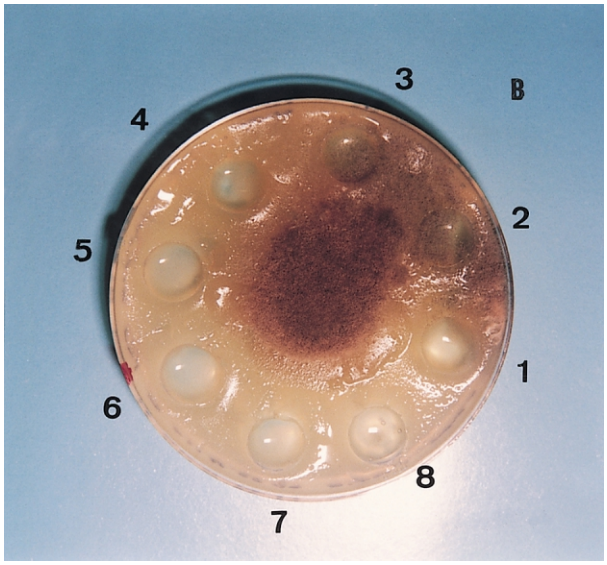

Fig. 2. Growth of *Botrytis cinerea* for 13 days on agar plates in the presence of hydrogen peroxide: 1 = 0.1 M; 2 = 0.2 M; 3 = 0.5 M; 4 = 1.0 M; 5 = 1.5 M; 6 = 2 M; 7. = 4 M; 8 = 6,4 M. The figure shows the ability of the fungus to cope with the presence of high hydrogen peroxide concentrations.

by internal or external factors, are far from clear at present, and measured enzyme activities can be expected to show great variability (Gil-ad et al., 2000).

Hydrogen peroxide is a stress factor in fungi, which acts as a trigger controlling their reaction to the environment. Consider, for example, that yeast cells have a major yeast stress-response regulon controlled by the H_2O_2-inducible *Yap1* transcription factor (Lee et al., 2000). Over all, yeasts respond to H_2O_2 by inducing the formation of some 115 proteins and the repression of 52 others (Godon et al., 1998). In contrast, the superoxide ion seems to stimulate defense gene activation in higher plants (Nuernberger et al., 1997; Durrant et al., 2000). We suggest that host-produced AOS may control the enzymatic responses of necrotrophic pathogens that enables them to survive in the AOS-rich environment of the infected host plant. Thus, H_2O_2 formation correlated positively with growth of *B. cinerea* (Govrin and Levine, 2000). In contrast, the growth of a virulent form of *Pseudomonas syringae* was inhibited in the same system when the HR was induced with an avirulent strain of the pathogen. At present, there are few tools for addressing these speculations, or for assigning a definite task for the depletion of AOS to any one of the enzymes we have discussed.

Acknowledgements

This work has been supported in part by a grant from The European Common Market (FAIR5-PL97-3351) awarded to A.M.M. Additional support for N.L.G. was provided by the Center for Absorption in Science in the Ministry of Absorption of the State of Israel.

References

Baker, C.J., Deahl, K., Domek, J., Orlandi, E.W., 2000. Scavenging of H_2O_2 and production of oxygen by horseradish peroxidase. Arch. Biochem. Biophys. 382, 232–237.

Brash, A.R., 1999. Lipoxygenase: occurrence, functions, catalysis and acquisition of substrate. J. Biol. Chem. 274, 23679–23682.

Beligni, M.V., Lamattina, L., 1999. Nitric oxide counteracts cytotoxic processes mediated by reactive oxygen species in plant tissues. Planta 208, 337–344.

Bolwell, G.P., 1999. Role of reactive oxygen species and NO in plant defence responses. Curr. Opin. Plant Biol. 2, 287–294.

Bussink, H.-J., Oliver, R., 2001. Identification of two highly divergent catalase genes in the fungal pathogen, *Cladosporium fulvum*. Eur. J. Biochem. 268, 15–24.

Chaturvedi, S., Lowry, C.V., Abramova, N., Rodeghier, B., Hamilton, A.J., Hobby, P., Chaturvedi, V., 1999. Characterization of Cu,Zn superoxide dismutase (SOD1) gene of *Cryptococcus neoformans*. Abstr. Gen. Meeting Am. Soc. Microbiol. 99, 298.

Choi, G.J., Lee, H.J., Cho, K.Y., 1997. Involvement of catalase and superoxide dismutase in resistance of *Botrytis cinerea* to dicarboximide fungicide Vinclozolin. Pesticide Biochem. Physiol. 59, 1–10.

Deighton, N., Muckenschnabel, I., Goodman, B.A., Williamson, B., 1999. Lipid peroxidation and the oxidative burst associated with infection of *Capsicum annuum* by *Botrytis cinerea*. Plant J. 20, 485–492.

Delledonne, M., Xia, Y., Dixon, R.A., Lamb, C., 1998. Nitric oxide functions as a signal in plant resistance. Nature 394, 585–588.

DeLuca, D.C., Dennis, R., Smith, W.G., 1995. Inactivation of an animal and a fungal catalase by hydrogen peroxide. Arch. Biochem. Biophys. 320, 129–134.

Duran-Patron, R., Hernadez-Galan, R., Rebordinos, L.G., Cantoral, J.M., Collado, I.G., 1999. Structure activity relationships of new phytotoxic metabolites with the Botryane skeleton from *Botrytis cinerea*. Tetrahedron 55, 2389–2400.

Durner, J., Wendelhenne, D., Klessig, D.F., 1998. Defense gene induction in tobacco by nitric oxide, cyclic GMP and cyclic ADP-ribose. Proc. Natl. Acad. Sci. USA 95, 10328–10333.

Durrant, W.E., Rowland, O., Piedras, P., Hammond-Kosack, K.E., Jones, J.D.G., 2000. cDNA-AFLP reveals a striking overlap in race-specific resistance and wound response gene expression profiles. Plant Cell 12, 963–977.

Emri, T., Pócsi, I., Szentirmai, A., 1997. Glutathione metabolism and protection against oxidative stress caused by peroxides in *Penicillium chrysogenum*. Free Radical Biol. Med. 23, 809–814.

Emri, T., Pócsi, I., Szentirmai, A., 1999. Analysis of the oxidative stress response of *Penicillium chrysogenum* to menadione. Free Radical Res. 38, 125–132.

Eshdat, Y., Doron, H., Zehava, F., Gozal, B.H., 1997. Plant glutathione peroxidases. Physiol. Plant. 100, 234–240.

Ferrari, R.P., Laurenti, E., Ghibaudi, R.M., Casella, L., 1997. Tyrosinase-catecholic substrates in vitro model: kinetic studies on the o-quinone/o-semiquinone radical formation. J. Inorg. Chem. 68, 61–69.

Fridovich, I., 1997. Superoxide anion radical [O_2], superoxide dismutases, and related matters. J. Biol. Chem. 272, 18515–18517.

Gil-ad, N.L., Mayer, A.M., 1999. Evidence for rapid breakdown of hydrogen peroxide by *Botrytis cinerea*. FEMS Microbiol. Lett. 176, 455–461.

Gil-ad, N.L., Bar-Nun, N., Noy, T., Mayer, A.M., 2000. Enzymes of *Botrytis cinerea* capable of breaking down hydrogen peroxide. FEMS Microbiol. Lett. 176, 455–461.

Gilchrist, D.G., 1998. Programmed cell death in plant disease: the purpose and promise of cellular suicide. Ann. Rev. Phytopathol. 36, 393–414.

Godon, C., Lagniel, G., Lee, J., Buhler, J.-M., Kieffer, S., Perrot, M., Boucherie, H., Toledano, M.B., Labarre, J., 1998. The H_2O_2 stimulon in *Saccharomyces cerevisiae*. J. Biol. Chem. 273, 22480–22489.

Govrin, E.M., Levine, A., 2000. The hypersensitive response facilitates plant infection by the necrotrophic pathogen *Botrytis cinerea*. Curr. Biol. 10, 751–757.

Greenberg, J.T., 1997. Programmed cell death in plant-pathogen interactions. Ann. Rev. Plant Physiol. Plant Molec. Biol. 48, 525–545.

Hager, L.P., Morris, D.R., Brown, F.S., Eberwein, H., 1966. Chloroperoxidase II: Utilisation of halogen anions. J. Biol. Chem. 241, 1769–1777.

Halliwell, B., Gutteridge, J.M.C., 1998. Free Radicals in Biology and Medicine. Clarendon, Oxford.

Hutcheson, S.W., 1998. Current concepts of active defense in plants. Ann. Rev. Phytopathol. 36, 59–90.

Hwang, C.S., Rhie, G., Kim, S.T., Kim, Y.R., Huh, W.K., Baek, Y.U., Kang, S.O., 1999. Copper- and zinc-containing superoxide dismutase and its gene from *Candida albicans*. Biochim. Biophys. Acta 1427, 245–255.

Jakubowski, W., Bilinski, T., Bartosz, G., 1999. Sensitivity of antioxidant-deficient yeast *Saccharomyces cervisiae* to peroxynitrite and nitric oxide. Biochim. Biophys. Acta 1472, 395–398.

Jocelyn, P.C., 1970. The enzymatic oxidation of glutathione in rat liver homogenates. Biochem. J. 117, 947–949.

Kelly, R.L., Reddy, C.A., 1986. Purification and characterization of glucose oxidase from ligninolytic cultures of *Phanerochaete chrysosporium*. J. Bacteriol. 166, 269–274.

Kono, Y., Yamamoto, H., Takeuchi, M., Komada, H., 1995. Alterations in superoxide dismutase and catalase in *Fusarium oxysporum*. Biochim. Biophys. Acta 1268, 35–40.

Lamb, C., Dixon, R.A., 1997. The oxidative burst in plant disease resistance. Ann. Rev. Plant Physiol. Plant Mol. Biol. 48, 251–275.

Lamboy, J.S., Staples, R.C., Hoch, H.C., 1995. Superoxide dismutase: a differentiation protein expressed in *Uromyces* germlings during early appressorium development. Exp. Mycol. 19, 284–296.

Lapinskas, P., Ruis, H., Culotta, V., 1993. Regulation of *Saccharomyces cerevisiae* catalase gene expression by copper. Curr. Gen. 24, 388–393.

Lee, J., Godon, C., Lagniel, G., Spector, D., Garin, J., Labarre, J., Toledano, M.B., 2000. Yap1 and Skn7 control two specialized oxidative stress response regulons in yeast. J. Biol. Chem. 274, 16040–16046.

Leshem, Y.Y., 1996. Nitric oxide in biological systems. Plant Growth Regul. 18, 155–159.

Leshem, Y.Y., Wills, R.B.H., Ku, V.V.-V., 1998. Evidence for the function of the free radical gas-nitric oxide ($NO^{\bullet}$)-as an endogenous maturation and senescence regulating factor in higher plants. Plant Physiol. Biochem. 36, 825–833.

Levine, A., Tenhaken, R., Dixon, R., Lamb, C., 1994. H_2O_2 from the oxidative burst orchestrates the plant hypersensitive disease resistance response. Cell 79, 583–593.

Lin, C.T., Lin, M.T., Sheu, D.C., Duan, K.J., 1994. Cloning and characterization of a copper/zinc-superoxide dismutase gene from *Aspergillus japonicus*. Taiwania 39, 73–79.

Liu, S., Oeljeklaus, S., Gerhardt, B., Tudzynski, B., 1998. Purification and characterization of glucose oxidase of *Botrytis cinerea*. Physiol. Mol. Plant Pathol. 53, 123–132.

Liu, X.F., Elashvili, I., Gralla, E.B., Valentine, J.S., Lapinskas, P., Culotta, V.C., 1992. Yeast lacking superoxide dismutase: isolation of genetic suppressors. J. Biol. Chem. 267, 18298–18302.

Lu, H., Higgins, V.J., 1999. The effect of hydrogen peroxide on the viability of tomato cells and of the fungal pathogen *Cladosporium fulvum*. Physiol. Mol. Plant Pathol. 54, 131–143.

Luttik, M.A.H., Overkamp, K.M., Koetter, P., DeVries, S., Van Dijken, J.P., Pronk, J.T., 1998. The *Saccharomyces cerevisiae* NDE1 and NDE2 genes encode separate mitochondrial NADH dehydrogenases catalyzing the oxidation of cytosolic NADH. J. Biol. Chem. 273, 24529–24534.

Maxwell, D.P., Wang, Y., McIntosh, L., 1999. The alternative oxidase lowers mitochondrial reactive oxygen production in plant cells. Proc. Nat. Acad. Sci., USA 96, 8271–8276.

Mayer, A.M., 1987. Polyphenoloxidases in plants, recent progress. Phytochemistry 26, 11–20.

Mittler, R., Herr, E.H., Orvar, B.L., Van Camp, W., Willekens, H., Inzé, D., Ellis, B.E., 1999. Transgenic tobacco plants with reduced capability to detoxify reactive oxygen intermediates are hyper-responsive to pathogen infection. Proc. Natl. Acad. Sci., USA 96, 14165–14170.

Morris, D.R., Hager, L.P., 1966. Chloroperoxidase I: isolation and properties of the crystalline glycoprotein. J. Biol. Chem. 241, 1763–1768.

Nakayama, T., Amachi, T., 1999. Fungal peroxidase: its structure, function, and application. J. Mol. Catalysis B Enzym. 6, 185–198.

Nuernberger, T., Wirtz, W., Nennstiel, D., Hahlbrock, K., Jabs, T., Zimmermann, S., Scheel, D., 1997. Signal perception and intracellular signal transduction in plant pathogen defense. J. Receptor Signal Trans. Res. 17, 127–136.

Picard, M., Gross, J., Lubbert, E., Tolzer, S., Krauss, S., van Pee, K.-H., Berkessel, A., 1997. Metal-free bacterial haloperoxidases as usual hydrolases: Activation of hydrogen peroxide by the formation of peracetic acid. Angew. Chem. Int. Ed. Engl. 36, 1196–1199.

Rhie, G.E., Hwang, C.S., Brady, M.J., Kim, S.T., Kim, Y.R., Huh, W.K., Baek, Y.U., Lee, B.H., Lee, J.S., Kang, S.O., 1999. Manganese-containing superoxide dismutase and its gene from *Candida albicans*. Biochim. Biophys. Acta 1426, 409–419.

Ruiz-Dueñas, F.J., Guillén, F., Camarero, S., Pérez-Boada, M., Martínez, M.J., Martínez, A.T., 1999. Regulation of peroxidase transcript levels in liquid cultures of the ligninolytic fungus *Pleurotus eryngii*. Appl. Environ. Microbiol. 65, 4458–4463.

Stakman, E.C., 1915. Relation between *Puccinia graminis* and plants highly resistant to its attack. J. Agric. Res. 4, 193–299.

Staples, R.C., Mayer, A.M., 1995. Putative virulence factors of *Botrytis cinerea* acting as a wound pathogen. FEMS Microbiol. Lett. 134, 1–7.

Tamura, H., Mizutani, A., Yukioka, H., Miki, N., Ohba, K., Masuko, M., 1999. Effect of methoxyiminoacetamide fungicide, SSF129, on respiratory activity in *Botrytis cinerea*. Pesticide Sci. 55, 681–686.

Umbach, A.L., Siedow, J.N., 2000. The cyanide-resistant alternative oxidase from the fungus *Pichia stipitis* and *Neurospora crassa* are monomeric and lack regulatory features of the plant enzyme. Arch. Biochem. Biophys. 378, 234–245.

Van der Vlugt-Bergmans, C.J.B., Wagemakers, C.A.M., Dees, D.C.T., van Kan, J.A.L., 1997. Catalase A from *Botrytis cinerea* is not expressed during infection on tomato leaves. Physiol. Mol. Plant Path. 50, 1–15.

Van Schijndel, J.W.P.M., Vollenbroek, E.G.M., Wever, R., 1993. The chloroperoxidase from the fungus *Curvularia inaequalis*, a novel vanadium enzyme. Biochim. Biophys. Acta 1161, 249–256.

Von Goenner, M., Schloesser, E., Neubacher, H., 1993. Evidence from electron-spin resonance for the formation of free radicals during infection of *Avena sativa* by Drechslera spp. Physiol. Mol. Plant Pathol. 42, 405–412.

Von Tiedemann, A., 1997. Evidence for a primary role of active oxygen species in induction of host cell death during infection of bean leaves with *Botrytis cinerea*. Physiol. Mol. Plant Pathol. 50, 151–166.

Wojtaszek, P., 2000. Nitric oxides in plants To NO or not to NO. Phytochemistry 54, 1–4.

Wysong, D.R., Christin, L., Sugar, A.M., Robbins, P.W., Diamond, R.D., 1998. Cloning and sequencing of a *Candida albicans* catalase gene and effects of disruption of this gene. Infec. Immun. 66, 1953–1961.

Yu, I.C., Parker, J., Bent, A.F., 1998. Gene-for-gene disease resistance without the hypersensitive response in *Arabidopsis* dnd1 mutant. Proc. Natl. Acad. Sci., USA 95, 7819–7824.

Zeng, L.H., Wu, J., Fung, B., Tong, J.H., Mickle, D., Wu, T.W., 1997. Comparative protection against oxyradicals by three flavonoids on cultured endothelial cells. Biochem. Cell Biol. 75, 717–720.

PERGAMON

Phytochemistry 58 (2001) 43–46

PHYTOCHEMISTRY

www.elsevier.com/locate/phytochem

Cloning of parsley flavone synthase I

Stefan Martens[a], Gert Forkmann[a], Ulrich Matern[b,*], Richard Lukačin[b]

[a]*Technische Universität München, Wissenschaftszentrum für Ernährung, Landnutzung und Umwelt, Department für Pflanzenwissenschaften, Lehrstuhl für Zierpflanzenbau, Am Hochanger 4, D-85350 Freising, Germany*

[b]*Institut für Pharmazeutische Biologie, Philipps-Universität Marburg, Deutschhausstrasse 17 A, D-35037 Marburg, Germany*

Received 19 March 2001; received in revised form 6 April 2001

Abstract

A cDNA encoding flavone synthase I was amplified by RT-PCR from leaflets of *Petroselinum crispum* cv. Italian Giant seedlings and functionally expressed in yeast cells. The identity of the recombinant, 2-oxoglutarate-dependent enzyme was verified in assays converting (2*S*)-naringenin to apigenin. © 2001 Elsevier Science Ltd. All rights reserved.

Keywords: *Petroselinum crispum*; Apiaceae; Flavonoid biosynthesis; Flavone synthase I cloning; 2-Oxoglutarate-dependent dioxygenase; Heterologous expression

During the last decade considerable progress has been achieved towards elucidating the mode of action and molecular architecture of 2-oxoglutarate-dependent dioxygenases. These enzymes catalyze diverse reactions, such as the hydroxylation, desaturation, epoxidation or cyclization of substrates, and the activities depend on ferrous iron and molecular oxygen which is reduced during catalysis by two electrons provided by decarboxylation of the cosubstrate (Prescott, 1993; DeCarolis and DeLuca, 1994; Prescott and John, 1996). Although 2-oxoglutarate is the common cosubstrate, some closely related dioxygenases mobilize the electrons from decarboxylation of the substrate itself, e.g. isopenicillin *N*-synthase (Baldwin and Abraham, 1988) and 4-hydroxyphenylpyruvate dioxygenase (Bradley et al., 1986; Rüetschi et al., 1992), or by the oxidation of ascorbate as in ethylene biosynthesis (Zhang et al., 1995; Lay et al., 1996). These latter enzymes may nevertheless classify with the 2-oxoglutarate-dependent dioxygenases stricto sensu in one category of intermolecular dioxygenases. Intermolecular dioxygenases fulfill a variety of pivotal functions in primary and secondary metabolism in bacteria (Omura et al., 1984; Salowe et al., 1990) and fungi, including the cyclization and ring expansion reactions in penicillin/cephalosporin biosynthesis (Baldwin and Abraham, 1988), as well as in mammalian tissues (Lindstedt et al., 1977; Kivirikko et al., 1989; Stenflo et al., 1989). Furthermore, these enzymes catalyze numerous reactions in plants, e.g. in the formation of hydroxyproline-rich glycoproteins (Tanaka et al., 1980), of gibberellins (Hedden and Graebe, 1982) and the secondary metabolites scopolamine (Hashimoto and Yamada, 1986), vindoline (DeCarolis et al., 1990) or of various flavonoids (Forkmann et al., 1980; Britsch et al., 1981; Lukačin and Britsch, 1997; Lukačin et al., 2000 a,b,c).

Five 2-oxoglutarate-dependent dioxygenases have been identified so far from flavonoid biosynthesis, which include the widely distributed anthocyanidin synthase (Menssen et al., 1990), flavanone 3β-hydroxylase (Forkmann et al., 1980; Britsch et al., 1981; Lukačin and Britsch, 1997; Lukačin et al., 2000 a,b,c) and flavonol synthase (Britsch et al., 1981; Holton et al., 1993). Another dioxygenase, catalyzing the 6-hydroxylation of partially methylated flavonols, was reported recently from *Chrysosplenium americanum* (Anzelotti and Ibrahim, 2000), while flavone synthase I, FNS I, appears to be confined to species of the Apiaceae (Britsch, 1990). FNS I had been characterized in 1981 as a soluble enzyme from parsley, in contrast to the microsomal flavone synthase II, FNS II, from other plants (Kochs and Grisebach, 1987; Martens and Forkmann, 1998), and was partially purified through six-steps of fractionation from irradiated cell cultures (Britsch, 1990). This

* Corresponding author. Tel.: +49-6421-282-2461; fax: +49-6421-282-6678.

E-mail address: matern@mailer.uni-marburg.de (U. Matern).

0031-9422/01/$ - see front matter © 2001 Elsevier Science Ltd. All rights reserved.
PII: S0031-9422(01)00191-1

enzyme was then employed in kinetic studies aiming at the reaction mechanism, which revealed that synthetic 2-hydroxynaringenin did not compete with flavanone substrates. Accordingly, the 2,3-desaturation of flavanones by FNS I was postulated to proceed by direct abstraction of the vicinal hydrogen atoms (Britsch, 1990), which would assign FNS I to a distinct desaturase subgroup among the 2-oxoglutarate-dependent dioxygenases. An analogous reaction mechanism, exluding the successive hydroxylation and dehydratation, was proposed for the desaturation of alkanes to olefines suggesting a reaction *via* radical intermediates (Mansuy, 1998). The exact course of FNS I catalysis requires further experimental support, but appears to proceed analogous to that of the cytochrome P450-dependent FNS II expressed in many plants except for the Apiaceae. The first full size FNS II cDNAs were recently cloned from *Gerbera hybrida* (Martens and Forkmann, 1999), *Antirrhinum majus* and *Torenia hybrida* (Akashi et al., 1999) by differential display PCR and expressed in yeast cells. As anticipated for a P450-dependent monoxygenase, this FNS II converted labelled flavanones to the corresponding flavones apparently without any intermediate (Martens and Forkmann, 1999).

The common mode of oxygen activation by intermolecular dioxygenases, particularly among the 2-oxoglutarate-dependent enzymes, seems to predict a high degree of homology at the DNA and polypeptide levels. However, only 30% similarity was observed in the polypeptide sequences of, for example, flavanone 3β-hydroxylase from *Petunia hybrida* and hyoscyamine 6β-hydroxylase from *Hyoscyamus niger* (Britsch et al., 1992), and the similarity of prolyl 4-hydroxylase with lysyl hydroxylase from chicken (Myllylä et al., 1991) or of fungal isopenicillin *N*-synthase with desacetoxycephalosporin C synthase ranged only at approx. 20% (Britsch et al., 1993). Nevertheless, superimposing the structural models of the penicillin and cephalosporin synthases revealed an almost identical architecture for these two enzymes (Lloyd et al., 1999), and comparison of the CD spectra of *Petunia* flavanone 3β-hydroxylase and isopenicillin *N*-synthase suggested the same pattern of helical, non-helical and β-sheet motifs for the *Petunia* dioxygenase (Lukačin et al., 2000b). Flavanone 3β-hydroxylase and FNS I both use 2-oxoglutarate as the cosubstrate and depend on the same flavanone substrates (Fig. 1). Accordingly, a thorough examination of the sequential and spatial differences of these two enzymes, together with in vitro mutagenesis studies, might be rather helpful to pinpoint the putative substrate binding sites and to explain the formation of flavones and flavonols, respectively.

Based on alignments of fourteen intermolecular dioxygenase polypeptides from public data bases two conserved sequence motifs were chosen, and, similar to the previous cloning of flavonol synthase (Fig. 1) from *Petunia hybrida* (Holton et al., 1993), degenerate oligonucleotide primers were designed for the cloning of FNS I. In combination with oligo(dT), the primers were employed for RT-PCR amplification of cDNAs from total RNA that had been extracted from young leaflets at four stages of development of flavone-producing *Petroselinum crispum* cv. Italian Giant plants (Martens and Forkmann, 1999). A whole set of intermolecular dioxygenase cDNAs was amplified, and the full-size

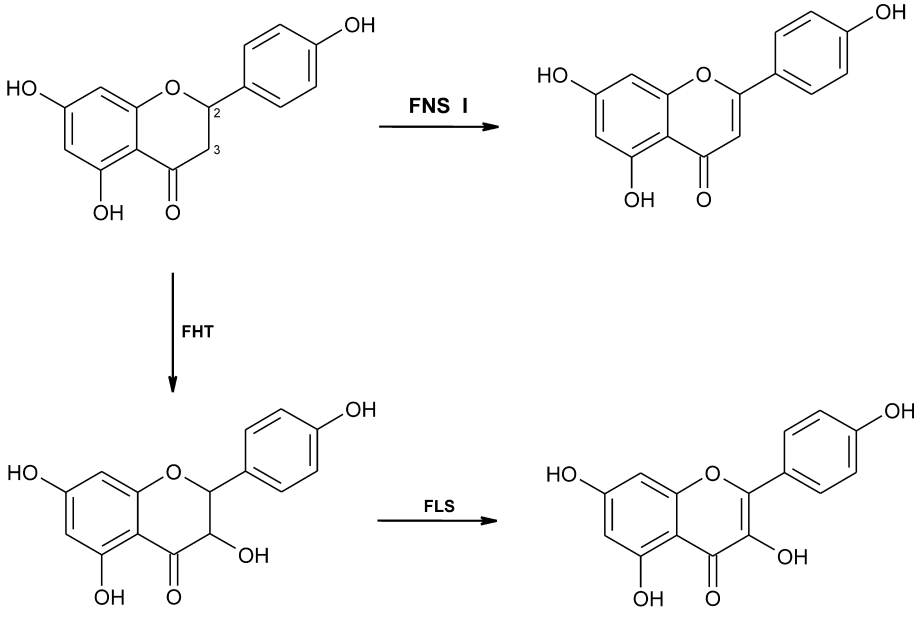

Fig. 1. Reaction catalyzed by flavone synthase I (FNS I), converting (2*S*)-naringenin to apigenin, in comparison to the activities of flavanone 3β-hydroxylase (FHT) and flavonol synthase (FLS), which sequentially convert (2*S*)-naringenin to dihydrokaempferol and kaempferol.

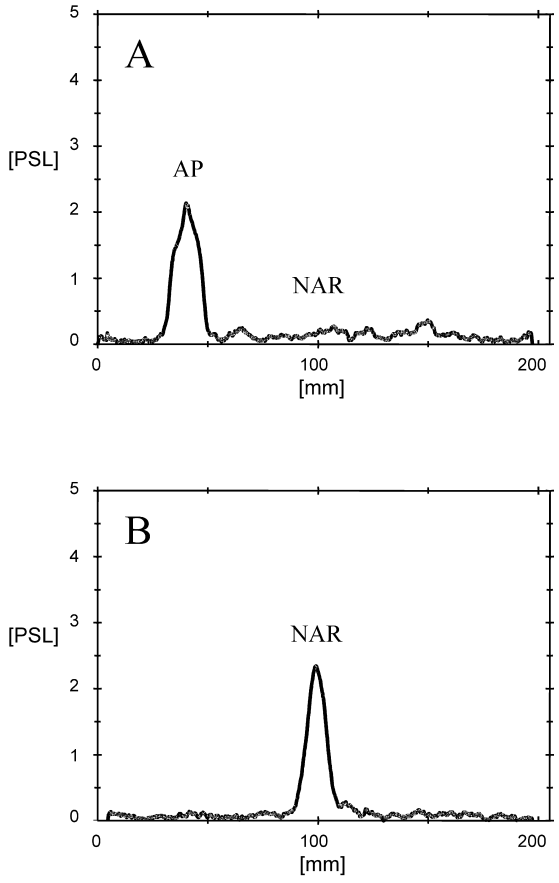

Fig. 2. Catalytic activity of parsley FNS I expressed in yeast cells. Crude extracts from yeast cells expressing the FNS I from the cDNA inserted in the pYES2 expression vector (A) or harbouring the FNS I cDNA in the inverse orientation (B) were incubated with (2*S*)-[4a,6-8-^{14}C]naringenin (NAR) as described for the native plant enzyme (Britsch, 1990). Subsequently, the incubations were extracted with ethyl acetate, the extracts were separated by thin-layer chromatograpy on cellulose in 30% aqueous acetic acid (v/v), and the radioactivity was spotted by a phosphorimager (Martens and Forkmann, 1998). The product was identified by cochromatography with authentic apigenin (AP).

clones were generated by the 5′-RACE technique. In addition to flavanone 3β-hydroxylase, flavonol synthase, 1-aminocyclopropane-1-carboxylate oxidase and two not yet fully characterized 2-oxoglutarate-dependent dioxygenases, FNS I was also recognized among the cDNA clones. The FNS I cDNA was unequivocally identified by expression in yeast strain INVSc1, using the expression vector pYES2 (Invitrogen, Groningen, The Netherlands), and the efficient conversion of naringenin to apigenin by the recombinant enzyme (Fig. 2 A). The identity of the reaction product was confirmed by direct comparison of the retention time on reversed phase HPLC in water/acetonitrile 7:3 and the ESI–MS spectrum with the mobility and fragmentation pattern of authentic apigenin (data not shown). The FNS I polypeptide was also recognized in Western blots by a FNS I polyclonal rabbit antiserum (Lukačin et al., unpublished). Moreover, the yeast strain transfected with the pYES2 vector hosting the FNS I cDNA in the inverse orientation did not express flavone synthase activity (Fig. 2 B). Recombinant FNS I lacked flavonol synthase activity (Fig. 1), and the sequences of these two enzymes differ considerably. Thus, soluble FNS I prevailing in the Apiaceae was cloned for the first time and has become available in quantity for mechanistic studies as well as for the convenient preparative synthesis of radiolabeled flavones which enable further biosynthetic and biotechnological studies. The evolutionary context for the expression of the soluble synthase exclusively in the Apiaceae remains to be established. In addition, the recombinant enzyme may be of value for the production of flavone-nutraceuticals due to their antioxidant and anticancer potentials (Harborne and Williams, 2000).

Acknowledgements

We are indebted to Dr. L. Britsch, Dr. R. Zimmermann and Dr. H. Müller (Merck KGaA, Darmstadt) for the ESI–MS analysis of apigenin as the product of the recombinant parsley FNS I.

References

Akashi, T., Fukuchi-Mizutani, M., Aoki, T., Ueyama, Y., Yonekura-Sakakibara, K., Tanaka, Y., Kusumi, T., Ayabe, S., 1999. Molecular cloning and biochemical characterization of novel cytochrome P450, flavone synthase II, that catalyzes direct conversion of flavanones to flavones. Plant Cell Physiology 40, 1182–1186.

Anzelotti, D., Ibrahim, R., 2000. Novel flavonol 2-oxoglutarate-dependent dioxygenase: affinity purification, characterization, and kinetic properties. Archives of Biochemistry and Biophysics 382, 161–172.

Baldwin, J.E., Abraham, E., 1988. The biosynthesis of penicillins and cephalosporins. Natural Product Reports 5, 129–145.

Bradley, F.C., Lindstett, S., Lipscomb, J.D., Que Jr., L., Roe, A.L., Rundgren, M., 1986. 4-Hydroxyphenylpyruvate is an iron-tyrosinate protein. Journal of Biological Chemistry 261, 11693–11696.

Britsch, L, Heller, W., Grisebach, H., 1981. Conversion of flavanone to flavone, dihydroflavonol and flavonol with an enzyme system from cell cultures of parsley. Zeitschrift für Naturforschung 36c, 742–750.

Britsch, L., 1990. Purification and characterization of flavone synthase I, a 2-oxoglutarate-dependent desaturase. Archives of Biochemistry and Biophysics 276, 348–354.

Britsch, L., Ruhnau-Brich, B., Forkmann, G., 1992. Molecular cloning, sequence analysis, and in vitro expression of flavanone 3β-hydroxylase from *Petunia hybrida*. Journal of Biological Chemistry 267, 5380–5387.

Britsch, L., Dedio, J., Saedler, H., Forkmann, G., 1993. Molecular characterization of flavanone 3β-hydroxylase: consensus sequence, comparison with related enzymes and the role of conserved histidines. European Journal of Biochemistry 217, 745–754.

DeCarolis, E., Chan, F., Balsevich, J., DeLuca, V., 1990. Isolation and characterization of a 2-oxoglutarate-dependent dioxygenase involved in the second-to-last step in vindoline biosynthesis. Plant Physiology 94, 1323–1329.

DeCarolis, E., DeLuca, V., 1994. 2-Oxoglutarate-dependent dioxygenase and related enzymes: biochemical characterization. Phytochemistry 36, 1093–1107.

Forkmann, G., Heller, W., Grisebach, H., 1980. Anthocyanin biosynthesis in flowers of *Matthiola incana*. Flavanone 3- and flavonoid 3′-hydroxylases. Zeitschrift für Naturforschung 35c, 691–695.

Harborne, J.B., Williams, C.A., 2000. Advances in flavonoid research since 1992. Phytochemistry 55, 481–504.

Hashimoto, T., Yamada, Y., 1986. Hyoscyamine 6β-hydroxylase, a 2-oxoglutarate-dependent dioxygenase, in alkaloid producing root cultures. Plant Physiology 81, 619–625.

Hedden, P., Graebe, J.E., 1982. Cofactor requirements for the soluble oxidases in the metabolism of the C20-gibberellins. Journal of Plant Growth Regulation 1, 105–116.

Holton, T.A., Brugliera, F., Tanaka, Y., 1993. Cloning and expression of flavonol synthase from *Petunia hybrida*. Plant Journal 4, 1003–1010.

Kivirikko, K.I., Myllylä, R., Pihlajaniemi, T., 1989. Protein hydroxylation: prolyl 4-hydroxylase, an enzyme with four cosubstrates and a multifunctional subunit. FASEB Journal 3, 1609–1617.

Kochs, G., Grisebach, H., 1987. Induction and characterization of a NADPH-dependent flavone synthase from cell cultures of soybean. Zeitschrift für Naturforschung 42c, 343–348.

Lay, V.J., Prescott, A.G., Thomas, P.G., John, P., 1996. Heterologous expression and site directed mutagenesis of the 1-aminocyclopropane-1-carboxylate oxidase from kiwi fruit. European Journal of Biochemistry 242, 228–234.

Lindstedt, G., Lindstedt, S., Nordin, I., 1977. Purification and properties of γ-butyrobetaine hydroxylase from *Pseudomonas* sp AK 1. Biochemistry 16, 2181–2188.

Lloyd, M.D., Lee, H.-J., Harlos, K., Zhang, Z.-H., Baldwin, J.E., Schofield, C.J., Charnock, J.M., Garner, C.D., Hara, T., Terwisscha van Scheltinga, A.C., Valegård, K., Viklund, J.A.C., Hajdu, J., Andersson, I., Danielsson, Å., Bhikhabhai, R., 1999. Studies on the active site of deacetoxycephalosporin C synthase. Journal of Molecular Biology 287, 943–960.

Lukačin, R., Britsch, L., 1997. Identification of strictly conserved histidine and arginine residues as part of the active site in *Petunia hybrida* flavanone 3β-hydroxylase. European Journal of Biochemistry 249, 748–757.

Lukačin, R., Gröning, I., Schiltz, E., Britsch, L., Matern, U., 2000a. Purification of recombinant flavanone 3β-hydroxylase from *Petunia hybrida* and assignment of the primary site of proteolytic degradation. Archive of Biochemistry and Biophysics 375, 364–370.

Lukačin, R., Gröning, I., Pieper, U., Matern, U., 2000b. Site-directed mutagenesis of the active site serine 290 in flavanone 3β-hydroxylase from *Petunia hybrida*. European Journal of Biochemistry 267, 853–860.

Lukačin, R., Urbanke, C., Gröning, I., Matern, U., 2000c. The monomeric polypeptide comprises the functional flavanone 3β-hydroxylase from *Petunia hybrida*. FEBS Letters 467, 353–358.

Mansuy, D., 1998. The great diversity of reactions catalyzed by cytochromes P450. Comparative Biochemistry and Physiology Part C 121, 5–14.

Martens, S., Forkmann, G., 1998. Genetic control of flavone synthase II activity in flowers of *Gerbera* hybrids. Phytochemistry 49, 1953–1958.

Martens, S., Forkmann, G., 1999. Cloning and expression of flavone synthase II from *Gerbera* hybrids. Plant Journal 20, 611–618.

Menssen, A., Höhmann, S., Martin, W., Schnable, P.S., Peterson, P.A., Saedler, H., Gierl, A., 1990. The En/Spm transposable element of *Zea mays* contains splice sites at the termini generating a novel intron from a dSpm element in the A2 gene. EMBO Journal 9, 3051–3057.

Myllylä, R., Pihlajaniemi, T., Pajunen, L., Turpeenniemi-Hujanen, T., Kivirikko, K.I., 1991. Molecular cloning of chick lysyl hydroxylase. Journal of Biological Chemistry 266, 2805–2810.

Omura, S., Tomoda, H., Yamamoto, S., Tsukui, M., Tanaka, H., 1984. Studies on two dioxygenases involved in the synthesis of tylosin in *Streptomyces fradiae*. Biochimica et Biophysica Acta 802, 141–147.

Prescott, A.G., 1993. A dilemma of dioxygenases (or where biochemistry and molecular biochemistry fail to meet). Journal of Experimental Botany 44, 849–861.

Prescott, A.G., John, P., 1996. Dioxygenases: molecular structure and role in plant metabolism. Annual Reviews of Plant Physiology and Plant Molecular Biology 47, 245–271.

Rüetschi, U., Odelhög, B., Lindstedt, S., Barros-Söderling, J., Persson, B., Jórnvall, H., 1992. Characterization of 4-hydroxyphenylpyruvate dioxygenase: primary structure of the *Pseudomonas* enzyme. European Journal of Biochemistry 205, 459–466.

Salowe, S.P., Marsh, E.N., Townsend, C.A., 1990. Purification and characterization of clavaminate synthase from *Streptomyces clavuligerus* an unusual oxidative enzyme in natural product biosynthesis. Biochemistry 29, 6499–6508.

Stenflo, J., Holme, E., Lindstedt, S., Chandramouli, N., Tsai Huang, L.H., Tam, J.P., Merrifield, R.B., 1989. Hydroxylation of aspartic acid in domains homologous to the epidermal growth factor precursor is catalyzed by a 2-oxoglutarate-dependent dioxygenase. Proceedings of the National Academy of Sciences USA 86, 444–447.

Tanaka, M., Shibata, H., Uchida, T., 1980. A new prolyl hydroxylase acting on poly-L-proline from suspension cultered cells of *Vinca rosea*. Biochimica et Biophysica Acta 616, 188–198.

Zhang, Z., Schofield, C.J., Baldwin, J.E., Thomas, P., John, P., 1995. Expression, purification and characterization of 1-aminocyclopropane-1-carboxylate oxidase from tomato in *Escherichia coli*. Biochemical Journal 307, 77–85.

PERGAMON

Phytochemistry 58 (2001) 47–51

PHYTOCHEMISTRY

www.elsevier.com/locate/phytochem

First cyclotide from *Hybanthus* (Violaceae)

Adriana M. Broussalis[a,1], Ulf Göransson[b,1], Jorge D. Coussio[a], Graciela Ferraro[a], Virginia Martino[a], Per Claeson[b,*]

[a]*Instituto de Química y Metabolismo del Fármaco (IQUIMEFA) (UBA-CONICET), Cátedra de Farmacognosia, Facultad de Farmacia y Bioquímica, Universidad de Buenos Aires, Argentina*

[b]*Division of Pharmacognosy, Department of Medicinal Chemistry, Uppsala University, Biomedical Centre, Box 574, SE-751 23 Uppsala, Sweden*

Received 26 January 2001; received in revised form 23 March 2001

Abstract

Hypa A, a novel macrocyclic polypeptide containing 30 amino acid residues, has been isolated from the *n*-butanol extract of the Argentine plant *Hybanthus parviflorus*. The sequence, cyclo-(SCVYIPCTITALLGCSCKNKVCYNGIPCAE), was determined by automated Edman degradation, quantitative amino acid analysis and nanospray MS/MS^2. Three intramolecular disulfide bridges stabilize the cyclic peptide backbone of hypa A. Using these structural features to classify the peptide as a cyclotide, we extended the distribution of that substance class to a new genus, and now propose a uniform nomenclature for cyclotides. © 2001 Elsevier Science Ltd. All rights reserved.

Keywords: *Hybanthus parviflorus* (Mutis ex L. F.) Baill.; Violaceae; Violetilla; Isolation; Primary structure; Cyclotides; Macrocyclic polypeptides; Hypa A; LCQ

1. Introduction

The generic name 'cyclotides' (cyclic peptides) has been given to a rapidly emerging family of macrocyclic polypeptides, which are approximately 30 amino acid residues in length and are cyclized via the amide bonds of the peptide backbone (Craik et al., 1999). Their known taxonomic distribution has been limited to genera of Violaceae and Rubiaceae (Table 1). Recently, the characteristic cyclic cystine knot has also been found in peptides isolated from the family Cucurbitaceae (Hernandez et al., 2000). To further investigate the occurrence of cyclotides within Violaceae, we examined *Hybanthus parviflorus* (Mutis ex L. F.) Baill.

H. parviflorus is a perennial shrub, widely distributed in the tropical and subtropical regions of America from Colombia to Argentina (Correa, 1988). In annual cultivations, it is a weed that grows on stubble, walls, rubble and wasteland (Zuloaga and Morrone, 1999). In several South American countries, including Colombia, Chile, Peru and Argentina, it is used as an emetic and purgative drug, and has substituted for ipecacuanha in medicine (Soukup, 1986; Murillo, 1889; Rutter, 1990; García Barriga, 1992; Mazorca, 1997). In Argentina, it is known under the name 'violetilla'.

In this study, we report the occurrence of the cyclotide hypa A in *H. parviflorus*, together with a modified sample clean-up and capture procedure. We also propose a principle for uniform naming of new members of this growing family of peptides.

2. Results and discussion

In our previous work on cyclotides from the Violaceae (Claeson et al., 1998; Göransson et al., 1999), we have used a fractionation protocol originally developed for polypeptides in general from plant biomass (Claeson et al., 1998). Here we utilise the pronounced lipophilic nature of the cyclotides by exchanging two steps in the original protocol, gel filtration on Sephadex G-10 and solid phase extraction on RP-18 silica, for a simple solvent–solvent partitioning between water and butanol. The butanolic fraction is then directly amenable to high-performance chromatography techniques (i.e. RP–HPLC).

* Corresponding author. Tel.: +46-18-471-44-79; fax: +46-18-50-91-01.

E-mail address: per.claeson@fkog.uu.se (P. Claeson).

[1] These authors contributed equally to this work.

0031-9422/01/$ - see front matter © 2001 Elsevier Science Ltd. All rights reserved.
PII: S0031-9422(01)00173-X

Table 1
The taxonomic distribution of known cyclotides

Family	Taxa	Reference
Violaceae	*Hybanthus parviflorus*	This work
	Leonia cymosa C. Martius	(Hallock et al., 2000)
	Viola arvensis Murray	(Göransson et al., 1999; Claeson et al., 1998)
	V. odorata Linn.	(Craik et al., 1999)
	V. hederacea Labill.	(Craik et al., 1999)
Rubiaceae	*Chassalia parvifolia* K. Schum.	(Gustafson et al., 2000; Gustafson et al., 1994)
	Oldenlandia affinis DC.	(Craik et al., 1999; Gran, 1973a,b; Sletten and Gran, 1973)
	Palicourea condensate Standl.	(Bokesch et al., 2001)
	Psychotria longipes Muell. Arg.	(Witherup et al., 1994)
Cucurbitaceae	*Momordica chinensis* Hort.	(Hernandez et al., 2000)

Thus, in this investigation of *H. parviflorus*, the plant material was first defatted with CH_2Cl_2 and then extracted with EtOH:H_2O 1:1. The acidified extract was filtered through polyamide to remove tannins before being partitioned between H_2O and *n*-BuOH. The *n*-BuOH extractives were subjected to repeated RP-HPLC to yield a homogeneous substance with an experimentally determined molecular mass of 3143 Da [M]. In comparison to the calculated theoretical mass given by the quantitative amino acid and Edman sequencing analyses (Table 2), a difference of 24 Da was observed. This agrees with previously isolated cyclotides, and is readily explained by the macrocyclic structure. Ring closure of the N- and C-terminals and the six cysteines engaged in three disulfide bridges corresponds to a mass loss of 24 Da.

The peptide was then reduced and alkylated with 4-vinylpyridine to yield the *S*-(ß-4-pyridylethyl) cysteine (PEC) derivative. The experimentally determined mass was 3780 Da [M], which agrees with the theoretical mass (3780 Da [M]) of a derivative with all six cysteines alkylated by 4-vinylpyridine. Subsequent digestion with endoproteinase Glu-C provided a single linear alkylated peptide (observed [M], 3798 Da; calculated [M], 3798 Da). The complete sequence of this derivative was then determined by automated Edman degradation and verified by MS^2. The results are shown in Table 2 and in Figs. 1 and 2.

Overall, this novel peptide exhibited a high degree of sequence similarity with the previously known cyclotides from Rubiaceae and Violaceae (Craik et al., 2001), and was 90% identical with the closest homologue, cycloviolacin O1, isolated from *V. odorata*. The disulfide arrangement in hypa A is most probably identical with the one reported from the NMR-structure of cycloviolacin O1 (Craik et al., 1999), i.e. C2–C17, C7–C22 and C15–C28. Moreover, the alignment placed the peptide in subfamily 1, the bracelet cyclotides, distinguished from the Moebius subfamily 2 by the lack of a *cis*-amide bond in a Trp-Pro sequence (Craik et al., 1999).

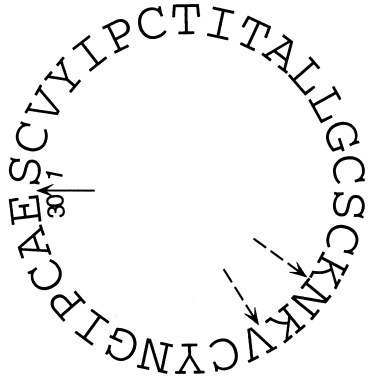

Fig. 1. The amino acid sequence of the cyclotide hypa A. The cleavage site of endoproteinase Glu-C, marked with an arrow, was chosen as an arbitrary starting point of the numbering of the amino acids (trypsin cleavage sites are marked with dashed arrows).

Cyclotides have hitherto been found in *Leonia* and *Viola* of the Violaceae family. This identification (the first) of a member of this substance class in *Hybanthus* supports chemotaxonomically the placing of *H. parviflorus* in Violaceae.

The total number of known cyclotides now exceeds 40, and that figure will no doubt grow. With the principles for naming them having varied considerably, we propose that the trivial name should be constructed as an indicative and pronounceable acronym of the Latin binomial of the plant from which the cyclotide was first isolated, followed by a letter indicating the order of appearance. By these principles, this first cyclotide from *Hybanthus parviflorus* is named hypa A.

3. Experimental

For HPLC, a Shimadzu LC-10 system was used, equipped with a SPD-M10Avp photodiode array detector. UV data were collected between 200 and 300 nm, 250×4.6 (id) and 250×10 (id) mm Rainin Dynamax (C_{18}, 5 μm, 300 Å) columns were used for analytical and

Table 2
The amino acid (aa) composition and molecular weight of hypa A. Residues from amino acid analysis are listed to the left, and the residues from sequencing, to the right

Amino acid	Hypa A	
Asp/Asn (D/N)	2.0	2 N
Thr (T)	1.9	2
Ser (S)	2.0	2
Glu/Gln (E/Q)	1.0	1 E
Pro (P)	2.0	2
Gly (G)	2.1	2
Ala (A)	2.0	2
Cys (C)	5.0[a]	6[b]
Val (V)	2.0	2
Ile (I)	2.8	3
Leu (L)	2.0	2
Tyr (Y)	1.8	2
Lys (K)	2.0	2
No aa:s	30	
M_r		
Calculated [M][c]	3143	
MS [M][d]	3143	

[a] Half-cystine was determined as cysteic acid with a separate sample following oxidation with performic acid.
[b] Cysteine, as (pyridylethyl)cysteine, following alkylation with 4-vinylpyridine.
[c] Calculated using average masses with the total sum from amino acid composition adjusted to the macrocyclic structure (−18 Da) and three disulfide bridges (−6 Da).
[d] Determined by nanospray MS.

preparative RP–HPLC. For MS and MS^2, a nanospray-ion trap MS (Protana's NanoES source mounted on a Finnigan LCQ MS) was used. All samples were sprayed in 50% MeOH, 1% HOAc, the capillary temperature was set to 230°C and the spray voltage to 0.8 kV. Average isotopic masses were used for all calculated molecular weights.

3.1. Plant material

Aerial parts of *H. parviflorus* [syn. *Ionidium glutinosum* Ventetat, *Viola parvifolia* Roemer & Schultes (Ballard and Jorgensen, 1997)] were collected along the road No.12 and its intersection with Arroyo Feliciano, Department La Paz, Entre Ríos Province, Argentina, during October 1998. A voucher specimen, identified by Dr. Juan de Dios Muñoz, is deposited at the herbarium of the Facultad de Ciencias Agrarias, Universidad Nacional de Entre Ríos, Paraná, Argentina with the collection number Muñoz 1514 (ERA). After sun and oven drying at a temperature no more than 60°C, the plant material was ground to a fine powder.

3.2. Extraction and isolation

Powdered aerial plant material (30.9 g) was extracted by maceration for 1 h with 300 ml of CH_2Cl_2 in a beaker mounted on a shaking table. This procedure was

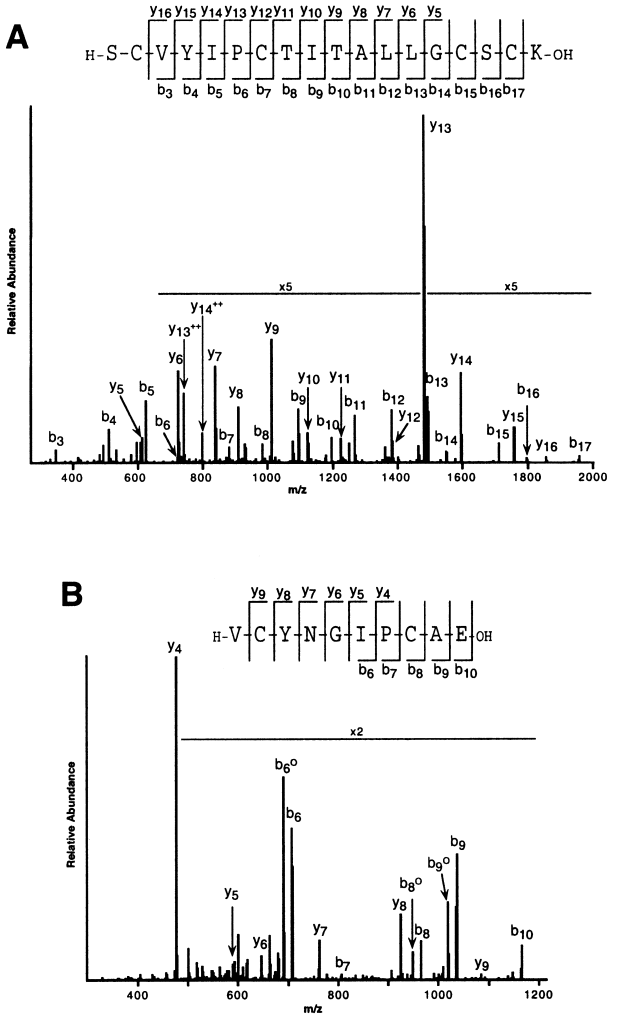

Fig. 2. MS^2-confirmation of the amino acid sequence after digestion with trypsin and endoproteinase Glu-C. Enzymatic peptides were isolated by RP-HPLC and analysed with nanospray-ion trap MS^2 (35% CID; observed fragment masses are listed in the Experimental section). The two peptides sequenced here cover 28 out of 30 amino acids. The remaining dipeptide, N19-K20, was confirmed in MS^2 fragmentation of a 30 amino acid linear peptide produced by partial digestion with trypsin (N19–K18, data not shown). (A) The fragmentation spectra of the ion 1052.5 $[M+2H]^{2+}$. Assignment of the b (N-terminal fragments) and y series (C-terminal fragments) verifies 18 amino acids, S1 to K18. (B) Fragmentation of the ion 1183.3 $[M+H]^+$, verifies the 10 amino acids before the cleavage point of GluC, V21 to E30 (b^O is b-H_2O). The assignment of this peptide is not as straightforward as in (A), due to the lack of basic amino acids.

repeated 7 times, and the CH_2Cl_2-soluble extractives were discarded. The plant residue was dried overnight at room temperature and macerated 3 times in an analogous manner with 400 ml of EtOH:H_2O 1:1.

The combined alcoholic extracts were evaporated to dryness in vacuo, then tannins were removed by dissolving the extract in 2% AcOH and passing it through 31 g of polyamide gel (Polyamide 6S Riedel-de Haën, Seelze, Germany) as described previously (Claeson et al., 1998). The yield was 4.5 g of lyophilized powder. A portion, 42 mg, of the tannin-free extract was dissolved

in H_2O (10 ml) and partitioned 3 times against *n*-BuOH (10 ml). The butanolic phases were combined to yield 0.84 mg of extractives after removal of the solvent, which was then subjected to preparative RP-HPLC using a 250×10 (i.d.) mm column eluted with a linear gradient from 25% CH_3CN, 0.1% TFA to 60% CH_3CN/0.1%TFA (v/v) over 30 min at a flow rate of 4 ml/min.

For final purification by RP–HPLC, we used a 250×4.6 (i.d.) mm column eluted with a gradient of 45–48% organic modifier (CH_3CH/*i*-PrOH, 6/4), 0.1% TFA, over 40 min at a flow rate of 1 ml/min. The yield of hypa A was 0.2 mg, as determined by quantitative amino acid analysis.

3.3. Determination of primary structure

Quantitative amino acid analysis was done at the Amino Acid Analysis Centre, Department of Biochemistry, Uppsala University. The peptide was hydrolysed for 24 h at 110°C with 6 N HCl containing 2 mg/ml phenol; the hydrolysates were analysed with an amino acid analyser using ninhydrin detection.

For the sequence analysis, the peptide was reduced with dithioerythritol in 0.25 M Tris–HCl containing 1 mM EDTA and 6 M guanidine-HCl (pH 8.5; 24°C; 2 h). The reduced peptide was subsequently alkylated to its PEC derivative by adding 4-vinylpyridine to the solution (37°C; 1 h). Desalting and isolation of the alkylated peptide was done using gel filtration on a Superdex Peptide HR 10/30 column (Amersham Pharmacia Biotech, Uppsala, Sweden) in 40% CH_3CN in 0.1% aqueous TFA.

The cyclic PEC derivative was digested with endoproteinase Glu-C (sequencing grade, Promega Co., WI, USA) in 50 mM ammonium bicarbonate (pH 7.8; 37°C; 4 h). The linear peptide was isolated using gradient RP-HPLC [250×4.6 (i.d.) mm, H_2O/CH_3CN in 0.1% TFA], and its amino acid sequence was determined by automated Edman degradation using a protein sequencer.

We then verified the sequence by MS^2 analyses of endoproteinase Glu-C and tryptic fragments (sequencing grade modified trypsin, Promega Co., WI, USA; 50 mM NH_4HCO_3 pH 7.8; 37°C; 4 h) of the cyclic peptide alkylated with iodoacetamide. Experimental masses $[M+H]^+$ of assigned MS^2-fragments (nomenclature according to Biemann, 1990): Fig. 2A, b-series: 1958.0 (b_{17}), 1796.7 (b_{16}), 1710.7 (b_{15}), 1549.5 (b_{14}), 1492.5 (b_{13}), 1379.5 (b_{12}), 1266.5 (b_{11}), 1195.4 (b_{10}), 1094.3 (b_9), 981.1 (b_8), 878.7 (b_7), 720.3 (b_6), 623.1 (b_5), 510.0 (b_4), 346.9 (b_3), y-series: 1855.9 (y_{16}), 1758.9 (y_{15}), 1594.7 (y_{14}), 1480.7 (y_{13}), 1384.8 (y_{12}), 1223.5 (y_{11}), 1122.4 (y_{10}), 1009.5 (y_9), 908.4 (y_8), 837.3 (y_7), 724.1 (y_6), 611.2 (y_5); Fig. 2B, b-series: 1165.4 (b_{10}), 1036.3 (b_9), 965.3 (b_8), 805.3 (b_7), 707.1 (b_6), y-series: 1084.3 (y_9), 923.1 (y_8), 760.2 (y_7), 646.1 (y_6), 589.5 (y_5), 476.1 (y_4).

Acknowledgements

We thank Dr. Juan de Dios Muñoz at the herbarium of the Facultad de Ciencias Agrarias, Universidad Nacional de Entre Ríos, Paraná for identifying the voucher specimen, Prof. Ernst Oliw, Dept. of Pharmaceutical Biosciences, Uppsala University, for technical advice concerning LCQ MS, and Dr. Åke Engström in the Dept. of Medical Biochemistry and Microbiology, Uppsala University for assistance with Edman sequencing. We also thank the Swedish Institute, Stockholm, for a scholarship that enabled one of us (A.M.B.) to spend a sabbatical leave from the University of Buenos Aires at Uppsala University.

References

Ballard, H.E., Jorgensen, P.M., 1997. A new name for an endemic Ecuadorian violet. Novon 7 (1), 13.

Biemann, K., 1990. Nomenclature for peptide fragment ions. Method Enzymol. 193, 886–887.

Bokesch, H.R., Pannell, L.K., Cochran, P.K., Sowder, R.C., McKee, T.C., Boyd, M.R., 2001. A novel anti-HIV macrocyclic peptide from *Palicourea condensata*. J. Nat. Prod. 64, 249–250.

Claeson, P., Göransson, U., Johansson, S., Luijendijk, T., Bohlin, L., 1998. Fractionation protocol for the isolation of polypeptides from plant biomass. J. Nat. Prod. 61, 77–81.

Correa, M.N., 1988. Flora Patagónica, Parte V Dicotiledones dialipétalas. Colección Científica del INTA, Buenos Aires.

Craik, D.J., Daly, N.L., Bond, T., Waine, C., 1999. Plant cyclotides: a unique family of cyclic and knotted proteins that defines the cyclic cystine knot structural motif. J. Mol. Biol. 294, 1327–1336.

Craik, D.J., Daly, N.L., Waine, C., 2001. The cystine knot motif in toxins and implications for drug design. Toxicon. 39, 43–60.

García Barriga, H., 1992. Flora Medicinal de Colombia, Botánica Médica, Tomo Segundo. Tercer Mundo Editores, Colombia.

Göransson, U., Luijendijk, T., Johansson, S., Bohlin, L., Claeson, P., 1999. Seven novel macrocyclic polypeptides from *Viola arvensis*. J. Nat. Prod. 62, 283–286.

Gustafson, K.R., Walton, L.K., Sowder, R.C., Johnson, D.G., Pannell, L.K., Cardellina, J.H., Boyd, M.R., 2000. New circulin macrocyclic polypeptides from *Chassalia parvifolia*. J. Nat. Prod. 63, 176–178.

Gustafson, K.R., Sowder, R.C., Henderson, L.E., Parsons, I.C., Kashman, Y., Cardellina, J.H., McMahon, J.B., Buckheit, R.W., Pannell, L.K., Boyd, M.R., 1994. Circulin A and circulin B — novel HIV-inhibitory macrocyclic peptides from the tropical tree *Chassalia parvifolia*. J. Am. Chem. Soc. 116, 9337–9338.

Gran, L., 1973a. Oxytocic principles of *Oldenlandia affinis*. Lloydia 36, 174–178.

Gran, L., 1973b. On the effect of a polypeptide isolated from "Kalata-kalata" (*Oldenlandia affinis* DC) on the oestrogen dominated uterus. Acta Pharmacol. Toxicol. 33, 400–408.

Hallock, Y.F., Sowder, R.C., Pannell, L.K., Hughes, C.B., Johnson, D.G., Gulakowski, R., Cardellina, J.H., Boyd, M.R., 2000. Cycloviolins A-D, anti-HIV macrocyclic peptides from *Leonia cymosa*. J. Org. Chem. 65, 124–128.

Hernandez, J.F., Gagnon, J., Chiche, L., Nguyen, T.M., Andrieu, J.P., Heitz, A., Hong, T.T., Pham, T.T.C., Nguyen, D.L., 2000. Squash trypsin inhibitors from *Momordica cochinchinensis* exhibit an atypical macrocyclic structure. Biochemistry 39, 5722–5730.

Mazorca, A., 1997. Vademecum de Malezas Medicinales de la Argentina, Indígenas y Exóticas. Orientación Gráfica Editora SRL, Buenos Aires.

Murillo, A., 1889. Plantes médicinales du Chili. In: Roger, A. (Ed.), Exposition Universelle de Paris. Imprimerie de Lagny, Chernoviz, pp. 18.

Rutter, R.A., 1990. Catálogo de Plantas Utiles de la Amazonia Peruana. Ministerio de Educación, Lima.

Sletten, K., Gran, L., 1973. Some molecular properties of kalatapeptide B-1. Medd. Nor. Farm. Selsk. 35, 69–82.

Soukup, J., 1986. Vocabulario de los Nombres Vulgares de la Flora Peruana y Catálogo de los Géneros. Editorial Salesiana, Lima.

Witherup, K.M., Bogusky, M.J., Anderson, P.S., Ramjit, H., Ransom, R.W., Wood, T., Sardana, M., 1994. Cyclopsychotride-A, a biologically active, 31-residue cyclic peptide isolated from *Psychotria longipes*. J. Nat. Prod. 57, 1619–1625.

Zuloaga, F.O., Morrone, O., 1999. Catálogo de las Plantas Vasculares de la República Argentina II, Monographs in Systematic Botany from the Missouri Botanical Garden 74. Missouri Botanical Garden Press, St. Louis.

PERGAMON

Phytochemistry 58 (2001) 53–58

PHYTOCHEMISTRY

www.elsevier.com/locate/phytochem

7-Deoxyloganin 7-hydroxylase in *Lonicera japonica* cell cultures

Nobuyuki Katano[a], Hirobumi Yamamoto[b], Reiko Iio[a], Kenichiro Inoue[a,*]

[a]*Department of Pharmacognosy, Gifu Pharmaceutical University, 6-1 Mitahora-higashi 5 chome, Gifu 502-8585, Japan*
[b]*Medicinal Plant Garden, School of Pharmaceutical Sciences, Nagasaki University, 1-14 Bunkyo-machi, Nagasaki 852-8521, Japan*

Received 3 January 2001; received in revised form 30 March 2001

Abstract

The activity of 7-deoxyloganin 7-hydroxylase, an enzyme catalyzing the conversion of 7-deoxyloganin into loganin, was detected in a microsomal preparation from the cell suspension cultures of *Lonicera japonica*. It was dependent on NADPH and molecular oxygen. The enzymatic reaction was inhibited by carbon monoxide as well as by several cytochrome P450 inhibitors, especially ketoconazole, indicating that the reaction was mediated by cytochrome P450. The enzyme showed substrate specificity for 7-deoxyloganin. The K_m values for 7-deoxyloganin and NADPH were estimated as 170 and 18 μM, respectively, from Lineweaver–Burk plots. © 2001 Elsevier Science Ltd. All rights reserved.

Keywords: *Lonicera japonica*; Caprifoliaceae; Cell suspension cultures; Loganin; 7-Deoxyloganin; Iridoid glucoside; 7-Deoxyloganin 7-hydroxylase; Cytochrome P450; Enzyme; Biosynthesis

1. Introduction

Secologanin, a secoiridoid glucoside, is a pivotal terpenoid intermediate in the biosynthesis of monoterpenoid indole alkaloids such as reserpine, ajmaline, ajmalicine, vincristine and vinblastine, which are biosynthesized via strictosidine, an alkaloidal glucoside, formed from secologanin and tryptamine (Zenk, 1977, 1980). *Lonicera japonica* (Caprifoliaceae) is known to contain loganin, an iridoid glucoside, as the main constituent as well as other derivatives of secologanin (Kawai et al., 1988). Our earlier studies demonstrated that the cell suspension cultures of *L. japonica* lacked the capability of secologanin biosynthesis but had the ability to convert 7-deoxyloganin and loganin into secologanin (Yamamoto et al., 1999). In our subsequent paper (Yamamoto et al., 2000), secologanin synthase, the enzyme catalyzing the conversion of loganin into secologanin was characterized as a cytochrome P450 dependent monooxygenase. Some possible radical-initiating mechanisms for this conversion were also proposed instead of the ionic ring-fission process proposed by Battersby (1967), which remained unsolved through many years in spite of several efforts (Battersby et al., 1981; Inoue et al., 1981, 1989).

As mentioned above, loganin is a biosynthetic intermediate just preceding secologanin. It is presumed that hydroxylation at the 7-position of the iridoid, which leads to loganin or loganic acid, takes place at either 7-deoxyloganin or deoxyloganic acid. Uesato et al. (1986) reported that hydroxylation proceeded at the stage of 7-deoxyloganic acid on the basis of administering various labeled compounds to *Galium* species, which contain both iridoid and secoiridoid glucosides (Bock et al., 1976; Bianco et al., 1978; Uesato et al., 1984). On the other hand, the conversion of 7-deoxyloganin into loganin was observed in cell suspension cultures of *L. japonica* (Yamamoto et al., 1999), suggesting that hydroxylation takes place at 7-deoxyloganin. The same result was also obtained in monoterpenoid indole alkaloid biosynthesis by Battersby et al. (1970). In the present paper, we describe the characterization of 7-deoxyloganin 7-hydroxylase from *L. japonica* cultured cells.

2. Results and discussion

2.1. Detection and preparation of 7-deoxyloganin 7-hydroxylase from Lonicera japonica cell suspension cultures

It is known that in plants, hydroxylation reactions at saturated carbons are catalyzed by either cytochrome

* Corresponding author. Tel.: +81-58-237-3931; fax: +81-58-237-5979.
E-mail address: inoueken@gifu-pu.ac.jp (K. Inoue).

0031-9422/01/$ - see front matter © 2001 Elsevier Science Ltd. All rights reserved.
PII: S0031-9422(01)00181-9

P450 dependent-mono-oxygenases, P450 dependent-peroxygenases (Bolwell et al., 1994) or 2-oxoglutarate-utilizing dioxygenases (Hashimoto and Yamada, 1986; De Carolis and De Luca, 1994). In order to investigate the properties of 7-deoxyloganin 7-hydroxylase, we first examined the cofactor requirement of the hydroxylase by using the cell-free extract prepared as described in the ''Experimental''. NADPH, NADH, FAD, FMN and H_2O_2 were used as potential cofactors for mono-oxygenase and peroxygenase, and $FeSO_4$ + Na ascorbate + 2-oxoglutarate as cofactors for dioxygenase. The enzymatic reaction proceeded only in the assay system containing NADPH or NADH and the specific activity (1.66 pkat/mg protein) was higher with NADPH. The enzymatic product detected by HPLC was identified by comparison of its UV absorption spectrum and LC–MS to those of loganin. No conversion was observed with the cell-free extract denatured by heating (data not shown).

2.2. Localization and reaction parameters of 7-deoxyloganin 7-hydroxylase

The subcellular localization of 7-deoxyloganin 7-hydroxylase in *L. japonica* cells was investigated. The cell-free extract was centrifuged at 100,000 × *g*. The precipitate was washed twice by homogenization in the same buffer followed by centrifugation at 100,000 × *g*. Even after washing twice, the hydroxylase activity still remained in the microsomal fraction, indicating that 7-deoxyloganin 7-hydroxylase was tightly associated with the membrane fraction. At the same time, secologanin synthase activity was also measured because this enzyme, a cytochrome P450 monooxygenase, was known to be included in the same fraction (Yamamoto et al., 2000). Secologanin, however, was not detectable because the amounts of secologanin formed from 7-deoxyloganin through loganin by two enzymes would still be beyond the limits of detection.

The hydroxylase activity of the microsomal fraction was stable upon storage at −84°C for at least 6 months.

The requirement of cofactors for 7-hydroxylase activity was studied in some detail using a microsomal preparation. Of the five cofactors used in this study, NADPH, NADH, NADP, NAD and FAD, NADPH was essential for enzymatic activity. As compared to NADPH, ca. 45% of the activity was detected with NADH and only ca. 10% with NADP or NAD (data not shown).

The optimal pH for the activity of 7-deoxyloganin 7-hydroxylase was 7.5 (in Tris–HCl buffer) with half-maximal values at 7.1 (in phosphate buffer) and 9.4 (in glycine–NaOH buffer). The pH optimum found was similar to those reported for cytochrome P450-dependent monoterpenoid hydroxylases such as sabinene hydroxylase (pH 7.4; Karp et al., 1987) and (−)-limonene C-3 and C-6 hydroxylase (pH 7.4; Karp et al., 1990), camphor hydroxylase (pH 7.0; Funk and Croteau, 1993) and (+)-limonene-6-hydroxylases (pH 7.2–7.4; Bouwmeester et al., 1999).

In the time-course of the amounts of loganin formed by 7-deoxyloganin 7-hydroxylase, the reaction proceeded linearly for ca. 10 min and then with a slow upward hyperbolic shaped-curve until after 1 h (data not shown).

2.3. Characterization of 7-deoxyloganin 7-hydroxylase

The effect of molecular oxygen on 7-hydroxylase activity was examined (Table 1). The substitution of nitrogen for air reduced the enzymatic activity by ca. 50%. An absolute requirement for oxygen was demonstrated by the removal of oxygen from the assay system by addition of the glucose oxidase/catalase system (Kochs and Grisebach, 1987), where the activity was reduced to ca. 6% of the control. This inhibition was not observed when glucose oxidase was denatured by heating. These results suggest that the hydroxylation is catalyzed by cytochrome P450.

To confirm this assumption, the effects of carbon monoxide (Omura and Sato, 1964) and several cytochrome P450 inhibitors (Fujita et al., 1982; Rossi, 1983; Wendorff and Matern, 1986; Lamberts et al., 1987) on the enzyme activity were investigated. As shown in Table 1, the reaction was inhibited by ca. 60% by CO/O_2 gas mixture in the dark and this inhibition was partially reversible upon illumination with white light. Six well-known cytochrome P450 inhibitors were also examined. Of these, ketoconazole had the strongest inhibitory effect (93% inhibition at the concentration of 0.01 mM and complete at 0.1 mM). In addition, miconazole, metyrapone, ancymidol and cytochrome c at concentrations of 0.01 and 0.1 mM inhibited 7-hydroxylation by 78.5 and 26.2, 92.4 and 73.6, 77.0 and 58.4, as well as 59.6 and 44.9%, respectively. The 7-hydroxylation activity was not inhibited by potassium cyanide, a potent inhibitor of peroxidases (Fujita et al., 1982). These results demonstrated that 7-deoxyloganin

Table 1
Influence of different treatments on 7-deoxyloganin 7-hydroxylase activity from *Lonicera japonica* cell suspension cultures

Treatment	Relative activity (%)
Air (dark)	100[a]
Air (light[b])	93.4
N_2 (dark)	50.9
N_2 (light[b])	42.0
Air + glucose + glucose oxidase + catalase	6.2
Air + glucose + boiled glucose oxidase + catalase	101.6
$CO/O_2 = 9/1$ (dark)	41.8
$CO/O_2 = 9/1$ (light[b])	59.4

[a] The enzyme activity of the control was 5.28 pkat/mg protein.
[b] White light (20,000 lx).

7-hydroxylase was a microsomal cytochrome P-450 mono-oxygenase.

2.4. Kinetic parameters of 7-deoxyloganin 7-hydroxylase

Kinetic parameters of 7-deoxyloganin 7-hydroxylase for 7-deoxyloganin and NADPH were determined by Lineweaver–Burk plots. The K_m values for 7-deoxyloganin and NADPH were 170 μM and 18 μM, respectively. The K_m value for 7-deoxyloganin was ten-fold higher than those reported for other terpenoid hydroxylases such as geraniol-10-hydroxylase (15 μM) (Hallahan et al., 1992) and (-)-limonene C-3, C-6 and C-7 hydroxylases (18, 20 and 21 μM) (Karp et al., 1990), indicative of the low affinity of 7-deoxyloganin for 7-deoxyloganin 7-hydroxylase.

2.5. Substrate specificity of 7-deoxyloganin 7-hydroxylase

The substrate specificity of the 7-hydroxylase was studied. The following substrates were used: the 11-carbomethoxy-type substrates, 7-deoxyloganin, 8-epi-7-deoxyloganin, 10-deoxygeniposide, mussaenoside and adoxoside; the 11-carboxyl-type substrates, 7-deoxyloganic acid, 8-epi-7-deoxyloganic acid, 10-deoxygenipo sidic acid, mussaenosidic acid and adoxosidic acid; the 11-aldehyde-type substrates, 5-deoxystansioside and boschnaloside; the 11-alcohol-type substrates, 7,8-dehydro-11-hydroxy-iridodial glucoside, 11-hydroxyiridodial glucoside; the 11-methyl-type substrates, iridodial glucoside (Fig. 1 for their structures). Of these 7-deoxy compounds, only two compounds, 7-deoxyloganin and 7-deoxyloganic acid, were hydroxylated and the production of loganic acid from 7-deoxyloganic acid was only ca. 50% of that of loganin from 7-deoxyloganin.

The conversion of 7-deoxyloganin into loganin, previously observed from administration experiments to *L. japonica* cultured cells (Yamamoto et al., 1999), was also confirmed in the present study at the enzyme level. 7-Deoxyloganic acid is presumed to be an intermediate just before 7-deoxyloganin. However, our above results, coupled with those of administration experiments to *Galium mollugo* (Uesato et al., 1986), suggest that *L. japonica* cells might include the following two biosynthetic pathways; one is the pathway in which methylation of deoxyloganic acid precedes hydroxylation of the resulting ester leading to loganin (not via loganic acid). The other is the pathway via loganic acid formed by 7-hydroxylation of 7-deoxyloganic acid leading to loganin. Madyastha et al. (1973) reported that the methyltransferase from *Catharanthus roseus* plant catalyzed the conversion of loganic acid into loganin but not that of deoxyloganic acid into deoxyloganin. Thus, the biosynthetic pathway to loganin remains unclear. Further information on loganin biosynthesis in *L. japonica* cultured cells requires detailed studies involving the administration of several substrates into the cultured cells, the purification and substrate specificity of the methyltransferase as well as the separation of cytochrome P450 dependent mono-oxygenases; this work is now in progress.

3. Experimental

3.1. Plant material and culture method

The origin and subculturing of cell suspension cultures of *Lonicera japonica* were described in our previous paper (Yamamoto et al., 1999). Fresh cells (1.5 g) were transferred to 20 ml of Murashige-Skoog liquid medium (Murashige and Skoog, 1962) containing 10 μM naphthaleneacetic acid and 10 μM 6-benzylaminopurine, and were agitated on a rotary shaker at a speed of 100 rpm at 23°C in the dark and subcultured every 2 weeks.

3.2. Enzyme preparation

All enzyme preparation operations were carried out at 4°C. Nine-day-old cultured *L. japonica* cells (20 g) were homogenized in 20 ml of 100 mM potassium phosphate buffer (pH 6.5) containing 10 mM DTT and 2 g PVPP with a teflon homogenizer. The homogenate was centrifuged at 12,000 × *g* for 20 min. The supernatant was applied to a PD-10 column (Amersham Pharmacia Biotech, UK) previously equilibrated with 100 mM Tris–HCl buffer (pH 7.5) containing 10 mM DTT and then the enzyme preparation was eluted with 3.5 ml of the same buffer. The eluted solution was used as the cell-free extract.

For the microsomal preparation, the above 12,000 × *g* supernatant was centrifuged at 100,000 × *g* for 30 min. The pellet was washed twice with 100 mM Tris–HCl buffer (pH 7.5) containing 10 mM DTT and then resuspended in 4 ml of the same buffer containing 10 mM DTT. This suspension was used as the microsomal fraction and was either used directly for assays, or frozen in liquid nitrogen after an addition of 10% (v/v) glycerol to the suspension and stored at −84°C.

Protein contents were determined according to the method of Bradford (1976), using bovine serum albumin as standard (Sigma, USA).

3.3. Enzyme assay for cofactor requirement

The incubation mixture contained 250 nmol 7-deoxyloganin, 200 μl cell-free extract (1.42 pkat/mg protein), various cofactors and was adjusted to a total volume of 250 μl with 100 mM Tris–HCl buffer (pH 7.5) containing 10 mM DTT. The cofactors used in this experiment were 250 nmol NADPH, 250 nmol NADH, 250 nmol

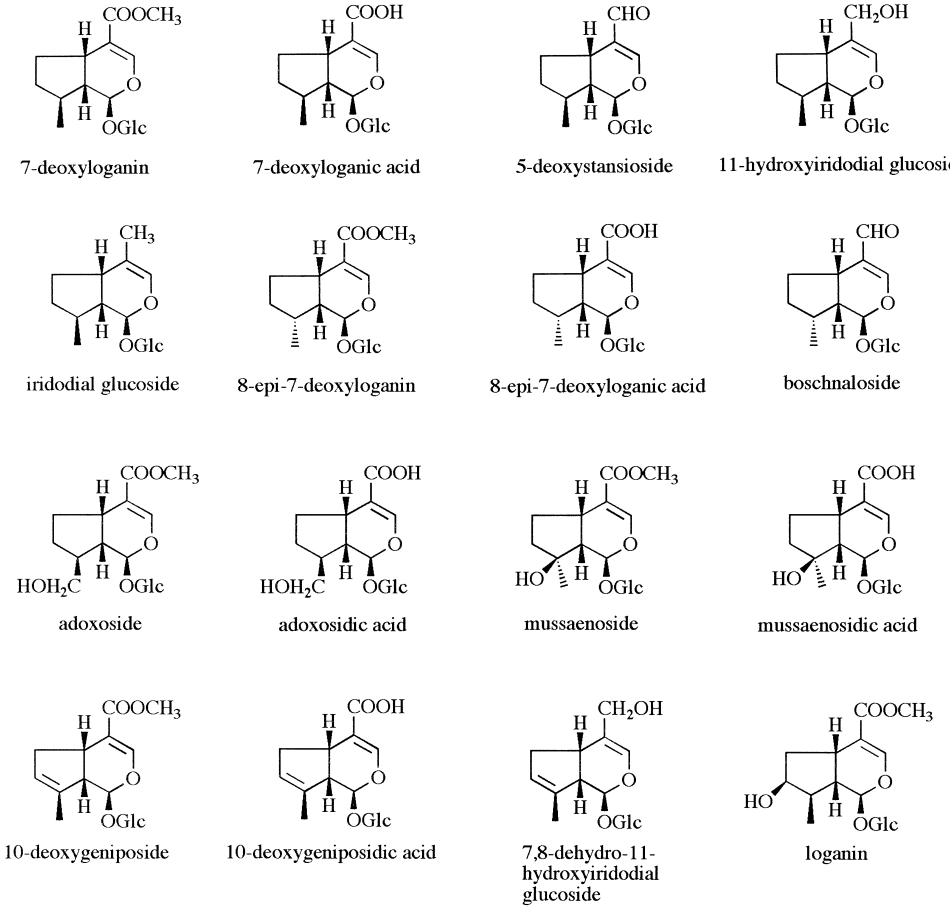

Fig. 1. Structures of substrates used for the experiments on substrate-specificity for 7-deoxyloganin 7-hydroxylase.

FAD, 250 nmol FMN, 250 nmol NADPH + 2.5 nmol FAD, 250 nmol NADPH + 2.5 nmol FMN, 250 nmol NADH + 2.5 nmol FAD, 250 nmol NADH + 2.5 nmol FMN, 40 nmol $FeSO_4$ + 400 nmol sodium ascorbate + 100 nmol 2-oxoglutarate or 250 nmol H_2O_2. The reaction was initiated by the addition of each cofactor to the mixture and after the incubation for 30 min at 30°C, terminated by boiling the reaction mixture on a water bath for 5 min. The mixture was centrifuged at 15,000 × *g* for 5 min and the supernatant was analyzed by reversed phase HPLC. The assays were performed in duplicate.

3.4. Standard enzyme assay

The incubation mixture contained the same components as described above except for the use of 200 µl of the microsomal fraction as the enzyme and 250 nmol NADPH as cofactor. After incubation for 10 min at 30°C, the mixture was treated and analyzed as described above. The assays were performed in duplicate.

3.5. pH-Optimum determination

Determination of the pH-optimum was carried out as described for the standard assay, but using the following three buffers: 200 mM potassium phosphate buffer (pH 5.0–7.5), 200 mM Tris–HCl buffer (pH 7.0–9.0) and 200 mM glycine–NaOH buffer (pH 8.5–10.0).

3.6. Oxygen dependence

The 20 ml test tubes containing all the reaction components of the standard enzyme assay except for NADPH were sealed with septum caps, and 60 ml of N_2, CO/O_2 (9:1) mixture or air were slowly bubbled into the mixture on ice, respectively.

The reaction was initiated by the addition of 250 nmol NADPH, treated and analyzed as described above. The assays were performed in duplicate. To examine the effect of the light on the inhibition by CO, the tubes were kept in the System Biotron (20,000 lx of fluorescent lights) for 10 min at 30°C. Tubes covered with aluminium foil were also kept in the same chamber as the dark condition. Additionally, to examine the photochemical effect on the enzyme activities under air or under nitrogen, the tubes containing the standard incubation mixture were kept in the same chamber.

For the oxygen consumption experiments, an enzyme assay lacking NADPH was preincubated at 30°C with 10 nmol glucose, 10 unit glucose oxidase (Nacalai Tesque,

Japan) and 20 unit catalase (Sigma, USA) (Kochs and Grisebach, 1987). After 5 min, the incubation was initiated by addition of 250 nmol NADPH and continued as described above. As a comparative experiment, heat-inactivated glucose oxidase was used.

3.7. Inhibition experiments

The P450 inhibitors, ketoconazole, miconazole, metyrapone, ancymidol and cytochrome c were tested. Metyrapone and cytochrome c were dissolved in H_2O and others were dissolved in DMSO. KCN was dissolved in 100 mM Tris–HCl buffer (pH 7.5). The concentrations of inhibitors were adjusted to 1 or 0.1 mM with each solvent. The incubation mixture contained 250 nmol 7-deoxyloganin, 250 nmol NADPH, 175 μl enzyme (24.95 pkat/mg protein) and 25 μl the solution of each inhibitor in total volume of 250 μl and continued as described above.

3.8. HPLC analysis

The amount of loganin was determined by reversed phase HPLC using Bio-Sil C18 HL 90-5 S column (5 μm, 4.6×250 mm, Bio-Rad, USA) in an oven at 40°C, with a CH_3CN/H_2O linear gradient solvent system, from 10% MeCN to 30% MeCN in 40 min at a flow rate of 1.0 ml/min, monitoring the absorption at 240 nm. The quantities were calculated from the peak area at 240 nm recorded by Chromatopac C-RA4 (Shimadzu, Japan). Rt. of loganin, 12.8 min, Rt. of 7-deoxyloganin, 32.8 min.

3.9. Identification of the reaction product

The identification of the product was carried out on the basis of UV and MS spectra obtained with Shimadzu SPDM-6A HPLC-photodiode array system (Shimadzu, Japan) as well as Shimadzu high performance liquid chromatograph–mass spectrometer LCMS-QP8000. The HPLC condition for the LC–MS system were as follows: column, Shim-pack VP-ODS (5 μm, 2.0×150 mm); solvent, CH_3CN/H_2O; linear gradient solvent system, from 10% MeCN to 30% MeCN in 30 min at a flow rate of 0.2 ml/min, monitoring the absorption at 240 nm oven temp., 40°C, Rt. of loganin, 9.5 min. Negative FAB–MS m/z; 389 ($[M-H]^-$).

3.10. Determination of kinetic parameters

The apparent Michaelis constant (K_m) and maximal reaction velocity (V_{max}) for 7-deoxyloganin was determined by Lineweaver–Burk plots at 0.04, 0.08, 0.16, 0.32 mM, using 250 nmol NADPH and those for NADPH at 0.02, 0.04, 0.08, 0.16 mM, using 250 nmol 7-deoxyloganin. K_m and V_{max} values for 7-deoxyloganin were 170 μM and 12.47 pkat/mg protein and for NADPH 18 μM and 8.33 pkat/mg protein, respectively.

Acknowledgements

We are grateful to Ms. K. Arakawa, Kyoto Analytical Applications Center, Shimadzu Corporation for the measurement of LC–MS spectrum. Financial support by Japanese Bioindustry Association is gratefully acknowledged.

References

Battersby, A.R., 1967. Biosynthesis of the indole and colchicum alkaloids. Pure and Applied Chemistry 14, 117–136.

Battersby, A.R., Burnett, A.R., Parsons, P.G., 1970. Preparation and isolation of deoxyloganin: its role as precursor of loganin and the indole alkaloids. Journal of the Chemical Society Chemical Communications, 826–827.

Battersby, A.R., Westcott, N.D., Glusenkamp, K.-H., Tiezte, L.-F., 1981. Untersuchungen zur Biogenese der Indolalkaloide. Synthese und Verfüetterung radioaktiv markierter Hydroxyloganin-Derivate. Chemische Berichte 114, 3439–3447.

Bianco, A., Guiso, M., Iavarone, C., Passacantilli, P., 1978. Iridoids XXV. New iridoid glucosides from Rubiaceae. Gazzetta Chimica Italiana 108, 13–16.

Bock, K., Jensen, S.J., Nielsen, B.J., 1976. Secogalioside, an iridoid glucoside from *Galium album* Mill. and carbon-13 NMR spectra of some secoiridoid glucosides. Acta Chemica Scandinavica Ser. B 30, 743–748.

Bolwell, G.P., Bozak, K., Zimmerlin, A., 1994. Plant cytochrome P450. Phytochemistry 37, 1491–1506.

Bouwmeester, H.J., Konings, C.J.M., Gershenzon, J., Karp, F., Croteau, R., 1999. Cytochrome P-450 dependent (+)-limonene-6-hydroxylation in fruits of caraway (*Carum carvi*). Phytochemistry 50, 243–248.

Bradford, M.M., 1976. A rapid and sensitive method for the quantitation of microgram quantities of protein utilizing the principle of protein-dye binding. Analytical Biochemistry 72, 248–254.

De Carolis, E., De Luca, V., 1994. 2-Oxoglutarate-dependent dioxygenase and related enzymes: biochemical characterization. Phytochemistry 36, 1093–1107.

Fujita, M., Oba, K., Uritani, I., 1982. Properties of a mixed function oxygenase catalyzing ipomeamarone 15-hydroxylation in microsomes from cut-injured and *Ceratocystis fimbriata*-infected sweet potato root tissues. Plant Physiology 70, 573–578.

Funk, C., Croteau, R., 1993. Introduction and characterization of a cytochrome P-450-dependent camphor hydroxylase in tissue cultures of common sage (*Salvia officinalis*). Plant Physiology 101, 1231–1237.

Hallahan, D.L., Dawson, G.W., West, J.M., Wallsgrove, R.M., 1992. Cytochrome P-450 catalyzed monoterpene hydroxylation in *Nepeta mussinii*. Plant Physiology and Biochemistry 30, 435–443.

Hashimoto, T., Yamada, Y., 1986. Hyoscyamine 6β-hydroxylase, a 2-oxoglutarate-dependent dioxygenase, in alkaloid-producing root cultures. Plant Physiology 81, 619–625.

Inoue, K., Takeda, Y., Tanahashi, T., Inouye, H., 1981. On the possibility of the intermediacy of 10-hydroxyloganin in the biosynthesis of secologanin. Chemical Pharmaceutical Bulletin 29, 981–990.

Inoue, K., Tanahashi, T., Inouye, H., Kuwajima, H., Takaishi, K., 1989. Intermediacy of 6-hydroxyloganin in the ring cleavage course of loganin to secologanin. Phytochemistry 28, 2971–2979.

Karp, F., Harris, J.L., Croteau, R., 1987. Metabolism of monoterpenes: demonstration of the hydroxylation of (+)-sabinene to (+)-*cis*-sabinol by an enzyme preparation from sage (*Salvia officinals*) leaves. Archives of Biochemistry and Biophysics 256, 179–193.

Karp, F., Mihaliak, C.A., Harris, J.L., Croteau, R., 1990. Monoterpene biosynthesis: specificity of the hydroxylations of (−)-limonene by enzyme preparations from peppermint (*Mentha piperita*), spearmint (*Mentha spicata*), and perila (*Perilla frutescens*) leaves. Archives of Biochemistry and Biophysics 276, 219–226.

Kawai, H., Kuroyanagi, M., Ueno, A., 1988. Iridoid glucosides from *Lonicera japonica* THUNB. Chemical Pharmaceutical Bulletin 36, 3664–3666.

Kochs, G., Grisebach, H., 1987. Induction and characterization of a NADPH-dependent flavone synthase from cell cultures of soybean. Zeitschrift für Naturforschung 42c, 343–348.

Lamberts, S.W.J., Bons, E.G., Bruining, H.A., de Jong, F.H., 1987. Differential effects of the imidazole derivatives etomidate, ketoconazole and miconazole and of metyrapone on the secretion of cortisol and its precursors by human adrenocortical cells. The Journal of Pharmacology and Experimental Therapeutics 240, 259–264.

Madyastha, K.M., Guarnaccia, R., Baxter, C., Coscia, C.J., 1973. *S*-Adenosyl-L-methionine: loganic acid methyltransferase. The Journal of Biological Chemistry 248, 2497–2501.

Murashige, T., Skoog, F., 1962. Revised medium for rapid growth and bioassays with tobacco tissue cultures. Physiologia Plantarum 15, 473–497.

Omura, T., Sato, R., 1964. The carbon monoxide-binding pigment of liver microsomes I. Evidence for its hemoprotein nature. The Journal of Biological Chemistry 239, 2370–2378.

Rossi, M., 1983. Strctural studies of metyrapone: a potent inhibitor of cytochrome P-450. Journal of Medicinal Chemistry 26, 1246–1252.

Uesato, S., Miyauchi, M., Itoh, H., Inouye, H., 1986. Biosynthesis of iridoid glucosides in *Galium mollugo*, *G. spurium var. echinospermon* and *Deutzia crenata*. Intermediacy of deoxyloganic acid, loganin and iridodial glucoside. Phytochemistry 25, 2515–2521.

Uesato, S., Ueda, S., Inouye, H., Kuwajima, H., Yatsuzuka, M., Takaishi, K., 1984. Iridoid glucosides from *Gallium mollugo*. Phytochemistry 23, 3535–3537.

Yamamoto, H., Katano, N., Ooi, A., Inoue, K., 1999. Transformation of loganin and 7-deoxyloganin into secologanin by *Lonicera japonica* cell suspension cultures. Phytochemistry 50, 417–422.

Yamamoto, H., Katano, N., Ooi, A., Inoue, K., 2000. Secologanin synthase which catalyzes the oxidative cleavage of loganin into secologanin is a cytochrome P450. Phytochemistry 53, 7–12.

Wendorff, H., Matern, U., 1986. Differential response of cultured parsley cells to elicitors from two non-pathogenic strains of fungi. European Journal of Biochemistry 161, 391–398.

Zenk, M.H., 1977. Isovimcoside (Strictosidine), the key intermediate in the enzymatic formation of indole alkaloids. FEBS Letters 79, 233–237.

Zenk, M.H., 1980. Enzymatic synthesis of ajmalicine and related indole alkaloids. Journal of Natural Products 43, 438–451.

PERGAMON

Phytochemistry 58 (2001) 59–66

PHYTOCHEMISTRY

www.elsevier.com/locate/phytochem

Purification and characterization of two α-amylase inhibitors from seeds of tepary bean (*Phaseolus acutifolius* A. Gray)

Tsuyoshi Yamada[a], Kazumi Hattori[a], Masao Ishimoto[b,*]

[a]*Graduate School of Agricultural Sciences, Nagoya University, Chikusa, Nagoya, 464-8601, Japan*
[b]*National Agricultural Research Center for Western Region, Fukuyama, Hiroshima 721-8514, Japan*

Received 16 November 2000; received in revised form 2 March 2001

Abstract

Two proteinaceous α-amylase inhibitors termed αAI-Pa1 and αAI-Pa2 were purified from seeds of a cultivated tepary bean (*Phaseolus acutifolius* A. Gray, cv. PI311897). The two inhibitors differed in their specificity towards α-amylases of insect pests such as bruchids, although neither showed any inhibitory activity against α-amylases of mammalian, bacterial or fungal origin. αAI-Pa2 resembles two common bean inhibitors, αAI-1 and αAI-2, in several characteristics such as N-terminal amino acid sequences and oligomeric structure being composed of α and β subunits. In contrast αAI-Pa1 is composed of a single glycopolypeptide with a molecular mass of 35 kDa, and its N-terminal amino acid sequence resembled that of seed lectins in tepary bean and common bean. The information on the two tepary bean α-amylase inhibitors may be useful not only for providing insight into critical structure for the specificity towards different α-amylase enzymes but also for enhancing insect resistance in crops. © 2001 Elsevier Science Ltd. All rights reserved.

Keywords: *Phaseolus acutifolius*; Leguminosae; α-Amylase inhibitor; Lectin; Insect resistance; Bean weevil; Bruchid

1. Introduction

Seeds of common bean (*Phaseolus vulgaris* L.) contain proteinaceous inhibitors of the digestive enzyme α-amylase. The common bean α-amylase inhibitor (αAI) does not inhibit the activity of plant, fungal and bacterial α-amylase, but inhibits the activity in mammals and some insects (Powers and Whitaker, 1977a; Powers and Culbertson, 1983; Freis and Rupmnow, 1984). Due to its inhibitory specificity, αAI has drawn attention as an insecticidal protein (Chrispeels and Raikhel, 1991) and as an antinutritional factor for humans and livestock (Layer et al., 1985). In conventional and molecular breeding, bean αAI is a powerful tool to control insect pests, such as bean weevils (bruchids). The inhibitor prevents insect growth through the inhibition of starch digestion in the gut. As a result, insect larvae starve to death. This insecticidal effect has been confirmed by the bioassay of bruchids on artificial bean containing purified αAI and by the expression of the cDNA encoding αAI in the pea (*Pisum sativum*) and azuki bean (*Vigna anguralis*) (Ishimoto and Kitamura, 1988; Huesing et al., 1991; Shade et al., 1994; Schroeder et al., 1995; Ishimoto et al., 1996). Transgenic crops accumulating αAI became resistant to several species of bruchids such as pea weevil (*Bruchus pisorum*) and azuki bean weevil (*Callosobruchus chinensis*).

Two allelic variants of αAI are found in common bean. αAI-1, which is found in most common beans, has been purified and characterized comprehensively from several bean varieties (Marshall and Lauda, 1975; Powers and Whitaker, 1977b; Lajolo and Finardi Filho, 1985). αAI-1 inhibits larval gut α-amylase of azuki bean weevil and cowpea weevil (*C. maculatus*) as well as mammalian α-amylase (Ishimoto and Kitamura, 1989). The second variant, αAI-2, has initially been found in some wild common beans resistant to Mexican bean weevil (*Zabrotes subfasciatus*), which is a storage pest of common beans, and specifically inhibits the larval α-amylase of *Z. subfasciatus* (Minney et al., 1990; Ishimoto and Kitamura, 1993). The cDNAs of the two inhibitors have been isolated and were shown to share 78% amino acid sequence identity (Hoffman et al., 1982; Mirkov et al., 1994; Suzuki et al., 1994).

* Corresponding author. Tel.: +81-849-23-4100; fax: +81-849-24-78930.
E-mail address: ishimoto@affrc.go.jp (M. Ishimoto).

0031-9422/01/$ - see front matter © 2001 Elsevier Science Ltd. All rights reserved.
PII: S0031-9422(01)00178-9

In addition to common bean, αAI is distributed in some other legumes of the genus *Phaseolus* such as scarlet runner bean (*P. coccineus*) and tepary bean (*P. acutifolius*) (Pueyo et al., 1993; Ishimoto and Chrispeels, 1996; Pueyo and Delgado-Salinas, 1997). In inhibitory specificity to α-amylase enzymes, scarlet runner bean αAI resembles αAI-1, while tepary bean αAI is different from the other bean inhibitors (Ishimoto and Chrispeels, 1996). The seed extract of tepary bean inhibited α-amylase of both *C. chinensis* and *Z. subfasciatus* but not mammalian α-amylases. An α-amylase inhibitor protein was purified from a tepary bean cultivar and its primary characteristics reported (Blanco-Labra et al., 1996), indicating that αAI was active against a large number of insect α-amylases, as compared with the other inhibitors purified from common beans. Because of its wide specificity toward insect enzymes, tepary bean αAI may be a source of factors important to the production of insect-resistant plants by conventional breeding and genetic engineering and may provide new information on the structure of αAI as it relates to the specificity and insecticidal activity. In contrast to αAI-1 and αAI-2, there is little information on the biochemical properties of tepary bean αAI. In the present paper, we describe the purification, characterization, and primary structure of tepary bean αAI.

2. Results and discussion

Tepary bean seed extracts showed a specificity for α-amylase inhibitory activity different from that of well-known common bean inhibitors, αAI-1 and αAI-2 (Table 1). αAI-1 inactivates the α-amylases of *C. chinensis*, *C. maculatus* and mammals, while αAI-2 shows specific inhibition towards the larval α-amylase of *Z. subfasciatus*. The specificity of the seed extracts from tepary beans suggested genetic variation in the α-amylase inhibitor as in common bean, and we classified the tepary bean accessions into two genotypes, αAI-Pa1 and αAI-Pa2. αAI-Pa1 inhibited the α-amylase activity of *C. chinensis*, but not porcine pancreatic α-amylase, while αAI-Pa2 inhibited the α-amylase activity of *Z. subfasciatus* in addition to *C. chinensis*.

The α-amylase inhibitor in common bean seeds can be visualized by immunoblotting with antibodies raised against αAI-1. Subunits of αAI-1 and αAI-2 were detected at around 14–20 kDa (Fig. 1, lanes 1, 2 and 4). The anitibodies cross-reacted with other α-amylase inhibitor-related proteins (around 29 kDa) such as arcelin in a breeding line, TAr4 (lane 2), and α-amylase inhibitor-like protein (AIL) in a breeding line, TO (lane 3), and Shiro-kinugasa (lane 4), while no seed extracts of tepary bean had proteins that intensely cross-reacted with the antibodies. Only a few faint polypeptide bands were detected at around 29 kDa. It is not clear whether the less-intense bands in tepary bean reflect the lower abundance in their seeds or the structural difference of the tepary bean α-amylase inhibitor from common bean inhibitors. Among tepary bean accessions used here, cultivar PI311897 classified as αAI-Pa2 type showed inhibitory activity against both *C. chinensis* and *Z. subfasciatus*. Therefore, we purified α-amylase inhibitor protein from seeds of PI311897.

We initially tried to purify the α-amylase inhibitor protein from tepary bean seeds by the method used for purifying αAI-1 and αAI-2 (Suzuki et al., 1993). The inhibitor protein in tepary bean, however, did not bind

Table 1
Inhibitory activity of seed extracts from the common bean *(Phaseolus vulgaris)* and the tepary bean *(Phaseolus acutifolius)* against different α-amylase preparations[a]

Variety, line or accession	Type of αAI	Source of α-amylase		
		Porcine pancreas	Azuki bean weevil (*Callosobruchus chinensis*)	Mexican bean weevil (*Zabrotes subfasciatus*)
Common bean				
Taisho-kintoki (Tk)	αAI-l	**99.5**[b]	**66.8**	0
TAr4	αAI-2	0	0	**99.1**
TO	null	0	0	0
Shiro-kinugasa (Sk)	αAI-1	**99.4**	**54.5**	0
Tepary bean (Wild)				
G40072	αAI-Pal	2.7	**40.5**	0
G40074 (Cultivated)	αAI-Pal	0	**34.1**	0
P1311897	αAI-Pa2	0	**45.5**	**100**
P1321437	αAI-Pal	0	**58.1**	0
Nayarit	αAI-Pal	0	**40.8**	0

[a] Two independent experiments were performed. Inhibitory activity (%) shows the relative value against activity of α-amylase preparations without preincubation with any inhibitor.
[b] Bold indicates more than 30% inhibition.

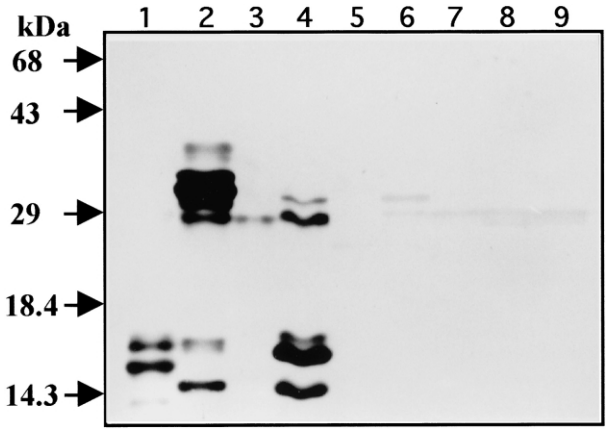

Fig. 1. Immunoblot analysis of α-amylase inhibitor (αAI)-related proteins in bean seed extracts. Polypeptides were separated by SDS-PAGE and detected by antibodies against αAI-1. Lanes 1–4: common bean (*Phaseolus vulgaris*), 1: Taisho-kintoki; 2: TAr4; 3: TO; 4: Shiro-kinugasa. Lanes 5–9: tepary bean (*Phaseolus acutifolius*), 5: G40072; 6: G40074; 7: PI311897; 8: PI321437; 9: Nayarit. Molecular weight markers are indicated on the left.

to a column of DEAE-Sephacel equilibrated with 20 mM PBS, pH 6.7. Therefore, the unadsorbed fraction was applied to a column of Concanavalin A (ConA)-Sepharose. The inhibitory activity against larval α-amylase of *C. chinensis* and *Z. subfasciatus* was detected in the fraction obtained by elution with 0.1 M α-methyl-D-mannopyranoside from the immobilized lectin. This fraction was dialyzed against a 50 mM acetate buffer (pH 3.6) and then applied to a CM-Sepharose column equilibrated with the same buffer. Three peaks were eluted with a linear gradient of NaCl, when proteins were monitored at 280 nm (Fig. 2A). The inhibitory activity against *Z. subfasciatus* was observed in the second peak while the inhibitory activity against *C. chinensis* was mainly observed in the third peak (Fig. 2B). On the SDS–PAGE gel, the protein in the second peak gave three polypeptides in the range of 14–18 kDa (Fig. 3, lane 4), and the protein in the third peak was composed of a single polypeptide band at 35 kDa (Fig. 3, lane 3). Thus, we identified two different α-amylase inhibitors coexisting in seeds of a tepary bean, cv. PI311897, classified as αAI-Pa2 type and re-designated the purified inhibitor proteins as αAI-Pa1 (active against *C. chinensis* α-amylase) and αAI-Pa2 (active against *Z. subfasciatus* α-amylase). Molecular weight of αAI-Pa1 was determined as 39.6 kDa by gel filtration chromatography, while molecular weight of αAI-Pa2 was esitimated as 28.1 kDa. Blanco-Labra et al. (1996) isolated tepary bean αAI from a different cultivar. The tepary bean αAI seems to be similar to αAI-Pa1 in primary structure, being a single glycopolypeptide with a molecular mass of 35 or 38 kDa and a monomer of about 39 kDa.

The two purified α-amylase inhibitors were analyzed for inhibitory activity against three α-amylase preparations, those of *C. chinensis*, *Z. subfasciatus* and porcine

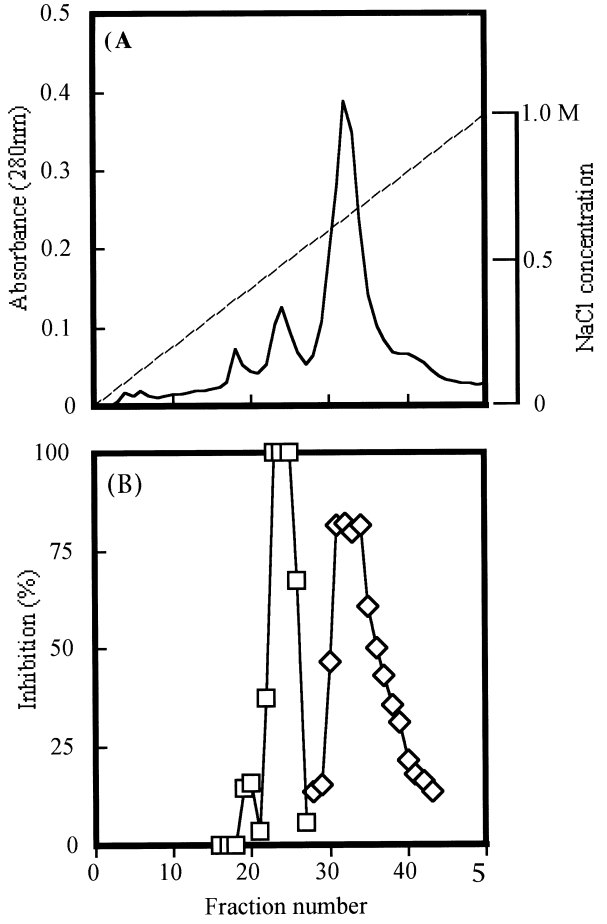

Fig. 2. Separation of two fractions showing α-amylase inhibitory activity on a column of CM-Sepharose. Column chromatography was performed with a linear gradient from 0 to 1.0 M NaCl. (A) Eluted protein was monitored at 280 nm. (B) Each fraction (10 ml) was pooled and measured for inhibitory activity against the larval α-amylases of *Callosobruchus chinensis* (◇) and *Zabrotes subfasciatus* (□). Inhibition (%) shows the relative value against one unit of each α-amylase activity without pre-incubation with any fraction.

pancreas (Fig. 4). αAI-Pa1 only inhibited *C. chinensis* α-amylase, which lost approximately 80% of its activity on addition of more than 3μg of αAI-Pa1 (Fig. 4A). αAI-Pa2 was highly active against *Z. subfasciatus* α-amylase (Fig. 4B), which was nearly completely inhibited on pre-incubation with not less than 1 μg of αAI-Pa2. αAI-Pa2 also inhibited *C. chinensis* α-amylase activity. Three micrograms of αAI-Pa2 inhibited nearly half of the activity of *C. chinensis* α-amylase, although the inhibitory effect was not increased even after incubation with an excess amount (5 μg) of the inhibitor (Fig. 4B).

The specificity of the two tepary bean α-amylase inhibitors, αAI-1 and αAI-2 was analyzed in detail using 9 α-amylase preparations (Table 2). There was no effect on fungal and bacterial α-amylases by the inhibitors. And while αAI-1 inhibited mammalian and coleopteran α-amylases, it did not inhibit the α-amylase activity of *Z. subfasciatus*, which is known to be a storage pest of the common bean. The other three αAIs did not inhibit

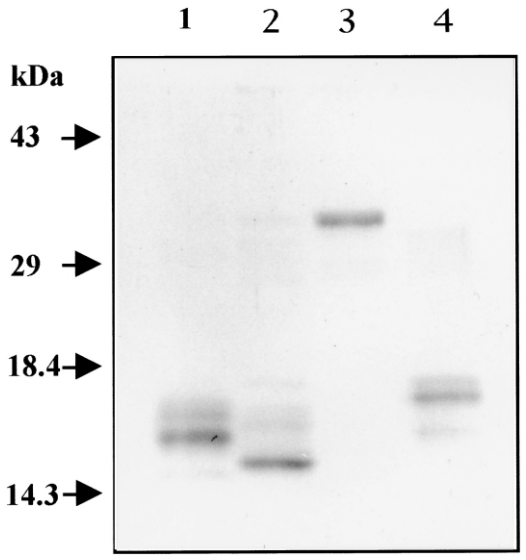

Fig. 3. SDS–PAGE analysis of purified α-amylase inhibitor proteins. Five micrograms of each protein was applied to a 13.5% polyacrylamide gel. Lane 1: αAI-1; 2: αAI-2; 3: αAI-Pa1; 4: αAI-Pa2. Molecular weight markers are indicated on the left.

the mammalian α-amylases. αAI-2 showed no evident inhibitory activity against the α-amylases except *Z. subfasciatus* α-amylase. αAI-Pa1 inhibited the α-amylase activity of *C. chinensis*, *C. maculatus*, *T. molitor*, and *T. confusum* but not *Z. subfasciatus*. On the other hand, the tepary bean αAI purified by Blanco-Labra et al. (1996) showed strong inhibitory activity against the α-amylase of *Z. subfasciatus* In spite of the molecular weight similarity between the tepary bean αAI and αAI-Pa1, they differ from each other on the inhibitory specificity to α-amylase enzymes. It appears more likely that at least three variants of αAI are found in tepary bean. αAI-Pa2 was active against all insect α-amylases tested, but its inhibition of the *C. chinensis* or *C. maculatus* α-amylase was less than 50%. *C. maculatus* larvae have at least four isozymes of α-amylase in the gut, and αAI-1 and wheat α-amylase inhibitor inhibited only some of these isozymes (Campos et al., 1989). αAI-Pa2 may inhibit a part of α-amylase isozymes of *C. maculatus* and *C. chinensis*, resulting in half of the original activity even after incubation with an excess amount of αAI-Pa2.

The purified αAI-Pa2 yielded three polypeptide bands on a SDS-PAGE gel (Fig. 3, lane 4). The two polypeptides with a higher molecular mass had an identical N-terminal amino acid sequence, showing high homology with the α-subunits of αAI-1 and αAI-2, while the lowest molecular mass polypeptide had high similarity to the β-subunits (Fig. 5B). In the case of αAI-1, post-translational maturation of the αAI precursor is essential to the development of an active form composed of two subunits, α- and β-subunits. (Altabella and Chrispeels, 1990; Santino et al., 1992; Pueyo et al., 1993). A

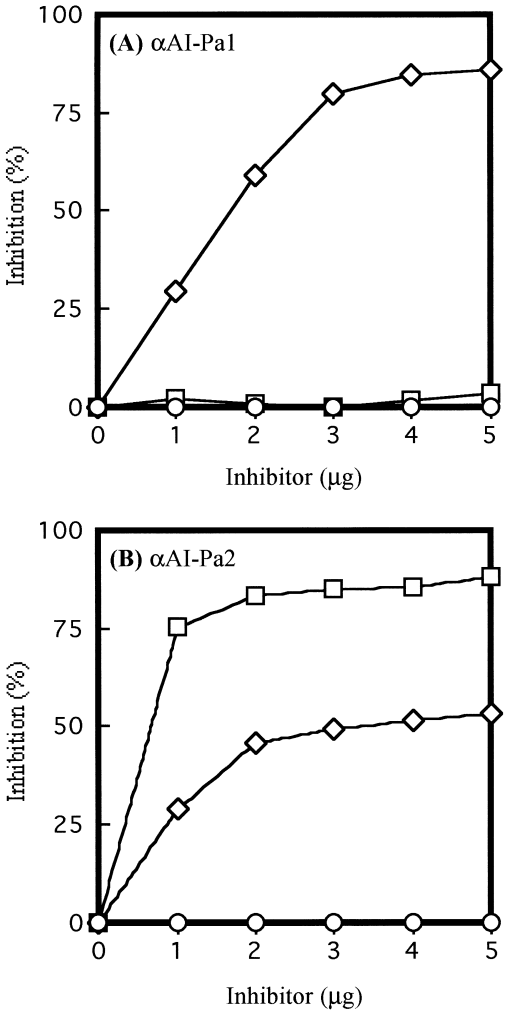

Fig. 4. α-Amylase inhibitory activity of αAI-Pa1 (A) and αAI-Pa2 (B) against α-amylase preparations from *Callosobruchus chinensis* (◇), *Zabrotes subfasciatus* (□) and porcine pancreas (○). Inhibition (%) shows the relative value against one unit of each α-amylase activity without pre-incubation with any fraction.

conformational change during the processing results in the creation of an active site filling the whole-substrate docking region of the α-amylase enzyme (Bompard-Golles et al., 1996). αAI-Pa2 is also composed of two subunits whose N-terminal amino acid sequences were similar to the α- or β-subunit of αAI-1 and αAI-2, suggesting that αAI-Pa2 is also proteolyticaly processed.

In contrast to αAI-Pa2, αAI-Pa1 is a single glycopolypeptide with a molecular mass of about 35 kDa. A similar α-amylase inhibitor was isolated from a different tepary bean cultivar (Blanco-Labra et al., 1996). These results indicate that αAI-Pa1 and an analogous inhibitor seem not to need the processing for the activation and the new group of αAI is widespread in tepary bean. The N-terminal amino acid sequence of αAI-Pa1 had high homology with seed lectin in tepary bean (TEPL) and common bean (PHA-L) (Fig. 5A) (Hoffman and Donaldson, 1985; Pratt et al., 1990), although αAI-Pa1

Table 2
Inhibitory activity of purified α-amylase inhibitor proteins against each α-amylase preparation[a]

Source of α-amylase preparations	α-Amylase inhibitor protein			
	αAI- 1	αAI-2	αAI-Pa1	αAI-Pa2
Mammals				
Porcine pancreas	**100**[b]	ND[b]	ND	ND
Human saliva	**100**	ND	ND	ND
Insects				
C. chinensis	**77.4**	14.6	**79.4**	**49.5**
C.maculatus	**83.1**	11.3	**86.5**	**46.1**
Z. subfasciatus	ND	**81.3**	ND	**85.0**
Tenebrio molitor	**61.4**	ND	**66.5**	**80.0**
Tribolium confusum	**81.4**	ND	**80.4**	**68.9**
Microorganisms				
Aspergillus oryzae	ND	ND	ND	ND
Bacillus lichenoformis	ND	ND	ND	ND

[a] Three micrograms of purified inhibitor was used for each assay. Inhibitory activity (%) shows the relative value against activity of α-amylase preparations without preincubation with any inhibitor. All values represent the average of two independent experiments. ND, no detectable inhibitory activity.
[b] Bold indicates more than 30% inhibition.

(A) αAI-Pa1 and a large (α) subunit of αAI-Pa2

	1								10
αAI-Pa1	S	N	**D**	I	**S**	**F**	**N**	**F**	D	R--
αAI-Pa2	**A**	**C**	**D**	**T**	**S**	**F**	**N**	**F**	**H**	**S**--
αAI-1(α subunit)	**A**	T	E	**T**	**S**	**F**	**N**	I	D	A--
αAI-2(α subunit)	**A**	S	**D**	**T**	**S**	**F**	**N**	**F**	Y	**S**--
TEPL	**A/S**	N	**D**	I	**S**	**F**	**N**	**F**	Q	R--
PHA-L	S	N	**D**	I	Y	**F**	**N**	**F**	Q	R--
PHA-E	**A**	S	Q	**T**	**S**	**F**	S	**F**	Q	R--
Arc1	S	N	**D**	A	**S**	**F**	**N**	V	E	T--

(B) A small (β) subunit of αAI-Pa2

	1								10
αAI-Pa2	**S**	**A**	**I**	**G**	**L**	**D**	**F**	**A**	**L**	**V**--
αAI-1(β-subunit)	**S**	**A**	V	**G**	**L**	**D**	**F**	V	**L**	**V**--
αAI-2(β-subunit)	**S**	V	**I**	**G**	**L**	**D**	**F**	A	**L**	**V**--

Fig. 5. Comparison of N-terminal amino acid sequences of two α-amylase inhibitors (αAI-Pa1 and αAI-Pa2) purified from a tepary bean (PI311897) and other αAI-related proteins. αAI-1 (Hoffman et al., 1982); αAI-2 (Mirkov et al., 1994; Suzuki et al., 1994); PHA-E: erythroagglutinating PHA subunit (Hoffman and Donaldson, 1985); PHA-L: leucoagglutinating PHA subunit (Hoffman and Donaldson, 1985) and Arc1: arcelin1 in the common bean (Osborn et al., 1988); TEPL: tepary bean lectin (Pratt et al., 1990). Identical amino acids to those of αAI-Pa2 are indicated in bold.

showed no agglutination of rabbit erythrocytes at any dilution. The lectin-related defense proteins, αAI and arcelin, isolated from common bean and tepary bean share a high degree of sequence identity in amino acid sequence (Mirkov et al., 1994). In common bean, the genes for lectin, αAI, and arcelin are encoded at a single locus (Nodari et al., 1993), suggesting that these homologous genes have evolved through duplication and divergence of an ancestral gene. αAI-Pa1 and αAI-Pa2 may have arisen through a similar evolutional process, and αAI-Pa1 may provide new information on the essential structure and evolution of αAI, because αAI-Pa1 is an unprocessed αAI.

The introduction of cDNA encoding αAI-1 into pea and azuki bean protected the seeds from attack by bruchid larvae, indicating the usefulness of bean αAI in pest management (Schroeder et al., 1993, 1995; Ishimoto et al., 1996; Morton et al., 2000). Because of the antinutrient effect of the common bean α-amylase inhibitor in mammals (Pusztai et al., 1995), however, consumers would likely be apprehensive of transgenic crops expressing αAI-1. Recently, Pusztai et al. (1999) reported that diets containing transgenic peas expressing αAI-1 at a moderate level (~300 g/kg) did not have major harmful effects on growth, metabolism, and health in rats, suggesting that it would be safe to use them in the diets of mammals, including farm animals. αAI-Pa1 and αAI-Pa2 are only active against insect α-amylases, having broad specificity towards storage pest α-amylases. Therefore, tepary bean αAIs have potential for crop protection from seed-eating insects by genetic engineering. Further studies on novel types of bean inhibitors such as αAI-Pa1 should elucidate the relationship between specificity and structure.

3. Experimental

3.1. Materials

Two wild accessions (G40072 and G40074) and 3 cultivated accessions (PI311897, PI321437 and Nayarit) of tepary bean were obtained from the Centro International de Agricultura Tropical (CIAT) in Cali, Columbia. Two common bean cultivars, Taisho-kintoki (containing αAI-1) and Shiro-kinugasa (containing αAI-1) were obtained from Hokkaido Prefectural Tokachi Agricultural Experiment Station in Memuro, Japan. Each near isogenic line, TO line (lacking αAI) or TAr4 line (containing αAI-2), was developed by backcrossing five times Taisho-kintoki into either an αAI-lacking cultivar (Ofuku-5) or a wild common bean accession (G12953). A laboratory colony of *C. chinensis* was obtained from the National Institute of Agro-Environmental Sciences, Tsukuba, Japan. Colonies of *C. maculatus* and *Z. subfasciatus* were obtained from the University of Tsukuba, Tsukuba, Japan. Larvae of yellow mealworm (*Tenebrio molitor*) and confused flour beetle (*Tribolium confusum*) were provided by the National Food Research Institute, Tsukuba, Japan. Porcine pancreatic α-amylase (Type I-A), human salivary α-amylase (type IX-A), fungal α-amylase from *Aspergillus oryzae*, and bacterial α-amylase from *Bacillus licheniformis* were purchased from Sigma

(St. Louis, MO). Phytohemagglutanin-P (PHA-P) from *Phaseolus vulgaris* was purchased from Wako Pure Chem. (Kyoto, Japan). DEAE-Sephacel, ConA-Sepharose, CM-Sepharose CL-6B, Superose 12, Superdex 200 were purchased from Amersham Pharmacia Biotech (Buckinghamshire, England). BCA protein assay kit was purchased from Pierce (Rockford, IL). Polyvinylidene difluoride (PVDF) membrane was from Bio-Rad (Hercules, CA). All other chemicals and reagent used were of analytical grade.

3.2. Seed protein extraction

The distal portion (50 mg) of individual dry seeds was ground with a mortar and pestle in 500 μl of 20 mM sodium phosphate buffer (PBS) pH 6.8. The supernatant was obtained by centrifugation at 15,000×*g* for 5 min at 4°C. The protein content in each seed extract was determined with a BCA protein assay kit, and then diluted to an adequate concentration for the analysis of inhibitory activity or immunoblotting.

3.3. α-Amylase inhibition assay

The α-amylases of three bruchid species, *C. chinensis*, *C. maculatus* and *Z. subfasciatus*, were prepared by homogenization of dissected larval guts as described previously (Ishimoto and Chrispeels, 1996), except for the use of 20 mM PBS buffer (pH 5.8). The larval α-amylases of *T. molitor* and *T. confusum* were prepared by homogenization of whole larvae with the above buffer. α-Amylase activity was measured with a modification of the Bernfeld method (Bernfeld, 1955) at pH 5.8 for insect α-amylases or at pH 6.8 for mammal, fungal and bacterial α-amylases. One unit of α-amylase activity is defined as the amount of enzyme that liberates 1 μmol of maltose at 37°C in 5 min under the assay condition. To analyze the inhibitory activity, seed extract or purified α-amylase inhibitor was pre-incubated with one unit of each α-amylase preparation prior to the addition of substrate solution.

3.4. Hemagglutination assay

Hemagglutination activity was measured using a serial dilution of rabbit erythrocytes. Five millilitres of rabbit blood was centrifuged at 1,500 *g* and 4°C for 10 min to remove the plasma. The erythrocytes were suspended in 5 ml of 50 mM sodium phosphate buffer, pH 6.7, containing 0.15 M NaCl, centrifuged at 1000 *g* and 4°C for 10 min, and washed three times with the same buffer. Finally, erythrocytes were resuspended to 3% (v/v) in the same buffer. The hemagglutination activity of each purified inhibitor was measured in microtiter plates. Each protein sample was serially diluted from the original concentration, 28 μg in 40 μl, and then mixed well with an equal volume of erythrocyte suspension. After 2 h at room temperature, agglutination was observed. PHA-P was used as a standard.

3.5. Electrophoresis and immunoblotting

Sodium dodecyl sulfate polyacrylamide gel electrophoresis (SDS-PAGE) (13.5% acrylamide) was performed according to the method of Laemmli (Laemmli, 1970). After separation by SDS-PAGE, polypeptides were transferred onto a PVDF membrane, and reacted with polyclonal antibodies against αAI-1 (Ishimoto et al., 1996). Goat anti-rabbit IgG coupled to horseradish peroxidase (Cappel) was used as secondary antibody for the detection of the products obtained with αAI-1 antibodies.

3.6. Purification of α-amylase inhibitor protein

α-Amylase inhibitor was purified from seeds of a tepary bean cultivar PI311897. Seed flour (20 g) was extracted with 200 ml of 20 mM sodium phosphate buffer (PBS), pH 6.7 at 4°C for 3 h. After centrifugation, the supernatant was fractionated by ammonium sulfate precipitation with 20–60% saturation. The precipitate was collected by centrifugation, dissolved with 50 ml of 20 mM PBS and dialyzed against the same buffer for 24 h. This material was applied to a column of DEAE-Sephacel equilibrated with 20 mM PBS (pH 6.7). The unadsorbed fraction was pooled and applied to a column of ConA-Sepharose equilibrated with 20 mM PBS (pH 6.7) containing 0.5 M NaCl. The adsorbed fraction was eluted with the same buffer containing 0.1 M α-methyl-D-mannopyranoside. The eluate was dialyzed against a 50 mM acetate buffer (pH 3.6), and this material was applied to a column of CM-Sepharose CL-6B equilibrated with the same buffer. The adsorbed material was eluted with a linear gradient from 0 to 1.0 M NaCl in the same buffer. The fractions showing αAI activity were dialyzed against distilled water, and lyophilized. The lyophilized material was dissolved in 50 mM PBS (pH 6.7) containing 0.15 M NaCl and was purified by gel filtration on a column of Superose 12 equilibrated with the same buffer.

αAI-1 and αAI-2 were purified from common bean cultivars, Taisho-kintoki and TAr4, according to the method of Suzuki et al. (1993).

3.7. Estimation of molecular weight

Molecular weight of αAI-Pa1 and αAI-Pa2 were estimated by gel filtration chromatography of a Superdex 200 column (1×30 cm). Proteins were eluted with 50 mM PBS (pH 6.7) containing 0.15 M NaCl at a flow rate of 0.5 ml/min, and monitored by absorbance at 280 nm. The following proteins were used as standard samples,

bovine serum albumin (67 kDa), ovalbumin (43 kDa), chymotrypsinogen A (25 kDa), myoglobin equine (17.8 kDa), and ribonuclease A (12.3 kDa). Blue dextran was used to measure the void volume.

3.8. N-terminal amino acid sequencing

After separation of the purified αAIs by SDS-PAGE, the polypeptides were transferred onto a PVDF membrane and detected by Coomassie brilliant blue staining. The bands corresponding to the αAI subunits were cut out and the N-terminal amino acid sequences were determined with a gas-phase protein sequencer 492 (Applied Biosystems).

Acknowledgements

We thank Dr. K. Fujii, University of Tsukuba, for providing us with colonies of *C. maculatus* and *Z. subfasciatus*.

References

Altabella, T., Chrispeels, M.J., 1990. Tobacco plants transformed with the bean αai gene express an inhibitor of insect α-amylase in their seeds. Plant Physiology 93, 805–810.

Bernfeld, P., 1955. Amylases, α- and β-. In: Colowick, S.P., Kaplan, N.O. (Eds.), Methods in Enzymology, Vol. 1. Academic Press, New York, pp. 149–158.

Blanco-Labra, A., Sandoval-Cardoso, L., Mendiola-Olaya, E., Valdes-Rodriguez, S., Lopez, M.G., 1996. Purification and characterization of a glycoprotein α-amylase inhibitor from tepary bean seeds (*Phaseolus acutifolius* A. Gray). Journal of Plant Physiology 149, 650–656.

Bompard-Golles, C., Rousseau, P., Rougé, P., Payan, F., 1996. Substrate mimicry in the active center of a mammalian α-amylase: structural analysis of an enzyme-inhibitor complex. Structure 4, 1441–1452.

Campos, F.A.P., Xavier-Filho, J., Silva, C.P., Ary, M.B., 1989. Resolution and partial characterization of proteinases and α-amylase from midguts of larvae of the bruchid beetle *Callosobruchus maculatus* (F.). Comparative Biochemistry and Physiology 92B, 51–57.

Chrispeels, M.J., Raikhel, N.V., 1991. Lectins, lectin genes, and their role in plant defense. Plant Cell 3, 1–9.

Freis, J.M., Rupmnow, J.H., 1984. Purification and partial characterization of two α-amylase inhibitors from black bean (*Phaseolus vulgaris*). Journal of Food Biochemistry 8, 281–301.

Hoffman, L.M., Donaldson, D.D., 1985. Characterization of two *Phaseolus vulgaris* phytohemagglutinin genes closely linked on the chromosome. EMBO Journal 4, 883–889.

Hoffman, L.M., Ma, Y., Barker, R.F., 1982. Molecular cloning of *Phaseolus vulgaris* lectin mRNA and use of cDNA as probe to estimate lectin transcript levels in various tissues. Nucleic Acids Research 10, 7819–7828.

Huesing, J.E., Shade, R.E., Chrispeels, M.J., Murdock, L.L., 1991. α-Amylase inhibitor, not phytohemagglutinin, explains the resistance of common bean seeds to cowpea weevil. Plant Physiology 96, 993–996.

Ishimoto, M., Chrispeels, M.J., 1996. Protective mechanism of the Mexican bean weevil against high levels of α-amylase inhibitor in the common bean, *Phaseolus vulgaris*. Plant Physiology 111, 393–401.

Ishimoto, M., Kitamura, K., 1988. Identification of the growth inhibitor on azuki bean weevil in kidney bean (*Phaseolus vulgaris* L.). Japanese Journal of Breeding 38, 367–370.

Ishimoto, M., Kitamura, K., 1989. Growth inhibitory effects of an α-amylase inhibitor from kidney bean, *Phaseolus vulgaris* (L.), on three species of bruchids (Coleoptera: Bruchidae). Applied Entomology and Zoology 24, 281–286.

Ishimoto, M., Kitamura, K., 1993. Specific inhibitory activity and inheritance of an α-amylase inhibitor in a wild common bean accession resistant to the Mexican bean weevil. Japanese Journal of Breeding 43, 69–73.

Ishimoto, M., Sato, T., Chrispeels, M.J., Kitamura, K., 1996. Bruchid resistance of transgenic azuki bean expressing seed α-amylase inhibitor of common bean. Entomologia Experimentalis et Applicata 79, 309–315.

Laemmli, U.K., 1970. Cleavage of structure proteins during assembly of the head of bacteriophage T4. Nature 22, 680–685.

Lajolo, F.M., Finardi Filho, F., 1985. Partial characterization of the amylase inhibitor of black beans (*Phaseolus vulgaris*), variety Rico 23. Journal of Agriculture and Food Chemistry 33, 132–138.

Layer, P., Carlson, G.L., DiMagno, E.P., 1985. Partially purified white bean amylase inhibitor reduces starch digestion in vitro and inactivates introduodental amylase in humans. Gastroenterology 88, 1895–1902.

Marshall, J.J., Lauda, C.M., 1975. Purification and properties of phaseolamin, an inhibitor of α-amylase, from the kidney bean, *Phaseolus vulgaris*. The Journal of Biological Chemistry 250, 8030–8037.

Minney, B.H.P., Gatehouse, A.M.R., Dobie, P., Dendy, J., Cardona, C., Gatehouse, J.A., 1990. Biochemical basis of seed resistance to *Zabrotes subfasciatus* (bean weevil) in *Phaseolus vulgaris* (common bean); a mechanism for arcelin toxicity. Journal of Insect Physiology 36, 757–767.

Mirkov, T.E., Wahlstrom, J.M., Hagiwara, K., Finardi-Filho, F., Kjemtrup, S., Chrispeels, M.J., 1994. Evolutionary relationships among proteins in the phytohemagglutinin-arcelin-α-amylase inhibitor family of the common bean and its relatives. Plant Molecular Biology 26, 1103–1113.

Morton, R.L., Schroeder, H.E., Bateman, K.S., Chrispeels, M.J., Armstrong, E., Higgins, T.J.V., 2000. Bean α-amylase inhibitor 1 in transgenic peas (*Pisum sativum*) provides complete protection from pea weevil (*Bruchus pisorum*) under field conditions. Proc. Natl. Acad. Sci. USA 97, 3820–3825.

Nodari, R.O., Tsai, S.M., Gilbertson, R.L., Gepts, P., 1993. Towards an integrated linkage map of common bean 2. Development of an RFLP-based linkage map. Theoretical and Applied Gnetics 85, 513–520.

Osborn, T.C., Alexander, D.C., Sun, S.S.M., Cardona, C., Bliss, F.A., 1988. Insecticidal activity and lectin homology of arcelin seed protein. Science 240, 207–210.

Powers, J.R., Culbertson, J.D., 1983. Interaction of a purified bean (*Phaseolus vulgaris*) glycoprotein with an insect amylase. Cereal Chem. 60, 427–429.

Powers, J.R., Whitaker, J.R., 1977a. Effect of several experimental parameters on combination of red kidney bean (*Phaseolus vulgaris*) α-amylase inhibitor with porcine pancreatic α-amylase. Journal of Food Biochemistry 1, 239–260.

Powers, J.R., Whitaker, J.R., 1977b. Purification and some physical and chemical properties of red kidney bean (*Phaseolus vulgaris*) α-amylase inhibitor. Journal of Food Biochemistry 1, 217–238.

Pratt, R.C., Singh, N.K., Shade, R.E., Murdock, L.L., Bressan, R.A., 1990. Isolation and partial characterization of a seed lectin from tepary bean that delays bruchid beetle development. Plant Physiology 93, 1453–1459.

Pueyo, J.J., Delgado-Salinas, A., 1997. Presence of α-mylase inhibitor in some members of the subtribe Phaseolinae (Phaseoleae: Fabaceae). American Journal of Botany 84, 79–84.

Pueyo, J.J., Hunt, D.C., Chrispeels, M.J., 1993. Activation of bean

(*Phaseolus vulgaris*) α-amylase inhibitor requires proteolytic processing of the proprotein. Plant Physiology 101, 1341–1348.

Pusztai, A., Bardocz, G.G.S., Alonso, R., Chrispeels, M.J., Schroeder, H.E., Tabe, L.M., Higgins, T.J.V., 1999. Expression of the insecticidal bean α-amylase inhibitor transgene has minimal detrimental effect on the nutritional value of peas fed to rats at 30% of the diet. Journal of Nutrition 129, 1597–1603.

Pusztai, A., Grant, G., Duguid, T., Brown, D.S., Peumans, W.J., Van Damme, E.J.M., Bardocz, S., 1995. Inhibition of starch digestion by α-amylase inhibitor reduces the efficiency of utilization of dietary proteins and lipids and retards the growth of rats. Journal of Nutrition 125, 1554–1562.

Santino, A., Daminati, M.G., Vitale, A., Bollini, R., 1992. The α-amylase inhibitor of bean seed: two-step proteolytic maturation in the protein storage vacuoles of the developing cotyledon. Physiologia Plantrum 85, 425–432.

Schroeder, H.E., Gollash, S., Moore, A., Tabe, L.M., Craig, S., Hardie, D.C., Chrispeels, M.J., Spencer, D., Higgins, T.J.V., 1995. Bean α-amylase inhibitor confers resistance to the pea weevil (*Bruchus pisorum*) in transgenic peas (*Pisum sativum* L.). Plant Physiology 107, 1233–1239.

Schroeder, H.E., Schotz, A.H., Wardley-Richardson, T., Spencer, D., Higgins, T.J.V., 1993. Transformation and regeneration of two cultivars of pea (*Pisum sativum* L.). Plant Physiology 101, 751–757.

Shade, R.E., Schroeder, H.E., Pueyo, J.J., Tabe, L.M., Murdock, L.L., Higgins, T.J.V., Chrispeels, M.J., 1994. Transgenic pea seeds expressing the α-amylase inhibitor of the common bean are resistant to bruchid beetles. Bio/Technology 12, 793–796.

Suzuki, K., Ishimoto, M., Kikuchi, F., Kitamura, K., 1993. Growth inhibitory effect of an α-amylase inhibitor from the wild common bean resistant to the Mexican bean weevil (*Zabrotes subfasciatus*). Japanese Journal of Breeding 43, 257–265.

Suzuki, K., Ishimoto, M., Kitamura, K., 1994. cDNA sequence and deduced primary structure of an α-amylase inhibitor from a bruchid-resistant wild common bean. Biochimica et Biophysica Acta 1206, 289–291.

PERGAMON

Phytochemistry 58 (2001) 67–73

PHYTOCHEMISTRY

www.elsevier.com/locate/phytochem

Characterization of α-galactosidases from germinating soybean seed and their use for hydrolysis of oligosaccharides

Valéria Monteze Guimarães[a,*], Sebastião Tavares de Rezende[b], Maurilio Alves Moreira[b], Everaldo Gonçalves de Barros[b], Carlos Roberto Felix[a]

[a]*Departamento de Biologia Celular, Universidade de Brasília, Brasília, DF, 70.910-900, Brazil*
[b]*BIOAGRO/DBB/DBG, Universidade Federal de Viçosa, Viçosa, MG, 36.571-000, Brazil*

Received 16 November 2000; received in revised form 22 February 2001

Abstract

Raffinose oligosaccharides (RO) are the major factors responsible for flatulence following ingestion of soybean derived products. Removal of RO from seeds or soymilk would then have a positive impact on the acceptance of soy-based foods. Enzymic hydrolysis of the RO is accomplished by α-galactosidase. While the content of RO decreases during seed germination, the activity of α-galactosidase increases substantially. Two α-galactosidases were isolated from germinating seeds by partition in an aqueous two-phase system followed by ion-exchange and affinity chromatography. One of the enzyme preparations (P1) showed a single protein with M_r of 33 kDa, and the second (P2) had two proteins with M_r of 31 and 33 kDa. Maximal activities against the synthetic substrate ρ-nitrophenyl-α-D-galactopyranoside (ρNPGal) were detected at pH 5.0–5.5 and 45–50°C. Both enzymes were fairly stable at 40°C, but lost most of their activities after 30 min at 50°C. The K_m values for hydrolysis of ρNPGal by the P1 and P2 enzymes were 1.55 and 0.76 mM, respectively. The K_m values determined for hydrolysis of raffinose and melibiose by the P2 enzyme were 5.53 and 5.34 mM, respectively and galactose was a competitive inhibitor ($K_i = 0.65$ mM). To different extents, both enzymes were sensitive to inhibition by galactose, melibiose, $CuSO_4$, and SDS. Sucrose and β-mercaptoethanol showed discrete inhibitory effects on both enzymes. © 2001 Elsevier Science Ltd. All rights reserved.

Keywords: *Glycine max* L.; Leguminosae; α-Galactosidase; Raffinose oligosaccharides; Flatulence

1. Introduction

Soybean (*Glycine max* L.) is an excellent source of proteins for human and animal use. Nevertheless, due to its raffinose oligosaccharides (RO) content, mainly raffinose [α-D-galactopyranosyl-(1,6)-α-D-glucopyranosyl-β-D-fructofuranoside] and stachyose [α-D-galactopyranosyl-(1,6)-α-D-galactopyranosyl-(1,6)-α-D-glucopyranosyl-β-D-fructofuranoside], the legume has not been used to its full potential. Since humans and other monogastric animals lack the enzyme α-galactosidase (E.C. 3.2.1.22, α-D-galactoside galactohydrolase), necessary for hydrolysis of the α-1,6 linkages present in RO (Gitzelmann and Auricchio, 1965), these sugars pass intact into the large intestine where anaerobic micro-organisms ferment then and cause flatulence. It is suggested that blocking the expression of the galactinol synthase gene which codes for the key enzyme on the synthetic route of the RO in the seeds, could decrease RO content and reduce flatulence caused by legumes (De Lumen, 1992). On the other hand, enzymic conversion of these RO in soymilk may be a rational alternative to improve the nutritional quality of this low-cost, high-quality protein supplement for humans and animals (Cruz and Park, 1982; De Rezende and Felix, 1997; Sanni et al., 1997). Hydrolysis of RO may be achieved either by α-galactosidase, invertase or both. While α-galactosidase hydrolyses the α-1,6 linkage of raffinose producing galactose and sucrose, the invertase hydrolyses the α-1,2 linkage producing melibiose and fructose. α-Galactosidase enzymes are widely distributed in microorganisms (De Rezende and Felix, 1999), plants and animals (Dey and Pridham, 1972). However, no economically efficient enzymic process using either indigenous or recombinant soybean α-galactosidase to reduce RO in soymilk has yet been

* Corresponding author. Present address: Universidade Federal de Viçosa, Instituto de Biotechnologia a Agropecuaria, BIOAGRO, 36.571-000 Viçosa, MG, Brazil. Fax: +55-31-3899-2864.
E-mail address: srezende@mail.ufv.br (V.M. Guimarães).

0031-9422/01/$ - see front matter © 2001 Elsevier Science Ltd. All rights reserved.
PII: S0031-9422(01)00165-0

proposed. Here we report on the characterization of α-galactosidases from germinating soybean seeds, and on the possibility of using these enzymes for hydrolysis of the RO present in soymilk.

2. Results and discussion

The RO content in germinating soybean seeds decreased during germination (Fig. 1). Consistently, the activity against the synthetic substrate (*ρ*-nitrophenyl-α-D-galactopyranoside) *ρ*NPGal (Fig. 1), and the content of soluble fructose (not shown) increased confirming hydrolysis of the fructose-containing oligosaccharides. The results confirm previous reports that RO are used as an energy source during seed germination (Porter et al., 1990; Avigad and Dey, 1997).

Most of the α-galactosidase activity (80%) present in the seed crude extract partitioned into the upper phase of an aqueous two-phase system (ATPS), which contained 12% NaCl. Chromatography of the resulting ATPS enzyme sample on a CM-Sepharose column (Fig. 2) resulted in the separation of two protein fractions (P1 and P2). SDS–PAGE analysis revealed that while the P1 active fraction contained a single protein with M_r of 33 kDa, the P2 active fraction contained two

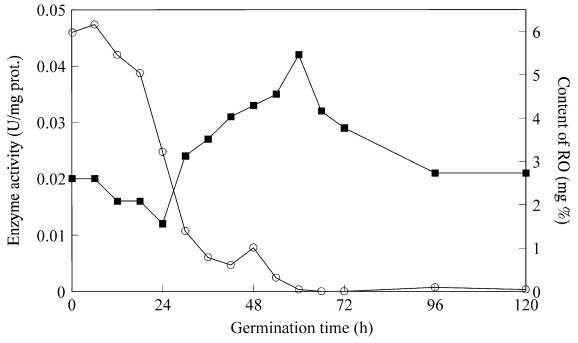

Fig. 1. α-Galactosidase activity (■) and content of raffinose oligosaccharides (raffinose + stachyose) (○) in soybean seeds after germination.

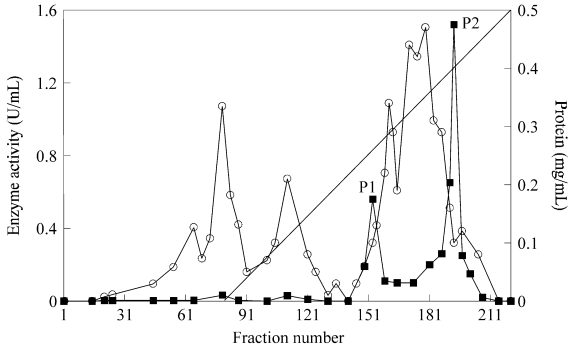

Fig. 2. Elution profile of the α-galactosidase from germinating soybean seeds on a CM-Sepharose columm. (■) enzyme activity; (○) protein concentration and (—) linear gradient of NaCl.

protein forms with M_r of 31 and 33 kDa. Affinity chromatography of the enzyme fractions resulted in further purification of the enzyme forms as indicated by their higher specific activities (Table 1). The electrophoretic profile of the two enzyme preparations in SDS-polyacrylamide gel (Fig. 3) confirmed the presence of a single protein band in the P1 fraction (33 kDa), and a broad band corresponding to the two protein forms of 31 and 33 kDa in P2. It was previously reported that the cotyledonary α-galactosidases from *Vigna unguiculata* have M_r of 33 kDa (Oliveira-Neto et al., 1998). In addition, a recombinant protein from *Glycine max* produced in *Pichia pastoris* purified by affinity chromatography showed a relative molecular mass of 39.8 kDa under reducing conditions, and of 38 kDa under non-reducing conditions as judged by electrophoretic analysis (Davis et al., 1996). Another α-galactosidase purified to near electrophoretic homogeneity from dry soybean seeds was shown to be monomeric at pH 7.0 with a molecular mass of 40 kDa, and to be tetrameric at pH 4.0 with a molecular mass of about 160 kDa (Porter et al., 1990). Both the tetrameric and monomeric forms were enzymically active but displayed different kinetic properties (Campillo and Shannon, 1982). It is not clear whether the 31 kDa protein present in the P2 enzyme preparation reported here is also active. *Phaseolus vulgaris* has two α-galactosidase isoenzymes with molecular masses of 38.3 and 39.6 kDa which co-migrate after several salt precipitation and chromatographic procedures (Dhar et al., 1994). The 31 and 33 kDa proteins, which could not be separated even after affinity chromatography, might well be isoforms, but additional studies are needed to characterize the 31 kDa protein.

Substantial activity against *ρ*NPGal was observed for both enzyme preparations in the temperature range of 20–70°C and in the pH range of 6.5–7.0. Maximal substrate hydrolysis by the P1 and P2 enzymes were achieved at the temperature of 45 and 50°C, respectively. The optima pH for the P1 and P2 enzymes were 5.0 and 5.5, respectively. These pH optima and temperature values are close to those determined for hydrolysis of *ρ*NPGal and melibiose by a crude α-galactosidase from germinating soybean seed (Cruz and Silva, 1986), by the cotyledonary α-galactosidases from *V. unguiculata* (Oliveira-Neto et al., 1998) and by the fungal raffinose-hydrolysing enzymes (De Rezende and Felix, 1999). The K_m and V_{max} values calculated by the Lineweaver–Burk plot for hydrolysis of *ρ*NPGal by the P2 and P1 enzymes were 0.76 mM and 1.76 μmol min^{-1} ml^{-1}, and 1.55 mM and 2.43 μmol min^{-1} ml^{-1}, respectively. These values are comparable to those determined for hydrolysis of the same substrate by a crude α-galactosidase from germinating soybean seed (Cruz and Silva, 1986). Both the P1 and P2 α-galactosidases were moderately thermostable. The enzymes retained about 50% of their original activity following incubation for 2 h at 40°C

Table 1
Summary of the purification steps of the α-galactosidases from germinating soybean seeds

Purification step	Total protein (mg)	Total activity (U)	Specific activity (U/mg protein)	Purification (fold)	Recovery (%)
Crude extract	21488.0	574.9	0.026	–	–
Upper layer of ATPS	1203.4	401.9	0.33	12.7	69.9
Dialyzed sample	728.5	263.5	0.36	13.9	45.8
CM-sepharose					
P1	12.6	42.0	3.33	128	7.3
P2	9.6	88.0	9.2	352	15.3
Con-A (P1)	0.48	6.8	14.2	545	1.2
Con-A (P2)	0.18	11.25	62.50	2404	2.00

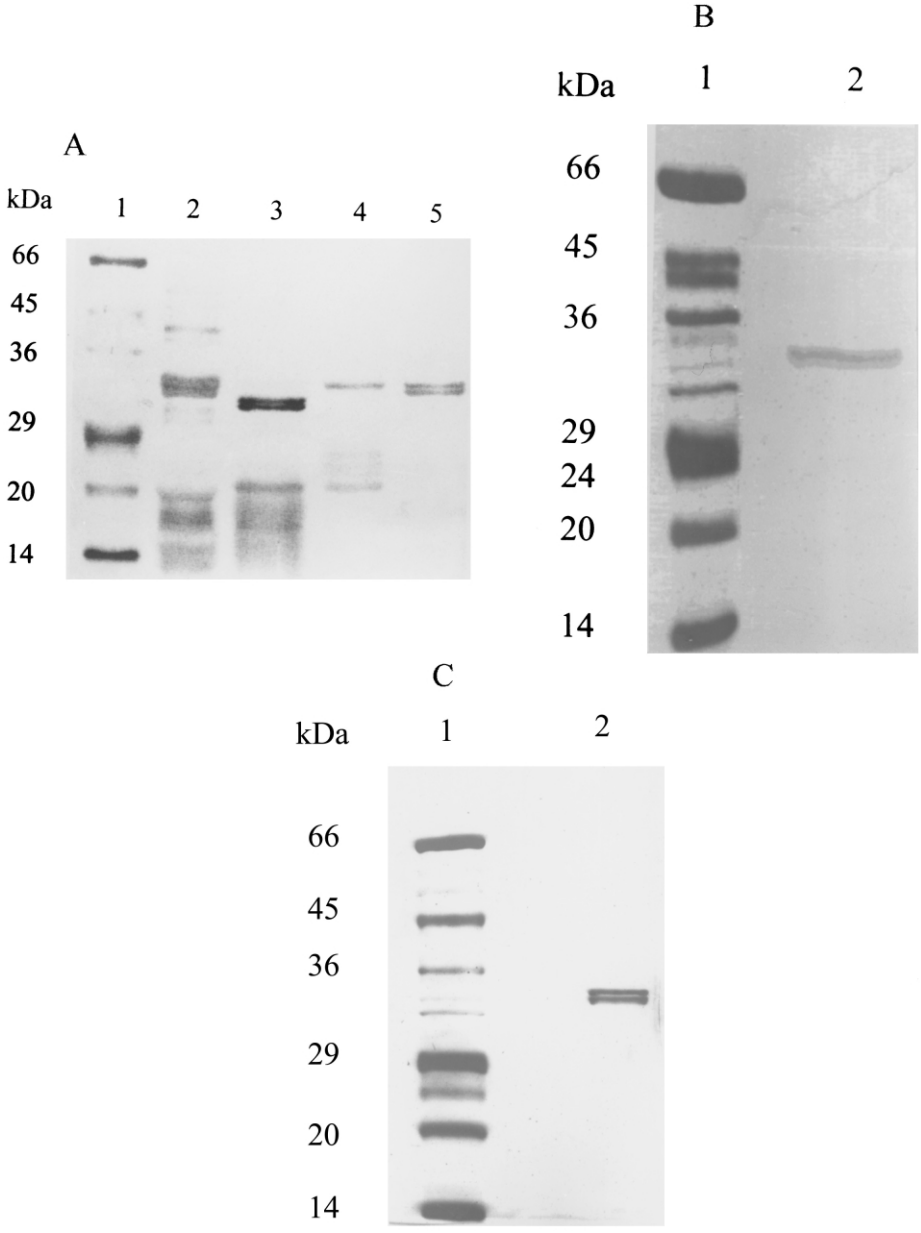

Fig. 3. SDS–PAGE of different purification steps of α-galactosidases from germinating soybean seeds. Lanes are as follows: A: 1, molecular mass standards; 2, crude extract; 3, upper phase of ATPS; 4, enzyme preparation P1 from CM-Sepharose; 5, and P2, enzyme preparation P2 from CM-Sepharose; B: 1, molecular mass standards; 2, P1 eluted through ConA; C, 1, molecular mass standards; 2, P2 eluted through ConA.

(Fig. 4), but 90% of the activity was lost by both enzyme preparations following 45 min of incubation at 50°C (Fig. 5).

The activities of the P1 and P2 α-galactosidases against other substrates are shown in Table 2. Both enzymes were able to hydrolyze melibiose, raffinose and stachyose. However, the affinities for these substrates were much lower in comparison to that against ρNPGal. The K_m and V_{max} values for hydrolysis of melibiose by the P2 enzyme were 5.34 mM and 0.13 μmol min^{-1} ml^{-1}, respectively. Values for raffinose were 5.53 mM and 0.43 μmol min^{-1} ml^{-1}, respectively. The K_m value for hydrolysis of raffinose is close to that determined for the α-galactosidase purified from dry soybean seeds (Porter et al., 1990), but much lower than those reported for hydrolysis of raffinose by enzymes from *Aspergillus fumigatus* (De Rezende and Felix, 1999) and *Trichoderma reesei* (Zeilinger et al., 1993). Lactose and synthetic substrates containing β-linkage were hydrolyzed by the P1 enzyme but not by the P2 enzyme. None of the enzyme preparations showed substantial activity against sucrose and cellobiose and the synthetic substrates containing xylose ρNP-X, arabinose ρNP-A and mannose ρNP-M (Table 2).

The P1 and P2 α-galactosidases showed distinct sensitivities to simple sugars and mono and divalent ions (Table 3). The P1 enzyme showed very low or no inhibition by galactose, glucose, sucrose, melibiose, magnesium, potassium, sodium, calcium and β-mercaptoethanol, but was highly inhibited by copper and SDS. The P2 enzyme was only partially inhibited by galactose, melibiose, copper, and SDS. This is in agreement with the results reported for the cotyledonary α-galactosidases from *V. unguiculata* (Oliveira-Neto et al., 1998). Inhibition by galactose was found to be competitive and the K_i value was 0.65 mM as determined by the Dixon plot. In a previous work Porter et al. (1990) reported that galactose competitively inhibited (K_i of

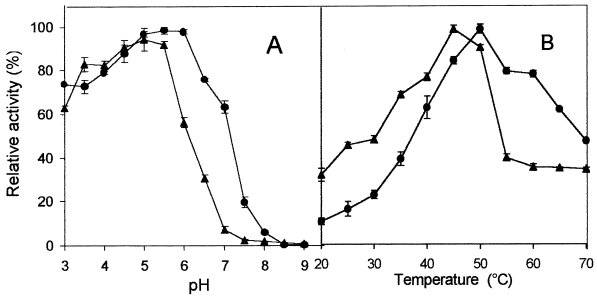

Fig. 4. pH (A) and temperature (B) influences on the activity of α-galactosidases (P1, ▲; P2, ●) from germinating soybean seeds.

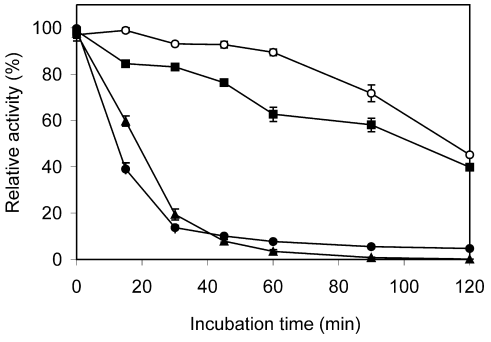

Fig. 5. Temperature influences on the stability of the α-galactosidase from germinating soybean seeds. Enzyme preparations were pre-incubated at 40°C P1 (■), P2 ○ or 50°C P1 (●), P2 (▲) for up to 2 h and the assays run at 37°C.

Table 2
Hydrolysis of several substrates by the α-galactosidases from germinating soybean seeds

Substrate	Concentration (mM)	Relative activity (%) ± S.D.	
		P1	P2
ρNP-α-Gal	0.5	100±0.98	100±0.89
Melibiose	40	6.89±0.27	10.09±0.20
Raffinose	40	11.82±0.49	54.31±0.46
Stachyose	40	5.02±0.06	10.52±0.15
Lactose	40	6.20±0.13	1.29±0.12
Maltose	40	3.97±0.17	1.60±0.12
Cellobiose	40	0.37±0.02	0.55±0.05
Sucrose	40	0	0
ρNP-β-Gal[a]	0.5	5.50±0.130	0
ρNP-β-Gal[a]	0.5	5.65±0.34	0
ρNP-α-Glc[a]	0.5	0	0
ρNP-X[a]	0.5	0	0
ρNP-A[a]	0.5	0	0
ρNP-M[a]	0.5	0	0

[a] ρNP-β-Gal, *para*-nitrophenyl-β-D-galactopyranoside; *o*NP-β-Gal, *ortho*-nitrophenyl-β-D-galactopyranoside; ρNP-α-Glc, *para*-nitrophenyl-α-D-glycopyranoside; ρNP-X, *para*-nitrophenyl-α-D-xylopyranoside; ρNP-A, *para*-nitrophenyl-α-D-arabinopyranoside; ρNP-M, *para*-nitrophenyl-α-D-mannopyranoside.

Table 3
Effect of simple sugars, ions, sodium dodecylsulphate and β-mercaptoethanol on α-galactosidases from germinating soybean seeds

Effector[a]	Relative activity (%) ± S.D.	
	P1	P2
–	100±0.92	100±0.100
D-Galactose	83.02±1.02	31.52±0.18
D-Glucose	108.35±0.79	97.16±0.93
Sucrose	89.48±1.25	89.66±1.86
Melibiose	84.17±1.23	64.08±0.66
$CuSO_4$	5.52±0.47	51.68±1.48
$MgCl_2$	95.77±0.95	96.47±1.70
KCl	98.71±2.00	103.36±1.01
NaCl	99.36±1.5	98.71±0.66
$CaCl_2$	95.11±0.70	102.15±1.72
SDS	1.94±0.11	62.64±0.15
β-Mercaptoethanol	88.71±1.25	88.37±0.55

[a] The final concentration of SDS was 1 mM. The final concentrations of all the other effectors were 2 mM.

0.12 mM) the α-galactosidase purified from dry soybean seeds with raffinose as substrate.

As the enzymes were able to hydrolyze also melibiose, raffinose and stachyose, the ability of P1 and P2 to hydrolyse RO present in the soybean aqueous extract (soymilk) was tested. Sucrose, raffinose and stachyose were present in dried soymilk at the concentrations of 10.25, 1.33 and 8.47 mg% (w/w), respectively. No change was observed for the amount of the RO in the control reactions. The P1 enzyme could not hydrolyze the RO present in soymilk, in contrast the P2 enzyme reduced considerably the amount of raffinose (by 73.3%) and stachyose (by 40.6%) after an incubation period of 8 h at 30°C. Hydrolysis of RO in soymilk by enzymic treatment was tested in 1982 by Cruz and Park (1982), and later by other researchers (Mulinami et al., 1997; Sanni et al., 1997; Scalabrini et al., 1998). However, no reliable, inexpensive and efficient enzymic process with indigenous or recombinant enzymes is available so far. In general, the enzymes suggested for this purpose are of microbial origin and therefore present the disadvantage of having no GRAS (generally regard as safe) status. The results presently reported indicate that the soybean seed α-galactosidases or the corresponding genes may be used for establishment of a process to improve the nutritional value of soymilk. Cloning of the genes encoding the P1 and P2 α-galactosidases is underway.

3. Experimental

3.1. Plant material and enzyme preparation

Soybean seeds (*G. max* L. Merr. cv. Doko) were allowed to germinate for 54 h, on a water-soaked filter paper (Germitest) at 27°C, and then frozen at −20°C. The frozen pre-germinated seeds (400 g fresh weight) were powdered in a blender and then resuspended in 800-ml of 0.1 M citric acid containing 0.05 M sodium phosphate, pH 5.5, and incubated with agitation for 1 h at 4°C. The suspension was then filtered through cheesecloth, the filtrate centrifuged (15,300 *g*) for 40 min at 4°C, and the supernatant used as a crude enzyme preparation.

3.2. α-Galactosidase assay

The enzyme was assayed using a reaction system (1 ml final volume) containing 650–750 μl of 0.1 M sodium acetate buffer, pH 5 (except when stated), 0–100 μl of enzyme preparation and 250μl of 2 mM ρ-nitrophenyl α-D-galactopyranoside (ρNPGal) or, other synthetic substrates. Reaction was conducted for 15 min at 37°C and stopped by the addition of 1 ml of 0.5 M sodium carbonate. The reaction was shown to be a first order reaction over a 60-min period. One unit (U) of enzyme was defined as the amount of protein necessary to produce one μmol of ρ-nitrophenol per min. For determination of thermal stability the enzyme fractions were pre-incubated for several time periods at either 40 or 50°C, and the residual activity was determined using the standard assay. The activities against raffinose, stachyose and sucrose were assayed for 20 min at 37°C using a reaction mixture containing 500 μl of 0.1 mM sodium acetate buffer, pH 5.0, 100μl of enzyme extract, and 400 μl of a 0.1 M substrate solution. The amount of reducing sugar produced was determined by adding 1 ml of 3,5-dinitrosalicylate reagent according to Miller (1956). The activities against melibiose, lactose, maltose and cellobiose were assayed using the same reaction conditions and substrate concentrations used for raffinose, stachyose and sucrose. In this case, the amount of glucose formed was determined by the glucose–oxidase method (Bergmeyer and Bernt, 1974). The data presented for all α-galactosidase activity determinations are mean values of triplicate assays in which the standard deviations were always smaller than 10%.

3.3. α-Galactosidase purification

The soybean enzyme was purified by separation on an ATPS (Hustedt et al., 1985) followed by two chromatography procedures. The ATPS consisted of 224 g of a 50% (w/w) polyethyleneglycol (PEG 1500) solution, 280 g of a 40% (w/w) monobasic and dibasic sodium phosphate solution, pH 5.0, 84 g of sodium chloride, and 112 g of crude enzyme extract. Samples (50 g each) of the aqueous mixture was transferred to centrifuge tubes which were vortex mixed for 1 min and then centrifuged for 5 min at 4100 *g* and 8°C. The volumes of the upper and lower phases were determined in graduated tubes, and collected separately. Protein and enzyme partition coefficients in the ATPS were calculated by measuring the amount of protein and enzyme in each phase. The effect of NaCl on the partition coefficient was investigated using 0, 3, 6, 9 and 12% NaCl in the ATPS. The upper phase resulting from the ATPS containing the enzyme was dialyzed overnight against 50 mM sodium acetate buffer, pH 4.0, and loaded onto a CM-Sepharose Fast Flow column (3×13 cm) equilibrated with 0.1 M sodium acetate buffer, pH 4.0. The proteins were eluted at 4°C at a flow rate of 40 ml/h, with a linear gradient formed with 300 ml of the acetate buffer and 300 ml of the same buffer containing 0.8 M NaCl. Five-ml fractions were collected. Fractions containing α-galactosidase activity were pooled and mixed with equal volume of sodium acetate buffer, pH 5.0, containing 1 mM each of $MnCl_2$, $MgCl_2$ and $CaCl_2$, and 0.9% NaCl. The resulting enzyme preparations where then chromatographed on a concanavalin-A Sepharose column (2×15.5 cm) equilibrated with the acetate ion-contain-

ing buffer. Proteins were recovered with 150 ml of equilibrating buffer containing 0.1 M methyl α-D mannoside.

3.4. Electrophoresis analysis

Enzyme preparations were analyzed by SDS–PAGE (12.5% gels) as described by Laemmli (1970). Proteins were silver-stained according to Blum et al. (1987).

3.5. Enzyme characterization

Kinetic experiments were performed at 37°C and pH 5.0. The Michaelis–Menten constant (K_m) and V_{max} for substrate hydrolysis and the inhibition constant (K_i) for galactose were calculated by the Lineweaver–Burk plot and Dixon plot, respectively. The substrate concentrations were: 0.025, 0.05, 0.1, 0.15, 0.25, 0.50, 0.75, 1.0, 1.5, and 2.0 mM in the case of ρNPGal, 0.25, 0.5, 1.5, 2.5, 5.0, 10.0, 20.0, and 40.0 mM for melibiose and raffinose. For K_i determination for galactose, the following ρNPGal concentrations were used: 0.05, 0.1, 0.2, 0.3, 0.4, 0.5, and 1.0 mM. The galactose concentrations used were 0.25, 0.5, and 1.0 mM. The effect of ions, simple sugars and reducing agent on the enzyme activity was tested by the standard assay with enzyme samples preincubated with each of the compounds tested for 15 min at 37°C.

3.6. Treatment of soybean milk with α-galactosidase

Soymilk was prepared from dry seeds (50 g). The seeds were chopped, homogenized in 400 ml water at 80°C, incubated for 10 min at 85°C, and filtered through cheese-cloth. Soymilk samples (2 ml) were then incubated with either water or 2 U of purified α-galactosidase for zero or 8 h with shaking (100 rpm) at 30°C. Each reaction mixture was dried and the soluble sugars extracted from 20 mg of dried powder with organic solvents according to Saravitz et al. (1987). The solvent was evaporated at 40°C and the sugars resuspended in 1 ml water. The sugars were analyzed by HPLC on a Shimadzu series 10A chromatograph using an analytical column [aminopropil (-NH_2)] eluted with an acetonitrile–water isocratic mixture (80:20 v/v). Individual sugars were automatically identified and quantified by comparison with retention times and known concentrations of standard sugars. Gentiobiose was used as an internal standard as it does not interfere with the other sugars and it is not found in soybean seeds.

3.7. Protein determination

Protein was quantified by the Coomassie Blue binding method (Bradford, 1976) with bovine serum albumin as standard.

Acknowledgements

V.M.G. gratefully acknowledges financial support from the Coordenação de Aperfeiçoamento de Pessoal de Nível Superior (CAPES, Brasil) and from the Universidade Federal de Goiás. This work was partially supported by a grant to CRF (FAPDF, No. 193.000.237/96).

References

Avigad, G., Dey, P.M., 1997. Carbohydrate metabolism: storage carbohydrates, In: Dey, P.M., Harborne, J.B. (Ed.), Plant Biochemistry, Academic Press, San Diego, pp. 143–204.

Bergmeyer, H.U., Bernt, E., 1974. Determination of glucose with oxidase and peroxidase. In: Bergmeyer, H.U. (Eds.), Methods of Enzymatic Analysis, Verlag Chemie, Weinheim, pp. 1205–1215.

Blum, H., Beier, H., Gross, H., 1987. Improved silver staining of plant proteins, RNA and DNA in polyacrylamide gels. Electrophoresis 8, 93–99.

Bradford, M.M., 1976. A rapid and sensitive method for quantification of microgram quantities of protein utilizing the principle dye binding. Anal. Biochem. 72, 680–685.

Campillo, H., Shannon, L.M., 1982. An α-galactosidase with hemagglutinin properties from soybean seeds. Plant Physiol. 69, 628–631.

Cruz, R., Park, Y.K., 1982. Production of α-galactosidase and its application to the hydrolysis of galactoligosaccharides in soybean milk. J. Food Sci. 47, 1973–1975.

Cruz, R., Silva, A.L., 1986. Soybean (*Glycine max*), endogenous alpha-galactosidase and invertase during the germinative process. Arq. Biol. Technol. 29, 435–443.

Davis, M.O., Hata, D.J., Johnson, S.A., Walker, J.C., Smith, D.S., 1996. Cloning, expression and characterization of a blood group B active recombinant α-D-galactosidase from soybean (*Glycine max*). Biochem. Mol. Biol. Int. 39, 471–485.

De Lumen, O.B., 1992. Molecular strategies to improve protein quality and reduce flatulence in legumes: a review. Food Structure 11, 33–46.

De Rezende, S.T., Felix, C.R., 1997. Raffinose-hydrolyzing activity of *Aspergillus fumigatus*. Biotech. Letters 19, 217–220.

De Rezende, S.T., Felix, C.R., 1999. Production and characterization of raffinose-hydrolysing and invertase activities of *Aspergillus fumigatus*. Folia Microbiol. 44, 191–195.

Dey, P.M., Pridham, J.B., 1972. Biochemistry of α-galactosidases. Adv. Enzymol. 36, 91–130.

Dhar, M., Mitra, M., Hata, J., Butnariu, O., Smith, D., 1994. Purification and characterization of *Phaseolus vulgaris* α-D-galactosidase isozymes. Biochem. Mol. Biol. Int. 34, 1055–1062.

Gitzelmann, R., Auricchio, S., 1965. The handling of soy α-galactoside by a normal and galactosemic child. Pediatrics 36, 231–232.

Hustedt, H., Kroner, K.K., Kula, M.R., 1985. Applications of phase partitioning in biotechnology. In: Walter, H., Brooks, D.E., Fisher, D. (Eds.), Partitioning in Aqueous Two-Phase Systems, Academic Press, Orlando.

Laemmli, U.K., 1970. Cleavage of structural of structural protein during the assembly of the head of bacteriophage T4. Nature 227, 680–685.

Miller, G.L., 1956. Use of dinitrosalicylic acid reagent for determination of reducing sugar. Anal. Chem. 31, 426–428.

Mulimani, V.H., Thippeswamy, S., Ramalingam, 1997. Effect of soaking, cooking and crude α-galactosidase treatment on the oligosaccharide content of soybean flour. Food Chem. 59, 279–282.

Oliveira-Neto, O.B., Gomes-Filho, E., Prisco, J.T., Enéas-Filho, J., 1998. Partial purification and properties of cotyledonary α-galacto

sidase from three cultivars of *Vigna unguiculata*. R. Bras. Fisiol. Veg. 10, 91–96.

Porter, J.E., Herrmann, K.M., Ladish, M.R., 1990. Integral kinetics of α-galactosidase purified from *Glycine max* for simultaneous hydrolysis of stachyose and raffinose. Biotechnol. Bioeng. 35, 15–22.

Sanni, A.I., Onilude, A.A., Ogundoye, O.R., 1997. Effect of bacterial galactosidase treatment on the nutritional status of soybean seeds and its milk derivative. Nahrung 41, 18–21.

Saravitz, D.M., Pharr, D.M., Carter Jr., T.E., 1987. Galactinol synthase activity and soluble sugars developing seeds of four soybean genotypes. Plant Physiol. 83, 185–189.

Scalabrini, P., Rossi, M., Spettoli, P., Matteuzzi, D., 1998. Characterization of *Bifidobacterium* strains for use in soymilk fermentation. Int. J. Food Microbiol. 39, 213–219.

Zeilinger, S., Kristufek, D., Arisan-Atac, I., Hodits, R., Kubicek, C.P., 1993. Conditions of formation, purification, and characterization of an α-galactosidase of *Trichoderma reesei* RUT C-30. Appl. Environ. Microbiol. 59, 1347–1353.

PERGAMON

Phytochemistry 58 (2001) 75–79

PHYTOCHEMISTRY

www.elsevier.com/locate/phytochem

Effect of the *Cnr* mutation on carotenoid formation during tomato fruit ripening

P.D. Fraser[a], P. Bramley[a], G.B. Seymour[b,*]

[a]*School of Biological Sciences, Royal Holloway, University of London, Egham, Surrey TW20 OEX, UK*
[b]*Horticulture research International, Wellesbourne, Warwick CV35 9EF, UK*

Received 13 December 2000; received in revised form 27 March 2001

Abstract

The characteristic pigmentation of ripe tomato fruit is due to the deposition of carotenoid pigments. In tomato, numerous colour mutants exist. The *Cnr* tomato mutant has a colourless, non-ripening phenotype. In this work, carotenoid formation in the *Cnr* mutant has been studied at the biochemical level. The carotenoid composition of Ailsa Craig (AC) and *Cnr* leaves was qualitatively and quantitatively similar. However, *Cnr* fruits had low levels of total carotenoids and lacked detectable levels of phytoene and lycopene. The presence of normal tocopherols and ubiquinone-9 levels in the ripe *Cnr* fruits suggested that other biosynthetically related isoprenoids were unaffected by the alterations to carotenoid biosynthesis. In vitro assays confirmed the virtual absence of phytoene synthesis in the ripe *Cnr* fruit. Extracts from ripe fruit of the *Cnr* mutant also revealed a reduced ability to synthesise the carotenoid precursor geranylgeranyl diphosphate (GGPP). These results suggest that besides affecting the first committed step in carotenoid biosynthesis (phytoene synthase) the *Cnr* mutation also affects the formation of the isoprenoid precursor (GGPP).
© 2001 Elsevier Science Ltd. All rights reserved.

Keywords: *Lycopersicon esculentum*; Solanaceae; Tomato ripening; Pleiotropic mutant; Pigments

1. Introduction

Carotenoid pigments are synthesised by all higher plants, algae, and some bacteria and fungi (Britton et al., 1995). Although essential for human health, carotenoids can not be synthesised de novo in the body and must be acquired from the diet (Parker, 1996). Tomato fruit and its products (e.g. ketchup, juices, soups and sauces) are the principal source of carotenoids in the western diet. Lycopene, the predominant carotenoid found in tomato, is a powerful antioxidant and may prevent the onset of serious disease states such as prostate cancer (Giovannucci et al., 1995). In addition, β-carotene is a provitamin A carotenoid and its deficiency can cause xerophthalmia, blindness, and premature death (Mayne, 1996). It is not surprising therefore, that the regulation of carotenoid biosynthesis in higher plants and especially crop plants, has become an area of considerable interest.

In higher plants, carotenoid biosynthesis and sequestration occurs in the plastid. In photosynthetic tissues, this occurs in the chloroplasts, while in non-photosynthetic plant tissues such as fruits and flowers carotenoid accumulation occurs in chromoplasts. Carotenoid formation utilizes the ubiquitous isoprenoid precursor geranylgeranyl pyrophosphate (GGPP). Two molecules of GGPP are condensed to form phytoene and this reaction is catalysed by phytoene synthase (PSY). Phytoene is then converted to lycopene in a series of dehydrogenation reactions, which introduce four double bonds into the phytoene molecule. This conversion is performed by the sequential action of phytoene and ζ-carotene desaturase enzymes respectively. The biosynthesis of β-carotene and α-carotene and xanthophylls then proceeds following the scheme shown in Fig. 1. Genes encoding the majority of the enzymes in the carotenoid biosynthetic pathway have been cloned. The ripening enhanced cDNA pTOM5 was identified as *Psy-1* in transgenic experiments (Bramley et al., 1992). The same sequence restores lycopene accumulation in transgenic *yellow-flesh* mutants identifying the mutation as a lesion in a *Psy-1* gene (Fray and Grierson, 1993). In both transgenic

* Corresponding author. Tel.: +44-1789-470382; fax: +44-1789-470552.
E-mail address: graham.seymour@hri.ac.uk (G.B. Seymour).

0031-9422/01/$ - see front matter © 2001 Elsevier Science Ltd. All rights reserved.
PII: S0031-9422(01)00175-3

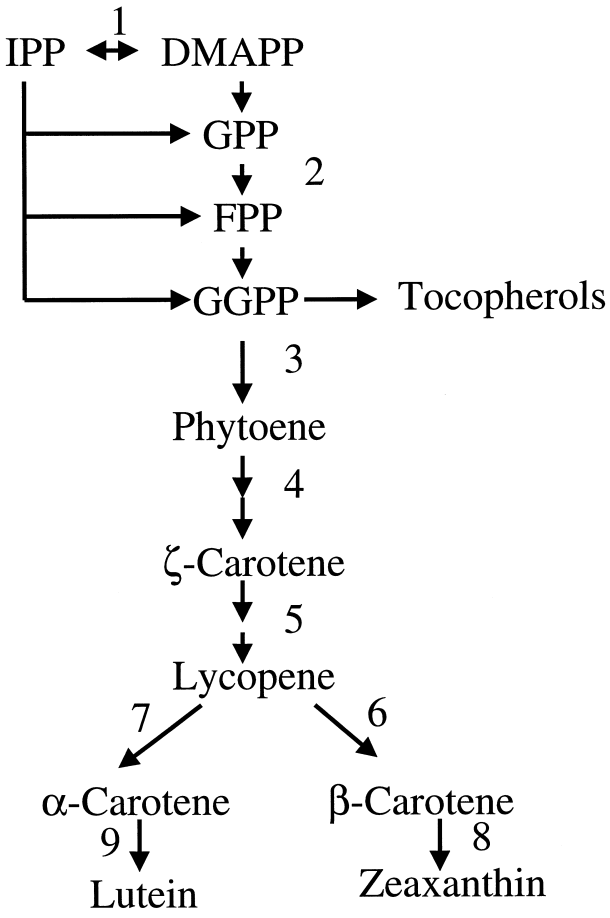

Fig. 1. Summary of the biosynthetic pathway for carotenoids. Numbers indicate enzyme responsible for the conversion. 1. Isopentenyl diphosphate isomerase. 2. Geranylgeranyl diphosphate synthase. 3. Phytoene synthase. 4. Phytoene desaturase. 5. ζ-Carotene desaturase. 6. β-Cyclase. 7. β- and ε-Cyclase. 8. β-Hydroxylase. 9. β- and ε-Hydroxylase.

plants containing *Psy-1* in an antisense orientation and in the *yellow flesh* mutant there are virtually no carotenoids in the ripe fruits (Fray and Grierson, 1993), although carotenoid levels in leaf and green fruit are essentially unaffected. This is due to the presence of another phytoene synthase, *Psy-2*, which is principally responsible for phytoene formation in chloroplast containing tissues (Fraser et al., 1999).

The regulation of carotenoid biosynthesis in higher plants is poorly understood. Tomato ripening mutants such as high-pigment (*hp*) (Yen et al., 1997) and colourless non-ripening (*Cnr*) (Thompson et al., 1999) are useful tools for exploring the regulation of this process. In *hp,* the level of carotenoids is twice that in normal fruits, but with a quantitatively very similar pattern (Bramley, 1997). This difference almost certainly reflects an increase in plastid number (Yen et al., 1997). The *hp* gene maps to chromosome 2 and is not allelic with any known carotenoid biosynthetic genes. In the *Cnr* mutant, carotenoid biosynthesis is all but abolished resulting in mature fruit with a white pericarp. This mutation also has other pleiotropic effects including altered fruit softening (Thompson et al., 1999). Like *hp,* the *Cnr* mutation maps to chromosome 2 in a location devoid of other known fruit ripening genes.

The purpose of this study was to characterise carotenoid biosynthesis in developing and ripening *Cnr* fruits at the biochemical level, in order to provide a greater insight into the mechanism of action of the C*nr* mutation.

2. Results and discussion

2.1. Carotenoid and isoprenoid analysis of Ailsa Craig (AC) and Cnr tissues

HPLC-PDA (photodiode array) analysis of carotenoids extracted from AC and *Cnr* chloroplast-containing tissues (leaf and developing fruit) show a very similar pigment profile (Table 1). The predominant pigment was the xanthophyll lutein (55–80%) also present in appreciable amounts were violaxanthin and β-carotene. Although not drastically reduced, less total carotenoid was found in the leaf and mature green fruit stage of the *Cnr* mutant (70 and 57% less respectively). As fruit ripening proceeded the characteristic accumulation of lycopene was not observed in the *Cnr* mutant, the intermediate phytoene also appeared to be absent. The total carotenoid content of AC fruit was 100-fold higher than in the mutant (Table 1), confirming previous data (Thompson et al., 1999). The profile of carotenoids in the ripe Cnr fruit resembles that found in green fruit or leaf tissue (Fig. 2, Table 1). However, the mature green and ripe Cnr fruits appear to lack violaxanthin, which would presumably result in an inhibition of ABA biosynthesis. Determination of other related isoprenoids e.g. tocopherols and ubiquinone-9 revealed no differences between *Cnr* and AC fruits (Table 2). The apparent reduction in leaf carotenoid levels in *Cnr* may reflect an affect of the mutation in tissues other than fruits. The data for the leaf samples was, however, quite variable due probably to effects of position of leaf with respect to others in the canopy and leaf carotenoid levels requires further investigation.

Comparison of the carotenoids present in AC and the *Cnr* mutant indicates that *Cnr* lacks the characteristic accumulation of ripening (or chromoplast) related carotenoids (e.g. lycopene and phytoene). Previous studies (Thompson et al., 1999) have shown that *Psy*-1 is not expressed in the *Cnr* mutant fruit. Characterisation of AC and *Cnr* carotenoids supports the absence of *Psy*-1 expression and show that *Psy-2* can not compensate for its absence in the formation of carotenoid in ripe fruit, as postulated previously (Fraser et al., 1999). Both *Psy-1* down-regulated mutants (Bramley et al., 1992; Fray and Grierson, 1993) and the *Cnr* have a characteristic

Table 1
Carotenoid content of Ailsa Craig and *Cnr* leaves and fruit. The tissue samples were prepared from three fruit or leaves. Fruits were cut in half, the seeds removed and freeze dried from which a ground powder was produced. Determinations were carried out in triplicate

	Carotenoid (μg/g DW)						
	Phytoene (%)	Phytofluene (%)	Lycopene (%)	β-Carotene (%)	Lutein (%)	Violaxanthin (%)	Total
AC							
Leaf	0	0	0	514±15 (30)	953±6 (55)	260±6.52 (15)	1727±27
IMG	0	0	0	20±7 (32)	40.4±15 (65)	1.1±0.46 (1.7)	62.0±22
MG	0	0	0	11±0.7 (31)	23.2±1.4 (67)	0.7±0.1 (2.0)	35.0±2.2
B	14±1.10 (8.6)	0	31.0±1.0 (19)	84±1 (52)	32.9±1.3 (20)	0.82±0.03 (0.8)	161.8±4.4
B+7	238±12 (5.6)	17±1.4 (0.4)	3746±326 (87)	200±9 (4.7)	20.4±2.4 (0.5)	3.9±0.04 (0.09)	4225±351
Cnr							
Leaf	0	0	0	312±97 (31)	536±166 (54)	153±49 (15)	1000.9±312
IMG	0	0	0	29.1±8.4 (37)	45.3±0.7 (58)	3.7±0.2 (4.7)	78.1±9.3
MG	0	0	0	4.1±0.04 (20)	16±0.26 (80)	0	20.1± 0.3
B	0	0	0	12.7±1.0 (26)	36.9±3.0 (74)	0	49.6±4
B+7	0	0	0	14.0±2.7 (37)	23.7±4.5 (63)	0	37.7±7.2

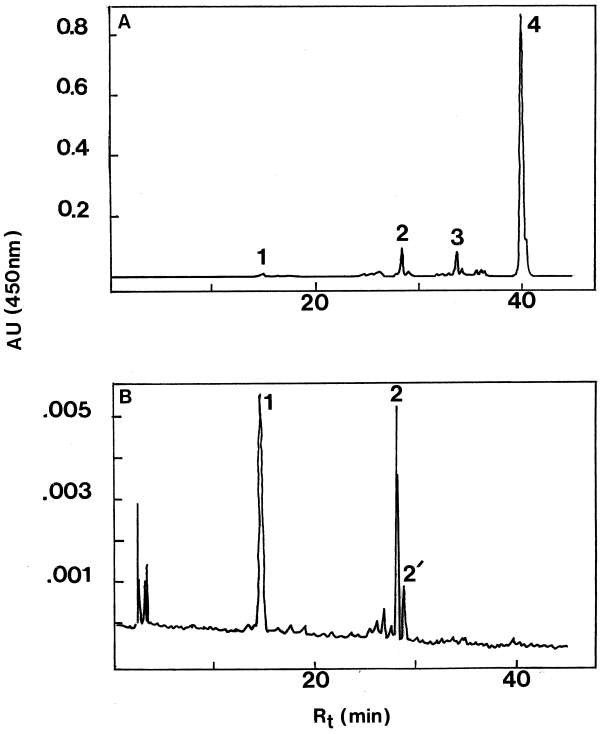

Fig. 2. HPLC trace of major carotenoids from (A) AC (B+7) and (B) *Cnr* (B+7). Peaks correspond to (1) lutein, (2) β-carotene, (2′) *cis*-β-carotene, (3) *cis*-lycopene and (4) lycopene. Traces were recorded at 450 nm.

yellow skin colour. This is due to the presence of the flavonoid naringen chalcone and not the presence of carotenoids (Bolwell, Fraser and Bramley, unpublished data).

Structurally, tocopherols possess a prenyl moiety, which is derived from GGPP. In *Cnr* tocopherols were not affected, suggesting that a pool of GGPP is available and that the *Cnr* mutation does not result in an absolute block in the formation of GGPP during fruit ripening. Unlike both the carotenoids and tocophorols, which are synthesised in the plastid from isopentenyl pyrophosphate (IPP) formed by the 'Rohmer' pathway, ubiquinone is a non-plastidic isoprenoid derived from IPP resulting from the mevalonate pathway. In the *Cnr* mutant ubiquinone content was unaffected.

Table 2
Levels of selected isoprenoids in red ripe (breaker+7) from Ailsa Craig and *Cnr* pericarp. The tissue samples were prepared from three fruit or leaves. Fruits were cut in half, the seeds removed and freeze dried from which a ground powder was produced. Determinations were carried out in triplicate

	Isoprenoid μg/g DW	
	Tocopherols	Ubiquinone- 9
AC Breaker+7	6.0±1.0	79±7.4
Cnr Breaker+7	7.3±2.0	75±17

2.2. In vitro analysis of phytoene synthesis from IPP

In order to confirm phytoene synthase as the biochemical block in *Cnr*, in vitro analysis was performed. Stromal extracts were prepared from both the AC and *Cnr*. The ability of these extracts to incorporate the precursor isopentenyl pyrophosphate (IPP) was determined. Data were expressed on a protein and fresh weight (FW) basis to eliminate possible discrepancies that may result from alterations in textural properties of the *Cnr* mutant. Comparisons clearly show (Table 3) that phytoene formation from [^{14}C]-IPP is significantly reduced (27-fold) in the *Cnr* mutant. Although not reduced as dramatically (5-fold), the levels of GGPP are also affected in *Cnr*. In contrast the total acid hydrolysable prenyl phosphates formed from IPP are not affected in the *Cnr* mutant. These data confirm that phytoene formation in the *Cnr* fruit is virtually abolished. Furthermore, besides

Table 3
In vitro analysis of phytoene formation in red ripe fruit of Ailsa Craig and *Cnr*

	IPP isomerase activity		Formation from IPP			
			GGPP		Phytoene	
	dpm/g FW	dpm/mg Protein	dpm/g FW	dpm/mg Protein	dpm/g FW	dpm/mg Protein
AC	799±129	$6.0\times10^{6}\pm1.0$	68.0±22	$3.3\times10^{5}\pm0.7$	4.1±0.6	$3.0\times10^{4}\pm0.4$
Cnr	1186±190	$3.0\times10^{6}\pm0.5$	18±4.0	$6.7\times10^{4}\pm1.3$	0.47±0.1	$1.1\times10^{3}\pm0.2$

phytoene synthesis, it would appear that the formation of GGPP is also reduced in the mutant. The reduction in GGPP does not, however, affect tocopherols suggesting that another pool of GGPP separate from that utilized for carotenoid biosynthesis is available. To date only one GGPP synthase has been isolated from tomato (Römer et al., 1993) but several GGPP synthases have been identified in *Arabidopsis* (Scolnik and Bartley, 1996). It is, therefore, feasible that alternative GGPP synthase(s) exist in tomato one of which is responsible for the supply of GGPP into the carotenoid pathway.

The *Cnr* mutation is the result of a lesion in a single gene which has pleiotropic effects on ripening including abnormal softening and colour development . The *Cnr* gene is likely to be involved in the regulation of normal ripening in tomato (Thompson et al., 1999). Data presented in this article show that carotenoid formation is an important component of the co-ordinated fruit ripening processes upon which the *Cnr* gene product exerts its effects. Typically PSY-1 is regarded as the most influential step for carotenoid formation in tomato, but the biochemical data obtained from the *Cnr* mutant suggest that an accessible pool of GGPP is a prerequisite for carotenoid accumulation. Future isolation of the *Cnr* gene could provide an important tool in the engineering of quality traits into tomato fruit.

3. Experimental

3.1. Plant material, radiolabelled substrates and reagents

Tomato (*Lycoperiscon esculentum* Mill. cv Ailsa Craig) fruit and a near isogenic line of *Cnr,* produced by back-crossing five times to Ailsa Craig, followed by selfing to generate a homozygous mutant line.mutant line, were grown in a heated greenhouse using standard cultural practices with regular additions of N,P,K fertilizer and supplementary lighting when required. Fruits were harvested at the following days post anthesis (DPA): immature green (IMG, c. 20 days DPA), mature-green (MG, 35 DPA), breaker (B, 49 DPA) and breaker + 7 (B + 7, 56 DPA). The radiolabelled [1-^{14}C]-IPP (2.2 GBq/mmol) was purchased from Amersham International, Amersham, Bucks, UK. Biochemical reagents were supplied by Sigma, Poole, UK, unless otherwise stated.

3.2. Extraction, separation, and identification of carotenoids and isoprenoids

Procedures for the solvent extraction, HPLC separation, identification (PDA) and quantification are provided in Fraser et al. (2000a).

3.3. Preparation of subcellular extracts

Pericarp tissue typically from three to four tomatoes (65–100 g per tomato) were homogenised in a Waring blender at 4°C. The homogenisation buffer contained 0.4 M sucrose, 1 mM EDTA, and 1 mM DTT, buffered with 50 mM Tris–HCl (pH 8.0). Ice-cold buffer was added until it covered the pericarp tissue (about 1:3/1:4 fruit vol: buffer). The mixture was left for 20 min before homogenising for two 3 s bursts. The suspension was filtered through cotton wool sandwiched by two layers of muslin. The filtrate (homogenate) was subjected to further subcellular fractionation as described in Fraser et al. (2000b).

3.4. In vitro assays

[^{14}C]-Isopentenyl diphosphate (19 kBq) was used to ascertain incorporation into prenyl diphosphates as well as phytoene. Incubations were buffered with 0.4M Tris–HCl (pH 8.0), containing 1 mM DTT, 4 mM $MgCl_2$, 6 mM $MnCl_2$, 3 mM ATP, 0.1%(w/v) Tween 60, 1 mM KF and substrate. The total volume of the buffer mixture was 150 μl, to which 150 μl of the enzyme preparation was added. Incubations were shaken for 3–4 h at 28°C unless stated otherwise. Radiolabelled products were separated and identified as described in Fraser et al. (2000b).

3.5. Other determinations

Protein contents were estimated as detailed previously (Lowry et al., 1951). Prior to determination, proteins were precipitated (Wessel and Flugge, 1984). Determination of

radioactivity by liquid scintillation counting was carried out according Bramley et al., 1973).

Acknowledgements

This work was funded in part by the UK Biotechnology and Biological Sciences Research Council (GBS), an EU Programme PL 962077 (P.B.) and The Royal Society G503 (P.D.F.).

References

Bramley, P.M., 1997. The regulation and genetic manipulation of carotenoid biosynthesis in tomato fruit. Pure and Applied Chemistry 69, 2159–2162.

Bramley, P.M., Davies, B.H., Rees, A.F., 1973. Colour quenching by carotenoids. In: Crook, M.A., Johnson, P. (Eds.), Liquid Scintillation Counting, Vol. 3. Heyeden, London, pp. 76–85.

Bramley, P.M., Teulieres, C., Blain, I., Bird, C., Schuch, W., 1992. Biochemical characterisation of transgenic tomato plants in which carotenoid synthesis has been inhibited through expression of antisense RNA to pTOM5. Plant Journal 2, 343–349.

Britton, G., Liaaen-Jensen, S., Pfander, H., 1995. Carotenoids. In: Britton, G., Liaaen-Jensen, S., Pfander, H. (Eds.), Isolation and Analysis, Vol. 1A. Birkhäuser, Basel, pp. 13–15.

Fraser, P.D., Kiano, J.W., Truesdale, M.R., Schuch, W., Bramley, P.M., 1999. Phytoene synthase-2 enzyme activity in tomato does not contribute to carotenoid synthesis in ripening fruit. Plant Molecular Biology 40, 687–698.

Fraser, P.D., Pinto, M.E.S., Holloway, D.E., Bramley, P.M., 2000a. Application of high-performance liquid chromatography with photodiode array detection to the metabolic profiling of plant isoprenoids. Plant Journal 24 (4), 1–10.

Fraser, P.D., Schuch, W., Bramley, P.M., 2000b. Phytoene synthase from tomato (*Lycopersicon esculentum*) chloroplasts — partial purification and biochemical properties. Planta 211 (3), 361–369.

Fray, R.G., Grierson, D., 1993. Identification and genetic analysis of normal and mutant phytoene synthase genes of tomato by sequencing, complementation and co-suppression. Plant Molecular Biology 22, 589–602.

Giovannucci, E., Ascherio, A., Rimm, E.B., Stampfer, M.J., Colditz, G.A., Willett, W.C., 1995. Intake of carotenoids and retinol in relation to risk of prostate-cancer. Journal of the National Cancer Institute 87, 1767–1776.

Lowry, O.H., Rosenbrough, N.J., Farr, A.L., Randall, R.J., 1951. Protein measurement with the Folin phenol reagent. Journal of Biological Chemistry 193, 265–275.

Mayne, S.T., 1996. Beta-carotene, carotenoids, and disease prevention in humans. FASEB Journal 10, 690–701.

Parker, R.S., 1996. Carotenoids. 4. Absorption, metabolism, and transport of carotenoids. FASEB Journal 10, 542–551.

Römer, S., Hugueney, P., Bouvier, F., Camara, B., Kuntz, M., 1993. Expression of the genes encoding the early carotenoid biosynthetic enzymes in *Capsicum annuum*. Biochemical and Biophysical Research Communications 196, 1414–1421.

Scolnik, P.A., Bartley, G.E., 1996. A table of some cloned plant genes involved in isoprenoid biosynthesis. Plant Molecular Biology Reporter 14, 305–319.

Thompson, A.J., Tor, M., Barry, C.S., Vrebalov, J., Orfila, C., Jarvis, M.C., Giovannoni, J.J., Grierson, D., Seymour, G.B., 1999. Molecular and genetic characterisation of a novel pleiotropic tomato-ripening mutant. Plant Physiology 120, 383–389.

Wessel, D., Flugge, U.I., 1984. A method for the quantitative recovery of protein in dilute-solution in the presence of detergents and lipids. Analytical Biochemistry 138, 141–143.

Yen, H.C., Shelton, B.A., Howard, L.R., Lee, S., Vrebalov, J., Giovannoni, J.J., 1997. The tomato *high-pigment (hp)* locus maps to chromosome 2 and influences — plastome copy number and fruit quality. Theoretical and Applied Genetics 95, 1069–1079.

PERGAMON

Phytochemistry 58 (2001) 81–89

PHYTOCHEMISTRY

www.elsevier.com/locate/phytochem

Effect of culture conditions on the synthesis of vitamin D_3 metabolites in *Solanum glaucophyllum* grown in vitro

Alejandro Curino, Lorena Milanesi, Silvia Benassati, Mario Skliar, Ricardo Boland*

Departamento de Biología, Bioquímica y Farmacia, Universidad Nacional del Sur. San Juan 670, 8000 Bahia Blanca, Argentina

Received 27 July 2000; received in revised form 15 November 2000

Abstract

In cultured *Solanum glaucophyllum* we have recently described the operation of a light-independent pathway of 1α,25-dihydroxy-vitamin D_3 (1α,25$(OH)_2D_3$) biosynthesis which involves similar intermediates as in vertebrates. In this work we investigated factors influencing the formation of 1α,25$(OH)_2D_3$ and related sterols in *S. glaucophyllum* grown in vitro in darkness. Callus tissue and cells cultured in Murashige and Skoog medium in the absence of light were employed. Lipids were extracted with chloroform–methanol. The remaining water soluble fraction was incubated with β-glucosidase to release vitamin D_3 compounds from their glycoconjugated derivatives followed by organic solvent extraction. Vitamin D_3 derivatives were isolated by Sephadex LH-20 and high-performance liquid chromatography (HPLC). HPLC or competitive protein binding assays with intestine 1α,25$(OH)_2D_3$ receptor and serum vitamin D binding protein were used to quantify the metabolites. The levels of 1α,25$(OH)_2D_3$ in calli varied according to the tissue explant origin, e.g. stem > leaf > fruit. For all organs, the metabolite was mainly present as free sterol (> 80% of total). There were larger amounts of 25$(OH)D_3$ than 1α,25$(OH)_2D_3$. It was found that Ca^{2+}, auxin and kinetin are important factors upregulating 1α,25$(OH)_2D_3$ synthesis in *S. glaucophyllum* tissue and cells. Irradiation with UV light increased vitamin D_3 but not 1α,25$(OH)_2D_3$ levels. In agreement with these results, incubation of cells with [^{3}H]25$(OH)D_3$ revealed a low conversion rate to [^{3}H]1α,25$(OH)_2D_3$. The operation of a light-dependent pathway formation of vitamin D_3 coupled to higher expression of 25$(OH)D_3$-1α-hydroxylase may account for the large concentrations of 1α,25$(OH)_2D_3$ normally found in differentiated field-grown plants. © 2001 Elsevier Science Ltd. All rights reserved.

Keywords: *Solanum glaucophyllum*; Solanaceae; In vitro cultures; Synthesis; Vitamin D_3 metabolites; Calcitriol

1. Introduction

Solanum glaucophyllum Desf. (*Solanum malacoxylon* Send.) is a plant native to South America which causes calcinosis in animals (Worker and Carrillo, 1967; Morris, 1982). Early studies correlated this property to the existence in the plant of the hormonally active form of vitamin D_3, 1α,25-dihydroxy-vitamin D_3 [1α,25$(OH)_2D_3$; calcitriol] (Wasserman et al., 1976). It was subsequently reported that *S. glaucophyllum* also contains vitamin D_3 and 25-hydroxy-vitamin D_3 (Esparza et al., 1982). Vitamin D_3 derivatives have been detected in several members of the Solanaceae as well as species belonging to other families (Boland, 1986; Prema and Raghuramulu, 1994; Aburjai et al., 1998; Skliar et al., 2001). Studies with in vitro systems have shown that vitamin D sterols stimulate root development (Buchala and Schmid, 1979; Talmon et al., 1989) through activation of the Ca^{2+} messenger system (Vega and Boland, 1986; Vega et al., 1988), suggesting a physiological function for these compounds in plants. Congruent with the participation of a photolytic reaction in the generation of vitamin D_3, it has been reported that the vitamin D activity of *Trisetum flavescens*, when tested in rachitic rats, is dependent on UV light exposure (Zucker et al., 1980; Rambeck et al., 1981). Further metabolism of the sterol through a pathway similar to that occurring in animals has been suggested by the detection of vitamin D_3-25-hydroxylase and 25$(OH)D_3$-1α-hydroxylase activities in *S. glaucophyllum* leaf extracts and subcellular fractions (Esparza et al., 1982).

* Corresponding author. Tel.: +54-291-459-5100; fax: +54-291-459-5130.

E-mail address: rboland@criba.edu.ar (R. Boland).

0031-9422/01/$ - see front matter © 2001 Elsevier Science Ltd. All rights reserved.
PII: S0031-9422(01)00090-5

There is controversial evidence regarding the native structure and the tissue distribution of $1\alpha,25(OH)_2D_3$ and related metabolites in *S. glaucophyllum*. On the basis of their solubility properties it has been reported that vitamin D_3 derivatives are mainly found as glycoconjugates (Humphreys, 1973; Wasserman et al., 1976; Esparza et al., 1982). However, other lines of evidence are indicative of the presence of free vitamin D_3 sterols (Masselin et al., 1969; Procsal et al., 1976). Also, in contradiction to the initial belief that $1\alpha,25(OH)_2D_3$ was exclusively localized in the leaves of *S. glaucophyllum,* the application of sensitive assay procedures has allowed detection of this metabolite in all plant organs (Weissenberg et al., 1989). The first aspect is of pharmacological importance as free secosterols act faster and more potently than the corresponding glycosides (De Boland et al., 1978) and the second of economical significance when considering *S. glaucophyllum* tissues as a source of calcitriol for use in medicine and animal husbandry (Boland, 1986).

Recent studies have shown the presence of 7-dehydrocholesterol, vitamin D_3, $25(OH)D_3$ and $1\alpha,25(OH)_2D_3$ in *S. glaucophyllum* callus and cell cultures (Weissenberg et al., 1989; Aburjai et al., 1996; Curino et al., 1998), confirming that the plant itself, and not opportunistic organisms, is able to produce these sterols. More important, calcitriol formation in *S. glaucophyllum* grown in vitro under strict conditions of darkness could be shown, suggesting that a metabolic route independent of light is also operative in the generation of vitamin D_3 compounds (Curino et al., 1998). As UV irradiation of cultures increased only slightly the concentration of $1\alpha,25(OH)_2D_3$ the question arose as to whether either photolytic cleavage of 7-dehydrocholesterol or the following hydroxylations of vitamin D_3 and $25(OH)D_3$ would be limiting the efficiency of the light-dependent synthetic pathway of $1\alpha,25(OH)_2D_3$ in culture systems. The elucidation of this aspect as well as the identification of medium constituents influencing calcitriol synthesis in *S. glaucophyllum* in vitro may help to optimize conditions for its biotechnological production, i.e. as a potentially convenient alternative to the expensive chemical procedures designed to cover the widespread medical application of the secosteroid hormone and analogs (Bouillon et al., 1995).

In view of the above considerations, in the present work we measured in *S. glaucophyllum*, grown in the field or green-house and in vitro, the relative contents of free and glycoconjugated $1\alpha,25(OH)_2D_3$ from different plant organs, and examined the effects of UV light on the levels of $1\alpha,25(OH)_2D_3$ and its precursors. The latter study led us to measure the activity of $25(OH)D_3$-1α-hydroxylase in cultured *S. glaucophyllum*. In addition, we investigated the influence of medium concentration of Ca^{2+} and plant growth factors on calcitriol production.

2. Results and discussion

2.1. Distribution of free and conjugated forms of $1\alpha,25(OH)_2D_3$ in calli and organs from *S. glaucophyllum*

Previous studies have shown that calli derived from leaves *of S. glaucophyllum* synthesize $1\alpha,25(OH)_2D_3$ in vitro (Weissenberg et al., 1989; Aburjai et al., 1996; Curino et al., 1998). The ability of calli derived from other organs of the plant to produce the sterol was studied. The levels of both free and glycoconjugated $1\alpha,25(OH)_2D_3$ generated by the in vitro systems under darkness were quantitatively evaluated using a specific radioreceptor assay. As shown in Fig. 1, the amounts of metabolite in calli derived from stem and leaves were appreciably more elevated than in calli derived from fruits and roughly comparable to those found in the tissues of origin. However, fruits from *S. glaucophyllum* grown in the field contained considerably higher concentrations of $1\alpha,25(OH)_2D_3$. The latter is in agreement with the results of a previous study reporting the presence of calcitriol bioactivity in all vegetative organs of the plant, the berries being the highest accumulating tissue (Weissenberg et al., 1989). The differences in calcitriol levels observed between in vitro and in vivo conditions are in accordance with observations made with other plant secondary products and may be explained by cell transformation occurring upon culture. The distribution of free $1\alpha,25(OH)_2D_3$ and the corresponding glycosidic derivatives in calli from stem, leaf and fruit was 94/6, 80/20 and 78/22%, respectively. In tissues obtained from the plant the free form of the metabolite was also predominant (Fig. 1). Although it has been reported that $1\alpha,25(OH)_2D_3$, $25(OH)D_3$ and vitamin D_3 are mainly present as glycosides in *S. glaucophyllum* leaves (Humphreys, 1973; Wasserman et al., 1976; Esparza et al., 1982), our data are in agreement with various lines of evidence supporting the existence of free secosterols in the plant. Thus, it was early found that the ether soluble fraction of *S. glaucophyllum* exhibited vitamin D_3-like activity when given to animals (Masselin et al., 1969). In addition, other workers observed that plant extracts not hydrolyzed with glycosidases had the ability to compete with $[^3H]1\alpha,25(OH)_2D_3$ for binding to the chick intestine vitamin D receptor, known to interact with the hormonal metabolite with high specificity (Procsal et al., 1976). Weissenberg et al. (1989) have detected both $1\alpha,25(OH)_2D_3$ and $1\alpha,25(OH)_2D_3$-glycoside in *S. glaucophyllum* cultivated in the field, the free form prevailing in some tissues. Greater amounts of $1\alpha,25(OH)_2D_3$ than its glycoside counterpart have been detected also in several different plant species, e.g. *Cestrum diurnum* (Prema and Raghuramulu, 1994), *Lycopersicon esculentum* (Prema and Raghuramulu, 1996), *Nicotiana glauca* (Skliar et al., 2001), *Solanum tuberosum*, *Solanum melongena* and *Cucurbita pepo* (Aburjai et al.,

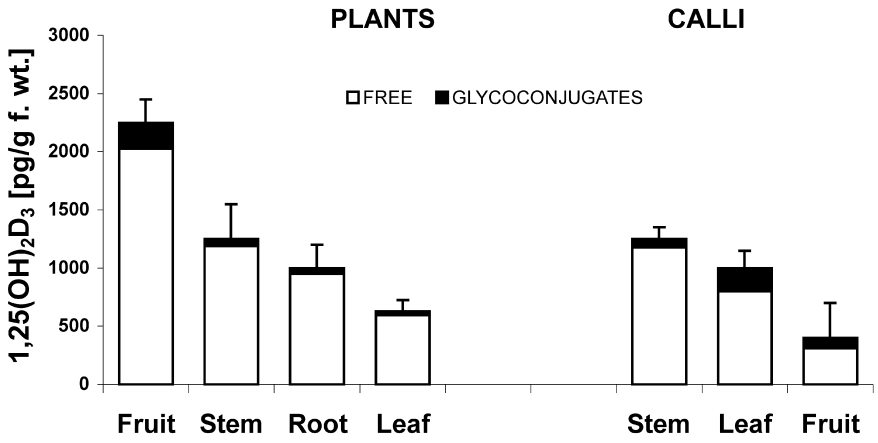

Fig. 1. Concentration of free and glycosidic $1\alpha,25(OH)_2D_3$ in *Solanum glaucophyllum* tissues and calli from different primary explants. Lipids were extracted with chloroform–methanol (1:2) by the Bligh and Dyer (1959) procedure. The remaining water soluble fraction was incubated with β-glucosidase to release sterols from their glyconjugated derivatives followed by organic solvent extraction. The $1\alpha,25(OH)_2D_3$ content of extracts was measured by radioreceptor assays as described in Experimental. Values are average of three determinations.

1998). In callus and cell suspension cultures derived from *S. glaucophyllum* leaves shown to contain 1α, $25(OH)_2D_3$, 7-dehydrocholesterol, vitamin D_3 and $25(OH)D_3$, again the free forms of these metabolically related vitamin D sterols are more abundant than their glycosides (Weissenberg et al., 1989; Aburjai et al., 1996; Curino et al., 1998). Comparison of the experimental conditions among the various studies cited brings about the possibility that formation of glycoconjugates of vitamin D_3 compounds in plants occurs to a great extent during drying and storage of collected tissues at the expense of the content of free sterols. In our work, *S. glaucophyllum* leaves were obtained in the field under dry-ice and stored lyophilized at −80°C until extraction, while calli were immediately extracted after removal from the culture medium. In contrast, investigations reporting the presence of substantial amounts of glycoside derivatives of $1\alpha,25(OH)_2D_3$ have used plant material oven-dried (60°C) for prolonged periods of time (Wasserman et al., 1976; Esparza et al., 1982; Weissenberg et al., 1989).

As recently reported (Curino et al., 1998), using a highly specific in vitro radioreceptor assay we have detected lower levels of $1\alpha,25(OH)_2D_3$ in field- and culture-grown *Solanum glaucophyllum* (Fig. 1) than those reported in other studies (Aburjai et al., 1996, 1997). Our results were validated by measuring the ability of plant and callus/cell extracts to stimulate intestinal ^{45}Ca absorption in vitamin D-deficient chicks (data not shown). Factors which may explain these differences are the distant geographic locations of the plants used for direct analysis or generation of cultures (Puche et al., 1980), the specifity/sensitivity of the assay procedures used to quantitate the metabolite (Boland, 1986) and, as addressed below, the culture medium composition.

2.2. Modulation by plant growth factors and calcium of $1\alpha,25(OH)_2D_3$ production in cultured *S. glaucophyllum*

Culture conditions are known to influence plant secondary product metabolism. In connection to the present work, it has been reported that *S. glaucophyllum* calli grown in Gamborg et al. (1968) medium synthesize greater amounts of cholesterol, 7-dehydrocholesterol and vitamin D_3 sterols than in Murashige and Skoog (1962) medium (Suardi et al., 1994; Aburjai et al., 1996). In agreement with this observation, significantly higher levels of $1\alpha,25(OH)_2D_3$ could be detected in the former than in the latter culture solution (Curino et al., 2001). As both media have a different content of plant growth factors and calcium, we investigated the effects of culturing *S. glaucophyllum* in the presence of varying concentrations of auxin (2,4-D), kinetin and Ca^{2+} on the formation of $1\alpha,25(OH)_2D_3$. The studies with plant hormones comprised four different treatment conditions, as follows: A: 0.5 mg/l 2,4-D + 0.2 mg/l kinetin; B: 1.0 mg/l 2,4-D + 0.4 mg/l kinetin; C: 2.5 mg/l 2,4-D + 1.0 mg/l kinetin, and D: 0.5 mg/l 2,4-D + 2.0 mg/l kinetin. The concentrations of metabolite were determined by radioreceptor assays and the results obtained were expressed relative to the standard condition A used in the other experiments included in the present investigations. As shown in Fig. 2, 1.7-, 4.2- and 17.9-fold increases in $1\alpha,25(OH)_2D_3$ levels could be measured for treatments B, C and D, respectively, as compared to condition A. Less evident changes were detected when cell suspensions were used instead of calli, e.g. 1.3-fold for B, 1.4-fold for C and 3.1-fold for D (Fig. 2). Similar relative increases were detected for calcitriol secreted into the culture medium (data not given). These results show then a clear stimulation by the plant growth factor binary

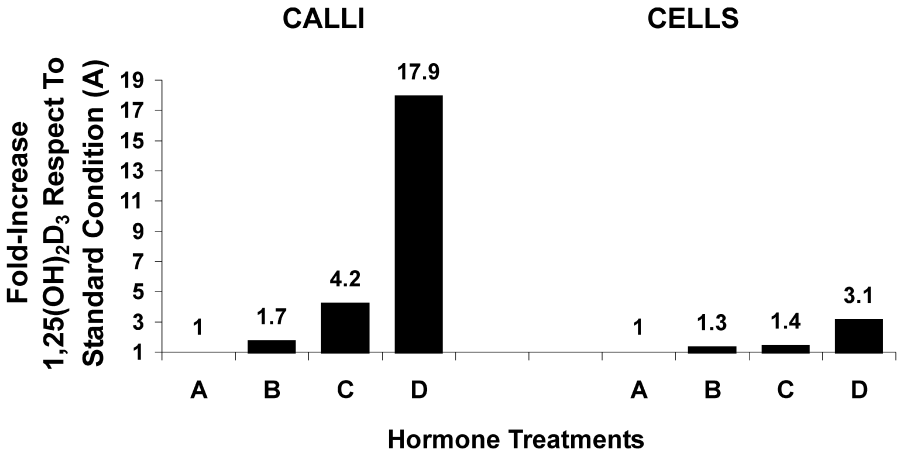

Fig. 2. Effect of plant growth regulators on the $1\alpha,25(OH)_2D_3$ content of cultured *Solanum glaucophyllum* calli and cells. Levels of free $1\alpha,25(OH)_2D_3$ in lipid extracts were measured as in Fig. 1. Values are average of three determinations. A = 0.5 mg/l 2,4D + 0.2 mg/l kinetin; B = 1 mg/l 2,4D + 0.4 mg/l kinetin; C = 2.5 mg/l 2,4D + 1 mg/l kinetin; D = 0.5 mg/l 2,4D + 2 mg/l kinetin.

mixture of $1\alpha,25(OH)_2D_3$ synthesis in *S. glaucophyllum*. As suggested by the data obtained with condition D, kinetin may play a major role in upregulating the production of the metabolite.

Regarding the influence of medium calcium concentration on calcitriol production by *S. glaucophyllum* grown in vitro, the studies performed with calli showed that media deprived of Ca^{2+} contained low levels of calcitriol. When using cation concentrations of 1, 8 and 13 mM the levels of metabolite detected by radioreceptor assays were increased 2.6-, 4.8- and 1.7-fold, respectively (Fig. 3). However, when similar experiments were performed with cell suspensions, only at 13 mM Ca^{2+} a significant increase in $1\alpha,25(OH)_2D_3$ was observed (1.7-fold). Contrary to our observations, an inverse relationship between medium Ca^{2+} concentrations and $1\alpha,25(OH)_2D_3$ formation has been reported before (Aburjai et al., 1997), curiously compared by these authors with Ca^{2+} regulation of calcitriol synthesis in animals which is known to be mediated by parathyroid hormone.

2.3. Effect of UV irradiation on the levels of vitamin D_3 and hydroxylated metabolites of S. glaucophyllum grown in vitro and in vivo

The operation of the light-dependent pathway in the generation of vitamin D_3 sterols was reinvestigated measuring the effects of UV irradiation on the levels of $25(OH)D_3$ and vitamin D_3, in addition to $1\alpha,25(OH)_2D_3$, in view that the concentration of calcitriol could not be altered previously by this treatment (Curino et al., 1998). In this study, calli were irradiated with UV light for 5, 10 and 15 days. The concentrations of vitamin D_3, $25(OH)D_3$ and $1\alpha,25(OH)_2D_3$ were measured by HPLC after prepurification of lipid extracts as described in the Experimental, and compared to those of non-irradiated calli. As shown in Table 1, the irradiation procedure induced marked increases in the levels of vitamin D_3 with respect to the tissue non-exposed to UV light; however, considerable less significant relative changes were observed for its mono- and dihydroxylated derivatives.

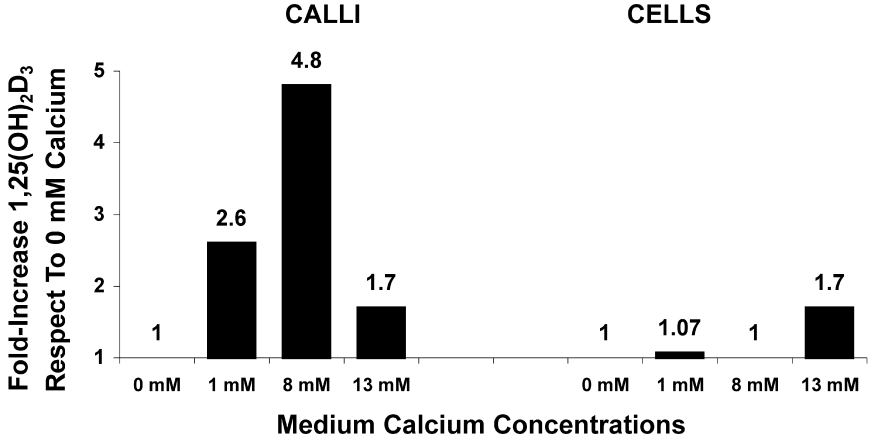

Fig. 3. Influence of medium calcium concentration on $1\alpha,25(OH)_2D_3$ production by cultured *Solanum glaucophyllum* calli and cells. Levels of free $1\alpha,25(OH)_2D_3$ in lipid extracts were measured as in Fig. 1. Values are average of two determinations.

In contrast, UV irradiation of mature *S. glaucophyllum* plants markedly increased the amounts of 1α, $25(OH)_2D_3$ and less significantly the quantities of 25(OH) D_3 and vitamin D_3, in comparison to non-irradiated plants (Fig. 4). These results together with those obtained by UV exposure of calli suggest that in the less differentiated cultured plant cells low activity and/or expression of the vitamin D_3 and $25(OH)D_3$ hydroxylases and not the photolytic breakdown of 7-dehydrocholesterol hinder the production of $1\alpha,25(OH)_2D_3$ in vitro. Specially, the reaction catalyzed by the 25-hydroxy-vitamin D_3-1α-hydroxylase could be the most rate limiting step as the application of a novel DBP-based competitive binding assay for $25(OH)D_3$ applied for the first time in plant tissues (see Experimental) revealed 8-10 fold higher levels of $25(OH)D_3$ than 1α, $25(OH)_2D_3$.

Table 1
Effect of ultraviolet light irradiation on the content of vitamin D_3, $25(OH)D_3$ and $1\alpha,25(OH)_2D_3$ of cultured *Solanum glaucophyllum* calli

	Percent increase above control		
Irradiation times (days)	Vitamin D_3	$25(OH)D_3$	$1,25(OH)_2D_3$
5	350	28	32
10	556	5	37
15	280	0	22

2.4. Detection of $25(OH)D_3$-1α- hydroxylase activity in *S. glaucophyllum* cell suspensions

25-Vitamin D_3-1α-hydroxylase assays were performed by incubating *S. glaucophyllum* cells in culture medium containing $[^3H]25(OH)D_3$ for 2–18 h followed by isolation of $[^3H]1\alpha,25(OH)_2D_3$ according to Bligh and

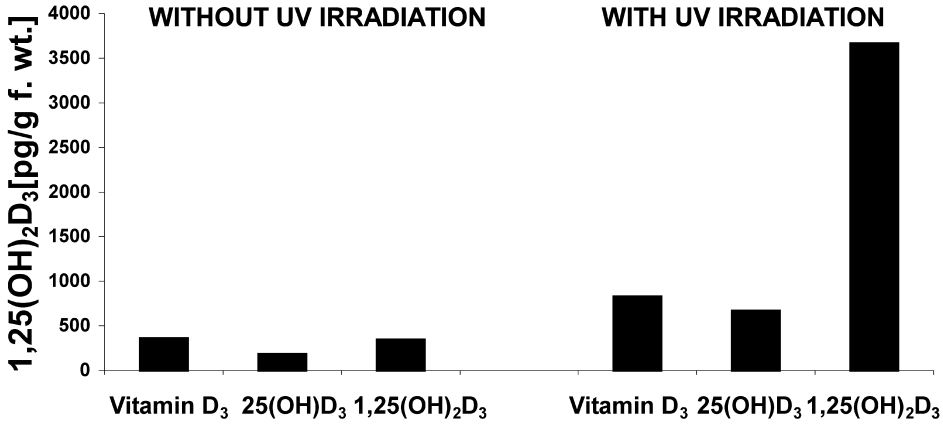

Fig. 4. Ultraviolet light irradiation of *Solanum glaucophyllum* increases its $1\alpha,25(OH)_2D_3$ leaf content. *S. glaucophyllum* plants grown in the greenhouse were either kept under darkness or irradiated with ultraviolet light for 7 days. Free $1\alpha,25(OH)_2D_3$ was quantified as in Fig. 1. Results from a typical experiment are shown.

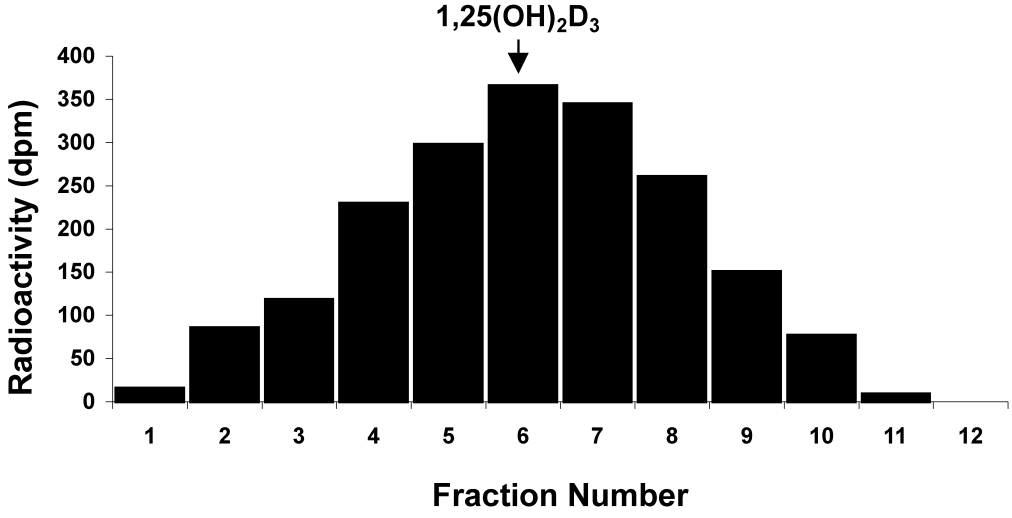

Fig. 5. 25-Hydroxy-vitamin D_3-1α-hydroxylase activity of cultured *Solanum glaucophyllum* cells. Cells were incubated in culture medium containing $[^3H]25(OH)D_3$ for 2 h followed by isolation of $[^3H]1\alpha,25(OH)_2D_3$ produced by Sephadex LH-20 followed by HPLC as indicated in Experimental. HPLC fractions of 0.2 ml were collected. Only the radioactivity of the $1\alpha,25(OH)_2D_3$ fraction of the entire chromatogram is shown.

Dyer (1959), Sephadex LH-20 chromatography and HPLC. The conversion of [^{3}H]25(OH)D_3 to [^{3}H]1α,25(OH)$_2D_3$ was time-dependent but as shown in Fig. 5, low 1α-hydroxylase levels were detected, supporting the interpretation in the section above. Furthermore, when compared with *S. glaucophyllum* leaves (Esparza et al., 1982) the activity of the enzyme was ca. 7 times lower (6 vs 40 pmol/mg prot./h, respectively).

3. Conclusions

In conclusion, the results of this study show that 1α,25(OH)$_2D_3$ and related vitamin D_3 compounds are present mainly as unconjugated forms in *S. glaucophylllum* calli and cells. The precursor 25(OH)D_3 is in greater concentration than the former metabolite. So culture preparations of *S. glaucophyllum* may represent a readily source of both metabolites for pharmacological use. The synthesis of 25(OH)D_3 and 1α,25(OH)$_2D_3$ in cultures strictly kept under darkness, confirms the participation of an non-photolytic reaction capable of opening the B ring in the absence of light (Curino et al., 1998). Of interest, this non-photolytic reaction leading to synthesis of 1α,25(OH)$_2D_3$ can be upregulated by the medium levels of calcium and growth factors. The alternative light-dependent generation pathway of 1α,25(OH)$_2D_3$ appears to operate efficiently in differentiated field-grown plants. The lack of significant effects of UV light irradiation on 1α,25(OH)$_2D_3$ production in cultured material may be explained by low levels of hydroxylase enzymes converting vitamin D_3 into 25(OH)D_3 and 1α,25(OH)$_2D_3$. Clearly of biotechnological importance are the development of experimental maneuvers to upregulate the expression and activity of vitamin D_3-25-hydroxylase and 25(OH)vitamin-D_3-1α hydroxylase in order to increase hormone synthesis for human and animal applications.

4. Experimental

4.1. Materials

Solvents used for isolation and chromatographic procedures were HPLC grade (J.T. Baker Co., Phillipsburg, NJ, USA). Compounds for culture media, purified almond β-glycosidase, salicin (2-[hydroxymethyl] phenyl β-D-glucopyranoside) and Sephadex LH-20 were obtained from Sigma-Aldrich Co. (St. Louis, MO, USA). The LiChroCART cartridge and the Nucleosil C_{18} column for HPLC analysis were from Merck Co. (Darmstadt, Germany) and Sigma-Aldrich, respectively. Other reagents were of analytical grade. [^{3}H]25(OH)-vitamin D_3 (171 Ci/mmol) and [^{3}H]1α,25(OH)$_2D_3$ (171 Ci/mmol) were purchased from New England Nuclear (Chicago, IL, USA). Non-radioactive, chemically synthetized, vitamin D_3, 25(OH)-vitamin D_3, and 1α,25(OH)$_2D_3$ were a gift from Dr. Lise Binderup, Leo Pharmaceutical Products Ltd. (Ballerup, Denmark). Purified human serum vitamin D binding protein was generously provided by Dr. H. van Baelen (Laboratorium voor Experimentele Geneeskunde en Endocrinologie, Katholieke Universiteit Leuven, 3000 Leuven, Belgium).

4.2. Plant material

S. glaucophyllum was collected from fields located in Monte Hermoso and Ensenada (Buenos Aires Province, Argentina). For determination of the vitamin D_3 metabolite content of tissues, the plants were immediately placed in dry ice. Fruits, stems, roots and leaves were separated followed by lyophilization. Lyophilized tissues were kept at −80°C until analyzed. To obtain green-house material, young plants were transplanted intact with soil from the field into pots and watered daily.

4.3. Cultures

To culture *S. glaucophyllum* tissue (callus), aseptic stem, root, fruit and leaf explants from plants grown in the greenhouse were inoculated in solidified (0.8% agar) Murashige–Skoog or Gamborg media supplemented with 2,4-dichlorophenoxyacetic acid (2,4-D) and kinetin, 0.5 mg/l and 0.2 mg/l, respectively, or as otherwise indicated in the experiments testing the influence of the concentrations of these hormones on 1α,25(OH)$_2D_3$ production. The tissue was grown at 25°C under complete darkness. The calli started to develop after approximately 15 days. Subculture was performed when all the surface of culture flasks was covered with tissue (ca. 2 months).

Cell suspensions were initiated by mechanical dispersion of calli and then cultured in 125 ml Erlenmeyer flasks containing 50 ml of liquid Murashige-Skoog medium supplemented with hormone as above, without agar. The cells were grown in culture chambers with constant agitation (100 rpm) at 25°C in strict darkness. The growth of cultures was evaluated by counting cell numbers, protein content, cellular weight and packed cell volume (PCV). Typical growth curves were obtained.

4.4. Irradiation experiments

Calli and cell cultures grown under darkness were placed in a Dubnoff incubator at 25°C, with shaking in the case of cell suspensions, and exposed to a Osram UV lamp (400 W) with a 280–450 nm emission wavelength range for a single period of 1 or 1.5 h daily during 5, 10 and 15 days. Cultures grown in parallel under identical conditions without receiving UV light were used for comparison. Green-house plants were kept in a dark room under glass covered with aluminum foil for

7 days. During this interval irradiated plants were exposed to UV light 1.5 h/day.

4.5. Extraction and chromatography of free vitamin D_3 metabolites

Free vitamin D_3-related compounds present in *S. glaucophyllum* callus and cell cultures and plant leaves were extracted following essentially the method of Bligh and Dyer. Briefly, the samples were homogenized with chloroform-methanol (1:2, v/v; 3.6 ml/g) using an Ultraturrax homogenizer (Janke and Kunkel, Germany) for 2 min at maximum speed. The suspension was further homogenized for 30 s with chloroform and then with water (1.2 ml/g each). The final homogenate was centrifuged in a Sorvall rotor SS-34 (Du Pont Co., Delaware, USA) at 4385 *g* during 10 min and the lower lipid soluble phase was collected. The upper phase containing polar compounds was saved to determine the amounts of glycoside derivatives of $1\alpha,25(OH)_2D_3$.

When the lipid extracts were used for $1,25(OH)_2D_3$ radioaceptor assays, they were evaporated by flushing nitrogen at 35°C and then dissolved in an appropriate volume of isopropanol.

Prior to HPLC, the lipid extracts were passed through a Sephadex LH-20 column (1×15 cm) using hexane–chloroform–methanol (9:1:1, v/v/v) as the solvent system. The fractions which eluted with similar retention times as authentic standards of vitamin D_3, $25(OH)D_3$ and $1,25(OH)_2D_3$ were collected. Each fraction was further resolved by high performance liquid chromatography (HPLC). HPLC was performed with an Isco Model 2360 gradient programmer equipped with an Isco Model V^4 multiwavelength programmable detector set at 265 nm and a pump Isco Model 2350 (Isco Co., Lincoln, NE, USA). A reversed-phase LiChroCART (4 mm×25 cm) cartridge or a Nucleosil C_{18} column (4.6 mm×25 cm) were eluted isocratically with methanol–water (86:14, v/v), (75:25, v/v) and (86:14, v/v) to isolate vitamin D_3, $25(OH)D_3$ and $1,25(OH)_2D_3$, respectively. The elution times of the plant vitamin D_3 sterols were similar to those of synthetic samples of vitamin D_3 (80.1 min), $25(OH)D_3$ (34.7 min) and $1,25(OH)_2D_3$ (8.9 min). Spectroscopic analysis of these HPLC compounds gives molecular ion and fragmentation peak patterns which match exactly those of authentic standards of the corresponding vitamin D_3 metabolite (Curino et al., 1998). Vitamin D_3, $25(OH)D_3$ and $1,25(OH)_2D_3$ were quantified on the basis of their absorption at 265 nm in the HPLC detector. $1,25(OH)_2D_3$ and $25(OH)D_3$ were also measured by radioreceptor and competitive protein binding assays, respectively, as indicated below.

4.6. $1,25(OH)_2D_3$ radioreceptor assays

The $1,25(OH)_2D_3$ content of lipids extracts from *S. glaucophyllum* and chromatographic fractions derived therefrom was measured by a specific radioreceptor assay. The $1,25(OH)_2D_3$ receptor preparation was obtained by homogenization of mucosa from duodena of 4 week-old vitamin D-deficient chicks in TEKDP buffer (10 mM TrisCl, pH 7.4; 1.5 mM EDTA; 0.3 M KCl; 2 mM dithiothreitol; 0.3 mM phenylmethylsulfonylfluoride) followed by centrifugation at 100,000 *g* during 60 min. The supernatant was collected and stored at −80°C until use. Binding assays were performed incubating the samples with 5.87×10^{-10} M $[^3H]1\alpha,25(OH)_2D_3$ for 4 h at 0°C. Free from bound radioactive steroid was separated by the hydroxylapatite procedure (Wecksler and Norman, 1979).

4.7. Quantification of $1\alpha,25(OH)_2D_3$-glycoside

To quantify glycoside derivatives of $1\alpha,25(OH)_2D_3$, the upper polar phase obtained after Bligh and Dyer (1959) fractionation of *Solanum glaucophyllum* tissue and calli (see above) was concentrated to eliminate methanol and the remaining aqueous fraction incubated with β-glycosidase for 4 h under nitrogen in 0.4 M acetate buffer pH 5.0 at 37°C. The activity of the enzyme was checked prior to the experiments by measuring the hydrolysis rate of the synthetic glycosidic substrate salicin under the same conditions for incubation of the aqueous fraction. The sterols released from their glycoconjugates by this procedure were extracted with Bligh and Dyer (1959) as described above.

4.8. In vivo measurement of $1\alpha,25(OH)_2D_3$ levels in whole extracts of S. glaucophyllum using intestinal calcium absorption (ICA) assays

Vitamin D-deficient 4-week-old chicks fed a diet free of vitamin D_3 (Reichel et al., 1987; Massheimeret et al., 1997) were used. *S. glaucophyllum* tissue and callus were extracted for 45 min at 38°C with H_2O (1 ml/g FW) under nitrogen followed by centrifugation and lyophilization of the supernatant to a small volume. Twenty hours before the assay, the chicks, which had been fed a Ca^{2+}-deficient diet for 48 h, were administered intramuscularly with the concentrated extracts. At the time of assay, the chicks were lightly anesthetized with ether, the duodenal loop was exposed, and 5 μCi of ^{45}Ca was injected into the duodenum. After 30 min, blood was collected for analysis. For quantification of the responses, chicks administered with known amounts of $1\alpha,25(OH)_2D_3$ (4–600 pmol) were assayed in parallel.

4.9. $25(OH)_2D_3$ binding assays

The $25(OH)D_3$ content of lipid extracts from *S. glaucophyllum* and chromatographic fractions derived therefrom was measured by a competitive protein binding assay using purified human serum vitamin D binding

protein (DBP). The binding assays were performed incubating the samples in barbital buffer pH 8.6 containing 8.2×10^{-10} M [^{3}H]25(OH)D_3 (380,000 dpm/ml) and 31.3 ng DBP/ml, during 3 h at 0°C. Free from bound radioactive steroid was separated as in 1,25$(OH)_2D_3$ radioreceptor assays.

4.10. Measurement of 25(OH)-vitamin D_3-1α-hydroxylase activity

S. glaucophyllum cells cultured for 5 days were resuspended (230,000 cells/ml) in Murashige and Skoog (1962) medium containing 4×10^{-5} M [^{3}H]25(OH)D_3 (33,000 dpm/ml) and incubated during 2, 7 or 19 h at 25°C with shaking, using a final volume of 3 ml. To stop the reaction the samples were extracted according to Bligh and Dyer (1959). Non-radioactive 1,25$(OH)_2D_3$ was added to the concentrated lipid extract followed by Sephadex LH-20 and HPLC chromatography as described above. The HPLC fraction which comigrated with 1α,25$(OH)_2D_3$ was collected and the radioactivity measured by liquid scintillation spectrometry.

Acknowledgements

This research was supported by grants from the Agencia Nacional de Promoción Científica y Tecnológica, Comisión de Investigaciones Científicas de la Provincia de Buenos Aires and Universidad Nacional del Sur, Argentina. We thank Drs. R. Bouillon and H. van Baelen (Leuven, Belgium) for the generous gift of purified human serum vitamin D binding protein. We dedicate this contribution to the late research teammate and friend Lic. Margarita Esparza whose memory has inspired our work.

References

Aburjai, T., Bernasconi, S., Manzocchi, L., Pelizzoni, F., 1996. Isolation of 7-dehydrocholesterol from cell cultures of *Solanum malacoxylon*. Phytochemistry 43, 773–776.

Aburjai, T., Bernasconi, S., Manzocchi, L., Pelizzoni, F., 1997. Effect of calcium and cell immobilization on the production of cholecalciferol and its derivatives by *Solanum malacoxylon* cell cultures. Phytochemistry 46, 1015–1018.

Aburjai, T., Al-Khalil, S., Abuirjeie, M., 1998. Vitamin D_3 and its metabolites in tomato, potato, egg plant and zucchini leaves. Phytochemistry 49, 2497–2499.

Bligh, E.G., Dyer, W.J., 1959. A rapid method of total lipid extraction and purification. Canadian Journal of Biochemistry and Physiology 37, 911–917.

Boland, R.L., 1986. Plants as source of vitamin D_3 metabolites. Nutrition Reviews 44, 1–8.

Bouillon, R., Okamura, W.H., Norman, A.W., 1995. Structure-function relationships in the vitamin D endocrine system. Endocrine Reviews 16 (2), 200–257.

Buchala, A.J., Schmid, A., 1979. Vitamin D and its analogues as a new class of plant growth substances affecting rhizogenesis. Nature 280, 230–231.

Curino, A., Skliar, M., Boland, R., 1998. Identification of 7-dehydrocholesterol, vitamin D_3, 25(OH)-vitamin D_3 and 1,25$(OH)_2$-vitamin D_3 in *Solanum glaucophyllum* cultures grown in the absence of light. Biochimica et Biophysica Acta 1425, 485–492.

Curino, A., Milanesi, L., Skliar, M., Benassati, S., Boland, R., 2000. Regulation of vitamin D_3 metabolite synthesis in cultured *Solanum glaucophyllum*. In: Norman, A.W., Bouillon, R., Thomasset, M. (Eds.), Vitamin D Endocrine System. Structural, Biological, Genetic and Clinical Aspects, University of California Riverside Press, USA, pp. 973–976.

De Boland, A.R., Skliar, M.I., Gallego, S., Esparza, M., Boland, R., 1978. Calcified Tissue Research 26, 215–219.

Esparza, M.S., Vega, M., Boland, R., 1982. Synthesis and composition of vitamin D_3 metabolites in *Solanum malacoxylon*. Biochimica et Biophysica Acta 719, 633–640.

Gamborg, O., Hiller, R.A., Ojima, K., 1968. Nutrient requirements of suspension cultures of soybean root cells. Experimental Cell Research 50, 155–158.

Humphreys, D.J., 1973. Studies on the active principle of Solanum malacoxylon. Nature New Biology 246, 155–157.

Masselin, J.N., Abadie, G.J., Monesiglio, J.C., Rossi, F.M., 1969. Acción del extracto etéreo del duraznillo blanco (*Solanum malacoxylon*). Revista Investigaciones Agropecuarias. INTA (Argentina) Serie 4, Patología Animal 8, 1–19.

Massheimer, V., Vazquez, G., Picotto, G., Skliar, M., Benassati, S., Curino, A., Torneiro, M., Fall, Y., Vitale, C., Mouriño, A., Boland, R., 1997. Substitution at the side chain of 1,25$(OH)_2D_2$ generates analogs having increased non-genomic activity and target cell selectivity than the animal hormone 1,25$(OH)_2D_3$. In: Norman, A.W., Bouillon, R., Thomasset, M. (Eds.), Vitamin D. Chemistry, Biology and Clinical Applications of the Steroid Hormone. California University Press, USA, pp. 373–374.

Morris, K.M.L., 1982. Plant induced calcinosis: a review. Veterinary Human Toxicolology 24, 34–48.

Murashige, T., Skoog, F., 1962. A revised medium for rapid growth and bioassays with tobacco tissue cultures. Physiologia Plantarum 15, 473–497.

Prema, T.P., Raghuramulu, N., 1994. Free vitamin D_3 metabolites in *Cestrum diurnum* leaves. Phytochemistry 37, 677–681.

Prema, T.P., Raghuramulu, N., 1996. Vitamin D_3 and its metabolites in the tomato plant. Phytochemistry 42, 617–620.

Procsal, D.A., Henry, H.L., Hendrickson, T., Norman, A., W., 1976. 1,25-dihydroxyvitamin D_3-like component present in the plant *Solanum glaucophyllum*. Endocrinology 99, 437–444.

Puche, R.C., Massoni, A.M., Alloatti, D.A., Roveri, E., 1980. The antirachitic activity of *Solanum glaucophyllum* leaves. Planta Medica 40, 378–381.

Rambeck, W.A., Kreutzberg, O., Bruns-Droste, C., Zucker, H., 1981. Vitamin D_3 in the grass *Trisetum flavescens*. Zeitschrift für Pflanzenphysiologie 104, 9–16.

Reichel, H., Koeffler, H.P., Bishop, J.E., Norman, A.W., 1987. 25-hydroxyvitamin D_3 metabolism by lipopolysaccharide-stimulated normal human macrophages. Journal of Clinical Endocrinology Metabolism 64, 1–9.

Skliar, M., Curino, A., Milanesi, L., Benassati, S., Boland, R., 2000. *Nicotiana glauca*: Another plant species containing vitamin D_3 metabolites. Plant Science 156, 193–199.

Suardi, M.L., Bernasconi, S., Pelizzoni, F., Racchi, M.L., 1994. In vitro cultures of *Solanum malacoxylon* Sendt.: nutritional requirements and sterol production. Plant Cell, Tissue Organ Culture 36, 9–14.

Talmon, M., Vega, R., Boland, R., 1989. Cytohistological studies on the action of vitamin D_3 and stigmasterol on *Phaseolus vulgaris* roots growing in vitro. Plant Science 59, 183–190.

Vega, M., Boland, R., 1986. Vitamin D_3 induces de novo synthesis of

calmodulin in *Phaseolus vulgaris* root segments growing in vitro. Biochimica et Biophysica Acta 881, 364–374.

Vega, M., Fernandez, L., Boland, R., 1988. Mediation of sterol-induced calmodulin synthesis in *Phaseolus vulgaris* roots by Ca^{2+} and its possible relationship to plant growth regulators. Physiologia Plantarum 75, 499–505.

Wasserman, R.H., Henion, J.D., Haussler, M.R., McCain, T.A., 1976. Calcinogenic factor in *Solanum malacoxylon*: evidence that it is 1,25-dihydroxyvitamin D_3-glycoside. Science 194, 853–854.

Wecksler, W.R., Norman, A.W., 1979. An hydroxylapatite batch assay for the quantitation of 1,25-dihydroxyvitamin D_3-receptor complexes. Analytical Biochemistry 92, 314–323.

Weissenberg, M., Levy, A., Wasserman, H., 1989. Distribution of calcitriol activity in *Solanum glaucophyllum* plants and cell cultures. Phytochemistry 28, 795–798.

Worker, N.A., Carrillo, B.J., 1967. ''Enteque seco'', calcification and wasting in grazing animals in the Argentine. Nature (London) 215, 72–74.

Zucker, H., Stark, H., Rambeck, W.A., 1980. Light-dependent synthesis of cholecalciferol in a green plant. Nature 283, 68–69.

PERGAMON

Phytochemistry 58 (2001) 91–100

PHYTOCHEMISTRY

www.elsevier.com/locate/phytochem

Seasonal variation in leaf glucosinolates and insect resistance in two types of *Barbarea vulgaris* ssp. *arcuata*

Niels Agerbirk*, Carl E. Olsen, Jens K. Nielsen

Chemistry Department, Royal Veterinary and Agricultural University, Thorvaldsensvej 40, DK-1871 Frederiksberg, C, Denmark

Received 13 November 2000; received in revised form 19 March 2001

Abstract

Leaves from natural populations of *Barbarea vulgaris* ssp. *arcuata* (Brassicaceae) in Denmark were examined for glucosinolate content and resistance to the crucifer specialist flea beetle *Phyllotreta nemorum*. Two types of the plant (P- and G-type) could be recognized. Leaves of the G-type contained the glucosinolates (only side chains mentioned): (*S*)-2-hydroxy-2-phenylethyl- (**2S**), indol-3-ylmethyl- (**4**) and in trace amount (*R*)-2-hydroxy-2-phenylethyl- (**2R**), 2-phenylethyl- (**1**) and 4-methoxyindol-3-ylmethyl- (**5**). Leaves of the P-type were dominated by **2R** and **4**, and had only trace amounts of **1**, **2S**, and **5** but contained in addition the previously unknown (*R*)-2-hydroxy-2-(4-hydroxyphenyl)ethyl- (**3R**). The epimer, (*S*)-2-hydroxy-2-(4-hydroxyphenyl)ethyl- (**3S**) was found in populations believed to be hybrids, and in *B. orthoceras*. **2S**, **2R**, desulfo **2S**,-**2R**, -**3S** and -**3R** were isolated and identified by NMR and MS. Acylated glucosinolates or allylglucosinolate were not detected in leaves. The glucosinolate content in August was variable, 3–46 μmol/ g dry wt, but was low in most populations, 3–15 μmol/g dry wt. In general, the glucosinolate content increased during the autumn, to 35–75 μmol/g dry wt in November. The G-type was resistant to neonate larvae of *Phyllotreta nemorum* in August and September (survival in 3-day bioassay typically 0%), and gradually lost the resistance in October and November (survival in 3-day bioassay 40-90%), and there was no correlation between glucosinolate content and resistance. Neither did glucosinolates explain the difference in resistance between the P-type (always susceptible) and the G-type (resistant in the summer season). © 2001 Elsevier Science Ltd. All rights reserved.

Keywords: *Barbarea vulgaris* ssp. *arcuata*; Brassicaceae; *Phyllotreta nemorum*; Coleoptera; Glucosinolates; Insect resistance; Seasonal regulation

1. Introduction

Barbarea vulgaris R. Br. ssp. *arcuata* (Opiz.) Simkovics (Brassicaceae) is a biannual or perennial plant. The leaves of first year rosettes stay green in the autumn, and may often stay green during the winter. Early in the following spring, the flowering shoot with bright yellow flowers is rapidly developed. These are the reasons for the common names of *B. vulgaris*; ''Wintercress'' and ''Yellow Rocket'' (MacDonald and Cavers, 1991).

As a glucosinolate containing plant, *B. v.* ssp. *arcuata* is a potential host plant for the characteristic fauna of crucifer adapted, glucosinolate-requiring insects. It is a very variable plant and its interactions with Danish populations of the flea beetle *Phyllotreta nemorum* L. (Coleoptera: Chrysomelidae: Alticinae) are rather complex. Genetic differences have been found in the resistance of the plant towards flea beetles, as well as in counteradaptations of the flea beetles to the plant defences (Nielsen, 1997a). The plant could be divided into two types: The P-type had pubescent leaves and was a suitable host plant for all flea beetle larvae throughout the year. The G-type had glabrous leaves and was resistant to the most common flea beetle genotype during the summer period. But some flea beetle genotypes were able to live on the G-type even in the summer period, and it was shown that the ability of these larvae to live on the plant was controlled by major, dominant genes (R-genes), specific for the defences of the G-type (Nielsen, 1997b, 1999). These genes were rare in most flea beetle populations, but frequent in two populations which utilized the G-type of *B. vulgaris* ssp. *arcuata* as a natural host plant (de Jong and Nielsen, 1999). The finding that a single dominant gene enabled flea beetles to overcome the resistance, suggested that a single biochemical factor was responsible for resistance.

* Corresponding author. Tel.: +45-35-28-24-38; fax: +45-35-28-23-98.

E-mail address: nia@kvl.dk (N. Agerbirk).

0031-9422/01/$ - see front matter © 2001 Elsevier Science Ltd. All rights reserved.
PII: S0031-9422(01)00151-0

The chemical basis of resistance in the G-type of *B. v.* ssp. *arcuata* to flea beetles is yet unknown. A seasonal variation in resistance has been demonstrated in rosette leaves from plants grown under uniform conditions in a common garden experiment. These plants were resistant during the summer period, but there was a gradual loss of resistance from September to November (Nielsen, 1997a). The uniform conditions in the common garden experiment were quite different from conditions in natural habitats where *B. v.* ssp. *arcuata* plants may vary tremendously in appearance. New plants may germinate throughout the year, and plants that have germinated in the spring and contain more than 20 large rosette leaves co-occur at the end of the season with plants which have germinated recently and contain only 1–6 small leaves. Moreover, new cauline rosettes may be formed from the root neck of plants that have flowered earlier in the year (MacDonald and Cavers, 1974). It was the aim of the present experiments to investigate whether there was a seasonal variation in resistance in all types of leaves occurring in natural habitats, and whether the changes in resistance were correlated with chemical changes in the plants.

Plant resistance to insects is often related to their content of secondary metabolites, which influence insect behaviour and performance on the plants (Fritz and Simms, 1992). *B. v.* ssp. *arcuata* and other crucifers contain a group of sulfur containing secondary metabolites known as the glucosinolates. The predominating glucosinolate in several species of *Barbarea* is (*S*)-2-hydroxy-2-phenylethylglucosinolate (**2S**, glucobarbarin) (Kjær and Gmelin, 1957; Jensen, 1990; Anderson et al., 1999). Leaves and seeds of the G-type of *B. v.* ssp. *arcuata* have been reported to contain mainly this compound while the epimer (*R*)-2-hydroxy-2-phenylethylglucosinolate (**2R**, glucosibarin) is the predominating compound in the P-type (Huang et al., 1994; Nielsen, 1997a). It was not known whether this chemical difference was a reliable character for the two types under natural conditions, or whether the seasonal variation in resistance of the G-type to flea beetles could be explained by changes in glucosinolate levels.

In the present study, leaves of *B. v.* ssp. *arcuata* were collected at seven natural growth sites once a month from August to November. Each leaf sample was subjected to measurements of (1) insect resistance, (2) numbers of hairs on the leaf margin, (3) leaf size and (4) glucosinolate content. The localities were chosen as sites where the G-type (localities 1–4) or the P-type (localities 5–7) was growing. The study tested four questions: (1) Can the existence of two plant types be confirmed in natural populations, and is there a consistent difference in glucosinolate structures between the two types? (2) Can the difference in insect resistance between the two types be explained by glucosinolate content? (3) Is the decline in insect resistance during the autumn in the G-type correlated with environmental or developmental factors? (4) Can the decline in insect resistance in the autumn be explained by changes in glucosinolate content?

Table 1
Seasonal variation in survival of *Phyllotreta nemorum* larvae in rosette leaves of *Barbarea vulgaris* ssp. *arcuata* collected from natural growth sites

Locality	Germination time[a]	Leaf position	Survival (*S*); mean number of hairs[b] (*H*) and mean leaf area (*A*; cm^2) in different months							
			August		September		October		November	
			S(%)	(*H*; *A*)	*S* (%)	(*H*; *A*)	*S* (%)	(*H*; *A*)	S (%)	(*H*; *A*)
1	Spring	Lower	8	(0; 40)	5	(0; 47)	82	(0; 31)	–	
1	Spring	middle	0	(0; 48)	0	(0; 30)	72	(0; 28)	65	(0; 31)
1	Spring	Upper	0	(0; 20)	0	(0; 18)	62	(0; 14)	68	(0; 10)
2	Spring	Middle	0	(0.3; 22)	0	(0.1; 31)	63	(0; 38)	85	(0; 19)
3	Spring	Middle	0	(14; 34)	3	(0.9; 36)	35	(0.9; 28)	63	(2.5; 12)
3	Summer	Middle[c]	0	(1.1; 9)	13	(6.8; 5)	55	(0; 4)	–	
3a	Spring	Middle	5	(58; 13)	55	(25; 37)	–		–	
3a	Summer	Middle[c]	–		33	(54; 15)	70	(30; 13)	90	(13; 13)
4	Spring	Middle	0	(0; 32)	0	(0; 46)	48	(0; 34)	73	(0; 19)
4	June	Middle	0	(0.7; 20)	13	(0.3; 36)	80	(0; 26)	55	0; 22)
4	Summer	Middle[c]	–		0	(0; 13)	40	(0; 13)	40	(0; 8)
4	Cauline	Middle[c]	–		0	(0; 20)	40	(0; 11)	73	(0; 13)
5	Spring	Middle	88	(139; 20)	90	(105; 28)	85	(36; 25)	88	(7.9; 12)
6	Spring	Middle	87	(121; 25)	93	(116; 28)	–		80	(13; 19)
7	Summer	Middle[c]	87	(179; 14)	93	(23; 15)	–		–	
7	Cauline	Middle[c]	93	(103; 16)	93	(40; 14)	–		85	(26; 11)

[a] Cauline rosettes are formed from the root neck of plants which had flowered earlier in May–June the same year.
[b] No. of hairs were counted on one fourth of the leaf margin as shown in Fig. 2.
[c] These rosettes were small, so almost all leaf positions were sampled except the very upper and lower leaves.

2. Results and discussion

2.1. Seasonal variation in resistance

Plants from four localities (1–4) were resistant to *P. nemorum* larvae in August and September, and belonged to the G-type according to counts of hairs along the leaf margin. Plants from three localities (5–7) were susceptible during this period, and were of the P-type according to counts of hairs along the leaf margin (Table 1). A small population (3a), growing a few hundred meters from locality 3, was intermediate since at least one third of the larvae survived in leaves collected in September. This population was also intermediate with respect to hairiness (Table 1).

Resistance in the G-type (localities 1–4) was not correlated with leaf size or plant age since small as well as large leaves, and young as well as old rosettes were resistant in August–September. Lower leaves from large rosettes that germinated in spring (locality 1) tended to be slightly less resistant than middle and upper leaves (Table 1). There were no differences between rosettes which originated from germinating seeds and cauline rosettes formed from the root neck of plants which had flowered earlier in the season (localities 4 and 7).

Plants from localities 1–4, corresponding to the G-type, gradually lost their resistance during October and November. The loss of resistance was not correlated with plant age or development, as it occurred in young as well as older rosettes, in upper as well as lower leaves, in cauline as well as first year rosettes, and independent of leaf size (Table 1). Plants from localities 5–7 (P-type) remained susceptible to *P. nemorum* larvae in October and November, and there was no seasonal variation in resistance in plants from these localities. Plants collected late in the season at localities 5–7 (P-type) were less hairy than those collected in August and September, but they remained more hairy than those collected in localities 1–4 (G-type) (Table 1).

The loss of resistance in the G-type of *B. vulgaris* ssp. *arcuata* in late autumn was confirmed for wild populations. As the loss of resistance was not correlated with plant age or-development, we suggest that it was regulated by environmental factors associated with the season, such as temperature or day length. Previous studies (Nielsen, 1997a) were unable to distinguish between effects of environmental and developmental factors on plant resistance.

2.2. Identification of glucosinolates

The glucosinolates **1**, **2S**, **2R**, **3S**, **3R**, **4** and **5** were detected in leaves of the P- and G-type of *Barbarea vulgaris* ssp. *arcuata*, collected at different growth sites (Table 2, Fig. 1). The phenolic glucosinolates **3S** and **3R** have not previously been described from the genus *Barbarea*, while the glucosinolates **1**, **2S**, **2R**, **4** and **5** are well established constituents of *Barbarea vulgaris* (Jensen, 1990; Sørensen, 1990; Huang et al., 1994; Andersson et al., 1999).

The absolute configurations of **2S** and **2R** at C-2 (Fig. 1) could be concluded from comparisons with reported NMR spectra of authentic **2R** and **2S** (Jensen, 1990; Sørensen, 1990). The absolute configurations at C-2 of **2R** and **2S** were originally proved by comparison of the enantiomeric phenyloxazolidine-2-thiones, produced by enzymatic hydrolysis of **2R** and **2S**, with the synthetic enatiomers of phenyloxazolidine-2-thione (Kjær and Gmelin, 1957; Gmelin et al., 1970). The chemical shift of H-1′, the anomeric proton, was approximately 0.23 ppm further downfield in **2R**, compared to **2S**. And the chemical shifts of H-1a and H-1b differed

Table 2
^{13}C NMR data for the intact glucosinolates **2S** and **2R**, and for the desulfoglucosinolates d**2S**, d**2R**, and d**3R** in D_2O (δC/ppm)

	2S[a]	**2R**[a]	d**2S**[a]	d**2R**[a]	d**3R**[a]
Thioglucosyl moiety					
C-1′	82.5	82.7	82.4	82.5	82.5
C-2′	72.7	72.8	72.9	73.0	73.0
C-3′	77.8	77.8	77.9	77.9	77.9
C-4′	69.9	69.9	70.0	69.9	69.9
C-5′	81.1	80.9	81.0	80.8	80.8
C-6′	61.5	61.3	61.5	61.4	61.3
Side chain and C-0					
C-0	161.0	161.2	152.8	153.0	153.0
C-1	42.1	41.7	41.9	41.4	41.3
C-2	72.0	71.6	72.4	72.2	71.8
C-1″	143.0	142.9	143.1	143.0	134.7
C-2″ + C-6″	126.9*	127.0*	126.9*	127.0*	128.6
C-3″ + C-5″	129.7*	129.6*	129.7*	129.6*	116.3
C-4″	129.3	129.1	129.2	129.1	156.5

[a] Chemical shifts labeled with an asterisk may be interchanged.

by 0.15 ppm in **2S**, giving rise to two double doublets, while the corresponding protons in **2R** had identical shifts, giving rise to a single doublet (Table 2).

MS proposed that **3R** was a hydroxylated form of the co-occurring **2R**, as the molecular mass of desulfo **3R** was 16 higher than for desulfo **2R**. ^{1}H and ^{13}C NMR confirmed this hypothesis, as the spectra were mostly identical to the spectra of **2R**, but with characteristic differences due to the hydroxy group in the *para* position relative to the alkyl group: An aromatic doublet in the ^{1}H NMR spectrum indicated a *p*-substituted aromatic ring, and the ^{13}C NMR spectrum showed a signal at 156.5 ppm, characteristic of a phenolic carbon (Tables 2 and 3). A HMBC spectrum confirmed the position of the phenolic C-4″ carbon.

In a few samples, **3S** was detected as a minor compound by HPLC of desulfoglucosinolates, tentatively identified by comparison of its diode array UV spectrum with that of authentic desulfo **3S**. Authentic desulfo **3S** could be isolated in sufficient amounts from desulfoglucosinolates prepared from leaves of *Barbarea orthoceras* Ledeb., and was identified by ^{1}H NMR and MS as an epimer of desulfo **3R** (Table 3). **3S** was not previously known to occur in *B. orthoceras*, but a screening of different *Barbarea* species showed that *B. orthoceras* contained **3S** in addition to **2S** (Agerbirk et al., unpublished).

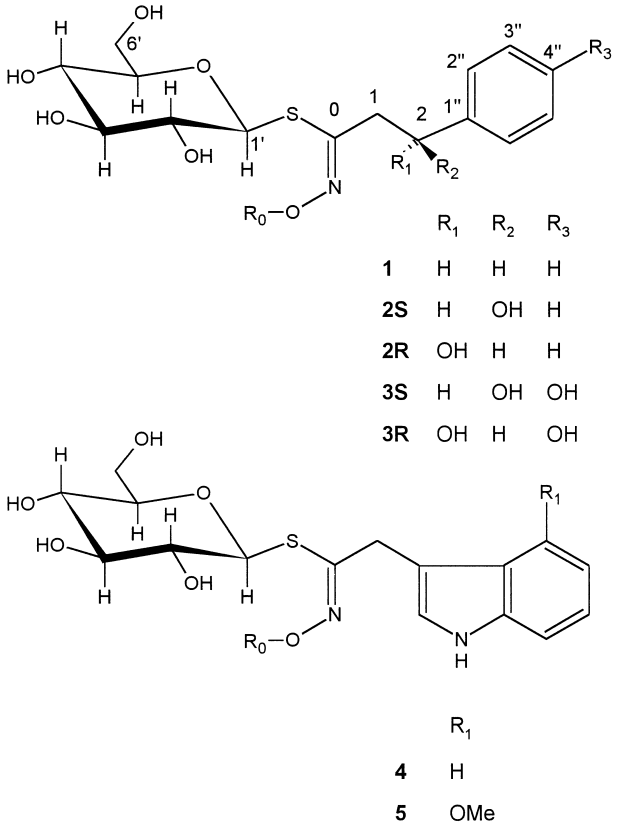

	R_1	R_2	R_3
1	H	H	H
2S	H	OH	H
2R	OH	H	H
3S	H	OH	OH
3R	OH	H	OH

	R_1
4	H
5	OMe

Fig. 1. Glucosinolates identified in *Barbarea* leaves. For glucosinolates, $R_0 = SO_3^-$. For desulfoglucosinolates, $R_0 = H$.

The diode array UV spectra of the two phenolic desulfoglucosinolates desulfo **3R** and **3S** were identical, and showed characteristic bands at 224 nm and 272 nm which can be attributed to the hydroxyphenyl group. This feature was helpful in the routine identification of the compounds, but indicates that the assumption of an identical HPLC response factor at 229 nm of desulfo benzylglucosinolate and desulfo **3R** and **3S** may have led to a moderate overestimation of **3R** and **3S**.

The biological occurrence of **2S** with **3S**, and **2R** with **3R** suggested a common biosynthetic basis of the 2-hydroxylation, and thus a common absolute configuration at C-2. Comparison of ^{1}H NMR spectra of the four desulfo derivatives confirmed this hypothesis. The significant difference in the chemical shift of the anomeric proton (H-1′) of **2S** and **2R**, was also found for desulfo **2S** and desulfo **2R**, and indeed for desulfo **3S** and desulfo **3R**: The H-1′ signal was 0.19–0.27 ppm further downfield in the (*R*)-isomers. The chemical shift of H-1a was also lower in desulfo **2S** and-**3S** than in desulfo **2R** and-**3R**. And while one of the H-6′ signals was unaltered in all four desulfoglucosinolates, the chemical shift of the other (H-6′b) was higher in desulfo **2S** and-**3S** than in desulfo **2R** and **3R** (Table 3). A model suggested that the 2-OH group can be spatially close to the 1′ and 6′ positions in the thioglucoside moiety, thus explaining the particular effects on these positions (data not shown).

Finally, the empirical relationship (Jensen, 1990; Sørensen, 1990) between absolute configuration and relative HPLC retention time on reversed phase columns for epimeric 2-hydroxydesulfoglucosinolates ("*R* is rapid, *S* is slow"), supported the proposed absolute configurations: On the Supelcosil LC-ABZ column, which carries an amide-C16 stationary phase, desulfo **3R** eluted at 12.6 min, desulfo **3S** at 13.5 min, desulfo **2R** at 17.8 min and desulfo **2S** at 19.3 min in a typical run. Based on the empirical NMR- and HPLC relationships, it is concluded that desulfo **3R** is desulfo (*R*)-2-hydroxy-2-(4-hydroxyphenyl)ethylglucosinolate (desulfo *p*-hydroxyglucosibarin), and desulfo **3S** is desulfo (*S*)-2-hydroxy-2-(4-hydroxyphenyl)ethylglucosinolate (desulfo *p*-hydroxyglucobarbarin). The existence of the corresponding intact glucosinolates in the extracted plant material was deduced, based on the binding of the native compounds to an anion exchange column, and the release of the desulfoglucosinolates after sulfatase treatment. This is to our knowledge the first report of chain-elongated phenolic glucosinolates, but a related glucosinolate, (*R*)-2-hydroxy-2-(4-methoxyphenyl)ethylglucosinolate, has been identified in seeds of *Arabis hirsuta* (Kjær and Schuster, 1972), which is phylogenetically close to *Barbarea* (Koch et al., 1999).

The identification of **1** and **5** in leaves was tentative as the levels were low. Several small, presumably non-glucosinolate peaks were observed in the chromatograms.

Allylglucosinolate (“sinigrin”) is sometimes claimed to be a constituent of *B. vulgaris* (MacDonald and Cavers, 1991; Senatore et al., 2000), but was not detected in any of the investigated leaf samples.

Isoferuloyl-**2S** or -**2R** have been reported from seeds of several *Barbarea* species (Andersson et al., 1999), and can be detected by e.g. electrophoresis of intact glucosinolates, but not by the desulfoglucosinolate method (Sørensen, 1990). Upon electrophoresis of extracts of seeds of both the P-type and the G-type, isoferuloyl-**2S** and -**2R** could be detected by a pink colour in UV light, changing to yellow with NH_3 vapour. But isoferuloyl substituted glucosinolates- or any other acylated glucosinolates visible in UV light after paper electrophoresis-were not detected in any of the leaf extracts, with a detection limit estimated to 0.2 μmol/g dry wt (10% of the concentration in seeds, reported as 2 μmol/g dry wt, Andersson et al., 1999). This finding is in agreement with the result that acylated glucosinolates quickly disappear during germination (H. Sørensen, 1999, personal communication).

2.3. Differential content of glucosinolates in the P- and G-types of B. v. ssp. arcuata, and its relation to insect resistance

The distinction of two types of *B. v.* ssp. *arcuata*, based on different leaf pubescence, and insect resistance in the summer period, was supported by structural differences in the accumulated leaf glucosinolates. The P-type (localities 5–7) preferentially accumulated 2-hydroxyglucosinolates with *R* configuration (**2R**, **3R**), while the G-type (localities 1–4) preferentially accumulated the epimer **2S** (Table 4). This difference was reflected in the concentration of **2S** relative to the sum of **2R** and **2S**, which differed significantly between the two types, independent of season and leaf type (Table 5). Furthermore, all populations of the P-type accumulated the *p*-hydroxylated glucosinolate **3R** during the autumn, while *p*-hydroxylated glucosinolates were only rarely detected in the G-type (see later).

However, the apparent hybridisation of the two types, which was detected at localities 3 and 3a, is an exception to the distinction of two types. The relative concentration of **2S** was around 50% in pooled leaves from localities 3a (Tables 4 and 5). When leaves from individual plants were later analysed, some were dominated by only **2R** or **2S** as found for the pure types. But most of the individual plants apparently contained the sum of the biosynthetic capabilities outlined above, as **2R**, **2S**, **3R** and **3S** were all accumulated in significant amounts in individual leaves (data not shown). This result, and observations of hairiness and insect resistance mentioned above, suggests that the plants at locality 3a are hybrids between the P- and the G-type. The hybrids seem to have inherited the ability to produce both epimers of 2-hydroxylated glucosinolates (from both parents), as well as the ability to produce *p*-hydroxylated glucosinolates (from the P-type). The presence of **3S** in these supposed hybrid plants suggest that the enzyme which catalyses *p*-hydroxylation is not specific for the configuration of the 2-hydroxygroup. At the nearby locality 3, the *p*-hydroxylated glucosinolate **3S** was detected in a few samples otherwise dominated by **2S**, as expected if a gene for *p*-hydroxylation [or a gene channelling a *p*-hydroxylated precursor into glucosinolate biosynthesis (Bak et al., 1999)] had been introduced to a genotype with ability for 2-hydroxylation in *S*-configuration. This observation suggests that the responsible gene from the P-type has been transferred to an otherwise morphologically and chemically typical G-type. Apparent hybridisation between the two types is rare in Denmark (Nielsen, unpublished), since most populations consist of either the P-type or the G-type (Nielsen, unpublished).

Table 3
^{1}H NMR data for the intact glucosinolates **2S** and **2R**, and for the desulfoglucosinolates d**2S**, d**2R**, d**3S** and d**3R** in D_2O (δH/ppm, multiplicity, (J/Hz))

	2S	**2R**	d**2S**	d**2R**	d**3S**	d**3R**
Thioglucosyl moiety						
H-1′	4.8[a]	5.03 *d* (9)	4.82[b] *d*	5.01 *d* (10)	4.70[b] *d*	4.97 *d* (10)
H-2′- H-5′	3.38–3.52 *m*	3.40–3.57 *m*	3.41–3.56 *m*	3.41–3.56 *m*	3.34–3.48 *m*	3.40–3.55 *m*
H-6′a	3.66–3.71 *m*	3.66 *dd* (13, 5)	3.68 *dd* (13, 5)	3.68 *dd* (13, 6)	3.68 *dd* (13, 5)	3.68 *dd* (13, 5)
H-6′b	3.87 d (12)	3.81 *dd* (13, 2)	3.86 *dd* (12, 1)	3.83 *dd* (13, 2)	3.87 *d* (12)	3.82 *d* (13)
Side chain						
H-1a	3.09 *dd* (16, 8)	3.19 *d* (7)	2.95 *dd* (15, 6)	3.02 *dd* (15, 6)	2.92 *dd* (15, 6)	2.98 *dd* (15, 6)
H-1b	3.24 *dd* (16, 5)	do.[c]	3.11 *dd* (15, 8)	3.11 *dd* (15, 7)	3.09 *dd* (15, 7)	3.09 *dd* (15, 7)
H-2	5.23 *dd* (8, 5)	5.25 *t* (7)	5.15 *t* (7)	5.14 *t* (6)	5.06 *t* (6)	5.07 *t* (7)
H-2″ + H-6″	7.4–7.5 *m*	7.4–7.5 *m*	7.37–7.47 *m*	7.36–7.44 *m*	7.30 *d* (9)	7.30 *d* (9)
H-3″ + H-5″	do.[c]	do.[c]	do.[c]	do.[c]	6.89 *d* (9)	6.89 *d* (9)
H-4”	do.[c]	do.[c]	do.[c]	do.[c]	–	–

[a] Overlap with water signal at 4.76 ppm.
[b] Hidden under water signal, revealed by COSY.
[c] do. = ditto.

Table 4
Seasonal variation in glucosinolate content in leaves of *Barbarea vulgaris* collected at seven different localities. Zero ("0") signifies "not detected". The limit of detection was about 0.05 μmol/g dry wt for the first five glucosinolates, and 0.01 μmol/g dry wt for **4** and **5**. When different leaf types from the same locality contained similar concentrations of glucosinolates, the average value is given

Locality	N	Month	Glucosinolates, μmol/g dry wt							
			1	**2R**	**2S**	**3R**	**3S**	**4**	**5**	Total
1	3	Aug.	0.09	0.48	44	0	0	1.3	0.12	46
	3	Sep.	0.02	0.24	22	0	0	0.68	0.08	23
	3	Oct.	0.10	0.32	33	0	0	1.7	0.06	35
	2	Nov.	0.25	0.43	44	0	0	2.8	0	47
2	1	Aug.	0	tr.[c]	2.3	0	0	0.20	0.07	3
	1	Sep.	0	0	0.62	0	0	0.06	0.08	1
	1	Oct.	0	tr.[c]	12	0	0	1.4	0.10	14
	1	Nov.	0.75	0.33	31	0	0	3.4	0.00	35
3	2	Aug.	0	0.90	7.6	0	0	0.56	0.02	9
	3	Sep.	0.32	1.5	43	0	Var.[a]	1.4	0.14	47
	2	Oct.	0.12	3.1	42	0	Var.[a]	2.4	0.07	48
3A	2	Aug.	0	1.9	2.6	0.03	0	0.25	0.02	5
	2	Sep.	0	19	15	0.75	0.18	1.5	0.13	37
	1	Oct.	0	20	18	1.4	0.38	2.8	0.13	43
4	1	Aug.	0	0.25	14	0	0	0.67	0.22	15
	4	Sep.	0.38	0.24	8.8	0	0	0.49	0.16	10
	4	Oct.	0	0.37	29	0	0	1.5	0.08	31
	4	Nov.	0	0.52	35	0	0	1.8	0.03	37
5	1	Aug.	0.10	7.1	0.04	0.43	0	0.54	0.03	8
	1	Sep.	0	7.8	0.09	0.64	0	0.85	0.07	9
	1	Oct.	0.09	16	0.10	2.1	0	2.0	0.07	20
	1	Nov.	0.58	43	0.32	5.7	tr.[c]	4.9	0.08	55
6	1	Aug.	0	35	0.34	0.94	0	2.3	0.02	39
	1	Sep.	0	20	0.17	1.1	0	2.2	0.14	24
	1	Oct.	0.21	34	0.28	3.1	0	3.3	0.13	41
	1	Nov.	0.43	32	0.30	7.6	tr.[c]	3.7	0.11	44
7	1	Aug.	0.09	2.7	0.22	0.05	0	0.14	0.01	3
	1	Aug.[b]	0	37	1.5	1.3	0	2.6	0.06	43
	2	Sep.	0	20	0.59	1.9	0	1.6	0.06	24
	2	Oct.	0.67	63	2.4	5.3	tr.[c]	4.4	0.05	76
	1	Nov.[b]	0.33	56	0.54	14	0.25	4.0	0.03	75

[a] Variable: 0.2 and 0.9 μmol/g dry wt detected in two samples, but absent from the remaining samples.
[b] Cauline rosettes.
[c] tr. = trace.

Table 5
Content (μmol/ g dry wt) of **2S** relative to the sum of **2R** and **2S**, in pooled leaves of each of the examined populations of *Barbarea vulgaris* ssp. *arcuata*. As the ratio of **2R** to **2S** did not vary with month or leaf type, results from the entire experimental period and for all examined leaf types were pooled

Locality	Type	[**2S**]/([**2R**] + [**2S**]) × 100%		
		Mean	S.D.	N
1	G	98.0	0.11	11
2	G	98.9	–	1
3	G	93.5	4.5	7
3a	"Hybrid"	51.3	11	5
4	G	98.5	0.77	10
5	P	0.83	0.24	5
6	P	0.89	0.06	4
7	P	4.1	3.2	7

The differences in resistance between the G- and P-type could not be attributed to differences in glucosinolate content. High levels of **2S** did not deter *P. nemorum* larvae, since high levels were found in susceptiple leaves collected in November. Furthermore, high levels of **2R** were not invariably correlated with susceptibility, since hybrid leaves collected at locality 3a in September were resistant although they contained high levels of **2R**, and since P-type leaves from locality 7 with widely different levels of **2R** were accepted by *P. nemorum* larvae to a similar extent (Tables 1 and 4). Differential effects of **2R** and **2S** had previously been mentioned as factors influencing oviposition behaviour of *Pieris* species on *Barbarea* plants (Huang et al., 1994).

2.4. Seasonal variation in glucosinolate content and its relation to insect resistance

The glucosinolate content in August was very variable, 3–46 μmol/ g dry wt, but was low in most populations, 3–15 μmol/g dry wt. The levels of all major glucosinolates increased from August to November in plants from five localities (2, 3, 4, 5 and 7), and increased from September to November in plants from the remaining two localities (1 and 6). The concentration-increase of the phenolic glucosinolate **3R** in the P-type was especially distinct during the autumn (Table 4).

Two observations demonstrate that glucosinolates are not the defensive compounds that confer resistance in the G-type of *B. v.* ssp. *arcuata* to *P. nemorum* larvae. First, the levels of glucosinolates increased in several populations at the same time as resistance decreased. Second, the resistance levels were consistently high in all populations of the G-type in August, although glucosinolate levels were variable during this period (Tables 1 and 4).

Glucosinolates are considered to be defensive compounds that protect the plants from a range of generalist herbivores and pathogens (Louda and Mole, 1991; Bennet and Wallsgrove, 1994). The role of these compounds in defences against specialized insects is far less clear, and many specialized insects are insensitive to changes in concentrations of these compounds (Nielsen et al., 2001). Although glucosinolates are obligate feeding stimulants for larvae of *P. nemorum* (Nielsen, 1989), low levels of glucosinolates were apparently sufficient for feeding stimulation: Low levels of glucosinolates in the P-type in August did not result in reduced larval acceptance of these susceptiple plants (localities 5 and 7). On the other hand, high levels of glucosinolates in the G-type in August did not result in increased larval acceptance of these resistant plants (locality 1).

2.5. Seasonal regulation of defence chemistry

Two types of chemical defence in *B. vulgaris* foliage were studied: Glucosinolates, and the unidentified compounds conferring resistance to *P. nemorum* and probably other specialist insects as well (Chew, 1981; Idris and Grafius, 1996). Our results suggest a seasonal regulation of defences: One or more seasonally dependent environmental signals seemed to (1) induce general glucosinolate biosynthesis; (2) induce a particular side chain modification (*p*-hydroxylation in the P-type) and (3) reduce the level of the *P. nemorum* resistance factor (in the G-type). The seasonal variation of insect resistance may be an adaptation to the seasonal variation in insect activity (Nielsen, 1997a).

Winter types of oilseed rape accumulate high levels of glucosinolates late in the year (Giamoustaris et al., 1994), while there is a decline in glucosinolate levels late in the season in *Cardamine cordifolia* and in *Dentaria* species (Feeny and Rosenberry, 1982; Louda and Rodman, 1983; Rodman and Louda, 1985). Rosette leaves of oilseed rape and *B. vulgaris* may remain green throughout the winter, while leaves of *Dentaria* and *Cardamine* species wilt late in the season. The physiological or defensive functions of the accumulation of glucosinolates in overwintering leaves of *B. vulgaris* and oilseed rape is to our knowledge unknown.

3. Experimental

3.1. Plants

Leaves of *B. vulgaris* ssp. *arcuata* were collected from seven localities on the Danish island Zealand. 1: Herlev (old grass field; accession No. 3), 2: Gl. Svebølle (waste area, accession No. 6), 3: Ejby (waste area; accession No. 8), 4: Kværkeby (wet meadow), 5: Tissø (wet meadow close to a lake; accession No. 9), 6: Trundholm Mose (meadow) and 7: Skellingsted (dry slope; close to accession No. 10). Accession numbers refer to Nielsen (1997a). Plants from Ejby and Kværkeby (localities 3 and 4) are natural host plants for populations of *P. nemorum* (with R-genes) (de Jong and Nielsen, 1999).

Leaf samples were collected once a month from August to November. Eight leaves from each sample were used in bioassays with *P. nemorum* larvae. The width (*a*) and length (*b*) of the end lobe of these eight leaves were measured, and the number of hairs on one fourth of the leaf margin (*c*) was counted (Fig. 2). The correlation between width × length ($a \times b$) and leaf area was determined using linear regression on data from a larger leaf sample (60 leaves) where *a* and *b*, as well as leaf area was measured (on a LiCor Model 3100 area meter). Leaves for glucosinolate analyses were lyophilized and stored at −20°C until the analyses could be performed.

B. orthoceras, for the isolation of desulfoglucosinolates from leaves, was grown from seeds collected at Wolcott, Vermont, USA, 1994, kindly provided by F.

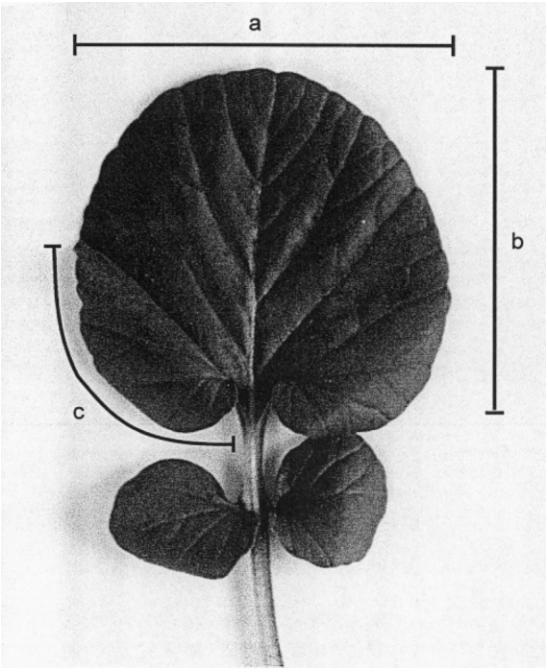

Fig. 2. Leaf of *Barbarea vulgaris* ssp. *arcuata*, showing width (a), length (b) and the basal fourth of the end lobe margin for counts of hairs (c).

Chew (Chew, 1981). *B. vulgaris* ssp. *arcuata* type P, for the isolation of desulfoglucosinolates from roots, was grown from seeds collected by J. K. Nielsen at Trundholm Mose, Denmark, 1997. Voucher specimens from the investigated populations of *B. vulgaris* ssp. *arcuata* type P and *B. vulgaris* ssp. *arcuata* type G have previously been deposited at the Botanical Museum in Copenhagen (Nielsen, 1997a). A voucher specimen of *B. orthoceras* has now additionally been deposited.

3.2. Insects and bioassays

P. nemorum was reared in the laboratory as described previously (Nielsen, 1978). The larvae belonged to a line (ST) which did not contain any R-genes conferring resistance to defences in the G-type of *B. v.* ssp. *arcuata* (Nielsen, 1999). A three-day bioassay was performed as described by de Jong and Nielsen (1999). Single leaves were presented to inexperienced, neonate larvae in small plastic vials (20–160 ml depending on the size of the leaf; 5 larvae per leaf). A piece of moist filter paper provided sufficient humidity to keep the leaves fresh. After three days at 24±2°C and a photoperiod of 18 h light and 6 h darkness, the number of surviving larvae was counted under a preparation microscope.

3.3. Spectroscopy

NMR spectra of intact glucosinolates were recorded on a Bruker AC250P spectrometer, while NMR spectra of desulfoglucosinolates were recorded on a Bruker Avance 400 spectrometer. Chemical shifts are based on dioxane as internal reference (δ_H (dioxane) = 3.75, δ_C(dioxane) = 67.4). Assignments were based on COSY, HSQC and HMBC spectra. UV spectra of desulfoglucosinolates were measured with the HPLC diode array detector.

Electrospray-ionisation MS of desulfoglucosinolates were measured in H_2O-AcCN (1:1) + 1% NH_3, with a "Platform LC" from Micromass Ltd, Manchester, UK, except desulfo **3R**, which was obtained in 50 μM NaOAc-MeOH 1:1 with a Bruker Esquire-LC ion trap mass spectrometer.

3.4. Glucosinolates

Glucosinolates (gls) were determined by conversion to desulfogls and analysis by HPLC with UV detection, following the principles described by Sørensen (1990). Ca. 100 mg dry wt of leaf material, omitting the petioles, was weighed and extracted three times with 3 × 3 ml of boiling 70% aq. MeOH with a T25 Basic homogenizer from Janke & Kunkel, Staufen, Germany. As internal standard, 100 µl of a 5 mM solution of benzylgls (Merck, Darmstadt, Germany) was added to the boiling extract. The crude extract was brought to 10 ml in a volumetric flask, from which 4 ml was applied to a 0.1 g dry wt column of DEAE Sephadex A-25 (Pharmacia, Uppsala, Sweden) on OAc^- form (achieved by incubation overnight with 3 ml of aq. 0.5 M HOAc–NaOAc pH 5.0, followed by a wash with water). The column was washed with 5×2 ml water followed by 2×2 ml of 0.02 M HOAc–NaOAc pH 5.0. Then, 0.5 ml of *Helix pomatia* sulfatase (Sigma) dissolved (2.5 mg/ml) in 0.02 M HOAc–NaOAc buffer was applied to the column, which was left overnight. The resulting desulfogls were eluted with 5×1 ml of water, and subjected to HPLC analysis. The HPLC apparatus was a LC-10AT with a SPD-M10AVP diode array detector, both from Shimadzu, Kyoto, Japan, equipped with a Supelcosil LC-ABZ column, 25 cm × 4.6 mm, 5 µm, from Supelco, Bellefonte, PA. The flow rate was 1 ml/min, and the desulfogls were eluted with water for 2 min followed by a linear gradient of MeOH from 0 to 60% in 48 min, followed by a brief wash with MeOH and equilibration with water.

For quantification, UV detection at 229 nm (bandwidth 8 nm) was employed. The response factors reported by Buchner (1987) were used: desulfobenzylgls: 0.95, desulfo **4**: 0.29, desulfo **5**: 0.25. Desulfobenzylgls and the desulfogls from **1**, **2S**, **2R**, **3S** and **3R** were assumed to have identical response factors at 229 nm. The purity of commercial benzylgls used as internal standard was found to be 90% by UV ($\varepsilon_{227.5}$ = 8870 M^{-1} cm^{-1}, Thies, 1988), this was considered in the calculation of absolute gls concentrations.

The completeness of binding and the sulfatase reaction, the complete elution also of desulfo **4**, and the overall linearity of the gls determination, was confirmed by appropriate controls. The relative standard deviation on the determination was tested for a leaf sample of the G-type analysed six times, and found to be 12, 8 and 14% for **2R**, **2S** and **4**, respectively. Other samples were only analysed once or twice. The detection limit was around 0.05 μmol/g dry wt for aliphatic gls, 0.01 μmol/g dry wt for the indoles.

In addition, the possibility of acylated gls was tested by high voltage paper electrophoresis of crude extracts at pH 1.9 (Olsen and Sørensen, 1981), followed by inspection in UV light with and without NH_3 vapour.

3.5. Purification of glucosinolates and desulfoglucosinolates

Intact **2R** and -**2S** were purified from seeds of the two plant types, as described by Thies (1988). Desulfogls for NMR were purified by preparative HPLC: Desulfo **2S** and -**3S** were obtained from leaves of *B. orthoceras*. Desulfo **2R**, -**4** and -**5** were purified from roots of *B. vulgaris* ssp. *arcuata* type P. Spectroscopic identification of **4** and **5** has been published elsewhere (Agerbirk et al., 2001). **3R** was purified from leaves collected at locality 6 in November.

3.6. Desulfo *2S*

Amorphous solid. UV: 228 nm (*sh*), 260 nm (*sh*). ESMS, pos. mode, cone voltage 110 V, *m/z*: 360 $[M+H]^+$, 382 $[M+Na]^+$, 342 $[M–H_2O+H]^+$, 198 $[M–C_6H_{10}O_5+H]^+$, 180 $[M–C_6H_{10}O_5–H_2O+H]^+$.

3.7. Desulfo *2R*

Amorphous solid. UV: 228 nm (*sh*), 260 nm (*sh*). ESMS, pos. mode, *m/z*: 382 $[M+Na]^+$.

3.8. Desulfo *3S*

Amorphous solid. UV: 224 nm (100%), 272 nm (12%, 281 nm (*sh*, 8%). ESMS, cone volt. 25 V, pos. mode, *m/z*: 376 $[M+H]^+$, 398 $[M+Na]^+$, 414 $[M+K]^+$, 358 $[M–H_2O+H]^+$, and neg. mode, *m/z* (rel. int.): 374 $[M–H]^-$.

3.9. Desulfo *3R*

Amorphous solid. UV: 224 nm (100%), 272 nm (12%, 281 nm (*sh*, 8%). ESMS, cone volt. 25 V, pos. mode, *m/z*: 376 $[M+H]^+$, 398 $[M+Na]^+$, 414 $[M+K]^+$, 358 $[M–H_2O+H]^+$, and neg. mode, *m/z* (rel. int.): 374 $[M–H]^-$.

Acknowledgements

The assistance of K.B.H. Herath, Boyce Thompson Institute for Plant Research at Cornell University, with electrospray mass spectrometry, and of Lena Rasmussen, Celestin A. Gnahore, Lars Borup and Hanne O. Frandsen with glucosinolate isolation and analysis, is gratefully acknowledged. We thank the Department of Agricultural Sciences, RVAU, for access to the Licor Area meter. The Danish Agricultural and Veterinary Research Council supported this research.

References

Agerbirk, N., Petersen, B.L., Olsen, C.E., Halkier, B.A., Nielsen, J.K., 2001. 1,4-Dimethoxyglucobrassicin in *Barbarea* and 4-hydroxyglucobrassicin in *Arabidopsis* and *Brassica*. J. Agric. Food Chem. 49, 1502–1507.

Andersson, A.A.M., Merker, A., Nilsson, P., Sørensen, H., Åman, P., 1999. Chemical composition of the potential new oilseed crops *Barbarea vulgaris*, *Barbarea verna* and *Lepidium campestre*. J. Sci. Food Agric. 79, 179–186.

Bak, S., Olsen, C.E., Petersen, B.L., Møller, B.L., Halkier, B.A., 1999. Metabolic engineering of *p*-hydroxybenzylglucosinolate in *Arabidopsis* by expression of the cyanogenic CYP79A1 from *Sorghum bicolor*. Plant. J. 20, 663–671.

Bennet, R.N., Wallsgrove, R.M., 1994. Secondary metabolites in plant defence mechanisms. New Phytol. 127, 617–633.

Buchner, R., 1987. Approach to determination of HPLC response factors for glucosinolates. In: Wathelet, J.-P. (Ed.), Glucosinolates in Rapeseed: Analytical Aspects. Martinus Nijhoff Publishers, Dordrecht, The Netherlands., pp. 50–58.

Chew, F., 1981. Coexistence and local extinction in two pierid butterflies. Am. Naturalist 118, 655–672.

Feeny, P., Rosenberry, L., 1982. Seasonal variation in the glucosinolate content of North American *Brassica nigra* and *Dentaria* species. Biochem. Syst. Ecol. 10, 23–32.

Fritz, R.S., Simms, E.L. (Eds.), 1992. Plant Resistance to Herbivores and Pathogens. University of Chicago Press, Chicago.

Gmelin, R., Kjær, A., Schuster, A., 1970. Glucosinolates in seeds of *Sibaria virginica* (L.) Rollins: two new glucosinolates. Acta Chem. Scand. 24, 3031–3037.

Giamoustaris, A., Magrath, R., Mithen, R., 1994. Modifying the aliphatic glucosinolate content of oilseed rape and its effect upon pest and pathogen interactions. Asp. Appl. Biol. 39, 125–132.

Huang, X., Renwick, J.A.A., Sachev-Gupta, K., 1994. Oviposition stimulants in *Barbarea vulgaris* for *Pieris rapae* and *P. napi oleracea*: Isolation, identification and differential activity. J. Chem. Ecol. 20, 423–438.

Idris, A.B., Grafius, E., 1996. Effects of wild and cultivated host plants on oviposition, survival, and development of diamondback moth (Lepidoptera: Plutellidae) and its parasitoid *Diadegma insulare* (Hymenoptera: Ichneumonidae). Environ. Entomol. 25, 825–833.

Jensen, S.K., 1990. Characterization and properties of epimeric 2-hydroxy substituted glucosinolates. In: Biochemical and Physiological Investigations of the Meal and Syrup Fractions from Aqueous Enzymatic Rapeseed Processing. PhD thesis. Royal Veterinary and Agricultural University, Denmark, pp. 57–71.

de Jong, P.W., Nielsen, J.K., 1999. Polymorphism in a flea beetle for the ability to use an atypical host plant. Proc. Roy. Soc. Lond. B 266, 103–111.

Kjær, A., Gmelin, R., 1957. *Iso*-Thiocyanates XXVIII. A new *iso*-thiocyanate glucoside (glucobarbarin) furnishing (−)-5-phenyl-2-

oxazolidinethione upon enzymatic hydrolysis. Acta Chem. Scand. 11, 906–907.

Kjær, A., Schuster, A., 1972. Glucosinolates in seeds of *Arabis hirsuta* (L.) Scop.: some new, naturally derived isothiocyanates. Acta Chem. Scand. 26, 8–14.

Koch, M., Bishop, J., Michell-Olds, T., 1999. Molecular systematics and evolution of *Arabidopsis* and *Arabis*. Plant Biol. 1, 529–537.

Louda, S., Mole, S., 1991. Glucosinolates: chemistry and ecology. In: Rosenthal, A., Berenbaum, M.R. (Eds.), Herbivores, their interaction with Secondary Plant Metabolites. Academic Press, San Diego, pp. 124–157.

Louda, S.M., Rodman, J., 1983. Ecological patterns in the glucosinolate content of a native mustard, *Cardamine cordifolia*, in the Rocky Mountains. J. Chem. Ecol. 9, 397–422.

MacDonald, M.A., Cavers, P.B., 1974. Cauline rosettes, an asexual means of reproduction and dispersal occurring after seed formation in *Barbarea vulgaris* (yellow rocket). Can. J. Bot. 52, 913–918.

MacDonald, M.A., Cavers, P.B., 1991. The biology of Canadian weeds. 97. *Barbarea vulgaris* R. Br. Can. J. Bot. 71, 149–166.

Nielsen, J.K., 1978. Host plant discrimination within Cruciferae: feeding responses of four leaf beetles (Coleoptera: Chrysomelidae) to glucosinolates, cucurbitacins and cardenolides. Entomol. Exp. Appl. 24, 41–54.

Nielsen, J.K., 1989. The effect of glucosinolates on responses of young *Phyllotreta nemorum* larvae to non-host plants. Entomol. Exp. Appl. 51, 249–259.

Nielsen, J.K., 1997a. Variation in defences of the plant *Barbarea vulgaris* and in counteradaptations by the flea beetle *Phyllotreta nemorum*. Entomol. Exp. Appl. 82, 25–35.

Nielsen, J.K., 1997b. Genetics of the ability of *Phyllotreta nemorum* larvae to survive in an atypical host plant, *Barbarea vulgaris* ssp. *arcuata*. Entomol. Exp. Appl. 82, 37–44.

Nielsen, J.K., 1999. Specificity of a Y-linked gene in the flea beetle *Phyllotreta nemorum* for defences in *Barbarea vulgaris*. Entomol. Exp. Appl. 91, 359–368.

Nielsen, J.K., Hansen, M.L., Agerbirk, N., Petersen, B.L., Halkier, B.A., 2001. Responses of the flea beetle species *Phyllotreta nemorum* and *P. cruciferae* to metabolically engineered *Arabidopsis thaliana* with an altered glucosinolate profile. Chemoecology 11, 75–83.

Olsen, O., Sørensen, H., 1981. Recent advances in the analysis of glucosinolates. J. Am. Oil Chem. Soc. 58, 857–865.

Rodman, J.E., Louda, S.M., 1985. Seasonal flux of isothiocyanate-yielding glucosinolates in roots, stems and leaves of *Cardamine cordifolia*. Biochem. Syst. Ecol. 13, 405–412.

Senatore, F., D'Agostino, M., Dini, I., 2000. Flavonoid glycosides of *Barbarea vulgaris* L. (Brassicaceae). J. Agric. Food Chem. 48, 2659–2662.

Sørensen, H., 1990. Glucosinolates: structure, properties, function. In: Shahidi, F. (Ed.), Canola and Rapeseed. Production, Chemistry, Nutrition and Processing Technology. Van Nostrand Reinhold, New York, pp. 149–172.

Thies, W., 1988. Isolation of sinigrin and glucotropaeolin from cruciferous seeds. Fat Sci. Technol. 90, 311–314.

PERGAMON

Phytochemistry 58 (2001) 101–115

PHYTOCHEMISTRY

www.elsevier.com/locate/phytochem

Taxonomy of gymnospermae: multivariate analyses of leaf fatty acid composition

Sébastien Mongrand[a,*], Alain Badoc[b], Brigitte Patouille[c], Chantal Lacomblez[c], Marie Chavent[c], Claude Cassagne[a], Jean-Jacques Bessoule[a]

[a]*Laboratoire de Biogenèse Membranaire-CNRS-UMR 5544, Université Victor Segalen-Bordeaux II, 146 rue Lé Saiǵnat, 33076 Bordeaux Cedex, France*
[b]*Laboratoire de Mycologie et Biotechnologie végétale, Université Victor Segalen-Bordeaux II, 146, rue Léo Saignat, 33076 Bordeaux Cedex, France*
[c]*Laboratoire de Mathématiques appliquées, CNRS-UMR 5466, Universités Bordeaux I - V. Segalen-Bordeaux II 146, rue Léo Saignat, 33076 Bordeaux Cedex, France*

Received 28 November 2000; received in revised form 13 March 2001

Abstract

The fatty acid composition of photosynthetic tissues from 137 species of gymnosperms belonging to 14 families was determined by gas chromatography. Statistical analysis clearly discriminated four groups. Ginkgoaceae, Cycadaceae, Stangeriaceae, Zamiaceae, Sciadopityaceae, Podocarpaceae, Cephalotaxaceae, Taxaceae, Ephedraceae and Welwitschiaceae are in the first group, while Cupressaceae and Araucariaceae are mainly in the second one. The third and the fourth groups composed of Pinaceae species are characterized by the genera *Larix,* and *Abies* and *Cedrus*, respectively. Principal component and discriminant analyses and divisive hierarchical clustering analysis of the 43 Pinaceae species were also performed. A clear-cut separation of the genera *Abies, Larix,* and *Cedrus* from the other Pinaceae was evidenced. In addition, a mass analysis of the two main chloroplastic lipids from 14 gymnosperms was performed. The results point to a great originality in gymnosperms since in several species and contrary to the angiosperms, the amount of digalactosyldiacylglycerol exceeds that of monogalactosyldiacylglycerol. © 2001 Elsevier Science Ltd. All rights reserved.

Keywords: Gymnospermae; Chemotaxonomy; Plant lipids; Plant fatty acids; Δ5-Olefinic fatty acids; Anteiso 17:0 fatty acid; Multivariate analysis; Divisive hierarchical analysis

1. Introduction

The gymnosperms represent an ecologically, morphologically and taxonomically very diverse botanical group. However, in the northern hemisphere, although one tree out of two is a conifer, the gymnosperms do not represent many different species. Indeed, according to one of the most recent gymnosperm databases (Earle, 1999), 873 species are referenced among 14 families. Nevertheless, many complex subfamilial and tribal classification problems remain to be solved. Elsewhere, information on the chemotaxonomic and phylogenetic relationships between angiosperm families were obtained by studying the leaf fatty acid composition of 468 species (Mongrand et al., 1998). This work clearly evidenced that the fatty acid composition of photosynthetic tissues can be a powerful tool for chemotaxonomic studies, and could be used for the classification of gymnosperms.

It is known that gymnosperm leaves contain branched-17:0 fatty acid, and quite high amounts of short and very long chain fatty acids (Jamieson and Reid, 1972; Vickery et al., 1984; Itabashi and Takagi, 1982). It has also been shown that seeds (e.g. Wolff et al., 1997b) and leaves (Jamieson and Reid, 1972) of gymnosperms contain Δ5-olefinic acid. These fatty acids are characteristic of mosses, ferns and gymnosperms (Karunen, 1990). Angiosperms, with a few exception such as the Ranunculaceae (Aitzetmüller, 1996), have lost the ability to synthesize such fatty acids. Hence, Δ5 fatty acids could be considered as an archaic fatty acid marker.

Even so, the fatty acid composition of gymnosperm leaves has been determined for only approximately 50 species belonging to only 8 of the 14 families in the gymnosperm classes (Jamieson and Reid, 1972; Vickery

* Corresponding author at: Laboratory of Plant Molecular Biology, Pr Nam-Hai Chua, The Rockefeller University, Box 162, 1230, York Avenue, 10021 New York, NY, USA. Tel.: +1-212-327-8093; fax: +1-212-327-8327.
E-mail address: mongras@rockvax.rockefeller.edu (S. Mongrand).

0031-9422/01/$ - see front matter © 2001 Elsevier Science Ltd. All rights reserved.
PII: S0031-9422(01)00139-X

et al., 1984; Itabashi and Takagi, 1982; Grahl-Nielsen et al., 1991; Mongrand et al., 1998). In other words, the leaf fatty acid composition of a high number of gymnosperm genera (and even of entire families: e.g. Podocarpaceae, Araucariaceae, Cephalotaxaceae) is still almost completely unknown. Therefore the aim of the present study was to analyze the fatty acid composition of 137 species belonging to each of the 14 gymnosperm families. Principal component and discriminant analyses were performed using the fatty acid composition of photosynthetic tissues of gymnosperms to establish relationships between and within the different families.

2. Results and discussion

2.1. Fatty acid composition of leaves

The word gymnosperm — also synonymous with Pinophyta Cronquist, Takht. et Zimmerm. ex Reveal or Gymnospermae — is used *s.l.* in the present paper. Hence, this group contains the gymnosperms *s. str.* (i.e. conifers and others), the former pre-spermatophytes (i.e. Ginkgoales) and previously termed chlamydosperms (i.e. Gnetales). In the present study, 137 plants distributed among the 14 gymnosperm families have been analyzed. Table 1 shows the overall leaf fatty acid composition of these gymnosperm species determined by gas chromatography. Orders, families, and sub-families are listed according to the classification of Earle (1999). Species names are according to Farjon's nomenclature (1998).

The fatty acid compositions of gymnosperm and angiosperm photosynthetic tissues are similar in that the major fatty acids are linolenic (C18:3), linoleic (C18:2) and palmitic (C16:0) acids. However, in most cases, the gas chromatography patterns of fatty acids from the photosynthetic tissues of gymnosperms (e.g. Fig. 1) showed the presence of a higher number of molecules than that observed with angiosperm species, with as many as 26 different fatty acids detected. In gymnosperm leaves, several unusual fatty acids with a *cis*-5 ethylenic bond (also called Δ5-olefinic acids, or Δ5-unsaturated polymethylene-interrupted fatty acid) were detected as widely described for gymnosperm oils (e.g. Wolff et al., 1996). The role of these fatty acids remains unknown but it has been hypothesized that it might be related to a cold acclimatization (Wolff et al., 1997c). Most of these fatty acids have 18 and 20 carbon atoms: *all cis*-Δ5, 9–18:2 (taxoleic), *all cis*-Δ5, 9, 12–18:3 (pinolenic), *all cis*-Δ5, 9, 12, 15–18:4 (coniferonic), *all cis*-Δ5, 11–20:2, *all cis*-Δ5,11, 14–20:3 (sciadonic or podocarpic), and *all cis*-Δ5, 11, 14, 17–20:4 (juniperonic). A few species do not contain any Δ5 fatty acids such as *Welwitschia mirabilis*. The Δ5, 11, 14, 17–20:4 fatty acid is detected in almost all of the gymnosperm species. By contrast, C18-Δ5 fatty acids are not uniformly distributed in the gymnosperm kingdom, and are almost exclusively present in Pinaceae. Hence, the C18-Δ5 fatty acids could be a powerful chemometric tool to discriminate Pinaceae among the gymnosperm families.

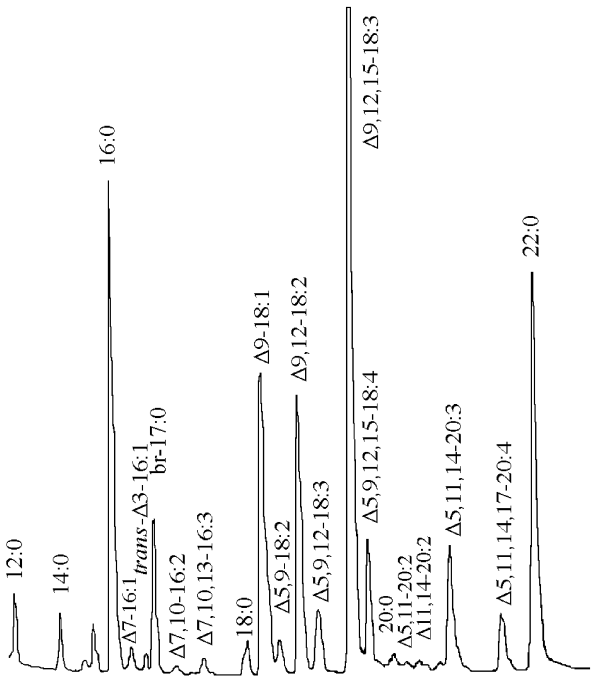

Fig. 1. Gas chromatography pattern of leaf fatty acid methyl esters of *Abies concolor* (Gord.) Lindl. ex Hildebr. (Pinaceae Abietoideae).

Another unusual fatty acid present in gymnosperm leaves is the branched-17:0 acid (also called 14-methyl-palmitic acid, or anteiso 17:0). This peculiar fatty acid has also been identified in the wood of several pines (Zinkel and Foster, 1980), in *Ginkgo biloba* seed oil (Hierro et al., 1996) and in conifer needles (Jamieson and Reid, 1972). Its role as well as the pathway of its biosynthesis remain totally unknown (Wolff et al., 1997a). From our results, br-17:0 fatty acid appeared particularly present in *Abies* (ca. 4%) and *Picea* (ca. 2%), while this fatty acid was not — or only poorly — detected in Ginkgoaceae, Sciadopityaceae, and Gnetales. Interestingly, some Araucariaceae and Podocarpaceae (e.g. *Araucaria montana*, *Podocarpus nivalis*) contain relatively high amounts of br-17:0 acid.

Small amounts of *cis*-Δ11-18:1 fatty acid were detected in some species, but this fatty acid never rose above 0.2% of the total fatty acid content. Higher amounts of short chain fatty acids (C12:0, C14:0) were detected, particularly in *Microbiota decussata* leaves. Like the short chain fatty acids, very long chain fatty acids, *i.e.* C20:0 (arachidic) and C22:0 (behenic) were detected in almost all of the gymnosperm photosynthetic tissues in which they could reach 30–40% of the total fatty acid content (*Cedrus libani, Tetraclinis articulata*), in contrast with what is observed with angiosperms leaves. Relatively high amounts of very long chain fatty acids were

Table 1
Overall fatty acid composition of gymnosperm leaves. Comparison with fatty acid composition of gymnosperm oils[c]

PINOPHYTA Cronquist, Takht. et Zimmerm. ex Reveal		(a)[c]	12:0	14:0	(b)[d]	16:0	16:1 (c)[e]	br-17:0 (d)[f]	16:2 Δ7,10	16:3 Δ7, 10, 13	18:0	18:1 Δ9	18:2 Δ5, 9	18:2 Δ9, 12	18:3 Δ5, 9, 12	18:3 Δ9, 12, 15	18:4 Δ5, 9, 12, 15	20:0	20:1 Δ11	20:2 Δ5, 11	20:2 Δ11, 14	20:3 Δ5, 11, 14	20:4 Δ5, 11, 14, 17	22:0	22:1	(e)[g]
GINKGOALES																										
GINKGOACEAE Engler																										
Ginkgo biloba L.	1	3	0.5	1.2	1.0	23.6	2.6	–[a]	–	4.5	1.5	5.8	2.4	5.5	–	41.5	–	1.6	–	1.5	–	2.0	2.3	2.6	–	–
Ginkgo biloba L.	2	2	0.8	0.2	2.3	24.8	3.2	–	0.3	4.4	1.4	5.2	2.1	6.8	–	39.3	–	1.0	–	1.6	1.1	1.9	2.1	1.1	–	0.4
CYCADALES																										
CYCADACEAE Lindl.																										
Cycas armstrongii Miq.	3	1	–	1.4	1.5	18.5	2.7	1.0	1.3	2.3	5.0	7.3	–	13.2	0.6	43.0	0.2	1.1	–	0.4	–	–	–	0.5	–	–
Cycas revoluta Thunb.	4	3	–	1.2	1.5	15.6	2.0	1.3	0.8	3.0	2.1	5.1	0.8	17.0	0.6	33.6	0.4	1.7	–	1.0	0.6	1.4	3.6	4.9	–	1.7
Cycas siamensis Miq.	5	1	–	1.5	1.4	20.3	2.9	1.2	0.4	3.6	2.6	10.1	0.5	14.4	0.3	38.3	0.3	0.2	–	0.3	tr.	0.6	0.5	0.5	–	–
STANGERIACEAE L. A. S. Johnson																										
Stangerioideae																										
Stangeria eriopus (Kunze) Baill.	6	10	0.5	0.8	6.9	20.2	13.7	6.4	0.7	0.8	1.2	3.8	–	7.5	–	22.6	0.8	1.2	2.6	1.8	0.9	4.4	1.0	2.2	–	–
Stangeria eriopus (Kunze) Baill.	7	5	1.9	2.2	2.1	23.4	2.3	–	0.4	1.9	4.6	9.4	–	10.5	–	32.4	–	1.8	–	1.3	0.3	2.3	1.9	1.1	–	–
Bowenioideae																										
Bowenia spectabilis Hook. ex J. D. Hook.	8	4	2.2	1.1	1.7	15.1	1.6	1.7	1.7	0.8	4.0	7.8	–	16.3	–	36.5	–	4.4	–	1.8	–	1.5	–	1.8	–	–
ZAMIACEAE Horianow																										
Encephalartoideae																										
Dioon edule Lindl.	9	1	0.6	1.2	1.7	18.3	1.1	0.5	0.5	1.8	2.7	8.1	tr.	17.0	0.5	33.1	1.3	1.2	0.4	0.5	0.4	1.4	5.0	2.8	–	–
Encephalartos lebomboensis Verdoorn	10	1	0.8	1.1	1.7	21.3	0.5	–	1.6	0.9	4.9	12.6	–	9.6	1.1	24.9	0.5	0.8	0.4	0.4	0.9	3.9	4.9	7.9	–	–
Lepidozamia hopei Regel	11	1	0.5	0.9	1.5	17.6	tr.	0.2	1.5	1.1	3.7	8.3	–	12.8	0.2	40.1	0.4	0.2	tr.	0.6	0.4	2.8	4.6	2.0	–	0.4
Macrozamia moorei F. Muell. ex C. Moore	12	1	0.3	0.5	1.2	18.3	0.6	0.6	0.3	1.7	3.1	7.2	–	19.9	0.2	36.9	–	0.4	–	0.4	0.4	2.0	4.8	1.2	–	–
Zamioideae																										
Ceratozamia robusta Miq.	13	1	0.4	2.0	2.1	18.2	2.3	1.2	0.9	1.5	1.9	9.9	0.5	18.9	0.2	34.2	0.2	–	–	0.5	0.2	2.5	1.2	1.1	–	tr.
Microcycas calocoma (Miq.) A. DC.	14	1	0.8	2.4	tr.	17.7	0.5	tr.	1.6	0.7	3.5	10.4	0.6	4.0	tr.	47.9	0.4	0.5	tr.	0.4	0.4	1.6	3.1	2.6	0.6	–
Zamia furfuracea L. f. in Ait.	15	1	0.2	0.5	1.6	15.7	2.0	0.2	0.7	1.8	1.9	7.7	–	5.8	0.2	41.0	0.7	5.9	0.4	1.3	0.4	1.7	6.0	4.4	–	–
PINALES (Coniferales)																										
PINACEAE Lindley																										
Pinoideae																										
Pinus cembra L.	16	1	2.5	2.5	2.2	13.3	0.9	2.2	1.1	1.4	1.2	3.6	0.8	8.4	2.2	29.1	3.2	5.0	0.7	0.7	1.2	5.7	3.2	8.9	–	–
Pinus griffithii Mc Clell.	17	3	5.5	2.8	0.7	9.6	1.1	1.0	0.7	1.6	2.8	8.1	2.3	12.4	5.4	27.5	1.8	2.6	0.3	0.4	0.7	3.8	1.9	6.7	–	0.4
Pinus strobiformis Engelm.	18	1	4.8	4.8	0.9	11.5	1.6	0.7	0.3	1.6	1.1	4.0	0.4	9.5	1.3	27.5	1.4	3.9	0.3	tr.	0.9	3.9	3.9	14.6	–	0.7
Pinus aristata Engelm.	19	1	2.5	1.4	1.2	12.7	1.7	0.4	0.3	2.1	1.2	4.0	0.5	13.4	2.2	29.0	1.9	8.4	0.2	tr.	1.1	4.8	1.7	9.1	–	0.2
Pinus monophylla Torr. et Frém.	20	3	4.3	1.9	0.5	11.9	1.2	tr.	0.2	2.0	1.3	10.2	0.9	15.1	1.9	27.2	0.9	3.6	0.2	tr.	1.0	4.1	2.1	7.5	–	1.9
Pinus bungeana Zucc. ex Endl.	21	1	6.0	1.5	0.2	11.5	1.4	0.3	0.2	2.0	0.9	10.8	0.8	16.4	2.3	25.6	1.7	1.2	1.1	0.5	1.6	4.8	0.9	5.4	0.6	2.4
Pinus nigra Arn. subsp. *laricio* (Poir.) Maire	22	3	3.9	3.5	1.2	11.7	3.8	2.4	3.4	0.9	2.5	3.0	0.8	8.5	1.6	26.7	0.8	6.5	0.2	3.9	0.6	6.2	1.6	5.9	–	0.3
Pinus resinosa Ait.	23	1	0.3	0.3	1.0	13.5	2.2	0.9	0.2	2.5	0.8	4.4	0.5	13.8	4.7	29.4	2.8	4.7	0.2	tr.	1.0	6.4	2.9	7.1	–	0.3
Pinus sylvestris L.	24	3	1.3	0.9	1.4	16.2	0.7	1.0	0.5	3.0	1.8	2.5	0.7	12.4	2.5	32.9	1.3	4.0	tr.	tr.	1.3	6.8	2.6	4.9	–	1.2

(*continued on next page*)

Table 1 (*continued*)

PINOPHYTA Cronquist, Takht. et Zimmerm. ex Reveal		(a)[c]	12:0	14:0	(b)[d]	16:0	16:1 (c)[e]	br-17:0 (d)[f]	16:2 Δ7,10	16:3 Δ7, 10, 13	18:0	18:1 Δ9	18:2 Δ5, 9	18:2 Δ9, 12	18:3 Δ5, 9, 12	18:3 Δ9, 12, 15	18:4 Δ5, 9, 12, 15	20:0	20:1 Δ11	20:2 Δ5, 11	20:2 Δ11, 14	20:3 Δ5, 11, 14	20:4 Δ5, 11, 14, 17	22:0	22:1	(e)[g]
Pinus jeffreyi Grev. et Balf.	25	1	8.9	2.9	0.5	9.8	0.4	0.6	0.6	1.4	0.8	3.8	0.2	8.7	1.1	17.9	1.2	15.1	1.5	0.9	0.8	6.1	1.5	14.5	0.3	0.4
Pinus palustris Mill.	26	1	3.1	2.7	0.6	12.7	1.3	1.0	1.2	1.3	1.4	1.7	0.6	10.3	0.6	26.5	0.6	22.7	–	0.3	0.4	4.7	1.9	–	–	4.4
Pinus pinaster Ait.	27	3	8.3	1.9	0.8	8.7	0.8	0.4	0.8	0.5	2.1	5.3	0.2	12.6	–	16.0	–	23.4	–	–	1.1	6.2	1.6	8.5	–	0.9
Pinus halepensis Mill.	28	3	5.1	1.4	0.9	13.3	2.0	0.4	0.2	4.2	2.1	2.6	–	9.8	–	33.2	2.4	6.4	0.8	0.6	0.9	5.9	1.1	5.9	–	0.7
Pinus pinea L.	29	3	5.8	3.6	9.4	12.5	2.0	0.3	0.3	3.0	1.1	3.9	–	8.9	–	31.2	–	–	tr.	0.4	0.7	5.1	1.4	9.9	–	0.4
Piceoideae																										
Picea abies (L.) H. Karst.	30	3	3.3	3.3	1.3	13.0	1.5	2.0	0.3	2.1	0.7	3.2	1.1	8.1	2.0	32.5	3.8	2.4	0.8	1.2	0.8	3.6	1.3	6.9	–	4.9
Picea asperata Mast.	31	1	0.5	0.6	1.0	12.0	0.6	1.7	0.3	0.6	1.0	2.7	2.0	8.3	1.8	16.5	1.8	20.1	0.3	0.4	–	3.5	0.6	23.7	–	–
Picea chihuahuana Martínez	32	1	0.3	0.4	0.7	12.4	1.3	1.6	0.3	1.0	1.1	5.9	1.3	13.5	3.5	29.8	3.5	6.9	1.3	–	–	4.7	1.0	9.3	–	–
Picea glauca (Moench) Voss	33	1	0.6	0.6	1.0	12.5	–	2.1	0.8	0.6	1.3	3.1	0.7	9.6	2.5	16.0	3.3	7.5	1.4	–	0.6	4.8	1.5	29.2	–	–
Picea omorica (Pancic) Purk.	34	1	0.3	0.5	0.8	10.4	0.7	1.5	0.4	0.8	0.7	3.0	0.9	8.0	2.1	12.6	2.3	2.8	3.1	0.7	2.9	2.9	0.6	41.0	–	1.0
Picea sitchensis (Bong.) Carr.	36	1	1.7	4.8	1.1	11.6	1.2	2.6	0.4	1.3	0.8	2.0	0.6	13.0	4.1	34.2	6.6	1.7	–	–	0.7	3.1	1.1	6.4	–	0.3
Picea torano (Sieb. ex K. Koch) Koehne	35	1	1.9	1.9	0.8	9.4	0.9	2.3	0.4	1.2	1.2	11.9	1.8	15.5	5.0	28.4	4.1	4.8	–	0.2	0.4	1.6	0.9	5.7	–	–
Laricoideae																										
Larix decidua Mill.	37	3	–	5.5	0.7	16.8	2.5	0.7	1.0	4.2	0.9	4.1	1.2	6.0	1.1	45.9	2.6	1.0	–	–	0.4	2.4	2.1	0.5	–	0.3
Larix gmelinii (Rupr.) Kuzen.	38	1	0.5	0.8	1.8	21.1	–	0.9	0.4	3.4	2.7	3.5	–	7.8	1.7	40.2	3.6	1.6	–	–	–	3.3	5.3	1.5	–	–
Larix kaempferi (Lamb.) Carr.	40	1	3.3	0.6	1.9	20.3	1.8	0.8	0.5	2.3	2.5	6.2	1.5	9.0	3.1	34.4	2.7	0.8	0.7	–	–	2.8	1.7	2.4	–	0.7
Larix laricina (Du Roi) K. Koch	39	1	0.9	0.6	1.6	20.7	3.0	1.9	0.9	4.4	1.1	3.3	0.3	6.5	1.0	40.5	4.2	1.8	–	–	0.5	3.8	2.1	0.9	–	–
Larix lyallii Parl.	41	1	2.6	0.6	1.8	21.9	2.3	1.2	0.5	3.3	2.3	6.4	1.4	2.6	4.4	35.8	2.9	0.9	0.7	0.7	1.0	4.1	1.9	0.8	–	–
Larix sibirica Ledeb.	42	1	tr.	1.5	0.7	11.2	1.9	0.8	0.2	4.0	1.8	2.8	1.6	7.2	4.5	38.4	5.9	8.5	–	–	–	6.2	1.7	0.9	–	0.2
Pseudotsuga macrocarpa (Vasey) Mayr	44	1	1.8	2.4	0.9	12.2	1.2	1.3	0.2	1.9	0.8	4.1	0.6	7.1	1.0	36.7	3.6	3.2	–	0.8	0.3	4.2	3.7	11.9	–	–
Pseudotsuga menziesii (Mirb.) Franco var. *glauca* (Beissn.) Franco	43	1	3.8	2.4	1.1	10.8	1.3	2.1	0.3	1.3	0.9	2.8	0.4	10.5	1.4	16.5	6.1	5.4	–	0.6	1.6	6.2	1.6	22.6	–	–
Pseudotsuga menziesii (Mirb.) Franco	45	3	0.4	2.8	0.8	12.3	0.9	2.5	0.5	–	1.9	5.4	0.8	9.2	1.0	20.8	2.5	4.7	–	–	2.6	6.8	3.4	20.6	–	–
Abietoideae																										
Abies alba Mill.	46	1	1.2	1.0	1.9	12.0	0.9	3.6	0.7	1.3	2.7	10.8	1.7	8.6	2.0	22.6	3.3	1.6	2.1	–	–	3.9	1.5	16.6	–	–
Abies cephalonica Loud.	47	2	5.5	2.0	1.3	9.1	0.5	3.1	0.5	0.8	1.8	6.0	1.7	5.8	1.5	28.1	3.1	0.4	–	tr.	0.9	2.4	2.7	22.1	–	0.5
Abies concolor (Gord.) Lindl. ex Hildebr.	48	1	2.3	0.7	1.0	11.1	1.3	3.4	0.2	0.5	1.0	9.9	1.1	7.9	2.2	32.2	3.4	0.9	0.4	0.4	0.4	4.1	2.0	13.4	–	–
Abies grandis (Dougl. ex D. Don) Lindl.	49	1	1.0	0.8	1.2	13.5	1.0	5.3	0.2	0.8	1.5	8.9	3.0	5.7	2.6	24.6	4.9	1.6	0.7	1.9	0.9	3.9	2.5	12.9	–	1.4
Abies pinsapo Boiss.	50	12	0.4	0.8	1.1	13.0	–	2.0	–	0.7	2.2	11.7	2.1	6.0	1.1	25.5	1.8	2.2	1.1	1.1	0.3	3.2	1.8	21.8	–	–
Abies sachalinensis (F. Schmidt) Mast.	51	1	9.6	5.6	2.6	12.4	1.7	4.9	0.5	1.0	1.9	10.4	4.2	10.0	4.6	10.0	3.6	1.0	0.5	0.4	0.2	2.7	1.2	10.9	–	–
Abies veitchii Lindl.	52	1	1.3	1.0	1.4	13.6	4.7	5.5	0.7	0.8	4.6	3.2	3.2	14.0	4.7	11.6	3.6	2.4	2.0	–	1.0	3.9	1.2	8.7	–	–
Abies vejarii Martínez	53	1	5.9	3.1	1.2	12.4	1.1	3.5	0.3	0.7	1.9	7.2	1.9	9.2	2.9	18.2	11.0	2.0	1.0	1.1	0.7	3.9	1.5	9.0	–	0.4
Cedrus atlantica (Endl.) Manet. ex Carr. 'Glauca'	54	3	0.6	0.6	0.8	11.3	0.7	1.4	0.3	1.0	0.9	5.0	1.8	7.4	2.1	33.0	3.3	6.3	1.7	2.1	1.2	2.8	1.1	12.9	–	1.6
Cedrus libani A. Rich.	55	3	0.5	0.5	0.6	10.9	0.6	1.0	0.2	0.9	1.0	5.5	0.8	6.1	0.6	23.5	0.9	8.0	1.4	–	–	2.7	0.7	32.8	–	0.9
Cedrus deodara (Roxb.) G. Don	56	3	6.5	1.2	0.4	7.8	0.8	0.5	0.2	1.1	tr.	3.3	1.7	6.7	3.8	25.4	0.6	7.9	–	–	–	9.7	2.5	20.0	–	–
Keteleeria evelyniana Mast.	57	8	1.1	0.6	1.6	17.3	2.0	0.5	–	1.0	1.9	9.1	0.2	5.5	–	30.9	–	0.4	–	1.9	–	3.0	3.1	20.0	–	–

(*continued on next page*)

Table 1 (*continued*)

PINOPHYTA Cronquist, Takht. et Zimmerm. ex Reveal		(a)[c]	12:0	14:0	(b)[d]	16:0	16:1 (c)[e]	br-17:0 (d)[f]	16:2 Δ7,10	16:3 Δ7, 10, 13	18:0	18:1 Δ9	18:2 Δ5, 9	18:2 Δ9, 12	18:3 Δ5, 9, 12	18:3 Δ9, 12, 15	18:4 Δ5, 9, 12, 15	20:0	20:1 Δ11	20:2 Δ5, 11	20:2 Δ11, 14	20:3 Δ5, 11, 14	20:4 Δ5, 11, 14, 17	22:0	22:1	(e)[g]
Pseudolarix amabilis (J. Nelson) Rehd.	58	1	1.7	1.7	0.6	18.5	2.4	0.9	0.9	1.7	1.3	3.4	2.0	8.7	4.2	31.7	4.7	0.3	–	–	–	6.2	6.3	–	–	2.7
Tsuga canadensis (L.) Carr.	59	1	3.8	2.7	1.5	13.1	1.9	1.8	0.3	0.4	2.2	4.4	tr.	14.5	2.6	37.9	1.2	1.6	tr.	–	0.5	4.7	2.6	1.9	–	0.3
SCIADOPITYACEAE Luerss.																										
Sciadopitys verticillata (Thunb.) Sieb et Zucc.	60	6	1.9	1.3	0.8	25.4	1.3	–	tr.[b]	1.7	1.3	3.4	–	25.6	–	23.6	–	1.3	0.5	0.3	1.2	3.3	4.4	–	2.6	–
PODOCARPACEAE Endl.																										
Podocarpoideae																										
Dacrydium cupressinum Sol. ex G. Forst.	61	1	1.8	1.8	0.6	21.0	1.8	–	0.4	0.8	1.4	4.6	–	11.4	0.5	36.1	–	1.0	0.3	0.3	0.4	4.1	5.2	6.7	–	–
Decussocarpus minor (Carr.) C. N. Page	62	8	0.6	–	1.7	23.8	0.6	–	0.8	0.7	2.0	6.3	–	22.5	–	31.3	–	1.8	–	–	–	3.9	3.1	1.1	–	–
Microstrobos fitzgeraldi (F. Muell.) J. Gardenet L. A. S. Johnson	63	9	0.2	1.1	7.3	17.2	12.6	–	0.8	1.3	1.3	1.7	tr.	12.2	–	21.9	2.5	0.9	0.5	1.7	0.9	2.8	3.0	2.3	5.3	2.4
Podocarpus chinensis Wall. ex J. Forb.	65	3	0.9	4.3	0.8	21.8	1.6	–	0.5	0.9	2.1	8.2	–	5.3	–	31.6	–	3.1	–	–	1.5	6.5	3.4	2.2	1.3	3.9
Podocarpus macrophyllus (Thunb.) Sweet	67	1	–	1.8	2.9	23.8	1.4	1.0	0.2	0.6	1.6	3.7	–	11.3	–	32.7	–	3.3	–	–	–	10.5	4.1	–	–	1.2
Podocarpus nivalis Hook.	68	1	0.5	0.4	–	17.8	0.7	16.0	0.5	tr.	1.4	2.4	–	13.0	–	26.3	5.4	2.8	0.8	2.5	1.6	3.6	4.3	–	–	–
Podocarpus salignus D. Don	69	1	2.3	5.8	1.1	19.5	1.4	0.2	0.6	0.7	1.1	4.6	0.2	14.2	–	36.9	–	0.4	0.2	0.3	0.6	3.5	2.9	0.3	2.5	0.5
Prumnopitys andina (Poepp. ex Endl.) de Laub.	64	1	1.6	2.2	1.1	18.6	1.8	0.4	0.4	0.8	1.6	5.6	–	12.3	tr.	37.1	–	5.1	–	–	–	4.1	3.5	2.3	–	1.5
Prumnopitys ferruginea (G. Benn ex D. Don) de Laub.	66	2	0.5	1.0	1.1	23.4	1.3	–	1.0	1.4	1.8	6.6	–	19.1	–	33.5	1.2	1.6	0.6	–	2.5	2.5	0.9	–	–	–
Prumnopitys taxifolia (Banks et Sol. ex D. Don) de Laub.	70	1	–	0.4	11.1	14.6	1.6	5.9	0.2	0.6	1.2	2.9	–	13.0	–	35.3	1.2	0.5	–	0.6	1.1	1.9	3.4	0.7	–	4.0
ARAUCARIACEAE Henkel et W. Hoscht.																										
Agatheae																										
Agathis australis (D. Don) Loud.	71	2	3.1	0.9	1.0	13.5	1.3	–	–	0.9	1.3	6.4	–	8.0	–	27.5	–	3.5	3.2	1.4	12.9	4.6	6.1	4.5	–	–
Agathis robusta (C. Moore) F. M. Bailey	72	10	2.5	1.2	1.1	19.8	1.6	0.3	0.3	1.5	1.1	9.7	–	15.6	–	41.8	–	0.9	–	0.3	0.2	0.9	0.7	0.6	–	–
Agathis moorei (Lindl.) Mast.	73	10	0.4	0.6	1.0	22.5	1.0	–	0.7	1.3	2.0	7.9	–	7.1	–	40.6	–	3.1	–	–	0.7	2.0	2.5	1.6	–	5.0
Araucarieae																										
Araucaria angustifolia (Bertol.) Kuntze	74	1	tr.	0.9	0.8	14.7	0.3	0.4	2.3	2.4	0.7	2.3	0.7	6.4	–	41.0	–	4.3	3.1	–	10.1	4.1	3.3	2.0	–	–
Araucaria angustifolia (Bertol.) Kuntze	75	3	tr.	1.0	0.7	13.2	1.3	0.3	0.2	1.7	1.1	2.3	0.9	6.2	1.9	34.6	–	tr.	1.0	0.9	8.9	5.0	6.3	9.9	–	2.3
Araucaria cunninghamii Sweet.	76	10	0.3	0.5	25.4	14.3	2.9	4.1	2.4	0.6	1.5	4.0	–	4.8	12.3	2.5	4.9	4.9	–	5.6	3.3	1.3	4.5	–	–	
Araucaria araucana C. Koch	77	3	1.2	0.4	1.2	15.5	18.8	0.5	0.8	1.3	1.0	4.5	–	8.9	–	30.1	–	0.9	2.6	2.6	1.4	3.9	2.7	1.4	–	–
Araucaria luxurians (Brongn. et Gris) deLaub.	78	10	0.3	–	5.8	21.9	6.9	6.4	–	0.5	1.6	4.0	–	10.4	–	30.2	0.7	2.8	1.1	–	0.6	3.0	0.8	3.3	–	–
Araucaria montana Brongn. et Gris	79	10	0.2	0.3	0.5	7.8	5.3	35.2	0.2	0.3	0.6	1.2	–	2.9	–	11.3	8.9	1.1	15.8	1.8	2.0	1.5	0.5	1.8	–	0.6

(*continued on next page*)

Table 1 (*continued*)

PINOPHYTA Cronquist, Takht. et Zimmerm. ex Reveal		(a)[c]	12:0	14:0	(b)[d]	16:0	16:1 (c)[e]	br-17:0 (d)[f]	16:2 Δ7,10	16:3 Δ7, 10, 13	18:0	18:1 Δ9	18:2 Δ5, 9	18:2 Δ9, 12	18:3 Δ5, 9, 12	18:3 Δ9, 12, 15	18:4 Δ5, 9, 12, 15	20:0	20:1 Δ11	20:2 Δ5, 11	20:2 Δ11, 14	20:3 Δ5, 11, 14	20:4 Δ5, 11, 14, 17	22:0	22:1	(e)[g]
CEPHALOTAXACEAE Neger																										
Cephalotaxus fortunei Hook.	80	2	tr.	3.0	0.9	17.1	1.2	0.9	0.2	3.0	0.8	5.8	–	8.9	–	40.6	tr.	2.4	1.2	1.2	0.5	4.4	4.8	2.4	–	0.6
Cephalotaxus harringtonii (Knight ex Forb.) K. Koch 'Fastigiata'	81	1	tr.	1.4	1.2	19.7	1.1	0.2	0.3	2.8	1.0	4.6	0.4	9.4	1.1	42.8	–	0.8	tr.	0.9	0.2	3.2	4.6	1.2	2.4	0.7
Cephalotaxus harringtonii (Knight ex Forb.) K. Koch var. *harringtonii*	82	3	0.3	0.3	1.3	20.0	1.6	0.4	0.3	2.6	0.8	3.3	–	6.8	tr.	45.9	–	0.6	–	1.0	0.2	3.8	4.7	0.8	2.7	2.4
Cephalotaxus sinensis (Rehd. et E. H. Wilson) Li	83	1	tr.	2.6	0.7	25.5	1.5	–	0.4	1.8	1.6	4.7	–	10.2	–	36.2	–	1.2	–	–	–	5.0	6.8	1.7	–	–
CUPRESSACEAE Rich. ex Bartling																										
Metasequoieae																										20.05
Metasequoia glyptostroboides Hu et Cheng	84	1	3.2	3.2	1.0	15.7	1.7	tr.	0.2	1.7	0.6	1.2	–	6.9	–	54.1	–	0.5	–	0.2	0.2	3.2	3.4	0.6	–	2.6
Sequoieae																										
Sequoia sempervirens (D. Don) Endl.	85	1	11.0	2.9	0.9	12.3	1.4	–	0.7	1.2	0.8	1.1	–	9.0	–	39.1	–	11.2	–	–	0.2	2.8	1.7	3.7	–	–
Sequoiadendron giganteum (Lindl.) Buchholz	86	1	2.8	1.7	0.8	14.0	1.3	tr.	0.3	1.7	1.1	2.7	tr.	14.7	0.6	35.7	–	4.6	–	tr.	0.7	5.9	3.7	7.1	–	0.3
Taxodieae																										
Taxodium distichum (L.) Rich. var. *imbricatum* (Nutt.) Croom	87	1	0.6	0.6	1.0	22.2	1.9	–	–	1.5	1.4	2.8	–	15.2	–	41.3	–	3.5	–	–	–	3.3	2.4	2.2	–	–
Taxodium distichum (L.) Rich. var. *distichum*	88	2	3.0	3.0	1.0	23.6	2.0	0.4	0.4	1.1	2.2	3.7	–	10.5	–	41.8	–	1.5	–	–	–	–	–	1.6	–	4.3
Taxodium mucronatum Ten.	89	1	0.2	2.2	0.2	16.1	2.3	0.8	0.1	1.4	1.3	3.3	–	9.9	–	45.6	–	2.5	–	1.3	–	6.8	4.7	–	–	0.8
Cryptomerieae																										
Cryptomeria japonica (Thunb. ex L.f.) D. Don	90	3	0.4	3.1	1.5	10.0	1.1	1.1	4.9	1.0	1.5	2.3	–	10.2	0.2	23.3	–	8.9	4.1	1.6	10.6	3.2	2.8	3.8	–	4.2
Cunninghamieae																										
Cunninghamia konishii Hayata	91	1	2.1	2.3	1.3	16.5	1.6	0.3	0.3	1.9	0.8	1.2	–	7.2	tr.	47.8	–	1.5	tr.	tr.	0.4	2.4	3.5	7.2	–	1.3
Cunninghamia lanceolata (Lamb.) Hook.	92	1	0.9	0.9	1.2	16.3	2.2	0.2	0.3	2.0	1.0	1.1	–	8.8	–	52.3	tr.	1.9	–	–	–	6.5	4.2	–	–	–
Athrotaxeae																										
Athrotaxis laxifolia Hook.	93	1	0.9	0.9	3.2	17.3	0.6	0.6	0.4	0.5	1.0	1.3	tr.	10.0	0.3	35.0	tr.	8.0	0.2	0.2	0.4	4.6	4.2	9.4	–	0.5
Taiwania cryptomerioides Hayata	94	1	1.3	1.3	1.0	17.2	1.7	0.3	0.2	2.8	0.8	1.5	–	16.7	–	38.4	–	1.5	tr.	tr.	0.3	1.6	4.2	8.6	–	0.4
Cupressoideae																										
Cupressus bakerii Jeps.	95	1	1.4	1.4	0.9	15.6	1.8	0.9	0.5	3.9	1.6	2.5	0.2	16.9	tr.	31.9	tr.	2.7	0.2	0.8	0.9	8.0	4.6	2.0	0.5	0.6
Cupressus dupreziana A. Camus	96	1	1.3	3.1	1.3	16.6	1.2	0.6	0.3	0.7	1.3	3.5	–	17.1	0.4	37.8	–	1.1	0.5	0.4	0.3	5.2	2.6	4.0	–	0.9
Cupressus funebris Endl.	97	2	3.3	2.4	1.0	13.9	1.5	0.9	1.8	2.7	1.4	6.1	–	6.9	–	28.9	–	–	3.6	–	2.2	4.5	5.0	11.4	–	2.4
Cupressus goveniana Gord. var. *goveniana*	99	1	3.1	3.1	1.1	15.5	2.7	1.2	0.3	2.5	1.7	3.4	0.6	15.4	0.6	28.3	1.6	4.6	tr.	tr.	0.8	5.5	3.0	2.2	–	2.6
Cupressus lusitanica Mill.	98	2	1.1	1.3	1.1	15.8	1.6	0.9	0.8	2.5	1.7	4.9	1.8	16.7	–	30.7	–	1.4	0.2	tr.	tr.	5.7	2.4	4.0	4.2	1.0

(*continued on next page*)

Table 1 (*continued*)

PINOPHYTA Cronquist, Takht. et Zimmerm. ex Reveal		(a)[c]	12:0	14:0	(b)[d]	16:0	16:1 (c)[e]	br-17:0 (d)[f]	16:2 Δ7,10	16:3 Δ7, 10, 13	18:0	18:1 Δ9	18:2 Δ5, 9	18:2 Δ9, 12	18:3 Δ5, 9, 12	18:3 Δ9, 12, 15	18:4 Δ5, 9, 12, 15	20:0	20:1 Δ11	20:2 Δ5, 11	20:2 Δ11, 14	20:3 Δ5, 11, 14	20:4 Δ5, 11, 14, 17	22:0	22:1	(e)[g]
Cupressus sempervirens L.	100	3	3.9	1.0	0.8	15.8	1.1	0.6	0.3	2.0	1.5	2.6	0.4	20.1	–	32.1	–	2.5	–	0.2	0.4	4.4	3.3	5.8	–	1.4
Cupressus torulosa D. Don	101	1	0.3	2.3	0.2	14.5	1.3	0.2	0.3	3.3	1.1	1.7	–	12.0	–	33.3	0.2	2.9	2.2	5.3	1.6	6.9	2.9	7.5	–	–
Chamaecyparis lawsoniana (A. Murr.) Parl.	102	2	tr.	4.3	1.1	11.6	11.0	3.0	1.5	2.3	1.1	1.4	–	10.0	0.2	28.3	0.9	10.7	–	–	1.7	4.9	2.0	3.6	–	0.5
Chamaecyparis pisifera (Sieb. et Zucc.) Endl. 'Boulevard'	118	3	4.1	4.1	2.3	11.6	3.6	0.4	0.3	1.8	1.2	1.6	0.3	9.5	–	34.4	1.1	5.4	0.6	1.3	1.3	4.7	3.6	5.2	–	1.7
x *Cupressocyparis notabilis* A. F. Mitchell	103	1	2.6	2.6	2.3	17.3	1.9	0.9	0.2	3.5	1.5	2.7	0.2	16.0	0.2	30.8	tr.	1.7	tr.	0.2	0.4	6.6	4.1	3.5	–	0.7
x *Cupressocyparis ovensii* A. F. Mitchell	104	1	tr.	1.1	–	12.5	0.2	4.7	0.3	2.0	1.2	2.6	tr.	18.2	–	22.4	2.7	2.7	2.6	0.5	1.1	9.8	4.6	6.8	2.2	1.8
Fokienia hodginsii (Dunn) A. Henry et H. H. Thomas	105	8	2.5	0.3	1.4	13.0	0.8	–	1.0	0.7	2.1	6.8	–	11.1	3.3	25.2	–	14.2	–	0.7	–	3.4	3.2	10.5	–	-
Thujoideae																										
Austrocedrus chilensis (D. Don) Pic. Serm. et Bizzarri	116	1	3.3	2.2	1.8	20.8	1.3	0.4	0.4	1.7	1.3	2.2	–	12.7	–	23.0	–	9.1	tr.	0.2	0.5	5.2	3.6	9.8	–	0.5
Calocedrus decurrens (Torr.) Florin	106	1	tr.	2.2	1.1	11.4	0.5	–	1.5	3.8	1.1	2.6	–	10.4	–	27.0	–	13.2	1.4	–	8.5	–	4.0	10.1	–	–
Calocedrus decurrens (Torr.) Florin 'Aureovariegata'	107	1	3.0	1.5	0.5	10.1	0.9	0.2	0.3	1.9	0.7	2.1	–	7.7	–	25.1	–	12.0	4.4	3.1	1.4	4.1	4.5	12.7	–	3.9
Thuja koraiensis Nakai	108	1	6.1	10.9	4.0	11.8	8.9	0.3	tr.	0.9	1.0	1.6	–	13.8	–	20.9	0.2	2.2	1.4	0.9	1.2	6.4	3.1	3.9	–	0.4
Thuja occidentalis L.	109	3	tr.	1.1	1.3	14.9	2.0	0.5	0.3	2.2	0.9	2.3	–	14.8	–	27.4	–	5.5	1.7	–	4.6	5.6	3.4	9.6	–	0.4
Platycladus orientalis (L.) Franco	110	3	4.8	3.0	2.2	12.6	1.4	0.7	0.2	2.9	1.0	2.9	–	12.1	0.9	31.8	–	5.5	–	tr.	0.5	5.9	4.0	7.2	–	0.3
Thuja plicata Donn ex D. Don	111	2	0.4	2.1	2.8	15.3	1.5	1.0	0.8	0.8	1.1	2.4	–	12.5	–	32.0	1.1	3.0	2.6	–	–	6.1	4.2	9.2	–	1.2
Thuja standishii (Gord.) Carr.	112	1	0.5	2.8	6.8	12.3	9.0	2.2	0.4	5.4	0.9	1.3	tr.	11.1	–	28.5	tr.	2.2	1.5	0.9	0.7	4.2	3.6	4.7	–	0.5
Thujopsis dolabrata (Thunb. ex L. f.) Sieb. et Zucc.	113	1	1.9	1.9	4.8	11.7	7.6	0.7	tr.	1.1	0.6	0.9	tr.	9.6	–	29.0	–	4.2	0.2	0.2	0.3	3.4	2.9	18.3	–	–
Microbiota decussata Kom.	123	1	23.0	14.5	2.8	6.6	6.9	0.6	0.8	1.3	1.5	1.5	0.9	9.7	–	12.7	–	1.5	1.2	–	2.0	6.9	1.8	1.4	–	2.4
Callitroideae																										
Callitris preissii Miq.	114	1	5.1	5.1	1.0	15.2	0.7	0.6	0.6	2.4	1.5	3.2	–	9.8	1.1	37.9	–	0.3	–	0.3	0.3	2.4	2.5	9.9	–	–
Diselma archeri Hook. f.	115	9	1.8	2.3	0.9	22.1	1.5	0.5	tr.	1.3	1.8	6.1	tr.	12.6	tr.	26.0	1.2	4.7	0.9	–	tr.	5.2	4.1	6.3	–	–
Tetraclinis articulata (Vahl) Mast.	117	1	4.4	4.4	0.6	12.5	0.8	0.4	0.3	1.6	2.0	4.2	–	7.9	–	28.8	–	8.5	–	0.9	0.3	–	0.9	20.2	–	1.3
Widdringtonia schwarzii Mast.	122	7	3.1	0.5	0.4	14.9	2.6	1.9	–	1.0	2.0	4.3	–	8.9	–	33.0	–	7.8	–	0.7	–	4.2	3.4	9.9	1.4	–
Juniperoideae																										
Juniperus communis L.	119	3	0.6	0.5	1.3	12.6	–	1.7	0.3	1.0	2.6	5.2	–	10.9	–	21.3	1.8	8.6	1.4	1.1	15.7	3.6	3.1	4.7	–	2.1
Juniperus chinensis L. 'Pfitzeriana' Spaeth.	120	3	4.7	4.7	0.7	12.9	1.1	0.6	0.3	1.7	1.2	2.9	0.6	8.9	0.2	22.7	0.4	8.2	tr.	tr.	0.8	7.4	5.6	10.6	1.6	1.6
Juniperus sabina L.	121	3	4.0	2.0	2.3	19.0	5.9	0.9	0.3	1.1	1.4	2.5	0.2	7.8	0.3	24.2	–	4.0	–	–	–	4.1	4.7	8.4	–	6.8
TAXACEAE Gray																										
Torreyeae																										
Torreya californica Torr.	124	1	1.4	1.4	1.5	18.0	1.5	0.5	1.1	3.8	2.1	2.8	tr.	13.1	0.4	35.5	–	2.8	0.2	0.3	0.8	6.1	3.7	2.9	–	–
Taxeae																										
Taxus baccata L.	125	3	0.4	0.4	1.8	17.9	0.8	0.6	0.2	3.3	0.6	6.8	–	9.5	tr.	43.7	–	0.5	0.2	0.7	0.4	4.4	5.3	1.6	–	0.7
Taxus baccata L.	126	2	0.6	2.8	1.0	25.9	0.9	3.5	–	4.1	1.8	4.5	–	8.1	–	25.6	–	4.1	–	–	–	4.3	2.6	10.2	–	–
Taxus baccata L. 'Lutea'	127	3	–	1.1	1.3	19.7	0.9	1.9	0.4	4.1	0.9	6.7	0.2	13.4	0.4	35.7	–	0.5	tr.	0.3	0.4	3.3	5.0	1.0	–	2.7

(*continued on next page*)

Table 1 (*continued*)

PINOPHYTA Cronquist, Takht. et Zimmerm. ex Reveal		(a)[c]	12:0	14:0	(b)[d]	16:0	16:1 (c)[e]	br-17:0 (d)[f]	16:2 Δ7,10	16:3 Δ7, 10, 13	18:0	18:1 Δ9	18:2 Δ5, 9	18:2 Δ9, 12	18:3 Δ5, 9, 12	18:3 Δ9, 12, 15	18:4 Δ5, 9, 12, 15	20:0	20:1 Δ11	20:2 Δ5, 11	20:2 Δ11, 14	20:3 Δ5, 11, 14	20:4 Δ5, 11, 14, 17	22:0	22:1	(e)[g]
Taxus baccata L. 'Fastigiata' Loud.	128	3	tr.	0.2	1.3	19.3	1.8	0.5	0.3	4.1	0.7	3.7	tr.	7.3	tr.	44.7	–	0.4	–	1.6	tr.	3.5	4.3	0.9	3.9	1.1
Taxus brevifolia Nutt.	129	1	0.1	1.1	0.7	14.1	0.8	0.3	0.2	9.5	0.3	2.4	0.1	5.4	0.3	52.1	0.3	2.5	0.9	1.3	0.6	2.5	3.3	1.4	–	–
Taxus cuspidata Sieb. et Zucc.	130	1	0.7	1.0	1.1	17.6	0.7	0.4	0.3	3.4	0.7	4.4	tr.	9.9	0.2	40.2	0.4	1.8	0.2	0.7	0.4	5.8	6.8	3.1	–	0.2
GNETALES																										
EPHEDRACEAE Dumortier																										
Ephedra chilensis Presl	131	1	–	0.6	1.0	15.2	0.9	–	0.2	0.3	1.2	6.2	1.0	29.8	0.2	29.8	0.6	0.9	0.4	0.8	0.7	3.3	2.3	2.5	–	2.3
Ephedra distachya L.	132	3	0.5	0.7	0.4	20.1	1.2	–	–	0.6	3.3	7.6	–	27.7	tr.	28.4	–	1.7	–	tr.	1.2	3.4	0.8	2.1	–	0.5
Ephedra equisetina Bunge	133	1	0.4	0.4	0.9	15.4	1.0	–	0.3	0.3	1.5	4.3	5.4	16.6	1.3	37.6	1.2	1.8	0.6	1.0	1.1	3.1	3.5	2.0	–	0.4
Ephedra fragilis Desf.	134	2	0.5	0.4	1.4	18.0	1.5	–	–	0.6	2.2	7.5	1.0	16.7	–	43.2	0.3	0.9	–	1.0	–	–	1.2	1.2	1.8	1.7
Ephedra gerardiana Wall. ex C. A. Mey.	135	1	–	0.9	0.6	17.9	0.7	–	0.5	0.4	2.3	7.0	tr.	19.3	tr.	37.5	0.3	1.4	0.2	0.2	0.9	4.2	2.5	3.1	–	–
GNETACEAE Lindl.																										
Gnetum gnemon L.	136	11	1.1	0.3	1.0	17.0	0.9	0.5	–	0.4	3.2	8.2	1.1	2.8	4.2	29.9	3.5	10.9	–	0.7	–	1.6	12.9	–	–	–
WELWITSCHIACEAE Markgraf																										
Welwitschia mirabilis Hook. f.	137	5	0.4	1.0	1.1	23.9	1.7	0.4	1.2	0.5	1.9	11.7	–	7.6	–	45.6	–	0.9	0.9	–	0.3	–	–	0.4	–	0.4
GYMNOSPERM OILS																										
Pinus sylvestris L.		13	–	tr.	–	3.4	0.2	tr.	–	tr.	1.9	15.9	2.8	44.1	20.7	0.4	tr.	0.6	1.2	0.6	1.1	6.5	–	0.3	–	–
Fokienia hodginsii (Dunn) A. Henry et H. H. Thomas		13	1.4	–	–	6.0	1.5	–	–	1.5	3.0	10.2	–	29.0	0.2	36.5	3.2	2.3	0.8	1.0	0.4	0.6	1.2	–	1.0	–
Austrocedrus chilensis (D.Don) Pic. Serm. et Bizzarri		13	–	–	–	5.4	–	–	tr.	–	1.6	16.3	–	30.2	–	29.3	1.1	0.3	1.5	1.0	1.5	3.1	8.4	tr.	tr.	–
Prumnopitys andina (Poepp. ex Endl.) de Laub.		13	tr.	–	–	5.6	tr.	–	–	–	3.9	32.9	–	30.3	–	0.2	0.3	0.8	2.4	0.9	5.7	15.6	1.3	–	–	–
Taxus chinensis (Pilg.) Rehd.		13	–	tr.	–	3.2	–	–	–	–	1.0	34.0	16.8	33.5	3.5	2.1	0.4	0.2	1.6	0.3	0.7	2.5	0.2	–	–	–

[a] –: Not detected.

[b] tr.: Trace, percentage less than 0.05%.

[c] (a): Origin of gymnosperm leaves: (1): Arboretum of Chèvreloup (Muséum National d'Histoire Naturelle, Paris, France); (2): Botanical garden of Bordeaux (France); (3): Botanical garden of Talence (France); (4): Provided by Mr. Bernard Bouet (Parc Floral Phoenix de Nice, France); (5): Botanical garden Les Cèdres (Saint-Jean-Cap-Ferrat, France); (6): Arboretum of Barres (Nogent-sur-Vernisson, France); (7): Villa Thuret (INRA Antibes, France); (8): Botanical garden of Nancy (France); (9): Botanical garden of Brest (France); (10): Bocca alla Leccie San Nicolao (Corse, France); (11): National Botanic Garden of Belgium (Domain of Bouchout, Meise); (12): Maymou tree nursery (Bayonne, France); (13): Gymnosperm oils are provided by Dr. Robert L. Wolff (University Bordeaux 1, France).

[d] (b): Undetermined short chain fatty acid eluting just before 16:0 acid (probably 15:0 or branched 15:0).

[e] (c): Sum of the *cis*-Δ7 and the *trans*-Δ3 C_{16} fatty acids.

[f] (d): Anteiso C_{17} fatty acid (14-methylhexadecanoic acid).

[g] (e): Undetermined very long chain fatty acid.

detected in different genera of Pinaceae (*Pinus, Picea, Pseudotsuga, Abies, Cedrus, Keteleeria*) and in Cupressaceae (*Thujopsis, Tetraclinis*). The various elongation products of oleic (C18:1), linoleic (C18:2) and linolenic (C18:3) acids — namely *all cis*-Δ11–20:1 (gondoic), *all cis*-Δ11, 14–20:2 (bishomo-linoleic) and *all cis*-Δ11, 14, 17–20:3 (bishomo-a-linolenic) acids, respectively — were also detected. In addition, *Welwitschia mirabilis* leaves contained two undetermined fatty acids (probably with 16 carbon atoms) eluted just before and after C16:3. These fatty acids represented 2.4 and 2.0% of the total fatty acids, respectively.

Our study also focused on the presence or the absence of *all cis*-Δ7, 10, 13-hexadecatrienoic acid (C16:3) in gymnosperm leaves. The presence of this fatty acid in leaves of some angiosperms (called "16:3 plants") indicates the existence of a "prokaryotic" galactolipid biosynthesis pathway which is probably inherited from cyanobacteria (for review see Browse and Somerville, 1991). In "16:3 angiosperms" (e.g. *Arabidopsis thaliana*, spinach, tomato), the content in 16:3 fatty acid can account for 17% of total fatty acids as it was observed for example in Apiaceae leaves (e.g. Rullkötter et al., 1975; Mongrand et al., 1998; Mongrand, 1998). Table 1 shows that the percentage of 16:3 fatty acid in gymnosperm leaves never reached the values obtained with photosynthetic tissues of "16:3" angiosperms. In gymnosperms, the highest levels of C16:3 were detected in *Ginkgo biloba*, *Larix laricina*, *Thuja standishii* and *Taxus brevifolia* (4.5, 4.4, 5.4 and 9.5%, respectively), but in most cases this fatty acid represented only around 0.5-3% of the total fatty acids.

2.2. Fatty acid composition of leaf gymnosperm galactolipids

The fatty acid composition of the two main leaf lipids digalactosyldiacylglycerol (MGD) and monogalactosyldiacylglycerol (DGD) from 14 gymnosperm species was then determined. Results are shown in Table 2. It was found that C16 and C18 poly-unsaturated *omega* 3 fatty acids (C16:3, C18:3) could reach 75% of the total fatty acids associated with galactolipids. However as already noted by Jamieson and Reid (1972), the amount of polyunsaturated fatty acids was slightly lower in gymnosperm than in angiosperm tissues. Furthermore, the analysis of the fatty acid composition of gymnosperm galactolipids showed that: (i) only small amounts of both long- and short-chain fatty acids and of Δ5-olefinic acids were esterified to galactolipids; (ii) C16:3 fatty acid levels were higher in MGD than in DGD; (iii) As in angiosperm leaves, DGD from gymnosperm photosynthetic tissues contained a large amount of palmitic acid (C16:0), probably esterified to the *sn*-1 position of the glycerol backbone (Roughan and Slack, 1982). However, MGD from some gymnosperm leaves also contained a high amount of palmitic acid, in contrast with that was observed in angiosperm tissues

Another difference with angiosperms appeared when the mass of both of the galactolipids was calculated from that of each fatty acid determined by gas chromatography. In gymnosperms, the ratio MGD/DGD varied from 0.28 to 1.52, so in some species, the amount of DGD is higher than that of MGD (Table 2). In *Cupressus dupreziana* and *C. bakerii* (Cupressaceae), DGD was 3-fold more concentrated than MGD. These results underline an originality of gymnosperms since unlike in angiosperm leaves, the amount of DGD does not exceed that of MGD (Roughan and Batt, 1969).

2.3. Multivariate analyses

A statistical analysis was performed to try to separate the orders and the families within the gymnosperm phylum by using only the 137 fatty acid compositions determined in this study (see Experimental). Thereafter, to obtain more details within a given family, the statistical analysis was performed for the 44 taxa of Pinaceae. Although the data on the types and distribution of fatty acids did not provide an unequivocal guide to the classification of plants, many correlations of taxonomic significance became apparent.

Principal component analysis (PCA) applied to the whole series of gymnosperms was carried out after ruling out *Araucaria montana* (see Experimental). The results show that the first two axes explain 25.4 and 11.1% of the total variation. Although these percentages are low, the analysis provides a global statistical distinction between four groups (Fig. 2): the first includes the Ginkgoaceae, Cycadaceae, Stangeriaceae, Zamiaceae, Sciadopityaceae, Podocarpaceae, Cephalotaxaceae, Taxaceae, Ephedraceae and Welwitschiaceae; the second contains most of the Araucariaceae and Cupressaceae. Both of the other groups contain the Pinaceae species with the genus *Larix* in group 3, and the genera *Abies* and *Cedrus* in group 4. *Gnetum gnemon* is in group 3, not far from the Ephedraceae. Groups 1 and 4 are separated by axis 1 and groups 2 and 3 by axis 2. It must be noted that the statistical analysis clearly shows that the variables associated with *all cis*-Δ5, 9–18:2, *all cis*-Δ5, 9, 12–18:3 and *all cis*-Δ; 5, 9, 12, 15–18:4 are strongly correlated, that can reflect a likely common metabolic pathway of these fatty acids. Nevertheless, our results did not allow us to conclude whether a specific C18 or C20 Δ5 desaturase is responsible for the synthesis of the very long chain Δ5 fatty acids, or whether the very long chain fatty acids were first synthesized before to be desaturated.

In Fig. 2, it appeared that (i) all seven of the eight genera of Zamiaceae (*Chigua* was not studied) belong to the statistical group 1, which underlines a very homogeneous leaf fatty acid composition in this family. In

Table 2
Fatty acid composition of galactolipids of gymnosperm leaves. All resuls are in duplicate

		14:0	(a)[c]	16:0	16:1 (b)[d]	br-17:0 (c)[e]	16:2	16:3	18:0	18:1 Δ9	18:2 Δ9, 12	18:3 Δ9, 12, 15	20:0	20:4 Δ5, 11, 14, 17	22:0	MGD/DGD
Ginkgo biloba L.	MGD	0.5	1.5	4.5	0.9	–[a]	–[a]	9.8	0.7	1.5	1.0	76.6	0.6	0.4	1.9	1.33
	DGD	0.5	1.4	25.0	0.5	–[a]	0.8	2.1	3.4	3.0	2.4	58.0	0.5	0.7	0.9	
Cycas revoluta Thunb.	MGD	0.5	1.4	3.9	5.5	–[a]	–[a]	9.3	0.9	1.3	13.6	61.8	0.8	–[a]	1.0	1.52
	DGD	0.6	1.7	19.2	1.7	–[a]	2.3	1.3	3.4	3.0	14.9	47.8	2.3	0.3	1.4	
Zamia furfuracea L. f. in Ait.	MGD	0.2	2.4	4.3	4.6	2.0	–[a]	4.3	1.3	1.1	3.7	70.3	–[a]	1.9	3.9	1.28
	DGD	0.5	1.2	23.1	3.3	–[a]	–[a]	–[a]	5.1	3.8	7.1	48.4	0.9	1.6	1.8	
Pinus cembra L.	MGD	0.7	3.1	4.4	4.8	–[a]	–[a]	15.9	8.1	–[a]	7.5	41.0	8.9	–[a]	5.5	0.75
	DGD	0.8	2.4	13.8	4.8	–[a]	2.4	2.5	4.1	3.7	8.6	49.8	4.6	–[a]	2.5	
Pinus halepensis Mill.	MGD	0.4	1.7	3.5	1.7	–[a]	–[a]	13.0	1.0	1.5	2.7	69.9	2.7	–[a]	1.9	0.95
	DGD	0.4	1.6	18.1	1.1	–[a]	1.4	4.8	3.3	2.8	6.2	57.3	3.0	–[a]	–[a]	
Larix sibirica Ledeb.	MGD	2.4	6.2	11.1	6.2	–[a]	–[a]	8.0	3.1	4.7	2.7	40.2	8.9	2.3	4.2	0.71
	DGD	1.4	4.2	17.4	3.0	–[a]	–[a]	3.3	3.4	2.8	2.5	54.3	4.5	–[a]	3.3	
Cedrus deodara (Roxb.) G. Don	MGD	0.5	1.9	4.1	1.4	–[a]	–[a]	5.3	0.7	1.1	2.4	78.1	2.1	0.3	2.0	1.45
	DGD	0.7	2.2	22.0	2.0	–[a]	1.0	2.0	2.0	1.9	4.1	54.4	4.4	2.9	0.6	
Prumnopitys andina (Poepp. ex Endl.) de Laub.	MGD	1.7	2.1	11.1	–[a]	2.2	–[a]	2.0	2.7	2.1	4.4	68.7	2.9	–[a]	–[a]	0.60
	DGD	1.1	0.8	25.7	0.9	0.6	–[a]	–[a]	2.8	1.7	4.4	58.0	0.9	2.8	0.2	
Cephalotaxus harringtonii (Knight ex Forb.) K. Koch 'Fastigiata'	MGD	1.1	3.2	4.7	–[a]	–[a]	–[a]	6.4	1.1	2.3	1.5	62.8	5.0	7.2	4.8	0.41
	DGD	0.4	1.0	24.5	1.7	0.5	0.5	2.0	1.1	3.4	2.8	59.4	0.4	1.2	1.2	
Cupressus bakerii Jeps.	MGD	1.5	6.7	8.4	2.6	–	–[a]	8.4	1.8	3.9	7.9	44.5	6.7	1.4	6.4	0.33
	DGD	0.5	1.9	17.0	2.6	–[a]	–[a]	4.5	1.8	1.7	6.5	60.4	1.9	–[a]	1.2	
Cupressus dupreziana A. Camus	MGD	–[a]	–[a]	22.3	–[a]	–[a]	–[a]	–[a]	7.9	7.1	6.1	56.6	–[a]	–[a]	–[a]	0.28
	DGD	–[a]	–[a]	19.7	–[a]	–[a]	–[a]	–[a]	2.5	1.9	2.8	73.0	–[a]	–[a]	–[a]	
Taxus brevifolia Nutt.	MGD	1.5	4.1	7.3	1.6	–[a]	–[a]	7.0	1.7	2.6	2.7	62.7	3.8	–[a]	4.9	0.52
	DGD	0.7	1.7	18.7	2.4	–[a]	–[a]	2.1	1.3	2.1	3.0	60.2	2.4	1.5	3.9	
Ephedra chilensis Presl	MGD	1.0	3.0	3.6	–[a]	–[a]	–[a]	–[a]	1.5	3.3	7.7	73.2	4.4	–[a]	2.3	0.46
	DGD	0.5	1.3	14.1	–[a]	–[a]	tr.[b]	–[a]	3.3	3.7	8.2	65.6	1.7	–[a]	1.2	
Welwitschia mirabilis Hook. f.	MGD	0.8	0.8	7.5	–[a]	1.5	–[a]	–[a]	1.9	3.7	7.4	76.3	–[a]	–[a]	–[a]	0.85
	DGD	1.0	0.5	23.6	–[a]	0.4	–[a]	–[a]	2.4	11.2	8.1	50.2	1.7	–[a]	0.9	

[a] – : Not detected.
[b] tr. : Trace, percentage less than 0.05%.
[c] (a): Undetermined short chain fatty acid eluting just before 16:0 acid (probably 15:0 or branched15:0).
[d] (b): Sum of the *cis*-Δ7 and the *trans*-Δ3 C_{16} fatty acids.
[e] (c): Anteiso C_{17} fatty acid (14-methylhexadecanoic acid).

addition, their content in Δ7, 10, 13–16:3 is low contrary to the neighboring Cycadaceae family; (ii) the separation of the Pinaceae, an exclusively northern family, from other conifers is in good agreement with the multivariate analyses of the fatty acid composition of seed oils (Imbs and Pham, 1996; Wolff et al., 1997b) and with results obtained after comparison of 18S rRNA sequence data (Chaw et al., 1995); (iii) The Podocarpaceae, a morphologically and ecologically very diverse family, appears homogeneous in view of the leaf fatty acid composition. These results are in agreement with the comparison of 18S rDNA sequence data which support the monophyly of Podocarpaceae (Kelch, 1998); (iv) The species of the cosmopolitan Cupressaceae family *s.l* (i.e. including Taxodiaceae *s. str*. and Cupressaceae *s. str*.) are closely related (Wolff et al., 1997b), and form a monophyletic lineage. According to Brunsfeld et al. (1994) and Stefanovic et al. (1998), Cupressaceae *s. str*. are monophyletic and derive from the Taxodiaceae. Our results do not contradict this view since the Cupressaceae *s. str*. analyzed in this paper belong to group 2 (with the exclusion of some *Cupressus* species). The other genera are distributed between groups 1 and 2. The monotypic *Metasequoia* from eastern Asia clearly belongs to group 1, contrary to the monotypic genera *Sequoia* and *Sequoiadendron* from North western America. These results are not in agreement with data for *rbc*L and *mat*K, which strongly support a clade for these three genera (Brunsfeld et al., 1994; Gadek et al., 1997); (v) Ephedraceae, Gnetaceae and Welwitschiaceae (a monospecific family) together form the order of Gnetales, and the analysis of morphological and ribosomal

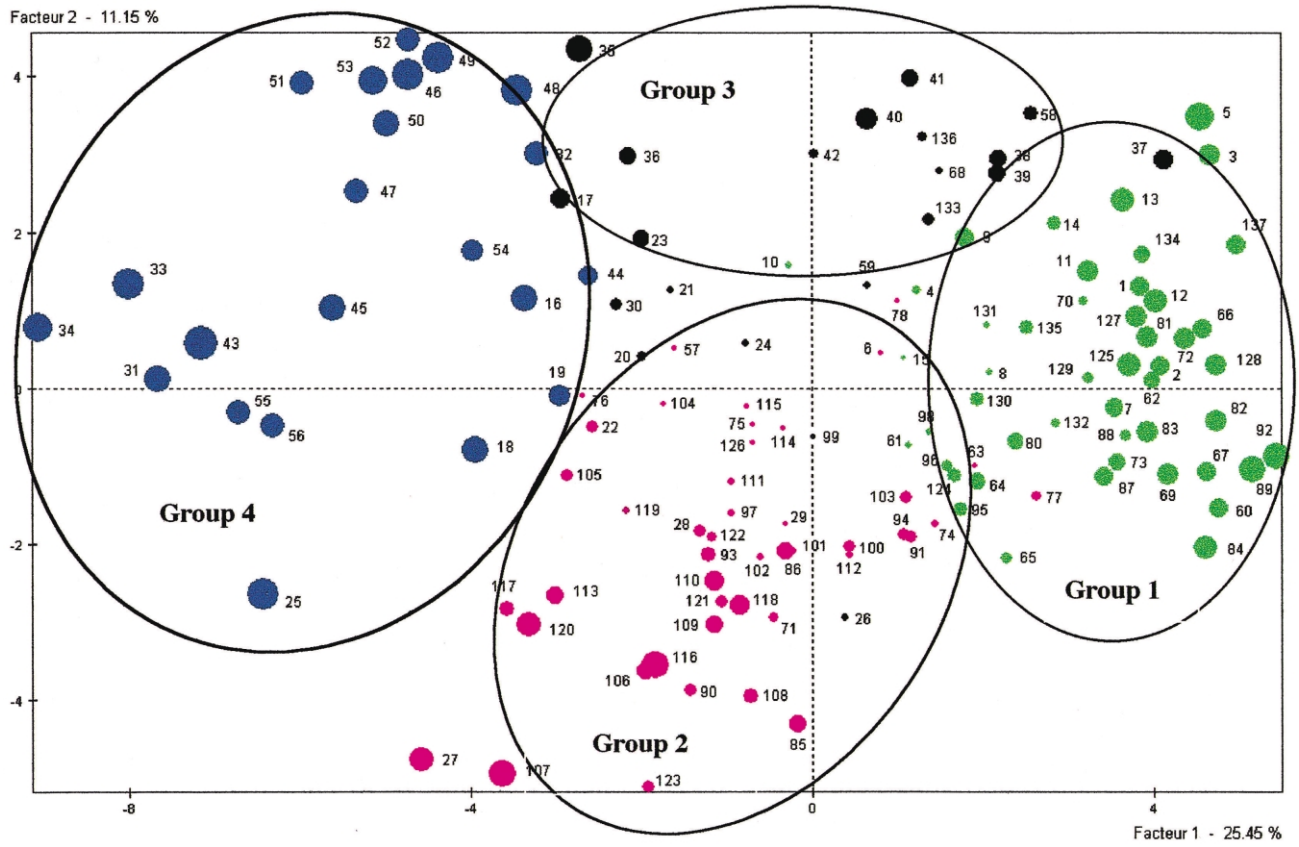

Fig. 2. Principal component and hierarchic analysis of 137 gymnosperm taxa, indexed from 1 to 137 according to Table 1. Four groups were evidenced by the hierarchic analysis. The size of each dot represents the quality of representation.

RNA data shows that these plants can be regarded as the closest living relatives of angiosperms (Doyle et al., 1994). For example, the internal transcribed spacer 1 region of rDNA of *Welwitschia* is the shortest among the Gnetales, so that its length is close to that of the longest one in the angiosperms (Liston et al., 1996). Despite obvious morphological differences, this group is widely regarded as monophyletic (Crane et al., 1995). Nevertheless, the analysis of *rbc*L gene sequences also shows that *Gnetum* and *Welwitschia* are more closely related to each other than either is to *Ephedra* (Hasebe et al., 1992). From our results it appears that the genera *Gnetum* belongs to group 3, whereas *Ephedra* and *Welwitschia* belong to group 1. In addition, both the leaves and seed oil (Aitzetmüller and Vosmann, 1998) of *Welwitschia* do not contain sciadonic and juniperonic acids whereas *Ephedra* species do. Moreover, unlike *Ephedra, Gnetum* and *Welwitschia* seed oils contain cyclopropenoic fatty acid which is known to be present in the angiosperm order Malvales (Aitzetmüller and Vosmann, 1998). Hence it appears that the monophyletic or the polyphyletic origin of Gnetales requires further consideration.

Principal component and discriminant analyses of the 44 Pinaceae taxa were also performed. Results are shown Fig. 3. Because of their very peculiar fatty acid composition, *Pinus pinaster* and *P. palustris* were omitted from these analyses and are shown as illustrative species. Under these conditions, the first and second axes explain 34.7 and 11.9% of the total variation, respectively. The most discriminant variables along axis 1 are 20:0, 22:0, 16:0, 18:0 and *all cis*-Δ7, 10, 13–16:3. Axis 1 clearly discriminates group 1 from the others. Along axis 2, br-17:0, which is at the highest level in the genus *Abies*, makes it possible to discriminate this genus from other Pinaceae. In other words, the analysis allows a clear-cut distinction between three groups: group 1 containing the genera *Larix, Pinus* and some *Picea* species; group 2 strongly clustering the genus *Abies*; and finally group 3 composed of the genera *Picea* and *Cedrus*. These results differ somewhat from those obtained by Wolff et al. (1997b), who carried out a multivariate analysis of the fatty acid composition of 58 Pinaceae seed oils. These authors observed 4 groups: *Cedrus*, *Abies*, *Larix* plus *Picea*, and *Pinus*, this last group including *Tsuga* and *Pseudotsuga*. Except for the genus *Abies,* our results did not make it possible a so-clear distinction; in addition *Larix* and *Picea* in one hand, and *Tsuga* and *Pseudotsuga* in an other hand appeared to be in a closer relationship than that was observed in Wolff et al. (1997b).

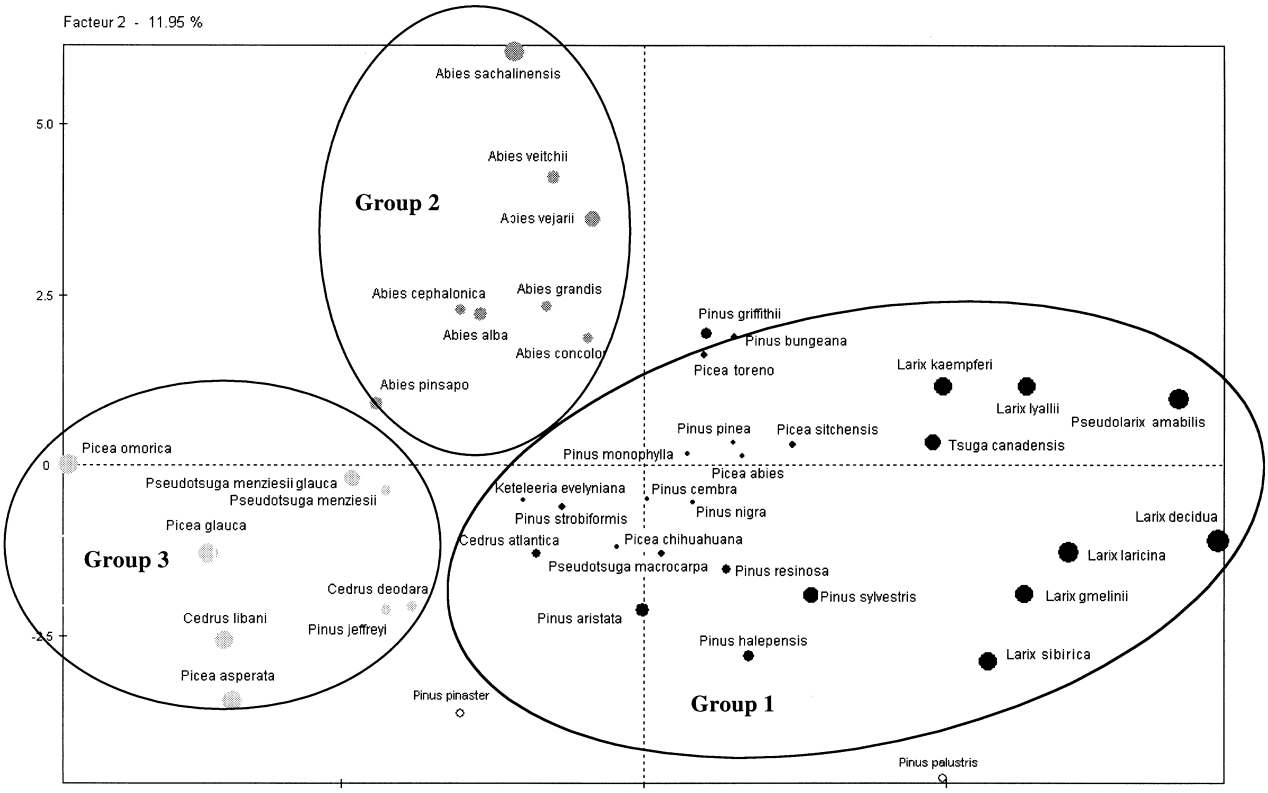

Fig. 3. Principal component and hierarchic analysis of 44 Pinaceae taxa. Three groups were evidenced by the hierarchic analysis. The size of each dot represents the quality of representation.

The Ward hierarchical clustering method — used in the previous two-step statistical analysis (Fig. 3) — is an agglomerative clustering algorithm which starts with n singleton clusters (each consisting of one element of the data set) and merges two clusters on the basis of a similarity measure. Another statistical method — termed "divisive hierarchical clustering method" — was also performed. This method reverses the process of agglomerative clustering by starting with all elements in one cluster (the 44 Pinaceae), and by dividing successively each cluster into two smaller ones, until a suitable stopping rule prevents further divisions (Chavent, 1997, 1998). The divisive clustering method — used to define a 5-cluster partition of the 44 Pinaceae — is closed in a non-supervised context to the segmentation methods (Breiman et al., 1984). During the hierarchy construction, each split is carried out by selecting one single variable (which is selected optimally) and its binary transformation. In the latter case, each cluster is characterized by a conjunction of logical properties both necessary and sufficient for membership in the cluster. An easily interpretable classification is obtained, and the resulting hierarchical tree is the decision tree presented in Fig. 4. This method makes it possible to divide the Pinaceae family into 5 clear-cut classes separating the genera *Larix*/*Pseudolarix* in group 1, *Abies* in group 4, and *Cedrus*/*Pseudotsuga* in group 5. The genera *Pinus* and *Picea* are distributed in groups 2 and 5. *Tsuga* and *Pseudotsuga* are not clustered in the same group and the genus *Keteleeria* is isolated with *Pinus pinea* in group 3.

3. Experimental

3.1. Material

Solvents used were of analytical grade. Thin layer chromatography plates were high-performance TLC (HPTLC) silica-gel 60F254 plates (Merck).

3.2. Plant material

Samples of gymnosperm photosynthetic tissues were collected during spring and summer 1998 from adult plants in the Arboretums of Chèvreloup (Muséum National d'Histoire Naturelle, Paris) and Barres (Nogent-sur-Vernisson, France), in the French botanical gardens of the cities of Bordeaux, Brest, Nancy, San Nicolao and Talence, in the National Botanic Garden of Belgium, in the Botanical garden of Les Cèdres (Saint-Jean-Cap-Ferrat, France), in the Villa Thuret (INRA Antibes, France), in the Maymou tree nursery (Bayonne, France) and in a private collection via Mr. B. Bouet.

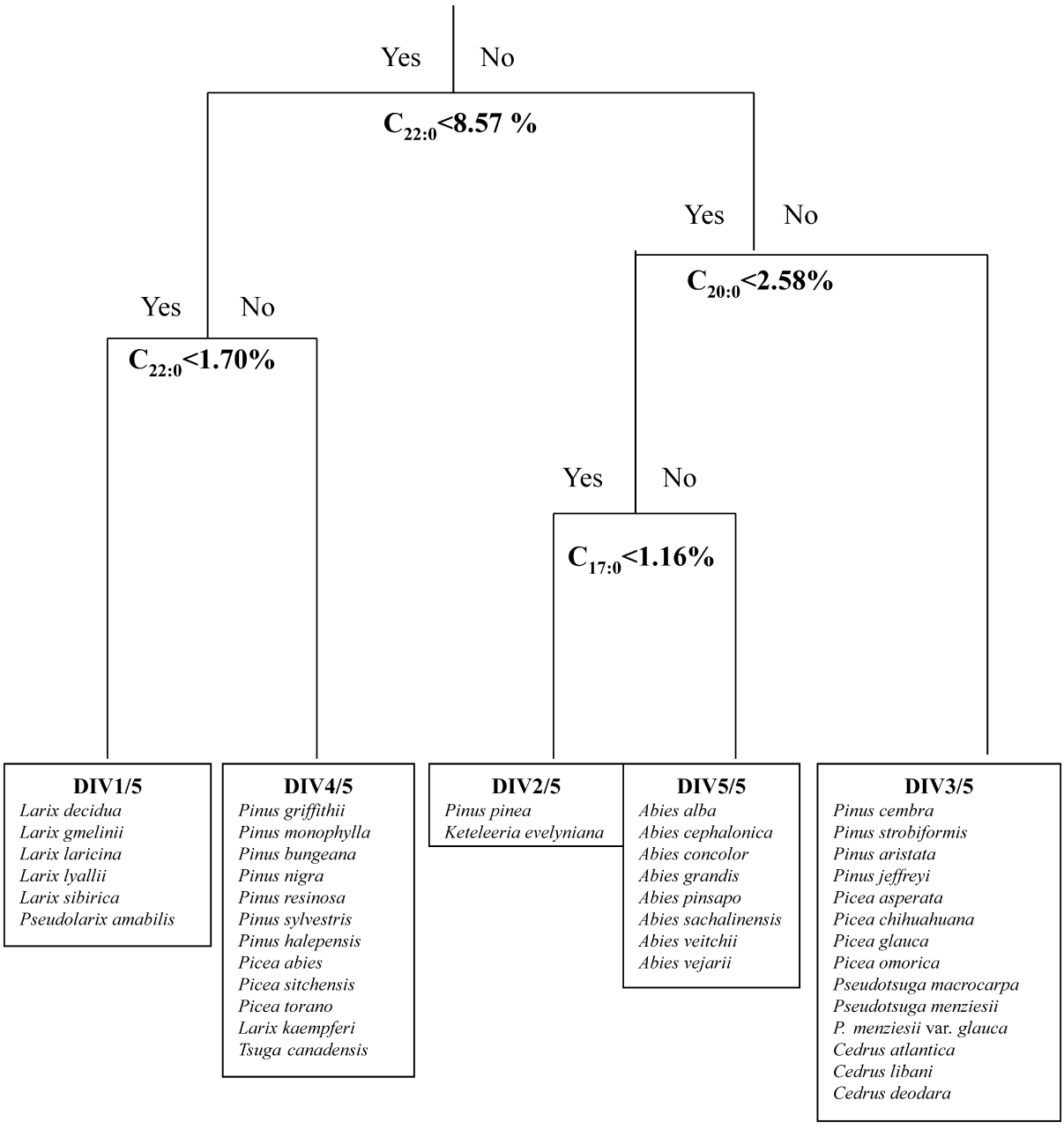

Fig. 4. Divisive hierarchical clustering method performed on the 44 taxa of Pinaceae. This method provides a 5-cluster partition.

3.3. Fatty acid analysis

Fatty acids of gymnosperm leaf lipids were analyzed by GLC after conversion to the corresponding methyl esters. The procedure used was described by Browse et al. (1986) and used hot methanolic H_2SO_4 to digest fresh photosynthetic tissue and simultaneously convert fatty acids of leaf lipids to methyl esters. Samples (approx. 250 mg of fresh tissue) were placed in screw-capped tubes. After addition of 1 ml MeOH, 2.5% H_2SO_4 (v/v), tubes were heated to 80°C for 1 h. After samples were cooled, 500 μl hexane and 1 ml H_2O were added. Fatty acid methyl esters were extracted into hexane by vigorous shaking, then a two-phase system was established by centrifugation (1500 *g*, 10 min). A sample (1 μl) was taken directly from the hexane phase and used for GC analysis on a 15 m×0.53 mm Carbowax column (Altech). The gas chromatograph used (Helwet Packard 5890 series II) was fitted with flame-ionization detector and electronic integrator (Hewlett Packard 3396 series III). The GC was programmed for an initial temp. of 160° for 1 min, followed by a 20° min^{-1} ramp to 190° and a secondary ramp of 5° min^{-1} to 210°. This final temp. was maintained constant for a further 5 min. The retention times of Δ5-olefinic fatty acids were determined by comparison with the well-known fatty acid composition of different gymnosperm

oil seeds: *Pinus sylvestris*, *Fokienia hodginsii*, *Austrocedrus chilensis*, *Prumnopitys andina* and *Taxus chinensis* (Wolff and Bayard, 1995; Wolff et al., 1998; Wolff et al., 1999a,b; Dr. R.L. Wolff, personal communication). Other fatty acid peaks were quantified and identified by comparison of their retention times with standards (Sigma Chemical Co., St. Louis, MO, USA). Because of the very close proximity of the the *cis*-Δ7 and the *trans*-Δ3 C16 peaks which didn't allow us to clearly separate them for all of the analyses carried out, the percentages of C16:1 in Table 1 represents the sum of these two peaks. It can be noted that the differences of C16:1 amount between the various species are mainly due to the *cis*-Δ7 C_{16} fatty acids. Several analyses of the same sample led to similar results. The fatty acid composition of photosynthetic tissue at various stage of development showed no significant differences.

3.4. Analysis of fatty acid galactolipids (MGD, DGD)

Two hundred and fifty milligrams of gymnosperm leaves were harvested and ground at −80°C with 6 ml of $CHCl_3$–MeOH-HCOOH (10:10:1) as described by Miquel and Browse (1992). Tubes were stored overnight at −20°C. The extraction procedure was continued by adding 2.2 ml of $CHCl_3$–MeOH–H_2O (5:5:1). The organic phase was washed with 3 ml of 0.2 M H_3PO_4–1 M KCl (Hajra, 1974). Lipids were recovered in the organic phase, dried and redisolved in 500 μl of $CHCl_3$–MeOH (2:1). Individual lipids were purified from the extracts by monodimensional TLC using the solvent system $CHCl_3$–MeOH–H_2O (65:25:2). To avoid any fatty acid contamination by silica of the TLC plates (mainly oleic and palmitic acids), we used plates previously washed by carrying out a chromatography for 3 h using $CHCl_3$–MeOH (2:1) as solvent. After chromatography, lipids were localized by spraying plates with a solution of 0.01% (w/v) primuline in 80% acetone, followed by visualization under UV light (366 nm). The silica gel zones corresponding to MGD and DGD, determined according to standards, were scraped from the plates and placed in 1 ml of methanolic H_2SO_4 reagent to convert galactolipid fatty acids to methyl esters. The analytical procedure was continued as described above.

3.5. Statistical analyses

Three data sets were studied by a two-step statistical analysis. The first data table is composed of 137 rows corresponding to the 137 plants, and 24 columns corresponding to 24 fatty acids (*Araucaria montana* was omitted during the calculation process because of its very high percentage of br-17:0). Because of the skewness of the distribution of the 24 numeric variables, the Box–Cox transformation $y = (x^a - 1)/a$ was performed on the 24 variables with $a = 1/2$ (Jobson, 1992a). The measurement was stretched and the distribution shapes were more normal-like. A third data table was extracted from this second data table which corresponds to 44 taxa of Pinaceae. The following two-step statistical process was applied to the three data tables: (1) a Principal Component Analysis (PCA) (Hotelling, 1933; Jobson 1992b) was performed, in order to visualize and reduce the dimension of the three data sets; this PCA was non-normalized, so the principal components were computed on the variance-covariance matrix, instead of the usual correlation matrix; (2) the Ward hierarchical clustering methods (Ward, 1963; Jain and Dubes, 1988) were performed on the species described by the 10 first principal components; the 4-cluster partitions were taken into account for each of the three data sets. The results were obtained with the Data Analysis software SPAD (Lebart et al., 1996).

The divisive clustering method (Chavent, 1997, 1998) used to define a 5-cluster partition of the 44 Pinaceae is in a non-supervised context, close to the segmentation methods (Breiman et al., 1984). During the hierarchy construction, each split is carried out by selecting one single variable (which is selected optimally) and its binary transformation. In the latter case, each cluster is characterized by a conjunction of logical properties both necessary and sufficient for membership in the cluster. Results are presented as a hierarchical decision tree.

Acknowledgements

This work was in part supported by the Conseil Régional d'Aquitaine. S.M. was supported by a grant from the Ministère de la Recherche et des Technologies, France. The authors are highly indebted to Dr. Robert L. Wolff (University Bordeaux 1) for helpful discussion and for providing gymnosperm oils. Acknowledgments to Mr. Bernard Bouet (Parc Floral Phoenix, Nice, France), Mr. Elmar Robbrecht (National Botanic Garden of Belgium), Mrs. Suzanne Marnier-Lapostolle (Botanical garden Les Cèdres, Saint-Jean-Cap-Ferrat, France), Mrs. Catherine Ducatillion (Villa Thuret, INRA Antibes, France), to the Arboretums of Chèvreloup (Muséum National d'Histoire Naturelle, Paris) and Barres (Nogent-sur-Vernisson), to the botanical gardens of the cities of Bordeaux, Brest, Nancy, San Nicolao and Talence, to the Maymou tree nursery (Bayonne, France), who kindly provided the samples analyzed in the present study.

References

Aitzetmüller, K., 1996. 30. Seed fatty acids, chemotaxonomy and renewable resources. Oils-Fat-Lipids, Proceedings of the 21st World Congress of the International Society of Fat Research. 1995 Vol. 1, pp. 117–120.

Aitzetmüller, K., Vosmann, K., 1998. Cyclopropenoic fatty acids in gymnosperms: the seed oil of *Welwitschia*. Journal of the American Oil Chemists Society 75 (12), 1761–1765.

Breiman, L., Friedman, J.H., Olshen, R.A., Stone, C.J., 1984. Classification and Regression Trees. Chapman & Hall.

Browse, J., Somerville, C., 1991. Glycerolipid synthesis: biochemistry and regulation. Annual Review of Plant Physiology, Plant Molecular Biology 42, 467–506.

Browse, J., McCourt, P.J., Somerville, C.R., 1986. Fatty acid composition of leaf lipids determined after combined digestion and fatty acid methyl ester formation from fresh tissue. Analytical Biochemistry 152 (1), 141–145.

Brunsfeld, S.J., Soltis, P.E., Soltis, D.E., Gadek, P.A., Quinn, C.J., Strenge, D.D., Ranker, T.A., 1994. Phylogenetic relationships among the genera of Taxodiaceae and Cupressaceae: evidence from *rbc*L sequences. Systematic Botany 19 (2), 253–262.

Chavent, M., 1997. Analyse des données symboliques; une méthode décisive de classification. PhD thesis, Univ. Paris IX-Dauphine.

Chavent, M., 1998. A monothetic clustering method. Pattern Recognition Letters 19, 989–996.

Chaw, S.M., Sung, H.M., Long, H., Zharkikh, A., Li, W.H., 1995. The phylogenetic positions of the conifer genera *Amentotaxus*, *Phyllocladus*, and *Nageia* inferred from 18S rRNA sequences. Journal of Molecular Evolution 41, 224–230.

Crane, P.R., Friis, E.M., Pedersen, K.R., 1995. The origin and early diversification of angiosperms. Nature 374 (6517), 27–33.

Doyle, J.A., Donoghue, M.J., Zimmer, E.A., 1994. Integration of morphological and ribosomal RNA data on the origin of Angiosperms. Annals of Missouri Botantical Garden 81, 419–450.

Earle, C.J., 1999. In: Earle, C.J. (Ed.), Gymnosperm Database. http://www.geocities.com/~earlecj/pinophyta.htm.

Farjon, A., 1998. World Checklist and Bibliography of Conifers. Royal Botanic Gardens, Kew, UK.

Gadek, P., Alpers, D., Quinn, C., 1997. Combined morphological and molecular analysis of Cupressaceae s.l. American Journal of Botany 84 (Suppl. 6), 195–196, Abstract 567.

Grahl-Nielsen, O., Mjaavatten, O., Øvstedal, D.O., 1991. A chemometric comparison between *Picea abies* and *P. obovata* (Pinaceae) in Norway. Nord. J. Bot 11 (6), 613–618.

Hajra, A.K., 1974. Extraction of acyl and alkyl dihydroxyacetone phosphate from incubation mixtures. Lipids 9 (8), 502–505.

Hasebe, M., Ito, M., Kofuji, R., Iwatsuki, K., Ueda, K., 1992. Phylogenetic relationships in Gnetophyta deduced from *rbc*L gene sequences. Botantical Magazing (Tokyo) 105 (1079), 385–391.

Hierro, M.T.G., Robertson, G., Christie, W.W., Joh, Y.G., 1996. The fatty acid composition of the seeds of *Ginkgo biloba*. Journal of the American Oil Chemists Society 73 (5), 575–579.

Hotelling, H., 1933. Analysis of a complex of statistical variables into principal components. Journal of Educational Psychology 24, 417–441.

Imbs, A.B., Pham, L.Q., 1996. Fatty acids and triacylglycerols in seeds of Pinaceae species. Phytochemistry 42 (4), 1051–1053.

Itabashi, Y., Takagi, T., 1982. *Cis*-5-olefinic nonmethylene-interrupted fatty acids on lipids of seeds, arils and leaves of japanese yew. Yakagaku 31, 574–579.

Jain, A.K., Dubes, R.C., 1988. Algorithms for Clustering Data. Prentice Hall, Englewood Cliffs, NJ.

Jamieson, G.R., Reid, E.H., 1972. The leaf lipids of some conifer species. Phytochemistry 11 (1), 269–275.

Jobson, J.D., 1992. Applied Multivariate Data Analysis, Volume I: Regression and Experimental Design. Springer Verlag, Berlin.

Jobson, J.D., 1992. Applied Multivariate Data Analysis, Volume II: Categorical and Multivariate Methods. Springer Verlag, Berlin.

Karunen, P., 1990. Galactolipid fatty acids of bryophytes. Plant Lipid Biochem., Struct. Util., Proc. Int. Symp. Plant Lipids 9, 30–32.

Kelch, D.G., 1998. Phylogeny of Podocarpaceae: comparison of evidence from morphology and 18S rDNA. American Journal of Botany 85, 986–996.

Lebart, L., Morineau, A., Lambert, T., Pleuvret, P., 1996. SPAD version 3. Système pour l'Analyse des données. CISIA, Saint-Mandé.

Liston, A., Robinson, W.A., Oliphant, J.M., Alvarez-Buylla, E.R., 1996. Length variation in the nuclear ribosomal DNA internal transcribed spacer region of non-flowering seed plants. Systematic Botany 21, 109–120.

Miquel, M., Browse, J., 1992. *Arabidopsis* mutants deficient in polyinsaturated fatty acids synthesis. Biochemical and genetic characterization of a plant oleoyl-phosphatidylcholine desaturase. Journal of Biological Chemistry 267, 1502–1509.

Mongrand, S., 1998. De l'origine des lipides chloroplastiques eucaryotiques. Etude in vivo. Distribution dans le règne végétal des lipides procaryotiques plastidiaux. PhD thesis, Univ. Bordeaux 2.

Mongrand, S., Bessoule, J.J., Cabantous, F., Cassagne, C., 1998. The C16:3/C18:3 fatty acid balance in photosynthetic tissues from 468 plant species. Phytochemistry 49, 1049–1064.

Roughan, P.G., Batt, R.D., 1969. The glycerolipid composition of leaves. Phytochemistry 8, 363–369.

Roughan, P.G., Slack, C.R., 1982. Cellular organization of glycerolipid metabolism. Annual Review Plant Physiology 33, 97–132.

Rullkötter, J., Heinz, E., Tulloch, A.P., 1975. Combination and positional distribution of fatty acids in plant digalactosyl diglycerides. Zeitschrift für Pflanzenphysiologie 76 (2), 163–175.

Stefanovic, S., Jager, M., Deutsch, J., Broutin, J., Masselot, M., 1998. Molecular phylogeny of conifers based on 28S rDNA gene sequences. American Journal of Botany 85 (Suppl. 6), 159, Abstract 459.

Vickery, J.R., Whitfield, F.B., Ford, G.L., Kennett, B.H., 1984. The fatty acid composition of Gymnospermae seed and leaf oils. Journal of the Americal Oil Chemists Society 61, 573–575.

Ward, J.H., 1963. Hierarchical grouping to optimize an objective function. Journal of the American Statistical Association 58, 236–244.

Wolff, R.L., Bayard, C.C., 1995. Fatty acid composition of some pine seed oils. Journal of the American Oil Chemists Society 72, 1043–1046.

Wolff, R.L., Deluc, L.G., Marpeau, A.M., 1996. Conifer seeds: oil content and fatty acid composition. Journal of the American Oil Chemists Society 73, 765–771.

Wolff, R.L., Christie, W.W., Coakley, D., 1997a. The unusual occurrence of 14-methylhexadecanoic acid in Pinaceae seed oils among plants. Lipids 32, 971–973.

Wolff, R.L., Deluc, L.G., Marpeau, A.M., Comps, B., 1997b. Chemotaxonomic differentiation of conifer families and genera based on the seed oil fatty acid compositions: multivariate analyses. Trees 12, 57–65.

Wolff, R.L., Comps, B., Marpeau, A.M., Deluc, L.G., 1997c. Taxonomy of *Pinus* species based on the seed oil fatty acid compositions. Trees 12, 113–118.

Wolff, R.L., Pédrono, F., Marpeau, A.M., Christie, W.W., Gunstone, F.D., 1998. The seed fatty acid composition and the distribution of Δ5-olefinic acids in the triacylglycerols of some Taxaceae (*Taxus* and *Torreya*). Journal of the American Oil Chemists Society 75, 1637–1641.

Wolff, R.L., Pédrono, F., Marpeau, A.M., Gunstone, F.D., 1999a. The seed fatty acid composition and the distribution of *Δ*5-olefinic acids in the triacylglycerols of some Taxares (*Cephalotaxus* and *Podocarpus*). Journal of the American Oil Chemists Society 76, 469–473.

Wolff, R.L., Pédrono, F., Marpeau, A.M., 1999b. *Fokienia hodginsii* seed oil, another source of *all-cis* 5,9,12,15-18:4 (coniferonic) acid. Journal of the American Oil Chemists Society 76, 535–536.

Zinkel, D.F., Foster, D.O., 1980. Oil precursors in the sapwood of four southern pines. Tappi 63, 137–139.

PERGAMON

Phytochemistry 58 (2001) 117–120

PHYTOCHEMISTRY

www.elsevier.com/locate/phytochem

Occurrence and characterization of oils rich in γ-linolenic acid (III): the taxonomical value of the fatty acids in *Echium* (Boraginaceae)

J.L. Guil-Guerrero[a,*], F. Gómez-Mercado[b], I. Rodríguez-García[c], P. Campra-Madrid[a], F. García-Maroto[d]

[a]*Departamento de Ingeniería Química, Universidad de Almería, E-04071 Almería, Spain*
[b]*Departamento de Biología Vegetal, Universidad de Almería, E-04071 Almería, Spain*
[c]*Departamento de Química Orgánica, Universidad de Almería, E-04071 Almería, Spain*
[d]*Departamento de Bioquímica, Universidad de Almería, E-04071 Almería, Spain*

Received 11 October 2000; received in revised form 30 March 2001

Abstract

Fourteen species of the genus *Echium* (Fam. Boraginaceae) collected in the Macaronesia were surveyed in a search for high levels of γ-linolenic acid (GLA, 18:3ω6) in the seed oil. High amounts of this fatty acid were found in all of them, ranging from 18.85% (*E. pitardii* var. *pitardii*) to 27.42% (*E. gentianoides*) on total seed fatty acids. The GLA content related to total seed weight was also significant, ranging from 1.26% (*E. handiense*) to 8.22% (*E. gentianoides*). In addition, considerable amounts of stearidonic acid (SA, 18:4ω3) were detected, ranging from 3.78% (*E. bonnetii* var. *bonnetii*) to 8.81% (*E. pininana*) on total fatty acids. Besides all the perennial species, the four herbaceous *Echium* taxa endemic to the Macaronesia also showed high GLA percentages. This is in contrast to the low GLA level found in continental *Echium* species, all of them bearing an herbaceous habit. These results are in good agreement with the available genetic data and show the ability of GLA to discriminate between Macaronesian and continental *Echium* species. The analysis of five other Macaronesian species belonging to plant families rich in GLA are also reported. © 2001 Elsevier Science Ltd. All rights reserved.

Keywords: Boraginaceae; *Echium*; γ-Linolenic acid; Macaronesia; Stearidonic acid; Fatty acid; Seed oil

1. Introduction

Seeds from Macaronesian *Echium* (ME) species (Fam. Boraginaceae) have been recently identified as among the richest sources of γ-Linolenic acid (GLA, 18:3ω6) found so far in nature, which are also rich in stearidonic acid (SA, 18:4ω3) (Guil-Guerrero et al., 2000a). In that study a partial survey of the genus covering 18 endemic species was made, all of them bearing a perennial woody habit. However, a number of *Echium* species from the Macaronesian area remained untested.

Finding of species producing high amounts of GLA is a great interest due to its pharmaceutical and dietary importance in addition to the use of GLA as a purified product in clinic and dietary investigations (Gunstone, 1992; Horrobin, 1992). Moreover, high GLA percentages in the oil make easier the purification bioprocess (Guil-Guerrero et al., 2000b).

A total of 27 *Echium* taxa at the specific level was reported to be present in the Macaronesia. All except *E. plantagineum*, which seems to be introduced by man, are exclusively from this area (Bramwell, 1972). Genetic studies based on the analysis of the mitochondrial genome indicated that all the island *Echium* plants descend from an herbaceous continental ancestor, through a single and relatively recent colonisation event followed by a rapid speciation process (Böhle et al., 1996). While all except two Macaronesian *Echium* species are woody perennials, continental species are herbaceous plants. Previous data (Guil-Guerrero et al., 2000a, 2001c) showed important ifferences in the fatty acid profile between European and North-African *Echium* plants (Continental Echium, CE) and their ME relatives thus an increase in the GLA content of the ME species — up to 100% as compared to the CE- in expense of a decrease of the α-linolenic acid (ALA, 18:3ω3) amount was obsered.

* Corresponding author. Tel.: +34-950-015586; fax: +34-950-015484.

E-mail address: jlguil@ual.es (J.L. Guil-Guerrero).

0031-9422/01/$ - see front matter © 2001 Elsevier Science Ltd. All rights reserved.
PII: S0031-9422(01)00184-4

In this paper we report the fatty acid composition of 14 endemic *Echium* species, including two herbaceous taxa that were remaining, essentially complete the analysis of the whole genus in the area. In addition, the analysis of five Macaronesian and north-african endemic species belonging to other genera from the families rich in GLA is also reported. The results are discussed in relation to the available genetic data besides to a possible evolutionary role of the fatty acid profile.

2. Results and discussion

Seed oil content and fatty acid composition of the 14 endemic *Echium* species here analyzed are given in Table 1. Seed oil content ranged from 6.28% in *E. handiense* to 29.97% in *E. gentianoides*. The percentage of GLA ranged between 17.83% of total fatty acids in *E. virescens* var. *angustissimum* to 27.42% in *E. gentianoides*. The percentage on total seed weight varied from 1.26% GLA in *E. handiense* to 8.22% GLA in *E. gentianoides*.

The amounts determined for other polyunsaturated fatty acids on total oil were in good agreement with previous reports for other plants of the same genus (Wolf et al., 1983; Tsevegsüren and Aitzetmüller, 1996; Guil-Guerrero et al., 2000a). SA ranged from 3.48% in *E. x bond-spranguei* to 8.81% in *E. pininana*. Linoleic acid (LA, 18:2ω6) ranged from 15.97% in *E. handiense* to 30.22% in *E. bonnetii* var. *bonnetii*. α-Linolenic acid (ALA, 18:3ω3) ranged from 16.52% in *E. bonnetii* var. *bonnetii* to 27.07% in *E. webbii*. For monounsaturated fatty acids we obtained similar values to those reported in other species from this group. Oleic acid (OA, 18:1ω9) ranged from 10.31% in *E. webbii* to 22.18% in *E. x bond-spranguei*. Other monounsaturated fatty acids

Table 1
Fatty acids composition for potential sources of GLA from Macaronesia

Seed	% seed oil	% GLA seed	Fatty acid percentages in the oil												
			16:0	18:0	18:1ω9	18:2ω6	18:3ω6	18:3ω3	18:4ω3	20:0	20:1ω9	22:0	22:1ω9	24:0	24:1ω9
Endemic Echium species															
Sect. *Echium*															
E. pitardii var. *pitardii*	21.88	4.04	6.81	3.80	12.97	24.03	18.85	25.91	5.74	0.20	0.73	0.12	0.13	0.06	0.12
E. p. var.*macrantha*	23.45	4.49	7.11	3.68	13.85	26.14	19.16	23.42	4.97	0.14	0.67	0.08	0.12	0.06	0.10
E. bonnetii var. *bonnetii*	16.39	3.52	7.34	3.64	14.54	30.22	21.46	16.52	3.78	0.83	0.09	0.22	0.15	0.19	0.09
E. b. var. *fuerteventurae*	12.44	2.13	9.76	3.69	13.11	26.73	20.30	16.78	4.23	0.97	0.80	0.39	0.26	0.32	0.21
Sect. *Gigantea*															
E. brevirame	10.68	2.47	7.93	4.43	11.64	27.96	23.14	19.49	3.97	0	0.86	0.35	0	0	0
Sect. *Virescentia*															
E. x bond-spranguei	17.35	3.92	6.95	3.71	22.18	29.87	22.57	19.3	3.48	0	0.83	0	0	0	0
E. virescens var. *angustissimum*	22.84	3.79	8.37	5.27	15.11	22.35	17.83	24.32	6.21	0	0.12	0	0	0	0
E. webbii	18.27	3.98	6.70	4.07	10.31	21.51	21.78	27.07	7.10	0	0.16	0	0.17	0	0
E. bethencourtianum	9.32	2.19	8.92	5.91	12.91	24.63	23.50	19.63	4.44	0	0	0	0	0	0
E. handiense	6.28	1.26	7.09	3.37	20.56	15.97	20.00	21.82	7.79	0	0.91	0	0.39	0	0
Sect. *Gentianiodea*															
E. gentianoides	29.97	8.22	6.19	4.04	10.47	20.12	27.42	21.78	7.03	0.15	1.29	0	0.5	0	0.26
Sect. *Simplicia*															
E. pininana	9.70	2.27	7.65	3.93	11.16	17.43	23.40	24.87	8.81	0.25	1.17	0.26	0.27	0	0.31
E. wildprettii ssp. *trichosiphon*	6.98	1.71	9.34	4.12	13.78	18.18	24.48	19.13	6.92	0.5	1.47	0.59	0.28	0	0.5
Sect. *Decaisnea*															
E. decaisnei ssp. *purpuriense*	20.11	4.37	7.62	3.25	12.96	25.87	21.72	21.79	4.45	0.18	0.84	0.12	0.24	0.06	0.24
Other endemic species from Macaronesia area															
Scrophulariaceae															
Isoplexis chalcantha	2.05	0.03	32.90	10.42	9.56	3.65	1.61	4.42	0	0	0	0	0	0	0
Scrophularia smithii	23.28	1.41	11.19	2.61	14.39	63.76	6.07	0.53	0	0.44	0.20	0.21	0.27	0	0.23
Kickxia heterophylla	27.95	0.04	9.73	3.75	15.90	67.55	0.15	0.58	0.27	0.37	0.11	0.19	0.28	0.11	0.11
Boraginaceae															
Myosotis latifolia	35.57	1.58	7.49	4.63	24.43	23.17	4.44	15.77	7.95	0.67	5.17	0.43	3.05	0	2.13
Heliotropium erosum	7.78	0.11	8.40	4.21	18.82	60.91	1.46	2.17	0.39	0.29	0.23	0.20	0.00	0	0

(20:1ω9, 22:1ω9 and 24:1ω9) were found in low amounts in agreement to the composition reported for other Boraginaceae species (Wolf et al.,1983; Tsevegsüren and Aitzetmüller, 1996; Guil-Guerrero et al., 2000a, 2001). Results for saturated fatty acids also agree with the reports mentioned above. Palmitic acid (16:0), for instance, ranged from 6.19% in *E. gentianoides* to 9.76% in *E. bonnetii* var. *fuerteventurae*.

Among *Echium* species five showed GLA values above 23% in a seed oil, and four showed GLA percentages in total seeds above 4% in a seed dry weight. For these species, the high relative amount of GLA in oil is paralleled by a high oil content within the seed (>20%). *E. gentianoides* seed oil was the richest source of GLA, with 8.22% of GLA on the total seed weight. Except for *E.handiense* and *E. wildprettii* ssp. *trichosiphon* seeds of all the surveyed *Echium* species have more than 2% (w/w) of GLA. Seed oils of all the surveyed *Echium* species, except those of *E. virescens* var. *angustissimum*, *E. pitardii* var. *pitardii*, and *E. pitardii* var. *macrantha*, have more than 20% of GLA.

Four herbaceous varieties (*E. bonnetii* var. *bonnetii*; *E. bonnetii* var. *fuerteventurae*; *E. pitardii* var. *pitardii* and *E. pitardii* var. *macrantha*) showed GLA contents in good agreement to those of other species from the Macaronesian sections behaving as perennial shrubs. Nevertheless, due to their herbaceous habit they have been included within the *Echium* section (Bramwell, 1972), a taxonomical group that gather herbaceous continental plants showing GLA percentages in the oil below a 12% (Guil-Guerrero et al., 2001). This is in good agreement with genetic data from Böhle et al. (1996), that groups *E. bonnetti* in a cluster together with the perennial ME, and apart from the herbaceous CE plants. A good example, that can be considered as a negative control, is *E. plantagineum*, an herbaceous plant which is considered as a continental island invasor. This species exhibits a low GLA level (9% GLA on a seed oil) (Guil-Guerrero et al., 2000a) and genetically lies far away from the ME group (Böhle et al., 1996). These data argue in favour of the usefulness of the fatty acid composition, and in particular of GLA, as a taxonomic marker as it has been claimed by other authors (Velasco and Goffman, 1999). On the other hand, these data indicate that it could be more appropriate to include the herbaceous ME in a new taxonomical group. Variability of the GLA content at the infraspecific level, as in the case of *E. virescens* var. *angustissimum* (17.83%) vs. *E. virescens* var. *virescens* (24.00%) (Guil-Guerrero et al., 2000a), or *E. wildprettii* ssp. *trichosiphon* (24.86%) vs. *E. wildprettii* ssp. *wildprettii* (15.16%) (Guil-Guerrero et al., 2000a) is probably reflecting the rapid diversification of the ME species.

The conspicuous presence of a high GLA level in the seeds of ME plants raises the question of whether this characteristic conferred to them a selective advantage during evolution. Conversely, in a neutral hypothesis, one can think that time since the island colonisation event took place (less than 20 millions years ago according to genetic estimations) was not enough for the loss of this character that was present in the common ancestor of the ME. Nevertheless, it remains intriguing why none of the CE plants that we have analysed do not show a high GLA level. Perhaps, a high GLA content is deleterious for the seeds of CE plants in their particular environmental conditions. In this context it is known that fatty acid composition in lipids determines the fluidity of structures where they are present. To test whether a high GLA content, at the expense of a reduction in the ALA amount, could have an influence on the fluidity of the seed content we have measured a "melting range" (oils are complex mixtures and therefore have no defined melting points) of the oils of several *Echium* species, and the results corroborate this idea. Thus, the seed oil from the mediterranean *E. sabulicola* (10% GLA) (Guil-Guerrero et al., 2001) melted in the range 13–18°C, while those from the Macaronesian *E. fastuosum* (18–22°C) and *E. nervosum* (19–25°C) had higher melting ranges (both 25% GLA, Guil-Guerrero et al., 2000a). An explanation for these data is that substitution of ALA by GLA at the second position of the storage lipids raises the melting point due to the particular spatial configuration of the GLA, in which the double bonds are more distant to the terminal methyl of the molecule than in the ALA. Considering these data, one can speculate that an increase in the proportion of GLA at the second position of tryglicerides in CE plants would reduce the fluidity of the seed oil. As the average continental temperature all year long is supposed to be lower than at the Macaronesian area, the high GLA content might affect negatively the mobilisation of tryglycerides during the seed germination of CE plants.

Although it has been reported that environmental factors such as soil type and temperature, can affect to GLA and other polyunsaturated fatty acids contents in the seed oil of *Boraginaceae* or *Onagraceae* (Gunstone, 1992), in our experience those factors do not seem to affect significatively the profiles found in *Echium* plants. For instance, seeds from *E. gentianoides* collected from different locations and times were analyzed with similar results for the fatty acid profiles (less than 1% variation of the GLA content). The same was true for other plants such as *E. fastuosum* and *E. virescens* var. *angustissimum*, as we could establish from other experiments. Thus, in the absence of a more exhaustive study, we can assume a constancy in the seed fatty acid profile in plants belonging to this genus.

Table 1 also shows the fatty acid profile of other endemic species from the Macaronesian area, belonging to families which are considered as good sources of GLA. Note that the small GLA percentages are in good

agreement with previous reports from European species (Wolf et al., 1983; Tsevesüren and Aitzetmüller, 1996; Guil-Guerrero et al., 2001). This indicates that, in some way, the characteristic fatty acid profile of the ME species could be restricted in the area to these plants.

The results of the present work indicate that ME species shown here had a high percentage of GLA in the seed oil, with *E. gentianoides* as the species showing the higher amount among them. The possibility of finding plant species with a much higher GLA content seems to be unlikely, due to the fact that the GLA in Boraginaceae is mainly found at the second position of triglycerides (Gunstone, 1992) and that, consequently, impose a theoretical limit around 33%. In addition, we found that the endemic herbaceous ME have percentages of GLA in the range found for the woody perennial ME species. This finding possesses agronomic interest as annual species producers of GLA have obvious advantages in the cultivation compared to the perennial shrubs, due to their shorter biological cycle.

3. Experimental

3.1. Materials

Mature seeds were collected at maturity in the natural habitats of these plants. Seeds of *E. brevirame*, *E. gentianoides*, *E. x bond-spraguei*, *E. webbi*, *E. bethercoutianum*, *E. wildpretti* ssp. *trichosiphon*, *E. pininana*, *Scrophularia smithii* and *Myosotis latifolia* were collected in La Palma island in June 1999. Seeds of *E. pitardii* var. *pitardii*, *E. pitardii* var. *macrantha*, *E. decaisnei* ssp. *purpuriense* and *Kickxia heterophylla* were gathered from Lanzarote island in April 2000. Seeds of *E. bonnetii* var. *bonnetii*, *E. bonnetii* var. *fuerteventurae*, *E. handiense*, and *Heliotropium erosum* were collected from Fuerteventura island in April 2000. Seeds of *Isoplexis chalcantha* were gathered from Gran Canaria island in May 2000. Seeds of *E. virescens* var. *angustissimum* were collected from Tenerife island in July 2000. Precautions accomplishing the harvesting were taken as previously reported (Guil-Guerrero et al., 2000a).

Oil extraction and transesterification, gas-liquid chromatography (GLC) and GC–mass spectrometry, were made as is previously reported (Guil-Guerrero et al., 2000a). Melting ranges of oils were determined by freezing the oils at −78°C and slowly rising the temperature until they become liquids.

References

Böhle, U.R., Hilger, H.H., Martin, W.F., 1996. Island colonization and evolution of the insular woody habit in *Echium* L. (Boraginaceae). Proc. Natl. Acad. Sci. USA 93, 11740–11745.

Bramwell, D., 1972. A revision of the genus *Echium* in Macaronesia. Lagascalia 2, 37–115.

Guil-Guerrero, J.L., Gómez-Mercado, F., García-Maroto, F., Campra-Madrid, P., 2000. Occurrence and characterization of oils rich in γ-linolenic acid (I): *Echium* seeds from Macaronesia. Phytochemistry 53, 451–456.

Guil-Guerrero, J.L., Campra-Madrid, P., Belarbi, E.H., 2000b. γ-Linolenic acid purification from seed oil sources by argentated silica gel chromatography column. Process Biochem. 36, 341–354.

Guil-Guerrero, J.L., García-Maroto, F.F., Giménez-Giménez, A., 2001. Fatty acids profiles in organs from forty-nine plant species that are potential new sources of γ-linolenic acid. J. Am. Oil Chem. Soc., in press.

Gunstone, F.D., 1992. γ-Linolenic acid. Occurrence and physical and chemical properties. Prog. Lipid Res. 31, 145–161.

Horrobin, D.F., 1992. Nutritional and medical importance of γ-linolenic acid. Prog. Lipid Res. 31, 163–194.

Tsevegsüren, N., Aitzetmüller, K., 1996. γ-Linolenic and stearidonic acids in Mongolian Boraginaceae. J. Am. Oil Chem. Soc. 73, 1681–1684.

Velasco, L., Goffman, F.D., 1999. Chemotaxonomic significance of fatty acids and tocopherols in Boraginaceae. Phytochemistry 52, 423–426.

Wolf, R., Kleiman, B., England, R.E., 1983. New sources of γ-linolenic acid. J. Am. Oil Chem. Soc. 60, 1858–1860.

PERGAMON

Phytochemistry 58 (2001) 121–127

PHYTOCHEMISTRY

www.elsevier.com/locate/phytochem

Constituents of *Eugenia sandwicensis* with potential cancer chemopreventive activity

Jian-Qiao Gu[a], Eun Jung Park[a], Lumonadio Luyengi[a], Michael E. Hawthorne[b], Rajendra G. Mehta[b], Norman R. Farnsworth[a], John M. Pezzuto[a,b], A. Douglas Kinghorn[a,*]

[a]*Program for Collaborative Research in the Pharmaceutical Sciences and Department of Medicinal Chemistry and Pharmacognosy, College of Pharmacy, University of Illinois at Chicago, 833 South Wood Street, Chicago, IL 60612, USA*

[b]*Department of Surgical Oncology, College of Medicine, University of Illinois at Chicago, 840 South Wood Street, Chicago, IL 60612, USA*

Received 31 January 2001; received in revised form 19 March 2001

Abstract

A triterpenoid, 3β-*cis*-*p*-coumaroyloxy-2α,23-dihydroxyolean-12-en-28-oic acid (**1**), and two natural products, 3β-*trans*-*p*-coumaroyloxy-2α,23-dihydroxyolean-12-en-28-oic acid (**2**) and 23-*trans*-*p*-coumaroyloxy-2α,3β-dihydroxyolean-12-en-28-oic acid (**3**), were isolated from a chloroform-soluble extract of the stems of *Eugenia sandwicensis*, along with 10 known compounds. Of these compounds, **2** showed significant inhibitory activity (79.2% at 4 μg/ml) in a 7,12-dimethylbenz[*a*]anthracene-induced mouse mammary organ culture assay system of relevance to cancer chemoprevention. Gallic acid was isolated as an antioxidative constituent of an ethyl acetate-soluble extract of *E. sandwicensis* stems. Isolates **1**–**3** were characterized on the basis of spectral and chemical evidence. © 2001 Elsevier Science Ltd. All rights reserved.

Keywords: *Eugenia sandwicensis*; Myrtaceae; Triterpenoids; 3β-*cis*-*p*-Coumaroyloxy-2α,23-dihydroxyolean-12-en-28-oic acid; 3β-*trans*-*p*-Coumaroyloxy-2α,23-dihydroxyolean-12-en-28-oic acid; Gallic acid; Mouse mammary organ culture assay; Antioxidant assay

1. Introduction

The genus *Eugenia* of the Myrtaceae comprises over 500 species, and is most common in tropical and subtropical America and tropical Asia, with a few species occurring in Australia and Africa (Hillebrand, 1888). Previously, coumarins (Lowry, 1968; Yazaki, 1977), ellagic acid (Yazaki, 1977), flavonoids and their glycosides (Mitscher et al., 1973; Painuly and Tandon, 1983a), hydrolysable tannins (Nonaka et al., 1987; Lee et al., 1997), steroids (Govindachari et al., 1969; Schapoval et al., 1994), and triterpenoids of the lupane (Yazaki, 1977) and ursane (Painuly and Tandon, 1983b) types have been found as constituents of this genus. *Eugenia sandwicensis* A. Gray, collected in Hawaii, is a perennial woody tree or shrub. Up to the present, no chemical and biological work has been carried out on this plant.

As part of an ongoing collaborative search for novel chemopreventive principles from plants (Kinghorn et al., 1998; Pezzuto et al., 1999), the methanolic extract of the stems of *E. sandwicensis* showed significant biological activities in preliminary screening, in both a 7,12-dimethylbenz[*a*]anthracene (DMBA)-induced mouse mammary organ culture model (Mehta and Moon, 1991) and a 1,2-diphenyl-2-picrylhydrazyl (DPPH) free-radical scavenging antioxidative assay (Fujita et al., 1988). The compounds responsible for the significant activities exhibited in the mouse mammary organ culture assay and the DPPH assay were partitioned selectively into subsequent chloroform- and ethyl acetate-soluble extracts, respectively. This paper describes the isolation, structure elucidation, and evaluation of biological activities in the mouse mammary organ culture assay of one triterpene derivative (**1**) and two triterpenoid natural products (**2** and **3**) from the chloroform-soluble extract of *E. sandwicensis* stems. Also, 10 known compounds were obtained from this extract, and gallic acid was isolated as an antioxidative principle from an ethyl acetate-soluble extract of the stems.

* Corresponding author. Tel.: +1-312-996-0914; fax: +1-312-996-7107.

E-mail address: kinghorn@uic.edu (A.D. Kinghorn).

0031-9422/01/$ - see front matter © 2001 Elsevier Science Ltd. All rights reserved.
PII: S0031-9422(01)00180-7

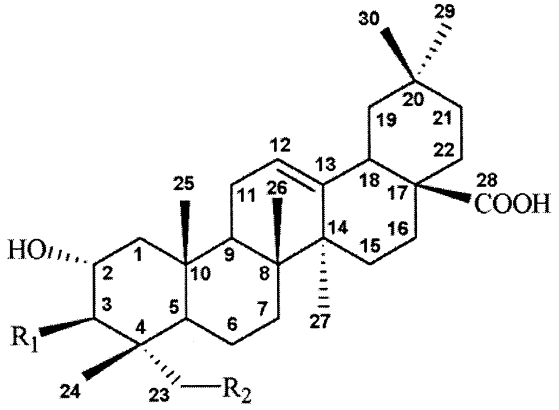

	R_1	R_2
1	*cis-p*-coumaroyloxy	OH
2	*trans-p*-coumaroyloxy	OH
3	OH	*trans-p*-coumaroyloxy

2. Results and discussion

Ten compounds of previously known structure were isolated from the $CHCl_3$ extract of the stems of *E. sandwicensis*, as described in the Experimental section, and were identified, in turn, as alphitolic acid (Yaguchi et al., 1988), arjunolic acid (Jayasinghe et al., 1993), betulinic acid (Ikuta and Itokawa, 1988), 3-*epi*-betulinic acid (Kitajima et al., 1990), 2α,3α-dihydroxylup-20(29)-en-28-oic acid (Kumar et al., 1985), 3β,23-dihydroxylup-20(29)-en-28-oic acid (Ikuta and Itokawa, 1988), hederagenin (Ikuta and Itokawa, 1988), maslinic acid (Tchivounda et al., 1991), β-sitosteryl 3-*O*-β-D-glucopyranoside (Fujita and Nakayama, 1993), and syringaldehyde (Kokpol et al., 1993), by comparison of their physical and spectral data with reported values. Among these isolates, arjunolic acid was the major compound found in this investigation, in a yield of greater than 0.06% w/w of the dried plant material.

Compound **1** was obtained as a white amorphous powder. A molecular formula was deduced as $C_{39}H_{54}O_7$ from the HRFABMS data at *m/z* 657.3763 $[M+Na]^+$ ($C_{39}H_{54}O_7Na$ calcd for 657.3767). This compound exhibited UV maxima at 223 and 312 nm, suggesting the presence of considerable conjugation in the molecule. In the IR spectrum, absorption bands at 3330 (OH), 1695 (ester carbonyls), 1604 and 1514 cm^{-1} (trisubstituted double bond and aromatic ring) were apparent. The EIMS of **1** exhibited characteristic ion peaks at *m/z* 248 and 203, due to *retro*-Diels–Alder type fragmentation of an olean-12-en-28-oic acid or an urs-12-en-28-oic acid unit bearing no other oxygenated substituent in any of the C, D or E rings (Bombardelli et al., 1974).

Interpretation of the ^1H and ^{13}C NMR spectral data of **1** with the use of ^1H–^1H COSY, HOHAHA, HMQC, HMBC, and NOESY experiments, and comparison with arjunolic acid (Jayasinghe et al., 1993), which, as mentioned, was also obtained in the present investigation, allowed full assignment of chemical shifts (Tables 1 and 2). Two methine protons at δ_H 5.80 (1H, *d*, $J=9.9$ Hz) and δ_H 4.39 (1H, *td*, $J=4.5$, 9.9 Hz) assigned to H-3 and H-2 were determined from the ^1H–^1H COSY and HOHAHA spectra, and were in conformity with a *trans*-diequatorial (2α,3β) configuration of two oxygen-bearing groups. The ^1H NMR spectrum also revealed a hydroxymethylene (CH_2OH) group (δ_H 3.60, 3.50, each $J=11$ Hz), which was confirmed by a HMQC experiment from the correlations of these two protons with the carbon signal of C-23 (δ_C 64.7). Moreover, the aromatic protons at δ_H 8.10 and 7.10 (each 2H, *d*, $J=8.5$ Hz) of a *p*-disubstituted benzene ring suggested the presence of a *p*-substituted *cis*-cinnamoyl moiety in **1**. Had the configuration of H-2′ and H-3′ been *trans*, a characteristic *J* value of about 16 Hz would have been expected (Lee, 1998). This ester substituent was placed at C-3 as a result of the downfield shift observed for H-3 in the ^1H NMR spectrum, compared with that of arjunolic acid (Jayasinghe et al., 1993), and the correlations between H-3 (δ_H 5.80) and C-2 (δ_C 66.7), C-4 (δ_C

Table 1
^1H NMR spectral data for compounds **1–3**[a]

No.	**1**	**2**	**3**
1	1.39[b], 2.33[b]	1.43[b], 2.34[b]	1.40[b], 2.32[b]
2	4.39 *td* (4.5, 9.9)	4.43[b]	4.22[b]
3	5.80 *d* (9.9)	5.79 *d* (9.7)	4.01 *d* (9.4)
5	1.83[b]	1.85[b]	1.68[b]
6	1.34[b], 1.70[b]	1.40[b], 1.74[b]	1.46[b], 1.68[b]
7	1.27[b], 1.63[b]	1.34[b], 1.70[b]	1.32[b], 1.68[b]
9	1.92[b]	1.93[b]	1.90[b]
11	1.97[b]	2.02[b]	2.01[b]
12	5.43 *br s*	5.44 *br s*	5.45 *t-like*
15	1.09[b], 2.12[b]	1.11[b], 2.12[b]	1.10[b], 2.10[b]
16	1.11[b], 1.96[b]	1.16[b], 2.01[b]	1.15[b], 2.00[b]
18	3.33 *d* (12)	3.34 *d* (12)	3.27 *dd* (3.9, 14)
19	1.21[b], 1.73[b]	1.27[b], 1.78[b]	1.23[b], 1.73[b]
21	1.13[b], 1.39[b]	1.15[b], 1.41[b]	1.14[b], 1.40[b]
22	1.76[b], 1.99[b]	1.79[b], 2.00[b]	1.79[b], 2.00[b]
23a	3.50 *d* (11)	3.48 *d* (11)	4.44 *d* (11)
23b	3.60 *d* (11)	3.63 *d* (11)	4.70 *d* (11)
24	0.90 *s*	0.95 *s*	1.06 *s*
25	1.04 *s*	1.08 *s*	1.04 *s*
26	1.00 *s*	1.02 *s*	1.02 *s*
27	1.18 *s*	1.23 *s*	1.21 *s*
29	0.89 *s*	0.92 *s*	0.88 *s*
30	0.99 *s*	1.00 *s*	0.97 *s*
2′	6.07 *d* (13)	6.64 *d* (16)	6.63 *d* (16)
3′	6.89 *d* (13)	7.95 *d* (16)	7.95 *d* (16)
2″/6″	8.10 *d* (8.5)	7.53 *d* (8.0)	7.56 *d* (8.8)
3″/5″	7.10 *d* (8.5)	7.15 *d* (8.0)	7.16 *d* (8.8)

[a] Chemical shifts (ppm) were recorded at 300 MHz using C_5D_5N as solvent and TMS as internal standard. Coupling constants are listed in parenthesis in Hz. Assignments were based on COSY, HMQC and HMBC experiments.

[b] Multiplicity patterns were unclear due to signal overlapping.

Table 2
^{13}C NMR spectral data for compounds **1–3**[a]

No.	1	2	3
1	48.4 *t*[b]	48.0 *t*	47.8 *t*
2	66.7 *d*	66.4 *d*	68.4 *d*
3	79.7 *d*	79.7 *d*	77.4 *d*
4	43.7 *s*	43.6 *s*	43.2 *s*
5	48.1 *d*	47.9 *d*	48.5 *d*
6	18.3 *t*	18.0 *t*	18.7 *t*
7	33.4 *t*	33.2 *t*	33.1 *t*
8	39.8 *s*	39.3 *s*	39.9 *s*
9	47.2 *d*	47.0 *d*	48.0 *d*
10	38.2 *s*	37.9 *s*	38.3 *s*
11	24.0 *t*	23.6 *t*	24.0 *t*
12	122.0 *d*	121.6 *d*	122.4 *d*
13	145.5 *s*	145.4 *s*	144.9 *s*
14	42.3 *s*	42.0 *s*	42.2 *s*
15	28.4 *t*	28.2 *t*	28.2 *t*
16	23.9 *t*	23.6 *t*	23.6 *t*
17	46.8 *s*	46.5 *s*	46.6 *s*
18	42.2 *d*	41.9 *d*	42.0 *d*
19	46.6 *t*	46.4 *t*	46.3 *t*
20	31.0 *s*	30.8 *s*	30.9 *s*
21	34.4 *t*	34.2 *t*	34.2 *t*
22	32.8 *t*	32.5 *t*	33.2 *t*
23	64.7 *t*	64.5 *t*	66.5 *t*
24	14.9 *q*	14.6 *q*	14.1 *q*
25	17.2 *q*	17.0 *q*	17.3 *q*
26	17.6 *q*	17.3 *q*	17.5 *q*
27	26.1 *q*	25.9 *q*	26.0 *q*
28	180.2 *s*	180.2 *s*	180.2 *s*
29	33.3 *q*	33.1 *q*	33.2 *q*
30	23.9 *q*	23.6 *q*	23.8 *q*
1′	167.5 *s*	168.2 *s*	167.4 *s*
2′	116.9 *d*	115.4 *d*	115.3 *d*
3′	143.9 *d*	144.8 *d*	145.1 *d*
1″	126.6 *s*	125.7 *s*	126.1 *s*
2″/6″	133.9 *d*	130.3 *d*	130.7 *d*
3″/5″	115.9 *d*	116.6 *d*	116.9 *d*
4″	160.6 *s*	161.3 *s*	161.5 *s*

[a] Carbon chemical shifts (ppm) were recorded at 75.6 MHz using C_5D_5N as solvent and TMS as internal standard. Assignments were based on COSY, HMQC and HMBC experiments.
[b] Carbon multiplicity.

43.7), C-23 (δ_C 64.7), C-24 (δ_C 14.9) and C-1′ (δ_C 167.5) of the *p*-coumaric acid unit in the HMBC spectrum. Moreover, the structure of the *p*-coumaroyl moiety was confirmed by the correlations between H-2′ (δ_H 6.07) and C-1″ (δ_C 126.6), and those of H-3′ (δ_H 6.89) and C-2‴/C-6″ (δ_C 133.9). The relative configuration of H-2, H-3 and H-23 and the other spatial information of compound **1** were further supported by a NOESY experiment, wherein NOEs were observed between H-24 (δ_H 0.90) and H-2 (δ_H 4.39), between H-3 (δ_H 5.80) and H-9 (δ_H 1.92), and between H-23 (δ_H 3.60, 3.50) and H-5 (δ_H 1.83) (Fig. 1). Therefore, based on all the above evidence, the structure of the new compound **1** was assigned as 3β-*cis*-*p*-coumaroyloxy-2α,23-dihydroxyolean-12-en-28-oic acid.

The natural product **2** was obtained as a pale yellowish powder and its molecular formula was deduced as $C_{39}H_{54}O_7$ by the HRFABMS data at *m*/*z* 657.3787 $[M+Na]^+$ ($C_{39}H_{54}O_7Na$ calcd for 657.3767). Compound **2** was characterized as 3β-*trans*-*p*-coumaroyloxy-2α,23-dihydroxyolean-12-en-28-oic acid, by comparison of its NMR spectroscopic data with those of compound **1** (Tables 1 and 2). Compound **2** was previously characterized as its C-28,C-4″-dimethylated derivative (Tapondjou et al., 1995; Lee, 1998), but not in its natural form. When the C-28,C-4″-dimethylated derivative was prepared from **2** as described in Section 3, the spectral data of the methylate were comparable with literature values.

The natural product **3** was obtained as a pale yellowish powder and its molecular formula was deduced as $C_{39}H_{54}O_7$ by the HRFABMS data at *m*/*z* 657.3751 $[M+Na]^+$ ($C_{39}H_{54}O_7Na$ calc. for 657.3767). Compound **3** was also previously characterized as its C-28,C-4″-dimethylated derivative (Lee, 1998). In a similar manner to compound **2**, the new natural product **3** was characterized as 23-*trans*-*p*-coumaroyloxy-2α,3β-dihydroxyolean-12-en-28-oic acid, and its ^{1}H NMR and ^{13}C NMR spectroscopic data are also assigned in Tables 1 and 2, respectively.

Compounds **1–3** were evaluated for potential to inhibit the development of DMBA-induced preneoplastic mammary lesions using a mouse mammary organ culture assay system (Mehta and Moon, 1991). The results summarized in Table 3 illustrate that compound **2** exhibited significant inhibitory activity (79.2% at 4 μg/ml) while compounds **1** and **3** were inactive. This is the first oleanane ester triterpenoid found to inhibit DMBA-induced preneoplastic lesions in this test system. Therefore, compound **2** appears worthy of additional biological evaluation to further define its promise as a cancer chemopreventive agent.

The sole compound from the EtOAc extract of *E. sandwicensis* stems found to be active in the DPPH antioxidant assay (Fujita et al., 1988) was obtained as yellowish needles and identified as gallic acid, by a comparison of the physical and spectral data with reported values (Sakar et al., 1993) and direct comparison with an authentic sample. It exhibited potent antioxidative activity with an IC_{50} value of 3.6 μg/ml in a DPPH assay system. This compound is among the most active substance we have evaluated in this system to date. However, gallic acid was inactive when tested in the above-mentioned mouse mammary organ culture assay system.

3. Experimental

3.1. General

Mps were determined using a Fisher–Johns melting point apparatus and are uncorrected. Optical rotations

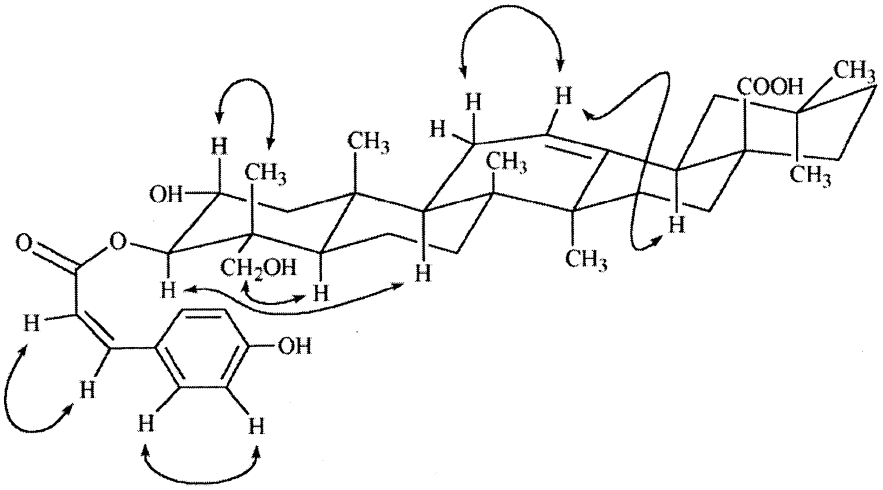

Fig. 1. Selective NOESY correlations for **1.**

Table 3
Effects of compounds **1**–**3** on DMBA-induced preneoplastic lession with mouse mammary gland organ culture

Compound	Concentration (μg/ml)	Inhibition (%)[a]
1	10	36.6
2	4	79.2
3	10	48.1

[a] Pure compounds are considered active if they exhibit >60% inhibition at 10 μg/ml.

were measured with a Perkin-Elmer 241 polarimeter using MeOH as solvent. UV spectra were recorded on a Beckman DU-7 spectrometer using MeOH as solvent. IR spectra were recorded on a JASCO FT/IR-410 spectrometer. EIMS (70 eV) were obtained using a Finnigan MAT-90 mass spectrometer, and HRFABMS using a VG 7070-HF mass spectrometer. The ^{1}H NMR and ^{13}C NMR spectra were recorded in C_5D_5N with TMS as internal standard, using a Brüker Avance DPX-300 instrument operating at 300 and 75.6 MHz, respectively. HMBC and NOESY experiments were performed on a Brüker Avance DRX-500 instrument operating at 500.2 MHz with a TAXI probe.

Open column chromatography (CC): silica gel (200–400 mesh, Natland International Corporation, Morrisville, NC); Sephadex LH-20 (Sigma). Semi-preparative HPLC: a YMC-pack ODC-AQ column (5 μm, 25×2 cm i.d., YMC Co., Ltd., Wilmington, NC) and a YMC-guardpack ODC-AQ guard column (5 μm, 5×2 cm i.d.); two Waters 515 HPLC pumps; a Waters 2487 dual λ absorbance detector; a Millennium chromatography manager system (Waters, Milford, MA). Preparative TLC: Kieselgel 60 F_{254} (Merck) plates (silica gel, 0.5 mm layer thickness, 20×20 cm). TLC: Kieselgel 60 F_{254} (Merck) plates (silica gel, 0.25 mm layer thickness), with compounds visualized by dipping plates into either 10% (v/v) H_2SO_4 or phosphomolybolic acid reagent (Aldrich, Milwaukee, WI) followed by charring at 110°C for 5–10 min.

3.2. Mouse mammary gland organ culture assay

This assay was carried out according to an established protocol (Mehta and Moon, 1991). In brief, BALB/c female mice were pretreated for 9 days with 1 μg of estradiol and 1 mg of progesterone. On the 10th day, the mice were sacrificed and the second pair of thoracic mammary glands were dissected on silk and transferred to 60-mm culture dishes containing 5 ml of Waymouth's 752/1 MB medium supplemented with streptomycin, penicillin and glutamine. The glands were incubated for 10 days (37°C, 95% O_2 + 5% CO_2) in the presence of growth-promoting hormones (5 μg of insulin, 5 μg of prolactin, 1 μg of aldosterone, and 1 μg of hydrocortisone per ml of medium). Glands were exposed to 2 μg/ml DMBA between 72 and 96 h. After the exposure, glands were rinsed and transferred to new dishes with fresh medium. The fully differentiated glands were then permitted to regress by withdrawing all hormones except insulin for 14 additional days. Test compounds were present in the medium during days 1–10 of culture; mammary glands were scored for incidence of lesions.

3.3. Assay for DPPH free radical scavenging potential

This assay is based on the scavenging activity of stable 1,1-diphenyl-2-picrylhydrazyl (DPPH) free radicals and was carried out according to established protocols (Fujita et al., 1988). In brief, reaction mixtures containing test samples (dissolved in DMSO) and 300 μM DPPH ethanolic solution in 96-well microtiter plates were incubated at 37°C for 30 min. Absorbances were then measured at 515 nm, and percent inhibition by

sample treatment was calculated. IC_{50} values denote the concentration of sample required to scavenge 50% of DPPH free radicals.

3.4. Plant material

The stems of *E. sandwicensis* were collected on the island of Kauai, Hawaii in June 1978 and identified by Dr. Yoneo Sagawa. A voucher specimen (accession no. CH-2507) is deposited at the Harold L. Lyon Arboretum, University of Hawaii, Honolulu, HI.

3.5. Extraction and isolation

The milled air-dried stems of *E. sandwicensis* (1.9 kg) were extracted with MeOH (6 L×3) at room temperature and the solution was evaporated in vacuo. On drying, this initial methanolic extract exhibited significant inhibitory activity (62.5% inhibition at a concentration of 10 μg/ml) in the mouse mammary gland organ culture assay and antioxidative activity (13.6 μg/ml) in the DPPH free-radical scavenging bioassay. The dried MeOH extract (296 g) was resuspended in 10% H_2O in MeOH (700 ml) and partitioned with petroleum ether (1 L×2) to afford a petroleum ether soluble-residue (8 g). To the aqueous MeOH layer was added H_2O (300 ml), and this was then partitioned with $CHCl_3$ (1 L×2) to afford a $CHCl_3$-soluble extract (12 g). The aqueous MeOH layer was further partitioned with EtOAc (1 l×2) to afford an EtOAc-soluble extract (46 g).

The $CHCl_3$ extract (12 g), with 50% inhibitory activity at a concentration of 10 μg/ml in the mouse mammary gland organ culture assay, was subjected to silica gel CC and eluted with increasing concentrations of MeOH in $CHCl_3$ from 1 to 50% to give six fractions (I–VI). Fraction I (500 mg) was subjected to silica gel CC eluted with mixtures of petroleum ether and acetone in a step-gradient mode to afford 3-*epi*-betulinic acid (10 mg, eluted with petroleum ether/acetone 10:1 v/v) and betulinic acid (5 mg, eluted with petroleum ether/acetone 8:1 v/v). Similarly, fraction II (1.0 g) was subjected to silica gel CC eluted with mixtures of *n*-hexane and acetone to yield five subfractions (VII-XI). Syringaldehyde (3 mg) was obtained from subfraction VIII (130 mg, eluted with *n*-hexane/acetone 5:1 v/v), which was further subjected to silica gel CC eluted with mixtures of *n*-hexane and EtOAc (2.5:1 v/v). 2α,3α-Dihydroxylup-20(29)-en-28-oic acid (12 mg) was obtained from subfraction X (100 mg, eluted with *n*-hexane/acetone 2.5:1 v/v), which was subjected to preparative TLC on silica gel developed with $CHCl_3$/acetone (3:2) and then followed by Sephadex LH-20 CC eluted with MeOH. In turn, fraction III (1.5 g) was subjected to silica gel CC eluted with mixtures of *n*-hexane and EtOAc to afford alphitolic acid (90 mg, eluted with *n*-hexane/EtOAc 5:1 v/v) and a subfraction XI (500 mg, eluted with *n*-hexane/EtOAc 3:1→2.5:1 v/v), which was further subjected to silica gel CC eluted with mixtures of *n*-hexane and acetone to afford four further subfractions (XI–XIV). Three compounds, 3β,23-dihydroxylup-20(29)-en-28-oic acid (9.2 mg), hederagenin (25 mg), and maslinic acid (5 mg) were isolated from subfraction XII (80 mg, eluted with *n*-hexane/acetone 3.5:1 v/v), and were purified by semi-preparative HPLC eluted with mixtures of MeOH and H_2O (85:15) (flow rate, 8 ml/min; detection wavelength, 205 and 280 nm) at room temperature. Compounds **1** (5 mg) and **2** (20 mg) were obtained from subfraction XIII (50 mg, eluted with *n*-hexane/acetone 3:1 v/v) by preparative TLC on silica gel developed twice with $CHCl_3$-MeOH (15:1). Fraction IV (560 mg) was subjected to silica gel CC and eluted with mixtures of *n*-hexane and acetone to afford three further subfractions (XV–XVII). Compound **3** (10 mg) was obtained from subfraction XVI (23 mg, eluted with *n*-hexane/acetone 2:1 v/v) by preparative TLC developed with $CHCl_3$–MeOH (10:1, R_f 0.45). Finally, arjunolic acid (1.2 g) and β-sitosteryl 3-*O*-β-D-glucopyranoside (10 mg) were crystallized in $CHCl_3$–MeOH from fractions V and VI.

The EtOAc-soluble extract (46 g) exhibited 12.5% inhibitory activity at a concentration of 10 μg/ml in the mouse mammary organ culture assay, and was deemed to be of no further interest in this regard. However, since it exhibited an IC_{50} 8.6 μg/ml in the DPPH free-radical scavenging assay, it was subjected to silica gel CC eluted with mixtures of $CHCl_3$ and MeOH to obtain 13 fractions (XVIII–XXX). Gallic acid (35 mg) was purified from fraction XXII (200 mg, eluted with $CHCl_3$/MeOH 5:1 v/v) by activity-guided fractionation, and finally purified by Sephadex LH-20 CC eluted with MeOH.

3.5.1. 3β-cis-p-Coumaroyloxy-2α,23-dihydroxyolean-12-en-28-oic acid (*1*)

White amorphous powder ($CHCl_3$–MeOH), mp 252°C (dec), $[\alpha]_D^{20}$ +34.9° (MeOH, *c* 0.032). UV λ_{max} MeOH nm (log ε): 229 (4.09), 312 (4.28). IR ν_{max} (dried film) cm^{-1}: 3600–3100, 1695, 1604, 1514, 1456, 1168, 1049, 830, 757. HRFABMS *m/z*: 657.3763 ($C_{39}H_{54}O_7Na$ calc. 657.3767). EIMS *m/z* (rel. int.): 634 ($[M]^+$ 0.08), 616 (0.02), 598 (0.02), 588 (0.07), 572 (0.05), 422 (2.5), 315 (4.2), 248 (88), 203 (58), 147 (34). ^1H NMR: Table 1. ^{13}C NMR: Table 2.

3.5.2. 3β-trans-p-Coumaroyloxy-2α,23-dihydroxyolean-12-en-28-oic acid (*2*)

Pale yellowish amorphous powder ($CHCl_3$–MeOH), mp 252°C (dec), $[\alpha]_D^{20}$ +25.5° (MeOH, *c* 0.047). UV λ_{max} MeOH nm (log ε): 229 (4.05), 312 (4.29). IR ν_{max} (dried film) cm^{-1}: 3600-3100, 3273, 1694, 1514, 1454, 1390, 1168, 1049, 831, 754. HRFABMS *m/z*: 657.3787 ($C_{39}H_{54}O_7Na$ calc. 657.3767). EIMS *m/z* (rel. int.): 634 ($[M]^+$ 0.07), 452 (3), 387 (17), 248 (100), 203 (79), 147 (71). ^1H NMR: Table 1. ^{13}C NMR: Table 2.

*3.5.3. 23-trans-p-Coumaroyloxy-2α,3β-dihydroxyolean-12-en-28-oic acid (**3**)*

White amorphous powder ($CHCl_3$–MeOH), mp 210–214°C. $[\alpha]_D^{20}$ +21.8° (MeOH, *c* 0.055). UV λ_{max} MeOH nm (log ε): 229 (4.07), 313 (4.34). IR ν_{max} (dried film) cm^{-1}: 3341, 1697, 1604, 1515, 1456, 1261, 1168, 1029, 832, 755. HRFABMS *m/z*: 657.3751 ($C_{39}H_{54}O_7Na$ calc. 657.3767). EIMS *m/z* (rel. int.): 634 ($[M]^+$ 0.05), 452 (2), 387 (17), 248 (73), 203 (58), 147 (100). ^1H NMR: Table 1. ^{13}C NMR: Table 2.

3.5.4. Methyl 3β-(trans-4-methoxycinnamoyloxy)-2α,23-dihydroxyolean-12-en-28-oate

A stirred mixture of **2** (7.0 mg, 0.011 mol), anhydrous K_2CO_3 (7.6 mg, 0.055 mol), CH_3I (15.6 mg, 0.142 mol) in acetone (4 ml) was heated under reflux for 5 h. After cooling, the mixture was filtered and the filtrate evaporated to give the title compound (6.7 mg, 92%). Its physical and spectral data were comparable with literature values (Lee, 1998).

3.5.5. Methyl 23-(trans-4-methoxycinnamoyloxy)-2α,3β-dihydroxyolean-12-en-28-oate

A stirred mixture of **3** (9.0 mg, 0.014 mol), anhydrous K_2CO_3 (9.8 mg, 0.071 mol), CH_3I (20.2 mg, 0.14 mol) in acetone (4 ml) was heated under reflux for 5 h. After cooling, the mixture was filtered and the filtrate evaporated to give the title compound (9.3 mg, 99%). Its physical and spectral data were comparable with literature values (Lee, 1998).

3.5.6. Identification of known compounds

Alphitolic acid (Yaguchi et al., 1988), arjunolic acid (Jayasinghe et al., 1993), betulinic acid (Ikuta and Itokawa, 1988), 3-*epi*-betulinic acid (Kitajima et al., 1990), 2α,3α-dihydroxylup-20(29)-en-28-oic acid (Kumar et al., 1985), 3β,23-dihydroxylup-20(29)-en-28-oic acid (Ikuta and Itokawa, 1988), hederagenin (Ikuta and Itokawa, 1988), maslinic acid (Tchivounda et al., 1991), β-sitosteryl 3-*O*-β-D-glucopyranoside (Fujita and Nakayama, 1993), and syringaldehyde (Kokpol et al., 1993) were identified by comparison with reported data.

Acknowledgements

We are grateful to Dr. Yoneo Sagawa, University of Hawaii, Honolulu, HI for collecting and identifying the plant material with financial support of the National Cancer Institute, Bethesda, Maryland. We thank Mr. Richard Dvorak of the Department of Medicinal Chemistry and Pharmacognosy, University of Illinois at Chicago (UIC) for recording the EIMS, and Dr. Rob Kleps of the Research Resource Center, UIC for facilitating the running of the 500 MHz NMR spectra. We also thank Mr. Keith Fagerquist of the Mass Spectrometry Service Laboratory, Department of Chemistry, University of Minnesota for recording the HRFABMS. This research was supported by program project P01 CA48112, funded by the National Cancer Institute, NIH, Bethesda, MD.

References

Bombardelli, E., Bonati, A., Gabetta, H., Mustich, G., 1974. Triterpenoids of *Terminalia sericea*. Phytochemistry 13, 2559–2562.

Fujita, T., Nakayama, M., 1993. Monoterpene glucosides and other constituents from *Perilla frutescens*. Phytochemistry 34, 1545–1548.

Fujita, Y., Uehara, I., Morimoto, Y., Nakashima, M., Hatano, T., Okuda, T., 1988. Studies on inhibition mechanism of antioxidation by tannins and flavonoids. II. Inhibition mechanism of caffeetannins isolated from leaves of *Artemisia* species. Yakugaku Zasshi 108, 129–135.

Govindachari, T.R., Jadhav, S.J., Joshi, B.S., Kamat, V.N., Mohamed, P.A., Parthasarathy, P.C., Patankar, S.J., Rane, D.F., Viswanathan, N., 1969. Chemical investigation of some Indian plants: part IV. Indian Journal of Chemistry 7, 308–310.

Hillebrand, W.F., 1888. Flora of the Hawaiian Islands: A Description of Their Phanerogams and Vascular Cryptogams. Williams & Norgate, London, pp. 128–129.

Ikuta, A., Itokawa, H., 1988. Triterpenoids of *Paeonia japonica* callus tissue. Phytochemistry 27, 2813–2815.

Jayasinghe, L., Wannigama, G.P., Macleod, J.K., 1993. Triterpenoids from *Anamirta cocculus*. Phytochemistry 34, 1111–1116.

Kinghorn, A.D., Fong, H.H.S., Farnsworth, N.R., Mehta, R.G., Moon, R.C., Moriarty, R.M., Pezzuto, J.M., 1998. Cancer chemopreventive agents discovered by activity-guided fractionation: A review. Current Organic Chemistry 2, 597–612.

Kitajima, J., Shindo, M., Tanaka, Y., 1990. Two new triterpenoid sulfates from the leaves of *Schefflera octophylla*. Chemical and Pharmaceutical Bulletin 38, 714–716.

Kokpol, U., Chavasiri, W., Chittawong, V., Bruce, M., Cunningham, G.N., Miles, D.H., 1993. Long chain aliphatic alcohols and saturated carboxylic acids from heartwood of *Rhizophora apiculata*. Phytochemistry 33, 1129–1131.

Kumar, N.S., Muthukuda, P.M., Wazeer, M.I.M., 1985. A lupenediol from *Euonymus revolutus*. Phytochemistry 24, 1337–1340.

Lee, C.K., 1998. New triterpenes from the heartwood of *Melaleuca leucadendron* L. Journal of the Chinese Chemical Society 45, 303–306.

Lee, M.H., Nishimoto, S., Yang, L.L., Yen, K.Y., Hatano, T., Yoshida, T., Okuda, T., 1997. Two macrocyclic hydrolysable tannin dimers from *Eugenia uniflora*. Phytochemistry 44, 1343–1349.

Lowry, J.B., 1968. The distribution and potential taxonomic value of alkylated ellagic acids. Phytochemistry 7, 1803–1813.

Mehta, R.G., Moon, R.C., 1991. Characterization of effective chemopreventive agents in mammary gland *in vitro* using an initiation-promotion protocol. Anticancer Research 11, 593–596.

Mitscher, L.A., Wu, W.N., Beal, J.L., 1973. The isolation and structural characterization of 5-*O*-methyldesmethoxymatteucinol from *Eugenia javanica*. Lloydia 36, 422–425.

Nonaka, G.I., Ishimaru, K., Watanabe, M., Nishioka, I., Yamauchi, T., Wan, A.S.C., 1987. Tannins and related compounds. LI. Elucidation of the stereochemistry of the triphenoyl moiety in castalagin and vescalagin, and isolation of 1-*O*-galloyl castalagin from *Eugenia grandis*. Chemical and Pharmaceutical Bulletin 35, 217–220.

Painuly, P., Tandon, J.S., 1983a. Two 3-*C*-methylflavone glycosides from *Eugenia kurzii*. Phytochemistry 22, 243–245.

Painuly, P., Tandon, J.S., 1983b. A new triterpene from *Eugenia kurzii* Duthie. Indian Journal of Chemistry 22B, 284–285.

Pezzuto, J.M., Song, L.L., Lee, S.K., Shamon, L.A., Mata-Greenwood, E., Jang, M., Jeong, H.J., Pisha, E., Mehta, R.G., Kinghorn,

A.D., 1999. Bioassay methods useful for activity-guided isolation of natural product cancer chemopreventive agents. In: Hostettmann, K., Gupta, M.P., Marston, A. (Eds.), Chemistry, Biological and Pharmacological Properties of Medicinal Plants from the Americas. Harwood Academic Publishers, Amsterdam, pp. 81–110.

Sakar, M.K., Petereit, F., Nahrstedt, A., 1993. Two phloroglucinol glucosides, flavan gallates and flavonol glycosides from *Sedum sediforme* flowers. Phytochemistry 33, 171–174.

Schapoval, E.E.S., Silveira, S.M., Miranda, M.L., Alice, C.B., Henriques, A.T., 1994. Evaluation of some pharmacological activities of *Eugenia uniflora* L. Journal of Ethnopharmacology 44, 137–142.

Tapondjou, A.L., Ngounou, N.F., Lontsi, D., Sondengam, B.L., Martin, M.T., Bodo, B., 1995. Pentacyclic triterpenes from *Myrianthus liberecus*. Phytochemistry 40, 1761–1764.

Tchivounda, H.P., Koudogbo, B., Besace, Y., Casadevall, B.E., 1991. Triterpene saponins from *Cylicodiscus gabunensis*. Phytochemistry 30, 2711–2716.

Yaguchi, Y., Sakurai, N., Nagai, M., Inoue, T., 1988. Constituents of *Myrica rubra*. III. Structures of two glycosides of myricanol. Chemical and Pharmaceutical Bulletin 36, 1419–1424.

Yazaki, Y., 1977. Polyphenols and triterpenoids of *Eugenia gustavioides* wood. Phytochemistry 16, 138–139.

PERGAMON

Phytochemistry 58 (2001) 129–135

PHYTOCHEMISTRY

www.elsevier.com/locate/phytochem

Stress induced carbazole phytoalexins in *Glycosmis* species

Thomas Pacher[a], Markus Bacher[1,b], Otmar Hofer[b], Harald Greger[a,*]

[a]*Comparative and Ecological Phytochemistry Department, Institute of Botany, University of Vienna, Rennweg 14, A-1030 Wien, Austria*
[b]*Institute of Organic Chemistry, University of Vienna, Währingerstrasse 38, A-1090 Wien, Austria*

Received 28 November 2000; received in revised form 4 April 2001

Abstract

Induced formation of a series of carbazole alkaloids was observed in leaves of *Glycosmis parviflora* and *G. pentaphylla* after wounding, UV-irradiation, and particularly after inoculation with the fungus *Botrytis cinerea*. Chemical variation between different provenances and even individuals of *G. parviflora* led to an accumulation of different derivatives from which three proved to be undescribed natural products. Their structures were identified by spectroscopic methods and named carbalexins A, B, and C. Bioautographic tests on TLC plates with *Cladosporium herbarum* exhibited strong antifungal activity for the new carbalexins as well as for the already known 2-hydroxy-3-methylcarbazole, but only weak effects for the pyranocarbazole glycoborinine. Detailed experiments with marked infection areas confirmed the restricted accumulation of carbazole derivatives which could not be detected in non-infected areas of the same leaf. Apart from carbazoles, in some individuals of *G. parviflora* an additional accumulation of the pyranoquinolones flindersine and methylflindersine was induced, which supports the already previously discussed biogenetic connections between carbazoles and prenylated quinolones. © 2001 Elsevier Science Ltd. All rights reserved.

Keywords: *Glycosmis parviflora*; *G. pentaphylla*; Rutaceae; Carbazoles; Quinolones; Antifungal; Antibacterial; Cytotoxic; Phytoalexins; Stress metabolites

1. Introduction

The formation of 3-methylcarbazole alkaloids represents a rare biogenetic trend mainly restricted to the four Rutaceae genera *Clausena*, *Glycosmis*, *Micromelum*, and *Bergera* (formerly section Bergera of the genus *Murraya*) (Kong et al., 1986; Samuel et al., 2001), and is known elsewhere only from *Ekebergia senegalensis* of the related family Meliaceae (Lontsi et al., 1985). Although the biosynthesis of this type of carbazoles is not yet entirely understood, it most likely derives from the anthranilic acid pathway via prenylated quinolones (Kong et al., 1986). Biogenetically 3-methylcarbazoles can be clearly separated from all other carbazole structures known from micro-organisms which are formed either via the polyketide or tryptophan pathway (Chakraborty and Roy, 1991). Based on literature and our current comparative phytochemical analyses within many *Glycosmis* species, carbazoles were shown to be mainly accumulated in the stem bark and to a lesser extent in the roots (Bhattacharrya et al., 1985; Chowdhury et al., 1987; Jash et al., 1992; Vajrodaya, 1998; Lukaseder, 2000) but they were only rarely found in the leaves (Kamaruzzman et al., 1989; Greger et al., 1992). However, we show that wounding, UV-irradiation, and infection with the fungus *Botrytis cinerea* resulted in an accumulation of carbazoles in the leaves of two *Glycosmis* species. Since the isolated compounds displayed pronounced antifungal activity in bioautographic tests on TLC plates and were accumulated only in the area of infection, they were regarded as a new class of phytoalexins. Especially different provenances of the more widespread *G. parviflora* (Sims) Little (syn.: *G. citrifolia* (Willd.) Lindley) responded clearly with the formation of a series of carbazoles (Fig. 1). Various accumulation trends towards different carbazole derivatives were observed between different geographical provenances and even different individuals. Three compounds were shown to be hitherto undescribed natural compounds named carbalexins A (**1**), B (**2**), and C (**3**) from which however, carbalexin B (**2**) was already previously reported as a synthetic product

* Corresponding author. Tel.: +43-1-4277-54070; fax: +43-1-4277-9541.

E-mail address: greger@s1.botanik.univie.ac.at (H. Greger).

[1] Current address: Novartis, Brunnerstrasse 59, A-1235 Vienna, Austria.

0031-9422/01/$ - see front matter © 2001 Elsevier Science Ltd. All rights reserved.
PII: S0031-9422(01)00186-8

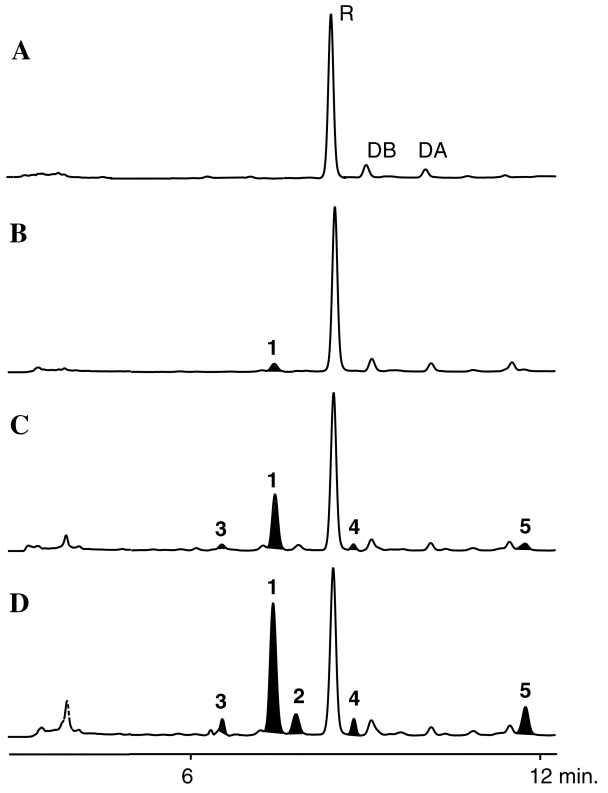

Fig. 1. Chronological composite of HPLC profiles obtained from combined leaves of different individuals of *G. parviflora* (RUT-69) after inoculation with *B. cinerea* : (A) untreated leaves without carbazoles, (B) after 2 days with small amount of carbalexin A (**1**), (C) and (D) different carbazoles were progressively accumulated after 3 and 4 days, respectively. **1**–**3** = carbalexins A-C, **4** = 2-hydroxy-3-methylcarbazole, **5** = glycoborinine, R = ritigalin, DA = dehydrothalebanin A, DB = dehydrothalebanin B. Mobile phase was MeOH (gradient 60–100%) in aqueous buffer (see Experimental).

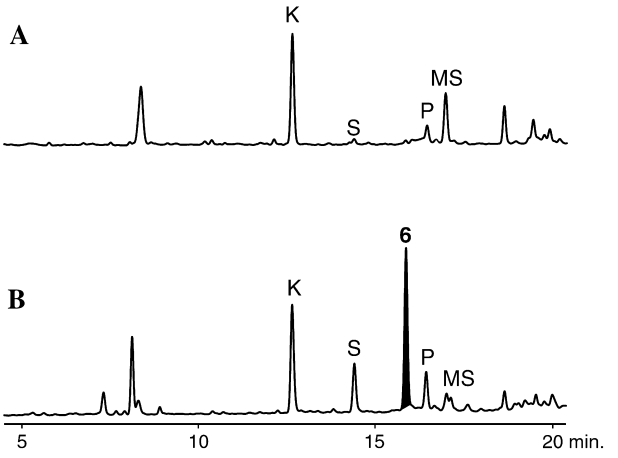

Fig. 2. HPLC comparison of lipophilic crude extracts of dried leaf parts from herbarium material of one individual of *G.* ex aff. *mauritiana* collected in Sri Lanka (WU, HG20-A). (A) Profile of an intact terminal leaf and (B) an infested basal leaf accumulating the carbazole glycozolidol (**6**). K = kokusaginine, S = sinharine, MS = methylsinharine, P = phenaglydon. Mobile phase was acetonitrile (gradient 20–60%) in aqueous buffer (see Experimental).

(Mester et al., 1980). A similar multi component response was also detected in *G. pentaphylla* (Retz.) DC. collected in Sri Lanka. In this case, however, only small quantities of carbazoles were formed. In light of these results the previously published carbazole glycozolidol (**6**) from the leaves of *G.* ex aff. *mauritiana* (Lam.) Tanaka (erroneously reported as *G. cyanocarpa* (Bl.) Spreng.) (Greger et al., 1992) is now also suggested to be formed after induction. In fact, a reinvestigation of small samples of corresponding herbarium material has shown that glycozolidol was only accumulated in infested older leaves, whereas younger intact leaves of the same individual did not contain any carbazole (Fig. 2). However, it should be pointed out that in this case only dried material was used and no induction experiments could be carried out with fresh leaves.

Although some 300 structures of phytoalexins were already isolated after experiments with approximately 900 species belonging to 40 plant families (Harborne, 1999), no carbazoles were described so far as phytoalexins. Moreover, only few reports on phytoalexins in the family Rutaceae were known, focussing only on the root bark of *Citrus limon* where the coumarins scoparone (Afek and Sztejnberg, 1988), xanthyletin (Khan et al., 1985), and seselin (Vernenghi et al., 1987) as well as the acetophenone xanthoxylin (Hartmann and Nienhaus, 1974) were isolated. The present paper reports on different induction experiments on different provenances of *G. parviflora* and one from *G. pentaphylla*. We also describe herein antifungal activity of the isolated carbazoles against the test fungus *C. herbarum* by bioautographic tests on TLC plates as well as structure elucidation of the new phytoalexins by spectroscopic methods.

2. Results and discussion

HPLC profiles of lipophilic crude extracts of freshly harvested leaves of *G. parviflora* and *G. pentaphylla* showed clear chemical differences after wounding, UV-irradiation and especially after inoculation of the leaves with aqueous spore suspensions of *Botrytis cinerea*. Besides the constitutive metabolites, consisting of the previously published amides ritigalin (Hofer et al., 1995) and dehydrothalebanins A and B (Greger et al., 1996) in *G. parviflora* (Fig. 1) and the well-known alkaloids arborine, skimmianine, and arborinine (Mester, 1983; Greger et al., 1993) in *G. pentaphylla*, both species additionally produced a series of carbazoles. Fungal infection mostly resulted in higher levels of accumulation than mere wounding or UV-irradiation. However, in wounded leaves, later infection can never be completely excluded during storing in a humid chamber. Comparisons of three provenances of *G. parviflora* originating from south China (Kwangchou), Indonesia

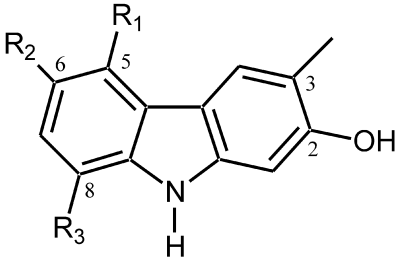

		R_1	R_2	R_3
1	carbalexin A	OCH_3	H	H
2	carbalexin B	H	H	OCH_3
3	carbalexin C	H	OCH_3	H
4	2-hydroxy-3-methylcarbazole	H	H	H

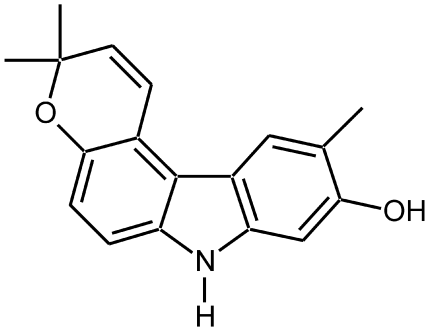

5 glycoborinine

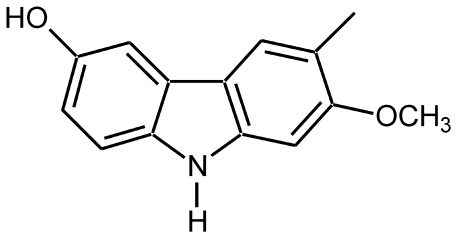

6 glycozolidol

(Java), and USA (California) as well as between different individuals from the same provenance showed chemical variation in accumulating different carbazoles. However, carbalexin A (**1**) was the most common and dominating derivative. In general, the individuals from south China (RUT-69) showed the highest degree of carbazole accumulation, whereas those from USA (RUT-402) and Indonesia (RUT-331, RUT-333) deviated by a rather weak phytoalexin response mostly leading only to small amounts of carbalexin A (**1**). Compared with individuals from south China, these provenances could also be distinguished by greater amounts of the two amides dehydrothalebanin A and B.

To confirm the role of carbazoles as phytoalexins only a limited area of a leaflet (ca. 1 cm^2) of a pinnate leaf of *G. parviflora* was infected with *B. cinerea*. After 4 days of incubation the leaf was separated into different parts around the infection zone which were subsequently extracted for comparative HPLC analyses. Importantly, only the extract from the infected zone showed an accumulation of carbazoles **1**–**5** with a preponderance of **1**, whereas those from the surrounding areas exhibited profiles identical to untreated leaves.

Besides the formation of different carbazoles, some individuals of *G. parviflora* additionally accumulated quinoline alkaloids after elicitation. They were identified as flindersine and methylflindersine by co-chromatography with authentic samples. However, in contrast to the carbazoles they did not show any antifungal activity against *C. herbarum*. With regard to previous findings of that species it should be pointed out that the chemical profile reported for a Taiwanese collection, published as the synonym *G. citrifolia* (Wu et al., 1995), completely deviated from all our samples derived from different geographical provenances. With respect to the many acridones already reported for other Taiwanese collections of *G. citrifolia* (e.g. Furukawa et al., 1984), which could never be detected in our provenances, it was tempting to suggest that all these collections did not belong to *G. parviflora* but to *G. erythrocarpa* (Hay.) Hayata. The latter species is widely distributed and endemic in Taiwan (Stone, 1985). This taxonomic confusion was probably caused by the Flora of Taiwan (Anon, 1993), where the old synonym *G. citrifolia* is erroneously used instead of *G. erythrocarpa*.

In order to obtain sufficient amounts of the new carbazoles for isolation and structure elucidation as well as for subsequent bioassays, fresh leaves from different individuals of the Chinese provenance (RUT-69), cultivated in the Botanical Garden of the University of Vienna, were collected and combined. Subsequently they were cut into small pieces and sprayed with an aqueous suspension of conidiospores of *B. cinerea*. After 4 days in a moist chamber the infected leaves were extracted with MeOH and analyzed by preparative MPLC linked with UV detection. Based on spectral characteristics and on comparison with already published data, compounds **4** and **5** were readily identified as the known carbazoles 2-hydroxy-3-methylcarbazole (**4**) (Mester et al., 1979; Bhattacharyya et al., 1986) and glycoborinine (**5**) (Chakravarty et al., 1999). However, compounds **1**–**3** proved to be new natural products.

They could already be distinguished by characteristic UV spectra showing three distinct maxima at 330, 293, and 239 nm (MeOH) for carbalexin A (**1**) and only two at 310 and 231 nm for carbalexin C (**3**). Carbalexin B (**2**), by contrast, was characterized by an intermediate spectrum with only a weak maximum at 330 nm but two strong ones at 299 and 235 nm. The IR spectra of all three compounds showed typical signals at 3598–3616 cm^{-1} ($CHCl_3$) for phenolic hydroxy groups and at 3468–3474 cm^{-1} for >N–H stretching. In addition, a prominent signal in the range of 1046–1108 cm^{-1} was also characteristic for this type of carbazole. From the ^1H NMR spectra of compounds **1**–**3** it followed immediately that they are, like the already known derivatives **4** and **5**, 2-hydroxy-3-methylcarbazoles. This was indicated by the methyl singlet at δ ca. 2.40 ppm and the two characteristic aromatic singlets at δ ca. 6.85 (H-1) and ca. 7.7–8.0 ppm (H-4). While in compound **4**, the previously reported 2-hydroxy-3-methylcarbazole (Bhattacharyya et al., 1986), one aromatic ring was not further substituted, the ^1H NMR spectra of compounds **1**–**3** were characterized by an additional methoxy group at that ring. The EIMS spectra were very similar and showed molecular ions of $m/z = 227$ (100%), which suggested also a series of three isomeric methoxy-hydroxy-methylcarbazoles. The coupling patterns of the three remaining A ring protons in combination with NOE measurements allowed the determination of the structures of the compounds and the assignments of all proton resonances. Carbalexins A (**1**) and B (**2**), were characterized by three neighbouring protons (*d*, *dd*, and *d*, with *ortho* couplings of 8.0 Hz and *meta* couplings <1 Hz), which left only positions 5 and 8 for the methoxy group. Irradiation at the methoxy resonance of **1** resulted in strong effects at the characteristic low-field singlet at $\delta = 8.02$ ppm (H-4) and the dublet at $\delta = 6.65$ ppm (consequently H-6), proving position 5 for the methoxy group. In the case of compound **2** only the dublet at $\delta = 6.83$ ppm (H-7) showed a strong effect which is only compatible with the 8-methoxy derivative. Irradiation of the methoxy group in carbalexin C (**3**) gave strong NOEs for the characteristic low-field signal at $\delta = 7.44$ ppm (H-5, *d* with a *meta* coupling of 2.5 Hz) and the *dd* at $\delta = 6.96$ ppm (consequently H-7, $J = 8.6$ and 2.5 Hz), which proved position 6 for the methoxy substituent.

Because of the weak phytoalexin response in *G. pentaphylla* (RUT-202), the additionally accumulated carbazoles could not be isolated and were only identified by HPLC comparison with authentic samples. In addition to the constitutive metabolites, consisting of the quinazoline arborine, the furoquinoline skimmianine, and the acridone arborinine, mainly carbalexin C (**3**) and glycoborinine (**5**) were additionally formed in different individuals, sometimes accompanied by traces of carbalexin A (**1**). However, in contrast to *G. parviflora* carbalexin C (**3**) was dominating in most individuals.

To determine the antifungal activity of carbazoles **1**–**5**, bioassays were carried out on TLC plates sprayed with a conidiospore suspension of *C. herbarum*. Definite amounts from 50 to 3 μg showed nearly the same activity for all the new carbalexins A–C (**1**–**3**) as well as for compound **4**. All four compounds exhibited clear inhibition zones even at the lowest concentration. In contrast, glycoborinine (**5**) showed very weak activity only at the higher doses (Fig. 3). In addition to antifungal properties, the most prominent phytoalexin carbalexin A (**1**) was also tested against the bacterium *Staphylococcus aureus* on TLC plates as well as screened for cytotoxicity against brine shrimp nauplii (*Artemia salina*) in a micro-dilution assay. In this case compound **1** also showed a strong antibacterial activity with inhibition zones even at the lowest concentration at 3 μg, but only a weak cytotoxic effect with LC_{50} at 36 and LC_{90} at 108 ppm. The antibacterial activity of hydroxycarbazoles was already observed in the case of glycozolidol (**6**), which was especially effective against Gram-positive bacteria (Battacharyya et al., 1985). In contrast to the carbazoles, the induced pyranoquinolones did not exhibit any antifungal activity and hence could not be interpreted as phytoalexins.

The present data again showed that the type of phytoalexin produced in plants is often related to existing preinfectional agents present in a given relationship (Harborne, 1999). Carbazoles represent a class of secondary metabolites typical for *Glycosmis* and closely related genera grouped together in the tribe Clauseneae of the Rutaceae subfamily Aurantioideae (Kong et al., 1986; Samuel et al., 2001). However, extensive studies within the genus *Glycosmis* showed that they are mainly accumulated in the stem and root bark (Chowdhury et al., 1987; Vajrodaya, 1998; Lukaseder, 2000). Their presence in the leaves (Kamaruzzman et al., 1989; Greger et al., 1992) might have been caused by extracting larger quantities of plant material containing leaves infested with different organisms. This hypothesis could now be supported by a reinvestigation of *G.* ex aff. *mauritiana* where the previously reported glycozolidol (**6**) (Greger et al., 1992) was only found in infested older leaves (Fig. 2). Preliminary inoculation studies with fresh leaves of many *Glycosmis* species showed however, that the formation of carbazole phytoalexins is probably restricted to only a few species. Chromosome counts have shown that all provenances of *G. parviflora* and *G. pentaphylla* from Sri Lanka deviate from the other species by higher numbers, being hexaploid ($2n = 54$) in the former and pentaploid ($2n = 45$) in the latter species (Lambrou, unpubl.). Hence, it is tempting to speculate about a link between the additional formation of carbazoles and polyploidy.

Regarding the bioactivity of hydroxy-3-methylcarbazoles, one would suggest that their antifungal and antibacterial properties were due to the free phenolic hydroxy group at C-2. However, the very weak activity

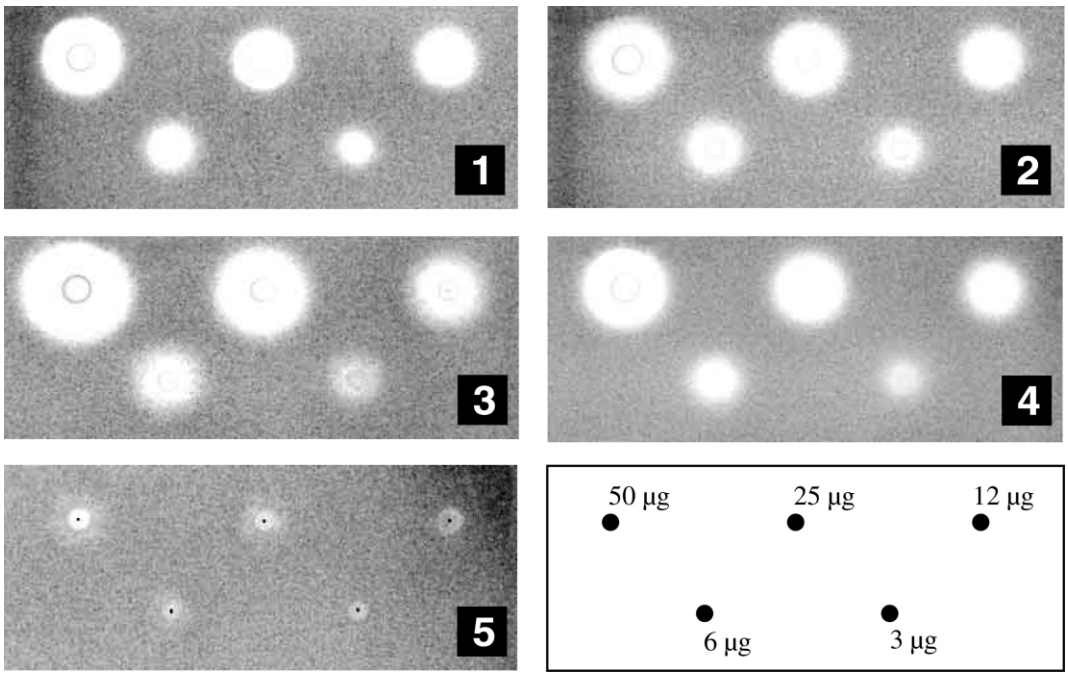

Fig. 3. Bioautographic comparison of different antifungal activities of five carbazole phytoalexins by direct spraying of TLC plates with a conidial suspension of the test fungus *Cladosporium herbarum*. (**1**) Carbalexin A, (**2**) carbalexin B, (**3**) carbalexin C, (**4**) 2-hydroxy- 3-methylcarbazole, (**5**) glycoborinine. The quantities used for each plate for serial dilution are indicated in the box.

of glycoborinine (**5**) (Fig. 3), containing such a hydroxy group but an additionally condensed pyran ring in aromatic ring A, clearly demonstrated that other substitutions in the molecule also play an important role in bioactivity. With regard to the still unknown biosynthesis of carbazoles, their co-occurrence with pyranoquinolones in infected leaves of *G. parviflora* deserves special attention and supports the hypothesis of a common biosynthetic origin. In this context it should also be pointed out, that the very rare phenanthridine alkaloid phenaglydon (Wurz et al., 1993) was also detected in the leaves of *G.* ex aff. *mauritiana* (Greger et al., 1992) (Fig. 2). This compound is also characterized by a methyl group in aromatic ring B, which suggests a similar ring closure with a prenyl group as in 3-methylcarbazoles. A possible close biogenetic relation of phenaglydon towards prenylated quinolones was already mentioned previously (Wurz et al., 1993).

3. Experimental

3.1. General

NMR: Bruker, DRX 250. MS: Finnigan MAT 900 S, IR: Perkin-Elmer 16PC FT-IR. UV: Hewlett-Packard, 8452A diode array spectrophotometer. HPLC: Hewlett-Packard 1090 II, UV diode array detection at 230 nm, column 250 × 4 mm, Hypersil BDS C-18, 5 µm, mobile phase MeOH (gradient 60–100%) or acetonitrile (gradient 20–60%) in aqueous buffer (0.015 M *o*-phosphoric acid, 0.0015 M tetrabutylammonium hydroxide, pH 3), flow rate 1 ml/min.

3.2. Plant material

Fresh leaves of *G. parviflora* and *G. pentaphylla* were collected from plants grown from seeds and cultivated in the Botanical Garden of the University of Vienna (HBV). Seeds from *G. parviflora* were obtained from (i) Botanical Garden Kwangchou, south China (RUT-69), (ii) Citrus Research Institute Riverside, California, USA (RUT-402), (iii) Botanical Garden Bogor, Java, Indonesia (RUT-331, RUT-333). Seeds from *G. pentaphylla* were collected by the late Professor S. Balasubramaniam in the campus of the University of Peradeniya, Sri Lanka (RUT-202). Plants were kept in the greenhouse during winter. Voucher specimens are deposited at the Herbarium of the Institute of Botany, University of Vienna (WU).

3.3. Induction of carbazoles

3.3.1. Fungal infection

Freshly harvested leaves were cut into small strips of 1–2 mm and divided into three portions from which one, serving as control, was immediately homogenized and extracted with MeOH. The second portion was placed on moistened blotters in the bottom of a plastic chamber and sprayed with a spore suspension of *Botrytis cinerea*. After incubation for 4 days at room temperature the leaf strips were homogenized and extracted

as above. The third portion was treated in the same manner but without fungal infection.

3.3.2. UV-irradiation

Freshly harvested intact leaves were irradiated with UV light (254 nm) at each surface for 1/2 h and transferred into a moist chamber. For control, intact leaves were directly placed in a humid chamber without UV light. After 4 days both samples were homogenized and extracted as mentioned above.

3.4. Extraction and isolation

Infected leaves from different provenances and individuals of *G. parviflora* and *G. pentaphylla* were ground and extracted separately with MeOH at room temp. for 3 days, filtered and conc. The aqueous residues were extracted with $CHCl_3$ and the conc. $CHCl_3$ fractions were used for comparative HPLC and preliminary bioassays. For preparative isolation infected leaves of different individuals of the Chinese *G. parviflora* (RUT-69) were combined (92 g) and treated in the same way. The lipophilic crude extract was evapd to dryness under reduced pressure (980 mg), and roughly separated by column chromatography (Merck silica gel 60, 35–70 mesh) with hexane, Et_2O and MeOH. The combined fractions eluted with 50% Et_2O in hexane, 100% Et_2O, and 5% MeOH in Et_2O (210 mg) were further separated by MPLC (400 × 40 mm column, Merck LiChroprep Si 60, 25–40 μm, UV-detection, 254 nm) to yield 14 mg impure carbalexin A (**1**), 2 mg carbalexin B (**2**), 2 mg carbalexin C (**3**), 2.5 mg 2-hydroxy-3-methlycarbazole (**4**), and 4 mg glycoborinine (**5**). Final purification of carbalexin A (**1**) was achieved by prep TLC (Merck, Si gel 60, 0.5 mm; CH_2Cl_2 : Et_2O = 85 : 15) to give 10 mg pure compound. In addition, 60 mg nearly pure ritigalin was isolated from the unpolar CC fractions eluted with 25% Et_2O in hexane. Small amounts of dehydrothalebanin A and B, and flindersine together with methylflindersine were isolated with 50% Et_2O in hexane and 10% MeOH in Et_2O, respectively, and were identified by HPLC comparison with authentic samples.

3.5. Fungal and bacterial bioassays

Definite amounts of pure compounds were applied on TLC plates (Merck, Si gel 60, 2.5 mm) in a twofold dilution series from 50 to 3 μg and sprayed either with an aqueous spore suspension of *C. herbarum* containing malt bouillon (Merck) as nutrient or with a freshly prepared bacterial suspension of *S. aureus* in nutrient broth (Merck). Plates for antifungal bioassays were incubated in moist chambers for 3 days in the dark at room temp. For antibacterial tests the plates were incubated for 18 h at 37°C, sprayed with 3-(4-iodophenyl)-2-(4-nitro-phenyl)-5-phenyl-2H-tetrazoliumchloride (3 mg/ml H_2O), stored for another 3 h and sprayed with 70% EtOH to stop bacterial growth. White inhibition zones of different size indicated the degree of antifungal activity on the dark mycelial layer, and white zones on a pinkish background were indicative for antibacterial activity.

3.6. Brine shrimp toxicity assay

Tests were performed in triplicate in 96-well microplates as described by Solis et al. (1993). Brine shrimp (*Artemia salina*) eggs were purchased and kept in artificial, aerated seawater at room temp. After 48 h, 10–15 freshly hatched nauplii were added to each well containing different concentrations (100–3.12 ppm) of carbalexin A (**1**). 1% DMSO was added to improve solubility. After 24 h the number of killed nauplii in each well was counted and compared to controls. LC_{50} and LC_{90} values were calculated by probit analysis with 95% confidence intervals.

3.7. Carbalexin A, 2-hydroxy-5-methoxy-3-methylcarbazole (*1*)

Colourless crystals from $CHCl_3$, mp 178–180°C. UV λ^{MeOH} nm 330, 317, 293, 239. IR ν^{CHCl4} cm^{-1} 3614 *w*, 3482 *w*, 2930 *m*, 2856 *w*, 1640 *w*, 1616 *m*, 1586 *w*, 1506 *m*, 1466 *s*, 1450 *w*, 1436 *w*, 1348 *w*, 1326 *s*, 1268 *m*, 1230 *w*, 1206 *w*, 1164 *w*, 1128 *m*, 1104 *s*, 1008 *w*, 978 *w*, 890 *w*, 834 *w*. ^{1}H NMR ($CDCl_3$) δ = 8.02 (*s*, 1H, 4-H), 7.89 (*br s*, 1H, NH), 7.25 (*dd*, 1H, *J* = 8.0 and 8.0 Hz, 7-H), 6.98 (*d*, 1H, *J* = 8.0 Hz, 8-Hz), 6.82 (*s*, 1H, 1-H), 6.65 (*d*, 1H, *J* = 8.0 Hz, 6-H), 4.07 (*s*, 3H, 5-OCH_3), 2.41 (*s*, 3H, 3-CH_3). EIMS (70 eV, 100°C) *m/z* : 227 (100%) M^+, 212 (41), 197 (27), 184 (37), 154 (7), 114 (12). HR-MS: M_{exp} 227.0947, M_{calc} 227.0946 for $C_{14}H_{13}NO_2$.

3.8. Carbalexin B, 2-hydroxy-8-methoxy-3-methylcarbazole (*2*)

Colourless crystals from $CHCl_3$, mp 196–198°C. UV λ^{MeOH} nm 330, 317 *sh*, 299, 251 *sh*, 239 *sh*, 235. IR ν ^{CHCl3} cm^{-1} 3616 *m*, 3468 *w*, 2974 *m*, 2924 *m*, 2894 *w*, 1638 *w*, 1578 *w*, 1508 *w*, 1466 *w*, 1448 *m*, 1390 *s*, 1304 *w*, 1264 *m*, 1254 *s*, 1142 *w*, 1088 *m*, 1046 *s*, 918 *w*, 876 *m*. ^{1}H NMR ($CDCl_3$) δ = 8.04 (*br s*, 1H, NH), 7.76 (*s*, 1H, 4-H), 7.55 (*d*, 1H, *J* = 8.0 Hz, 5-H), 7.11 (*dd*, 1H, *J* = 8.0 and 8.0 Hz, 6-H), 6.87 (*s*, 1H, 1-H), 6.83 (*d*, 1H, *J* = 8.0 Hz, 7-H), 4.00 (*s*, 3H, 8-OCH_3), 2.40 (*s*, 3H, 3-CH_3). EIMS (70 eV, 100°C) *m/z* : 227 (100%) M^+, 212 (28), 184 (26), 154 (7), 83 (7), 71 (5), 57 (7). HR-MS: M_{exp} 227.0949, M_{calc} 227.0946 for $C_{14}H_{13}NO_2$.

3.9. Carbalexin C, 2-hydroxy-6-methoxy-3-methylcarbazole (*3*)

Colourless oil. UV λ ^{MeOH} nm 310, 263 *sh*, 231. IR ν^{CHCl3} cm^{-1} 3598 *w*, 3474 *w*, 2928 *m*, 2856 *w*, 1640 *m*,

1592 *w*, 1488 *s*, 1468 *s*, 1436 *m*, 1382 *w*, 1332 *w*, 1294 *s*, 1276 *w*, 1170 *w*, 1146 *m*, 1132 *m*, 1108 *s*, 1034 *w*, 1014 *m*, 860 *w*, 842 *w*. ^{1}H NMR ($CDCl_3$) $\delta = 7.74$ (*s*, 1H, 4-H), 7.70 (*br s*, 1H, NH), 7.44 (*d*, 1H, $J = 2.5$ Hz, 5-H), 7.25 (*d*, 1H, $J = 8.6$ Hz, 8-H), 6.96 (*dd*, 1H, $J = 8.6$ and 2.5 Hz, 7-H), 6.82 (*s*, 1H, 1-H), 3.91 (*s*, 3H, 6-OCH_3), 2.40 (*s*, 3H, 3-CH_3). EIMS (70 eV, 100°C) *m*/*z* : 227 (100%) M^+, 212 (71), 184 (38), 154 (11), 114 (17), 97 (10), 83 (16), 71 (22), 57 (38). HR-MS: M_{exp} 227.0946, M_{calc} 227.0946 for $C_{14}H_{13}NO_2$.

Acknowledgements

The authors are grateful to the late Professor S. Balasubramaniam, Department of Botany, University of Peradeniya, Sri Lanka and Professor R. Scora from the Citrus Research Institute in Riverside, California for providing *Glycosmis* seeds. Dr. M. Lambrou from the Institute of Botany, University of Vienna is acknowledged for the determination of chromosome numbers. This project was funded by the Austrian National Committee for the Intergovernmental Programme 'Man and Biosphere'.

References

Afek, U., Sztejnberg, A., 1988. Scoparone, a phytoalexin associated with resistance of citrus to *Phytophthora citrophora*. Phytopathology 78, 1678–1682.

Anon, 1993. Flora of Taiwan, 2nd Edition, Vol. III. Editorial Committee of the Flora of Taiwan, Taipei, ROC, p. 519.

Bhattacharyya, P., Chakrabartty, P.K., Chowdhury, B.K., 1985. Glycozolidol, an antibacterial carbazole alkaloid from *Glycosmis pentaphylla*. Phytochemistry 24, 882–883.

Bhattacharyya, P., Jash, S.S., Chowdhury, B.K., 1986. A biogenetically important carbazole alkaloid from *Murraya koenigii* Spreng. Chemistry and Industry, 246.

Chakraborty, D.P., Roy, S., 1991. Carbazole alkaloids III. In: Herz, W., Kirby, G.W., Steglich, W., Tamm, Ch. (Eds.), Progress in the Chemistry of Organic Natural Products, Vol. 57. Springer, Wien, New York, pp. 71–152.

Chakravarty, A.K., Sarkar, T., Masuda, K., Shiojima, K., 1999. Carbazole alkaloids from roots of *Glycosmis arborea*. Phytochemistry 50, 1263–1266.

Chowdhury, B.K., Mustapha, A., Garba, M., Bhattacharyya, P., 1987. Carbazole and 3-methylcarbazole from *Glycosmis pentaphylla*. Phytochemistry 26, 2138–2139.

Furukawa, H., Wu, T.S., Kuoh, C.S., Sato, T., Nagai, Y., Kagei, K., 1984. Acridone alkaloids. Part XII. The structure of glycobismine-A, the first naturally occurring "binary" acridone alkaloid containing acarbon linkage. Chemical and Pharmaceutical Bulletin 32, 1647–1649.

Greger, H., Hofer, O., Kählig, H., Wurz, G., 1992. Sulfur containing cinnamides with antifungal activity from *Glycosmis cyanocarpa*. Tetrahedron 48, 1209–1218.

Greger, H., Zechner, G., Hofer, O., Hadacek, F., Wurz, G., 1993. Sulphur-containing amides from *Glycosmis* species with different antifungal activity. Phytochemistry 34, 175–179.

Greger, H., Zechner, G., Hofer, O., Vajrodaya, S., 1996. Bioactive amides from *Glycosmis* species. Journal of Natural Products 59, 1163–1168.

Harborne, J.B., 1999. The comparative biochemistry of phytoalexin induction in plants. Biochemical Systematics and Ecology 27, 335–367.

Hartmann, G., Nienhaus, F., 1974. Xanthoxylin from the bark of *Phytophthora*- and *Hendersonula*-infected *Citrus limon*. Phytopathologische Zeitschrift 81, 97–113.

Hofer, O., Zechner, G., Wurz, G., Hadacek, F., Greger, H., 1995. Ritigalin, a new thiocarbonic acid amide from *Glycosmis* species. Monatshefte für Chemie 126, 365–368.

Jash, S.S., Biswas, G.K., Bhattacharyya, S.K., Bhattacharyya, P., Chakraborty, A., Chowdhury, B.K., 1992. Carbazole alkaloids from *Glycosmis pentaphylla*. Phytochemistry 31, 2503–2505.

Kamaruzzman Roy, S., Chakraborty, D., P., 1989. Mupamine from *Glycosmis pentaphylla*. Phytochemistry 28, 677–678.

Khan, A.J., Kunesch, G., Chuilan, S., Revise, A., 1985. Xanthyletin, a new phytoalexin of citrus. Fruits 40, 807–811.

Kong, Y.C., Cheng, K.F., Ng, K.H., But, P.P.H., Li, Q., Yu, S.X., Chang, H.T., Cambie, R.C., Kinoshita, T., Kan, W.S., Waterman, P.G., 1986. A chemotaxonomic division of *Murraya* based on the distribution of the alkaloids yuehchukene and girinimbine. Biochemical Systematics and Ecology 14, 491–497.

Lontsi, D., Ayafor, J.K., Sondengam, B.L., Connolly, J.D., Rycroft, D.S., 1985. Ekeberginine, a new carbazole alkaloid from *Ekebergia senegalensis* (Meliaceae). Tetrahedron Letters 26, 4249–4252.

Lukaseder, B., 2000. Vergleichende HPLC-Analysen in der Gattung *Glycosmis* (Rutaceae). Isolierung und Identifizierung charakteristischer Inhaltsstoffe. MSc thesis, University of Vienna, Austria.

Mester, I., Bergenthal, D., Reisch, J., 1979. Inhaltsstoffe aus *Clausena anisata* (Willd.) Oliv. (Rutaceae), III [1,2] ^{13}C-NMR-Spektren des Mupamins, des Carbazols und einiger Carbazol-Derivate. Zeitschrift für Naturforschung 34b, 650–652.

Mester, I., Choudhury, M. K., Reisch, J., 1980. Synthese des Mupamins. Liebigs Annalen der Chemie 241–245.

Mester, I., 1983. Structural diversity and distribution of alkaloids in the Rutales. In: Waterman, P.G., Grundon, M.L. (Eds.), Chemistry and Chemical Taxonomy of the Rutales. Academic Press, London, New York., pp. 31–96.

Samuel, R., Ehrendorfer, F., Chase, M.W., Greger, H., 2001. Phylogenetic analyses of Aurantioideae (Rutaceae) based on non-coding plastid DNA sequences and phytochemical features. Plant Biology 3, 77–87.

Solis, P.N., Wright, C.W., Anderson, M.M., Gupta, M.P., Phillipson, J.D., 1993. A microwell cytotoxicity assay using *Artemia salina* (brine shrimp). Planta Medica 59, 250–252.

Stone, B.C., 1985. A conspectus of the genus Glycosmis Correa: studies in Malesian Rutaceae, III. Proceedings of the Academy of Natural Sciences of Philadelphia 137, 1–27.

Vajrodaya, S., 1998. Comparative phytochemical analyses within the genus *Glycosmis* (Rutaceae-Citroideae). PhD thesis, University of Vienna, Austria.

Vernenghi, A., Ramiandrasoa, F., Chuilon, S., Ravise, A., 1987. Phytoalexines des *Citrus*: seselin proprietes inhibitrices et modulation de synthese. Fruits 42, 103–111.

Wu, T.S., Chang, F.C., Wu, P.L., 1995. Flavonoids, amidosulfoxides and an alkaloid from the leaves of *Glycosmis citrifolia*. Phytochemistry 39, 1453–1457.

Wurz, G., Hofer, O., Greger, H., 1993. Structure and synthesis of phenaglydon, a new quinolone derived phenanthridine alkaloid from *Glycosmis cyanocarpa*. Natural Product Letters 3, 177–182.

PERGAMON

Phytochemistry 58 (2001) 137–142

PHYTOCHEMISTRY

www.elsevier.com/locate/phytochem

Structure and characterization of the crown gall opines heliopine, vitopine and ridéopine

William Scott Chilton[a,*], Annik Petit[b], Mary-Dell Chilton[c], Yves Dessaux[b]

[a]*Department of Botany, North Carolina State University, Raleigh, NC 27695, USA*
[b]*Institut des Sciences Végétales, CNRS, Avenue de la Terrasse F91198, Gif-sur-Yvette, France*
[c]*Syngenta Biotechnology Unit, Research Triangle Park, PO Box 12257, NC 27709, USA*

Received 12 October 2000; received in revised form 26 January 2001

Abstract

The crown gall opines heliopine from tumors induced by octopine type *Agrobacterium tumefaciens* strains A6, A136(pTiB6-806), E9, A652 and 1590-1 and vitopine from tumor induced by grapevine strains S4 and T2 are identical to synthetic N^2-(1′*R*-carboxyethyl)-L-glutamine. Tumors produced by strains S4 and T2 do not contain octopine or lysopine, but they do contain heliopine and the new opine ridéopine identified as *N*-(4′-aminobutyl)-D-glutamic acid. Grapevine strains S4 and T2 grow normally on tumor heliopine or synthetic heliopine and on tumor and synthetic ridéopine as well as on ridéopine lactam as sole carbon source. While octopine strains A6 and A136(pTiB6-806) do not grow on heliopine, mutant colonies do appear after a few weeks. Heliopine catabolism by octopine strains is not induced by octopine. © 2001 Elsevier Science Ltd. All rights reserved.

Keywords: Crown gall; *Agrobacterium tumefaciens*; Grapevine strains; Opines; Ridéopine; *N*-(4′-Aminobutyl)-D-glutamic acid; Heliopine; Vitopine; N^2-(1′*R*-Carboxyethyl)-L-glutamine

1. Introduction

Crown gall disease is induced at plant wound sites by the soil bacterium *Agrobacterium tumefaciens* possessing a tumor-inducing Ti-plasmid. A portion of the Ti-plasmid DNA (T-DNA) is transferred from the bacterial plasmid into the host plant cell where the T-DNA is integrated into host plant chromosomal DNA by an illegitimate recombination process. Some of the transferred genes encode enzymes responsible for the synthesis of plant hormones out of control of normal regulation by the plant, causing abnormal cell divisions that produce a plant gall. Other transferred genes encode biosynthetic enzymes capable of tying up plant metabolites into a class of compounds called opines that are not catabolizable by the host plant, but are catabolizable by the tumor-inducing bacterial strain. More than two dozen crown gall opines have been structurally characterized (Dessaux et al., 1992). They are typically reductive conjugates of L-amino acids and common carbonyl compounds of primary metabolism (e.g. pyruvate, α-ketoglutarate or glucose). There are also several structurally uncharacterized opines or incompletely characterized opines (Chang and Chen, 1983; Chilton et al., 1984b, 1995). These include heliopine from tumors incited by octopine strains A6NC and B6 (Chang et al., 1989) and vitopine from tumors induced by some grapevine strains (Szegedi et al., 1988).

Heliopine is present in some octopine type tumors in which octopine synthase (lysopine dehydrogenase), a T-DNA encoded enzyme, reductively conjugates pyruvate with four basic L-amino acids. In addition to the better-known octopine, an arginine reductive conjugate, and lysopine, a lysine conjugate, these tumors also contain small amounts of the ornithine and histidine conjugates octopinic acid and histopine, all products of the enzyme octopine synthase. A few octopine strains also have been shown to reductively conjugate pyruvate and methionine to produce methiopine (Otten and Szegedi, 1985). In all of these opines the newly generated alanyl asymmetric center has R-chirality (D-alanyl). Tumors induced on sunflower (*Helianthus annuus* L.) by *A. tumefaciens* A6NC, B6, 15955, W1 and 27 also contain acidic iminodiacids derived from neutral and acidic amino acids (Chang et al., 1989). The major new opine

* Corresponding author. Tel.: +1-919-515-3792; fax: +1-191-515-3436.

0031-9422/01/$ - see front matter © 2001 Elsevier Science Ltd. All rights reserved.
PII: S0031-9422(01)00166-2

in the acidic iminodiacid fraction of A6NC-induced tumor was identified as N^2-(1-carboxyethyl)-glutamine (heliopine) by oxidative cleavage to alanine and glutamine. Chang et al. (1989) reported that tumors induced by an octopine synthase deletion mutant of A6NC were devoid of heliopine. Octopine synthase purifed from B6 sunflower tumor has substate specificity for L-arginine, L-ornithine, L-lysine, L-histidine, L-methionine and L-glutamine (Kemp, 1982). Different octopine strains induce tumors containing opines derived from various combination of these six L-amino acids, presumably reflecting availability of the precursors in the gall cells. The stereochemistry of heliopine has not been investigated, although evidence that it is synthesized by octopine synthase strongly suggests that heliopine is the D-alanyl reductive conjugate of pyruvate and L-glutamine.

The new opine, vitopine, was first reported to be present in tumors induced on *Kalanchoe daigremontiana* by three biotype 3 grapevine (*Vitis vinifera*, Vitaceae) isolates of *A. tumefaciens* (Szegedi et al., 1988). Like other iminodiacids, vitopine chelates silver ion and has anionic electrophoretic mobility at pH 2.8. However vitopine is resolvable from other opines of this class (*S*,*S*-leucinopine, *S*,*S*-succinamopine and R^{asn}, S^{gln}-succinamopines). Vitopine has not been structurally characterized. We report here the full stereochemistry of heliopine, the identity of heliopine and vitopine, and the structure and stereochemistry of a further new opine, ridéopine, discovered in the course of the present work on vitopine-type tumors.

2. Results

2.1. Structure and synthesis of ridéopine

Ridéopine (**1**) is readily detectable with the ninhydrin reagent without heating, indicating the presence of a primary amine. The NMR of ridéopine in D_2O (pH 1) indicated a glutamic acid substituted with an aminobutyl group on the amine: 4-aminobutyl moiety: α′-CH_2, 3.15, *t*; β′,γ′-CH_2CH_2,1.78, *br*; δ′-CH_2, 3.03, *t*; glutamic acid moiety: α-CH, 3.96; *t*; β-CH_2, 2.1-3.4, *m*; γ-CH_2, 2.61, t. Racemic ridéopine was synthesized by reductive amination of putrescine with α-ketoglutaric acid. Synthetic *N*-(4′-aminobutyl)-D,L-glutamic acid had the same NMR spectrum and electrophoretic mobility between pH 1.8 and 10.8 as tumor ridéopine

Ridéopine, like other glutamyl and glutaminyl opines, is readily converted to a lactam. Lactamization creates an amide chromophore whose n–π^* circular dichroism has been correlated with chirality at the α-carbon of the glutamyl moiety (Goodman et al., 1969). Previous work has shown that lactams with L-glutamyl chiral center have a positive CD extremum near 215 nm (L-glutamic acid lactam, *S*,*S*-succinopine lactam, agropinic acid), while those with D-glutamyl configuration have a negative CD extremum ca. 215 nm ($S^{asp}R^{glu}$-succinopine lactam, nopaline lactam; Chilton et al., 1984b, 1985b). Ridéopine lactam (**2**) from S4 *Datura* tumor has a negative CD at 215 nm. Therefore, the natural opine induced by *A. tumefaciens* strains S4 and T2 is R-ridéopine (**1**).

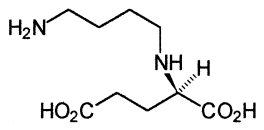

1: Rideopine

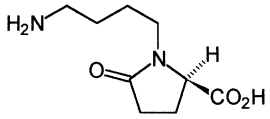

2: Rideopine lactam

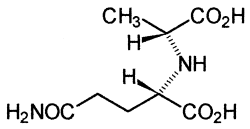

3: Heliopine

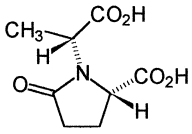

4: Heliopine lactam

2.2. Catabolism of ridéopine

Catabolism of S4-induced, tumor-extracted ridéopine in liquid medium was monitored by high voltage paper electrophoresis (HVPE). Grapevine strains S4 and T2 catabolized all of the opine within 72 h. None of the other assayed strains degraded this compound within 7 days whether they were nonpathogenic (C58C1) or pathogenic *A. tumefaciens* (C58, B6s3, ACH5, R10, Bo542, ANT4) or *A. rhizogenes* (15834, 2659, 8196, 1724) isolates.

A similar result was observed when tumor-extracted ridéopine was substituted with racemic ridéopine which was not degraded by any of the assayed strains (C58C1, C58, ACH5, ANT4) except S4 and T2. Surprisingly, in liquid culture the ridéopine strains S4 and T2 completely consumed both enantiomers of this opine. In addition, strains S4 and T2 were able to grow on agar plates containing racemic ridéopine as the sole carbon source. Strains S4 and T2 can also grow on racemic ridéopine lactam as the sole carbon source in liquid culture, but they utilize only one enantiomer. The residual enantiomer of ridéopine lactam not catabolized by strain S4 and T2 has positive CD extremum at 215 nm, indicating that these strains catabolize only R-ridéopine lactam (**2**), the lactam of R-ridéopine produced in the S4 and T2 tumors.

2.3. Identity and stereochemistry of heliopine and vitopine

The proton NMR spectra of heliopine isolated from tobacco tumors incited by *A. tumefaciens* A6 and A136 (pTi B6-806) and from sunflower tumors incited by *A. tumefaciens* A6 are identical to those of vitopine isolated from *Datura stramonium* tumors incited by grapevine strains S4 and T2. The spectra in D_2O at pH 2 are

consistent with structure **3**, N^2-(1′-carboxyethyl)-glutamine: carboxyethyl moiety: α′ 3.91 ppm, *q*; β′ 1.53, *d*; glutamine moiety: α CH, 3.82 ppm, *t*; β CH_2, 2.20, *m*; γ CH_2, 2.52, *t*. Heliopine isolated from A6 and A136 (pTiB6-806) tobacco tumors and from A6 sunflower tumors was indistinguishable electrophoretically at pH 2.8 from vitopine purified from *Datura stramonium* tumors incited by *A. tumefaciens* S4. Heliopine lactam (**4**) and vitopine lactam, prepared by heating in aqueous acid, also comigrated at pH 2.8, 4.0 and 10.8. Thus, heliopine and vitopine are identical. Since the structure (without stereochemistry) of heliopine has been published (Chang et al., 1989), we use the name heliopine in preference to vitopine (Szegedi et al., 1988).

All four diastereomers of heliopine were prepared pairwise by reductive alkylation of pyruvic acid and L-glutamine or D-glutamine. In addition single-isomer N^2-(1′*R*-carboxyethyl)-L-glutamine was prepared by alkylation of L-glutamine with 2*S*-bromopropionic acid. This single-isomer heliopine comigrated electrophoretically at pH 2.5 with S4, A6 and A277 tumor heliopine and with the slower, barely resolved isomer of the diastereomeric pair prepared by reductive alkylation. For better resolution of diastereomers by HVPE the heliopines were converted to the conformationally less flexible lactams which enhances the difference in pKa_2, providing better resolution of the more mobile erythro heliopine lactam, **4**, from the threo lactam (isoheliopine lactam). The circular dichroism spectrum of natural heliopine lactam from both S4 *Datura* and A6 tobacco tumors had the positive CD extremum at 215 nm expected for L-glutamyl lactams (Goodman, 1969; Chilton et al., 1984a, 1985b). Thus, the tumor heliopine from both octopine type tumors and from heliopine type tumors is the erythro isomer N^2-(1′*R*-carboxyethyl)-L-glutamine, **3**.

2.4. Catabolism of opines by heliopine type strains S4 and T2

Catabolism of synthetic, single isomer heliopine (*N*-[1′*R*-carboxyethyl]-L-glutamine) in liquid medium was monitored by HVPE. Grapevine heliopine strains S4 and T2 catabolized all of the heliopine within 72 h. The same strains grown on a 1:1 mixture of heliopine and isoheliopine [N^2-(1′*S*-carboxyethyl)-L-glutamine] selectively catabolized heliopine within 72 h but did not reduce the concentration of isoheliopine within 1 week. Neither strain was able to catabolize either of the isomeric N^2-(1′-carboxyethyl)-D-glutamines. Strains S4 and T2 also catabolized heliopine lactam [*N*-(1′*R*-carboxyethyl)-L-pyroglutamic acid], within 72 h in liquid culture, but not the 1′*S*-isomer. Growth of heliopine type strains S4 and T2 was tested on agar plates containing other opines as sole carbon source. Neither of these strains grew on plates containing octopine, nopaline, agropine, agropinic acid or mannopine as sole carbon source. They were not tested for ability to grow on cucumopine, mikimopine, R^{asn},S^{gln}-succinamopine or *S*,*S*-leucinopine.

2.5. Catabolism of heliopine by diverse opine type strains of A. tumefaciens

None of the nopaline [A136 (pTi K27), A136 (pTi 223), A136 (pTi T37, T37Braun, C58, IIBV7], mannopine [C58C1 (pRi 8196)], chrysopine (ANT4), or leucinopine [A136(pTi Bo542)] type strains grew on heliopine as sole carbon source. Typical octopine strains did not grow at all within 1 week in liquid culture containing as sole carbon source the heliopine isomeric pair prepared from L-glutamine. These strains were tested for growth on solid medium containing the same isomers. There was no detectable confluent growth after one week, but isolated mutant colonies were detected after several weeks. Several mutant colonies of B6 and R10 were picked, purified and found able to grow rapidly on heliopine in liquid medium as well as on agar. Each of the eight mutants picked utilized the natural heliopine, *N*-(1′*R*-carboxyethyl)-L-glutamine, and not the 1′S-isomer. To test whether heliopine is a non-inducing substrate for uptake and catabolism by the octopine pathway, the original wild type octopine strains were inoculated into liquid medium containing heliopine and isoheliopine plus octopine to induce the octopine-utilization pathway. None of the octopine strains tested was able to utilize heliopine (or isoheliopine) after consuming octopine (Table 1).

3. Discussion

Glutamine derivatives are known to undergo slow lactamization. Thus aging solutions of glutamine-derived opines contain some opine lactam. Nonenzymatic lactamization occurs in the tumor as well. Therefore, it is not surprising that mannopine, nopaline, succinamopine, leucinopine and heliopine strains causing synthesis of glutamine-type opines in tumors can also catabolize the corresponding glutamyl opine lactam. (Chilton et al., 1984a, 1985b, 1995). Strains S4 and T2 that catabolize heliopine [N^2-(1′*R*-carboxyethyl)-L-glutamine] conform to this pattern and catabolize heliopine lactam [N^2-(1′*R*-carboxyethyl)-L-glutamic lactam but none of the other three lactam diastereomers. *A. tumefaciens* S4 and T2 also catabolize R-ridéopine and *R*-ridéopine lactam, but not *S*-rideopine lactam. This makes evolutionary sense because the tumors they incite contain *R*-rideopine and not *S*-ridéopine, consequently no *S*-ridéopine lactam. However these strains catabolize *both* enantiomers of unlactamized ridéopine, even though they induce tumors containing only *R*-ridéopine. Catabolism of the S-enantiomer may be accomplished by the transport

Table 1
Growth of *Agrobacterium tumefaciens* strains on octopine and heliopine

		Utilization in liquid culture				Growth on agar plates	
			Opine cocktail				
Strain (plasmid)	Opine type[a,b]	HEL only	HEL	+	OCT	HEL	HEL + trace of OCT[e]
A136(pTiB6-806)	OCT[c]	–	–		+	Mutants	NT
A6	OCT[c,d]	–	–		+	Mutants	NT
B6	OCT[c,d]	–	–		+	Mutants	–
IDI	OCT	–	–		+	NT	–
K301	OCT	–	–		+	NT	–
K768	OCT	–	–		+	NT	–
R10	OCT	–	–		+	Mutants	–
15955	OCT[d]	–	–		+	Mutants	–
T13	OCT, CUC	NT	NT		NT	–	NT
S4	HEL, RID	+	NT		NT	+	NT
T2	HEL, RID	+	NT		NT	+	NT

[a] CUC = cucumopine; OCT = octopine; HEL = heliopine; RID = ridéopine.
[b] Tumors induced by octopine strains also contain lysopine.
[c] Strain inducing tumors containing heliopine in addition to octopine and lysopine (this work).
[d] Strain inducing tumors containing heliopine in addition to octopine and lysopine (Chang et al., 1989).
[e] Octopine pathway induced by addition of 0.05 mg/ml octopine; plates scored after 48–72 hours, before appearance of mutants would be noted.

and catabolic machinery responsible for the uptake and degradation of the *R*-enantiomer. Alternatively, degradation of the *S*-enantiomer could occur via some L-amino acid catabolic enzyme of primary metabolism.

The high frequency with which heliopine-utilizing mutants of octopine strains B6 and R10 appeared was reminiscent of the mannityl opine constitutive mutants that appeared when mannopine strains were grown on mannopine analogs which turned out in most cases to be non-inducing substrates for the catabolic pathway involved (Chilton and Chilton, 1984). We reasoned that uptake and catabolism of heliopine, a structural analog of octopine, might be facilitated by induction of the octopine uptake and catabolism pathway. According to this hypothesis, the heliopine catabolizing mutants might be constitutive for octopine utilization. However, because of the failure of strains A6, B6 and 15955 to consume heliopine after induction with octopine, we cannot declare these strains (which produce heliopine along with octopine and lysopine in the tumors they induce) to be heliopine strains in the classical sense that S4 and T2 may be called heliopine strains. Octopine strains A6, B6 and 15955 do produce mutants that consume heliopine. The failure of unmutated strains A6, B6 and 15955 to catabolize heliopine after completing catabolism of octopine indicates that induction of the octopine uptake and catabolism pathway is not sufficient to permit catabolism of heliopine by these octopine strains. If induction is required for catabolism of heliopine by these mutants, heliopine, but not octopine must presumbably act as the inducer. It is unclear what aspect of the utilization process is acquired in our mutant octopine strains that consume heliopine, but we have seen that mutation has left octopine catabolism unimpared.

Methiopine is another example of a non-catabolized octopine analog produced by octopine-lysopine dehydrogenase in some octopine strains. Enzyme kinetic studies showed that partially purified lysopine dehydrogenase isolated from B6S3 tobacco tumor accepts glutamine and methionine in addition to the four basic amino acids and reductively conjugates them with pyruvate to make heliopine and methiopine (Otten et al., 1977). Methiopine was later shown to be present in octopine tumors induced by octopine strains A6 and B6 (Otten and Szegedi, 1985). Similar to our finding with heliopine, methiopine was not catabolized by the tumor inducing strains even after induction with octopine. However cell lysates of octopine-induced strains were able to catabolize [^{35}S]methiopine, leading later authors to refer to methiopine as a "pseudo-opine" (Firmin et al., 1985).

We have now identified the glutamine conjugate of pyruvic acid (heliopine) as a true opine, not of octopine strains but of the grapevine strains S4 and T2. It appears to us that production of the gratuitous opine analogs heliopine and methiopine in tumors induced by various octopine strains is a result of unselected "substrate promiscuity" of octopine-lysopine dehydrogenase. We speculate that such gratuitous analogs may be an intermediate step toward evolution of new opine type *Agrobacterium* strains.

4. Experimental

4.1. Opine catabolism and analysis

Opine catabolism experiments were carried out on agar plates containing AT medium (Guyon et al., 1980)

and 1 mg/ml of each opine diastereomer as sole carbon source, or in some cases with the addition of 0.05 mg/ml octopine as inducer. No growth was detected on control plates containing 0.05 mg/ml octopine as sole carbon source. Plates were observed for growth in the confluent area at 24 and 48 h and for isolated mutant colonies in diluted streaks after one or more weeks. Catabolism in liquid culture was conducted in AT medium containing 1 mg/ml of each opine diastereomer as described in previous work (Chilton and Chilton, 1984, Chilton et al., 1984a). *A. tumefaciens* strains S4 and T2 required the addition of 0.1 mg/ml yeast extract (Difco) for growth on AT medium. Tubes containing 3 ml of medium were inoculated with 100 ul of the appropriate *Agrobacterium* strain grown overnight at 28°C on a rotary drum. Aliquots (0.1 ml) were collected at intervals up to 168 h, centrifuged and analyzed by HVPE.

High voltage electrophoreses were performed on Whatman 3MM paper at 50 V/cm under Stoddard standard solvent or Isopar H (Exxon) as heat transfer liquid for 30–40 min. The pH 1.9 HVPE buffer was prepared by adding HCO_2H to 2 M HOAc. The pH 2.8 and 4.0 buffers were prepared by titration of 0.1 M HCO_2H or 0.1 M HOAc with NaOH, and the pH 10.8 buffer was prepared by titrating 0.1 M NH_4OH with HOAc. Heliopine was detected using Ag chelation with $AgNO_3$-mannitol reagent (Chilton et al., 1984b), and heliopine lactam was visualized using aniline-xylose reagent for acidity (Zweig and Sherma, 1972). Heliopine was generally lactamized before analysis to achieve better resolution of isomers. For this purpose 0.05 ml aliquots from catabolism experiments were added to 0.1 ml 6 M HCl in a microcentrifuge tube and heated at 100°C for 1 h. Aqueous HCl was evaporated, and the microcentrifuge tube was then placed in a vacuum dessicator over NaOH to remove HCl which interferes in the electrophoretic analysis. Ridéopine was detected with ninhydrin.

4.2. Purification of vitopine (heliopine) and ridéopine from strain S4 tumors

Tumors initiated by strain S4 on *Datura stramonium* (15 g, f.w.) were minced and extracted with 300 ml water for 5 min at 100°C. The aqueous extract was filtered and sterilized at 105°C for 20 min. No loss of opines was detectable by electrophoresis at pH 1.9. The sterilized tumor extract was inoculated with strain C58.00, lacking both the tumor-inducing plasmid and the cryptic plasmid and incubated at 28°C for 68 h. after which time HVPE showed that all amino acids had been metabolized and that the concentrations of vitopine and ridéopine were undiminished. Bacteria were removed by centrifugation and the water was evaporated to give 380 mg of brown residue from 15 g tumor (f.w.). The brown residue (140 mg) was dissolved in water and passed through a 12 ml column of Dowex $50H^+$. The column was then washed with 4 bed volumes of distilled water to remove any neutral compounds, followed by 20 bed volumes of water to remove the iminodiacid fraction in which vitopine appeared. The column was then washed with 3% aqueous ammonia to remove ridéopine. HVPE analysis showed that the iminodiacid fraction contained vitopine (pH 2.8, Ag chelation) and the ammonia fraction contained ridéopine (pH 1.9, ninhydrin)

Pure vitopine (9 mg), containing no ninhydrin positive substances was obtained following preparative HVPE at pH 2.8. The ridéopine fraction contained a small amount of a ninhydrin positive substance which was removed by preparative HVPE (pH 1.9) to give 10 mg pure ridéopine. NMR spectroscopic characterization of these opines is reported in Section 2.

4.3. Purification of heliopine from tumors induced by octopine strains

The pKa_1 of α,α′-iminodiacids like heliopine is so low that the first carboxyl ionization is complete at pH 2, and the isoelectric point for iminodiacids lacking a second basic group is below 2. Consequently, opines such as succinamopine, leucinopine, and heliopine can be eluted from a cation exchange column with a large volume of distilled water in the acidic iminodiacid fraction free of amino acids (Chilton et al., 1984a, 1985a. 1985b). Opines with a second basic group such as octopine, lysopine and nopaline are not eluted by distilled water, but are eluted along with amino acids by dilute, aqueous ammonia. Heliopine was isolated from tobacco tumors incited by *A. tumefaciens* strains A652, A6, E9 and 1590-1 and from sunflower tumor incited by strain A6 by absorption onto cation exhange resin and elution in 20 bed volumes of distilled water as described for vitopine isolation (above). These preparations contained heliopine, pyroglutamic acid (derived from glutamic acid still held on the cation exchange resin) and another, unidentified iminodiacid of slightly lower HVPE mobility than heliopine at pH 2.8. Heliopine from tobacco tumors induced by strain A6 and pTiA136 were further purified by preparative HVPE at pH 2.8 to remove the unidentified iminodiacid and pyroglutamic acid. Oxidation of heliopine from A6 and pTiA136 tobacco tumors with potassium permanganate gave alanine and glutamine as described earlier (Chang, 1989).

4.4. Synthesis of racemic ridéopine

A semi-crystalline putrescine-putrescine carbonate mixture (1.47 g, ca. 12 mmole) and 2.62 g (18 mmole) α-ketoglutaric acid dissolved in 40 ml water was reduced by gradual addition of 0.75 g (12 mmole) sodium cyanoborohydride with periodic addition of HOAc as necessary to maintain pH 6.0–6.8. After several hours, the reaction solution was added to a 50-ml slurry of Dowex $50H^+$ to

destroy borohydride. After hydrogen evolution ceased, the resin was placed in a column and washed with water until the effluent was no longer acidic. Ridéopine eluted with 3% ammonia was electrophoretically pure and did not contain any of the putrescine dialkylation product.

4.5. Synthesis of heliopine diastereomer pairs

A mixture of N^2-(1′*R*-carboxyethyl)-L-glutamine (heliopine) and N^2-(1′*S*-carboxyethyl)-L-glutamine (isoheliopne) was prepared by reductive amination of L-glutamine with excess α-ketoglutaric acid as described for synthesis of ridéopine. A mixture of N^2-(1′*R*-carboxyethyl)-D-glutamine and N^2-(1′*S*-carboxyethyl)-D-glutamine was similarly prepared from D-glutamine.

4.6. Synthesis of N^2-(1′*R*-carboxyethyl)-L-glutamine (heliopine)

L-Glutamine (1.50 g, 10 mmole) was dissolved in 10 ml H_2O by addition of 5 ml 2.5 M NaOH. The solution was adjusted to pH 7. Optically active 2*S*-bromo-propionic acid (Aldrich Chemical Co., 2.595 g, 17 mmole) was added, followed by dropwise addition of 3.86 ml (22.5 mmole) NaOH (final pH 9). Subsequently NaOH was added over the next 2 days as necessary to maintain pH 9. A total of 39 mmole NaOH was consumed (theoretical 38 mmole). The reaction solution was acidified to pH 1 and passed through a Dowex $50H^+$ column. After washing the column with distilled water, the synthetic, single-isomer heliopine was eluted with 3% ammonia. HVPE (pH 2.8) showed only heliopine and no glutamine in the dried product, while pH 2.8 HVPE of its lactam, N^2-(1′*R*-carboxyethyl)-L-pyroglutamic acid, showed the presence of only the more mobile isomer of heliopine lactam comigrating with tumor heliopine lactam and tumor vitopine lactam. Synthetic, single-isomer heliopine (842 mg) crystallized from concentrated aqueous solution. A further 95 mg of heliopine was recovered on evaporation of the mother liquor.

References

Chang, C.-C., Jayaswal, R.K., Chen, C.-M., Gelvin, S.B., 1989. Altered iminodiacid synthesis and transcription in crown gall tumors with transposon Tn5 insertions in the 3′ end of the octopine synthase gene. Journal of Bacteriology 171, 5922–5927.

Chang, C.-C., Chen, C.-M., 1983. Evidence for the presence of N^2-(1′,3′-dicarboxypropyl)-L-amino acids in crown gall tumors induced by *Agrobacterium tumefaciens* strains 181 and EU6. FEBS Letters 162, 432–435.

Chilton, W.S., Chilton, M.-D., 1984. Mannityl opine analogs allow isolation of catabolic pathway regulatory mutants. Journal of Bacteriology 158, 650–658.

Chilton, W.S., Rinehart, K.L., Chilton, M.-D., 1984a. Structure and stereochemistry of succinamopine. Biochemistry 23, 3290–3297.

Chilton, W.S., Tempé, J., Matzke, M., Chilton, M-D., 1984b. Succinamopine: a new crown gall opine. Journal of Bacteriology 157, 357–362.

Chilton, W.S., Hood, E., Chilton, M.-D., 1985a. Absolute stereochemistry of leucinopine, a crown gall opine. Phytochemistry 24, 221–224.

Chilton, W.S., Hood, E., Rinehart, K.L., Chilton, M.-D., 1985b. L,L-Succinamopine: an epimeric crown gall opine. Phytochemistry 24, 2945–2948.

Chilton, W.S., Stomp, A.M., Beringue, V., Bouzar, H., Vaudequin-Dransart, V., Petit, A., Dessaux, Y., 1995. The chrysopine family of Amadori-type crown gall opines. Phytochemistry 40, 619–628.

Dessaux, Y., Petit, A., Tempé, J., 1992. Opines in Agrobacterium biology. In: Verma, D.P.S. (Ed.), Molecular Signals in Plant Microbe Communications. CRC Press, Boca Raton, pp. 109–136.

Firmin, J.L., Stewart, I.M., Wilson, K.E., 1985. N^2-(1′-Carboxyelthyl)methionine, a "pseudo-opine" in octopine-type crown-gall tumours. Biochemistry Journal 232, 431–434.

Goodman, M., Toniolo, C., Falcetta, J., 1969. Conformational aspects of polypeptide structure. XXX. Rotatory properties of cyclic and bicyclic amides. Restricted and rigid model compounds for peptide chromophores. Journal of the American Chemical Society 91, 1816–1823.

Guyon, P, Chilton, M.-D., Petit, A., Tempé, J., 1980. Agropine in "null typeø crown gall tumors: evidence for generality of the opine concept. Proceedings of the National Academy of Science USA 77, 2693–2697.

Kemp, J.D., 1982. Enzymes in octopine and nopaline metabolism. In: Kahl, G., Schell, J.S. (Eds.), Molecular Biology of Plant Tumors. Academic Press, NY, pp. 462–474.

Otten, L., Szegedi, E., 1985. Crown galls induced by octopine-degrading biotype 3 strains of *Agrobacterium tumefaciens* contain a new form of lysopine dehydrogenase. Plant Science 40, 81–85.

Otten, L., Vreugdenhil, V., Schilperoort, R.A., 1977. Properties of D(+)-lysopine dehydrogenase from crown gall tumor tissue. Biochimica Biophysica Acta 485, 268–277.

Szegedi, E., Czakó, X., Otten, L., Koncz, C.S., 1988. Opines in crown gall tumors induced by biotype 3 isolates of *Agrobacterium tumefaciens*. Physiological and Molecular Plant Pathology 32, 237–247.

Zweig, G., Sherma, J., 1972. Handbook of Chromatography, Volume II. CRC Press, Cleveland, OH, p. 144.

PERGAMON

Phytochemistry 58 (2001) 143–152

PHYTOCHEMISTRY

www.elsevier.com/locate/phytochem

The antioxidant activity of aqueous spinach extract: chemical identification of active fractions

Margalit Bergman[a], Lucy Varshavsky[a], Hugo E. Gottlieb[b], Shlomo Grossman[a,*]

[a]*Faculty of Life Sciences, Bar-Ilan University, Ramat Gan 52900, Israel*
[b]*Department of Chemistry, Bar-Ilan University, Ramat Gan 52900, Israel*

Received 28 September 2000; received in revised form 11 March 2001

Abstract

In previous studies we have elucidated the presence of powerful, natural antioxidants (NAO) in water extracts of spinach leaves and demonstrated their biological activity in both in vitro and in vivo systems. In the present study, the chemical identity of several of these antioxidant components is presented. Spinach leaves were extracted with water and the 20,000 g supernatant which contained the antioxidant activity was extracted with a water:acetone (1:9) solution. The 20,000 g supernatant obtained was further purified on reverse phase HPLC using C-8 semi-preparative column. Elution with 0.1% TFA resulted in five hydrophilic peaks. Elution with acetonitrile in TFA resulted in seven additional hydrophobic peaks. All the peaks were detected at 250 nm. All the fractions obtained showed antioxidant activity when tested using three different assays. Based on ^{1}H and ^{13}C NMR spectroscopy four of the hydrophobic fractions were identified as glucuronic acid derivatives of flavonoids and three additional fractions as *trans* and *cis* isomers of *p*-coumaric acid and others as *meso*-tartarate derivatives of *p*-coumaric acid. The present study demonstrates for the first time the presence of both flavonoids and *p*-coumaric acid derivatives as antioxidant components of the aqueous extract of spinach leaves. © 2001 Published by Elsevier Science Ltd.

Keywords: Antioxidants; Flavonoids; Coumaric acid; Spinach

1. Introduction

Over the past several years, there has been an extraordinarily rapid growth in our knowledge of free radical chemistry and its possible involvement in both normal essential biology and age related disease and dysfunction. Oxidative stress, induced by oxygen radicals, is believed to be a primary factor in various degenerative diseases of the central nervous system, as well as in the normal process of aging (Ramarathnam et al., 1996). The reactive oxygen species formed during normal metabolic processes can easily initiate the peroxidation of membrane lipids, leading to the accumulation of lipid peroxides.

Antioxidants are compounds that inhibit or delay the oxidation of other molecules by inhibiting the initiation or propagation of oxidizing chain reactions. Natural antioxidants constitute a broad range of compounds including phenolic compounds, nitrogen compounds, and carotenoids (Velioglu et al., 1998). In addition, ascorbic acid has been shown to have antioxidant properties. The main role of antioxidants is to help the body protect itself against damage caused by reactive oxygen species and degenerative diseases (Shahidi, 1996).

Antioxidant activity is essential for life, to counteract the strongly oxidizing environment in which we live (Velioglu et al., 1998). Many biological functions, such as protection from mutagenesis, carcinogenesis and aging, among others, are due to antioxidative effects (Cook and Samman, 1996; Huang et al., 1992). The antioxidant activity of several plant materials has recently been described (Oomah and Mazza, 1994; Al-Saikhan et al., 1995; Yen and Duh, 1995; Amarowicz et al., 1996; Cao et al., 1996; Wang et al., 1996). Recently we have reported the presence of a series of powerful water soluble natural antioxidants in spinach leaves and

* Corresponding author. Tel.: +972-3-5318050; fax: +972-3-6356869.
E-mail address: grossms@mail.biu.ac.il (S. Grossman).

0031-9422/01/$ - see front matter © 2001 Published by Elsevier Science Ltd.
PII: S0031-9422(01)00137-6

described their potential biological activity (Grossman et al., 1994; Lomnitski et al., 2000a,b,c; Zurovsky et al., 1994, 1995; Zurovsky and Gispaan, 1995). In the present study we describe for the first time the isolation and chemical identification of several of these antioxidant components.

2. Results

2.1. Fractionation of spinach extracts, and antioxidant activity

Previous results from our lab showed that the water extract from spinach leaves, which exhibits antioxidant activity, contained two main fractions: a low molecular weight (under 1000 Da) fraction, which is water soluble, and another fraction which consists of components over 1000 M_W and is water insoluble. Moreover, the HPLC profile using a reverse phase C_{18} column indicated that a significant amount of the first fraction was not eluted from the column (Reznik, 1990). These findings indicate that the antioxidants from spinach contain both hydrophilic and hydrophobic constituents. Since the antioxidants we described appeared to comprise both hydrophobic and hydrophilic fractions, we first tested the solubility of the antioxidants present in the aqueous spinach extract in various solvents. A combination of 1:9 (water:acetone) was found to be optimal for extracting the activity (not shown).

To further fractionate the extract, the acetone was evaporated and the residue was applied onto an analytical reverse phase C_8 HPLC column. The profile obtained at the detection wavelength 250 nm showed a high resolution separation. Moreover, all the fractions isolated exhibited antioxidant activity. In order to enable the chemical structure analysis of these fractions, we decided to use a semi-preparative column. The absorption profile obtained at 250 nm is shown in Fig. 1. Elution with 0.1%TFA (solvent A) resulted in five main peaks. Elution with a gradient of acetonitrile resulted in many additional peaks. According to their chromatographic behavior we divided these peaks into 2 main groups: hydrophilic (for those eluted only with solvent A) and hydrophobic (for the remaining part of gradient).

These various eluted fractions were collected, and each whole fraction was assayed for antioxidant activity using three different assays (Fig. 2a, b and c). These results indicate that the hydrophobic elution contained at least 10 active fractions while the hydrophilic elution contained fewer. The different pattern of the active fractions obtained in the pollarographic assay (Fig. 3c) is probably due to the fact that this assay is more specific compared to the other two assays (TBA and FOX), since it is based on the inhibition of linoleic acid oxidation induced by the lipoxygenase enzyme.

Although, in general, the profile obtained from the semi-preparative column resembled that of the analytical separation, several additional active fractions were detected. The UV spectra of all detected peaks were determined and our results indicated that many of the hydrophobic peaks exhibit additional absorbance at 310 nm. Therefore, we used this wavelength for detection while collecting the hydrophobic peaks (Fig. 3).

Based on their spectra, we could divide the main hydrophobic peaks into two groups: group 1, with two

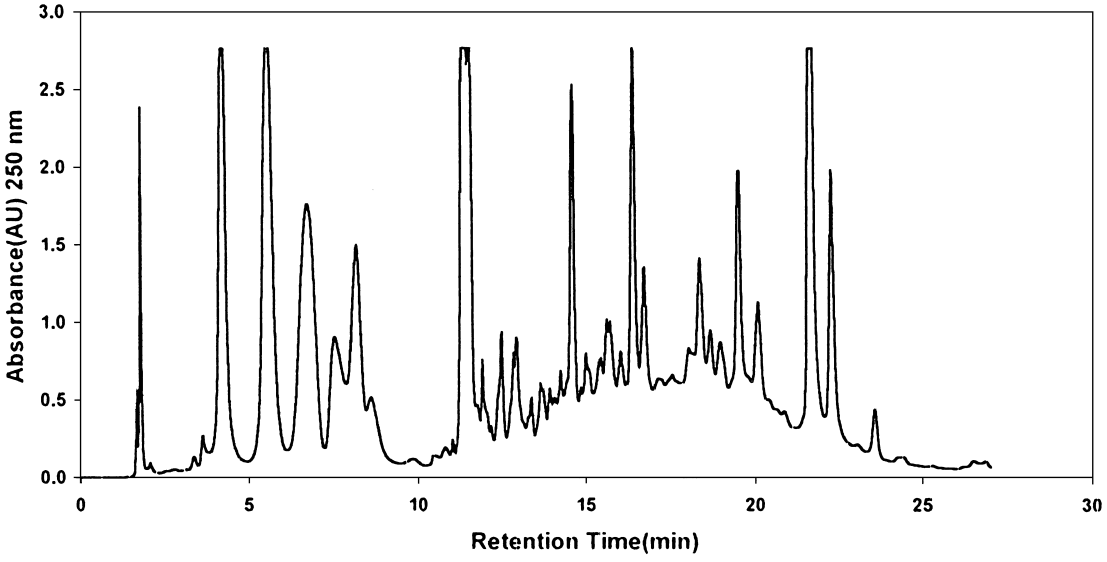

Fig. 1. Reversed phase HPLC profile of natural antioxidants (NAO) isolated from spinach leaves, detected at 250 nm. The residue of an acetone: water extract of a water soluble antioxidant from spinach leaves was applied to a semipreparative LiChrocart 250-10 RP-8 column. Solutions: A, 0.1% TFA in water; B, CH_3CN; run conditions: 0–5 min/100% A (0.1% TFA); 5–27 min/100–56%/A (linear gradient) at a flow rate of 6 ml/min.

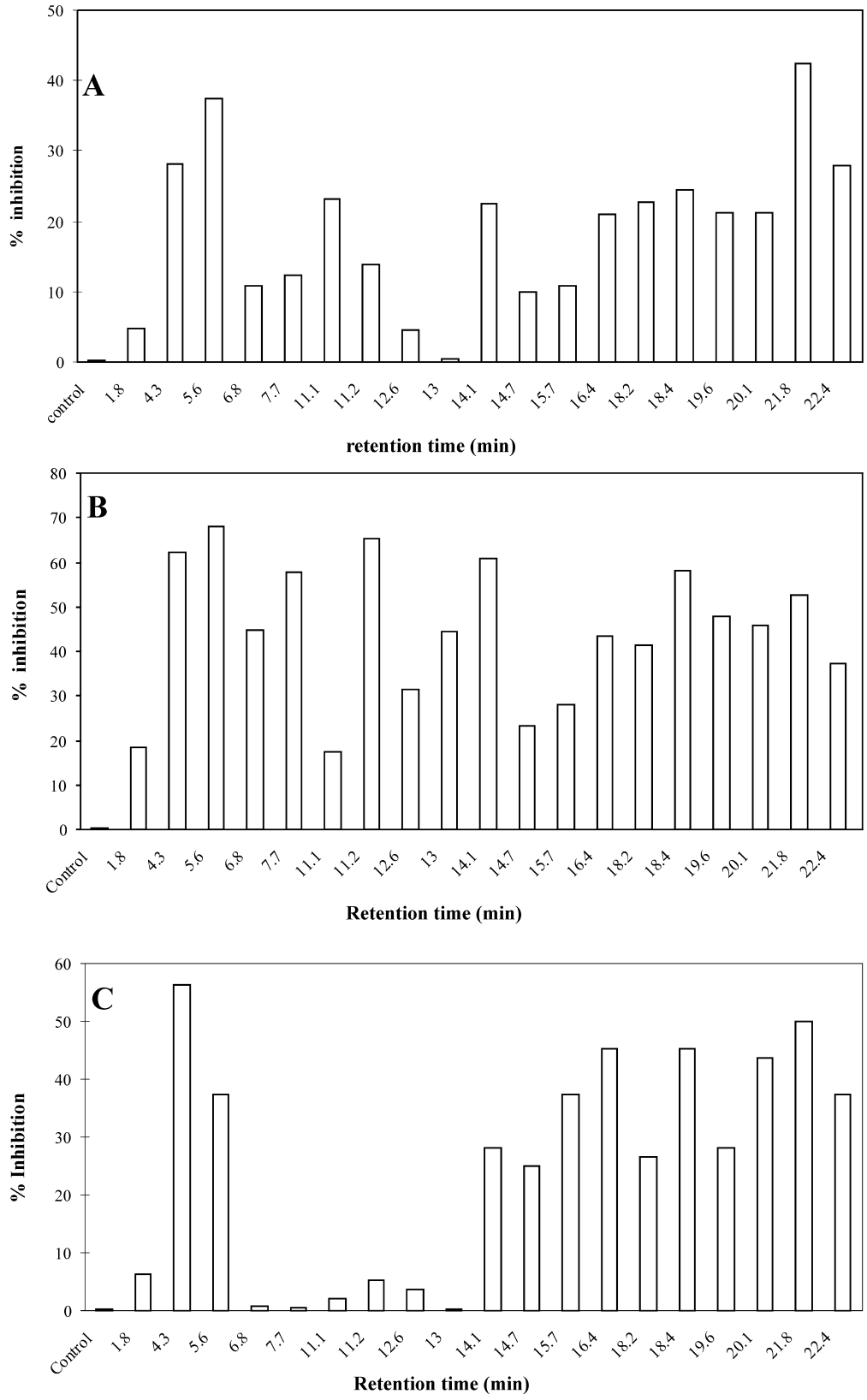

Fig. 2. Antioxidant activity of fractions obtained from HPLC separation. (A) Percentage of inhibition of linoleic acid auto-oxidation for 24 h at 37°C, as measured by the FOX method. (B) Percentage of inhibition of linoleic acid auto-oxidation measured by MDA assay. (C) Percentage of inhibition of linoleic acid oxidation induced by lipoxygenase as measured polarographically.

maxima — at 280 and 350 nm, and group 2, with a single maximum at 314 nm (Fig. 4).

2.2. Spectroscopic identification of antioxidant peaks

Some of the main hydrophobic peaks were then studied in an attempt to determine their chemical nature and structure. Once pure fractions were isolated, their structure was determined mainly by NMR spectroscopy.

The most abundant of the relatively hydrophobic substances were eluted at 21.68 min. The UV spectrum of this peak corresponded to the smooth line trace in Fig. 4, and enough material was obtained to take both ^{1}H and ^{13}C NMR spectra (Table 1). We were also able to establish $^{1}H\times^{1}H$, one-bond $^{13}C\times^{1}H$, and long-range $^{13}C\times^{1}H$ correlations via 2D NMR experiments (COSY, HMQC and HMBC, respectively). These spectra allowed us to unambiguously determine the structure of this material as **1**, a conjugate between a flavone and glucuronic acid (most importantly, a correlation was found between C-4′ and H-1″). A literature search revealed that this compound has been previously described (Aritomi and Kawasaki, 1984; Ferreres et al., 1997). Our more modern techniques permit unambiguous assignment of all the proton and carbon NMR peaks.

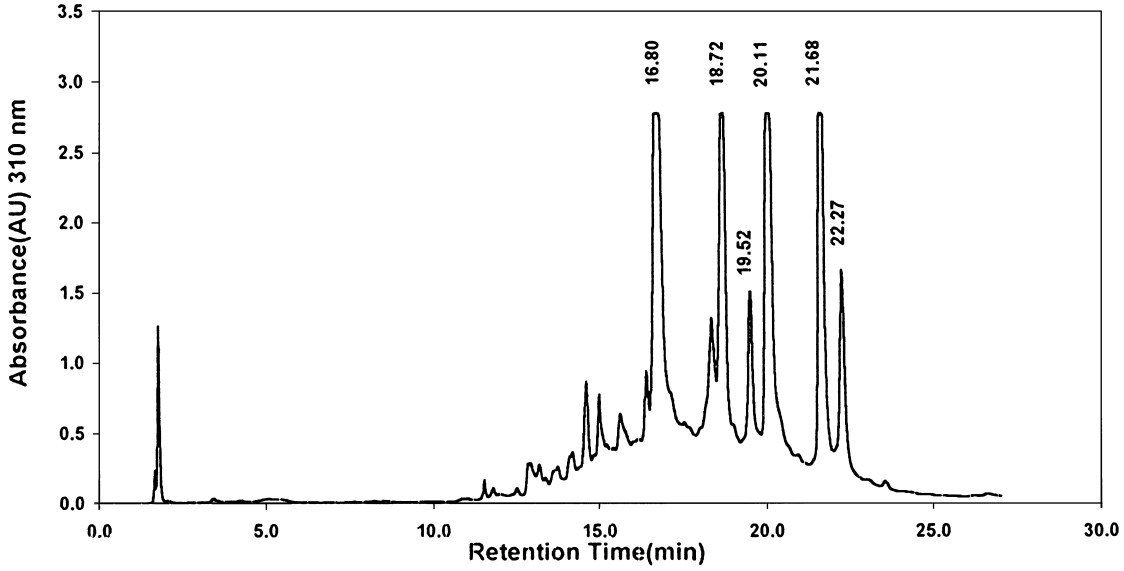

Fig. 3. Reversed phase HPLC pattern of NAO from spinach detected at 310 nm. HPLC conditions were identical to those described for Fig. 1.

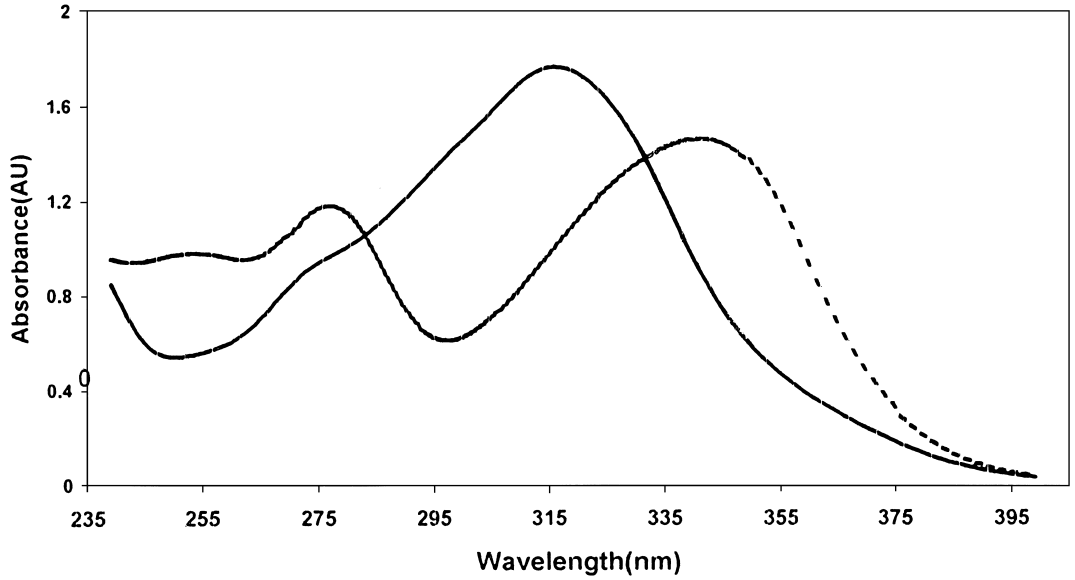

Fig. 4. Spectra of the components eluted from semipreparative HPLC column. — Coumaric acid derivatives; - - - - flavonoids.

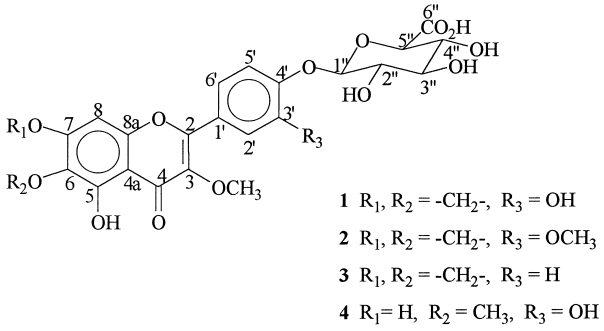

Two other peaks had UV traces virtually identical to that of 1. The ^{1}H NMR spectrum of the fraction eluting at 22.27 min showed this was a mixture of two flavonoids, both glucuronic acid conjugates very similar to **1**. Compound **2** (ca. 85%) only differed from the former in that it was methoxylated at the 3′-OH position; this was confirmed by the detection of through-space interactions (NOESY experiment) between this additional methoxy moiety and H-2′, as well as between the anomeric hydrogen (H-1″) and H-5′. The minor constituent, **3**, lacked this 3′ substituent and the B ring showed a symmetrical AA′XX′ pattern.

The most polar of this family of compounds, eluting at 19.5 min, had structure **4,** similar to **1** but with the 6,7-methylenedioxy unit replaced by 6-methoxy-7-hydroxy substitution; the location of the "new" methoxy moiety at position 7 was ascertained from a long-range coupling interaction (HMBC experiment) between the methoxy protons and C-6, the second of the three adjacent oxygenated ring A carbons, located at δ 132.8 (see Table 2). In view of the small amounts of material isolated, we were not able to determine direct ^{13}C spectra for **2**–**4**. For flavonoid **4**, however, many of the carbon chemical shifts could be inferred from the two-dimensional HMQC and HMBC. While compounds **2** (Aritomi and Kawasaki, 1984; Ferreres et al., 1997) and **4** (Aritomi et al., 1986; Wagner et al., 1977) have been previously reported we find no previous reference to minor constituent **3**.

Another set of peaks in the liquid chromatograph had UV spectra similar to the solid trace in Fig. 4. The ^{1}H NMR spectrum of the fraction eluting at 18.72 min showed it was composed of an ca. 85/15 mixture of two very simple substances; the spectra immediately suggested them to be the *trans* and *cis* isomers of *p*-coumaric acid (**5**), characterized by vicinal olefinic coupling

Table 1
NMR data for the components eluted from a semipreparative HPLC column[a]

	1		**2**	**3**	**4**	
	^{1}H	^{13}C	^{1}H	^{1}H	^{1}H	^{13}C[b]
2	–	157.44	–	–	–	[c]
3	–	140.24	–	–	–	140.0
3-OMe	3.81, *s* 3H	60.69	3.84, *s* 3H	3.82, *s* 3H	3.81, *s* 3H	60.7
4	–	180.65	–	–	–	[c]
4a	–	108.97	–	–	–	106.7
5	–	142.46	–	–	–	[c]
6	–	131.24	–	–	–	132.8
6-OMe	–	–	–	–	3.88, *s* 3H	61.0
OCH_2O	6.10, *s* 2H	104.38	6.11, *s* 2H	6.11, *s* 2H	–	–
7	–	156.18	–	–	–	159.3[d]
8	6.68, *s*	90.46	6.75, *s*	6.73, *s*	6.53, *s*	95.1
8a	–	153.93	–	–	–	154.0[d]
1′	–	126.62	–	–	–	127.0
2′	7.64, *d* 2.2	117.33	7.77, *d* 2.1	8.09 (AA′XX′)	7.65, *d* 2.2	117.4
3′	–	148.32	–	–	–	148.0
3′-OMe	–	–	3.95, *s* 3H	–	–	–
4′	–	148.96	–	–	–	149.0
5′	7.25, *d* 8.8	117.82	7.28, *d* 8.7	7.24 (AA′XX′)	7.29, *d* 8.7	118.1
6′	7.59, *dd* 8.8, 2.2	121.93	7.73, *dd* 8.7, 2.1	8.09 (AA″XX″)	7.61, *dd* 8.7, 2.2	121.7
1″	5.03, *d* 7.7	103.25	5.14, *d* 7.7	5.14, *d* 7.7	5.01, *d* 7.6	103.6
2″	3.60, *dd* 9.3, 7.7	74.52	3.60, *dd* 9.1, 7.7	[e]	3.60, *dd* 9.3, 7.6	[c]
3″	3.55, *t* 9.1	76.98	3.53, *t* 9.1	[e]	3.54, *t* 9.1	[c]
4″	3.64, *dd* 9.6, 8.9	73.06	3.64, *t* 9.4	[e]	3.63, *dd* 9.7, 9.0	[c]
5″	4.03, *d* 9.6	76.71	4.01, *d* 9.8	4.01, *d* 9.8	3.99, *d* 9.7	[c]
6″	–	172.36	–	–	–	[c]

[a] In CD_3OD.
[b] Chemical shifts measured indirectly from HMQC and HMBC spectra.
[c] Not detected.
[d] Assignment may be reversed.
[e] Superimposed on the peaks of **2**.

constants of 16 and 12.5 Hz, respectively (Table 2). A commercial sample of *trans*-*p*-coumaric acid gave a ^{1}H spectrum identical to the natural product; the ^{13}C chemical shifts of the latter are also listed in the table.

We cannot exclude the possibility that coumaric acid is formed by hydrolysis of its esters or that the *cis*/*trans* mixture observed for the acid and its derivatives (vide infra) was generated by light-induced isomerisation. However, we are quite convinced both reactions are unlikely in view of our isolation procedures (see Experimental).

The fraction eluting at 16.8 min had very similar spectra, also showing a mixture of *trans* and *cis* *p*-coumarate fragments. The ^{1}H spectrum had an additional pair of doublets for each isomer; a ^{13}C spectrum indicated this to be a tartaric acid derivative, with two oxymethines and two carboxylate groups. This fraction, therefore, corresponds to *trans*- and *cis*-forms of compound **6** (see Table 2).

Table 2
NMR data for *p*-coumaric acid derivatives[a]

	5			**6**			**7**		
	trans		*cis*	*trans*		*cis*	*trans*		*cis*
δ, J_{HH}	^{1}H	^{13}C	^{1}H	^{1}H	^{13}C	^{1}H	^{1}H	^{13}C[b]	^{1}H
1	–	127.17	–	–	127.19	–	–	127.2	–
2/6	7.45	131.06	7.61	7.49	131.38	7.70	7.49	131.4	7.69
3/5	6.80	116.76	6.73	6.81	116.93	6.75	6.81	116.9	6.75
4	–	161.04	–	–	161.53	–	–	161.4	–
7	7.60	146.68	6.82	7.72	147.74	6.94	7.68	147.7	6.97
8	6.28	115.49	5.75	6.41	114.39	5.88	6.39	114.4	5.82
$J_{7,8}$ (Hz)	16	–	12.5	16	–	12.5	16	–	12.5
9	–	171.06	–	–	168.13	–	–	168.2	–
1′	–	–	–	–	170.34	–	–	170.1	–
2′	–	–	–	5.56	75.50	5.52	5.70	73.3	5.72
3′	–	–	–	4.67	72.04	4.64	5.66	73.7	5.61
$J_{2',3'}$ (Hz)	–	–	–	2.5	–	2.5	2	–	2
4′	–	–	–	–	173.53	–	–	170.6	–
CH$_3$CO	–	–	–	–	–	–	2.15	20.7	2.12
CH$_3$*CO*	–	–	–	–	–	–		171.5	

[a] In CD_3OD.
[b] Chemical shifts measured indirectly from HMQC and HMBC spectra.

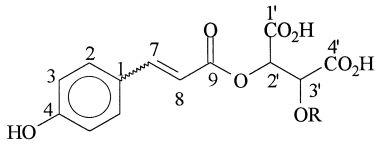

6 R = H
7 R = $COCH_3$

The least polar of this group of peaks (retention time 20.11 min) had a very similar ^{1}H NMR spectrum, with the addition of only a methyl group at δ 2.12 (δ 2.15 for the minor constituent) and strong deshielding of one of the tartarate methines, suggesting acetylation of **6** at position 3'. The structure was confirmed as an 85/15 mixture of *trans*- and *cis*- forms of **7,** with the aid of 2D ^{13}C×^{1}H correlation experiments (HMQC and HMBC). The carbon chemical shifts measured indirectly via these techniques are also shown in Table 2. A literature search revealed that *trans*-**6** and **7** had been previously identified in spinach leaves (Tadera and Mitsuda, 1970). These authors unambiguously assigned a *meso* configuration to the tartrate moieties, based on the value of $^3J_{2',3'}$. Using the same criterion, we can also establish **6** and **7** as having *meso*-tartarate residues. As far as we can tell, the *cis*-isomers have not been previously reported.

Based on ^{1}H NMR and ^{13}C NMR spectra the most active hydrophilic fraction (RT 5.6, Fig. 1a and b) was identified as uridine. Commercial sample of uridine exhibited similar antioxidant activity compared to the RT 5.6 fraction.

2.3. Synergism of antioxidant effects

In order to test the possibility of a synergistic effect among the antioxidant fractions isolated by HPLC, we took representative samples of the three main categories of the antioxidant fractions after HPLC separation (Fig. 1). The three fractions selected were RT 5.6 (uridine), RT 20.11 (*p*-coumaric) and RT 21.8 (flavonoid). From the hydrophilic group we chose the most active fraction and the two others were chosen as representatives of the two other groups. Each fraction was tested for its antioxidant activity in the TBA and FOX assays, and a mixture of these fractions was also analyzed as shown in Table 3.

Table 3
Synergism of antioxidant effects

Fractions[a]	Retention time (min)	% Inhibition (FOX)	% Inhibition (TBA)
Flavonoid	21.68	5.3±0.13	5.4±0.21
p-Coumaric acid	20.11	6.9±0.15	7.3±0.42
Hydrophilic (uridine)	5.60	5.3±0.20	5.0±0.14
Mixture[b]	–	35±0.21	34.5±0.41

[a] Fractions were taken from HPLC separation based on their retention time (Fig. 1).
[b] The mixture contained all the three fractions together (flavonoid, *p*-coumaric acid and hydrophilic). Inhibition of linoleic acid oxidation was followed by the FOX and TBA assays as described in Experimental.

The antioxidant activity obtained from the combination of these fractions was at least double the sum of activity of the three fractions, when each was assayed individually.

The antioxidant activity of the isolated purified fractions was compared on a molar basis to that of other known antioxidants and the IC_{50} values obtained are presented in Table 4. The data obtained show that the antioxidant potential of the purified aromatic polyphenol

Table 4
The IC_{50} values of purified fractions isolated from spinach (HPLC — Fig. 1) in comparision to other antioxidants. The antioxidant activity was measured by both TBA and FOX assays as described in Experimental

Fractions and antioxidants	Retention time (min)	IC_{50} (μM)
Flavonoid	21.8	15
p-Coumaric acid	20.1	18
Hydrophilic	5.60	120
EGCG (epigallocatechin gallate)	–	20
Vitamin E (trolox)	–	12
BHT (butylated hydroxytoluene)	–	100

fractions of spinach is similar to that of EGCG and vitamin E and even superior to that of BHT.

3. Discussion

We have previously shown that spinach contains a very effective natural antioxidant system (NAO) capable of preventing lipid peroxidation both in plant and animal systems (Grossman et al., 1994). The potential physiological role of NAO as an antioxidant was shown in several in vitro and in vivo systems (Grossman et al., 1994; Lomnitski et al., 2000a,b,c; Reznik, 1990; Zurovsky et al., 1994, 1995; Zurovsky and Gispaan, 1995). We have shown its efficacy in preventing lipid peroxidation in the skin of mice, rats and humans (Grossman et al., 1994; Renzik, 1990). Zurovsky et al. have shown the beneficial effect of NAO in preventing metabolic damage to the kidney, following exposure to hyperoxia,-induced by reperfusion in the rat (Zurovsky et al., 1995; Zurovsky and Gispaan, 1995). Recently, the efficacy of NAO in preventing LPS-induced hepatic injury both in rats and rabbits was demonstrated (Ben-Shaul et al., 1999; Lomnitski et al., 2000a,b,c). Moreover, NAO is very active in reducing the cardiotoxicity induced by antitumoral agents (Breitbart et al., 1999). In all these studies, the isolated fraction A from a water extract of spinach leaves was used (Grossman et al., 1994).

In the present study, a comprehensive investigation was performed to isolate and identify the active antioxidant components present in spinach leaves. Although this goal is not yet complete, we were able to characterize several antioxidant components, among them at least two whose structure was not previously described in spinach (structure **3** of the flavonoid, and the *cis-trans*-isomers **6** and **7** of the *meso*-tartarate residues).

Using a combination of solvents (1:9, water:acetone), a significant part of the antioxidant activity present in spinach leaves was extracted and resolved into several active peaks by HPLC on a C-8 column. High resolution separation of the active antioxidant peaks was obtained with a semi-preparative C-8 column in the HPLC separations (Figs. 1 and 3).

The identification of the chemical structure of the various fractions was based mainly on NMR spectroscopy. The active antioxidant peaks identified can be separated into three categories of chemicals: (a) flavonoid derivatives (b) coumaric acid derivatives (c) and hydrophilic components, one of them was identified as the nucleoside, uridine.

The possible presence of flavonoid-like compounds in spinach was first reported by Weatherby and Cheng (1943). Williams islolated a flavonoid. Zane and Wender (1961) established the structure of isolated flavonol from spinach leaves as patuletin and also described the presence of spinacetin in this extract. Aritomi et al. (Aritomi et al., 1986; Aritomi and Kawasaki, 1984) reported the presence of seven flavonol glycosides in methanolic extract of spinach leaves. Recently, Ferreres et al. (1997) isolated and identified five novel naturally occurring flavonoids from alcoholic extracts of spinach leaves. In all these studies there was no reference to the possible biological or physiological role of these compounds. The main goal of the present study was to identify the active components which comprise the powerful antioxidant activity present in aqueous spinach leaf extracts. Our NMR data indicate that several of the flavonoids, compounds **1**, **2** and **4**, which were described previously, and the new naturally occurring compound **3** described in this study, are present in the water extract of spinach leaves and contribute to its antioxidant activity (Fig. 2).

For some time it has been recognized that several classes of flavonoid show antioxidant activity toward a variety of easily oxidizable compounds (Larson, 1988). Early work of Clemetson and Andersen showed that many flavonoids and other plant phenolic compounds protect against ascorbic acid destruction (Clemetson and Andersen, 1966). The past two decades have witnessed a renewed interest in the study of flavanoids and of their biological interactions with mammalian cells and tissues. Flavonoids are known to display a broad array of pharmacological and biochemical actions (Middleton and Kandaswami, 1992, 1993). The flavonoids are typical phenolic compounds and powerful chain- breaking antioxidants (Lea and Swoboda, 1956; Clemetson and Andersen, 1966; Hughes and Wilson, 1977; Baumann et al., 1980b; Jones and Hughes, 1984; Torel et al., 1986; Pratt, 1992). It was reported that lipid peroxidation can be inhibited by flavonoids, possibly through their activity as strong $O_2^{\cdot -}$ scavengers (Baumann et al., 1980b) and singlet oxygen quenchers (Sorata et al., 1984). Recently, the ability of eight structurally related naturally occurring flavonoids to inhibit lipid peroxidation and mitochondrial membrane permeability transition was described (Santos et al., 1998). It was suggested that flavonoids have multiple biological

activities including potent anti-allergic, anti-inflammatory, and antiviral actions, which may result, at least in part, from their antioxidant and free radical-scavenging abilities (Kahl, 1991; Middleton and Kandaswami, 1993; van Acker et al., 1996; Santos et al., 1998). We have shown here that the flavonoid-containing fractions from the spinach extract inhibited lipid peroxidation in all three assays used in this study. Moreover, the spinach flavonoids significantly inhibited soybean lipoxygenase activity. These data are in agreement with other studies (Baumann et al., 1980a; Robak et al., 1988; Laughton et al., 1991) which demonstrated inhibition of lipoxygenases by flavonoids from other sources.

In addition to the flavonoids, the spinach extract was found to contain derivatives of the isomers of *p*-coumaric acid (**5, 6** and **7**), while **6** and **7** have *meso*-tartarate residues. Moreover, **7** was confirmed to be a mixture of *trans* and *cis* isomers. The *cis* isomer had not been previously reported in spinach. The presence of *p*-coumaroyl-meso-tartaric acid detected in spinach leaves in large amounts was reported by Winter and Herrmann (1986). As can be seen from Fig. 2, these *p*-coumaric derivatives are very strong antioxidants. The ability of some phenolic compounds to act as antioxidants has been previously shown (Clemetson and Andersen, 1966). In a recent publication, Velioglu et al. (1998) studied the antioxidant activity and total phenolics of 28 plant products including seeds, fruits, vegetables and medicinal plants and reported a significant correlation between total phenolics and antioxidative activity. The antitumor activity of a polyphenolic fraction isolated from grape seeds has also been demonstrated (Zhao et al., 1999).

In summary, the present study demonstrates for the first time the presence of both flavonoids and p-coumaric acid derivatives as antioxidant components of the aqueous extract of spinach leaves. About seven individual active fractions were isolated in the aromatic polyphenol group (Figs. 1 and 3). Although each isolated fraction exhibits antioxidant activity (Fig. 2), we may assume that the combination of these fractions contributes to the synergistic efficacy of the NAO extract as a powerful antioxidant in protecting against oxidation damages in biological systems that we tested. As shown in Table 4 several of the isolated antioxidants are as active as other known antioxidants such as EGCG (green tea) and the water soluble derivative of vitamin E. The aromatic polyphenols that we isolated are all glycosylated. This is expected to increase their intestinal absorption and bio-availability in a manner similar to the flavonoid quercetin, which was shown to be absorbed in much greater amounts than the pure aglycone (Hollman and Katan, 1999). We are currently pursuing the chemical identification of the isolated hydrophilic fractions (Fig. 1, RT 3.5–11.5). Preliminary results indicate the presence of amino acids, sugars, organic and nucleic acids in these fractions. The main active fraction was identified as uridine. Determination of the exact chemical structure of the other fractions and their antioxidative nature remains to be completed.

4. Experimental

4.1. Chemicals

All the standard chemicals used and Soybean Lipoxygenase (Type II) were obtained from Sigma Chemical (St. Louis, MO). Organic solvents were purchased from Merck (Darmstadt, Germany) for HPLC analyses and from Bio labs (Jerusalem, Israel) for acetone extraction.

4.2. Antioxidant preparation and purification

Spinach extract was prepared at room temperature (25°C). Fresh leaves of spinach (*spinacia oleracea*) were mixed 1:1 (w/v) with distilled water and homogenized in a blender for about 5 min. The homogenate was filtered through two layers of cheesecloth and centrifuged at 20,000×*g* for 10 min. The supernatant was collected. The concentration of solids in the supernatant was about 3%, as determined by reflectometry. The supernatant was concentrated to 25% by evaporation at 80°C. One ml of this supernatant was mixed with 9 ml of acetone AR for 5 min by stirring. This mixture was centrifuged at 20,000×*g* for 10 min. The supernatant was collected and the acetone was evaporated at 85°C; this residue was used for HPLC analysis and separation.

4.3. HPLC analysis and separation

LaChrom chromatography system was used with LaChrom L-7450 Diode Array Detector (DAD); data for each run was documented by the HSM program included with the LaChrom software. For analytical separations, a LiChrocart 125-4 column was used, packed with Lichrospher 100, RP8, 5 um. For semipreparative separation, a LiChrocart 250-10 column was used packed with the same resin. Solutions: A 0.1% TFA in water; B CH3CN; The running conditions were as follows: 0–5 min/100% A; 5–27 min/100–56%/A (linear gradient); flow rate:1 ml/min (for the analytical column) and 6 ml/min (for the semipreparative column); detection was at 254 or 310 nm. Using the DAD, we were able to analyze the run at any wavelength and to see the spectrum of any peak.

4.4. Antioxidant activity of peaks eluted from HPLC

The peaks were collected to clean tubes and acetonitrile (CH_3CN) was evaporated in a Speed Vac Plus SC110A (Savant), and freeze dried. The dried peaks were diluted in 100 μl of water and equal volumes were taken for antioxidant activity assays.

4.5. Determination of antioxidant activity

Antioxidant activity was determined by measuring the inhibition of auto-oxidation of linoleic acid at 37°C for 24 h. Linoleic acid was prepared in Tween 20 as described by Grossman and Zakut (1979). In brief, a stock solution of 3×10^{-2} M linoleic acid was prepared by addition of 3 nmoles of linoleic acid to 50 ml of distilled water containing 1 ml of Tween 20. Three to 5 ml of 1 N NaOH were added in order to clarify the resulting emulsion and the volume was adjusted to 100 ml with distilled water. This stock solution was diluted with 100 mM of phosphate buffer pH 7.0 to 7.5×10^{-3} M. The solution was stored at 4°C for up to two weeks. One ml of this solution was used for the auto-oxidation assay. It was incubated at 37°C for 24 h in the presence or absence of antioxidants, and from this solution 25–100 μl were taken for TBA assay and 2–5 μl for the FOX determination.

The level of auto-oxidation was measured by two methods: (a) the Thiobarbituric acid (TBA) assay measuring malonedialdehyde (MDA) and, (b) the ferrous oxidation in the presence of xylenol orange (FOX method) for measuring peroxide levels. TBA was reacted colorimetrically with MDA according to the method of Wasowicz et al. (1993). The colored product was monitored at 532 nm.

In the FOX method (Wolff, 1994), peroxides mediate the oxidation of Fe^{+2} to Fe^{+3} under acid conditions. In the presence of xylenol orange, Fe^{+3} forms a blue-purple complex with absorption at 560 nm.

4.6. The polarographic method

In some cases antioxidant activity was determined as inhibition of soybean lipoxygenase oxidation of linoleic acid using the polarographic method in which oxygen consumption during lipoxygenase activity is determined (Grossman and Zakut, 1979).

Lipoxygenase activity was determined using a YSI Biological Oxygen Monitor (Yellow Springs Instrument, Ohio) equipped with Clark electrode in a closed chamber. The substrate for Lipoxygenase activity was Linoleic acid, 7.5×10^{-3} M, in 50 mM phosphate buffer, pH 6.5. To assay lipoxygenase activity, 0.9 ml of linoleic acid (7.5×10^{-3} M) were added to the oxygen monitor chamber containing 50 μl of lipoxygenase (1 mg/10 ml) in phosphate buffer pH 6.5, and 50 μl of antioxidant fractions after HPLC analysis. Oxygen consumption was recorded.

4.7. Identification of molecular structure of HPLC peaks by NMR

NMR spectra were run, in CD_3OD solutions, on a Bruker DMX-600 instrument, operating at 600.1 and 150.9 MHz (^1H and ^{13}C, respectively). In all cases chemical shifts are given in ppm units downfield from internal TMS and coupling constants are reported in Hz.

References

Al-Ssikhan, M.S., Howard, L.R., Miller Jr, L.C., 1995. Antioxidant activity and total phenolics in different genotypes of potato (*Solanum tuberosum*, L.). J. Food Sci. 60, 341–343.

Amarowicz, R., Wanasunddara, U.N., Karamac, M., Shahidi, F., 1996. Antioxidant activity of ethanolic extract of mustard seed. Nahrung 40, 261–263.

Aritomi, M., Kawasaki, T., 1984. Three highly oxygenated flavone glucuronides in leaves of *spinacia oleracea*. Phytochemistry 23, 2043–2047.

Aritomi, M., Kokori, T., Kawasaki, T., 1986. Flavonol glycosides in leaves of *Spinacia oleracea*. Phytochemistry 25, 231–234.

Baumann, J., von Bruchhausen, F., Wurm, G., 1980a. Flavonoids and related compounds as inhibition of arachidonic acid peroxidation. Prostaglandins 20, 627–639.

Baumann, J., Wurm, G., von Bruchhausen, F., 1980b. Prostaglandin synthetase inhibition by flavonoids and phenolic compounds in relation to their O_2 — scavenging properties. Arch. Pharm. (Weinheim) 313, 330–337.

Ben-Shaul, V., Sofer, Y., Bergman, M., Zurovsky, Y., Grossman, S., 1999. Lipopolysaccharide-induced oxidative stress in the liver: comparison between rat and rabbit. Shock 12, 288–293.

Breitbart, E., Sofer, Y., Kalechman, Y., Sredni, B., Grossman, S., 1999. The effect of water-soluble antioxidant on prevention of the doxorubin toxic effect on the immune system and the heart. 90th AOCS Annual Meeting, Orlando, USA.

Cao, G.H., Sofic, E., Prior, R.L., 1996. Antioxidant capacity of tea and vegetables. J. Agric. Food Chem. 44, 3426–3431.

Clemetson, C.A., Andersen, L., 1966. Plant polyphenols as antioxidants for ascorbic acid. Ann. N.Y. Acad. Sci. 136, 341–376.

Clemetson, C.A., Andersen, L., 1996. Plant polyphenols as antioxidants for ascorbic acid. Ann. N.Y. Acad. Sci. 136, 341–376.

Cook, N.C., Samman, S., 1996. Flavonoids chemistry, metabolism, cardioprotective effects and dietary sources. Nutr. Biochem. 7, 66–76.

Ferreres, F., Castaner, M., Tomas-Barbern, A., 1997. Acylated flavonol glycosides from spinach leaves (*Spinacia oleraceas*). Phytochemistry 45, 1701–1705.

Grossman, S., Reznik, R., Tamari, T., Albeck, M., 1994. New plant water soluble antioxidant (NAO) from spinach. In: Asada, K., Toshikawa, T. (Eds.), Frontiers of Reactive Oxygen Species in Biology and Medicine. Elsevier Science, Amsterdam, The Netherlands, pp. 343–344.

Grossman, S., Zakut, R., 1978. Determination of the activity of lipoxygenase (lipoxidase). In: Glick, D. (Ed.), Methods of Biochemical Analysis. pp. 308–329.

Hollman, P.C., Katan, M.B., 1999. Dietary flavonoids: intake, health effects and bioavailability. Food Chem. Toxicol. 37, 937–942.

Huang, M.-T., Ho, C.-T., Lee, C.Y., 1992. Phenolic compound in food and their effects on health. II. Antioxidant and cancer prevention. In: ACS SYmposium Series 507, American Chemical Society, Washington, DC.

Hughes, R.E., Wilson, H.K., 1977.In: Ellis, G.P., West, G.B.(Eds.), Progress in Medicinal Chemistry. Elsevier, Amsterdam, p. 285–301.

Jones, E., Hughes, R.E., 1984. The influence of bioflavonoids on the absorption of vitamin C. IRCS Med. Sci. 12, 320.

Kahl, R., 1991. Protective and adverse biological actions of phenolic antioxidants. In: Sies, H. (Ed.), Oxidative Stress: Oxidants and Antioxidants. Academic Press, London, pp. 245–273.

Larson, R.A., 1988. The antioxidant of higher plants. Phytochemistry 27, 969–978.

Laughton, M.J., Evans, P.J., Moroney, M.A., Hoult, J.R., Halliwell, B., 1991. Inhibition of mammalian 5-lipoxygenase and cyclo-oxygenase by flavonoids and phenolic dietary additives. Relationship to antioxidant activity and to iron ion-reducing ability. Biochem. Pharmacol. 42, 1673–1681.

Lea, C.H., Swoboda, P.A.T., 1956. Antioxidant activity of flavonols, gossypetin and quercetagetin. Chem. Ind. 1426.

Lomnitski, L., Carbonatto, M., Ben-Shaul, V., Peano, S., Conz, A., Corradin, L., Maronpot, R.R., Grossman, S., Nyska, A., 2000a. The prophylactic effects of natural water-soluble antioxidant from spinach and apocynin in a rabbit model of lipopolysaccharide-induced endotoxemia. Toxicol. Pathol. 28, 588–600.

Lomnitski, L., Foley, J., Grossman, S., Ben-Shaul, V., Maronpot, R., Moomaw, C., Carbonatto, M., Nyska, A., 2000b. Effects of apocynin and natural antioxidants from spinach on iNOS and COX-2 induction in LPS-induced hepatic injury in rat. Pharmacol. Toxicol. 87, 18–25.

Lomnitski, L., Nyska, A., Ben-Shaul, V., Maronpot, R.R., Haseman, J.K., Harrus, T.L., Bergman, M., Grossman, S., 2000c. Effects of antioxidants apocynin and the natural water-soluble antioxidant from spinach on cellular damage induced by lipopolysaccharide in the rat. Toxicol. Pathol. 287, 580–587.

Middleton Jr, E., Kandaswami, C., 1992. Effects of flavonoids on immune and inflammatory cell functions. Biochem. Pharmacol. 43, 1167–1179.

Middleton Jr, E., Kandaswami, C., 1993. The impact of plantvonoids on mammalian biology; implication for immunity, inflammation and cancer. In: Harborne, J.B. (Ed.), The Flavonoids: Advances in Research Since 1986. Chapman & Hall, London, pp. 619–652.

Oomah, B.D., Mazza, G., 1994. Flavonoid and antioxidant activities in buckwheat. J. Agric. Food Chem. 7, 1746–1750.

Pratt, D.E., 1992. In Huang, M.-T., Ho C.-H., Lee C.Y. (Eds.), Phenolic Compounds in Food and their Effects on Health II. American Chemical Society, Washington, pp. 54.

Ramarathnam, N., Ochi, H., Takeuchi, M., 1996. Antioxidant defense in vegetable extracts. In: Shahidi, F.(Ed.), Natural Antioxidants Chemistry, Health Effects and Applications. pp. 76–78.

Reznik, R., 1990. Plant water soluble antioxidants characterization and biological activity *in vivo*. PhD thesis, Ba-Ilan University, Ramat-Gan, Israel.

Robak, J., Shridi, F., Wolbis, M., Krolikowska, M., 1988. Screening of the influence of flavonoids on lipoxygenase and cyclooxygenase activity, as well as on nonenzymic lipid oxidation. Pol. J. Pharmacol. Pharm. 40, 451–458.

Santos, A.C., Uyemura, S.A., Lopes, J.L., Bazon, J.N., Mingatto, F.E., Curti, C., 1998. Effect of naturally occurring flavonoids on lipid peroxidation and membrane permeability transition in mitochondria. Free Radic. Biol. Med. 24, 1455–1461.

Shahidi, F., 1996. Natural Antioxidants. In: Shahidi, F.(Ed.), Natural Antioxidants Chemistry, Health Effects and Applications. pp. 1–11.

Sorata, Y., Takahama, U., Kimura, M., 1984. Protective effect of quercetin and rutin on photosensitized lysis of human erythrocytes in the presence of hematoporphyrin. Biochim. Biophys. Acta 799, 313–317.

Tadera, K., Mitsuda, H., 1970. New *p*-coumaryl derivatives isolated from spinach leaves. II. Determination of chemical structure. Agric. Biol. Chem. 34, 517–522.

Torel, J., Cillard, J., Cillard, P., 1986. Antioxidant activity of flavonoids and reactivity with peroxy radica. Phytochemistry 25, 383–386.

van Acker, S.A., van den Berg, D.J., Tromp, M.N., Griffioen, D.H., van Bennekom, W.P., van der Vijgh, W.J., Bast, A., 1996. Structural aspects of antioxidant activity of flavonoids. Free Radic. Biol. Med. 20, 331–342.

Velioglu, Y.S., Mazza, G., Gao, Y.L., Oomah, B.D., 1998. Antioxidant activity and total phenolics in selected fruits, vegetables and grain products. J. Agric. Food Chem. 46, 4113–4117.

Wagner, H., Maurer, I., Farkas, L., Streilisky, J., 1977. Synthese von polyhydroxy-flavonomethylathern mit potentieller cytotoxischer wirksamkeit — 1. Tetrahedron 33, 1405–1409.

Wang, H., Cao, G.H., Prior, R.L., 1996. Total antioxidant capacity of fruits. J. Agric. Food Chem. 44, 701–705.

Wasowicz, W., Neve, J., Peretz, A., 1993. Optimized steps in fluorometric determination of thiobarbituric acid-reactive substances in serum: importance of extraction pH and influence of sample preservation and storage. Clin. Chem. 39, 2522–2526.

Weatherby, L., Cheng, L., 1943. Determination of flavons or quercetin-like substances in certain naturally occurring products. J. Biol. Chem. 48, 707.

Winter, M., Hermann, K., 1986. Esters and glucosides of hydroxycinnamic acids in vegetables. J. Agric. Food Chem. 34, 616–620.

Wolff, S.P., 1994. Ferrous ion oxidation in presence of ferric ion indicator xylenol orange for measurement of hydroperoxides. In: Packer, L.(Ed.), Methods in Enzymology. Academic Press, pp. 182–189.

Yen, G., Duh, P.D., 1995. Antioxidants activity of methanolic extracts of peanut hulls from various cultivars. Am. Oil Chem. Soc. 72, 1065–1067.

Zane, A., Wender, S.H., 1961. Flavanols in spinach leaves. J. Org. Chem. 26, 4718.

Zhao, J., Wang, J., Chen, Y., Agarwal, R., 1999. Anti-tumor-promoting activity of a polyphenolic fraction isolated from grape seeds in the mouse skin two-stage initiation-promotion protocol and identification of procyanidin B5-3′-gallate as the most effective antioxidant constituent. Carcinogenesis 20, 1737–1745.

Zurovsky, Y., Eligal, Z., Grossman, S., 1995. Unilateral renal ischemia reperfusion in the rat: effect of blood volume trapped in the kidney, sucrose infusion, and antioxidant treatments. Exp. Toxicol. Pathol. 47, 471–478.

Zurovsky, Y., Eligal, Z., Grossman, S., Bergman, M., Gafter, U., 1994. Glycerol-induced augmentation of sensitivity to endotoxin in rats. Toxicon 32, 17–26.

Zurovsky, Y., Gispaan, I., 1995. Antioxidant attenuate endotoxin induced acute renal failure in the rats. Am. J. Kid. Dis. 25, 51–57.

PERGAMON

Phytochemistry 58 (2001) 153–157

PHYTOCHEMISTRY

www.elsevier.com/locate/phytochem

Isolation of an anti-HIV diprenylated bibenzyl from *Glycyrrhiza lepidota*

Kirk P. Manfredi[a,*], Vasanti Vallurupalli[a], Maria Demidova[a], Kelly Kindscher[b], Lewis K. Pannell[c]

[a]*Department of Chemistry, University of Northern Iowa, Cedar Falls, IA 50614, USA*
[b]*Kansas Biological Survey, University of Kansas, 2041 Constant Avenue, Lawrence, KS 66047-2906, USA*
[c]*Laboratory of Bioorganic Chemistry, NIDDK, Bethesda, MD 20892-0805, USA*

Received 5 September 2000; received in revised form 9 March 2001

Abstract

The organic soluble extract from the leaves of *Glycyrrhiza lepidota* showed moderate activity in the US National Cancer Institute in vitro anti-HIV-1 bioassay. Chromatographic separation of this extract resulted in the identification of a new diprenylated bibenzyl as the compound responsible for the observed anti-viral activity. Extensive spectroscopic experiments provide the complete ^{1}H NMR and ^{13}C NMR spectral assignments to support the proposed structure. Known compounds glepidotin B and glepidotin A were also isolated from the extract and shown to be inactive in the anti-viral assay. © 2001 Elsevier Science Ltd. All rights reserved.

Keywords: *Glycyrrhiza lepidota*; Fabaceae; Prenylated; Glepidotin; HIV-1

1. Introduction

Over the past several years, this laboratory has been investigating the chemistry of medicinal native plants of the North American prairie. Plant collection was guided by historical accounts of plant medicinal uses by early European settlers traveling across the plains and by indigenous North Americans (Dilwyn, 1980). The ethnobotanical literature cites 203 plant species used for medicinal purposes by the Indian tribes of the Prairie Bioregion of North America (Kindscher, 1992). With the ethnobotanical uses of plants for medicinal purposes clearly documented, a study of native prairie plants as sources of new pharmaceuticals was begun. The initial investigation examined the anti-HIV activity of 22 species of medicinal plants using the US National Cancer Institute's (US NCI) in vitro AIDS anti-viral assay (Weislow et al., 1989). The assay results identified three organic extracts as "active" in the anti-HIV screen (Kindscher et al., 1998). An active extract was defined as a crude extract that showed at least 50% growth inhibition in HIV-infected white blood cells compared to the non-infected control at a maximum test concentration of 250 μg/ml. One of the three active species was *Glycyrrhiza lepidota* (wild licorice). This communication describes the isolation and structure elucidation of the diprenylated bibenzyl **1** responsible for the observed anti-HIV activity.

The genus *Glycyrrhiza* ("sweet root") is a member of the Fabaceae family and contains 18 species world-wide (Mabberly, 1997). *Glycyrrhiza lepidota* (common names: wild licorice, American licorice, and desert root) is the only member of the genus native to North America and is widely distributed throughout the western United States and Canada. It is a perennial herb that grows to 0.3–1.1 m in height. Its use by native North Americans has been well documented (Gilmore, 1977; Camazine and Bye, 1980; Munson, 1981). The antimicrobial agents from *G. lepidota* have been previously studied (Mitscher et al., 1983; Gollapudi et al., 1989). In the work by Mitscher et al. (1983) antimicrobial bioassay-guided fractionization afforded the flavanol glepidotin A (**2**), the flavanol glepidotin B (**3**), and the prenylated bibenzyl glepidotin C (**4**). Additionally, a number of other flavanoids and bibenzyls were isolated and identified that had been previously isolated from *G. glabra* (Saitoh et al., 1976; Mitscher et al., 1980), *Helichrysum umbraculigerum* (Bohlmann and Hoffmann, 1979), and *Radula camplanata* (Asakawa et al., 1978).

* Corresponding author. Tel.: +1-319-273-2437; fax: +1-319-273-7127.
E-mail address: manfredi@uni.edu (K.P. Manfredi).

0031-9422/01/$ - see front matter © 2001 Elsevier Science Ltd. All rights reserved.
PII: S0031-9422(01)00177-7

2. Results and discussion

The dried leaves of *G. lepidota* were extracted with both water and CH_2Cl_2:MeOH (1:1) . Both the aqueous and organic extracts were submitted for in vitro screening against HIV-1 as previously described by Wieslow et al. (1989). The water extract was inactive in the assay while the organic extract gave an EC_{50} of 30 μg / ml in duplicate testing. Subsequent bioassay-guided fractionation (LH-20) yielded one active fraction which was then subjected to normal phase HPLC purification to yield three pure compounds.

The first eluting compound from HPLC was identified as glepidotin B (**2**) based on its high resolution accurate mass, ^{13}C, and ^{1}H NMR spectral characteristics. The coupling constant of 13.4 Hz and the lack of a NOE between H-2 and H-3 suggested a *trans* stereochemistry. The second eluting compound was identified as glepidotin A (**3**). Subsequent in vitro assay for anti-HIV activity showed that neither of these two compounds were responsible for the observed anti-viral activity of the parent fraction.

The third compound isolated proved to be somewhat difficult to work with. After its initial purification by HPLC and removal of solvent, spectral data (^{1}H and ^{13}C NMR, IR and UV) could be obtained if the experiments were performed immediately after solvent removal. However, if the solvent was removed and the sample stored overnight, only about 50% would re-dissolve in the NMR solvent ($CDCl_3$ or CD_3OD) the next day. The insoluble material appeared as a white film on the flask. Attempts to dissolve this material in any common solvent (e.g. DMSO, THF, H_2O) failed. It was determined that if the sample was stored dry for any extended period of time (i.e. over approximately 6 h), substantial decomposition occurred and reisolation by HPLC was required with a concomitant loss of material. Eventually it was determined that the material could be stored for long periods of time in solution without decomposition. Therefore, once isolated, **1** would be quickly weighed and stored in solution ($CDCl_3$) for subsequent experiments.

The ^{1}H NMR spectrum of **1** showed a four-proton multiplet at δ 2.82. A subsequent ^{1}H–^{1}H COSY analysis showed no coupling outside the multiplet which suggested an isolated pair of non-equivalent methylene protons. This observation initially led us to believe that the compound was the earlier isolated bibenzyl **4**. However, high resolution mass spectrometry indicated a molecular formula of $C_{24}H_{30}O_3$. This molecular formula suggested a diprenylated bibenzyl. Two prenyl groups could be identified from two methyl groups at δ 1.76 and δ 1.78 and an overlapping six-proton methyl singlet at δ 1.73 ppm thus accounting for the expected four methyl groups. The one-proton signals for the prenyl olefin triplets were at δ 5.25 and δ 5.45. There was a substantial difference between the chemical shifts of the prenyl methylene groups, δ 3.39 and δ 4.45 ppm, which suggested that one of the prenyl groups was bonded to an oxygen (Williams and Flemming, 1989). Analysis of the aromatic region of the ^{1}H NMR 1D and ^{1}H–^{1}H COSY spectra identified an isolated *meta* coupled spin system at δ 6.29 and δ 6.34. This suggested that one of the aromatic rings was 1,2,3,5-tetra-substituted. Four other aromatic protons appeared as a triplet at δ 7.15 ($J = 7.65$), a *meta* coupled doublet of triplets at δ 6.78 ($J = 7.65$, 1.02), and a pair of overlapping signals centered at δ 6.66 and δ 6.65. The signal at δ 6.66 was a poorly resolved, finely coupled triplet while the one centered at δ 6.65 appeared as an unresolved mulitplet. Careful examination of the ^{1}H–^{1}H COSY identified the proton signal centered at δ 6.65 as being coupled to the triplet at δ 7.15. This implied that the proton at δ 6.66 showed only *meta* coupling. These observations suggested that this ring was *meta* disubstituted with the resonance centered at δ 6.66 corresponding to the isolated proton.

In order to establish the ring substitution patterns, a HMBC experiment was performed. Shown in Fig. 1 are the key long range correlations. Essential to establishing the structure was the correlation from the non-oxygenated prenyl methylene protons at δ 3.39 to C-1 and C-3. The oxygen-bonded prenyl methylene protons at δ 4.45 ppm also correlated to C-3, thus establishing the ether oxygen carbon at δ 157.0. This indicated that the tetra-substituted ring had the two prenyl groups *ortho* to each other and a hydroxy group *ortho* to the non-oxygenated prenyl group. These HMBC data, in combination with the 1D proton data, established the substitution pattern for the tetra-substituted ring as shown in Fig. 1. This is also consistent with the substitution previously established for glepidotin C (**4**) (Gollapudi et al., 1989).

The *meta* substitution pattern on the other aromatic ring had been established from its ^{1}H–^{1}H COSY spectrum. The results of the HMBC experiment confirmed the assignment of the signal at δ 6.66 to be assigned to H-2″ based on its long range correlation to the hydroxyl bearing carbon at δ 155.3 (C-3″) and the bibenzyl carbon at δ 37.7 (C-1″a). The assignment of the H-6″ signal at δ 6.78 was established based on its long range correlation to the same bibenzyl carbon as H-2″ (C-1″a). Given in Table 1 are the complete ^{1}H and ^{13}C NMR spectra assignments for **1** based on the acquired HMBC, ^{13}C–^{1}H HETCOR, and ^{1}H–^{1}H COSY experiments.

Compound **1** is, therefore, 2-(3-methyl-2-butenyl)-3-*O*-(3-methyl-2-butenyl)-5-[2-(3-hydroxyphenyl)ethyl]-1, 3-benzenediol. However, Mitscher et al. (1980, 1983) have established the common name ''glepidotins'' for bibenzyls and flavanols from *G. lepidota*. Therefore, we refer to this compound as glepidotin D.

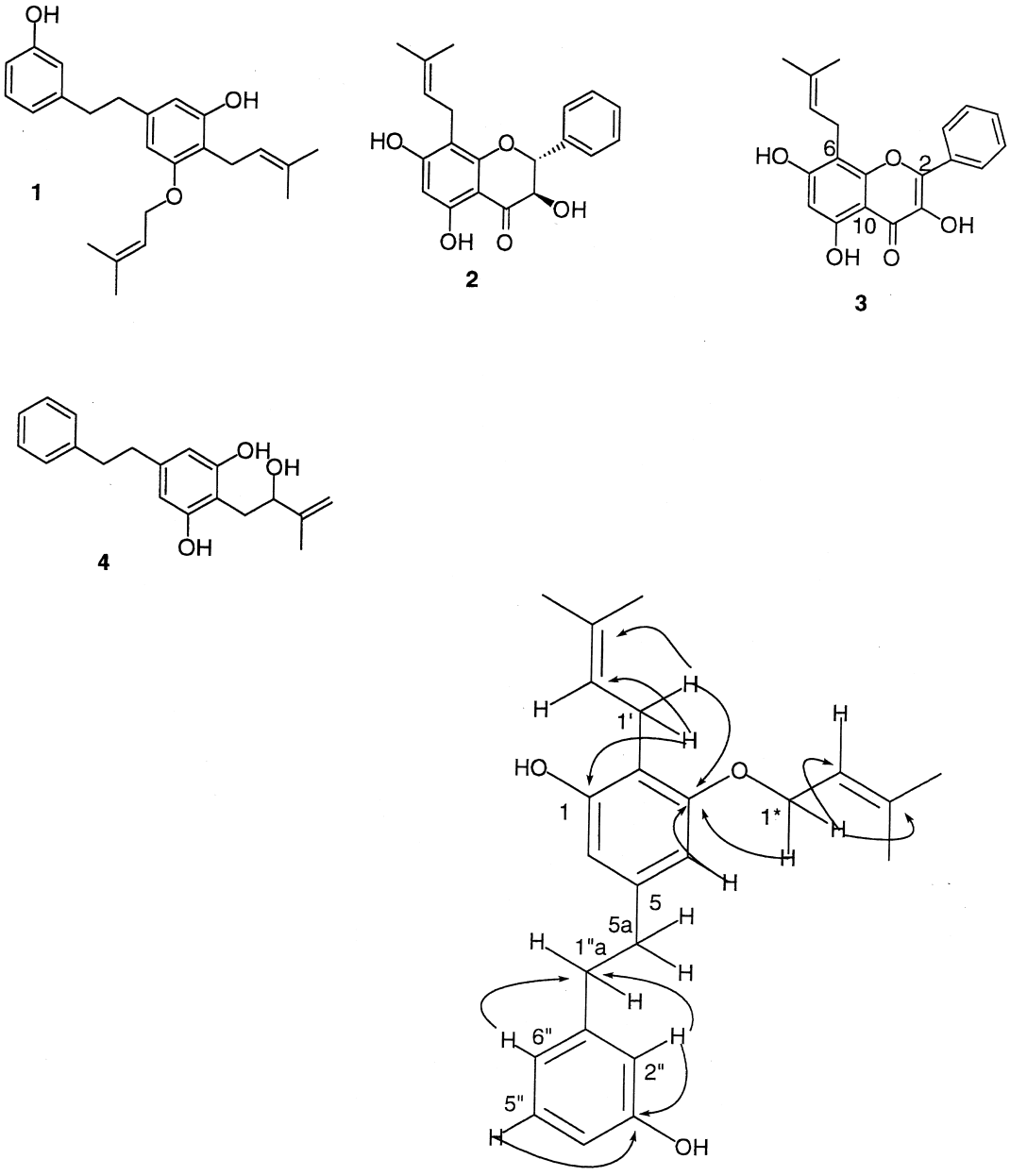

Fig. 1. Key long range HMBC correlations for **1**.

3. Biological activity

In conjuction with the Laboratory of Drug Discovery, Research and Development (LDDRD) at the US NCI, an in vitro assay against HIV-1 was performed. Compound **1** achieved an EC_{50} of 2.0 μg/ml and an IC_{50} of 5.0 μg/ml. The activity of **1** is a full order of magnitude greater than that of the crude extract and supports the hypothesis that the observed anti-HIV activity may solely be due to **1**. We were unable to isolate any glepidotin C (**4**) from the plant to determine if this related compound possessed anti-viral properties. The activity associated with this compound may be suspect because of its instability. However, we have determined that it is stable for prolonged periods of time in organic solvents, but are unsure of its stabilty under the assay conditions. Because of the instability of compound **1** and its small therapuetic index (TI: EC_{50}/IC_{50}) no further testing in the anti-viral assays is planned.

4. Experimental

4.1. General

NMR experiments were acquired on a Tecmag Aquerius (GE QE 300) at 300 or 75 MHz. The inverse-detected HMBC experiment was acquired on a Varian

Table 1
^1H and ^{13}C spectral assignments for **1** ($CDCl_3$)

Carbon	^1H (ppm, *m*, *J*)	^{13}C (ppm)	Long range (HMBC)
1		155.3	
2		113.1	
3		157.0	
4	6.29 (*d*, 1.02)	105.1	157.0, 113.1, 108.7, 37.4
5		141.0	
6	6.34 (*d*, 1.02)	108.7	155.3, 113.1, 105.1, 37.4
1″		143.8	
2″[a]	6.66 (*dt*)	112.8	155.5, 115.4, 37.7
3″		155.5	
4″[a]	6.65 (*t*)	115.4	155.5, 112.8
5″	7.15 (*t*, 7.65)	129.5	155.5, 143.8
6″	6.78 (*dt*, 7.65,1.1)	120.9	115.4, 112.8, 37.7
1″a, 5a[b]	2.82 (*m*)	37.4, 37.7	37.7, 37.4, 143.8, 141.0, 108.7, 112.8, 120.9
1′	3.39 (*d*, 7.14)	22.3	157.0, 155.3, 134.1
2′	5.25 (*t*, 7.14)	122.3	17.7, 25.8
3′		134.1	
4′, 5′	1.73, 1.78 (*s*)	25.8, 17.8	134.1, 137.2, 120.2, 122.3
1*	4.45 (*t*, 6.63)	65.4	157.0, 137.2, 120.2
2*	5.45 (*t*, 6.63)	120.2	18.7, 25.8
3*		137.2	
4*, 5*	1.76, 1.73 (*s*)	18.2, 25.8	134.1, 137.2, 20.2, 122.3
OH	4.42 (*s*, *br*)		
OH	4.70 (*s*, *br*)		

[a] Because these signals overlapped, the coupling constants could not be determined from the 1D ^1H NMR spectrum at 300 MHz.

[b] These carbons and hydrogens could not be resolved. The long range correlations must be assigned based on the proposed structure.

VXR 500 at LDDRD at the US NCI in Frederick, Maryland. All chemical shifts are reported in ppm relative to TMS. Mass spectral data were obtained on a JOEL SX 102 mass spectrometer operating at 10 kV (NIDDK, US NIH, Bethesda, Maryland). Samples for FABMS were desorbed from a nitrobenzyl alcohol matrix using 6 keV xenon atoms. Accurate mass FAB was performed at a resolution of 10,000. IR data were acquired on a Galaxy series 2020 FT–IR spectrometer. HPLC chromatography was performed on an ISCO gradient HPLC with a ISCO V-4 UV detector. All solvents were purchased from Fisher Scientific and were HPLC grade. HPLC columns were either Altech (Econosil) or Rainin (Varian) Dynamax.

4.2. Biological testing

The anti-HIV assay was carried out at LDDRD at the US NCI in Frederick, Maryland as previously described by Wieslow et al. (1989). The assay involves the killing of T4 (CD4+) lymphoid cells (CEM-SS line) by HIV-1 (RF strain). The EC_{50} is the concentration at which a compound or fraction inhibits the killing of the lymphoid cells by 50% relative to the HIV infected, non-treated lymphoid cells. The IC_{50} is a measure of the compound's or fraction's toxicity to uninfected lymphoid cells. The growing lymphoid cells were pelleted from the growth medium, infected at a multiplicity of infection (MOI) of 0.05 at room temperature for 45 min with constant shaking. The infected cells were then diluted in the growth medium to yield a desired concentration of infected cells of 5000 cells/well after inoculation into individual wells of a 96-well microtiter plate. The extracts, fractions and compounds were dissolved in H_2O–DMSO and incubated for 6 days at 37°C. (Typically, fractions and extracts were tested at an initial concentration of 250 μg /ml and serially diluted. Pure compounds were tested at an initial concentration of 100 μg/ml.) After incubation, cell viability and growth were measured using the XTT-tetrazolium method as described. *G. lepidota* extract and subsequent fractions were tested through the high-flux assay lab by SAIC Frederick, PO Box B, Frederick, MD. Pure compounds were tested by Dr. Robert Gulowkoski at LDDRD. To avoid decomposition associated with **1** when stored neat, all samples were sent to LDDRD in $CDCl_3$ solutions in sealed tubes.

4.3. Plant material

G. lepidota was collected and identified by Hillary Loring at a location 1 km west and 0.5 km north of Brookville, KS. Plant identification follows the *Flora of the Great Plains* (Great Plains Flora Association, 1986). A voucher specimen is archived at the R.L. McGregor Herbarium at the University of Kansas.

4.4. Extraction and isolation

The air-dried leaves and stems of *G. lepidota* (500 g) were chopped into small pieces and covered with CH_2Cl_2:MeOH (1:1) for 24 h. The solvent was then removed and the plant material covered with MeOH. After another 24 h, this MeOH extract was added to the CH_2Cl_2:MeOH extract and the solvent removed at reduced pressure. The plant material was then extracted with H_2O and freeze-dried. Small samples of the organic and aqueous extract were submitted for HIV testing. All activity was associated with the organic phase (EC_{50} = 30 μg/ml). The crude organic extract (5.4 g) was dissolved in MeOH (100 ml) and H_2O (10 ml). This suspension was then extracted with three aliquots (50 ml each) of hexane, which was removed at reduced pressure to give a residue (1.0 g). Water was then added to the aqueous layer to bring the total H_2O content to 20% and then extracted with CCl_4 which was removed at reduced pressure to give extract (1.8 g). (CCl_4 extraction has now been eliminated in our lab due to environmental concerns.) Water was then added to the aqueous layer to bring the total concentration to 30%, and extracted with $CHCl_3$ to give a residue (0.90 g). The methanol was then removed from the aqueous layer under reduced pressure and the subsequent water layer

extracted with EtoAc to give a residue (0.28 g). The aqueous layer was then freeze dried to give a residue (1.3 g). Subsequent anti-HIV assay indicated that all of the activity was associated with the CCl_4 fraction. The CCl_4 fraction was then applied to a Sephadex LH-20 column (Pharmacia-Upjohn; 100×2.5 cm i.d.; 1:1 CH_2Cl_2:MeOH). Collected fractions were analyzed by TLC using a (H_2SO_4–EtOH–H_2O–vanillin) spray reagent and UV for visualization. Like fractions were combined and assayed (8 total).

4.5. Glepidotin B (2)

Compound **2** (32 mg) was isolated using HPLC purification on a silica HPLC column and a solvent gradient of hexane : 2-propanol (6% 2-propanol increasing to 15%). HRMS (FAB) calc. for $C_{20}H_{21}O_5$ (M + H) 341.1389, obs. 341.1379. ^{13}C NMR spectral data (75 Mhz, $CDCl_3$): δ 196.0 (*s*, C-4), 164.6, 161.2, 161.0 (*s*, C-5, C-7, C-9), 136.1 (*d*, C-2″), 136.0 (*s*, C-1′), 129.3 (*d*, C-4′) 128.7, 127.5 (4C, *d*, C-2′, 3′, 5′,6′), 121.0 (*d*, C-2″) 107.5 (*s*, C-6), 100.8 (*s*, C-10) 96.0 (*d*, C-8), 83.3 (*d*, C-3), 72.5 (*d*, C-2), 25.8 (*t*, C-1″), 21.0, 18.0 (*q*, C-4″, C-5″). Its ^1H NMR and IR spectral data were identical to those reported by Mitscher et al. (1983).

4.6. Glepidotin A (3)

Compound **3** (56 mg) was isolated using the same solvent gradient as above, with **3** eluting 0.5 min after **2**. HRMS (FAB) calcd. for $C_{20}H_{19}O_5$ $(M-H)^+$ 339.1227, obs. 339.1234. All spectral data were consistent with that previously reported by Mitscher et al. (1983).

4.7. Glepidotin D (1)

Compound **1** (18 mg) was isolated using the same HPLC solvent system as for **2** and **3**, and eluted approximately 0.1 min after **3**. Attempts to eliminate traces of **3** were initially thwarted by the apparent decomposition of **1** when it was stored neat for any length of time (>6 h). An insoluble white material formed on the walls of the flask which could not be dissolved in any common solvent. To circumvent this problem, repurification of **1** was accomplished by keeping the compound in a small amount of hexane-isopropanol HPLC solvent. Once purified, **1** could be stored in solution without appreciable decomposition as measured by periodic ^1H NMR spectral comparisons. The ^1H and ^{13}C NMR spectral data are given in Table 1. IR spectral data (neat, thin film, NaCl, ν_{max} cm^{-1}): 3382, 1588, 1489, 1453, 737, 697. EIMS (probe) 70 eV, *m*/*z* (rel. int): 366 $[M]^+$ (18), 298 (33), 69 (100). HRMS (FAB) calc. for $C_{24}H_{31}O_3$ $(M-H)^+$ 367.2273, obs. 367.2260.

Acknowledgements

The authors would like to thank Dr. Kirk Gustafson from the US NCI LDDRD, Frederick, Maryland for performing the HMBC experiments. Dr. Michael R. Boyd is acknowledged for use of the anti-HIV assay and Dr. Robert Gulowkoski for running the assay. Dr. John Cardellina is also acknowledged for helpful discussions. Dr. Hillary Lorring is acknowledged for plant collection. Financial support for this work was provided by the Iowa Carver Foundation, College of Natural Sciences at UNI and the Graduate College at UNI. The Office of International Programs is acknowledged for support of M.D. who was a summer undergraduate student from Herzen State University, Saint Petersburg, Russia.

References

Asakawa, Y., Kusube, E., Takematsu, T., Suire, C., 1978. New bibenzyls from *Radula complanata*. Phytochemistry 17, 2115–2117.

Bohlmann, F., Hoffmann, E., 1979. Cannabigerol-ähnliche Verbindungen aus *Helichrysum umbraculigerum*. Phytochemistry 18, 1371–1474.

Camazine, S., Bye, R.A., 1980. A study of the medical and ethnobotany of the Zuni Indians of New Mexico. J. Ethnopharmacol. 2, 365–388.

Dilwyn, R. J., 1980. Lakota names and traditional uses of prairie plants by Sicangu (Brule) people in the Rosebud Area. South Dakota. Rosebud Educational Society, St. Francis, SD.

Gilmore, M., 1977. Uses of Plants by Indians of the Missouri River Region. University of Nebraska Press, Lincoln, NB.

Gollapudi, S.R., Telikepalli, H., Keshavarz-Shokri, A., Vander Velde, D., Mitscher, L.A., 1989. Glepidotin C: a minor antimicrobial bibenzyl from *Glycyrrhiza lepidota*. Phytochemistry 28, 3556–3557.

Kindscher, K., 1992. Medicinal Wild Plants of the Prairie. University Press of Kansas, Lawrence, KS.

Kindscher, K., Manfredi, K.P., Britton, M., Demidova, M., Hurlburt, P.D., 1998. Testing prairie plants with ethnobotanical importance for anti-cancer and anti-AIDS compounds. J. Ethnobiol. 18, 229–245.

Mabberly, D.J., 1997. The Plant Book. Cambridge University Press, Cambridge, UK, p. 305.

Mitscher, L.A., Park, Y.H., Clark, D., Beal, J.L., 1980. Antimicrobial agents from higher plants. Antimicrobial isoflavanoids and related substances from *Glycyrrhiza glabra* L. var. *typica*. J. Nat. Prod. 43, 259–269.

Mitscher, L.A., Rao, R.G.S., Khanna, I., Veysoglu, T., Drake, S., 1983. Antimicrobial agents from higher plants: Prenylated flavanoids and other phenols from *Glycyrrhiza lepidota*. Phytochemistry 22, 573–576.

Munson, P.J., 1981. Contributions to Osage and Lakota ethnobotany. Plains Anthropologist 26, 229–240.

Saitoh, T., Kinoshita, T., Shibata, S., 1976. Chemical studies on the Oriental plant drugs XL. The occurrence of an isoflavene and the corresponding isoflavone in licorice root. Chem. Pharm. Bull. 24, 991–994.

Weislow, O.S., Kiser, R., Fine, D.L., Bader, J., Shoemaker, R.H., Boyd, M.R., 1989. New soluble-formazan assay for HIV-1 cytopathic effects: application to high flux screening of synthetic and natural products for AIDS-antiviral activity. J. Natl. Cancer Inst. 81, 577–586.

Williams, D.H., Flemming, I., 1989. Spectroscopic Methods in Organic Chemistry. McGraw-Hill, London, p. 135.

PERGAMON

Phytochemistry 58 (2001) 159–165

PHYTOCHEMISTRY

www.elsevier.com/locate/phytochem

Betalains of *Celosia argentea*

Willibald Schliemann[a,*], Yizhong Cai[b], Thomas Degenkolb[c], Jürgen Schmidt[c], Harold Corke[b]

[a] *Abteilung Sekundärstoffwechsel, Leibniz-Institut für Pflanzenbiochemie, Weinberg 3, D-06120 Halle (Saale), Germany*
[b] *Department of Botany, The University of Hong Kong, Pokfulam Road, Hong Kong SAR, People's Republic of China*
[c] *Abteilung Natur- und Wirkstoffchemie, Leibniz-Institut für Pflanzenbiochemie, Weinberg 3, D-06120 Halle (Saale), Germany*

Received 28 January 2001; received in revised form 15 March 2001

Abstract

The betalains of yellow, orange and red inflorescences of common cockscomb (*Celosia argentea* var. *cristata*) were compared and proved to be qualitatively identical to those of feathered amaranth (*Celosia argentea* var. *plumosa*). In addition to the known compounds amaranthin and betalamic acid, the structures of three yellow pigments were elucidated to be immonium conjugates of betalamic acid with dopamine, 3-methoxytyramine and (*S*)-tryptophan by various spectroscopic techniques and comparison to synthesized reference compounds; the latter two are new to plants. Among the betacyanins occurring in yellow inflorescences in trace amounts, the presence of 2-descarboxy-betanidin, a dopamine-derived betacyanin, has been ascertained. The detection of high dopamine concentration may be of toxicological relevance in use of yellow inflorescences as a vegetable and in traditional Chinese medicine, common uses for the red inflorescences of common cockscomb. © 2001 Elsevier Science Ltd. All rights reserved.

Keywords: *Celosia argentea* var. *cristata*; *Celosia argentea* var. *plumosa*; Amaranthaceae; Common cockscomb; Feathered amaranth; Betalains; Betaxanthins; Miraxanthin V; Dopamine; 3-Methoxytyramine

1. Introduction

The plant genus *Celosia* consisting of about 60 species in the family Amaranthaceae (Caryophyllales) is native in subtropical and temperate zones of Africa, South America and South East Asia. *Celosia argentea* var. *cristata* (L.) Kuntze, (*Celosia cristata* L.) (common cockscomb), and *Celosia argentea* var. *plumosa* (Burvenich) Voss, (*Celosia plumosa* Burvenich) (feathered amaranth), are widespread ornamental plants. Seedlings, young leaves and inflorescences are used as a vegetable in China and other countries (Palada and Crossman, 1999), and also dried leaves, inflorescences and seeds are used in traditional Chinese medicine (Wong, 1994; Xu, 1996). Among the garden varieties, inflorescence colour variation from yellow to various shades of red and violet occurs. At an early date (Wehmer, 1929) it was claimed that red inflorescences of common cockscomb contain a nitrogen-containing pigment. Later, amaranthin and betanin were found in red inflorescences, whereas violet ones contain additional hydroxycinnamoyl-amaranthins (celosianins) (Piattelli and Minale, 1964; Minale et al., 1966). The structures of the latter were presumed to be identical with compounds from cell suspension cultures of *Chenopodium rubrum* L. identified as 2″-*O*-*E*-(4-coumaroyl)-amaranthin (celosianin I) and 2″-*O*-*E*-feruloyl-amaranthin (celosianin II) (Bokern and Strack, 1988; Strack et al., 1988). Protein extracts from inflorescences of *C. plumosa* catalysed the transfer of ferulic acid from 1-*O*-feruloyl-β-glucose to amaranthin forming celosianin II (Bokern et al., 1992). The knowledge of betaxanthins in the Amaranthaceae family is very limited (Reznik, 1975), although betalamic acid has been electrophoretically detected in *Celosia* species (Reznik, 1978). Yellow betaxanthin-synthesizing seedlings of *C. plumosa* reacted upon illumination with a 3–4-fold increase in betaxanthin content (Giudici de Nicola et al., 1973, 1974). Dopa feeding to inflorescences of *Amaranthus caudatus* and *Celosia argentea* did not induce betaxanthin formation (Rink and Böhm, 1991), whereas the administration of this central intermediate to seedlings of *A. caudatus* led to the occurrence of a betaxanthin

* Corresponding author. Tel.: +49-345-5582-1530; fax: +49-345-5582-1009.
E-mail address: wschliem@ipb-halle.de (W. Schliemann).

0031-9422/01/$ - see front matter © 2001 Elsevier Science Ltd. All rights reserved.
PII: S0031-9422(01)00141-8

mixture (French et al., 1974; Colomas, 1977; Bianco-Colomas, 1980) from which vulgaxanthin II [(*S*)-Glu-BX] and miraxanthin II [(*S*)-Asp-BX] were identified by comparison to authentic samples, but dopaxanthin [(*S*)-Dopa-BX] was entirely absent (Giudici de Nicola et al., 1975). Cell cultures of *A. caudatus* and *Celosia argentea* showed only pigmentation by betalains in auxin-free, but GA_3-containing nutrient solutions (Constabel and Nassif-Makki, 1971; Böhm and Rink, 1988). As no betaxanthins from *Celosia* have so far been identified, structural elucidation of the betaxanthins of two *Celosia* varieties was performed, which led to two new betaxanthins. In addition, the levels of pharmacologically active precursors were determined.

2. Results and discussion

HPLC analysis of extracts prepared from differently pigmented inflorescences of *C. cristata* and *C. plumosa* (Fig. 1) confirmed the presence of the already known amaranthin (**1**) and its (2*S*,15*R*)-isoform (**1′**) as well as betalamic acid (**2**), but celosianins and also betanin, formerly claimed to be a minor constituent (Piattelli and Minale, 1964), were not found. The main pigment **1** in extracts from inflorescences, red leaves and epidermal layers of the stem of red flowering *C. cristata* was accompanied by minor unknown betaxanthins (Table 1). In contrast, these pigments are the major components (**3**–**5**) in yellow- and orange-coloured inflorescences (Fig. 2). The same held true also in yellow and orange-red inflorescences of *C. plumosa* which showed a qualitatively identical betalain pattern. Compounds **1** and **2** were readily identified by UV-vis spectroscopy and co-chromatography (HPLC) with authentic standards from callus culture of *Chenopodium rubrum* (Bokern et al., 1992) and hypocotyls of fodder beets (Schliemann et al., 1999) as amaranthin (**1**) and betalamic acid (**2**). The identification of **1** was corroborated by LC–MS of the purified

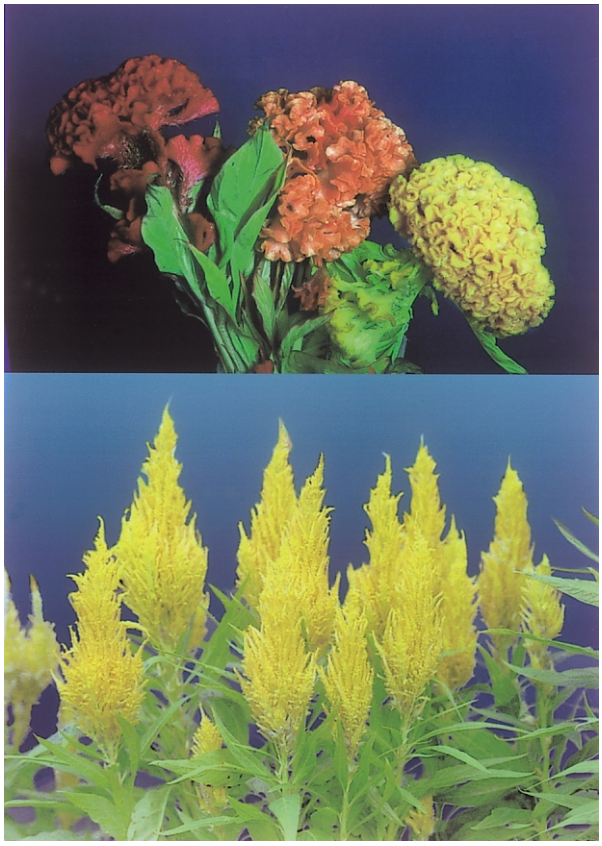

Fig. 1. Flowering *Celosia argentea* var. *cristata* (L.) Kuntze (red, orange, yellow) (above) and *Celosia argentea* var. *plumosa* (Burvenich) Voss (yellow) (below).

compound giving the expected protonated molecular ion $[M+H]^+$ (**1**, *m*/*z* 727) (Table 2). Furthermore, the collision induced dissociation (CID) mass spectrum of *m*/*z* 727 gave the main fragments *m*/*z* 551 $[betanin+H]^+$ and *m*/*z* 389 $[betanidin+H]^+$ indicative for the presence of **1**. Finally, high-resolution LC–ESI–TOF–MS yielded *m*/*z* 727.1913 ($C_{30}H_{35}N_2O_{19}$, calculated mass: 727.1829) completing the structure elucidation of **1** as amaranthin.

Table 1
Betalain content of differently coloured inflorescences and tissues of two *Celosia argentea* varieties

Plant parts	Total betalain content [nmol (g fr. wt)$^{-1}$]	Betalain content [nmol (g fr. wt)$^{-1}$]				
		1/1′	**2**	**3**	**4**	**5**
Celosia argentea var. *cristata* (L.) Kuntze						
Inflorescence, yellow	92.1	3.5	12.1	58.0	16.1	2.4
Inflorescence, orange	228.2	96.8	35.0	80.8	12.2	3.4
Inflorescence, red	396.0	373.6	10.2	10.2	1.8	0.2
Leaf, red	493.5	480.8	10.5	2.0	0.2	Trace
Epidermal layers of stem, red	230.3	213.0	15.7	1.6	n.d.[a]	Trace
Celosia argentea var. *plumosa* (Burvenich) Voss						
Inflorescence, yellow	456.5	Trace	19.6	364.4	59.2	13.3
Inflorescence, orange-red	621.5	208.3	11.0	330.3	62.5	9.4

[a] n.d., Not detected.

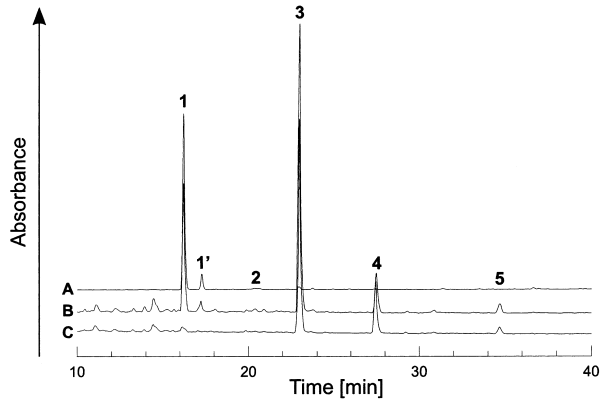

Fig. 2. HPLC elution profiles of betalains from inflorescences of *Celosia argentea* var. *cristata* (L.) Kuntze. A, red inflorescences (maxplot detection 400–650 nm; full scale: 1.55 AU); B, orange inflorescences (470 nm; full scale: 0.255 AU); **C**, yellow inflorescences (470 nm; full scale: 0.185 AU). Peak numbers correspond to the numbers in Tables 1 and 2 and Fig. 3.

From the retention time and the characteristic HPLC-PDA data (R_t 23.0 min; λ_{max} 261/457 nm), compound **3** was suggested to be miraxanthin V (dopamine-derived betaxanthin, dopamine-BX), recently found as the major betaxanthin in hairy root cultures of yellow beets (Schliemann et al., 1999). Co-chromatography (HPLC) with synthetically prepared authentic standard and LC–MS giving the protonated molecular ion $[M+H]^+$ at m/z 347 confirmed the suggestion. The CID mass spectrum of m/z 347 was shown to be identical in its fragmentation pattern with recently published data (Schliemann et al., 1999). Additionally, ESI–TOF–MS yielding m/z 347.1264 ($C_{17}H_{19}N_2O_6$, calculated mass: 347.1238) supported the structural elucidation of **3** as miraxanthin V. For compound **4** a similar structure was suggested because the UV-vis spectral data were identical with **3**, but showed a longer retention time than **3** (Fig. 2). This lower polarity observed could be caused by the lack of a hydroxyl group in the aromatic amine moiety (tyramine instead of dopamine) or by modification of a hydroxyl group with an acyl or alkyl residue. The first proposal could be disproved as synthesized miraxanthin III (tyramine-BX) (R_t 26.6 min; λ_{max} 262/457 nm) did not coelute with compound **4**. Subsequently, the betaxanthins derived from 4-methoxy-3-hydroxy-phenylethylamine and 3-methoxy-4-hydroxy-phenylethylamine (3-methoxytyramine) were prepared and used as reference compounds in co-injection experiments. Both compounds were identical with compound **4** with respect to UV-vis data (λ_{max} 261/457 nm). 4-Methoxy-3-hydroxy-phenylethylamine-BX eluted at R_t 29.2 min, clearly different from **4**, whereas 3-methoxy-4-hydroxy-phenylethylamine-BX (3-methoxytyramine-BX) showed complete co-elution with the endogenous betaxanthin. This chromatographical identity was supported by comparison of the mass spectral data of the standard compound with that of compound **4**. Both compounds showed in LC–MS a protonated molecular ion at m/z 361 ($[M+H]^+$) indicative for a methyl derivative of **3** (m/z 347). In the CID mass spectrum of m/z 361 the fragment ion at m/z 151 represents the deaminated component conjugated with betalamic acid in **4**, whereas the fragment ion at m/z 211 is the complementary aminated betalamic acid. In addition, the fragment at m/z 317 ($[M+H\text{-}CO_2]^+$) can be explained by the loss of a carboxyl group from the molecular ion. In LC–ESI–TOF–MS the protonated molecular ion was found at m/z 361.1417 ($C_{18}H_{21}N_2O_6$, calculated mass: 361.1394) confirming the structure elucidation of **4** as 3-methoxytyramine-BX, a new betaxanthin.

One of the most unpolar betaxanthins synthesized so far as a reference compound (Trezzini and Zryd, 1991; Schliemann et al., 1999) is (*S*)-tryptophan-BX [(*S*)-Trp-BX]. As compound **5** showed in our RP-HPLC system a long retention time (R_t 34.7 min), a comparison to betaxanthins synthesized from (*S*)-Trp and tryptamine was performed. Whereas tryptamine-BX was different from **5** with respect to both retention time and UV-vis data (R_t 37.8 min; λ_{max} 217/262/456 nm), the corresponding data for (*S*)-Trp-BX matched with compound **5** and both betaxanthins co-eluted in HPLC. In LC–MS the protonated molecular ion was found at m/z 398 ($[M+H]^+$), expected for (*S*)-Trp-BX. In the CID mass spectrum of m/z 398 the fragment ion at m/z 188 represents the deaminated (*S*)-Trp conjugated to betalamic acid in **5**, whereas the fragment ion at m/z 211 is the complementary aminated betalamic acid. In addition, the fragment at m/z 354 ($[M+H\text{-}CO_2]^+$) can be

Table 2
Retention time, HPLC-PDA and MS data of betalains from inflorescences of two *Celosia argentea* varieties

Peak	R_t (min)	HPLC–PDA (λ_{max}, nm)	LC–MS m/z $[M+H]^+$	Betalain
1	16.2	270/294/541	727	Amaranthin
1′	17.2	270/294/540	n. d.[a]	Isoamaramthin
2	20.4	249/405	n.d.	Betalamic acid
3	23.0	261/457	347	Miraxanthin V (Dopamine-BX[b])
4	27.5	261/457	361	3-Methoxytyramine-BX
5	34.7	218/264/471	398	(*S*)-Tryptophan-BX

[a] n.d., Not determined.
[b] BX, betaxanthin.

explained by the loss of a carboxyl group from the molecular ion. The fragments at m/z 130 and 180 are typical Trp ions in ESI–CID-spectra of Trp conjugates (Schmidt et al., 1995). By ESI–TOF–MS the protonated molecular ion was found at m/z 398.1327 ($C_{20}H_{20}N_3O_6$, calculated mass: 398.1347) completing the structure elucidation of **5** as (*S*)-Trp-BX, a new betaxanthin from plants.

A hypothetical scheme (Fig. 3) illustrates the proposed steps of betaxanthin biosynthesis in *Celosia*. In addition to the known pathway, a methylation step has to be included which is required for the formation of **4**. The question arises whether **4** is formed by methylation of the main compound **3** or by methylation of a biosynthetic intermediate. An indication for the latter option would be the detection of 3-methoxytyramine in the extract. The analysis of the extract from yellow inflorescences of common cockscomb with respect to the precursors of betaxanthins **3**–**5** gave the results shown in Table 3. All three precursors, dopamine, 3-methoxytyramine and (*S*)-Trp could be detected and quantified in comparison with standard compounds. 3-Methoxytyramine was found to be present at low concentration, but in the same order of magnitude as the derived betaxanthin **4**. Therefore, it is most probable that the methylation takes place at the catecholic level rather than at the betaxanthin level. 3-Methoxytyramine is a known dopamine catabolite in humans and animals (Bidard and Cronenberger, 1977; Faraj et al., 1981; Fitoussi et al., 1998), but it was found for the first time in plants as a constituent of cactus alkaloids from *Trichocereus pachanoi* (Agurell, 1969; Crosby and McLaughlin, 1973). Cacti, like *Celosia*, belong to the Caryophyllales, and therefore, it may be speculated about the occurrence of cactus alkaloid-derived betaxanthins in cactus species. In contrast to the relatively

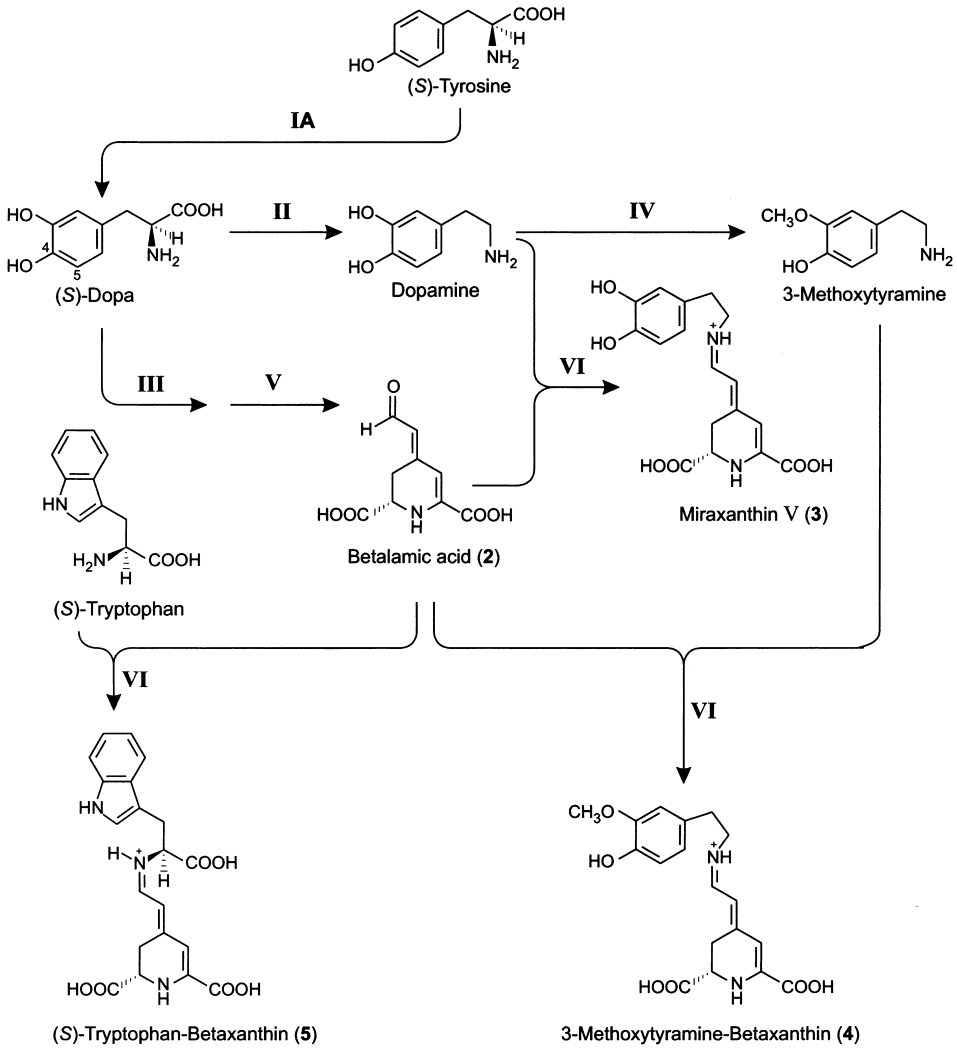

Fig. 3. Proposed scheme of betaxanthin biosynthesis in *Celosia*. Enzymatically catalysed steps: IA — hydroxylating activity of the tyrosinase; II — Dopa decarboxylase; III — dopa dioxygenase; IV — *O*-methyltransferase. Spontaneous steps: V — cyclization reaction; VI — condensation reaction (aldimine formation). Compound numbers of this scheme correspond to peak numbers in Tables 1 and 2 and Fig. 2.

Table 3
Content and HPLC data of dopamine, 3-methoxytyramine and (*S*)-tryptophan in yellow inflorescences of *Celosia argentea* var. *cristata* (L.) Kuntze

Precursor	Content [nmol (g fr. wt)$^{-1}$]	R_t (min)	HPLC–PDA (λ_{max}, nm)
Dopamine	41150	5.7	220sh/278
3-Methoxytyramine	35	10.9	223/277
(*S*)-Tryptophan	283	21.5	216/276

low concentration of 3-methoxytyramine and (*S*)-Trp, the precursor of **3**, dopamine, occurs in thousand-fold higher concentration than 3-methoxytyramine. Due to its various biological actions, these high dopamine concentrations found may be toxicologically relevant when yellow inflorescences are consumed as a vegetable or used as material in traditional Chinese medicine.

Recently, the rare betacyanins derived from 2-descarboxy-*cyclo*-Dopa were isolated from hairy root cultures of yellow beets and their origin from dopamine elucidated (Kobayashi et al., 2001). As extracts from yellow *Celosia* inflorescences also contain high concentration of dopamine, the occurrence of this type of compounds seems probable. By isolation of betacyanins occurring in trace amounts in yellow inflorescences of *C. cristata* and co-injection with a hairy root extract from yellow beets the presence of 2-descarboxy-betanidin was ascertained. The distribution of the occurrence of 2-descarboxy-betanidin, isolated for the first time from flowers of *Carpobrotus acinaciformis* (L.) L. Bol. (Aizoaceae) (Piattelli and Impellizzeri, 1970), identified recently together with its glucoside and corresponding malonyl derivative from beet cultures (Chenopodiaceae) (Schliemann et al., 1999; Kobayashi et al., 2001) has to be expanded now to the Amaranthaceae.

The betalain content of differently coloured inflorescences and tissues of the two *Celosia* varieties presented in Table 1 reveals that all tissues of red *C. cristata* contain minor amounts of the betaxanthins **3**–**5** which are the major compounds in the yellow and orange/orange-red inflorescences. This colour change implies a gradual reversion of the pigments' biosynthesis, from Dopa via *cyclo*-Dopa to amaranthin on the one side to betaxanthins (**3**, **4**) derived from Dopa via dopamine on the other side. The betalain patterns in the two *Celosia* varieties are qualitatively the same, and a direct comparison of the concentrations between them is not reasonable because *C. cristata* was grown in Halle (Germany), and *C. plumosa* in Wuhan (China) under different climatic conditions.

In summary, the presented data describe the betalain patterns of two *Celosia* varieties. In addition to amaranthin and betalamic acid, the structures of three betaxanthins are elucidated by comparison with synthetic standards and using MS techniques as miraxanthin V, 3-methoxytyramine-BX and (*S*)-tryptophan-BX, with the latter two newly described from plant origin. Evidence is obtained for the occurrence of the dopamine-derived 2-descarboxy-betanidin. Furthermore, the detection of 3-methoxytyramine may be indicative for a methylation reaction on a catecholic intermediate rather than at the miraxanthin V level.

3. Experimental

3.1. Plant material

Common cockscombs [*Celosia argentea* var. *cristata* (L.) Kuntze] (yellow, orange and red) were grown from seeds and then further cultivated in the institute's experimental garden (Halle, Germany). Two yellow- and orange-red-coloured inflorescence genotypes of *Celosia argentea* var. *plumosa* (Burvenich) Voss were selected from the genetic resource collections of the Hubei Academy of Agricultural Sciences, Wuhan, China. All genotypes were planted in the field in Wuhan in 1999. Plant materials were harvested at full bloom. Callus cultures of *Chenopodium rubrum* (Bokern et al., 1992), hairy root cultures of yellow beet (*Beta vulgaris* L. subsp. *vulgaris*, Garden Beet Group "Golden Beet") (Schliemann et al., 1999) and fodder beets (*Beta vulgaris* L. subsp. *vulgaris*, Fodder Beet Group "Altamo") were cultivated as recently described (Schliemann et al., 1999).

3.2. Isolation, quantification and purification of betalains

The materials were frozen in liquid N_2, homogenized in a mortar and extracted with 80% aq. MeOH (containing 50 mM ascorbate) for 30 min [3 ml (g fr. wt)$^{-1}$]. After centrifugation at 14,000 *g* for 10 min at 4°C, the supernatant was removed and its betalain content was quantified photometrically at 540 nm (betacyanins) and 475 nm (betaxanthins) using the molar extinction coefficients described (amaranthin, 56.6×10^6 cm^2 mol^{-1}, Piattelli et al., 1969; the mean molar extinction coefficient for betaxanthins, 48×10^6 cm^2 mol^{-1}, Girod and Zryd, 1991). For the calculation of the composition of extracts containing both amaranthin and betaxanthins as well as betalamic acid, amaranthin (from *Chenopodium rubrum* callus culture), miraxanthin V (from hairy root culture of yellow beets) and betalamic acid (from yellow fodder beets) were isolated by semi-prep. HPLC (solvent system 1), their absorbancies measured and aliquots of known content analyzed by HPLC (solvent system 2). The peak areas of analyzed extracts were used to calculate the individual betalain content expressed in nmol (g fr. wt)$^{-1}$. All experiments were performed in duplicate. For LC–MS and LC–ESI–TOF–MS amaranthin and the betaxanthins **3**–**5** were isolated by semi-prep. HPLC (solvent system 1).

3.3. Isolation of betalamic acid and preparation of standard betaxanthins

Yellow hypocotyls (50 g) of fodder beet seedlings (*Beta vulgaris* L. subsp. *vulgaris*, Fodder Beet Group "Altamo") (4-weeks-old) were frozen in liquid N_2, homogenized in a mortar and extracted for 30 min with 150 ml aq. 80% MeOH containing 50 mM Na-ascorbate (pH 8.2). After centrifugation (14,000 *g*; 10 min at 4°C) the supernatant was concentrated to 20 ml in vacuo at 30°C. Betalamic acid was isolated by semi-prep. HPLC (solvent system 3) and the acidic eluate (10 nmol) was added directly to 10 μmol of the amino acid or amine, respectively. After evaporation of the reaction mixtures in vacuo to dryness, the residues containing the betaxanthins formed were dissolved in 100 μl water and used for co-injection experiments either directly or after purification by semi-prep. HPLC (solvent system 1).

3.4. Quantification of catecholamines and (S)-tryptophan

For quantification of dopamine, 3-methoxytyramine and (*S*)-Trp 50 μl extract from yellow inflorescences of *C. cristata* (in the case of dopamine only 5 μl) was separated by HPLC (solvent system 2) with detection of the native fluorescence emission at 314 nm (Steiner et al., 1999) and absorbance at 280 nm. The endogenous compounds were identified and quantified with reference to the corresponding standard compounds. The experiments were performed in duplicate.

3.5. HPLC

Analytical and semi-prep. HPLC was performed with a system from Waters (Milford, MA, USA), including the separation module 2690. The liquid chromatograph was equipped with a 5-μm Nucleosil C_{18} column (250×4 mm i.d.; Macherey-Nagel, Düren, Germany). The following solvent and gradient systems were used. Solvent system 1: A: 1% aq. HOAc; B: acetonitrile; gradient: linear gradient from 100% A to 24% B in (A + B) within 40 min; the flow rate was 1 ml min^{-1}. Solvent system 2: A: 1.5% aq. H_3PO_4 B: acetonitrile; gradient as in solvent system 1. Solvent system 3: A: 1% aq. HOAc; B: acetonitrile; gradient: linear gradient from 5 to 18% B in (A + B) within 10 min. The betalains were detected at 540, 460 and 405 nm or by maxplot detection between 400 and 650 nm (photodiode array detection). The injection volume was 20 μl in analytical (solvent system 2) and 100 μl in semi-prep. work (solvent systems 1 and 3).

3.6. LC–MS

Positive ion electrospray ionization mass spectra were recorded on a Finnigan MAT TSQ 7000 instrument [electrospray voltage 4.5 kV; capillary 220°C; sheath gas N_2] coupled to a Micro-Tech Ultra-Plus Micro LC system equipped with a 4-μm C_{18} column (100×1 mm i.d, ULTRASEP). For LC, a gradient system starting from 10% B (0.2% aq. AcOH in acetonitrile) in 90% A (0.2% aq. AcOH) to 50% B in (A + B) within 10 min was used, followed by 10 min isocratic elution at a flow rate of 70 μl min^{-1} (injection volume: 2 μl). The CID mass spectra during the LC run were obtained under the following conditions: collision energy (collision cell) −25 eV; collision gas: argon; collision pressure: 1.8 mT. All mass spectra are averaged and background subtracted.

Positive LC–ESI–TOF mass spectra were recorded on an API QSTAR Pulsar instrument (Perkin Elmer Sciex, Foster City, USA) [electrospray voltage: 5.5 kV; sheath gas: N_2] coupled to an Ultimate micro-HPLC system (Software Ultichrom 2.5)(LC Packings, Amsterdam, Netherlands) equipped with a 3-μm Fusica C_{18} column (150 ×0.3 mm i.d, PepMap). For LC, a gradient system starting from 100% A [0.05% aq. HCOOH/acetonitrile (95/5)] to 100% B [HCOOH/ acetonitrile (0.05/99.95)] within 20 min was used, at a flow rate of 4 μl min^{-1} (injection volume: 0.5 μl).

Compound **1** (amaranthin), (*m/z*, rel. int.): 727 $[M+H]^+$ (100); ESI–CID–MS of *m/z* 727: 551 [betanin + H]$^+$ (8), 389 [betanidin + H]$^+$ (100); ESI–TOF–MS: *m/z* 727.1913 (calc. for $C_{30}H_{35}N_2O_{19}$: 727.1829, Δ 8.4 mmu). Compound **3** (miraxanthin V), (*m/z*, rel. int.): 347 $[M+H]^+$ (100); ESI–CID–MS of *m/z* 347: 303 [M + H-CO_2]$^+$ (18), 211 [aminated betalamic acid + H]$^+$ (30), 137 [deaminated dopamine + H]$^+$ (100, base peak). ESI–TOF–MS: *m/z* 347.1264 (calc. for $C_{17}H_{19}N_2O_6$: 347.1238; Δ 2.6 mmu). Compound **4** (3-methoxytyramine-BX), (*m/z*, rel. int.): 361 $[M+H]^+$ (100); ESI–CID–MS of *m/z* 361: 317 [M + H-CO_2]$^+$ (8), 211 [aminated betalamic acid + H]$^+$ (18), 151 [deaminated 3-methoxytyramine + H]$^+$ (100, base peak), 119 (6). ESI–TOF–MS: *m/z* 361.1417 (calc. for $C_{18}H_{21}N_2O_6$: 361.1394; Δ 2.3 mmu). Compound **5** [(*S*)-tryptophan-BX], (*m/z*, rel. int.): 398 $[M+H]^+$ (100); ESI–CID–MS of *m/z* 398: 354 [M + H-CO_2]$^+$ (5), 269 (80), 211 [aminated betalamic acid + H]$^+$ (89), 188 [deaminated Trp + H]$^+$ (52), 130 (45). ESI-TOF-MS: *m/z* 398.1327 (calc. for $C_{20}H_{20}N_3O_6$: 398.1347; Δ 2.0 mmu).

Acknowledgements

The authors thank Barbara Kolbe [Institut für Pflanzenbiochemie (IPB), Halle, Germany] for skillful technical assistance. Furthermore, we are grateful to Christine Kaufmann and Annett Kohlberg (IPB) for the figures and photographs. This work was supported by the Hong Kong Research Grants Council and the Deutsche Forschungsgemeinschaft (Bonn, Germany).

References

Agurell, S., 1969. Cactaceae alkaloids. I. Lloydia 32, 206–216.

Bianco-Colomas, J., 1980. Qualitative and quantitative aspects of betalains biosynthesis in *Amaranthus caudatus* L. var. *pendula* seedlings. Planta 149, 176–180.

Bidard, J.N., Cronenberger, L., 1977. Effect of benzatropine on the *O*-methylation of striatal dopamine. C. R. Acad. Sci. Hebd. Seances Acad. Sci. D. 284, 485–487.

Böhm, H., Rink, E., 1988. Betalains. In: Constabel, F., Vasil, I.K. (Eds.), Cell Culture and Somatic Cell Genetics of Plants, Vol. 5. Academic Press, New York–London, pp. 449–463.

Bokern, M., Heuer, S., Strack, D., 1992. Hydroxycinnamic acid transferases in the biosynthesis of acylated betacyanins: purification and characterization from cell cultures of *Chenopodium rubrum* and occurrence in some other members of the Caryophyllales. Bot. Acta 105, 146–151.

Bokern, M., Strack, D., 1988. Synthesis of hydroxycinnamic acid esters of betacyanins via 1-*O*-acylglucosides of hydroxycinnamic acids by protein preparations from cell suspension cultures of *Chenopodium rubrum* and petals of *Lampranthus sociorum*. Planta 174, 101–105.

Colomas, J., 1977. Séparation des pigments bétalaiques par une méthode fondée sur la chromatographie sur gel de Séphadex appliquée à des plantules d'*Amaranthus caudatus* L. var. *pendula*. Z.-Pflanzenphysiol. 85, 227–232.

Constabel, F., Nassif-Makki, H., 1971. Betalainbildung in *Beta*-Calluskulturen. Ber. Dtsch. Bot. Ges. 84, 629–636.

Crosby, D.M., McLaughlin, J.L., 1973. Cactus alkaloids. XIX. Crystallization of mescaline HCl and 3-methoxytyramine HCl from *Trichocereus pachanoi*. Lloydia 40, 416–418.

Faraj, B.A., Lawson, D.H., Nixon, D.W., Murray, D.R., Camp, V.M., Ali, F.M., Black, M., Staciarini, W., Tarcan, Y., 1981. Melanoma detection by enzyme-radioimmunoassay of L-dopa, dopamine, and 3-*O*-methyldopamine in urine. Clin. Chem. 27, 108–112.

Fitoussi, N., Sotnik-Barkai, I., Tornatore, C., Herzberg, U., Yadid, G., 1998. Dopamine turnover and metabolism in the striatum of parkinsonian rats. Neuroscience 85, 405–413.

French, C.J., Pecket, R.C., Smith, H., 1974. Effect of exogenous DOPA and tyrosine on amaranthin synthesis and pigment type in *Amaranthus*. Phytochemistry 13, 1505–1511.

Girod, P.-A., Zryd, J.-P., 1991. Secondary metabolism in cultured red beet (*Beta vulgaris* L.) cells: differential regulation of betaxanthin and betacyanin biosynthesis. Plant Cell Tiss. Org. Cult. 25, 1–12.

Giudici de Nicola, M., Amico, V., Piattelli, M., 1974. Effect of white and far-red light on betalain formation. Phytochemistry 13, 439–442.

Giudici de Nicola, M., Amico, V., Sciuto, S., Piattelli, M., 1975. Light control of amaranthin synthesis in isolated *Amaranthus* cotyledons. Phytochemistry 14, 479–481.

Giudici de Nicola, M., Piattelli, M., Amico, V., 1973. Photocontrol of betaxanthin synthesis in *Celosia plumosa* seedlings. Phytochemistry 12, 353–357.

Kobayashi, N., Schmidt, J., Wray, V., Schliemann, W., 2001. Formation and occurrence of dopamine derived betacyanins. Phytochemistry 56, 429–436.

Minale, L., Piattelli, M., De Stefano, S., Nicolaus, R.A., 1966. Pigments of Centrospermae — VI. Acylated betacyanins. Phytochemistry 5, 1037–1052.

Palada, M.C., Crossman, S.M.A., 1999. Evaluation of tropical leaf vegetables in the Virgin Islands. In: Janick, J. (Ed.), Perspectives on New Crops and New Uses. ASHS Press, Alexandria, pp. 388–393.

Piattelli, M., Giudici de Nicola, M., Castrogiovanni, V., 1969. Photocontrol of amaranthin synthesis in *Amaranthus tricolor*. Phytochemistry 8, 731–736.

Piattelli, M., Impellizzeri, G., 1970. 2-Descarboxybetanidin, a minor betacyanin from *Carpobrotus acinaciformis*. Phytochemistry 9, 2553–2556.

Piattelli, M., Minale, L., 1964. Pigments of Centrospermae — II. Distribution of betacyanins. Phytochemistry 3, 547–557.

Reznik, H., 1975. Betalaine. Beri. Dtsch. Bot. Ges. 88, 179–190.

Reznik, H., 1978. The occurrence of betalamic acid in the order Centrospermae. Z. Pflanzenphysiol. 87, 95–102.

Rink, E., Böhm, H., 1991. Effect of DOPA feeding on betaxanthins in various species of Centrospermae. Phytochemistry 30, 1109–1112.

Schliemann, W., Kobayashi, N., Strack, D., 1999. The decisive step in betaxanthin biosynthesis is a spontaneous reaction. Plant Physiol. 119, 1217–1232.

Schmidt, J., Kramell, R., Schneider, G., 1995. Liquid chromatography/electrospray tandem mass spectrometry of amino acid conjugates of jasmonic acid under positive and negative ionisation. Eur. Mass Spectrom. 1, 573–581.

Steiner, U., Schliemann, W., Böhm, H., Strack, D., 1999. Tyrosinase involved in betalain biosynthesis of higher plants. Planta 208, 114–124.

Strack, D., Bokern, M., Marxen, N., Wray, V., 1988. Feruloylbetanin from petals of *Lampranthus* and feruloylamaranthin from cell suspension cultures of *Chenopodium rubrum*. Phytochemistry 27, 3529–3531.

Trezzini, G.F., Zryd, J.-P., 1991. Characterization of some natural and semi-synthetic betaxanthins. Phytochemistry 30, 1901–1903.

Wehmer, C., 1929. Die Pflanzenstoffe, 2nd Edition, Vol. I. Fischer Verlag, Jena, p. 299.

Wong, K.-Y., 1994. Chinese Herbal Medicine. Wokman Press, Hong Kong.

Xu, G. J., 1996. Ji Guan Zi (No. 12768), Ji Guan Hua (No. 12769) and Ji Guan Miao (No. 12770). In: Yan, Y.Q., Yu, C.L., Huang, T.K. (Eds.), Encyclopedia of Chinese Medicine, Vol. 2. China Medicine Sci. Technol., Beijing, pp. 509–511.

PERGAMON

Phytochemistry 58 (2001) 167–172

PHYTOCHEMISTRY

www.elsevier.com/locate/phytochem

Acylated flavone *C*-glycosides from *Cucumis sativus*

Mamdouh M. Abou-Zaid[a,*], Domenic A. Lombardo[a], Geoffrey C. Kite[b], Renée J. Grayer[b], Nigel C. Veitch[b]

[a]*Natural Resources Canada, Canadian Forest Service, Great Lakes Forestry Centre, 1219 Queen Street East, Sault Ste. Marie, Ontario, P6A 5M7, Canada*
[b]*Jodrell Laboratory, Royal Botanic Gardens, Kew, Richmond, Surrey, TW9 3DS, UK*

Received 19 January 2001; received in revised form 22 March 2001

Abstract

Leaves of *Cucumis sativus* plants treated with silicon and infected with *Sphaerotheca fuliginea* yielded five new acylated flavone *C*-glycosides identified as isovitexin 2″-*O*-(6‴-(*E*)-*p*-coumaroyl)glucoside (**6**), isovitexin 2″-*O*-(6‴-(*E*)-*p*-coumaroyl)glucoside-4′-*O*-glucoside (**7**), isovitexin 2″-*O*-(6‴-(*E*)-feruloyl)glucoside-4′-*O*-glucoside (**11**), isoscoparin 2″-*O*-(6‴-(*E*)-*p*-coumaroyl)glucoside (**9**), and isoscoparin 2″-*O*-(6‴-(*E*)-feruloyl)glucoside-4′-*O*-glucoside (**12**). The known flavone-glycosides isovitexin (**1**), saponarin (**2**), saponarin 4′-*O*-glucoside (**3**), vicenin-2 (**4**), apigenin 7-*O*-(6″-*O*-*p*-coumaroylglucoside) (**5**), isovitexin 2″-*O*-(6‴-(*E*)-feruloyl)glucoside (**8**) and isoscoparin 2″-*O*-(6‴-(*E*)-feruloyl)glucoside (**10**), were also identified in this plant material. © 2001 Elsevier Science Ltd. All rights reserved.

Keywords: *Cucumis sativus*; Cucurbitaceae; Cucumber; Acylated flavone *C*-glycosides

1. Introduction

The *Cucurbitaceae* is characterised chemically by the presence of cucurbitacins, bitter-tasting triterpenoids that are present in high concentrations in root tissue and toxic to mammals (Hegnauer, 1964, 1989). In contrast, the fruits of many species in this family are edible and used as foods, including pumpkin, marrow and zucchini (*Cucurbita* spp.), watermelon (*Citrullus lanatus* (Thunb.) Matsum. & Nakai), melon (*Cucumis melo* L.) and cucumber (*Cucumis sativus* L.). The phenolic constituents of these valuable crop plants have not been investigated extensively, although there is some evidence for their involvement in mechanisms of resistance to fungal infection in *C. sativus* (Menzies et al., 1991; Daayf et al., 1997). In a recent investigation, a flavonol phytoalexin (7-*O*-methoxy-3,5,3′,4′-tetrahydroxyflavone) was identified in seedlings of *C. sativus* treated with silicon and infected with *Sphaerotheca fuliginea* (Schlechtend.:Fr) Poll., a fungus causing powdery mildew (Fawe et al., 1998). A role for Si in mediating the accumulation of this compound was also demonstrated. The present report describes a more extensive survey of the flavonoids of this plant material. Among these are five new acylated flavone *C*-glycosides that were identified using a combination of LC–MS and NMR techniques.

2. Results and discussion

A MeOH extract of fresh leaves of *C. sativus* from plants treated with silicon (as potassium silicate) and infected with *Sphaerotheca fuliginea* yielded flavone *C*-glycosides **1**–**7** by column chromatography and semi-preparative HPLC. The purified fractions of **6** and **7** also contained **8**–**10** and **11**–**12**, respectively, as minor components. Five of the compounds were identified as isovitexin (**1**), saponarin (**2**), saponarin 4′-*O*-glucoside (**3**), vicenin-2 (**4**) and apigenin 7-*O*-(6″-*O*-*p*-coumaroylglucoside) (**5**), on the basis of chemical and spectroscopic data (see Experimental section). These flavone *C*-glycosides are well-known from other plant sources (Harborne and Baxter, 1999). Gallic acid and *p*-coumaric acid were also identified as constituents of the leaves of *C. sativus* by the same methods.

Acid hydrolysis (2 M HCl) of **6** and **7** afforded isovitexin, vitexin, glucose and *p*-coumaric acid in each case. The UV spectra of both compounds were similar,

* Corresponding author. Tel.: +705-759-5740; fax: +705-759-5700.

E-mail address: mabouzai@nrcan.gc.ca (M.M. Abou-Zaid).

0031-9422/01/$ - see front matter © 2001 Elsevier Science Ltd. All rights reserved.
PII: S0031-9422(01)00156-X

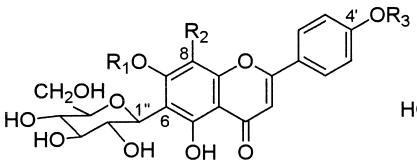

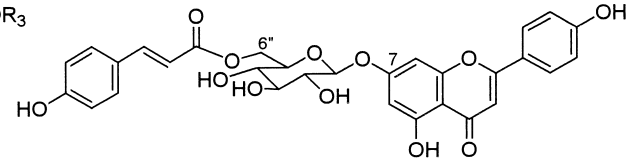

	R_1	R_2	R_3
1	H	H	H
2	Glc	H	H
3	Glc	H	Glc
4	H	Glc	H

5

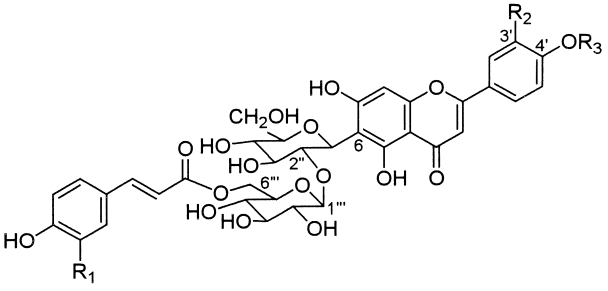

	R_1	R_2	R_3
6	H	H	H
7	H	H	Glc
8	OCH_3	H	H
9	H	OCH_3	H
10	OCH_3	OCH_3	H
11	OCH_3	H	Glc
12	H	OCH_3	Glc

and characteristic for flavonoid glycosides acylated by hydroxycinnamic acids (Markham, 1982). The 1D ^{1}H NMR spectrum of **6** acquired in DMSO-d_6 at 37°C contained a significant number of exchange-broadened resonances, a feature observed previously in some flavone *C*-glycosides (Markham and Geiger, 1993; Lewis et al., 2000). One of these resonances, corresponding to 5-OH, appeared as two components which coalesced at 50°C. An acceptable level of spectral resolution overall was achieved at 60°C, the temperature used for all subsequent NMR measurements. The molecular structure of **6** was obtained using 1D ^{1}H, 1D XSROESY, 1D ^{13}C, DEPT, DQF-COSY, HSQC and HMBC experiments. Characteristic ^{1}H and ^{13}C chemical shift values and coupling constant data indicated that the structure was based on that of isovitexin (apigenin 6-*C*-β-glucopyranoside) (Agrawal, 1989; Markham and Geiger, 1993). This was confirmed by the detection of a long-range ^{1}H–^{13}C connectivity (HMBC) from the anomeric proton of the *C*-β-glucopyranosyl moiety at δ 4.71 (*d*, $J=9.9$ Hz, H-1″) to the ^{13}C resonance at δ 107.9 (C-6). The remaining resonances of the primary sugar residue (6-*C*-Glc) were assigned from DQF-COSY, HSQC and HMBC data using the anomeric proton at δ 4.71 as a starting point (Table 1). A second anomeric sugar proton was noted in the 1D ^{1}H NMR spectrum at δ 4.28 (*d*, $J=7.3$ Hz), with a ^{13}C resonance at δ 105.2 by HSQC. Assignment of the corresponding set of sugar resonances identified their origin as a second β-glucopyranosyl moiety *O*-linked to the *C*-β-glucopyranose (Table 1). The precise nature of the linkage between the two sugar residues was determined using ^{1}H–^{1}H dipolar connectivities detected in 1D XSROESY experiments (Gradwell et al., 1997). Strong ROE connectivities were found between the resonances of the two anomeric protons indicating that the interglycosidic linkage was 1‴→2″. This was also evident from the significant downfield shifts experienced by H-2″ and C-2″ in comparison to their values in the

NMR spectra of isovitexin (Agrawal, 1989). The β-configuration of the two glucose moieties was confirmed by observation of ROE connectivities from H-1″ to H-3″ and H-5″, and H-1‴ to H-3‴ and H-5‴.

The remaining resonances in the 1D ^{1}H NMR spectrum of **6** were typical of those of (*E*)-*p*-coumaric acid (Table 1). A weak ROE connectivity was detected between one of the 6‴-CH_2 protons of the *O*-linked β-glucopyranose at δ 3.89 and the α-CH resonance of the *p*-coumaric acid moiety at δ 6.07. In addition, the ^{13}C resonance of C-6‴ was downfield shifted to 62.4 ppm. These observations indicated that the *O*-linked β-glucopyranose was acylated by (*E*)-*p*-coumaric acid at the 6‴ position. APCI–MS (negative mode) of **6** gave a deprotonated molecule ($[M-H]^-$) at *m*/*z* 739 which together with NMR data indicated an empirical formula of $C_{36}H_{36}O_{17}$. MS–MS of the deprotonated molecule gave three major product ions at *m*/*z* 593, 413 and 293, which were in accordance with cleavage of the ester bond of the acyl (coumaroyl) moiety (fragmentation Y_3), cleavage of the glycosidic bond at C-2″ (fragmentation Y_2), and fragmentation Y_2 plus elimination of a 120 Da ring fragment from the *C*-linked glucose (fragmentation Y_1), respectively (Fig. 1a). Minor product ions at *m*/*z* 619 (fragmentation Y_1) and *m*/*z* 473 (fragmentations $Y_1 + Y_3$) were also present. The molecular structure of **6** was, therefore, confirmed as isovitexin 2″-*O*-(6‴-(*E*)-*p*-coumaroyl)-β-glucopyranoside on the basis of both MS and NMR data.

Table 1
^{1}H and ^{13}C NMR chemical shift assignment and coupling constant data for flavone *C*-glycosides **6** and **7** (δ in DMSO-d_6 at 60°C)

		6		**7**	
	Atom	δ ^{1}H	δ ^{13}C	δ ^{1}H	δ ^{13}C
	2		163.5		162.7
	3	6.47 *br s*	102.8	6.54 *br s*	103.7
	4		181.7		181.6
	5	13.55 *br s* (OH)	160.5	13.47 *br s* (OH)	160.7
	6		107.9		108.1
	7		163.3		164.1
	8	6.40 *s*	93.5	6.39 *s*	93.4
	9		156.4		156.5
	10		103.2		103.0
	1′		121.4		124.3
	2′, 6′	7.71 *d* (8.9)	128.2	7.81 *d* (8.9)	127.9
	3′, 5′	6.85 *d* (8.9)	115.7	7.12 *d* (8.9)	116.5
	4′		160.7		160.1
6-*C*-Glc	1″	4.71 *d* (9.9)	71.2	4.72 *d* (9.9)	71.3
	2″	4.35 *br s*	80.8	4.36 *br s*	80.6
	3″	3.48 *m*	78.4	3.48 *m*	78.4
	4″	3.24 *m*	70.1	3.25 *m*	70.1
	5″	3.23 *m*	81.3	3.23 *m*	81.3
	6″	3.69 *m*	61.2	3.69 *m*	61.2
		3.46 *m*		3.46 *m*	
2″-*O*-Glc	1‴	4.28 *d* (7.3)	105.2	4.30 *d* (7.3)	105.2
	2‴	2.94 *m*	74.3	2.95 *m*	74.3
	3‴	3.12 *m*	76.2	3.12 *m*	76.3
	4‴	3.04 *m*	69.0	3.03 *m*	69.0
	5‴	3.03 *m*	73.4	3.03 *m*	73.4
	6‴	3.89 *m*	62.4	3.88 *m*	62.4
		3.75 *m*		3.75 *m*	
4′-*O*-Glc	1⁗			5.00 *d* (7.3)	100.2
	2⁗			3.32 *m*	73.1
	3⁗			3.35 *m*	76.4
	4⁗			3.24 *m*	69.7
	5⁗			3.42 *m*	77.0
	6⁗			3.74 *m*	60.7
				3.54 *m*	
Coum.	α	6.07 *d* (15.9)	113.8	6.08 *d* (15.9)	113.8
	β	7.19 *d* (15.9)	144.1	7.19 *d* (15.9)	144.1
	1		125.1		125.1
	2, 6	7.32 *d* (8.6)	129.9	7.32 *d* (8.6)	129.9
	3,5	6.78 *d* (8.6)	115.6	6.79 *d* (8.6)	115.7
	4		159.4		159.5
	CO		166.1		166.1

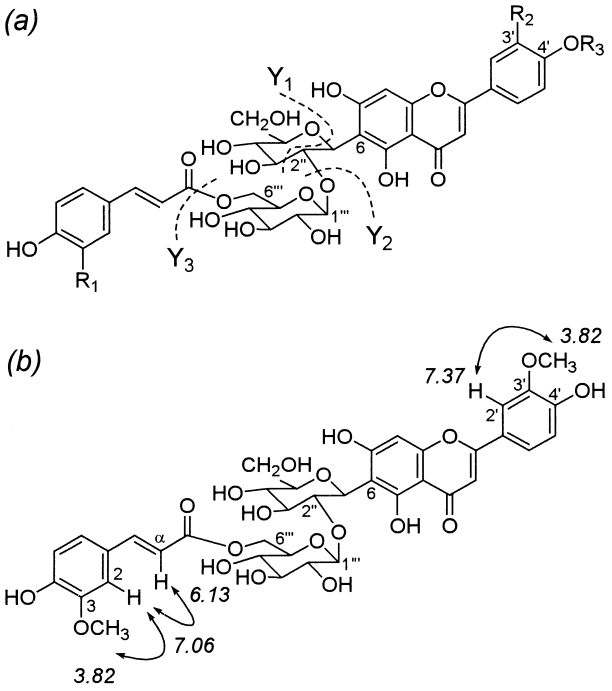

Fig. 1. (a) Fragmentation patterns Y_1–Y_3 observed for **6**–**12** in MS–MS experiments; (b), Summary of ^{1}H–^{1}H ROE connectivities observed for **8**–**10** in 1D XSROESY NMR experiments. The corresponding proton chemical shift values are given for reference. Although compound **10** (the dimethoxy derivative of **6**) is shown here, the NMR data for the 'feruloyl' and 'flavone' parts of the molecule are also valid for compounds **8** and **9**, respectively (the monomethoxy derivatives of **6**).

were assigned from DQF-COSY, HSQC and HMBC data, and were typical of those for an *O*-linked β-glucopyranoside. Site selective excitation of the anomeric proton resonance at δ 5.00 using 1D XSROESY gave a strong ROE connectivity to the H-3′,5′ resonance at δ 7.12. This confirmed the site of attachment of the additional *O*-Glc residue to be at C-4′. The resonance assignments of the NMR spectra of **6** and **7** (Table 1) were similar with the exception of the downfield shifts of H-3′,5′ and H-2′,6′ in **7** due to substitution of 4′-OH by *O*-Glc. APCI–MS (negative mode) of **7** gave a deprotonated molecule ($[M–H]^-$) at *m*/*z* 901, which together with NMR data indicated an empirical formula of $C_{42}H_{46}O_{22}$. MS–MS of the deprotonated molecule gave only one major product ion, at *m*/*z* 739 $[(M–H)–162]^-$, corresponding to loss of the C-4′ glucopyranosyl group. Collision induced dissociation (CID) of this ion in a MS^3 experiment yielded the same array of product ions as in the CID spectrum of deprotonated **6**. Compound **7** was therefore identified as isovitexin 2″-*O*-(6‴-(*E*)-*p*-coumaroyl)-β-glucopyranoside-4′-*O*-β-glucopyranoside, the 4′-*O*-glucoside of **6**.

Further analysis of the samples containing **6** and **7** by reverse phase HPLC/APCI–MS (negative mode) showed that neither gave a chromatographically pure peak. Minor components with slightly shorter retention times and giving deprotonated molecules at *m*/*z* 769 (**8** and **9**) and 799 (**10**) eluted within the peak of **6**, and components giving deprotonated molecules at *m*/*z* 931 (**11** and **12**) eluted within **7**. The similarities observed in the CID spectra of the minor components compared to **6** and **7** indicated that they might be methoxy derivatives of these compounds. This was supported by the observation of minor component resonances in the NMR spectra of the samples of both **6** and **7** at chemical shift values typical of $ArOCH_3$ (δ_H 3.82 and δ_C 55.7).

MS–MS of deprotonated **10** (60 Da greater than **6**) gave three major product ions, all 30 Da greater than those observed in the CID spectrum of **6**, and a minor product ion at $[(M–H)–120]^- = m/z$ 679 (i.e. a Y_1 cleavage). These data were in accordance with **10** being a dimethoxy derivative of **6** with one methoxy group located on the aglycone moiety and one on the acyl moiety (suggesting a feruloyl group). The location of a methoxy group on the aglycone moiety was further supported by a MS^3 experiment in which CID of the 'aglycone' product ion at *m*/*z* 323 (generated by Y_1+Y_2 cleavage) showed the loss of a methyl radical. On the basis of the fragmentation shown by **6** and **10**, the negative ion CID spectrum of the peak at *m*/*z* 769, observed in the LC–MS analysis of **6**, was in accordance with it being a mixed spectrum of two methoxy derivatives of **6**. One (**9**) showed a Y_3 cleavage product at $[(M–H)–146^-] = m/z$ 623, in accordance with the loss of a coumaroyl moiety, and the loss of a methyl radical from the aglycone ion, as shown by a MS^5 (*m*/*z* 796→623→443→323) experiment to ensure the fragmented ion was pure. The other (**8**) showed a Y_3 cleavage product at $[(M–H)–176]^- = m/z$ 593, consistent with the loss of a feruloyl moiety, and no loss of methyl radical from the aglycone ion.

The precise location of the methoxy groups in **8**–**10** was established using 1D XSROESY experiments, as illustrated in Fig. 1b. Site selective excitation of the minor proton resonance at δ 3.82 (corresponding to the coincident methoxy resonances of **8**–**10**) gave ROE connectivities to δ 7.06 and 7.37. Similarly, site selective excitation of δ 7.06 (which was not obscured by the resonances of **6**, the major component of the sample) gave ROE connectivities to resonances at δ 6.13 (*d*, *J* = 15.9 Hz) and 3.82 (*s*). The resonance at δ 6.13 was located in the 1D ^1H NMR spectrum of the sample as a low intensity signal appearing slightly downfield of α-CH of the coumaroyl group of **6** at δ 6.08 (*d*, *J* = 15.9 Hz), and with the same multiplet structure. This allowed the ROE connectivities to be assigned as H-2 (δ 7.06) to α-CH (δ 6.13) and 3-OCH_3 (δ 3.82), and confirmed the presence of a feruloyl group (Fig. 1b). Compound **8**, the monomethoxy derivative of **6** with the OCH_3 group located on the acyl moiety was therefore confirmed to be isovitexin 2″-*O*-(6‴-(*E*)-feruloyl)-β-glucopyranoside. The minor component resonance at δ 7.37, although obscured by H-2,6 of the coumaroyl group of **6**, was assigned to H-2′ of the flavone. This was supported by data obtained from an analogous set of 1D XSROESY experiments for the sample containing **7** (and **11** and **12** as minor components), where the equivalent minor component resonance at δ 7.41 appeared as a low-intensity doublet with *J* = 2.2 Hz (satisfied only by H-2′). Compound **9**, the monomethoxy derivative of **6** with the OCH_3 group located on the flavone moiety was therefore identified as 3′-methoxyisovitexin 2″-*O*-(6‴-(*E*)-*p*-coumaroyl)-β-glucopyranoside (= isoscoparin 2″-*O*-(6‴-(*E*)-*p*-coumaroyl)-β-glucopyranoside). The dimethoxy derivative of **6**, compound **10**, was identified as 3′-methoxyisovitexin 2″-*O*-(6‴-(*E*)-feruloyl)-β-glucopyranoside (isoscoparin 2″-*O*-(6‴-(*E*)-feruloyl)-β-glucopyranoside).

The minor components **11** and **12** observed in the LC–MS analysis of the sample containing **7** (both giving deprotonated molecules at *m*/*z* 931) were resolved chromatographically. Both generated a $[(M–H)–162]^-$ product ion in MS–MS experiments, like **7**, and in MS^3 experiments the CID spectra of these ions, at *m*/*z* 769, were the same as the CID spectra of deprotonated **8** and **9**, respectively. These data suggested that **11** and **12** were the 4′-*O*-glucosides of **8** and **9**. Site selective excitation of the minor component methoxy resonances for **11** and **12** at δ 3.82 was carried out by 1D XSROESY as before. This gave ROE connectivities to minor component resonances at δ 7.09 and 7.41 (*d*, *J* = 2.2 Hz) (analogous to δ 7.06 and 7.37 in the sample containing **6** and

8–**10**), and a much weaker connectivity to δ 5.00, the anomeric proton of the 4′-*O*-glucosyl group. The two methoxy derivatives **11** and **12**, were therefore identified as isovitexin 2″-*O*-(6‴-(*E*)-feruloyl)-β-glucopyranoside-4′-*O*-β-glucopyranoside, and 3′-methoxyisovitexin 2″-*O*-(6‴-(*E*)-*p*-coumaroyl)-β-glucopyranoside-4′-*O*-β-glucopyranoside (isoscoparin 2″-*O*-(6‴-(*E*)-feruloyl)-β-glucopyranoside-4′-*O*-β-glucopyranoside). Deprotonated molecules of an equivalent glucoside of **10** were not observed in the LC–MS analysis.

Compounds **6** and **7** have not been reported previously in the literature, and are new examples of acylated flavone *C*-glycosides. Of the minor components **8**–**12**, only two (**8** and **10**) are known, and were isolated originally from methanolic extracts of the rice plant, *Oryza sativa* (Besson et al., 1985). Earlier work on *Cucumis* flavonoids appears to be relatively limited. Monties et al. (1976) partially characterised four flavone *C*-glucosides from *C. melo* as 6-*C*-diglucosylapigenin, 6-*C*-diglucosylluteolin, and the caffeic acid esters of these compound, and Saunders and McClure (1976) reported orientin in *C. maxima*. It is interesting to note in the context of the present study that the acylated flavone *C*-glucosides **6**–**12** were only detected in extracts of leaves of *C. sativus* that had been treated with silicon and infected with *Sphaerotheca fuliginea*, a causative agent of powdery mildew. This may indicate that they are accumulated as a response to stress conditions experienced by the plant.

3. Experimental

3.1. General

^{1}H NMR (500 and 300 MHz) and ^{13}C NMR (125 and 75 MHz) spectra were recorded in DMSO-d_6, with the residual solvent resonances used as internal standards at δ 2.50 and 39.5, respectively. Negative ion APCI-mass spectra were obtained with a quadrupole ion-trap instrument (Finnigan LCQ) using a vaporiser temperature of 550°C, sheath and auxiliary nitrogen gas pressures of 80 and 20 psi, a needle current of 5 μA, and a heated capillary temperature of 150°C. Samples were introduced by direct infusion, or via an HPLC fitted with a Merck LiChrospher 250×4.6 (i.d.) mm (5 μm particle size) C18 column using a 20 min linear gradient of 25–100% methanol in 1% aqueous acetic acid at 1 ml/min. MS^n experiments were performed in the ion trap using an ion isolation width of 5 Da and a collision energy of 50%.

3.2. Plant material

Seeds of cucumber, *Cucumis sativus* L. cv. Mustang, were sown in rockwool cubes and watered with distilled water until emergence. Seedlings were transferred individually to 500 ml jars containing nutrient solutions to which silicon (1.7 mM) had been added in the form of potassium silicate, and placed in a growth chamber (16 h photophase of ca. 145 μE m^{-2} s^{-1}, 23°C day/19°C night). Plants were grown until the fourth leaf had fully expanded, following which a conidial suspension of the biotrophic powdery mildew fungus *Sphaerotheca fuliginea* was sprayed onto the adaxial leaf surfaces until run-off, as described previously (Fawe et al., 1998). Non-treated control plants grown as above but without the addition of silicon were transferred to a similar growth chamber to minimise cross-infection. After 3 weeks both treated and untreated leaves were harvested and immediately frozen in liquid nitrogen. Leaf samples were stored at −80°C prior to analysis.

3.3. Extraction and isolation procedures

Infected leaf material of *C. sativus* grown in the presence of silicon was ground to a fine powder in liquid nitrogen (amount equivalent to 2.2 kg fr. wt). This was extracted at room temp. in two stages; first by steeping for 24 h in 100% MeOH and decanting the solvent, and second by steeping the residue for an additional 24 h in 50% aqueous MeOH (10 g fr. wt/100 ml solvent). Combined methanolic extracts were evaporated under reduced pressure to near dryness and the residue freeze-dried to yield 257 g crude extract. 200 g of this material was redissolved in a minimum quantity of MeOH and adsorbed onto polyvinylpolypyrrolidone (PVPP) packed in a Buchner funnel (2 l). The initial elution solvent was H_2O, followed by aq. EtOH (20, 50, 70%) and finally 100% EtOH. The 50% aq. EtOH bulk fraction was further chromatographed on a PVPP column using CH_2Cl_2–EtOH–MeCOEt–Me_2CO (1:1:1:1), yielding a mixture of flavone glycosides. Separation by low pressure liquid chromatography (Chemco low-prep. pump) using a MeOH-water gradient afforded **1**–**5**. Final purification of these compounds was achieved by column chromatography using Sephadex LH-20 (50×1 cm i.d.) with MeOH as eluting solvent, and gave **1** (28.0 mg), **2** (3.3 mg), **3** (2.4 mg), **4** (18.4 mg) and **5** (8.1 mg). Identification was achieved by standard procedures (Mabry et al., 1970; Markham, 1982), including acid hydrolysis in 2 M and 0.1 M HCl, alkaline hydrolysis, H_2O_2 oxidation, UV spectroscopy (with the use of shift reagents), MS, and comparison of ^{1}H and ^{13}C NMR spectra with literature data (Agrawal, 1989; Markham and Geiger, 1993). Compounds **6** and **7** were also present in the 50% aq. EtOH bulk fraction, but required further separation by HPLC (see Section 3.4).

3.4. Analytical and semi-prep. HPLC

A Waters Delta Prep 4000 LC system equipped with a 996 photodiode array detector was used for HPLC. For analytical work, dilute solutions of freeze-dried crude

extracts (10 mg ml^{-1}; both with and without spiking by standards) were passed through Acrodisc filters (0.45 μm) and 10 μl aliquots injected onto a Waters reverse-phase analytical column of 150×3.9 mm (i.d.) packed with Nova-Pak C18 material (4 μm, 60 Å). A gradient profile using two solvents was applied at room temp. (Van Sumere et al., 1993), with solvent A = 5% aq. HCO_2H, solvent B = CH_3CN:MeOH (5:95) and a flow rate of 0.9 ml min^{-1}. Compounds of interest were detected on the basis of characteristic UV-vis spectra (spectral range 220–390 nm) and retention time. Semi-prep. HPLC was carried out using two Waters prep. cartridges in series, each of 100×25 mm (i.d.), and packed with Nova-Pak HR C18 material (6 μm, 60 Å). A gradient profile using two solvents was applied at room temp. (Grayer and Veitch, 1998), with solvent A = H_2O, solvent B = MeOH and a flow rate of 3 ml min^{-1}. This procedure was applied to those fractions identified from analytical HPLC as containing the acylated flavone *C*-glycosides **6** and **7** (recognised from their distinctive UV-vis spectra). Repeated cycles of semi-prep. HPLC gave **6** (15.0 mg) and **7** (13.6 mg) in quantities sufficient for spectroscopic analysis and with a purity of ca. 90–95%.

3.5. Isovitexin 2″-O-(6‴-(E)-p-coumaroyl)-β-glucopyranoside (6)

Yellow solid; UV λ_{max} MeOH nm: 273, 294*sh*, 321; + NaOMe 280, 335*sh*, 380 (increased intensity); + $AlCl_3$ 280, 305, 330, 356*sh*, 384*sh*; + $AlCl_3$ and HCl 282, 302, 330, 382*sh*; + NaOAc 279, 298*sh*, 309*sh*, 375; + NaOAc and H_3BO_3 274, 319; ^1H NMR (DMSO-d_6): see Table 1; ^{13}C NMR (DMSO-d_6): see Table 1; APCI–MS (negative mode) *m*/*z*: 739 $[M\text{-}H]^-$.

3.6. Isovitexin 2″-O-(6‴-(E)-p-coumaroyl)-β-glucopyranoside-4′-O-β-glucopyranoside (7)

Yellow solid; UV λ_{max} MeOH nm: 278, 316; + NaOMe 269*sh*, 282*sh*, 293, 308*sh*, 363 (no change in intensity); + $AlCl_3$ 283*sh*, 305, 325, 385*sh*; + $AlCl_3$ and HCl 283*sh*, 305, 325, 382*sh*; + NaOAc 280, 303*sh*, 312*sh*, 380*sh*; + NaOAc and H_3BO_3 280, 303*sh*, 315; ^1H NMR (DMSO-d_6): see Table 1; ^{13}C NMR (DMSO-d_6): see Table 1; APCI–MS (negative mode) *m*/*z*: 901 $[M–H]^-$.

Acknowledgements

We thank the Canadian Biotechnology Strategy Fund, the Canadian Ministry of External Affairs (DFAIT program 'Going Global' — European Section) and the Integrated Forest Pest Management Network for financial support. Access to NMR facilities was kindly provided by the Biomedical NMR Centre, National Institute for Medical Research, Mill Hill, London, UK.

References

Agrawal, P.K., 1989. Carbon-13 NMR of Flavonoids. Elsevier, Amsterdam. pp. 283–364.

Besson, E., Dellamonica, G., Chopin, J., Markham, K.R., Kim, M., Koh, H.-S., Fukami, H., 1985. C-Glycosylflavones from *Oryza sativa*. Phytochemistry 24, 1061–1064.

Daayf, F., Schmidtt, A., Bélanger, R.R., 1997. Evidence of phytoalexins in cucumber leaves infected with powdery mildew following treatment with leaf extracts of *Reynoutria sachalinensis*. Plant Physiology 113, 719–727.

Fawe, A., Abou-Zaid, M., Menzies, J.G., Bélanger, R.R., 1998. Silicon-mediated accumulation of flavonoid phytoalexins in cucumber. Phytopathology 88, 396–401.

Gradwell, M.J., Kogelberg, H., Frenkiel, T.A., 1997. Applying excitation sculpting to construct singly and doubly selective 1D NMR experiments. Journal of Magnetic Resonance 124, 267–270.

Grayer, R.J., Veitch, N.C., 1998. An 8-hydroxylated external flavone and its 8-*O*-glucoside from *Becium grandiflorum*. Phytochemistry 47, 779–782.

Harborne, J.B., Baxter, H., 1999. The Handbook of Natural Flavonoids, Vol. 1. Wiley, Chichester, UK.

Hegnauer, R., 1964. Chemotaxonomie der Pflanzen, Vol. 3. Birkhäuser, Basel. pp. 608–625.

Hegnauer, R., 1989. Chemotaxonomie der Pflanzen, Vol. 8. Birkhäuser, Basel. pp. 363–375.

Lewis, K.C., Maxwell, A.R., McLean, S., Reynolds, W.F., Enriquez, R.G., 2000. Room-temperature (^1H, ^{13}C) and variable-temperature (^1H) NMR studies on spinosin. Magnetic Resonance in Chemistry 38, 771–774.

Mabry, T.J., Markham, K.R., Thomas, M.B., 1970. The Systematic Identification of Flavonoids. Springer, Berlin.

Markham, K.R., 1982. Techniques of Flavonoid Identification. Academic Press, London.

Markham, K.R., Geiger, H., 1993. ^1H nuclear magnetic resonance spectroscopy of flavonoids and their glycosides in hexadeuterodimethylsulfoxide. In: Harborne, J.B. (Ed.), The Flavonoids: Advances in Research since 1986. Chapman and Hall, London, pp. 441–497.

Menzies, J.G., Ehret, D.L., Glass, A.D.M., Samuels, A.L., 1991. The influence of silicon on cytological interactions between *Sphaerotheca fuliginea* and *Cucumis sativus*. Physiological and Molecular Plant Pathology 39, 403–414.

Monties, B., Bouillant, M.-L., Chopin, J., 1976. C-diholosylflavones dans les feuilles du melon (*Cucumis melo*). Phytochemistry 15, 1053–1056.

Saunders, J.A., McClure, J.W., 1976. The distribution of flavonoids in chloroplasts of twenty five species of vascular plants. Phytochemistry 15, 809–810.

Van Sumere, C., Faché, P., Vande Casteele, K., De Cooman, L., Everaert, E., De Loose, R., Hutsebaut, W., 1993. Improved extraction and reversed phase-high performance liquid chromatographic separation of flavonoids and the identification of *Rosa* cultivars. Phytochemical Analysis 4, 279–292.

PERGAMON

Phytochemistry 58 (2001) 173–177

PHYTOCHEMISTRY

www.elsevier.com/locate/phytochem

3(2H)-Benzofuranones and chromanes from liquid cultures of the mycoparasitic fungus *Coniothyrium minitans*

Koichi Machida[a], Latchezar S. Trifonov[a], William A. Ayer[a,*], Zheng-Xiang Lu[b], André Laroche[b], Hung Chang Huang[b], Kuo Joan Cheng[b], Jennifer L. Zantige[b]

[a]*Department of Chemistry, University of Alberta, Edmonton, Alberta, T6G 2G2, Canada*
[b]*Agriculture and Agri-Food Canada, Lethbridge Research Center, Lethbridge, Alberta, T1J 4B1, Canada*

Received in revised form 5 January 2001

Abstract

Two 3(2H)-benzofuranones and three chromanes were isolated from the mycoparasitic fungus *Coniothyrium minitans*. Their structures and absolute stereochemistry were determined by spectroscopic methods. © 2001 Published by Elsevier Science Ltd.

Keywords: *Coniothyrium minitans*; Benzofuranones; Chromanes; Circular dichroism; Absolute configuration

1. Introduction

The fungus *Coniothyrium minitans* Campbell (Cm) is an aerobic mycoparasite capable of attacking the fungal plant pathogen *Sclerotina sclerotiorum* (Lib) de Bary (Huang and Hoes, 1976) resulting in the degradation of sclerotia (Huang and Kokko, 1987) and hyphae (Huang and Kokko, 1988) of the pathogen. Different strains of *C. minitans* have been identified based on morphological features such as color of cultures grown on artificial media (Huang, 1981). These features are, however, developmentally regulated or influenced by genotypic traits and environmental interaction. Jones et al. (1974) reported that β-1,3-endo- and exo-glucanases from *C. minitans* were responsible for the degradation of cell-wall glucans of *S. sclerotiorum*. *C. minitans* is used as a biological agent against Sclerotinia wilt of sunflower (Huang, 1980) and lettuce drop (Budge et al., 1995) caused by *S. sclerotiorum*. The plant pathogen *S. sclerotiorum*, commonly known as a white mold fungus, causes major losses in oilseed and pulse crops (Purdy, 1979) and no effective plant resistance has been identified so far. Whether metabolites of *C. minitans* might play a role in attacking and colonizing *S. sclerotiorum* is still unknown. In this paper we report the isolation and characterization of secondary metabolites produced when *C. minitans* is grown in artificial medium in which the only source of carbon is a sterilized powder made from sclerotia of *S. sclerotiorum*.

2. Results and discussion

The culture of *Coniothyrium minitans* strain LRS2130 was filtered and the filtrate was concentrated and extracted with EtOAc. The crude EtOAc extract was subjected to flash chromatography on silica gel with petroleum ether–CH_2Cl_2–EtOH gradient to give eight fractions. Further preparative TLC or HPLC purification of these fractions provided the new metabolites **1**–**5**, the common metabolites tyrosol, thriptophol, indole-3-carboxylic acid, and uracil, as well as dibutylphthalate and bis-(2-ethylhexyl)phthalate which are probably artifacts. In this study we report the structure elucidation of compounds **1**–**5**.

Compound **1** was isolated as an amorphous powder. The molecular formula, $C_{10}H_{10}O_3$, was established from the HREIMS spectrum. The ^{1}H NMR spectrum of **1** showed signals for three adjacent aromatic protons [δ 6.82, 6.84 (each 1H, *br d*, $J = 7.9$ Hz, 7.47 (1H, *t*, $J = 7.9$ Hz)] and two methyl group singlets. The ^{13}C NMR spectrum showed, in addition to the signals for a 1,2,3-trisubstituted phenyl ring, signals for two methyl groups, of a quaternary carbon atom (δ 102.7), and of a carbonyl group. Therefore, the structure of **1** was

* Corresponding author. Tel.: +1-780-492-5476; fax: +1-780-492-8231.
E-mail address: bill.ayer@ualberta.ca (W.A. Ayer).

0031-9422/01/$ - see front matter © 2001 Published by Elsevier Science Ltd.
PII: S0031-9422(01)00129-7

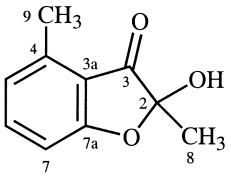

1

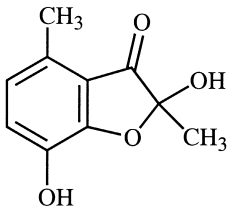

2

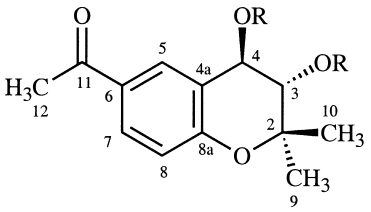

3: R = H
3a: R = *p*-$O_2NC_6H_4CO$

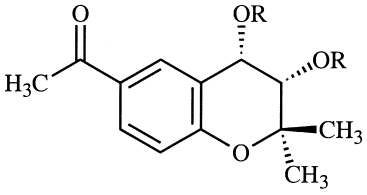

4: R = H
4a: R = *p*-$O_2NC_6H_4CO$

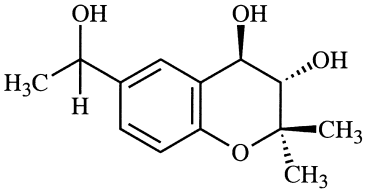

5

established as 2-hydroxy-2,4-dimethyl-3(2H)-benzofuranone.

Compound **2** was isolated as an amorphous yellow powder with a molecular formula $C_{10}H_{10}O_4$ as determined by HREIMS. Its ^1H and ^{13}C NMR spectra were similar to those of **1** and of cycloarthropsone isolated from liquid cultures of the fungus *Arthropsis truncata* (Ayer et al., 1992). The ^1H and ^{13}C NMR spectra, however, lacked signals due to an (E)-propenyl moiety at C-4 in cycloarthropsone and instead showed signals of an aromatic methyl group [δ_H 2.42 (3H, *s*), δ_C 17.1]. Furthermore, the HREIMS spectrum displayed the characteristic loss of hydroxyl and acetyl groups (see Experimental), which suggested that compound **2** is 2,7-dihydroxy-2,4-dimethyl-3(2H)-benzofuranone. This structure was confirmed by the HMBC spectrum which placed the aromatic methyl group at C-4 (cross peak between the methyl group signal (δ_H 2.42) and C-3a (δ_C 118.7)).

Compound **3** was isolated as an amorphous powder, $[\alpha]_D$ +39.0°C. Its molecular formula, $C_{13}H_{16}O_4$, was determined by HREIMS. The ^1H NMR spectrum of **3** showed signals for two methyl groups, one acetyl group, two mutually coupled methine protons at δ 3.52 and 4.55 (each 1H, J = 8.5 Hz) and three aromatic protons characteristic of a 1,2,4-trisubstituted phenyl ring. The ^1H NMR spectroscopic data were similar to those of *trans*-2,2-dimethyl-3,4,7-trihydroxy-6-acetylchromane isolated from *Helianthella quinquenervis* (Herz and Kulanthaivel, 1984), except for the aromatic proton signals. The HMBC spectrum positioned the acetyl group at C-6 (cross peak between H-5 (δ 8.15) and C-4 (δ 69.6). From the above data, the structure of compound **3** was established as that of 2,2-dimethyl-3,4-dihydroxy-6-acetylchromane. The relative stereochemistry of the two hydroxyl groups at C-3 and C-4 was determined as *trans* on the basis of the coupling constant $J_{H\text{-}3,H\text{-}4}$ = 8.5 Hz. A W-type long range coupling between H-3 and one of the methyl signals on C-2 (δ 1.21) was observed. Furthermore, the conformation of the pyrane ring was deduced from the ^1H–^1H COSY and the TROESY spectra. The TROESY spectrum showed a cross peak between H-4 and the methyl signal at δ 1.21. The above information indicated that the relationship between H-3 and methyl group at δ 1.21 to be quasi-trans axial and between H-4 and this methyl group to be 1,3-di-quasi axial in a pyrane ring with a half-chair conformation. The absolute configuration of **3** was derived from the CD spectrum of the corresponding p-nitrobenzoate (**3a**) which showed a negative first Cotton effect ($\Delta\varepsilon$ −9.92 at 270 nm) and a positive second Cotton effect ($\Delta\varepsilon$ + 4.10 at 243 nm) (Harada and Nakanishi, 1983; Jennings, 1982). Hence, **3** is (3*S*, 4*R*)-6-acetyl-3,4-dihydroxy-2,2-dimethylchromane.

Compound **4** was isolated as an amorphous powder, $[\alpha]_D$ −25.6°C. Its ^1H NMR spectrum closely resembled that of **3**, except that the proton signals at H-3 (δ 3.73) and H-4 (δ 4.85) were shifted downfield and their coupling constant (J = 4.2 Hz) was significantly smaller than that of **3** which indicates that **4** is a *cis*-diol. The stereochemistry of **4** was further supported by the

TROESY spectrum which showed correlations between H-4 and one of the methyl group signals (δ 1.29), and between H-3 and H-4. This leaves 3-OH and the methyl group at δ 1.29 in quasi-*trans*-axial orientation. Furthermore, the *p*-nitrobenzoate derivative **4a** showed a negative first ($\Delta\varepsilon$ −9.89 at 275 nm) and a positive second ($\Delta\varepsilon$ +5.39 at 250 nm) Cotton effect which is consistent with the absolute configuration (3*S*,4*S*)-6-acetyl-3,4-dihydroxy-2,2-dimethylchromane for compound **4**.

Compound **5** was isolated as an inseparable mixture (2:1) of two isomers. The molecular formula, $C_{13}H_{18}O_4$, was deduced from the HREIMS spectrum. Its ^1H and ^{13}C NMR spectra were similar to those of **3**. The ^1H NMR spectrum of **5**, however, lacked the signals due to the C-6 acetyl group of **3** and instead showed signals of an oxygenated methine proton [δ 4.76 (1H, *q*, $J=6.5$ Hz)] and a methyl group [δ 1.41 (3H, *d*, $J=6.5$ Hz)]. Furthermore, the ^1H NMR spectrum of **5** showed two sets of H-5, H-7 and H-8 signals, and H-5 and H-7 were shifted upfield compared with those of **3**. The relative stereochemistry of **5** at C-3 and C-4 was established as *trans* on the basis of the vicinal coupling $J_{H\text{-}3,H\text{-}4}=8.5$ Hz which is identical to the same coupling of the diol **3**. Compound **5** is, therefore, a mixture of epimers at C-11 of *trans*-6-(1-hydroxyethyl)-3,4-dihydroxy-2,2-dimethylchromane. The absolute configuration at C-3 and at C-4 was not determined since there was insufficient quantity of this compound available.

This is the first report of the isolation of metabolites from fungi of the genus *Coniothyrium*. Evaluation of the biological activity of the new metabolites is currently in progress.

3. Experimental

3.1. General experimental procedures

The HREIMS, LRESMS and HRESMS were recorded on an AEI-50 mass spectrometer. Optical rotations were determined with a Perkin Elmer 241 polarimeter with a cell length of 10 cm and CD spectra were measured on a Jasco ORD-CD spectrometer with a cell path of 1 mm. UV spectra were measured on a Hewlett Packard Diode Array UV–vis spectrometer (ICP) with a cell path of 1 mm. ^1H NMR, ^{13}C NMR, TROESY, ^1H–^1H COSY, HMQC and HMBC spectra were recorded on Brüker AM-200, AM-300, Varian IINOVA 300 and 500 spectrometers. Chemical shifts are given on a δ (ppm) scale and the solvent signal was used as reference. Carbon multiplicities were measured with APT and HMQC sequences. Pre-coated TLC plates, SIL G-25, 20×20 cm, 0.25 mm layer (Macherey-Nagel) were used for preparative TLC. Column chromatography (C.C.) was carried out on silica gel 60 (EM Science; 230–400 mesh) and Sephadex LH-20 (Pharmacia Fine Chemicals). Preparative HPLC was carried out on a Waters HPLC system (pump, 600E; detector, 490E) using Waters μ-Bondapak C_{18} (7.8 mm i.d.× 30 cm) column. SKB refers to Skelly Oil Company light petroleum, bp 60–68°C.

3.1.1. Fungal growth

Coniothyrium minitans strain LRS2130 was originally isolated from sclerotia of *S. sclerotiorum* produced on a diseased sunflower plant in Manitoba, Canada and stock cultures were lyophilized (Huang, 1981). Voucher specimens are deposited at the Lethbridge Research Centre, Agriculture and Agri-Food, Canada, as LRS2130 and at ATCC (Manassas, VA) as ATCC 74417. The fungus was grown in shake cultures (140 rpm) using modified Czapek-Dox medium (per litre: $NH_4H_2PO_4$, 2.0 g, K_2HPO_4, 1.0 g, $MgSO_4.7H_2O$, 0.5 g, KCl, 0.5 g, $FeSO_4$, 0.01 g, 1 ml 1% $ZnSO_4$, 1 ml 0.5% $CuSO_4$ and 1% dry powder of sclerotia of *S. sclerotiorum* as carbon source). Cultures were grown in 4 l brown glass bottles for 12 days at 20°C.

3.1.2. Isolation of metabolites

The mycelium was separated by filtration and the broth (80 l) was concentrated under reduced pressure to approximately 1/10 of its original volume. The broth was extracted by stirring with an equal volume of EtOAc (3 times). Due to poor separation, each extraction had to be filtered through celite to result in definitive layers. The EtOAc extract was dried (anhydr $MgSO_4$) and filtered with the solvent evaporated under reduced pressure to afford 5.84 g of crude EtOAc extract. The latter was subjected to flash column chromatography (C.C.) on silica gel using SKB–CH_2Cl_2–EtOH of increasing polarity, and the eluate was separated into eight fractions [fr. 1 (131 mg), fr.2 (150 mg), fr.3 (2600 mg), fr.4 (1104 mg), fr.5 (538 mg), fr.6 (469 mg), fr.7 (133 mg) and fr. 8 (187 mg)]. Fraction 1 (80 mg) was subjected to preparative TLC with benzene–EtOAc (10:0.5). The UV-active zone at R_f 0.28 gave pure dibutylphthalate (1.5 mg). The UV-active fraction of R_f 0.44 gave a crude product which was further subjected to preparative HPLC (solvent: MeOH, UV detection: 220 nm, flow rate: 1.5 ml/min) to give pure bis-(2-ethylhexyl)phthalate (Rt 11.0 min, 4.0 mg). Fr. 2 (80.0 mg) was subjected to preparative TLC with benzene–EtOAc (10:1, two-fold development). The UV-active zone at R_f 0.45 gave a crude product which was further purified by preparative TLC with hexane–Et_2O (8:5, three-fold development, R_f 0.49) to give pure **1** (1.5 mg). Fraction 3 (2600 mg) was applied to a silica gel column using SKB–EtOAc (5:1, 4:1, 3:1, 3:2, 1:1, 1:2 and 1:4) and EtOAc as eluant, with it separated into seven fractions [fr. 3-1 (99.7 mg), fr. 3-2 (103.0 mg), fr. 3-3 (83.6 mg), fr. 3-4 (83.3 mg), fr. 3-5 (928.6 mg), fr. 3-6 (155.5 mg) and fr.3-7 (1109.4 mg)]. Fraction 3-5 (200 mg) was subjected

to preparative HPLC [solvent: MeOH–H_2O (2:3), UV detection: 215 nm, flow rate: 1.5 ml/min) to give pure tyrosol (Rt 11.0 min, 4.0 mg) and **3** (Rt 27.6 min, 3.0 mg) and a mixture of three compounds (Rt 18.0–20.2 min). This mixture was further purified by preparative HPLC [solvent: CH_3CN–H_2O (2:3) and MeOH–H_2O (2:3); UV detection: 215 nm] to give pure indole-3-carboxylic acid (15.0 mg), tryptophol (5.0 mg) and **2** (3.0 mg). The remainder of fr. 3-5 was combined with fr. 3-4 (fr. 3-4, 5). Fraction 3-4,5 (810 mg) was applied to a Sephadex LH-20 column eluted with 50% MeOH, and the eluate was separated into five fractions [fr. 3-4,5-1 (410 mg), fr. 3-4,5-2 (188 mg), fr. 3-4,5-3 (68 mg), fr. 3-4,5-4 (24 mg) and fr. 3-4,5-5 (10 mg)]. Fraction 3-4,5-2 (100 mg) was subjected to preparative HPLC [solvent: MeOH–H_2O (2:3), UV detection: 280 nm, flow rate: 1.25 ml/min] to give pure **2** (Rt 24.4 min, 6.0 mg), **3** (Rt 35.6 min, 5.0 mg) and **4** (Rt 29.0 min, 2.0 mg). Fractions 3-4,5-3 and 3-4,5-4 were purified by preparative TLC with hexane-acetone (1:1), respectively. The UV active zone at R_f 0.38 gave tryptophol (2.0 mg) while the zone at R_f 0.24 gave indole-3-carboxylic acid (6.0 mg). Fraction 3-6 (148.0 mg) was crystallized from MeOH to afford pure uracil (5.0 mg). The remainder of fr. 3-6 was subjected to Sephadex LH-20 chromatography (50% of MeOH as eluant) to give three fractions (Frs. 3-6-1 ~ 3-6-3). Fraction 3-6-2 (23.8 mg) was purified by preparative HPLC [solvent: MeOH–H_2O (3:2), UV detection: 220 nm, flow rate: 1.5 ml/min] to give **5** (Rt 25.0 min, 2.0 mg).

*3.1.2.1. 2-Hydroxy-2,4-dimethyl-3(2H)-benzofuranone (**1**).* Amorphous powder; $[\alpha]_D$ −15.0°C (*c* 0.02, MeOH); UV λ_{max}(MeOH) nm (log ε): 216 *sh* (4.07), 256 (3.65), 340 (3.16), 342 (3.14); ^{1}H NMR (300 MHz, $CDCl_3$): δ 1.63 (3H, *s*, 8-CH_3), 2.56 (3H, *br s*, 9-CH_3), 6.82, 6.84 (each 1H, *br d*, *J* = 7.9 Hz, H-5,7), 7.47 (1H, *t*, *J* = 7.9 Hz, H-6); ^{13}C NMR (125.7 MHz, $CDCl_3$): δ 17.9 (C-9), 22.7 (C-8), 102.7 (C-2), 110.5 (C-7), 114.5 (C-3a), 123.7 (C-5), 138.5 (C-6), 141.0 (C-4), 170.4 (C-7a), 199.3 (C-3); HREIMS *m*/*z* (rel. int.): $[M]^+$ 178.0630 (15, $C_{10}H_{10}O_3$ required 178.0630), 161.0598 (6, $C_{10}H_9O_2$ required 161.0603), 135.0445 (100, $C_8H_7O_2$ required 135.0446), 118.0419 (16, C_8H_6O required 118.0419), 107.0496 (15, C_7H_7O required 107.0497), 90.0468 (23, C_7H_6 required 90.0469), 77.0395 (17, C_6H_5 required 77.0391).

*3.1.2.2. 2,7-Dihydroxy-2,4-dimethyl-3(2H)-benzofuranone (**2**).* Amorphous yellow powder; $[\alpha]_D$ −7.03°C (*c* 0.37, MeOH); UV λ_{max}(MeOH) nm (log ε): 204 (3.90), 208 (3.91), 232 (3.76), 274 (3.69), 358 (3.18); ^{1}H NMR (300 MHz, CD_3OD): δ 1.52 (3H, *s*, 8-CH_3), 2.42 (3H, *br s*, 9-CH_3), 6.65 (1H, *dq*, *J* = 7.9, 0.8 Hz, H-5), 6.98 (1H, *d*, *J* = 7.9 Hz, H-6); ^{13}C NMR (75.5 MHz, CD_3OD): δ 17.1 (C-9), 22.1 (C-8), 104.9 (C-2), 118.7 (C-3a), 124.0 (C-5), 125.0 (C-6), 130.9 (C-4), 142.6 (C-7), 160.6 (C-7a), 202.6 (C-3); HREIMS *m*/*z* (rel. int.): $[M]^+$ 194.0586 (17, $C_{10}H_{10}O_4$ required 194.0579), 177.0553 (9, $C_{10}H_9O_3$ required 177.0552), 151.0392 (100, $C_8H_7O_3$ required 151.0395), 134.0371 (3, $C_8H_6O_2$ required 134.0368), 123.0445 (12, $C_7H_7O_2$ required 123.0446), 106.0418 (15, C_7H_6O required 106.0419), 77.0390 (15, C_6H_5 required 77.0391).

*3.1.2.3. (3S,4R)-6-Acetyl-3,4-dihydroxy-2,2-dimethylchromane (**3**).* Amorphous powder; $[\alpha]_D$ +39.0°C (*c* 0.42, MeOH); UV λ_{max}(MeOH) nm (log ε): 223 (4.01), 276 (4.07) ; ^{1}H NMR (300 MHz, CD_3OD): δ 1.21 (3H, *s*, 9-CH_3), 1.46 (3H, *s*, 10-CH_3), 2.54 (3H, *s*, 12-CH_3), 3.52 (1H, *d*, *J* = 8.5 Hz, H-3), 4.55 (1H, *d*, *J* = 8.5 Hz, H-4), 6.80 (1H, *d*, *J* = 8.6 Hz, H-8), 7.81 (1H, *dd*, *J* = 8.6, 2.2 Hz, H-7), 8.15 (1H, *d*, *J* = 2.2 Hz, H-5); ^{13}C NMR (50.3 MHz, CD_3OD): 19.7 (C-9), 26.4 (C-12), 27.1 (C-10), 69.6 (C-4), 76.4 (C-3), 81.0 (C-2), 117.9 (C-8), 126.0 (C-4a), 130.7, 131.0 (C-5 and 7), 131.2 (C-6), 158.5 (C-8a), 199.4 (C-11); HREIMS *m*/*z* (rel. int.): $[M]^+$ 236.1044 (64, $C_{13}H_{16}O_4$ required 236.1049), 221.0808 (10, $C_{12}H_{13}O_4$ required 221.0814), 203.0696 (9, $C_{12}H_{11}O_3$ required 203.0708), 178.0621 (16, $C_{10}H_{10}O_3$ required 178.0630), 165.0552 (100, $C_9H_9O_3$ required 165.0552), 149.0241 (62, $C_8H_5O_3$ required 149.0239), 123.0440 (25, C_7H_7O required 123.0446), 105.0339 (7, C_7H_5O required 105.0340), 77.0394 (19, C_6H_5 required 77.0391); CD: $\Delta\varepsilon_{300}$ +0.65 (MeOH, *c* 0.00093 M).

*3.1.2.4. Preparation of diester of **3**.* To a solution of **3** (2.0 mg, 0.0085 mmol) and 4-dimethylaminopyridine (1.0 mg) in pyridine (1.0 ml) and dry CH_2Cl_2 (1.0 ml) was added *p*-nitrobenzoyl chloride (5.9 mg, 0.032 mmol). The reaction mixture was kept at Rt for 2 days, then the mixture was diluted with 15 ml of EtOAc and washed with 8 ml of 5% Na_2CO_3 solution and then with water. The organic layer was separated and the solvent was removed under vacuum. The residue was subjected to preparative TLC with hexane-acetone (1:1). The UV-active zone (R_f 0.55) was extracted with EtOAc to give 3.0 mg (66.2%) of diester **3a** as a colorless solid, $[\alpha]_D$ −56.7° (*c* 0.3, MeOH); UV λ_{max}(MeOH) nm (log ε): 222 sh (4.25), 262 (4.53); ^{1}H NMR (300 MHz, $CDCl_3$): δ 1.51, 1.57 (each 3H, *s*, 9, 10-CH_3), 2.50 (3H, *s*, 12-CH_3), 5.66 (1H, *d*, *J* = 6.1 Hz, H-3), 6.45 (1H, *d*, *J* = 6.1 Hz, H-4), 7.02 (1H, *d*, *J* = 8.3 Hz, H-8), 7.90 (1H, *dd*, *J* = 2.2 Hz, H-5), 7.92 (1H, *dd*, *J* = 8.3, 2.2 Hz, H-7), 8.12–8.28 (8H, *m*); HREIMS *m*/*z* (rel. int.): $[M]^+$ 534.1270 (0.5, $C_{27}H_{22}O_{10}N_2$ required 534.1274); CD: $\Delta\varepsilon_{270}$-9.92, $\Delta\varepsilon_{243}$ +4.10 (MeOH, c 0.00028 M).

*3.1.2.5. (3S,4S)-6-Acetyl-3,4-dihydroxy-2,2-dimethylchromane (**4**).* Amorphous powder; $[\alpha]_D$ −25.6°C (*c* 0.09, MeOH); UV λ_{max} (MeOH) nm (log ε): 202 (4.07), 225 (3.89), 280 (3.95); ^{1}H NMR (300 MHz, CD_3OD): δ 1.29 (3H, *s*, 9-CH_3), 1.47 (3H, *s*, 10-CH_3), 2.54 (3H, *s*,

12-CH_3), 3.73 (1H, *d*, $J=4.0$ Hz, H-3), 4.85 (1H, *d*, $J=4.0$ Hz, H-4), 6.80 (1H, *d*, $J=8.6$ Hz, H-8), 7.81 (1H, *dd*, $J=8.6$, 2.1 Hz, H-7), 8.18 (1H, *d*, $J=2.1$ Hz, H-5); ^{13}C NMR (75.5 MHz, CD_3OD): δ 24.8, 25.0 (C-9 and 10), 26.3 (C-12), 65.7 (C-4), 72.1 (C-3), 80.3 (C-2), 117.7 (C-8), 124.4 (C-4a), 130.5, 131.3 (C-5 and 7), 131.1 (C-6), 160.0 (C-8a), 199.5 (C-11); HREIMS *m*/*z* (rel. int.): $[M]^+$ 236.1045 (56, $C_{13}H_{16}O_4$ required 236.1048), 221.0814 (6, $C_{12}H_{13}O_4$ required 221.0814), 203.0703 (4, $C_{12}H_{11}O_3$ required 203.0708), 178.0627 (11, $C_{10}H_{10}O_3$ required 178.0630), 165.0548 (100, $C_9H_9O_3$ required 165.0552), 149.0233 (63, $C_8H_5O_3$ required 149.0238), 123.0445 (21, C_7H_7O required 123.0446), 105.0340 (4, C_7H_5O required 105.0340), 77.0390 (16, C_6H_5 required 77.0391); CD: $\Delta\varepsilon_{285}$ −0.56 (MeOH, *c* 0.00076 M).

*3.1.2.6. Preparation of diester of **4***. To a solution of **4** (0.5 mg, 0.0021 mmol) and 4-dimethylaminopyridine (0.5 mg) in pyridine (0.5 ml) and dry CH_2Cl_2 (0.5 ml) was added *p*-nitrobenzoyl chloride (1.5 mg, 0.0081 mmol). The reaction mixture was kept at Rt for 2 days. The crude product was purified by preparative TLC with hexane-acetone (1:1) (R_f 0.56) to give 1.0 mg (88%) of diester **4a** as a colorless solid, $[\alpha]_D$ −58.9°C (*c* 0.09, MeOH); UV λ_{max}(MeOH) nm (log ε): 225 *sh* (4.00), 261 (4.27); ^{1}H NMR (300 MHz, $CDCl_3$): δ 1.54, 1.56 (each 3H, *s*, 9,10-CH_3), 2.52 (3H, *s*, 12-CH_3), 5.75 (1H, *d*, $J=4.2$ Hz, H-3), 6.55 (1H, *d*, $J=4.2$ Hz, H-4), 7.04 (1H, *d*, $J=8.2$ Hz, H-8), 7.92–8.22 (10H, *m*); HREIMS *m*/*z* (rel. int.): $[M]^+$ 534.1243 (2, $C_{27}H_{22}O_{10}N_2$ required 534.1274); CD: $\Delta\varepsilon_{275}$-9.89, $\Delta\varepsilon_{250}$ +5.39 (MeOH, *c* 0.00034 M).

*3.1.2.7. Trans-6-(1-hydroxyethyl)-3,4-dihydroxy-2,2-dimethylchromane (**5**)*. Amorphous powder; $[\alpha]_D$ +13.3°C (*c* 0.12, MeOH); UV λ_{max}(MeOH) nm (log ε): 227 (3.77), 280 (3.19), 287 (3.17); ^{1}H NMR (300 MHz, CD_3OD): δ 1.16 (3H, *s*, 9-CH_3), 1.41 (3H, *s*, 10-CH_3), 1.41 (3H, *d*, $J=6.5$ Hz, 12-CH_3), 3.50 (1H, *d*, $J=8.5$ Hz, H-3), 4.55 (1H, *d*, $J=8.5$ Hz, H-4), 4.76 (1H, *q*, $J=6.5$ Hz, H-11), 6.675 (1/3H, *d*, $J=8.4$ Hz, H-8), 6.68 (2/3H, *d*, $J=8.4$ Hz, H-8), 7.14 (1/3H, *dd*, $J=8.4$, 2.2 Hz, H-7), 7.15 (2/3H, *dd*, $J=8.4$, 2.2 Hz, H-7), 7.44 (1H, *m*, H-5); ^{13}C NMR (125.7 MHz, CD_3OD): δ 19.3 (C-9), 25.37, 25.43 (C-12), 27.15, 27.18 (C-10), 70.30, 70.31, 70.59, 70.64 (C-4 and C-11), 77.1 (C-3), 79.6 (C-2), 117.4, 117.5 (C-8), 125.4 (C-4a), 126.3, 126.5, 127.2, 127.4 (C-5 and C-7), 139.5 (C-6), 152.9 (C-8a); HREIMS *m*/*z* (rel. int.): $[M]^+$ 238.1203 (59, $C_{13}H_{18}O_4$ required 238.1205), 223.0968 (33, $C_{12}H_{15}O_4$ required 223.0970), 167.0709 (82, $C_9H_{11}O_3$ required 167.0708), 151.0396 (100, $C_8H_7O_3$ required 151.0395), 149.0604 (69, $C_9H_9O_2$ required 149.0603), 123.0446 (25, $C_7H_7O_2$ required 123.0446), 95.0497 (21, C_6H_7O required 95.0497), 77.0392 (26, C_6H_5 required 77.0391).

Acknowledgements

The financial support from the Natural Sciences and Engineering Research Council of Canada and from Agriculture and Agri-Food Canada is gratefully acknowledged.

References

Ayer, W.A., Craw, P.A., Neary, J., 1992. Metabolites of the fungus *Arthtropsis truncata*. Can. J. Chem. 70 (5), 1338–1347.

Budge, S.P., McQuilken, M.P., Fenlon, J.S., Whipps, J.M., 1995. Use of *Coniothyrium minitans* and *Gliocladium virens* for biological control of *Sclerotinia sclerotiorum* in glasshouse lettuce. Biol. Control 5 (4), 513–522.

Harada, N., Nakanishi, K., 1983. Circular Dichroic Spectroscopy. University Science Books, CA.

Herz, W., Kulanthaivel, P., 1984. Chromans from *Helianthella quinquenervis*. Phytochemistry 23 (2), 435–437.

Huang, H.C., 1980. Control of sclerotinia wilt on sunflower by hyperparasites. Can. J. Plant Pathol. 2 (1), 26–32.

Huang, H.C., 1981. Distribution of *Cobiothyrium minitans* in Manitoba sunflower fields. Can. J. Plant Pathol. 3 (4), 219–222.

Huang, H.C., Hoes, J.A., 1976. Penetration and infection of *Sclerotinia sclerotiorum* by *Coniothyrium minitans*. Can. J. Bot. 54 (5), 406–410.

Huang, H.C., Kokko, E.G., 1987. Ultrastructure of hyperparasitism of *Coniothyrium minitans* on sclerotia of *Sclerotinia sclerotiorum*. Can. J. Bot. 65 (11), 2483–2489.

Huang, H.C., Kokko, E.G., 1988. Penetration of hyphae of *Sclerotinia sclerotiorum* by *Coniothyrium minitans* without the formation of appressoria. Phytopathol. Zeit. 123 (1), 133–139.

Jennings, R.C., 1982. Synthesis, resolution and absolute configuration of the diol metabolites of precocene I. Tetrahedron Lett. 23 (26), 2693–2696.

Jones, D., Gordon, A.H., Bacon, J.S.D., 1974. Co-operative action by endo- and exo-beta-(1,3)-glucanases from parasitic fungi in the degradation of cell-wall glucans of *Sclerotinia sclerotiorum*. Biochem. J. 140 (1), 47–55.

Purdy, L.H., 1979. *Sclerotinia sclerotiorum*: History, diseases, symptomatology, host range, geographic distribution, and impact. Phytopathology 69 (8), 875–880.

PERGAMON

Phytochemistry 58 (2001) 179–183

PHYTOCHEMISTRY

www.elsevier.com/locate/phytochem

Cytotoxic 7,20-epoxy *ent*-kauranoids from *Isodon xerophilus*

Ai-Jun Hou[a], Qin-Shi Zhao[a], Ma-Lin Li[b], Bei Jiang[a], Zhong-Wen Lin[a], Han-Dong Sun[a,*], Yi-Ping Zhou[b], Yang Lu[c], Qi-Tai Zheng[c]

[a]*Laboratory of Phytochemistry, Kunming Institute of Botany, Academia Sinica, Kunming 650204, Yunnan, People's Republic of China*
[b]*Yunnan Laboratory of Pharmacology for Natural Products, Kunming Medical College, Kunming 650031, Yunnan, People's Republic of China*
[c]*Institute of Materia Medica, Chinese Academy of Medical Sciences, Beijing 100050, People's Republic of China*

Received 12 October 2000; received in revised form 1 February 2001

Abstract

Four 7,20-epoxy *ent*-kaurane diterpenoids, xerophilusins G (**1**) and I–K (**2**–**4**), were isolated from the leaves of *Isodon xerophilus*, along with four known ones, enanderianin C (**5**), rosthorin A (**6**), longikaurin B (**7**), and rabdoternin D (**8**). Their structures were determined primarily using NMR spectroscopic techniques. The structure and stereochemistry of **3** were confirmed by X-ray crystallography. Compounds **4** and **7** exhibited broad cytotoxicity against four kinds of human tumor cells (K562, HL-60, HCT, and MKN-28 cells) in the range of 2.23–15.35 and 0.30–8.61 μg/ml, respectively. © 2001 Elsevier Science Ltd. All rights reserved.

Keywords: *Isodon xerophilus*; Labiatae; *ent*-Kaurane diterpenoids; Xerophilusins G, I–K

1. Introduction

In the course of searching for biologically active diterpenoids from *Isodon* species, we have discovered a series of *ent*-kaurane diterpenoids with antitumor activity from *Isodon xerophilus* (C.Y. Wu and H.W. Li) H. Hara (Labiatae) (Hou et al., 2000). Continuing phytochemical investigation on this plant led to the isolation of four new 7,20-epoxy *ent*-kauranoids, xerophilusins G (**1**) and I–K (**2**–**4**), along with four known ones, enanderianin C (**5**) (Wang et al., 1998a), rosthorin A (**6**) (Li and Wang, 1984), longikaurin B (**7**) (Takeda et al., 1988) and rabdoternin D (**8**) (Takeda et al., 1994). Compounds **1**, **2**, and **5** are three of a few compounds having 1β substituents (Wang et al., 1997, 1998b). Compounds **1**–**7** were tested for their cytotoxicity toward K562, HL-60, HCT, and MKN-28 cells. This paper describes the structural characterization of **1**–**4** and the biological evaluation of **1**–**7**.

2. Results and discussion

After chromatographic purification on silica gel, the EtOAc soluble portion of the Me_2CO extract of *I. xerophilus* yielded four new diterpenoids, xerophilusins G (**1**) and IK (**2**–**4**), as well as four known ones, enanderianin C (**5**), rosthorin A (**6**), longikaurin B (**7**) and rabdoternin D (**8**).

Xerophilusin G (**1**), colorless needles, had a molecular formula of $C_{22}H_{30}O_8$ established by positive HRFABMS (obsd 423.1955, calc. 423.2019). Its UV (λ_{max} at 237.5 nm), IR (ν_{max} at 1704 and 1642 cm^{-1}), and NMR [^1H NMR δ 6.21 and 5.44 (each 1H, *s*); ^{13}C NMR δ 209.3 (*s*), 152.9 (*s*), and 119.6 (*t*)] spectra showed an *exo*-methylene group conjugated with a carbonyl group on a five-membered ring. In addition, the ^{13}C NMR and DEPT spectra exhibited signals of an acetoxyl group [δ 170.9 (*s*) and 20.8 (*q*)], one methyl, six methylenes (including two oxygenated ones), six methines (including three oxygen-bearing ones), and four quaternary carbons (including a ketalic group at δ 98.9). These facts and the degree of unsaturation indicated the presence of a pentacyclic ring system. Considering the types of diterpenoids in the *Isodon* genus (Takeda et al., 1992; Wang et al., 1998b), the basic skeleton of **1** was considered to be 7β-hydroxy-7α, 20-epoxy-*ent*-kaur-16-en-15-one, which was substituted by three hydroxyl and one acetoxyl groups.

One oxygenated group was possibly at C-19 because only one methyl at δ 27.6 (Me-18) was observed. The methylene at δ 67.2 (C-19) and the correlation between Ha,b-19 and the ester carbonyl at δ 170.9 in HMBC spectrum proved the acetoxyl group at C-19. The signals at δ 3.63 (1H, *br s*) and δ 64.6 (*d*) and the downfield

* Corresponding author. Tel.: +86-871-5150660; fax: +86-871-5216343.
E-mail address: hdsun@mail.kib.ac.cn (H.-D. Sun).

0031-9422/01/$ - see front matter © 2001 Elsevier Science Ltd. All rights reserved.
PII: S0031-9422(01)00164-9

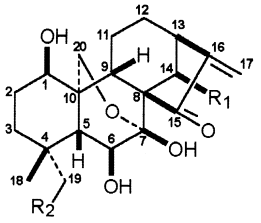

1: R_1 = OH, R_2 = OAc
2: R_1 = H, R_2 = H
5: R_1 = H, R_2 = OAc

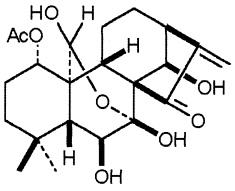

3

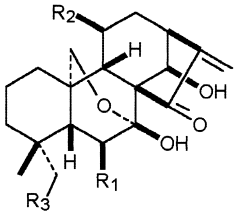

4: R_1 = OH, R_2 = OAc, R_3 = H
6: R_1 = OH, R_2 = OH, R_3 = H
7: R_1 = OH, R_2 = H, R_3 = OAc
8: R_1 = OAc, R_2 = OH, R_3 = H

shift of C-10 in NMR spectra suggested one hydroxyl group at C-1. The broad singlet of H-1 resulted from the β-orientation of 1-OH (Wang et al., 1997). On the basis of ^{1}H–^{1}H COSY and HMQC spectra, the other two hydroxyls were assigned to C-6 and C-14. According to the NOE effects (H-6α with Me-18 and Ha-19; H-14α with H-11α and H-20a), the two hydroxyls at C-6 and C-14 both had β-orientation. In conclusion, xerophilusin G (**1**) was elucidated as 1β, 6β, 7β, 14β-tetrahydroxy-19-acetoxy-7α, 20-epoxy-*ent*-kaur-16-en-15-one.

Xerophilusin I (**2**), isolated as an amorphous powder, had a molecular weight of 349.2039 (positive HRFABMS) corresponding to $C_{20}H_{29}O_5$. The difference between **2** and enanderianin C (**5**) was that Me-19 in **2** was unsubstituted, which was explained by the following findings. In the ^{13}C NMR spectrum of **2**, no signals attributed to an acetoxyl group were observed while a methyl signal at δ 23.1 replaced the signal at δ 67.1 (*t*, C-19) in **5**. Furthermore, the signals of C-3 and Me-18 in **2** shifted downfield without the γ-steric compression effect of OAc. A comparison of the ^{1}H NMR spectroscopic data showed that the absence of two AB-type doublets and a 3H singlet of OAc, and the presence of a methyl signal at δ 1.14 (Me-19) were notable characteristics of **2**. Therefore, xerophilusin I (**2**) was identified as 1β, 6β, 7β-trihydroxy-7α, 20-epoxy-*ent*-kaur-16-en-15-one.

Xerophilusin J (**3**), colorless needles, had a molecular formula of $C_{22}H_{30}O_8$ inferred from positive HRFABMS (obsd 423.2007, calc. 423.2019). Its UV, IR and NMR spectroscopic data, and the degree of unsaturation indicated that **3** was a 7β-hydroxy-7α, 20-epoxy-*ent*-kaur-16-en-15-one. The NMR spectra of **3** also suggested the presence of an acetoxy-bearing methine and two secondary hydroxyl groups. Moreover, the signals at δ 6.09 (1H, *s*) and δ 92.9 (*d*) were assigned to a hemiacetal structure at C-20. ^{1}H–^{1}H COSY, HMQC, and HMBC techniques disclosed that the acetoxyl and two hydroxyl groups were located at C-1, C-6 and C-14, respectively. The α-oriented 1-OAc was determined mainly through the peak form (*dd*) and the coupling constants (J = 4.9, 11.5 Hz) of H-1. The β-orientation of 6-OH and 14-OH was determined by the ROESY correlations: H-6α with Me-19; H-14α with H-11α and H-20. The *R* form of C-20 was also defined by the cross peaks of H-20 with H-11α and H-14α in the ROESY spectrum. Thus, xerophilusin J (**3**) was established as 1α-acetoxy-6β, 7β, 14β, 20(*R*)-tetrahydroxy-7α, 20-epoxy-*ent*-kaur-16-en-15-one, which was further confirmed by X-ray crystallographic analysis (Fig. 1).

Xerophilusin K (**4**), $C_{22}H_{30}O_7$ (positive HRFABMS, obsd 407.2061 calc. 407.2070), was isolated as colorless needles. The ^{1}H and ^{13}C NMR spectra of **4** were very similar to those of rosthorin A (**6**) (Li and Wang, 1984). However, observed in the ^{1}H NMR spectrum of **4** were the appearances of a signal due to an acetyl group (δ 2.07) and the downfield shift of the signal assigned to H-11 ($\Delta\delta$ + 0.99 ppm). Accordingly, xerophilusin K (**4**) was presumed as 11-acetylated rosthorin A as verified by the downfield shift of C-11 ($\Delta\delta$ + 3.0 ppm) and the upfield shift of C-9 ($\Delta\delta$ −6.1 ppm) and C-12 ($\Delta\delta$ −4.7 ppm) in the ^{13}C NMR spectrum of 4. Consequently, xerophilusin K (**4**) was assigned as 6β, 7β, 14β-trihydroxy-11β-acetoxy-7α,20-epoxy-*ent*-kaur-16-en-15-one.

Compounds **1**–**7** were examined for their cytotoxicity against four kinds of human tumor cells. From Table 1, it is noticeable that most of these compounds were more cytotoxic against K562, HL-60, and MKN-28 cells than HCT cells. The IC_{50} values of **4** and **7** against four kinds of tumor cells were all less than 16 μg/ml (2.23–15.35 and 0.30–8.61 μg/ml, respectively), indicating their broad cytotoxic activity. Compounds **2**, **3** and **5** exhibited significant inhibitory effects on K562, HL-60, and MKN-28

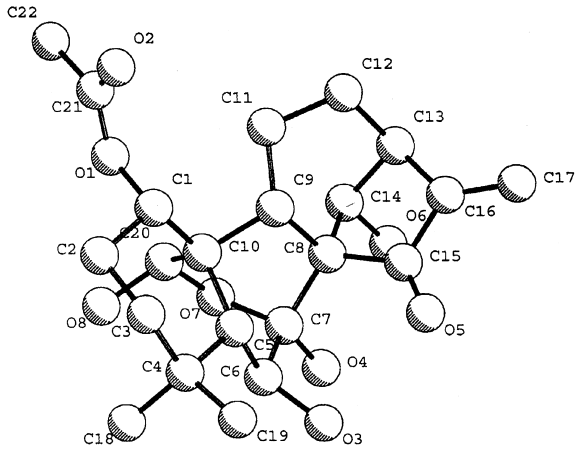

Fig. 1. Stereostructure of **3**.

cells with IC_{50} values lower than 5 μg/ml. However, they were inactive to HCT cells. Compound **1** was non-cytotoxic against K562, HCT, and MKN-28 cells, but it had the selectivity on HL-60 cells (IC_{50} = 3.93 μg/ml).

3. Experimental

3.1. General

All melting points were measured on an XRC-1 micro melting point apparatus and are uncorrected. Optical rotations were taken on a SEPA-300 polarimeter. IR spectra were measured on a Bio-Rad FTS-135 spectrometer with KBr pellets. UV spectra were obtained on a UV 210A spectrometer. MS were recorded on a VG Auto Spec-3000 spectrometer. 1D- and 2D-NMR spectra were run on a Bruker AM-400 and DRX-500 instrument with TMS as internal standard, respectively.

3.2. Plant material

The leaves of *I. xerophilus* were collected in Yuanyang prefecture of Yunnan Province in November 1998, and air-dried. The identity of plant material was verified by Professor Zhong-Wen Lin, and a voucher specimen (KIB 98-11-25 Lin) is deposited in the Herbarium of the Department of Taxonomy, Kunming Institute of Botany, Academia Sinica.

3.3. Extraction and isolation

The dried and powdered leaves (8.3 kg) were extracted with 70% ag. Me_2CO and filtered. The filtrate was concentrated and extracted with EtOAc and *n*-BuOH, successively. A portion (440 g) of the EtOAc extract (660 g) was applied to a Si gel column eluting with a $CHCl_3$–Me_2CO (1:0–0:1) gradient system to yield fractions I–VII. All fractions were collected and combined by monitoring with TLC. From fraction VI, **6** (1.1 g) was obtained as colorless needles by recrystallization in MeOH. The mother liquor was applied to MCI-gel CHP-20P column chromatography developing with MeOH–H_2O (6:4–9:1). The elute from MeOH–H_2O (8:2) was further purified by a Si gel column (petroleum ether–ether 7:3) to produce five fractions (combined by monitoring with TLC). Purification of the second fraction, using petroleum ether–isopropyl alcohol (4:1) on a Si gel column, gave **1** (3.3 g), **2** (35 mg), and **4** (88 mg). The third fraction afforded **3** (76 mg) and **5** (141 mg) after repeated Si gel column chromatography (petroleum ether–EtOAc 3:2; $CHCl_3$–Me_2CO 9:1) and recrystallization in MeOH. Fraction VII was fractionated by a combination of Si gel column chromatography and recrystallization to give **7** (260 mg) and **8** (98 mg).

Table 1
Antitumor properties of compounds **1**–**7**

Compound	M.W.	IC_{50} (μg/ml)			
		K562	HL-60	HCT	MKN-28
1	422	138.84	3.93	ND[a]	ND
2	348	2.75	0.19	ND	0.07
3	422	4.26	2.08	ND	1.54
4	406	2.95	2.29	15.35	2.23
5	406	1.17	0.87	52.78	1.86
6	364	5.20	>1000	13.69	0.92
7	406	0.30	0.44	8.61	0.46
Mitoxantrone	444.5	0.29	0.29	1.54	0.02

[a] ND: not determined (if the inhibitory rate was less than 40% within the testing concentration, the IC_{50} value was not calculated).

3.4. Xerophilusin G (*1*)

Colorless needles (MeOH): mp 216–218°C; $[\alpha]_D^{23}$ −116.3 (C_5H_5N,*c* 0.43); UV (MeOH) λ_{max} nm (log ε): 237.5 (3.94); IR (KBr) ν_{max} cm^{-1}: 3484, 2950, 2893, 1730, 1704, 1642, 1404, 1375, 1250, 1189, 1091; ^1H NMR (C_5D_5N, 400 MHz) δ 6.21 (1H, *s*, H-17a), 5.44 (1H, *s*, H-17b), 5.21 (1H, *s*, H-14α), 4.78 (1H, ABd, *J* = 11.2 Hz, H-19a), 4.47 (1H, ABd, *J* = 11.2 Hz, H-19b), 4.44 (1H, *d*, *J* = 5.9 Hz, H-6α), 4.22 (1H, ABd, *J* = 10.1 Hz, H-20a), 4.14 (1H, ABd, *J* = 10.1 Hz, H-20b), 3.63 (1H, *br s*, H-1α), 3.17 (1H, *d*, *J* = 9.4 Hz, H-13α), 2.66 (1H, *dd*, *J* = 5.9, 12.5 Hz, H-9β), 2.37 (1H, overlap, H-12α), 2.34 (1H, *d*, *J* = 5.9 Hz, H-5β), 2.11 (1H, *m*, H-11β), 2.05 (1H, *dd*, *J* = 5.4, 13.6 Hz, H-3α), 1.99 (3H, *s*, OAc), 1.90 (1H, *m*, H-11α), 1.77 (2H, overlap, H-2α,β), 1.67 (1H, *d*, *J* = 13.6 Hz, H-3β), 1.53 (1H, *m*, H-12β), 1.43 (3H, *s*, Me-18); ^{13}C NMR data, see Table 2; EIMS *m*/*z* (rel. int):

Table 2
^{13}C NMR spectroscopic data for compounds **1**–**4** in C_5D_5N (100 MHz, δ in ppm)

Carbon	**1**	**2**	**3**	**4**
1	64.6 *(d)*	64.8 *(d)*	77.3 *(d)*	29.2 *(t)*
2	27.4 *(t)*	27.6 *(t)*	26.5 *(t)*	18.9 *(t)*
3	28.6 *(t)*	34.5 *(t)*	40.0 *(t)*	41.3 *(t)*
4	37.8 *(s)*	34.2 *(s)*	33.1 *(s)*	34.1 *(s)*
5	56.6 *(d)*	56.4 *(d)*	60.1 *(d)*	60.8 *(d)*
6	73.6 *(d)*	74.7 *(d)*	74.8 *(d)*	73.7 *(d)*
7	98.9 *(s)*	96.4 *(s)*	99.7 *(s)*	98.3 *(s)*
8	62.3 *(s)*	59.9 *(s)*	62.9 *(s)*	62.1 *(s)*
9	48.0 *(d)*	46.0 *(d)*	55.3 *(d)*	54.8 *(d)*
10	41.3 *(s)*	41.4 *(s)*	44.2 *(s)*	37.9 *(s)*
11	16.3 *(t)*	16.3 *(t)*	20.1 *(t)*	64.7 *(d)*
12	30.3 *(t)*	30.0 *(t)*	30.9 *(t)*	37.4 *(t)*
13	44.0 *(d)*	35.3 *(d)*	43.4 *(d)*	43.7 *(d)*
14	74.0 *(d)*	27.0 *(t)*	73.0 *(d)*	73.7 *(d)*
15	209.3 *(s)*	211.0 *(s)*	209.6 *(s)*	208.2 *(s)*
16	152.9 *(s)*	154.2 *(s)*	153.2 *(s)*	151.4 *(s)*
17	119.6 *(t)*	116.2 *(t)*	119.9 *(t)*	120.6 *(t)*
18	27.6 *(q)*	33.7 *(q)*	35.7 *(q)*	33.3 *(q)*
19	67.2 *(t)*	23.1 *(q)*	23.4 *(q)*	22.4 *(q)*
20	66.7 *(t)*	66.0 *(t)*	92.9 *(d)*	66.8 *(t)*
OAc	170.9 *(s)*	–	170.4 *(s)*	169.9 *(s)*
	20.8 *(q)*	–	21.5 *(q)*	21.2 *(q)*

422 $[M]^+$ (85), 404 $[M–H_2O]^+$ (10), 362 $[M–AcOH]^+$ (100), 344 $[M–AcOH–H_2O]^+$ (11), 326 (6), 313 (11), 298 (7), 267 (9), 255 (6), 241 (12); positive HRFABMS *m/z*: 423.1955 (calc. for $C_{22}H_{31}O_8$, 423.2019).

3.5. Xerophilusin I (**2**)

White amorphous powder: $[\alpha]_D^{23}$ −146.3 (C_5H_5N,*c* 0.41); UV (MeOH)λ_{max} nm (log ε): 240.5 (3.98); IR (KBr) ν_{max} cm^{-1}: 3464, 3359, 3233, 2930, 1707, 1642, 1453, 1333, 1274, 1193, 1061; ^1H NMR (C_5D_5N, 400 MHz) δ 5.94 (1H, *s*, H-17a), 5.24 (1H, *s*, H-17b), 4.31 (1H, *d*, *J* = 5.1 Hz, H-6α), 4.12 (1H, ABd, *J* = 9.8 Hz, H-20a), 4.08 (1H, ABd, *J* = 9.8 Hz, H-20b), 3.66 (1H, *br s*, H-1α), 2.92 (1H, *dd*, *J* = 3.8, 9.2 Hz, H-13α), 2.53 (1H, *dd*, *J* = 3.8, 12.2 Hz, H-14β), 2.51 (1H, *dd*, *J* = 5.3, 12.5 Hz, H-9β), 2.38 (1H, *d*, *J* = 12.2 Hz, H-14α), 2.21 (1H, *m*, H-3α), 2.13 (1H, *d*, *J* = 5.1 Hz, H-5β), 2.12 (1H, overlap, H-12α), 2.11 (1H, overlap, H-11β), 1.86 (1H, *m*, H-11α), 1.74 (2H, *m*, H-2α,β), 1.36 (1H, *m*, H-12β), 1.30 (3H, *s*, Me-18), 1.22 (1H, *d*, *J* = 13.2 Hz, H-3β), 1.14 (3H, *s*, Me-19); ^{13}C NMR data, see Table 2; EIMS *m/z* (rel. int): 348 $[M]^+$ (100), 330 $[M–H_2O]^+$ (36), 320 (5), 312 $[M-2\times H_2O]^+$ (24), 297 (21), 284 (30), 269 (46), 256 (32), 243 (37); positive HRFABMS *m/z*: 349.2039 (calc. for $C_{20}H_{29}O_5$, 349.2015).

3.6. Xerophilusin J (**3**)

Colorless needles (MeOH): mp 165–166°C; $[\alpha]_D^{23}$ −80.7 (C_5H_5N,*c* 0.41); UV (MeOH) λ_{max} nm (log ε): 232.5 (3.47); IR (KBr) ν_{max} cm^{-1}: 3430, 2951, 1733, 1643, 1459, 1374, 1245, 1084, 1037; ^1H NMR (C_5D_5N, 400 MHz) δ 6.28 (1H, *s*, H-17a), 6.09 (1H, *s*, H-20), 5.50 (1H, *s*, H-17b), 5.17 (1H, *s*, H-14α), 4.95 (1H, *dd*, *J* = 4.9, 11.5, H-1β), 4.68 (1H, *m*, H-6α), 3.12 (1H, *d*, *J* = 9.3 Hz, H-13α), 2.39 (1H, *m*, H-2α), 2.27 (1H, *m*, H-12α), 2.01 (1H, overlap, H-9β), 1.99 (3H, *s*, OAc), 1.94 (1H, *m*, H-11α), 1.92 (1H, *m*, H-2β), 1.73 (1H, *d*, *J* = 9.3 Hz, H-5β), 1.53 (3H, *s*, Me-19), 1.43 (1H, overlap, H-12β), 1.43 (3H, *s*, Me-18), 1.42 (2H, overlap, H-3α,β), 1.41 (1H, overlap, H-11β); ^{13}C NMR data, see Table 2; EIMS *m/z* (rel. int): 422 $[M]^+$ (2), 404 $[M–H_2O]^+$ (18), 386 $[M-2\times H_2O]^+$ (4), 371 (1), 362 $[M–AcOH]^+$ (7), 344 $[M–AcOH–H_2O]^+$ (72), 326 (26), 315 (33), 298 (61), 280 (39), 269 (67); positive HRFABMS *m/z*: 423.2007 (calc. for $C_{22}H_{31}O_8$, 423.2019).

3.7. Xerophilusin K (**4**)

Colorless needles (MeOH): mp 189–190°C; $[\alpha]_D^{23}$ −44.3 (C_5H_5N,*c* 0.30); UV (MeOH) λ_{max} nm (log ε): 237.5 (3.79); IR (KBr) ν_{max} cm^{-1}: 3445, 2931, 1734, 1642, 1372, 1247, 1178, 1090, 1019; ^1H NMR (C_5D_5N, 400 MHz) δ 6.31 (1H, *s*, H-17a), 5.56 (1H, *s*, H-17b), 5.41 (1H, *m*, H-11α), 5.14 (1H, *s*, H-14α), 4.19 (1H, *d*, *J* = 5.8 Hz, H-6α), 4.17 (1H, ABd, *J* = 10.3 Hz, H-20a), 4.07 (1H, ABd, *J* = 10.3 Hz, H-20b), 3.18 (1H, *d*, *J* = 9.0 Hz, H-13α), 3.15 (1H, *m*, H-12α), 2.15 (1H, *d*, *J* = 9.3 Hz, H-9β), 2.07 (3H, *s*, OAc), 1.52 (1H, *m*, H-12β), 1.50 (1H, *d*, *J* = 5.8 Hz, H-5β), 1.34 (1H, *m*, H-3α), 1.29 (1H, overlap, H-1α), 1.26 (2H, *m*, H-2α,β), 1.24 (1H, overlap, H-1β), 1.23 (3H, s, Me-18), 1.11 (1H, *m*, H-3β), 1.05 (3H, *s*, Me-19); ^{13}C NMR data, see Table 2; EIMS *m/z* (rel. int): 406 $[M]^+$ (48), 360 (3), 346 $[M\text{-}AcOH]^+$ (9), 328 $[M\text{-}AcOH\text{-}H_2O]^+$ (8), 315 (3), 285 (6), 257 (7), 215 (10); positive HRFABMS *m/z*: 407.2061 (calc. for $C_{22}H_{31}O_7$ 407.2070).

3.8. X-ray crystallographic analysis of **3**

The compound crystallizes in the monoclinic group $P2_1$, *a* = 6.410 (1) Å, *b* = 11.841 (2) Å, *c* = 14.212 (3) Å, β = 97.34 (1)Å, V = 1069.9 (3) $Å^3$, *Z* = 2 and with the calculated density of 1.367 g/cm^3. The structure was solved by direct methods (SHELXS-86). The final R-factor is 0.087 with R_w 0.090 and *S* 3.108. All measurements were made on a MAC DIP 2030K imaging plate area detector with graphite monochromated Mo–Ka radiation.

3.9. Cytotoxicity against four kinds of human tumor cell

The cytotoxicity assay was performed in a method of MTT, the experimental details of which have been reported previously (Hou et al., 2000).

Acknowledgements

The authors appreciate the assistance of the analytical group in the laboratory of Phytochemistry, Kunming Institute of Botany, Academia Sinica, for the spectral measurements. Crystallographic data for the structure reported in this paper have been deposited with the Cambridge Crystallographic Data Centre. Copies of the data can be obtained, free of charge, on application to the Director, CCDC, 12 Union Road, Cambridge CB2 1EZ, UK (Fax: +44-(0)1223-336033 or e-mail: deposit@ccdc.cam.ac.uk).

References

Hou, A.J., Li, M.L., Jiang, B., Lin, Z.W., Ji, S.Y., Zhou, Y.P., Sun, H.D., 2000. New 7,20:14,20-diepoxy *ent*-kauranoids from *Isodon xerophilus*. J. Nat. Prod. 63 (5), 599–601.

Li, G.Y., Wang, Y.L., 1984. Studies on the diterpenoids of *Rabdosia rosthornii*. Acta Pharmaceutica Sinica 19 (8), 590–592.

Takeda, Y., Fujita, T., Shingu, T., 1988. Structure elucidation of longikaurin A and longikaurin B, new biologically active diterpenoids from *Rabdosia longituba* and chemical conversion of oridonin into dihydrolongikaurin A. J. Chem. Soc. Perkin Trans. I, 379–383.

Takeda, Y., Ikawa, A., Matsumoto, T., Terao, H., Otsuka, H., 1992. Diterpenoids having *ent*-kaurene and *ent*-spiro-*seco*-kaurene skeletons from *Rabdosia longituba*. Phytochemistry 31 (5), 1687–1690.

Takeda, Y., Takeda, K.I., Fujita, T., Sun, H.D., Minami, Y., 1994. Rabdoternins D-G, *ent*-7β,20-epoxykaurenes from *Rabdosia ternifolia*. Phytochemistry 35 (6), 1513–1516.

Wang, J., Lin, Z.W., Shingu, T., Sun, H.D., 1997. Four new compounds from *Isodon eriocalyx*. Chin. Chem. Lett. 8 (7), 603–606.

Wang, Y.H., Chen, Y.Z., Lin, Z.W., Sun, H.D., 1998a. A new 1β-hydroxy-*ent*-kaurenoid from *Isodon enanderianus*. Chin. Chem. Lett. 9 (8), 733–734.

Wang, Y.H., Chen, Y.Z., Lin, Z.W., Sun, H.D., Fan, J.S., 1998b. 7,20-Epoxy-*ent*-kaurenoids from *Isodon enanderianus*. Phytochemistry 48 (7), 1267–1269.

PERGAMON

Phytochemistry 58 (2001) 185–186

PHYTOCHEMISTRY

www.elsevier.com/locate/phytochem

Book reviews

Biochemistry & Molecular Biology of Plants
B.B. Buchanan, W. Gruissem and R.L. Jones (Eds.), American Society of Plant Physiologists. 2000. 1367 pp. ISBN 0-943088-39-9, $100

This is the book we have been waiting for! Whether we are teachers at undergraduate or postgraduate level or researchers trying to attract high calibre graduate students, we have all encountered the same problem no doubt. This is the fact that plant biochemistry has always suffered for being rather a Cinderella subject in the eyes of students doing general biochemistry degrees, with the result that there is often a low enrollment for courses. Perhaps part of the reason for this is the lack of a text book which could sell the subject like many of the sumptuously produced Biochemistry volumes or other volumes such as Alberts et al., *The Molecular Biology of the Cell*. Well here it is at last! Students nowadays have such sophisticated imagery thrown at them all the time through media and the net, so we desperately needed a textbook that was up to these standards of illustration to make the subject attractive. Regrettable but necessary in this day and age, where scholarship alone is insufficient to enthuse. This is not to denigrate the texts that addressed the subject in a general way and that we all know and love; the two Bonner and Varners, Goodwin and Mercer and more recently Harborne and Dey. Indeed, there is a touching connection and reminder that the concept for this volume lay with a third edition of Bonner and Varner before Joe's untimely death and it is nice to see the dedication up front. It is just that we needed a book to get the student hooked in the first place in the 21st century. It is not just at the undergraduate level, of course, at postgraduate it is often difficult to get the best students to take up research in plants — they all want to cure cancer. Then there is a knock-on effect that some of the best students do not subsequently follow careers in plant biochemistry. This Cinderella aspect even persists in certain societies and in journals where plants have a low profile. This was one of the reasons for founding *Phytochemistry* in the first place (J.B. Harborne 2001. Phytochemistry 56, 219–221). Also it is kind of fitting that this book should have been published in the year of the completion and release of the *Arabidopsis* genome. Some sections of the media flagged this up by saying it was the most important genome to be sequenced, even more so than the human genome, since we ultimately depend on plants for our existence. Hopefully this sort of attention may divert more talent towards plants and this is certainly the book to support and encourage that.

My emphasis on appearance should not detract from the fact that this a work of scholarship. Inevitably things cannot be treated in depth and it is acceptable that treatment of controversial subjects has to be compromised. However, the range of subjects and the breadth of treatment is astonishing. This massive undertaking is organised into 24 chapters in 5 parts dealing with compartmentation, cellular dynamics, energy provision, metabolism and the environment and agriculture. All the contributors, including three *Phytochemistry* board members, are first rate experts in their respective fields and have been assisted by a panel of reviewers to produce outstanding chapters. It is a joy to open at any page and pleasing to the eye — I do not think any double page lacks an illustration. The standard of illustrations is simply first class. It would be invidious to select any one chapter, although we will all have our individual favorites. It will also please the phytochemist. There is ample treatment of biochemistry and there is no shortage of biochemical pathways and chemical structures. Biochemistry gets equal treatment with plant physiology and molecular biology. Chapters have a core text with technical, anecdotal and supplementary information being supplied in a familiar "Box" format. It is up-to-date in all specialist areas and excellent as a core reference on any subject in the biochemistry and molecular biology of plants. For the researcher it is also educational and superb for browsing and for catching up on developments outside one's immediate field.

So Bob, Russell and Wilhelm and all the contributors, a huge thank you! You have suddenly made my job one heck of a lot easier! There's one big problem, however, how do we prevent it going "missing"? Perhaps it should be supplied with a chain and a lock!

G. Paul Bolwell
Division of Biochemistry
School of Biological Sciences
Royal Holloway, University of London
Egham, Surrey, TW20 0EX, UK
E-mail address: phytochemistry@rhul.ac.uk

PII: S0031-9422(01)00095-4

Evolution of Metabolic Pathways, Recent Advances in Phytochemistry volume 34
J.T. Romeo, R. Ibrahim, L. Varin and V. de Luca (Eds.), Pergamon Press, Amsterdam, 2000. 480 pp. $222.50. ISBN 0-08-043860-1

This volume of essays is derived from a symposium held by the PSNA in Montreal, Canada and contains 14 contributions on the biosynthetic pathways of secondary metabolites in plants. The book is appropriately dedicated to the memory of Arthur Neish (1916–1972), who pioneered the application of radiolabelled precursors to plant biosynthesis. The most important and admirable feature in many of these chapters is the assembly of comparative data for various key enzymes which are involved in the biosynthesis of many different end products, from alkaloids and flavonoids to stilbenoids and terpenoids. Thus, I. Schröder discusses the functional diversity and evolution of chalcone synthases, while R.A. Kohn and F. Durst cover the multifarious plant cytochrome P450 oxidases. Two-oxo acid-dependent dioxygenases are ably reviewed by A.G. Prescott and the range and diversity of acyl transferases are described by B. St. Pierre and V. de Luca. There are also chapters considering the evolution of glycosyltransferases (T. Vogt) and of methyltransferases (R.K. Ibrahim and I. Muzac). These are all pioneering contributions. A stimulating opening chapter by B.B. Jarvis entitled 'The role of natural products in evolution' sets the scene for these subsequent contributions.

There are further chapters in this volume which are devoted in turn to biosynthetic aspects of phenolics (H.A. Stafford), cyanogenic glycosides (B.L. Moller), terpenoids in conifers (J. Gershenzon) and brassinosteroids (G. Adam). Altogether, this symposium proceedings provides an important summary of our present knowledge on the comparative biochemistry of secondary metabolism in plants. Also, it tells us where we still lack information and where the experiments of the future will be done.

Jeffrey B. Harborne
Department of Botany
The University of Reading
Whiteknight, Reading RG6 6AS, UK

PII: S0031-9422(01)00136-4

Biodiversity: New Leads for the Pharmaceutical and Agrochemical Industries
S.K. Wrigley, M.A. Hayes, R. Thomas, E.J.T. Chrystal and N. Nicholson (Eds.); Proceedings of the International Meeting held 5–8 September 1999 at the University of St. Andrews. Royal Society of Chemistry, Cambridge, 2000, 313 + vi pp. ISBN 0-85404-830-8, £59.50

Biodiversity, its maintenance, management and commercial importance, are currently hot topics, and rightly so. The profile of a publication is thus enhanced if reference to Biodiversity appears in the title. Unfortunately this can lead to a bit of a let down when the reader finds that for the most part the papers included in this publication are really about drug discovery and the role of secondary metabolites, past, present and future.

What I was hoping for, from the title, was encapsulated in the contribution of Reddell and Gordon (CSIRO, Australia) who explored the hypothesis that ecology can provide new leads, hinting at different chemical diversities in different biomes and different ecological strategies. Unfortunately for the most part authors were really discussing chemical diversity which, unfortunately, seems to have come to be considered as synonymous with biodiversity, which it clearly is not.

However, when I recovered from my disappointment and browsed the many chapters on chemical diversity I am pleased to report that the quality was generally good and the various chapters did cover many different types of biota and revealed them to be excellent sources of bioactive leads. As an information source and as part of an argument to convince the doubters of the continued role of natural products in drug discovery this is a useful and worthwhile contribution and I shall be pleased to have it in my own personal library.

There are 21 Chapters that have been divided into six sections: (a) history, diversity and discovery (6 chapters), (b) microbial natural products discovery (3 chapters), (c) marine natural products (3 chapters), plant natural products (4 chapters), biosynthesis (2 chapters) and synthesis (3 chapters). Chapters are well illustrated and typographical errors are rare.

Peter G. Waterman
Centre for Phytochemistry and Phytopharmacology
Southern Cross University
PO Box 157, Lismore, NSM 2480, Australia
E-mail address: pwaterma@scu.edu.au

PII: S0031-9422(01)00155-8

PERGAMON

Phytochemistry 58 (2001) 187–202

PHYTOCHEMISTRY

www.elsevier.com/locate/phytochem

Review

Visible light-dependent degradation of lipidic phytoplanktonic components during senescence: a review

Jean-François Rontani*

Laboratoire d'Océanographie et de Biogéochimie (UMR 6535), Centre d'Océanologie de Marseille (OSU), campus de Luminy case 901, 13288 Marseille, France

Received 27 February 2001; received in revised form 18 April 2001

Abstract

Though most of the organic components of phytoplankton are susceptible to being photodegraded during senescence, until recent years there has been very little research in this area. Recently, however, there have been a renewal of interest, and the heterogeneous visible light-induced degradative reactions of lipidic compounds associated with phytodetritus have been studied. The present paper reviews the results obtained in the course of these studies. In the first part, the production and quenching of excited states of chlorophyll and toxic oxygen species (singlet oxygen, superoxide ion, hydroxyl radical and hydrogen peroxide) in healthy and senescent phytoplanktonic cells are discussed. Then, the photo-oxidation of the main lipidic cell components (chlorophyll, chlorophyll phytyl chain, carotenoids, sterols, unsaturated fatty acids, alkenones and unsaturated alkenes) in senescent phytoplanktonic cells is examined. Emphasis is given to the degradation rates and the mechanisms of visible light-induced degradation of the main lipidic components of phytoplankton and to the structure of the photoproducts formed. In each case, the selectivity of these compounds is discussed in order to select a ''pool'' of photoproducts able to act as tracers of photo-oxidative alterations in the marine medium. This ''pool'' of photoproducts could provide very useful information concerning the physiological state of phytoplanktonic communities and current environmental problems related to ozone depletion. © 2001 Elsevier Science Ltd. All rights reserved.

Keywords: Visible light-induced degradation; Lipids; Phytodetritus; Senescence; Tracers of photo-oxidative alterations

Contents

1. Introduction 188

2. Different photo-oxidation mechanisms 188
   2.1. Direct photo-oxidative reactions 188
   2.2. Indirect photo-oxidative reactions 188

3. The photoprotective system of healthy cells 188

4. The photodynamic effect 189

5. Visible light-dependent photodegradation of the main lipidic components of phytoplankton during senescence 191
   5.1. Chlorophylls 191
   5.2. Carotenoids 193
   5.3. Sterols 194
   5.4. Unsaturated fatty acids 194

* Tel.: +33-4-91-82-96-23; fax: +33-4-82-65-48.
E-mail address: rontani@com.univ-mrs.fr

0031-9422/01/$ - see front matter © 2001 Elsevier Science Ltd. All rights reserved.
PII: S0031-9422(01)00202-3

5.5. Alkenones 198
5.6. Unsaturated hydrocarbons 199

6. Conclusions 199

Acknowledgements 200

References 200

1. Introduction

To date, due to the lack of adequate tracers, the role played by the photochemical processes during the degradation of phytoplankton in the euphotic layer of the oceans has been virtually ignored. Owing to the problem of stratospheric ozone depletion, some studies have recently examined the degradative effects of enhanced UV-B doses on phytoplanktonic lipids (Skerratt et al., 1998). However, photochemical damages in phytoplanktonic cells are not a monopoly of UV radiation (Nelson, 1993). In fact, due to the presence of chlorophylls [which are very efficient photosensitizers (Foote, 1976)], numerous organic components of phytoplankton are susceptible to being photodegraded during senescence by photosynthetically active radiation (PAR) (Rontani et al., 1998).

The present paper reviews this particular aspect of photodegradation processes, i.e. **the heterogeneous visible light-induced degradative reactions associated with phytodetritus**. Emphasis is given to the degradation rates and the mechanisms of visible light-induced degradation of the main lipidic components of phytoplankton and to the structure of the photoproducts formed. In each case, the selectivity of these compounds is discussed in order to select a "pool" of photoproducts able to act as tracers of photo-oxidative alterations in the marine medium.

It is hoped that this short review will stimulate research in this very interesting area and that the questions raised will be answered in the near future.

2. Different photo-oxidation mechanisms

2.1. Direct photo-oxidative reactions

These processes involve light-absorbing entities called chromophores, which undergo oxidative change as a direct consequence of absorbing photons (Zafiriou et al., 1984). In the marine environment, comparatively few natural molecules of known structure can react in this way (carbonyl compounds, thryptophane, thiamine, vitamin B12, pigments, polyunsaturated fatty acids, etc.) (Zafiriou et al., 1984). In contrast, these reactions must play an important role in the photochemistry of coloured complex organic molecules of unknown structure such as humic and fulvic acids (Zafiriou, 1977; Zafiriou et al., 1984).

2.2. Indirect photo-oxidative reactions

Indirect processes are common in natural waters and are particularly important since they can alter molecules that resist direct photo-oxidative reactions, such as transparent species or chromophores whose reactive states are inefficiently populated by absorption (Zafiriou et al., 1984). These reactions involve substances called photosensitizers. These compounds have two systems of electronically excited states, the singlet (^{1}sens) and the triplet (^{3}sens) (Foote, 1976). Most photosensitized oxidations occur by way of a triplet state (Gollnick, 1968). Many dyes, pigments and aromatic hydrocarbons are very effective sensitizers (Foote, 1976). ^{3}Sens can react: either directly with another molecule, to give radicals after hydrogen atom or electron transfer (type I processes) (Gollnick, 1968) (Fig. 1), or with oxygen (type II processes) (Fig. 1). In this case, the excitation is transferred from the sensitizer to the oxygen, to produce an electronically excited singlet state of oxygen ($^1O_2$). Less efficient electron transfer from sensitizer to oxygen can also occur, affording superoxide ion ($O_2^{\bullet -}$) (Foote, 1976).

3. The photoprotective system of healthy cells

The organisation of the pigments in the lipo-protein membranes of the chloroplasts consists of a series of pigment-protein complexes which cooperate together to promote electron flow (Halliwell, 1987).When a chlorophyll molecule absorbs a quantum of light energy, an excited singlet state (^{1}Chl) is formed. In healthy cells the primary route for energy from the ^{1}Chl is the fast reactions of photosynthesis (Foote, 1976). However, a small proportion (less than 0.1%) of ^{1}Chl may undergo intersystem crossing to form the longer live triplet state (^{3}Chl) (Knox and Dodge, 1985) (Fig. 2). ^{3}Chl is not only potentially damaging itself in type I reactions (Knox and Dodge, 1985), but it may also generate toxic oxygen species ($^1O_2$ and $O_2^{\bullet -}$) by reaction with ground state oxygen ($^3O_2$) (Type II processes) (Fig. 1). Formation of an active complex between ^{3}Chl and $^3O_2$ can also oxidize HO^- to the extremely powerful oxidizing agent $HO^{\bullet}$

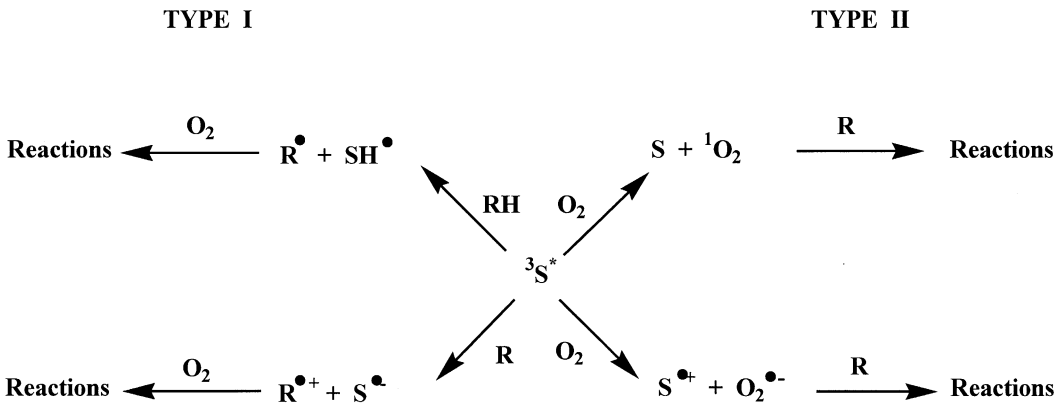

Fig. 1. Reactions of the triplet sensitizer [reprinted from Rontani (1999), with permission from Springer].

(Harbour and Bolton, 1978; Chauvet et al., 1981). Superoxide ion ($O_2^{\bullet -}$) may subsequently disproportionate to $^1O_2$ and hydrogen peroxide (H_2O_2) in the presence of a proton donor [Eqs. (1) and (2)] (Foote, 1976).

$$O_2^{-\bullet} + H^+ \rightleftharpoons HOO^\bullet \quad (1)$$

$$2HOO^\bullet \longrightarrow H_2O_2 + {}^1O_2 \quad (2)$$

In the presence of Fe^{+3}, $O_2^{\bullet -}$ also intereacts with H_2O_2 to give hydroxyl radicals (Haber–Weiss reaction) (Leshem, 1988).

$$O_2^{-\bullet} + H_2O_2 \xrightarrow{Fe^{+3}} HO^\bullet + HO^- + O_2 \quad (3)$$

In view of their susceptibility to oxidative damage, one would expect to find many antioxidant protective mechanisms in chloroplasts. Carotenoids quench ^{3}Chl and $^1O_2$ by energy transfer mechanisms (Fig. 2) at very high rates (Foote, 1976). Tocopherols can remove $^1O_2$, $O_2^{\bullet -}$, $HOO^\bullet$ and $HO^\bullet$ by acting as sacrificial scavengers, these processes resulting in the irreversible oxidation of the tocopherol molecule (Halliwell, 1987). In common with carotenoids, tocopherols and ascorbic acids are also efficient physical deactivators (i.e. "quenchers") of $^1O_2$ (Halliwell, 1987). Superoxide dismutase enzyme (SOD) and ascorbic acid may also scavenge $O_2^{\bullet -}$ (Halliwell, 1987), while catalase activity by virtue of its lowering H_2O_2 levels provides less substrate for $HO^\bullet$ in the Haber–Weiss reaction (Leshem, 1988).

4. The photodynamic effect

As we can see in Section 3, in healthy cells the primary route for energy from the ^{1}Chl is the fast reactions of photosynthesis. In senescent phytoplanktonic cells this pathway would not be functional; thus an accelerated rate of formation of ^{3}Chl would be expected (Nelson, 1993). The rate of formation of ^{3}Chl and toxic oxygen species ($^1O_2$, $O_2^{\bullet -}$, $HO^\bullet$, H_2O_2) might then exceed the quenching capacity of the photoprotective system and photodegradation can occur (Merzlyak and Hendry, 1994) (Fig. 3). In phytodetritus, when the ordered structure of

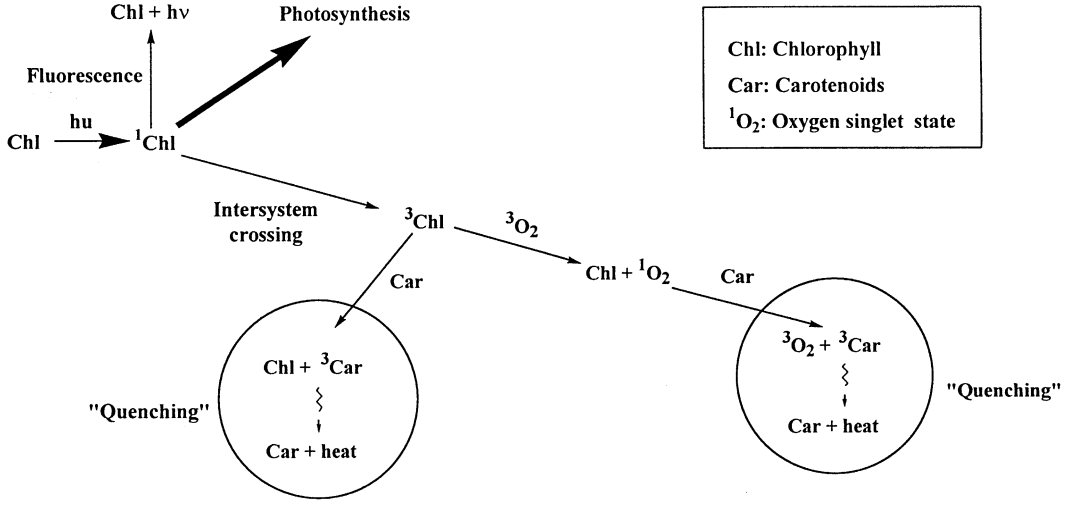

Fig. 2. Potential pathways for chlorophyll excitation energy in healthy phytoplanktonic cells (simplified scheme taking into account only the involvement of singlet oxygen).

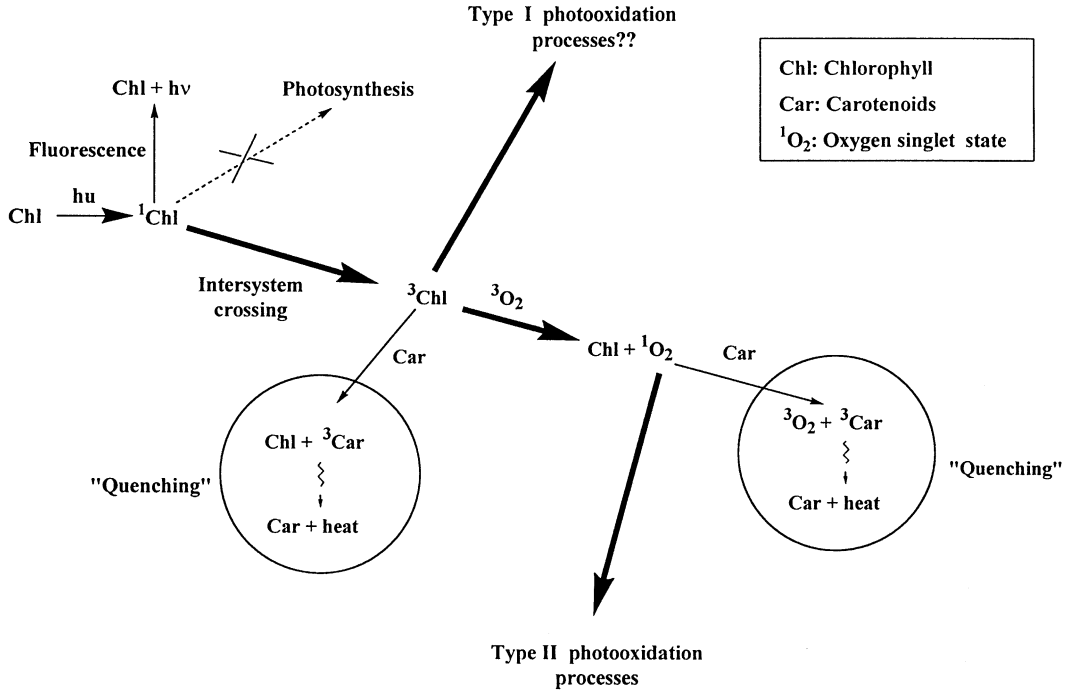

Fig. 3. Potential pathways for chlorophyll excitation energy in senescent phytoplanktonic cells (simplified scheme taking into account only the involvement of singlet oxygen).

Table 1
Calculated rate constants for light-dependent degradation of lipid components in killed cell experiments at 20°C

	Chlorophyll-*a*	Chlorophyll-*b*	β-Carotene	Phytol	Sterols	Unsaturated fatty acids			*n*-Alkenones		*n*-Alkenes mono, di and tri-unsaturated		
						$C_{18:1}$	$C_{18:2}$	$C_{18:3}$	$C_{37:2}$	$C_{37:3}$	C_{37}–C_{38}	C_{31}–C_{33}	C_{17}–C_{29}
Dunaliella tertiolecta	0.34[a,h]	0.26[a,h]	0.37[b,h]	0.08[a,h]									
	0.19[b,h]	0.12[b,h]		0.03[c,h]									
Dunaliella sp.				0.05[d,h]	0.03[d,h,j]	0.05[d,h]	0.13[d,h]	0.32[d,h]					
Phaeodactylum tricornutum	0.56[c,h]			0.15[d,i]	0.01[d,h]	0.03[d,h]	0.06[d,h]						
				0.16[c,i]									
Skeletonema costatum	0.37[a,h]		0.43[b,h]	0.10[a,h]	0.09[e,h,j]								
	0.29[b,h]												
Emiliania huxleyi PC 221	0.47[a,h]			0.12[a,h]	0.02[f,h]				0.002[f,h]	0.003[f,h]			
Emiliania huxleyi CS 57									0[g,k]	0[g,k]	0[g,k]	0.3 — 0.8[g,i]	
Thalassiosira rotula	0.31[a,h]			0.09[a,h]									
Nannochloropsis salina													⩽0.25[g,i]

[a] Cuny et al., 1999.
[b] Nelson, 1993.
[c] Rontani et al., 1995.
[d] Rontani et al., 1998.
[e] Rontani et al., 1997a.
[f] Rontani et al., 1997b.
[g] Mouzdahir et al., 2001.
[h] First-order kinetic (mol^{-1} m^2).
[i] Second-order kinetic (μmol^{-1} 1 mol^{-1} m^2).
[j] Mean values.
[k] No significant degradation.

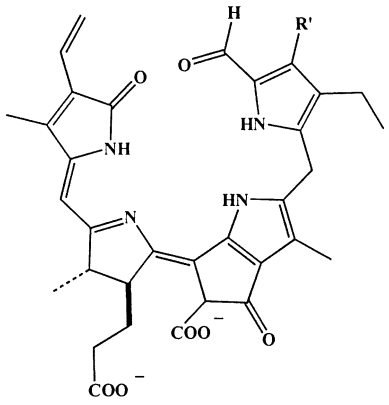

1a: (R = CH_3)
1b: (R = CHO)

Fig. 4. Red bilin derivative detected in the algae *Chlorella protothecoides*.

the thylakoid membranes has been disrupted, pigments tend to remain associated with other hydrophobic cellular components such as membrane lipids (Nelson, 1993). The photo-oxidative effect of chlorophyll sensitization might be strongly amplified within such a hydrophobic micro-environment. Moreover, the lifetime of $^1O_2$ produced from sensitizers in a lipid-rich hydrophobic environment could be longer, and its potential diffusive distance greater, than if produced by sensitizers in aqueous solution (Suwa et al., 1977).

5. Visible light-dependent photodegradation of the main lipidic components of phytoplankton during senescence

5.1. Chlorophylls

Irradiation of killed phytoplanktonic cells by the light used for their growth results in rapid degradation of chlorophylls (Nelson, 1993; Rontani et al., 1995). The light-dependent degradation rates obtained in detrital chlorophytes and diatoms showed a good fit to first-order kinetics (Table 1). The photochemical degradation of chlorophylls has so far been studied almost exclusively with respect to the porphyrin moiety of the molecule, which is the more reactive. In the older literature, light and oxygen were considered as essential for the degradation of the chlorophyll macrocycle in living organisms (Hendry et al., 1987). From the present point of view, this dogma must be called into question since enzymatic degradation of chlorophyll in bleaching cells of algae also takes place in darkness (Engel et al., 1991; Kräutler et al., 1991). It was postulated that these enzymes degrade chlorophyll because the senescent cells must try to eliminate dangerous photodynamic molecules which are liberated upon the mobilisation of the corresponding apoproteins (Gossauer and Engel, 1996). There is a great deal known about the structure of the photoproducts of the chlorophyll tetrapyrrolic structure, probably due to the instability of these substances (Merzlyak and Hendry, 1994). Recently, the 19-formyl-1[21*H*,22*H*]bilinone derivatives **1a** and **1b** (Fig. 4) have been identified in senescent cells of the microalgae *Chlorella protothecoides* (Engel et al., 1991; Iturraspe et al., 1994). These compounds represent the first examples of natural products whose structure corresponds to those of the in vitro photo-oxidation products of chlorophyll macrocycle (Fuhrhop et al., 1974). Unfortunately, enzymatic degradation of chlorophyll yields similar products (Gossauer and Engel, 1996) (Fig. 5). Despite some recent progress regarding intermediary photoproducts, no stable and specific markers of the chlorophyll macrocycle photodegradation could be characterised.

The isoprenoid phytyl side-chain of chlorophyll, which is generally considered to be the major source of acyclic isoprenoids with twenty or fewer carbon atoms in the biosphere (Volkman and Maxwell, 1986), is also sensitive to photochemical processes. In fact, in phytodetritus the visible light-dependent degradation rates were only 3–4 times higher for the chlorophyll tetrapyrrolic structure than for its phytyl side-chain (Table 1). It was previously demonstrated that the photosensitized oxidation (involving $^1O_2$) of the phytol moiety of chlorophyll-*a* or -*b* leads to the production of photoproducts of type **a** and **b** (Fig. 6) quantifiable after alkaline hydrolysis

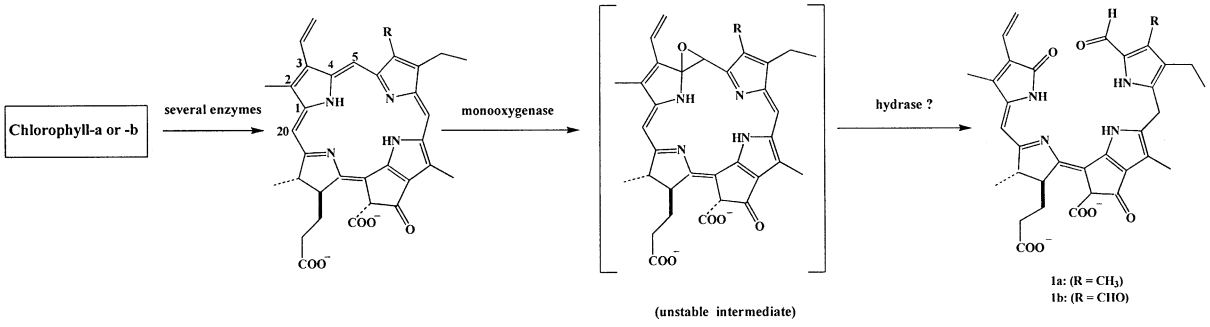

Fig. 5. Suggested pathway of the enzymatic degradation of chlorophylls (adapted from Gossauer and Engel, 1996).

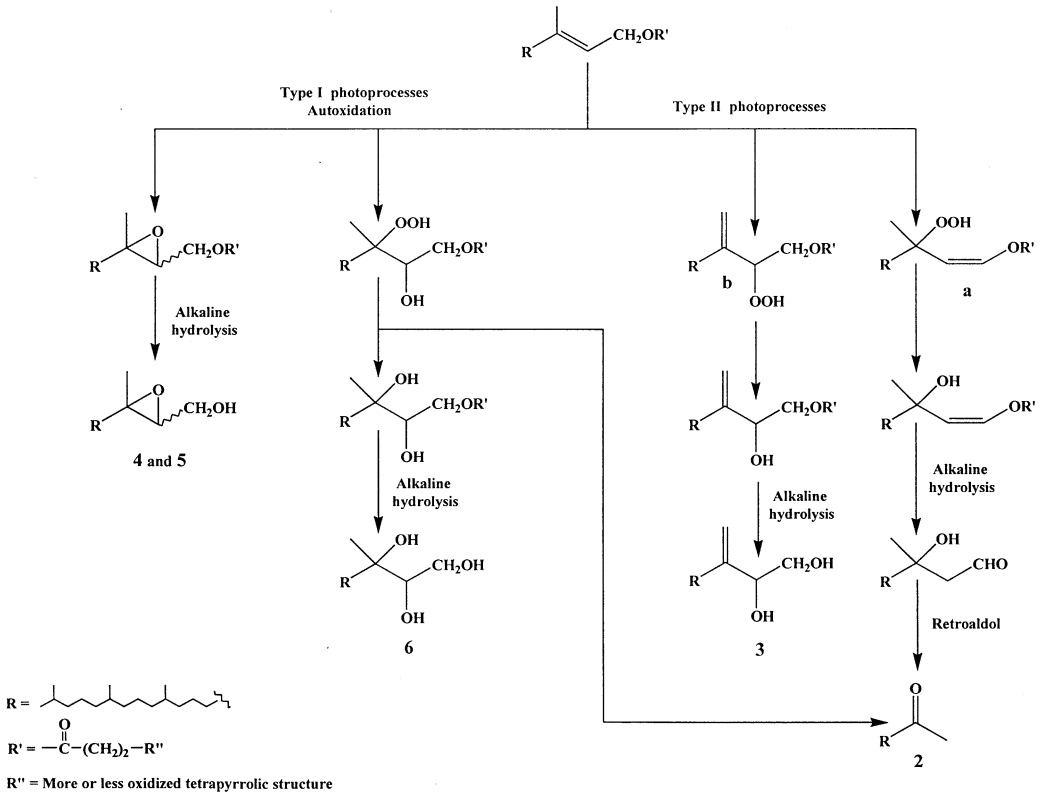

Fig. 6. Photo- and auto-oxidation of chlorophyll phytyl chain and reactions of oxidation products during alkaline hydrolysis [adapted from Rontani et al. (1991) and Rontani and Aubert (1994)].

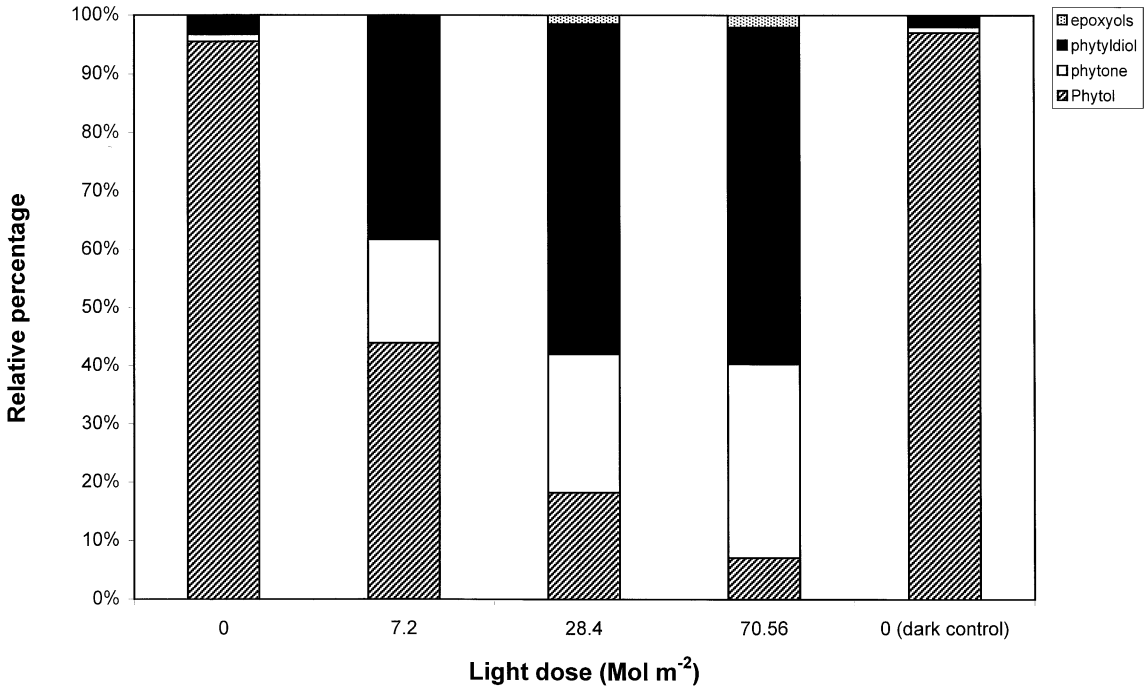

Fig. 7. Photodegradation of chlorophyll phytyl chain during *Dunaliella* sp. incubations [adapted from Rontani et al., (1998)].

respectively in the form of 6,10,14-trimethylpentadecan-2-one (phytone) (**2**) and 3-methylidene-7,11,15-trimethylhexadecan-1,2-diol (phytyldiol) (**3**) (Fig. 6) (Rontani et al., 1991). In contrast, oxy-free radical oxidation of the phytyl chain and subsequent alkaline hydrolysis affords mainly *Z* and *E* 3,7,11,15-tetramethyl-2,3-epoxyhexadecan-1-ols (**4** and **5**), 3,7,11,15-tetramethylhexadecan-1,2,3-triol (**6**) and the ketone **2**

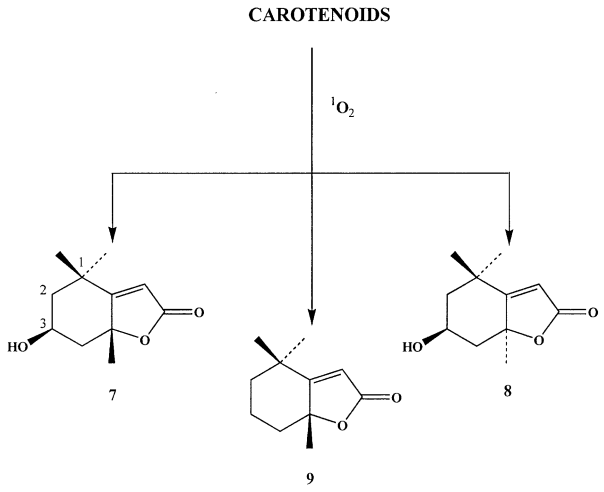

Fig. 8. Structure of the main carotenoid photoproducts.

(Fig. 6) (Rontani and Aubert, 1994). Analysis of isoprenoid photoproducts of chlorophyll after irradiation of killed phytoplanktonic cells by visible light clearly established that the photodegradation of the chlorophyll phytyl side-chain in phytodetritus involved mainly $^1O_2$ and to a small degree free-radicals (Fig. 7) (Rontani et al., 1995). Phytyldiol (**3**), which is a stable, specific (Rontani et al., 1996) and widely distributed (Rontani et al., 1994; Cuny and Rontani, 1999) chlorophyll phytyl side-chain photoproduct, appeared to be a suitable biogeochemical marker of chlorophyll photodegradation. Consequently the molar ratio of phytyldiol (**3**) to phytol named **CPPI** (**C**hlorophyll **P**hytyl side-chain **P**hotodegradation **I**ndex) has been proposed as a useful tool relating to the photodegradation of chlorophylls with a phytyl side-chain in aquatic ecosystems (Cuny et al., 1999).

5.2. Carotenoids

In phytodetritus, chlorophylls and carotenoids remain in a close molecular-scale association at relatively high localized concentrations, even though the structure of the thylakoid membrane has been disrupted (Nelson, 1993). Thus, the sensitized photo-oxidation of carotenoid is enhanced. In a previous paper, Nelson (1993) determined the visible light-dependent degradation rates of carotenoids in killed chlorophyte and diatom cells (Table 1). Using D_2O (which prolongs $^1O_2$ lifetime) and radical scavengers, Takahama (1983) demonstrated that carotenoid photobleaching in isolated chloroplasts involves $^1O_2$ and radical chain reactions. The photosensitized oxidation (involving $^1O_2$) of carotenoids in solvents has been studied (Iseo et al., 1972) and loliolide (**7**), *iso*-loliolide (**8**) and dihydroactinidiolide (**9**) (Fig. 8) were identified as major photo-products, depending on the functionality of carotenoids at C-3. Recently, loliolide (**7**) and *iso*-loliolide (**8**) have been detected in killed cells of *Dunaliella* sp. irradiated by visible light (Rontani et al., 1998). During this study, the production of lesser amounts of these compounds has been also observed after dark axenic incubations of killed cells and attributed to the action of peroxidases (Huff, 1982). Loliolides have been also detected in situ in suspended particles (Repeta, 1989) and in sediments (Klock et al., 1984; Repeta, 1989); however, due to their apparent production by anaerobic bacteria (Repeta, 1989) and during dark incubations of killed phytoplanktonic cells (Rontani et al.,

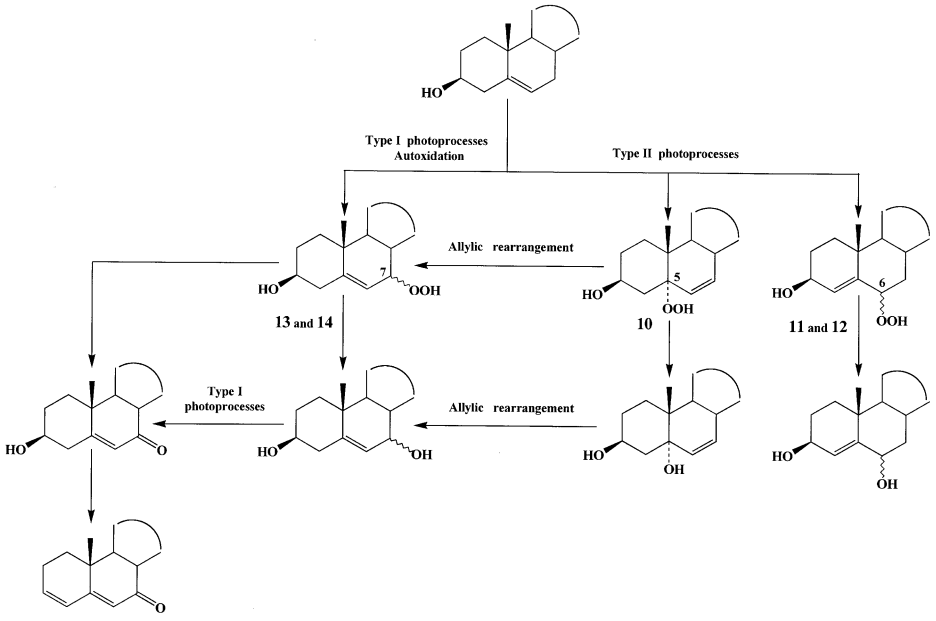

Fig. 9. Photo- and auto-oxidation of sterols (only the major oxidation products are shown) [adapted from Rontani (1999)].

1998), these compounds cannot constitute unequivocal indicators of photo-oxidative processes.

5.3. Sterols

As important unsaturated components of biological membranes, sterols are highly susceptible to photo-oxidative degradation during the senescence of phytoplankton. Type I (free radical) (Rontani et al., 1993) and type II ($^1O_2$) photo-oxidation (Nickon and Bagli, 1961; Kulig and Smith, 1973) of these compounds have been extensively studied in solution. Type II ($^1O_2$) photo-oxidation of sterols gives mainly Δ^6-5α-hydroperoxides (**10**) and to a lesser extent Δ^4-6α/6β-hydroperoxides (**11** and **12**) (Nickon and Bagli, 1961; Kulig and Smith, 1973), whereas type I (free radical) photoreactions (Rontani et al., 1993) and autooxidative processes (Smith, 1981) give Δ^5-7α/7β-hydroperoxides (**13** and **14**) (Fig. 9). Δ^6-5α-hydroperoxysterols (**10**) are relatively unstable and may undergo allylic rearrangement to Δ^5-7α-hydroperoxysterols (**13**), which in turn epimerize to the corresponding 7β-hydroperoxides (**14**) (Fig. 9) (Smith, 1981).

Irradiation by visible light of killed cells of *Skeletonema costatum*, *Dunaliella* sp., *Phaeodactylum tricornutum* and *Emiliania huxleyi* (Rontani et al., 1997a,b; 1998) resulted in a quick photodegradation of the sterol components of these algae. The light-dependent degradation rates thus obtained (Table 1) show a good fit to apparent first-order kinetics. The results obtained clearly established that the photo-oxidation of sterols in senescent cells of phytoplankton involves singlet oxygen-mediated photoprocesses. These processes produce 6-hydroperoxides in considerably higher yields [ratio Δ^4-6-hydroperoxides/Δ^6-5-hydroperoxides = 0.34 in killed cells of *Skeletonema costatum* (Rontani et al., 1997a)] than in homogeneous solutions (Kulig and Smith, 1973). This confirms previous observations made by Korytowski et al. (1992) in cell membranes. Allylic rearrangement does not occur significantly in killed cells of phytoplankton. Korytowski et al. (1992) have observed that Δ^6-5α-hydroperoxides are more stable in membranes containing unsaturated phospholipids than in those containing saturated phospholipids. This stability was attributed either to hydrogen bonding between the unsaturated fatty acyl chain of phospholipids and Δ^6-5α-hydroperoxides which could hinder the allylic rearrangement, or to differences of polarity in the carbon 7–10 zone of the fatty acyl chain [where sterols tend to localize in phospholipid/sterol bilayers (MacIntosch, 1978)]. On the basis of these hypotheses, the lack of allylic rearrangement in phytodetritus can be correlated with the well-known high Δ^9 unsaturated fatty acid content of phytoplankton (Kawamura and Gagosian, 1987; Stephanou, 1992). It is also interesting to note that the reduction of hydroperoxysterols to the corresponding diols (Fig. 9) weakly operates in killed phytoplanktonic cells (Rontani et al., 1997a).

Recently, significant amounts of Δ^6-5α- and Δ^4-6α/6β-hydroperoxysterols have been detected in marine recent sediments (Rontani and Marchand, 2000). These results show that photodegradation of Δ^5-stenols in senescent or dead phytoplanktonic cells plays a role in the degradation of these compounds in the marine environment. The surprising preservation of hydroperoxysterols observed in these sediments was attributed to the weak reducing properties of sulfides towards these compounds. These photoproducts, which are present mainly in esterified and bound forms, could also be protected in intact phytoplanktonic membranes of well-silicified diatoms. Indeed, it is generally considered that most of the bound materials observed in sediments represent the contents of intact biological debris (Cranwell, 1978; Sun et al., 1993). If Δ^6-5α-hydroperoxysterols are particularly stable in phytodetritus, they decay slowly in the sediment to their corresponding Δ^5-7α/7β-derivatives, which are not selective markers. Consequently, Δ^4-6α/6β-hydroperoxysterols (or the corresponding Δ^4-6α/6β-hydroxysterols) may be considered as more reliable *in situ* markers of photodegradation processes than Δ^6-5α-hydroperoxysterols (Korytowski et al., 1992).

5.4. Unsaturated fatty acids

Since damaging effects of $^1O_2$ are primarily concerned with the oxidation of membrane lipids (Percival and Dodge, 1983), chloroplast membrane components are particularly susceptible to type II photo-oxidation (Heath and Packer, 1968). This is the case for unsaturated fatty acids, which generally predominate in algal lipids, particularly in the photosynthetic membranes (Woods, 1974). In killed phytoplanktonic cells, the photodegradation rates of unsaturated fatty acids show a good fit to apparent first-order kinetics and logically increase with their unsaturation degree (Rontani et al., 1998) (Table 1). Singlet oxygen-mediated photo-oxidation of monounsaturated fatty acids involves a direct reaction of $^1O_2$ with the carbon-carbon double bond by a concerted "ene" addition (Frimer, 1979), and leads to the formation of hydroperoxides at each unsaturated carbon. Thus, oleic acid produces a mixture of 9- and 10-hydroperoxides (**15** and **16**) with an allylic *trans* double bond (Frankel et al., 1979) (Fig. 10). These two hydroperoxides may undergo highly stereoselective radical allylic rearrangement respectively to 11-*trans* and 8-*trans* hydroperoxides (**17** and **18**) (Fig. 10) (Porter et al., 1995). Frankel et al. (1977) and Garwood et al. (1977) reported that autoxidation of oleic acid yields mainly a mixture of 8-*trans*, 8-*cis*, 9-*trans*, 10-*trans*, 11-*trans* and 11-*cis* hydroperoxides (**15**–**20**), with minor amounts of 9-*cis* and 10-*cis* hydroperoxides (Fig. 10).

The visible light-induced degradation of mono-unsaturated fatty acids in killed phytoplanktonic cells has recently been studied (Rontani, 1998; Rontani et al., 1998). Comparison of the isomeric distribution of Δ^9 octadecenoic acid (oleic acid) hydroperoxides (quantified after reduction to their corresponding secondary alcohols) obtained in killed cells (Fig. 11) and after oxidation with radicals and $^1O_2$ (Fig. 10) made it possible to show that the photodegradation of mono-unsaturated fatty acids in phytodetritus involves mainly singlet oxygen. The 9- and 10- allylic hydroperoxides (**15** and **16**) thus formed may undergo three main degradative processes: (i) highly stereoselective free radical allylic rearrangement respectively to 11-*trans* and 8-*trans* hydroperoxides (**17** and **18**), (ii) homolysis of the O–O bond leading to carbonyl (dehydration), alcoholic (reduction), fragmentation (β-scission) or oxirane (radical cyclization) products (Frimer, 1979), and (iii) heterolysis of the O–O bond leading to the formation of two carbonyl fragments (Hock cleavage), this proton-catalysed cleavage being initiated by migration of groups to positive oxygen (Frimer, 1979).

The free radical nature of the allylic hydroperoxide rearrangement is supported by the observation that the rearrangement is catalysed by free radical initiators or light and inhibited by phenolic antioxidants (Porter et al., 1995). This allylic rearrangement weakly intervenes in killed phytoplanktonic cells (Fig. 11). This could be attributed to the relatively high localized lipidic concentrations present in phytodetritus (Nelson, 1993), which favoured the dimerisation of hydroperoxides. Hydrogen atom abstraction to form allylperoxyl radicals does indeed occur readily from hydroperoxide monomers but not from hydroperoxide dimers (Porter et al., 1995). Homolysis of the O–O bond of mono-unsaturated acids deriving allylic hydroperoxides in phytodetritus involves mainly reduction to hydroxyacids (**21**) and dehydration to ketoacids (**22**) (Fig. 12). The presence of allylic ketoacids (**22**), which was not easy to prove since these compounds do not survive alkaline hydrolysis of killed cells, has been recently demonstrated thanks to deuterium labelling (Rontani, unpublished results). Proton-catalysed cleavage of allylic hydroperoxides involves mainly the migration of the vinyl group (Frimer, 1979). According to this pathway, allylic hydroperoxides resulting from the light-induced oxidation of phytoplanktonic mono-unsaturated fatty acids affords C_7–C_{12} ω-oxocarboxylic acids (**23**) and C_6–C_{11} aldehydes (**24**) (Rontani, 1998; Rontani et al., 1998) (Fig. 12). In the presence of peroxides or molecular oxygen such compounds are easily oxidized respectively

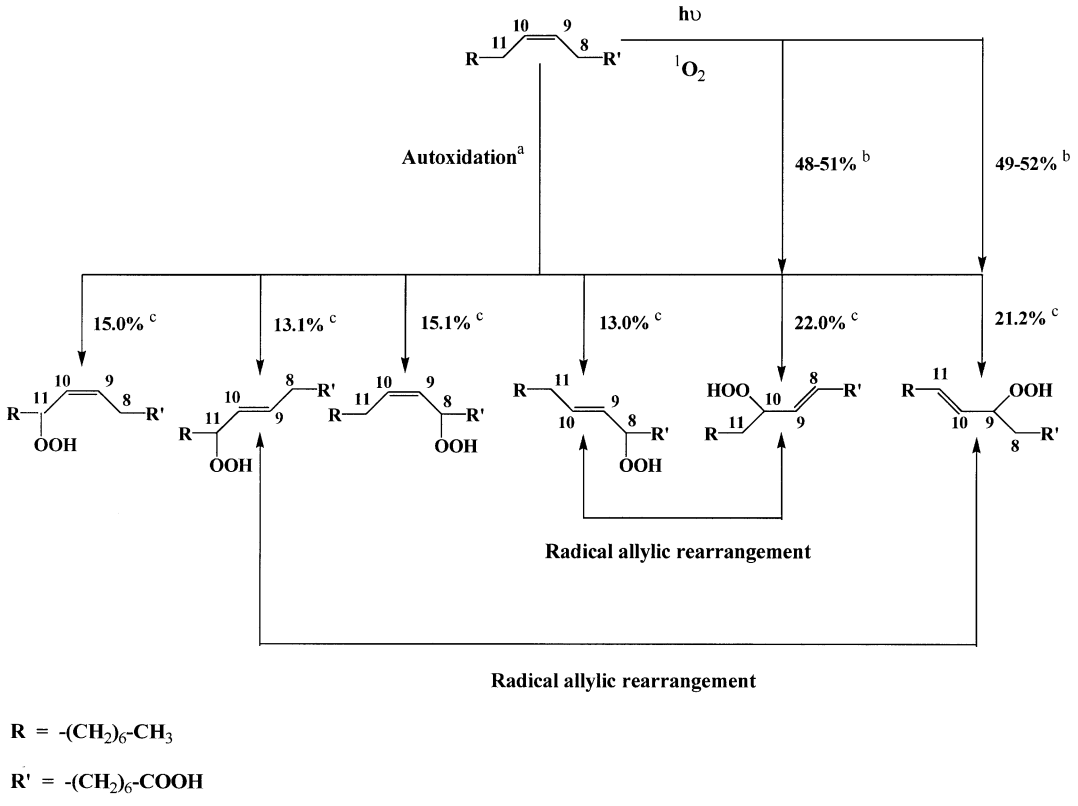

Fig. 10. Hydroperoxides from autoxidation and singlet oxygen-mediated photo-oxidation of octadec-9-enoic acid [reprinted from Marchand and Rontani (2001), with permission from Elsevier Science Ltd]. [a]Cis-9 and 10 hydroperoxides (which represent less than 1% of autoxidation products) have been omitted in order to simplify the scheme. [b]From Frankel, 1998. [c]At 14 °C (values extrapolated from the data of Frankel et al., 1984 and Porter et al., 1994).

to ω-dicarboxylic (**25**) and carboxylic acids (**26**) (Fig. 12).

Significant amounts of photo-oxidation products of phytoplanktonic mono-unsaturated acids have been recently detected in particulate matter and sediment samples (Marchand and Rontani, 2001). Deuterium labelling showed that isomeric hydroperoxyacids are relatively stable in the water column. During early diagenesis, hydroperoxides undergo heterolytic cleavage to aldehydes and ω-oxocarboxylic acids or homolytic cleavage and subsequent transformation to the corresponding alcohols or ketones.

The detection of homologous series of ω-oxocarboxylic acids (with C_9 as the most abundant species) and their corresponding α,ω-dicarboxylic acids in marine sediments (Kawamura et al., 1990; Stephanou, 1992) and sediment traps (Kawamura et al., 1990) was interpreted as indicative of atmospheric transport of unsaturated fatty acid photo-oxidation products rather than of an autochthonous formation (Kawamura et al., 1990; Stephanou and Stratigakis, 1993). The production of similar compounds recently observed during the irradiation of senescent phytoplanktonic cells (Rontani, 1998; Rontani et al., 1998) and attributed to heterolytic cleavage of allylic hydroperoxides (Rontani, 1998) calls into question the use of these compounds as tracers of atmospheric input to the sea, since the photosensitized oxidation of unsaturated fatty acids in senescent phyto-

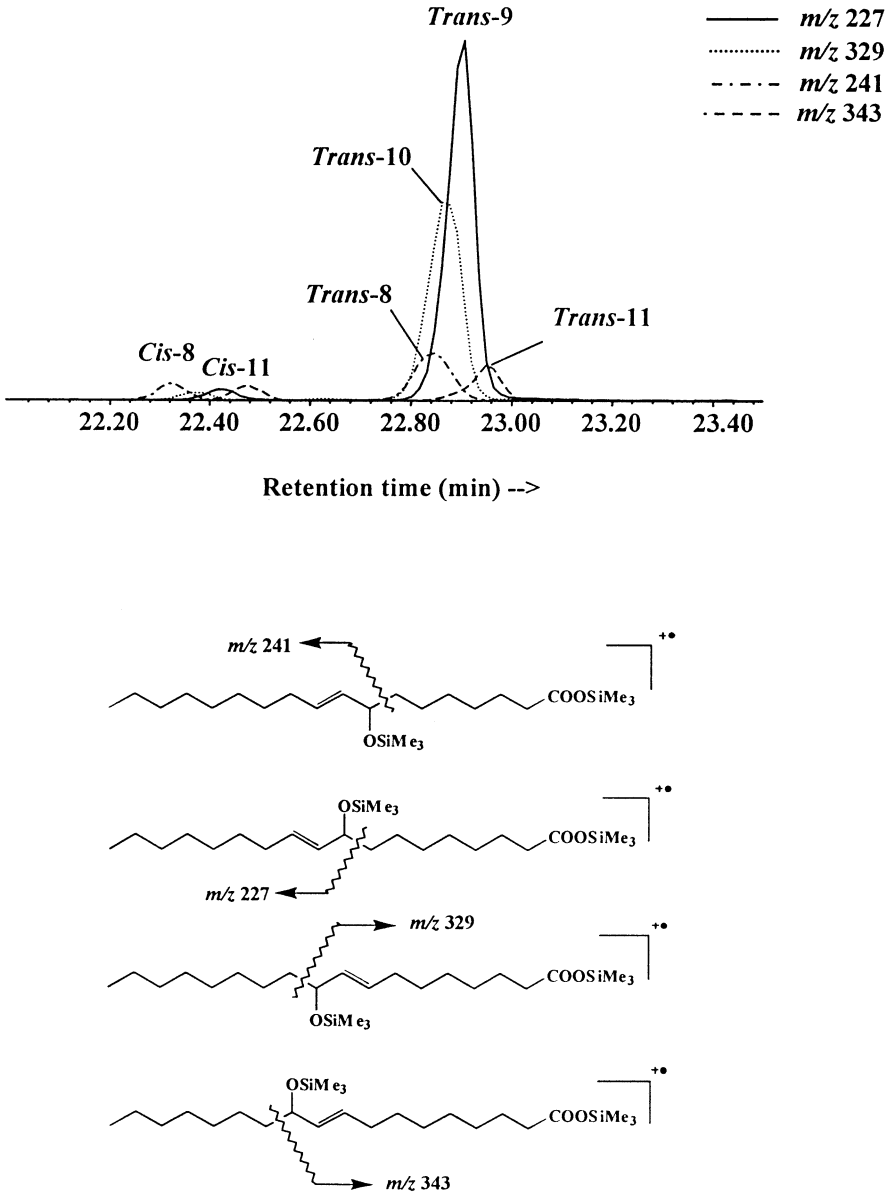

Fig. 11. Mass chromatograms of *m*/*z* 227, 241, 329 and 343 revealing the presence of four octadec-9-enoic acid deriving isomeric hydroxyacids in a reduced ($NaBH_4$) extract of *Dunaliella* sp. killed cells exposed to 66 mol m^{-2} (PAR) [adapted from Rontani (1998)].

planktonic cells, which can act throughout the euphotic layer of the oceans, must constitute a significant source of ω-oxocarboxylic and α,ω-dicarboxylic acids in the marine environment. Moreover, it is important to note that heterolytic cleavage of allylic hydroperoxides produced by autoxidation of Δ^9 unsaturated acids also results in the production of ω-oxocarboxylic and α,ω-dicarboxylic acids (with C_9 as the more abundant species) (Marchand and Rontani, 2001). It is clear that these compounds could not be considered any longer as specific tracers of photo-oxidative degradation of biogenic unsaturated fatty acids but only of their oxidation.

In contrast, the distribution pattern of allylic hydroxyacids (resulting from the reduction of the corresponding hydroperoxides), which is well preserved in recent sediments (Table 2) (Marchand and Rontani, 2001), allows easy differentiation between autoxidative and photo-oxidative processes.

Taking into account the high amounts of photoproducts of mono-unsaturated fatty acids detected in the particulate matter samples, and the well known increasing photo-oxidation rates (Rontani et al., 1998) of fatty acids with their degree of unsaturation, it can be concluded that considerable amounts of poly-unsaturated fatty acids must be photo-oxidized in the marine environment. However, at this time photo-oxidation products of this kind of fatty acids could not be detected in natural samples. This is possibly due to: (i) the instability of the hydroperoxides formed, or (ii) the involvement of cross-linking reactions leading to the formation of macromolecular structures (Neff et al., 1988) nonamenable by gas chromatography. The characterisation and quantification of such structures (which could play a

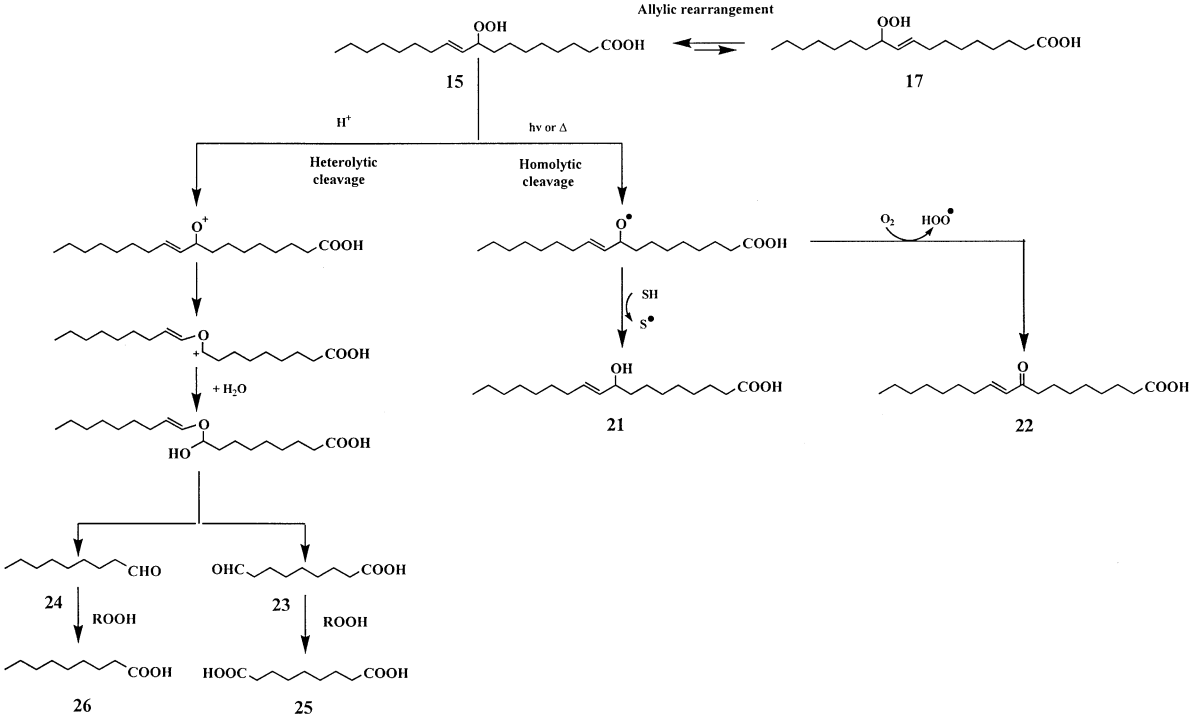

Fig. 12. Proposed pathways for the degradation of 9-hydroperoxyoctadec-10-enoic acid in killed cells of *Dunaliella* sp. [adapted from Rontani (1998)].

Table 2
Relative percentages of allylic hydroxyacids resulting from oxidation of oleic acid detected in upper sediment of the SOFI station [reprinted from Marchand and Rontani (2001), with permission from Elsevier Science Ltd]

Sediment slice (cm)	% of *cis*-8 and -11 allylic hydroxyacids	% of *trans*-9 and -10 allylic hydroxyacids	% of *trans*-8 and -11 allylic hydroxyacids
0–2	13	70	17
2–4	11	69	20
4–6	10	72	18
6–8	10	70	20
8–10	13	63	24
10–12	ND[a]	ND	ND

[a] ND, not determined (concentrations of oxidation products too low).

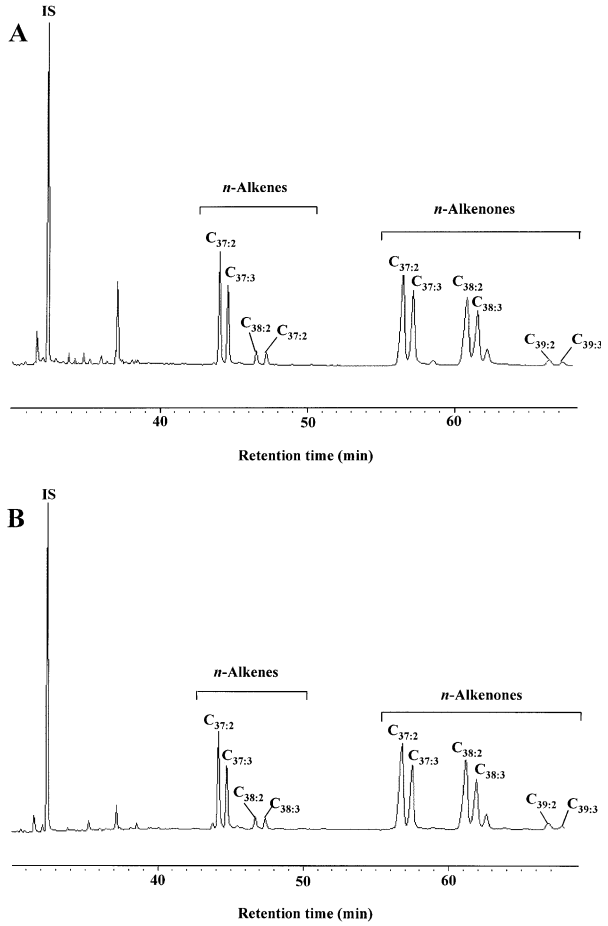

Fig. 13. Partial gas chromatograms of the unsaponifiable fractions obtained after exposure of *Emiliania huxleyi* CS-57 at 20°C for 20 days to different light regimes: (A) without irradiation under sterile conditions and (B) after exposure to 194 mol m^{-2} (PAR). (IS = internal standard) [adapted from Mouzdahir et al. (2001)].

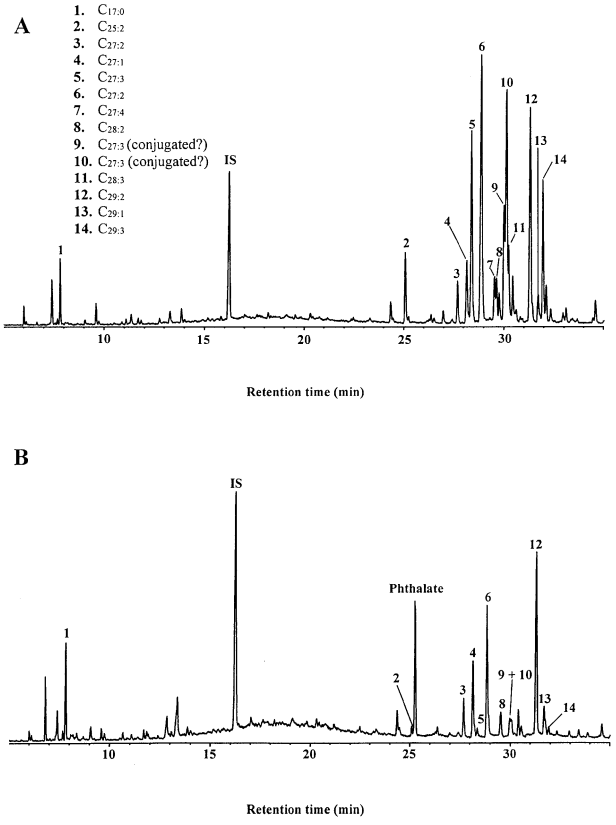

Fig. 14. Gas chromatograms of the unsaponifiable fractions obtained after exposure of *Nannochloropsis salina* CCAP849/4 at 20°C for 19 days to different light regimes: (A) without irradiation under sterile conditions and (B) after exposure to 185 mol m^{-2} (PAR) (IS = internal standard) [reprinted from Mouzdahir et al. (2001), with permission from Elsevier Science Ltd].

role in the formation of humic substances (Harvey et al., 1983) in particulate matter or senescent phytoplanktonic samples constitutes an exciting challenge for the future.

5.5. Alkenones

The alkenones comprise an unusual class of long-chain unsaturated methyl and ethyl ketones that are synthesized by a limited number of haptophyte microalgae (Volkman et al., 1980; 1995; Marlowe et al., 1984). The relative abundance of the two main $C_{37:2}$ and $C_{37:3}$ alkenones expressed as the $U^{k'}_{37}$ index $[C_{37:2}]/([C_{37:2}]+[C_{37:3}])$ is now widely used for reconstructing sea surface paleotemperatures (Rosell-Melé et al., 1995).

In recent work, we studied the photodegradation of these compounds in order to determine if photochemical processes could appreciably modify $U^{k'}_{37}$ ratios during algal senescence (Rontani et al., 1997b). In solution, singlet oxygen-mediated photochemical processes degraded alkenones more slowly than fatty acids with the same unsaturation degree. This difference of reactivity was attributed to: (i) the *trans* configuration of the alkenone double bonds (Rechka and Maxwell, 1988), which is known to be less reactive towards singlet oxygen (Hurst et al., 1985), and (ii) the separation of the double bonds by five saturated carbons in the alkenone structure. Though selective, photochemical degradation of alkenones is not fast enough in killed cells of *Emiliania huxleyi* to induce significant modifications of the $U^{k'}_{37}$ ratio before the photodestruction of the photosensitizing substances (Fig. 13) (Rontani et al., 1997b; Mouzdahir et al., 2001). This poor photo-reactivity was attributed not only to the *trans* configuration of the double bonds of alkenones, but also to a localisation of these compounds elsewhere than in cell membranes (Rontani et al., 1997b; Mouzdahir et al., 2001), which could significantly decreases the likelihood of interaction between singlet oxygen and alkenones. This latter hypothesis is well supported by the results of Conte and Eglinton (1993), who failed to detect alkenones in the membranes of *Emiliania huxleyi* after cell fractionation.

5.6. Unsaturated hydrocarbons

The visible light-induced degradation of *n*-alkenes has been studied in killed cells of the Prymnesiophycea *Emiliania huxleyi* and the Eustigmatophycea *Nannochloropsis salina* (Mouzdahir et al., 2001). In *Emiliania huxleyi* killed cells, minor C_{31} and C_{33} *n*-alkenes were strongly photodegraded, while the major C_{37} and C_{38} *n*-alkenes appeared particularly recalcitrant towards photochemical processes (Fig. 13). These differences of photoreactivity imply distinct biological syntheses and/or functions for these two groups of hydrocarbons in *Emiliania huxleyi* cells. As in the case of the corresponding alkenones (see Section 5.5), the particular photochemical recalcitrance of C_{37} and C_{38} *n*-alkenes has been attributed to the chemical structure and localization of these hydrocarbons in the cells. Irradiation of dead cells of *Nannochloropsis salina* resulted in a strong modification of the hydrocarbon fraction (Fig. 14). It did not provide evidence of a significant light-dependent degradation of monounsaturated hydrocarbons; this result was attributed to the terminal position of the double bond in these compounds (Gelin et al., 1997), which is poorly reactive towards singlet oxygen (Hurst et al., 1985). In contrast, di-, tri-, and tetraenes were strongly photodegraded during irradiation (Fig. 14). The visible light-dependent degradation of phytoplanktonic *n*-alkenes showed apparent second-order kinetics with respect to light exposure, and the half-life doses obtained logically decrease with increasing number of double bonds in these compounds (Mouzdahir et al., 2001). During this study, products deriving from *n*-alkene photodegradation could not be detected.

Wakeham et al. (1991) previously observed in the Black Sea decreasing concentrations of C_{31}–C_{33} alkenes with increasing depth, while C_{37}–C_{39} alkenes persisted both in the water column and in the sediment. These authors invoked selective degradation to explain the observed depth profiles. The strong differences of photoreactivity of these two groups of *n*-alkenes observed well support this hypothesis.

6. Conclusions

It is generally considered that approximately 95% of the total particulate organic matter consists of particles < 20 μm having settling velocities of less than 1 m d^{-1} (MacCave, 1975). Consequently, the bulk of the organic particulate matter has a fairly long residence time within the euphotic layer. Assuming a surface daily irradiance of 60 mol m^{-2} (PAR) (a value representative of mid-latitude waters under a clear summer day (Nelson, 1993)), it clearly appears that most of the phytoplanktonic lipids (half-life doses ranging from 1 to 350 mol m^{-2}) (Table 3) may be significantly photodegraded in the upper portion of the euphotic zone during senescence. Some of the more reactive lipids (chlorophylls,

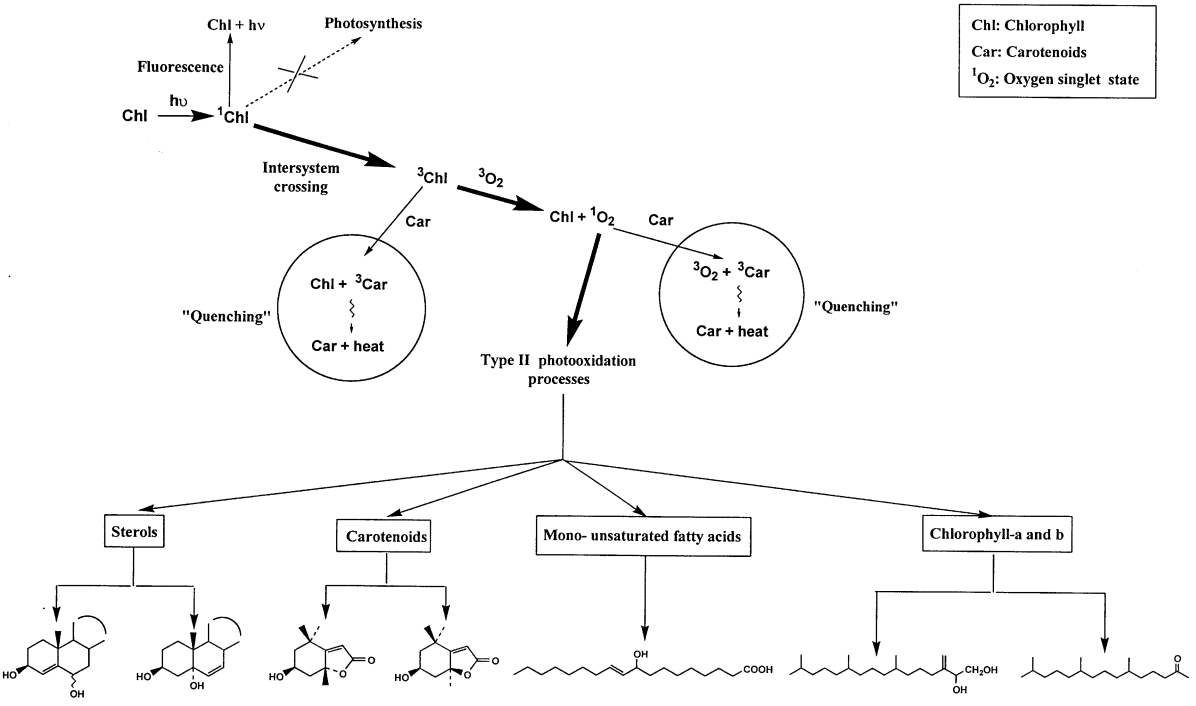

Fig. 15. Photodegradation of lipid compounds in senescent cells of phytoplankton (simplified scheme taking into account only the involvement of singlet oxygen) [adapted from Rontani et al. (1998)].

Table 3
Half-life doses ($D_{1/2}$) for visible light-dependent degradation of lipidic phytoplanktonic components

Compound	$D_{1/2}$ (mol m^{-2})
Chlorophyll-*a*	4–1[a–c]
Chlorophyll-*b*	3–6[a,b]
β-Carotene	1–2[b]
Sterols	8–64[d–f]
Phytol	4–24[a,c,d]
Mono-unsaturated fatty acids	14–23[d]
Di-unsaturated fatty acids	5–12[d]
Tri-unsaturated fatty acids	2[d]
Di-unsaturated *n*-alkenes	10–342[g]
Tri-unsaturated *n*-alkenes	7–16[g]
Tetra-unsaturated *n*-alkenes	2[g]
$C_{37:2}$ alkenone	346[f]
$C_{37:3}$ alkenone	231[f]

[a] Cuny et al., 1999.
[b] Nelson, 1993.
[c] Rontani et al., 1995.
[d] Rontani et al., 1998.
[e] Rontani et al., 1997a.
[f] Rontani et al., 1997b.
[g] Mouzdahir et al., 2001.

carotenoids, polyunsaturated fatty acids and *n*-alkenes) (Table 3) may be photodegraded even near the limit of the euphotic layer (daily irradiance 0.6 mol m^{-2}). However, under such low light conditions, particle sinking or biologically mediated degradation may have a greater impact on lipid concentration than light-dependent degradation processes (Vernet and Mitchell, 1990).

Probably due to its long lifetime in hydrophobic micro-environments (Suwa et al., 1977), singlet oxygen plays a key role in the photodegradation of most of the lipidic phytoplanktonic components (i.e. chlorophyll phytyl chain, carotenoids, sterols and unsaturated fatty acids). Consequently, we propose a scheme for the photodegradation of lipid compounds in senescent cells of phytoplankton that involves activation by $^1O_2$ (Fig. 15).

After elimination of the insufficiently specific and stable photoproducts, we selected 3-methylidene-3,11,15-trimethylhexadecan-1,3-diol (**3**) (Fig. 6), 6α/6β-hydroxysterols (**11** and **12**) (Fig. 9) and allylic hydroxyacids (**21**) (Fig. 13) to constitute a "pool" of useful markers of photodegradative alterations. This "pool" of photoproducts could provide very useful information concerning the physiological state of phytoplanktonic communities and current environmental problems related to ozone depletion.

In fact, since photoxidative degradation of lipidic components of phytoplankton intervene mainly in senescent cells, the proportion of photo-oxidation products relative to their parent lipidic components could be indicative of the physiological state of phytoplanktonic communities.

Atmospheric scattering is most pronounced in the blue and UV region of the solar light. Consequently, ozone depletion results in the exposure of phytoplankton to enhanced UV-B and blue light doses. If UV-B has been shown to reduce the survival, growth and production of phytoplankton (Skerratt et al., 1998), enhancement of the light doses in the blue region must result in the production of higher amounts of excited chlorophylls and thus to enhanced photodegradation of the lipidic components of phytoplankton. Consequently, photo-oxidation products of lipidic components of phytoplankton could give interesting information about ozone depletion.

Acknowledgements

Financial support over many years from the Groupement de Recherche HYCAR 1123 (CNRS/Elf Aquitaine) is gratefully acknowledged. Thanks are due to Mr. M. Paul for his careful reading of the English.

References

Chauvet, J.-P., Villain, F., Viovy, R., 1981. Photooxidation of chlorophyll and pheophytin. Quenching of singlet oxygen and influence of the micellar structure. Photochemistry and Photobiology 34, 557–565.

Conte, M.H., Eglinton, G., 1993. Alkenone and alkenoate distributions within the euphotic zone of the eastern North Atlantic: correlation with production temperature. Deep-Sea Research 40, 1935–1961.

Cranwell, P.A., 1978. Extractable and bound lipid components in a freshwater sediment. Geochimica et Cosmochimica Acta 42, 1523–1532.

Cuny, P., Rontani, J.-F., 1999. On the widespread occurrence of 3-methylidene-7,11,15-trimethylhexadecan-1,2-diol in the marine environment: a specific isoprenoid marker of chlorophyll photodegradation. Marine Chemistry 65, 155–165.

Cuny, P., Romano, J.-C., Beker, B., Rontani, J.-F., 1999. Comparison of the photodegradation rates of chlorophyll chlorin ring and phytol side chain in phytodetritus: is the phytyldiol versus phytol ratio (CPPI) a new biogeochemical index? Journal of Experimental Marine Biology and Ecology 237, 271–290.

Engel, N., Jenny, T.A., Mooser, V., Gossauer, A., 1991. Chlorophyll catabolism in *Chlorella protothecoides*. Isolation and structure elucidation of a red biline derivative. FEBS Letters 293, 131–133.

Foote, C.S., 1976. Photosensitized oxidation and singlet oxygen: consequences in biological systems. In: Pryor, W.A. (Ed.), Free Radicals in Biology. Academic Press, New York, pp. 85–133.

Frankel, E.N., 1998. Lipid Oxidation. The Oily Press, Dundee, pp. 1–302.

Frankel, E.N., Garwood, R.F., Khambay, B.P.S., Moss, G., Weedon, B.C.L., 1984. Stereochemistry of olefin and fatty acid oxidation. III. The allylic hydroperoxides from the autoxidation of methyl oleate. Journal of the Chemical Society Perkin Transactions I, 2233–2240.

Frankel, E.N., Neff, W.E., Bessler, T.R., 1979. Analysis of autoxidized fats by gas chromatography-mass spectrometry: V. Photosensitized oxidation. Lipids 14, 961–967.

Frankel, E.N., Neff, W.E., Rohwedder, W.K., Khambay, B.P.S., Garwood, R.F., Weedon, B.C.L., 1977. Analysis of autoxidized fats by gas chromatography-mass spectrometry: I. Methyl oleate. Lipids 12, 901–907.

Frimer, A.A., 1979. The reaction of singlet oxygen with olefins: the question of mechanism. Chemical Review 79, 359–387.

Fuhrhop, J.-H., Wasser, P. K. W., Subramanian, J., Schrader, U., 1974. Formylbiliverdine und ihre Metallkomplexe. Liebigs Annalen der Chemie, 1450–1466.

Garwood, R.F., Khambay, B.P.S., Weedon, B.C.L., Frankel, E.N., 1977. Allylic hydroperoxides from the autoxidation of methyl oleate. Journal of the Chemical Society Chemical Communications 364–365.

Gelin, F., Boogers, I., Noordeloos, A.A.M., Sinninghe Damsté, J.S., Riegman, R., De Leeuw, J.W., 1997. Resistant biomacromolecules in marine microalgae of the classes Eustigmatophyceae and Chlorophyceae: geochemical implications. Organic Geochemistry 26, 659–675.

Gollnick, K., 1968. Type II photooxygenation reactions in solution. Advances in Photochemistry 6, 1–122.

Gossauer, A., Engel, N., 1996. Chlorophyll catabolism — structures, mechanisms, conversions. Journal of Photochemistry and Photobiology B32, 141–151.

Halliwell, B., 1987. Oxidative damage, lipid peroxidation and antioxidant protection in chloroplasts. Chemistry and Physics of Lipids 44, 327–340.

Harbour, J.R., Bolton, J.R., 1978. The involvement of the hydroxyl radical in the destructive photo-oxidation of chlorophylls in vivo and in vitro. Photochemistry and Photobiology 28, 231–234.

Harvey, G.R., Boran, D.A., Chesal, L.A., Tokar, J.M., 1983. The structure of marine fulvic and humic acids. Marine Chemistry 12, 119–132.

Heath, R.L., Packer, L., 1968. Photoperoxidation in isolated chloroplasts. II. Role of electron transfer. Archives of Biochemistry and Biophysics 125, 850–857.

Hendry, G.A.F., Houghton, J.D., Brown, S.B., 1987. The degradation of chlorophyll — a biological enigma. New Phytologist 107, 255–302.

Huff, A., 1982. Peroxidase-catalyzed oxidation of chlorophyll by hydrogen peroxide. Phytochemistry 21, 261–265.

Hurst, J.R., Wilson, S.L., Schuster, G.B., 1985. The ene reaction of singlet oxygen: kinetic and product evidence in support of a perepoxide intermediate. Tetrahedron 41, 2191–2197.

Iseo, S., Hyeon, S.B., Katsumura, S., Sakan, T., 1972. Photooxygenation of carotenoids. II — The absolute configuration of loliolide and dihydroactinidiolide. Tetrahedron Letters 25, 2517–2520.

Iturraspe, J., Engel, N., Gossauer, A., 1994. Chlorophyll catabolism. Isolation and structure elucidation of chlorophyll-b catabolites in *Chlorella protothecoides*. Phytochemistry 35, 1387–1390.

Kawamura, K., Gagosian, R.B., 1987. Implications of ω-oxocarboxylic acids in the remote marine atmosphere for photo-oxidation of unsaturated fatty acids. Nature 325, 330–332.

Kawamura, K., Handa, N., Nozaki, Y., 1990. ω-Oxocarboxylic acids in the sediment trap and sediment samples from the North Pacific: implication for the transport of photo-oxidation products to deep-sea environments. Geochemical Journal 24, 217–222.

Klock, J., Baas, M., Cox, H.C., de Leeuw, J.W., Schenck, P.A., 1984. Loliolides and dihydroactinidiolide in a recent marine sediment probably indicate a major transformation pathway of carotenoids. Tetrahedron Letters 25, 5577–5580.

Knox, J.P., Dodge, A.D., 1985. Singlet oxygen and plants. Phytochemistry 24, 889–896.

Korytowski, W., Bachowski, G.J., Girotti, A.W., 1992. Photoperoxidation of cholesterol in homogeneous solution, isolated membranes, and cells: comparison of the 5α- and 6β-hydroperoxides as indicators of singlet oxygen intermediacy. Photochemistry and Photobiology 56, 1–8.

Kräutler, B., Jaun, B., Amrein, W., Bortlik, K., Schellenberg, M., Matile, P., 1991. Breakdown of chlorophyll: constitution of a secoporphinoid chlorophyll metabolite isolated from senescent barley leaves. Plant Physiology and Biochemistry 30, 333–346.

Kulig, M.J., Smith, L.L., 1973. Sterol metabolism. XXV. Cholesterol oxidation by singlet molecular oxygen. Journal of Organic Chemistry 20, 3639–3642.

Leshem, Y.Y., 1988. Plant senescence processes and free radicals. Free Radical Biology and Medicine 5, 39–49.

MacCave, I.N., 1975. Vertical flux of particles in the ocean. Deep-Sea Research 31, 329–352.

MacIntosh, T.J., 1978. The effect of cholesterol on the structure of phosphatidylcholine bilayers. Biochimica et Biophysica Acta 513, 43–58.

Marchand, D., Rontani, J.-F., 2001. Characterisation of photo-oxidation and autoxidation products of phytoplanktonic monounsaturated fatty acids in particulate matter and recent sediments. Organic Geochemistry 32, 287–304.

Marlowe, I.T., Green, J.C., Neal, A.C., Brassell, S.C., Eglinton, G., Course, P.A., 1984. Long-chain (nC_{37}–C_{39}) alkenones in the Prymnesiophyceae. Distribution of alkenones and other lipids and their taxonomic significance. British Phycology Journal 19, 203–216.

Merzlyak, M.N., Hendry, G.A.F., 1994. Free radical metabolism, pigment degradation and lipid peroxidation in leaves during senescence. Proceedings of the Royal Society of Edinburgh 102B, 459–471.

Mouzdahir, A., Grossi, V., Bakkas, S., Rontani, J.-F., 2001. Visible light-dependent degradation of long-chain alkenes in killed cells of *Emiliania huxleyi* and *Nannochloropsis salina*. Phytochemistry 56, 677–684.

Neff, W.E., Frankel, E.N., Fujimoto, K., 1988. Autoxidative dimerization of methyl linolenate and its monohydroperoxides, hydroperoxy epidioxides and dihydroperoxides. Journal of the American Oil Chemical Society 65, 616–623.

Nelson, J.R., 1993. Rates and possible mechanism of light-dependent degradation of pigments in detritus derived from phytoplankton. Journal of Marine Research 51, 155–179.

Nickon, A., Bagli, J.F., 1961. Reactivity and geometry in allylic systems. I. Stereochemistry of photosensitized oxygenation of monoolefins. Journal of the American Chemical Society 83, 1498–1508.

Percival, M.P., Dodge, A.D., 1983. Photodynamic damage to chloroplast membranes, photooxidized oxidation of chloroplast acyl lipids. Plant Science Letters 29, 255–264.

Porter, N.A., Mills, K.A., Carter, R.L., 1994. A mechanistic study of oleate autoxidation: competing peroxyl H-atom abstraction and rearrangement. Journal of the American Chemical Society 116, 6690–6696.

Porter, N.A., Caldwell, S.E., Mills, K.A., 1995. Mechanisms of free radical oxidation of unsaturated lipids. Lipids 30, 277–290.

Rechka, J.A., Maxwell, J.R., 1988. Characterisation of alkenone temperature indicators in sediments and organisms. Organic Geochemistry 13, 727–734.

Repeta, D.J., 1989. Carotenoid diagenesis in recent marine sediments. II — Degradation of fucoxanthin to loliolide. Geochimica et Cosmochimica Acta 53, 699–707.

Rontani, J.-F., 1998. Photodegradation of unsaturated fatty acids in senescent cells of phytoplankton: photoproduct structural identification and mechanistic aspects. Journal of Photochemistry and Photobiology 114A, 37–44.

Rontani, J.-F., 1999. Photodegradation of lipidic compounds during the senescence of phytoplankton. In: Boule, P. (Ed.), The Handbook of Environmental Chemistry. Springer, Berlin Heidelberg, pp. 264–282.

Rontani, J.-F., Aubert, C., 1994. Effect of oxy-free radicals upon the phytyl chain during chlorophyll-a photodegradation. Journal of Photochemistry and Photobiology A79, 167–172.

Rontani, J.-F., Baillet, G., Aubert, C., 1991. Production of acyclic isoprenoid compounds during the photodegradation of chlorophyll-a in seawater. Journal of Photochemistry and Photobiology A51, 369–377.

Rontani, J.-F., Beker, B., Raphel, D., Baillet, G., 1995. Photodegradation of chlorophyll phytyl chain in dead phytoplanktonic cells. Journal of Photochemistry and Photobiology 85A, 137–142.

Rontani, J.-F., Cuny, P., Aubert, C., 1997a. Rates and mechanism of light-dependent degradation of sterols in senescent cells of phytoplankton. Journal of Photochemistry and Photobiology 111A, 139–144.

Rontani, J.-F., Cuny, P., Grossi, V., 1998. Identification of a pool of lipid photoproducts in senescent phytoplanktonic cells. Organic Geochemistry 29, 1215–1225.

Rontani, J.-F., Cuny, P., Grossi, V., Beker, B., 1997b. Stability of long-chain alkenones in senescing cells of *Emiliania huxleyi*: effect of photochemical and aerobic microbial degradation on the alkenone unsaturation ratio ($U^{k'}_{37}$). Organic Geochemistry 26, 503–509.

Rontani, J.-F., Grossi, V., Faure, R., Aubert, C., 1994. "Bound" 3-methylidene-7,11,15-trimethylhexadecan-1,2-diol: a new isoprenoid marker for the photodegradation of chlorophyll-a in seawater. Organic Geochemistry 21, 135–142.

Rontani, J.-F., Marchand, D., 2000. Photoproducts of phytoplanktonic sterols: a potential source of hydroperoxides in marine sediments? Organic Geochemistry 31, 169–180.

Rontani, J.-F., Raphel, D., Aubert, C., 1993. Photodegradation of cholesterol induced by anthraquinone. Journal of Photochemistry and Photobiology A72, 189–193.

Rontani, J.-F., Raphel, D., Cuny, P., 1996. Early diagenesis of the intact and photooxidized chlorophyll phytyl chain in a recent temperate sediment. Organic Geochemistry 24, 825–832.

Rosell-Melé, A., Eglinton, G., Pflaumann, U., Sarnthein, M., 1995. Atlantic core-top calibration of the $U^{k'}_{37}$ index as a sea-surface paleotemperature indicator. Geochimica et Cosmochimica Acta 59, 3099–3107.

Skerratt, J.H., Davidson, A.D., Nichols, P.D., MacMeekins, T.A., 1998. Effect of UV-B on lipid content of three Antarctic marine phytoplankton. Phytochemistry 49, 999–1007.

Smith, L.L., 1981. The Autoxidation of Cholesterol. Plenum, New York, pp. 119–132.

Stephanou, E.G., 1992. α,ω-Dicarboxylic acid salts and α,ω-dicarboxylic acids: photo-oxidation products of unsaturated fatty acids present in marine aerosols and marine sediments. Naturwissenschaften 79, 128–131.

Stephanou, E.G., Statigakis, N., 1993. Oxocarboxylic and α,β-dicarboxylic acids: photo-oxidation products of biogenic unsaturated fatty acids present in urban aerosols. Environmental Science and Technology 27, 1403–1407.

Sun, M.-Y., Lee, C., Aller, R.C., 1993. Laboratory studies of oxic and anoxic degradation of chlorophyll-a in Long Island Sound sediments. Geochimica et Cosmochimica Acta 57, 147–157.

Suwa, K., Kimura, T., Schaap, A.P., 1977. Reactivity of singlet molecular oxygen with cholesterol in a phospholipidic membrane matrix: a model for oxidative damage of membranes. Biochemistry and Biophysic Research Communications 75, 785–792.

Takahama, U., 1983. Effects of deuterium oxide and free radical scavengers on carotenoid photobleaching in spinach chloroplasts. Plant and Cell Physiology 24, 495–500.

Vernet, M., Mitchell, B.G., 1990. RACER: phaeopigment photo-oxidation during the spring bloom in northern Gerlache Strait. Antarctic Journal of United States 25, 162–164.

Volkman, J.K., Barrett, S.M., Blackburn, S.I., Sikes, E.L., 1995. Alkenones in *Gephyrocapsa oceanica*: implications for studies of paleoclimate. Geochimica et Cosmochimica Acta 59, 513–520.

Volkman, J.K., Eglinton, G., Corner, E.D.S., Forsberg, T.E.V., 1980. Long-chain alkenes and alkenones in the marine coccolithophorid *Emiliania huxleyi*. Phytochemistry 19, 2619–2622.

Volkman, J.K., Maxwell, J.R., 1986. Acyclic isoprenoids as biological markers. In: Johns, R.B. (Ed.), Biological Markers in the Sedimentary Record. Elsevier, Amsterdam, pp. 1–46.

Wakeham, S.G., Beier, J.A., Clifford, C.H., 1991. Organic matter sources in the Black Sea as inferred from hydrocarbon distributions. In: Izdar, E., Murray, J.W. (Eds.), Black Sea Oceanography. Kluwer Academic, The Netherlands, pp. 319–341.

Wood, B.J.B., 1974. Fatty acids and saponifiable lipids. In: Steward, W.D. (Ed.), Algal Physiology and Biochemistry. University of California Press, Berkeley, pp. 236–265.

Zafiriou, O.C., 1977. Marine organic photochemistry previewed. Marine Chemistry 5, 497–522.

Zafiriou, O.C., Joussot-Dubien, J., Zepp, R.G., Zika, R.G., 1984. Photochemistry of natural waters. Environmental Science and Technology 18, 358. A–371A.

PERGAMON

Phytochemistry 58 (2001) 203–212

PHYTOCHEMISTRY

www.elsevier.com/locate/phytochem

Purification and characterization of a Ca^{2+}-dependent protein kinase from sandalwood (*Santalum album* L.): evidence for Ca^{2+}-induced conformational changes

Veena S. Anil, K. Sankara Rao*

Department of Biochemistry, Indian Institute of Science, Bangalore-560 012, India

Received in revised form 16 January 2001; accepted 10 May 2001

Abstract

An early development-specific soluble 55 kDa Ca^{2+}-dependent protein kinase has been purified to homogeneity from sandalwood somatic embryos and biochemically characterized. The purified enzyme, swCDPK, resolved into a single band on 10% polyacrylamide gels, both under denaturing and non-denaturing conditions. swCDPK activity was strictly dependent on Ca^{2+}, $K_{0.5}$ (apparent binding constant) for Ca^{2+}-activation of substrate phosphorylation activity being 0.7 μM and for autophosphorylation activity ~50 nM. Ca^{2+}-dependence for activation, CaM-independence, inhibition by CaM-antagonist (IC_{50} for W7 = 6 μM, for W5 = 46 μM) and cross-reaction with polyclonal antibodies directed against the CaM-like domain of soybean CDPK, confirmed the presence of an endogenous CaM-like domain in the purified enzyme. Kinetic studies revealed a K_m value of 1.3 mg/ml for histone III-S and a V_{max} value of 0.1 nmol min^{-1} mg^{-1}. The enzyme exhibited high specificity for ATP with a K_m value of 10 nM. Titration with calcium resulted in the enhancement of intrinsic emission fluorescence of swCDPK and a shift in the λ_{max} emission from tryptophan residues. A reduction in the efficiency of non-radiative energy transfer from tyrosine to tryptophan residues was also observed. These are taken as evidence for the occurrence of Ca^{2+}-induced conformational change in swCDPK. The emission spectral properties of swCDPK in conjunction with Ca^{2+} levels required for autophosphorylation and substrate phosphorylation help understand mode of Ca^{2+} activation of this enzyme. © 2001 Elsevier Science Ltd. All rights reserved.

Keywords: *Santalum album* L.; Santalaceae; Sandalwood; Signal transduction; Protein purification; Calmodulin-like domain protein kinase; Ca^{2+}-dependent protein kinase; Enzyme activation; Conformational changes

1. Introduction

In plants, calcium acts as a second messenger in the regulation of a variety of physiological and metabolic processes (Marme and Dieter, 1983; Malho and Trewavas, 1996; Sanders et al., 1999; Trewavas, 1999; Anil and Sankara Rao, 2000). To understand the downstream events in Ca^{2+}-mediated signaling, analogy has been drawn with animal systems wherein the Ca^{2+}-message is perceived by proteins that bind Ca^{2+}, and transduced via protein kinases. Plants predominantly exhibit a calcium-dependent, CaM-independent protein kinase activity. This activity was first purified from soybean (Harmon et al., 1986; Putnam-Evans et al., 1990) and later identified and/or purified from a host of other plant species (Roberts, 1993). The enzyme, calcium-dependent protein kinase (CDPK) is now classified into a novel family of calcium-regulated protein kinases found only in plants (Roberts, 1993) and protists (Zhao et al., 1994). CDPKs have the common feature of a C-terminal CaM-like domain that can directly bind Ca^{2+}, thereby making CaM unnecessary for their activation (Harper et al., 1991). This unique family of protein kinases is now implicated in the regulation of diverse metabolic and physiological processes (Harmon et al., 2000).

We have earlier identified a 55 kDa sandalwood (*Santalum album* L.) CDPK (swCDPK) that exhibits preferential accumulation and activity only in embryos, seedlings and endosperm tissues (Anil et al., 2000). The developmentally regulated expression of swCDPK suggests its involvement in the processes of embryogenesis, seed development and germination. Furthermore, a second messenger role for

* Corresponding author. Tel.: +91-80-3092821; fax: +91-80-3600683/3600085.

E-mail address: baradwaj@biochem.iisc.ernet.in (K. Sankara Rao).

0031-9422/01/$ - see front matter © 2001 Elsevier Science Ltd. All rights reserved.
PII: S0031-9422(01)00231-X

Ca^{2+} and a probable intermediary role for swCDPK during sandalwood somatic embryogenesis have been earlier determined (Anil and Sankara Rao, 2000). Knowledge of the biochemical properties of this development-specific kinase would help in understanding modes of regulation of enzyme activity.

Therefore, in this study, we report purification of swCDPK and biochemical characterization of this purified enzyme. swCDPK exhibits both Ca^{2+}-dependent autophosphorylation and substrate phosphorylation activities. However, these activities differ in their Ca^{2+} requirement for activation, autophosphorylation having a 14-fold lower calcium requirement as compared to substrate phosphorylation activity. The study is the first to provide fluorescence spectral evidence for Ca^{2+}- induced conformational changes in CDPK. Interestingly, half-maximal change in conformation was observed at Ca^{2+} concentrations 10 fold lower than that required for substrate phosphorylation activity. Furthermore, the Ca^{2+}-induced changes in tryptophan emission spectra indicate occurrence of at least two distinct changes in conformation/Ca^{2+}-enzyme complexes at low (10–100 nM) and high (>100 nM) calcium levels.

2. Results

2.1. Purification

swCDPK was purified to homogeneity from torpedo/cotyledonary stage somatic embryos following three chromatographic procedures. The ammonium sulfate fraction was subjected to anion-exchange chromatography using DEAE-cellulose. The enzyme activity eluted with 0.4 M NaCl, 20 of the initial fractions showing Ca^{2+}-dependent protein kinase activity were pooled and processed for the next chromatographic step. The DEAE eluant was subjected to hydroxyapatite column chromatography. There was no loss of kinase activity in the wash with 5 mM K_2HPO_4 in buffer B. The kinase activity was eluted from the column, first with a step elution of 25 mM K_2HPO_4 followed by gradient elution with 25–300 mM K_2HPO_4 in buffer B. A minor protein peak that eluted with 25 mM K_2HPO_4 exhibited strong Ca^{2+}-dependent kinase activity. The fractions comprising this peak were pooled and processed for the next chromatographic step. Most of the bound proteins that eluted from the hydroxyapatite column at a higher concentration of phosphate as a second peak showed negligible Ca^{2+}-dependent kinase activity. The final purification was achieved by fractionation on Cibacron Blue–Sepharose. The wash with 0.6 M NaCl eliminated minor contaminants that were present in the hydroxyapatite pool. swCDPK was eluted as a single small peak comprising of three fractions in buffer containing 0.2% CHAPS.

The standard purification of swCDPK was 375-fold, yielding 75 μg (Table 1) from 30 g of starting material. The percentage recovery of protein kinase activity was approximately 10%, the final specific activity in the presence of micromolar Ca^{2+} being 35–43 pmol min^{-1} mg^{-1} (Table 1). Fig. 1A shows the silver staining pattern after SDS–PAGE analysis of pools from different steps of purification. Though only a single major protein band is seen in the hydroxyapatite pool, a minor high molecular weight contaminant was visualized when the gel was developed for longer time, during silver staining. The Blue–Sepharose column eluant resolved into a single protein band at 55 kDa (Fig. 1A). The three Blue–Sepharose fractions that comprised the activity peak resolved into a single protein band under non-denaturing conditions as well (Fig. 1B). This band cross-reacted strongly with polyclonal antibodies raised against the CaM-like domain of soybean CDPK (Fig. 1C), suggesting that the purified protein was an immunological homologue of soybean CDPK. As the purified preparation resolved into a single band both under denaturing and non-denaturing conditions, it is most likely that the band represents a single protein.

2.2. Calcium ion dependency

swCDPK displayed Ca^{2+}-dependent substrate phosphorylation activity (Fig. 2A). Fig. 2B shows the in-gel phosphorylation of histone III-S in a Ca^{2+}-dependent manner. Substrate phosphorylation activity was

Table 1
Purification of swCDPK from sandalwood somatic embryos

S1. No.	Purification	Protein (mg)	Specific activity pmol^{32}P/min/mg		Sensitivity			
			$+Ca^{2+}$	$-Ca^{2+}$	*x*-fold	EA (u)[a]	Purification (*x*-fold)	Percentage recovery
(1)	Crude	259.3	0.116	0.02	6	1.15	1	100
(2)	80% NH_4SO_4	157.5	0.165	0.023	7	1.65	1.4	87
(3)	DEAE cellulose	81.4	0.189	0.012	16	1.8	1.6	52
(4)	Hydroxyapatite	0.9	8.0	0.13	61	80	70	24
(5)	CB-Sepharose	0.075	43.07	0.53	80	430.7	374.5	11

[a] One unit of enzyme activity (u) = 0.1 pmol^{32}P/min/mg; EA, enzyme activity; TA, total activity.

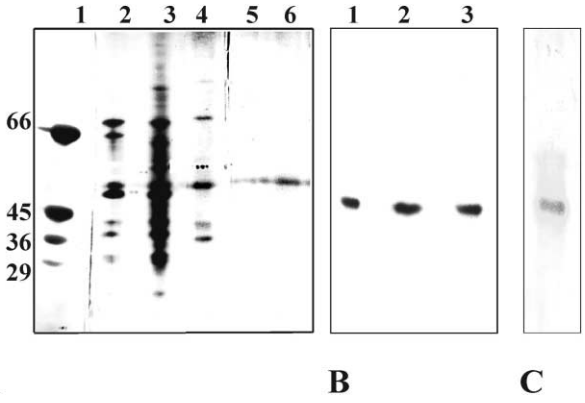

Fig. 1. Analysis of purification pools by gel electrophoresis and western blotting. A. Proteins from different stages of purification were resolved in a 10% polyacrylamide gel containing SDS and visualized by silver staining. Lane 1, molecular weight markers indicated in kilodaltons; lane 2, crude supernatant (10 μg); lane 3, ammonium sulfate fraction (10 μg); lane 4, DEAE pool (1 μg); lane 5, hydroxyapatite pool (0.25 μg); lane 6, Blue–Sepharose fraction (0. 25 μg). B. swCDPK (0.5 μg) was resolved on a non-denaturing 10% polyacrylamide gel and silver stained; lanes 1, 2 and 3 represent fractions 4, 5 and 6 respectively eluted from the Blue–Sepharose column. C. The resolved protein (1 μg) on the non-denaturing gel was analyzed by western blotting using polyclonal antibodies directed against the CaM-like domain of soybean CDPK.

stimulated 80–100 fold in the presence of Ca^{2+} ion, showing a half-maximal activation at 0.7 μM Ca^{2+} (Fig. 2C). The steep increase in histone phosphorylation activity with micromolar Ca^{2+} in a linear plot indicates the cooperative nature of this Ca^{2+}-dependent activation (Fig. 2C, inset). Autophosphorylation activity of swCDPK was observed at nanomolar concentrations of Ca^{2+}, half-maximal activation requiring only 40–50 nM Ca^{2+} (Fig. 3).

2.3. Kinetic properties

From the plot of $1/v$ versus 1/[histone III-S] (figure not shown), the K_m of swCDPK for histone III-S was estimated to be 1.3 mg/ml and the V_{max} value extrapolated from this plot was 0.1 nmol min^{-1} mg^{-1}. The plot of $1/v$ versus 1/[ATP] (figure not shown) indicated that swCDPK has high specificity for ATP, exhibiting a K_m of 10 nM. The turnover number (k_3) of swCDPK was 1×10^2 min^{-1} and the specificity constant (k_3/K_m) for histone III-S and ATP was calculated to be 1.6×10^6 and 1×10^{10} M^{-1} min^{-1} respectively. The observed high specificity for ATP and the low turnover number of swCDPK are different from those of other well characterized CDPKs (Putnam-Evans et al., 1990; DasGupta, 1994; Ganguly and Singh, 1998; Anil, 2000).

2.4. Effect of salt, Mg^{2+}, and pH on swCDPK activity

swCDPK activity was inhibited above 10 mM NaCl, complete inhibition occurring at 100 mM NaCl (figure not shown). swCDPK requires Mg^{2+} for activity, optimal histone III-S phosphorylation occurring only in the

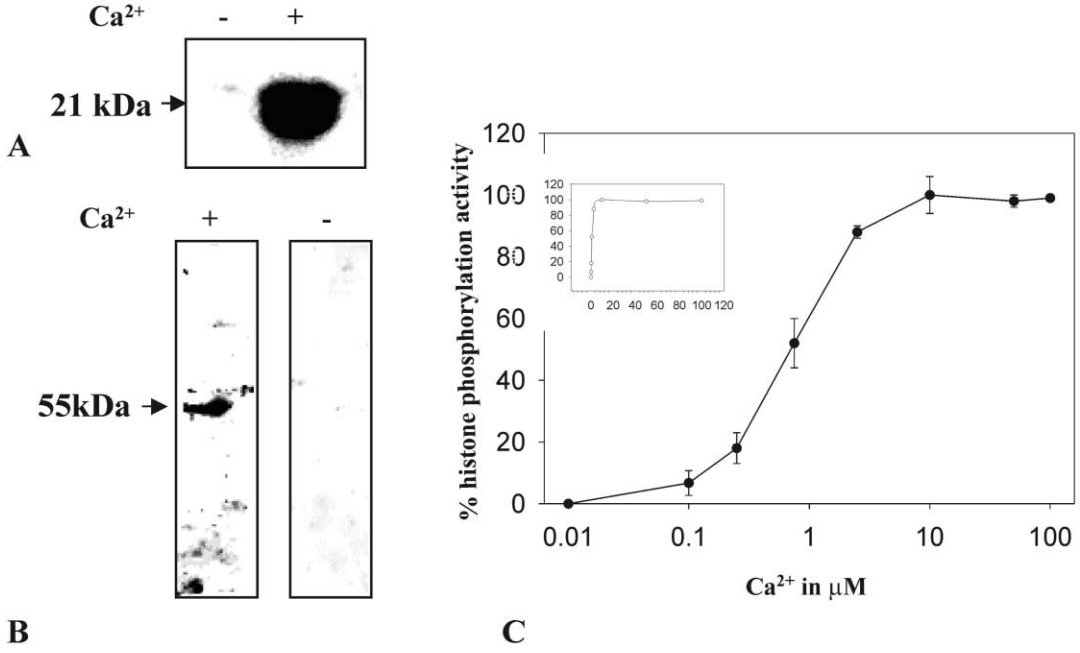

Fig. 2. Ca^{2+}-dependent substrate phosphorylation activity of swCDPK. A. swCDPK (50 ng) was assayed for histone phosphorylation activity as outlined in 'Experimental'. The reaction mix was then resolved by SDS 10% (w/v) polyacrylamide gel electrophoresis. The autoradiogram shows the position of phosphorylated histone III-S in the presence of Ca^{2+}. B. Autoradiogram represents the Ca^{2+}-dependent in-gel phosphorylation of histone III-S. C, Effect of Ca^{2+} on the activity of swCDPK (50 ng). Percentage activity is deduced relative to the activity obtained under standard assay conditions.

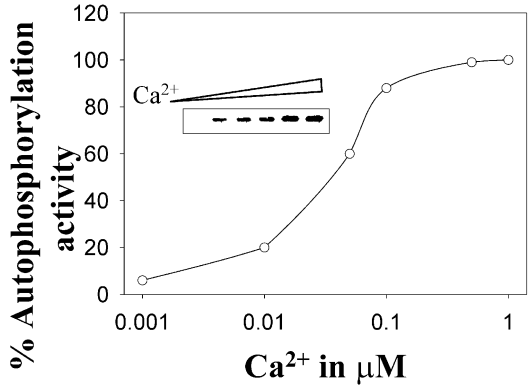

Fig. 3. Effect of Ca^{2+} on swCDPK autophosphorylation activity. Autophosphorylation of swCDPK (50 ng) was monitored at different concentrations of calcium in assay buffer. The phosphorylated swCDPK was resolved in a 10% (w/v) polyacrylamide gel containing SDS and visualized by phosphorimager. The percentage activity as a function of Ca^{2+} concentration was plotted using the photostimulated luminescence minus background (PSL–BG) emitted by phosphorylated swCDPK bands. One hundred per cent activity represents a PSL–BG of 70. Inset is a representative autoradiogram showing increase in swCDPK autophosphorylation within a range of 0.001–1 μM Ca^{2+}.

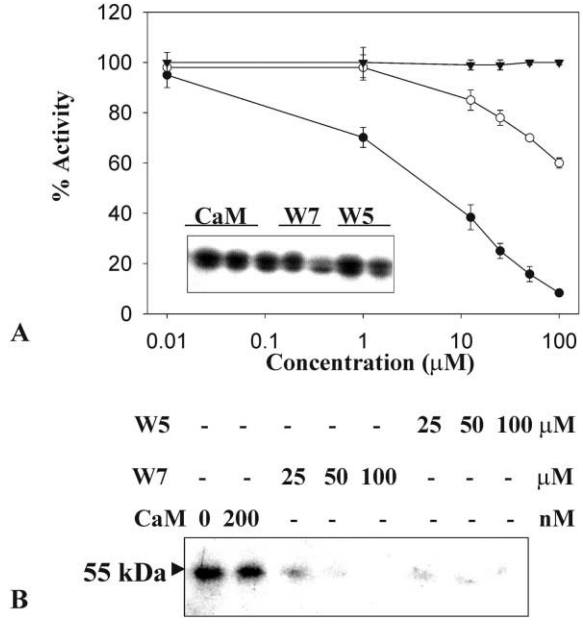

Fig. 4. Effect of CaM, W7 and W5 on swCDPK activity: Protein kinase assays were performed under standard assay conditions using 50 ng purified enzyme and amounts of CaM or inhibitors as indicated. A. Effect of increasing concentrations of CaM (▼), W5 (O), and W7 (●) on histone phosphorylation activity. Inset is a representative autoradiogram showing position of phosphorylated histone III-S in presence of CaM (0, 100 and 200 μM), W7 (0 and 10 μM) and W5 (0 and 10 μM). B. Effect of increasing concentrations of CaM, W7 and W5 on the autophosphorylation activity of swCDPK.

presence of 5–10 mM Mg^{2+} (figure not shown). However, inhibition of activity was observed above 10 mM Mg^{2+}. Purified swCDPK exhibited broad pH optima between pH 6.8 and 8.5, highest activity being observed at pH 7.2 (figure not shown).

2.5. Effect of calmodulin, and CaM-antagonists W7 and W5 on swCDPK activities

Exogenous calmodulin (CaM) did not enhance substrate phosphorylation activity of swCDPK (Fig. 4A). However, CaM- antagonist, *N*-(6-aminohexyl)-5-chloro-1-naphthalene sulfonamide (W7) and its less potent analogue W5 (Fig. 4A) inhibited activity. W7 inhibited with an IC_{50} of 6 μM and W5 inhibited with an IC_{50} of 46 μM. The autophosphorylation of swCDPK also remained unaffected by exogenous CaM, and was inhibited by both W7 and W5 (Fig. 4B). Although W5 has lower affinity towards CaM, it inhibits, albeit to a lesser extent, CaM-dependent enzymes and CDPKs (Harmon et al., 1986). The inhibition by W7 and W5 thus indicates that swCDPK has an endogenous CaM-like domain that regulates both substrate and autophosphorylation activities of the enzyme.

2.6. Phosphoamino acid analysis

Hydrolyzed phosphorylated histone III-S and autophosphorylated swCDPK were subjected to PC so as to identify the phosphorylated amino acid residues. swCDPK phosphorylated the substrate histone III-S exclusively on serine residues and autophosphorylated itself exclusively on threonine residues (Fig. 5).

2.7. Autophosphorylation versus substrate phosphorylation activity of swCDPK

Autophosphorylation reactions carried out in the presence of the exogenous substrate histone III-S resulted in a reduction in the autophosphorylation of swCDPK with increasing concentrations of histone III-S (Fig. 6).

2.8. Spectral properties

The absorption spectra of swCDPK shows that the enzyme exhibits maximum absorption (λ_{max}) at 290 nm, suggesting the presence of a number of tryptophan residues (Spectra not shown). Titration of swCDPK with Ca^{2+} enhanced the emission fluorescence intensity when excited at 280 nm, reaching saturation at approximately 1 μM calcium (Fig. 7A). Plot of the fluorescence intensity values at λ_{max} as a function of Ca^{2+}concentration (Fig. 7B) shows that the Ca^{2+} concentration required for half-maximal-enhancement of fluorescence intensity is 64 nM. The ratio of the fluorescence intensity at 350 nm and 310 nm, that represents emission by tryptophans and tyrosines respectively (Fig. 7A) underwent a reduction from 1.9 to 1.4 with addition of Ca^{2+}. A similar Ca^{2+}-induced fluorescence enhancement was observed when swCDPK was excited at 295 nm (Fig. 7C). The

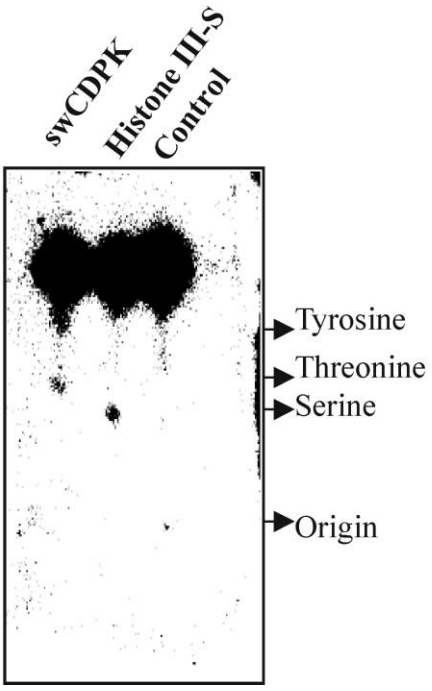

Fig. 5. Identification of phosphorylated amino acids. Phosphorylated histone III-S/phosphorylated swCDPK was hydrolyzed in 6 M HCl. The hydrolysates were resolved by PC. The position of standards is indicated by arrows. swCDPK, position of phosphorylated amino acid by autophosphorylation activity; histone III-S, position of phosphorylated amino acid by substrate phosphorylation activity; control, assay performed in the absence of the enzyme, the intense signal on autoradiogram represents the position of unreacted γ-^{32}P ATP.

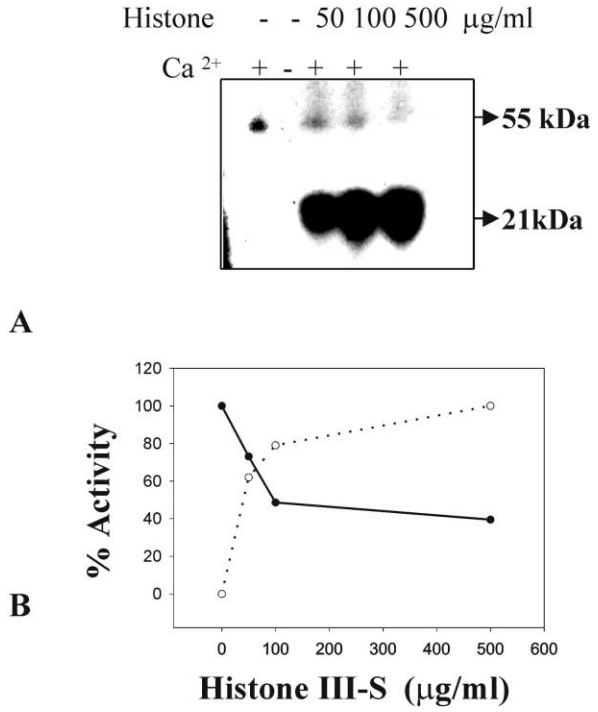

Fig. 6. Effect of histone III-S on autophosphorylation activity of swCDPK. Standard autophosphorylation assays were performed with 50 ng of purified swCDPK with different concentrations of histone III-S. The assay mixture was resolved in a 10% polyacrylamide gel containing SDS. The phosphorylated proteins were visualized by a phosphorimager. A. Autoradiogram shows the effect of increasing concentrations of histone III-S on autophosphorylation of 55 kDa swCDPK; B. Change in percentage autophosphorylation (●) by substrate phosphorylation (O). Percentage activity is derived from the photostimulated luminescence minus background (PSL–BG) of different phosphorylated bands in 'A'. One hundred per cent autophosphorylation represents a PSL–BG of 65 and 100% histone phosphorylation represents a PSL–BG of 790.

fluorescence spectra also showed a shift of λ_{max} from 350 to 367.5 nm with addition of Ca^{2+} (Fig. 7C). In addition, a change in spectral shape was observed above 100 nM Ca^{2+} (Fig. 7C). Fig. 7D clearly shows breaks or discontinuity in the plots representing fluorescence intensity values or λ_{max} as a function of [Ca^{2+}], at low (10–100 μM) and high (>100 μM) Ca^{2+} levels. These observations not only are clear evidence for Ca^{2+}-induced conformational change in swCDPK, but also imply the formation of at least two kinds of Ca^{2+}-enzyme complexes.

3. Discussion

This paper describes the purification and characterization of an early development-specific CDPK from sandalwood. Activation by sub-micromolar Ca^{2+}, independence of exogenous CaM and inhibition by CaM-antagonists of both substrate- and autophosphorylation activities are clear indicators for the presence of an endogenous CaM-like Ca^{2+}-binding domain in the purified enzyme. Furthermore, cross-reaction with antibodies raised against the CaM-like domain of soybean CDPK confirms the existence of an endogenous CaM-like structure. This structural feature acts as a diagnostic character for classifying this developmentally regulated sandalwood enzyme as a member of the CDPK family.

swCDPK exhibited divergent and similar biochemical properties with the prototype, soybean CDPK, and other CDPKs. swCDPK is a Ser/Thr protein kinase that exhibits a Ca^{2+} requirement for substrate phosphorylation activity comparable to that of other CDPKs (Harmon et al., 2000). The inhibition of substrate phosphorylation activity by salt (Section 2.4) implies ionic interactions between the positively charged substrate and the enzyme's active site. In corroboration, the inhibition of activity above 10 mM Mg^{2+} (Section 2.4) also suggests the disruption of ionic interaction between the enzyme and the substrate. Nonetheless, the possibilities of salt-induced conformational changes that result in the inhibition of activity cannot be ruled out from the present study. Highest activity that was obtained at about pH 7 (Section 2.4) indicates the presence of histidine residues at the enzyme's active site. The pH optimum (6.8–8.5) of swCDPK is comparable to that of soybean CDPK (Putnam-Evans et al., 1990), but differs from the alkaline pH

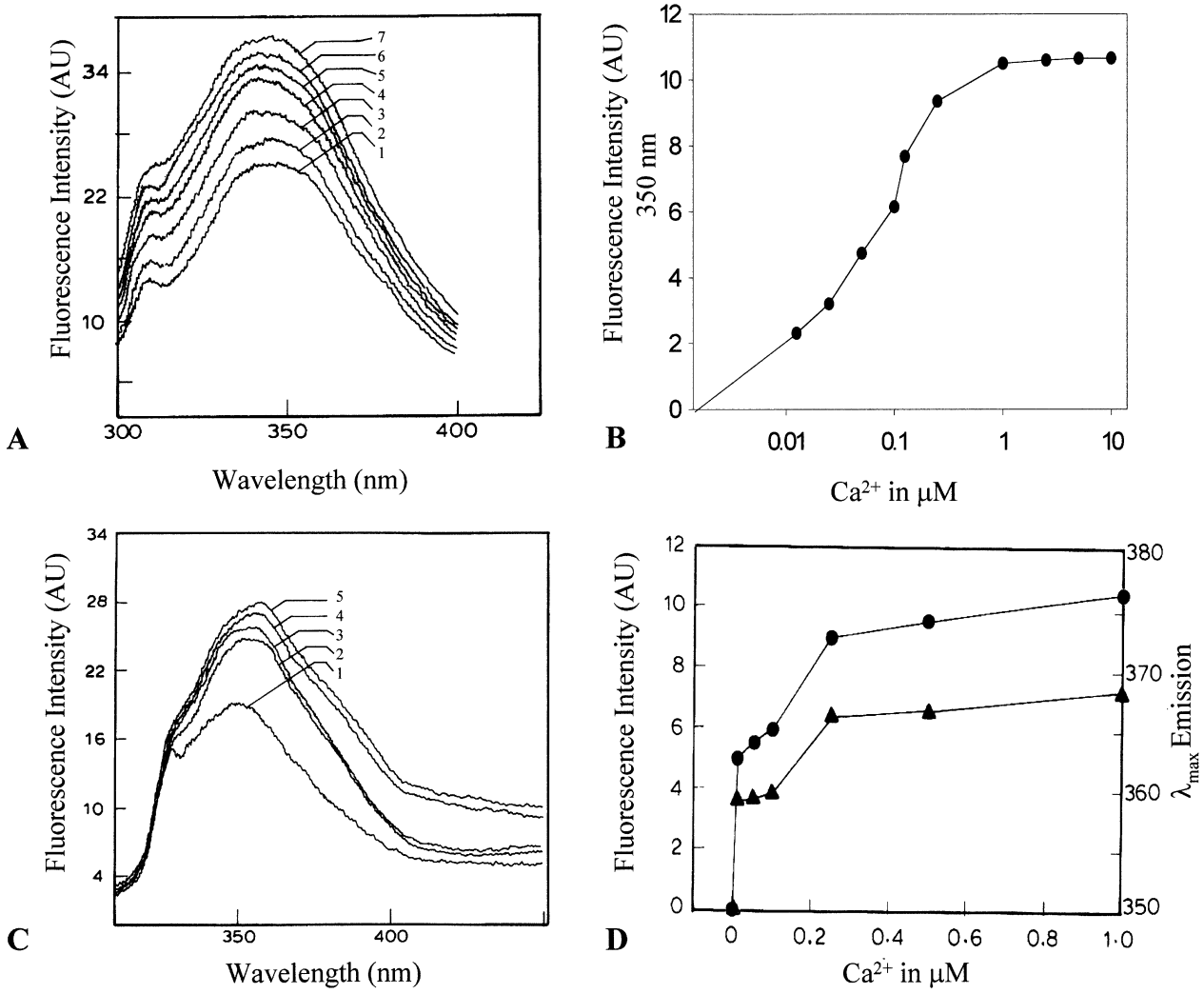

Fig. 7. Spectral properties of swCDPK. A. Change in fluorescence emission spectra of swCDPK (9 nM) with increasing Ca^{2+} at excitation wavelength of 280 nm. Numbers 1–7 represent [Ca^{2+}] of 0, 0.01, 0.05, 0.1, 0.125, 0.25 and 1 μM, respectively (overlapping spectra obtained at Ca^{2+} concentrations between 1 and10 μM are not shown); B. A replot of A showing fluorescence intensity at λ_{max} emission plotted as a function of Ca^{2+} concentration; C. Changes in fluorescence emission spectra of swCDPK (9 nM) with increasing Ca^{2+} at excitation wavelength of 295 nm. Numbers 1–5 represent [Ca^{2+}] of 0, 0.01, 0.1, 0.25 and 1 μM; D. Replot of values obtained from C representing fluorescence intensity (●) or λ_{max} emission (▲) plotted as a function of [Ca^{2+}].

requirement of groundnut CDPK (DasGupta, 1994). These variations in pH optima among CDPKs might indicate variations in the amino acid composition at their active sites.

Histone III-S was found to be the preferred exogenous substrate for swCDPK than histone VII-S, kemptide, BSA, casein or phosvitin (data not shown). Nonetheless swCDPK has a comparatively higher K_m for histone III-S than most other CDPKs (Putnam-Evans et al., 1990; Binder et al., 1994; Saha and Singh, 1995; Ganguly and Singh, 1998). This to some extent explains the low activity and as a result the low V_{max} value exhibited by swCDPK. It is plausible that some members of the CDPK family such as swCDPK and some isoforms of CDPK from potato (MacIntosh et al., 1996) and maize (Ogawa et al., 1998), that exhibit lower specific activity in the order of pmol min^{-1} mg^{-1}, are so designed as to regulate specific signaling pathways, thus having implications at the cellular level. However, it remains to be determined whether swCDPK exhibits higher specificity and different kinetic properties to its hitherto not identified in vivo substrate(s). Kinetic studies further reveal that swCDPK has high specificity for ATP, exhibiting a K_m of only 10 nM. Such a high affinity for ATP has not been reported for other CDPKs and is rather unusual for protein kinases. However, similar K_m values for ATP have been reported earlier in the case of cyclic AMP-dependent protein kinase (Cook et al., 1982; Whitehouse and Walsh, 1983).

There is no consensus on the regulatory role of autophosphorylation in CDPKs as both stimulatory (Chaudhuri et al., 1999) and inhibitory (Saha and

Singh, 1995) effects of autophosphorylation on substrate phosphorylation activity have been reported. The present finding that increasing histone III-S in the reaction inhibits the autophosphorylation of swCDPK (Fig. 6) suggests that the enzyme preferably phosphorylates the substrate rather than itself. This therefore implies that autophosphorylation may not be a prerequisite for substrate phosphorylation activity. However, another plausible explanation for this observation is the occurrence of ATP depletion in the assay that could have led to the ~2-fold increase in substrate phosphorylation over a 10-fold substrate range, catalyzed by a smaller population of autophosphorylated enzyme. In addition preautophosphorylation of swCDPK with 1mM cold ATP was neither inhibitory nor stimulatory for the enzyme's substrate phosphorylation activity (data not shown). With the available data a regulatory role for swCDPK-autophosphorylation therefore cannot be elucidated and requires further study. Nonetheless, the lower calcium requirement for autophosphorylation in comparison to that for substrate phosphorylation activities of swCDPK could be a mechanism of regulation shared by some members of the CDPK family. Similarly, soybean isoforms CDPK α,-β,-γ, also show a 1.3–3.3-fold decrease in the Ca^{2+}-requirement for autophosphorylation ($K_{0.5}=0.03$, 0.3 and 0.3 μM respectively) from that required for substrate phosphorylation ($K_{0.5}=0.06$, 0.4 and 1 μM respectively) (Lee et al., 1998). However, the 14-fold difference in the Ca^{2+} requirement for autophosphorylation ($K_{0.5}=\sim 50$ nM) and substrate phosphorylation ($K_{0.5}=700$ nM) of swCDPK is comparatively higher and physiologically significant as the $K_{0.5}$ values can be correlated with the resting $[Ca^{2+}]_{cyt}$ of ~30–50 nM and stimulus-induced elevation of ~600–800 nM in sandalwood embryogenic cells (Anil and Sankara Rao, 2000). Therefore, in the light of the low calcium requirement for autophosphorylation of swCDPK, it is likely that the enzyme is in an autophosphorylated state at resting levels of $[Ca^{2+}]_{cyt}$. Substrate phosphorylation becomes possible only upon stimulus-induced calcium elevation. In addition, the ~64 nM calcium required for half maximal change in fluorescence enhancement (Fig. 7B) is comparable to that required for autophosphorylation and is approximately 10-fold lower than that required for substrate phosphorylation activity of swCDPK. The fluorescence spectral data (Fig. 7) in conjunction with autophosphorylation properties of the enzyme suggest that low Ca^{2+} levels induce changes in conformation that can stimulate autophosphorylation activity.

According to the 'release of inhibition' model proposed by Huang et al. (1996), Ca^{2+}-binding to CDPK induces the interaction of the CaM-like domain to the autoinhibitory-junction domain (Harper et al., 1994; Harmon et al., 1994), releasing the autoinhibitor from the catalytic domain, thereby activating the enzyme. This model thus implies that Ca^{2+}-induced conformational changes are a necessary prerequisite for enzyme activation. In corroboration, CD analysis of a *Plasmodium falciparum* CDPK (PfCPK) has shown that a change from zero to saturating calcium induces a 16% decrease in the mean molar ellipticity at 222 nm (Zhao et al., 1994). Nevertheless there is lack of information concerning Ca^{2+}-induced conformational changes in plant CDPKs. The present study exploits the intrinsic fluorescence properties of swCDPK to gain insights into this phenomenon. Calcium titration of swCDPK not only results in the enhancement of fluorescence intensity but also in a reduction in the ratio of fluorescence intensity emitted at 350–310 nm (excitation $\lambda=280$ nm). This increased emission from tyrosines at 310 nm could be reflective of minor differences in the abilities of tyrosines to ionize, but it also suggests a decrease in the efficiency of non-radiative energy transfer from tyrosine residues to tryptophan residues. This reduction in energy transfer can be attributed to an increase in the relative distances between tyrosine and tryptophan residues brought about by Ca^{2+} binding. Corroboratively, the shift in λ_{max} emission observed when excited at 295 nm (Fig. 7C) indicates that Ca^{2+}-binding of swCDPK results in tryptophan residues shifting to a much lesser hydrophobic environment. The spectral shift as well as the prominent change in the spectral shape above 100 nM Ca^{2+} (Fig 7C) implies that further changes in conformation occur at higher Ca^{2+} levels. Corroboratively, the discontinuity in the plots of fluorescence intensity at λ_{max} or shift in λ_{max} as a function of $[Ca^{2+}]$(Fig. 7D) clearly indicate distinct changes in conformation of swCDPK at low and high concentrations of calcium. This suggests that at least two distinct Ca^{2+}-enzyme complexes are formed at different calcium concentrations. Considerable variation in the affinity for Ca^{2+} between the four Ca^{2+}-binding sites of vertebrate CaM (Klee and Vanaman, 1982) gives further support to this. Therefore, the monitoring of Ca^{2+}-induced conformational changes in swCDPK with step-wise increases in $[Ca^{2+}]$ within the physiological range provides new insights into this process.

In conclusion, the data presented confirms the identity of swCDPK as a CaM-like domain protein kinase. Nonetheless, considerable variations with respect to enzymatic properties such as a higher sensitivity to W7 inhibition ($IC_{50}=6$ μM), much higher specificity for ATP ($K_m=10$ nM) and a low turnover number ($1\times10^2 min^{-1}$) renders swCDPK a unique member of this family of kinases. Furthermore, biochemical and fluorescence spectral properties of the enzyme suggest the occurrence of considerable changes in conformation and activation of autophosphorylation at low levels of Ca^{2+}. Variation in the affinity to Ca^{2+} among the Ca^{2+}-binding sites of swCDPK could be the probable reason for activation of autophosphorylation- and substrate

phosphorylation activities at two different ranges of Ca^{2+}. However, elucidation of the role of autophosphorylation is necessary for complete understanding of the mechanism of regulation of enzyme activity.

4. Experimental

4.1. Chemicals

Histone III-S, Chelex 100, leupeptin, aprotinin, PMSF, ATP, phosphotyrosine, phosphothreonine, phosphoserine, DEAE-cellulose and other chemicals used were purchased from Sigma chemical company, USA, unless mentioned otherwise. Bovine serum albumin (BSA) fraction V was obtained from Boehringer Mannheim. Hydroxyapatite was purchased from Bio-Rad, USA. HRP conjugated goat anti-rabbit IgG was purchased from Bangalore Genie. Radioactive isotope, γ-^{32}P-ATP (5000 Ci/mmol) was obtained from BRIT, Hyderabad. Cibacron Blue-Sepharose 6B was prepared according to the method of Hughes et al., 1982.

4.2. Plant material

Endosperm explants from mature sandalwood fruits were cultured on MS medium (Murashige and Skoog, 1962) as described by Anil and Sankara Rao (2000), to sequentially induce embryogenic callus, callus proliferation, and embryogenesis. Torpedo- and cotyledonary stage somatic embryos that differentiate from the embryogenic calli, were harvested and used for protein purification.

4.3. Substrate phosphorylation assay

In a total volume of 0.15 ml, the assay mixture contained 1.4 mg ml^{-1} histone III-S in Ca/EGTA buffer (50 mM Hepes pH 7.2, 10 mM $MgCl_2$, 0.25 mM ethyleneglycol-bis (β-aminoethyl ether)-*N*,*N*,*N*′,*N*′-tetra acetic acid.[-EGTA]) with or without 0.2 mM $CaCl_2$ and 50 ng of purified swCDPK. The reaction was initiated with addition of 10 nM γ-^{32}P-ATP (5000 nCi/pmol) and incubated at 30 °C for 6 min. Termination of the reaction, spotting of the mixture on glass fiber filters and washing of the filters were carried out according to the method of Putnam-Evans et al. (1990). Counts were recorded on an LKB liquid scintillation counter. Assays were also performed with varying concentration of Ca^{2+}, W7 and CaM in the assay mixture. During purification, 5 μl of each fraction was assayed in Ca/EGTA buffer as described earlier using histone III-S as the exogenous substrate.

4.4. Purification of swCDPK

All steps of purification were performed at 4°C unless mentioned otherwise. Sandalwood torpedo/cotyledonary stage somatic embryos (30 g) were homogenized in liquid nitrogen using pestle and mortar and suspended in 3 volumes of cold buffer A (20 mM Tris, pH 7.2, 2.5 mM EDTA) containing 1 mM PMSF and 20 μg/ml aprotinin. The crude homogenate was centrifuged at 13,650 *g* at 4 °C for 30 min to separate cell debris from the crude supernatant. The crude supernatant was then subjected to 80% ammonium sulfate fractionation. The precipitated proteins were dissolved in buffer A containing 1 mM PMSF and 20 μg/ml aprotinin and dialyzed against 5 l of buffer A twice overnight.

The dialysate was applied on a DEAE-cellulose column (50 ml) equilibrated with buffer A. The column was washed with 100 ml of buffer A containing 0.05 M NaCl and the bound proteins eluted with 100 ml of buffer A containing 0.4 M NaCl. Fractions containing Ca^{2+}-dependent kinase activity were pooled and 1mM PMSF and 20 μg/ml aprotinin added. The pool was then dialyzed overnight against 5 l of buffer B (20 mM Tris, pH 7.2, 0.25 mM EDTA and 0.25 mM $CaCl_2$), twice overnight. The DEAE-pool was applied to a 15 ml hydroxyapatite column, equilibrated with buffer B. The column was washed with 2 column volumes of buffer B containing 5 mM K_2HPO_4. The kinase was eluted first with 20 ml of buffer B containing 25 mM K_2HPO_4 followed by a linear gradient of K_2HPO_4 (25–300 mM) in buffer B. Fractions having kinase activity were pooled. Protease inhibitors (1 mM PMSF, 20 μg/ml aprotinin and 10 μg/ml leupeptin) were added to this pool, followed by dialysis against 5 l of buffer C (20 mM Tris, pH 7.2, 0.2 mM EDTA and 5.5 mM $MgCl_2$), twice overnight.

The hydroxyapatite pool was applied to a 2 ml Cibachron Blue-Sepharose column, equilibrated with buffer C. The column was washed with 5 column volumes of buffer C containing 0.6 M NaCl. swCDPK was eluted with buffer C containing 0.2% CHAPS (buffer D). The purified preparation was stored in buffer D containing 10% glycerol at −80 °C until use. Spectroscopic measurements were carried out with freshly eluted enzyme in buffer D.

4.5. Electrophoresis and protein determination

Electrophoresis on 10% polyacrylamide gels was performed according to the method of Laemmli (Laemmli, 1970) and protein concentrations were measured according to the method of Bradford (Bradford, 1976) using BSA as standard.

4.6. Autophosphorylation assay

Purified swCDPK was assayed to determine Ca^{2+}-dependent autophosphorylation activity. The reaction was carried out as described by Anil et al. (2000), following which, the reaction mixture containing swCDPK

was resolved on a 10% SDS polyacrylamide gel at 45 V overnight. The gels were exposed to Kodak X-ray film for 24 h or visualized by phosphor imager. This assay was also performed in the presence of varying concentrations of Ca^{2+}, W7, CaM and histone III-S.

4.7. In-gel histone phosphorylation assay

In-gel phosphorylation of histone III-S was carried out according to the method described by McCurdy and Harmon (1992). SDS 10% polyacrylamide gel was polymerized in the presence of 0.5 mg/ml histone III-S. The purified preparation was incubated for 2 min in Laemmli's sample buffer at 70 °C. After resolving the protein on the gel, the gel was washed with six changes of 50 mM Hepes buffer (pH 7.2) for a period of 6 h to renature the proteins. The gel was then cut into strips and the CDPK kinase activity of the resolved enzyme was determined following the method of Harmon et al., (1986). The gel strips were washed to remove unreacted γ-^{32}P-ATP as described by Anil et al. (2000).

4.8. Phosphoamino acid analysis

Substrate phosphorylation and autophosphorylation assays were performed as described above. The phosphorylated swCDPK and phosphorylated histone III-S were subjected to acid hydrolysis in 6 M HCl by boiling at 100 °C under vacuum for 2 h. After mixing the hydrolysates with standard phosphoserine, phosphothreonine and phosphotyrosine, they were chromatographed on Whatman 3MM paper using a solvent system comprising of *n*-propanol and 0.5 N HCl (2:1). They were then rechromatographed with *n*-butanol, acetic acid and water (100:22:50) in the same direction. Radiolabeled amino acids were visualized by autoradiography, and standard phosphoamino acids by ninhydrin staining.

4.9. Western blot analysis

Purified swCDPK was resolved on a non-denaturing polyacrylamide gel and transferred to nitrocellulose membrane following standard conditions (Towbin et al., 1979). The immobilized protein was then subjected to western blot analysis as described by Anil et al. (2000), using polyclonal antibodies directed against the CaM-like domain of soybean CDPK (Bachmann et al., 1996).

4.10. Spectral studies

A Shimadzu UV spectrophotometer was used to study the absorption spectral properties of swCDPK between the range of 200–340 nm. Fluorescence spectroscopic studies were carried out in a RF5000 Shimadzu spectrofluorimeter, using excitation wavelengths of 280 and 295 nm, and fluorescence spectra recorded between 300 and 400 nm. Changes in fluorescence spectra of swCDPK with Ca^{2+}-titration were recorded.

Acknowledgements

We thank Professor S.K. Podder for valuable suggestions and critical reading of the manuscript, Professor A. C. Harmon for the gift of polyclonal anti-soybean CDPK and Professor C. Jayabaskaran for helpful discussions. This work was supported by the Department of Science and Technology and the Council of Scientific and Industrial Research, Government of India.

References

Anil, V.S., Sankara Rao, K., 2000. Calcium-mediated signaling during sandalwood somatic embryogenesis. Role for exogenous calcium as second messenger. Plant Physiology 123, 1301–1312.

Anil, V.S., Harmon, A.C., Sankara Rao, K., 2000. Spatio-temporal accumulation and activity of calcium-dependent protein kinases during embryogenesis, seed development and germination in sandalwood. Plant Physiology 122, 1035–1043.

Anil V.S., 2000. Study of Ca^{2+}-mediated signal transduction during embryogenesis in sandalwood (*Santalum album* L.) and characterization of an early development-specific CDPK. PhD thesis, Indian Institute of Science.

Bachmann, M., Shiraishi, N., Campbell, W.H., Yoo, B., Harmon, A.C., Huber, S.C., 1996. Identification of Ser-543 as the major regulatory phosphorylation site in spinach leaf nitrate reductase. Plant Cell 8, 505–517.

Binder, B.M., Harper, J.F., Sussman, M.R., 1994. Characterization of an *Arabidopsis* calmodulin-like domain protein kinase purified from *Escherichia coli* using affinity sandwich technique. Biochemistry 33, 2033–2041.

Bradford, M.M., 1976. A rapid and sensitive method for the quantitation of micrograms of protein utilizing the principle of protein-dye binding. Analytical Biochemistry 72, 248–254.

Chaudhuri, S., Seal, A., DasGupta, M., 1999. Autophosphorylation-dependent activation of a calcium-dependent protein kinase from groundnut. Plant Physiology 120, 859–866.

Cook, P.F., Neville, M.E., Varna, K.E., Hartl, F.T., Roskoski, J.R., 1982. Adenosine cyclic 3′,5′-monophosphate dependent protein kinase: kinetic mechanism for the bovine skeletal muscle catalytic subunit. Biochemistry 21, 5794–5799.

DasGupta, M., 1994. Characterization of a calcium-dependent protein kinase from *Arachis hypogea* (Groundnut) seeds. Plant Physiology 104, 961–969.

Ganguly, S., Singh, M., 1998. Characterization of a second calcium-dependent protein kinase from winged bean. Phytochemistry 48, 61–70.

Harmon, A.C., Gribskov, M., Harper, J.F., 2000. CDPKs—a kinase for every Ca^{2+} signal? Trends in Plant Science 5, 154–159.

Harmon, A.C., Yoo, B., McCaffery, C., 1994. Pseudosubstrate inhibition of CDPK, a protein kinase with a calmodulin-like domain. Biochemistry 33, 7278–7287.

Harmon, A.C., Putnam-Evans, C., Cormier, M.J., 1986. Calcium-dependent but Calmodulin independent protein kinase from soybean. Plant Physiology 83, 830–837.

Harper, J.F., Huang, J., Lloyd, S.J., 1994. Genetic identification of an autoinhibitor in CDPK, a protein kinase with a calmodulin-like domain. Biochemistry 33, 7267–7277.

Harper, J.F., Sussman, M.R., Schaller, G.E., Putnam-Evans, C., Charbonneau, H., Harmon, A.C., 1991. A calcium-dependent protein kinase with a regulatory domain similar to calmodulin. Science 252, 951–954.

Huang, J., Teyton, L., Harper, J.F., 1996. Activation of a Ca^{2+}-dependent protein kinase involves intramolecular binding of a calmodulin-like regulatory domain. Biochemistry 35, 13222–13230.

Hughes, P., Lowe, C.R., Sherwood, R.F., 1982. Metal ion-promoted binding of proteins to immobilized triazine dye affinity adsorbents. Biochemica et Biophysica Acta 700, 9–100.

Klee, C.D., Vanaman, T.C., 1982. Calmodulin. In: Anfinsen, C.B., Richards, F.M. (Eds.), Advances in Prot. Chemistry, Vol 35. pp. 213-321.

Laemmli, U.K., 1970. Cleavage of structural proteins during the assembly of the head of bacteriophage T4. Nature 227, 680–685.

Lee, J., Yoo, B., Harmon, A.C., 1998. Kinetic and calcium-binding properties of three calcium-dependent protein kinase isoenzymes from soybean. Biochemistry 37, 6801–6809.

MacIntosh, G.C., Ulloa, R.M., Raices, M., Tellez-Inon, M.T., 1996. Changes in calcium-dependent protein kinase activity in in vitro tuberization in potato. Plant Physiology 112, 1541–1550.

Malho, R., Trewavas, A.J., 1996. Localized apical increases of cytosolic free calcium control pollen tube orientation. Plant Cell 8, 1935–1949.

Marme, D., Dieter, P., 1983. In: Cheung, W. Y. (Ed.), Calcium and Cell function. Academic Press, New York, Vol. 4, pp. 263–311.

McCurdy, D.W., Harmon, A.C., 1992. Calcium-dependent protein kinase in the green alga *Chara*. Planta 188, 54–61.

Murashige, T., Skoog, G., 1962. A revised medium for rapid growth and bioassays with tobacco tissue cultures. Physiologia Plantarum 15, 473–497.

Ogawa, N., Yabuta, N., Ueno, Y., Izui, K., 1998. Characterization of a maize Ca^{2+}-dependent protein kinase phosphorylating phosphoenolpyruvate carboxylase. Plant Cell Physiology 39, 1010–1019.

Putnam-Evans, C.L., Harmon, A.C., Cormier, M.J., 1990. Purification and characterization of a novel calcium-dependent protein kinase from soybean. Biochemistry 29, 2488–2495.

Roberts, D.M., 1993. Protein kinases with calmodulin-like domains: novel targets of calcium signals in plants. Current Opinion in Cell Biology 5, 242–246.

Saha, P., Singh, M., 1995. Characterization of a winged bean (*Psophocarpus tetragonolobus*) protein kinase with calmodulin-like domain: regulation by autophosphorylation. Biochemical Journal 305, 205–210.

Sanders, D., Brownlee, C., Harper, J.F., 1999. Communicating with calcium. Plant Cell 11, 691–706.

Towbin, H., Staehelin, T., Gordon, T., 1979. Electrophoretic transfer of proteins from polyacrylamide gel to nitrocellulose sheets: Procedure and some applications. Proceedings of the National Academy of Sciences of the United States of America 76, 4350–4354.

Trewavas, A., 1999. Le calcium, c'est la vie: calcium makes waves. Plant Physiology 120, 1–6.

Whitehouse, S., Walsh, D.A., 1983. $Mg.ATP^2$-dependent interaction of the inhibitor protein of the CAMP-dependent protein kinase with the catalytic subunit. Journal of Biological Chemistry 258, 3682–3692.

Zhao, Y., Pokutta, S., Maurer, P., Lindt, M., Franklin, R.M., Kappes, B., 1994. Calcium-binding properties of a calcium-dependent protein kinase from *Plasmodium falciparum* and the significance of individual calcium-binding sites for kinase activation. Biochemistry 33, 3714–3721.

PERGAMON

Phytochemistry 58 (2001) 213–219

PHYTOCHEMISTRY

www.elsevier.com/locate/phytochem

Characteristics of an α-galactosidase associated with grape flesh

Han-Chul Kang[a,*], Seon-Hwa Lee[b]

[a]*Department of Plant Nutrition, National Institute of Agricultural Science and Technology, Rural Development Administration, Suwon 441-707, South Korea*

[b]*National Horticultural Research Institute, Rural Development Administration, Suwon 440-310, South Korea*

Received 1 September 2000; received in revised form 4 April 2001

Abstract

α-Galactosidase activity in grape flesh (*Vitis venifera* L. Muscat of Alexandria) was characterized by a marked increase in its activity 4 weeks after fruit bearing. After 12 weeks the specific activity of the enzyme had increased 15-fold. Several other glycosidases were measured at different stages of fruit development but none showed the increased levels of activity displayed by this α-galactosidase. α-Galactosidase activity (unit/g·fresh wt) increased by 52% during postharvest storage, whereas the unripe grape showed a "stagnancy" for 10–15 days prior to the increase. An α-galactosidase was partially purified ca. 103-fold from grape flesh of *Vitis labruscana* Honey black, by a procedure involving ammonium sulfate fractionation, Biogel P-60, melibiose-agarose, and Sephacryl S-200 chromatographic separations. The enzyme was effectively separated by affinity chromatography on melibiose-agarose, and was a monomer of 40–45 kDa as determined by SDS-PAGE and Sephacryl S-200 chromatographic analysis. The hydrolysis rate of *p*-nitrophenyl-α-D-Gal (PNP-α-D-Gal) was 4.2 times higher than that of PNP-β-D-Gal, implying an apparent α-anomer specificity, and natural oligosaccharides such as melibiose, stachyose, and raffinose were also considerably hydrolyzed. The enzyme was active over a narrow pH range with an optimal hydrolysis of stachyose and PNP-α-D-Gal at pH 6.0 and 7.0, respectively. EDTA or 1,10-phenanthroline did not substantially affect enzyme activity. © 2001 Elsevier Science Ltd. All rights reserved.

Keywords: *Vitis veniferae*; Vitaceae; Grape; α-Galactosidase

1. Introduction

α-Galactosidase (E.C. 3.2.1.22, α-D-galactoside galactohydrolase) is one of the exoglycosidases, capable of hydrolysing α-1,6 linked α-galactoside residues. α-Galactosidases are widely distributed in intra- or extracellular forms in microorganisms, plants and animals. The enzyme in plants, especially, has been greatly investigated from seeds in relation to germination (Dey and Pridam, 1969; Barham et al., 1971; McCleary and Matheson, 1974; Dey et al., 1983; Corchette and Guerra, 1987) and is also found in leaves and other tissues (Gatt and Baker, 1970; Thomas and Webb, 1978; Smart and Pharr, 1980; Gaudreault and Webb, 1983; Burns, 1990). Diverse forms of α-galactosidase occur occasionally in many plants, having molecular weights ranging from 25 to 270 kDa and different properties (Dey and Pridam, 1969, 1972; Thomas and Webb, 1977; Hankins et al., 1980; Smart and Pharr, 1980; Dey et al., 1983; Mujer et al., 1984; Haibath et al., 1991; Chrost and Schmitz, 1997; Irving et al., 1997). α-Galactosidases are generally involved in metabolic utilization of oligosaccharides such as raffinose, stachyose, melibiose, and galactomannan, that are even more widely distributed in storage organs such as seeds, roots, and tubers (McCleary and Matheson, 1974; Kandler and Hopf, 1980). α-Galactosidases have been implicated with the metabolism of galactolipids (Sastry and Kates, 1964; Pridam and Dey, 1974). In addition to these hydrolysis reactions, transglycosylation is catalyzed by the enzyme with somewhat broad acceptor specificity (Dey and Pridam, 1972).

Despite this wide distribution and diversity, α-galactosidases seem to be less abundant in fruits compared with other plant organelles. Biochemical/physiological aspects in fruits differ from those of other tissues or organelles in plants, and hence other types of α-galactosidase may be present in grape. Characterization of α-galactosidase in grape flesh would be helpful in understanding the physiological role of the enzyme. In this

* Corresponding author. Tel.: +82-31-290-0260; fax: +82-31-290-0261.

E-mail address: hckang3436@hanmail.net (H.-C. Kang).

0031-9422/01/$ - see front matter © 2001 Elsevier Science Ltd. All rights reserved.
PII: S0031-9422(01)00207-2

paper, we partially purified an α-galactosidase associated with grape flesh and present some of its biochemical characteristics.

2. Results and discussion

2.1. α-Galactosidase activity from grape flesh

The glycosidase activities of flesh (mesocarp plus placental tissue) from *Vitis venifera* L. Muscat of Alexandria are shown in Table 1. Of the various glycosidases assayed, α-galactosidase was the most active, followed by α-mannosidase, as measured by the assays at pH 5.0 or 7.0. Significant activities of α- and β-glucosidase, and β-galactosidase were found at acidic or neutral pH. Glycosidases were also evaluated from the flesh of other grape cultivars, Honey black, Marguerite, Edelweiss, Agawan, Egiodola, Green hungarian, and Takasumi at pH 7.0. For all of the strains tested, α-galactosidase was the most active, although other glycosidases also showed significant activities (data not shown). Fig. 1 shows the variation in the specific activities of galactosidase, glucosidase, and α-mannosidase in flesh from Muscat of Alexandria at different stages of fruit development. These glycosidase activities were scarcely found at the unripe stage (approximately up to 4 weeks from fruit bearing). After this stage, the activities increased rapidly to different extents. Approximately 15 times increase in α-galactosidase activity was observed during the ripening stage from 4 to 12 weeks. The most prominent increase was found at the mid-term of ripening stage (4–8 weeks from fruit bearing). The expression of α-galactosidase in the flesh was characterised by an increase in activity per g·fresh wt as well as in the activity per mg·protein along with the ripening stage. These results suggest that α-galactosidase might play an important role in grape flesh during fruit development. The marked expression of α-galactosidase synchronizing with the ripening stage could be correlated with the report of Gross (1986) that applied galactose stimulated ethylene production and promoted ripening of mature green tomatoes. But the results presented here do not elucidate any role for the α-galactosidase in the grape flesh. Putative variation of α-galacto sidase during postharvest storage at 4°C was assessed from the flesh of Honey black harvested after 9 or 12 weeks from fruit bearing (Fig. 2). In the latter grape, the α-galactosidase activity (unit/g· flesh wt) increased by 52% of control after 15 days of storage and then declined slowly. The unripe grapes harvested after 9 weeks, however, showed a "stagnancy" for 10–15 days of storage before an increase in activity occurred, and then the activity slowly increased albeit to a lesser extent than the more ripe grape.

Table 1
Distribution of glycosidases in grape flesh (*Vitis venifera* L. Muscat of Alexandria). The activity was measured for the grape harvested after 3 months from fruit bearing. The enzyme assay was run by hydrolysis of PNP-glycosides (2 mM) in 50 mM Na-acetate (pH 5.0) or K-phosphate (pH 7.0) containing 0.5% glycerol. Glycosidase activities were represented as units per g·fresh wt. Soluble solids content of the grape berry was 17.1°Bx. Activity values were expressed as means ± S.E. of three independent experiments

Substrate	Glycosidase activity (unit/g·flesh wt)	
	pH 5.0	pH 7.0
PNP-α-D-Gal	545.6±26.5	814.2±31.6
PNP-β-D-Gal	206.4±18.4	190.8± 9.5
PNP-α-D-Glc	195.4±12.0	374.1±11.7
PNP-β-D-Glc	201.9±10.2	309.0±22.1
PNP-α-L-Fuc	49.2± 4.3	101.4± 2.5
PNP-β-D-Fuc	31.3± 2.5	55.4± 3.1
PNP-α-D-Man	398.3±22.3	569.8±18.4
PNP-α-L-Ara	8.9± 0.2	6.1± 0.6
PNP-α-L-Rha	0.6± 0.1	0.8± 0.2
PNP-β-D-GlcUA	0.4± 0.1	0.5± 0.1
PNP-α-D-GlcNAc	2.4± 0.2	0.9± 0.2
PNP-β-D-GlcNAc	1.6± 0.1	0.7± 0.1
PNP-β-D-GalNAc	57.4± 2.4	63.3± 4.5
Polygalacturonic acid[a]	5.9± 0.5	7.7± 0.2

[a] The polygalacturonase activity was measured using 2-cyanoacetamide (Gross, 1982).

2.2. Purification of α-galactosidase

Purification of α-galactosidase was performed using flesh of *Vitis labruscana* Honey black. With regard to

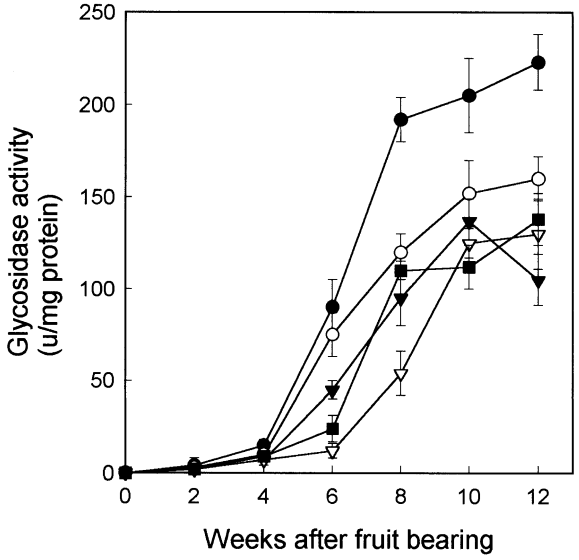

Fig. 1. Occurrence of glycosidases at different stages of fruit development. Glycosidase activities in grape flesh (*Vitis venifera* L. Muscat of Alexandria) was assessed up to 3 months after fruit bearing. α-Galactosidase (-●-), β-galactosidase (-▽-), α-mannosidase (-○-), α-glucosidase (-■-), and β-glucosidase (-▼-) activities were measured using PNP-glycosides and represented as unit per mg·protein. Activities per g·fresh wt increased also gradually along with the ripening stage (These data are not represented in the figure). Each value was the average of three replicate assays.

the α-galactosidase extraction from grape flesh, we note that homogenization of grape flesh with 0.2 M Na_2CO_3 resulted in an increase in α-galactosidase activity (unit/g·fresh wt) by 3.1 times compared with the extraction without Na_2CO_3. Alternatively, addition of 0.05 N NaOH caused the enzyme activity to increase as much as 2.8 times. Thus, the increase of ionic strength and/or the augmentation of pH (pH was elevated to 5.1 from 3.9.) appeared to release more α-galactosidase from the grape flesh. The α-galactosidase from grape flesh was stable during the initial steps of the purification procedures. The stability gradually decreased as the purification steps proceeded and dilution of the enzyme also accelerated a decrease in activity (data not shown). Stabilization or restoration of activity was attempted by adding dithiothreitol (2 and 10 mM) or EDTA (1 and 5 mM), but the stability of α-galactosidase was not affected by these compounds. The activity loss was considerably prevented by addition of glycerol in the equilibration/elution buffers during the purification procedure.

The enzyme was partially purified by salting out with ammonium sulfate and using chromatographic steps involving Biogel P-60, melibiose-agarose, and Sephacryl S-200 columns respectively. A peak of α-galactosidase activity was resolved on melibiose-agarose chromatography.

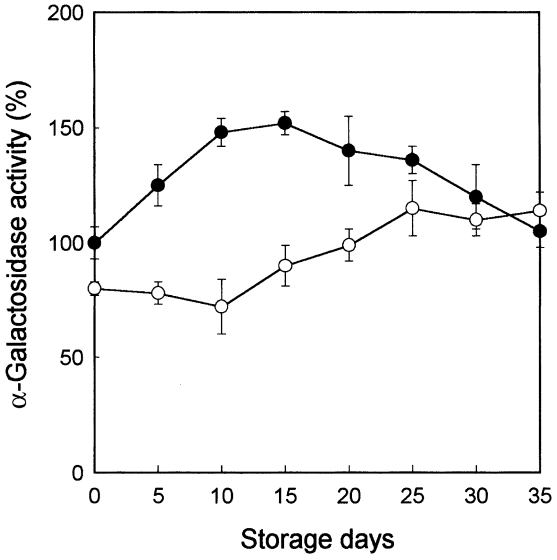

Fig. 2. Activity variation of α-galactosidase during postharvest storage. Grapes (Honey black) were collected after 9 weeks (-○-) and 12 weeks (-●-) and stored at 4°C. The fruits reached each storage day were stored at −70°C. The α-galactosidase activity in flesh was measured at the same time. One hundred per cent activity of α-galactosidase was 109 unit/g·fresh wt. The α-galactosidase activity increased more rapidly at room temperature than at 4°C. Difficulties in storage at room temperature hampered the test for more prolonged intervals (data not shown). Protein concentration was roughly consistent during postharvest storage. Soluble solid contents increased parallel with the storage days as follows: from 12.1 to 14.5 and from 14.7 to 18.1°Bx in grapes harvested after 9 and 12 weeks, respectively. Each value was the average of three replicate assays.

The fractions obtained from the affinity chromatography were further purified using Sephacryl S-200 chromatography (Fig. 3). This gel chromatography was the final step in the purification of α-galactosidase because its instability impeded any further chromatography. Specific activity of the enzyme was increased more than 103-fold by the purification procedure (Table 2). SDS-PAGE analysis of the main fractions with peak activity from the Sephacryl S-200 chromatography showed one major band with a monomeric molecular mass of 45 kDa and some faint bands (Fig. 4). Affinity chromatography on melibiose-agarose was crucial for enzyme purification. Even though melibiose (6-*O*-α-D-galactopyranosyl-D-glucose) might not be perfect as an affinity ligand for chromatography, this carbohydrate seems to be effective for the enzyme purification in

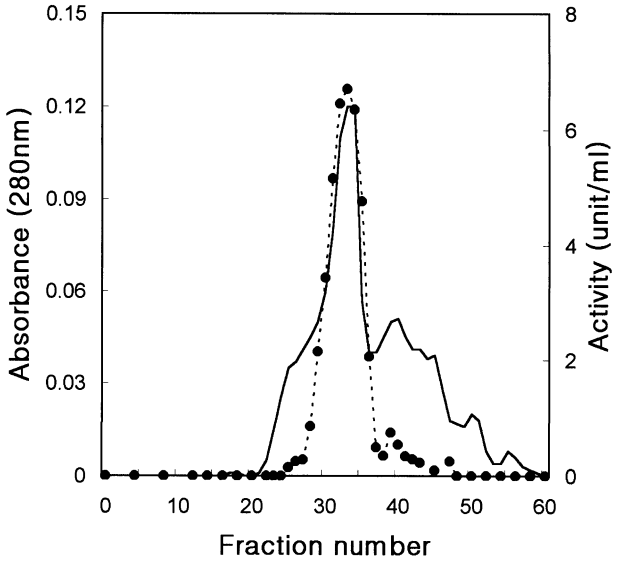

Fig. 3. Elution profile of α-galactosidase from Sephacryl S-200 chromatography. The active fractions from melibiose-agarose chromatography were loaded onto a Sephacryl S-200 column that was equilibrated with K-phosphate buffer (pH 7.0, 50 mM) containing 2% glycerol. Proteins were eluted using the same buffer along with measurement of absorbance at 280 nm (—). The α-galactosidase activity (unit/ml, -●-) was monitored using PNP-α-D-Gal as a substrate. One fraction volume was 5 ml.

Table 2
Purification summary of α-galactosidase from grape flesh of *Vitis labruscana* Honey black[a]

Purification step	Total protein (mg)	Total activity (μ)	Specific activity (μ/mg protein)	Purification fold
Crude extract	980.1	490.1	0.50	1.00
Ammonium sulfate	275.4	294.7	1.07	2.14
Biogel P-60	64.2	201.9	3.14	6.28
Melibiose-agarose	5.8	140.5	24.22	48.44
Sephacryl S-200	1.9	98.0	51.58	103.16

[a] α-Galactosidase assay used 2 mM PNP-α-D-Gal as a substrate.

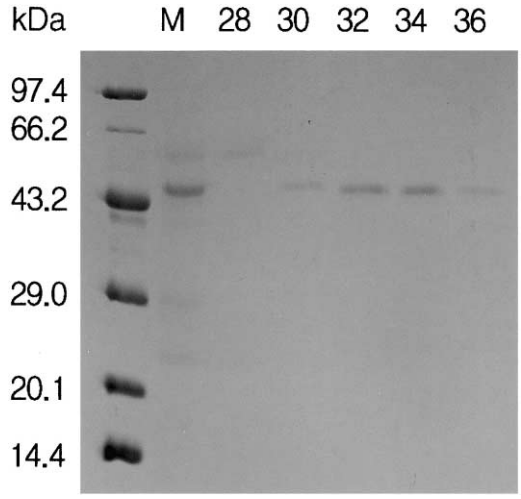

Fig. 4. SDS-polyacrylamide gel electrophoresis of purified α-galactosidase from the grape flesh. Outer left lane: reference proteins consisted of phosphorylase b (M_r; 97,400), BSA (66,200), ovalbumin (43,000), carbonic anhydrase (29,000), trypsin inhibitor (20,100), and lysozyme (14,400). Other lanes: M, the active fraction from melibiose-agarose chromatography; 28–36, the fraction numbers from the Sephacryl S-200 chromatography. The gel was stained with Coomassie Brilliant Blue R-250 and then with silver nitrate. Some faint bands (35 and 38 kDa) were observed in lanes 34 and 36 (not very visible in gel photo).

view of 7.7 times increase in specific activity during the stage from Biogel P-60 to affinity chromatography. The enzyme was stored in 20% glycerol at −70°C, and over 85% of the initial activity was retained after 3 months.

2.3. Substrate specificity of α-galactosidase

The purified α-galactosidase was assayed using different PNP-glycosides (Table 3a). The PNP-α-D-Gal was hydrolyzed more efficiently by the purified galactosidase than any other substrate tested, and *o*-nitrophenyl α-D-Gal (ONP-α-D-Gal) was also easily hydrolyzed. β-D-gal was scarcely hydrolyzed, showing 16% of the α-D-Gal hydrolysis (control), and the extent of 6-*O*-β-D-Gal-β-D-Gal was similarly low. Another galactose-related compounds such as β-D-Lac, Lac-*N*-bioside, and β-D-GalUA were rarely hydrolyzed, resulting in 4.3–12.6% activity of the control, and β-D-GalNAc was not efficiently hydrolyzed. The rapid hydrolysis of α-D-Gal and low hydrolysis of β-D-Gal suggest that the galactosidase is α-anomer specific.

Table 3b shows the hydrolysis of a range of natural or synthetic di-polysaccharides related with galactose. The activity represented as amount of galactose liberated was compared with the hydrolysis of ONP-α-D-Gal (control). ONP-α-D-Gal was used as a control substrate in place of PNP-α-D-Gal since *p*-nitrophenol was an inhibitor of the galactose dehydrogenase used to measure the galactose released (Bhalla and Dalling, 1984). Considerable liberations of galactose were obtained from natural oligosaccharides such as melibiose, stachyose, and raffinose, and the hydrolysis extent from stachyose was the most, showing 32.4% of control. A synthetic disaccharide, 4-*O*-α-D-Gal-D-Gal, was also significantly hydrolyzed. Poly-galacturonic acid was not effectively

Table 3a
Substrate specificity of α-galactosidase assayed using PNP-glycosides. The purified α-galactosidase was assayed for its activity using different PNP-glycosides (2 mM) in K-phosphate (50 mM, pH 7.0) containing 0.5% glycerol. The activities measured by the standard assay method were compared with the hydrolysis of PNP-α-D-Gal (100%), which was 49 units/mg·protein. All values were the mean of two replicate assays

Substrates	Relative activity (%)
PNP-α-D-Gal	100.0
ONP-α-D-Gal[a]	78.2
PNP-β-D-Gal	16.0
PNP-β-D-Lac	4.3
PNP-Lac-*N*-bioside	4.7
PNP-β-D-GalUA	12.6
PNP-6-*O*-β-D-Gal-β-D-Gal	16.1
PNP-α-D-Glc	7.0
PNP-β-D-Glc	6.2
PNP-α-L-Fuc	0
PNP-β-D-Fuc	0
PNP-α-D-Man	3.7
PNP-α-L-Ara	<1.0
PNP-α-L-Rha	0
PNP-β-D-GlcUA	<1.0
PNP-α-D-GlcNAc	<1.0
PNP-β-D-GlcNAc	<1.0
PNP-β-D-GalNAc	<1.0

[a] ONP-α-D-Gal is *o*-nitrophenyl α-D-galactopyranoside.

Table 3b
Substrate specificity of α-galactosidase for natural or synthetic carbohydrates. The purified α-galactosidase was incubated with galactose related carbohydrates (2 mM) in K-phosphate (50 mM, pH 6.0) containing 0.5% glycerol, and estimation of galactose released was performed as described in Experimental. Polygalacturonic acid was used as a substrate for polygalacturonase assay, and the activity determined using 2-cyanoacetamide. The activities were compared with the hydrolysis of ONP-α-D-Gal (100%), which was 42 units/mg · protein. All values were the mean of three replicate assays

Substrates	Free galactose released (%)
ONP-α-D-Gal	100.0
Melibiose	17.1
D-Lactose	7.6
Lactulose	2.0
Lacto-*N*-tetraose	2.7
Lactobionic acid	7.1
Melibionic acid	3.0
3-*O*-β-D-Gal-D-Ara	<1.0
4-*O*-α-D-Gal-D-Gal	26.7
4-*O*-β-D-Gal-D-Man	12.7
4-*O*-β-D-Gal-D-Glc	11.3
Stachyose	32.4
Raffinose	19.8
Polygalacturonic acid	<1.0

hydrolyzed, suggesting that the purified enzyme is not a polygalacturonase. Rapid hydrolysis of the synthetic substrate PNP-α-D-Gal and relatively slow hydrolysis of the oligosaccharides were similar to the α-galactosidase from *Cucurbita pepo* leaves (Thomas and Webb, 1977).

2.4. Other characteristics

Apparent molecular mass of the α-galactosidase was also determined by a gel filtration chromatography. The 34th fraction obtained from the final chromatographic step was co-injected with size marker onto a Sephacryl S-200 column. This protein mixture was eluted along with monitoring of the activity (unit/ml) peak, and the molecular mass was calculated to be ca. 40 kDa. On the analogy of the result from this gel chromatography, the 45 kDa band in the SDS-PAGE (Fig. 4) was considered as an α-galactosidase since 40 kDa of molecular mass determined from the chromatography approached to this value and the intensities of the 45 kDa bands were roughly proportional to the activity profile.

The α-galactosidase was further characterized by measuring its activity in buffers of varying pH using 2 mM PNP-α-D-Gal or stachyose as substrates (Fig. 5-A and B). When PNP-α-D-Gal was used as a substrate, the optimum pH for the activity was estimated to be around 7.0. But the pH profile assayed with a natural substrate, stachyose, resulted in a lowered pH optimum of 6.0. The pH for half maximal activity was ca. 4.5–5.2 and the activity rapidly increased from pH 4.0 to 6.0–7.0. This rapid increase in the activity up to pH 6.0–7.0 could have a correlation with the environment of grape since pH in flesh increases into a weaker acidity as ripening proceeds. Thus, increase in pH during ripening might be an important factor of α-galactosidase regulation in the grape flesh. However, it was not confirmed in this experiment whether such pH variation play an exclusive role in the enzyme activation.

The requirement of divalent cations for the α-galactosidase activity was examined using 1 mM Mg^{2+}, Co^{2+}, Zn^{2+}, Fe^{2+}, Cu^{2+}, Mn^{2+}, Cd^{2+}, and Ca^{2+} with chloride ion as a counter part ion. Addition of Fe^{2+} ion to the assay mixture in the absence of EDTA elevated the α-galactosidase activity by 46%. Other cations did not significantly increase or decrease the activity, except 49% inhibitory effect by Cd^{2+} (detailed data not shown). 1, 10-Phenanthroline or EDTA (0.5 and 2.0 mM) resulted in only a slight decrease in activity ranging from 90 to 98% of the initial activity (detailed data not shown).

Heat stability was examined with the 36th fraction from the Sephacryl S-200 chromatography. The enzyme was preincubated at 30, 45, or 60°C for 10 min and assayed using PNP-α-D-Gal. The activity decreased to 62% of the initial activity when preincubated at 60°C (detailed data not shown).

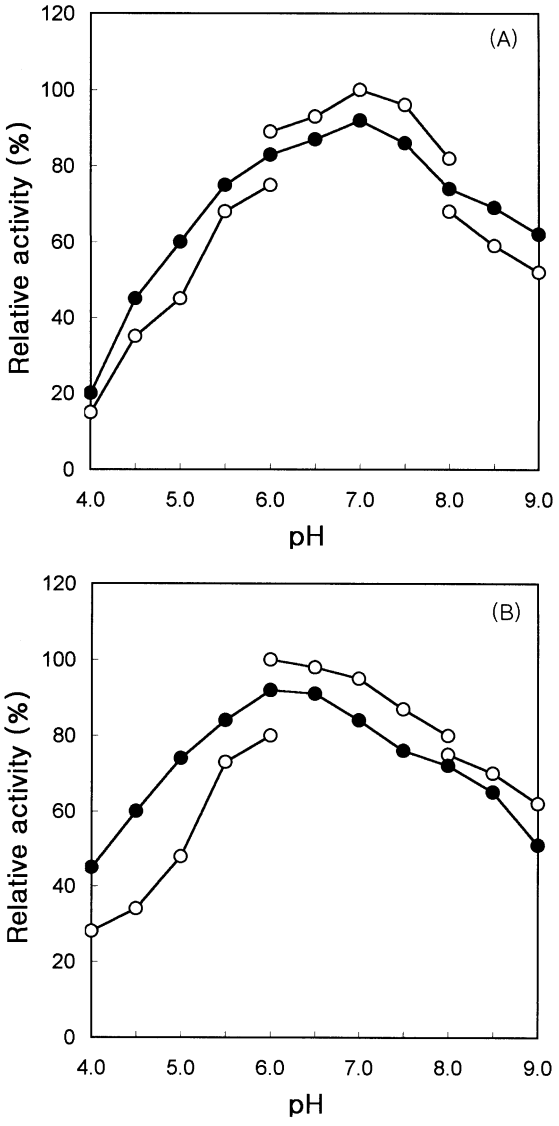

Fig. 5. Effect of pH on the hydrolysis of synthetic and natural substrates by α-galactosidase. The purified α-galactosidase was assayed using the following two series of buffers (1 ml) supplemented with 0.5% glycerol. (1) A three-buffer mixture (25 mM acetic acid, 25 mM Mes, and 50 mM Tris, -●-) titrated to the indicated pH values with KOH or HCl. (2) Acetate buffer 50 mM, pH 4.0–6.0; K-phosphate 50 mM, pH 6.0–8.0; Tris–HCl 50 mM, pH 8.0–9.0 (-○-). The pH effect was examined using PNP-α-D-Gal (A) and stachyose (B) as substrates. The relative activities calculated by two replicate assays were compared with the maximum activities (100%) that were equivalent to 39 and 14 units/mg·protein for (A) and (B), respectively.

3. Experimental

3.1. Plant materials

Grapevines of 4–5 year old *Vitis* cultivars (Muscat of Alexandria, Agawan, Marguerite, Edelweiss, Egiodola, Green hungarian, Honey black, and Takasumi) were cultivated in a greenhouse under ca. 14 h of daylight and 10 h of darkness at temperatures ranging from 18 to 31°C. Healthy, unblemished grapes were harvested up

to 3 months at intervals of 2 weeks after fruit bearing. After surface sterilization with 60% ethanol, fruits were rinsed with sterile water and immediately stored at −70°C until needed.

In order to test variations in α-galactosidase activities during postharvest storage, several bunches of grapes (*Vitis labruscana* Honey black) harvested after 9 or 12 weeks after fruit bearing were stored for 5 weeks at 4°C. Infection was minimized by repetitive rinses using 60% aq. ethanol and sterile water every 5 days during storage. At intervals of 5 days, the grapes were randomly picked from the bunches and immediately stored at −70°C until a simultaneous assay of α-galactosidase activity in flesh could be carried out. The grapes stored at −70°C just after harvest were used as controls for measuring the initial activity of the flesh.

3.2. Measurement of glycosidases

Grape flesh, separated from whole grapes, was mixed with 2% glycerol, and then directly homogenized for 30 s. The resulting paste was filtered through two layers of nylon cloth, and the filtrate was centrifuged at 8000 *g* for 20 min. After eliminating pellets, the supernatant was used for measurement of glycosidase activity in flesh. The standard assay of glycosidase was performed using PNP-glycosides as substrate. Enzyme samples were added to K-phosphate (50 mM, pH 7.0, in 1 ml of final volume) containing 0.5% glycerol. Reactions were initiated by adding 2 mM (final concentration) of substrate. After 30 min of incubation at 37°C, release of *p*-nitrophenol from the hydrolysis of substrate was detected spectrophotometrically by measuring the increase in absorbance at 410 nm (molar extinction coefficient = 1.84×10^4 M^{-1} cm^{-1}). Eventually, hydrolysis of di-, oligo-, and polysaccharides by α-galactosidase was examined by measurement of the galactose content using galactose dehydrogenase according to the method of Kurz and Kurt (1974). Enzyme sample was added to 400 μl of K-phosphate (50 mM, pH 6.0) containing 0.5% glycerol and 2 mM substrates. After incubation for 60 min at 37°C, the reaction was stopped by boiling for 5 min. The hydrolysed sample was cooled and put together with 570 μl Tris/HCl (0.1 M, pH 8.6), 20 μl of 15 mM NAD, and 10 μl galactose dehydrogenase solution (Sigma. from *Pseudomonas fluorescens*, 8.5 units/ml), with the incubation then further continued for 60 min at 37°C. The difference in Abs_{340nm} was measured from zero to the final incubation time. Quantitative analyses were performed from a calibration curve of galactose from 0 to 100 nmol. One unit of enzyme activity, in the method using PNP-glycosides, was expressed as the release of one μmol of free *p*-nitrophenol/min and specific activity as the amount released/min/mg·protein. Activity units from the method using galactose dehydrogenase were defined in the same way, except galactose was released in place of *p*-nitrophenol. Separate blanks were used for each enzyme and substrate preparation.

The pH effect of α-galactosidase was examined with 2 mM PNP-α-D-Gal or stachyose using the following buffers of similar ionic strengths: a three-buffer mixture (25 mM acetic acid, 25 mM Mes, and 50 mM Tris; Ellis and Morrisson, 1982) titrated to different pH values with KOH or HCl. Another buffer series was also used for this pH experiment: acetate buffer 50 mM, pH 4.0–6.0; K-phosphate 50 mM, pH 6.0–8.0; Tris/HCl 50 mM, pH 8.0–9.0. All buffers contained 0.5% glycerol. Hydrolysis of PNP-α-D-Gal in these buffers was determined by the standard assay method as described. The enzyme assay with stachyose was carried out in 500 μl of the two series buffers. After incubation for 1 h, each reaction mixture (200 μl) was taken to minimize the pH effect of these buffers on the subsequent galactose dehydrogenase. These samples were each added to 800 μl of the reaction mixtures for the galactose dehydrogenase assay. Further incubation and determination of galactose were performed as described. Non-enzymatic hydrolysis of PNP-α-D-Gal occurred slightly at alkaline pH, and these values were subtracted.

3.3. Extraction and purification of α-galactosidase

All purification procedures were carried out at 4°C. Grape flesh (2.6 kg) from *Vitis labruscana* Honey black was homogenized for 30 s in the presence of 0.2 M Na_2CO_3, 1% (w/v) insoluble polyvinylpolypyrrolidone, and 5% glycerol. The homogenate was filtered through two layers of nylon cloth. The resulting filtrate was centrifuged at 8000 *g* for 20 min and the pellet discarded. The supernatant was fractionated with ammonium sulfate at 30–55% saturation. The precipitate was recovered by centrifugation at 10,000 *g* for 20 min and resuspended in 100 ml of 40 mM potassium phosphate buffer (pH 7.0) containing 2% glycerol (buffer A). Clarification was done by dialysis with the same buffer and insoluble materials were removed by centrifugation at 10,000 *g* for 20 min.

The clarified supernatant was applied to a Biogel P-60 (Bio-Rad) column equilibrated with buffer A. Proteins were eluted with the same buffer at a flow rate of 12 ml/h. An additional aim of this step prior to affinity chromatography was to minimize various small substances such as pigments, which may interfere with chromatographic behavior by nonspecific adsorption. α-Galactosidase activity was monitored using PNP-α-D-Gal as a substrate throughout the purification procedures including this step.

The active fractions obtained were loaded onto a melibiose-agarose (Sigma) column (2 × 10 cm) equilibrated with buffer A. After washing the column, proteins were eluted with 200 ml of buffer A containing a linear gradient of K-phosphate (0–500 mM) at a flow rate of 15

ml/h. Fractions with α-galactosidase activity were collected and clarified by centrifugation for next step.

The pooled fractions from the affinity chromatography were further purified using Sephacryl S-200 (Pharmacia) chromatography. Proteins were eluted with 50 mM K-phosphate buffer (pH 7.0) containing 2% glycerol at a flow rate of 12 ml/h. Purification was followed by monitoring the absorbance at 280 nm and assaying enzyme activity. Except for physiological aspects, all of the experiments on α-galactosidase were performed using this sample obtained from this chromatography.

3.4. Native molecular mass determination

The apparent molecular mass of the purified α-galactosidase was estimated by gel filtration chromatography using a Sephacryl S-200 column (2 × 90 cm), which was equilibrated with 50 mM K-phosphate buffer (pH 7.0) containing 2% glycerol. The following proteins were co-injected with the enzyme to the column for the calibration: aldolase (M_r; 158,000), phosphorylase b (97,400), BSA (66,200), ovalbumin (43,000), and cytochrome c (12,000). The proteins were eluted with the same buffer at a flow rate of 12 ml/h. Along with measuring Abs_{280nm}, the activity peak was monitored by assaying the enzyme activity using PNP-α-D-Gal as substrate.

3.5. Other analytical methods

Soluble solid contents were measured with a refractometer using 50 μl of flesh juice, that was prepared by slightly grinding and subsequent centrifugation at 10,000 *g* for 5 min. Reducing sugars produced from the hydrolysis of polygalacturonic acid were measured using 2-cyanoacetamide (Gross, 1982). SDS-PAGE was performed according to the method of Laemmli (1970). A slab gel that consisted of 12.5% acrylamide resolving gel and 5% acrylamide stacking gel was used, with the gel stained with Coomassie Brilliant Blue R-250 and then with silver nitrate (Wray et al., 1981). Protein concentrations were determined by the dye-binding assay of Bradford (1976) using BSA as a standard protein.

References

Barham, D., Dey, P.M., Griffiths, D., Pridam, J.B., 1971. Studies on the distribution of α-galactosidases in seeds. Phytochemistry 10, 1759–1763.

Bhalla, P.L., Dalling, M.J., 1984. Characteristics of a β-galactosidase associated with the stroma of chloroplast prepared from mesophyll protoplast of the primary leaf of wheat. Plant Physiol. 76, 92–95.

Bradford, M.M., 1976. A rapid and sensitive method for the quantitation of microgram quantities of proteins utilizing the principle of protein-dye binding. Anal. Biochem. 72, 248–254.

Burns, J.K., 1990. α- And β-galactosidase activities in juice vesicles of stored Valencia oranges. Phytochemistry 29, 2425–2429.

Chrost, B., Schmitz, K., 1997. Changes in soluble sugar and activity of α-galac-tosidases and acid invertase during muskmelon (*Cucumis melo* L.) fruit development. J. Plant Physiol. 151, 41–50.

Corchette, M., Guerra, H., 1987. α- And β-galactosidase activities in protein bodies and cell walls of lentil seed cotyledons. Phytochemistry 26, 927–932.

Dey, P.M., Del Campillo, E.M., Lezica, R.P., 1983. Characterization of a glycoprotein α-galactosidase from lentil seeds (*Lens culinaris*). J. Biol. Chem. 258, 923–929.

Dey, P.M., Pridam, J.B., 1969. Purification and properties of α-galactosidases from *Vicia faba* seeds. Biochem. J. 113, 49–55.

Dey, P.M., Pridam, J.B., 1972. Biochemistry of α-D-galactosidase.. In: Meister, A. (Ed.), Advances in Enzymology, Vol. 36. Academic, New York, pp. 91–130.

Ellis, K.J., Morrisson, J.F., 1982. Buffers of constant ionic strength for studying pH-dependent processes. Methods Enzymol. 87, 405–426.

Gatt, S., Baker, E.A., 1970. Purification and separation of α- and β-galactosidases from spinach leaves. Biochim. Biophys. Acta 206, 125–135.

Gaudreault, P.R., Webb, J.A., 1983. Partial purification and properties of an alkaline α-galactosidase from mature leaves of *Cucurbita pepo*. Plant Physiol. 71, 662–668.

Gross, K.C., 1982. A rapid and sensitive spectrophotometric method for assaying polygalacturonase using 2-cyanoacetamide. HortScience 17, 933–934.

Gross, K.C., 1986. Promotion of ethylene evolution and ripening of tomato fruit by galactose. Plant Physiol. 79, 306–307.

Haibath, F., Hata, J., Mitra, M., Dhar, M., Harmata, M., Sun, P., Smith, D., 1991. Purification and characterization of a *Coffea canephora* α-D-galactosidase isozyme. Biochem. Biophys. Res. Commun 181, 1564–1571.

Hankins, C.N., Kindinger, J.I., Shannon, L.M., 1980. Legume α-galactosidases which have hemagglutinin properties. Plant Physiol. 65, 618–622.

Irving, D.E., Hurst, P.L., Ragg, J.S., 1997. Changes in carbohydrates and carbohydrate metabolism enzymes during the development, maturation, and ripening of buttercup squash (*Cucurbita maxima* D. Delica). J. Am. Soc. Hort. Sci. 122, 310–314.

Kandler, O., Hopf, H., 1980. Occurrence, metabolism and function of oligosaccharides. In: Stumpf, P.K., Conn, E.E. (Eds.), The Biochemistry of Plants. A Comprehensive Treatise, Vol. 3. Academic, New York, pp. 221–270.

Kurz, G., Kurt, W., 1974. D-Galactose UV-assay with galactose dehydrogenase. In: Bergmeyer, H.U. (Ed.), Methods of Enzymatic Analysis, Vol. 3. Academic, New York, pp. 1279–1287.

Laemmli, U.K., 1970. Cleavage of structural proteins during the assembly of the head of bacteriophage. Nature 227, 680–685.

McCleary, B.V., Matheson, N.K., 1974. α-D-galactosidase activity and galactomannan and galactosylsucrose oligosaccharide depletion in germinating legume seeds. Phytochemistry 13, 1747–1757.

Mujer, C.V., Ramirez, D.A., Mendoza, E.M.T., 1984. Coconut α-D-galactosidase isoenzymes: isolation, purification and characterization. Phytochemistry 23, 1251–1254.

Pridam, J.B., Dey, P.M., 1974. The nature and function of higher plant α-galactosidases. In: Pridam, J.B. (Ed.), Plant Carbohydrate Biochemistry. Academic, New York, pp. 83–96.

Sastry, P.S., Kates, M., 1964. Hydrolysis of monogalactosyl and digalactosyl diglycerides by specific enzymes in runner-bean leaves. Biochemistry 3, 1280–1287.

Smart, E.L., Pharr, D.M., 1980. Characterization of α-galactosidase from cucumber leaves. Plant Physiol. 66, 731–734.

Thomas, B., Webb, J.A., 1977. Multiple forms of α-galactosidase in mature leaves of *Cucurbita pepo*. Phytochemistry 16, 203–206.

Thomas, B., Webb, J.A., 1978. Distribution of α-galactosidase I in *Cucurbita pepo*. Plant Physiol. 62, 713–717.

Wray, W., Boulikas, T., Wray, V.P., Hancock, B., 1981. Silver staining of proteins in polyacrylamide gels. Anal. Biochem. 118, 197–203.

PERGAMON

Phytochemistry 58 (2001) 221–225

PHYTOCHEMISTRY

www.elsevier.com/locate/phytochem

Endogenous lectin as a possible regulator of the hydrolysis of physiological substrates by soybean seed acid phosphatase

Hiroshi Aoyama[a], Alexandre D.M. Cavagis[a], Eulázio M. Taga[b], Carmen V. Ferreira[a,*]

[a]*Departamento de Bioquimica, Instituto de Biologia, Universidade Estadual de Campinas (UNICAMP), 13083-970 Campinas, São Paulo, Brazil*
[b]*Departamento de Ciências Biológicas, Faculdade de Odontologia de Bauru, Universidade de São Paulo (USP), 17043-101 Bauru, São Paulo, Brazil*

Received 11 May 2000; received in revised form 11 January 2001

Abstract

The effects of two lectins concanavalin A (conA) and soybean agglutinin, on soybean seed acid phosphatase activity were investigated using *p*-nitrophenylphosphate (pNPP), pyrophosphate (PPi) and phosphoenolpyruvate (PEP) as substrates. Of the four acid phosphatase isoforms (AP1, AP2, AP3A and AP3B) purified from soybean seeds, only AP1 was activated 40 and 60% by conA and soybean agglutinin, respectively. Both lectins affected some of the kinetic parameters of AP1. The activation by lectins was not affected by 1 mM Ca^{2+} or Mn^{2+} but glucose and methylmannopyranoside (100 mM) prevented activation by conA. Under the same conditions, galactose had no effect. These results suggest that plant acid phosphatases may be regulated by lectins, the effects vary according to the substrate used. © 2001 Elsevier Science Ltd. All rights reserved.

Keywords: *Glycine max*; Leguminosae; Soybean agglutinin; Concanavalin A; Soybean seed; Acid phosphatase; Lectins

1. Introduction

Acid phosphatases (E.C. 3.1.3.2) are a group of enzymes that catalyze the hydrolysis of phosphate monoesters. These enzymes are widely distributed among mammalian tissues, plants and microorganisms. In particular, plant acid phosphatases have been characterized in roots (Penheiter et al., 1997), tubers (Gellatly et al., 1994), bulbs (Guo and Pesacreta, 1997), seeds (Park and Van Etten, 1986; Ullah and Gibson, 1988; Malhotra and Kayastha, 1990; Ferreira et al., 1998; Granjeiro et al., 1999), aleurone layer (Gabard and Jones, 1986), leaves (Staswick et al., 1994), maize scutellum (Rossi et al., 1981) and suspension cells (Lefebvre et al., 1990; Duff et al., 1989). These phosphatases, usually present in multiple forms, display different biochemical properties and exhibit a broad specificity at pH optima below 6.0. Many roles have been ascribed to acid phosphatases in plants, including participation on signal transduction (Plaxton, 1996), regulation of metabolism by protein dephosphorylation (Duff et al., 1994) and the release of inorganic phosphate from organic phosphate in the environment. Phosphorus not only plays a vital role in energy transfer and in metabolic regulation, but it is also an important constituent of phospholipids and nucleic acids. The growth and development of plants is particularly dependent upon the availability of phosphate (Lefebvre et al., 1990).

Lectins are proteins that bind to carbohydrates with considerable specificity through hydrogen bonds, metal coordination, van der Waals and hydrophobic interactions. These proteins occur in a variety of organisms and are involved in numerous cellular processes. In the seeds of many plants, lectins can account for as much as 10% of the total nitrogen of mature seed extracts, and may be involved in protein storage (Ferens and Morawieka, 1985). Ferens and Morawieka (1985) reported a 20% activation of rye germ acid phosphatase by conA; a similar activation of this enzyme from *Pleurotus ostreatus* was also observed by Corand and Rüdiger (1994).

We have previously purified four acid phosphatase isoforms from soybean seeds, and found that they all contain a carbohydrate moiety in their structures (Ferreira et al., 1998). In this report, we describe the effects of concanavalin A and soybean agglutinin on the activity of

Abbreviations: conA, concanavalin A; PPi, inorganic pyrophosphate; PEP, phosphoenolpyruvate; pNPP, *p*-nitrophenylphosphate.

* Corresponding author. Fax: +55-19-3788-7840.
E-mail address: carmenv@unicamp.br (C.V. Ferreira).

0031-9422/01/$ - see front matter © 2001 Elsevier Science Ltd. All rights reserved.
PII: S0031-9422(01)00190-X

these phosphatases. Kinetic parameters were determined in the presence of lectins, using potential physiological substrates, such as PPi and PEP.

2. Results and discussion

The lectin conA was used in order to allow us to compare our results with other reports, whereas soybean agglutinin was tested because of its possible participation in the in vivo regulation of soybean acid phosphatase. The isoforms AP1, AP2, AP3A and AP3B contain 30, 28, 18 and 10% carbohydrate, respectively, in their structures (Ferreira et al., 1998). The carbohydrate composition of isoform AP1 consists of mannose (8.3%), galactosamine (50.3%), glucosamine (32.1%), glucose (5.1%) and galactose (4.2%) (not shown).

Although there are several reports of acid phosphatases from plant tissues (Guo and Pesacreta, 1997; Duff et al., 1994), little is known of their regulation by endogenous compounds.

Table 1 shows that conA and soybean agglutinin increased the activity of AP1 by 40 and 60%, respectively, when pNPP was used as substrate, but had no effect on the other isoforms. The extent of activation of AP1 by conA was substrate-dependent. Thus, 50 μg caused 20, 60 and 80% activation of AP1 with PEP, pNPP and PPi, respectively (Fig. 1A). No significant effect was observed when PEP was used as substrate, suggesting that the presumed conformational change in AP1 produced by conA was not sufficient to increase PEP hydrolysis. It is also possible that the high affinity of AP1 for PEP may have prevented activation by the lectin (Ferreira et al., 1999). In contrast to conA, the activation by soybean agglutinin was independent of the substrate used (Fig. 1B). In addition, soybean agglutinin significantly increased the activation by about 60% seen with PEP as substrate. These results agree with an previous demonstration that PEP may be a physiological substrate for the AP1 isoform (Ferreira et al., 1999), and suggest that the specificity for PEP in vivo may be increased by the presence of this lectin.

The activation by both lectins was concentration-dependent up to about 50 μg (Fig. 1). Additional activation was observed after preincubating the enzyme with conA (Fig. 2), although the pattern of the curves was similar to those obtained in the absence of preincubation (Figure 1A). In contrast to our results, Ferens and Morawieka (1985) reported that rye germ acid phosphatase was activated by conA only after preincubation for 15 min.

The activation by conA was prevented when glucose or mannose, but not lactose, was present in the assay medium (Table 2). In contrast to lactose, glucose and mannose can efficiently bind to conA. The divalent cations Ca^{2+} and Mg^{2+} had no effect on the activation by conA (Table 2). A similar result was obtained for the activation by soybean agglutinin (Table 3), although in this case, only galactose prevented the activation by soybean agglutinin, in agreement with this lectins preferential binding to this sugar.

Table 4 shows the effect of the two lectins on the K_m, V_{max} and specificity constant (V_{max}/K_m) of soybean seed AP1 acid phosphatase with different substrates. Both lectins increased enzyme specificity, but this effect was higher with PEP in the presence of soybean agglutinin, thus reinforcing the data in Fig. 1B. The acid phosphatase AP1 showed a particularly high affinity in the presence of soybean agglutinin, as suggested by the very low K_m. PPi, another potential physiological substrate, showed specificity constants with both similar to those obtained with PEP and soybean agglutinin.

These results show that the effects of lectins depend on the substrate used rather than being caused by enzyme stabilization, AP1 was not stabilized by these proteins (data not shown). Soybean agglutinin had a strong effect on the specificity of PEP and PPi, since with these substrates, the specificity constants for AP1 were at least 10 times higher than that for the synthetic substrate pNPP. This observation suggested that soybean seed lectin may play an important role in the regulation of a specific acid phosphatase isoform, in addition to its function as a storage protein. The increase in plant acid phosphatase activity, during germination could thus be associated with the nature of the lectin constituents of the seed.

Some authors have reported the presence of hydrolytic enzymes (acid phosphatases, proteinases and α-D-mannosidase) in the protein bodies and that levels of the enzymes are elevated during germination (Asghar and Demason, 1992; Elpidina et al., 1992, 1993). It is possible that soybean lectin may contribute to the increase in acid phosphatase activity during germination. This activation may be important in the role of these enzymes in phosphorus aquisition, an important nutrient for plant development and growth.

Table 1
Effect of conA and soybean agglutinin on the activity of acid phosphatase isoforms[a]

Isoform	Relative activity (%)	
	conA	Soybean agglutinin
AP1	137 (±4)	160 (±7)
AP2	94 (±5)	90 (±2)
AP3A	103 (±3)	110 (±6)
AP3B	98 (±6)	102 (±3)

[a] The isoforms were incubated for 10 min (period of the enzyme assay) in the absence and in the presence of 50 μg conA or soybean agglutinin and the enzyme activities determined measuring the pNP released. The activities in the absence of lectins were considered as 100%. All data were obtained in triplicate and shown with their standard deviations (in parentheses).

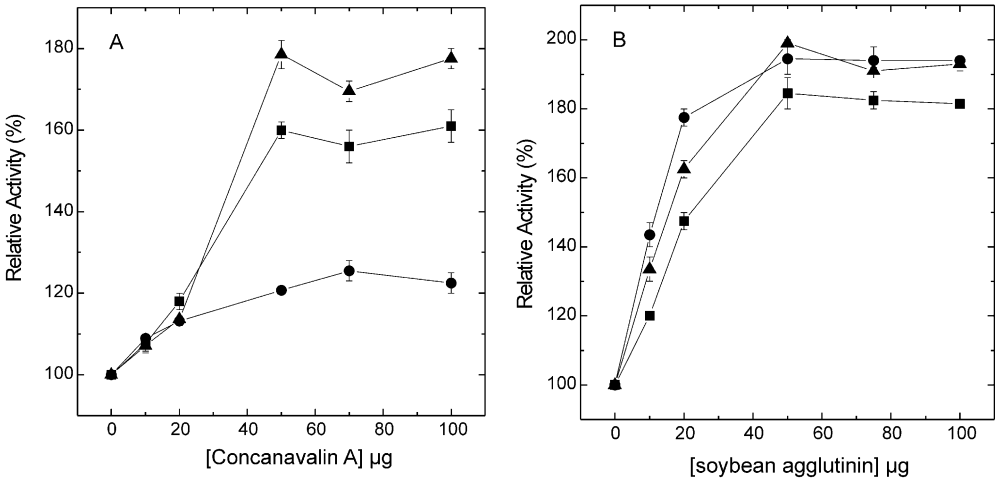

Fig. 1. Effect of conA and soybean agglutinin on the activity of soybean seed acid phosphatase (AP1). The incubation mixture included pNPP (■), PPi (▲) or PEP (●) as substrate, in the presence of increasing concentrations of conA (A) and soybean agglutinin (B). The samples were incubated with the lectins for 10 min (period of the enzyme assay). The activity in the absence of lectin was considered as 100%. The experiments were performed in triplicate and bars represent the standard deviations.

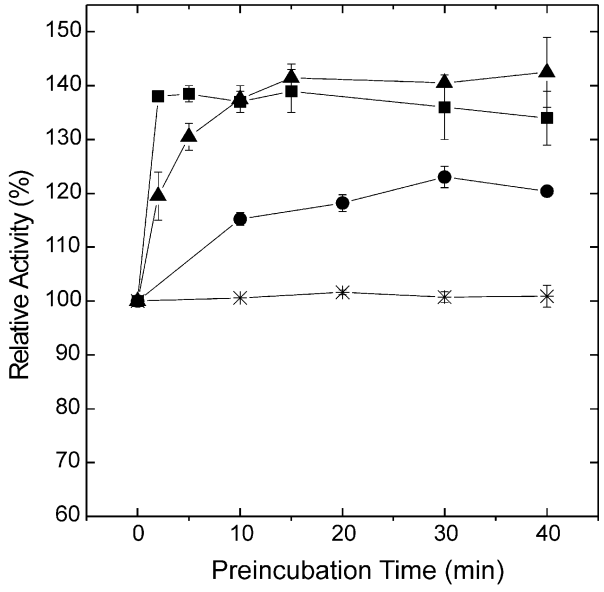

Fig. 2. Effect of preincubation of conA with the acid phosphatase. The AP1 was incubated with or without conA (50 µg), and enzyme activity was determined with pNPP (■), PPi (▲) or PEP (●) as substrates. The activity in the presence of lectin and without preincubation was considered as 100% (*). The experiments were performed in triplicate and bars represent the standard deviations.

3. Experimental

3.1. Plant materials

Soybean seed acid phosphatases (AP1, AP2, AP3A and AP3B) were purified 910-, 180-, 15- and 73-fold, with specific activities of 50, 10, 0.8 and 4 µmol min^{-1} mg^{-1} of protein, using pNPP as substrate, as previously described (Ferreira et al., 1998).

Table 2
Effect of different compounds on AP1 acid phosphatase activity in the presence of ConA[a]

Compound	Relative activity (%)
Control	100
conA	139 (±5)
conA + Ca^{2+} + Mn^{2+} (1 mM)	147 (±5)
Glucose 100 mM	99 (±4)
conA + glucose 100 mM	104 (±2)
Methylmannopyranoside 100 mM	95 (±6)
conA + methylmannopyranoside 100 mM	100 (±3)
Lactose 100 mM	97 (±5)
conA + lactose 100 mM	135 (±6)

[a] The compounds were added to the assay medium containing pNPP, as described in Experimental. The enzyme activity in the absence of the compounds was considered as 100%. All data were obtained in triplicate and shown with their standard deviations (in parentheses).

3.2. Chemicals

pNPP, PEP, PPi, conA and soybean agglutinin were obtained from Sigma Chemical Company. All other chemicals were of the highest purity available.

3.3. Enzyme assay

The amounts of AP1, AP2, AP3A and AP3B used in the assays were 0.06, 0.5, 3.2 and 2.2 µg, respectively, with equal activities in all assays. The reaction mixture (1 ml) containing 100 mM sodium acetate buffer (pH 5.0), 5 mM pNPP, and enzyme was incubated for 10 min at 37°C, and then terminated by the addition of 1 ml of 1 M NaOH. The relative absorbance was read at 405 nm. The molar extinction coefficient of *p*-nitrophenolate ion, at 405 nm, in alkaline medium is 18,000 M^{-1} cm^{-1}.

Table 3
Effect of different compounds on the AP1 acid phosphatase activity in the presence of soybean agglutinin[a]

Compound	Relative activity (%)
Control	100
Soybean agglutinin	169 (±4)
Soybean agglutinin + Ca^{2+} + Mn^{2+} (1 mM)	160 (±5)
Glucose 100 mM	100 (±6)
Soybean agglutinin + glucose 100 mM	150 (±5)
Methylmannopyranoside 100 mM	99 (±7)
Soybean agglutinin + methylmannopyranoside 100 mM	167 (±6)
Lactose 100 mM	98 (±5)
Soybean agglutinin + lactose 100 mM	132 (±6)
Galactose 100 mM	99 (±4)
Soybean agglutinin + galactose 100 mM	95 (±8)

[a] The compounds were added to the assay medium, as described in Experimental, using pNPP as substrate. The activity in the absence of compounds was considered as 100%. All data were obtained in triplicate and shown with their standard deviations (in parentheses).

Table 4
Effect of conA and soybean agglutinin on the kinetic parameters of the soybean seed acid phosphatase[a]

Substrate	Control	conA	Soybean agglutinin
	V_{max}/K_m	V_{max}/K_m	V_{max}/K_m
pNPP	114/0.49 (233)	162/0.10 (1620)	180/0.10 (1800)
PPi	121/0.13 (930)	175/0.05 (17,500)	200/0.02 (20,000)
PEP	89/0.23 (387)	120/0.08 (1500)	190/0.01 (19,000)

[a] The assay conditions were as described in Experimental. K_m (mM) and V_{max} (μmol min^{-1}) values were calculated from Lineweaver–Burk plots, and are given as ratios. The specificity constant values are shown in parentheses. All data were obtained in triplicate.

When PEP and PPi were used as substrates, the activities were assayed by measuring the amount of phosphate released. The incubation mixtures were as described for pNPP, using 10 mM PEP or PPi. After a 10 min incubation at 37C, the reaction was stopped by addition of 1 ml of 3% ammonium molybdate (in 200 mM acetate buffer, pH 4.0), followed by addition of 0.1 ml of ascorbic acid (in 200 mM acetate buffer, pH 4.0). The color was developed for 30 min and the relative absorbance was read at 700 nm. The amount of inorganic phosphate produced was calculated using a molar extinction coefficient of 4000 M^{-1} cm^{-1} (Lowry and Lopez, 1945).

Acknowledgements

This work was supported by grants from Fundação de Amparo à Pesquisa do Estado de São Paulo (Proc. 1997/6360-4 and 1999/12940-9), Conselho Nacional de Desenvolvimento Científico e Tecnológico (Proc. 521654/95-5), and Fundo de Apoio ao Ensino e a Pesquisa/Unicamp. The authors thank Dr. Ladaslav Sodek (Instituto de Biologia, Unicamp) for critically reading the manuscript.

References

Asghar, R., Demason, D.A., 1992. Differential activities of acid phosphatase from adaxial and abaxial regions of *Lupinus luteus* (Fabaceae) cotyledons. Am. J. Bot. 79, 1134–1144.

Corand, F., Rüdiger, H., 1994. The lectin from *Pleurotus ostreatus*: purification, characterization and interaction with a phosphatase. Phytochemistry 30, 277–283.

Duff, S.M.G., Lefebvre, D.D., Plaxton, W.C., 1989. Purification and characterization of a phosphoenolpyruvate phosphatase from *Brassica nigra* suspension cells. Plant Physiol. 90, 734–741.

Duff, S.M.G., Sarath, G., Plaxton, W.C., 1994. The role of acid phosphatases in plant phosphorus metabolism. Physiol. Plant. 90, 791–800.

Elpidina, E.N., Dunaevskii, Y.E., Belozerskii, M.A., 1992. Isolation and characterization of protein-storing organelles from buckwheat seedlings. Biochemistry (Moscow) 57, 527–534.

Elpidina, E.N., Dunaevskii, Y.E., Belozerskii, M.A., Durant, M., Cerletti, P., 1993. Isolation and characterization of protein bodies from cotyledons of dry *Lupinus albus* seeds. Biochemistry (Moscow) 57, 440–443.

Ferens, M., Morawieka, B., 1985. Rye germ acid phosphatase: properties of the enzyme and its activation by lectins. Phytochemistry 24, 2839–2842.

Ferreira, C.V., Granjeiro, J.M., Taga, E.M., Aoyama, H., 1998. Multiple forms of soybean seed acid phosphatases. Purification and characterization. Plant Physiol. Biochem. 36, 487–494.

Ferreira, C.V., Taga, E.M., Aoyama, H., 1999. Glycolysis intermediates as substrates of acid phosphatases from soybean seeds. Plant Sci. 147, 49–54.

Gabard, K.A., Jones, R.L., 1986. Localization of phytase and acid phosphatase isoenzymes in aleurone layers of barley. Physiol. Plant 67, 182–192.

Gellatly, K., Moorhead, G.B.G., Duff, S.M.G., Lefebvre, D.D., Plaxton, W.C., 1994. Purification of a potato tuber acid phosphatase having characteristics of a protein tyrosine phosphatase. Plant Physiol. 106, 223–232.

Granjeiro, P.A, Ferreira, C.V., Granjeiro, J.M., Taga, E.M., Aoyama, H., 1999. Purification and kinetic properties of castor bean seed acid phosphatase containing sulphydryl groups. Physiol. Plant. 107, 151–158.

Guo, J., Pesacreta, T.C.J., 1997. Purification and characterization of an acid phosphatase from the bulb of *Allium cepa* L. var. sweet spanish. Plant Physiol. 151, 520–527.

Lefebvre, D.D., Duff, S.M.G., Fife, C., Plaxton, W.C., 1990. Response to phosphate deprivation in *Brassica nigra* suspension cells. Enhancement of intracellular, cell surface and secreted phosphatase activities compared to increases in Pi-absorption rate. Plant Physiol. 93, 504–511.

Lowry, O.H., Lopez, J.A., 1945. The determination of inorganic phosphate in the presence of labile phosphate esters. J. Biol. Chem. 162, 421–424.

Malhotra, O.P., Kayastha, A.M., 1990. Isolation and characterization of phosphoenolpyruvate phosphatase from germinating mung beans (*Vigna radiata*). Plant Physiol. 93, 194–200.

Park, H.S.C., Van Etten, R., 1986. L, Purification and characterization of homogeneous sunflower seed acid phosphatase. Phytochemistry 25, 351–357.

Penheiter, A.R., Duff, S.M., Sarath, G., 1997. Soybean root nodule and acid phosphatase. Plant Physiol. 114, 597–604.

Plaxton, W.C., 1996. The organization and regulation of plant glycolysis. Ann. Rev. Plant Physiol. Plant Mol. Biol. 47, 185–214.

Rossi, A., Palma, M.S., Leone, F.A., Brigliador, M.A., 1981. Properties of acid phosphatase from scutella of germinating maize seeds. Phytochemistry 20, 1823–1826.

Staswick, P.E., Papa, C., Huang, J., Rhee, Y., 1994. Purification of the major soybean leaf acid phosphatase that is increased by seed-pod removal. Plant Physiol. 104, 49–57.

Ullah, A.H.J., Gibson, D.M., 1988. Purification and characterization of acid phosphatase from cotyledons of germinating soybean seeds. Arch. Biochem. Biophys. 260, 514–520.

PERGAMON

Phytochemistry 58 (2001) 227–232

PHYTOCHEMISTRY

www.elsevier.com/locate/phytochem

Modification of fatty acids changes the flavor volatiles in tomato leaves

Chunlin Wang[a], Jinsong Xing[a], Chee-Kok Chin[a,*], Chi-Tang Ho[b], Charles E. Martin[c]

[a]*Department of Plant Science, Rutgers, The State University of New Jersey, 59 Dudley Road, New Brunswick, NJ 08901-8520, USA*
[b]*Department of Food Science, Rutgers, The State University of New Jersey, 65 Dudley Road, New Brunswick, NJ 08901-8520, USA*
[c]*Department of Cell Biology and Neuroscience, Rutgers, The State University of New Jersey, 604 Allison Road, Piscataway, NJ 08854-8002, USA*

Received 15 December 2000; received in revised form 13 April 2001

Abstract

Expression of the yeast Δ9 desaturase gene in tomato (*Lycopersicon esculentum* Mill.) resulted in changes in the profiles of fatty acids in tomato leaves. Transgenic leaves displayed a dramatic increase in *cis*-Δ9 16:1, which only existed in a small quantity in control leaves. Also higher, but not as dramatic, were 18:1 and 16:3 fatty acids. Several fatty acids, viz. 16:0, 18:0, and 18:3 declined in transgenic leaves. Changes in fatty acids were accompanied by changes in certain volatile compounds derived from fatty acids. On a percentage basis, most notable increases (>3-fold) were 1-hydroxy-2-butanone, 1-penten-3-ol, heptanal, 3-hexen-1-ol, 2-octanol,*cis*-3-hexenal, hexanal and 2-nonenal. Several flavor compounds not known to be biochemically derived from fatty acids, viz. 2-ethyl-furan, 5-ethyl-2- [5H]-furanone, eugenol, and 2-ethylthiophene also showed sharp increases in transgenic leaves. © 2001 Published by Elsevier Science Ltd.

Keywords: Tomato; *Lycopersicon esculentum*; Solanaceae; Fatty acid; Lipid; Flavor; Hexenal; Transgenic plant

1. Introduction

Plant leaves are an important constituent of our diet. Their desirability is affected by many factors, one of the most consequential being flavor. Many volatile compounds, including fatty acid derivatives, terpenoids, phenylpropanoids, and benzenoids contribute to leaf flavor. Some of these compounds are used as flavoring agents in manufactured products and thus have additional economical value. However, many valuable leaf volatiles are only present in minute quantities, making utilization of most leaves economically impractical. Although chemical synthesis could be used to produce many of these compounds, consumers in general prefer natural products. Conventional plant breeding has been used to empirically alter plant flavor. With the advancement of genetic engineering, another option is available, i.e. to genetically modify specific pathways that produces the compound of interest.

Leaf volatiles derived from fatty acids constitute a conspicuous component of a leaf flavor profile. Most of these volatiles are formed through the lipoxygenase/hydroperoxide lyase enzyme pathway (Stone et al., 1975; Galliard et al., 1977; Vick and Zimmerman, 1986). It usually begins with release of free fatty acids from lipids by lipases, then peroxidation of specific double bonds of polyunsaturated fatty acids, such as linoleic and linolenic acids, by lipoxygenase to produce the corresponding hydroperoxides. These hydroperoxides are then converted to various C6 and C9 aldehydes by hydroperoxide lyase. The aldehydes can subsequently be reduced by alcohol dehydrogenase to form corresponding alcohols (Vick and Zimmerman, 1986). Only polyunsaturated fatty acids serve as substrates for lipoxygenases in this pathway. Our laboratory has previously demonstrated that supply of linolenic acid fatty acids is a limiting factor in the production of *cis-3*-hexenal by cultured alfalfa cells (Chou and Chin, 1994). Thus, increasing the level of polyunsaturated fatty acids may increase the flavor compounds derived from these acids.

Fatty acids in plants are first produced in saturated forms, which are later desaturated to mono- and

* Corresponding author. Tel.: +1-732-932-9711x238; fax: +1-732-932-9441.
E-mail address: chin_c@aesop.rutgers.edu (C.-K. Chin).

0031-9422/01/$ - see front matter © 2001 Published by Elsevier Science Ltd.
PII: S0031-9422(01)00233-3

polyunsaturated fatty acids. Desaturation starts with the conversion of 16:0-acyl carrier protein (ACP) and 18:0-ACP into 16:1-ACP and 18:1-ACP respectively by a soluble plastid Δ-9 desaturase (McKeon and Stumpf, 1982; Shanklin and Sommerville, 1991). Further desaturation of 18:1-ACP is accomplished by two desaturases: the Δ12 desaturase adding the second double bond at Δ12 position of 18:1 to form 18:2, and the Δ15 desaturase adding the third double bond at Δ15 position to form 18:3. For most plants, the levels of monounsaturated fatty acids are lower than that of saturated and polyunsaturated fatty acids, inferring that the first desaturation by Δ9 desaturase is a limiting factor in polyunsaturated fatty acid production. We have previously observed that the levels of 18:2 in tomato fruit could be dramatically increased by expressing the yeast Δ9 desaturase gene in tomato (Wang et al., 1996).

Concomitantly, certain flavor compounds derived from fatty acids, most notably *cis*-3-hexenol, 1-hexanol, hexanal, *cis*-3-hexenal, and 2-nonenal were also elevated. Tomato fruit and leaf have different fatty acid and flavor volatile profiles. Here, we report that expression of the yeast Δ9 desaturase gene in tomato also alters the profiles of fatty acids and flavor volatiles in tomato leaves.

2. Results

2.1. Expression of the yeast Δ9 desaturase gene alters fatty acid profile

Fig. 1 shows the levels of various fatty acids in the leaves of control and 2 transgenic (T4 and T5) plants expressing the yeast Δ9 desaturase gene. Predominant fatty acids in the control leaves were 18:3, 18:2, and 16:0. Leaves from both transgenic plants displayed dramatic increases in*cis*-Δ9 16:1, which only existed in small quantity in control leaves. Also higher, but not as dramatic, were 18:1 and16:3 fatty acids. Several fatty acids, viz. 16:0, 18:0, and 18:3 declined in transgenic leaves.

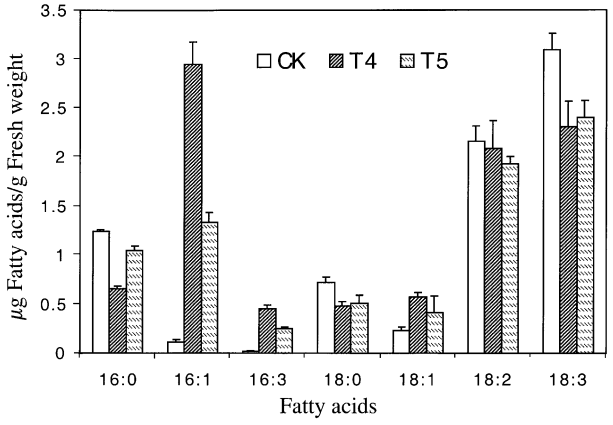

Fig. 1. Fatty acids in control (CK) and transgenic (T4 and T5) tomato leaves.

The much higher increase in 16:1 than 18:1 likely reflects the relative availability of substrates to the yeast Δ9 desaturase and not the substrate specificity of the enzyme. The yeast Δ9 desaturase is a cytochrome b5-dependent endoplasmic reticulum (ER) enzyme that converts 16:0-CoA and 18:0-CoA to 16:1-CoA and 18:1-CoA respectively (Stukey et al., 1990). As the yeast Δ9 desaturase lacks the known characteristics of the chloroplast targeting sequences, it is expected to be located in the cytosol and not in the chloroplasts (Heijne and Nishikawa, 1991). Consequently, it can only utilize the fatty acids in the cytosol as substrates. Fatty acid synthesis in plants has been found to be almost exclusively localized in the plastids (Ohlrogge and Browse, 1995). Some of the synthesized fatty acids, mostly 18:1 and 16:0, are subsequently exported to the cytosol (Ohlrogge and Browse, 1995). The availability of the exported saturated 16:0 could explain the sharp increase in 16:1. The smaller increase in 18:1 indicates that 18:0 was also exported to the cytosol, albeit presumably at a level significantly less than 16:0. Generally, 18-carbon fatty acids, except 18:1, declined in transgenic leaves. This could be a consequence of shunting of 16:0, the precursor of 18-carbon fatty acids, to 16:1. The increase in unsaturated fatty acids exceeded the decline in saturated fatty acids indicating an overall increase of total fatty acids on per fresh weight basis in transgenic leaves.

2.2. Expression of the yeast Δ9 desaturase gene alters the profile of volatile compounds

The identities of the major volatile compounds and their concentrations are shown in Table 1. Oxygenated aliphatic compounds constitute 18% of the total volatile compounds in control leaves. Most of these compounds are likely derived from unsaturated fatty acids. This group of compounds increased 3.2- and 2.7-fold in the T4 and T5 leaves respectively, supporting the contention that changes in the levels of fatty acids can significantly alter the levels of compounds derived from them. By far the most abundant oxygenated aliphatic compound found in tomato leaves was *trans*-2-hexenal. The levels of *trans*-2-hexenal were significantly higher in transgenic than in control leaves. *trans*-2-Hexenal was likely an artifact of GC thermal conversion of *cis*-3-hexenal (Karmas et al., 1993). Thus, the amounts of *trans*-2-hexenal reported here should represent a sum of *cis*-3-hexenal and *trans*-2-hexenal. *Cis*-3-hexenal is derived from linolenic acid in a 2-step process. Linolenic acid is first converted to linolenic acid 13-hydroperoxide (13-Ln OOH) by lipoxygenase, and 13-Ln OOH is in turn converted by hydroperoxide lyase to *cis*-3-hexenal (Hatanaka et al., 1977, 1986). Unlike lipoxygenase in tomato fruits, lipoxygenase in tomato leaves has not been extensively studied. The overwhelming amount of *cis*-3-hexenal produced by tomato leaves suggests that

Table 1
Volatile compounds in the control and transgenic tomato leaves

Compound	Control (CK) (ppb)	T4 (ppb)	T4/CK (fold)	T5 (ppb)	T5/CK (ppb)	Fatty acid (precursor)
Oxygenated aliphatic compounds						
trans-2-Hexenal	10983.8	37537.9	3.42	32538.5	2.96	18:3
1-Hexanol	717.9	827.0	1.15	798.0	1.11	16:1, 18:2
cis-3-Hexenal	701.6	2621.7	3.74	2232.0	3.18	18:3
Nonanal	297.1	446.4	1.50	450.1	1.51	18:2
Unknown aldehyde mw 148	227.2	580.4	2.55	321.3	1.41	
Heptanal	147.3	697.5	4.74	423.4	2.87	16:1
1-Penten-3-one	111.1	110.5	0.99	120.2	1.08	
3-Hexen-1-ol	102.4	453.1	4.42	126.1	1.23	18:3
2-Ethyl-1-hexanol	88.6	73.7	0.83	89.1	1.01	
Decanal	68.7	99.3	1.45	65.2	0.95	18:1
2-Octanol	64.9	260.0	4.01	189.9	2.93	
2-Penten-1-ol	51.2	118.3	2.31	111.1	2.17	
Octanal	46.2	65.8	1.42	78.8	1.71	18:1
3-Methyl-1-butanol	16.4	20.8	1.27	11.1	0.68	
2-Methyl-1-butanol	16.2	20.1	1.24	10.2	0.63	
2-Nonenal	15.0	45.8	3.05	65.3	4.35	16:1
Hexanal	13.7	50.2	3.66	61.3	4.47	16:1, 18:2
2-Heptanol	10.0	15.6	1.56	16.7	1.67	
1-Penten-3-ol	8.7	44.6	5.13	52.2	6.03	18:3
Undecanal	6.2	6.7	1.08	9.1	1.47	
1-Hydroxy-2-butanone	0.0	6.7	∞	4.2	∞	
Aliphatic hydrocarbons						
Cyclohexan	68.1	69.9	1.03	58.1	0.85	
Hexadecane	34.6	20.0	0.58	26.8	0.77	
Octane	31.3	52.4	1.67	48.0	1.53	
Tetradecane	28.7	17.9	0.62	21.7	0.76	
Dodecane	23.4	25.0	1.07	24.3	1.04	
Nonane	21.2	21.2	1.00	22.3	1.05	
1-Nonene	13.4	7.5	0.56	9.6	0.72	
Aromatic compounds						
Methyl salicylate	97.4	270.1	2.77	289.6	2.97	
Guaiacol	21.2	22.3	1.05	27.0	1.27	
Diethylnaphthalene	18.7	17.9	0.96	11.4	0.61	
2-Ethylthiopene	13.7	50.2	3.66	62.3	4.55	
Eugenol	12.5	78.1	6.25	92.3	7.38	
Isopropylbenzenaldehyde	12.5	27.9	2.23	26.8	2.14	
2-Ethyl-furan	11.6	421.9	36.37	357.1	30.78	
5-Ethyl-2-[5H]-furanone	11.2	110.4	9.86	102.0	9.11	
Benzaldehyde	5.0	4.5	0.90	0.0	0.00	
Monoterpenoids						
β-phelladrene	32682.9	20402.9	0.62	25978.0	0.79	
2-Carene	11940.1	10828.1	0.91	11360.9	0.95	
α-phelladrene	2372.0	2169.6	0.91	2356.7	0.99	
α-pinene	1822.7	809.2	0.44	777.5	0.43	
β-myrcene	1184.8	756.7	0.64	656.2	0.55	
m-Cymene	962.5	1583.7	1.65	1449.3	1.51	
p-Cymene	641.7	689.7	1.07	654.4	1.02	
3,7-Dimethyl-1,3,7-octatriene	443.2	350.4	0.79	332.9	0.75	
Terpinolene	248.4	166.3	0.67	150.9	0.61	
Terpinene	157.3	90.4	0.57	85.2	0.54	
Isoterpinolene	78.7	43.5	0.55	53.4	0.68	
Sabinene	76.2	78.1	1.02	92.8	1.22	
3-Carene	41.2	21.1	0.51	40.8	0.99	
3,7-Dimethyl-1-octanol	32.5	54.7	1.68	29.1	0.90	
Isolimonene	23.7	14.5	0.61	6.0	0.25	
Camphene	18.7	19.0	1.02	21.7	1.16	

Table 1 (*continued*)

Compound	Control (CK) (ppb)	T4 (ppb)	T4/CK (fold)	T5 (ppb)	T5/CK (ppb)	Fatty acid (precursor)
Limonene oxide	8.7	8.9	1.02	6.7	0.77	
β-cyclocitral	7.5	22.3	2.97	62.1	8.28	
Sesquiterpenoids						
β-caryophyllene	7400.7	7206.5	0.97	7455.0	1.01	
α-caryophellene	1269.7	1482.1	1.17	1198.0	0.94	
Isoledene	89.9	98.2	1.09	95.3	1.06	
9,10-Dehydroisolongifolene	20.0	22.3	1.12	32.0	1.60	
γ-elemene	18.7	44.6	2.39	38.4	2.05	
Carophyllene oxide	11.2	33.5	2.99	28.9	2.58	
δ-selinene	7.5	7.8	1.04	7.5	1.00	

tomato leaves possess lipoxygenase active in production Δ^6 13-Ln OOH, the substrate of *cis*-3-hexenal. The lipoxygenase/hydroperoxide lyase pathway that produces hexenal from linolenic acid can also produce hexanal from linoleic acid (Hatanaka et al., 1986). However, in spite of the similar levels of linolenic and linoleic acids in tomato leaves, the amount of hexanal found was only a small fraction of that of hexenal. This discrepancy may be explained by the specificity of the tomato leaf hydroperoxide lyase, which has a strong preference towards 13-Ln OOH over linoleic acid 13-hydroperoxide (13-La OOH) (100% against 9.8%). The specificity of tomato leaf hydroperoxide lyase may also explain the low amounts of 9-carbon aldehydes in tomato leaves. Tomato leaf hydroperoxide lyase is only active against 13-La OOH and 13-Ln OOH, but has no activity against 9-La OOH and 9-Ln OOH (Fauconnier et al., 1997).

As hexenal is derived from linolenic acid, we expected a positive correlation of linolenic acid and hexenal. Instead, we observed that the sharp increase in the levels of hexenal in transgenic leaves was associated with a reduction in 18:3. This appears to suggest that hexenal production in tomato leaves is not limited by 18:3. We have previously proposed that hexenal production could also be limited by hydroperoxide lyase activity (Chou and Chin, 1994). Thus, a stimulation of hydroperoxide lyase activity could produce an increase in hexenal. Indeed, expression of the yeast Δ9 desaturase in planta has been found to affect enzyme activity. Specifically, expression of the yeast Δ9 desaturase gene in eggplant leaves has been found to increase the activity of phospholipase A_2, an enzyme that releases free fatty acids from phospholipids (Xing and Chin, 2000). It would be of interest to examine whether the transgenic leaves also have higher lipid hydroperoxide lyase activity.

Compared to C6 aldehydes, the amounts of other aliphatic compounds found in tomato leaves were relatively insignificant. Nonetheless, several of these compounds showed significant increases in transgenic leaves. There were moderate increases in nonanal, and octanal, which could be formed by autooxidation of 18:1 fatty acid (Frankel, 1977; Gardner, 1989). Other oxygenated aliphatic compounds, including heptanal, 2-octanol, and 2-nonenal that showed significant increase, could be formed by autooxidation of palmitoleic acid following the pattern of autooxidation of 18:1 (Frankel, 1977). If so, the sharp increase in palmitoleic acid in transgenic leaves may explain the multi-fold increases of these compounds.

In addition to aliphatic compounds, a number of monoterpenes, sesquiterpenes, and aromatic compounds were found in tomato leaves. Most dramatically, two aromatic compounds, 2-ethylfuran and 5-ethyl-2 [5H] furanone, were present in minute amounts in control leaves but showed dramatic increases of >36-fold and >9-fold, respectively, in transgenic leaves. It is not clear how these 2 compounds are being synthesized in plants. Two monoterpenes, viz. ß-phelladrene and 2-carene (Buttery et al., 1987) existed in relatively high amounts in control leaves but the amounts declined in the transgenic leaves.

This study lends support to the contention that changes in fatty acids can lead to changes in lipid-derived flavor compounds, even though changes of flavor volatiles did not always correlate with the levels of the fatty acid precursors. Since fatty acids of a plant can be changed by the expression of a specific gene in the fatty acid pathway, engineering fatty acid metabolism could be an effective approach in flavor modification.

It should be pointed out that compound identification in this study was based on mass spectra matching with that of the National Institute of Standards and Technology mass spectral library. Thus, the probability of misidentification of certain compounds cannot be ruled out.

3. Experimental

3.1. Production of transgenic plants

Open-pollinated tomato (*Lycopersicon esculentum*) line PSR55809 from the New Jersey Agricultural

Experimental Station was used in this study. The transformation procedure was as previously described (Wang et al., 1996). *Agrobacterium tumefaciens* LBA 4404 containing the yeast Δ9 desaturase and NPTII gene sequence driven by CaMV 35S promoters (Polashock et al., 1992) was used to infect tomato cotyledon segments. Kanamycin resistant plantlets regenerated were subjected to Southern blotting (Southern, 1975). Fifteen kanamycin-resistant and Southern blot positive plants were produced. Eleven of these plants displayed dramatically higher levels of 16:1 fatty acid, (over 10-fold increase, data not shown). Plantlets with high levels of palmitoleic were multiplied in vitro and later transplanted to greenhouse. Two of the high 16:1 plants, T4 and T5, were selected and propagated by cuttings for this study.

3.2. Fatty acid analysis

Fatty acid analysis was carried out with leaf preparations with a protocol according to Browse et al. (1986). A Shimadzu 17A gas chromatograph equipped with a FID detector and HP-2330 capillary column (30m × 1.5 mm, 1 μm thick film) was used. Injector temperature was 230 °C, and detector temperature was 240 °C. A column temperature program was set initially at 170 °C and ramped at 3 °C/min to 210 °C 3 min after injection. The fatty acid methyl ester (FAME) peaks were identified with the authentic standards of FAME from Sigma Chemical.

3.3. Volatiles analysis

Tomato plants were maintained in a greenhouse and leaves were collected from 6 to 7-week-old plants. Leaves (10 g) were frozen (liquid nitrogen) in a mortar and pulverized with a pestle. The resulting slurry in liquid nitrogen was quickly transferred to a 250 ml Wheaton Purge and Trap apparatus and 50 ml of distilled water and 10 μl of 1000 ppm tridecane dissolved in methylene chloride were then added. Volatile compounds were trapped onto Tenax-Carbotrap tube, with a flow of nitrogen gas at 40 ml/min at 52 °C for 1 h. The trapped tube was dried at room temperature with nitrogen at a flow rate of 40 ml/min for 45 min. The trapped volatile compounds were thermally desorbed at 250 °C with a TD-4 short path thermal desorption system from SIS (Ringoes, New Jersey) and injected into a HP 6890 GC with a HP 6973 MS detector. The GC was equipped with a DB-1 capillary column (60m × 0.32 mm, 1 μm film thickness, J&W Scientific Co.). The injector temperature and the interface temperature were both set at 250 °C. The desorbed sample was frozen on the head of the column by a cryotrap with liquid CO_2 at −40 °C. A split ratio of 10:1 was used. Column temperature was programmed linearly 30 to 280 °C at 2 °C/min. The mass spectra were identified with the aid of the National Institute of Standards and Technology mass spectral library and the data of Buttery et al. (1987). Some of the peaks were also identified using authentic standards.

References

Browse, J., McCourt, P., Somerville, C.R., 1986. Fatty acid composition of leaf lipids determined after combined digestion and fatty acid methyl ester formation from fresh tissue. Analytical Biochemistry 152, 141–145.

Buttery, R.G., Ling, L.C., Light, D.M., 1987. Tomato leaf volatile aroma components. Journal of Agricultural and Food Chemistry 35, 1039–1042.

Chou, S.R., Chin, C., 1994. Control of the production of *cis*-3 hexenal, a lipid derived flavor compound by plant cell culture. In: Ho, C., Hartman, T.G. (Eds.), Lipids in Food Flavors. ACS Symposium Series, pp. 282-291.

Fauconnier, M.L., Perez, A.G., Sanz, C., Marlier, M., 1997. Purification and characterization of tomato leaf (*Lycopersicon esculentum* Mill.) hydroperoxide lyase. Journal of Agricultural and Food Chemistry 4, 4232–4236.

Frankel, E.N., 1997. Chemistry of autooxidation: mechanism, products and flavor significance. In: Min, D.B., Smouse, T.H. (Eds.), Flavor Chemists' of Fats and Oils. American Oil Chemistry Society, Champaign, IL, pp. 1–37. 1985.

Galliard, T., Matthew, J.A., Wright, A.J., Fishwick, M.J., 1977. The enzymic breakdown of lipids to volatile and non-volatile carbonyl fragments in disrupted tomato fruits. Journal of Science of Food and Agriculture 28, 863–868.

Gardner, H.W., 1989. Oxygen radical chemistry of polyunsaturated fatty acids. Free Radical Biology Medicine 7, 65–86.

Hatanaka, A., Kajiwara, T., Sekiya, J., Kido, Y., 1977. Formation of 12-oxo-trans-10-dodecenoic acid in chloroplasts from *Thea senensis* leaves. Phytochemistry 16, 1828–1829.

Hatanaka, A., Kajiwara, T., Sekiya, J., 1986. Fatty acid hydroperoxide lyase in plant tissues. In: Parliment, T.H., Croteau, R. (Eds.), Biogeneration of Aromas. ACS Symposium Series 317. American Chemical Society, Washington, DC, pp. 167–175.

Heijne, G.Von, Nishikawa, K., 1991. Chloroplast transit peptides. The perfect random coil? FEBS Lett. 278, 1–3.

Karmas, K., Hartman, T.G., Salinas, J.P., Lech, J., Rosen, T.R., 1993. Lipid-derived flavor compounds in fresh and dehydrated tomato product. In: Ho, C.T., Hartman, T.G. (Eds.), Lipids in Food Flavors. ACS Symposium Series 558, pp. 130–143.

McKeon, T.A., Stumpf, P.K., 1982. Purification and characterization of the stearoyl-acyl carrier protein desaturase and the acyl-acyl carrier protein thioesterase from maturing seeds of safflower. Journal of Biological Chemistry 257, 12141–12147.

Ohlrogge, J., Browse, J., 1995. Lipid biosynthesis. The Plant Cell 7, 957–970.

Polashock, J.J., Chin, C.K., Martin, C., 1992. Expression of the yeast Δ-9 fatty acid desaturase in *Nicotiana tabacum*. Plant Physiology 100, 894–901.

Shanklin, J., Somerville, C.R., 1991. Stearyl-acyl-carrier-protein desaturase from higher plants is structurally unrelated to the animal and fungal homologs. Proceedings of National Academy of Science USA 88, 2510–2514.

Southern, E.M., 1975. Detection of specific sequences among DNA fragments separated by gel electrophoresis. Journal of Molecular Biology 98, 503–517.

Stone, E.J., Hall, R.M., Kazeniac, S.J., 1975. Formation of aldehydes and alcohols in tomato fruits from the 14C labeled linolenic and linoleic acids. Journal of Food Science 40, 1138–1141.

Stukey, J.E., McDonough, V.M., Martin, C.E., 1990. Isolation and characterization of OLE 1, a gene affecting fatty acid desaturation from *Saccharomyces cerevisiae*. Journal of Biological Chemistry 265, 20144–20149.

Vick, B.A., Zimmerman, D.C., 1986. The lipoxygenase pathway. In: Stumpf, P.K., Mudd, J.B., Nes, W.D. (Eds.), The Metabolism, Structure, and Function of Plant Lipids. Plenum Press, New York and London, pp. 383–390.

Wang, C., Chin, C.K., Ho, C.-T., Hwang, C., Polashock, J.J., Martin, C.E., 1996. Changes of fatty acids and fatty acid-derived flavor compounds by expressing the yeast Δ-9 desaturase gene in tomato. Journal of Agricultural and Food Chemistry 44, 3399–3402.

Xing, J., Chin, C.K., 2000. Modification of fatty acids in eggplant affects its resistance to *Verticillium dahlia*. Physiological and Molecular Plant Pathology 56, 217–225.

PERGAMON

Phytochemistry 58 (2001) 233–238

PHYTOCHEMISTRY

www.elsevier.com/locate/phytochem

Roots and shoots of tomato produce 6-deoxo-28-norcathasterone, 6-deoxo-28-nortyphasterol and 6-deoxo-28-norcastasterone, possible precursors of 28-norcastasterone

Takao Yokota[a,*], Tatsuro Sato[b], Yasutomo Takeuchi[b], Takahito Nomura[a], Koyuru Uno[c], Tsuyoshi Watanabe[d], Suguru Takatsuto[c]

[a]*Department of Biosciences, Teikyo University, Utsunomiya 320-8551, Japan*
[b]*Center for Research on Wild Plants, Utsunomiya University, Mine-machi, Utsunomiya 321-8505, Japan*
[c]*Department of Chemistry, Joetsu University of Education, Joetsu-shi, Niigata 943-8512, Japan*
[d]*Tama Biochemical Co. Ltd., Shinjuku-ku, Tokyo 163-0704, Japan*

Received 30 January 2001; received in revised form 20 April 2001

Abstract

Roots and shoots of tomato (*Lycopersicon esculentum*) were investigated for the occurrence of biosynthetic precursors of 28-norcastasterone, a C_{27} brassinosteroid that we have shown to be present in shoots of tomato. A series of putative precursors, including 6-deoxo-28-norcathasterone, 6-deoxo-28-norteasterone, 3-dehydro-6-deoxo-28-norteasterone, 6-deoxo-28-nortyphasterol and 6-deoxo-28-norcastasterone, were synthesized and used as GC-MS standards, resulting in the identification of 6-deoxo-28-norcathasterone, 6-deoxo-28-nortyphasterol and 6-deoxo-28-norcastasterone in both roots and shoots. These findings indicate that the biosynthesis of 28-norcastasterone may parallel that of castasterone. The endogenous levels of brassinosteroids differed between roots and shoots, indicating that the biosynthesis of brassinosteroids is differently regulated between these tissues. Regulation of root growth by brassinosteroids is also discussed. © 2001 Elsevier Science Ltd. All rights reserved.

Keywords: Tomato; *Lycopersicon esculentum*; Solanaceae; Shoot; Root; Brassinosteroid; 6-Deoxo-28-norcathasterone; 6-Deoxo-28-norteasterone; 3-Dehydro-6-deoxo-28-norteasterone; 6-Deoxo-28-nortyphasterol; 6-Deoxo-28-norcastasterone; 28-Norcastasterone; Castasterone

1. Introduction

Unusual phenotypes such as dwarfism and leaf curling in the tomato mutants *dwarf* (Bishop et al., 1999) and *dumpy* (Koka et al., 2000) have recently been ascribed to brassinosteroid (BR) deficiency, while a similar appearance in the tomato mutant *curl-3* was attributed to insensitiveness to BRs (Koka et al., 2000). These findings revealed that BRs play an essential role in the growth and development of tomato. In tomato shoots, castasterone (**1**), a C_{28} BR, seems to be biologically active since brassinolide was not detected in this tissue (Yokota et al., 1997a,b; Bishop et al., 1999; Nomura et al., 2001). Castasterone is biosynthesized from campestanol through either early C-6 oxidation or late C-6 oxidation (Sakurai, 1999). GC–MS analyses of biosynthetic precursors of castasterone in tomato shoots led to the identification of 6-deoxoBRs rather than 6-oxoBRs, indicating that the late C-6 oxidation pathway is exclusively operative in this tissue (Yokota et al., 1996; Bishop et al., 1999; Nomura et al., 2001).

In addition to castasterone (**1**), tomato shoots contain 28-norcastasterone (**2**) which may be another bioactive BR with the same C_{27}-carbon skeleton as cholesterol, its endogenous level being comparable to that of castasterone (Bishop et al., 1999; Nomura et al., 2001). Since cholesterol, along with cholestanol, was detected in the shoots with the former being the major sterol, it is likely that the synthesis of 28-norcastasterone from cholesterol *via* cholestanol occurs through late C-6 oxidation in analogy to the biosynthesis of castasterone. To ascertain this hypothesis, we synthesized a series of putative C_{27} precursors of 28-norcastasterone that have a 6-deoxo structure and, using these chemicals as standards, analyzed

* Corresponding author. Tel.: +81-28-627-7209; fax: +81-28-627-7187.
E-mail address: yokota@nasu.bio.teikyo-u.ac.jp (T. Yokota).

0031-9422/01/$ - see front matter © 2001 Elsevier Science Ltd. All rights reserved.
PII: S0031-9422(01)00237-0

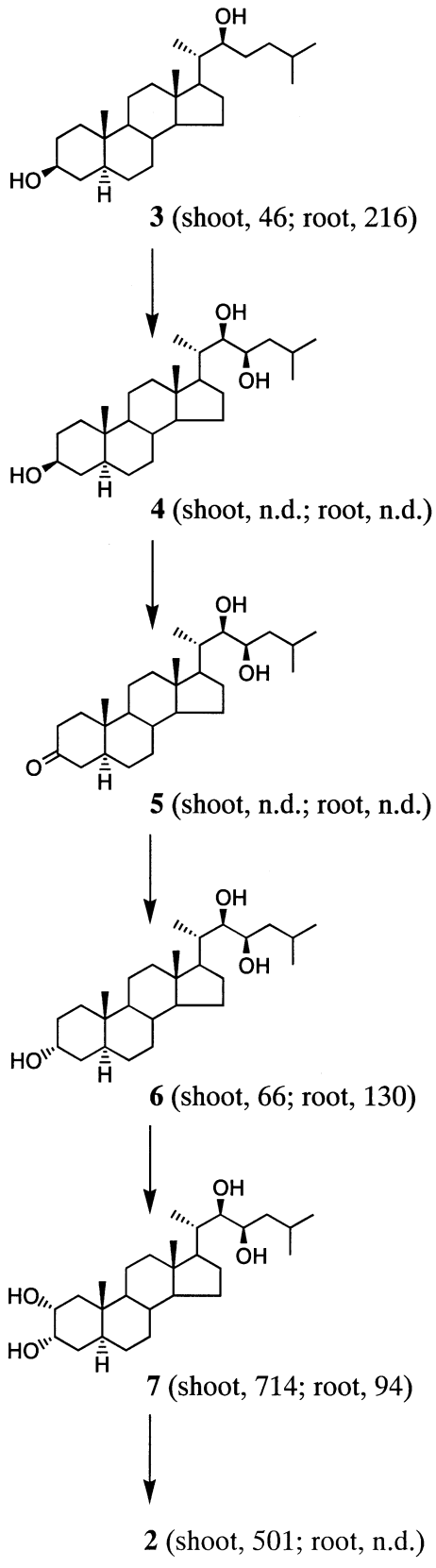

Fig. 1. Putative biosynthetic pathway of 28-norcastasterone (**2**) in tomato. The endogenous levels of BRs (ng/kg fresh weight) in shoots and roots of tomato are shown in parentheses.

the shoots and roots of tomato by GC–MS. In this paper, we report the successful identification of some 6-deoxo intermediates in these tissues and will discuss the biosynthesis of 28-norcastasterone by comparing our results with recent work on the putative biosynthetic pathway of 28-norcastasterone from castasterone in some plants, including tomato (Fujioka et al., 2000). Requirement of BRs in the root growth is also discussed.

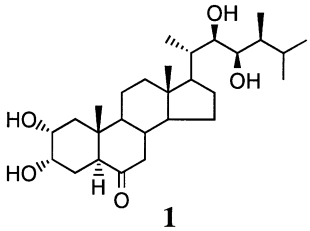

1

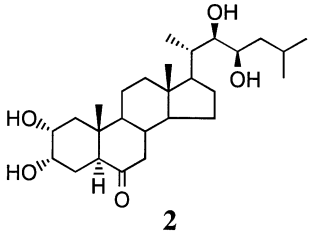

2

2. Results and discussion

28-Norcastasterone (**2**) was assumed to be derived from 6-deoxo-28-norcathasterone (**3**) via 6-deoxo-28-norteasterone (**4**), 3-dehydro-6-deoxo-28-norteasterone (**5**), 6-deoxo-28-nortyphasterol (**6**) and 6-deoxo-28-norcastasterone (**7**) (Fig. 1). These compounds were synthesized as described in Experimental. The Rts and mass spectra of these BRs were determined by GC–MS after being converted into appropriate derivatives (Table 1).

Tomato seedlings, grown hydroponically, were separated into shoots and roots. These tissues were extracted with methanol and subjected to solvent partitioning and then to chromatography on charcoal and/or Sephadex LH-20. The purified extracts were chromatographed on reversed phase HPLC. HPLC fractions corresponding to the Rts of compounds **2**–**7** were analyzed by selected ion monitoring (SIM) on the basis of the GC–MS data obtained for respective authentic specimens (Table 1). Ions characteristic of 6-deoxo-28-norcathasterone (**3**) bisTMSi ether, 6-deoxo-28-nortyphasterol (**6**) methaneboronate-TMSi ether and 6-deoxo-28-norcastasterone (**7**) bismethaneboronate were detected in the extracts obtained from shoots and roots of tomato with the Rts (Table 1) and intensities (Table 2) being comparable to authentic compounds. These results corroborate our hypothesis that 28-norcastasterone may be synthesized from 6-deoxo-28-norcathasterone. But to positively confirm this, feeding experiments will be needed in the

Table 1
GC–MS data for synthetic 28-norbrassinosteorids

Compound	Derivative	Rt	Ion (relative peak height)
6-Deoxo-28-norcathasterone (**3**)	BisTMSi ether	8′57″	533 (M^+-15, 1.3), 477 (1.3), 458 (2.3), 387 (1.1), 368 (4.6), 345 (2.4), 255 (7), 173 (100)
6-Deoxo-28-norteasterone (**4**)	Methaneboronate-TMSi ether	9′13″	516 (M^+, 100), 501 (58), 459 (13), 426 (58), 411 (36), 305 (29), 285 (12), 257 (19), 230 (26), 215 (80)
3-Dehydro-6-deoxo-28-norteasterone (**5**)	Methaneboronate	9′00″	442 (M^+, 100), 427 (12), 246 (18), 231 (92), 217 (17), 163 (16), 141 (14)
6-Deoxo-28-nortyphasterol (**6**)	Methaneboronate-TMSi ether	8′27″	516 (M^+, 65), 501 (17), 426 (100), 411 (61), 305 (17), 285 (11), 257 (11), 230 (29), 215 (85)
6-Deoxo-28-norcastasterone (**7**)	Bismethaneboronate	9′17″	484 (M^+, 100), 469 (24), 288 (21), 273 (89), 141 (15)

Table 2
GC–SIM data indicating the occurrence of 6-deoxo-28-norcathasterone (**3**), 6-deoxo-28-nortyphasterol (**6**) and 6-deoxo-28-norcastasterone (**7**) in tomato. Typical data obtained from analysis of shoots and roots of tomato are shown

Compound	Sample analyzed	Ions detected (relative peak area)			
6-Deoxo-28-norcathasterone (**3**) bisTMSi ether	Synthetic	533 (1)	368 (2)	255 (8)	173 (100)
	Extract	533 (1)	368 (2)	255 (4)	173 (100)
6-Deoxo-28-nortyphasterol (**6**) methaneboronate-TMSi ether	Synthetic	516 (32)	426 (61)	411 (48)	215 (100)
	Extract	516 (34)	426 (76)	411 (45)	215 (100)
6-Deoxo-28-norcastasterone (**7**) bismethaneboronate	Synthetic	484 (56)	469 (16)	288 (19)	273 (100)
	Extract	484 (59)	469 (15)	288 (16)	273 (100)

future. Although ions characteristic of 6-deoxo-28-norteasterone (**4**) methaneboronate-TMSi ether and 3-dehydro-6-deoxo-28-norteasterone (**5**) methaneboronate were not detectable, this does not contradict the present conclusion since corresponding C_{28} BRs, 6-deoxoteasterone and 3-dehydro-6-deoxoteasterone are also known to be scarce in tomato, pea and *Arabidopsis thaliana* (Nomura et al., 2001).

Recently, [26, 28-$^2H_6$] castasterone has been found to be converted with removal of C-28 to [26-$^2H_3$] 28-norcastasterone in seedlings of *A. thaliana,* and tomato, and cultured cells of *Catharanthus roseus* (Fujioka et al., 2000). On the basis of this evidence, it was postulated that 28-norcastasterone is synthesized from castasterone. Likewise, *Marchantia polymorpha* cells also remove C-28 of [26, 28-$^2H_6$]brassinolide to give [26-$^2H_3$]28-norbrassinolide (Kim et al., 2000). However, *Marchantia* cells cannot remove C-28 from unlabelled brassinolide and instead detach its C-26. Thus, there is the possibility that the removal of C-28 only occurs in [26, 28-$^2H_6$] BRs but not in unlabelled, natural BRs. The intermediary of castasterone in the biosynthesis of 28-norcastasterone, therefore, may remain ambiguous.

The present work demonstrates that roots can synthesize BRs, agreeing with the recent finding that maize roots produce castasterone (Kim et al., 2000), and suggesting that BRs are necessary for the growth of not only shoots, but also roots. In support of this, the pea mutant *lk* which is deficient in BRs (Yokota et al., 1997a,b) has unusually thick and less lateral roots (T. Yokota, unpublished). The levels of a series of 28-norBRs in shoots and roots of tomato are shown in Fig. 1. Quantification of **2** was made by GC–SIM using deuterated brassinolide as an internal standard. However, the levels of **3**–**7** were obtained only by comparing the areas of their molecular ions with those of authentic compounds, because appropriate deuterated standards were not available. Thus, the loss encountered during purification could not be compensated for and hence the values obtained for **3**–**7** were less than the actual ones. However, the data presented in Fig. 1 at least suggest that relative amounts of these BRs are significantly varied between shoots and roots. Thus, the biosynthesis of BRs seems to be differently regulated between shoots and roots.

Of further interest, the level of 28-norcastasterone (**2**) is high in shoots, but undetectable in roots (Fig. 1) and this relationship was also the case in the levels of castasterone which is abundant in shoots but only in a trace amount in roots (T. Yokota, to be published elsewhere), indicating that roots require 28-norcastasterone and castasterone to a much lesser extent than that required by shoots. Less requirement of endogenous gibberellin by roots has also been demonstrated in *Lactuca sativa* (Tanimoto, 1987, 1991), *Pisum sativum* (Tanimoto, 1991) and *Lemna minor* (Inada et al., 2000; Inada and Shimmen, 2000) by applying gibberellin A_3 to respective

seedlings treated with gibberellin biosynthesis inhibitors. In contrast to gibberellin, even low levels of brassinolide and/or 24-epibrassinolide have been known to be inhibitory to root growth of wheat, mung bean and maize (Roddick and Ikekawa, 1992), *A. thaliana* (Clouse et al., 1993) and tomato (Roddick, 1994) and hence, in roots, there seems to be a homeostasis keeping the levels of biologically active BRs very low. Conversely, one may propose that castasterone and 28-norcastasterone are biologically active in their own right (Yokota, 1997).

3. Experimental

3.1. Plant materials

Seeds of tomato (cv. Sekaiichi) were sown in vermiculite and grown for 31 days in a greenhouse under natural light: day, 23 °C (13 h); night, 20 °C (11 h). Seedlings were fed with Hyponex (×1000) 20 and 27 days after sowing. Seedlings were then grown for a further 15 days hydroponically using Tadano and Tanaka (1980) liquid medium. One hundred and ninety-six seedlings were separated into shoots (349 g) and roots (95 g).

3.2. Bioassay

To monitor the biological activity of BRs, sample aliquots were assayed by the rice lamina inclination test (Yokota et al., 1996).

3.3. Extraction and purification of BRs

Shoots and roots were subjected to the following purification procedures although charcoal chromatography was avoided in the case of roots. Plant tissues were homogenized in MeOH containing [$^2H_6$]-labeled internal standards (100 or 1000 ng) of C_{28}-BRs were added before reduction to an aq. residue. The latters were partitioned between EtOAc and 0.5 M K_2HPO_4. The EtOAc phases were evaporated to dryness and partitioned between hexane and 80% MeOH. The 80% MeOH phase was evaporated to dryness and the residual solid was purified on a column of charcoal (chromatography grade; Wako Pure Chemicals, Japan) which was eluted with MeOH–H_2O (6:4 and 8:2, v/v), MeOH, MeOH–$CHCl_3$ (9:1, 7:3, 5:5, 3:7, and 1:9, v/v) and $CHCl_3$. The MeOH–$CHCl_3$ (9:1–3:7) fractions were applied on a Sephadex LH-20 column (bed volume, 500 ml; Pharmacia) using MeOH–$CHCl_3$ (4:1) as a mobile phase. Successive 10-ml fractions were collected. Fractions 37–41 (shoots) and 37–40 (roots) were combined, dissolved in MeOH and passed through columns of diethylaminopropyl silica (Bondesil, Varian. Palo Alto, CA) and octadecyl silica (ODS-SS-1020-T; Senshu Science, Tokyo, Japan). Reversed-phase HPLC was carried out on a Senshu Pak ODS-3251-D column (250×8 mm i.d.; Senshu Science) eluted with an acetonitrile–H_2O gradient at a flow rate of 2.5 ml min^{-1}: 0–20 min, 45% acetonitrile; 20–40 min, 45–100% acetonitrile; 40–60 min, 100% acetonitrile. Fractions were collected every min. The column oven temp. was maintained at 40 °C. Based on bioassay and the HPLC Rts of authentic BRs, BR fractions were collected for analysis by GC–MS/SIM. The following fractions were analyzed: fr.14/15 (28-norcastasterone), fr. 35/36 (6-deoxo-28-norcastasterone), fr. 40 (6-deoxo-28-norteasterone), fr. 43 (3-dehydro-6-deoxo-28-norteasterone), fr. 45 (6-deoxo-28-nortyphasterol), fr. 48/49 (6-deoxo-28-norcathasterone).

3.4. GC–MS/SIM analysis of BRs

Methaneboronation was conducted by dissolving BRs in pyridine that contains 2 mg ml^{-1} methaneboronic acid prior to heating at 70 °C for 30 min. Further trimethylsilylation of methaneborones was conducted by reacting with *N*-methyl-*N*-trimethylsilyl-trifluoroacetamide (MSTFA) at room temp. for 10 min. 6-Deoxocathasterone was converted to a TMSi derivative with MSTFA–pyridine (1:4) at 70 °C for 30 min. GC–EI MS/SIM (70 eV) was carried out on a JMS AX 505W instrument (Jeol, Tokyo, Japan) fitted with a DB-5 column (0.25 mm i.d. ×15 m; 0.25 μm film thickness; J&W Scientific, Folsom, CA). The carrier gas was He at a flow rate of 1 ml min^{-1}, the injection port temp. was 280 °C, and samples were introduced by splitless injection. The column oven temp. was programmed at 170 °C for 1.5 min, before being elevated to 280 °C at 37 °C min^{-1}, and then to 300 °C at 1.5 °C min^{-1}. The amount of 28-norcastasterone was determined from a calibration curve constructed from the peak area ratios of the $[M]^+$ ions of 28-norcastasterone bismethaneboronates and [$^2H_6$]brassinolide bismethaneboronates. The contents of other 28-norBRs were calculated by comparing the peak areas of $[M]^+$ ions with those of authentic samples.

3.5. Synthesis of C_{27} BRs

Compound **3** was prepared from a known 22α-hydroxycholesterol (Ishiguro et al., 1978) by hydrogenation. **4**–**7** were synthesized from a known (22*R*, 23*R*)-dihydroxycholesterol (Takatsuto and Ikekawa, 1987) by using the same method as described for their corresponding 6-deoxo type C_{28} steroids (Takatsuto et al., 1997).

3.5.1. (22S)-5α-Cholestan-3β,22-diol (6-deoxo-28-norcathasterone **3**)

Mp 178–179 °C (MeOH). ^{1}H NMR spectral data (400 MHz, $CDCl_3$) δ 0.664 (3H, *s*, H-18), 0.806 (3H, *s*, H-19), 0.891 (9H, *d*, *J* = 6.35 Hz, H-21, H-26 and H-27), 3.542–3.650 (2H, *m*, H-3α and H-22). EIMS (probe) 70 eV, *m*/*z* (rel. int.): 404 $[M]^+$ (3), 386 (12), 371 (6), 353 (2), 333

(2), 315 (7), 304 (47), 289 (23), 271 (16), 257 (11), 248 (12), 234 (100), 215 (55), 165 (41), 147 (36), 135 (53), 121 (59), 107 (98).

*3.5.2. (22S,23R)-5α-Cholestan-3β,22,23-triol (6-deoxo-28-norteasterone **4**)*

Mp 213–214 °C (MeOH). ^{1}H NMR spectral data (400 MHz, $CDCl_3$) δ 0.674 (3H, *s*, H-18), 0.807 (3H, *s*, H-19), 0.891 (3H, *d*, $J=6.35$ Hz, H-21), 0.932 (3H, *d*, $J=6.84$ Hz, H-26 or H-27), 0.960 (3H, *d*, $J=6.84$ Hz, H-26 or H-27), 3.362 (1H, *m*, H-23), 3.542–3.660 (2H, *m*,H-3α and H-22). EIMS (probe) 70 eV, *m*/*z* (rel. int.): 420 $[M]^+$ (3), 402 (6), 384 (5), 334 (74), 333 (72), 315 (82), 297 (30), 274 (29), 257 (55), 233 (43), 215 (49), 109 (57), 107 (88), 95 (79), 81 (100), 69 (69). HR–EIMS, *m*/*z*: 420.3611 $[M]^+$ ($C_{27}H_{48}O_3$ requires: 420.3605).

*3.5.3. (22S,23R)-22,23-Dihydroxy-5α-cholestan-3-one (3-dehydro-6-deoxo-28-norteasterone **5**)*

Mp 146–147 °C (hexane). ^{1}H NMR spectral data (400 MHz, $CDCl_3$) δ 0.703 (3H, s, H-18), 0.898 (3H, *d*, $J=6.34$ Hz, H-21), 0.935 (3H, *d*, $J=6.34$ Hz, H-26 or H-27), 0.963 (3H, *d*, $J=6.83$ Hz, H-26 or H-27), 1.011 (3H, *s*, H-19), 3.363 (1H, *m*, H-23), 3.624 (1H, *m*, H-22). EIMS (probe) 70 eV, *m*/*z* (rel. int.): 418 $[M]^+$ (1), 400 (1), 332 (50), 331 (43), 313 (47), 302 (6), 273 (39), 271 (16), 257 (11), 231 (25), 203 (14), 109 (31), 107 (23), 95 (42), 81 (71), 69 (100). HR–EIMS, *m*/*z*: 418.3459 $[M]^+$ ($C_{27}H_{46}O_3$ requires: 418.3449).

*3.5.4. (22S,23R)-5α-Cholestan-3α,22,23-triol (6-deoxo-28-nortyphasterol **6**)*

Mp 213–214 °C (EtOH). ^{1}H NMR spectral data (400 MHz, $CDCl_3$) δ 0.677 (3H, *s*, H-18), 0.782 (3H, *s*, H-19), 0.894 (3H, *d*, $J=6.35$ Hz, H-21), 0.932 (3H, *d*, $J=6.84$ Hz, H-26 or H-27), 0.959 (3H, *d*, $J=6.35$ Hz, H-26 or H-27), 3.363 (1H, *m*, H-23), 3.618 (1H, *m*, H-22), 4.038 (1H, *m*, H-3 α). EIMS (probe) 70 eV, *m*/*z* (rel. int.): 420 $[M]^+$ (3), 402 (3), 384 (2), 334 (54), 333 (38), 315 (100), 297 (46), 274 (18), 257 (37), 233 (29), 215 (36), 109 (35), 107 (48), 95 (46), 81 (58), 69 (40). HR–EIMS, *m*/*z*: 420.3611 $[M]^+$ ($C_{27}H_{48}O_3$ requires: 420.3605).

*3.5.5. (22S,23R)-5α-Cholestan-2α,3α,22,23-tetraol (6-deoxo-28-norcastasterone **7**)*

Mp 218–219 °C (EtOH). ^{1}H NMR spectral data (400 MHz, $CDCl_3$) δ 0.675 (3H, *s*, H-18), 0.804 (3H, *s*, H-19), 0.894 (3H, *d*, $J=6.34$ Hz, H-21), 0.933 (3H, *d*, $J=6.34$ Hz, H-26 or H-27), 0.960 (3H, *d*, $J=6.35$ Hz, H-26 or H-27), 3.361 (1H, *m*, H-23), 3.625 (1H, *m*, H-22), 3.768 (1H, *m*, H-2 α), 3.963 (1H, *m*, H-3 α). EIMS (probe) 70 eV, *m*/*z* (rel. int.): 436 $[M]^+$ (2), 418 (2), 400 (2), 350 (58), 331 (100), 313 (92), 295 (21), 290 (16), 273 (31), 255 (18), 249 (18), 231 (29), 203 (13), 109 (37), 107 (39), 95 (59), 81 (65), 69 (54). HR–EIMS, *m*/*z*: 436.3559 $[M]^+$ ($C_{27}H_{48}O_4$ requires: 436.3554).

Acknowledgements

T.Y. is supported by a Grant-in-Aid for Scientific Research (11460057) from the Ministry of Education, Science, Sports and Culture of Japan and by the Human Frontier Science Program. T.N. is a Research Fellow of the Japan Society for the Promotion of Science for Young Scientists since 1998. We are thankful to Kyomi Shibata for GC–MS operation and Dr. Shozo Fujioka, RIKEN, Japan for mass spectrum of synthetic compounds.

References

Bishop, G., Nomura, T., Yokota, T., Harrison, K., Noguchi, T., Fujioka, S., Takatsuto, S., Jones, J.D.G., Kamiya, Y., 1999. The tomato DWARF enzyme catalyses C-6 oxidation in brassinosteroid biosynthesis. Proc. Natl. Acad. Sci. USA 96, 1761–1766.

Clouse, S.D., Hall, A.F., Langford, M., McMorris, T.C., Baker, M.E., 1993. Physiological and molecular effects of brassinosteroids on *Arabidopsis thaliana*. J. Plant Growth Regul. 12, 61–66.

Fujioka, S., Noguchi, T., Sekimoto, M., Takatsuto, S., Yoshida, S., 2000. 28-Norcastasterone is biosynthesized from castasterone. Phytochemistry 55, 97–101.

Inada, S., Shimmen, T., 2000. Regulation of elongation growth by gibberellins in root segments of *Lemna minor*. Plant Cell Physiol. 41, 932–939.

Inada, S., Tominaga, M., Shimmen, T., 2000. Regulation of root growth by gibberellin in *Lemna minor*. Plant Cell Physiol 41, 657–665.

Ishiguro, M., Saito, H., Sakamoto, A., Ikekawa, N., 1978. Studies on steroids. LI. Stereoselective introduction of 22- and 24-hydroxyl function in the steroidal side chain. Chem. Pharm. Bull. 26, 3715–3721.

Kim, S.-K., Chang, S.-C., Lee, E.-J., Chung, W.-S., Kim, Y.-S., Hwang, S., Lee, J.-S., 2000. Involvement of brassinosteroids in the gravitropic response of primary root of maize. Plant Physiol. 123, 997–1004.

Koka, C.V., Cerny, R.E., Gardner, R.G., Noguchi, T., Fujioka, S., Takatsuto, S., Yoshida, S., Clouse, S.D., 2000. A putative role for the tomato genes *DUMPY* and *CURL-3* in brassinosteroid biosynthesis and response. Plant Physiol. 122, 85–98.

Nomura, T., Sato, T., Bishop, G.J., Kamiya, Y., Takatsuto, S., Yokota, T., 2001. Accumulation of 6-deoxocathasterone and 6-deoxocastasterone in *Arabidopsis*, pea and tomato is suggestive of common rate-limiting steps in brassinosteroid biosynthesis. Phytochemistry 57, 171–178.

Roddick, J.G., Ikekawa, N., 1992. Modification of root and shoot development in monocotyledon and dicotyledon seedlings by 24-epibrassinolide. J. Plant Physiol. 40, 70–74.

Roddick, J.G., 1994. Comparative root growth inhibitory activity of four brassinosteroids. Phytochemistry 37, 1277–1281.

Sakurai, A., 1999. Biosynthesis. In: Sakurai, A., Yokota, T., Clouse, S.D. (Eds.), Brassinosteroids: Steroidal Plant Hormone. Springer, Tokyo, pp. 91–111.

Tadano, T., Tanaka, A., 1980. The effect of low phosphate concentrations in culture medium on early growth of several crop plants (in Japanese, translated by T.Y.). Jpn. J. Soil Sci. Plant Nutr. 51, 399–404.

Takatsuto, S., Ikekawa, N., 1987. Synthesis of 28-norbrassinolides and related 2-deoxysteroids. Chem. Pharm. Bull. 35, 3006–3010.

Takatsuto, S., Watanabe, T., Fujioka, S., Sakurai, A., 1997. Synthesis of new naturally-occurring 6-deoxo brassinosteroids. J. Chem. Res. (S) 134–135, (M) 0901–0924.

Tanimoto, E., 1987. Gibberellin-dependent root elongation in *Lactuca sativa*: recovery from growth retardant-suppressed elongation with thickening by low concentration of GA_3. Plant Cell Physiol 28, 963–973.

Tanimoto, E., 1991. Gibberellin requirement for the normal growth of roots. In: Takahashi, N., Phinney, B.O., MacMillan, J. (Eds.), Gibberellins. Springer, Tokyo, pp. 229–240.

Yokota, T., 1997. The structure, biosynthesis and function of brassinosteroids. Trend Plant Sci. 2, 137–143.

Yokota, T., Matsuoka, T., Koarai, T., Nakayama, M., 1996. 2-Deoxybrassinolide, a brassinosteroid from *Pisum sativum* seed. Phytochemistry 42, 509–511.

Yokota, T., Nomura, T., Kitasaka, Y., Takatsuto, S., Reid, J.B., 1997a. Biosynthetic lesions in brassinosteroid-deficient pea mutants. In: Proceedings of the 24th Annual Meeting of the Plant Growth Regulation Society of America, p. 24.

Yokota, T., Nomura, T., Nakayama, M., 1997b. Identification of brassinosteroids that appear to be derived from campesterol and cholesterol in tomato shoots. Plant Cell Physiol. 38, 1291–1294.

PERGAMON

Phytochemistry 58 (2001) 239–241

PHYTOCHEMISTRY

www.elsevier.com/locate/phytochem

5-Deoxy-7-methylbostrycoidin from cultured mycobionts from *Haematomma* sp.

Yuchiko Moriyasu[a], Hisashi Miyagawa[a,*], Nobuo Hamada[b], Hiromi Miyawaki[c], Tamio Ueno[a]

[a]*Division of Applied Life Sciences, Graduate School of Agriculture, Kyoto University, Kyoto 606-8502, Japan*
[b]*Osaka City Institute of Public Health and Environmental Sciences, 8-34, Tennoji-ku, Osaka 543-0026, Japan*
[c]*Faculty of Culture and Education, Saga University, Saga-shi 840-8502, Japan*

Received 21 November 2000; received in revised form 27 February 2001

Abstract

An unusual alkaloid, the 2-aza-anthraquinone derivative, 5-deoxy-7-methyl bostrycoidin, was identified in the cultures of the spore-derived mycobionts of the lichen *Haematomma* sp., but not in the natural lichen thallus. © 2001 Elsevier Science Ltd. All rights reserved.

Keywords: *Haematomma* sp.; Lichen; Mycobiont; Aza-anthraquinone; Bostrycoidin; nitrogen

1. Introduction

Lichens are distinctive organisms resulting from a symbiosis between algae and fungi. They are well known for their production of unique metabolites, generally referred to as lichen substances. Although the cooperative mechanisms for the biosyntheses of lichen substances are not fully understood, they are thought to be produced by the fungal portion (mycobiont) of the symbiotic system. However, it is very likely that the algal component (photobiont) has some role in their production, since there are many lichen substances characteristically produced in the symbiotic systems, and not in the isolated form. In this regard, the metabolic differences between the isolated fungal or algal cultures and the symbiotic form are likely to give us clues how these metabolic systems arise. Recent studies in our laboratories demonstrated that isolated lichen mycobionts are, in some cases, capable of producing new compounds under osmotically stressed conditions (Miyagawa et al., 1993, 1994, 1997; Tanahashi et al., 1997, 1999; Amano et al., 2000),which are not detected in the natural lichen specimens. These compounds are of interest, because they could be regarded as indicators of the "independent state" of the fungal mycobionts which are free from the interactions with the algal partners. In continuing the study of differences in secondary metabolism between lichens and mycobionts, we isolated and identified a bright yellow pigment produced by the spore-derived culture of the mycobiont from *Haematomma* sp., which was not detected in the natural lichen thallus. This paper describes the structural elucidation of this new and unusual pigment.

2. Results and discussion

The isolated mycobiont from *Haematomma* sp. was cultured on a malt-yeast extract medium supplemented with 10% sucrose. After a 7-month culture period, the mycobiont formed elevated round-shaped compact colonies on the agar slants. The brown colored colonies and culture medium were extracted in several groups using diethyl ether, and the production of a bright yellow pigment was detected in all the extracts by TLC analysis. The extract was then purified by chromatographic means to obtain compound **1** as a yellow powder.

The molecular formula of compound **1** was established to be $C_{16}H_{13}O_4N$ based on the HR–EI-mass spectrum ($[M]^+$ observed at m/z 283.0848, calculated

* Corresponding author. Tel./fax: +81-75-753-6123.
E-mail address: miyagawa@kais.kyoto-u.ac.jp (H. Miyagawa).

0031-9422/01/$ - see front matter © 2001 Elsevier Science Ltd. All rights reserved.
PII: S0031-9422(01)00167-4

283.0845); its degree of unsaturation was calculated to be 11. The presence of a hydrogen-bonded hydroxyl group was deduced from a characteristic signal observed in the ^{1}H NMR spectrum (δ H 12.87, s). In addition, signals assignable to two aryl methyl groups were observed in the ^{1}H (δ H 2.78, *s* and 2.22, *s*) and ^{13}C NMR (δ C 25.3 and 8.3). One methoxyl function was also identified from ^{1}H and ^{13}C NMR spectra (δ H 4.03, *s* and C 56.3).

The two carbon resonances at δ C 186.7 and 182.5, characteristic of anthraquinonoidal carbonyl δ C atoms, were assigned to C-10 and C-9, respectively. Treatment of **1** with acetic anhydride in the presence of catalytic amounts of sulfuric acid gave the monoacetylated derivative **2**, as evidenced by MS and NMR spectroscopic analyses. This suggested that only one hydroxyl group was present in **1**, assigned to that being hydrogen-bonded as mentioned above. On acetylation, the carbon resonance at C-9 shifted to higher field [$\Delta = -6.3$ ppm], revealing that the C-9 cabonyl group was involved in hydrogen bond formation.

The signals corresponding to the remaining eight carbon atoms resonated in the region from δ C 100 to 170 ppm. The proton resonances at δ H 9.42, 7.88 and 7.39, which showed no spin-interaction, were correlated by HMQC experiments with the methine signals at δ C 148.9, 118.5 and 102.7, respectively. These data, together with the presence of a nitrogen atom in the molecular formula, allowed the formulation of a 2-aza-anthraquinone ring. This structure is consistent with the degree of unsaturation calculated for this compound (Fig. 1).

The substitution pattern of the anthraquinone ring was determined from carbon-proton long range couplings observed in HMBC experiments and NOE correlations observed in NOESY spectra. The correlations are shown in Fig. 2. From these data this new pigment was formulated as **1**, or 3,7-dimethyl-8-hydroxy-6-meth oxy-2-aza-anthraquinone.

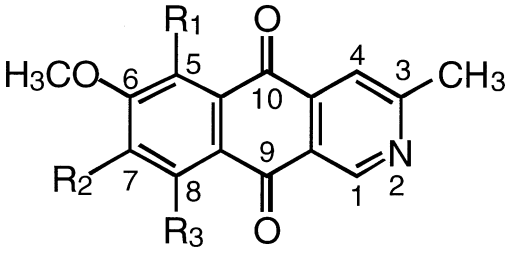

1 R_1 = H, R_2 = CH_3, R_3 = OH
5-deoxy-7-methylbostrycoidin

2 R_1 = H, R_2 = CH_3, R_3 = $OCOCH_3$
8-O-acetyl-5-deoxy-7-methylbostrycoidin

3 R_1 = OH, R_2 = H, R_3 = OH
bostrycoidin

Fig. 1. 2-Aza-anthraquinone derivatives.

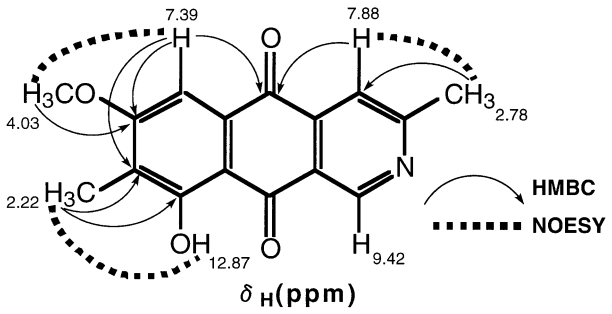

Fig. 2. HMBC and NOESY correlations of **1**.

It is noteworthy that compound **1** has not been described before and cannot be related to any known *N*-containing substances of lichen origin (Huneck and Yoshimura, 1996). Compound **1** rather has quite a similar structure to that of the antibiotic, bostrycoidin (**3**), produced by the fungus *Fusarium bostrycoides* (Arsenault, 1965), and thus, is named 5-deoxy-7-methyl bostrycoidin. No 5-deoxy-7-methylbostrycoidin was found in the lichen thallus, or the symbiotic form of fungi and algae, but atranorin was detected by TLC. It is interesting that without the algal counterpart, the isolated mycobiont produced a 2-aza-anthraquinone derivative, which is structurally related to bostrycoidin with an antibiotic activity (Cajori et al., 1954). It could be hypothesized that the metabolic capacity of fungi to produce this antibiotic compound, which is unfavorable for symbiosis, is suppressed by algae in this lichen symbiotic form.

Some *N*-containing compounds produced by lichens are biosynthetically related to amino acids (Begg et al., 1978; Huneck et al., 1992, 1993). In contrast, compound **1** appears to be formed biosynthetically from a heptaketide (Kurobane et al., 1980; Parisot et al., 1988) and is distinct from the *N*-containing lichen substances reported.

3. Experimental

3.1. General experimental procedures

The mycobiont of the lichen specimen was obtained from spores from apothecia in the thallus and was cultured in test tubes containing MY10 medium (malt extract 10 g, yeast extract 4 g, agar 15 g in 1 l H_2O, pH 7), supplemented with sucrose at a conc. of 100 g l^{-1}. The culture was maintained at 15°C in the dark for ca. 7 months. The culture media along with the entire mycelia were then extracted with diethyl ether and the extract was filtered to remove the debris. After evaporating the filtrate, the residue was subjected to column chromatography (Kieselgel 60) eluting with $CHCl_3$. The eluate (47 mg) containing the substance of interest was evaporated

and then applied to a 10×20 cm silicagel TLC plate of Merck 60 PF 254, 1.5 mm thick. The development was done twice in $CHCl_3$ and the zone containing the target compound was confirmed by its R_f value of 0.31 under UV light. The corresponding band was excised, with the compound of interest being extracted with $CHCl_3$. The yield of the pigment was 1.6 mg g^{-1} culture including both mycelia and the medium.

*3.1.1. 5-Deoxy-7-methylbostrycoidin (**1**)*

Yellow powder: mp 149–153° FAB–MS *m/z*: 283.0848 [M]$^+$, calc. for $C_{16}H_{13}O_4N$ 283.0845. EIMS 70 eV *m/z* (rel. int.): 283 [M]$^+$ (100), 282 [M–H]$^+$ (15), 268 [M–Me]$^+$ (17), 265 [M–H_2O]$^+$ (94), 254 [M–H-CO]$^+$ (37), 240 [M–Me–CO]$^+$ (12). UV $\lambda_{max}^{CHCl_3}$ nm (log ε): 591 (0.001), 420 (0.492), 325 (0.380), 286 (1.546), 246 (1.702). IR ρ_{max}^{Nujol} cm^{-1}: 4000–3300 (br, −OH), 1670 (>C=O), 1630 (>C=O), 1590 (>C=N−). ^{13}C NMR spectral data (75 MHz, $CDCl_3$): δ 8.3 (*s*, C-13), 25.3 (*s*, C-11), 56.3 (*s*, C-12), 102.7 (*s*, C-5), 110.1 (*s*, C-8a), 118.5 (*s*, C-4), 122.0 (*s*, C-7), 124.2 (*s*, C-1a), 131.8 (*s*, C-5a), 138.7 (*s*, C-4a), 148.9 (*s*, C-1), 162.2 (*s*, C-8), 163.7 (*s*, C-6), 165.7 (*s*, C-3), 182.5 (*s*, C-10), 186.7 (*s*, C-9). ^1H NMR spectral data (300 MHz, $CDCl_3$): δ 2.22 (3H, *s*, H-13), 2.78 (3H *s*, H-11), 4.04 (3H, *s*, H-12), 7.39 (1H, *s*, H-5), 7.88 (1H, *s*, H-4), 9.42 (1H, *s*, H-1), 12.87 (1H *s*, OH-8).

*3.1.2. 8-O-Acetyl-5-deoxy-7-methylbostrycoidin (**2**)*

A small amount of **1** was treated with Ac_2O containing a catalytic amount of sulfuric acid. After a chromatographic work-up, the product was analyzed by EIMS and ^1H NMR. EIMS 70 eV *m/z* (rel. int.): 325 [M]$^+$ (1), 283 [M–CH_3CO]$^+$ (100), 282 [M–CH_3CO–H]$^+$ (17), 268 [M–CH_3CO–Me]$^+$ (25), 265 [M–CH_3CO–H_2O]$^+$ (93), 254 [M–CH_3CO–H–CO]$^+$ (31). ^1H–NMR spectral data (300 MHz, $CDCl_3$): δ 2.20 (3H, *s*, H-13), 2.54 (3H, *s*, H-15), 2.82 (3H, *s*, H-11), 4.06 (3H, *s*, H-12), 7.68 (1H, *s*, H-5), 7.91 (1H, *s*, H-4), 9.37 (1H, *s*, H-1).

3.2. Biological material

Specimens of *Haematomma* sp. were collected at Suzaki City, Kochi Pref. Japan, altitude 30 m on 5 March 1998 and are deposited at Osaka City Institute of Public and Environmental Science under registration No. 9830572. Its identification was authorized by H. Miyawaki.

Acknowledgements

The authors express thanks to Dr. Naoshige Akimoto of the faculty of Pharmaceutical Science, Kyoto University, for the measurement of the mass spectra. This work was supported in part by a Grant-in-Aid for Scientific Research from the Ministry of Education, Science, Sports and Culture of Japan (No. 12660105).

References

Amano, T., Miyagawa, H.M., Ueno, T., Hamada, N., 2000. Production of 5,7-dihydroxy-6-hydroxymethyl-2-methoxy-1,4-naphthoquinone by the cultured lichen mycobiont of *Opegrapha* sp. No. 9771836. Zeitschrift für Naturfoschung 55b, 667–669.

Arsenault, G.P., 1965. The structure of bostrycoidin, β-aza-anthraquinone from *Fusarium solani* D_2 purple. Tetrahedron Letters 45, 4033–4037.

Begg, W.R., Elix, J.A., Jones, A.J., 1978. Nonacylic amids from lichens of the genus *Xanthoparmelia*. Tetrahedron Letters 12, 1047–1050.

Cajori, F.A., Otani, T.T., Hamilton, M.A., 1953. The isolation and some properties of an antibiotic from *Fusarium bostrycoides*. The Journal of Biological Chemistry 208, 107–114.

Huneck, S., Yoshimura, I., 1996. Identification of Lichen Substances. Springer, Berlin.

Huneck, S., Porzel, A., Schmidt, J., 1992. Hypothallin, ein weiterer Vertreter eines Aminosäure-aminoalkohol-esters aus der Krustenflechte *Schismatomma hypothallinum*. Zeitschrift für Naturforschung 47c, 785–790.

Huneck, S., Porzel, A., Schmidt, J., 1993. Structure and synthesis of arthonin, a lichen metabolite from *Arthonia endlicheri*. Tetrahedron Asymmetry 4, 303–311.

Kurobane, I., Vining, L.C., Mcinnes, A.G., Gerber, N.N., 1980. Metabolites from *Fusarium solani* related to dihydrofusarubin. The Journal of Antibiotics 33, 1376–1379.

Tanahashi, T., Kuroishi, M., Kuwahara, A., Nagakura, N., Hamada, N., 1997. Four phenolics from the cultured lichen mycobiont of *Graphis scripta* var. *pulverulenta*. Chemical and Pharmaceutical Bulletin 45, 1183–1185.

Tanahashi, T., Takenaka, Y., Ikuta, Y., Tani, K., Nagakura, N., Hamada, N., 1999. Xanthones from the cultured lichen mycobionts of *Pyrenula japonica* and *Pyrenula pseudobufonia*. Phytochemistry 52, 401–405.

Miyagawa, H., Hamada, N., Sato, M., Ueno, T., 1993. Hypostrepsilic acid, a new dibenzofuran from the cultured lichen mycobiont of *Evernia esorediosa*. Phytocemistry 34, 589–591.

Miyagawa, H., Yamashita, M., Ueno, T., Hamada, N., 1997. Hypostrepsilalic acid from a cultured lichen mycobiont of *Stereocaulon japonicum*. Phytochemistry 46, 1289–1291.

Miyagawa, H., Hamada, N., Sato, M., Ueno, T., 1994. Pigments from the cultured lichen mycobionts of *Graphis scripta* and *G. desquamescens*. Phytochemistry 36, 1319–1322.

Parisot, D., Devys, M., Barbier, M., 1988. Fusarbinoic acid, a new naphtoquinone from the fungus *Nectria haematococca*. Phytochemistry 27, 3002–3004.

PERGAMON

Phytochemistry 58 (2001) 243–248

PHYTOCHEMISTRY

www.elsevier.com/locate/phytochem

β-Fluoro-coniferyl alcohol does not inhibit lignin biosynthesis in suspension cultures of *Picea abies* (L.) Karst.

Mikaela Gustafsson[a], Anna Kärkönen[b], Liisa K. Simola[b], Teemu H. Teeri[c], Jussi Sipilä[a], Ilkka Kilpeläinen[c], Gösta Brunow[a,*]

[a]*Laboratory of Organic Chemistry, Department of Chemistry, University of Helsinki, PO Box 56, FIN-00014, Helsinki, Finland*
[b]*Department of Biosciences, Division of Plant Physiology, University of Helsinki, PO Box 56, FIN-00014, Helsinki, Finland*
[c]*Institute of Biotechnology, University of Helsinki, PO Box 56, FIN-00014, Helsinki, Finland*

Received 2 October 2000; received in revised form 14 May 2001

Abstract

A fluorinated analogue of coniferyl alcohol has been reported to be a specific inhibitor of oxidases involved in the biosynthesis of lignin. The *Z* isomer of β-fluoro-coniferyl alcohol was synthesized and used for the preparation of dehydrogenation polymers (DHPs) and was also tested on lignin producing suspension cultures of spruce (*Picea abies* (L.) Karst.). The growth of the cells or the production of lignin by the suspension cultures was not significantly affected by the addition of fluoroconiferyl alcohol. This analogue did not form polymers quite as easily as did coniferyl alcohol in oxidation with hydrogen peroxide and horseradish peroxidase. In both cases the β-fluoroconiferyl alcohol became incorporated in the polymeric product. We were unable to detect any specific inhibition of peroxidase activity, which is at variance with earlier reports of pronounced inhibition of lignin biosynthesis in poplar plantlets by fluoroconiferin, a potential inhibitor of oxidases involved in lignin biosynthesis. © 2001 Elsevier Science Ltd. All rights reserved.

Keywords: *Picea abies* (L.) Karst.; Spruce; Suspension cultures; Lignin synthesis; Inhibition; Fluoroconiferyl alcohol

1. Introduction

Fluorinated analogues of lignin precursors, so called monolignols, have been studied as possible inhibitors of peroxidase activity (Goldberg et al., 1988). Fluorine, being similar in size to hydrogen but very different in reactivity can, when substituted in a reactive position, give rise to analogues which may act as antimetabolites towards the fluorine-free parents (Welch, 1987). In monolignols, the β position in the side chain is the most reactive. Such fluoro analogues of cinnamic compounds have been reported to function as hydrogen donors for peroxidase reactions, forming "lignin-like" polymers (Goldberg et al., 1988). In a more recent report it was stated that β-fluoroconiferyl alcohol acts as a specific inhibitor of lignin biosynthesis in poplar shoots (Daubresse et al., 1997). In view of the importance for the study of lignin forming enzymes of finding a specific inhibitor of lignin polymerization, we have synthesized β-fluoroconiferyl alcohol and studied its effect on the lignin formation ability of suspension cultures of spruce as well as its reactivity in peroxidatic oxidation experiments. We could not observe any significant effects on lignin production in the suspension cultures after addition of the fluoro analogue of coniferyl alcohol.

2. Results

2.1. The preparation of β-fluoro coniferyl alcohol

The synthesis of the *Z* isomer coniferyl alcohol with a fluorine in the β position, using a Horner–Emmons reaction with phosphonofluoroacetate and vanillin acetate, has been mentioned in an article by Goldberg et al. (1988) but no physical or spectroscopic data for the product have been published. The Horner–Emmons is a general route for obtaining mainly the E isomer, which in this case has to be isomerized to the *Z* isomer by treatment with bromine. We have used a more direct stereoselective route to (*Z*)-2-fluoroalkenoates (Clemenceau and Cousseau, 1993) to prepare the acetate of (*Z*)-β-fluoro ethyl ferulate which we then reduced to the cor-

* Corresponding author.
E-mail address: gosta.brunow@helsinki.fi (G. Brunow).

0031-9422/01/$ - see front matter © 2001 Elsevier Science Ltd. All rights reserved.
PII: S0031-9422(01)00251-5

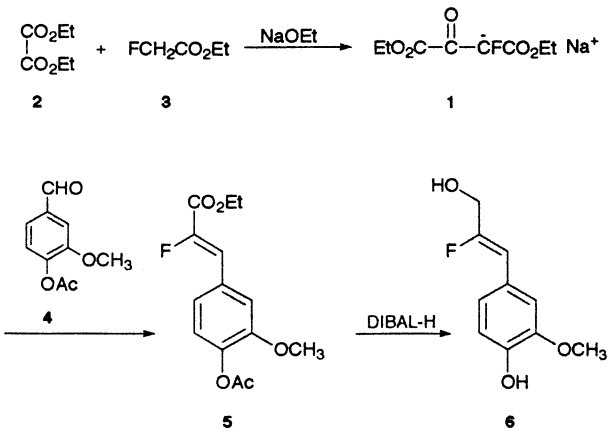

Scheme 1.

responding alcohol with DIBAL-H (Quideau and Ralph, 1992) in 86% yield (Scheme 1).

2.2. The preparation of DHPs

The synthetic lignins (DHPs) were prepared by oxidation with H_2O_2/horseradish peroxidase (HRP) at pH 4 using a suspension with cellulose powder to facilitate the isolation of the polymer. The experiments were carried out with fluoroconiferyl alcohol, coniferyl alcohol, and a mixture of the two. As can be seen in Table 1 the fluoro analogue formed less polymer and more unreacted starting material was left at the end of the reaction, compared to coniferyl alcohol, with the mixture being intermediate in reactivity (Table 1).

Mixtures of dimers isolated from an interrupted oxidation of fluoroconiferyl alcohol were analyzed by chromatography, NMR and mass spectrometry. NMR studies indicate that the main dimer is a β-5 product; the presence of β-O-4 and a β-β dimers were also indicated (the spectra will be published separately).

Table 1
Yields (%) of dehydrogenation polymers formed in H_2O_2/HRP oxidation of fluoroconiferyl alcohol (F-CA) and coniferyl alcohol (CA)

Starting material	Unreacted	EtAc-soluble	Dioxane-soluble
F-CA	31	31	38
CA	3	13	84
F-CA + CA	12	9	79

2.3. The suspension culture experiments

In the suspension cultures, the extracellular precipitate became visible on day 3 after initiation of the suspension culture regardless of the added compound. The chemical analysis of this extracellular lignin precipitate has been described (Brunow et al., 1993). In day 6 some of the suspension cultures showed signs of ageing so a 5-day culture period was used in the following replicate cultures.

Neither coniferyl alcohol nor fluoroconiferyl alcohol had a statistically significant effect on the fresh weight of the cells, on the pH of the nutrient medium at the end of culture, on the amount of secreted proteins in the medium or on the amount of extracellular precipitate formed according to variance analysis (Table 2). Also, the peroxidase isoenzyme pattern was similar as revealed by IEF and peroxidase activity staining, showing that the presence of this fluoro analogue did not induce secretion of any new peroxidase isoenzymes into the suspension culture medium (Fig. 1).

According to kinetic data nutrient medium peroxidases from cultures 1 and 2 showed a higher apparent utilization efficacy towards coniferyl alcohol, as evidenced for a higher value of V_{max}/K_m (Table 3): it was ca. 1.7-fold towards coniferyl alcohol compared to its fluorinated analogue. It should be noted that this apparent difference could be explained by the different stability of the radicals formed from the coniferyl alcohol and its fluoro analogue (Daubresse et al., 1997). However, for the nutrient medium peroxidases from culture 3 and for HRP types I and II the apparent utilization efficacy was similar for both the fluorinated analogue and for the coniferyl alcohol (Table 3). The substrate concentration of 150 μM inhibited coniferyl alcohol and fluoroconiferyl alcohol oxidation by nutrient medium peroxidases as well as by HRP (data not shown). K_m values calculated for coniferyl alcohol and fluoroconiferyl alcohol or their mixture were similar for nutrient medium peroxidases (20–50 μM), however, the affinity of HRP types I and II was over two-times higher for the fluorinated analogue

Table 2
Fresh weight of the cells, pH of the nutrient medium at the end of culture period, amount of secreted proteins in the nutrient medium and the amount of extracellular precipitate per 25 ml of suspension culture of *Picea abies* after 5 days in suspension culture[a]

	Fresh weight of the cells (g)	pH	Secreted proteins in the medium (mg/ml)	Extracellular precipitate (mg/25 ml culture)
Control	0.62±0.04	4.0±0.13	0.067±0.03	5.98±0.74
Coniferyl alcohol (0.1 mM)	0.62±0.03	4.0±0.14	0.078±0.02	5.53±0.69
Coniferyl alcohol (0.05 mM) + fluoroconiferyl alcohol (0.05 mM)	0.61±0.03	3.9±0.13	0.083±0.01	5.10±0.84
Fluoroconiferyl alcohol (0.1 mM)	0.61±0.04	3.8±0.10	0.080±0.01	4.20±0.61

[a] Means of 4 separate cultures±SE. The results of different treatments do not differ statistically significantly according to variance analysis.

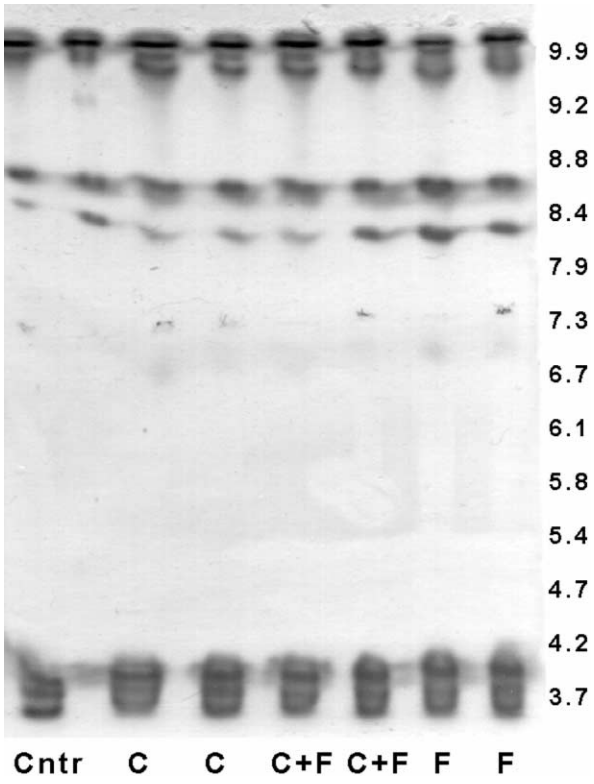

Fig. 1. Peroxidase isoenzymes from the nutrient media of fluoroconiferyl alcohol feeding experiment separated on polyacrylamide gel by isoelectric focusing (pH 3.5–10). Control culture (Cntr), 0.1 mM coniferyl alcohol (C), 0.05 mM coniferyl alcohol + 0.05 mM fluoroconiferyl alcohol (C + F), 0.1 mM fluoroconiferyl alcohol (F). The amounts of proteins loaded onto the gel were counted as 80 pkat of peroxidase activity. Peroxidases were visualised by activity staining with 3,3-diaminobenzidine and H_2O_2 as described in Experimental.

than for the non-fluorinated one (Table 3). The K_m value for HRP type I for the mixture of both substrates was in the middle of those of pure coniferyl alcohol or its analogue as a substrate. On the contrary, K_m values of HRP type II for the mixture of substrates and for the fluoro analogue were almost similar (159 and 197 μM, respectively; Table 3).

3. Discussion

Lignin precursors such as coniferyl alcohol are oxidized by many kinds of oxidizing enzymes, and no specificity has yet been established. The presence of a fluorine atom on the β-carbon of the side chain of coniferyl alcohol does not prevent the oxidation by peroxidases. Oxidation of fluoroconiferyl alcohol with hydrogen peroxide and horseradish peroxidase produced polymers albeit in smaller yields than with coniferyl alcohol itself. Analysis of dimers formed in the reaction indicated the formation of β-5, β-O-4 and β–β coupling products. The use of fluoroconiferyl alcohol in the kinetic assays showed that nutrient medium peroxidases used the native substrate coniferyl alcohol apparently more efficiently as a substrate its fluorinated analogue. In suspension cultures, however, the amount of precipitate formed was not statistically significantly decreased when the fluoroconiferyl alcohol was feeded to the cells. On the other hand, HRP preparations did not make any difference in the oxidizability between these substrates, as evidenced for the same V_{max}/K_m (Table 3). We were thus unable to reproduce in cell cultures the results of Daubresse et al. (1997) who observed a pronounced inhibition of lignin biosynthesis in feeding experiments with poplar plantlets with fluorooconiferin, that was designed as a potential inhibitor of oxidases involved in the biosynthesis of lignin.

4. Experimental

4.1. β-Fluoro coniferyl alcohol

The sodium salt of diethyl fluoro-oxaloacetate **1** was prepared from diethyl oxalate **2**, ethyl fluoroacetate **3** (Aldrich) and alcohol free sodium ethoxide, according to a published procedure (Blank et al., 1995).

The sodium salt of diethyl fluoro-oxaloacetate (8.58 g, 38 mmol) **1** was suspended in dry THF (100 ml) and cooled to 0 °C. Acetyl vanillin **4** (7.4 g, 38 mmol) in THF (40 ml) was added to the suspension with stirring (Clemencau and Cousseau, 1993). Then the reaction mixture was heated for 7 h at 80 °C. After a further 3 days at room temperature most of the THF was evaporated in vacuo and 100 ml diethyl ether was added. Then 50 ml saturated aq. $KHCO_3$ was added with stirring during 30 min. The organic layer was washed with water and with aqueous sodium bisulfite (10%). The organic layer was then dried ($NaSO_4$) and evaporated. The yield was 8.33 g (79%). The acetylated β-fluoro ethyl ferulate **5** was recrystallized from ethanol and water to give 5.3 g (50%) of light yellow crystals of melting point 63–66 °C.

Acetylated β-fluoro ethyl ferulate: δ_H (200 MHz) 1.39 (3H, *t*,–CH_3) 2.33 (3H, *s*,–$OCCH_3$) 3,86 (3H, *s*,–OCH_3) 4.36 (2H, *q*,–CH_2-) 6.89 (1H, *d*, α–CH) 7.05–7.31 (3H, *m*, arom.); δ_C(50 MHz) 14.3 (*s*, $OOCCH_3$) 20.8 (*s*, OCH_2CH_3) 56.0 (*s*, OCH_3) 62.1 (*s*,-OCH_2CH_3) 113.8 (*d*, C-α, J_{CF} = 9.6 Hz) 116.9 (*d*, ArC-2, J_{CF} = 4.55 Hz) 123.1(*s*, ArC-6) 123.4 (*d*, ArC-5, J_{CF} = 7.25) 130,0 (*d*, ArC-1, J_{CF} = 4.55) 140.8 (*d*, ArC-4, J_{CF} = 3.6) 147.0 (*d*, C-β, J_{CF} = 266) 151.2 (*s*, ArC-3) 161.3 (*d*, C-γ, J_{CF} = 40) *m*/*z* (%) 58 (11) 197 (13) 212 (27) 240(100) 282 (M^+,12) (HRMS: $C_{14}H_{15}O_5F$ requires M 282.0904. Found: M^+ 282.0901)

The ester was reduced using DIBAL-H (Aldrich) in toluene to give the β-fluoro coniferyl alcohol **6**, 86% yield. The recrystallized product (66%) had a melting point of 105–107 °C.

β-Fluoro coniferyl alcohol: δ_H (200 MHz) 3.90 (3H, *s*, OCH_3) 4.27 (2H, *d*, γCH_2) 5,70 (1H, *d*, α-CH) 6.85-7.14

Table 3
Apparent kinetic parameters in the oxidation of coniferyl alcohol and its fluorinated analogue by nutrient medium bulk peroxidases of three separate cultures (1-3) of *Picea abies* and by horseradish peroxidase (HRP) types I and II[a]

Substrate		Nutrient medium peroxidases				
		1	2	3	HRP I	HRP II
Coniferyl alcohol	K_m μM	18.6	46.7	33.9	208	328
	V_{max} nkatal×(g f. wt)$^{-1}$	22.7	129	32.6		
	μkatal×(mg protein)$^{-1}$				12.9	37.5
	V_{max}/K_m	1.2	2.8	1.0	0.06	0.11
Fluoroconiferyl alcohol	K_m μM	18.9	30.4	26.7	110	159
	V_{max} nkatal×(g f. wt)$^{-1}$	12.5	49.5	28.8		
	μkatal×(mg protein)$^{-1}$				7.7	20.4
	V_{max}/K_m	0.7	1.6	1.1	0.07	0.13
Coniferyl alcohol	K_m μM	18.7	17.5	35.5	176	197
+fluoroconiferyl alcohol (1:1)	V_{max} nkatal×(g f. wt)$^{-1}$	18.7	65.3	29.0		
	μkatal×(mg protein)$^{-1}$				9.8	22.4
	V_{max}/K_m	1.0	3.7	0.8	0.06	0.11

[a] Hanes plots were constructed from initial velocity data and K_m and V_{max} values determined after linear regression analysis. Rate values for nutrient medium peroxidases are normalized per gram of fresh tissue (Gonzàlez et al., 1999).

(3H, *m*, arom.); δ_C(50 MHz) 55.9 (*s*, OCH_3) 62.1 (*d*, C-γ, $J_{CF}=15.4$ Hz) 107.7 (*d*, C-α, $J_{CF}=6.9$ Hz) 111.0 (*d*, ArC-2, $J_{CF}=9.6$ Hz) 114.4 (*s*, ArC-6) 122.5 (*d*, ArC-3, $J_{CF}=5.9$ Hz) 125.1 (*d*, ArC-1, $J_{CF}=2.74$ Hz) 145.3 (*d*, ArC-4, $J_{CF}=2.75$ Hz) 146.4 (*s*, ArC-3) 156.7 (*d*, C-β, $J_{CF}=264$ Hz). *m/z* (%) 58 (33), 107 (12), 109 (24), 121 (13), 124 (14), 137 (52), 149 (45), 165 (11), 180 (28), 198 (M^+,100) (HRMS: $C_{10}H_{11}O_3F$ requires M 198.0692. Found: M^+ 198.0701).

4.2. Coniferyl alcohol

Ferulic acid was prepared from vanillin and malonic acid (Pearl and Beyer, 1951). The acid was methylated with concentrated sulfuric acid and methanol (Adler and Gustafsson, 1963). The methyl ester of ferulic acid was reduced with DIBAL-H in toluene to give coniferyl alcohol (Quideau and Ralph, 1992).

4.3. DHP

Three different DHPs were prepared; one from 1.53 mmol β-fluoro coniferyl alcohol, another from 1.53 mmol coniferyl alcohol and a third from a mixture of 0.77 mmol coniferyl alcohol and 0.77 mmol β-fluoro coniferyl alcohol. An enzyme (12 mg) (horseradish peroxidase 529 U/mg, RZ 1.29, Serva, E.C. 1.11.1.7) was added to a suspension of cellulose (10 mg) and buffer pH 4 (10 ml). The alcohol (in 1 ml acetone) and 1 ml 5% hydrogen peroxide (2 eq.) were added to the mixture continuously for 5 h. The enzyme (12 mg) was added after 2 h. The mixture was allowed to react overnight. The suspension was filtered and the solid was washed with small amounts of water and then fractionated into an ethyl acetate soluble and a dioxan soluble fraction. The unreacted alcohol was extracted from the aqueous phase with ethyl acetate. All the fractions were acetylated, and identified with NMR.

4.4. The suspension culture experiments

A chlorophyllous callus line of *Picea abies* (L.) Karst. was used for suspension cultures that were cultured in a liquid medium containing T-macroelements (NH_4^+/NO_3^-, 1:2) and SS-microelements (Simola and Santanen 1990; Simola et al., 1992). 2,4-Dichlorophenoxyacetic acid (0.5 μM) and kinetin (2.5 μM) were used as growth regulators. No organic nitrogen was added to the liquid medium. Cells were cultured in 100 ml Erlenmeyer flasks with a culture volume of 25 ml. For feeding experiments, cells were transferred to basic medium supplemented with (A) 0.1 mM coniferyl alcohol, (B) 0.1 mM fluoroconiferyl alcohol, (C) 0.05 mM coniferyl alcohol and 0.05 mM fluoroconiferyl alcohol, (D) control (distilled water). Stock solutions (5 mM) of coniferyl alcohol and fluoroconiferyl alcohol were made by dissolving them first to a small volume of acetone after which H_2O was added. They were filter-sterilized into the autoclaved medium. Cultures were incubated in a shaker (100 rpm) at 25°C in 18 h light/6 h dark photoperiod (20–30 μmol m^{-2} s^{-1} Osram L36/30, Warmton Warm White). Three separate cultures were made with 3–5 replicates in each treatment.

In order to reduce the variation in replicate cultures, a fourth repetition was made with a modified method with 9 replicates. Suspension cultures were initiated normally. On day 1, A_{262} was measured to check the amount of lignin precursors secreted into the nutrient medium. Culture flasks of the same absorbance were divided into four groups and coniferyl alcohol and fluoroconiferyl

alcohol were added to the treatment bottles. The cultures were allowed to grow for 4 days (5-day culture in total) after which the nutrient medium was collected.

4.5. Isolation of proteins from culture medium

The nutrient medium was collected after 5 or 6 days in culture. Because on day 6 some of the suspension cultures showed signs of ageing, a 5-day culture period was used in the following replicate cultures. The nutrient medium was decanted, filtered through glass wool and the extracellular precipitate collected using centrifugation (12,000 *g*, 15 min at 4 °C). The pellet was washed twice with distilled water, freeze-dried, quantified and stored at −20 °C for NMR studies. pH of the nutrient medium was measured, the medium was frozen and stored at −80 °C until used. The cells were washed in a Büchner funnel with distilled water and the fresh weight of the cells was measured. The viability of cells was checked by staining with Evans Blue (Yeoman, 1986).

After quick thawing the nutrient medium was centrifuged for 45 min at 4 °C at 12,000 *g*. The supernatant was concentrated over 10-fold using an Amicon ultra-filtration apparatus (YM 10 membrane) and passed through Sephadex G-25 columns (PD10, Pharmacia) pre-equilibrated with 50 mM Tris–HCl buffer, pH 7.5 containing 0.5 mM $CaCl_2$, 5 mM $Na_2B_4O_7$, 30 mM NaCl and 0.5 mM phenylmethylsulfonyl fluoride (PMSF; modified from Fagerstedt et al., 1998). Peroxidase activity measurements were made using concentrated bulk proteins of the nutrient medium.

4.6. Enzyme assays and quantitation of protein

Kinetic behaviour of nutrient medium peroxidases was studied with coniferyl alcohol and its fluorinated analogue as hydrogen donors at 262 nm. Assays were carried out in a volume of 1.0 ml in a Shimadzu UV-2100 spectrophotometer at 25 °C. The reaction mixture contained coniferyl alcohol and/or fluoroconiferyl alcohol (5–100 μM), and 250 μM H_2O_2 in 45 μM Na-citrate buffer, pH 5.0. The activities were determined using nutrient medium protein fractions of three separate cultures and horseradish peroxidase type I (HRP, Sigma P-8125) and type II (Sigma P-8250). Hanes plots were constructed from initial velocity data and K_m and V_{max} values determined after linear regression analysis by Shimadzu UVPC Optional Kinetics Software. Because bulk proteins of nutrient medium were used, rate values are normalized per gram of fresh tissue (Gonzàles et al., 1999). The extinction coefficient for coniferyl alcohol was estimated and was found to be 14,000 M^{-1} cm^{-1}.

Protein contents of the nutrient medium and enzyme samples were determined with the Bio-Rad microassay procedure (Bradford, 1976) using bovine serum albumin (Sigma) as a standard.

4.7. Isoelectric focusing (IEF)

IEF was accomplished with a Multiphor II apparatus (Pharmacia) in a 4% polyacrylamide gel containing Ampholine with a pH range of 3.5–10.0 according to the manufacturer's instructions. Peroxidase was visualized in the gel by staining with 50 mM Na-citrate buffer, pH 5.0 containing 0.03% 3,3-diaminobenzidine, 10 mM $CaCl_2$ and 10 mM H_2O_2 (Sato et al., 1993). After pre-incubation for 20 min in staining buffer without H_2O_2 the reaction was started by addition of H_2O_2.

Acknowledgements

The tissue culture work was funded by the Finnish Forest Cluster Research Programme WOOD WISDOM supported by The National Technology Agency, Tekes; and the Finnish Academy of Sciences. We thank Ms Maaret Mustonen for skillful technical assistance.

References

Adler, E., Gustafsson, B., 1963. Darstellung der *threo*- und *erythro*-Formen des *D,L*-Guaiacylglycerins und des *D,L*-Veratrylglycerins. Acta Chem. Scand. 17, 27–31.

Blank, I., Mager, J., Bergmann, E.D., 1955. Studies of organic fluorine compounds. Part IV. Synthesis of esters of fluoro-oxalic and fluoropyruvic acid. J. Chem. Soc., 2190–2193.

Bradford, M.M., 1976. A rapid and sensitive method for the quantitation of microgram quantities of proteins utilizing the principle of protein-dye binding. Anal. Biochem. 72, 248–254.

Brunow, G., Kilpeläinen, I., Lapierre, C., Lundquist, K., Simola, L.K., Lemmetyinen, J., 1993. The chemical structure of extracellular lignin released by cultures of *Picea abies*. Phytochemistry 32, 845–850.

Clemenceau, D., Cousseau, J., 1993. An expedient stereoselective access to (Z)-2-fluoroalkenoates. Tetrahedron Lett. 34, 6903–6906.

Daubresse, N., Chupeau, Y., Francesch, C., Lapierre, C., Pollet, B., Rolando, C., 1997. Rational design, synthesis and biological evaluation of the first inhibitor of lignin polymerization. Chem. Commun., 1489–1490.

Fagerstedt, K., Saranpää, P., Piispanen, R., 1998. Peroxidase activity, isoenzymes and histological localization in sapwood and heartwood of Scots pine (*Pinus sylvestris* L.). J. For. Res. 3, 43–47.

Goldberg, R., Pang, A., Pierron, M., Catesson, A.-M., Czaninski, Y., Franchesch, C., Rolando, C., 1988. Investigation of lignification by means of fluorinated analogues of ferulic acid and coniferyl alcohol. Phytochemistry 27, 1647–1651.

Gonzàlez, L.F., Rojas, M.C., Perez, F.J., 1999. Diferulate and lignin formation is related to biochemical differences of wall-bound peroxidases. Phytochemistry 50, 711–717.

Pearl, I.A., Beyer, D.L., 1951. Reactions of vanillin and its derived compounds. XI. Cinnamic acids derived from vanillin and its related compounds. J. Org. Chem. 16, 216–220.

Quideau, S., Ralph, J., 1992. Facile large-scale synthesis of coniferyl, sinapyl, and *p*-coumaryl alcohols. J. Agric. Food Chem. 40, 1108–1110.

Sato, Y., Sugiyama, M., Górecki, R.J., Fukuda, H., Komamine, A., 1993. Interrelationship between lignin deposition and the activities of peroxidase isoenzymes in differentiating tracheary elements of *Zinnia*. Analysis using L-α-aminooxy-β-phenylpropionic acid and 2-aminoindan-2-phosphonic acid. Planta 189, 584–589.

Simola, L.K., Santanen, A., 1990. Improvement of nutrient medium for growth and embryogenesis of megagametophyte and embryo callus lines of *Picea abies*. Physiol. Plant. 80, 27–35.

Simola, L.K., Lemmetyinen, J., Santanen, A., 1992. Lignin release and photomixotrophism in suspension cultures of *Picea abies*. Physiol. Plant. 84, 374–379.

Welch, J.T., 1987. Advances in the preparation of biologically active organofluorine compounds. Tetrahedron 43, 3123–3197.

Yeoman, M.M., 1986. Plant Cell Culture Technology. Botanical Monographs. Vol. 23. Blackwell Scientific Publications, Oxford. ISBN 0-632-013, pp. 112–113.

PERGAMON

Phytochemistry 58 (2001) 249–256

PHYTOCHEMISTRY

www.elsevier.com/locate/phytochem

Effects of ajugarins and related neoclerodane diterpenoids on feeding behaviour of *Leptinotarsa decemlineata* and *Spodoptera exigua* larvae

Cristina Caballero[a], Pedro Castañera[a,*], Félix Ortego[a], Gianfranco Fontana[b], Paola Pierro[b], Giuseppe Savona[b], Benjamín Rodríguez[c]

[a]*Departamento de Biología de Plantas, Centro de Investigaciones Biológicas, CSIC, Velàzquez 144, E-28006 Madrid, Spain*
[b]*Dipartimento di Chimica Organica "E. Paternò", Università di Palermo, Parco d'Orleans 2, I-90128 Palermo, Italy*
[c]*Instituto de Química Orgánica, CSIC, Juan de la Cierva 3, E-28006 Madrid, Spain*

Received 15 March 2001; received in revised form 11 May 2001

Abstract

Three naturally occurring ajugarins and seven semisynthetic derivatives of them, possessing different functionalities in the decalin part, together with two natural furoneoclerodane diterpenes, have been assessed as feeding behavior modifying agents of larvae of the generalist *Spodoptera exigua* and a specialist like *Leptinotarsa decemlineata*. Ajugarin I and some of its derivatives exhibited a significant antifeedant activity against larvae of *S. exigua* in both choice and no-choice assays. Conversely, the furoneoclerodane diterpenes only presented antifeedant activity against larvae of *L. decemlineata*. These results indicate that the biological action of the tested substances is strongly modulated by minimal structural variations, which are also responsible for the specificity of action.
© 2001 Elsevier Science Ltd. All rights reserved.

Keywords: Diterpenes; Ajugarins; Furoneoclerodanes; Antifeedant activity; *Leptinotarsa decemlineata*; *Spodoptera exigua*

1. Introduction

Clerodanes are a large group of naturally occurring diterpenoids isolated mainly from Compositae and Labiatae plants (Merritt and Ley, 1992; Rodríguez-Hahn et al., 1994). These compounds have attracted interest in the last years on account of their biological activities against some economically important lepidopteran (Simmonds and Blaney, 1992; Rodríguez et al., 1999), coleopteran (Ortego et al., 1995; López-Olguín et al., 1999) and orthopteran (Hanson et al., 1982) pests. Among these substances, ajugarins I (**1**) (Kubo et al., 1976; Savona et al., 1984; Beauchamp et al., 1996) and II (**2**) (Kubo et al., 1976; Beauchamp et al., 1996; Bruno et al., 2000) and deacetylajugarin II (**3**) (Savona et al., 1984; Fontana et al., 1998) are neoclerod-13-en-15,16-olide derivatives that have been shown to have significant insect antifeedant properties against larvae of the lepidopteran *Spodoptera littoralis* (Boisduval) (Kubo et al., 1976; Simmonds et al., 1989; Cole et al., 1990; Simmonds and Blaney, 1992; Bremner et al., 1998), *S. frugiperda* (J. E. Smith) (Simmonds and Blaney, 1992; Bruno et al., 2000), *S. exempta* (Walker) (Kubo et al., 1976) and *Helicoverpa* (*Heliothis*) *armigera* (Hübner) (Simmonds et al., 1989; Bruno et al., 2000).

The interesting insect antifeedant action of ajugarins, together with the uncertain knowledge available on the structure–activity relationships of these substances (Kubo et al., 1983; Simmonds and Blaney, 1992), prompted us to undertake some chemical transformations of **2** and **3** in order to establish how the functionalities of their decalin part modulate feeding behavior of larvae of the specialist *Leptinotarsa decemlineata* (Say) (Coleoptera: Chrysomelidae) and the generalist *Spodoptera exigua* (Hübner) (Lepidoptera: Noctuidae). In addition to the neoclerod-13-en-15,16-olide derivatives **1**–**10**, we have also tested teumassilenins A and C (**11** and **12**, respectively), recently isolated (Fontana et al., 1998) from *Teucrium massiliense* L. (Labiatae), whose structures possess a β-

* Corresponding author. Tel.: +34-91-5611800; fax: +34-91-5627518.
E-mail address: castan@cib.csic.es (P. Castañera).

0031-9422/01/$ - see front matter © 2001 Elsevier Science Ltd. All rights reserved.
PII: S0031-9422(01)00253-9

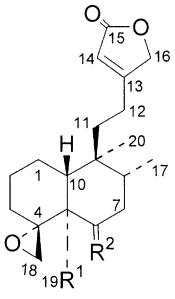

	R^1	R^2
1	CH_2OAc	α-OAc, β-H
2	CH_2OAc	α-OH, β-H
3	CH_2OH	α-OH, β-H
4	CH_2OH	α-OAc, β-H
5	CHO	α-OH, β-H
6	CH_2OAc	O
7	CHO	α-OAc, β-H

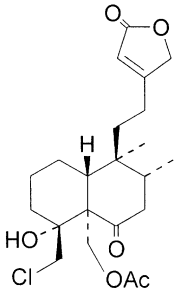

8

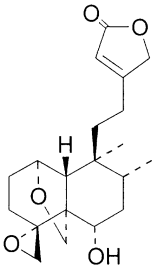

9

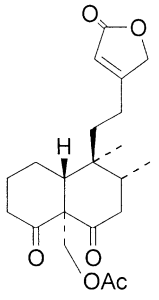

10

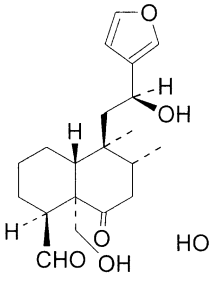

11

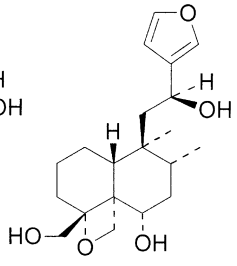

12

substituted furan ring instead of the α,β-unsaturated γ-lactone of **1**–**10**.

2. Results and discussion

Deacetylajugarin II (**3**) (Savona et al., 1984; Fontana et al., 1998), one of the major constituents of the acetone extract of the aerial parts of *Teucrium massiliense* (0.73% on dry plant material), was used as the starting material for obtaining compounds **1**, **2** and **4**–**10**. Ajugarin I (**1**) was prepared by treatment of **3** with acetic anhydride-pyridine at room temperature for 24 h (Savona et al., 1984). Reaction of **3** with the same reagent for 1.5 h yielded a mixture of three compounds, which were easily separated by column chromatography giving unreacted **3** (41%), ajugarin II (**2**, 32%) (Kubo et al., 1976; Beauchamp et al., 1996; Bruno et al., 2000) and compound **4** (24.5%). Selective oxidation of **3** with the Dess–Martin periodinane (Dess and Martin, 1991) gave the aldehyde **5** in almost quantitative yield (96%), whereas oxidation of **2** with chromium trioxide-pyridine (Poos et al., 1953) yielded the expected 6-keto derivative **6** (79%). Treatment of **4** with the Dess–Martin periodinane gave the 19-aldehyde **7** in poor yield (30%), probably due to the steric hindrance caused by the acetoxyl group at the C-6α position. Best results (60% yield of **7**) were achieved by using 4-methylmorpholine-*N*-oxide (NMO) and catalytic amounts of tetrapropylammonium perruthenate (TPAP) as an oxidizing reagent (Ley et al., 1994). The chlorohydrin derivative **8** was obtained in poor yield (22%, see Experimental) by treating ajugarin II (**2**) with pyridinium chlorochromate (PCC), which produces the oxidation of the C-6α hydroxyl group and the oxirane-opening by attack of the nucleophile (Cl^-) on the primary center of the epoxide (C-18) (Rodríguez et al., 1994). Remote oxidation of **3** with iodobenzene diacetate (IBD)-iodine (Majetich and Wheless, 1995) gave the 1α,19-epoxy derivative **9** in 72% yield. Treatment of ajugarin II (**2**) with an excess of Jones' reagent (Bowers et al., 1953) gave the 18-nor-neoclerodane derivative **10** (56%), via oxidation of the C-6α hydroxyl group and opening of the 4α,18-oxirane, followed by oxidation of the resulting glycol to an α-hydroxycarboxylic acid, which undergoes decarboxylation to yield **10** (Chen et al., 1995).

The structures of all the above compounds are strongly supported by their ^1H and ^{13}C NMR, IR and mass spectra, and other analytical data (see Experimental Section). The derivatives **4**–**10** have not been described previously.

Among the compounds tested (**1**–**12**) we have found an outstanding differential antifeedant pattern depending on the insect species. The two naturally occurring furoneoclerodane diterpenes (**11** and **12**), possessing a β-substituted furan ring in which the C-13–C-16 carbon atoms are involved, showed antifeedant activity against last instar larvae of the specialist *L. decemlineata*, but no activity was detected on *S. exigua* (Table 1). On the contrary, compounds possessing a β-substituted α,β-unsaturated γ-lactone instead of the furan ring, like natural ajugarin I (**1**) and the semisynthetic derivatives **4**, **8** and **10**, only showed antifeedant effect on the fifth instar larvae of the generalist *S. exigua* (Table 1). These results indicated that the antifeedant action on *L. decemlineata* larvae is associated with the presence of a furan ring in the molecule of the active compounds (**11** and **12**), whereas the rest of the chemical structure does not play a significant role for such biological effect. The 12*S*-hydroxyl group of **11** and **12**, however, could also be an important structural feature for the mode of action of these compounds at a molecular level, because it modifies drastically the reactivity of the furan.

Ajugarin I (**1**) showed antifeedant activity against larvae of *S. exigua* in both choice and no-choice assays (Table 1). Deacetylation at C-19 (**4**) resulted in a decrease of the activity and no antifeedant effect was observed when there is an α-hydroxyl function (**2**) or a ketone (**6**) at the C-6 position, or when both C-6α and C-19 sub-

Table 1
Effect of compounds **1–12** on the feeding behaviour of *Leptinotarsa decemlineata* and *Spodoptera exigua* larvae

Compound[a]	*Leptinotarsa decemlineata*			*Spodoptera exigua*		
	No-choice bioassay AI[b]	Choice bioassay AI[c]	Choice/ no choice SI[d]	No-choice bioassay AI[b]	Choice bioassay AI[c]	Choice/ no choice SI[d]
1	5.30±6.27	26.78±8.64	−7.62±7.77	70.04±6.78[e]	67.90±17.18	15.51±8.88
2	−12.70±9.01	31.39±17.72	6.87±6.98	8.30±9.83	25.12±9.75	−8.79±19.81
3	11.25±8.43	13.70±11.84	−12.78±9.74	−22.39±7.45	9.67±6.63	−31.68±6.30
4	5.30±5.60	26.78±5.43	−7.62±5.04	30.97±9.15	57.12±9.11[e]	−11.34±9.12
5	9.03±17.64	46.14±7.98	−23.00±7.33	24.53±14.08	38.46±13.82	−10.82±15.28
6	−9.22±7.25	39.92±7.05	−18.06±5.90	34.29±22.98	25.80±12.21	23.04±19.27
7	16.11±5.52	8.62±11.62	7.95±8.42	14.90±16.82	39.46±8.78	37.33±9.91
8	29.36±11.74	33.06±16.26	25.76±18.04	29.95±16.60	91.36±6.20[e]	1.96±16.23
9	5.51±12.93	28.49±12.57	−16.04±26.00	−16.11±19.15	26.07±14.18	−22.14±12.23
10	−13.77±6.26	36.42±15.95	2.24±18.06	9.88±19.56	72.87±13.36[e]	−8.78±11.23
11	75.62±8.58[e]	88.19±6.35[e]	12.03±9.21	−26.25±9.56	10.45±10.45	−3.04±7.18
12	67.64±12.30[e]	73.71±19.74[e]	43.80±11.24	15.99±7.34	13.74±9.14	−23.89±10.35

[a] At 1000 ppm.
[b] Average antifeedant index $[(C-T)/C]\times 100\% \pm$ standard error ($n = 10$). C and T represent consumption of control and treatment disks, respectively.
[c] Average antifeedant index $[(C-T)/C+T)]\times 100\% \pm$ standard error ($n = 10$). C and T represent consumption of control and treatment disks, respectively, within each arena.
[d] Average suppression index $[(C-T)/C]\times 100\% \pm$ standard error ($n = 10$). T represents consumption of both treated and untreated disks in test arenas and C in control arenas that contain untreated leaf disks only.
[e] Antifeedant activity considered for indexes over 50%.

stituents are deacetylated (**3**) (Table 1). Moreover, transformation of the C-19 acetoxyl group into an aldehyde (**5** and **7**) or a 1α,19-ether function (**9**), together with deacetylation at the C-6α position in the case of **5** and **9**, also caused the loss of the activity (Table 1). These results suggest that both acetoxyl groups at the C-6α and C-19 positions play a major role in the antifeedant activity of ajugarin I (**1**) against this species. However, when the C-19 acetoxyl group was maintained, but the functionality at C-6 was a ketone and the 4α,18-epoxide was replaced by a chlorohydrin (**8**) or it was eliminated giving the 18-nor-4-oxo derivative **10**, a very high antifeedant activity was found in choice assays for these compounds (Table 1). This suggests that **8** and **10** act predominantly as feeding deterrents of *S. exigua* in a choice situation, but the larvae will feed on it when other resources are not available, as compared with ajugarin I (**1**). The effect of ajugarins **1**–**10** on the feeding behavior of *S. exigua* larvae (Table 1) establishes that the activity is strongly dependent on the functionality of the *trans*-decalin part of the molecule, as has been suggested previously (Kubo et al., 1983). In addition, the furoneoclerodanes **11** and **12** have no activity on *S. exigua* (Table 1), as reported for some related diterpenoids tested against other lepidopteran species (Simmonds and Blaney, 1992).

The data presented in this study on the antifeedant activity of compounds **1**–**12** against *L. decemlineata* and *S. exigua* larvae, reveal that minimal structural changes in the substance can account for large variations in the activity and cause remarkable differences of specificity between both insect species.

3. Experimental

3.1. General

Mps uncorr. ^{1}H NMR chemical shifts are reported with respect to residual $CHCl_3$ (δ 7.25). ^{13}C NMR chemical shifts are reported with respect to solvent signals (δ_{CDCl_3} 77.00). ^{13}C NMR assignments were determined by gHSQC and gHMBC spectra. MS were recorded in the positive EI mode and no fragments below m/z 50 were registered. Merck Si gel no. 7734 (70-230 mesh) deactivated with 15% H_2O, w/v, was used for column chromatography.

Deacetylajugarin II (**3**) and teumassilenins A (**11**) and C (**12**) were available from our previous studies on *T. massiliense* (Savona et al., 1984; Fontana et al., 1998). Ajugarin I (**1**) was obtained from **3** as described previously (Savona et al., 1984).

3.2. Preparation of 19-acetoxy-4α,18-epoxy-6α-hydroxyneoclerod-13-en-15,16-olide [ajugarin II (**2**)] and 6α-acetoxy-4α,18-epoxy-19-hydroxyneoclerod-13-en-15,16-olide (**4**) from deacetylajugarin II (**3**)

Treatment of **3** (1 g, 2.85 mmol) with Ac_2O-pyridine (1:1, 20 ml) at room temperature for 1.5 h yielded, after workup in the usual manner, a mixture of **2**, **4**, and starting material (**3**). Column chromatography of this mixture [gradient of elution from EtOAc–petroleum ether (2:1) to 100% EtOAc] gave, in order of increasing chromatographic polarity, **4** (275 mg, 0.70 mmol, 24.5%), **2** (362 mg, 0.92 mmol, 32.3%), and **3** (411 mg, 1.17 mmol, 41.1%).

Table 2
^{1}H NMR spectral data of compounds **2** and **4–10**[a]

	2	**4**	**5**	**6**	**7**	**8**	**9**	**10**
H								
1α	~1.55[b]	~1.54[b]	1.76, *qd*	~1.62[b]	[c]	[c]	–	1.91, *dddd*
1β	~1.55[b]	~1.54[b]	1.48, *dddd*	~1.62[b]	[c]	[c]	4.33, *br d*	~1.71[b]
2α	~2.00[b]	2.00, *ddddd*	2.02, *ddddd*	~1.98[b]	[c]	[c]	~1.56[b]	~2.16, *m*
2β	1.40, *qdd*	1.39, *ddddd*	1.36, *qt*	~1.40[b]	[c]	[c]	~1.56[b]	~1.69[b]
3α	~2.10[b]	2.35, *dddd*	2.60, *tdd*	~2.26[b]	2.51, *tdd*	[c]	~2.41[b]	2.62, *ddd*
3β	1.10, *ddd*	1.07, *ddd*	1.09, *ddd*	~1.01[b]	~1.06[b]	[c]	~1.18[b]	2.38, *ddd*
6β	35.2, *ddd*	4.77, *ddd*	3.65, *dd*	–	4.88, *dd*	–	3.65, *ddd*[d]	–
7α	~1.56[b]	~1.57[b]	1.67, *ddd*	2.76, *t*	[c]	2.49, *dd*	~1.56[b]	2.46, *dd*
7β	~1.56[b]	~1.57[b]	1.79, *ddd*	~2.24[b]	[c]	2.30, *dd*	~1.56[b]	2.39, *dd*
8β	~1.64[b]	~1.55[b]	~1.61[b]	~1.92[b]	[c]	[c]	~1.60[b]	~2.04[b]
10β	1.32, *dd*	1.32, *dd*	1.32, *ddd*	~1.80[b]	[c]	[c]	1.57, *br s*	2.05, *dd*
11A	~1.55[b]	~1.55[b]	~1.63[b]	~1.66[b]	[c]	[c]	[c]	~1.69[b]
11B	~1.55[b]	~1.55[b]	~1.63[b]	~1.66[b]	[c]	[c]	2.04, *ddd*	~1.69[b]
12A	~2.10[b]	2.10, *dddd*	2.09, *dddd*	~2.09[b]	~2.10[b]	[c]	2.28, *m*	~2.10[b]
12B	2.26, *dddd*	2.24, *dddd*	2.28, *dddd*	~2.25[b]	~2.25[b]	[c]	2.28, *m*	2.28, *dddd*
14	5.82, *quint*	5.83, *quint*	5.82, *quint*	5.84, *quint*	5.86, *quint*	5.87, *quint*	5.84, *quint*	5.84, *quint*
16 (2H)	4.72, *d*	4.72, *d*	4.72, *d*	4.73, *d*	4.75, *d*	4.76, *d*	4.73, *d*	4.72, *d*
Me-17	0.84, *d*	0.82, *d*	0.88, *d*	0.90, *d*	0.87, *d*	0.92, *d*	0.88, *d*	0.90, *d*
18A	2.42, *d*	2.24, *d*	2.54, *d*	2.25, *d*	2.34, *d*	3.88, *d*	2.70, *d*	–
18B	3.21, *dd*	2.92, *dd*	3.26, *dd*	3.37, *dd*	3.01, *dd*	3.95, *br d*	3.31, *dd*	–
19A	4.52, *d*	4.03, *ddd*[e]	10.22, *d*	4.79, *s*	10.20, *s*	4.56, *d*	4.07, *d*	4.60, *d*
19B	4.56, *br d*	4.30, *dd*[f]	–	4.79, *s*	–	4.83, *d*	4.16, *d*	4.76, *d*
Me-20	0.74, *s*	0.70, *s*	0.71, *s*	1.01, *s*	0.77, *s*	1.04, *s*	0.96, *s*	0.99, *s*
OAc	2.08, *s*	2.03, *s*	–	2.07, *s*	2.04, *s*	2.02, *s*	–	2.01, *s*
6α (OH)[g]	3.40, *s*	–	3.62, *s*	–	–	–	2.82, *d*	–
19 (OH)[g]	–	2.37, *dd*	–	–	–	–	–	–
$J_{H,H}$ (*Hz*)								
1α,1β	[b]	[b]	13.3	[b]	[b]	[b]	–	13.7
1α,2α	4.1	4.2	4.1	[b]	[b]	[b]	–	3.4
1α,2β	13.3	13.2	13.3	[b]	[b]	[b]	–	13.4
1α,10β	12.5	11.5	13.3	[b]	[b]	[b]	–	12.0
1β,2α	2.8	2.9	2.9	[b]	[b]	[b]	4.6	[b]
1β,2β	4.3	5.2	4.1	[b]	[b]	[b]	<0.3	[b]
1β,10β	3.4	4.4	4.2	[b]	[b]	[b]	<0.3	3.2
2α,2β	13.3	13.1	13.3	[b]	[b]	[b]	[b]	13.0
2α,3α	4.2	4.4	4.1	[b]	4.2	[b]	[b]	6.7
2α,3β	3.1	2.7	2.9	[b]	[b]	[b]	[b]	2.9
2β,3α	13.3	13.4	13.3	[b]	13.0	[b]	[b]	12.7
2β,3β	3.5	4.2	4.1	[b]	[b]	[b]	[b]	4.7
3α,3β	13.1	13.6	13.3	[b]	13.0	[b]	[b]	13.2
6β,7α	10.6	8.9	11.0	–	8.7	–	11.8	–
6β,7β	4.5	5.7	4.6	–	7.7	–	5.6	–
7α,7β	[b]	[b]	13.5	13.5	[b]	15.5	[b]	15.9
7α,8β	[b]	[b]	12.1	13.5	[b]	13.8	[b]	11.5
7β,8β	[b]	[b]	3.2	[b]	[b]	4.0	[b]	5.2
8β,17	6.2	6.3	6.7	6.7	6.0	6.7	6.8	6.8
11A,11B	[b]	[b]	[b]	[b]	[b]	[b]	12.6	[b]
11A,12A	[b]	9.8	12.8	[b]	[b]	[b]	[b]	[b]
11A,12B	4.5	4.5	5.0	[b]	[b]	[b]	[b]	4.6
11B,12A	[b]	4.5	3.2	[b]	[b]	[b]	4.8	[b]
11B,12B	9.8	9.8	9.5	[b]	[b]	[b]	7.1	8.1
12A,12B	13.6	13.5	13.7	[b]	[b]	[b]	[b]	14.0
12A(B),14	1.6	1.4	1.4	1.4	1.4	1.4	1.6	1.7
14,16A(B)	1.7	1.7	1.8	1.6	1.7	1.7	1.7	1.9
16A,16B	0	0	0	0	0	0	0	0
18A,18B	3.5	3.7	3.4	5.5	4.0	11.8	3.7	–
18B,3α	2.4	2.2	2.3	2.3	2.6	<0.6	2.1	–
19A,19B	12.0	12.0	–	0	–	11.7	9.4	12.0
19A,6β	0	1.5	0	–	0	0	0	–

(*continued on next page*)

Table 2 (*continued*)

	2	4	5	6	7	8	9	10
19B,6β	0.4	0	–	–	–	0	0	–
6β,6α (OH)[g]	0	–	0	–	–	–	1.6	–
19A,19 (OH)[g]	–	11.4	–	–	–	–	–	–
19B,19 (OH)[g]	–	1.4	–	–	–	–	–	–
19,10β	0	0	1.1	0	0	0	0	0

[a] At 500 MHz (**2**, **4, 5** and **10)** or 300 MHz **(6–9),** in $CDCl_3$ solution; chemical shifts are reported in δ values. All these assignments were in agreement with HSQC and HMBC spectra.
[b] Overlapped signal; approximate δ value was measured from the HSQC spectrum.
[c] Not measured due to overlapping.
[d] Collapsed into a *dd* ($J=$ 11.8, 5.6 Hz) after addition of D_2O.
[e] Collapsed into a *dd* ($J=$ 12.0, 1.5 Hz) after addition of D_2O.
[f] Collapsed into a *d* ($J=$ 12.0 Hz) after addition of D_2O.
[g] Interchangeable with D_2O.

Ajugarin II (**2**): colorless needles (EtOAc–petroleum ether), mp 179–181 °C; $[\alpha]_D^{23}$ +17.7° ($CHCl_3$,*c* 0.261); ν_{max}^{KBr} cm^{-1}: 3460 (OH), 1785, 1755, 1640 (α,β-unsaturated γ-lactone), 1730, 1235 (OAc), 2960, 1450, 1390, 1375, 1325, 1165, 1040, 1020, 885, 850, 840; ^1H NMR: Table 2; ^{13}C NMR: Table 3; EIMS *m*/*z* (rel. int.): 392 $[M]^+$ (2), 362 (2), 361 (2), 332 (3), 320 (22), 319 (100), 301 (13), 189 (9), 167 (12), 165 (11), 147 (10), 123 (19), 121 (12), 119 (10), 107 (11), 105 (12), 98 (11), 95 (13), 93 (15), 91 (15), 81 (11), 79 (15), 69 (10), 63 (13), 55 (17). (Found: C, 67.51; H, 8.31. Calc. for $C_{22}H_{32}O_6$: C, 67.32; H, 8.22%.)

These data for **2** were in agreement with those reported for natural and semisynthetic ajugarin II [mp 188–189 °C, $[\alpha]_D^{24}$ +14.6° ($CHCl_3$,*c* 0.025)] (Kubo et al., 1976; Beauchamp et al., 1996; Bruno et al., 2000), and the present unequivocal and complete assignment of its ^1H and ^{13}C NMR spectra (Tables 2 and 3, respectively), based on two-dimensional NMR experiments, completes and corrects previous data reported by other authors (e.g. the chemical shifts of the C-7, C-8, C-13 and C-15 carbons) (Bruno et al., 2000).

Compound **4**: colorless needles (EtOAc–petroleum ether), mp 249–251 °C; $[\alpha]_D^{23}$ +5.5° ($CHCl_3$,*c* 0.272); ν_{max}^{KBr} cm^{-1}: 3620, 3590 (OH), 3130, 1795, 1760, 1630 (α,β-unsaturated γ-lactone), 3070 (oxirane), 1740, 1245 (OAc), 2960, 1455, 1370, 1170, 1125, 1080, 1040, 1010,

Table 3
^{13}C NMR spectral data of compunds **2** and **4–10**[a]

C	2	4	5	6	7	8	9	10
1	20.8, *t*	21.0, *t*	21.0, *t*	21.6, *t*	21.2, *t*	21.1, *t*	77.7, *d*	20.4, *t*
2	25.0, *t*	25.0, *t*	24.8, *t*	24.8, *t*	24.9, *t*	21.6, *t*	38.2, *t*	25.9, *t*
3	31.9, *t*	32.3, *t*	31.7, *t*	33.1, *t*	32.4, *t*	29.5, *t*	28.0, *t*	38.6, *t*
4	66.8, *s*	65.5, *s*	66.3, *s*	61.5, *s*	63.9, *s*	76.9, *s*	65.6, *s*	205.3, *s*
5	45.2, *s*	46.2, *s*	54.5, *s*	54.3, *s*	54.9, *s*	57.5, *s*	51.9, *s*	64.2, *s*
6	73.4, *d*	74.3, *d*	73.2, *d*	206.6, *s*	72.2, *d*	212.6, *s*	68.1, *d*	203.8, *s*
7	34.7, *t*	32.6, *t*	34.8, *t*	44.4, *t*	33.8, *t*	45.8, *t*	32.4, *t*	43.6, *t*
8	33.9, *d*	34.5, *d*	34.3, *d*	38.0, *d*	34.4, *d*	36.1, *d*	35.8, *d*	35.9, *d*
9	38.6, *s*	38.2, *s*	39.1, *s*	38.9, *s*	38.7, *s*	38.4, *s*	36.8, *s*	38.8, *s*
10	47.3, *d*	47.8, *d*	49.1, *d*	51.0, *d*	49.7, *d*	45.9, *d*	54.9, *d*	51.8, *d*
11	34.8, *t*	34.6, *t*	34.5, *t*	35.4, *t*	34.2, *t*	35.0, *t*	32.7, *t*	35.5, *t*
12	22.1, *t*	22.0, *t*	22.1, *t*	22.0, *t*	21.9, *t*	21.6, *t*	23.1, *t*	21.8, *t*
13	169.9, *s*	169.7, *s*	169.6 s	169.2, *s*	169.3, *s*	168.9, *s*	169.8, *s*	169.0, *s*
14	115.4, *d*	115.4, *d*	115.5, *d*	115.6, *d*	115.4, *d*	115.7, *d*	115.5, *d*	115.6, *d*
15	173.5, *s*	173.6, *s*	173.5, *s*	173.4, *s*	173.6, *s*	173.4, *s*	173.6, *s*	173.4, *s*
16	72.9, *t*	72.9, *t*	72.8, *t*	72.9, *t*	72.9, *t*	72.9, *t*	72.9, *t*	72.9, *t*
17	15.4, *q*	15.3, *q*	15.4, *q*	15.8, *q*	15.3, *q*	15.5, *q*	15.3, *q*	15.9, *q*
18	48.7, *t*	47.5, *t*	50.4, *t*	48.9, *t*	49.8, *t*	48.3, *t*	53.2, *t*	–
19	62.0, *t*	61.6, *t*	205.1, *d*	62.7, *t*	203.9, *d*	61.8, *t*	71.4, *t*	62.7, *t*
20	17.6, *q*	17.3, *q*	18.8, *q*	17.9, *q*	18.6, *q*	16.8, *q*	16.8, *q*	17.8, *q*
$CH_3\underline{C}OO$	171.0, *s*	169.5, *s*	–	171.0, *s*	170.1, *s*	170.0, *s*	–	170.6, *s*
$\underline{C}H_3COO$	21.1, *q*	21.3, *q*	–	20.8, *q*	21.1, *q*	21.0, *q*	–	20.7, *q*

[a] At 125.7 MHz, in $CDCl_3$ solution; chemical shifts are reported in, δ values. All these assignments were in agreement with HSQC and HMBC spectra. Multiplicities were determined from HSQC data.

960, 890, 855, 845; ^{1}H NMR: Table 2; ^{13}C NMR: Table 3; EIMS *m/z* (rel. int.): 392 $[M]^+$ (1), 361 (12), 332 (3), 331 (5), 320 (21), 319 (100), 301 (17), 289 (23), 191 (11), 189 (13), 147 (8), 136 (8), 123 (12), 121 (11), 107 (10), 105 (10), 95 (10), 93 (12), 91 (14), 79 (14), 67 (11), 55 (15). (Found: C, 67.21; H, 8.13. $C_{22}H_{32}O_6$ requires: C, 67.32; H, 8.22%.)

3.3. Preparation of 4α,18-epoxy-6α-hydroxy-19-oxoneoclerod-13-en-15,16-olide (5) from deacetylajugarin II (3)

To a stirred solution of **3** (120 mg, 0.342 mmol) in dry CH_2Cl_2 (5 ml) an excess of the Dess–Martin periodinane (157 mg, 0.37 mmol) (Dess and Martin, 1991) was added at room temperature under Ar. After 20 h, the reaction mixture was filtered through a short column of Si gel and the solvent was evaporated under vacuum. The residue was then subjected to column chromatography (EtOAc as eluent) yielding pure **5** (115 mg, 0.330 mmol, 96.4%) as colorless needles (EtOAc–petroleum ether): mp 163–165 °C; $[\alpha]_D^{23}$ +25.1° ($CHCl_3$,*c* 0.422); ν_{max}^{KBr} cm^{-1}: 3460 (OH), 3110, 1775, 1750, 1645 (α,β-unsaturated γ-lactone), 3070 (oxirane), 2770, 1715 (aldehyde), 2970, 2880, 1460, 1395, 1330, 1260, 1135, 1060, 1020, 915, 880; ^{1}H NMR: Table 2; ^{13}C NMR: Table 3; EIMS *m/z* (rel. int.): 349 $[MH]^+$ (1), 302 (2), 287 (4), 275(2), 231 (3), 211 (10), 191 (17), 189 (21), 173 (14), 171 (11), 163 (12), 161 (11), 159 (10), 149 (14), 147 (17), 145 (18), 138 (34), 136 (20), 135 (18), 123 (24), 122 (33), 121 (43), 98 (44), 95 (47), 93 (70), 91 (84), 81 (57), 79 (100), 77 (62), 67 (64), 55 (87). (Found: C, 69.09; H, 8.17. $C_{20}H_{28}O_5$ requires: C, 68.94; H, 8.10%.)

3.4. Preparation of 19-acetoxy-4α,18-epoxy-6-oxoneoclerod-13-en-15,16-olide (6) from ajugarin II (2)

To a solution of **2** (80 mg, 0.20 mmol) in dry pyridine (8 ml) a mixture of CrO_3 (200 mg) and pyridine (2 ml) was added, and the reaction mixture was stirred at room temperature for 20 h under Ar (Sarett oxidation procedure, Poos et al., 1953). Then, the reaction mixture was poured into H_2O (50 ml) and extracted with EtOAc (4×25 ml). The extracts were dried ($MgSO_4$) and evaporated to dryness. The residue was chromatographed (Si gel column, petroleum ether–Me_2CO from 20 to 40% in Me_2CO as eluent), giving unreacted **2** (12 mg, 0.03 mmol, 15%, less polar constituent) and **6** (63 mg, 0.16 mmol, 79.1%) as colorless needles (EtOAc–*n*-hexane): mp 147–148 °C; $[\alpha]_D^{22}$ +11.9° ($CHCl_3$, *c* 0.184); ν_{max}^{KBr} cm^{-1}: 3100, 1780, 1750 br, 1645 (α,β-unsaturated γ-lactone), 1740, 1250 (OAc), 1725 (ketone), 2960, 2950, 1450, 1370, 1215, 1140, 1035, 905, 885, 865; ^{1}H NMR: Table 2; ^{13}C NMR: Table 3; EIMS *m/z* (rel. int.): $[M]^+$ absent, 330 $[M–AcOH]^+$ (1), 317 $[M–CH_2OAc]^+$ (100), 299 (13), 289 (20), 189 (17), 137 (13), 121 (11), 105 (10), 93 (10), 91 (15), 81 (11), 79 (14), 69 (13), 67 (11), 55 (15). (Found: C, 67.76; H, 7.61. $C_{22}H_{30}O_6$ requires: C, 67.67; H, 7.74%.)

3.5. Preparation of 6α-acetoxy-4α,18-epoxy-19-oxoneoclerod-13-en-15,16-olide (7) from compound 4

To a stirred solution of **4** (60 mg, 0.153 mmol) in dry CH_2Cl_2 (10 ml) NMO (20 mg, 0.170 mmol), TPAP (3 mg, 0.0084 mmol), and powdered molecular sieve (4 Å, 77 mg) were added (Ley et al., 1994). The reaction mixture was stirred at room temperature under Ar for 2 h, and then filtered through a pad of Celite. Removal of the solvent under vacuum, followed by column chromatography of the residue [EtOAc–petroleum ether (4:1) as eluent] yielded **7** (36 mg, 0.09 mmol, 60.3%) and unreacted **4** (9 mg, 0.02 mmol, 15%).

Oxidation of **4** with the Dess–Martin periodinane, as described above for **3**, gave **7** in 30% yield after 24 h of reaction.

Compound **7** was crystallized from EtOAc–*n*-hexane: colorless needles, mp 233–235 °C; $[\alpha]_D^{23}$ +38.1° ($CHCl_3$, *c* 0.063); ν_{max}^{KBr} cm^{-1}: 3130, 1790, 1750, 1635 (α,β-unsaturated γ-lactone), 2780, 1725 (aldehyde), 1740, 1240 (OAc), 2990, 2950, 2880, 1445, 1375, 1175, 1120, 1030, 1015, 1000, 890, 860; ^{1}H NMR: Table 2; ^{13}C NMR: Table 3; EIMS *m/z* (rel. int.): $[M]^+$ absent, 330 $[M\text{-}AcOH]^+$ (2), 319 (64), 302 (32), 301 (30), 290 (55), 289 (100), 287 (25), 205 (23), 193 (29), 191 (48), 189 (46), 187 (30), 173 (47), 171 (32), 163 (39), 159 (49), 145 (44), 136 (59), 121 (62), 105 (55), 93 (51), 91 (72), 79 (68), 67 (47), 55 (62). (Found: C, 67.54; H, 7.82. $C_{22}H_{30}O_6$ requires: C, 67.67; H, 7.74%.)

3.6. Preparation of 19-acetoxy-18-chloro-4α-hydroxy-6-oxoneoclerod-13-en-15,16-olide (8) from ajugarin II (2)

To a stirred solution of **2** (76 mg, 0.19 mmol) in dry CH_2Cl_2 (5 ml) an excess of PCC (85 mg, 0.39 mmol) and powdered molecular sieve (4 Å, 30 mg) were added, and the reaction mixture was stirred under Ar at room temperature. After 5 days, the mixture was filtered through a short column of Si gel and the filtrate was evaporated to dryness. Then, the residue was subjected to column chromatography [EtOAc–petroleum ether (1:1) as eluent] yielding starting material (**2**, 36 mg, 0.09 mmol, 47.3%, most polar constituent) and compound **8** (18 mg, 0.04 mmol, 21.7%): colorless needles (EtOAc–*n*-hexane), mp 154–156 °C; $[\alpha]_D^{22}$ −41.7° ($CHCl_3$, *c* 0.285); ν_{max}^{KBr} cm^{-1}: 3490, 3460 (OH), 1790, 1755, 1635 (α,β-unsaturated γ-lactone), 1745, 1245 (OAc), 1700, 1690 (chelated ketone), 2960, 2930, 1450, 1385, 1335, 1180, 1130, 1035, 1010, 890, 790, 730, 630; ^{1}H NMR: Table 2; ^{13}C NMR: Table 3; EIMS *m/z* (rel. int.): $[M]^+$ absent, 391 $[M\text{-}Cl]^+$ (12), 377 (12), 317 (100), 305 (18), 301 (35), 289 (15), 271 (11), 269 (10), 205 (14), 201 (11), 189 (23), 187 (13), 165 (21), 149 (31), 137 (24), 121 (21), 95 (23), 93 (20), 91 (27), 81 (30), 79 (29), 69 (32), 67 (26), 57 (25),

55 (41). (Found: C, 61.68; H, 7.41; Cl, 8.21. $C_{22}H_{31}ClO_6$ requires: C, 61.89; H, 7.32; Cl, 8.30%.)

3.7. Preparation of 1α,19;4α,18-diepoxy-6α-hydroxyneoclerod-13-en-15,16-olide (9) from deacetylajugarin II (3)

Compound **3** (100 mg, 0.286 mmol) was dissolved in dry benzene (40 ml) and treated with IBD (94 mg, 1 eq.) and I_2 (73 mg, 1 eq.) (Majetich and Wheless, 1995). The reaction mixture was heated at 50 °C under Ar while it was irradiated with a 200 W tungsten lamp. After 35 min, the reaction mixture was poured into an aqueous saturated solution of $Na_2S_2O_3$ to eliminate the excess of I_2, and extracted with EtOAc (4×30 ml). The organic extract was dried (Na_2SO_4) and the solvents removed under vacuum. The residue was then chromatographed (Si gel column, gradient of elution petroleum ether–EtOAc from 20 to 70% in EtOAc) to give **9** (72 mg, 0.207 mmol, 72.4%): colorless fine needles (EtOAc– *n*-hexane), mp 148–151 °C; $[\alpha]_D^{22}$ −15.9° ($CHCl_3$, *c* 0.169); $\nu_{max}^{KBr}cm^{-1}$: 3510, 3490 (OH), 3100, 1780, 1750, 1640 (α,β-unsaturated γ-lactone), 2940, 2880, 1455, 1445, 1365, 1320, 1160, 1130, 1050, 1015, 900, 880, 865, 640; ^1H NMR: Table 2; ^{13}C NMR: Table 3; EIMS *m*/*z* (rel. int.): $[M]^+$ absent, 316 $[M\text{-}CH_3OH]^+$ (1), 287 (3), 219 (5), 205 (6), 191 (8), 177 (9), 175 (10), 173 (16), 149 (15), 135 (17), 133 (18), 121 (28), 119 (25), 111 (43), 105 (40), 98 (38), 95 (39), 93 (39), 91 (68), 85 (36), 81 (54), 79 (65), 77 (50), 69 (59), 67 (69), 57 (34), 55 (100). (Found: C, 68.79; H 8.16. $C_{20}H_{28}O_5$ requires: C, 68.94; H, 8.10%.)

3.8. Preparation of 19-acetoxy-4,6-dioxo-18-nor-neoclerod-13-en-15,16-olide (10) from ajugarin II (2)

To a solution of **2** (60 mg, 0.153 mmol) in Me_2CO (10 ml) an excess (0.5 ml) of Jones' reagent (Bowers et al., 1953) was added at 0 °C with stirring. The reaction mixture was then stirred at room temperature for 2.5 h and the excess of Jones' reagent was destroyed by addition of EtOH (5 ml). Then, the reaction was diluted with H_2O (50 ml). Extraction with EtOAc (4×20 ml), and workup as usual gave a residue which was subjected to column chromatography [petroleum ether–EtOAc (7:3) as eluent] yielding **10** (32 mg, 0.085 mmol, 55.6%): colorless prisms (EtOAc– *n*-hexane), mp 176–177 °C; $[\alpha]_D^{22}$ +8.2° ($CHCl_3$, *c* 0.294); ν_{max}^{KBr} cm^{-1}: 3140, 1805, 1775, 1655 (α,β-unsaturated γ-lactone), 1750,1245 (OAc), 1740, 1715 (ketones), 2995, 1460, 1395, 1210, 1160, 1045, 1000, 910, 895; ^1H NMR: Table 2; ^{13}C NMR: Table 3; EIMS *m*/*z* (rel. int.): 376 $[M]^+$ (9), 346 (16), 334 (80), 329 (15), 316 (15), 305 (25), 303 (30), 288 (60), 275 (19), 274 (19), 260 (18), 224 (63), 206 (29), 205 (37), 177 (28), 169 (30), 165 (54), 137 (100), 123 (36), 121 (31), 119 (29), 109 (63), 105 (32), 98 (39), 95 (32), 69 (66), 67 (43), 55 (86). (Found: C, 66.87; H, 7.46. $C_{21}H_{28}O_6$ requires: C, 67.00; H,7.50%.)

3.9. Insects for the bioassays

Newly ecdysed fourth instar larvae of *L. decemlineata* were obtained from a colony reared on potato, *Solanum tuberosum*, cv. Kennebec, at 25±2 °C, 90±10% rh and 16:8 h (L:D) photoperiod in a environmental chamber. This colony is renewed annually with wild adults collected from potato fields. *S. exigua* eggs were obtained from the University of Leiden (The Netherlands). The larvae were reared on a semi-artificial diet (Poitout and Bues, 1970) under environmental conditions identical to those described for *L. decemlineata*.

3.10. Feeding experiments

Assays were performed in plastic Petri dishes (15×90 mm), coated on their bottom half with about 20 ml of a 2.5% agar solution (Escoubas et al., 1993). Potato and sugar beet leaf disks (1.77 cm^2) for *L. decemlineata* and *S. exigua*, respectively, were cut with a cork borer No. 15 and fit into holes punched in the agar layer.

The disks were treated on the upper surface with 20 μl of an acetone solution containing 1000 ppm of the test compound or the solvent carrier alone. After complete evaporation of the solvent, newly emerged fourth instar *L. decemlineata* larvae and fifth instar *S. exigua* were starved for 6 h, and placed in each dish in a growth chamber at 26±0.5 °C and 85±10% rh, where they were allowed to feed. In the choice assay, three treated and three control disks were alternately arranged in each arena. For the no-choice assays, six treated or control disks were used in each arena. Feeding was terminated after the consumption of 50% of the disks (control plus treated) in the choice assay and when larvae had ingested about 75% of the control disks in the no-choice assay. Ten replications per treatment were used in all assays.

Feeding indexes were calculated on a dry weight basis. For each assay, initial dry weight of the leaf disks was estimated with 100 leaf disks to calculate the ratio of fresh to dry weight. At the end of the experiment, the uneaten leaf disks were oven dried at 60 °C for 2 days and weighed. The antifeedant index (AI) was calculated in the no-choice assay by the equation $[(C-T)/C]\times100\%$ (Bentley et al., 1984), and in the choice assay by the equation $[(C-T)/(C+T)]\times100\%$ (Simmonds et al., 1989), where *C* and *T* represent the consumption in control and treated disks, respectively. The suppression index (SI) was determined by the equation $[(C-T)/C]\times100\%$, where *T* represents consumption of both treated and untreated leaf disks in choice arenas, and C represents the consumption in control arenas that contain untreated leaf disks only (Raffa and Frazier, 1988). No antifeedant activity was considered for indexes below 50%.

Acknowledgements

We thank N. J. De Boer for providing the eggs of *S. exigua*. This work was supported by funds from the Spanish Comisión Asesora de Investigación Científica y Técnica (grant AGF98-0805) and from the Italian Ministero dell'Università e della Ricerca Scientifica e Tecnologica (MURST).

References

Beauchamp, P.S., Bottini, A.T., Caselles, M.C., Dev, V., Hope, H., Larter, M., Lee, G., Mathela, C.S., Melkani, A.B., Millar, P.D., Miyatake, M., Pant, A.K., Raffel, R.J., Sharma, V.K., Wyatt, D., 1996. Neo-clerodane diterpenoids from *Ajuga parviflora*. Phytochemistry 43, 827–834.

Bentley, M.D., Leonard, D.E., Stoddard, W.F., Zalkow, L.H., 1984. Pyrrolizidine alkaloids as larval feeding deterrents for spruce budworm, *Choristoneura fumiferana* (Lepidoptera: Tortricidae). Annals of the Entomological Society of America 77, 393–397.

Bowers, A., Halsall, T.G., Jones, E.R.H., Lemin, A. J., 1953. The chemistry of the triterpenes and related compounds. Part XVIII. Elucidation of the structure of polyporenic acid C. Journal of the Chemical Society 2548–2560.

Bremner, P.D., Simmonds, M.S.J., Blaney, W.M., Veitch, N.C., 1998. Neo-clerodane diterpenoid insect antifeedants from *Ajuga reptans* CV catlins giant. Phytochemistry 47, 1227–1232.

Bruno, M., Rosselli, S., Pibiri, I., Piozzi, F., Simmonds, M.S.J., 2000. Hydrogenation derivatives of neo-clerodanes and their antifeedant activity. Heterocycles 53, 599–612.

Chen, H.-M., Min, Z.-D., Iinuma, M., Tanaka, T., 1995. Clerodane diterpenoids from *Ajuga decumbens*. Chemical and Pharmaceutical Bulletin 43, 2253–2255.

Cole, M.D., Anderson, J.C., Blaney, W.M., Fellows, L.E., Ley, S.V., Sheppard, R.N., Simmonds, M.S.J., 1990. Neo-clerodane insect antifeedants from *Scutellaria galericulata*. Phytochemistry 29, 1793–1796.

Dess, D.B., Martin, J.C., 1991. A useful 12-I-5 triacetoxyperiodinane (the Dess–Martin periodinane) for the selective oxidation of primary or secondary alcohols and a variety of related 12-I-5 species. Journal of the American Chemical Society 113, 7277–7287.

Escoubas, P., Lajide, L., Mitzutani, J., 1993. An improved leaf-disk antifeedant bioassay and its application for the screening of Hokkaido plants. Entomologia Experimentalis et Applicata 66, 99–107.

Fontana, G., Paternostro, M.P., Savona, G., Rodríguez, B., de la Torre, M.C., 1998. Neoclerodane diterpenoids from *Teucrium massiliense*. Journal of Natural Products 61, 1242–1247.

Hanson, J.R., Rivett, D.E.A., Ley, S.V., Williams, D.J., 1982. The X-ray structure and absolute configuration of insect antifeedant clerodane diterpenoids from *Teucrium africanum*. Journal of the Chemical Society, Perkin Transactions 1, 1005–1008.

Kubo, I., Lee, Y.-W., Balogh-Nair, V., Nakanishi, K., Chapya, A., 1976. Structure of ajugarins. Journal of the Chemical Society, Chemical Communications1976, 949–950.

Kubo, I., Fukuyama, Y., Chapya, A., 1983. Structure of ajugarin-V. Chemistry Letters, 223–224.

Ley, S.V., Norman, J., Griffith, W.P., Marsden, S.P., 1994. Tetrapropylammonium perruthenate, Pr_4N^+ RuO_4^-, TPAP: A catalytic oxidant for organic synthesis. Synthesis, 639–666.

López-Olguín, J., de la Torre, M.C., Ortego, F., Castañera, P., Rodríguez, B., 1999. Structure-activity relationships of natural and synthetic neo-clerodane diterpenes from *Teucrium* against Colorado potato beetle larvae. Phytochemistry 50, 749–753.

Majetich, G., Wheless, K., 1995. Remote intramolecular free radical functionalizations: an update. Tetrahedron 51, 7095–7129.

Merritt, A.T., Ley, S.V., 1992. Clerodane diterpenoids. Natural Product Reports 9, 243–287.

Ortego, F., Rodríguez, B., Castañera, P., 1995. Effects of neo-clerodane diterpenes from *Teucrium* on feeding behavior of Colorado potato beetle larvae. Journal of Chemical Ecology 21, 1375–1386.

Poitout, S., Bues, R., 1970. Elevage de plusieurs espèces de Lépidoptères Noctuidae sur milieu artificiel riche et sur milieu artificiel simplifié. Annales de Zoologie et Ecologie Animale 2, 79–91.

Poos, G.I., Arth, G.E., Beyler, R.E., Sarett, L.H., 1953. Approaches to the total synthesis of adrenal steroids. Journal of the American Chemical Society 75, 422–429.

Raffa, K.F., Frazier, J.L., 1988. A generalized model for quantifying behavioral de-sensitization to antifeedants. Entomologia Experimentalis et Applicata 46, 93–100.

Rodríguez, B., Rodríguez, B., de la Torre, M.C., Simmonds, M.S.J., Blaney, W.M., 1999. From a phagostimulant natural product to semisynthetic antifeedants against *Spodoptera littoralis* larvae: chemical transformations of the neoclerodane diterpenoid scutegalin B. Journal of Natural Products 62, 594–600.

Rodríguez, B., de la Torre, M.C., Perales, A., Malakov, P.Y., Papanov, G.Y., Simmonds, M.S.J., Blaney, W.M., 1994. Oxirane-opening reactions of some 6,19-oxygenated 4α,18-epoxy-neo-clerodanes isolated from *Teucrium*. Biogenesis and antifeedant activity of their derivatives. Tetrahedron 50, 5451–5468.

Rodríguez-Hahn, L., Esquivel, B., Cárdenas, J., 1994. Clerodane diterpenoids in Labiatae. In: Herz, W., Kirby, G.W., Moore, R.E., Steglich, W., Tamm, Ch. (Eds.), Progress in the Chemistry of Organic Natural Products, Vol. 63. Springer, Vienna, pp. 107–196.

Savona, G., Bruno, M., Piozzi, F., Servettaz, O., Rodríguez, B., 1984. Neo-clerodane diterpenoids from *Teucrium massiliense*. Phytochemistry 23, 849–852.

Simmonds, M.S.J., Blaney, W.M., 1992. Labiate-insect interactions: effects of Labiate-derived compounds on insect behaviour. In: Harley, R.M., Reynolds, T. (Eds.), Advances in Labiate Science, Vol. 1. Botanic Gardens, Kew, UK, pp. 375–392.

Simmonds, M.S.J., Blaney, W.M., Ley, S.V., Savona, G., Bruno, M., Rodríguez, B., 1989. The antifeedant activity of clerodane diterpenoids from *Teucrium*. Phytochemistry 28, 1069–1071.

PERGAMON

Phytochemistry 58 (2001) 257–262

PHYTOCHEMISTRY

www.elsevier.com/locate/phytochem

Syringicin, a new α-elicitin from an isolate of *Phytophthora syringae*, pathogenic to citrus fruit

Renato Capasso[a,*], Gennaro Cristinzio[b], Antimo Di Maro[c], Pasquale Ferranti[d], Augusto Parente[e]

[a]*Dipartimento di Scienze Chimico-Agrarie, Università di Napoli "Federico II", 80055 Portici, Italy*
[b]*Dipartimento di Arboricoltura, Botanica e Patologia Vegetale, Università di Napoli "Federico II", 80055 Portici, Italy*
[c]*Dipartimento di Chimica Organica e Biologica, Università di Napoli "Federico II", 80100 Napoli, Italy*
[d]*Dipartimento di Scienza degli Alimenti, Università di Napoli "Federico II", 80055 Portici Italy*
[e]*Dipartimento di Scienze della Vita, Seconda Università di Napoli, 81100 Caserta, Italy*

Received 23 January 2001; received in revised form 18 April 2001

Abstract

The primary structure of syringicin (syr), a new acidic α-elicitin, isolated from culture filtrates of *Phytophthora syringae*, causal agent of citrus fruit rot, has been determined using a combined approch based on Edman degradation and MALDI-MS (TTCTT TQQTA AYVAL VSILS DSSFN QCATD SGYSM LTATA LPTTA QYKLM CASTA CKTMI TKIVS LNAPD CELTV PTSGL VLNVY SYANG FSSTC ASL). Syr has 98 amino acids with a M_r of 10194.6±0.2, which was determined by electrospray ionisation-mass spectrometry (ES-MS) and in agreement with three disulphide bridges, located between Cys3-Cys71, Cys27-Cys56 and Cys51-Cys95. Syr induces a hypersensitive response and electrolyte leakage in tobacco. These are characteristic elicitor properties of the group and in agreement with the molecular mechanism recently proposed for this kind of protein. Finally, its possible applications in biological agriculture and biomedicine are briefly discussed. © 2001 Elsevier Science Ltd. All rights reserved.

Keywords: *Phytophthora syringae*; Citrus fruits; Elicitins; Amino acid sequence; Syringicin; Biological activity

1. Introduction

An approach to controlling plant diseases is to induce natural plant defence mechanisms without relying on synthetic pesticides.

In this view, proteins with elicitor activity named elicitins have been isolated from the culture filtrates of several *Phytophthora* species. Elicitins, 98 amino acid proteins with a M_r of about 10 kDa, are divided into α-elicitins and β-elicitins, of acid and basic nature, respectively (Ponchet et al., 1999; Churngchow and Rattarasarn, 2000).

Their characteristic biological activities are the induction of a hypersensitive response (HR) and systemic acquired resistance (SAR) in tobacco, with the formation of phytoalexins, PR proteins and salycilic acid (Ricci, 1997). Both types induce electrolyte leakage from the same plant cell (Zimmermann et al., 1998).

Moreover, they induce protection against phytopathogenic micro-organisms in tobacco and in some species of *Brassicaceae* (Kamoun et al., 1993; Bonnet et al., 1996; Blancard et al., 1998; Keizer et al., 1998; Tepfer et al., 1998; Keller et al., 1999). Churngchow and Rattarasarn (2000) have recently reported that palmivorein, a new α-elicitin purified from *Phytophthora palmivora*, isolated from rubber tree leaf, is also active on *Hevea* and a susceptible rubber clone.

The secondary and tertiary structure of some α-elicitins was also assessed by ^{1}H NMR (Bovaziz et al., 1994; Fefeu et al., 1997; Gooley et al., 1998) and X-ray diffraction studies (Boissy et al., 1996).

The gene (Inf1) encoding the α-elicitin infestin in *Phytophthora infestans* was identified and cloned (Kamoun et al., 1998). In addition, a mutant of a phytopathogenic *P. infestans* lacking Inf1 proved to be virulent to a tobacco species (*Nicotiana benthamiana*) (Kamoun et al., 1997), indicating an in vivo defence

* Corresponding author. Tel.: +39-081-7785205; fax: +39-081-7755130.

E-mail addresses: capasso@unina.it (R. Capasso), cristinz@unina.it (G. Cristinzio), antimo@unina.it (A. Di Maro), ferranti@unina.it (P. Ferranti), augusto.parente@unina2.it (A. Parente).

0031-9422/01/$ - see front matter © 2001 Elsevier Science Ltd. All rights reserved.
PII: S0031-9422(01)00201-1

mechanism of the protein and, in all likelihood, of all elicitins.

It has recently been found that the bioactivity of the elicitins is correlated to the interaction of an elicitin-sterol complex with its plant plasmalemma receptor, which is proposed to be an allosteric calcium channel (Ponchet et al., 1999). The property of these proteins to load sterols has been exploited for the preparation of anticholesteremic agents, and their medical use has recently been patented (Mikes et al., 1998).

In a previous paper we reported the isolation and biochemical characterisation of elicitin 172, produced by an isolate pathogenic to tomato (Capasso et al., 1999). Elicitin 172 proved to be identical to parasiticein (Ricci et al., 1992) and elicitin 310 (Mouton-Perronet et al., 1995).

Here we describe the primary structure of syr, a new α-elicitin purified from the culture filtrates of *P. syringae,* which is the causal agent of rot of citrus fruit, and compare it to the other known α-elicitins (Huet et al., 1994; Churngchow and Rattarasarn, 2000).

Moreover, we report and discuss its elicitor activity identified by the usual HR and the electrolyte leakage test on tobacco (*Nicotiana tabacum* L., cv. Rustica).

We also briefly describe its potential applications in biological agriculture and biomedicine.

2. Results and discussion

The purification of syr was performed by a procedure slightly more simple than the one used for elicitin 172 (Capasso et al., 1999). The last step was low pressure chromatography through a reverse phase column (Lichroprep RP-18), giving rise to a very sharp and intense peak (Fig. 1). The protein (20 mg per litre of culture filtrate of *Phytophthora syringae*) was obtained in high purity grade as shown by native or SDS–PAGE.

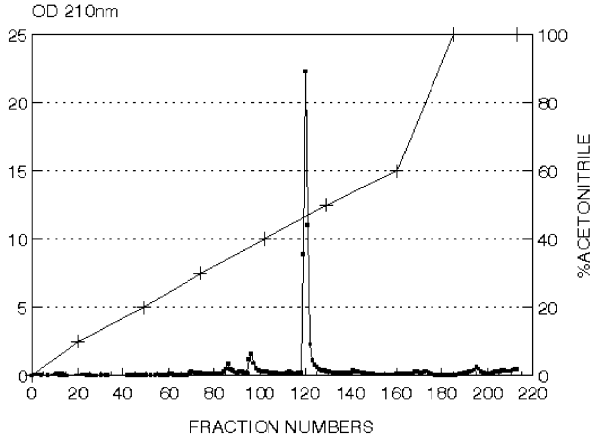

Fig. 1. Chromatogram of α-syringicin obtained by step-wise elution from an RP-HPLC C-18 column (31×2.5 cm), using H_2O/CH_3CN as eluant, under low pressure (3 bar). Flow rate: 15 ml/min; fractions of 5 ml.

After staining the tricine–SDS–PAGE electrophoregram with silver nitrate or with Coomassie blue, a single band appeared. Its apparent M_r was 10 kDa. The protein appeared as a single band in correspondence of 10 kDa on SDS-PAGE, even after heating in presence of 2-mercaptoethanol.

The protein, analysed by ES–MS, exhibited the characteristic bell-shaped distribution of multiple charged ions from which a M_r of 10194.6 ± 0.2 was calculated.

The experimental amino acid composition (Ala12, Asx7, Cys6, Glx5, Gly3, Ile3, Leu10, Lys3, Met3, Phe2, Pro3, Ser13, Thr17, Tyr5, Val6) of the purified syringicin account for a total of 98 amino acid residues and a M_r of 10195, considering the presence of three disulphide bridges.

Therefore, here we consider that threonine, serine and alanine are the most abundant amino acid residues; that the acidic nature, indicated by the theoretical pI value 4.31 and confirmed by the native alkaline PAGE, is consistent with the presence of seven Asx and five Glx and of only three lysyl residues and the absence of hystidinyl and arginyl residues.

The UV absorbance with a maximum at 277 nm (not shown) is in accordance with the presence of phenylalanyl and tyrosinyl residues and the absence of tryptophan.

Automated Edman degradation both on the native and *S*-pyridylethylated protein, allowed the N-terminal sequence of syr to be identificated up to residue 30. The rest of the syr sequence came from the CB-peptides (Fig. 2).

Native syr was treated with CNBr, *S*-pyridylethylated and then subjected to RP–HPLC chromatography, which furnished all CB-peptides.

CB-1 (positions 1-35), CB-2 (36-50) and CB-3 (51-59) were completely sequenced by Edman degradation, while CB-4 (60-98) was sequenced up to residue 94. The last four residues of syr were obtained by combining CPaseA digestion with MALDI–MS analysis as already reported for elicitin 172 (Capasso et al., 1999). In particular,

```
1         10        20        30        40        50
*         *         *         *         *         *
TTCTTTQQTAAYVALVSILSDSSFNQCATDSGYSMLTATALPTTAQYKLM
<=============================>
<---------------CB-1------------><-----CB-2----->

51        60        70        80        90      98
*         *         *         *         *       *
CASTACKTMITKIVSLNAPDCELTVPTSGLVLNVYSYANGFSSTCASL
<-CB-3-><-------------CB-4------------------>
                                            <<<<
```

Fig. 2. Complete amino acid sequence of syringicin. Automated Edman degradation (<====>, <——–>) and CPase A digestion (<<<<), and MALDI–MS were employed for sequence determination. CB-peptides are numbered according to their position in the polypeptide chain. Alignment of CB peptides 2 and 3 was obtained by homology with other elicitins. CB, Cyanogen bromide.

aliquots of CB-4 peptide, incubated with the enzyme, were analysed at five minute intervals and the amino acid residues removed in sequence from the C-terminus were identified by the mass change relatively to the mass (4259.14) of *S*-pyridylethylated CB-4 peptide, as shown in Table 1. Therefore, the C-terminal sequence was determined as Cys-Ala-Ser-Leu, which is characteristic for all α-elicitins, with the exception of cactorein (cact).

The alignment of CB-2 and CB-3 peptides was inferred from the sequence homology with elicitin. The complete sequence of syr is reported in Fig. 2.

Syr contains no Trp, His and Arg residues. Furthermore, as found for all other known α-elicitins, the six cysteine residues are located in positions 3, 27, 51, 56, 71 and 95 and are, very likely, engaged in disulphide bridges. This conclusion is based on the negative reaction of native syr with Nbs_2 [5,5′-(ditiobis(2-nitrobenzoic acid)] (Parente et al., 1985), showing no free sulphydryl groups and confirmed by the value for the M_r of 10194.6±0.2, found for the native syr by mass spectrometry (see above). The three disulphide bridges are located, in all likelihood, between Cys3-Cis71, Cys27-Cys56 and Cys51-Cys95, as demonstrated for capsicein (Bovaziz et al., 1994), from which syr differs only in four amino acid positions (i.e. positions 1, 57, 68 and 93; Fig. 3).

Table 1
Time course digestion of CB-4 peptide with CPase A

t (min)	M_r (u)	ΔM_r	Removed residue
0	4259.14	–	–
5	4146.14	113.0	Leu/Ile
10	4059.04	87.1	Ser
15	3987.64	71.4	Ala
20	3779.54	208.1	Cys (pyridylethyl)

The comparison of the primary structure of syr with all other known α-elicitins allowed us to assess the novelty of this protein, as shown in Fig 3. In particular, cact from *P. cactorum* shows the higher number of amino acid differences (thirteen) and caps, from *P. capsicum,* the lower one (four). The other α-elicitins with known amino acid sequence show intermediate amino acid differences: (i) twelve [α-drechselerin (dre-α) from *P. drechseleri*]; (ii) nine [parasiticein (Ricci et al., 1992); elicitin 310 (Mouton-Perronet et al., 1995) and elicitin 172 (Capasso et al., 1999)]; and seven [α-megaspermin (meg-α) from *P. megasperma* and infestin (inf.) from *P. infestans*].

Palmivorein, isolated from *Phytophthora palmivora* and sequenced up to residue 26, shows, with respect to syr, an amino acid replacement in position 22 (Ser replaced by Thr, see Fig. 3). When we compare the amino acid composition of syr with that of palmivorein we found six amino acid differences: Ala (+2), Val (+1), Pro (−2) and Asx (−1).

The identification of syr as α-elicitin was also confirmed by the hypersensitive response (HR) (Ricci, 1997) and the electrolytes leakage (Zimmermann et al., 1998) induced on tobacco.

In fact, from 1 to 20 μM, syr induced necrosis in tobacco. When applied to the leaves at 1 μM, syr

```
                1       10          20          30          40
                *        *          *           *           *
Syr             TTCTTTQQTA AYVALVSILS DSSFNQCATD SGYSMLTATA
Elic-172        TTCTTTQQTA AYVALVSILS DTSFNQCSTD SGYSMLTATS
Cact            ATCTSSQQTA AYVALVSILS DTSFNQCSTD SGYSMLTATS
Caps            ATCTTTQQTA AYVALVSILS DSSFNQCATD SGYSMLTATA
Dre-α           TTCTSTQQTA AYVTLVSILS DSSFNQCATD SGYSMLTATS
Meg-α           TTCTSTQQTA AYVTLVSILS DSSFNQCATD SGYSMLTATA
Inf             TTCTTSQQTV AYVALVSILS DTSFNQCSTD SGYSMLTATS
Pal             TTCTTTQQTA AYVALVSILS DTSFNQ

                41      50          60          70          80
                *        *          *           *           *
Syr             LPTTAQYKLM CASTACKTMI TKIVSLNAPD CELTVPTSGL
Elic-172        LPTTEQYKLM CASTACKTMI NKIVTLNPPD CELTVPTSGL
Cact            LPTTAQYTLM CGSTACKTMI NKIVSLNPPN CELTVPTSGL
Caps            LPTTAQYKLM CASTACNTMI TKIVSLNPPD CELTVPTSGL
Dre-α           LPTDAQYKLM CSSTACNTMI KKIVSLNAPN CDLTVPTSGL
Meg-α           LPTTAQYKLM CASTACNTMI KKIVTLNPPD CELTVPTSGL
Inf             LPTTRQYKLM CASTACKTMI NKIVSLNAPD CELTVPTSGL

                81      90        98
                *        *        *
Syr             VLNVYSYANG FSSTCASL
Elic-172        VLNVFTYANG FSSTCASL
Cact            VLNVYSYANG FSTTCSSL
Caps            VLNVYSYANG FSATCASL
Dre-α           VLNVYEYANG FSTKCASL
Meg-α           VLNVYSYANG FSATCASL
Inf             VLNVYSYANG FSSTCASL
```

Fig. 3. Comparison of syr with the all known α-elicitin sequences.

induced necrosis estimated in amount of 1 in the relative evaluation scale (see experimental) and 4 when applied at 20 μM; when tobacco leaves were immersed in a solution of syr at 1 μM, little necrotic spots appeared on tobacco leaves (1); at 10 μM, necrosis was observed on entire leaves (4). These data indicate that syr induced in tobacco a weak HR at 1μM, whereas the highest HR was obtained at 10 μM.

As expected, syr significantly stimulates the electrolytes leakage through the cell membranes of tobacco plant tissues (Fig. 4) at 0.02 mM, which is the lowest concentration used in our experiments.

It is also noteworthy that, even if syr stimulates the electrolyte leakage from tobacco with increasing intensity, corresponding to the concentration values of 0.1 and 0.2 mM, as shown by the two respective curves in Fig. 4, however, these converge to the same value after 9 h, and remain constant for an extended period of time. This result is fully consistent with the molecular mechanism of elicitins, recently proposed by Ponchet et al. (1999). These authors report that four elicitin molecules, loaded with an ergosterol molecule, which is trapped from a plant cell, interact with the calcium channel of the plant cell plasmalemma, triggering the considered biological and physiological responses. At 0.1 mM, all tobacco cells have, in all likelihood, the site saturated in nine hours, while at 0.02 mM only a part, in our experimental conditions.

In conclusion, syr is a new α-elicitin (see Fig. 2) with the closest primary structure to caps and the farthest from cact (Fig. 3).

The structural specificity of the elicitins produced by the different species of *Phytophthora* suggests that syr also could be used as a taxonomic marker for *P. syringae*.

Furthermore, syr could be used to extend the studies on triggering the resistance of tobacco and other plants towards many pathogenic microrganisms, using directly the protein or by means of the preparation of transgenic plants, as already performed in the last decade for other well known elicitins (Kamoun et al., 1993; Bonnet et al., 1996; Blancard et al., 1998; Tepfer et al., 1998; Keller et al., 1999; Churngchow and Rattarasarn, 2000).

Finally, the property of elicitins as sterol carriers has recently been exploited, by patenting the use of some of them, including caps, as anticholesteremic agents (Mikes et al., 1998), suggesting a similar use for syr for their high analogy.

3. Experimental

3.1. General

Protein was estimated by the Bradford method (Bradford, 1976) using bovine serum albumin as a standard. UV (Perkin Elmer): H_2O.

3.2. Production of culture filtrates

A pathogenic strain of *Phytophthora syringae* was isolated from Citrus lemon plants in Meta di Sorrento and deposited in the culture collection at the Dipartimento di Aboricoltura, Botanica and Patologia Vegetale, Università di Napoli "Federico II", 80055 Portici, and numbered Ph 254. The stock culture was maintained on V-8 agar Petri plates. Liquid cultures were obtained by growing the fungus in flasks containing ASYT medium composed of: L-asparagine, 1 g; sucrose, 10 g; yeast extract, 5 g; thiamine, 0.001 g; $KH_2PO_4 \cdot 7H_2O$, 0.5 g; distilled water, 1000 ml. The flasks were incubated and stirred for 12 days at 26°C. Then, the culture fluid was strained through cheese cloth and filter

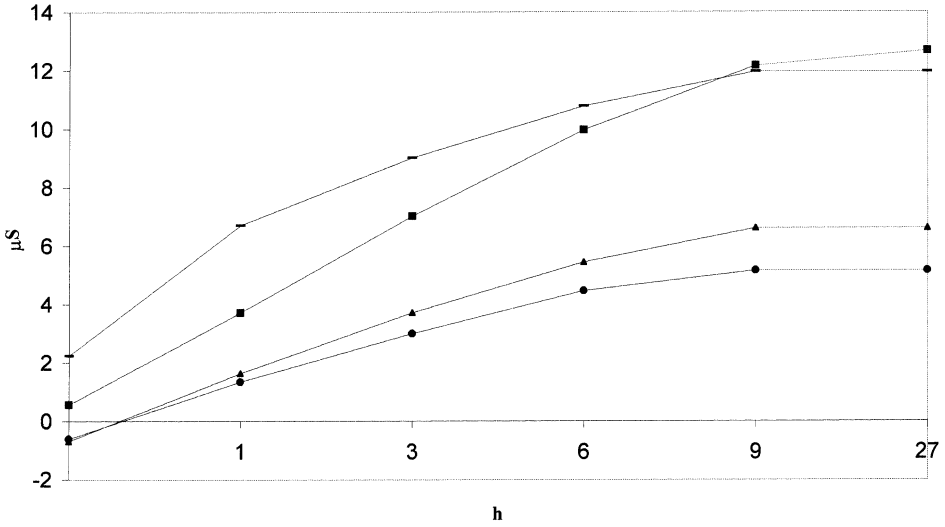

Fig. 4. Electrolytes leakage curves stimulated by syr on tobacco (*Nicotiana tabacum* L., cv. Rustica) leaf discs: the curves are corresponding to concn 0.2 mM (–), 0.1mM (■), 0.02 mM (▲) and control (0.0 mM) (●).

paper, sterilised by filtration through a 0.22 μm membrane and stored at −20°C.

3.3. SDS–PAGE

Polyacrylamide gel electrophoresis in the presence of SDS, using also tricine–SDS or tricine–SDS with urea 6 M and alkaline PAGE performed at pH 8.3 with glycine were performed as reported for elicitin 172 (Capasso et al., 1999).

3.4. Purification of syringicin

Syringicin was purified using a four-step procedure. This is slightly more simple than that used for the purification of elicitin 172 (Capasso et al., 1999), which consisted of five steps. The only difference regarding the purification of syringicin was the elimination of the rechromatography (fourth step) of the raw elicitin through a Sephadex G 50 column, which was directly substituted by the chromatography through a Lichroprep RP-18 column (Merck). In particular, the partially pure syingicin (19 mg each time of a raw sample of 38 mg coming out from the third step) was eluted stepwise with H_2O containing CH_3CN (0, 1, 5, 10, 20, 30, 40, 50 and 100% of acetonitrile in water, 150 ml every step) at low pressure (3 bar). Fractions of 5 ml were collected and monitored by UV absorbance at 210 nm. The purity of syr in every step was controlled by SDS–PAGE, whereas alkaline native PAGE was only used for the monitoring the purity after the final purification step.

3.5. Electrospray–mass spectrometry (ES–MS)

Syr was analysed by ES–MS using a Platform single quadrupole mass spectrometer (micromass). Aliquots (1 μg/10 μl) of protein solution were injected into the ion source at a flow rate of 2 μl/min. The mass spectrometer was scanned from m/z 1000 to 2500 at 10 s/scan, using a capillary voltage of 3.6 kV and a cone voltage of 40 V.

3.6. Cyanogen bromide cleavage

Cleavage of native syr with cyanogen bromide was carried out in 70% formic acid as already reported (Parente et al., 1993).

3.7. S-Pyridylethylation

Samples of native (10 μg) or CNBr-treated (25 μg) syr were *S*-pyridylethylated as previously reported (Scudiero et al., 1995). At the end of the incubation time the modified syr absorbed on ProSorb™ to remove reagents and solvent. The modified protein was then sequenced at the N-terminus. CNBr-treated syr, after *S*-pyridylethylation, was brought to 50% formic acid and chromatographed by RP-HPLC on a Beckman C_{18} column, using acetonitrile containing 0.1% TFA as eluant.

3.8. Amino acid composition

Samples of native syr were hydrolysed at 110°C for 20 h in the presence of 0.02% phenol. Amino acid analyses were obtained with an amino acid analyser (Beckman) equipped with the post-column, ninhydrin detection system. Chemicals and experimental were as suggested by the manufacturer.

3.9. pI Determination

Theorical pI was determined by CHARGPRO in PC-GENE software package.

3.10. Amino acid sequencing

Samples of native, *S*-pyridylethylated syr or CB-peptides were sequenced by automated Edman degradation on a pulsed phase sequencer (Model 473A; Applied Biosystems) as previously reported (Parente et al., 1993).

3.11. CPase A digestion and MALDI–mass spectrometry (MALDI–MS)

Cyanogen bromide peptide CB-4 was dissolved in 0.02 M ammonium bicarbonate and incubated with CPase A (Sigma; final enzyme: substrate ratio of 1:50, w:w), at 37°C. Aliquots of 10 μl were removed from the incubation mixture after 0, 5, 10, 15 and 20 min and analysed by MALDI-MS. The timed aliquots (1 μl, about 0.5 μg) of CPase A-treated CB-4 peptide were prepared in the following way, using α-cyano-4-hydroxycinnamic acid (Fluka) as matrix. The sample was loaded on the target and dried. Then 1 μl of a mixture composed by 0.1% TFA in water–ethanol–10 μg/μl of matrix in H_2O (l:1:1; v/v). The sample was analysed using a Voyager (Persective Biosystem) mass spectrometer in linear mode.

3.12. Hypersensitivity induction assay

Induction of hypersensitivity by pure syr was determined by infiltrating sterile distilled water solutions of protein into tobacco leaves (*Nicotiana tabacum* L., cv. Rustica). A hypersensitive response (HR) was scored when a brown necrosis occurred in the infiltrated area 48 h after inoculation. HR was scored on the basis of necrotic areas: 0 = necrosis of 0–5% infiltrated tissues; 1 = 6–25% infiltrated tissues; 2 = 26–50% infiltrated tissues; 3 = 51–75% infiltrated tissues; 4 = 76–100% infiltrated tissues. To test the induction of distal HR, petiole dip assays (Huet et al., 1992) were carried out on cut tobacco leaves. Leaf petioles were dipped into a 50 ml-solution of protein. The solution was taken up after

about 2 h. Then the leaves were transferred to sterile water. Necrotic lesions were visible after 24–48 h and ranged from minute necrotic spots to large, confluent necrotic areas.

3.13. Electrolytes leakage assay (LEA)

Thirty tobacco leaf discs (5 mm diameter) were incubated overnight in 0.0, 0.2, 1.0 and 2.0 mg/ml (corresponding to 0.0, 0.02, 0.1 and 0.2 mM, respectively) of syr, respectively. Than six leaf disks were transferred in sterile distilled water 20 ml and the corresponding conductance was measured in microsiemens using a conductivity meter CRISON 525 with 20 electrodes (range 20 μS–200 mS cm; $K=1$) connected to a computer with a specific program. Each value was the mean of at least five replicate samples and was calculated as the difference from the reading at the beginning of the assay, after 1, 3, 6, 9 and 27 h. These values where then corrected by subtracting those obtained for the control.

Acknowledgements

This work was supported by grants from the University of Naples "Federico II"; from the "Seconda Università di Napoli"; from the Italian Ministry of University and Scientific and Technological Research (PRIN 99). The authors are grateful to Miss. Giuseppina Travaglione and Mr. Luigi Battista for the technical assistance. DISCA contribution No. 193.

References

Blancard, D., Coubard, C., Bonnzet, P., Lenoir, M., Ricci, P., 1998. Mis en evidence d'une protection non specifique induite par la cryptogeine sur feuiles de tabac vis-à-vis de 5 champignons phytopathogenes. Ann. Tabac. 30, 11–20.

Boissy, G., de la Fortelle, E., Kahn, R., Huet, J.-C., Bricogne, G., Pernollet, J.-C., Brunie, S., 1996. Crystal structure of a fungal elicitor secreted by *Phytophthora cryptogea*, a member of a novel class of plant necrotic proteins. Structure 4, 1429–1439.

Bonnet, P., Bourdon, E., Ponchet, M., Blein, J.-P., Ricci, P., 1996. Acquired resistance triggered by elicitins in tobacco and other plants. J. Plant Pathol. 102, 181–192.

Bovaziz, S., Vanheijenoort, C., Huet, J.-C., Pernollet, J.-C., Guittet, E., 1994. Resonance assignment, cysteine-pairing elucidation and secondary-structure determination of capsicein, an alpha-elictin by three-dimensional ^{1}H NMR. Eur. J. Biochem. 220, 427–438.

Bradford, M.M., 1976. A rapid and sensitive method for the quantitation of microgram quantities of protein utilizing the principle of protein-dye binding. Anal. Biochem. 72, 248–254.

Capasso, R., Cristinzio, G., Evidente, A., Visca, C., Ferranti, P., Del Vecchio, Blanco, F., Parente, A., 1999. Elicitin 172 from an isolate of *Phytophthora nicotianae*, pathogenic to tomato. Phytochemistry 50, 703–709.

Churngchow, N., Rattarasarn, M., 2000. The elicitin secreted by *Phytophthora palmivora*, a rubber tree pathogen. Phytochemistry 54, 33–38.

Fefeu, S., Bovaziz, S., Huet, J.-C., Pernollet, J.-C., Guittet, E., 1997. Three-dimensional solution structure of *beta*-cryptogein, a *beta*-elicitin secreted by a phytopathogenic fungus *Phytophthora cryptogea*. Protein Sci. 6, 2279–2284.

Gooley, P.-R., Keniry, M.-A., Dimitrov, R.-A., Marsh, D.E., Keizer, D.-W., Gayler, K.-R., Grant, B.-R., 1998. The NMR solution structure and characterization of pH dipendent chemical shifts of the *beta*-elicitin cryptogein. J. Biomol. NMR 12, 523–534.

Huet, J.-C., Nespoulous, C., Pernollet, J.C., 1992. Structures of elicitin isoforms secreted by *Phytophthora drechseleri*. Phytochemistry 31, 1471–1476.

Huet, J.-C., Sallé-Tourne, M., Pernollet, J.-C., 1994. Amino acid sequence and toxicity of the α-elicitin secreted with ubiquitin by *Phytophthora infestans*. Molecular Plant-Microbe Interaction 7, 302–304.

Kamoun, S., Van West, P., de Jong, A.-J., de Groot, K.-E., Vleeshouvers, V.-G.-A.-A., Govers, F., 1997. A gene encoding a host-specific elicitor protein of *Phytophthora infestans* is down-regulated during infection of potato. Mol. Plant-Microbe Interac. 10, 13–20.

Kamoun, S., Van West, P., Vleeshouvers, V.-G.-A.-A., de Groot, K.-E., Govers, F., 1998. Resistance of *Nicotiana benthamania* to *Phytophthora infestans* is mediated by the recognition of the elicitor protein INF1. Plant Cell 10, 1413–1425.

Kamoun, S., Young, M., Glascock, C.-B., Tyler, B.-M., 1993. Extracellular protein elicitors from *Phytophthora*: host specificity and induction of resistance to bacterial and fungal phytopathogens. Mol. Plant-Microbe Interact. 6, 15–25.

Keizer, D.-W., Schuster, B., Grant, B.-R., Gayler, K.-R., 1998. Interaction between elicitins and radish *Raphanus sativus*. Planta 204, 480–489.

Keller, H., Pampoukdjian, N., Ponchet, M., Poupet, A., Delon, R., Verrier, J.-L., 1999. Pathogen-induced elicitin production in transgenic tobacco generates a hypersensitive response and non specific disease resistance. Plant Cell 11, 223–235.

Mikes, V., Blein, J.-P., Milat, M.-L., Ponchet, M., Ricci, P., 1998. Use of Elicitins as Lipid Carriers and Their Medical Use. Patent PCT Int. Appl. 31 pp Coden; PIXXD2.

Mouton-Perronet, F., Brunetau, M., Denoroy, L., Bouliteau, P., Ricci, P., Bonnet, P., Michel, G., 1995. Elicitin produced by an isolate of *Phytophthora parasitica* pathogenic to tobacco. Phytochemistry 38, 41–44.

Parente, A., Merrifield, B., Geraci, G., D'Alessio, G., 1985. Molecular basis of superreactivity of cysteine residues 31 and 32 of seminal rebonuclease. Biochemistry 24, 1098–1104.

Parente, A., Verde, C., Malorni, A., Montecucchi, P., Aniello, F., Geraci, G., 1993. Amino acid sequence of cooperative dimeric myoglobin from the radular muscles of marine gastropod *Nassa mutabilis*. Biochim. Biophys. Acta 1162, 1–9.

Ponchet, M., Panabieres, F., Milat, M.-L., Mikes, V., Montillet, J.-L., Suty, L., Triantaphylides, C., Tirilly, Y., Blein, J.-P., 1999. Are elicitins cryptograms in plant-Oomycete communications? Cell Mol. Life Sci. 56, 1020–1047.

Ricci, P., 1997. Induction of hypersensitive response (HR) and systemic acquired resistance (SAR) by fungal proteins: the case of elicitins. In: Stacey, G., Keen, N.T. (Eds.), Plant Microbe Interactions, Vol. 3. Chapman and Hall, New York, pp. 53–75.

Ricci, P., Trentin, F., Bonnet, P., Venard, P., Mouton-Perronnet, F., Bruneteau, M., 1992. Differential production of parasiticein an elicitor of necrosis and resistance in tobacco, by isolates of *Phytophthora parasitica*. Plant Pathol. 41, 298–307.

Scudiero, R., Capasso, C., Del Vecchio Blanco, F., Savino, G., Capasso, A., Parente, A., Parisi, E., 1995. Isolation and primary structure determination of a metallothionein from *Paracentrotus lividus (Echinodermata echinoidea)*. Comp. Biochem. Physiol. 111B, 329–336.

Tepfer, D., Bounteaux, C., Vigon, C., Aymes, S., Perez, V., O' Donohue, M.-J., 1998. *Phytophthora* resistance through production of a fungal protein elicitor (*beta*-cryptogein) in tobacco. Mol. Plant-Microbe Interac. 11, 64–67.

Zimmermann, S., Franchisse, J.-M., Thomine, S., Barbier Brygoo, H., Guern, J., 1998. Elicitor-induced chloride efflux and anion channels in tobacco cell suspensions. Plant Physiol. Biochem. 36, 665–674.

PERGAMON

Phytochemistry 58 (2001) 263–268

PHYTOCHEMISTRY

www.elsevier.com/locate/phytochem

Changes in membrane lipid and free fatty acid composition during low temperature preconditioning against SO_2 injury in coleus

Helen A. Norman[a,*,1], Donald T. Krizek[b,2], Roman M. Mirecki[b,3]

[a]*Weed Science Laboratory, Agricultural Research Service, US Department of Agriculture, Beltsville, MD 20705, USA*
[b]*Climate Stress Laboratory, Agricultural Research Service, US Department of Agriculture, Beltsville, MD 20705, USA*

Received 28 December 2000; received in revised form 19 April 2001

Abstract

The effects of a low temperature (13 °C) treatment known to provide protection against sulphur dioxide (SO_2) injury were assessed on leaf lipid composition in two cultivars of *Coleus blumei* Benth, found previously to differ in sensitivity to SO_2 and other environmental stresses. After 5 days growth at 13 °C, there were significant differences in membrane lipid fatty acid composition as well as in free fatty acid (FFA) levels between SO_2-sensitive 'Buckley Supreme' ('BS') and SO_2-insensitive 'Marty' ('M'). Molecular species of chloroplast galactolipids in 'M' contained increased levels of linolenic acid (18:3). In the leaf FFA pools, the saturated components, palmitic (16:0) and stearic (18:0) acids, were predominant at 20 °C. After temperature hardening at 13 °C, the total amount of FFAs decreased in 'M' but increased in 'BS.' These modifications in lipid composition suggest an additional mechanism for cultivar differences in tolerance to SO_2 and other stressors in coleus. Published by Elsevier Science Ltd.

Keywords *Coleus blumei*; Labiatae; Cross protection; Lipid metabolism; SO_2-membrane interactions; SO_2 tolerance; Stress tolerance; Temperature hardening

1. Introduction

The physiological and morphological effects of sulfur dioxide (SO_2) on higher plants have been investigated extensively (Peiser and Yang, 1985; Darrall, 1989). The phenomenon of cross-protection against SO_2 by drought, salinity, low temperature, and other environmental factors is well documented (Kobriger and Tibbitts, 1985; Krizek et al., 1986, 2001; Menser et al., 1963). There are several reports which suggest that abscisic acid (ABA) may be involved in this phenomenon (Kondo and Sugahara, 1978; Krizek et al., 1986, in press; Terry et al., 1988), causing closure of the stomates and a corresponding reduction in uptake of SO_2 and a decrease in visible leaf injury (Krizek et al., 1986, in press).

Genotypic differences in SO_2 sensitivity under natural and experimental conditions have been reported for several ornamental plants, including poinsettia (Krizek et al., 1985b, 1986) and other species (Semeniuk and Heggestad, 1981; Unsworth and Ormrod, 1982). Published studies have demonstrated considerable genetic variability within cultivars of *Coleus blumei* Benth. in their responses to different environmental stresses. These include ozone (Semeniuk and Heggestad, 1981), SO_2 (Krizek et al., 2001; Semeniuk and Heggestad, 1981), UV-B radiation (Semeniuk and Stewart, 1979), water stress (Terry et al., 1988), chilling (Moline and Semeniuk, 1983; Krizek et al., 1985a), and aluminum stress (Krizek et al., 1997).

Krizek et al. (1985b) have suggested that both morphological and physiological properties of stomata may

Chemical names: (16:0), palmitic acid; (18:0), stearic acid; (18:3), linolenic acid; DGDG, digalactosyldiacylglycerol; FFA, free (unesterified) fatty acids; MDA, malondialdehyde; MGDG, monogalactosyldiacylglycerol; PC, phosphatidylcholine; PE, phosphatidyl ethanolamine; PG, phosphatidylglycerol; PI, phosphatidylinositol; PS, phosphatidylserine; SL, sulpholipid; SO_2, sulphur dioxide

* Corresponding author. Tel.: +1-301-595-9121; fax: +1-301-504-6491.

E-mail address: nhelenanorman@aol.com (H.A. Norman).

[1] Present address: 10403 A, 46th Ave., Apt. 107, Beltsville, MD 20705, USA.

[2] Present address: Sustainable Agricultural Systems Laboratory, Agricultural Research Service, US Department of Agriculture, Rm. 342, Bldg. 001, BARC-West, Beltsville, MD 20705, USA.

[3] Present address: Phytonutrients Laboratory, Agricultural Research Service, US Department of Agriculture, Bldg. 308, BARC-East, Beltsville, MD 20705, USA.

0031-9422/01/$ - see front matter Published by Elsevier Science Ltd.
PII: S0031-9422(01)00242-4

contribute to the differential sensitivity to SO_2 observed between certain poinsettia cultivars. A subsequent study (Krizek et al., 1986) showed that poinsettia plants subjected to soil moisture stress prior to SO_2 fumigation were equally protected compared with well-watered plants given exogenous applications of ABA, suggesting a protective role for ABA in certain cultivars of poinsettia.

Reducing the growth temperature from 20 to 13 °C for 5 days prior to fumigation (at 27 °C) provided effective protection against subsequent SO_2 exposure in 'Buckley Supreme' ('BS'), a drought- and SO_2-sensitive cultivar of coleus (Krizek et al., 2001). ABA was found to play a major role in this low temperature-induced phytoprotection (Krizek et al., 2001). After 5 days growth at 13 °C, the levels of ABA were significantly increased over those in plants maintained at 20 °C. This was associated with a decrease in stomatal conductance and transpiration rate and a corresponding decrease in SO_2 injury in 13 °C-treated plants.

There are many citations in the literature on changes in plant membrane polyunsaturated fatty acids in response to a shift in growth temperature. It is well known that lipids enriched in polyunsaturated FA are potentially subject to damage by peroxidative reactions (Khan and Malhotra, 1977; Sandmann and Gonzales, 1989). One of the primary modes of action of air pollution injury in plants has been identified as the generation of free radicals and the resultant peroxidation of cellular components (Asada, 1980; Peiser and Yang, 1985; Lee et al., 1992). We have, therefore, included lipid analyses in our investigations of differential SO_2 tolerance in coleus.

The present study was conducted to determine: (a) whether changes in membrane lipid composition occur during a low temperature pretreatment known to provide cross protection against SO_2 and other environmental stresses, and (b) whether alterations in lipids may also be related to the differential SO_2 sensitivity between coleus cultivars. The composition of leaf FFA as well as membrane lipids were included in these analyses since FFA are also potential substrates for SO_2-induced peroxidation, and if elevated levels of polyunsaturated FFA in chloroplasts were accessible to superoxide ions and other reactive oxygen species, then SO_2 sensitivity may be increased.

2. Results and discussion

The molecular species composition of leaf galactolipids, monogalactosyldiacylglycerol (MGDG) and digalactosyldiacylglycerol (DGDG), after 5 days growth of each cultivar at 20 or 13 °C are recorded in Tables 1 and 2, respectively. In the shorthand notation used to define molecular species, pairs of numbers representing fatty acids and separated by a slash, represent the components in the *sn*-1 and *sn*-2 positions, respectively, of the molecular species. The major MGDG molecular species in leaves of each cultivar was 18:3/18:3 at both 20 and 13 °C (Table 1). In plants maintained at 20 °C, this component was about 10% lower in 'BS' compared with 'M', and the relative amount of 18:2/18:3 MGDG was increased. This latter molecular species is a precursor for desaturation of 18:2 at the *sn-2* position to form 18:3/18:3 MGDG in the chloroplast (Norman and St. John, 1986). The relative amount of 16:0/18:3 MGDG was less in 'BS' at 20 °C compared to the level in 'M' and the 16:0/18:2 molecular species was correspondingly increased.

Plants of both cultivars showed an increase in 18:3/18:3 MGDG in response to 5 days of temperature preconditioning at 13 °C. This could be predicted from previous studies reporting temperature-induced changes in the fatty acid composition of membrane lipids of some plant species. The increases in 18:3/18:3 MGDG in coleus were accompanied by decreases in 18:2/18:3, 18:2/18:2, and 16:0/18:2 molecular species (Table 1). The amounts of these three MGDG components, however, differed between the two cultivars, with 'M' maintaining a relative enrichment in 18:3/18:3 MGDG. The corresponding DGDG molecular species showed the same trends between the two cultivars and in response to low temperature pretreatment (Table 2). The total and relative amounts of galactolipids showed little or no difference between cultivars or treatments (Tables 1 and 2).

The composition of PC was also compared at the molecular species level in the two cultivars. In plants grown at either 20 or 13 °C, 18:3/18:3 PC was relatively higher in leaves of SO_2-insensitive 'M' than in SO_2-sensitive 'BS,' and levels of 18:2/18:3 PC and 18:2/18:2 PC were lower (Table 3). In contrast to the composition of the galactolipids, the distribution of the 16:0/18:3 and 16:0/18:2 molecular species of PC was not significantly different between the cultivars grown at 20 °C. Temperature pretreatment at 13 °C for 5 days increased 18:3/18:3 PC in both cultivars and caused declines in the corresponding 18:2-containing molecular species (Table 3). Only in the leaves of 'M,' however, did the amount of 16:0/18:3 PC increase and 16:0/18.2 PC decrease. In contrast to the galactolipids, analyses of the levels of individual phospholipids revealed an increase in PC in 'M' after 5 days at 13 °C (Tables 3 and 4).

In coleus plants grown at 20 °C, there were no differences between cultivars in the leaf FFA pool size or composition (Table 5). The major components were the saturated fatty acids, 16:0 and 18:0. After 5 days at 13 °C, 'BS' showed an increase in total FFA (on a per mg chlorophyll basis); there was a decline in the relative amount of the unsaturated components of the FFA pool due to increases (both relative and absolute) in

Table 1
Molecular species composition of MGDG from 'Buckley Supreme' and 'Marty' coleus leaves after 5 days at 20 or 13 °C[a]

Molecular species	20 °C		13 °C	
	Buckley Supreme	Marty	Buckley Supreme	Marty
wt.% Total MGDG				
18:3/18:3	63.8±1.5	71.7±1.1	70.6±1.5	80.6±1.4
18:2/18:3	13.4±0.6	8.9±0.5	10.1±0.3	5.3±0.3
18:2/18:2	3.4±0.3	2.5±0.3	3.0±0.4	1.0±0.1
18:1/18:1	2.1±0.2	1.6±0.2	1.9±0.2	0.9±0.1
16:0/18:3	6.0±0.5	9.2±0.5	7.1±0.4	8.8±0.3
16:0/18:2	10.4±0.4	5.3±0.4	6.5±0.3	3.0±0.2
16:0/18:1	0.9±0.1	0.8±0.1	0.0±0.1	0.4±0.1
μmol MGDG/g dry wt				
	182.0±5.0	186.4±5.8	178.8±6.7	180.6±4.5

[a] Means ± S.E. of four analyses each of three plant samples.

Table 2
Molecular species composition of DGDG from 'Buckley Supreme' and 'Marty' coleus leaves after 5 days at 20 or 13 °C[a]

Molecular species	20 °C		13 °C	
	Buckley Supreme	Marty	Buckley Supreme	Marty
wt.% Total DGDG				
18:3/18:3	55.8±1.1	64.6±0.9	63.9±0.8	72.5±1.4
18:2/18:3	9.9±0.4	5.5±0.3	6.3±0.5	2.9±0.2
18:1/18:3	1.8±0.2	2.0±0.2	1.5±0.2	2.4±0.3
18:1/18:2	1.6±0.2	1.5±0.3	1.1±0.1	0.8±0.1
16:0/18:3	6.5±0.4	10.0±0.5	7.3±0.4	11.0±0.4
16:0/18:2	21.7±1.1	14.5±1.0	17.4±0.9	9.0±0.9
16:0/18:1	2.7±0.3	1.9±0.2	2.5±0.2	1.0±0.1
μmol DGDG/g dry wt				
	102.6±2.0	108.3±3.5	104.4±0.5	102.0±2.0

[a] Means ± S.E. of four analyses each of three plant samples.

Table 3
Molecular species composition of PC from 'Buckley Supreme' and 'Marty' coleus leaves after 5 days at 20 or 13 °C[a]

Molecular species	20 °C		13 °C	
	Buckley Supreme	Marty	Buckley Supreme	Marty
wt.% Total PC				
18:3/18:3	12.2±0.8	17.9±1.0	17.1±0.7	25.8±1.1
18:2/18:3	15.7±0.5	12.4±0.6	13.2±0.4	9.0±0.6
18:2/18:2	12.9±0.4	8.3±0.5	9.1±0.5	5.9±0.5
18:1/18:3	1.5±0.2	2.7±0.2	2.9±0.2	3.0±0.2
18:1/18:2	2.8±0.1	2.5±0.1	3.0±0.3	2.6±0.1
18:1/18:1	2.3±0.2	3.6±0.3	2.7±0.2	3.2±0.2
16:0/18:3	24.0±0.7	25.2±0.8	24.9±0.5	31.4±1.0
16:0/18:2	28.6±0.6	27.4±0.7	27.1±0.4	19.1±0.7
μmol PC/g dry wt				
	33.2±3.0	32.3±3.5	34.9±2.7	47.2±2.5

[a] Means ± S.E. of four analyses each of three plant samples.

Table 4
Polar lipid content of leaves from 'Buckley Supreme' and 'Marty' coleus leaves after 5 days at 20 or 13 °C[a]

Lipid class	20 °C		13 °C	
	Buckley Supreme	Marty	Buckley Supreme	Marty
% Total polar lipid				
MGDG	47.2±1.5	46.8±1.0	46.5±1.4	45.5±1.3
DGDG	26.6±0.9	27.2±1.1	27.2±1.4	25.7±1.6
SL	3.8±0.3	3.7±0.2	4.0±0.3	3.5±0.3
PC	8.6±0.5	8.1±0.4	9.1±0.4	11.9±0.4
PE	3.9±0.3	4.2±0.3	3.4±0.2	4.0±0.4
PG	6.7±0.4	6.5±0.4	6.4±0.5	6.2±0.5
PI	1.7±0.2	1.8±0.3	2.0±0.2	1.8±0.2
PS	1.5±0.1	1.7±0.2	1.4±0.2	1.4±0.2
Total μmol polar lipid/g dry wt				
	387.5±20.3	397.4±15.8	383.1±16.0	392.0±18.2

[a] Means ± S.E. of four analyses each of three plant samples.

16:0 and 18:0. Conversely, in 'M,' the total FFA pool was reduced by approximately 45% at 13 °C and the new pool was depleted in the saturated fatty acid components. The absolute amount of unesterified 18:3 declined in 'M' but showed no significant change in 'BS' (data not shown).

There was no visible leaf curling, senescence, or abscission, in either 'M' or 'BS' after growth at 13 °C for 5 days. We used lipid peroxidation as a parameter to assess any indication of intercellular low temperature damage by estimating total peroxides in leaf extracts. There was no detectable increase in MDA accumulation in plants of either cultivar after 5 days at 13 °C as compared to 20 °C. MDA levels were approximately the same in both cultivars at 20 °C, while at 13 °C, MDA levels in 'M' tended to decline (Table 6).

The precise mode of action of SO_2 in plant cells is still largely uncertain despite considerable research in this area, and in related fields examining plant cross-tolerance to environmental stresses (Menser et al., 1963; Kobriger and Tibbitts, 1985; Krizek et al., 1985a, 1986, 2001; Terry et al., 1988). There is growing evidence, however, that one of the prominent effects of SO_2 in plant cells involves the initiation of a free radical generating mechanism resulting in peroxidative destruction of cellular constituents (Peiser and Yang, 1985). The multiple effects of both SO_2 and sulphite on the plant include pigment destruction (Peiser and Yang, 1985), depletion of cellular lipids (Khan and Malhotra, 1977), and peroxidation of polyunsaturated fatty acids (Sandmann and Gonzales, 1989).

The fact that coleus cultivars such as 'BS' and 'M' are fundamentally different in their response to temperature hardening and a wide range of environmental stresses, including SO_2, chilling, drought, and UV-B radiation (Semeniuk and Stewart, 1979; Semeniuk and Heggestad,

Table 5
Effect of temperature pre-conditioning for 5 days at 13 or 20 °C on free fatty acid (FFA) composition in leaves of 'Buckley Supreme' and 'Marty' coleus[a]

FFA	20° C		13° C	
	Buckley Supreme	Marty	Buckley Supreme	Marty
wt.% Total FFA				
14:0	4.8±0.4	5.3±0.3	2.8±0.2	1.9±0.2
16:0	40.6±0.9	41.5±0.7	50.3±0.8	32.5±1.0
16:1	3.5±0.3	3.0±0.4	0.9±0.2	0.8±0.1
18:0	29.5±1.0	28.7±1.2	36.0±0.9	33.9±0.8
18:1	9.8±0.4	10.4±0.4	4.3±0.3	15.6±0.6
18:2	9.6±0.5	9.2±0.3	4.2±0.2	13.1±0.4
18:3	2.2±0.3	1.9±0.2	1.5±0.1	2.2±0.2
μmol FFA/mg chlorophyll				
	0.87±0.03	0.84±0.04	1.32±0.07	0.46±0.02

[a] Data are expressed as a percentage of total FFA (wt) and on an absolute basis (μmol per mg chlorophyll). Means ± S.E. of four analyses each of three plant samples.

Table 6
Lipid peroxidation products in leaves of 'Buckley Supreme' and 'Marty' coleus grown for 5 days at 20 or 13 °C[a]

Growth temperature °C	nmol MDA equiv./g fr. wt	
	Buckley Supreme	Marty
20	68.5±0.7	67.9±1.0
13	67.2±0.9	53.0±0.8

[a] Means ± S.E. of four analyses each of three plant samples.

1981; Terry et al., 1988; Krizek et al., 2001) suggest a commonality in stress adaptation.

We proposed that cellular differences in sensitivity to oxidative stress between these two coleus cultivars may serve as one basis for their genotypic differences in SO_2 sensitivity (Krizek et al., 2001). Differences in lipid composition between SO_2-sensitive 'BS' and SO_2-insensitive 'M' would appear to support this hypothesis. Our data on differences in ascorbate and ascorbate peroxidase between the two coleus cultivars (Krizek et al., in press) also implicate some role for antioxidants. Lee et al. (1992) have suggested that free-radical scavenging enzymes or endogenous antioxidant compounds are more important than stomatal restriction of pollutant diffusion to sensitive leaf mesophyll sites in determining genotype differences in response to SO_2 and O_3.

Temperature-induced changes in plant lipid fatty acid composition have been a subject of numerous investigations. An increase in the degree of unsaturation in response to a reduction in growth temperature, as seen in coleus, is a predictable, although certainly not a universally occurring response. The increases seen in molecular species containing linolenic acid in coleus grown at 13 °C (Tables 1, 2 and 4) suggest that both of the coleus cultivars employed have some ability to adapt to low temperature by altering membrane lipid composition. Inherent differences were found in membrane lipids of the two cultivars when grown at 20 °C; cultivar 'M' which is the least sensitive to the air pollutants SO_2 and O_3, contained elevated levels of the 18:3/18:3 molecular species of MGDG. The direct precursor proposed is 18:2/18:3 MGDG (Norman and St. John, 1986), and this was correspondingly at lower levels in 'M,' possibly due to an increase in the activity of a specific chloroplast desaturase.

Reactions leading to the biosynthesis of the 18:3/18:3 molecular species of DGDG and PC are less certain (Heemskerk and Wintermans, 1987). Both lipid components were increased in 'M' relative to 'BS,' again implying a difference in activities of specific enzymes regulating levels of membrane polyunsaturated fatty acids, or possibly enhanced 18:3 peroxidation in 'BS,' although there was no evidence of an increase in peroxidation products as measured by MDA (Table 6).

We propose that there is a protective mechanism in 'M' for membrane lipids. Growth at 13 °C for 5 days, a pretreatment which decreases visible injury during subsequent SO_2 fumigation (Krizek et al., 2001), increased the 18:3/18:3 molecular species of MGDG, DGDG, and PC in both cultivars. Collectively, our data could be interpreted to indicate that coleus plants with membrane lipids enriched in 18:3 will be predictably less sensitive to SO_2. Without further knowledge, this might appear contradictory, since this fatty acid is a preferred substrate for SO_2-induced lipid peroxidation (Sandmann and Gonzales, 1989). Therefore, the increase in 18:3 (as in 'M' relative to 'BS' at 20 °C, and in both cultivars grown at 13 °C as opposed to 20 °C) may require a concomitant enhancement of protective mechanisms to reduce enzymatic and nonenzymatic peroxidation of fatty acids, particularly within the chloroplast, where the galactolipids are modified. Mechanisms possibly required to protect 18:3 synthesized in response to reduced growth temperature may also protect the plant during subsequent SO_2 fumigation. For example, low temperature can increase the levels of cellular antioxidants including glutathione (de Kok and Oosterhuis, 1983; Alscher, 1989; Alscher et al., 1987). SO_2 damage involves membrane lipid peroxidation and several independent studies have implicated cellular glutathione as an antioxidant in SO_2 tolerance (Alscher, 1989; Sandman and Gonzales, 1989; Madamanchi and Alscher, 1991). However, we found little evidence for changes in glutathione metabolism in coleus (Krizek et al., 2001).

Unesterified fatty acids typically constitute an extremely low proportion of the total fatty acid complement of plant cells (1–2%). Elevated levels of polyunsaturated FFA particularly within the chloroplast stroma would be unfavorable considering that they are a substrate for peroxidation. The changes in the total FFA pool seen

here in coleus possibly reflect cultivar differences in the rates of lipid metabolism at 13 °C. The analyses of lipid peroxidation products in coleus cultivars maintained at 20 °C or transferred to 13 °C showed no large difference between cultivars, and no indication of any enhanced peroxidation resulting from lowered growth temperature (Table 6). Conversely, peroxidation products tended to decline at 13 °C in 'M.' In the present paper, changes in fatty acid composition gave no evidence for loss of linolenic acid. Although FFA complements were essentially identical in 'BS' and 'M' at 20 °C, differences in pool size and composition were found in plants grown at 13 °C (Table 5). Currently, we have insufficient data to interpret these changes, although they do imply a differential lipid metabolic response to lowered growth temperature between the two cultivars. One explanation to offer is that the overall changes seen in FFA composition at 13 °C constitute part of an adaptive mechanism modifying lipid metabolism which operates at different levels in the two coleus cultivars.

3. Experimental

3.1. Plant material

Cultivars of coleus compared in this study were identified previously (Terry et al., 1988; Krizek et al., in press) as differing in sensitivity to various environmental stresses, with 'Buckley Supreme' ('BS') (a red pigmented cultivar) being highly sensitive and 'Marty' ('M') (a red and yellow pigmented cultivar), being relatively insensitive. Reducing the growth temperature from 20 to 13 °C for 5 days prior to SO_2 fumigation was shown to increase SO_2 tolerance in both cultivars (Krizek et al., in press).

3.2. Culturing procedures

Cuttings from clonal stocks of coleus cultivars were propagated in a charcoal-filtered greenhouse on a hot pad (25 °C) under mist in a synthetic peat-vermiculite mix (Jiffy Mix, Jiffy Products of America, West Chicago, IL, USA).[4] After 2 weeks, cuttings were selected for uniformity and transplanted to pots containing the same peat-vermiculite mix. Plants were maintained in the greenhouse under a 16 h photoperiod [25 μmol m^{-2} s^{-1} supplemental photosynthetic photon flux (PPF), provided by General Electric 200 W, 130 V incandescent lamps], at 28 ± 3 °C day temperature, 21 ± 2 °C night temperature, ambient CO_2 and ambient relative humidity.

[4] Use of a company or product name by USDA does not imply approval or recommendation of the product to the exclusion of others which may also may be suitable.

3.3. Temperature preconditioning

At 10 days after transplanting, the cuttings were preconditioned for 5 days in Revco (Asheville, NC) Model 511-38 growth chambers maintained at constant temperatures of either 13 or 20 ± 0.5 °C, 70 ± 5% relative humidity and ambient CO_2. Plants were grown under a 16 h photoperiod at 320 ± 35 μmol m^{-2} s^{-1} of PPF provided by General Electric 1500 mA cool white fluorescent lamps.

3.4. Lipid analyses

Pairs of leaves from the lower and middle nodes were removed from three plants of each cultivar from each treatment. The leaves collected from an individual plant were combined and treated as one sample. The tissue was boiled in isopropanol for 5 min, and then lipids were extracted using a modification of the procedure of Folch et al. (1957). Separation into neutral lipid, galactolipid, and phospholipid classes was achieved using silica Sep-Pak cartridges (Waters Assoc., Milford, MA) (Norman and St. John, 1987). Individual galactolipid and phospholipid components were resolved by TLC on silica gel H using $CHCl_3$–HOAc–MeOH–H_2O (75:25:5:1.1) as developing solvent, and then eluted from the silica gel (Norman and St. John, 1986).

Galactolipids were quantified based on sugar content according to Roughan and Batt (1968), and lipid phosphorus was determined using the procedure of Marinetti (1962). Lipid molecular species were resolved by isocratic HPLC procedures (Smith et al., 1985; Norman and St. John, 1987), employing a 25 cm×4.6 mm i.d. Beckman Ultrasphere (5 μm) reversed-phase C-18 column, and quantitated directly using a Tracor 945 Flame Ionization LC Detector (Tracor Instruments, Austin, TX) operated as previously described (Norman and St. John, 1986). Neutral lipid fractions were redissolved in hexane and FFA extracted according to Anderson and McCarty (1972). FA methyl esters were prepared directly with boron trifluoride/methanol (Sigma Chemical Co., St. Louis, MO) (Morrison and Smith, 1964). GLC analysis was performed on a Hewlett Packard (model 5880A) gas chromatograph using previous specifications (Norman and St. John, 1986). Chlorophyll was assayed spectrophotometrically (Arnon, 1949). Data represent the means ± S.E. of four analyses each of three plant samples.

3.5. Measurement of lipid peroxidation

The extent of lipid peroxidation was estimated by measuring the thiobarbituric acid (TBA) reactive substances, primarily malondialdehyde (MDA), in aqueous 5% (w/v) trichloroacetic acid (TCA) extracts of leaf tissue (Heath and Packer, 1968; Buege and Aust, 1978).

The extracts were centrifuged (8000 *g*, 10 min) and then 1 ml aliquots were combined with 4 ml of TBA reagent [0.5% (w/v) TBA in 20% (w/v) TCA], boiled at 100 °C for 20 min, and immediately cooled on ice. After centrifugation for 15 min at 8000 *g*, the absorbance was determined at 532 nm and values corrected by subtracting the absorbance value at 600 nm. The concentration of MDA was calculated using the extinction coefficient of Heath and Packer (1968).

Acknowledgements

The authors thank Ruth Magnum for her expert technical assistance in running the lipid analyses and to Randy Rowland for his help in preparing the graphical abstract.

References

Alscher, R.G., 1989. Biosynthesis and antioxidant function of glutathione in plants. Physiol. Plant 77, 457–464.

Alscher, R., Bower, J.L., Zipfel, W., 1987. The basis for differential sensitivities of photosynthesis to SO_2 in two cultivars of pea. J. Exp. Bot. 38, 99–108.

Anderson, M.M., McCarty, R.E., 1972. Rapid and sensitive assay for free fatty acids using Rhodamine 6G. Anal. Biochem. 45, 260–270.

Arnon, D.I., 1949. Copper enzymes in isolated chloroplasts, polyphenol-oxidase in *Beta vulgaris*. Plant Physiol 24, 1–15.

Asada, K., 1980. Formation and scavenging of superoxide in chloroplasts, with relation to injury by sulfur dioxide. Res. Rep. Natl. Inst. Environ. Stud. 11, 165–179.

Buege, J.A., Aust, S.D., 1978. Microsomal lipid peroxidation. Methods Enzymol. 52, 302–310.

Darrall, N.M., 1989. The effect of air pollutants on physiological processes in plants. Plant, Cell Environ. 12, 1–30.

de Kok, L.J., Oosterhuis, F.A., 1983. Effects of frost-hardening and salinity on glutathione and sulfhydryl levels and on glutathione reductase activity in spinach leaves. Physiol. Plant 58, 47–51.

Folch, J., Lees, M., Sloane-Stanley, G.H., 1957. A simple method for the isolation and purification of total lipids from animal tissues. J. Biol. Chem. 226, 497–509.

Heath, R.L., Packer, L., 1968. Photoperoxidation in isolated chloroplasts. I. Kinetics and stoichiometry of fatty acid peroxidation. Arch. Biochem. Biophys. 125, 189–198.

Heemskerk, J.W.M., Wintermans, J.F.G.M., 1987. Role of the chloroplast in the leaf acyl-lipid synthesis. Physiol. Plant 70, 558–568.

Khan, A.A., Malhotra, S.S., 1977. Effects of aqueous sulphur dioxide on pine needle glycolipids. Phytochemistry 16, 539–543.

Kobriger, J.M., Tibbitts, T.W., 1985. Effect of relative humidity prior to and during exposure on response of peas to ozone and sulfur dioxide. J. Am. Soc. Hort. Sci. 110, 21–24.

Kondo, N., Sugahara, K., 1978. Changes in transpiration rate of SO_2-resistant and-sensitive plants with SO_2 fumigation and the participation of abscisic acid. Plant Cell Physiol. 19, 365–373.

Krizek, D.T., Foy, C.D., Mirecki, R.M., 1997. Influence of aluminum stress on shoot and root growth of contrasting genotypes of coleus. J. Plant Nutr. 20, 1045–1060.

Krizek, D.T., Mirecki, R.M., Semeniuk, P., 1986. Influence of soil moisture stress and abscisic acid pretreatment in modifying SO_2 sensitivity in poinsettia. J. Am. Soc. Hort. Sci. 111, 446–450.

Krizek, D.T., Semeniuk, P., Moline, H.E., Mirecki, R.M., Abbott, J.A., 1985a. Chilling injury in coleus as influenced by photosynthetically active radiation, temperature, and abscisic acid pretreatment. I. Morphological and physiological responses. Plant, Cell Environ. 8, 135–142.

Krizek, D.T., Wergin, W.P., Semeniuk, P., 1985b. Morphological and physiological properties of poinsettia leaves and bracts in relation to sulfur dioxide sensitivity. Envir. Exp. Bot. 25, 165–173.

Krizek, D.T., P.A. Terry, Upadhyaya, A., Caldwell, C.R., Mirecki, R., 2001. Changes in abscisic acid, stomatal conductance, and antioxidants during low temperature preconditioning against SO_2 injury in contrasting cultivars of coleus. Biotronics 30.

Lee, E.H., Kramer, G.F., Rowland, R.A., Agrawal, M., 1992. Antioxidants and growth regulators counter the effects of O_3 and SO_2 in crop plants. Agric. Ecosystems Environ. 38, 99–106.

Madamanchi, N.R., Alscher, R.G., 1991. Metabolic bases for differences in sensitivity of two pea cultivars to sulfur dioxide. Plant Physiol. 97, 88–93.

Marinetti, G.V., 1962. Chromatographic separation, identification and analysis of phosphatides. J. Lipid Res. 3, 1–11.

Menser, H.A., Heggestad, H.E., Street, O.E., Jeffrey, R.N., 1963. Response of plants to air pollutants. Effects of ozone on tobacco plants preconditioned by light and temperature. Plant Physiol. 38, 605–609.

Moline, H.E., Semeniuk, P., 1983. Variation in sensitivity of coleus seedlings to chilling injury. HortScience 18, 80–81.

Morrison, W.R., Smith, L.M., 1964. Preparation of fatty acid methyl esters and dimethyl acetals from lipids with boron trifluoride methanol. J. Lipid Res. 5, 600–608.

Norman, H.A., St. John, J.B., 1986. Metabolism of unsaturated monogalactosyldiacylglycerol molecular species in *Arabidopsis thaliana* reveals different sites and substrates for linolenic acid synthesis. Plant Physiol. 81, 731–736.

Norman, H.A., St. John, J.B., 1987. Differential effects of a substituted pyridazinone, BASF 13-338, on pathways of monogalactosyldiacylglycerol synthesis in Arabidopsis. Plant Physiol. 85, 684–688.

Peiser, G.D., Yang, S.F., 1985. Biochemical and physiological effects of SO_2 on nonphotosynthetic processes in plants. In: Winner, W.E., Mooney, H.A., Goldstein, R.A. (Eds.), Sulphur Dioxide and Vegetation. Stanford University Press, Stanford, CA, pp. 148–161.

Roughan, P.G., Batt, R.D., 1968. Quantitative analysis of sulfolipid (sulfoquinovosyl diglycerides) and galactolipids (monogalactosyl and digalactosyl diglycerides) in plant tissues. Anal. Biochem. 22, 74–88.

Sandmann, G., Gonzales, H.G., 1989. Peroxidative processes induced in bean leaves by fumigation with sulphur dioxide. Environ. Pollut. 56, 145–154.

Semeniuk, P., Heggestad, H.E., 1981. Differences among coleus cultivars in tolerance to ozone and sulfur dioxide. J. Hered. 72, 459–460.

Semeniuk, P., Stewart, R.N., 1979. Comparative sensitivity of cultivars of coleus to increased UV-B radiation. J. Am. Soc. Hort. Sci. 104, 471–474.

Smith, L.A., Norman, H.A., Cho, S.H., Thompson Jr., G.A., 1985. Isolation and quantitative analysis of phosphatidylglycerol and glycolipid molecular species using reverse phase high performance liquid chromatography with flame ionization detection. J. Chromatogr. 346, 291–300.

Terry, P.H., Krizek, D.T., Mirecki, R.M., 1988. Genotype variation in coleus in the ability to accumulate abscisic acid in response to water deficit. Physiol. Plant 72, 441–449.

Unsworth, M.H., Ormrod, D.P. (Eds.), 1982. Effects of Gaseous Air Pollution in Agriculture and Horticulture. Butterworths, London.

PERGAMON

Phytochemistry 58 (2001) 269–276

PHYTOCHEMISTRY

www.elsevier.com/locate/phytochem

Macrocyclic trichothecenes are undetectable in kudzu (*Pueraria montana*) plants treated with a high-producing isolate of *Myrothecium verrucaria*

H.K. Abbas[a,*], H. Tak[b], C.D. Boyette[a], W.T. Shier[a,c], B.B. Jarvis[b]

[a]*US Department of Agriculture, Agricultural Research Service, Southern Weed Science Research Unit, Stoneville, MS 38776, USA*
[b]*Department of Chemistry and Biochemistry, University of Maryland, College Park, MD 20748, USA*
[c]*College of Pharmacy, University of Minnesota, Minneapolis, MN 55455, USA*

Received 30 November 2000; received in revised form 5 April 2001

Abstract

Myrothecium verrucaria was found to be an effective pathogen against kudzu grown in the greenhouse and the field. *M. verrucaria* produced large amounts of macrocyclic trichothecenes when cultured on solid rice medium, including epiroridin E (16.8 mg/g crude extract), epiisororidin E (1 mg/g), roridin E (8.7 mg/g), roridin H (31.3 mg/g), trichoverrin A (0.6 mg/g), trichoverrin B (0.1 mg/g), verrucarin A (37.4 mg/g), and verrucarin J (2.2 mg/g). Most of these toxins were also isolated from *M. verrucaria* spores and mycelia grown on potato dextrose agar medium, including epiroridin E (32.3 mg/g), epiisororidin E (28.6 mg/g), roridin E (0 mg/g), roridin H (60 mg/g), trichoverrin A (1.3 mg/g), trichoverrin B (1.8 mg/g), verrucarin A (13.8 mg/g), and verrucarin J (131 mg/g). When *M. verrucaria* was cultured on liquid media, the numbers but not the amounts of toxins decreased. Only epiroridin E (28.3 mg/g), epiisororidin E (29.6 mg/g), verrucarin B (195 mg/g) and verrucarin J (52.6 mg/g) were measured when the fungus was cultured on cornsteep medium. On soyflour–cornmeal broth *M. verrucaria* produced several toxins, including epiroridin E (58.1 mg/g), epiisororidin E (5.8 mg/g), verrucarin B (29.9 mg/g) and verrucarin J (32 mg/g). In contrast, no macrocyclic trichothecenes were detected by HPLC analysis of plant tissues of kudzu, sicklepod, and soybean treated with aqueous suspensions of *M. verrucaria* spores formulated with a surfactant. Chloroform–methanol extracts of kudzu leaves and stems treated with *M. verrucaria* spores were less cytotoxic to four cultured mammalian cell lines than the corresponding extracts from control plants. Purified macrocyclic trichothecenes (verrucarin A and T-2 toxin) were very cytotoxic to the same cell lines ($\leqslant 2$ ng/ml). These results show that neither intact macrocyclic trichothecenes nor toxic metabolites could be detected in plant tissues after treatment with *M. verrucaria* spores. These results argue for both safety and efficacy for the use of *M. verrucaria* in biological control of kudzu and other noxious weeds, and support proceeding to animal feeding trials for further evaluation of safety. © 2001 Elsevier Science Ltd. All rights reserved.

Keywords: Macrocyclic trichothecenes; Mycotoxins; Natural products; Kudzu (*Pueraria montana*); Mycoherbicide; *Myrothecium verrucaria*; Phytotoxins; Phytotoxicity; Cytotoxicity; Biological control

1. Introduction

Myrothecium verrucaria is a fungal pathogen that has been known to attack important crop and ornamental plants including beet, marigold, sunflower, zinnia, peanut, cotton, red clover, and potato (Cunfer et al., 1969; Walker and Tilley, 1997). *M. verrucaria* also attacks important weed plants such as redroot pigweed, cocklebur, velvetleaf, and johnsongrass (Yang and Jong, 1995a,b; Walker and Tilley, 1997). A few reports have shown the potential of various isolates of *M. verrucaria* for use in biological control of weeds (Sutton and Peng, 1993; Zhang et al., 1994). Recently, it has been reported (Boyette et al., 1999) that *M. verrucaria* is also pathogenic to kudzu (*Pueraria montana*). Kudzu is an exotic invasive vine that is responsible for massive economic and aesthetic losses every year in the southern US. Kudzu, native to eastern Asia, was introduced into the eastern and southern US in the 1800s (Beckwith and Dangerfield, 1996; Piper, 1920). It was originally promoted for

* Corresponding author. Present address: USDA-ARS, CG & PRU, P.O. Box 345, Stoneville, MS 38776, USA. Tel.: +1-662-686-5313; fax: +1-662-686-5218.

0031-9422/01/$ - see front matter © 2001 Elsevier Science Ltd. All rights reserved.
PII: S0031-9422(01)00214-X

erosion control and as an inexpensive forage for livestock (Bailey, 1944; McKee and Stephens, 1943). It is now present from Florida to New York, westward to central Oklahoma and Texas, with heavy infestations in Alabama, Georgia and Mississippi (Everest et al., 1991; US Congress, 1993). Kudzu grows up the sides of buildings, along fences and on telephone poles, and dies in the winter, leaving behind ugly, brown foliage (Miller, 1997). *M. verrucaria* has been shown in preliminary experiments to cause 90% mortality to kudzu plants in the greenhouse and the field (Boyette et al., 1999). Other weed species such as sicklepod, leafy spurge (*Euphorbia esula* L.) (Yang and Jong, 1995a) and plumeless thistle (*Carduus acanthoides* L.) (Yang and Jong, 1995b) are also susceptible to isolates of *M. verrucaria*. Fortunately, the pathogen has shown no toxic or pathogenic effects to oak, sycamore and other forestry trees (unpublished data). The potential of *M. verrucaria* spore suspensions as a bioherbicide has been limited by its broad host range, and because isolates produce macrocyclic trichothecene toxins in culture (Jarvis et al., 1985; Jarvis, 1991; Grove, 1993). The toxins include verrucarin A, B and J, and roridin A, D, E, H and J, which are known to be toxic to cultured mammalian cells as well as phytotoxic (Mortimer et al., 1971; Busam and Habermehl, 1982; Cutler and Jarvis, 1985; Jarvis et al., 1988; Schiefer et al., 1989; Jarvis, 1991). However, macrocyclic trichothecenes have not been isolated from plants infected with high toxin-producing strains of *Myrothecium* sp. (Bean et al., 1984). The present study was designed to evaluate the production of macrocyclic trichothecenes by *M. verrucaria* on a variety of culture media, and to determine the fate of these toxins in kudzu plants treated with spore suspensions of the same isolate.

2. Results and discussion

A culture of the fungus *M. verrucaria,* originally obtained from naturally infected sicklepod (*Senna obtusifolia* L.), exhibited potential application as a biocontrol agent for use against sicklepod and kudzu. Published studies (Jarvis et al., 1982; Bloem et al., 1983; Lee and Mirocha, 1984) and previous experience in this laboratory (Abbas et al., 1988) indicate that isolates of *M. verrucaria* vary widely in terms of toxin production when cultured on various media [solid, liquids, potato dextrose agar (PDA)]. Some isolates produced large numbers and quantities of toxins on solid media such as rice, whereas others produced more in liquid media. The toxin-producing capabilities of the *M. verrucaria* isolate used in this study were initially characterized with respect to its ability to produce macrocyclic trichothecene toxins on both solid and liquid media. *M. verrucaria* produced large quantities of numerous toxins when cultured on solid rice medium (Table 1). These toxins were epiroridin E, epiisororidin E, roridin E, roridin H, trichoverrin A, trichoverrin B, verrucarin A, verrucarin B, and verrucarin J. Several toxins were present at high levels in spores and mycelia of *M. verrucaria* grown on PDA, including epiroridin E, epiisororidin E, roridin H, trichoverrin A, trichoverrin B, verrucarin A, and verrucarin J (Table 1). *M. verrucaria* also produced macrocyclic trichothecenes when cultured in two different liquid media. However, fewer toxins were produced in liquid media than on solid rice substrate, or were present in spores and mycelia. The fungus produced the following four toxins in cornsteep liquor and soyflour liquid media: epiroridin E, epiisororidin E, verrucarin B and verrucarin J (see Table 1). Verrucarin A was not produced in either liquid medium.

In greenhouse experiments, the isolate of *M. verrucaria* was active in controlling kudzu in the absence of dew, using conidia suspensions formulated in 0.2% Silwet L-77 surfactant. Potted kudzu plants at the 3- to 5-true leaf stage developed disease symptomatology of *M. verrucaria* infection, including necrotic flecking, within 6 h after treatment with conidia suspensions at temperatures 28–35 °C. Disease symptoms progressed from infected leaves to necrotic stem lesions within 48 h. Based on the disease symptoms, treated kudzu plants were harvested for toxin analysis. At 24 h, infection percentages were 50% in treated trays with symptoms including wilted leaves and petioles and necrotic lesions. The roots of the same plants showed no disease symptomatology. At 72 h, infection was present in 70% of treated kudzu plants, which exhibited more pronounced disease symptoms than at 24 h, including necrotic lesions on stems, but the roots remained healthy. At 120 h, 95% of treated kudzu plants were diseased. From 168 h to 14 days, 100% of treated kudzu plants were diseased, while the roots remained healthy. All control kudzu plants for each time period remained healthy, and showed minimal or no damage from 0.2% Silwet L-77. Plants treated in the field, including kudzu, sicklepod, and soybean also showed symptoms of disease at either high or low dose treatment levels. At 72 h, low dose level (1.0×10^6 conidia/ml) plots had an infection rate from 20 to 30%, and high dose level (2.0×10^7 conidia/ml) plots were 80 to 100% infected. At 5, 7, 10, and 14 days, diseased and non-diseased tissues were taken for toxin analysis. The roots of the plants species in the field were not evaluated for disease symptoms or toxin content.

None of the plant tissues studied (leaves and stems and greenhouse plant roots) of kudzu, soybean or sicklepod contained any macrocyclic trichothecenes detectable by HPLC analysis at any time after treatment, despite their presence in the *M. verrucaria* spore and mycelia preparations used for treatment. Similarly, all kinds of tissues of each plant species (kudzu, soybean, sicklepod) were negative by HPLC analysis for other toxins examined in this study (Fig. 1). To eliminate the

possibility that toxic derivatives or metabolites were present in the tissues of treated plants, but were not detected by HPLC because their HPLC elution times differed from available standards, we examined tissue extracts for in vitro toxicity to cultured mammalian cells. The results of these studies are presented in Tables 2–4. Extracts from kudzu foliage tissues (leaves and stems) treated with fungal *M. verrucaria* at 2×10^7 conidia/ml in 0.2% Silwet L-77 generally caused less cytotoxicity to the four mammalian cell lines tested (Table 2) than extracts prepared in the same manner from untreated control tissues. Also, sicklepod and soybean foliage treated with fungal *M. verrucaria* at 2×10^7 conidia/ml in 0.2% Silwet L-77 generally caused less cytotoxicity to four cell lines tested (Tables 3 and 4) in comparison to extracts prepared in the same manner from untreated control tissues. We speculate that low levels of cytotoxicity observed in control tissues results from phytoalexins produced from progenitors during sampling and extraction, and the generally lower levels of cytotoxicity in *M. verrucaria*-treated tissues reflects prior depletion of phytoalexin progenitors in response to exposure to *M. verrucaria*. Consistent with this, the most toxic extract from *M. verrucaria*-treated kudzu tissues was obtained after 14 days recovery time following treatment (Table 2). The purified toxins verrucarin A,

Table 1
Toxin production by *Myrothecium verrucarin* grown in culture on various substrates

Toxin	Mycotoxin level (mg per gram extract)[a]						
	Solid rice media	Liquid[b]		Spores and mycelia[c]	Plant tissues[d]		
		CSL	SF		Kudzu	Sicklepod	Soybean
Epiroridin E	17	28	58	32	<0.01	<0.01	<0.01
Epiisororidin E	1.0	29.6	5.8	29	<0.01	<0.01	<0.01
Isororidin E	<0.01	<0.01	<0.01	<0.01	<0.01	<0.01	<0.01
Roridin E	8.7	<0.01	<0.01	<0.01	<0.01	<0.01	<0.01
Roridin H	31.3	<0.01	<0.01	60	<0.01	<0.01	<0.01
Trichoverrin A	0.6	<0.01	<0.01	1.3	<0.01	<0.01	<0.01
Trichoverrin B	0.1	<0.01	<0.01	1.8	<0.01	<0.01	<0.01
Verrucarin A	37.4	<0.01	<0.01	14	<0.01	<0.01	<0.01
Verrucarin B	<0.01	195	30	<0.01	<0.01	<0.01	<0.01
Verrucarin J	2.2	57	32	131	<0.01	<0.01	<0.01

[a] Limit of detection was 5 ng.
[b] CSL = cornsteep liquor; SF = soyflour–cornmeal broth.
[c] Spores (conidia) and mycelia were grown in plastic Petri dishes (9 cm inside diameter) containing Difco potato dextrose agar (PDA).
[d] Plant tissues include every part of the plant (leaves, stems, and roots) whether severely damaged or moderately damaged.

Table 2
Cytotoxicity of extracts from kudzu leaves treated with *Myrothecium verrucaria*

Kudzu extract[a] and toxin controls	% of plants infected	Harvesting time (day)	Approximate IC_{50} (mg/ml)[b]			
			H4TG	MDCK	NIH3T3	KA3IT
Control (0.2% SW)	0	1	35	35	40	20
M. verrucaria + 0.2% SW	50	1	20	15	30	15
Control (0.2% SW)	0	3	35	50	60	50
M. verrucaria + 0.2% SW	70	3	20	20	40	15
M. verrucaria + 0.2% SW	94	5	15	35	40	20
M. verrucaria + 0.2% SW	100	7	15	35	40	20
Control (0.2% SW)	0	10	15	40	75	30
M. verrucaria + 0.2% SW	100	10	20	20	40	20
M. verrucaria + 0.2% SW	100	14	7	5	10	5
Control (DMSO)	–	–	–	–	–	–
Verrucarin A	–	–	2 ng/ml	0.5 ng/ml	1.5 ng/ml	1 ng/ml
Roridin E	–	–	3.5 ng/ml	1.5 ng/ml	4 ng/ml	3.5 ng/ml
T-2 toxin	–	–	2 ng/ml	ND	ND	0.75 ng/ml

[a] SW = Silwet L-77, an organo-silicone surfactant (Union Carbide, Tarrytown, NY). Each sample was extracted with MeOH–chloroform, 1:1, v/v, dried, and redissolved in growth media containing 0.5% DMSO for cytotoxicity testing.
[b] The concentration of toxin which causes a 50% reduction in cell number after 5 days in culture. Cell lines used were H4TG, thioguanine-resistant rat hepatoma cells; MDCK, Madin-Darby canine kidney cells; NIH3T3; NIH Swiss mouse embryo fibroblasts, and KA31T, Kirsten strain of Moloney sarcoma virus-transformed 3T3 cells.

Table 3
Cytotoxicity of extracts from sicklepod treated with *Myrothecium verrucaria*

Sicklepod extract[a] and toxin controls	% of plants infected	Harvesting time (day)	Approximate IC_{50} (mg/ml)[b]			
			H4TG	MDCK	NIH3T3	KA3IT
Control (0.2% SW)	0	1	0.1	0.35	0.2	0.2
M. verrucaria + 0.2% SW	50	1	0.05	0.5	0.35	0.35
Control (0.2% SW)	0	3	0.1	0.35	0.2	0.2
M. verrucaria + 0.2% SW	70	3	0.05	0.5	0.35	0.35
M. verrucaria + 0.2% SW	95	5	0.05	0.35	0.35	0.35
M. verrucaria + 0.2% SW	100	7	0.15	0.75	0.5	0.2
Control (0.2% SW)	0	10	0.2	0.75	0.5	0.5
M. verrucaria + 0.2% SW	100	10	0.1	0.5	0.2	0.2
M. verrucaria + 0.2% SW	100	14	ND	ND	ND	ND
Control (DMSO)	–	–	–	–	–	–
Verrucarin A	–	–	2 ng/ml	1 ng/ml	2 ng/ml	1 ng/ml
Roridin E	–	–	4 ng/ml	2 ng/ml	4 ng/ml	4 ng/ml
T-2 toxin	–	–	2 ng/ml	ND	ND	1 ng/ml

[a] SW = Silwet L-77, an organo-silicone surfactant (Union Carbide, Tarrytown, NY). Each sample was extracted with MeOH–chloroform, 1:1, v/v, dried, and redissolved in growth media containing 0.5% DMSO for cytotoxicity testing.

[b] The concentration of toxin which causes a 50% reduction in cell number after 5 days in culture. Cell lines used were H4TG, thioguanine-resistant rat hepatoma cells; MDCK, Madin-Darby canine kidney cells; NIH3T3; NIH Swiss mouse embryo fibroblasts, and KA31T, Kirsten strain of Moloney sarcoma virus-transformed 3T3 cells.

Table 4
Cytotoxicity of extracts from soybean treated with *Myrothecium verrucaria*

Soybean extract[a] and toxin controls	% of plants infected	Harvesting time (day)	Approximate IC_{50} (mg/ml)[b]			
			H4TG	MDCK	NIH3T3	KA3IT
Control (0.2% SW)	0	1	0.2	1.0	0.75	0.75
M. verrucaria + 0.2% SW	50	1	0.5	1.5	1.0	0.5
Control (0.2% SW)	0	3	0.5	1.0	0.75	0.5
M. verrucaria + 0.2% SW	70	3	0.05	0.07	0.07	0.15
M. verrucaria + 0.2% SW	95	5	0.2	0.05	0.1	0.07
M. verrucaria + 0.2% SW	100	7	0.1	0.07	0.15	0.07
Control (0.2% SW)	0	10	0.2	1.5	0.5	1.0
M. verrucaria + 0.2% SW	100	10	0.05	0.01	0.04	0.02
M. verrucaria + 0.2% SW	100	14	0.2	0.15	0.2	0.15
Control (DMSO)	–	–	–	–	–	–
Verrucarin A	–	–	2 ng/ml	1 ng/ml	2 ng/ml	1 ng/ml
Roridin E	–	–	4 ng/ml	2 ng/ml	4 ng/ml	4 ng/ml
T-2 toxin	–	–	2 ng/ml	ND	ND	1 ng/ml

[a] SW = Silwet L-77, an organo-silicone surfactant (Union Carbide, Tarrytown, NY). Each sample was extracted with MeOH–chloroform, 1:1, v/v, dried, and redissolved in growth media containing 0.5% DMSO for cytotoxicity testing.

[b] The concentration of toxin which causes a 50% reduction in cell number after 5 days in culture. Cell lines used were H4TG, thioguanine-resistant rat hepatoma cells; MDCK, Madin-Darby canine kidney cells; NIH3T3; NIH Swiss mouse embryo fibroblasts, and KA31T, Kirsten strain of Moloney sarcoma virus-transformed 3T3 cells.

roridin E and T-2 toxin were very cytotoxic to the four cell lines used (Table 2). The IC_{50} of these toxins were $\leqslant 4$ ng/ml while the IC_{50} of kudzu plant tissues extracted with C:M, 1:1 was $\geqslant 5$ mg/ml.

These results demonstrate that *M. verrucaria* is an effective pathogen against kudzu and sicklepod, causing disease on all kudzu plants after 96 h. Therefore, *M. verrucaria* shows good potential for control of these noxious weeds. The isolate of *M. verrucaria* used in this study was found to produce large amounts of macrocyclic trichothecenes in culture. These toxins, specifically verrucarin A and roridin E, have proven to be very toxic to plants and animals (Cutler and Jarvis, 1985; Bean et al., 1988; Jarvis and Acierto, 1989). Toxin production has caused concern about the safety for animals and humans of using *M. verrucaria* in biological control. Although the amounts and numbers of toxins produced varied with substrate, none of these toxins were detected in the tissues of treated kudzu plants. To ensure that kudzu was not unique in this, soybean and sicklepod, which are in the same family (Leguminosae) as kudzu, were also studied. No toxins were isolated from *M. verrucaria*-treated sicklepod or soybean. These results are in agreement with previous reports (Bean et

al., 1984; Kuti et al., 1987) on watermelon, muskmelon and cucumber (all from the family "Cucurbitaceae") infected with *Myrothecium* species. These investigators were also unable to detect macrocyclic trichothecenes in infected tissues. However, there are numerous reports of macrocyclic trichothecenes being produced by fungal endophytes in shrubs known as *Baccharis* spp. (Busam and Habermehl, 1982; Jarvis, 1992; Jarvis et al., 1996; Rizzo et al., 1997). These toxins may have been made by the plants using genes for trichothecene biosynthetic enzymes acquired from fungi, but it is also possible that the toxins may be metabolites of trichothecenes produced by contaminating fungi. The failure to find in treated tissue either intact trichothecenes by HPLC, or toxic metabolites by cytotoxicity tests in the present study supports the case for using *M. verrucaria* as a biological control agent. The results support animal feeding trials as the appropriate next step in evaluating safety. Additional studies are needed to quantitate the extent of colonization of kudzu tissues after treatment with *M. verrucaria* conidia preparations. The results obtained to date provide evidence for both safety and efficacy for the use of *M. verrucaria* in biological control of kudzu and other noxious weeds.

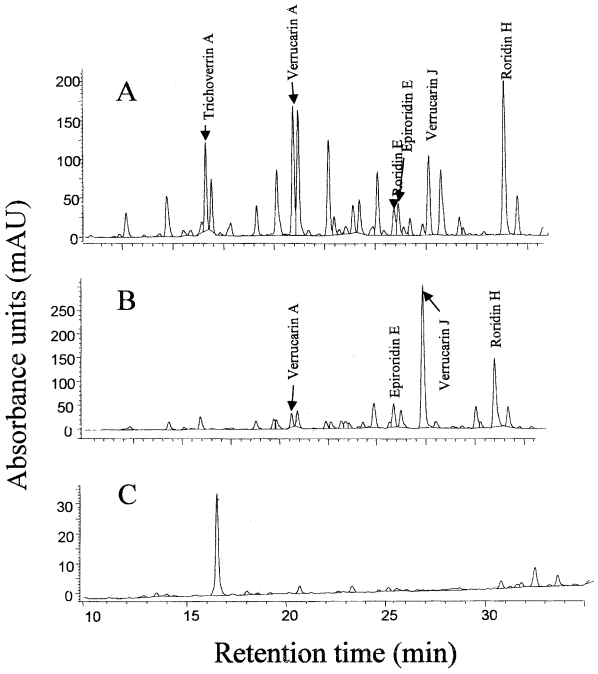

Fig. 1. HPLC chromatographs of extracts from (A) rice culture medium infected with *Myrothecium verrucaria* spores, (B) rice culture medium infected with *M. verrucaria* fungal mycelia, and (C) kudzu plant tissue treated with *M. verrucaria* conidia. Note the presence of various macrocyclic trichothecenes in the extracts of moldy rice culture medium infected with spores or mycelia. No toxins were detected in the extract of kudzu tissues treated with this fungus.

3. Experimental

3.1. Mycotoxin production on rice culture media

Converted long-grain enriched parboiled rice (200 g; Uncle Ben's Inc., Greenville, MS) was mixed with 120 ml of distilled water in one liter flasks, and allowed to stand about 1 h until the water was absorbed. The flasks were shaken to uniformly distribute the moist substrates, closed with light cotton stoppers and autoclaved 60 min at 15 lb pressure. Immediately after autoclaving, the flasks were shaken vigorously to break up clumps. They were allowed to stand 24 h and the autoclaving and shaking process was repeated. The flasks were inoculated when cool with *M. verrucaria* (International Mycological Institute, Bakeham Lane, Egham, Surrey, UK; holding IMI No. 361690) maintained in stock cultures on sterile soil or silica gel in small test tubes. The flasks were incubated for 3 to 4 weeks either in the laboratory at 22–24°C, or in an incubator at 28°C with 12 h light intervals. Daily shaking for the first few days was used to enable the fungus to penetrate the rice uniformly. The fungus-infested rice was removed from the flasks and air dried on a screen-bottomed tray. Five grams of mouldy rice were ground to the consistency of flour using a Stein Mill grinder (Fred Stein Laboratories, Inc., Atchison, KS), and samples taken for chemical analyses (Abbas et al., 1984; 1988). All operations with fungal cultures and spores were carried out in a vented hood to prevent exposure to investigators and facilities.

3.2. Mycotoxin standards

Verrucarin A and J, roridin E and isororidin E were purchased in analytically pure form from Sigma Chemical Co., St Louis, MO. An additional 55 mycotoxin standards were prepared in the laboratory of B.B. Jarvis, Department of Biochemistry and Chemistry, University of Maryland, College Park, MD (Jarvis and Wang, 1999).

3.3. Extraction and determination of mycotoxins

Dried, ground moldy rice cultures (5 g) of *M. verrucaria* were extracted with methanol:chloroform, 1:1 (v/v) at a ratio of 1 g mouldy rice to 5 ml extracting solvent, using ultrasound agitation for 1 h, or homogenization for 3 to 5 min with a Brinkmann Polytron PT 3000 at 27.8×1000 rpm. The flask and contents were allowed to sit overnight (4°C) before filtration and concentration of the organic extract. The concentrated organic extract was dissolved in a minimum amount of methylene chloride and applied to a polyethyleneimine column (Jarvis, 1992). Elution of the column with methylene chloride gave fractions which were analyzed by reversed phase HPLC on a HP-1100 system using an 150×2.0 mm, 3 μ C-18 column and a UV–vis diode array detector at 260

nm (Hinkley and Jarvis, 2000). Samples (5 μl) were eluted with gradients of 25 to 100% acetonitrile in water as the mobile phase. Peak assignments were made by a combination of retention times and UV spectra compared to purified trichothecene standards. Extraction efficiencies of 90–95% were obtained in plant tissues for the various macrocyclic trichothecenes.

3.4. Mycotoxin production in liquid media

This study evaluated *M. verrucaria* fermentation in two liquid media, cornsteep medium according to the method of Jarvis et al. (1986), and cornmeal–soyflour medium according to the method of Walker and Riley (1982). Fermentation in cornsteep medium was carried out in two stages. Five inoculum cultures were prepared in Erlenmeyer flasks (500 ml) each containing 100 ml of cornsteep medium (15.6 g of glucose and 10 ml of cornsteep liquor per l water) autoclaved at 121°C for 20 min. The flasks were inoculated with one or two 1 cm^2 pieces of PDA agar (Difco) medium from plates carrying *M. verrucaria* mycelium and conidia (spores), and shaken at 150 rpm at 28°C for 3 days to produce the inoculum for the production phase. Five Erlenmeyer flasks (4 l) each containing 1 l of production medium (1.0 g $NH_4H_2PO_4$, 3.0 g K_2HPO_4, 5.0 g NaCl, 0.2 g $MgSO_4$–$7H_2O$, 40 g sucrose and 10 g glycerol per l of water) were autoclaved for 30 min at 121°C, and one inoculum culture was poured into each flask. The cultures were incubated with shaking (150 rpm, 28°C) for 7 days, and the mycelium and the fermentation beer harvested separately by centrifuging for 10 min at 10,000 rpm and filtering through glass wool. The mycelium was soaked in acetone three times and homogenized at high speed using Polytron PT 3000, for 3 to 5 min and centrifuged. All the acetone extracts were combined and the acetone removed on a rotary evaporator. The aqueous concentrate was extracted with ethyl acetate three times. Ethyl acetate extracts were combined and dried over Na_2SO_4, filtered and evaporated. The fermentation beer was extracted with ethyl acetate. The ethyl acetate extract was dried over Na_2SO_4, filtered and evaporated. The material obtained from the mycelium and the fermentation beer were combined to give 9 g of total extract. The toxin content of these extracts was determined by HPLC as described above.

The second medium consisted of cornmeal (0.44 g), soyflour (3.75 g), sucrose (7.5 g) and calcium carbonate (0.75 g) in 600 ml of deionized water. Aliquots of 50 ml were placed in 300 ml Erlenmeyer flasks and autoclaved. The flasks were inoculated with one or two 1 cm^2 pieces of PDA agar medium from plates carrying *M. verrucaria* mycelium and conidia (spores), and incubated with shaking at 150 rpm for 7 to 10 days at 28°C. When the fungal biomass formed, the same procedure was followed for extraction and determination of toxin content as described above for cornsteep medium.

3.5. Determination of mycotoxins in fungal spores and mycelia

Spores and mycelia of *M. verrucaria* for this study were produced on Petri dishes (9 cm inside diameter) containing 20 to 25 ml PDA as described in detail previously (Abbas and Riley, 1996). After inoculation Petri dishes were incubated 12 days at 28°C with 12 h light and 12 h dark cycles. Spores and mycelia were harvested from agar surfaces using a plastic scraper and transferred to a sterile beaker. Five hundred grams (wet weight) of mycelium was obtained from 500 Petri dishes. The mycelium sample was mixed well, and an aliquot of 5 g was taken for extraction and mycotoxin analysis by the same procedure as described above for mycelium from liquid cultures.

3.6. Determination of mycotoxin from infected plant tissues

Kudzu (*Pueraria montana*), sicklepod [*Senna obtusifolia* (L.) Irwin and Barneby], and soybean [*Glycine max* (L.) Merr.] were used in this study. Kudzu seedlings (2 to 3 true leaf stage) were grown from seed (Adams-Briscoe Seed Co., Jackson, GA 30233) in 30×60 cm plastic trays containing a 1:1 commercial potting mix (Jiffy mix®): soil combination supplemented with a controlled-release 13:13:13 (N:P:K) fertilizer. Sicklepod and soybean seedlings were grown from seed (collected locally, Stoneville, MS 38776) in the field during the growing season. All plants were kept outdoors. Seedlings at the 1st to 3rd leaf growth stage were inoculated by aerosol sprayers until foliage was fully wetted with 2×10^7 conidia/ml suspended in 0.2% aqueous Silwet L-77 surfactant. Control (non-infected) groups received 0.2% Silwet L-77 surfactant only. Following inoculation, infected and non-infected plants were sampled at the following times: 0, 1, 2, 3, 4, 5, 7, 10, and 14 days. Each sample was divided based on disease symptoms into two groups: (i) severely infected (total necrosis, brown dry tissues, dead) and (ii) moderately or partially infected tissue (minimal necrosis, green, healthy tissue to partially-infected leaves). Also, root samples were kept separate from the above-ground samples for each treatment and species. Root samples were washed with water to remove dirt before storage inside plastic bags. Samples were brought to the laboratory and each sample was cut into small pieces prior to processing for analyses. Half of each sample was frozen in liquid nitrogen and lyophilized. The other halves of the samples were put into paper bags and dried in an oven at 70–75 °C for 72 h. Each dried sample was ground to the consistency of powder using a Stein Mill grinder before analysis. All samples were stored at −20 °C. Aliquots of 5 g were taken for mycotoxin analyses using the same procedure as described above.

3.7. Cytotoxicity assay

The mammalian permanent cell line 3T3 Swiss mouse fibroblasts (strain NIH3T3) was obtained from S. Aaronson, National Cancer Institute, Bethesda, MD, USA, and KA31T was obtained from R. Pollack, Columbia University, New York, NY. Rat hepatoma cell line H4TG and dog kidney cell line MDCK were purchased from the American Type Culture Collection, Rockville, MD, USA. The cells were cultured and the cytotoxicity assays were conducted as described previously (Abbas et al., 1995; Shier et al., 1991).

Acknowledgements

The authors thank Bobbie J. Johnson, Jimmey R. McAlpine, and Mary V. Duke, USDA-ARS, Stoneville, MS, for their valuable technical assistance.

References

Abbas, H.K., Tanaka, T., Shier, W.T., 1995. Biological activities of synthetic analogues of *Alternaria alternata* toxin (AAL-toxin) and fumonisin in plant and mammalian cell cultures. Phytochemistry 40, 1681–1689.

Abbas, H.K., Mirocha, C.J., Meronuk, R.A., Pokorny, J.D., Gould, S.L., Kommedahl, T., 1988. Mycotoxins and *Fusarium* species associated with infected ears of corn in Minnesota. Appl. Environ. Microbiol. 54, 1930–1933.

Abbas, H.K., Mirocha, C.J., Shier, W.T., 1984. Mycotoxins produced from fungi isolated from foodstuffs and soil: comparison of toxicity in fibroblasts and rat feeding test. Appl. Environ. Microbiol. 48, 654–661.

Abbas, H.K., Riley, R.T., 1996. The presence and phytotoxicity of fumonisins and AAL-toxin in *Alternaria alternata*. Toxicon 34, 133–136.

Bailey, R.Y., 1944. Kudzu for erosion control in the Southeast. USDA Farm Bull., 1840, 31 pp.

Bean, G.A., Fermando, T., Jarvis, B.B., Bruton, B., 1984. The isolation and identification of the trichothecene metabolites from a plant pathogenic strain of *Myrothecium roridum*. J. Nat. Prod. 47, 727–729.

Bean, G.A., Kuti, J.O. and Ng, N.J., 1988. Trichothecenes and their possible role in pathogenicity of *Myrothecium roridium*. In: Aibara, K., Kumagai, S., Ohtsubo, K., Yoshizawa, T., (Eds.), Proc. Jap. Assoc. Mycotox, Special Issue No. 1, Tokyo, pp. 204–207.

Beckwith, J.R., Dangerfield, C.W., 1996. Forest resources one-lines. Extn. For. Res. Unit, Bull. For., 96-040, Georgia Coop. Extn. Serv., Univ. GA Press, Athens, GA.

Bloem, R.J., Smitka, T.A., Bunge, R.H., French, J.C., Mazzola, E.P., 1983. Roridin L-2, a new trichothecene. Tetrahedron Lett. 24, 249–252.

Boyette, C.D., Walker, H.L., Abbas, H.K. 1999. Biological control of kudzu (*Pueraria montana*) with an endemic fungal pathogen. Proc. South. Weed Sci. Soc. 52, 237.

Busam, L., Habermehl, G.G., 1999. Accumulation of mycotoxins by *Baccharis coridifolia*: a reason for livestock poisoning. Naturwissenschaften 69, 392–393.

Cunfer, B.M., Graham, J.H., Lukezic, F.L., 1969. Studies on the biology of *Myrothecium roridium* and *M. verrucaria* pathogenic on red clover. Phytopathology 59, 1306–1309.

Cutler, H.G., Jarvis, B.B., 1985. Preliminary observations on the effects of macrocyclic trichothecenes on plant growth. Environ. and Experiment. Botany 25, 115–128.

Everest, J.W., Miller, J.H., Ball, D.M., Patterson, M.G., 1991. Kudzu in Alabama, Circ. ANR-65. Ala. Coop. Ext. Serv., 8 pp.

Grove, J.F., 1993. Macrocyclic trichothecenes. Natural Prod. Rep., pp. 429–448.

Hinkley, S.F., Jarvis, B.B., 2000. Method for *Stachybotrys* toxins. In: Trucksess, M.W., Pohland, A.E. (Eds.), Methods in Molecular Biology: The Mycotoxin Protocols, Vol. 157. Humana Press, Totowa, NJ, pp. 173–194.

Jarvis, B.B., 1991. Macrocyclic trichothecenes. In: Sharma, R.P., Salunkhe, D.K. (Eds.), Mycoyoxins and Phytoalexins in Human and Animal Health. CRC Press, Boca Raton, FL, pp. 261–421.

Jarvis, B.B., 1992. Macrocyclic trichothecenes from Brazilian *Baccharis* species: from microanalysis to large scale isolation. Phytochem. Anal. 3, 241–249.

Jarvis, B.B., Acierto, A.M., 1989. Anticancer properties of trichothecenes. In: Beasley, V.R. (Ed.), Trichothecene Mycotoxicosis: Pathophysiologic Effects, Vol. 1. CRC Press, Boca Raton, FL, pp. 73–105.

Jarvis, B.B., Comezoglu, F.T., Lee, Y-W., Flippen-Anderson, J.L., Gilardi, R.D., d George, C.F., 1986. Novel macrocyclic trichothecenes from *Myrothecium roridum*. Bull. Soc. Chim. Belg. 95, 681–697.

Jarvis, B.B., Kuti, J.O., Bean, G.A., 1988. Phytotoxicity of macrocylic trichothecenes toward *Baccharis* cell lines. Proc. Jpn Assoc. Mycotoxicol. 1, 199–202.

Jarvis, B.B., Pavanasasivam, G.P., Bean, G.A., 1985. Mycotoxin production from *Myrothecium* species. In: Lacey, J. (Ed.), Trichochecenes and Other Mycotoxins. John Wiley and Sons Ltd, New York, pp. 221–231.

Jarvis, B.B., Stahly, G.P., Pavanasasivam, P., Midiwo, J.O., DeSilva, T., Holmlund, C.E., Mazzola, E.P., Geohegan Jr., R.F., 1982. Isolation and characterization of the trichoverroids and new roridins and verrucarins. J. Org. Chem. 47, 1117–1124.

Jarvis, B.B., Wang, S., Cox, C., Rao, M.M., Philip, V., Varaschin, M.S., Barros, C.S., 1996. Brazilian *Baccharis* toxins: livestock poisoning and the isolation of macrocyclic trichothecene glucosides. Natural Toxins 4, 8–71.

Jarvis, B.B., Wang, S.J., 1999. Stereochemistry of the roridins. Diastereomers of roridin E. J. Nat. Prod. 62, 1284–1289.

Kuti, J.O., Ng, T.J., Bean, G.A., 1987. Reactions of muskmelon cultigens to *Myrothecium roridum*. Hort. Sci. 22, 635–637.

Lee, Y-W., Mirocha, C.J., 1984. Production of nivalenol and fusarenone-X by *Fusarium roseum* Fn-2B on a rice substrate. Appl. Environ. Microbiol. 48, 857–858.

McKee, R., Stephens, J.L., 1943. Kudzu as a farm crop. USDA Bull. No. 1923, 13 pp.

Miller, J.H., 1997. Kudzu eradication and management. In: Hoots, D., Baidwin, J. (Eds.), Kudzu: The Vine to Love or Hate. Suntop Press, Virginia Beach, VA, pp. 137–149.

Mortimer, P.H., Campbell, J., DiMenna, M.E., White, E.P., 1971. Experimental myrotheciotoxicoses and poisoning in ruminants by verrucarin A and roridin A. Res. Vet. Sci. 12, 508–515.

Piper, C.V. 1920. Kudzu. USDA Dept. Circular, 89, 7 pp.

Rizzo, I., Varsavky, E., Haidukowski, M., Frade, H., 1997. Macrocyclic trichothecenes in *Baccharis-Coridifolia* plants and endophytes and *Baccharis-Artemisioides* Plants. Toxicon. 35, 753–757.

Schiefer, H.B., Hancock, D.S., Jarvis, B.B., 1989. Toxicology of novel macrocyclic trichothecenes, baccharinoid B4, myrotoxin B and roritoxin B. J. Vet. Med. A. 36, 152–160.

Shier, W.T., Abbas, H.K., Mirocha, C.J., 1991. Toxicity of the mycotoxins fumonisins B1 and B2 and *Alternaria alternata* f. sp. *lycopersici* toxin (AAL) in cultured mammalian cells. Mycopathologica 116, 97–104.

Sutton, J.C., Peng, G., 1993. Biocontrol of *Botrytis cinerea* in strawberry leaves. Phytopathology 83, 615–621.

US Congress, Office Technol. Assess., 1993. Harmful, non-indigenous species in the United States. OTA-F-565, 391 pp.

Walker, H.L., Riley, J.A., 1982. Evaluation of *Alternaria cassiae* for the biocontrol of sicklepod (*Cassia obtusifoloa*). Weed Science 30, 651–654.

Walker, H.L., Tilley, A.M., 1997. Evaluation of an isolate of *Myrothecium verrucaria* from sicklepod (*senna obtusifolia*) as a potential mycoherbicide agent. Biological Control 10, 104–112.

Yang, S.-M., Jong, S.C., 1995a. Host range determination of *Myrothecium verrucaria* isolated from leafy spurge. Plant Disease 79, 994–997.

Yang, S.-M., Jong, S.C., 1995b. Factors infuencing pathogenicity of *Myrothecium verrucaria* isolated from *Euphorbia esula* on species of *Euphorbia*. Plant Disease 79, 998–1002.

Zhang, P.G., Sutton, J.C., Hopkin, A.A., 1994. Evaluation of micro-organisms for biocontrol of *Botrytis cinerea* in container-grown black spruce seedlings. Can. J. For. Res. 24, 1312–1316.

PERGAMON

Phytochemistry 58 (2001) 277–280

PHYTOCHEMISTRY

www.elsevier.com/locate/phytochem

Effects of water-deficit on lipids of safflower aerial parts

Ibtissem Hamrouni[a], Hammadi Ben Salah[b], Brahim Marzouk[a,*]

[a]*INRST, Laboratoire d'Adaptation et d'Amélioration des Plantes, BP 95 2050 Hammam-Lif, Tunisia*
[b]*Laboratoire des Cultures Industrielles, INRAT 45, Rue Hedy Karray 2080 Ariana, Tunisia*

Received 8 September 2000; received in revised form 7 February 2001

Abstract

Three-week-old plants of safflower (*Carthamus tinctorius* L.) were subjected to a water-deficit stress. The lipid composition of the shoot parts of both control (well-watered) and water stressed plants was analyzed. Experimental data revealed that moderate stress induced an increase in total lipid content within all lipidic classes. However, severe water-deficit induced a sharp decrease in the total lipid content and specially in polar lipids, particularly in phosphatidylethanolamine, phosphatidylcholine, monogalactosyl-diacylglycerol and digalactosyl-diacylglycerol. Also, the content of neutral lipids was increased. Concerning the fatty acid composition, water-deficit induced a decrease in their degree of unsaturation expressed by a reduction in the proportions of linolenic (18:3) and linoleic (18:2) acids and most of lipidic classes. © 2001 Elsevier Science Ltd. All rights reserved.

Keywords: Carthamus tinctorius L.; Compositeae; Safflower; Drought-stress; Fatty acids; Lipids

1. Introduction

Among the different environmental stresses, drought is the constraint which induces a highly negative effect on crop production. When subjected to this constraint, plants manifest a wide range of behaviors varying from great sensitivity to high tolerance.

Belhassen et al. (1995) reported three adaptive strategies used by plants in response to drought:

- escaping by reducing their life cycle to a short period,
- avoidance of dehydration which allows plants to maintain a high water potential,
- tolerance of dehydration by establishing a wide range of physiological and biochemical changes allowing the plant to resist a low water potential (mechanical resistance, membrane degradation mechanisms etc.).

Previous workers reported that tolerance of plants to environmental stresses induced a variation in their glycerolipidic composition which could result in a decrease or even of an inhibition of the biosynthesis of many lipidic classes and/or an acceleration of their degradation (Stuiver et al., 1981; Hegazy and Lösel, 1992; Selstam et al., 1992; Navari-Izzo et al., 1993; Aid et al., 1995). Regarding drought, many studies showed that this stress could induce serious alterations of phospholipid and galactolipid contents on one hand and an increase of the neutral lipid content on the other hand (Navari-Izzo et al., 1989). Also, it was reported that water deficit could induce a reduction in the level of free sterols in corn plants (Quartacci et al., 1995). Similar results were found in rape roots (Svenningson and Liljenberg, 1986). In addition, it was reported that water deficiency leads to a decrease of the degree of fatty acids unsaturation explained by the fact that drought inhibits the biosynthesis of polyunsaturated fatty acids and desaturase activities (Pham-Thi et al., 1985).

The aim of the present work was to study the effect of water deficit on the glycerolipids of safflower (*Carthamus tinctorius* L.) shoot parts.

2. Results

2.1. Effect of water deficit on fatty acids and on total lipids

Safflower (*Carthamus tinctorius* L.) is a plant which uses the "eukaryotic" desaturation pathway. Therefore, the fatty acid composition of the shoot part lipids was

* Corresponding author. Fax: +216-1-430-934.
E-mail address: brahim.marzouk@inrst.rnrt.tn (B. Marzouk)

0031-9422/01/$ - see front matter © 2001 Elsevier Science Ltd. All rights reserved.
PII: S0031-9422(01)00210-2

Table 1
Effect of water-deficit on total fatty acid composition of safflower aerial parts[a]

Treatment[b]	% Of total fatty acids					
	16:0	16:1	18:0	18:1	18:2	18:3
C	14.6±1.6	0.7±0.1	2.0±0.3	4.9±0.6	23.2±2.4	54.3±3.5
MS	14.7±2.0	0.6±0.2	2.6±0.6	9.0±0.4	22.6±3.7	50.4±2.6
SS	28.4±2.4	0.3±0.1	20.4±1.3	7.0±0.6	12.9±1.7	30.8±1.8

[a] Results are given as % of total fatty acids. Values are means of six plants±S.D.
[b] C, control; MS, mild stress; SS, severe stress.

characterized by an appreciable content of linoleic acid (18:2) at 23.2% of the total fatty acids. In addition, the other main fatty acids were scored: 18:3 (the major component), 16:0, 16:1, 18:0, and 18:1 (Table 1).

The total fatty acid composition of safflower was affected by drought. There was an increase in the proportion of both palmitic (16:0) and stearic (18:0) acids as well as a decrease in those of linoleic (18:2) and linolenic (18:3) acids in accordance to the degree of severity of the stress (Table 1).

Based on our experimental data, it was shown that the content of total lipids of safflower aerial parts, as measured by total fatty acid content (mg g^{-1} dry wt.), increases by about 15% in mildly stressed plants, nevertheless, it declines sharply in severely stressed plants (Table 2).

2.2. Effect of water deficit on the main glycerolipids

The analysis of the main glycerolipidic components showed that the moderate water stress led to an increase of both phospholipid (PL) and galactolipid (GL) contents of 37.4% and 5.4%, respectively. However, the severe water stress induced a depressive effect for both groups. For the severe stress, the decrease reached 6.5% for PL and 49.4% for GL (Table 2).

Among the different phospholipids, the significant variation concerned the phosphatidylcholine (PC) class which showed an increase of its content for about 40.4% in mild stressed plants. For the severely stressed plants, the PC content was decreased of 22.1% in comparison to the control level (Table 2).

For the two main galactolipids of aerial parts, we observed that the digalactosyldiacylglycerol (DGDG) was the most affected by water deficit. In the case of mild stress, its content was decreased of about 23%. This decrease was more significant when the degree of water stress was increased (Table 2). For severely stressed plants, the decrease reached 70.7% compared to the control (Table 2). Likewise, for the monogalactosyldiacylglycerol (MGDG), was less affected by water deficit. In fact, at a mild stress, the MGDG content was increased for about 42%, but as soon as the water deficiency became severe, its content was sharply decreased by 21.4% compared to the control (Table 2).

Regarding the neutral lipids, their levels increased under severe water stress and reached 180% compared to the control (Table 2). This was due, mainly, to a similar increase of the triacylglycerol (TAG) content which was also increased by about 487% in the severely stressed plants (Table 2).

These results are similar to those obtained by Svenningson and Liljenberg (1986), who reported a significant decrease in total lipids, galactolipid and phospholipid contents and an increase of neutral lipids of rape roots submitted to drought treatment. In the same way, it has been shown (Hubac et al., 1989) that water deficit resulted in a large decrease in various lipidic classes (MGDG, PC and PE), while the TAG amounts increased considerably at the level of two *Lupinus albus* genotypes leaves.

2.3. Effect of water deficit on the degree of fatty acid unsaturation

The computation of the double binding index (DBI) calculated according to Rie De Vos et al. (1993) showed a decrease in these parameters for all lipidic classes and which was more pronounced in plants under severe stress. This decrease was confirmed by a

Table 2
Effect of water-deficit upon the lipid content (mg g^{-1} dry wt.) of safflower aerial parts[a]

	Control	Mild stress	Severe stress
Total lipids	16.05±2.97	20.95±3.04	12.15±1.12
Phospholipids	5.16±0.46	7.09±1.56	4.80±0.52
PC	2.41±0.36	3.37±0.59	1.87±0.17
PE	0.78±0.04	0.88±0.03	0.70±0.03
PG	0.94±0.03	1.24±0.07	0.89±0.02
Galactolipids	8.71±0.82	9.18±0.41	4.41±2.18
MGDG	3.78±0.33	5.38±0.58	2.97±0.20
DGDG	4.92±0.38	3.80±0.33	1.44±0.28
Neutral lipids	2.47±0.75	6.14±0.89	6.92±0.90
TAG	0.76±0.12	2.14±0.17	4.46±0.38

[a] Results are means of six plants ±S.D.

significant reduction in the rates of 18:3 and 18:2 in all lipidic classes in parallel with an increase in both of 16:0 and 18:0 with extending stress severity (Table 3). Overall, these results showed that water stress tends to reduce the degree of unsaturation of safflower aerial part lipids. Seqqat Dakhma et al. (1995) have also reported a decrease in the unsaturated lipids of rape leaves subjected to water deficit.

3. Discussion

Severe water deficit induced a large decline in the levels of total lipids in the aerial parts of safflower. The amounts of galactolipids (MGDG and DGDG) and phospholipids (PC, PG and PE) which are the major lipidic classes present, decreased significantly in response to water deficit (Table 2). Such results are in agreement with previous works (Pham, Thi et al., 1985-1992; Quartacci et al., 1995).

The decrease in galactolipids (main chloroplastic lipids) indicated that water stress could affect the photosynthesis, since the structure of chloroplastic membranes could be affected.

The reduction in PC under drought conditions was explained by Thomas et al. (1982) by the fact that water stress stimulates the mobilization of choline for the biosynthesis of glycine-betaine, an osmoregulative substance elaborated by stressed corn plants leaves.

The increase in polar lipids of moderately stressed plants indicates that a mild water deficit activates the biosynthesis of new membranes.

Fatty acid composition of the main lipids of safflower aerial parts was also affected by water deficit. The major variation consisted in a decrease of the unsaturated acids (18:2 and 18:3) in a favor of an increase in saturated ones (16:0 and 18:0). These results are in agreement with those obtained by Pham-Thi, et al. (1985) in cotton leaves submitted to water stress.

The decrease in the level of polar lipids is accompanied by an increase in the neutral lipids, particularly in triacylglycerols of safflower aerial parts subjected to drought conditions. Triacylglycerol accumulation have been previously reported in two *Lupinus albus* genotypes submitted to water deficit (Hubac, et al., 1989).

Overall, tolerance of safflower towards drought is expressed by structural modifications; which allow the plants to adjust their membranous fluidity by not only an appropriate rearrangement of their glycerolipids but also by an adjustment of their unsaturated fatty acid composition.

4. Experimental

4.1. Plant material

Safflower (*Carthamus tinctorius* L.) plants were cultivated in clay pots (20 cm diameter) filled by commercial standard compost and kept in a greenhouse under controlled conditions: 14 h day length at 26–30°, 10 h night at 8–12°, relative humidity 60%. Plants were irrigated 3× per week and used for experiment when they were three weeks old.

Table 3
Fatty acid composition and DBI variation of different glycerolipids from safflower aerial parts after water-deficit stress

		% Of total fatty acids						
Lipid	Treatment	16:0	16:1	18:0	18:1	18:2	18:3	DBI
MGDG	C	6.5±0.6	0.2±0.1	1.5±0.7	13.6±0.9	11.0±0.6	67.2±3.8	2.37±0.10
	MS	13.0±1.2	2.8±0.5	3.6±0.5	19.5±2.2	11.7±0.8	49.4±3.2	1.93±0.10
	SS	17.7±2.7	1.0±0.3	4.1±0.5	39.0±3.2	17.3±1.0	20.9±1.8	1.37±0.06
DGDG	C	21.9±2.0		5.5±0.6	4.1±0.5	15.3±1.1	53.0±2.6	1.93±0.10
	MS	23.3±1.9		3.5±0.8	22.4±3.6	14.7±1.0	36.0±2.1	1.59±0.07
	SS	29.2±3.5	0.4±0.1	7.8±0.9	37.4±1.7	13.6±0.9	11.5±1.5	0.99±0.02
PC	C	27.8±3.4		1.1±0.3	3.9±0.5	38.6±1.9	28.6±2.6	1.66±0.10
	MS	39.1±2.4		1.9±0.2	5.0±0.4	31.4±2.2	22.6±2.4	1.35±0.20
	SS	70.2±3.0		6.9±1.0	7.7±0.4	12.2±1.7	3.0±0.5	0.40±0.10
PG	C	16.2±1.8	41.6±3.4	1.7±0.6	8.6±0.7	18.7±1.0	13.0±0.6	1.26±0.06
	MS	26.6±1.0	29.9±2.0	4.2±0.4	18.0±1.1	11.5±1.4	9.7±1.0	1.00±0.06
	SS	33.5±4.6	27.3±1.0	14.0±1.7	11.6±0.7	3.6±0.6	9.9±0.8	0.75±0.03
PE	C	30.0±2.1		1.5±0.4	5.2±0.9	40.5±2.0	22.7±2.4	1.54±0.04
	MS	42.9±2.8		3.5±0.9	18.1±2.6	25.8±3.2	9.6±0.9	0.98±0.03
	SS	26.7±2.4	33.3±3.3	16.0±1.2	15.6±1.2	3.9±0.5	4.4±0.4	0.69±0.04
NL	C	14.1±1.2	4.4±0.8	9.2±1.4	40.4±2.2	16.1±1.4	15.7±1.0	1.24±0.06
	MS	11.9±1.1	5.5±0.6	6.6±0.9	44.8±3.0	17.3±1.0	13.9±1.5	1.26±0.03
	SS	16.3±1.0	1.2±0.4	47.7±3.2	20.9±3.0	7.1±1.0	6.8±0.8	0.56±0.02

4.2. Drought treatments

Water treatment was started when the second leaf emerged. Water deficit was realised by withholding irrigation during different times according to the desired stress. Watering was suspended for six days for mildly stressed plants (MS, leaf water potential $\psi = -7.2$ bar) and 10 days for severely stressed ones (SS, leaf water potential $\psi = -8.8$ bar). Control plants (C, well hydrated) were irrigated twice a week and maintained a leaf water potential ($\psi = -6.7$ bar). Leaf water potentials were measured by a pressure chamber (Scholander et al., 1965). After seven weeks of treatment, a sample of six plants was used.

4.3. Lipid extraction

Plant material was fixed by boiling water to inactivate the tissue phospholipases (Benson, 1964). Total lipids were extracted by pouring the sample into a mixture of $CHCl_3$–MeOH–H_2O (1:1:1) (Bligh and Dyer, 1959). Finally, the water of fixation was added to collect the lipids which have been swept along by the fixation. After a centrifugation step at 2000 rpm during 15 min, two phases have been obtained and the chloroform phase (lower phase) containing the lipids was dried under N_2 then the residue was dissolved in a known volume of toluol–EtOH (4:1).

4.4. Lipid analysis

Polar lipids were separated by TLC on silica gel plates 60 (Merck) in a mixture of $CHCl_3$–Me_2CO–MeOH–HOAc–H_2O (1:4:2:2:1) (Lepage 1967)., Lipid spots were detected by brief exposure to I_2 vapor. The identification was made by comparison to a reference lipids and by specific stains for phospholipids and galactolipids. Fatty acids from total lipids and lipidic classes were transmethylated according to the procedure described by (Carreau and Dubacq, 1978) . Fatty acid Me esters were analyzed by FID–GC on a capillary column (30 m $\times$0.25 μm $\times$250 μm) with a stationary phase made of PEG. Carrier gas N_2, flow rate 1.5 ml min^{-1}. The analysis was performed under this temps program: oven temps isotherm at 150° for 1 min, from 150 to 200° at the rate of 15° min^{-1}, from 200 to 225° at the rate of 2° min^{-1} and isotherm at 225° during 2 min. Injector and detector temps were held, respectively, at 250 and 275°. In order to measure the amounts of fatty acids, 17:0 was added as int. standard before methylation. Calculation of fatty acid quantities was performed using a HP-Chemstation software.

References

Aid, F., Demandre, C., Kesri Ben Hassaine, G., Mazliak, P., 1995. Effects of heat shock on the molecular species of rape polar lipids. In: Kader, J.C., Mazliak, P. (Eds.), Plant Lipid Metabolism. Dordrecht, Netherlands, pp. 387–389.

Belhassen, E., This, D., Monneveux, P., 1995. L'adaptation génétique face aux contraintes de sécheresse. Cah. Agri. 4, 251.

Benson, A.A., 1964. Plant membrane lipids. Ann. Rev. Plant. Physiol. 15, 1.

Bligh, E.G., Dyer, W.J., 1959. A rapid method of total lipid extraction. Can. J. Biochem. Physiol. 37, 911.

Carreau, J.P., Dubacq, J.P., 1978. Adaptation of macroscale method to the micro-scale for fatty acid methyl transesterification of biological lipid extracts. J. Chromatogr. 151, 384.

Hegazy, H.S.O., Lösel, D., 1992. Effects of bacterial infection on plant lipid metabolism. In: Chérif, A., Ben Miled Daoud, D., Marzouk, B., Smaoui, A., Zarrouk, M., (Eds.). Metabolism, Structure and Utilization of Plant Lipids. CNP Tunisia.

Hubac, C., Guerrier, D., Ferran, J., Trémolières, A., 1989. Change of leaf lipid composition during water stress in two genotypes of *Lupinus albus* resistant or susceptible to drought. Plant. Physiol. Biochem. 27, 737.

Lepage, M., 1967. Identification and composition of turnip root lipids. Lipids 2, 244.

Navari-Izzo, F., Quartacci, M.F., Izzo, R., 1989. Lipid changes in maize seedlings in response to field water deficits. J. Exp. Bot. 40, 675.

Navari-Izzo, F., Quartacci, M.F., Melfi, D., Izzo, R., 1993. Lipid composition of plasma membranes isolated from sunflower seedlings grown under water stress. Physiol. Plant. 87, 508.

Pham-Thi, A.T., Borrel-Flood, C., Veira Da Silva, J., Justin, A.M., Mazliak, P., 1985. Effect of water stress on lipid metabolism in cotton leaves. Physiol. Plant. 24, 723.

Pham Thi, A.T., Borrel-Flood, C., Veira Da Silva, J., Justin, A.M., Mazliak, P. 1992. Water stress stimulates the degradation of polyunsaturated molecular species of *Vigna unguiculata* galactolipids. In: Chérif, A., Ben Miled Daoud, D., Marzouk, B., Smaoui, A., Zarrouk, M. (Eds.), Metabolism, Structure and Utilization of Plant Lipids. CNP Tunisia.

Quartacci, M.F., Pinzino, C., Sgherri, C.L.M., Navari-Izzo, F., 1995. Lipid composition and protein dynamics in thylakoids of two wheat cultivars differently sensitive to drought. Plant. Physiol. 108, 1991.

Rie De Vos, C.H., Ten Bookum, W.M., Voojis, R., Schat, H., Deko, L.J., 1993. Effect of copper on fatty acid composition and peroxydation of lipids in the roots of copper tolerant and sensitive *Silene cucubalus*. Plant Physiol. Biochem. 31, 151.

Scholander, P.F., Hammel, H.J., Hemmingsen, E.A., Bradstreet, E.D., 1965. Sap pressure in vascular plants. Sciences 148, 339–346.

Selstam, E., Mattsson, A., Dormling, I., Ekberg, I., 1992. Shortening of daylength induces increased fatty acid unsaturation of membrane lipid in *Picea abies*. In: Chérif, A., Ben Miled Daoud, D., Marzouk, B., Smaoui, A. Zarrouk, M. (Eds.), Metabolism, Structure and Utilization of Plant Lipids. CNP Tunisia.

Seqqat Dakhma, W., Zarrouk, M., Chérif, A., 1995. Effects of drought-stress on lipids of rape leaves. Phytochemistry 40, 1383.

Stuiver, C.E.E., Kuiper, P.J.C., Marscner, H., Kylin, A., 1981. Effects of salinity and replacement of K^+ by Na^+ on lipid composition in two sugar beet in bred lines. Physiol. Plant. 52, 77.

Svenningson, H., Liljenberg, C., 1986. Membrane lipid changes in root cells of rape (*Brassica napus*) as a function of water deficit stress. Physiol. Plant 68, 53.

Thomas, H., Giddings Jr., J., Hanson, A.D., 1982. Water stress provokes a generalized increase in phosphatidylcholine turnover in barely leaves. Planta 155, 493.

PERGAMON

Phytochemistry 58 (2001) 281–289

PHYTOCHEMISTRY

www.elsevier.com/locate/phytochem

Amino acids in seeds and seedlings of the genus *Lens*

Pascale Rozan, Yu-Haey Kuo, Fernand Lambein*

Laboratory of Physiological Chemistry, Faculty of Medicine and Health Sciences, Ghent University, Jozef Kluyskensstraat 27, B-9000 Ghent, Belgium

Received 19 June 2000; received in revised form 17 April 2001

Abstract

The amino acid content of seeds and 4-day-old seedlings were studied in five species of lentil: *Lens culinaris, L. orientalis, L. ervoides, L. nigricans* and *L. odemensis*. Free amino acid and also total protein amino acid content after HCl hydrolysis were determined by HPLC. The nonprotein UV-absorbing amino acids were determined by capillary zone electrophoresis (CZE). The content of free protein amino acids in seeds varied among species and increased dramatically after germination. Asparagine is quantitatively most important in both seed and seedling. The content of free nonprotein amino acids is variable in seeds and seedlings. γ-Hydroxyarginine, γ-hydroxyornithine, α-aminobutyric acid and taurine were found in both seeds and seedlings. Homoarginine was found in four species but not in *L. orientalis* while γ-aminobutyric acid (GABA), α-aminoadipic acid (α-aaa) and three isoxazolinone derivatives: β-(isoxazolin-5-on-2-yl)-alanine (BIA), γ-glutamyl-BIA (γ-glu-BIA) and 2-carboxymethyl-isoxazolin-5-one (CMI) were found exclusively in the seedlings. CMI was identified for the first time in lentil species. Lathyrine, β-(2-aminopyrimidine-4-yl)-alanine, which was reported to be in the seeds of some *Lathyrus* species was confirmed to be present also in the seedling of *L. culinaris* (trace amount), *L. nigricans* and *L. odemensis*. Trigonelline (*N*-methyl-nicotinic acid), a plant hormone, is present both in seeds and seedlings in different concentrations except in *L. ervoides*. The different combination of nonprotein amino acids among the species gives indication of their genetic relationship and might partly explain the varying compatibility for interspecies crossing. © 2001 Elsevier Science Ltd. All rights reserved.

Keywords: *Lens culinaris*; *Lens orientalis*; *Lens ervoides*; *Lens odemensis*; *Lens nigricans*; *Leguminosae*; Lentil seedling; Nonprotein amino acids; Isoxazolinone; Chemotaxonomy

1. Introduction

Lentil is a common grain legume known since biblical times. The seedlings are also sold as a fresh food commodity and contribute to the increasing varieties of seedlings now offered to consumers. The chemical composition of seedlings can be dramatically different from the seeds and the nutritional value of these seedlings is not well known.

The different species of the genus *Lens* (*L.*) are mainly studied to check the intra and interspecific variation in the genus. Wild lentil is potentially an important source of genetic variability for the improvement of the cultivated lentil (Ferguson and Robertson, 1999). Sharma et al. (1995) found that *L. orientalis* (Boiss.) Schmalh [present nomenclature: *L. orientalis* (Boiss.) Ponert; Ferguson (1998)] is most similar to the cultivated lentil and that *L. ervoides* (Brign.) Grande is the most divergent wild taxon, followed by *L. nigricans* (M. Bieb) Godron. Abo-Elwafa et al. (1995) found that the intraspecific variations were lower in *L. ervoides* than in cultivated lentils. *L. orientalis* is the most likely candidate as progenitor of the cultivated species (Abo-Elwafa et al., 1995; Ahmad et al., 1996). The origin of the cultivated lentil from the taxon *L. orientalis* has been proven by morphological evidence and breeding experiments. This wild form exhibits variability in many characters and is distributed over a vast area from the Middle East to central Asia (Ladizinsky, 1999). Abbo and Ladizinsky (1994) studied the hybrid embryo abortion that is an effective crossing barrier in the genus *Lens*. It divides the genus into two crossing groups: the *culinaris* and the *nigricans* groups.

L. culinaris Medik. (present nomenclature *L. culinaris* Medikus ssp *culinaris,* Ferguson 1998), the most commonly consumed lentil, has been best studied for its

* Corresponding author: Tel.: +32-9-264-92-78; fax: +32-9-233-88-31.

E-mail address: fernand.lambein@rug.ac.be (F. Lambein).

0031-9422/01/$ - see front matter © 2001 Elsevier Science Ltd. All rights reserved.
PII: S0031-9422(01)00200-X

content of nutrients such as carbohydrates (Vidal-Valverde and Frias, 1992; Frias et al., 1996) and vitamins including thiamin, riboflavin and niacin (Prodanov et al., 1997) but also for the presence of antinutritional factors such as trypsin inhibitor (Frias et al., 1995). Weder and Kahleyss (1998) isolated four trypsin-chymotrypsin inhibitors from *L. culinaris* cultivated in Syria. The content of total amino acids including protein amino acids and nonprotein amino acids in lentils is not well studied. During the development of plants important physiological changes occur involving also changes in amino acid content. As contribution to the better phytochemical and nutritional knowledge of this genus, we studied the free amino acids and total protein amino acids in five species of the genus *Lens*. Both HPLC and CZE methods were used to obtain the most accurate evaluation of the amino acids in seeds and seedlings. The nomenclature of the ILDIS database is followed for the four species accepted in this source, recent adaptations by Ferguson (1998) are given in parenthesis when appropriate. *L. odemensis* Ladizinsky is not listed in the ILDIS database and in the literature it is sometimes given the status of a subspecies of *L. culinaris*. Two recently described taxa *L. tomentosus* Ladizinsky (not listed in the ILDIS database) and *L. lamottei* Czefranova (Ferguson, 1998) were not available at the time of the experiments.

2. Results and discussion

All the following results are given in mg/g dry wt.

2.1. Free amino acid content

In non-germinated dry seeds only small amounts of free amino acids were found (Table 1). The major amino acids found in all five species were asparagine, alanine, aspartic and glutamic acids. As in most legumes the sulphur-amino acids methionine and cysteine were the limiting essential amino acids.

After 4 days of germination the content of free amino acids increased dramatically (Table 2). The seedlings were the sites of high amino acid biosynthetic activity resulting in high content of free protein amino acids (Sutcliffe and Bryant, 1977), supporting the synthesis of proteins and the development of the plant. On the other hand during the germination storage protein can undergo proteolysis and results in the increase of free amino acids (Lea and Joy, 1983).

Asparagine was quantitatively by far the most important protein amino acid found in all lentil seedlings studied (Table 2). This was also the case in other commercially available seedlings such as adzuki, kamut, chickpea, mungbean, garden pea and pintobean (Rozan et al., 1999, 2000). The highest content of asparagine was found in *L. nigricans* and the lowest in *L. culinaris* (62.24 and 18.96 mg/g dry wt, respectively).

2.2. Total amino acid content

In nongerminated seeds the total amino acid content was rather different for each species (Table 3). Asparagine and glutamine were hydrolysed to aspartic and glutamic acids respectively, the results were expressed as

Table 1
Free amino acids in the seeds of 5 lentil species (mg/g of dry wt ± S.D.)[a]

	L. culinaris	*L. ervoides*	*L. nigricans*	*L. odemensis*	*L. orientalis*
Arg	0.10±0.00	0.13±0.05	0.09±0.01	0.12±0.01	0.19±0.11
His	0.22±0.05	ND	0.20±0.01	0.17±0.02	0.08±0.07
Ile	ND[b]	0.12±0.19	0.16±0.00	0.20±0.11	Trace
Leu	ND	0.05±0.09	0.05±0.09	0.02±0.04	ND
Lys	Trace	ND	0.02±0.01	Trace	0.02±0.03
Met	ND	ND	ND	ND	ND
Cys	ND	ND	ND	ND	ND
Phe	Trace	0.12±0.07	0.03±0.01	Trace	0.06±0.07
Tyr	Trace	ND	0.05±0.00	ND	ND
Pro	0.17±0.03	0.28±0.03	0.44±0.02	0.58±0.19	0.53±0.04
Ser	ND	ND	0.02±0.00	0.11±0.09	ND
Thr	0.03±0.04	Trace	0.12±0.01	0.09±0.01	0.10±0.03
Val	Trace	0.02±0.01	0.05±0.00	0.03±0.03	Trace
Trp	ND	0.09±0.08	0.05±0.00	0.01±0.02	0.06±0.06
Ala	0.45±0.08	0.20±0.08	0.61±0.06	0.48±0.07	0.76±0.19
Asp	0.18±0.01	0.21±0.01	0.50±0.02	0.68±0.05	0.21±0.01
Asn	0.51±0.04	0.50±0.04	1.86±0.10	0.78±0.10	1.96±0.15
Glu	0.48±0.05	0.46±0.03	0.73±0.05	2.00±0.16	0.63±0.093
Gln	ND	ND	ND	0.09±0.06	ND
Gly	0.05±0.00	0.01±0.01	0.09±0.03	0.06±0.00	0.06±0.02

[a] Standard deviation (three replicates).
[b] ND = not detected.

Table 2
Free amino acids in the seedlings (4-day-old) of 5 lentil species (mg/g of dry wt±S.D.)[a]

	L. culinaris	*L. ervoides*	*L. nigricans*	*L. odemensis*	*L. orientalis*
Arg	0.94±0.03	1.12±0.08	2.44±0.13	0.77±0.03	0.87±0.08
His	0.68±0.10	1.60±1.10	0.90±0.21	0.45±0.42	1.55±0.16
Ile	2.06±0.04	0.99±0.07	3.65±0.11	2.28±0.07	1.08±0.15
Leu	2.05±0.14	0.77±0.12	2.27±0.16	1.68±0.06	0.70±0.03
Lys	0.93±0.21	0.54±0.04	3.59±0.71	1.32±0.19	0.73±0.05
Met	0.26±0.07	0.12±0.01	0.25±0.05	0.15±0.05	0.11±0.09
Cys	ND[b]	ND	ND	ND	ND
Phe	2.32±0.51	1.93±0.35	4.90±0.48	3.29±0.74	1.17±0.23
Tyr	1.10±0.09	1.35±0.15	3.03±0.30	1.44±0.16	0.19±0.01
Pro	3.24±0.01	3.64±1.83	4.42±0.30	4.91±0.14	2.55±0.25
Ser	2.64±0.11	3.10±0.35	5.63±0.35	4.02±0.14	1.97±0.20
Thr	1.18±0.03	1.15±0.22	2.22±0.28	1.31±0.38	0.72±0.14
Val	2.83±0.45	1.86±0.36	5.80±0.83	3.55±0.59	1.87±0.06
Trp	0.52±0.11	0.70±0.09	0.87±0.10	0.69±0.14	0.23±0.05
Ala	3.21±1.13	2.80±0.53	5.89±0.48	4.72±0.54	2.40±0.32
Asp	0.32±0.01	0.80±0.04	1.68±0.08	1.77±0.13	0.38±0.05
Asn	18.96±0.40	36.72±1.87	62.24±0.45	37.19±1.86	25.05±1.26
Glu	3.15±0.18	2.86±0.22	4.26±0.04	4.11±0.29	1.67±0.13
Gln	1.00±0.58	0.55±0.23	1.33±0.57	1.60±0.12	ND
Gly	1.23±0.28	0.69±0.11	1.96±0.86	1.29±0.57	0.59±0.46

[a] Standard deviation (three replicates).
[b] ND = not detected.

Table 3
Protein amino acids in the seeds of 5 lentil species (mg/g dry wt±S.D.)[a]

	L. culinaris	*L. ervoides*	*L. nigricans*	*L. odemensis*	*L. orientalis*
Arg	10.61±0.48	12.05±0.77	7.48±1.37	9.10±0.32	14.04±0.83
His	8.74±0.32	9.75±0.56	4.94±4.31	6.84±2.37	3.95±6.85
Ile	6.26±0.25	8.59±1.01	7.76±1.22	5.06±0.34	9.58±0.85
Leu	10.64±2.15	14.07±1.22	11.74±1.69	8.09±1.06	15.86±1.52
Lys	4.54±0.92	9.48±1.05	6.14±0.87	5.69±0.66	12.64±1.08
Met	1.49±0.22	1.74±0.41	1.22±0.96	1.18±0.34	1.63±0.14
Cys	0.40±0.12	0.53±0.15	0.47±0.03	0.44±0.28	0.39±0.06
Phe	6.70±0.51	9.37±1.29	9.46±1.33	5.55±0.77	10.64±2.08
Tyr	6.34±1.11	6.65±1.05	6.35±0.94	5.05±1.26	7.53±1.29
Pro	11.11±1.14	11.54±0.66	10.52±0.78	8.88±1.04	11.36±0.50
Ser	11.38±0.65	14.10±0.70	8.70±0.89	11.20±0.60	15.60±0.73
Thr	5.57±0.17	6.31±0.83	4.56±1.11	5.62±0.63	7.57±0.39
Val	8.54±0.48	9.60±0.91	8.64±1.79	7.24±0.22	11.64±0.90
Trp	ND[b]	ND	ND	ND	ND
Ala	20.42±4.09	16.01±1.04	22.47±2.75	21.32±5.76	39.81±3.46
ASX	10.96±1.27	17.42±2.94	7.68±2.12	11.17±0.24	26.10±2.17
GLX	26.55±1.34	32.62±3.53	19.95±3.84	24.22±0.57	42.27±2.81
Gly	9.77±1.01	11.48±0.45	7.89±0.59	10.22±0.91	12.66±0.51

[a] Standard deviation (three replicates).
[b] ND = not detected.

ASX and GLX. In all species the amino acids present in low concentrations were methionine and cysteine, while tryptophan was not detected after hydrolysis. Tyrosine was lowest (5.05±1.26 mg/g) in *L. odemensis* and lysine was lowest in *L. culinaris* (4.54±0.92 mg/g). High levels of alanine, ASX, GLX, glycine, serine, leucine, proline and arginine were found in all the species examined. These results confirmed the earlier report of Lea and Joy (1983) that over half of the protein nitrogen in legume seeds is in the form of ASX, GLX, arginine and leucine.

In 4-day-old seedlings the content of most protein amino acids increased, especially alanine and ASX (Table 4). The essential amino acids such as Ile, Leu, Lys, Phe, Tyr, Thr and Val increased after germination in *L. culinaris* and *L. nigricans* except cysteine but this could be a methodological limitation. Also the results

Table 4
Protein amino acids in the seedlings (4-day-old) of 5 lentil species (mg/g dry wt ± S.D.)[a]

	L. culinaris	*L. ervoides*	*L. nigricans*	*L. odemensis*	*L. orientalis*
Arg	12.11 ± 1.48	10.45 ± 0.35	13.50 ± 1.44	9.83 ± 3.05	11.18 ± 1.00
His	10.79 ± 3.90	9.02 ± 1.07	0.56 ± 0.18	9.27 ± 1.23	9.70 ± 0.35
Ile	11.44 ± 1.72	8.43 ± 0.53	12.01 ± 1.54	8.69 ± 0.95	8.87 ± 0.78
Leu	17.10 ± 1.63	12.93 ± 0.22	17.66 ± 1.77	12.53 ± 1.35	14.71 ± 3.83
Lys	16.99 ± 1.64	12.31 ± 0.91	16.66 ± 2.20	0.22 ± 0.02	12.00 ± 1.10
Met	1.02 ± 0.86	1.52 ± 0.27	1.06 ± 0.38	1.59 ± 0.24	0.25 ± 0.25
Cys	ND[b]	0.22 ± 0.03	0.49 ± 0.06	0.30 ± 0.11	ND
Phe	11.56 ± 2.36	10.16 ± 0.25	13.82 ± 1.25	5.11 ± 0.75	11.45 ± 0.00
Tyr	7.70 ± 1.35	7.68 ± 0.85	8.45 ± 1.99	6.67 ± 1.22	10.06 ± 3.06
Pro	10.84 ± 0.69	9.87 ± 0.27	12.05 ± 1.06	9.00 ± 1.20	8.93 ± 0.91
Ser	15.54 ± 1.95	13.25 ± 0.18	18.35 ± 1.89	12.82 ± 1.34	14.69 ± 0.59
Thr	7.14 ± 1.45	6.26 ± 0.28	8.65 ± 1.19	6.42 ± 0.69	6.18 ± 0.90
Val	13.23 ± 2.52	10.89 ± 0.63	15.16 ± 2.33	11.53 ± 1.51	11.78 ± 0.93
Trp	ND	ND	ND	ND	ND
Ala	36.76 ± 7.17	34.90 ± 1.05	60.21 ± 7.26	44.13 ± 7.82	37.14 ± 5.55
ASX	41.39 ± 4.67	26.71 ± 1.35	45.58 ± 4.99	29.16 ± 3.05	43.17 ± 3.12
GLX	34.12 ± 3.87	22.41 ± 0.53	32.13 ± 4.52	20.10 ± 1.69	19.59 ± 0.86
Gly	10.77 ± 0.77	9.44 ± 0.46	12.32 ± 1.16	9.97 ± 1.33	10.49 ± 0.24

[a] Standard deviation (three replicates).
[b] ND = not detected.

for methionine and tryptophan might be underestimated due to HCl hydrolysis.

2.3. Nonprotein amino acid content

To study the nonprotein amino acids in seeds and seedlings, two methods were combined: HPLC to determine the content of amino acids and trigonelline (Rozan et al., 2000, 2001), and capillary zone electrophoresis (CZE) to determine the content of isoxazolinones. The CZE-method will be published elsewhere.

The results are given in Table 5. In lentil seeds we found trigonelline as well as some nonprotein amino acids such as γ-hydroxyarginine, γ-hydroxyornithine, homoarginine, α-aminobutyric acid and taurine. In lentil seedling we found more nonprotein amino acids comparing to the seeds. These include α-aminoadipic acid (a higher homologue of glutamate), γ-aminobutyric acid (GABA), lathyrine and isoxazolinone derivatives. Fig. 1 presents the structures of the nonprotein amino acids and trigonelline found in these 5 *Lens* species.

In this study, trigonelline was found in all species except in *L. ervoides*. The concentration of trigonelline was variable (Table 5). For *L. nigricans*, no difference in trigonelline content was observed before and after the germination of seeds, for *L. culinaris* and *L. orientalis* the content of trigonelline in seedlings was lower than that in seeds while for *L. odemensis* trigonelline increased after germination. Trigonelline can be considered as a multifunctional natural plant hormone: it has a function as a cell cycle regulator during the early growth of many legume root meristems and also as osmoregulator in salt-stressed legumes (Tramontano and Jouve, 1997).

The total content of nonprotein amino acids in non-germinated seeds was very low and variable between the species. The species *ervoides* contained less nonprotein amino acids than the four other species. The content of α-aminoadipic acid was not detected in non-germinated seeds and increased after germination to about 4 mg/g of dry wt in each species. Bridges et al. (1991) found a gliotoxic activity of α-aminoadipic acid in cultures of neonatal rat astrocytes.

The nonprotein amino acid *erythro*-γ-hydroxyarginine or 2(*S*),4(*R*)-4-hydroxyarginine (Bell et al., 1999) is a specific metabolite in the genus *Lens* and its content in the seeds and in the seedlings is very different among the species (Table 5). Sulser and Sager (1976) found γ-hydroxyarginine (γ-OH-Arg), γ-hydroxyornithine (γ-OH-Orn) and homoarginine (Har) in 5 different varieties of *L. culinaris* seeds. In our study γ-OH-Arg was present in the nongerminated seeds of all five species studied and it increased after 4 days of germination. γ-OH-Orn which eluted out about 1 min after isoleucine in our HPLC system was detected in all our samples of seeds and seedlings in low concentration. γ-OH-Orn is a metabolite of γ-OH-Arg. We also confirmed the presence of Har in four of the lentil species studied except in *L. orientalis*. The seed of *L. ervoides* contained highest concentration of Har.

One of the major peaks in seed extracts was identified as a sulphur-containing amino acid taurine (2-aminoethanesulphonic acid). Taurine is the most abundant nonprotein amino acid in human organisms and is the metabolic product of cysteine after oxidation and decarboxylation (Bezkorovainy and Rafelson, 1996). Taurine has been identified in the seeds of bean (*Phaseolus*

Table 5
Free nonprotein amino acids[a] and trigonelline in the seeds and seedlings (4-day-old) of 5 lentil species (mg/g dry wt ± S.D.)[b]

	L. culinaris	*L. ervoides*	*L. nigricans*	*L. odemensis*	*L. orientalis*
Nongerminated seeds					
Trigonelline	11.85±1.48	ND[c]	8.31±2.10	1.80±0.44	18.15±5.91
γ-OH-Arg	2.52±0.07	Trace	2.04±0.14	0.75±0.03	5.73±3.77
γ-OH-Orn	0.01±0.00	0.01±0.00	0.04±0.00	0.02±0.00	0.04±0.03
α-Aminobutyric acid	0.01±0.00	0.01±0.00	0.02±0.00	0.02±0.00	0.03±0.00
Taurine	0.03±0.00	0.01±0.00	0.21±0.01	0.19±0.00	0.05±0.00
Har	Trace	0.06±0.00	0.01±0.01	Trace	ND
Seedlings					
Trigonelline	6.42±0.28	ND	8.68±1.92	10.57±7.43	2.52±1.13
γ-OH-Arg	11.35±0.45	1.32±1.23	11.75±0.79	4.74±0.63	18.05±1.00
γ-OH-Orn	0.05±0.04	0.07±0.01	0.11±0.03	0.08±0.07	0.14±0.03
α-Aminobutyric acid	0.04±0.00	0.06±0.01	0.07±0.05	0.07±0.01	0.04±0.01
Taurine	0.18±0.00	0.02±0.00	0.20±0.01	0.26±0.05	0.05±0.00
Har	Trace	Trace	Trace	Trace	ND
α-aaa	3.15±1.12	3.61±0.80	4.54±0.56	4.00±0.20	2.57±0.18
GABA	1.64±0.04	1.00±0.20	2.04±0.25	1.26±0.15	0.78±0.15
Lathyrine	Trace	ND	0.77±0.04	0.20±0.01	ND
BIA	0.27±0.01	0.27±0.01	0.43±0.01	0.24±0.01	0.15±0.00
γ-glu-BIA	0.41±0.02	0.09±0.02	0.24±0.01	0.03±0.00	ND
CMI	0.66±0.02	1.03±0.01	1.21±0.01	0.56±0.02	0.22±0.01

[a] Abbreviations: see Fig. 1.
[b] Standard deviation (three replicates).
[c] ND = not detected.

vulgaris L.) and pea (*Pisum sativum* L.) and also in several other plant genera (Kataoka and Ohnishi, 1986; Lähdesmäki, 1986; Stintzing et al., 1999). We confirmed the presence of taurine in all five *Lens* species studied and the concentration in *L. nigricans* and in *L. odemensis* was at least 10–20 times higher than in pea and bean reported by Lähdesmäki (1986). The metabolism and physiological role of taurine in plants is not established and is worth further study because legume seeds in general are low in sulphur-containing amino acids methionine and cysteine. In animals taurine was reported to have multiple functions as neuromodulator, cell membrane stabilizer, antioxidant, detoxifier, bile acid conjugator and osmoregulator (Zelikovic et al., 1990). Another major compound in the seeds with elution time at 29.7 min and absorption max of 265 nm in HPLC analysis is still unknown. The UV absorption spectrum is similar to trigonelline and is not an amino acid.

Arginine is one of the most versatile amino acids in animal cells, serving as a precursor for the synthesis not only of proteins but also of nitric oxide, urea, polyamines, proline, glutamate, creatine and agmatine (Wu and Morris, 1998). There is no information whether γ-hydroxyarginine might affect any of these various physiological functions. While a variety of toxic synthetic analogues of arginine such as *N*-methyl-L-arginine and *N*-nitro-L-arginine are often used in pharmacological studies (Hobbs et al., 1999), the natural occurring homoarginine (high concentration in *Lathyrus sativus* seeds consumed in some countries) and γ-hydroxyarginine are rarely used (Jyothi and Rao, 1999). Buga et al. (1998) found that γ-hydroxyarginine inhibits Caco-2 tumor cell proliferation.

For each species, the total nonprotein amino acids increased dramatically during germination. α-Aminoadipic acid (α-aaa) and γ-aminobutyric acid (GABA) were found in all five lentil species studied only after germination. Homoarginine was found in trace amounts. Two unknowns with elution times of 29.2 and 32.6 min respectively in HPLC analysis were also found in the seedlings. The peak with elution time of 29.2 min is confirmed to be lathyrine, β-(2-amino-pyrimidine-4-yl)alanine, a heterocyclic nonprotein amino acid previously found in some *Lathyrus* species (Brown and Turan, 1996). The standard lathyrine after PITC derivatization was co-eluted out in HPLC at the same position and both peaks have the same absorption spectra and max at 230 nm. Additional analysis by high voltage paper electrophoresis and two-dimensional TLC indicated the presence of the typical bright tomato-red colour of lathyrine at the RF value of authentic lathyrine after ninhydrin spray. Lathyrine was mainly found in the seedling of *L. nigricans* and *L. odemensis*. In *L. culinaris* only trace amount of lathyrine was present. α-Aminobutyric acid was present in all five species of lentil seeds and seedlings studied.

The isoxazolinones were mainly found in the tribe *Vicieae* (Lambein et al., 1990a). These compounds were mostly absent from the dry seeds but their concentration in seedlings can be very high: up to 10% of the dry wt of the seedling axes of some *Lathyrus* species (Lambein et al., 1976, 1992b, 1993). Ten different isoxazolinones

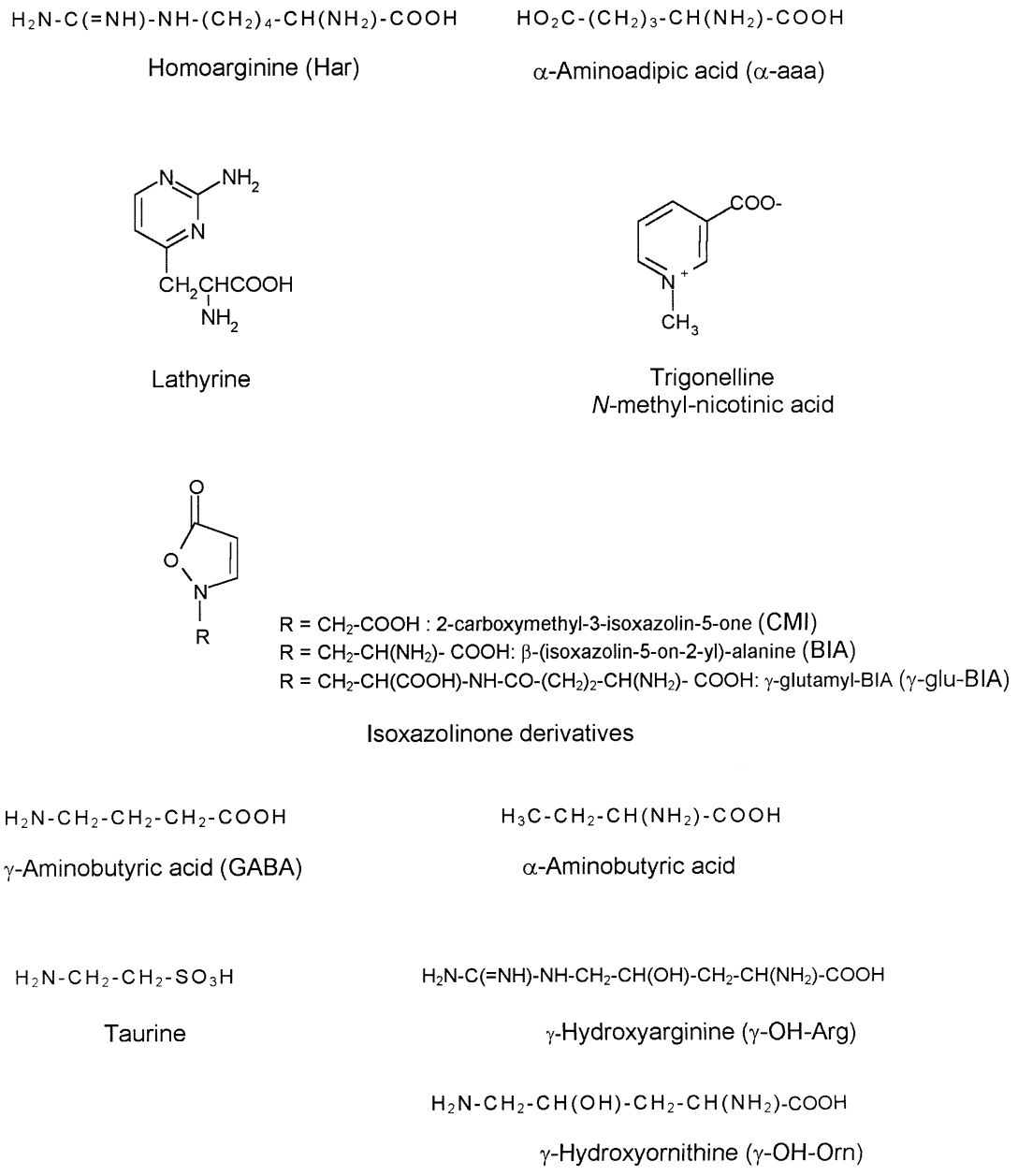

Fig. 1. Structures of nonprotein amino acids and trigonelline found in lentil seeds or seedlings.

were identified from *Lathyrus* species. In the genus *Lens*, three major isoxazolinones were detected in the seedlings by the CZE method. HPLC also permitted to detect these compounds but the number of peaks obtained by HPLC was too numerous to allow a correct quantification of the isoxazolinone compounds that were present in much lower concentrations.

The isoxazolinones detected were BIA (β-(isoxazolin-5-on-2-yl)-alanine), γ-glu-BIA (γ-glutamyl-BIA) and CMI (2-carboxymethyl-3-isoxazolin-5-one). BIA and γ-glu-BIA were previously reported in *L. culinaris* (Kuo et al., 1998; Rozan et al., 2000, 2001). The concentration of BIA ranged between 0.15 mg/g dry wt (*L. orientalis*) and 0.43 mg/g (*L. nigricans*) (Table 5). BIA is the metabolic precursor of γ-glu-BIA and of 3-*N*-oxalyl-L-2, 3-diaminopropanoic acid (β-ODAP) in grass pea (*Lathyrus sativus* L.) seedlings (Lambein et al., 1990b; Kuo et al., 1998). β-ODAP, a neurotoxic nonprotein amino acid, is present in *Lathyrus sativus* seeds and overconsumption of these seeds is responsible for lathyrism (a human irreversible neurodegenerative disease) in India, Bangladesh and Ethiopia. The most recent epidemic of lathyrism occurred in Ethiopia since 1997 after a drought and famine (Getahun et al., 1999). In *L. culinaris* BIA was metabolized to γ-glu-BIA and to four unknown amino acids while ODAP was not found (Kuo et al., 1998).

Riepe et al. (1995) reported that BIA itself is slightly neurotoxic, at concentrations of 0.5–2.0 mM it produced

a concentration-dependent neurodegeneration in mouse cortical explants.

A metabolite of BIA, γ-glu-BIA was first isolated from *L. culinaris* and from *Lathyrus sativus* (Lambein et al., 1992a) and in this study it was found in four of the five species examined. In *L. nigricans* and *L. culinaris* 0.24 and 0.41 mg/g dry wt were found respectively and lower concentrations were present in *L. odemensis* and *L. ervoides*. The physiological role of γ-glu-BIA in the plant is not known. Kusama et al. (2000) found in cultured cortical neurons of the rat that γ-glu-BIA showed weak antagonistic effects against NMDA receptors, and weak agonistic effects at AMPA receptors and cloned glutamate transporter.

CMI which is not an amino acid was the major isoxazolinone compound in all five species of *Lens* studied. CMI was first isolated from *Lathyrus odoratus* seedlings (Van Rompuy et al., 1974) and this is the first report of its detection in lentil seedlings. The biological activity of CMI has not been studied.

In this study we found less than 2% of the dry weight as total isoxazolinones in 4-day-old lentil seedling which is lower than in *Lathyrus* seedlings, but similar to pea seedlings.

3. Conclusion

This study showed some qualitative differences in composition of nonprotein amino acids among the five species of lentil studied: the absence of homoarginine and γ-glu-BIA in *L. orientalis;* the absence of trigonelline in *L. ervoides*. Phylogenetic classification on the basis of this phytochemical information from nonprotein amino acids composition is not an easy task. This was done before on the basis of distribution of nonprotein amino acids in seeds of the two major genera of the tribe *Vicieae (Lathyrus* and *Vicia)* (Bell, 1971). However, when seedlings of the genus *Lathyrus* were screened for a larger number of nonprotein amino acids including isoxazolinones, mostly unique combinations were found (Lambein et al., 1986). In the present study *L. orientalis* showed most different from the other four species studied by the absence of homoarginine, lathyrine and isoxazolinone derivative γ-glu-BIA. *L. nigricans* and *L. odemensis* seem to be more closely related by the presence of higher level of taurine and lathyrine. It was suggested by Simola (1986) that the different qualitative composition of nonprotein amino acids contributes to the barrier against interspecies crossing in some legume genera. In this case lathyrine or taurine might contribute to the crossing incompatibility between certain species of *Lens*.

Most studies on lentils are related to genetic aspects and their nutritional value is less mentioned whereas *L. culinaris* is consumed all over the world. The nongerminated lentil seeds contain some nonprotein amino acids with known or proposed physiological effects such as γ-hydroxyarginine and homoarginine affecting the biosynthesis of NO. The isoxazolinones, α-aminoadipic acid, GABA and lathyrine were only found after germination. The presence of taurine is mostly overlooked in common food legumes including pea, bean and lentil which are known to be low in sulphur-containing amino acids methionine and cysteine. Over-consumption of these seedlings, sold on the European market as new healthy food, might involve health problems. Especially for vegetarians and for those who can not afford animal protein, legumes are the main source of dietary protein. Seedlings of the garden pea, lentil and mungbean (*Vigna radiata* L.) are commonly available as fresh product for human consumption among a large diversity of seedlings. These contain secondary metabolites that are absent from the seeds and on which there is insufficient nutritional, toxicological or pharmacological information.

4. Experimental

4.1. Plant material

Five species of lentil seeds: *Lens culinaris*, *L. ervoides*, *L. nigricans, L. odemensis* and *L. orientalis* were obtained from ICARDA (Aleppo, Syria). The seeds were kept in moist condition in the cold room for 8 days to activate the process of germination and then germinated in the dark at 20°C with constant humidity. The seedlings were harvested after 4 days of germination. In this study the cotyledons and seedling axes were not separated.

Nongerminated seeds and seedlings were lyophilised before analysis. For each species, 4 extractions were done: one extraction for free amino acids analysis and another extraction after hydrolysis for total amino acids analysis in both seeds and seedlings. Each analysis was done in triplicate.

4.2. Protein hydrolysis

The dry weights of the samples varied from 10 to 87 mg. Fifty microlitres of DL-allylglycine (300 μmol/ml, Sigma) were added to samples as internal standard. Protein hydrolysis was done following a classical method with 6 N HCl for 24 h at 100°C in a vacuum-closed vial. Hydrolysates were dried under vacuum and rinsed twice with water.

4.3. Extraction of amino acids

This step was done for the free amino acids and total amino acid content. The dry weight of the free amino acid samples varied from 19 to 185 mg.

Fifty microlitres of DL-allylglycine (100 μmol/ml) was added to samples used for free amino acid extraction as internal standard. Four millilitres of 70% EtOH were added to the samples (protein hydrolysates and free amino acid samples). After keeping overnight at +4°C the samples were centrifuged (34,800 *g*, 20 min) and the pellets were washed twice with 70% EtOH. The supernatants were pooled and concentrated under vacuum and finally stored at −20°C.

4.4. High-performance liquid chromatography (HPLC) analysis

The free amino acid and trigonelline content of the extracts were analyzed by a HPLC gradient system with precolumn phenylisothiocyanate (PITC) derivatization (Khan et al., 1994). Buffer A (0.1 M NH_4OAc, pH 6.5) and Buffer B (0.1 M NH_4OAc, containing ACN and MeOH; 44:46:10; v:v; pH 6.5) were used.

Sample preparation was done as described in one of our previous studies (Rozan et al., 2000). A standard protein amino acid mixture (Food hydrolysate A 9656, Sigma) was prepared as above. Trigonelline and lathyrine were purified from plant extracts; α-aminoadipic acid, homoarginine (Sigma) and taurine (NBC) were used as standards. Standard γ-hydroxyarginine was kindly provided by Prof. E. A. Bell (King's College, London) and γ-hydroxyornithine was obtained by enzymatic reaction of arginase (ICN Biomedicals) with γ-hydroxyarginine as substrate. DL-allylglycine (Sigma) was used as the internal standard with a recovery of 90.5%. The results were analysed by Millennium software (Waters, version 1.10).

4.5. Capillary zone electrophoresis (CZE) analysis

The capillary electrophoresis instrument used was a Quanta 4000E (Waters) equipped with a Mercury lamp and a filter at 254 nm (Chowdhury et al., in preparation). Sodium-barbiturate 4 mM was used as the internal standard. Standards of BIA, γ-glu-BIA were previously isolated from *Lathyrus sativus*, CMI from *Lathyrus odoratus*. The results were analysed by Millennium software (version 3.1).

Acknowledgements

This work was supported by the Agro-industrial research development of EC (FAIR No. CT98-5001) and by a grant from the Flemish Science Foundation. ICARDA in Aleppo, Syria, is acknowledged for freely supplying seed materials. Professor Dr. E.A. Bell of King's College, London is thanked for a sample of standard γ-hydroxyarginine. Dr. W. Erskine of ICARDA is acknowledged for taxonomic clarifications. M.Sc. Delphin Diasolua Ngudi is thanked for performing the arginase test to localize the peak of γ-hydroxyornithine.

References

Abbo, S., Ladizinsky, G., 1994. Genetical aspects of hybrid embryo abortion in the genus *Lens* L.. Heredity 72, 193–200.

Abo-Elwafa, A., Murai, K., Shimada, T., 1995. Intra- and inter-specific variations in *Lens* revealed by RAPD markers. Theor. Appl. Genet. 90, 335–340.

Ahmad, M., McNeil, D.L., Fautrier, A.G., Armstrong, K.F., Paterson, A.M., 1996. Genetic relationships in *Lens* species and parentage determination of their interspecific hybrids using RAPD markers. Theor. Appl. Genet. 92, 1091–1098.

Bell, E.A., 1971. Comparative biochemistry of non-protein amino acids. In: Harborne, J.B., Boulter, D., Turner, B.L. (Eds.), Chemotaxonomy of the Leguminosae. Academic, London, pp. 179–206.

Bell, E.A., Lyddiard, J.R.A., Malik, M.A., Motevalli, M., Nunn, P.B., O'Brien, P., Perera, K.P.W.C., 1999. X-ray single-crystal structure of 2(*S*),4(*R*)-4-hydroxyarginine from *Lens culinaris* seeds. Phytochemistry 50, 1201–1204.

Bezkorovainy, A., Rafelson Jr. M.E., 1996. Protein and amino acid metabolism. In: Concise Biochemistry. Marcel Dekker, New York, pp. 535–579.

Bridges, R.J., Hatalski, C., Shim, S.N., Nunn, P.B., 1991. Gliotoxic properties of the *Lathyrus* excitotoxin β-*N*-oxalyl-L-α,β-diaminopropionic acid β-(L-ODAP). Brain Res. 561, 262–268.

Brown, E.G., Turan, Y., 1996. Lathyrine biosynthesis and the origin of the precursor 2-amino-4-carboxypyrimidine in *Lathyrus tingitanus*. Phytochemistry 43, 1029–1031.

Buga, G.M., Wei, L.H., Bauer, P.M., Fukuto, J.M., Ignarro, L.J., 1998. *N*-γ-Hydroxy-L-arginine and nitric oxide inhibit Caco-2 tumor cell proliferation by distinct mechanisms. Am. J. Physiol. — Regulatory Integrative and Comparative Physiol. 44, R1256–R1264.

Ferguson, M.E., 1998. Studies of Genetic Variation within the Genus *Lens*. PhD thesis. School of Biological Sciences, University of Birmingham, Birmingham, UK.

Ferguson, M.E., Robertson, L.D., 1999. Morphological and phenological variation in the wild relatives of lentil. Genet. Resour. Crop Evol. 46, 3–12.

Frias, J., Diaz-Pollan, C., Hedley, C.L., Vidal-Valverde, C., 1995. Evolution of trypsin inhibitor activity during germination of lentils. J. Agric. Food Chem. 43, 2231–2234.

Frias, J., Diaz-Pollan, C., Hedley, C.L., Vidal-Valverde, C., 1996. Evolution and kinetics of monosaccharides, disaccharides and α-galactosides during germination of lentils. Z. Lebensm. Unters. Forsch. 202, 35–39.

Getahun, H., Mekonnen, A., Tekle Haimanot, R., Lambein, F., 1999. Epidemic of neurolathyrism in Ethiopia. Lancet 354, 306–307.

Hobbs, A.J., Higgs, A., Moncada, S., 1999. Inhibition of nitric oxide synthase as a potential therapeutic target. Annu. Rev. Pharmacol. Toxicol. 39, 191–220.

Jyothi, P., Rao, S.L.N., 1999. Sustained nitric oxide generation with L-homoarginine. Res. Comm. Biochem. Cell Mol. Biol. 3, 223–232.

Kataoka, H., Ohnishi, N., 1986. Occurrence of taurine in plants. Agric. Biol. Chem. 50, 1887–1888.

Khan, J.K., Kuo, Y.H., Kebede, N., Lambein, F., 1994. Determination of non-protein amino acids and toxins in *Lathyrus* by high performance liquid chromatography with precolumn phenylisothiocyanate derivatization. J. Chromatogr. A 687, 113–119.

Kuo, Y.-H., Ikegami, F., Lambein, F., 1998. Metabolic routes of β-(isoxazolin-5-on-2-yl)-L-alanine (BIA), the precursor of the neurotoxin ODAP (β-*N*-oxalyl-L-α,β-diaminopropionic acid), in different legume seedlings. Phytochemistry 49, 43–48.

Kusama, T., Kusama-Eguchi, K., Ikegami, F., Yamamoto, A., Kuo, Y.-H., Lambein, F., Watanabe, K., 2000. Effects of β-ODAP, the *Lathyrus sativus* neurotoxin, and related compounds on cloned glutamate receptors and transporters expressed in *Xenopus oocytes*. Research Comm. Pharmacol. Toxicol. 5, 37–56.

Ladizinsky, G., 1999. Identification of the lentil's wild genetic stock. Genet. Resour. Crop Evolution 46, 115–118.

Lähdesmäki, P., 1986. Determination of taurine and other acidic amino acids in plants. Phytochemistry 25, 2409–2411.

Lambein, F., De Bruyn, A., Ikegami, F., Kuo, Y.-H., 1986. Distribution and biosynthesis of isoxazolinone derivatives in the genus *Lathyrus*. In: Kaul, A.K., Comb, D. (Eds.), *Lathyrus* and Lathyrism. Third World Medical Research Foundation, New York, pp. 246–256.

Lambein, F., Khan, J.K., Becu, C., De Bruyn, A., 1992a. Characterization of γ-glutamyl-β-(isoxazolinonyl)-alanine from *Lathyrus sativus* and its decarboxylation product from *Lathyrus odoratus*. Phytochemistry 31, 887–892.

Lambein, F., Khan, J.K., Kuo, Y.-H., 1992b. Free amino acids and toxins in *Lathyrus sativus* seedlings. Planta Med. 58, 380–381.

Lambein, F., Khan, J.K., Kuo, Y.-H., Campbell, C.G., Briggs, C.J., 1993. Toxins in the seedlings of some varieties of grass pea (*Lathyrus sativus*). Natural Toxins 1, 246–249.

Lambein, F., Kuo, Y.-H., Ikegami, F., Murakoshi, I., 1990a. Toxic and non-toxic nonprotein amino acids in the *Vicieae*. In: Lubec, G., Rosenthal, G.A. (Eds.), Amino Acids: Chemistry, Biology and Medicine. Escom, Leiden, pp. 21–28.

Lambein, F., Kuo, Y.-H., Van Parijs, R., 1976. Isoxazolin-5-ones. Chemistry and biology of a new class of plant products. Heterocycles 4, 567–593.

Lambein, F., Ongena, G., Kuo, Y.-H., 1990b. β-Isoxazolinone-alanine is involved in the biosynthesis of the neurotoxin β-*N*-oxalyl-L-α,β-diaminopropionic acid. Phytochemistry 29, 3793–3796.

Lea, P.J., Joy, K.W., 1983. Amino acid interconversion in germinating seeds. In: Nozzolillo, C., Lea, P.J., Loewus, F.A. (Eds.), Recent Advances in Phytochemistry, Vol. 17. Plenum, New York, pp. 77–109.

Prodanov, M., Sierra, I., Vidal-Valverde, C., 1997. Effect of germination on the thiamine, riboflavin and niacin contents in legumes. Z. Lebensm. Unters. Forsch. A 205, 48–52.

Riepe, M., Spencer, P.S., Lambein, F., Ludolph, A.C., Allen, C.N., 1995. In vitro toxicological investigations of isoxazolinone amino acids of *Lathyrus sativus*. Natural Toxins 3, 58–64.

Rozan, P., Kuo, Y.-H., Lambein, F., 1999. Free amino acids present in edible seed sprouts sold for human consumption. Amino Acids 17, 101–102.

Rozan, P., Kuo, Y.-H., Lambein, F., 2000. Free amino acids present in commercially available seedlings sold for human consumption. A potential hazard for consumers. J. Agric. Food Chem. 48, 716–723.

Rozan, P., Kuo, Y.-H., Lambein, F., 2001. Nonprotein amino acids in edible lentil and garden pea seedlings. Amino Acids 20, 319–324.

Sharma, S.K., Dawson, I.K., Waugh, R., 1995. Relationships among cultivated and wild lentils revealed by RAPD analysis. Theor. Appl. Genet. 91, 647–654.

Simola, L.K., 1986. Structural and chemical aspects of evolution of *Lathyrus* species. In: Kaul, A.K., Combes, D. (Eds.), *Lathyrus* and Lathyrism. Third World Medical Research Foundation, New York, pp. 225–239.

Stintzing, F.C., Schieber, A., Carle, R., 1999. Amino acid composition and betaxanthin formation in fruits from *Opuntia ficus-indica*. Planta Med. 65, 632–635.

Sulser, H., Sager, F., 1976. Identification of uncommon amino acids in the lentil seed (*Lens culinaris Med.*). Experientia 32, 422–423.

Sutcliffe, J.F., Bryant, J.A., 1977. 3-Biochemistry of germination and seedling growth. In: Cox, Wyman L.T.D. (Ed.), The Physiology of the Garden Pea. Academic, London, pp. 45–83.

Tramontano, W.A., Jouve, D., 1997. Trigonelline accumulation in salt-stressed legumes and the role of other osmoregulators as cell cycle control agents. Phytochemistry 44, 1037–1040.

Van Rompuy, L., Lambein, F., De Gussem, R., Van Parijs, R., 1974. The isolation and structure analysis of 2-(2-cyanoethyl)-3-isoxazolin-5-one, 2-(β-D-glucopyranosyl)-3-isoxazolin-5-one and 2-carboxymethyl-3-isoxazolin-5-one from *Lathyrus odoratus*. Biochem. Biophys. Res. Comm. 56, 199–205.

Vidal-Valverde, C., Frias, J., 1992. Changes in carbohydrates during germination of lentils. Z. Lebensm. Unters. Forsch. 194, 461–464.

Weder, J.K.P., Kahleyss, R., 1998. Isolation and characterisation of four trypsin-chymotrypsin inhibitors from lentil seeds. J. Sci. Food Agric. 78, 429–434.

Wu, G.Y., Morris, S.M., 1998. Arginine metabolism: nitric oxide and beyond. Biochem. J. 336, 1–17.

Zelikovic, I., Chesney, R.W., Friedman, A.L., Ahlfors, C.E., 1990. Renal immaturity causes taurine depletion in very low birth weight infants fed with prolonged total parental nutrition. In: Lubec, G., Rosenthal, G.A. (Eds.), Amino Acids — Chemistry, Biology and Medicine. Escom, Leiden, pp. 1095–1103.

PERGAMON

Phytochemistry 58 (2001) 291–297

PHYTOCHEMISTRY

www.elsevier.com/locate/phytochem

Antibacterial halogenated metabolites from the Malaysian *Laurencia* species☆

Charles Santhanaraju Vairappan[a], Motonari Daitoh[a], Minoru Suzuki[a,*], Tsuyoshi Abe[b], Michio Masuda[c]

[a]*Division of Material Science, Graduate School of Environmental Earth Science, Hokkaido University, Sapporo 060-0810, Japan*
[b]*The Hokkaido University Museum, Sapporo 060-0810, Japan*
[c]*Division of Biological Sciences, Graduate School of Science, Hokkaido University, Sapporo 060-0810, Japan*

Received in revised form 18 April 2001

Abstract

Two halogenated C_{15} acetogenins, named lembyne-A and lembyne-B, have been isolated from an unrecorded *Laurencia* species collected off the Malaysian waters. Their structures were deduced on the basis of spectroscopic evidence. Previously known elatol and iso-obtusol showed potent antibacterial activity against some marine bacteria. © 2001 Elsevier Science Ltd. All rights reserved.

Keywords: *Laurencia*; Rhodomelaceae; Red alga; Sesquiterpene; C_{15} acetogenin; Halogenated compound; Chemotaxonomy; Antibacterial activity

1. Introduction

In the marine ecosystem, seaweeds are directly exposed and are susceptible to ambient microorganisms such as bacteria, fungi and viruses. In Japan, disease caused by pathogenic species of marine bacteria such as *Vibrio* (Ando and Inoue, 1961), *Alteromonas* (Yumoto et al., 1989; Sawabe et al., 1992), and *Pseudoalteromonas* (Sawabe et al., 1998; Sawabe et al., 2000) have appeared in the kelp *Laminaria* species. The selective occurrence and the dynamics of these infections and the ability of the seaweed to survive these diseases have urged us to delve into the possible existence of an inherently available antibacterial defense mechanism in seaweed (Vairappan et al., in press). To date, it is well known that many species of the red algal genus *Laurencia* (Rhodomelaceae, Ceramiales) produce numerous halogenated secondary metabolites with diverse structural features (Erickson, 1983). Although the function of these secondary metabolites has not been clearly studied, it is suggested that these metabolites serve as feeding deterrents against marine herbivores (Hay et al., 1987; Kurata et al., 1998). Furthermore, some halogenated metabolites from *Laurencia* have been shown to have antibacterial activity against terrestrial bacteria (Waraszkiewicz and Erickson, 1974; Wratten and Faulkner, 1977; Carter et al., 1978; Caccamese et al., 1980; König and Wright, 1997), thus suggesting that halogenated compounds have the potential to function as chemical defense substances against pathogenic marine bacteria. In the course of our continuing chemotaxonomic studies of *Laurencia* species, we previously reported chemical components of *Laurencia* specimens collected from the Malaysian coasts; *Laurencia snackeyi* (Weber-van Bosse) Masuda (Masuda et al., 1997), which produced brominated sesquiterpenes, and *Laurencia similis* Nam *et* Saito (Masuda et al, 1999), which produced polybrominated indoles. As part of our chemical analyses of *Laurencia* species from the Malaysian waters, we examined samples of *Laurencia majuscula* (Harvey) Lucas harvested from five locations and a sample of an unrecorded *Laurencia* species. *L. majuscula* contained known chamigrane-type sesquiterpenes, elatol (**1**) (Sims et al., 1974) and iso-obtusol (**2**) (González et al., 1979), as its common metabolites. The unrecorded *Laurencia*

☆ Part 3 in the series "Chemical compositions of *Laurencia* species from the Malaysian waters". Part 1, Masuda et al., 1997. Part 2, Masuda et al., 1999.

* Corresponding author. Tel.: +81-11-706-2272; fax: +81-11-706-4862.

E-mail address: misu@ees.hokudai.ac.jp (M. Suzuki).

0031-9422/01/$ - see front matter © 2001 Elsevier Science Ltd. All rights reserved.
PII: S0031-9422(01)00243-6

contained two new halogenated metabolites, named lembyne-A (**3**) and lembyne-B (**4**), along with elatol (**1**). In this paper we describe the isolation and structure elucidation of these halogenated compounds and their antibacterial activity against marine bacteria isolated from algal habitats in the Malaysian coastal waters.

2. Results and discussion

2.1. Laurencia majuscula

Pulau Tikus and Pulau Nunuyan Laut specimens contained elatol (**1**) as the major metabolite. Specimens that were collected from Pulau Satang Besar, Pulau Bankawan and Pulau Redang contained iso-obtusol (**2**) as their major metabolite. These results indicated that the chemical compositions of the Malaysian *L. majuscula* specimens closely resemble that of the Gran Canarian *L. majuscula* (Masuda et al., 1998).

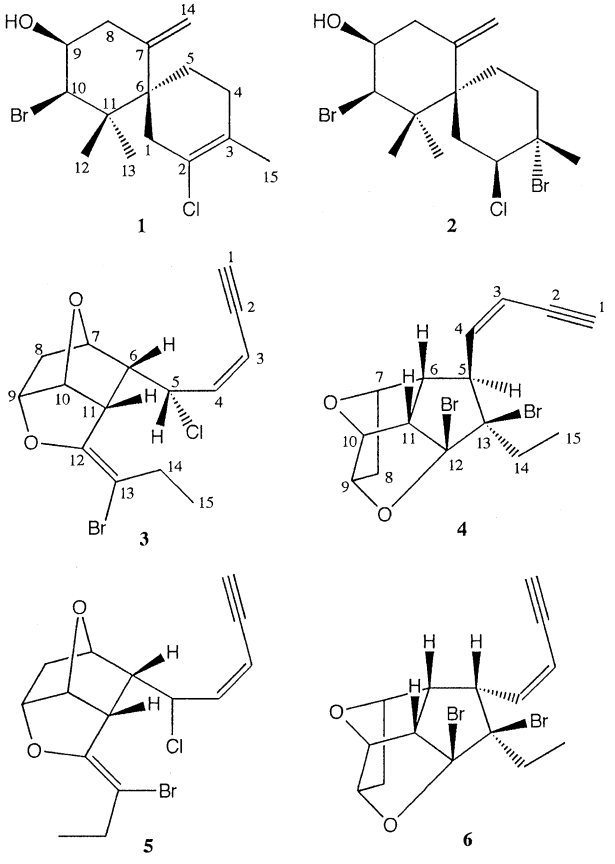

2.2. Laurencia species

The unrecorded *Laurencia* sp. collected at Pulau Lembu, Kedah, Malaysia, on 29 December 1997, was extracted with methanol. The methanol extract was fractionated by CC over silica gel with a step gradient (hexane and EtOAc). The fraction eluted with hexane–EtOAc (9:1) was further subjected to prep. TLC with hexane–EtOAc (3:1) to give elatol (**1**) in 38% yield based on the weight of the extract. In addition, the fraction eluted with hexane–EtOAc (75:25) was further subjected to prep. TLC with chloroform to give lembyne-A (**3**) (1.7%) and lembyne-B (**4**) (0.9%).

Lembyne-A (**3**), $[\alpha]_D^{24}$ +197.6° ($CHCl_3$), was assigned the molecular formula $C_{15}H_{16}BrClO_2$ (HR–EIMS). The IR spectrum showed signals due to a terminal acetylenic group at ν_{max} 3200 and 2100 cm^{-1} and a vinyl ether stretching at 1685 and 1210 cm^{-1}. Strong C–O bands (1175–1117 cm^{-1}) with no hydroxyl or carbonyl absorptions suggested that both oxygens were involved in ether links. The presence of a 1-buten-3-ynyl moiety was evident from the ^1H NMR spectrum (Table 1) [δ_H 2.71 (1H, *dd*, $J=2.4$ and 0.9 Hz), 5.00 (1H, *br dd*, $J=10.5$ and 2.4 Hz) and 5.40 (1H, *ddd*, $J=10.5$, 10.5 and 0.9 Hz)]. The *J*-value (10.5 Hz) for H-3 and H-4 indicated the geometry of the double bond at C-3 to be *Z* (Suzuki and Kurosawa, 1987). Interpretation of the ^1H–^1H COSY spectrum enabled the partial structural units **a** and **b** to be considered (Fig. 1).

The ^{13}C NMR spectrum (Table 1) showed the presence of three oxygen-bearing methine carbons at δ_C 78.66 (C-7), 80.51 (C-9), and 85.08 (C-10). In addition, the presence of a trisubstituted vinyl ether moiety (partial structural unit **c**) was also shown by two quaternary carbons at δ_C 149.37 and 102.47 (Suzuki et al., 1983). These chemical shift values indicated that the ethereal oxygen atom is attached to C-12 and a halogen atom to C-13. Another substituent at C-13 can be shown to be the ethyl group (**b**) by analyses of the HMBC spectrum, which is summarized in Table 1, indicating a cross peak between the quaternary carbon at C-13 (δ_C 102.47) and the terminal methyl group (H_3–15). Furthermore, the substituent at C-5 was shown to be a chlorine atom by the halogen-induced ^{13}C isotope shifts (Sergeyev et al., 1995; Raynes et al., 1997; Suzuki et al., 1999). The methine carbon at C-5 (δ_C 55.88) showed an isotope shift of 8 ppb with relative intensities of about 3:1 induced by ^{35}Cl and ^{37}Cl, according to natural isotopic abundance of its halogen atom; ^{35}Cl (75.711%)/^{37}Cl (24.229). Hence, the chlorine atom is linked to C-5 and the bromine atom to C-13.

Lembyne-A (**3**), which has seven degrees of unsaturation, should have two ether linkages. Judging from the ^1H NMR spectroscopic data, **3** has no 1,2-disubstituted oxirane (Tori et al., 1964) or 1,3-disubstituted oxetane (Pretsch et al., 2000; Irie et al., 1970) ring, leading to a planar formula **d** derived by bonding between C-9 and C-12 and between C-7 and C-10. The formula **d** was confirmed by the HMBC spectrum (Table 1).

A literature survey indicated that lembyne-A (**3**) has the same carbon skeleton as maneonenes, maneonene-

Table 1
^{13}C NMR (100 MHz, DEPT), ^{1}H NMR (400 MHz) and HMBC data[a] for lembyne-A (**3**)

C[b]	^{13}C (δ)	^{1}H (δ)	Multiplicity, J (Hz)	HMBC correlations
1	78.41	2.71	*dd*, $J=2.4$, 0.9	
2	86.88			
3	111.31	5.00	*dd*, $J=10.5$, 2.4	H-1, H-4, H-5
4	141.74	5.40	*ddd*, $J=10.5$, 10.5, 0.9	H-3, H-5
5	55.88	4.85	*dd*, $J=10.5$, 10.5	H-3, H-4, H-7
6	54.58	2.34	*dddd*, $J=10.5$, 9.5, 4.4, 0.9	H-4, H-5, H-7, H_2-8, H-10, H-11
7	78.66	3.81	*dd*, $J=4.9$, 4.4	H-6, H_2-8, H-9, H-10, H-11
8	36.55	1.76	*d*, $J=14.2$	H-6, H-10
		1.29	*dddd*, $J=14.2$, 7.8, 4.9, 0.9	
9	80.51	4.14	*dd*, $J=7.8$, 4.9	H-7, H_2-8, H-10, H-11
10	85.08	4.47	*dd*, $J=4.9$, 4.9	H-7, H_2-8, H-11
11	43.35	2.82	*dd*, $J=9.5$, 4.9	H-5, H-6, H-7, H-9, H-10
12	149.37			H-9, H_2-14
13	102.47			H_2-14, H_3-15
14	30.95	2.55	*dq*, $J=14.6$, 7.3	H_3-15
		2.46	*dq*, $J=14.6$, 7.3	
15	15.06	1.18	*dd*, $J=7.3$, 7.3	H_2-14

[a] Measured in benzene-d_6.
[b] Assingments were made with the aid of the HSQC spectrum.

A, -B and -C, isolated from the Hawaiian *Laurencia nidifica* (Waraszkiewicz et al., 1978). Detailed comparisons of the spectral data of **3** with those of maneonenes showed that **3** corresponds to none of the maneonenes.

A study of the molecular models indicated that three oxolane rings in **3** should be proposed as shown in formula **d**. The relative stereochemistries were determined by detailed analysis of the coupling constants in the ^{1}H NMR spectrum as well as from analysis of the NOESY spectrum. The coupling constants, $J_{6,7}=4.4$ Hz and $J_{6,11}=9.5$ Hz, reflecting a ca. 30° dihedral angle between H-6 and H-7 and a ca. 0° angle between H-6 and H-11, were identical to those of *cis*-meneonene-C (**5**). Thus H-6 has an *exo*-configuration, which was also confirmed by NOEs between H-6/H-7 and H-6/H-11. Furthermore, the coupling constant, $J_{5,6}=10.5$ Hz, indicated that the rotation of the C-5–C-6 bond is restricted due to steric hindrance by both the chlorine atom and the conjugated enyne moiety. The conformation between H-5 and H-6 should adopt a *cis*-eclipsed form, which was supported by a NOE between H-5 and H-6. In addition, a NOE between H-4 and H-7 showed that the configuration between C-5 and C-6 is *threo* as shown in formula **e** (Fig. 1). The assignment of the *Z*-configuration to the vinyl ether moiety was made by a NOE between H-11 and H_2-14. Thus lembyne-A has the relative stereochemistry, 5*S**, 6*R**, 7*R**, 9*R**, 10*R** and 11*S**, as shown in formula **3**.

Lembyne-B (**4**), oil, $[\alpha]_D^{24}$ + 157.1° ($CHCl_3$), was assigned the molecular formula $C_{15}H_{16}Br_2O_2$ (HREIMS). The presence of a (*Z*)-1-buten-3-ynyl moiety was also evident from the ^{1}H NMR spectrum (Table 2). The ^{1}H–^{1}H COSY spectrum showed the presence of the same spin systems (**a** and **b**) as in the case of lembyne A (**3**). Since

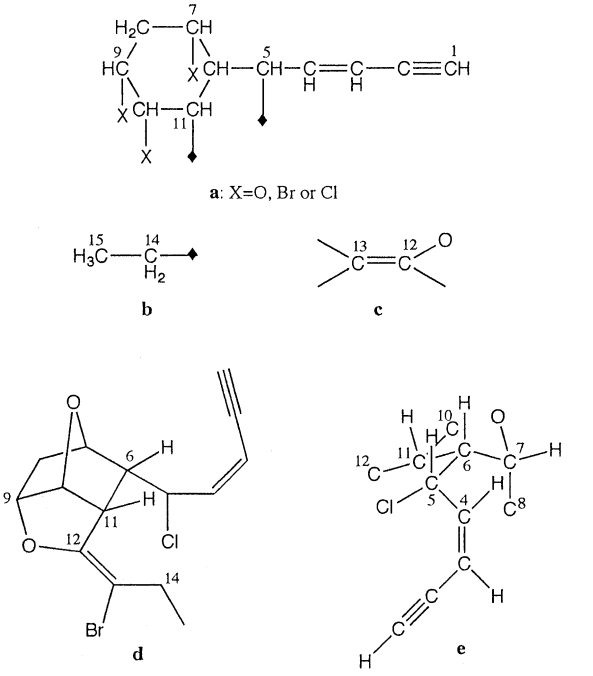

Fig. 1. Partial and planar structures and conformation for lembyne-A (**3**).

the IR spectrum showed no hydroxyl and carbonyl absorptions, both oxygen atoms were suggested to be involved in ether linkages. The ^{13}C NMR spectrum (Table 2) showed fourteen carbon atoms including three oxygen-bearing methine carbons (C-7, C-9 and C-10) which could be correlated with three oxymethine signals in the ^{1}H NMR spectrum by the HSQC measurement. Therefore, the remaining oxygen-bearing carbon must be a quaternary carbon.

Table 2
^{13}C NMR (100 MHz, DEPT), ^{1}H NMR (400 MHz) and HMBC data[a] for lembyne-B (**4**)

C[b]	^{13}C (δ)	^{1}H (δ)	Multiplicity, J (Hz)	HMBC correlations
1	84.38	2.67	*dd*, $J = 1.9, 0.9$	
2	84.08			
3	113.03	5.34	*dd*, $J = 10.7, 1.9$	H-1, H-5
4	141.85	5.47	*ddd*, $J = 10.7, 9.7, 0.9$	H-5, H-6
5	51.47	3.81	*dd*, $J = 9.7, 6.3$	H-3, H-4, H_2-14
6	52.44	1.96	*dddd*, $J = 10.7, 6.3, 5.4, 0.9$	H-4, H-5, H_2-8, H-10, H-11
7	78.63	4.15	*ddd*, $J = 5.4, 5.4, 0.9$	H-5, H_2-8, H-9, H-10, H-11
8	38.58	2.11	*d*, $J = 13.6$	H-6, H-7, H-10
		1.21	*dddd*, $J = 13.6, 5.9, 5.4, 0.9$	
9	81.83	4.31	*ddd*, $J = 5.9, 4.9, 0.9$	H-7, H_2-8, H-10, H-11
10	85.08	5.00	*dd*, $J = 4.9, 4.9$	H-7, H_2-8,
11	60.19	2.93	*dd*, $J = 10.7, 4.9$	H-6, H-7, H-9
12	108.66			H-6, H-9, H_2-14
13				
14	34.24	2.12	*dq*, $J = 13.7, 7.3$	H-5, H_3-15
		1.96	*dq*, $J = 13.7, 7.3$	
15	13.01	0.75	*dd*, $J = 7.3, 7.3$	H_2-14

[a] Measured in benzene-d_6.
[b] Assingments were made with the aid of the HSQC spectrum.

Since there were no halogen-bearing methine signals in the ^{1}H NMR spectrum, the two bromine atoms were assumed to be attached to quaternary carbons. The chemical shift value of δ_C 108.66 suggested the presence of a quaternary carbon with both bromine and oxygen atoms. Furthermore, a missing quaternary carbon should have a remaining bromine atom adjacent to the isolated ethyl group. Since lembyne-B (**4**) has seven degrees of unsaturation, **4** should be a tetracyclic compound. Detailed analysis of the HMBC spectrum (Table 2) of **4** indicated the existence of a ether linkage between C-7 and C-10 by cross-peaks between H-7/C-10 and H-10/C-7. Moreover, in the HMBC spectrum, the above-mentioned quaternary carbon at δ_C 108.66 displayed cross peaks to H-6 and H-9. This result indicated that this quaternary carbon should be adjacent to C-11, leading to the extended partial structure **f** (Fig. 2). In addition, the cross peaks between H-5/C-14, H_2-14 /C-5 and H_2-14/C-12 showed that the missing quaternary carbon with Br and Et group should be inserted between C-5 and C-12, hence giving rise to the planar formula **g**, which has the same carbon framework as isomaneonenes (-A and -B) isolated from the Hawaiian *Laurencia nidifica* (Waraszkiewicz et al., 1978).

The relative stereochemistry of lembyne-B (**4**) came from analysis of the NOESY spectrum. NOEs between H-5/H_{endo}-8, H-5/H_2-14 and H-4/H-6 were indicative that the conjugated enyne side chain and the ethyl group are in the *exo*- and *endo*-configurations, respectively. Thus lembyne-B has (5*R**, 6*R**, 7*R**, 9*R**, 10*R**, 11*S**, 12*S** and 13*R**)-configuration as shown in formula **4**, i.e., it is a stereoisomer of isomaneonene-A (**6**) at C-5.

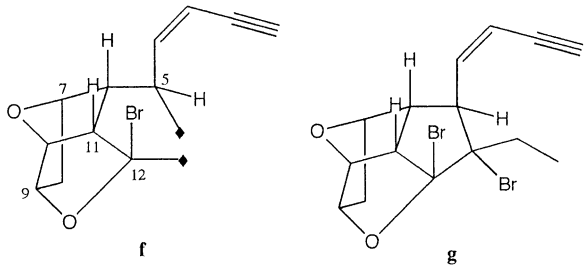

Fig. 2. Partial and planar structures for lembyne-B (**4**).

2.3. Antibacterial activity

The antibacterial activity of the isolated halogenated metabolites was tested against 13 species of marine bacteria isolated from algal habitats in the Malaysian coastal waters. The results of the paper disc diffusion assay are shown in Table 3. Elatol (**1**) showed antibacterial activity against all the 13 species of bacteria tested. It showed minimum inhibitory concentration (MIC) values of 5, 5 and 10 μg/disc against *Clostridium cellobioparum*, *Proteus mirabilis*, and *Flavobacterium helmiphilum* and 15–30 μg/disc against the remaining bacteria. On the other hand, iso-obtusol (**2**) showed MIC values of 10 and 15 μg/disc against *Clostridium cellobioparum* and *Proteus mirabilis*, while those against other bacteria were 40–60 μg/disc. Comparatively, lembyne-A (**3**) showed weaker antibacterial activity with MIC values in the range of 20–60 μg/disc.

"*Corps en cerise*" in superficial cortical cells has been thought to be the site of synthesis and/or storage of halogenated secondary metabolites of *Laurencia* (Young

Table 3
Antibacterial activities of the halogenated compounds against marine bacteria isolated from algal habitats in the Malaysian coastal waters[a]

Test bacteria	Compounds[b]		
	Elatol (**1**)	Iso-obtusol (**2**)	Lembyne-A (**3**)
Chromobacterium violaceum	+ +	+	+
Clostridium fallax	+	–	–
Clostridium novyi	+	–	–
Clostridium sordellii	+	–	–
Clostridium cellobioparum	+ + + +	+ + +	+ +
Escherichia coli	+	+	–
Enterobacter aerogenes	+	–	–
Flavobacterium helmiphilum	+ + +	+	+
Shigella flexneri	+	–	–
Proteus mirabilis	+ + + +	+ +	+
Vibrio cholerae	+	–	–
Vibrio parahaemolyticus	+	+	+
Vibrio vulnificus	+	–	–

[a] Inhibiton zone diameter; + + + +: 25–30 mm, + + +: 19–24 mm, + +: 12–18 mm, +: 7–12 mm, –: no inhibition.
[b] Compound concentration: 90 μg disc^{-1}.

et al., 1980). These intracellular inclusions are present in all investigated *Laurencia* species that produce halogenated secondary metabolites, whereas the *Laurencia* species without these intracellular inclusions does not produce any halometabolites. Hence, halogenated metabolites of "*corps en cerise*" in superficial cortical cells would appear to inhibit the growth of any penetrating marine bacteria.

These findings are the first report on the possible role of halogenated metabolites as antibacterial defense agents in *Laurencia* spp. against the marine bacteria in these algal habitats.

3. Experimental

3.1. General

^{1}H (400 MHz) and ^{13}C NMR (100 MHz); $CDCl_3$ unless otherwise stated, TMS as int. standard (coupling constant, *J* in Hz). The ^{13}C NMR isotope shifts measurements were deduced from ^{13}C NMR spectra taken in the bilevel complete decoupled mode using JEOL JNM-EX-400 spectrometer. The operating frequency was 100.4 MHz. The spectra were obtained using a 2500 Hz spectral window and acquisition time of 52 s and the number of points acquired was 131 K. The FID was zero-filled to 262 K data points (digital resolution was 0.0095 Hz/Pt). The standard Lorentzian-Gaussian resolution enhancement procedure was used before Fourier transformation to achieve a better separation of ^{37}Cl/^{35}Cl splittings. In the spectrum of lembyne-A, the signal of δ_C 55.90 ppm (C-5) showed an isotopic shift of 8 ppb (0.786 Hz) and a peak intensity ratio of 3.04:1. The isotope shift of the signal for C-13 could not be obtained because the respective carbon was not visible in the ^{13}C NMR spectrum. Low and high resolution MS: 70 eV; Optical rotations: $CHCl_3$; CC: silica gel (Merck, Kieselgel 60, 70-230 mesh); prep. TLC: silica gel 60 F_{254} (Merck). All known metabolites were identified by comparison of the spectral data with those of the authentic specimens. Yields are based on the weights of the extracts.

3.2. Collection

Samples of *Laurencia majuscula* were collected from five different sites in Malaysia: Pulau Tikus (Sandakan, Sabah (6°04′06″N, 117°57′48″E); 14 May 1998), Pulau Satang Besar (Kuching, Sarawak (1°47′20″N, 110°09′53″E); 23 May 1998), Pulau Bankawan (Sandakan, Sabah (6°04′56″N, 117°59′50″E); 17 May 1998), Pulau Nunuyan Laut (Sandakan, Sabah (5°56′00″N, 118°06′36″E); 18 May 1998) and Pulau Redang (Terengganu (5°45′17″N, 103°01′16″E), 24 May 1999). While the unrecorded *Laurencia* species was harvested from Pulau Lembu (Kedah (6°04′20″N, 100°03′21″E); 29 December 1997). The voucher specimens are deposited in the Herbarium (SAP) of the Graduate School of Science, Hokkaido University.

3.3. Extraction and separation of L. majuscula

The partially dried sample (40 g) from Pulau Satang Besar was soaked in methanol for 1 week. The MeOH soln was concentrated in vacuo and partitioned between Et_2O and H_2O. The Et_2O soln was washed with water, dried over anhydrous Na_2SO_4 and evaporated to leave a dark green oil (842 mg). The extract was fractioned by Si gel column chromatography with a step gradient (hexane and EtOAc). The fraction eluted with hexane–EtOAc (3:1) was repeatedly submitted to prep. TLC with hexane–EtOAc (3:1) or chloroform to give elatol (**1**) (35 mg) and iso-obtusol (**2**) (193 mg).

Extraction and separation of other samples were carried out in the same manner as described above. Pulau Tikus and Pulau Nunuyan Laut specimens contained elatol (**1**) as the major metabolite. Pulau Tikus specimen (dried alga, 5g); elatol (**1**) (27 mg) and iso-obtusol (**2**) (1.0 mg); Pulau Nunuyan Laut specimen (dried alga, 10 g): **1** (64 mg) and **2** (1.0 mg). Specimens from Pulau Bankawan and Pulau Redang contained iso-obtusol (**2**) as the major metabolite. Pulau Bankawan specimen (dried alga, 20 g): **2** (32 mg) and **1** (13 mg): Pulau Redang specimen (dried alga, 40 g): **2** (230 mg) and **1** (182 mg).

3.4. Elatol (*1*)

Oil; $[\alpha]_D^{24}$ +75.3° (MeOH; *c* 0.318); ^{13}C NMR ($CDCl_3$), CH_3: δ 20.13 (C-15), 21.46 (C-12 or C-13),

24.94 (C-13 or C-12), CH_2: δ 26.33 (C-5), 30.06 (C-4), 38.71 (C-8), 39.33 (C-1), 116.60 (C-14), CH: δ 71.57 (C-10), 72.89 (C-9), C: δ 43.85 (C-6), 49.88 (C-11), 124.86 (C-2), 128.76 (C-3), 141.49 (C-7). The ^{1}H NMR spectrum was identical to that of authentic sample.

3.5. Iso-obtusol (*2*)

Mp 109–113 °C; $[\alpha]_D^{26}$ +24.8° ($CHCl_3$; *c* 0.48); ^{13}C NMR ($CDCl_3$), CH_3: δ 25.58 (C-12 or C-13), 25.98 (C-13 or C-12), 33.74 (C-15), CH_2: δ 26.27 (C-1 or C-5), 33.96 (C-4), 34.58 (C-5 or C-1), 40.01 (C-8), 114.53 (C-14), CH: δ 65.79 (C-2), 70.40 (C-9), 77.08 (C-10), C: δ 44.32 (C-11), 44.56 (C-6), 71.85 (C-3), 148.07 (C-7). The ^{1}H NMR spectrum was identical to that of an authentic sample.

3.6. Extraction and separation of Laurencia species

The partially dried unrecorded *Laurencia* sp. (40 g) was soaked in methanol for one week. The MeOH soln was concentrated in vacuo and partitioned between Et_2O and H_2O. The Et_2O soln was washed with water, dried over anhydrous Na_2SO_4 and evaporated to leave a dark green oil (500 mg). The extract was fractionated by Si gel column chromatography with a step gradient (hexane and EtOAc). The fraction eluted with hexane–EtOAc (9:1) was further submitted to prep. TLC with hexane–EtOAc (3:1) to give elatol (**1**) (190 mg). Further separation of the fraction eluated with hexane–EtOAc (8:2) under the above-mentioned TLC yielded lembyne-A (**3**) (8.5 mg) and lembyne-B (**4**) (4.5 mg).

3.7. Lembyne-A (*3*)

Mp 95–96 °C; $[\alpha]_D^{24}$ +197.6° ($CHCl_3$; *c* 0.70); IR ν_{max} ($CHCl_3$) cm^{-1} : 3200, 2100, 1685, 1210, 1175, 1158, 1117, 1080, 1032, 1020, 1010, 982, 967, 950, 821, 805, 790; ^{1}H and ^{13}C NMR spectra, Table 1; LR–EIMS *m*/*z* (rel. int.): 346, 344, 342 (9:35:27) $[M]^+$, 309, 307 (99:100) $[M\text{-}Cl]^+$, 265, 263 (24:28), 201, 199 (18:16) $[M–C_5H_4Cl–C_2H_5–O]^+$, 159 (34), 122 (29), 115 (20), 91 (25), 81 (20), 79 (22), 77 (31), 69 (27), 65 (18), 41 (24), 39 (21); HR-EIMS *m*/*z*: 342.0013. Calc. for $C_{15}H_{16}{}^{79}Br\ {}^{35}Cl\ O_2$, 342.0022 [M].

3.8. Lembyne-B (*4*)

Oil; $[\alpha]_D^{24}$ +157.1° ($CHCl_3$; *c* 0.10); IR ν_{max} (neat) cm^{-1} : 3300, 2150, 1280, 1262, 1250, 1100, 1050, 1020, 1003, 959, 935, 890, 879, 820, 807, 785, 752; ^{1}H and ^{13}C NMR spectra, Table 2; LR–EIMS *m*/*z* (rel. int.): 390, 388, 386 (7:14:7) $[M]^+$, 309, 307 (98:100) $[M\text{-}Br]^+$, 227 (57) $[M\text{-}Br\text{-}HBr]^+$, 202, 200 (42:42), 141 (20), 107 (28), 79 (23), 77 (24), 65 (13), 41 (11), 39 (11); HR–EIMS *m*/*z*: 387.9482. Calc. for $C_{15}H_{16}{}^{79}Br^{81}BrO_2$, 387.9497 [M].

3.9. Antibacterial bioassays

Antibacterial bioassays were carried out using 13 species of marine bacteria isolated from an algal bed at Penang Island, Malaysia (Vairappan and Suzuki, 2000 and unpublished data). These bacteria are *Chromobacterium violaceum*, *Clostridium fallax*, *Clostridium novyi*, *Clostridium sordellii*, *Clostridium cellobioparum*, *Escherichia coli*, *Enterobacter aerogenes*, *Flavobacterium helmiphilum*, *Shigella flexneri*, *Proteus mirabilis*, *Vibrio cholerae*, *Vibrio parahaemolyticus* and *Vibrio vulnificus*. One loopful of each organism was precultured in 20 ml of peptone water (3% NaCl) overnight. The turbidity of the culture was adjusted to an optical density (OD) McFarland 0.5 (Sonnenwirth and Jarett, 1980; Hindler et al., 1990). Then 0.1 ml of the precultured bacterial suspension was used to seed Nutrient Agar plates (3% NaCl). Paper discs (Whatman, 6 mm) impregnated with various amounts of the respective pure compounds were placed on the seeded agar plates and the diameters of the inhibitory zones were measured after the plates were incubated at 28 °C for 24 h.

Acknowledgements

This study was supported in part by a Grant-in-Aid for Scientific Research (No. 09041134) from the Ministry of Education, Science, Sports and Culture of Japan and also by the Sasakawa Scientific Research Grant from the Japan Science Society (No. 12-300).

References

Ando, Y., Inoue, K., 1961. Decomposition of alginic acid by microorganism—IV. On the *Vibrio*-type bacteria, newly isolated from the decaying *Laminaria*. Nippon Suisan Gakkaishi 27, 339–341.

Caccamese, S., Azzolina, R., Duesler, E.N., Paul, I.C., Rinehart Jr., K.L., 1990. Laurencienyne, a new acetylenic cyclic ether from the marine red alga *Laurencia obtusa*. Tetrahedron Letters 21, 2299–2302.

Carter, G.T., Rinehart Jr., K.L., Li, L.H., Kuentzel, S.L., Connor, J.L., 1978. Brominated indoles from *Laurencia brongniartii*. Tetrahedron Letters, 4479–4482.

Erickson, K.L., 1983. Constituents of *Laurencia*. In: Scheuer, P.J. (Ed.), Marine Natural Products: Chemical and Biological Perspectives, Vol. V. Academic Press, New York, pp. 131–257.

González, A.G., Martín, J.D., Martín, V.S., Martinez-Ripoli, M., Fayos, J., 1979. X ray studies of sesquiterpene constituents of the alga *L. obtusa* leads to structure revision. Tetrahedron Letters, 2717–2718.

Hay, M.E., Fenical, W., Gustafson, K., 1987. Chemical defense against diverse coral-reef herbivors. Ecology 68, 1581–1591.

Hindler, J.A., González, A.H., Drake, T.A., 1990. Stability of viable-bacterium counts in liquid media used for preparation of inocula and subsequent impact on antimicrobial susceptibility test results. Journal of Clinical Microbiology 28, 1271–1275.

Irie, T., Izawa, M., Kurosawa, E., 1970. Lauretin, a constituent from *Laurencia nipponica* Yamada. Tetrahedron 26, 851–870.

König, G.M., Wright, A.D., 1997. Sesquiterpene content of the antibacterial dichloromethane extract of the marine alga *Laurencia obtusa*. Planta Medica 63, 186–187.

Kurata, K., Taniguchi, K., Agatsuma, Y., Suzuki, M., 1998. Diterpenoid feeding-deterrents from *Laurencia saitoi*. Phytochemistry 47, 363–369.

Masuda, M., Kawaguchi, S., Takahashi, Y., Okamoto, K., Suzuki, M., 1999. Halogenated secondary metabolites of *Laurencia similis* (Rhodomelaceae, Rhodophyta). Botanica Marina 42, 199–202.

Masuda, M., Kogame, K., Arisawa, S., Suzuki, M., 1998. Morphology and halogenated secondary metabolites of three Gran Canarian species of *Laurencia* (Ceramiales, Rhodophyta). Botanica Marina 41, 265–277.

Masuda, M., Takahashi, Y., Okamoto, K., Matsuo, Y., Suzuki, M., 1997. Morphology and halogenated secondary metabolites of *Laurencia snackeyi* (Weber-van Bosse) stat. nov. (Ceramiales, Rhodophyta). European Journal of Phycology 32, 293–301.

Pretsch, E., Bühlmann, P., Affolter, C. 2000. Structure Determination of Organic Compounds. Springer, p. 205.

Raynes, W.T., Sergeyev, N.M., Sandor, P., Grayson, M., 1997. ^{81}Br-^{79}Br induced ^{13}C isotope shift and line broadening in the ^{13}C NMR spectrum of methyl bromide. Magnetic Resonance in Chemistry 35, 141–143.

Sawabe, T., Ezura, Y., Kimura, T., 1992. Characterization of an alginolytic marine bacterium from decaying Rishiri-konbu *Laminaria japonica* var. *ochotensis*. Nippon Suisan Gakkaishi 58, 141–145.

Sawabe, T., Makino, H., Tatsumi, M., Nakano, K., Tajima, K., Iqbal, M.M., Yumoto, I., Ezura, Y., Christen, R., 1998. *Pseudoalteromonas bacteriolytica* sp. nov., a marine bacterium that is the causative agent of red spot disease of *Laminaria japonica*. International Journal of Systematic Bacteriology 48, 769–774.

Sawabe, T., Narita, M., Tanaka, R., Onji, M., Tajima, K., Ezura, Y., 2000. Isolation of *Pseudoalteromonas elyakovii* strains from spot-wounded fronds of *Laminaria japonica*. Nippon Suisan Gakkaishi 66, 249–254.

Sergeyev, N.M., Sandor, P., Sergeyeva, N.D., Raynes, W.T., 1995. ^{37}Cl/^{35}Cl- induced ^{13}C isotope shift in chlorinated methanes. Journal of Magnetic Resonance (Series A) 115, 174–182.

Sims, J.J., Lin, G.H.Y., Wing, R.M., 1974. Marine natural product X. Elatol, a halogenated sesquiterpene alcohol from the red alga *Laurencia elata*. Tetrahedron Letters, 3487–3490.

Sonnenwirth, C.A., Jarett, L., 1980. Gradwohl's Clinical Laboratory Methods and Diagnosis, 8th ed. The C. V. Mosby Company, St Louis. pp. 1959–1970.

Suzuki, M., Kurosawa, E., 1987. (3*E*)-Laureatin and (3*E*)-isolaureatin, halogenated C_{15} non-terpenoid compounds from the red alga *Laurencia nipponica* Yamada. Bulletin of the Chemical Society of Japan 60, 3791–3792.

Suzuki, M., Kurosawa, E., Furusaki, A., Matsumoto, T., 1983. The structures of (3Z)-epoxyvenustin, (3Z)-venustin, and (3Z)-venustinene, new halogenated C15-nonterpenoids from the red alga *Laurencia venusta* Yamada. Chemistry Letters, 779–782.

Suzuki, M., Nakano, S., Takahashi, Y., Abe, T., Masuda, M., 1999. Bisezakyne-A and-B, halogenated C_{15} acetogenins from a Japanese *Laurencia* species. Phytochemistry 51, 657–662.

Tori, K., Komeno, T., Nakagawa, T., 1964. Nuclear magnetic resonance studies on steriods. III. Steroidal epoxides and episulfides. The Journal of Organic Chemistry 29, 1136–1141.

Vairappan, C.S., Suzuki, M., 2000. Dynamics of total surface bacteria and bacterial species counts during desiccation in the Malaysian sea lettuce, *Ulva reticulata* (Ulvales, Chlorophyta). Phycological Research 48, 55–61.

Vairappan, C. S., Suzuki, M., Motomura, T., Ichimura, T., 2001. Pathogenic bacteria associated with lesions and thallus bleaching symptoms in the Japanese kelp, *Laminaria religiosa* Miyabe. Hydrobiologia, in press.

Waraszkiewicz, S. M., Erickson, K. L., 1974. Halogenated sesquiterpenoids from the Hawaiian marine alga *Laurencia nidifica*: nidificene and nidifidiene. Tetrahedron Letters, 2003–2006.

Waraszkiewicz, S.M., Sun, H.H., Erickson, K.L., Finer, J., Clardy, J., 1978. C_{15} halogenated compounds from the Hawaiian marine alga *Laurencia nidifica*. Maneonenes and isomaneonenes. The Journal of Organic Chemistry 43, 3194–3204.

Wratten, S.J., Faulkner, D.J., 1977. Metabolites of the red alga *Laurencia subopposita*. The Journal of Organic Chemistry 42, 3343–3349.

Young, D.N., Howard, B.M., Fenical, W., 1980. Subcellular localization of brominated secondary metabolites in the red alga *Laurencia snyderae*. Journal of Phycology 16, 182–185.

Yumoto, I., Ezura, Y., Kimura, T., 1989. Distribution of the *Alteromonas* sp., the causative agent of red-spot on the culture bed of makonbu *Laminaria japonica*, in the coastal area of Funka Bay. Nippon Suisan Gakkaishi 55, 453–462.

PERGAMON

Phytochemistry 58 (2001) 299–304

PHYTOCHEMISTRY

www.elsevier.com/locate/phytochem

Antialgal furano-diterpenes from *Potamogeton natans* L.

Marina DellaGreca[a], Antonio Fiorentino[b,*], Marina Isidori[b], Pietro Monaco[a], Fabio Temussi[a], Armando Zarrelli[a]

[a]*Dipartimento di Chimica Organica e Biochimica, Università Federico II, Complesso Universitario di Monte Sant'Angelo, Via Cinthia, I-80126, Napoli, Italy*

[b]*Dipartimento di Scienze della Vita, II Università di Napoli, Via Vivaldi 43, I-81100, Caserta, Italy*

Received 26 February 2001; received in revised form 18 April 2001

Abstract

Six furano-*ent*-labdanes, 19-acetoxy-15,16-epoxy-8(17),13(16),14-*ent*-labdatrien-20-al, 15,16-epoxy-12-oxo-8(17),13(16),14-*ent*-labdatrien-20,19-olide, 12(*S*)-hydroxy-15,16-epoxy-8(17),13(16),14-*ent*-labdatrien-20,19-olide, 10α,19-dihydroxy-15,16-epoxy-8(17),13(16),14-nor-*ent*-labdatriene, 19,20-dihydroxy-15,16-epoxy-8(17),13(16),14-*ent*-labdatriene, 15,16-epoxy-12-oxo-8(17),13(16),14-*ent*-labdatrien-19,20-olide, were isolated, together with the known potamogetonin, from the aquatic plant *Potamogeton natans*. Their structures were determined on the basis of their chemical and spectral data. The compounds showed in vitro phytotoxicity against *Raphidocelis subcapitata*, a microalga used in aquatic tests. © 2001 Elsevier Science Ltd. All rights reserved.

Keywords: *Potamogeton natans*; Potamogetonaceae; *Raphidocelis subcapitata*; *ent*-Labdanes; Furano-diterpenes; Antialgal activity; Spectroscopic analysis

1. Introduction

Chemical interactions between aquatic plants and microalgae play an important role in aquatic ecosystems since the production of metabolites by the macrophytes might control the algal growth (Fitzgerald, 1969). Hasler and Jones (1949) observed that the algal population decreased when plants belonging to the Potamogetonaceae were present in the aquatic systems. The ability of some natural products to inhibit the in vitro development of the microalgae has been reported copiously (DellaGreca et al., 1996 and ref. cit.) and in a previous paper we showed that bioactive products isolated from *Pistia stratiotes* are released into the environment (DellaGreca et al., 1999).

Recently we investigated *Potamogeton natans*, a freshwater Potamogetonacea, distributed throughout the Mediterranean basin (Cangiano et al., 2001). The phytochemical study has already led to the isolation of several diterpene lactones, some of them showing a high antialgal activity.

2. Results and discussion

In pursuing the chemical investigation of *P. natans*, we isolated the potamogetonin (**1**) (Smith et al., 1976) and six new furanoid *ent*-labdanes **2**–**7**, identified by their spectroscopic features.

Spectral data of compound **1** were in good agreement with those of the revised structure of potamogetonin (Hasegawa and Hirose, 1983), but there were some differences in the chemical shift assignments. Our assignments, based on 2D NMR experiments (H–H COSY, DEPT, HMBC, HMQC, and NOESY), are reported in Table 1. The methylene signals at δ 36.0 and 41.8, ascribed to C-3 and C-1, as well as those at δ 23.7 and 25.7, ascribed to C-11 and C-12, were exchanged on the basis of the HMBC experiment. In fact the signal at δ 36.1, showing interaction with the H-2 at δ 1.70, was attributed to the C-1, while the signal at δ 41.2, correlated with the H-1, H-18 and H-19, was attributed to the C-3. The same spectrum showed the interaction of the carbon at δ 23.8 with the H-11, H-14 and H-16 signals and of the carbon at δ 25.8 with the H-9 and H-12. These observations are in agreement with the exchange of the carbon assignments at C-11 and C-12.

The EI mass spectrum of compound **2** showed a molecular ion at m/z 358, which, together with the

* Corresponding author. Tel.: +39-0823-274576; fax: +39-0823-274571.

E-mail address: antonio.fiorentino@unina2.it (A. Fiorentino).

0031-9422/01/$ - see front matter © 2001 Elsevier Science Ltd. All rights reserved.
PII: S0031-9422(01)00203-5

Table 1
NMR data for compound **1**[a]

Position	Potamogetonin[b] δ_C	**1** DEPT	δ_C	δ_H	HMBC (C→H)
1	41.8	CH_2	36.1	1.25[c]	2
				2.30[c]	
2	20.9	CH_2	21.0	1.40[c]	
				1.70[c]	1, 3
3	36.0	CH_2	41.2	1.44[c]	
				1.65[c]	1, 18, 19
4	33.4	C	33.5	–	5, 6, 18, 19
5	49.4	CH	49.6	1.45[c]	3, 18, 19
6	28.1	CH_2	28.2	1.40[c]	5, 7
				2.10[c]	
				1.90	
7	36.9	CH_2	37.1	2.51[c]	17
8	145.2	C	145.3	–	7, 9, 11, 17
9	51.6	CH	51.2	1.78[c]	7, 11, 12, 17
10	51.2	C	52.8	–	11
11	23.7	CH_2	25.8	2.12[c]	9, 12
				2.50[c]	
12	25.7	CH_2	23.8	2.15[c]	11, 14, 16
				2.60[c]	
13	125.2	C	125.2	–	11, 12, 14, 15, 16
14	111.0	CH	111.0	6.27 *dd* (0.9, 1.6)	12, 15, 16
15	142.7	CH	142.7	7.34 *dd* (1.3, 1.6)	14, 16
16	138.8	CH	139.0	7.20 *dd* (0.9, 1.3)	12, 14, 15
17	108.2	CH_2	108.4	4.84 *brs*	7, 9, 11
				4.96 *brs*	
18	23.7	CH_3	23.8	0.91 *s*	19
19	76.4	CH_2	76.5	3.98 *d* (11.9)	3, 18
				4.17 *dd* (2.1,11.9)	
20	172.9	C	173.0	–	5, 18, 19

[a] Values were recorded at 400 MHz for ^1H and 100 MHz for ^{13}C in $CDCl_3$ with *J* values in Hz in parentheses.
[b] Assignments proposed by Hasegawa and Hirose, 1983.
[c] Overlapped with other signals.

elemental analysis, defined the molecular formula as $C_{22}H_{30}O_4$. The spectroscopic data indicate that the compound contains a $\Delta^{8,17}$ exocyclic methylene group. In fact, the ^1H NMR (Table 2) showed two broad singlets at δ 4.96 and 4.64, the ^{13}C NMR (Table 3) exhibited a quaternary and a methylene carbon at δ 145.6 and 108.0, and the IR spectrum showed ν_{max} bands at 2962, 1619 and 896 cm^{-1}. The presence of a furano group was indicated by the chemical shifts of H-14, H-15 and H-16 protons at δ 6.23, 7.34 and 7.17 in the ^1H NMR, and by the signals of the corresponding carbons in the ^{13}C NMR spectrum at δ 110.8, 142.9 and 138.9. The IR absorptions at 1733 and 1713 cm^{-1} indicated the presence of two carbonyl groups in the molecule. The ^1H NMR also showed a singlet proton at δ 9.82, a methylene group as two double doublets at δ 3.85 and 3.75, and two methyl singlets at δ 2.01 and 0.98.

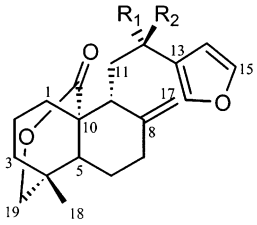

1 R_1 =R_2 = H
3 R_1 =R_2 = O
4 R_1 =OH, R_2 = H
8 R_1 =H, R_2 = OH

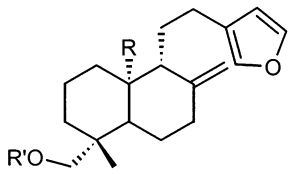

2 R = CHO R' = Ac
5 R = OH R' = H
6 R = CH_2OH R' = H

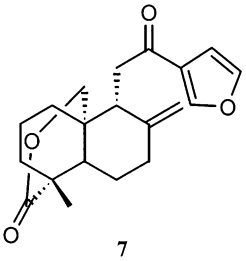

7

Treatment of compound **2** with $NaBH_4$ and subsequent hydrolysis gave a diol **6**. The same product was obtained from the reduction of potamogetonin **1**. The identical values of the optical rotation of the reduction products indicated that they belong to the same *ent*-labdane series.

On the basis of a HMBC experiment, the formyl group was located at the C-10 carbon, while the acetylated function was located at C-4. In fact, the H-18 methyl protons at δ 0.98 were heterocorrelated to the C-19 acetoxymethyl carbon at δ 20.9, while the H-19 protons at δ 3.75 and 3.85 were correlated to the C-18 carbon at δ 26.7. All five protons gave cross peaks with the C-4 carbon at δ 37.4. The formyl proton at δ 9.82 gave interactions with the C-5, C-9 and C-10 carbons at δ 54.5, 52.7 and 53.7, respectively.

In accordance with the assigned structure, the formyl H-20 proton gave NOE with the H-19 at δ 3.85 and the acetyl protons at δ 2.01.

Compound **3** was identified as the 12-oxo derivative of potamogetonin. In the IR spectrum, bands of a γ-lactone and a α,β-unsaturated ketone group at 1720 and 1677 cm^{-1}, respectively, were evident.

In the ^{13}C NMR two carbonyl groups at δ 173.6 and 194.8 were present. This latter was attributed to the C-12 because of the presence, in the ^1H NMR (Table 2), of two double doublets at δ 3.80 and 3.34, attributed to the diasterotopic H-11 protons, and because of the downfield shifts of the H-14 and H-16 proton, at δ 6.80 and 8.20. The ^{13}C NMR data (Table 3) were in agreement with those reported by Hasegawa and Hirose (1983), for its enantiomer.

Compound **4** showed 20 carbon signals in the ^{13}C NMR spectrum (Table 3), which, along with the mole-

Table 2
Selected ^{1}H NMR chemical shifts for labdanes **2**–**8**[a]

Position	**2**	**3**	**4**	**5**	**6**	**7**	**8**
11	1.55 *m*	3.34 *dd* (3.9, 18.1)	2.28 *m*	nd[b]	nd	nd	2.23 *m*
	1.83 *m*	3.80 *dd* (9.0, 18.1)	2.66 *m*				2.81 *m*
12	2.27 *m*		4.67 *d* (9.0)	nd	nd	nd	4.70 dd (5.0, 10.0)
	2.58 *m*						
14	6.23 *dd* (0.9, 1.6)	6.80 *dd* (0.8, 1.7)	6.43 *dd* (0.7, 1.9)	6.26 *dd* (0.8, 1.8)	6.25 *dd* (0.9, 1.8)	6.78 *dd* (1.0, 1.9)	6.42 *dd* (0.7, 1.8)
15	7.34 *dd* (1.3, 1.6)	7.43 *dd* (1.3, 1.7)	7.40 *dd* (1.2, 1.9)	7.36 *dd* (1.4, 1.8)	7.36 *dd* (1.3, 1.8)	7.46 *dd* (1.5, 1.9)	7.40 *dd* (1.2, 1.8)
16	7.17 *dd* (0.9, 1.3)	8.20 *dd* (0.8, 1.3)	7.39 *dd* (0.7, 1.2)	7.20 *dd* (0.8, 1.4)	7.20 *dd* (0.9, 1.3)	8.09 *dd* (1.0, 1.5)	7.34 *dd* (0.7, 1.2)
17	4.64 *brs* 4.96 *brs*	4.61 *s* 4.79 *s*	4.76 *s* 4.96 *s*	4.81 *s* 5.13 *d* (1.1)	4.83 *s* 4.95 *s*	4.46 *s* 4.88 *s*	4.97 *s*
18	0.98 *s*	0.93 *s*	0.92 *s*	0.80 *s*	1.02 *s*	1.22 *s*	0.89 *s*
19	3.75 *d* (11.5)	4.18 *d* (11.8)	4.03 *d* (11.8)	3.20 *d* (11.5)	3.58 *d* (11.6)	–	4.00 d (11.5)
	3.85 *dd* (1.6, 11.5)	4.23 *dd* (1.8, 11.8)	4.19 *dd* (2.0, 11.8)	3.54 *dd* (1.5, 11.5)	3.77 *d* (11.6)		4.16 *dd* (1.5, 11.5)
20	9.82 *s*	–	–	–	3.80 *m*	4.19 *d* (11.6)	–
						4.43 *dd* (1.9, 11.6)	
Ac	2.01 *s*	–	–	–	–	–	–

[a] Values were recorded at 400 MHz in $CDCl_3$ with *J* values in Hz in parentheses.
[b] nd = Not determined.

Table 3
^{13}C NMR chemical shifts assignments for labdanes **2**–**8**[a]

Position	**2**	**3**[b]	**4**	**5**	**6**	**7**[c]	**8**
1	31.9	36.4	36.0	37.7	36.3	38.1	35.9
2	19.2	20.9	20.9	19.8	18.8	21.1	20.8
3	36.6	41.1	41.1	38.2	38.5	39.7	41.0
4	37.4	33.5	33.5	38.1	38.8	43.6	33.7
5	54.5	49.2	49.5	53.6	55.2	49.0	50.9
6	24.4	27.6	28.0	23.8	23.6	26.5	27.8
7	38.2	36.4	36.9	35.9	34.5	35.8	36.8
8	145.6	146.6	145.9	148.4	151.8	146.5	145.8
9	52.7	46.2	48.1	53.3	55.5	45.2	49.0
10	53.7	50.4	50.8	74.1	44.6	37.9	50.9
11	24.1	36.4	34.3	23.0	26.2	36.0	34.1
12	22.8	194.8	65.1	25.5	24.8	192.7	66.1
13	124.7	128.0	130.0	125.0	125.0	127.6	128.3
14	110.8	108.7	108.4	110.8	110.9	108.6	108.2
15	142.9	144.2	143.3	142.8	142.8	144.4	143.5
16	138.9	147.4	138.6	138.8	138.8	146.8	139.7
17	108.0	107.9	108.7	109.6	106.1	109.1	108.6
18	26.7	23.6	23.7	27.8	27.9	23.1	23.6
19	66.5	76.7	76.5	68.6	67.4	176.0	76.4
20	206.8	173.6	173.2	–	65.8	73.1	178.0
Ac1	173.0	–	–	–	–	–	–
Ac2	20.9	–	–	–	–	–	–

[a] Values were recorded at 100 MHz in $CDCl_3$.
[b] Assignments in accordance with Hasegawa and Hirose, 1983.
[c] Assignments in accordance with Hasegawa and Hirose, 1985.

cular ion at *m*/*z* 330 in the EI–MS spectrum, justified a molecular formula $C_{20}H_{26}O_4$. The IR spectrum, besides the signals of the exocyclic methylene, of the furano and of the γ-lactone groups, showed a band at 3290 cm^{-1} attributable to a hydroxyl group. In the ^{1}H NMR (Table 2) the furano protons H-14, H-15 and H-16 were present at δ 6.43, 7.40 and 7.39, the broad singlets H-17 methylene at δ 4.96 and 4.76, the H-19 protons at δ 4.19 and 4.03 and a doublet at δ 4.67 attributable to a proton geminal with a hydroxyl function. This latter proton linked to the carbon at δ 65.1, was heterocorrelated, in the HMBC spectrum, to the furano carbon 13 at δ 130.0 and to the H-11 at δ 2.66 and 2.28, in the H–H COSY. These data located the hydroxyl group at the C-12 carbon univocally. Accordingly, the $NaBH_4$ reduction of ketone **3** gave compound **4**. The configuration of the natural product at C-12 was established by Mosher's method (Dale and Mosher 1973; Othani et al., 1991). The R-MTPA and S-MTPA esters showed a difference in the chemical shift of +0.094 and +0.153 ppm for the H-11 methylene and of −0.07 ppm for the H-14 proton in agreement with the *S* configuration.

Compound **5** had a molecular formula $C_{19}H_{28}O_3$ in accordance with the molecular ion at *m*/*z* 304 in the EI–MS spectrum and 19 carbon signals in the ^{13}C NMR (Table 3). The IR spectrum showed signals for the furano, exocyclic methylene and hydroxyl groups. The ^{1}H NMR spectrum (Table 2) showed a methyl singlet at δ 0.80 and two diasterotopic hydroxymethyl protons at δ 3.54 and 3.20 besides the H-14, H-15 and H-16 furano protons at δ 6.26, 7.36 and 7.20, respectively, and the H-17 methylene signals at δ 5.13 and 4.81. Both the methyl and hydroxymethyl groups were located at C-4 on the basis of the heterocorrelation of their protons, in the HMBC spectrum, with the same carbon at δ 38.1. The compound, after acetylation by Ac_2O in dry pyridine, still showed a hydroxyl absorption in the IR spectrum at 3392 cm^{-1}, attributable to a hindered alcoholic function. In the ^{13}C NMR spectrum, a quaternary carbon at δ 74.1 suggested that this function might be at the C-10 carbon. *Nor*-diterpenes with a hydroxyl group at C-4, have often been isolated from natural sources and data indicate that they are formed by autoxidation of the corresponding aldehydes (Caputo et al., 1974). Accordingly compound **5** was obtained from aldehyde **2** by autoxidation at the light and successive alkaline hydrolysis.

Compound **6** was identified as 19,20-dihydroxy-15,16-epoxy-8(17),13(16),14-*ent*-labdatriene. It had spectral data identical to those reported by Hasegawa and Hirose (1983) for 19,20-dihydroxy-15,16-epoxy-8(17),13(16),14-labdatriene, obtained from chemical reduction of methyl 15,16-epoxy-20-oxo-8(17),13(16),14-labdatrien-19-oate. The opposite rotation indicates that **6** belongs to the *ent*-labdane series.

Compound **7** was easily identified as the isomer of **3**. The spectroscopic data were in accordance with the labdane sciadinone, already isolated from *Sciadopitys verticillata* (Hasegawa and Hirose, 1985 and ref. cit.) unless in the opposite rotation, which confirmed the *ent*-labdane skeleton.

The phytotoxicity profile of these new naturally occurring diterpenes from *P. natans* was determined by the toxicity tests, described in the experimental section, with the unicellular green alga *Raphidocelis subcapitata* (CCAP 278/4, formerly *Selenastrum capricornutum*). Comparison of the toxicity of chemicals after the calculation of their respective median inhibition concentrations (IC_{50}) in μmol/l with the 95% confidence limits, revealed that the toxicity was highly dependent not only on the skeleton but even on the kind of substituent (Table 4).

The most active compounds were **4**, with IC_{50} of 4.40, and **5** with IC_{50} of 2.84. The less active compounds were **2** with IC_{50} of 58.27, and **7** so that it was not possible to estimate the IC_{50} value at the tested concentrations, because of a lack of further available samples. Even compound **3** is not reported in Table 4, because it showed a biostimulation up to the concentration of 25.85 μmol/l and only a slight inhibition of algal growth (8%) at the highest tested concentration (60.89 μmol/l).

3. Experimental

3.1. General experiment procedures

NMR spectra were recorded at 400 MHz for ^1H and 100 MHz for ^{13}C on a Bruker AC400 spectrometer with 0.05 M solns. in $CDCl_3$ at 37 °C. Proton-detected heteronuclear correlations were measured using HMQC (optimised for $^1J_{HC} = 145$ Hz) and HMBC (optimised for $^1J_{HC} = 7$ Hz). Optical rotations were measured on a Perkin-Elmer 343 polarimeter. IR spectra were determined in $CHCl_3$ solns. on a FT–IR Perkin-Elmer 1740 spectrometer. UV spectra were obtained on a Perkin-Elmer Lambda 7 spectrophotometer in EtOH solns. EI–MS spectra were obtained with a Kratos MS 80 apparatus. The HPLC apparatus consisted of a pump (Shimadzu LC-10AD), a refractive index detector (Shimadzu RID-10A) and a recorder Shimadzu Chromatopac C-R6A. Preparative HPLC was performed using RP-8 (Luna 10 μm, 250×10 mm i.d., Phenomenex) columns. Analytical TLC was performed on Merk Kieselgel 60 F_{254} or RP-18 F_{254} plates with 0.2 mm layer thickness. Spots were visualised by UV light or by spraying with H_2SO_4–AcOH–H_2O (1:20:4). The plates were then heated for 5 min at 110°C. Prep. TLC was performed on Merck Kieselgel 60 F_{254} plates, with 0.5 or 1 mm film thickness. Flash column chromatography (FCC) was performed on Merck Kieselgel 60 (230–400 mesh) at medium pressure. Column chromatography (CC) was performed on Merck Kieselgel 60 (70–240 mesh) or on Sephadex LH-20® (Pharmacia).

Table 4
IC_{50} values of diterpenes from *Potamogeton natans* (μmol/l)

Compounds	IC_{50}	95% Confidence limits
1	28.58	23.85–36.63
2	58.27	37.94–89.49
4	4.40	3.11–6.21
5	2.84	2.04–3.95
6	18.45	13.73–24.81

3.2. Plant material

Plants of *Potamogeton natans* were collected from the Volturno River, near Naples (Italy), and identified by Professor Antonino Pollio. A voucher specimen is deposited at the Dipartimento di Biologia Vegetale of University Federico II of Naples.

3.3. Extraction and isolation

The air dried and powdered plant material (13 kg) was sequentially and exhaustively extracted with light petrol, EtOAc and MeOH. The extracts were frozen and stored at −80°C until used.

3.3.1. Light petrol extract fractionation

The light petrol extract (66 g) was chromatographed on silica gel to give fractions A and B. Fraction A eluted with hexane–EtOAc (19:1) was chromatographed using hexane–EtOAc (17:3) as eluent to give pure compounds **1** (125 mg) and **2** (57 mg). Fraction B eluted with hexane–EtOAc (17:3) was filtered on Sephadex LH-20 using hexane–$CHCl_3$–MeOH (3:1:1) as eluent. The elute purified by prep. TLC, using a mixture of C_6H_6–EtOAc (19:1) as eluent, gave pure **3** (85 mg) and **7** (4 mg).

3.3.2. EtOAc extract fractionation

The EtOAc extract (79 g) was chromatographed on silica gel with hexane and EtOAc solns. to give fractions C and D. Fraction C, eluted with hexane–EtOAc (4 : 1), was chromatographed on Sephadex LH-20 with hexane-$CHCl_3$–MeOH (3:1:1). The elute, purified by HPLC using a preparative RP-8 column and a mixture of

MeOH–H_2O (4:1) as eluent, gave pure **4** (35 mg) and **5** (11 mg). Fraction D was chromatographed on prep. TLC [$CHCl_3$–EtOAc (3:1)] to give compound **6** (31 mg).

3.4. Compound characterisation

3.4.1. 15,16-Epoxy-8(17),13(16),14-ent-labdatrien-20,19-olide (1)

White amorphous powder; $[\alpha]_D^{25}$ −29.7° ($CHCl_3$, c 0.34); spectral data: see Table 1.

3.4.2. 19-Acetoxy-15,16-epoxy-8(17),13(16),14-ent-labdatrien-20-al (2)

White amorphous powder; $[\alpha]_D^{25}$ −17.1° ($CHCl_3$, *c* 0.52); UV (EtOH) λ_{max} (log ε): 207 (3.95); IR ν_{max} ($CHCl_3$) cm^{-1}: 2962, 1733, 1713, 1619, 1509, 896, 875; ^1H NMR: see Table 2; ^{13}C NMR: see Table 3; EI–MS: *m/z* 358 $[M]^+$, 343 $[M–CH_3]^+$, 329 $[M–CHO]^+$, 298 $[M–AcOH]^+$, 81 $[C_5H_5O$, pyrylium ion$]^+$; elemental analysis: found: C, 73.86; H, 8.37. $C_{22}H_{30}O_4$ requires: C, 73.71; H, 8.44%.

3.4.3. 15,16-Epoxy-12-oxo-8(17),13(16),14-ent-labdatrien-20,19-olide (3)

Colourless oil; $[\alpha]_D^{25}$ +22.5° ($CHCl_3$, *c* 0.43); UV (EtOH) λ_{max} (log ε): 204 (3.89), 252 (1.95); IR ν_{max} ($CHCl_3$) cm^{-1}: 2969, 1720, 1677, 1615, 1500, 895, 873; ^1H NMR: see Table 2; ^{13}C NMR: see Table 3; EI-MS: *m/z* 328 $[M]^+$, 313 $[M–CH_3]^+$, 247 $[M–C_5H_5O]^+$, 81 $[C_5H_5O$, pyrylium ion$]^+$; elemental analysis: found: C, 73.02; H, 7.36. $C_{20}H_{24}O_4$ requires: C, 73.15; H, 7.37%.

3.4.4. 12(S)-Hydroxy-15,16-epoxy-8(17),13(16),14-ent-labdatrien-20,19-olide (4)

Colourless oil; $[\alpha]_D^{25}$ −25.7° ($CHCl_3$, *c* 0.31); UV (EtOH) λ_{max} (log ε): 204 (4.01); IR ν_{max} ($CHCl_3$) cm^{-1}: 3290, 2944, 1728, 1620, 1500, 891, 875; ^1H NMR: see Table 2; ^{13}C NMR: see Table 3; EI–MS *m/z*: 330 $[M]^+$, 315 $[M–CH_3]^+$, 312 $[M–H_2O]^+$, 249 $[M–C_5H_5O]^+$, 81 $[C_5H_5O$, pyrylium ion$]^+$; elemental analysis: found: C, 72.65; H, 7.96. $C_{20}H_{26}O_4$ requires: C, 72.70; H, 7.93%.

3.4.5. 10α,19-Dihydroxy-15,16-epoxy-8(17),13(16),14-nor-ent-labdatriene (5)

Colourless oil; $[\alpha]_D^{25}$ −4.1° ($CHCl_3$, c 0.21); UV (EtOH) λ_{max} (log ε): 205 (3.89); IR ν_{max} ($CHCl_3$) cm^{-1}: 3392, 2934, 1642, 1463, 890, 878; ^1H NMR: see Table 2; ^{13}C NMR: see Table 3; EI–MS *m/z*: 304 $[M]^+$, 289 $[M–CH_3]^+$, 286 $[M–H_2O]^+$, 223 $[M–C_5H_5O]^+$, 81 $[C_5H_5O$, pyrylium ion$]^+$; elemental analysis: found: C, 74.90; H, 9.29. $C_{19}H_{28}O_3$ requires: C, 74.96; H, 9.27%.

3.4.6. 19,20-Dihydroxy-15,16-epoxy-8(17),13(16),14-ent-labdatriene (6)

Colourless oil; $[\alpha]_D^{25}$ −20.4° ($CHCl_3$, c 0.38); UV (EtOH) λ_{max} (log ε): 204 (3.68); IR ν_{max} ($CHCl_3$) cm^{-1}: 3525, 2931, 1637, 1513, 889, 876; ^1H NMR: see Table 2; ^{13}C NMR: see Table 3; EI-MS *m/z*: 318 $[M]^+$, 303 $[M–CH_3]^+$, 300 $[M–H_2O]^+$, 237 $[M–C_5H_5O]^+$, 81 $[C_5H_5O$, pyrylium ion$]^+$; elemental analysis: found: C, 75.33; H, 9.54. $C_{20}H_{30}O_3$ requires: C, 75.43; H, 9.50%.

3.4.7. 15,16-Epoxy-12-oxo-8(17),13(16),14-ent-labdatrien-19,20-olide (7)

Colourless oil; $[\alpha]_D^{25}$ +65.3° ($CHCl_3$, *c* 0.04); UV (EtOH) λ_{max} (log ε): 205 (3.99), 249 (2.09); IR ν_{max} ($CHCl_3$) cm^{-1}: 2970, 1719, 1680, 1610, 1498, 893, 871; ^1H NMR: see Table 2; ^{13}C NMR: see Table 3; EI–MS *m/z*: 328 $[M]^+$, 313 $[M–CH_3]^+$, 247 $[M–C_5H_5O]^+$, 81 $[C_5H_5O$, pyrylium ion$]^+$; elemental analysis: found: C, 73.06; H, 7.34. $C_{20}H_{24}O_4$ requires: C, 73.15; H, 7.37%.

3.5. Preparation of compound 4

$NaBH_4$ (8 mg) was added to a soln. of **3** (30 mg) in MeOH (2.5 ml) and the reaction mixture was stirred for 5 h at room temperature. The hydride in excess was quenched with AcOH (2 drops). The mixture was then directly purified by prep. TLC with C_6H_6–EtOAc (17:3) to give, beside the unreacted **3** (11 mg), compound **4** (5 mg) and its epimer **8** (10 mg). Compound **8** had $[\alpha]_D^{25}$ −13.3° (*c* 0.01, $CHCl_3$); ^1H NMR: see Table 2; ^{13}C NMR: see Table 3.

3.6. Preparation of compound 6

$LiAlH_4$ (15 mg) was added to a soln. of **1** (30 mg) in dry Et_2O (5 ml) and the reaction mixture was stirred for 6 h at room temperature. After the hydride in excess had been destroyed, the mixture was purified by prep. TLC [$CHCl_3$–EtOAc (3:1)] to give compound **6** (23 mg).

The analogue reduction of aldehyde **2** with $NaBH_4$, after alkaline hydrolysis, gave the same compound **6**.

3.7. Preparation of (R) and (S)-MTPA esters of 4

To a soln. of pure **4** (1.5 mg) in dry pyridine (50 μl) (*S*)-(+)-MTPA-Cl (5 μl) was added. After 4 h under magnetic stirring at room temperature, Et_2O (5 ml) and water (5 ml) were added to the reaction mixture. The organic layer gave a crude ester which was purified by prep. TLC eluting with hexane–EtOAc (5:1). The (*S*)-MTPA ester had the ^1H NMR spectral data (400 MHz, $CDCl_3$): δ 6.45 (1H, *s*, H-14), 5.95 (1H, *d*, *J* = 10.5 Hz, H-12), 5.01 (1H, *s*, H-17), 4.69 (1H, *s*, H-17), 4.18 (1H, *dd*, *J* = 1.5, 11.6 Hz, H-19), 4.01 (1H, *d*, *J* = 11.6 Hz, H-19), 2.65 (1H, *m*, H-11), 2.11 (1H, *m*, H-11), 0.90 (3H, *s*, H-18). The (*R*)- MTPA ester of **4** was prepared using the same procedure. ^1H NMR (400 MHz, $CDCl_3$): δ 6.38 (1H, *s*, H-14), 5.91 (1H, *dd*, *J* = 4.7, 10.5 Hz, H-12), 5.02 (1H, *s*, H-17), 4.76 (1H, *s*, H-17), 4.14 (1H, *dd*, *J* = 1.5, 11.5 Hz, H-19), 3.98 (1H, *d*, *J* = 11.5 Hz, H-19), 2.75 (1H, *m*, H-11), 2.26 (1H, *m*, H-11), 0.89 (3H, *s*, H-18).

3.8. Preparation of compound 5

Pure aldehyde **2** (30 mg) was dissolved in C_6H_6 and the soln. evaporated in a large flask to obtain a thin layer. After 2 days at room temperature, the autoxidation mixture was dissolved in peroxides-free Et_2O and the ether soln. extracted with 10% Na_2CO_3 aq. The residue was purified by prep. TLC with hexane–Me_2CO (4:1) to give compound **5** (4 mg).

3.9. Bioassay

The freshwater toxicity test Algaltoxkit F™ (Creasel, Belgium) with the alga *Raphidocelis subcapitata* currently used for aquatic toxicity assays was applied for the antialgal activity. This test is a 0–72 h algal growth inhibition assay and is independent on the live culture stocks of the alga that is immobilized on beads of alginate. Pure chemicals (99%) were dissolved in DMSO and then diluted in bidistilled water to make the final stock solns. The highest DMSO concentration in the test solns. did not exceed 0.01% (v/v). Blanks were carried out to detect whether the DMSO concentrations might cause toxicity. The dilution water used for the test solns. was the OECD medium (OECD, 1994). The alga was inoculated (1×10^4 cells/ml) in 25 ml of test soln. prepared in five concentrations for each chemical and three replicates included the control. Details on the toxicity test procedures are given in DellaGreca et al., (2000). The cell density was measured at 0 time and every 24 h for 3 days by an electronic particle dual threshold counter (Coulter Counter Z2, 100 μm capillary) and from these data the algal growth inhibition was calculated by integrating the mean values from t_0 to t_{72} h (area under the curve), calculating the median inhibition (IC_{50}) in μmol/l and then operating the log-transformation (OECD, 1994).

References

Cangiano, T., DellaGreca, M., Fiorentino, A., Isidori, M., Monaco, P., Zarrelli, A., 2001. Lactone diterpenes from the aquatic plant *Potamogeton natans*. Phytochemistry 56, 469–473.

Caputo, R., Mangoni, L., Monaco, P., Previtera, L., 1974. Autoxidation of terpenic aldehydes — III. Gaz. Chim. Ital 104, 1269–1278.

Dale, J.A., Mosher, H.S., 1973. Nuclear magnetic resonance enantiomer reagents. Configurational correlations via nuclear magnetic resonance chemical shifts of diastereomeric mandelate, O-methylmandelate, and α-methoxy-α-trifluoromethylphenylacetate (MTPA) esters. J. Am. Chem. Soc. 95, 512–519.

DellaGreca, M., Fiorentino, A., Isidori, M., Monaco, P., Zarrelli, A., 2000. Antialgal ent-labdane diterpenes from *Ruppia maritima*. Phytochemistry 55, 909–913.

DellaGreca, M., Fiorentino, A., Monaco, P., Pinto, G., Pollio, A., Previtera, L., 1996. Action of antialgal compounds from *Juncus effusus* L. on *Selenastrum capricornutum*. J. Chem. Ecol 22, 587–603.

DellaGreca, M., Fiorentino, A., Monaco, P., Previtera, L., Pinto, G., Pollio, A., 1999. Release of potential allelochemical from aquatic plants. In: Macias, F.A., Galindo, J.C.G., Molinillo, J.M.G., Cuttler, H.G. (Eds.), Recent Advances in Allelopathy — A Science for the Future, Vol. 1. Academic Cadiz, pp. 255–262.

Fitzgerald, G.P., 1969. Some factore if the competition or antagonism among bacteria, algae and aquatic weeds. J. Phicol., 351–359.

Hasegawa, S., Hirose, Y., 1983. The structure of potamogetonin. Chem. Letters, 1–4.

Hasegawa, S., Hirose, Y., 1985. Diterpenes from the seed of *Sciadopitys verticillata*. Phytochemistry 24, 2041–2046.

Hasler, A.D., Jones, E., 1949. Demonstration of the antagonistic action of large aquatic plants on algae and rotifers. Ecology 30, 359–365.

Organization for Economic Cooperation and Development, 1994. Algal growth inhibition test. OECD Guideline 201. Paris, France.

Othani, I., Kusumi, T., Kashman, Y., Kakisawa, H., 1991. High-Field NMR application of Mosher's method. The absolute configurations of marine terpenoids. J. Am. Chem. Soc. 113, 4092-4096.

Smith, C.R., 1976. Jr. , Madrigal, R. V., Weisleder, D., Mikolajczak, K. L., Highet, R. J., Potamogetonin, a new furanoid diterpene. Structural assignment by carbon-13 and proton magnetic resonance J. Org. Chem. 41, 593–596.

PERGAMON

Phytochemistry 58 (2001) 305–310

PHYTOCHEMISTRY

www.elsevier.com/locate/phytochem

Chlamydocin analogues from the soil fungus *Peniophora* sp.: structures and plant growth-retardant activity

Hiroko Tani[a], Yuzo Fujii[b], Hiromitsu Nakajima[a,*]

[a]*Department of Agricultural Chemistry, Faculty of Agriculture, Tottori University, Koyama, Tottori 680-8553, Japan*
[b]*Department of Materials Science, Yonago National College of Technology, Yonago, Tottori 683-0854, Japan*

Received 29 December 2000; received in revised form 21 March 2001

Abstract

Three chlamydocin analogues that show activity for reducing the height of rice seedlings without blotch and wilting were isolated from the culture filtrate of the soil fungus *Peniophora* sp. and were characterized by spectral data and chemical conversion. For two of these, it is their first isolation as natural products. The proposed role of the functional groups of the 2-amino-8-oxodecanoic acid moiety of these analogues is discussed in terms of growth retardant activity. © 2001 Elsevier Science Ltd. All rights reserved.

Keywords: Rice plant; *Oryza sativa*; Gramineae; *Peniophora* sp.; Chlamydocin; Plant growth regulators; Structural elucidation

1. Introduction

Use of plant growth regulators to control plant height during rice production could reduce lodging, permit higher nitrogen application rates, and increase yields. Most nitrogen recommendations are based on an application rate that will produce the maximum yield without lodging. Because lodging generally results in lower yield and grain quality, a plant shortener or stalk stiffener would be valuable for the rice industry (Eastin, 1983). We, therefore, conducted a screening-based search among the metabolites produced by soil fungi for natural plant growth regulators which would control rice plant height. We found that cladospolide B and zygosporine D act as rice plant growth retardants (Fujii et al., 1995, 2000). Recently we found a fungus, identified as *Peniophora* sp., whose culture filtrate had activity to reduce the height of rice seedlings without causing either blotch or wilting. From their spectroscopic data three active metabolites (**1**, **2** and **3**) (Fig. 1) isolated from the filtrate were shown to be analogues of chlamydocin (Closse and Huguenin, 1974). Compound **1** is the same as the chlamydocin analogue reported by Gupta et al. (1994). Ours is the first isolation of compounds **2** and **3** as natural products, whereas **2** was reported earlier as a chemical conversion product of chlamydocin (Closse and Huguenin, 1974).

2. Results and discussion

The fungus, whose metabolites reduced the height of rice seedlings in the screening, did not form spores in many trials, making identification of the fungus difficult. Eventually, it was determined to be *Peniophora* sp. on the basis of electron microscopy observations and its 18S rRNA gene sequence. Electron microscopy showed that this fungus has a dolipore-parethesome septum in its hyphae, indicative that it belongs to the holobasidiomycetes (Khan and Kimbrough, 1982). The sequence of its 18S rRNA gene (1737 bases) was determined (data not shown) and a BLAST similarity search of the sequence showed that *Peniophora nuda* is the most closely related fungus (97% similarity).

The fungus was grown on malt extract medium without shaking at 24°C for 14 days in the dark. Metabolites extracted from the culture filtrate and purified by chromatography gave compounds **1**, **2** and **3** in respective yields of 3.3, 0.42 and 0.07 mg/l of medium. Compound **1** had the molecular formula $C_{28}H_{40}N_4O_6$ from its HREIMS, with a molecular ion peak at m/z 528.2955, and NMR spectroscopic data. The IR spectrum of **1**

* Corresponding author. Tel.: +81-857-31-5362; fax: +81-857-31-5362.
E-mail address: nakajima@muses.tottori-u.ac.jp (H. Nakajima).

0031-9422/01/$ - see front matter © 2001 Elsevier Science Ltd. All rights reserved.
PII: S0031-9422(01)00209-6

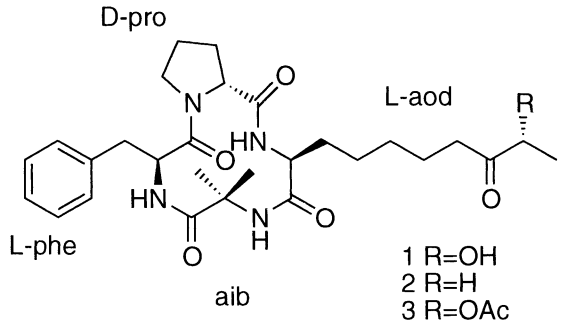

Fig. 1. Chemical structures of compounds **1**–**3**.

showed absorption bands at 3454 cm^{-1} for hydroxyl and/or amide groups, at 1697 cm^{-1} for a ketone carbonyl group, and at 1667 cm^{-1} for amide carbonyl groups. A ketone carbonyl carbon resonance appeared at δ 212.4 in its ^{13}C NMR spectrum, and four amide carbonyl carbon resonances at δ 171.9, 172.8, 174.3, and 175.6. Acetylation of **1** gave a monoacetate, suggesting it has one hydroxyl group. Structural clarifications were based on ^{1}H–^{1}H COSY, HMQC and HMBC data. Analysis of the NMR spectral data (Table 1) for compound **1** suggested that it was the same as the chlamydocin analogue isolated from *Verticillium coccosporum* by Gupta et al. (1994). The reported spectral data, however, were insufficient for unambiguous identification because the NMR data were recorded in C_6D_6 and the optical rotation was not described. We therefore collected NMR spectral data in C_6D_6 and found them identical to the reported data, indicative that compound **1** has the same structure and same relative stereochemistry as the reported analogue. To confirm the absolute stereochemistry of **1**, acid hydrolysis of the compound was carried out. HPLC analysis after derivatizing the hydrolyzate with (+)-1-(9-fluorenyl)ethyl chloroformate (Hayashi and Sasagawa, 1993) showed that the phenylalanine derivative in the hydrolyzate had the same retention time as the L-phenylalanine derivative, evidence that the stereochemistry of the phenylalanine in **1** is L, the same as the reported configuration. Thus **1** was definitively identified as the same as the chlamydocin analogue reported by Gupta et al. (1994).

Compound **2** was characterized as follows: it had the molecular formula $C_{28}H_{40}N_4O_5$ on the basis of its HREIMS data, which showed a molecular ion peak at m/z 512.3001. Its NMR spectral data were similar to those of **1**, indicating that **2** is also a chlamydocin analogue. Its structure was clarified by comparing its NMR spectral data (Table 1) with those for **1**. The carbon resonance (δ 72.6) produced by an oxygenated methine carbon (C-9 of 2-amino-8-oxodecanoic acid (aod)), present in the ^{13}C NMR spectrum of **1**, was absent. Instead, there was a carbon resonance (δ 35.9) due to a methylene carbon in the ^{13}C NMR spectrum of **2**. Furthermore, its ^{1}H NMR spectrum showed a two-proton quartet signal at δ 2.41 and a three-proton triplet signal at δ 1.05, whose signals were coupled. These findings indicate that compound **2** has a structure in which the hydroxyl at the C-9 of aod in compound **1** has been lost. Loss of chirality at the C-9 of aod changed the shape of the proton signal (H-7 of aod) from the AB type triplet in compound **1** to a simple triplet in compound **2**. The amino acid sequence of compound **2** was confirmed from the HMBC correlations between the NH of aod and C-1 of pro, between the NH of 2-aminoisobutyric acid (aib) and C-1 of aod, and between the NH of phe and C-1 of aib. NOE data support this sequence (Fig. 2). The fact that the NOE data for compound **2** are almost the same as those reported for compound **1** suggests that the compounds have the same relative stereochemistry. Compound **2** has been obtained from chlamydocin by chemical conversion (Closse and Huguenin, 1974), but there were insufficient spectroscopic data for unequivocal characterization. Ours is the first report of compound **2** as a natural product and of its full spectroscopic data.

The structure of compound **3** was determined as follows: on the basis of its HREIMS, which showed a molecular ion peak at m/z 570.3035, and its NMR spectral data, this compound has the molecular formula $C_{30}H_{42}N_4O_7$. The NMR spectrum is similar to that of **1**, evidence that **3** also is a chlamydocin analogue. Its structure was established by comparing its NMR spectral data (Table 1) with those for **1** and by chemical conversion. Two new additional carbon resonances (δ 170.4 and 20.7), not observed in the ^{13}C NMR spectrum of **1**, were present in the ^{13}C NMR spectrum of **3**, and an additional new three proton singlet signals appeared at δ 2.15 in its ^{1}H NMR spectrum. These findings indicate there is an additional acetyl group in **3**. Furthermore, the hydroxyl methine proton signal produced by the H-9 of aod was shifted down field (δ 4.23 in the ^{1}H NMR spectrum of **1** to δ 5.08 in that of **3**), indicative that the acetoxyl group is attached to the C-9 of aod. To verify this, compound **1** was acetylated by the usual method. The resulting product was identical in all respects to **3**. Compound **3**, therefore, is a new compound, never before reported.

Plant growth retardant activities for compounds **1**–**3** in a microdrop bioassay (Murakami, 1968) of rice seedlings (*Oryza sativa* L. cv. Koshihikari) are shown in Table 2. Administration of 10 nmol/plant of **1** or **2**

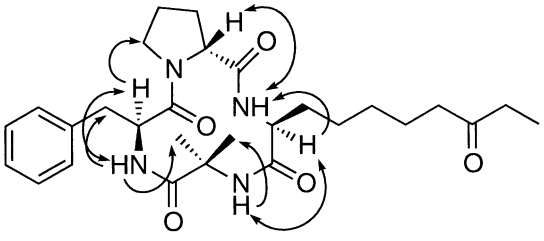

Fig. 2. Key NOE correlations in compound **2**.

Table 1
NMR spectral data for compounds **1**–**3**

Unit position		**1**		**2**		**3**	
		δ_C	δ_H[a]	δ_C	δ_H[a]	δ_C	δ_H[a]
aod	1	174.3		174.4		174.4	
	2	54.3	4.18 (1H, *ddd*, 10.2, 7.8, 7.6)	54.3	4.18 (1H, *ddd*, 10.3, 7.6, 7.6)	54.3	4.18 (1H, *ddd*, 10.2, 7.6, 7.6)
	3	28.74	1.64 (1H, *m*)	28.8	1.56 (1H, *m*)	28.74	1.64 (1H, *m*)
			1.79 (1H, *m*)		1.78 (1H, *m*)		1.79 (1H, *m*)
	4	25.2	1.33 (2H, *m*)	25.3	1.28 (2H, *m*)	25.2	1.33 (2H, *m*)
	5	28.69	1.29 (2H, *m*)	28.7	1.28 (2H, *m*)	28.62	1.29 (2H, *m*)
	6	23.2	1.63 (2H, *m*)	23.6	1.56 (2H, *m*)	22.9	1.63 (2H, *m*)
	7	37.2	2.41 (1H, *ddd*, 17.3, 7.3, 7.3)	42.1	2.40 (2H, *t*, 7.6)	37.9	2.40 (1H, *ddd*, 17.6, 7.3, 7.3)
			2.50 (1H, *ddd*, 17.3, 7.3, 7.3)				2.51 (1H, *ddd*, 17.6, 7.3, 7.3)
	8	212.4		211.7		207.6	
	9	72.6	4.23 (1H, *q*, 7.1)	35.9	2.41 (2H, *q*, 7.3)	74.6	5.08 (1H, *q*, 7.1)
	10	19.8	1.37 (3H, *d*, 7.1)	7.8	1.05 (3H, *t*, 7.3)	16.1	1.39 (3H, *d*, 7.1)
	NH		7.13 (1H, *d*, 10.2)		7.09 (1H, *d*, 10.3)		7.08 (1H, *d*, 10.2)
	CH_3CO					170.4	
	CH_3CO					20.7	2.15 (3H, *s*)
aib	1	175.6		175.6		175.6	
	2	58.8		58.8		58.8	
	3	23.5	1.77 (3H, *s*)	23.5	1.77 (3H, *s*)	23.5	1.77 (3H, *s*)
	4	26.4	1.34 (3H, *s*)	26.4	1.34 (3H, *s*)	26.4	1.34 (3H, *s*)
	NH		6.00 (1H, *s*)		5.95 (1H, *s*)		5.93 (1H, *s*)
phe	1	172.8		172.8		172.8	
	2	53.4	5.15 (1H, *ddd*, 10.2, 10.2, 5.8)	53.4	5.16 (1H, *ddd*, 10.2, 10.2, 5.6)	53.4	5.16 (1H, *ddd*, 10.0, 10.0, 5.8)
	3	35.8	2.95 (1H, *dd*, 13.6, 5.8)	35.8	2.95 (1H, *dd*, 13.5, 5.6)	35.8	2.95 (1H, *dd*, 13.6, 5.8)
			3.25 (1H, *dd*, 13.6, 10.2)		3.26 (1H, *dd*, 13.6, 10.2)		3.26 (1H, *dd*, 13.6, 10.0)
	4	137.0		137.0		137.0	
	5, 9	129.0	7.22 (2H, *m*)	129.0	7.22 (2H, *m*)	129.0	7.22 (2H, *m*)
	6, 8	128.6	7.29 (2H, *m*)	128.6	7.28 (2H, *m*)	128.6	7.29 (2H, *m*)
	7	126.7	7.20 (1H, *m*)	126.7	7.19 (1H, *m*)	126.7	7.20 (1H, *m*)
	NH		7.51 (1H, *d*, 10.2)		7.51 (1H, *d*, 10.2)		7.51 (1H, *d*, 10.0)
pro	1	171.9		171.8		171.9	
	2	57.7	4.65 (1H, *dd*, 7.8, 2.2)	57.8	4.66 (1H, *dd*, 7.8, 2.2)	57.7	4.66 (1H, *dd*, 8.0, 2.7)
	3	24.7	1.74 (1H, *m*)	24.7	1.78 (1H, *m*)	24.7	1.74 (1H, *m*)
			2.31 (1H, *m*)		2.31 (1H, *m*)		2.31 (1H, *m*)
	4	25.0	1.75 (1H, *m*)	25.0	1.78 (1H, *m*)	25.0	1.75 (1H, *m*)
			2.16 (1H, *m*)		2.17 (1H, *m*)		2.16 (1H, *m*)
	5	46.9	3.21 (1H, *ddd*, 10.2, 7.3, 7.3)	47.0	3.22 (1H, *ddd*, 10.2, 7.3, 7.3)	46.9	3.22 (1H, *ddd*, 10.2, 7.6, 7.6)
			3.86 (1H, *ddd*, 10.2, 9.0,4.9)		3.86 (1H, *ddd*, 10.2, 8.5, 5.1)		3.85 (1H, *ddd*, 10.2, 8.3, 4.9)

[a] Intensities, multiplicities and *J* values (Hz) shown in parentheses.

reduced the second leaf sheath length of the treated plants, respectively to 73 and 71% of the value for the water control. The same amount of **3** produced 83% growth of the second leaf sheath length in the treated as compared to control plants. Interestingly, compound **2** was more active than **3** and as active as **1**. This suggests that the hydroxyl group at the C-9 of aod in **1** is not important for plant growth retardation and that the acetoxyl group at the C-9 of aod in **3** reduced activity. It is noteworthy that the metabolites had this effect with causing neither blotch nor wilting.

Cyclic tetrapeptides, which have both proline and an adjacent novel amino acid, 2-amino-9, 10-epoxy-8-oxodecanoic acid, include Cyl-2 from *Cylindrocladium scoparium*

Table 2
Effects of compounds **1**–**3** on second leaf sheath length of rice (*Oryza sativa* L. cv. Koshihikari) seedlings

Amount (nmol/plant)	Second leaf sheath length[a]		
	1	**2**	**3**
0	100 (49.2 mm)	100 (49.2 mm)	100 (46.8 mm)
0.3	94.5±2.1	95.3±2.9	100.0±4.9
1	81.6±1.3	84.8±3.2	100.4±6.3
3	78.3±1.4	79.1±3.5	94.0±1.8
10	73.0±1.4	71.0±3.2	82.9±3.1
30	57.6±3.0	59.6±5.2	79.1±3.1

[a] Values are presented as percentage of the control. Data are mean ± standard error ($n=5$).

(Takayama et al., 1984), chlamydocin from *Diheterospora chlamydosporia* (Closse and Huguenin, 1974), and HC toxin from *Helminthosporium carbonum* (Walton et al., 1982), all of which are reported to have phytotoxic activity. A chlamydocin analogue that has 2-amino-9-hydroxy-8-oxodecanoic acid instead of 2-amino-8, 9-epoxy-8-oxodecanoic acid has phytotoxic activity (Gupta et al., 1994). This means that the phytotoxicity is not produced by the epoxide function of aod. Our present findings show that the 9-hydroxyl of aod is not essential for the retardant activity, and thus the 9-hydroxyl of aod may also not be essential for phytotoxicity. It is necessary to determine the role of the ketone function at the C-8 of aod in the retardant activity. An investigation to clarify this role is in progress.

3. Experimental

3.1. General experimental procedures

Optical rotation was measured with a Horiba SEPA-200 polarimeter. UV spectra were recorded with a Hitachi U-2001 spectrophotometer, and IR spectra with a JASCO FT/IR 7000 spectrometer. NMR spectra were measured with a Jeol Lambda 400 NMR spectrometer. Chemical shifts were referenced to $CDCl_3$ (δ_H 7.26, δ_C 77.0). Mass spectra were obtained with a Jeol AX505HA spectrometer (direct probe, 70 eV). Unless otherwise noted, HPLC was carried out with a Cosmosil 5C_{18}–AR column (Nacalai Tesque, 10×250 mm), 70 wt.% MeOH as the solvent, a flow rate of 1.0 ml/min, and monitoring at 220 nm.

3.2. Fungal material

The fungal isolate, obtained from a soil sample collected in Tottori Prefecture, Japan was found to be very close to *Peniophora nuda* based on electron microscopic observations and the sequence of its 18S rRNA gene: for the electron microscopy study the fungus was grown on PDA medium at 25°C for 7 days. Sections prepared according to the procedure reported (Suh et al., 1993) were observed with a Jeol JEM-1010 transmission electron microscope at 100 kV. For analysis of the l8S rRNA sequence, the isolate was grown in YM medium (0.3% yeast extract, 0.3% malt extract, 0.5% peptone, 1% glucose; pH 5.6) at 25°C for 3 days with shaking. Mycelia were collected by centrifugation, freeze-dried, and disrupted in liq. N_2. Genomic DNA was obtained with a Dneasy Plant Mini Kit (QIAGEN GmbH, Hilden, Germany). The PCR used genomic DNA as the template and NS1 and NS8 (White et al., 1990) as the PCR primers. Amplification conditions were 94°C for 1 min, followed by 30 cycles of 94°C for 1 min, 52°C for 30 s, 72°C for 2 min, and lastly 72°C for 2 min. PCR products were purified with a QIAquick PCR purification kit (QIAGEN GmbH, Hilden, Germany) and directly sequenced. NS1-8 were the sequencing primers (White et al., 1990). All the sequencing reactions were done with a Perkin-Elmer BigDye Terminator Kit, and the sequence determination with a Perkin-Elmer ABI PRISM 377 sequencer.

3.3. Fermentation and extraction

The fungus was grown without shaking at 24°C for 14 days in the dark in 500 ml conical flasks (100) containing liquid medium (200 ml/flask) composed of glucose (30 g/1), peptone (3 g/l), the extract from 50 g/l of malt, and H_2O. Metabolites were extracted from the culture filtrate with EtOAc (3×10 l) after adjusting the pH to 2.0 with HCl. The EtOAc solution was washed with 1 M $NaHCO_3$ (2×0.5 volume), dehydrated over Na_2SO_4 and concentrated to dryness for a residue (1.6 g).

3.4. Purification

The residue (1.6 g) was subjected to silica gel column chromatography (Daisogel IR-60, 16×230 mm), with 200 ml (40 ml×5) each of 30, 40 and 60% acetone in *n*-hexane as eluant. The first fraction (143 mg), eluted with 40% acetone in *n*-hexane, was further purified by Sephadex LH-20 column chromatography (20×370 mm, MeOH). Five milliliter portions of the eluate were collected. Fraction 18 was dried by evaporation, giving **1** as a colorless oil (66 mg). The third fraction (48 mg), eluted with 30% acetone in *n*-hexane and purified by HPLC, gave **2** as a colorless oil (8.4 mg, R_t 30.7 min). The fourth fraction (39 mg), eluted with 30% acetone in *n*-hexane and purified by HPLC, gave **3** as a colorless oil (1.5 mg, R_t 26.9 min).

3.5. Compound *1*

$[\alpha]_D^{23}$ −51° (EtOH; *c* 0.10). UV λ_{max} nm (log ε): 237 (3.58), 205 (4.26). IR ν_{max} (film) cm^{-1}: 3454, 3288, 1697, 1667, 1622, 1528. ^1H NMR and ^{13}C NMR data: see Table 1. ^1H–^{13}C HMBC correlations: aod H-2/aod C-1, aod C-3; aod H-3/aod C-4; aod H-4/aod C-3; aod H-5/aod C-3; aod H-6/aod C-4, aod C-7; aod H-7/aod C-5, aod C-6, aod C-8; aod H-9/aod C-8, aod C-10; aod H-10/aod C-8, aod C-9; aib H-3/aib C-1, aib C-2, aib C-4; aib H-4/aib C-1, aib C-2, aib C-3; aib NH/aib C-2, aib C-3, aod C-1; phe H-2/phe C-1; phe H-3/phe C-1, phe C-2, phe C-4, phe C-5,9; phe H-5,9/phe C-3; pro H-2/pro C-3, pro C-4, pro C-5; pro H-3/pro C-1, pro C-5; pro H-5/pro C-3, pro C-4. EIMS *m*/*z*: $[M]^+$ 528 (26), 498 (8), 485 (20), 471 (27), 428 (50), 426 (15), 409 (28), 343 (7), 330 (23), 314 (15), 269 (14), 229 (26), 219 (10), 172 (14), 120 (37), 70 (100), 58 (66). HR–EIMS *m*/*z*: 528.2955 (calc. for $C_{28}H_{40}N_4O_6$, 528.2948).

3.6. Compound 2

$[\alpha]_D^{23}$ −55.6° (EtOH; *c* 0.36). UV λ_{max} nm (log ε): 237 (3.56), 205 (4.02). IR ν_{max} (film) cm^{-1}: 3453, 3310, 1692, 1667, 1628, 1530. ^1H NMR and ^{13}C NMR data: see Table 1. ^1H–^{13}C HMBC correlations: aod H-2/aod C-1, aod C-3, pro C-1; aod H-7/aod C-5; aod H-9/aod C-8; aod H-10/aod C-8; aod NH/pro C-1; aib H-3/aib C-1, aib C-2; aib H-4/aib C-1, aib C-2; aib NH/aib C-3, aib C-4, aod C-1; phe H-2/phe C-1, aib C-1; phe H-3/phe C-1, phe C-2; phe NH/aib C-1; pro H-2/pro C-1, pro C-4; pro H-5/pro C-4. EIMS *m/z*: $[M]^+$ 512 (16), 456 (14), 455 (16), 413 (13), 412 (44), 400 (11), 393 (22), 315 (18), 314 (51), 253 (22), 252 (11), 229 (26), 201 (10), 156 (21), 131 (12), 120 (37), 91(10), 70 (100), 58 (59), 57 (24). HR–EIMS *m/z*: 512.3001 (calc. for $C_{28}H_{40}N_4O_5$, 512.2999).

3.7. Compound 3

$[\alpha]_D^{23}$ −45.7° (EtOH; c 0.21). UV λ_{max} nm (log ε): 237 (3.52), 211(4.00). IR ν_{max} (film) cm^{-1}: 3456, 1705, 1690, 1456, 1032. ^1H NMR and ^{13}C NMR data: see Table 1. ^1H–^{13}C HMBC correlations: aod H-2/aod C-1, aod C-3; aod H-4/aod C-3, aod C-4; aod H-5/aod C-4; aod H-6/aod C-4; aod H-7/ aod C-5, aod C-6, aod C-8; aod H-9/aod C-8, aod C-10, aod CH_3CO; aod H-10/aod C-8, aod C-9; aod NH/pro C-1; aod CH_3CO/aod CH_3CO; aib H-3/aib C-1, aib C-2, aib C-4; aib H-4/aib C-1, aib C-2, aib C-3; aib NH/aib C-2, aib C-3, aib C-4, aod C-1; phe H-2/phe C-1, phe C-3; phe H-3/ phe C-1, phe C-2, phe C-4, phe C-5,9; phe H-5,9/phe C-3, phe C-6,8, phe C-7; phe 6,8/phe C-4; phe H-7/phe C-5,9, phe C-6,8; phe NH/aib C-1; pro H-2/pro C-3, pro C-4, pro C-5; pro H-3/pro C-1; pro H-5/pro C-3, pro C-4. EIMS *m/z*: $[M]^+$ 570 (24), 514 (20), 513 (29), 512 (13), 470 (47), 451 (26), 412 (18), 372 (43), 314 (31), 311 (19), 310 (12), 229 (28), 214 (20), 120 (34), 70 (100), 58 (55). HR–EIMS *m/z*: 570.3035 (calc. for $C_{30}H_{42}N_4O_7$, 570.3054).

3.8. Acetylation of compound 1

Compound **1** (9.5 mg) was treated overnight with 1 ml of acetic anhydride and 0.5 ml of pyridine. The product was purified by HPLC, giving compound **3** (8.8 mg).

3.9. Amino acid analysis

Compound **1** (0.6 mg) was hydrolysed in 0.12 ml of 6 N HCl at 110°C for 20 h. The reaction mixture was dried by evaporation and dissolved in 50 μl of 0.1 M borate buffer (pH 9.0). Ten microliters of CH_3CN and 2 μl of (+)-1-(9-fluorenyl)ethyl chloroformate (Aldrich, 18 mM in acetone) were added to 10 μl of the hydrolysate solution, after which the mixture was kept at 50°C for 15 min. The reaction was terminated by adding 25 μl of 100 mM cysteic acid in 0.1 M borate buffer (pH 9.0). Before HPLC analysis, the reaction mixture was diluted with 153 μl of 0.1 M NaOAc buffer (pH 4.0) (Hayashi and Sasagawa, 1993). Analytical HPLC employed a Shim Pack CLC-C8 (Shimadzu, 6.0×150 mm) column. Derivatives were detected with a Shimadzu RF 550 fluorescence detector (excitation: 260 nm; emission: 315 nm). Two solvents were used; solvent A consisting of THF–NaOAc buffer (pH 4.0) (25:75, v/v) and solvent B consisting of THF–NaOAc buffer (pH 5.1) (50:50, v/v). Gradient elution conditions were 0–25 min, 0–60% B; 25–80 min, 60% B; 80–90 min, 60–100% B; 90–95 min, 100% B; 95–100 min, 100–0% B. The flow rate was 0.8 ml/min. Under these conditions the R_t of D-phenylalanine derivative was 81.4 min and that of the L-form 85.6 min.

3.10. Biological assays

Compounds **1**–**3** were evaluated for their ability to retard the growth of rice plants. Rice seeds (*Oryza sativa* L. cv Koshihikari) were soaked in H_2O for 48 h at 28°C under fluorescent light. Sets of six germinated seeds were planted on 1% agar medium in 30 ml beakers then incubated for 48 h under continuous light. A 1 μl drop of 50% aq. MeOH containing a certain amount of the test compound was placed between the shoot and first leaf of each seedling. After incubation for 72 h under continuous light, the length of the second leaf sheath of the seedling was measured.

Acknowledgements

We thank Dr. Yukihiro Sugimoto of the Arid Land Research Center of this university for his assistance in measuring the NMR and Miss Izumi Sugimoto of this laboratory for her technical assistance. This investigation was supported in part by a Grant-in-Aid for Scientific Research (No. 11660111) to H.N. from the Ministry of Education, Science and Culture of Japan.

References

Closse, A., Huguenin, R., 1974. Isolierung und Strukturaufklärung von Chlamydocin. Helvetica Chimica Acta 57, 533–545.

Eastin, E.F., 1983. Plant growth regulators in rice. In: Nickell, L.G. (Ed.), Plant Growth Regulating Chemicals, Vol. II. CRC Press, Boca Raton, FL, pp. 150–160.

Fujii, Y., Fukuda, A., Hamasaki, T., Ichimoto, I., Nakajima, H., 1995. Twelve-membered lactones produced by *Cladosporium tenuissimum* and the plant growth retardant activity of cladospolide B. Phytochemistry 40, 1443–1446.

Fujii, Y., Tani, H., Ichinoe, M., Nakajima, H., 2000. Zygosprin D and two new cytochalasins produced by the fungus *Metarrhizium anisopliae*. Journal of Natural Products 63, 132–135.

Gupta, S., Peiser, G., Nakajima, T., Hwang, Y., 1994. Characterization of a phytotoxic cyclotetrapeptide, a novel chlamydocin analogue, from *Verticillium coccosporum*. Tetrahedron Letters 35, 6009–6012.

Hayashi, T., Sasagawa, T., 1993. A method for identifying the carboxy terminal amino acid of a protein. Analytical Biochemistry 209, 163–168.

Khan, S.R., Kimbrough, J.W., 1982. A reevaluation of the basidiomycetes based upon septal and basidial structures. Mycotaxon 15, 103–120.

Murakami, Y., 1968. A new rice seedling test for gibberellins, 'microdrop method' and its use for testing extracts of rice and morning glory. Botanical Magazine Tokyo 81, 33–43.

Suh, S.-O., Hirata, A., Sugiyama, J., Komagata, K., 1993. Septal ultrastructure of basidiomycetous yeasts and their taxonomic implications with observations on the ultrastructure of *Erythrobasidium hasegawaianium* and *Sympodiomycopsis paphopedili*. Mycologia 85, 30–37.

Takayama, S., Isogai, A., Nakata, M., Suzuki, H., Suzuki, A., 1984. Structure of Cyl-1, a novel cyclotetrapeptide from *Cylindrocladium scoparium*. Agricultural and Biological Chemistry 48, 839–842.

Walton, J.D., Earle, E.D., Gibson, B.W., 1982. Purification and structure of the host-specific toxin from *Helminthosporium carbonum* race 1. Biochemical and Biophysical Research Communications 107, 785–794.

White, T.J., Bruns, T., Lee, S., Taylor, J.W., 1990. Amplification and direct sequencing of fungal ribosomal RNA genes for phylogenetics. In: Innis, M.A., Gelfand, D.H., Sninsky, J.J., White, T.J. (Eds.), PCR Protocols, a Guide to Methods and Applications. Academic Press, New York, pp. 315–322.

PERGAMON

Phytochemistry 58 (2001) 311–314

PHYTOCHEMISTRY

www.elsevier.com/locate/phytochem

Insecticidal compounds from *Kalanchoe daigremontiana* × *tubiflora*

Unang Supratman, Tomoyuki Fujita, Kohki Akiyama, Hideo Hayashi*

Division of Applied Biological Chemistry, Graduate School of Agriculture and Life Sciences, Osaka Prefecture University, 1-1 Gakuen-cho, Sakai, Osaka 599-8531, Japan

Received 20 November 2000; received in revised form 23 February 2001

Abstract

Methyl daigremonate, an insecticidal bufadienolide, was isolated from the leaves of *Kalanchoe daigremontiana*×*tubiflora* (Crassulaceae) along with four known bufadienolides. Its structure was established by spectroscopic analysis, and insecticidal activities were assessed against the third instar larvae of silkworm (*Bombyx mori*). The results suggest that the orthoester and α-pyrone moieties played an important role in the activity. © 2001 Elsevier Science Ltd. All rights reserved.

Keywords: *Kalanchoe daigremontiana* × *tubiflora*; Crassulaceae; Bufadienolide; Methyl daigremonate; Insecticidal activity

1. Introduction

In the course of our continuing search for novel insecticidal compounds from Indonesian medicinal plants, we isolated and described two insecticidal bufadienolides, bryophyllins A (**1**) and C (**2**), along with an inactive bufadienolide, bersaldegenin-3-acetate (**3**), from the leaves of *Kalanchoe pinnata* (Supratman et al., 2000). In the further screening for insecticidal compounds from Indonesian *Kalanchoe* (syn. *Bryophyllum*) species, we found that the methanolic extract of the leaves of *Kalanchoe daigremontiana* × *tubiflora* exhibited an insecticidal activity against silkworm.

K. daigremontiana × *tubiflora* (Crassulaceae) is a hybrid plant between *K. daigremontiana* and *K. tubiflora*. Both *Kalanchoe* species are widely distributed in tropical and subtropical countries (Beckett, 1990). The plant is used in Indonesian folk medicine for the treatment of infections, rheumatism, cough, fever and inflammation (Hutapea, 1994). Previous phytochemical studies on both *K. daigremontiana* and *K. tubiflora* reported the presence of sterols (Kalinowska et al., 1990) and bufadienolides (Wagner et al., 1985, 1986; Capon et al., 1986), but the phytochemistry of *K. daigremontiana* × *tubiflora* is still unknown. We now report on the isolation and structural elucidation of a new insecticidal bufadienolide derivative.

2. Results and discussion

Repeated column chromatography of the methanolic extract of fresh leaves of *K. daigremontiana* × *tubiflora* by bioassay-guided fractionation resulted in the isolation of four bufadienolide derivatives (Fig. 1) together with bryophyllin A (**1**). Based on their spectral evidence and a detailed comparison with published data, compounds **4**–**6** were identified as bersaldegenin-1,3,5-orthoacetate (Kupchan and Ognyanov, 1969; Wagner et al., 1986), daigremontianin (Wagner et al., 1985), and bersaldegenin-1-acetate (Kupchan et al., 1971; Wagner et al., 1986), respectively.

Compound **7** was isolated as colorless prisms from chloroform-methanol; mp 258–261°C, $[\alpha]_D^{20}$ −41.7° ($CHCl_3$; *c* 0.024). The molecular formula of **7** was established to be $C_{27}H_{34}O_9$ by HREIMS data (*m*/*z* 502.2185) together with ^1H and ^{13}C NMR spectral data (Table 1), thus requiring 11 degrees of unsaturation. The UV spectrum showed an absorption maximum at 296 nm (log ε 4.02), indicating the presence of a conjugated carbonyl group. The IR spectrum showed bands which were ascribed to hydroxyls (ν_{max} 3544 and 3478 cm^{-1}), an aldehyde (ν_{max} 1714 cm^{-1}), a conjugated ester (ν_{max} 1692 and 1168 cm^{-1}), and an ether group (ν_{max} 1134 and 1109 cm^{-1}). The ^{13}C NMR together with the DEPT spectra revealed 27 carbon signals including characteristic signals due to an orthoester [δ_C 25.6 (*q*), 66.3 (*d*), 71.1 (*d*), 73.2 (*s*), and 111.0 (*s*)], an aldehyde [δ_C 206.2 (*d*)], an ester carbonyl [δ_C 167.9 (*s*)], three sp^2 methines [δ_C 146.3 (*d*), 141.7 (*d*), and 112.0 (*d*)], one sp^2

* Corresponding author. Tel.: +81-722-54-9471; fax: +81-722-54-9471.

E-mail address: hayashi@biochem.osakafu-u.ac.jp (H. Hayashi).

0031-9422/01/$ - see front matter © 2001 Elsevier Science Ltd. All rights reserved.
PII: S0031-9422(01)00199-6

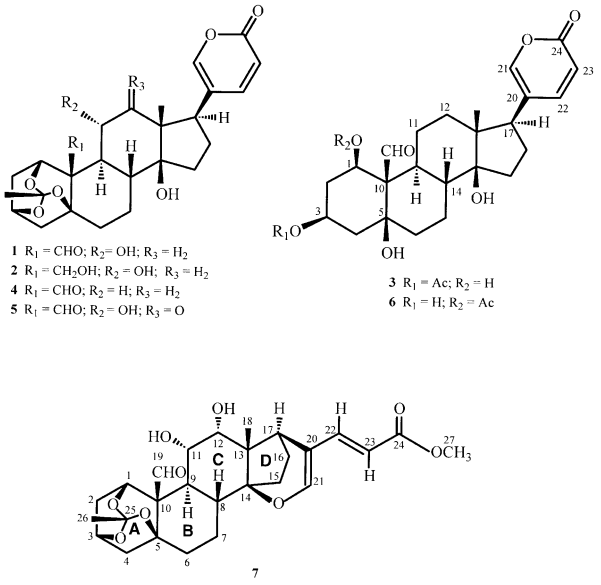

Fig. 1. Structures of bufadienolides derivatives.

quaternary carbon [δ_C 121.3 (*s*)], one carbomethoxyl [δ_C 51.4 (*q*)], one methyl [δ_C 8.8 (*q*)], six methylenes, five methines, and three quaternary carbons, indicating **7** to be a pentacyclic structure with an orthoester moiety.

The ^{1}H NMR spectrum of **7** was quite similar to that of bryophyllin A (**1**), particularly the signals in the A, B, and C rings of **1** (Supratman et al., 2000). The essential differences between the ^{1}H NMR spectra of **1** and **7** consisted of the absence of an α-pyrone ring and appearance of a *trans* olefine [δ_H 5.75 (1H, *d*, J=15.3 Hz) and 7.18 (1H, *d*, J=15.3 Hz)], an olefinic [δ_H 6.54 (1H, *s*)], a carbomethoxyl [δ_H 3.73 (3H, *s*)], and one oxygenated proton [δ_H 3.52 (1H, *dt*, J=5.2, 11.6 Hz)] in the ring C, suggesting that **7** was an α-pyrone opening compound of bufadienolide.

The ^{1}H–^{1}H COSY spectrum of **7** showed correlations in C_1–C_2–C_3–C_4, C_6–C_7–C_8–C_9–C_{11}–C_{12}, and C_{15}–C_{16}–C_{17}, supporting the presence of steroidal structure like that in **1** and remained the cholane skeleton. To determine the connectivity of the partial structure due to an α-pyrone ring cleavage, HMBC experiments were carried out, and the results are shown in Table 1. The carbomethoxyl signal was correlated to an ester carbonyl (δ_C 167.9), and the signals of H-23 (δ_H 5.75) and H-22 (δ_H 7.18) were correlated to the carbonyl and another olefinic carbons at C-20 and C-21, indicating that a conjugated ester was built up at C-21, C-20, C-22, C-23, and C-24. The signal of H-21 (δ_H 6.54) was correlated with C-14 (δ_C 92.8), suggesting that an ether bridge was formed between C-21 and C-14. Other correlations from H-21 to C-20 (δ_C 121.3), and from H-17 to C-13 (δ_C 47.1) and C-14 (δ_C 92.8), also supported the presence of a dihydropyran ring made up of C-21, C-20, C-17, C-13, and C-14. Two oxygenated protons at δ_H 3.89 (δ_C 68.3) and δ_H 3.52 (δ_C 69.0) are mutually coupled, and the signal at δ_H 0.98 (Me-18) was correlated to the oxygenated carbon at δ_C 69.0, while the signal at δ_H 1.95 (H-9) was correlated to the oxygenated carbon at δ_C 68.3, indicating that the signals at δ_C 68.3 and 69.0 were assigned to secondary hydroxyls at C-11 and C-12, respectively. The relative configuration of A and B rings was determined to be the same as those of **1** on the basis of NOESY experiments (Fig. 2). In the differential NOE spectrum, irradiation of the H_3-18 at δ_H 0.98 enhanced the signal intensity of two methine protons (H-8 and H-11), indicating that H_3-18, H-8, and H-11 have a 1,3-diaxial relationship to each other. The relative configuration of a hydroxyl at C-12 was assigned to be α configuration on the basis of ^{1}H–^{1}H coupling constant and NOESY correlation. Consequently, the structure of new insecticidal bufadienolide derivative **7** was determined to be methyl [1β,3β,5β,11α,12α]-(22*E*)-1,3,5-ethylidynetris(oxy)-14,21-epoxy-11,12-dihydroxy-19-oxo-

Table 1
NMR spectral data for compound **7**[a]

Position	^{13}C NMR δ_C (mult.)	^{1}H NMR δ_H (integral, mult., J Hz)	HMBC (^{1}H to ^{13}C)
1	71.1 (*d*)	4.56 (1H, *d*, 3.9)	3, 5, 25
2	27.1 (*t*)	1.61 (1H, *m*) 2.51 (1H, *ddd*, 3.9, 6.4, 14.0)	
3	66.3 (*d*)	4.32 (1H, *m*)	
4	28.4 (*t*)	1.62 (1H, *m*) 2.02 (1H, *m*)	5, 10
5	73.2 (*s*)		
6	41.2 (*t*)	2.09 (1H, *m*) 2.17 (1H, *m*)	5, 9, 10
7	30.6 (*t*)	1.92 (1H, *m*) 1.97 (1H, *m*)	8, 14
8	35.7 (*d*)	1.42 (1H, *dd*, 3.4, 10.7)	9, 14
9	43.6 (*d*)	1.95 (1H, *t*, 10.7)	8, 11
10	51.3 (*s*)		
11	68.3 (*d*)	3.89 (1H, *dt*, 5.2, 10.7)	
12	69.0 (*d*)	3.52 (1H, *d*, 5.2)	
13	47.1 (*s*)		
14	92.8 (*s*)		
15	34.5 (*t*)	1.96 (1H, *m*) 2.20 (1H, *m*)	14, 16
16	32.2 (*t*)	2.01 (1H, *m*) 2.05 (1H, *m*)	13, 14
17	39.0 (*d*)	2.74 (1H, *d*, 5.6)	12, 13, 14, 16, 20, 21, 22
18	8.8 (*q*)	0.98 (3H, *s*)	12, 13, 14, 17
19	206.2 (*d*)	10.28 (1H, *d*, 1.8)	10
20	121.3 (*s*)		
21	146.3 (*d*)	6.54 (1H, *s*)	14, 17, 20, 22
22	141.7 (*d*)	7.18 (1H, *d*, 15.3)	17, 21, 23, 24
23	112.0 (*d*)	5.75 (1H, *d*, 15.3)	20, 21, 24
24	167.9 (*s*)		
25	111.0 (*s*)		
26	25.6 (*q*)	1.44 (3H, *s*)	25
27	51.4 (*q*)	3.73 (3H, *s*)	24

[a] Taken in $CDCl_3$ at 500 MHz for ^{1}H and at 125 MHz for ^{13}C.

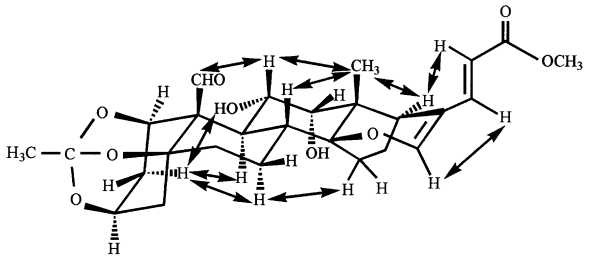

Fig. 2. NOE correlations observed in the NOESY and differential NOE spectra of **7**.

5β,14β-chola-20,22-dien-24-oate, and was named methyl daigremonate.

To determine whether **7** is a natural metabolite or an artifact during the extraction or separation process, identification of **7** was attempted from the acetone extract of the plant. The acetone extract afforded a compound whose HPLC retention time and mass spectrum were identical to those of **7**. Thus, it was confirmed that **7** should be a natural metabolite. The presence of bufadienolides in the parental generation of the hybrid known was not examined in this study.

Compounds **4**–**7** were evaluated for insecticidal activity against the third instar larvae of silkworm. The insecticidal activities of compounds **4**–**7**, and three previously isolated bufadienolides (**1**, **2** and **3**) (Supratman et al., 2000) are shown in Table 2. All bufadienolides having an orthoacetate and α-pyrone moiety showed strong activity, while non-orthoacetate bufadienolides **3** and **6** showed no activity. Methyl daigremonate **7**, an α-pyrone opening type of bufadienolide, showed weak activity. These results suggested that the orthoacetate and α-pyrone moieties were important structural components for insecticidal activity. In addition, daigremontianin (**5**) having oxygenated substituents at C-11 and C-12 showed the strongest activity among these compounds, indicating that oxygenated substituents at C-11 and C-12 on C-ring enhanced the insecticidal activity.

Table 2
Insecticidal activity of bufadienolides

Compounds	LD_{50} μg/g of diet
Bryophyllin A (**1**)	3
Bryophyllin C (**2**)	5
Bersaldegenin-3-acetate (**3**)	>100
Bersaldegenin-1,3,5-orthoacetate (**4**)	16
Daigremontianin (**5**)	0.9
Bersaldegenin-1-acetate (**6**)	>100
Methyl daigremonate (**7**)	82

3. Experimental

3.1. General

Melting points were uncorr.; optical rotation was measured with a Horiba model SEPA-300 polarimeter; UV spectra were recorded on a Hitachi model U-3210 spectrophotometer; IR spectra on a Perkin-Elmer 1760X in KBr; mass spectra were recorded with a JEOL JMS-DX300 and Kratos PC-Kompact MALDI instruments; ^{1}H and ^{13}C NMR spectra were obtained with a JEOL JNM A-500 spectrometer using TMS as internal standard. Chromatographic separations were carried out on Wakogel C-200 (Wako Pure Chemical Industries), silica gel 60 (Merck), and Chromatorex ODS (Fuji Silysia, Japan) adsorbents.

3.2. Plant material

Leaves of *K. daigremontiana* × *tubiflora* were collected from plantation trees growing in Bandung District, West Java, Indonesia in September 1999 and identified by staff of the Laboratory of Plant Taxonomy at Bandung Institute of Technology, Bandung, Indonesia. A voucher specimen (No. 10184) was deposited at the herbarium of the Bandung Institute of Technology.

3.3. Extraction and isolation

Fresh leaves of *K. daigremontiana* × *tubiflora* were exhaustively extracted with MeOH at room temp. The MeOH extract was evap. in vacuo to yield a dark brown residue (182.3 g) that was partitioned between CH_2Cl_2 and H_2O to afford an active CH_2Cl_2 extract (21.5 g). This CH_2Cl_2 extract was subjected to CC on Wakogel C-200 (*n*-hexane–EtOAc–MeOH) to obtain two active fractions, I (100% EtOAc and 10% MeOH eluates, 3.1 g) and II (20% MeOH eluate, 2.5 g). These fractions were separately subjected to CC on silica gel 60 eluted with $CHCl_3$ and an increasing ratio of MeOH. The active fraction (259 mg) from fraction I was successively subjected to silica gel flash-chromatography with $CHCl_3$–MeOH (49:1) and *n*-hexane–Me_2CO (7:3) as eluant. This was followed by crystallization in MeOH to yield bersaldegenin-1,3,5-orthoacetate (**4**, 11.4 mg), daigremontianin (**5**, 14.6 mg), and bryophyllin A (**1**, 6.2 mg). The active fraction (138 mg) from fraction II was then successively subjected to silica gel flash-chromatography with $CHCl_3$–MeOH (19:1) and *n*-hexane–Me_2CO (6:4) as eluant, and then subjected to CC on ODS with MeOH–H_2O (6:4). Finally, bersaldegenin-1-acetate (**6**, 5.5 mg) and methyl daigremonate (**7**, 9.1 mg) were obtained by crystallization from $CHCl_3$–MeOH.

3.4. Methyl daigremonate (7)

Colorless prisms ($CHCl_3$–MeOH), mp 258–261°C. $[\alpha]_D^{20}$ −41.7° ($CHCl_3$; *c* 0.024). HPLC (R_t 10.9 min, Inertsil ODS, 10.0×250 mm; CH_3CN–H_2O = 4:6, 0.8 ml/min, A_{296} nm). UV λ_{max}^{MeOH} nm (log ε): 297 (4.02); IR ν_{max}^{KBr} (cm^{-1}): 3544, 3478, 2924, 1714, 1692, 1618, 1339,

1168, 1134, 1109. ^{1}H NMR ($CDCl_3$) and ^{13}C NMR ($CDCl_3$) (Table 1). HREIMS [found m/z 502.2185 (M^+); calc. for $C_{27}H_{34}O_9$, 502.2202]. EIMS m/z (rel. int): 502 (100), 484 (32), 406 (30), 378 (28), 278 (92), 207 (45).

3.5. Identification of 7 from acetone extract

The fresh leaves of *K. daigremontiana* × *tubiflora* (35 g) collected at the same place in June 2000 were exhaustively extracted with Me_2CO at room temp. The Me_2CO extract was separated as mentioned above except for using Me_2CO instead of MeOH. The CH_2Cl_2 extract (2.4 g) was subjected to CC on Wakogel C-200 (*n*-hexane–EtOAc–Me_2CO by stepwise elution) to obtain 11 fractions. The 20% Me_2CO eluate was separated by preparative HPLC using Inertsil ODS (10.0×250 mm, CH_3CN–H_2O = 4:6, 0.8 ml/min, A_{296} nm) to give a compound (R_t 10.9 min). The retention time and mass spectrum of the isolated compound were identical with those of compound **7**.

3.6. Insecticidal activity (Hayashi et al., 1989)

Larvae of *Bombyx mori* were used for the bioassay, and were cultured on an artificial diet purchased from Nippon Nosan Kogyo Co., Ltd. One hundred microlitres of MeOH extract or a certain amount of the sample to be tested were added to one gram of the diet in a petri dish. After removing the solvent, ten larvae of the third instar stage were introduced into the petri dish. Thirty larvae (three petri dishes) were treated at each dosage, and the mortality rate of the silkworm was observed after 24 h. MeOH was used as a control treatment. The insecticidal activities of tested compounds at each dose were examined by triplicate experiments. The average mortality rate of each dose were determined and used for determining of LD_{50} values by using logarithmic increment.

Acknowledgements

The authors express their gratitude to Dr. Kazuhiro Irie of the Division of Applied Life Sciences in the Graduate School of Agriculture at Kyoto University for the MS measurements.

References

Beckett, K.A., 1990. The Australian and New Zealand Encyclopedia of House Plants, Vol. 1. Simon and Schuster, Australia, pp. 312–314.

Capon, R.J., MacLeod, J.K., Oelrichs, P.B., 1986. Bryotoxins B and C, toxic bufadienolide orthoacetates from flowers of *Bryophyllum tubiflorum* (Crassulaceae). Aust. J. Chem. 39, 1711–1715.

Hayashi, H., Takiuchi, K., Murao, S., Arai, M., 1989. Structure and insecticidal activity of new indole alkaloids, okaramines A and B, from *Penicillium simplicissimum* AK-40. Agric. Biol. Chem. 53, 461–469.

Hutapea, J.R., 1994. Inventory of Indonesian Medicinal Plants, Vol. 3. Research and Development Agency, Ministry of Health, Jakarta, Indonesia, (pp. 117–118).

Kalinowska, M., Nes, W.R., Crumley, F.G., Nes, W.D., 1990. Stereochemical differences in the anatomical distribution of C-24 alkylated sterols in *Kalanchoe daigremontiana*. Phytochemistry 29, 3427–3434.

Kupchan, S.M., Ognyanov, I., 1969. The isolation and structural elucidation of a novel naturally-occurring bufadienolide orthoacetate. Tetrahedron Lett. 21, 1709–1712.

Kupchan, S.M., Ognyanov, I., Moniot, L., 1971. Tumor inhibitors. LXIV. Isolation and structural elucidation of novel bufadienolides, the cytotoxic principles of *Bersama abyssinica*. Bioorg. Chem. 1, 13–31.

Supratman, U., Fujita, T., Akiyama, K., Hayashi, H., 2000. New insecticidal bufadienolide, bryophyllin C, from *Kalanchoe pinnata*. Biosci. Biotechnol. Biochem. 64, 1309–1311.

Wagner, H., Fischer, M., Lotter, H., 1985. Isolation and structure determination of daigremontianin, a novel bufadienolide from *Kalanchoe daigremontiana*. Planta Med. 169–170.

Wagner, H., Lotter, H., Fischer, 1986. Die toxischen und sedierend wirkenden bufadienolide von *Kalanchoe daigremontiana* Hamet et Peer. Helv. Chim. Acta 69, 359–367.

PERGAMON

Phytochemistry 58 (2001) 315–320

PHYTOCHEMISTRY

www.elsevier.com/locate/phytochem

Identification and quantification of catecholamines in potato plants (*Solanum tuberosum*) by GC–MS

Jan Szopa[a,*], Grzegorz Wilczyński[a,b], Oliver Fiehn[b], Andreas Wenczel[a], Lothar Willmitzer[b]

[a]*Institute of Biochemistry and Molecular Biology, University of Wrocław, Przybyszewskiego 63, 51-148 Wrocław, Poland*
[b]*Max Planck Institute of Molecular Plant Physiology, Am Mühlenberg 1, 14476 Golm, Germany*

Received 2 February 2001; received in revised form 3 May 2001

Abstract

Dopamine, norepinephrine, and normetanephrine were identified by GC–MS in potato (*Solanum tuberosum* L.) plants, the latter was new for plants. The highest amount of catecholamines was found in leaves. A developmental stage dependent variation in potato leaf catecholamines accumulation was also observed with highest level in third leaves. Catecholamine contents decrease during cold storage of tubers to undetectable levels. Mechanical wounding of leaves led to a small increase in the level of catecholamines investigated. © 2001 Published by Elsevier Science Ltd.

Keywords: Potato; *Solanum tuberosum*; Solanaceae catecholamines; Dopamine; Norepinephrine; Normetanephrine; GC–MS

1. Introduction

Catecholamines are a group of biogenic amines possessing a 3,4-dihydroxysubstituted phenyl ring. Dopamine (**1**), norepinephrine (**2**), epinephrine and their derivatives are widespread in animals and have also been detected in 44 plant families (Smith, 1977). They are formed in plants from tyrosine, either via tyramine or via dihydroxyphenylalanine (dopa) (Smith, 1980). In banana fruits, dopamine is formed by the hydroxylation of tyramine and further hydroxylated to norepinephrine (Fig. 1). In marine alga (*Monostroma fuscum*) and in Scotch broom (*Cytisus scoparius*) dopamine is formed by decarboxylation of dopa (Smith, 1980). Thus, the biosynthetic pathway of catecholamines in plants is similar to that in animals.

The physiological role of catecholamines in animal cells is well studied. Both epinephrine and norepinephrine are synthesized and released from the medulla of the mammalian adrenal gland. Catecholamine catabolism starts via methylation of the hydroxyl group of the catechol ring followed by oxidation to homovanillic acid and vanillylmandelic acid and subsequent secretion via urine (Smith, 1980). In contrast to the vast amount of knowledge concerning the role and action of catecholamines in mammals, very little is known of the role catecholamines play in plants. Several reports suggest that catecholamines are precursors for alkaloids, the hallucinogen mescaline, identified in several species of cacti (Lundstrom, 1983) and tetrahydroisoquinoline alkaloids (Guinaudeau and Bruneton, 1993), both derived from dopamine. Norepinephrine is believed to be a precursor for berberastine, an alkaloid of *Hydrastis canadensis* (Smith, 1980). Other reports suggest that catecholamines may interact with plant hormones (Dai et al., 1993; Protacio et al., 1992). Most of the data describing the presence of catecholamines in plants have arisen using co-chromatography (either HPLC or TLC) as the criterion for identification (Kuklin and Conger, 1995; Smith, 1977; Wilczyński et al., 1998). To the best of our knowledge, no data have been published that unequivocally demonstrate the chemical nature of the compounds by either NMR or mass spectrometry. The lack of such an analytical system has also made difficult the analysis of large numbers of samples with respect to the variations in levels and types of catecholamines present.

In this study, a fast and highly reliable method allowing the unequivocal detection of catecholamines

* Corresponding author. Tel.: +48-71-3247202; fax: +48-71-3252930.
E-mail address: szopa@biochem.microb.uni.wroc.pl (J. Szopa).

0031-9422/01/$ - see front matter © 2001 Published by Elsevier Science Ltd.
PII: S0031-9422(01)00232-1

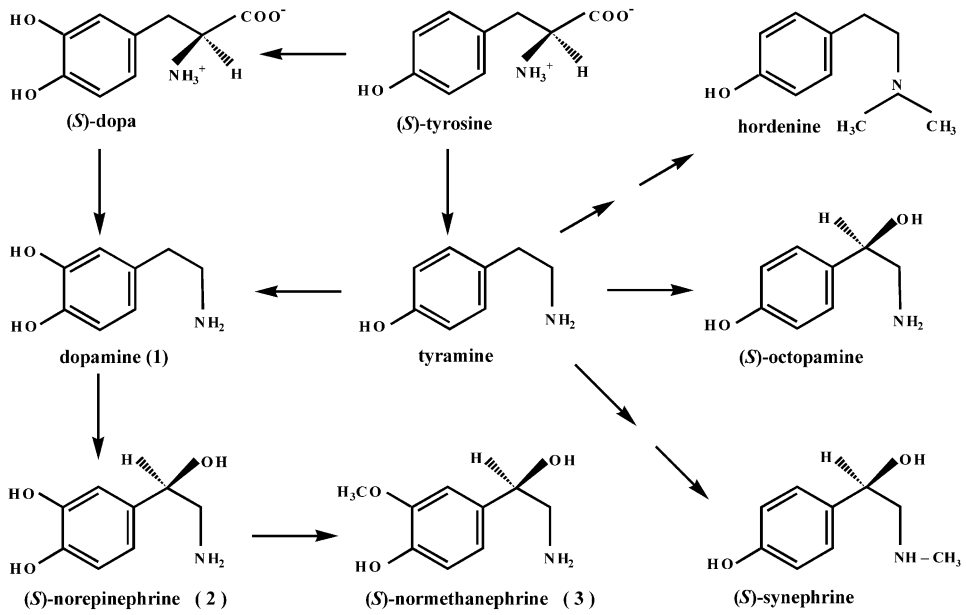

Fig. 1. The biosynthetic pathway of catecholamines in higher plants.

such as **1**, **2**, epinephrine, and their catabolites was developed based on gas chromatography coupled to mass spectrometry (GC–MS). In a second step, this method was applied using potato plants in a variety of physiological states to test whether or not the level of catecholamines correlates in some way with certain developmental, and/or environmental changes. Analysis of a variety of tissues from potato plants definitively revealed the presence of the catecholamines **1**, **2**, and normethanephrine (**3**). Furthermore, some of the data obtained suggest a physiological role of these catecholamines in plants.

2. Results and discussion

Gas chromatography coupled to mass spectrometry allows the quantitative and unequivocal identification of the catecholamines dopamine, norepinephrine, and normetanephrine in plant extracts.

In order to develop an easy and reliable assay for the qualitative and quantitative determination of catecholamines in plants, a sensitive GC–MS method based on the analysis of the trimethylsilylated catecholamine derivatives was developed to monitor the presence and concentration of these compounds and related metabolites. Based on the retention times and the mass spectra of standards, the presence of **1**–**3** of potato leaves was clearly detected (Figs. 2 and 3). The stereochemistry of the identified compounds has not been determined. However, epinephrine, the most prominent hormone of the catecholamine class in mammals, was not detectable. Although the possibility of its presence in the plant extracts analyzed cannot be excluded, epinephrine levels

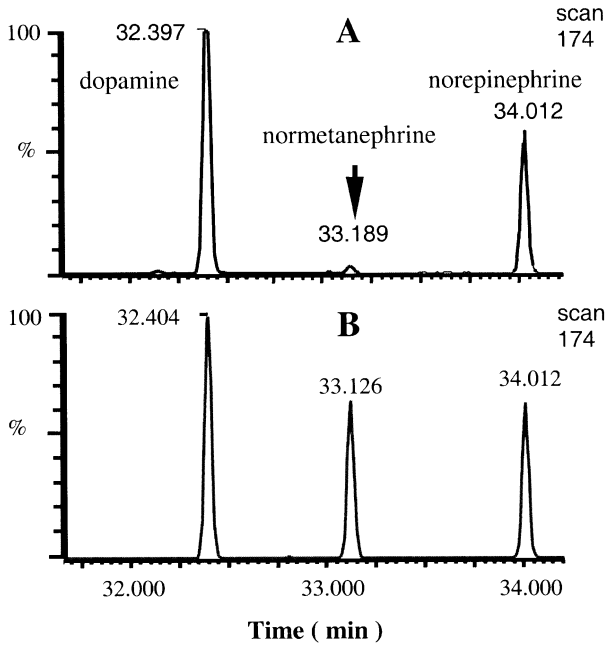

Fig. 2. Chromatographic resolution and single ion monitoring (*m*/*z* 174) of catecholamines in potato leaves. Only a part of chromatogram is shown. (A) potato leaves extract; (B) dopamine, normetanephrine and norepinephrine standards.

would be lower than 20 ng g^{-1} fresh weight as based on recovery and spiking experiments.

In addition, neither homovanillic acid nor vanillylmandelic acid catabolites of **1** and **2**/epinephrine, respectively, were detectable in the extracts analyzed, whereas both octopamine and tyramine, two further derivatives of tyrosine (Fig. 1) with signalling functions in animal systems (Osborne, 1996), were present at levels high enough to be easily identified (not shown). The

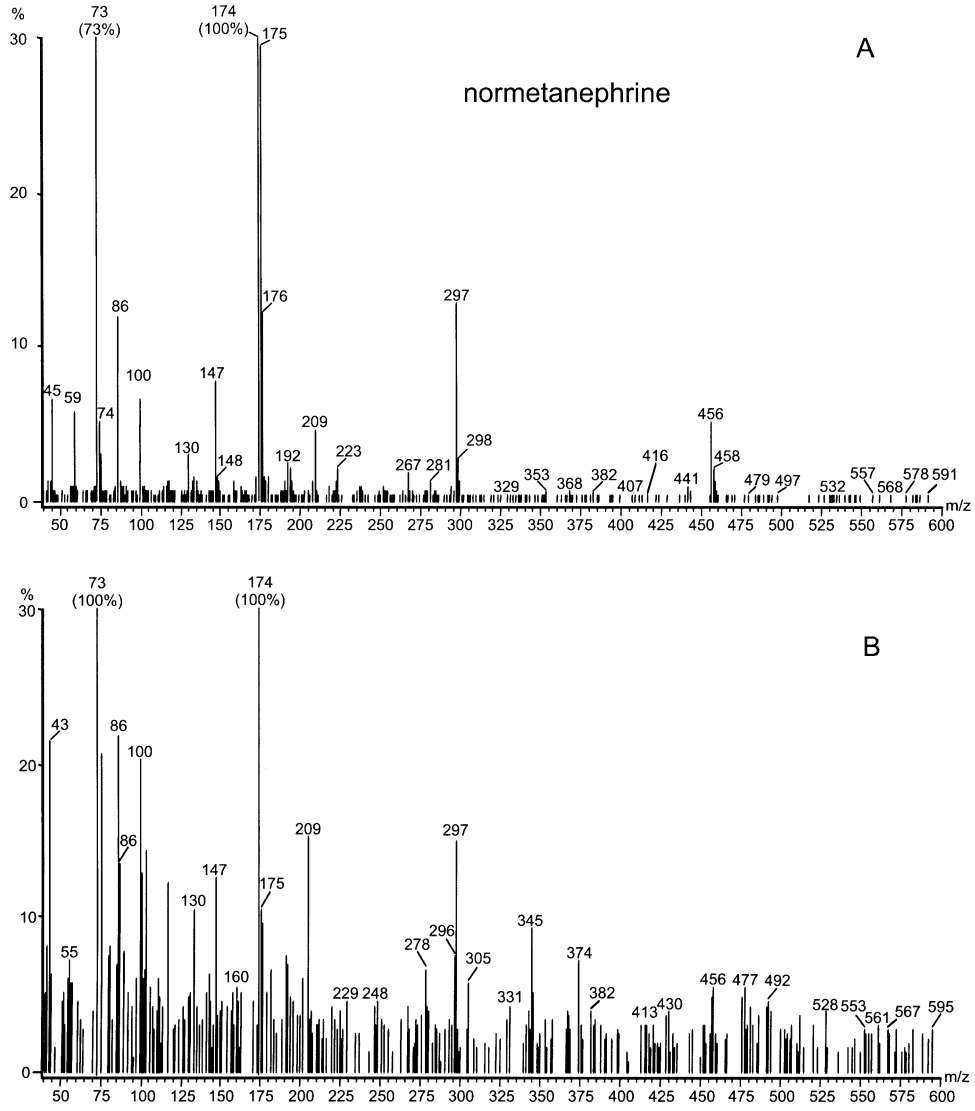

Fig. 3. Comparison of the mass spectra: (A) normetanephrine standard (Sigma); (B) compound from leaf.

catecholamine catabolites homovanillic acid and vanillylmandelic acid are either not present in potatoes or their amounts are below the detection limits.

The content of catecholamines differs significantly between different organs of potato and varies between leaves in different developmental stages.

In order to approach the question concerning possible physiological function of endogenous catecholamines, potato leaves in different developmental stages, tubers, and flowers were analyzed for their content of the various catecholamines.

As shown in Fig. 4, fully developed green leaves (third leaves) contain the highest amounts of catecholamines, whereas significantly lower amounts were found in younger, developing leaves and in older leaves. The contents determined ranged from 1.9–6.9 μg g^{-1} fresh weight for **1**, 2.5–8.4 μg g^{-1} fresh weight for **2**, and 0.2–0.7 μg g^{-1} fresh weight for **3**.

A 10-fold lower amount of **1** and **2** was found for both developing tubers and flowers (Fig. 5). Neither epinephrine nor the catabolites homovanillic acid or vanillylmandelic acid were detected in flower or tuber extracts.

Wounding of leaves consistently leads to a rapid but small increase in norepinephrine.

In mammalian systems, catecholamines serve as stress hormones, displaying a rapid transient increase as a result of stress. In order to see whether or not a similar response occurs in plants, leaves of several plants were wounded and the catecholamine levels prior to and 5, 10 and 30 min after wounding were determined.

Data obtained from three independent experiments are summarized in Fig. 6. Although the data vary, there is a consistent trend towards increasing levels of the three catecholamines analyzed, this is best seen in case of **2**. Potato leaf wounding leads to increase in catecholamine

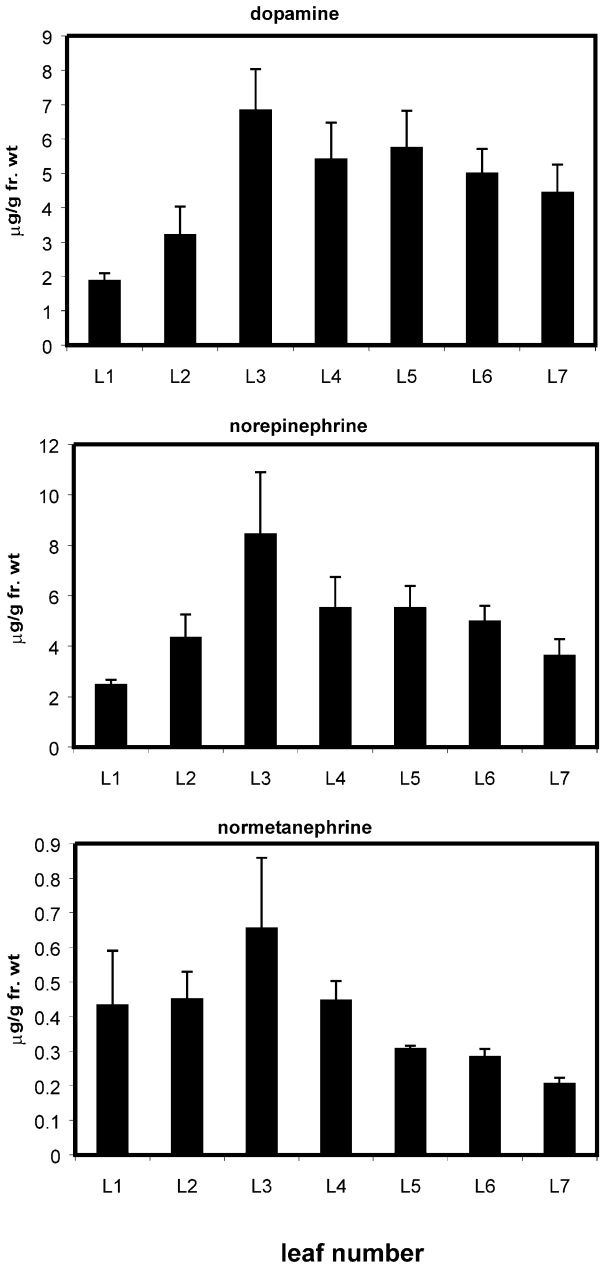

Fig. 4. Catecholamine levels in different leaves of potato plants. L1, 1st leaf from the top of the plant.

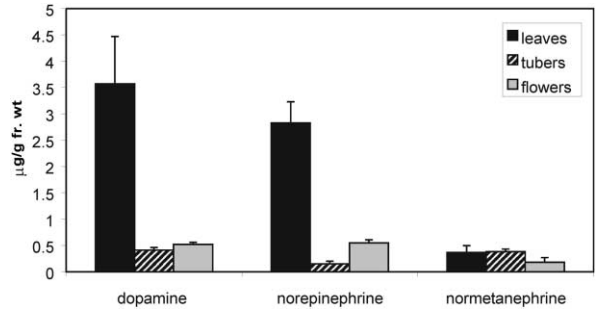

Fig. 5. Catecholamine contents in leaves (average value), tubers, and flowers of potato plant.

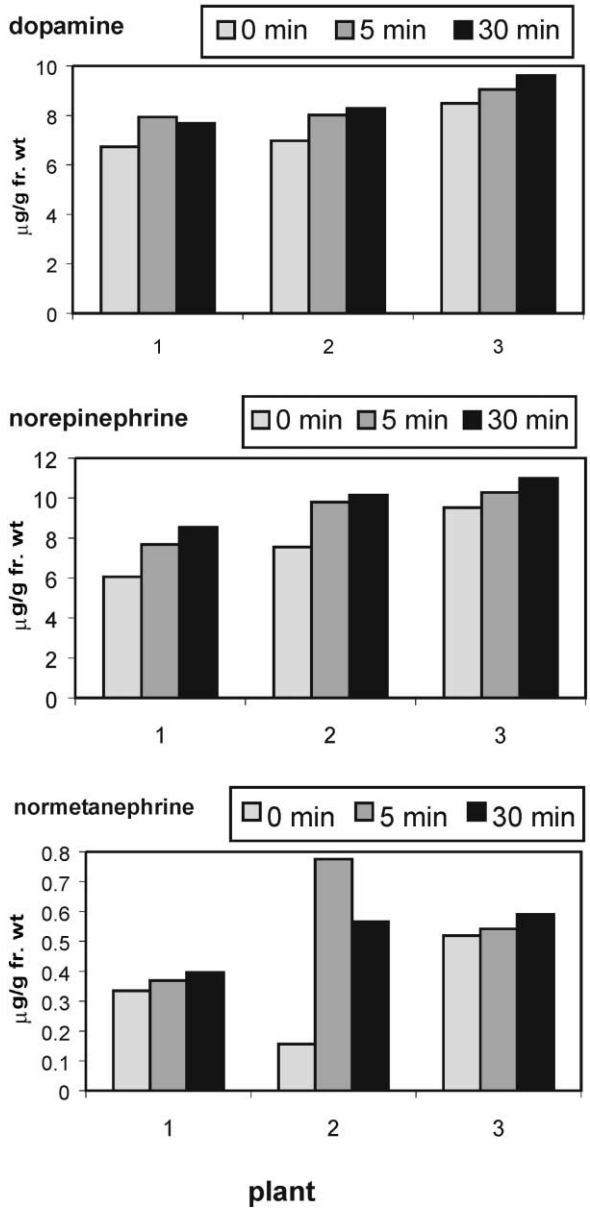

Fig. 6. The effect of leaf wounding on catecholamine levels.

levels. Tyr-dopa decarboxylase is the first key enzyme on the plant catecholamines biosynthesis pathway. Recently the involvement of this enzyme was implicated in plant wounding responses (Park et al., 1999). This observation together with our results may lead to the conclusion that catecholamines or their metabolites may be involved in stress responses.

Storage of tubers at 4 °C leads to decreases in dopamine, norepinephrine, and normetanephrine.

Potato tubers stored at 4 °C react to the low temperature by increasing their solute contents and respiration through starch degradation (Hill et al., 1996). Since one of the best understood examples of the hormonal action of epinephrine and norepinephrine in mammals is the degradation of glycogen, we decided to analyze tubers

undergoing starch degradation for the content of catecholamines.

The data summarized in Fig. 7 show the decrease in **1**–**3** with the time of cold storage, after two months to undetectable levels. Surprisingly, potato tubers when stored at room temperature for the same period of time show almost no decrease in the content of all three catecholamines. The potential correlations between carbohydrate synthesis and metabolism with catecholamine levels remain to be investigated.

3. Experimental

3.1. Plant material

Potato plants (*Solanum tuberosum* L. cv. Desiree) were obtained from Saatzucht Fritz Lange KG (Bad Schwartau, Germany). Plants were cultivated in a greenhouse in soil under a 16 h light (22 °C)/8 h dark (15°C) regime. Plants were grown in individual pots and were watered daily. Leaves were harvested from plants 50 days old. Potato leaves were wounded mechanically. The samples were taken at three time points after 0, 5 and 30 min after wounding. Tubers were harvested three months after transfer of the plants grown in tissue culture to the greenhouse. Tubers were stored than at 4 °C or at room temperature (25 °C) prior to experiments.

3.2. Tissue extraction, derivatization and GC–MS quantification

For GC–MS analysis, frozen plant tissue was powdered in liquid N_2, extracted with MeOH (4 ml g^{-1} fr. wt.), heated for 15 min at 70 °C and centrifuged (5 min, 12,000 *g*). Samples were diluted with H_2O to 50% methanol concentration and extracted with $CHCl_3$ (1:1 v/v). Portion of water phase was dried under vacuum and used for derivatisation. Ribitol was used as an internal standard added directly to the sample homogenate (30 μg g^{-1} fr. wt.).

To the dried extracts, 100 μl methoxyamine hydrochloride (20 mg ml^{-1}) was added and incubated for 90 min at 37 °C. Afterwards, the samples were derivatised with 100 μl *N*-methyl-*N*-trimethylsilyltrifluoroacetamide at 37 °C for 90 min (2 μl of sample was used for analysis). A gas chromatograph GC8000 and AS2000 autosampler (all ThermoQuest, Manchester, UK) combined with a Fisson quadrupole mass spectrophotometer (Voyager), equipped with SPB 50 (Supelco, Bellefonte, CA) fused silica capillary column (30 m×0.25 mm, film thickness 0.25 μm), was used. Dopamine, norepinephrine, and normetanephrine (Sigma) were used as standards. The recovery samples were spiked with dopamine, norepinephrine, and normetanephrine and estimated recoveries were 80, 93 and 85%, respectively. For the quantification (MassLab software-ThermoQuest, Manchester, UK) of catecholamines the corresponding calibration curves ranging from 10 to 1500 ng were used. The following ions were used for quantification: ribitol *m*/*z* 307; 319, dopamine *m*/*z* 174; 426, norepinephrine *m*/*z* 174; 355, normetanephrine *m*/*z* 174; 297. The amounts of catecholamines were determined from the ratio of peak areas of catecholamines to peak area of internal standard (ribitol) and plotted against the amounts ratios using the calibration curves. The curves were fitted by linear regression. The instrument settings were done as recently described (Roessner et al., 2000). The results are the average of three determinations, with S.D. represented by the bars above the graph except for Fig. 6 where the three independent experiments are shown.

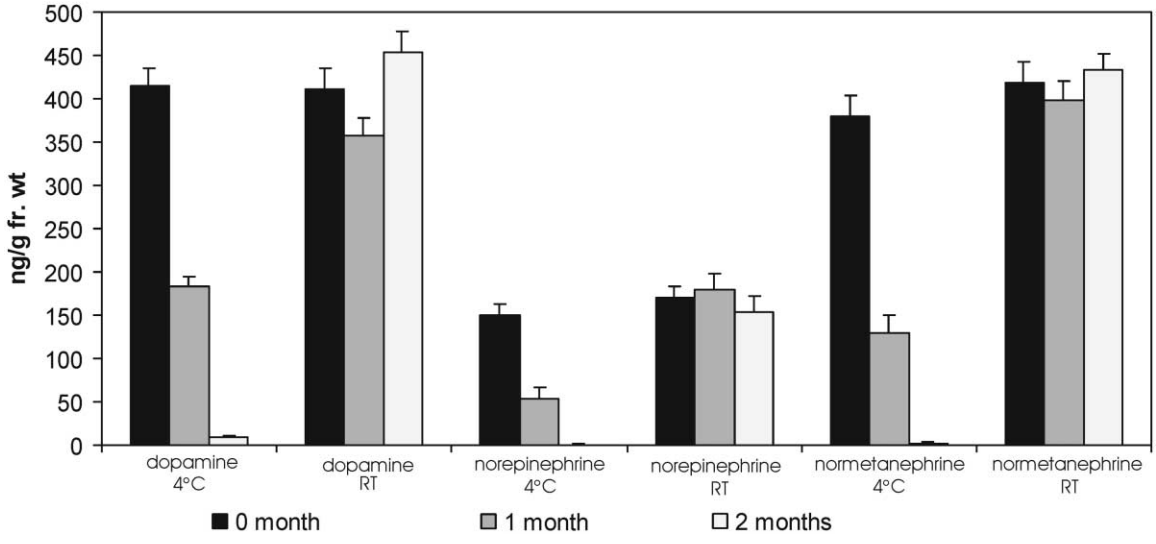

Fig. 7. Catecholamine levels in tubers stored at 4 °C and room temperature for different periods of time.

Acknowledgements

The authors wish to thank C. Wagner and K. Bieberich for help with the GC–MS analysis and M. McKenzie and A. Fernie for linguistic advice. This study was financed by grant 6P04A 02018 from KBN and partially Max Planck Gesellschaft, G.W. was supported by a Max Planck Fellowship.

References

Dai, Y.R., Michaels, P.J., Flores, H.E., 1993. Stimulation of ethylene production by catecholamines and phenylethylamine in potato cell suspension cultures. Plant Growth Reg. 12, 219–222.

Guinaudeau, H., Bruneton, J., 1993. Isoquinoline alkaloids. In: Waterman, P.G. (Ed.), Alkaloids and Sulphur Compounds, In: Dey, P.M., Harborne, J.B. (Eds.), Methods in Plant Biochemistry, Vol. 8. Academic Press, London, pp. 373–419.

Hill, L.M., Reimholz, R., Schroder, R., Nielsen, T.H., Stitt, M., 1996. The onset of sucrose accumulation in cold-stored potato tubers is caused by an increased rate of sucrose synthesis and coincides with low levels of hexose-phosphates, an activation of sucrose phosphate synthase and the appearance of a new form of amylase. Plant, Cell Environ. 19, 1223–1237.

Kuklin, A.I., Conger, B.V., 1995. Catecholamines in plants. J. Plant Growth Reg. 14, 91–97.

Lundstrom, J., 1983. Simple isoquinoline alkaloids. In: Brossi, A. (Ed.), The Alkaloids, Vol. 21. Academic Press, New York, pp. 255–327.

Osborne, R.H., 1996. Insect neurotransmission: Neurotransmitters and their receptors. Pharmacol. Ther. 69, 117–142.

Park, S.U., Johnson, A.G., Penzes-Yost, C., Facchini, P.J., 1999. Analysis of promoters from tyrosine/dihydroxyphenylalanine decarboxylase and berberine bridge enzyme genes involved in benzylisoquinoline alkaloid biosynthesis in opium poppy. Plant Mol. Biol. 40, 121–131.

Protacio, C.M., Dai, Y.-R., Lewis, E.F., Flores, H.E., 1992. Growth stimulation by catecholamines in plant tissue-organ cultures. Plant Physiol. 98, 89–96.

Roessner, U., Wagner, C., Kopka, J., Trethewey, R.N., Willmitzer, L., 2000. Simultaneous analysis of metabolites in potato tuber by gas chromatography-mass spectrometry. Plant J. 23, 131–138.

Smith, T.A., 1977. Phenethylamine and related compounds in plants. Phytochemistry 16, 9–16.

Smith, T.A., 1980. Plant amines. In: Bell, E.A., Charlwood, B.V. (Eds.), Secondary Plant Products, Encyclopedia of Plant Physiology New Series, Vol. 8. Springer Verlag, Berlin, pp. 433–440.

Wilczyński, G., Kulma, A., Feiga, I., Wenczel, A., Szopa, J., 1998. Manipulating of 14-3-3 protein expression results in the changes of catecholamine content in potato plant. Cell. Mol. Biol. Lett. 3, 75–91.

PERGAMON

Phytochemistry 58 (2001) 321–327

PHYTOCHEMISTRY

www.elsevier.com/locate/phytochem

A flavonol glycoside-lignan ester and accompanying acylated glucosides from *Monochaetum multiflorum*

Jose H. Isaza, Hideyuki Ito, Takashi Yoshida*

Faculty of Pharmaceutical Sciences, Okayama University, Tsushima, Okayama 700-8530, Japan

Received 23 January 2001; received in revised form 12 April 2001

Abstract

Four acylated glycosides along with six known glycosides were isolated from the leaves of *Monochaetum multiflorum*. The new compounds were characterized as 4-*O*-(6′-*O*-galloyl-β-glucopyranosyl)-*cis*-*p*-coumaric acid, 6′-*O*-galloylprunasin, benzyl 6′-*O*-galloyl-β-glucopyranoside, and a novel diester of tetrahydroxy-μ-truxinic acid with 2 mol of hyperin (monochaetin), based on NMR and MS spectral data and chemical evidence. © 2001 Elsevier Science Ltd. All rights reserved.

Keywords: *Monochaetum multiflorum*; Melastomataceae; Galloylglucoside; Galloylprunasin; Di-hyperin ester of tetrahydroxy-μ-truxinic acid

1. Introduction

As part of a phytochemical study on Colombian melastomataceous plants, we previously reported the isolation and structural elucidation of new oligomeric hydrolyzable tannins, nobotanins O and P, along with known ellagitannins characteristic of this family, from *Tibouchina multiflorum* (Yoshida et al., 1999). Chromatographic analysis by HPLC suggested that *Monochaetum multiflorum* (Bompl.) Naudin, a shrub endemic to Colombia, is also rich in polyphenols. The aerial part of the plant has been traditionally used as a topical treatment for infections and skin injuries in parts of Colombia. However, its chemical constituents have been little investigated. Here, we report the isolation and characterization of ten compounds (**1**–**10**), including four new acylated glycosides (**7**–**10**) from the leaves of *M. multiflorum*; one of these is a novel flavonol glycoside diester of a lignan possessing a cyclobutane ring.

2. Results and discussion

Dried leaves of *M. multiflorum* were extracted with aqueous acetone. The concentrated solution was subjected to extraction successively with Et_2O, EtOAc and *n*-BuOH. The EtOAc extract was submitted to column chromatography over Toyopearl HW-40, followed by gel chromatography on MCI gel CHP-20P and preparative HPLC to yield 10 glycosidic compounds (**1**–**10**). Six among them were identified as trifolin (**1**) (Barbera et al., 1986), hyperin (**2**) (Bennini et al., 1992), quercetin 3-(6′-*O*-caffeoyl)-β-D-galactoside (**3**) (Shigematsu et al., 1982), isoquercitrin (**4**), quercetin 3-(6′-*O*-caffeoyl)-β-D-glucopyranoside (**5**) (Lin and Wang, 1987) and 4-*O*-β-D-glucopyranosyl-2-*O*-methylphloroacetophenone (**6**) (Konda et al., 1991) by spectroscopic means and comparison with reference samples or reported data.

Compound **7**, $[\alpha]_D$ −14.3°, was obtained as an amorphous powder. The molecular formula, $C_{22}H_{22}O_{12}$, was established by HRESIMS. The ^1H NMR spectrum indicated the presence of a galloyl group (δ 7.13, 2H, *s*), a 1,4-disubstituted benzene ring (δ 7.04, 7.71, each 2H, *d*, $J=8.5$ Hz), vinyl protons (δ 5.83, 6.84, each 1H, *d*, $J=12.5$ Hz), and signals characteristic of a $^4C_1$-glucopyranosyl residue. The coupling constant of the signal at δ 5.03 (*d*, $J=7.5$ Hz) assignable to an anomeric proton of the glucose indicated a β-configuration for the glucosidic linkage. These spectral features as well as two carboxyl carbon signals at δ 166.9 and 167.9 in the ^{13}C NMR spectrum indicated that **7** is a galloyl ester of 4-*O*-β-glucopyranosyl-*cis*-*p*-coumaric acid. The NOESY spectrum of **7** verified this structure, with NOE correlations in a sequence of the signals of δ 5.83↔δ 6.84↔δ

* Corresponding author. Tel.: +81-86-251-7936; fax: +81-86-251-7936.

E-mail address: yoshida@pheasant.pharm.okayama-u.ac.jp (T. Yoshida).

0031-9422/01/$ - see front matter © 2001 Elsevier Science Ltd. All rights reserved.
PII: S0031-9422(01)00247-3

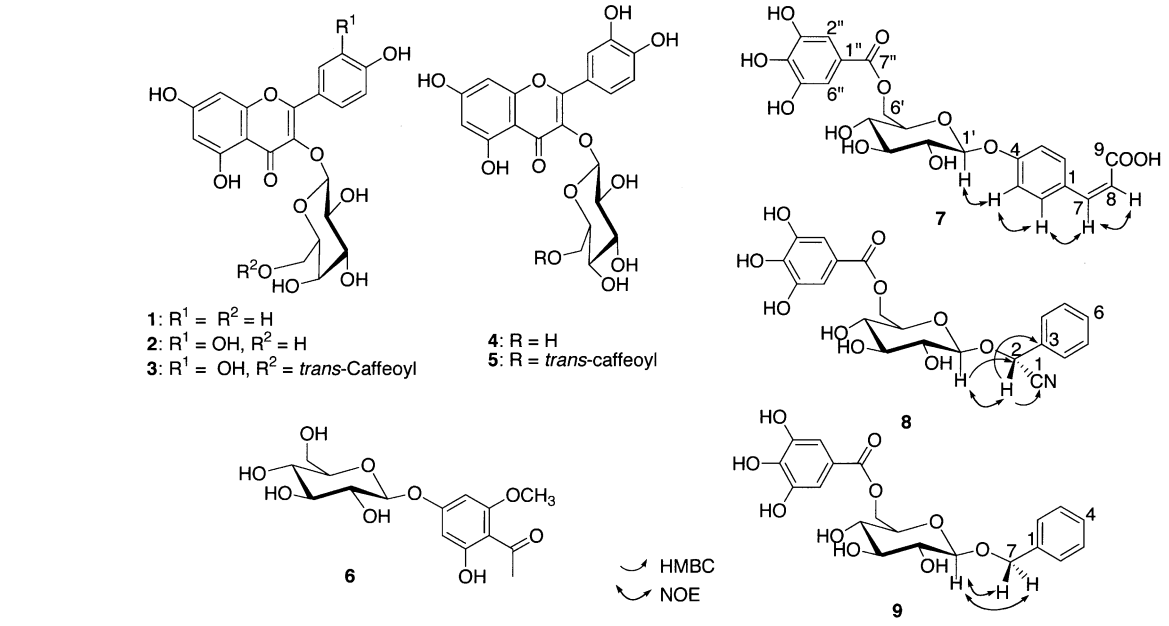

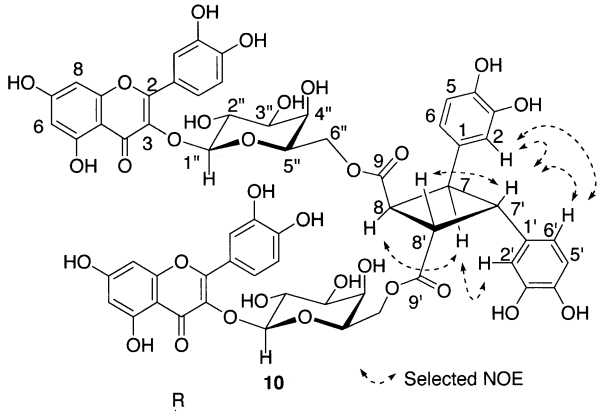

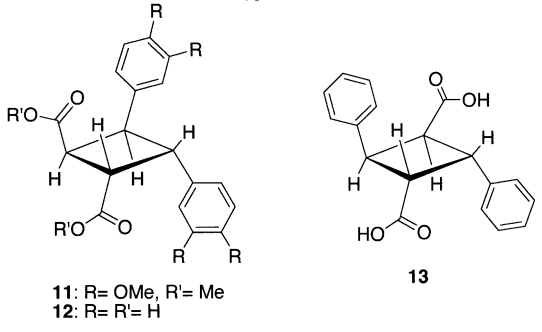

7.71↔δ 7.04↔δ 5.03 as shown in formula (**7**). The location of the galloyl unit at O-6 of the glucopyranose core was evident from low-field shifts of the H-6′ signals (δ 4.63, 4.28). Furthermore, the galloylglucose carbon signals observed in the ^{13}C NMR spectrum of **7** were almost superimposable on those reported for 6-*O*-galloylglucose (Nonaka and Nishioka, 1983) except for a large downfield shift for the anomeric carbon. Based on these data, compound **7** was identified as 4-*O*-(6′-*O*-galloyl-β-glucopyranosyl)-*cis*-*p*-coumaric acid, which is a new compound though 4-*O*-β-glucopyranosyl-*cis*-*p*-coumaric acid has been described in the literature (Lemmich, 1995).

Compound **8**, $[\alpha]_D$ −17.0°, was obtained as an amorphous powder. Its ESIMS showed an $[M+NH_4]^+$ peak at *m*/*z* 465 and the molecular formula was determined as $C_{21}H_{21}NO_{10}$ by HRESIMS. The ^{1}H NMR spectrum of **8** showed signals ascribable to a galloyl (δ 7.17, 2H, *s*), a monosubstituted benzene ring (δ 7.53, 2H, *dd*, *J*=2, 7.5 Hz; 7.41–7.44, 3H, *m*) and a sugar residue. A methine proton was also observed as a singlet at δ 5.82. The presence of a 6-*O*-galloylated $^4C_1$-glucopyranose residue was suggested by the ^{13}C NMR spectrum which showed sugar signals similar to those of **7**, although the chemical shift of an anomeric proton signal (δ 4.40) in **8** markedly differed from that in **7** (δ 5.03). Based on these spectral characteristics along with the signal at δ 118.8 assignable to a nitrile carbon, compound **8** was assumed to be 6′-*O*-gallate of prunasin (Seigler, 1975) or its (2*S*) isomer, sambunigrin (Jensen and Nielsen, 1973), which was substantiated by correlations in HMBC and NOESY as shown in the formula. The configuration at C-2 was confirmed to be *R* by production of prunasin, $[\alpha]_D$ −26.0°, along with gallic acid upon enzymatic hydrolysis of **8** with tannase. The difference in the chemical shifts of the anomeric protons in **7** and **8** can be explained by an anisotropic effect of the benzene ring directly attached to the glucose in **7**.

Compound **9**, $[\alpha]_D$ −29.4°, had the molecular formula $C_{20}H_{22}O_{10}$ as revealed by HRESIMS. The ^{1}H and ^{13}C NMR spectra of **9** closely resembled those of **8** except for the presence of a methylene group [δ_H 4.61, 4.82 (each *d*, *J*=12 Hz); δ_C 70.9] instead of the cyano group at the benzyl position in **8**. Both methylene protons disclosed clear NOEs with an anomeric proton. There-

fore, compound **9** was characterized as benzyl 6′-*O*-galloyl-β-glucopyranoside.

Compound **10**, $[\alpha]_D$ −25.0°, obtained as a yellow amorphous powder, had the UV absorption characteristic of a flavonol skeleton (λ_{max} 358, 286 *sh*, 267 *sh*, 258 nm). A characteristic feature on normal phase HPLC was the longer retention time than for the flavonoid glycosides **1**–**5**, suggesting a larger molecular size than the ordinary flavonoid. Its ESIMS exhibited an $[M+H]^+$ peak at *m*/*z* 1253 and the molecular formula was established as $C_{60}H_{52}O_{30}$ by HRESIMS. Although the ^1H and ^{13}C NMR spectra of **10** were complicated because most signals appeared in pairs having close chemical shifts and some were overlapped, full assignment of the signals was achieved by means of ^1H-^1H COSY, TOCSY, ^1H *J*-resolved and HMQC spectroscopy at an elevated temperature (50 °C) in DMSO-d_6. These ^1H and ^{13}C NMR (Table 1) spectra included pairs of signals similar to those of quercetin 3-*O*-galactoside (hyperin **2**), suggesting that **10** contains two hyperin moieties. This was also substantiated by MS fragmentation showing a successive loss of quercetin (Q) (*m*/*z* 951 $[M+H–Q]^+$, 645 $[M+H–2Q]^+$) as well as a base peak at *m*/*z* 303 $[Q+H]^+$. Large downfield shifts of the galactose C-6 methylene protons relative to the corresponding signals of **2** (δ 3.28 for **2**→δ 3.52, 3.62 for **10**; δ 3.45 for **2**→δ 3.71, 3.84 for **10**) indicated that both galactose cores are acylated at *O*-6. The presence of a di-(3,4-dihydroxyphenyl)cyclobutane dicarboxyl moiety (lignan) as an acyl unit in the molecule was indicated by the following observations. (1) The ^1H NMR spectrum showed two ABX-type aromatic proton signals and an AA′BB′ system of methine proton signals [each ddd, $J=10.5$ Hz (*cis*), $J=7.0$ Hz (*trans*), $J=2.0$ Hz (long range)], which is characteristic of tetrasubstituted cyclo butane protons (Montaudo and Caccamese, 1973). (2) In the ^{13}C NMR spectrum, signals due to an acyl moiety, $C_{18}H_{14}O_6$, were observed as nine paired-varieties with close proximity, among which seven partly overlapping pairs are of sp^2 carbons including ester carbonyl carbons (δ 171.0, 171.2) and two pairs are of sp^3 carbons (δ 40.1, 40.4; 46.1, 46.3). These carbon signals were assignable to those of a cyclobutane ring possessing two 3,4-dihydroxyphenyl and two ester substituents by HMQC and DEPT. Based on these data, the acyl unit in **10** was deduced to be either μ-truxinyl-type ([7.7′, 8.8′]-lignan) or α-truxillyl-type ([7.8′, 8.7′]-lignan) (Ben-Efraim and Green, 1974), the former being preferred because of the close similarity of chemical shifts and coupling patterns of the cyclobutyl protons to those reported for μ-truxinic acid (**12**) (or its enantiomer) rather than α-truxillic acid (**13**) (Ben-Efraim and Green, 1974). The proposed lignan structure in **10** was substantiated by the HMBC spectrum (Table 2), which revealed three-bond correlations among most of the protons and carbons including those between the proton [H-7 (H-7′)] on the phenyl bearing-carbon and the carboxyl-bearing carbons [C-8′ (8)] (Table 2). The HMBC spectrum also showed correlations of the carboxyl carbons with the C-6 methylene protons of both galactoses. The configuration of the substituents on the cyclobutane ring was established by the NOESY spectrum which showed clear NOE correlations among H-2(6)/H-6′ (2′) and H-2 (2′)/H-7′ (H-7), which are only possible in a μ-truxinate arrangement. These correlations revealed the preferred eclipsed conformation between H-7 and H-6, and between H-7′ and H-6′, which was consistent with the minimal steric energy model calculated by MM2. A similar feature was reported for the μ-truxinic acid moiety of sargerinic acid (Lu and Foo, 1999).

Table 1
^{13}C NMR spectral data[a] for the flavonol glycoside moiety of **10** and **3**

	10	**3**
Quercetin moiety		
C-2	156.34[b], 156.25[b]	156.2
C-3	133.7, 133.6	133.4
C-4	177.4, 177.4	177.4
C-5	161.26, 161.25	161.1
C-6	98.8, 98.8	98.6
C-7	164.2, 164.1	164.2
C-8	93.57, 93.55	93.4
C-9	156.34[b], 156.34[b]	156.2
C-10	104.0, 104.0	103.8
C-1′	121.20, 121.18	121.0
C-2′	116.14, 116.13	115.1
C-3′	144.82, 144.81	144.7
C-4′	148.5, 148.5	148.4
C-5′	115.3, 115.3	115.9
C-6′	121.86, 121.84	121.9
Galactose moiety		
C-1″	102.0, 101.9	101.8
C-2″	71.0, 71.0	71.2
C-3″	72.9, 72.8	73.2
C-4″	68.4, 67.7	67.9
C-5″	73.0, 72.5	75.7
C-6″	62.0, 63.3	60.1

[a] 126 MHz, DMSO-d_6, 50 °C.
[b] Interchangeable.

Acid hydrolysis of a methylated derivative of **10** followed by remethylation yielded an optically inactive methyl ester (**11**) and penta-*O*-methylquercetin. The ^1H NMR spectral data for **11** were as expected for a symmetrical structure, and included a single carbomethoxyl signal at δ 3.37, shifted upfield by the shielding effect of the *cis*-β-phenyl group (Ben-Efraim and Green, 1974). Based on these data, the structure (**10**) for monochaetin was established as shown in the formula.

Monochaetin is most plausibly formed from **3** via a [2+2] photochemical addition process. Dimeric products having a cyclobutane ring produced from various phenylpropanoid acids have been reported (Atta-ur-Rahman et al., 1998; Lu and Foo, 1999; Seidel et al.,

Table 2
^1H and ^{13}C NMR data and HMBC correlations for the μ-truxinyl moiety of **10**

Position	δ_H	δ_C	Observed three-bond correlation
1 (1′)		129.6 (129.5)	H-5 (H-5′), H-8 (H-8′)
2 (2′)	6.52 (6.54)		C-7 (C-7′)
		114.8 (114.9)	H-7 (H-7′)
3 (3′)		144.8	H-5, H-5′
4 (4′)		144.1 (144.0)	H-2 (H-2′), H-6 (H-6′)
5 (5′)	6.59 (6.56)		C-1 (C-1′, C-3′)
		115.2	
6 (6′)	6.30 (6.25)		C-4, C-2′
		118.3 (118.1)	H-7 (H-7′)
7 (7′)	3.89 (3.87)		C-2 (C-2′), C-6 (C-6′)
			C-8′ (C-8), C-9 (C-9′)
		40.3 (40.1)	H-2 (H-2′), H-6(H-6′), H-8′ (H-8)
8 (8′)	3.54 (3.46)		C-1 (C-1′), C-7′ (C-7), C-9′ (C-9)
		46.2 (46.3)	H-7′ (H-7)
9 (9′)		171.0 (171.2)	H-7 (H-7′)
			Galactose H-6″ 3.52, 3.84 (3.62, 3.71)

2000; Sudo et al., 2000; Wang et al., 2000). However, only a few diflavonoid esters of dicarboxylic acid are known (Itokawa et al., 1981; Horie et al., 1986). More notably, only stachysetin isolated from *Stachys aegyptiaca* (Labiatae) was reported as a flavone glycoside truxinate ester (El-Ansari et al., 1995). Monochaetin is thus the second analogue of such a flavonoid cyclodimer in the μ-truxinate form.

3. Experimental

3.1. General

^1H (500 MHz) and ^{13}C (126 MHz) NMR spectra were recorded on a Varian VXR-500 spectrometer. ESI–MS was performed with a Micromass Auto Spec OA–Tof mass spectrometer using 0.1% NH_4OAc in 50% MeOH as solvent, at a flow rate of 0.02 ml min^{-1}. Optical rotations were conducted on a JASCO DIP-1000 polarimeter. Normal phase (NP) HPLC was performed on a YMC Pack Sil A-003 column (5 μm, 4.6 mm i.d. × 250 mm), flow rate 1.5 ml min^{-1}, detected with UV 280 nm. Mobile phases: (NP-1) *n*-hexane–MeOH–THF–HCOOH (55:33:11:1) containing oxalic acid (450 mg l^{-1}), (NP-2) *n*-hexane–MeOH–THF–HCOOH (60:45:15:1) containing oxalic acid (500 mg 1.2 l^{-1}) and (NP-3) *n*-hexane–MeOH–THF–HCOOH (47:39:13:1) containing oxalic acid (450 mg l^{-1}). Analytical reversed-phase HPLC was performed on a J'sphere ODS M-80 column (4.6 mm i.d. × 250 mm), flow rate 1.0 ml min^{-1}, 40 °C, detector UV 280 nm; Mobile phases: (RP-1) 0.01 M H_3PO_4–0.01 M KH_2PO_4–EtOH–EtOAc (42.5:42.5:10:5) and (RP-2) 0.01 M H_3PO_4–0.01 M KH_2PO_4–MeCN (42.5:42.5:15). Preparative HPLC was carried out on a J'sphere ODS M-80 column (10 mm i.d. × 250 mm, 4 μm, 80 Å,), detector MCPD 240–400 nm, flow rate 3.0 ml min^{-1}, 40 °C, mobile phase RP-2.

3.2. Plant material

The leaves of *Monochaetum multiflorum* were collected near Manizales City, Caldas, Colombia and identified by Dr. Gustavo Lozano C. A voucher specimen was deposited at Herbario Nacional de Colombia (COL) (voucher No. 361696).

3.3. Extraction and isolation

Dried leaves (400 g) of *M. multiflorum* were homogenized in 70% aqueous acetone, filtered and concentrated in vacuo. The concentrated solution was subjected to liquid-liquid partition to give Et_2O (4.6 g), EtOAc (13.4 g), *n*-BuOH (33.8 g) extracts and aqueous residue (54.3 g). The EtOAc extract (10.2 g) was fractionated on a Toyopearl HW-40 (coarse grade) column (2.2 cm i.d. × 45 cm) with aq. MeOH and a mixture of acetone–MeOH–H_2O in a step-wise gradient mode to produce four fractions, (A) 40% MeOH (3.9 g), (B) 70% MeOH (2.2 g), (C) acetone–MeOH–H_2O (2:5:3) (3.4 g) and (D) acetone–H_2O (7:3) (0.7 g).

Fraction A (3.5 g) was applied to a Toyopearl HW-40 (coarse grade) column (2.2 cm i.d. × 45 cm), this being eluted with a step-wise water–MeOH gradient from 20 to 70% MeOH (CC-1-1). Fractions showing similar HPLC patterns were pooled and further purified on a YMC ODS AQ120 S-50 column (1.1 cm i.d. × 45 cm), eluting with a binary step-wise gradient from water to MeOH. In this way, fractions (281 mg) eluted with 20% MeOH yielded **6** (36 mg) and the 25% MeOH eluate (105 mg) gave **7** (9.0 mg), **8** (21 mg), and **9** (10 mg). The 30% eluate afforded 1 g of a mixture of **1**, **2** and **4**, from which 50 mg was subjected to preparative HPLC (RP-2) to give **1** (2.5 mg), **2** (23 mg) and **4** (15 mg). The 40–50% MeOH eluate yielded 428 mg of a mixture, which after purification with a combination of MCI gel CHP-20P,

YMC ODS and preparative HPLC (RP-2) gave **1** (0.5 mg), **2** (7 mg), **4** (5.0 mg) and **10** (9.0 mg).

Fraction B (2.0 g) from CC-1, (70% MeOH fraction) was separated on a Toyopearl HW-40C (CC-1-2) eluted with a binary step-wise gradient of MeOH (20–70%) collecting each 5 ml fraction. Fractions 351–460 (380 mg) (Fr. B-1) and 501–530 (91.6 mg) (Fr. B-2) eluted with 40% MeOH were further independently purified on an MCI-gel CHP-20P (1.1 cm i.d. × 45 cm) chromatographic column eluted with a step-wise gradient of EtOH (5 → 60%). Fraction B-1 yielded **1** (0.2 mg), **2** (14 mg), **5** (12 mg) and **10** (59 mg) when eluted with 30% EtOH. Fraction B-2 afforded a mixture (29 mg) of **3** and **5**, when eluted with 30% EtOH. Final purification was performed by preparative RP-HPLC as described above to obtain **3** (7 mg) and **5** (10 mg).

3.4. Quercetin 3-(6″-O-trans-caffeoyl)-β-D-galactopyranoside (3)

A yellow powder, UV λ_{max} MeOH nm (log ε): 366 *sh* (4.15), 335 (4.32), 301 (4.20), 267.0 *sh* (4.24), 253.5 (4.32); MeOH + $AlCl_3$: 440 (426), 354.5 (4.21), 303 *sh* (4.09), 2.74.5 (4.37); MeOH + $AlCl_3$ + HCl: 405 (4.11), 333.0 (4.25), 302 *sh* (4.20), 271.5 (4.35). ESIMS *m/z*: 627 $[M+H]^+$. ^{1}H NMR (DMSO-d_6): δ 12.61 (1H, *s*, 5-OH), 7.65 (1H, *dd*, *J* = 1.5, 8.5 Hz, H-6′), 7.50 (1H, *d*, *J* = 1.5 Hz, H-2′), 6.80 (1H, *d*, *J* = 8.5 Hz, H-5′), 6.36 (1H, *d*, *J* = 1.5 Hz, H-8), 6.15 (1H, *d*, *J* = 1.5 Hz, H-6) (quercetin moiety), 5.39 (1H, *d*, *J* = 8 Hz, H-1″), 4.10 (1H, *dd*, *J* = 4.5, 11.5 Hz, H-6″), 4.04 (1H, *dd*, *J* = 7.5, 11.5 Hz, H-6″), 3.67 (1H, *m*, H-5″), 3.66 (1H, *d*, *J* = 3 Hz, H-4″), 3.56 (1H, *br t*, *J* = 8.5 Hz, H-2″), 3.42 (1H, *dd*, *J* = 3, 10 Hz, H-3″) (galactose moiety), 7.30 (1H, *d*, *J* = 16 Hz, H-7‴), 6.96 (1H, *br s*, H-2‴), 6.81 (1H, *d*, *J* = 8 Hz, H-5‴), 6.74 (1H, *br d*, *J* = 8 Hz, H-6‴), 6.04 (1H, *d*, *J* = 16 Hz, H-8‴) (caffeoyl moiety).

3.5. 4-O-(6′-O-Galloyl-β-D-glucopyranosyl)-cis-p-coumaric acid (7)

A white amorphous powder, $[\alpha]_D$ −14.3° (*c* 1.1, MeOH). UV λ_{max} MeOH nm (log ε): 269 (3.49). ESIMS *m/z*: 501 $[M+Na]^+$. HRESIMS *m/z*: 501.0992 $[M+Na]^+$, calc. for $C_{22}H_{22}O_{12}$ + Na, *m/z* 501.1009. ^{1}H NMR (Me_2CO-d_6 + D_2O): δ 7.71 (2H, *d*, *J* = 8.5 Hz, H-2, 6), 7.13 (2H, *s*, H-2″, 6″), 7.04 (2H, *d*, *J* = 8.5 Hz, H-3, 5), 6.84 (1H, *d*, *J* = 12.5 Hz, H-7), 5.83 (1H, *d*, *J* = 12.5 Hz, H-8), 5.03 (1H, *d*, *J* = 7.5 Hz, glucose (glc) H-1′), 3.49–3.57 (3H, overlapped with HDO, glc H-2′–4′), 4.63 (1H, *dd*, *J* = 2, 12 Hz, glc H-6′), 4.28 (1H, *dd*, *J* = 8, 12 Hz, glc H-6′). ^{13}C NMR (Me_2CO-d_6 + D_2O): δ 167.9 (C-9), 166.9 (C-7″), 159.2 (C-4), 146.0 (2C, C-3″, 5″), 142.9 (C-7), 138.8 (C-4″), 132.9 (2C, C-2, 6), 129.9 (C-1), 121.5 (C-1″), 118.7 (C-8), 116.6 (2C, C-3, 5), 109.9 (2C, C-2″, 6″), 101.5 (glc C-1′), 77.7 (glc C-3′), 75.1 (glc C-5′), 74.5 (glc C-2′), 71.1 (glc C-4′), 64.5 (glc C-6′).

3.6. 6′-O-Galloylprunasin (8)

A white amorphous powder, $[\alpha]_D$ −17.0° (*c* 1.9, MeOH). UV λ_{max} MeOH nm (log ε): 269 (2.8), 351 (2.4). ESIMS *m/z*: 465 $[M+NH_4]^+$. HRESIMS *m/z*: 465.1487 $[M+NH_4]^+$, calc. for $C_{21}H_{21}NO_{10}$ + NH_4, *m/z* 465.1509. ^{1}H NMR (Me_2CO-d_6 + D_2O): δ 7.53 (2H, *dd* *J* = 2, 7.5 Hz, H-4, 8), 7.41–7.44 (3H, *m*, H-5–7), 7.17 (2H, *s*, H-2″, 6″), 5.82 (1H, *s*, H-2), 4.59 (1H, *dd*, *J* = 2, 12 Hz glc H-6′), 4.40 (1H, *d*, *J* = 7.5 Hz, glc H-1′), 4.36 (1H, *dd*, *J* = 6, 12 Hz, glc H-6′), 3.57 (1H, *ddd*, *J* = 2, 6, 10 Hz, glc H-5′), 3.48 (1H, *t*, *J* = 10 Hz, glc H-4′), 3.39 (1H, *t*, *J* = 9 Hz, glc H-3′), 3.36 (1H, *dd*, *J* = 7.5, 9 Hz, glc H-2′). ^{13}C NMR (Me_2CO-d_6 + D_2O): δ 167.1 (C-7″), 146.0 (2C, C-3″, 5″), 138.9 (C-4″), 134.4 (C-3), 130.5 (C-6), 129.8 (2C, C-5, 7), 128.5 (2C, C-4, 8), 121.4 (C-1″), 118.8 (C-1), 109.8 (2C, C-2″, 6″), 101.9 (glc C-1′), 77.4 (glc C-3′), 75.3 (glc C-5′), 74. 2 (glc C-2′), 70.8 (glc C-4′), 68.2 (C-2), 64.3 (glc C-6′).

3.7. Enzymatic hydrolysis of 8

An aqueous solution of **8** (4.1 mg ml^{-1}) was incubated at 37 °C with tannase prepared from *Aspergillus niger* (Yoshida et al., 1989), and the progress of the reaction was followed by HPLC (RP-2) until the starting material disappeared. After 18 h, prunasin and gallic acid were detected. Prunasin was isolated by preparative HPLC (RP-2) and identified by co-chromatography with an authentic sample, and by comparing its optical rotation and ^{1}H NMR spectrum with those reported in the literature.

Prunasin: $[\alpha]_D$ −26.0° (*c* 0.5, MeOH) Lit. $[\alpha]_D$ −30.1° (Seigler, 1975). ^{1}H NMR (Me_2CO-d_6 + D_2O): δ 7.60 (2H, *dd*, *J* = 1, 8 Hz, H-4, 8), 7.45–7.49 (3H, *m*, H-5-7), 5.95 (1H, *s*, H-2), 4.38 (1H, *d*, *J* = 7.5 Hz, glc H-1′), 3.86 (1H, *dd*, *J* = 2.5, 12 Hz, glc H-6′), 3.66 (1H, *dd*, *J* = 6, 12 Hz, glc H-6′), 3.27–3.33 (4H, *m*, glc H-2′-5′).

3.8. Benzyl 6′-O-galloyl-β-D-glucopyranoside (9)

A white amorphous powder, $[\alpha]_D$ −29.4° (*c* 1.7, MeOH). UV λ_{max} MeOH nm (log ε): 272 (3.68). ESIMS *m/z*: 440 $[M+NH_4]^+$. HRESIMS *m/z*: 440.1555 $[M+NH_4]^+$, calc. for $C_{20}H_{22}O_{10}$ + NH_4, *m/z* 440.1557. ^{1}H NMR (Me_2CO-d_6 + D_2O): δ 7.36 (2H, *dd*, *J* = 1.5, 8.5 Hz, H-2, 6), 7.28 (2H, *ddd*, *J* = 1.5, 7.0, 8.5 Hz, H-3, 5), 7.24 (1H, *dt*, *J* = 1.5, 7 Hz, H-4), 7.16 (2H, *s*, galloyl), 4.82, 4.61 (each 1H, *d*, *J* = 12 Hz, H-7), 4.57 [1H, *dd*, *J* = 2, 12 Hz, glc H-6′], 4.40 (1H, *d*, *J* = 8 Hz, glc H-1′), 4.37 (1H, *dd*, *J* = 6, 12 Hz, glc H-6′), 3.29 (1H, *dd*, *J* = 8, 9 Hz, glc H-2′), 3.42 (1H, *t*, *J* = 9 Hz, glc H-3′), 3.44 (1H, *t*, *J* = 9 Hz, glc H-4′), 3.58 (1H, *ddd*, *J* = 2, 6, 9 Hz, glc H-5′). ^{13}C NMR (Me_2CO-d_6 + D_2O) : δ 167.0 (C-7″), 146.0 (2C, C-3″, 5″), 138.9 (C-1), 138.8 (C-4″), 128.9 (2C, C-3, 5), 128.7 (2C, C-2, 6), 128.2 (C-4), 121.6 (C-

1″), 109.8 (2C, C-2″, 6″), 102.9 (glc C-1′), 77.0 (glc C-3′), 75.0 (glc C-5′), 74.7 (glc C-2′), 71.2 (glc C-4′), 70.9 (C-7), 64.5 (glc C-6′).

3.9. Monochaetin (**10**)

A yellow amorphous powder, $[\alpha]_D$ +25.0° (*c* 1.0, MeOH). UV λ_{max} MeOH nm (log ε): 358 (4.61), 286 *sh* (4.46), 267 *sh* (4.67), 258 (4.71); MeOH + $AlCl_3$: 430 (471), 339 *sh* (4.21), 298 *sh* (4.50), 275 (4.84); MeOH + $AlCl_3$ + HCl: 402 (4.59), 367 *sh* (4.50), 198 *sh* (4.38), 271 (4.78); MeOH + AcONa: 273.0 (4.79), 321.0 (4.46), 394.8 (4.57); MeOH + AcONa + H_3BO_3: 260.5 (4.79), 291.5 (4.51), 377.7 (4.62). ESIMS *m/z*: 1253 $[M+H]^+$, 951 $[M+H\text{-quercetin (Q)}]^+$, 645 $[M+H\text{-2Q}]^+$, 303 $[Q+H]^+$. HRESIMS *m/z*: 1253.2689 $[M+H]^+$, calc. for $C_{60}H_{52}O_{30}+H$, *m/z* 1253.2622. ^{1}H NMR (DMSO-d_6, 50 °C): δ 12.56 (2H, *s*, 5-OH), 6.19, 6.20 (1H each, *d*, *J* = 2.0 Hz, H-6), 6.35, 6.37 (1H each, *d*, *J* = 2.0 Hz, H-8), 7.51, 7.52 (1H each, *d*, *J* = 2 Hz, H-2′), 6.79, 6.81 (1H each, *d*, *J* = 8.5 Hz, H-5′), 7.58, 7.59 (1H each, *dd*, *J* = 2, 8.5 Hz, H-6′) (quercetin moieties), 5.24, 5.26 (1H each, *d*, *J* = 7.5 Hz, H-1″), 3.52, 3.54 (1H each, *dd*, *J* = 7.5, 9.5 Hz, H-2″), 3.29, 3.32 (1H each, *dd*, *J* = 3, 9.5 Hz, H-3″), 3.40 (2H, *br d*, *J* = 3 Hz, H-4″), 3.11, 3.12 (1H each, *m*, H-5″), 3.52 (1H, dd, *J* = 5, 10.5 Hz, H-6″), 3.62 (1H, dd, *J* = 7, 11.5 Hz, H-6″), 3.84 (1H, dd, *J* = 6.5, 10.5 Hz, H-6″), 3.71 (1H, dd, *J* = 5, 11.5 Hz, H-6″) (galactose moieties), 6.52, 6.54 (1H each, *d*, *J* = 2.0 Hz, H-2, 2′), 6.56, 6.59 (1H each, *d*, *J* = 8.0 Hz, H-5, 5′), 6.25, 6.30 (1H each, *dd*, *J* = 2, 8 Hz, H-6, 6′), 3.87, 3.89 (1H each, *ddd*, *J* = 2, 7, 10.5 Hz, H-7, 7′), 3.46, 3.54 (1H each, *ddd*, *J* = 2, 7, 10.5 Hz, H-8, 8′) (μ-truxinoyl moiety). ^{13}C NMR (DMSO-d_6, 50 °C): see Tables 1 and 2.

3.10. Methylation and hydrolysis of monochaetin (**10**)

A solution of **10** (17.9 mg) in MeOH (0.5 ml) and trimethylsilyldiazomethane (2.0 M solution in hexane) (0.5 ml) was left standing for 1 h. The solvent was removed under an N_2 stream, and this process of methylation was repeated three times. The reaction mixture was directly hydrolyzed in 2.0 M HCl–MeOH for 2 h. After evaporation and remethylation, the residue was separated by preparative TLC [Si gel, benzene–acetone (2:1)] to yield compounds **11** (0.6 mg) and penta-*O*-methylquercetin (2.2 mg).

3.10.1. Dimethyl 3,3′,4,4′-tetramethoxy-μ-truxinate (**11**)

A white amorphous powder, $[\alpha]_D$ 0.0° (*c* 0.1, MeOH). UV λ_{max} EtOH nm (log ε): 230 (3.66), 280 (3.16). ESI–MS *m/z*: 445 $(M+H)^+$. ^{1}H NMR ($CDCl_3$): δ 6.81 (2H, *d*, *J* = 2.0 Hz, H-2, 2′), 6.83 (2H, *d*, *J* = 8.0 Hz, H-5, 5′), 6.86 (2H, *dd*, *J* = 2, 8 Hz, H-6, 6′), 4.38 (2H, *dd*, *J* = 7.5, 10.5 Hz, H-7, 7′), 3.90 (2H, *dd*, *J* = 7.5, 10.5 Hz, H-8, 8′), 3.37 (6H, *s*, 2 × CH_3OCO–), 3.87, 3.90 (6H each *s*, 4 × CH_3O–).

3.10.2. Penta-O-methylquercetin

^{1}H NMR ($CDCl_3$): δ 7.72 (1H, *d*, *J* = 2.0 Hz, H-2′), 7.70 (1H, *dd*, *J* = 2, 9, Hz, H-6′), 6.98 (1H, *d*, *J* = 9.0 Hz, H-5′), 6.51 (1H, *d*, *J* = 2.5 Hz, H-8), 6.35 (1H, *d*, *J* = 2.5 Hz, H-6), 3.97, 3.96, 3.96, 3.91, 3.88 (3H each, *s*, 5 × CH_3O–).

Acknowledgements

This work was supported in part by a Grant-in-Aid (No. 09672143) for Scientific Research from the Ministry of Education, Culture, Sports, Science and Technology of Japan. The authors are grateful to the SC-NMR Laboratory of Okayama University for the NMR measurements. One of us (J.H.I.) thanks Universidad Tecnológica de Pereira in Colombia for study commission.

References

Atta-ur-Rahman Khattak, K. F., Nighat, F., Shabbir, M., Hemalal, K. D., Tillekeratne, L. M., 1998. Dimeric tropane alkaloids from *Erythroxylum moonii*. Phytochemistry 48 (2), 377–383.

Barbera, O., Sanz, J.F., Sanchez-Parareda, J., Alberto Marco, J., 1986. Further flavonol glycosides from *Anthyllis onobrychioides*. Phytochemistry 25 (10), 2361–2365.

Ben-Efraim, D.A., Green, B.S., 1974. The use of mid-points or average NMR chemical shifts in stereochemical assignments. Tetrahedron 30, 2357–2364.

Bennini, B., Chulia, A.J., Kaouadji, M., Thomasson, F., 1992. Flavonoid glycosides from *Erica cinerea*. Phytochemistry 31 (7), 2483–2486.

El-Ansari, M.A., Nawwar, M.A., Saleh, N.A.M., 1995. Stachysetin, A, diapigenin-7-glucoside-*p*, *p*′-dihydroxytruxinate from *Stachys aegyptiaca*. Phytochemistry 40 (5), 1543–1548.

Horie, T., Tsukayama, M., Yamada, T., Miura, I., Nakayama, M., 1986. Three flavone glycosides from *Citrus sudachi*. Phytochemistry 25 (11), 2621–2624.

Itokawa, H., Sato, H., Takeya, K., 1981. Structures of isoagastachoside and agastatin, new glucosylflavones isolated from *Agastache rugosa*. Chemical and Pharmaceutical Bulletin 29 (6), 1777–1779.

Jensen, S.R., Nielsen, B.J., 1973. Cyanogenic glucosides in *Sambucus nigra*. Acta Chemica Scandinavica 27, 2661–2685.

Konda, Y., Funano, N., Harigaya, Y., Li, X., Zhang, D., Onda, M., 1991. A phenolic glycoside from *Artemisia sacrorum*. Journal of Heterocyclic Chemistry 28, 1949–1951.

Lemmich, J., 1995. Monoterpene, chromone and coumarin glucosides of *Diplolophium buchananii*. Phytochemistry 38 (2), 427–432.

Lin, Y.-L., Wang, K.-J., 1987. Studies on the constituents of *Pittosporum pentandrum*. Journal of the Taiwan Pharmaceutical Association 39 (1), 33–41.

Lu, Y., Foo, L.Y., 1999. Rosmarinic acid derivatives from *Salvia officinalis*. Phytochemistry 51 (1), 91–94.

Montaudo, G., Caccamese, S., 1973. Structure and conformation of chalcone photodimers and related compounds. Journal of Organic Chemistry 33 (4), 710–716.

Nonaka, G., Nishioka, I., 1983. Tannins and related compounds. X. Rhubarb (2): Isolation and structures of a glycerol gallate, gallic

acid glucoside gallates, galloylglucoses and isolindleyin. Chemical and Pharmaceutical Bulletin 31 (5), 1652–1658.

Seidel, V., Francois, B., Waterman, P.G., 2000. (*Rel*)-1β, 2α-Di-(2, 4-dihydroxy-6-methoxybenzoyl)-3β, 4α-di-(4-methoxyphenyl)-cyclobutane and other flavonoids from the aerial parts of *Goniothalamus gardneri* and *Goniothalamus thwaitesii*. Phytochemistry 55 (5), 439–446.

Seigler, D.S., 1975. Isolation and characterization of naturally occurring cyanogenic compounds. Phytochemistry 14 (1), 9–29.

Shigematsu, N., Kouno, I., Kawano, N., 1982. Quercetin 3-(6″-caffeoylgalactoside) from *Hydrocotyle sibthorpioides*. Phytochemistry 21 (8), 2156–2158.

Sudo, H., Ide, T., Otsuka, H., Hirata, E., Takushi, A., Shinzato, T., Takeda, Y., 2000. Megastigmane, benzyl and phenethyl alcohol glycosides, and 4, 4′-dimethoxy-β-truxinic acid catalpol diester from the leaves of *Premna subscandens* MERR. Chemical and Pharmaceutical Bulletin 48 (4), 542–546.

Wang, Q., Terreaux, C., Marston, A., Tan, R.-X., Hostettmann, K., 2000. Lignans from *Mosla scabra*. Phytochemistry 54 (8), 909–912.

Yoshida, T., Amakura, Y., Yokura, N., Ito, H., Isaza, J.H., Remirez, S., Pelaez, D.P., Renner, S.S., 1999. Oligomeric hydrolysable tannins from *Tibouchina multiflora*. Phytochemistry 52 (8), 1661–1666.

Yoshida, T., Tanaka, K., Chen, X.-M., Okuda, T., 1989. Tannins of rosaceous medicinal plants. V. Hydrolyzable tannins with dehydrodigalloyl group from *Rosa laevigata* Michx. Chemical and Pharmaceutical Bulletin 37 (4), 920–924.

PERGAMON

Phytochemistry 58 (2001) 329–332

PHYTOCHEMISTRY

www.elsevier.com/locate/phytochem

3-Monoterpenyl-2,4-dioxygenated quinoline alkaloids from the aerial parts of *Halfordia kendack*

Nasim Sultana[a], Peter G. Waterman[b,*]

[a]*Department of Chemistry, BCSIR Laboratories, Dhanmondi, Dhaka-1205, Bangladesh*
[b]*Centre for Phytochemistry, Southern Cross University, PO Box 157, Lismore, NSW 2480, Australia*

Received 11 January 2001; received in revised form 11 April 2001

Abstract

The aerial parts of *Halfordia kendack* (Rutaceae) have yielded the known alkaloid *trans*-erioaustralasine ({*rel*}-1-acetoxymethyl-4.8′-epoxy-3-(1′β,2′β-epoxy-3′β,4′α-*para*-menthyl-3′-yl)quinolin-2-one) together with four new alkaloids. The latter were characterised by spectroscopic methods as *trans*-deacetoxyerioaustralasine ({*rel*}-1-methyl-4.8′-epoxy-3-(1′β,2′β-epoxy-3′β,4′α-*para*-menthyl-3′-yl)quinolin-2-one), *trans*-deacetoxyerioaustralasine hydrate ({*rel*}-1-methyl-4.8′-epoxy-3-(1′α,2′α-dihydroxy-3′β,4′α-*para*-;menthyl-3′-yl)quinolin-2-one), *trans*-erioaustralasine hydrate ({*rel*}-1-acetoxymethyl-4.8′-epoxy-3-(1′α,2′α-dihydroxy-3′β,4′α-*para*-menthyl-3′-yl) quinolin-2-one) and *trans*-1-epi-deacetoxyerioaustralasine hydrate ({*rel*}-1-acetoxymethyl-4.8′-epoxy-3-(1′β,2′α-dihydroxy-3′β,4′α-*para*-menthyl-3′-yl)quinolin-2-one). © 2001 Elsevier Science Ltd. All rights reserved.

Keywords: *Halfordia kendack*; Rutaceae; 3-Monoterpenyl 2,4-dioxygenated quinoline alkaloids; *trans*-Erioaustralasine derivatives

1. Introduction

The small genus *Halfordia* F. Muell. (Rutaceae) is restricted in distribution to the rain forests of Australia, New Guinea and New Caledonia (Richards, 1991). Previous studies on two species, *H. kendack* (Mountr.) Guillaumin. and *H. scleroxyla* F. Muell., have led to the isolation of furoquinoline alkaloids typical of the Rutaceae together with more unusual 5-phenyloxazole alkaloids and a series of 3,4-dioxygenated furanocoumarins (Gray, 1983; Mester, 1983). While the Rutaceae are a rich source of coumarins, the latter are currently unique in the family because of the presence of C-3 and C-4 oxygenation.

We have now been able to re-examine *H. kendack* from material collected in Queensland, Australia. As well as re-isolating the previously reported halfordin we were able to obtain, as a major constituent, a new furanocoumarin possessing the very unusual 2,4-diketo A-ring (Sultana et al., 2000). In this paper we report on the investigation of the alkaloids of the same collection and the surprising isolation of a series of 3-monoterpenyl quinoline alkaloids.

2. Results and discussion

The ground aerial parts were extracted with hexane and then with chloroform. Vacuum chromatography followed by gel filtration and then column chromatography gave the previously reported coumarins from the hexane extract together with very small amounts of the two alkaloids **3** and **4**. Similar treatment of the chloroform extract yielded **1** and **2** as the major alkaloids together with a small amount of **5**. The major alkaloid (**1**) proved to be identical to *trans*-erioaustralasine which had previously been reported from *Eriostemon australasius* var. *banksii* (Da Cunha et al., 1993). The ^{1}H and ^{13}C NMR data obtained are recorded in Tables 1 and 2 and are reproduced here to allow comparison with data obtained for the other, novel, alkaloids. The second major alkaloid gave spectral data very similar to that of **1** but lacked the *N*-acetoxymethyl substituent which was replaced by resonances for an *N*-methyl

* Corresponding author. Tel.: +61-2-6622-3211; fax: +61-2-6622-3459.
E-mail address: pwaterma@scu.edu.au (P.G. Waterman).

0031-9422/01/$ - see front matter © 2001 Elsevier Science Ltd. All rights reserved.
PII: S0031-9422(01)00196-0

Table 1
^{1}H NMR chemical shift data for the alkaloids of *Halfordia kendack*[a]

H/C	1	2	3	4	5
5	7.96 *dd* (8.0, 1.5)	7.96 *dd* (8.0, 1.5)	7.98 *dd* (8.0, 1.4)	7.98 *dd* (8.0, 1.4)	7.96 *dd* (8.0, 1.5)
6	7.24 *td* (7.2, small)	7.22 *ddd* (8.0, 7.2, 0.8)	7.21 *ddd* (8.0, 7.1, 0.9)	7.24 *t* (7.5)	7.21 *ddd* (8.0, 7.2, 0.9)
7	7.55 *ddd* (8.4, 7.2, 1.4)	7.55 *ddd* (8.6, 7.2, 1.6)	7.54 *ddd* (8.6, 7.1, 1.6)	7.54 *ddd* (8.4, 7.4, 1.5)	7.54 *ddd* (8.8, 7.2, 1.6)
8	7.33 (*d*, 8.4)	7.33 *d* (8.4)	7.24 *d* (8.4)	7.34 *d* (8.4)	7.24 *d* (8.8)
2′	3.79 *s*	3.79 *s*	5.78 *t* (1.9)	5.65 *s*	5.12 *s*
3′	2.79 *d* (12.2)	2.79 *d* (12.0)	3.57 *dd* (11.4, 2.6)	3.53 *dd* (11.5, 2.6)	3.20 *dd* (11.8, 1.8)
4′	1.50 *td* (12.0, *sm*)	1.52 *td* (12.0, *sm*)	2.18 *ddd* (11.7, 11.6, 3.7)	2.18 *td* (12.0, 3.7)	2.08 *td* (12.0, 3.0)
5′	1.60 *m*	1.60 *ddt* (13.6, 6.5, *sm*)	1.61 *dd* (12.4, 3.6)	1.63 *m*	1.61 *m*
	1.22 *m*	1.24 *tdd* (12.1, 12.0, 5.2)	1.26 *m*	1.25 *m*	1.26 *m*
6′	2.26 *dd* (14.9, 5.2)	2.27 *dd* (14.9, 5.1)	1.94 *td* (13.0, 5.0)	1.94 *td* (13.2, 4.5)	1.81 *ddd* (13.5, 13.2, 4.5)
	1.79 *dddd* (12.1, 11.9, 6.4, 2.8)	1.79 *dddd* (14.9, 11.9, 6.4, 2.8)	1.73 *m*	1.73 *m*	1.68 *m*
7′α-Me	1.32 *s*	1.32 *s*	1.36 *s*		
7′β-Me	1.47 *s*	1.46 *s*			
8′α-Me	1.55 *s*	1.54 *s*	1.57 *s*	1.57 *s*	1.54 *s*
8′β-Me	1.13 *s*	1.12 *s*	1.22 *s*	1.23 *s*	1.19 *s*
N–Me	3.72 *s*	3.60 *s*	3.60 *s*		
N–CH_2	6.40 *d* (9.2)			6.35 *d* (9.2)	
	6.31 *d* (9.2)			6.31 *d* (9.2)	
$COCH_3$	2.11 *s*			2.11 *s*	

[a] All spectra run in $CDCl_3$.

group (Tables 1 and 2). Consequently this new alkaloid must be *trans*-deacetoxyerioaustralasine (**2**).

The minor alkaloid **3** revealed a M^+ 18 daltons more than **1** and **2** suggesting the addition of the elements of water (supported by a band at 3370 cm^{-1} in the IR spectrum). The loss of the resonance for the H-2′ epoxy proton and its replacement by a resonance at δ 5.78 (Table 1) further indicated that the 1′,2′-epoxy group had been hydrated to form the 1′,2′-diol. The relative stereochemistry across the ring junction remained *trans* ($J_{3',4'} = 11.4$ Hz) and that between H-2′ and H-3′ has to be cis as $J_{2',3'}$ was small. This left the stereochemistry at C-1′ to be resolved. This was achieved by means of a NOESY experiment (Fig. 1) which showed correlations between the 7′-Me and H-2′ and H-3′. This requires the 7′-Me to be axial on C-1′ and establishes the structure as **3**.

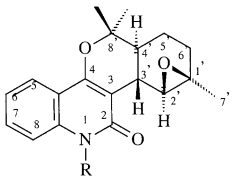

1 R = CH_2OCOCH_3
2 R = CH_3

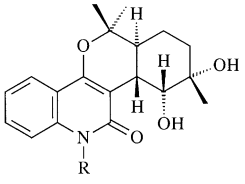

3 R = CH_3
4 R = CH_2OCOCH_3

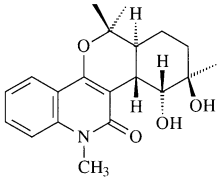

5

Table 2
^{13}C NMR chemical shift data for the alkaloids of *Halfordia kendack*[a]

	1	2	3	5
2	162.2	162.4	162.9	163.1
3	105.6	106.2	106.3	106.2
4	157.8	156.5	157.4	158.5
4a	117.0	116.8	116.9	117.1
5	123.7	123.4	123.4	123.4
6	122.6	121.6	121.7	121.8
7	131.2	130.7	130.6	130.5
8	113.8	113.9	114.0	114.0
8a	138.1	139.4	139.1	139.0
1′	57.8	57.8	72.5	71.9
2′	62.2	62.6	65.4	72.6
3′	36.1	36.4	36.1	36.6
4′	44.5	44.7	40.1	39.7
5′	22.4	22.5	22.9	22.9
6′	31.2	31.3	33.0	33.5
7′α-Me	23.7	23.7		28.6
7′β-Me	29.5			
8′	81.1	80.5	79.8	80.1
8′α-Me	27.4	27.5	27.6	27.7
8′β- Me	19.9	19.7	19.8	19.7
N–Me	29.3	29.4	29.3	
N–CH_2	66.2			
C=O	170.7			
CH_3	21.1			

[a] All spectra run in $CDCl_3$.

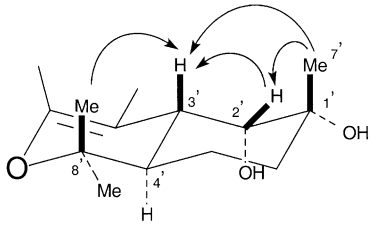

Fig. 1. NOESY correlations of **3**.

A second minor alkaloid (**4**) was identical to **3** accept for the replacement of the *N*-methyl resonances with those for an *N*-acetoxymethyl group. The final alkaloid (**5**) had the same M_r as **3** and the NMR spectra (Tables 1 and 2) confirmed it to be identical to **3** except for the stereochemistry at C-1′.

The isolation of these 3-monoterpenyl-quinoline alkaloids from *Halfordia kendack* was somewhat surprising as they had been found only in *Eriostemon banksii* (formerly *E. australasius* subsp. *banksii*), another Australian Rutaceae but a genus not thought to be at all closely allied to *Halfordia*.

3. Experimental

3.1. General

Melting points are uncorrected. UV spectra were run in methanol and IR spectra as liquid films. HR–EIMS spectra were obtained at 70 eV. NMR spectra were recorded at 400 MHz (^{1}H), 500 MHz (^{1}H–nOe) and 100.56 MHz (^{13}C) using the solvent as internal standard. Vacum liquid chromatography (VLC) and column chromatography were performed on Merck (7736) silica gel 60 H (0.04–0.005 mm) and Merck (7734) silica gel (0.063–0.2 mm), respectively. Analytical TLC and PTLC were performed on precoated Merck F_{254} silica gel plates and spraying with anisaldehyde-H_2SO_4 and Dragendroff's reagents. Gel filtration chromatography (GFC) was performed on Sephadex LH-20 (0.25–1 mm).

3.2. Plant material

Aerial parts of *H. kendack* were collected in southern Queensland in March 1992. A voucher specimen (W.J. MacDonald — 4775) has been deposited at the Queensland Herbarium, Brisbane (BRI).

3.3. Extraction and isolation

The dried, ground plant material (244 g) was sequentially extracted in a Soxhlet with *n*-hexane, $CHCl_3$ and MeOH. The extracts were filtered and evaporated to a gummy mass in a rotary evaporator under vacuum at a maximum temperature of 40°C.

The *n*-hexane extract (6.82 g) was fractionated by VLC over silica gel using solvents of increasing polarity. After removal of coumarins elution with 30–35% EtOAc in *n*-hexane followed by gel filtration of the eluate on Sephadex LH-20 column eluting with $CHCl_3$ and finally rechromatography of the alkaloid fraction over silica gel column with *n*-hexane containing ethylacetate gave **3** (6.1 mg) and then **4** (1 mg).

The $CHCl_3$ extract (6.60 g) was similarly fractionated by VLC and the eluate from 25–30% EtOAc in *n*-hexane was first chromatographed over silica gel with *n*-hexane containing increasing amount of EtOAc to give two alkaloidal-rich fractions. The less polar of these was first treated by gel filtration (Sephadex LH-20) eluting with $CHCl_3$ and then by CC over silica gel to give **1** (12.2 mg). The second subfraction was further fractionated by CC to give **2** (28.6 mg). The VLC fraction from 1 to 4% MeOH in EtOAc was further treated by gel filtration and CC using an EtOAc:MeOH gradient yielded **5** (6 mg).

3.3.1. Trans-erioaustrasine (*1*)

Amorphous solid, UV, $[\alpha]_D = +103°$ (*c*. 0.06 in $CHCl_3$ at 29.6°C) {lit. $[\alpha]_D = +130°$ (*c*. 0.96 in $CHCl_3$)} IR, ^{1}H NMR, ^{13}C NMR, EIMS in agreement with literature data (Da Cunha et al., 1993).

3.3.2. Trans-deacetoxyarioaustrasine (*2*)

Needles from EtOAc, mp 190–192°C. $[\alpha]_D$ + 244° (*c*. 0.242 in $CHCl_3$ at 29.6°C). $[\alpha]_D$ +125° (*c*. 0.08 in $CHCl_3$ at 29.6°C). UV λ_{max} (log ε) (MeOH) nm: 235 (3.84), 276 (3.68), 286 (3.68), 318 (3.65), 331 (3.55). IR (liquid film) ν_{max} cm^{-1}: 1629, 1593, 1502, 1462, 1417, 1386, 1328, 1312, 1271, 1253, 1213, 1196, 1164, 1123, 1099, 1043, 1017, 882, 806, 754. ^{1}H NMR — see Table 1, ^{13}C NMR — see Table 2. EIMS *m*/*z* (rel. int.); 325 [M^+] (100), 310 [M-CH_3]$^+$ (20), 282 [M-CH_3CO]$^+$ (49), 255 (42), 242 (45), 226 (20), 200 (21) 143 (30); found for M^+ 325.16832, $C_{20}H_{23}NO_3$, 325.16779.

3.3.3. Trans-deacetoxyaustralasine hydrate (*3*)

Amorphous, $[\alpha]_D$ +125° (*c*. 0.032 in $CHCl_3$ at 29.6°C) UV λ_{max} (log ε) (MeOH) nm: 234 (3.55), 275 (3.31), 286 (3.32), 317 (3.29), 332 (3.18). IR (liquid film) ν_{max} cm^{-1}: 3370, 1611, 1587, 1502, 1462, 1416, 1390, 1333, 1317, 1283, 1260, 1240, 1213, 1165, 1139, 1107, 1025, 999, 905, 871, 754. ^{1}H NMR — see Table 1. ^{13}C NMR — see Table 2. EIMS *m*/*z* (rel. int.); 343 [M^+] (29), 325 [M–H_2O]$^+$ (50), 310 [M–H_2O–CH_3]$^+$ (71), 308 [M–H_2O–OH]$^+$ (100), 282 [M–H_2O–CH_3CO]$^+$ (50), 240 (31), 226 (42), 200 (34); found for M^+ 343.18722, $C_{20}H_{25}NO_4$, 343.17836.

3.3.4. Trans-australasine hydrate (*4*)

Amorphous, UV λ_{max} (log ε) (MeOH) nm: 234 (4.17), 275 (3.98), 285 (3.99), 317 (3.90), 324 (3.77). IR (liquid film) ν_{max} cm^{-1}: 3406, 1745, 1623, 1595, 1575, 1502, 1462, 1389, 1371, 1333, 1287, 1232, 1200, 1167, 1139, 1107, 1023, 965, 904, 873 and 757. ^{1}H NMR ($CDCl_3$) — Table 1.

3.3.5. Trans-1′-epideacetoxyaustralasine hydrate (*5*)

Amorphous. UV λ_{max} (log ε) (MeOH) nm: 233 (3.93), 276 (3.45), 287 (3.46), 317 (3.44), 329 (3.34). IR (liquid

film) ν_{max} cm^{-1}: 3396, 1717, 1700, 1668, 1616, 1586, 1502, 1560, 1418, 1389, 1333, 1209, 1163, 1108, 1039, 1019, 905, 863, 752. ^1H NMR — see Table 1, ^{13}CNMR — see Table 2. EIMS *m*/*z* (rel. int.); 343 [M^+] (3), 325 [M–H_2O]$^+$ (100), 310 [M–H_2O–CH_3]$^+$ (14), 282 [M–H_2O–CH_3CO]$^+$ (18), 242 (26); found for M^+ 343.18722, $C_{20}H_{25}NO_4$, 343.17836.

Acknowledgements

N.S. thanks the Bangladesh Council of Scientific and Industrial Research (BCSIR) for the award of a scholarship. Mr. W.J. MacDonald of the Queensland Herbarium is thanked for the collection of plant material.

References

Da Cunha, E.V.L., Armstrong, J.A., Gray, A.I., Hockless, D.C.R., Waterman, P.G., White, A.H., 1993. 3-Monoterpenyl 2,4-dioxygenated quinoline alkaloids from the aerial parts of *Eriostemon australasius* subsp. *banksii* (Rutaceae). Australian Journal of Chemistry 46, 1507–1514.

Gray, A.I., 1983. Coumarins and chromones of the Rutales. In: Waterman, P.G., Grundon, M.F. (Eds.), Chemistry and Chemical Taxonomy of the Rutales. Academic, London, pp. 97–146.

Mester, I., 1983. Alkaloids in the Rutales. In: Waterman, P.G., Grundon, M.F. (Eds.), Chemistry and Chemical Taxonomy of the Rutales. Academic, London, pp. 31–96.

Richard, P.G., 1991. In: Harden, G.J. (Ed.), Flora of New South Wales, Vol. 2. NSWU, Sydney, pp. 271–272.

Sultana, N., Skelton, B.W., Waterman, P.G., White, A.H., 2000. 3,5-Dimethoxy-3-(1,1-dimethylprop-2-enyl)-3,4-dihydropsoralen-4-one: an unusual furanocoumarin derivative from *Halfordia kendack*. Phytochemistry 55, 675–678.

PERGAMON

Phytochemistry 58 (2001) 333–336

PHYTOCHEMISTRY

www.elsevier.com/locate/phytochem

Megastigmane and iridoid glucosides from *Clerodendrum inerme*

Tripetch Kanchanapoom[a,b], Ryoji Kasai[a], Phannipha Chumsri[c], Yoshikazu Hiraga[d], Kazuo Yamasaki[a,*]

[a]*Institute of Pharmaceutical Sciences, Faculty of Medicine, Hiroshima University, 1-2-3 Kasumi, Minami-ku, Hiroshima 734-8551, Japan*
[b]*Department of Pharmaceutical Botany and Pharmacognosy, Faculty of Pharmaceutical Sciences, Khon Kaen University, Khon Kaen 40002, Thailand*
[c]*Department of Pharmacognosy, Faculty of Pharmacy, Mahidol University, Bangkok 10400,Thailand*
[d]*Department of Chemistry, Graduate School of Science, Hiroshima University 1-3-1, Kagamiyama, Higashi-Hiroshima 739-8526, Japan*

Received 2 January 2001; received in revised form 16 March 2001

Dedicated to Professor Vichiara Jirawongse on the occasion of his 83rd birthday

Abstract

From the aerial parts of *Clerodendrum inerme*, two megastigmane glucosides (sammangaosides A and B) and a iridoid glucoside (sammangaoside C) were isolated together with 15 known compounds. The structural elucidations were based on analyses of physical and spectroscopic data. © 2001 Published by Elsevier Science Ltd.

Keywords: *Clerodendrum inerme*; Verbenaceae; Megastigmane glucoside; Iridoid glucoside; Sammangaosides A–C

1. Introduction

As part of our ongoing study on Thai medicinal plants, we investigated the constituents of *Clerodendrum inerme* Gaertn. (Verbenaceae, Thai name: Sam-ma-nga) collected in the Botanical gardens, Faculty of Pharmaceutical Sciences, Khon Kaen University, Thailand. *C. inerme* is a shrub distributed in South and South-east Asia, Australia and Pacific islands. In Thai traditional medicine, the fresh leaves are externally used for treating skin diseases. In preliminary studies of this plant, flavones (Vendantham et al., 1977) a clerodane diterpene (Achari et al., 1990), a neolignan (Spencer and Flippen-Anderson, 1981), a phenylpropanoid (Fauvel et al., 1989) and iridoid glycosides (Calis et al., 1994a,b) have been isolated. The present study deals with the isolation and structural elucidations of two new megastigmane glucosides (**6**, **7**) and one new iridoid glucoside (**10**), together with 15 known compounds; phenylpropanoid glycosides (**1–3**), phenylethanoid glycosides (**4**, **5**, **15**), iridoid glucosides (**8**, **9**), neolignan glucosides (**11**, **12**), benzyl alcohol glycosides (**13**, **14**), aliphatic glucoside (**16**) and hydroquinone glycosides (**17**, **18**).

2. Results and discussion

The methanolic extract of the aerial part of *C. inerme* was suspended in H_2O and defatted with Et_2O. The aqueous layer was subjected to a column of highly porous copolymer of styrene and divinylbenzene, and eluted with H_2O, MeOH and Me_2O, successively. The fraction eluted with MeOH was repeatedly chromatrographed on columns of silica gel and RP-18, then by HPLC-ODS to afford 18 compounds (**1–18**). Fifteen were identified as known compounds; verbascoside (**1**), isoverbascoside (**2**), leucosceptoside A (**3**) (Miyase et al., 1982), decaffeoylverbascoside (**4**), darendoside B (**5**) (Calis et al., 1993), monomelittoside (**8**) (Chaudhuri and Sticher, 1980), melittoside (**9**) (Swiatek et al., 1981), (7*S*, 8*R*)-dehydrodiconiferyl alcohol 9-*O*-β-glucopyranoside (**11**) (Binns et al., 1987), (7*S*, 8*R*)-dehydrodiconiferyl alcohol 4-*O*-β-glucopyranoside (**12**) (Yoshizawa et al., 1990), benzyl alcohol β-glucopyranoside (**13**) (Miyase et al., 1987), benzyl alcohol β-(2′-*O*-β-xylopyranosyl) glucopyranoside (**14**) (Sudo et al., 2000), salidroside (**15**) (Nonaka et al., 1982), (*Z*)-3-hexenyl-β-glucopyranoside (**16**) (Mizutani et al., 1988) and 2,6-dimethoxy-*p*-hydroquinone 1-*O*-β-glucopyranoside (**17**) (Otsuka et al., 1989), seguinoside K (**18**) (Zhong et al., 1999) by physical data and spectroscopic evidences.

The molecular formula of compound **6** was determined as $C_{19}H_{32}O_8$ by HR–FAB mass spectrometry.

* Corresponding author. Tel.: +81-82-257-5285; fax: +81-82-257-5289.
E-mail address: yamasaki@pharm.hiroshima-u.ac.jp (K. Yamasaki).

0031-9422/01/$ - see front matter © 2001 Published by Elsevier Science Ltd.
PII: S0031-9422(01)00208-4

Inspection of the ^{13}C NMR spectrum indicated the presence of one β-glucopyranosyl unit together with 13 carbon signals for the aglycone moiety which suggested it to possess the megastigmane skeleton. Compound **6** showed the same planar structure as 3-hydroxy-5,6-epoxy-β-ionyl-9-*O*-β-glucopyranoside, previously isolated from flue-cured tobacco (Kodama et al., 1981) and the absolute configuration at C-9 was confirmed to be *R* (Sudo et al., 2000). Comparison of the ^{1}H and ^{13}C NMR spectral data of **6** with those of 3-hydroxy-5,6-epoxy-β-ionyl-9-*O*-β-glucopyranoside (Sudo et al., 2000) revealed the same relative arrangement of the ring carbons and protons. The difference of the chemical shifts at C-9 (δ 74.7) and 10 (δ 22.4,) with C-9 (δ 76.9) and C-10 (δ 21.0) of the reported data from the ^{13}C NMR spectrum led to conclude the absolute configuration at C-9 to be *S* (Pabst et al., 1992; Takeda et al., 1997). Therefore, the structure of **6** was assigned as (3*S*, 5*R*, 6*S*, 7*E*, 9*S*)-3-hydroxy-5,6-epoxy-β-ionyl-9-*O*-β-glucopyranoside, named sammangaoside A.

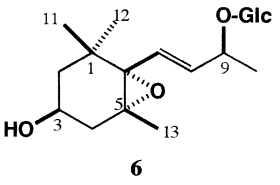

6

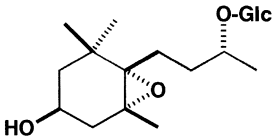

7

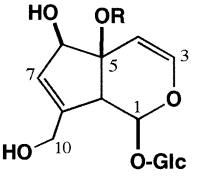

	R
8	**H**
9	**Glc**
10	**Glc (3'–1")-Glc**

The molecular formula of compound **7** was determined as $C_{19}H_{34}O_8$ by HR–FAB mass spectrometry. The ^{1}H and ^{13}C NMR spectral data indicated it to be a megastigmane glucoside. Inspection of the FAB mass spectrometry revealed the two mass units larger than **6** and the signals for the double bond were not observed in the ^{1}H and ^{13}C NMR spectra, indicating the presence of the saturated side chain. The chemical shifts for the signals attributed to the ring were coincident with those of **6**, deduced from the ^{1}H and ^{13}C NMR spectral data. The absolute configuration at C-9 was assigned to be *R* from the chemical shifts at C-9 and 10 (δ 77.8 and 21.8, respectively) (Pabst et al., 1992; Takeda et al., 1997). Consequently, (3*S*, 5*R*, 6*S*, 9*R*)-3-hydroxy-5,6-epoxy-β-dihydroionyl-9-*O*-β-glucopyranoside, was proposed for sammangaoside B.

The molecular formula of compound **10** was determined as $C_{27}H_{42}O_{20}$ by HR–FAB mass spectrometry. The ^{13}C NMR spectrum was very similar to that of **9** (Table 2) except that the ^{13}C NMR signals for one more glucopyranosyl unit were observed. The additional unit was assigned to be attached at C-3″ of the second glucopyranose on C-5 by HMQC and HMBC experiments, in which long-range correlations were observed between (i) H-1‴ (δ 4.54) and C-3″ (δ 88.3), and (ii) H-1″ (δ 4.74) and C-3″ (δ 88.3), C-5 (δ 79.8) as shown in Fig. 1. Moreover, the chemical shifts of C-3″, C-2″ and C-4″ were changed by +10.0,− 0.7 and−1.5 ppm, respectively. Therefore, the structure of compound **10** was elucidated as melittoside 3″-*O*-β-glucopyranoside, named sammangaoside C.

3. Experimental

3.1. General

NMR spectra were recorded in CD_3OD using a JEOL JNM A-400 spectrometer (400 MHz for ^{1}H NMR and 100 MHz for ^{13}C NMR) and JNM-ECP 500 (500 MHz for ^{1}H NMR and 125 MHz for ^{13}C NMR) with tetramethylsilane (TMS) as internal standard. MS were recorded on a JEOL JMS-SX 102 spectrometer. Preparative HPLC was carried out on columns of ODS (150 ×20 mm i.d., YMC) with a Tosoh refraction index (RI-8) detector. The flow rate was 6 ml/min. For CC, silica gel G 60 (Merck), RP-18 (50 μm, YMC) and highly porous copolymer of styrene and divinylbenzene (Mitsubishi Chem. Ind. Co. Ltd) were used. The solvent systems were: (I) EtOAc–MeOH–H_2O (4:1:0.1), (II) EtOAc–MeOH–H_2O (7:3:0.3), (III) EtOAc–MeOH–H_2O (6:4:1), (IV) 15–70% MeOH, (V) 10–50% MeOH, (VI) 10% MeCN, (VII) 20% MeCN, and (VIII) 6% MeCN. The spray reagent used was 10% H_2SO_4 in ethanol.

3.2. Plant material

The aerial part of *Clerodendrum inerme* was collected in August, 1999 from the Botanical gardens, Faculty of

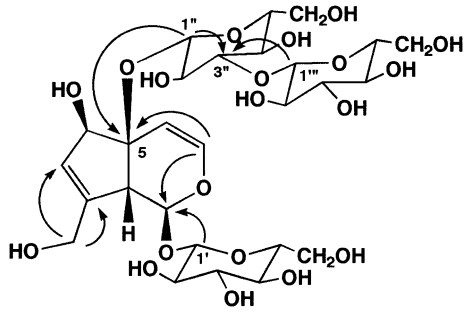

10

Fig. 1. The HMBC correlations of compound **10**.

Pharmaceutical Sciences, Khon Kaen University, Thailand. The identification of the plant was confirmed by Professor Vichiara Jirawongse, Department of Pharmaceutical Botany and Pharmacognosy, Faculty of Pharmaceutical Sciences, Khon Kaen University. A voucher sample is kept in the Herbarium of the Faculty of Pharmaceutical Sciences, Khon Kaen University, Thailand.

3.3. Extraction and isolation

The dried aerial part (880 g) of *C. inerme* was extracted with hot MeOH. After removal of the solvent by evaporation, the residue (90.0 g) was defatted with Et_2O. The aqueous layer was subjected to column chromotography, using highly porous copolymer of styrene and divinylbenzene, eluted with H_2O, MeOH and Me_2CO, successively. The fraction eluted with MeOH (17.5 g) was subjected to silica gel column chromotography (systems I, II and III, respectively) affording seven fractions. Fraction 2 (3.12 g) was applied to a RP-18 column using system IV, then followed by prep. HPLC–ODS (system VI and VII) to provide compounds **1** (456 mg), **2** (183 mg), **3** (10 mg), **4** (9 mg), **5** (5 mg), **6** (11 mg), **7** (6 mg), **11** (5 mg), **13** (13 mg), **14** (5 mg), **15** (8 mg), **16** (24 mg), **17** (13 mg) and **18** (4 mg). Fraction 4 (1.74 g) was further separated on a RP-18 column (system IV) and purified by prep. HPLC–ODS (system VII) to give compound **12** (7 mg). Fraction 5 (2.73 g) was similarly subjected to RP-18 column (system IV), then followed by prep. HPLC–ODS (system VII) to afford compounds **8** (50 mg). Fraction 6 (4.8 g) was purified by using columns of RP-18 (system V) and prep. HPLC–ODS (system VIII) to give compounds **9** (1.0 g) and **10** (10 mg).

3.4. Sammangaoside A (6)

Amorphous, $[\alpha]_D^{20}$ −99.1° (MeOH, *c* 0.8); ^{1}H NMR (CD_3OD): δ 6.04 (1H, *d*, *J* = 15.6 Hz, H-7), δ 5.56 (1H, *dd*, *J* = 15.6, 7.6 Hz, H-8), δ 4.52 (1H, *m*, H-9), δ 4.27 (1H, *d*, *J* = 7.5 Hz, H-1′ Glc), δ 3.73 (1H, *m*, H-3), δ 2.28 (1H, *dd*, *J* = 14.2, 1.7 Hz, H-4e), δ 1.61 (1H, *dd*, *J* = 14.2, 9.3 Hz, H-4a), δ 1.56 (1H, *bd*, *J* = 10.7 Hz, H-2e), δ 1.27 (3H, *d*, *J* = 6.3 Hz, H-10), δ 1.24 (3H, *s*, H-13), δ 1.20 (1H, *bt*, *J* = 11.0 Hz, H-2a), δ 1.08 (3H, *s*, H-11), δ 0.93 (3H, *s*, H-12); ^{13}C NMR (CD_3OD): Table 1; Negative HR–FAB–MS, *m*/*z*: 387.2039 $[M–H]^-$ ($C_{19}H_{31}O_8$ requires 387.2019)

3.5. Sammangaoside B (7)

Amorphous, $[\alpha]_D^{20}$ −35.0° (MeOH, *c* 0.4); ^{1}H NMR (CD_3OD): δ 4.30 (1H, *d*, *J* = 7.8 Hz, H-1′ Glc), δ 3.76 (1H, *m*, H-9), δ 3.67 (1H, *m*, H-3), δ 2.21 (1H, *dd*, *J* = 14.0, 1.8 Hz, H-4e), δ 1.98 (1H, *m*, H-7), δ 1.77 (1H, *m*, H-8), δ 1.63 (1H, *m*, H-8), δ 1.59 (1H, *dd*, *J* = 14.0, 9.2 Hz, H-4a), δ 1.57 (1H, *m*, H-7), δ 1.47 (1H, *bd*, *J* = 12.6 Hz, H-2e), δ 1.35 (3H, *s*, H-13), δ 1.23 (3H, *d*, *J* = 6.2 Hz, H-10), δ 1.18 (3H, *s*, H-11), δ 1.16 (1H, *dd*, *J* = 12.6, 11.0 Hz, H-2a), δ 1.03 (3H, *s*, H-12); ^{13}C NMR (CD_3OD): Table 1; Negative HR–FAB–MS, *m*/*z*: 389.2142 $[M–H]^-$ ($C_{19}H_{33}O_8$ requires 389.2175).

Table 1
^{13}C NMR spectral data of compounds **6** and **7** (CD_3OD, 100 MHz)

C	6	7
1	35.9	36.6
2	47.9	47.9
3	64.5	64.4
4	41.6	42.6
5	68.1	67.4
6	71.1	70.8
7	129.6	27.9
8	136	34.4
9	74.7	77.8
10	22.4	21.8
11	30.1	29.5
12	25	25.9
13	20.7	21.3
1′	101.3	103.8
2′	75	75.3
3′	78.3	78.2
4′	71.8	71.7
5′	78.1	77.8
6′	62.8	62.8

Table 2
^{13}C NMR spectral data of compounds **9** and **10** (CD_3OD, 100 MHz)

C	9	10[a]
1	94.2	93.8
3	143.4	143.4
4	105.2	105
5	80	79.8
6	79.9	79.6
7	128.1	128
8	147.3	147.6
9	51.5	51.4
10	60.9	60.9
1''	98.1	98
2''	74.8	74.9
3''	78.4	78.2a
4′	71.6	71.6b
5′	77.1	77.2
6′	32.7	62.8c
1″	99.6	99.3
2″	75.1	74.4 (−0.7)
3″	78.2	88.3 (+10.0)
4″	70.8	69.3 (−1.5)
5″	78.1	77.8
6″	62.1	62
1‴		105.2
2‴		75.5
3‴		78.5a
4‴		71.7b
5‴		77.8
6‴		62.6c

[a] a–c, assignment may be interchangeable.

3.6. Sammangaoside C (**10**)

Amorphous, $[\alpha]_D^{20}$ −36.1° (MeOH, *c* 0.7); ^{1}H NMR (CD_3OD): δ 6.65 (1H, *d*, *J* = 6.7 Hz, H-3), δ 5.79 (1H, *bs*, H-7), δ 5.63 (1H, *d*, *J* = 3.7 Hz, H-1), δ 5.15 (1H, *dd*, *J* = 6.4, 1.1 Hz, H-4), δ 4.74 (1H, *d*, *J* = 7.8 Hz, H-1″ Glc), δ 4.59 (1H, *d*, *J* = 7.8 Hz, H-1′ Glc), δ 4.54 (1H, *d*, *J* = 7.8 Hz, H-1‴ Glc); ^{13}C NMR (CD_3OD): Table 2; Negative HR–FAB–MS, *m*/*z*: 685.2204 $[M–H]^-$ ($C_{27}H_{41}O_{20}$ requires 685.2191).

Acknowledgements

We would like to thank the Research Center for Molecular Medicine, Hiroshima University for the use of its NMR facilities. Also, we are grateful to Mr. Bamrung Thavinchiua of the Department of Pharmaceutical Botany and Pharmacognosy, Faculty of Pharmaceutical Sciences, Khon Kaen University, Thailand, for help in obtaining the plant material.

References

Achari, B., Chaudhuri, C., Saha, C.R., Dutta, P.K., Pakrashi, S.C., 1990. A clerodane diterpene and other constituents of *Clerodendron inerme*. Phytochemistry 29, 3671–3673.

Binns, A.N., Chen, R.H., Wood, H.N., Lynn, D.G., 1987. Cell division promoting activity of naturally occurring dehydrodiconiferyl glucosides: do cell wall components control cell division? Proceedings of the National Academy Sciences of the United States of America 84, 980–984.

Calis, I., Hosny, M., Yuruker, A., 1994. Inerminosides A1, C and D, three iridoid glycosides from *Clerodendrum inerme*. Phytochemistry 37, 1083–1085.

Calis, I., Hosny, M., Yuruker, A., Wright, A.D., Sticher, O., 1994. Inerminosides A and B, two novel complex iridoid glycosides from *Clerodendrum inerme*. Journal of Natural Products 57, 494–500.

Calis, I., Saracoglu, I., Basaran, A.A., Sticher, O., 1993. Two phenethyl alcohol glycosides from *Scutellaria orientalis* subsp. *pinnatifida*. Phytochemistry 32, 1621–1623.

Chaudhuri, R.K., Sticher, O., 1980. Globularifolin, a new acyl iridoid glucoside from *Globularia corifolia*. Helvetica Chemica Acta 63, 117–120.

Fauvel, M.T., Gleye, J., Andary, C., 1989. Verbascoside: a constituent of *Clerodendrum inerme*. Planta Medica 55.

Kodama, H., Fujimori, T., Kato, K., 1981. Isolation of a new terpene glucoside, 3-hydroxy-5,6-epoxy-β-ionyl-β-D-glucopyranoside from flue-cured tobacco. Agricultural and Biological Chemistry 45, 941–944.

Miyase, T., Koizumi, A., Ueno, A., Noro, T., Kuroyanagi, M., Fukushima, S., Akiyama, Y., Takemoto, T., 1982. Studies on the acyl glycosides from *Leucoseptrum japonicum* (Miq.) Kitamura et Murata. Chemical and Pharmaceutical Bulletin 30, 2732–2737.

Miyase, T., Ueno, A., Takizawa, N., Kobayashi, H., Karasawa, H., 1987. Studies on the glycosides of *Epimedium graniflorum* Morr. var. *thunbergianum* (Miq.) Nakai. Chemical and Pharmaceutical Bulletin 35, 1109–1117.

Mizutani, K., Yuda, M., Tanaka, O., Saruwatari, Y.-I., Fuwa, T., Jia, M-R, Ling, Y.-K., Pu, X.-F., 1988. Chemical studies on Chinese traditional medicine dangshen. I. Isolation of (*Z*)-3-(*E*)-2-hexenyl β-D-glucosides. Chemical and Pharmaceutical Bulletin 36, 2689–2690.

Nonaka, G.-I., Nishimura, H., Nishioka, I., 1982. Tannins and related compounds IV. Seven new phenol glucoside gallates from *Quercus stenophylla* Makino. Chemical and Pharmaceutical Bulletin 30, 2061–2067.

Otsuka, H., Takeuchi, M., Inoshiri, S., Sato, T., Yamasaki, K., 1989. Phenolic compounds from *Coix lachryma-jobi*. var. *ma-yuen*. Phytochemistry 30, 883–886.

Pabst, A., Barron, D., Semon, E., Schreier, P., 1992. Two diastereomeric 3- oxo-α-ionol β-D-glucosides from raspberry fruit. Phytochemistry 31, 1649–1652.

Spencer, G.F., Flippen-Anderson, J.L., 1981. Isolation and X-ray structure determination of a neolignan from *Clerodendron inerme* seeds. Phytochemistry 20, 2757–2759.

Sudo, H., Ide, T., Otsuka, H., Hirata, E., Takushi, A., Shinzato, T., Takeda, Y., 2000. Megastigmane, benzyl and phenethyl alcohol glycosides, and 4,4′-dimethoxy-β-truxinic acid catalpol diester from the leaves of *Premna subscandens* Merr. Chemical and Pharmaceutical Bulletin 48, 542–546.

Swiatek, L., Lehmann, D., Chudhuri, R.K., Sticher, O., 1981. Occurrence of milittoside in the seeds of *Plantago media*. Phytochemistry 20, 2023–2324.

Takeda, Y., Zhang, H., Matsumoto, T., Otsuka, H., 1997. Oosio, Y, Honda, G Tabata, M., Fujita, T, Sun, H., Sezik, E, Yesilada, E., Megastigmane glycosides from *Salvia nemorosa*. Phytochemistry 44, 117–120.

Vendantham, T.N.C., Subramanian, S.S., Harborne, J.B., 1977. 4′-Methylscutellarein and pectolinarigenin from *Clerodendron inerme*. Phytochemistry 16, 294.

Yoshizawa, F., Deyama, T., Takizawa, N., Usmanghani, K., Ahmad, M., 1990. The constitutents of *Cistanche tubulosa* (Schrenk) Hook.f. II. Isolation and structures of a new phenylethanoid glycoside and a new neolignan glycoside. Chemical and Pharmaceutical Bulletin 38, 1927–1930.

Zhong, X.-N., Otsuka, H., Ide, T., Hirata, E., Takeda, Y., 1999. Hydroquinone diglycosides acyl esters from the leaves of *Myrsine seguinii*. Phytochemistry 52, 923–927.

PERGAMON

Phytochemistry 58 (2001) 337–341

PHYTOCHEMISTRY

www.elsevier.com/locate/phytochem

Iridoid glucosides from *Barleria lupulina*

Tripetch Kanchanapoom[a,b], Ryoji Kasai[a], Kazuo Yamasaki[a,*]

[a]*Institute of Pharmaceutical Sciences, Faculty of Medicine, Hiroshima University, 1-2-3 Kasumi, Minami-ku, Hiroshima 734-8551, Japan*
[b]*Department of Pharmaceutical Botany and Pharmacognosy, Faculty of Pharmaceutical Sciences, Khon Kaen University, Khon Kaen 40002, Thailand*

Received 29 December 2000; received in revised form 12 April 2001

Dedicated to Professor Vichiara Jirawongse on the occasion of his 83rd birthday

Abstract

From the aerial part of *Barleria lupulina*, 8-*O*-acetyl-6-*O*-*trans*-*p*-coumaroylshanzhiside, saletpangponosides A–C and 8-*O*-acetylmussaenoside were isolated together with 13 known compounds. The structural elucidations were based on analyses of physical and spectroscopic data. © 2001 Elsevier Science Ltd. All rights reserved.

Keywords: *Barleria lupulina*; Acanthaceae; Iridoid glucosides; Saletpangponosides A–C; Shanzhiside derivatives; 8-*O*-Acetylmussaenoside

1. Introduction

As part of our ongoing study on Thai medicinal plants, we investigated the constituents of *Barleria lupulina* Lindl. (Acanthaceae, Thai name: Sa-let-pang-pon, Chong-ra-ar) collected in the Botanical gardens, Faculty of Pharmaceutical Sciences, Khon Kaen University, Thailand. *B. lupulina* is a small shrub, distributed in the South-east Asia region. In Thai traditional medicine, the plant is externally used as an antiinflammatory for insect bite, herpes simplex and herpes zoster. In preliminary investigations nine iridoid glucosides (Suksamrarn 1986; Byrne et al., 1987; Tuntiwachwuttikul et al., 1998) have been isolated. In addition, some anti-HSV-2 (herpes simplex virus type 2) activity of organic extracts of the plant have been reported (Yoosook et al., 1999). The present study deals with the isolation and structure elucidation of iridoid glucosides (**1**–**12**), of which five are new (**5**–**8**, **12**), together with six other known compounds; phenylpropanoid glycosides (**13**–**15**), lignan glucoside (**16**), aliphatic glycoside (**17**) and benzyl alcohol glycoside (**18**) from the aerial part of this plant.

2. Results and discussion

The methanolic extract of the aerial part of *B. lupulina* was suspended in H_2O and defatted with Et_2O. The aqueous layer was subjected to column chromatography using a highly porous copolymer of styrene and divinylbenzene, and eluted with H_2O, MeOH and Me_2CO, successively. The fraction eluted with MeOH was repeatedly subjected to column chromatography using silica gel and octadecylsilyl silica gel, then by preparative HPLC-ODS to afford 18 compounds (**1**–**18**). Thirteen were known compounds; shanzhiside methyl ester (**1**), 8-*O*-acetylshanzhiside methyl ester (barlerin) (**2**), 6-*O*-acetylshanzhiside methyl ester (**3**), 6,8-*O*,*O*-diacetylshanzhiside methyl ester (acetylbarlerin) (**4**) (Damtoft et al., 1982; Byrne et al., 1987), ipolamiide (**9**) (Damtoft et al., 1984b), ipolamiidoside (**10**) (Byrne et al., 1987), phlorigidoside B (**11**) (Takeda et al., 2000), forsythoside B (**13**) (Endo et al., 1982), verbascoside (**14**) (Andary et al., 1982), poliumoside (**15**) (Andary et al., 1985), (+)-lyoniresinol 3a-*O*-β-glucopyranoside (**16**) (Achenbach et al., 1992), (3*R*)-1-octen-3-yl-β-primeveroside (**17**) (Yamamura et al., 1998) and benzyl alcohol β-(2′-*O*-β-xylopyranosyl) glucopyranoside (**18**) (Sudo et al., 2000) by physical data and spectroscopic evidences.

The molecular formula of compound **5** was determined as $C_{27}H_{32}O_{14}$ by HR–FAB mass spectrometry. Inspection of the ^{13}C NMR spectral data revealed the

* Corresponding author. Tel.: +81-82-257-5285; fax: +81-82-257-5289.
E-mail address: yamasaki@pharm.hiroshima-u.ac.jp (K. Yamasaki).

0031-9422/01/$ - see front matter © 2001 Elsevier Science Ltd. All rights reserved.
PII: S0031-9422(01)00236-9

presence of one β-glucopyranosyl unit, one coumaroyl moiety and one acetyl group in addition to eleven carbon signals for the aglycone moiety. The coumaroyl moiety was assigned as *trans* by the coupling constant of the α and β protons in the ^{1}H NMR spectrum (δ 6.28 and 7.56, $J = 15.9$ Hz). The ^{1}H and ^{13}C NMR spectral data were very similar to those of 8-*O*-acetyl-6-*O*-*trans*-*p*-coumaroylshanzhiside methyl ester (Tuntiwachwuttikul et al., 1998), except for lacking the methoxy signal due to the carbomethoxy group, which established the presence of a carboxyl group. On the basis of these spectral data, the structure of compound **5** was determined as 8-*O*-acetyl-6-*O*-*trans*-*p*-coumaroylshanzhiside.

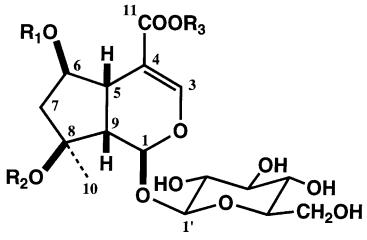

	R_1	R_2	R_3
1	H	H	Me
2	H	Ac	Me
3	Ac	H	Me
4	Ac	Ac	Me
5	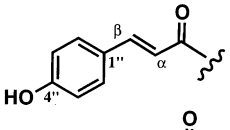	Ac	H
6	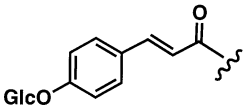	Ac	Me
7	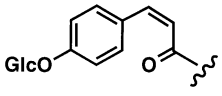	Ac	Me
8	H	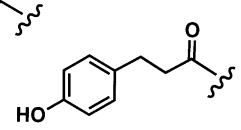	Me

The molecular formula of compound **6** was determined as $C_{34}H_{44}O_{19}$ by HR–FAB mass spectrometry. The ^{1}H and ^{13}C NMR spectral data showed the presence of two β-glucopyranosyl units, one *trans*-coumaroyl moiety, as well as the signals for an acetyl group and a carbomethoxy group. The ^{1}H and ^{13}C NMR spectra were very similar to those of 8-*O*-acetyl-6-*O*-*trans*-*p*-coumaroylshanzhiside methyl ester (Tuntiwachwuttikul et al., 1998), except for a set of additional signals arising from a β-glucopyranosyl moiety in **6**. The additional glucopyranosyl unit was assigned to be attached at C-4″ (δ 160.9) of the coumaroyl moiety because the chemical shifts of C-4″, C-3″,5″ (δ 118.0) changed by +0.2 and-2.6 ppm, respectively. Moreover, the HMBC spectrum provided further confirmation with a significant correlation between H-1‴ (δ 4.93, *d*, $J = 7.6$ Hz) of this glucopyranosyl unit and C-4″ of the coumaroyl moiety. Consequently, the structure of compound **6** was assigned as 6-*O*- (4″-*O*-β-glucopyranosyl)-*trans*-*p*-coumaroyl-8-*O*-acetylshanzhiside methyl ester, named saletpangponoside A.

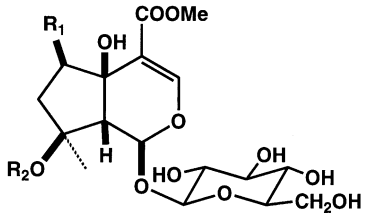

	R_1	R_2
9	H	H
10	H	Ac
11	OH	Ac

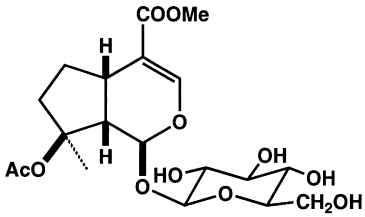

12

The molecular formula of compound **7** had the same elemental composition as **6**, $C_{34}H_{44}O_{19}$, by HR–FAB mass spectrometry. The ^{1}H and ^{13}C NMR spectral data were very similar to those of **6**. The only significant difference was the coupling constants of the olefinic protons (δ 5.86 and 6.94, $J = 12.9$ Hz). Therefore, the structure of compound **7** was determined as the *cis* isomer of **6**, named saletpangponoside B.

The molecular formula of compound **8** was determined as $C_{26}H_{34}O_{13}$ by HR–FAB mass spectrometry. The ^{1}H and ^{13}C NMR spectral data indicated that **8** is a derivative of shanzhiside methyl ester (**1**), with an ester moiety on the 8-hydroxy group because of the downfield shift of C-8 (+10.5 ppm). The ester moiety showed the presence of an AA′BB′ system (δ 6.64 and 6.98, $J = 8.6$ Hz from ^{1}H NMR), two methylenes (δ 2.49 and δ 2.76 from ^{1}H NMR, and δ 38.2 and 31.2 from ^{13}C NMR) and a carbonyl carbon (δ 175.0), identified as a *p*-dihydrocoumaroyl moiety. The complete assignments were confirmed by the HMBC spectrum, in which H-α (δ 2.49) showed a three bond correlation to C-1″ (δ 132.6), and H-β (δ 2.76) showed the significant correlation to C-2″,6″ (δ 130.3). Thus, the structure of compound **8**

was elucidated as 8-*O*-*p*-dihydrocoumaroylshanzhiside methyl ester, named saletpangponoside C.

The molecular formula of compound **12** was determined as $C_{19}H_{28}O_{11}$ by HR–FAB mass spectrometry. The ^1H and ^{13}C NMR spectra indicated an iridoid structure. The chemical shifts were very similar to those of mussaenoside (Damtoft et al., 1984a) except that the acetyl group was observed in the spectra. The attachment of the acetyl group was assigned to C-8 (δ 91.0), the carbon signal of which was shift to downfield by 10.6 ppm. Therefore, the structure of compound **12** was identified as 8-*O*-acetylmussaenoside.

3. Experimental

3.1. General

NMR spectra were recorded in CD_3OD using a JEOL JNM A-400 spectrometer (400 MHz for ^1H NMR and 100 MHz for ^{13}C NMR) with tetramethylsilane (TMS) as internal standard. MS were recorded on a JEOL JMS-SX 102 spectrometer. Optical rotations were measured with a Union PM-1 digital polarimeter. Preparative HPLC was carried out on columns of ODS (20×150 mm i.d., YMC) with a Tosoh refraction index (RI-8) detector. For CC, silica gel G 60 (Merck), YMC-gel ODS (50 mm, YMC), and highly porous copolymer of styrene and divinylbenzene (Mitsubishi Chem. Ind. Co. Ltd) were used. The solvent systems were: (I) EtOAc–MeOH (9:1), (II) EtOAc–MeOH–H_2O (4:1:0.1), (III) EtOAc–MeOH–H_2O (7:3:0.3), (IV) 20–35% MeCN, (V) 15% MeCN, (VI) 25% MeCN, (VII) 10–35% MeCN, (VIII) 10% MeCN and (IX) 40% MeOH. The spray reagent used for TLC was 10% H_2SO_4 in 50% EtOH.

3.2. Plant material

Barleria lupulina Lindl. was collected in September 1999 from the Botanical gardens, Faculty of Pharmaceutical Sciences, Khon Kaen University, Thailand. The identification of the plant was confirmed by Prof. Vichiara Jirawongse, Department of Pharmaceutical Botany and Pharmacognosy, Faculty of Pharmaceutical Sciences, Khon Kaen University. A voucher sample (KKU-0018) is kept in the Herbarium of the Faculty of Pharmaceutical Sciences, Khon Kaen University, Thailand.

Table 1
^1H NMR spectral data of compounds **5**–**8** and **12** (400 MHz, CD_3OD)

H	5	6	7	8	12
1	5.89, *d* (2.7)[b]	5.85, *d* (3.2)	5.85, *d* (3.2)	5.82, *d* (2.4)	5.71, *d* (3.4)
3	7.49, *d* (1.5)	7.48, *d* (1.5)	7.50, *d* (1.5)	7.38, *d* (1.5)	7.43, *d* (1.0)
5	3.33*[a]	3.30*	3.25*	2.94*	3.12, *m*
6	5.40, *m*	5.34, *m*	5.34, *m*	4.25, *m*	1.75, *m*
7	2.37, *bd* (15.4)	2.38, *bd* (15.4)	2.38, *bd* (15.6)	2.11, *bd* (14.9)	2.05, *m*
	2.05, *dd* (15.4, 5.3)	2.09, *dd* (15.4, 5.3)	2.09, *dd* (15.6, 5.4)	1.97, *dd* (14.9, 5.4)	
9	3.01, *dd* (8.5, 2.7)	3.00, *dd* (8.6, 3.2)	2.90, *dd* (8.6, 3.2)	2.94*	2.68, *dd* (8.5, 3.4)
10	1.51, *s*	1.53, *s*	1.53, *s*	1.38, *s*	1.54, *s*
COOMe		3.65, *s*	3.68, *s*	3.66, *s*	3.69, *s*
1′	4.65, *d* (7.8)	4.63, *d* (8.1)	4.66, *d* (7.8)	4.59, *d* (7.8)	4.59, *d* (7.8)
2′	3.18, *dd* (9.0, 7.8)	3.16, *dd* (9.0, 8.1)	3.22, *dd* (9.0, 7.8)	3.14, *dd* (9.0, 7.8)	3.14, *dd* (9.0, 7.8)
3′	3.37, *dd* (9.0, 9.0)	3.34*	3.34*	3.32, *dd* (9.0, 8.8)	3.32, *dd* (9.0, 8.8)
4′	3.26, *dd* (9.0, 9.0)	3.23, *dd* (9.5, 9.5)	3.26*	3.22, *dd* (9.5, 8.8)	3.22, *dd* (9.5, 8.8)
5′	3.31, *m*	3.31, *m*	3.31, *m*	3.26, *m*	3.26, *m*
6′	3.88, *dd* (12.2, 2.2)	3.88, *dd* (11.9, 2.2)	3.90, *dd* (12.0, 2.0)	3.85, *dd* (12.2, 2.2)	3.85, *dd* (12.2, 2.2)
	3.66, *dd* (12.2, 6.1)	3.66, *dd* (11.9, 6.1)	3.71, *dd* (12.0, 5.6)	3.61, *dd* (12.2, 6.4)	3.61, *dd* (12.2, 6.4)
2″,6″	7.40, *d* (8.6)	7.53, *d* (8.8)	7.65, *d* (8.8)	6.98, *d* (8.5)	
3″,5″	6.77, *d* (8.6)	7.08, *d* (8.8)	7.07, *d* (8.8)	6.64, *d* (8.5)	
α	6.28, *d* (15.9)	6.37, *d* (15.9)	5.86, *d* (12.9)	2.49, *m*	
β	7.56, *d* (15.9)	7.61, *d* (15.9)	6.94, *d* (12.9)	2.76, *m*	
1‴		4.93, *d* (7.6)	4.96, *d* (7.6)		
2‴		3.42*	3.48*		
3‴		3.34*	3.34*		
4‴		3.40*	3.45*		
5‴		3.26*	3.28*		
6‴		3.81, *dd* (12.0, 2.0)	3.87, *dd* (12.0, 1.7)		
		3.64, *dd* (12.0, 6.4)	3.71, *dd* (12.0, 5.6)		
OAc		1.92, *s*	1.89, *s*		1.99, *s*

[a] *Chemical shift obtained approximately from HSQC.
[b] *J* (Hz) in parentheses.

3.3. Extraction and isolation

The dried aerial part (900 g) of *B. lupulina* was extracted with hot MeOH. After removal of the solvent by evaporation, the residue (100 g) was defatted with Et_2O. The aqueous layer was subjected to a column of highly porous copolymer of styrene and divinylbenzene and eluted with H_2O, MeOH and Me_2CO, successively. The fraction eluted with MeOH (29.0 g) was subjected to a column of silica gel (systems I, II and III, respectively) affording five fractions. Fraction 2 (7.4 g) was applied to a RP-18 column using system IV to provide six fractions, together with compound **4** (5.1 g). Fractions 2–5 were purified by prep. HPLC–ODS (system VI) to afford compounds **8** (43 mg) and **12** (27 mg). Fraction 3 (8.4 g) was subjected to a column of RP-18 (system IV) to give eight fractions, along with compounds **2** (2.6 g) and **10** (596 mg). Fractions 3-1 and 3-2 were further purified by prep. HPLC-ODS (system V) to provide compound **3** (398 mg). Fraction 3-8 was purified by prep. HPLC-ODS (system VI) to afford compound **16** (92 mg). Fraction 4 (8.2 g) was applied to a RP-18 column (system VII) to afford fifteen fractions, and compound **1** (1.9 g). Fraction 4-5 was purified by prep. HPLC–ODS (system VIII) to give compounds **9** (50 mg) and **18** (59 mg). Fraction 4-8 was purified by prep. HPLC–ODS (system V) to provide compounds **11** (32 mg) and **17** (27 mg). Fraction 4-9 was further purified by prep. HPLC-ODS (system IX) to give compounds **13** (162 mg), **14** (73 mg) and **15** (138 mg). Finally, fractions 4-13 and 4-14 were purified by prep. HPLC-ODS (system VI) to provide compound **5** (23 mg), **6** (90 mg) and **7** (73 mg).

Table 2
^{13}C NMR spectral data of compounds **5–8** and **12** (100 MHz, CD_3OD)

C	5	6	7	8	12
1	95.3	95.4	95.4	95.7	95.5
3	154.6	154.5	154.5	153.6	153.0
4	108.4	108.5	108.4	109.8	112.2
5	39.8	39.9	39.8	42.2	32.9
6	78.8	78.9	78.8	76.0	29.7
7	45.2	45.1	45.0	47.7	39.6
8	89.6	89.6	89.6	89.7	91.0
9	50.3	50.3	50.3	49.9	51.0
10	21.9	21.8	21.8	22.2	21.2
11	169.7	168.4	168.4	169.0	169.0
OMe		51.9	51.9	51.8	51.7
1′	100.3	100.3	100.3	100.4	100.2
2′	74.6	74.6	74.5	74.7	74.7
3′	77.8	77.9	77.8	78.0	78.0
4′	71.5	71.6	71.6	71.4	71.6
5′	78.2	78.3	78.3	78.2	78.3
6′	62.9	62.9	62.9	63.0	62.9
1″	127.0	129.8	130.3	132.6	
2″,6″	131.1	130.8	132.9	130.3	
3″,5″	115.4	118.0	117.1	116.2	
4″	161.1	160.9	159.7	156.7	
α	116.8	117.2	118.8	38.2	
β	146.5	145.9	144.0	31.2	
CO	168.5	168.1	167.4	175.0	
1‴		101.8	101.9		
2‴		74.8	74.8		
3‴		77.9	77.8		
4‴		71.2	71.2		
5‴		78.1	78.1		
6‴		62.4	62.4		
Oac	173.0	172.9	172.9		173.0
	22.2	22.3	22.2		22.2

3.4. 8-O-Acetyl-6-O-trans-p-coumaroylshanzhiside (*5*)

Amorphous powder, $[\alpha]_D^{21}$ −75.6° (MeOH, *c* 1.58); ^1H NMR (CD_3OD): Table 1 and ^{13}C NMR (CD_3OD): Table 2; negative HR–FAB–MS, *m/z*: 579.1710 $[M–H]^-$ ($C_{27}H_{31}O_{14}$ requires 579.1713).

3.5. Saletpangponoside A (*6*)

Amorphous powder, $[\alpha]_D^{21}$ −90.3° (MeOH, *c* 1.79); ^1H NMR (CD_3OD): Table 1 and ^{13}C NMR (CD_3OD): Table 2; negative HR–FAB–MS, *m/z*: 755.2413 $[M–H]^-$ ($C_{34}H_{43}O_{19}$ requires 755.2398).

3.6. Saletpangponoside B (*7*)

Amorphous powder, $[\alpha]_D^{21}$ −104.8° (MeOH, *c* 2.43); ^1H NMR (CD_3OD): Table 1 and ^{13}C NMR (CD_3OD): Table 2; negative HR–FAB–MS, *m/z*: 755.2413 $[M–H]^-$ ($C_{34}H_{43}O_{19}$ requires 755.2398).

3.7. Saletpangponoside C (*8*)

Amorphous powder, $[\alpha]_D^{21}$ −58.9° (MeOH, *c* 2.86); ^1H NMR (CD_3OD): Table 1 and ^{13}C NMR (CD_3OD): Table 2; negative HR–FAB–MS, *m/z*: 553.1979 $[M–H]^-$ ($C_{26}H_{33}O_{13}$ requires 553.1921).

3.8. 8-O-Acetylmussaenoside (*12*)

Amorphous powder, $[\alpha]_D^{21}$ −53.2° (MeOH, *c* 1.84); ^1H NMR (CD_3OD) Table 1 and ^{13}C NMR (CD_3OD): Table 2; negative HR–FAB–MS, *m/z*: 431.1576 $[M–H]^-$ ($C_{19}H_{27}O_{11}$ requires 431.1553).

Acknowledgements

We would like to thank the Research Center for Molecular Medicine, Hiroshima University for the use of its NMR facilities. Also, we are grateful to Mr. Bamrung Thavinchiua of the Department of Pharmaceutical Botany and Pharmacognosy, Faculty of Pharmaceutical Sciences, Khon Kaen University, Thailand, for help in obtaining the plant material.

References

Achenbach, H., Lowel, M., Waibel, R., Gupta, M., Solis, P., 1992. New lignan glucosides from *Stemmadenia minima*. Planta Medica 58, 270–272.

Andary, C., Wylde, R., Heitz, A., Rascol, J.P., Roussel, J.L., Laffite, C., 1985. Poliumoside, a caffeic glycoside ester from *Teucrium belion*. Phytochemistry 24, 362–364.

Andary, C., Wylde, R., Laffite, C., Privat, G., Winternitz, F., 1982. Structure of verbascoside and orobanchoside, caffeic acid sugar esters from *Orobanche rapum-genistae*. Phytochemistry 21, 1123–1127.

Byrne, L.T., Sasse, J.M., Skelton, B.W., Suksamrarn, A., White, A.H., 1987. The minor iridoid glucosides of *Barleria lupulina*: isolation, crystal structure and plant growth-inhibiting properties of 6-*O*-acetylshanzhiside methyl ester. Australian Journal of Chemistry 40, 785–794.

Damtoft, S., Hansen, S.B., Jacobsen, B., Jensen, S.R., Nielsen, B.J., 1984a. Iridoid glucosides from *Melampyrum*. Phytochemistry 23, 2387–2389.

Damtoft, S., Jensen, S.R., Nielsen, B.J., 1982. Structural revision of barlerin and acetyl barlerin. Tetrahedron Letters 23, 4155–4156.

Damtoft, S., Jensen, S.R., Nielsen, B.J., 1984b. The identity of the iridoid glucoside tarphetalin with ipolamiide. Phytochemistry 23, 907–908.

Endo, K., Takahashi, K., Abe, T., Hikino, H., 1982. Structure of forsythoside B, an antibacterial principle of *Forsythia koreana* stems. Heterocycles 19, 261–264.

Sudo, H., Ide, T., Otsuka, H., Hirata, E., Takushi, A., Shinzato, T., Takeda, Y., 2000. Megastigmane, benzyl alcohol and phenethyl alcohol glycosides, and 4,4′-dimethoxy-β-truxinic acid catapol diester from the leaves of *Premna subscandens* Merr. Chemical and Pharmaceutical Bulletin 48, 542–546.

Suksamrarn, A., 1986. Iridoid glucosides from *Barleria lupulina*. Journal of Natural Products 49, 179.

Takeda, Y., Matsumura, H., Masuda, T., Honda, G., Otsuka, H., Takaishi, Y., Sezik, E., Yesilada, E., 2000. Phlorigidosides A-C, iridoid glucosides from *Phlomis rigida*. Phytochemistry 53, 931–935.

Tuntiwachwuttikul, P., Pancharoen, O., Taylor, W.C., 1998. Iridoid glucosides of *Barleria lupulina*. Phytochemistry 49, 163–166.

Yamamura, S., Ozawa, K., Ohtani, K., Kasai, R., Yamasaki, K., 1998. Antihistaminic flavones and aliphatic glycosides from *Mentha spicata*. Phytochemistry 48, 131–136.

Yoosook, C., Panpisutchai, Y., Chaichana, S., Santisuk, T., Reutrakul, V., 1999. Evaluation of anti-HSV-2 activities of *Barleria lululina* and *Clinacanthus nutans*. Journal of Ethnopharmacology 67, 179–187.

PERGAMON

Phytochemistry 58 (2001) 343–349

PHYTOCHEMISTRY

www.elsevier.com/locate/phytochem

Synthesis and biological activity of 26-norbrassinolide, 26-norcastasterone and 26-nor-6-deoxocastasterone

Tsuyoshi Watanabe[a,*], Takahiro Noguchi[a], Takao Yokota[b], Kyomi Shibata[b], Hiroyuki Koshino[c], Hideharu Seto[c], Seong-Ki Kim[d], Suguru Takatsuto[e]

[a]*Tama Biochemical Co. Ltd., 2-7-1 Nishishinjuku Shinjuku-ku, Tokyo 163-0704, Japan*
[b]*Department of Biosciences, Teikyo University, Utsunomiya 320-8551, Japan*
[c]*RIKEN (The Institute of Physical and Chemical Research), Wako-shi, Saitama 351-0198, Japan*
[d]*Department of Life Science, Chung-Ang University, Seoul 156-756, South Korea*
[e]*Department of Chemistry, Joetsu University of Education, Joetsu-shi, Niigata 943-8521, Japan*

Received 28 December 2000; received in revised form 12 April 2001

Abstract

26-Norbrassinolide, identified as a metabolite of brassinolide in cultured cells of the liverwort, *Marchantia polymorpha,* as well as 26-norcastasterone and 26-nor-6-deoxocastasterone were synthesized. Synthesis of these new brassinosteroids was conducted by employing the orthoester Claisen rearrangement and asymmetric dihydroxylation as key reactions. The modified rice lamina inclination test indicated that these three 26-norbrassinosteroids were less active than their corresponding C_{28} brassinosteroids. Growth-promoting activities were also examined by using the brassinosteroid-deficient, dwarf mutant *lkb* of garden pea (*Pisum sativum* L.). In this assay, 26-norbrassinolide was as effective as brassinolide and 26-norcastasterone was more effective than castasterone although 26-nor-6-deoxocastasterone was much less effective than 6-deoxocastasterone. Therefore, removal of C-26 of brassinosteroids does not necessarily reduce the biological activity. The role of C-26 removal in *Marchantia* cells remains unclear. © 2001 Elsevier Science Ltd. All rights reserved.

Keywords: *Marchantia polymorpha*; Synthesis; Biological activity; Rice; *Oryza sativa*; Gramineae; Rice lamina inclination test; Pea dwarf mutant; *Pisam sativum*; Leguminosae; Brassinosteroids; 26-Norbassinolide; 26-Norcastasterone; 26-Nor-6-deoxocastasterone

1. Introduction

Brassinosteroids (BRs) are steroidal plant hormones with plant growth promoting activity. More than 40 natural BRs have been characterized (Fujioka, 1999). The biosynthetic pathway of C_{28} BRs including brassinolide (BL) and related BRs has been elucidated by using cultured cells of *Catharanthus roseus* (Fujioka and Sakurai, 1997a) and seedlings of *Arabidopsis thaliana* (Noguchi et al., 2000). At present, it is known that BL is converted from castasterone (CS), which, in turn, is synthesized from campestanol through either early C-6 oxidation and/or late C-6 oxidation pathways (Fujioka and Sakurai, 1997a). These pathways seem to occur widely in the plant kingdom because of the ubiquitous presence of the intermediates involved (Fujioka and Sakurai, 1997b). Moreover, various genes involved in BR biosynthesis have been characterized by investigating a number of BR-deficient dwarf mutants of Arabidopsis, pea, and tomato (Yokota, 1997; Altmann, 1998; Clouse and Feldmann, 1999). In addition to de novo synthesis of BRs, the metabolism and catabolism are important factors controlling the levels of endogenous BRs (Crozier et al., 1999; Yokota, 1999). Recently, we found that BL was metabolized to 26-norbrassinolide (26-norBL) with removal of C-26 in cultured cells of the liverwort, *Marchantia polymorpha* (Kim et al., 2000a). In tomato cells, C-26 hydroxylation occurs presumably as a deactivation process (Winter et al., 1997). Recently the *bas1-D phyB-4* Arabidopsis mutant was found to have enhanced C-26 hydroxylation in response to BL (Neff et al., 1999). These findings suggest that loss or modification of C-26 has an important role in the metabolism of BRs.

In the present work, we give the full account of the synthesis of 26-norBL, that was used as an authentic compound to identify the *Marchantia* metabolite by

* Corresponding author. Fax: +81-463-95-0610.
E-mail address: watanabe_t@tama-bc.co.jp (T. Watanabe).

0031-9422/01/$ - see front matter © 2001 Elsevier Science Ltd. All rights reserved.
PII: S0031-9422(01)00213-8

GC–MS (Kim et al., 2000a). Furthermore, we have synthesized 26-norcastasterone (26-norCS) and 26-nor-6-deoxocastasterone (26-nor-6-deoxoCS), the presence of which in plants should be also suspected. In order to investigate whether or not the removal of C-26 is a deactivation step, we examined the biological activity of these compounds using the modified rice lamina inclination test and the pea growth test using the BR-deficient dwarf mutant *lkb*.

2. Results and discussion

2.1. Synthesis of 26-norbrassinosteroids

First, we synthesized 26-norCS **2** from the known allylic 22-alcohol **7** (Watanabe et al., 1997) by applying the method used to construct the side chain of BL in which orthoester Claisen rearrangement and asymmetric dihydroxylation were key reactions (Scheme 1). The orthoester Claisen rearrangement of **7** using triethyl orthoacetate gave the ester **8** in 98% yield. The ethoxycarbonyl group of **8** was reduced with $LiAlH_4$ to give the alcohol **9**. The hydroxyl group of **9** was removed by reducing its sulfonate to give the 26-nor compound **10**. Transformation of **10** to the 2,22*E*-dien-6-one **12** was attained in 82% yield using a conventional procedure (Watanabe et al., 1997). Introduction of two vicinal diols into **12** was elaborated through asymmetric dihydroxylation using 1,4-bis(9-*O*-dihydroquinidinyl)phthalazine as a chiral ligand to give **2** in 67% yield. To determine the stereochemistry of the C-22 and -23 positions of **2**, **2** was derivatized to the bisacetonide **4** whose NMR spectra gave well-defined signals and its NMR spectra were compared with those of the known compound **5** (Takatsuto et al., 1984) and its stereoisomer **6** (Watanabe and Takatsuto, unpublished data, Fig. 1). Direct and long-range heteronuclear ^{1}H–^{13}C correlations obtained by HMQC and HMBC techniques resulted in complete assignment of the ^{1}H and ^{13}C NMR signals. ^{1}H and ^{13}C signals in the vicinity of the side chain diol moiety of **4** were almost superimposable with those of **5** but not with those of **6** (Table 1). Consequently, the stereochemistry of the side chain in **4** was determined to be (22*R*, 23*R*) configuration.

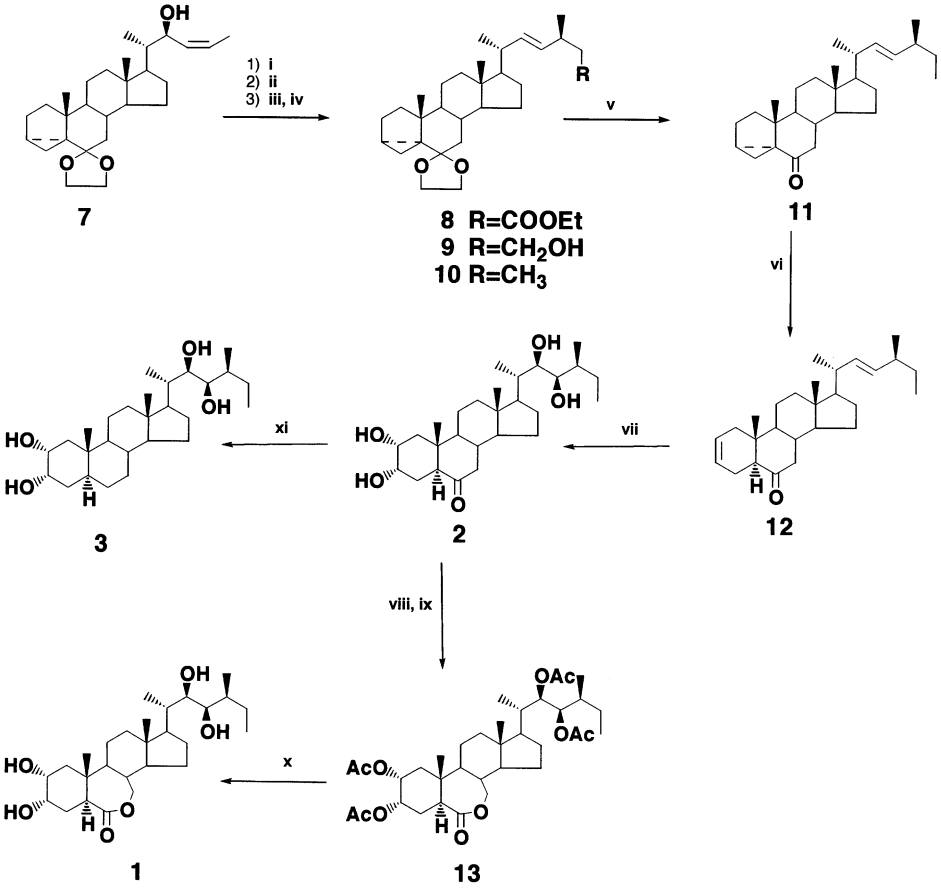

Scheme 1. Reagent and conditions: (i) $MeC(OEt)_3$, acetic acid, xylene, reflux, 2 h; (ii) $LiAlH_4$, THF, reflux, 2 h; (iii) $MeSO_2Cl$, Et_3N, CH_2Cl_2, room temp., 2 h; (iv) $LiAlH_4$, THF, room temp., overnight; (v) 1 M H_2SO_4, acetone, room temp., 2 h; (vi) PPTS, LiBr, DMAc, 160°C, 5 h; (vii) OsO_4, $K_3[Fe(CN)_6]$, 1,4-bis(9-*O*-dihydroquinidinyl)phthalazine, K_2CO_3, methanesulfonamide, *t*-BuOH–H_2O, room temp., 3 days; (viii) acetic anhydride, Et_3N, CH_2Cl_2, room temp., overnight; (ix) CF_3COOOH, CH_2Cl_2, Na_2HPO_4, 0°C, 3 h; (x) K_2CO_3, 70% MeOH, reflux, 6 h; (xi) $N_2H_2{\cdot}H_2O$, NaOH, diethylene glycol, reflux, 2 h.

Table 1
Selected ^{1}H and ^{13}C NMR spectral data of compounds **4**, **5** and **6**[a]

Atom	Compound		
	4	**5**	**6**
17-H	1.55: *m*	1.52: *m*	1.19: *m*
20-H	1.45: *m*	1.43: *m*	1.80: *m*
21-H_3	0.98: *d, J* = 6.8	0.98: *d, J* = 6.4	1.03: *d, J* = 7.3
22-H	3.89: *br d, J* = 7.8	3.84: *br d, J* = 8.8	3.91: *dd, J* = 6.3 and 2.9
C-17	53.37	53.42	52.34
C-20	36.72	36.21	39.66
C-21	12.68	12.68	14.84
C-22	80.22	80.57	83.20

[a] ^{1}H NMR (600 MHz; δ: multiplicity, J in Hz) and ^{13}C NMR (150 MHz; δ) were measured in $CDCl_3$.

Furthermore, acetylation of **2** followed by Baeyer–Villiger oxidation gave 26-norBL tetraacetate **13**, which was then deprotected to afford 26-norBL **1** in 50% yield from **2** (Takatsuto et al., 1984). 26-Nor-6-deoxoCS **3** was subjected to the Huang Minlon reaction (Mori et al., 1984) to give **2** in 38% yield.

2.2. Biological activity of 26-norbrassinosteroids

The rice lamina inclination test is very sensitive to BRs (Wada et al., 1981), and has been used to evaluate biological potency of natural and synthetic BRs. Kim et al. (2000a) already demonstrated using this bioassay that the activity of 26-norBL was 10-fold lower than BL. Recently this bioassay was greatly sensitized by utilizing auxin-BR synergism in intact rice seedlings (Fujioka et al., 1998). Thus this rice bioassay was applied to the new 26-norBRs synthesized. When comparing dosages which caused 50% degree of the maximum inclination angle, 26-norBL was 13 times less active than BL, being in accord with the previously published data (Kim et al., 2000a). Similarly, 26-norCS was 7 times less active than CS, and 26-nor-6-deoxoCS was 80 times less active than 6-deoxoCS (Fig. 2). The strength of biological activities of 26-norBRs were in the following order; 26-norBL > 26-norCS > 26-nor-6-deoxoCS. The same relationship has been observed between corresponding C_{28} BRs (Fujioka et al., 1998). Thus, removal of C-26 of the C_{28} BRs is suggested to be a deactivation step. A similar deactivation due to another demethylation of C-28 of CS is also suggested by the fact that 28-norCS is converted from CS in some higher plants and 28-norCS is ca. 10 times less active than CS in this rice bioassay (Fujioka et al., 2000).

Dwarfism of BR-deficient mutants such as the Arabidopsis *det2* (Li et al., 1996) and pea *lkb* mutant (Nomura et al., 1999) can be rescued by application of brassinolide and its precursors. Based on the above-mentioned result by the rice bioassay, it is expected that respective biological activities of the 26-norBRs are lower than those of the corresponding C_{28} BRs in this growth test. So, we examined the growth-promoting activities of 26-norBRs using the *lkb* mutant. Results are shown in Fig. 3. Although 26-nor-6-deoxoCS had very weak activity, and its activity was much lower than that of 6-deoxoCS, 26-norBL showed strong activity that was comparable to that of BL, and 26-norCS was more active than CS and its activity was nearly equivalent to that of BL. Therefore, it was found that removal of C-26 does not necessarily reduce biological activity of BRs as far as the pea *lkb* bioassay data indicate.

Contradictory data obtained between two bioassay systems suggest that biological activities of BRs cannot be discussed only by a single bioassay system. In support of this, structure–activity relationships of BRs have been known to vary in different bioassay systems. For example, the biological activity of 28-norBL is about one-order of magnitude lower than that of BL in the rice lamina inclination test (Takatsuto et al., 1983a; Wada et al., 1983) and tomato growth test (Takatsuto et al., 1983b), but it is comparable to BL in the radish growth test (Takatsuto et al., 1983b).

In conclusion, we were unable to make clear the roles of C-26 elimination of BRs in *Marchantia* cells. Roles of BR in the growth and development of *M. polymorpha* also remain to be studied although BRs are endogenous in *M. polymorpha* (Kim et al., 2000b).

3. Experimental

3.1. General

Mps were determined under a hot-stage microscope (Yanaco micro melting point apparatus) and were uncorrected. ^{1}H and ^{13}C NMR spectra were recorded

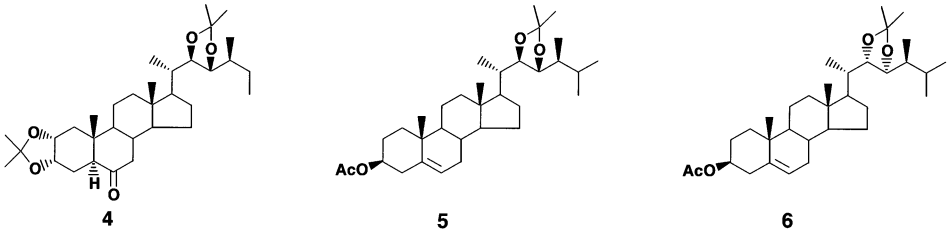

Fig. 1. Structure of 26-norcastasterone bisacetonide **4**, compounds **5** and **6**.

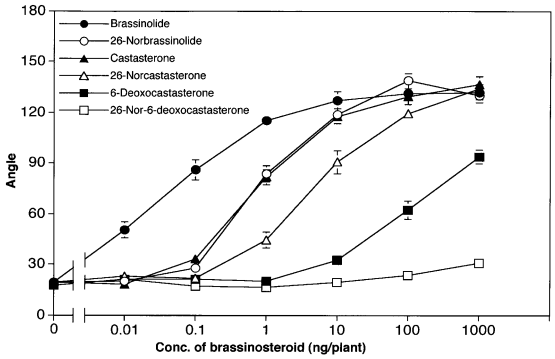

Fig. 2. Rice lamina inclination test of 26-norbrassinosteroids by co-application of the test sample with indole-3-acetic acid (5 μg/plant). Each data point represents the mean of 20–24 replicates ±S.E.

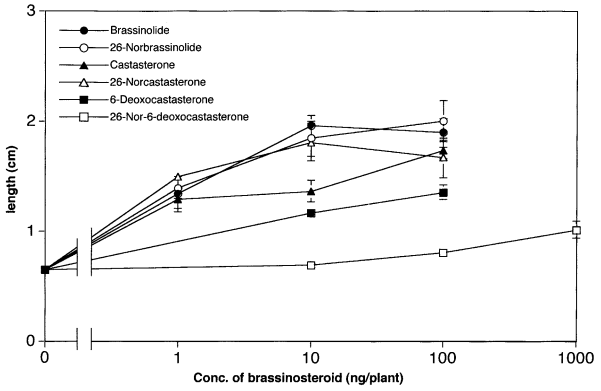

Fig. 3. Effect of 26-norbrassinosteroids on the fifth internode length of *lkb* of pea. Each data point represents the mean of 8 replicates ±S.E.

on a JEOL A400, ECP500 and A600 spectrometers in $CDCl_3$ with tetramethylsilane as an internal standard. HR–MS was recorded on JEOL JMS-AX505H and JMS-AX505HA mass spectrometers.

Silica gel (Kieselgel 60, 70-230 mesh, Merck) was used for column chromatography. Reactions were monitored by TLC on silica gel plates (Kieselgel 60 F_{254}, 0.25 mm thickness, Merck). Spots were visualized with 1% Ceric sulphate–10% aq. H_2SO_4 solution, followed by heating. All purified compounds showed a single spot by TLC analysis.

3.2. Synthesis of 26-norbrassinosteroids

3.2.1. Ethyl (22E,24R)-3α,5-cyclo-6,6-ethylenedioxy-26-nor-5α-ergost-22-en-27-oate **8**

A mixture of the known allylic alcohol **7** (632.6 mg, 1.526 mmol), triethyl orthoacetate (7.0 ml), acetic acid (3 drops) and xylene (5.0 ml) was refluxed under Ar atmosphere for 5 h. MeOH was added and the solvent was removed in vacuo to give a residue, which was applied to a column of silica gel (2.0 cm i.d. ×20 cm). Elution with hexane–EtOAc (50:1) afforded **8** (726.5 mg, 98.2%) as an oil; TLC: hexane–EtOAc (10:1) $R_F = 0.65$; ^{1}H NMR spectral data (500 MHz, $CDCl_3$): δ 0.33 (1H, *t*, *J* = 4.3 Hz, 4-H), 0.61 (1H, *dd*, *J* = 8.3 and 4.7 Hz, 4-H), 0.71 (3H, *s*, 18-H_3), 0.98 (3H, *d*, *J* = 6.6 Hz, 28-H_3), 1.00 (3H, *s*, 19-H_3), 1.01 (3H, *d*, *J* = 6.6 Hz, 21-H_3), 1.26 (3H, *t*, *J* = 7.0 Hz, $OCH_2C\underline{H}_3$), 2.25 (2H, *m*, not assigned), 2.59 (1H, *m*, not assigned), 3.74 (1H, *q*, *J* = 7.0 Hz, ketal ethylene), 3.84 (1H, *q*, *J* = 5.7 Hz, ketal ethylene), 3.90 (1H, *q*, *J* = 8.0 Hz, ketal ethylene), 4.03 (1H, *m*, ketal ethylene), 4.11 (2H, *m*, $OC\underline{H}_2CH_3$) and 5.23 (2H, *m*, 22 and 23-H). HR–EIMS $[M]^+$ *m/z:* 484.3562 (calc. 484.3553) for $C_{31}H_{48}O_4$.

3.2.2. (22E,24S)-3α,5-Cyclo-6,6-ethylenedioxy-26-nor-5α-ergost-22-en-27-ol **9**

The ester **8** (691.5 mg, 1.427 mmol) in THF (70 ml) was treated with $LiAlH_4$ (200 mg, 5.270 mmol) at 0 °C to room temperature under Ar atmosphere for 5 h. Work-up (hexane and EtOAc extraction) was followed by chromatography on silica gel (2.0 cm i.d. ×20 cm). Elution with hexane–EtOAc (10:1) afforded **9** (621.3 mg, 98.4%) as an oil; TLC: toluene–EtOAc (3:1) $R_F = 0.38$; ^{1}H NMR spectral data (500 MHz, $CDCl_3$): δ 0.33 (1H, *t*, *J* 3.9 Hz, 4-H), 0.61 (1H, *dd*, *J* = 8.0 and 4.7 Hz, 4-H), 0.72 (3H, *s*, 18-H_3), 0.98 (3H, *d*, *J* = 7.0 Hz, 28-H_3), 1.00 (3H, *d*, *J* = 7.3 Hz, 21-H_3), 1.01 (3H, *s*, 19-H_3), 3.65 (2H, *m*, 27-H_2), 3.75 (1H, *q*, *J* = 7.5 Hz, ethylene ketal), 3.84 (1H, *q*, *J* = 6.5 Hz, ethylene ketal), 3.91 (1H, *qd*, *J* = 6.7 and 1.3 Hz, ethylene ketal), 4.02 (1H, *qd*, *J* = 6.0 and 1.7 Hz, ethylene ketal) and 5.17 (1H, *dd*, *J* = 15.3 and 8.0 Hz, 22-H) and 5.23 (1H, *dd*, *J* = 5.3 and 8.3 Hz, 23-H). HR–EIMS $[M]^+$ *m/z:* 442.3454 (calc. 442.3447) for $C_{29}H_{46}O_3$.

3.2.3. (22E,24S)-3α,5-Cyclo-6,6-ethylenedioxy-26-nor-5α-ergost-22-ene **10**

The alcohol **9** (601.7 mg, 1.359 mmol) was dissolved in CH_2Cl_2 (50 ml) and triethylamine (3.0 ml) and then treated with methanesulfonyl chloride (0.5 ml) at 0 °C for 2 h. Work-up (CH_2Cl_2) gave a corresponding sulfonate, which was treated with $LiAlH_4$ (200 mg, 5.270 mmol) in THF (50 ml) at 0 °C to room temperature overnight. Work-up (hexane and EtOAc extraction) was followed by chromatography on silica gel (2.0 cm i.d. ×20 cm). Elution with hexane–EtOAc (100:1) afforded **10** (543.5 mg, 93.7% in two steps) as an oil; TLC: toluene $R_F = 0.70$; δ_H (500 MHz): 0.33 (1H, *t*, *J* = 4.1 Hz, 4-H), 0.61 (1H, *dd*, *J* = 7.8 and 4.6 Hz, 4-H), 0.73 (3H, *s*, 18-H_3), 0.83 (3H, *t*, *J* = 7.4 Hz, 27-H_3), 0.92 (3H, *d*, *J* = 6.9 Hz, 28-H_3), 0.99 (3H, *d*, *J* = 6.4 Hz, 21-H_3), 1.01 (3H, *s*, 19-H_3), 3.74 (1H, *q*, *J* = 6.4 Hz, ketal ethylene), 3.85 (1H, *q*, *J* = 6.5 Hz ketal ethylene), 3.91 (1H, *qd*, *J* = 6.4 and 1.4 Hz, ketal ethylene), 4.02 (1H, *qd*, *J* = 6.3 and 1.8 Hz, ketal ethylene) and 5.14 (2H, *m*, 22 and 23-H). HR–EIMS $[M]^+$ *m/z:* 426.3496 (calc. 426.3498) for $C_{29}H_{46}O_2$.

3.2.4. (22E,24S)-3α,5-Cyclo-26-nor-5α-ergost-22-en-6-one **11**

A solution of the compound **10** (513.5 mg, 1.110 mmol) in acetone (30 ml) was treated with 1 M H_2SO_4 (1.0 ml) at room temperature for 1 h. Work-up (EtOAc

extraction) was followed by chromatography on silica gel (2.0 cm i.d. ×20 cm). Elution with hexane–EtOAc (50:1) afforded **11** (435.4 mg, 94.5%), mp 120–121°C (from MeOH); TLC: hexane–EtOAc (20:1) $R_F = 0.14$; δ_H (500 MHz): 0.73 (3H, *s*, 18-H_3), 0.83 (3H, *t*, $J = 7.5$ Hz, 27-H_3), 0.93 (3H, *d*, $J = 6.7$ Hz, 28-H_3), 1.01 (3H, *s*, 19-H_3), 1.01 (3H, *d*, $J = 6.7$ Hz, 21-H_3), 2.43 (1H, *dd*, $J = 14.7$ and 2.4 Hz, 7β-H) and 5.15 (2H, *m*, 22 and 23-H). HR–EIMS $[M]^+$ *m/z:* 382.3244 (calc. 382.3236) for $C_{27}H_{42}O$.

3.2.5. (22E,24S)-26-Nor-5α-ergosta-2,22-dien-6-one 12

A mixture of **11** (424.7 mg, 1.292 mmol), pyridinium *p*-toluenesulfonate (55 mg, 0.219 mmol), LiBr (450 mg, 5.18 mmol) and *N,N*-dimethylacetamide (20 ml) was heated at 160°C under Ar atmosphere for 5 h. Work-up (hexane extraction) was followed by chromatography on silica gel (2.0 cm i.d. ×25 cm). Elution with toluene afforded **12** (368.9 mg, 86.9%), mp 109–111 °C (from MeOH); TLC: hexane–EtOAc (20:1) $R_F = 0.29$; δ_H (500 MHz): 0.68 (3H, *s*, 18-H_3), 0.71 (3H, *s*, 19-H_3), 0.83 (3H, *t*, $J = 7.3$ Hz, 27-H_3), 0.93 (3H, *d*, $J = 6.7$ Hz, 28-H_3), 1.01 (3H, *d*, $J = 6.7$ Hz, 21-H_3), 2.35 (2H, *m*, 5-H), 5.15 (2H, *m*, 22 and 23-H), 5.57 (1H, *m*, 2-H) and 5.69 (1H, *ddd*, $J = 9.5$, 4.9 and 1.9 Hz, 3-H). HR–EIMS $[M]^+$ *m/z*: 382.3228 (calc. 382.3236) for $C_{27}H_{42}O$.

3.2.6. (22R,23R,24S)-2α,3α,22,23-Tetrahydroxy-26-nor-5α-ergostan-6-one, 26-norcastasterone 2

A mixture of **12** (207.9 mg, 0.5434 mmol), $K_3[Fe(CN)_6]$ (3.5 g, 10.63 mmol), K_2CO_3 (1.5 g, 10.85 mmol), methanesulfonamide (365.0 mg, 3.84 mmol), 1,4-bis(9-*O*-dihydroquinidinyl)phthalazine (270.0 mg, 0.347 mmol) and $K_2OsO_4 \cdot 2H_2O$ (71.0 mg, 0.193 mmol) in *t*-BuOH–H_2O (65 ml, 1:1) was stirred at room temperature in the dark for 3 days. Sodium hydrogen sulphite (1.0 g, powder) was added and the mixture was stirred further for 1 h. Work-up (EtOAc extraction) was followed by chromatography on silica gel (2.0 cm i.d. ×25 cm). Elution with CH_2Cl_2–EtOH (50:1) afforded **2** (164.1 mg, 67.0%), mp 275–276 °C (from EtOAc–EtOH); TLC: CH_2Cl_2–EtOH (15:1) $R_F = 0.17$; δ_H (400 MHz): 0.69 (3H, *s*, 18-H_3), 0.76 (3H, *s*, 19-H_3), 0.84 (3H, *d*, $J = 6.4$ Hz, 28-H_3), 0.92 (3H, *d*, $J = 6.4$ Hz, 21-H_3), 0.94 (3H, *t*, $J = 7.2$ Hz, 27-H_3), 2.30 (1H, *dd*, $J = 13.0$ and 4.6 Hz, 7β-H), 2.69 (1H, *dd*, $J = 12.2$ and 2.6 Hz, 5-H), 3.57 (2H, *br s*, 22 and 23-H), 3.77 (1H, *m*, 2-H) and 4.05 (1H, *br s*, 3-H). HR–FABMS $[M + Na]^+$ *m/z*: 473.3263 (calc. 473.3243) for $C_{27}H_{46}O_5Na$.

3.2.7. (22R,23R,24S)-2α,3α,22,23-Tetra-acetoxy-26-nor-B-homo-7-oxa-5α-ergostan-6-one 13

26-Norcastasterone **2** (50.7 mg, 0.1125 mmol) was dissolved in a mixture of CH_2Cl_2 (10 ml) and triethylamine (5.0 ml) and then treated with acetic anhydride (0.5 ml) at 0 °C at room temperature overnight. Work-up (CH_2Cl_2 extraction) was followed by chromatography on silica gel (1.0 cm i.d. ×20 cm). Elution with toluene–EtOAc (5:1) afforded tetracetate (62.7 mg, 90.1%), mp 187–189 °C (from MeOH); TLC: toluene–EtOAc (2:1) $R_F = 0.60$; δ_H (400 MHz): 0.70 (3H, *s*, 18-H_3), 0.83 (3H, *s*, 19-H_3), 0.94 (3H, *t*, $J = 7.2$ Hz, 27-H_3), 0.95 (3H, *d*, $J = 6.4$ Hz, 28-H_3), 1.02 (3H, *d*, $J = 6.8$ Hz, 21-H_3), 2.00 (3H, *s*, acetyl), 2.01 (3H, *s*, acetyl), 2.02 (3H, *s*, acetyl), 2.09 (3H, *s*, acetyl), 2.32 (1H, *dd*, $J = 13.2$ and 4.8 Hz, 7β-H), 2.56 (1H, *dd*, $J = 11.4$ and 4.2 Hz, 5-H), 4.95 (1H, *ddd*, $J = 12.4$, 4.8 and 3.2 Hz, 2-H), 5.19 (2H, *m*, 22 and 23-H) and 5.38 (1H, *d*, $J = 3.2$ Hz, 3-H). HR–FABMS $[M + Na]^+$ *m/z:* 641.3632 (calc. 641.3666) for $C_{35}H_{54}O_9Na$.

Trifluoroacetic anhydride (5.0 ml) was added at 0 °C to a mixture of 30% H_2O_2 (0.8 ml) and CH_2Cl_2 (3.0 ml) and then stirred at 0 °C for 15 min. The prepared trifluoroperacetic acid solution was added to a mixture of the tetracetate (56.7 mg, 0.09163 mmol) and disodium hydrogen phosphate (0.8 g) in CH_2Cl_2 (10.0 ml) at 0 °C for 3 h. After adding saturated aqueous sodium hydrogen sulphite (5.0 ml) the mixture was stirred at 0 °C for 1 h. Work-up (CH_2Cl_2 extraction) was followed by chromatography on silica gel (1.0 cm i.d. ×20 cm). Elution with toluene–EtOAc (7:1) afforded **13** (46.1 mg, 79.3%), mp 248–249 °C (from MeOH); TLC: toluene–EtOAc (2:1) $R_F = 0.38$; δ_H (400 MHz): 0.74 (3H, *s*, 18-H_3), 0.93 (3H, *l*, $J = 7.4$ Hz, 27-H_3), 0.95 (3H, *d*, $J = 6.8$ Hz, 28-H_3), 0.99 (3H, *s*, 19-H_3), 1.01 (3H, I, $J = 6.8$ Hz, 21-H_3), 2.00 (3H, *s*, acetyl), 2.01 (3H, *s*, acetyl), 2.02 (3H, *s*, acetyl), 2.11 (3H, *s*, acetyl), 2.99 (1H, *dd*, $J = 12.0$ and 4.4 Hz, 5-H), 4.04 (1H, *dd*, $J = 12.8$ and 9.0 Hz, 7α-H), 4.12 (1H, *d*, $J = 11.2$ Hz, 7β-H), 4.87 (1H, *ddd*, $J = 13.2$, 4.8 and 2.8 Hz, 2-H), 5.19 (2H, *m*, 22 and 23-H) and 5.36 (1H, *d*, $J = 0.8$ Hz, 3-H). HR–FABMS $[M + Na]^+$ *m/z:* 657.3611 (calc. 657.3615) for $C_{35}H_{54}O_{10}Na$.

3.2.8. (22R,23R,24S)-2α,3α,22,23-Tetrahydroxy-26-nor-B-homo-7-oxa-5α-ergostan-6-one, 26-norbrassinolide 1

A solution of the compound **13** (39.2 mg, 0.06175 mmol) was treated with K_2CO_3 (150 mg, 1.09 mmol) in 70% aq. MeOH (20 ml) with refluxing for 6 h. Work-up (EtOAc extraction) was followed by chromatography on silica gel (1.0 cm i.d. ×25 cm). Elution with CH_2Cl_2–EtOH (20:1) afforded **1** (20.2 mg, 70.1%), mp 286–287 °C (from EtOAc); TLC: CH_2Cl_2–EtOH (5:1) $R_F = 0.40$; δ_H (400 MHz): 0.72 (3H, *s*, 18-H_3), 0.84 (3H, *d*, $J = 6.4$ Hz, 28-H_3), 0.91 (3H, *d*, $J = 7.2$ Hz, 21-H_3), 0.93 (3H, *s*, 19-H_3), 0.95 (3H, *t*, $J = 6.8$ Hz, 27-H_3), 3.12 (1H, *dd*, $J = 12.2$ and 5.2 Hz, 5-H), 3.56 (2H, *m*, *brs*, 22 and 23-H), 3.72 (1H, *m*, 2-H), 4.03 (1H, *br s*, 3-H) and 4.11 (2H, *m*, 7-H_2). HR–FABMS $[M + Na]^+$ *m/z:* 489.3210 (calc. 489.3192) for $C_{27}H_{46}O_6Na$.

3.2.9. (22R,23R,24S)-2α,3α,22,23-Tetrahydroxy-26-nor-5α-ergostane, 6-deoxo-26-norcastasterone 3

A mixture of the 26-norcastasterone **2** (11.0 mg, 0.02441 mmol), $N_2H_2 \cdot H_2O$ (300 μl), NaOH (350 mg,

8.75 mmol) and diethylene glycol (2.0 ml) was stirred at reflux temperature for 2 h. The excess $N_2H_2{\cdot}H_2O$ and H_2O were removed by concentrating in vacuo and the residue was stirred at 200 °C for 30 min. Work-up (EtOAc ectraction) was followed by chromatography on silica gel (1.2 cm i.d. ×15 cm). Elution with CH_2Cl_2–EtOH (20:1) afforded **3** (4.0 mg, 37.5%), mp 254–256 °C (from EtOAc); TLC: CH_2Cl_2–EtOH (15:1) $R_F = 0.21$; δ_H (400 MHz): 0.67 (3H, *s*, 18-H_3), 0.80 (3H, *s*, 19-H_3), 0.84 (3H, *d*, $J = 6.8$ Hz, 28-H_3), 0.90 (3H, *d*, $J = 6.4$ Hz, 21-H_3), 0.94 (3H, *t*, $J = 6.8$ Hz, 27-H_3), 3.57 (2H, *m*, *br s*, 22 and 23-H), 3.76 (1H, *m*, 2-H) and 3.96 (1H, *br s*, 3-H). HR–EIMS $[M]^+$ *m/z:* 436.3548 (calc. 436.3553) for $C_{27}H_{48}O_4$.

3.2.10. (22R,23R,24S)-2α,3α,22,23-Bisisopropylidene-dioxy-26-nor-5α-ergostan-6-one **4**

A mixture of the 26-norcastasterone **2** (10.8 mg, 0.02397 mmol), *p*-toluenesulfonic acid (1.0 mg, 6.4 μmol) and acetone (5.0 ml) was stirred at room temperature for 2 h. Work-up (EtOAc extraction) was followed by chromatography on silica gel (1.2 cm i.d. ×15 cm). Elution with hexane–EtOAc (10:1) afforded **4** (12.0 mg, 94.3%), mp 147–149 °C (from acetone); TLC: toluene–EtOAc (2:1) $R_F = 0.60$; δ_H (600 MHz): 0.66 (3H, *s*, 18-H_3), 0.67 (3H, *s*, 19-H_3), 0.92 (3H, *t*, $J = 7.1$ Hz, 27-H_3), 0.95 (3H, *d*, $J = 6.4$ Hz, 28-H_3), 0.98 (3H, *d*, $J = 6.8$ Hz, 21-H_3), 1.34 (3H, *s*, acetonide), 1.35 (3H, *s*, acetonide), 1.38 (3H, *s*, acetonide), 1.51 (3H, *s*, acetonide), 2.32 (1H, *dd*, $J = 12.7$ and 4.4 Hz, 7β-H), 2.55 (1H, *dd*, $J = 12.7$ and 3.9 Hz, 5-H), 3.60 (1H, *dd*, $J = 7.8$ and 4.8 Hz, 23-H), 3.89 (1H, *br d*, $J = 7.8$ Hz, 22-H), 4.10 (1H, *ddd*, $J =$ 10.3, 6.4 and 4.9 Hz, 2-H) and 4.28 (1H, *ddd*, $J = 4.9$, 4.4 and 1.5 Hz, 3-H). δ_C (150 MHz): 11.67 (C-27), 11.71 (C-18), 12.68 (×2) (C-19 and C-21), 14.21 (C-28), 21.13 (C-11), 22.57 (C-4), 23.88 (C-15), 26.53 (acetonide methyl), 26.58 (C-25), 27.25 (×2) (acetonide methyl), 27.76 (C-16), 28.65 (acetonide methyl), 36.72 (C-20), 37.25 (C-24), 37.62 (C-8), 39.14 (C-12), 41.11 (C-1), 42.51 (C-10), 42.80 (C-13), 46.90 (C-7), 51.48 (C-5), 53.31 (C-9), 53.37 (C-17), 56.40 (C-14), 72.15 (C-3), 72.35 (C-2), 80.22 (C-22), 81.11 (C-23), 107.65 (acetonide), 107.89 (acetonide), 211.45 (C-6). HR–FABMS $[M + Na]^+$ *m/z*: 553.3871 (calc. 553.3869) for $C_{33}H_{54}O_5Na$.

3.2.11. (22R,23R,24S)-2β-Acetyloxy-22,23-isopropylidene-dioxy-ergost-5-ene **5**

δ_H (600 MHz): 0.69 (3H, *s*, 18-H_3), 0.86 (3H, *d*, $J = 6.3$ Hz, 26-H_3), 0.89 (3H, *d*, $J = 6.8$ Hz, 28-H_3), 0.94 (3H, *d*, $J = 6.8$ Hz, 27-H_3), 0.98 (3H, *d*, $J = 6.4$ Hz, 21-H_3), 1.02 (3H, I, 19-H_3), 1.34 (3H, *s*, acetonide), 1.37 (3H, *s*, acetonide), 2.03 (3H, *s*, acetyl), 2.32 (2H, *m*, 4-H_2), 3.74 (1 H, *dd*, $J = 8.8$ and 4.4 Hz, 23-H), 3.84 (1H, *br d*, $J = 8.8$ Hz, 22-H), 4.61 (1H, *m*, 3-H) and 5.37 (1H, *m*, 6-H). δ_C (150 MHz): 9.97 (C-28), 11.60 (C-18), 12.68 (C-21), 18.44 (C-26), 19.33 (C-19), 21.04 (C-11), 21.18 (C-27), 21.43 (acetyl methyl), 24.16 (C-15), 27.27 (×2) (acetonide methyl), 27.76 (C-2), 27.99 (C-16), 30.64 (C-25), 31.85 (C-7), 31.92 (C-8), 36.21 (C-20), 36.57 (C-10), 36.95 (C-1), 38.10 (C-4), 39.50 (C-12), 40.60 (C-24), 42.26 (C-13), 49.94 (C-9), 53.42 (C-17), 56.42 (C-14), 73.96 (C-3), 79.12 (C-23), 80.57 (C-22), 107.51 (acetonide), 122.56 (C-6), 139.69 (C-5), 170.51 (acetyl carbonyl). HR–FABMS $[M + Na]^+$ *m/z*: 537.3917 (calc. 537.3920) for $C_{33}H_{54}O_4Na$.

3.2.12. (22S,23S,24S)-2β-Acetyloxy-22,23-isopropyl-idenedioxy-ergost-5-ene **6**

δ_H (600 MHz): 0.72 (3H, *s*, 18-H_3), 0.81 (3H, *d*, $J = 7.3$ Hz, 28-H_3), 0.85 (3H, *d*, $J = 6.4$ Hz, 26-H_3), 0.92 (3H, *d*, $J = 6.8$ Hz, 27-H_3), 1.03 (3H, *d*, $J = 7.3$ Hz, 21-H_3), 1.02 (3H, *s*, 19-H_3), 1.36 (3H, *s*, acetonide), 1.41 (3H, *s*, acetonide), 2.03 (3H, *s*, acetyl), 2.32 (2H, *m*, 4-H_2), 3.72 (1H, *dd*, $J = 6.8$ and 6.3 Hz, 23-H), 3.91 (1H, *dd*, $J = 6.3$ and 2.9 Hz, 22-H), 4.61 (1H, *m*, 3-H) and 5.37 (1H, *m*, 6-H). δ_C (150 MHz): 11.02 (C-28), 11.64 (C-18), 14.84 (C-21), 16.43 (C-26), 19.29 (C-19), 21.00 (C-11), 21.45 (acetyl methyl), 22.02 (C-27), 24.57 (C-15), 26.89 (C-25), 27.61 (acetonide methyl), 27.76 (×2) (C-2 and acetonide methyl), 28.52 (C-16), 31.80 (C-7), 31.87 (C-8), 36.56 (C-10), 37.00 (C-1), 38.10 (C-4), 39.60 (C-12), 39.66 (C-20), 41.97 (C-24), 42.98 (C-13), 49.97 (C-9), 52.34 (C-17), 56.30 (C-14), 73.94 (C-3), 80.81 (C-23), 83.20 (C-22), 107.22 (acetonide), 122.54 (C-6), 139.64 (C-5), 170.55 (acetyl carbonyl). HR–FABMS $[M + Na]^+$ *m/z*: 537.3919 (calc. 537.3920) for $C_{33}H_{54}O_4Na$.

3.3. Bioassay method

The rice lamina inclination test was carried out as described by Fujioka et al. (1998). Normal rice (*Oryza sativa* cv. Akinishiki) was used in our experiment. Totally 20–24 seedlings were used for each treatment.

The pea growth test using the dwarf mutant *lkb* was done as previously reported (Nomura et al., 1999). A total of 8 plants were used for each treatment. The fourth stems were treated with BRs when the third leaves were just expanded and the lengths of the fourth and fifth internodes were measured. Because the fifth internodes were more sensitive, their lengths were employed to evaluate biological activities. This bioassay was repeated three times.

Acknowledgements

The authors thank Professor T. Yoshikawa and Dr. M. Hirotani of Kitasato University for the measurement of mass spectra.

References

Altmann, T., 1998. Recent advances in brassinosteroid molecular genetics. Curr. Opin. Plant Biol. 1, 378–383.

Clouse, S.D., Feldmann, K.A., 1999. Molecular genetics of brassinosteroid action. In: Sakurai, A., Yokota, T., Clouse, S.D. (Eds.), Brassinosteroids. Springer, Tokyo, pp. 163–189.

Crozier, A., Kamiya, Y., Yokota, T., 1999. The biosynthesis of plant hormones (Chapter 17). In: Buchanan, B.B., Gruissem, W., Jones, R.L. (Eds.), Biochemistry and Molecular Biology of Plants. American Society of Plant Physiologists, Maryland, pp. 850–929.

Fujioka, S., 1999. Natural occurrence of brassinosteroids in the Plant Kingdom. In: Sakurai, A., Yokota, T., Clouse, S.D. (Eds.), Brassinosteroids: Steroidal Plant Hormones. Springer, Tokyo, pp. 21–45.

Fujioka, S., Sakurai, A., 1997a. Biosynthesis and metabolism of brassinosteroids. Physiol. Plant. 100, 710–715.

Fujioka, S., Sakurai, A., 1997b. Brassinosteroids. Nat. Prod. Rep. 14, 1–10.

Fujioka, S., Noguchi, T., Sekimoto, M., Takatsuto, S., Yoshida, S., 2000. 28-Norcastasterone is biosynthesized from castasterone. Phytochemistry 55, 97–101.

Fujioka, S., Noguchi, T., Takatsuto, S., Yoshida, S., 1998. Activity of brassinosteroids in the dwarf rice lamina inclination bioassay. Phytochemistry 49, 1841–1888.

Kim, T.-W., Chang, S.C., Choo, J., Watanabe, T., Takatsuto, S., Yokota, T., Lee, J.S., Kim, S.Y., Kim, S.-K., 2000a. Brassinolide and [26, 28-$^{2}H_{6}$]brassinolide are differently demethylated by loss of C-26 and C-28, respectively, in *Marchantia polymorpha*. Plant Cell Physiol. 41, 1171–1174.

Kim, S.-K., Chang, S.C., Lee, E.J., Chung, W.-S., Kim, Y.-S., Hwang, S., Lee, J.S., 2000b. Involvement of brassinosteroids in the gravitropic response of primary root of maize. Plant Physiol. 123, 997–1004.

Li, J., Nagpal, P., Vitart, V., McMorris, T.C., Chorry, J., 1996. A role for brassinosteroids in light-dependent development of Arabidopsis. Science 272, 398–401.

Mori, K., Sakakibara, M., Okada, K., 1984. Synthesis of naturally occurring brassinosteroids employing cleavage of 23, 24-epoxides as key reactions: synthesis of brassinolide, castasterone, dolicholide, dolichosterone, homodolicholide, homodolichosterone, 6-deoxocastasterone and 6-deoxodolichosterone. Tetrahedron 40, 1767–1782.

Neff, M.M., Nguyen, S.M., Malancharuvil, E.J., Fujioka, S., Noguchi, T., Seto, H., Tsubuki, M., Honda, T., Takatsuto, S., Yoshida, S., Chory, J., 1999. *BAS1:* a gene regulating brassinosteroid levels and light responsiveness in Arabidopsis. Proc. Natl. Acad. Sci., USA 96, 153–316.

Noguchi, T., Fujioka, S., Choe, S., Takatsuto, S., Tax, F.E., Yoshida, S., Feldmann, K.A., 2000. Biosynthetic pathways of brassinolide in Arabidopsis. Plant Physiol. 124, 201–209.

Nomura, T., Kitasaka, Y., Takatsuto, S., Reid, J.B., Fukami, M., Yokota, T., 1999. Brassinosteroid/sterol synthesis and plant growth as affected by *lka* and *lkb* mutations of pea. Plant Physiol. 119, 1517–1526.

Takatsuto, S., Yazawa, N., Ishiguro, M., Morisaki, M., Ikekawa, N., 1984. Stereoselective synthesis of plant growth-promoting steroids, brassinolide, castasterone, typhasterol and their 28-nor analogues. J. Chem. Soc., Perkin Trans. 1 139–146.

Takatsuto, S., Yazawa, N., Ikekawa, N., Morisaki, T., Abe, H., 1983a. Synthesis of (24*R*)-28-homobrassinolide and structure–activity relationships of brassinosteroids in rice lamina inclination test. Phytochemistry 22, 1393–1397.

Takatsuto, S., Yazawa, N., Ikekawa, N., Takematsu, T., Takeuchi, Y., Koguchi, M., 1983b. Structure–activity relationship of brassinosteroids. Phytochemistry 22, 2437–2441.

Yokota, T., 1997. The structure, biosynthesis and function of brassinosteroids. Trends Plant Sci. 2, 137–143.

Yokota, T., 1999. Brassinosteroids. In: Hooykaas, M.A., Hall, M.A., Libbenga, K.R. (Eds.), Biochemistry and Molecular Biology of Plant Hormones. Elsevier Science, Amsterdam, pp. 277–293.

Wada, K., Marumo, S., Ikekawa, N., Morisaki, N., Mori, K., 1981. Brassinolide and homobrassinolide promotion of lamina inclination of rice seedlings. Plant Cell Physiol. 22, 323–326.

Wada, K., Marumo, S., Mori, K., Takatsuto, S., Morisaki, M., Ikekawa, N., 1983. The rice lamina inclination–promoting activity of synthetic brassinolide analogues with a modified side-chain. Agric. Biol. Chem. 47, 1139–1141.

Watanabe, T., Takatsuto, S., Fujioka, S., Sakurai, A., 1997. Improved synthesis of castasterone and brassinolide. J. Chem. Res. (S), 360–361.

Winter, J., Schneider, B., Strack, D., Adam, G., 1997. Role of a cytochrome P450-dependent monooxygenase in the hydroxylation in cultured *Zinnia* cells. Phytochemistry 45, 233–237.

PERGAMON

Phytochemistry 58 (2001) 351–355

PHYTOCHEMISTRY

www.elsevier.com/locate/phytochem

Eucalyptus camaldulensis: volatiles from immature flowers and high production of 1,8-cineole and β-pinene by in vitro cultures

Andreas Giamakis[a], Ourania Kretsi[b], Ioanna Chinou[b], Caroline G. Spyropoulos[a,*]

[a]*Division of Botany, Department of Biology, University of Athens, Athens 157 71, Greece*
[b]*Division of Pharmacognosy, School of Pharmacy, University of Athens, Athens 157 71, Greece*

Received 7 December 2000; received in revised form 5 April 2001

Abstract

Calli of *Eucalyptus camaldulensis* Dehn were induced, for the first time, from immature flowers and stamens and established in the presence of 2,4-D and BA, under dark and light conditions. Immature flowers, of the same type used for callus induction, were submitted to hydrodistillation while the induced calli were extracted with *n*-pentane. The constituents of the *n*-pentane extracts and of the hydrodistillate were identified by GC–MS. The main constituents of the hydrodistillate from immature flowers were 1,8-cineole (34.7%), β-pinene (7.7%), and spathulenol (9.5%). The *n*-pentane extract from calli developed from stamens consisted only of alkanes, alkenes and alcohols, while that of calli developed from immature flowers consisted mainly of monoterpenes (92.08–96.56%). The main monoterpenes produced in these calli, cultured in darkness and under light conditions, were 1,8-cineole, 62.70 and 69.26% as well as β-pinene, 27.09 and the 25.31%, respectively. © 2001 Elsevier Science Ltd. All rights reserved.

Keywords: *Eucalyptus camaldulensis*; Myrtaceae; Callus cultures; Immature flowers; Monoterpenes; Sesquiterpenes; Stamens; Volatiles; 1,8-Cineole; β-Pinene

1. Introduction

Eucalyptus is one of the world's most important and most widely planted genera. Among its main uses is the production of essential oils, which are used for medicinal and pharmaceutical purposes (Ghisalberti, 1996; Leung and Foster, 1996). One of the most important compounds extracted from *Eucalyptus* is 1,8-cineole, mainly due to its antibacterial and expectorant properties (Leung and Foster, 1996). It is reported to be particularly abundant in leaves and its content in the essential oil of different *Eucalyptus* species varies between 25 and 90%. Apart from 1,8-cineole, the essential oil of leaves from *Eucalyptus* species contains, in relatively high amounts, several monoterpene hydrocarbons, (α-pinene, limonene, *p*-cymene, β-pinene, α-phellandrene, camphene, γ-terpinene, etc., with the first three in major amounts) and in lower percentage several sesquiterpene hydrocarbons (aromadendrene, allo-aromadendrene, globulol, etc.), oxygenated monoterpenes (e.g. myrtenal, carvone and pinocarvone) and others (Nicole et al., 1998; Pagula et al., 2000). Although there are many reports on the essential oil composition of *Eucalyptus* aerial parts (Nicole et al., 1998; Pagula et al., 2000), to our knowledge, there is no report on the composition of volatiles from immature flowers. Furthermore, although there are many reports on the uses of *Eucalyptus* species cell culture for the biotransformation of several terpenoid metabolites (Orihara and Furuya, 1994; Orihara et al., 1994), there is no report on the production of monoterpenes and sesquiterpenes by tissue cultures of this species. In this paper, we report the essential oil composition of immature flowers from *E. camaldulensis*, a species that is widely cultivated in Greece, and the production of monoterpenes and sesquiterpenes by tissue cultures.

2. Results and discussion

2.1. Composition of the essential oil from immature flowers

In the essential oil isolated from immature *E. camaldulensis* flowers 42 compounds were identified, corresponding

* Corresponding author. Tel.: +30-1-727-4653; fax: +30-1-727-4702.
E-mail address: cgspyro@atlas.uoa.gr (C.G. Spyropoulos).

0031-9422/01/$ - see front matter © 2001 Elsevier Science Ltd. All rights reserved.
PII: S0031-9422(01)00193-5

to 82.5% of the total oil (total oil 0.81 mg g^{-1} fr. wt). Among these 18.6% were monoterpene hydrocarbons, 50.0% were oxygenated monoterpenes, while the rest were sesquiterpene hydrocarbons (1.2%) and oxygenated sesquiterpenes (12.7%). 1,8-Cineole (34.7%, 0.28 mg g^{-1}), β-pinene (7.7%, 0.06 mg g^{-1}) and spathulenol (9.46%, 0.08 mg g^{-1}) were determined as the most abundant constituents (Table 1). 1,8-Cineole was also the major component of the leaf oil (Leung and Foster, 1996). In lower, but significant, amounts were the monoterpenes terpinen-4-ol (3.6%), α-pinene (3.3%), cryptone (3.2%), *trans*-pinocarveol (1.9%), α-terpineol (1.8%), and myrtenal (1.5%). Most of the constituents of the essential oil from immature flowers were the same as those from leaves collected from the same tree at the same period (Kretsi et al., 2000). However, the terpenes, caryophyllene oxide (2.4%), γ-terpinene (0.5%), *trans*-sabinene hydrate (0.3%), *cis*-sabinene hydrate (0.2%) *trans*-linalool oxide (0.1%), bornyl acetate (0.1%), α-gurjunene (0.1%), β-caryophyllene (0.2%) and viridiflorol (0.2%) were detected exclusively in immature flowers.

2.2. Tissue culture

Immature flowers and stamens were cultured in seven media, which differed in their concentrations of BA and 2,4-D. Callus formation was observed under the binocular microscope 5 or 6 days after the start of immature stamen or flower culture, irrespectively of the culture medium. Calli from immature flowers, depending on the culture medium seemed to originate either from the ovule (media 5 and 7) or from the stamen filament. They had a yellow-brownish color, and those cultured under dim light conditions were yellow-green.

Calli from immature stamens had a similar appearance with those from immature flowers and seemed to originate from the stamen filament. Although callus initiation was not affected by the concentration of the growth factors in the culture medium, callus growth rate was higher in those media that contained both growth factors (media 5, 6, and 7). Calli were subcultured every 2 months, and after 2 subcultures calli from media 5, 6, and 7 were combined and extracted with *n*-pentane.

2.3. Analysis of the n-pentane extract from calli developed from immature stamens and flowers

Table 2 shows the results of the analysis of the *n*-pentane extracts from calli, which were developed from immature stamens and flowers of *E. camaldulensis* and cultured under dark or light conditions. The percent concentration of the identified volatile constituents from calli that derived from immature stamens and cultured in darkness were not the same as those cultured under light conditions. In calli derived from stamens, 15 compounds were identified corresponding to the 65.7% of

Table 1
Volatile constituents of the hydrodistillate and the *n*-pentane extract from *Eucalyptus camaldulensis* immature flowers[a]

Constituents	1 (%)	2 (%)	KI	DB5[b]
Monoterpene hydrocarbons	18.5			
α-Pinene	3.3	3.51	939	319
β-Pinene	7.7	10.33	980	386
Sabinene	3.2		976	379
α-Thujene	0.6	0.77	931	307
α-Phellandrene	2.1	2.14	1005	435
β-Myrcene	0.5	0.56	991	408
α-Terpinene	0.2	0.26	1018	457
γ-Terpinene	0.5	0.41	1062	545
α-Terpinolene	0.5	0.48	1088	608
P-Cymene	9.32	9.33	1026	471
Oxygenated monoterpenes	50.0			
Carvone	0.10	0.14	1242	984
1-Terpineol	0.6	0.52	1134	712
Cuminal	0.94	1.01	1239	977
trans-Sabinene hydrate	0.3	0.23	1097	629
cis-Sabinene hydrate	0.2	0.21	1068	560
cis-*p*-Menth-2-en-1-ol	0.9	0.77	1121	682
Piperitone	0.1	0.13	1252	1011
α-Campholenal	0.1	0.13	1125	692
1,8-Cineole	34.7	36.80	1033	485
cis-Linalool oxide	0.1	0.09	1074	574
Linalool	0.5	0.42	1098	632
β-Thujone	0.1	–	1114	667
α-Fenchol	0.3	0.22	1112	664
trans-Pinocarveol	1.9	1.00	1139	724
Terpin-4-ol	3.6	3.29	1177	820
Cryptone	3.2	2.47	–	–
α-Terpineol	1.8	1.43	1189	852
Myrtenal	1.5	1.15	1193	864
Borneol	0.3	0.21	1165	789
trans-Carveol	0.2	0.15	1217	923
Bornyl acetate	0.1	0.09	1285	1099
p-Cymen-7-ol	0.23	0.10	1287	1106
Thymol	0.24	0.25	1290	1113
Phellandral	0.2	0.25	–	–
Sesquiterpene hydrocarbons	1.2			
Alloaromadendrene	0.2	0.21	1461	1546
Bicyclogermacrene	0.4	0.38	1494	1632
α-Gurjunene	0.1	0.09	1409	1421
β-Caryophyllene	0.2	0.22	1418	1442
d-Guaiene	0.1	–	–	–
1(5), 6-Guaiadiene	0.2	–	–	–
Aromadendrene	0.21	0.24	1439	1491
Oxygenated sesquiterpenes	12.7			
Spathulenol	9.5	10.18	1576	1825
Isospathulenol	0.1	0.12		
2*Z*, 6*E*-Farnesol	0.1		1697	2106
Caryophyllene oxide	2.4	2.54	1581	1837
Viridiflorol	0.2		1590	1859
τ-Muurolol	0.2		1641	1976
Lepidozenal	0.3	0.37		
Total	82.7	92.92		

[a] 1, Hydrodistillate; 2, *n*-pentane extract; KI, Kovats indices.

[b] J & W DB5, 0.26 mm i.d. × 30 m, 0.25 μm coating thickness fused silica capillary column (Adams, 1995).

Table 2
Composition of the *n*-pentane extract of calli, which were developed from immature stamens and flowers

	Peak-area ratio (×100)			
	Calli from stamens		Calli from flowers	
Constituents	Dark	Light	Dark	Light
Alkanes				
Nonane	1.21	0.70		
Decane	2.01	0.95		
Undecane	3.19	1.64		
Dodecane	4.09	2.86		
Tridecane	4.67	4.02	0.12	tr
Tetradecane	4.20	4.16	0.13	tr
Pentadecane	3.48	3.81	0.13	tr
Hexadecane	2.52	2.99	0.11	tr
Heptadecane	1.73	2.10	0.09	tr
Octadecane	1.14	1.33		
Cyclododecane			0.10	
Cyclotetradecane	10.30	10.02		
Alkenes				
1-Octadecene	5.05	5.08	0.85	0.25
5-*E*-Octadecene	7.85	17.09	1.97	0.69
1,13-Tetradecadiene	tr	6.63	0.96	0.23
Squalene			0.12	tr
Alcohols				
9-*Z*-Octadecen-1-ol	14.24	19.01	2.70	0.73
Monoterpene hydrocarbons				
α-Pinene			1.22	1.12
Camphene			0.51	0.46
β-Pinene			27.09	25.31
Myrcene			0.35	0.32
Oxygenated monoterpenes				
Isocineole			0.09	0.09
1,8-Cineole			62.70	69.26
Myrtenol			0.12	tr
Sesquiterpenes				
Bicyclogermacrene			0.09	tr
Oxygenated sesquiterpenes				
Spathulenol			0.12	tr
trans-Pinocarveol			0.11	0.11
Total	65.68	82.39	99.68	98.57

the total extract for those cultured in darkness, while the identified volatiles of calli cultured under light conditions corresponded to the 82.4% of the total extract. These compounds, irrespective of the culture conditions, were alkanes, alkenes, and aliphatic alcohol hydrocarbons. The major compounds were the alkenes 1-octadecene (5.1% under either dark or light conditions) and 5-octadecene (7.9 and 17.1%, under dark and light conditions, respectively). No mono- or sesquiterpenes were detected. Generally, with the exception of few examples (Zito et al., 1991; Figuiredo et al., 1995; Hosokawa and Fukunaga, 1995), there is lack of success in de novo production of monoterpene and sesquiterpene compounds by undifferentiated tissue cultures. One explanation could be the fact that their site of production is not physically separated from their storage site and, as a result, they are exposed to enzymatic degradation (Alves-Pereira and Fernandes-Ferreira, 1998).

In contrast to calli, which were developed from stamens, the volatiles from calli derived from immature flowers (0.17 mg g^{-1} fr. wt in darkness and 0.15 mg g^{-1} fr. wt under light conditions) were mainly monoterpenes. In the extract of calli cultured under dark and light conditions, 21 compounds were identified, corresponding to the 99.7 and 98.6% of the total extract, respectively. The two major compounds identified in the *n*-pentane extract of calli grown either in darkness or under light conditions, corresponding to 89.8 and 94.8% of the total, respectively, were the oxygenated monoterpene 1,8-cineole (62.7%, 0.11 mg g^{-1} fr. wt and 69.3%, 0.1 mg g^{-1} fr. wt, respectively) and the monoterpene β-pinene (27.1 and 25.5%, respectively). In lower amounts were determined α-pinene (1.2 and 1.1%, respectively) and the terpenoids, camphene, myrcene, isocineole, myrtenol, bicyclogermacrene, spathulenol, and *trans*-pinocarveol (in less than 1%). Apart from *iso*-cineole, these constituents were also determined in the essential oil from immature flowers.

In order to check whether extraction with *n*-pentane underestimated the number and the amounts of terpenoids in calli, we determined also the constituents of the *n*-pentane extract of immature flowers. As shown in Table 1, the constituents of the *n*-pentane extract were almost identical with those of hydrodistillate and in comperable amounts.

Our results showed that a very important role on the production of monoterpenes and sesquiterpenes by *E. camaldulensis* calli played the kind of explant used for callus development. On the other hand, light conditions did not considerably affect the production of these compounds by calli developed from immature flowers. It is remarkable that undifferentiated calli are capable of producing high amounts of monoterpenoid compounds (approx. one third of that produced by the explant). This makes immature flowers from *E. camaldulensis* an interesting candidate plant material for the development of calli able to produce high percentages of two important monoterpenes.

3. Experimental

3.1. Plant material

Fresh immature flowers were collected from *E. camaldulensis* in the University Campus of the University of Athens, Zografou, Athens, at the beginning of September 2000. Dr. L. Koumpli-Sovantzi identified a voucher specimen which it has been deposited in her herbarium (KS6187) kept in ATHU.

3.2. Initiation of cultures from immature flowers and stamens

Immature flowers were collected from a tree in the University Campus, at the beginning of April 2000. They were surface sterilized with 70% ethanol for 1.5 min and 10% common bleach for 4 min, and then rinsed three times with distilled sterile water. A batch of flowers was cut in half while from another batch stamens were dissected. Half flowers and stamens were placed separately, under sterile conditions, in petri dishes containing MS (Murashige and Skoog, 1961) supplemented with 8% agar, 2% sucrose, in the presence of either BA, 2,4-D, or both: media 1, 2 and 3 contained only 0.01, 0.1 and 0.5 mg l^{-1} BAP, respectively, medium 4 contained only 0.01 mg l^{-1} 2,4-D, while media 5, 6, and 7 contained both growth factors at concentrations of 0.01, 0.05 and 0.05 mg l^{-1} 2,4-D and 0.1, 0.01 and 0.1 mg l^{-1}, respectively. The pH of the culture media was adjusted to 5.8. The explants were incubated at 25°C in continuous darkness or in 16 h light (3200 lux). Calli were initiated 6 days after the start of flower or stamen culture.

3.3. Identification of volatiles from calli of immature stamens and flowers and of the essential oil from immature flowers

Two weeks after callus initiation (observation under the binocular microscope) calli with (stamens) or without the explant (immature flowers) were transferred to petri dishes with the same culture medium and cultured under the same conditions. After two subcultures, calli that were cultured in media 5, 6, and 7 were collected and extracted with *n*-pentane.

Fresh immature flowers (200 g fr. wt) were submitted to steam distillation for 3 h in 1 l water, in a Clevenger modified apparatus with a water-cooled oil receiver to reduce hydrodistillation-overheating artifacts. The essential oils were taken in pesticide analysis grade diethyl ether and were subsequently dried over anhydrous sodium sulfate and stored at 4–6°C until they were analyzed. The oil was light yellow with distinct sharp odor.

In all cases, the *n*-pentane extracts from calli, which were developed from flowers and stamen and the obtained essential oil of the fresh immature flowers of *E. camaldulenis* were then subjected to GC–MS analysis.

3.4. GC–MS analysis

Analysis was performed with a Hewlett Packard 6890 chromatograph linked to a Hewlett Packard 5973 mass spectrometer system operating on EI mode (equipped with a split/ splitless injector (200°C) 1/10 split ratio), and a 30 m long, 0.25 mm i.d., 0.25 μm film thickness HP 5MS capillary column. The ionization energy was 70 eV. The temperature of the injection block was 200°C. The GC oven temperature was programmed as follows: initial temperature 60°C (for 5 min) followed by a temperature increase of 3°C min^{-1} up to 280°C. The carrier gas was He. Identification of the volatile components was established using a Wiley MS data library as well as\by comparison of Kovats indices (Adams, 1995) and GC–MS data with those of authentic samples.

3.5. Kovats indices

Values were determined relative to the retention times of a series of *n*-paraffin hydrocarbons (Van den Dool, 1963) on a Hewlett Packard 6890 GC. Analytical conditions were identical to those used for the GC–MS analysis.

Acknowledgements

A research grant from the General Secretary of Research and Technology to C.G.S. is gratefully acknowledged.

References

Adams, R.P., 1995. Identification of Essential Oil Components by Gas Chromatography/Mass Spectrometry. Allured Publishing Corporation, Carol Stream, IL, USA.

Alves-Pereira, I.M.S., Fernandes-Ferreira, M., 1998. Essential oils and hydrocarbons from leaves and calli of *Origanum vulgare* ssp. *virens*. Phytochemistry 48, 795–799.

Figueiredo, A.C., Salome, M., Pais, S., Scheffer, J.J.C., 1995. Composition of the essential oil from cell suspension cultures of *Achillea millefolium* spp. *millefolium*. Plant Cell, Tissue and Organ Culture 40, 113–118.

Ghisalberti, E.L., 1996. Bioactive acylphloroglucinol derivatives from *Eucalyptus* species. Phytochemistry 41, 7–22.

Hosokawa, K., Fugunaga, Y., 1995. Production of essential oils by flowers of *Hyacynthus orientalis* L. regenerated in vitro. Plant Cell Reports 14, 575–579.

Kretsi, O., Tsiri, D., Harvala, E., Ganis-Spyropoulos, C., Chinou, I.B. 2000. Essential oils and hydrocarbons from leaves and calli of *Eucalyptus camaldulensis*. 48th Annual Congress, Society for Medicinal Plant Research, Zurich, Switzerland 4–September 2000.

Leung, A.Y., Foster, S., 1996. Encyclopedia of common natural ingredients used in food, drugs, and cosmetics, 2nd Edition. John Willey & Sons, pp. 232–233.

Murashige, T., Skoog, G., 1962. A revised medium for rapid growth and bioassay with tobacco cultures. Physiol. Plant. 15, 473–479.

Nicole, D., Dunlop, P.J., Bignell, C.M., 1998. A study of the variation with time of the compositions of the essential leaf oils of 16 *Eucalyptus* species. Flavour Fragr. J. 13, 324–328.

Orihara, Y., Fyruya, T., 1994. Biotransformation of 1,8-cineole by cultured cells of *Eucalyptus perinniana*. Phytochemistry 35, 641–644.

Orihara, Y., Saiki, K., Fyruya, T., 1994. Biotransformation of caryophyllene oxide by cultured cells *Eucalyptus perinniana*. Phytochemistry 35, 635–639.

Pagula, P.F., Baser, K.H.C., Kürkçüoglu, M., 2000. Essential oil composition of *Eucalyptus camaldulensis* Dehn. from Mozambique. J. Essent. Oil Res. 12, 333–335.

Van den Dool, H., Kratz, P.D., 1963. A generalization of the retention index system including linear temperature programmed gas–liquid partition chromatography. J. Chromatogr. 11, 463–471.

Zito, S.W., Srivastava, V., Adebayo-Olojo, E., 1991. Incorporation of [1-^{14}C]-isopentenyl pyrophosphate into monoterpenes by a cell-free homogenate prepared from callus cultures of *Chrysanthemum cinerariaefolium*. Planta Med. 57, 425–427.

PERGAMON

Phytochemistry 58 (2001) 357–362

PHYTOCHEMISTRY

www.elsevier.com/locate/phytochem

Anti-inflammatory tetramers of resveratrol from the roots of *Vitis amurensis* and the conformations of the seven-membered ring in some oligostilbenes

Kai-Sheng Huang, Mao Lin*, Gui-Fang Cheng

Institute of Materia Medica, Chinese Academy of Medical Sciences and Peking Union Medical College, 1 Xian Nong Tan Street, Beijing 100050, People's Republic of China

Received 21 November 2000; received in revised form 11 April 2001

Abstract

Five resveratrol tetramers, amurensins I–M, were isolated from the roots of *Vitis amurensis* (Rupr.), together with five known resveratrol tetramers, (+)-hopeaphenol, isohopeaphenol, vitisin A, (+)-vitisifuran A, and heyneanol A. Their structures and stereochemistry were determined by chemical and spectroscopic methods, especially by use of 2D NMR analysis. Some of them had an ampelopsin A or a balanocarpol unit, in which the conformations of the seven-membered carbon ring were described for the first time. The anti-inflammatory activities of the tetramers were also tested. Among them, (+)-hopeaphenol, isohopeaphenol, vitisin A, (+)-vitisifuran A and heyneanol A showed potent inhibition on the biosynthesis of leukotriene B_4 (LTB_4), and amurensins I and L showed strong antagonism of the histamine acceptor. © 2001 Elsevier Science Ltd. All rights reserved.

Keywords: *Vitis amurensis*; Vitaceae; Oligostilbenes; Resveratrol; Amurensins I–M; Structural elucidation; Conformation

1. Introduction

Hopeaphenol was the first resveratrol tetramer isolated from *Hopea odorata* (thingan) and *Balanocarpus heimii* (chengal) (Coggon et al., 1965), whose structure was determined by X-ray crystallographic analysis (Coggon et al., 1966). Kawabata and his colleagues reported its NMR spectroscopic data (Kawabata et al., 1992). In this study, besides the resveratrol dimers and trimers reported previously (Huang and Lin, 1999; Huang et al., 1999, 2000), ten resveratrol tetramers including five new compounds amurensins I–M (**1**–**5**), were isolated from the roots of *Vitis amurensis*. The known tetramers were determined to be (+)-hopeaphenol, isohopeaphenol (Ito et al., 1997), vitisin A (Oshima et al., 1993), (+)-vitisifuran A (Ito et al., 1999) and heyneanol A (Li et al., 1996) by comparison of their chemical and spectral data with those in the literature.

2. Results and discussion

Amurensin I (**1**) was obtained as a brown amorphous powder, exhibiting strong blue violet fluorescence under UV-254 light, $[\alpha]_D^{20}$ −128.2° (*c* 0.12, MeOH). Its molecular formula of $C_{56}H_{38}O_{12}$ was determined by the high resolution FAB–MS *m*/*z* 903.2385 $[MH]^+$ (calc. for $C_{56}H_{39}O_{12}$, 903.2442), corresponding to a resveratrol tetramer. The ^1H NMR spectrum of **1** contained the signals for an 8b-dehydroxybalanocarpol unit [δ 7.63 (2H, *d*, $J=8.5$ Hz), 7.03 (2H, *d*, $J=8.5$ Hz), 6.33 (2H, *d*, $J=8.8$ Hz), 6.22 (2H, *d*, $J=8.8$ Hz), 6.39 (1H, *d*, $J=2.2$ Hz), 6.35 (1H, *d*, $J=2.2$ Hz), 5.72 (1H, *d*, $J=2.1$ Hz), 4.42 (1H, *d*, $J=2.1$ Hz), 5.63 (1H, *d*, $J=10.1$ Hz), 5.59 (1H, *d*, $J=10.1$ Hz), 5.52 (1H, *d*, $J=4.5$ Hz), 2.98 (1H, *dd*, $J=4.5$, 11.3 Hz)]. The other signals were similar to those of malibatol B (Dai et al., 1998), but there were three hydroxy groups less than in malibatol, suggesting that an extra ring (ring D_4) was formed by the connectivity of C-2d and C-14d to satisfy the ^1H NMR patterns. The two units were bonded at C-8b and C-8c to form **1**, which was confirmed by ^1H–^1H COSY (H-7b→H-8b→H-8c→H-7c) and long range CH correlations (H-8b/C-8c and H-8c/C-8b) in the HMBC spectrum. The up-field

* Corresponding author. Tel.: +86-10-63165326; fax: +86-10-63017757.

E-mail address: linmao@imm.ac.cn (M. Lin).

0031-9422/01/$ - see front matter © 2001 Elsevier Science Ltd. All rights reserved.
PII: S0031-9422(01)00224-2

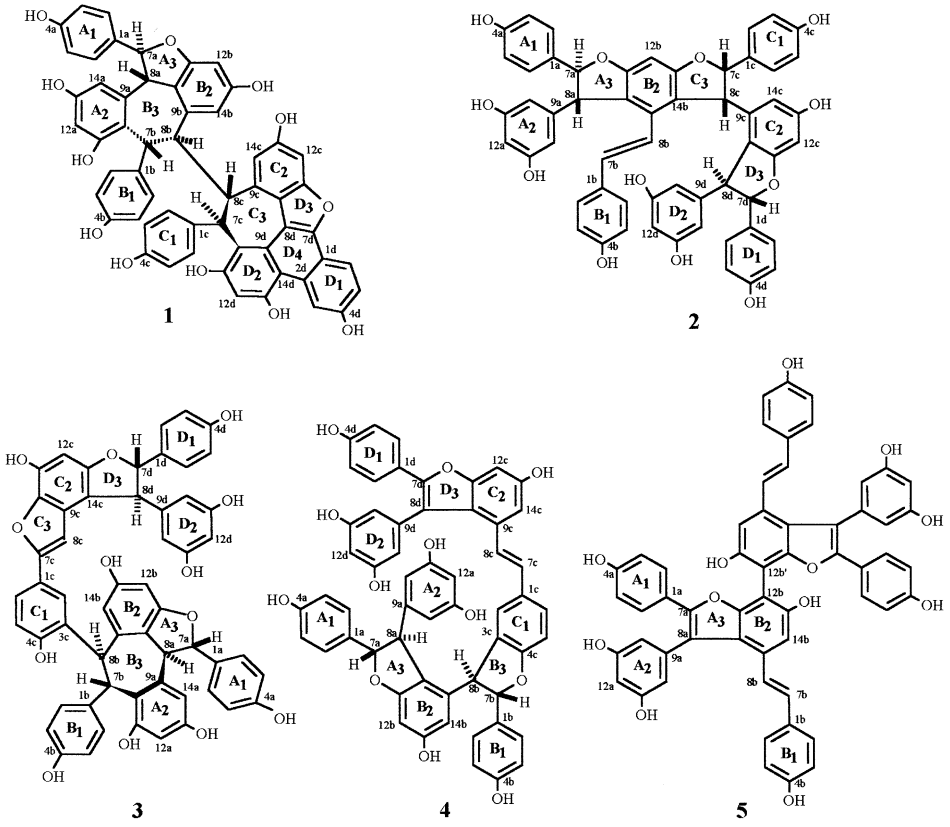

shift of H-14b (δ 4.42) was due to the shielding effect of ring C_2 which can be observed clearly from the molecular model, and the down-field shift of H-3d, 5d, 6d (δ 9.49, 7.25, 8.20) was due to the strong deshielding effect of the highly unsaturated ring system in the structure. The NOE interaction between H-8a and H-2(6)a suggested a *trans* orientation of ring A_3. The NOE enhancements between H-8a/H-8c, H-7b/H-8c, H-8b/H-14b, H-8c/H-14c verified the relative configuration of *rel*-(7a*S*, 8a*S*, 7b*R*, 8b*S*, 7c*R*, 8c*S*) for **1**. In a previous paper (Sotheeswaran and Pasupathy, 1993), it was proposed that all naturally occurring oligomers of resveratrol with dihydrobenzofuran moieties were formed from reveratrol via the dimer ε-viniferin, the absolute configuration of **1** was tentatively assigned as (7a*S*, 8a*S*, 7b*R*, 8b*S*, 7c*R*, 8c*S*) because only (+)-ε-viniferin was isolated from this plant.

Amurensin J (**2**) was obtained as a yellowish amorphous powder, exhibiting strong blue fluorescence under UV-254 light, $[\alpha]_D^{20}$ +174.9° (*c* 0.12, MeOH). The high resolution FAB–MS *m*/*z* 907.2699 $[MH]^+$ (calc. for $C_{56}H_{43}O_{12}$, 907.2755) was in agreement with the molecular formula $C_{56}H_{42}O_{12}$, which corresponds to a resveratrol tetramer. In the ^1H NMR spectrum of **2** at room temperature in acetone-d_6, several protons appeared as very broad signals. This resulted in many difficulties for the structural elucidation because they did not give cross-peaks in the 2D NMR spectra. Considering that the reason for the broad signals was probably spatial congestion, the ^1H and ^1H–^1H COSY spectra of **2** were carried out at a temperature of 100 °C, resulting in improved resolution. The ^1H NMR spectrum of **2** at 100 °C in DMSO-d_6 showed signals for four 1-substituted 4-hydroxybenzene moieties (ring A_1, B_1, C_1, D_1) at δ 7.13 (2H, *d*, *J* = 8.4 Hz) and 6.76 (2H, *d*, *J* = 8.4 Hz) δ 6.96 (2H, *d*, *J* = 8.4 Hz) and 6.72 (2H, *d*, *J* = 8.4 Hz) δ 6.81 (2H, *d*, *J* = 8.2 Hz) and 6.52 (2H, *d*, *J* = 8.2 Hz), δ 6.62 (2H, *d*, *J* = 8.6 Hz) and 6.57 (2H, *d*, *J* = 8.6 Hz); signals for two 1-substituted 3,5-dihydroxybenzene moieties (rings A_2, D_2) at δ 5.78 (2H, *br s*) and 6.04 (1H, overlap), δ 6.04 (2H, *br s*) and 6.04 (1H, overlap); two *meta*-coupled signals at δ 6.22 (1H, *br s*) and 5.98 (1H, *br s*) for ring C_2; one singlet for ring B_2 at δ 6.25; and three sets of signals for the dihydrobenzofuran moieties (rings A_3, C_3, D_3) at δ 5.33 (1H, *d*, *J* = 4.5 Hz) and 4.34 (1H, *d*, *J* = 4.5 Hz), δ 5.13 (1H, *br s*) and 3.61 (1H, *br s*), δ 4.92 (1H, *d*, *J* = 7.7 Hz) and 4.55 (1H, *d*, *J* = 7.7 Hz). The ^{13}C NMR spectrum in DMSO-d_6 revealed the presence of six aliphatic carbons besides 50 aromatic and olefinic carbons. The ^1H and ^{13}C NMR patterns menttioned above were similar to those of flexuosol A (Li et al., 1998), and the CH long range correlations between H-7a/C-2(6), 9a, 10b, H-12b/C-10b, 14b, H-8b/C-10b, 14b, H-8c/C-14b, 13b, 10c, 14c, H-10(14)d/C-8d observed in the HMBC spectrum (measured at 70 °C in DMSO-d_6) supported the same planar structure of **2** as flexuosol A, thus **2** was a stereomer of flexuosol A. Since amurensin B (Huang and Lin, 1999; Huang et al., 1999), a resveratrol trimer with a *cis*-dihydrobenzofuran moiety was iso-

lated from this plant, it was proposed that **2** was derived from amurensin B through addition of a resveratrol unit. The strong NOE interaction between H-7c and H-8c supported a *cis* relationship between H-7c and H-8c. The *trans* orientations between H-7a/H-8a, H-7d/H-8d were confirmed by the NOE interactions between H-7a/H-2(6)a, H-8a/H-2(6)a, H-7d/H-2(6)d, H-8d/H-2(6)d in the NOESY spectrum. Based on consideration of the biosynthesis of naturally occurring oligostilbenes (Sotheeswaran and Pasupathy, 1993) the absolute configuration of **2** was tentatively assigned as (7a*S*, 8a*S*, 7c*S*, 8c*R*, 7d*S*, 8d*S*).

Amurensin K (**3**) was obtained as a brown amorphous powder, exhibiting blue fluorescence under UV-254 light, $[\alpha]_D^{20}$ +195.3° (*c* 0.34, MeOH). A molecular formula of $C_{56}H_{40}O_{13}$ was determined from its high resolution FAB–MS *m*/*z* 921.2566 $[MH]^+$ (calc. for $C_{56}H_{41}O_{13}$, 921.2523), corresponding to a resveratrol tetramer with an extra oxygen atom. The ^1H NMR spectrum of **3** showed similar spectral patterns to those of vitisin A (Oshima et al., 1993) containing the signals of an ampelopsin A unit, except that resonances for two *trans* olefinic protons were not observed. The 37 degrees of unsaturation of **3** were one more degree than the 36 of vitisin A. Therefore, it was proposed that a five-membered ring could be formed between C-7c and C-10c, to account for the additional oxygen atom present in **3**. This supposition regarding the planar structure of **3** was confirmed by the CH long range couplings between H-8a/C-1a, 10a, 10b, H-7b/C-10a, 11a, 9b, H-8b/C-10b, 2c, H-8c/C-7c, 10c, H-12c/C-10c, 14c, H-8d/C-14c, 1d, 10(14)d observed in the HMBC spectrum. The NOEs observed between H-7d/H-10(14)d, and H-8d/H-2(6)d indicated a *trans* orientation for the H-7d and H-8d protons. The *trans* relationship between H-7a/H-8a was revealed by strong NOE between H-8a/H-2(6)a, and the NOEs between H-8a/H-2(6)b and H-8b/H-2(6)b confirmed the *trans* orientation between H-8a/H-7b as well as H-7b/H-8b. Thus, the absolute configuration of **3** could tentatively be assigned as (7a*S*, 8a*S*, 7b*S*, 8b*R*, 7d*S*, 8d*S*), considering the biosynthesis of the oligostilbenes.

Amurensin L (**4**) was obtained as a pale yellow amorphous powder, exhibiting strong white fluorescence under UV-254 light, $[\alpha]_D^{30}$ −116.5° (c 0.058, MeOH). The high resolution FAB–MS *m*/*z* 905.2587 $[MH]^+$ (calc. for $C_{56}H_{41}O_{12}$, 905.2598) gave a molecular formula of $C_{56}H_{40}O_{12}$, which together with the ^1H and ^{13}C NMR spectra suggested that **4** was a resveratrol tetramer. The UV spectrum (λ_{max} 340 nm) revealed the presence of a strong conjugated system in the structure. The ^1H and ^{13}C NMR spectral data (Table 2) of **4** were similar to those of heyneanol A (Li et al., 1996) except that **4** showed only four aliphatic proton signals for two dihydrobenzofuran moieties in the ^1H NMR spectrum and two quaternary carbon signals more than in heyneanol A in the ^{13}C NMR spectrum. This suggested that one dihydrobenzofuran moiety was transformed into an unsaturated benzofuran moiety in **4**, consequently the signals of H-2(6)d were shifted to lower field at δ 7.47. In the HMBC spectrum of **4**, long-range couplings between H-8a/C-9b, H-8a/C-10b, H-8b/C-9b, H-8b/C-10b indicated that rings A_3 and B_3 were dihydrobenzofuran rings, the ring D_3 was a benzofuran ring, and thus the planar structure of amurensin L was as shown in **4**. The relative stereochemistry of **4** was determined on the basis of NOESY experiments. The NOEs between H-7a and 10(14)a; H-7b and 14b; suggested a *trans* orientation of rings A_1 and A_2, and B_1 and B_2, respectively. The NOE between H-8a and H-8b suggested a *cis* orientation between these two protons. Since only (+)-ε-viniferin was isolated from this plant, the absolute configurations of **4** could tentatively be assigned as (7a*S*, 8a*S*, 7b*S*, 8b*S*).

Amurensin M (**5**), obtained as a greenish amorphous powder, exhibited strong white fluorescence under UV-254 light. The high resolution FAB–MS *m*/*z* 903.2484 $[MH]^+$ (calc. for $C_{56}H_{39}O_{12}$, 903.2442) was in agreement with a molecular formula of $C_{56}H_{38}O_{12}$, corresponding to a resveratrol tetramer. Its ^1H and ^{13}C NMR patterns were relatively simple in contrast to the molecular formula, and the presence of a strong ion peak at *m*/*z* 452 in FAB–MS indicated that **5** was composed of two equivalent units. The ^1H and ^{13}C NMR data were similar to those of amurensin H (Huang et al., 1999) except that two *meta*-coupled doublets in amurensin H were transformed into a singlet in **5**. Thus, it was proposed that **5** should be a dimer of amurensin H through formation of a bond between C-12b and C-12b′. This was substantiated by the appearance of a quaternary carbon signal at δ 104.0 in the ^{13}C NMR spectrum of **5**. Amurensin M is the first resveratrol tetramer with a completely unsaturated ring system.

Ampelopsin A (**6**) (Oshima et al., 1990) and balanocarpol (**7**) (Diyasena et al., 1985; Dai et al., 1998) shared the same planar structure. However, the chemical shifts of H-8a (δ 4.10), H-2(6)a (δ 7.07), C-7a (δ 88.4), C-8a (δ 49.5) and the coupling constant between H-7a/H-8a (11.4 Hz) in **6** (Huang and Lin, 1999) were markedly different from those (δ 5.14 for H-8a, δ 7.46 for H-2(6)a, δ 93.0 for C-7a, δ 52.2 for C-8a, *J* 7a, 8a = 9.2 Hz) in **7** (Diyasena et al., 1985). It was considered that a mere change in the *cis* or *trans* configuration between H-7b and H-8b of **6** and **7** would not result in all of these differences after reasonable analysis of the NMR spectral data for both **6** and **7**. Therefore, it was proposed that the conformations of ring B_3 in compounds **6** and **7** were different, one in a pseudo-boat conformation and the other in a pseudo-chair conformation. The NOE interactions (Fig. 1) between H-7a/H-14a, H-8a/H-2(6)a, H-8a/H-2(6)b, H-8b/H-2(6)b, H-8b/H-14b of **6** required ring B_3 to be in a preferred pseudo-boat conformation, while a preferred pseudo-chair conformation of ring B_3 in **7** would satisfy the NOEs between H-7a/H-2(6)a, H-7a/H-2(6)b, H-8a/H-8b, H-8a/H-14a, H-7b/H-8b of 7

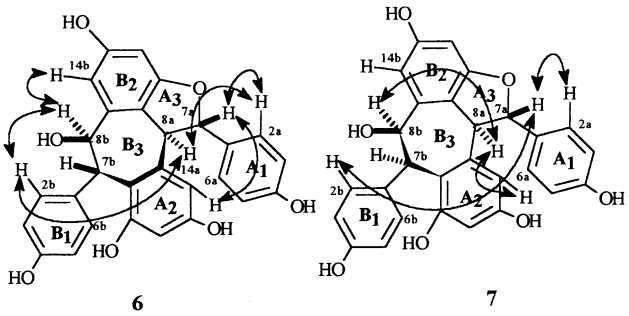

Fig. 1. Significant NOE interactions of compounds **6** and **7**.

(Fig. 1). The obvious downfield shifts of H-8a and H-2(6)a in **7** were due to the deshielding effect of ring A_2, and different conformation of ring B_3 were responsible for the variety of coupling constants between H-7a and H-8a in **6** and **7**. Thus, the stereostructures of **6** and **7** are suggested as shown. The energy-minimized conformations of compounds **6** and **7** were calculated with an Alchemy 3.0 molecular modeling program (Fig. 2), and the results confirmed the above deduction.

(+)-Hopeaphenol and isohopeaphenol were obtained as pale white amorphous powders, whose spectral data were identical with those reported previously (Ito et al., 1997). In both (+)-hopeaphenol and isohopeaphenol, the vicinal coupling constants between H-7b and H-8b were almost zero, H-7b and H-8b appearing as singlets. Consequently, it was impossible that the vicinal dihedral angles between H-7b and H-8b are nearly 90°in both (+)-hopeaphenol and isohopeaphenol if the conformations of ring B_3 were the same. The NMR spectral data of (+)-hopeaphenol and isohopeaphenol were similar to those of **6** and **7**, respectively. It was found that the pseudo-boat conformation of ring B_3 satisfied the 90° angle of *trans* H-7b and H-8b, and that the pseudo-chair conformation satisfied the 90° angle of *cis* H-7b and H-8b from molecular models. It was determined that ring B_3 had a pseudo-boat conformation in (+)-hopeaphenol and a pseudo-chair conformation in isohopeaphenol; (+)-hopeaphenol was the dimer of **6** and isohopeaphenol was the dimer of **7**.

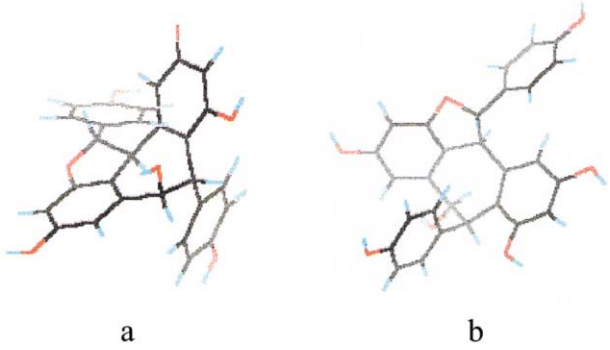

Fig. 2. Energy-minimized stereostructure of **6** with a pseudo-boat conformation (a) and **7** with a pseudo-chair conformation (b) (MM^+ calculation using the Alchemy 3.0 molecular modeling program).

The ^1H and ^{13}C NMR spectral data of vitisin A (Oshima et al., 1993) were the same as those of γ-2-viniferin (Korhammer et al., 1995). Consequently, it was suggeated that vitisin A and γ-2-viniferin had the same structure with a pseudo-boat conformation of the seven-membered ring. Considering that a part of its NMR spectral data were similar to those of **6**, the correct structure was determined to be vitisin A, and we concluded that the structure of γ-2-viniferin was erroneously elucidated. In the reported oligostilbenes containing a seven-membered ring, only isohopeaphenol was the analogue of **7**; and amurensin I reported in this paper was the second one, the others were analogues of **6**.

Since the alcoholic extract of the roots of *Vitis amurensis* showed anti-inflammatory activity, the activities of these tetramers on the inhibition of leukotriene B_4 (LTB_4) biosynthesis and histamine receptor antagonism were tested (Yang et al., 1995). (+)-Hopeaphenol, isohopeaphenol, vitisin A, (+)-vitisifuran A and heyneanol A exhibited a strong inhibitory effect on the biosynthesis of LTB_4 at concentrations of 10^{-5} mol L^{-1} with inhibitory rates of 56, 60, 63, 72 and 76%, respectively. The inhibitory rates of histamine receptor antagonism for compounds **1**, **2**, **4** and **5** at concentrations of 10^5 mol L^1 were 65, −45, −39, and 74%, respectively, compounds **1** and **5** showed potent activity.

3. Experimental

3.1. General experimental procedures

Optical rotations were determined on a Perkin-Elmer digital polarimeter. UV spectra were taken on a Shimadzu UV-300 spectrophotometer. IR spectra were run on a Perkin-Elmer 683 infrared spectrometer recorded in KBr pellet. The NMR spectra were carried out on a Bruker AM-500 using TMS as internal standard. The FAB–MS spectra were taken on an Autospec-Ulma-Tof mass spectrometer.

3.2. Plant material

The roots of *Vitis amurensis* Rupr. were collected from Huairou, Beijing in May 1997, and identified as *Vitis amurensis* by Professor W.Z. Song of our institute. A voucher specimen (97021) was deposited in the herbarium of the Institute of Materia Medica, Chinese Academy of Medical Sciences and Peking Union Medical College.

3.3. Extraction and isolation

Dried and powdered roots of *Vitis amurensis* (20 kg) were extracted with 95% EtOH. The extract was concentrated in vacuo to yield a gum (2.2 kg), which was

mixed with silica gel (60–100 mesh), and the column was eluted successfully with $CHCl_3$, EtOAc, Me_2CO, MeOH, respectively, to give four fractions. The EtOAc fraction (640 g) was subjected to silica gel column chromatography eluted with $CHCl_3$–MeOH (100:1–100:30) to give: A (27.5 g), B (30 g), C (25 g), D (230 g) and E (210 g). Fraction E was further divided into three fractions E_1–E_3 by column chromatography (ODS, RP-18, MeOH–H_2O = 6:4–4:6); (+)-hopeaphenol (840 mg, 0.0042%) and isohopeaphenol (680 mg, 0.0032%) were obtained from fraction E_1, and **1** (10 mg, 0.00005%) and **5** (18 mg, 0.00009%) from section E_2 by MPLC (ODS, RP-18, 40–63 μm, MeOH:H_2O of 4:6). Fraction D was further divided into fractions D_1–D_4 by column chromatography (silica gel, 100–200 mesh, cyclohexane—Me_2CO). Fraction D_1 was subjected to ODS RP-18 column eluted with MeOH–H_2O (6:4) to afford

Table 1
^1H and ^{13}C NMR spectral data for compounds **1** and **2**[a]

Position	**1**		**2**		
	^1H[b]	^{13}C[b]	^1H[c]	^1H[b]	^{13}C[d]
1a		133.9			131.9
2(6)a	7.63 *d* (8.5)	130.6	7.13 *d* (8.4)	7.21 *d* (8.4)	126.3
3(5)a	7.03 *d* (8.5)	116.6	6.76 *d* (8.4)	6.84 *d* (8.4)	115.1[e]
4a		158.7			157.2
7a	5.63 *d* (10.1)	93.8	5.33 *d* (4.5)	5.39 *d* (4.3)	92.5
8a	5.59 *d* (10.1)	54.3	4.34 *d* (4.5)	4.37 *br s*	55.8
9a		141.0			145.6
10a		118.3	6.04 *br s*	6.17 *d* (2.1)	105.2[f]
11a		158.7			158.5
12a	6.39 *d* (2.2)	103.2	6.07 overlap	6.17 *t* overlap	100.9
13a		156.9[e]			158.5
14a	6.35 *d* (2.2)	107.7	6.04 br s	6.17 *d* (2.1)	105.2[f]
1b		137.4			128.2
2(6)b	6.33 *d* (8.8)	129.9	6.62 *d* (8.6)	6.73 *d* (8.6)	127.0
3(5)b	6.22 *d* (8.8)	115.1	6.57 *d* (8.6)	6.64 *d* (8.6)	115.1[e]
4b		155.2			156.9
7b	5.52 *d* (4.5)	42.8	6.26 *d* (16.6)	6.30 *br d* (16.6)	132.8
8b	2.98 *dd* (4.5, 11.3)	57.3	6.06 *d* (16.6)	6.07 *br d* (16.6)	120.2
9b		141.4			131.5
10b		116.0			117.8
11b		160.3			161.0
12b	5.72 *d* (2.1)	94.9	6.25 *s*	6.28 *s*	90.6
13b		158.5			161.0
14b	4.42 *d* (2.1)	109.6			117.2
1c		136.2			130.8
2(6)c	6.37 *d* (8.6)	129.4	6.96 *d* (8.4)	7.04 *d* (8.5)	127.8
3(5)c	6.22 *d* (8.6)	114.7	6.72 *d* (8.4)	6.77 *d* (8.5)	115.2[e]
4c		155.5			157.1
7c	5.79 *d* (5.4)	42.5	4.92 *d* (7.7)	4.95 *br s*	90.6
8c	4.18 *dd* (5.4, 11.3)	51.0	4.55 *d* (7.7)	4.63 *d* (8.4)	54.6
9c		139.1			139.4
10c		118.3			118.4
11c		156.3			161.3
12c	6.70 *d* (1.9)	96.1	6.22 *br s*	6.29 *d* (2.2)	95.5
13c		158.0[f]			158.3
14c	6.26 *d* (1.9)	113.2	5.98 *br s*	6.15 *d* (2.2)	108.2
1d		127.4			132.1
2d		133.7	6.81 *d* (8.2)	6.7–6.9 *br*	127.4
3d	9.49 *d* (2.4)	115.9	6.52 *d* (8.2)	6.5–6.7 *br*	115.2[e]
4d		156.8[e]			157.4
5d	7.25 *dd* (8.7, 2.4)	116.1	6.52 *d* (8.2)	6.5–6.7 *br*	115.2[e]
6d	8.20 *d* (8.7)	121.6	6.81 *d* (8.2)	6.7–6.9 *br*	127.4
7d		151.6	5.13 *br s*	5.19 *br s*	92.1
8d		115.7	3.61 *br s*	3.60 *br s*	55.8
9d		133.6			146.5
10d		114.7	5.78 *br s*	5.91 *d*, (2.2)	105.0[f]
11d		156.3			158.4
12d	7.09 *s*	102.7	6.04 overlap	6.17 overlap	100.9
13d		157.9[f]			158.4
14d		112.3	5.78 *br s*	5.91 *d*, (2.2)	105.0[f]

[a] All assignments were confirmed by ^1H–^1H COSY, ^1H–^{13}C COSY, HMBC and NOESY spectra.
[b] In $(CD_3)_2CO$ at room temperature.
[c] In DMSO-d_6 at 100 °C.
[d] In DMSO-d_6 at room temperature.
[e] May be interchanged within the same column.
[f] May be interchanged within the same column.

Table 2
^1H and ^{13}C NMR spectra data for compounds **3**–**5**[a]

Position	3		4		5	
	^1H	^{13}C	^1H	^{13}C	^1H	^{13}C
1a		130.8		134.2		123.1
2(6)a	7.15 *d* (8.6)	130.1	7.25 *d* (8.5)	127.9	7.35 *d* (8.7)	128.1
3(5)a	7.03 *d* (8.6)	116.0	6.90 *d* (8.5)	116.4	6.79 *d* (8.7)	115.8
4a		158.5		158.2[b]		157.9
7a	5.80 *d* (11.7)	88.5	5.41 *d* (4.6)	94.1		150.1
8a	4.24 *d* (11.7)	49.5	4.56 *d* (4.6)	57.0		117.0
9a		142.0		147.3		137.9
10a		120.0[b]	6.13 *d* (2.2)	107.0	6.58 *d* (2.1)	109.6
11a		158.7		160.1		160.3
12a	5.98 *d* (2.0)	100.9	6.22 *t* (2.2)	102.5	6.62 *t* (2.1)	102.8
13a		156.5				160.3
14a	6.21 *d* (2.0)	104.7	6.13 *d* (2.2)		6.58 *d* (2.1)	109.6
1b		135.0		132.4[c]		129.9
2(6)b	7.02 *d* (8.7)	128.8	6.66 *d* (8.7)	127.6	7.13 *d* (8.7)	128.5
3(5)b	6.66 *d* (8.7)	115.4	6.60 *d* (8.7)	115.9	6.67 *d* (8.7)	116.1
4b		156.5		157.8		157.9
7b	5.39 *d* (3.9)	40.7	5.53 *d* (4.6)	91.3	7.07 *d* (16.2)	128.9
8b	5.51 *d* (3.9)	41.4	4.35 *d* (4.6)	52.1	7.16 *d* (16.2)	122.5
9b		141.0		142.2		132.2
10b		120.1b		119.8		122.2
11b		160.2		162.5		153.8
12b	6.05 *d* (2.2)	96.1	6.31 *d* (2.1)	96.5		104.0
13b		157.8		160.3		153.9
14b	6.11 *d* (2.2)	109.9	6.18 *d* (2.1)	107.0	7.40 *s*	107.6
1c		122.2		130.0		
2c	6.56 *br s*	129.1	6.81 *br s*	126.1		
3c		133.2		132.5[c]		
4c		155.9		159.7		
5	6.85 *d* (8.4)	116.2	6.73 *d* (8.4)	110.6		
6c	7.33 *dd* (8.4, 2.2)	124.3	6.97 *dd* (8.4, 1.9)	126.0		
7c		158.8	6.78 *d* (16.2)	129.2		
8c	5.89 *s*	97.9	6.96 *d* (16.2)	123.4		
9c		127.7		132.7		
10c		140.0		122.2		
11c		143.1		155.9		
12c	6.32 *s*	94.0	6.88 d (2.1)	97.4		
13c		157.1		156.4		
14c		110.2	7.06 *d* (2.1)	107.6		
1d		133.1		123.4		
2(6)d	7.18 *d* (8.5)	128.3	7.47 *d* (8.9)	128.3		
3(5)d	6.81 *d* (8.5)	116.0	6.79 *d* (8.9)	116.2		
4d		158.2		158.3[b]		
7d	5.35 *d* (7.3)	94.0		150.2		
8d	4.43 *d* (7.3)	57.4		117.1		
9d		145.8		138.0		
10(14)d	6.20 *d* (2.2)	107.1	6.46 *d* (2.2)	109.9		
11(13)d		159.2		160.4		
12d	6.32 *t* (2.2)	102.4	6.56 *t* (2.2)	103.2		

[a] All assignments were confirmed by ^1H–^1H COSY, ^1H–^{13}C COSY, HMBC and NOESY spectra.
[b,c] May be interchanged within the same column.

vitisin A (25 mg, 0.00013%) and **4** (25 mg, 0.00013%), and was further purified by MPLC (ODS, RP-18, 40–63 μm, MeOH–H_2O = 5.5:4.5). Fraction D_2 was subjected to MPLC (ODS, RP-18, 40-63 μm, MeOH:H_2O of 1:1) to afford **2** (39 mg, 0.0002%) and **3** (14 mg, 0.00007%). (+)-Vitisifuran A (35 mg, 0.00018%) was obtained from fraction D_3 using the same method as above, and heyneanol A (10 g, 0.05%) from fraction C by column chromatography (silica gel, 100–200 mesh, cyclohexane:acetone, 1:1)

3.4. Amurensin I (*1*)

Brown amorphous powder; $[\alpha]_D^{20}$ −128.2° (*c* 0.12, MeOH); HRFAB–MS *m/z* 903.2385 $[MH]^+$ (calc. for $C_{56}H_{39}O_{12}$, 903.2442); UV λ_{max}^{MeOH} (log ε): 280 (4.5), 334 (4.0), 348 (4.1), 377 (3.5) nm; IR ν_{max}^{KBr}: 3359, 1693, 1612, 1512, 1450, 1365, 1221, 1173, 1134, 1082, 1007, 833 cm^{-1}; ^1H NMR and ^{13}C NMR spectral data, see Table 1.

3.5. Amurensin J (*2*)

Yellowish amorphous powder; $[\alpha]_D^{20}$ +174.9° (*c* 0.12, MeOH); HRFAB–MS *m/z* 907.2699 $[MH]^+$ (907.2755 calc. for $C_{56}H_{43}O_{12}$); UV λ_{max}^{MeOH} (log ε): 285 (4.4) 310 *sh* (4.2) nm; IR ν_{max}^{KBr}: 3410, 1614, 1514, 1446, 1338, 1238, 1157, 1122, 1080, 997, 833 cm^{-1}; ^1H NMR and ^{13}C NMR spectral data, see Table 1.

3.6. Amurensin K (*3*)

Brown amorphous powder; $[\alpha]_D^{20}$ +195.3° (c 0.34, MeOH); HRFAB–MS *m/z* 921.2566 $[MH]^+$ (921.2523 calc. for $C_{56}H_{41}O_{13}$); UV λ_{max}^{MeOH} (log ε): 285 (4.7), 310 (4.6), 320 (4.6) nm; IR ν_{max}^{KBr}: 3378, 1613, 1512, 1447, 1338, 1234, 1157, 998, 833 cm; ^1H NMR and ^{13}C NMR spectral data, see Table 2.

3.7. Amurensin L (*4*)

Pale yellow amorphous powder, $[\alpha]_D^{30}$ −116.5° (*c* 0.058, MeOH). HRFAB–MS *m/z* 905.2587 $[MH]^+$ (905.2598 calc. for $C_{56}H_{41}O_{12}$); UV λ_{max}^{MeOH} (log ε): 285 (4.6), 340 (4.4) nm; IR ν_{max}^{KBr} cm^{-1}: 3386, 1697, 1612, 1516, 1442, 1336, 1236, 1153, 999, 835^{-1}; ^1H NMR and ^{13}C NMR spectral data, see Table 2.

3.8. Amurensin M (*5*)

Greenish amorphous powder; HRFAB–MS *m/z* 903.2484 $[MH]^+$ (903.2442 calc. for $C_{56}H_{39}O_{12}$); UV λ_{max}^{MeOH} (log ε): 316 (4.6), 338 (4.6), 380 (4.6) nm; IR ν_{max}^{KBr}: 3379, 1603, 1512, 1439, 1367, 1236, 1171, 1078, 997, 837 cm^{-1}; ^1H NMR and ^{13}C NMR spectral data, see Table 2.

Acknowledgements

This research program was supported by the National Natural Science Foundation of China. The authors are grateful to Professor X.T. Liang of our institute for valuable advice on structural elucidation. The authors also thank Lin-Ning Yu and Man Kong of the Department of Instrumental Analysis, Institute of Materia Medica, Chinese Academy of Medical Sciences and Peking Union Medical College, for the measurement of NMR spectra.

References

Coggon, P., Janes, N.F., King, F.E., King, T.J., Molyneux, R.J., Morgan, J.W.W., 1965. Hopeaphenol, an extractive of the heartwood of *Hopea ordorata* and *Balanocarpus heimii*. Journal of the Chemical Society, 406–409.

Coggon, P., King, T.J., Wallwork, S.C., 1966. The structure of hopeaphenol. JCS Chemical Communication, 439–440.

Dai, J.-R., Hallock, Y.F., Cardellina II, J.H., Boyd, M.R., 1998. HIV-inhibitory and cytotoxic oligostilbenes from leaves of *Hopea malibato*. Journal of Natural Products 61, 351–353.

Diyasena, M.N.C., Sotheeswaran, S., Surendrakumar, S., Balasubramanian, S., Bokel, M., Kraus, W., 1985. Balanocarpol, a new polyphenol from *Balanocarpus zeylanicus* (Trimen) and *Hopea jucunda* (Thw.) (Dipterocarpaceae). Journal of the Chemical Society, Perkin Trans I, 1807–1809.

Huang, K.S., Lin, M., 1999. Oligostilbenes from the roots of *Vitis amurensis*. Journal of Asian Natural Products Research 2, 21–28.

Huang, K.S., Lin, M., Wang, Y.-H., 1999a. Synthesis of amurensin H, a new resveratrol dimer from the roots of *Vitis amurensis*. Chinese Chemical Letters 10, 817–820.

Huang, K.-S., Lin, M., Yu, L.N., Kong, M., 2000. Four novel oligostilbenes from the roots of *Vitis amurensis*. Tetrahedron 56, 1231–1239.

Ito, J., Niwa, M., Oshima, Y., 1997. A new hydroxystilbene tetramer named isohopeaphenol from *Vitis vinifera* 'Kyohou'. Heterocycles 45, 1809–1813.

Ito, J., Takaya, Y., Oshima, Y., Niwa, M., 1999. New oligostilbenes having a benzofuran from *Vitis vinifera* 'Kyohou'. Tetrahedron 55, 2529–2544.

Kawabata, J., Fukushi, E., Hara, M., Mizutani, J., 1992. Detection of connectivity between equivalent carbons in a C2 molecule using isotopomeric asymmetry: identification of hopeaphenol in *Carex pumila*. Magnetic Resonance in Chemistry 30, 6–10.

Korhammer, S., Reniero, F., Mattivi, F., 1995. An oligostilbene from *Vitis* roots. Phytochemistry 38, 1501–1504.

Li, W.W., Ding, L.S., Li, B.G., Chen, Y.Z., 1996. Oligostilbenes from *Vitis heyneana*. Phytochemistry 42, 1163–1165.

Li, W.W., Li, B.G., Chen, Y.Z., 1998. Flexuosol A, a new tetrastilbene from *Vitis flexuosa*. Journal of Natural Products 61, 646–647.

Oshima, Y., Deno, Y., Hikino, H., Yang, L.-L., Yen, R.-Y., 1990. Ampelopsins A, B and C, new oligostilbenes of *Ampelopsis brevipedunculata* var. *hancei*. Tetrahedron 46, 5121–5126.

Oshima, Y., Kamijou, A., Moritani, H., Namao, K., Ohizumi, Y., 1993. Vitisin A and *cis*-vitisin A, strongly hepatotoxic plant oligostilbenes from *Vitis coignetiae* (Vitaceae). Journal of Organic Chemistry 58, 850–853.

Sotheeswaran, S., Pasupathy, V., 1993. Distribution of resveratrol oligostilbenes in plants. Phytochemistry 32, 1083–1092.

Yang, D.X., He, K.Q., Cheng, G.F., 1995. Effect of tremulacin on actions of SRS-A and histamine. Acta Pharmaceutica Sinica 30, 254–257.

PERGAMON

Phytochemistry 58 (2001) 363–367

PHYTOCHEMISTRY

www.elsevier.com/locate/phytochem

Triterpenoids from *Adiantum caudatum*

Keiko Tsuzuki[a], Ayumi Ôhashi[a], Yôko Arai[a], Kazuo Masuda[a], Akihito Takano[a], Kenji Shiojima[a,*], Hiroyuki Ageta[a], Shao-Qing Cai[b]

[a]*Shôwa Pharmaceutical University, 3-Chome, Higashitamagawagakuen, Machida, Tokyo 194-8543, Japan*
[b]*Beijing Medical University, Beijing, China*

Received 11 September 2000; received in revised form 31 January 2001

Abstract

Three triterpenoids, 8α-hydroxyfernan-25,7β-olide, 3α-hydroxy-4α-methoxyfilicane and 19α-hydroxyferna-7,9(11)-diene were isolated from the fresh fronds of *Adiantum caudatum*. Their structures were elucidated by spectroscopic techniques. Thirteen known triterpenoids were also identified from this fern. © 2001 Elsevier Science Ltd. All rights reserved.

Keywords: *Adiantum caudatum*; Adiantaceae; Triterpenoid; 9α-Hydroxyfernan-25,7β-olide; 3α-Hydroxy-4β-methoxyfilicane; 19α-Hydroxyferna-7,9(11)-diene

1. Introduction

In the course of chemotaxonomic studies of Adiantaceous ferns, we reported the presence of a large number of triterpenoids belonging to hopane and migrated hopane skeleta (Ageta et al., 1964, 1966, 1968; Ageta and Iwata, 1966). Recently we reported a triterpenoid ether having a fernane skeleton from *A. cuneatum* Langsd. et Fisch (Shiojima et al., 1997a,b,c; Nakane et al., 1999). In a continuation of our study, we have now investigated *Adiantum caudatum* L. (cultivated), resulting in the isolation of three new triterpenoids, characterized as 8α-hydroxyfernan-25,7β-olide (**1**), 3α-hydroxy-4β-methoxyfilicane (**2**) and 19α-hydroxyferna-7,9(11)-diene (**3**), along with 13 known triterpenoids. We report herein the isolation of the constituents and structure elucidation of **1**, **2** and **3**.

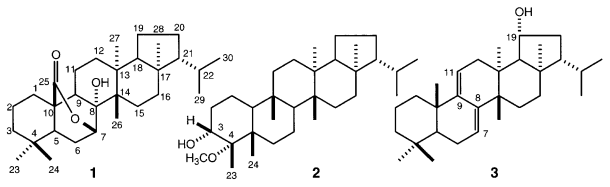

2. Results and discussion

The dried fronds of *A. caudatum* were extracted with *n*-hexane and the extract was subjected to silica gel chromatography generating seven fractions. The individual fractions were subjected to rechromatography and preparative HPLC to obtain a total of 16 compounds: new compounds **1**–**3**, and known triterpenoids; neohop-13(18)-ene (**4**), fern-7-ene (**5**), fern-8-ene (**6**), fern-9(11)-ene (**7**), ferna-7,9(11)-diene (**8**), filic-3-ene (**9**), 17β,21β-epoxyhopane (**10**), adiantone (**11**), isoadiantone (**12**), 19α-hydroxyfern-7-ene (**13**), 19α-hydroxyfern-9(11)-ene (**14**), 19α-hydroxyfern-9(11)-ene (**15**) and 19α-hydroxyadiantone (**16**). Known triterpenoids (**4**–**16**) were identified with authentic samples.

Compound **1**, mp 268–271°C, $[\alpha]_D^{23}$ −21.6°, (EtOH; *c* 0.4) was obtained as colorless needles, and its molecular formula was found to be $C_{30}H_{48}O_3$ by high resolution MS (HR–MS M^+ at *m*/*z* 456.3604, calc. 456.3603). Its IR spectrum showed absorption at γ_{max}^{KBr} cm^{-1}; 3470 and 1730 due to a hydroxyl and a six membered ring lactone groups. The ^1H NMR spectra of **1** indicated the presence of five tertiary and two secondary methyl groups, and a methine proton attached to oxygen (Table 1). As the ^1H (Table 1) and ^{13}C (Table 2) NMR spectroscopic data of **1** were not conclusive in the determination of the structure of the compound, its 2D NMR spectra were recorded. Detailed analysis of the heteronuclear multiple bond correlation (HMBC) spectrum of the compound

* Corresponding author. Tel.: +81-3-42-721-1595; fax: +81-3-42-721-1595.
E-mail address: y-arai@ac.shoyaku.ac.jp (K. Shiojima).

0031-9422/01/$ - see front matter © 2001 Elsevier Science Ltd. All rights reserved.
PII: S0031-9422(01)00198-4

Table 1
^{1}H NMR spectral data[b] for **1**, **2** and **3** (500 MHz, $CDCl_3$, δ)

Proton	1	2	3
23	0.848 *s*	1.153 *s*	0.862 *s*
24	0.883 *s*	1.084 *s*	0.916 *s*
25	–	0.887 *s*	0.916 *s*
26	1.153 *s*	0.887 *s*	0.885 *s*
27	1.088 *s*	0.965 *s*	1.089 *s*
28	0.758 *s*	0.780 *s*	1.110 *s*
29	0.848 *d* (6.4)[a]	0.881 *d* (6.7)	0.939 *d* (6.4)
30	0.824 *d* (6.4)	0.822 *d* (6.7)	0.864 *d* (6.4)
3	–	3.803 *dd* (2.8, 2.9)	
5α	1.66 *s*	–	–
7α	4.315 *dd* (4.5, 4.5)	–	5.436 *dd* (2.6, 2.6)
9α	2.71 *s*	–	
11	–	–	5.195 *dd* (2.4, 2.4)
19β	–	–	4.347 *dd* (8.2, 5.8, 2.6)
OMe	–	3.176 *s*	–

[a] Multiplicity and coupling constant (*J*, Hz) are shown in parentheses.

[b] Assignments were made on the basis of distortionless enhancement by polarization transfer (DEPT), ^{1}H–^{1}H COSY, ^{1}H–^{13}C COSY, HMBC and NOESY spectra.

revealed that it possesses a fernane skeleton (partial structure as obtained from HMBCs shown in Fig. 1) with an unusual lactone linkage between C-25 and C-7, and a hydroxyl group at C-8 of the molecule as would be evident from the two- and three-bond correlation of protons with the carbons viz.: δ 1.66 (H-5α) with 33.39 (C-4), 29.71 (C-6), 66.60 (C-7), 46.77 (C-9), 50.00 (C-10), 20.47 (C-23), 32.03 (C-24) and 179.70 (C-25); δ 4.315 (H-7α) with 45.49 (C-5), 29.71 (C-6), 88.38 (C-8) and 46.77 (C-9); δ 2.71 (H-9α) with 45.49 (C-5), 60.60 (C-7), 88.38 (C-8), 50.00 (C-10), 16.47 (C-11) and 179.70 (C-25), and δ 1.153 (H_3-26) with 88.38 (C-8), 36.97 (C-13), 44.06 (C-14) and 33.06 (C-15). The mass fragment ions at *m*/*z* (rel. int.) 441 $[M–CH_3]^+$ (14), 438 $[M–H_2O]^+$ (27), 423$[M–H_2O\text{-}CH_3]^+$ (45), 411 [**a**, $M–CO_2H]^+$ (31), 394 [**a**-OH]$^+$ (47), 379 [**a**-OH–$CH_3]^+$ (52), 285 [**b**]$^+$ (14), 241 [**b**-$CO_2]^+$ (43), 239 [**b**-HCOOH]$^+$ (39), 227 [**c**]$^+$ (56), 225 [**c**-H_2]+(37), 215[**d**]$^+$ (22), 213 [**d**-$H_2]^+$ (24), and 191 [**e**]$^+$ (100) (Fig. 2.) also supported the assigned structure. The relative stereochemistry at most of the chiral center of **1** was established by the NOE interactions observed in its NOESY spectrum as depicted in Fig. 1. Configuration of the tertiary hydroxyl group at C-8 was determined by the down field shifts of methyl proton signals at δ 1.153 (H_3-26, C-14) and δ.1.088 (H_3-27, C-13) compare with those of fernenes (Ageta et al., 1994). Thus, the structure of **1** was proved as 8α-hydroxyfernan-25,7β-olide.

Table 2
^{13}C NMR spectral data[a] (125 MHz, $CDCl_3$, δ)

Carbon	1	2	9	3	8
1	18.38	15.27	17.50	37.44	37.44
2	27.83	30.54	27.22	19.09	19.10
3	41.61	71.21	120.30	42.42	42.46
4	33.39	79.30	144.33	36.66	33.35
5	45.49	42.69	38.44	48.51	48.54
6	29.71	33.60	38.73	24.27	24.25
7	66.60	17.43	18.27	118.64	117.37
8	88.38	48.57	49.36	146.42	146.24
9	46.77	37.40	37.62	140.43	140.00
10	50.00	50.74	57.16	33.34	33.35
11	16.47	35.67	35.20	112.64	113.27
12	31.41	28.54	28.47	36.79	37.51
13	36.97	39.03	39.06	37.34	36.86
14	44.06	40.21	40.22	41.09	40.17
15	33.06	29.04	29.13	28.49	28.56
16	35.41	35.76	35.66	37.55	36.19
17	42.63	42.77	42.77	42.42	43.08
18	54.41	51.77	51.76	56.13	52.32
19	20.22	19.91	19.93	71.76	20.15
20	28.14	28.44	28.42	42.05	28.32
21	59.43	60.10	60.09	59.70	59.68
22	30.71	30.79	30.77	30.48	48.57
23	20.47	13.89	17.94	32.83	30.76
24	32.03	18.24	20.65	22.07	22.07
25	179.70	20.58	20.61	20.44	22.14
26	19.45	16.08	16.08	20.83	20.89
27	22.97	15.83	15.65	16.58	16.62
28	14.78	16.37	16.34	16.58	14.03
29	22.07	21.95	21.95	22.23	23.01
30	22.91	22.91	22.91	22.97	20.41
OMe	–	49.80	–	–	

[a] Assignments were made on the bases of DEPT, ^{1}H–^{1}H COSY, ^{1}H–^{13}C COSY and HMBC spectra.

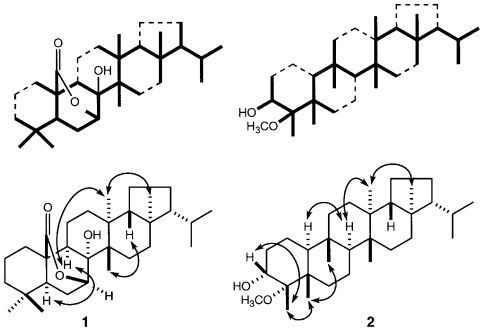

Fig. 1. Partial structures of **1** and **2** derived from HMBC spectrum and NOEs obtained from NOESY spectrum.

Compound **2**, $C_{31}H_{54}O_2$ (HR–MS; M^+ at *m*/*z* 458.4103, calc. 458.4124), mp 198–204°C, $[\alpha]_D^{23}$ +18.7° (EtOH; *c* 0.3), showed strong absorption bands at γ_{max}^{KBr} cm^{-1}; 3300 and 1080 for a hydroxyl group in its IR spectrum. Its ^{1}H NMR spectroscopic data (Table 1) displayed, besides the signals for six tertiary and two secondary methyl groups, a hydroxymethine proton at δ 3.803 (*dd* J = 2.8, 2.8 HZ) and OMe protons at δ 3.176.

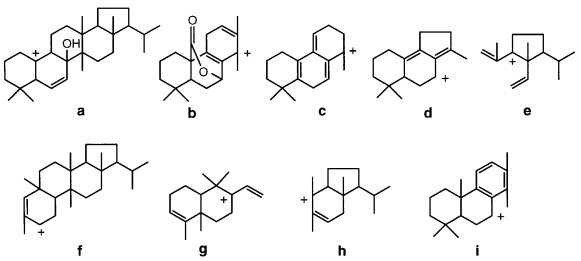

Fig. 2. MS fragment ions of **1**, **2** and **3**.

Its ^{13}C NMR chemical shifts were found to be close to those of filicane (**9**) (Table 2) except those of ring A carbons including that **2** might be a filicane derivative with an oxygen function located in ring A. Detailed analysis of the correlations observed in its HMBC spectrum revealed the presence of the partial structure shown in Fig. 1. Moreover the correlation of the OMe protons with C-3 (δ 71.2), C-4 (δ 79.3), C-5 (δ 42.7) and C-23 (δ 13.9) established that the OMe group is attached to C-4 and the OH group must be located at C-3. The above structural assignment was also supported from the mass spectrum which exhibited besides, the base peak at *m/z* 458 $[M]^+$, the other prominent peaks at *m/z* (rel. int.) 443 $[M–CH_3]^+$ (48), 341 $[\mathbf{f}]^+$ (78), 217 $[\mathbf{g}]^+$ (10), 205 $[\mathbf{h}]^+$ (34), and 191 $[\mathbf{e}]^+$ (28) (Fig. 2). Finally, the relative stereochemistry of **2** was deduced from its NOESY spectrum which showed NOEs connecting δ 3.80 (H-3β) — 1.15 (H_3-23) — 1.08 (H_3-24) — 0.88 (H_3-25), and δ 1.77 (H-10α) — 1.28 (H-8α) — 0.97 (H_3-27) — 0.780 (H_3-28) (Fig 1). Based on the above evidence, the structure of **2** can be represented as 3α-hydroxy-4-methoxyfilicane.

Compound **3**, mp 213–214°C, $[\alpha]_D^{23}$ −180.0°, $C_{30}H_{48}O$ (HR MS; M^+ at *m/z* 424.3704, calc. 424.3705) showed besides the signals for six tertiary and two secondary methyl groups, signals for a carbinyl proton at δ 4.35 (*ddd* J = 8.2, 5.8, 2.6 HZ) and two olefin protons at δ 5.2 (*dd* J = 2.4, 2.4 HZ) and 5.4 (*dd* J = 2.6, 2.6 HZ) in its ^1H NMR spectrum (Table 1). The diagnostic UV absorption bands λ_{max} nm (ε); 232 (30,900), 238 (28,400) and 247 (18,200) suggested that the two double bonds were conjugated and they constituted a heteroannular diene system (Ageta et al., 1964). A comparison its ^{13}C NMR spectrum (Table 2) with those of ferna-7,9(11)-diene (**8**) and 19α-hydroxyfern-9(11)-ene (**14**) (Tanaka et al., 1998) revealed that compound **3** possesses a 19-hydroxyferna-7,9(11)-diene structure. The configuration of the hydroxyl group at C-19 was established to be α by comparison of the chemical shift and coupling constant of H-19 of **3** at δ 4.35 (*ddd* J = 8.2, 5.8, 2.6 Hz) with those of **14** at δ 4.33 (*ddd* J = 8.2, 5.8, 2.6 Hz). The assigned structure of **3** was corroborated by its mass spectrum which showed formation of the diagnostic ion at *m/z* 255 $[\mathbf{I}]^+$ (52) (Fig. 2) (Shiojima et al., 1992). Based on the above observations, **3** could be represented by 19α-hydroxyferna-7,9(11)-diene.

Of these three new compounds, **1** seems to be the most interesting, since a triterpenoid with a lactone ring, as in **1**, has so far not been reported from fern species. The fact that the isolation of 19α-hydroxyadiantone (**16**) in the highest yield from this fern is next to from *Adiantum edgeworthii* HOOK (Shiojima and Ageta, 1994) might support the morphological close relation of both ferns. Also, adiantone (**11**) is the most common triterpenoid among *Adiantum* ferns.

3. Experimental

3.1. General

Uncorr. mps; EI–MS: 30 eV; TLC: on precoated Kiesel gel 60. ^1H NMR (270 MHz for identification and 500 MHz for structure determination) and ^{13}C NMR (125 MHz) spectra: in $CDCl_3$ (TMS as internal standard); HPLC: reversed phase C_{18} column, RI detector, CH_3CN: $CHCl_3$ (9:1); CC: Si gel 60 (230–400 mesh, Merck) and 20% $AgNO_3$-impregnated silica gel (Mallincrodt); GC: 1.4% SE-30 on Chromosorb G Oven: 260°C (cholestane as internal standard).

3.2. Plant material

The material was grown in the green-house of our university in September 1994. The fern is widely distributed in the Old World tropics and cultivated as a foliage plant. The voucher specimen has been deposited in the herbarium of Showa Pharmaceutical University, Tokyo.

3.3. Extraction and separation

The fresh fronds (2.96 kg) were cut into small pieces, then extracted (3×) with *n*-C_6H_{14} using the modified Soxhlet extraction method to give extract (27.3 g) together with separated aqueous filter (2 l). The extract was heated in C_6H_6 until reflux began this being maintained for 1 h. The resulting suspension was then allowed to stand at room temp. for 1 day. The insoluble materials were removed by filtration (fraction A, abbreviated as fr.A) and the filtrate was evaporated to dryness to afford a gummy residue which was subjected to silica gel chromatography to give seven fractions: fr. B (eluted with *n*-C_6H_{14}), fr. C [*n*-C_6H_{14}–C_6H_6 (8:2)], fr. D [*n*-C_6H_{14}–C_6H_6 (1:1)], fr. E (C_6H_6), fr. F [C_6H_6–Et_2O (9:1)] and fr. G and fr. H (Et_2O).

3.4. Isolation of 8α-hydroxyfernan-25,7β-olide (1)

Fr. F was applied to silica gel eluted with C_6H_6, with fractions of interest being subjected to preparative HPLC followed by crystallization from Et_2O–MeOH to give 8α-hydroxyfernan-25,7β-olide (**1**, 16 mg).

*3.4.1. 8α-Hydroxyfernan-25,7β-olide (**1**)*

Mp 268–271°C. $[\alpha]_D$ −21.6°, (EtOH; *c* 0.4). γ_{max} cm^{-1}; 3470 and 1730. EI–MS *m/z* (rel. int.): 456 $[M]^+$ (**15**), 441 $[M- CH_3]^+$ (14), 438 $[M- H_2O]^+$ (27), 423 $[M–H_2O–COCH_3]^+$ (45), 411 (31), 191 (100). EI–HRMS; M^+ *m/z* : 456.3604 (calc. for $C_{30}H_{48}O_3$: 456.3603). ^1H NMR and ^{13}C NMR spectral analysis: Tables 1 and 2.

*3.5. Isolation of 3α-hydroxy-4-methoxyfilicane (**2**), 19α-hydroxyferna-7,9(11)-diene (**3**) and, isolation and identification of other known oxidized triterpenoids*

Repeated recrystallization of fr. D from MeOH–$CHCl_3$ gave adiantone (**11**, 840 mg). The filtrate was evaporated and the residue was applied to silica gel, 20% $AgNO_3$-impregnated silica gel eluted with? Fractions of interest were then subjected to preparative HPLC followed by recrystallization from MeOH-$CHCl_3$ to give 17β,21β-epoxyhopane (**10**, 3 mg), isoadiantone (**12**, 5 mg), 19α-hydroxyfern-7-ene (**13**, 9 mg), 19α-hydroxyfern-9(11)-ene (**14**, 3 mg), 3α-hydroxy-4-methoxyfilicane (**2**, 3 mg), 19α - hydroxyfern - 9(11) - ene (**15**, 30mg) and 19α - hydroxyferna-7,9(11)-diene (**3**, 8 mg).

Chromatography of fr. A on silica gel eluted with C_6H_6–Ex_2O (9:1), followed by recrystallization of the fractions of interest from $CHCl_3$–MeOH gave 19α-hydroxyadiantone (**16**, 1.50 g) in pure form.

*3.5.1. 19α-Hydroxyferna-7,9(11)-diene (**2**)*

Mp 198–204°C. $[\alpha]_D$ +18.7° (EtOH; *c* 0.3). γ_{max} cm^{-1}; 3300 and 1080. EI–MS *m/z* (rel. int.): 458 $[M]^+$ (100), 443 $[M–CH_3]^+$ (48), 341 (78), 205 (34), 191 (28). λ_{max} nm (ε): 232 (30900), 238 (28400), 247 (18200). EI–HRMS; M^+ *m/z*: 458.4103 (calc. for $C_{31}H_{54}O_2$: 458.4124). ^1H NMR and ^{13}C NMR spectral analysis: Tables 1 and 2.

*3.5.2. 3α-Hydroxy-4-methoxyfilicane (**3**)*

Mp 213–214°C. $[\alpha]_D$ −180.0° (EtOH; *c* 0.3). EIMS *m/z* (rel. int.): 424 $[M]^+$ (100), 409 $[M–CH_3]+$(20), 406 $[M–H_2O]^+$ (14), 391 $[M–H_2O–CH_3]^+$ (26), 255 (52). EI–HRMS; M^+ *m/z*: 424.3704 (calc. for $C_{30}H_{48}O$: 424.3705). ^1H NMR and ^{13}C NMR spectral analysis: Tables 1 and 2.

*3.5.3. 17β,21β-Epoxyhopane (**10**)*

Mp 286–287°C. Compound **10** was identified by comparison with literature data (Shiojima et al., 1990).

*3.5.4. Adiantone (**11**)*

Mp 229–231°C. Compound **11** was identified by comparison with literature data (Ageta and Iwata, 1966).

*3.5.5. Isoadiantone (**12**)*

Mp 236–237°C. Compound **12** was identified by comparison with literature data (Ageta and Iwata, 1966).

*3.5.6. 19α-Hydroxyfern-7-ene (**13**)*

Mp 244–246°C. Compound **13** was identified by comparison with literature data (Tanaka et al., 1998).

*3.5.7. 19α-Hydroxyfern-9(11)-ene (**14**)*

Mp 254–255°C. Compound **14** was identified by comparison with literature data (Tanaka et al., 1998).

*3.5.8. 28-Hydroxyfern-9(11)-ene (**15**)*

Mp 159–161°C. Compound **15** was identified by comparison with literature data (Nakane et al., 1999).

*3.5.9. 19α-Hydroxyadiantone (**16**)*

Mp 281–283°C. Compound **16** was identified by comparison with literature data (Shiojima and Ageta, 1994).

3.6. Isolation and identification of triterpenoid hydrocarbons

Chromatography of Fr. B on 20% $AgNO_3$-impregnated silica gel using n-C_6H_{14} as eluant, followed by recrystallization from Me_2CO gave six triterpenoid hydrocarbons in pure form viz. neohop-13(18)-ene (**4**, 4 mg), fern-7-ene (**5**, 141 mg), fern-8-ene (**6**, 3 mg), fern-9(11)-ene (**7**, 23 mg), ferna-7,9(11)-diene (**8**, 8 mg) and filic-3-ene (**9**, 322 mg). Compounds **4**–**9** were identified by direct comparison with literature data (Ageta et al., 1994).

*3.6.1. Neohop-13(18)-ene (**4**)*

Mp 194–195°C.

*3.6.2. Fern-7-ene (**5**)*

Mp 213–214°C.

*3.6.3. Fern-8-ene (**6**)*

Mp 190–191°C.

*3.6.4. Fern-9(11)-ene (**7**)*

Mp 170–171°C.

*3.6.5. Ferna-7,9(11)-diene (**8**)*

Mp 200–202°C.

*3.6.6. Filic-3-ene (**9**)*

Mp 232–234°C.

Acknowledgements

We thank Mr. Y. Takase and Dr. Hideki Suzuki of the Central Analysis Center of our university for the measurements of MS and NMR spectra.

References

Ageta, H., Iwata, K., Natori, S., 1964. Fern constituents: adianene, filicene, 7-fernene, isofernene and diploptene, triterpenoid hydrocarbons isolated from *Adiantum monovhlamys*. Tetrahedron Letters, 3413–3418.

Ageta, H., Iwtata, K., Arai, Y., 1966. Fern constituents: hydroxyadiantone and ketohakonanol isolated from *Adiantum monovhlamys*. Tetrahedron Letters, 5679–5684.

Ageta, H., Iwata, K., 1966. Fern constituents: adipedatol and other triterpenoids isolated from *Adiantum pedatum*. Tetrahedron Letters, 6069–6074.

Ageta, H., Shiojima, K., Arai, Y. 1968. Fern consituents: neohopene, hopene II, neohopadiene and fernadiene isolated from *Adiantum* species. JCS Chemical Communications, 1105–1107.

Ageta, H., Shiojima, K., Arai, Y., Suzuki, H., Kiyotani, T., 1994. NMR spectra of triterpenoid II. Hopenes and migrated hopenes. Chemical and Pharmaceutical Bulletin (Tokyo) 42, 39–44.

Nakane, T., Arai, Y., Masuda, K., Ishizaki, Y., Ageta, H., Shiojima, K., 1999. Fern constituents: six new triterpenoid alcohols from *Adiantum capillus-veneris*. Chemical and Pharmaceutical Bulletin (Tokyo) 47, 543–547.

Shiojima, K., Masuda, K., Ageta, H., 1990. Ozone-oxidation products of triterpenoid hydrocarbons belonging to the hopane and migrated hopane series. Chemical and Pharmaceutical Bulletin (Tokyo) 38, 79–85.

Shiojima, K., Arai, Y., Masuda, K., Takase, Y., Ageta, T., Ageta, H., 1992. Mass spectra of pentacyclic triterpenoids. Chemical and Pharmaceutical Bulletin (Tokyo) 40, 1683–1690.

Shiojima, K., Ageta, H., 1994. Fern constituents: triterpenoids isolated from the leaves of *Adiantum edgeworthii*. Structure of 19a-hydroxyadiantone and fern-9(11)-en-25-oic acid. Chem. Pharm. Bull. 42, 45–47.

Shiojima, K., Arai, Y., Nakane, T., Ageta, H., 1997. Fern constituents: *Adiantum cuneatum* I. Three new triterpenoids, glaucanol-B acetate, 7b,25-epoxyfern-8-ene and 25-norfern-7-en-10b-yl formate. Chemical and Pharmaceutical Bulletin (Tokyo) 45, 636–638.

Shiojima, K., Arai, Y., Nakane, T., Ageta, H., 1997. Fern constituents: *Adiantum cuneatum* II. Six new triterpenoids, neohop-18-en-12a-ol, 13-epineohop-18-en-12a-ol, neohop-13,18-en-19a-ol, fern-7-en-25-ol, fern-9(11)-en-25-ol and adian-5-en-25-ol. Chemical and Pharmaceutical Bulletin (Tokyo) 45, 639–642.

Shiojima, K., Arai, Y., Nakane, T., Ageta, H., Cai, S.-Q., 1997. Fern constituents: *Adiantum cuneatum* III. Four new triterpenoids, 4,23-Bisnor-3,4-secofilic-5(24)-en-3-al, 4,23-bisnor-3,3-dimethoxy-3,4-secofilic-5(24)-ene, 7b-25-epoxyfern-9(11)-en-8a-ol and 7a,8a-epoxyfernan-25-ol. Chemical and Pharmaceutical Bulletin (Tokyo) 45, 1608–1610.

Tanaka, Y., Kitajima, J., Ageta, H., 1998. Pharmacognostical studies on "Ku-tui-po" III. Constituents of the rhizomes of *Davallia solida*. Natural Medicines 52, 409–413.

PERGAMON

Phytochemistry 58 (2001) 369–374

PHYTOCHEMISTRY

www.elsevier.com/locate/phytochem

Taxane diterpenoids from the bark of *Taxus yunnanensis*

Shenghong Li[a], Hongjie Zhang[b,1], Ping Yao[b], Handong Sun[a], Harry H.S. Fong[b,*]

[a]*Laboratory of Phytochemistry, Kunming Institute of Botany, Academia Sinica, Kunming 650204, Yunnan, China*
[b]*Program for Collaborative Research in the Pharmaceutical Sciences, College of Pharmacy, University of Illinois at Chicago, 833 S. Wood Street, Chicago, IL 60612, USA*

Received 30 August 2000; received in revised form 4 April 2001

Abstract

Further investigation on the alcohol extract of the barks of *Taxus yunnanensis* led to the isolation of four taxoids, namely, 7β-xylosyl-taxol D, taxuyunnanines P, Q and R, along with the known taxuyuntin G (**2**). Four are rearranged taxoids with an 11(15→1)-*abeo*taxoid skeleton and an opened oxetane ring moiety. Structures were determined by spectroscopic and chemical means. © 2001 Elsevier Science Ltd. All rights reserved.

Keywords: *Taxus yunnanensis*; Taxaceae; Bark; *abeo*Taxoids; 7β-Xylosyl-taxol D; Taxuyunnanines P–R; Taxuyuntin G

1. Introduction

Since the discovery of the anticancer agent paclitaxel in 1971 (Wani et al., 1971), nearly 400 taxoids have been reported. Our previous studies on *Taxus yunnanensis* Cheng et L.K. Fu have resulted in the isolation of paclitaxel, and 41 other taxoids from the root (Zhang et al., 1993, 1994a,b, 1995a,b, 1997; Xiang et al., 1999); two new bacctin III type (Li et al., 1998) and five new rearranged taxoids (Li et al., 2000) from the bark. Investigation on the more polar part of the alcohol extract of the bark of *T. yunnanensis* afforded a new paclitaxel related compound, 7β-xylosyl-taxol D (**1**), and three new 11(15→1)-*abeo*-taxoids, taxuyunnanines P–R (**3**–**5**), together with a known *abeo*taxoid, taxuyuntin G (**2**) (Fig. 1). This paper deals with the isolation and structure elucidation of these compounds.

2. Results and discussion

7β-Xylosyl-taxol D (**1**) was assigned a molecular formula of $C_{49}H_{61}NO_{18}$ based on its HRFABMS (*m*/*z* 952.4054 ($[M+H]^+$, calc. 952.3967). The ^1H NMR (Table 1) spectrum showed the presence of four characteristic taxane methyl (δ 1.17, 1.16, 1.95 and 1.72) and two acetyl methyl (δ 2.34 and 2.18) groups; a xylosyl group, and a complex side chain of *N*-butanoylphenylisoserine as found in taxol D and its derivatives (Appendino et al., 1994; Guo et al., 1995). A detailed comparison of the ^1H NMR spectral data of **1** and those of 7β-xylosyl-10-deacetyl-taxol D (Guo et al., 1995) indicated that, except for the existence of an additional acetyl group in **1**, the two compounds were very much alike. In the lowfield region, the sharp proton signal at δ 5.37 (1H, *s*) of 7β-xylosyl-10-deacetyl-taxol D was found to have shifted to δ 6.50, which suggested that the additional acetyl group in **1** is positioned at C-10. Since the ^{13}C NMR data of 7β-xylosyl-10-deacetyl-taxol D are not available in the literature for comparative purposes, ^{13}C and 2D NMR (including ^1H–^1H COSY, HMQC, HMBC) experiments were carried out to confirm the proposed structure for **1** and for its unambiguous assignments. The presence of an acetoxy group at C-10 was confirmed by the ^1H–^{13}C long-range correlation of H-10 with an acetyl carbonyl carbon in the HMBC spectrum.

Compound **2** was identified as the known taxayuntin G by comparison of its spectroscopic data (^1H and ^{13}C NMR and FABMS) with those previously reported in the literature (Yue et al., 1995).

Taxuyunnanine P (**3**), $C_{24}H_{38}O_{10}$ (HRFABMS: *m*/*z* 485.2401 ($[M-H]^+$, calc. 485.2487), showed both ester (1718 and 1271 cm^{-1}) and free hydroxyl (3399 cm^{-1}) absorptions in its IR spectrum. Its ^1H NMR spectrum

* Corresponding author. Tel.: +1-312-996-5972; fax: +1-312-413-5894.

E-mail addresses: zhanghj@uic.edu (H. Zhang), hfong@uic.edu (H.H.S. Fong).

[1] Also corresponding author. Tel.: +1-312-996-7868; fax: +1-312-413-5894.

0031-9422/01/$ - see front matter © 2001 Elsevier Science Ltd. All rights reserved.
PII: S0031-9422(01)00218-7

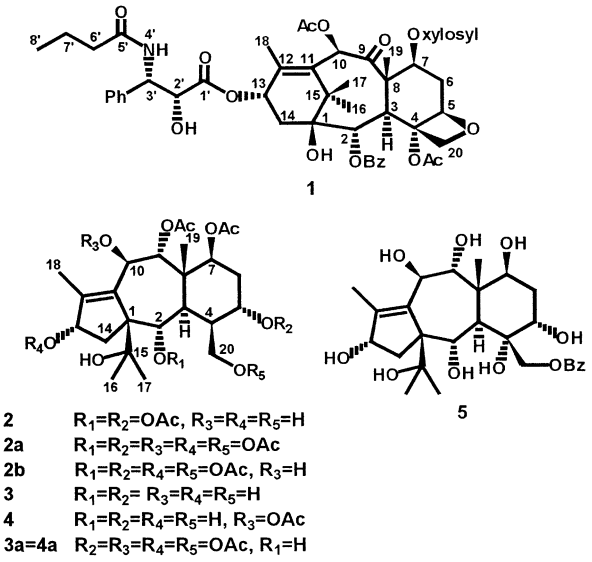

Fig. 1. Compounds **1**–**5** isolated from *Taxus yunnanensis*.

(Table 1) indicated the presence of four taxoid methyl groups at δ 1.40, 1.03, 1.85 and 1.02 (singlets) ascribable to Me-16, -17, -18 and -19, respectively, together with two acetyl methyl groups at δ 2.07 (3H, *s*) and 2.06 (3H, *s*). The ^{13}C NMR (Table 2) spectrum disclosed the existence of two olefinic quaternary carbons at δ 140.0 (C-11) and 145.8 (C-12), one oxygen-bearing quaternary carbon at δ 77.3 (C-15), and a quaternary carbon at δ 69.5 (C-1). These data suggested a 5/7/6 membered 11 (15→1)-*abeo*taxoid skeleton, which was confirmed by the long-range ^{1}H–^{13}C correlation of H-10 [δ 4.58 (1H, *d*, J = 10.1 Hz)] to C-1 in the HMBC spectrum. The COSY, HMQC and HMBC experiments showed that, unlike normal taxoids or *abeo*taxoids, the C-4 of **3** was a methine carbon instead of an oxygen-bearing quaternary carbon; and H-3 of **3** was a doublet of doublets rather than a simple doublet. The relationships of H-2/H-3/H-4/H_2-20 were well displayed in the ^{1}H–^{1}H COSY spectrum. Thus, **3**, like **2**, belongs to the rare group of *abeo*taxoids devoid of an oxygenated substituent at C-4. The opened oxetane ring system was inferred from the relatively highfield chemical shift of C-20 [δ 63.5 (*t*)] in the ^{13}C NMR spectrum and six double bond equivalents in its molecular formula. The downfield chemical shifts of H-7 [δ 5.38 (1H, *dd*, J = 4.8, 11.5 Hz)] and H-9 [δ 5.55 (1H, *brd*, J = 10.00 Hz)] in the ^{1}H NMR, combined with the HMBC correlations of H-7 and H-9 signals with the two carbonyl carbon resonances at δ 172.1 and 173.0, affixed the two acetyl groups to C-7 and C-9, respectively. The relative stereochemistry of **3** was established by comparison of its coupling constants with those of **2** (Yue et al., 1995). Thus, the structure of taxuyunnanine P was established as 7β, 9α-diacetoxy-2α, 5α, 10β, 13α, 15, 20-hexahydroxy-11(15→1)*abeo*taxa-11-*ene* (**3**).

Taxuyunnanine Q (**4**) has the molecular formula of $C_{26}H_{40}O_{11}$ as shown by its HRFABMS (*m*/*z* 527.2464 ([M–H]$^{+}$, calc. 527.2492). Analysis of the IR and NMR spectra (including ^{1}H, ^{13}C, COSY, HMQC and HMBC) (Tables 1 and 2) implied that **4** is an *abeo*taxoid related to **3**, differing in the presence of an additional acetyl

Table 1
^{1}H NMR spectral data of compounds **3**–**5** ([a] 400 MHz, [b]500 MHz, δ_H in ppm, J in Hz)

Proton	**3**[a]	**4**[a]	**5**[b]
H-2	4.47 (1H, *d*, 8.2)	4.52 (1H, *d*, 8.2)	4.49 (1H, *d*, 7.7)
H-3	2.57 (1H, *dd*, 4.7, 8.2)	2.50 (1H, *dd*, 4.7, 8.3)	2.62 (1H, *d*, 7.4)
H-4	2.19 (1H, *m*)	2.18 (1H, *m*)	
H-5	3.97 (1H, *brd*, 2.2)	3.99 (1H, *brd*, 2.3)	3.98 (1H, *brs*)
H-6a	1.88 (1H, *m*)	1.87 (1H, *m*)	1.91 (2H, *m*, H_2-6)
H-6b	1.67 (1H, *m*)	1.76 (1H, *m*)	
H-7	5.38 (1H, *dd*, 4.8, 11.5)	5.45 (1H, *dd*, 4.9, 11.4)	4.16 (1H, *dd*, 5.2, 11.0)
H-9	5.55 (1H, *brd*, 10.0)	5.66 (1H, *brd*, 10.1)	4.00 (1H, *d*, 10.4)
H-10	4.58 (1H, *d*, 10.1)	6.17 (1H, *d*, 10.7)	4.45 (1H, *d*, 10.0)
H-13	4.41 (1H, *t*, 7.5)	4.43 (1H, *t*, 7.4)	4.47 (1H, *t*, 8.8)
H-14a	4.41 (1H, *t*, 7.5)	2.33 (1H, *dd*, 7.7, 15.3)	2.05 (1H, *dd*, 6.9, 14.0)
H-14b	1.71 (1H, *dd*, 7.7, 14.6)	1.78 (1H, *dd*, 8.1, 14.3)	1.82 (1H, *dd*, 7.6, 14.1)
Me-16	1.40 (3H, *s*)	1.28 (3H, *s*)	1.36 (3H, *s*)
Me-17	1.03 (3H, *s*)	1.25 (3H, *s*)	1.08 (3H, *s*)
Me-18	1.85 (3H, *s*)	1.85 (3H, *s*)	1.86 (3H, *s*)
Me-19	1.02 (3H, *s*)	1.03 (3H, *s*)	1.29 (3H, *s*)
H-20a	3.84 (1H, *dd*, 5.4, 10.6)	3.86 (1H, *dd*, 6.0, 11.0)	4.96 (1H, *d*, 12.1)
H-20b	3.48 (1H, *dd*, 8.4, 10.5)	3.47 (1H, *dd*, 8.6, 10.4)	4.65 (1H, *d*, 12.0)
OAc	2.07 (3H, *s*)	2.03 (3H, *s*)	
	2.06 (3H, *s*)	1.97 (3H, *s*)	
		1.92 (3H, *s*)	
Obz			8.03 (2H, *d*, 7.4)
			7.59 (1H, *t*, 7.4)
			7.46 (2H, *t*, 7.5)

Table 2
^{13}C NMR spectral data of compounds **3**–**5** (125 MHz, δ_C in ppm)

Carbon	**3**[b]	**4**[b]	**5**[b]
1	69.5 *s*	69.3 *s*	69.5 *s*
2	66.6 *d*	67.3 *d*	69.5 *d*
3	41.7 *d*	41.1 *d*	44.8 *d*
4	47.2 *d*	47.2 *d*	77.6 *s*
5	68.9 *d*	68.8 *d*	69.8 *d*
6	33.6 *t*	33.4 *t*	34.9 *t*
7	71.5 *d*	71.3 *d*	70.5 *d*
8	45.1 *s*	45.3 *s*	44.1 *s*
9	81.2 *d*	78.4 *d*	81.7 *d*
10	68.2 *d*	70.4 *d*	70.1 *d*
11	140.0 *s*	135.9 *s*	139.9 *s*
12	145.8 *s*	151.3 *s*	145.9 *s*
13	78.5 *d*	77.8 *d*	78.3 *d*
14	40.3 *t*	40.6 *t*	39.8 *t*
15	77.3 *s*	77.9 *s*	77.6 *s*
16	27.0 *q*	27.3 *q*	26.6 *q*
17	28.0 *q*	28.0 *q*	28.2 *q*
18	11.3 *q*	11.9 *q*	11.3 *q*
19	14.5 *q*	14.4 *q*	15.3 *q*
20	63.5 *t*	63.5 *t*	67.0 *t*
OAc	173.0 *s*; 172.1 *s*	172.1 *s*; 171.8 *s*; 170.2 *s*	
	21.8 *q*; 21.5 *q*	21.6 *q*; 21.0 *q*; 20.8 *q*	
OBz-1′			168.2 *s*
2′			131.4 *s*
3′			130.7 (2C, *d*)
4′			129.5 (2C, *d*)
5′			134.3 *d*

group at C-10. In the ^1H NMR spectrum, the H-10 signal moved downfield from δ 4.58 (1H, *d*, $J=10.1$ Hz) in **3** to δ 6.17 (1H, *d*, $J=10.7$ Hz) in **4**. This assignment was confirmed by the HMBC cross-peak signal of H-10 to an acetyl carbonyl carbon at δ 170.2. Compound **4** was deduced to have the same relative stereochemistry as **3** by virtue of their similar coupling patterns, and was identified as 7β, 9α, 10β-triacetoxy-2α, 5α, 13α, 15, 20-pentahydroxy-11(15→1)*abeo*taxa-11-*ene* (**4**).

Theoretically, compounds **2**, **3** and **4** can be converted to the same heptacetate, which would confirm their proposed structures. Accordingly, they were subjected to acetylation experiments. Under normal conditions, only **2** yielded the expected heptacetate product (**2a**) plus a hexacetate (**2b**). Compounds **3** and **4** afforded the same hexacetate product (**3a**=**4a**) with the hydroxy group at C-2 remained unacetylated even under more vigorous conditions. The failure of **3** and **4** to form heptacetates may be caused by the steric hindrance around the 2-OH group or due to the formation of a hydrogen-bond between the 2-OH and one of the other oxy-groups.

Taxuyunnanine R (**5**), $C_{27}H_{37}O_{10}$ established by HR–FABMS: *m*/*z* 521.2371 $[M-H]^+$, calc. 521.2387. The IR spectrum showed carbonyl, hydroxyl and ester groups at 1711, 3385 and 1279 cm^{-1}, respectively. As in the case of isolates **2**–**4**, spectral features of 11(15→1)-*abeo*taxoids were clearly evident in the NMR (Tables 1 and 2) spectra of **5**. However, contrary to the protonated C-4 in **2**–**4**, the C-4 of **5** was an oxygenated quaternary carbon: the H-3 (δ 2.62) of **5** was a doublet instead of the doublet of doublet found in **2**–**4**; and the H_2-20 were a pair of AB doublets instead of two doublet of doublets. The downfield chemical signals of H_2-20 [δ 4.96 (1H, *ABd*, $J=12.1$ Hz) and 4.65 (1H, *ABd*, $J=12.0$ Hz)] suggested that the benzoxy group could be assigned to C-20. Confirmation for this linkage was achieved by a HMBC experiment, in which the H_2-20 and aromatic protons at δ 8.03 (2H, *d*, $J=7.4$ Hz) correlated with the carbonyl carbon signal at δ 168.2 simultaneously. It is interesting to note that although compound **5** possessed nine oxygenated carbons (one oxymethylene, six oxymethines and two oxyquaternary carbons), there was only one ester substitute group (benzoate) present. Normally, such a highly oxygenated taxane would contain two or more esterified substituents.

In order to determine the relative stereochemistry of compound **5**, a ROESY experiment was performed (Fig. 2). The orientation of the benzoxymethyl at C-4 was established as β due to the NOE correlation between H_2-20 and Me-19. NOE correlations of H-2 with Me-16, 17 and 19, H-7 with H-3, H-9 with H-2 and Me-19, H-10 with H-3 and Me-18, and H-13 with Me-16 and 17, fixed the orientation of the hydroxy groups at C-2, C-7, C-9, C-10 and C-13 as α-, β-, α-, β- and α-, respectively. The configuration of the 5-OH was assigned an α-orientation due to its small coupling constant (H-5, *brs*). Hence the structure of taxuyunnanine R was deduced as 20-benxoxyl-2α, 4α, 5α, 7β, 9α, 10β, 13α, 15-octahydroxy-11(15→1)*abeo*taxa-11-*ene* (**5**).

With the exception of **1**, the isolates obtained in this study belong to the rare 11(15→1)-*abeo*taxoids possessing an opened oxetane ring moiety. To-date, only a few such taxoids have been reported. Further, *abeo*taxoids with a C-4 methine are rarer still (Baloglu and Kingston, 1999; Parmar et al., 1999). To our knowledge, taxuyunnanine R is the most highly oxygenated *abeo*taxoid isolated to-date that contains only a single ester substituent.

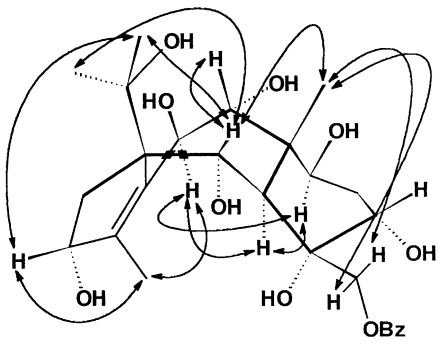

Fig. 2. Significant ROESY correlations of compound **5**.

3. Experimental

3.1. General

1D and 2D NMR experiments were performed either on a Bruker AM-400 or DRX-500 spectrometer. Unless otherwise specified, chemical shifts (δ) were expressed in ppm with reference to the solvent signals. FABMS and HRFABMS were taken on a VG Auto Spec-3000 or on a Finnigan MAT 90 instrument. IR spectra were recorded on a Bio-Rad FTS-135 spectrometer with KBr pellets. UV spectral data were obtained on a UV 210A spectrometer. Optical rotations were carried out on a HORIBA SEPA-300 High Sensitive Polarimeter or Perkin-Elmer model 241 Polarimeter. Column chromatography was performed either on Si gel (200–300 mesh, Qingdao Marine Chemical Inc., China), Si gel H (10–40 μm, Qingdao Marine Chemical Inc., China), Lichroprep RP_{18} gel (40–63 μm, Merck, Darmstadt, Germany), or on. MCI gel (70–150 μm, Mitsubishi Chemical Corporation, Tokyo, Japan). Fractions were monitored by TLC and spots were visualized by heating Si gel plates sprayed with 10% H_2SO_4 in EtOH.

3.2. Plant material

The barks of *T. yunnanensis* Cheng et L. K. Fu (Taxaceae) were collected in Lijiang Prefecture of Yunnan Province of Peoples Republic of China. A voucher specimen has been deposited at the Yunnan Academy of Forestry, Kunming, Yunnan, People's Republic of China.

3.3. Extraction and isolation

Dried bark (50 kg) was milled, extracted and fractionated by silica gel column chromatography as described previously. Briefly, the $CHCl_3$ fraction was successively chromatographed over three columns of silica gel. Fractions 14–29 from the third silica gel column were combined (4.9 g) and chromatographed on silica gel, eluted with $CHCl_3$–*iso*-PrOH (9:1) (Li et al., 2000). The more polar fractions obtained were combined and sequentially re-chromatographed on RP_{18} Si gel eluted with MeOH–H_2O (1:1) and acetonitrile–H_2O (2:8), and on silica gel eluted with petroleum ether–*iso*-PrOH (8:2) to yield compounds **1** (14 mg) and **2** (2 mg). A post Frs. 14–29 combined fraction (14.0 g) obtained from the third silica gel column referred to above was further fractionated successively on MCI gel with Me_2CO–H_2O (2:8), on silica gel with petroleum ether–*iso*-PrOH (8:2) and on silica gel with $CHCl_3$–*iso*-PrOH (7:1) as eluting solvents to provide compound **4** (5 mg). A second post Frs. 14–29 fraction (10.0 g) was also subjected to extensive chromatography on MCI gel using Me_2CO–H_2O (2:8), on silica gel using $CHCl_3$–MeOH (9:1), on silica gel using $CHCl_3$–*iso*-PrOH (5:1) and on RP_{18} gel using acetonitrile–H_2O (1:5) as eluents, stepwise, to afford Compounds **3** (13 mg) and **5** (3 mg).

7β-Xylosyl-taxol D (**1**): white powder, $[\alpha]_D^{28}$: −25.0° (*c* 0.25 MeOH). UV (MeOH) λ_{max} (log ε): 202 (4.3), 229 (4.2). IR (KBr) ν_{max} (cm^{-1}): 3440, 2935, 1723, 1654, 1519, 1453, 1373, 1316, 1247, 1179, 1106, 1071, 1048, 981, 709. Positive FABMS *m/z* (%): 952 ($[M+H]^+$, 4), 894 (2), 820 (1), 760 (1), 642 (2), 569 (1), 510 (2), 405 (2), 327 (4), 286 (16), 252 (35), 206 (16), 176 (7), 136 (12), 105 (100), 77 (15). HR–FABMS *m/z* 952.4054 ($C_{49}H_{62}NO_{18}$, calc. 952.4093). ^1H NMR (500 MHz, CD_3OD) δ: 5.65 (1H, *d*, *J* = 7.1 Hz, H-2), 3.82 (1H, *d*, *J* = 7.5 Hz, H-3), 4.97 (1H, *d*, *J* = 8.0 Hz, H-5), 2.68 (1H, *m*, H-6a), 1.92 (1H, *m*, H-6b), 4.27 (1H, *dd*, *J* = 6.9, 10.6 Hz, H-7), 6.50 (1H, *s*, H-10), 6.11 (1H, *t*, *J* = 9.2 Hz, H-13), 2.25 (1H, *m*, H-14a), 2.04 (1H, *m*, H-14b), 1.17 (3H, *s*, Me-16), 1.16 (3H, *s*, Me-17), 1.95 (3H, *s*, Me-18), 1.72 (3H, *s*, Me-19), 4.19 (2H, *m*, H_2-20), 4.58 (1H, *d*, *J* = 4.6 Hz, H-2′), 5.45 (1H, *d*, *J* = 4.6 Hz, H-3′), 2.27 (2H, *m*, H_2-6′), 1.61 (2H, *m*, H_2-7′), 0.91 (3H, *t*, *J* = 7.5 Hz, Me-8′), 2.34 (3H, *s*, 4-OAc), 2.18 (3H, *s*, 10-OAc); 3′-Ph: 7.41 (4H, *m*), 7.27 (1H, *t*, *J* = 7.0 Hz); 2-OBz: 8.10 (2H, *dd*, *J* = 1.5, 8.5 Hz), 7.66 (1H, *t*, *J* = 7.5 Hz), 7.56 (2H, *t*, *J* = 7.5 Hz); 7-xylosyl: 4.24 (1H, *d*, *J* = 7.3 Hz, H-1″), 3.06 (1H, *dd*, *J* = 7.4, 8.9 Hz, H-2″), 3.28 (1H, *t*, *J* = 8.9 Hz, H-3″), 3.42 (1H, *ddd*, *J* = 5.3, 8.8 Hz, 10.0, H-4″), 3.81 (1H, *dd*, *J* = 5.2, 11.5 Hz, H-5″a), 3.18 (1H, *dd*, *J* = 10.2, 11.5 Hz, H-5″b). ^{13}C NMR (125 MHz, CD_3OD) δ: 78.8 (*s*, C-1), 76.1 (*d*, C-2), 47.9 (*d*, C-3), 82.1 (*d*, C-4), 85.4 (*d*, C-5), 36.5 (*t*, C-6), 80.6 (*d*, C-7), 58.8 (*s*, C-8), 204.6 (*s*, C-9), 77.2 (*d*, C-10), 134.8 (*s*, C-11), 142.0 (*s*, C-12), 72.3 (*d*, C-13), 36.5 (*t*, C-14), 44.6 (*s*, C-15), 22.1 (*q*, Me-16), 26.9 (Me-17),14.9 (*q*, Me-18), 11.8 (*q*, Me-19), 77.5 (*t*, Me-20); 2-OBz: 167.6 (*s*), 131.3 (*s*),131.2 (2C, *d*), 129.7 (2C, *d*), 134.6 (*d*); OAc: 172.0 (*s*), 171.7 (*s*), 23.2 (*q*), 21.1 (*q*); C-13 side chain moiety: 174.4 (*s*, C-1′), 74.7 (*d*, C-2′), 56.8 (*d*, C-3′), 175.9 (*s*, C-5′), 20.4 (*t*, C-6′), 38.9 (*t*, C-7′), 14.0 (*q*, C-8′), 3′-Ph: 140.2 (*s*), 129.7 (2C, *d*), 128.4 (2C, *d*), 128.9 (*d*); 7-xylosyl moiety: 104.9 (*d*, C-1″), 74.8 (*d*, C-2″), 77.4 (*d*, C-3″), 70.9 (*d*, C-4″), 66.8 (*t*, C-5″).

Taxayuntin G (**2**): colorless prism. Negative FABMS *m/z* (%): 569 $[M-H]^+$ (100), 527 (18), 449 (8), 389 (10), 325 (8), 245 (4), 153 (11), 97 (6). ^1H NMR (400 MHz, acetone-d_6) δ: 5.78 (1H, *d*, *J* = 8.1 Hz, H-2), 2.84 (1H, *dd*, *J* = 4.4, 8.1 Hz, H-3), 1.95 (1H, *m*, H-4), 5.07 (1H, *brt*, *J* = 2.7 Hz, H-5), 1.93 (1H, *m*, H-6a), 1.73 (1H, *m*, H-6b), 5.25 (1H, *dd*, *J* = 4.9, 11.6 Hz, H-7), 5.61 (1H, *d*, *J* = 10.0 Hz, H-9), 4.61 (1H, *d*, *J* = 10.0 Hz, H-10), 4.55 (1H, *t*, *J* = 7.2 Hz, H-13), 2.18 (1H, *dd*, *J* = 7.1, 14.4 Hz, H-14a), 1.76 (1H, *dd*, *J* = 7.1, 14.4 Hz, H-14b), 1.19 (3H, *s*, Me-16), 0.95 (3H, *s*, Me-17), 1.93 (3H, *s*, Me-18), 1.04 (3H, *s*, Me-19), 3.44 (2H, *m*, H_2-20); OAc: 2.11, 2.07, 2.05, 2.03 (each in 3H of singlet). ^{13}C NMR (100 MHz, acetone-d_6) δ: 69.3 (*s*, C-1), 69.5 (*d*, C-2), 42.2 (*d*, C-3), 46.6 (*d*, C-4), 72.6 (*d*, C-5), 30.4 (*t*, C-6), 70.8 (*d*, C-7), 44.8 (*s*, C-8), 80.7 (*d*, C-9), 68.1 (*d*, C-10), 138.5 (*s*, C-

11), 145.8 (*s*, C-12), 77.5 (*d*, C-13), 41.1 (*t*, C-14), 76.6 (*s*, C-15), 25.5 (*q*, Me-16), 28.2 (*q*, Me-17), 11.2 (*q*, Me-18), 14.6 (*q*, Me-19), 62.0 (*t*, C-20); OAc: 173.3 (*s*), 172.7 (*s*), 172.2 (*s*), 171.9 (*s*), 21.6 (*q*, 2C), 21.3 (*q*, 2C).

Acetylation of **2**: The sample of **2** (2 mg) in dissolved in pyridine (0.3 ml) and Ac_2O (0.3 ml) was stirred for 24 h at room temperature, and worked-up to give a mixture (3 mg) of **2a** and **2b**, which was purified by Si gel CC, eluting with $CHCl_3$–Me_2CO (5:1) to provide **2a** (1 mg) and **2b** (1 mg). **2a**: Negative FABMS *m*/*z* (%): 695 $[M–H]^+$ (3), 653 (2), 554 (2), 461 (3), 369 (6), 276 (22), 244 (10), 184 (100), 151 (25), 192 (25), 59 (47). ^1H NMR (400 MHz, CD_3OD) δ: 5.91 (1H, *d*, $J=8.4$, H-2), 2.75 (1H, *dd*, $J=4.6$, 8.4, H-3), 2.13 (1H, *m*, H-4), 5.07 (1H, *brdd*, $J=2.7$, 5.3, H-5), 2.02 (1H, *m*, H-6a), 1.87 (1H, *m*, H-6b), 5.38 (1H, *dd*, $J=5.0$, 11.5, H-7), 5.87 (1H, *d*, $J=10.7$, H-9), 6.28 (1H, *d*, $J=10.7$, H-10), 5.66 (1H, *t*, $J=7.2$, H-13), 2.60 (1H, *dd*, $J=7.1$, 14.5, H-14a), 1.78 (1H, *dd*, $J=7.9$, 14.5, H-14b), 1.26 (3H, *s*, Me-16), 1.09 (3H, *s*, Me-17), 1.91 (3H, *s*, Me-18), 1.22 (3H, *s*, Me-19), 4.21 (1H, *dd*, $J=8.5$, 11.9, H-20a), 3.91 (1H, *d*, $J=11.8$, H-20b); OAc: 2.18 (3H, *s*), 2.11 (3H, *s*), 2.09 (3H, *s*), 2.06 (6H, *s*), 2.03 (3H, *s*), 1.98 (3H, *s*). **2b**: Negative FABMS *m*/*z* (%): 654 $[M]^+$ (5), 612 (1), 476 (6), 325 (3), 185 (5), 119 (6), 59 (100). ^1H NMR (400 MHz, CD_3OD) δ: 5.83 (1H, *d*, $J=8.2$ Hz, H-2), 2.79 (1H, *dd*, $J=4.5$, 8.2 Hz, H-3), 2.18 (1H, *m*, H-4), 5.05 (1H, *brdd*, $J=2.7$, 5.4 Hz, H-5), 2.03 (1H, *m*, H-6a), 1.81 (1H, *m*, H-6b), 5.30 (1H, *dd*, $J=5.0$, 11.7 Hz, H-7), 5.72 (1H, *d*, $J=10.2$ Hz, H-9), 4.68 (1H, *d*, $J=10.2$ Hz, H-10), 5.64 (1H, *t*, $J=7.0$ Hz, H-13), 2.40 (1H, *dd*, $J=7.0$, 14.4 Hz, H-14a), 1.75 (1H, *dd*, $J=7.7$, 14.4 Hz, H-14b), 1.23 (3H, *s*, Me-16), 1.07 (3H, *s*, Me-17), 1.93 (3H, *brd*, $J=0.8$ Hz, Me-18), 1.13 (3H, *s*, Me-19), 4.21 (1H, *dd*, $J=8.5$, 12.1 Hz, H-20a), 3.91 (1H, *d*, $J=11.9$ Hz, H-20b); OAc: 2.17 (3H, *s*), 2.11 (6H, s), 2.09 (3H, *s*), 2.07 (3H, *s*), 2.06 (3H, *s*).

Taxuyunnanine P (**3**): white powder, $[\alpha]_D^{28}$: −12.7° (*c* 0.65, MeOH). UV (MeOH) λ_{max} (log ε): 208 (4.1). IR (KBr) ν_{max} (cm^{-1}): 3399, 2928, 1718, 1653, 1440, 1376, 1271, 1159, 1061, 1028, 984, 943, 605. Negative FABMS *m*/*z* (%): 485 $[M–H]^+$ (47), 425 (30), 339 (92), 325 (100), 311 (63), 277 (19), 185 (55), 127 (15), 92 (57), 80 (18), 60 (15). HR–FABMS *m*/*z* 485.2401 ($C_{24}H_{37}O_{10}$, calc. 485.2387). ^1H NMR data: see Table 1. ^{13}C NMR data: see Table 2.

Taxuyunnanine Q (**4**): white powder, $[\alpha]_D^{28}$: −44.0° (*c* 0.25, MeOH). UV (MeOH) λ_{max} (log ε): 204 (4.4). IR (KBr) ν_{max} (cm^{-1}): 3413, 2935, 1748, 1654, 1438, 1374, 1261, 1067, 1031, 943, 903, 602. Negative FABMS *m*/*z* (%): 527 ($[M–H]^+$, 100), 468 (14), 409 (3), 345 (2), 311 (3), 244 (5), 152 (8). HR–FABMS *m*/*z* 527.2464 ($C_{26}H_{39}O_{11}$, calc. 527.2492). ^1H NMR data: see Table 1. ^{13}C NMR data: see Table 2.

Acetylation of **3** and **4**: samples of **3** or **4**, 2 mg each, was acetylated separately in 0.6 ml pyridine–Ac_2O (1:1) in the same manner as that of **2** to give **3a** (3 mg) and **4a** (3 mg) respectively. The 2-OH groups of **3** and **4** were not acetylated after 24 h. The ratio of Ac_2O–pyridine was then changed from 1:1 to 5:1, and then to 10:1, and the reaction was allowed to proceed for four days. However, the 2-OH remained unacetylated. **3a** and **4a**: Negative FABMS *m*/*z* (%): 654 $[M]^+$ (3), 536 (2), 475 (3), 415 (1), 339 (7), 119 (6), 59 (100). ^1H NMR (400 MHz, CD_3OD) δ: 4.53 (1H, *d*, $J=8.1$ Hz, H-2), 2.49 (1H, *dd*, $J=4.9$, 8.1 Hz, H-3), 2.28 (1H, *m*, H-4), 5.02 (1H, *brdd*, $J=2.8$, 5.2 Hz, H-5), 2.00 (1H, *m*, H-6a), 1.85 (1H, *m*, H-6b), 5.33 (1H, *dd*, $J=4.9$, 11.6 Hz, H-7), 5.69 (1H, *brd*, $J=10.3$ Hz, H-9), 6.19 (1H, *d*, $J=10.8$ Hz, H-10), 5.60 (1H, *t*, $J=7.5$ Hz, H-13), 2.43 (1H, *dd*, $J=7.2$, 14.5 Hz, H-14a), 1.69 (1H, *dd*, $J=7.9$, 14.5 Hz, H-14b), 1.31 (3H, *s*, Me-16), 1.28 (3H, *s*, Me-17), 1.84 (3H, *s*, Me-18), 1.04 (3H, *s*, Me-19), 4.23 (1H, *t*, $J=10.4$ Hz, H-20a), 4.31 (1H, *d*, $J=9.8$ Hz, H-20b); OAc: 2.12 (3H, *s*), 2.06 (3H, *s*), 2.04 (3H, *s*), 2.03 (6H, *s*), 1.99 (3H, *s*), 1.94 (3H, *s*).

Taxuyunnanine R (**5**): white powder, $[\alpha]_D^{28}$: −5.0° (*c* 0.10, MeOH). UV (MeOH) λ_{max} (log ε): 212 (4.2), 229 (4.3). IR (KBr) ν_{max} (cm^{-1}): 3385, 2978, 1711, 1610, 1452, 1279, 1177, 1113, 1068, 1027, 936, 784, 708, 611. Negative FABMS *m*/*z* (%): 521 ($[M–H]^+$, 100), 504 (13), 417 (19), 399 (11), 325 (22), 311 (19), 297 (8), 181 (36), 121(79), 71 (10), 59 (30). HR–FABMS *m*/*z* 521.2371 ($C_{27}H_{37}O_{10}$, calc. 521.2387). ^1H NMR data: see Table 1. ^{13}C NMR data: see Table 2.

Acknowledgements

The authors wish to thank the members of the analytical group of the Phytochemistry Laboratory of Kunming Institute of Botany, Academic Sinica, for measurement of the spectral data. This project was supported by grants from the National Science Foundation of China (3950081), the Young Academic and Technical Leader Raising Foundation of Yunnan Province (awarded to H.-J.Z.), and the Special Supported Bioscience and Biotechnique Foundation of Academia Sinica (STZ-11).

References

Appendino, G., Cravotto, G., Enriu, R., Gariboldi, P., Barboni, L., Torregiani, E., Gabetta, B., Zini, G., Bombardelli, E., 1994. The chemistry and occurrence of taxane derivatives. 14. Taxoids from the roots of *Taxus*×*media* cv. Hicksii. Journal of Natural Products 57, 607.

Baloglu, E., Kingston, D.G.I., 1999. The taxane diterpenoids. Journal of Natural Products 62, 1448.

Guo, Y.W., Diallo, B., Jaziri, M., Vanhaelen-Fastre, R., Vanhaelen, M., Ottinger, R., 1995. Two new taxoids from the stem bark of *Taxus baccata*. Journal of Natural Products 58, 1906.

Li, S.H., Zhang, H.J., Yao, P., Sun, H.D., 1998. Two new taxoids from *Taxus yunnanensis*. Chinese Chemical Letter 9, 1017.

Li, S.H., Zhang, H.J., Yao, P., Sun, H.D., Fong, H.H.S., 2000. Rearranged taxanes from the bark of *Taxus yunnanensis*. Journal of Natural Products 63, 1488.

Parmar, V.S., Jha, A., Bisht, K.S., Taneja, P., Singh, S.K., Kumar, A., Jain, R., Olsen, C.E., 1999. Constituents of the yew trees. Phytochemistry 50, 1267.

Wani, M.C., Taylor, H.L., Wall, M.E., Coggon, P., McPhail, A.T., 1971. Plant antitumor agents. VI. The isolation and structure of taxol, a novel antileukemic and antitumor agent from *Taxus brevifolia*. Journal of American Chemical Society 93, 2325.

Xiang, W., Zhang, H.J., Sun, H.D., Yao, P., Li, L., 1999. Study on the chemical constituents of the root of *Taxus yunnanensis*. Chinese Traditional and Herbal Drugs 30, 46.

Yue, Q., Fang, Q.C., Liang, X.T., 1995. Taxayuntin G: a new taxoid from *Taxus yunnanensis*. Chinese Chemical Letter 6, 225.

Zhang, H.J., Mu, Q., Xiang, W., Yao, P., Sun, H.D., Takeda, Y., 1997. Intramolecular transesterified taxanes from *Taxus yunnanensis*. Phytochemistry 44, 911.

Zhang, H.J., Sun, H.D., Takeda, Y., 1995a. Four new taxanes from the roots of *Taxus yunnanensis*. Journal of Natural Products 58, 1153.

Zhang, H.J., Takeda, Y., Matsumoto, T., Minami, Y., Yoshida, K., Xiang, W., Mu, Q., Sun, H.D., 1994a. Taxol related diterpenoids from the roots of *Taxus yunnanensis*. Heterocycles 38, 975.

Zhang, H.J., Takeda, Y., Minami, Y., Yoshida, K., Unemi, N., Mu, Q., Xiang, W., Matsumoto, T., Sun, H.D., 1993. Taxanes from the roots of *Taxus yunnanensis*. Acta Botanical Yunnica 15, 424.

Zhang, H.J., Takeda, Y., Minami, Y., Yoshida, K., Matsumoto, T., Xiang, W., Mu, Q., Sun, H.D., 1994b. Three new taxanes from the roots of *taxus yunnanensis*. Chemistry Letter, 957.

Zhang, H.J., Takeda, Y., Sun, H.D., 1995b. Taxanes from *Taxus yunnanensis*. Phytochemistry 39, 1147.

PERGAMON

Phytochemistry 58 (2001) 375–376

PHYTOCHEMISTRY

www.elsevier.com/locate/phytochem

Book reviews

Two Thousand Years of Natural Products Research — Past, Present and Future
T.J.C. Luijendijk (Ed.), Phytoconsult Publishers, Leiden, The Netherlands, 2000, 295 pp., ISBN 90-805866-1-2, 130 NGL

The idea of holding a Millennium meeting to celebrate 2000 years of natural product research seems to have been a good one. In the event, this congress organised by four relevant scientific societies, held in Amsterdam in July 1999, was very successful and it attracted over a thousand participants drawn from 62 countries. Whether the proceedings of this meeting is likely to attract a similar-sized audience is more problematical. The contents consist of 14 unrelated essays, which cannot hope to draw attention to more than a fraction of our current phytochemical knowledge.

A major theme in several papers is the search for new compounds of useful biological activities in tropical plants. Separate chapters deal with biologically active constituents from African plants, from Latin American plants and from Asian tropical forest plants. The chapter from Latin America includes an extensive list of research workers and local firms involved in the exploitation of the local floras. A further chapter reports on recent advances in the synthesis of taxol, the well known anti-cancer agent from *Taxus brevifolia*. The history of medicinal plant research is reviewed in chapters on plant alkaloids and on botanical illustrations of herbals.

The remaining chapters in this symposium volume concentrate on plant-microbial signalling, on allelopathic effects and on flavonoid researches. I particularly appreciated a review by D. Joulain on the use of natural products in modern perfumery. Professor Arnold Vlietinck, the current chairman of the Phytochemical Society of Europe, had the formidable task of bringing all the themes of this book together in a final chapter. In his contribution, he forecasts an exciting future for the phytochemical research of the twenty-first century.

Jeffrey B. Harborne
Department of Botany
The University of Reading
Reading RG6 6AS, UK

PII: S0031-9422(01)00157-1

Saffron. *Crocus sativus* L.
M. Negbi (Ed.), Harwood Academic Publishers. Amsterdam, The Netherlands, 1999, 154 pp., £49.00 or US$80.00, ISBN 90-5702-394-6

This book constitutes volume 8 in the series edited by Roland Hardman, *Medicinal and Aromatic Plants — Industrial Profiles* in which other plants of industrial interest have been the topic of the 7 previous volumes (Valerian, Perilla, Poppy, Cannabis, Neem, Ergot and Caraway). This pretends to be a comprehensive book on saffron. After an introductory chapter by the editor, this is divided into three main sections. The first details the botany, including taxonomy, reproduction biology and chemistry. The second deals with the present state of saffron cultivation in different countries (Azerbaijan, Greece, Italy and Morocco) and with saffron technology. The third section describes futuristic aspects of saffron cultivation, usage and industry. Every chapter is produced by a different author and contains an abstract and an individual list of references. It is a pity that there are no chapters with information about the main saffron producing countries (Iran, Spain and India). The editor recognises that the appeals to saffronologists in these countries did not produce any results, and therefore, the book is not as complete as it should be. The chapter on reproduction biology is especially interesting with nice colour pictures from different *Crocus* species and pollen grains as well as micrographs of the fertilisation process. The chapter on Chemistry is probably too short, although it includes a large number of references in which the information will be available. The chapters on the production of saffron in different countries provides a beautiful description of the methods and practices used in different countries for saffron cultivation, harvesting and processing (drying, storage, etc.). There is a short, but

useful, chapter on saffron technology, including short references to picking, separation, drying, milling, packaging and marketing. Chapter 10 reviews the biological effects of saffron and its components in studies in vivo and in vitro, mainly related to its anticarcinogenic properties. In chapter 11 an interesting approach to mechanized cultivation and harvesting is presented. This is a key topic in saffron production, as a reduction in man hours would be essential for the future of this crop. In chapters 12 and 13 plant breeding to improve saffron production and quality and the in vitro propagation and secondary metabolite production are reviewed.

This book can be recommended as a valuable source of information for those researchers interested in spice cultivation and processing, especially to those dealing with saffron. It can be also useful to those dealing with spice quality control. As a volume within the series *Medicinal and Aromatic Plants — Industrial Profiles* the whole collection will be very useful for postgraduate students in agronomy and industrial research, and to phytochemists, pharmacologists and food technologists that are interested in the specific species included in this collection.

F.A. Tomas-Barberan
CEBAS (CSIC)
PO Box 4195
30080 Murcia, Spain
E-mail address: fatomas@natura.cebas.csic.es

PII: S0031-9422(01)00197-2

Flavonoids of the Sunflower Family (Asteraceae)
B.A. Bohm, T.F. Stuessy, Springer-Verlag, Wien, 2001, 831 pp., 398 DM. ISBN 3-211-83479-6

This book is unique in providing the first comprehensive compilation of available flavonoid data for a large plant family, in this case the Asteraceae. It is not an easy read but it will provide an invaluable source of references to the enormous number of flavonoid constituents discovered in the family during the chemosystematic investigations carried out over the last ca 40 years. This is a very specialized book aimed at two limited audiences: flavonoid chemists working on the chemotaxonomy of the Asteraceae and taxonomists wishing to access flavonoid data for comparison with molecular and morphological data. It is divided into six sections. Section I (two chapters) provides an introduction to the morphology, distribution, classification, phylogeny and biogeography of the family for the benefit of the non-taxonomists. Section II introduces the uses, structural variation, biosynthesis and biological functions of flavonoids, in four chapters, to the non-chemist. The largest Section III (10 chapters), includes comprehensive flavonoid data with text and tables for each tribe. On the whole the data in this section appear to be accurate but I did notice that a 1999 reference to *Tanacetum parthenium* in the text had been omitted from the corresponding table. Section IV (6 chapters) considers the efficacy of flavonoids at subfamilial, tribal, subtribal, generic, specific and infraspecific levels. This section contains much useful information and includes some discussion of the flavonoid data in the light of the new macromolecular perspectives on the higher level classification of the Asteraceae. However, it proves rather tedious reading with many annoying back references to previous sections/chapters. The last two short sections, V and VI (2 chapters each), deal with flavonoids as indicators of the evolutionary process and flavonoids and phylogeny, respectively. These two sections are rather light weight and disappointing. There are 136 pages of references, a very useful key to the common names of those flavonoids included in the book and three indexes: subject, chemical and taxon.

I recommend this book as a novel and useful addition to the literature of plant chemosystematics.

Christine A. Williams
Department of Botany, School of Plant Sciences
The University of Reading Whiteknights, PO Box 221
Reading, RG6 6AS,UK
E-mail address: christine.williams@reading.ac.uk

PII: S0031-9422(01)00206-0

PERGAMON

Phytochemistry 58 (2001) 375–376

PHYTOCHEMISTRY

www.elsevier.com/locate/phytochem

Book reviews

Two Thousand Years of Natural Products Research — Past, Present and Future
T.J.C. Luijendijk (Ed.), Phytoconsult Publishers, Leiden, The Netherlands, 2000, 295 pp., ISBN 90-805866-1-2, 130 NGL

The idea of holding a Millennium meeting to celebrate 2000 years of natural product research seems to have been a good one. In the event, this congress organised by four relevant scientific societies, held in Amsterdam in July 1999, was very successful and it attracted over a thousand participants drawn from 62 countries. Whether the proceedings of this meeting is likely to attract a similar-sized audience is more problematical. The contents consist of 14 unrelated essays, which cannot hope to draw attention to more than a fraction of our current phytochemical knowledge.

A major theme in several papers is the search for new compounds of useful biological activities in tropical plants. Separate chapters deal with biologically active constituents from African plants, from Latin American plants and from Asian tropical forest plants. The chapter from Latin America includes an extensive list of research workers and local firms involved in the exploitation of the local floras. A further chapter reports on recent advances in the synthesis of taxol, the well known anti-cancer agent from *Taxus brevifolia*. The history of medicinal plant research is reviewed in chapters on plant alkaloids and on botanical illustrations of herbals.

The remaining chapters in this symposium volume concentrate on plant-microbial signalling, on allelopathic effects and on flavonoid researches. I particularly appreciated a review by D. Joulain on the use of natural products in modern perfumery. Professor Arnold Vlietinck, the current chairman of the Phytochemical Society of Europe, had the formidable task of bringing all the themes of this book together in a final chapter. In his contribution, he forecasts an exciting future for the phytochemical research of the twenty-first century.

Jeffrey B. Harborne
Department of Botany
The University of Reading
Reading RG6 6AS, UK

PII: S0031-9422(01)00157-1

Saffron. *Crocus sativus* L.
M. Negbi (Ed.), Harwood Academic Publishers. Amsterdam, The Netherlands, 1999, 154 pp., £49.00 or US$80.00, ISBN 90-5702-394-6

This book constitutes volume 8 in the series edited by Roland Hardman, *Medicinal and Aromatic Plants — Industrial Profiles* in which other plants of industrial interest have been the topic of the 7 previous volumes (Valerian, Perilla, Poppy, Cannabis, Neem, Ergot and Caraway). This pretends to be a comprehensive book on saffron. After an introductory chapter by the editor, this is divided into three main sections. The first details the botany, including taxonomy, reproduction biology and chemistry. The second deals with the present state of saffron cultivation in different countries (Azerbaijan, Greece, Italy and Morocco) and with saffron technology. The third section describes futuristic aspects of saffron cultivation, usage and industry. Every chapter is produced by a different author and contains an abstract and an individual list of references. It is a pity that there are no chapters with information about the main saffron producing countries (Iran, Spain and India). The editor recognises that the appeals to saffronologists in these countries did not produce any results, and therefore, the book is not as complete as it should be. The chapter on reproduction biology is especially interesting with nice colour pictures from different *Crocus* species and pollen grains as well as micrographs of the fertilisation process. The chapter on Chemistry is probably too short, although it includes a large number of references in which the information will be available. The chapters on the production of saffron in different countries provides a beautiful description of the methods and practices used in different countries for saffron cultivation, harvesting and processing (drying, storage, etc.). There is a short, but

useful, chapter on saffron technology, including short references to picking, separation, drying, milling, packaging and marketing. Chapter 10 reviews the biological effects of saffron and its components in studies in vivo and in vitro, mainly related to its anticarcinogenic properties. In chapter 11 an interesting approach to mechanized cultivation and harvesting is presented. This is a key topic in saffron production, as a reduction in man hours would be essential for the future of this crop. In chapters 12 and 13 plant breeding to improve saffron production and quality and the in vitro propagation and secondary metabolite production are reviewed.

This book can be recommended as a valuable source of information for those researchers interested in spice cultivation and processing, especially to those dealing with saffron. It can be also useful to those dealing with spice quality control. As a volume within the series *Medicinal and Aromatic Plants — Industrial Profiles* the whole collection will be very useful for postgraduate students in agronomy and industrial research, and to phytochemists, pharmacologists and food technologists that are interested in the specific species included in this collection.

F.A. Tomas-Barberan
CEBAS (CSIC)
PO Box 4195
30080 Murcia, Spain
E-mail address: fatomas@natura.cebas.csic.es

PII: S0031-9422(01)00197-2

Flavonoids of the Sunflower Family (Asteraceae)
B.A. Bohm, T.F. Stuessy, Springer-Verlag, Wien, 2001, 831 pp., 398 DM. ISBN 3-211-83479-6

This book is unique in providing the first comprehensive compilation of available flavonoid data for a large plant family, in this case the Asteraceae. It is not an easy read but it will provide an invaluable source of references to the enormous number of flavonoid constituents discovered in the family during the chemosystematic investigations carried out over the last ca 40 years. This is a very specialized book aimed at two limited audiences: flavonoid chemists working on the chemotaxonomy of the Asteraceae and taxonomists wishing to access flavonoid data for comparison with molecular and morphological data. It is divided into six sections. Section I (two chapters) provides an introduction to the morphology, distribution, classification, phylogeny and biogeography of the family for the benefit of the non-taxonomists. Section II introduces the uses, structural variation, biosynthesis and biological functions of flavonoids, in four chapters, to the non-chemist. The largest Section III (10 chapters), includes comprehensive flavonoid data with text and tables for each tribe. On the whole the data in this section appear to be accurate but I did notice that a 1999 reference to *Tanacetum parthenium* in the text had been omitted from the corresponding table. Section IV (6 chapters) considers the efficacy of flavonoids at subfamilial, tribal, subtribal, generic, specific and infraspecific levels. This section contains much useful information and includes some discussion of the flavonoid data in the light of the new macromolecular perspectives on the higher level classification of the Asteraceae. However, it proves rather tedious reading with many annoying back references to previous sections/chapters. The last two short sections, V and VI (2 chapters each), deal with flavonoids as indicators of the evolutionary process and flavonoids and phylogeny, respectively. These two sections are rather light weight and disappointing. There are 136 pages of references, a very useful key to the common names of those flavonoids included in the book and three indexes: subject, chemical and taxon.

I recommend this book as a novel and useful addition to the literature of plant chemosystematics.

Christine A. Williams
Department of Botany, School of Plant Sciences
The University of Reading Whiteknights, PO Box 221
Reading, RG6 6AS,UK
E-mail address: christine.williams@reading.ac.uk

PII: S0031-9422(01)00206-0

PERGAMON

Phytochemistry 58 (2001) 377

PHYTOCHEMISTRY

www.elsevier.com/locate/phytochem

Corrigendum

Corrigendum to "A chalcone and a dihydrochalcone from *Uvaria dulcis*" [Phytochemistry 53 (2000) 511–513]☆

Kan Chantrapromma[a,*], Yanisa Rat-A-pa[a], Chatchanok Karalai[a], Vitchu Lojanapiwatana[a], Vatcharee Seechamnanturakit[b]

[a]*Department of Chemistry, Faculty of Science, Prince of Songkla University, Hatyai, Songkhla 90112, Thailand*
[b]*Scientific Equipment Centre, Prince of Songkla University, Hatyai, Songkhla 90112, Thailand*

The dihydrochalcone identified was previously reported by A. Sinz et al. "Phenolic compounds from *Anomianthus dulcis*", Phytochemistry 50 (1999) 1069–1072. The spectral data of the chalcone and dihydrochalcone are inverted in our publication.

Table 1 following gives the correct assignments. The *Uvaria dulcis* and *Anomianthus dulcis* are the same plant species. The authors apologize for any inconvenience this has caused.

Table 1
^{1}H NMR (δ values) for the chalcone (**1**), dihydrochalcone (**2**) and the flavanone (**3**) in $CDCl_3$

Position	**1**	**2**	**3**
2′–OH	14.06 (*s*, D_2O-exchangeable)	13.80 (*s*, D_2O-exchangeable)	–
3′–OH	5.10 (*s*, D_2O-exchangeable)	5.10 (*s*, D_2O-exchangeable)	5.1 (*br.s*, D_2O-exchangeable)
4′,6′–OCH_3	3.86 (*s*), 3.93 (*s*)	3.86 (*s*), 3.93 (*s*)	3.83 (*s*), 3.90 (*s*) (at positions 5 and 7)
5′	5.97 (*s*)	5.91 (*s*)	6.08 (1H-6)
α	7.77 (*s*, 1Hα, 1H*β*)	3.35 (*t*, $J_{AB}=7.7$, 2H)	2.83–3.0 (*m*, 2H-3)
β		2.95 (*t*, $J_{AB}=7.7$, 2H)	5.37 (*d.d*, $J=4$, $10H_2$, 1H-2)
5 Ar–H (ring B)	7.21–7.70 (*m*)	7.15 (*m*)	7.33 (*s*)

☆ PII of original article: S0031-9422(99)00477-X

* Corresponding author.

0031-9422/01/$ - see front matter
PII: S0031-9422(01)00153-4

PERGAMON

Phytochemistry 58 (2001) 379–387

PHYTOCHEMISTRY

www.elsevier.com/locate/phytochem

Characterization of peroxidase-mediated chlorophyll bleaching in strawberry fruit

Gustavo A. Martínez[a,*], Pedro M. Civello[a], Alicia R. Chaves[b], María C. Añón[b]

[a]*Instituto de Investigaciones Biotecnológicas-Instituto Tecnológico de Chascomús (IIB-INTECH), UNSAM-CONICET, Camino de Circunvalación Laguna Km 6, 7130 Chascomús, Argentina*

[b]*Centro de Investigación y Desarrollo en Criotecnología de Alimentos (CIDCA), Facultad de Ciencias Exactas, UNLP, CONICET, 47 y 116, 1900 La Plata, Argentina*

Received 2 January 2001; received in revised form 9 May 2001

Abstract

Peroxidase (POX) from strawberry fruits was analyzed for its capacity to bleach chlorophyll. The partially purified enzyme preperation catalyzed the bleaching of chlorophylls and their derivatives in the presence of H_2O_2 and phenolic compounds. The optimal reaction conditions were 35 °C, pH 5.2 and ionic strength equal to 0.2. The maximum activity was observed at 1 mM of H_2O_2, while higher concentrations inhibited enzyme activity. Compounds with a high affinity to the heme group, radical scavengers and reducing agents, showed an inhibitory effect. Phenolic compounds such as umbelliferone, naringenin and *p*-substituted monophenols acted as cofactors. Instead, other phenolic compounds tested such as caffeic acid, catechin, ellagic acid, esculin and quercetin inhibited the activity of POX on chlorophylls. Phenolic compounds extracted from strawberry fruits showed an inhibitory effect on POX-chlorophyll bleaching activity, although this effect decreased markedly during ripening. POX showed higher affinity for compounds derived from chlorophyll ***a*** than from chlorophyll ***b***, and the enzyme preferentially degraded chlorophyll derivatives with the Mg^{2+} ion present and the phytol group removed. The POX-chlorophyll bleaching activity was found in all ripening stages from small green to ripe, the highest activity corresponding to large green fruits. © 2001 Elsevier Science Ltd. All rights reserved.

Keywords: *Fragaria* x *ananassa*; Rosaceae; Strawberry; Chlorophyll; Peroxidase; Phenolic compounds

1. Introduction

Chlorophyll (Chl) degradation is a characteristic symptom of leaf senescence and fruit ripening. During senescence, chlorophyll-protein complexes are disassembled and the pigments liberated. Free chlorophylls (Chls) are highly photoactive compounds that can generate free radicals, causing damage to cell membranes (Matile et al., 1996). It has been suggested that two types of reactions are involved in Chl catabolism (Shioi et al., 1995). Type I reactions include the loss of phytol, Mg^{2+}, and other modifications of the side chains that do not involve the breaking of the tetrapyrrolic ring present in chlorophylls. Chlorophyllase, which removes the phytol and produces chlorophyllides (Chlds), has been involved in the first step of Chl breakdown (Trebitsh et al., 1993; Matile et al., 1996). Another enzyme involved in chlorophyll catabolism is Mg-dechelatase, which eliminates Mg^{2+} from Chl or Chld to produce pheophytin (Phe) or pheophorbide (Pheo), respectively (Langmeier et al., 1993; Vicentini et al., 1995). Further catabolism of Pheo involves the elimination of $-COOCH_3$ to form pyropheophorbide, and oxidation to form hydroxypheophorbide (Shioi et al., 1991) or the formation of C-13^2-carboxylpyropheophorbide by the action of pheophorbidase (Watanabe et al., 1999). Type II reactions involve the oxidative cleavage (bleaching) of the tetrapyrrole ring. It has been reported that the cleavage of Phe ***a*** by a pheophorbide ***a*** oxygenase is the key regulatory step in the Chl catabolism pathway (Matile and Schellemberg, 1996; Hörtensteiner et al., 1998; Matile et al., 1999). However, other oxidative enzymes such as lipoxygenase (Orthoefer and Dugan, 1973), Chl oxidase, and peroxidase also appear to be involved in Chl bleaching.

* Corresponding author. Postal address: Camino de Circunvalacion Laguna Km 6, (7130) Chascomus, Argentina. Tel.: +54-2241-424049; fax: +54-2241-424048.

E-mail address: gmartinez@intech.gov.ar (G.A. Martínez).

0031-9422/01/$ - see front matter © 2001 Elsevier Science Ltd. All rights reserved.
PII: S0031-9422(01)00266-7

Peroxidase (POX) is a ubiquitous enzyme located in several subcellular compartments, including chloroplasts (Johnson-Flanagan and McLachlan, 1990; Kuroda et al., 1990). Although the role of POX in Chl degradation 'in vivo' is controversial (Matile et al., 1999), many studies have supported its possible participation in Chl catabolism (Matile, 1980; Huff, 1982; Johnson-Flanagan and McLachlan, 1990; Johnson-Flanagan and Spencer; 1996; Maeda et al., 1998). Probably, the controversy has been caused by the existence of different chlorophyll degradation pathways (Amir-Shapira et al., 1987; Trebitsh et al., 1993) and the presence of multiple POX isoenzymes with uneven capacities to degrade chlorophylls (Kuroda et al., 1990; Adachi et al., 1996).

Strawberry is classified as a non-climacteric fruit, and neither the respiration rate nor ethylene production increase as the fruit changes its color, texture and flavor (Abeles and Takeda, 1990). The chlorophyll content diminishes very quickly as the fruit ripens (Given et al., 1988; Martínez et al., 1994; Perkins-Veazie, 1995), and the chloroplasts disintegrate during the process (Gross, 1982; Perkins-Veazie, 1995) without conversion into chromoplasts or gerontoplasts, as occurs in tomato fruits and leaves respectively (Matile et al., 1996). These characteristics make strawberry fruit an interesting model system in which to study chlorophyll degradation during fruit ripening.

In the present work, we have partially characterized the activity of strawberry peroxidase for bleaching chlorophyll, determined the influence of phenolic compounds on this activity and analyzed the change of POX bleaching activity during ripening.

2. Results and discussion

We have previously reported the presence of two cationic peroxidase isoenzymes in strawberry fruit, both of which are associated with membranes and show maximum activity at the green ripening stage (Civello et al., 1995). It has been suggested that cationic peroxidases, located in the chloroplast, are involved in Chl bleaching (Kuroda et al., 1990). In order to analyze strawberry POX activity on chlorophylls, extracts from green fruits were prepared and partially purified by means of $(NH_4)_2SO_4$ fractionation. The absorption spectrum of complete reaction mixtures (enzyme extract, chlorophyll, H_2O_2, and *p*-coumaric acid) showed a progressive reduction of the absorbance at 669 nm (Fig. 1). According to previous reports, this effect is due to the cleavage of the tetrapyrrolic ring present in chlorophylls (Huff, 1982). Different reaction mixtures were prepared to verify the activity of POX. Complete mixtures degraded Chl at a constant rate during the first 100 s, but then the reaction rate decreased (Fig. 2a). This is probably due to the diminution of H_2O_2 concentration, since the replenishment of H_2O_2 restored the initial bleaching rate. No chlorophyll degradation was observed in the absence of H_2O_2 or the inclusion of boiled extracts, while a low Chl bleaching activity was found in the absence of phenolic cofactors. The effect of H_2O_2 concentration on chlorophyll-bleaching activity was assayed (Fig. 2b). The chlorophyll-bleaching rate was extremely low in the absence of H_2O_2, increased to reach a maximum at 1.0 mM and then decreased slightly at 2.5 mM H_2O_2. Higher concentrations of H_2O_2 were inhibitory and the activity decreased to zero at 50 mM (data not shown). The inhibitory effect of high concentrations of H_2O_2 on peroxidase activity has been attributed to damage caused to the heme group present in the enzyme (Sánchez-Romero et al., 1995).

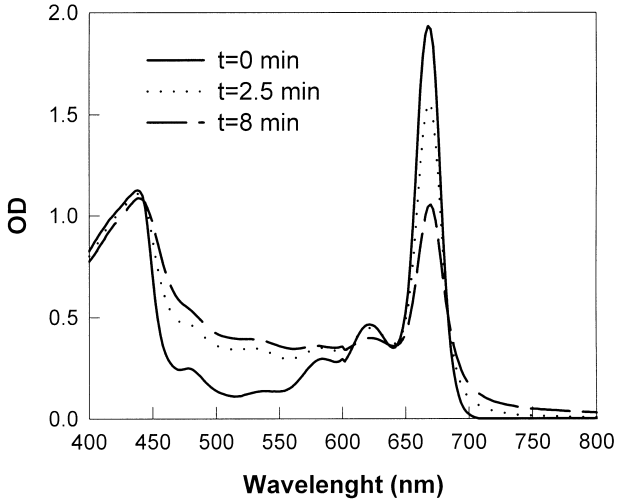

Fig. 1. Changes in the absortion spectra of the complete reaction mixture (enzymatic extract + chlorophyll ***a*** + H_2O_2 + *p*-coumaric acid) after incubation for different times.

2.1. Enzyme characterization

Peroxidase-chlorophyll bleaching activities were measured at different temperatures and pHs (Fig. 3a and b). A steep increase in enzyme activity was found when the temperature rose from 20 to 35 °C, whereas higher temperatures caused diminution of the activity. The activity at 35 °C was nearly twofold higher than at 25 °C, the temperature mostly used to measure POX–Chl-bleaching activity (Kuroda et al., 1990; Adachi and Shimokawa, 1995). The optimum pH was determined to be pH 5.2, being 50% of activity at 3.2 and 6.2. The optimum pH range for POX–Chl bleaching activity is lower than 6.0, the optimum pH for POX–guaiacol activity (Civello et al., 1995), suggesting that the value depended on the hydrogen donor. The highest activity was found at an ionic strength of $\mu = 0.2$ (Fig. 3c), similar to that reported for POX obtained from orange flavedo (Huff, 1982).

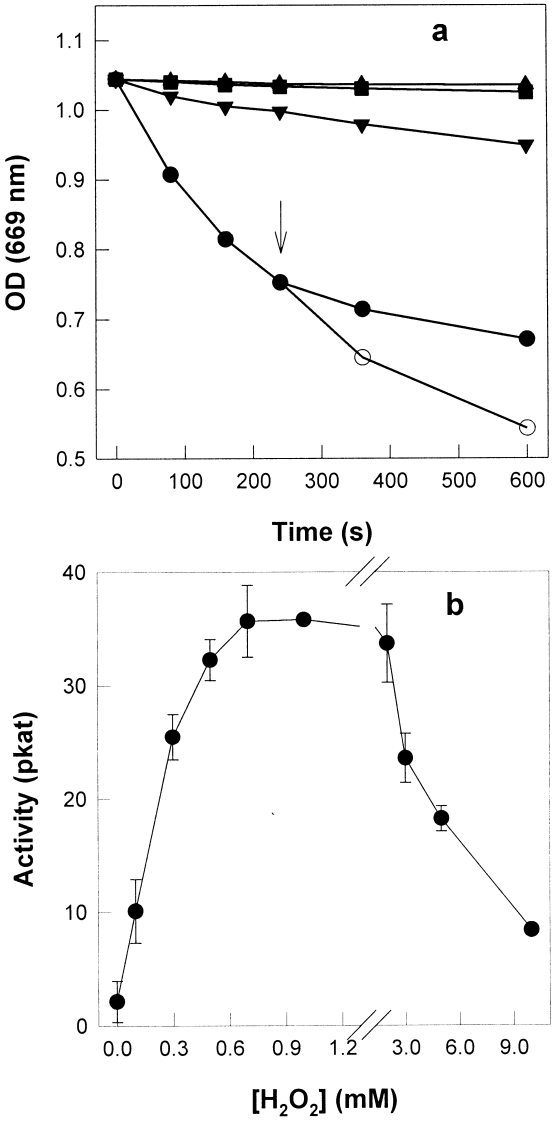

Fig. 2. (a) Time courses of chlorophyll *a* degradation. (▲) Reaction mixtures without H_2O_2. (■) Reaction mixtures with boiled enzymatic extract. (▼) Reaction mixtures without *p*-coumaric acid. (●) Complete reaction mixtures (enzymatic extract + chlorophyll *a* + H_2O_2 + *p*-coumaric acid). (○) Complete reaction mixtures after replenishing H_2O_2. (b) Effect of (H_2O_2) on POX-Chl bleaching activity. Vertical bars denote ± standard deviation when it exceeds the symbol size.

2.2. Substrate specificity

The determination of apparent kinetic parameters (K_m and V_{max}) was performed by using Chls and their derivatives as substrates (Table 1). The K_m value corresponding to Chl *a* was lower than that of Chl *b*, while the V_{max} was higher, indicating that POX from strawberry fruit has higher affinity for Chl *a*. Peroxidase extracted from orange flavedo has been assayed with both chlorophylls, and a preferential degradation of Chl *a* was also reported (Huff, 1982). The fact that Chl *b* can be transformed in Chl *a* (Ohtosuka et al., 1997) suggests that Chl *b* could be degraded after its transformation into Chl *a*. The absence of Mg^{2+} ion in Phe a diminished the affinity for the substrate (higher K_m), although the V_{max} increased. The removal of the phytol group from chlorophylls a and b increased both the affinity and the V_{max}. When catalytic power (V_{max}/K_m) was calculated, the highest value corresponded to Chld *a*, which was 5-fold higher than that of Chl *a*. These results suggest that strawberry fruit POX can preferentially degrade chlorophyll derivatives with the Mg^{2+} ion present and the phytol group removed. It is worth pointing out that chlorophyllase, the enzyme necessary to remove phytol group from chlorophylls, has been found in strawberry fruit and that the enzyme shows highest affinity for Chl *a* (Martínez et al., 1995). Together, the data suggest that the catabolism of both Chls could start from Chl *a* in strawberry fruit.

Table 1
Apparent kinetic constants of different substrates of the POX bleaching system

Compound	K_m (μM)	V_{max} (μM/min)	V_{max}/K_m
Chlorophyll *a*	16.1±2.0	2.6±0.2	0.161
Chlorophyll *b*	66.6±2.1	1.0±0.1	0.015
Pheophytin *a*	59.9±2.4	4.6± 0.3	0.077
Chlorophyllide *a*	10.3±2.0	6.1±0.6	0.588
Chlorophyllide *b*	36.9±3.8	1.3±0.2	0.035

2.3. Effect of inhibitory compounds

Several compounds were analyzed as possible inhibitors of chlorophyll bleaching (Table 2). Although Mn^{2+} ion has been reported to strongly inhibit POX–Chl bleaching activity in other systems (Adachi and Shimokawa, 1995), the ion at 1 mM concentration caused only a slight inhibition in this study. Compounds with high affinity for the heme group (N_3^- and CN^-) induced a high inhibition, confirming the involvement of peroxidase in Chl bleaching. Free radical scavengers such as hydroquinone, *n*-propyl gallate, tiron and α-tocopherol inhibited Chl bleaching, suggesting the participation of free radicals as intermediate products. In addition, strong inhibition of Chl bleaching activity was found when reducing agents such as cysteine, dithiothreitol (DTT), glutathione and ascorbic acid were present at 1 mM concentration. In the cases of cysteine, DTT and ascorbic acid, a lag period ranging from 30 to 240 s was observed, after which the Chl bleaching started (data not shown). Higher concentrations of reducing agents induced longer lag periods and a lower POX activity once the reaction started. This low POX activity could be due to the diminution of H_2O_2 concentration, caused by its consumption during the oxidation of cysteine or DTT. Considering that some plant peroxidases also possess a thiol oxidase activity (Pichorner et al., 1992), another possibility is that the enzyme preferably oxidizes

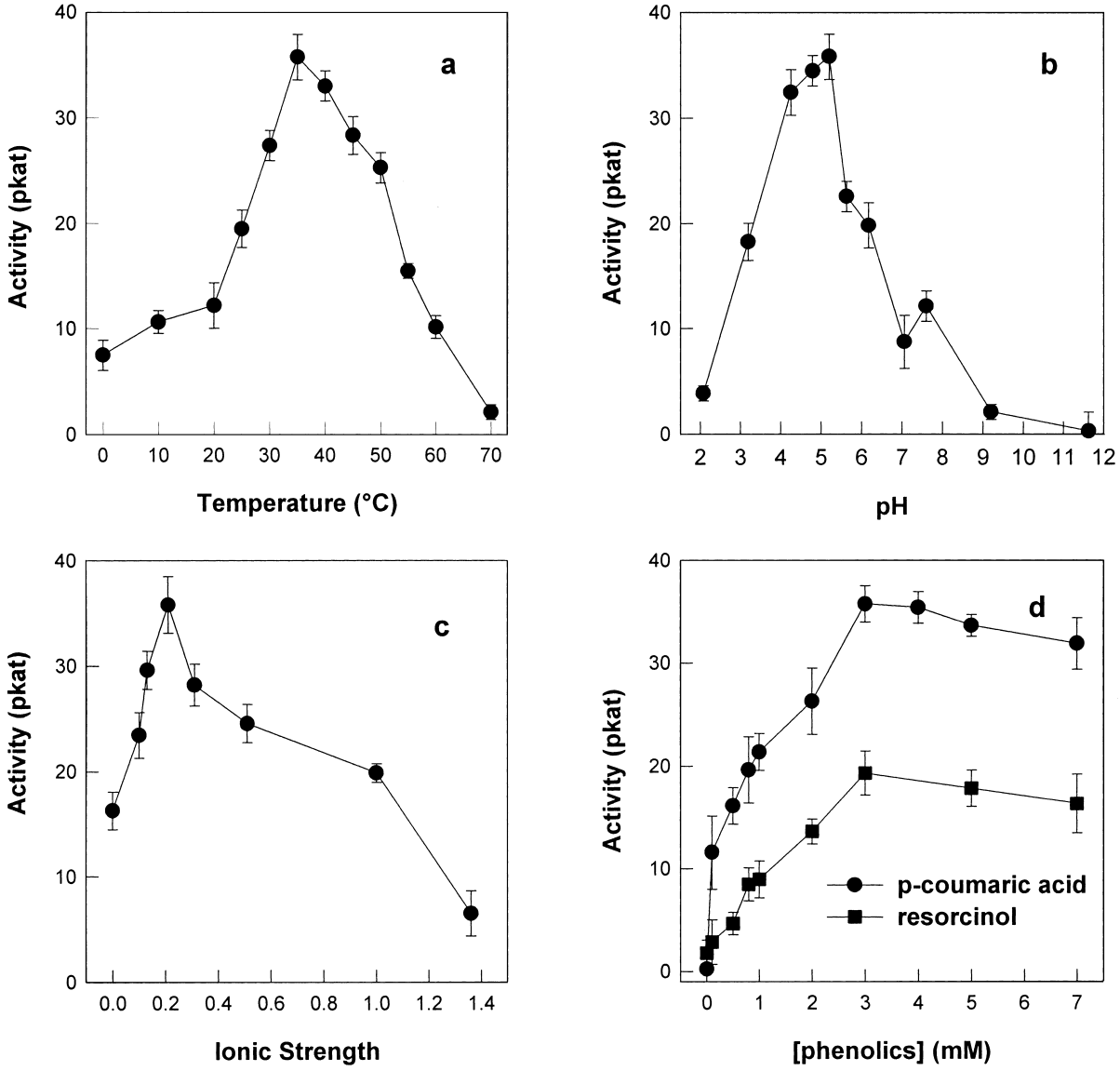

Fig. 3. (a) Effect of temperature on POX–Chl bleaching activity. (b) Effect of pH on POX–Chl bleaching activity. (c) Effect of ionic strength of reaction mixture on POX–Chl bleaching activity. (d) Effect of concentration of phenolic compounds on POX–Chl bleaching activity. Vertical bars denote ± standard deviation when it exceeds the symbol size.

cysteine or DTT instead of chlorophyll. Among the reducing agents tested, the highest inhibition of Chl bleaching was caused by ascorbic acid. It has been reported that ascorbic acid delays the senescence of oat leaves and decreases the chlorophyll loss (Borracino et al., 1994). The content of several antioxidant compounds, including ascorbic acid, decrease during fruit ripening (Baldwin, 1993; Markus et al., 1999). Probably, this compound could inhibit POX 'in vivo', therefore delaying the chlorophyll degradation process. During the course of leaf senescence, the antioxidant defense system, including catalase, is impaired while the activity of H_2O_2-producer enzymes is enhanced, which generates an appropriate environment to increase the chlorophyll bleaching (Hideg, 1997). β-Carotene, which has been mentioned previously as an inhibitor of Chl bleaching (Kato and Shimizu, 1985), did not show any effect in our system.

2.4. Effect of phenolic compounds

As shown in Fig. 2a, POX–Chl bleaching activity is enhanced by the inclusion of *p*-coumaric acid in the mixture reaction. This compound along with resorcinol has been reported among the most effective phenolic cofactors of peroxidase in the Chl bleaching reaction (Kato and Shimizu, 1985). Therefore, we assayed their effect on POX–Chl bleaching activity present in strawberry fruit (Fig. 3d). Either *p*-coumaric acid or resorcinol was more effective at a concentration of 3 mM, while

Table 2
Effect of inhibitors on POX–Chl bleaching activity. Different compounds were added to a control mixture reaction (POX extracted from SG fruits + chlorophyll *a* + H_2O_2 + *p*-coumaric acid) and the remaining enzyme activity was measured

Compound	Concentration (mM)	Activity (pkat)	Inhibition (%)
Control reaction (no addition)		39.03	0
Mn^{2+}	1	35.45	9.1
NaN_3	1	11.46	70.6
NaCN	0.1	0.36	99.0
L-Cysteine	1	3.94	89.9
DTT	1	8.23	78.9
Glutathione	1	17.19	55.9
Ascorbic Acid	1	2.15	94.5
Hydroquinone	1	0.72	98.2
n-Propyl gallate	1	1.79	95.4
Tiron	1	ND[a]	100
Triethylenediamine	5	39.03	0
α-Tocopherol	0.1	16.47	57.8
ß-Carotene	0.1	40.10	0

[a] ND: not detected.

Table 3
Effect of phenolic compounds on POX–Chl bleaching activity. Different phenolic compounds were added to a mixture reaction (POX extracted from SG fruits + chlorophyll *a* + H_2O_2 + phenolic) and the enzyme activity measured

		Activity (pkat)
Monophenols and derivatives	Phenol 2 mM	17.54
	2-4 Dichlorophenol 2 mM	12.17
	p-Coumaric acid 2 mM	26.14
	p-Hydroxibenzoic acid 2 mM	9.31
	m-Hydroxibenzoic acid 2 mM	0.36
	o-Cresol 2 mM	0.36
	p-Cresol 2 mM	3.58
Diphenols and derivatives	Catechol 2 mM[a]	ND[b]
	Guaiacol 2 mM[a]	ND
	Resorcinol 2 mM	13.60
	Caffeic acid 2 mM[a]	ND
	Ellagic acid 2 mM	ND
	Hydroquinone 2 mM	ND
	Chlorogenic acid 2 mM	ND
Triphenols and derivatives	Pyrogallol 2 mM[a]	0.36
	Gallic acid 2 mM[a]	7.52
Coumarins and derivatives	Umbelliferone 1.2 mM	3.94
	Eesculin 1.2 mM	ND
Flavonoids and derivatives	Rutin 0.1 mM	0.36
	Quercetin 0.1 mM	ND
	Catechin 0.5 mM	ND
	Epicatechin 0.5 mM	ND
	Naringenin 1 mM	1.07

[a] Phenolic compounds that showed oxidation.
[b] ND, not detected.

higher concentrations slightly decreased the activity. In addition, the effect of several phenolic compounds on POX–Chl bleaching activity was analyzed (Table 3). The highest enzyme activities were found with phenol or *p*-substituted monophenol (*p*-coumaric acid, *p*-hydroxybenzoic acid and *p*-cresol), in agreement with reports from other systems (Kato and Shimizu, 1985). Low activities were observed with *o*- or *m*-substituted monophenol (*m*-hydroxibenzoic acid and *o*-cresol), while compounds with *o*- and *p*- substitutions in the same compound (e.g. 2,4-dichlorophenol) induced a POX bleaching activity similar to that found with *p*-monophenol. Among diphenols, only resorcinol (a *m*-diphenol) was effective to induce Chl bleaching. When *o*- or *p*-diphenols or their derivatives were used (catechol, guaiacol, caffeic acid, ellagic acid, hydroquinone and chlorogenic acid), no activity was detected. In the case of catechol, guaiacol, caffeic acid and chlorogenic acid, an enhanced absorption in the blue region of the spectrum was observed, probably due to the phenolic oxidation. Regarding triphenols and derivatives, a mild oxidation of pyrogallol and gallic acid and a short lag initial phase were observed, after which the Chl bleaching reaction started. Among natural coumarines, flavonoids and their derivatives, only umbelliferone and naringenin were effective as cofactors, coincidently with reports in other plant systems (Kato and Shimizu, 1985; Yamauchi and Watada, 1994). Finally, catechin and epicatechin showed oxidation as occurred with other diphenols. When mixtures containing some of the non-effective phenolic compounds (caffeic acid, catechin, ellagic acid, esculin, and quercetin) were added with *p*-coumaric acid, a measurably enzyme activity was recovered, indicating that their inhibitory effect is reversible (data not shown). In summary, phenolic compounds could act differently probably depending on their chemical structures. Some of the phenolics can activate POX–Chl bleaching while others inhibit the reaction through competition with Chl as substrate or by scavenging free radicals.

Strawberry fruit have high concentration of phenolics, which could regulate the activity of POX–Chl bleaching. It has been shown that phenolic compounds inhibit the POX (Zieslin and Ben-Zaken, 1993) and lipoxygenase activity (Richard-Forget et al., 1990), and that they can act as radical scavengers (Rice-Evans et al., 1997). In order to analyze the effect of strawberry endogenous phenolic compounds, we prepared crude extracts with and without PVPP, a phenolic adsorbent, and measured guaiacol–POX and POX–Chl bleaching activities (Table 4). The removal of phenolics by PVPP increased markedly the POX activity with both substrates, suggesting that endogenous phenolic compounds could act as inhibitors. Partial recovery of activity was achieved when extracts were prepared without PVPP and then dialyzed, probably due to the removal of some of the inhibitory compounds. The fact that the enzyme activity was only partially recovered could be due to oxidized phenolic-mediated protein modification or to the presence of high

Table 4
Effect of addition of PVPP in the buffer extraction on guaiacol–POX activity and POX–Chl bleaching activity

	Guaiacol (pkat)	Chlorophyll (pkat)
With PVPP	98.4±14.4	39.03±3.94
Without PVPP	16.9±3.1	1.07±0.36
Without PVPP, dialyzed	61.4±9.4	22.56±3.22

molecular mass inhibitors in the extract. According to Huff (1982), these non-dialyzable inhibitory compounds could be polyphenols of high molecular mass.

As the amount and composition of phenolic compounds changes during strawberry fruit ripening, we extracted phenolic compounds at several ripening stages and then assayed their effect on POX–Chl bleaching activity (Tables 5 and 6). The concentration of phenolic compounds decreased six-fold during the course of ripening, from 11.4 mg phenol per gram of fruit in 'small green' fruit to 1.8 mg phenol per gram of fruit in the ripe stage. Phenolic compounds extracted from fruit at several ripening stages were used to prepare reaction mixtures at the same total phenolics concentration (19 μg/ml). These mixtures were used to test the effect of the endogenous phenolic compounds on POX–Chl bleaching activity. A lag phase was found in all cases, after which the Chl bleaching started and a residual activity could be measured. A shortening of lag phase and an increase of residual activity were found as phenolic extracts from more advanced ripening stages were used.

Table 5
Change in phenolic compound content during strawberry fruit ripening

Ripening stage	Concentration of phenolics (mg phenol/g fresh weight)
Small green	11.4±0.5
Large green	6.1±0.4
White	2.3±0.1
Turning	2.1±0.1
Ripe	1.8±0.1

Table 6
Effect of phenolic extracts on POX–Chl bleaching activity. Phenolic compounds extracted from strawberry fruit at different ripening stages were added to a control mixture reaction (POX extracted from SG fruits + chlorophyll ***a*** + H_2O_2 + *p*-coumaric acid) and the effect on lag phase length and residual activity was measured. The concentration of phenolics added was 19 μg per ml of mixture reaction in all cases

Ripening stage	Lag phase (s)	Residual activity (pkat)
Control reaction (no addition)	0	39.03±3.94
Small green	150±10	18.97±1.07
Large green	140±10	21.12±0.72
White	100±10	22.20±1.07
Turning	75±8	23.27±1.07
Ripe	65±7	24.34±1.07

Therefore, the inhibitory effect of endogenous phenolic compounds on POX–Chl bleaching activity decreases during strawberry fruit ripening, probably due to changes in both the amount and the type of phenolic compounds. These results suggest a role for phenolics as regulators of the POX–Chl bleaching activity during strawberry fruit ripening. Schuster and Herrmann (1985) detected esters of *p*-coumaric acid and *p*-hydroxybenzoic acid in strawberry fruit, two of the phenolic compounds that induced POX activity on chlorophyll in this study. As well, ellagic acid, an inhibitor of POX-Chl bleaching, was found in strawberries and its concentration decreased during fruit ripening (Maas et al., 1991).

2.5. Change of chlorophyll content and POX–Chl bleaching activity during ripening

Strawberry fruit changes dramatically over a short period during ripening and, once the SG stage is reached, a rapid loss of chlorophylls is observed. The total chlorophyll content per gram of fruit decreased gradually during ripening, with the level of Chl ***a*** being higher than that of Chl ***b*** at all the stages analyzed (Fig. 4a). Peroxidase chlorophyll bleaching activity was

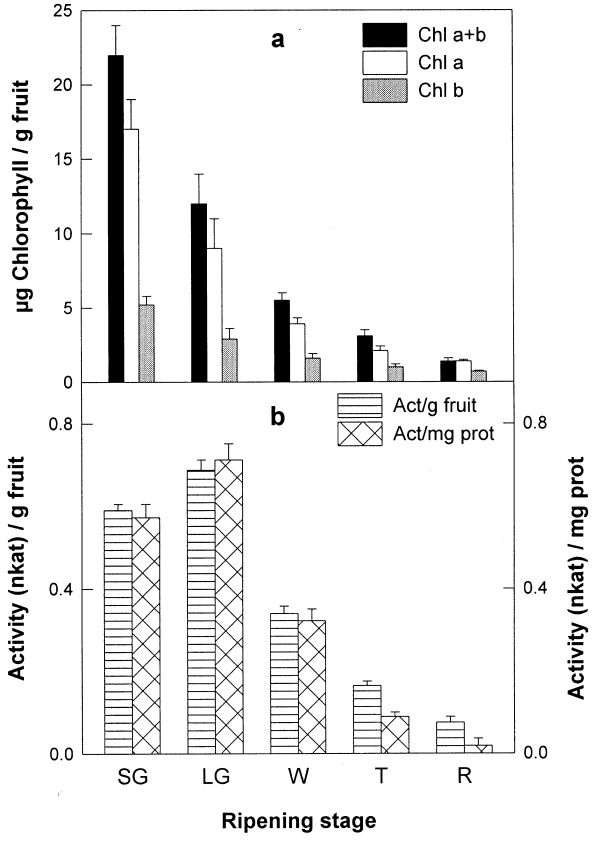

Fig. 4. (a) Changes in chlorophyll content during ripening of strawberry fruit. Chlorophyll ***a*** + ***b***, ■. Chlorophyll ***a*** □ Chlorophyll ***b*** ▒. (b) Changes in POX–Chl bleaching activity during ripening of strawberry fruit. Activity per gram of fruit ▤; activity per mg of protein ▩. SG: small green; LG: large green; W: white; T: turning; R: red.

detected in all ripening stages analyzed (Fig. 4b). It was present in SG strawberries before the onset of ripening, increased in LG fruits and then decreased until the end of fruit ripening.

'In vitro' POX–Chl bleaching activity is high from SG to W stages, coincidently with the period when most of the fruit chlorophyll is degraded. In addition, we have found a diminution along ripening of inhibitory phenolic compounds on POX–Chl bleaching activity, in agreement with findings reported in citrus (Baldwin, 1993). Together, the results encourage further analysis of POX participation in Chl bleaching during strawberry fruit ripening, although more research is needed to prove the 'in vivo' role of peroxidase in chlorophyll degradation.

3. Experimental

3.1. Plant material

Strawberry fruits (*Fragaria×ananassa*, Duch., cv. Selva), grown in a greenhouse, were obtained from local producers. Fruits were harvested and classified according to the external coloration degree and size into different ripening stages: small green (SG), large green (LG), white (W), turning (T) and red (R). Fruits were washed and drained and, after removing calyxes and peduncles, were used immediately or frozen at −60 °C.

3.2. Enzyme extraction

Extractions were performed according to Civello et al. (1995) with slight modifications. Fresh or frozen green strawberries (25 g) were homogenized in an Omnimixer homogenizer with 100 ml of the following extraction buffer: 0.02 M Na_2HPO_4, 0.08 M NaH_2PO_4, 0.2% (v/v) Triton X-100, 1 M NaCl, 30 g/l polyvinylpolypyrrolidone (PVPP), pH 6.0. The mixture was stirred for 1 h at 4 °C and then centrifuged at 9000 *g* for 20 min at the same temperature. Solid $(NH_4)_2SO_4$ was added up to 45% saturation to the extract. The mixture was stirred for 5 h at 4 °C and then centrifuged at 9000 *g* for 1 h at the same temperature. The supernatant was treated with $(NH_4)_2SO_4$ to reach 90% saturation and the resulting mixture was stirred at 4 °C overnight. The suspension was centrifuged at 9200 *g* at 4 °C during 1 h. The retained pellet was dissolved in 20 ml of 0.02 M Na_2HPO_4–0.08 M NaH_2PO_4 buffer (pH 6.0) and dialyzed against the same buffer at 4 °C overnight.

3.3. Determination of peroxidase chlorophyll-bleaching activity

Determination of activities was done according to Huff (1982) with slight modifications. The following reaction mixture was used: 0.2 M sodium phosphate buffer (pH 5.2), 0.3% (v/v) Triton X-100, 1 mM H_2O_2, 3 mM *p*-coumaric acid, 20 μM chlorophyll ***a*** (dissolved in acetone) and enzymatic extract, containing 30 μg of total protein, in a final volume of 1 ml. The mixture was incubated at 35 °C and the reaction was started by adding H_2O_2. The degradation of chlorophylls and their derivatives was evaluated by measuring the decrease of OD at: 669 nm for chlorophyll ***a*** and chlorophyllide ***a***, 649 nm for chlorophyll ***b*** and chlorophyllide ***b*** and 672 nm for pheophytin ***a***. Assays at pH different from 6.0 were carried out by adjusting the pH of the mixture with suitable amounts of 1.0 M NaOH, 1.0 M HCl and 0.5 M NaCl to keep the ionic strength constant. Assays at different ionic strengths were carried out by adding suitable amounts of 4 M NaCl to the reaction mixture.

3.4. Determination of peroxidase–guaiacol activity

The activity of peroxidase using guaiacol as substrate was done according to Civello et al. (1995).

3.5. Protein dosage

Protein concentrations of the extracts were measured by the modified Lowry method described by Potty (1969), measuring OD at 750 nm and using bovine albumin as standard.

3.6. Extraction and measurement of phenolic compounds

Extractions were performed according to Gil et al. (1997) with slight modifications. Samples of 10 g of frozen strawberries were mixed with 30 ml of acetone and homogenized in an Omnimixer. The mixture was centrifuged at 9000 *g* for 10 min at 4 °C. The pellet was re-extracted with 30 ml of acetone and supernatants were pooled (crude extract). This crude extract was extracted three times with 20 ml of hexane to eliminate chlorophylls. The aqueous-acetone phase was evaporated under nitrogen stream at 40 °C until 1 ml. Four milliliters of 3% (v/v) formic acid were added to the concentrate and then passed through a C_{18} Sep-Pak cartridge (Waters), previously activated with 5 ml methanol followed by 5 ml water and then 5 ml of 3% (v/v) formic acid. Phenolics were adsorbed on the column while sugars and other water-soluble compounds were eluted with 10 ml of 3% (v/v) aqueous formic acid. Then, phenolics were recovered with 1.8 ml of 3% (v/v) formic acid in methanol (purified extract). Total phenolic compounds of crude and purified extracts were determined with Folin–Ciocalteau reagent according to Zieslin and Ben-Zaken (1993). Ten microliters of crude extract or a dilution (1:6) of purified extract were mixed with 1.11 ml of water and 200 μl of 1 N Folin–Ciocalteau reagent. After 3 min at 25 °C, 1.5 ml of saturated solution of Na_2CO_3 was added and the reaction mixture was incubated for 1 h at the same

temperature. The content of phenolic compounds was expressed as milligrams of phenol per g of fresh weight, using phenol as standard.

3.7. Extraction and measurement of chlorophylls

Frozen strawberries were homogenized with four volumes of acetone in an Omnimixer. The suspensions were centrifuged at 5000 *g* for 5 min at 4 °C and the chlorophylls (Chls) in the supernatant determined according to Lichtenthaler (1987).

3.8. Preparation of chlorophylls ***a*** and ***b*** and derivatives

Three spinach leaves were homogenized in an Omnimixer with 60 ml of acetone and the resulting suspension was vacuum-filtered through filter paper. The acetone solution obtained was mixed with 50 ml of petroleum ether and 50 ml of saturated NaCl solution to extract the chlorophylls. The ether phase was separated, washed twice with 50 ml of saturated NaCl solution and then evaporated under nitrogen stream. Chlorophylls were redissolved in a solution of 5% (v/v) acetone in hexane and purified by passage through a powdered sucrose column using 5% (v/v) acetone in hexane as mobile phase. Solvents were evaporated under a nitrogen stream and chlorophylls were stored at −20 °C until used. Purified chlorophylls were redissolved in acetone for their use. Chl ***a*** and Chl ***b*** obtained by this procedure were about 98% and 93% pure, respectively. Chlorophyllides (Chld) ***a*** and ***b*** were prepared from purified Chl ***a*** and Chl ***b*** by using chlorophyllase obtained from orange flavedo according to Huff (1982). Pheophytin (Phe) ***a*** was prepared by treating Chl ***a*** with HCl solution, according to Lichtenthaler (1987).

References

Abeles, F., Takeda, F., 1990. Cellulase activity and ethylene in ripening strawberry and apple fruit. Scientia Horticulturae 42, 269–275.

Adachi, M., Shimokawa, K., 1995. Evidence for the involvement of superoxide anion in the ethylene-induced chlorophyll **a** catabolism of *Raphanus sativus* cotyledons. Phytochemistry 39, 527–530.

Adachi, M., Tsuzuki, E., Shimokawa, K., 1996. Effect of ethylene on degreening of intact radish (*Raphanus sativus* L) cotyledons. Scientia Horticulturae 65, 1–9.

Amir-Shapira, D., Goldschmidt, E., Altman, A., 1987. Chlorophyll catabolism in senescing plant tissues: in vivo breakdown intermediates suggest different degradative pathways for *Citrus* fruits and parsley leaves. Proceedings of the National Academy of Sciences USA 84, 1901–1905.

Baldwin, E., 1993. Citrus fruit. In: Seymour, G., Taylor, J., Tucker, G. (Eds.), Biochemistry of Fruit Ripening. Chapman & Hall, London, pp. 107–149.

Borracino, G., Mastropasqua, L., De Leonardis, S., Dipierro, S., 1994. The role of the ascorbic acid system in delaying the senescence of oat (*Avena sativa* L.) leaf segments. Journal of Plant Physiology 144, 161–166.

Civello, P., Martínez, G., Chaves, A., Añón, M., 1995. Peroxidase from strawberry fruit (*Fragaria ananassa,* Duch.): partial purification and determination of some properties. Journal of Agricultural and Food Chemistry 43, 2596–2601.

Gil, M., Holcroft, D., Kader, A., 1997. Changes in strawberry anthocyanins and other polyphenols in response to carbon dioxide treatments. Journal of Agricultural and Food Chemistry 45, 1662–1667.

Given, N., Venis, M., Grierson, D., 1988. Hormonal regulation of ripening in the strawberry, a non-climateric fruit. Planta 174, 402–406.

Gross, J., 1982. Changes of chlorophyll and carotenoids in developing strawberry fruits (*Fragaria ananassa*) cv. Tenira. Gartenbauwissenschaft 47, 142–144.

Hideg, E., 1997. Free radical production in photosynthesis under stress conditions. In: Pessarakli, M. (Ed.), Handbook of Photosynthesis. Marcel Dekker, New York, pp. 897–910.

Hörtensteiner, S., Wütrich, K., Matile, P., Ongania, K., Kräutler, B., 1998. The key step in chlorophyll breakdown in higher plants. Journal of Biological Chemistry 273, 15335–15339.

Huff, A., 182. Peroxidase-catalysed oxidation of chlorophyll by hydrogen peroxide. Phytochemistry 21, 261–265.

Johnson-Flanagan, A., McLachlan, G., 1990. Peroxidase-mediated chlorophyll bleaching in degreening canola (*Brassica napus*) seeds and its inhibition by sublethal freezing. Physiologia Plantarum 80, 453–459.

Johnson-Flanagan, A., Spencer, N., 1996. Chlorophyllase and peroxidase activity during degreening of maturing canola (*Brassica napus*) and mustard (*Brassica juncea*) seed. Physiologia Plantarum 97, 353–359.

Kato, M., Shimizu, S., 1985. Chlorophyll metabolism in higher plants VI. Involvement of peroxidase in chlorophyll degradation. Plant Cell Physiology 26, 1291–1301.

Kuroda, M., Ozawa, T., Imagawa, H., 1990. Changes in chloroplast peroxidase activities in relation to chlorophyll loss in barley leaf segments. Physiologia Plantarum 80, 555–560.

Langmeier, M., Ginsburg, S., Matile, P., 1993. Chlorophyll breakdown in senescent leaves: demonstration of Mg-dechelatase activity. Physiologia Plantarum 89, 347–353.

Lichtenthaler, H., 1987. Chlorophylls and carotenoids: pigments of photosynthetic biomembranes. Methods in Enzymology 148, 350–382.

Maas, J., Wang, S., Galletta, G., 1991. Evaluation of strawberry cultivars for ellagic acid content. HortScience 26, 66–68.

Maeda, Y., Kurata, H., Adachi, M., Shimokawa, K., 1998. Chlorophyll catabolism in ethylene-treated *Citrus unshiu* fruits. Journal of the Japanese Society for Horticulturae Science 67, 497–502.

Markus, F., Daood, H., Kapitany, J., Biacs, P., 1999. Change in the carotenoid and antioxidant content of spice red pepper (Paprika) as a function of ripening and some technological factors. Journal of Agricultural and Food Chemistry 47, 100–107.

Martínez, G., Chaves, A., Añón, M., 1994. Effect of gibberellic acid on ripening of strawberry fruits (*Fragaria ananassa* Duch.). Journal of Plant Growth Regulation 13, 87–91.

Martínez, G., Civello, P., Chaves, A., Añón, M., 1995. Partial characterization of chlorophyllase from strawberry fruit (*Fragaria ananassa*, Duch.). Journal of Food Biochemistry 18, 213–226.

Matile, P., 1980. Catabolism of chlorophyll. Involvement of peroxidase. Zeitschrift für Pflanzenphysiologie 99, 475–478.

Matile, P., Hörtensteiner, S., Thomas, H., Kräutler, B., 1996. Chlorophyll breakdown in senescent leaves. Plant Physiology 112, 1403–1409.

Matile, P., Schellemberg, M., 1996. The cleavage of phaeophorbide **a** is located in the envelope of barley gerontoplasts. Plant Physiology and Biochemistry 34 (1), 55–59.

Matile, P., Hörtensteiner, S., Thomas, H., 1999. Chlorophyll degradation. Annual Review of Plant Physiology and Plant Molecular Biology 50, 67–95.

Ohtosuka, T., Ito, H., Tanaka, A., 1997. Conversion of chlorophyll **b** to chlorophyll **a** and the assembly of chlorophyll with apoproteins by isolated chloroplasts. Plant Physiology 113, 137–147.

Orthoefer, F., Dugan, L., 1973. The coupled oxidation of chlorophyll **a** with linoleic acid catalysed by lipoxidase. Journal of the Science of Food and Agriculture 24, 357–365.

Perkins-Veazie, P., 1995. Growth and ripening of strawberry fruit. Horticultural Reviews 17, 267–297.

Pichorner, H., Couperus, A., Korori, S., Eberman, R., 1992. Plant peroxidase has a thiol oxidase function. Phytochemistry 31, 3371–3376.

Potty, V., 1969. Determination of protein in the presence of phenols and pectins. Analytical Biochemistry 29, 535–539.

Rice-Evans, C., Miller, N., Paganga, G., 1997. Antioxidant properties of phenolic compounds. Trends in Plant Science 2, 152–159.

Richard-Forget, F., Gauillard, F., Hughes, M., Jean-Marc, T., Boivin, P., Nicolas, J., 1990. Inhibition of horse bean and germinated barley lipoxigenases by some phenolic compounds. Journal of Food Science 60, 1325–1329.

Sánchez-Romero, C., García-Gómez, L., Pliego-Alfaro, F., Heredia, A., 1995. One-step purification of an avocado peroxidase. Plant Physiology and Biochemistry 33, 531–537.

Schuster, B., Herrmann, K., 1985. Hydroxybenzoic and hydroxycinnamic acid derivatives in soft fruits. Phytochemistry 24, 2761–2764.

Shioi, Y., Masuda, T., Takamiya, K., Shimokawa, K., 1995. Breakdown of chlorophylls by soluble proteins extracted from leaves of *Chenopodium album*. Journal of Plant Physiology 145, 416–421.

Shioi, Y., Tatsumi, Y., Shimokawa, K., 1991. Enzymatic degradation of chlorophyll in *Chenopodium album*. Plant Cell Physiology 32, 87–93.

Trebitsh, T., Goldschmidt, E., Riov, J., 1993. Ethylene induces de novo synthesis of chlorophyllase, **a** chlorophyll degrading enzyme in citrus fruit peel. Proceedings of the National Acadeny of Science USA 90, 9441–9445.

Vicentini, F., Iten, F., Matile, P., 1995. Development of an assay for Mg-dechelatase of oilseed rape cotyledons, using chlorophyllin as the substrate. Physiologia Plantarum 94, 57–63.

Watanabe, K., Ohta, H., Tsuchiya, T., Mikami, B., Masuda, T., Shioi, Y., Takamiya, K., 1999. Purification and some properties of pheophorbidase in *Chenopodium album*. Plant Cell Physiology 40, 104–108.

Yamauchi, N., Watada, A., 1994. Effectiveness of various phenolic compounds in degradation of chlorophyll by in vitro peroxidase-hyrogen peroxide system. Journal of the Japanese Society for Horticultural Science 63, 439–444.

Zieslin, N., Ben-Zaken, R., 1993. Peroxidase activity and presence of phenolic substances in peduncles of rose flowers. Plant Physiology and Biochemistry 31, 333–339.

PERGAMON

Phytochemistry 58 (2001) 389–394

PHYTOCHEMISTRY

www.elsevier.com/locate/phytochem

Altritol synthesis by *Notheia anomala*

John A. Raven[a,b,*], John Beardall[a], J.A. Chudek[c], Charles M. Scrimgeour[d], Margaret N. Clayton[a], Shona G. McInroy[b]

[a]*School of Biological Sciences, Monash University, Clayton, Vic 3800, Australia*
[b]*Division of Environmental and Applied Biology, School of Life Sciences, University of Dundee, Dundee DD1 4HN, UK*
[c]*Division of Physical and Inorganic Chemistry, School of Life Sciences, University of Dundee, Dundee DD1 4HN, UK*
[d]*Scottish Crop Research Institute, Invergowrie, Dundee DD2 5DA, UK*

Received 19 March 2001; received in revised form 11 June 2001

Abstract

The linear hexitol altritol has only been identified in six genera, all of them in the order Fucales of the brown algae. Five of these genera are closely related according to molecular phylogenetic and other data, while the sixth (*Notheia*) is an obligate epiphyte on two other altritol-containing genera with which it is symphanic. The possibility that *Notheia* obtains altritol from the algae on which it is epiphytic rather than by synthesizing altritol independently was investigated by supplying ^{13}C-inorganic carbon in the light followed by mass spectrometric and nuclear magnetic resonance analysis. *Notheia* separated from the phorophyte *Hormosira* during exposure to ^{13}C showed ^{13}C enrichment in both altritol and mannitol, while the *Hormosira* only showed significant labelling of mannitol. These data show that altritol can be synthesized by *Notheia*, with implications for the number of gains and losses of the capacity to synthesize altritol in the evolution of the Fucales. © 2001 Published by Elsevier Science Ltd.

Keywords: *Hormosira banksii*; Hormosiraceae; Fucales; Phaeophyceae; *Notheia anomala*; Chemotaxonomy; Linear hexitols; Altritol; Mannitol; Epiphyte; Phorophyte

1. Introduction

Six-carbon sugar alcohols with the empirical formula $C_6H_{14}O_6$ occur widely in living organisms. Mannitol, sorbitol and dulcitol (Fig. 1) occur in many algae, fungi and embryophytes, with (for example) mannitol as a ubiquitous component of the Phaeophyceae (Heterokontophyta) as well as occurring in some members of the Chlorophyta, Rhodophyta and Embryophyta (Kremer, 1980; Raven et al., 1990; Reed et al., 1985, 1995, Wright et al., 1987). They have functions such as compatible solutes and organic C and energy reserves, although these two functions cannot occur simultaneously for sugar alcohols in the compartments of high enzyme content and diversity such as the cytosol, stroma and mitochondrial matrix. These sugar alcohols can also function in organic C and energy transfer in lichens with green algal photobionts and in parasitism of vascular plants by other vascular plants, and as free radical scavengers. There is considerable knowledge of the pathways by which these sugar alcohols are synthesized and degraded, with aldose and ketose six-carbon sugars of appropriate stereochemistry as substrates for reductive synthesis of the sugar alcohols and as products of their oxidation.

The hexitol altritol (Fig. 1) (isomeric with mannitol, sorbitol and dulcitol) was first discovered as a natural product in the North-East Atlantic brown seaweed *Himanthalia elongata* by Chudek et al. (1984) but not in any of the 12 species of sympatric brown algae that were examined (Reed et al., 1985). It was subsequently found to be present in four other species of brown algae, all from the southern hemisphere, i.e. *Bifurcariopsis capensis* (South Africa) and *Hormosira banksii*, *Notheia anomala* and *Xiphophora chondrophylla* (South-Eastern Australia, and New Zealand) but not in the eight other species of southern hemisphere brown algae which were examined (Wright et al., 1987). The other species of *Xiphophora* (*X. gladiata*) has not yet been examined for the

* Corresponding author at second address. Fax: +44-1382-344275.
E-mail address: j.a.raven@dundee.ac.uk (J.A. Raven).

0031-9422/01/$ - see front matter © 2001 Published by Elsevier Science Ltd.
PII: S0031-9422(01)00286-2

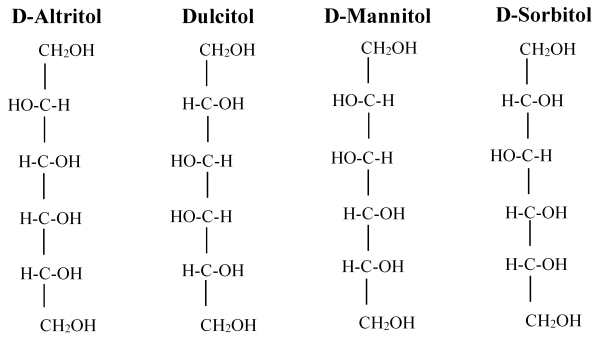

Fig. 1. Structure of altritol, dulcitol, mannitol and sorbitol. In all three cases of optically active hexitols the naturally occurring isomer is the D-form shown here, although D-altritol is equivalent to L-talitol.

occurrence of altritol. All of these algae are members of the Fucales, although the inclusion of *Notheia* involves modification of the definition of the order to include organisms with an anisogamous as well as those with an oogamous diplontic life cycle. Altritol was not detected in the brown algae from orders other than the Fucales which were examined by Reed et al. (1985) and Wright et al. (1987), so that the ability to synthesize altritol is relatively rare.

An estimate of the number of times that the capacity to synthesize altritol has evolved can be made from the molecular phylogeny of the Fucales sensu lato. A large number of genera are included in an analysis based on large and small subunit rDNA genes (de Reviers and Rousseau, 1999; Rousseau and de Reviers, 1999). A smaller data set, but with more overtly rigorous analysis, is that of Serrâo et al. (1999) based on ITS (internal transcribed spacer) 1 and 2 sequences. These analyses show that *Bifurcariopsis*, *Himanthalia*, *Hormosira* and *Xiphophora* are the four earliest-branching genera in the fucacean clade, and that *Notheia* is distantly related to the other altritol-containing genera, although it is a member of the Fucales sensu lato (Fig. 2). The rather distant relationship of *Notheia* to the other altritol-containing genera lends credence to the possibility that altritol synthesis only evolved once, since *Notheia* always grows in nature as an epiphyte on the two genera of altritol-containing brown algae which are geographically accessible, i.e. *Hormosira* and *Xiphophora*

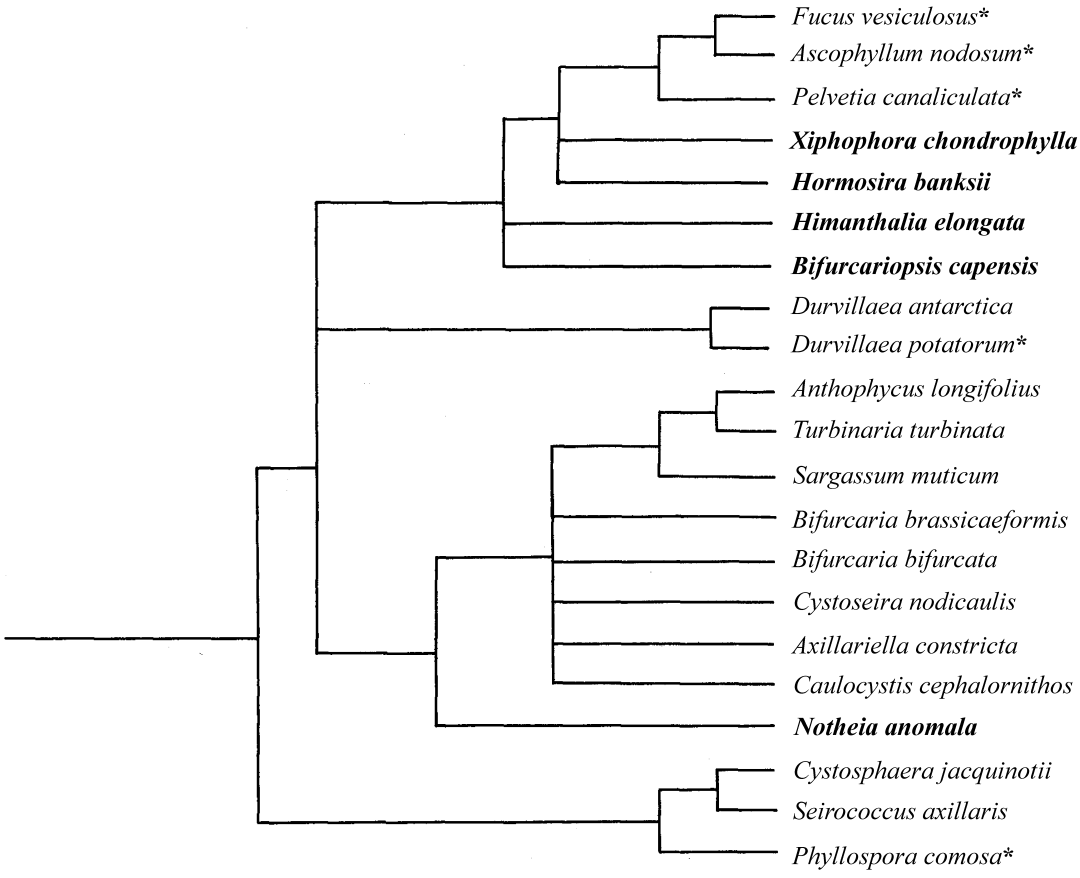

Fig. 2. Phylogeny of the Fucales based on molecular genetic and other evidence, modified, with permission, from de Reviers and Rousseau (1999). The Fucaceae sensu stricto shown here are the genera *Ascophyllum*, *Fucus* and *Pelvetia*, while the Fucaceae *sensu lato* also include *Bifurcariopsis*, *Himanthalia*, *Hormosira* and *Xiphophora* (see de Reviers and Rousseau, 1999). Organisms reported to contain altritol are indicated by bold type, and genera reported to lack detectable quantities of altritol are indicated by an asterisk; other genera in this Figure have not been tested (Chudek et al., 1984; Reed et al., 1985; Wright et al., 1987). Reed et al. (1985) did not find altritol in *Halidrys siliquosa*, a member of the Cystoseiraceae-Sargassaceae clade, which is represented here by the clade containing the genera from *Anthophycus* to *Caulocystis*.

(Raven et al., 1995; de Reviers and Rousseau, 1999). Accordingly, it is possible that *Notheia* obtains the altritol it contains from its phorophyte (Raven et al., 1995; de Reviers and Rousseau, 1999). In this case, altritol synthesis could have had one origin (at the divergence of the Fucaceae *sensu lato* clade from the rest of the Fucales) and one loss (at the origin of the clade of Fucaceae containing *Pelvetia*, *Fucus* and *Ascophyllum*) (Fig. 2; Fig. 7 of de Reviers and Rousseau, 1999; see also Serrâo et al., 1999).

The alternative is that *Notheia* can make its own altritol, which is consistent with the photosynthetic capacity of *Notheia*, which is higher than that of the *Hormosira* on which it is growing on a dry or fresh matter basis and similar to that of *Hormosira* on a surface area or chlorophyll basis (Raven et al., 1995). This alternative is also consistent with the structure of the holdfast attaching *Notheia* to *Hormosira* which resembles that of an attaching rather than that of an absorbing organ. If *Notheia* can make its own altritol, then the most economical hypothesis as to gains and losses of the capacity to synthesize altritol is that there was a single origin of the capacity to make altritol in the clade containing all of the Fucales other than the early-branching Seirococcaceae (Fig. 7 of de Reviers and Rousseau, 1999). This hypothesises losses of the capacity to synthesise altritol after *Notheia* branches from Cystoseiraceae-Sargassaceae clade, in the clade leading to *Durvillaea*, and, as in the hypothesis that *Notheia* obtains all of its altritol from the phorophyte, at the origin of the clade of the Fucaceae containing *Pelvetia*, *Fucus* and *Ascophyllum* (Fig. 2; Fig. 7 of de Reviers and Rousseau, 1999). An alternative phylogeny also based on large and small subunit rDNA (Figs. 1 and 2 of Rousseau and de Reviers, 1999) has an earlier branching of *Durvillaea*, such that altritol synthesis was gained after the rest of the Fucales branched from the Seirococcaceae and *Durvillaea* clades, with the need for only two losses, one after *Notheia* branches from the Cystoseiraceae-Sargassaceae clade, and at the origin of the Fucaceae *sensu stricto*.

A second evolutionary possibility predicated, as in the last paragraph, on the ability of *Notheia* to synthesise altritol, involves two evolutionary gains of the ability to synthesize altritol, i.e. at the branching of *Notheia* from the Cystoseiraceae-Sargassaceae clade and at the branching of the Fucaceae *sensu lato* at the unresolved trichotomy giving rise to the Fucaceae *sensu lato*, *Durvillaea* and the *Notheia* plus Cystoseiraceae-Sargassaceae clade (Fig. 7 of de Reviers and Rousseau, 1999). This possibility involves only one loss of the capacity to synthesize altritol, i.e. that at the origin of the Fucaceae *sensu lato* which is also required in the original suggestion that *Notheia* obtained its altritol from the phorophyte and could not synthesize altritol.

In summary, the hypothesis that *Notheia* obtains its altritol entirely from the phorophyte requires as a minimum one gain and one loss of the capacity to make altritol. The alternative view that *Notheia*, as well as *Bifurcariopsis*, *Himanthalia*, *Hormosira* and *Xiphophora*, can synthesize altritol, requires as a minimum either one gain and two or three losses, or two gains and one loss, of the capacity to synthesize altritol.

In the absence of any knowledge of the pathway of altritol synthesis there are no enzymological or molecular genetic means to distinguish the capacity of *Notheia* to synthesize altritol from its obtaining altritol from the phorophyte. Similarly, it has not so far proved possible to culture *Notheia* for more than a few days independently of altritol-containing phorophytes, and thus to determine whether or not free-living *Notheia* synthesises altritol from measurements (e.g. using NMR: Chudek et al., 1984) of the altritol content of *Notheia* cultured from zygotes growing independently of a phorophyte. Accordingly, this paper reports a study of the ability of *Notheia* detached from *Hormosira*, as well as the *Hormosira* on which it had been growing, to incorporate ^{13}C-labelled inorganic C, *via* photosynthesis, into altritol. The use of ^{13}C label permits the use of ^{13}C NMR to measure the synthesis of altritol, just as ^{13}C at the natural abundance level was used in the original detection and quantification of altritol (Chudek et al., 1984; Reed et al., 1985; Wright et al., 1987). Incorporation of ^{13}C-enriched inorganic C by photosynthesis has been used to study turnover of altritol and mannitol in *Himanthalia elongata* (Reed et al., 1995); the experiments showed that altritol turned over less rapidly than mannitol.

2. Results

Table 1 shows the C and N contents of the dried algal material, and three representations of the ^{13}C content of the algal material. The C and N contents of the algae on a dry matter basis are similar to those reported earlier for *Hormosira* and *Notheia* from Victoria (Raven et al., 1995). The measured $\delta^{13}C$, and the $^{13}C/^{12}C$ ratios and the ^{13}C mol% in excess of the natural abundance level computed from the $\delta^{13}C$, show the ^{13}C enrichment of the algal carbon which occurred in the 52 h labelling period. The ^{13}C mol% in excess of the natural abundance level is higher in the *Notheia* than in the *Hormosira*. This is in accord with the observed greater photosynthetic rate of *Notheia* than of *Hormosira* on a dry matter and on an organic C basis at inorganic carbon and light saturation (Raven et al., 1995). The maximum mole per cent ^{13}C enrichment does not exceed 1.8 in *Hormosira* and 3.8 in *Notheia*, i.e. much lower than the 99.5 mol% ^{13}C enrichment in the inorganic C. However, these rather low enrichments of organic C are not unexpected in view of measured inorganic C fixation rates on an algal organic C basis (Raven et al., 1995),

Table 1
C and N contents, $\delta^{13}C$, $^{13}C/^{12}C$ ratio, and mole per cent excess ^{13}C above natural abundance level for *Hormosira* and *Notheia* incubated in ^{13}C-labelled inorganic C. The ^{13}C mole excess values were calculated using the natural abundance $^{13}C/^{12}C$ values for *Hormosira* and *Notheia* of 0.011115 and 0.01189 respectively (computed from $\delta^{13}C$ values in Raven et al., 1995)

Alga	Conditions during incubation	mg C/g dry matter	mg N/g dry matter	δ ^{13}C	$^{13}C/^{12}C$ ratio	^{13}C mole per cent in excess of the natural abundance value
Hormosira (1)	Detached (from *Notheia* (1))	321; 331	7.4; 7.8	1500; 1500	0.0284; 0.0284	1.64; 1.80
Hormosira (2)	Detached (from *Notheia* (2))	330; 350	8.7; 9.1	1500; 1520	0.0284; 0.0286	1.80; 1.82
Hormosira (3)	Detached (from *Notheia* (3))	332; 333	9.4; 9.4	1260; 1270	0.0257; 0.0257	1.52; 1.52
Notheia (1)	Detached (from *Hormosira* (1))	332; 341	17.2; 17.7	3150; 3170	0.0472; 0.0474	3.84; 3.86
Notheia (2)	Detached (from *Hormosira* (2))	331; 336	14.4; 14.5	2760; 2170	0.0427; 0.0433	3.33; 3.41
Notheia (3)	Detached (from *Hormosira* (3))	333; 339	14.7; 15.0	2780; 2760	0.0430; 0.0433	3.38; 3.41
Hormosira (4)	Attached to *Notheia* (4)	334; 336	8.3; 8.4	1140; 1150	0.0240; 0.0244	1.34; 1.38
Hormosira (5)	Attached to *Notheia* (5)	346; 352	7.5; 7.7	443; 446	0.0164; 0.0164	0.54; 0.54
Notheia (4)	Attached to *Hormosira* (4)	338; 342	11.3; 11.5	2180; 2190	0.0360; 0.0361	2.63; 2.64
Notheia (5)	Attached to *Hormosira* (5)	352; 364	13.4; 13.5	2210; 2220	0.0365; 0.0366	2.68; 2.68

and the turnover of sugar alcohols in *Fucus spiralis* and *Himanthalia elongata* (Wright et al., 1989; Reed et al., 1995) would be expected to yield a much higher enrichment in sugar alcohols than the average in algal organic C. It is not clear why the ^{13}C labelling of both *Hormosira* and *Notheia* is higher in the specimens in which epiphyte and phorophyte were separated before labelling than when the algae were separated after the ^{13}C labelling.

^{13}C spectra of both *Hormosira* and *Notheia* showed resonances which could be attributed to mannitol and altritol. In the enriched *Hormosira* samples the altritol was present only in trace quantities (in spectra of extracts of natural *Hormosira* the mannitol to altritol ratio was ~2:1, see Table 2) while in the equivalent enriched *Notheia* samples altritol made up approximately 47% of the total polyol content (ratio in natural material ~1:1, Table 2). The marked change in the ratios from natural to enriched indicate that in *Hormosira* only mannitol carbons are enriched while in *Notheia* enrichment is in both of the polyols. In *Hormosira* mannitol in the ^{13}C-labelled sample is enriched to 20–30 times natural abundance level. In *Notheia* mannitol is enriched to 20–25 times the natural abundance levels, while altritol enrichment is to 10 times the natural abundance value.

Table 2
Intensities of the C_3 in mannitol and the C_6 in altritol measured with respect to the intensity of the acetate resonance normalised to 1.0, for samples of natural abundance and enriched *Hormosira* and *Notheia*. Intensities are in arbitrary units with a machine precision of ±0.2. Sample numbers are as in Table 1, i.e. the data shown here are for the epiphyte and phorophyte separated prior to incubation in ^{13}C-inorganic C

	Hormosira				*Notheia*			
	Natural abundance	Enriched			Natural abundance	Enriched		
		(1)	(2)	(3)		(1)	(2)	(3)
Mannitol	0.5	15.3	13.3	11.5	0.5	11.3	10.2	12.8
Altritol	0.3	0.2	0.3	0.4	0.6	6.5	6.0	6.0

Around each of the resonances which would be expected for natural abundance spectra of mannitol (C1,6, 64.6 ppm; C2,5, 72.2 ppm; C3,4, 70.7) and altritol (C1, 64.4 ppm; C2, 71.8 ppm; C3, 72.2 ppm; C4, 73.0 ppm; C5, 74.0 ppm; C6, 63.4 ppm) were a number of smaller peaks (Fig. 3). These were attributable to the effect of carbon–carbon splitting, not normally observed in natural abundance ^{13}C spectra, where the probability of adjacent labelled (^{13}C) carbons is 1:10,000, but clearly seen here. Measurement of the intensities of individual carbons was difficult due to line overlap but it would appear that their intensities relative to the standard acetate are equal in both mannitol and altritol, indicating that labelling was equal in all carbons when averaged over all of the sugar alcohol molecules. However, the line splitting shows that labelling is not uniform throughout each polyol molecule. Analysis of the splitting exhibited by carbons 2 and 5 in mannitol in *Hormosira* sample (1) indicates the presence of a singlet, no labelled carbons adjacent; a doublet ($J_{CC} = 40.9$ Hz), one labelled carbon adjacent and a triplet ($J_{CC} = 42.4$ Hz), 2 labelled carbons adjacent. Thus, the line splitting implies that there are polyol molecules with a mixture of ^{13}C and ^{12}C molecules, with more ^{13}C than the natural abundance level (i.e. synthesized from ^{13}C-labelled photosynthate) but with more ^{12}C than would be expected from the 99% ^{13}C-enriched inorganic C substrate supplied for photosynthesis. This implies dilution of the supplied ^{13}C with ^{12}C before the polyols are synthesized, the ^{12}C coming from the (minimal) residual inorganic C

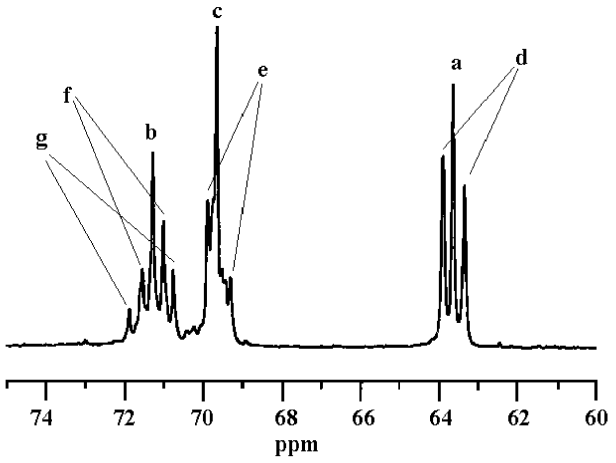

Fig. 3. ^{13}C {H} spectrum of *Hormosira* after photosynthesis in ^{13}C-HCO_3^--enriched medium; only resonances associated with mannitol are observed. Peak (a) resonances for C atoms 1 and 6, (b) for C atoms 2 and 5, and (c) for C atoms 3 and 4. In unenriched samples only these three resonances are observed. The resonances marked (d) and (e) indicate enrichment of at least one C adjacent to C atoms 1 and/or 6 and C atoms 3 and/or 4 respectively. Resonances marked (f) and (g) show the doublet and triplet [central band under (b)], described in the text; these, together with resonance (b) indicates that C atoms 2 and 5 are present in molecules where no neighbouring C atoms are enriched [singlet (b)], where one is enriched [doublet (f)] and where two are enriched [triplet (g)].

in the 'CO_2-free' seawater (see Experimental), and from CO_2 generated within the thallus by respiration of substrates with no significant ^{13}C enrichment (see Table 1 for enrichment of whole-alga organic C) rather than dilution of the supplied ^{13}C by atmospheric air (see Experimental).

3. Discussion

The data reported in this paper clearly show that *Notheia anomala* can synthesise altritol from products of its own photosynthesis when it is detached from its phorophyte *Hormosira banksii*. The data showing labelling of altritol in *Notheia* when the *Hormosira*/*Notheia* combination is incubated in the ^{13}C-enriched inorganic C and only separated after labelling is consistent with the ability of *Notheia* to synthesise altritol, but on its own would be inconclusive since translocation of altritol from phorophyte to epiphyte has not been ruled out. An absence of ^{13}C labelling of altritol when detached *Notheia* were incubated with ^{13}C-labelled inorganic C would not be regarded as conclusive evidence that *Notheia* was unable to synthesise altritol, since some hypothetical labile 'host factor' could be invoked as necessary to permit altritol synthesis in *Notheia*. However, there is no need to hypothesise such a host (phorophyte) factor since detached *Notheia* can synthesis altritol.

The finding that *Notheia* can synthesise altritol means that the first hypothesis as to the phylogeny of altritol synthesis in the Fucales which was proposed in the Introduction can be eliminated. As for the alternative hypotheses, the data presented in this paper do not distinguish between the suggestions of a single gain of the ability to synthesise altritol and three losses of this synthetic ability from the alternative of two gains of the ability to synthesise altritol and a single loss of this synthetic ability.

4. Experimental

4.1. General experimental procedures

Seawater containing ^{13}C inorganic C was prepared by removing inorganic C from 4 dm^3 seawater by adjusting pH to 3.8, purging overnight with CO_2-free air then readjusted to the starting pH (8.17) with freshly made up NaOH solution (1 kmol m^{-3}) and 1.25 g of $NaHCO_3$ which was 99 at.% ^{13}C (Sigma). This gave an added inorganic C concentration of 3.67 mol m^{-3}, with a residual inorganic C concentration prior to ^{13}C addition of less than 40 mmol m^{-3}. Triplicate samples of Hormosira phorophytes (5.91–6.37 g fresh weight) from which the *Notheia* epiphytes had been detached were incubated in 500 cm^3 aliquots of the labelling solution. Triplicate samples of the *Notheia* epiphytes (6.01–6.25 g fresh weight) which had been detached from *Hormosira* were also incubated in aliquots of the ^{13}C solution. Duplicate samples of *Hormosira* bearing *Notheia* (11.60 and 11.81 g fresh weight) were incubated in further aliquots. Samples were incubated in 0.5 dm^3 conical flasks containing 0.5 dm^3 of the ^{13}C-enriched seawater; there was minimal air space above the aqueous phase and the flasks were sealed with a double layer of Parafilm. Incubation conditions were 100 μmol photon m^{-2} s^{-1} continuous photosynthetically active radiation at 16 °C for 52 h. At the end of the incubation the specimens were removed from the labelling solution, washed briefly with unlabelled seawater and dried at 60 °C. Drawdown of inorganic carbon by photosynthesis during incubation was indicated by increase in pH of the incubation medium to 8.64–9.04 (*Hormosira* alone), 9.32–9.66 (*Notheia* alone) and 9.47–9.63 (*Hormosira* plus *Notheia*), despite the initial inorganic C concentration of almost twice that of normal seawater. Some loss of photosynthetic performance during the 52 h incubation was indicated by the decrease in F_v/F_m (a function of the quantum yield of net electron transport through reaction centres of photosystem two: Falkowski and Raven, 1997) from 0.67 to 0.54 for *Hormosira* and from 0.60 to 0.53 for *Notheia*.

The enrichment of ^{13}C algal bulk organic carbon was determined on 1 mg dry matter samples of algae on a

Europa 20–20 isotope ratio mass spectrometer coupled to an ANCA-SL sample converter. This procedure provided values for the C and N contents of the specimens as well as $\delta^{13}C$ of the organic carbon. Computation of the $^{13}C/^{12}C$ ratio of the algal material from the $\delta^{13}C$ involved the use of the known $^{13}C/^{12}C$ of the Pee–Dee Belemnite standard for the $\delta^{13}C$ measurements, i.e. 0.011365. Estimation of the mol percent ^{13}C in the algal material in excess of the natural abundance ^{13}C levels in the algae were performed using $\delta^{13}C$ values for the algae from Raven et al. (1995).

The remainder of the ^{13}C-labelled specimens were individually extracted in boiling 80% v/v aqueous ethanol, followed by overnight extraction in the same solvent at room temperature (Wright et al., 1989; Reed et al., 1995). An internal standard containing 50.0 mg of 20.7 mol percent ^{13}C-enriched sodium acetate was added to each sample vial at the beginning of the extraction procedure. The extract was filtered through a Whatman GF/C filter and then dried by rotary evaporation. The material was then redissolved in 1 cm^3 of D_2O, the deuterium signal of which was used as a field lock.

Samples were placed into 5mm OD NMR tubes and $^{13}C\{^1H\}$ NMR spectra were acquired on a Bruker AVANCE DPX 300 FT NMR spectrometer, resonating at ^{13}C: 75.42 MHz; ^1H: 299.90 MHz. Data were accumulated into 64 k data points using a 30° (5.3 μs) pulse width; a 3.4 s repetition time and a 24 kHz sweep width, these parameters were designed to allow the relative intensities of the polyol resonances to be measured. Data were transformed into 32 k words using 3 Hz line broadening. Resonance frequencies were measured with regard to external TMS; line intensities with regard to the acetate resonance, integral 1.0.

4.2. Biological materials

Hormosira banksii (Turner) Decaisne with epiphytic *Notheia anomala* Harvey and Bailey was collected from rock pools at Sorrento Ocean Beach (Sorrento, Victoria, Australia; 38° 28′S; 144° 43′E) on 16 March 2000 at low tide (13.45). Seawater temperature at the time of sampling was 16–17 °C; air temperatures during the day were 22–23 °C for the prior 3–4 days, after three weeks of much higher temperatures. The samples were taken to the laboratory in a cool box and incubated overnight in aerated seawater before being used in labelling experiments.

A voucher specimen of *Notheia anomala* on *Hormosira banksii* collected from Sorrento is deposited in the Algal Herbarium, School of Biological Sciences, Monash University. The specimen number is 2770 and the collector/identifier is M. Forbes.

Acknowledgements

The assistance of Christine Ashburner, Dr. Antionetta Quigg and Dr. Erica Young is greatly appreciated. We are greatly indebted to Mrs. R. L. MacKay who ran the NMR spectra, and to the authors and publishers of de Reviers and Rousseau (1999) for permission to reproduce the material shown in Fig. 2.

References

Chudek, J.A., Foster, R., Davison, I.R., Reed, R.H., 1984. Altritol in the brown alga *Himanthalia elongata*. Phytochemistry 23, 1081–1082.

Falkowski, P.G., Raven, J.A., 1997. Aquatic Photosynthesis. Blackwell Science, Malden, MA.

Kremer, B.P., 1980. Taxonomic implications of algal photoassimilate patterns. British Phycological Journal 15, 399–409.

Raven, J.A., Johnston, A.M., MacFarlane, J.J., 1990. Carbon metabolism. In: Cole, M., Sheath, R.G. (Eds.), Biology of the Red Algae. Cambridge University Press, Cambridge, pp. 171–198.

Raven, J.A., Beardall, J., Johnston, A.M., Kübler, J.E., Geoghegan, I., 1995. Inorganic carbon acquisition by *Hormosira banksii* (Phaeophyta: Fucales) and its epiphyte *Notheia anomala* (Phaeophyta: Fucales). Phycologia 34, 256–277.

Reed, R.H., Davison, I.R., Chudek, J.A., Foster, R., 1985. The osmotic role of mannitol in the Phaeophyceae: an appraisal. Phycologia 24, 35–47.

Reed, R.H., Wright, P.J., Chudek, J.A., Hunter, G., 1995. Turnover of hexitols in the marine macroalga *Himanthalia elongata* (Phaeophyta, Fucales). European Journal of Phycology 30, 169–177.

de Reviers, B., Rousseau, F., 1999. Towards a new classification of the brown algae. In: Round, F.E., Chapman, D.J. (Eds.), Progress in Phycological Research. Vol. 13. Biopress Ltd, Bristol, pp. 107–201.

Rousseau, F., de Reviers, B., 1999. Phylogenetic relationships within the Fucales (Phaeophyceae) based on partial SSU & LSU rDNA sequence data. European Journal of Phycology 34, 53–64.

Serrâo, E.A., Alice, L.A., Brawley, S.H., 1999. Evolution of the Fucaceae (Phaeophyceae inferred from nrDNA-ITS. Journal of Phycology 35, 382–394.

Wright, P.J., Clayton, M.N., Chudek, J.A., Foster, R., Reed, R.H., 1987. Low molecular weight carbohydrates in marine brown algae from the southern hemisphere: the occurrence of altritol in *Bifurcariopsis capensis*, *Hormosira banksii*, *Notheia anomala* and *Xiphophora chondrophylla*. Phycologia 26, 429–434.

Wright, P.J., Chudek, J.A., Foster, R., Reed, R.H., 1989. Turnover of the intracellular mannitol pool of *Fucus spiralis* L. (Fucales, Phaeophyta) during osmotic shock. Journal of Experimental Botany 40, 1347–1353.

PERGAMON

Phytochemistry 58 (2001) 395–401

PHYTOCHEMISTRY

www.elsevier.com/locate/phytochem

Production of loline alkaloids by the grass endophyte, *Neotyphodium uncinatum*, in defined media

Jimmy D. Blankenship[a], Martin J. Spiering[a], Heather H. Wilkinson[a,1], Franklin F. Fannin[b], Lowell P. Bush[b], Christopher L. Schardl[a,*]

[a]*Department of Plant Pathology, University of Kentucky, Lexington, KY 40546-0091, USA*
[b]*Department of Agronomy, University of Kentucky, Lexington, KY 40546-0091, USA*

Received 27 February 2001; received in revised form 18 May 2001

Abstract

Lolines (saturated 1-aminopyrrolizidines with an oxygen bridge) are insecticidal alkaloids produced in symbioses of certain *Epichloë* (anamorph-*Neotyphodium*) species (fungal endophytes) with grasses, particularly of the genera *Lolium* and *Festuca*. Prior to the present study, it was unknown whether lolines were of plant or fungal origin. *Neotyphodium uncinatum*, the common endophyte of meadow fescue (*Lolium pratense* = *Festuca pratensis*) produced loline, *N*-acetylnorloline, and *N*-formylloline when grown in the defined minimal media at pH 5.0–7.5, with both organic and inorganic nitrogen sources and sugars as carbon sources. In contrast, lolines were not detected in complex medium cultures. GC–MS and ^{13}C NMR spectroscopic analyses confirmed the identity of the alkaloids isolated from the defined medium cultures. Lolines accumulated to ca. 700 mg/l (4 mM) in cultures with 16.7 mM sucrose and 15–30 mM asparagine, ornithine or urea. Kinetics of loline production and fungal growth were assessed in defined medium with 16.7 mM sucrose and 30 mM ornithine. The alkaloid production rate peaked after the onset of stationary phase, as is common for secondary metabolism in other microbes. © 2001 Elsevier Science Ltd. All rights reserved.

Keywords: *Neotyphodium uncinatum*; Clavicipitaceae; Epichloë endophyte; *Lolium pratense*; *Festuca pratensis*; Poaceae; Meadow fescue; Fungal fermentation; 1-Aminopyrrolizidines; Loline alkaloids

1. Introduction

Loline alkaloids (saturated 1-aminopyrrolizidines with an oxygen bridge) (Fig. 1) have been identified in some grass-endophyte associations (Siegel et al., 1990), but are absent in most other organisms. These grasses are naturally infected with symbiotic endophytic fungi, especially *Epichloë* spp. and their asexual derivatives (*Neotyphodium* spp.), which grow in the intercellular spaces (apoplast) of host plants. In these symbioses, an array of other anti-herbivore alkaloids is produced. Three of the alkaloid classes commonly found in endophyte–grass associations—peramine (a pyrrolopyrazine), ergot alkaloids, and lolitrems (indolediterpenes)—are of known fungal origin because these are reported to accumulate in fermentation cultures (Bacon, 1988; Rowan, 1993, Gurney et al., 1994; Porter, 1994). The lolines are produced in a number of grass-endophyte symbioses: *Lolium arundinaceum* (= *Festuca arundinacea*) with *Neotyphodium coenophialum* (Siegel et al., 1990), *Lolium giganteum* (= *Festuca gigantea*) with *Epichloë festucae* (Leuchtmann et al., 2000), *Lolium pratense* (= *Festuca pratensis*) with *Neotyphodium uncinatum* (Bush et al., 1993; Justus et al., 1997), *L. pratense* with *Neotyphodium siegelii* (Craven et al., 2001), and endophyte-infected *Festuca argentina* (Casabuono and Pomilio, 1997), *Lolium temulentum* (Dannhardt and Steidt, 1985), *Poa autumnalis* (Siegel et al., 1990), and *Stipa robusta* (TePaske et al., 1993). The plants, *Argyreia mollis* (Convolvulaceae) and *Adenocarpus* spp. (Fabaceae) have also been reported to contain loline alkaloids, although endophytes have not been implicated (Hartmann and Witte, 1995; Tofern et al., 1999).

The lolines are secondary metabolites and have an unusual structure consisting of a saturated necine ring with an –NRR′ substituent at C1 and an oxygen bridge

* Corresponding author. Tel.: +1-859-257-8758; fax: +1-859-323-1961.

E-mail address: schardl@pop.uky.edu (C.L. Schardl).

[1] Current address: Department of Plant Pathology and Microbiology, Texas A&M University, College Station, 77843, USA.

0031-9422/01/$ - see front matter © 2001 Elsevier Science Ltd. All rights reserved.
PII: S0031-9422(01)00272-2

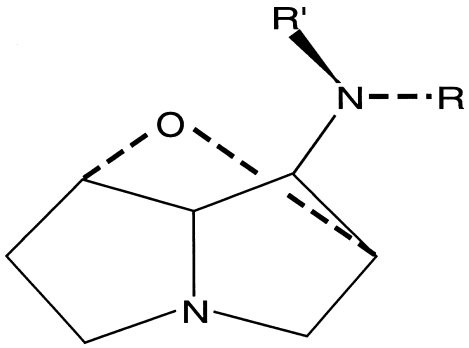

	R	R'
Loline (**1**)	H	CH_3
N-Acetylnorloline (**2**)	$COCH_3$	H
N-Formylloline (**3**)	CHO	CH_3
N-Formylloline (**3'**)	CH_3	CHO

Fig. 1. Structures of loline alkaloids.

between C2 and C7 (Yates et al., 1990; Powell and Petroski, 1992). Lolines thus differ from most plant pyrrolizidines, which are synthesized from homospermidine (Böttcher et al., 1993) and have a $-CH_2OR$ group at C1. Nothing is known about the biosynthesis of the endophyte-associated lolines, but based on this difference, the loline alkaloids have been suggested to be derived from spermidine or spermine (Bush et al., 1993). The alkaloids are found throughout the plant in these associations and have protective effects for the plant due to their anti-invertebrate and feeding deterrent activities (Patterson et al., 1991; Justus et al., 1997; Dougherty et al., 1998; Wilkinson et al., 2000). Lolines are broad-spectrum insecticides (Siegel and Bush, 1997); and in grasses symbiotic with strains of *E. festucae* segregating for loline alkaloid expression, accumulation of these alkaloids was clearly associated with activity against certain aphid species (Wilkinson et al., 2000). Thus, the loline alkaloids are of great interest as natural plant protectants. Although studies do indicate immunosuppressive effects in mice (Dew et al., 1990) and depressed feed intake has been observed in rats fed loline alkaloids (Jackson et al., 1996), it has not been conclusively shown that the loline alkaloids at in planta levels are toxic to mammalian herbivores (Siegel and Bush, 1997). Lolines do not share the same potent anti-mammalian hepatotoxicity and carcinogenicity as plant pyrrolizidines, 1-hydroxymethylpyrrolizidines, which contain C-1,2 unsaturation in the necine ring (Hincks et al., 1991); cytochrome P450 converts the 1-hydroxymethylpyrrolizidines to more bioactive forms, which to varying degrees are capable of crosslinking of DNA (Kim et al., 1999).

Loline alkaloid expression correlates with fungal genotype, and in some grass-endophyte symbiota levels can exceed 2% plant dry mass (Craven et al., 2001). Until the present study lolines have been the only grass-endophyte associated alkaloid class reported in the literature that was not observed in fungal cultures (Porter, 1994). Knowledge of the origin of lolines would be beneficial for elucidating the biosynthetic pathway and its regulation, identifying biosynthesis genes, and expanding biotechnological possibilities for these alkaloids.

Since lolines were only detected in endophyte-infected plants, we hypothesized the endophyte was responsible for their production, and that cultures that adequately mimic the internal environment of the plant may stimulate loline production. In this paper, it is demonstrated that three of the loline alkaloids found in plant tissue—loline (**1**), *N*-acetylnorloline (**2**), and both rotamers of *N*-formylloline (**3** and **3′**)—are produced by *N. uncinatum* under certain minimal medium conditions.

2. Results

The common endophyte of *L. pratense, N. uncinatum,* was examined for potential production of loline alkaloids in culture because grasses symbiotic with this species accumulate lolines at high levels. In a minimal medium modified from Chung and Schardl (1997), with mannitol as the carbon source and asparagine as the nitrogen source, *N. uncinatum* produced **1**, **2**, **3**, and **3′**. The identities of these alkaloids were confirmed by GC–MS and ^{13}C NMR spectroscopic analyses. Another loline alkaloid, *N*-acetylloline, is (together with **3** and **3′**) one of the most abundant alkaloids in *L. pratense–N. uncinatum* symbiota (Siegel et al., 1990), but was not detected in the culture. No loline alkaloids were detected from the cultures grown in potato dextrose broth (PDB).

Various carbon sources typically present in plant apoplasts were examined. Initially, mannitol was chosen because it is a good carbon source for growth of the related endophyte, *N. coenophialum* (Kulkarni and Nielsen, 1986). Fructose, glucose, and sucrose were then tested as alternative carbon sources because sucrose is a major transport sugar in the apoplast, while glucose and fructose are produced from sucrose by the action of invertase secreted by endophytes (Lam et al., 1994). As shown in Fig. 2, sucrose was the best of these carbon sources for loline production, giving a range of 500–750 $\mu g\ ml^{-1}$ (up to 4 mM) total of **2**, **3**, and **3′**. This was a 12-fold increase of production over cultures with mannitol. Glucose or fructose also tended to increase production only slightly compared to mannitol cultures, but not to the level obtained using sucrose.

Nitrogen sources tested were asparagine, arginine, ornithine, glutamine, ammonium sulfate, and urea, in cultures at pH 5.5 with sucrose as carbon source.

Nitrogen concentration was maintained at 30 mM total nitrogen atoms. In this experiment, cultures with urea as the sole nitrogen source yielded the greatest overall level of loline alkaloid production, ca. 425 μg ml^{-1} of culture filtrate (Fig. 3). Ornithine as the sole nitrogen source also gave much greater levels than expressed in cultures with asparagine or arginine. The level of loline alkaloid production at day 20 was 5-fold greater when ornithine rather than asparagine was the nitrogen source (Fig. 3).

Altering concentrations of phosphate between 6.8 and 68 mM, $MgSO_4$ between 0.2 and 4.0 mM, mannitol between 8.3 and 16.7 mM, or asparagine between 15 and 30 mM had only slight effects on loline alkaloid production levels (data not shown).

To determine how loline alkaloid production and growth may be related, a time course experiment was conducted with medium containing 16.7 mM sucrose and 30 mM ornithine (Figs. 4 and 5) (these carbon and nitrogen sources were chosen for the time course because they promote loline alkaloid production and are known substituents of plant apoplasts; Pate, 1973). The proportion of **2** to **3** with **3′** in this experiment (Fig. 4a and b) was consistent with levels obtained in similar experiments. (Levels of **1** were characteristically very low, so they are not included in Fig. 4.) The maximum rate of loline alkaloid accumulation (Fig. 4a and b) consistently occurred after cessation of the fungal growth with onset of stationary phase (Fig. 5a). A slight increase in pH occurred whether the initial pH was 5.5

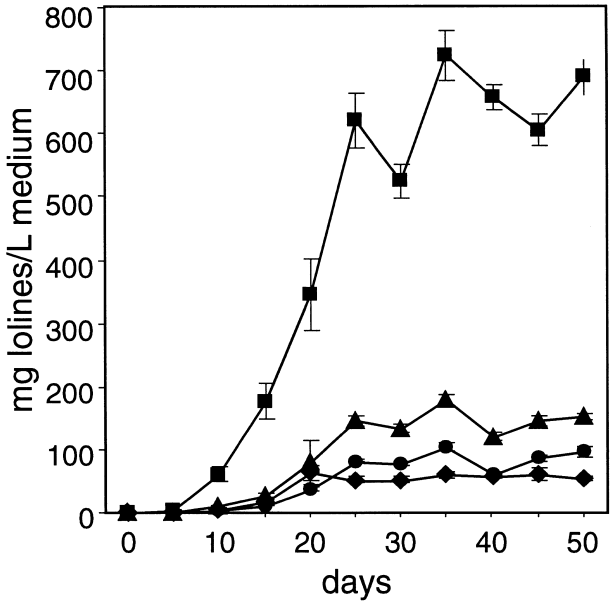

Fig. 2. Effect of carbon source on loline production. Carbon sources were ◆ 16.7 mM mannitol, ▲ 16.7 mM glucose, ● 16.7 mM fructose, or ■ 16.7 mM sucrose. Asparagine concentration was at 15 mM; pH 5.5. Means ($n=5$) are indicated with error bars equal to ± 1 S.D. S.D. smaller than the symbol are not shown.

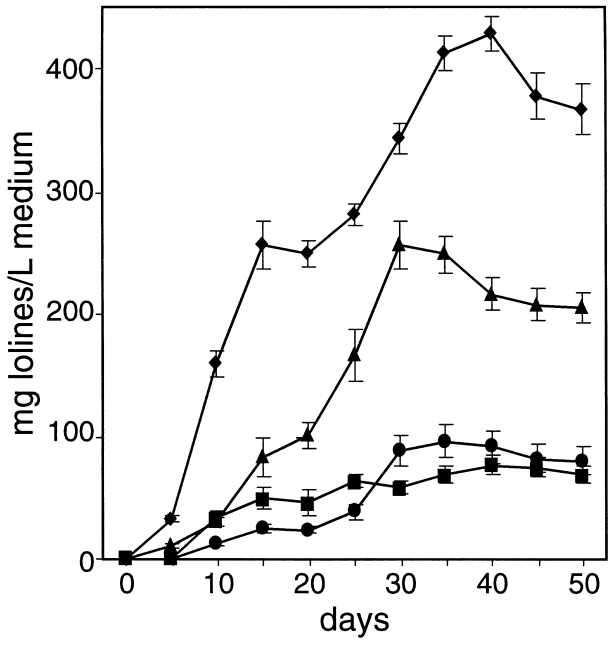

Fig. 3. Effect of nitrogen source on loline production. Nitrogen sources were ▲ 15 mM ornithine, ● 15 mM asparagine, ■ 7.5 mM arginine, or ◆ 15 mM urea. Sucrose concentration was 16.7 mM, and pH was 5.5. Means ($n=4$, except urea $n=3$) are indicated with error bars equal to ± 1 S.D.

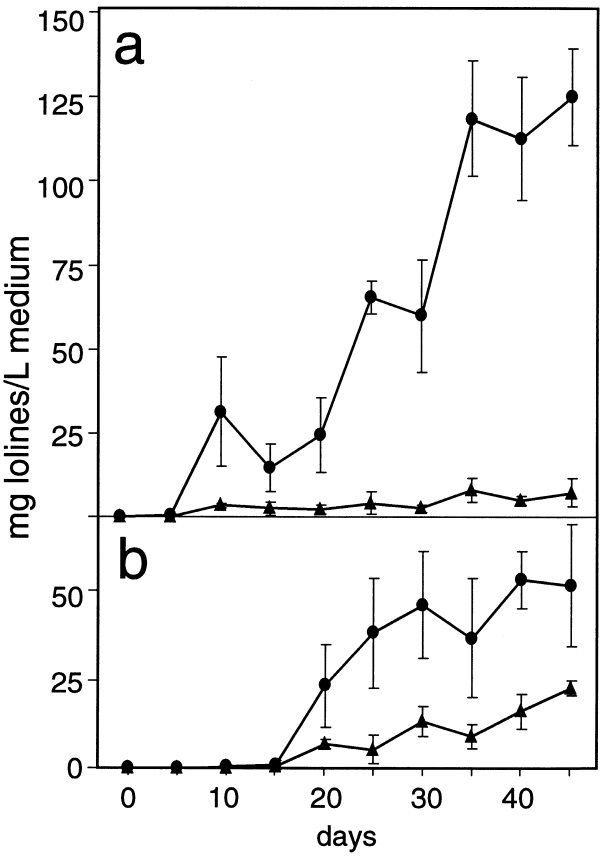

Fig. 4. Levels of ▲ *N*-acetylnorloline and ● *N*-formylloline in cultures. (a) Production at pH 5.5. (b) Production at pH 7.0. Means ($n=4$) are indicated with error bars equal to ± 1 S.D.

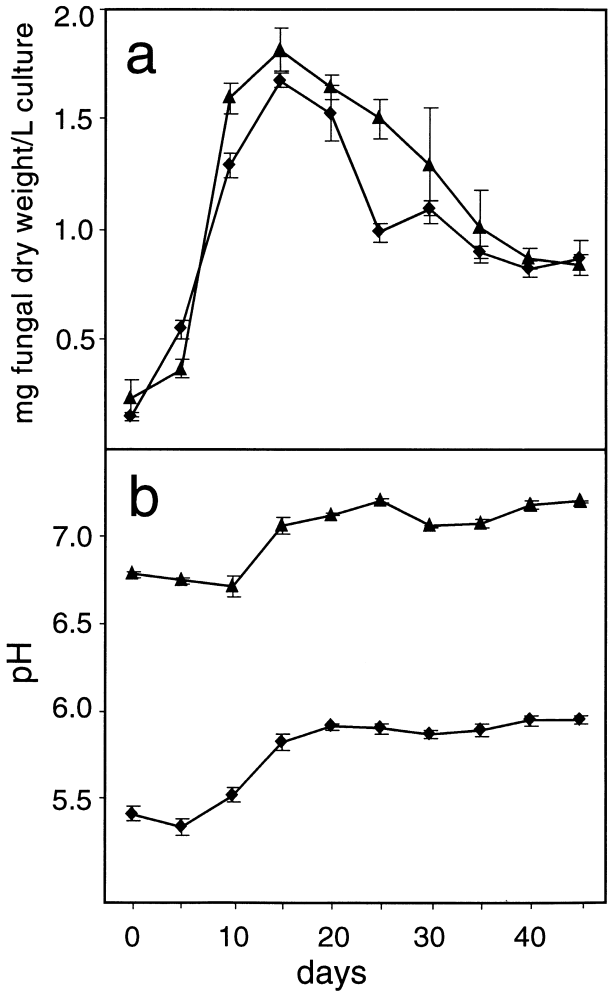

Fig. 5. Comparison of loline production at pH ◆ 5.5 and ▲ 7.0. (a) Growth of *Neotyphodium uncinatum*. (b) Change in pH of culture medium. Carbon and nitrogen sources were 16.7 mM sucrose and 30 mM ornithine, respectively. Means ($n=4$) are indicated with error bars equal to ± 1 S.D.

or 7.0 (Fig. 5b), and the change coincided with the onset of loline production (Fig. 4a and b) and slowing of fungal growth (Fig. 5a).

Other grass endophytes known to produce lolines in planta—*E. festucae* from *L. giganteum* (Leuchtmann et al., 2000), *N. coenophialum* from *L. arundinaceum* (Siegel et al., 1990), and *N. siegelii* from *L. pratense* (Craven et al., 2001)—were also tested for production. These fungi were cultured under the preferred conditions established for *N. uncinatum* (including 20 mM sucrose and 30 mM ornithine), but lolines were not detected in these cultures.

3. Discussion

The *Epichloë* and *Neotyphodium* species, closely related fungi that live as endophytes of grasses, have been implicated in the production of the ergot, lolitrem, and peramine alkaloids (Porter, 1994). Previously, lolines were never observed outside the grass-endophyte symbiota (Schardl and Phillips, 1997). Thus, prior to this study it was not established whether the plant or fungus, or the combination of both, produced the loline alkaloids. By establishing culture conditions for production of the loline alkaloids (specifically *N*-formylloline, *N*-acetylnorloline, and loline) by *N. uncinatum,* it was demonstrated that this fungus has the full biosynthetic capacity for some of the most common loline alkaloids found *in planta.* The observed correspondence of maximal loline production with the stationary phase was in keeping with secondary metabolism in other microorganisms (Campbell, 1984).

Nitrogen sources for these experiments were chosen to test organic and inorganic nitrogen and also based on the known precursors of polyamines and plant pyrrolizidines (Böttcher et al., 1993). Ammonium sulfate was used as an inorganic nitrogen source with levels of production comparable to those with asparagine, glutamine, and arginine. Cultures with urea as nitrogen source yielded the highest levels of lolines, but urea was not examined further because its levels in plant apoplast and xylem are unknown. Arginine and ornithine are apoplast substituents in grasses (Pate, 1973), and ornithine is a direct precursor in the polyamine biosynthetic pathway. It has been proposed, based on structures of the lolines, that spermidine, spermine, or both could be precursors to the lolines (Siegel and Bush, 1997). Arginine and ornithine are closely related, and removal of the urea group from arginine yields ornithine in the urea cycle. A determinant step in polyamine synthesis is decarboxylation of ornithine to form putrescine, which is converted to spermidine with the addition of a propylamine group from decarboxylated *S*-adenosylmethionine. Adding an additional propylamine group to spermidine yields spermine. These propylamine groups ultimately derive from aspartate, which is readily derived from asparagine. Preliminary feeding studies with ^{13}C-labelled ornithine and aspartate confirmed that these are likely loline alkaloid precursors (J.D.B. and C.L.S., unpubl. data).

The absence of *N*-acetylloline in culture, the other major loline alkaloid produced in planta, remains to be explained. Alternative possibilities are that the fungus does not express the necessary enzyme to convert loline (or other lolines) to *N*-acetylloline, or that the plant is responsible for the conversion. Another surprising observation is that no other fungal endophyte that produces the loline alkaloids in planta produced measurable quantities in culture, even under conditions favorable for production by *N. uncinatum*. A possibility is that only *N. uncinatum* has the full competence to produce lolines outside its host, whereas in other grass-endophyte symbiota loline alkaloid production may be accomplished by both symbiotic partners. A more likely possibility, however, is simply that the culture conditions promoting production by *N. uncinatum* were unsuitable for production by the other endophytes.

Now that it has been shown that some common loline alkaloids can be produced by cultured *N. uncinatum*, work is underway on the biosynthetic pathway for loline alkaloids. The high level of their production in culture will significantly facilitate studies of the pathway and will aid in identifying and characterizing the genes that may be responsible.

4. Experimental

4.1. General experimental procedure

For gas chromatography, all samples were run on a Hewlett Packard (Avondale, PA) 5890 Series II Plus GC equipped with a flame ionization detector and a J&W Scientific Inc. (Rancho Cordova, CA) fused silica capillary column (SE 30, 60 m×0.30 mm inner diameter with 0.25 μm film thickness of dimethylpolysiloxane). Nitrogen was used as the carrier gas at a flow rate of 20.4 ml min^{-1}. The run parameters were an initial column temperature of 110 °C, an injection temperature of 250 °C, a detector temperature of 325 °C, a 2.2-min purge time, and a 4 °C min^{-1} increase in column temperature to 188 °C. Between each sample run, the column was purged at 280 °C for 5 min. ^{13}C NMR spectroscopic analysis employed a Varian Gemini 200 equipped with VNMR 6. 1B software (Varian Inc., Palo Alto, CA). Samples of purified alkaloids in 750 μl D_2O (Cambridge Isotopes Laboratories, Inc., Andover, MA) were prepared in 5 mm×17.8 cm NMR tubes (Wilmad, Beuna, NJ) and 10 μl methanol added as an internal standard. ^{13}C NMR spectroscopic conditions were at 200 mHz, ambient temperature, and proton decoupling. Chemicals for these experiments were obtained from Sigma-Aldrich (Milwaukee, WT).

4.2. Fungal isolate isolation

Cultures were obtained by growing *Neotyphodium uncinatum* (W. Gams Petrini et Schmidt) Glenn Bacon et Hanlin (voucher specimen CBS 102646 at Centraalbureau Voor Schimmelcultures) out of an infected plant (number 167 in our plant collection) of *Lolium pratense* (Huds.) Darbysh. [*Festuca pratensis* Huds., realigned with genus *Lolium* by Darbyshire (1993).] Leaf blades were sterilized in 50-ml Costar tubes with 95% ethanol for 1 min, followed by a rinse of sterile water, then soaked for 2 min in 5.25% sodium hypochlorite. The leaf blades were then rinsed with sterile water, cut into 2-mm sections, and plated on potato dextrose agar (PDA, Difco Laboratories, Detroit, MI) with penicillin (167 units ml^{-1}) and streptomycin (76.3 units ml^{-1}). After 14 days, 5 pieces of fungal mycelium grown out (approximately 0.5 cm) of the plant material was removed from the agar and homogenized in 10 ml of the minimal medium in an Omni Homogenizer Model 17105 (Omni International, Waterbury, CT) with six 10-s bursts. The ground mycelium was drop-inoculated onto PDA and grown for 7 days, then 1.5–2 cm plugs were cut out of the agar, homogenized in minimal medium, and 1 ml used to inoculate each 30 ml minimal medium culture for study. Large differences in alkaloid expression between experiments most likely were due to unavoidable differences in inoculum density and physiological condition of the source mycelium, so employing a single source of inoculum for each experiment minimized variation between replicates. Cultures of *Epichloë festucae* Leuchtm. Schardl et Siegel (CBS 102474) from *Lolium giganteum* (L.) Darbysh. (= *Festuca gigantea* L.), *Neotyphodium coenophialum* (Morgan-Jones et W. Gams) Glenn Bacon et Hanlin (American Type Culture Collection accession ATCC 90664) from *Lolium arundinaceum* (Schreb.) Darbysh. (= *Festuca arundinacea* Schreb.), and *Neotyphodium siegelii* K. D. Craven Leuchtm. et Schardl (ATCC 74483) from *L. pratense* were obtained similarly (Craven et al., 2001).

4.3. Culture medium

The defined media used in these experiments were adapted from Chung and Schardl (1997) with modifications. The 10× stock solutions of basal salts—300 mM K_2HPO_4 and 300 mM KH_2PO_4 in water purified by Milli-Q (Nanopure, Model D4751, Barnstead/Thermolyne, Dubuque, IA)—were mixed to the desired pH (4.5–8.0 as specified). Then, 2(*N*-morpholino)ethanesulfonic acid (MES) was added to the basal salt solution to 300 mM, and pH readjusted with NaOH. MES was used to prevent the drastic pH increase that sometimes occurred in cultures with only phosphate as buffer. Final concentrations in the minimal medium were 30 mM potassium phosphate and 30 mM MES. The carbon sources were added to a conc. of 8.3 mM, and nitrogen sources were added to give 30 mM nitrogen atoms, except where otherwise specified. To the medium were added $MgSO_4$ to 2 mM, thiamine to 0.6 μM, and a solution of trace elements (from 1000×stock) to give 3.6 μM H_3BO_3, 1 μM $CuSO_4$, 0.7 μM KI, 0.8 μM FeNa-ethylenediaminetetraacetic acid, 1 μM $MnSO_4$, 0.5 μM $NaMoO_4$, and 0.4 μM $ZnSO_4$ (Kulkarni and Nielsen, 1986). Basal salts and MES in purified water were autoclaved together, and the $MgSO_4$ was autoclaved separately to prevent precipitation of salts. Carbon source, nitrogen source, thiamine, and trace elements were filter-sterilized together then combined with the basal salts and $MgSO_4$ solution. After preliminary trials with cultures in Erlenmeyer flasks proved inconsistent, 100×25 mm polystyrene petri plates (Fisherbrand, Fisher Scientific, Pittsburgh, PA) were used for the 30 ml cultures in all experiments reported here. The cultures were incubated at 21 °C with 100 rpm rotary shaking.

4.4. Sampling from cultures

Aliquots of medium from each culture were transferred into 1.7-ml Eppendorf (Brickmann Instruments, Inc., Westbury, NY) microcentrifuge tubes that had been pretreated at 100 °C for 2 days to remove extractable contaminants that otherwise interfered with the analysis. Prior to day 20 of culture, 1 ml aliquots were sampled; thereafter, aliquots were 0.5 ml. For fungal biomass and loline level determinations, 30-ml cultures were harvested for each time point and filtered through tared Whatmann no. 1 filter paper (Whatmann Limited, England). Then the mycelium on each filter was oven dried (37 °C, 2 days) and weighed, and the culture filtrate was frozen and freeze-dried for later analysis of lolines.

4.5. Alkaloid analysis

For GC analysis, freeze-dried samples were extracted using a modified procedure from Yates et al. (1990) and Robbins et al. (1972). One-tenth volume of a saturated sodium bicarbonate solution (0.25 g ml^{-1} in H_2O) was added to each dried filtrate and the tubes were vortexed. Chloroform (1 ml), with 14.2 mg l^{-1} of quinoline (RR $t=7.60$) as the internal standard was added to each tube. The suspension was vortexed, then shaken 30 min on a platform shaker. The $CHCl_3$ layer was transferred to a capped glass vial. Levels for lolines from GC analysis in these experiments are reported as the total of **2** (RR $t=16.75$) and **3** with **3′** (RR $t=17.44$), because the levels of **1** (RR $t=9.21$) were always very low.

For analysis by GC–MS and ^{13}C NMR spectroscopy, loline alkaloids were isolated using modifications of the procedure of Petroski et al. (1989). Fungal culture filtrates were freeze-dried, then extracted with 1 ml satd. sodium bicarbonate (aq.) and 30 ml $CHCl_3$. The aqueous layer was discarded and the organic solvent evaporated in a stream of nitrogen gas to yield a brown oil. One ml $CHCl_3$ was added to the oil and 500 μl of this mixture was spotted onto a K6F Silica gel 60A TLC plate (Whatmann Inc, Clifton, NJ). After drying, the plate was developed in a chromatography chamber with 140 ml of a 50:50:1 (by volume) mixture of CH_3OH, $CHCl_3$ and satd. NH_3OH. Loline alkaloids were visualized as dark brown spots after exposing the plate to iodine vapor. R*f* values for **1**, **2**, and **3** with **3′** were determined as 0.26, 0.37, and 0.49, respectively. The visible spots corresponding to the loline alkaloids (**1**, **2**, and **3** with **3′**) on the plate were scraped off individually and alkaloids eluted with purified H_2O, extracted with $CHCl_3$ and solvent removed by a stream of N_2 gas. These purified samples were then used in GC–MS and ^{13}C NMR analysis.

4.6. Alkaloid purification and identification:

Loline (**1**) was isolated by separation of the alkaloids by TLC and extracted from the silica with H_2O, and because of its volatility, conc. HCl was added to yield the salt form, which was recrystallized with EtOH: ^{13}C NMR (D_2O, 200 MHz), 29.2 (C6), 34.0 (NMe), 55.5 (C5), 61.8 (C3), 63.8 (C1), 70.1 (C8), 71.9 (C2), 80.9 (C7); EIMS *m*/*z* 154 $[M]^+$ (0), 123(58), 110 (7), 95 (75), 82 (100).

N-Acetylnorloline (**2**) was purified as a clear oil after being separated from the other alkaloids by TLC, extracted from the plate with H_2O followed by extraction with $CHCl_3$ which was removed with a stream of nitrogen gas: ^{13}C NMR (D_2O, 200 MHz), 24.2 (MeC=O), 35.1 (C6), 54.8 (C5), 58.4 (C1), 61.4 (C3), 70.1 (C8), 74.1 (C2), 81.6 (C7), 171.9 (HC=O); EIMS *m*/*z* 182 $[M]^+$ (0), 153 $[M\text{-}29]^+$ (8), 139 (0), 123 (9), 110 (0), 95 (30), 82 (100), 69 (22).

N-Formylloline (**3**) was purified as a viscous brown oil similar to purification of **2**: ^{13}C NMR (D_2O, 200 MHz), 32.0 (C6), 34.8 (NMeth), 54.1 (C5), 59.7 (C3), 65.5 (C1), 67.8 (C8), 74.3 (C2), 83.2 (C7), 165.1 (HC=O); EIMS *m*/*z* 182 $[M]^+$ (0), 154 $[M\text{-}28]^+$ (25), 123 (13), 110 (13), 95 (28), 82 (100).

N-Formylloline (**3′**) extracted with **3** as a brown oil: ^{13}C NMR (D_2O, 200 MHz), 30.4 (NMeth), 31.7 (C6), 54.3 (C5), 60.6 (C3), 63.0 (C1), 68.6 (C8), 73.5 (C2), 81.4 (C7), 167.0 (HC=O); EIMS *m*/*z* 182 $[M]^+$ (0), 154 $[M\text{-}28]^+$ (25), 123 (13), 110 (13), 95 (28), 82 (100).

Acknowledgements

We thank Dr. Mark S. Meier and Mr. John Layton for their expert advice on ^{13}C NMR analysis, and we thank Dr. Harold H. Burton, Dr. Peter A. Crooks and Dr. Xiaochen Wei for their expert advice on GC–MS. Capable assistance was kindly provided by Mr. A.D. Byrd, Ms. J.L. Dueñas, Ms. D.W. Franks, Mr. W. Hollin, Ms. A.C. Mallory, Ms. S.A. Mathews, and Ms. S. Van Orden. This research was supported by National Science Foundation grant IBN-9808554 to C.L.S. and L.P.B., and the United States Department of Agriculture NRI grant 96-35303-3578 to H.H.W.

References

Bacon, C.W., 1988. Procedure for isolating the endophyte from tall fescue and screening isolates for ergot alkaloids. Applied and Environmental Microbiology 54, 2615–2618.

Böttcher, F., Adolph, R.D., Hartmann, T., 1993. Homospermidine synthase, the first pathway-specific enzyme in pyrrolizidine alkaloid biosynthesis. Phytochemistry 32, 679–689.

Bush, L.P., Fannin, F.F., Siegel, M.R., Dahlman, D.L., Burton, H.R., 1993. Chemistry, occurrence, and biological effects of saturated pyrrolizidine alkaloids associated with endophyte grass interactions. Agriculture, Ecosystems, and Environment 44, 81–102.

Campbell, I.M., 1984. Secondary metabolism and microbial physiology. Advances in Microbial Physiology 25, 2–59.

Casabuono, A.C., Pomilio, A.B., 1997. Alkaloids from endophyte-infected *Festuca argentina*. Journal of Ethnopharmacology 57, 1–9.

Chung, K.R., Schardl, C.L., 1997. Vegetative compatibility between and within *Epichloë* species. Mycologia 89, 558–565.

Craven, K.D., Blankenship, J.D., Leuchtmann, A., Hignight, K., Schardl, C.L., 2001. Hybrid fungal endophytes symbiotic with the grass *Lolium pratense*. Sydowia 53, 44–73.

Dannhardt, G., Steidt, L., 1985. Alkaloids of *Lolium temulentum*: isolation, identification, and pharmacological activity. Planta Medica 51, 212–214.

Darbyshire, S.J., 1993. Realignment of *Festuca* subgenus *Schedonorus* with genus *Lolium* (Poaceae). Novon 3, 239–243.

Dew, R.K., Boissonneault, G.A., Gay, N., Boling, J.A., Cross, R.J., Cohen, D.A., 1990. The effect of the endophyte (*Acremonium coenophialum*) and associated toxin(s) on the serum titer response to immunization and spleen cell flow cytometry analysis and response to mitogens. Veterinary Immunology and Immunopathology 26, 285–295.

Dougherty, C.T., Knapp, F.W., Bush, L.P., Maul, J.E., Van Willigen, J., 1998. Mortality of horn fly (Diptera: Muscidae) larvae in bovine dung supplemented with loline alkaloids from tall fescue. Journal of Medical Entomology 35, 798–803.

Gurney, K.A., Mantle, P.G., Penn, J., Garthwaite, I., Towers, N.R., 1994. Loss of toxic metabolites from *Acremonium lolii*, the endophyte of ryegrass, following mutagenesis. Naturwissenschaften 81, 362–365.

Hartmann, T., Witte, L., 1995. Chemistry, biology and chemoecology of the pyrrolizidine alkaloids. In: Pelletier, S.W. (Ed.), The Alkaloids: Chemical and Biological Perspectives, Vol. 9. Springer, New York, pp. 155–231.

Hincks, J.R., Kim, H.Y., Segall, H.J., Molyneux, R.J., Stermitz, F.R., Coulombe, R.A., 1991. DNA cross-linking in mammalian cells by pyrrolizidine alkaloids: Structure-activity relationships. Toxicology and Applied Pharmacology 111, 90–98.

Jackson, J.A., Varney, D.R., Petroski, R.J., Powell, R.G., Bush, L.P., Siegel, M.R., Hemken, R.W., Zavos, P.M., 1996. Physiological responses of rats fed loline and ergot alkaloids from endophyte-infected tall fescue. Drug and Chemical Toxicology 19, 85–96.

Justus, M., Witte, L., Hartmann, T., 1997. Levels and tissue distribution of loline alkaloids in endophyte-infected *Festuca pratensis*. Phytochemistry 44, 51–57.

Kim, H.Y., Stermitz, F.R., Li, J.K.K., Coulombe, R.A., 1999. Comparative DNA crosslinking by activated pyrrolizidine alkaloids. Food and Chemical Toxicology 37, 619–625.

Kulkarni, R.K., Nielsen, B.D., 1986. Nutritional requirements for growth of a fungus endophyte of tall fescue grass. Mycologia 78, 781–786.

Lam, C.K., Belanger, F.C., White, J.F., Daie, J., 1994. Mechanism and rate of sugar uptake by *Acremonium typhinum*, an endophytic fungus infecting *Festuca rubra*: evidence for presence of a cell wall invertase in endophytic fungi. Mycologia 86, 408–415.

Leuchtmann, A., Schmidt, D., Bush, L.P., 2000. Different levels of protective alkaloids in grasses with stroma-forming and seed-transmitted *Epichloë/Neotyphodium* endophytes. Journal of Chemical Ecology 26, 1025–1036.

Pate, J.S., 1973. Uptake, assimilation and transport of nitrogen compounds by plants. Soil Biology and Biochemistry 5, 109–119.

Patterson, C.G., Potter, D.A., Fannin, F.F., 1991. Feeding deterrency of alkaloids from endophyte-infected grasses to Japanese beetle grubs. Entomologia Experimentalis et Applicata 61, 285–289.

Petroski, R.J., Yates, S.G., Weisleder, D., Powell, R.G., 1989. Isolation, semi-synthesis, and NMR spectral studies of loline alkaloids. Journal of Natural Products 53, 810–817.

Porter, J.K., 1994. Chemical constituents of grass endophytes. In: Bacon, C.W., White Jr., J.F. (Eds.), Biotechnology of Endophytic Fungi of Grasses. CRC, Boca Raton, FL, pp. 103–123.

Powell, R.G., Petroski, R.J., 1992. The loline group of pyrrolizidine alkaloids. In: Pelletier, S.W. (Ed.), The Alkaloids: Chemical and Biological Perspectives, Vol. 8. Springer, Berlin, pp. 320–338.

Robbins, J.D., Sweeny, J.G., Wilkinson, S.R., Burdick, D., 1972. Volatile alkaloids of Kentucky 31 tall fescue seed (*Festuca arundinacea* Schreb.). Journal of Agricultural and Food Chemistry 20, 1040–1042.

Rowan, D.D., 1993. Lolitrems, peramine, and paxilline—mycotoxins of the ryegrass–endophyte interaction. Agriculture Ecosystems and Environment 44, 103–122.

Schardl, C.L., Phillips, T.D., 1997. Protective grass endophytes: where are they from and where are they going? Plant Disease 81, 430–438.

Siegel, M.R., Bush, L.P., 1997. Toxin production in grass/endophyte associations. In: Carroll/Tudzynski (Ed.), The Mycota V, Part A: Plant Relationships. Springer, Berlin, Heidelberg, pp. 185–207.

Siegel, M.R., Latch, G.C.M., Bush, L.P., Fannin, F.F., Rowan, D.D., Tapper, B.A., Bacon, C.W., Johnson, M.C., 1990. Fungal endophyte-infected grasses: alkaloid accumulation and aphid response. Journal of Chemical Ecology 16, 3301–3315.

TePaske, M.R., Powell, R.G., Clement, S.L., 1993. Analyses of selected endophyte-infected grasses for the presence of loline-type and ergot-type alkaloids. Journal of Agricultural and Food Chemistry 41, 2299–2303.

Tofern, B., Kaloga, M., Witte, L., Hartmann, T., Eich, E., 1999. Phytochemistry and chemotaxonomy of the Convolvulaceae part 8—occurrence of loline alkaloids in *Argyreia mollis* (Convolvulaceae). Phytochemsitry 51, 1177–1180.

Wilkinson, H.H., Siegel, M.R., Blankenship, J.D., Mallory, A.C., Bush, L.P., Schardl, C.L., 2000. Contribution of fungal loline production to protection from aphids in a grass fungus mutualism. Molecular Plant-Microbe Interactions 13, 1027–1033.

Yates, S.G., Petroski, R.J., Powell, R.G., 1990. Analysis of loline alkaloids in endophyte-infected tall fescue by capillary gas chromatography. Journal of Agricultural and Food Chemistry 38, 182–185.

PERGAMON

Phytochemistry 58 (2001) 403–413

PHYTOCHEMISTRY

www.elsevier.com/locate/phytochem

Cytoplasmic accumulation of flavonoids in flower petals and its relevance to yellow flower colouration

Kenneth R. Markham[a,*], Kevin S. Gould[b], Ken G. Ryan[a]

[a]*Industrial Research Ltd., PO Box 31310, Lower Hutt, New Zealand*
[b]*School of Biological Sciences, University of Auckland, Private Bag 92019, Auckland, New Zealand*

Received 16 February 2001; received in revised form 6 June 2001

Abstract

It is widely accepted that the mix of flavonoids in the cell vacuole is the source of flavonoid based petal colour, and that analysis of the petal extract reveals the nature and relative levels of vacuolar flavonoid pigments. However, it has recently been established with lisianthus flowers that some petal flavonoids can be excluded from the vacuolar mix through deposition in the cell wall or through complexation with proteins inside the vacuole, and that these flavonoids are not readily extractable. The present work demonstrates that flavonoids can also be compartmented within the cell cytoplasm. Using adaxial epidermal peels from the petals of lisianthus (*Eustoma grandiflorum*), *Lathyrus chrysanthus* and *Dianthus caryophyllus*, light and laser scanning confocal microscopy studies revealed a significant concentration of petal flavonoids in the cell cytoplasm of some tissues. With lisianthus, flavonoid analyses of isolated protoplasts and vacuoles were used to establish that ca 14% of petal flavonoids are located in the cytoplasm (cf. 30% in the cell wall and 56% in the vacuole). The cytoplasmic flavonoids are predominantly *acylated* glycosides (cf. non-acylated in the cell wall). Flavonoid aggregation on a cytoplasmic protein substrate provides a rational mechanism to account for how colourless flavonoid glycosides can produce yellow colouration in petals, and perhaps also in other plant parts. High vacuolar concentrations of such flavonoids are shown to be insufficient. © 2001 Elsevier Science Ltd. All rights reserved.

Keywords: Compartmentation; Cytoplasm; Flavonoids; Petals; *Eustoma grandiflorum*; Lisianthus; *Lathyrus chrysanthus*; Yellow colouration; Flavonoid-protein binding

1. Introduction

In discussions of flower colour chemistry and its manipulation, it is commonly presumed that flavonoid pigments mix freely with one another in the aqueous environment of the cell vacuole (Brouillard, 1988; Brouillard and Dangles, 1994; Mol, 1991; Norback et al., 1998). However in the course of recent studies of flower colour at the cellular level it has been established that flavonoid pigment types can be selectively compartmentalised within a petal cell, such that not all come in contact with one another in situ (Markham et al., 2000a,b). This can have a significant influence on flower colour since intermolecular interactions such as copigmentation and aggregation within the vacuole have a marked influence on colour hue, intensity and stability (Brouillard and Dangles, 1994). The observation (Markham et al., 2000a) that anthocyanins with specific structural features may be excluded from vacuolar solution through binding to protein to form insoluble anthocyanic vacuolar inclusions (AVIs), is a good example of this. Another example is the selective compartmentalisation of non-acylated flavonol glycosides in the cell walls of petal cells (Markham et al., 2000b). In both cases certain flavonoids are not available to interact freely with other pigments in the vacuole and thus to influence vacuolar colour.

Flavonoids are currently thought to be synthesized within the cell cytoplasm (Ibrahim, 1990, 1992; Stafford, 1990; Hrazdina, 1992; Marrs et al., 1995), perhaps on or in association with the endoplasmic reticulum (Hrazdina and Wagner, 1985; Hrazdina et al., 1987; Ibrahim et al., 1987; Hrazdina, 1992), and then transported to the vacuole via this membrane or via vesicles budded from it (Pecket and Small, 1980; Small and Pecket, 1982). Passage into the vacuole in maize (Marrs et al., 1995) and other plants (Alfenito et al., 1998) is thought to be effected by glutathionation which allows recognition

* Corresponding author. Tel:. +64-4-5690577; fax: +64-4-5690055.

0031-9422/01/$ - see front matter © 2001 Elsevier Science Ltd. All rights reserved.
PII: S0031-9422(01)00276-X

and vacuolar entry of the conjugate via the glutathione pump, although aspects of this mechanism have recently been questioned (Mueller et al., 2000). The presence of flavonoids within the cytoplasm is thus normally considered to be transitory, the cytoplasm not being a repository unless this transport system is disabled, as in the maize "*Bronze-2*" mutant. In this mutant, the "*Bronze-2*" gene, which encodes for a glutathione S-transferase, is not functional and the non-glutathionated cyanidin-3-glucoside consequently accumulates in the cytoplasm (Marrs et al., 1995).

The transitory nature of flavonoids in the cytosol has been noted by Grandmaison and Ibrahim (1996) who used immunogold-labeled monospecific polyclonal antibodies to detect the subcellular localization of quercetin sulphates in leaves of *Flaveria chloraefolia*. A consistent association of the label with the nuclei was observed together with some diffuse labeling in the cytoplasm. Subsequently, quercetin-3-sulphate was shown to exhibit strong affinity for a specific (ca. 30 kD) protein isolated from a total nuclear protein extract from this plant. In a more recent study (Hutzler et al., 1998) involving confocal laser scanning microscopy to detect the subcellular location of flavonoids rendered visible with ammonia or diphenylboric acid 2-aminoethyl ester (commonly referred to as "NA"), flavonoids were detected in both the cell walls and vacuoles, and were found associated with the nucleus in a variety of plants. In the same study, fluorescence attributable to the presence of flavonoids was also observed in the cytoplasm of spruce needle epidermal cells.

Published evidence for the accumulation of significant quantities of flavonoids in the cytoplasm is thus sparse, indicating perhaps that this phenomenon is uncommon in green leaves. In flowers, a knowledge of any sub-cellular compartmentation of specific flavonoid types is of particular significance in view of the potential influence on colour at the cellular level. Recent pigment work on lisianthus (*Eustoma grandiflorum*) petals (Markham et al., 2000b) has established for the first time, the existence of cell-wall sited flavonoids in petal cells. Evidence cited in support of this finding included images from confocal laser scanning microscopy (CLSM) of NA-treated epidermal peels. The yellow-orange fluorescence observed in cell-walls, indicative of the presence of flavonoids (in this case flavonol-*O*-glycosides), was also observed in a thin "brighter region lining the inner surface" of the cell wall. An explanation given for this was that it might indicate the presence of flavonoids in the thin band of cytoplasm surrounding the vacuole. Here, we provide further evidence in support of this concept based on light microscopy and chemical studies.

Yellow flowers most commonly derive their colour from carotenoid pigmentation. However there are examples in which yellow colouration results from the presence of "yellow" flavonoids such as aurones, chalcones and highly oxygenated flavonols (Brouillard, 1988). Of more interest, and as yet without adequate explanation, are the few reported flowers which derive yellow colouration from "colourless" flavonoids such as the flavonols, kaempferol and quercetin, e.g. *Lathyrus chrysanthus* (Markham et al., 1992), *Camellia chrysantha* (Hwang et al., 1992) and *Eustoma grandiflorum* (lisianthus) (Davies et al., 1993; Markham and Ofman, 1993). Although simple flavonols are converted into yellow ionised forms at very high or low pHs, such pHs are not found in petal tissue which is commonly in the 3–7 pH range (Brouillard and Dangles, 1994). This pH range, however, does not exclude another possible yellowing mechanism, that of molecular aggregation, which can occur on surfaces or at high concentrations. This mechanism was proposed by Smith and Markham (1998) who demonstrated through fluorescence and reflectance studies, that kaempferol and quercetin glycosides exist to a significant extent in their yellow (λ_{max} ca. 450 nm for 7-*O*-glycosides) enolic tautomer form when aggregated on a suitable matrix or, to a lesser extent, in a concentrated solution. Evidence presented in the current paper relating to studies on several yellow flowers, demonstrates a correlation between cytoplasmic compartmentation of "colourless" flavonoids and yellow petal colour. It is proposed that the adoption by these flavonoids of their yellow tautomeric or pyrylium forms, is brought about by interaction with protein in the cytoplasm.

2. Results and discussion

2.1. Microscopy studies

Oblique and transverse sections through petals of white and purple lisianthus (*Eustoma grandiflorum*), yellow *Lathyrus chrysanthus* and yellow carnation (*Dianthus caryophyllus*), were stained with NA and examined by epifluorescence microscopy for yellow-green to orange fluorescence. This stain is widely used for the detection of flavones and flavonols, the presence of which is evidenced by yellow-green to orange fluorescence under UV light (Markham, 1982; Sheahan and Rechnitz, 1993; Hutzler et al., 1998). In petals from all flower types, epidermal cells were identified in which such fluorescence was concentrated in regions peripheral to the vacuole, and commonly in irregular patches (e.g. Fig. 1A–C). Varying levels of fluorescence were also visible in the vacuoles. That these irregular patches of fluorescent tissue are indeed cytoplasmic and not associated with the cell wall, was evident from a confocal laser scanning micrograph of the transverse section of purple lisianthus petal in which plasmolysis had occurred (Fig. 1D). A clear dark space is visible, which separates the cell wall from the fluorescing cytoplasm. Furthermore, in a mix of protoplasts prepared from purple lisianthus petals

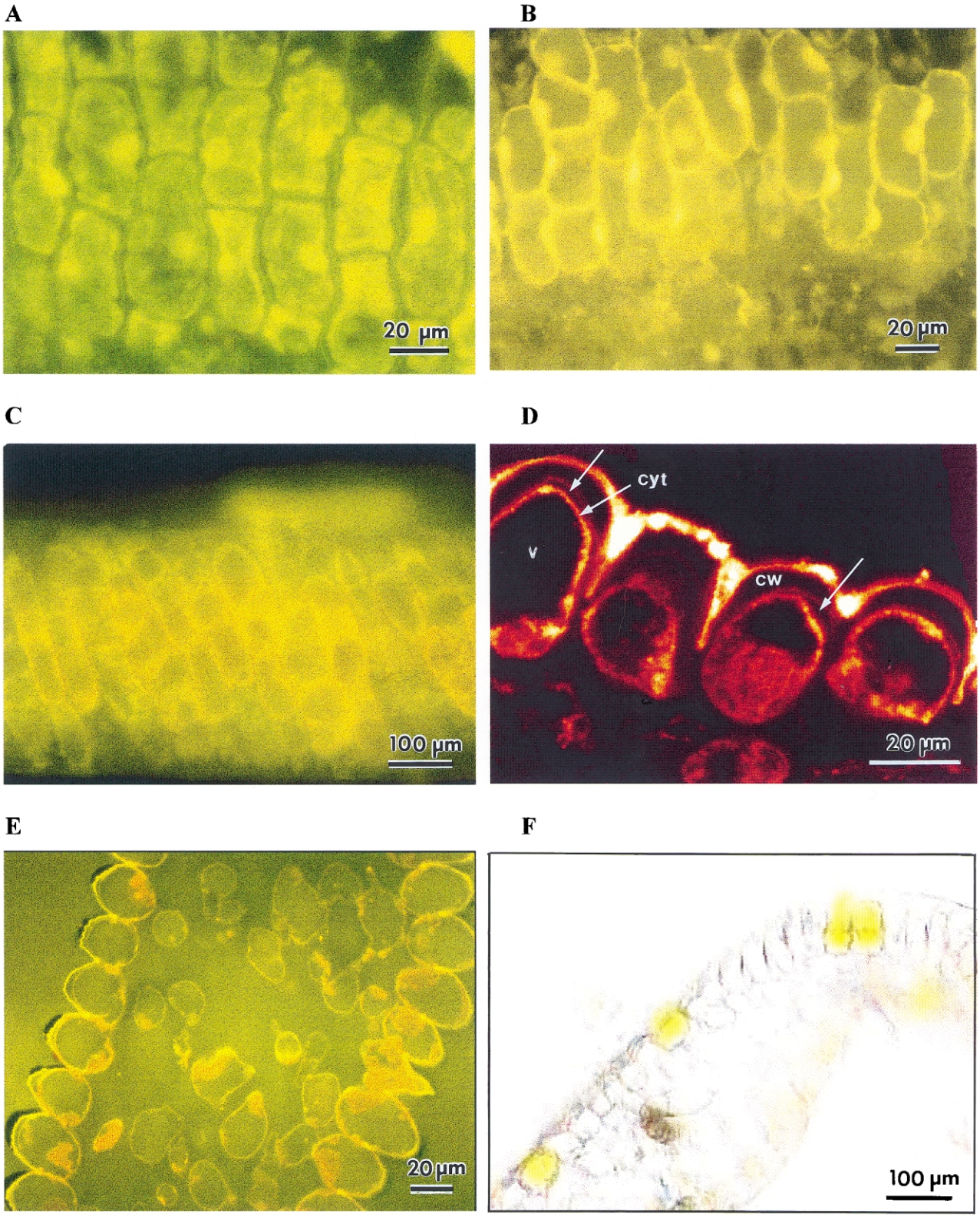

Fig. 1. (A), (B) NA-treated oblique hand-sections through the epidermis of the inner petal region of white lisianthus (*Eustoma grandiflorum*). (C) NA-treated oblique hand-section through the epidermis of a standard petal of *Lathyrus chrysanthus*. (D) Adaxial epidermal cells in the inner petal region of white lisianthus (*Eustoma grandiflorum*) viewed by CLSM after staining with NA (Abbreviations: v = vacuole, cyt = cytoplasm, cw = cell wall. Unlabelled arrows indicate examples of plasmolysis). (E) NA-treated transverse section through the inner petal region of white lisianthus (*Eustoma grandiflorum*). (F) Transverse section through a standard petal of *Lathyrus chrysanthus*.

and stained with NA, some protoplasts displayed blobs and/or streaks of fluorescent tissue on or near the surface, rather than a uniform fluorescence throughout the vacuole (data not shown). This relative lack of fluorescence in the vacuole is also a feature of the examples selected for Figs. 1A–C.

The data from these microscopy studies are thus in accord with previous observations using CLSM, which indicate the presence of flavonoids in the thin layer of cytoplasm surrounding the vacuole (Markham et al., 2000b).

2.2. Intracellular flavonoid distribution in lisianthus petal epidermal tissue

Previous work on the flavonoids of lisianthus flowers has established that the acyanic flavonoids in white and purple flowers are present at about the same levels and possess the same structures (Markham and Ofman, 1993). All are flavonol-tri-*O*-glycosides, the major of which are a 1:2 mix of the non-acylated kaempferol- and isorhamnetin-3-*O*-rhamnogalactoside-7-*O*-rhamnosides and their acylated (4^{Gal}-linked *p*-coumaroyl and ferulyl) derivatives. In order to study the nature of any flavonol glycosides located in the cytoplasm, the approach chosen was to compare the flavonoid composition of protoplasts with that of the vacuoles isolated from them. The flavonoids lost from the protoplast in the production of intact vacuoles would be those sited in the cytoplasm. Protoplasts (Fraction A) were prepared enzymatically from purple lisianthus adaxial epidermal peels, and vacuoles were isolated from these in varying yield. The best yields were in fractions containing, 50% intact vacuoles plus anthocyanic vacuolar inclusions (AVIs) from ruptured vacuoles (Fraction B), and 70% intact vacuoles plus 30% protoplasts (Fraction C). The flavonoid content of each fraction was analysed by HPLC on a reversed phase column. Under the conditions used, acylated flavonol glycosides as a group were well separated from their non-acylated analogues with retention times in excess of 33 min (non-acylated <26 min—see Fig. 2). They were also readily distinguishable from their on-line measured absorption spectra which exhibit hydroxycinnamoyl absorption in the 290–330 nm region.

The HPLC patterns of flavonol glycosides in fractions A (protoplasts), B (vacuoles plus AVIs) and C (7:3, vacuoles:protoplasts) were qualitatively the same and the major peaks in all three were peaks 1–6 (see Fig. 2). Fraction B (Fig. 2) in effect reflects the flavonol pattern of pure vacuoles, since the contaminating AVIs have been shown to contain anthocyanins but no flavonols (Markham et al., 2000a), and fraction C is intermediate between A and B in that it represents a mix of the flavonols from protoplasts and vacuoles. Thus, the *range* of flavonol glycosides present in the vacuoles is the same as that for the intact protoplasts. The main difference

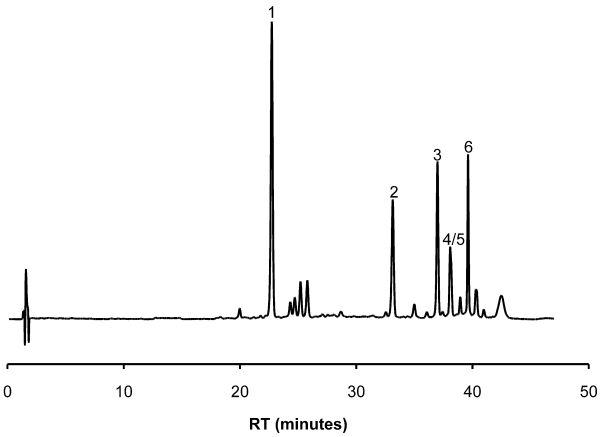

Fig. 2. HPLC profile (352 nm) of the flavonol glycosides from vacuoles (Fraction B) of white lisianthus, *Eustoma grandiflorum*. Peaks with retention times (RT) between 20 and 30 min represent unacylated glycosides and those with RTs between 30 and 45 min represent acylated (hydroxycinnamoyl) glycosides. Structures (see Markham et al., 2000b): 1-kaempferol-3-*O*-[6-*O*-rhamnosylgalactoside]-7-*O*-rhamnoside, 2-kaempferol-3-*O*-[6-*O*-rhamnosyl-4-*O*-*E*-caffeoylgalactoside]-7-*O*-rhamnoside, 3-kaempferol-3-*O*-[6-*O*-rhamnosyl-4-*O*-*E*-*p*-coumaroylgalacto-side]-7-*O*-rhamnoside, 4-isorhamnetin-3-*O*-[6-*O*-rhamnosyl-4-*O*-*E*-*p*-coumaroylgalactoside-7-*O*-rhamnoside, 5-kaempferol-3-*O*-[6-*O*-rhamnosyl-4-*O*-*E*-ferulylgalactoside]-7-*O*-rhamnoside, 6-kaempferol-3-*O*-[6-*O*-rhamnosyl-4-*O*-*Z*-*p*-coumaroylgalactoside]-7-*O*-rhamnoside.

between the flavonol profiles of the vacuoles (B) and the protoplasts (A) is in the *ratio* of total acylated to total non-acylated flavonol glycosides. Quantification by integration of the HPLC peaks demonstrates that vacuoles have a ratio of 1.4:1, and protoplasts a ratio of 2:1. This indicates that the cytoplasm contains a predominance of acylated glycosides. The mix of vacuoles and protoplasts in Fraction C gave a ratio of 1.7:1 which, as expected, falls between the Fraction A and Fraction B ratios. This ratio compares well with the theoretical ratio of 1.6:1 calculated from the ratios determined for pure vacuoles (Fraction B) and pure protoplasts (Fraction A).

The approximate ratio of acylated to non-acylated flavonol glycosides that must be present in the cytoplasm to effect a change in ratio from 2:1 (protoplasts) to 1.4:1 (vacuoles), can be estimated if the relative volumes of vacuole and cytoplasm in a typical epidermal cell are known. The transverse section (Fig. 1E) and the CLSM images [Fig. 1D, and also Fig. 2 (Markham et al., 2000b), which represent optical 'cross-sections' through these cells] suggest that the cytoplasmic volume is about 10% of the vacuolar volume. Assuming this to be typical, the protoplast is thus comprised of about nine parts vacuole and one part cytoplasm. Nine times the vacuolar ratio of 1.4:1 totals 12.6:9, and to convert this to the required protoplast ratio of 2:1 would require that the cytoplasm ratio be 7.4:1, i.e. the total vacuole plus cytoplasm content would equal 20:10. On this basis the cytoplasm located flavonoids would appear to be predominantly (ca. 90%) acylated flavonol glycosides.

Previous work with lisianthus has established that about 30% of the flavonol glycosides biosynthesized in the petal are sequestered into the plant cell wall and that these are exclusively non-acylated (Markham et al., 2000b). The remaining 70% comprise a 2:1 mix of acylated:non-acylated flavonol glycosides (≡ protoplasts). From the observed reduction of this ratio to 1.4:1 in the vacuole, it follows that 30% ((2–1.4)/2×100) of the acylated glycosides, that is 14% of the total petal flavonoids (30% of 67% ×70/100), are retained in the cytoplasm and the remaining 56% transported into the vacuole. The distribution of flavonol glycosides in the epidermal tissue of the lisianthus petals studied is, therefore, *approximately*:

Cell wall	30%	(comprising flavonol-*O*-glycosides)
Cytoplasm	14%	(comprising acylated flavonol-*O*-glycosides)
Vacuole	56%	(comprising 1.4:1, acylated: non-acylated flavonol-O-glycosides)

The glutathione transport system in this tissue is thus apparently capable of transporting both acylated and non-acylated glycosides from the cytoplasm to the vacuole. Retention of a portion of the acylated glycosides in the cytoplasm therefore, may result from competitive binding to cytoplasmic materials. Differences between the protein binding characteristics of acylated and non-acylated flavonoid glycosides have been reported previously. Alluis and Dangles (1999), using a model system involving bovine serum albumin (BSA), chrysin-7-glucoside and its *p*-methoxycinnamate, concluded that flavonoid glycosides bearing aromatic acyl groups can bind with very high affinity and may act as potent bidentate ligands. The acylated flavonoid glycosides found in the cytoplasm of lisianthus are of this general type.

2.3. Intercellular flavonoid distribution and yellowing in *L. chrysanthus* petal epidermal tissue

Examination of epidermal peels and transverse sections of "standard" petals under the light microscope established that yellow colouration occurs essentially only in the adaxial epidermis (Fig. 1F), and therein, in groups of cells. Other cells are colourless (= "white"). Groups of white and yellow cells were separated by manual excision from epidermal peels and their contents analysed by high performance liquid chromatography (HPLC). The white cells were found to be devoid of flavonoids, while the yellow cells contained the major flavonol glycosides (the 3-glucoside-7-rhamnosides of quercetin and isorhamnetin) previously identified in these petals (Markham et al., 1992). This was confirmed by measuring the in situ absorption spectra of groups of cells predominantly of each colour type, which showed for the yellow cells (Fig. 3), strong blue absorption with a peak at 370–375 nm and a shoulder at ca. 440 nm, the intensity of this shoulder varying with the proportion of yellow cells. White cells in contrast, exhibited no absorption at or above 350 nm (data not shown). The absorption of the yellow cells is at surprisingly long wavelengths, since the spectra of the isolated flavonol glycosides in water exhibit peaks at ca. 352 nm, with little or no absorption at or beyond 400 nm (Markham et al., 1992). Additionally, the absorption level for the yellow cells is very high, considering that the flavonoids producing this are contained within the pathlength of a single cell. The actual flavonoid concentration in a typical yellow cell was established after determining that the depth/pathlength of an average yellow cell was ca. 0.005 cm. This figure was used as the pathlength (l) to calculate the flavonoid concentration (c) from a single cell UV-visible transmission spectrum, using the Beer-Lambert law:

$$\text{Optical density} = \log_{10} I_{\text{incident}}/I_{\text{transmitted}} = \varepsilon \times c \times l$$

An area of petal predominant in yellow cells was found to transmit about 5% of incident light at 400 nm. Thus, using an $I_{\text{incident}}\backslash I_{\text{transmitted}}$ of 95/5, and an extinction coefficient (ε) of 14,300 (measured for the major flavonoid glycoside in *L. chrysanthus*), a concentration of 1.8×10^{-2} m l^{-1} is indicated. With the major components possessing molecular weights of ca. 600, this equates to a concentration of about 11 g l^{-1} of flavonoids in an average yellow cell.

In order to establish whether the spectral shift (i.e. yellowing) of the flavonol glycosides in situ could be a concentration effect, the absorption of a clarified, concentrated aqueous extract from *L. chrysanthus* petals was measured. The concentration used (44 g l^{-1} of flavonols—see Markham et al., 1992, for components) was equivalent to 4× that measured in vivo and the spectra were measured on a solution sandwiched between glass slides to reduce the pathlength. Under these conditions, the extract exhibited a $\lambda_{\max}$ at 364 nm, with no sign of a longer wavelength shoulder, compared with 352 nm when diluted 4000× with water. Thus, although a 12 nm bathochromic shift is produced on concentration, the in vivo spectrum could not be reproduced by these means. Deposition of this same concentrated extract on a substrate such as a cellulose sheet however, produced intense yellowing, and the visible absorptance spectrum (Fig. 4) approximated to that of the yellow petal itself ($\lambda_{\max}$ ca. 400 nm. Data not shown), with visible absorptance out to beyond 400 nm. These findings indicate that although the degree of yellow colouration seen in *L. chrysanthus* petals cannot be produced by increasing the flavonoid concentration in solution, it can be produced through flavonoid aggregation on a substrate.

2.4. The proposed significance of cytoplasm sited flavonoids to yellow flower colouration

Evidence from the microscopy and chemical studies described above, establishes that about 14% of the total

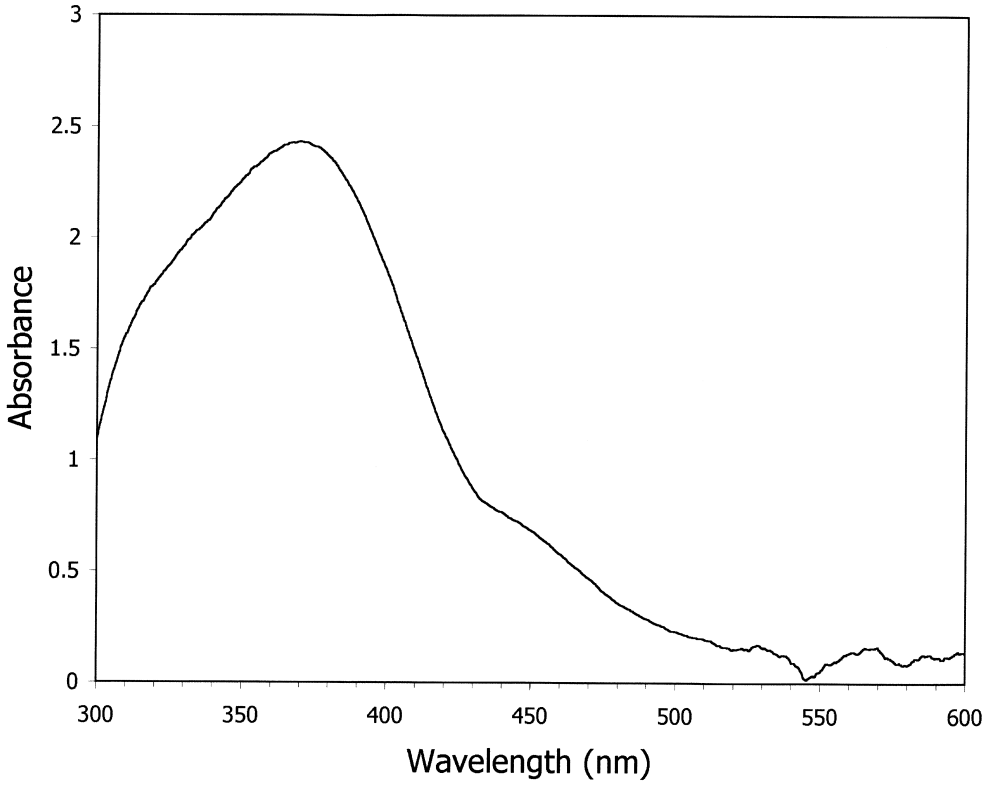

Fig. 3. UV-visible absorption spectrum of a group of yellow cells in an epidermal peel from a *Lathyrus chrysanthus* standard petal.

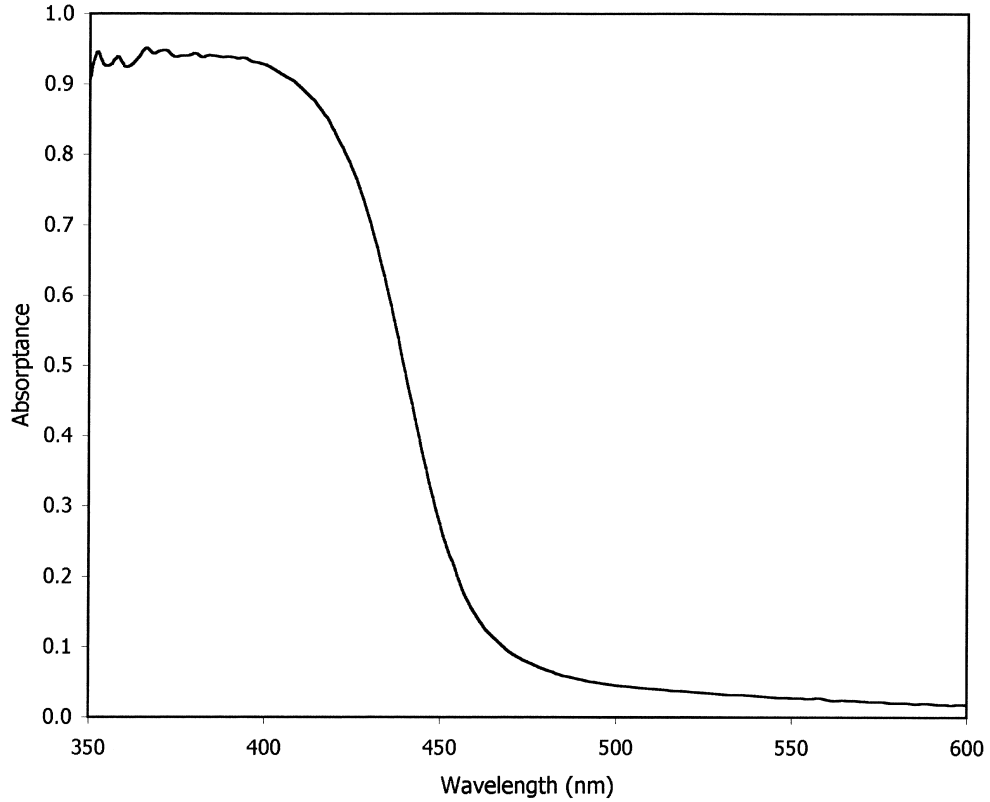

Fig. 4. Absorptance spectrum of an extract of *Lathyrus chrysanthus* standard petals deposited on a sheet of cellulose filter paper.

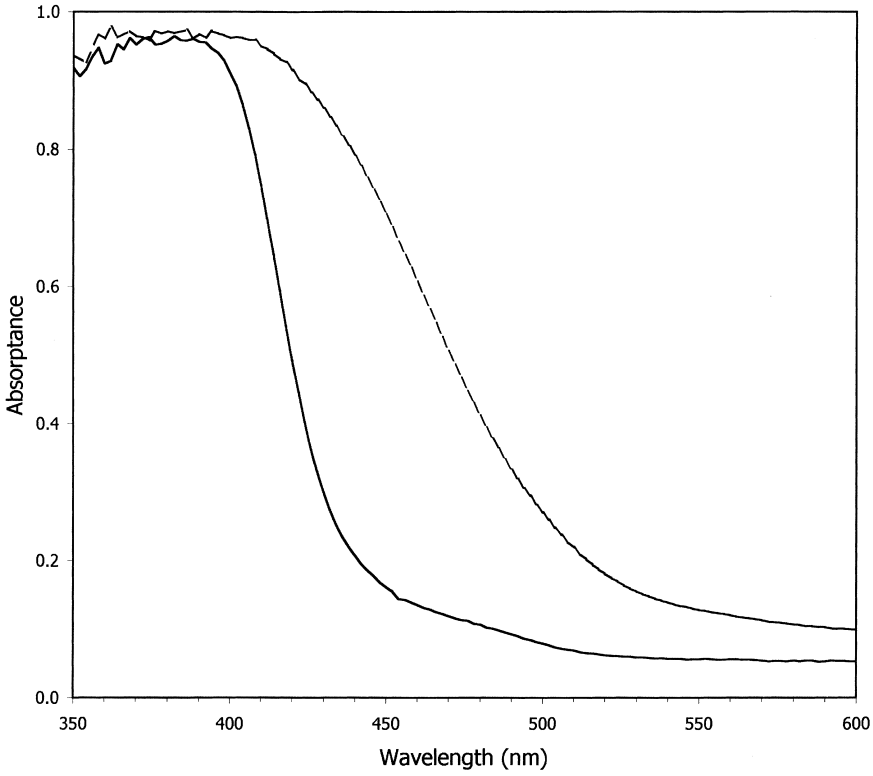

Fig. 5. Absorptance spectra of fresh (lower intensity curve) and dry (higher intensity curve) white lisianthus, *Eustoma grandiflorum*, petals.

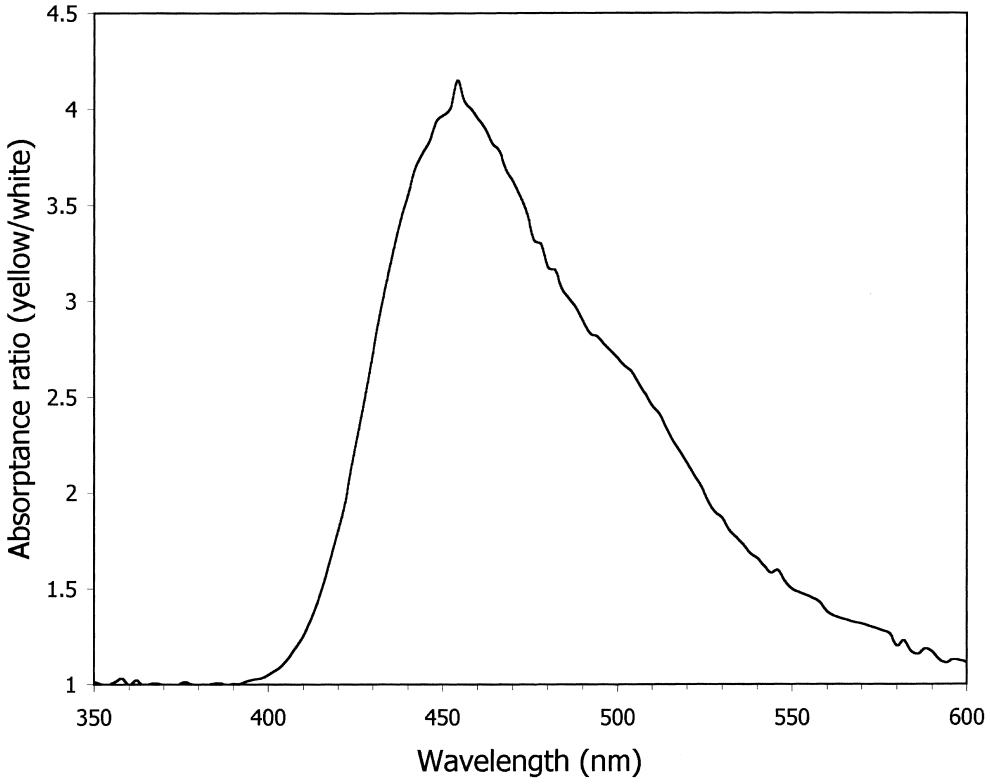

Fig. 6. A plot of the ratios of absorptances of dry white lisianthus petals : fresh white lisianthus petals at wavelengths between 350 and 600 nm. Absorptance data used, was that depicted in Fig. 5.

petal flavonols are concentrated in the cytoplasm of the adaxial epidermal cells of lisianthus petals. In white petals however (where vacuolar staining with NA can be seen as it is not obscured by the presence of anthocyanins), this cytoplasmic concentration is evident mainly in cells from the base (or "inner" region) of the petal. Significantly, this is the yellow region (see Davies et al., 1993). Epidermal cells from the rest of the petal tend to exhibit NA-induced fluorescence evenly throughout the vacuole. The whole petal however, turns a more uniform yellow when it is left to dry (i.e. when the flavonol glycosides throughout the petal are concentrated). No change in the HPLC measured flavonoid profile was evident after this drying. The extent of the observed yellowing was quantified using an integrating sphere and spectroradiometer to compare its absorptance spectrum with that of the "outer" zone of an undried white petal. A marked bathochromic shift was evident in the spectrum of the yellowed petal relative to that of the fresh petal (Fig. 5), such that the difference between the spectra (= Absorptance ratios) produced a single visible maximum at ca. 450 nm (Fig. 6). This difference spectrum is consistent with the visible spectrum measured by Smith and Markham (1998) for the enolic tautomer forms of kaempferol and quercetin glycosides, and thus supports the contention that such yellow forms may be produced in petals by aggregation.

The data resulting from the study of yellow *L. chrysanthus* petals also support a flavonol aggregation explanation for petal yellowing, rather than alternative mechanisms such as cell shape or vacuolar pH. Epidermal cell shape for example is unlikely to be influential as no differences were observed between yellow and white petal zones, and the measured petal vacuolar pH of 6.7 failed to induce yellowing in petal extracts. However, as with lisianthus, microscopic inspection indicated considerable concentration of flavonol glycosides in the cytoplasm of standard petals (Fig. 1C). That a high concentration of these flavonol glycosides in the vacuole at the measured in vivo pH of 6.7 cannot alone account for this yellowing, was demonstrated by reconstituting the petal extract at a flavonol concentration 4× higher than that in vivo (see above). In contrast, the greater degree of aggregation achievable on a substrate did produce yellowing akin to that seen in the petal itself. Thus flavonol glycoside aggregation on a cytoplasmic matrix, through which single cell absorption spectra would be measured, may well account for the bathochromic spectral shift observed in situ in this petal (Fig. 3).

On the basis of the data presented here, it is proposed that yellow colouration in flowers can result from aggregation of (colourless) flavonol glycosides on a protein matrix in epidermal cell cytoplasm. The well established affinity between polyphenolics and appropriately structured proteins (Dangles et al., 1999; Haslam et al., 1999; Siebert, 1999; Wang and Goodman, 1999) provides a plausible mechanism for such aggregation. Binding of flavonoids to cytoplasmic protein however is unlikely to be indiscriminate, in view of the toxic effect this would have within the cell. The binding is more likely to be via a specific site or sites on a protein subgroup, much as has been observed for the binding of flavonols to protein of nuclear origin (Grandmaison and Ibrahim, 1996). Perhaps exemplifying this is our finding that kaempferol-3-*O*-rutinoside-7-*O*-rhamnoside, a lisianthus-type flavonol, produced yellowing (= interaction) with only one of three proteins investigated. When this flavonol was applied to glass slides upon which each of the three proteins, collagen, lysozyme and neutral polyarginine were deposited, conversion to its yellow form (λ_{max}365, 400 nm) was observed on polyarginine, but not on the other two proteins or on glass itself. Whilst this study is only preliminary, yellowing of flavonols with various substrates has previously been ascribed to the adoption of some pyrylium or enolic tautomer character by the bound flavonoid. Pyrylium involvement was inferred from fluorescence studies on the quercetin/BSA complex model system (Dangles et al., 1999), and the enolic tautomer concept from a study of quercetin and kaempferol glycosides deposited on cellulose (Smith and Markham, 1998). In both studies enhancement of flavonol fluorescence at ca. 530 nm (with excitation at 450 nm) was observed. This general mechanism for producing yellow colouration from (colourless) flavonol glycosides in petals, may also account for other examples of unexplained yellowing credited to the presence of (colourless) flavonol glycosides, for example in anthers (Napoli et al., 1999) and in seed coats (Beninger et al., 1998).

3. Experimental

3.1. Plant material

The lisianthus (*Eustoma grandiflorum*) lines used in this study were the purple No. 54 and the white Wakasaki (see Deroles et al., 1998 for further details) and were supplied by Crop & Food Research, Palmerston North, New Zealand. The yellow *Lathyrus chrysanthus* petals were the same as used in earlier studies (Markham et al., 1992) and were supplied by Hammett Plant breeders (NZ) Ltd., Auckland, New Zealand. Yellow *Dianthus caryophyllus* flowers were purchased from a local outlet. Epidermal peels were prepared using adhesive tape as described previously (Markham et al., 2000b).

3.2. Microscopy

Absorbance spectra of transverse and paradermal sections of petals were obtained using a Zeiss compound

microscope, modified such that all glass components were removed and a front-surfaced mirror incorporated to optimise the transmission of UV. Zeiss quartz objectives (40×) were used as condenser and objective. The light source was provided by a 100 W xenon arc lamp fitted with a UG5 filter. Specimens were mounted in water on quartz microscope slides and covered with quartz coverslips. The spectral absorbance of groups of cells was measured using an ocean optics spectrophotometer, connected to the microscope phototube via a fibre optic cable. A reference solution of rutin (λ_{max} 360 nm) was used to check the accuracy of the equipment.

The depth/pathlength of an average yellow cell in the epidermis of *L. chrysanthus* was determined by comparing the microscopically enlarged image of a transverse section of petal (Fig. 1F) with that of a similarly enlarged (134×) 1 mm graduated scale.

Fresh sections of the plant material were examined for the presence of flavonols using epifluorescence microscopy with a Zeiss filterset 09 (excitation: 450 nm; beamsplitter: 510 nm; emission 520 nm) in a Zeiss Axioplan 2 microscope. Sections were then treated for approx. 15 min with a saturated solution of NA (diphenylboric acid 2-amino ethyl ester) (Sigma) in 10% aqueous sucrose, and examined for yellow-green fluorescence.

CLSM of NA stained samples was carried out on a Leica TCS 4D using a 40×/1.Ona oil immersion objective. The filter block used a 488 nm excitation filter, a 488 nm dichroic mirror and a fluorescein isothiocyanate band pass suppression filter.

3.3. Protoplast and vacuole preparation from Lisianthus No. 54 petals

(Methodology based on that described by Martinoia et al. (1981) and Atsumi (1980). Whole petal adaxial epidermal peels prepared by the adhesive tape method (Markham et al., 2000a) were floated, ruptured side down, on an enzyme solution containing 1% cellulase, 0.05% pectolyase, and 0.4 M sucrose in a buffer solution made up from 0.04 M Na_2HPO_4 and 0.02 M citric acid in the ratio of about 5.8:4.2 (pH 5.6). After incubation at 25 °C for ca. 5 h, the mix was filtered through a 50μm stainless steel mesh into a centrifuge tube and stored overnight in the refrigerator to allow the protoplasts to settle. The separated protoplasts were washed twice with buffer solution. A portion was set aside for analysis (Fraction A) and the remainder were ruptured to isolate cell vacuoles using a solution comprising 12 mM Tris–HCl (pH 8.0), 1 mM EDTA and 0.15 M sucrose and monitored under a dissecting microscope. The process of vacuole liberation was usually maximised after about 10 min. Cellular debris was removed by centrifugation (800 rpm) on a Percoll gradient (comprising 2 mls each of 10, 20 and 30% Percoll solutions in the pH 5.6 buffer), for 8–10 min. Vacuoles together with intact protoplasts were recovered as a red band on the Percoll gradient near the 20–30% boundary. AVIs formed an overlapping band just below this boundary. This procedure was carried out several times with fresh protoplasts to maximise yield (which was assessed microscopically). The two best fractions obtained were comprised of 50% intact vacuoles plus 50% AVIs (from broken vacuoles) (Fraction B), and 70% intact vacuoles plus 30% protoplasts (Fraction C). Freezing of these fractions led to protoplast and vacuole rupture. Each fraction was diluted with water and the non-phenolic constituents removed by passing the sample through a cartridge of reversed phase silica and washing with water. A methanol wash eluted the flavonoids which were then analysed by HPLC on a reversed phase column.

3.4. HPLC analyses

HPLC analyses were carried out using a Waters 600E solvent delivery system, Waters 996 diode array detector, and a Jasco 851-AS intelligent sampler, results being analysed using Waters Millennium 2010 software. An injection volume of 20 μl was used with a Merck LiChrospher 100RP-18 endcapped column (5 μl, 4×119 mm). Elution (0.8 ml/min, 30°) was performed using a solvent system comprising solvent A (1.5% H_3PO_4) and solvent B (HOAc–CH_3CN–H_3PO_4–H_2O (20:24:1.5:54.5)) mixed using a linear gradient starting with 80% A, decreasing to 33% at 30 min, 10% A at 33 min, and 0% A at 39.3 min. Flavonols were detected at 352 nm. Retention times and on-line absorption spectra were recorded for all major peaks. Acylated flavonol glycosides were distinguished by the presence of an absorption peak at 320–330 nm (with a shoulder at ca. 350 nm) compared with 350–360 nm for flavonol glycosides. Ratios of acylated: non-acylated flavonols were determined by summation of the integrals of HPLC peaks eluting before 26 min (non-acylated) and after 33 min (acylated). For fractions A, B and C (Section 3.3) the sums of integrals for acylated:non-acylated flavonoid peaks were: for fraction A; 274:136, fraction B; 303:208 and fraction C; 361:212.

3.5. Flavonol-protein studies

Aqueous solutions of collagen (Sigma, Type III), lysozyme (ex saliva) and polyarginine (Sigma) adjusted to pH7 with 1 N HCl, were spread onto separate microscope slides and left to dry. Kaempferol-3-*O*-rutinoside-7-*O*-rhamnoside in MeOH was applied to each of the dried protein layers and to the surface of a clean microscope slide. Visible change was evident only with neutral polyarginine, and the visible absorption of λ_{max} 365, 400 nm compared with λ_{max} 355 nm for the flavonol on glass alone.

3.6. Reflectance measurements

Reflectance (and absorptance) spectra of petals, and flavonoids deposited on substrates, were determined using an external integrating sphere connected via a fibre optic cable to a Li-Cor 1800 spectroradiometer (Lincoln, Nebr.) and compared with those of a barium sulphate standard. Reflectance and transmittance are defined as the proportions of incident, diffuse light that is reflected from, and transmitted through the petal, respectively. Absorptance was calculated as:

$$\text{Absorptance} = 1 - \text{reflectance} - \text{transmittance}$$

Preparation of samples was as follows. (a) Pure flavonoid glycosides or mixtures from extracts were applied in solution to Whatman No. 1 filter paper, repeatedly with drying, until a visible yellow spot was evident. Reflectance spectra were measured on the dried yellow spot. (b) A white lisianthus flower (Wakasaki) was held at room temperature for several weeks in a vase without water. Reflectance spectra were obtained for petals from both the original white flower and the dry (yellowed) flower.

Acknowledgements

The authors would like to thank Kevin Mitchell of Industrial Research for carrying out the HPLC analyses, Dr. Geoff Rickards of the School of Biological Sciences, Victoria University of Wellington, New Zealand for the CLSM measurements, Deborah Huff for the isolation of quantities of lisianthus protoplasts and vacuoles, Crop & Food Research, Palmerston North, New Zealand for the supply of lisianthus petals, Dr Keith Hammett of Hammett Plant Breeders (NZ) Ltd, Auckland, New Zealand for the supply of *L. chrysanthus* petals, and the NZ Royal Society administered Marsden Fund for financial support (Programme IRL701).

References

Alfenito, M.R., Souer, E., Goodman, C.D., Buell, R., Mol, J., Koes, R., Walbot, V., 1998. Functional complementation of anthocyanin sequestration in the vacuole by widely divergent glutathione S-transferases. Plant Cell 10, 1135–1149.

Alluis, B., Dangles, O., 1999. Acylated flavone glucosides: synthesis, conformational investigation and complexation properties. Helv. Chim. Acta 82, 2201–2212.

Atsumi, S., 1980. Relation between auxin autotrophy and tryptophan content in sunflower crown gall cells in culture. Plant Cell Physiol 21, 1031–1039.

Beninger, C.W., Hosfield, G.L., Nair, M.G., 1998. Flavonol glycosides from the seed coat of a new Manteca-type dry bean (*Phaseolus vulgaris L*). J. Agric. Food Chem. 46, 2906–2910.

Brouillard, R., 1998. Flavonoids and flower colour. In: Harborne, J.B. (Ed.), The Flavonoids — Advances in Research since 1980. Chapman and Hall, London, pp. 525–538.

Brouillard, R., Dangles, O., 1994. Flavonoids and flower colour. In: Harborne, J.B. (Ed.), The Flavonoids — Advances in Research Since 1986. Chapman and Hall, London, pp. 565–586.

Dangles, O., Dufour, C., Bret, S., 1999. Flavonol-serum albumin complexation. Two electron oxidation of flavonols and their complexes with serum albumin. J. Chem. Soc., Perkin Trans. 2, 737–744.

Davies, K.M., Bradley, J.M., Schwinn, K.E., Markham, K.R., Podivinsky, E., 1993. Flavonoid biosynthesis in flower petals of five lines of lisianthus (*Eustoma grandiflorum*. Grise). Plant Sci. 95, 67–77.

Deroles, S.C., Bradley, M.J., Schwinn, K.E., Markham, K.R., Bloor, S.J., Manson, D.G., Davies, K.M., 1998. An antisense chalcone synthase cDNA leads to novel colour patterns in lisianthus (*Eustoma grandiflorum*) flowers. Mole. Breeding 4, 59–66.

Grandmaison, J., Ibrahim, R.K., 1996. Evidence for nuclear protein binding of flavonol sulphate esters in *Flaveria chloraefolia*. J. Plant Physiol 147, 653–660.

Haslam, E., Williamson, M.P., Baxter, N.J., Charlton, A.J., 1999. Astringency and polyphenol protein interactions. In: Kluwer, R. (Ed.), Phytochemicals in Human Health Protection, Nutrition and Plant Defense. Plenum Publishers, New York.

Hrazdina, G., 1992. Compartmentation in aromatic metabolism. In: Stafford, H.A., Ibrahim, R.K. (Eds.), Phenolic metabolism in Plants—Recent Advances in Phytochemistry, Vol. 26. Plenum Press, New York, pp. 1–23.

Hrazdina, G., Wagner, G.J., 1985. Compartmentation of plant phenolic compounds; sites of synthesis and accumulation. In: Van Sumere, C.F., Lea, P.J. (Eds.), The Biochemistry of Plant Phenolics, Annu. Proc. Phytochem. Soc. Eur. Clarendon Press, Oxford, pp. 119–129.

Hrazdina, G., Zobel, A.M., Hoch, H.C., 1987. Biochemical, immunological and immunocytochemical evidence for the association of chalcone synthase with endoplasmic reticulum membranes. Proc. Natl. Acad. Sci., USA 84, 8966–8970.

Hutzler, P., Fischbach, R., Heller, W., Jungblut, T.P., Reuber, S., Schmitz, R., Veit, M., Weissenböck, G., Schnitzler, J.P., 1998. Tissue localization of phenolic compounds in plants by confocal laser scanning microscopy. J. Exp. Bot 49, 953–965.

Hwang, Y.J., Yoshikawa, K., Miyajima, I., Okubo, H., 1992. Flower colours and pigments in hybrids with *Camellia chrysantha*. Scientia Horticulturae 51, 251–259.

Ibrahim, R.K., 1990. Immunocytochemical localization of plant secondary metabolites and the enzymes involved in their biosynthesis. Phytochem. Anal 1, 49–59.

Ibrahim, R.K., 1992. Immunolocalization of flavonoid conjugates and their enzymes. In: Stafford, H.A., Ibrahim, R.K. (Eds.), Phenolic Metabolism in Plants—Recent Advances in Phytochemistry, Vol. 26. Plenum, New York, pp. 25–61.

Ibrahim, R.K., De Luca, V., Khouri, H., Latchinian, L., Brisson, L., Charest, P.M., 1987. Enzymology and compartmentation of polymethylated flavonol glucosides in *Chrysoplenium americanum*. Phytochemistry 26, 1237–1245.

Markham, K.R., Ofman, D.J., 1993. Lisianthus flavonoid pigments and factors influencing their expression in flower colour. Phytochemistry 34, 679–685.

Markham, K.R., 1982. Techniques of Flavonoid Identification. Academic Press, London.

Markham, K.R., Gould, K.S., Winefield, C.S., Mitchell, K.A., Bloor, S.J., Boase, M.R. 2000. Anthocyanic vacuolar inclusions—their nature and significance in flower colouration. Phytochemistry, 55, 327–336.

Markham, K.R., Hammett, K.R.W., Ofman, D.J. 1992. Floral pigmentation in two yellow-flowered *Lathyrus* species and their hybrid. Phytochemistry 31, 549–554.

Markham, K.R., Ryan, K.G., Gould, K.S. and Rickards, G.K. 2000, Cell wall sited flavonoids in lisianthus flower petals. Phytochemistry 54, 681–687.

Marrs, K.A., Alfenito, M.R., Lloyd, A.M., Walbot, V., 1995. A glutathione S-transferase involved in vacuolar transfer encoded by the maize gene *Bronze-2*. Nature 375 397–400.

Martinoia, E., Heck, U., Wiemken, A., 1981. Vacuoles as storage compartments for nitrate in barley leaves. Nature 289, 292–293.

Mol, J., 1991. Flower colour manipulation: a floral facelift. Endeavour, New Series, 15, 42–47.

Muellar, L.A., Goodman, C.D., Silady, R.A., Walbot, V., 2000. AN9, a petunia glutathione S-transferase required for anthocyanin sequestration, is a flavonoid-binding protein. Plant Physiol 123, 1561–1570.

Napoli, C.A., Fahy, D., Wang, H.-Y., Taylor, L.P.White anther: a petunia mutant that abolishes pollen flavonol accumulation, induces male sterility, and is complemented by a chalcone synthase transgene. Plant Physiol 120, 615–622.

Norbaek, R., Christensen, L.P., Brandt, K., 1998. An investigation of flower colour and breeding of anthocyanins in species and hybrids of *Alstroemeria*. Plant Breeding 117, 63–67.

Pecket, R.C., Small, C.J., 1980. Occurrence, location and development of anthocyanoplasts. Phytochemistry 19, 2571–2576.

Sheahan, J.J., Rechnitz, G.A., 1993. Differential visualization of transparent testa mutants in *Arabidopsis thaliana*. Anal. Chem. 65, 961–963.

Siebert, K.J., 1999. Effects of protein-polyphenol interactions on beverage haze, stabilization, and analysis. J. Agric. Food Chem. 47, 353–362.

Small, C.J., Pecket, R.C., 1982. The ultrastructure of anthocyanoplasts in red cabbage. Planta 154 97–99.

Smith, G., Markham, K.R., 1998. Tautomerism of flavonol glycosides: relevance to plant UV protection and flower colour. J. Photochem. Photobiol. A: Chem. 118, 99–105.

Stafford, H.A., 1990. Flavonoid metabolism. CRC Press, Florida, pp. 202–207.

Wang, W., Goodman, M.T., 1999. Antioxidant property of dietary phenolic agents in a human LDL-oxidation ex vivo model: interaction of protein binding activity. Nutr. Res. 19, 191–202.

PERGAMON

Phytochemistry 58 (2001) 415–422

PHYTOCHEMISTRY

www.elsevier.com/locate/phytochem

Probing the role of calmodulin in Al toxicity in maize

Renato A. Jorge[a,*], Marcelo Menossi[b,c], Paulo Arruda[b,c]

[a]*Universidade Estadual de Campinas, UNICAMP, Instituto de Química, Departamento de Físico-Química, Campinas, SP, Brazil*
[b]*Universidade Estadual de Campinas, UNICAMP, Centro de Biologia Molecular e Engenharia Genética, Campinas, SP, Brazil*
[c]*Universidade Estadual de Campinas, UNICAMP, Instituto de Biologia, Departamento de Genética e Evolução, Campinas, SP, Brazil*

Received 19 January 2001; received in revised form 11 April 2001

Abstract

The role of calmodulin on Al toxicity was studied in two maize (*Zea mays* L.) inbred lines, Cat 100-6 (Al-tolerant) and S 1587-17 (Al-sensitive). Increasing levels of Al induced the release of malate at similar rate by roots of both genotypes, while the exudation of citrate, a stronger Al-binding compound, was 3.5 times higher in Cat 100-6 seedlings exposed to 16.2×10^{-6} Al^{3+} activity. The calmodulin inhibitor trifluoperazine significantly reduced the root growth in both genotypes, mimicking the main effect of Al. However, when Cat 100-6 and S 1587-17 seedlings were challenged with Al in conjunction with trifluoperazine, no further reduction in root growth or any other effect of Al toxicity was observed. The rate of Al-induced citrate exudation by both genotypes was not affected by treatment with trifluoperazine or calmidazolium, another calmodulin inhibitor. The Al^{3+} interaction with cytoplasmic CaM was estimated using models for the binding of Al^{3+} and Mg^{2+} with CaM and physiological concentrations of citrate, CaM, $InsP_3$, ATP, ADP, Al^{3+} and Mg^{2+}. In this simulation, Al^{3+} associated with citrate and $InsP_3$, but not with CaM. We conclude that calmodulin is not relevant to the physiological processes leading to the Al tolerance in maize, nor is it a primary target for Al toxicity. © 2001 Elsevier Science Ltd. All rights reserved.

Keywords: Aluminum toxicity; Calmodulin; Maize; *Zea mays*; Gramineae; Organic acids; Tolerance

1. Introduction

Calcium is an important cellular messenger involved in many biological events. CaM plays a key role in signal transduction pathways because the Ca^{2+} signals generated by $InsP_3$ are translated into intracellular responses by Ca^{2+}-CaM complexes (Garret and Grisham, 1995; Lu et al., 1996). Studies using CaM inhibitors in plants indicate that several responses to environmental stress are dependent on CaM. For instance, Facchini et al., (1996) and Mahady and Beecher (1994) used the CaM inhibitors TFP and W7 to show that CaM was involved in the release of alkaloids in response to fungal attack, and Gong et al., (1997) observed that heat tolerance in maize seedlings decreased in the presence of W7.

Aluminum toxicity in acid soils is the main factor affecting plant productivity (Taylor, 1991; Kochian, 1995). At toxic levels, Al^{3+} inhibits root growth as a consequence of root tip destruction (Delhaize et al., 1993a). Although Al^{3+} tolerance has been observed in several species, the pathways leading to this tolerance are not well understood (Jones and Kochian, 1997). It has been proposed that tolerant plants can detoxify Al^{3+} within the plant cell, or exclude Al^{3+} from the root (Kochian, 1995). The internal mechanism of tolerance requires that Al^{3+} be immobilized in the cytoplasm by chelating compounds, polypeptides or by compartmentalization in the vacuole. The exclusion mechanism proposes that Al^{3+} be immobilized in the cell wall by the formation of a rhizosphere pH barrier or by root exudation of Al-chelating compounds such as organic acids or polypeptides (Kochian, 1995). The latter mechanism has been demonstrated in tolerant plants where the release of citrate and/or malate (Jorge and Arruda, 1997; Pellet et al., 1995, Delhaize et al., 1993b) suggests a signaling process mediated by the Al^{3+}. Recently, Ryan et al. (1997) devised an ion channel that is induced by Al^{3+} and may be responsible for the

Abbreviations: CaM, calmodulin; Citr, citrate; CMZ, calmidazolium; $InsP_3$, inositol 1,4,5-triphosphate; TFP, trifluoperazine; TR1C, N-terminal half-fragment domain of calmodulin; TR2C, C-terminal half-fragment domain of calmodulin; RRG, relative root growth

* Corresponding author. Fax: +55-19-37883023.
E-mail address: rjorge@iqm.unicamp.br (R.A. Jorge).

0031-9422/01/$ - see front matter © 2001 Elsevier Science Ltd. All rights reserved.
PII: S0031-9422(01)00258-8

organic acids released by wheat roots following Al stress.

Although Al can enter the root symplasm (Lazof et al., 1994), no relationship between the accumulation of Al in the symplasm and toxicity has been established. Al^{3+} may interact with intracellular target sites such as calmodulin (Haug and Vitorello, 1996), plasma membrane lipids (Jones and Kochian, 1997), Ca^{2+}-ATPases and various components of the phosphoinosite signaling pathway (Haug et al., 1994; Jones and Kochian, 1995), to influence the function of intracellular sites. However, the assumption that calmodulin act as a primary site for Al toxicity is still controversial (Jones and Kochian, 1997).

The goal of this work was to analyze the physiological basis of the Al tolerance seen in two tropical maize lines and to evaluate whether calmodulin plays a role in this response. We observed that Al^{3+}-tolerant plants released higher levels of citrate than their Al-sensitive counterparts and that this response was not mediated by CaM. The data obtained were compatible with results from simulations using models from the literature for the interaction of Al^{3+} and Mg^{2+} with CaM, and estimated cytoplasmatic concentrations of citrate, CaM, $InsP_3$, ATP, ADP, Al^{3+} and Mg^{2+}.

2. Results and discussion

2.1. Al tolerance in maize

The inhibition of root growth is a primary effect of Al toxicity (Delhaize et al., 1993a). The relative root growth (RRG) of Cat 100-6 (Al-tolerant) and S 1587-17 (Al-sensitive) grown in complete nutrient solution containing Al^{3+} is shown in Fig. 1.

The two genotypes showed a clear difference in root growth in the presence of 36 μM $AlCl_3$, which corresponds to 16.2×10^{-6} Al^{3+} activity (see Experimental). Although Al^{3+} reduced the RRG of the sensitive and tolerant lines after 12 h, the effect on S1587-17 was greater. In contrast, Cat 100-6 sustained a RRG of around 0.8, indicating that this maize line was able to overcome the toxic effects of Al^{3+}. As the incubation progressed, several symptoms caused by Al toxicity were observed in the roots of S 1587-17, including the swelling of root cells, the destruction of apical meristems and the induction of secondary meristems that were also destroyed (results not shown). Moon et al. (1997) observed the same effects with these maize lines when using another nutrient solution and different growth conditions.

The two genotypes also differed when treated with hematoxylin, which binds to Al and allows the visualization of Al in the apoplast (Delhaize et al., 1993a). After 6 h in the presence of Al, both lines showed an intense color, indicating the binding of Al to the apoplasm.

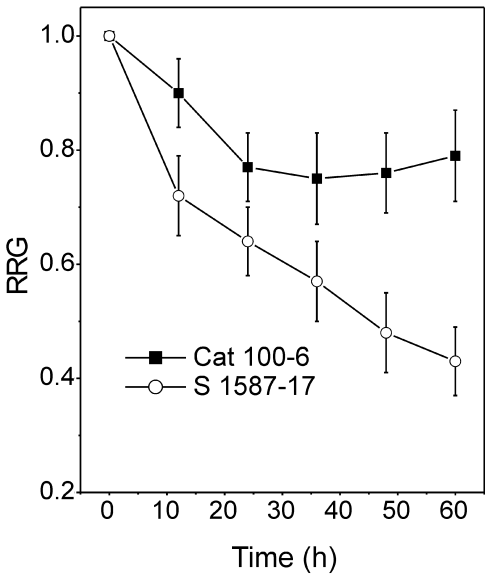

Fig. 1. Time course of Al^{3+} inhibition of relative root growth (RRG) in maize seedlings. Cat 100-6 and S 1587-17 seedlings were exposed to 36 μM $AlCl_3$ in growth solutions and the root growth at various times was used to calculate the RRG. The data are the mean ± S.D. ($n=10$).

After 24 h in the presence of Al, the apical region of tolerant plants was no longer stained with hematoxylin, in contrast to the sensitive roots that remained colored (data not shown). Similar results were also observed for other maize genotypes (Pellet et al., 1995; Jorge and Arruda, 1997). Together, these results indicate that Al tolerance in Cat 100-6 is mediated by an Al exclusion mechanism.

The differences in observed Al^{3+}-tolerance between the two maize inbred lines may be related to the release of organic acids by roots, as observed in several species (Myasaka et al., 1991; Pellet et al., 1995, Jorge and Arruda, 1997). These compounds can bind Al^{3+} to prevent the internalization of the ion, thereby alleviating Al toxicity. To evaluate this hypothesis, the amounts of malate, citrate, isocitrate, succinate, fumarate and oxaloacetate present in the growth solution containing different Al^{3+} activities were determined enzymatically (Jorge and Arruda, 1997). Of the anions analyzed, only a small amount of malate was detected in the exudates of Cat 100-6 and S 1587-17 grown in the absence of Al^{3+} (Fig. 2). Both tolerant and sensitive plants showed a dose-dependent exudation of malate up to 48 μM (21.5×10^{-6} Al^{3+} activity). In contrast, citrate exudation was strikingly different between the two lines. In S 1587-17, the velocity of citrate exudation was constant at the Al concentrations tested, whereas the exudation in Cat 100-6 responded to increasing concentrations of Al^{3+}. At 16.2×10^{-6} Al^{3+} activity, the tolerant line released 3.5 times more citrate than the sensitive line.

Considering that the binding of citrate to Al is stronger than that of malate (Martell et al., 1996), it can be inferred that the exclusion of Al^{3+} in Cat 100-6 is

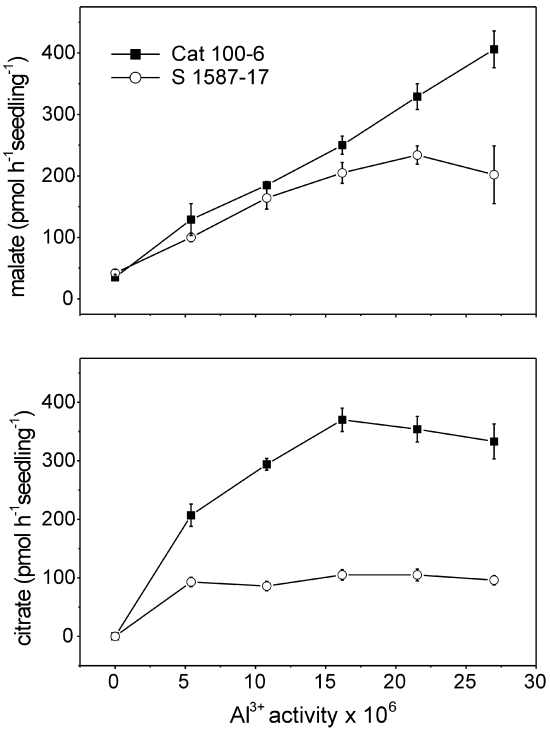

Fig. 2. Dose–response curves for citrate and malate release by intact Cat 100-6 and S 1587-17 roots in response to Al^{3+}. Seedlings were grown in nutrient solution containing increasing Al^{3+} activities. After 24 h incubation, the organic acids released into the nutrient solution were determined. The data are the mean ± S.D. ($n=2$).

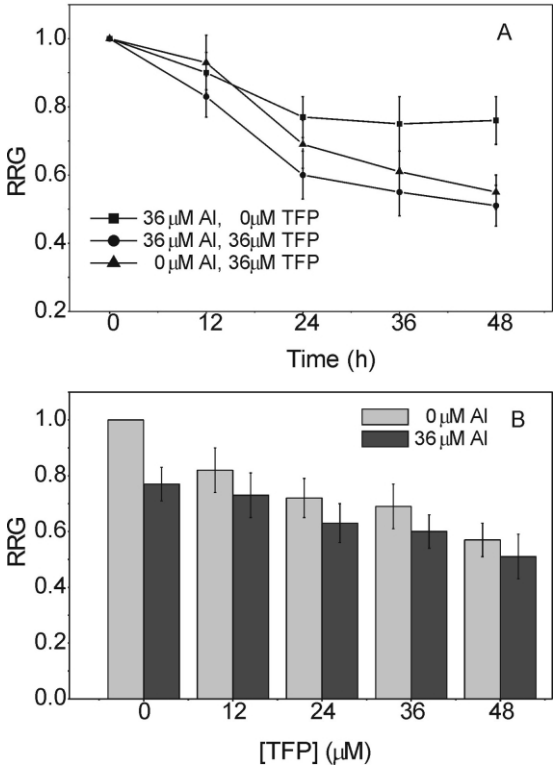

Fig. 3. Effect of TFP and Al^{3+} on RRG in the Al-tolerant maize line Cat 100-6. Seedling RRG was measured as before, in 50 ml recipients under slight agitation at pH 4.1. The data are the mean ± S.D. ($n=10$). (A) Root growth was measured over time at a fixed concentrations of Al^{3+} and TFP as indicated in the figure. (B) After 24 h incubation, root growth was measured with and without 36 μM Al^{3+} and at variable concentrations of TFP.

mediated by the release of citrate by roots. This strategy for overcoming Al toxicity has also been observed in other maize germplasms (Pellet et al., 1995, Jorge and Arruda, 1997). Moreover, the roots transgenic tobacco plants expressing a bacterial citrate synthase gene release up to fourfold more citrate than control plants and show increased tolerance to Al^{3+} (Fuente et al., 1997).

2.2. Effects of calmodulin inhibitors on Al tolerance

To assess the relevance of CaM on the mechanism(s) of Al tolerance Cat100-6 roots, seedlings were exposed to Al in combination with TFP. This compound binds to CaM, causing changes in the protein structure that block interactions with target enzymes (Vandonselaar et al., 1994).

While the RRG of tolerant plants remained practically unchanged by Al^{3+} treatment, 36 μM TFP reduced the RRG to 0.55 after 48 h (Fig. 3A). This inhibition was concentration-dependent up to at least 48 μM (Fig. 3B). A similar effect of TFP on root growth was also observed in *Arabidopsis thaliana* (Sinclair et al., 1996) and in another maize germplasm (Stinemetz et al., 1992). This inhibition probably involves the stabilization-destabilization of cortical microtubules which participate in such diverse processes as the orientation of cellulose microfibrils and chromosome segregation (Goddard et al., 1994), and is at least partly mediated by Ca^{2+}/CaM (Fisher et al., 1996). At the TFP concentrations used, the addition of 36 μM Al^{3+} caused no significant decrease in RRG (Fig. 3B) nor did it trigger the typical effects of Al toxicity (the swelling of the root tip and induction of secondary meristems; data not shown).

CaM antagonists can affect the activation of plant defenses in response to external harmful agents. For example, the release of alkaloids from *Sanguinaria canadensis* and *Papaver somniferum* cells in response to fungi elicitors is blocked by TFP and W7, another CaM inhibitor (Mahady and Beecher, 1994; Facchini et al., 1996). To further evaluate the involvement of CaM in Al^{3+} tolerance, the effects of TFP and CMZ on citrate release was examined. CMZ is 26 times more powerful than TFP in inhibition of CaM-dependent functions (Gietzen et al., 1981) and also more specific (Tuana and Maclennan, 1984). Seedlings were treated with TFP and CMZ in the presence of Al. The rate of citrate release by Al^{3+}-tolerant seedlings does not depend on the concentration of the CaM inhibitors (Fig. 4). The lower levels of citrate in the CMZ-treated seedlings reflected the lower Al concentration used (24 μM); at 36 μM Al^{3+}, the citrate exudation was similar to that of the TFP-treated seedlings as shown in Fig. 4 (results not shown).

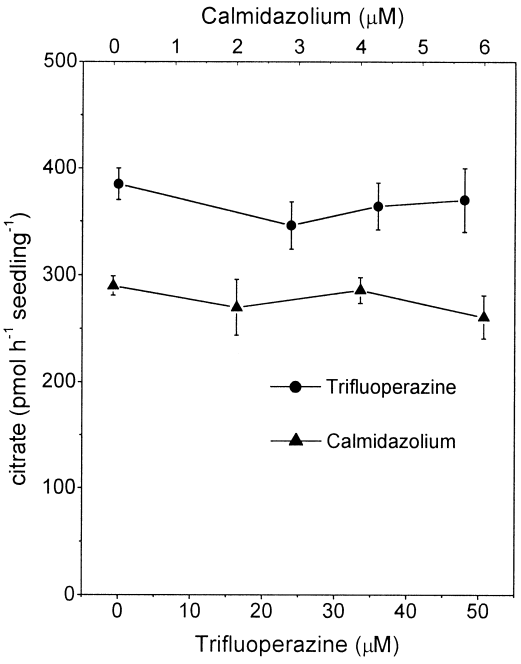

Fig. 4. Citrate exudation by maize roots incubated with calmidazolium (CMZ) and trifluoroperazine (TFP). Intact Cat 100-6 roots were exposed to 36 μM $AlCl_3$, and variable concentrations of TFP and CMZ, for 24 h. The data are the mean ± S.D. ($n=2$).

The rate of citrate release in the presence and absence of calmodulin inhibitors, together with the effect of TFP and Al on root growth, showed that CaM was not involved in the mechanism of Al tolerance.

2.3. The binding of Al to CaM in the symplasm

The most critical aspect of the hypothesized role of CaM as a primary site for Al toxicity is the binding of Al to CaM. This binding has been questioned and the involvement of calmodulin in Al tolerance in vivo is controversial. A study of wheat has indicated that CaM levels are similar in Al-tolerant and Al-sensitive lines and that Al does not induce CaM accumulation, although the results are not incompatible with the hypothesis that CaM is the primary target of Al^{3+} toxicity (Larkin, 1987). The replacement of calmodulin-dependent by calmodulin-independent NAD kinases could be responsible for the differences in tolerance between the two wheat lines (Slaski, 1989). Equilibrium dialysis studies demonstrated that Al^{3+} binds tightly to CaM (Siegel et al., 1983). Moreover, Al/CaM molar ratio of 2:1 induced a major structural change and a molar ratio of 4:1 totally inhibited the activity of the Ca/CaM-dependent phosphodiesterase (Siegel and Haug, 1983). However, Al^{3+} concentrations below 10^{-5} mol l^{-1} neither displaced Ca^{2+} bound to CaM nor depressed the Ca/CaM-dependent and basal phosphodiesterase activities, and failed to mimic the effects of chlorpromazine, another CaM inhibitor (Richardt et al., 1985). Indeed, Al^{3+} binding may not displace Ca^{2+} from the specific Ca^{2+}-binding domain on CaM (Weis and Haug, 1987). Studies with electron paramagnetic resonance spectroscopy, have failed to show a strong Al^{3+} interaction with CaM at pH 6.5 in methionine or tyrosine spin-labeled CaM (You and Nelson, 1991).

So far, no evidence was found that there is enough free Al^{3+} in the cell to interact with CaM. Under physiological conditions, the interaction of Al^{3+} with CaM must take into account the presence of other cytoplasmic components which could also bind to Al^{3+}, such as citrate and phosphate groups (such as $InsP_3$, ATP and ADP). Moreover, Mg^{2+} may compete with Al^{3+} for binding to these compounds, as seen in the association constants in aqueous medium (Table 1). In addition, Mg^{2+} is present at a high concentration in the cytoplasm and has similar ionic radii to Al^{3+}.

The interaction of Al^{3+} with CaM in the cytoplasm can be simulated using estimated cytoplasmic concentrations of citrate, CaM, $InsP_3$, ATP, ADP, Al^{3+} and Mg^{2+} and using the Geochem 2.0 software (Parker et al., 1995). For this simulation models for the binding of Al^{3+} and Mg^{2+} to CaM are necessary. CaM contains two globular domains linked by a flexible tether. These domains, which can be separated by tryptic digestion, are denoted TR1C (N-terminal domain) and TR2C (C-terminal domain). The calcium bindings in these domains is similar to those in the intact protein (Linse et al., 1991). Each domain contains two binding sites with a high affinity for Ca^{2+} (log Ka = 6.0–7.0). Sites III and IV in the C domain have greater affinity than sites I and II in the N domain (Linse et al., 1991). Haug and Vitorello (1996) proposed that the sites of Al^{3+} binding are not the four sites that bind Ca^{2+} and that Al^{3+} will bind to CaM using the same sites for Mg^{2+}. The model of the binding of Al^{3+} to CaM must take into account the models for the binding of Mg^{2+} with CaM. Three conflicting models for the interaction between Mg^{2+} and Ca^{2+} with CaM have been described in the literature: (1) competition between Ca^{2+} and Mg^{2+} for the two sites located in the terminal N domain (Malmendal et al., 1998), (2) direct competition between Ca^{2+} and Mg^{2+} for all four CaM sites (Tsai et al., 1987), and (3) no competition between the two ions for the Ca-specific sites (Gilli et al., 1998). The first model is based on NMR spectroscopy observations showing that Mg^{2+} only binds to the two sites in the TR1C (Malmendal et al., 1998). The absence of binding to the TR2C domain would explain why Mg^{2+} does not induce the same global structural changes provoked by Ca^{2+} in the protein (Malmendal et al., 1998). A later study on the interdependence of the Ca^{2+}/Mg^{2+} bound at the two sites located in the TR1C domain suggested that each site could bind to either Ca^{2+} or Mg^{2+}, but not both simultaneously (Malmendal et al., 1999). The second model is also based on NMR spectroscopy and involves

Table 1
Log β_{pqr} used in the simulation of the composition of the Al-complex. The general formula of the complex was $M_pL_qH_r$, where *p,q,r* refers to the numbers of metal ions (*M*), ligand molecules (*L*) and protons (H^+), respectively. A positive value of *r* indicates that the ligand is protonated and a negative value of *r* indicates the ionization of the ligand. The numbers in parentheses in the seventh column represented (*p,q,r*). β_{pqr} is the overall association constant

				p,q,r			
				120	12-1	Others	References
Metal-L	*1 1 0*	*1 1 1*	*1 1-1*				
Al-$InsP_3$	13.4	19.0	5.8			−1.8 (11–2)	Mernissi et al.,1995
Al-ATP	7.92	11.3	2.46	12.5	4.84		Kiss et al.,1991
Al-ADP	7.8	11.0	2.90	12.2	5.0		Kiss et al.,1991
Al-CaM 1	5.92	–	–	–	–		Haug and Vitorello,1996
Al-CaM 2	6.22						Haug and Vitorello,1996
Mg-Citr	2.7	6.5				7.3 (112)	Piispanen and Lajunen, 1995
Mg-$InsP_3$	4.4	12.2	18.5				Bieth et al., 1990[a]
Mg-ATP	4.5	2.3				6.3 (210)	Alberty, 1998
Mg-ADP	3.4	1.60					Alberty, 1998
Mg-CaM 1	3.10						Malmendal et al.,1998
Mg-CaM 2	2.7						Malmendal et al.,1998
Ligand	*0 1 1*	*0 1 2*	*0 1 3*				
CaM 1	6.2						Mladen et al., 1986
CaM 2	6.2						Mladen et al., 1986
Citr	5.7	10.0	13.0				Gregor and Powell, 1986
ATP	6.7	10.8					Alberty (1998)
ADP	6.5	10.5					Alberty (1998)

[a] Estimated values of D-*myo*-inositol 1,2,6-trisphosphate.

the suggestion that the occupation of all four sites by Mg^{2+} could cause small structural changes in the protein, as well as a minimal activation of the protein targets of CaM (Tsai et al., 1987). In the third model, in which the Ca^{2+}/CaM and Mg^{2+}/CaM complexes were characterized by flow dialysis and isothermal microcalorimetry, Mg^{2+} would bind to the auxiliary sites present on CaM (Gilli et al., 1998). The third model is compatible with the supposition of Haug and Vitorello (1996) in which Al^{3+} apparently does not displace Ca^{2+} from its specific sites.

We have simulated the interaction of Al^{3+} with CaM under physiological conditions for the three models. In this simulation, it was supposed that Al^{3+} would compete with Mg^{2+} for the same sites as described by the three models for the competition between Mg^{2+} and Ca^{2+}. Table 1 shows the association constants of the various compounds with Al^{3+}, Mg^{2+} and H^+, which were used with the Geochem 2.0 software. The association constants for Mg^{2+}/CaM refer to the first model.

Kiss et al (1994) estimated the concentrations of the cytoplasmic components in plasma as: total Al (Al^{3+}, $Al(OH)^{2+}$ $Al(OH)_2^+$ and aluminum complexes) = 1 μM, total phosphate (organic and inorganic, and 100 μM of ATP) = 10 mM, small molecular weight ligands containing oxygen-donating atoms (citrate, lactate, etc.) = 100 μM, while Jones and Kochian (1997), based on the work of Lazof et al. (1994) and Martin (1992), have presented the following estimates for plants (root epidermis cells) and animals (blood serum): total Al = 50 μM and citrate = 50–1000 μM. Fisher et al. (1996) estimated cellular CaM at 1 μM. In the present paper, the following initial concentrations were used: CaM = 1 and 50 μM, total Al = 1 and 50 μM, citrate = 0–100 μM; $InsP_3$ = ATP = ADP = 100 and 1000 μM, Mg^{2+} = 1000 μM.

The percentage distribution of Al-citrate and Al-$InsP_3$ complexes at equilibrium based on the above concentrations according to the first model is shown in Fig. 5. In this simulation, Al is associated with citrate and $InsP_3$, but not with CaM. The same results were observed for 1 μM CaM and 100 μM $InsP_3$, ATP and ADP. The binding of Al to ATP and ADP was maximum (0.4%) at 0 μM citrate (not shown in the Fig. 5 for clarity). The concentration of Al-CaM 1 and Al-CaM 2 complexes was minimal (log [Al-$CaM_{1\ or\ 2}$] = −12 to −14), indicating that it would be difficult for Al to bind to CaM under the conditions prevailing in the cytoplasm. This simulation was compatible with the previous results at pH 6.5, which suggested that at a high molar concentration (9:1 for citrate: aluminum and 10:1 for citrate:calmodulin), citrate blocked the binding of Al^{3+} to CaM (Suhayda and Haug, 1985, 1986) and also protected the calmodulin phosphodiesterase from damage caused by Al^{3+} (Suhayda and Haug, 1985). The simulation using the second and third models and the association constants for Mg^{2+} with CaM reported by Tsai et al. (1987) or by Gilli et al. (1998), respectively, produced the same results as obtained with the first model (data not shown).

Jones et al. (1998a,b) found that Al can disrupt cellular Ca^{2+} homeostasis in *Arabidopsis thaliana* root

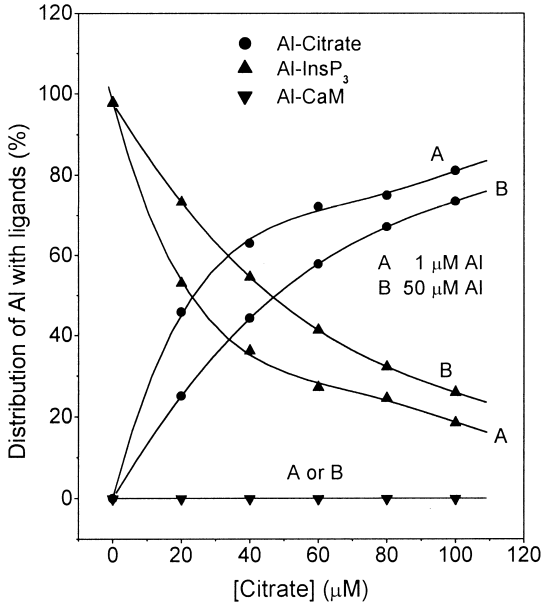

Fig. 5. Al–citrate and Al–$InsP_3$ complex composition at equilibrium based on initial physiological concentrations at pH 7.0 as determined using Geochem 2.0 software. The two CaM sites (CaM 1 and CaM 2) in the N terminal domain, which bind to Mg^{2+}, were considered to be independent, although the figure represents the sum of both sites. In all cases, [CaM 1]= [CaM 2]=50 μM, $[Al]_{total}$=1.0 and 50 μM, [$InsP_3$], [ATP] and [ADP]=1000 μM, and [Mg^{2+}]=1000 μM.

hairs and tobacco culture cells, and suggested that several intracellular sites could be targets for Al toxicity. Recently, Ma et al. (2000) reported evidence that Al inactivates extracellular CaM, leading to the inhibition of germination and pollen tube elongation in *Sorbaria kirilowi* Maxium. However, the role of extracellular CaM on Al^{3+} toxicity in the root apex remains to be proven.

Our results and the simulations using three models indicate that under normal intracellular conditions, CaM is not a primary target for Al toxicity. Our results also indicate that the processes leading to Al^{3+} tolerance in maize are not controlled by CaM.

3. Experimental

3.1. Plant material

The maize (*Zea mays* L.) inbred lines Cat 100-6, (Al-tolerant) and its somaclonal variant S1587-17, (Al-sensitive) (Moon et al., 1997) were obtained from the Germplasm Bank of the Universidade Estadual de Campinas, Campinas, Brazil. The plants were grown in the field and self-pollinated.

3.2. Seedling growth in nutrient solution

Seeds were surface-sterilized with 0.5% (v/v) sodium hypochlorite for 20 min, rinsed eight times with sterile water and germinated between layers of moist filter paper at 30 °C for 60 h.

Following germination, the seedlings were grown in opaque plastic receptacles containing 250 ml of aerated complete nutrient solution (Delhaize et al., 1993a) with small modifications (Jorge and Arruda, 1997). The pH was adjusted to 4.1 with HCl. The Al^{3+} solution was prepared freshly from $AlCl_3$ and standardized according to Kinnunem and Merikanto (1955). In all experiments, the seedlings were exposed to 16 h of light daily at room temperature (~26 °C).

The length of the main roots (n=10) was measured with a ruler and the roots then returned to the nutrient solution. Relative root growth is the mean of the quotients between the root growth of each seedling under a given a treatment and the mean root growth of all seedlings grown in control solution.

To study organic acid exudation, maize seedlings were grown in opaque plastic recipients with 25 ml of complete nutrient solution. To prevent microbial degradation of organic acids exuded by the roots, all the procedures were done under sterile conditions and the $AlCl_3$ solution was filter sterilized to avoid the formation of polynuclear compounds during autoclaving (Delhaize et al., 1993b). TFP and CMZ solutions were also filter sterilized and added to the nutrient solution. UV spectroscopy showed that TFP and CMZ did not interact with Al^{3+} or any other ions of the nutrient solution (data not shown). After 24 h incubation under constant agitation, the solution from each recipient was filtered (0.45 μm), frozen at −20 °C and completely freeze-dried. The organic acid levels were analyzed by enzymatic methods (see below).

3.3. Determination of organic acids in the growth solution

Malate, succinate, oxalate, citrate and isocitrate levels were determined according to Delhaize et al. (1993b), with minor modifications (Jorge and Arruda, 1997) using an HP array diode (HP, USA) spectrophotometer.

3.4. Bacterial control

In the experiments involving the quantification of organic acid exudation, contamination by microorganism was evaluated by plating one aliquot of the growth solution of each treatment in a Petri dish containing LB. In general, 20,000–30,000 bacteria/ml were observed. This concentration did not cause degradation of short chain organic acids, since preliminary experiments with 2000–70,000 bacteria/ml did not affect the amount of malate or citrate detected in the solution containing 36 μM $AlCl_3$ (data not shown).

3.5. Al^{3+} chemical activity

Al^{3+} in liquid media or in soil can be complexed by several ligands. As a result, Al^{3+} toxicity is better

Table 2
Total concentration and free activities of Al^{3+} in the nutrient solutions used to measure organic acid exudation and root growth in the presence and absence of $AlCl_3$ at pH 4.1. For the calculation of the Al^{3+} activity (a non-dimensional quantity), a 1 mol l^{-1} solution was used as standard

Al (μmol l^{-1})	Free Al^{3+} activity ($\times 10^6$)
0	0.0
12	5.4
24	10.8
36	16.2
48	21.5
60	27.0

reflected by the chemical activity of the Al^{3+} ion rather than its total molar concentration. The activities of the ionic species in the growth solutions at pH 4.1 were calculated using the Geochem 2.0 software (Parker et al., 1995).

Table 2 shows the concentrations of $AlCl_3$ used and the respective free Al^{3+} activities in the nutrient solutions.

3.6. Hematoxylin staining of maize roots

Intact roots from Al-tolerant and Al-sensitive root tips grown in nutrient solution with or without $AlCl_3$ were stained with hematoxylin according to Delhaize et al. (1993a).

Acknowledgements

This work was supported by grants from INCO-DC (ICA4-CT2000-30017) and PADCT/CNPq (62.0472/98.7) to M.M, INCO-DC (ERBIC19-CT-9600 89) to P.A, and FAEP-UNICAMP (Project No. 1124/95) to R.A.J. M.M received a post-doctoral fellowship from FAPESP.

References

Alberty, R.A., 1998. Change in the binding of hydrogen ions and magnesium ions in the hydrolysis of ATP. Biophys. Chem. 70, 109–119.

Bieth, H., Jost, P., Spiess, B., 1990. Complexation studies in inositol-phosphates. I. Ca(II) and Mg (II) complexes of D-*myo*-inositol 1,2,6-trisphosphate. J. Inorg. Biochem. 39, 59–73.

Delhaize, E., Craig, S., Beaton, C.D., Bennet, R.J., Jagadish, V.C., Randall, P.J., 1993a. Aluminum tolerance in wheat (*Triticum aestivum* L.) I. Uptake and distribution of aluminum in root apices. Plant Physiol. 103, 685–693.

Delhaize, E., Ryan, P.R., Randall, P.J., 1993b. Aluminum tolerance in wheat (*Triticum aestivum* L.). II. Aluminum-stimulated excretion of malic acid from root apices. Plant Physiol. 103, 695–702.

Facchini, P.J., Johnson, A.G., Poupart, J., De Luca, V., 1996. Uncoupled defense gene expression and antimicrobial alkaloid accumulation in elicited opium poppy cell cultures. Plant Physiol. 111, 687–797.

Fisher, D.D., Gilroy, S., Cyr, R.J., 1996. Evidence for opposing effects of calmodulin on cortical microtubules. Plant Physiol. 112, 1079–1087.

Fuente, J.M., Ramírez, -R.V., Cabrera-P, J.L., Herrera-E, L., 1997. Aluminum tolerance in transgenic plants by alteration of citrate synthesis. Science 276, 1566–1568.

Garret, R.H., Grisham, C.M., 1995. Molecular Aspects of Cell Biology. Saunders College Publishing, Orlando.

Gietzen, K., Wüthrich, A., Bader, H., 1981. R 243571: a new powerful inhibitor of red blood cell Ca^{++}-transport ATPase and of calmodulin-regulated functions. Biochem. Biophys. Res. Commun. 101, 418–425.

Gilli, R., Lafitte, D., Lopez, C., Kilhoffer, M.-C., Makarov, A., Briand, C., Haiech, J., 1998. Thermodynamic analysis of calcium and magnesium binding to calmodulin. Biochemistry 37, 5450–5456.

Goddard, R.H., Wick, S.W., Silfow, C.D., Snustad, D.P., 1994. Microtubule components of the plant-cell cytoskeleton. Plant Physiol. 104, 1–6.

Gong, M., Chen, N., Song, Y., Li, Z., 1997. Effect of calcium and calmodulin on intrinsic heat tolerance in relation to antioxidant systems in maize seedlings. Aust. J. Plant Physiol. 24, 371–379.

Gregor, J.E., Powell, H.K., 1986. Aluminium (III)-citrate complexes: a potentiometric and ^{13}C NMR study. Aust. J. Chem. 39, 1851–1864.

Haug, A., Shi, B., Vitorello, V., 1994. Aluminum interaction with phosphoinositide-associated signal transduction. Arch. Toxicol. 68, 1–7.

Haug, A., Vitorello, V., 1996. Aluminium coordination to calmodulin: thermodynamic and kinetic aspects. Coord. Chem. Rev. 149, 113–124.

Jones, D.L., Kochian, L.V., 1995. Aluminum inhibition of the inositol 1,4,5-trisphosphate signal transduction pathway in wheat roots: a role in aluminum toxicity? Plant Cell 7, 1913–1922.

Jones, D.L., Kochian, L.V., 1997. Aluminum interaction with plasma membrane lipids and enzyme metal binding sites and its potential role in Al cytotoxicity. FEBS Lett. 400, 51–57.

Jones, D.L., Gilroy, S., Larsen, P.B., Howell, S.H., Kochian, L.V., 1998a. Effect of aluminum on cytoplasmatic Ca^{2+} homeostasis in root hairs of *Arabidopsis thaliana* (L.). Planta 206, 378–387.

Jones, D.L., Kochian, L.V., Gilroy, S., 1998b. Aluminum induces a decrease in cytosolic calcium concentration in BY-2 tobacco cell cultures. Plant Physiol. 116, 81–89.

Jorge, R.A., Arruda, P., 1997. Aluminum-induced organic acids exudation by roots of an Al-tolerant tropical maize variety. Phytochemistry 45, 675–681.

Kinnunem, J., Merikanto, B., 1955. EDTA titrations using zincon as indicator. Chem. Anal. 44, 50.

Kiss, T., Sóvágó, I., Martín, R.B., 1991. Al^{3+} binding by adenosine 5′-phosphates: AMP, ADP and ATP. Inorg. Chem. 30, 2130–2132.

Kiss, T., Sóvágó, I., Martín, R.B., Pursiainen, J., 1994. Ternary complex formation between Al(III)-adenosine-5′-phosphates and carboxylic acid derivatives. J. Inorg. Biochem. 55, 53–65.

Kochian, L.V., 1995. Cellular mechanisms of aluminum toxicity and resistance in plants. Ann. Rev. Plant Physiol. Plant Mol. Biol. 46, 237–260.

Larkin, P.J., 1987. Calmodulin levels are not responsible for aluminium tolerance in wheat. Aust. J. Plant Physiol. 14, 377–385.

Lazof, D.B., Goldsmith, J.G., Rufty, T.W., Linton, R.W., 1994. Rapid uptake of aluminum into cells of soybean root tips. Plant Physiol. 106, 1107–1114.

Linse, S., Helmersson, A., Forsén, S., 1991. Calcium binding to calmodulin and its globular domains. J. Biol. Chem. 266, 8050–8054.

Lu, Y., Hidaka, H., Feldman, L.J., 1996. Characterization of calcium/calmodulin-dependent protein kinase homolog from maize roots showing light-regulated gravitropism. Planta 199, 18–24.

Ma, G.L., Fan, Q.S., Yu, Z.Q., Zhou, H.L., Zhang, F.S., Sun, D.Y., 2000. Does aluminum inhibit pollen germination via extracellular calmodulin? Plant Cell Physiol. 41, 372–376.

Mahady, G.B., Beecher, C.W.W., 1994. Elicitor-stimulated benzophenanthridine alkaloid biosynthesis in bloodroot suspension cultures is mediated by calcium. Phytochemistry 37, 415–419.

Malmendal, A., Evenäs, J., Thulin, E., Gippert, G.P., Drakenberg, T., 1998. When size is important. Accommodation of magnesium in a calcium regulatory domain. J. Biol. Chem. 273, 28994–29001.

Malmendal, A., Linse, S., Evenäs, J., Forsén, S., Drakenberg, T., 1999. Battle for the EF-hands: magnesium-calcium interference in calmodulin. Biochemistry 38, 11844–11850.

Martell, A.E., Hancock, R.D., Smith, R.M., Motekaitis, R.J., 1996. Coordination of Al (III) in the environment and in biological systems. Coord. Chem. Rev. 149, 311–328.

Martin, R.B., 1992. Aluminium speciation in biology. In: Chadwick, D. J., Whelan, J. (Eds.), Aluminium in Biology and Medicine. John Wiley & Sons, New York, pp. 5–25.

Mernissi, -A.K., Bieth, H., Schlelwer, G., Spiess, B., 1995. Complexation studies on inositol-phosphates. VI. Al^{3+} Complexes of DL-*myo*-inositol 1,4,5-triphosphate and D-*myo*-inositol 1,2,6-triphosphate. J. Inorg. Biochem. 57, 127–135.

Mladen, M., Schaer, J., Comte, M., Cox, J.A., 1986. Calcium-proton and calcium-magnesium antagonisms in calmodulin: microcalorimetric and potentiometric analyses. Biochemistry 25, 6279–6287.

Moon, D.H., Ottoboni, L.M.M., Souza, A.P., Sibov, S.T., Gaspar, M., Arruda, P., 1997. Somaclonal variation-induced aluminum-sensitive mutant from an aluminum-tolerant maize inbred line. Plant Cell Reports 15, 686–691.

Myasaka, S.C., Buta, J.G., Howell, R.K., Foy, C.D., 1991. Mechanism of aluminum tolerance in snapbeans: root exudation of citric acid. Plant Physiol. 96, 737–743.

Parker, D.R., Norvell, W.A., Chaney, R.L., 1995. Geochem-PC: a chemical speciations program for IBM and compatible personal computers. In: Loeppert, R.H., Schwab, A.P., Goldberg, S. (Eds.), Chemical Equilibrium and Reaction Models. Soil Sci. Soc. Am. Spec. Publ. 42, ASA and SSA, Madison, WI, pp. 253–269.

Pellet, D.M., Grunes, D.L., Kochian, L.V., 1995. Organic acid exudation as an aluminum-tolerance mechanism in maize (*Zea Mays* L). Planta 196, 788–795.

Piispanen, J., Lajunen, L.H.J., 1995. Complex formation equilibria of some aliphatic α-hydroxycarboxylic acids. 1. The determination of protonation constants and the study of calcium (II) and magnesium (II) complexes. Acta Chem. Scand. 49, 235–240.

Richardt, G., Federolf, G., Habermann, E., 1985. The interaction of aluminum and other metal ions with calcium-calmodulin dependent phosphodiesterase. Arch. Toxicol. 57, 257–259.

Ryan, P.R., Skerrett, M., Findlay, G.P., Delhaize, E., Tyerman, S.D., 1997. Aluminum activates an anion channel in the apical cells of wheat roots. Proc. Natl. Acad. Sci. 94, 6547–6552.

Siegel, N., Coughlin, R.T., Haug, A., 1983. A thermodynamic and electron paramagnetic resonance study of structural changes in calmodulin induced by aluminum binding. Biochem. Biophys. Res. Commun. 115, 512–517.

Siegel, N., Haug, A., 1983. Aluminum interaction with calmodulin: evidence for altered structure and function from optical and enzymatic studies. Biochim. Biophys. Acta 744, 36–45.

Sinclair, W., Oliver, I., Maher, P., Trewavas, A., 1996. The role of calmodulin in the gravitropic response of *Arabidopsis thaliana agr*-3 mutant. Planta 199, 343–351.

Slaski, J.J., 1989. Effect of aluminum on calmodulin-dependent and calmodulin-independent NAD kinase activity in wheat (*Triticum aestivum* L.) root tips. J. Plant Physiol. 133, 696–701.

Stinemetz, C.L., Hasenstein, K.H., Young, L.M., Evans, M.L., 1992. Effect of calmodulin antagonists on the growth and graviresponsiveness of primary roots of maize. Plant Growth Regul. 11, 419–427.

Suhayda, C.G., Haug, A., 1985. Citrate chelation as a potential mechanism against aluminum toxicity in cells: the role of calmodulin. Can. J. Biochem. Cell Biol. 63, 1167–1175.

Suhayda, C.G., Haug, A., 1986. Organic acids reduce aluminum toxicity in maize root membranes. Physiol Plant 68, 189–195.

Taylor, G.J., 1991. Current views of the aluminum stress response: the physiological basis of tolerance. Curr. Top. Plant Biochem. Physiol. 10, 57–93.

Tsai, M.D., Drakenberg, T., Thulin, E., Forsen, S., 1987. Is the binding of magnesium (II) to calmodulin significant? An investigation by magnesium-25 nuclear magnetic resonance. Biochemistry 26, 3635–3643.

Tuana, B.S., Maclennan, D.H., 1984. Calmidazolium and compound 48/80 inhibit calmodulin-dependent protein phosphorylation and ATP-dependent Ca^{++}-ATPase activity in skeletal muscle sarcoplasmic reticulum. J. Biol. Chem. 259, 6979–6983.

Vandonselaar, M., Hickie, R.A., Quail, J.W., Delbaere, L.T.J., 1994. Trifluoperazine-induced conformational change in Ca^{2+}-calmodulin. Nature Struct. Biol. 1, 795–801.

Weis, C., Haug, A., 1987. Aluminum-induced conformational-changes in calmodulin alter the dynamics of interaction with melittin. Arch. Biochem. Biophys. 254, 304–312.

You, G., Nelson, D.J., 1991. Al^{3+} versus Ca^{2+} ion binding to methionine and tyrosine spin-labeled bovine brain calmodulin. J. Inorg. Biochem. 41, 283–291.

PERGAMON

Phytochemistry 58 (2001) 423–428

PHYTOCHEMISTRY

www.elsevier.com/locate/phytochem

Soybean sterol composition and utilization by *Phytophthora sojae*

Julie A. Marshall, Allen L. Dennis, Toshihiro Kumazawa, Ann M. Haynes, W. David Nes*

Department of Chemistry and Biochemistry, Texas Tech University, Lubbock, TX 79409-1061, USA

Received 11 January 2001; received in revised form 19 April 2001

Abstract

The sterol fraction of *Glycine max* (soybean) was found to contain a mixture of 13 major sterols which differed dramatically in composition between seeds and shoots. Typical C4-desmethyl Δ^5-sterols, including sitosterol, predominate the sterol mixture of shoots, whereas C4-methyl sterol intermediates, cycloartenol and 24(28)-methylene cycloartanol, accumulate in seeds. The significance of modified sterol profile of shoot compared to seed was relevant to the physiology of *Phytophthora sojae*, a phytopathogen of soybean shown to be auxotrophic for sterol. Sterols native to the host plant containing a C4-methyl group, such as cycloartenol, were not utilized by the fungus. Alternatively, all Δ^5-sterols added to the culture media of *P. sojae* supported normal growth and promoted viable oospore production. The results demonstrate the importance of sterols in plant–fungal interactions and offer the possibility of bioengineering the phytosterol pathway for resistance to phytopathogens which scavenge specific sterols of the host plant to complete the life cycle. © 2001 Elsevier Science Ltd. All rights reserved.

Keywords: Soybean; *Glycine max*; Leguminosae; Host-pathogen interactions; Oomycetes; *Phytophthora sojae*; Sitosterol; Sterol

1. Introduction

The pythiaceous fungi (*Phytophthora* and *Pythium*) are a less-advanced group of phytopathogens which cannot synthesize sterols (Nes, 1987). This unusual defect in phytosterol synthesis by pythiaceous fungi has evolved into a nutritional dependency for Δ^5-sterols which can be acquired from the host during infection (Hendrix, 1970; Nes et al., 1982; Nes and Stafford, 1983). In the case of *Phytophthora sojae* which attacks soybean (*Glycine max*) (Erwin and Ribiero, 1996), Erwin et al. (1968) observed that the Δ^5-phytosterol, sitosterol can promote vegetative growth and sexual reproduction in an analogous manner to its effect on *P. cactorum* physiology (Nes et al., 1982). Based on these findings, we considered a hypothesis that Phytophthora-soybean interactions can be impaired by limiting sitosterol availability to the fungus. To test our proposal, we determined the phytosterol composition of soybean at two stages of development, one stage where no disease occurs — the seed, and a second stage where disease can cause serious crop losses — the shoot, and evaluated these materials as supplements in the growth media of *P. sojae*. Our results indicate that phytosterol intermediates which accumulate in seeds, C4-methyl sterols, can offer protection to disease and that limiting sitosterol availability can retard growth and interrupt oospore production.

2. Results and discussion

2.1. Sterol composition of soybean

The sterol composition of soybean seeds and shoots was determined by a combination of TLC, GLC, HPLC and MS as described in our earlier publications (Guo et al., 1995; Xu et al., 1988). In addition, the stereochemistry of the 24-alkyl group in the sterol side chain of material which had been purified by reversed-phase HPLC was established unambiguously by ^{1}H NMR (Guo et al., 1995). As shown in Table 1, the sterols of seeds and shoots are the same, but the proportion of the various sterols in the mixture and the total amount of sterol in each plant part differ significantly from seed to shoot (6-day seedling). To our knowledge, the elevated C4-methyl

* Corresponding author. Tel.: +1-806-742-1673; fax: +1-806-742-01350.

E-mail address: u0nes@ttacs.ttu.edu (W.D. Nes).

0031-9422/01/$ - see front matter © 2001 Elsevier Science Ltd. All rights reserved.
PII: S0031-9422(01)00219-9

Table 1
Sterol composition of soybean shoots and seeds

Sterol	Structure	MW M^+	% Total sterol	
			Shoot	Seed
Cycloartenol	**1**	426	1	19
24(28)-Methylenecycloartenol	**2**	440	5	26
Obtusifoliol	**3**	426	1	tr.
14α,24-Dimethylcholest-8-enol	**4**	412	tr.	2
24(28)-Methylenelophenol	**5**	412	1	3
24(28)Z-Ethylidienelophenol	**6**	426	1	2
Isofucosterol	**7**	412	tr.	3
Sitosterol	**8**	414	61	23
Stigmasterol	**9**	412	17	3
Campesterol	**10**	400	5	9
24-Epicampesterol	**11**	400	5	9
Desmosterol	**12**	384	tr.	tr.
Cholesterol	**13**	386	tr.	0
Total sterol (μg/seedling)			23	60

sterol content of soybean seeds (at ca. 46% of total sterol) is the highest amount of sterol intermediates so far detected from crop plants. From our experience in analyzing phytosterol compositions of vascular plants, the amount of sterol intermediates in seeds is generally 10–20% of the total sterol mixture (Nes, 1990). The major sterols of soybean seeds were determined to be cycloartenol (**1**, Fig. 1) and 24(28)-methylene cycloartanol (**2**) whereas the major sterol of shoots was sitosterol (**9**). Fenner et al. (1986) determined that the shoot sterols of soybean remained in the same proportion to each other during the course of plant development.

2.2. Sterol biosynthetic capabilities of *P. sojae*

P. sojae was cultured initially in liquid culture on a maintenance medium to establish the native sterol composition of the mycelia. A non-saponifable lipid extract of the mycelia was analyzed by GC–MS and found to contain an identical sterol composition to that of the growth media viz., sitosterol, stigmasterol, campesterol and cholesterol (cf. Nes, 1987). Within the limits of detection of our chromatographic system no ergosterol was detected. These observations suggest the fungus lacks an active biosynthetic pathway to sterols. To confirm that *P. sojae* cannot synthesize sterol, the fungus was cultured in liquid medium with 10 ppm [2-^{3}H]lanosterol (9 Ci/Mol) derived from synthesis (Le and Nes, 1986) or [11–^{14}C] squalene (55 Ci/Mol, obtained from Research Products International Corp.). Both compounds were absorbed by the mycelia to ca. 5% of the fresh weight. The labeled material was recovered from the mycelia in unchanged form as indicated by a single band of radioactivity migrating on TLC plates corresponding to standards of lanosterol ($R_f = 0.5$) and squalene ($R_f = 0.9$), respectively (Xu et al., 1988). The radiotracer studies involving *P. sojae* are in agreement with our earlier observations with *P. cactorum* that Phytophthora cannot synthesize sterols de novo (Nes et al., 1986; Nes, 1987). In related studies, we (Nes et al. 1982; Stafford and Nes, 1983) and Gottleib et al. (1978) found that *P. cactorum* and *P. infestans* can synthesize squalene but are unable to epoxidize the olefin to squalene oxide. Thus, the defect in the conversion of squalene to squalene oxide is likely the impaired step in the isoprenoid-sterol pathway responsible for sterol auxotrophy in this class of fungi.

To determine whether the fungus can metabolize sterols at all, the fungus was cultured on minimal broth with several soybean sterols, including cycloartenol, 24(28)-methylene cycloartanol, 24(28)-methylene lophenol, obtusifoliol, 24(28)-methylene cholesterol, sitosterol, and cholesterol (Fig. 1), and two sterols typically synthesized by fungi, lanosterol and ergosterol (Fig. 2). Each of the sterols was recovered from the fungus in unchanged form, except for ergosterol (M^+ 396 amu) which was metabolized to brassicasterol (M^+ 398 amu), the $\Delta^{5,22}$-analog of ergosterol, in 30% yield. The structure of brassicasterol was confirmed by its relative chromatographic mobility on TLC and HPLC and mass spectrum fragmentation pattern compared to that of an authentic specimen (Nes and Le, 1990). From these analyses, it would appear that *P. sojae*, like *P. cactorum* (Nes et al., 1982), has a limited number of enzymes than can act on the sterol substrate. In contrast to insects which are similarly auxotrophic for phytosterols (Nes et al., 1997) and convert sitosterol to cholesterol for hormonal purposes (Ikekawa et al., 1993), species of Phytophthora apparently utilize sitosterol in unchanged form to promote growth and sexual reproduction. These data and the fact sterols accumulate in mycelial membranes (Nes et al., 1982) indicate the primary role of sterols absorbed by Phytophthora is to affect membrane structure and function.

2.3. Sterol structure requirement of *P. sojae*

P. sojae was found to grow and reproduce sexually on a semisynthetic diet containing sitosterol as first reported by Erwin et al. (1968). We have now determined the amount of sitosterol required to promote maximal growth (as measured by hyphal extension) and oospore production is 10 mg/l or 0.001% of the diet (Figs. 3 and 4). In place of sitosterol a series of sterols were added to the fungal diet and their nutritional effects were evaluated. The sterols were chosen based on their relative position in the soybean sterol pathway as either a C4-methyl sterol intermediate or C4-desmethyl sterol end product. None of the C4-methyl sterol intermediates, cycloartenol **1**, 24(28)-methylene cycloartanol **2**, obtusifoliol **3** or 24(28)-methylene lophenol **5** promoted significant growth or induced functional oospore production. Sitosterol **8**, 24(28)-methylene cholesterol **14** and cholesterol **13** were absorbed by the mycelia to simi-

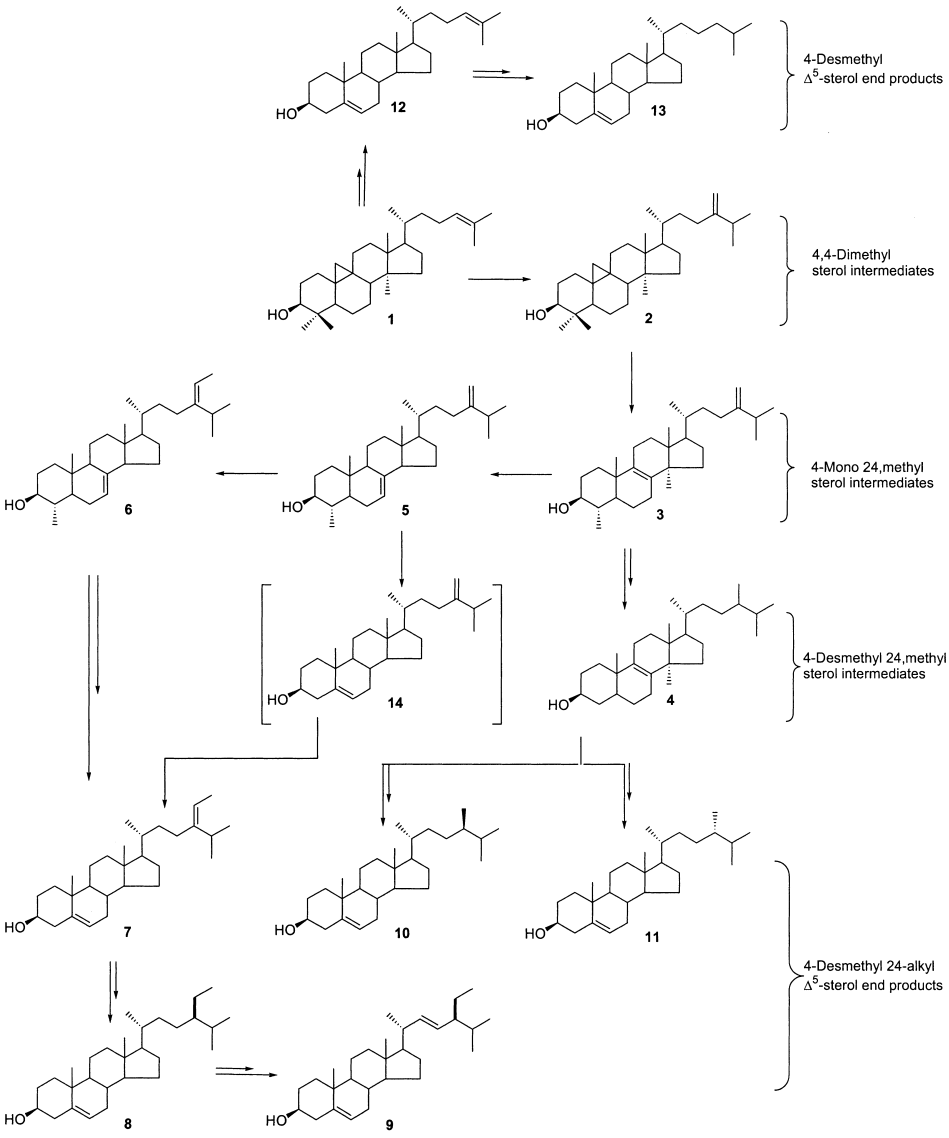

Fig. 1. Hypothetical sterol pathway in soybean. Compounds illustrated are: **1** cycloartenol, **2** 24(28)-methylene cycloartenol, **3** obtusifoliol, **4** 14, 24-dimethyl cholest-8-enol, **5** 24(28)-methylene lophenol, **6** 24Z-ethylidene lophenol, **7** isofucosterol, **8** sitosterol, **9** stigmasterol, **10** campesterol, **11**, 24-epicampsterol, **12** desmosterol, **13** cholesterol, **14** 24(28)-methylene cholesterol. Bracketed compound **14** represents a suspected intermediate in the pathway.

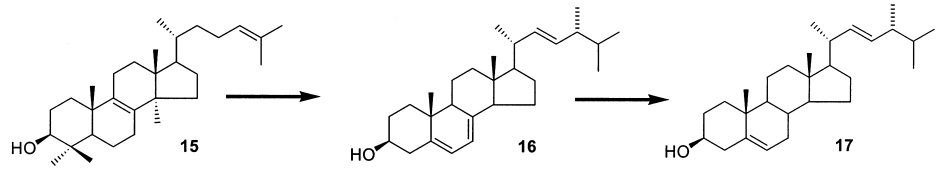

Fig. 2. Hypothetical pathway of fungal sterol biosynthesis. Compounds illustrated are: **15** lanosterol, **16** ergosterol and **17** brassicasterol.

lar levels, ca. 70 μg/g fr. wt, and cycloartenol and 24(28)-methylene lophenol were absorbed to a level of ca. 3 μg/g fr. wt. The amount of sterol absorbed by the mycelium was not necessarily limiting to phytosterol action, since cholesterol and 24(28)-methylene cholesterol were found to induce about half the number of oospores as were generated by treatment with sitosterol. These observations are similar to sterol-structure activity relationships observed with *P. cactorum* (Nes et al., 1982)

To establish the importance of sitosterol availability on *P. sojae* physiology the diet of *P. sojae* was supplemented first with different proportions of cycloartenol and sitosterol then with an equivalent amount of similar sterol types synthesized in the shoot and seed (Table 2).

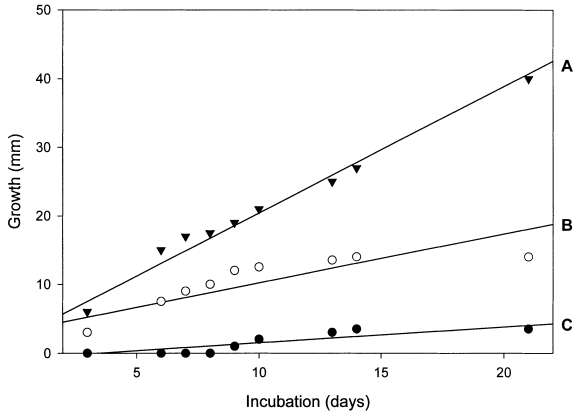

Fig. 3. Growth analysis (measured as hyphal extension) of *Phytophthora sojae* treated with 10 ppm sitosterol **A**, cycloartenol **B** or no sterol **C**. Petri plates were inoculated in the center of the plate with mycelia obtained from a maintenance culture using a 8 mm cork borer.

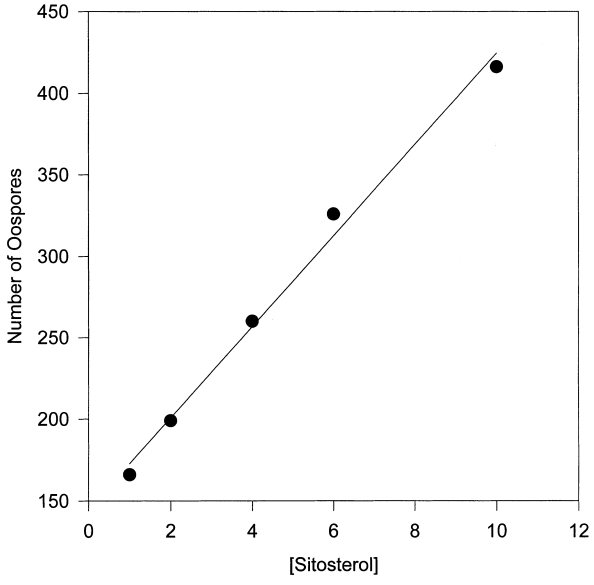

Fig. 4. Plot of increasing numbers of oospores per transect as a function of increasing amounts of sitosterol supplemented to the medium of *Phytophthora sojae*. The number of oopsores per transect remained constant at ca. 450 at higher levels of sitosterol treatment, ca. 15 or 25 ppm. Oospores were counted at 21 days of culture incubation. Microscope (Olympus Model CHT) settings for counting oospores were 40×.

Fungal growth was found to be significantly impaired at a 30/70 mixture of sitosterol to cycloartenol, which corresponds to ca. 50% the growth of sitosterol-treated mycelia. At a 10/90 mixture of the same set of sterols, growth of the mycelia was about the same as the 30/70 mixture of sitosterol to cycloartenol (data not shown). Growth of the fungus on a diet supplemented with 100% cycloartenol was very poor and not much better than the growth of a sterol-less diet, as reported in Fig. 3. *P. sojae* fed shoot or seed soybean sterol grew in a manner similar to mycelia fed a 50/50 mixture of sitosterol to cycloartenol. The number of oospores

Table 2
Phytophthora sojae utilization of cycloartenol spared with sitosterol

Sitosterol:cycloartenol ratio[a]	Oospores[b]	Sterol supplement[c]	
		Sitosterol	Cycloartenol
100:0	437	70	0
90:10	400	69	0
70:30	340	32	0
50:50	262	23	2
30:70	167	11	3
10:90	0[d]	5	3
0:100	0	0	3
NSF-shoot	423	58	0
NSF-seed	156	13	2

[a] Total sterol added to media at 10 ppm.
[b] Oospores per transect.
[c] μg/g fr. wt of mycelia.
[d] Media contained many aborted oogonia.

dropped from a maximum number of 437 to 0 as the proportion of sitosterol to cycloartenol was modified (Table 2). In the case of shoot sterol-treated mycelia where "sitosterol" levels are high in the sterol mixture, the number of oospores is high. However, in seed sterol-treated mycelia where "sitosterol" levels are low the number of oospores is also low. There is a clear correspondence between the amount of sitosterol in the sterol mixture, that amount of sitosterol absorbed by the mycelium and the number of oospores produced (Table 2). Whereas cycloartenol can be harmful to oospore production (Fig. 5), the amount of cycloartenol accumulated by the cells can be controlled as indicated by the limited absorption of C4-methyl sterols by the fungus.

One explanation for the low accumulation of cycloartenol by *P. sojae* is that species of Phytophthora synthesize a sterol carrier protein which can discriminate structural features of the sterol molecule. Indeed, Boissy et al. (1999) recently identified a pathogenic elicitin protein secreted by Phytophthora species which acts as a sterol carrier protein, favoring the binding over sitosterol to cholesterol and ergosterol. This sterol carrier protein is considered to facilitate movement of the host's sterol to the fungus. We hypothesize that a sterol carrier protein from *P. sojae* will be found to bind sitosterol with much greater efficacy than cycloartenol.

For these reasons, we assume that the unusual mixture of sterol in the seed fails to provide the necessary type or amount of phytosterol for *P. sojae* to grow and reproduce whereas the sterol mixture of the shoot can provide the nutritional sterol. Since the sterol methyl transferase (SMT) enzyme activity can regulate the cycloartenol-sitosterol pathway in soybean (Nes, 2000), it seems reasonable to hypothesize that bioengineering soybean to generate altered SMT levels could impair carbon flux thereby causing a change in phytosterol homeostasis to protect the plant from fungal attack.

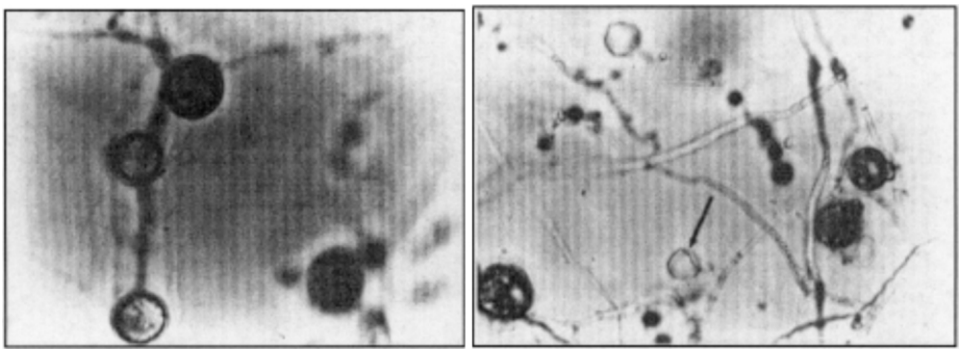

Fig. 5. Micrographs of normal oospores from (left picture) sitosterol-treated cultures and (right picture) aborted oospores from cycloartenol-treated cultures.

3. Experimental

3.1. General

The first set of experiments was designed to establish that *P. sojae* cannot synthesize sterols *de novo* and therefore, as in the case of other pythiaceous fungi, will require sterol to grow and reproduce sexually. To pursue these studies, *P. sojae* was cultured in two ways: Firstly, a maintenance system was developed which consisted of V8 juice/yeast potato dextrose medium added to agar distributed in 30 ml aliquots to 85 mm Petri plates. Secondly, a minimal broth was established which consisted of a synthetically compounded media to which was added sterol at 10 ppm (Nes et al., 1982).

P. sojae strain P7225 was obtained from Dr. Donald Erwin (Department of Plant Pathology at U.C. Riverside). The experimental methods for culturing *P. sojae* on solid and liquid substrates, determining growth rates, counting oospores and for isolating, identifying and quantifying sterols were as described in our earlier publications (Nes et al., 1982). Mycelia were grown in the dark at ambient temperature for 21 days. The sterols used in this study were from soybean or the Nes collection (Xu et al., 1988; Guo et al., 1995). Methods and instrumentation for mass spectroscopic and proton nuclear magnetic resonance spectroscopic analysis of sterols were as described (Guo et al., 1995). Samples for radiotracer analysis were dissolved in 5 ml of Scinti-Verse BD cocktail (Fisher). Radioactivity measurements were obtained on a Beckman LS 6500 liquid counter.

Soybean seeds strain DP3478 were purchased from Delta Pine and Land Co (Lubbock, Texas). Seeds were soaked in a 10% bleach solution for 10 min and washed. These seeds were imbibed with water and grown for 6 days in the dark. The resulting shoots were removed from the seeds and saponified in 10% methanolic KOH. The total sterol fraction was obtained from the non-saponifiable lipid fraction in the usual manner and purified into individual compounds by a combination of TLC and HPLC (Xu et al., 1988; Guo et al., 1995).

Acknowledgements

The financial support of the Texas Higher Education Coordinating Board Advanced-Technology Program (W.D.N.), the ARCS Foundation Inc. (J.A.M.), and a Texas Tech University Chancellor's Fellowship (A.L.D.) is gratefully acknowledged.

References

Boissy, G., O'Donohue, Gaudemer, O., Perez, V., Pernollet, J-C., Brunie, S., 1999. The 2.1 Å structure of an elicitin-ergosterol complex: a recent addition to the sterol carrier protein family. Protein Science 8, 1191–1199.

Erwin, D.D., Patridge, J.E., McCormick, W.H., 1968. Mycelial growth and production of oospores as affected by β-sitosterol, and the germination of oospores of *Phytophthora megasperma* var. *sojae* (Abst.). Phytopathology 58, 1049.

Erwin, D.C., Ribero, O.K., 1996. Phytophthora Disease Worldwide. American Phytopathology Society Press, St. Paul, MI, pp. 46–48.

Fenner, G.P., Patterson, G.W., Koines, P.M., 1986. Sterol composition during the life cycle of soybean and squash. Lipids 21, 48–51.

Gottlieb, D., Knauss, R.J., Wood, S.G., 1978. Differences in the sterol synthesizing pathways of sterol producing and non-sterol producing fungi. Phytopathology 68, 1168–1169.

Guo, D., Venkatramesh, M., Nes, W.D., 1995. Developmental regulation of sterol biosynthesis in *Zea mays*. Lipids 30, 203–219.

Hendrix, J.W., 1970. Sterols in growth and reproduction of *Pythium* and *Phytophthora* sp. Phytopathology 8, 111–130.

Ikekawa, N., Morisaki, M., Fujimoto, Y., 1993. Sterol Metabolism in insects: dealkylation of phytosterol to cholesterol. Acc. Chem. Res. 26, 139–146.

Le, P.H., Nes, W.D., 1986. Sterols: trittium labeling and selective oxidations. Chem. Phys. Lipids 40, 57–69.

Nes, W.D., 1987. Biosynthesis and requirement for sterols in the growth and reproduction of Oomycetes. ACS Symp. Ser. 325, 304–328.

Nes, W.D., 1990. Control of sterol biosynthesis and its importance to developmental regulation and evolution. Rec. Adv. Phytochem. 24, 283–327.

Nes, W.D., 2000. Sterol methyl transferase: enzymology and inhibition. Biochim. Biophys. Acta. 55711, 1–26.

Nes, W.D., Le, P.H., 1990. Evidence for separate intermediates in the biosynthesis of multiple 24β-methyl sterol end products by *Gibberella fujikuroi*. Biochim. Biophys. Acta 1042, 119–125.

Nes, W.D., Le, P.H., Berg, L.R., Patterson, G.W., Kerwin, J.L., 1986. A comparison of cycloartenol and lanosterol biosynthesis and metabolism by the Oomycetes. Experientia 42, 556–558.

Nes, W.D., Lopez, M., Zhou, W., Guo, D., Dowd, P.F., Norton, R.A., 1997. Sterol utilization and metabolism by *Heliothis zea*. Lipids 32, 1317–1323.

Nes, W.D., Saunders, G.A., Heftmann, E., 1982. Role of steroids and triterpenoids in the growth and reproduction of *Phytophthora cactorum*. Lipids 17, 178–183.

Nes, W.D., Stafford, A.E., 1983. Evidence for metabolic and functional discrimination of sterols by *Phytophora cactorum*. Proc. Natl. Acad. Sci. (USA) 80, 3227–3231.

Stafford, A.E., Nes, W.D., 1983. Biosynthesis of long chain fatty alcohols in *Phytophthora cactorum*. Experimental Mycology 7, 374–379.

Xu, S., Norton, R.A., Crumley, F.G., Nes, W.D., 1988. Comparison of the chromatographic properties of sterols, select additional steroid and triterpenoids: gravity flow liquid chromatography, thin layer chromatography, gas–liquid and high performance liquid chromatography. J. Chromatogr. 452, 377–398.

PERGAMON

Phytochemistry 58 (2001) 429–440

PHYTOCHEMISTRY

www.elsevier.com/locate/phytochem

Fragrance chemistry and pollinator affinities in Nyctaginaceae

Rachel A. Levin[a,*,1], Robert A. Raguso[b], Lucinda A. McDade[c]

[a]*Department of Ecology and Evolutionary Biology, University of Arizona, Tucson, AZ 85721, USA*
[b]*Department of Biology, Coker Life Sciences Building, University of South Carolina, Columbia, SC 29208, USA*
[c]*Academy of Natural Sciences, 1900 Ben Franklin Parkway, Philadelphia, PA 19103, USA*

Received 5 December 2000; received in revised form 11 May 2001

Abstract

We present results of dynamic head-space collections and GC–MS analyses of floral and vegetative fragrances for 20 species in three genera of Nyctaginaceae: *Acleisanthes*, *Mirabilis* and *Selinocarpus*. Most of the species included in this study are either hawkmoth or noctuid moth-pollinated. A wide variety of compounds were observed, including mono- and sesquiterpenoids, aromatics (both benzenoids and phenylpropanoids), aliphatic compounds, lactones, and nitrogen-bearing compounds. Intraspecific variation in fragrance profiles was significantly lower than interspecific variation. Each species had a unique blend of volatiles, and the fragrance of many species contained species-specific compounds. The fragrance profiles presented here are generally consistent with previous studies of fragrance in a variety of moth-pollinated angiosperms. © 2001 Elsevier Science Ltd. All rights reserved.

Keywords: *Acleisanthes*; *Mirabilis*; *Selinocarpus*; Nyctaginaceae; Four o'clock; Floral fragrance; Pollination; Hawkmoths

1. Introduction

In many pollination interactions, floral fragrance appears to act in concert with visual cues to attract floral visitors (see review by Dobson, 1994). Consequently, a number of studies have examined the relationship of fragrance composition to type of floral visitor (Knudsen and Tollsten, 1993, 1995; Borg-Karlson et al., 1994; Kaiser and Tollsten, 1995; Bestmann et al., 1997; Dobson et al., 1997; Miyake et al., 1998; Grison et al., 1999). The fragrances of hawkmoth-pollinated flowers in a number of plant families have been of particular interest (Knudsen and Tollsten, 1993; Kaiser and Tollsten, 1995; Raguso and Pichersky, 1995; Barthlott et al., 1997; Miyake et al., 1998). Such flowers often have similar morphologies, with long, tubular perianths that are usually white, occasionally yellow or pink (Grant, 1983; Haber and Frankie, 1989). Because these flowers generally emit fragrance at night, when most hawkmoths are active, it has been suggested that convergent evolution for hawkmoth attraction in various angiosperm families may involve scent chemistry as well as floral morphology (Nilsson et al., 1985; Knudsen and Tollsten, 1993; Miyake et al., 1998). To date there has been some support for this idea (Kaiser, 1993; Knudsen and Tollsten, 1993; Miyake et al., 1998); oxygenated terpenoids and nitrogen-bearing compounds are frequently present in the fragrance of hawkmoth-pollinated flowers. However, the high degree of among species variation in fragrance chemistry identified in these studies suggests that convergence is but one of several factors affecting scent chemistry.

Nyctaginaceae are a small family of trees, shrubs, and herbs, distributed mainly in tropical and subtropical regions of the New World. This family is commonly called the Four o'clock family, as most species have flowers that open in the late afternoon to early evening. Further, the flowers of many species are pollinated by hawkmoths (Grant, 1983; Grant and Grant, 1983; Martínez del Río and Búrquez, 1986; Hodges, 1995). Thus, it is an ideal group in which to examine volatiles produced from hawkmoth-pollinated flowers.

Here we present results of head-space volatile collections from flowers and vegetation of species in three genera of Nyctaginaceae: *Acleisanthes*, *Mirabilis*, and

* Corresponding author. Tel.: +1-301-238-3444, x114; fax: +1-301-238-3059.
E-mail address: rlevin@lms.si.edu (R.A. Levin).
[1] Current address: Laboratory of Molecular Systematics, Smithsonian Museum Support Center, 4210 Silver Hill Road, Suitland, MD 20746, USA.

0031-9422/01/$ - see front matter © 2001 Elsevier Science Ltd. All rights reserved.
PII: S0031-9422(01)00257-6

Selinocarpus (Table 1). This is the first report of fragrance compounds for any Nyctaginaceae except *Mirabilis jalapa* (Heath and Manukian, 1994). In particular, we investigated within versus among species variation in fragrance compounds for 20 species of Nyctaginaceae. The prediction was that intraspecific variation would be less than interspecific variation, supporting the premise that species have distinct fragrance profiles. Further, we asked how fragrances differed within and among the three genera, and how these differences are related to pollinator affinities.

2. Results and discussion

Our analyses identified a wide variety of volatile compounds across all 20 species examined (Table 2), including representatives of at least seven different biosynthetic classes: monoterpenoids, sesquiterpenoids, fatty acid and amino acid-derived aliphatic compounds and lactones, benzenoids, phenylpropanoids, and nitrogen-bearing compounds [the nitrogen-bearing compounds are known to result from three different biosynthetic pathways (Radwanski and Last, 1995; Wink, 1997)]. The most commonly occurring fragrance compounds were 4,8-dimethyl-nona-1,3,7-triene (present in all species), and *trans*-β-ocimene, *cis*-3-hexenyl acetate, and methyl salicylate (found in 18 of 20 species). There was also a preponderance of *cis*-3-hexenyl esters across all three genera, including both aliphatic and aromatic compounds; these may be the products of a single enzyme or a group of similar enzymes reacting with multiple substrates (see Wang and Pichersky, 1999; Dudareva and Pichersky, 2000).

2.1. Intraspecific vs. interspecific variation

Intraspecific variation in floral and vegetative fragrance quality (types of compounds) and quantity (amounts of compounds) was significantly lower than interspecific variation [$P < 0.0001$, Wilcoxon Signed Ranks Test (SPSS Inc., 1999); mean% dissimilarity of relative amounts of volatiles within species = 12.0 (S.D. = 6.8) vs. among species = 19.1 (S.D. = 7.3)]. These results are consistent with those of Barkman et al. (1997), who found that whereas intraspecific variation was substantial in *Cypripedium* (Orchidaceae), it was not as great as interspecific variation. Thus, it is reasonable to conclude that each species has its own characteristic fragrance profile, which can then be compared to the fragrance profiles of other taxa (Table 2). It should be noted that the interspecific comparisons spanned a wide range of phylogenetic relationships (i.e., some species were more closely related than others; Levin, 2000), and it would be ideal to control for degree of phylogenetic relatedness (Levin, 2001). Levin (2000) has shown that *Acleisanthes* and *Selinocarpus* species together form a monophyletic group, although

Table 1
Species included in this study, and their known pollinator affiliations[a]

Species	Likely pollinators	Evidence
Genus *Acleisanthes* A. Gray		
A. acutifolia Standl.	Hawkmoths	Floral morphology
A. crassifolia A. Gray	Hawkmoths	Pers. observations[a]
A. longiflora A. Gray	Hawkmoths	Pers. observations; Spellenberg and Delson, 1977
A. obtusa (Choisy) Standl.	Hawkmoths	Pers. observations
A. wrightii (A. Gray) Benth. & Hook.	Hawkmoths	Pers. observations
Genus *Mirabilis* L.		
M. alipes (S. Watson) Pilz	Noctuid moths, hawkmoths	Pers. observations
M. bigelovii A. Gray	Noctuid moths	Floral morphology
M. greenei S. Watson	Hawkmoths	Floral morphology
M. jalapa L.	Hawkmoths	Martínez del Río and Búrquez, 1986
M. longiflora L.	Hawkmoths	Grant and Grant, 1983
M. macfarlanei Constance & Rollins	Bees	Barnes, 1996
M. multiflora (Torrey) A. Gray	Hawkmoths	Pers. observations; Cruden, 1970; Hodges, 1995
M. pudica Barneby	Noctuid moths	Pers. observations
M. triflora Benth.	Hummingbirds	Pilz, 1978
Genus *Selinocarpus* A. Gray		
S. angustifolius Torrey	Noctuid moths	Floral morphology
S. chenopodioides A. Gray	Noctuid moths, hawkmoths, long-tongued flies	Pers. observations
S. lanceolatus Wooton	Hawkmoths	Floral morphology
S. parvifolius (Torrey) Standl.	Hawkmoths	Pers. observations
S. purpusianus Heimerl	Hawkmoths	Pers. observations; Fowler and Turner, 1977
S. undulatus Fowler & Turner	Noctuid moths	Floral morphology

[a] Personal observations by R. Levin include floral visitation, examination of visitors for pollen carriage, and microscopic study of stigmas for the presence of moth scales. In addition to nocturnal floral anthesis, floral morphological traits used as evidence of hawkmoth pollination included a tubular perianth >2 cm long; a perianth < 2 cm long suggested noctuid moth pollination.

Table 2
Mean percentage of each compound out of the total amount of volatiles found in the floral and vegetative fragrance of each species[a]

Compound[b]	RT	Aac $n=1$[c,d]	Acr $n=5$[d]	Alo $n=4$	Aob $n=5$	Awr $n=5$	Mal $n=7$	Mbi $n=1$[d]	Mgr $n=6$	Mja $n=1$	Mlo $n=2$	Mmf $n=1$[d]	Mmu $n=5$	Mpu $n=5$	Mtr $n=2$[e]	San $n=3$	Sch $n=9$	Sla $n=4$	Spa $n=4$	Spu $n=4$	Sun $n=4$
Total amount[f]		611.06	56.77	553.90	99.87	135.84	9.84	63.73	0.32	6.66	7.13	0.19	4.87	13.92	0.96	3.30	174.31	61.44	415.36	333.46	1.85
% Floral[g]		18.18	99.53	92.23	69.73	17.98	94.61	95.92	13.71	92.05	94.22	54.95	99.47	100.00	73.99	5.23	82.17	83.87	64.14	96.65	40.04
Total no. cmpds[h]		60	62	47	73	108	29	41	5	21	27	6	30	32	24	36	63	51	63	81	39
# Floral cmpds[i]		13	59	25	55	33	23	34	1	15	22	2	29	32	17	8	50	47	43	77	17
Amount floral/μg floral mass[j]		575.54	26.49	233.74	102.59	10.4	8.43	75.78	0.04	3.84	5.59	0.13	2.84	9.75	3.52	0.90	236.49	43.59	352.81	334.63	3.42
Monoterpenoids/irregular terpenes																					
α-Pinene*[k]	2.50	0.32	**Trace**[l,m]	Trace	0.32	0.06	–	–	–	–	–	–	–	–	**Trace**	0.29	–	**0.40**	Trace	**Trace**	0.57
Camphene*	2.95	0.67	–	**Trace**	**1.15**	**0.31**	–	–	–	–	–	–	–	–	–	0.25	–	**4.39**	–	–	0.54
β-Pinene*	4.00	–	Trace	Trace	1.13	0.02	–	–	–	–	–	–	–	**0.03**	–	0.45	–	**0.56**	**0.06**	**Trace**	0.14
Sabinene*	4.10	0.15	–	**Trace**	6.50	**Trace**	–	–	–	–	–	–	–	–	–	**0.29**	–	–	0.08	**Trace**	–
2-Carene*	4.43	–	–	–	–	–	–	–	–	–	**15.10**	–	–	–	–	–	–	–	–	–	–
Phellandrene*	5.10	–	–	–	–	–	–	–	–	–	0.65	–	–	–	–	–	–	–	–	–	–
Myrcene*	5.14	1.09	**0.59**	Trace	**1.26**	0.31	**0.31**	**0.08**	–	0.58	–	–	–	**0.30**	–	2.80	–	**3.09**	0.63	**0.73**	1.27
α-Terpinene*	5.45	–	–	–	**Trace**	**0.04**	–	–	–	–	**0.23**	–	–	–	–	–	–	–	–	–	–
Limonene*	5.75	0.54	0.32	0.24	15.26	2.29	–	0.14	–	–	3.89	**43.35**	**1.94**	**0.88**	**4.76**	3.14	0.25	**6.87**	0.58	**0.07**	9.85
β-Terpinene	5.90	–	–	–	–	–	–	–	–	–	**9.91**	–	–	–	–	1.39	–	–	–	–	–
cis-β-Ocimene*	6.53	0.16	**0.18**	Trace	**0.13**	0.05	**1.05**	**0.13**	–	**1.31**	**0.83**	–	–	**0.02**	–	4.68	0.10	**1.52**	0.33	**1.05**	1.41
trans-β-Ocimene*	6.97	**1.50**	**10.08**	0.43	**5.39**	0.82	**60.79**	**7.21**	–	**38.10**	**3.44**	–	**1.72**	**2.24**	**1.30**	12.14	0.76	**5.87**	0.76	**57.81**	3.45
α-Terpinolene*	7.31	0.06	**Trace**	–	**0.28**	0.06	–	0.01	–	–	**0.24**	–	**Trace**	**0.08**	–	–	–	**0.94**	0.15	Trace	–
6-Methyl-5-hepten-2-one	8.27	–	–	**6.16**	**4.99**	–	**1.34**	–	4.36	–	–	0.52	–	**0.76**	–	–	**0.58**	**3.67**	0.72	**0.10**	5.53
α-Pinene epoxides	8.57, 9.16	–	–	–	–	–	–	–	–	–	–	–	–	–	–	–	–	–	–	**0.14**	–
2,7-Methyl Octadiene	8.63	–	–	–	–	0.03	–	–	–	–	–	–	–	–	–	–	–	–	–	–	–
Allo-Ocimene*	8.80	–	**Trace**	–	**0.02**	**Trace**	–	**0.02**	–	**Trace**	–	–	–	–	–	**0.52**	–	–	–	**0.16**	–
Cinerone/piperitenone	9.26, 9.9	–	–	–	–	–	–	–	–	–	–	–	–	–	–	–	–	–	–	**0.15**	–
Furanoid linalool oxides*	9.8, 10.3	–	–	–	–	0.03	**7.18**	–	–	–	–	–	–	**4.16**	–	–	–	–	–	–	**2.28**
Menthatriene	9.91	–	–	–	–	–	**0.61**	–	–	–	–	–	–	–	–	–	–	**Trace**	–	**0.17**	–
Santene*	10.68	–	–	–	–	**Trace**	–	–	–	–	–	–	–	–	–	–	–	–	–	–	–
Octadiene	11.07	–	–	–	–	–	**0.47**	–	–	–	–	–	–	–	–	–	–	–	–	**0.07**	–
Linalool*	11.25	0.19	**0.32**	0.51	**0.80**	2.52	**0.66**	**0.38**	–	–	–	–	0.53	**2.00**	8.55	1.85	**0.92**	**3.93**	**1.21**	**0.30**	3.72
Isocitronellen	11.67	–	–	–	–	–	–	–	–	–	–	–	–	–	–	–	–	**0.31**	**0.76**	–	–
4-Terpineol*	11.95	–	–	–	–	–	–	–	–	–	–	–	–	–	–	–	–	–	–	–	**7.93**
cis-Citral*	12.76	–	**Trace**	–	–	**0.03**	–	–	–	–	**Trace**	–	–	–	–	–	–	–	–	**0.08**	–
Limonene diepoxides	13-13.9	–	–	–	**0.08**	**Trace**	–	–	–	–	–	–	–	–	**0.80**	**0.91**	–	–	–	**0.07**	–
Eucarvone*	13.44	–	–	–	–	–	–	–	–	–	–	–	–	–	–	–	–	–	–	**0.11**	–
(−)-Verbenone*	13.54	–	–	–	–	–	–	–	–	–	–	–	–	–	–	–	–	–	–	**0.73**	–
trans-Citral*	13.61	–	–	–	–	0.06	–	–	–	–	–	–	–	–	–	–	–	–	–	–	–
Pyranoid linalool oxides*	13.7, 13.9	–	–	–	–	–	**10.60**	–	–	–	–	–	**0.68**	**20.04**	–	–	–	–	–	–	**1.70**
Nerol*	14.3	2.72	–	–	–	–	–	**0.03**	–	–	**0.49**	–	**0.35**	–	**3.59**	8.27	**7.02**	–	–	–	**2.81**
α-Ionone*	14.46	–	–	–	–	–	–	–	–	–	–	–	–	–	–	–	–	–	–	**0.08**	–
Carveol*	14.57	–	**0.03**	–	–	**0.05**	–	**0.05**	–	–	–	–	–	–	–	–	**0.09**	–	–	**0.04**	–

(*continued on next page*)

Table 2 (*continued*)

Compound[b]	RT	Aac $n=1$[c,d]	Acr $n=5$[d]	Alo $n=4$	Aob $n=5$	Awr $n=5$	Mal $n=7$	Mbi $n=1$[d]	Mgr $n=6$	Mja $n=1$	Mlo $n=2$	Mmf $n=1$[d]	Mmu $n=5$	Mpu $n=5$	Mtr $n=2$[e]	San $n=3$	Sch $n=9$	Sla $n=4$	Spa $n=4$	Spu $n=4$	Sun $n=4$
Thujol	16.38	–	**0.15**	–	–	–	–	–	–	–	–	–	–	–	–	–	–	–	–	**0.05**	–
Unknowns with 150 as mol. ion																					
150,135,43,67,55[n]	7.76	–	–	–	–	–	–	–	–	–	–	–	–	–	–	–	–	**Trace**	**Trace**	**0.02**	–
150,39,95,77,91	11.07	–	–	–	–	–	–	–	–	–	–	–	–	–	–	–	–	–	–	**0.08**	–
150,39,41,91,79,107,135	17.18	–	–	–	–	0.16	–	–	–	–	–	–	–	–	–	–	–	–	–	**0.36**	–
150,41,107,53,79,135,91	19.18	–	–	–	–	0.20	–	–	–	–	–	–	–	–	–	–	–	–	–	–	–
Other unknowns		1.37	**0.10**	**0.09**	1.34	0.38	**1.41**	**0.02**	–	3.12	**0.46**	–	–	**0.05**	**Trace**	0.72	**Trace**	**1.65**	**0.31**	**1.43**	**10.83**
Total%		8.78	11.76	7.44	38.65	7.42	84.41	8.07	4.36	43.11	35.25	43.87	5.23	30.56	19.03	37.71	9.73	33.21	5.57	63.83	52.02
Sesquiterpenoids																					
4,8-dimethyl-nona-1,3,7-triene*	7.76	0.84	**0.47**	**0.20**	**0.68**	**Trace**	**5.03**	**23.84**	**13.71**	0.81	**4.41**	**11.60**	**5.18**	**12.25**	2.93	15.23	1.29	**10.37**	0.53	**0.02**	**2.01**
Other likely homoterpenes	10.47, 14.10, 14.41	–	**0.14**	**0.02**	**0.06**	0.21	**0.74**	–	–	–	–	–	–	**0.21**	**1.04**	0.93	**Trace**	**0.14**	–	–	–
α-Cubebene*	9.95	0.02	–	–	–	Trace	–	–	–	–	–	–	–	–	–	–	–	–	–	–	–
δ-Elemene*	10.23	0.05	–	0.04	Trace	**0.12**	–	–	–	–	–	–	–	–	–	–	**0.15**	**0.44**	**0.08**	–	–
α-Copaene*	10.54	0.16	**0.03**	–	**Trace**	0.12	–	–	–	–	**0.31**	–	–	–	–	–	–	–	–	–	–
β-Bourbonene*	10.84, 10.92	0.74	–	–	–	0.51	–	–	–	–	–	–	–	–	–	2.42	–	–	–	–	Trace
α-Gurjunene	11.06	–	–	–	–	0.02	–	–	–	–	–	–	–	–	–	Trace	–	–	–	–	–
β-Cubebene*	11.17	0.42	**0.01**	–	–	0.03	–	**0.01**	–	–	–	–	–	–	–	–	–	–	–	–	–
α-Bergamotene*	11.60	–	**0.04**	–	**1.42**	–	**0.29**	–	–	–	**0.65**	–	–	–	–	–	**0.20**	–	–	–	–
β-Elemene*	11.70	6.86	**0.04**	–	–	12.74	–	0.30	–	–	–	–	–	–	–	–	–	–	–	**0.04**	–
Caryophyllene*	11.98	7.36	**3.52**	–	**1.52**	4.35	–	**24.85**	–	–	**0.93**	–	**0.40**	–	–	9.84	0.73	**2.19**	**0.41**	–	–
Chamigrene	12.30	**Trace**	–	–	–	–	–	–	–	–	**Trace**	–	–	–	–	1.07	–	Trace	**0.08**	–	**0.47**
β-Selinene	12.48	0.63	–	–	–	0.17	–	–	–	–	–	–	–	–	–	–	–	–	–	**Trace**	–
β-Farnesene*	12.7, 13.1	1.06	**Trace**	**0.26**	**1.36**	0.05	–	**0.09**	–	–	–	–	**Trace**	–	–	–	**0.12**	–	–	–	–
α-Humulene*	12.9	4.11	**0.22**	–	**1.11**	11.73	–	**4.38**	–	–	**Trace**	–	–	–	–	2.37	0.14	–	**0.14**	–	–
β-Cadinene*	13.11	–	–	–	–	0.07	–	–	–	–	–	–	–	–	–	–	–	–	–	–	–
Germacrene D*	13.4, 13.7	12.27	–	**Trace**	**2.34**	1.57	–	–	–	–	**Trace**	–	–	–	–	4.11	**0.01**	**1.26**	**0.18**	–	–
α-Farnesene*	13.48–13.80	–	**2.00**	**0.52**	**18.95**	0.07	**0.42**	**0.02**	–	**37.03**	**4.37**	–	–	**0.97**	–	–	**0.53**	–	**0.09**	**2.63**	**0.52**
δ-Guaiene*	13.52	7.72	–	–	–	–	–	–	–	–	–	–	–	–	–	–	–	–	–	–	–
Junipene	13.54	**0.70**	–	–	–	2.99	–	–	–	–	–	–	–	–	–	–	**0.49**	–	–	–	–
γ-Cadinene*	14.02	8.01	–	–	**Trace**	6.83	–	–	–	–	–	–	–	–	–	–	0.01	–	**0.06**	–	–
α-Muurolene*	14.33	0.58	–	–	–	0.22	–	–	–	–	–	–	–	–	–	–	–	–	–	–	–
Calamenene*	14.79	0.78	–	–	–	0.16	–	–	–	–	–	–	–	–	–	–	–	–	–	–	–
Geranyl acetone*	14.95	–	–	0.45	–	–	0.10	–	–	–	–	–	**0.45**	**0.35**	1.28	1.38	**0.63**	**1.02**	0.36	**0.08**	**2.46**
Caryophyllene oxides*	16.2, 16.5	6.18	**0.12**	–	**Trace**	**3.75**	–	**2.39**	–	–	–	–	–	–	–	–	**0.23**	–	–	–	–
Nerolidol*	16.46–16.87	**2.55**	**0.14**	**80.46**	**1.06**	0.28	–	**0.05**	–	**0.21**	–	–	–	–	–	–	**0.14**	–	**Trace**	**0.01**	–
1,5-Cyclo-undecadiene[o]	16.69	–	–	–	–	0.06	–	–	–	–	–	–	–	–	–	–	–	–	–	–	–
12-Oxabicyclo dodecadiene[p]	17.04	0.57	**0.01**	–	–	0.98	–	**0.58**	–	–	–	–	–	–	–	–	–	–	–	–	–

(*continued on next page*)

Table 2 (*continued*)

Compound[b]	RT	Aac $n=1$[c,d]	Acr $n=5$[d]	Alo $n=4$	Aob $n=5$	Awr $n=5$	Mal $n=7$	Mbi $n=1$[d]	Mgr $n=6$	Mja $n=1$	Mlo $n=2$	Mmf $n=1$[d]	Mmu $n=5$	Mpu $n=5$	Mtr $n=2$[e]	San $n=3$	Sch $n=9$	Sla $n=4$	Spa $n=4$	Spu $n=4$	Sun $n=4$
Germacrone	17.33	–	–	–	–	0.05	–	–	–	–	–	–	–	–	–	–	–	–	–	–	–
Carotol	17.60	–	–	–	–	0.07	–	–	–	–	–	–	–	–	–	–	–	–	–	–	–
Spathulenol	17.78	–	–	–	–	0.11	–	–	–	–	–	–	–	–	–	–	–	–	–	–	–
Aromadendrene epoxide	17.99	–	–	–	–	0.22	–	–	–	–	–	–	–	–	–	–	–	–	–	–	–
δ-Cadinol	18.28	–	–	–	–	9.14	–	–	–	–	–	–	–	–	–	–	–	–	–	–	–
Guaiol	18.34	–	–	–	–	0.22	–	–	–	–	–	–	–	–	–	–	–	–	–	–	–
Aristolene	18.41	–	–	–	–	0.35	–	–	–	–	–	–	–	–	–	–	–	–	–	–	–
α,β-Eudesmol	18.73, 18.86	2.11	–	–	–	10.41	–	–	–	–	–	–	–	–	–	–	–	–	–	–	–
Farnesol*	18.9–19.8	0.64	**0.19**	**0.95**	**3.02**	**3.55**	–	–	–	–	–	–	–	–	–	–	–	–	–	–	–
Nerolidol epoxyacetate	21.58	–	–	–	–	0.12	–	–	–	–	–	–	–	–	–	–	–	–	–	–	–
Unknown sesquiterpenoids																					
204,41,107,81,91,67,121	13.85	–	**0.05**	**Trace**	–	**0.09**	–	**0.03**	–	–	–	–	–	–	–	2.34	–	–	–	–	**0.30**
222,43,161,55,81,91,207,105,119	15.36, 15.75	1.27	**0.08**	–	**0.08**	0.15	–	**Trace**	–	0.70	–	–	–	–	–	**0.44**	–	–	–	**0.03**	–
222,81,41,55,93,121,69,136,109	15.87	–	**Trace**	–	**0.31**	**1.02**	–	–	–	–	–	–	–	–	**1.55**	–	–	–	0.12	**0.04**	–
222,41,81,55,93,69,109,161,121,207	15.90	–	–	–	–	**0.66**	–	–	–	–	–	–	–	–	–	–	–	–	–	–	–
220,43,79,93,55,69,109,121	16.50	–	–	–	–	**2.55**	–	–	–	–	–	–	–	–	–	–	–	–	–	–	–
222,81,43,161,105,71,91,55,119,207	17.07	0.41	–	–	–	**0.44**	–	–	–	–	–	–	–	–	–	–	–	–	–	–	–
222,41,119,161,55,179,105,81,95,204	17.16	–	–	–	–	0.33	–	–	–	–	–	–	–	–	–	–	–	–	–	–	–
Other unknowns		5.10	–	–	**Trace**	2.60	–	**Trace**	–	–	–	–	–	–	–	–	–	–	–	–	–
Total %		71.14	7.08	82.90	31.92	79.13	6.58	56.55	13.71	38.75	10.69	11.60	6.03	13.78	6.80	40.13	4.66	15.42	2.04	2.86	5.77
Aliphatic compounds																					
2-Hexenal*	6.21	–	–	0.05	**0.24**	–	–	–	–	–	–	–	–	–	–	–	–	**0.44**	0.70	–	–
cis-3-Hexenyl acetate*	7.95	2.16	**9.52**	3.27	2.00	5.73	3.33	**29.00**	52.43	3.44	–	–	**6.49**	**31.22**	**5.51**	11.66	9.28	7.71	15.04	1.08	11.19
trans-2-Hexenyl acetate*	8.18	0.01	**0.04**	–	Trace	0.01	–	**0.43**	–	–	–	–	–	–	–	–	0.76	–	–	–	–
1-Hexanol*	8.42	–	**0.23**	0.51	1.06	0.05	Trace	0.13	11.35	–	–	21.65	**1.63**	**0.34**	–	–	**0.93**	**3.26**	0.74	**0.08**	**1.91**
1-Octen-3-ol acetate*	8.87	–	–	–	–	0.25	–	**0.37**	–	–	–	–	–	–	–	–	–	–	–	–	–
cis-3-Hexen-1-ol*	8.95	0.22	**5.08**	1.03	0.86	0.91	1.68	3.21	18.15	**0.79**	0.94	19.39	**12.89**	**12.95**	**17.83**	1.44	3.43	7.49	13.96	0.34	2.90
cis-3-Hexenyl propionate*	8.97	–	–	0.03	–	–	–	–	–	–	–	–	–	–	–	–	–	**0.29**	**0.46**	–	–
Butanoic acid, 3-hexenyl ester	9.04, 10.1	–	**0.13**	**0.20**	–	0.02	–	**0.04**	–	–	–	–	**1.35**	**1.55**	**12.64**	–	**0.05**	**3.20**	**4.85**	**0.16**	–
trans-2-Hexen-1-ol*	9.37	–	**0.03**	–	–	Trace	0.19	**0.26**	–	–	–	–	**0.76**	**0.21**	–	–	0.37	–	–	–	–
7-Octen-4-ol	9.89	**0.31**	**0.13**	Trace	**6.64**	0.36	–	0.30	–	–	0.25	–	–	–	**7.74**	–	**1.68**	**0.62**	–	–	0.55
cis-3-Hexenyl 2-methyl butanoate	10.27, 10.48	–	**0.09**	0.10	**Trace**	0.04	–	**0.11**	–	**0.43**	–	–	**1.34**	**2.74**	**11.02**	–	**0.12**	**2.19**	**5.16**	0.11	–
2-Nonenal	11.14	–	**Trace**	–	**0.53**	–	–	–	–	–	–	–	–	–	1.77	–	–	**Trace**	0.01	–	1.68
cis-3-Hexenyl 3-methyl butanoate	11.40	–	**Trace**	–	–	–	–	–	–	–	–	–	–	–	–	**0.20**	–	–	**0.17**	–	–
Butanoic acid, 2-hexenyl ester	11.76	–	–	**2.07**	–	–	–	–	–	–	–	–	–	–	–	–	–	–	–	–	–
2,6-Nonadienal	11.80	–	–	–	–	–	–	–	–	–	–	–	–	–	–	–	–	–	–	–	5.48
Hexanoic acid, 3-hexenyl ester	12.07, 12.65	–	**0.02**	–	–	**Trace**	–	–	–	–	–	–	–	–	–	–	–	**0.92**	**2.26**	–	–
Isobutyl tiglate	12.22	–	–	–	–	–	–	–	–	–	–	–	–	–	–	–	–	–	**0.26**	–	–

(*continued on next page*)

Table 2 (*continued*)

Compound[b]	RT	Aac $n=1$[c,d]	Acr $n=5$[d]	Alo $n=4$	Aob $n=5$	Awr $n=5$	Mal $n=7$	Mbi $n=1$[d]	Mgr $n=6$	Mja $n=1$	Mlo $n=2$	Mmf $n=1$[d]	Mmu $n=5$	Mpu $n=5$	Mtr $n=2$[e]	San $n=3$	Sch $n=9$	Sla $n=4$	Spa $n=4$	Spu $n=4$	Sun $n=4$
cis-3-Hexenyl tiglate	12.83	–	**0.02**	–	–	**Trace**	–	**0.05**	–	–	–	–	**0.32**	–	–	–	**0.29**	**5.22**	**31.11**	**0.13**	–
Heptanoic acid, 3-hexenyl ester	13.42	–	**Trace**	–	–	–	–	–	–	–	–	–	–	–	–	–	–	**0.25**	**0.38**	–	–
Hexyl butanoate	15.32	–	0.14	–	**0.07**	–	–	–	–	–	–	–	–	–	–	–	–	–	–	–	**4.04**
cis-Jasmone*	16.1	**0.14**	**16.83**	**Trace**	**Trace**	**0.84**	–	–	–	**1.32**	**4.09**	–	–	–	–	–	**0.45**	–	**0.37**	**24.71**	–
Benzyl Tiglate	17.56	–	–	–	–	–	–	–	–	–	–	–	–	–	–	–	**0.49**	–	**0.09**	–	–
Methyl caprate	18.55	–	–	–	**0.18**	–	–	–	–	–	–	–	–	–	–	–	–	–	–	–	–
Unknowns		Trace	**0.14**	0.16	**0.29**	0.04	–	**0.22**	–	–	–	–	**0.53**	–	–	–	0.54	**Trace**	0.49	**1.20**	0.39
Total%		2.84	32.40	7.42	11.88	8.25	5.19	34.11	81.93	5.97	5.28	41.04	25.31	49.02	56.50	13.31	18.37	31.60	76.04	27.80	28.15
Benzenoids																					
Anisole*	8.37	0.13	**0.17**	–	–	0.13	–	–	–	–	**2.38**	–	–	–	–	3.40	**0.78**	–	–	–	–
Benzyl methyl ether*	9.10	–	–	–	–	–	–	–	–	–	–	–	–	–	–	–	**0.48**	–	–	–	–
Other benzyl ethers	10.75, 13.34	–	–	–	–	–	–	–	–	–	–	–	–	–	–	–	–	–	–	**0.47**	–
Benzaldehyde*	11.05	–	–	0.18	1.67	–	**0.54**	–	–	–	–	–	**0.91**	**0.37**	–	–	**2.32**	–	0.30	–	5.25
Methyl benzoate*	12.33	**0.18**	**44.44**	**0.62**	**8.05**	–	–	Trace	–	**0.44**	–	–	**44.53**	–	**0.75**	1.00	**35.90**	**1.93**	**0.36**	**Trace**	**1.16**
Phenyl acetaldehyde*	12.54	–	–	**0.04**	**0.05**	–	**1.74**	–	–	–	–	–	–	**1.67**	–	–	**0.09**	**0.24**	0.05	–	–
Ethyl benzoate*	12.9	–	**0.16**	–	–	–	–	–	–	–	–	–	**0.09**	–	–	–	**0.07**	**0.05**	–	–	–
Salicylaldehyde	13.00	–	–	0.01	**Trace**	–	–	–	–	–	–	–	–	–	–	–	0.17	**0.65**	**Trace**	**Trace**	–
Benzyl acetate*	13.59	–	–	**0.07**	**0.92**	–	0.10	**0.09**	–	**5.31**	–	–	**1.27**	**0.33**	1.20	**0.63**	**0.45**	–	**0.03**	**0.03**	–
Propyl benzoate*	13.95	–	–	–	–	–	–	–	–	–	–	–	–	–	–	–	**0.03**	–	–	–	–
Methyl salicylate*	14.20	2.54	**0.19**	0.18	**0.83**	0.06	**0.50**	**0.86**	–	**0.57**	0.03	–	**2.81**	**0.21**	8.14	1.59	**2.80**	0.92	0.23	0.05	1.20
Isobutyl benzoate*	14.32	–	**0.12**	–	**Trace**	–	–	–	–	–	–	–	–	–	–	–	**0.16**	**Trace**	**0.02**	**0.11**	–
Phenethyl acetate*	14.60	–	–	**Trace**	–	–	**0.16**	–	–	–	–	–	–	**0.18**	–	**Trace**	–	–	–	–	Trace
Butyl benzoate*	15.14	–	**0.09**	–	**0.03**	**0.04**	–	–	–	–	–	–	–	–	–	–	**0.33**	**0.45**	**0.08**	**0.05**	–
Benzyl butanoate*	15.18	–	–	–	**Trace**	**0.02**	–	–	–	**0.27**	–	–	–	–	–	–	**0.06**	–	–	Trace	–
Benzyl alcohol*	15.25	–	–	0.15	**1.02**	–	**0.03**	–	–	**1.67**	–	3.48	**1.54**	**0.17**	**4.14**	**2.22**	**1.28**	**0.72**	0.10	**0.09**	4.13
Benzyl 3-methylbutanoate	15.42	–	–	–	**0.01**	**0.20**	–	–	–	–	–	–	–	–	–	–	**0.21**	–	–	**0.03**	–
Isopropyl salicylate	15.47	–	–	–	–	–	–	–	–	–	–	–	–	–	–	–	**0.05**	–	–	–	–
2-Phenylethanol*	15.54	–	**Trace**	**0.07**	**0.12**	**Trace**	**0.43**	–	–	–	–	–	–	**0.93**	–	–	**0.26**	**0.23**	**0.27**	**0.07**	**0.47**
Pentyl benzoate*	15.68	**0.42**	**0.08**	–	**0.02**	**0.16**	–	–	–	–	–	–	–	–	–	–	**0.25**	–	**0.10**	**0.12**	–
Hexyl benzoate*	16.26	–	**0.01**	–	–	–	–	–	–	–	–	–	**Trace**	–	–	–	**0.62**	–	**0.04**	**0.01**	–
Tolyl/Allyl benzoate	16.89	–	**0.21**	–	**Trace**	**Trace**	–	–	–	–	–	–	–	–	–	–	**0.15**	**Trace**	**0.21**	**0.12**	–
Cyclohexyl benzoate	17.23	–	**0.36**	–	**0.04**	**Trace**	–	**0.13**	–	–	–	–	**1.31**	–	**Trace**	–	**0.70**	–	**0.07**	**0.25**	–
cis-3-Hexenyl benzoate*	17.62–17.96	**1.72**	**2.21**	**0.08**	**0.23**	**0.25**	–	**0.14**	–	**0.27**	–	–	**7.87**	**0.28**	2.14	–	**3.09**	**1.13**	**3.73**	**1.88**	–
Phenethyl benzoate	17.80	–	–	–	–	–	–	–	–	–	–	–	–	**0.83**	–	–	–	–	–	–	–
Benzyl benzoate*	22.30	–	**0.21**	**Trace**	**4.03**	0.21	–	–	–	**3.63**	–	–	**1.43**	**0.14**	**1.30**	–	**7.41**	–	–	**0.32**	–
Unknown: 105, 77, 41, 51, 67	15.20	–	–	–	–	–	–	–	–	–	–	–	–	–	–	–	–	**0.13**	**0.12**	–	–
Other Unknowns		–	**Trace**	–	**0.05**	–	–	–	–	–	–	–	**Trace**	–	–	–	–	–	–	–	–
Total %		4.99	48.26	1.41	17.07	1.09	3.51	1.22	–	12.17	2.40	3.48	61.75	5.12	17.68	8.85	57.67	6.45	5.71	3.62	12.22
Phenylpropanoids																					
Eugenol*	18.20	**2.53**	–	–	–	–	–	–	–	–	–	–	–	–	–	–	**0.05**	–	–	–	–
Eugenol acetate/Isoeugenol*	19.07	–	–	–	–	**0.08**	–	–	–	–	–	–	–	–	–	–	–	–	–	–	–
Isoeugenol*	19.88	**6.55**	–	–	–	**2.91**	–	–	–	–	–	–	–	–	–	–	**Trace**	–	–	–	–

(*continued on next page*)

Table 2 (*continued*)

Compound[b]	RT	Aac $n=1$[c,d]	Acr $n=5$[d]	Alo $n=4$	Aob $n=5$	Awr $n=5$	Mal $n=7$	Mbi $n=1$[d]	Mgr $n=6$	Mja $n=1$	Mlo $n=2$	Mmf $n=1$[d]	Mmu $n=5$	Mpu $n=5$	Mtr $n=2$[e]	San $n=3$	Sch $n=9$	Sla $n=4$	Spa $n=4$	Spu $n=4$	Sun $n=4$
Vanillin*	21.70	–	–	–	–	**0.20**	–	–	–	–	–	–	–	–	–	–	–	–	–	–	–
Vanillyl methylketone	22.50	–	–	–	–	**0.19**	–	–	–	–	–	–	–	–	–	–	–	–	–	–	–
Total %		9.07	–	–	–	3.38	–	–	–	–	–	–	–	–	–	–	0.05	–	–	–	–
Lactones																					
4,4-Dimethyl but-2-enolide	12.17	–	–	–	–	–	–	–	–	–	–	–	–	–	–	–	–	–	–	**0.05**	–
Butyrolactone	12.40	–	–	–	–	–	–	–	–	–	–	–	–	–	–	–	–	–	**0.09**	–	–
γ-Vinyl-γ-valerolactone	12.90	–	–	**0.41**	–	–	–	–	–	–	–	–	–	–	–	–	–	–	–	–	**1.13**
γ-Caprolactone	13.30	–	–	–	**Trace**	–	–	–	–	–	–	–	–	–	–	–	–	**0.56**	**0.34**	–	–
δ-Octalactone	16.22	–	–	–	–	–	–	–	–	–	–	–	–	–	–	–	–	**0.62**	**0.26**	–	–
δ-Nonalactone	18.41	–	–	–	–	–	–	–	–	–	–	–	–	–	–	–	–	**0.10**	**0.26**	–	–
7-Decen-5-olide	19.00	**2.96**	–	–	–	–	–	–	–	–	–	–	–	–	–	–	–	**9.87**	**9.44**	–	–
Total %		2.96	–	0.41	Trace	–	–	–	–	–	–	–	–	–	–	–	–	11.15	10.39	0.05	1.13
Nitrogen-bearing compounds																					
Methyl nicotinate*	14.15	–	–	–	–	–	–	–	–	–	–	–	–	–	–	–	**8.89**	–	–	–	–
Phenylacetonitrile*	15.88	**0.12**	**Trace**	0.06	–	0.05	–	**0.04**	–	–	–	–	–	**1.52**	–	–	**0.54**	**2.18**	**0.22**	**0.06**	0.42
Methyl anthranilate*	18.93	–	–	–	**0.10**	–	–	–	–	–	**31.31**	–	–	–	–	–	–	–	–	–	–
Indole*	20.76	–	**0.48**	–	**0.26**	**0.45**	**0.30**	**0.02**	–	–	**15.07**	–	**1.68**	–	–	–	**0.09**	–	**0.03**	**Trace**	–
Total%		0.12	0.49	0.06	0.36	0.49	0.30	0.06	–	–	46.38	–	1.68	1.52	–	–	9.52	2.18	0.25	0.06	0.42
Unknowns		0.10	–	0.36	0.12	0.24	–	–	–	–	–	–	–	–	–	–	–	–	–	1.77	0.30

[a] Abbreviations: *Acleisanthes acutifolia* (Aac), *A. crassifolia* (Acr), *A. longiflora* (Alo), *A. obtusa* (Aob), *A. wrightii* (Awr), *Mirabilis alipes* (Mal), *M. bigelovii* (Mbi), *M. greenei* (Mgr), *M. jalapa* (Mja), *M. longiflora* (Mlo), *M. macfarlanei* (Mmf), *M. multiflora* (Mmu), *M. pudica* (Mpu), *M. triflora* (Mtr), *Selinocarpus angustifolius* (San), *S. chenopodioides* (Sch), *S. lanceolatus* (Sla), *S. parvifolius* (Spa), *S. purpusianus* (Spu), *S. undulatus* (Sun).

[b] Compounds within classes are listed according to retention time (RT); for each class its percentage of the total is given.

[c] Sample size (n) is the number of individuals from which fragrance was collected; unless otherwise noted, only one fragrance collection per individual was included.

[d] Only one plant was available, but multiple collections were made of this plant.

[e] Multiple collections from two plants were made during both the day and night for this diurnal species.

[f] Total amount is the mean total unit area (as integrated peak area; see Experimental) of all volatiles produced per 12 h, divided by 10^6 for ease of presentation.

[g] % Floral is the percentage of the total volatiles emitted by flowers.

[h] The total number of both floral and vegetative compounds.

[i] The total number of compounds produced solely or mainly from flowers.

[j] The amount of floral volatiles (an average of the total unit area) was adjusted to give the amount released per mg of floral tissue.

[k] Asterisks indicate compounds for which we have retention times from standards and agreement with mass spectral libraries.

[l] Trace = $<0.01\%$ of volatiles emitted.

[m] Entries in bold identify solely or mainly floral compounds.

[n] Mass fragments for unknowns are listed with the molecular ion first (if known or inferred), followed by the base peak and other fragments in order of decreasing abundance.

[o] 1,5-Cyclo-undecadiene, 8,8-dimethyl-9-methylene.

[p] 12-Oxabicyclo 9.1.0 dodeca-3,7-diene,1,5,5,8-tetramethyl-,1R-(1R@,3E,7E,11R@).

each genus separately is not monophyletic; all *Mirabilis* species also form a monophyletic group. Further, the amount of intraspecific variation varied among taxa. In particular, species that produce many different volatiles have necessarily more sources of variation and, thus, higher levels of intraspecific variation relative to other species. For example, the fragrance profile of *A. wrightii* contains the most compounds (Table 2), and this species also has one of the highest levels of intraspecific variation (mean% intraspecific dissimilarity = 23.5, S.D. = 3.5). By contrast, *Mirabilis* species released fewer volatiles than *Acleisanthes* and *Selinocarpus* species and had fairly low levels of intraspecific variation (mean% intraspecific dissimilarity = 8.8, S.D. = 4.2) compared to *Acleisanthes* and *Selinocarpus* species (mean% intraspecific dissimilarity = 14.1, S.D. = 7.3).

Further exploration of intraspecific variation can be accomplished by comparing our fragrance results for *Mirabilis jalapa* to those previously published (Heath and Manukian, 1994). Despite methodological differences (we sampled the fragrance from one individual whereas they sampled from 12) and selective reporting of fragrance compounds by Heath and Manukian (1994), the results of our two studies are generally consistent. Our study confirms the presence of *trans*-β-ocimene as the major component of the fragrance of *M. jalapa* (38% of total volatiles emitted; Table 2). In further agreement with the previous study, we found *cis*-3-hexenyl acetate and myrcene. Our study did not detect benzaldehyde and indole; this may not be surprising, as Heath and Manukian (1994) report that neither of these compounds was found in all of their *M. jalapa* fragrance samples. We did find other compounds not reported by Heath and Manukian (1994), including α-farnesene (37%) and benzyl acetate (5%) (Table 2).

2.2. Volatiles in taxa with diurnal pollination

The two species in this study known to be pollinated by animals other than moths (Table 1), *Mirabilis triflora* and *M. macfarlanei*, had low total volatile production (Table 2). One of these species, *M. triflora*, is hummingbird-pollinated. Hummingbirds have been shown to ignore fragrance while nectar-foraging (Bené, 1945; van Riper, 1960), and hummingbird-pollinated flowers are generally described as scentless (Faegri and van der Pijl, 1979). Nevertheless, flowers of *M. triflora* released some fragrance (Table 2). It is possible that volatile compounds that are no longer necessary for pollinator attraction may be retained for herbivore deterrence (Mullin et al., 1991; Berenbaum and Seigler, 1992; Dobson, 1994). However, as its closest relatives also produce fragrance (Levin, 2000), the emission of floral volatiles in *M. triflora* may suggest more about its phylogenetic heritage than an absence of strong selection against fragrance production due to its mode of pollination (Levin, 2001).

Mirabilis macfarlanei has been shown to be mainly bee-pollinated (Barnes, 1996). In addition to low overall volatile production, its flowers also released few compounds, with the monoterpene limonene as the main compound (43%; Table 2). This compound is known to be perceived by bees (reviewed by Dobson, 1994), and in combination with visual cues it may be sufficient for attraction.

2.3. Volatiles in moth-pollinated taxa

The majority of species in this study are moth-pollinated (Table 1) and have a clearly discernible and detectable fragrance, but there are many quantitative and qualitative differences among them. One notable finding is that *Acleisanthes* and *Selinocarpus* species generally emit higher total amounts of volatiles than do *Mirabilis* species (Table 2). Also, there are substantial differences in the number of fragrance compounds emitted (Table 2), with *Acleisanthes* and *Selinocarpus* species averaging twice as many compounds (mean = 62) as *Mirabilis* species (mean = 24; conservatively, the average number of compounds = 30 when include only moth-pollinated *Mirabilis* and also exclude *M. greenei*, which has a very weak fragrance, see below).

In terms of biosynthetic classes, fragrances of *Mirabilis* species also are less diverse, with no species producing either phenylpropanoids or lactones (Table 2). The presence of compounds from these two biosynthetic classes appears to be phylogenetically informative, being characteristic of closely related species (Levin, 2000) within both *Acleisanthes* (phenylpropanoids) and *Selinocarpus* (lactones). Interestingly, most of the lactones observed do not appear to have been reported previously from floral fragrances (Knudsen et al., 1993).

In addition to the identity of individual fragrance compounds, the source of the volatiles should also be considered when comparing fragrance profiles among species, as both vegetative and floral volatiles are known to attract floral visitors (Raguso, 2001). For example, crepuscular hawkmoths respond to fragrance from close range (0–10 m) by approaching its source and then probing at bright objects (Brantjes, 1978; Raguso and Willis, in press); they do not functionally distinguish between floral and vegetatively-derived odors. *Acleisanthes acutifolia* and *A. wrightii* have very fragrant vegetation, with most of the total volatile production emanating from vegetation rather than from flowers (ca. 82%; Table 2). Specifically, sesquiterpenoids are released in large amounts from the vegetation of both species. A similar situation is found in *Selinocarpus angustifolius* and *S. undulatus*, where the vegetation is characterized by the emission of high amounts of mono- and sesquiterpenoids. In addition to terpenoids, lipoxygenase-derived "green leaf volatiles" (mainly compounds with a *cis*-3-hexenyl moiety) are often released from vegetation (Hatanaka et al., 1986;

Croft et al., 1993), and these compounds are also emitted vegetatively in *A. acutifolia*, *A. wrightii, S. angustifolius* and *S. undulatus*. Phylogenetic history may explain some of these patterns in fragrance chemistry (Levin, 2001). Interestingly, *S. angustifolius* and *S. undulatus* are strongly supported as sister species, and *A. wrightii* and *A. acutifolia* are also very closely related (Levin, 2000).

Whether floral or vegetative volatiles dominate the fragrance profile depends on the species; among all twenty species the volatiles emitted from flowers varied from 5-100% of the total amount of fragrance emitted (Table 2). Across all taxa some compounds are mainly emitted by flowers (Table 2). These floral compounds include the lactones and phenylpropanoids, the isoleucine-derived tiglates (Hill et al., 1980), *cis*-jasmone, the majority of the benzenoid compounds, and most of the nitrogen-bearing compounds.

The amount of each floral compound produced per μg of floral mass varies substantially among species (Table 2). Although compounds such as *trans*-β-ocimene, nerolidol, *cis*-jasmone, and methyl benzoate are emitted by flowers of many species, the amount produced can differ greatly. This finding suggests that simply the presence of these compounds, rather than their amounts, may be sufficient for moth attraction.

In general, our results are consistent with other studies that have detected floral fragrance in moth-pollinated taxa; however, the one exception is the absence of fragrance in *Mirabilis greenei*. In addition to its low volatile production, of the five volatile compounds collected from this species, only the homoterpene 4,8-dimethylnona-1,3,7-triene was likely to be floral, with the others emitted from the vegetation (Table 2). This lack of fragrance is surprising if this species is indeed moth-pollinated. However, any interpretation of the fragrance of *M. greenei* should be considered preliminary, as the fragrance samples from this species were collected in the field when temperatures were unusually low (these conditions were unique to this species' fragrance collection); low temperatures have been reported to inhibit volatile production (Jakobsen and Olsen, 1994).

2.4. Fragrance and pollination

Several authors have suggested a link between the presence of particular fragrance compounds and moth pollination (Nilsson et al., 1985; Kaiser, 1993; Knudsen and Tollsten, 1993; Miyake et al., 1998). Kaiser (1993) described moth-pollinated flowers as having a "'white-floral'" odor, containing acyclic terpene alcohols such as linalool and nerolidol and simple aromatic alcohols like benzyl alcohol, 2-phenylethanol, and their esters. Jasmonates, tiglates, lactones, and nitrogen-bearing compounds are also prevalent in a variety of moth-pollinated flowers (Kaiser, 1993). Knudsen and Tollsten (1993) obtained results consistent with Kaiser (1993) in their survey of hawkmoth and noctuid moth-pollinated flowers among 15 species in 12 genera and 9 plant families, but they additionally suggested that hawkmoth-pollinated flowers can be distinguished from noctuid moth-pollinated flowers by the presence of geraniolic compounds and oxygenated sesquiterpenes.

The fragrances of all of the moth-pollinated (i.e., both hawkmoth and noctuid moth-pollinated) species included in this study (except *M. greenei*) are similar in containing mono- and sesquiterpenoids, aliphatic compounds, benzenoids, and nitrogen-bearing compounds. These fragrance profiles are consistent with the descriptions of moth-pollinated fragrances reported by Kaiser (1993), and to some extent support the suggestion of Knudsen and Tollsten (1993) that the specific presence of oxygenated sesquiterpenes is more characteristic of hawkmoth-pollinated than noctuid moth-pollinated species. Of the 12 taxa in our study that are likely to be hawkmoth-pollinated, eight had fragrances that contained at least one oxygenated sesquiterpene. However, the fragrances of two likely noctuid moth-pollinated species, *Selinocarpus angustifolius* and *S. undulatus*, also contained oxygenated sesquiterpenes (Tables 1 and 2). Further, we observed that these two *Selinocarpus* species emitted the lowest total amount of volatiles and had the least diversity of compounds compared to other *Selinocarpus*. Based on floral morphology, *Selinocarpus chenopodioides* would appear to be noctuid moth-pollinated, but the white-lined sphinx moth (*Hyles lineata*) has also been observed visiting its flowers, and may move pollen (Table 1; Levin, 2001). Interestingly, flowers of this species emit a fragrance similar to that of hawkmoth-pollinated *Selinocarpus* species in that they produce large amounts of a variety of volatiles, including oxygenated sesquiterpenes (Table 2). Thus, while pollination by smaller insects may be occurring, the flowers are also attractive to hawkmoths. By contrast, the flowers of *Mirabilis alipes*, which are likely noctuid moth-pollinated, emit a low diversity of volatiles and lack oxygenated sesquiterpenoids. However, flowers of *M. alipes* also attract *Hyles lineata*, although the hawkmoths collected while visiting this species did not carry any pollen (Table 1; Levin, 2001). In general, results of this study suggest that a diversity of compounds may attract moths, and oxygenated sesquiterpenes, while commonly found in fragrances of hawkmoth-pollinated taxa, are not restricted to the fragrances of these species.

2.5. Conclusions

The fragrance profiles we observed in Nyctaginaceae are generally consistent with the "'white-floral'" odor described by Kaiser (1993) and the fragrances of moth-pollinated plants reported by Knudsen and Tollsten (1993) and Miyake et al. (1998). However, the floral volatiles reported here and in previous studies are not unique to fragrances of hawkmoth-pollinated flowers;

for example, many of these volatiles have also been reported from beetle-pollinated flowers (Azuma et al., 1997). In addition to the chemical similarities of fragrance across moth-pollinated taxa, there are many differences that give flowers of each species their distinctive odor. These include species-specific compounds (e.g., vanillin in *A. wrightii* and methyl nicotinate in *S. chenopodioides*), compounds shared by closely related species (e.g., δ-octalactone and δ-nonalactone in *S. lanceolatus* and *S. parvifolius*), and species-specific blends of more ubiquitous compounds.

Fragrance plays diverse roles in hawkmoth pollination, attracting moths from a distance (Tinbergen, 1958; Haber, 1984), combining with visual cues to elicit floral approaches and feeding (Brantjes, 1978; Raguso and Willis, 2001), and facilitating associative learning and discrimination (Daly and Smith, 2000). Among diverse hawkmoth-pollinated flowers, the presence of common classes of compounds, such as oxygenated terpenoids and aromatic esters, combined with the species-specific nature of each blend documented in our study and its antecedents, provides a complex ecological signal with the potential to support all of these functions.

3. Experimental

3.1. Study taxa

Fragrance was collected from multiple individuals (sample sizes are given in Table 2) of each of the 20 Nyctaginaceae species (Table 1), the majority of which are found in the Chihuahuan Desert in southwestern North America. These taxa were chosen because of the prevalence of hawkmoth pollination and multiple evolutionary losses of this pollination system (Levin, 2001). Vouchers of all species included in this study are housed in the herbarium at the University of Arizona (ARIZ; see Table 2 in Levin, 2000).

3.2. Volatile collection

Fragrance was collected in the field using dynamic head-space collection methods (see Raguso and Pellmyr, 1998, and references therein). Flowers on a living plant were enclosed within a polyacetate bag (Reynolds® oven bags) where volatile compounds emitted from the plant accumulated and were trapped in adsorbent cartridges through the use of a battery operated diaphragm pump (KNF Neuberger, Inc.). Glass cartridges were packed with 100 mg of the adsorbent Porapak®Q (80–100 mesh), and the pump pulled air over the flowers and into the adsorbent trap at a flow rate of ca. 250 ml/min. Fragrance collections typically commenced at floral anthesis and continued for 12 h. Most of the species included in this study have nocturnal floral anthesis, such that fragrance collection usually began at dusk and ended early the following morning. As all these species have flowers that last only one day, this collection period generally encompassed the entire period during which a flower was open. For a few species, we were unable to collect floral fragrance in the field, and instead did so in the greenhouse using the same protocol as outlined above. In general one fragrance collection was made per individual plant, and the number of flowers included for each fragrance collection was noted. After fragrance collection, flowers were removed from the plants and weighed to obtain an average fresh wt per flower for each species.

Simultaneous collections of ambient and vegetative volatiles were used to distinguish between truly floral compounds, compounds emitted from the vegetation, and ambient contaminants. The architecture of these plants made it impossible to avoid trapping vegetative volatiles while also collecting volatiles from a number of flowers. Ideally the mass of vegetation from which fragrance was collected would have been quantified; however, this would have required destructive sampling of plants (in many cases fragrance was collected from an entire plant), which was not feasible.

3.3. Chemical and data analysis

After the 12 h collection period, cartridges were wrapped in aluminum foil and kept chilled. They were then eluted with 3 ml of hexane, and the eluate was stored frozen in glass vials. Before GC–MS analysis, samples were concentrated to 75 μl with N_2. One microliter (occasionally 3 μl) aliquots of each sample were injected into a Shimadzu GC-17A equipped with a Shimadzu QP5000 quadrupole electron impact MS as a detector. All analyses were done using splitless injections on a polar GC column [diameter 0.25 mm, length 30 m, film thickness 0.25 μm (EC WAX); Alltech Associates, Inc.]. The carrier gas was helium with a flow rate of 1 ml/min and a split ratio of 12. The injector temp. was 240 °C and detector temp. was 260 °C. The oven program began with injection at 60 °C and a constant temp. for 3 min. The temp. then increased by 10 °C per min until 260 °C, where it was held for 7 min. The column pressure at injection was 60.6 kilo Pascals (kPa); the pressure then increased to 400 kPa for 48 s followed by a decrease to 60.6 kPa for 2 min (this pressure pulse was included for peak sharpening at the suggestion of L. Evanicke, Shimadzu Scientific Instruments, Inc.) and then an increase of 3.9 kPa per min until 132.9 kPa, where it was held for 7 min.

Compounds were tentatively identified using computerized mass spectral libraries [Wiley and NIST libraries (> 120,000 mass spectra)]. The identity of many compounds was also verified using retention times of known standards (Table 2). To ensure that even small quantities

of compounds were detected, we searched for the presence of specific mass fragments using single ion chromatograms (SIC). For example, the nitrogen-bearing compounds indole and phenylacetonitrile often were present in very small amounts; by searching for the molecular ion (117 Da) at the appropriate retention times, we were able to detect trace amounts of these compounds. Quantification of compound amounts was achieved by integrating individual GC peak areas of the total ion chromatograms (TIC) using Shimadzu's Class-5000 software (Shimadzu Co., 1993–1996). For each species these compound areas were averaged across individuals and divided by the total average amount of volatiles produced to yield the relative amount (mean percentage) of each compound present in the floral and vegetative fragrance per 12 h collection period (Table 2). For volatiles released mainly or solely from flowers, compound areas were standardized by adjusting for the number and mass of flowers sampled to yield the amount present per μg of floral mass (Table 2).

3.4. Intraspecific vs. interspecific variation

To compare intraspecific variation in fragrance profiles to interspecific variation, we used the relative amounts of both floral and vegetative volatiles for each individual (rarely were multiple samples from the same individual included, see Table 2) to calculate a dissimilarity matrix based on Euclidean distance (SPSS Inc., 1999). Variables were standardized to have a mean of zero and a standard deviation of one. We then used a Wilcoxon Signed Rank Test (SPSS Inc., 1999) to compare the pair-wise% dissimilarities between individuals within a species to those between individuals among species. A lower dissimilarity between conspecific individuals than between individuals among species would suggest that interspecific variation is greater than intraspecific variation in fragrance profiles.

Acknowledgements

We are grateful to T. Tully, A. Boyd, M. Manktelow, D. Hearn, and A. Chetochine, without whose assistance these fragrance collections could not have been made. We thank Big Bend National Park, the Jornada LTER, and J. Duft for access to plants, and A. Le Duc and M. Fishbein for providing seeds. For use of a GC–MS and injection of many of the samples we thankfully acknowledge E. Pichersky and J. D'Auria, University of Michigan. This manuscript was greatly improved by J.S. Miller, who read an early version of the manuscript, and by three anonymous reviewers. The main source of funding for this research was provided by the National Science Foundation DEB9806840 to L.A.M. and R.A.R. Further support was provided by small grants to R.A.L. from the American Society of Plant Taxonomists, Sigma Xi, the Department of Ecology and Evolutionary Biology at the University of Arizona, and the University of Arizona Research Training Group in the Analysis of Biological Diversification (NSF DIR-9113362, BIR-9602246). This paper is part of a dissertation by R.A.L. submitted in partial fulfillment of the requirements for the degree of doctor of philosophy, University of Arizona.

References

Azuma, H., Toyota, M., Asakawa, Y., Yamaoka, R., Garcia-Franco, J.G., Dieringer, G., Thien, L.B., Kawano, S., 1997. Chemical divergence in floral scents of *Magnolia* and allied genera (Magnoliaceae). Plant Species Biol. 12, 69–83.

Barkman, T.J., Beaman, J.H., Gage, D.A., 1997. Floral fragrance variation in *Cypripedium*: Implications for evolutionary and ecological studies. Phytochemistry 44, 875–882.

Barnes, J. L., 1996. Reproductive ecology, population genetics, and clonal distribution of the narrow endemic: *Mirabilis macfarlanei* (Nyctaginaceae). Master's thesis, Utah State University, Logan, Utah.

Barthlott, W., Porembski, S., Kluge, M., Hopke, J., Schmidt, L., 1997. *Selenicereus wittii* (*Cactaceae*): an epiphyte adapted to Amazonian Igapó inundation forests. Plant Syst. Evol. 206, 175–185.

Bené, F., 1945. The role of learning in the feeding behavior of Black-chinned Hummingbirds. The Condor 47, 3–22.

Berenbaum, M., Seigler, D., 1992. Biochemicals: engineering problems for natural selection. In: Roitberg, B.D., Isman, M.B. (Eds.), Insect Chemical Ecology: An Evolutionary Approach. Chapman & Hall, New York, pp. 89–121.

Bestmann, H.J., Winkler, L., von Helversen, O., 1997. Headspace analysis of volatile flower scent constituents of bat-pollinated plants. Phytochemistry 46, 1169–1172.

Borg-Karlson, A.-K., Valterová, I., Nilsson, L.A., 1994. Volatile compounds from flowers of six species in the family Apiaceae: bouquets for different pollinators? Phytochemistry 35, 111–119.

Brantjes, N.B.M., 1978. Sensory responses to flowers in night-flying moths. In: Richards, A.J. (Ed.), The Pollination of Flowers by Insects. Academic Press, London, pp. 13–19.

Croft, K.P.C., Jüttner, F., Slusarenko, A.J., 1993. Volatile products of the lipoxygenase pathway evolved from *Phaseolus vulgaris* (L.) leaves inoculated with *Pseudomonas syringae* pv *phaseolicola*. Plant Physiol. 101, 13–24.

Cruden, R.W., 1970. Hawkmoth pollination of *Mirabilis* (Nyctaginaceae). Bull. Torr. Bot. Club 97, 89–91.

Daly, K., Smith, B.H., 2000. Associative olfactory learning in the moth *Manduca sexta*. J. Exp. Biol. 203, 2025–2038.

Dobson, H.E.M., 1994. Floral volatiles in insect biology. In: Bernays, E.A. (Ed.), Insect-Plant Interactions, Vol. V. CRC Press, Boca Raton, pp. 47–81.

Dobson, H.E.M., Arroyo, J., Bergström, G., Groth, I., 1997. Interspecific variation in floral fragrances within the genus *Narcissus* (Amaryllidaceae). Biochem. Syst. Ecol. 25, 685–706.

Dudareva, N., Pichersky, E., 2000. Biochemical and molecular genetic aspects of floral scents. Plant Physiol. 122, 627–633.

Faegri, K., van der Pijl, L., 1979. The Principles of Pollination Ecology, 3rd Edition. Pergamon, Oxford.

Fowler, B.A., Turner, B.L., 1977. Taxonomy of *Selinocarpus* and *Ammocodon* (Nyctaginaceae). Phytologia 37, 177–208.

Grant, V., 1983. The systematic and geographical distribution of hawkmoth flowers in the temperate North American flora. Bot. Gaz. 144, 439–449.

Grant, V., Grant, K.A., 1983. Hawkmoth pollination of *Mirabilis longiflora* (Nyctaginaceae). Proc. Nat. Acad. Sci. 80, 1298–1299.

Grison, L., Edwards, A.A., Hossaert-McKey, M., 1999. Interspecies variation in floral fragrances emitted by tropical *Ficus* species. Phytochemistry 52, 1293–1299.

Haber, W.A., 1984. Pollination by deceit in a mass-flowering tropical tree *Plumeria rubra* L. (Apocynaceae). Biotropica 16, 269–275.

Haber, W.A., Frankie, G.W., 1989. A tropical hawkmoth community: Costa Rican dry forest Sphingidae. Biotropica 21, 155–172.

Hatanaka, A., Kajiwara, T., Sekiya, J., 1986. Fatty acid hydroperoxidase lyase in plant tissues: volatile aldehyde formation from linoleic and linolenic acid. In: Parliament, T.H., Croteau, R. (Eds.), Biogeneration of Aromas. American Chemical Society, Washington, DC, pp. 167–175.

Heath, R.R., Manukian, A., 1994. An automated system for use in collecting volatile chemicals released from plants. J. Chem. Ecol. 20, 593–607.

Hill, R.K., Rhee, S.-W., Leete, E., McGaw, B.A., 1980. Stereospecificity of enzymatic dehydrogenation during tiglate biosynthesis. J. Am. Chem. Soc. 102, 7344–7348.

Hodges, S.A., 1995. The influence of nectar production on hawkmoth behavior, self-pollination, and seed production in *Mirabilis multiflora* (Nyctaginaceae). Am. J. Bot. 82, 197–204.

Jakobsen, H.B., Olsen, C.E., 1994. Influence of climatic factors on emission of flower volatiles in situ. Planta 192, 365–371.

Kaiser, R., 1993. The Scent of Orchids: Olfactory and chemical investigations. Elsevier, Amsterdam.

Kaiser, R., Tollsten, L., 1995. An introduction to the scent of cacti. Flav. Fragr. J. 10, 153–164.

Knudsen, J.T., Tollsten, L., 1993. Trends in floral scent chemistry in pollination syndromes: floral scent composition in moth-pollinated taxa. Bot. J. Linn. Soc. 113, 263–284.

Knudsen, J.T., Tollsten, L., 1995. Floral scent in bat-pollinated plants: a case of convergent evolution. Bot. J. Linn. Soc. 119, 45–57.

Knudsen, J.T., Tollsten, L., Bergström, L.G., 1993. Floral scents—a checklist of volatile compounds isolated by head-space techniques. Phytochemistry 33, 253–280.

Levin, R.A., 2000. Phylogenetic relationships within Nyctaginaceae tribe Nyctagineae: evidence from nuclear and chloroplast genomes. Systematic Botany 25, 738–750.

Levin, R.A., 2001. Relationships among fragrance, phylogeny and pollination in southwestern Nyctaginaceae. PhD. diss. University of Arizona, Tucson, AZ.

Martínez Del Río, C., Búrquez, A., 1986. Nectar production and temperature dependent pollination in *Mirabilis jalapa* L. Biotropica 18, 28–31.

Miyake, T., Yamaoka, R., Yahara, T., 1998. Floral scents of hawkmoth-pollinated flowers in Japan. J. Plant Res. 111, 199–205.

Mullin, C.A., Alfatafta, A.A., Harman, J.L., Serino, A.A., Everett, S.L., 1991. Corn rootworm feeding on sunflower and other Compositae: influence of floral terpenoid and phenolic factors. In: Hedin, P.A. (Ed.), Naturally Occurring Pest Bioregulators. American Chemical Society, Washington, DC, pp. 278–292.

Nilsson, L.A., Jonsson, L., Rason, L., Randrianjohany, E., 1985. Monophily and pollination mechanisms in *Angraecum arachnites* Schltr. (Orchidaceae) in a guild of long-tongued hawk-moths (Sphingidae) in Madagascar. Biol. J. Linn. Soc. 26, 1–19.

Pilz, G.E., 1978. Systematics of *Mirabilis* subgenus Quamoclidion (Nyctaginaceae). Madroño 25, 113–132.

Radwanski, E.R., Last, R.L., 1995. Tryptophan biosynthesis and metabolism: biochemical and molecular genetics. The Plant Cell 7, 921–934.

Raguso, R.A., 2001. Floral scent, olfaction and scent-driven foraging behavior. In: Chittka, L., Thomson, J. (Eds.), Cognitive Ecology of Pollination: Animal Behavior and Floral Evolution. Cambridge University Press, Cambridge, pp. 83–105.

Raguso, R.A., Pellmyr, O., 1998. Dynamic headspace analysis of floral volatiles: a comparison of methods. Oikos 81, 238–254.

Raguso, R.A., Pichersky, E., 1995. Floral volatiles from *Clarkia breweri* and *C. concinna* (Onagraceae): recent evolution of floral scent and moth pollination. Plant Syst. Evol. 194, 55–67.

Raguso, R.A., Willis, M.W., 2001. The importance of olfactory and visual cues in nectar foraging by nocturnal hawkmoths. In: Boggs, C.L., Watt, W.B., Ehrlich, P.R. (Eds.), Proceedings of the Third Symposium on Butterfly Ecology and Evolution. University of Chicago Press, Chicago, in press.

Shimadzu Co., 1993–1996. Class-5000, Version 2.0.0. Shimadzu Chemical Laboratory Analysis System & Software.

Spellenberg, R., Delson, R. K., 1977. Aspects of reproduction in Chihuahuan Desert Nyctaginaceae. In: Wauer, R. H., Riskind, D. H. (Eds.), Transactions of the Symposium on the Biological Resources of the Chihuahuan Desert Region United States and Mexico. US Department of the Interior, pp. 273–287.

SPSS Inc., 1999. SPSS for Windows, Version 10.0.5. SPSS Inc., Chicago.

Tinbergen, N., 1958. Curious Naturalists. Doubleday & Co., Garden City, NY.

van Riper, W., 1960. Does a hummingbird find its way to nectar through its sense of smell? Sci. Am. 202, 157–166.

Wang, J., Pichersky, E., 1999. Identification of specific residues involved in substrate discrimination in two plant *O*-methyltransferases. Arch. Biochem. Biophys. 368, 172–180.

Wink, M., 1997. Special nitrogen metabolism. In: Dey, P.M., Harborne, J.B. (Eds.), Plant Biochemistry. Academic Press, San Diego, pp. 439–486.

PERGAMON

Phytochemistry 58 (2001) 441–449

PHYTOCHEMISTRY

www.elsevier.com/locate/phytochem

Isolation, characterization, and systematic significance of 2-pyrone-4,6-dicarboxylic acid in Rosaceae

Sonja Wilkes, Heinrich Glasl*

Institut für Pharmazeutische Biologie und Phytochemie der Westfälischen Wilhelms-Universität Münster, Hittorfstraße 56, D-48149 Münster, Germany

Received 12 February 2001; received in revised form 14 May 2001

Abstract

2-Pyrone-4,6-dicarboxylic acid was isolated from *Potentilla anserina*. Until now this substance was only found in bacteria and not in higher plants. By sterile cultivation it was verified that this compound is genuine also in plants. In addition the systematic relevance of 2-pyrone-4,6-dicarboxylic acid within the Rosaceae was tested. The compound seems to be a chemotaxonomic marker for the *Rosoideae sensu stricto* proposed by Morgan et al. (Morgan, D.R., Soltis, D.E., Robertson, K.R., 1994. Systematic and evolutionary implications of *rbc*L sequence variation in Rosaceae. American Journal of Botany 81, 890–903). © 2001 Elsevier Science Ltd. All rights reserved.

Keywords: 2-Pyrone-4,6-dicarboxylic acid; *Potentilla anserina* L.; *Potentilla recta* L.; Rosaceae; Chemotaxonomy

1. Introduction

Some bacterial strains degrade aromatic, especially phenolic substances to 2-pyrone-4-6-dicarboxylic acid (Fig. 1), e.g. *Pseudomonas* (Kersten et al., 1982; Samejima et al., 1987) or *Micrococcus* (Eaton and Ribbons, 1982a,b). The central metabolites of this reactions are protocatechuic or gallic acid followed by 2-pyrone-4,6-dicarboxylic acid. Until now these ring fission reactions resulting in 2-pyrone-4,6-dicarboxylic acid have been known only from bacteria. We recently found 2-pyrone-4-6-dicarboxylic acid in *Potentilla anserina* L. in the family Rosaceae, a member of higher plants (Wilkes and Glasl, 2000).

The family Rosaceae has been often and well studied systematically. Several different compounds are used as taxonomic markers like cyanogenic glycosides (Fikenscher et al., 1981), flavonoids (Harborne, 1967; Challice, 1972), tannins (Okuda et al., 1992) and sorbitol (Wallaart, 1980). We tried to find out if 2-pyrone-4,6-dicarboxylic acid has any taxonomic significance for the family Rosaceae.

2. Results and discussion

2.1. Isolation and characterization of 2-pyrone-4-6-dicarboxylic acid from Potentilla anserina L.

HPLC analysis of crude methanol–water extract of *Potentilla anserina* L. showed a major signal at 315 nm. For isolation and structural elucidation lyophilised plant material was extracted with acetone–water and ethanol–water mixtures. After removing the organic solvents the aqueous extract was prefractionated by partition between ether and ethylacetate. The compound was obtained in a pure form from the ethylacetate fraction after column chromatography on Sephadex LH-20 and preparative HPLC on RP-18 material.

For structure elucidation the compound was subjected to UV and NMR spectroscopy and mass spectrometry. The data are mostly in good agreement with published literature data only the assignment of the ^{13}C NMR signals of C-7 and C-8 had to be exchanged after viewing the HMBC data (Maruyama, 1979; Samejima et al., 1987).

2.2. Detection of 2-pyrone-4,6-dicarboxylic acid in sterile cultivated Potentilla recta seedlings

To establish that the isolated compound originated from the plant and not from bacteria or parasitic fungi

* Corresponding author. Tel.: +49-251-83-33378; fax: +49-251-83-38341.

E-mail address: glasl@uni-muenster.de (H. Glasl).

0031-9422/01/$ - see front matter © 2001 Elsevier Science Ltd. All rights reserved.
PII: S0031-9422(01)00256-4

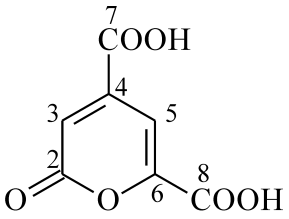

Fig. 1. 2-Pyrone-4,6-dicarboxylic acid.

living on the plants, experiments under sterile conditions were necessary. HPLC analysis of sterile seedlings (3–5 cm) of *Potentilla recta* L. detected 2-pyrone-4,6-dicarboxylic acid. *Potentilla recta* was used because seeds of *Potentilla anserina* were not available.

2.3. Occurence of 2-pyrone-4,6-dicarboxylic acid in several members of the family Rosaceae

2-Pyrone-4,6-dicarboxylic acid is a central catabolite of several aromatic or phenolic substances in bacteria (Eaton and Ribbons, 1982a,b; Samejima et al., 1987; Rosazza et al., 1995). Many members of the family *Rosaceae* contain phenolic substances like flavonoids, hydroxycinnamic acids or tannins (Hegnauer, 1973, 1990). Further investigations are necessary to determine whether 2-pyrone-4-6-dicarboxylic acid is a catabolic substance of these phenolic compounds in *Potentilla anserina*.

The systematic significance of 2-pyrone-4,6-dicarboxylic acid in the Rosaceae was studied in more detail. Eighty-three species of the Rosaceae were collected during two seasons (1999 and 2000) with an emphasis on the genus *Potentilla* (Table 1).

In this paper we follow the systematic classification of Schulze-Menz (1964), who divided the family into the subfamilies *Spiraeoideae, Rosoideae, Maloideae* and *Prunoideae*, basing the classification on fruit types and the habit of the plants (woody or herbaceous). We tried to get many tribes and genera described by Schulze-Menz (1964) to get a nearly complete sampling of the family Rosaceae (Table 2).

Aerial parts of the plants were harvested as far as possible during the flowering period. The fresh plants

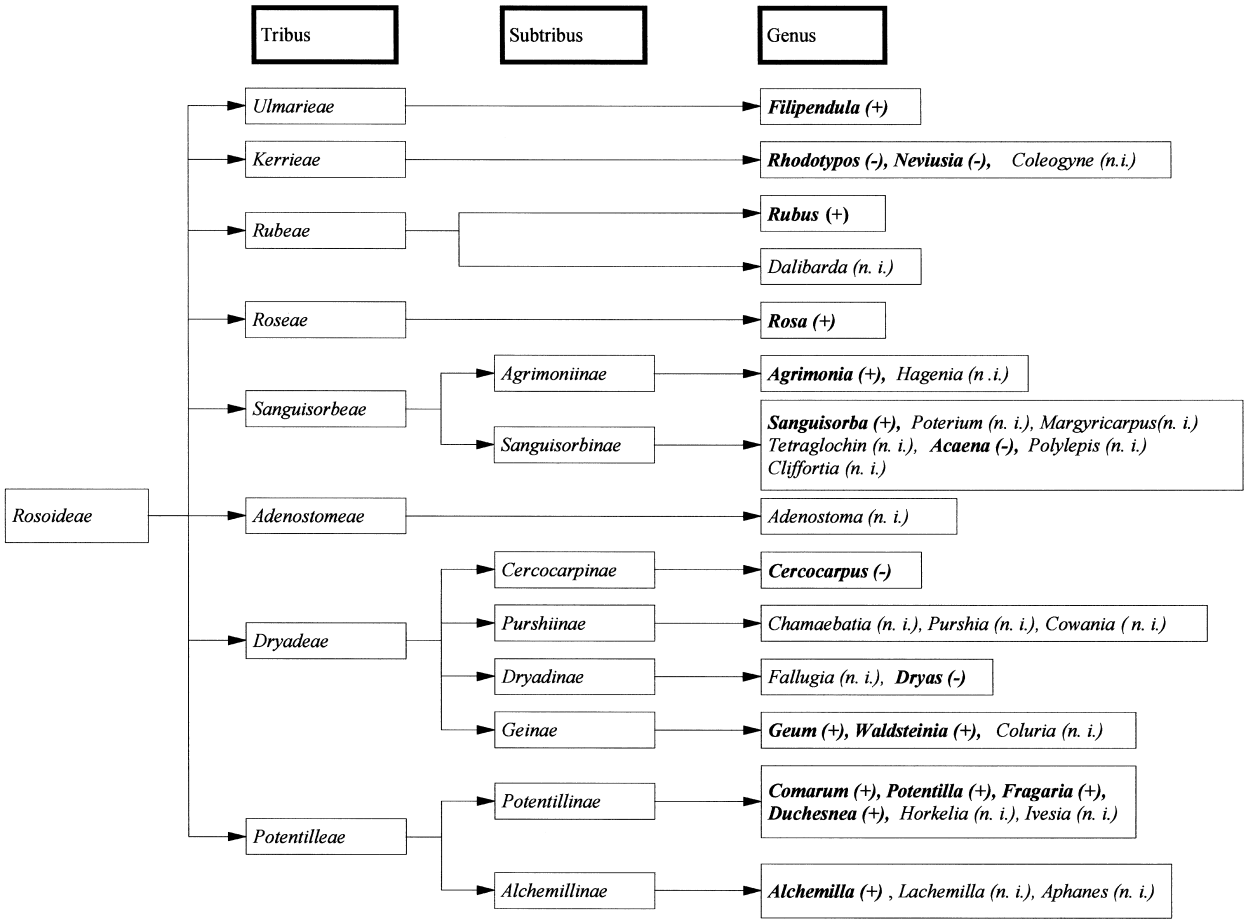

Fig. 2. Classification of the *Rosoideae* proposed by Schulze-Menz (1964). +/−: 2-Pyrone-4,6-dicarboxylic acid existing/not existing, n. i.: not investigated.

Table 1
List of all plants checked for 2-pyrone-4,6-dicarboxylic acid. The systematic of Schulze-Menz (1964) was used, the valid plant names were taken from Encke et al. (1994a)[a]

No.	Species	Harvested	Plant material	HN
Subfamily: *Spiraeoideae*				
1	*Quillaja saponaria* Mol.	4.5.1999 IG	L, B	
2	*Exochorda giraldii* Hesse var. *wilsonii* Rehd.	19.4.1999 IG	L, Fl, B	
3	*Exochorda serratifolia* S.Moore	11.4.1999 IG, IG-No. 27057	L, Fl, B	110
4	*Gillenia trifoliata* (L.) Moench	26.5.1999 IG, IG-No. 27099	L, B	107
5	*Spiraea chamaedryfolia* L. emend. Jacq.	9.4.1999 IG	L, Fl, B	153
6	*Aruncus dioicus* (Walt.)Fern.	16.6.1999 IG	H	154
Subfamily: *Rosoideae*				
7	*Filipendula ulmaria* (L.) Maxim.	5.6.2000 IG	H	155
8	*Rhodotypos scandens* (Thunb.) Mak.	19.4.1999 IG; IG-No.: 27097	L, Fl, B	106
9	*Kerria japonica* (L.) DC.	2.5.1999 Münster north	L, Fl, B	156
10	*Neviusia alabamensis* A. Gray	26.5.1999 IG; IG-No.: 28854	L, Fl, S	108
11	*Rubus fruticosus* L.	26.5.1999 IG	L, Fl, S	157a
12	*Rubus idaeus* L.	26.5.1999 IG	L, Fl, S	157b
13	*Rubus illecebrosus* Focke	29.6.1999 BG	H	157c
14	*Rosa damascena* Mill. "Trigintipetala"	26.5.1999 IG	L, Fl, S	158a
15	*Rosa jundzillii* Bess.	29.6.1999 BG	L, Fl, B	158b
16	*Rosa omeiensis* Rolfe. *forma pteracantha* (Franch.) Rehd et Wils.	29.6.1999 BG	L, Fl, B	
17	*Rosa rugosa* Thungb.	16.6.1999 IG	L, Fl, S	158c
18	*Agrimonia eupatoria* L.	22.6.1999 IG	H	159a
19	*Agrimonia procera* Wallr.	16.6.1999 IG	H	159b
20	*Sanguisorba canadensis* L.	29.6.1999 BG	H	160a
21	*Sanguisorba obtusa* Maxim.	29.6.1999 BG	L, St	160c
22	*Sanguisorba officinalis* L.	18.5.1999 BG	H	160d
23	*Acaena microphylla* Hook.	29.6.1999 BG	H	161
24	*Cercocarpus betuloides* Nutt ex Torr. et A. Gray	4.5.1999 IG	L, B	
25	*Dryas octopetala* L.	18.5.1999 BG	H, R, F	162
26	*Geum rivale* L.	29.6.1999 BG	H (faded)	163a
27	*Geum urbanum* L.	26.5.1999 IG	H	163b/c
28	*Waldsteinia ternata* (Steph.) Fritsch	18.5.1999 BG	L, R	
29	*Potentilla anserina* L.	21.5.1999 IG	H	86
30	*Potentilla argentea* L.	16.6.1999 IG; IG-No.: 16.94	H	164a
31	*Potentilla aurea* L.	22.6.1999 IG; IG-No.: 36.95	L, St	86c
32	*Potentilla calycina* Boiss.	19.5.1999 BG	H	164b
33	*Potentilla crantzii* (Crantz.) Beck et Fritsch	28.4.1999 IG	H	164n
34	*Potentilla erecta* (L.) Raeusch.	16.6.1999 IG	H	15a-c
35	*Potentilla fruticosa* L.	16.6.1999 IG	L, St	
36	*Potentilla grandiflora* L.	20.5.1999 IG; IG-No.: 39.97	H	164c/d
37	*Potentilla neumannia* Rchb.	19.4.1999 IG	H	164l/m
38	*Potentilla norvegica* L.	16.6.1999 IG	H	164e
39	*Potentilla (Comarum) palustris* (L.) Scop.	20.5.1999 IG	H	164f
40	*Potentilla recta* L.	16.6.1999 IG; IG-No.:5.94	H	86e
41	*Potentilla reptans* L.	28.8.2000 IG		164g/h
42	*Potentilla rupestris* L.	18.5.1999 BG	H	164i
43	*Fragaria ananassa* (Duch.) Guedes	26.5.1999 IG	H	165
44	*Fragaria vesca* L.	30.4.1999 IG	H	
45	*Duchesnea indica* (Andr.) Focke	16.6.1999 IG	H (faded)	
46	*Alchemilla conjunca* Bab.	29.6.1999 BG	H	166a
47	*Alchemilla xanthochlora* Rothm.	28.4.1999 IG	H	
Subfamily: *Maloideae*				
48	*Cydonia oblonga* Mill.	27.4.1999 IG	L, Fl, Sp	
49	*Coenomeles speciosa* (Sweet) Nakai	19.4.1999 IG	L, Fl, B	167
50	*Pyrus communis* L.	11.4.1999 IG	L, Fl, Sp	
51	*Malus domestica* Borkh.	27.4.1999 IG	L, Fl, Sp	
52	*Sorbus aucuparia* L.	2.5.1999 Münster north	L, Fl, St	168
53	*Sorbus domestica* L.	27.4.1999 IG	L, St	
54	*Eriobotrya japonica* (Thunb.) Lindl.	4.5.1999 IG	L	
55	*Amelanchier ovalis* Medik.	11.4.1999 IG	L, Fl, B	

(*continued on next page*)

No.	Species	Harvested	Plant material	HN
56	*Photinia villosa* var. *laevigata* (Thumb.) DC	18.5.1999 BG	L, Fl, B	
57	*Stranvaesia davidiana* Decne.	18.5.1999 BG	B, Fl (buds)	169a/b
58	*Osteomeles schwerinae* Schneid.	16.6.1999 IG	L, Fl, St	
59	*Cotoneaster dammeri* Schneid. "Skolgholm"	29.6.1999 BG	L, B	
60	*Cotoneaster lucidus* Schlechtend. Franch.	18.5.1999 BG	L, Fl, B	170a/b
61	*Cotoneaster. roseus* Edgew.	18.5.1999 BG	L, Fl, B, F(green)	170c
62	*Pyracantha coccinea* M. J. Roem.	29.6.1999 BG	L, F, B	171
63	*Mespilus germanica* L.	20.5.1999 IG	L, Fl, St	
64	*Crataegus crus-galli* L.	31.5.1999 Münster north	L, Fl, B	172
65	*Crataegus monogyna* Jacq. Emend.Lindm.	28.4.1999 IG	L, Fl, St	143a
66	*Crataegus nigra* Waldst. et Kit.	30.4.1999 IG	L, Fl, St	145a
67	*Crataegus pedicellata* Sarg.	30.4.1999 IG	L, Fl, Sp	
68	*Crataegus submollis* Sarg.	28.4.1999 IG	L, Fl, St	
69	*Aronia prunifolia* (Marsh.) Rehd.	26.5.1999 IG	L, F, St	123
Subfamily: *Prunoideae*				
70	*Prunus avium* L.	28.4.1999 IG	L, St	
71	*Prunus cerasifera* Ehrh. F. *atropurpurea* var. *pissardii*	29.6.1999 BG	L, F, B	
72	*Prunus cerasus* L.	30.4.1999 IG	L, Fl, Sp	
73	*Prunus domestica* L. ssp. *syriaca* (Borkh.) Janchen	11.4.1999 IG	L, Fl, B	
74	*Prunus dulcis* (Mill.) D.A. Webb. var. *dulcis*	27.4.1999 IG	L, St	
75	*Prunus laurocerasus* L.	27.4.1999 IG	L, Fl, B	
76	*Prunus lusitanica* L.	22.6.1999 IG	L, Fl, St	
77	*Prunus padus* L.	18.5.1999 BG	L, F (green), St	173a
78	*Prunus serrulata* Lindl. Sorte: Kanzan	29.6.1999 BG	L, B	
79	*Prunus spinosa* L.	26.5.1999 IG	L, F, St	173b
80	*Prinsepia uniflora* Batal.	19.4.1999 IG; IG-No.: 28027	L, Fl, B	109
81	*Oemleria cerasiformis* (Torr.et A. Gray ex Hook et Arn.) Landon	11.4.1999 IG; IG-No.: 29160	L, Fl (faded), B	88

[a] Abbreviations: IG: Garden of the Institut für Pharmazeutische Biologie und Phytochemie; BG: Botanical Garden, Westfälische Wilhelms-Universität Münster; H: herb, all overhead parts; L: leaves; Fl: flower; S: shoot; St: this year's shoot or twig; Sp: spur shoot; B: branch or twig in general, mostly older than one year; R: roots; F: fruit; HN: herbarium number (Institut für Pharmazeutische Biologie und Phytochemie).

were frozen at −30 °C, lyophilised and finally pulverised followed by extraction with acetone–water mixtures. The solvent was removed and the rest was filled up to a definite volume with water and filtered. A solid phase extraction (RP-18 material) of this crude extract was necessary for the following HPLC analysis.

2-Pyrone-4,6-dicarboxylic acid was found in all 14 investigated *Potentilla* species and in many members of the *Rosoideae*. This compound was found exclusively in the *Rosoideae* and not in any other subfamily. The distribution of 2-pyrone-4,6-dicarboxylic acid among the *Rosoideae* does not correspond to this classification (Schulze-Menz, 1964) (see Fig. 2). The tribe *Dryadeae* includes subtribes with or without 2-pyrone-4,6-dicarboxylic acid. The subtribes *Cercocarpinae* and *Dryadinae* contain no 2-pyrone-4,6-dicarboxylic acid while the subtribe *Geinae* includes two genera with a relative high amount of this substance (2% dry wt, see Table 3). The genera *Sanguisorba* and *Acaena* are combined in the *Sanguisorbinae*. However, *Acaena* contains no 2-pyrone-4,6-dicarboxylic acid whereas *Sanguisorba* does. 2-Pyrone-4,6-dicarboxylic acid is obviously limited to the *Rosoideae* but it does not occur in every member of the subfamily.

The classification of Schulze-Menz (1964) is only one of many suggested classifications of the Rosaceae. Morgan et al. (1994) investigated the family *Rosaceae* without viewing the traditional circumscriptions. The characteristic he used for determining phylogenetic relationships in this family was *rbc*L sequence variation. As a result the *Rosoideae* proposed by Schulze-Menz (1964) do not form a monophyletic group. *Rbc*L evidence splits *Rosoideae* according to chromosome numbers. *Rosoideae* with $x=7$ or 8 form a monophyletic group (*Rosoideae sensu stricto*) while traditional *Rosoideae* with $x=9$ are dispersed throughout the rest of the family.

Of the taxa of Rosaceae investigated for the presence of 2-pyrone-4,6-dicarboxylic acid, the only ones that the compound was found in are members of the *Rosoideae s. str.* proposed by Morgan et al. (1994). No genus outside the *Rosoideae s. str.* was found containing 2-pyrone-4,6-dicarboxylic acid. Therefore 2-pyrone-4,6-dicarboxylic acid seems to be a specific content of the *Rosoideae s. str.* and is perhaps a systematic marker for the *Rosoideae s. str.* proposed by Morgan et al. (1994) (see Fig. 3). In addition, two genera not investigated by Morgan et al. (1994), *Sanguisorba* and *Duchesnea*, contain 2-pyrone-

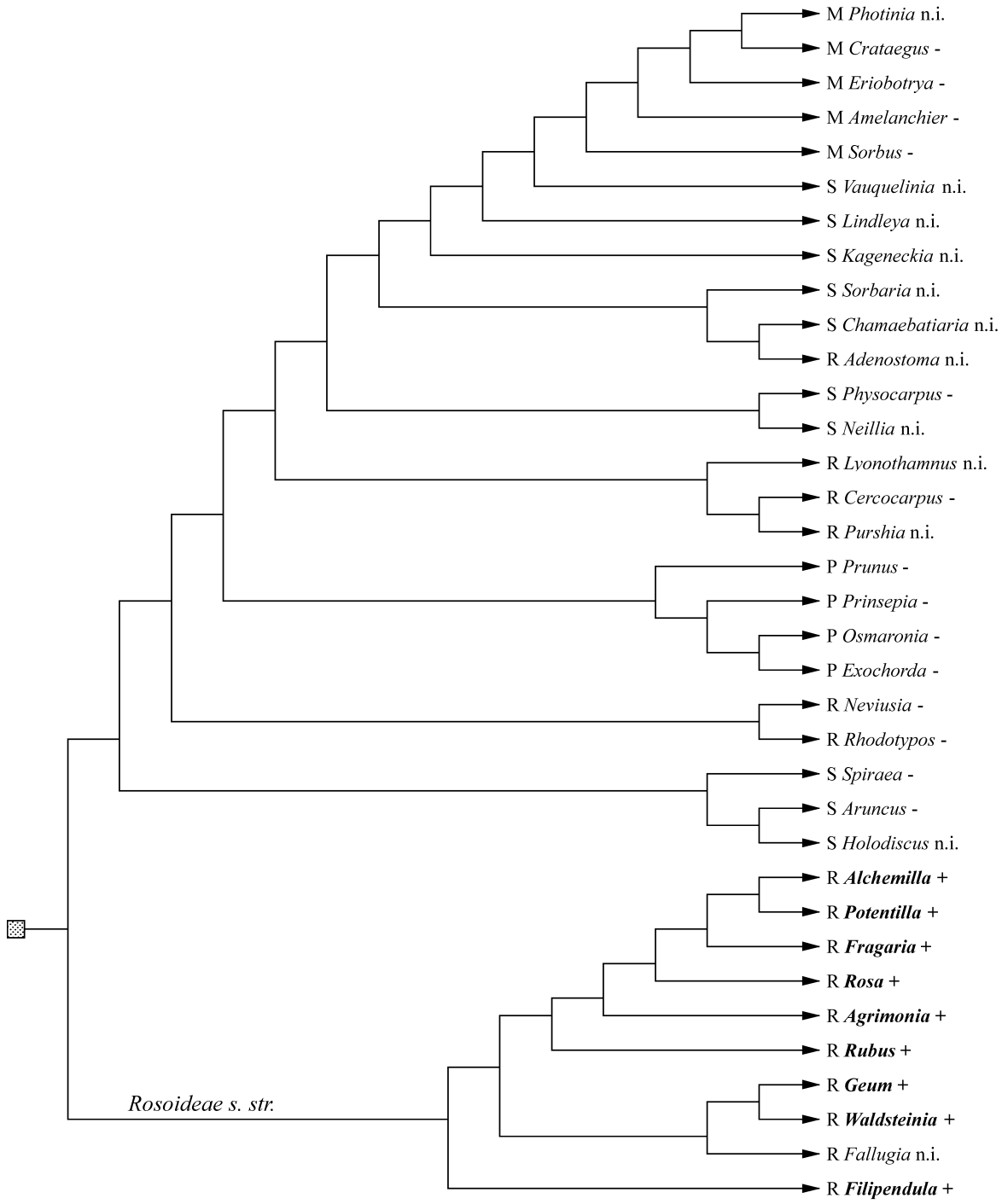

Fig. 3. Phylogenetic relationships in Rosaceae suggested by *rbc*L sequence variation (Morgan et al., 1994). +/−: 2-Pyrone-4,6-dicarboxylic acid existing/ not existing; n.i.: not investigated. S: *Spiraeoideae*; R: *Rosoideae*; M: *Maloideae*; P: *Prunoideae* from Schulze-Menz (1964).

4,6-dicarboxylic acid as well suggesting that they might also belong in *Rosoideae s. str*.

The amount of 2-pyrone-4,6-dicarboxylic acid within the investigated species varies (see Table 3). Most species contain 0.1–0.5% of the compound but species of the genera *Geum* and *Waldsteinia* show a much higher amount of 2 and 1,3% respectively. *Geum* and *Waldsteinia* are close relatives in both systematic systems so the occurrence of high amounts of 2-pyrone-4,6-dicarboxylic acid supports their relationship.

The distribution of 2-pyrone-4,6-dicarboxylic acid within a single plant differs (see Table 4). In *Potentilla*

Table 2
Classification of the Rosaceae used for screening of 2-pyrone-4,6-dicarboxylic acid proposed by Schulze-Menz (1964). Genera used in this investigation are shown in bold type

Subfamily *Spiraeoideae*	
Tribus *Quillajeae*	Genera: ***Quillaja***, *Kageneckia, Vauquellinia*
Tribus *Exochordeae*	Genera: ***Exochorda***, *Lindleya*
Tribus *Gillenieae*	Genera: ***Gillenia***, *Spiraeanthus*
Tribus *Sorbarieae*	Genera: *Sorbaria, Chamaebatiaria, Lyonothamnus*
Tribus *Neillieae*	Genera: *Physocarpus, Neillia, Stephanandra*
Tribus *Spiraeeae*	Genera: ***Spiraea***, ***Aruncus***, *Sibiraea*
Tribus *Holodisceae*	Genera: *Holodiscus*
Subfamily: *Rosoideae*	
Tribus *Ulmarieae*	Genera: ***Filipendula***
Tribus *Kerrieae*	Genera: ***Rhodotypos***, ***Kerria***, ***Neviusia***, *Coleogyne*
Tribus *Rubeae*	Genera: ***Rubus***, *Dalibarda*
Tribus *Roseae*	Genera: ***Rosa***
Tribus *Sanguisorbeae*	Genera: ***Agrimonia***, *Hagenia*, ***Sanguisorba***, *Poterium, Margyricarpus, Tetraglochin*, ***Acaena***, *Polylepis, Cliffortia*
Tribus *Adenostomeae*	Genera: *Adenostoma*
Tribus *Dryadeae*	Genera: ***Cercocarpus***, *Chamaebatia, Purshia, Cowania, Fallugia*, ***Dryas***, ***Geum***, ***Waldsteinia***, *Coluria*
Tribus *Potentilleae*	Genera: ***Comarum***, ***Potentilla***, ***Fragaria***, ***Duchesnea***, *Horkelia, Ivesia*, ***Alchemilla***, *Lachemilla, Aphanes*
Subfamily *Maloideae*	
Tribus *Maleae*	Genera: ***Cydonia***, ***Chaenomeles***[a], ***Pyrus***, ***Malus***, ***Sorbus***, ***Eriobotrya***, ***Amelanchier***, Raphiolepis, ***Photinia***[b], *Stranvaesia*, ***Osteomeles***[c]
Tribus *Crataegeae*	Genera: ***Cotoneaster***, ***Pyracantha***, ***Mespilus***, ***Crataegus***
Subfamily *Prunoideae*	
	Genera: ***Osmaronia***[a], *Maddenia, Pygeum*, ***Prunus***, ***Prinsepia***

[a] Today is *Chaenomeles Choenomeles* and *Osmaronia Oemleria* (Encke et al., 1994).
[b] *Aronia* belongs to the genus *Photinia* (Royal Botanic Gardens, Kew, http://www.rbg.kew.org.uk/).
[c] *Osteomeles* is not described by Schulze-Menz, but this genus also belongs to the Rosaceae (Royal Botanic Gardens, Kew, http://www.rbg.kew.org.uk/).

anserina the leaves have the highest concentration of 2-pyrone-4,6-dicarboxylic acid while the shoots and seeds contain lower concentrations.

3. Conclusion

2-Pyrone-4,6-dicarboxylic acid was isolated from *Potentilla anserina* L. It is a genuine compound of several members of the *Rosoideae* and it seems to be a taxonomic marker for the *Rosoideae s. str.* proposed by Morgan et al. (1994).

4. Experimental

4.1. General experimental procedures

^{1}H, ^{13}C and APT NMR spectra were recorded at ambient temperature at 200 respectively 50 MHz on a Varian Gemini 200 spectrometer relative to MeOH ($\delta = 3.35$ ppm). HSQC and HMBC spectra were recorded at 600 MHz on Varian Unity 600. MS was recorded on a GCQ Finnigan - MAT at 70 eV. UV spectroscopy was made on a Shimadzu UV-visible recording spectrophotometer in MeOH, 0.1 N HCl and 0.1 N NaOH. HPLC was made on Waters System (analytic: In-Line Degasser, 717 plus Autosampler, 600 Controller, 996 Photodiode Array Detector, Waters software, column: ProSep C-18 150×4 mm, 5 μm, endcapped, Latek Eppelheim; preparative: In-Line Degasser, Automated Gradient Controller, 515 HPLC Pump, Lambda Max Model 481 LC Spectrophotometer, column: Knauer Refill C-18 250×20 mm, 7 μm).

4.2. Plant material

Aerial plant material of *Potentilla anserina* L. for isolation of 2-pyrone-4,6-dicarboxylic acid was harvested in the garden of the institute in summer 1997. Seeds of *Potentilla recta* L. were purchased from Bornträger GmbH, D-67591 Offstein. Plants for screening were collected in the Botanical Garden of the university, the garden of the institute and in the environs of Münster (see Fig. 2 for the place of collection, collection time and herbarium number). The species were determined using Rothmaler (1995) or the determination was taken from the gardens.

4.3. HPLC analysis of crude Potentilla anserina L. extract

Three grams of lyophilised and pulverised *Potentilla anserina* L. were extracted with 40 ml 80% aq. MeOH

Table 3
Amounts of 2-pyrone-4,6-dicarboxylic acid in *Rosoideae* s. str. numbering, see Table 1

No.	Species	2-Pyrone-4,6-dicarboxylic acid (mg/100 g)
7	*Filipendula ulmaria* (L.) Maxim.	14±5
11	*Rubus fruticosus* L.	268±7
12	*Rubus idaeus* L.	120±1
13	*Rubus illecebrosus* Focke	153±1
14	*Rosa damascena* Mill. ‚Trigintipetala“	235±3
15	*Rosa jundzillii* Bess.	149±1
16	*Rosa omeiensis* Rolfe. *forma pteracantha* (Franch.) Rehd et Wils.	44±1
17	*Rosa rugosa* Thungb.	121±2
18	*Agrimonia eupatoria* L.	434±1
19	*Agrimonia procera* Wallr.	597±22
20	*Sanguisorba canadensis* L.	372±15
21	*Sanguisorba obtusa* Maxim.	289±45
22	*Sanguisorba officinalis* L.	19±2
26	*Geum rivale* L.	2092±56
27	*Geum urbanum* L.	2055±92
28	*Waldsteinia ternata* (Steph.) Fritsch	1296±16
29	*Potentilla anserina* L.	291±1
30	*Potentilla argentea* L.	353±2
31	*Potentilla aurea* L	232±14
32	*Potentilla calycina* Boiss.	159±4
33	*Potentilla crantzii* (Crantz.) Beck et Fritsch	125±2
34	*Potentilla erecta* (L.) Raeusch.	214±3
35	*Potentilla fruticosa* L.	97±3
36	*Potentilla grandiflora* L.	241±5
37	*Potentilla neumannia* Rchb.	244±10
38	*Potentilla norvegica* L.	384±24
39	*Potentilla palustris* (L.) Scop.	335±2
40	*Potentilla recta* L	464±1
41	*Potentilla reptans* L.	236±1
42	*Potentilla rupestris* L.	207±1
43	*Fragaria ×ananassa* (Duch.) Guedes	238±9
44	*Fragaria vesca* L.	214±1
45	*Duchesna indica* (Andr.) Focke	177±1
46	*Alchemilla conjunca* Bab.	202±20
47	*Alchemilla xanthochlora* Rothm.	247±2

Table 4
Amounts of 2-pyrone-4,6-dicarboxylic acid in parts of the plant *Potentilla anserina*

Part of the plant	2-Pyrone 4,6-dicarboxylic acid (mg/100 g)
Shoot (runner)	162±2
Shoot (flower)	160±1
Leaves	427±14
Flowers	272±6
Epigeal parts	216±1
Seed (*Potentilla recta*)	107±1

with Ultra Turrax. After filtration the extract was evaporated nearly to dryness and was filled up with water to 10.0 ml. The extract was held overnight at 8 °C and filtrated. Five microliters were used for HPLC. Analytical HPLC was made with a gradient of CH_3CN/0.1% aq. TFA (flow: 2 ml/min; 0 min: 0/100; 20 min: 7/93; 35 min: 25/75; 40 min: 50/50); 45 min: 100/0. Retention time of 2-pyrone-4,6-dicarboxylic acid: 5.6 min.

4.4. Preparative extraction and separation

Fresh plant material of *Potentilla anserina* (16 kg) was frozen with liquid nitrogen, crushed, lyophilised (3.7 kg) and extracted with aq. Me_2CO (70%, 54 l) followed with aq. EtOH (50%, 45 l) with an Ultra-Turrax homogenizer. After removing the organic solvent at 40 °C under vacuum the aqueous solution was allowed to stand overnight at 8 °C, filtered to remove chlorophyll and defatted with petrol. The crude extract (28 l) was concentrated (6.5 l) by lyophilisation and extracted successively with Et_2O (9 l) and EtOAc (12 l) setting the crude extract before to pH = 2 with HCl. Twenty grams of the dry EtOAc-fraction (82 g) were fractionated on a Sephadex LH-20 column (5×62 cm) using 80% aq. EtOH (6 l). The fraction from elution volume 200–1400 ml contains 2-pyrone-4,6-dicarboxylic acid (2061 mg). A small portion of

this fraction (150 mg) was purified by HPLC using CH_3CN/0.1% aq. TFA (gradient 20/80 to 50/50, 20 min., 7 ml/min.) to yield 2-pyrone-4,6-dicarboxylic acid (10.5 min).

4.5. Analytical extraction and quantification

The fresh plants were frozen at −30 °C and lyophilised without crushing. The plant material was pulverised. Three grams of the powder were extracted four times with 40 ml 70% aq. Me_2CO in ultrasound (3 min.). The extract was evaporated nearly to dryness and was filled up with water to 10 ml. The extract was held overnight at 8 °C and filtered. Two hundered and fifty microliters of the crude extract were taken for solid-phase extraction at LiChrolut® RP-18 (500 mg, Merck). Before use, the columns were cleaned and prepared by eluting 1 ml water, 1 ml Me_2CO and 2 ml water. Then the extract was given up to the column followed by elution three times with 250 µl water. This extract was collected and used for HPLC. Analytical HPLC was made with a gradient of CH_3CN / 0,1% aq. TFA (flow: 2 ml/min; 0 min: 0/100; 5 min: 0/100; 15 min: 7/93; 25 min: 100/0). Calibration was made with freshly isolated 2-pyrone 4,6-dicarboxylic acid (0.1–0.0005 mg/run, four concentrations, $R^2 = 0.9994$).

4.6. Sterile cultivation of Potentilla recta

Seeds of *Potentilla recta* were sterilised 30 min with 5% aq. NaOCl and washed with sterile water before transferring them to the culture medium (Vermiculite; 0.51 g KNO_3, 1.18 g $Ca(NO_3)_2{*}4H_2O$, 0.49 g $MgSO_4{*}7H_2O$, 0.136 g KH_2PO_4 2.5 ml Fe-EDTA (Gamborg, 1966), 0.1 ml microsalts (Gamborg, 1966), all per l). The seedlings were harvested after the second primary leaf emerged (10–12 weeks). Detection of 2-pyrone-4,6-dicarboxylic acid was done as in *Analytical extraction and quantification* above. The seed and the seedlings were tested for sterility by transferring them to a solid culture medium containing 0.9% agar, 3% saccharose, 2% 2,4-D, microsalts (Murashige and Skoog, 1962) and organic compounds (Gamborg et al., 1968). Bacteria and fungi contamination was not detectable.

4.7. NMR, MS and UV

The spectral properties (MS, UV, ^{1}H NMR) of 2-pyrone-4,6-dicarboxylic acid were essentially those reported by Maruyama (1979): EI–MS:184 (5.3%) $[M]^+$139 (100%): 184–45 $[M - COOH]^+$, 111 (6.6%): 184–45–28 $[M–COOH–CO]^+$, 95 (1.5%): 184–45–44 $[M–COOH–CO_2]^+$. UV $\lambda^{MeOH\text{-}max.}$ nm: 316 ($\varepsilon = 4927$), 212 ($\varepsilon = 8218$); $\lambda^{0,1n\ HCl\text{-}max}$ nm: 315 ($\varepsilon = 5506$), 214; $\lambda^{0,1n\ NaOH\text{-}max}$ nm: 353, 220. ^{1}H NMR (CD_3OD): δ 7.44 (*d*, H-3, *J* (3-5) 1.16 Hz), *δ* 7.07 (*d*, H-5, *J* (5-3) 1.17 Hz). ^{13}C NMR data are shown in Samejima et al. (1987) but not in complete. The complete assignment of the carbons C-7 and C-8 was determined by ^{13}C NMR, APT, HSQC and HMBC: ^{13}C NMR (CD_3OD): *δ* 161.7 (*s*, C-2), *δ* 109.8 (*s*, C-3), *δ* 145.8 (*s*, C-4), *δ* 122.7 (*s*, C-5), *δ* 151.3 (*s*, C-6), *δ* 165.1 (*s*, C-7); *δ* 162.1 (*s*, C-8). The data are in good agreement with those published by Samejima et al. (1987).

Acknowledgements

Our thanks are due to Dr. I. Rath and Professor W. Barz, Münster, for sterile cultivation and the Botanischer Garten der Westfälischen Wilhelms-Universität Münster for the kind gift of several Rosaceae species. Thanks also to Dr. D. Bergenthal and Dr. Bergander, Münster, for NMR-spectra and T. Meiners, Münster, for mass spectrometry.

References

Challice, J.S., 1972. Phenolic compounds of the subfamily Pomoideae: a chemotaxonomic survey. Phytochemistry 12, 1095–1101.

Eaton, R.W., Ribbons, D.W., 1982a. Metabolism of dibutylphthalate and phthalate by *Micrococcus* sp. strain 12B. Journal of Bacteriology 151, 48–57.

Eaton, R.W., Ribbons, D.W., 1982b. Metabolism of dimethylphthalate by *Micrococcus* sp. strain 12B. Journal of Bacteriology 151, 465–467.

Encke, F., Buchheim, G., Seybold, S., 1994. Zander Handwörterbuch der Pflanzennamen. Vol. 15. Aufl. Eugen Ulmer, Stuttgart.

Fikenscher, L.H., Hegnauer, R., Ruijgrok, H.W.L., 1981. Die Verbreitung der Blausäure bei den Cormophyten. Planta Medica 41, 313–327.

Gamborg, O.L., Miller, R.A., Ojima, K., 1968. Nutrient requirements of suspension cultures of soybean root cells. Exp. Cell Res. 50, 151–158.

Gamborg, O.L., 1966. Aromatic metabolism in plants II. Enzymes of the shikimate pathway in suspension cultures of plant cells. Canadian Journal of Biochemistry 44, 791–799.

Harborne, J.B., 1967. Comparative Biochemistry of Flavonoids. Academic, London. pp. 154–160.

Hegnauer, R., 1973. Chemotaxonomie der Pflanzen, Bd. 6. Birkhäuser, Basel–Boston, Berlin.

Hegnauer, R., 1990. Chemotaxonomie der Pflanzen, Bd. 9. Birkhäuser, Basel–Boston, Berlin.

Kersten, P.J., Dagley, S., Whittaker, J.W., Arciero, D.M., Lipscomb, J.D., 1982. 2-Pyrone-4,6-dicarboxylic acid, a catabolite of gallic acid in *Pseudomonas* species. Journal of Bacteriology 152, 1154–1162.

Maruyama, K., 1979. Isolation and identification of the reaction product of α-hydroxy-γ-carboxymuconic ε-semialdehyde dehydrogenase. Journal of Biochemistry 86, 1671–1677.

Morgan, D.R., Soltis, D.E., Robertson, K.R., 1994. Systematic and evolutionary implications of *rbc*L sequence variation in Rosaceae. American Journal of Botany 81, 890–903.

Murashige, T., Skoog, F., 1962. A revised medium for rapid growth and bioassay with tobacco tissue cultures. Physiology of Plants 15, 473–497.

Okuda, T., Yoshida, T., Hatano, T., Iwasaki, M., Kubo, M., Orime, T., Yoshizaki, M., Naruhashi, N., 1992. Hydrolysable tannins as chemotaxonomic markers in the Rosaceae. Phytochemistry 31, 3091–3096.

Rosazza, P.N., Huang, Z., Volm, T., Rousseau, B., 1995. Review:

Biocatalytic transformations of ferulic acid: an abundant aromatic natural product. Journal of Industrial Microbiology 15, 457–471.

Rothmaler, W., 1995. Gefäßpflanzen: Atlasband. Exkursionsflora von Deutschland, Bd. 3, 9. Aufl. Gustav Fischer, Jena–Stuttgart.

Samejima, M., Tatarazako, N., Arakawa, T., Saburi, Y., Yoshimoto, T., 1987. Metabolism of 3,4-dimethoxycinnamic acid and ferulic acid by mutant strains derived from *Pseudomonas* sp. TMY1009. Mokuzai Gakkaishi 33, 728–734.

Schulze-Menz, G.K., 1964. Rosaceae. In: Melchior, H. (Ed.), Engler's Syllabus der Pflanzenfamilien. Vol. II. Gebrueder Bornträger, Berlin, pp. 209–218.

Wallaart, R.A., 1980. Distribution of sorbitol in Rosaceae. Phytochemistry 19, 2603–2610.

Wilkes, S., Glasl, H., 2000. Isolation and characterization of 2-pyrone-4,6-dicarboxylic acid from *Potentilla anserina* L. and its occurrence in other *Potentilla* species. Poster at the Annual Meeting of the Deutsche Pharmazeutische Gesellschaft, Münster.

PERGAMON

Phytochemistry 58 (2001) 451–454

PHYTOCHEMISTRY

www.elsevier.com/locate/phytochem

Betaine distribution in the Malvaceae

Gerald Blunden[a,*], Asmita V. Patel[a], Nigel J. Armstrong[a], John Gorham[b]

[a]*School of Pharmacy and Biomedical Sciences, University of Portsmouth, St Michael's Building, White Swan Road, Portsmouth, Hampshire PO1 2DT, UK*

[b]*School of Biological Sciences, University of Wales, Bangor, Gwynedd LL57 2UW, UK*

Received 11 February 2001; received in revised form 22 May 2001

Abstract

Aerial parts of 26 taxa, distributed in 18 genera and all 5 tribes of the Malvaceae have been examined for the presence of betaines. Glycinebetaine was obtained in high yield (0.5–4.6%, dry weight) from all the plants studied, except *Abelmoschus moschatus*, in extracts of which glycinebetaine was not detected. Trigonelline was recorded for 16 of the plants tested, but the yields were low (0.005–0.07%, dry weight). Roots and flowers of a few of the species were also examined for betaines. The same compounds as those found in the aerial parts were usually detected, but the glycinebetaine contents of the roots and flowers were considerably lower. © 2001 Elsevier Science Ltd. All rights reserved.

Keywords: Malvaceae; Betaines; Glycinebetaine; Trigonelline; Chemotaxonomy

1. Introduction

The taxonomic value of betaines, particularly at the generic level, has been reported, for example, for the Graminae (Wyn Jones and Storey, 1981), marine algae (Blunden et al., 1982, 1992; Blunden and Gordon, 1986), the Labiatae (Blunden et al., 1996), the Capparaceae (McLean et al., 1996), the Amaranthaceae (Blunden et al., 1999) and the Bromeliaceae (Adrian-Romero and Blunden, 2001).

For the Malvaceae, Wyn Jones and Storey (1981) reported glycinebetaine in two species of *Abutilon* and a Dragendorff-positive compound in *Lavatera plebeja*. Later, Popp et al. (1984) recorded high concentrations of methylated onium compounds for *Hibiscus tilaceus*, and Poljakoff-Mayer et al. (1994) isolated glycinebetaine in a yield of about 1%, dry weight, from the seeds of *Kosteletzkya virginica*, prior to germination. Gorham (1995) found glycinebetaine in most of the Malvaceae he investigated and another unidentified betaine was detected in several of the plants examined; no yields were given for any of the species. In a later paper, Gorham (1996) reported glycinebetaine in all but 3 of over 100 species of Malvaceae investigated. He concentrated on *Gossypium* species, which were found to contain large amounts of glycinebetaine (>20 mmol kg^{-1}, fresh weight). In this current investigation we have isolated, characterized and quantified the betaines present in 18 genera of Malvaceae, representing all 5 tribes listed by Jury (1993).

2. Results and discussion

Malvaceae is a family comprised of 75 genera distributed in tropical and temperate areas (Willis, 1973). Classification of the family poses many problems and opinions differ as to deliniation of genera and tribes, but most treatments recognize 5 tribes (Jury, 1993). Aerial parts of 26 taxa, included in 18 genera of the Malvaceae and distributed in all 5 tribes, were extracted and the extracts examined for the presence of betaines; these were detected by TLC in all the extracts (Table 1). The betaines were isolated by preparative TLC and characterized from TLC, ^{1}H NMR spectroscopic and, when possible, FAB mass spectrometric data. Glycinebetaine was found in all the species tested, except *Abelmoschus moschatus*. In an earlier study of the family, Gorham (1995) also reported the absence of glycinebetaine from this species. High yields of glycinebetaine were obtained, ranging from 0.5% of the dry weight of *Malvastrum*

* Corresponding author. Tel.: +44-2392843593; fax: +44-2392843565.

0031-9422/01/$ - see front matter © 2001 Elsevier Science Ltd. All rights reserved.
PII: S0031-9422(01)00263-1

Table 1
Betaines in the Malvaceae

Species	Place of collection	Date of collection	Glycinebetaine yield (%, dry weight)	Trigonelline yield (%, dry weight)
Abutileae				
Abutilon x *hybridum* Hort. 'Canary Bird'	Greenway Gardens Nursery, Churston Ferrers, Devon	February 2000	2.3	nd[a]
Abutilon x *hybridum* 'Louise Marignac'	Greenway Gardens Nursery, Churston Ferrers, Devon	February 2000	0.9	0.01
A. vitifolium Presl	Greenway Gardens Nursery, Churston Ferrers, Devon	February 2000	0.9	nd
A. vitifolium 'Tennants White'	Greenway Gardens Nursery, Churston Ferrers, Devon	February 2000	1.0	nd
Modiola caroliniana G. Don.	Cambridge University Botanic Garden	September 2000	0.5	nd
Sida hermaphrodita Rusby = *S.napaea* Cav.	Cambridge University Botanic Garden	September 2000	1.0	0.007
Hibisceae				
Abelmoschus moschatus Medik.	Havant, Hampshire (grown from seed)	July 2000	nd	0.07
Gossypium armourianum Kearney	Bangor, Gwynedd	July 2000	0.7	nd
Hibiscus esculentus Linn. Fruits	Purchased in a supermarket	May 2000	0.07	0.05
H. rosa-sinensis Linn.	Havant, Hampshire	May 2000	4.6	0.1
H. rosa-sinensis Flowers	Havant, Hampshire	June 2000	1.1	0.02
H. syriacus Linn. (stems only)	Greenway Gardens Nursery, Churston Ferrers, Devon	February 2000	1.2	nd
Lagunaria patersonii G. Don.	Greenway Gardens Nursery, Churston Ferrers, Devon	February 2000	1.0	0.007
Malopeae				
Kitaibela vitifolia Willd.	Chipchase Castle Nursery, Wark, Hexham, Northumberland	July 2000	1.1	0.009
Malveae				
Alcea rosea Linn.	Havant, Hampshire	January 2000	1.9	0.03
A. rosea Roots	Havant, Hampshire	January 2000	0.04	nd
Althaea officinalis Linn.	Mill Hill Plants, East Stoke, Newark, Nottinghamshire	July 2000	0.8	nd
Callirhoë involucrata A. Gray	A. & A. Thorp, Theddingworth, Leicestershire	July 2000	0.7	0.02
C. involucrata Roots	A. & A. Thorp, Theddingworth, Leicestershire	July 2000	0.6	0.009
Hoheria lyallii Hook. f. (stems only)	Greenway Gardens Nursery, Churston Ferrers, Devon	February 2000	1.0	0.006
H. sexstylosa Colenso	Greenway Gardens Nursery, Churston Ferrers, Devon	February 2000	3.2	0.005
Lavatera cretica Linn.	Havant, Hampshire (grown from seed)	April 2000	0.9	0.03
Malva moschata Linn.	Warblington, Hampshire	July 2000	0.5	0.01
M. sylvestris Linn.	Havant, Hampshire	January 2000	1.9	0.07
M. sylvestris Roots	Havant, Hampshire	May 2000	0.05	0.002
M. sylvestris Flowers	Havant, Hampshire	May 2000	1.0	0.001
Malvastrum lateritium Nichols.	Greenway Gardens Nursery, Churston Ferrers, Devon	February 2000	0.5	0.02
Plagianthus regius Hochr.	Greenway Gardens Nursery, Churston Ferrers, Devon	February 2000	0.7	nd
Sidalcea candida A. Gray	Chipchase Castle Nursery, Wark, Hexham, Northumberland	July 2000	1.6	0.01
S. reptans Greene	A. & A. Thorp, Theddingworth, Leicestershire	July 2000	1.5	nd
S. reptans Root	A. & A. Thorp, Theddingworth, Leicestershire	July 2000	1.2	nd
Ureneae				
Goethea strictiflora Hook.	Cambridge University Botanic Garden	September 2000	0.7	0.01

[a] nd, not detected (limits of detection for glycinebetaine and trigonelline are approximately 0.0008 and 0.001%, dry weight, respectively). Unless otherwise stated, aerial parts of the plant were used.

lateritium, *Malva moschata* and *Modiola caroliniana* to 4.6% of the dry weight of *Hibiscus rosa-sinensis*. Trigonelline was detected in 16 of the plants tested, including *Abelmoschus moschatus*, 1 sample of *Abutilon x hybridum*, *Alcea rosea* and *Lavatera cretica*, for all of which an unidentified betaine was recorded by Gorham (1995). It is thus highly probable that this unidentified compound was trigonelline. The highest yield of trigonelline was from *Abelmoschus moschatus* (0.07%), but usually the values were very low and with such small amounts, the ^{1}H NMR spectroscopic assay procedure is subject to considerable error. Because of the low trigonelline contents and the small amount of plant material available of several of the species, confirmation of the identity of trigonelline by FAB mass spectometry was obtained only for *A. moschatus*, *Alcea rosea* and *Malva sylvestris*. Trigonelline was recorded for *Kitaibelia vitifolia*, *Malva moschata* and *M. sylvestris*, whereas Gorham (1995) did not detect the unidentified betaine in these species. In addition to the genera reported in this current study, 10 species of *Kosteletzkya* have recently been examined by Gorham (unpublished data) and all yielded more than 1%, dry weight, glycinebetaine. Trigonelline was detected in only two of the species examined (*K. racemosa* and *K. grantii*).

For a few of the species investigated (*Alcea rosea*, *Callirhoë involucrata*, *Malva sylvestris* and *Sidalcea reptans*), both aerial parts and roots were examined for betaines. In all cases, the yield of glycinebetaine was noticeably lower in the roots than in the aerial parts (Table 1). Moreover, although trigonelline was isolated from the aerial parts of *A. rosea* and *C. involucrata*, this betaine was not detected in the roots. The roots and aerial parts of *Salicornia europaea* L. (Chenopodiaceae) were also examined and, again, the glycinebetaine content of the aerial parts (1.5%) was higher than that of the roots (1.1%).

The flowers of *Hibiscus rosa-sinensis* and *Malva sylvestris* and the fruits of *H. esculentus* were tested for the presence of betaines. Glycinebetaine and trigonelline were detected, but in lower concentrations than those reported for the 'aerial parts', which excluded flowers and fruits (Table 1).

Rhodes and Hanson (1993) divided the betaine-yielding families and genera into those which accumulate betaines and those which do not. With the exception of *Abelmoschatus moschatus*, the results for all the species recorded here show that the Malvaceae should be classified as a betaine-accumulating family. *A. moschatus* was also the exception among the species tested in not containing glycinebetaine. Unlike some families examined, for example the Labiatae (Blunden et al., 1996) and Capparaceae (McLean et al., 1996), in which species in different genera often contain significantly different betaines, in the Malvaceae, all species tested, including examples in all 5 tribes (Jury, 1993), showed very similar betaine compositions.

3. Experimental

3.1. Plant material

The species examined and their places of collection are given in Table 1. Voucher samples of the plants studied are maintained in the herbarium of the Hampshire County Council Museums Service, Winchester, Hampshire, UK (Index Herbariorum code HCMS; accession number Bi 2000. 16).

3.2. Extraction, isolation, characterization and quantitative estimation of betaines

The plant materials were oven dried at 40 °C, powdered and extracted for 6 h with 80% MeOH. The methods of extraction, purification of the extracts by passage through a column of cation exchange resin, two-way TLC examination and isolation of the Dragendorff-positive compounds by prep.TLC have been described previously (Blunden et al., 1981, 1985).

The isolated compounds were identified by TLC, using appropriate reference compounds, ^{1}H NMR spectroscopy (D_2O; 270 or 400 MHz) and, when possible, FAB mass spectrometry.

Estimation of the content of each betaine present in the extracts was achieved using the ^{1}H NMR spectroscopic assay procedure of Blunden et al. (1986). With the quantities of dry plant material extracted (0.5–3 g), the limits of detection for glycinebetaine and trigonelline are approximately 0.0008 and 0.001%, respectively.

Acknowledgements

We thank the following for the supply of plant materials: the Director, University of Cambridge Botanic Garden; Mr. R. Clark, Greenway Gardens Nursery, Churston Ferrers, Devon; Mill Hill Plants, East Stoke, Newark, Nottinghamshire; A. & A. Thorp, Theddingworth, Leicestershire; and Chipchase Castle Nursery, Wark, Hexham, Northumberland. We are grateful to Mr. S. Sumner for technical assistance.

References

Adrian-Romero, M., Blunden, G., 2001. Betaine distribution in the Bromeliaceae. Biochemical Systematics and Ecology 29, 305–311.

Blunden, G., Cripps, A.L., Gorden, S.M., Mason, T.G., Turner, C.H., 1986. The characterisation and quantitative estimation of betaines in commercial seaweed extracts. Botanica Marina 29, 155–160.

Blunden, G., El Barouni, M.M., Gorden, S.M., McLean, W.F.H., Rogers, D.J., 1981. Extraction, purification and characterisation of Dragendorff-positive compounds from some British marine algae. Botanica Marina 24, 451–456.

Blunden, G., Gorden, S.M., 1986. Betaines and their sulphonio analogues in marine algae. In: Round, F.E., Chapman, D.J. (Eds.),

Progress in Phycological Research, Vol 4. Biopress, Bristol, pp. 39–80.

Blunden, G., Gorden, S.M., McLean, W.F.H., Guiry, M.D., 1982. The distribution and possible taxonomic significance of quaternary ammonium and other Dragendorff-positive compounds in some genera of marine algae. Botanica Marina 25, 563–567.

Blunden, G., Gorden, S.M., Smith, B.E., Fletcher, R.L., 1985. Quaternary ammonium compounds in species of the Fucaceae (Phaeophyceae) from Britain. British Phycological Journal 20, 105–108.

Blunden, G., Smith, B.E., Irons, M.W., Yang, M.-H., Roch, O.G., Patel, A.V., 1992. Betaines and tertiary sulphonium compounds from 62 species of marine algae. Biochemical Systematics and Ecology 20, 373–388.

Blunden, G., Yang, M.-H., Janicsák, G., Máthé, I., Carabot-Cuervo, A., 1999. Betaine distribution in the Amaranthaceae. Biochemical Systematics and Ecology 27, 87–92.

Blunden, G., Yang, M.-H., Yuan, Z.-X., Smith, B.E., Patel, A.V., Cegarra, J.A., Máthé, I., Janicsák, G., 1996. Betaine distribution in the Labiatae. Biochemical Systematics and Ecology 24, 71–81.

Gorham, J., 1995. Betaines in higher plants-biosynthesis and role in stress metabolism. Society of Experimental Biology Seminar Series 56, 173–203.

Gorham, J., 1996. Glycinebetaine is a major nitrogen-containing solute in the Malvaceae. Phytochemistry 43, 367–369.

Jury, S.L., 1993. Malvaceae. In: Heywood, V.H. (Ed.), Flowering Plants of the World.. B.T. Batsford, London, pp. 94–95.

McLean, W.F.H., Blunden, G., Jewers, K., 1996. Quaternary ammonium compounds in the Capparaceae. Biochemical Systematics and Ecology 24, 427–434.

Poljakoff-Mayber, A., Somers, G.F., Werker, E., Gallagher, J.L., 1994. Seeds of *Kosteletzkya virginica* (Malvaceae)—their structure, germination, and salt tolerance. 2. Germination and salt tolerance. American Journal of Botany 81, 54–59.

Popp, M., Larher, F., Weigel, P., 1984. Chemical composition of Australian mangroves. III. Free amino acids, total methylated onium compounds and total nitrogen. Zeitschrift für Pflanzenphysiologie 114, 15–25.

Rhodes, D., Hanson, A.D., 1993. Quaternary ammonium and tertiary sulphonium compounds in higher plants. Annual Reviews of Plant Physiology and Plant Molecular Biology 44, 357–383.

Willis, J.C., 1973. Dictionary of the Flowering Plants and Ferns, 8th edition. Cambridge University Press, Cambridge, pp. 708–709.

Wyn Jones, R.G., Storey, R., 1981. Betaines. In: Paleg, L.G., Aspinall, D. (Eds.), Physiology and Biochemistry of Drought Tolerance in Plants. Academic Press, Sydney, pp. 171–204.

PERGAMON

Phytochemistry 58 (2001) 455–462

PHYTOCHEMISTRY

www.elsevier.com/locate/phytochem

Calystegine distribution in some solanaceous species

Khalid Bekkouche[a], Youssef Daali[b], Samir Cherkaoui[b], Jean-Luc Veuthey[b], Philippe Christen[b,*]

[a]*Laboratory of Medicinal Plants and Phytochemistry, Department of Biology, Faculty of Sciences-Semlalia, PO Box 2390, Marrakech, Morocco*
[b]*Laboratory of Pharmaceutical Analytical Chemistry, University of Geneva, Bd d'Yvoy 20, 1211 Geneva 4, Switzerland*

Received 29 January 2001; received in revised form 7 June 2001

Abstract

The distribution of eight calystegines (A_3, A_5, B_1, B_2, B_3, B_4, C_1 and N_1) and their content was investigated by gas chromatography coupled to mass spectrometry (GC–MS) in *Datura metel*, *Atropa belladonna*, *Hyoscyamus albus*, *Mandragora autumnalis*, *Solanum sodomaeum*, *Withania somnifera*, *Withania frutescens* and *Brunfelsia nitida*. The most frequently encountered calystegines were A_3, B_1, B_2 and B_3, while distribution of N_1 and C_1 was more limited. In all the investigated samples, calystegines A_5 and B_4 were never detected. This report focuses for the first time on calystegines in *Withania* and *Brunfelsia* genera and in *Mandragora autumnalis and Solanum sodomaeum* species. © 2001 Published by Elsevier Science Ltd.

Keywords: *Atropa*; *Brunfelsia*; *Datura*; *Hyoscyamus*; *Mandragora*; *Solanum*; *Withania*; Solanaceae; GC–MS; Calystegines

1. Introduction

In the last 10 years, a large number of nitrogen-containing polyhydroxylated heterocyclic compounds have been isolated from plants (Nash et al., 1996). These natural products are competitive inhibitors of various glycosidases. The most efficient compounds are used to treat various diseases including diabetes, cancer, and viral infections (Jacob, 1995). Furthermore, these compounds exhibit additional activities, such as immunomodulatory properties and inhibition of glycolipid synthesis (Jacob, 1995). Among these metabolites, a new class of nortropane polyhydroxylated alkaloids, called calystegines, has recently been isolated from different species belonging to the Solanaceae, Convolvulaceae and Moraceae (Tepfer et al., 1988; Goldmann et al., 1990; Nash et al., 1993; Asano et al., 1994a,b; Schimming et al., 1998). Calystegines have been suggested to be nutritional mediators in the plant rhizosphere (plant-bacteria relationship) (Tepfer et al., 1988). Moreover, they possess glycosidase inhibiting properties (Asano et al., 1995, 1997a,b) and an allelopathic activity (Goldmann et al., 1996). To date, 14 calystegines have been isolated (Asano et al., 1997a,b). From a biosynthetic point of view, it is assumed that calystegines originate from the tropane alkaloid pathway (Dräger et al., 1994) although the exact details have not yet been confirmed.

Most calystegines have been isolated in several solanaceous species and found to occur in the following genera: *Atropa* (Tepfer et al., 1988; Molyneux et al., 1993; Dräger et al. 1994, 1995; Dräger, 1995; Nash et al., 1997), *Datura* (Nash et al., 1993), *Lycium* (Asano et al., 1997b), *Physalis* (Asano et al., 1995), *Hyoscyamus* (Dräger et al., 1994; Asano et al., 1996b), *Mandragora* (Dräger et al., 1995), *Scopolia* (Asano et al., 1996a), *Duboisia* (Kato et al., 1997), *Solanum* (Nash et al, 1993; Dräger et al., 1995; Keiner and Dräger, 2000) and *Nicandra* (Griffiths et al., 1996). In contrast, and to our knowledge, the occurrence of calystegines in *Brunfelsia* and *Withania* genera has not been reported. This paper discusses calystegine distribution in 8 solanaceous species belonging to 7 different genera. Particular attention is given to the occurrence of calystegines A_3, A_5, B_1, B_2, B_3, B_4, C_1 and N_1 (Fig. 1), which were identified by GC–MS, with authentic samples as reference material.

* Correspondence author. Tel.: +41-22-702-65-61; fax: +41-22-781-51-93.
E-mail address: philippe.christen@pharm.unige.ch (P. Christen).

0031-9422/01/$ - see front matter © 2001 Published by Elsevier Science Ltd.
PII: S0031-9422(01)00283-7

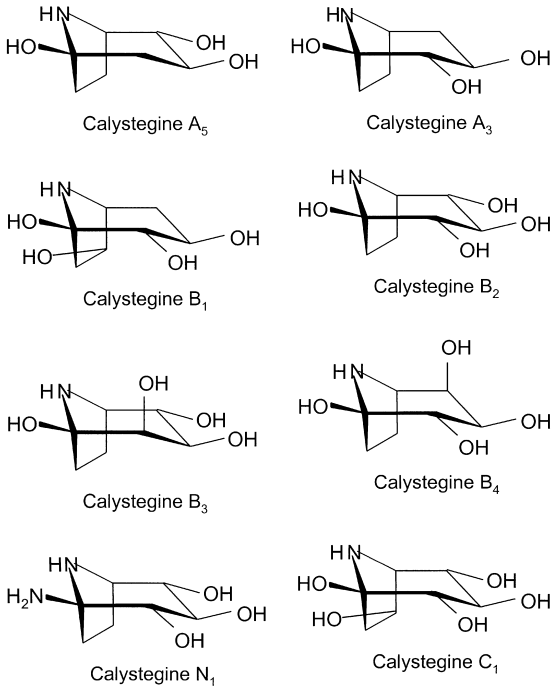

Fig. 1. Structures of investigated calystegines.

2. Results and discussion

Fig. 2 illustrates a typical gas chromatogram of a silylated calystegine standard mixture composed of calystegines A_3, A_5, B_1, B_2, B_3, B_4, C_1 and N_1 with octadecane as internal standard. The method allowed a good separation of the investigated compounds in less than 19 min . As expected, calystegines A (3 OH groups) eluted faster than calystegines B (4 OH groups) and calystegines C (5 OH groups). Indeed, since TMS derivatization occurs on the hydroxy groups, interaction of derivatized calystegines with the hydrophobic stationary phase increases with the number of hydroxy groups. The calystegine profile and the amount of individual alkaloid in each species are reported in Table 1 and Fig. 3. Calystegines were identified by comparing their retention times and mass spectra with those of silylated reference compounds, although no statement can be made on the absolute configuration of the alkaloids, nor even on their enantiomeric purity. Important qualitative and quantitative variations were observed among the species. The absence of reference material precluded the identification of other calystegines. None of the investigated calystegines were detected in *Datura metel* L. Tetrahydroxylated calystegine B_2 was present in all other species and its content varied significantly (from 19.1 to 110.9 μg/g dry wt.). The most frequently encountered calystegines were B_2, B_3, A_3 and B_1, while calystegines B_4 and A_5 were never observed.

Table 1
Distribution of calystegines in the investigated Solanaceae species

Plant species	Organ	Calystegines							
		A_3	A_5	B_1	B_2	B_3	B_4	C_1	N_1
Atropa belladonna	Aerial parts	+	–	+	+	+	–	–	+
Hyoscyamus albus	Leaves	+	–	+	+	+	–	–	+
Mandragora autumnalis	Leaves	–	–	–	+	+	–	–	–
Mandragora autumnalis	Roots	+	–	+	+	+	–	–	–
Solanum sodomaeum	Leaves	–	–	–	+	+	–	–	–
Withania frutescens	Leaves	+	–	+	+	+	–	+	+
Withania somnifera	Leaves	–	–	–	+	–	–	+	–
Brunfelsia nitida	Leaves	+	–	+	+	+	–	+	–
Datura metel	Leaves	–	–	–	–	–	–	–	–

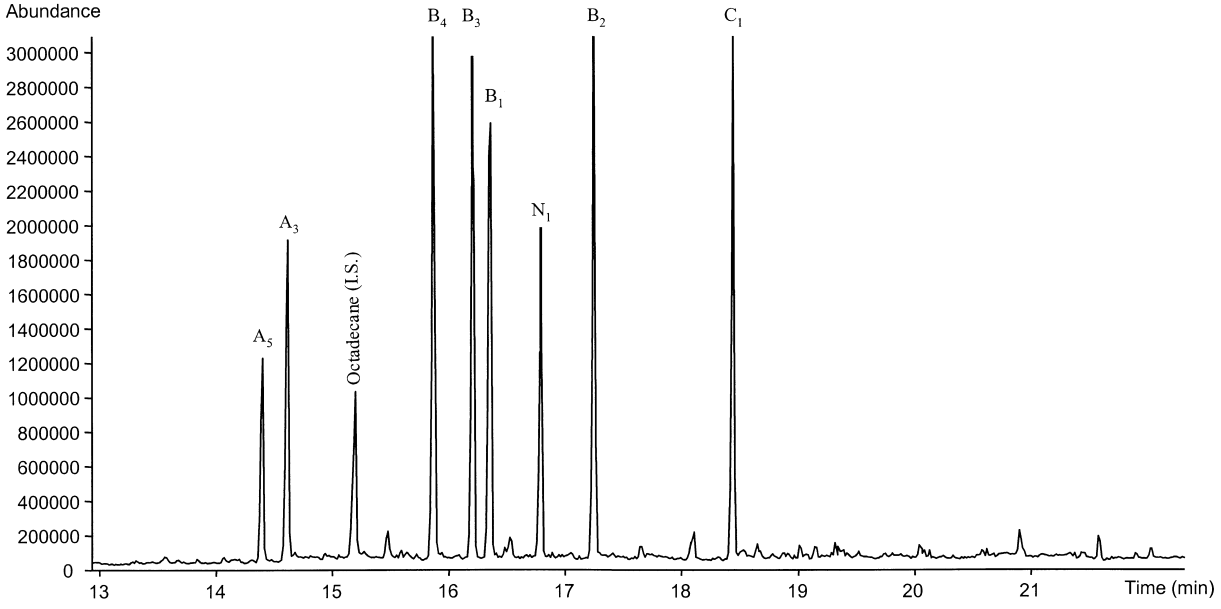

Fig. 2. Typical GC–MS chromatogram of a mixture of silylated standard calystegines with octadecane as internal standard.

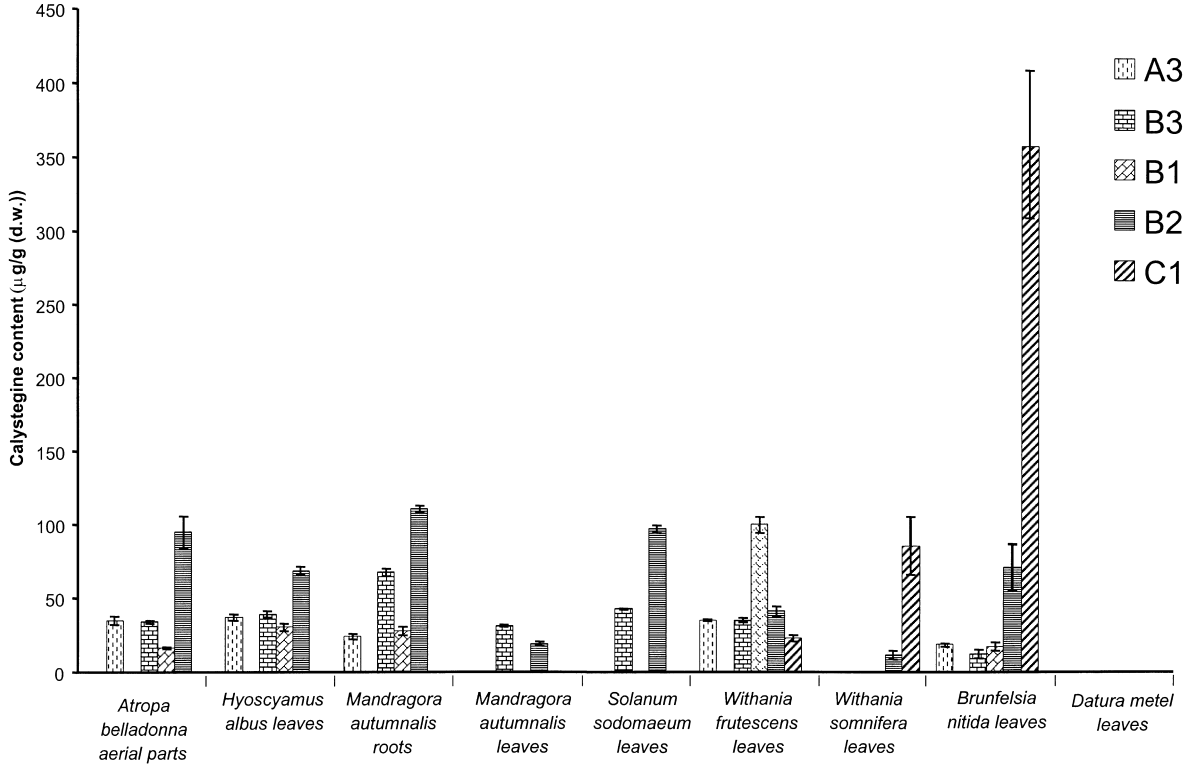

Fig. 3. Calystegine content in eight Solanaceae species.

In the aerial parts of *Atropa belladonna* L., the major compounds were A_3, B_2, B_3 and B_1. Calystegine B_4, previously reported by Nash et al. (1997), was not identified in our extract and calystegine N_1 was detected at a very low level. Calystegines N_1 and B_3 are reported in this species for the first time.

The presence of A_3 and other calystegines of the B-group in cultured roots of *Hyoscyamus albus* L. has already been reported elsewhere (Dräger et al., 1994). However, to the best of our knowledge, N_1 is reported in this species for the first time. Calystegines B_3 and B_2 were detected in leaves and roots of *Mandragora autumnalis* Bertol. B_1 and A_3 were also observed in the latter organ. Analogous studies (Dräger et al., 1995) reported the presence of calystegines B_1, B_2 and A_3 in leaves and roots of *M. officinarum*.

Calystegines B_2 and B_3 were detected in the leaves of *Solanum sodomaeum* L. which is consistent with similar articles reporting the presence of these metabolites in other *Solanum* species (Nash et al., 1993; Dräger et al., 1995; Keiner and Dräger, 2000).

The calystegine profiles of the two *Withania* species were found to be very different. Whilst calystegines B_2 and C_1 were identified in *W. somnifera* L. only, the calystegine spectrum of *W. frutescens* L. was more complex. All the investigated alkaloids, except A_5 and B_4, were found in the leaves *of W. frutescens*. This is the first time that calystegines are reported in the subtribe Solaninae of the Solanaceae family. Calystegines A_3, B_1, B_2, B_3 and C_1 were unambiguously identified in the leaves of *Brunfelsia nitida* Benth. The latter compound was in a high amount (357 μg/g dry wt.), and the most abundant calystegine found in all the investigated species. To the best of our knowledge, this class of compounds has not been reported in this genus before.

To date, calystegine N_1 has been isolated from *Hyoscyamus niger* (Asano et al., 1996b) and *Lycium chinense* (Asano et al., 1997b) only. In our study, this calystegine was found in three other species, *A. belladonna, H. albus* and *W. frutescens*. The distribution of pentahydroxlated calystegine C_1 was more limited as this compound was only found in *B. nitida*, *W. somnifera* and *W. frutescens*. Previous studies have also reported the presence of C_1 in *H. niger* (Asano et al., 1996b), *Duboisia leichhardtii* (Kato et al., 1997) and *Capsicum sp.* (Asano et al., 1997a).

It is noteworthy that most chromatograms of the different investigated species showed additional unidentified compounds with a similar fragmentation pattern to that of calystegines. Fig. 4 shows the chromatogram of *H. albus* leaf extract. Beside calystegines A_3, B_1, B_2, B_3 and N_1, some other peaks (X_1 and X_2) with specific calystegine MS profiles are also present. As shown in Fig. 5, calystegine N_1 (Fig. 5a) and unidentified compound X_1 (Fig. 5b) exhibit similar MS patterns. Beside fragment ions at m/z 390, 375 and 300,

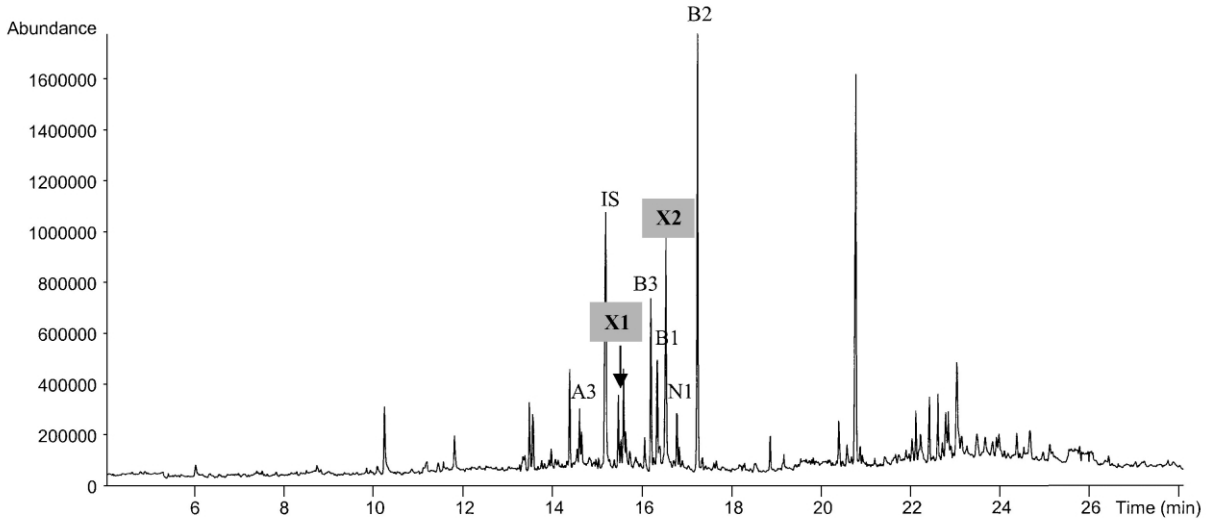

Fig. 4. Calystegine chromatogram from *Hyoscyamus albus* leaf extract.

corresponding to the molecular ion and to the loss of a methyl and dimethylsilyl groups, respectively, other fragments at *m*/*z* 186 and 83, specific of the exocyclic N-group, are found. Indeed, only calystegines belonging to the N-group exhibit such fragments which can be mainly attributed to the underivatized exocyclic amino group, as shown in the suggested fragmentation pattern of calystegines N_1 and X_1 (Fig. 6). As a result, unidentified peak X_1 may correspond to a new calystegine of the N-group, where the NH_2 function is located on the Δ^1-pyrrolinium skeleton at a different position to that of calystegine N_1. Moreover, fragment *m*/*z* 217 is typical of polyhydroxy compounds, as already described elsewhere (DeJongh et al., 1969).

Compound X_2 (Fig. 4) may correspond to a calystegine with a particular hydroxylation pattern. Its mass spectrum (Fig. 5C) clearly demonstrates that this compound does not belong to the N-group. To assess our assumption, further studies are to be performed. In particular isolation and structure characterization of these compounds should be carried out.

Before an overall chemotaxonomic conclusion regarding the occurrence of calystegines throughout this family can be drawn, further detailed phytochemical studies are required.

3. Experimental

3.1. Chemicals

Standard calystegines (A_3, A_5, B_1, B_2, B_3, B_4, $C_1$and N_1) were kindly donated by Dr. N. Asano (Hokuriku University, Kanazawa, Japan). All other chemicals and solvents were of analytical grade.

3.2. Plant material

Roots or aerial parts from wild plants were collected in different localities of Morocco for *Mandragora autumnalis*, *Datura metel*, *Hyoscyamus albus*, *Withania somnifera, Withania frutescens* and *Solanum sodomaeum*. Voucher specimens have been deposited in the Herbarium, Faculty of Sciences-Semlalia, Marrakech, Morocco. Seeds of *Brunfelsia nitida* and *Atropa belladonna* were provided by the Fairchild Tropical Garden, Miami, Florida. Plants were grown at the Station Fédérale de Recherches Agronomiques, Centre des Fougères, in Conthey, Switzerland.

3.3. Extraction

Air-dried and powdered plant material (20 g) was exhaustively extracted using Ultra-Turrax® homogenisation with water/methanol (80/20, v/v) for 30 min. After centrifugation, the supernatant was evaporated to dryness and applied to a cation exchange column (Dowex 50W X8-400 H^+ form). The column was washed with water to remove non-binding contaminants. Calystegines and bound compounds were eluted with 2 N NH_4OH. The concentrated residue was applied to an anion exchange column (Amberlite IRA-400 Cl^- form) and eluted with water to obtain a purified plant extract.

3.4. GC–MS procedure

GC–MS experiments were carried out essentially as described by Dräger (1995) without further validation from our side. An HP 5890 series II gas chromatograph and a HP 5972 mass selective detector (Hewlett-

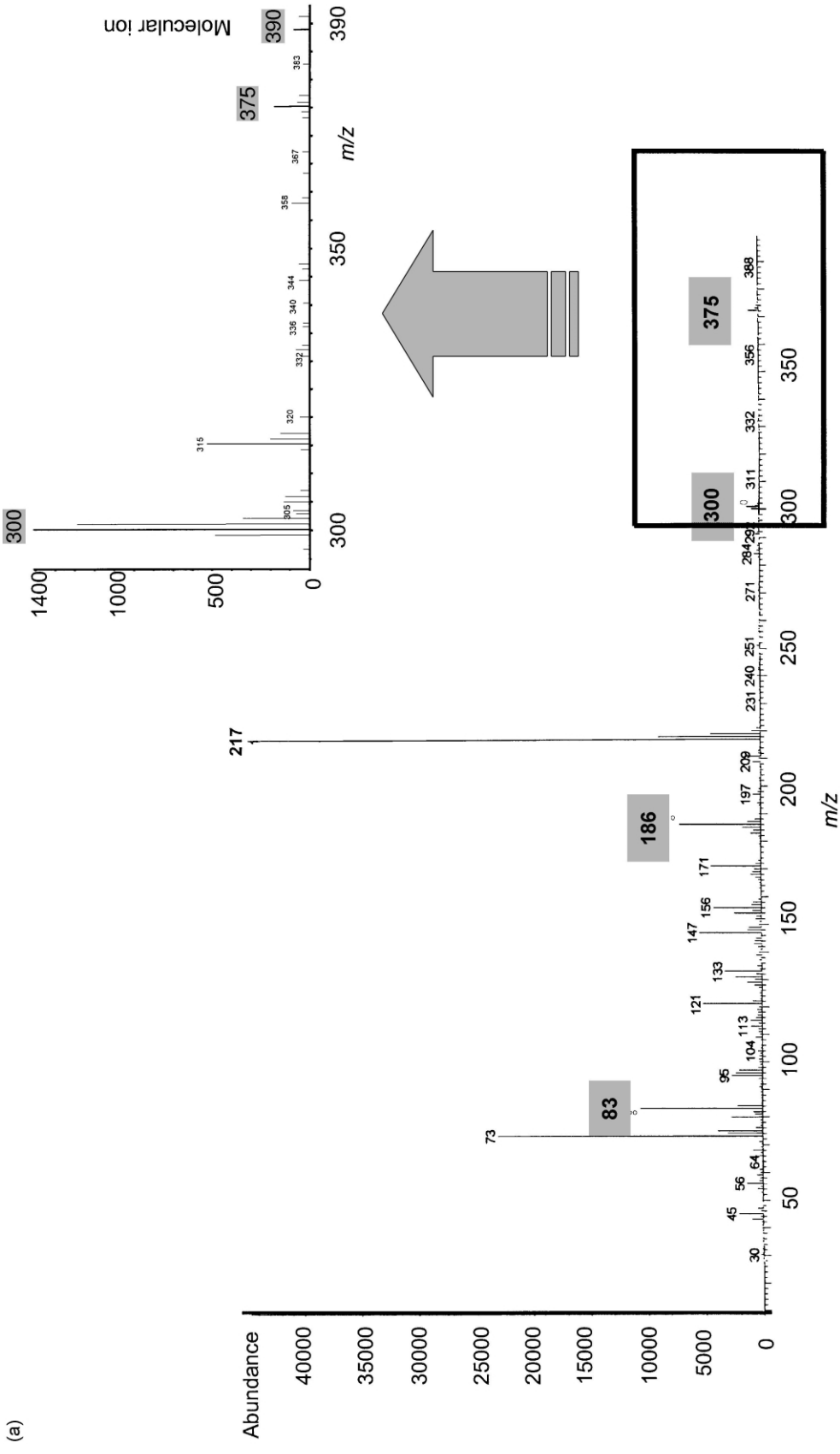

Fig. 5. Mass spectra of calystegines N_1 (a), X_1 (b) and X_2 (c).

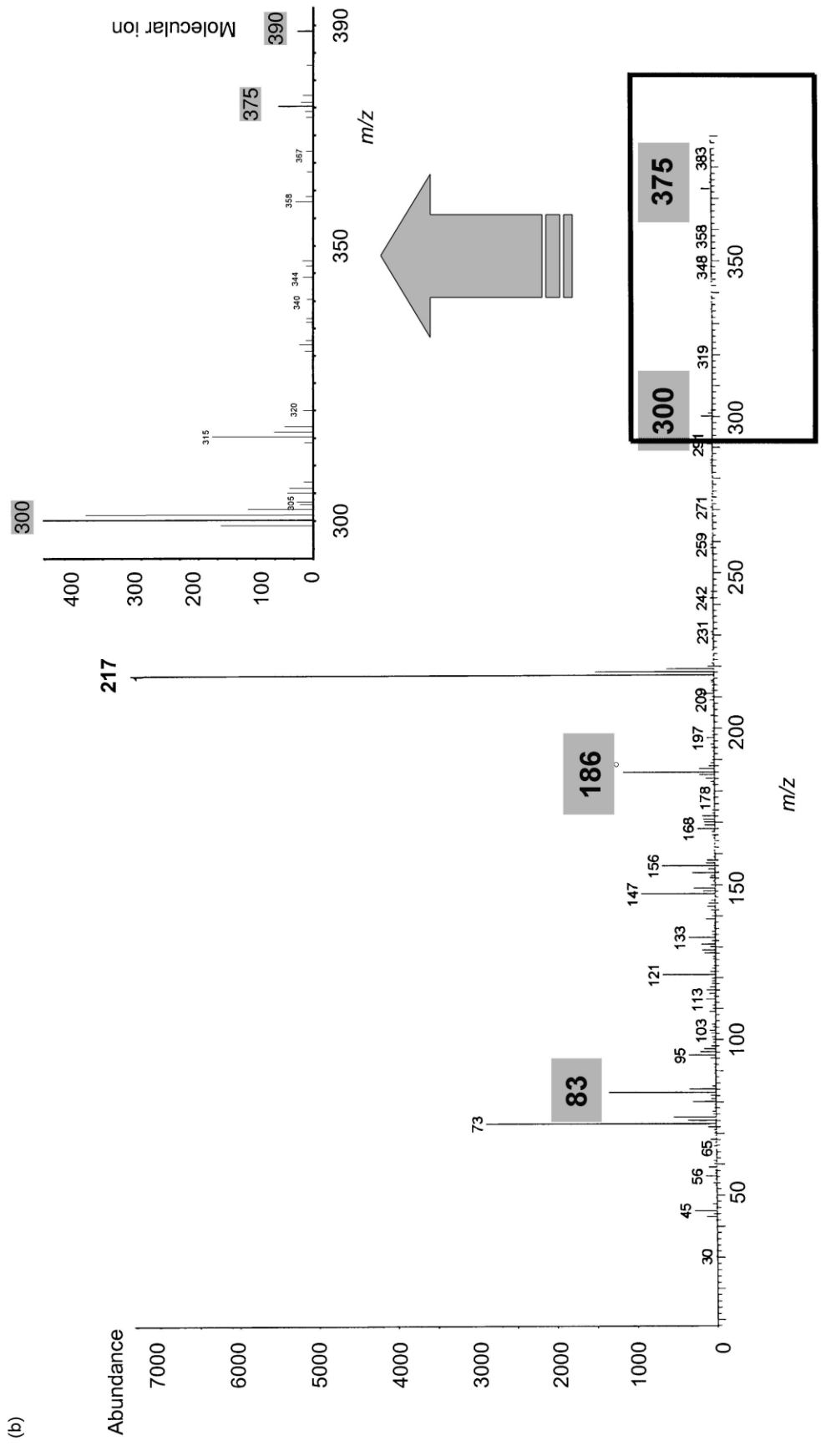

Fig. 5 (*continued*).

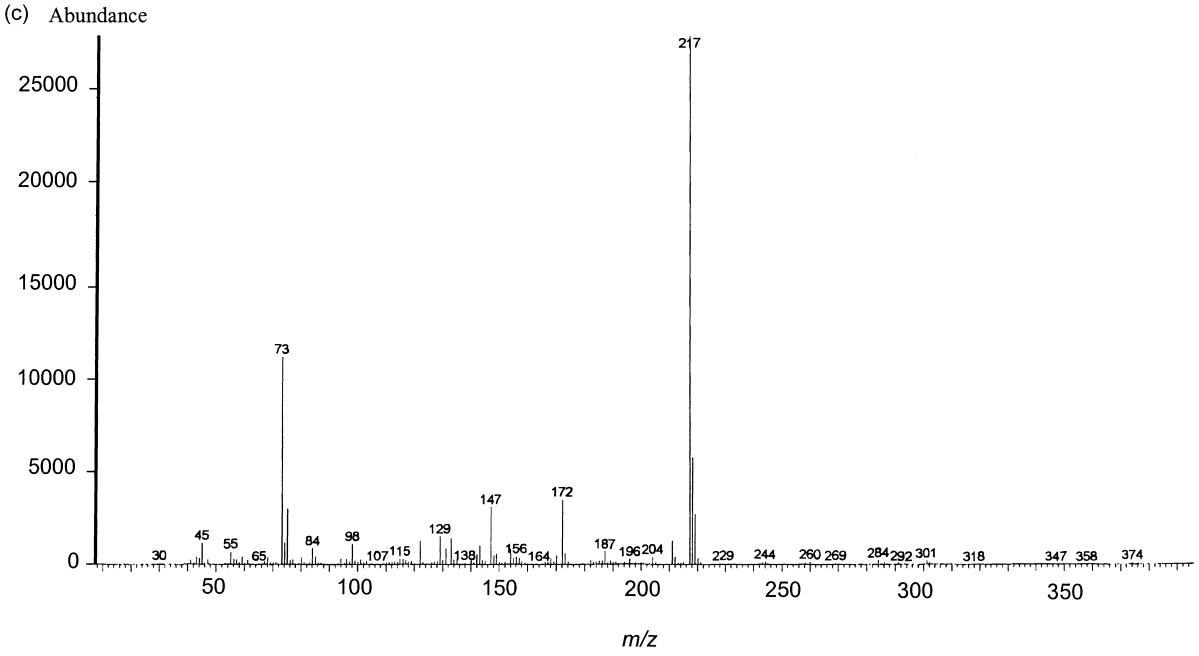

Fig. 5 (*continued*).

Packard) in the EI mode at 70 eV were used. Helium was used as carrier gas at a flow rate of 1 ml/min. The injection was performed in splitless mode at 250 °C and the injected volume was 1 μl. The column was a HP5-MS fused silica capillary (30 m × 0.25 mm i.d.) coated with a phenyl-methyl silicone phase (film thickness 0.25 μm).

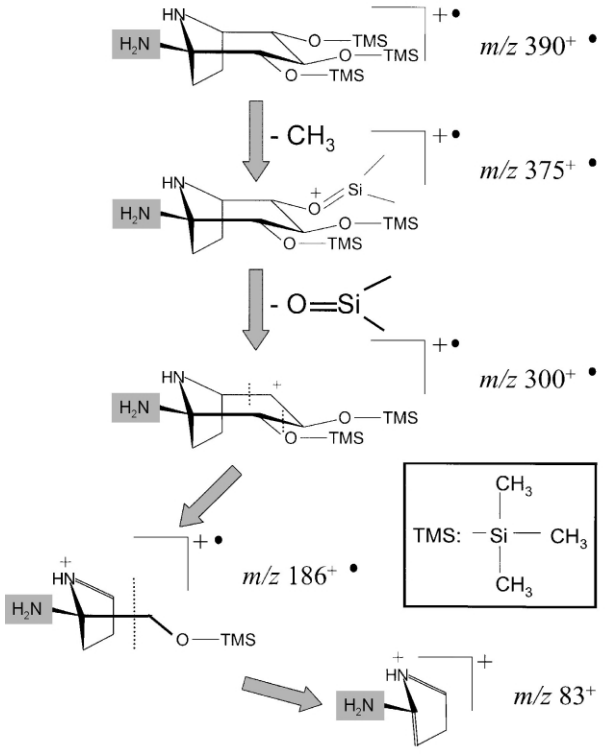

Fig. 6. Suggested fragmentation patterns of calystegines N_1 and X_1.

The temperature program was isothermal 100 °C for 5 min, 100–270 °C at 10 °C min^{-1} and isothermal 270 °C for 5 min. GC–MS interface was heated at 280 °C. Full-scan mode was used and the run time was 25 min.

3.4.1. Derivatization

In order to analyse calystegines by GC, a derivatization procedure was applied to form trimethylsilyl (TMS) ether derivatives, according to the procedure described elsewhere (Dräger, 1995). The reference compounds or the purified plant extract were dissolved in pyridine (1 ml) and mixed with hexamethyldisilazane (HMDS) and trimethylchlorosilane (10:1) to 2 ml and kept at 60 °C for 30 min. After evaporation to dryness under nitrogen at 50 °C, the residue was dissolved in heptane. An octadecane stock solution in heptane was added to the samples as internal standard to a final concentration of 100 μg/ml. The solutions were filtered through a 0.45 μm microfilter and 1 μl of each solution was subjected to GC–MS.

3.4.2. Calibration curves and quantitation

Calibration curves, reporting peak area ratio as a function of silylated calystegine concentration, were established between 10 and 200 μg/ml, in the presence of 100 μg/ml of octadecane as internal standard. No calibration curve was performed for calystegine N_1 which was only available in a small amount. In the studied concentration range, linearity was demonstrated with correlation coefficients higher than 0.992 for all the selected compounds (Table 2). The limit of detection (LOD), defined as the lowest concentration of analyte that can be clearly detected, is estimated as three times

Table 2
Regression data for the calibration curves

	Calystegines						
	A_3	A_5	B_1	B_2	B_3	B_4	C_1
Range (μg/ml)	10–200	10–200	10–200	10–200	10–200	10–200	10–200
Line	$y = 0.4944 + 0.0343\ x$	$y = -0.2159 + 0.0195\ x$	$y = -0.2071 + 0.0344\ x$	$y = -0.1795 + 0.0372\ x$	$y = -0.2867 + 0.0364\ x$	$y = -0.3910 + 0.0405\ x$	$y = 0.0574 + 0.0318\ x$
Determination coefficient (r^2)	0.9943	0.9927	0.9927	0.9979	0.9930	0.9942	0.9928
LOD (μg/ml)	2	2	1	1	1	1	1
LOQ (μg/ml)	6	6	3	3	3	3	3

the signal-to-noise ratio. LOD values were 2 μg/ml, for A_3 and A_5 and 1 μg/ml for all other standards giving a limit of quantification (LOQ) values of 6 μg/ml for A_3 and A_5 and 3 μg/ml for all other calystegines (Table 2).

Acknowledgements

The authors are grateful to Dr. N. Asano, Faculty of Pharmaceutical Sciences, Hokuriku University, Kanazawa, Japan for his kind gift of calystegines, and K.B. acknowledges the Swiss Government (Commission Fédérale des Bourses) for the award of a research fellowship during the development of this work.

References

Asano, N., Kato, A., Kizu, H., Matsui, K., Watson, A.A., Nash, R.J., 1996a. Calystegine B_4, a novel trehalase inhibitor from *Scopolia japonica*. Carbohydrate Research 293, 195–204.

Asano, N., Kato, A., Matsui, K., Watson, A.A., Nash, R.J., Molyneux, R.J., Kackett, L., Topping, J., Winchester, B., 1997a. The effects of calystegines isolated from edible fruits and vegetables on mammalian liver glycosidases. Glycobiology 7, 1085–1088.

Asano, N., Kato, A., Miyauchi, M., Kizu, H., Timomori, T., Matsui, K., Nash, R.J., Molyneux, R.J., 1997b. Specific α-glycosidase inhibitors, *N*-methylcalystegines-structure/activity relationships of calystegines from *Lycium chinense*. European Journal of Biochemistry 248, 296–303.

Asano, N., Kato, A., Oseki, K., Kizu, H., Matsui, K., 1995. Calystegins of *Physalis alkekengi* var. *francheti* (Solanaceae), structure determination and their glycosidase inhibitory activities. European Journal of Biochemistry 229, 369–376.

Asano, N., Kato, A., Yokoyama, Y., Miyauchi, M., Yamamoto, M., Kizu, H., Matsui, K., 1996b. Calystegin N_1, a novel nortropane alkaloid with a bridgehead amino group from *Hyoscyamus niger*: Structure determination and glycosidase inhibitory activities. Carbohydrate Research 284, 169–178.

Asano, N., Oseki, K., Tomioka, E., Kizu, H., Matsui, K., 1994a. N-Containing sugars from *Morus alba* and their glycosidase inhibitory activities. Carbohydrate Research 259, 243–255.

Asano, N., Tomioka, E., Kizu, H., Matsui, K., 1994b. Sugars with nitrogen ring isolated from the leaves of *Morus bombycis*. Carbohydrate Research 253, 235–245.

DeJongh, D.C., Radford, T., Hribar, J.D., Hanessian, S., Bieber, M., Dawson, G., Sweeley, C.C., 1969. Analysis of trimethylsilyl derivatives of carbohydrates by gas chromatography and mass spectrometry. Journal of American Chemical Society 91, 1728–1740.

Dräger, B., 1995. Identification and quantification of calystegines, polyhydroxyl nortropane alkaloids. Phytochemical Analysis 6, 31–37.

Dräger, B., Funk, C., Höhler, A., Mrachatz, G., Nahrstedt, A., Portsteffen, A., Schaal, A., Schmidt, R., 1994. Calystegines as a new group of tropane alkaloids in Solanaceae. Plant Cell, Tissue and Organ Culture 38, 235–240.

Dräger, B., van Almsick, A., Mrachatz, G., 1995. Distribution of Calystegines in several Solanaceae. Planta Medica 61, 577–579.

Goldmann, A., Message, B., Tepfer, D., Molyneux, R.J., Duclos, O., Boyer, F.D., Pan, Y.T., Elbein, A.D., 1996. Biological activities of the nortropane alkaloid, calystegine B_2, and analogs: structure-function relationships. Journal of Natural Products 59, 1137–1142.

Goldmann, A., Milat, M.L., Ducrot, P.H., Lallemand, J.Y., Maille, M., Lepingle, A., Charpin, I., Tepfer, D., 1990. Tropane derivatives from *Calystegia sepium*. Phytochemistry 29, 2125–2127.

Griffiths, R.C., Watson, A.A., Kizu, H., Asano, N., Sharp, H.J., Jones, M.G., Wormald, M.R., Fleet, G.W.J., Nash, R.J., 1996. The isolation from *Nicandra physalodes* and identification of the 3-*O*-(-D-glucopyranoside of 1α,2β,3α,6α-tetrahydroxy-nor-tropane (calystegine B_1). Tetrahedron Letters 37, 3207–3208.

Jacob, G.S., 1995. Glycosylation inhibitors in biology and medicine. Current Biology 5, 605–611.

Kato, A., Asano, N., Kizu, H., Matsui, K., Suzuki, S., Arisawa, M., 1997. Calystegine alkaloids from *Duboisia leichhardtii*. Phytochemistry 45, 425–429.

Keiner, R., Dräger, B., 2000. Calystegine distribution in potato tubers and plants. Plant Science 150, 171–179.

Molyneux, R.J., Pan, Y.T., Goldmann, A., Tepfer, D.A., Elbein, A.D., 1993. Calystegins, a novel class of alkaloid glycosidase inhibitors. Archives of Biochemistry and Biophysics 304, 81–88.

Nash, R.J., Rothschild, M., Porter, E.A., Watson, A.A., Waigh, R.D., Waterman, P.G., 1993. Calystegines in *Solanum* and *Datura* species and the death's-head hawk-moth (*Acherontia atropus*). Phytochemistry 34, 1281–1283.

Nash, R.J., Watson, A.A., Asano, N., 1996. Polyhydroxylated alkaloids that inhibit glycosidases. In: Pelletier, S.W. (Ed.), Alkaloids : Chemical and Biological Perspectives, Vol. 11. Pergamon, Oxford, pp. 346–376.

Nash, R.J., Watson, A.A., Winters, A.L., Fleet, G.W.J., Wormad, M.R., Dealler, S., Lees, E., Asano, N., Kizu, H., 1997. Novel biologically-active alkaloids from British plants. Special Publication. Royal Society of Chemistry 200, 106–113.

Schimming, T., Tofern, B., Mann, P., Richter, A., Jennett-Siems, K., Dräger, B., Asano, N., Gupta, M.P., Correra, M.D., Eich, E., 1998. Distribution and taxonomic significance of calystegines in the Convolvulaceae. Phytochemistry 49, 1989–1995.

Tepfer, D.A., Goldman, A., Pamboukdjian, N., Maille, M., Lepingle, A., Chevalier, D., Denarie, J., Rosenberg, C., 1988. A plasmid of *Rhizobium meliloti* 41 encodes catabolism of two compounds from root exudate of *Calystegia sepium*. Journal of Bacteriology 170, 1153–1161.

PERGAMON

Phytochemistry 58 (2001) 463–474

PHYTOCHEMISTRY

www.elsevier.com/locate/phytochem

Semisynthetic derivatives of *ent*-kauranes and their antifeedant activity

Maurizio Bruno[a,*], Sergio Rosselli[a], Ivana Pibiri[a], Franco Piozzi[a,b], Maria Luisa Bondì[b], Monique S.J. Simmonds[c]

[a]*Department of Organic Chemistry, Palermo University, Viale delle Scienze, Parco d'Orleans II, 90128 Palermo, Italy*
[b]*I.C.T.P.N.-C.N.R., via U. La Malfa 153, 90146 Palermo, Italy*
[c]*Jodrell Laboratory, Royal Botanic Gardens, Kew, Richmond, Surrey TW9 3AB, UK*

Received 28 November 2000; received in revised form 9 May 2001

Abstract

Chemical modification of functional groups on linearol yielded several *ent*-kaurane derivatives. These compounds were tested for their antifeedant activity against larvae of *Spodoptera littoralis*. Although linearol did not influence the feeding behaviour of larvae, some of its derivatives showed significant antifeedant activity. © 2001 Elsevier Science Ltd. All rights reserved.

Keywords: Lamiaceae; *ent*-Kaurane; Diterpenoids; Linearol; Chemical modifications; *Spodoptera littoralis*; Antifeedant

1. Introduction

ent-Kauranes are naturally occurring diterpenoids isolated from several families, such as Asteraceae and Lamiaceae. These compounds have attracted interest because of their structures and their biological activities as anti-tumorals, anti-HIV and anti-bacterials (Hanson, 1999).

The genus *Sideritis* (family Lamiaceae) is a rich source (Gonzales et al., 1990) of *ent*-kauranes. In a previous paper we described the isolation and identification (Bondì et al., 2000) of many *ent*-kauranes from several Turkish species of *Sideritis*. In the same paper, the antifeedant activity against larvae of *Spodoptera frugiperda* and *S. littoralis* was described. One of the diterpenes, sideroxol (**1**), isolated from *Sideritis akmanii* and *S. rubriflora* had potent antifeedant activity against *S. frugiperda*.

We were able to isolate large amounts of another *ent*-kaurane, linearol (**2**), from species of *Sideritis* (Bondì et al., 2000). This provided us with enough starting material to plan a structure–activity study in which we would modify the different functional groups on the *ent*-kaurane skeleton to evaluate their importance in the antifeedant activity of these compounds.

2. Results and discussion

Linearol (**2**), possessing an exocyclic double bond between carbons 16 and 17, was subjected to catalytic hydrogenation on 10% Pd/C. The reduction that diastereoselectively happened from the sterically less congested side (Piozzi et al., 1971), yielded a mixture of two compounds. After separation, the less polar compound was identified as 16-α-H dihydrolinearol (**3**); the second one (**4**), surprisingly was the transacetylated product of the former, in which the acetyl group migrated from position 18 to position 3.

Since the antifeedant sideroxol (**1**) had an epoxy group we performed an epoxidation on the double bond of linearol. Treatment with 3-chloroperbenzoic acid (MCPBA) in CH_2Cl_2 allowed us to generate, diastereoselectively, the epoxy ring (Piozzi et al., 1973; Gonzales et al., 1990). Also in this case, as described before, we obtained two compounds: epoxylinearol (**5**) and the 18→3 transacetylated product (**6**). Both **5** and **6** were subjected to acetylation to give the same triacetylderivative (**7**).

Next, in order to remove the exocyclic double bond we performed an ozonolysis. Treatment of **2** with ozone

* Corresponding author. Tel.: +39-091-596905; fax: +39-091-596825.
E-mail address: bruno@dicpm.unipa.it (M. Bruno).

0031-9422/01/$ - see front matter © 2001 Elsevier Science Ltd. All rights reserved.
PII: S0031-9422(01)00252-7

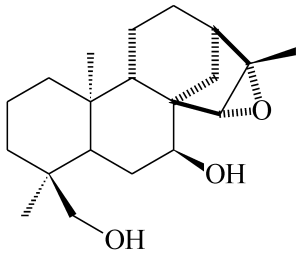

1

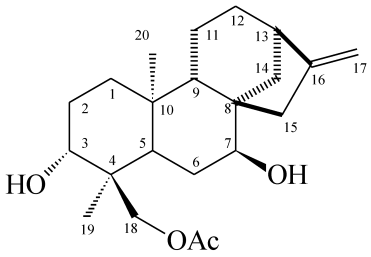

2

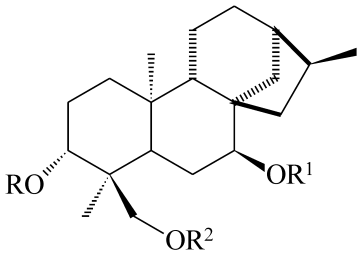

	R	R^1	R^2
3	H	H	Ac
4	Ac	H	H

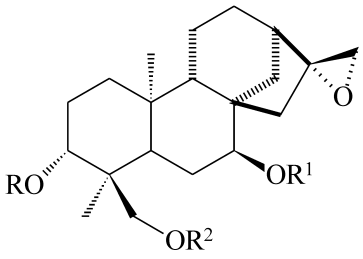

	R	R^1	R^2
5	H	H	Ac
6	Ac	H	H
7	Ac	Ac	Ac

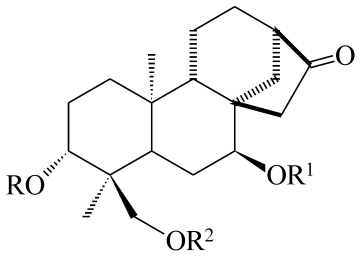

8 R = R^1 = H R^2 = Ac

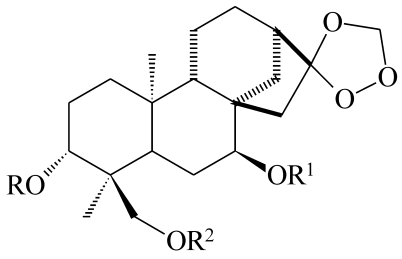

9 R = R^1 = H R^2 = Ac

in CH_2Cl_2 resulted in a mixture of two products. One of them was the expected ketone (**8**), the other one showed in ^{1}H NMR spectrum a signal at δ 5.01 (*br s*, 2H) for acetalic protons and in ^{13}C NMR spectrum two signals at ppm 116.0 (*s*) and 93.2 (*t*) for two carbons bearing two oxygens. Therefore this compound was assigned the structure of ozonide (**9**). Furthermore, **9** was transformed to ketone (**8**) by reduction with Zn/AcOH. Isolation of ozonides is not common, due to their instability; in fact, we could not store **9** as after a few hours it started to decompose.

The composition of ester moieties on neoclerodane diterpenoids influences their antifeedant activity (Rodríguez et al., 1999). Therefore, to evaluate the effect of different esters on the activity of *ent*-kauranes, esterification reactions were undertaken on the two free hydroxyl groups of linearol.

Treatment of linearol with propanoyl chloride, triethylamine (TEA), 4-dimethylaminopyridine (DMAP) in CH_2Cl_2 gave 3,7-dipropanoate ester (**10**) and a mono esterified derivative. The ^{1}H and ^{13}C NMR spectra of the latter compound showed signals at δ 3.60 (*t*, J = 3.8 Hz, H-7) and at δ 4.86 (*dd*, J = 11.2 and 5.2 Hz, H-3) and ppm 76.7 (*d*, C-7) and 74.2 (*d*, C-3), clearly indicating that only 3-OH was esterified; therefore, we assigned to it structure (**11**). Similarly, we prepared

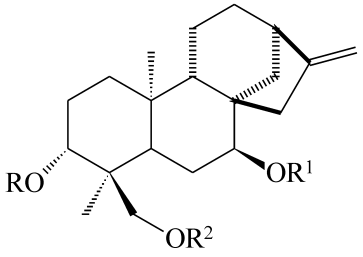

	R	R^1	R^2
10	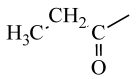	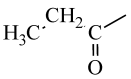	Ac
11	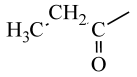	H	Ac
12	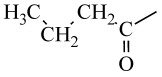	H	Ac
13	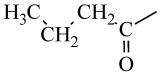	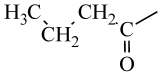	Ac
14	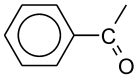	H	Ac
15	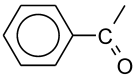	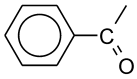	Ac
16	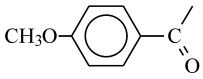	H	Ac
17	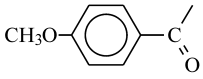	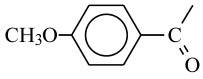	Ac
18	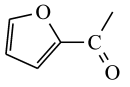	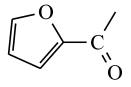	Ac
19	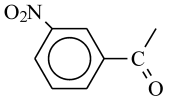	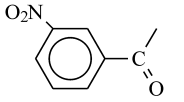	Ac
20	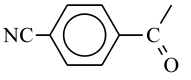	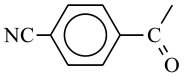	Ac
21	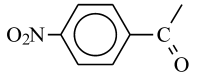	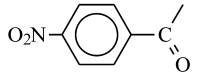	Ac
22	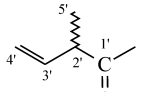	H	Ac
25	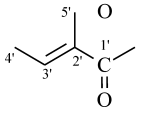	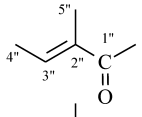	Ac
26	Ac	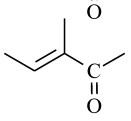	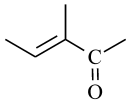

3-mono- and 3,7-diester derivatives (**12**), (**13**), (**14**), (**15**), (**16**) and (**17**) using different acyl chlorides such as butanoyl, benzoyl and 4-methoxybenzoyl chlorides. The same reactions performed with 2-furoyl chloride, 3-nitrobenzoyl chloride, 4-cyanobenzoyl chloride and 4-nitrobenzoyl chloride allowed us to isolate compounds (**18**), (**19**), (**20**) and (**21**) in which both hydroxyl groups were esterified. Monoacyl derivatives were not obtained.

Acylation of linearol with tigloyl chloride was not an easy transformation. In fact, treatment of **2** with tiglic acid chloride, TEA, DMAP in CH_2Cl_2 gave an inseparable mixture of two compounds. The ^1H and ^{13}C NMR spectra showed that esterification was achieved only in position 3 (δ_H 4.86 *dd*, H-3; δ_C 74.3 *d*/74.4 *d* C-3) and that the ester moiety was the $\Delta_{3'\text{-}4'}$ isomer of tiglate (δ_C 137.2 *d*/137.1 *d*, C-3′; 115.9 *t*/115.7 *t*, C-4′). There-

fore, compound (**22**) was an epimeric mixture at C-2′ due to the formation of a stereogenic center, a consequence of isomerization. Isomerization of a tigloyl moiety has been already observed by other authors (Hatakeyama et al., 1985).

A different behaviour was observed when linearol and tigloyl chloride were refluxed in toluene for 30 min. In this case an inseparable mixture of di-tiglates (**23**) and (**24**) was obtained, in which the double bond between carbons 16 and 17 was hydrated to give a tertiary hydroxyl group in C-16 (δ_H 1.35, CH_3-17; δ_C 78.6 *s*/78.7 *s*, C-16, 24.3 *q*, C-17). Compound (**23**) was an isomer of **24** in which the acetyl group migrated to position 3 and the tiglic ester was at position 18. Finally, by refluxing linearol, TEA and tigloyl chloride in toluene for 24 h two compounds were isolated. The more polar one was identified as 3,7-ditigloyl-linearol (**25**); the other one (**26**) was the transesterification isomer of the former with the tigloyl moiety in position 18 and the acetyl in position 3.

3. Biological activity

The effects of compounds (**2**–**8**, **10**, **11**, **13**–**22**, **25**–**26**) on the feeding behaviour of larvae of *S. littoralis* are reported in Table 2. Linearol did not influence the feeding behaviour of *S. littoralis*. However, modification to the substitutions on the molecule resulted in a range of analogue esters that differ in their activity when tested at 100 ppm. We selected this dose to allow us to better discriminate among the effects of different substances although, in our experience, many diterpenes show activity at 1000 ppm.

Compounds with a ketone or epoxide group had significant antifeedant activity except for **7**. Modification to the substitutions at R (C-3), R^1 (C-7) or R^2 (C-18) altered the activity of the compounds but there were no clear trends in structure–activity relationship. For example, increasing the length of the substitution at R (**11** vs. **22**), when the substitutes at R^1 and R^2 did not change, resulted in an increase in antifeedant activity. However, the activity of compounds varied when similar substitutes were added to both R and R^1, while R^2 was an acetyl group. Of the compounds tested, **26** was the most active; this was the only compound in which the substitution at R^2 was neither an hydroxy nor an acetyl group. This suggests that the composition and position of the functional groups at C-3, C-7 and C-18 modulate the activity of the compound. This is supported by previous research into the antifeedant activity of *neo*-clerodanes from *Teucrium* (Simmonds et al., 1989; Simmonds and Blaney, 1992), *Scutellaria* (Cole et al., 1990) or *Salvia* (Simmonds et al., 1996). Whilst there appears to be no clear structure–activity relationship the

Table 1a
^{13}C NMR spectral data of compounds[a]

C	2	3	4	5	6	7	8	9
1	38.2, *t*	38.4, *t*	38.4, *t*	38.3, *t** [b]	38.0, *t**	37.5, *t**	37.9, *t*	37.8, *t*
2	26.0, *t*	26.4, *t*	23.4, *t*	26.4, *t*	23.3, *t*	22.7, *t*	26.2, *t**	26.1, *t**
3	71.5, *d*	72.3, *d*	74.5, *d*	72.1, *d*	74.4, *d*	73.5, *d*	71.7, *d*	71.8, *d*
4	41.2, *s*	41.8, *s*	41.6, *s*	41.8, *s*	41.6, *s*	40.1, *s*	41.5, *s*	41.4, *s*
5	37.9, *d*	38.2, *d*	37.3, *d*	38.1, *d*	37.2, *d*	39.4, *d*	37.7, *d*	37.8, *d*
6	26.9, *t*	27.2, *t*	26.5, *t*	27.4, *t*	26.6, *t*	23.9, *t*	26.4, *t**	26.7, *t**
7	76.3, *d*	77.1, *d*	77.0, *d*	76.6, *d*	76.5, *d*	78.9, *d*	75.8, *d*	76.1, *d*
8	47.6, *s*	48.5, *s*	48.5, *s*	49.0, *s*	49.1, *s*	47.5, *s*	46.2, *s*	46.6, *s*
9	49.9, *d*	51.4, *d*	51.5, *d*	50.1, *d*	49.7, *d*	49.9, *d*	49.0, *d*	50.0, *d*
10	38.4, *s*	38.7, *s*	38.4, *s*	38.8, *s*	38.5, *s*	38.4, *s*	38.7, *s*	38.5, *s*
11	17.5, *t*	18.3, *t*	18.3, *t*	18.9, *t*	18.9, *t*	18.6, *t*	17.9, *t*	17.3, *t*
12	33.2, *t*	26.3, *t*	26.3, *t*	29.3, *t*	29.4, *t*	28.9, *t*	29.6, *t*	25.6, *t*
13	43.4, *d*	39.5, *d*	39.5, *d*	42.4, *d*	42.5, *d*	42.1, *d*	47.3, *d*	43.3, *d*
14	38.0, *t*	39.8, *t*	39.8, *t*	37.2, *t**	37.1, *t**	36.8, *t**	35.5, *t*	35.9, *t*
15	44.7, *t*	44.4, *t*	44.3, *t*	45.0, *t*	44.9, *t*	44.7, *t*	51.3, *t*	46.5, *t*
16	154.9, *s*	34.4, *d*	34.4, *d*	66.2, *s*	66.3, *s*	65.5, *s*	222.2, *s*	116.0, *s*
17	103.0, *t*	15.6, *q*	15.6, *q*	50.3, *t*	50.3, *t*	50.5, *t*		93.2, *t*
18	65.8, *t*	66.1, *t*	64.2, *t*	65.9, *t*	63.8, *t*	64.6, *t*	65.7, *t*	65.8, *t*
19	11.9, *q*	11.8, *q*	12.7, *q*	11.9, *q*	12.9, *q*	12.7, *q*	11.8, *q*	11.7, *q*
20	17.6, *q*	18.1, *q*	18.1, *q*	18.2, *q*	18.2, *q*	18.0, *q*	18.2, *q*	17.8, *q*
OAc	172.2, *s*	171.8, *s*	171.7, *s*	171.8, *s*	171.8, *s*	170.4, *s*	171.8, *s*	171.8, *s*
	20.5, *q*	21.1, *q*	21.2, *q*	21.1, *q*	21.2, *q*	20.9, *q*	21.0, *q*	21.0, *q*
						170.3, *s*		
						20.9, *q*		
						169.8, *s*		
						20.7, *q*		

[a] $CDCl_3$ solution.
[b] *, These assignments may be reversed.

data from *neo*-clerodanes suggests that the composition of the substitution at C-4 (C-18) is important. Many of the *neo*-clerodanes with potent antifeedant activity have an epoxide substitution at C-4 but, to date, no *ent*-kauranes with an epoxide at this position have been tested for antifeedant activity against *S. littoralis*. However, sideroxol, one of the most potent *ent*-kaurane diterpenoids tested for antifeedant activity in the binary choice assay used in this study, has an epoxide at C-15–C-16. Although this compound showed potent antifeedant activity, this was against larvae of *Spodoptera frugiperda* (Feeding Index = 54 (4.3), $P < 0.05$) not *S. littoralis* (Feeding Index = 9 (15.9), (Bondì et al., 2000). In the present study no compounds had the C-15–C16 epoxide present in sideroxol, but the two compounds with an epoxide at C-16 (**5** and **6**) had antifeedant feeding activity against *S. littoralis* (Table 2). However, the antifeedant activity of the *ent*-kauranes cannot be totally determined by the presence of an epoxide, as other active antifeedant compounds (**8**, **14**, **18**, **20**, **21** and **26**) lacked this group. Whether the presence of a C-15–C-16 epoxide or addition of an epoxide at C-4 would enhance the activity of the *ent*-kaurenes justifies investigation.

A comparison of the activity of compounds **25** with **26**, the most potent antifeedant in the present study, illustrates how altering the position of substitutions on the molecule can alter its potency. For example, exchange of the acetyl group at C-18 (**25**) with the tigloyl group at C-3 (**26**) resulted in a significant increase in antifeedant activity. This would suggest that the position of these groups influence the ability of the molecule to stimulate receptors on the taste neurones of *S. littoralis*. The position of these groups alters the polarity of the molecule, as compound **26** is less polar

Table 1b
^{13}C NMR spectral data of compounds[a]

C	10	11	12	13	14	15	16	17	18
1	38.1, *t** [b]	38.4, *t**	38.4, *t**	38.1, *t**	38.3, *t**	37.8, *t**	38.3, *t**	38.0, *t*	37.7, *t**
2	23.0, *t*	23.0, *t*	23.0, *t*	23.1, *t*	23.0, *t*	22.9, *t*	23.1, *t*	23.1, *t*	23.0, *t*
3	73.5, *d*	74.2, *d*	74.1, *d*	73.5, *d*	75.1, *d*	74.2, *d*	74.7, *d*	74.0, *d*	74.3, *d*
4	40.4, *s*	40.5, *s*	40.5, *s*	40.4, *s*	40.7, *s*	40.3, *s*	40.7, *s*	40.3, *s*	40.2, *s*
5	39.8, *d*	38.0, *d*	38.0, *d*	39.9, *d*	38.1, *d*	39.4, *d*	38.1, *d*	39.6, *d*	39.2, *d*
6	24.3, *t*	27.0, *t*	27.0, *t*	24.4, *t*	27.0, *t*	23.9, *t*	27.0, *t*	24.1, *t*	23.9, *t*
7	78.9, *d*	76.7, *d*	76.6, *d*	78.8, *d*	76.5, *d*	79.7, *d*	76.5, *d*	79.4, *d*	79.9, *d*
8	46.8, *s*	47.9, *s*	47.9, *s*	46.8, *s*	47.9, *s*	47.0, *s*	47.9, *s*	47.1, *s*	46.7, *s*
9	50.9, *d*	50.0, *d*	50.0, *d*	51.0, *d*	49.9, *d*	51.3, *d*	50.0, *d*	51.4, *d*	50.8, *d*
10	38.6, *s*	38.6, *s*	38.6, *s*	38.7, *s*	38.6, *s*	38.5, *s*	38.6, *s*	38.6, *s*	38.4, *s*
11	17.7, *t*	17.8, *t*	17.8, *t*	17.8, *t*	17.8, *t*	17.8, *t*	17.8, *t*	17.9, *t*	17.7, *t*
12	33.2, *t*	33.5, *t*	33.5, *t*	33.3, *t*	33.4, *t*	33.1, *t*	33.4, *t*	33.2, *t*	33.0, *t*
13	43.5, *d*	43.5, *d*	43.6, *d*	43.5, *d*	43.5, *d*	43.3, *d*	43.5, *d*	43.4, *d*	43.2, *d*
14	37.7, *t**	37.7, *t**	37.7, *t**	37.7, *t**	37.7, *t**	37.7, *t**	37.7, *t**	38.0, *t*	37.6, *t**
15	44.9, *t*	44.9, *t*	45.0, *t*	45.0, *t*	44.9, *t*	45.1, *t*	44.9, *t*	45.3, *t*	45.0, *t*
16	154.0, *s*	154.8, *s*	154.8, *s*	154.1, *s*	154.7, *s*	153.6, *s*	154.8, *s*	153.9, *s*	153.6, *s*
17	103.8, *t*	103.6, *t*	103.6, *t*	103.9, *t*	103.5, *t*	103.9, *t*	103.5, *t*	103.9, *t*	103.8, *t*
18	65.0, *t*	64.6, *t*	64.7, *t*	65.2, *t*	65.0, *t*	64.6, *t*	65.0, *t*	64.8, *t*	64.5, *t*
19	12.9, *q*	13.0, *q*	13.0, *q*	12.9, *q*	13.2, *q*	13.1, *q*	13.2, *q*	13.3, *q*	12.9, *q*
20	18.0, *q*	17.8, *q*	17.8, *q*	18.0, *q*	17.8, *q*	17.8, *q*	17.8, *q*	17.9, *q*	17.7, *q*
OAc	170.5, *s*	171.5, *s*	171.4, *s*	170.5, *s*	171.4, *s*	170.5, *s*	171.5, *s*	170.7, *s*	170.4, *s*
	20.8, *q*	21.1, *q*	21.1, *q*	20.9, *q*	21.0, *q*	19.2, *q*	21.0, *q*	19.6, *q*	19.5, *q*
C=O′					165.7, *s*	165.6, *s*	165.5, *s*	165.5, *s*	157.9, *s*
C=O″						165.1, *s*		165.1, *s*	157.6, *s*
1′	173.8, *s*	173.8, *s*	173.0, *s*	173.1, *s*	130.5, *s*	130.6, *s*	123.0, *s*	123.1, *s*	
2′	27.9, *t*	27.9, *t*	36.6, *t*	36.7, *t*	129.4, *d*	129.4, *d*	131.4, *d*	131.5, *d*	144.7, *s*
3′	9.2, *q*	9.2, *q*	18.5, *t*	18.5, *t*	128.2, *d*	128.3, *d*	113.5, *d*	113.7, *d*	117.5, *d*
4′			13.6, *q*	13.8, *q*	132.8, *d*	132.8, *d*	163.2, *s*	163.3, *s*	111.7, *d*
5′					128.2, *d*	128.3, *d*	113.5, *d*	113.7, *d*	146.1, *d*
6′					129.4, *d*	129.4, *d*	131.4, *d*	131.5, *d*	
1″	173.5, *s*			172.8, *s*		130.3, *s*		122.8, *s*	
2″	27.9, *t*			36.5, *t*		129.3, *d*		131.4, *d*	144.5, *s*
3″	9.1, *q*			18.5, *t*		128.1, *d*		113.5, *d*	117.5, *d*
4″				13.7, *q*		132.7, *d*		163.2, *s*	111.5, *d*
5″						128.1, *d*		113.5, *d*	145.9, *d*
6″						129.3, *d*		131.4, *d*	
OCH_3'							55.3, *q*	55.4, *q*	
OCH_3''								55.3, *q*	

[a] $CDCl_3$ solution.
[b] *, These assignments may be reversed.

than **25**. Thus, whether changes in the polarity of the compound rather than the position or composition of specific functional groups on the molecule influence activity is not known.

To test the effect of compounds on insect feeding we usually test compounds dry on an inert substrate (glass–fibre discs). This avoids interactions between the test compound and compounds in leaf material but it also avoids problems associated with having to apply solvents to the insect mouth parts that we know could themselves modulate feeding by damaging insect taste neurones, such as high concentrations of ethanol. In our bioassay we apply a set aliquot (100 μl) of test compounds to the discs and always start with a dose of 100 ppm. The test compound is dissolved in an appropriate solvent, which will differ among compounds. An aliquot (100 μl) of the solvent is also applied to the control discs. The discs are dried before being presented to the insect. Although this type of bioassay is only suitable for a range of lepidopteran larvae and locusts it does enable us to provide quantitative comparative data about the potency of compounds for use in structure–activity relationship studies. However, the influence that compounds have on the acceptance or rejection of the discs by insects could depend on their solubility in the saliva produced during feeding or in the fluid that bathes their taste receptors. The composition of these fluids could be modified by the diet the insects are reared on, which is why we try and standardise the diet fed to our insects (Simmonds et al., 1992). As yet we known very little about the role these fluids have in modulating the ability of insects to detect compounds in their food and thus feeding behaviour of leaf chewing insects (Chapman and de Boer, 1995).

Table 1c
^{13}C NMR spectral data of compounds[a]

C	**19**	**20**	**21**	**22A >**	**22B <**	**23 >**	**24 <**	**25**	**26**
1	37.9, *t** [b]	37.7, *t**	38.0, *t**	38.3, *t**	38.3, *t**	37.8, *t*	37.8, *t*	38.0, *t**	38.1, *t**
2	22.8, *t*	22.7, *t*	23.0, *t*	22.9, *t*	22.8, *t*	22.9, *t*	22.9, *t*	23.1, *t*	23.1, *t*
3	75.3, *d*	75.0, *d*	75.5, *d*	74.3, *d*	74.4, *d*	74.2, *d*	73.7, *d*	73.9, *d*	74.4, *d*
4	40.5, *s*	40.3, *s*	40.6, *s*	40.7, *s*	40.6, *s*	40.3, *s*	40.3, *s*	40.5, *s*	40.5, *s*
5	39.7, *d*	39.5, *d*	39.9, *d*	38.0, *d*	38.0, *d*	39.9, *d*	39.5, *d*	39.7, *d*	40.2, *d*
6	23.9, *t*	23.7, *t*	24.0, *t*	26.9, *t*	26.9, *t*	24.1, *t*	23.9, *t*	24.1, *t*	24.3, *t*
7	81.2, *d*	80.9, *d*	81.4, *d*	76.6, *d*	76.6, *d*	79.7, *d*	79.4, *d*	79.2, *d*	79.4, *d*
8	46.8, *s*	46.7, *s*	47.0, *s*	47.9, *s*	47.9, *s*	48.0, *s*	47.9, *s*	47.1, *s*	47.2, *s*
9	51.3, *d*	51.1, *d*	51.5, *d*	50.0, *d*	50.0, *d*	48.3, *d*	48.3, *d*	51.3, *d*	51.3, *d*
10	38.5, *s*	38.4, *s*	38.6, *s*	38.6, *s*	38.6, *s*	38.5, *s*	38.5, *s*	38.7, *s*	38.7, *s*
11	17.8, *t*	17.6, *t*	17.9, *t*	17.8, *t*	17.8, *t*	17.6, *t*	17.6, *t*	17.9, *t*	17.9, *t*
12	33.0, *t*	32.9, *t*	33.1, *t*	33.4, *t*	33.4, *t*	26.8, *t*	26.8, *t*	33.3, *t*	33.3, *t*
13	43.2, *d*	43.0, *d*	43.3, *d*	43.5, *d*	43.5, *d*	51.9, *d*	51.9, *d*	43.5, *d*	43.5, *d*
14	37.6, *t**	37.5, *t**	37.8, *t**	37.6, *t**	37.6, *t**	35.9, *t*	35.8, *t*	37.9, *t**	37.9, *t**
15	45.1, *t*	45.0, *t*	45.2, *t*	44.9, *t*	44.9, *t*	54.2, *t*	54.2, *t*	45.3, *t*	45.3, *t*
16	153.2, *s*	153.1, *s*	153.2, *s*	154.8, *s*	154.8, *s*	78.6, *s*	78.7, *s*	154.1, *s*	154.1, *s*
17	104.1, *t*	104.0, *t*	104.3, *t*	103.6, *t*	103.6, *t*	24.3, *q*	24.3, *q*	103.8, *t*	103.8, *t*
18	64.5, *t*	64.3, *t*	64.7, *t*	64.5, *t*	64.6, *t*	65.1, *t*	65.0, *t*	65.2, *t*	65.3, *t*
19	13.0, *q*	12.9, *q*	13.1, *q*	13.0, *q*	13.0, *q*	12.8, *q*	13.1, *q*	13.2, *q*	12.9, *q*
20	17.8, *q*	17.6, *q*	17.9, *q*	17.8, *q*	17.8, *q*	18.2, *q*	18.1, *q*	18.0, *q*	18.1, *q*
OAc	170.0, *s*	169.9, *s*	170.1, *s*	171.4, *s*	171.4, *s*	170.5, *s*	170.7, *s*	170.7, *s*	170.5, *s*
	19.5, *q*	19.4, *q*	19.7, *q*	21.1, *q*	21.1, *q*	21.1, *q*	20.2, *q*	20.3, *q*	21.1, *q*
′C=O	163.5, *s*	163.9, *s*	163.9, *s*						
″C=O	163.1, *s*	163.4, *s*	163.5, *s*						
1′	132.3, *s*	134.2, *s*	136.0, *s*	173.6, *s*	173.7, *s*	166.7, *s*	167.3, *s*	167.4, *s*	167.0, *s*
2′	124.2, *d*	129.8, *d*	130.6, *d*	44.1, *d*	43.9, *d*	128.5, *s*	128.8, *s*	128.9, *s*	128.6, *s*
3′	148.2, *s*	132.1, *d*	123.6, *d*	137.2, *d*	137.1, *d*	136.2, *d*	137.0, *d*	136.8, *d*	136.3, *d*
4′	127.3, *d*	116.2, *s*	150.5, *s*	115.9, *t*	115.7, *t*	12.0, *q*	12.1, *q*	12.2, *q*	12.1, *q*
5′	129.7, *d*	132.1, *d*	123.6, *d*	16.5, *q*	16.7, *q*	14.3, *q*	14.3, *q*	14.3, *q*	14.3, *q*
6′	134.9, *d*	129.8, *d*	130.6, *d*						
1″	132.0, *s*	133.9, *s*	135.7, *s*			167.0, *s*	167.5, *s*	167.7, *s*	167.6, *s*
2″	124.2, *d*	129.7, *d*	130.5, *d*			129.0, *s*	129.1, *s*	129.2, *s*	129.2, *s*
3″	148.0, *s*	131.9, *d*	123.4, *d*			136.5, *d*	136.7, *d*	136.6, *d*	136.6, *d*
4″	127.1, *d*	116.0, *s*	150.4, *s*			12.0, *q*	12.1, *q*	12.0, *q*	12.0, *q*
5″	129.5, *d*	131.9, *d*	123.4, *d*			14.3, *q*	14.3, *q*	14.3, *q*	14.3, *q*
6″	134.9, *d*	129.7, *d*	130.5, *d*						
CN′		117.6, *s*							
CN″		117.5, *s*							

[a] $CDCl_3$ solution.
[b] *, These assignments may be reversed.

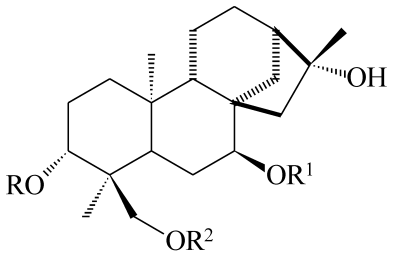

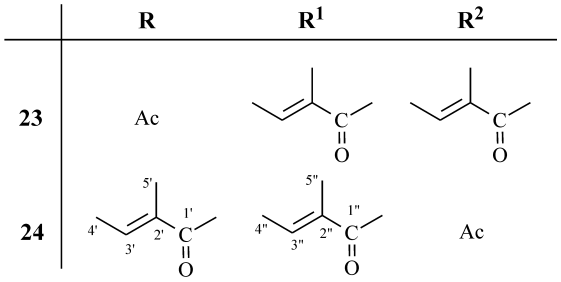

Table 2
Effect of compounds (100 ppm) on the feeding behaviour of final stadium larvae of *Spodoptera littoralis* ($n = 10$–15)

Compound	Feeding Index[a]	
	Mean	(SEM)
2	6.8	(12.91)
3	−9.4	(10.22)
4	19.5	(21.34)
5	39.0	(19.06)*
6	47.7	(25.06)*
7	22.6	(12.76)
8	42.4	(18.88)*
10	−37.5	(18.64)$^{\#}$
11	−1.6	(18.93)
13	0.0	(29.81)
14	27.7	(11.76)*
15	23.4	(12.54)
16	22.0	(14.07)
17	−6.0	(12.27)
18	48.3	(19.57)*
19	21.5	(13.32)
20	44.6	(11.55)*
21	34.0	(17.82)*
22	36.6	(25.91)
25	−15.5	(8.21)
26	74.1	(12.93)**

[a] Feeding Index ((C−T)/(C+T))%; significant antifeedant activity *$P < 0.05$, **$P < 0.01$; significant phagostimulant activity $^{\#}P < 0.05$, Wilcoxon matched-pairs test.

Despite these limitations in our knowledge the present study has shown that *ent*-kauranes can have potent antifeedant activity in a binary choice bioassay. For example, compound **26** at 100 ppm has elicited a higher Feeding Index than ajugarin I (Feeding Index = 43 (7.3), Simmonds et al., 1989) but not a high as Jodrellin B (Feeding Index = 100 (0.0), Cole et al., 1990) against *S. littoralis*. Further research is required to understand the molecular mechanism associated with the observed behavioural responses to these and other diterpenoids and whether different species of insects will show similar behavioural responses to these compounds.

4. Experimental

4.1. General experimental procedures

IR spectra (film) were registred on a Shimadzu FT–IR 8300 spectrophotometer. ^{1}H NMR spectra were recorded in $CDCl_3$ solution using a Bruker AC 250 E apparatus at 250 MHz and chemical shifts were reported with respect to residual $CHCl_3$ (δ 7.27). ^{13}C NMR spectra were recorded in $CDCl_3$ on the same apparatus at 62.7 MHz and chemical shifts were reported with respect to solvent signals (δ_{CDCl_3} 77.0). ^{13}C NMR assignments were determined by DEPT spectra. MS were recorded on a Finnigan TSQ70 instrument (70 eV, direct inlet). Melting points were determined on a Kofler block and are uncorrected. Merck Si gel no. 7734 (70–230 mesh) deactivated with 15% H_2O wt./v was used for column chromatography. An ozone generator Fischer 500 M has been used to perform ozonolysis. Linearol was isolated from the following species: *Sideritis akmanii, S. niveotomentosa, S. brevidens, S. rubriflora* and *S. gulendamii* (Bondì et al., 2000).

CH_2Cl_2 was dried by distillation over calcium hydride. Toluene was dried by distillation over molecular sieves (3 Å).

4.2. Reduction of linearol (2) to compounds 3 and 4

To a solution of **2** (50 mg) in MeOH (20 ml) was added Pd/C 10% (30 mg). This solution was subjected to a H_2 pressure (3 atm) in a Parr apparatus for 24 h. After filtration, the solvent was evaporated to give a mixture which was resolved by CC (silica gel, petrol–EtOAc 3:2 as eluent) yielding compound **3** (34 mg) and **4** (14 mg) in order of increasing polarity.

Compound **3**: amorphous solid. IR ν_{max} (film) cm^{-1}: 3423, 2970, 2930, 2840, 1712, 1438, 1373, 1255, 1172, 1039, 1018, 979. EI–MS *m/z* (rel. int.): 364 $[M]^+$ (1), 346 $[M–H_2O]^+$ (5), 328 $[M–2(H_2O)]^+$ (14), 304 $[M–AcOH]^+$ (20), 286 $[M–AcOH–H_2O]^+$ (56), 268 $[M–AcOH–2(H_2O)]^+$ (100), 255 (42), 235 (83), 217 (36). ^{1}H NMR ($CDCl_3$): δ 3.52 (*dd*, 1H, $J = 9.0$ and 5.4 Hz, H-3β), 3.59 (*t*, 1H, $J = 3.0$ Hz, H-7α), 1.01 (*d*, 3H, $J = 6.4$ Hz, Me-17), 4.07 (*d*, 1H, $J = 11.6$ Hz, H_A-18), 3.96 (*d*, 1H, $J = 11.6$ Hz, H_B-18), 0.75 (*s*, 3H, Me-19), 1.05 (*s*, 3H, Me-20), 2.09 (*s*, 3H, OAc). ^{13}C NMR: Table 1a.

Compound **4**: amorphous solid. IR ν_{max} (film) cm^{-1}: 3430, 2970, 2930, 2840, 1715, 1438, 1373, 1258, 1170, 1036, 1020, 985. EI–MS *m/z* (rel. int.): $[M]^+$ absent, 346 $[M–H_2O]^+$ (2), 328 $[M–2(H_2O)]^+$ (2), 304 $[M–AcOH]^+$

(4), 286 $[M–AcOH–H_2O]^+$ (10), 268 $[M–AcOH–2(H_2O)]^+$ (10), 255 (100), 241 (30), 213 (21). ^1H NMR ($CDCl_3$): δ 4.91 (*dd*, 1H, $J=11.2$ and 5.4 Hz, H-3β), 3.60 (*t*, 1H, $J=3.0$ Hz, H-7α), 1.01 (*d*, 3H, $J=6.4$ Hz, Me-17), 3.33 (*d*, 1H, $J=12.4$ Hz, H_A-18), 2.99 (*d*, 1H, $J=12.4$ Hz, H_B-18), 0.67 (*s*, 3H, Me-19), 1.08 (*s*, 3H, Me-20), 2.07 (*s*, 3H, OAc). ^{13}C NMR: Table 1a.

4.3. Epoxidation of linearol (2) to compounds (5) and (6)

To a solution of **2** (250 mg) in CH_2Cl_2 (15 ml) was added MCPBA 70% (170 mg). After stirring overnight, the solution was extracted with a saturated aqueous solution of $NaHCO_3$ (3×10 ml) and washed with H_2O (3×10 ml). The organic layer was dried with dry Na_2SO_4 and evaporated under reduced pressure giving a residue which was purified by CC (silica gel, diethyl ether as eluent) yielding compounds **5** (140 mg) and **6** (92 mg).

Compound **5**: amorphous solid. IR ν_{max} (film) cm^{-1}: 3480, 3267, 3040, 2931, 2866, 1714, 1384, 1371, 1255, 1049, 1018. EI–MS *m/z* (rel. int.): 378 $[M]^+$ (1), 360 $[M–H_2O]^+$ (5), 318 $[M–AcOH]^+$ (36), 300 $[M–H_2O–AcOH]^+$ (55), 282 $[M–AcOH–2(H_2O)]^+$ (97), 270 (100), 249 (96), 231 (41), 121 (85). ^1H NMR ($CDCl_3$): δ 3.54 (*dd*, 1H, $J=9.0$ and 5.2 Hz, H-3β), 3.73 (*t*, 1H, $J=3.8$ Hz, H-7α), 2.91 (*d*, 1H, $J=4.5$ Hz, H_A-17), 2.82 (*d*, 1H, $J=4.5$ Hz, H_B-17), 4.06 (*d*, 1H, $J=11.8$ Hz, H_A-18), 3.99 (*d*, 1H, $J=11.8$ Hz, H_B-18), 0.77 (*s*, 3H, Me-19), 1.08 (*s*, 3H, Me-20), 2.08 (*s*, 3H, OAc). ^{13}C NMR: Table 1a.

Compound **6**: amorphous solid. IR ν_{max} (film) cm^{-1}: 3388, 3040, 2933, 2868, 1724, 1369, 1250, 1053, 1024, 1004, 953, 736. EI–MS *m/z* (rel. int.): 378 $[M]^+$ (1), 360 $[M–H_2O]^+$ (2), 318 $[M–AcOH]^+$ (4), 300 $[M–AcOH–H_2O]^+$ (12), 282 $[M–AcOH–2(H_2O)]^+$ (22), 270 (100), 255 (40), 213 (11), 182 (12), 159 (12), 145 (19), 119 (22). ^1H NMR ($CDCl_3$): δ 4.90 (*dd*, 1H, $J=11.2$ and 5.2 Hz, H-3β), 3.72 (*t*, 1H, $J=3.8$ Hz, H-7α), 2.91 (*d*, 1H, $J=4.6$ Hz, H_A-17), 2.79 (*d*, 1H, $J=4.6$ Hz, H_B-17), 3.29 (*d*, 1H, $J=12.6$ Hz, H_A-18), 2.96 (*d*, 1H, $J=12.6$ Hz, H_B-18), 0.67 (*s*, 3H, Me-19), 1.07 (*s*, 3H, Me-20), 2.05 (*s*, 3H, OAc). ^{13}C NMR: Table 1a.

4.4. Acetylation of compounds 5 and 6

Fifty milligrams of compounds **5** and **6** were treated separately with 5 ml of a mixture of pyridine–acetic anhydride (3:2) yielding, after evaporation under reduced pressure, the same compound **7** (98% yield).

Compound **7**: amorphous solid. IR ν_{max} (film) cm^{-1}: 3040, 2939, 2868, 1734, 1732, 1371, 1246, 1030, 962, 902, 734. EI–MS *m/z* (rel. int.): 462 $[M]^+$ (1), 402 $[M–AcOH]^+$ (2), 342 $[M–2(AcOH)]^+$ (5), 329 (2), 300 (2), 282 $[M–3(AcOH)]^+$ (23), 269 (10), 119 (8), 95 (12), 43 (100). ^1H NMR ($CDCl_3$): δ 4.65 (*dd*, 1H, $J=11.2$ and 5.2 Hz, H-3β), 4.79 (*t*, 1H, $J=3.8$ Hz, H-7α), 2.80 (*d*, 1H, $J=4.5$ Hz, H_A-17), 2.72 (*d*, 1H, $J=4.5$ Hz, H_B-17), 3.84 (*d*, 1H, $J=11.9$ Hz, H_A-18), 3.44 (*d*, 1H, $J=11.9$ Hz, H_B-18), 0.75 (*s*, 3H, Me-19), 1.04 (*s*, 3H, Me-20), 1.95 (*s*, 3H, OAc), 1.94 (*s*, 3H, OAc), 1.92 (*s*, 3H, OAc). ^{13}C NMR: Table 1a.

4.5. Ozonolysis of 2 to compounds 8 and 9

A current of O_2/O_3 (30 l/h) was bubbled into a solution of **2** (300 mg) in dry CH_2Cl_2 at −78 °C for 30 min. After evaporation of the solvent under reduced pressure, the residue was purified by CC (silica gel, gradient elution from petrol ether–AcOEt 2:3 to pure AcOEt) giving, in order of increasing polarity, 87 mg of compound **8** and 186 mg of compound **9**.

Compound **8**: white crystals, mp 155–158 °C. IR ν_{max} (film) cm^{-1}: 3433, 2935, 2870, 1732, 1720, 1371, 1251, 1047, 837, 734. EI–MS *m/z* (rel. int.): 364 $[M]^+$ (1), 346 $[M–H_2O]^+$ (4), 328 $[M–2(H_2O)]^+$ (5), 304 $[M–AcOH]^+$ (6), 286 $[M–AcOH–H_2O]^+$ (18), 268 $[M–AcOH–2(H_2O)]^+$ (10), 235 (15), 217 (11), 119 (13), 107 (20), 95 (26), 43 (100). ^1H NMR ($CDCl_3$): δ 3.51 (*dd*, 1H, $J=9.0$ and 5.2 Hz, H-3β), 3.66 (*t*, 1H, $J=3.8$ Hz, H-7α), 2.37 (*m*, 1H, H-13), 2.10 (*br s*, 2H, H-15), 3.99 (*d*, 1H, $J=11.6$ Hz, H_A-18), 3.92 (*d*, 1H, $J=11.6$ Hz, H_B-18), 0.72 (*s*, 3H, Me-19), 1.06 (*s*, 3H, Me-20), 2.02 (*s*, 3H, OAc). ^{13}C NMR: Table 1a.

Compound **9**: white solid, mp 88–92. IR ν_{max} (film) cm^{-1}: 3445, 2937, 2870, 1735, 1372, 1248, 1040, 1005, 956, 734. EI–MS *m/z* (rel. int.): $[M]^+$ absent, 364 $[M–CH_2O_2]^+$ (1), 346 $[M–CH_2O_2–H_2O]^+$ (1), 304 $[M–CH_2O_2–AcOH]^+$ (3), 286 $[M–CH_2O_2–AcOH–H_2O]^+$ (5), 268 $[M–CH_2O_2–AcOH–2(H_2O)]^+$ (3), 245 (7), 227 (10), 145 (12), 119 (10), 107 (15), 91 (20), 43 (100). ^1H NMR ($CDCl_3$): δ 3.48 (*dd*, 1H, $J=9.0$ and 5.2 Hz, H-3β), 3.55 (*t*, 1H, $J=3.8$ Hz, H-7α), 5.01 (*br s*, 2H, H-17), 3.91 (*d*, 1H, $J=11.6$ Hz, H_A-18), 3.89 (*d*, 1H, $J=11.6$ Hz, H_B-18), 0.67 (*s*, 3H, Me-19), 0.98 (*s*, 3H, Me-20), 2.00 (*s*, 3H, OAc). ^{13}C NMR: Table 1a.

4.6. Transformation of compound 9 into compound 8

Twenty milligrams of ozonide **9** were dissolved in 10 ml of glacial acetic acid and added to zinc powder. After 30 min the conversion of **9** to **8** was complete. This was confirmed by TLC comparison with an authentic sample of **8**.

4.7. General esterification procedure

Linearol (150 mg) was solubilized in 10 ml of dry CH_2Cl_2 and added with 1 eq. of DMAP (56 mg), 25 eq. of TEA (1.5 ml) and the appropriate acyl chloride (4 eq.) at room temperature under argon atmosphere. After stirring overnight, the reaction was subjected to usual work-up adding H_2O and extracting with AcOEt; finally, the organic layer was dried over Na_2SO_4 and

evaporated under reduced pressure. Generally, the residue was purified by CC (silica gel, mixtures of petrol–AcOEt as eluent). This procedure gave the following ester derivatives:

Compounds **10** and **11**. Treatment of **2** with propanoyl chloride gave a mixture of two compounds which were separated by CC (silica gel, petrol ether–AcOEt 4:1 as eluent) giving 125 mg of **10** and 47 mg of **11**.

Compound **10**: amorphous solid. IR ν_{max} (film) cm^{-1}: 2937, 2858, 1732, 1660, 1462, 1371, 1230, 1195, 1178, 1150, 1070, 1041, 1024, 875. EI–MS *m/z* (rel. int.): 474 $[M]^+$ (1), 400 $[M–CH_3CH_2COOH]^+$ (9), 340 $[M–CH_3CH_2COOH–AcOH)]^+$ (2), 326 $[M–2(CH_3CH_2COOH)]^+$ (93), 283 (2), 266 $[M–2(CH_3CH_2COOH)–AcOH]^+$ (82), 253 (28), 185 (22), 119 (31), 105 (28), 43 (100). ^1H NMR ($CDCl_3$): δ 4.77 (*dd*, 1H, $J=11.2$ and 5.2 Hz, H-3β), 4.77 (*t*, 1H, $J=3.8$ Hz, H-7α), 2.70 (*m*, 1H, H-13), 2.17 (*dt*, 1H, $J=17$ and 2.2 Hz, H_A-15), 2.13 (*dt*, 1H, $J=17$ and 2.2 Hz, H_B-15), 4.82 (*br s*, 1H, H_A-17), 4.81 (*br s*, 1H, H_B-17), 3.92 (*d*, 1H, $J=11.8$ Hz, H_A-18), 3.53 (*d*, 1H, $J=11.8$ Hz, H_B-18), 0.83 (*s*, 3H, Me-19), 1.09 (*s*, 3H, Me-20), 2.02 (*s*, 3H, OAc), 2.31 (*q*, 2H, $J=7.5$ Hz, H-2′), 1.16 (*t*, 3H, $J=7.5$ Hz, H-3′), 2.30 (*q*, 2H, $J=7.5$ Hz, H-2″), 1.11 (*t*, 3H, $J=7.5$ Hz, H-3″). ^{13}C NMR: Table 1b.

Compound **11**: amorphous solid. IR ν_{max} (film) cm^{-1}: 3435, 2937, 2858, 1730, 1660, 1462, 1423, 1371, 1230, 1180, 1041, 1024. EI–MS *m/z* (rel. int.): 418 $[M]^+$ (1), 400 $[M–H_2O]^+$ (2), 344 $[M–CH_3CH_2COOH)]^+$ (2), 326 $[M–CH_3CH_2COOH–H_2O]^+$ (37), 284 $[M–CH_3CH_2COOH–AcOH]^+$ (10), 266 $[M–CH_3CH_2COOH–AcOH–H_2O]^+$ (42), 251 (23), 149 (32), 121 (35), 93 (35), 43 (100). ^1H NMR ($CDCl_3$): δ 4.86 (*dd*, 1H, $J=11.2$ and 5.2 Hz, H-3β), 3.60 (*t*, 1H, $J=3.8$ Hz, H-7α), 2.69 (*m*, 1H, H-13), 2.26 (*br s*, 2H, H-15), 4.83 (*br s*, 1H, H_A-17), 4.80 (*br s*, 1H, H_B-17), 4.08 (*d*, 1H, $J=11.6$ Hz, H_A-18), 3.54 (*d*, 1H, $J=11.6$ Hz, H_B-18), 0.84 (*s*, 3H, Me-19), 1.09 (*s*, 3H, Me-20), 2.07 (*s*, 3H, OAc), 2.32 (*q*, 2H, $J=7.5$ Hz, H-2′), 1.14 (*t*, 3H, $J=7.5$ Hz, H-3′). ^{13}C NMR: Table 1b.

Compounds **12** and **13**. Treatment of **2** with butanoyl chloride gave a mixture of two compounds which were separated by CC (silica gel, petrol ether–AcOEt 4:1 as eluent) giving 50 mg of **12** and 120 mg of **13**.

Compound **12**: amorphous solid. IR ν_{max} (film) cm^{-1}: 3440, 2937, 2858, 1725, 1660, 1458, 1425, 1367, 1235, 1185, 1020. EI–MS *m/z* (rel. int.): 432 $[M]^+$ (1), 414 $[M–H_2O]^+$ (1), 344 $[M–CH_3CH_2CH_2COOH)]^+$ (2), 326 $[M–CH_3CH_2CH_2COOH–H_2O]^+$ (30), 284 $[M–CH_3CH_2CH_2COOH–AcOH]^+$ (7), 266 $[M–CH_3CH_2CH_2COOH–AcOH\text{-}H_2O]^+$ (50), 149 (42), 121 (30), 93 (20), 71 (33), 43 (100). ^1H NMR ($CDCl_3$): δ 4.87 (*dd*, 1H, $J=11.2$ and 5.2 Hz, H-3β), 3.60 (*t*, 1H, $J=3.8$ Hz, H-7α), 2.69 (*m*, 1H, H-13), 2.27 (*br s*, 2H, H-15), 4.83 (*br s*, 1H, H_A-17), 4.80 (*br s*, 1H, H_B-17), 4.08 (*d*, 1H, $J=11.7$ Hz, H_A-18), 3.53 (*d*, 1H, $J=11.7$ Hz, H_B-18), 0.83 (*s*, 3H, Me-19), 1.09 (*s*, 3H, Me-20), 2.07 (*s*, 3H, OAc), 2.27 (*t*, 2H, $J=7.5$ Hz, H-2′), 0.95 (*t*, 3H, $J=7.5$ Hz, H-4′). ^{13}C NMR: Table 1b.

Compound **13**: amorphous solid. IR ν_{max} (film) cm^{-1}: 2931, 2875, 2856, 1732, 1658, 1460, 1371, 1232, 1193, 1174, 1041, 873, 754. EI–MS *m/z* (rel. int.): $[M]^+$ absent, 414 $[M–CH_3CH_2CH_2COOH]^+$ (6), 354 $[M–CH_3CH_2CH_2COOH–AcOH)]^+$ (2), 326 $[M–2(CH_3CH_2CH_2COOH)]^+$ (82), 266 $[M–2(CH_3CH_2CH_2COOH)–AcOH]^+$ (100), 253 (29), 185 (20). ^1H NMR ($CDCl_3$): δ 4.78 (*dd*, 1H, $J=11.2$ and 5.2 Hz, H-3β), 4.77 (*t*, 1H, $J=3.8$ Hz, H-7α), 2.71 (*m*, 1H, H-13), 2.16 (*dt*, 1H, $J=17$ and 2.2 Hz, H_A-15), 2.12 (*dt*, 1H, $J=17$ and 2.2 Hz, H_B-15), 4.82 (*br s*, 1H, H_A-17), 4.81 (*br s*, 1H, H_B-17), 3.90 (*d*, 1H, $J=11.7$ Hz, H_A-18), 3.54 (*d*, 1H, $J=11.7$ Hz, H_B-18), 0.83 (*s*, 3H, Me-19), 1.11 (*s*, 3H, Me-20), 2.03 (*s*, 3H, OAc), 2.28 (*t*, 4H, $J=7.3$ Hz, H-2′ and H-2″), 0.97 (*t*, 3H, $J=7.5$ Hz, H-4′), 0.93 (*t*, 3H, $J=7.5$ Hz, H-4″). ^{13}C NMR: Table 1b.

Compounds **14** and **15**. Treatment of **2** with benzoyl chloride gave a mixture of two compounds which were separated by CC (silica gel, petrol ether–AcOEt 4:1, petrol–AcOEt 3:2 as eluent) giving 37 mg of **14** and 180 mg of **15**.

Compound **14**: white crystals, mp 176–180 °C. IR ν_{max} (film) cm^{-1}: 3527, 2933, 2858, 1743, 1716, 1655, 1600, 1450, 1273, 1250, 1176, 1115, 943, 736, 711. EI–MS *m/z* (rel. int.): 466 $[M]^+$ (1), 448 $[M–H_2O]^+$ (2), 344 $[M–C_6H_5COOH]^+$ (2), 326 $[M–C_6H_5COOH–H_2O]^+$ (35), 284 $[M–C_6H_5COOH–AcOH]^+$ (10), 266 $[M–C_6H_5COOH–AcOH–H_2O]^+$ (37), 176 (22), 149 (47), 105 (93), 84 (100). ^1H NMR ($CDCl_3$): δ 5.09 (*dd*, 1H, $J=11.2$ and 5.2 Hz, H-3β), 3.59 (*t*, 1H, $J=3.8$ Hz, H-7α), 2.67 (*m*, 1H, H-13), 2.26 (*br s*, 2H, H-15), 4.81 (*br s*, 1H, H_A-17), 4.79 (*br s*, 1H, H_B-17), 4.17 (*d*, 1H, $J=11.7$ Hz, H_A-18), 3.56 (*d*, 1H, $J=11.7$ Hz, H_B-18), 0.98 (*s*, 3H, Me-19), 1.11 (*s*, 3H, Me-20), 2.03 (*s*, 3H, OAc), 8.00 (*dd*, 2H, $J=7.0$ and 1.6 Hz, H-2′ and H-6′), 7.41 (*td*, 2H, $J=7.0$ and 1.6 Hz, H-3′ and H-5′), 7.51 (*tt*, 1H, $J=7.0$ and 1.6 Hz, H-4′). ^{13}C NMR: Table 1b.

Compound **15**: white crystals, mp 175–178 °C. IR ν_{max} (film) cm^{-1}: 3060, 2933, 2860, 1743, 1716, 1658, 1600, 1450, 1276, 1249, 1176, 1114, 879, 738, 711. EI–MS *m/z* (rel. int.): $[M]^+$ absent, 448 $[M–C_6H_5COOH]^+$ (3), 388 $[M–C_6H_5COOH–AcOH]^+$ (2), 326 $[M–2(C_6H_5COOH)]^+$ (58), 266 $[M–2(C_5H_6COOH)–AcOH]^+$ (70), 251 (32), 185 (32), 119 (18), 105 (100). ^1H NMR ($CDCl_3$): δ 5.02 (*dd*, 1H, $J=11.2$ and 5.2 Hz, H-3β), 5.02 (*t*, 1H, $J=3.8$ Hz, H-7α), 2.75 (*m*, 1H, H-13), 2.35 (*dt*, 1H, $J=17$ and 2.2 Hz, H_A-15), 2.20 (*dt*, 1H, $J=17$ and 2.2 Hz, H_B-15), 4.83 (*br s*, 1H, H_A-17), 4.76 (*br s*, 1H, H_B-17), 3.80 (*d*, 1H, $J=11.7$ Hz, H_A-18), 3.60 (*d*, 1H, $J=11.7$ Hz, H_B-18), 0.99 (*s*, 3H, Me-19), 1.21 (*s*, 3H, Me-20), 1.12 (*s*, 3H, OAc), 8.05 (*dd*, 2H, $J=7.0$ and 1.6 Hz, H-2′ and H-6′), 7.46 (*td*, 2H, $J=7.0$ and 1.6 Hz, H-3′ and H-5′), 7.54 (*tt*, 1H, $J=7.0$ and 1.6 Hz, H-4′), 7.96 (*dd*, 2H, $J=7.0$ and 1.6 Hz, H-2″ and H-6″), 7.40 (*td*, 2H, $J=7.0$ and 1.6 Hz, H-3″ and H-5″), 7.51 (*tt*, 1H, $J=7.0$ and 1.6 Hz, H-4″). ^{13}C NMR: Table 1b.

Compounds **16** and **17**. Treatment of **2** with 4-methoxybenzoyl chloride gave a mixture of two compounds which were separated by CC (silica gel, petrol ether–AcOEt 4:1, petrol ether–AcOEt 3:2 as eluent) giving 60 mg of **16** and 175 mg of **17**.

Compound **16**: white crystals, mp 187–190 °C. IR ν_{max} (film) cm^{-1}: 3508, 2931, 2856, 1740, 1700, 1654, 1606, 1579, 1512, 1317, 1270, 1256, 1167, 1101, 1029, 869, 771, 736. EI–MS *m/z* (rel. int.): 496 $[M]^+$ (2), 478 $[M–H_2O]^+$ (6), 418 $[M–H_2O–AcOH]^+$ (16), 344 $[M–CH_3OC_6H_5COOH]^+$ (3), 326 $[M–CH_3OC_6H_5COOH–H_2O]^+$ (32), 284 $[M–CH_3OC_6H_5COOH–AcOH]^+$ (18), 266 $[M–CH_3OC_6H_5COOH–AcOH–H_2O]^+$ (80), 253 (60), 135 (100). ^1H NMR ($CDCl_3$): δ 5.06 (*dd*, 1H, *J* = 11.2 and 5.2 Hz, H-3β), 3.58 (*t*, 1H, *J* = 3.8 Hz, H-7α), 2.67 (*m*, 1H, H-13), 2.26 (*br s*, 2H, H-15), 4.81 (*br s*, 1H, H_A-17), 4.78 (*br s*, 1H, H_B-17), 4.16 (*d*, 1H, *J* = 11.7 Hz, H_A-18), 3.56 (*d*, 1H, *J* = 11.7 Hz, H_B-18), 0.97 (*s*, 3H, Me-19), 1.14 (*s*, 3H, Me-20), 2.03 (*s*, 3H, OAc), 7.95 (*d*, 2H, *J* = 6.8 Hz, H-2′ and H-6′), 6.90 (*d*, 2H, *J* = 6.8 Hz, H-3′ and H-5′), 3.83 (*s*, 3H, OME′). ^{13}C NMR: Table 1b.

Compound **17**: white crystals, mp 83–86 °C. IR ν_{max} (film) cm^{-1}: 3064, 2935, 2860, 1743, 1708, 1658, 1606, 1581, 1512, 1461, 1317, 1270, 1257, 1166, 1101, 1029, 877, 771, 736. EI–MS *m/z* (rel. int.): $[M]^+$ absent, 478 $[M–CH_3OC_6H_5COOH]^+$ (3), 326 $[M–2(CH_3OC_6H_5COOH)]^+$ (76), 266 $[M–2(CH_3OC_5H_6COOH)–AcOH]^+$ (100), 251 (28), 135 (96). ^1H NMR ($CDCl_3$): &*delta*; 4.97 (*dd*, 1H, *J* = 11.2 and 5.2 Hz, H-3β), 4.97 (*t*, 1H, *J* = 3.8 Hz, H-7α), 2.73 (*m*, 1H, H-13), 2.32 (*dt*, 1H, *J* = 17 and 2.2 Hz, H_A-15), 2.18 (*dt*, 1H, *J* = 17 and 2.2 Hz, H_B-15), 4.82 (*br s*, 1H, H_A-17), 4.74 (*br s*, 1H, H_B-17), 3.76 (*d*, 1H, *J* = 11.7 Hz, H_A-18), 3.60 (*d*, 1H, *J* = 11.7 Hz, H_B-18), 0.97 (*s*, 3H, Me-19), 1.20 (*s*, 3H, Me-20), 1.20 (*s*, 3H, OAc), 8.00 (*d*, 2H, *J* = 6.8 Hz, H-2′ and H-6′), 6.94 (*d*, 2H, *J* = 6.8 Hz, H-3′ and H-5′), 7.91 (*d*, 2H, *J* = 6.8 Hz, H-2″ and H-6″), 6.87 (*d*, 2H, *J* = 6.8 Hz, H-3″ and H-5″), 3.84 (*s*, 3H, OME′), 3.82 (*s*, 3H, OME″). ^{13}C NMR: Table 1b.

Compound **18**. Treatment of **2** with 2-furoyl chloride gave 187 mg of **18**. Amorphous solid. IR ν_{max} (film) cm^{-1}: 3124, 3064, 2937, 2862, 1744, 1714, 1660, 1579, 1569, 1471, 1394, 1299, 1232, 1180, 1120, 1041, 1012, 975, 885, 763, 736, 702. EI–MS *m/z* (rel. int.): $[M]^+$ absent, 438 $[M–C_4H_3OCOOH]^+$ (2), 326 $[M–2(C_4H_3OCOOH)]^+$ (50), 266 $[M–2(C_4H_3OCOOH)–AcOH]^+$ (52), 251 (16), 185 (14), 95 (100). ^1H NMR ($CDCl_3$): δ 4.95 (*dd*, 1H, *J* = 11.2 and 5.2 Hz, H-3β), 4.91 (*t*, 1H, *J* = 3.8 Hz, H-7α), 2.67 (*m*, 1H, H-13), 2.25 (*dt*, 1H, *J* = 17 and 2.2 Hz, H_A-15), 2.10 (*dt*, 1H, *J* = 17 and 2.2 Hz, H_B-15), 4.77 (*br s*, 1H, H_A-17), 4.70 (*br s*, 1H, H_B-17), 3.77 (*d*, 1H, *J* = 11.7 Hz, H_A-18), 3.54 (*d*, 1H, *J* = 11.7 Hz, H_B-18), 0.88 (*s*, 3H, Me-19), 1.11 (*s*, 3H, Me-20), 1.37 (*s*, 3H, OAc), 7.13 (*m*, 1H, H-3′), 6.47 (*m*, 1H, H-4′), 7.54 (*m*, 1H, H-5′), 7.04 (*m*, 1H, H-3″), 6.42 (*m*, 1H, H-4″), 7.49 (*m*, 1H, H-5″). ^{13}C NMR: Table 1b.

Compound **19**. Treatment of **2** with 3-nitrobenzoyl chloride gave 220 mg of **19**. Amorphous solid. IR ν_{max} (film) cm^{-1}: 3085, 3064, 2937, 2864, 1747, 1732, 1658, 1616, 1537, 1479, 1440, 1260, 1234, 1136, 1041, 837, 775, 719. EI–MS *m/z* (rel. int.): $[M]^+$ absent, 493 $[M–NO_2C_6H_4COOH]^+$ (3), 433 $[M–NO_2C_6H_4COOH–AcOH]^+$ (3), 326 $[M–2(NO_2C_6H_4COOH)]^+$ (53), 266 $[M–2(NO_2C_6H_4COOH)–AcOH]^+$ (100), 251 (45), 150 (67), 119 (24), 83 (86). ^1H NMR ($CDCl_3$): δ 5.00 (*dd*, 1H, *J* = 11.2 and 5.2 Hz, H-3β), 5.03 (*t*, 1H, *J* = 3.8 Hz, H-7α), 2.72 (*m*, 1H, H-13), 2.33 (*dt*, 1H, *J* = 17 and 2.2 Hz, H_A-15), 2.17 (*dt*, 1H, *J* = 17 and 2.2 Hz, H_B-15), 4.80 (*br s*, 1H, H_A-17), 4.73 (*br s*, 1H, H_B-17), 3.86 (*d*, 1H, *J* = 11.7 Hz, H_A-18), 3.54 (*d*, 1H, *J* = 11.7 Hz, H_B-18), 1.00 (*s*, 3H, Me-19), 1.20 (*s*, 3H, Me-20), 1.17 (*s*, 3H, OAc), 8.81 (*br s*, 1H, H-2′), 8.41 (*br d*, 1H, *J* = 7.5, H-4′), 7.70 (*t*, 1H, *J* = 7.5, H-5′), 8.37 (*br d*, 1H, *J* = 7.5, H-6′), 8.70 (*br s*, 1H, H-2″), 8.34 (*br d*, 1H, *J* = 7.5, H-4″), 7.60 (*t*, 1H, *J* = 7.5, H-5″), 8.24 (*br d*, 1H, *J* = 7.5, H-6″). ^{13}C NMR: Table 1c.

Compound **20**. Treatment of **2** with 4-cyanobenzoyl chloride gave 232 mg of **20**. Amorphous solid. IR ν_{max} (film) cm^{-1}: 3064, 2937, 2862, 2231, 1744, 1716, 1658, 1610, 1569, 1309, 1276, 1234, 1176, 1041, 1015, 862, 767, 736. EI–MS *m/z* (rel. int.): $[M]^+$ absent, 326 $[M–2(NCC_6H_4COOH)]^+$ (24), 266 $[M–2(NCC_6H_4COOH)–AcOH]^+$ (44), 251 (20), 185 (16), 130 (100). ^1H NMR ($CDCl_3$): δ 4.96 (*dd*, 1H, *J* = 11.2 and 5.2 Hz, H-3β), 4.98 (*t*, 1H, *J* = 3.8 Hz, H-7α), 2.70 (*m*, 1H, H-13), 2.28 (*dt*, 1H, *J* = 17 and 2.2 Hz, H_A-15), 2.13 (*dt*, 1H, *J* = 17 and 2.2 Hz, H_B-15), 4.78 (*br s*, 1H, H_A-17), 4.71 (*br s*, 1H, H_B-17), 3.79 (*d*, 1H, *J* = 11.7 Hz, H_A-18), 3.52 (*d*, 1H, *J* = 11.7 Hz, H_B-18), 0.94 (*s*, 3H, Me-19), 1.15 (*s*, 3H, Me-20), 1.14 (*s*, 3H, OAc), 8.12 (*br d*, 2H, *J* = 6.8 Hz, H-2′ and H-6′), 7.75 (*br d*, 2H, *J* = 6.8 Hz, H-3′ and H-5′), 8.00 (*br d*, 2H, *J* = 6.8 Hz, H-2″ and H-6″), 7.66 (*br d*, 2H, *J* = 6.8 Hz, H-3″ and H-5″). ^{13}C NMR: Table 1c.

Compound **21**. Treatment of **2** with 4-nitrobenzoyl chloride gave 260 mg of **21**. Amorphous solid. IR ν_{max} (film) cm^{-1}: 3057, 2935, 2862, 1743, 1722, 1656, 1606, 1529, 1344, 1276, 1234, 1118, 1103, 1041, 1014, 873, 842, 785, 736, 719. EI–MS *m/z* (rel. int.): $[M]^+$ absent, 493 $[M–NO_2C_6H_4COOH]^+$ (1), 433 $[M–NO_2C_6H_4COOH–AcOH]^+$ (2), 326 $[M–2(NO_2C_6H_4COOH)]^+$ (40), 266 $[M–2(NO_2C_6H_4COOH)–AcOH]^+$ (100), 251 (57), 185 (35), 150 (82). ^1H NMR ($CDCl_3$): δ 5.02 (*dd*, 1H, *J* = 11.2 and 5.2 Hz, H-3β), 5.04 (*t*, 1H, *J* = 3.8 Hz, H-7α), 2.77 (*m*, 1H, H-13), 2.33 (*dt*, 1H, *J* = 17 and 2.2 Hz, H_A-15), 2.20 (*dt*, 1H, *J* = 17 and 2.2 Hz, H_B-15), 4.85 (*br s*, 1H, H_A-17), 4.77 (*br s*, 1H, H_B-17), 3.86 (*d*, 1H, *J* = 11.7 Hz, H_A-18), 3.59 (*d*, 1H, *J* = 11.7 Hz, H_B-18), 1.00 (*s*, 3H, Me-19), 1.22 (*s*, 3H, Me-20), 1.21 (*s*, 3H, OAc), 8.23 (*br d*, 2H, *J* = 6.8 Hz, H-2′ and H-6′), 8.33 (*br d*, 2H, *J* = 6.8 Hz, H-3′ and H-5′), 8.11 (*br d*, 2H, *J* = 6.8 Hz, H-2″ and H-6″), 8.24 (*br d*, 2H, *J* = 6.8 Hz, H-3″ and H-5″). ^{13}C NMR: Table 1c.

Compound **22**. Treatment of **2** with tigloyl chloride gave 92 mg of **22** an unsemixture of two compounds in a 3:2 ratio. Amorphous solid. IR ν_{max} (film) cm^{-1}: 3531, 2981, 2935, 2877, 1732, 1656, 1639, 1458, 1371, 1250, 1193, 1049, 995, 977, 873, 756. EI–MS *m/z* (rel. int.): 444 $[M]^+$ (1), 426 $[M–H_2O]^+$ (3), 344 $[M–C_4H_7COOH]^+$ (8), 326 $[M–C_4H_7COOH\text{-}H_2O]^+$ (92), 284 $[M–C_4H_7COOH–AcOH]^+$ (23), 266 $[M–C_4H_7COOH–H_2O–AcOH]^+$ (100), 253 (32), 223 (14), 83 (40). ^1H NMR ($CDCl_3$): δ 4.86 (*dd*, 1H, $J=11.2$ and 5.2 Hz, H-3β), 3.57 (*t*, 1H, $J=3.8$ Hz, H-7α), 2.66 (*m*, 1H, H-13), 2.25 (*br s*, 2H, H-15), 4.80 (*br s*, 1H, H_A-17), 4.77 (*br s*, 1H, H_B-17), 4.07 (*d*, 1H, $J=11.6$ Hz, H_A-18), 3.45 (*d*, 0.6H, $J=11.6$ Hz, H_B-18, 22A epimer), 3.49 (*d*, 0.4H, $J=11.6$ Hz, H_B-18, 22B epimer), 0.81 (*s*, 3H, Me-19), 1.07 (*s*, 3H, Me-20), 2.04 (*s*, 3H, OAc), 3.11 (*br quint*, 1H, $J=7.0$ Hz, H-2′), 5.87 (*m*, 1H, H-3′), 5.08 (*br d*, 1H, $J=10.0$ Hz, H_A-4′), 5.12 (*br d*, 1H, $J=17.2$ Hz, H_B-4′), 1.24 (*d*, 1.8H, $J=7.0$ Hz, Me-5, 22A epimer), 1.25 (*d*, 1.2H, $J=7.0$ Hz, Me-5′, 22B epimer). ^{13}C NMR: Table 1c.

Compounds **23** and **24**. Treatment of **2** (150 mg) with 287 mg of tigloyl chloride in refluxing toluene for 30 min gave 140 mg of an unresolvable mixture of **23** and **24** in a 55:45 ratio. Amorphous solid. IR ν_{max} (film) cm^{-1}: 3435, 2935, 2868, 1733, 1708, 1652, 1380, 1270, 1139, 1072, 1028, 732. EI–MS *m/z* (rel. int.): 544 $[M]^+$ (1), 526 $[M–H_2O]^+$ (3), 426 $[M–H_2O–C_4H_7COOH]^+$ (4), 366 $[M–H_2O–C_4H_7COOH–AcOH]^+$ (15), 344 $[M–2(C_4H_7COOH)]^+$ (7), 326 $[M–H_2O–2(C_4H_7COOH)]^+$ (33), 284 $[M–2(C_4H_7COOH)–AcOH]^+$ (97), 266 $[M–2(C_4H_7COOH)–H_2O–AcOH]^+$ (100), 225 (20). ^1H NMR ($CDCl_3$): δ 4.88 (*dd*, 0.55H, $J=11.2$ and 5.2 Hz, H-3β of **23**), 4.82 (*dd*, 0.45H, $J=11.2$ and 5.2 Hz, H-3β of **24**), 4.78 (*t*, 1H, $J=3.8$ Hz, H-7α), 1.35 (*s*, 3H, Me-17), 3.83 (*d*, 0.55H, $J=12.0$ Hz, H_A-18 of **23**), 3.78 (*d*, 0.45H, $J=12.0$ Hz, H_A-18 of **24**), 3.58 (*d*, 0.55H, $J=12.0$ Hz, H_B-18 of **23**), 3.54 (*d*, 0.45H, $J=12.0$ Hz, H_B-18 of **24**), 0.84 (*s*, 1.35H, Me-19 of **24**), 0.86 (*s*, 1.65H, Me-19 of **23**), 1.13 (*s*, 3H, Me-20), 1.99 (*s*, 1.65H, OAc of **23**), 1.82 (*s*, 1.35H, OAc of **24**), 6.69 (*qq*, 1.55H, $J=7.0$ and 1.0 Hz, H-3′ and H-3″ of **23** and H-3″ of **24**), 6.82 (*qq*, 0.45H, $J=7.0$ and 1.0 Hz, H-3′ of **24**), 1.77 (*br d*, 6H, $J=7.0$ Hz, Me-4′ and Me-4″), 1.71 (*br s*, 6H, Me-5′ and Me-5″). ^{13}C NMR: Table 1c.

Compounds **25** and **26**. Treatment of **2** (150 mg) with 287 mg of tigloyl chloride and 1.5 ml of TEA in refluxing toluene for 24 h gave a mixture of two compounds which were separated by CC (silica gel, gradient elution from petrol ether to petrol ether–AcOEt 3:2) giving 50 mg of **25** and 70 mg of **26**.

Compound **25**. Amorphous solid. IR ν_{max} (film) cm^{-1}: 2931, 2858, 1745, 1707, 1653, 1630, 1265, 1236, 1137, 1074, 1021, 732. EI–MS *m/z* (rel. int.): 526 $[M]^+$ (1), 426 $[M–C_4H_7COOH]^+$ (8), 366 $[M–C_4H_7COOH–AcOH]^+$ (10), 326 $[M–2(C_4H_7COOH)]^+$ (90), 266 $[M–2(C_4H_7COOH)–AcOH]^+$ (100), 251 (26), 226 (15). ^1H NMR ($CDCl_3$): δ 4.80 (*dd*, 1H, $J=11.2$ and 5.2 Hz, H-3β), 4.77 (*t*, 1H, $J=3.8$ Hz, H-7α), 2.71 (*m*, 1H, H-13), 2.22 (*dt*, 1H, $J=17$ and 2.2 Hz, H_A-15), 2.10 (*dt*, 1H, $J=17$ and 2.2 Hz, H_B-15), 4.81 (*br s*, 1H, H_A-17), 4.76 (*br s*, 1H, H_B-17), 3.78 (*d*, 1H, $J=11.8$ Hz, H_A-18), 3.56 (*d*, 1H, $J=11.8$ Hz, H_B-18), 0.87 (*s*, 3H, Me-19), 1.13 (*s*, 3H, Me-20), 1.84 (*s*, 3H, OAc), 6.86 (*qq*, 1H, $J=7.0$ and 1.0 Hz, H-3′), 6.79 (*qq*, 1H, $J=7.0$ and 1.0 Hz, H-3″), 1.76 (*br d*, 6H, $J=7.1$ Hz, Me-4′ and Me-4″), 1.78 (*br s*, 6H, Me-5′ and Me-5″). ^{13}C NMR: Table 1c.

Compound **26**. Amorphous solid. IR ν_{max} (film) cm^{-1}: 2925, 2856, 1745, 1709, 1653, 1630, 1269, 1238, 1140, 1074, 1026, 756, 732. EI–MS *m/z* (rel. int.): 526 $[M]^+$ (1), 426 $[M–C_4H_7COOH]^+$ (10), 366 $[M–C_4H_7COOH–AcOH]^+$ (20), 326 $[M–2(C_4H_7COOH)]^+$ (80), 266 $[M–2(C_4H_7COOH)–AcOH]^+$ (100), 251 (30), 226 (20). ^1H NMR ($CDCl_3$): δ 4.89 (*dd*, 1H, $J=11.2$ and 5.2 Hz, H-3β), 4.77 (*t*, 1H, $J=3.8$ Hz, H-7α), 2.71 (*m*, 1H, H-13), 2.21 (*dt*, 1H, $J=17$ and 2.2 Hz, H_A-15), 2.12 (*dt*, 1H, $J=17$ and 2.2 Hz, H_B-15), 4.81 (*br s*, 1H, H_A-17), 4.76 (*br s*, 1H, H_B-17), 3.87 (*d*, 1H, $J=12.0$ Hz, H_A-18), 3.59 (*d*, 1H, $J=12.0$ Hz, H_B-18), 0.87 (*s*, 3H, Me-19), 1.14 (*s*, 3H, Me-20), 2.01 (*s*, 3H, OAc), 6.73 (*qq*, 2H, $J=7.0$ and 1.0 Hz, H-3′ and H-3″), 1.75 (*br d*, 6H, $J=7.1$ Hz, Me-4′ and Me-4″), 1.74 (*br s*, 6H, Me-5′ and Me-5″). ^{13}C NMR: Table 1c.

4.8. Antifeedant bioassay

Compounds were exposed to final stadium larvae of *Spodoptera littoralis* in a binary choice test using glass-fibre discs (Simmonds et al., 1990). All compounds were tested at 100 ppm as this is the dose used to compare activity among compounds (Rodríguez et al., 1999; Bondì et al., 2000). The majority of compounds were tested against insects from 2–3 generations, therefore, each compound was tested against either 10 or 15 insects. All discs were treated with 100 μl sucrose (0.05 M), and then the treatment discs were treated with 100 μl of one of the test compounds. The control discs were treated with an aliquot (100 μl) of the solvent used to dissolve the test compound. Larvae were taken from a colony fed on a wheat-germ based diet (Simmonds et al., 1992). Larvae 24–36 h into the final stadium were removed from food 2–3 h prior to the bioassay. These larvae were placed individually in Petri dishes (9.1 cm diam.) with a pair of discs: one treatment (T) and one control (C) disc. The discs were dried and weighed before and after being exposed to the insects. The amount eaten of each disc was used to calculate a Feeding Index $[(C-T)/(C+T)]\%$. A positive Index indicates an antifeedant and a negative Index a phagostimulant. The data did not differ significantly among generations and were pooled for analysis using the Wilcoxon matched-pairs test.

Acknowledgements

This paper was supported by MURST research funds. We thank Mrs. M. Yule and Dr. P. Green for support in rearing the insects. The insects bioassays were carried out at RBG Kew under a MAFF, Plant Health Great Britain licence.

References

Bondì, M.L., Bruno, M., Piozzi, F., Baser, K.H.C., Simmonds, M.S.J., 2000. Diversity and antifeedant activity of diterpenes from Turkish species of *Sideritis*. Biochem. Syst. Ecol. 28, 299–303.

Chapman, R.F., de Boer, G., 1995. Regulatory Mechanisms in Insect Feeding. Chapman & Hall, New York.

Cole, M.D., Anderson, J.C., Blaney, W.M., Fellows, L.E., Ley, S.V., Sheppard, R.N., Simmonds, M.S.J., 1990. Neo-clerodane insect antifeedant from *Scutellaria galericulata*. Phytochemistry 29, 1793–1976.

Gonzales, A.G., Luis, J.G., Ravelo, A.G., 1990. Plantas Ibericoamericanas Fuentes de Moleculas Bioactivas, Vol. 2, Labiatae. Romero, Tenerife, Spain.

Hanson, J.R., 1999. Diterpenoids. Nat. Prod. Rep. 16, 209–219.

Hatakeyama, S., Matsui, Y., Suzuki, M., Sakurai, K., Takano, S., 1985. Enantioselective synthesis of (+)-citreoviral using asymmetric hydroxylation of tiglate esters. Tetrahedron Lett. 26, 6485–6488.

Piozzi, F., Savona, G., Marino, M.L., 1973. Cyclic carbonate formed during performic acid oxidation of atractyligenin. Tetrahedron 29, 621–624.

Piozzi, F., Venturella, P., Bellino, A., Paternostro, M.P., 1971. Revised structures for candicandiol and epicandicandiol. Chem. Ind. 1971, 962.

Rodríguez, B., Rodríguez, B., de la Torre, M.C., Simmonds, M.S.J., Blaney, W.M., 1999. From a phagostimulant natural product to semisynthetic antifeedants against *Spodoptera littoralis* larvae: chemical transformations of the neoclerodane diterpenoid scutegalin B. J. Nat. Prod. 62, 594–600.

Simmonds, M.S.J., Blaney, W.M., 1992. Labiate-insect interactions: effects of labiate-derived compounds on insect behaviour. In: Harvey, R.M., Reynolds, T. (Eds.), Advances in Labiate Science. Royal Botanic Garden, Kew, England, pp. 375–392.

Simmonds, M.S.J., Blaney, W.M., Ley, S.V., Savona, G., Bruno, M., Rodríguez, B., 1989. The antifeedant activity of clerodanes from *Teucrium*. Phytochemistry 28, 1069–1071.

Simmonds, M.S.J., Blaney, W.M., Fellows, L.E., 1990. Behavioral and electrophysiological study of antifeedant mechanisms associated with polydroxy alkaloids. J. Chem. Ecol. 16, 3167–3196.

Simmonds, M.S.J., Blaney, W.M., Schoonhoven, L.M., 1992. Effects of larval diet and larval age on the responsiveness of taste neurones to sucrose. J. Insect. Physiol. 38, 249–257.

Simmonds, M.S.J., Blaney, W.M., Esquivel, B., Rodriguez-Hahn, L., 1996. Effect of clerodane-type diterpenoids isolated from *Salvia* spp. on the feeding behaviour of *Spodoptera littoralis*. Pestic. Sci. 47, 17–23.

PERGAMON

Phytochemistry 58 (2001) 475–480

PHYTOCHEMISTRY

www.elsevier.com/locate/phytochem

Dihydroagarofuran alkaloid and triterpenes from *Maytenus heterophylla* and *Maytenus arbutifolia*

Khaled Y. Orabi[a,*], Saleh I. Al-Qasoumi[a], Mahmoud M. El-Olemy[a], Jaber S. Mossa[a], Ilias Muhammad[b]

[a]*Department of Pharmacognosy, College of Pharmacy, King Saud University, PO Box 2457, Riyadh 11451, Saudi Arabia*
[b]*National Center for Natural Products Research, Research Institute of Pharmaceutical Sciences, School of Pharmacy, University of Mississippi, University, MS 38677, USA*

Received 13 September 2000; received in revised form 1 March 2001

Abstract

The antimicrobially active EtOH extracts of *Maytenus heterophylla* yielded a new dihydroagarofuran alkaloid,1β-acetoxy-9α-benzoyloxy-2β,6α-dinicotinoyloxy-β-dihydroagarofuran, together with the known compounds β-amyrin, maytenfolic acid, 3α-hydroxy-2-oxofriedelane-20α-carboxylic acid, lup-20(29)-ene-1β,3β-diol, (−)-4′-methyl*epi*gallocatechin, and (−)-*epi*catechin. In addition, β-amyrin, (−)-*epi*catechin and (−)-4′-methyl*epi*gallocatechin were isolated from *Maytenus arbutifolia*. The structure elucidation of the isolated compounds was based primarily on 1D and 2D NMR analyses, including HMQC, HMBC, and NOESY correlations. Maytenfolic acid showed moderate antimicrobial activity by inhibiting the growth of *Candida albicans, Cryptococcus neoformans, Staphylococcus aureus* and *Pseudomonas aeruginosa*. © 2001 Published by Elsevier Science Ltd.

Keywords: *Maytenus heterophylla*; *Maytenus arbutifolia*; Celastraceae; Alkaloid; Dihydroagarofuran; Heterophylline; Triterpenes; Antimicrobial

1. Introduction

Plants of the genus *Maytenus* are extensively investigated for bioactive compounds as they are widely used in folk medicine as an antiseptic, antiasthmatic, fertility-regulating agent, antitumor, as well as for stomach problems (Flores, 1984; Ghazanfar, 1994). They exhibited diverse types of secondary metabolites, including triterpenes (Shirota et al., 1996), oligo-nicotinated sesquiterpenes and sesquiterpene pyridine alkaloids (Corsino et al.,1998), phenolic glucosides (Sannomiya et al., 1998) and agarofurans (Gonzalez et al., 1993), with an interesting spectrum of biological activities (Lee et al., 1982; Kuo et al., 1990; Gonzalez et al., 1996; Nakamura et al., 1997). Earlier investigation on the Saudi species *M. undata* yielded antiinflamatory and antibacterial 12-oleanene and secooleanene triterpene acids (Muhammad et al., 2000), while *M. heterophylla* and *M. arbutifolia* of South African origin afforded friedelane triterpenes and spermidine alkaloids (Kupchan et al., 1974; Wagner and Burghart, 1977).

A bioautography (antimicrobial)-guided examination of *M. heterophylla* (Eckl. & Zeyh.) and *M. arbutifolia* (A. Rich.) Wilezek., led to the isolation of a new dihydroagarofuran alkaloid **1**, as well as the triterpenes maytenfolic acid, 3α-hydroxy-2-oxofriedelane-20α-carboxylic acid (**2**), and lup-20(29)-ene-1β,3β-diol. The present study represents the isolation, characterization and antimicrobial activity of the isolated compounds.

2. Results and discussions

The antimicrobially active EtOH extract of *M. heterophylla* was subjected to flash-chromatography, followed by Centrifugal Preparative TLC (see Experimental) to give the dihydroagarofuran alkaloid **1**, maytenfolic acid, 3α-hydroxy-2-oxofriedelane-20α-carboxylic acid (**2**), lup-20(29)-ene-1β,3β-diol, β-amyrin (Doddrell et al., 1974), (−)-*epi*catechin (Mossa et al., 1992) and (−)-4′-methyl*epi*gallocatechin (Monache et al., 1967). Maytenfolic acid, 3α-hydroxy-2-oxofriedelane-20α-carboxylic

* Corresponding author. Tel.: +966-1-467-7259; fax: +966-1-467-7245.
E-mail address: kyorabi@ksu.edu.sa (K.Y. Orabi).

0031-9422/01/$ - see front matter © 2001 Published by Elsevier Science Ltd.
PII: S0031-9422(01)00277-1

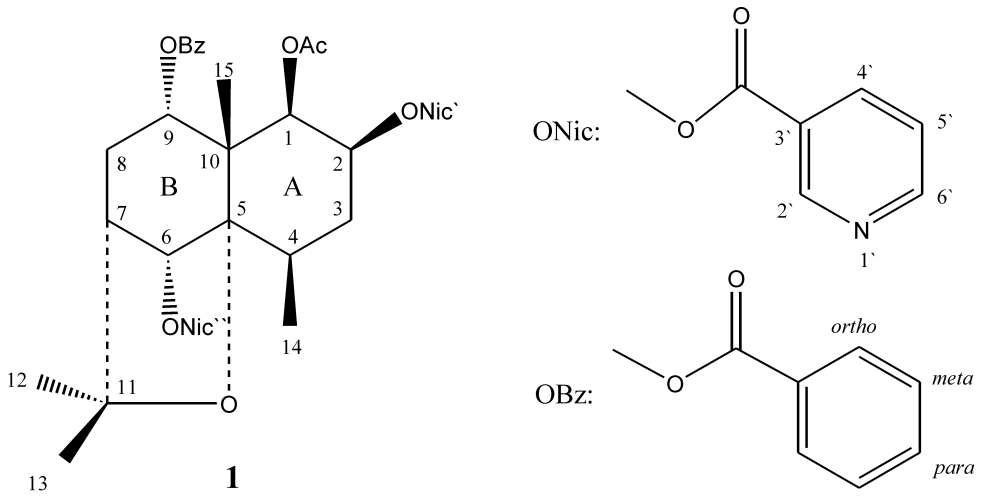

1

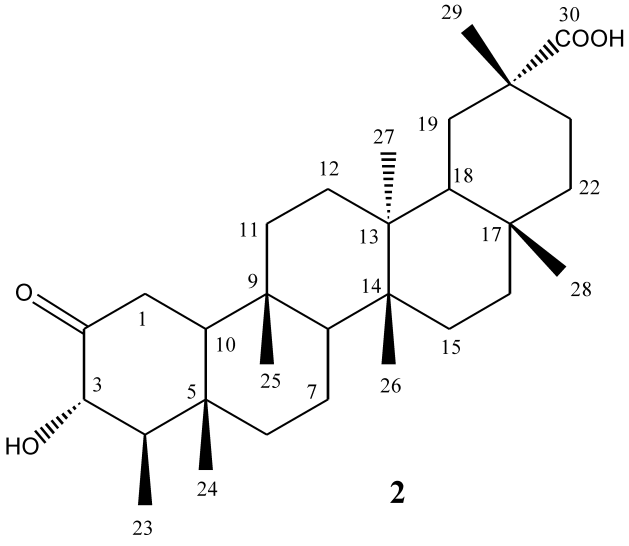

2

acid (**2**), and lup-20(29)-ene-1β,3β-diol were analyzed for the molecular formulas $C_{30}H_{48}O_4$, $C_{30}H_{48}O_4$ and $C_{30}H_{50}O_2$, respectively, by EIMS. The carbon skeleta of 12-oleanen-30-oic acid (for maytenfolic acid), 2-oxo-friedelan-30-oic acid (for **2**) and 3-hydroxylupane (for lup-20(29)-ene-1β,3β-diol) were suggested from their ^{1}H and ^{13}C NMR data (Nozaki et al., 1982; Chen et al., 1983; Nick et al., 1994, 1995). They were identified by comparison of their physical (mp and $[\alpha]_D$) and ^{1}H NMR data with those reported previously for maytenfolic acid (Nozaki et al., 1982), 3α-hydroxy-2-oxo-friedelane-20α-carboxylic acid (De Sousa et al., 1990) and lup-20(29)-ene-1β,3β-diol (Savona et al., 1987), respectively. Their structures were further substantiated by complete ^{13}C NMR assignments, which have not been previously reported for 2, using 2D NMR COSY, HETCOR, HMQC, HMBC and NOESY experiments.

Compound **1** was isolated as a crystalline solid, mp 132–135 °C, $[\alpha]_D$ +63.2^0 (*c* 1.00, $CHCl_3$), analyzed for *m/z* 642 $[C_{36}H_{38}N_2O_9]$ by EIMS. It exhibited UV (λ_{max} at 264, 258 and 234 (*sh*) nm) and IR (ν_{max} at 1734, 1710, 1705, 1593 and 1423 cm^{-1}) absorption bands for multi-carbonyl esters and aromatic ring(s). Fragment peaks at *m/z* 106 $[C_5H_4NCO]^+$, 78 $[C_5H_4N]^+$, 105 $[C_6H_5CO]^+$ and 43 $[C_2H_3O]^+$ in the MS indicated the presence of nicotinoyl, benzoyl and acetyl ester groups. The carbon skeleton of the dihydroagarofuran sesquiterpene was suggested from its ^{1}H- and ^{13}C NMR data (Gonzalez et al., 1987; He and Wu, 1994) (Table 1). The ^{13}C NMR spectra showed 36 carbon resonances; five quartets, two

Table 1
NMR data of compound **1**[a]

Position	δ_H (*mult.*, *J*, Hz)	δ_C	HMBC[c]
1	5.74 (*d*, 2.8)	71.5[b]	2, 3, 15, 1-OC=O
2	5.92 (*br s*)	71.8	1, 2-OC=O
3	2.03 (*ddd*, 13.9, 13.1, 2.1), 2.56 (m)	31.5	1, 4, 5, 14
4	2.59 (*m*)	34.4	2
5	-	90.0	
6	5.72 (*s*)	80.8	5, 8, 10, 11, 6-OC=O
7	2.43 (*br s*)	49.4	
8	2.25 (*dd*, 16.5, 3.1), 2.56 (*m*)	32.1	6, 11
9	5.04 (*d*, 6.8)	73.3	5, 7, 8, 15, 9-OC=O
10	-	50.4	
11	-	83.5	
12	1.45 (*s*)	26.4	
13	1.45 (*s*)	31.3	
14	1.31 (*d*, 7.5)	19.5	5
15	1.62 (*s*)	21.1	
1-OC=O	-	170.0	
CH_3	1.58 (*s*)	20.8	
2-OC=O	-	164.8	
2′	9.24 (*s*)	151.1	
3′	-	126.5	
4′	8.31 (*dd*, 7.9, 1.6)	137.5	2-OC=O
5′	7.42 (*m*)	124.1	
6′	8.81 (*br s*)	154.3	
6-OC=O	–	165.2	
2″	9.14 (*s*)	151.0	
3″	–	126.2	
4″	8.21 (*dd*, 7.2, 1.6)	137.5	
5″	7.37 (*dd*, 7.2, 5.1)	123.9	
6″	8.74 (*br s*)	153.8	
9-OC=O	–	165.8	
ipso	–	129.7	
ortho	8.05 (*d*, 8.1)	130.5	9-OC=O
meta	7.43 (*dd*, 7.6, 7.6)	128.7	
para	7.55 (*dd*, 7.6, 7.6)	133.8	

[a] All spectra were recorded at 500 MHz (^{1}H) and 125 MHz (^{13}C); assignments were aided by 2D NMR COSY, HMQC and HMBC experiments.
[b] ^{13}C NMR multiplicities were determined by DEPT 135^O.
[c] Protons correlating with carbon resonance.

triplets, nineteen doublets, and ten singlets. Its ^{1}H NMR spectrum showed signals for one acetyl group, one benzoyl group, two nicotinyl groups, four methyl groups, two sets of methylene protons, and six methine protons. Spectral data proved collectively that compound **1** is a tetrasubstituted dihydroagarofuran sesquiterpene alkaloid. The substitution pattern of ring A was established from the COSY and HMBC spectra. The signal at δ_H 5.74 was assigned to H-1 as it showed ^3J-correlations with δ_C 170.0 (1-OC=O) and 21.1 (C-15) and ^2J-correlations with δ_C 71.8 (C-2). From the COSY spectrum, H-2 was also assigned at δ_H 5.92, since it couples with two methylene protons (δ_H 2.03 and 2.56, H-3), which in turn couple with a methine proton (δ_H 2.59, H-4) that couples with a methyl group (δ_H 1.31, CH_3-14). These assignments were further supported, from the HMBC spectra, by the presence of a ^2J-correlation between H-2 and an oxygenated doublet carbon resonating at δ_C 71.5 (C-1). This carbon showed another ^3J-correlation with H-3, which showed several long range correlations with an oxygenated singlet carbon resonating at δ_C 90.0 (C-5), a quartet carbon resonating at δ_C 19.5 (CH_3-14) and a doublet carbon resonating at δ_C 34.4 (C-4). Other ^{1}H and ^{13}C-resonances were similar to those of ring A in cangorin J (Itokawa et al., 1994). Therefore, the ring A substituents were determined to be 1β-acetoxy, 2β-nicotinoyloxy and 4β-methyl groups. The stereochemical disposition of these substituents was determined from both the similarity in coupling constants and patterns of ring A protons of **1** and those of cangorin J, and from the NOESY spectra. These showed strong cross peaks between H-1 (δ_H 5.74) and H-2 (δ_H 5.92), H-2 and H-3 (δ_H 2.03, 2.56) and H-4 (δ_H 2.59), and H-14 (δ_H 1.31) and H-15 (δ_H 1.62).

The proton signal at δ_H 5.04 (*d*, $J=6.8$ Hz) showed ^3J-correlations with δ_C 165.8 (9-OC=O), δ_C 21.1 (C-15), δ_C 90.0 (C-5) and δ_C 49.4 (C-7). Consequently, this proton was assigned to be H-9. From the COSY spectrum, this proton couples with two methylene protons (H-8) resonating at δ_H 2.25 (*dd*, $J=16.5$, 3.1 Hz) and δ_H 2.56 (*m*); moreover, from the HETCOR spectrum, H-7 was assigned to resonate at δ_H 2.43 as a broad singlet. These assignments were further confirmed by the presence of long range correlations between C-8 (δ_C 32.1, *t*) and H-9, and between C-11 (δ_C 83.5, *s*) and H-8. The proton signal resonating at δ_H 5.72 was determined to be H-6. This proton showed long range correlations with C-8 (δ_C 32.1), C-10 (δ_C 50.4), C-11 (δ_C 83.5), C-5 (δ_C 90.0) and 6-OC=O (δ_C 165.2). Other ^{1}H- and ^{13}C-resonances were almost identical to those of ring B in wilforcidine, isolated from *T. wilfordii* (He and Wu, 1994). Similarity in coupling constants and patterns of ring B protons of **1** and those of wilforcidine determined the substituents of ring B to be 6α-nicotinoyloxy and 9α-benzoyloxy groups. The NOESY spectra showed correlations between H-6 (δ_H 5.72) and H-14 (δ_H 1.31), H-15 (δ_H 1.62) and H-8 (δ_H 2.56), H-7 (δ_H 2.43) and H-8 (δ_H 2.25, 2.56), H-9 (δ_H 5.04) and H-8 (δ_H 2.56) and H-15 (δ_H 1.62), and H-15 and the acetate methyl protons (δ_H 1.58).

Unambiguous assignments of other protons and carbons were made possible from the COSY, HETCOR and HMBC spectra. Compound **1** can thus be identified as 1β-acetoxy-9α-benzoyloxy-2β,6α-dinicotinoyloxy-β-dihydroagarofuran. The key ^3J HMBC correlations of **1** are shown in Table 1. A related positional isomer of compound **1**, namely, 1β-acetoxy-8α-benzoyloxy-9α,13-dinicotinoyloxy-β-dihydroagarofuran, was recently isolated from the Chinese species of *Celastrus angulatus* seed (Tu et al., 1993).

Maytenfolic acid, 3α-hydroxy-2-oxofriedelane-20α-carboxylic acid (**2**), lup-20(29)-ene-1β,3β-diol were tested for antimicrobial activity against bacteria and fungi

and maytenfolic acid showed the most prominent antimicrobial activity by inhibiting the growth of *Staphylococcus aureus, Pseudomonus aeruginosa*, *Candida albicans* and*Cryptococcus neoformans* with MIC values of 12.5 μg/ml (Table 2). The friedelane acid **2** was less active against these organisms with a MIC values in the range of 12.5–50 μg/ml, while lup-20(29)-ene-1β,3β-diol and agarofuran alkaloid **1** were inactive. The antibacterial 12-oleanenes and 3,4-secooleanenes were also isolated from another Saudi species of *M. undata* (Muhammad et al., 2000) and from *D. papuana* (Nick et al., 1994, 1995).

Maytenfolic acid, previously isolated from *M. diversifolia*, showed significant inhibitory activity against P-388 lymphocytic leukemia in BDF_1 mice (Nozaki et al., 1982). 3α-Hydroxy-2-oxofriedelane-20α-carboxylic acid (**2**), was previously isolated from another Celastraceae, *A. populena* (De Sousa et al., 1990), while lup-20(29)-ene-1β,3β-diol was not previously reported from Celastraceae. β-Amyrin, (-)-*epi*catechin and (-)-4′-methyl*epi*-gallocatechin were also isolated from *M. arbutifolia*.

3. Experimental

3.1. General

Mp: uncorr.; IR: KBr; NMR: were taken on a Bruker Avance DRX-500 instrument at 500 MHz (^1H) and 125 MHz (^{13}C) in $CDCl_3$, using TMS as int. standard. Multiplicity determinations (DEPT) and 2D NMR spectra (COSY, HETCOR, HMBC and NOESY) were run using standard Bruker software; MS: were obtained by direct injection using a Shimadzu GC/MS QP 500 and Quattro LC triple quadrupole tandem MS/MS with electrospray (Z-spray) ion source; UV spectra were obtained on an UV-160 IPC UV-visible spectrophotometer using either $CHCl_3$ or MeOH solutions; Optical rotation measurements were taken on a Perkin-Elmer 241 MC polarimeter in $CHCl_3$ at ambient temp.; TLC: silica gel 60 F_{254} plates. solvent: $CHCl_3$–MeOH (4:1); CC: flash-silica gel G (J.T. Baker, 40 μm); Centrifugal preparative TLC (CPTLC, using Chromatotron®, Harrison Research Inc. Model 7924): 2 mm silica gel PF 254 Chromatotron rotor, using a N_2 flow rate of 4 ml min^{-1}. The isolated compounds were visualized by observing under UV-254 nm, followed by spraying with either Dragendorff's or 1% vanillin-H_2SO_4 spray reagents.

Table 2
Antimicrobial activities of maytenfolic acid (MA), **2**, and lup-20(29)-ene-1β,3β-diol (LPD)[a]

	MIC (in μg/ml)			
Compounds	*S. aureus*	*P. aeruginosa*	*C. neoformans*	*C. albicans*
MA	12.5	12.5	>12.5	>12.5
2	>12.5	>25	>50	>50
LPD	(−)	(−)	(−)	(−)

[a] MIC values after 48 h of incubation at 37 °C. (−): Inactive

3.2. Plant material

The aerial parts and stem bark of *M.heterophylla* and *M. arbutifolia* were collected in February 1997 from the Abha and Albaha regions of Saudi Arabia, respectively. Both are shrubs or small trees widespread in southwestern Arabian Peninsula (Collenette, 1985). The plants were identified by Dr. Sultanul Abidin of Medicinal, Aromatic and Poisonous Plants Research Center, College of Pharmacy, King Saud University. Voucher specimens (*M. heterophylla* 13987, *M. arbutifolia* 13418) were deposited at the herbarium of the College of Pharmacy, King Saud University, Riyadh, Saudi Arabia.

3.3. Extraction method and bioautography

M. heterophylla dried ground leaves (1.5 kg) were percolated at room temperature with 95% EtOH to yield a green residue (115 g). On the other hand, dried powdered stem bark (250 g) of *M. heterophylla* were extracted by percolation with ethyl acetate to afford a brownish residue (10 g). *M. arbutifolia* dried powdered leaves (225 g) were extracted by percolation with 95% EtOH to yield a green residue (50 g). All of the crude extracts showed animicrobial activities against*Bacillus subtilis*,*S. aureus*, *C. albicans*, and *C. neoformans* using the agar dilution assay (Mitscher et al., 1985). Furthermore, these three extracts were separately subjected to bioautography (Hamburger and Cordell, 1987) on Si-gel plates (5×10 cm; solvent: $CHCl_3$–MeOH (9:1) for *M. heterophylla* stem bark; $CHCl_3$–MeOH (4:1) for *M. heterophylla* leaves; $CHCl_3$–MeOH–HCOOH (8:2:0.01) for *M. arbutifolia* leaves), using *B. subtilis* as the test organism. Two major clear elongated zones with R_f values between 0.15–0.30 and 0.55–0.60 were observed for *M. heterophylla* leaves after 24 h of incubation, two zones with R_f values between 0.10–0.25 and 0.45–0.60 were also observed for *M. heterophylla* stem bark, while a single elongated zone with R_f value corresponded to 0.25–0.35 was observed for *M. arbutifolia* leaves.

3.4. Isolation of compounds

A part of the active EtOH extract of *M. heterophylla* leaves (30 g) was flash-chromatographed over Si gel (40 μm, 750 g), using $CHCl_3$–Me_2CO as eluant, to give several mixtures that were pooled by TLC characteristics. Mixtures that eluted with 5–7% Me_2CO–$CHCl_3$ were further subjected to repeated CC over Si-gel, followed by CPTLC (using a Chromatotron®) on 2 mm Si-gel PF_{254} disc, using $CHCl_3$–Me_2CO as eluant, to afford β-amyrin (50 mg), lup-20(29)-ene-1β,3β-diol (30 mg, R_f 0.32) and **1**

(50 mg, R_f 0.28). Further elution of the flash-CC, using 12–15% Me_2CO–$CHCl_3$, afforded (−)-4′-methyl*epi*-gallocatechin (15 mg), followed by (−)-*epi*catechin (18 mg). Likewise, the active ethyl acetate extract of *M. heterophylla* stem bark afforded maytenfolic acid (25 mg, R_f 0.57) and **2** (30 mg, R_f 0.38). A similar isolation procedure adopted for the EtOH extract of *M. arbutifolia* leaves afforded β-amyrin (200 mg), (−)-*epi*catechin (20 mg) and (−)-4′-methyl*epi*gallocatechin (60 mg). The identity of (−)-*epi*catechin (Mossa et al., 1992) were confirmed by direct comparison with an authentic sample.

3.5. 1β-Acetoxy-9α-benzoyloxy-2β,6α-dinicotinoyloxy-β-dihydroagarofuran (heterophylline) (1)

Mp 132–135 °C; $[\alpha]_D$ +63.2° (*c* 1.00, $CHCl_3$); UVλ_{max} (logε) ($CHCl_3$) 264 (3.74), 258 (3.72), 234 (4.10) nm; IR ν_{max} (KBr) 2950, 1734, 1710, 1705 (C=O), 1593 cm^{-1}; ^1H and ^{13}C NMR: Table 1; MS: (*m*/*z*) 642 ($C_{36}H_{38}N_2O_9$; $[M]^+$).

3.6. Maytenfolic acid

Needles, mp: 285–287 °C, $[\alpha]_D$ +45.7° (*c* 0.13, MeOH) [Lit. (Nozaki et al., 1982) mp: 281–282 °C, $[\alpha]_D$ +34.2°]; MS: (*m*/*z*) 472 ($C_{30}H_{48}O_4$; $[M]^+$).

3.7. 3α-Hydroxy-2-oxofriedelane-20α-carboxylic acid (2)

Needles, mp 305–307 °C [Lit. (De Sousa et al., 1990) mp: 313–315 °C]; $[\alpha]_D$ +90° (*c* 0.10, $CHCl_3$); ^{13}C-NMR: 36.5 (C-1), 212.3 (C-2), 77.3 (C-3), 54.8 (C-4), 39.6 (C-5), 40.9 (C-6), 17.9 (C-7), 51.0 (C-8), 38.3 (C-9), 60.9 (C-10), 35.0 (C-11), 29.7 (C-12), 38.0 (C-13), 39.5 (C-14), 30.1 (C-15), 36.5 (C-16), 30.5 (C-17), 44.7 (C-18), 30.6 (C-19), 40.6 (C-20), 29.7 (C-21), 37.1 (C-22), 11.2 (C-23), 14.6 (C-24), 18.1 (C-25), 18.2 (C-26), 16.6 (C-27), 32.2 (C-28), 32.1 (C-29), 182.4 (C-30); MS: (*m*/*z*) 472 ($C_{30}H_{48}O_4$; $[M]^+$).

3.8. Lup-20(29)-ene-1β,3β-diol

Needles, mp 245–247 °C, $[\alpha]_D$ +13.0° (*c* 1.00, $CHCl_3$)] [Lit. (Savona et al., 1978) mp: 249–250 °C; $[\alpha]_D$ +11.0 °C (*c* 0.10, $CHCl_3$)]; EIMS: (*m*/*z*) 442 ($C_{30}H_{50}O_2$; $[M]^+$).

3.9. Antimicrobial activity

The preliminary antimicrobial activity of the extracts/fractions were determined by using agar dilution technique (Mitscher et al., 1985) and the MIC values of maytenfolic acid and **2** were determined by two-fold serial broth microdilution assay (Hufford et al., 1975). The test organisms used were ATCC strains of *C. albicans* (# 10231), *C. neoformans* (# 90113), *S. aureus* (#29213) and *P. aeruginosa* (# 15442). Amphotericin B and chloramphenicol were used as positive controls, while DMSO as a negative control.

Acknowledgements

The authors thank Mr. Humayun H. Mirza and Mr. Mustafa O. Khaled, College of Pharmacy, King Saud University, Riyadh, Saudi Arabia for their valuable technical assistance, Dr. Mohamed Rashed, King Faisal Specialist Hospital and Research Center, Riyadh, for obtaining some the mass spectra and Mr. Frank T. Wiggers, School of Pharmacy, University of Mississippi, USA, for recording the NMR spectra.

References

Chen, T.K., Ales, D.C., Baenziger, N.C., Wiemer, D.F., 1983. Anti-repellent triterpenoids from *Cordia alliodora*. J. Org. Chem. 48, 3525–3531.

Collenette, S., 1985. An Illustrated Guide to the Flowers of Saudi Arabia. Scorpion Publishing, London, UK, pp. 113–114.

Corsino, J., Furlam, M., Bolzani, V.D.A.S., Pereira, A.M.S., Franca, S.E., 1998. Further sesquiterpene pyridine alkaloids from *Maytenus aquifolium*. Phytochemistry 49, 2181–2183.

De Sousa, J.R., Silva, G.D.F., Pedersoli, J.L., Alves, R.J., 1990. Friedelane and oleanane triterpenoids from *Austroplenckia populena*. Phytochemistry 29, 3259–3261.

Doddrell, D.M., Khong, P.W., Lewis, K.G., 1974. The stereochemical dependence of ^{13}C chemical shifts in olean-12-ene and urs-12-ene as an aid to stereochemical assignments. Tetrahedron Letters 27, 2381–2384.

Flores, A.F. 1984. Advances in economic botany. In: Prance, G.T., Kallunti, J.A. (Eds.), Ethnobotany in the New Tropics New York, pp. 1–8.

Ghazanfar, S.A., 1994. Handbook of Arabian Medicinal Plants. CRC Press, Boca Raton, p. 83.

Gonzalez, A.G., Jimenez, I.A., Ravelo, A.G., Sazatornil, G., Bazzocchi, I.L., 1993. New sesquiterpene with antifeedent activity from *Maytenus canariensis* (Celastraceae). Tetrahedron 49, 697–702.

Gonzalez, A.G., Alvarenga, N.L., Ravelo, A.G., Jimenez, I.A., Bazzocchi, I.L., Canela, N.J., Moujir, L.M., 1996. Antibiotic phenol nor-triterpenes from *Maytenus canariensis*. Phytochemistry 43, 129–132.

Gonzalez, A.G., Gonzalez, C.M., Bazzocchi, I.L., Ravelo, A.G., Luis, J.G., Dominguez, X.A., 1987. Sesquiterpene alkaloids from celastraceae. Phytochemistry 26, 2133–2135.

Hamburger, M.O., Cordell, G.A., 1987. A direct bioautographic TLC assay for compounds possessing antibacterial activity. J. Nat. Prod. 50, 19–22.

He, Z.-H., Wu, H.-M., 1994. Wilforcidine, a new alkaloid from *Tripterygium wilfordii*. J. Nat. Prod. 57, 305–307.

Hufford, C.D., Funderburk, M.J., Morgan, J.M., Robertson, L.W., 1975. Two antimicrobial alkaloids from heartwood of *Liriodendron tulipifera*. J. Pharm. Sci. 4, 789–792.

Itokawa, H., Shiota, O., Morita, H., Takeya, K., 1994. Cangorins F-J, additional oligo-nicotinated sesquiterpenes polyesters from *Maytenus ilicifolia*. J. Nat. Prod. 57, 460–470.

Kuo, Y.H., Chen, C.H., Kuo, L.M.Y., King, M.L., Wu, T.S., Haruna, M., Lee, K.H., 1990. Antitumor agents, 112. Emarginatine B, a

novel potent cytotoxic sesquiterpene pyridine alkaloid from *Maytenus emarginata*. J. Nat. Prod. 53, 422–428.

Kupchan, S., Morris, H., Harold, P.J., Smith, R.M., Karim, A., Malcolm, W., Court, W.A., Yatagai, M., 1974. Celacinnine, a novel macrocyclic alkaloid prototype. J. Chem. Soc., Chem. Commun. 9, 329–330.

Lee, K.H., Nozaki, H., Hall, I.H., Kasai, R., Hirayama, T., Suzuki, H., Wu, R.Y., Huang, H.C., 1982. Antitumour agents, 60. Maytansine, an antileukemic principle from *Maytenus diversifolia*. J. Nat. Prod. 45, 509–510.

Mitscher, L.A., Leu, R.-P., Bathala, M.S., Wu, W.-N., Beal, J., 1985. Antimicrobial agents from higher plants. 1. Introduction, rationale and methodology. Lloydia 35, 157–166.

Monache, F.D., d'Albuguerque, I.L., Ferrari, F., Bettolo, G.B., 1967. A new catechin and a dimeric proanthocyanidin from *Ouratea* sp. Tetrahedron Letters 43, 4211–4214.

Mossa, J.S., Muhammad, I., El-Feraly, F.S., Hufford, C.D., 1992. 3β-Dihydroxyabieta-8,11,13-triene-1-one and other constituents from *Juniperus excelsa* leaves. Phytochemistry 31, 2789–2792.

Muhammad, I., El-Sayed, K.A., Mossa, J.S., Al-Said, M.S., El-Feraly, F.S., Clark, A.M., Hufford, C.D., Oh, S., Mayer, A.M.S., 2000. Bioactive 12-oleanene and secooleanene triterpene acids from *Maytenus undata*. J. Nat. Prod. 63, 605–610.

Nakamura, M., Nakasumi, T., Yoshizawa, T., Minagawa, Y., Nakagawa, K., 1997. Eur. Pat. Appl., Application: EP 96-106838 960430. CAN 127, 70825.

Nick, A., Wright, A.D., Rali, T., Sticher, O., 1995. Antibacterial triterpenoids from *Dillenia papuana* and their structure activity relationship. Phytochemistry 40, 1691–1695.

Nick, A., Wright, A.D., Sticher, O., Rali, T., 1994. Antibacterial triterpenoid acids from *Dillenia papuana*. J. Nat. Prod. 57, 1245–1250.

Nozaki, H., Suzuki, H., Lee, K.-H., McPhail, A.T., 1982. Structure and stereochemistry of maytenfolic acid and maytenfoliol, two new antileukemic triterpenes from *Maytenus diversifolia*: x-ray crystal structure. J. Chem. Soc., Chem. Commun. 1048–1051.

Sannomiya, M., Vilegas, W., Rastrelli, L., Pizza, C., 1998. A flavonoid glycoside from *Maytenus aquifolium*. Phytochemistry 49, 237–239.

Savona, G., Bruno, M., Rodriguez, B., Marco, J.L., 1987. Triterpenoids from *Salvia deserta*. Phytochemistry 26, 3305–3308.

Shirota, O., Tamemura, T., Morita, H., Takeya, K., Itokawa, H., 1996. Triterpenes from Brazilian medicinal plant chuchuhausi (*Maytenus krukovii*). J. Nat. Prod. 59, 1072–1075.

Tu, Y., Song, Q., Wu, X., Huang, G., Ma, Y., Chen, Y., 1993. Sesquiterpene constituents from *Celastrus angulatus*. Huaxue Xuebao 51, 404–408.

Wagner, H., Burghart, J., 1977. Chemical constituents of the Celastraceae. IV. Spermidine alkaloids and triterpenes from *Maytenus heterophylla* and *Pleurostylia africana*. Planta Medica 32A, 9–14.

PERGAMON

Phytochemistry 58 (2001) 481–487

PHYTOCHEMISTRY

www.elsevier.com/locate/phytochem

Germacrenes from fresh costus roots

Jan-Willem de Kraker[a,b], Maurice C.R. Franssen[a,*], Aede de Groot[a], Toshiro Shibata[c], Harro J. Bouwmeester[b]

[a]*Laboratory of Organic Chemistry, Wageningen University, Dreijenplein 8, 6703 HB Wageningen, The Netherlands*
[b]*Plant Research International, PO Box 16, 6700 AA Wageningen, The Netherlands*
[c]*Hokkaido Experimental Station for Medicinal Plants, National Institute of Health Sciences, 108 Ohashi, Nayoro, Hokkaido, 096-0065, Japan*

Received 20 March 2001; received in revised form 21 May 2001

Abstract

Four germacrenes, previously shown to be intermediates in sesquiterpene lactone biosynthesis, were isolated from fresh costus roots (*Saussurea lappa*). The structures of (+)-germacrene A, germacra-1(10),4,11(13)-trien-12-ol, germacra-1(10),4,11(13)-trien-12-al, and germacra-1(10),4,11(13)-trien-12-oic acid were deduced by a combination of spectral data and chemical transformations. Heating of these compounds yields (−)-β-elemene, (−)-elema-1,3,11(13)-trien-12-ol, (−)-elema-1,3,11(13)-trien-12-al, and elema-1,3,11(13)-trien-12-oic acid respectively, in addition to small amounts of their diastereomers. Acid induced cyclisation of the germacrenes yields selinene, costol, costal, and costic acid respectively. It is highly probable that the elemenes reported in literature for costus root oil are artefacts. © 2001 Elsevier Science Ltd. All rights reserved.

Keywords: *Saussurea lappa*; Asteraceae; Sesquiterpenes; Sesquiterpene lactone biosynthesis; Germacrenes; Elemenes; Eudesmanes

1. Introduction

Saussurea lappa Clarke, is a member of the Asteraceae indigenous to parts of India and Pakistan where it grows in the Himalayas at 2500–3500 m elevation. The dried 4–5 year old roots of this plant are known as costus roots and have a reputation for their medicinal properties as well as their fragrance. Attempts are being made to cultivate this plant, since it has become an endangered species due to ruthless collection from forest areas (Paul et al., 1960; Hatakeyama et al., 1989; Ayaz, 1996).

Various studies have shown that costus roots are extremely rich in sesquiterpene lactones (3% of fresh weight), of which the most important are dehydrocostus lactone and (+)-costunolide (**5**) (Paul et al., 1960; Somasekar Rao et al., 1960). The latter is the structurally simplest sesquiterpene lactone and is generally accepted as the common intermediate in the biosynthesis of most sesquiterpene lactones (Herz, 1977; Fischer, 1990). Costunolide (**5**) is presumably formed from farnesyl diphosphate (FPP) via (+)-germacrene A (**1**) (Fig. 1). Enzyme activities that introduce a carboxylic function in the isopropenyl side chain of (+)-germacrene A yielding germacra-1(10),4,11(13)-trien-12-oic acid (**4**) have recently been identified in chicory (*Cichorium intybus* L.), a vegetable rich in sesquiterpene lactones (de Kraker et al., 1998, 2001). Currently, investigations concerning the pathway for sesquiterpene lactones in chicory are hampered by the lack of a source of germacrene intermediates **1–4**, in particular germacrene acid (**4**). These germacrene compounds are themselves not present in chicory (Sannai et al., 1982), and to our knowledge only the isolation of (+)-germacrene A (**1**) from various plant species (e.g. Wichtman and Stahl-Biskup, 1987) and the partial purification of germacra-1(10),4,11(13)-trien-12-al (**3**) from *Vernonia glabra* (Steetz) (Bohlmann et al., 1983) have been described. A reason for the scarcity of reports on these germacrenes might be their instability. They are susceptible to proton-induced cyclisations and to heat induced (e.g. steam distillation, GC-analysis) Cope rearrangement yielding the eudesmane or elemene framework, respectively (Fig. 2) (Southwell, 1970; Takeda, 1974; Wichtman and Stahl-Biskup, 1987; Teisseire, 1994; de Kraker et al., 1998, 2001).

* Corresponding author. Tel.: +31-317-482976; fax: +31-317-484914.
E-mail addresses: maurice.franssen@bio.oc.wag-ur.nl (M.C.R. Franssen), h.j.bouwmeester@plant.wag-ur.nl (H.J. Bouwmeester).

0031-9422/01/$ - see front matter © 2001 Elsevier Science Ltd. All rights reserved.
PII: S0031-9422(01)00291-6

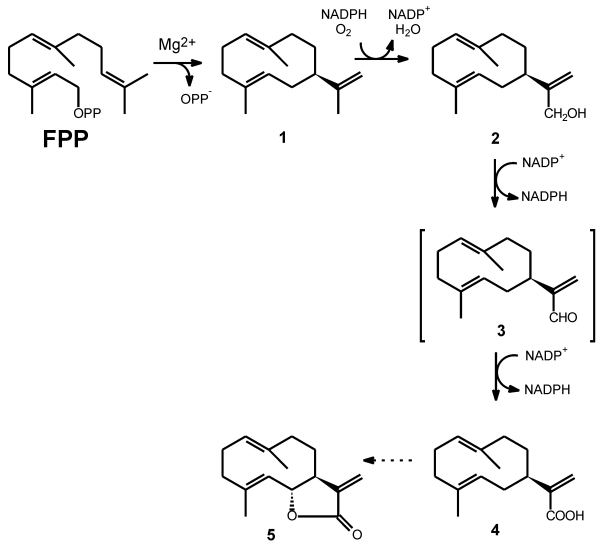

Fig. 1. Biosynthetic route from FPP to (+)-costunolide (**5**) via (+)-germacrene A (**1**), germacra-1(10),4,11(13)-trien-12-ol (**2**), germacra-1(10),4,11(13)-trien-12-al (**3**), and germacra-1(10),4,11(13)-trien-12-oic acid (**4**). Only the last step (dotted arrow) has not yet been demonstrated.

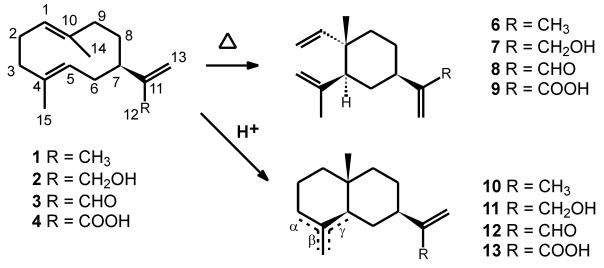

Fig. 2. Heat induced Cope-rearrangement of **1–4** yields (−)-β-elemene (**6**), (−)-elema-1,3,11(13)-trien-12-ol (**7**), (−)-elema-1,3,11(13)-trien-12-al (**8**), and elema-1,3,11(13)-trien-12-oic acid (**9**); acidic conditions are expected to give selinene (**10**), costol (**11**), costal (**12**), and costic acid (**13**).

The presence of β-elemene (**6**), (−)-elema-1,3,11(13)-trien-12-ol (**7**), and (−)-elema-1,3,11(13)-trien-12-al (**8**) in commercially available costus root oil has drawn our attention to these roots (Klein and Thömel, 1976; Maurer and Grieder, 1977). Since this oil is obtained by steam distillation and elemenes are generally considered to be artefacts, we assumed that costus roots originally contain the corresponding germacrenes **1–3**. The reported isolation of costic acid (**13**) from costus roots also suggests the presence of germacrene acid (**4**) (Bawdekar and Kelkar, 1965), since HCl was used in the isolation procedure which might have initiated the cyclisation of germacrene acid.

The aim of the present research was to investigate the presence of the germacrenes **1–4** in fresh costus roots, and to develop a mild isolation procedure for these compounds so that they can be used for further studies on sesquiterpene lactone biosynthesis.

2. Results and discussion

Et_2O extracts of commercially available dried costus roots, costus resinoid and costus root oil were screened on GC–MS for the presence of germacrene A (**1**). This germacrene can be measured as a well resolved peak at a GC-injection port temperature of 150 °C. The more polar germacrenes **2–4** cannot be measured as a real peak, because they will rearrange during migration through the GC-column to their faster migrating elemenes and will be observed as a broad "hump" in the baseline such as described for hedycaryol and 7-hydroxygermacrene (Stahl, 1984; de Kraker et al., 1998, 2001). Yet, in all of these extracts we would detect only the Cope-rearrangement product β-elemene (**6**). It was concluded that the germacrene A originally present in these materials had been exposed to heat and that the commercially available materials are not suitable for the isolation of germacrenes. Interestingly, in the resinoid and dried roots the previously unreported elema-1,3,11(13)-trien-12-oic acid (**9**) was detected in addition to (−)-elema-1,3,11(13)-trien-12-ol (**7**) and (−)-elema-1,3,11(13)-trien-12-al (**8**).

In contrast, the Et_2O extract of fresh costus roots did contain germacrene A (**1**), whereas no (−)-β-elemene (**6**) was observed. At the applied GC-injection port temperature of 150 °C, also the foreseen "broad humps" of the oxygenated germacrenes **2–4** were visible in the GC-chromatogram instead of sharp peaks of the oxygenated elemenes **7–9**.

In order to isolate germacrenes **1–4**, 300 g of fresh costus roots was powdered in liquid N_2 and extracted with Et_2O. The organic extract was shaken with aq Na_2CO_3 to remove germacrene acid (**4**) and other acidic/polar compounds; the lactones (mainly costunolide and dehydrocostus lactone, 1.5 g) were partially removed by crystallisation from pentane (Somasekar Rao et al., 1960). Germacrenes **1–3** could be selectively extracted from pentane with aq $AgNO_3$ (Southwell, 1970; Minnaard, 1997), because of the complex-formation between the Ag^+-ions and the diene-ring system present in the germacrenes. Subsesquent flash column chromatography of the obtained crude germacrene-mixture in combination with a second $AgNO_3$ extraction yielded: 1.5 mg germacrene A (**1**), 1.5 mg germacrene aldehyde (**3**), and a mixture of germacrene alcohol (**2**) with β-costol (**11**), hedycaryol, costunolide (**5**), and dehydrocostus lactone. The isolated germacrene A contained a small impurity of 4% (determined by GC–MS) humulene that is extracted with aq $AgNO_3$ as well due to the presence of a cylic diene moiety. Purification of the germacrene alcohol (**2**) was more elaborate because β-costol (**10**) with its two adjacent exocyclic bond is also extracted with aq $AgNO_3$, whereas α- and γ-costol are not. Furthermore germacrene alcohol, in our hands, could hardly be separated from costunolide on silica gel. Argentation chromatography yielded 3 mg of germacrene alcohol (**2**)

that was, however, unlike the isolated germacrenes **1**, **3** and **4**, contaminated with elematrien-12-ol (**7**) (approx. 30%).

The germacrene acid (**4**) containing alkaline (Na_2CO_3) extracts were carefully brought to pH 6 and extracted with Et_2O. As expected from the protocol of Bawdekar and Kelkar (1965), the sesquiterpenoid acids did not dissolve in aq $NaHCO_3$ and acidification to a lower pH was not necessary, thus preventing the undesired cyclisation of germacrene acid to costic acid (**13**). Extraction with aq $AgNO_3$ and column chromatography yielded 1.5 mg of germacrene acid (**4**).

GC-analyses of germacrene aldehyde (**3**) at a GC-injection port temperature of 150 °C results in a "broad hump" is (Fig. 3 A) that displays the mass spectrum of elematrien-12-al (**8**) over its entire range. At a GC-injection port temperature of 250 °C a sharp peak of elematrien-12-al is visible instead (Fig. 3B), because the germacrene aldehyde is immediately rearranged in the GC-injection port and not during its migration through the GC-column (de Kraker et al., 2001). In the presence of *p*-toluenesulfonic acid the germacrene aldehyde is completely cyclised to costal (**12**) (Fig. 3C). This indicates that the sample is free of elemene aldehyde, because the elemene aldehyde does not cyclise to costal. ^{1}H NMR of the germacrene aldehyde confirmed that it did not contain any of its Cope rearrangement product, since a double doublet at δ 5.85 of $C_2{=}C_1H{-}C_{10}$ typical for the elemene aldehyde was clearly missing. Unfortunately, in solution many germacrenes show broadened NMR signals or even multiple NMR signals, due to the existence of different conformations of the ten-membered ring (Fig. 4) (Takeda, 1974; Minnaard, 1997). This hinders a complete interpretation of the NMR. Most striking is the presence of two aldehyde proton signals of similar height at δ 9.37 and δ 9.35 that cannot be due to coupling with a proton at C_{13}, accompanied by two very small signals at δ 9.47 and δ 9.45 (ratio 1:1:0.01:0.01).

The existence of different germacrene conformations also explains the formation of a small amount of diastereomeric elematrien-12-al during the Cope rearrangement of germacrene aldehyde (Fig. 3B). Cope rearrangement is a stereospecific reaction that preferably proceeds via a chair-like transition state (March, 1992), via either the UU or DD conformation of the germacrene (Fig. 4). However, the UU conformation with the isopropenal group in the equatorial position predominates and consequently the diastereomer of **8** will be formed only in low yield (Takeda, 1974; Piet et al., 1995; Minnaard, 1997). Small amounts of diastereomeric elemenes were also detected for the GC-injection port induced Cope rearrangement of germacrene A, germacratrien-12-ol

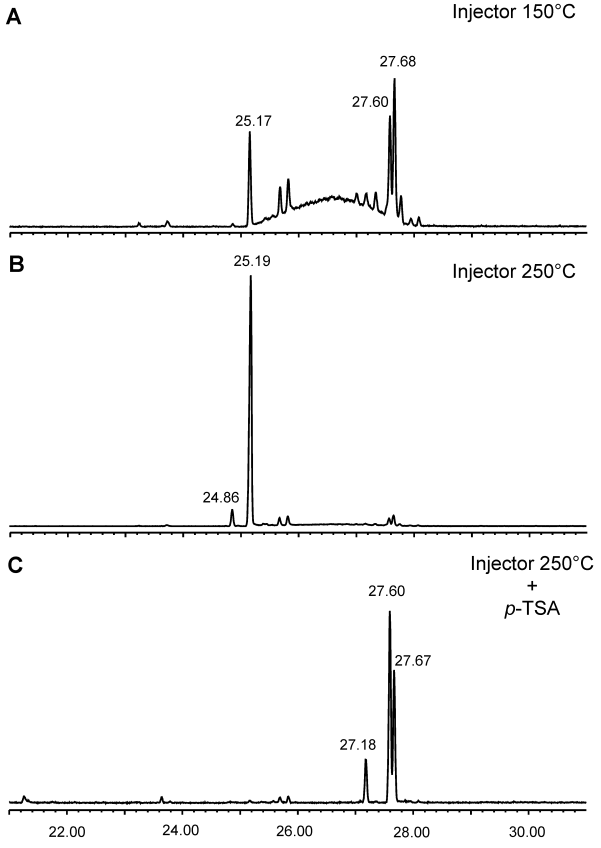

Fig. 3. GC–MS analyses of the germacrene aldehyde (**3**) at an injection port temperature of 150 °C (A) yields a broad hump that starts at the position of elematrien-12-al (**12**) (25.17 min). Injection at an temperature of 250 °C (B) gives almost complete rearrangement of **3** to elematrien-al (**12**) (25.19), whereas a small amount of diastereomeric elemene aldehyde can also be detected (24.86). In the presence of *p*-toluenesulfonic acid (C) the germacrene aldehyde (**3**) is completely converted into costal (**8**): γ-costal (27.18 min), β-costal (27.60 min), and α-costal (27.67 min).

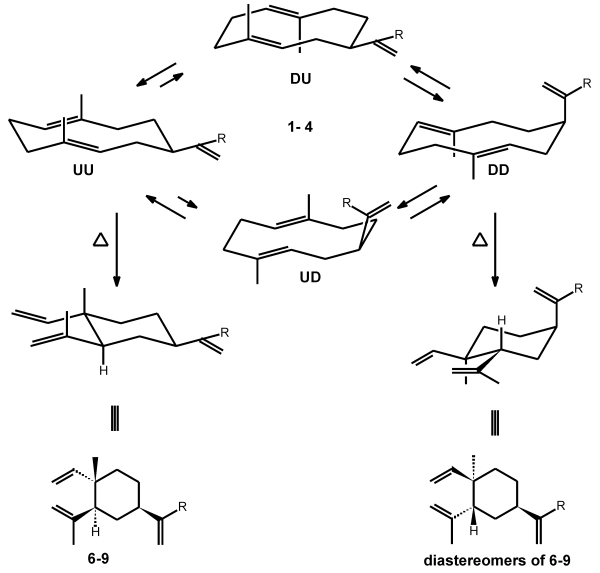

Fig. 4. Conformations of germacrenes **1–4** denoted as UU, UD, DU, and DD. U (up) and D (down) refer to the orientation of the C-14 and C-15 methyl groups. Both conformations UU and DD will easily undergo Cope rearrangement, however, the UU conformation is predominant and will yield elemenes **6–9**, whereas the diastereomeric elemenes that origin from the DD conformation will hardly be formed.

and germacratrien-12-oic acid. These diastereomers have a mass spectrum very similar to their true elemene and typically constitute only 2–7% of the total amount of Cope rearrangement product formed. Although we failed to detect the β-elemene diastereomer before (de Kraker et al., 1998), small amounts of it are not unusual in samples containing β-elemene/germacrene A (Dr. M. A. Posthumus, personal communication). The structure of the elematrien-12-ol diastereomer has tentatively been assigned by Maurer and Grieder (1977).

When the injection port temperature of the GC was varied between 150 and 250 °C, germacrene alcohol (**2**) and germacrene acid (**4**) showed chromatogram patterns similar to that of germacrene aldehyde (**3**). Both germacrene A (**1**) and germacrene acid (**4**) were completely converted into their eudesmane analogues (**10** and **13**, respectively) in the presence of *p*-toluenesulfonic acid. However, the GC-chromatogram of the germacrene alcohol (**2**) still showed a peak of elematrien-12-ol (**7**) after acid treatment, indicating that isolated sample of germacrene alcohol is actually a mixture of germacrene- and elemene alcohol. This was confirmed by ^{1}H NMR that showed a double doublet ($J=18$ and 10 Hz) at δ 5.81 typical for elematrien-12-ol (Maurer and Grieder, 1977). It is not known whether the presence of elematrien-12-ol is caused by an intrinsic higher instability of the germacrene alcohol and/or by the more difficult and time-consuming purification of this compound. Although less likely, we cannot rule out that the elematrien-12-ol was already present in the crude plant material. In this respect it is remarkable that the germacratrien-12-ol produced in an enzyme assay from germacrene A (de Kraker et al., 2001) was free of any elematrien-12-ol and could be fully cyclised into costol (**11**), notwithstanding the fact that the germacratrien-12-ol had been exposed to 30 °C, a temperature unlikely to occur in costus roots that are underground.

The ^{1}H NMR of germacrene acid (**4**) was free of the double doublet at δ 5.85 from elematrien-12-oic acid (**9**) (de Kraker et al., 2001), but once again only few signals could be assigned. Similar observations were made by Zdero et al. (1991) for 3α- and 3β-acetoxygermacra-1(10)-,4,11(13)trien-12-oic acid whose structures could only be resolved after Cope-rearrangement to their corresponding elemene derivatives.

The isolation under mild conditions from fresh costus roots of (+)-germacrene A (**1**), germacra-1(10),4,11(13)-trien-12-al (**3**), and germacra-1(10),4,11(13)-trien-12-oic acid (**4**) clearly demonstrates that their reported elemene derivatives (**6–9**) are indeed heat-induced artefacts formed during drying of the roots or the manufacturing of costus resinoid/oil as literature on germacrenes suggests (e.g. Bohlmann et al., 1983; Wichtman and Stahl-Biskup, 1987; Teisseire, 1994). Very similar, has for example, been reported for the Australian shrub *Phebalium ozothamnoides* F. Muell whose main essential oil component is elemol, whereas the petroleum extract of macerated leaves yields hedycaryol instead (Southwell, 1970). Only in the case of germacra1(10),4,11(13)-trien-12-ol (**2**), it cannot completely be ruled out that a small quantity of its corresponding elemene is already present in fresh costus roots. The presence of elemenes instead of germacrenes was the only significant difference between an Et_2O-extract from fresh costus roots and the commercial costus root oil,[1] such as thoroughly described by Maurer and Grieder (1977). It is less certain whether the eudesmanes **10–13** have to be regarded as artefacts as well. Although they can be formed from germacrenes under acidic conditions, maybe during storage in the plant—an enzyme specifically producing β-selinene from FPP has been isolated from *Citronella mitis* fruits (Belingheri et al., 1992). It cannot be ruled out that costus root also contain such an enzyme and the eudesmanes present are genuine enzymatic products.

The presence of germacrenes **1–4** together with vast amounts of costunolide (**5**) in costus roots supports the pathway for costunolide as depicted in Fig. 1. The isolated germacrene acid (**4**) is currently being used to investigate the formation of costunolide (**5**) during sesquiterpene lactone biosynthesis in chicory.

3. Experimental

3.1. General experimental procedures

^{1}H NMR and ^{13}C NMR: recorded at 400 MHz with C_6D_6 as solvent and TMS as internal standard. GC–MS: HP 5890 series II gas chromatograph and HP 5972A mass selective detector (70 eV), equipped with a capillary HP5-MS column (30 m×0.25 mm, film thickness of 0.25 μm) at a helium flow rate of 0.969 ml min^{-1}, programmed at 55 °C for 4 min followed by a ramp of 5 °C min^{-1} to 280 °C, and a standard injection port temperature of 250 °C. CC: Silica gel flash (Janssen, 0.035–0.07 nm, pore 6 nm; column width 1.8 cm) (Still et al., 1978). 5% $AgNO_3$/Silica gel was prepared according to Maurer and Grieder (1977). TLC: Silica gel (Merck) 60 F254, eluent EtOAc–hexane (1:4); spray of 5 ml *p*-anisaldehyde in 5 ml H_2SO_4 and 95 ml EtOH, 1–2 min heating at 120 °C.

3.2. Plant material

Seeds of *Saussurea lappa* Clarke were introduced from Hortus Botanicus Vilr, Moscow (USSR) to the fields of Hokkaido Experimental Station for Medicinal Plants (Japan) in 1981 (Accession No. 9678-81) (Hatakeyama

[1] Less volatile compounds like fatty acids are not taken into account, because they are for obvious reasons not present in the costus oil that is produced by steam-distillation.

et al., 1989). Five-year old roots were harvested in August 2000 and transported by courier to The Netherlands. Upon arrival they were cut into pieces, powdered in liquid N_2 with a Waring blender and stored at −80 °C. Dried costus roots were obtained via internet from gaines.com (El Cajon CA, USA) and ginseng4less.com (Petaluma CA, USA).

3.3. Chemicals and reference compounds

Costus resinoid and costus oil were obtained from Pierre Chauvet SA (Seillans, France). Costunolide (**5**) and dehydrocostus lactone were isolated from costus resinoid according to Fischer et al. (1990) making use of the described TLC-spot colour (Asakawa et al., 1981), and recrystallised in pentane; NMR date were identical to those reported in literature (Kuroda et al., 1987; Takahashi et al., 1987). Standards of (−)-elema-1,3,11(13)-trien-12-al (**8**) [NMR in C_6D_6 did not markedly differ from those recorded in $CDCl_3$ (Maurer and Grieder, 1977; Bohlmann et al., 1983)], elema-1,3,11(13)-trien-12-oic acid (**9**) and costal (**12**) were isolated/synthesised as previously described (de Kraker et al., 2001). A mixture of α- and γ-costic acid (**13**) was synthesised from a mixture of α- and γ-costal with $NaClO_3$ (de Kraker et al., 2001). (−)-Elema-1,3,11(13)-trien-12-ol (**7**) was a gift of Dr. B. Maurer (Firmenich SA, Geneva, Switzerland), standards of (+)-germacrene A (**1**) and (−)-β-elemene (**6**) were a gift of Professor W. A. König (Hamburg University, Germany).

3.4. Screening of crude materials for the presence of germacrene A (*1*)

Samples of dried costus roots were powdered in liquid N_2, and 0.2 g of powdered root was shaken in 3 ml Et_2O and centrifuged after 5 min. The Et_2O was passed through a Pasteur pipette with 0.4 g silica gel. A spatula tip of costus resinoid and a droplet of costus oil were also dissolved in 3 ml of Et_2O and passed over silica gel. The Et_2O extracts were screened at an injection port temperature of 150 °C for a germacrene A (**1**) peak that should be replaced by a peak of β-elemene (**6**) at an injection port temperature of 250 °C (de Kraker et al., 1998).

3.5. Isolation of germacrenes *1–3*

Powdered fresh costus root (300 g) was extracted twice with 500 ml of Et_2O at 6 °C; the Et_2O was filtered and the volume reduced to 75 ml by rotary evaporation at room temperature. The concentrate was extracted with 5% aq Na_2CO_3 (3×50 ml). The aq Na_2CO_3 layers were combined and stored at 4 °C. The Et_2O layer was washed with brine, dried with Na_2SO_4, and the solvent removed yielding 2.8 g of a yellow-brown solid. Lactones (1.5 g) were partially removed by dissolving the residue in pentane and cooling at −20 °C, after which the crystallised lactones were filtered off and the solvent removed in vacuo. This procedure was repeated twice. The obtained oil was dissolved in 15 ml pentane and extracted with 20% aq. $AgNO_3$ (4×10 ml). The Ag^+ ions were complexed by adding carefully 10 ml of aq. NH_3 (25%) on ice, after which the water layer was extracted with pentane (3×50 ml) (Southwell, 1970). The pentane layers were washed with brine and dried with Na_2SO_4 yielding 100 mg of a yellow oil. This oil was chromatographed with 350 ml pentane–CH_2Cl_2 (3:7) after which the column was eluted with CH_2Cl_2. Fractions of 10 ml were collected and monitored by GC–MS and TLC; costunolide and dehydrocostus lactone could easily be distinguished by their greenish-blue (R_f 0.30) and blue (R_f 0.35) spots respectively. After removal of aplotaxene [a major constituent of costus root oil (Klein and Thömel, 1976; Maurer and Grieder, 1977)] by a second silver-ion extraction (4×1.5 ml 20% aq. $AgNO_3$, etc.), fractions 2+3 yielded 4 mg of germacrene A (**1**) with an impurity of 4% of humulene. Fractions 19–33 yielded, after a second silver-ion extraction, 1.5 mg germacratrien-12-al (**3**). Fractions 40–64 contained a mixture of costunolide (**5**), dehydrocostus lactone, β-costol (**11**), hedycaryol and germacrene alcohol (**2**). Attempts to separate the latter from β-costol and costunolide by column chromatography on silica gel using pentane–CH_2Cl_2 (1:9) or Et_2O–pentane (1:4) failed. Column chromatography on 5% $AgNO_3$-silica gel (10 gram) was more successful: costol and subsesquently costunolide were eluted with Et_2O (400 ml), whereas germacratrien-12-ol (2 mg, of which ≈ 30% elematrien-12-ol) was eluted with 150 ml MeOH–Et_2O (1:9).

3.6. Isolation of germacra-1(10),4,11(13)-trien-12-oic acid (*4*)

The aq. $NaCO_3$ layers (150 ml) were carefully acidified on ice to pH 6 with 5 M HCl and extracted with Et_2O (4×60 ml). The Et_2O layers were washed with brine, dried with Na_2SO_4, concentrated to 15 ml, and extracted with 20% aq $AgNO_3$ (4×10 ml). The Ag^+ ions were precipitated with 35 ml 2 M NaCl, and the remaining solution was extracted with Et_2O (4×50 ml). After washing with brine and drying with Na_2SO_4, 20 mg of a yellow solid was obtained that mainly contained germacratrien-12-oic acid (**4**), costunolide (**5**) and dehydrocostus lactone. Column chromatography with 350 ml of EtOAc–pentane (1:4) removed the lactones after which the germacrene acid was eluted with 100 ml EtOAc. The last minor impurities were removed by column chromatography with Et_2O–pentane (1:4; 400 ml), and 1.5 mg of germacratrien-12-oic acid was obtained.

3.7. Acid induced cyclisation of germacrenes

A small amount (≈ 10 nmol) of germacrene (**1–4**) was dissolved in 2 ml of CH_2Cl_2 and a crystal of *p*-toluenesulphonic acid was added (Minnaard, 1997). After 7 min at room temperature, the solution was washed with 1 ml of $NaHCO_3$ (satd.) and passed through a Pasteur pipette filled with 0.25 g $MgSO_4$. The solvent was reduced to 100 μl under a stream of N_2 and the sample was analysed by GC–MS. In case of germacratrien-12-oic acid (**4**) $NaHCO_3$ was replaced by NaH_2PO_4. The experiments were repeated with elemenes **6–9** that did not cyclise.

3.8. Compound characterisation

3.8.1. Germacrene A (*1*), 4 mg

Colourless oil, purple TLC-spot R_f 0.75, R_I 1511, EIMS *m/z* (rel int) M^+ 204 (8), $[M–Me]^+$ 189 (37), 93 (100), 67 (99), 68 (94), 107 (79), 81 (77), 41 (68), 79 (67), 105 (59), 91 (57), 53 (54), 147 (47), 119 (43), 121 (41), 55 (41), 161 (36), 133 (36). Cope rearrangement to **6**, R_I 1396, EIMS *m/z* (rel int) M^+ 204 (1), $[M–Me]^+$ 189 (28), 93 (100), 81 (96), 67 (83), 68 (76), 41(67), 79 (64), 107 (63), 53 (51), 91 (48), 147 (45), 121 (42), 105 (42), 55 (41), 161 (31), 119 (31), 133 (29); and diastereomer of **6**, R_I 1388, EIMS *m/z* (rel int) M^+ 204 (1), $[M–Me]^+$ 189 (23), 93 (100), 81 (78), 67 (61), 68 (58), 41 (52), 79 (51), 107 (50), 91 (41), 121 (35), 161 (34), 55 (33), 53 (32), 105 (31), 119 (27), 133 (23), 147 (21). Cyclisation yields **10**, R_I 1479 (γ), 1491 (β) and 1500 (α) [MS-data are comparable with those of Maurer and Grieder (1977) and were used in combination with the R_I's reported by Adams (1995) to determine the elution order].

3.8.2. Germacra-1(10),4,11(13)-trien-12-ol (*2*), 2 mg, mixture with 7 (≈ 30%)

Colourless/slightly yellow oil, pink/purple TLC-spot R_f 0.29, R_I 1673 to ± 1806. Cope rearrangement to **7**, R_I 1673 EIMS *m/z* (rel int) M^+ 220 (1), $[M–Me]^+$ 205 (4), 79 (100), 81 (94), 41 (91), 91 (90), 67 (86), 93 (85), 55 (69), 105 (66), 53(60), 119 (58), 77 (55), 68 (53), 189 (42), 121 (37), 133 (35), 145 (33), 163 (25), 161 (25); and diastereomer of **7**, R_I 1657, EIMS *m/z* (rel int) M^+ 220 (1), $[M–Me]^+$ 205 (3), 81 (100), 41 (94), 79 (92), 93 (78), 67 (78), 91 (71), 69 (70), 55 (63), 105 (55), 119 (50), 77 (46), 53 (45), 161 (28), 133 (24), 145 (18), 189 (15). Cyclisation yields **11**, R_I 1755 (γ), 1775 (β) and 1781 (α) [MS-data are comparable with those of Maurer and Grieder (1977) and used to determine elution order].

3.8.3. Germacra-1(10),4,11(13)-trien-12-al (*3*), 1.5 mg

Colourless/slightly yellow oil with strong mossy odour, pink spot R_f 0.58, R_I 1585 to ± 1715. ^1H NMR δ 9.35 (*s*) 9.37 (*s*), 9.45 (*s*) and 9.47 (*s*) (ratio 1:1:0.01:0.01, 1H, H-12); 5.77 (*br s*) and 5.72 (*s*) (ratio 1:1, 1H, H-13); 5.36 (*br s*) and 5.33 (*s*) (ratio 1:1, 1H, H′-13); 5.22 (*br s*,1H, H-1); 4.84 (*br d*, J = 13.3 Hz) and 4.62 (*br d*, J = 10.3 Hz) (ratio 1:1, 1H, H-5) 2.75–2.55 (*br m*, 1H, H-7). Cope rearrangement to **8**, R_I 1585 EIMS *m/z* (rel int) M^+ 218 (1), $[M–Me]^+$ 203 (12), 81 (100), 67 (70), 79 (68), 41 (63), 91 (56), 53 (50), 93 (46), 95 (38), 77 (38), 55 (37), 107 (37), 105 (35), 119 (27), 161 (25), 121 (24); and diastereomer of **8**, R_I 1570 EIMS *m/z* (rel int) M^+ 218 (ND), $[M–Me]^+$ 203 (8), 81 (100), 79 (64), 67 (60), 41 (57), 91 (48), 93 (43), 95 (41), 53 (40), 77 (36), 105 (36), 107 (35), 68 (34), 55 (34), 119 (25), 121 (22), 175 (22). Cyclisation yields **12**, R_I 1673 (γ), 1692 (β) and 1695 (α) [MS-data are comparable with those of Maurer and Grieder (1977) and used to determine elution order].

3.8.4. Germacra-1(10),4,11(13)-trien-12-oic acid (*4*), 1.5 mg

White crystals, blue TLC-spot (note: **9** gives pink spot) R_f 0.18, R_I 1771 to ± 1845. ^1H NMR δ 6.44-6.37 (*m*) and 6.36 (*s*) (ratio 1:1, 1H, H-13); 5.44 (*br m*) and 5.38 (*s*) (ratio 1:1, 1H, H′-13); 5.30–5.15 (*br s*, 1H, H-1); 4.85 (*br m*) and 4.63 (*br d*, J = 10.6 Hz) (ratio 1:1, 1H, H-5); 2.75-2.55 (*br m*, 1H, H-7). Cope rearrangement to **9**, R_I 1771 EIMS *m/z* (rel int) M^+ 234 (1), $[M–Me]^+$ 219 (7), 81 (100), 67 (50), 79 (47), 41 (43), 68 (40), 91 (38), 53 (34), 93 (29), 105 (29), 55 (26), 77 (26), 107 (26), 121 (23), 119 (19), 69 (17), 177 (15); and diastereomer of **9**, R_I 1750 EIMS *m/z* (rel int) M^+ 234 (ND), $[M–Me]^+$ 219 (4), 81 (100), 79 (67), 41 (58), 67 (56), 107 (55), 91 (49), 93 (49), 53 (41), 55 (40), 68 (39), 105 (38), 121 (35), 162 (33), 147 (26), 119 (25), 163 (25). Cyclisation yields **13**; R_I 1854 (γ), EIMS *m/z* (rel int) M^+ 234 (26), $[M–Me]^+$ 219 (100), 91 (57), 41 (35), 79 (35), 81 (34), 105 (34), 147 (34), 107 (32), 93 (31), 55 (30), 77 (30), 173 (25); R_I 1876 (β), EIMS *m/z* (rel int) M^+ 234 (25), $[M–Me]^+$ 219 (67), 91 (100), 79 (95), 93 (85), 41 (78), 121 (78), 77 (63), 81 (63), 55 (61), 67 (59), 105 (55), 107 (55), 53 (45), and R_I 1879 (α), EIMS *m/z* (rel int) M^+ 234 (27), $[M–Me]^+$ 219 (100), 91 (57), 79 (46), 41 (38), 81 (37), 107 (36), 105 (35), 93 (35), 55 (29), 205 (26) (elution order of isomers presumed to be the same as for **10–12**).

Acknowledgements

The authors are most grateful to Dr. B. Maurer for the gift of elematrien-12-ol and to Professor Dr. W. A. König for the gift of the germacrene A and β-elemene standard. We would also like to thank Dr. M. A. Posthumus for the GC–MS analyses of the costus root oil and resinoid, A. van Veldhuizen for recording NMR data, Dr. J. B. P. A. Wijnberg for his help in the interpretation of the NMR data, and ing. F. W. A. Verstappen for technical assistance.

References

Adams, R.P., 1995. Identification of Essential Oil Components by Gas Chromatography/Mass Spectroscopy. Allured Publishing Corporation, Carol Stream.

Ayaz, M., 1996. Use and survival of kuth (*Saussurea lappa*) a plant of medicinal and economic value in Pakistan. Pak. J. Forest. 46, 9–24.

Asakawa, Y., Matsuda, R., Toyota, M., Hattori, S., Ourisson, G., 1981. Terpenoids and bibenzyls of 25 liverwort *Frullania* species. Phytochemistry 20, 2187–2194.

Bawdekar, A.S., Kelkar, G.R., 1965. Terpenoids—LXVIII: structure and absolute configuration of costic acid—a new sesquiterpene acid from costus root oil. Tetrahedron 21, 1521–1528.

Belingheri, L., Cartayrade, A., Pauly, G., Gleizes, M., 1992. Partial purification and properties of the sesquiterpene β-selinene cyclase from *Citronella mitis* fruits. Plant Sci. 84, 129–136.

Bohlmann, F., Ates, N., Jakupovic, J., 1983. Hirsutinolides from South African *Vernonia* species. Phytochemistry 22, 1159–1162.

Fischer, N.H., 1990. Sesquiterpene lactones: biogenesis and biomimetic transformations. In: Towers, G., Towers, H. (Eds.), Biochemistry of the Mevalonic Acid Pathway to Terpenoids. Plenum, New York, pp. 161–201.

Fischer, N.H., Weidenhamer, J.D., Riopel, J.L., Quijano, L., Menalaou, M.A., 1990. Stimulation of witchweed germination by sesquiterpene lactones: a structure activity study. Phytochemistry 29, 2479–2483.

Hatakeyama, Y., Kumagai, T., Yoneda, K., 1989. Studies on the cultivation and breeding of wild medicinal plants: I. Trial cultivation of *Saussurea lappa* Clarke. Shoyakugaku Zasshi 43, 246–249.

Herz, W., 1977. Sesquiterpene lactones in the compositae. In: Heywood, V.H., Harborne, J.B., Turner, B.L. (Eds.), The Biology and Chemistry of the Compositae. Academic, London, pp. 337–357.

Klein, E., Thömel, F., 1976. Über neue Inhaltstoffe von Costuswurzelöl. Tetrahedron 32, 163–165.

de Kraker, J.-W., Franssen, M.C.R., de Groot, Ae., König, W.A., Bouwmeester, H.J., 1998. (+)-Germacrene A biosynthesis: the committed step in the biosynthesis of sesquiterpene lactones in chicory. Plant. Physiol. 117, 1381–1392.

de Kraker, J.-W., Franssen, M.C.R., Dalm, M.C.F., de Groot, Ae., Bouwmeester, H.J., 2001. Biosynthesis of germacrene A carboxylic acid in chicory roots: demonstration of cytochrome P450 (+)-germacrene A hydroxylase and $NADP^+$-dependent sesquiterpenoid dehydrogenase(s) involved in sesquiterpene lactone biosynthesis. Plant. Physiol. 125, 1930–1940.

Kuroda, M., Yoshida, D., Kodama, H., 1987. Bio-antimutagenic effects of sesquiterpene lactones from costus root oil. Agric. Biol. Chem. 51, 585–587.

March, J. 1992. Advanced Organic Chemistry, 4th Edition. Wiley-Interscience, New York, pp. 1132.

Maurer, B., Grieder, A., 1977. Sesquiterpenoids from costus root oil (*Saussurea lappa* Clarke). Helv. Chim. Acta 60, 2177–2190.

Minnaard, A., 1997. Germacrene Sesquiterpenes, Synthesis and Role in Biosynthesis. PhD thesis, Wageningen University, Wageningen, The Netherlands.

Paul, A., Bawdekar, A.S., Joshi, R.S., Somesekar Roa, A., Kelkar, G.R., Bhattacharyya, S.C., 1960. Terpenoids XX: examination of costus root oil. Perf. Ess. Oil Rec. 15, 115–120.

Piet, D.P., Minnaard, A.J., van der Heyden, K.A., Franssen, M.C.R., Wijnberg, J.B.P.A., de Groot, Ae., 1995. Biotransformation of (±)-4,8-dimethylcyclodeca-3(*E*),7(*E*)-dien-1β-ol and (+)-hedycaryol by *Cichorium intybus*. Tetrahedron 51, 243–254.

Sannai, A., Fujimori, T., Kato, K., 1982. Studies on flavor components of roasted chicory root. Agric. Biol. Chem. 46, 429–433.

Stahl, E., 1984. Das ätherische Öl aus *Thymus praecox* spp. *articus* isländischer Herkunft. Planta Med. 50, 157–160.

Still, W.C., Kahn, M., Mitra, A., 1978. Rapid chromatographic technique for preparative separations with moderate resolution. J. Org. Chem. 43, 2923–2925.

Somasekar Roa, A., Kelkar, G.R., Bhattacharyya, S.C., 1960. Terpenoids—XXI: the structure of costunolide, a new sesquiterpene lactone from costus root oil. Tetrahedron 9, 275–283.

Southwell, I.A., 1970. A new occurrence of hedycaryol, the precursor of elemol in *Phebalium ozothamnoides* (Rutaceae). Phytochemistry 9, 2243–2245.

Takahashi, T., Nemoto, H., Kanda, Y., Tsuji, J., Fukazawa, Y., Okajima, T., Fujise, Y., 1987. Macroring contraction methodology 3: total syntheses of costunolide and haageanolide using transannular [2,3]-Wittig rearrangement of 13-membered diallylic ethers as key reaction. Tetrahedron 43, 5490–5520.

Takeda, K., 1974. Stereospecific Cope rearrangement of the germacrene-type sesquiterpenes. Tetrahedron 30, 1525–1534.

Teisseire, P.J., 1994. Chemistry of Fragrant Substances. VCH, New York, pp. 193–289.

Wichtman, E.-M., Stahl-Biskup, E., 1987. Composition of the essential oils from caraway herb and root. Flavor Fragrance J. 2, 83–89.

Zdero, C., Bohlmann, F., Anderberg, A., King, R.M., 1991. Eremophilane derivatives and other constituents from *Haeckeria* species and further Australian inuleae. Phytochemistry 30, 2643–2650.

PERGAMON

Phytochemistry 58 (2001) 489–492

PHYTOCHEMISTRY

www.elsevier.com/locate/phytochem

Coexistence of chrysanthenone, filifolone and (*Z*)-isogeranic acid in hydrodistillates. Artefacts!

Nigist Asfaw[a], Hans J. Storesund[a,*], Lars Skattebøl[b], Arne J. Aasen[a]

[a]*School of Pharmacy, University of Oslo, PO Box 1068, Blindern, N-0316 Oslo, Norway*
[b]*Department of Chemistry, University of Oslo, PO Box 1033, Blindern, N-0315 Oslo, Norway*

Received 19 March 2001; received in revised form 11 May 2001

Abstract

Hydrodistilled oil from leaves of the Ethiopian plant *Laggera tomentosa* has been shown to contain (−)-chrysanthenone (5%), (−)/(+)-filifolone (92:8; 8%) and (*Z*)-isogeranic acid (8%)—all likely to be artefacts. The main constituent of the oil, (+)-chrysanthenone (53%), is believed to be the precursor undergoing thermal and solvolytic reactions during the hydrodistillation process.
© 2001 Published by Elsevier Science Ltd.

Keywords: *Laggera tomentosa*; Asteraceae; Chrysanthenone; Filifolone; (*Z*)-Isogeranic acid; Hydrodistillation; Artefacts

1. Introduction

The common procedure for isolation of essential oil from plant material involves hydrodistillation. Recently we reported (Asfaw et al., 1999) that hydrodistillation of the Ethiopian plant *Laggera tomentosa* Sch. Bip. ex Oliv. & Hiern yielded chrysanthenone (**1**, 58%), isochrysanthenone (**2**, 5%) and filifolone (**3**, 8%). Further analysis of the hydrodistillate of the oil revealed the presence of an acidic component identified as (*Z*)-isogeranic acid (**4**, 8%).

Enantioselective GC analyses of the ketones in the hydrodistilled oil showed enantiomerically pure (−)-isochrysanthenone ($[\alpha]_D^{21}$ −67 ° ($CHCl_3$; c 0.47)) while chrysanthenone ($[\alpha]_D^{21}$ +97.6 ° ($CHCl_3$; *c* 4.0)) and filifolone ($[\alpha]_D^{22}$ −636 ° ($CHCl_3$; *c* 0.30)) were found to be enantiomeric mixtures with a (+)/(−) ratio of 92:8 and 8:92, respectively.

The presence of filifolone (**3**) in plant material has frequently been reported after Beereboom (1965) first synthesised the cyclobutanone by cyclisation of geranic acids. Its natural occurrence was first published by Bates et al. (1967) who found the (+)-enantiomer (“D-filifolone”; $[\alpha]_D^{24}$ +307 °) in the Australian plant *Zieria smithii* Andrews and the (−)-enantiomer (“L-filifolone”; $[\alpha]_D^{25}$ −270 °) in the Arizonian sage *Artemisia filifolia* (Torrey). In the essential oil obtained by hydrodistillation of *Z. smithii*, D-filifolone co-occurred with (−)-**1** ($[\alpha]_D$ −88 °; Penfold et al., 1939). Bates et al. (1967) reported that (−)-**1** isomerised to racemic **3** during gas chromatography. They did not, however, record any isolation procedure for “L-filifolone”. A more detailed work by Torrance (1973) on *Artemisia filifolia* established the presence of (−)-**3** in the hydrodistillate together with several other monoterpenoids including (−)-verbenone but not chrysanthenone (**1**). The thermal instability of **1** to yield racemic **3** suggests, according to Bates et al., that the filifolone in *Zieria smithii* might conceivably be an artefact. However, due to the presence of optically active **3** in the plant oil, they concluded, nevertheless, the latter to be a natural constituent of the plant since a mechanistic route from (−)-**1** to optically active **3** seemed “difficult to imagine”. In a later work on *Zieria smithii* by Flynn and Southwell (1987), the authors suggest that milder isolation techniques may reveal that (+)-**1** is the heat and photo labile precursor of (−)-**3**.

2. Results and discussion

The reported coexistence of naturally occurring chrysanthenone (**1**) and filifolone (**3**) in the essential oil of *Z.*

* Corresponding author. Tel.: +47-22855002; fax: +47-22855947.
E-mail address: h.j.storesund@farmasi.uio.no (H.J. Storesund).

0031-9422/01/$ - see front matter © 2001 Published by Elsevier Science Ltd.
PII: S0031-9422(01)00254-0

smithii as well as in oils of other plants, where hydrodistillation method of isolation had been employed (Uchio, 1978; Weyerstahl et al., 1999; Kalemba and Kusewicz, 2000), may be challenged as pentane/ether extractions at room temperature of the leaves of *L. tomentosa* provided extracts containing barely detectable amounts of filifolone and (*Z*)-isogeranic acid. Increased amounts of chrysanthenone (72% as compared to 58% in the hydrodistillate) were instead recorded. Interestingly, enantioselective GC analysis of the extract revealed the presence of (+)-**1** of >99% optical purity implying that ca 16% racemisation had taken place during the hydrodistillation (see above). (*Z*)-Isogeranic acid (**4**) was isolated from the hydrodistilled oil by flash chromatography and identified by GC–MS and NMR. The spectroscopic data were in agreement with those reported for the acid by Weyerstahl et al. (1987).

In a study of cyclobutanones Erman et al. (1971) report 29% racemisation as the sole reaction on thermolysis of (−)-**1** in refluxing cyclohexane (81 °C) for 25 h. Similar treatment of (+)-**3** in the same solvent gave high yield of recovered starting material with complete retention of configuration. Furthermore, thermolysis of **1** in refluxing methanol (65 °C) for 16 h was reported by the same authors to yield ca 50% of the methyl ester of **4** in addition to recovered **1** (ca 50%) of unquoted optical purity. Filifolone (**3**) was not, however, detected. On the other hand, treatment of **1** ($[\alpha]_D^{25}$ −12.3 ° ($CHCl_3$)) in glacial acetic acid at 60 ° for 77 h was reported to produce 71% of **3** ($[\alpha]_D^{25}$ +24.2 ° ($CHCl_3$; *c* 0.24)) and partially racemised starting material together with some other minor products. Unlike Bates et al. (1967) we found no evidence for thermolysis of **3** — neither racemisation nor isomerisation to chrysanthenone—under the chromatographic conditions employed. However, nearly complete racemisation of chrysanthenone and partial isomerisation to racemic filifolone were observed during preparative GC conditions (Scheme 1).

To visualise the racemisation process of chrysanthenone (**1**) and its isomerisation to filifolone (**3**) at elevated temperatures (i.e. GC conditions) the achiral ketene **5** (Scheme 1) is a likely intermediate for both reactions as depicted by reaction path ii. The ketene may either revert to racemic **1** or undergo [2+2] cycloaddition to produce racemic **3**. Of the two competing reactions the cycloaddition reaction has the higher energy of activation and is probably important only at temperatures above 200 °C. However, the observed racemisation of **1** in cyclohexane at 81 °C and the formation of the methyl ester of (*Z*)-isogeranic acid (**4**) on treatment of **1** at 65 °C in MeOH, suggest thermal cleavage of **1** to the ketene **5** even at moderate temperatures, and thus explain the presence of (−)-**1** and (*Z*)-isogeranic acid (**4**) in the hydrodistilled oil from *L. tomentosa* (reaction path i). Consequently, both compounds (−)-**1** and **4** are most likely artefacts.

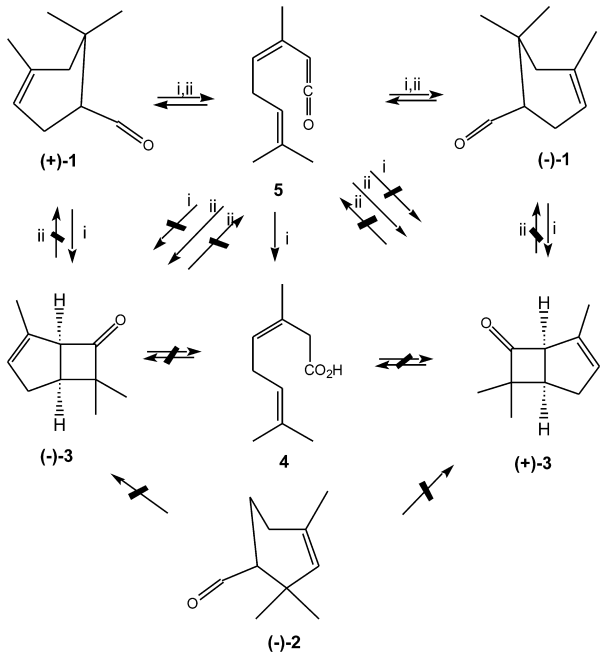

Scheme 1. (i) Hydrodistillation, (ii) 260 °C/preparative GC.

The presence of (−)-**3** with 84% e.e. was more difficult to rationalise. A route involving the achiral ketene **5** can be ruled out for obvious reasons. Chrysanthenone (**1**) with the same enantiomeric excess as that of **3**, though with opposite sign, seems nevertheless to be an attractive alternative, considering the observations of Erman et al., (1971) on acetic acid treatment of **1** (see above). On the other hand, it cannot be excluded that the essential oil might contain constituents, which might produce **3** with the observed stereochemistry under hydrodistillation conditions. Initially, our approach was that **3** might constitute a part of a larger molecule which might liberate optically active **3** in the boiling water. In order to examine such a possibility Soxhlet extractions of dried plant material using pentane, ether and methanol were carried out, followed by column chromatographic separation into fractions that were individually subjected to hydrodistillation. It turned out that only fractions containing chrysanthenone (**1**) and isochrysanthenone (**2**) produced **3** and **4** during the distillation. A sample containing **1** (92%), **2** (4%) and trace amounts of **3** and **4** was prepared by irradiation of (−)-verbenone (Erman, 1967), and for comparison hydrodistilled in the same way. Analysis of the distillate revealed unchanged contents of **2**, significant amounts of **4** (15%) and **3** (4%), and a marked reduction in the amount of **1** (57%) This result strongly suggests a relationship between chrysanthenone and filifolone/(*Z*)-isogeranic acid. This is further substantiated by enantioselective GC analyses of the hydrodistilled fractions from the plant oil and from the synthetic material, containing compounds **1** and **3**; the fractions invariably showed the enantiomeric ratio of (+)-**1**/(−)-**1** to be equal to the ratio of (−)-**3**/(+)-**3**.

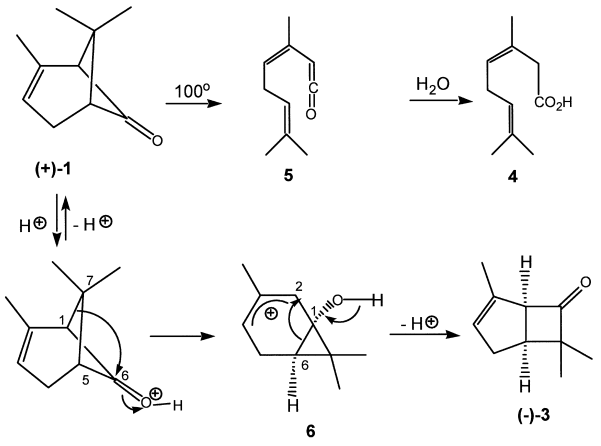

Scheme 2.

Thus under hydrodistillation conditions, (−)-**3** seems to originate exclusively from (+)-**1** while the (−)-enantiomer is apparently the sole precursor of (+)-**3** as shown in path i (Scheme 1). Accordingly, none of the enantiomers of filifolone (**3**) are naturally occurring constituents of *L. tomentosa*.

Scheme 2 illustrates how the above reactions may proceed in order to preserve optical activity *en route* from (+)-**1** to (−)-**3** in an assumed acid catalysed rearrangement. Bearing in mind that the treatment of **1** in refluxing methanol gave high yield of the methyl ester of **4** but no filifolone (Erman et al., 1971), we may now attribute its absence to lack of an acid catalyst. Returning to *L. tomentosa*, the first step in the hydrodistillation of **1** is consequently believed to be a thermally induced rearrangement of the ketone to the ketene **5**, which by water addition provides the acid catalyst necessary for the subsequent transformations of **1** to the observed products. The latter pathway is believed to involve two consecutive 1.2 alkyl shifts—migration of the 1.7 bond in (+)-**1** affords the optically active allylic carbocation **6**, which by a shift of the 1.6 bond provides (−)-**3**.

Our results show that the analytical data of the constituents of a plant obtained from hydrodistillation must be treated with great caution if labile compounds are present in the plant material. Accordingly, comparative routine analysis of the essential oil from cold pentane/ether extractions of the plant is strongly recommended in order to minimise confusion caused by formation of artefacts.

3. Experimental

3.1. Plant material

L. tomentosa was collected on 18 October 1998 near Chancho, about 40 km Northwest of Addis Ababa, Ethiopia. A voucher specimen has been authenticated and deposited at the National Herbarium, Biology Department, Addis Ababa University.

3.2. Isolation and analysis

3.2.1. Hydrodistillation

Fresh leaves (1.2 kg) of *L. tomentosa* were hydrodistilled for 3 h using a Clevenger-type apparatus to yield 2.0 ml of oil (0.16% v/w). Chrysanthenone-enriched fractions from *L. tomentosa*—contaminated with trace amounts of filifolone (**3**) and *Z*-isogeranic acid (**4**, <0.1%) and isochrysanthenone (**2**, 5–11%)[1] were hydrodistilled in a similar way. Chrysanthenone (from irradiation of verbenone), containing small amounts of compounds **3**, **4** and **2** (4%), was hydrodistilled as described above.

3.2.2. Cold extraction

L. tomentosa fresh leaves (50 g) were soaked in pentane (100 ml) for 24 h at room temperature. The extract was drained and the remaining material was subsequently soaked in ether (100 ml) for 24 h at room temperature. Both extracts were analysed by GC before and after removal of solvent.

3.2.3. Soxhlet extraction

Samples of powdered leaves (10–50 g) were extracted successively by pentane, ether and methanol using Soxhlet for periods of 3 h. Each extract was separated into fractions by flash chromatography using pentane, ether and methanol as eluents followed by hydrodistillation of the fractions. Hydrodistilled fractions containing filifolone (**3**) and *Z*-isogeranic acid (**4**) were registered.

3.2.4. GC analysis

The samples were analysed by GC and enantioselective GC. A Supelcowax 10 (30 m×0.25 mm, 0.2 μm film thickness) fused silica capillary column with helium as carrier gas at a flow rate of 1 ml min^{-1}, and with a split ratio of 82, was used for GC analysis. The column temperature was programmed from 70 °C (5 min), 70–180 °C (5 min), 180–240 °C (10 min) and 240 °C (10 min). An FID detector was used at a temperature of 260 °C and the injector temperature was 210 °C. Enantioselective GC analyses were performed on a CP Chirasil-DEX CB (25 m×0.25 mm, 0.25 μm film thickness) fused silica capillary column temperature programmed as follows: 100 °C (10 min), 1.5 °C min^{-1} to 180 °C (15 min). Carrier gas flow rate was 1 ml min^{-1}. Injector and detector temperatures were 210 and 260 °C, respectively. Preparative GC was conducted on a Hewlett Packard GC instrument equipped with a glass column (15% OV-17; 2.26 m×4 mm). Injector and detector temperatures were 260 °C. The column temperature for sample analysis of

[1] All compositional % quoted in this work are based upon relative amounts from GC analyses.

chrysanthenone and filifolone was 150 and 200 °C, respectively. Nitrogen was used as a carrier gas at a flow rate of 100 ml min^{-1}.

Acknowledgements

N.A. is grateful to the University of Oslo for financial support. We thank Professor Sebsebe Demissew, the National Herbarium, Addis Ababa University, Addis Ababa, Ethiopia for the collection and proper identification of the plant material.

References

Asfaw, N., Storesund, H.J., Skattebøl, L., Aasen, A.J., 1999. (1*S*,5*R*)-(−)-2,4,4-Trimethylbicyclo[3.1.1]hept-2-en-6-one, from the essential oil of the Ethiopian plant *Laggera tomentosa*. Phytochemistry 52, 1491–1494.

Bates, R.B., Onore, M.J., Paknikar, S.K., Steelink, C., 1967. D- and L-Filifolones, monoterpenoid cyclobutanones with the bicyclo[3.2.0] heptane ring system. Chem. Commun., 1037–1038.

Beereboom, J.J., 1965. The cyclization of geranic acids. Preparation of a cyclobutanone. J. Org. Chem., 4230–4234 (and references cited therein).

Erman, W.F., 1967. Photochemical transformations of unsaturated bicyclic ketones. Verbenone and its photodynamic products of ultraviolet irradiation. J. Am. Chem. Soc. 89, 3828–3841.

Erman, W.F., Treptow, R.S., Bakuzis, P., Wenkert, E., 1971. Acid-catalyzed rearrangements of cyclobutanones. J. Am. Chem. Soc. 93, 657–665.

Flynn, T.M., Southwell, J.A., 1987. Essential oil constituents of the genus *Zieria*. Phytochemistry 26, 1673–1686.

Kalemba, D., Kusewicz, D., 2000. Composition and antimicrobial activity of the essential oil of *Artemisia selengensis* Turcz. Presented at the ISEO 2000 31st International Symposium on Essential Oils. Hamburg, 10–13 September.

Penfold, A.R., Ramage, G.R., Simonsen, J., 1939. 1-Δ^3-Carene-5: 6-epoxide, a constituent of the oil from *Zieria Smithii*. J. Chem. Soc., 1496–1504.

Torrance, S.J., 1973. Chemical constituents of *Artemisia filifolia*. Diss. Abstr. Int. B 34 (6), 2536.

Uchio, Y., 1978. Constituents of the essential oil of *Chrysanthemum japonense*. Nojigiku alcohol and its acetate. Bull. Chem. Soc. Japan 51, 2342–2346.

Weyerstahl, P., Kaul, V.K., Weirauch, M., Marschall-Weyerstahl, H., 1987. Volatile constituents of *Artemisia vestita* oil. Planta Med., 66–72.

Weyerstahl, P., Marschall, H., Wahlburg, H.-C., Christiansen, C., Rustaiyan, A., Mirdjalili, F., 1999. Constituents of the essential oil of *Pulicaria gnaphalodes* (Vent.) Boiss. from Iran. Flav. Fragr. J. 14, 121–130.

PERGAMON

Phytochemistry 58 (2001) 493–500

PHYTOCHEMISTRY

www.elsevier.com/locate/phytochem

Acylated anthocyanidin 3-sophoroside-5-glucosides from *Ajuga reptans* flowers and the corresponding cell cultures

Norihiko Terahara[a,*], Alfons Callebaut[b], Riichiro Ohba[c], Tadahiro Nagata[d], Mayumi Ohnishi-Kameyama[d], Masahiro Suzuki[d]

[a]*Department of Food Science and Technology, College of Horticulture, Minami-Kyushu University, Takanabe, Miyazaki 884-0003, Japan*
[b]*Instituut voor Scheikundig Onderzoek, Leuvensesteenweg 17, B-3080 Tervuren, Belgium*
[c]*Department of Applied Microbial Technology, Sojo University, Ikeda 4-22-1, Kumamoto 860-0082, Japan*
[d]*National Food Research Institute, Ministry of Agriculture, Forestry, and Fisheries, Tsukuba, Ibaraki 305-8642, Japan*

Received in revised form 23 January 2001

Abstract

Four anthocyanins from *Ajuga reptans* flowers and its cell cultures were isolated, and a fifth was also characterized by HPLC-mass spectrometry. By means of chemical and spectroscopic analyses, their structures were identified as delphinidin 3-(*p*-coumaroyl-feruloyl)sophoroside-5-malonylglucoside, delphinidin 3-(diferuloyl)sophoroside-5-malonylglucoside, and cyanidin 3-(di-*p*-coumaroyl)sophoroside-5-glucoside, respectively. The other two were tentatively identified as delphinidin 3-(diferuloyl)sophoroside-5-glucoside and cyanidin 3-(feruloyl-*p*-coumaroyl)sophoroside-5-malonylglucoside. In neutral aqueous solution, the crude extract from *A. reptans* flower cell cultures and the major anthocyanin cyanidin 3-(di-*p*-coumaroyl)sophoroside-5-malonylglucoside were more stable than cyanidin 3-glucoside, and also prevented more efficiently peroxidation than did the latter. *A. reptans* flower cell culture anthocyanins may have a potential as natural colorants for food utilities or other purposes. © 2001 Elsevier Science Ltd. All rights reserved.

Keywords: *Ajuga reptans* L.; Lamiaceae; Cell culture; Flavonoid; Anthocyanin; Acylated anthocyanidin 3-Sophoroside-5-glucosides; Stability; Antioxidative activity

1. Introduction

In recent years, many studies of anthocyanin production by plant cell, tissue and organ cultures have been conducted in either the biochemical or the food chemical fields (Yamamoto et al., 1981; Harborne et al., 1983; Tamura et al., 1989; Calsteren et al., 1991; Takahashi et al., 1991; Mori et al., 1993; Sakamoto et al., 1993; Baker et al., 1994; Cormier et al., 1994; Tholakalabavi et al., 1994). *Ajuga reptans* L., (Lamiaceae), is a plant grown in Europe, North America and West Asia, and is called "Bugle" in France, "Günsel" in Germany and "Seiyo-Kiransou" in Japan. It has bluish-purple flower and reddish-purple leaf colored with anthocyanin pigments. The cell cultures of the flower and leaf produce acylated anthocyanins (Callebaut et al., 1990a,b, 1993) under appropriate conditions. In the flower culture system, both the composition and the amounts of anthocyanins produced were shown to be stable (Callebaut et al, 1997). Thus, it is a good anthocyanin producing system and a suitable tool to investigate anthocyanin modification (Callebaut et al., 1996). A preliminary examination showed that the major pigments of the flower cell cultures were cyanidin 3-sophoroside-5-glucoside-based, and resembled more the pigments of the leaf or the leaf cultures rather than those of the flower itself, i.e. delphinidin 3-sophoroside-5-glucoside-based (Callebaut et al., 1990a, 1993).

Recently, the major anthocyanins of *A. reptans* flower and flower cell cultures were determined as delphinidin 3-(di-*p*-coumaroyl)sophoroside-5-malonylglucosides and cyanidin 3-(di-*p*-coumaroyl)sophoroside-5-malonylglucosides, respectively (Terahara et al., 1996). The leaf culture of the related species *A. pyramidalis* Metallica Crispa was shown to produce the same type of anthocyanins. It mainly accumulated cyanidin 3-(diferulyl)sophoroside-5-malonylglucoside (Madhavi et al., 1996).

We have now established the structures of three new anthocyanins from *A. reptans* flower and the

* Corresponding author. Tel.: +81-983-22-6615; fax: +81-983-22-0295.
E-mail address: terahara@nankyudai.ac.jp (N. Terahara).

0031-9422/01/$ - see front matter © 2001 Elsevier Science Ltd. All rights reserved.
PII: S0031-9422(01)00172-8

corresponding cell cultures by chemical and spectroscopic methods comprising HPLC-electrospray ionization mass spectrometry (LC–ESIMS), FABMS, Electrospray Ionization Fourier transform Ion Cyclotron Resonance Mass Spectrometry (ESI/FT–ICRMS) and various NMR spectroscopic methods. For application of cell culture anthocyanins as food colorants, the stability and the antioxidative activity of the crude extract were also examined, together with the major anthocyanin cyanidin 3-(di-*p*-coumaroyl)sophoroside-5-malonylglucoside, its deacylated derivative cyanidin 3-sophoroside-5-glucoside and cyanidin 3-glucoside .

2. Results and discussion

By HPLC analysis under improved conditions, *A. reptans* flower crude extract contained more than seven anthocyanins, and the corresponding cell cultures contained more than 16, as shown in Fig. 1.

Preliminary acid hydrolysis of *A. reptans* flower crude extract gave predominantly delphinidin (Dp) and to a lesser extent cyanidin (Cy). In contrast, the flower crude extract c gave mainly Cy and a lower amount Dp (Callebaut et al., 1993; Terahara et al., 1996). These extracts were purified and isolated through several forms of column chromatography as in the previous report (Terahara et al., 1996). Three anthocyanins **1**–**3** were isolated from *A. reptans* flowers, and one (**4**) from the corresponding cell cultures.

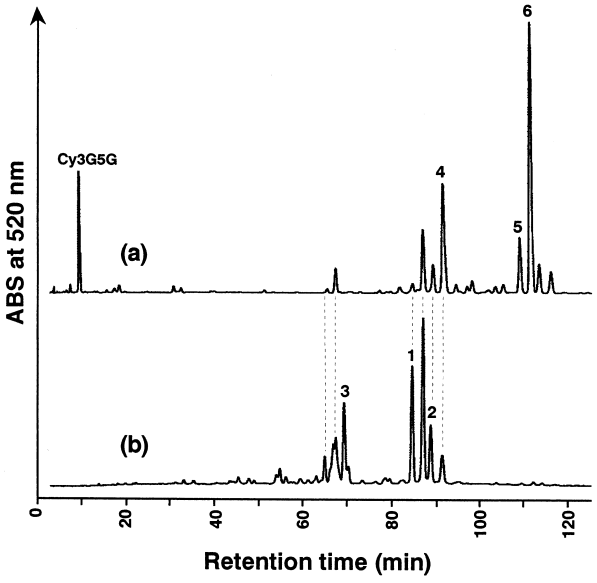

Fig. 1. Anthocyanin compositions of the crude extracts from (a) flower cell culture and (b) flower of A. reptans. HPLC was run on Inertsil ODS-2 column at 35°C with a flow rate of 1 ml min^{-1} monitoring at 530 nm. Cy3G5G indicates cyanidin 3,5-diglucoside. Anthocyanin six indicates cyanidin 3-(di-*p*-coumaroyl)sophoroside-5-malonylglucoside determined on a previous experiment (Terahara et al., 1996).

On acidic hydrolysis, **1**–**3** gave Dp and **4** gave Cy as aglycons, respectively. All the hydrolysates gave only glucose (G) as the released sugar component. In the UV-VIS spectra of **1**–**4**, the presence of the characteristic absorptions around 315 nm (**1** and **4**) and 325 nm (**2** and **3**) suggested that these were acylated with hydroxycinnamic acids such as *p*-coumaric acid (P) and ferulic acid (F), respectively. The numbers of bound hydroxycinnamic acids in all pigments could be estimated as 2 moles, when the values (about 160%) of $E_{acid.max}$ /$E_{VIS.max}$ (a ratio of absorbances at hydroxycinnamic acid absorption maximum and at visible absorption maximum) were compared with Harborne's data (1958). Especially, **2** and **3** have two ferulic acids because of a characteristic bathochromic shift of $\lambda_{acid.max}$ of about 10 nm compared with *p*-coumaric absorption. On alkaline hydrolysis, the acylating acids from **1** were identified as P, F and malonic acid (m), from **2** as F and m, from **3** as F, and from **4** as P by TLC and HPLC. Other than organic acids, the alkaline hydrolysis of **1**–**3** and **4** gave the deacylated anthocyanins delphinidin 3-sophoroside-5-glucoside (Dp3S5G) and cyanidin 3-sophoroside-5-glucoside (Cy3S5G), respectively. The 3,5-disubstitution patterns of **1**–**4** were also confirmed from the values (about 12%) of E_{440}/$E_{VIS.max}$ (a ratio of absorbances at 440 nm and visible absorption maxima), similar to those of common delphinidin 3,5-diglucoside and cyanidin 3,5-diglucoside (Cy3G5G) which are 10 and 13%, respectively (Harborne, 1958).

FABMS spectra of **1**–**4** were measured under a positive mode with a linked-scan of the molecular cations. Moreover, **5**, in addition to **4**, could be characterized by HPLC-electrospray ionization mass spectrometry (LC-ESIMS) in *A. reptans* flower cell culture crude extract. LC-ESIMS is a powerful tool for analysis of bio-molecules like anthocyanins, since it can separate chromatographically and simultaneously ionized unstable compounds softly, and then clearly gives the fragment ions as well as the molecular ions (Whitehouse et al., 1985; Sakairi and Kambara, 1988; Balidi et al., 1995). On FABMS and LC-ESIMS measurements, anthocyanins **1**, **2** and **5** were respectively determined as mono-malonylated. The molecular weight of each anthocyanin, the construction of partial structures, and the molecular formula based on the molecular ion and its fragmentation patterns could be determined as shown in Fig. 2. It shows that each molecular ion is decomposed to the aglycone via two routes. One is the pathway releasing the hexosyl-hexoside (glucosyl-glucoside) fragment (GG) diacylated with ferulic or *p*-coumaric acid (**1** and **5**: PGFG, **2** and **3**: FGFG, and **4**: PGPG), and followed by the elimination of glucose (**3** and **4**: G) or malonylglucose (**1**, **2** and **5**: mG) fragment. The other route is a reversed order case. The result indicates that each anthocyanin has two structural units (PGFG/FGFG/PGPG and mG/G) in

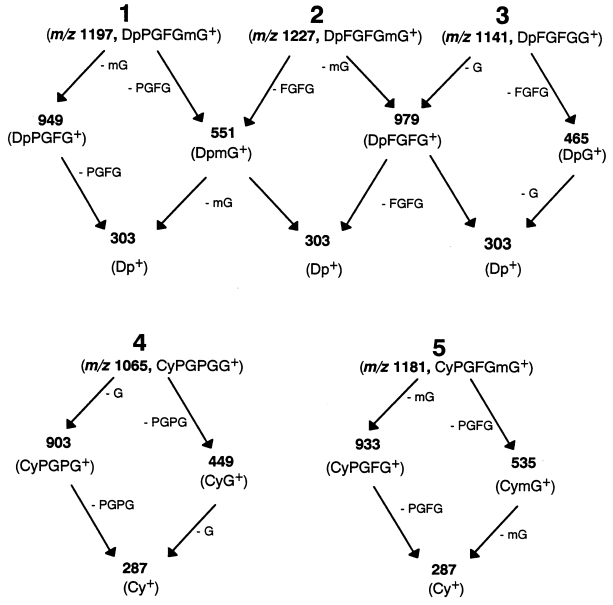

Fig. 2. Mass fragmentation patterns of *Ajuga reptans* flower and the cell culture anthocyanins. The values in the scheme show mass numbers (m/z) of molecular and fragment cations from the anthocyanins **1**–**5**. Abbreviations: Dp = delphinidin, Cy = cyanidin, G = glucose, F = ferulic acid, P = *p*-coumaric acid, and m = malonic acid.

the molecule. Combined with previous data (Terahara et al., 1996), the structural compositions of **1**–**5** can be deduced as DpPGFGmG, DpFGFGmG, DpFGFGG, CyPGPGG and CyPGFGmG, respectively. Thus the molecular formulas of **1**–**5** were respectively determined as $C_{55}H_{57}O_{30}^{+}$, $C_{56}H_{59}O_{31}^{+}$, $C_{53}H_{57}O_{28}^{+}$, $C_{51}H_{53}O_{25}^{+}$ and $C_{55}H_{57}O_{29}^{+}$. The molecular formulas of **1**, **2** and **4** were verified by high-resolution mass measurement using an electrospray ionization Fourier-transform ion cyclotron resonance mass spectrometer (ESI-FTICRMS) within an error of 5×10^{-4} (0.4 ppm) in mass assignment on the samples. ESI–FTICR mass spectrometry allows for high-resolution and accurate mass analyses of many biomolecules (Green et al., 1998).

Since anthocyanin **3** was obtained in insufficient amounts and **5** was not isolated, only **1**, **2** and **4** were used for further examinations.

Determination of detailed chemical structures of **1**, **2** and **4** were performed through ^{13}C and ^{1}H NMR analyses using DQF–COSY, NOESY, ROESY, 2D-HOHAHA, HSQC and HMBC methods as previously reported (Terahara et al., 1996). The assigned data are depicted in Table 1. At low field (δ_H 7–9 ppm) in the ^{1}H NMR spectra, the aglycone and hydroxycinnamoyl protons occurred as well separated signals, and at high field (δ_H 3–6 ppm), glucosyl (and malonyl) protons were observed as overlapping signals. In the low field area, four singlets of **1** and **2** were assigned to the protons of a Dp-unit having a symmetric B-ring, while three singlets, two doublets, and one double-doublet of **4** are to Cy-unit protons. In **1**, **2** and **4**, two pairs of characteristic doublets with large coupling constants ($J = 16$ Hz) were allocated to two pairs of olefinic α- and β-protons of *trans* (*E*)-hydroxycinnamoyl moieties. The superimposed proton signals at high field were assigned with the aid of HOHAHA spectra. As three anomeric protons of a-, b- and c-glucoses (G_a-1-H, G_b-1-H and G_c-1-H) in each pigment were characteristic doublets shifted to lower field with large coupling constants (7–8 Hz) and the glucosyl ring protons had large coupling constants (7–9 Hz), all sugars have a β-D-glucopyranosyl configuration. Proton and carbon signals of a-glucose (G_a-2-H/C) of each anthocyanin shifted to lower magnetic field (chemical shift differences ($\Delta\delta_H$): from +0.5 to +1.0 ppm, $\Delta\delta_C$: from +7.6 to +10.1 ppm) from those of G_b-2-H/C and G_c-2-H/C, indicating G_a-2-OH was glycosylated with G_b. Thus, the connectivity of G_a and G_b was deduced as 2-*O*-(β-D-glucopyranosyl)-β-D-glucopyranoside, a sophoroside. All glucosyl 6-methylene protons/carbons in **1** and **2** were also observed at lower field ($\Delta\delta_H$: from +0.4 to +0.8 ppm, $\Delta\delta_C$: from +6.5 to +10.1 ppm) compared with those of Cy3S5G (Terahara et al., 1996), indicating that the 6-OH positions of G_a, G_b and G_c were acylated. Similarly only G_a and G_b in **4** were observed at lower magnetic field, indicating that the 6-OH of G_a and G_b were acylated, but that G_c-6-OH was not. Malonyl methylene protons and carbons were observed at δ_H 3.38 (δ_C 41.33) and δ_H 3.39 (δ_C 41.29) ppm in **1** and **2**, respectively, but were not observed in **4**. At lower field, δ_C 166–168 ppm, four (**1** and **2**) and two (**4**) ^{13}C-signals could be easily assigned to carbonyl carbons of two hydroxycinnamoyl and one malonyl (not observed in **4**) moieties.

Connectivities of the three sugar moieties in **1**, **2** and **4** were unequivocally determined from NOESY and/or ROESY spectra. Cross-peaks of intense NOEs between Dp/Cy-4-H and G_a-1-H, Dp/Cy-6-H and G_c-1-H, and G_a-2-H and G_b-1-H proved that G_a, G_b and G_c were glycosylated to Dp/Cy-3-OH, Dp/Cy-5-OH and G_a-2-OH, respectively. Hence these basic structures are Dp/Cy 3-{G_b-(1→2)-G_a}-5-G_c that is Dp/Cy3S5G. The connectivity was also supported by the observation of weak NOEs between Dp/Cy-B-ring protons (2′- and 6′-H /2′-, 6′- and 5′-H) and G_b-1-H, showing that G_b was spatially close to the Dp/Cy-B-rings, respectively. Similarly, the connecting positions on the sugars of the acyl residues in **1**, **2** and **4** were mainly determined by HMBC spectra. In **1** and **2**, malonic acid was linked to G_c-6-OH due to the presence of ^{1}H–^{13}C cross-peaks between G_c-6-H and malonyl-carbonyl carbon. In **1**, **2** and **4**, the cross-peaks between G_a-6-H and hydroxycinnamic acid-I-carbonyl carbon and between G_b-6-H and acid-II-carbonyl carbon provided decisive proof that acids-I and-II were respectively linked to G_a-6-OH and G_b-6-OH.

In conclusion, the new anthocyanins **1**, **2** and **4** were unambiguously determined as 3-*O*-{2-*O*-(6-*O*-*E*-feruloyl-β-D-glucopyranosyl)-(6-*O*-*E*-*p*-coumaroyl-β-D-

Table 1
^{13}C and ^{1}H NMR spectral data of anthocyanins from *Ajuga reptans* flowers and the corresponding cell cultures (δ ppm from internal standard TMS)[a]

Assignment	**1**		**2**		**4**	
	δ_C	δ_H	δ_C	δ_H	δ_C	δ_H
Aglycon-2	161.85	–	161.96	–	162.59	–
3	145.22	–	145.15	–	144.29	–
4	145.06	8.71 *s*	145.07	8.74 *s*	133.23	8.82 s
5	154.90	–	154.90	–	155.50	–
6	105.30	6.93 *s*	105.30	6.92 *s*	105.18	6.93 s
7	167.41	–	167.36	–	167.96	–
8	96.19	6.92 *s*	96.82	6.91 *s*	96.46	6.94 s
9	155.06	–	155.07	–	155.44	–
10	111.75	–	111.66	–	111.94	–
1′	118.32	–	118.34	–	119.73	–
2′	111.20	7.79 *s*	111.20	7.79 *s*	117.82	8.02 *d* (1)
3′	146.70	–	146.70	–	146.58	–
4′	149.56	–	149.56	–	155.38	–
5′	146.70	–	146.70	–	117.26	7.10 *d* (9)
6′	111.55	7.79 *s*	111.66	7.79 *s*	127.90	8.27 *dd* (1, 9)
G_a-1	98.55	5.76 *d* (7)	101.89	5.76 *d* (7)	99.48	5.68 *d* (7)
2	83.30	4.15 *t* (8)	83.31	4.15 *t* (7)	81.87	4.06 *t* (8)
3	73.95	3.76 *t* (9)	73.96	3.75 *t* (8)	74.30	3.75 *t* (9)
4	69.69	3.48 *t* (9)	69.31	3.51 *t* (8)	70.01	3.48 *t* (9)
5	75.87	4.10 *m*	75.90	3.98 *m*	76.33	3.93 m
6a	63.42	4.29 *m*	63.43	4.46 *m*	63.33	4.40 br*d* (11)
6b	63.42	4.43 *brd* (10)	63.43	4.27 *brd* (11)	63.33	4.30 *dd* (7, 12)
G_b-1	104.96	4.78 *d* (8)	104.97	4.78 *d* (8)	104.76	4.82 *d* (8)
2	73.22	3.12 *t* (8)	73.19	3.12 *t* (8)	74.30	3.13 *d* (8)
3	75.06	3.22 *m*	75.04	2.93 *m*	74.96	3.26 m
4	69.03	2.99 *m*	69.00	2.89 *m*	69.70	3.18 m
5	75.82	3.22 *m*	75.78	2.98 *m*	76.37	3.26 m
6a	61.67	3.63 *brd* (10)	61.66	3.63 *m*	62.75	3.99 *dd* (4, 10)
6b	61.67	3.81 *brd* (10)	61.66	3.87 *m*	62.75	3.93 m
G_c-1	101.96	5.04 *d* (8)	102.52	5.03 *d* (8)	102.42	5.04 *d* (8)
2	73.22	3.56 *t* (8)	73.19	3.54 *t* (8)	73.50	3.54 *t* (8)
3	74.30	3.39 *t* (9)	74.32	3.38 *t* (8)	76.17	3.39 *t* (9)
4	69.98	3.28 *t* (9)	69.74	3.27 *t* (9)	70.04	3.28 *t* (9)
5	75.91	3.73 *m*	75.37	3.70 *m*	77.96	3.47 m
6a	64.42	4.10 *dd* (6, 11)	64.16	3.98 *m*	61.12	3.56 m
6b	64.42	4.42 *brd* (10)	64.16	4.41 *brd* (11)	61.12	3.80 *brd* (10)
Acid-I-1	125.65	–	125.64	–	125.27	–
2	130.46	7.31 *d* (8)	129.59	7.14 *s*	130.50	7.38 *d* (8)
3	115.76	6.72 *d* (8)	115.70	–	116.13	6.79 *d* (8)
4	159.98	–	159.52	–	160.19	–
5	115.76	6.72 *d* (8)	115.70	6.74 *d* (9)	116.13	6.79 *d* (8)
6	130.46	7.31 *d* (8)	125.91	6.95 *d* (9)	130.50	7.38 *d* (8)
α	113.79	6.13 *d* (16)	114.11	6.14 *d* (16)	114.07	6.03 *d* (16)
β	144.47	7.16 *d* (16)	144.56	7.16 *d* (16)	144.94	7.25 *d* (16)
C=O	166.37	–	166.38	–	166.60	–
OCH_3	–	–	55.74	3.81 *s*	–	–
Acid-II-1	125.06	–	123.06	–	125.27	–
2	123.29	7.13 *s*	121.70	7.06 *s*	130.72	7.34 *d* (8)
3	115.70	–	115.60	–	116.08	6.77 *d* (8)
4	159.98	–	159.64	–	160.19	–
5	116.02	6.91 *d* (8)	116.57	6.68 *d* (9)	116.08	6.77 *d* (8)
6	130.46	6.79 *d* (8)	129.59	6.92 *d* (9)	130.72	7.34 *d* (8)
α	116.56	6.13 *d* (16)	112.39	6.31 *d* (16)	113.93	6.23 *d* (16)

continued on next page

Table 1 (*continued*)

Assignment	**1**		**2**		**4**	
	δ_C	δ_H	δ_C	δ_H	δ_C	δ_H
β	144.41	7.35 *d* (16)	143.72	7.40 *d* (16)	145.44	7.37 *d* (16)
C=O	166.74	–	166.80	–	166.89	–
OCH_3	55.84	3.81 *s*	55.85	3.75 *s*	–	–
Mal-CH_2-	41.33	3.38 *s*	41.29	3.39 *s*	–	–
C=O	167.01	–	167.00	–	–	–
C=O	168.14	–	168.19	–	–	–

[a] Abbreviations: G = glucose; Mal = malonic acid; *s* = singlet; *d* = doublet; *t* = triplet; *m* = multiplet; *brd* = broad doublet and brt = broad triplet. Values in parentheses indicate coupling constants (*J* in Hz).

glucopyranosyl)}-5-*O*-(6-*O*-malonyl-β-D-glucopyranosyl) delphinidin, 3-*O*-{2-*O*-(6-*O*-*E*-feruloyl-β-D-glucopyranosyl)-(6-*O*-*E*-feruloyl-β-D-glucopyranosyl)}-5-*O*-(6-*O*-malonyl-β-D-glucopyranosyl) delphinidin, and 3-*O*-{2-*O*-(6-*O*-*E*-*p*-coumaroyl-β-D-glucopyranosyl)-(6-*O*-*E*-*p*-coumaroyl - β-D-glucopyranosyl)}-5-*O*-(β-D-glucopyranosyl) cyanidin, respectively. The anthocyanins **3** and **5** were tentatively determined as 3-(di-feruloyl)sophorosyl-5-glucosyl delphinidin and 3-(feruloyl-*p*-coumaroyl)sophorosyl-5-malonylglucosyl cyanidin, respectively (Fig. 3).

The stability and antioxidative activity of *A. reptans* flower cell culture crude extract, its major anthocyanin cyanidin 3-(di-*p*-coumaroyl)sophoroside-5-malonylglucoside (**6**) whose structure had been already determined (Terahara et al., 1996), and the deacylated derivative Cy3S5G were compared with cyanidin 3-glucoside (Cy3G) in neutral aqueous solution. The stability could be evaluated on the basis of the half-life ($t_{1/2}$) which was defined as the time to reach 50% residual color. As shown in Fig. 4, **6** ($t_{1/2} > 600$ min) and the cell culture crude extract ($t_{1/2} = 270$ min) were more stable than Cy3G ($t_{1/2} = 80$ min) and Cy3S5G ($t_{1/2} = 15$ min). Comparison of the stability of **6** and Cy3S5G suggested that the two *p*-coumaric acids protect the aglycone nucleus by a sandwich type hydrophobic stacking mechanism, and inhibit the attack of a water molecule that leads to a loss of color (Brouillard, 1983; Goto and Kondo, 1991).

The antioxidative activity of the cell culture crude extract and **6** were measured as the inhibitory ratio to β-carotene bleaching induced with linoleic acid peroxidation by lipoxygenase (Igarashi et al., 1989, 1993). As shown in Fig. 5, **6** and the cell culture crude extract showed weaker antioxidative activity than a natural antioxidant α-tocopherol and a synthetic antioxidant BHT. However, **6** demonstrated stronger activity than non-acylated anthocyanins Cy3G5G, Cy3S5G and Cy3G which had strong antioxidative activity as reported by Tsuda et al. (1994), and than other polyphenols like *p*-coumaric acid and (+)-catechin. The difference of antioxidative activity between **6** and Cy3S5G was considered that the

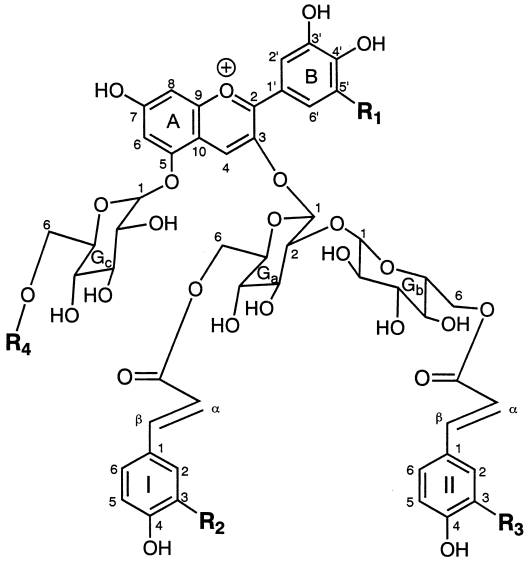

Fig. 3. Structures of *Ajuga reptans* flower and the cell culture anthocyanins. The anthocyanins **3** and **5** are the tentative structures.

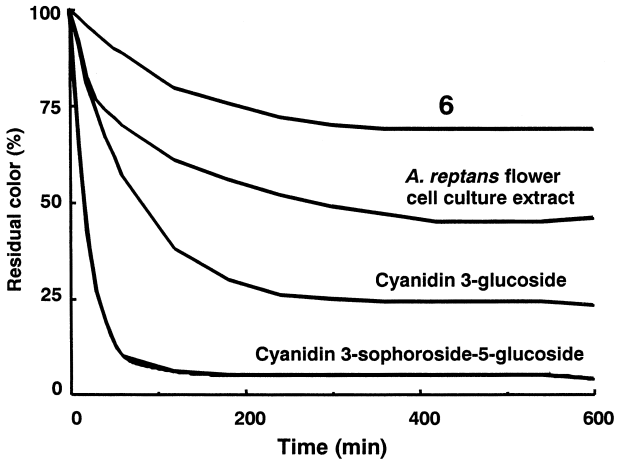

Fig. 4. Stability of *Ajuga reptans* flower culture anthocyanins in neutral aqueous solution at room temperature. Anthocyanin **6** indicates cyanidin 3-(di-*p*-coumaroyl)sophoroside-5-malonylglucoside.

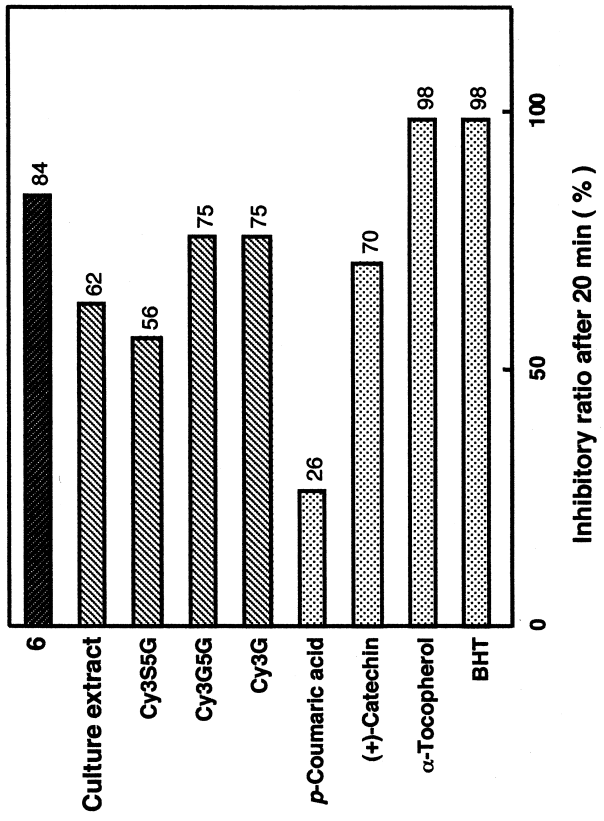

Fig. 5. Antioxidative activity of *Ajuga reptans* flower culture anthocyanins on β-carotene bleaching by linoleic acid — lipoxygenase system. Abbreviations: Crude extract = *A. reptans* flower cell culture extract, **6** = cyanidin 3-(di-*p*-coumaroyl)sophoroside-5-malonylglucoside, Cy3S5G = cyanidin 3-sophoroside-5-glucoside, Cy3G5G = cyanidin 3,5-diglucoside, Cy3G = cyanidin 3-glucoside, and BHT = butylated hydroxytoluene.

two intramolecular *p*-coumaric acids synergistically operated with **6** to prevent lipid peroxidation (Tamura and Yamagami, 1994). Therefore, hydroxycinnamic acid moieties in anthocyanins from *A. reptans* flower cell culture could play important roles for enhancement of stability and antioxidative activity.

Thus, *A. reptans* flower cell cultures are an excellent anthocyanin source for natural colorants of foods or others, because they produce anthocyanins with a constant composition and amount for a long time (Callebaut et al., 1997), and the produced anthocyanins have higher stability and antioxidative activity than Cy3G which is major anthocyanin in a purple corn pigment used currently as a commercially available food colorant.

3. Experimental

3.1. General procedures

All the reagents and solvents employed were of analytical grade and used without further purification. TLC, analytical HPLC and preparative HPLC were run under established conditions (Terahara et al., 1996). However, in order to get better resolution, the analytical HPLC elution mode was improved by using a linear gradient elution for 140 min from 18 to 46% solvent B (1.5% H_3PO_4, 20% AcOH, 25% MeCN in H_2O) in solvent A (1.5% H_3PO_4 in H_2O) on Inertsil ODS-2 column (4.6 i.d.×250 mm, GL Sciences Inc.) at 35°C with a flow rate of 1 ml min^{-1} monitoring at 530 nm. UV-VIS spectra were recorded on MPS-2000 spectrophotometer (Shimadzu Co., Ltd.) in 0.01% HCl–MeOH. FABMS spectra were measured on a JMS SX102 (Jeol Co., Ltd.) in MeOH with *m*-nitrobenzyl alcohol as a matrix in the positive mode and a linked scan method. ^{13}C (150.8 MHz) and ^{1}H (600.1 MHz) NMR spectra were run on alpha-600 (Jeol Co., Ltd.) in DMSO-*d*6: CF_3COOD = 9:1. LC–ESIMS analysis was performed on a PU-980 Intelligent pump system (Jasco Co., Ltd.) and run on a L-column ODS (4.6 i.d.×250 mm, Chemical Inspection and Testing Institute, Japan) at 40°C with a flow rate of 1 ml min^{-1} with detection at 530 nm by a UV–visdetector (UV-970, Jasco Co., Ltd.) coupled with an electrospray ionization (ESI) interfaced mass spectrometer Platform (VG biotech Co., Ltd.). It eluted with a linear gradient for 30 min from 15 to 20% solvent B (MeCN) in solvent A (0.4% HCOOH). Electrospray ionization Fourier-transform ion cyclotron resonance mass spectra (ESI–FTICRMS) were measured on ApexII mass spectrometer (Bruker Daltonics, Inc., USA) in 50%MeOH in 1%AcOH. Spectronic 20A (Shimadzu Co., Ltd.) was used for colorimetric measurements of antioxidative activity assay.

3.2. Plant materials

Anthocyanin producing cell cultures were induced from young flowers according to previous reports (Callebaut et al., 1990a, 1993).

3.3. Isolation and preparation of pigments

Isolation and preparation of anthocyanins of *A. reptans* flower and the cell cultures were carried out as was previously reported (Terahara et al., 1996). Three anthocyanins **1**–**3** were isolated from *A. reptans* flowers and one (**4**) from the cell cultures as red amorphous powders of trifluoroacetic acid (TFA) salts. The crude pigment of *A. reptans* flower cell cultures was prepared as described in the report (Terahara et al., 1996). Cy3S5G were prepared by alkaline deacylation of the major culture anthocyanin, **6**. Cy3G5G and Cy3G were isolated from *A. reptans* flower cell culture crude extract and a purple corn, respectively.

3.4. Pigment composition

As shown in Fig. 1, *A. reptans* flower cell culture crude extract contained anthocyanins at retention times

(contents%); Cy 3G5G: 8.4 (8%), 63.9 (1%), 65.8 (3%), **1**: 82.6 (1%), 85.0 (7%), **2**: 87.2 (4%), **4**: 89.5 (16%), **5**: 106.4 (7%), **6**: 108.8 (34%), unknown: 110.6 (4%) and unknown: 113.3 (3%) min. *A. reptans* flower crude extract contained anthocyanins at retention times (contents%); 63.9 (3%), 65.8 (12%), **3**: 67.9 (10%), **1**: 82.6 (16%), 85.0 (24%), **2**: 87.2 (8%) and **4**: 89.5 (5%) min.

3.5. FABMS analytical data

FABMS spectra of isolated anthocyanins gave m/z as follows; **1**: 1197 ($M = DpPGFGmG = C_{55}H_{57}O_{30})^+$, 949 ($DpPGFG = C_{46}H_{45}O_{22})^+$, 551 ($DpmG = C_{24}H_{23}O_{15})^+$, 303 ($Dp = C_{15}H_{11}O_7)^+$, 177 ($F = C_{10}H_9O_3)^+$, 147 ($P = C_9H_7O_2)^+$; **2**: 1227 ($M = DpFGFGmG = C_{56}H_{59}O_{31})^+$, 979 ($DpFGFG = C_{47}H_{47}O_{23})^+$, 551 ($DpmG_c = C_{24}H_{23}O_{15})^+$, 303 ($Dp = C_{15}H_{11}O_7)^+$, 147 ($P = C_9H_7O_2)^+$; **3**: 1141 ($M = DpFGFGG = C_{53}H_{57}O_{28})^+$, 979 ($DpFGFG = C_{47}H_{47}O_{23})^+$, 465 ($DpG = C_{21}H_{21}O_{12})^+$, 303 ($Dp = C_{15}H_{11}O_7)^+$, 147 ($P = C_9H_7O_2)^+$; **4**: 1065 ($M = CyPGPGG = C_{51}H_{53}O_{25})^+$, 903 ($CyPGPG = C_{45}H_{43}O_{20})^+$, 449 ($CyG_c = C_{21}H_{21}O_{11})^+$, 287 ($Cy = C_{15}H_{11}O_6)^+$, 147 ($P = C_9H_7O_2)^+$.

3.6. High-resolution mass data

ESI–FTICRMS afforded accurate mass assignments for single charged ions of anthocyanins at a mass resolution in excess of 2×10^4, and with an error of about 0.4 ppm as follows; **1**: obsd. m/z 1197.29338 (calc. 1197.29292 as $M^+ = C_{55}H_{57}O_{30}^+$); **2**: 1227.30389 (calc. 1227.30348 as $M^+ = C_{56}H_{59}O_{31}^+$); **4**: 1065.28738 (calc. 1065.28704 as $M^+ = C_{51}H_{53}O_{25}^+$).

3.7. LC–ESIMS analytical data

The crude extract from *A. reptans* flower cell culture crude extract gave the following mass numbers at retention times (m/z of molecular and fragment ions); $DpPGPGG^+$: 14.8 (1081: $M^+ = C_{51}H_{53}O_{26}^+$, 919, 465, 303), $CyPGPGG^+$ (**4**): 22.3 (1065: $M^+ = C_{51}H_{53}O_{25}^+$, 903, 449, 287), $DpPGPGmG^+$: 24.7 (1167: $M^+ = C_{54}H_{55}O_{29}^+$, 551, 303), $CyPGFGmG^+$ (**5**): 32.3 (1181: $M^+ = C_{55}H_{57}O_{29}^+$, 933: $CyPGFG^+ = C_{46}H_{45}O_{21}^+$, 535: $CymG^+ = C_{24}H_{23}O_{14}^+$, 287: $Cy^+ = C_{15}H_{11}O_6^+$), $CyPGPGmG^+$: 33.8 (1151: $M^+ = C_{54}H_{55}O_{28}^+$, 903, 535, 287) min

3.8. UV–vis spectral data

UV–vis spectra gave following data; **1**: λ_{max} (0.01% HCl–MeOH) nm: 542 (shifted bathochromically by 53 nm with $AlCl_3$), 316, $E_{440}/E_{VIS.max} = E_{440}/E_{542} = 11\%$, $E_{acid.max}/E_{VIS.max} = E_{316}/E_{542} = 164\%$; **2**: λ_{max} (0.01% HCl–MeOH) nm: 542 (shifted bathochromically by 53 nm with $AlCl_3$), 325, $E_{440}/E_{VIS.max} = E_{440}/E_{542} = 13\%$, $E_{acid.max}/E_{VIS.max} = E_{325}/E_{542} = 184\%$; **3**: λ_{max} (0.01% HCl–MeOH) nm: 544 (shifted bathochromically by 50 nm with $AlCl_3$), 284, 326, $E_{440}/E_{VIS.max} = E_{440}/E_{544} = 12\%$, $E_{acid.max}/E_{VIS.max} = E_{316}/E_{544} = 141\%$; **4**: λ_{max} (0.01% HCI–MeOH) nm: 527 (shifted bathochromically by 50 nm with $AlCl_3$), 299, 314, $E_{440}/E_{VIS.max} = E_{440}/E_{527} = 19\%$, $E_{acid.max}/E_{VIS.max} = E_{314}/E_{527} = 158\%$.

3.9. Stability test

Citric acid 1-hydrate (Chameleon), and disodium hydrogenphosphate 12-water (Chameleon) were used for McIlvaine (10^{-1} M citrate — 2×10^{-1} M phosphate) buffer components. Each anthocyanin mono-TFA salt (10^{-6} mol) and the cell culture crude extract (5 mg) were dissolved in 20 ml of pH 7.0 McIlvaine buffer solution (pure anthocyanin concentration: 5×10^{-5} M, the cell culture crude extract: 25×10^{-2} mg ml^{-1}), and the VIS spectra (400–700 nm) were measured automatically at appropriate time intervals. Based on the absorbance at $\lambda_{VIS.max}$ of each spectrum, the residual color (%) was calculated as percent of the initial absorbance (=100%). The stability of the anthocyanin could be evaluated on the basis of the half-life ($t_{1/2}$), defined as the time to reach 50% residual color.

3.10. Antioxidative activity assay

β-Carotene (Wako Pure Chemical) was used as indicator for antioxidative activity. Linoleic acid (Nippon Oil & Fats Co., EXTRA LINOLEIC-90) was used as model lipid for peroxidation with lipoxygenase (lipoxydase from soybean, Boehringer Ingelheim Bioproducts). *p*-Coumaric acid (Tokyo Chemical), (+)-catechin (Extrasynthese) and α-tocopherol (Wako Pure Chemical) were used as natural antioxidants, and butylated hydroxytoluene (BHT, Wako Pure Chemical) as synthetic antioxidant. Each sample solution was tested according to the modified method of Igarashi et al. (1989). Four milliliters of 150 μg ml^{-1} linoleic acid in pH 7.0 McIlvaine buffer (containing 0.8 mg ml^{-1} of Tween 80), 300 μl of 50 μg ml^{-1} β-carotene in acetone, and 200 μl of 1 mM-substrate ethanol solution (concentration of the cell culture crude extract: 1 mg ml^{-1}) were mixed in a test tube. To this solution, 500 μl of 100 μg ml^{-1} lipoxygenase aqueous solution was added and shaken immediately. Final sample concentration was 40 μM (or 40 μg ml^{-1}), and pH of the test solution was about 7.2. The mixture was kept standing at 20°C, then measured the residual β-carotene content at 460 nm at appropriate interval times. A reaction mixture without substrate was similarly treated and used as a control in colorimetry. The antioxidative power of substrates was evaluated with inhibitory ratio (IR%) between each substrate and control.

Acknowledgements

We are grateful to Dr. Y. Kato, San-Ei Gen FFI Inc., for measurement of LC-ESIMS, and to Dr. Y. Inoue, Bizen Chemical Co., Ltd., for providing pure linoleic acid sample to us. We also thank the San-Ei Gen Foundation for Food Chemical Research for financial support.

References

Baker, D.C., Dougall, D.K., Glassgen, W.E., Johnson, S.C., Metzger, J.W., Rose, A., Seitz, H.U., 1994. Effects of supplied cinnamic acids and biosynthetic intermediates on the anthocyanins accumulated by wild carrot suspension cultures. Plant Cell Tissue and Organ Culture 39, 79–91.

Balidi, A., Romani, A., Mulinacci, N., Vincieri, F.F., Casetta, B., 1995. HPLC/MS application to anthocyanins of *Vitis vinifera* L. Journal of Agricultural and Food Chemistry 43, 2104–2109.

Brouillard, R., 1983. The *in vivo* expression of anthocyanin colour in plants. Phytochemistry 22, 1311–1323.

Callebaut, A., Hendrickx, G., Voets, A.M., Motte, J.C., 1990a. Anthocyanins in cell cultures of *Ajuga reptans*. Phytochemistry 29, 2153–2158.

Callebaut, A., Voets, A.M., Motte, J.C., 1990b. Anthocyanin production by plant cell cultures on media based on milk whey. Biotechnology Letters 12, 215–218.

Callebaut, A., Decleire, M., Vandermeiren, K.I., 1993. *Ajuga reptans* (Bugle): *in vitro* production of anthocyanins. In Bajay, Y. P. S. (Ed.), Biotechnology in Agriculture and Forestry. Springer-Verlag, Berlin, pp. 1–22.

Callebaut, A., Terahara, N., Decleire, M., 1996. Anthocyanin acyltransferases in cell cultures of *Ajuga reptans*. Plant Science 118, 109–118.

Callebaut, A., Terahara, N., de Haan, M., Decleire, M., 1997. Stability of anthocyanin composition in *Ajuga reptans* callus and cell suspension cultures. Plant Cell Tissue and Organ Culture 50, 195–201.

Calsteren, M.-R.V., Cormier, F., Do, C.B., Laing, R.R., 1991. ^{1}H and ^{13}C NMR assignments of the major anthocyanins from *Vitis vinifera* suspension culture. Spectroscopy (Ottawa) 9, 1–15.

Cormier, F., Do, C.B., Nicolas, Y., 1994. Anthocyanin production in selected cell lines of grape (*Vitis vinifera* L). In Vitro Cellular and Developmental Biology Plant 3, 171–173.

Goto, T., Kondo, T., 1991. Structure and molecular stacking of anthocyanins — flower color variation. Angewandte Chemie, International Edition in English 30, 17–33.

Green, M.K., Vestling, M.M., Johnston, M.V., Larsen, B.S., 1998. Distinguishing small molecular mass differences of proteins by mass spectrometry. Analytical Biochemistry 260, 204–211.

Harborne, J.B., 1958. Spectral methods of characterizing anthocyanins. Biochemical Journal 70, 22–28.

Harborne, J.B., Mayer, A.M., B.-Nun, N., 1983. Identification of the major anthocyanin of carrot cells in tissue culture as cyanidin 3-(sinapoylxyosylglucosylgalactoside). Zeitschrift fur Naturforschung 38c, 1055–1056.

Igarashi, K., Takanashi, K., Makino, M., Yasui, T., 1989. Antioxidative activity of major anthocyanin isolated from wild grapes (*Vitis coignetiae*). Nippon Shokuhin Kogyo Gakkaishi 36, 852–856.

Igarashi, K., Yoshida, T., Suzuki, E., 1993. Antioxidative activity of nasunin in Chouja-nasu (little eggplant, *Solanum melongena* L. 'Chouja'). Nippon Shokuhin Kogyo Gakkaishi 40, 138–143.

Madhavi, D.L., Juthangkoon, S., Lewen, K., Berber-Jimenez, M.D., Smith, M.A.L., 1996. Characterization of anthocyanins from *Ajuga pyramidalis* Metallica Crispa cell cultures. Journal of Agricultural and Food Chemistry 44, 1170–1176.

Mori, T., Sakurai, M., Shigeta, J., Yoshida, K., Kondo, T., 1993. Formation of anthocyanins from cells cultured from different parts of strawberry plants. Journal of Food Science 58, 788–792.

Sakairi, M., Kambara, H., 1988. Characteristics of a liquid chromatography/atmospheric pressure ionization mass spectrometer. Analytical Chemistry 60, 774–780.

Sakamoto, K., Iida, K., Sawamura, K., Hajiro, K., Asada, Y., Yoshikawa, T., Furuya, T., 1993. Studies on plant tissue cultures. Part 82. Effects of nutrients on anthocyanin production in cultured cells of *Aralia cordata*. Phytochemistry 33, 357–360.

Takahashi, A., Takeda, K., Ohnishi, T., 1991. Light-induced anthocyanin reduces the extent of damage to DNA in UV-irradiated *Centaurea cyanus* cells in culture. Plant and Cell Physiology 32, 541–547.

Tamura, H., Fujiwara, M., Sugisawa, H., 1989. Production of phenylpropanoids from cultured callus tissue of the leaves of akachirimenshiso (*Perilla* sp.). Agricultural and Biological Chemistry 53, 1971–1973.

Tamura, H., Yamagami, A., 1994. Antioxidative activity of monoacylated anthocyanins isolated from Muscat Bailey A grape. Journal of Agricultural and Food Chemistry 42, 1612–1615.

Terahara, N., Callebaut, A., Ohba, R., Nagata, T., Suzuki, M., 1996. New triacylated anthocyanins from *Ajuga reptans* L. flowers and the flower cultures. Phytochemistry 42, 199–203.

Tholakalabavi, A., Zwiazek, J.J., Thorpe, T.A., 1994. Effect of mannitol and glucose-induced osmotic stress on growth, water relations, and solute composition of cell suspension cultures of poplar (*Populus deltoides* var *occidentalis*) in relation to anthocyanin accumulation. In Vitro Cellular and Developmental Biology Plant 3, 164–170.

Tsuda, T., Watanabe, M., Ohshima, K., Norinobu, S., Choi, S.W., Kawakishi, S., Osawa, T., 1994. Antioxidative activity of the anthocyanin pigments cyanidin 3-*O*-β-D-glucoside and cyanidin. Journal of Agricultural and Food Chemistry 42, 2407–2410.

Whitehouse, C.W., Dreyer, R.N., Yamashita, M., Fenn, J.B., 1985. Electrospray interface for liquid chromatographs and mass spectrometers. Analytical Chemistry 57, 675–679.

Yamamoto, Y., Mizuguchi, R., Yamada, Y., 1981. Chemical constituents of cultured cells of *Euphorbia tirucalli* and *E. millii*. Plant Cell Reports 1, 29–30.

PERGAMON

Phytochemistry 58 (2001) 501–508

PHYTOCHEMISTRY

www.elsevier.com/locate/phytochem

Isolation of solasodine and other steroidal alkaloids and sapogenins by direct hydrolysis-extraction of *Solanum* plants or glycosides therefrom

Martin Weissenberg*

Laboratory of Natural Products Chemistry, Department of Plant Genetics, Institute of Field Crops, Agricultural Research Organization, The Volcani Center, PO Box 6, Bet Dagan 50 250, Israel

Received 16 January 2001; accepted 1 March 2001

Abstract

Concomitant extraction and hydrolysis of *Solanum* steroidal glycoalkaloids in a two-phase system containing an aqueous mineral acid and an organic water immiscible solvent, and having a boiling point under 100°C, is described. It is essentially a "one-pot" process, combining direct acid hydrolysis of the glycosides in the plant material and in situ extraction of the released aglycones after alkali treatment, in a single step, the various ingredients being added simultaneously or sequentially, as required. Application of the process to fruits, leaves, and tissue cultures of *Solanum khasianum* Clarke plants, either fresh or in dried, finely ground form, using a two-phase aqueous hydrochloric acid-toluene system, proved to be very suitable for continuous production of pure solasodine which is a valuable raw steroid for the preparation of steroidal drugs. Pure *Solanum* glycoalkaloids were also prepared and hydrolysed accordingly. The process has analytical applications too, and could be extended in a general way to glycosides in other series for preparation of their related aglycones. © 2001 Elsevier Science Ltd. All rights reserved.

Keywords: *Solanum* spp; Solanaceae; Spirosolane and solanidane derivatives; Steroidal glycoalkaloids; Solamargine; Solasonine; β-Solamarine; Solaverbascine chacotrioside and solatrioside; Tomatine; Aglycones; Solasodine; Tomatidenol; Solaverbascine; Tomatidine; Solanidine; Plant glycosides; Two-phase acid hydrolysis

1. Introduction

Proliferation of papers dealing with simultaneous isolation and hydrolysis of *Solanum* glycoalkaloids using either single-phase (Löken and Sollins, 1970; Hardman and Williams, 1976; Panina et al., 1976; Weston, 1976; Pandeya et al., 1981; Chandler and Dodds, 1983; Ntahomvukiye et al., 1983; Chungath and Nair, 1989; Kittipongpatana et al., 1999) or two-phase (van Gelder, 1984) solvent systems, prompts us to report our own results which have been patented (Weissenberg, 1982) and only briefly reviewed at the time (Chem. Abstr., 1983 [see Weissenberg, 1982]; Harrison, 1984), and thus apparently underexposed to general attention. Our investigation was part of an extensive study concerned with the development of high-yielding varieties and mutants of solasodine-bearing *Solanum khasianum* Clarke plants (Yaniv et al., 1981) as a convenient source of 16-dehydropregnenolone acetate (DPA), which is a starting material for anti-fertility and anti-inflammatory steroidal drugs (Mann, 1978).

In *S. khasianum* plants, solasodine (**1**) occurs mainly as triosides solasonine (**2**) and solamargine (**3**) (Figs. 1 and 2). The reported procedures for preparation of solasodine were reviewed (Weston, 1976; Mann, 1978; Crabbe and Fryer, 1983), and include either enzymatic hydrolysis of solasodine glycosides by fermentation of plant raw material (Fonin et al., 1996), or their extraction by means of aqueous and/or alcoholic acids; simultaneously with, or subsequent to the extraction, occurred hydrolysis of the glycoalkaloids by which the sugar moiety is split off. In these acid extraction methods, the separation of the plant material from the liquid phase after the extraction is slow and tedious. Alternatively, extraction might be carried out with an alcohol alone, whereby the extracted material is isolated by precipitation with an alkali, and is then subjected to

* Fax: +972-3-6350491.

0031-9422/01/$ - see front matter © 2001 Elsevier Science Ltd. All rights reserved.
PII: S0031-9422(01)00185-6

	Compound	Rings A/B Juncture	Other Substituents	R	X_1	X_2	Chiral Centers
1	Solasodine	Δ^5		OH	NH	CH_2	22R, 25R
2	Solasonine	Δ^5		O-Solatriosyl	NH	CH_2	22R, 25R
3	Solamargine	Δ^5		O-Chacotriosyl	NH	CH_2	22R, 25R
4	Solasodiene	Δ^5	Δ^3	H	NH	CH_2	22R, 25R
5	Tomatidenol	Δ^5		OH	CH_2	NH	22S, 25S
6	α-Solamarine	Δ^5		O-Solatriosyl	CH_2	NH	22S, 25S
7	β-Solamarine	Δ^5		O-Chacotriosyl	CH_2	NH	22S, 25S
8	Tomatidine	5α-H		OH	CH_2	NH	22S, 25S
9	Tomatine	5α-H		O-Lycotetraosyl	CH_2	NH	22S, 25S
10	Solaverbascine	Δ^5	16β-OH	OH	NH	CH_2	22S, 25R
11	Solaverbascine solatrioside	Δ^5	16β-OH	O-Solatriosyl	NH	CH_2	22S, 25R
12	Solaverbascine chacotrioside	Δ^5	16β-OH	O-Chacotriosyl	NH	CH_2	22S, 25R

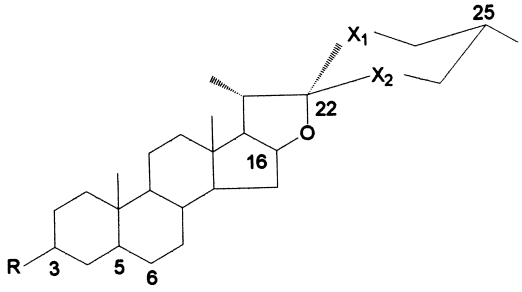

Fig. 1. Structure of spirosolane aglycones and glycosides.

hydrolysis with an alcoholic acid solution. The free base obtained according to either of these methods is precipitated from alcoholic acid solution by alkalinisation, and the raw material prepared in this way is then purified.

All these methods require at some stage boiling with an aqueous or alcoholic acid solution. It has been found that following this process, the yield of **1** is significantly reduced due to the occurrence of side reactions that leads to degradation products (Weston, 1976; Crabbe and Fryer, 1983). They include 3,5-solasodiene (**4**), which is formed by dehydration of solasodine upon boiling with acids. As a result, the crude material is obtained in only moderate yields as a brown-greenish powder contaminated with by-products, pigments, salts, sapogenins, and a fair amount of **4**. The latter, of course, is useless as a steroidal drug precursor being devoid of a 3-oxygenated function, and the purification of the crude **1** thus obtained proved to be laborious, to involve loss of material, and finally to afford modest yields of a satisfactory raw product. The object of our study was to provide a simplified and improved process for the isolation of alkaloidal steroids from plant material that contains them in glycoside form. The present communication describes the process, as well as its preparative and analytical applications.

2. Results and discussion

The process is based on the different solubility in certain selected solvents of the polar glycoalkaloids and the

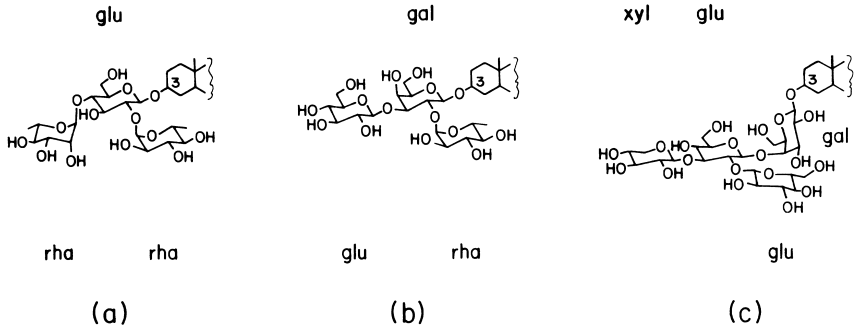

Fig. 2. Carbohydrate moieties attached to the position 3 in the steroidal framework of some spirosolane glycoalkaloids. (a) chacotriose; (b) solatriose; (c) lycotetraose. glu = D-glucose; gal = D-galactose; xyl = D-xylose; rha = L-rhamnose.

apolar aglycones. Thus, it has been found that pure aglycones can be obtained in high yield by conducting the hydrolysis of their corresponding glycosides in a two-phase liquid system comprising an aqueous solution of a mineral acid and a water immiscible organic solvent, and having a boiling point at a temperature below 100°C. Following reflux of the reaction mixture, the glycosides undergo hydrolysis in the aqueous acid phase, and the aglycone set free by alkalinisation is simultaneously extracted into the organic phase of the liquid system, thus being protected from further contact, with the acid phase. Prior to alkalinisation, the presence of the organic solvent suppresses the side reactions of the solasodine salt and of the partially hydrolysed products formed, prevents their precipitation, and thus ensures complete hydrolysis. Moreover, the temperature of the reaction mixture in the two-phase liquid system is, as a rule, lower than in the one-phase process, which is also a contributory factor to the decrease of side reactions. Following alkalinisation, the alkaloidal steroid is selectively removed into the organic solvent phase from which it can be readily recovered, either by direct crystallisation from the concentrated extract, or by extraction with an aqueous acid followed by alkalinisation of the aqueous acid extract. In both cases, the crude product consisting of colourless crystalls or amorphous precipitate, respectively, of solasodine, is obtained in over 90% recovery, and is sufficiently pure to serve as the starting material for conversion into DPA. Other examples of alkaloidal steroids that could be isolated in accordance with this process beside the previously mentioned solasodine (**1**), are the latter 22S,25S isomer tomatidenol (**5**) which occurs as glycosides α- and β-solamarines (**6** and **7,** respectively) in *S. dasyphyllum* Thonn. and *S. dulcamara* L., and its 5,6-saturated derivative tomatidine (**8**) which occurs as a 3β-lycotetraoside (tomatine, **9**) in *Lycopersicon esculentum* Mill (Figs. 1 and 2). All these spirosolane aglycones can be readily degraded to 16-dehydropregnane derivatives. Solaverbascine (**10**), a 16β-hydroxy derivative of **1** occurring in *S. verbascifolium L. (*Adam et al., 1980), was prepared in the same way both from its solatrioside (**11**) and chacotrioside (**12**) synthesised in turn by reduction with sodium borohydride of **2** and **3**, respectively (see Experimental).

Among the various mineral acids that are suitable as the aqueous acid component of the two-phase system in the process, hydrochloric acid and sulphuric acid may be mentioned in particular. The organic water-immiscible solvents that were evaluated comprise aromatic hydrocarbons such as benzene, toluene, and xylene, as well as halogenated aliphatic hydrocarbons like chloroform, carbon tetrachloride, and ethylene dichloride. The preferred solvent was toluene, used in a 1:1 v/v mixture with hydrochloric acid whose concentration is from 3.5 to 7% by weight, and preferably about 5% by weight. Such a two-phase system has a first boiling point at about 85°C.

In a preliminary attempt, purified mixtures of glycoalkaloids **2**, **3**, **6** and **7** (see Experimental) were refluxed for 3 h under stirring in the above mentioned two-phase liquid system; the reaction mixture was then alkalinised by addition of 40% w/v aqueous sodium hydroxide solution, and further refluxed under stirring. Phase separation and concentration in vacuo of toluene afforded the aglycones **1** and **5**, respectively. TLC monitoring of the process indicates that hydrolysis of the glycosides proceeds smoothly to yield the corresponding aglycones, practically free of dehydration products (TLC and NMR evidence).

Application of the process to fruits, leaves, and tissue cultures of various *Solanum* plants, either fresh or in dried, finely ground form (see Experimental), proved to be very suitable for continuous operation. It is essentially a ''one-pot'' process combining direct hydrolysis of steroidal glycoalkaloids in the plant material and in situ extraction of the released aglycones in a single step, the various ingredients being added into one vessel simultaneously or sequentially, as required. In experiments done with *S. khasianum* fruits, pure solasodine readily crystallised out from the concentrated toluene extracts, and the distilled off, or remaining mother liquor solvent may be recovered and recycled. As expected, work with fresh plant material avoids the time and energy-consuming steps of drying and milling.

In practicing the process, certain conditions proved to be imperative in order to obtain optimal yield and purity of the desired aglycone: (a) when processing oven-dried or lyophylised plant material, it should be finely ground before being submitted to hydrolysis; (b) the stirring of the two-phase system should be very efficient during the hydrolysis stage, and just moderate during alkalinisation in order to avoid formation of emulsions; (c) the proportions (by weight and volume) between plant material and reactants, the reaction duration, and the choice of the reagents, should be kept under the limits underlined in the Experimental section; (d) toluene is suggested as the solvent of choice since it leads to a two-phase system having an optimal boiling point, and has low propensity to emulsion formation. Besides, it allows spontaneous separation of crystalline solasodine from concentrated extracts. All the same, slight variations in the selection of appropriate solvents and conditions permit extension of this method to other saponins and glycosides of plant origin, substantially, as described.

Further application of this process for analytical purposes, which will be described elsewhere, enabled extensive screenings of large *Solanum* plant populations, as well as analyses of solasodine derivatives like immunogenic protein conjugates and inclusion complexes with cyclodextrin, prepared in connection with other works (Weissenberg, unpublished results). Among the solasodine-bearing *Solanum* plants examined, *S. khasianum* appears to be the best suited for the commercial production of **1**–**3**, as it was found to contain about 6% of **1** in dry whole fruits, most of it in the mucilage layer of the fruit (Yaniv et al., 1981). Spineless lines with high **1** content and concentrated fruit set were developed (A. Levy, unpublished results), and optimal cultivation practices were established for its eventual large-scale cultivation (Yaniv et al., 1983, 1984).

Besides its potential value as a raw starting material for synthesis of steroidal drugs, solasodine has been shown to possess some biological activity like antifungal (Wolters, 1976; Nes et al., 1982; Rowan et al., 1983; Kusano et al., 1987b), insect growth regulation (Raja et al., 1987; Kaur et al., 1988), and enzyme inhibition (Kusano et al., 1987a). Also it is noteworthy mentioning several reports on solasodine pharmacological effects, including significant cytotoxic activity in vitro against a variety of cancer cell lines (Lin et al., 1990; Nakamura et al., 1996), and DNA repair-deficient yeast mutants (Kim et al., 1996). It was also found to heal various *Herpes* skin lesions (Chataing et al., 1997), to inhibit *Trypanosoma cruzi* growth in vitro (Chataing et al., 1998), to inhibit proliferation of murine spleen cell cultures (Bähr and Hänsel, 1982), to mobilise glucocorticoids from the adrenals of rats (Dároczy and Hernádi, 1971), and to exhibit an antihepatotoxic effect on mice (Lin et al., 1988), It had an antiartherosclerotic effect on cholesterol-fed rabbits (Dixit et al., 1992), a hypotensive effect on cat (Basu and Lahiri, 1977), and an antispermatogenic effect on humans and bovines (Kanwar et al., 1990), Rhesus monkey (Dixit et al., 1989), and dog (Dixit and Gupta, 1982), respectively. On the other hand, a relatively low teratogenicity (Gaffield and Keeler, 1996), embryotoxicity (Friedman et al., 1992), and benign hapatomegaly (Friedman et al., 1996) were also noted. Likewise, intravenously injected solasodine was found to be excreted slowly in humans and in Syrian hamster (Claringbold et al., 1980). The occurrence, biological properties and ecological relevance of *Solanum* glycoalkaloids including **2**, **3**, **7**, **11** and **12**, have recently been assessed (Roddick et al., 2001).

3. Experimental

3.1. General

Mps, uncorr. ^{1}H and ^{13}C NMR at 400 and 100 MHz, respectively, in $CDCl_3$ or C_5D_5N. FAB–MS, glycerol matrix. TLC: precoated Kieselgel 60 F_{254} aluminium sheets (Merck), detection I_2 vapours. CC: silica gel 60, 70-230 mesh (Merck) or Al_2O_3 activity III (Woelm).

3.2. Plant material

Leaves and fruits of *S. khasianum, S. laciniatum* Ait., *S. aviculare Forst., S. marginatum* L., *S. mammosum* L. and *L. esculentum* were obtained from plants grown in an experimental field at the Volcani Center, Agricultural Research Organization, Bet Dagan, Israel, and harvested at about 8 months after sowing (courtesy of Professor A. Levy, Department of Plant Genetics, the Volcani Center, Agricultural Research Organization). A sample of purified *S. dulcamara* glycoalkaloids mixture was obtained through the courtesy of Professor J.F. Verbist, Faculty of Pharmacy, University of Nantes, France.

3.3. Reference compounds

Solasodine (**1**), tomatidine (**8**), tomatine (**9**), and solanidine were of commercial origin (Sigma, St. Louis, MO, USA). Pure reference samples of tomatidenol (**5**) and β-solamarine (**7**) were kindly provided by Dr. I. Merfort, University of Düsseldorf, Germany, and by Dr. M. Suffness, NCI, NIH, Bethesda, MD, USA, respectively. The following compounds were prepared in our laboratory according to published procedures:

3.3.1. (22R,25R)-Spirosola-3,5-diene (Solasodiene, 4)

This compound was prepared from solasodine refluxed with conc. HCl in MeOH by a modification of the method of Uskert (1963), and identified by comparison (mp, ^{1}H NMR) with reported data (Bird et al., 1979).

*3.3.2. (22S,25R)-22,26-Epiminocholest-5-ene-3β,16β-diol (Solaverbascine, Dihydrosolasodine A, **10**)*

This compound was prepared by reaction of **1** with $NaBH_4$ in MeOH for 3 h at room temp. according to Bird et al. (1979), and identified by comparison of physical and spectral data with reported data for solaverbascine isolated from *S. verbascifolium* (Adam et al., 1980), and for the synthetic compound (Bird et al., 1979).

3.4. Preparation of glycoalkaloids

*3.4.1. Solasonine (**2**) and Solamargine (**3**)*

Dried, finely ground berries of *S. khasianum* (150 g) were submitted to a preliminary purification which involved defatting with petroleum ether, and pigments removal with CH_2Cl_2. Subsequent exhaustive extraction with hot EtOH and evaporation of the solvent under reduced pressure afforded a crude glycosides extract (23.5 g) which was subjected to alumina CC. Elution with H_2O-satd *n*-BuOH yielded **3** (7.8 g) followed by mixtures of **3** and **2**, and finally **2** (2.8 g). The separation was monitored by TLC. Compounds **2** and **3** were repeatedly recrystallised from aqueous MeOH, and their identity ascertained by comparing physical and spectral data (mp, ^1H and ^{13}C NMR, and FAB–MS) with reported assignments (Fukuhara and Kubo, 1991). The mixtures of **2** and **3** were collected and rechromatographed on subsequent batches. Berries of *S. marginatum* were similarly processed; however, work with leaves of *S. laciniatum* or other species, which of course, do have a higher pigment content, would require an alkali treatment of the EtOH extract before CC, in order to have them removed.

*3.4.2. β-Solamarine (**7**)*

A purified glycoalkaloids mixture of *S. dulcamara* was subjected to repeated alumina CC (elution with H_2O-satd *n*-BuOH) monitored by TLC, followed by repeated prep. TLC ($CHCl_3$–MeOH–1% aq. NH_3 2:2:1) of the combined fractions enriched in **7**, which finally afforded pure **7** crystallised from MeOH–Me_2CO, and identified by comparison (mp, TLC) with reported data (Boll, 1962), and with an authentic sample. Since spectral data of **7** do not appear to have been reported previously, we note herein the positive FAB–MS, *m/z* (rel.int.) 868 $[M+H]^+$(100), 850 $[M+H-H_2O]^+$ (5), 722 $[M+H-C_6H_{10}O_4]^+$ (8), 704 $[M+H-C_6H_{12}O_5]^+$ (8), 414 $[C_{27}H_{43}NO_2+H]^+$(13); negative FAB–MS, *m/z* 866 $[M-H]^+$ (100), 720 $[M-H-C_6H_{10}O_4]^+$(12). ^{13}C NMR(C_5D_5N, TMS), aglycone signals: δ16.19 (C-21), 16.86 (C-18), 19.42 (C-19), 19.80 (C-27), 21.17 (C-11), 27.07 (C-23), 29.26 (C-24), 30.18 (C-2), 31.42 (C-25), 31.61 (C-8), 32.42 (C-7), 33.15 (C-15), 37.17 (C-10), 37.52 (C-1), 38.98 (C-4), 40.13 (C-12), 40.73 (C-13), 43.01 (C-20), 50.38 (C-9), 50.58 (C-26), 56.05 (C-14), 62.22 (C-17), 78.10 (C-3), 78.63 (C-16), 99.44 (C-22), 121.85 (C-6), 140.82 (C-5); oligosaccharide signals: δ100.28, 78.10, 77.87, 78.72, 76.94, 61.31 (glucose, C-1–C-6), 102.92, 72.57, 72.85, 74.13, 69.56, 18.52 (4-*O*-rhamnose, C-1–C-6), 102.08, 72.54, 72.75, 73.93, 70.45, 18.67 (2-*O*-rhamnose, C-1–C-6). ^1H NMR (C_5D_5N, TMS), aglycone signals: δ0.81(27-H_3), 0.87(18-H_3), 1.05(19-H_3), 1.08(21-H_3), 2.95(26-H_2), 3.80(3α-H), 4.11(16α -H), 5.32(6-H); oligosaccharide signals: δ4.94(glucose, H-1), 5.87 (4-*O*-rhamnose, H-1), 6.41 (2-*O*-rhamnose, H-1).

*3.4.3. (22S,25R)-16β-Hydroxy-3β-{O-α-L-rhamnopyranosyl-(1→2)-[O-β-D-glucopyranosyl-(1→3)]-β-D-galactopyranosyloxy}-22,26-epiminocholest-5-ene (solaverbascine 3β-O-solatrioside, **11**)*

To a solution of **2** (200 mg) in MeOH (40 ml) was added $NaBH_4$ (200 mg) and the reaction mixture was stirred for 1 h at room temp., then concentrated in vacuo, treated with ice-H_2O and extracted with *n*-BuOH (3×50 ml). The organic phase was washed with H_2O, and the solvent evapd in vacuo. The residue (186 mg, homogeneous on TLC) was treated with MeOH to give pure **11**, amorphous (92 mg); positive FAB–MS, *m/z* 886 $[M+H]^+$ (100), 868 $[M+H-H_2O]^+$(5), 416 $[C_{27}H_{45}NO_2+H]^+$(4); negative FAB–MS, *m/z* 884 $[M-H]^+$(7), 367 (100). ^{13}C NMR (C_5D_5N,TMS), aglycone signals: δ13.48 (C-18), 17.19 (C-21), 19.42 (C-19), 19.70 (C-27), 21.12 (C-11), 28.90 (C-23), 30.19 (C-2), 31.95 (C-25), 32.19 (C-8), 32.30 (C-7), 34.32 (C-24), 35.61 (C-15), 37.07 (C-10 and C-20), 37.53 (C-1), 38.84 (C-4), 40.44 (C-12), 42.75 (C-13), 50.52 (C-9), 54.74 (C-26), 55.19 (C-14), 59.22 (C-17), 61.77 (C-22), 71.21 (C-16), 78.38 (C-3), 121.96 (C-6), 140.93 (C-5); oligosaccharide signals: δ100.44, 76.53, 84.89, 70.45, 75.06, 62.57 (galactose, C-1–C-6), 105.87, 74.97, 78.54, 71.66, 77.59, 61.77 (glucose, C-1–C-6), 102.22, 72.61, 72.87, 74.22, 69.46, 18.64 (rhamnose, C-1–C-6). ^1H NMR (C_5D_5N, TMS), aglycone signals: δ0.73 (27-H_3), 0.75 (18-H_3), 1.09 (19-H_3), 1.10 (21-H_3), 2.80 (26-H_2), 3.80 (3α-H), 4.43 (16α-H), 5.34 (6-H); oligosaccharide signals: δ4.93 (glucose, H-1), 5.20 (galactose, H-1), 6.32 (rhamnose, H-1).

*3.4.4. (22S,25R)-16β-Hydroxy-3β-{O-α-L-rhamnopyranosyl-(1→2)-[O-α-L-rhamnopyranosyl-(1→4)]-β-D-glucopyranosyloxy}-22,26-epiminocholest-5-ene (solaverbascine 3β-O-chacotrioside, **12**)*

Compound **3** (200 mg) in MeOH (40 ml) was treated with $NaBH_4$ (200 mg) for 2 h at room temp., and the reaction mixture processed as described for **11**. The crude product (195 mg, homogeneous on TLC) was treated with EtOH with a few drops of H_2O to give pure **12** amorphous (119 mg), positive FAB–MS, *m/z* 870 $[M+H]^+$ (100), 852 $[M+H-H_2O]^+$(7), 724 $[M+H-C_6H_{10}O_4]^+$ (8), 706 $[M+H-C_6H_{12}O_5]^+$ (7), 416 $[C_{27}H_{45}NO_2+H]^+$ (3), 398 $[416-H_2O]^+$(6); negative FAB–MS, *m/z* 868 $[M-H]^+$(100), 722 $[M-H-C_6H_{10}O_4]^+$(16). ^{13}C NMR

(C_5D_5N,TMS), aglycone signals: δ13.48 (C-18), 17.19 (C-21), 19.42 (C-19), 19.70 (C-27), 21.13 (C-11), 28.92 (C-23), 30.21 (C-2), 31.93 (C-25), 32.21 (C-8), 32.28 (C-7), 34.33 (C-24), 35.62 (C-15), 37.06 (C-10 and C-20), 37.53 (C-1), 39.01 (C-4), 40.44 (C-12), 42.75 (C-13), 50.55 (C-9), 54.73 (C-26), 55.20 (C-14), 59.23 (C-17), 62.67 (C-22), 71.21 (C-16), 78.17 (C-3), 122.02 (C-6), 140.84 (C-5); oligosaccharide signals: δ100.31, 77.97, 77.81, 78.73, 76.93, 61.35 (glucose, C-1–C-6), 102.03, 72.75, 72.84, 73.93, 70.45, 18.65 (4-*O*-rhamnose, C-1–C-6), 102.94, 73.75, 72.54, 74.15, 69.53, 18.50 (2-*O*-rhamnose, C-1–C-6). ^{1}H NMR (C_5D_5N, TMS), aglycone signals: δ0.73 (27-H_3), 0.75 (18-H_3), 1.08 (19-H_3), 1.10 (21-H_3), 2.79 (26-H_2), 3.80 (3α-H), 4.42 (16α-H), 5.33 (6-H); oligosaccharide signals: δ 4.95 (glucose,H-1), 5.89 (4-*O*-rhamnose, H-1), 6.43 (2-*O*-rhamnose, H-1).

3.5. Isolation of solasodine and/or other steroidal alkaloids by direct hydrolysis- extraction of Solanum plants

3.5.1. From dried plant material

A suspension of dried, finely ground powder of different *Solanum* fruits and/or leaves (100 g) in toluene (300 ml), H_2O (200 ml) and conc. HCl (32%, 100 ml), was refluxed under stirring for 5 h. The reaction mixture was subsequently alkalinised with 40% aq. NaOH (200 ml) and refluxed again under stirring for 2 h. Following phase separation, the upper, pale-yellow toluene layer was siphoned out, and the remaining dark brown aqueous mixture was extracted three times with 100 ml portions of toluene. The combined toluene extracts were clarified with charcoal, then concentrated in vacuo to small volume. Further treatment involved either direct crystallisation of the cooled concentrate, or alternatively extraction with an equal volume of 25% aq. HOAc by stirring twice for 1 h at room temp. In the case of direct crystallisation, the mother liquor resulted following filtration of the colourless crystalline solasodine was subjected to extraction with dilute HOAc as described above. In both cases, the aqueous acid extract was separated off from the toluene layer and then alkalinised with 25% aq. NH_3. The mixture was briefly heated, then cooled at room temp. The solasodine which precipitated was filtered off, washed with cold H_2O and dried in air. The directly crystallised solasodine had mp 199–200°C, and the purity of both crystalline and precipitate samples was ascertained by TLC and NMR evidence, and by comparison with an authentic sample. The procedure gave consistently colourless and crystalline solasodine in 90–95% recovery, out of 5% content for *S. khasianum* fruits, 2.5–4% for *S. marginatum* fruits, 1.5% for *S. laciniatum* leaves, which solasodine contents were previously assayed by spectrophotometric analysis (Weissenberg, unpublished). The toluene recuperated during the process by concentration or by phases separation, was recirculated. Similarly processed *L. esculentum* (tomato) and *Solanum tuberosum* L. (potato) plants afforded pure tomatidine and solanidine, respectively, characterised by comparison with authentic samples.

3.5.2. From fresh plant material

The procedure is identical to that used in the previous example, Section 3.5.1, except that fresh fruits of different *Solanum* plants were processed instead of the dried, milled plant powder. Thus, fresh green-yellow fruits (containing about 80% moisture) were cut into slices, taking care to discard, as much as possible, seeds and retaining the richest glycoalkaloids-containing sap next to seeds. The slices were homogenised in a blender to a thick slurry which was transferred to the reaction vessel with a minimal volume of H_2O. Alternatively, the fresh fruits could be processed in a press to a past consisting of juice and pulp, which was subsequently homogenised and transferred as above. Proper amounts of conc. HCl and toluene were then added in proportion to the water content of the slurry, such as to obtain a 1:1 v/v mixture of toluene and aqueous phase, with about 5% acid concentration. The process was further carried out as described in Section 3.5.1.

3.5.3. From pure glycoalkaloids

Pure samples of glycoalkaloids solasonine (**2**), solamargine (**3**), β-solamarine (**7**), solaverbascine solatrioside(**11**), solaverbascine chacotrioside (**12**), were submitted to the two-phase hydrolysis as described in Section 3.5.1, to give quantitatively the pure aglycones: solasodine (**1**) from **2** and **3**, identified as described in Section 3.5.1; tomatidenol (**5**) from **7**, identified and characterised by comparing mp, TLC, and ^{1}H NMR with reported data (Kaneko et al., 1981), and with an authentic sample. ^{13}C NMR (C_5D_5N, TMS): δ15.91(C-21),16.74 (C-18),19.35(C-19), 19.43(C-27), 20.91 (C-11), 26.67 (C-23), 28.57 (C-24), 31.05 (C-2), 31.42 (C-25), 31.65 (C-8), 32.12 (C-7), 32.78 (C-15), 36.67 (C-10), 37.25 (C-1), 39.96 (C-4), 40.61 (C-12), 41.76 (C-13), 43.03 (C-20), 50.14 (C-9), 50.25 (C-26), 56.02 (C-14), 61.93 (C-17), 71.68 (C-3), 78.52 (C-16), 99.13 (C-22), 121.38 (C-6), 140.87 (C-5); solaverbascine (**10**) from **11** and **12**, identified by comparison with an authentic sample synthesised from **1** as described in Section 3.3.

Acknowledgements

The author is indebted to Professor J.F. Verbist, Faculty of Pharmacy, University of Nantes, France, to Dr. I. Merfort, University of Düsseldorf, Germany, and to Dr. M. Suffness, the Natural Products Branch, Division of Cancer Treatment, NCI, NIH, Bethesda, MD, USA, for their kind gifts of *S. dulcamara* glycosides mixture, tomatidenol, and β-solamarine samples,

respectively. Also to Ms. Irit Schaeffler, for skillful assistance in the chemical work; to the Mass Spectrometry Center under the direction of Professor A. Mandelbaum, the Technion-Israel Institute of Technology, Haifa, for the FAB-MS determinations; to Mr. Mircea Gruenberg, the Department of Organic Chemistry, the Weizmann Institute of Science, Rehovot, for the NMR spectra. Finally to Professor A. Levy of our Department for his kind cooperation in developing and making available all plant samples, including spineless, high solasodine-yieding *S. khasianum* cultivars.

References

Adam, G., Huong, H.Th., Khoi, N.H., 1980. Solaverbascine — a new 22, 26 — epiminocholestane alkaloid from *Solanum verbascifolium*. Phytochemistry 19, 1002–1003.

Bähr, V., Hänsel, R., 1982. Immunomodulating properties of 5,20α (*R*)-dihydroxy-6α,7α-epoxy-1-oxo-(5α)-witha-2,24-dienolide and solasodine. Planta Med. 44, 32–33.

Basu, A., Lahiri, S.C., 1977. Some pharmacological actions of solasodine. Ind. J. Exp. Biol. 15, 285–289.

Bird, G.J., Collins, D.J., Eastwood, F.W., Exner, R.H., Romanelli, M.L., Small, D.D., 1979. The synthesis of (25*R*)-22α*N*-[15,17α-$^2H_2$]-spirosol-5-en-3β-ol ([15,17α-$^2H_2$] solasodine) and assignment of the ^{13}C NMR spectra of solasodine and its derivatives. Aust. J. Chem. 32, 783–796.

Boll, P.M., 1962. Alkaloidal glycosides from *Solanum dulcamara*. II. Three new alkaloidal glycosides and a reassessment of Soladulcamaridine. Acta Chem. Scand. 16, 1819–1830.

Chandler, S., Dodds, J., 1983. Solasodine production in rapidly proliferating tissue cultures of *Solanum laciniatum* Ait. Plant Cell Reports 2, 69–72.

Chataing, B., Concepción, J.L., de Cristancho, N.B., Usubillaga, A., 1997. Estudio clinico de la efectividad de extractos alcaloideos obtenidos de los frutos del *Solanum americanum* Miller sobre el *Herpes simplex, Herpes zoster* y *Herpes genitalis*. Rev. Facultad de Farmacia U.L.A. 32, 18–25.

Chataing, B., Concepción, J.L., Lobatón, R., Usubillaga, A., 1998. Inhibition of *Trypanosoma cruzi* growth in vitro by *Solanum* alkaloids: a comparison with ketoconazole. Planta Med. 64, 31–36.

Chungath, J.I., Nair, P.B., 1989. Modified extraction method and determination of solasodine from *Solanum xanthocarpum* at different stages of fruit development. Ind. Drugs 26, 295–297.

Claringbold, W.D.B., Few, J.D., Brace, C.J., Renwick, J.H., 1980. The disposition and metabolism of ^3H-solasodine in man and Syrian hamster. J. Steroid Biochem. 13, 889–895.

Crabbe, P.G., Fryer, C., 1983. Modeling of acid hydrolysis of solasodine glycosides. Part I: formation of solasodine by glycosidic hydrolysis. A.I.Ch.E.J. 29, 572–579.

Dároczy, A., Hernádi, F., 1971. On the "glucocorticoid-like" effects of Solanum alkaloids. Acta Biochim. Biophys. Acad. Sci. Hung. 6, 327–331.

Dixit, V.P., Gupta, R.S., 1982. Antispermatogenic/antiandrogenic properties of solasodine ($C_{27}H_{43}O_2N$) obtained from *Solanum xanthocarpum* berries on the male genital tract of dog (Canis-familiaris). A histophysiological approach. Int. J. Androl. 5, 295–307.

Dixit, V.P., Gupta, R.S., Gupta, S., 1989. Antifertility plant products: testicular cell population dynamics following solasodine administration in rhesus monkey (*Macca mulatta*). Andrologia 21, 542–546.

Dixit, V.P., Varma, M., Mathur, N.T., Mathur, R., Sharma, S., 1992. Hypocholesterolaemic and antiatherosclerotic effects of solasodine ($C_{27}H_{43}O_2N$) in cholesterol fed rabbits. Phytother. Res. 6, 270–273.

Fonin, V.S., Shain, S.S., Vandyshev, V.V., 1996. Enzymatic hydrolysis of steroid glycosides in plant raw material for medicinal use. Prikl. Biokhim. Mikrobiol. 32, 514–518.

Friedman, M., Rayburn, J.R., Bantle, J.A., 1992. Structural relationships and developmental toxicity of *Solanum* alkaloids in the frog teratogenesis assay- *Xenopus*. J. Agric. Food Chem. 40, 1617–1624.

Friedman, M., Henika, P.R., Mackey, B.E., 1996. Feeding of potato, tomato, and eggplant alkaloids affects food consumption and body and liver weights in mice. J. Nutr. 126, 989–999.

Fukuhara, K., Kubo, I., 1991. Isolation of steroidal glycoalkaloids from *Solanum Incanum* by two countercurrent chromatographic methods. Phytochemistry 30, 685–687.

Gaffield, W., Keeler, R.F., 1996. Craniofacial malformations induced in hamsters by steroidal alkaloids. J. Nat. Toxins 5, 25–38.

Hardman, R., Williams, T.G., 1976. A titrimetric determination of solasodine for aqueous incubates of *Solanum* fruits. Planta Med. 30, 66–71.

Harrison, D.M., 1984. Steroidal alkaloids. Natur. Prod. Reports 1, 219–224.

Kaneko, K., Nakaoka, U., Tanaka, M., Yoshida, N., Mitsuhashi, H., 1981. Two steroidal alkaloids, hapepunine and amakorinine, from the mature *Fritillaria camtschatcensis*. Phytochemistry 20, 157–160.

Kanwar, U., Batla, A., Sanyal, S.N., Ranga, A., 1990. Glycolytic enzyme activities of human and bovine spermatozoa treated in vitro with solasodine. J. Ethnopharmacol. 28, 49–52.

Kaur, A., Raja, S.S., Thakur, S.S., Rao, B.K., 1988. Insect growth regulating activity of solasodine on *Dysdercus* Similis. Comp. Physiol. Ecol. 13, 195–197.

Kim, Y.C., Che, Q.-M., Gunatilaka, A.A.L., Kingston, D.G.I., 1996. Bioactive steroidal alkaloids from *Solanum umbelliferum*. J. Nat. Prod. 59, 283–285.

Kittipongpatana, N., Porter, J.R., Hock, R.S., 1999. An improved high performance liquid chromatographic method for the quantification of solasodine. Phytochem. Anal. 10, 26–31.

Kusano, G., Takahashi, A., Nozoe, S., Sonoda, Y., Sato, Y., 1987a. Solanum alkaloids as inhibitors of enzymatic conversion of dihydrolanosterol into cholesterol. Chem. Pharm. Bull. 35, 4321–4323.

Kusano, G., Takahashi, A., Sugiyama, K., Nozoe, S., 1987b. Antifungal properties of Solanum alkaloids. Chem. Pharm. Bull. 35, 4862–4867.

Lin, C.-N., Chung, M.-I., Gan, K.-H., 1988. Novel antihepatotoxic principles of *Solanum incanum*. Planta Med. 54, 222.

Lin, C.-N., Lu, C.-M., Cheng, M.-K., Gan, K.-H., 1990. The cytotoxic principles of *Solanum incanum*. J. Nat. Prod. 53, 513–516.

Löken, B., Sollins, I.V., 1970. Method for obtaining solanum alkaloids and sapogenines from plant materials. US patent 3,510,400; 5 pp.

Mann, J.D., 1978. Production of solasodine for the pharmacological industry. Adv. Agronomy 30, 207–245.

Nakamura, T., Komori, C., Lee, Y.-y., Hashimoto, F., Yahara, S., Nohara, T., Ejima, A., 1996. Cytotoxic activities of *Solanum* steroidal glycosides. Biol. Pharm. Bull. 19, 564–566.

Nes, W.D., Hanners, P.K., Bean, G.A., Patterson, G.W., 1982. Inhibition of growth and sitosterol-induced sexual reproduction in *Phytophtora cactorum* by steroidal alkaloids. Phytopathology 72, 447–450.

Ntahomvukiye, D., Van Puyvelde, L., De Kimpe, N., Schamp, N., 1983. Extraction de la solasodine du *Solanum adoense* Hochst au Rwanda (Afrique Centrale). Pl. Med. Phyt. 17, 18–21.

Pandeya, S.C., Saratbabu, G.V., Bhatt, A.B., 1981. A quick method for estimation of solasodine in leaves and berries of *Solanum sysimbrifolium* Lamk. Indian J. Exper. Biol. 19, 1207–1208.

Panina, V.V., Glyzina, G.S., Avilova, O.P., Prashchurovich, A.K., Kogan, L.M., 1976. Method of determining solasodin content in lobed nightshade. Khim.-Farm.Zh. 10, 135–141.

Raja, S.S., Kaur, A., Thakur, S.S., 1987. Juvenomimetic effects of solasodine on *Chilo Partellus*. Curr. Sci. 56, 913–915.

Roddick, J.G., Weissenberg, M., Leonard, A.L., 2001. Membrane disruption and enzyme inhibition by naturally-occurring and modified chacotriose-containing *Solanum* steroidal glycoalkaloids. Phytochemistry 56, 603–610.

Rowan, D.D., Macdonald, P.E., Skipp, R.A., 1983. Antifungal stress metabolites from *Solanum Aviculare*. Phytochemistry 22, 2102–2104.

Uskert, A., 1963. Über die Dinitrophenyläther von Sterolen und Aminosterolen. Acta Chim. Hung. 35, 107–118.

Van Gelder, W.M.J., 1984. A new hydrolysis technique for steroid glycoalkaloids with unstable aglycones from *Solanum* spp. J. Sci. Food Agric. 35, 487–494.

Weissenberg, M., 1982. Isolation of alkaloidal steroids from plants. Israeli patent 58, 227; 14 pp; Chem. Abstr. 99, 28002, 1983.

Weston, R.J., 1976. An investigation of methods for isolation of the steroidal alkaloid solasodine from native New Zealand *Solanum* species. J. Appl. Chem. Biotechnol. 26, 657–666.

Wolters, B. 1976. Serienversuche Über Transformation und Abbau sekundärer Pflanzenstoffe durch Mikroorganismen mittels DC-fertigfolien als Substanzträger. Planta Med. 29, 41–53.

Yaniv, Z., Weissenberg, M., Palevitch, D., Levy, A., 1981. Effect of seed number and fruit weight on content and localisation of glycoalkaloids in *Solanum khasianum*. Planta Med. 42, 303–306.

Yaniv, Z., Palevitch, D., Weissenberg, M., 1983. Growth and solasodine production by *Solanum khasianum* Clarke and *Solanum laciniatum* Ait. under water stress. Acta Hort. 132, 217–222.

Yaniv, Z., Palevitch, D., Weissenberg, M., 1984. The effect of water stress on growth and solasodine content in *Solanum khasianum*. Planta Med. 45, 60–65.

PERGAMON

Phytochemistry 58 (2001) 509–516

PHYTOCHEMISTRY

www.elsevier.com/locate/phytochem

Glycoside esters from lichens of central Asia

Tomáš Řezanka[a,*], Irene A. Guschina[b]

[a]*Institute of Microbiology, Vídeňská 1083, 14220 Prague, Czech Republic*
[b]*Institute of Ecology of the Volga River Basin of the Russian Academy of Sciences, Togliatti 445003, Russia*

Received 5 December 2000; received in revised form 17 May 2001

Abstract

Ten compounds isolated from the extract of the central Asian lichens comprised new glycosides and glycoside esters having 18*R*-hydroxy-dihydroalloprotolichesterinic, 18*S*-hydroxy-dihydroprotolichesterinic and 18*S*-hydroxy-neodihydroprotolichesterinic acids, as the aglycones and a saccharide moiety linked at C-18 and also at C-21 made by glucose, xylose or rhamnose. The structures were elucidated using extensive spectroscopic analysis (1D and 2D NMR, MS, IR, UV and ORD) and by biochemical methods. © 2001 Elsevier Science Ltd. All rights reserved.

Keywords: Glycoside esters; Lichens of central Asia; NMR, MS, IR, ORD and UV spectra

1. Introduction

The lichens of the genera *Acarospora gobiensis, Cladonia furcata, Lecanora fructulosa, Leptogium saturninum, Peltigera canina, Rhizoplaca peltata, Xanthoparmelia camtschadalis, X. tinctina* and *Xanthoria elegans* are a central Asia species found in Tian-Shan mountains. The present study is the general phytochemical investigation carried out on these species and we report herein on the isolation and structure elucidation of seven new glycosides and glycoside esters.

Although many tens of thousands of plant glycosides and glycoside esters have been discovered in nature (Ikan, 1999), only a few of these have as yet been identified from lichens. These include, e.g. 1-(*O*-β-D-glucopyranosyl)-3*S*,25*R*-hexacosanediol from *Solorina crocea* (Huneck and Yoshimura, 1996), galapagin, lobodirin, mollin and roccellin (Huneck et al. 1992).

In our continuing search for unusual bioactive compounds from central Asian lichens (Řezanka and Dembitsky, 1998, 1999; Řezanka and Guschina, 1999, 2000a,b), we have examined the nine above-mentioned lichens. The ten compounds isolated from the extract of the thallus comprised new glycosides (**4**–**10**) having 18*R*-hydroxy-dihydroalloprotolichesterinic, 18*S*-hydroxy-dihydroprotolichesterinic and 18*S*-hydroxy-neodihydroprotolichesterinic acids as the aglycones and an oligosaccharide moiety linked at C-18 and C-21 made by glucose, xylose or rhamnose.

2. Results and discussion

In recent papers (Řezanka and Gushina, 2000a,b), we reported the isolation of lichen's acids, i.e. hydroxy-murolic, hydroxy-protoconstipatic, hydroxy-allo-murolic acids and their glycosides from the water–methanolic extract of the central Asian lichens. All nine lichen species were extracted independently and the extracts were also chromatographed separately by means of column chromatography over Sephadex LH-20 eluted with EtOH-i-PrOH (fraction 1), EtOH (fraction 2) and then MeOH (fraction 3). Repeated RP–HPLC of fraction 1 afforded new compounds (**1**), together with (**2**) and (**3**) (Table 1). Fraction 2 accounted for the largest amount of the EtOH extract by weight. Repeated column chromatography of this fraction afforded compounds (**4**–**6**) (Table 1). Fraction 3 was also purified by a further RP–HPLC method to give compounds (**7**–**10**) (Table 1). Comparing their spectral data, i.e. predominantly 1D and 2D NMR, MS, IR, UV and ORD with previously reported data performed the identification of the above-mentioned compounds. All compounds (**1**–**10**) are new natural products.

* Corresponding author. Tel.: +420-2-4752300; fax: +420-2-4752347.

E-mail address: rezanka@biomed.cas.cz (T. Řezanka).

0031-9422/01/$ - see front matter © 2001 Elsevier Science Ltd. All rights reserved.
PII: S0031-9422(01)00261-8

Table 1
Occurrence of acids and their derivatives from lichens of Tian Shan mountains

Name of lichen	Name of compounds; mg/100 g of dry weight									
	1	**2**	**3**	**4**	**5**	**6**	**7**	**8**	**9**	**10**
Acarospora gobiensis	22.5	–[a]	–	8.7	–	–	–	–	–	–
Cladonia furcata	–	24.3	–	–	0.5	–	–	2.9	0.8	–
Lecanora fructulosa	–	13.5	–	–	3.8	–	–	3.4	1.9	–
Leptogium saturninum	–	–	19.8	–	–	6.8	7.1	–	–	3.9
Peltigera canina	–	–	25.4	–	–	0.9	0.9	–	–	1.4
Rhizoplaca peltata	–	19.1	–	–	4.2	–	–	6.3	1.4	–
Xanthoparmelia camtschadalis	–	22.7	–	–	0.2	–	–	5.7	3.1	–
X. tinctina	13.8	–	–	1.8	–	–	–	–	–	–
Xanthoria elegans	10.3	–	–	2.9	–	–	–	–	1.7	–

[a] –, Less than 0.1 mg/100 g of dry weight.

The unknown compound **1** isolated as white solid crystals was 18*R*-hydroxy-dihydroalloprotolichesterinic acid and was identified by comparison of its ^{1}H, ^{13}C NMR, MS, and ORD data with our and previously published values for dihydroalloprotolichesterinic acid (Huneck and Takeda, 1992). The HREIMS of **1** showed a molecular ion at *m/z* 370.5293. These data are consistent with the molecular formula of $C_{21}H_{38}O_5$. The ^{13}C NMR spectrum of **1** showed 21 signals corresponding to 21 carbons of acid, and DEPT measurements revealed the presence of two methyl groups, 13 methylenes, four methines (two bearing oxygen), and two oxygenated quaternary carbons at δ 170.1 and 177.5 assigned to carboxylic acid and lactone, respectively. The ^{1}H NMR spectrum of **1** showed signals at δ 2.93 (1H, *dq*, $J=7.0$, 7.5 Hz, H-2), 3.30 (1H, *dd*, $J=7.0$, 8.0 Hz, H-3), and 4.64 (1H, *ddd*, $J=8.0$, 8.0, 5.0 Hz, H-4), typical for a trisubstituted γ-butyrolactone acid. Examination of NMR, MS, and physical data for compound **1** showed that they are very similar to the data of (−)-dihydropertusaric and dihydroalloprotolichesterinic acids. The relative stereochemistry of **1** was assigned on the basis of the 2D NOESY spectrum, which exhibited the presence of NOEs, indicating that the Me on C-2 (C-20), H-3 and H-4 are oriented on the same side of the molecule, while H-2 has the same orientation as the lipophilic side chain (Fig. 1), suggesting that **1** have the following relative stereo configuration, i.e. 2*R*,3*S*,4*S*. The presence of signals at δ 1.17 (3H, *d*, $J=6$ Hz, H-19) and 3.74 (1H, *m*, H-18) were of the terminal hydroxyethyl group. The absolute configuration at C-18 of all three acids, i.e. **1**, **2** and **3** was determined by the modified Mosher's method (Ohtani et al., 1991a,b; Rieser et al., 1992).

Treatment of each hydroxy acid with (*R*)-(−)-MTPACl or (*S*)-(+)-MTPACl converted them into the (*S*)- and (*R*)-2-methoxy-2-trifluoromethylphenylacetic acid (MTPA) esters (**1s**, **2s** and **3s** and **1r**, **2r** and **3r**, respectively). The values of $\Delta\delta=[\delta(S\text{-MTPA ester})-\delta(R\text{-MTPA ester})]$ in the ^{1}H NMR spectra suggested that the absolute configuration at C-18 of compound **1** was (*R*) while that of **2** and **3** were (*S*) (Ohtani et al., 1991b). The data are shown in Table 7.

Compound **2**, i.e. 18*S*-hydroxy-dihydroprotolichesterinic acid, had according to the high-resolution mass spectrum the formula $C_{21}H_{38}O_5$. Its UV spectrum showed a maximum at 207 nm (log ε 2.74), indicative of a saturated γ-lactone. The ^{1}H NMR spectrum (Table 2) and ORD data (Fig. 2) of 18*S*-hydroxy-dihydroprotolichesterinic acid gave the structure and absolute configuration shown in formula 2 (Fig. 1). The ORD curve of compounds **2** is very similar to the ORD curve of (−)-dihydroprotolichesterinate (Huneck and Takeda, 1992), thus proving the same relative and absolute configuration of both compounds. Contrary to this the ORD spectra of 18*R*-hydroxy-dihydroalloprotolichesterinic acid (**1**) and 18*S*-hydroxy-neodihydroprotolichesterinic acid (**3**)

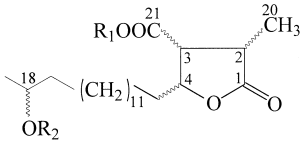

Compound	R_1	R_2	Carbon 2	Carbon 3	Carbon 4	Carbon 18
1	H	H	*R*	*S*	*S*	*R*
2	H	H	*S*	*R*	*S*	*S*
3	H	H	*R*	*R*	*S*	*S*
4	Rha	H	*R*	*S*	*S*	*R*
5	Glc	H	*S*	*R*	*S*	*S*
6	Glc	H	*R*	*R*	*S*	*S*
7	Rha	Glc	*R*	*S*	*S*	*R*
8	Glc	Xyl	*S*	*R*	*S*	*S*
9	Glc	Rha	*R*	*R*	*S*	*S*
10	Glc	Glc	*R*	*R*	*S*	*S*

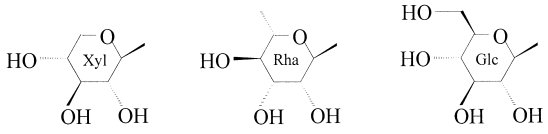

Fig. 1. The structures of hydroxy-lichesterinic acids (**1**, **2** and **3**) and their glycosides and glycoside esters (**4**–**10**) from lichens.

Table 2
^{1}H NMR spectral data of 18*R*-hydroxydihydroalloprotolichesterinic acid (**1**), 18*S*-hydroxydihydroprotolichesterinic acid (**2**) and 18*S*-hydroxyneodihydroprotolichesterinic acid (**3**), solvent see Experimental

H No.	**1**	**2**	**3**
2	2.93 (1H, *dq*, $J_{2,3}=7.0$, $J_{2,20}=7.5$)	2.97 (1H, *dq*, $J_{2,3}=9.0$, $J_{2,20}=7.5$)	2.99 (1H, *dq*, $J_{2,3}=11.1$, $J_{2,20}=7.2$)
3	3.30 (1H, *dd*, $J_{3,2}=7.0$, $J_{3,4}=8.0$)	3.12 (1H, *dd*, $J_{3,2}=9.0$, $J_{3,4}=6.5$)	3.30 (1H, *dd*, $J_{3,2}=11.1$, $J_{3,4}=9.5$)
4	4.64 (1H, *ddd*, $J_{4,3}=8.0$, $J_{4,5}=8.0$ and 5.0)	4.70 (1H, *ddd*, $J_{4,3}=6.5$, $J_{4,5}=8.0$ and 4.5)	4.44 (1H, *ddd*, $J_{4,3}=9.5$, $J_{4,5}=8.0$ and 4.0)
5	1.66 (2H, *m*)	1.69 (2H, *m*)	1.71 (2H, *m*)
6–16	1.26 (22H, *m*)	1.28 (22H, *m*)	1.27 (22H, *m*)
17	1.53 (2H, *m*)	1.58 (2H, *m*)	1.56 (2H, *m*)
18	3.74 (1H, *m*)	3.81 (1H, *m*)	3.78 (1H, *m*)
19	1.17 (3H, *d*, $J=6$)	1.16 (3H, *d*, $J=6$)	1.18 (3H, *d*, $J=6$)
20	1.31 (3H, *d*, $J_{20,2}=7.5$)	1.29 (3H, *d*, $J_{20,2}=7.5$)	1.33 (3H, *d*, $J_{20,2}=7.2$)

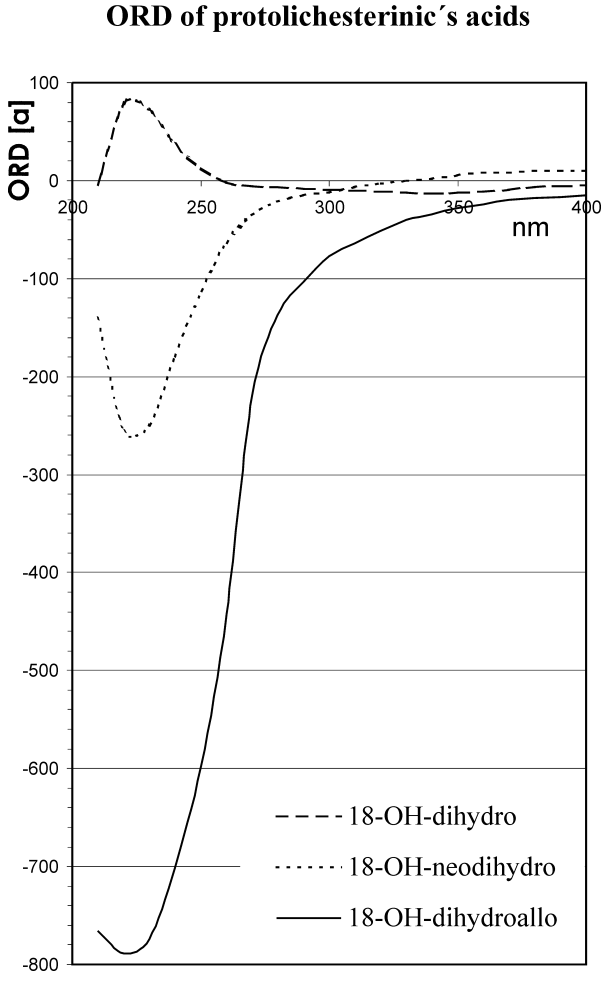

Fig. 2. The ORD spectra of lichen's acids [18*R*-hydroxy-dihydroalloprotolichesterinic (**1**), 18*S*-hydroxy-dihydroprotolichesterinic (**2**) and 18*S*-hydroxy-neodihydroprotolichesterinic (**3**)].

were quite different (Fig. 2). As Table 2 shows, the signal of H-18 in **2** (δ 3.81) is shifted downfield in relation to the chemical shift of H-18 in dihydroprotolichesterinic acid (δ 1.26) (Huneck and Takeda, 1992). The deshielding of the H-18 through the OH group in 2 causes this shift. Hence dihydro acid has relative stereochemistry 2*S*,3*R*,4*S*,18*S*.

HREIMS of compounds **3** showed the molecular ion at 370.5295 corresponding to the formula $C_{21}H_{38}O_5$, which implies three unsaturated sites. Its IR spectrum displayed two, intense carbonyl absorption, the stronger at 1740 cm^{-1} (lactone) and the second at 1705 cm^{-1} (acid). The remaining unsaturation was assigned to the lactone ring.

The spectrum of **3** showed double quartet (1H) at δ 2.99 ppm as well as a double doublet (1H) at δ 3.30 ppm and also signal at δ 4.44 (1H, *ddd*). The high relative values of coupling constants ($J_{2,3}=11.1$ Hz and $J_{3,4}=9.5$ Hz) indicate trans orientations of hydrogen on C-2, the hydrogen on C-3 and also the hydrogen on C-4. The absolute configuration on C-18 determined by Mosher's method is *S*. For data of chemical shifts, see Table 7. Thus, the structure of compound **3** is 18*S*-hydroxy- neodihydroprotolichesterinic acid.

Treatment of esters (**4**–**10**) with esterase (E.C. 3.1.1.1, from porcine liver) gave compounds (**4a**–**10a**) and free sugars. Their analysis by GC–MS according to Gerwig et al. (1978) indicated that the ester bound sugars were rhamnose (**4** and **7**) and glucose (**5**, **6**, **8**–**10**). According to ^{1}H NMR and ORD spectra, free acids **4a**–**6a** were identical with compounds **1**–**3**. Enzymatic hydrolysis of the compounds **7a**–**10a** by β-glucosidase (E.C. 3.2.1.21) liberated free sugars, i.e. glucose from **7** and **10**, xylose from **8** and rhamnose from **9**, and aglycones **7b**–**10b**. The latter were again identical with free acids **1** and **3**, according of their ^{1}H NMR and ORD spectra.

The combined positive ion HRFABMS (see Experimental) and NMR data (Tables 3 and 4) confirmed the molecular formula and identity of the acids and sugars present. The positive HRFABMS of al three esters (**4**–**6**) showed pseudomolecular ions $(M+H)^+$ and the negative ion FABMS spectra $(M-H)^-$ and $(M-H-146)^-$ for a deoxyhexosyl unit (**4**) and $(M-H-162)^-$ for a hexosyl unit (**5** and **6**). Substitution of the sugar at C-21 of the acid was unambiguously established from correlations of this carbon with the appropriate anomeric protons in the 2D HMBC NMR spectra.

Analysis of the ^{13}C NMR chemical shifts of sugar moieties (**7**–**10**), conducted by a combination of homo-

Table 3
^{13}C NMR spectral data of compounds **1**–**6**, solvent see Experimental

C No.	1	2	3	4	5	6
1	177.5, *s*	178.9, *s*	177.8, *s*	177.7, *s*	178.0, *s*	177.9, *s*
2	36.4, *d*	36.0, *d*	36.8, *d*	36.1, *d*	35.4, *d*	36.4, *d*
3	51.8, *d*	52.0, *d*	51.5, *d*	50.9, *d*	50.1, *d*	50.0, *d*
4	77.5, *d*	79.3, *d*	78.6, *d*	77.1, *d*	78.2, *d*	78.2, *d*
5	31.2, *t*	32.1, *t*	32.3, *t*	31.9, *t*	32.2, *t*	31.7, *t*
6	25.6, *t*	25.8, *t*	24.6, *t*	25.9, *t*	25.4, *t*	25.6, *t*
7–15			28.1–29.8			
16	25.1, *t*	25.5, *t*	24.9, *t*	25.3, *t*	25.9, *t*	25.3, *t*
17	38.1, *t*	38.5, *t*	38.6, *t*	38.7, *t*	38.5, *t*	38.4, *t*
18	68.5, *d*	68.8, *d*	68.6, *d*	68.0, *d*	68.1, *d*	68.8, *d*
19	22.8, *q*	23.4, *q*	22.9, *q*	22.4, *q*	23.4, *q*	23.0, *q*
20	12.8, *q*	13.9, *q*	14.9, *q*	12.9, *q*	13.4, *q*	13.9, *q*
21	170.1, *s*	168.7, *s*	169.5, *s*	163.7, *s*	162.8, *s*	163.0, *s*
1′	–	–	–	95.7, *d*	95.7, *d*	95.2, *d*
2′	–	–	–	73.7, *d*	73.9, *d*	75.0, *d*
3′	–	–	–	70.8, *d*	78.7, *d*	77.7, *d*
4′	–	–	–	75.2, *d*	71.2, *d*	71.1, *d*
5′	–	–	–	68.0, *d*	78.3, *d*	78.1, *d*
6′	–	–	–	18.6, *q*	62.4, *t*	62.4, *t*

and heteronuclear COSY spectra, indicated their unsubstituted nature (Huneck and Takeda, 1992).

These data indicated that one monosaccharide was linked to the C-18 position of the aglycone, the other monosaccharide being linked to the C-21 of the aglycone through an ester bond.

Comparison of the ^{13}C NMR chemical shifts of glycoside **7** with those of **1** (Tables 3 and 6) revealed that a glycosidation shift at C-19 (3.6 ppm) larger than that at C-17 (3.1 ppm) was observed in pyridine-(d_5) as solvent. Application of the glycosidation shift rule (Seo et al., 1978; Tori et al., 1977; Kasai et al., 1977) to these shifts indicated the configuration at C-18 of glycoside **7** to be *R*; the glycoside **7** was thus confirmed to be 18*R*-glycoside. In the spectrum of **8**, **9** and **10**, the glycosidation shift is the opposite (Δ at C_{19} = 3.5–3.7 ppm and Δ at C_{17} = 3.8–4.1 ppm), and the configuration in **8**, **9** and **10** is thus *S*.

A correlation in the HMQC spectrum of **7** showed that the rhamnose residue was attached to the carboxylic group of the aglycone by an ester linkage. HMBC experiments showed that the second sugar (glucose) was connected by a glycosidic bond to hydroxyl group on C-18.

The chemical shifts of C-18 δ 76.6 and C-21 δ 163.8 indicated that **8** was at the same time a glycoside and glycoside ester, with xylose linked to C-18 and glucose to C-21, as indicated from their ^{13}C NMR data (Table 4).

Compound **9** again contained two sugar residues in a HMQC NMR experiment. The anomeric ^{13}C-NMR signals gave cross-peaks with anomeric protons and long-range ^{1}H–^{13}C correlations were observed between the signals at δ_C 163.4 and δ_H 6.25, δ_C 77.1 and δ_H 5.82. Accordingly, the glucose unit was again linked to C-21 of the aglycone, while the rhamnose units were linked to the C-18 position of the aglycone. These linkages were confirmed from the NOESY spectrum of **9**.

The HMBC spectrum of **10** showed that one glucose unit was at the C-21 position of the aglycone and another glucose exhibited correlation peaks between H-1 δ 5.14 of glucose and C-18 δ 77.2 of the aglycone. The names of compounds **4**–**10** are given in Experimental.

To summarize the present study, the chemical structures and structural relationships among the new 10 component of lichen acids produced by lichens from Central Asia are shown in Fig. 1.

We have isolated three hydroxy substituted γ-lactonic carboxylic acids of which only the optical antipode, i.e. neodihydromurolic acid has previously been described (Huneck et al., 1979). The absolute configuration of the hydroxyl group of all three acids (**1**–**3**) were determined and also the all three were described for the first time in

Table 4
^{1}H NMR spectral data of compounds **4**–**6**, solvent see Experimental

H No.	4	5	6
2	2.88 (1H, *dq*, $J_{2,3}$ = 7.0, $J_{2,20}$ = 7.5)	2.91 (1H, *dq*, $J_{2,3}$ = 9.0, $J_{2,20}$ = 7.5)	2.92 (1H, *dq*, $J_{2,3}$ = 11.1, $J_{2,20}$ = 7.2)
3	3.24 (1H, *dd*, $J_{3,2}$ = 7.0, $J_{3,4}$ = 8.0)	3.09 (1H, *dd*, $J_{3,2}$ = 9.0, $J_{3,4}$ = 6.5)	3.26 (1H, *dd*, $J_{3,2}$ = 11.1, $J_{3,4}$ = 9.5)
4	4.57 (1H, *ddd*, $J_{4,3}$ = 8.0, $J_{4,5}$ = 8.0 and 5.0)	4.65 (1H, *ddd*, $J_{4,3}$ = 6.5, $J_{4,5}$ = 8.0 and 4.5)	4.40 (1H, *ddd*, $J_{4,3}$ = 9.5, $J_{4,5}$ = 8.0 and 4.0)
5	1.68 (2H, *m*)	1.67 (2H, *m*)	1.70 (2H, *m*)
6–16	1.26 (22H, *m*)	1.26 (22H, *m*)	1.26 (22H, *m*)
17	1.54 (2H, *m*)	1.57 (2H, *m*)	1.56 (2H, *m*)
18	3.76 (1H, *m*)	3.80 (1H, *m*)	3.79 (1H, *m*)
19	1.16 (3H, *d*, *J* = 6)	1.17 (3H, *d*, *J* = 6)	1.17 (3H, *d*, *J* = 6)
20	1.30 (3H, *d*, $J_{20,2}$ = 7.5)	1.31 (3H, *d*, $J_{20,2}$ = 7.5)	1.32 (3H, *d*, $J_{20,2}$ = 7.2)
1′	6.18 (1H, *d*, *J* = 1.7)	6.31 (1H, *d*, *J* = 8.0)	6.30 (1H, *d*, *J* = 7.8)
2′	4.20 (1H, *dd*, *J* = 1.7, 3.4)	4.22, (1H, *dd*, *J* = 8.0, 9.0)	4.23 (1H, *dd*, *J* = 7.8, 9.1)
3′	4.41 (1H, *dd*, *J* = 3.4, 9.0)	4.28, (1H, *t*, *J* = 9.0)	4.24 (1H, *t*, *J* = 9.1)
4′	4.08 (1H, *t*, *J* = 9.0)	4.37 (1H, *dd*, *J* = 9.0, 10.0)	4.31 (1H, *dd*, *J* = 9.1, 10.2)
5′	4.77 (1H, *dq*, *J* = 9.0, 6.5)	4.03 (1H, *ddd*, *J* = 9.6, 6.1, 2.3)	4.04 (1H, *m*)
6′	1.31 (3H, *d*, *J* = 6.5)	4.40 (1H, *dd*, *J* = 12.0, 5.0)	4.38 (1H, *dd*, *J* = 11.8, 4.8)
		4.43 (1H, *dd*, *J* = 12.0, 2.5)	4.44 (1H, *dd*, *J* = 11.8, 2.7)

Table 5
^{1}H NMR spectral data of compounds **7**–**10**, solvent see Experimental

H No.	**7**	**8**	**9**	**10**
2	2.89 (1H, *dq*, $J_{2,3}=7.0$, $J_{2,20}=7.5$)	2.92 (1H, *dq*, $J_{2,3}=9.0$, $J_{2,20}=7.5$)	2.94 (1H, *dq*, $J_{2,3}=11.1$, $J_{2,20}=7.3$)	2.95 (1H, *dq*, $J_{2,3}=11.1$, $J_{2,20}=7.3$)
3	3.28 (1H, *dd*, $J_{3,2}=7.0$, $J_{3,4}=8.0$)	3.10 (1H, *dd*, $J_{3,2}=9.0$, $J_{3,4}=6.5$)	3.27 (1H, *dd*, $J_{3,2}=11.1$, $J_{3,4}=9.5$)	3.26 (1H, *dd*, $J_{3,2}=11.1$, $J_{3,4}=9.5$)
4	4.58 (1H, *ddd*, $J_{4,3}=8.0$, $J_{4,5}=8.0$; 5.0)	4.64 (1H, *ddd*, $J_{4,3}=6.5$, $J_{4,5}=8.0$; 4.5)	4.39 (1H, *ddd*, $J_{4,3}=9.5$, $J_{4,5}=8.0$; 4.0)	4.40 (1H, *ddd*, $J_{4,3}=9.5$, $J_{4,5}=8.0$; 4.0)
5	1.67 (2H, *m*)	1.69 (2H, *m*)	1.71 (2H, *m*)	1.71 (2H, *m*)
6–16	1.26 (22H, *m*)	1.26 (22H, *m*)	1.26 (22H, *m*)	1.26 (22H, *m*)
17	1.73 (2H, *m*)	1.78 (2H, *m*)	1.76 (2H, *m*)	1.77 (2H, *m*)
18	3.98 (1H, *m*)	3.94 (1H, *m*)	3.96 (1H, *m*)	3.99 (1H, *m*)
19	1.24 (3H, *d*, $J=6$)	1.26 (3H, *d*, $J=6$)	1.25 (3H, *d*, $J=6$)	1.26 (3H, *d*, $J=6$)
20	1.31 (3H, *d*, $J_{20,2}=7.5$)	1.29 (3H, *d*, $J_{20,2}=7.5$)	1.33 (3H, *d*, $J_{20,2}=7.3$)	1.33 (3H, *d*, $J_{20,2}=7.3$)
1′	6.25 (1H, *d*, $J=1.6$)	6.28 (1H, *d*, $J=7.9$)	6.25 (1H, *d*, $J=8.0$)	6.29 (1H, *d*, $J=7.8$)
2′	4.26 (1H, *dd*, $J=3.5$, 1.6)	4.19 (1H, *dd*, $J=7.9$, 9.1)	4.20 (1H, *dd*, $J=8.0$, 9.0)	4.18 (1H, *dd*, $J=7.8$, 9.1)
3′	4.39 (1H, *dd*, $J=8.9$, 3.5)	4.26 (1H, *t*, $J=9.1$)	4.28 (1H, *t*, $J=9.0$)	4.29 (1H, *t*, $J=9.2$)
4′	4.12 (1H, *t*, $J=8.9$)	4.34 (1H, *t*, $J=9.1$)	4.31 (1H, *t*, $J=9.0$)	4.33 (1H, *t*, $J=9.2$)
5′	4.74 (1H, *dd*, $J=8.9$, 6.0)	4.03 (1H, *m*)	4.01 (1H, *m*)	4.01 (1H, *m*)
6′	1.36 (1H, *d*, $J=6.0$)	4.42 (1H, *dd*, $J=11.0$, 4.7);	4.44 (1H, *dd*, $J=10.8$, 5.5);	4.41 (1H, *dd*, $J=10.8$, 4.9);
		4.48 (1H, *dd*, $J=11.8$, 2.9)	4.47 (1H, *dd*, $J=11.3$, 3.7)	4.46 (1H, *dd*, $J=11.6$, 3.5)
1″	5.15 (1H, *d*, $J=7.9$)	4.92 (1H, *d*, $J=7.4$)	5.82 (1H, *d*, $J=1.5$)	5.14 (1H, *d*, $J=7.9$)
2″	4.04 (1H, *dd*, $J=9.0$, 7.9)	3.96 (1H, *dd*, $J=7.4$, 8.8)	4.06 (1H, *dd*, $J=3.0$, 1.5)	4.03 (1H, *dd*, $J=9.0$, 7.9)
3″	4.14 (1H, *dd*, $J=9.0$, 8.7)	4.04 (1H, *dd*, $J=8.8$, 8.2)	3.94 (1H, *dd*, $J=9.0$, 3.0)	4.13 (1H, *dd*, $J=9.2$, 9.0)
4″	4.21 (1H, *t*, $J=8.9$)	4.19 (1H, *ddd*, $J=10.5$, 8.2, 5.2)	4.02 (1H, *t*, $J=9.0$)	4.24 (1H, *dd*, $J=9.2$, 9.1)
5″	3.94 (1H, *m*)	3.68 (1H, *dd*, $J=10.7$, 10.5)	3.93 (1H, *dd*, $J=9.0$, 5,6)	3.98 (1H, *m*)
		4.35 (1H, *dd*, $J=10.7$, 5.2)		
6″	4.28 (1H, *dd*, $J=11.2$, 4.0);	–	1.33 (1H, *d*, $J=5.6$)	4.25 (1H, *dd*, $J=11.4$, 3.9);
	4.45 (1H, *dd*, $J=11.2$, 3.8)			4.50 (1H, *dd*, $J=11.4$, 4.1)

Table 6
^{13}C NMR spectral data of compounds **7**–**10**, solvent see Experimental

C No.	7	8	9	10
1	177.6, *s*	177.4, *s*	177.3, *s*	177.7, *s*
2	36.1, *d*	36.3, *d*	36.2, *d*	36.5, *d*
3	50.6, *d*	50.4, *d*	50.1, *d*	50.0, *d*
4	77.0, *d*	77.6, *d*	77.5, *d*	77.6, *d*
5	31.9, *t*	32.2, *t*	31.7, *t*	31.7, *t*
6	25.9, *t*	25.4, *t*	25.6, *t*	25.6, *t*
7–15		28.1–29.4		
16	26.6, *t*	26.5, *t*	25.3, *t*	25.9, *t*
17	35.0, *t*	34.4, *t*	34.5, *t*	34.8, *t*
18	76.5, *d*	76.6, *d*	77.1, *d*	77.2, *d*
19	19.2, *q*	19.7, *q*	19.4, *q*	19.3, *q*
20	12.6, *q*	12.8, *q*	12.9, *q*	13.4, *q*
21	163.7, *s*	163.8, *s*	163.4, *s*	164.0, *s*
1′	95.0, *d*	94.8, *d*	94.8, *d*	95.6, *d*
2′	72.8, *d*	75.7, *d*	75.7, *d*	74.1, *d*
3′	71.8, *d*	78.0, *d*	78.0, *d*	78.8, *d*
4′	73.5, *d*	71.3, *d*	71.6, *d*	71.0, *d*
5′	67.5, *d*	78.5, *d*	78.2, *d*	79.2, *d*
6′	18.5, *q*	62.3, *t*	62.1, *t*	62.0, *t*
1″	105.4, *d*	106.3, *d*	104.4, *d*	105.7, *d*
2″	75.4, *d*	75.3, *d*	72.7, *d*	75.5, *d*
3″	77.9, *d*	78.1, *d*	72.6, *d*	78.6, *d*
4″	71.5, *d*	71.1, *d*	73.8, *d*	71.6, *d*
5″	78.2, *d*	67.1, *t*	69.0, *d*	78.3, *d*
6″	62.7, *t*	–	18.5, *q*	62.6, *t*

Table 7
Stereochemical analysis of compounds **1**, **2** and **3** with (*R*)- and (*S*)-MTPA (Mosher) derivatives[a]

MTPA esters of compound No.	$\Delta\delta = \delta_{S\text{-ester}} - \delta_{R\text{-ester}}$ (Hz)		
	H-19	H-17	Carbinol configuration
1	+12.8	−30.1	*R*
2	−16.9	+26.7	*S*
3	−15.8	+34.2	*S*

[a] The aglycones from glycosides **4**–**10** are identical from **1** or **2** or **3**.

nature. Absolute new is the discovery of glycoside esters containing rhamnose, xylose and glucose.

3. Experimental

3.1. General experimental procedures

UV spectra were measured in heptane within the range of 200–350 nm by a Cary 118 (Varian) apparatus. Optical rotatory dispersion (ORD) measurement was carried out under a dry N_2 on a Jasco-500A spectropolarimeter at 24 °C. A Perkin-Elmer Model 1310 (Perkin-Elmer, Norwalk, CT, USA) IR spectrophotometer was used for scanning IR spectroscopy of acids and glycosides as neat films. NMR spectra were recorded on a Bruker AMX 500 spectrometer (Bruker Analytik, Karlsruhe, Germany) at 500.1 MHz (^1H), 125.7 MHz (^{13}C) in mixture of deuterated pyridine and CD_3OD (v/v 1:1). High- and also low-resolution MS were recorded using a VG 7070E- HF spectrometer (70 eV). HRFABMS (positive and/or negative ion mode) were obtained with a PEG-400 matrix. RP–HPLC was carried out using Shimadzu gradient LC system (Shimadzu, Kyoto, Japan). Gas chromatography analysis was made on a Hewlett Packard HP 5980 gas chromatograph (Hewlett Packard sro, Czech Republic).

3.2. Plant material

The specimens of *Acarospora gobiensis* H. Magn., *Cladonia furcata* (Huds.) Schrad, *Lecanora fructulosa* (Dicks.) Ach., *Leptogium saturninum* (Dicks.) Nyl., *Peltigera canina* (Neck.) Hoffm., *Rhizoplaca peltata* Ram., *Xanthoparmelia camtschadalis* Ach., *X. tinctina* Mah. et Gill., and *Xanthoria elegans* (Link.) Th. Fr. were collected in July 1996 along the shore of Lake Issyk Kul, Tian-Shan Mountains.

3.3. Extraction and isolation

All nine lichen species (100 g of air-dried lichens, see Řezanka and Guschina, 2000a) were extracted independently by the Blight and Dyer (1959) method and the extracts were also chromatographed separately be means of the column chromatography over Sephadex LH-20 eluted with EtOH-i-PrOH (fraction 1), EtOH (fraction 2) and then MeOH (fraction 3). Fraction 1 was further fractionated by RP–HPLC on a C18-Bondapak (Waters sro, Czech Republic) column (30 cm×7.8 mm, flow rate 2.0 ml/min) with ACN–H_2O (1:2) to yield compounds **1**–**3**. Fraction 2 was separated by RP-HPLC with ACN–H_2O (2:5) to yield the compounds **4**–**6**. Fraction 3 using ACN–H_2O (1:3), yielded compounds **7**–**10**.

The identification and the D or L configuration of sugars (i.e. D-xylose, L-rhamnose and D-glucose) was determined using GC–MS (according to the method of Gerwig et al., 1978), with some modifications, as previously described (Řezanka and Guschina, 2000a) with SPB-1 (Supelco) column (30 m×0.25 mm I.D.). The column temperature was programmed to rise 5 °C/min from 170 to 260 °C. The flow rate of the helium carrier gas through the column was 1.5 ml/min. The temperature of the injector was 270 °C.

3.4. Acid hydrolysis of *4*

The glycoside (~1 mg) was refluxed in 2 N HCl (0.5 ml) for 2 h. The aglycone was extracted three times with EtOAc (10 ml). After separating the organic layer, the

aqueous phase was neutralized with $NaHCO_3$ and lyophilized.

3.5. Enzymatic hydrolysis

A solution of glycoside (1 mg) in acetate buffer (pH 4.4, 10 ml) was treated with β-glucosidase (20 mg) for 48 h at 37 °C. The reaction solution was evaporated to dryness, and the residue was chromatographed on a column of silica gel (10 g), using CH_2Cl_2–MeOH–H_2O (90:10:1) to provide lichen's acids for ^{1}H NMR and ORD analysis.

Glycosides (~0.5 mg) were suspended in $(NH_4)_2SO_4$ solution of enzyme (E.C. 3.1.1.1, from porcine liver) at pH ~8 and incubated 15 min at 25 °C. Aglycone was extracted three times with EtOAc (10 ml). After separating the organic layer, the aqueous phase was neutralized with 0.5 N HCl and lyophilized.

3.6. (S)-MTPA and (R)-MTPA esters

(*S*)-MTPA esters of free acids (**1**–**3**) and aglycones from glucosides **4**–**10** (Ohtani et al., 1991a,b). To a CH_2Cl_2 solution (100 μl) of aglycone (0.3 mg), DMAP (1.0 mg), and Et_3N (2 μl) was added (*R*)-(−)-MTPACl (2.0 mg) at room temperature, and stirring was continued for 3 h. After evaporation of solvent, the residue was purified by Silica gel TLC (hexane–AcOEt, 2:1) to provide the (*S*)-MTPA ester as a colorless oil.

(*R*)-MTPA Esters of free acids (**1**–**3**) and of aglycones from glucosides **4**–**10**. Each aglycone (0.3 mg) was treated with (*S*)-(+)-MTPACl (2.0 mg) by the same procedure as described above to provide the (*R*)-MTPA ester as colorless oil.

18*R*-Hydroxydihydroalloprotolichesterinic acid **1**, white crystals, m.p. 143 °C, $[\alpha]_D^{24}$ −48° (*c* 0.19, $CHCl_3$), UV λ_{max} (EtOH, nm) 218 (log ε 2.28); ORD: $[\alpha]_{222}^{24}$ nm (−790), see also Fig. 2; IR (KBr) (cm^{-1}): 3450 (OH), 2950, 2920, 1740 (lactone), 1705 (acid); HREIMS *m/z*: 370.5293 (M^+, calc. for $[C_{21}H_{38}O_5]^+$ 370.5297; LREIMS *m/z* (%), 370 $[M]^+$ (2), 355 $[M–Me]^+$ (21), 352 $[M–H_2O]^+$ (56), 334 $[M–2xH_2O]^+$ (67), 326 $[M–CO_2]^+$ (14), 308 $[M–CO_2–H_2O]^+$ (58); ^{1}H and ^{13}C NMR spectra, see Tables 2 and 3.

18*S*-Hydroxydihydroprotolichesterinic acid **2**, white small needles, mp 105–107 °C, $[\alpha]_D^{24}$ +7.9° (*c* 0.10, $CHCl_3$), UV λ_{max} (EtOH, nm) 207 (log ε 2.74); ORD: $[\alpha]_{220}^{24}$ nm (+90), see also Fig. 2); IR (KBr) (cm^{-1}): 3450 (OH), 2950, 2920, 1740 (lactone), 1705 (acid); HREIMS *m/z*: 370.5301 (M^+, calc. for $[C_{21}H_{38}O_5]^+$ 370.5297; LREIMS *m/z* (%), 370 $[M]^+$ (3), 355 $[M–Me]^+$ (19), 352 $[M–H_2O]^+$ (67), 334 $[M–2xH_2O]^+$ (81), 326 $[M–CO_2]^+$ (10), 308 $[M–CO_2–H_2O]^+$ (51); ^{1}H and ^{13}C NMR spectra, see Tables 2 and 3.

18*S*-Hydroxyneodihydroprotolichesterinic acid **3**, white plates, mp 127.5 °C, $[\alpha]_D^{24}$ −28.5° (*c* 0.21, $CHCl_3$), UV λ_{max} (EtOH, nm) 217 (log ε 2.42); ORD: $[\alpha]_{220}^{24}$ nm (−260), see also Fig. 2; IR (KBr) (cm^{-1}): 3450 (OH), 2950, 2920, 1740 (lactone), 1705 (acid); HREIMS *m/z*: 370.5295 (M^+, calc. for $[C_{21}H_{38}O_5]^+$ 370.5297; LREIMS *m/z* (%), 370 $[M]^+$ (4), 355 $[M–Me]^+$ (17), 352 $[M–H_2O]^+$ (63), 334 $[M–2xH_2O]^+$ (73), 326 $[M–CO_2]^+$ (9), 308 $[M–CO_2–H_2O]^+$ (42); ^{1}H and ^{13}C NMR spectra, see Tables 2 and 3.

21-*O*-α-L-Rhamnopyranosyl-18*R*-hydroxydihydroalloprotolichesterinate **4**, colorless powder, mp 146.5 °C, $[\alpha]_D^{24}$ −188° (*c* 0.15, MeOH); UV 219 nm (log ε 3.88); IR (KBr) (cm^{-1}): 3400 (OH), 2950, 2920, 1750 (lactone), 1710 (ester); HRFABMS *m/z* 517.6801 $[M+H]^+$, calc. for $[C_{27}H_{49}O_9]^+$ 517.6807; negative LRFABMS *m/z* 515 $(M–H)^-$, 369 (M–H-146)$^-$ and ^{1}H and ^{13}C NMR spectra see Table 3 and 4.

21-*O*-β-D-Glucopyranosyl-18*S*-hydroxydihydroprotolichesterinate **5**, colorless powder, mp 157 °C, $[\alpha]_D^{24}$ −179° (*c* 0.14, MeOH); UV 218 nm (log ε 3.82); HRFABMS *m/z* 533.6806 $(M+H)^+$ calc. for $[C_{27}H_{49}O_{10}]^+$ 533.6800; negative LRFABMS *m/z* 531 $(M–H)^-$, 369 (M–H–162)$^-$, and ^{1}H and ^{13}C NMR spectra, see Table s3 and 4.

21-*O*-β-D-Glucopyranosyl-18*S*-hydroxyneodihydrolichesterinate (**6**), white amorphous powder, $[\alpha]_D^{23}$ −14°; HRFABMS *m/z* 533.6797 $(M+H)^+$, calculated for $[C_{27}H_{49}O_{10}]^+$ 533.6800; negative LRFABMS *m/z* 531 $(M–H)^-$, 369 (M–H–162)$^-$ and 353 (M–H–178)$^-$; and ^{1}H NMR and ^{13}C NMR spectra see Tables 3 and 4.

18-*O*-β-D-Glucopyranosyl-18*R*-hydroxydihydroalloprotolichesterinate 21-*O*-α-L-rhamnopyranoside (**7**), white amorphous powder, $[\alpha]_D^{23}$ −35°; HRFABMS *m/z* 679.8234 $(M+H)^+$, calc. for $[C_{33}H_{59}O_{14}]^+$ 679.8231; negative LRFABMS *m/z* 677 $(M–H)^-$, 531 (M–H–146)$^-$, 515 (M–H–162)$^-$, 499 (M–H–178)$^-$, 369 (M–H–162–146)$^-$; ^{1}H and ^{13}C NMR spectra, see Tables 5 and 6.

18-*O*-β-D-Xylopyranosyl-18*S*-hydroxydihydroprotolichesterinate 21-*O*-β-D-glucopyranoside (**8**), white powder, $[\alpha]_D^{23}$ −18°; HRFABMS *m/z* 665.7961 $(M+H)^+$, calc. for $[C_{32}H_{57}O_{14}]^+$ 665.7960; negative FABMS *m/z* 663 $(M–H)^-$, 501 (M–H–162)$^-$, 369 (M–H–162–132)$^-$; ^{1}H and ^{13}C NMR spectra, see Tables 5 and 6.

18-*O*-α-L-Rhamnopyranosyl-18*S*-hydroxyneodihydroprotolichesterinate 21-*O*-β-D-glucopyranoside (**9**), white powder, $[\alpha]_D^{23}$ −52.7°; HRFABMS *m/z* 679.8233 $(M+H)^+$, calc. for $[C_{33}H_{59}O_{14}]^+$ 679.8231; negative LRFABMS *m/z* 677 $(M–H)^-$, 515 (M–H–162)$^-$, 369 (M–H–162–146)$^-$; ^{1}H and ^{13}C NMR spectra, see Tables 5 and 6.

18-*O*-β-D-Glucopyranosyl-18*S*-hydroxyneodihydroprotolichesterinate 21-*O*-β-D-glucopyranoside (**10**), colorless powder, $[\alpha]_D^{23}$ −42.0°; HRFABMS *m/z* 695.8224 $(M+H)^+$, calc. for $[C_{33}H_{59}O_{15}]^+$ 695.8221; negative LRFABMS *m/z* 693 $(M–H)^-$, 531 (M–H–162)$^-$, 369 (M–H–162–162)$^-$; ^{1}H and ^{13}C NMR spectra, see Tables 5 and 6.

References

Blight, E.G., Dyer, W.J., 1959. A rapid method of total lipid extraction and purification. Can. J. Biochem. Physiol. 37, 911–917.

Gerwig, G.J., Kamerling, J.R., Vliegenthart, J.F.G., 1978. Determination of the D and L configuration of neutral monosaccharides by high-resolution capillary GLC. Carbohydr. Res. 62, 349–357.

Huneck, S., Jakupovic, J., Follmann, G., 1992. The final structures of the lichen chromones galapagin, lobodirin, mollin, and roccellin. Z. Naturforsch. 47b, 449–451.

Huneck, S., Schreiber, K., Höfle, G., Snatzke, G., 1979. Neodihydromurol- und Murolsäure, zwei neue γ-Lactoncarbonsäuren aus *Lecanora muralis*. J. Hattori Bot. Lab. 45, 1–23.

Huneck, S., Takeda, R., 1992. Zur Chemie der Proto- und allo-Protolichesterinsäure Z. Naturforsch. 47b, 842–854.

Huneck, S., Yoshimura, I., 1996. Identification of Lichen Substances. Springer Verlag, Berlin.

Ikan, R., 1999. Naturally Occurring Glycosides. John Wiley & Sons, New York.

Kasai, R., Suzuo, M., Asakawa, J., Tanaka, O., 1977. Carbon-13 chemical shifts of isoprenoid-β-D-glucopyranosides and-β-δ-mannopyranosides. Stereochemical influences of aglycone alcohols. Tetrahedron Lett., 175–178.

Ohtani, I., Kusumi, T., Kashman, Y., Kakisawa, H., 1991a. High-field FT NMR application of Mosher method—the absolute-configurations of marine terpenoids. J. Am. Chem. Soc. 113, 4092–4095.

Ohtani, I., Kusumi, T., Kashman, Y., Kakisawa, H., 1991b. A new aspect of the high-field NMR application of Mosher method—the absolute-configuration of marine triterpene Sipholenol-A. J. Org. Chem. 56, 1296.

Řezanka, T., Dembitsky, V.M., 1998. Brominated fatty acids from lichen *Acarospora gobiensis*. Phytochemistry 50, 97–99.

Řezanka, T., Dembitsky, V.M., 1999. Novel brominated lipidic compounds from lichens of Central Asia. Phytochemistry 51, 963–968.

Řezanka, T., Guschina, I.A., 1999. Brominated depsidones from *Acarospora gobiensis*, a lichen of Central Asia. J. Nat. Prod. 62, 1675–1677.

Řezanka, T., Guschina, I.A., 2000a. New glycosidic compounds of murolic, protoconstipatic and allo-murolic acids from lichens of Central Asia. Phytochemistry 54, 635–645.

Řezanka, T., Guschina, I.A., 2000b. Further glucosides of lichen's acids from Central Asian lichens. Phytochemistry 56, 181–188.

Rieser, M.J., Hui, Y., Rupprecht, J.K., Kozlowski, J.F., Wood, K.V., McLaughlin, J.L., Hanson, P.R., Zhuang, Z., Hoye, T.R., 1992. Determination of absolute-configuration of stereogenic carbinol centers in annonaceous acetogenins by ^{1}H NMR and ^{19}F NMR analysis of Mosher ester derivatives. J. Am. Chem. Soc. 114, 10203.

Seo, S., Tomita, Y., Tori, K., Yoshimura, Y., 1978. Determination of the absolute configuration of a secondary hydroxy group in a chiral secondary alcohol using glycosidation shifts in carbon-13 nuclear magnetic resonance spectroscopy. J. Am. Chem. Soc. 100, 3331–3339.

Tori, K., Seo, S., Yoshimura, Y., Arita, H., Tomita, Y., 1977. Glycosidation shifts in carbon-13 NMR spectroscopy: Carbon-13 signal shifts from aglycone and glucose to glucoside. Tetrahedron Lett., 179–182.

PERGAMON

Phytochemistry 58 (2001) 517–523

PHYTOCHEMISTRY

www.elsevier.com/locate/phytochem

Halogenated metabolites with antibacterial activity from the Okinawan *Laurencia* species

Charles Santhanaraju Vairappan[a,1], Minoru Suzuki[a,*], Tsuyoshi Abe[b], Michio Masuda[c]

[a]*Division of Material Science, Graduate School of Environmental Earth Science, Hokkaido University, Sapporo 060-0810, Japan*
[b]*The Hokkaido University Museum, Sapporo 060-0810, Japan*
[c]*Division of Biological Sciences, Graduate School of Science, Hokkaido University, Sapporo 060-0810, Japan*

Received 4 December 2000; received in revised form 19 April 2001

Abstract

The chemical compositions of five species of the red algal genus *Laurencia* from coastal waters of Okinawa Prefecture, Japan, have been investigated. A halogenated C_{15} acetogenin, (12*E*)-lembyne-A, was isolated from *L. mariannensis*, and a halogenated sesquiterpene, (6*R*,9*R*,10*S*)-10-bromo-9-hydroxy-chamigra-2,7(14)-diene, was first found from *L. majuscula* as a naturally occurring compound. *Laurencia nidifica* yielded previously known laurinterol and isolaurinterol. Samples of *L. cartilaginea* and *L. concreta* afforded no halogenated metabolites. The structures of these halogenated metabolites as well as their antibacterial activity against some marine bacteria are reported. © 2001 Elsevier Science Ltd. All rights reserved.

Keywords: *Laurencia*; Rhodomelaceae; Red alga; Sesquiterpene; C_{15} acetogenin; Halogenated compound; Chemotaxonomy; Antibacterial activity

1. Introduction

The red algal genus *Laurencia* is unique due to its ability to produce a wide variety of halogenated secondary metabolites with diverse structural features depending on the species and localities. Although the roles of these halogenated compounds are still a matter of speculation, their importance as chemical defense substances against marine herbivores is undeniable (Hay et al., 1987; Kurata et al., 1998).

Some halogenated metabolites have been shown to possess antibacterial activities against terrestrial bacteria (Waraszkiewicz and Erickson, 1974; Wratten and Faulkner, 1977; Carter et al., 1978; Caccamese et al., 1980; König and Wright, 1997a). More recently, we reported on the antibacterial potential of halogenated compounds isolated from the Malaysian *Laurencia* against marine bacteria from the algal habitat (Vairappan et al., 2001), suggesting the possible role played by these halogenated compounds as the seaweed's chemical defense substances.

As part of our continuing study on the chemical compositions of *Laurencia* species from the Okinawan waters, we harvested five species of *Laurencia*; *L. mariannensis* Yamada, *L. majuscula* (Harvey) Lucas, *L. nidifica* J. Agardh, *L. cartilaginea* Yamada, and *L. concreta* Cribb from four different sites. *Laurencia mariannensis* contained a new C_{15} acetogenin, (12*E*)-lembyne-A (**1**), along with 2-bromo-3-chloro-5-acetoxy-chamigra-7(14), 9-dien-8-one (**2**) that was previously isolated from the Okinawan sea hare *Aplysia dactylomela* (Sakai et al., 1986) and from the Okinawan *L. majuscula* collected at Taketomi (Masuda et al., 1997). *Laurencia majuscula* contained a brominated sesquiterpene, (6*R*,9*R*,10*S*)-10-bromo-9-hydroxy-chamigra-2,7(14)-diene (**3**), together with previously known (*Z*)-10,15-dibromo-9-hydroxy-chamigra-1,3(15),7(14)-triene (**4**) and (*E*)-10,15-dibromo-9-hydroxy-chamigra-1,3(15),7(14)-triene (**5**) from this species collected at Kochi Prefecture, Japan (Suzuki and Kurosawa, 1978; Suzuki et al., 1979). Metabolite **3** has not been previously found as a natural source. Furthermore, *L. nidifica* produced laurinterol (**6**) and isolaurinterol (**7**), characteristic metabolites of the Japanese *L. okamurae* Yamada (Suzuki and Kurosawa, 1979), while *L. cartilaginea* and *L. concreta* produced no halogenated secondary metabolites.

We report herein the chemical compositions of these *Laurencia* species, structures of halogenated compounds,

* Corresponding author. Tel.: +81-11-706-2272; fax: +81-11-706-4862.

E-mail address: misu@ees.hokudai.ac.jp (M. Suzuki).

[1] Present address: Borneo Marine Research Institute, University Malaysia Sabah, 88999 Kota Kinabalu, Sabah, Malaysia.

0031-9422/01/$ - see front matter © 2001 Elsevier Science Ltd. All rights reserved.
PII: S0031-9422(01)00260-6

and their antibacterial activity against marine bacteria isolated from the algal habitat.

2. Results and discussion

2.1. Laurencia mariannensis

A sample collected from Teruma, Yonashiro, was extracted with methanol. The methanol extract was fractionated by CC over silica gel with a stepped gradient (hexane and EtOAc). The fraction eluted with hexane–EtOAc (9:1) was further subjected to prep. TLC with hexane–EtOAc (3:1) to give 2-bromo-3-chloro-5-acetoxy-chamigra-7(14),9-dien-8-one (**2**) (Sakai et al., 1986; Masuda et al., 1997) in 14% yield based on the weight of the extracts. The fraction eluted with hexane–EtOAc (4:1) was also separated using prep. TLC with hexane–EtOAc (3:1) to give compound **1** (6%).

Compound **1**, oil, $[\alpha]_D^{24}$ +42° ($CHCl_3$), was assigned the molecular formula $C_{15}H_{16}BrClO_2$ (HRFDMS). Its IR spectrum revealed absorptions due to a terminal acetylenic group (ν_{max} 3310 cm^{-1}), a vinyl ether stretching (ν_{max} 1680 cm^{-1}), and C–O bands (ν_{max} 1110 and 1050 cm^{-1}). In addition, since there were no hydroxyl or carbonyl absorptions, both oxygens were suggested to be involved in ether links. The presence of a terminal conjugated enyne moiety, which is frequently encountered in *Laurencia* C_{15} acetogenins, was evident from the ^1H NMR spectrum (Table 1) [δ_H 3.31 (1H, *br s*), 5.58 (1H, *dd*, J=10.7, 1.5 Hz) and 6.06 (1H, *dd*, J=10.7, 10.7 Hz)]. Interpretation of the ^1H–^1H COSY spectrum showed the presence of a partial structure **1a**

Table 1
^{13}C NMR (100 MHz, DEPT), ^1H NMR (400 MHz), and HMBC spectral data[a] for **1**

C[b]	^{13}C (δ)	^1H (δ)	Multiplicity, J (Hz)	HMBC correlations
1	78.7	3.31	*br s*	
2	85.8			
3	110.9	5.58	*dd*, J=10.7, 1.5	H-1, H-4, H-5
4	142.2	6.06	*dd*, J=10.7, 10.7	H-3, H-5
5	54.9	4.72	*dd*, J=10.7, 10.7	H-3, H-4, H-7
6	54.2	2.74	*ddd*, J=10.7, 9.3, 4.4	H-4, H-5, H-7, H-10, H-11
7	77.9	4.29	*dd*, J=4.4, 4.4	H-6, H-9, H-10, H-11
8	36.8	1.92	*d*, J=13.6	H-6, H-7, H-10
		1.71	*m*	
9	81.5	4.67	*dd*, J=6.8, 4.9	H-7, H-10, H-11
10	84.2	5.13	*dd*, J=4.9, 4.9	H-7, H-9, H-11
11	45.2	3.46	*dd*, J=9.3, 4.9	H-5, H-6, H-7, H-9, H-10
12				
13	105.8			H_2-14, H_3-15
14	28.1	2.64	*dq*, J=14.6, 7.3	H_3-15
		2.38	*dq*, J=14.6, 7.3	
15	13.8	1.10	*dd*, J=7.3, 7.3	H_2-14

[a] Measured in chloroform-d_1.
[b] Assignments were made with the aid of the HSQC spectrum.

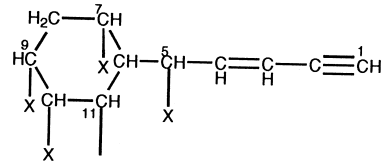

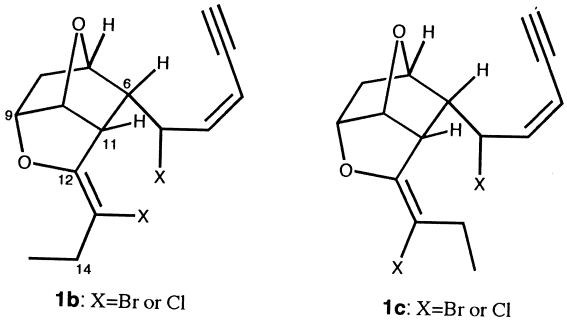

Fig. 1. Partial and planar structures for **1**.

(Fig. 1) together with an isolated ethyl group. The J-value (10.7 Hz) between H-3 and H-4 as well as the chemical shift value (δ_H 3.31) of the acetylenic proton indicated the geometry of the double bond at C-3 to be Z (Suzuki and Kurosawa, 1987).

The ^{13}C NMR spectrum (Table 1) revealed the presence of 14 carbon atoms, 12 of which were hydrogen-bearing carbons. Among 14 carbon atoms, three oxygen-bearing carbons were demonstrated by the signals at δ_C 77.9, 81.5 and 84.2 and further attributed to C-7, C-9 and C-10, respectively, by HSQC spectrum. Furthermore, based on the chemical shift values of H-5 (δ_H 4.72) and C-5 (δ_C 54.9), a halogen atom was deduced to be attached to C-5 position. The planar formula for compound **1** could be assigned by the HMBC spectrum whose results are summarized in Table 1. In the HMBC spectrum, cross peaks of C-7/H-10 and C-10/H-7 established the ether ring closure between C-7 and C-10. In addition, a cross peak between the terminal methyl group and the vinyl carbon at δ_C 105.8 indicated that the ethyl group was attached to the tetrasubstituted double bond. The chemical shift value (δ_C 105.8) of this vinyl carbon atom suggested that another substituent is a halogen atom (Suzuki et al., 1983). Therefore, this double bond had to be inserted between C-9 and C-11 to give a planar formula **1b** or **1c**. Facile loss of a chlorine atom on the FDMS is evident from the fragment ion of m/z 309, 307 $[M\text{-}Cl]^+$ which strongly suggested the presence of a vinyl bromide moiety in **1**. Hence the chlorine atom was linked to C-5 and the bromine atom to C-13.

The ^1H and ^{13}C NMR spectral data of **1** were very similar to those of lembyne-A (**1′**), which has recently been isolated from the Malaysian *Laurencia* sp. (Vairappan et al., 2001). The chemical shifts and coupling constants of the protons from C-1 to C-10 in the ^1H NMR spectrum of **1** are almost identical to those of **1′**. However,

distinct differences are observed in the chemical shift values of H-11 and H_2-14. The low-field chemical shift of the H-11 in **1** is due to the deshielding being caused by the bromine atom at C-13 that is situated close to the H-11. Furthermore, the large magnetic nonequivalence of the H_2-14 in **1** is attributed to the electronic influence of the oxygen atom that is *cis* to the ethyl group. Thus the stereochemistry of the vinyl ether moiety in **1** is established as *E*-configuration. In consequence, the structure of compound **1** must be represented by formula **1**, (12*E*)-lembyne-A, including the same relative stereochemistry, 5*S**, 6*R**, 7*R**, 9*R**, 10*R**, and 11*S**, as lembyne-A (**1′**).

(12*E*)-Lembyne-A (**1**) and lembyne-A (**1′**) have structures very similar to *cis*-maneonene-C (**1″**) and (12*Z*)-*cis*-maneonene-C (**1‴**), respectively, the latter of which was obtained from *cis*-maneonene-C by treatment with *p*-toluenesulfonic acid (Waraszkiewicz et al., 1978). However, there are some obvious differences between our ^{1}H and ^{13}C NMR spectral data (in C_6D_6) and the published data (Waraszkiewicz et al., 1978) along with their optical rotations (**1**: $[\alpha]_D$ +42°; **1′**: $[\alpha]_D$ +198°, **1b″**: $[\alpha]_D$ +336°, **1‴**: $[\alpha]_D$ +137 °C). Thus *cis*-maneonene-C and (12*Z*)-*cis*-maneonene-C may be a stereoisomer at C-5 of (12*E*)-lembyne-A and lembyne-A, respectively.

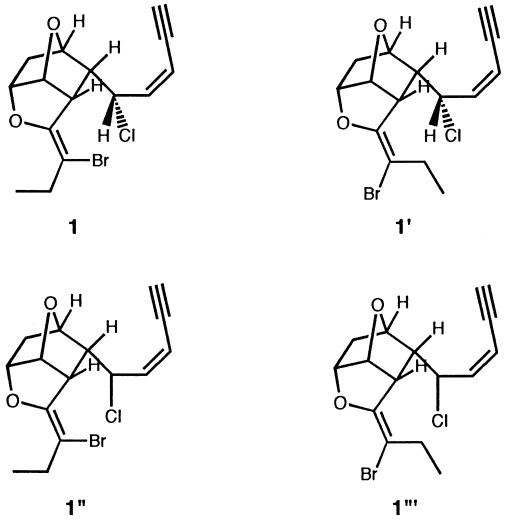

2.2. *Laurencia majuscula*

The methanol extract of a sample collected from Yagachi, Nago, was subjected to a combination of column and thick-layer chromatography to give 10-bromo-9-hydroxy-chamigra-2,7(14)-diene (**3**) (9%) along with previously known (*Z*)-10,15-dibromo-9-hydroxy-chamigra-1,3(15),7(14)-triene (**4**) (3%) and (*E*)-10,15-dibromo-9-hydroxy-chamigra-1,3(15),7(14)-triene (**5**) (4%), isolated from this species which had been collected at Kochi Prefecture, Japan (Suzuki and Kurosawa, 1978; Suzuki et al., 1979).

Compound **3**, oil, $C_{15}H_{23}OBr$, $[\alpha]_D^{25}$ −110° ($CHCl_3$), was readily assigned the planar structure by its 1D and 2D (^{1}H–^{1}H COSY, HSQC, and HMBC) NMR spectra. The relative configuration was determined by the NOESY spectrum. A NOE between H-10 and Hb-5 showed that the H-10 adopts an axial configuration and hence the bromine atom is equatorial. Since based on the *J*-value ($J_{9,10}$ = 2.9 Hz), the vicinal bromine and hydroxyl groups are in *cis*-configuration as in the case of compounds **4** and **5**, the C-9 hydroxyl group is axial. Furthermore, NOEs between Ha-14/Ha-1 and H_3-13 (one of *gem*-dimethyl)/Ha-4 also confirmed the stereochemistry of the spiro carbon at C-6. Thus the relative stereochemistry of **3** would be represented by formula **3a** as shown in Fig. 2.

A literature survey indicated that the ^{1}H and ^{13}C NMR spectral data of **3** were almost identical with those of deschloroelatol (**3′**), which has previously been isolated from *Laurencia obtusa* (Kennedy et al., 1988) and *L. rigida* (König and Wright, 1997b). However, judging from the signs of the optical rotations, compound **3** must be an enantiomer of deschloroelatol. Compound **3** had previously been obtained from obtusol as the partially dehalogenated compound by treatment with lithium aluminum hydride in ether (González et al., 1976). Co-occurrence of compound **3** with halochamigrenes **4** and **5** in the same alga also suggested that the absolute configurations of chiral centers at C-6, C-9, and C-10 are the same as those of **4** and **5**.

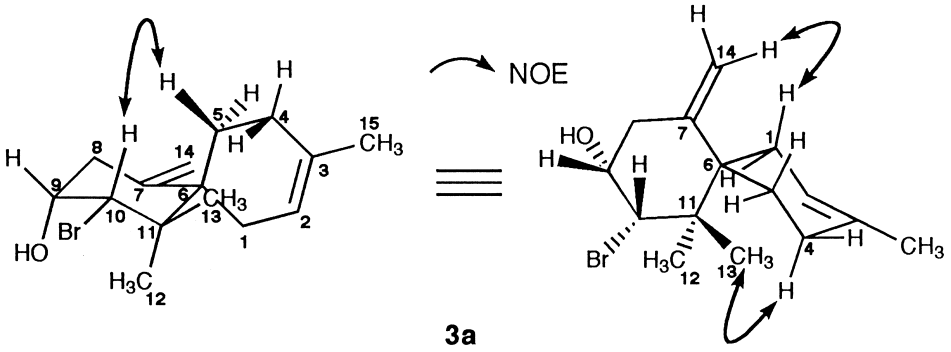

Fig. 2. Stereochemistry of 10-bromo-9-hydroxy-chamigra-2,7(14)-diene (**3**).

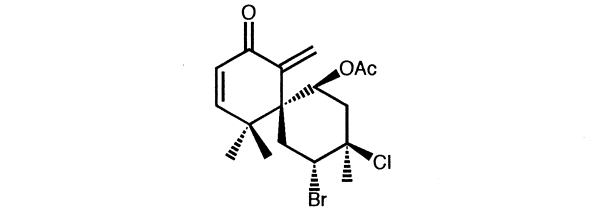

2

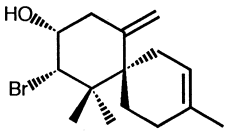

3

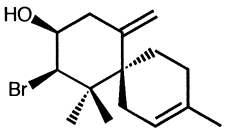

3'

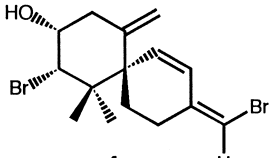

4

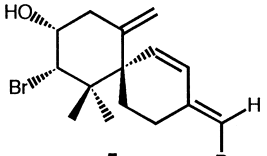

5

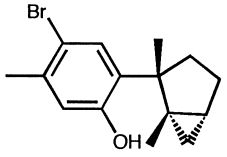

6

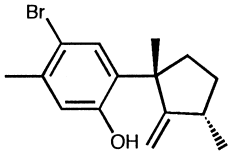

7

Accordingly, the structure of compound **3** should be (6*R*,9*R*,10*S*)-10-bromo-9-hydroxy-chamigra-2,7(14)-diene, which has not previously been found as a naturally occurring compound.

The difference of the chemical compositions in the samples from Yagachi, Nago (present study) and Taketomi island (Masuda et al., 1997) suggests that chemical races (Abe et al., 1999) are also present in *Laurencia majuscula*.

2.3. Laurencia nidifica

The methanol extract of a sample collected from Toyohara, Nago, gave laurinterol (**6**) (22%) and isolaurinterol (**7**) (4%) (Suzuki and Kurosawa, 1979). The chemical composition of *Laurencia nidifica* collected at two sites (Teruma and Toyohara) is different from that of a sample harvested from Goza, Mie Prefecture, Japan (Shizuri et al., 1984); it is, however, rather similar to that of a Hawaiian sample (a clumpy pink variety) from Oahu island (Waraszkiewicz and Erickson, 1974, 1975).

2.4. Laurencia cartilaginea and Laurencia concreta

No halogenated secondary metabolites were found in both extracts of *Laurencia cartilaginea* and *L. concreta*. As reported in a previous paper (Suzuki et al., 1987), a sample of *L. cartilaginea* collected at Sakurajima, Kagoshima Prefecture in Japan, close to the type locality, Moji, Fukuoka Prefecture, also showed the absence of halogenated compounds in its extract. Both *Laurencia* species have no "*corps en cerise*" (our unpublished observations). "*Corps en cerise*" are considered to be the sites of synthesis and/or storage for the halogenated secondary metabolites of *Laurencia* (Young et al., 1980). Although the Hawaiian *L. cartilaginea* was reported to produce halogenated chamigrane-type sesquiterpenes (Juagdan et al., 1997), the identification of their material seems to be questionable.

2.5. Antibacterial activity

The antibacterial activities of the isolated halogenated metabolites of Okinawan *Laurencia* were tested against eight species of marine bacteria. These were *Alcaligenes aquamarinus*, *Alteromonas* sp., *Azomonas agilis*, *Azotobacter beijerinckii*, *Erwinia amylovora*, *Escherichia coli*, *Halobacterium* sp., and *Halococcus* sp. All these bacteria were Gram-negative strains. The results of the paper disc diffusion assays are shown in Table 2. Prominent antibacterial activities were seen in compounds **1**, **3**, **6** and **7**, while **4** and **5** only showed very marginal activity. Compound **2** was inactive towards the bacteria tested. Compound **1** showed activity against *Alcaligenes aquamarinus*, *Azomonas agilis*, *Erwinia amylovora*, and *Escherichia coli*. Their minimum inhibitory concentration (MIC) values are in the range of 20–30 μg/disc as shown in Table 3. Compound **3** showed antibacterial activity against five species of bacteria, *Alcaligenes aquamarinus*, *Azomonas agilis*, *Azotobacter beijerinckii*, *Erwinia amylovora*, and *Escherichia coli*. Its MIC values were in the range of 10–30 mg/disc (Table 3). Compounds **6** and **7** showed better antibacterial activity than compounds **1** and **3**. Their antibacterial activities and respective MIC values are shown in Tables 2 and 3, respectively.

Table 2
Antibacterial activity of the halogenated compounds against marine bacteria isolated from algal habitats in the Japanese coastal waters

Test bacteria	Compounds[a]			
	1	**3**	**6**	**7**
Alcaligenes aquamarinus	+ +	+ +	–	–
Alteromonas sp.	–	–	+ +	+ + +
Azomonas agilis	+ +	+ +	+ + +	+ + +
Azobacter beijerinckii	–	+ +	+ +	–
Erwinia amylovora	+ +	+ +	+ + +	+ + +
Escherichia coli	+ +	+ +	+ +	+ + +
Halobacterium sp.	–	–	–	–
Halococcus sp.	–	–	–	–

[a] Inhibition zone diameter; + + +: 19–24 mm, + +: 12–18 mm, +: 7–12 mm, –: no inhibition. Concentration: 90 μg/disc.

Table 3
Minimal inhibitory concentration (MIC[a]) of the halogenated compounds against marine bacteria isolated from algal habitats in the Japanese coastal waters

Test bacteria	Compounds[a]			
	1	**3**	**6**	**7**
Alcaligenes aquamarinus	20	20	–	–
Alteromonas sp.	–	–	5	10
Azomonas agilis	30	20	5	5
Azobacter beijerinckii	–	15	15	–
Erwinia amylovora	30	15	5	5
Escherichia coli	30	10	5	10
Halobacterium sp.	–	–	–	–
Halococcus sp.	–	–	–	–

[a] Concentration: μg/disc. –: no inhibition.

The possibility that these halogenated compounds are involved in protecting these *Laurencia* species against bacterial intrusion is real when we look at the distribution of these compounds. Basically, halogenated compounds are reported to be contained in "*corps en cercise*" (Young et al., 1980), an unusually swollen refractile inclusion, that are located in the outer cortical layer and trichoblast cells of *Laurencia*. "*Corps en cercise*" are absent in the inner cortical layers, and their specific distribution pattern could be suggestive of their importance as barricades to withhold any bacterial intrusion.

3. Experimental

3.1. General

^{1}H (400 MHz) and ^{13}C NMR (100 MHz); $CDCl_3$ or C_6D_6, TMS as int. standard (coupling constant, *J* in Hz); low and high resolution MS: 70 eV; optical rotations: $CHCl_3$; CC: silica gel (Merck, Kieselgel 60, 70–230 mesh); prep. TLC: silica gel 60 F_{254} (Merck). All known metabolites were identified by comparison of the spectral data with those of the authentic specimens. Yields are based on the weights of the extracts.

3.2. Collection

Five *Laurencia* samples were collected from four sites in Okinawa Prefecture, Japan: *L. mariannensis* Yamada at Teruma, Yonashiro, on 4 June 1997; *L. majuscula* (Harvey) Lucas at Yagachi, Nago, on 6 June 1997; *L. nidifica* J. Agardh at Teruma,Yonashiro, on 4 June 1997, and Toyohara, Nago, on 5 June, 1997; *L. cartilaginea* Yamada at Yagachi, Nago, on 6 June 1997; *L. concreta* Cribb at Hedomisaki, Kunigami, on 6 June 1997. The voucher specimens are deposited in the Herbarium (SAP) of the Graduate School of Science, Hokkaido University.

3.3. Extraction and separation of Laurencia mariannensis

The partially dried alga (4 g) was soaked in methanol for one week. The MeOH soln was concentrated in vacuo and partitioned between Et_2O and H_2O. The Et_2O soln. was washed with water, dried over anhydrous Na_2SO_4, and evaporated to leave a dark green oil (65 mg). The extract was fractionated by Si gel column chromatography with a stepped gradient (hexane and EtOAc). The fraction eluted with hexane–EtOAc (9:1) was further submitted to prep. TLC with hexane–EtOAc (3:1) to give 2-bromo-3-chloro-5-acetoxy-chamigra-7(14),9-dien-8-one (**2**) (14%). Further separation of the fraction eluated with hexane–EtOAc (4:1) under the above-mentioned TLC yielded compound **1** (6%).

3.4. Compound *1*

Oil; $[\alpha]_D^{24}$ +42° ($CHCl_3$; *c* 0.02); IR ν_{max} (neat) cm^{-1}: 3310, 1680, 1110, 1050, 930, 880; ^{1}H and ^{13}C NMR spectra, Table 1; ^{1}H NMR spectrum (400 MHz, C_6D_6), δ 1.21 (3H, *dd*, *J* = 7.3, 7.3 Hz, H_3-15), 1.28 (1H, *m*, Ha-8), 1.78 (1H, *d*, *J* = 13.6 Hz, Hb-8), 2.41 (1H, *ddd*, *J* = 10.7, 9.3, 4.4 Hz, H-6), 2.50 (1H, *dq*, *J* = 14.6, 7.3 Hz, Ha-14), 2.71 (1H, *dd*, *J* = 2.4, 0.9 Hz, H-1), 2.84 (1H, *dq*, *J* = 14.6, 7.3 Hz, Hb-14), 3.39 (1H, *dd*, *J* = 9.3, 4.9 Hz, H-11), 3.85 (1H, *dd*, *J* = 4.9, 4.4 Hz, H-7), 4.18 (1H, *dd*, *J* = 6.8, 4.9 Hz, H-9), 4.52 (1H, *dd*, *J* = 4.9, 4.9 Hz, H-10), 4.86 (1H, *dd*, *J* = 10.7, 10.7 Hz, H-5), 5.02 (1H, *dd*, *J* = 10.7, 2.4 Hz, H-3), 5.43 (1H, *ddd*, *J* = 10.7, 10.7, 0.9 Hz, H-4); LR-FDMS *m*/*z* (rel. int.): 346, 344, 342 (30:90:76) $[M]^+$, 309, 307 (11:10) $[M–Cl]^+$; HR–FDMS *m*/*z*: 342.0013. Calc. for $C_{15}H_{16}{}^{79}Br^{35}ClO_2$, 342.0022 [M].

3.5. Extraction and separation of Laurencia majuscula

Extraction of partially dried alga (8 g) was carried out by conventional methods described above to yield a brownish green extract (95 mg). A combination of column and thick-layer chromatography of the MeOH extract gave three halochamigrenes, 10-bromo-9-hydroxy-chamigra-2,7(14)-diene (**3**) (9%), (*Z*)-10,15-dibromo-9-hydroxy-chamigra-1,3(15),7(14)-triene (**4**) (3%), and (*E*)-10,15-dibromo-9-hydroxy-chamigra-1,3(15),7(14)-triene (**5**) (4%).

3.6. 10-Bromo-9-hydroxy-chamigra-2,7(14)-diene (*3*)

Oil; $[\alpha]_D^{25}$ −110° ($CHCl_3$; *c* 0.20); IR ν_{max} (neat) cm^{-1}: 3550, 3450, 1640, 1395, 1365, 1220, 1200, 1180, 1085, 1070, 1035, 895, 830, 810; ^{1}H NMR (400 MHz, $CDCl_3$), δ 1.10 (6H, *s*, H_3-12 and H_3−13), 1.50 (3H, *br s*, H_3-15), 1.67 (1H, *m*, Hb-4), 1.75 (1H, *m*, Hb-5), 1.80 (1H, *m*, Ha-5), 1.84 (1H, *m*, Ha-4), 2.19 (1H, *m*, Hb-1), 2.20 (1H, *m*, Ha-1), 2.48 (1H, *dd*, *J* = 14.2, 2.9 Hz, Hb-8), 2.71 (1H, *dddd*, *J* = 14.2, 2.9, 2.9, 1.5 Hz, Ha-8), 4.16

(1H, *dd*, $J=2.9$, 2.9 Hz, H-9), 4.68 (1H, *d*, $J=2.9$ Hz, H-10), 4.80 (1H, *br s*, Hb-14), 5.10 (1H, *dd*, $J=1.5$, 1.5 Hz, Ha-14), 5.29 (1H, *br s*, H-2); ^{13}C NMR (100 MHz, $CDCl_3$), CH_3: δ 21.5 (C-13), 23.8 (C-15), 25.0 (C-12), CH_2: δ 26.6 (C-5), 28.5 (C-4), 30.9 (C-1), 38.8 (C-8), 116.5 (C-14), CH: δ 72.6 (C-10), 73.2 (C-9), 120.2 (C-2), C: δ 43.9 (C-11), 47.8 (C-6), 133.4 (C-3), 141.9 (C-7); LR–EIMS *m/z* (rel.int.): 300, 298 (14:15) $[M]^+$, 285, 283 (12:12) $[M-CH_3]^+$, 219 (21) $[M-Br]^+$, 217 (32) $[M-Br-H_2]^+$, 201 (100) $[M-Br-H_2O]^+$, 173 (27), 119 (64), 105 (54), 69 (52), 55 (45), 41 (44); HR–EIMS *m/z*: 298.0927. Calc. for $C_{15}H_{23}{}^{79}BrO$, 298.0933 [M]. The ^{1}H and ^{13}C NMR spectral data were almost identical with those reported in the literature for deschloroelatol (König and Wright, 1997b).

3.7. Extraction and separation of Laurencia nidifica

Extraction of partially dried alga (10 g) was carried out by conventional methods as described above to give a green oily extract (110 mg). A combination of column and thick-layer chromatography of the MeOH extracts gave laurinterol (**6**) (22%) and isolaurinterol (**7**) (4%).

3.8. Extraction and separation of Laurencia cartilaginea and Laurencia concreta

The MeOH extracts of both samples contained no halogenated compounds.

3.9. Antibacterial bioassay

Antibacterial bioassay was carried out using eight species of marine bacteria isolated from algal surfaces collected from the Japanese waters. These bacteria are *Alcaligenes aquamarinus*, *Alteromonas* sp., *Azomonas agilis*, *Azotobacter beijerinckii*, *Erwinia amylovora*, *Escherichia coli*, *Halobacterium* sp., and *Halococcus* sp. One loopful of each organism was precultured in 20 ml of peptone water (3% NaCl) overnight. The turbidity of the culture was adjusted to an optical density (OD) McFarland 0.5 (Sonnerwirth and Jarett, 1980; Hindler et al., 1990). Then 0.1 ml of the precultured bacterial suspension was used to seed Nutrient Agar plates (3% NaCl). Paper discs (Whatman, 6 mm) impregnated with various amounts of the respective pure compounds were placed on the seeded agar plates and the diameters of the inhibitory zones were measured after the plates were incubated at 28 °C for 24 h.

Acknowledgements

This study was supported in part by a Grant-in Aid for Scientific Research (No. 09839001) from the Ministry of Education, Science, Sports and Culture of Japan and also by the Sasakawa Scientific Research Grant from the Japan Science Society (No. 12-300).

References

Abe, T., Masuda, M., Suzuki, T., Suzuki, M., 1999. Chemical races in the red alga *Laurencia nipponica* (Rhodomelaceae, Ceramiales). Phycological Research 47, 87–95.

Caccamese, S., Azzolina, R., Duesler, E.N., Paul, I.C., Rinehart Jr., K.L., 1980. Laurencienyne, a new acetylenic cyclic ether from the marine red alga *Laurencia obtusa*. Tetrahedron Letters 21, 2299–2302.

Carter, G.T., Rinehart Jr., K.L., Li, L.H., Kuentzel, S.L., Connor, J.L., 1978. Brominated indoles from *Laurencia brongniartii*. Tetrahedron Letters, 4479–4482.

González, A.G., Darias, J., Díaz, A., Fourneron, J.D., Martín, J.D., Pérez, C., 1976. Evidence for the biogenesis of halogenated chamigrenes from the red alga *Laurencia obtusa*. Tetrahedron Letters, 3051–3054.

Hay, M.E., Fenical, W., Gustafson, K., 1987. Chemical defense against diverse coral-reef herbivores. Ecology 68, 1581–1591.

Hindler, J.A., Gonzalez, A.H., Drake, T.A., 1990. Stability of viable-bacterium counts in liquid media used for preparation of inocula and subsequent impact on antimicrobial susceptibility test results. Journal of Clinical Microbiology 28, 1271–1275.

Juagdan, E.G., Kalidindi, R., Scheuer, P., 1997. Two new chamigranes from an Hawaiian red alga, *Laurencia cartilaginea*. Tetrahedron 53, 521–528.

Kennedy, D.J., Selby, I.A., Thomson, R.H., 1988. Chamigrane metabolites from *Laurencia obtusa* and *L. scoparia*. Phytochemistry 27, 1761–1766.

König, G.M., Wright, A.D., 1997a. Sesquiterpene content of the antibacterial dichloromethane extract of the marine alga *Laurencia obtusa*. Planta Medica 63, 186–187.

König, G.M., Wright, A.D., 1997b. *Laurencia rigida*: chemical investigations of its antifouling dichloromethane extract. Journal of Natural Products 60, 967–970.

Kurata, K., Taniguchi, K., Agatsuma, Y., Suzuki, M., 1998. Diterpenoid feeding-deterrents from *Laurencia saitoi*. Phytochemistry 47, 363–369.

Masuda, M., Itoh, T., Matsuo, Y., Suzuki, M., 1997. Sesquiterpenoids of *Laurencia majuscula* (Ceramiales, Rhodophyta) from the Ryukyu Islands, Japan. Phycological Research 45, 59–64.

Sakai, R., Higa, T., Jefford, C.W., Bernardinelli, G., 1986. The absolute configurations and biogenesis of some new halogenated chamigrenes from the sea hare *Aplysia dactylomela*. Helvetica Chimica Acta 69, 91–105.

Shizuri, Y., Yamada, A., Yamada, K., 1984. Laurequinone, a cyclolaurane sesquiterpene from the red alga *Laurencia nidifica*. Phytochemistry 23, 2672–2673.

Sonnerwirth, C.A., Jarett, L., 1980. Gradwohl's Clinical Laboratory Methods and Diagnosis, 8th Edition. The C. V. Mosby Company, St. Louis, pp. 1959–1970.

Suzuki, M., Furusaki, A., Hashiba, N., Kurosawa, E. 1979. The structures and absolute stereochemistry of two halogenated chamigrenes from the red alga *Laurencia majuscula* Harvey. Tetrahedron Letters 879–882.

Suzuki, M., Kurosawa, E., 1978. Two new halogenated sesquiterpenes from the red alga *Laurencia majuscula* Harvey. Tetrahedron Letters, 4805–4808.

Suzuki, M., Kurosawa, E., 1979. Halogenated and non-halogenated aromatic sesquiterpenes from the red algae *Laurencia okamurai* Yamada. Bulletin of the Chemical Society of Japan 52, 3352–3354.

Suzuki, M., Kurosawa, E., 1987. (3E)-Laureatin and (3E)-isolaureatin, halogenated C-15 non-terpenoid compounds from the red alga *Laurencia nipponica* Yamada. Bulletin of the Chemical Society of Japan 60, 3791–3792.

Suzuki, M., Kurosawa, E., Furusaki, A., Matsumoto, T., 1983. The structures of (3*Z*)-epoxyvenustin, (3*Z*)-venustin, and (3*Z*)-venustinene, new halogenated C_{15}-nonterpenoids from the red alga *Laurencia venusta* Yamada. Chemistry Letters, 779–782.

Suzuki, M., Kurosawa, E., Kurata, K., 1987. (E)-Tridecyl-2-heptadecenal, an unusual metabolites from the red alga *Laurencia* species. Bulletin of the Chemical Society of Japan 60, 3793–3794.

Vairappan, C.S., Daitoh, M., Suzuki, M., Abe, T., Masuda, M., 2001. Antibacterial halogenated metabolites from the Malaysian *Laurencia* species. Phytochemistry, in press.

Waraszkiewicz, S.M., Erickson, K.L., 1974. Halogenated sesquiterpenoids from the Hawaiian marine alga *Laurencia nidifica*: nidificene and nidifidiene. Tetrahedron Letters, 2003–2006.

Waraszkiewicz, S.M., Erickson, K.L., 1975. Halogenated sesquiterpenoids from the Hawaiian marine alga *Laurencia nidifica*. II. Nidifidienol. Tetrahedron Letters, 281–284.

Waraszkiewicz, S.M., Sun, H.H., Erickson, K.L., Finer, J., Clardy, J., 1978. C_{15} halogenated compounds from the Hawaiian marine alga *Laurencia nidifica*. Maneonenes and isomaneonenes. The Journal of Organic Chemistry 43, 3194–3204.

Wratten, S.J., Faulkner, D.J., 1977. Metabolites of the red alga *Laurencia subopposita*. The Journal of Organic Chemistry 42, 3343–3349.

Young, D.N., Howard, B.M., Fenical, W., 1980. Subcellular localization of brominated secondary metabolites in the red alga *Laurencia snyderae*. Journal of Phycology 16, 182–185.

PERGAMON

Phytochemistry 58 (2001) 525–531

PHYTOCHEMISTRY

www.elsevier.com/locate/phytochem

Xyloglucan from the leaves of *Hymenaea courbaril*

Ana P. Busato[a], Carem G. Vargas-Rechia[b], Fany Reicher[a,*]

[a]*Departmento de Bioquímica, Universidade Federal do Paraná, CP 19046, 81531-990, Curitiba, Paraná, Brazil*
[b]*Departmento de Química e Física, Faculdade de Ciências Farmacêuticas de Ribeirão Preto- Universidade de São Paulo, 14040-903, Ribeirão Preto, São Paulo, Brazil*

Received 11 September 2000; received in revised form 5 February 2001

Abstract

A fucosylated xyloglucan was isolated from the leaves of *Hymenaea courbaril* by alkaline extraction, followed by ethanol precipitation and ion-exchange chromatography. The isolated polysaccharide showed Glc:Xyl:Gal:Fuc in molar ratio of 8:5:2.5:1 and $[\alpha]_D^{25}$ +40.5°. Composition and linkage analyses, supported by NMR spectroscopic measurements, showed that the polysaccharide has a glucan backbone which is highly substituted at *O*-6 with D-xylopyranose residues, about a half of which are substituted at *O*-2 by D-galactopyranosyl units. Some of the galactose residues are further substituted by L-fucopyranose at *O*-2. The M_r, as determined by HPSEC, was 49,500. © 2001 Elsevier Science Ltd. All rights reserved.

Keywords: *Hymenaea courbaril*; Caesalpiniaceae; Leaf polysaccharides; Cell wall; Hemicellulose; Fucosylated xyloglucan

1. Introduction

The primary cell wall is a dynamic and highly ordered complex network of several macromolecules, mainly polysaccharides, comprising pectic substances, hemicelluloses and fibrillar cellulosic material. Structural proteins and phenolic compounds are also present (Varner and Lin, 1989; McCann et al., 1995; Schindler, 1998). It plays an important role in controlling the growth rate of cells and morphogenetic processes, and acts as a barrier to plant pathogens (Keegstra et al., 1973).

Xyloglucan is a major hemicellulosic polysaccharide in Type I primary cell walls (Dicotyledoneae), which makes up about 20–25% (dry wt) (McNeil et al., 1984; Fry, 1989; Carpita and Gibeaut, 1993). It is also present as 2–5% of the Type II primary walls, the typical wall of Poaceae (Varner and Lin, 1989; Carpita, 1996). Xyloglucan was also found in gymnosperms (Kakegawa et al., 1998). Besides being a structural component of primary cell walls, xyloglucans play diverse important roles, namely the control of cell expansion, growth substance effects and as a reserve carbohydrate in seeds (Fry, 1989; Hayashi, 1989).

Xyloglucan is tightly bound to cellulose microfibrils by hydrogen bonds and forms a cellulose-xyloglucan network (Bauer et al., 1973; Hayashi et al., 1987; Carpita and Gibeaut, 1993). The dynamic nature of this cross-linking is proposed to be a major factor in controlling the rate of cell wall expansion, thereby regulating the plant cell wall (Bauer et al., 1973; Darvill et al., 1992). All xyloglucans, storage or structural, have a cellulosic backbone substituted at *O*-6 by α-D-xylopyranosyl units. Some xylosyl residues are further substituted at *O*-2 by β-D-galactopyranosyl units. In primary cells, some galactopyranosyl residues are substituted by fucopyranose (Fry, 1989; Carpita and Gibeaut, 1993).

Degradation and reconstruction of xyloglucan molecules, catalyzed by enzymes, such as endo-1,4-β-D-glucanases, xyloglucanases, α-L-fucosidase and xyloglucan endotransglycosylase are involved in the auxin- or acid-promoted breakdown of xyloglucans and regulate the ability to loosen the network in the cell wall and allow the cells to expand during growth (Hayashi et al., 1984; Nishitani and Tominaga, 1992; Fry et al., 1992). The nonasaccharide XXFG, an end-product of the digestion of xyloglucan by cellulase, has antiauxin activity in the pea stem segment straight-growth bioassay (York et al., 1984; McDougall and Fry, 1988). Substitution of the heptasaccharide XXXG core with one or two Gal residues to give XXLG and XLLG resulted in growth promotion

* Corresponding author. Tel.: +55-41-361-1661; fax: +55-41-266-2042.

E-mail address: reicher@bio.ufpr.br (F. Reicher).

0031-9422/01/$ - see front matter © 2001 Elsevier Science Ltd. All rights reserved.
PII: S0031-9422(01)00217-5

and *in vitro* stimulation of cellulase (McDougall and Fry, 1990). These oligosaccharides were also used to demonstrate their role as signal molecules in plant cells by ligand-binding experiments (Dunand et al., 2000).

Hymenaea courbaril, family Caesalpiniaceae, is a species that occurs abundantly throughout Brazilian forests. The seeds contain 40–45% xyloglucan, as reserve carbohydrate, whose structure consists of a cellulosic-type (1→4)-linked β-D-glucan main chain and side chains containing α-D-xylopyranosyl and β-D-galctopyranosyl-(1→2)-α-D-xylopyranosyl residues, each (1→6)-linked to the main chain (Lima et al., 1993, 1995). The ability of endoglucanase I of *Humicola insolens* to cleave the (1→4)-linked β-D-glucosyl residues of xyloglucan from *H. courbaril* seeds was carried out and the released oligomers examined in terms of their biological activity (Vargas-Rechia et al., 1998). The auxin activity of the xyloglucan oligosaccharides in their reduced form was investigated. The octasaccharide (XXLGol), at nanomolar concentrations, promoted growth of wheat coleoptiles, independent of the presence of 2,4-dichlorophenoxyacetic acid (2,4-D). In addition, a system of *Rubus fruticosus* protoplasts or cells was used to study the signalling effect of induction of glycohydrolases and significant responses were found. The octasaccharide has the ability to induce, at nanomolar concentrations, a rapid increase in a α-L-fucosidase and to modulate 2,4-D or gibberellic acid-induced α-L-fucosidase (Vargas-Rechia et al., 1998).

This paper reports the isolation, composition and structural features of *H. courbaril* leaf xyloglucan and its relation with the xyloglucan from seeds of the same species.

2. Results and discussion

2.1. Polysaccharide isolation

Powdered leaves were defatted (~20%) with ethanol, then toluene–ethanol and extracted with 2% EDTA. The residual solid was delignified with sodium chlorite–acetic acid (Wise et al., 1946) and then extracted with water. EDTA, sodium chlorite-acetic acid and water extracts were treated with ethanol, yielding fractions which were denominated EI, EII and EIII, respectively. The hemicelluloses were recovered from the residual holocellulose by sequential extraction with 1 M KOH (×3) and 4 M KOH (×3). The alkaline extracts were treated with HOAc to pH 5. No precipitation was observed due to acidification in 1 M KOH extracts, and further precipitation with ethanol gave rise to hemicellulosic fractions, denominated IHT, IIHT and IIIHT. The extracts obtained with 4 M KOH, when treated with HOAc gave rise to hemicellulose A precipitates (IHA, IIHA and IIIHA). Hemicelluloses B were isolated from the supernatant of the 4 M KOH fractions, by precipitation with EtOH (IHB, IIHB and IIIHB) (Whistler and Feather, 1965). Table 1 indicates the yield and composition of each fraction.

The protein content (Table 1) was determined using two methods and the results were significantly different. The differences are due to the interference of phenolic compounds, which react with the Folin–Ciocalteu reagent of the modified method of Lowry (Hartree, 1972). The Peterson (1977) method is also a modification of the Lowry method, but the protein is previous precipitated with sodium deoxycholate-trichloroacetic acid, so that the interfering substances remained in the supernatant. After solubilization of the protein precipitates using sodium dodecyl sulfate, the colorimetric reaction was also performed with the Folin–Ciocalteu reagent.

The fraction obtained in highest yield was IHT (14.1%, Table 1). However, its total sugar content was low and the protein content, obtained with the Hartree and Peterson methods, was 66.5 and 58.9%, respectively. The similarity of the values obtained by both methods confirms the high protein content. On the other hand, the interference of phenolic compounds was observed in EII, IHB, IIHB and IIIHB fractions.

Table 2 shows the monosaccharide composition of the fractions obtained. Fractions EI, EII and EIII are rich in uronic acid, galactose and arabinose, probably due to the presence of pectins. The sugar composition of fractions IHT, IIHT and IIIHT suggested that they contain a mixture of pectic and hemicellulosic polymers. Pectic polymers are predominant in IHT (41% uronic acid) and xylans in the other fractions (about 50% xylose).

The main monosaccharide component of hemicellulose A fractions (IHA, IIHA and IIHA) is xylose (Table 2), indicating the occurrence of xylans. The chemical structure of the first fraction (IHA) was determined (Busato et al., 2000). It is an acidic xylan, $[\alpha]_D^{25}$ −78° (0.5

Table 1
Composition of fractions obtained from the leaves of *Hymenaea courbaril*

Fraction	Extractant[a]	Yield[b] (%)	Total sugar[c] (%)	Protein[d] (%)	Protein[e] (%)
EI	2% EDTA	0.04	29.5	18.9	6.4
EII	2% $NaClO_2$	3.3	14.5	21.3	5.3
EIII	H_2O	0.4	29.1	18.1	10.9
I HT	1 M KOH	14.1	14.6	66.5	58.9
II HT	1 M KOH	2.5	23.1	49.6	35.0
III HT	1 M KOH	2.3	22.9	36.3	23.2
I HA	4 M KOH	1.7	71.7	3.9	3.5
II HA	4 M KOH	0.3	65.3	6.8	6.5
III HA	4 M KOH	0.08	53.6	6.9	3.8
I HB	4 M KOH	2.2	44.8	17.9	7.7
II HB	4 M KOH	1.4	34.7	15.8	4.1
III HB	4 M KOH	0.4	37.6	9.5	1.8

[a] At 25°C, except EII (70°C) and EIII (60°C).
[b] Based on defatted leaves.
[c] Dubois et al. (1956).
[d] Hartree (1972).
[e] Peterson (1977).

Table 2
Monosaccharide composition of fractions obtained from the leaves of *Hymenaea courbaril*

Fraction	Mol%[a]							
	Rha	Fuc	Ara	Xyl	Man	Gal	Glc	Uronic acids[b]
EI	5.4	0.4	16.3	1.8	0.5	20.6	10.9	44.1
EII	2.2	0.7	25.6	3.4	1.6	18.1	4.3	44.1
EIII	1.8	0.6	34.9	7.8	1.6	15.2	2.3	35.8
IHT	1.4	0.3	13.8	29.6	0.6	9.4	3.5	41.4
IIHT	1.6	0.5	15.0	49.1	0.6	9.5	4.4	19.3
IIIHT	1.4	0.3	13.6	50.7	1.7	8.9	2.3	21.1
IHA	0.7	–	0.6	90.4	0.2	0.6	0.4	7.1
IIHA	1.0	–	0.2	82.7	0.5	2.7	1.7	11.2
IIIHA	1.3	1.7	10.6	50.9	4.1	12.5	10.7	8.2
IHB	1.0	3.6	11.2	33.8	1.6	13.5	22.9	12.4
IIHB	2.2	1.5	23.9	6.9	1.3	22.3	8.4	23.5
IIIHB	2.0	1.4	21.8	19.8	1.4	21.3	8.5	23.8
Final residue	2.8	0.8	10.4	32.3	6.7	8.0	39.0	n.d.[c]

[a] Neutral sugar analyzed by GLC.
[b] Blumenkrantz and Asboe-Hansen (1973), based on total sugar.
[c] Not determined.

M NaOH; *c* 0.1), M_r 183,800, and is composed of a linear main chain of β-xylopyranosyl residues linked (1→4), substituted at *O*-2 with glucuronic acid and/or its 4-*O*-methyl derivative.

The final residue of alkaline extractions (28.6% yield; Table 2) contained 39.0% of glucose, probably from cellulose, and 32.3% of xylose, that indicates the presence of remaining xylans and xyloglucans.

Fraction IHB, extracted with 4 M KOH, was rich in xylose, glucose and contained fucose (Table 2), indicating the presence of xyloglucan, which could be present also as minor component in fractions IIHB and IIIHB. Most of the xyloglucan is strongly bound to cellulose and required 4 M KOH to be extracted. Once xyloglucan has been made soluble with alkali, it usually remains water-soluble even after neutralization, so that xyloglucan is a hemicellulose-B (Fry, 1989). Fraction IHB contained uronic acids (~12.4%) and was subjected to anion-exchange chromatography, in order to eliminate the acidic polymers (Table 3).

The column was eluted with water followed by saline solutions. The water-eluted fraction (52% yield; XG-1), showed Glc:Xyl:Gal:Fuc in a molar ratio of 7:5:3:1, respectively and a low amount of acidic residues (~4.1%). It was re-chromatographed on the same column. The purification steps increased the total sugar content in the purified sample, as observed in Table 3. Most protein and phenolic components were eliminated from original sample (IHB, Table 1). The protein content in the purified xyloglucan (78% yield, XG-2) was 2.3%. This fraction showed Glc:Xyl:Gal:Fuc in a molar ratio of 8:5: 2.5:1. The molar proportions are consistent with the ratio obtained for xyloglucans from other plant sources (Siddiqui and Wood, 1977; O'Neill and Selvendran, 1983; Buchala et al., 1993; Vincken et al., 1994; Cutillas-Iturralde et al., 1998).

Table 3
Fractionation of hemicellulose B (IHB) by DEAE-trisacryl

Fraction	Total sugar (%)	Mol%[a]							
		Rha	Fuc	Ara	Xyl	Man	Gal	Glc	Uronic acids[b]
IHB[c]	44.8	1.0	3.6	11.2	33.8	1.6	13.5	22.9	12.4
XG-1[d]	78.5	0.8	5.5	6.4	25.3	3.3	18.4	36.2	4.1
XG-2[e]	83.3	–	5.6	1.2	29.2	3.1	13.9	46.8	–

[a] Neutral sugar analyzed by GLC.
[b] Blumenkrantz and Asboe-Hansen (1973), based on total sugar.
[c] Original fraction.
[d] Obtained by elution of IHB with water.
[e] Obtained by rechromatography of XG-I under the same conditions.

The purified fraction also contained manosyl residues (3.1%, Table 3). The presence of mannose during xyloglucan purification has been previously described (O'Neill and Selvendran, 1983; Redgwell and Selvendran., 1986; Vincken et al., 1994,1996; Cutillas-Iturralde et al., 1998) and was said to be an impurity (Fry, 1989).

2.2. Fucosylated xyloglucan analysis

The purified xyloglucan was soluble in water. The polysaccharide showed a specific rotation of $[\alpha]_D^{25}$ + 40.5° (H_2O; *c* 0.5) that it is in close agreement with reported values for other fucosylated xyloglucans (Siddiqui and Wood, 1977; Watanabe et al., 1980).

Fraction XG-2 was analyzed by high performance size exclusion chromatography (HPSEC) with multidetection for molecular weight determination. HPSEC, using a light scattering detector, was considered by Rinaudo (1993) as the only valid method to characterize polysaccharides over a wide range of molecular weights. The molecular weight (M_r) of XG-2 fraction is 49,500 by this method. The elution profile of xyloglucan indicates its homogeneity (Fig. 1).

The purified xyloglucan was subjected to methylation analysis (Ciucanu and Kerek, 1984), and the results are shown in Table 4. The overall recoveries of methylated alditol acetates (Glc: Xyl: Gal: Fuc ratio 8: 4: 2: 1) were in good agreement with the ratio found for the original polysaccharide after hydrolysis, reduction and acetylation. The methylation analysis data show that the polysaccharide has a highly branched structure. The results suggest that the xyloglucan contains a (1→4)-glucan backbone, ~60% of the units of which were substituted at *O*-6. Terminal fucose, galactose and xylose both substituted at *O*-2 are present, suggesting the presence of Fuc*p*-(1→2)-Gal*p*(1→2)-Xyl*p*-(1→ as a side chain, and all sugars are in the pyranose form. The peak whose retention time is 737 s (Table 4) could be also, under the

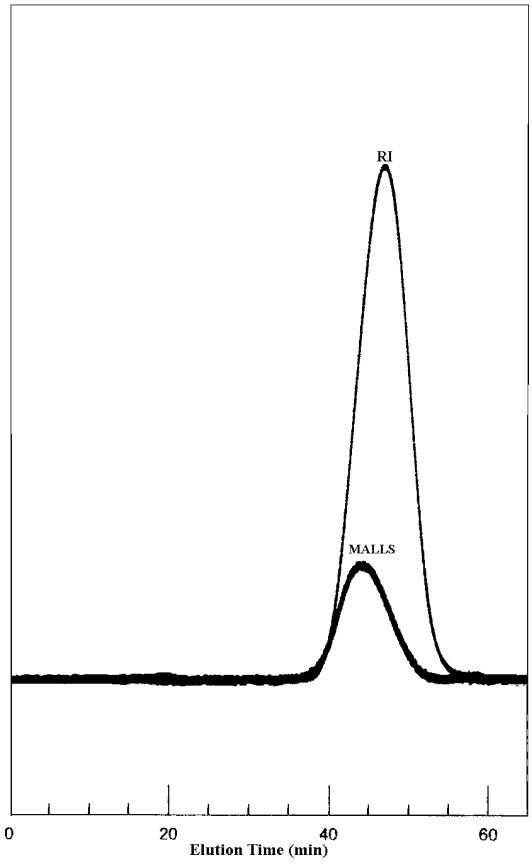

Fig. 1. High performance size exclusion chromatography (HPSEC) of the fraction XG-2, with light scattering (MALLS) and refractive index (RI) detection.

experimental conditions used, 2,3-Me_2Xyl, indicating 4-*O*-substituted xylopyranosyl or 5-*O*-substituted xylofuranosyl residues. However, this is not likely.

These data are consistent with those found for xyloglucans from other plant sources (Siddiqui and Wood, 1977; O'Neil and Selvendran, 1983, 1985; Stevens and Selvendran, 1984; Redgwell and Selvendran, 1986; Mabusela et al., 1990; Renard et al., 1992; Buchala et al., 1993; Vincken et al., 1994; Cutillas-Iturralde et al., 1998). In addition small amounts of 2,3,6-Me_3Gal and traces of 2,3,4-Me_3Glc were detected.

Table 4
Methylation analysis of xyloglucan (XG-2) from the leaves of *Hymenaea courbaril*

O-Methylated alditol acetate[a]	Linkage indicated	Mol%	RT[a]
2,3,4-Me_3Xyl	(Xyl*p*)1→	12.9	545
2,3,4-Me_3Fuc	(Fuc*p*)1→	6.5	552
2,3,4,6-Me_4Glc	(Glc*p*)1→	1.2	704
2,3,4,6-Me_4Gal	(Gal*p*)1→	3.9	711
3,4-Me_2Xyl	→2(Xyl*p*)1→	14.1	737
3,4,6-Me_3Gal	→2(Gal*p*)1→	7.3	864
2,3,6-Me_3Gal	→4(Gal*p*)1→	3.5	875
2,3,6-Me_3Glc	→4(Glc*p*)1→	17.2	888
2,3,4-Me_3Glc	→6(Glc*p*)1→	1.6	1009
2,3-Me_2Glc	→4(Glc*p*)1→ 6 ↑	31.8	1316

[a] Retention time in s.

Fig. 2 shows the ^{13}C NMR spectra of XG-2 fraction. In Table 5, the anomeric carbon chemical shifts of XG-2 are compared with those of xyloglucan obtained from the seeds of *H. courbaril* (Buchala et al., 1993; Lima et al., 1993). The well-defined anomeric signals at about 104.4, 102.4, 99.4, 98.9 ppm are attributed to terminal β-galactopyranosyl, β-glucopyranosyl and terminal and internal α-xylopyranosyl residues respectively. The anomeric carbon chemical shifts of XG-2 are compared with those of xyloglucan from the seeds (Lima et al., 1993) and they are closely related (Table 5). The other signals present in the anomeric region of ^{13}C NMR spectrum of the leaf xyloglucan, were not found in that of seeds. These are attributed to internal β-galactose and α-fucose, confirming the presence of Fuc*p*-(1→2)-Gal*p*(1→2)-Xyl*p*-(1→ as a side chain. It was also possible to distinguish signals from the C-4 and C-6 substituted β-glucopyranosyl residues at about 79.9 and 66.3 ppm respectively, and the latter is inverted in ^{13}C DEPT spectrum. The other signals that are inverted in ^{13}C DEPT spectra, between 61.6 and 60.2 ppm can be assigned to C-6 of β-galactopyranosyl, C-5 of α-xylopyranosyl and C-6 of β-glucopyranosyl units. The signal at high field (15.8 ppm) arises from C-6 of fucopyranosyl residues.

The structure of the xyloglucan from the leaves of *H. courbaril* is broadly typical of those xyloglucans detected in primary cell walls of other plants. It has a cellulosic backbone which is highly substituted at *O*-6 with D-xylopyranosyl residues, about a half of which are substituted by D-galactopyranosyl residues at *O*-2. Some of the galactosyl residues are further substituted at *O*-2 by L-fucose. The two most abundant subunits of type I cell wall xyloglucans are the nonasaccharide, XXFG, and the heptasaccharide, XXXG (Bauer et al., 1973; Hayashi et al., 1984; Guillén et al., 1995). However, the presence of a well-defined anomeric signal of terminal β-galactopyranose at ~104.4 ppm (Fig. 2, Table 5) could indicate that the xyloglucan from the

Table 5
Comparison of C-1 chemical shifts (δ) of ^{13}C NMR spectra for XG-2 fraction and xyloglucan from the seeds of *Hymenaea courbaril*[a]

	δ (ppm)	
C-1	Fraction XG-2	Seeds xyloglucan
Terminal β-D-galactose	104.4	104.5
Internal β-D-galactose	103.2	–
β-D-Glucose	102.4	102.5
α-L-Fucose	101.6	–
Terminal α-D-xylose	99.4	99.1
Internal α-D-xylose	98.9	98.7

[a] Lima et al. (1993).

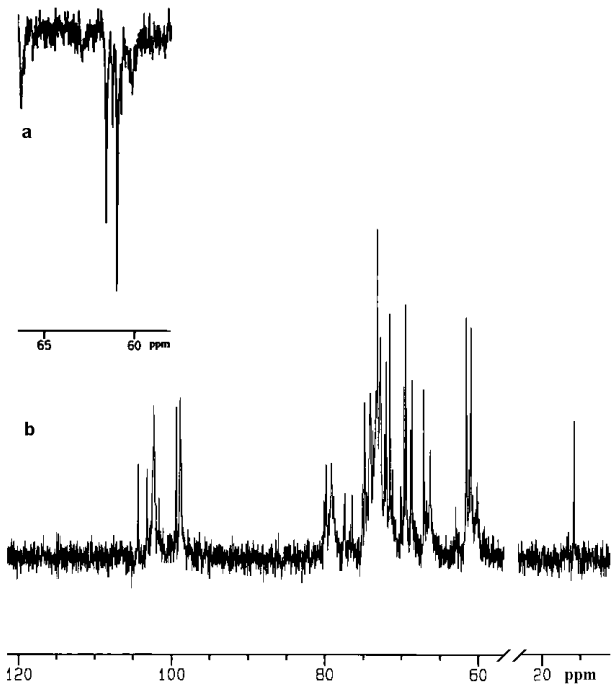

Fig. 2. (a) ^{13}C DEPT and (b) ^{13}C NMR spectrum of fraction XG-2 in D_2O, 50°C.

leaves of *H. courbaril* is also composed of some decasaccharide XLFG and/or nonasaccharide XLLG, in addition to XXFG and XXXG. These will be confirmed by future characterization of the oligosaccharides.

Comparative analysis of xyloglucans from seeds and leaf of *H. courbaril* gives rise results which are compatible with their functions, such as the differences observed in the M_r 300,000 for the polysaccharide from the seeds (Lima et al., 1993) and 49,500 for that obtained from the leaves. Another difference was observed in the $[\alpha]_D^{25}$ value, that was $+79.3°$ for the seeds xyloglucan (Lima et al., 1993) and $+40.5°$ for the leaf xyloglucan. The lower value obtained for the latter is probably due to the presence of α-L-fucosyl residues.

3. Experimental

3.1. General experimental procedures

Specific rotation was obtained, from a 0.5% solution, in water at 25°C, using an Autopol III automatic polarimeter.

Uronic acid was estimated according Blumenkrantz and Asboe-Hansen (1973), using galacturonic or glucuronic acids as standards. Total carbohydrate was determinated by the PhOH–H_2SO_4 method (Dubois et al., 1956), using glucose as standard, and protein content by the Hartree (1972) and Peterson (1977) methods, using BSA as standard.

Polysaccharide fractions were hydrolyzed with M TFA (5 h, at 100°C), except final residue with 72% H_2SO_4 (1 h, at 0°C) and then diluted to 8% (5 h, at 100°C) (Saeman et al., 1954). After removal of acid, monosaccharides were reduced with $NaBH_4$ and acetylated with Ac_2O–pyridine (1:1 v/v, 16 h, at 25°C). The resulting alditol acetates were analyzed by GLC, using a 5890 A II HP gas chromatograph at 220°C (FID and injector temperature, 250°C) with DB-210 capillary column (0.25 mm i.d.×30 m), film thickness 0.25 μm, the carrier gas being N_2 (2.0 ml/min).

The xyloglucan was methylated according to Ciucanu and Kerek (1984). The procedure was repeated until the products did not show OH absorption in the IR at 3400 cm^{-1}. The methylated polysaccharide was refluxed with 3% MeOH–HCl for 2 h and then hydrolyzed with 0.5 M H_2SO_4 (14 h, at 100°C). The resulting mixtures of *O*-methylated aldoses were reduced with $NaBH_4$ and then acetylated. The partially *O*-methylated alditol acetates were analyzed by capillary GC–MS, using a 3300 Varian gas chromatograph linked to an 810 R-12 Finnigan ion-trap mass spectrometer, using He as the carrier gas (2.0 ml/min). A capillary column of DB-210 (0.25 mm i.d.×30 m) was used. The former was held at 50°C during injection and then programmed at 40°C/min to 220°C (constant temperature).

The ^{13}C NMR and ^{13}C DEPT spectra were obtained with a DRX-400 Bruker spectrometer at 100 MHz in the Fourier transform mode, with complete proton decoupling at 50°C, using D_2O as solvent, contained in a tube of 0.5 cm i.d. Chemical shifts are reported as δ (ppm) relative to the resonance of DDS (sodium 4,4-dimethyl-4-silopentano-1-sulphonate), used as a internal standard ($\delta = 0$). The spectral width was 200 ppm.

High pressure size exclusion chromatography (HPSEC) was carried out on 5 mg/ml XG-2 fraction solutions, using a multidetection equipment in with a Waters 2410 differential refractometer (RI) and a Wyatt Technology Dawn F multi-angle laser light scattering (MALLS) detector were adapted on-line. Four Waters Ultrahydrogel 2000/500/250/120 columns were connected in series and coupled to the multidetection equipment. A 0.1 M $NaNO_3$ solution, containing NaN_3 (0.5 g/l), was used as eluent. The refractive index increment was determined by using a refractive index detector. The value of dn/dc (differential refractive index increment of the solvent-solute solution with respect to a change in solute concentration) was 0.172 at 633 nm.

3.2. Plant material

Hymenaea courbaril leaves were collected in August 1997, from the campus of the University of São Paulo, Ribeirão Preto, Brazil, where a voucher specimen is deposited in the Herbarium (SPFR), under the number 05312.

3.3. Polysaccharide extraction

Dry leaves (100 g) were triturated and extracted successively with absolute EtOH (170 h) and C_6H_5–CH_3:EtOH (2:1, 48 h) in a Soxhlet. The remaining solid material (80 g) was extracted with 2% EDTA (3 h, at 25°C), delignified with 2% aq. $NaClO_2$ and HOAc (6 h, at 70°C, pH 4) (Wise et al., 1946) and was submitted to aq. extraction at 60°C (6 h). The extracts were neutralized with 50% (v/v) HOAc, completely dialyzed against H_2O when necessary, conc., and pptd. with EtOH. The extracts were solubilized with H_2O and freeze-dried. The resulting holocellulose was then sucessively treated with 1 M KOH and 10 mM $NaBH_4$ (8 h, at 25°C, under a N_2 atmosphere, ×3). The alkaline extracts were adjusted with 50% (v/v) HOAc to pH 5, and then pptd. with EtOH, yielding IHT, IIHT and IIIHT fractions. The residue of 1M KOH extraction were treated with 4 M KOH and 10 mM $NaBH_4$ (8 h, at 25°C, under a N_2 atmosphere, ×3). The 4 M KOH extracts were acidified to pH 5 with 50% (v/v) HOAc, giving rise to hemicellulose A precipitation (IHA, IIHA and IIIHA fractions). Supernatants were dialysed against running water and treated with ethanol, giving rise to precipitation of hemicellulose B fractions, namely IHB, IIHB and IIHB (Whistler and Feather, 1965).

3.4. Xyloglucan isolation

Ion-exchange chromatography of the IHB fraction was carried out on a DEAE-Trisacryl (chloride form) column (23 × 0.8 cm) and eluted successively with H_2O, 0.5, 1 and 2 M NaCl, and 0.5 M NaOH. The collected fractions were analyzed for total sugar (Dubois, et al., 1956). After dialysis, polysaccharide fractions were recovered by pptn. with EtOH, solubilized with H_2O and then freeze-dried. The fraction eluted with H_2O (XG-1) was further purified by fractionation on the same column.

Acknowledgements

Financial support was provided by Conselho Nacional de Desenvolvimento Científico e Tecnológico (Brazil), Pronex-Carboidratos and the Universidade Federal do Paraná.

References

Bauer, W.D., Talmadge, K.W., Keegstra, K., Albersheim, P., 1973. The structure of plant cell walls. II. The hemicellulose of the walls of suspension-cultured sycamore cells. Plant Physiol. 51, 174–187.

Blumenkrantz, N., Asboe-Hansen, G., 1973. New method for quantitative determination of uronic acids. Anal. Biochem. 54, 484–489.

Buchala, A.J., Genoud, T., Roulin, S., Summermatter, K., 1993. Xyloglucans in different typs of cotton (*Gossypium* sp.) cells. Acta Bot. Neerl. 42, 213–219.

Busato, A.P., Vargas-Rechia, C.G., Reicher, F., 2000. Acidic xylan from the leaves of *Hymenaea courbaril*. In: Mattoso, L.H.C., Leão, A., Frollini, E. (Eds.), Natural Polymers and Composites. Embrapa, São Carlos-SP, Brazil, pp. 157–161.

Carpita, N.C., 1996. Structure and biogenesis of the cell wall of grasses. Annu. Rev. Plant Physiol. Plant Mol. Biol. 47, 445–476.

Carpita, N.C., Gibeaut, D.M., 1993. Structural models of primary cell walls in flowering plants: consistency of molecular structure with the physical properties of the walls during growth. Plant J. 3, 1–30.

Ciucanu, I., Kerek, V., 1984. A simple and rapid method for the permethylation of carbohydrates. Carbohydr. Res. 131, 209–217.

Cutillas-Iturralde, A., Peña, M.J., Zarra, I., Lorences, E.P., 1998. A xyloglucan from persimmon fruit cell walls. Phytochemistry 48, 607–610.

Darvill, A.G., Augur, C., Bergmann, C., Carlson, R.W., Cheong, J.-J., Eberhard, S., Hahn, M.G., Ló, V.-M., Marfá, V., Meyer, B., Mohnen, D., O'Neil, M.A., Spiro, M.D., VanHalbeek, H., York, W.S., Albersheim, P., 1992. Oligosaccharins-oligosaccharides that regulate growth, development and defence responses in plants. Glycobiology 2, 181–198.

Dubois, M., Gilles, K.A., Hamilton, J.K., Rebers, P.A., Smith, F., 1956. Colorimetric method for determination of sugars and related substances. Anal. Chem. 28, 350–356.

Dunand, C., Gautier, C., Chambat, G., Liénart, Y., 2000. Characterization of the binding of α-L-Fuc(1→2)-β-D-Gal(1→), a xyloglucan signal, in blackberry protoplasts. Plant Sci. 151, 183–192.

Fry, S.C., 1989. The structure and functions of xyloglucan. J. Exp. Bot. 40, 1–11.

Fry, S.C., Smith, R.C., Renwick, K.F., Martin, D.J., Hodge, S.K., Matthews, K.J., 1992. Xyloglucan endotransglycosylase, a new wall-loosening enzyme activity from plants. Biochem. J. 282, 821–828.

Guillén, R., York, W.S., Pauly, M., An, J., Impallomeni, G., Albersheim, P., Darvill, A.G., 1995. Metabolism of xyloglucan generates xylose-deficient oligosaccharide subunits of this polysaccharide in etiolated peas. Carbohydr. Res. 277, 291–311.

Hartree, E.F., 1972. Determination of protein: a modification of the Lowry method that gives a linear photometric response. Anal. Biochem. 48, 422–427.

Hayashi, T., 1989. Xyloglucans in the primary cell wall. Annu. Rev. Plant Physiology. Plant Mol. Biol. 40, 139–168.

Hayashi, T., Marsden, M.P.F., Delmer, D.P., 1987. Pea xyloglucan and cellulose. V. Xyloglucan-cellulose interactions in vitro and in vivo. Plant Physiol. 83, 384–389.

Hayashi, T., Wong, Y.-S., MacLachlan, G., 1984. Pea xyloglucan and cellulose. II. Hydrolysis by pea endo-1,4-β-glucanases. Plant Physiol. 75, 605–610.

Kakegawa, K., Edashige, Y., Ishi, T., 1998. Xyloglucan from xylem-differentiating zones of *Cryptomeria japonica*. Phytochemistry 47, 767–771.

Keegstra, K., Talmadge, K.W., Bauer, W.D., Albersheim, P., 1973. Structure of plant cell walls. III. A model of the walls of suspension-cultured sycamore cells based on interconnections of the macromolecular components. Plant Physiol. 51, 188–197.

Lima, N.N., Reicher, F., Corrêa, J.B.C., Ganter, J.L.M.S., Sierakowski, M.-R., 1993. Partial structure of a xyloglucan from the seeds of *Hymenaea courbaril* var. *stilbocarpa* (jatobá). Cien. Cult. 45, 22–26.

Lima, N.N., Reicher, F., Corrêa, J.B.C., Ganter, J.L.M.S., Sierakowski, M.-R., 1995. Oligosaccharides derived from the xyloglucan from the seeds of *Hymenaea coubaril* var. stilbocarpa. Int. J. Biol. Macromol. 17, 413–415.

Mabusela, W.T., Stephen, A.M., Botha, M.C., 1990. Carbohydrate polymers from *Aloe ferox* leaves. Phytochemistry 29, 3555–3558.

McCann, M.C., Roberts, K., Wilson, R.H., Gidley, M.J., Gibeaut, D.M., Kim, J-B., Carpita, N.C., 1995. Old and new ways to probe plant cell-wall architecture. Can. J. Bot. 73, 103–113.

McDougall, G.J., Fry, S.C., 1988. Inhibition of auxin-stimulated growth of pea stem segments by a specific nonasaccharide of xyloglucan. Planta 175, 412–416.

McDougall, G.J., Fry, S.C., 1990. Xyloglucan oligosaccharides promote growth and activate cellulase: evidence for a role of cellulase in cell expansion. Plant Physiol. 93, 1042–1048.

McNeil, M., Darvill, A.G., Fry, S.C., 1984. Structure and function of the primary cell walls of plants. Annu. Rev. Biochem. 53, 625–663.

Nishitani, K., Tominaga, R.J., 1992. Endo-xyloglucan transferase, a novel class of glycosyltransferase that catalyses transfer of a segment of xyloglucan molecule to another xyloglucan molecule. J. Biol. Chem. 267, 21058–21064.

O'Neill, M.A., Selvendran, R.R., 1983. Isolation and partial characterization of a xyloglucan from the cell walls of *Phaseolus coccineus*. Carbohydr. Res. 111, 239–255.

O'Neill, M.A., Selvendran, R.R., 1985. Structural analysis of the xyloglucan from *Phaseolus coccineus* cell-walls using cellulase-derived oligosaccharides. Carbohydr. Res. 145, 45–58.

Peterson, G.L., 1977. A simplification of the protein assay method of Lowry et al. which is more generally applicable. Anal. Biochem. 83, 346–356.

Redgwell, R.J., Selvendran, R.R., 1986. Structural features of cell-wall polysaccharides of onion *Allium cepa*. Carbohydr. Res. 157, 183–199.

Renard, C.M.G.C., Lomax, J.A., Boon, J.J., 1992. Apple fruit xyloglucans: a comparative study of enzyme digests of whole cell walls and alkali-extracted xyloglucans. Carbohydr. Res. 232, 303–320.

Rinaudo, M., 1993. Polysaccharide characterization in relation with some original properties. J. Appl. Poly. Sci.: Appl. Polym. Sympos. 52, 11–17.

Saeman, J.F., Moore, W.E., Mitchell, R.L., Millet, M.A., 1954. Techniques for determination of pulp constituents by quantitative paper chromatography. Tech. Assoc. Pulp. Pap. Ind. 37, 336–343.

Schindler, T.M.Z., 1998. The new view of primary cell wall. Pflanzenernähr. Bodenk. 161, 499–508.

Siddiqui, I.R., Wood, P.J., 1977. Structural investigation of sodium hydroxide-soluble rapeseed (*Brassica campestris*) polysaccharides. Carbohydr. Res. 53, 85–94.

Stevens, B.J.H., Selvendran, R.R., 1984. Hemicellulosic polymers of cabbage leaves. Phytochemistry 23, 339–347.

Vargas-Rechia, C., Reicher, F., Sierakowski, M.R., Heyraud, A., Driguez, H., Liénart, Y., 1998. Xyloglucan octasaccharide XXLGol derived from the seeds of *Hymenaea courbaril* acts as a signaling molecule. Plant Physiol. 116, 1013–1021.

Varner, J.E., Lin, L.-S., 1989. Plant cell architecture. Cell 56, 231–239.

Vincken, J.P., Beldman, G., Voragen, A.G.J., 1994. The effect of xyloglucans on the degradation of cell-wall-embedded cellulose by the combined action of cellobiohydrolase and endoglucanases from *Trichoderma viride*. Plant Physiol. 104, 99–107.

Vincken, J.P., Wijsman, A.J.M., Beldman, G., Niessen, W.M.A., Voragen, A.G.J., 1996. Potato xyloglucan is built from XXGG-type subunits. Carbohydr. Res. 288, 219–232.

York, W.S., Darvill, A.G., Albersheim, P., 1984. Inhibition of 2,4-dichlorophenoxyacetic acid-stimulated elongation of pea stem segments by a xyloglucan nonasaccharide. Plant Physiol. 75, 295–297.

Watanabe, T., Takahashi, K., Matsuda, K., 1980. Isolation and characterization of oligosaccharides from purified cellulase digest of jojoba (*Simmondsia chinensis*) seed xyloglucan. Agric. Biol. Chem. 44, 791–797.

Whistler, R.L., Feather, M.S., 1965. Extraction from annual plants with alkaline solutions. Methods Carbohydr. Chem. 5, 144–145.

Wise, L.E., Murphy, M., D'Addieco, A., 1946. Chlorite holocellulose, its fractionation and bearing on summative wood analysis and on studies on the hemicelluloses. Paper Trade J. 122, 35–46.

PERGAMON

Phytochemistry 58 (2001) 533–535

PHYTOCHEMISTRY

www.elsevier.com/locate/phytochem

Book reviews

Basil. The Genus *Ocimum*

R. Hiltunen and Y. Holm (Eds.). Harwood Academic Publishers, Amsterdam, 1999. 182 pp., ISBN 90-5702-432-2, EUR 66, £49 or $80

The last couple of decades have seen a surge of interest in medicinal and aromatic plants by industry, life and health sciences and the general public. However, the information on the ethnobotany, cultivation and processing of these plants is scattered in the scientific literature. For this reason, Harwood Academic Publishers have brought out a series of Industrial Profiles, which aim to provide an in-depth coverage of the major medicinal and aromatic plants that are of industrial importance. I was asked to give my views on Volume 10, *Basil. The genus Ocimum*. Several species of this genus in the plant family Lamiaceae (Labiatae) are economically important because of the production of essential oils, especially *Ocimum basilicum, O. americanum, O. x citriodorum* and *O. gratissimum*, and they also have been used medicinally for a large number of ailments and as insect repellents. Although the cultivation of basil is usually associated with warm climates such as India, Africa and the Mediterranean, the book is edited and most chapters are written by Finnish scientists. However, many species of basil can be successfully cultivated in greenhouse conditions in colder climates, and research teams in Finland have studied the cultivation and essential oils of basil plants for many years.

Estimates of the number of species in the genus vary widely, from 30 to 160. Industrial and economic papers on basil frequently do not follow the International Code of Botanical Nomenclature, and the same species is often referred to by more than one name. For this reason, the first chapter of the book is a useful overview of the classification and relationships of the genus, written by Kew taxonomists A. Paton, R. Harley and M. Harley. According to their treatment the genus now comprises 65 species. They also provide a key to all these species together with their geographic distribution, habitat and synonyms. Unfortunately, some other authors of the book do not seem to have read this chapter before submitting their manuscripts. For instance, they write about *O. sanctum* without referring to its correct name *O. tenuiflorum,* although this has been the botanically accepted name for the species for quite some time.

Many aspects of the production systems of basil are described in Chapter 2 by experts E. Putievski (Israel) and B. Galambosi (Finland), including ecology, propagation and pests and diseases. In the next three chapters, the editors R. Hiltunen and Y. Holm write about the chemical composition of the *Ocimum* species, their essential oils and bioactivity. For most readers of *Phytochemistry* these chapters will probably be the most interesting. All the different oils detected in the various species are described, including monoterpenoids, sesquiterpenoids and phenylpropanoids. The phenomenal number of different chemotypes found in the various species, especially *O. basilicum, O. americanum* and *O. gratissimum*, are also listed here and so is the variation in oil composition due to the environment. Medicinal and insect-deterrent properties of *Ocimum* species may be due to a large extent to the essential oils, although few of the other constituents in *Ocimum* have been investigated for their bioactivity. The chapter about these other types of compounds in *Ocimum* species, e.g. flavonoids, is already slightly out of date, as this area is currently actively explored by a number of research groups including our own. In the sixth and last chapter, S.M. Mäkinen and K.K. Pääkkönen give an interesting overview of the processing and use of basil in food.

I was not disappointed by the current volume, and found a lot of new information. The scientific level is much higher than that of most books on herbs, their constituents and uses. I would therefore like to recommend it to all researchers and graduates in botany, phytochemistry, pharmacognosy, agronomy, pharmacology and medicine interested in the subject, especially because the price of the book is quite reasonable.

Renée J. Grayer
Jodrell Laboratory
Royal Botanic Gardens, Kew
Richmond, Surrey TW9 3AB, UK
E-mail address: r.grayer@rbgkew.org.uk

PII: S0031-9422(01)00229-1

Ginseng: The Genus *Panax* Medicinal and Aromatic Plants—Industrial Profiles
Vol. 15, Edited by William E. Court, Harwood Academic Publishers, Amsterdam, The Netherlands, 2000. 266 + x pp. ISBN 90-5823-034-1. $95, £64, €86

This monograph is a superbly written treatise in the very important series on medicinal and aromatic plants from Harwood Academic. The overall series editor is Roland Hardman, and immense credit is due him for the selection of the overall editors of these monographs. In this case, the editor of the volume, William Court, is also the sole author of all but one of the ten chapters, and the result is an extraordinary effort.

Even thinking about writing a comprehensive volume on ginseng makes my head ache. This is a truly vast field of study, and much of the older literature is in the Korean, Chinese, and Japanese primary literature, and thus quite difficult to access. Consequently, an appreciation of these studies on this plant in its various forms, and its profound significance and almost mythical powers over the millennia, is more laborious than some of the other monographs. Anyone going to Korea for the first time can only be awed by the enormous commercial displays in department stores of this, the emperor of medicinal plants. These exhibits of the bottled, magnificently prepared, roots of ginseng, each costing thousands of dollars, and almost imitating the displays of fine, rare wine one might see in Europe, offers a new perspective on both the power of the doctrine of signatures and the deep cultural reverence this plant engenders.

This volume addresses the science behind the myths. Is ginseng a panacea? Does it really have anti-aging and anti-stress properties? Is the older root material more potent that the younger? Are all of the active compounds to be found in an aqueous extract? Can the various ginsengs in use be distinguished chemically?

Following an introductory chapter there is a botanical overview of the genus *Panax*, a chapter on the specialized growth and cultivation of ginseng, one on the tissue culture of ginseng by Čellárová and Kimáková and an overview of the substantial chemistry of the genus, highlighting the differences between the various species that are grown in the countries of eastern Asia. A thorough discussion of the pharmacology and therapeutics of ginseng is followed by an overview of the side effects of ginseng, and then there is a terrific compilation of the patents associated with ginseng. Finally, there are the other "ginsengs", those plants which in various systems of traditional medicine have been borrowing the claim to fame of ginseng, perhaps the most famous of which is *Eleutherococcus senticosus*, Siberian ginseng. The volume concludes with an index of author names and a general index. Each chapter is fully referenced.

Overall, the production values are high and there are a number of very attractive color plates of ginseng and its cultivation and propagation. The printing is clear and attractive, and the paper is of good quality. However, there are some irritating aspects which detract somewhat from the volume. Many of the structures in the chemistry chapter are of surprisingly poor quality and very difficult to read, and there is a substantial absence of commas, making for some long and awkward sentences. Most surprisingly, the volume I received had a number of pages which were completely out of sequence! On the other hand, the critical reviews of this field make for fascinating reading and consequently, this volume is recommended for all chemical libraries, and also for anyone interested in learning about this important genus of medicinal plants.

Geoffrey A. Cordell
College of Pharmacy
University of Illinois at Chicago
Chicago, IL 60612, USA
E-mail address: cordell@uic.edu

PII: S0031-9422(01)00227-8

Tea Tree—The Genus *Melaleuca*
Edited by Ion Southwell and Robert Lowe, Harwood Academic Publishers, The Netherlands, 1999, 285 pp., ISBN 9057024179

Interest in medicinal and aromatic plants is increasing in the pharmaceutical, cosmetic, and perfume industries as well as at universities and in the field of medicine. These plants yield, for example, gums, resins, essential oils, juices, and secondary metabolites (e.g. flavonoids, alkaloids, terpenes) which can be used in medicines and fragrances. All these natural products are available in international trade.

In the last ten years **tea tree oil** (TTO), as a naturally occurring agent, has become increasingly more popular for a wide range of health care products. To all appearances, the name **tea tree** arose when Captain James Cook, on his exploratory voyage to Australia in 1770, encountered a myrtaceous shrub (possibly a *Leptospermum* species) with leaves that were used by his sailors as a substitute for tea (*Camellia sinensis*). Today a variety of myrtaceous shrubs derived from the genera *Leptospermum*, *Melaleuca* and

Kunzea are collectively termed tea tree. All these myrtaceous shrubs produce an essential oil in their leaves known as tea tree oil. Throughout the present book "**Tea Tree—The Genus *Melaleuca***", the term "**tea tree oil**" is reserved for "Oil of Melaleuca — Terpinen-4-ol Type," which is derived from *Melaleuca alternifolia*, *M. linariifolia*, *M. dissitiflora* and other species of *Melaleuca*.

About 230 species of *Melaleuca* are known in the world. The most well-known is *Melaleuca alternifolia,* which, like most other *Melaleuca* species, is indigenous to Australia. Some *Melaleuca* species also come from neighboring regions in Indonesia and Papua New Guinea. Typically, the paper-like bark of the trees can be pulled off in large strips. Australian beekeepers are very fond of the blossoms (flowers) as the honey from these flowers is excellent. The leaves of most of the species contain essential oil.

Because of its antimicrobial activity against a wide range of bacteria and fungi, TTO is increasingly being used in cosmetics and other health care products as well as in nursing and traditional medical treatments. Clinical data have also shown beneficial effects in treating acne vulgaris, onychomycosis, and Tinea pedis. On the other hand, undesirable side effects such as allergic contact dermatitis or local skin irritations associated with the use of TTO have also been reported. It is assumed that oxidized monoterpenes are the sensitizing agents of the oil.

Various aspects of *Melaleuca* research are discussed in the present volume, which contains 16 chapters written by competent experts in the field of tea tree oil research. The primary focus of the individual contributions, which are based on the scientific literature up to 1998, is the commercially most important species *Melaleuca alternifolia*. A discussion of the botanic aspects of the plant and a systematic distinction from other *Melaleuca* species as well as the cultivation and diseases and their treatment have been included. Furthermore, production, distillation, analysis, and chemical structure of the essential oil of *M. alternifolia* and the toxicological and medical aspects of its use are presented. Aspects of marketing conclude the discussion of *M. alternifolia*. Fortunately, the authors (editors) have included a discussion of side effects which can develop as a result of uncritical use of the essential oil. They describe dermatotoxicologic and allergic reactions which can occur with the use of undiluted TTO or its use over longer periods of time.

In two chapters towards the end of the book, cajuput oil (derived from *M. cajuputi)* and naiouli oil (from *M. quinquenervia*) are discussed. Both of these essential oils are commercially available; however, they do not have the same economic value as the essential oil from *M. alternifolia*. In the last chapter the editors also present botanical and chemical data on other *Melaleuca* species (about 16) which could potentially be commercially produced.

The book is suitable for use both by the various industries (for example, the pharmaceutical, cosmetics, and perfume industries) and in academic research at universities. It contains good illustrations, informative tables, and a comprehensive index. The extensive list of references provides both expert and newcomer alike with a complete survey of the subject and also lends itself to a more intensive study of particular topics. The book can be recommended to all interested readers with no reservations.

Jürgen Reichling
Institute of Pharmaceutical Biology
INF 364, 69120
Heidelberg, Germany
E-mail address: juergen.reichling@tonline.de

PII: S0031-9422(01)00228-X

Ginseng: The Genus *Panax* Medicinal and Aromatic Plants—Industrial Profiles
Vol. 15, Edited by William E. Court, Harwood Academic Publishers, Amsterdam, The Netherlands, 2000. 266 + x pp. ISBN 90-5823-034-1. $95, £64, €86

This monograph is a superbly written treatise in the very important series on medicinal and aromatic plants from Harwood Academic. The overall series editor is Roland Hardman, and immense credit is due him for the selection of the overall editors of these monographs. In this case, the editor of the volume, William Court, is also the sole author of all but one of the ten chapters, and the result is an extraordinary effort.

Even thinking about writing a comprehensive volume on ginseng makes my head ache. This is a truly vast field of study, and much of the older literature is in the Korean, Chinese, and Japanese primary literature, and thus quite difficult to access. Consequently, an appreciation of these studies on this plant in its various forms, and its profound significance and almost mythical powers over the millennia, is more laborious than some of the other monographs. Anyone going to Korea for the first time can only be awed by the enormous commercial displays in department stores of this, the emperor of medicinal plants. These exhibits of the bottled, magnificently prepared, roots of ginseng, each costing thousands of dollars, and almost imitating the displays of fine, rare wine one might see in Europe, offers a new perspective on both the power of the doctrine of signatures and the deep cultural reverence this plant engenders.

This volume addresses the science behind the myths. Is ginseng a panacea? Does it really have anti-aging and anti-stress properties? Is the older root material more potent that the younger? Are all of the active compounds to be found in an aqueous extract? Can the various ginsengs in use be distinguished chemically?

Following an introductory chapter there is a botanical overview of the genus *Panax*, a chapter on the specialized growth and cultivation of ginseng, one on the tissue culture of ginseng by Čellárová and Kimáková and an overview of the substantial chemistry of the genus, highlighting the differences between the various species that are grown in the countries of eastern Asia. A thorough discussion of the pharmacology and therapeutics of ginseng is followed by an overview of the side effects of ginseng, and then there is a terrific compilation of the patents associated with ginseng. Finally, there are the other "ginsengs", those plants which in various systems of traditional medicine have been borrowing the claim to fame of ginseng, perhaps the most famous of which is *Eleutherococcus senticosus*, Siberian ginseng. The volume concludes with an index of author names and a general index. Each chapter is fully referenced.

Overall, the production values are high and there are a number of very attractive color plates of ginseng and its cultivation and propagation. The printing is clear and attractive, and the paper is of good quality. However, there are some irritating aspects which detract somewhat from the volume. Many of the structures in the chemistry chapter are of surprisingly poor quality and very difficult to read, and there is a substantial absence of commas, making for some long and awkward sentences. Most surprisingly, the volume I received had a number of pages which were completely out of sequence! On the other hand, the critical reviews of this field make for fascinating reading and consequently, this volume is recommended for all chemical libraries, and also for anyone interested in learning about this important genus of medicinal plants.

Geoffrey A. Cordell
College of Pharmacy
University of Illinois at Chicago
Chicago, IL 60612, USA
E-mail address: cordell@uic.edu

PII: S0031-9422(01)00227-8

Tea Tree—The Genus *Melaleuca*
Edited by Ion Southwell and Robert Lowe, Harwood Academic Publishers, The Netherlands, 1999, 285 pp., ISBN 9057024179

Interest in medicinal and aromatic plants is increasing in the pharmaceutical, cosmetic, and perfume industries as well as at universities and in the field of medicine. These plants yield, for example, gums, resins, essential oils, juices, and secondary metabolites (e.g. flavonoids, alkaloids, terpenes) which can be used in medicines and fragrances. All these natural products are available in international trade.

In the last ten years **tea tree oil** (TTO), as a naturally occurring agent, has become increasingly more popular for a wide range of health care products. To all appearances, the name **tea tree** arose when Captain James Cook, on his exploratory voyage to Australia in 1770, encountered a myrtaceous shrub (possibly a *Leptospermum* species) with leaves that were used by his sailors as a substitute for tea (*Camellia sinensis*). Today a variety of myrtaceous shrubs derived from the genera *Leptospermum*, *Melaleuca* and

PERGAMON

Phytochemistry 58 (2001) 537–542

PHYTOCHEMISTRY

www.elsevier.com/locate/phytochem

Cardiac glycosides from *Cryptostegia grandiflora*

M.S. Kamel[a,*], M.H. Assaf[a], Y. Abe[b], K. Ohtani[b], R. Kasai[b], K. Yamasaki[b]

[a]*Department of Pharmacognosy, Faculty of Pharmacy, Assiut University, Assiut 71526, Egypt*
[b]*Institute of Pharmaceutical Sciences, Hiroshima University, Faculty of Medicine, 1-2-3 Kasumi, Minami-Ku, Hiroshima 734, Japan*

Received 1 May 2001; received in revised form 25 June 2001

Abstract

From the leaves of *Cryptostegia grandiflora,* four new cardiac glycosides oleandrigenin 3-*O*-β-glucopyranosyl-(1→4)-β-cymaropyranosyl-(1→4)-β-digitoxopyranoside, cryptostigmin I, oleandrigenin 3-*O*-β-glucopyranosyl-(1→4)-α-rhamnopyranoside, cryptostigmin II, 16-propionylgitoxigenin 3-*O*-β-glucopyranosyl-(1→4)-α-rhamnopyranoside, cryptostigmin III and oleandrigenin 3-*O*-β-glucopyranosyl-(1→6)-β-glucopyranosyl-(1→4)-β-cymaropyranosyl-(1→4)-β-digitoxopyranoside, cryptostigmin IV have been isolated together with two known cardenolides subalpinosid and 16-*O*-acetyl-digitalinum verum. The structures of the isolated compounds were verified by means of MS and NMR spectral analyses. © 2001 Elsevier Science Ltd. All rights reserved.

Keywords: Cryptostegia grandiflora; Asclepiadaceae; Cardenolides; Cryptostigmin I–IV

1. Introduction

Cryptostegia grandiflora R.Br. (Asclepiadaceae) is an ornamental plant commonly cultivated in Egypt and warm countries (Metcalf and Chalk, 1950; Chopra et al., 1965; Hutchinson, 1973). The plant has a wide use in manufacturing of rubber and as a source of hydrocarbon fuels from its latex (Mehta et al., 1982). Three cardiac glycosides were isolated from *Cryptostegia madagascarensis* (14, 16-dianhydrogitoxigenin-3-rhamnoside, 16-propionylgitoxigenin-3-rhamnoside and 16-anhydrogitoxigenin-3-rhamnoside) (Sanduja et al., 1984) while few cardenolides (cryptograndoside A, B and digitalinum verum) have been already isolated and identified from *C. grandiflora* (Watt and Breyer, 1962). Moreover, the macro and micromorphological characters of the leaves and stems of *C. grandiflora* have been also investigated (Assaf, 1998). The present study deals with the isolation and structure elucidation of four new cardiac glycosides together with two known glycosides from the leaves of *C. grandiflora*.

2. Results and discussion

The ethanolic extract of the leaves of *C. grandiflora* was defatted with CH_2C1_2 and the aqueous layer was subjected to a column chromatography of Diaion HP-20. The 80% methanol eluate was repeatedly chromatographed on columns of silica gel and then by MPLC and HPLC to afford 6 glycosides.

Comparison of the NMR spectra of compound **1** with the published data revealed its structure as subalpinosid previously isolated from *Digitalis subalpina* (Lichius et al., 1991).

The molecular formula of compound **2** was deduced as $C_{44}H_{68}0_{17}$ from HR FAB–MS spectrometry (see Experimental section). The ^{13}C NMR spectrum (Tables 1 and 2) of **2** displayed the presence of one unsubstituted β-g1ucopyranosy1 unit from the signals at δ_c 104.3 (C-1), 74.9 (C-2), 78.2 (C-3 and 5), 71.9 (C-4) and 63.0 (C-6), one substituted β-digitoxopyranosyl unit from the signals at δ_c 96.5 (C-1), 38.9 (C-2), 71.8 (C-3), 83.0 (C-4), 67.5 (C-5) and 18.6 (C-6) and one substituted β-cymaropyranosyl unit from the signals at δ_c 101.3 (C-1), 37.2 (C-2), 78.5 (C-3), 83.4 (C-4), 68.5 (C-5), 18.7 (C-6) and 56.7 (OMe) (Bradbury and Jenkins, 1984) together with 25 carbon signals for the aglycone. The chemical shifts of the aglycone carbons were similar to those reported for 3-0 substituted oleandrigenin (Lichius et al., 1991). The downfield shifts of C-4 of the digitoxo- and

* Corresponding author. Tel.: +20-88-333196; fax: +20-88-332776.
E-mail address: mkamel@mailcity.com (M.S. Kamel).

0031-9422/01/$ - see front matter © 2001 Elsevier Science Ltd. All rights reserved.
PII: S0031-9422(01)00297-7

Table 1
^{13}C NMR spectral data of the aglycone moieties of compounds **2**–**5** (100 MHz, C_5D_5N)[a]

C	2	3	4	5
1	30.4	30.1	30.1	30.4
2	26.9	26.9	27.0	27.0
3	73.2	72.6	72.8	73.2
4	30.7	30.9	30.9	30.8
5	36.9	36.9	37.0	36.9
6	26.9	26.7	26.8	27.0
7	21.1[a]	21.1[a]	21.1[a]	21.1[a]
8	41.8	41.8	41.9	41.9
9	35.7	35.6	35.7	35.8
10	35.4	35.3	35.4	35.4
11	21.6[a]	21.6[a]	21.6[a]	21.6[a]
12	39.1	38.9	38.9	39.1
13	50.4	50.4	50.4	50.4
14	83.6	83.3	83.3	83.4
15	41.1	41.1	41.3	41.1
16	75.6	76.3	76.4	75.4
17	75.3	56.7	56.8	57.6
18	16.2	16.2	16.2	16.2
19	23.8	23.9	23.9	23.9
20	169.8	169.9	169.8	169.8
21	76.2	76.2	76.3	76.2
22	121.5	121.5	121.6	121.5
23	174.2	174.2	174.2	174.2
-COMe	170.2	170.3	173.7	170.2
-COMe	20.7	20.6		20.7
-$COCH_2$Me			9.1	
-$COCH_2$Me			27.7	

[a] a,b values may be interchangeable in each column.

Table 2
^{13}C NMR spectral data of the sugar moieties of compounds **2**–**5** (100 MHz, C_5D_5N)[a]

C[b]	2	3	4	5
Dig				
1	96.5			96.5
2	38.9			38.9
3	71.8			71.7
4	83.0			83.0
5	67.5			67.5
6	18.6			18.6
Cym				
1	101.3			101.4
2	37.2			37.4
3	78.5			78.5
4	83.4			83.7
5	68.5			68.5
6	18.7			18.7
OMe	56.7			56.8
Rha				
1		99.6	99.6	
2		71.4	71.4	
3		72.2	72.3	
4		85.1	85.2	
5		68.3	68.3	
6		18.4	18.4	
Glc				
	104.3	106.6	107.7	104.3
1	74.9	74.9	74.7	74.9
2	78.2	78.3[a]	78.4[a]	78.3[b]
3	71.9	72.4	72.5	72.1
4	78.2	78.4[a]	78.5[a]	77.4
5	63.0	62.5	62.6	70.2
6				
Glc				
1				105.1
2				74.9
3				78.2[b]
4				72.1
5				78.3[b]
6				62.8

[a] a,b: values may be interchangeable in each column.
[b] Dig: β-Digitoxopyranose, Cym: β-Cymaropyranose, Rha: α-Rhamnopyranose, Glc: β-Glucopyranose.

cymaropyranosyl units (δ_c 83.0 and 83.4 respectively) proved their substitution at C-4 of each unit (Bradbury and Jenkins, 1984). In the ^1H NMR spectrum of **2**, the doublet signal at δ_H 5.04 (1H) with *J* (constant) 7.8 Hz for the anomeric proton of the glucosyl residue indicated the β configuration. Moreover, the broad doublet signal at δ_H 5.39 (*J* constant 9.1 Hz) and the doublet of doublet signal at δ_H 4.71 (*J* constant 4.7 and *9.5* Hz) indicated the β configuration of the digitoxo- and cymaropyranosyl units respectively. The HMQC spectral data of **2** revealed the correlations between each carbon and its directly attached protons while H–H COSY interpreted the proton–proton couplings. The HMBC spectral analysis of **2** (Fig. 1) displayed significant correlation peaks between H-1 of the digitoxopyranosyl unit with C-3 of the aglycone as well as H-16 with COMe and H-22 with C-23. The negative FAB–MS spectrum of **2** exhibited M^+ at *m/z* 867 $[M–H]^-$ as well as a significant peak at *m/z* 705 $[M–H\text{-glucose}]^-$ and a peak at *m/z* 561 $[M–H\text{-(glucose + cymarose)}]^-$. Therefore, the internal sugar unit was confirmed as the digitoxopyranosyl unit and the structure of compound **2** was assigned as oleandrigenin 3-*O*-β-glucopyranosyl-(1→4)-β-cymaropyranosyl-(1→4)-β-digitoxopyranoside and named cryptostigmin I.

The molecular formula of compound **3** was deduced as $C_{37}H_{56}O_{15}$ from HR FAB–MS spectrometry (see Experimental section). ^{13}C NMR spectral data of **3** (Tables 1 and 2) were very similar to those of **2** in the aglycone moiety indicating the presence of 3-*O* substituted oleandrigenin as aglycone. The signals of the sugar moiety revealed the presence of a terminal β-glucopyranosyl unit in addition to α-substituted a rhamnopyranosyl unit from the signals at δ_c 99.6 (C-1), 71.4 (C-2), 72.2 (C-3), 85.1 (C-4), 68.3 (C-5) and 18.4 (C-6) (Breitmaier and Voelter, 1987). The downfield shift of C-4 of the rhamnopyranosyl unit (δ_c 85.1) indicated its substitution at this position. The β configuration of the glucopyranosyl unit was deduced from the doublet signal of its anomeric proton at δ_H 5.20 with *J* constant 7.7

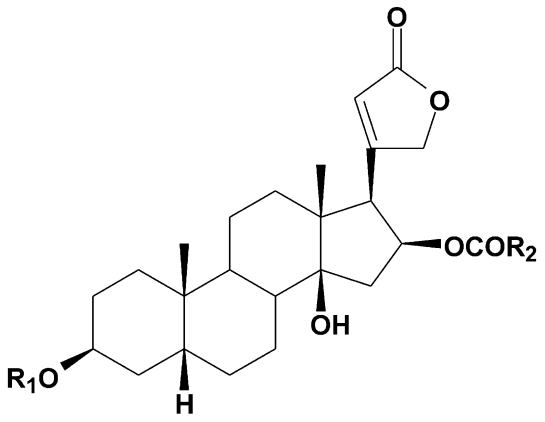

	R_1	R_2
(2)	— Dig —(4)— Cym —(4)— Glc	-CH_3
(3)	— Rha —(4)— Glc	-CH_3
(4)	— Rha —(4)— Glc	-CH_2-CH_3
(5)	—Dig—(4)— Cym —(4)— Glc—(6)—Glc'	-CH_3

Dig: β-digitoxopyranose, Cym: β-cymaropyranose, Rha: α-rhamnopyranose, Glc: β-glucopyranose

Hz in the ^{1}H NMR spectrum while the configuration of the rhamnopyranosyl unit was established from the upfield shift of its C-5 (δ_c 68.3) in the ^{13}C NMR spectrum (Kasai et al., 1979). The structural assignment was confirmed by carrying out 2D NMR techniques such as HMQC and H–H COSY. The HMBC spectral analysis of **3** (Fig. 1) displayed correlation peaks between H-3 and C-1 of the rhamnopyranosyl unit, the anomeric proton of the glucosyl residue and C-4 of the rhamnosyl unit, H-16 and both COMe and C-20, H-17 and COMe, H-21, 21′ with C-23 and H-22 with C-23. The negative FAB–MS spectrum of **3** showed significant peaks at m/z 739 [M–H]$^-$ and 577 [M–H-glucose]$^-$ confirming the sequence of the sugar moiety. Consequently, the structure of **3** was determined as oleandrigenin 3-*O*-β-glucopyranosyl-(1→4)-α-rhamnopyranoside and named cryptostigmin II.

The molecular formula of compound **4** was established as $C_{38}H_{58}O_{15}$ from HR FAB–MS spectrometry (see Experimental section). Inspection of ^{13}C NMR spectral data of **4** (Tables 1 and 2) revealed their similarity to those of **3** both in the aglycone and sugar moieties. However, the presence of a methylene signal at δ_c 27.7 and a methyl signal at δ_c 9.1 in addition to the absence of the methyl signal at δ_c 20.6 in compound **4** proved the presence of a propionyl instead of the acetyl moiety at C-16 of the aglycone. At the same time, ^{1}H NMR spectrum of compound **4** showed a quartet at δ_H 2.13 (J constant 7.3 Hz) and a triplet at δ_H 0.93 (J constant 7.6 Hz) for the the methylene and methyl groups of the propionyl moiety, respectively, in addition to the absence of the methyl singlet at δ_H 1.82 of the acetyl group when compared with compound **3**. Moreover, FAB–MS spectrum of **4** exhibited significant peaks at m/z 753 [M–H]$^-$, 591 [M–H-glucose]$^-$ and 445 [M–H-(glucose + rhamnose)]$^-$. Consequently, the structure of compound **4** was assigned as 16-propionylgitoxigenin 3-*O*-β-glucopyranosyl-(1→4)-α-rhamnopyranoside and named cryptostigmin III.

The molecular formula of compound **5** was determined as $C_{50}H_{78}O_{22}$ from HR FAB–MS spectrometry (see Experimental section). Inspection of ^{13}C NMR spectral data of **5** (Tables 1 and 2) revealed their similarity to those of **2** both in the aglycone and sugar moieties. However, the downfield shift of C-6 of the glucosyl unit to δ_c 70.2 (+ 7.2 ppm) revealed its substitution at this position with an additional glucopyranosyl unit from the signals at δ_c 105.1, 74.9, 78.2, 72.1, 78.3 and 62.8 (Bradbury and Jenkins, 1984). In the ^{1}H NMR spectrum of **5**, the doublet signals at δ_H 5.19 and 4.99 (each 1H) with J constant 7.8 Hz for each one of the anomeric protons of the glucosyl residues indicated the β configuration. Moreover, the broad doublet signal at

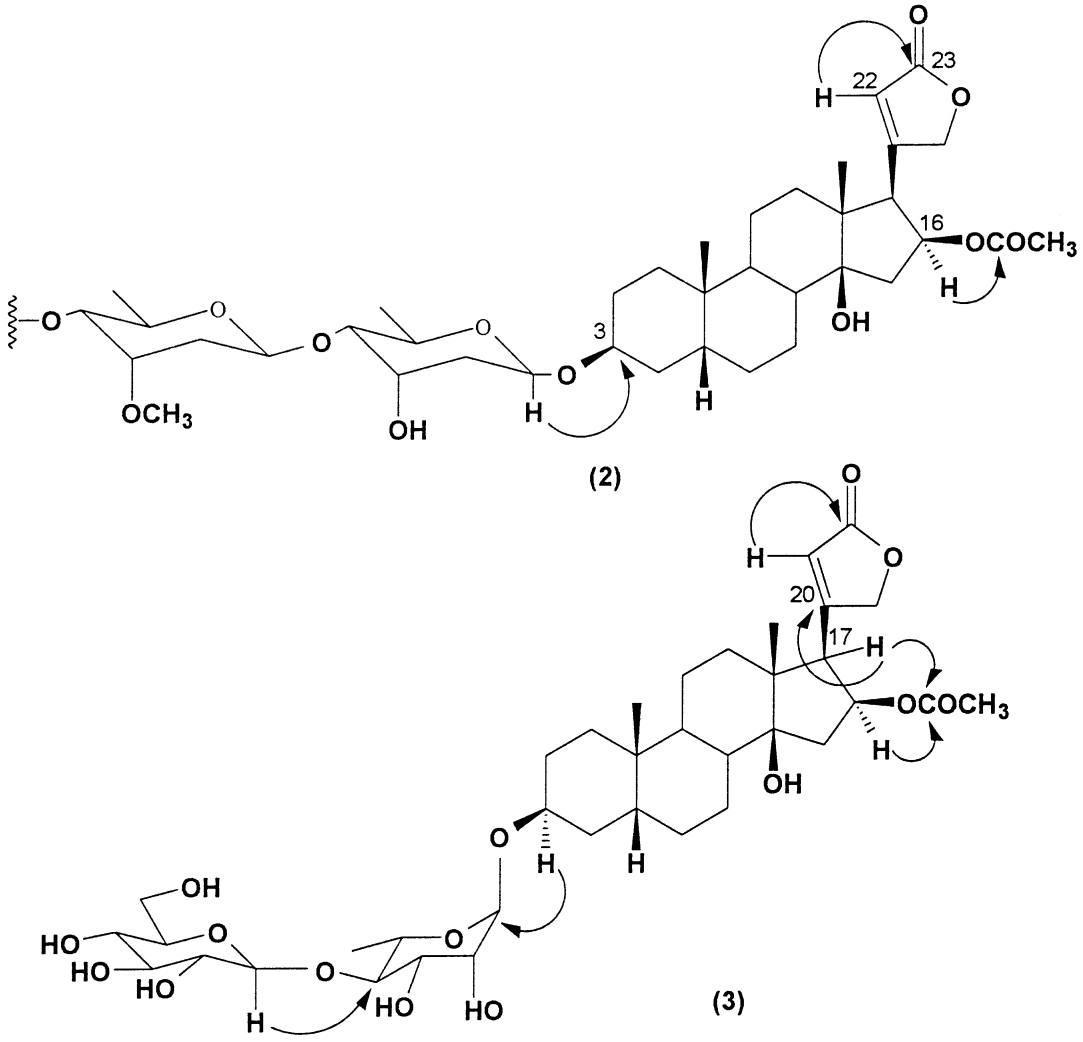

Fig. 1. Significant HMBC correlations of compounds **2** and **3**..

δ_H 4.79 (*J* constant 11.7 Hz) and the doublet of doublet signal at δ_H 4.73 (*J* constant 3.9 and 7.2 Hz) indicated the β configuration of the digitoxo- and cymaropyranosyl units respectively. FAB–MS spectrum of **5** exhibited significant peaks at *m/z* 1029 $[M–H]^-$, 867 $[M–H\text{-glucose}]^-$, 705 $[M–H\text{-(2 glucose)}]^-$ and 561 $[M–H\text{-(2 glucose + cymarose)}]^-$. Consequently, the structure of compound **5** was assigned as oleandrigenin 3-*O*-β-glucopyranosyl-(1→6)-β-glucopyranosyl-(1→4)-β-cymaropyranosyl-(1→4)-β-digitoxopyranoside and named cryptostigmin IV.

Comparison of the ^1H and ^{13}C NMR spectra of compound **6** with the published data deduced its structure as 16-*O*-acetyl-digitalinum verum previously isolated from *Addenium obesum* (Yamauchi and Abe, 1990).

3. Experimental

^1H and ^{13}C NMR (TMS as int. standard): 400 and 100 MHz, respectively were recorded on a JEOL JNM α-400 spectrometer. FAB–MS spectra were taken on a JEOL JMS-SX 102 spectrometer by direct inlet method at an ionizing voltage of 70 eV. Optical rotations were measured with a Union PM-I digital polarimeter. MPLC: RP-18 column (20 mm i.d. ×40 cm); flow rate of mobile phase 3 ml/min. HPLC: D-ODS-5 and polyamine columns (each 20 mm i.d. ×25 cm, YMC) with a Toyo Soda high speed chromatograph HLC-803 D pump and a Tosoh refraction index (R1-8) detector; flow rate of mobile phase 6 ml/min, injection vol. 0.8–1.0 ml. On the ODS column, 30% MeCN (I) and 25% MeCN (II) were used while 90% MeCN (III) and 85% MeCN (IV) were used on the polyamine column. CC: Kieselgel 60 (70-230 mesh, Merck) and Diaion HP 20 (Mitsubishi). TLC: silica gel 60 precoated plates F-254 and HPTLC using RP-18 precoated plates, F-254 s (Merck).

3.1. Plant material

Leaves of *C. grandi flora* R.Br. (Asclepiadaceae) were collected from the trees cultivated in the Experimental

Station of Faculty of Agriculture, Assiut University, Assiut, Egypt, in March 1997. The plant was identified by Professor N. El-Keltawi, Department of Horticulture, Faculty of Agriculture, Assiut University, Assiut, Egypt. A voucher specimen is deposited at the Herbarium of Department of Pharmacognosy, Faculty of Pharmacy, Assiut University, Assiut, Egypt.

3.2. Extraction and isolation of compounds (*1*–*6*)

The air-dried powdered leaves of *C. grandiflora* (2 kg) were extracted with 70% EtOH. The dried ethanolic extract (499 g) was suspended in H_2O and defatted successively with *n*-hexane and CH_2C1_2. The aq. fr. was applied to a column of Diaion HP-20 and eluted with H_20, 40% MeOH, 80% MeOH, MeOH and acetone successively. The 80% MeOH eluate (12 g) was chromatographed by silica gel CC using CH_2C1_2–MeOH–H_20 (85: 15: 1) and finally with (70 : 30 : 3) to give 4 fractions. Fraction 1 (760 mg) was separated by MPLC on RP-18 using 35% MeCN and HPLC using ODS column and solvent I to afford compounds **1** (white powder, 14 mg) and **6** (white powder, 53 mg). Fraction 2 (718 mg) was subjected to HPLC using polyamine column and solvent III to give compound **2** (white powder, 70 mg). Fraction 3 (610 mg) was separated by HPLC using polyamine column and solvent IV to afford compounds **3** (white powder, 149 mg) and **4** (white powder, 43 mg). Fraction 4 (2.5 g) was separated by MPLC on RP-18 using 30% MeCN as a solvent system and HPLC using ODS colunm and solvent II to afford compound **5** (white powder, 29 mg).

3.2.1. Compound (*2*)

Cryptostigmin I, $[\alpha]_D^{25}$ −15.4° (MeOH; *c* 5.70). HR FAB–MS (negative) *m/z*: 867.4371 $[M–H]^-$ $C_{44}H_{68}O_{17}$ (req. 867.4378). ^{13}C NMR (C_5D_5N, Tables 1 and 2). ^1H NMR (C_5D_5N): δ_H 6.30 (1H, *s*, H-22), 5.63 (1H, *m*, H-16), 5.40 (1H, *d*, *J* = 18.1 Hz, H-21), 5.39 (1H, *bd*, *J* = 9.1 Hz, H-1 Dig), 5.20 (1H, *d*, *J* = 18.1 Hz, H-21′), 5.04 (1H, *d*, *J* = 7.8 Hz, H-1 Glc), 4.71 (1H, *dd*, *J* = 4.7 and 9.5 Hz, H-1 Cym), 3.49 (3H, *s*, OMe), 3.35 (1H, *d*, *J* = 8.8 Hz, H-17), 2.77 (1H, *dd*, *J* = 8.6 and 14.6 Hz, H-15), 2.02 (1H, *d*, *J* = 13.2 Hz, H-15′), 1.82 (3H, *s*, COMe), 1.58 (3H, *d*, *J* = 5.4 Hz, Me-6 Cym), 1.42 (3H, d, *J* = 6.1 Hz, Me-6 Dig), 1.04 (3H, *s*, Me-18) and 0.84 (3H, *s*, Me-19).

3.2.2. Compound (*3*)

Cryptostigmin II, $[\alpha]_D^{25}$ −39.4° (MeOH; *c* 3.73). HR FAB–MS (negative) *m/z*: 739.3604 $[M–H]^-$ $C_{37}H_{56}O_{15}$ (req. 739.3541). ^{13}C NMR (C_5D_5N, Tables 1 and 2). ^1H NMR (C_5D_5N): δ_H 6.32 (1H, *bs,* H-22), 5.66 (1H, *m,* H-16), 5.40 (1H, *dd,* *J* = 1.8, 18.3 Hz, H-21), 5.32 (1H, *bs,* H-1 Rha), 5.22 (1H, *dd,* *J* = 1.5, 18.3 Hz, H-21′), 5.20 (1H, *d,* *J* = 7.7 Hz, H-1 Glc), 4.18 (1H, *m*, H-3), 3.37 (1H, *d,* *J* = 8.6 Hz, H-17), 2.78 (1H, *dd,* *J* = 9.5 and 15.7 Hz, H-15), 2.03 (1H, *dd,* *J* = 2.1, 15.3 Hz, H-15′), 1.82 (3H, *s,* COMe), 1.67 (3H, *d,* *J* = 6.4 Hz, Me-6 Rha), 1.05 (3H, *s,* Me-18) and 0.81 (3H, *s,* Me-19).

3.2.3. Compound (*4*)

Cryptostigmin III, $[\alpha]_D^{25}$ −41.3° (MeOH; *c* 2.01). HR FAB–MS (negative) *m/z*: 753.3683 $[M–H]$ $C_{38}H_{58}O_{15}$ (req. 753.3697). ^{13}C NMR (C_5D_5N, Tables 1 and 2). ^1H NMR (C_5D_5N): δ_H 6.32 (1H, *bs,* H-22), 5.70 (1H, *m,* H-16), 5.41 (1H, *d,* *J* = 18.3 Hz, H-21), 5.22 (1H, *d,* *J* = 18.3 Hz, H-21′), 5.20 (1H, *d,* *J* = 7.1 Hz, H-1 Glc), 3.40 (1H, *d,* *J* = 8.8 Hz, H-17), 2.80 (1H, *d,* *J* = 14.8 Hz, H-15), 2.13 (2H, *q*, *J* = 7.3 Hz, $COCH_2$), 2.10 (lH, *d*, *J* = 14.8 Hz, H-l5′), 1.68 (3H, *d,* *J* = 6.1 Hz, Me-6 Rha), 1.07 (3H, *s,* Me-18), 0.93 (3H, *t,* *J* = 7.6 Hz, CO–CH_2-Me) and 0.83 (3H, *s*, Me-19).

3.2.4. Compound (*5*)

Cryptostigmin IV, $[\alpha]_D^{25}$ −37.8° (MeOH; *c* 1.80). HR FAB–MS (negative) *m/z*: 1029.4891 $[M–H]$ $C_{50}H_{78}0_{22}$ (req. 1029.4906). ^{13}C NMR (C_5D_5N, Tables 1 and 2). ^1H NMR (C_5D_5N): δ_H 6.32 (1H, *s,* H-22), 5.40 (1H, *d,* *J* = 18.6 Hz, H-21), 5.22 (1H, *d,* *J* = 18.6 Hz, H-21′), 5.19 and 4.99 (each 1H, *d,* *J* = 7.8 Hz, H-1 Glc and Glc′), 4.79 (1H, *bd,* *J* = 11.7 Hz, H-1 Dig), 4.73 (1H, *dd,* *J* = 3.9 and 7.2 Hz, H-1 Cym), 3.60 (3H, *s,* OMe), 3.36 (lH, *d,* *J* = 9.1 Hz, H-17), 2.78 (1H, *dd,* *J* = 10.0 and 15.2 Hz, H-15), 2.04 (1H, *d,* *J* = 15.2 Hz, H-15′), 1.83 (3H, *s,* COMe), 1.57 (3H, *d,* *J* = 6.1 Hz, Me-6 Cym), 1.43 (3H, *d,* *J* = 6.4 Hz, Me-6 Dig), 1.05 (3H, *s,* Me-18) and 0.85 (3H, *s,* Me-19).

Acknowledgements

The authors are grateful to the Japan Society for Promotion of Science (JSPS) and a Grant-in-Aid, Ministry of Education and Culture, Japan for the financial support of this work. Also, we would like to thank the Research Center of Molecular Medicine of the Hiroshima University School of Medicine, Japan, for NMR measurements.

References

Assaf, M., 1998. Macro- and micromorphological study of the leaves and stems of *Cryptostegia grandiflora* R.Br. cultivated in Egypt. Bulletin of Pharmaceutical Sciences. Assiut University 21, 61–74.

Bradbury, H., Jenkins, J., 1984. Determination of the structures of trisaccharides by ^{13}C NMR spectroscopy. Carbohydr. Res. 126, 125–156.

Breitmaier, E., Voelter, W., 1987. Carbon-13 NMR Spectroscopy, 3rd Edition. Verlagsgesellschaft mbH, Weinheim, Germany. pp. 381–382.

Chopra, R., Badhwar, R., Ghosh, S., 1965. Poisonous Plants of India, Vol. I. Indian council of Agricultural Research, pp. 577–578.

Hutchinson, J., 1973. The families of flowering plants, 3rd Edition. The Clarendon Press, Oxford, p. 472.

Kasai, R., Okihara, M., Asakawa, J., Mizutani, K., Tanaka, O., 1979. ^{13}C NMR study of α- and β-anomeric pairs of D-mannopyranosides and L-rhamnopyranosides. Tetrahedron 35, 1427–1432.

Lichius, J., El Khyari, D., Wichtl, M., 1991. Subalpinosid (S1) a new oleandrigenin glycoside and other cardenolides from *Digitalis subalpina* var. *subalpina*. Planta Med. 57, 159–161.

Mehta, H., Doshi, A., Choudhari, P., Bokil, K., Rao, S., 1982. Liquid fuels from laticiferous plants. Ind. J. Technol. 20, 454–456.

Metcalf, C., Chalk, L., 1950. Anatomy of the dicotyledons, Vol II. The Clarendon Press, Oxford, p. 914.

Sanduja, R., Lo, W., Euler, K., Alam, M., 1984. Cardenolides of *Cryptostegia madagascarensis*. J. Nat. Prod. 47, 260–265.

Watt, J., Breyer, M., 1962. Medicinal and poisonous plants of southern and eastern Africa. Livingstone, London. p. 69.

Yamauchi, T., Abe, F., 1990. Cardiac glycosides and pregnanes from *Addenium obesum*. Chem. Pharm. Bull. 38, 669.

PERGAMON

Phytochemistry 58 (2001) 543–546

PHYTOCHEMISTRY

www.elsevier.com/locate/phytochem

Enmein type diterpenoids from *Isodon japonica*

Baolin Li[a,*], Xianhua Tian[b]

[a]*Department of Chemistry, Shaanxi Normal University, Xi'an 710062, People's Republic of China*
[b]*Life Science College, Shaanxi Normal University, Xi'an 710062, People's Republic of China*

Received 8 December 2000; received in revised form 19 April 2001

Abstract

Two enmein type diterpenoids, taibaijaponicains A and B, were isolated from the ethanol extract of the leaves and branches of *Isodon japonica*. Their structures are designated as 6β,11α-dihydroxy-16α-methoxymethyl-6,20-epoxy-6,7-*seco*-*ent*-kaur-15-one-1,7-olide and 3β-acetoxy-6β,11α-dihydroxy-16α-methoxymethyl-6,20-epoxy-6,7-*seco*-*ent*-kaur-15-one-1,7-olide, respectively, on the basis of detailed spectroscopic analyses. © 2001 Elsevier Science Ltd. All rights reserved.

Keywords: *Isodon japonica*; Labiatae; Taibaijaponicains A and B; Enmein type diterpenoids

1. Introduction

Enmein was first isolated from *Isodon japonica* in 1958. Enmein type diterpenoids are bitter constituents of the plants of genus *Isodon* (Labiatae). They have varied biological activities, i.e. anti-bacterial, anti-inflammatory, anti-tumor, etc. (Cheng et al., 1987). Previous studies on *I. japonica* led to the isolation of more than 16 diterpenoids (Fujita et al., 1973; Li et al., 1982; Liu et al., 1982; Zhao et al., 1984; Wang et al., 1987; Zhao and Li., 1987; Meng et al., 1989; Xu et al., 1996). A further study of the minor diterpenoid constituents of this species was aimed at finding substances with even higher biological activities. We have isolated two new enmein type diterpenoids, taibaijaponicains A (**1**) and B (**2**), together with six known diterpenoids, norhendosin A, rabdophyllin G, dihydroenmein, nodosin, enmein, rabdosin A, and two other known compounds, β-sitosterol and oleanolic acid. In this paper, we report the isolation and structure elucidation of the new diterpenoids by means of spectroscopic methods including 1D and 2D NMR spectroscopy.

2. Results and discussion

Taibaijaponicain A (**1**) was obtained as an amorphous powder. Its molecular formula was determined as $C_{21}H_{30}O_7$ by positive HR–FABMS ($[M+1]^+$ m/z 395.4644, calc. 395.4666) and FABMS ($[M+Li]^+$ m/z 401, $[M+Na]^+$ m/z 417). The ^1H, ^{13}C and DEPT NMR spectra of **1** (see Tables 1 and 2) showed signals for two methyl groups, one methoxy group, six methylene groups, seven methine groups, three quaternary carbons, one ketonic carbon and one ester carbonyl carbon. Taibaijaponicain A (**1**) contains a five-membered ketone group [ν_{max} 1765 cm^{-1}, δ_c 212.3(*s*)], δ-lactone [ν_{max} 1720 cm^{-1}, δ_H 4.77(1H, *dd*, $J=11.2$, 3.9 Hz), δ_c 171.2(s)], and a hemiacetal group [δ_H 5.27(1H, s), δ_c 102.6(d)]. In addition, the IR and ^1H NMR spectra also revealed that the compound possessed two hydroxyl groups [ν_{max} 3358 cm^{-1}, δ_H 5.27 (1H, s), 4.30 (1H, *ddd*, $J=10.6$, 8.8, 3.4 Hz)]. Considering the known structures of diterpenoids from the genus *Isodon*, these data suggest that **1** was an enmein type diterpenoid of pentacyclic 6,7-*seco*-*ent*-kaurane type, with one methoxy group and two hydroxyl groups.

Compound **1** did not show an absorption maximum band above 220 nm in the UV spectrum, which indicated the absence of a five-membered ketone conjugated with the *exo*-methylene group. The ^{13}C NMR spectroscopic data of **1** were very similar to those of nodosin (**3**) (Takeda et al., 1994) except for one more methoxyl group and one less C–C double bond. Comparison of their ^{13}C NMR spectral data indicated that the difference between **1** and **3** was only in the ring D. This meant that two hydroxyl groups were attached at C-6 and C-11, and a methoxyl group was in ring D in compound **1**. In the ^1H NMR spectrum of **1**, besides an AB peak at δ 3.92, 3.73 (each 1H, AB, *d*, $J=9.2$ Hz, H-20a, 20b),

* Corresponding author. Tel.: +86-29-5307788; fax: +86-29-5307774.
E-mail address: baolinli@snnu.edu.cn (B. Li).

0031-9422/01/$ - see front matter © 2001 Elsevier Science Ltd. All rights reserved.
PII: S0031-9422(01)00245-X

Table 1
^{1}H NMR and principal HMBC correlations of compounds **1** and **2** in acetone-d_6[a]

	1		**2**	
Proton	δ_H, mult, intgr, (*J*, Hz)	HMBC (carbon)	δ_H, mult, intgr, (*J*, Hz)	HMBC (carbon)
1β	4.77, *dd*, 1H, (11.2, 3.9)	(2), 3, 9, (10), 20	4.85, *dd*, 1H, (10.8, 3.6)	(2), 3, (10), 20
2α	1.82, *m*, 1H	(1), (3), 4, 9, 10	2.12, *m*, 1H	(1), (3), 4, 10
2β	1.78, *m*, 1H	(1), (3), 4, 9, 10	2.34, *m*, 1H	(1), (3), 4
3α	1.48, *m*, 1H	1, (2), (4), 19	4.79, *dd*, 1H, (3.5, 3.6)	(2), (4), 19, OAc(170.6 ppm)
3β	1.38, *m*, 1H	1, (2), (4), 19	–	–
5β	2.75, *s*, 1H	(4), (6), 9, (10), 20	2.73, *s*, 1H	(4), (6), 9, 10
6α	5.27, *s*, 1H	4, (5), 10, 20	5.26, *s*, 1H	(5), 10, 20
9α	2.14, *bs d*, 1H, (10.6)	1, (8), (10), (11), 12, 14, 15	2.13, *bs d*, 1H, (10.4)	(8), (10), (11), 12
11β	4.30, *ddd*, 1H, (10.6, 8.8, 3.4)	(9), 10, (12)	4.31, *ddd*, 1H, (10.4, 8.3, 3.1)	(9), 10, (12)
12α	2.40, *m*, 1H	(11), (13), 14	2.41, *m*, 1H	(11), (13), 14
12β	1.45, overlap, 1H	9, (11), (13)	1.44, overlap, 1H	n.o.[b]
13β	2.79, *m*, 1H	9, 11, (12), (14), 17	2.80, *m*, 1H	11, (12), (14), 16
14α	1.81, overlap, 1H	(8), (13)	1.82, *m*, 1H	n.o.
14β	1.48, overlap, 1H	(8), (13)	1.50, *m*, 1H	(8), (13)
16β	1.45, *m*, 1H	11, 12, (13), 14, MeO	1.47, *m*, 1H	(13), 14, 17
17a	3.64, 3.56, AB, dd, each 1H, (10.4, 4.5)	13, (16), MeO	3.65, 3.54, AB, *dd*, each 1H, (10.2, 4.3)	13, (16), MeO
17b		13, (16), MeO		13, (16), MeO
18	1.00, *s*, 3H	3, (4), 5, 19	1.01, *s*, 3H	(4), 5, 19
19	0.97, *s*, 3H	3, (4), 5, 18	0.98, *s*, 3H	3, (4), 5, 18
20a	3.92, 3.73, AB, d, each 1H, (9.2)	1, 9, (10), 11	3.93, 3.71, AB, d, each 1H, (9.1)	1, 6, 9, (10)
20b		9, (10)		6, 9, (10)
OCH_3	3.30, *s*, 3H	17	3.32, *s*, 3H	17
OAc	–	–	2.07, *s*, 3H	

[a] Two-bond correlations are indicated in parentheses.
[b] n.o. Indicates no clear correlations with this proton.

there was an AB peak at δ 3.64, 3.56 (each 1H, AB, *dd*, $J = 10.4$, 4.5 Hz, H-17a, 17b). In the HMBC spectrum of **1** (see Table 1), the signals at δ 3.64 and 3.56 correlated with the signals at δ 31.3 (*d*, C-13), 58.8 (*d*, C-16) and 56.4 (*q*, OCH_3); the signal at δ 2.79 (1H, *m*, H-13β) showed a correlation with the signals at δ 69.3 ppm (*t*, C-17), 32.6 ppm (*t*, C-12) and 35.0 ppm (*t*, C-14). These results suggested that the methoxyl group should be located at the C-17 position.

In enmein type diterpenoids, the ring A is in a chair conformation, the rings B_1 and D are in envelope conformations and ring B_2 is in a boat conformation. Ring C can adopt either a chair or boat conformation depending on the substituents present in ring C (Xu, 1985). In compound **1**, the coupling constant between H-5β (δ 2.75, *s*) and H-6 (δ 5.27, *s*) was zero, which indicated that its dihedral angle approximated 90°, consistent with a β-orientation of the hydroxyl group at C-6 of **1**. Ring C of **1** appears to be in a boat conformation judging from that the coupling constant of H-11 (δ 4.30, *ddd*, $J = 10.6$, 8.8, 3.4 Hz) with H-9α (δ 2.14, *bs d*, $J = 10.6$ Hz) and H-12α(δ 2.40, m), H-12β (δ 1.45, overlap). For a chair conformation of the ring C, the dihedral angles between H-9α and H-11, H-11 and H-12α or H-12β should approximate 60°, and all of their coupling constants should be less than 4 Hz. This fact suggests that the hydroxyl group at C-11 of **1** was in the α-orientation. These results were further verified by a NOESY experiment, where correlations are shown in Fig. 1. In addition, in the NOESY spectrum of **1**, the signal at δ 1.45 (1H, m, H-16) exhibited a NOE correlation with both the signals at δ 2.79 (1H, *m*, H-13β) and δ 1.81 (1H,

Table 2
^{13}C NMR spectral data for compounds **1** and **2** in acetone-d_6

Carbon	**1**	**2**
1	77.3, *d*	77.2, *d*
2	24.2, *t*	32.1, *t*
3	37.4, *t*	71.6, *d*
4	32.1, *s*	35.7, *s*
5	54.3, *d*	54.2, *d*
6	102.6, *d*	102.5, *d*
7	171.2, *s*	171.1, *s*
8	57.7, *s*	57.5, *s*
9	53.1, *d*	53.0, *d*
10	50.9, *s*	51.5, *s*
11	63.3, *d*	63.4, *d*
12	32.6, *t*	32.5, *t*
13	31.3, *d*	31.4, *d*
14	35.0, *t*	35.2, *t*
15	212.3, *s*	212.4, *s*
16	58.8, *d*	58.9, *d*
17	69.3, *t*	69.4, *t*
18	33.1, *q*	32.8, *q*
19	23.5, *q*	22.4, *q*
20	73.9, *t*	73.7, *t*
OMe	56.4, *q*	56.2, *q*
AcO		170.6, *s*
		20.9, *q*

overlap, H-14α). This indicated that C-17 was in the α-orientation. Therefore, taibaijaponicain A (**1**) was 6β, 11α-dihydroxy-16α-methoxymethyl-6,20-epoxy-6,7-*seco-ent*-kaur-15-one-1,7-olide.

Taibaijaponicain B (**2**) was obtained as an amorphous powder. Its molecular formula was determined as $C_{23}H_{32}O_9$ by FABMS ($[M+Li]^+$ *m/z* 459, $[M+Na]^+$ *m/z* 475). The IR, ^1H, ^{13}C and DEPT NMR data of **2** (see Tables 1 and 2) were very similar to those of taibaijaponicain A (**1**) except for the presence of one acetoxyl group in **2** [ν_{max} 1742 cm^{-1}, δ_H 2.07 (3H, *s*), δ_c 170.6 (*s*), 20.9(q)]. The ^{13}C NMR spectral data of **2** differed from those of **1** only at C-2, C-3 and C-4. The downfield shift of C-3 from δ 37.4 ppm in **1** to δ 71.6 ppm in **2** indicated that the acetoxyl group at C-3 in **2** had replaced the H in **1**. These assignments were further confirmed by the HMBC spectrum of **2** (see Table 1).

The relative configuration of the acetoxyl group at C-3 of **2** was established on the basis of the coupling constants of H-3 (δ 4.79, 1H, *dd*, $J=3.5$, 3.6 Hz) with H-2α (δ 2.12, 1H, *m*) and H-2β (δ 2.34, 1H, *m*). The coupling constants suggested that the dihedral angles between H-3 and H-2α, and H-2β approximated 60°, thus the H-3 was in the α-orientation and the acetoxyl group was in the β-orientation in compound **2**. On the basis of the above evidence, the structure of taibaijaponicain B (**2**) was determined to be 3β-acetoxy-6β,11α-dihydroxy-16α-methoxymethyl-6,20-epoxy-6,7-*seco-ent*-kaur-15-one-1,7-olide.

3. Experimental

3.1. General

FAB mass spectra were recorded on a ZAB-HS Instrument (data system: MASPEC II); HR–FAB mass spectrum was recorded in an Autospec 3000 instrument. IR spectra were recorded in KBr pellets on a Nicolet AVATAR 360 FT–IR spectrometer. The optical rotations were measured with a JASCO-20C polarimeter. NMR spectra were recorded on a Bruker AM-400 Instrument. The chemical shift values are given in ppm using TMS as the internal standard.

3.2. Plant material

The plant material of *I. japonica* was collected in Taibai Mountain, Shaanxi Province, PR China, in August 1997. A voucher specimen (SNU 97-08-03, Li) was deposited in the Herbarium of Department of Biology, Shaanxi Normal University.

3.3. Extraction and isolation

The dried powdered leaves and tender branches of *I. japonica* (7.0 kg) were extracted with 95% EtOH (18 l×2) at room temperature for 7 days. After removal of the solvent in vacuo, the residue was partitioned in H_2O and extracted with petroleum ether (4 l×3) and EtOAc (4 l×3), respectively. The EtOAc extract (130 g) was subjected to CC on silica gel (3 kg, 200–300 mesh), eluting with $CHCl_3$ and increasing proportions of Me_2CO (from $CHCl_3$ 100% to Me_2CO 100%). Fractions were combined by monitoring with TLC. All components were further purified by column chromatography and preparative TLC on silica gel to give β-sitosterol (1.13 g, 0.016%), oleanolic acid (2.6 g, 0.037%), norhendosin A (273 mg, 0.0039%), rabdophyllin G (67 mg, 0.00096%), dihydroenmein (315 mg, 0.0045%), nodosin (**3**, 110 mg, 0.0016%), enmein (384 mg, 0.0055%), taibaijaponicain A (**1**, 236 mg, 0.0034%), taibaijaponicain B (**2**, 89 mg, 0.0013%), rabdosin A (95 mg, 0.0014%), orderly.

3.4. Taibaijaponicain A (*1*)

An amorphous powder; $[\alpha]_D^{17}$ −104.7° (*c* 0.49, acetone); IR ν_{max}^{KBr} cm^{-1}: 3358, 2925, 2800, 1765, 1720, 1504, 1461, 1264, 1126, 1072 and 1050; FABMS *m/z*: 401 $[M+Li]^+$, 417 $[M+Na]^+$; HR–FABMS *m/z* 395.4644 $[M+1]^+$ for $C_{21}H_{30}O_7$ (calc. 395.4666); ^1H NMR spectral data (400 MHz) and principal HMBC correlations are listed in Table 1; DEPT, ^{13}C NMR spectral data are listed in Table 2. Most of the NOESY correlations are shown in Fig. 1.

3.5. Taibaijaponicain B (*2*)

An amorphous powder; $[\alpha]_D^{17}$ −98.6° (*c* 0.5, acetone); IR ν_{max}^{KBr} cm^{-1}: 3360, 2921, 1766, 1742, 1720, 1463, 1370,

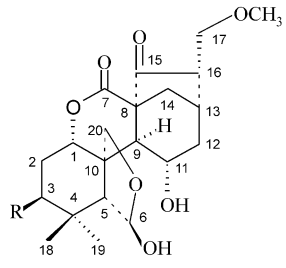

1. R=H
2. R=AcO

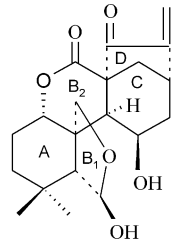

3

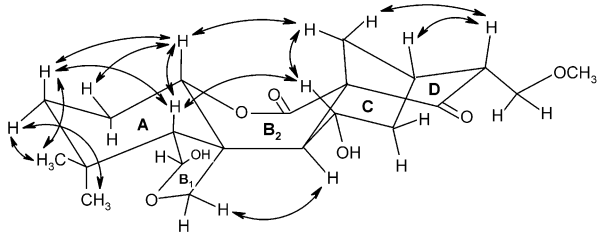
H
H
H

1264, 1052 and 908; FABMS m/z: 459 $[M+Li]^+$, 475 $[M+Na]^+$; ^1H NMR spectral data (400 MHz) and principal HMBC correlations are listed in Table 1; DEPT, ^{13}C NMR spectral data are listed in Table 2.

Acknowledgements

We are grateful for the financial support from the Natural Science Foundation of Shaanxi Province, PR China. We would like to thank Professor Xuan Tian, Department of Chemistry, Lanzhou University (PR China), for helpful discussions.

References

Cheng, P.Y., Guo, Y.W., Xu, M.J., 1987. Pharmaceutical prospects of *Rabdosia* species. Zhong Yao Tong Bao 12, 707.

Fujita, E., Taoka, M., Nagao, Y., Fujita, T., 1973. Terpenoids. XXV. J. Chem. Soc., Perkin Trans. 1, 16, 1760.

Li, J.C., Liu, C.J., An, X.Z., Wang, M.T., Zhao, T.Z., Yu, S.Z., Zhao, G.S., Chen, R.F., 1982. Study on the antitumor constituent of *Rabdosia japonica* (burm. f) Hara. I. Structure of rabdosins A and B. Yao Xue Xue Bao 17, 682.

Liu, C.J., Li, J.C., An, X.Z., Cheng, R.M., Chen, F.Z., Xu, Y.L., Wang, D.Z., 1982. Studies on the antitumor constituent of *Rabdosia japonica*. II. Structure of rabdosin C. Yao Xue Xue Bao 17, 750.

Meng, X.J., Wang, Q.G., Chen, Y.Z., 1989. Diterpenoids from *Rabdosia japonica*. Phytochemistry 28 (4), 1163.

Takeda, Y., Matsumoto, T., Otsuka, H., 1994. Longirabdolide C, a new diterpenoid from *Rabdosia longituba*. J Nat. Prod. 57 (5), 650.

Wang, M.T., Zhao, T.Z., Li, J.C., Liu, C.J., An, X.Z., 1987. Structures of rabdosinate and rabdosinatol. Acta Chim. Sin. 45 (9), 871.

Xu, F.M., Hu, H.P., Wang, Z.Q., 1996. Studies on diterpenoid constituents in *Rabdosia japonica* (Burm. f.) Hara. Zhong Guo Zhong Yao Za Zhi 21 (11), 678.

Xu, G.Y., 1985. ^1H NMR of *Rabdosia* diterpenoids. Acta Chim. Sin. 43, 35.

Zhao, Q.C., Li, C.S., 1987. Chemical contituents of *Rabdosia japonica* var. glaucocalyx. Zhong Yao Tong Bao 12 (5), 294.

Zhao, Q.Z., Chao, J.H., Wang, H.Q., Sun, H.D., 1984. Chemical constituent in *Rabdosia japonica*. Zhong Cao Yao 15 (2), 49.

PERGAMON

Phytochemistry 58 (2001) 547–551

PHYTOCHEMISTRY

www.elsevier.com/locate/phytochem

Essential oil analysis of 10 Piperaceae species from the Brazilian Atlantic forest

Paulo Roberto Dias dos Santos[a], Davyson de Lima Moreira[a,*], Elsie Franklin Guimarães[b], Maria Auxiliadora Coelho Kaplan[a]

[a]*Núcleo de Pesquisas de Produtos Naturais, Universidade Federal do Rio de Janeiro, CEP. 21941-590, Brazil*
[b]*Botânica Sistemática, Jardim Botânico do Rio de Janeiro, Rio de Janeiro, Brazil*

Received 30 November 2000; received in revised form 22 March 2001

Abstract

The volatile composition of ten Piperaceae species, comprising three genera (*Ottonia, Piper* and *Peperomia*) has been studied. The species were collected in a typical fragment of the Brazilian Atlantic forest, constantly being damaged by human action. The essential oils were obtained by hydrodistillation in a modified Clevenger-type apparatus and their analyses were performed by GC and GC/MS. Identification of the substances was made by comparison of mass spectra and retention indices with literature records. A great number of non-oxygenated monoterpenes and sesquiterpenes were identified. Most of these sesquiterpenes are derived from *E,E*-farnesyl-PP, suggesting a preference of these species to synthesize metabolites from this pathway. Arylpropanoids, although being common compounds produced by Piperaceae species, were not found in these oils. © 2001 Elsevier Science Ltd. All rights reserved.

Keywords: Piperaceae; *Piper*; *Peperomia*; *Ottonia*; Essential oil composition; Monoterpenes; Sesquiterpenes

1. Introduction

The family Piperaceae belonging to the superorder Nymphaeiflorae, order Piperales (Dahlgren, 1980), comprises about 5 genera and 1400 species (Joly, 1977). The genera *Piper* and *Peperomia* are the most representative of the Piperaceae (700 and 600 species, respectively). Some *Piper* species are used in folk medicine to treat many diseases while species of the genus *Peperomia* are mainly used as ornamentals (Duke, 1985). Analysis of volatile constituents from Piperaceae species has revealed the presence of monoterpenes, sesquiterpenes and arylpropanoids (apiol, dillapiol, myristicin, safrole, sarisan,) that have shown interesting biological properties (Parmar et al., 1997; Martins et al., 1998; Moreira et al., 1998). Recently we reported the presence of a butylbenzene derivative in the volatile fraction of *Ottonia anisum* (Moreira et al., 1997). The essential oil compositions of ten species from the Brazilian Atlantic forest, an ecosystem in constant change due to human devastation, were studied. These species are *Ottonia anisum* Sprengel, *Piper amplum* Kunth., *Piper arboreum* var. *arboreum* Yunck., *Piper dilatatum* L.C. Rich, *Piper goesii* Yunck., *Piper hispidum* var. *hispidum* Kunth., *Piper hoffmanseggianum* Rocker & Sehulter, *Piper mollicomum* Kunth., *Peperomia blanda* Kunth. and *Peperomia rupestris* var. *rupestris* Humb. Bonpl. & Kunth. The structures of the compounds in the volatile fractions of these ten species were elucidated satisfactorily by using GC and GC/MS analyses as well as by comparison of their mass spectra and RI values with literature data (McLafferty and Stanffer, 1989; Adams, 1995).

2. Results and discussion

GC/MS analyses and comparison of their MS and RI values with those in the literature permitted records allowed the identification of monoterpenes (acyclic and monocyclic) and sesquiterpenes (acyclic, monocyclic, bicyclic and tricyclic) in the essential oils. In total, 71 different compounds were identified (Tables 1 and 2, Fig. 1). The ketone, 2-tridecanone, was found in significant concentration (> 3%) in the essential oil of *Peperomia rupestris* var. *rupestris* (4.30%), *Piper dilatatum* (4.39%) and *P. mollicomum* (4.29%). The volatile fraction composition

* Corresponding author.
E-mail address: moreiradl@nppn.ufrj.br (D. de Lima Moreira).

0031-9422/01/$ - see front matter © 2001 Elsevier Science Ltd. All rights reserved.
PII: S0031-9422(01)00290-4

Table 1
Essential oil composition of the Piperaceae species

Compound	Percentage											
	RI*[a]	RI[lit.b]	Oan	Peb	Per	Pam	Par	Pdi	Pgo	Phi	Pho	Pmo
Monoterpene hydrocarbons												
α-Pinene	930–943	939	0.55	1.50	0.82	16.78	<0.01	17.7		1.37		
Camphene	944–948	953				0.55		0.26				
β-Pinene	967–979	980	0.23	1.71	0.77	0.27				0.28		
Myrcene	980–995	991			0.62			41.77				
α-Phellandrene	1008–1010	1005					0.28		0.16			
Limonene	1020–1032	1031			1.07	3.50	0.24	0.07				
1,8-Cineole	1026	1033						2.70				
(*Z*)-β-Ocimene	1036–1042	1040			3.13	1.08	2.33	0.55	1.14			
(*E*)-β-Ocimene	1049–1052	1050			1.39		1.42		0.51			
Linalool	1103	1098							0.24			
Perillene	1119	1099							0.20			
neo-Isopulegol acetate	1279	1273						<0.01				
Bornyl acetate	1282	1285				0.30						
Sesquiterpene hydrocarbons												
δ-Elemene	1324–1342	1339	1.09		3.40		3.14	0.35	5.90		3.32	0.43
α-Cubebene	1344	1351						0.19		0.42		
α-Copaene	1367–1377	1376	1.20	3.31	0.63	1.03	0.32	0.38	0.70	2.50		
β-Elemene	1386–1395	1391	2.54		1.15	0.36	0.50	0.36	1.17			0.87
(*E*)-Caryophyllene	1412–1424	1418	8.84	3.32	9.69	9.82	6.40	2.18	13.31	6.30	10.11	
Isobornyl isobutyrate	1439	1429			0.71							
β-Gurjunene	1422–1429	1432	0.41				<0.01	0.39	0.39	1.31		
γ-Elemene	1433–1438	1433					<0.01		0.22			
Neryl acetone	1431	1434						0.41				
α-*trans*-Bergamotene	1432–1436	1436		3.00				0.06		2.11		
α-Guaiene	1440	1439							0.24			
(*Z*)-β-Farnesene	1422–1439	1443	1.17									5.70
α-Caryophyllene	1446–1457	1454	6.90	3.30	1.90	2.45	1.20	0.81	3.25	9.21		4.23
(*E*)-β-Farnesene	1467	1458	1.06									
Seychellene	1455–1473	1460		3.60				0.09				
(*E*)-Muurola-4-(14),5-diene	1463–1460	1460							0.49			
9-*epi*-Caryophyllene	1453–1475	1467						2.15		1.31		
γ-Gurjunene	1475	1473								4.27		
Germacrene D	1476–1490	1480	10.49	3.50	14.95	5.28	3.59	0.43	28.87	7.11	4.95	3.65
Guaiene	1482–1498	1490		6.80	4.54					3.36		
Valencene	1496–1500	1491		3.70			0.40					
Bicyclogermacrene	1495–1508	1494	10.34					1.51				
Germacrene A	1502–1516	1503					3.32					
(*E,E*)-α-Farnesene	1491–1527	1508	1.57		2.65	3.74	0.53		14.09	5.62	7.21	2.03
γ-Cadinene	1510–1522	1513			0.90				2.23	3.03		0.92
Cubebol	1518	1514	2.58									
α-Methyl-ionone	1519	1518					0.39					
$C_{15}H_{24}$	1519	—							1.57			
δ-Cadiene	1520–1541	1524	0.68	3.50	2.73	1.36	1.65	1.41	3.75	3.95		2.29
α-Cadiene	1549	1538						0.55				
Elemol	1551–1556	1549			0.71		2.64					
Germacrene B	1549–1561	1556		3.40	1.93		1.31	0.12	2.42	1.56		1.17
(*E*)-Nerolidol	1559–1588	1564	11.28		0.95	8.30	0.91		2.60	2.50		23.20
Spathulenol	1562–1593	1576	0.52	3.30				0.23		4.05		
Thujopsan-2-α-ol	1581–1601	1581			1.30							
Caryophyllene oxide	1571–1586	1581		3.30		1.00		0.06		5.03		3.07
Globulol	1585–1592	1583				0.56		0.05		0.75		
Guaiol	1600–1606	1595			1.51						4.59	
Widdrol	1610	1597	0.72									
Humulene epoxide II	1597–1613	1606		3.80		0.99		0.06		3.62		2.29
10-*epi*-γ-Eudesmol	1612–1628	1619			5.48		4.37	0.38			15.95	
(1,10-di-*epi*)-Cubenol	1609	1614								1.09		

(*continued on next page*)

Table 1 (*continued*)

Compound	Percentage											
	RI*[a]	RI[lit.b]	Oan	Peb	Per	Pam	Par	Pdi	Pgo	Phi	Pho	Pmo
$C_{15}H_{22}O$	1623	–	3.15									
γ-Eudesmol	1626–1631	1630					14.61				8.51	
epi-α-Cadinol	1638	1640	0.34									
Hinesol	1630–1641	1641			5.94			0.21			19.33	
epi-α-Muurolol	1626–1630	1641							0.91	1.03		
Cubenol	1644–1646	1642	0.71						1.30			
β-Eudesmol	1643–1650	1649			2.76						8.14	
Kongol	1648	1650							0.38			
α-Eudesmol	1646–1653	1652			2.77		12.21				8.27	
α-Cadinol	1657–1665	1653	1.57						2.28			
$C_{15}H_{22}O$	1656	–					2.90					
α-Bisabolol	1670	1683	1.41									
Bulnesol	1664	1664					8.13					
$C_{15}H_{22}O$	1668	–					6.29					
epi-α-Bisabolol	1678	1686	5.54									
(*E,E*)-Farnesol	1689	1722							0.35			10.48
$C_{15}H_{22}O$	1695	–				2.69						
Other		–										
2-Tridecanone	1501	1492			4.30			4.39				4.29
2-Dodecanol	1507	–										0.66
2-Tetradecanol	1515	–			1.53							
2-Nonyl-1-ol	–	–						0.14				

[a] RT* = range of the samples retention indices.
[b] Rt^{lit} = retention indices published.

Table 2
Compound distrubution in the analysed essential oils

Species	Monoterpene (%)		Sesquiterpene (%)		Other[a] (%)	Total[b] (%)	N.[c]
	Non-oxy	Oxy	Non-oxy	Oxy			
Oan	0.78	0.00	49.09	25.49	0.00	75.36	25
Peb	3.21	0.00	40.84	10.40	0.00	54.45	16
Per	6.73	1.07	44.47	21.42	5.83	79.52	28
Pam	18.68	3.80	24.04	10.85	0.00	57.37	17
Par	4.04	0.24	22.59	43.26	0.00	70.13	26
Pdi	60.28	2.78	11.03	0.99	4.53	79.61	33
Pgo	2.01	0.24	77.03	7.82	0.00	87.10	25
Phi	1.65	0.00	52.06	18.07	0.00	71.78	23
Pho	0.00	0.00	25.59	64.79	0.00	90.38	10
Pmo	0.00	0.00	21.29	39.04	5.59	65.92	16

[a] Other substances as *n*-alcanes and ketones.
[b] Total of the identified substances.
[c] Number of identified substances.

of *Peperomia rupestris* var. *rupestris, Piper dilatatum*, *P. goesii* and *P. hoffmansegianum* were found to be rich and diversified with more than 80% of the structures oil constituents successfuly elucidated. The *Ottonia anisum* essential oil had *E*-nerolidol in great concentration (11.28%). Surprisingly, 1 - butyl - 3,4 - methylenedioxybenzene, the major compound (90.00%) identified in the *O. anisum* essential oil collected in Teresopolis (Moreira et al., 1997), was not found in this sample (Table 1). The volatile compositions of the studied *Peperomia* species showed sesquiterpenes as the major fraction (*Peperomia blanda*—51.24% and *Peperomia rupestris* var. *rupestris*—65.89%). Monoterpenes were also identified in these oils in minor amounts (*Peperomia blanda*—3.20% and *Peperomia rupestris*—8.51%). These results are in agreement with published data for some other Brazilian *Peperomia* (Tables 1 and 2, Fig. 1) (Moreira et al., 1999). The essential oil composition from the seven studied *Piper* species was mainly found to be sesquiterpenes (Tables 1 and 2, Fig. 1).

Analysis of the major compounds identified in the oils showed a preference of the Piperaceae (8 of 10 species) to

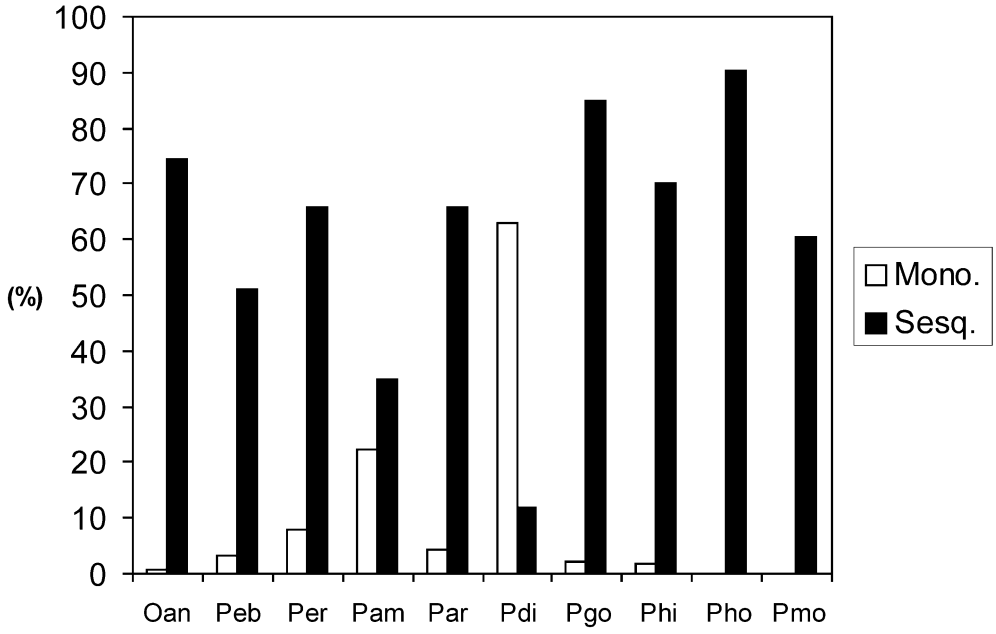

Fig. 1. Monoterpene and sesquiterpene distribution in the selected Piperaceae species for study. Mono. = monoterpenes; Sesq. = sesquiterpenes.

synthesize sesquiterpenes. Non-oxygenated sesquiterpenes were identified as the major compounds of the essential oil of *P. blanda* (guaiene: 6.80%), *P. rupestris* var. *rupestris* (germacrene D: 14.95%), *P. goesii* (gemacrene D: 28.87%), and *P. hispidum* var. *hispidum* (α-caryophyllene: 9.21%). Oxygenated sesquiterpenes were found in great amount in the oils of *O. anisum* (*E*-nerolidol: 11.28%), *P. mollicomum* (*E*-nerolidol: 23.20%), *P. arboreum* var. *arboreum* (γ-eudesmol: 14.61%), and *P. hoffmansegianum* (hinesol: 19.33%). Whereas monoterpenes were found as the major compounds in the essential oils of *P. amplum* (α-pinene: 16.78%) and *P. dilatatum* (myrcene: 41.77%).

The most frequent compounds identified in the oils were also sesquiterpenes. However, the non-oxygenated monoterpenes (*Z*)-β-ocimene (5/10)[1], α-pinene (6/10) and β-pinene (6/10) were well represented. Only 13 different types of sesquiterpenes were identified in at least 5 of the 10 studied species, and among them, 10 were non-oxygenated. A biosynthetic approach showed that the most common sesquiterpenes identified in the oils from these species have the *E*,*E*-farnesyl-PP as fundamental precursor (Dewick, 1997). In fact, a great number of the most representative sesquiterpenes (11 types), including those of higher occurrence (*E*-caryophyllene: 9/10 and gemacrene D: 10/10), are formed primarily from *E*,*E*-farnesyl-PP. This analysis also showed that only 2 different sesquiterpenes types originated from *E*,*Z*-farnesyl-PP reactions (α-copaene: 8/10 and δ-cadinene: 9/10).

Considering the average mono- and sesquiterpene contents for each studied Piperaceae genus (*Ottonia, Peperomia* and *Piper*), it is interesting that significant differences were not observed for the sesquiterpene fractions (oxygenated and non-oxygenated) but for monoterpenes, the non-oxygenated representatives were considerably more abundant (Table 2).

Our observations suggest the trend of these Piperaceae from the Brazilian Atlantic forest to give larger number of non-oxygenated sesquiterpenes derived from the *E*,*E*-farnesyl-PP precursor.

3. Experimental

3.1. Plant material

Leaves from *Ottonia anisum* Sprengel (Oan), *Piper amplum* Kunth. (Pam), *Piper arboreum* var. *arboreum* Yunck. (Par), *Piper dilatatum* L.C. Rich (Pid), *Piper goesii* Yunck. (Pgo), *Piper hispidum* var. *hispidum* Kunth. (Phi), *Piper hoffmanseggianum* Rocker & Sehulter (Pho), *Piper mollicomum* Kunth. (Pmo) and aerial parts of *Peperomia blanda* Kunth. (Peb) and of *Peperomia rupestris* var. *rupestris* Humb. Bonpl. & Kunth. (Per) were collected near Paraty, Rio de Janeiro State, Brazil, in May 1997. The plants were identified by the botanist Prof. Elsie F. Guimarães and botanical samples are found at the Herbarium of the Botanical Garden of Rio de Janeiro, Rio de Janeiro, Brazil.

3.2. Isolation of the essential oil

Each fresh plant material was submitted to hydrodistillation for one hour in a modified Clevenger-type apparatus. A sample of the obtained essential oils was dissolved in dichloromethane for GC and GC/MS analyses (Moreira et al., 1997).

[1] Frequence in the studied species.

3.3. Analysis of essential oil

GC analysis: GC analysis was performed using a Varian Star 3400 CX gas chromatograph, fused silica capillary column (DB-5, 30 m×0.20 mm), flame-ionization detector, hydrogen as carrier gas and temperature programming from 60 to 240 °C (3 °C/min). Retention times (RT) were measured in minutes and the relative amount in percent values of each compound in the mixture was obtained directely from the GC data.

3.3.1. GC/MS analysis

GC/MS analysis was performed using a HP5890 SII gas chromatograph coupled to a VG Autospec mass spectrometer at 70 eV, fused silica capillary column (DB-1, 30 m×0.20 mm), helium as carrier gas and temperature programming from 60 to 240 °C (3 °C/min).

3.3.2. Retention indices

Retention indices (RI) were calculated using GC data of a saturated aliphatic hydrocarbon homologous series within C_8 to C_{22}, performed in the same column and conditions as used in the GC analysis for the essential oils.

3.3.3. Compound identification

Identification of the substances was carried out primarily by comparing the mass spectra with a computer databank (National Institute for Standard Technology–NIST–62,235 compounds). Further visual comparison of the mass spectra with literature records and comparison of the RI permitted identification of the major compounds (McLafferty and Stanffer, 1989; Adams, 1995).

References

Adams, R.P., 1995. Identification of Essential Oil Components by Gas Chromatography/Mass Spectroscopy. Allured, Carol Stream, IL, USA.

Dahlgren, R.M.T., 1980. A revised system of classification of the angiosperms. Bot. J. Linn. Soc. 80 (2), 91–124.

Dewick, P.M., 1997. Medicinal Natural Products, A Biosynthetic Approach. John Wiley & Sons, UK, pp. 172–184.

Duke, J.A., 1985. Handbook of Medicinal Herbs. CRC, New York, pp. 378–383, 521, 563.

Joly, A.B., 1977. Botânica- Introdução à Taxonomia Vegetal. Companhia Editora Nacional, São Paulo, Brazil.

Martins, A.P., Salguero, L., Vila, R., Tomi, F., Cañigueral, S., Casanova, J., Proença da Cunha, A., Adzet, T., 1998. Essential oils from *Piper* species. Phytochemistry 49 (7), 2019–2023.

McLafferty, F.W., Stanffer, D.B., 1989. Registry of Mass Spectral Data, Vols I–II. Wiley-Interscience, New York.

Moreira, D.L., Guimarães, E.F., Kaplan, M.A.C., 1997. 1-Butyl-3,4-methylenedioxybenzene as the major constituent of essential oil from *Ottonia anisum* Sprengel (Piperaceae). J. Essent. Oil Res. 9, 565–568.

Moreira, D.L., Guimarães, E.F., Kaplan, M.A.C., 1998. Essential oil analysis of two *Piper* species (Piperaceae). An. Acad. Bras. Ci. 70 (4), 751–754.

Moreira, D.L., Guimarães, E.F., Kaplan, M.A.C., 1999. Essential oil analysis of four *Peperomia* species (Piperaceae). Acta Horticulturae 500 (1), 65–70.

Parmar, V.S., Jain, S.C., Bisht, K.S., Jain, R., Taneja, P., Jha, A., Tyagi, O.D., Prasad, A.K., Wengel, J., Olsen, C.E., Boll, P.M., 1997. Phytochemistry of the genus *Piper*. Phytochemistry 46 (4), 597–673.

PERGAMON

Phytochemistry 58 (2001) 553–556

PHYTOCHEMISTRY

www.elsevier.com/locate/phytochem

Bacopaside I and II: two pseudojujubogenin glycosides from *Bacopa monniera*

Ajit K. Chakravarty[a,*], Tapas Sarkar[a], Kazuo Masuda[b], Kenji Shiojima[b], Takahisa Nakane[c], Nobuo Kawahara[c]

[a]*Indian Institute of Chemical Biology, Calcutta 700 032, India*
[b]*Showa Pharmaceutical University, Machida, Tokyo 194-8543, Japan*
[c]*National Institute of Health Sciences, 1-18-1 Kamiyoga, Setagaya-ku, Tokyo 158-8501, Japan*

Received 13 October 2000; received in revised form 15 March 2001

Abstract

Two saponins, designated as bacopaside I and II, have been isolated from *Bacopa monniera* Wettst. and their structures have been elucidated as 3-*O*-α-L-arabinofuranosyl-(1→2)-[6-*O*-sulphonyl-β-D-glucopyranosyl-(1→3)]-α-L-arabinopyranosyl pseudojujubogenin **(1)** and 3-*O*-α-L-arabinofuranosyl-(1→2)-[β-D-glucopyranosyl (1→3)]-β-D-glucopyranosyl pseudojujubogenin **(2)** mainly on the basis of 2D NMR and other spectral analyses. © 2001 Elsevier Science Ltd. All rights reserved.

Keywords: *Bacopa monniera*; Scrophulariaceae; Saponins; Bacopaside I; Bacopaside II; Pseudojujubogenin; 2D NMR

1. Introduction

The reputation of *Bacopa monniera* Wettst. as a nervine tonic is well known in Indian traditional medicine (Chopra et al., 1969). Recent pharmacological studies indeed confirmed the activity (Singh and Dhawan, 1978, 1982; Singh et al., 1988). It was also confirmed that the activity was due to the saponins present in the alcoholic extract of the plant. Because of the presence of a large number of glycosidic constituents in the extract as an intimate mixture, two groups of workers could isolate and characterize only a part of the constituents (Jain and Kulshrestha, 1993; Rastogi et al., 1994; Garai et al., 1996a,b; Rastogi and Kulshrestha, 1998; Mahato et al., 2000). In view of the increasing interest on this herb drug, we undertook a thorough chemical re-investigation of the glycosidic fraction of the methanol extract of the plant and have been able to isolate two new pseudojujubogenin glycosides, designated as bacopaside I (**1**) and II (**2**). The present paper reports the isolation and structure elucidation of these two saponins.

2. Results and discussion

Bacopaside I (**1**) and II (**2**) were isolated from the dark green solid which separated out from the methanol extract of the plant on concentrating and cooling. While **1** was obtained by direct crystallization of a chromatographic fraction of the above mentioned green solid, **2** could be isolated by prep. HPLC of a less polar fraction of the chromatography (vide Experimental). Both the compounds gave a positive froth test for the saponins and Liebermann–Burchard test for triterpenes. The sugar constituents present in the saponins were identified to be glucose and arabinose by PC and GC of their acid hydrolysates. The absolute configuration of the sugars as D and L respectively were determined by the specific rotations (vide Experimental) of the sugars isolated by prep. paper chromatography of the hydrolysates.

^{13}C NMR spectrum (Table 1) of **1**, mp 260–261 °C (decomp.), $[\alpha]_D$ −35.6°, displayed signals for 46 carbons, of which 30 were assigned to the triterpene moiety and 16 to the sugar units indicating that there must be one unit of glucose and two units of arabinose in the molecule and this was corroborated by the GC analysis of their alditol acetates. Its 600 MHz ^{1}H NMR spec-

* Corresponding author. Fax: +91-33-4730-2840.
E-mail address: akchakravarty@iicb.res.in (A.K. Chakravarty).

0031-9422/01/$ - see front matter © 2001 Elsevier Science Ltd. All rights reserved.
PII: S0031-9422(01)00275-8

trum (Table 2) exhibited signals for seven methyl groups on tertiary carbons, two –CH_2–O–, one –CH–O– protons and one vinylic proton of a trisubstituted double bond, besides the protons of two arabinose and one glucose units. Moreover, the presence of a ketal group (δ_C 110.3 s) and an oxygenated quaternary carbon (δ_C 71.8 s) in the aglycone moiety was evident from its ^{13}C NMR spectrum (Table 1). Detailed analysis of the 2D HMBC spectrum of the compound clearly revealed that the compound is a saponin containing pseudojujubogenin (Garai et al., 1996a) as the aglycone and that a trisaccharide unit is attached through the oxygen at C-3 of the aglycone.

Of the two arabinose units of the trisaccharide moiety, one exists in pyranose form and the other in furanose form as would be evident from the splitting pattern and chemical shifts (Table 2) of their anomeric protons (Garai et al., 1996a). The chemical shifts of all the individual protons of the three sugar units were ascertained from a combination of 2D ^1H–^1H HOHAHA and ^1H–^1H COSY spectral analyses and accordingly ^{13}C chemical shifts of their attached carbons could be assigned unambiguously from the HMQC spectrum of the compound.

Having thus assigned all the ^{13}C and ^1H chemical shifts of the three sugar units (Tables 1 and 2), it is clear that the arabinofuranose and glucopyranose units are linked to C-2′ and C-3′ of the arabinopyranose unit. However, the exact positions of attachment of the two sugar units to arabinopyranose unit could be established from its HMBC spectrum as follows.

The HMBC correlations between (i) arabinofuranose anomeric proton (H-1″, δ 6.04) and C-2′ (δ 76.3) of arabinopyranose, (ii) glucopyranose anomeric proton (H-1‴, δ 4.99) and C-3′ (δ 84.1) of arabinopyranose, and (iii) anomeric proton (H-1′, δ 4.81) of arabinopyranose and C-3 (δ 88.7) of the aglycone conclusively proved that the arabinofuranose and glucopyranose units are linked respectively to C-2′ and C-3′ of the arabinopyranose

Table 1
^{13}C NMR chemical shifts[a] of bacopasides I (**1**) and II (**2**) in pyridine-d_5

Carbon	1	2	Carbon	1	2
1	38.7	38.7	26	26.1	26.1
2	26.7	26.7	27	18.5	18.5
3	88.7	89.1	28	27.7	27.8
4	39.8	39.7	29	16.6	16.6
5	56.1	56.1	30	65.8	65.9
6	18.3	18.3	3-*O*-Ara(p) **1**, 3-*O*-Glc **2**		
7	36.0	36.0	1′	105.4	105.1
8	37.5	37.5	2′	76.3	79.1
9	53.0	52.9	3′	84.1	88.7
10	37.2	37.1	4′	67.7	70.3
11	21.7	21.7	5′	65.4	77.9
12	28.6	28.6	6′	-	62.7
13	37.0	37.0	Ara(f)		
14	53.5	53.5	1″	110.0	109.9
15	36.9	36.9	2″	83.7	83.8
16	110.3	110.3	3″	77.6	77.8
17	51.3	51.2	4″	84.7	85.0
18	18.8	18.8	5″	61.8	62.1
19	16.4	16.3	Glc		
20	71.8	71.8	1‴	105.0	104.8
21	27.2	27.2	2‴	74.8	75.5
22	46.2	46.2	3‴	77.3	78.4
23	66.1	66.1	4‴	70.7	71.6
24	124.1	124.2	5‴	76.3	78.6
25	132.9	132.9	6‴	67.1	62.4

[a] Chemical shifts were assigned on the basis of 2D NMR, viz. ^1H–^1H COSY, HMQC, HMBC and NOESY spectral analyses. Spectra of **1** and **2** were recorded in 600 MHz and 500 MHz instruments respectively. Ara(p) = arabinopyranose; Ara(f) = arabinofuranose; Glc = glucopyranose.

Table 2
^1H NMR chemical shifts[a] of bacopasides I (**1**) and II (**2**) in pyridine-d_5

Proton	1	2	Proton	1	2
H_3-18	1.04*s*	0.98*s*	H-4′	4.58*br. s*	3.93*m*
H_3-19	0.69*s*	0.60*s*	H-5′	3.70d (11.7), 4.27*m*	3.82*m*
H_3-21	1.37*s*	1.32*s*	H-6′	–	4.18*m*, 4.45*m*
H_3-26	1.66*s*	1.62*s*	H-1″	6.04*br. s*	6.24*d* (3.0)
H_3-27	1.59*s*	1.54*s*	H-2″	4.97*m*	5.01*m*
H_3-28	1.22*s*	1.22*s*	H-3″	4.86*t* (7.4)	4.83*m*
H_3-29	1.03*s*	1.01*s*	H-4″	4.74*m*	4.79*m*
H_3-30	4.18*m*, 4.28*m*	4.14*m*, 4.24*m*	H-5″	4.23*m*, 4.32*br.d* (10.2)	4.18*m*, 4.30*dd* (12.0, 3.0)
H_3-23	3.86*d* (10.2), 4.70*d* (10.2)	3.82*dd* (11.0, 2.5), 4.67*dd* (11.0, 2.0)	H-1‴	4.99*d* (7.0)	5.18*d* (7.5)
H-3	3.22*dd* (11.7, 4.0)	3.22*dd* (11.5, 4.0)	H-2‴	3.78*t* (8.1)	3.96*m*
H-13	2.83*m*	2.78*m*	H-3‴	4.11*t* (8.8)	4.16*m*
H-24	5.83*d* (9.9)	5.80*d* (10.5)	H-4‴	4.14*m*	4.06*m*
H-1′	4.81*d* (5.8)	4.83*d* (8.0)	H-5‴	4.01*m*	3.96*m*
H-2′	4.52*t* (7.3)	4.05*m*	H-6‴	4.99*m*, 5.06*m*	4.16*m*, 4.52*m*
H-3′	4.21*m*	4.15*m*			

[a] Chemical shifts were assigned on the basis of 2D NMR, viz. ^1H–^1H COSY, HMQC, HMBC and NOESY spectral analyses. Spectra of **1** and **2** were recorded in 600 and 500 MHz instruments respectively.

which, in turn, is linked to C-3 of the aglycone. The above structural assignment was in total agreement with the NOE interactions observed in the NOESY spectrum of the compound.

Based on the above assigned structure, the molecular mass of the compound should be 898 ($C_{46}H_{74}O_{17}$). However, the positive and negative ion FAB mass spectra showed the molecular mass to be 978. This difference of 80 mass units could, however, be accommodated by assuming that the compound is a sulphate. This contention was indeed confirmed by high resolution positive ion FAB mass spectral analysis which showed $[M+H]^+$ ion at m/z 979.4592 and $[M+Na]^+$ ion at m/z 1001.4383 corresponding to the molecular formula $C_{46}H_{74}O_{20}S$.

Now, a careful look at the ^1H and ^{13}C chemical shifts of the compound revealed that the methylene protons (H_2-6‴) and carbon (C-6‴) of the glucopyranose unit experienced deshielding by more than 0.5 (Table 2) and 4.5 ppm (Table 1) respectively compared to those observed in **2** demonstrating that the sulphate group must be linked to C-6‴ of the glucopyranose unit. This was also supported by the observed up-field shift of C-5‴ signal by 2.3 ppm (γ effect) as against that of **2**.

Based on the above observations, bacopaside I may be represented as 3-*O*-α-L-arabinofuranosyl-(1→2)-[6-*O*-sulphonyl-β-D-glucopyranosyl-(1→3)]-α-L-arabinopyranosyl pseudojujubogenin (**1**).

Bacopaside II (**2**), mp 249–251 °C, $[\alpha]_D$ -34.3^0, showed in its positive ion high resolution FAB–MS, the $[M+H]^+$ at m/z 929.5110 corresponding to the molecular formula $C_{47}H_{76}O_{18}$. Of the 47 carbon signals in its ^{13}C NMR spectrum (Table 1), 17 signals were due to sugar units demonstrating the presence of two glucose and one arabinose units and this was indeed confirmed by the GC analysis of their alditol acetates. A comparison of the ^{13}C chemical shifts of the aglycone part of the compound with those of **1** (Table 1) revealed that this compound also contains pseudojujubogenin as the aglycone, and it differs from **1** only with respect to the trisaccharide moiety attached to C-3 of the aglycone.

For determining the linkages among the sugar units of the trisaccharide moiety, the ^{13}C and ^1H chemical shifts of the individual sugar units were assigned from a combination of 2D ^1H–^1H HOHAHA, ^1H–^1H COSY and HMQC spectral analyses (Tables 1 and 2). It was clear from the chemical shifts of the arabinose unit that it exists in the furanose form. That the arabinofuranose and one glucopyranose units are linked to C-2′ and C-3′ respectively of another glucopyranose unit became evident from the HMBC correlations between (i) the anomeric proton (H-1″, δ 6.24) of the arabinofuranose and C-2′ (δ 79.1) of the inner glucose, and (ii) the anomeric proton (H-1‴, δ 5.18) of the terminal glucose and C-3′ (δ 88.7) of the inner glucose. The correlation of the anomeric proton (H-1′, δ 4.83) of the inner glucose with C-3 (δ 89.1) of the aglycone demonstrated that the trisaccharide moeity is attached to C-3 of the aglycone through the inner glucose unit. The assigned linkages were also found to be in excellent agreement with the NOE interactions observed in the NOESY spectrum of the compound.

Based on the above evidence, bacopaside II may be represented as 3-*O*-α-L-arabinofuranosyl-(1→2)-[β-D-glucopyranosyl (1→3)]-β-D-glucopyranosyl pseudojujubogenin (**2**).

3. Experimental

The plant material was collected in May from the suburbs of Calcutta and supplied by M/s United Chemical and Allied Products, 10 Clive Row, Calcutta 700 001. A voucher specimen is available in the herbarium of the company. Mps: uncorr; IR: KBr discs; 1D and 2D NMR: 500 and 600 MHz in pyridine-d_5; GC: ECNSS-M, 3% on Gas-Chrom Q at 190 °C for alditol acetates which were identified by co-injection of the authentic samples; HPLC: C_{18} column (7 mm i.d.), H_2O–MeOH (30:70) as the mibile phase, UV absorbance detector (217 nm).

The air-dried and powdered arial parts of *Bacopa monniera* (4.4 kg) were successively extracted with petroleum ether (b.p. 60–80 °C) and MeOH in a percolator at room temp. The MeOH extract was concd. and kept overnight at room temp. The separated deep green solid was filtered, washed with MeOH and air dried to get a pasty solid (20 g). The solid was subjected to column chromatography over Si gel (1 kg) and eluted with $CHCl_3$ and $CHCl_3$–MeOH mixtures having increasing proportions of MeOH. Elution with $CHCl_3$–MeOH (9:1 and 4:1) gave fr. A and with $CHCl_3$–MeOH (7:3) afforded fr.B. The latter fraction on repeated crystallizations from MeOH yielded **1** (49 mg). Fr.A was further purified by repeated CC over Si gel and by precipitation from MeOH solution by addition of acetone to get a mixture of components (single spot in TLC) as white powder (3 g). A part (0.2 g) of this was then subjected to prep. HPLC to afford **2** (36 mg), besides the already known saponins, viz. bacopa saponin C (Garai et al., 1996a), bacoside A_3 (Rastogi et al., 1994) and 3-*O*-α-L-arabinofuranosyl-(1→2)-[β-D-glucopyranosyl-(1→3)]-α-L-arabinopyranosyl jujubogenin (Higuchi et al., 1984).

3.1. Bacopaside I (*1*)

White powder (MeOH), mp 260–261 °C (dec.), $[\alpha]_D$ −35.6° (MeOH, *c* 0.20). IR ν_{max} (KBr) cm^{-1}: 1221, 696 (sulphate). HR–FABMS (positive) m/z: 979.4592 $[M+H]^+$; calc. for $[C_{46}H_{74}O_{20}S+H]^+$: 979.4572. ^{13}C NMR: Table 1. ^1H NMR: Table 2.

3.2. Bacopaside II (2)

Amorphous powder, mp 249–251 °C, $[\alpha]_D$ −34.3° (MeOH, *c* 0.40). HR–FABMS (positive) *m/z*: 929.5110 $[M+H]^+$; calc. for $[C_{47}H_{76}O_{18}+H]^+$: 929.5109. ^{13}C NMR: Table 1. ^1H NMR: Table 2.

3.3. Hydrolysis of 1 and 2

Compounds **1** and **2** (20 mg each) were hydrolysed separately with 2 N HCl in aq. MeOH (10 ml) on a steam bath for 5 h. The reaction mixtures were cooled, diluted with water (10 ml) and extracted with $CHCl_3$. The aqueous parts were neutralised with Ag_2CO_3 and filtered. The filtrates were concd under reduced pressure and examined for sugars by PC (EtOAc–pyridine–H_2O; 2:1:2). Two spots were detected corresponding to arabinose (R_f 0.23) and glucose (R_f 0.19) in both cases. Small portions of the filtrate concentrates were reduced with $NaBH_4$, worked up as usual and the products were acetylated with Ac_2O–pyridine. The acetates were then subjected to GC analysis. Two peaks corresponding to glucitol acetate and arabinitol acetate in 1:2 ratio in case of **1** and in 2:1 ratio in case of **2** were observed.

The remaining portion of the filtrate concentrate obtained from **1** was subjected to prep. PC to obtain D-glucose, $[\alpha]_D$ +55° (H_2O, *c* 0.15) and L-arabinose, $[\alpha]_D$ +101° (H_2O, *c* 0.21). In an identical way, prep PC of the remaining portion of the filtrate concentrate obtained from the hydrolysate of **2** yielded D-glucose and L-arabinose.

References

Chopra, R.N., Chopra, I.C., Verma, B.S., 1969. Glossary of Indian Medicinal Plants. CSIR, New Delhi.

Garai, S., Mahato, S.B., Ohtani, K., Yamasaki, K., 1996a. Dammarane-type triterpenoid saponins from *Bacopa monniera*. Phytochemistry 42, 815–820.

Garai, S., Mahato, S.B., Ohtani, K., Yamasaki, K., 1996b. Bacopasaponin D—a pseudojujubogenin glycoside from *Bacopa monniera*. Phytochemistry 43, 447–449.

Higuchi, R., Kubota, S., Komori, T., Kawasaki, T., Pandey, V.B., Singh, J.P., Shah, A.H., 1984. Triterpenoid saponins from the bark of *Zizyphus joazeiro*. Phytochemistry 23, 2597–2600.

Jain, P., Kulshrestha, D.K., 1993. Bacoside A_1, a minor saponin from *Bacopa monniera*. Phytochemistry 33, 449–451.

Mahato, S.B., Garai, S., Chakravarty, A.K., 2000. Bacopasaponins E and F: two jujubogenin bisdesmosides from *Bacopa monniera*. Phytochemistry 53, 711–714.

Rastogi, S., Pal, R., Kulshrestha, D.K., 1994. Bacoside A_3–A triterpenoid saponin from *Bacopa monniera*. Phytochemistry 36, 133–137.

Rastogi, S., Kulshrestha, D.K., 1998. Bacoside A_2–A triterpenoid saponin from *Bacopa monniera*. Indian Journal of Chemistry 38B, 353–356.

Singh, H.K., Dhawan, B.N., 1978. The effect of *Bacopa monniera* on the learning ability of rats. Indian Journal of Pharmacology 10, 72.

Singh, H.K., Dhawan, B.N., 1982. Effect of *Bacopa monniera* extract on avoidance responses in rats. Journal of Ethnopharmacology 5, 205–214.

Singh, H.K., Rastogi, R.P., Srimal, R.C., Dhawan, B.N., 1988. Effect of bacosides A and B on avoidance responses in rats. Phytotheraphy Research 2, 70–75.

PERGAMON

Phytochemistry 58 (2001) 557–561

PHYTOCHEMISTRY

www.elsevier.com/locate/phytochem

Bufadienolides from *Drimia robusta* and *Urginea altissima* (Hyacinthaceae)

Tracy Pohl[a], Chantal Koorbanally[a], Neil R. Crouch[b], Dulcie A. Mulholland[a,*]

[a]*Natural Products Research Group, Department of Chemistry, University of Natal, Durban, 4041, South Africa*
[b]*Ethnobotany Unit, National Botanical Institute, PO Box 52099, Berea Road, Durban 4007, South Africa*

Received 16 August 2000; received in revised form 10 April 2001

Abstract

The bufadienolides, 6β-acetoxy-3β,8β,12β,14β-tetrahydroxybufa-4,20,22-trienolide (12β-hydroxyscillirosidin) (**1**) and 14β-hydroxybufa-4,20,22-trienolide 3β-*O*-{α-L-rhamnopyranosyl-[(1→4)-β-D-glucopyranosyl]-(1→3)-α-L-rhamnopyranoside} (urginin) (**2**) were isolated from *Drimia robusta* and *Urginea altissima*, respectively. © 2001 Elsevier Science Ltd. All rights reserved.

Keywords: *Drimia robusta*; *Urginea altissima*; Hyacinthaceae; Bufadienolides; 6β-Acetoxy-3β,8β,12β,14β-tetrahydroxybufa-4,20,22-trienolide (12β-hydroxyscillirosidin); 14β-Hydroxybufa-4,20,22-trienolide; 3β-*O*-{α-L-Rhamnopyranosyl-[(1→4)-β-D-glucopyranosyl](1→3)-α-L-rhamnopyranoside} (urginin)

1. Introduction

The subfamily Urgineoideae of the Hyacinthaceae, in which both the genera *Drimia* Jacq. ex Willd. and *Urginea* Steinh. have been placed, is phytochemically characterised by the presence of bufadienolides (Speta, 1998). *Urginea* is a heterogeneous, poorly understood genus in need of revision (Speta, 1998), and has at times been included in the genus *Drimia* (Jessop, 1977).

Drimia robusta Bak. from southern Africa is a heavily utilised Zulu medicinal plant (Cunningham, 1990) with preparations employed as diuretics (Van Wyk et al., 1997) emetics, expectorants (Watt and Breyer-Brandwijk, 1962), to treat febrile complaints (Hutchings et al., 1996), diseases of the uterus (Van Wyk et al., 1997) and to promote the healing of broken bones (Ndlovu, pers. commun.). Ethanolic and ethyl acetate extracts of *D. robusta* have, respectively, been found to possess anti-inflammatory and antibacterial activities and although Luyt and co-workers attributed this activity to the presence of proscillaridin A, this compound was not positively identified (Luyt et al., 1999).

Urginea altissima (L.f.) Bak. is extremely widespread, occurring throughout most of sub-Saharan Africa. Across its range, bulbs find both ethnomedical (Watt and Breyer-Brandwijk, 1962) and ethnoveterinary (Burkill, 1955) applications. In South Africa, bulb preparations are variously employed in the treatment of gout (Smith, 1966), rheumatism (Watt and Breyer-Brandwijk, 1962) and a range of respiratory complaints including asthma (Smith, 1966), influenza and bronchitis (Watt and Breyer-Brandwijk, 1962). Although Miyakado et al. (1975) have reported on the isolation and identification of the isoquinoline alkaloids lycorine and acetylcaranine from the bulbs of *U. altissima*, this finding is questionable. Verdcourt and Trump (1969) have pointed out that the cottony appearance of the torn leaf bases of *U. altissima* could lead to its confusion with some amaryllidaceous bulbs, including *Boophane* and *Crinum*, which is likely in this case. Unfortunately, no herbarium voucher was lodged to vouch for the correct identification of their material, which was sourced in Ethiopia. The report of typical Amaryllidaceae type alkaloids from the Hyacinthaceae prompted the reinvestigation of *U. altissima*.

Both *D. robusta* (syn. *D. alta* R.A.Dyer) and *U. altissima* are reportedly toxic (Steyn, 1936; Van der Walt and Steyn, 1943), exhibit digitalis-like action (Sapieka, 1951) and possess caustic saps.

* Corresponding author. Tel.: +27-31-260-1108; fax: +27-31-260-3091.

E-mail address: mulholld@nu.ac.za (D.A. Mulholland).

0031-9422/01/$ - see front matter © 2001 Elsevier Science Ltd. All rights reserved.
PII: S0031-9422(01)00225-4

2. Results and discussion

Compound **1** was isolated from the dichloromethane extract of *D. robusta*. High resolution mass spectrometry gave the highest peak at m/z 414.2056 g mol^{-1} which indicated a molecular formula of $C_{24}H_{30}O_6$. However, NMR spectroscopy indicated that this was not the molecular ion, but that a molecule of acetic acid had been lost giving the correct molecular formula $C_{26}H_{34}O_8$. Use was made of ^{1}H, ^{13}C, HSQC, HMBC, COSY, TOCSY and NOESY spectra to determine the structure of the compound and to assign all ^{1}H and ^{13}C NMR resonances (Table 1).

The presence of a bufadienolide side-chain at C-17 was indicated by coupled resonances at δ 7.94, 7.41 and 6.27 in the ^{1}H NMR spectrum ascribable to H-22, H-21 and H-23, respectively, and δ 123.8, 149.6, 148.1, 114.2, and 163.5 ascribable to C-20, 21, 22, 23 and 24, respectively, in the ^{13}C NMR spectrum. Two secondary hydroxy groups and a secondary acetoxy group were indicated by methine resonances at δ 67.1, 76.1 and 76.1 in the ^{13}C NMR spectrum and corresponding resonances at δ 4.10,

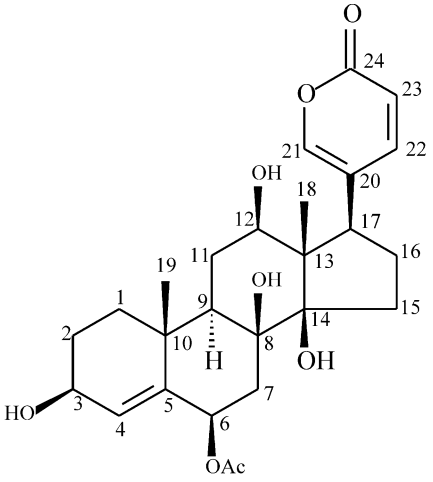

1

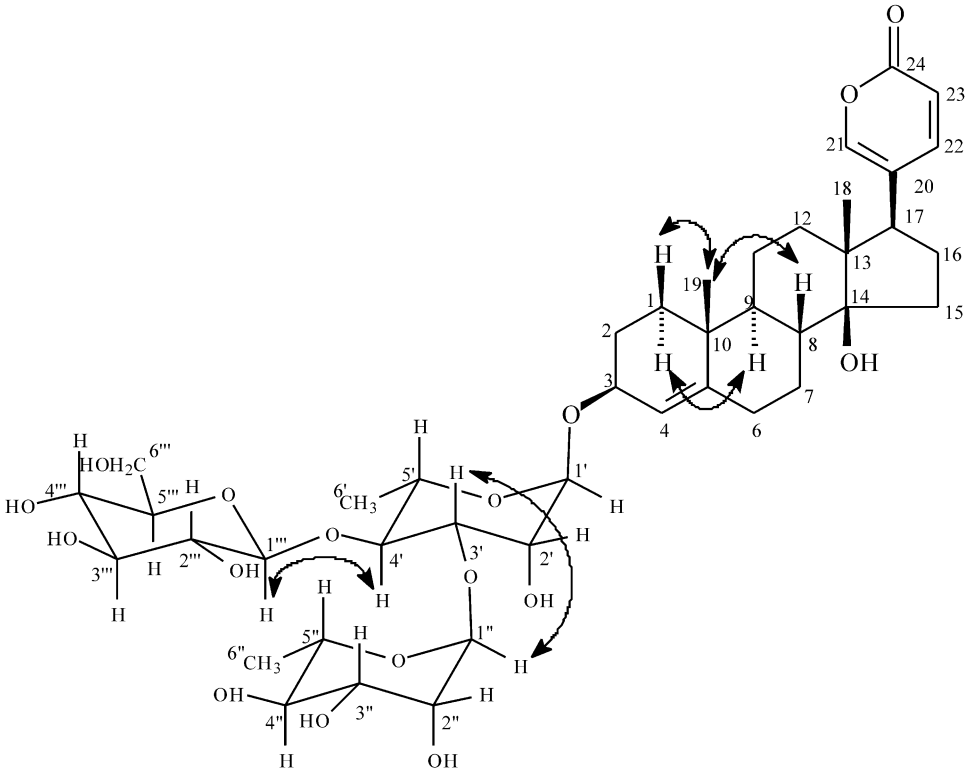

2 (Showing important NOE correlations)

3.43 and 5.43 and a three proton singlet at δ 1.99 at the ^{1}H NMR spectrum. The presence of two tertiary hydroxyl groups was indicated by carbon resonances at δ 75.7 and 85.6 and a trisubstituted alkene double bond was indicated by resonances at δ 133.3 (CH) and δ 140.7 (C). The alkene proton was present at δ 5.73 in the ^{1}H NMR spectrum and this proton was coupled to the methine resonance at δ 4.10. The TOCSY and HETCOR spectra indicated the presence of two further methylene groups in the same spin system and these were assigned to 2H-1, 2H-2 and the hydroxy group was placed at C-3 and the alkene group at C-4. The acetoxy group was placed at C-6. The H-6 resonance at δ 5.43 was coupled to 2H-7 and the HMBC spectrum showed ^3J correlation with H-4. The tertiary hydroxyl groups were placed at C-8 and C-14 as the TOCSY spectrum showed that H-17 was only coupled to 2H-16 and 2H-15 and that no coupling was present between 2H-7 and H-8. The COSY spectrum showed coupling between H-9 (δ 1.41), 2H-11 (δ 1.34 and 1.36) and H-12 at δ 3.43. Thus, the remaining hydroxyl group was placed at C-12.

The stereochemistry at C-8 and C-14 could not be confirmed but a literature search showed that bufadienolides in which hydroxy groups are present at these position have them in the β-orientation. The stereochemistry at C-3, C-6, and C-12 was determined from the NOESY spectrum. The resonance ascribed to H-9α gave a positive NOE correlation with H-17α and H-12α indicated that the hydroxyl group was present at C-12β. The methyl group protons of the acetate group at C-6 showed a positive NOE with 3H-19 at C-10β, indicating the acetate group was at C-6β. H-6α showed a positive NOESY interaction with H-4 and H-4 showed a positive correlation with H-3α. Thus, the hydroxyl group was placed at C-3β.

This compound (**1**) was reported previously from *Urginea sanguinea* (Krenn et al., 1993) and *Urginea maritima* (Kopp et al., 1996) but no spectroscopic or physical data was provided.

Compound **2** was isolated as the major constituent from the methanol extract of *U. altissima* with no other bufadienolides being isolated from this source. The ^{1}H NMR spectrum indicated the presence of a bufadienolide with resonances at δ 7.41, 7.97 and 6.26 assigned to H-21, H-22 and H-23. Coupled resonances at δ 4.08 and 5.31 and corresponding resonances at δ 74.0 (CH) and δ 120.4 (CH) in the ^{13}C NMR spectrum indicated the presence of an oxygen substituent at C-3 and a 4,5-double bond. A resonance at δ 84.6 was ascribed to C-14 on the basis of a ^3J HMBC correlation with 3H-18 and a hydroxyl group was placed at this position. The stereochemistry at C-8 and C-9 was determined using the NOESY spectrum. A positive NOE correlation between the 3H-19 methyl singlet resonance at C-10β and the H-8 multiplet indicated that H-8 was in the β configuration. Similarly, a positive NOE correlation observed between the 3H-19 singlet and the H-1 resonance at δ 1.78 allowed for the assignment of a β orientation to this proton and hence assignment of the α orientation to the other H-1 resonance at δ 1.32. A correlation between H-1α and the H-9 multiplet confirmed the α orientation of the H-9 proton.

The presence of three anomeric proton resonances at δ 4.55 (J = 7.9 Hz), δ 4.80 (J = 1.5 Hz) and δ 4.97 (J = 1.5 Hz) were indicative of a trisaccharide substituent at C-3β. In addition, the two doublet resonances at δ 1.23 (J = 6.0 Hz) and δ 1.27 (J = 5.5 Hz) confirmed the presence of two rhamnose molecules. The third sugar moiety was identified as a glucose molecule. Use of HSQC, HMBC and NOESY spectra and of literature ^{13}C NMR data enabled assignment of all the glycoside resonances and determination of the manner in which the sugar molecules were attached. A HMBC correlation between C-3 and H-1′ of one of the rhamnose molecules established that a rhamnose molecule was attached at C-3. HMBC correlations (both ^3J) between C-3′ and H-1′ of the first rhamnose molecule and H-1″ of the second rhamnose molecule established the attachment of the second rhamnose to C-3′ of the first. The downfield shift for C-3′ of δ 80.4 supported this. The glucose molecule was attached at C-4′ based on the C-4 downfield shift of δ 77.0. Resonances ascribed to C-3 and C-4 usually occur at about δ 71 and 72 [17]. The NOESY spectrum also confirmed the sugar substitution pattern as positive NOE correlations were observed between H-1″ and H-3′ and between H-1‴ and H-4′.

Confirmation of the glycosidic linkages was obtained from LC MS studies. A molecular ion peak was observed at m/z 838.6 which corresponds to the $C_{42}H_{62}O_{17}$ bufadienolide glycoside structure suggested by NMR studies. Successive MS–MS experiments produced fragment peaks at m/z 691.3 [M^+-147], m/z 675.4 [M^+-163], m/z 529.3 [M^+-147–162] and m/z 383.3 [M^+-147–163–145]. The peaks at m/z 691 and 675 correspond to the loss of a rhamnose and a glucose molecule from the glycoside, respectively. This confirmed that the sugars were not linked in a linear manner. The peak at m/z 529 corresponds to the loss of both a glucose and a rhamnose molecule and indicated that the sugar attached at C-3 was indeed a rhamnose molecule. In addition, the peak at m/z 383 confirmed the monohydroxybufatrienolide aglycone structure proposed by NMR studies.

3. Experimental

Fresh bulbs of both *D. robusta* Bak. and *U. altissima* (L.f.) Bak. were purchased at the Warwick Triangle Herbal Market in Durban, and vouchers retained in the Natal Herbarium (*Crouch 793*, NH and *Crouch 792*, NH, respectively).

The bulbs of *D. robusta* (3.5 kg) were macerated and extracted at room temperature with continuous agitation

Table 1
^1H, ^{13}C, HMBC and NOESY NMR data for compound **1** (CD_3OD, 400 MHz)

	^1H	^{13}C	HMBC C→H	NOESY
1	1.32 (α)	37.9	19	–
	1.82 (β)			
2	1.88, 1.60	27.9	4	3
3	4.10	67.1	–	2, 4
4	5.73, *s*	133.3	–	3, 6
5	–	140.7	7, 19	–
6	5.43, *br t* (J=2.5)	76.1	4	4, 7
7	2.32, 1.63	37.6	–	6
8	–	75.7	6	–
9	1.41, *dd* (J=1.2, 12.8)	47.9	1, 7, 11,19	12, 17
10	–	36.6	4, 19	–
11	1.92, 1.60	26.7	12	–
12	3.43, *dd* (J=3.6, 11.7)	76.1	9, 11, 17, 18	9, 17
$COCH_3$	–	170.1	$OCOCH_3$	–
$COCH_3$	1.99, *s*	20.4	–	–
13	–	55.4	11, 12, 17, 18	–
14	–	85.6	15, 18	–
15	1.66	33.9	–	–
16	2.10	29.1	17	17
17	3.04, *dd* (J=2.0, 7.5)	47.1	18	12, 16, 21
18	0.80, *s*	12.0	12	21, 22
19	1.34, *s*	21.7	–	–
20	–	123.8	17, 21, 23	–
21	7.41, *d* (J=1.7)	149.6	17, 22	17, 18
22	7.94, *d* (J=2.4)	148.1	17, 21	16, 18, 23
23	6.27, *d* (J=9.7)	114.2	–	22
24	–	163.5	21, 22, 23	–

for 24 h with dichloromethane. Repeated column chromatography of the extract over silica gel (Merck 9385) yielded compound **1** (12β-hydroxyscillirosidin). The bufadienolide isolated could be identified as a navy blue spot on the t.l.c. plate. The chromatographic techniques involved the use of a step-gradient solvent system using methylene chloride and methanol. Compound **1** eluted with an 18:2 methylene chloride–methanol solvent system.

The bulbs of *U. altissima* (3.2 kg) were macerated and freeze dried. The dried plant material was then extracted with ethanol at room temperature with continuous agitation for three days. The crude aqueous extract was acidified with conc. HCl to pH 2 and extracted with dichloromethane. The pH of the aqueous extract was then increased to pH 9 using 4 M NH_4OH and then followed by extraction, first with dichloromethane, and then with 50:50 dichloromethane:methanol. Thin layer chromatographic analysis of the two basic fractions indicated that they were very similar and they were thus combined. Repeated column chromatography of the basic fraction (4.36 g) over silica gel (Merck 9385) using a gradient solvent system, 100 dichloromethane →20:1 → 10:1 → 20:3 → 10:2 → 10:3 dichloromethane:methanol yielded the novel bufadienolide **2** called urginin.

NMR spectra were recorded on a Varian 400 MHz NMR spectrometer. IR spectra were recorded on a Shimadzu-IR spectrophotometer and mass spectra for **1** were recorded at the Cape Technikon on a Finnigan 1020 spectrometer. LC MS spectra for **2** were recorded on a Finnigan MAT LCQ spectrometer with an electrospray ionization source at the University of Lausanne, Switzerland.

Table 2
^1H, ^{13}C, HMBC and NOESY NMR data for compound **2** (CD_3OD, 400 MHz)

	^1H	^{13}C	HMBC C→H	NOESY
1	1.32 (α)	35.48	9, 19	19, 9
	1.78 (β)			
2	1.9 (α)	27.07	–	–
	1.5 (β)			
3	4.08, *bt* (J=7.5)	74.00	1′	4, 2α
4	5.31, *s*	120.40	–	3
5	–	147.31	19	–
6	2.09 (α)	32.41	4	–
	2.20 (β)			
7	1.74	28.70	–	–
8	1.70 (β)	42.22	–	–
9	1.09 (α)	50.38	19	–
10	–	37.51	4, 19	–
11	1.46	21.37	–	–
12	1.51	40.57	18	18
13	–	48.51	18	–
14	–	84.62	18	–
15	1.98	32.12	–	18, 21, 22
	1.64			
16	2.14	28.94	–	–
17	2.52, *bt* (J=6.8)	50.93	18	12, 16, 21
18	0.72, *brs*	16.24	–	12, 15, 21, 22
19	1.05, *brs*	18.46	–	–
20	–	123.78	17, 21, 23	–
21	7.41, *d* (J=1.5)	149.2	–	15β, 17, 18
22	7.97, *dd* (J=9.7, 2.6)	148.13	17, 21	15β, 18, 23
23	6.26, *d* (J=9.7)	114.26	–	22
24	–	163.6	21, 23	
1′	4.80, *d* (J=1.5)	99.54	–	3
2′	3.85, *brs*	71.44	1′	3′
3′	3.91**[a]	80.40	1′, 1″	1′, 2′, 4′
4′	3.74**	77.01*	6′	3′
5′	3.74	67.85*	1′, 4′	–
6′	1.27, *d* (J=6.2)	17.28	4′, 5′	–
1″	4.97, *d* (J=1.5)	103.31	–	2″, 3′
2″	4.01, *brs*	70.86	–	1″, 3″
3″	3.71	71.06	1″	2″
4″	3.37	72.85	2″, 6″	–
5″	3.81	69.05	1″	–
6″	1.23, *d* (J=6.2)	16.93	4″, 5″	–
1‴	4.55, *d* (J=7.9)	103.16	–	2‴, 5‴, 4′
2‴	3.14, *t* (J=8.4)	74.06	–	1‴, 3‴, 4‴
3‴	3.33	76.70	1‴	2‴
4‴	3.28	70.70	3‴	2‴, 6‴
5‴	3.20	76.70	6‴	2‴, 6‴
6‴	3.65, *dd* (J=5.5, 7.7)	61.97	4‴	4‴, 5‴
	3.82			

[a] *, ** Values may be interchanged.

NMR data for **1** and **2** are given in Tables 1 and 2, respectively.

12β-Hydroxyscillirosidin (**1**) (80.1 mg) powdery solid. HRMS: [M^+–CH_3COOH] at m/z 414.20568 g mol^{-1}

($C_{24}H_{30}O_6$ requires 414.20424). EIMS: 414 (100.00) M^+–CH_3COOH], 396 (42.49), 381 (10.71), 378 (11.45), 363 (7.64), 279 (9.13), 261 (12.76), 223 (17.35), 193 (29.70), 177 (34.45), 136 (59.47), 121 (37.15). IR: ν_{max} (NaCl) (cm^{-1}): 3450 (O–H stretching, H-bonded), 2948, 2876 (C–H aromatic and aliphatic stretches), 1711 (C=O stretch), 1379, 1252 (CH_2 and CH_3 bending), 1136, 1037 (C–O stretching).

Urginin (**2**) (100 mg) pale yellow crystals mpt. 178–182 °C (MeOH). $[\alpha]_D = -55.15°$ (c, 6.8×10^{-3} gml^{-1}). LCMS: m/z 838.6 [M^+], 691.3 [M^+–147], 675.4 [M^+-163], 529.3 [M^+-147–162] and 383.3 [M^+–147–163–145]. IR: ν_{max} (KBr) (cm^{-1}): 3444 (O–H stretching), 2935, 2872 (C–H aromatic and aliphatic stretching), 1717 (C=O stretching), 1043 (C–O stretching).

Acknowledgements

The Mazda Wildlife Fund is thanked for supporting the Ethnobotany Programme of the NBI and the DEAT for funding the development of MEDBASE, the National Medicinal Plants Database for South Africa. We are grateful to Tr. Dr. Elliot Ndlovu of Kamberg for providing current usage information, Mr. Dilip Jagjivan for running NMR spectra, Dr. P. Boshoff for mass spectrometric analysis, Mr. Bret Parel for technical assistance, and Professor K. Hostettmann and Professor A. Marston of the University of Lausanne for the kind use of their LC MS facilities. T.P. and C.K. gratefully acknowledge the National Research Foundation (NRF) for their postgraduate bursaries. This research was funded by the NRF and University of Natal Research fund.

We gratefully acknowledge the Wellcome Trust Equipment grant number 053547 for the provision of the 400 MHz NMR spectrometer.

References

Burkill, H.M., 1955. The useful plants of west tropical Africa. Vol. 3, 2nd Edition. Royal Botanic Gardens, Kew.

Cunningham, A.B., 1990. People and medicines: the exploitation and conservation of traditional Zulu medicinal plants. Mitteilungen aus dem Institut für Allgemeine Botanik Hamburg, 23b, 979–990.

Hutchings, A., Scott, A.H., Lewis, G., Cunningham, A.B., 1996. Zulu medicinal plants. An inventory. University of Natal Press, Pietermaritzburg.

Jessop, J.P., 1977. Studies in the bulbous Liliaceae in South Africa: 7. The taxonomy of *Drimia* and certain allied genera. Journal of South African Botany 43, 265–319.

Kopp, B., Krenn, L., Draxler, M., Hoyer, A., Terkola, R., Vallaster, P., Robien, W., 1996. Bufadienolides from *Urginea maritima* from Egypt. Phytochemistry 42 (2), 513–522.

Krenn, L., Kopp, B., Bamberger, M., Brustmann, E., Kubelka, W., 1993. Bufadienolides and a steroidal sapogenin from *Urginea sanguinea* (Hyacinthaceae). Natural Products Letters 3, 139–143.

Luyt, R.P., Jager, A.K., Van Staden, J., 1999. The rational use of *Drimia robusta* Bak. in traditional medicine. South African Journal of Botany 65 (4), 291–294.

Miyakado, M., Kaot, T., Ohno, N., Koshimizu, K., 1975. Alkaloids of *Urginea altissima* and their antimicrobial activity against *Phytophthora capsici*. Phytochemistry 14, 2717.

Ndlovu, E., pers. commun.

Sapieka, N., 1951. South African plants with digitalis-like action. South African Pharmaceutical Journal 17, 28–29, 54.

Smith, C.A., 1966. Common names of South African Plants. Botanical Survey Memoir 35. Department of Agriculture and Technical Services, Pretoria.

Speta, F., 1998. Hyacinthaceae. In: Kubitzki, K (Ed.), The Families and Genera of Vascular Plants III. Flowering Plants. Monocotyledons. Lilanae (Except Orchidaceae). Springer, Berlin, pp. 261–285.

Steyn, D.G., 1936. Recent investigations into the toxicity of known and unknown poisonous plants in the Union of South Africa. Onderstepoort Journal of Veterinary Science and Animal Industry 7 (1), 169–178.

Van der Walt, S.J., Steyn, D.G., 1943. Recent investigations into the toxicity of plants, etc., XIII. Onderstepoort Journal of Veterinary Science and Animal Industry 18 (1 and 2), 207–224.

Van Wyk, B.-E., Van Oudshoorn, B., Gericke, N., 1997. Medicinal Plants of South Africa. Briza Publications, Pretoria.

Verdcourt, B., Trump, E.C., 1969. Common Poisonous Plants of East Africa. Collins, London, p. 181.

Watt, J.M., Breyer-Brandwijk, M.G., 1962. The Medicinal and Poisonous Plants of Southern and Eastern Africa, 2nd Edition. E.&S. Livingston Ltd, London.

PERGAMON

Phytochemistry 58 (2001) 563–566

PHYTOCHEMISTRY

www.elsevier.com/locate/phytochem

Biflavonoids from the aerial part of *Stephania tetrandra*

Duanyun Si, Dafang Zhong*, Yi Sha, Wen Li

Laboratory of Drug Metabolism and Pharmacokinetics, Shenyang Pharmaceutical University, Shenyang 110016, PR China

Received in revised form 3 May 2001

Abstract

Investigation of the aerial part of *Stephania tetrandra* led to the isolation of two biflavonoids, stephaflavone A and stephaflavone B, with a 3–6″ linkage pattern, together with β-sitosterol. Their structures were established on the basis of their spectroscopic data and their physicochemical properties. © 2001 Elsevier Science Ltd. All rights reserved.

Keywords: *Stephania tetrandra*; Menispermaceae; Aerial part; Biflavonoids; Stephaflavone A; Stephaflavone B

1. Introduction

Different parts of a plant usually contain different types of secondary metabolites. Most of the known alkaloids from "*Fen Fang Ji*", a traditional Chinese medicine from the dried root of *Stephania tetrandra* S. Moore (Menispermaceae), were of the bisbenzylisoquinoline type (Hsing and Chang, 1957; Tomita et al., 1967; Hu and Zhao, 1986; Ogino et al., 1988, 1998; Deng et al., 1990). However, our previous paper showed that the aerial part of *S. tetrandra* mainly contained aporphinoid alkaloids (Si et al., 1992). In the present study on the same plant material, our attention shifted to the non-alkaloid constituents, which resulted in the isolation of two new biflavonoids. This is the first report about biflavonoids from Menispermaceae plants.

2. Results and discussion

The EtOH extract of the aerial part of *S. tetrandra* was subjected to silica gel chromatography to yield two new biflavonoids, stephaflavone A and B (**1** and **2**), and component, β-sitosterol. The identification of β-sitosterol was conducted on the basis of direct comparisons (mp., IR, MS, and co-TLC) with an authentic sample. The color reactions, UV absorption maxima, and IR absorption bands of **1** and **2** were very similar, which suggested that both compounds possessed an identical flavonoid system (Geiger and Quinn, 1975). The molecular ion of **1** at *m*/*z* 594 ($C_{34}H_{26}O_{10}$) showed it to be a methyl derivative of **2** (*m*/*z* 580, $C_{33}H_{24}O_{10}$).

The ^{13}C NMR spectrum of **1** showed signals for all 34 carbons of the molecule including four sp3 carbons for four methoxyl groups at δ 55.3–56.2 and thirty sp^2 carbons, including signals for two carbonyl groups at δ 181.1 and 182.0. The IR spectrum exhibited a broad OH absorption band at 3348 cm^{-1} and a hydrogen-bonded carbonyl band at 1652 cm^{-1}. These observations and selective molecular mass of 594 hinted that **1** could be a flavone-flavone based biflavonoid (Geiger and Quinn, 1982, 1988).

The ^1H NMR spectrum of **1** demonstrated the presence of two hydroxyl protons, twelve alkyl protons for four methoxyl groups, and twelve aromatic protons. The two hydroxyl protons resonated in the downfield region at δ 12.94 and 13.02, indicating the presence of two hydrogen-bonded hydroxyl groups at the 5 and 5″ positions. The presence of two sets of AA'XX' doublets at δ 7.81 (2H, *d*, $J = 8.8$ Hz) and 6.98 (2H, *d*, $J = 8.8$ Hz); δ 7.48 (2H, *d*, $J = 8.8$ Hz) and 6.78 (2H, *d*, $J = 8.8$ Hz) were ascribed to eight aromatic protons of rings B and ring E. Another two protons comprising a set of *meta*-coupled doublets appearing at δ 6.36 (1H, *d*, $J = 2.5$ Hz) and 6.47 (1H, *d*, $J = 2.5$ Hz) represented H-6 and H-8 of ring A, respectively. The remaining two aromatic singlets at δ 6.55 and 6.50 were assigned to H-3″ of ring F and H-6″ or H-8″ of ring D, which implied that either C-8″ or C-6″ of ring D was involved in the interflavonoid C–C linkage with C-3 of ring C. The structure of **1** was, therefore, composed of two 7,4′-dimethoxy-5-

* Corresponding author. Tel.: +86-24-2390-2539; fax: +86-24-2390-2539.

E-mail address: zhongdf@ihw.com.cn (D. Zhong).

0031-9422/01/$ - see front matter © 2001 Elsevier Science Ltd. All rights reserved.
PII: S0031-9422(01)00271-0

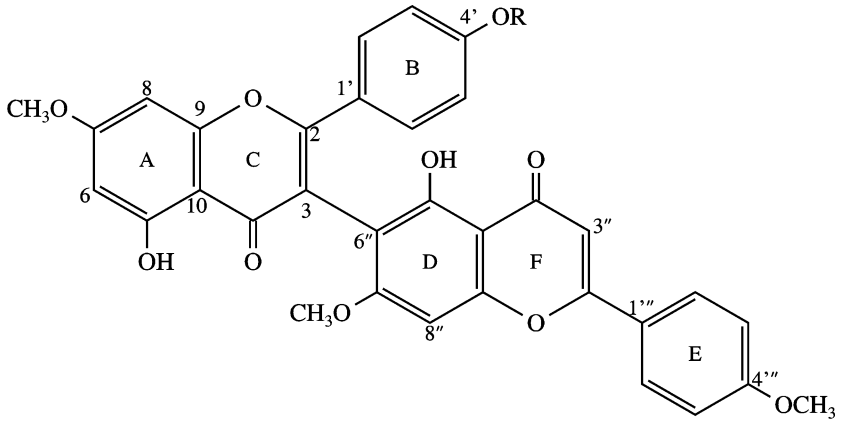

1 R = CH_3 2 R = H

hydroxylflavone units with a C–C linkage either between C-3 and C-6″ or between C-3 and C-8″.

On the basis of systematic ^{13}C NMR spectroscopic analysis of many naturally occurring flavonoids and biflavonoids, Chari et al. (1977) stated that the resonances for unsubstituted C-8 and C-6 of monomeric flavones, flavonols and flavanones with a 5,7-dioxy substitution were found between δ 90.0 and 100.0. The signal for C-6 is usually located at lower fields than that for C-8. This difference is about 4.8 ppm for flavones and flavonols. When the carbon atom at position 6 or 8 was substituted by an alkyl or aryl group, the signal for the quaternary C-substituted carbon atom shifts by 6.0–9.6 ppm downfield whereas the signal for a *meta*-unsubstituted carbon atom is not markedly altered. So, it is apparent that mere inspection of the ^{13}C NMR chemical shift values in the spectral region δ 90.0–100.0 of a biflavonoid can give a good indication of the linkage positions if ring A and/or ring D is involved in a C-C linkage. The DEPT spectra of **1** showed the presence of three methine signals between δ 90.0 to 100.0. The two upfield signals at δ 92.1 and 90.3 corresponded to C-8 of ring A and C-8″ of ring D. The remaining signal at δ 97.9 had to be ascribed to C-6 of ring A. The resonance of C-6″ in ring D appeared as a quaternary carbon atom at δ 105.6, suggested that **1** was a biflavone with a C–C linkage between C-3 and C-6″.

The HMBC spectrum of **1** further confirmed the involvement of C-3 and C-6″ in interflavonoid linkage as C-6″ showed correlations with H-8″ and the hydroxyl proton at position 5″ (Fig. 1). Thus, from the foregoing spectral studies, **1** was characterized as 5,5″-dihydroxy-7,4′,7″,4‴-tetramethoxy-[3→6″]-biflavone and designated stephaflavone A. The complete assignment of the proton and carbon shifts aided by DEPT, HMQC, and HMBC experiments are shown in Table 1.

The ^{13}C NMR spectrum of **2** closely resembled that of **1**, except that compound **2** contained only three methoxyl

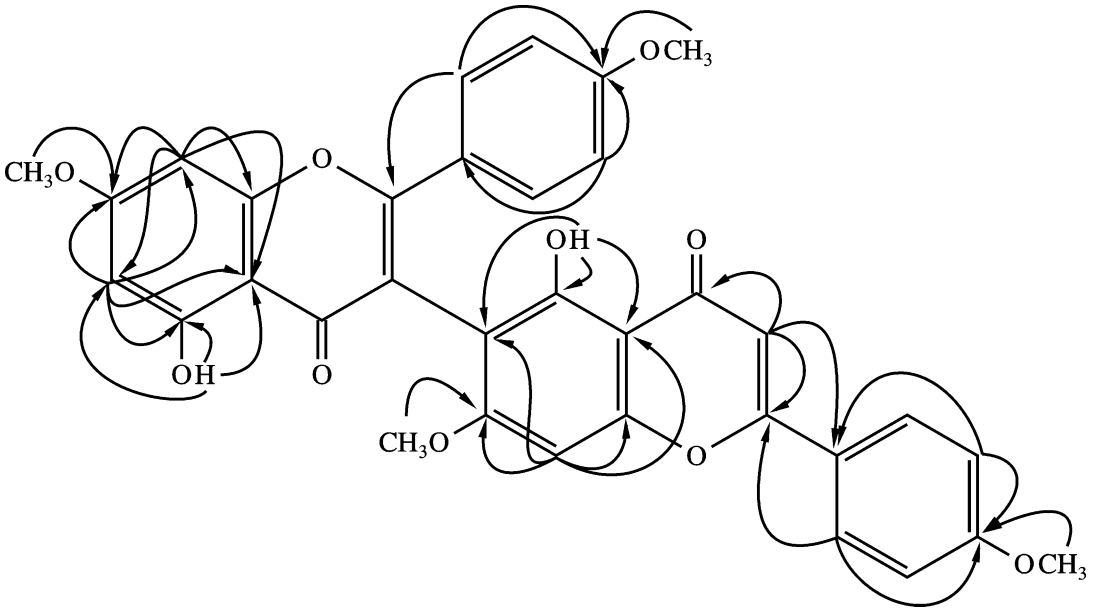

Fig. 1. Major HMBC correlations observed in compound **1**.

Table 1
NMR spectroscopic data for stephaflavone A and B[a]

Position	Stephaflavone A				Stephaflavone B	
	δ_C[b]	δ_H	HMBC[c]		δ_C[b]	δ_H
2	163.5 (*s*)				164.0 (*s*)	
3	111.8 (*s*)				111.2 (*s*)	
4	180.2 (*s*)				180.5 (*s*)	
5	162.3 (*s*)				162.0 (*s*)	
5-OH		12.94 (*s*)	5, 6, 10			12.86 (s)
6	97.9 (*d*)	6.36 (*d*, 2.5)	5, 7, 8, 10		98.2 (*d*)	6.37 (*d*, 2.5)
7	165.4 (*s*)				165.6 (*s*)	
7-OCH_3	55.5 (*q*)	3.87 (*s*)	7		55.8 (*q*)	3.87 (*s*)
8	92.1 (*d*)	6.47 (*d*, 2.5)	6, 7, 9, 10		92.3 (*d*)	6.46 (*d*, 2.5)
9	157.8 (*s*)				157.8 (*s*)	
10	105.3 (*s*)				105.3 (*s*)	
1′	125.5 (*s*)				124.3 (*s*)	
2′	129.5 (*d*)	7.48 (*d*, 8.8)	2, 4′, 6′		129.7 (*d*)	7.41 (*d*, 8.8)
3′	113.5 (*d*)	6.78 (*d*, 8.8)	1′, 4′		115.2 (*d*)	6.71 (*d*, 8.8)
4′	161.2 (*s*)				159.5 (*s*)	
4′-OCH_3	56.2 (*q*)	3.86 (*s*)	4′	4′-OH		
5′	113.5 (*d*)	6.78 (*d*, 8.8)	1′, 4′		115.2 (*d*)	6.71 (*d*, 8.8)
6′	129.5 (*d*)	7.48 (*d*, 8.8)	2, 2′,4′		129.7 (*d*)	7.41 (*d*, 8.8)
2″	163.8 (*s*)				164.1 (*s*)	
3″	104.3 (*d*)	6.55 (*s*)	2″, 4″, 1‴		104.0 (*d*)	6.57 (*s*)
4″	181.1 (*s*)				181.2 (*s*)	
5″	159.5 (*s*)				159.0 (*s*)	
5″-OH		13.02 (*s*)	5″, 6″, 10″			12.95 (*s*)
6″	105.5 (*s*)				105.5 (*s*)	
7″	163.3 (*s*)				163.5 (*s*)	
7″-OCH_3	55.8 (*q*)	3.76 (*s*)	7″		56.2 (*q*)	3.76 (*s*)
8″	90.3 (*d*)	6.50 (*s*)	6″, 7″, 9″, 10″		90.6 (*d*)	6.49 (*s*)
9″	157.9 (*s*)				158.0 (*s*)	
10″	105.1 (*s*)				105.0 (*s*)	
1‴	123.2 (*s*)				122.9 (*s*)	
2‴	127.8 (*d*)	7.81 (*d*, 8.8)	2″, 4‴, 6‴		128.0 (*d*)	7.83 (*d*, 8.8)
3‴	114.4 (*d*)	6.98 (*d*, 8.8)	1‴, 4‴		114.4 (*d*)	7.00 (*d*, 8.8)
4‴	162.6 (*s*)				162.7 (*s*)	
4‴-OCH_3	55.3 (*q*)	3.88 (*s*)	4‴		55.4 (*q*)	3.88 (s)
5‴	114.4 (*d*)	6.98 (*d*, 8.8)	1‴, 4‴		114.4 (*d*)	7.00 (*d*, 8.8)
6‴	127.8 (*d*)	7.81 (*d*, 8.8)	2″, 2‴, 4‴		128.0 (*d*)	7.83 (*d*, 8.8)

[a] 1D NMR data recorded in $CDCl_3$ at 89.61 MHz for ^1H and at 22.53 MHz for ^{13}C; 2D NMR data recorded in $CDCl_3$ at 300.13 MHz for ^1H and at 75.43 MHz for ^{13}C; δ_C and δ_H are in ppm, multiplicities and *J* values (in Hz) are shown in parentheses.
[b] Multiplicities determined by a DEPT experiment.
[c] Protons correlated with carbon atoms on position number.

groups, and there were small but significant differences in four signals for six carbon atoms of ring B. The resonances for C-1′, C-2′ (6′), C-3′ (5′), and C-4′ in **1** appeared at δ 125.5, 129.5, 113.5, 161.2, respectively, whereas in **2** at δ 124.3, 129.7, 115.2, and 159.5, respectively. These alterations suggested a 4′-OH substitution in ring B of **2** instead of a methoxyl group in **1** (Chari et al., 1977; Williams and Fleming, 1995). The ^1H NMR spectrum of **2** also appeared very similar to that of **1**. The slight differences were found at δ 7.41 (2H, *d*, $J=8.8$ Hz) and 6.71 (2H, *d*, $J=8.8$ Hz) for the four aromatic protons in ring B. These also supported the suggestion that the substituent at position 4′ was a hydroxyl group (Geiger and Quinn, 1982; Williams and Fleming, 1995). Thus, the chemical structure of **2** could be established as 5,4′,5″-trihydroxy-7,7″,4‴-trimethoxy-[3→6″]-biflavone and was designated stephaflavone B. The complete assignment of the proton and carbon shifts aided by the comparisons with NMR data of **1** are shown in Table 1.

3. Experimental

3.1. General

Mps were uncorr. UV spectra were obtained on a Shimadzu UV-300 spectrophotometer with 95% EtOH as solvent. IR spectra in KBr disk were recorded on a Nicolet 5S XC spectrometer. ^1H and ^{13}C NMR spectra were determined in $CDCl_3$, with TMS as int. standard,

on a JEOL FX90Q spectrometer for 1D determination and on a Bruker ARX-300 spectrometer for the 2D experiments. EI mass spectra were obtained on Nicolet FTMS-2000 and JMS DX 300 spectrometers. CC was conducted on silica gel H and TLC on silica gel G glass plates, and the latter was detected with conc. H_2SO_4. Silica gels H and G were purchased from the Qingdao Marine Chemical Factory, China.

3.2. Plant material

The aerial part of *S. tetrandra* was collected and identified as description in lit. (Si et al., 1992). A voucher specimen was deposited in the same place.

3.3. Extraction and isolation

Air-dried and ground plant material was extracted exhaustively with boiling EtOH, and the extract was evaporated in vacuo to afford a residue, which was extracted by refluxing with petroleum ether, and then with $CHCl_3$. The $CHCl_3$ fraction was concentrated to give a gum which was treated with 2% HCl. The insoluble mass was subjected to a column of silica gel H with an elution gradient of C_6H_6 and Me_2CO to give β-sitosterol and two combined similar fractions, which were purified by prep. TLC with C_6H_6–Me_2CO–HCOOH (8:1.8:0.2) as the developer to afford **1** (R_f = 0.55) and **2** (R_f = 0.43).

3.4. Stephaflavone A (*1*)

Yellow cubic crystals from C_6H_6, mp. 237–239 °C. UV λ_{max}^{EtOH} nm (log ε): 214 (4.64), 273 (4.63), 331 (4.63). IR ν_{max}^{KBr} cm^{-1}: 3448, 2935, 2841, 1652 (hydrogen-bonded carbonyl), 1604, 1511, 1488, 1452, 1439, 1351, 1259, 1179, 1167, 1126, 1054, 833. ^1H and ^{13}C NMR data, see Table 1. HREIMS *m/z*: $[M]^+$ 594.1490 (calc. 594.1526 for $C_{34}H_{26}O_{10}$). EIMS *m/z* (rel. int.): 594 (100), 579 (0.9), 565 (2.7), 564 (11.2), 563 (30), 548 (1.3), 533 (1.3), 520 (1.6), 505 (0.5), 487 (14.2), 462 (0.8), 429 (16.3), 428 (38.6), 427 (6.7), 297 (29.7), 296 (5.3), 281 (6.4), 268 (2.3), 167 (8.8), 166 (1.1), 138 (1.5), 135 (9.4), 132 (1.8), 117 (1.5), 110(1.1), 107 (1.4), 79 (1.1).

3.5. Stephaflavone B (*2*)

Yellow cubic crystals from $CHCl_3$, mp. 192–194 °C. UV λ_{max}^{EtOH} nm (log ε): 224 (4.51), 273 (4.57), 333 (4.61). IR ν cm^{-1}: 3450, 2915, 2849, 1654 (hydrogen-bonded carbonyl), 1597, 1509, 1487, 1471, 1458, 1443, 1342, 1258, 1209, 1180, 1172, 1122, 1056, 1022, 835. ^1H and ^{13}C NMR data, see Table 1. HREIMS *m/z*:$[M]^+$ 580.1271 (calcd. 580.1369 for $C_{33}H_{24}O_{10}$). EIMS *m/z* (rel. int.): 580 (89.2), 563 (15.5), 562 (13.9), 550 (34.2), 549 (99.0), 534 (13.3), 506 (16.9), 488 (22.6), 487 (78.7), 414 (100), 413 (19.2), 385 (13.6), 297 (26.6), 282 (20.5), 267 (10.2), 253 (6.7), 167 (27.5), 135 (19.1), 89 (8.8).

Acknowledgements

The authors are very grateful to Professor S. Zhao, Division of Phytochemistry, China Pharmaceutical University, PR China, for his advice and support of this work.

References

Chari, V.M., Ilyas, M., Wagner, H., Neszmelyi, A., Chen, F.C., Chen, L.K., Lin, Y.C., Lin, Y.M., 1977. ^{13}C-NMR spectroscopy of biflavanoids. Phytochemistry 16, 1273–1278.

Deng, J., Zhao, S., Lou, F., 1990. A new monoquaternary bisbenzylisoquinoline alkaloid from *Stephania tetrandra*. Journal of Natural Products 53, 993–994.

Geiger, H., Quinn, C., 1975. Biflavonoids. In: Harborne, J.B., Mabry, T.J., Mabry, H. (Eds.), The Flavonoids. Academic, New York, pp. 692–742.

Geiger, H., Quinn, C., 1982. Biflavonoids. In: Harborne, J.B., Mabry, T.J. (Eds.), The Flavonoids. Chapman and Hall, London, pp. 505–534.

Geiger, H., Quinn, C., 1988. Biflavonoids. In: Harborne, J.B. (Ed.), The Flavonoids. Chapman and Hall, London, pp. 99–124.

Hsing, C.-Y., Chang, C.-H., 1957. Constitution of fangchinoline. Acta Chimica Sinica 23, 405–410.

Hu, T., Zhao, S., 1986. The structures of oxofangchirine and stephenanthrine isolated from *Stephania tetrandra* S. Moore. Acta Pharmaceutica Sinica 21, 29–34.

Ogino, T., Sato, T., Sasaki, H., Chin, M., Mitsuhashi, H., 1988. Four new bisbenzylisoquinoline alkaloids from the root of *Stephania tetrandra* (Fen-Fang-Ji). Heterocycles 27, 1149–1154.

Ogino, T., Katsuhara, T., Sato, T., Sasaki, H., Okada, M., Muruno, M., 1998. New alkaloids from the root of *Stephania tetrandra* (Fen-Fang-Ji). Heterocycles 48, 311–317.

Si, D., Zhao, S., Deng, J., 1992. A 4,5-dioxoaporphine from the aerial part of *Stephania tetrandra*. Journal of Natural Products 55, 828–829.

Tomita, M., Kozuka, M., Lu, S.-T., 1967. Studies on the alkaloids of Menispermaceae plant. CCXXIX. Alkaloids of *Stephania tetrandra* S. Moore (Suppl. I). Yakugaku Zasshi 87, 316–318.

Williams, D.H., Fleming, I., 1995. Spectroscopic methods in Organic Chemistry, 5th Edition. McGraw-Hill, London, pp. 152–160.

PERGAMON

Phytochemistry 58 (2001) 567–569

PHYTOCHEMISTRY

www.elsevier.com/locate/phytochem

A cytotoxic diarylheptanoid from *Viscum cruciatum*

Carmen Martín-Cordero[a,*], Miguel López-Lázaro[a], María Angeles Agudo[a], Eduardo Navarro[b], Juan Trujillo[c], María Jesús Ayuso[a]

[a]*Laboratorio de Farmacognosia, Facultad de Farmacia, Universidad de Sevilla, 41012 Sevilla, Spain*
[b]*Departamento de Farmacología, Universidad de la Laguna, Canarias, Spain*
[c]*Instituto de Productos Naturales y Agrobiología de Canarias, C.S.I.C., La Laguna, Spain*

Received 30 March 2001; received in revised form 18 June 2001

Abstract

A diarylheptanoid, 1,7-di-(3′,4′-dihydroxyphenyl)-4-hepten-3-one, hirsutanone, has been isolated from the methanolic extract of the aerial parts of *Viscum cruciatum* (Viscaceae) and characterized by spectroscopic methods and chemical transformations. This compound showed cytotoxic activity against melanoma (UACC-62), renal (TK-10) and breast (MCF-7) cancer cell lines. © 2001 Elsevier Science Ltd. All rights reserved.

Keywords: *Viscum cruciatum*; Viscaceae; Diarylheptanoids; 1,7-Di-(3′,4′-dihydroxyphenyl)-4-hepten-3-one; Hirsutanone; ^{1}H and ^{13}C NMR spectra

1. Introduction

Viscum cruciatum is an evergreen hemiparasitic plant, characterized by its whorled leaves and its red berries ("*muérdago colorado*"), usually epiphyting various dicotyledonous trees and shrubs: *Retama sphaerocarpa* Boiss., *Olea europaea* L., *Rhamnus alaternus* L., *Rhamnus lycioides* L., *Prunus amygdalus* Stokes. In the course of our pharmacological and phytochemical studies on the extracts of *Viscum cruciatum,* we have reported the cytotoxic activity (Ayuso et al., 1987a,b; 1988) and we have isolated alkaloids and flavonoids (Martín-Cordero et al., 1989, 1993, 1997). None of them could be clearly shown to possess the established cytotoxic activity.

As part of our continuing study of *Viscum cruciatum* for novel compounds which might posess biological activity, we have undertaken a reexamination of the chemical constituents of the aerial parts of *Viscum cruciatum* and we examined its cytotoxic activity. We report here the isolation and characterization of 1,7-di-(3′,4′-dihydroxyphenyl)-4-hepten-3-one, hirsutanone (**1**) (Terazawa et al., 1984) and cytotoxic activity against three tumor cell lines.

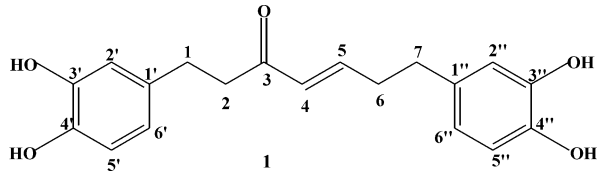

1

2. Results and discussion

From the methanolic extract of the aerial parts of *Viscum cruciatum* a diarylheptanoid (**1**) was isolated on Si gel column. The structural elucidation and the cytotoxic activity of compound (**1**) is described in the present study. This compound was not crystallized. Its IR spectrum showed an absorption at 3350 cm^{-1} corresponding to phenolic groups, a band at 1650 cm^{-1} of an α-β unsatured carbonyl group and another band at 1600 cm^{-1} was ascribed to double bonds. Its ^{1}H NMR spectrum showed multiplets at δ 2.78 and δ 2.43 corresponding to 8H which were attributed to four deshielded methylene groups. The ^{13}C NMR exhibited four signals at 30.0, 34.2, 34.8 and 42.1 that can be ascribed to four methylene groups, tentatively assigned in experimental section. A signal at 200.30 corresponded to a carbonyl of an α-β unsatured ketone. The remainder of the signals were attributable to two aromatic moieties and a double bond. The HRMS showed a molecular ion M^{+} at m/z 328.1307, corresponding to a molecular formula $C_{19}H_{20}O_5$.

* Corresponding author. Tel.: +34-5-423-37-65; fax: +34-5-423-37-65.
E-mail address: cordero@fafar.us.es (C. Martín-Cordero).

0031-9422/01/$ - see front matter © 2001 Elsevier Science Ltd. All rights reserved.
PII: S0031-9422(01)00293-X

By acetylation or methylation, compound **1** gave a tetraacetate ($C_{27}H_{20}O_9$) or a tetramethylether ($C_{23}H_{28}O_5$). The respective spectral data supported the structure thus proposed. Moreover, this same compound **1** was treated with dichloromethane/dimethylformamide and CsF to confirm that the phenolic groups were in *ortho* position (Clark et al., 1976).

The cytotoxic assays of isolated compound **1** were carried out according to the standard protocols established by the NCI (Monks et al., 1991). 1,7-di-(3′,4′-dihydroxyphenyl)-4-hepten-3-one, hirsutanone showed activity against cell lines tested, the GI_{50} values for TK-10 cells, MCF-7 cells and UACC-62 cells were 6.8, 1.9 and 4.8μg/ml, respectively. Etoposide was used as a positive control (GI_{50} values for TK-10 cells, MCF-7 cells and UACC-62 cells were 8.1, 0.33 and 0.97μg/ml, respectively).

Previous reports (Chun et al., 1999; Elattar and Virji, 2000; Hadi et al., 2000; Ramsewak et al., 2000) have pointed to the cytotoxicity of structurally related diarylheptanoids such as curcumin I (1,7-di-(4′-hydroxy-3′methoxyphenyl)-1,4,6-heptatrien-3-one-5-hydroxy), curcumin II (monodemethoxycurcumin) and curcumin III (bisdemethoxycurcumin) from *Curcuma longa* (Zingiberaceae). Curcumin I was found to be more active than other two as a cytotoxic agent (Ramsewak et al., 2000). The structural differences between curcumin I and the isolated compound (1,7-di-(3′,4′-dihydroxyphenyl)-4-hepten-3-one, hirsutanone) are the different substituents at the aromatic ring (C-4′, C-4″) and C-5 and two double bond of the aliphatic chain. In addition, diarylheptanoids such as yakuchinone A and B have the ability to suppress proliferation of human cancer cells via induction of apoptosis (Surh, 1999). These findings suggest that the isolation of an active diarylheptanoid from *Viscum cruciatum* may contribute to its cytotoxic activity.

Open chain diarylheptanoids were isolated previously from Aceraceae, Betulaceae, Zingiberaceae and Leguminosae family (Keserü and Nógrádi, 1995). It is the first report of diarylheptanoids in the Viscaceae and *Viscum* species.

3. Experimental

3.1. General experimental procedure

IR spectra were measured as KBr disc and $CHCl_3$. NMR spectra were taken in $CDCl_3$; ^{13}C NMR at 50 MHz and ^1H NMR at 200 MHz, using TMS as int. standard. MS were recorded at 70 eV. CC: silica gel.

3.2. Plant material

The aerial parts of *Viscum cruciatum* hemiparasitic of *Prunus amygdalus* Stokes were collected in January, during the fruiting period from Zahara de la Sierra (Cádiz, Spain). The identity was kindly verified by Dr. Santiago Silvestre (Department of Botany of the Faculty of Pharmacy, University of Sevilla) and a voucher specimen is deposited, labelled SEV. 82694.

3.3. Extraction and isolation

Air-dried, powdered aerial parts (250 g) of *Viscum cruciatum* were extracted by Soxhlet successively with $CHCl_3$ and MeOH. The MeOH extract (3.3 g) was chromatographed on Si gel column eluting gradient with *n*-hexane–EtOAc and $CHCl_3$–MeOH, the compound (**1**) was isolated from the intermediate fractions eluting with *n*-hexane–Et_2Ac.

3.3.1. 1,7-Di-(3′,4′-dihydroxyphenyl)-4-hepten-3-one (*1*)

Syrupy solid (210 mg) IR ν_{max}^{KBr} cm^{-1}: 3350, 3050, 2920, 1650, 1510. ^1H NMR (200 MHz, $CDCl_3$): δ 2.43–2.78 (8H, *m*, H-6, H-7, H-1, H-2), 6.05 (1H, *d*, $J=16.8$ Hz, H-4), 6.45–6.69 (6H, *m*, H-6′, H-6″, H-2′, H-2″, H-5′, H-5″), 6.86 (1H, *dt*, $J=6.5$, 16.8Hz, H-5). ^{13}C NMR (50 MHz, $CDCl_3$): δ 30.0 (*t*, C-1), 34.9 (*t*, C-6), 34.2 (*t*, C-7), 42.1 (*t*, C-2), 116.0 (*d*, C-5′, C-5″), 116.2 (*d*, C-2′, C-2″), 118.2 (*d*, C-6′, C-6″), 131.1 (*d*, C-4), 133.5 (*s*, C-1′, C-1″) 143.8 (*s*, C-4′, C-4″), 145.5 (*s*, C-3′, C-3″), 147.6 (*d*, C-5), 200.3 (*s*, C-3). EIMS *m*/*e* (rel. int. %) M^+ 328.1307 (calc. for $C_{19}H_{20}O_5$ 328.1310) 328 (20), 206 (19), 191 (18), 149(58), 148(38), 137 (28), 136 (28), 123 (100), 107 (22), 91 (36), 77 (58).

3.3.2. Acetylation of *1*

Fifty milligrams was carried out with Ac_2O–Pyr at room temperature and in the dark for 24 h. IR $\nu_{max}^{CHCl_3}$ cm^{-1}: 3010, 2920, 2823, 1760, 1660, 1620, 1500, 1368, 1256, 1180, 1110, 1010, 900. ^1H NMR (200 MHz, $CDCl_3$): δ 2.27 (12H, *s*), 3.0–2.4 (8H, *m*) 6.1 (1H, *d*, $J=16.8$ Hz), 6.8 (1H, *dt*, $J=6.5$, 16.8 Hz) 7.1–7.0 (6H, *m*). EIMS *m*/*e* (rel. int.%) M^+ 496.1729 (2) (calc. for $C_{27}H_{28}O_9$ 496.1733) 454 (10), 412 (20), 370 (17), 352 (12), 338 (26), 206 (18), 165 (20), 123 (100), 77 (11).

3.3.3. Methylation of *1*

Compound **1** (20 mg) was suspended in Me_2CO (30 ml) and K_2CO_3 (300 mg) and MeI (0.5 ml) was added. The mixture was refluxed for 14 h and extracted in the usual manner. The product was purified by CC to give the tetramethylether derivate. IR $\nu_{max}^{CHCl_3}$ cm^{-1}: 3000, 2960, 2940, 2840, 1660, 1620, 1590, 1510, 1460, 1258, 1155, 1135, 1030, 850. ^1H NMR (200 MHz, $CDCl_3$): δ 2.87–2.48 (8H, *m*), 3.85 (6H, *s*), 3.86 (6H, *s*), 6.11 (1H, *d*, $J=16$ Hz), 6.91–6.68 (7H, *m*). EIMS *m*/*e* (rel. int.%) M^+ 384.1935 (28) (calc. for $C_{23}H_{28}O_5$ 384.1936), 370 (4), 219 (6), 191 (4), 177 (14), 151 (100), 137 (26), 107 (33), 77 (21.).

3.3.4. Methylenedioxy derivate of *1*

The methylenedioxy derivate of **1** (50 mg) was obtained by the Clark method (Clark et al., 1976) and

purified by CC. IR $\nu_{max}^{CHCl_3}$ cm^{-1}: 2990, 2880, 2763, 1720, 1660, 1620, 1498, 1480, 1438, 1090, 1042, 937. ^1H NMR (200 MHz, $CDCl_3$): δ 2.49 (2H, *m*), 2.69 (2H, *m*), 2.81 (4H, *m*), 5.91 (2H, *s*), 5.92 (2H, *s*), 6.08 (1H, *d*, $J=16$ Hz), 6.90-6.60 (7H, *m*). EIMS *m*/*e* (rel. int. %) M^+ 352.1307 (13) (calc. for $C_{21}H_{20}O_5$ 352.1310), 204 (3), 203 (3), 160 (3), 135 (100), 105 (6), 91 (6), 77 (23).

3.4. Human tumor cell lines

The following three human cancer cell lines were used in these experiments: the human renal adenocarcinoma (TK-10), the human breast adenocarcinoma (MCF-7) and the human melanoma (UACC-62) cell lines. They were kindly provided by Dr. G. Cragg, Department of NCI, Maryland, USA. The human tumour cytotoxicities were determined following protocols established by the National Cancer Institute, National Institute of Health (Monks et al., 1991) TK-10, MCF-7 and UACC -62 cell lines were cultured in RPMI 1640 medium (Bio whittaker) containing 20% fetal calf serum, 2 mM L-glutamine, 100 U/ml penicillin and 100 μg/ml streptomycin. All cell lines were maintained at 37 °C in a 5% CO_2 atmosphere with 95% humidity. Maintenance cultures were passaged weekly, and the culture medium was changed twice a week. According to their growth profiles, the optimal plating densities of each cell line was determined (15×10^3, 5×10^3 and 100×10^3 cells/well for TK-10, MCF-7 and UACC-62, respectively) to ensure exponential growth throughout the experimental period and to ensure a linear relationship between absorbance at 492 nm and cell number when analysed by the SRB assay. Data for the isolated compound was analysed according to the standard protocols established by the NCI (Monks et al., 1991).

References

Ayuso, M.J., Martín-Cordero, C., Sáenz, M.T., 1988. Activité antimitotique de *Viscum cruciatum* Sieber parasite de *Olea europaea* subsp. *europaea* et de *Retama sphaerocarpa*. Fitoterapia 59, 222–226.

Ayuso, M.J., Martín-Cordero, C., Sáenz, M.T., 1987a. Activité antimitotique de *Viscum cruciatum* Sieber: etude comparative de deux échantillons récoltés sur *Rhamnus alaternus* L. et *Rhamnus lycioides* L. subsp. oleoides (L.) Jahandiez & Maire. Plantes Méd. et Phytothér 21, 177–182.

Ayuso, M.J., Sáenz, M.T., De Miguel, C., 1987b. Influence of the host plant in the cytostatic activity of *Viscum cruciatum* Sieber. Phytother. Res. 1, 93–94.

Clark, J.H., Herbert, L., Holland, H.L., Miller, J.M., 1976. Hydrogen bonding in organic synthesis IV: a simple, high-yield method for the methylenation of catechols. Tetrahedron Lett. 38, 3361–3364.

Chun, K.S., Sohn, Y., Kim, H.S., Park, K.K., Lee, J.M., Moon, A., Lee, S.S., Surh, Y.J., 1999. Anti-tumor promoting potential of naturally occurring diarylheptanoids structurally related to curcumin. Mutant. Res. 16, 49–57.

Elattar, T.M., Virji, A.S., 2000. The inhibitory effect of curcumin, genistein, quercetin and cisplatin on the growth of oral cancer cells in vitro. Anticancer Res. 20, 1733–1738.

Hadi, S.M., Asad, S.F., Singh, S., Ahmad, A., 2000. Putative mechanism for anticancer and apoptosis-inducing properties of plant derived poliphenolic compounds. IUBMB Life 50, 167–171.

Keserü, G.M., Nógrádi, M., 1995. Chemistry of natural diarylheptanoids. In: Atta-ur-Rahman, X. (Ed.), Studies in natural products chemistry Vol 17. Elsevier Science, Amsterdam, p. 357.

Martín-Cordero, C., Gil, A.M., Ayuso, M.J., 1993. Transfer of bipiperidyl and quinolizidine alkaloids to *Viscum cruciatum* (Loranthaceae) hemiparasitic on shrub of *Retama sphaerocarpa*. J. Chem. Ecol. 19, 2389–2393.

Martín-Cordero, C., Pedraza, M.A., Gil, A.M., Ayuso, M.J., 1997. Bipiperidyl and quinolizidine alkaloids in fruits of *Viscum cruciatum* Sieber parasitic on *Retama sphaerocarpa* Boissier. J. Chem. Ecol. 23, 1913–1916.

Martín-Cordero, C., Ayuso, M.J., Richomme, P., Bruneton, J., 1989. Quinolizidine alkaloids from *Viscum cruciatum*, hemiparasitic shrub of *Lygos sphaerocarpa*. Planta Med. 55, 196.

Monks, A., Scudeiro, D., Skehan, P., Shoemaker, R., Paull, K., Vistica, D., Hose, C., Jangley, J., Cronise, P., Vaigro-Wolff, A., Gray-Goodrich, M., Campell, H., Mayo, J., Boyd, M., 1991. Feasibility of a high-flux anticancer drug screen using a diverse panel of cultured human tumor cell lines. J. Natl. Cancer Inst. 83, 757–766.

Ramsewak, R.S., DeWitt, D.L., Nair, M.G., 2000. Cytotoxicity, antioxidant and anti-inflammatory activities of curcumins I-III from *Curcuma longa*. Phytomedicine 7, 303–308.

Surh, Y., 1999. Molecular mechanism of chemopreventive effects of selected dietary and medicinal phenolic substances. Mutant. Res. 428, 305–327.

Terazawa, M., Okuyama, H., Miyake, M., Sasaki, M., 1984. Phenolic compounds in living tissue of woods IV. Nippon Mokuzai Gakkaishi 30, 587–600.

PERGAMON

Phytochemistry 58 (2001) 571–575

PHYTOCHEMISTRY

www.elsevier.com/locate/phytochem

Cytotoxic coumarins from *Calophyllum dispar*

David Guilet[a], Denis Séraphin[a], David Rondeau[b], Pascal Richomme[a,*], Jean Bruneton[a]

[a]*SONAS, UFR des Sciences Pharmaceutiques, 16 Bd Daviers, F-49100 Angers, France*
[b]*SCAS, UFR Sciences, 2 Bd Lavoisiers, F-49045 Angers Cedex, France*

Received 15 March 2001; received in revised form 21 May 2001

Abstract

Six coumarins have been isolated from the fruits and the stem bark of *Calophyllum dispar* (Clusiaceae). The structures of these minor components were established by means of spectroscopic analysis, including extensive 2D NMR studies. Some of these coumarins exhibited a significant cytotoxic activity against KB cells. © 2001 Elsevier Science Ltd. All rights reserved.

Keywords: *Calophyllum dispar*; Coumarins; Clusiaceae

1. Introduction

The genus *Calophyllum* which comprises 200 species (Stevens, 1980) is widely distributed in the tropical rain forest where several species are used in folk medicine (Perry and Metzer, 1980). This genus is well known as a source of biologically active compounds such as coumarins (Kashman et al., 1992; Kawazu et al., 1972), xanthones (Reyes-Chilpa et al., 1997) and terpenoids (Cao et al., 1997). As part of our phytochemical study of *Calophyllum* species, we have described previously the isolation of twelve new 4-phenylcoumarins from *C. dispar* P. F. Stevens exhibiting cytotoxic activities (Guilet et al., 1999, 2001). In the present work, six new minor coumarins (**1**–**6**) were isolated and characterized from the stem bark and the fruits of the same species.

2. Results and discussion

Compound **1** was isolated as an amorphous residue from an EtOAc-soluble extract of the fruits of *C. dispar*. The UV absorptions of **1** characterized a 5,7-dioxygenated coumarin (Crichton and Waterman, 1978) whereas the ^{1}H and ^{13}C NMR spectra supported the presence of a monosubstituted phenyl group and a 3-methyl-1-oxobutyl moiety in the molecule. Through spectroscopic comparison (^{1}H NMR, MS, UV and IR), compound **1** appeared analogous to a synthetic coumarin previously described by Crombie et al. (1987). Total assignment of the ^{1}H and ^{13}C resonances of **1**, which we have named isodispar A, were finally completed (Tables 1 and 2) through its HMQC and HMBC data analysis. To the best of our knowledge, this compound has not been previously isolated from natural source.

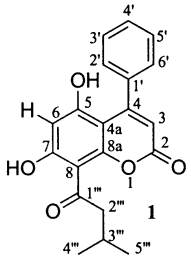

1

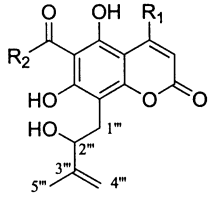

2 R_1 = Ph, R_2 = $CH(CH_3)_2$
3 R_1 = *n*-Pr, R_2 = $CHCH_3CH_2CH_3$
7 R_1 = Ph, R_2 = $CHCH_3CH_2CH_3$

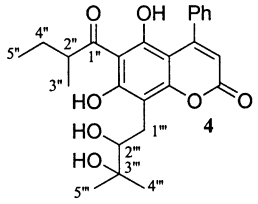

4

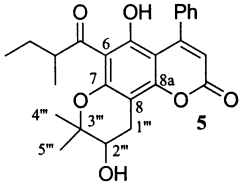

5

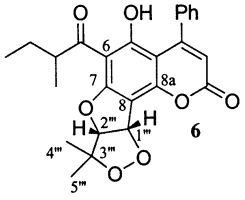

6

* Corresponding author. Tel.: +33-2-41-22-66-58; fax: +33-2-41-48-67-33.
E-mail address: pascal.richomme@univ-angers.fr (P. Richomme).

0031-9422/01/$ - see front matter © 2001 Elsevier Science Ltd. All rights reserved.
PII: S0031-9422(01)00285-0

Table 1
^{1}H NMR spectral data of compounds **1**–**6** (in $CDCl_3$, 500 MHz, values with TMS as internal standard)

H	1	2	3	4	5	6
3	6.02 *s*	5.97 *s*	5.94 *s*	5.97 *s*	5.96 *s*	6.01 *s*
OH-5	–	14.29 *s*	15.23 *s*	14.29 *s*	14.67 *s*	14.96 *s*
6	6.26 *s*	–	–	–	–	–
OH-7	14.77 *s*	10.20 *s*	10.00 *s*	10.26 *s*	–	–
2′,6′ [a]	7.43 *m*	7.33 *m*	2.97 *m*	7.32 *m*	7.33 *m*	7.30 *m*
3′,5′ [a]	7.56 *m*	7.42 *m*	1.65 *m*	7.41 *m*	7.41 *m*	7.42 *m*
4′	7.56 *m*	7.42 *m*	1.02 *t* (7.0)	7.41 *m*	7.41 *m*	7.42 *m*
2″	–	3.99 *h* (7.0)	3.90 *m*	3.84 *m*	3.64 *m*	3.58 *m*
3″	–	1.16 *d* (7.0)	1.19 *d* (7.0)	1.15 *d* (6.5)	1.16 *d* (6.5)	1.17 *d* (7.0)
4″	–	–	1.44 *m* 1.87 *m*	1.40 *m* 1.80 *m*	1.41 *m* 1.81 *m*	1.43 *m* 1.79 *m*
5′	–	–	0.93 *t* (7.5)	0.90 t (7.5)	0.93 *t* (7.0)	0.91 *t* (7.0)
1‴	–	3.05 *dd* (8.0/15.5)	2.95–3.00 m	2.61 *dd* (10.0/15.0)	3.35 *m*	6.22 *d* (6.0)
		3.32 *dd* (2.0/15.0)	3.26 *dd* (2.0/15.0)	3.37 *d* (15.0)		
2‴	3.19 *d* (6.5)	4.51 *d* (7.5)	4.46 *t* (8.5)	3.74 *dd* (7.0/8.0)	5.25 *d* (8.5)	5.48 *d* (6.0)
3‴	2.31 *m*	–	–	–	–	–
4‴	1.07 *d* (6.5)	4.94 *s* 5.03 *s*	4.90 *s* 5.00 *s*	1.36 *s*	1.36 *s*	1.48 *s*
5‴	1.07 *d* (6.5)	1.95 *s*	1.91 *s*	1.49 *s*	1.36 *s*	1.50 *s*

[a] For compounds **1**, **2** and **4**–**6.**

Table 2
^{13}C NMR spectral data of compounds **1**–**6** (in $CDCl_3$, 67.5 MHz, values with TMS as internal standard)

C	1	2	3	4	5	6
2	158.5	159.9	160.5	159.7	159.8	158.8
3	111.7	112.2	109.6	111.9	112.0	113.1
4	154.0	156.6	160.1	156.6	156.7	157.1
4a	100.8	102.1	103.2	101.9	102.5	102.4
5	159.6	163.4	164.4	163.5	165.0	166.5
6	101.4	106.9	107.4	107.6	102.8	103.2
7	168.8	162.1	161.5	162.4	163.9	164.6
8	104.9	104.7	104.6	105.3	104.6	102.9
8a	155.7	157.7	157.9	157.3	155.5	156.2
1′	136.3	139.4	38.6	139.1	139.1	139.0
2′	127.4	127.1	22.8	127.1	127.2	127.2
3′	129.6	127.7	14.0	127.6	127.6	127.7
4′	130.4	128.2	–	128.2	128.2	128.3
1″	–	212.3	212.7	212.1	209.6	209.3
2″	–	39.9	46.6	46.5	45.6	45.7
3″	–	19.2	16.6	16.5	16.5	16.7
4″	–	19.2	26.8	26.7	26.4	26.5
5″	–	–	11.9	11.8	11.7	11.9
1‴	205.8	28.7	28.8	26.0	27.1	81.8
2‴	53.5	77.7	77.6	80.6	89.0	99.4
3‴	25.5	146.0	146.0	73.2	83.0	85.7
4‴	22.6	111.1	111.0	26.7	19.9	18.4
5‴	22.6	18.7	18.7	22.2	20.5	23.6

Column chromatography of the EtOAc-soluble extract of the stem bark of *C. dispar* allowed isolation of the new compounds **2**–**6** and the known dihydroxycoumarin disparinol B (**7**). Compound **2** was obtained as an amorphous residue, and the alkaline shifts of its UV spectrum could readily be associated with a 6-acyl-5,7-dihydroxycoumarin chromophore (Crombie et al., 1967; Carpenter et al., 1971). The molecular formula of **2** ($C_{24}H_{24}O_6$) was established by HRFABMS analysis of its negative pseudomolecular ion $[M\text{-}H]^-$ at m/z 407.1530 ($\Delta + 3.5$ mmu). The molecular formula of **2** thus differed from that of disparinol B (**7**), previously isolated from *C. dispar* (Guilet et al., 1999), by the loss of a CH_2 moiety. Comparison of the ^{1}H and ^{13}C NMR spectra of **2** (tables 1 and 2) and **7**, then suggested that they were closely related, differing only in the nature of their acyl substituents. Interlocking DQF-COSY, HMQC and HMBC data of **2**, an isobutanoyl moiety was firmly characterized and therefore, this compound was identified as structure **2** which we have named disparinol D.

Compound **3**, crystallized as yellow needles (mp = 111–112 °C), and exhibited spectroscopic data closely related to those of disparinol D (**2**) and disparinol B (**7**). Its molecular formula $C_{22}H_{28}O_6$ was determined by HREIMS ($\Delta + 0.1$ mmu). An extensive NMR analysis of **3** then showed that this coumarin exhibited identical substituents with those of disparinol B (**7**) except for the 4-position (Tables 1 and 2). Examination of the contours maps of a gradient-selected DQF-COSY and a HMQC experiments then allowed us to distinguish a *n*-propyl system in the molecule. Long-range ^{1}H–^{13}C couplings deduced from the HMBC spectrum of **3** then confirmed the 4-position of this *n*-propyl substituent. Therefore, compound **3**, or disparpropylinol B, could be identified as the first representative of a new disparinol series exhibiting a 4-*n*-propyl substitution.

Compound **4** was obtained as an amorphous residue. In the presence of alkali, the bathochromic shifts of its UV spectrum suggested that **4**, like **2** and **3**, was a 6-acyl-5,7-dihydroxycoumarin chromophore. HRISMS analysis of its pseudomolecular ion $[M + H]^+$ indicated the composition $C_{25}H_{28}O_7$ ($\Delta + 1.4$ mmu). The ^{1}H NMR (Table 1), ^{13}C NMR (Table 2), and 2D-experiments (DQF-COSY, HMQC and HMBC) indicated the

presence of a monosubstituted phenyl group, an isopentanoyl moiety, and showed two chelated hydroxyl groups at δ_H 10.26 and 14.29, respectively. The molecular formula of **4** thus suggested that the remaining substitution of the coumarinic nucleus was a $C_5H_{11}O_2$ side chain. The presence of a 2,3-dihydroxy-3-methylbutyl moiety was then proved by HMQC and HMBC experiments. Long-range ^1H–^{13}C couplings deduced from the HMBC spectrum of **4** also revealed that the methylene group of this chain (δ_H 2.61 and 3.37) correlated with three coumarinic carbons C-7, C-8 and C-8a. The substitution at the 8-position of the coumarinic nucleus with a 2,3-dihydroxy-3-methylbutyl moiety was so established. Finally, from the aforementioned spectroscopic data, this compound was identified as structure **4**, which we have named dispardiol B.

Compound **5** was assigned the molecular formula $C_{25}H_{26}O_6$ by HREIMS ($[M]^+$ m/z 422.1747, Δ +1.7 mmu). As for compounds **3** and **4**, the acyl chain of **5** was established to be an isopentanoyl moiety (Table 1) located at C-6 after inspection of the UV spectrum (Crombie et al., 1967; Carpenter et al., 1971). Furthermore, a monosubsituted phenyl and a phenolic hydroxyl were also located at C-4 and C-5 through NMR evidences. The remaining ring system in **5** was characterized with chemical shifts at δ_H: 1.36 (6H, *s*, H-4‴ and H-5‴), 3.35 (2H, *m*, H-1‴) and 5.25 (1H, *br d*, J=8.5 Hz, H-2‴) and δ_C: 19.9 (C-4‴), 20.5 (C-5‴), 27.1 (C-1‴), 83.0 (C-3‴) and 89.0 (C-2‴), suggesting the presence of a 3-hydroxy-2,2-dimethyldihydropyran in the molecule. The HMBC data (Table 3) confirmed this hypothesis and **5** was concluded to be the mammea A/AB cyclo E, according to the nomenclature already proposed for related compounds (Crombie et al., 1966).

Compound **6** exhibited, in its HREIMS, a molecular ion $[M]^+$ at m/z 436.1528 associated with the molecular formula $C_{25}H_{24}O_7$ (Δ +0.6 mmu). The UV spectrum of **6** showed bathochromic shifts similar to those of 6-acyl-5,7-dioxycoumarin chromophores. The NMR data of **6** suggested the presence of a monosubstituted phenyl, a chelated phenolic hydroxyl (δ_H 14.96), and a 2-methyl-1-oxobutyl chain at the 4, 5 and 6 positions of the coumarin, respectively (Tables 1 and 2). The nature of the remaining susbtituents at the position 7 and 8 were then deduced from NMR evidences. Indeed, the ^1H NMR spectrum of **6** exhibited the presence of two coupled methines [δ_H 5.48 (1H, *d*, J=6 Hz, H-2‴) and 6.22 (1H, *d*, J=6 Hz, H-1‴)] and two methyls [δ_H 1.48 (3H, *s*, H-4‴) and 1.50 (3H, *s*, H-5‴)]. In the HMBC spectrum of **6** (Table 3), these methyls appeared to be long-range coupled with carbons at δ_C 85.7 (C-3‴) and 99.4 (C-2‴), while the methine proton signal at δ_H 6.22 (H-1‴) correlated with four carbons at δ_C 85.7 (C-3‴), 102.9 (C-8), 156.2 (C-8a) and 164.6 (C-7), the three latter resonances being associated with the coumarin nucleus. These elements suggested the presence of a trioxygenated isoprenic skeleton, link to the heterocycle *via* the methine at δ_H 6.22 (H-1‴). According to the molecular formula of **6**, this substituent also had to be a bicyclic structure. Furthermore, a significant correlation was observed between the proton signal at δ_H 5.48 (H-2‴) and the coumarinic carbon at δ_C 164.6 (C-7), implicating the presence, on one hand, of a dihydrofuran cycle and, on the other, of a dioxolane structure. This compound was thus identified as structure **6**, which we have named mammea A/AB dioxalanocyclo F.

It may be noticed that coumarins **2**–**6** did not present any significant optical activities, this point being already stressed for a number of coumarins isolated from the genera *Mammea* (Crombie et al., 1967; Carpenter et al., 1971) and *Mesua* (Morel et al., 1999). We thus may assume that the isoprenic moieties probably derive from non stereoselective functionalizations of the corresponding prenylated precursors, which may justify the racemic nature of **2** (Guilet, 2000). *A contrario*, coumarins substituted by an isopentanoyl moiety, probably issued from a chiral amino acid such as isoleucin (Kunesch and Polonsky, 1969), exhibit weak optical activities for highly concentrated solutions (Finnegan et al., 1972). It thus could be the same for compounds **3**–**6** isolated here in small amounts.

From a chemotaxonomic point of view, it should also be mentioned that the isoprenic moieties identified in

Table 3
Significant HMBC data (J=6 Hz) of compounds **2**, **5** and **6**

2		**5**		**6**	
H	Correlated C	H	Correlated C	H	Correlated C
3	2, 4a, 1′	3	2, 4a, 1′	3	2, 4a, 1′
OH-5	4a, 5, 6	OH-5	4a, 5, 6	OH-5	4a, 5, 6
H-2″ H-6″	4	H-2″ H-6″	4	H-2″ H-6″	4
H-3″ H-5″	1′	H-3″ H-5″	1′	H-3″ H-5″	1′
H-1″	7, 8, 8a, 2‴, 3‴	H-1″	7, 8, 8a, 2‴, 3‴	H-1″	7, 8, 8a, 3‴
H-2″	8, 1‴, 4‴, 5‴	H-2‴	7, 8, 1‴, 3‴, 4‴, 5‴	H-2‴	7, 8, 1‴, 3‴, 4‴, 5‴
H-4″	2‴, 3‴, 5‴	H-4‴	2‴, 3‴, 5‴	H-4‴	2‴, 3‴, 5‴
H-5″	2‴, 3‴, 4‴	H-5‴	2‴, 3‴, 4‴	H-5‴	2‴, 3‴, 4‴

Table 4
Cytotoxicity against KB cells of coumarins **1**–**3** and **7**

Compounds	**1**	**2**	**3**	**7**
ED_{50} (μg/ml)	8	21	4	7

compounds **5** and **6** are recorded here for the first time in the genus *Calophyllum*, whereas they were already identified in coumarins isolated from *Mammea americana* (Crombie et al., 1972).

The cytotoxic effect against KB cells of a number of these coumarins was finally evaluated (Table 4). Most of them tested exhibited a significant activity in this assay since these compounds inhibited 50% of the cellular growth at concentration ranging from 4 to 8 μg/ml.

3. Experimental

3.1. General

Melting points were determined on an Electrothermal 8100 melting point apparatus and are uncorrected. Optical rotations were measured on a Schmidt-Haensch-polartronic-I polarimeter. IR spectra were recorded on a Perkin Elmer 580 spectrophotometer and UV spectra were taken on a Hitachi U-2000 spectrophotometer. HREIMS (70 eV) were recorded on Varian MAT 311 spectrometer and HRFABMS were recorded on a Jeol JMS-700 spectrometer. NMR spectra were recorded in $CDCl_3$ solution on a Bruker Avance DRX 500 instrument, using TMS as the internal standard. Si gel 60 (Macherey-Nagel, 230–400 mesh) was used for column chromatography and precoated Si gel plates (Macherey-Nagel, SIL G/UV254, 0.25 mm) were used for preparative TLC. The compounds were detected under UV light at 254 and 366 nm.

3.2. Plant material

The stem bark and the fruits of *Calophyllum dispar* P. F. Stevens were collected from Terrangganu, Malaysia in October, 1994. An herbarium specimen (KL 4430) is deposited at the University of Kuala-Lumpur, Malaysia.

3.3. Extraction and isolation

The dried and powdered stem bark of *C. dispar* (5 kg) was extracted with EtOAc (7 l) for 72 h in a Soxhlet apparatus. After concentration, the extract gave a residue (238.85 g). A portion of the residue (87.50 g) was chromatographed over Si gel by MPLC, eluting with *n*-hexane and a 5% stepwise gradient of EtOAc (0–80% close up) to afford several fractions labeled, in order of elution A to I. Work-up of fraction F by repeated CC and prep. TLC using pentane-Me_2CO (93:7) led then to the isolation of **3** (32 mg, 0.037%), **6** (3 mg, 0.003%), and **2** (8 mg, 0.009%). Work-up of fraction G also by repeated CC and prep. TLC using $CHCl_3$–EtOAc (9:1) afforded **5** (10 mg, 0.011%) and **4** (4 mg, 0.005%).

The same procedure was applied to the dried and powdered fruits of *C. dispar* (140 g). After extraction with EtOAc, 4.60 g of residue were obtained and then chromatographed on Si gel by MPLC, eluting with *n*-hexane and a 5% stepwise gradient of EtOAc (0–80%) to afford several fractions labeled, in order of elution A to H. Work-up of fraction E by repeated CC and preparative TLC using *n*-hexane–EtOAc (9:1) led to the purification of **1** (13 mg, 0.28%).

3.3.1. Isodispar B, (5,7-dihydroxy-8-(2-methyl-1-oxo butyl)-4-phenyl-2H-[1]benzopyran-2-one, **1**)

UV λ_{max}^{EtOH} (log ε) nm: 222 (4.40), 292 (4.32), 329 (4.25); $\lambda_{max}^{EtOH+NaOH}$: 225 (4.34), 253 (4.21), 333 (4.45), 381 (3.93), 428 (4.01); IR ($CHCl_3$) ν_{max} cm^{-1}: 3500, 1684, 1622, 1594, 774, 700; ^1H NMR (500 MHz, $CDCl_3$) see Table 1 and ^{13}C NMR (125 MHz, $CDCl_3$) see Table 2; HR–FABMS $[M-H]^-$: *m*/*z* 337.1174 (calc. for $C_{20}H_{17}O_5$, 337.1076).

3.3.2. Disparinol D, (5,7-dihydroxy-8-(2-hydroxy-3-methylbut-3-enyl)-6-(2-methyl-1-oxopropyl)-4-phenyl-2H-[1]benzopyran-2-one, **2**)

$[\alpha]_D^{25}$ 0° ($c = 0.16$, $CHCl_3$); UV λ_{max}^{EtOH} (log ε) nm : 235 (3.75), 283 (3.89), 331 (3.46); $\lambda_{max}^{EtOH+NaOH}$: 258 (3.82), 306 (3.75), 391 (3.42), 409 (3.41); IR ($CHCl_3$) ν_{max} cm^{-1}: 3420, 1732, 1716, 1622, 1595, 756, 702; ^1H NMR (500 MHz, $CDCl_3$) see Table 1 and ^{13}C NMR (125 MHz, $CDCl_3$) see Table 2; HR–FABMS: $[M-H]^-$: *m*/*z* 407.1530 (calc. for $C_{24}H_{23}O_6$, 407.1495).

3.3.3. Disparpropylinol B, (5,7-dihydroxy-8-(2-hydroxy-3-methylbut-3-enyl)-6-(2-methyl-1-oxobutyl)-4-propyl-2H-[1]benzopyran-2-one, **3**)

Yellow crystals, mp 111–112 °C (*n*-hexane–EtOAc 9:1); $[\alpha]_D^{25}$ 0° ($c = 0.6$, $CHCl_3$); UV λ_{max}^{EtOH} (log ε) nm: 236 (3.96), 286 (4.20), 329 (3.85); $\lambda_{max}^{EtOH+NaOH}$: 237 (4.22), 301 (4.15), 372 (3.95), 404 (3.92); IR ($CHCl_3$) ν_{max} cm^{-1}: 3650, 1717, 1622, 1578, 758; ^1H NMR (500 MHz, $CDCl_3$) see Table 1 and ^{13}C NMR (125 MHz, $CDCl_3$) see Table 2; HR–EIMS $[M]^+$: *m*/*z* 388.1888 (calc. for $C_{22}H_{28}O_6$, 388.1886), EIMS *m*/*z*: 388 (20), 370 (70), 355 (27), 331 (13), 317 (100), 313 (31), 303 (22), 299 (55), 289 (26), 271 (35), 261 (32).

3.3.4. Dispardiol B, (5,7-dihydroxy-8-(2,3-dihydroxy-3-methylbutyl)-6-(2-methyl-1-oxobutyl)-4-phenyl-2H-[1]benzopyran-2-one, **4**)

$[\alpha]_D^{25}$ 0° ($c = 0.08$, $CHCl_3$); UV λ_{max}^{EtOH}(log ε) nm: 234 (4.22), 284 (4.43), 355 (3.93), 426 (3.59); $\lambda_{max}^{EtOH+NaOH}$: 238 (4.29), 279 (4.31), 381 (4.06), 410 (4.05); IR ($CHCl_3$) ν_{max} cm^{-1}: 3460, 1717, 1706, 1617, 768, 702; ^1H NMR

(500 MHz, $CDCl_3$) see Table 1 and ^{13}C NMR (125 MHz, $CDCl_3$) see Table 2; HR–LSIMS $[M+H]^+$: *m/z* 441.1927 (calc. for $C_{25}H_{29}O_7$, 441.1913).

*3.3.5. Mammea A/AB cyclo E, (9,10-dihydro-5,9-dihydroxy-8,8-dimethyl-6-(2-methyl-1-oxobutyl)-4-phenyl-2H,8H-benzo[1,2-b:5,6-b']-dipyran-2-one, **5**)*

$[\alpha]_D^{25}$ 0° (*c* = 0.2, $CHCl_3$); UV λ_{max}^{EtOH} (log ε) nm : 235 (4.11), 282 (4.37), 344 (3.94); $\lambda_{max}^{EtOH+NaOH}$: 254 (4.22), 282 (4.09), 313 (4.01), 426 (3.92); IR ($CHCl_3$) ν_{max} cm^{-1}: 3400, 1717, 1617, 1561, 768, 704; ^1H NMR (500 MHz, $CDCl_3$) see Table 1 and ^{13}C NMR (125 MHz, $CDCl_3$) see Table 2; HR–EIMS: $[M]^+$ *m/z* 422.1747 (calc. for $C_{25}H_{26}O_6$, 422.1730), EIMS *m/z*: 422 (75), 420 (20), 405 (10), 389 (13), 365 (94), 363 (50), 347 (40), 335 (12), 321 (14), 307 (33), 305 (20), 293 (100).

*3.3.6. Mammea A/AB dioxalanocyclo F, (7a,10a-dihydro-5-hydroxy-8,8-dimethyl-6-(2-methyl-1-oxobutyl)-4-phenyl-2H-8H-[1,2]-dioxolano[4'', 5'':4',5']furo[2',3':5,6]benzo[1,2-b]pyran-2-one, **6**)*

$[\alpha]_D^{25}$ 0° (*c* = 0.06, $CHCl_3$); UV λ_{max}^{EtOH} (log ε) nm: 230 (3.83), 281 (4.08), 346 (3.46); $\lambda_{max}^{EtOH+NaOH}$: 256 (4.00), 281 (3.98), 338 (3.34), 416 (3.56); IR ($CHCl_3$) ν_{max} cm^{-1}: 3440, 1717, 1617, 1559, 768, 702; ^1H NMR (500 MHz, $CDCl_3$) see Table 1 and ^{13}C NMR (125 MHz, $CDCl_3$) see Table 2; HR–EIMS $[M]^+$: *m/z* 436.1528 (calc. for $C_{25}H_{24}O_7$, 436.1522), EIMS *m/z*: 436 (41), 403 (25), 389 (57), 379 (61), 378 (41), 363 (20), 347 (37), 321 (90), 305 (45), 171 (30), 43 (100).

3.4. Cytotoxicity testing

The cytotoxicity assays were carried out in triplicate against human nasopharynx carcinoma KB cell lines. After 72 h incubation at 37 °C with or without test compounds, cell growth was estimated by colorimetric measurement of stained living cells by neutral red. The cultured cells were treated at five concentrations of pure test compounds ranging from 50 to 0.01 μg/ml. Optical density was determined at 540 nm on a Titertek Multiscan photometer. The ED_{50} value was defined as the concentration of sample necessary to inhibit the cell growth to 50% of the control. Doxorubicine, as positive control substance, presents an ED_{50} value of 0.058 μg/ml.

Acknowledgements

The authors express their thanks to C. Gaspard (GDR "Substances d'intérêt biologique", I.C.S.N., Gif-Sur-Yvette, France) who performed the cytotoxicity evaluation on KB cells.

References

Cao, S.G., Sim, G.Y., Goh, S.H., Xue, F., Mak, T.C., 1997. Gracilipense: a heterocyclic seco-trisnor oleanane from *Calophyllum gracilipes*. Tetrahedron Lett. 38, 4783–4786.

Carpenter, I., McGarry, E. J., Scheinmann, F., 1971. Extractives from Guttiferae. Part XXI. The isolation and structure of nine coumarins from the bark of *Mammea africana* G Don. J. Chem. Soc. (C), 3783–3790.

Crichton, E.G., Waterman, P.G., 1978. Dihydromammea C/OB: a new coumarin from the seed of *Mammea africana*. Phytochemistry 17, 1783–1786.

Crombie, L., Games, D.E., Haskins, N.J., Reed, G.F., 1972. Extractives of *Mammea americana* L. Part III. Identification of new coumarin relatives of mammea B/BA, B/BB, and B/BC having 5,6-annulation and higher oxidation levels. J. Chem. Soc. Perkin Trans. 1, 2241–2247.

Crombie, L., Games, D.E., McCormick, A., 1966. Isolation and structure of mammea B/BA, B/BB, B/BC, and C/BB: A group of 4-*n*-propyl and 4-*n*-amylcoumarin extractives of *Mammea americana* L. J. Chem. Soc. (C), 151–156.

Crombie, L., Games, D.E., McCormick, A., 1967. Extractives of *Mammea americana* L. Part I. The 4-*n*-alkylcoumarins. Isolation and structure of mammea B/BA, B/BB, B/BC, and C/BB. J. Chem. Soc. (C), 2545–2552.

Crombie, L., Jones, R.C.F., Palmer, C.J., 1987. Synthesis of the *Mammea* coumarins. Part 1. The coumarins of the mammea A, B, and C series. J. Chem. Soc. Perkin Trans. 1, 317–331.

Finnegan, R.A., Merkel, K.E., Back, N., 1972. Constituents of *Mammea americana* L. VII: novel structural variations on the mammein theme and antitumor activity of mammein and related coumarin and phloroglucinol derivatives. J. Pharm. Sci. 61, 1599–1603.

Guilet, D., Morel, C., Noyer, N., Cornec, M., Séraphin, D., Wiart, C., Hadi, A.H.A., Sevennet, T., Richomme, P., Bruneton, J., 1999. Four new 4-phenylcoumarins from *Calophyllum dispar*, isolation and hemisynthesis. Heterocycles 51, 67–76.

Guilet, D., 2000. Etude Phytochimique d'une Clusiaceae Malaise, le *Calophyllum dispar*. PhD thesis, Angers University, 291, Angers, France.

Guilet, D., Hélesbeux, J.-J., Séraphin, D., Sévenet, T., Richomme, P., Bruneton, J., 2001. Novel cytotoxic 4-phenylfuranocoumarins from *Calophyllum dispar*. J. Nat. Prod., in press.

Kashman, Y., Gustafson, K.R., Fuller, R.W., Cardellina, J.H., MacMahon, J.B., Currens, M.J., Buckheit, R.W., Hughes, S.H., Cragg, G.M., Boyd, M.R., 1992. The calanolides, a novel HIV-inhibitor class of coumarin derivatives from the tropical rainforest tree, *Calophyllum lanigerum*. J. Med. Chem. 35, 2735–2743.

Kawazu, K., Ohigashi, H., Takahashi, N., Mitsui, T., 1972. Piscicidal constituents of *Calophyllum inophyllum*. Bull. Inst. Chem. Res. Kyoto Univ. 50, 160–167.

Kunesch, G., Polonsky, J., 1969. Biosynthèse du calophyllolide, sur l'origine biogénétique du groupement tigloyle. Phytochemistry 8, 1221–1226.

Morel, C., Guilet, D., Oger, J.M., Séraphin, D., Sévenet, T., Wiart, C., Hadi, A.H.A., Richomme, P., Bruneton, J., 1999. 6-Acylcoumarins from *Mesua racemosa*. Phytochemistry 50, 1243–1247.

Perry, L.M., Metzer, J., 1980. Medicinal plants of east and southeast Asia. Mit Press, Cambridge, MA.

Reyes-Chipa, R., Jimenez-Estrada, M., Estrada-Muniz, E., 1997. Antifungal xanthones from *Calophyllum brasiliensis* heartwood. J. Chem. Ecol. 23, 1901–1911.

Stevens, P.F., 1980. A revision of the Old World species of *Calophyllum* (Guttiferae). J. Arnold Arbor 61, 117–690.

PERGAMON

Phytochemistry 58 (2001) 577–580

PHYTOCHEMISTRY

www.elsevier.com/locate/phytochem

Flavonol glycosides from the stems of *Trigonella foenum-graecum*

Yingmei Han[a], Sansei Nishibe[b,*], Yukari Noguchi[b], Zhexiong Jin[c]

[a]*Research Department of Chinese Materia Medicine, Pharmaceutical Institute of Tianjin, No. 308 Anshanxi Road, Nankai District, Tianjin 300193, China*
[b]*Faculty of Pharmaceutical Sciences, Health Sciences University of Hokkaido, Ishikari-Tobetsu, Hokkaido 061-0293, Japan*
[c]*Department of Chinese Medicine, Heilongjiang Commercial College, No. 138 Tongda Street, Daoli District, Harbin 150076, China*

Received 27 February 2001; received in revised form 4 May 2001

Abstract

Two kaempferol glycosides [kaempferol 3-*O*-β-D-glucosyl(1→2)-β-D-galactoside 7-*O*-β-D-glucoside and kaempferol 3-*O*-β-D-glucosyl(1→2)-(6''-*O*-acetyl)-β-D-galactoside 7-*O*-β-D-glucoside] as well as the quercetin glycoside [quercetin 3-*O*-β-D-glucosyl (1→2)-β-D-galactoside 7-*O*-β-D-glucoside] were isolated from the stems of *Trigonella foenum-graecum* L. (Leguminosae) along with a known kaempferol glycoside, lilyn [kaempferol 3-*O*-β-D-glucosyl(1→2)-β-D-galactoside]. Their structures were established by analysis of chemical and spectral evidence. © 2001 Elsevier Science Ltd. All rights reserved.

Keywords: *Trigonella foenum-graecum*; Leguminosae; Stems; Kaempferol glycosides; Quercetin glycoside

1. Introduction

Trigonella foenum-graecum L. (Leguminosae) has been widely cultivated in Asia, Africa and Mediterranean countries for the edible and medicinal values of its seeds (Yoshikawa et al., 1997). In Chinese traditional medicine, the seeds of this plant have been prescribed as a tonic and for stomach disorders, and the whole aerial part of the plant is used as a folk medicine for the treatment of renal diseases in the Northern-East region of China (Liu et al., 1990). Many phytochemical studies on constituents of the seeds have been reported (Varshney and Beg, 1978), but little research has been carried out on other parts of the plant. As part of studies for developing new sources of medicinal materials, we investigated phenolic components of the stems of this plant. Here we report on the isolation and structure elucidation of three new flavonol glycosides from the stems of *Trigonella foenum-graecum*.

2. Results and discussion

The concentrated methanolic extract from the stems of *Trigonella foenum-greacum* was fractionated by successive extraction with petroleum ether, ethyl acetate and *n*-BuOH. The *n*-BuOH extract was subjected to column chromatography (CC) on silica gel, followed by CC on Sephadex LH-20 to yield compound **1**. The aqueous fraction furnished compounds **2**, **3** and **4** by combination of CC on silica gel and Diaion HP-20 and final purification by preparative HPLC.

Complete acid hydrolysis of compounds **1**, **2** and **3** afforded kaempferol, glucose and galactose (TLC for sugars and HPLC, UV for aglycones), respectively.

Compound **1** was identified as kaempferol 3-*O*-β-D-glucosyl (1→2)-β-D-galactoside (lilyn) on the basis of acid hydrolysis, spectral data (UV, ^{1}H NMR,^{13}C NMR and FAB–MS), optical rotation value ($[\alpha]_D$) and comparison with published data (Nagy et al., 1984). This is the second example of isolation of compound **1** from a natural source.

A positive ion FAB-mass spectrum of compound **2** exhibited pseudomolecular ions at *m*/*z* 811 $[M+K]^+$ and *m*/*z* 795 $[M+Na]^+$, thus confirming its $[M]^+$ to be 772 (calc. for $C_{33}H_{40}O_{21}$). The fragment ions at *m*/*z* 449 $[M+H\text{-}324]^+$ and *m*/*z* 287 $[M+H\text{-}486]^+$ indicated successive loss of three hexosyl (glucosyl or galactosyl) moieties. The appearance of three anomeric proton signals in the ^{1}H NMR spectrum further confirmed that compound **2** is a kaempferol triglycoside. Three sugar moieties were identified as two glucoses and one galactose from the ^{13}C NMR spectral data. In the ^{13}C NMR spectrum, a downfield shift (compared with reported

* Corresponding author. Tel.: +81-1332-3-1211; fax: +81-1332-3-1338.

E-mail addresses: nishibe@hoku-iryo-u.ac.jp (S. Nishibe), hanyingmei@21cn.com (Y. Han).

0031-9422/01/$ - see front matter © 2001 Elsevier Science Ltd. All rights reserved.
PII: S0031-9422(01)00273-4

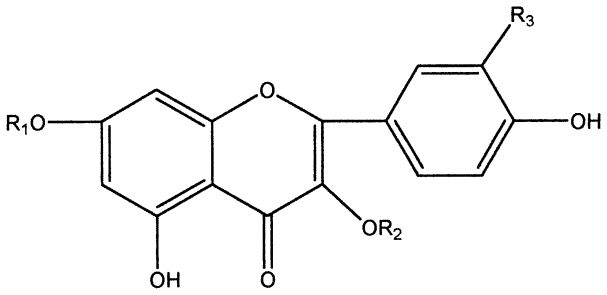

	R_1	R_2	R_3
1	H	glc(1-2)gal	H
2	glc	glc(1-2)gal	H
3	glc	glc(1-2)(6″-Ac)gal	H
4	glc	glc(1-2)gal	OH

data of unsubstituted galactosyl moiety) (Markham et al., 1978; Nagy et al., 1984) of C-2″ (from 71.4 to 80.5 ppm) and an upfield shift of C-1″ of galactosyl moiety (from 102.5 to 98.3 ppm) suggested the presence of a (1→2) linked glucosyl-galactosyl unit in this structure (Liu et al., 1994). The anomeric carbon (98.3 ppm) and proton shifts (5.66 ppm, 1H, *d*, $J=7.5$ Hz) of the galactosyl moiety indicated the direct connection of the galactosyl moiety at C-3 of the kaempferol moiety, which was confirmed by 2-D NMR spectroscopic and long-range ^{13}C–^{1}H shift correlation (COSY) spectral analyses. Comparison of the carbon shifts of the aglycone with those of published data for kaempferol 3-glycosides (Markham et al., 1978; Budzianowski, 1990) revealed an upfield shift of C-7 ($\Delta\delta$ 1.1 ppm) and downfield shifts at C-6 ($\Delta\delta$ 1.2 ppm), C-8 ($\Delta\delta$ 1.0 ppm) and C-10 ($\Delta\delta$ 1.8 ppm) implying glycosylation of C-7 of the aglycone. The H-6 (6.42 ppm) and H-8 (6.79 ppm) signals in the ^{1}H NMR spectrum supported further evidence for this assignment. An anomeric proton signal (5.05 ppm, 1H, *d*, $J=7.5$ Hz) in the ^{1}H NMR spectrum was assignable to the glucosyl moiety attached to C-7 position of the aglycone. The anomeric carbon shift (99.8 ppm) of a remaining glucosyl moiety agreed well with this assignment, which was confirmed by analysis of the 2-D NMR and long-range ^{13}C–^{1}H shift correlation (COSY) spectra. Therefore, compound **2** was established as kaempferol 3-*O*-β-D-glucosyl(1→2)-β-D-galactoside 7-*O*-β-D-glucoside, a new kaempferol glycoside.

Compound **3** was also confirmed as a kaempferol triglycoside on the basis of its fragmentation behavior in the FAB-mass spectrum and the appearance of three anomeric proton signals in the ^{1}H NMR spectrum. The ^{1}H NMR (δ 1.65 ppm), ^{13}C NMR (δ 20.4 and 169.3 ppm) and IR (1730 cm^{-1}) spectral data indicated the presence of an additional acetyl group in **3**. The ^{13}C NMR spectroscopic shifts of the aglycone corresponded well with those of **2**. In the ^{1}H NMR spectrum, the three anomeric proton signals were very close to those of the glycosyls in the spectrum of **2**. Except for a downfield shift of 3.0 ppm for C-6″ and an upfield shift of 2.8 ppm for C-5″ of the galactosyl moiety in 3, the ^{13}C NMR data of the sugar moieties of **3** showed great similarity to those of **2**. Thus, these data suggested the attachment of the acetyl group to C-6″ hydroxyl group of the galactosyl moiety (Mizuno et al., 1990). Hence, compound **3** was characterized as kaempferol 3-*O*-β-D-glucosyl (1→2)-(6″-*O*-acetyl)-β-D-galactoside 7-*O*-β-D-glucoside, an acetylated derivative of **2**.

Compound **4** released quercetin, glucose and galactose upon complete acid hydrolysis. The ^{1}H and ^{13}C NMR spectral data further confirmed the presence of the quercetin part in the structure. The ^{1}H and ^{13}C NMR spectral data of the sugar moieties of **4** resembled those of compound **2**. Carbon shifts of the aglycone showed typical 3,7-disubstitution of quercetin (Markham et al., 1978; Yasukawa et al., 1988). Thus, the structure of compound **4** was established as quercetin 3-*O*-β-D-glucosyl (1→2)- β-D-galactoside 7-*O*-β-D-glucoside, a new glycoside of quercetin.

3. Experimental

3.1. General

Mp:uncorr., optical rotations were measured on a Jasco DIP-360. UV spectra were recorded on Hitachi U-2000, whereas IR spectra were obtained on a Jasco VALOR-III. ^{1}H and ^{13}C NMR spectra were recorded in DMSO-d_6 or CD_3OD at 300.40 MHz, TMS was used as an internal standard. TLC was carried out on precoated silica gel 60 F254 and RP-8 plates (Merck). Preparative HPLC was performed on a GP RP-18 column (5 μm, 20×250 mm) at a flow rate of 6 ml/min and the purity of compounds was checked by HPLC on Nucleosil 5C18 column (4.6×150 mm).

3.2. Plant material

Trigonella foenum-graecum L. was collected in Heilongjiang province of China in July, 2000. Voucher specimens were deposited at the Department of Pharmacognosy, Faculty of Pharmaceutical Sciences, Health Sciences University of Hokkaido.

3.3. Extraction and isolation

The dried stems of *Trigonella foenum-graecum* (3.7 kg) were extracted with hot MeOH (37 l×3) and concentrated to a small volume under reduced pressure, then H_2O was added and the suspension was filtered. The filtrate was extracted with petroleum ether, EtOAc and *n*-BuOH, successively. The *n*-BuOH extract (20 g) was subjected to CC on silica gel eluted first with

$CHCl_3$, then with a gradient of $CHCl_3$–EtOH with increasing EtOH. A fraction collected from $CHCl_3$-EtOH (4:1) elution yielded compound **1** (177 mg) after repeated CC on Sephadex LH-20 with H_2O and H_2O–MeOH (95:5) as eluent. The aqueous layer (30 g) was applied to a silica gel column eluted with $CHCl_3$, $CHCl_3$–EtOH, EtOH to give 4 fractions. Fraction 3 (collected from EtOH) was applied to CC on Diaion HP-20 eluted with H_2O and a gradient of MeOH in H_2O. The fraction collected from 20% MeOH, was further subjected to preparative HPLC (RP-18 MeOH–H_2O–CH_3CN 20:300:20), to furnish compounds **2** (99 mg) and **4** (12 mg). Fraction 2 ($CHCl_3$–EtOH 45:55) afforded compound **3** (26 mg) after CC on Diaion HP-20 and purification by preparative HPLC (RP-18, MeOH–H_2O–CH_3CN 40:300:20).

3.4. Acid hydrolysis

Acid hydrolysis of compounds **1**–**4** were performed as described in the literature (Bashir et al., 1991); each compound was treated with 2 N HCl (1 h of reaction time, in a sealed vial, at 100 °C) and, after cooling, the reaction mixture was extruded with Et_2O. Sugars in the neutralized acidic phase were analyzed on cellulose TLC (Merck) by comparison with authentic samples [acetone-(2-propanol)-0.2 M lactic acid 4:4:2; detection with anilinephtalate reagent; glucose R_f: 0.3, galactose R_f: 0.24]. The aglycone residues were identified on HPLC (Nucleosil 5C-18, MeOH–H_2O–AcOH, 35:45:3) by comparison with authentic samples and combination of UV spectrum.

3.5. Kaempferol 3-O-β-D-glucosyl(1→2)-β-D-galactoside (*1*)

Light yellow amorphous powder. $[\alpha]_D^{26}$ −40° (MeOH, *c* 0.08); UV λ_{max}^{MeOH}nm (log ε): 267 (4.21), 302 sh (3.97), 350 (4.13); IR ν^{KBr} (cm^{-1}): 1655, 1608, 1508; FAB–MS *m/z* 649 $[M(C_{27}H_{30}O_{16})+K]^+$, *m/z* 633 $[M+Na]^+$, *m/z* 449 $[M+H\text{-}162]^+$, *m/z* 287 $[M+H\text{-}324]^+$; ^1H NMR (CD_3OD): 4.74 (1H, *d*, *J* = 6.0 Hz, H-1‴), 5.33 (1H, *d*, *J* = 7.4 Hz, H-1″), 6.17 (1H, *d*, *J* = 2 Hz, H-6), 6.37 (1H, *d*, *J* = 2 Hz, H-8), 6.88 (2H, *d*, *J* = 9 Hz, H-3′,5′), 8.07 (2H, *d*, *J* = 9 Hz, H-2′,6′); for ^{13}C NMR spectral data: Table 1.

3.6. Kaempferol 3-O-β-D-glucosyl(1→2)-β-D-galactoside 7-O-β-D-glucoside (*2*)

Amorphous powder. mp 220–222 °C; $[\alpha]_D^{26}$ −37° (H_2O, *c* 0.09); UV λ_{max}^{MeOH}nm (log ε): 267 (4.33), 320 sh (4.18), 352 (4.25); IR ν^{KBr} (cm^{-1}): 1655, 1603, 1494; FAB–MS: *m/z* 811 $[M(C_{33}H_{40}O_{21})+K]^+$, *m/z* 795 $[M+Na]^+$, *m/z* 449 $[M+H\text{-}324]^+$, *m/z* 287 $[M+H\text{-}486]^+$; ^1H NMR (DMSO-d_6):4.56 (1H, *d*, *J* = 7.7 Hz, H-1‴), 5.06 (1H, *d*, *J* = 7.5 Hz, H-1⁗), 5.66 (1H, *d*, *J* = 7.5 Hz H-1″), 6.42 (1H, *d*, *J* = 2 Hz, H-6), 6.7 8(1H, *d*, *J* = 2 Hz, H-8), 6.89 (2H, *d*, *J* = 9 Hz, H-3′,5′), 8.10 (2H, *d*, *J* = 9.0 Hz, H-2′,6′); for ^{13}C NMR spectral data: Table 1.

Table 1
^{13}C NMR spectral data for compounds **1** (CD_3OD) and **2**–**4** (DMSO-d_6)

C	1	2	3	4
2	158.5	156.2	156.1	156.4
3	134.9	133.2	133.1	133.4
4	179.8	177.7	177.7	177.7
5	163.1	160.9	160.9	160.9
6	99.9	99.4	99.3	99.3
7	166.1	162.8	162.9	162.8
8	94.7	94.5	94.6	94.4
9	158.8	156.0	155.9	155.9
10	105.7	105.6	105.5	105.6
1′	122.7	120.8	120.7	122.3
2′	132.4	131.2	131.2	115.4
3′	116.3	115.4	115.4	144.9
4′	161.5	160.2	160.2	148.8
5′	116.3	115.4	115.4	116.3
6′	132.4	131.2	131.2	121.0
3-Gal 1″	101.5	98.3	98.1	98.3
2″	80.2	80.5	80.7	80.9
3″	74.8	73.4	73.2	73.4
4″	70.0	67.7	68.0	67.7
5″	76.9	75.9	73.1	75.9
6″	62.6	60.0	63.0	60.0
2″-Glc 1″	104.7	104.3	104.6	104.5
2‴	75.4	74.5	74.5	74.5
3‴	77.9	76.5	76.5	76.4
4‴	71.3	69.7	69.6	69.6
5‴	78.2	77.0	77.1	76.8
6‴	61.9	60.7	60.7	60.7
7-Glc 1⁗		99.8	99.9	99.8
2⁗		73.1	73.1	73.2
3⁗		76.6	76.6	76.6
4⁗		69.7	69.6	69.6
5⁗		77.2	77.2	77.2
6⁗		60.8	60.8	60.7
Ac			20.4	
			169.3	

3.7. Kaempferol 3-O-β-D-glucosyl(1→2)-(6″-O-acetyl)-β-D-galactoside 7-O-β-D-glucoside (*3*)

Amorphous powder. mp: 200–203 °C; $[\alpha]_D^{26}$ −76° (MeOH, *c* 0.08); UV λ_{max}nm (log ε): 267 (4.35), 321 sh (4.17), 350 (4.28); IR ν^{KBr} (cm^{-1}): 1730, 1655, 1602, 1494; FAB–MS: *m/z* 853 $[M(C_{35}H_{42}O_{22})+K]^+$, *m/z* 837 $[M+Na]^+$, *m/z* 653 $[M+H\text{-}162]^+$, *m/z* 449 $[M+H\text{-}366]^+$, *m/z* 287 $[M+H\text{-}528]^+$; ^1H NMR (DMSO-d_6): 1.65 (3H, *s*, CH_3CO), 4.54 (1H, *d*, *J* = 7.7 Hz, H-1‴), 5.04 (1H, *d*, *J* = 7.1 Hz, H-1⁗), 5.60 (1H, *d*, *J* = 7.3 Hz, H-1″), 6.42 (1H, *d*, *J* = 2 Hz, H-6), 6.80 (1H, *d*, *J* = 2 Hz, H-8), 6.90 (2H, *d*, *J* = 9.0 Hz, H-3′,5′), 8.08 (2H, *d*, *J* = 9.0 Hz, H-2′,6′); for ^{13}C NMR spectral data: Table 1.

3.8. Quercetin 3-O-β-D-glucosyl(1→2)-β-D-galactoside 7-O-β-D-glucoside (**4**)

Amorphous powder. mp: 199–202 °C; $[\alpha]_D^{26}$ −37° (H_2O, *c* 0.09); UV λ_{max}^{MeOH}nm (log ε): 257 (4.35), 267 sh (4.30), 358 (4.21); IR ν^{KBr} (cm^{-1}): 1665, 1601, 1492; FAB–MS: *m/z* 827 $[M(C_{33}H_{40}O_{22})+K]^+$, *m/z* 811 $[M+Na]^+$, *m/z* 465 $[M+H\text{-}324]^+$, *m/z* 303 $[M+H\text{-}486]^+$; ^{1}H NMR (DMSO-d_6): 4.56 (1H, *d*, *J* = 7.4 Hz, H-1‴), 5.07 (1H, *d*, *J* = 8.3 Hz, H-1⁗), 5.64 (1H, *d*, *J* = 7.5 Hz, H-1″), 6.41 (1H, *d*, *J* = 2 Hz, H-6), 6.74 (1H, *d*, *J* = 2 Hz, H-8), 6.85 (1H, *d*, *J* = 8.6 Hz, H-5′), 7.56 (1H, *d*, *J* = 1.8 Hz, H-2′), 7.67 (1H, *dd*, $J_{H5',6'}$ = 8.6 Hz, $J_{H2',6'}$ = 1.8 Hz, H-6′); for ^{13}C NMR spectral data: Table 1.

Acknowledgements

Y. Han thanks the Japan-China Medical Association for the scholarship to study for one year in Health Sciences University of Hokkaido. We thank Professor T. Nikaido and Dr. K. Koike of School of Pharmaceutical Sciences, Toho University for FAB–MS measurements.

References

Bashir, A., Hamburger, M., Gupta, P.M., Solis, N.P., 1991. Flavonol glycosides from *Monnina sylvatica*. Phytochemistry 30, 3781–3784.

Budzianowski, A.J., 1990. Kaempferol glycosides from *Hosta ventricosa*. Phytochemistry 29, 3643–3647.

Liu, H., Zhang, T., Li, M., 1990. Clinical study of chronic renal failure patients treated with xiangcao infusion. Zhongyiyaoxinxi 7, 20–21.

Liu, Q., Liu, M., Mabry, J.T., Richard, A.D., 1994. Flavonol glycosides from *Cephalocereus senilis*. Phytochemistry 36, 229–231.

Markham, K.R., Ternai, B., Stanley, R., Geiger, H., Mabry, T.J., 1978. Carbon-13 NMR studies of flavonoids-III. Naturally occurring flavonoid glycosides and their acylated derivatives. Tetrahedron 34, 1389–1397.

Mizuno, M., Iinuma, M., Tanaka, T., Sakakibara, N., Murata, J., Frank, A.L., 1990. Two flavonol glycosides from the underground parts of *Vancouveria hexandra*. Phytochemistry 29, 1277–1281.

Nagy, E., Sere, I., Verzár-Petri, G., Neszmélyi, A., 1984. Kaempferol 3-*O*-[β-D-glucopyranosyl(1-2)β-D-galactopyranoside], a new flavonoid from *Lilium candidum* L. Z. Naturforsch. 39b, 1813–1815.

Yasukawa, K., Takido, M., 1988. Quercetin 3-rhamnosyl(1-2) galactoside from *Lysimachia vulgaris* var. *Davurica*. Phytochemistry 27, 3017–3018.

Yoshikawa, M., Murakami, T., Komatsu, H., Murakami, N., 1997. Medicinal foodstuffs.IV. Fenugreek seed. (1): structures of trigoneosides Ia, Ib, IIa, IIb, IIIa, and IIIb, new furostanol saponins from the seeds of Indian *Trigonella foenum-graecum* L. Chem. Pharm. Bull. 45, 81–87.

Varshney, I.P., Beg, M.F.A., 1978. Study of saponins from the seeds of *Trigonella foenum-graecum* Linn. Indian J. Chem. 16B, 1134–1136.

PERGAMON

Phytochemistry 58 (2001) 581–586

PHYTOCHEMISTRY

www.elsevier.com/locate/phytochem

Phenanthrene derivatives from the orchid *Coelogyne cristata*

P.L. Majumder*, S. Sen, S. Majumder

Department of Chemistry, University College of Science, 92, Acharya Prafulla Chandra Road, Calcutta 700 009, India

Received 14 February 2001; received in revised form 15 May 2001

Abstract

Coeloginanthridin, a 9,10-dihydrophenanthrene derivative, and coeloginanthrin, the corresponding phenanthrene analogue, were isolated from the orchid *Coelogyne cristata* which earlier afforded coelogin (**1a**) and coeloginin (**1b**). The structures of coeloginanthridin and coeloginanthrin were established as 3,5,7-trihydroxy-1,2-dimethoxy-9,10-dihydrophenanthrene (**2a**) and 3,5,7-trihydroxy-1,2-dimethoxyphenanthrene (**2c**), respectively, from spectral and chemical evidence including the conversion of coeloginanthridin triacetate (**2b**) to coeloginanthrin triacetate (**2d**) by dehydrogenation with DDQ. In the light of earlier reports on structurally similar compounds, **2a** and **2c** may have biological activities of phytoalexins and endogenous plant growth regulators.
© 2001 Published by Elsevier Science Ltd.

Keywords: Coelogyne cristata; Orchidaceae; Coeloginanthridin; Coeloginanthrin; Phenanthrene derivatives

1. Introduction

We reported earlier the isolation of a fairly large number of compounds from a series of Indian orchids. These compounds encompass a wide variety of stilbenoids, viz. stilbene (Majumder et al., 1998b), bibenzyls (Majumder et al., 1999a), phenanthrenes (Majumder and Sen, 1991) and 9,10-dihydrophenanthrenes (Majumder et al., 1996) and their dimers (Majumder and Banerjee, 1988; Majumder et al., 1998a, 1999b), phenanthropyrans and pyrones (Majumder and Sabzabadi, 1988; Majumder and Maiti, 1991) and their 9,10-dihydro derivatives (Majumder et al., 1999c), fluorenonone (Majumder and Chakraborty, 1989) and a few other polyphenolics (Majumder et al., 1994, 1995), several triterpenoids (Majumder and Ghosal, 1991), steroids of biogenetic importance (Majumder and Pal, 1990) and some simple aromatic compounds (Majumder and Lahiri, 1989). As part of this general programme of research we chemically investigated the orchid *Coelogyne cristata* which earlier afforded the first pair of naturally occurring 9,10-dihydrophenanthropyran and pyrone derivatives **1a** and **1b**, respectively (Majumder et al., 1982). Further investigation of this orchid has now resulted in the isolation of two new phenanthrene derivatives, designated coeloginanthridin and coeloginanthrin. The structures of coeloginanthridin and coeloginanthrin were established as **2a** and **2c**, respectively, from ^{1}H and ^{13}C NMR spectral and chemical evidence.

2. Results and discussion

Coeloginanthridin (**2a**), $C_{16}H_{16}O_5$ ([M^+] at m/z 288) showed UV absorptions [λ_{max}^{EtOH} 220.5, 275.5 and 298.5 nm (log ε 4.37, 4.02 and 3.90)] which are strikingly similar to those of 9,10-dihydrophenanthrene derivatives (Majumder et al., 1982). The UV spectrum of coeloginanthrin (**2c**), $C_{16}H_{14}O_5$ ([M^+] at m/z 286) [λ_{max}^{EtOH} 223.5, 260.5, 347 and 364 nm (log ε 4.53, 4.57, 3.63 and 3.64)], on the other hand, exhibited close resemblance to those of fully aromatic phenanthrene derivatives (Majumder and Kar, 1987).

The phenolic nature of both **2a** and **2c** was indicated by their characteristic colour reactions with $FeCl_3$ (violet) and phosphomolybdic acid reagent (deep blue), alkali-induced bathochromic shifts of their UV maxima and by their IR absorption bands [**2a**: ν_{max} 3240–3480 cm^{-1}; **2c**: ν_{max} 3220–3490 cm^{-1}]. The presence of three phenolic hydroxyl groups in both **2a** and **2c** was confirmed by the formation of their respective triacetyl derivatives [coeloginanthridin triacetate (**2b**), $C_{22}H_{22}O_8$

* Corresponding author. Tel.: +91-33-351-9754.
E-mail address: priyalalm@hotmail.com (P.L. Majumder).

0031-9422/01/$ - see front matter © 2001 Published by Elsevier Science Ltd.
PII: S0031-9422(01)00287-4

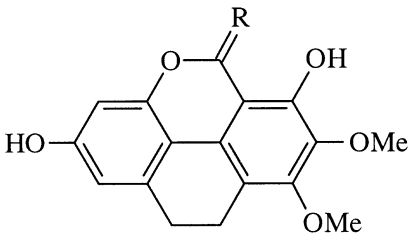

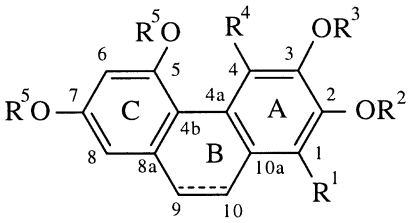

1a : R=H_2

1b : R=O

2a : R^1=OMe, R^2=Me, R^3=R^4=R^5=H, 9,10-dihydro-

2b : R^1=OMe, R^2=Me, R^3=R^5=Ac, R^4=H, 9,10-dihydro-

2c : R^1=OMe, R^2=Me, R^3=R^4=R^5=H, 9,10-dehydro-

2d : R^1=OMe, R^2=Me, R^3=R^5=Ac, R^4=H, 9,10-dehydro-

2e : R^1=R^3=R^5=H, R^2=Me, R^4=OMe, 9,10-dihydro-

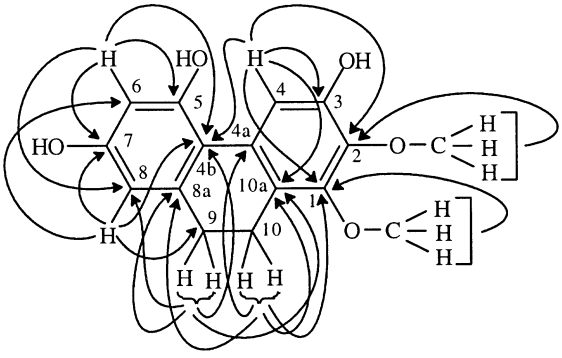

2a

(M^+) at *m*/*z* 414; coeloginanthrin triacetate (**2d**), $C_{22}H_{20}O_8$ ([M^+] at *m*/*z* 412)] with Ac_2O and pyridine. The presence of three phenolic hydroxyl groups in each of **2a** and **2c** was also corroborated by the ^{1}H NMR spectra of the compounds [**2a**: δ 5.76 (3H, *br. s*, disappeared on deuterium exchange); **2c**: δ 4.99, 5.65 and 5.70 (each 1H, *br.s*; also disappeared on dueterium exchange)].

The presence of two aromatic methoxyl groups in each compound was evident from the three-proton singlets at δ 3.83 and 3.95 (**2a**) and 4.00 and 4.10 (**2c**). The ^{1}H NMR spectrum of **2a** showed two two-proton multiplets at δ 2.57 and 2.62, which are typical of the protons of the two benzylic methylene groups of a 9,10-dihydrophenanthrene derivative (Majumder et al., 1982). The signals at δ 2.57 and 2.62 of **2a** were replaced by a pair of one-proton doublets at δ 7.35 and 7.85 (each having J=8.7 Hz), which are characteristic of H-9 and H-10 of a phenanthrene derivative (Majumder and Kar, 1987). This would suggest that **2a** is a 9,10-dihydrophenanthrene derivative and **2c** is the corresponding phenanthrene analogue. Furthermore, the ^{1}H NMR spectrum of **2a** exhibited a one-proton singlet at δ 7.52 corresponding to H-4 or H-5 of 9,10-dihydrohenanthrene derivative (Majumder and Lahiri, 1990), while the spectrum of **2c** was characterized by a one-proton singlet at δ 8.85 similar to that of the corresponding proton of a phenanthrene (Majumder and Lahiri, 1990). The relatively upfield shifts of these proton signals in the ^{1}H NMR spectra of both **2a** and **2c** by about 0.5 ppm (H-4 and H-5 of 9,10-dihydrophenanthrene normally appear at ca δ 8.0 and the corresponding protons

of phenanthrene usually resonate at ca δ 9.5) were attributed to the presence of electron-donating groups (OH or OMe) at *ortho* and *para* to these protons in both **2a** and **2c**. Now, if these downfield aromatic proton signals of **2a** and **2c** are assigned to H-4, then C-5 of both the compounds must be substituted by a hydroxyl or methoxyl group. Again, since the above downfield proton signals of both **2a** and **2c** appeared as sharp singlets, C-3 and C-2 of both the compounds must also be substituted by OH or OMe.

The remaining two aromatic protons of **2a** and **2c** appeared as a pair of doublets corresponding to the *meta*-coupled aromatic protons [**2a**: δ 6.29 and 6.33 (each 1H, *d*, $J=2.0$ Hz); **2c**: δ 6.55 and 6.75 (each ill-resolved *meta*-coupled doublets)]. The signals at δ 6.29 and 6.33 in the spectrum of **2a** resemble those of H-6 and H-8 of calaphenanthrenol (**2e**) (Yoshikawa et al., 1998) having two hydroxyl groups at C-5 and C-7. The corresponding signals at δ 6.55 and 6.75 of **2c** may be similarly assigned to H-6 and H-8 of the compound possessing a phenanthrene skeleton having two hydroxyl functions at C-5 and C-7. This would imply that while two hydroxyl groups in both **2a** and **2c** may be located at C-5 and C-7, the remaining hydroxyl function and the two methoxyl groups in each compound must be distributed between C-3, C-2 and C-1.

The relative positions of the hydroxyl and methoxyl groups in both **2a** and **2c** were ascertained by the observed changes in the chemical shifts of H-4, H-6 and H-8 of the compounds in the ^{1}H NMR spectra of their respective triacetyl derivatives **2b** and **2d**. It has been shown that H-5 of a 4-hydroxyphenanthrene and its 9,10-dihydro derivative is shifted upfield by ca 0.5 and 0.2 ppm, respectively on acetylation (Letcher and Nhamo, 1971; Letcher and Wong, 1978; Majumder and Lahiri, 1990). A similar upfield shift of H-4 was observed in **2b** and **2d** by 0.28 and 0.09 ppm, respectively, affirming the placement of one of the three hydroxyl groups at C-5 in both **2a** and **2c**. The relatively smaller upfield shifts of H-4 of both **2a** and **2c** than those usually observed on acetylation of their hydroxyl function at C-5 may be attributed to the presence of a hydroxyl group at C-3 in both the compounds, which on acetylation produces a deshielding effect on H-4. The remaining hydroxyl group in both **2a** and **2c** was placed at C-7 from the observed downfield shifts of H-6 (*ortho* to two hydroxyl groups at C-5 and C-7) and H-8 (*ortho* to one hydroxyl group at C-7 and *para* to another hydroxyl function at C-5) by 0.52 and 0.61 ppm, and 0.65 and 0.82 ppm, respectively, in the ^{1}H NMR spectra of their triacetyl derivatives **2b** and **2d**. The greater deshielding of H-6 and H-8 of **2c** in the spectrum of its triacetyl derivative **2d** may be partly attributed to the acetylation of its hydroxyl group at C-3, causing a deshielding of its H-9 by 0.23 ppm in the spectrum of **2d**. The two methoxyl groups in both **2a** and **2c** must then be placed at C-1 and C-2. Coeloginanthridin and coeloginanthrin may, therefore, be represented as 3,5,7-trihydroxy-1,2-dimethoxy-9,10-dihydrophenanthrene (**2a**) and 3,5,7-trihydroxy-1,2-dimethoxyphenanthrene (**2c**), respectively.

The structure of coeloginanthridin (**2a**) was also affirmed by the ^{13}C NMR spectral data of the compound and its triacetyl derivative **2b** (Table 1). The degree of protonation of the carbon atoms in **2a** and **2b** was determined by DEPT experiments and the carbon chemical shifts were assigned by comparison with the δ_C values of the structurally similar compound calaphenanthrenol (**2e**) (Yoshikawa et al., 1998). Thus, except that of C-8a, the δ_C values of C-4b, C-5, C-6, C-7 and C-8 of **2a** are essentially similar to those of the corresponding carbon atoms of **2e** supporting the placement of two hydroxyl groups at C-5 and C-7 in **2a**. The ^{13}C NMR chemical shift assignments of **2a** were confirmed by HMQC and HMBC experiments and on the basis of these experiments C-8a of **2a** was assigned the signal at δ_C 142.0. It appears from the following 2D NMR spectral analysis of coeloginanthridin (**2a**) that the signal at δ_C 131.4 earlier assigned to C-8a of calaphenanthrenol (**2e**) (Yoshikawa et al., 1998) should be interchanged with that at δ_C 142.0 assigned to its C-3.

The HMQC spectrum of **2a** (with J_{CH} parameter set to 160 Hz) showed correlations of the hydrogens at δ_H

Table 1
^{13}C NMR spectral data of compounds **2a, 2b** and **2e**

C	Chemical shift (δ, ppm)[a]		
	2a	**2b**	**2e**[b]
1	149.4	149.3	108.0
2	137.8	144.1	145.7
3	147.1	142.5	142.0
4	108.6	117.2	142.1
4a	128.7	128.4	119.2
4b	114.4	126.4	113.0
5	153.7	147.8	154.7
6	102.1	115.2	104.0
7	155.0	151.3	156.0
8	107.7	118.6	108.0
8a	142.0	141.7	131.4
9	30.1	29.6	31.6
10	21.3	21.4	30.5
10a	123.6	130.8	137.2
OMe	60.7 (OMe at C-1)	60.7 (2xOMe)	61.8 (OMe at C-4)
	60.9 (OMe at C-2)		56.4 (OMe at C-2)
OAc	–	168.6	–
	–	168.7	
	–	168.8	–
		20.6	
		20.9	
		21.0	

[a] Spectra were run in $CDCl_3$ and the chemical shifts were measured with $\delta_{(TMS)}=\delta_{(CDCl_3)}+76.9$ ppm.

[b] The carbon resonances of **2e** and their assignments shown here are those reported by (Yoshikawa et al., 1998).

2.57 (H_2-9), 2.62 (H_2-10), 7.52 (H-4), 6.29 (H-6), 6.33 (H-8), 3.83 (OMe) and 3.95 (OMe) with the carbon atoms at δ_C 30.1 (C-9), 21.3 (C-10), 108.6 (C-4), 102.1 (C-6), 107.7 (C-8), 60.7 and 60.9, respectively. In the HMBC spectrum of **2a** (with J_{CH} parameter set to 7 Hz), the signal at δ_H 2.57 (H_2-9) exhibited fairly strong 3-bond correlations with the carbon signals at δ_C 114.4, 107.7 and 123.6, which were thus assigned to C-4b, C-8 and C-10a, respectively. The signal at δ_H 2.57 (H_2-9) also showed a 2-bond correlation with the carbon at δ_C 142.0 assigned to C-8a. In aromatic compounds 3-bond ^1H-^{13}C correlations were found to be a common feature, while 2-bond and other long range (4-bond or more remote) correlations are usually not observed. However, in polyoxygenated phenanthrene derivatives such 2-bond and other long range correlations have sometimes been observed and were assumed to occur due to the presence of oxygenated functions like OH and OMe attached to the aromatic ring, which alter the electron distribution in favour of such couplings (Majumder et al., 1997).

In light of the observation that presence of a substituent like methoxyl group at C-1 in 9,10-dihydrophenenthrene derivatives causes an upfield shift of C-10 by ca 7 ppm as in coelogin (**1a**), coeloginin diacetate and coeloginin dimethyl ether (Majumder et al., 1982), the upfield benzylic methylene carbon at δ_C 21.3 of **2a** having a methoxyl group at C-1 must be assigned to C-10 which showed 1-bond correlation to the protons at δ_H 2.62. The signal at δ_H 2.62 of **2a** must then be assigned to its H_2-10 which showed 3-bond correlations with the carbons resonating at δ_C 142.0, 149.4 and 128.7, which may, therefore, be assigned to C-8a, C-1 and C-4a, respectively, of **2a**. The signal at δ_H 2.62 (H_2-10) also exhibited a 2-bond correlation with the carbon at δ_C 123.6 which has already been assigned to C-10a. Since both **2a** and **2e** have identical substituents in their ring C (OH at C-5 and C-7), the confirmation of the assignment of the carbon resonance at δ_C 142.0 of **2a** to its C-8a implies that the signal at δ_C 142.0 of **2e** (earlier attributed to its C-3) may, by analogy, be also assigned to its C-8a. The signal at δ_C 131.4 of **2e** (earlier assigned to its C-8a) would correspond to its C-3. The proton at δ_H 7.52 corresponding to H-4 showed 3-bond correlations with the carbons at δ_C 114.4 (C-4b), 123.6 (C-10a) and 137.8 which must correspond to C-2. H-4 (δ_H 7.52) also exhibited a 2-bond correlation with the carbon at δ_C 147.1 (C-3) and a weak 4-bond correlation with the carbon at δ_C 149.4 (C-1). The proton at δ_H 6.29 assigned to H-6 was found to exhibit 3-bond correlations with the carbons at δ_C 107.7 and 114.4 which were already assigned to C-8 and C-4b, respectively. H-6 (δ_H 6.29) also showed 2-bond correlations with the non-protonated carbons at δ_C 153.7 and 155.0, which corresponded to C-5 and C-7, respectively. Similarly, the proton at δ_H 6.33 assigned to H-8 showed 3-bond correlations with the carbons at δ_C 102.1 (C-6), 114.4 (C-4b) and 30.1 (C-9) and a weak 2-bond correlation with the carbon at δ_C 155.0 (C-7). The methoxyl protons at δ_H 3.83 and 3.95, which were associated with methoxyl carbons at δ_C 60.7 and 60.9, respectively, as evident from HMQC spectrum of **2a**, showed 3-bond correlations with the carbons at δ_C 149.4 (C-1) and 137.8 (C-2), respectively. All the above ^1H–^{13}C correlations observed in the HMBC spectra of **2a** are depicted in its structural diagram. The above spectral data thus unequivocally established the structure of coeloginanthridin (**2a**).

Although similar spectral analysis could not be made with coeloginanthrin (**2c**) due to paucity of material, the structure of the compound was confirmed by the conversion of coeloginanthridin triacetate (**2b**) to coeloginanthrin triacetate (**2d**) by dehydrogenation of the former to the latter with 2,3-dichloro-5,6-dicyano-1,4-benzoquinone (DDQ) in dry benzene. Acid-hydrolysis of the dehydrogenation product finally afforded coeloginanthrin (**2c**).

Coeloginanthridin (**2a**) and coeloginanthrin (**2c**) are thus two new additions to the growing lists of the naturally occurring 9,10-dihydrophenanthrenes and phenanthrenes respectively. In the light of the earlier reports that a variety of phenanthrene derivatives were found to be potent phytoalexins (Gaumann and Kern, 1959a,b; Gorham, 1980; Purkayastha, 1985, 1995), while several others were shown to act as endogenous plant growth regulators (Gorham, 1980), it would be interesting to study **2a** and **2c** for similar biological activities.

3. Experimental

Melting points: uncorr. CC: Silica gel (100–200 mesh). MPLC: silica gel (230–400 mesh). TLC: silica gel G. UV: 95% aldehyde-free EtOH. IR: KBr discs. ^1H and ^{13}C NMR: 300 and 75 MHz, respectively (for **2b**, **2c** and **2d**); 500 MHz (for ^1H, HMBC and HMQC of **2a**), 125 MHz (for ^{13}C NMR of **2a**). NMR spectra were recorded in $CDCl_3$ using TMS as internal standard and chemical shifts are expressed in δ (ppm). MS: direct inlet system, 70 eV. All analytical samples were routinely dried over P_2O_5 for 24 h in vacuo and were tested for purity by TLC and MS. The petrol used had bp 60–80 °C.

3.1. Plant materials

Coelogyne cristata was collected from Kalimpong (Darjeeling), India in October, 1998. A voucher specimen (Majumder s.n.) was deposited in the Herbarium of the Department of Botany, University of Calcutta (CUH).

3.2. Isolation of coeloginanthridin (**2a**) and coeloginanthrin (**2c**)

Air-dried finely powdered whole plant of *Coelogyne cristata* (5 kg) was kept soaked in MeOH (10 l) for 3 weeks. The MeOH extract was concentrated to ca. 100 ml, diluted with H_2O (750 ml) and exhaustively extracted with Et_2O. The Et_2O extract was fractionated into acidic and nonacidic fractions with 2 M NaOH. The aqueous alkaline solution was acidified in the cold with conc. HCl and the liberated solids were extracted with Et_2O, washed with H_2O, dried and the solvent removed. The residue was subjected to CC. The petrol–EtOAc (7:1) eluate gave a mixture of **1a** and **1b**. The above mixture of **1a** and **1b** was then subjected to CC and the early fractions of the petrol–EtOAc (7:1) eluate also gave a mixture of **1a** and **1b** containing predominantly **1b**. The later fractions of the same eluate also afforded a mixture of **1a** and **1b** containing mostly **1a**. The fractions containing mostly **1a** and those containing mostly **1b** were separately mixed together and evaporated. The two residues enriched with respect to **1a** and **1b** were then separately subjected to MPLC using petrol–EtOAc (5:1) as the solvent system. The early fractions of the residue containing mostly **1b** gave pure **1b**, while the later fractions of the same eluate gave pure **1a**. Similarly, MPLC of the residue containing mostly **1a** gave in the early fractions pure **1b**, while the later fractions afforded pure **1a**. The fractions containing pure **1b** and **1a** were separately mixed together and the solvent removed to give pure **1b** (0.3 g), crystallized from petrol–EtOAc in yellowish needles, mp 198 °C and pure **1a** (0.25 g), also crystallized from the same solvent mixture in fine colourless needles, mp 151 °C. Washing the main column with petrol–EtOAc (3:1) gave a gummy residue comprising mainly coeloginanthridin (**2a**) and coeloginanthrin (**2c**). The above mixture was subjected to MPLC using petrol–EtOAc (2:1) as the solvent system. The early fractions gave a residue which contained coeloginanthridin (**2a**) as the major constituent, while the later fractions gave a mixture containing mostly coeloginanthrin (**2c**). The above two mixtures were again separately subjected to MPLC using the same solvent system to give finally pure coeloginanthridin (**2a**) (0.10 g) and coeloginanthrin (**2c**) (0.02 g), both as semisolid mass.

Coeloginanthridin (**2a**) (found: C, 66.61; H, 5.48; $C_{16}H_{16}O_5$ requires: C, 66.67; H, 5.60%). UV $\lambda_{max}^{EtOH-0.1\ M\ NaOH}$ nm: 212.5, 286.0 and 311.5 (log ε 4.51, 3.98 and 4.00); IR ν_{max} cm^{-1}: 3240–3480 (OH), 1610, 1550, 1480, 880 and 840 (aromatic nucleus); MS *m*/*z* (rel. int.): 288 [M^+] (100), 273 (25), 258 (15) and 230 (10); ^1H NMR: δ 7.52 (1H, *s*; H-4), 6.33 and 6.29 (each 1H, *d*, $J=2.0$ Hz, H-8 and H-6), 5.76 (3H, *br*. *s*, 3xArOH), 3.95 and 3.83 (each 3H, *s*, 2xArOMe), 2.62 and 2.57 (each 2H, m, H_2-10 and H_2-9). Acetylation of coeloginanthridin (**2a**) with Ac_2O and pyridine in the usual manner gave coeloginanthridin triacetate (**2b**), also as a semisolid mass. (found: C, 63.71; H, 5.25; $C_{22}H_{22}O_8$ requires: C, 63.77; H, 5.35%). IR: ν_{max} cm^{-1}: 1215, 1220, 1225, 1745, 1755 and 1770 (OAc), 1615, 1600, 1580, 1475, 820, 775, 735, 715, 690 and 595 (aromatic nucleus); ^1H NMR: δ 7.43 (1H, *s*, H-4), 6.94 and 6.81 (each 1H, *d*, $J=2.34$ Hz, H-8 and H-6), 3.89 and 3.84 (each 3H, *s*, 2xArOMe), 2.80 and 2.77 (each 2H, *m*, H_2-10 and H_2-9), 2.35, 2.29 and 2.27 (each 3H, *s*, 3xOAc); MS *m*/*z* (rel. int.): 414 [M^+] (25), 372 (30), 330 (35), 288 (100), 273 (20), 258 (10) and 230 (10).

Coeloginanthrin (**2c**): (found: C, 67.02, H, 4.83. $C_{16}H_{14}O_5$ requires: C, 67.13; H, 4.93%). UV $\lambda_{max}^{EtOH-0.1\ M\ NaOH}$ nm: 212, 228.5, 277, 307 and 377 (log ε 4.47, 4.45, 4.44, 4.15 and 3.69); IR ν_{max} cm^{-1}: 3220–3490 (OH), 1625, 1615, 1585, 1480, 885, 840 and 650 (aromatic nucleus); MS *m*/*z* (rel. int.) 286 [M^+] (100), 271 (30), 256 (20) and 228 (10); ^1H NMR: δ 8.85 (1H, *s*, H-4), 7.85 and 7.35 (each 1H, *d*, $J=8.7$ Hz, H-10 and H-9), 6.75 and 6.55 (each 1H, ill-resolved *meta*-coupled *d*, H-8 and H-6), 5.70, 5.65 and 4.99 (each 1H, *br*.*s*, 3xArOH), 4.10 and 4.00 (each 3H, *s*, 2xArOMe). Acetylation of coeloginanthrin (**2c**) with Ac_2O and pyridine in the usual manner gave coeloginanthrin triacetate (**2d**), also as a semisolid mass. (found: *C*, 63.97; H, 4.78. $C_{22}H_{20}O_8$ requires: C, 64.07; H, 4.89%). IR ν_{max} cm^{-1}: 1205, 1220, 1230, 1775, 1780 and 1785 (OAc), 1615, 1585, 1555, 1485, 845, 820, 810, 765 and 740 (aromatic nucleus); ^1H NMR: δ 8.57 (1H, *s*, H-4), 8.08 and 7.67 (each 1H, *d*, $J=9.2$ Hz, H-10 and H-9), 7.57 and 7.20 (each 1H, ill-resolved *meta*-coupled d, H-8 and H-6), 4.07 and 4.03 (each 3H, *s*, 2xArOMe), 2.49, 2.42 and 2.36 (each 3H, s, 3xOAc); MS *m*/*z* (rel. int.) 412 [M^+] (35), 370 (30), 328 (20), 286 (100), 271 (25), 256 (10) and 228 (8).

3.3. Conversion of coeloginanthridin triacetate (**2b**) to coeloginanthrin triacetate (**2d**) by dehydrogenation with 2,3-dichloro-5,6-dicyano-1,4-benzoquinone (DDQ) and acid-hydrolysis of coeloginanthrin triacetate (**2d**) to coeloginanthrin (**2c**)

To a soln. of coeloginanthridin triacetate (**2b**) (0.03 g) in dry C_6H_6 (25 ml) was added 0.07 g of 2,3-dichloro-5,6-dicyano-1,4-benzoquinone. The resultant mixture was heated under reflux for 16 h. The solvent was removed under red. pres. to give a solid which was extracted with Et_2O, washed three times with 2 M aq. NaOH and then with H_2O, dried and the solvent removed. The residue was chromatographed. The petrol-EtOAc (10:1) eluate gave coeloginanthrin triacetate (**2d**) (0.018 g) as a semi-solid mass. To a soln. of 0.01 g of coeloginanthrin triacetate (**2d**) was added 5 ml of 2 M aq. methanolic HCl and the mixture was heated under reflux for 5 h. MeOH was removed under red. pres. and

the residue was extracted with Et_2O, washed with H_2O, dried and the solvent removed. The residue was chromatographed. The petrol–EtOAc (3:1) eluate gave coeloginanthrin (**2c**) (0.008 g) as a semi-solid mass.

Acknowledgements

The work was supported by C.S.I.R., New Delhi, India.

References

Gaumann, E., Kern, H., 1959a. Über die Isolierung and den Chemischen Nachweis des Orchinobs. Phytopathologische Zeitschrift 35, 347–356.

Gaumann, E., Kern, H., 1959b. Über chemische Abwehrreaktionen bei Orchideen. Phytopathologische Zeitschrift 36, 1–26.

Gorham, J., 1980. The Stilbenoids. Progress in Phytochemistry 6, 203–252.

Letcher, R.M., Nhamo, L.R.M., 1971. Chemical constituents of the combretaceae Part 1. Substituted phenanthrenes and 9,10-dihydrophenanthrenes from the heartwood of *Combretum apiculatum*. Journal of the Chemical Society (C) 3070–3076.

Letcher, R.M., Wong, K.M., 1978. Structure and synthesis of the phenanthrenes TaI and TaV from *Tamus communis*. Journal of the Chemical Society Perkin Trans. I 739–742.

Majumder, P.L., Bandyopadhyay, D., Joardar, S., 1982. Coelogin and coeloginin: two novel 9,10-dihydrophenanthrene derivatives from the orchid *Coelogyne cristata*. Journal of the Chemical Society Perkin Trans I 1131–1136.

Majumder, P.L., Banerjee, S., 1988. Structure of flavanthrin, the first dimeric 9,10-dihydrophenanthrene derivative from the orchid *Eria flava*. Tetrahedron 44, 7303–7308.

Majumder, P.L., Banerjee, S., Lahiri, S., Mukhoti, N., Sen, S., 1998a. Dimeric phenanthrenes from two *Agrostophyllum* species. Phytochemistry 47, 855–860.

Majumder, P.L., Banerjee, S., Sen, S., 1996. Three stilbenoids from the orchid *Agrostophyllum callosum*. Phytochemistry 42, 847–852.

Majumder, P.L., Chakraborty, J., 1989. Chemical constituents of the orchid *Dendrobium farmerii*: Further evidence for the revised structure of dengibsin. Journal of the Indian Chemical Society 66, 834–837.

Majumder, P.L., Ghosal, S., 1991. Arundinol, a new triterpene from the orchid *Arundina bambusifolia*. Journal of the Indian Chemical Society 68, 88–91.

Majumder, P.L., Guha, S., Sen, S., 1999a. Bibenzyl derivatives from the orchid *Dendrobium amoenum*. Phytochemistry 52, 1365–1369.

Majumder, P.L., Kar, A., 1987. Confusarin and confusaridin, two phenanthrene derivatives of the orchid *Eria confusa*. Phytochemistry 26, 1127–1129.

Majumder, P.L., Kar, A., Banerjee, S., Pal, A., Joardar, M., 1997. Application of 2D NMR spectroscopy in structural elucidation of some phenanthrene derivatives from Indian Orchidaceae plants. Journal of the Indian Chemical Society 74, 908–916.

Majumder, P.L., Lahiri, S., 1989. Chemical constituents of the orchid *Lusia indivisa*. Indian Journal of Chemistry 28B, 771–774.

Majumder, P.L., Lahiri, S., 1990. Lusianthrin and lusianthridin, two stilbenoids from the orchid *Lusia indivisa*. Phytochemistry 29, 621–624.

Majumder, P.L., Lahiri, S., Mukhoti, N., 1995. Chalcone and dihydrochalcone derivatives from the orchid *Lusia volucris*. Phytochemistry 40, 271–274.

Majumder, P.L., Lahiri, S., Pal, S., 1994. Occurrence of lignans in the Orchidaceae plants *Lusia volucris* and *Bulbophyllum triste*. Journal of the Indian Chemical Society 71, 645–647.

Majumder, P.L., Maiti, D.C., 1991. Isoflaccidinin and isooxoflaccidinin, stilbenoids from *Coelogyne flaccida*. Phytochemistry 30, 971–974.

Majumder, P.L., Pal, S., 1990. A steroidal ester from *Coelogyne uniflora*. Phytochemistry 29, 2717–2720.

Majumder, P.L., Pal, S., Majumder, S., 1999b. Dimeric phenanthrenes from the orchid *Bulbophyllum reptans*. Phytochemistry 50, 891–897.

Majumder, P.L., Roychowdhury, M., Chakraborty, S., 1998b. Thunalbene, a stilbene derivative from the orchid *Thunia alba*. Phytochemistry 49, 2375–2378.

Majumder, P.L., Sabzabadi, E., 1988. Agrostophyllin, a naturally occurring phenanthropyran derivative from *Agrostophyllum khasiyanum*. Phytochemistry 27, 1899–1901.

Majumder, P.L., Sen, R.C., 1991. Pendulin, A polyoxygenated phenanthrene derivative from the orchid *Cymbidium pendulum*. Phytochemistry 30, 2432–2434.

Majumder, P.L., Sen, S., Banerjee, S., 1999c. Agrostophyllol and isoagrostophyllol, two novel diastereomeric 9,10-dihydrophenanthropyran derivatives from the orchid *Agrostophyllum callosum*. Tetrahedron 55, 6691–6702.

Purkayastha, R.P., 1985. Phytoalexins. In: Mukerji, K.G., Pathak, N.C., Singh, V.P. (Eds.), Frontiers in Applied Microbiology. Vol. 1. Print House (India), Lucknow, pp. 363–407.

Purkayastha, R.P., 1995. Progress in Phytoalexin Research during the Past 50 Years. In: Daniel, M., Purkayastha, R.P. (Eds.), Handbook of Phytoalexin Metabolism and Action. Marcel Dekker, New York, pp. 1–39.

Yoshikawa, M., Murakami, T., Kishi, A., Sakurama, T., Matsuda, H., Nomura, M., Matsuda, H., Kubo, M., 1998. Novel indole S,*O*-bisdesmoside, calanthoside, the precursor glycoside of tryptanthrin, indirubin, and isatin, with increasing skin blood flow promoting effects, from two *Calanthe* species (Orchidaceae). Chemical and Pharmaceutical Bulletin 46, 886–888.

PERGAMON

Phytochemistry 58 (2001) 587–590

PHYTOCHEMISTRY

www.elsevier.com/locate/phytochem

An oligomer from flaxseed composed of secoisolariciresinoldiglucoside and 3-hydroxy-3-methyl glutaric acid residues

Afaf Kamal-Eldin[a,*], Nienke Peerlkamp[a], Pernilla Johnsson[a], Roger Andersson[a], Rolf E. Andersson[b], Lennart N. Lundgren[b], Per Åman[a]

[a]*Department of Food Science, Swedish University of Agricultural Sciences (SLU), 750 07 Uppsala, Sweden*
[b]*Department of Chemistry, Swedish University of Agricultural Sciences (SLU), 750 07 Uppsala, Sweden*

Received 29 January 2001; received in revised form 6 June 2001

Abstract

A straight-chain oligomeric structure composed of five secoisolariciresinoldiglucoside (SDG) residues interconnected by four 3-hydroxy-3-methyl glutaric acid (HMGA) residues (molecular weight ca. 4000 Da) was assigned to the main lignan of flaxseed on the basis of nuclear magnetic resonance spectroscopy (NMR). © 2001 Elsevier Science Ltd. All rights reserved.

Keywords: Flaxseed; *Linum usitatissimum*; Linaceae; Lignan; Oligomer; Secoisolariciresinoldiglucoside; 3-Hydroxy-3-methyl glutaric acid

1. Introduction

Within the paradigm of bioactive phytochemicals in foods, lignans may be appreciated as health-promoting dietary micronutrients (Bentsath et al., 1937; Mazur and Adlercreutz, 1998; Challem, 1999). Flaxseed (*Linum usitatissimum*, Linn., Linaceae) is one of the richest sources of lignans as its defatted flour may contain 1–4% of secoisolariciresinoldiglucoside (SDG) (Bakke and Klosterman, 1956; Johnsson et al., 2000; Westcott and Muir, 1996, 2000). SDG and its mammalian lignan metabolites produced by the intestinal microflora were reported to enhance health by having phytoestrogenic, anticarcinogenic and antiatherosclerotic effects (Axelson et al., 1982). Bakke and Klosterman (1956) noted that SDG is present in flaxseed in a tan polymeric powder that includes, inter alias, 3-hydroxy-3-methyl glutaric acid (HMGA) (Klosterman and Smith, 1954) and 4-*O*-β-D-glucopyranosyl-*p*-coumaric acid which they called linocinnamarin (Klosterman et al., 1955). We isolated and identified 4-*O*-β-D-glucopyranosyl ferulic acid as one of the components in the flaxseed polymer and suggested that SDG and other phenolic compounds of flaxseed exist in acylated forms (Johnsson et al., unpublished). Other phenolic compounds found to be present in flaxseeds include a SDG isomer (Bambagiotti-Alberti et al., 1994a,b), pinoresinoldiglucoside (Qiu et al., 1999), isolariciresinol (Meagher et al., 1999) and *p*-hydroxybenzoic, gentisic, vanillic, and sinapic acids in free and/or bound forms (Kozlowska et al., 1983; Dabrowski and Sosulski, 1984). In this paper, we used nuclear magnetic resonance spectroscopy to assign an average straight-chain oligomeric structure composed of five SDG residues interconnected by four HMGA residues to the main phenolic polymer in flaxseed.

2. Results and discussion

In a previous study, the major fraction of the 1,4-dioxane/ethanol (1:1, v/v)-extractable phenolic polymer in flaxseed was isolated by solid-phase extraction and analyzed by HPLC to show a relatively broad peak suggesting structural heterogeneity or differences in molecular weight (Johnsson et al., unpublished). In this study, ^{1}H NMR (Fig. 1) of this fraction showed, in the aromatic region, peaks due to SDG (δ 6.4–6.7 ppm) as well as to other phenolic compounds, most probably *p*-coumaric acid and ferulic acid moieties (δ 6.1–7.7 ppm).

* Corresponding author. Tel.: +46-18-672036; fax: +46-18-672995.
E-mail address: afaf.kamal-eldin@lmv.slu.se (A. Kamal-Eldin).

0031-9422/01/$ - see front matter © 2001 Elsevier Science Ltd. All rights reserved.
PII: S0031-9422(01)00279-5

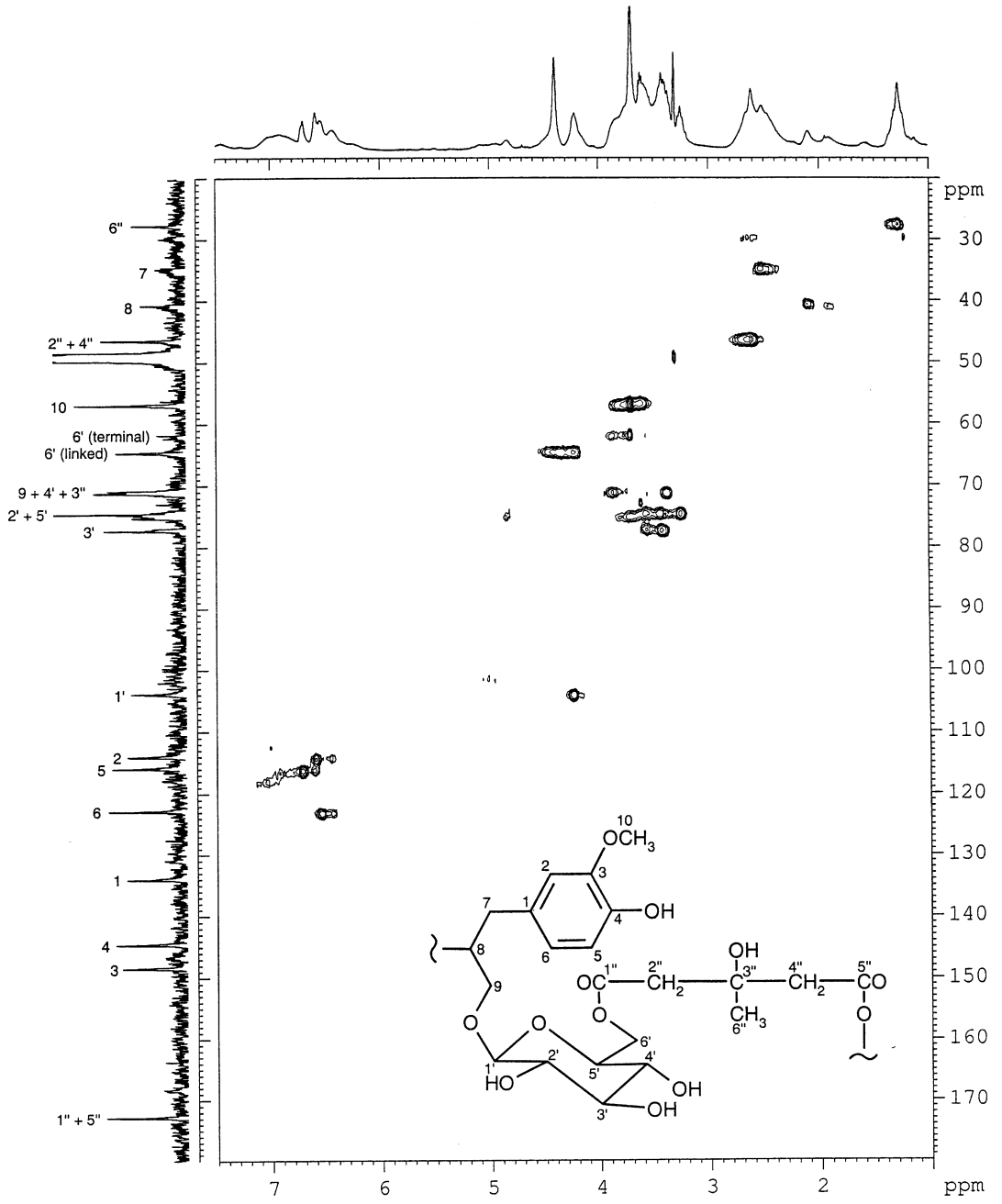

Fig. 1. ^{1}H NMR, ^{13}C NMR and HSQC–DEPT spectra of the oligomer composed of SDG (secoisolariciresinoldiglucoside) and HMGA (3-hydroxy-3-methyl glutaric acid) residues in flaxseed. Insert shows the numbering system used to assign ^{13}C NMR signals. For the complete structure of the oligomer, see Fig. 3.

Also observed were peaks corresponding to the aliphatic CH_3 (δ 1.28 ppm) and CH_2 (δ 2.61 ppm) groups of HMGA which has also been reported to be present in flaxseed (Klosterman and Smith, 1954; Bakke and Klosterman, 1956). ^{13}C NMR (Fig. 1) showed only peaks for SDG (Chimichi et al., 1999; Qiu et al., 1999) and HMGA residues but no visible peaks for the other phenols (mainly *p*-coumaric acid-*O*-glucoside and ferulic acid-*O*-glucoside) which also seem to exist in polymeric forms involving ester bonds. Very weak and broad NMR signals from these "other phenolic polymers" were visible in the phenolic region of ^{1}H NMR (Fig. 1) indicating a more rigid structure and, consequently, shorter relaxation times.

The fact that the carboxylic carbon signal of the isolated fraction was 2 ppm upfield ($\delta = 173$ ppm) as compared with that of the free HMGA ($\delta = 175$ ppm) suggests that HMGA is solely present in symmetrically esterified form. The HSQC–DEPT spectrum (Fig. 1) revealed that C-6 of the glucose in SDG gives two types of strong cross peaks; one peak (^{13}C: $\delta =$ 62.4 ppm, ^{1}H: $\delta = 3.8$ ppm) characteristic of a non-esterified $-CH_2OH$

group, and another (down-field) peak (^{13}C: $\delta =$ 64 ppm, ^{1}H: $\delta = 4.2$ ppm) characteristic of an ester-linked carbon (Farah et al., 1992). Since some of the C-6 of the glucose residues in SDG are ester-linked and some are not, some glucose residues must be in terminal position in the polymer. This finding is confirmed by TOCSY (Fig. 2) which showed two types of spin systems for the protons at positions 7, 8 and 9 where signals from the linked SDG were downfield compared to those from terminal SDG. HMBC (results not shown) revealed that the ester link is between the carboxylic carbon of HMGA (^{13}C: $\delta =$ 173 ppm) and some of the C-6 of glucose (^{1}H: $\delta =$ 4.2 ppm). Taken together, these results suggest a linear and symmetrical structure composed of SDG and HMGA units. On basis of HSQC–DEPT, the structure of the polymer was elucidated from two types of calculations: (i) the ratio of terminal versus linked glucose residues in the polymer, and (ii) the ratio between SDG and HMGA units. The ratio of terminal versus intermediate SDG groups was roughly calculated as 1:4 from the ^{13}C NMR spectrum by integration of the peaks at $\delta = 61.6$–62.3 ppm (terminal glucose) and $\delta =$ 64.6 ppm (linked glucose). Integration of peaks, in the ^{1}H NMR spectrum, at $\delta = 1.8$–2.1 ppm (two protons at positions 8 of SDG) and $\delta = 2.3$–2.9 ppm (four protons at positions 7 of SDG and the $-CH_2-$ groups of HMGA) gave the SDG/HMGA ratio as 0.56/0.44 from which the average number of SDG and HMGA molecules in this polymer can be calculated as 4.67 and 3.67, respectively. Both calculations support an average structure of ca. 4000 Da (Fig. 3), containing two terminal and eight linked glucose residues.

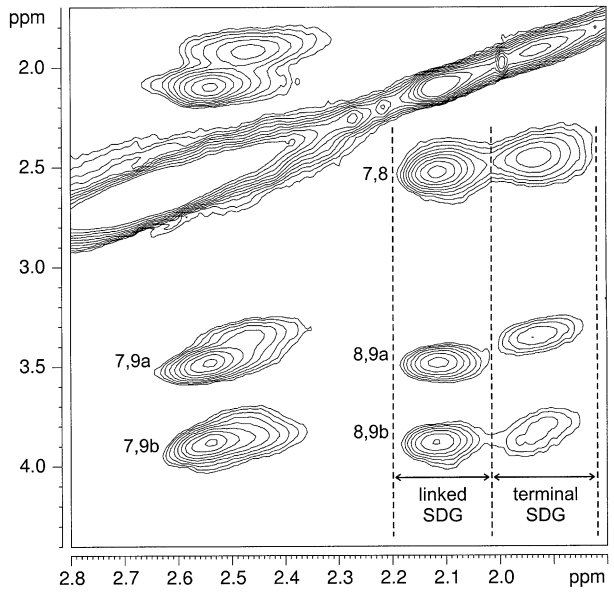

Fig. 2. Part of TOCSY spectrum of the oligomer isolated from flaxseed illustrating two spin systems (linked and terminal SDG) for the cross peaks between the protons at positions 7, 8 and 9. For numbering, see Fig. 1 and for the complete structure of the oligomer, see Fig. 3.

Structures containing glucose residues glycosidically linked to flavonoid residues and esterified at C-6 to malonate residues were found in red clover (Lin et al., 2000). Conjugation to malonate was thought to increase the solubility of phenolic aglycones for storage by the plant till further release, by hydrolysis, as phytoalexins in events of microbial or viral invasion of the cells. The polymeric structure of SDG–HMGA presented here is different from other known biopolyesters of plants, e.g. cutin and suberin (Kolattukudy, 1980) and cinnamate-containing arabinoxylan (Ishii, 1997). Since both SDG (Axelson et al., 1982, Westcott and Muir, 2000) and HMGA (Laurenti et al., 1990) are known for beneficial health effects, this oligomer might be of interest for nutritional and pharmaceutical applications. Knowledge about this structure is important from nutritional (bioavailability, bioconversion and bioactivity) as well as biochemical (biosynthesis and biosynthesis elicitors) points of view.

3. Experimental

A crude polymeric flaxseed extract was obtained by stirring of a sample of defatted flaxseed flour (50 g) twice with 1,4-dioxane/ethanol (1:1 v/v, 200 ml) at 60 °C for 7 hours as described earlier (Johnsson et al., 2000). Part of this polymeric extract, called whole polymer, was fractionated using pre-packed reversed-phase solid phase extraction column (1 g C18, Mega Bond Elut®, Varian, Harbor City, LA, USA) preconditioned with methanol (5 ml) followed by water (5 ml). An aqueous solution of the extracted polymer (0.1 g/ml, 5 ml) was loaded on the column, washed with 5 ml of 50% methanol and then

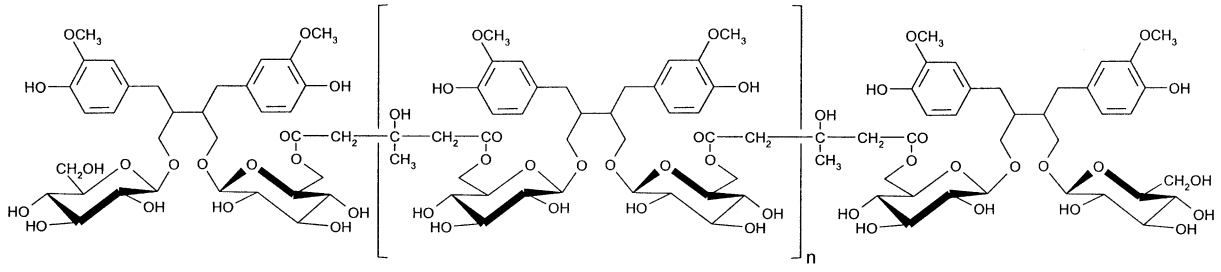

Fig. 3. The structure of a polymer composed of SDG and HMGA residues in flaxseed (average value of $n = 3$).

eluted with 60% methanol to obtain the major fraction of the polymer.

Before NMR analysis, the purified hygroscopic fraction was dried using a rotary evaporator, re-dissolved in either D_2O or a mixture of D_2O and CD_3OD and re-dried three times to exchange water followed by overnight incubation in a *vacuum* oven. All spectra (^1H MR, ^{13}C NMR, TOCSY, HMBC and HSQC-DEPT) were recorded at frequencies of 400 (^1H) and 100 (^{13}C) MHz on a Bruker DRX 400 instrument (Karlsruhe, Germany). Measurements were performed in a D_2O: CD_3OD mixture (1:1, v/v) at 60 °C. ^1H NMR chemical shifts were referenced to TMS while ^{13}C chemical shifts were referenced to the methyl group signals from residual methanol ($\delta = 49.0$ ppm). ^1H and ^{13}C NMR chemical shifts of the polymer, standard SDG (Johnsson et al., 2000) and HMGA (Sigma-Aldrich Chemie, Germany) were assigned by consideration of chemical shift values, coupling patterns and coupling constants, where appropriate. A sequence with pre-saturation of the water peak was used for ^1H NMR. TOCSY was recorded with a mixing time of 80 ms and HMBC was recorded with a delay of 65 ms for evolution of long range couplings and 164 scans over 256 increments. For HSQC–DEPT, the number of scans was 64 over 256 increments.

Acknowledgements

This project was financed by the Swedish Council for Forestry and Agricultural Research (SJFR). We thank Alternativ Förädling AB (Glanshammar, Sweden) for providing the flaxseed cake used in this study.

References

Axelson, M., Sjövall, J., Gustafsson, B.E., Setchell, K.D.R., 1982. Origin of lignans in mammals and identification of a precursor from plants. Nature 298, 659–660.

Bakke, J.E., Klosterman, H.J., 1956. A new diglucoside from flaxseed. Proc. North Dakota Acad. Sci. 10, 18–22.

Bentsath, A., Rusznyak, S., Szent-Györgi, A., 1937. Vitamin P. Nature 139, 326–327.

Bambagiotti-Alberti, M., Coran, S.A., Ghiara, C., Giannellini, V., Raffaelli, A., 1994a. Revealing the mammalian lignan precursor secoisolariciresinol diglucoside in flax by ion spray mass spectrometry. Rapid Commun. Mass Spectrom. 8, 595–598.

Bambagiotti-Alberti, M., Coran, S.A., Ghiara, C., Giannellini, V., Raffaelli, A., 1994b. Investigation of mammalian lignan precursors in flaxseed: first evidence of secoisolariciresinol diglucoside in two isomeric forms by liquid chromatography/mass spectrometry. Rapid Commun. Mass Spectrom. 8, 929–932.

Challem, J.J., 1999. Toward a new definition of essential nutrients: is it now time for a third 'vitamin' paradigm? Med. Hypothesis 52, 417–422.

Chimichi, S., Bambagiotti-Alberti, M., Coran, S.A., Giannellini, V., Biddau, B., 1999. Complete assignment of the ^1H and ^{13}C NMR spectra of secoisolariciresinol diglucoside, a mammalian lignan precursor isolated from *Linum usitatissimum*. Magn. Reson. Chem. 37, 860–863.

Dabrowski, K.J., Sosulski, F.W., 1984. Composition of free and hydrolyzable phenolic acids in defatted flours of ten oilseeds. J. Agric. Food Chem. 32, 128–130.

Farah, H., Andersson, R., Samuelsson, G., 1992. Microdotin A and B: two new aloin derivatives from *Aloe microdonta*. Planta Medica 58, 88–93.

Ishii, T., 1997. Structure and functions of feruloylated polysaccharides. Plant Sci. 127, 111–127.

Johnsson, P., Kamal-Eldin, A., Lundgren, L.N., Åman, P., 2000. HPLC method for analysis of secoisolariciresinol diglucoside in flaxseeds. J. Agric. Food Chem. 48, 5216–5219.

Klosterman, H.J., Smith, F., 1954. The isolation of β-hydroxy-β-methylglutaric acid from the seed of flax (*Linum usitatissimum*). J. Am. Chem. Soc. 76, 1229–1230.

Klosterman, H.J., Smith, F., Clagett, C.O., 1995. The constitution of Linocinnamerin. J. Am. Chem. Soc. 77, 420–421.

Kolattukudy, P.E., 1980. Biopolyester membranes of plants: cutin and suberin. Science 208, 990–1000.

Kozlowska, H., Zadernowski, R., Sosulski, F.W., 1983. Phenolic acids in oilseed flour. Nahrung 27, 449–453.

Laurenti, O., Albi, F., Artini, M., Bravi, C., Hurd, R., De Matti, G., 1990. Effects of HMGA in non-insulin-dependent diabetics with secondary dyslipidemia. Clin. Trials J. 27, 149–154.

Lin, I.-Z., He, X.-G., Lindenmaier, M., Yang, J., Cleary, M., Qiu, S.-X., Cordell, G.A., 2000. LC-ESI-MS study of the flavonoid glycoside malonates of red clover (*Trifolium pratense*). J. Agric. Food Chem. 48, 354–365.

Meagher, L.P., Beecher, G.R., Flanagan, V.P., Li, B.W., 1999. Isolation and characterisation of the lignans isolariciresinol and pinoresinol in flaxseed meal. J. Agric. Food Chem. 47, 3173–3180.

Mazur, W., Adlercreutz, H., 1998. Natural and anthropogenic environmental oestrogens: the scientific basis for risk assessment. Naturally occurring oestrogens in food. Pure Appl. Chem. 70, 1759–1776.

Qiu, S., Lu, Z., Luyengi, L., Lee, S.K., Pezzuto, J.M., Farnsworth, N.R., Thompson, L.U., Fong, H.S., 1999. Isolation and characterisation of flaxseed (*Linum usitatissimum*) constituents. Pharmaceutical Biol. 37, 1–7.

Westcott, N.D., Muir, A.D., 1996. Process for extracting and purifying lignans and cinnamic acid derivatives from flaxseed. PCT Patent No. WO9630468A2.

Westcott, N.D., Muir, A.D., 2000. Overview of flax lignans. INFORM 11, 118–121.

PERGAMON

Phytochemistry 58 (2001) 591–594

PHYTOCHEMISTRY

www.elsevier.com/locate/phytochem

Stilbenoids from the lianas of *Gnetum pendulum*

Xiao-Mei Li, Ying-Hong Wang, Mao Lin*

Institute of Materia Medica, Chinese Academy of Medical Sciences and Peking Union Medical College, No. 1 Xiannongtan Street, Beijing 100050, People's Republic of China

Received 11 January 2001; received in revised form 3 May 2001

Abstract

Two stilbenoids, gnetupendin A and B, were isolated from the lianas of *Gnetum pendulum* C. Y. Cheng, together with four known compounds, resveratrol, isorhapontigenin, shegansu B and β-daucosterol. Their structures were determined on the basis of analysis of spectral evidence, especially 2D NMR spectroscopic techniques. © 2001 Elsevier Science Ltd. All rights reserved.

Keywords: *Gnetum pendulum*; Gnetaceae; Gnetupendins A and B; Stilbenoid; Cyclo-oxgyenase-2 inhibitory activity

1. Introduction

Oligostilbenes have attracted much attention for their unique structures and various biological activities, including antifungal (Langcake and Pryce, 1977; Ducrot et al., 1998), protein kinase C inhibitory (Kulanthaivel et al., 1995), hepatoprotective and hepatotoxic (Oshima et al., 1995), anti-HIV, cytotoxic (Dai et al., 1998; Cichewicz et al., 2000) and cyclo-oxygenase (COX) and COX II inhibitory (Cichewicz et al., 2000) activities, etc.. Our research group has focused on naturally occurring oligostilbenes in recent years and three *Gnetum* species, *G. parvifolium*, *G. montanum* and *G. hainanense*, have been investigated (Li et al., 1991; Lin et al., 1991, 1992; Xu and Lin, 1997; Chen and Lin, 1998, 1999a,b; Huang et al., 2000a,b; Wang et al., 2001). As part of our systematic research on oligostilbene constituents, we investigated another Gnetum species, *G. pendulum*, and two stilbenoids, gnetupendin A and B were obtained together with resveratrol (Ingham, 1976), isorhapontigenin (3′,4,5′-trihydroxy-3-methoxystilbene) (Li et al., 1991), shegansu B (Zhou,and lin, 2000) and β-daucosterol (Chen and Lin, 1999a,b). The structures of the two stilbenoids, gnetupendin A (**1**) and B (**2**), contain a new stilbenoid skeleton in which the position 2 of 3,5-dihydroxybenzene ring (B) of the isorhapontigenin unit are substituted with a 4-hydroxybenzyl in **1** and a 3,4-dihydroxybenzyl group in **2** respectively. These are the first reports of this skeleton. Cyclo-oxygenase-2 inhibitory activity of **2** was tested.

2. Results and discussion

Gnetupendin A (**1**) was obtained as a pale yellow solid, exhibiting strong blue violet fluorescence under UV light at 254 nm. The high resolution EIMS *m/z* 364.1316 agreed with a molecular formula of $C_{22}H_{20}O_5$ (required 364.1311) with 13 degrees of unsaturation. The UV absorption spectrum of **1** at 228 and 325 nm suggested the presence of a stilbene skeleton (ring A and B) in **1**. The ^{1}H NMR spectrum of **1** (Table 1) showed eleven aromatic and olefinic protons and displayed the presence of ABX, AB and A_2B_2 systems respectively. Its spectrum showed signals as follows: an ABX system for ring A at δ 7.07 (1H, *br s,* H-2), 6.78 (1H, *d,* $J=8.4$ Hz, H-5) and 6.93 (1H, *dd*, $J=1.8$ and 8.4 Hz, H-6); an AB system for ring B at δ 6.41 (1H, *d*, $J=2.1$ Hz, H-12) and 6.68 (1H, *d*, $J=2.1$ Hz, H-14); an A_2B_2 system for ring C at δ 7.08 (2H, *br d*, $J=8.7$ Hz, H-17, 21) and 6.68 (2H, *br d*, $J=8.7$ Hz, H-18, 20); two *trans* olefinic protons at δ 6.85 (1H, *d*, $J=16.2$ Hz, H-7) and 7.24 (1H, *d*, $J=16.2$ Hz, H-8); one methoxyl singlet at δ 3.87 (3H, *s*, OCH_3) and one benzylic methylene singlet at δ 4.02 (2H, *s*, H-15). The ^{13}C NMR and DEPT spectra of **1** exhibited one methoxy group at δ 56.1 and one benzylic methylene group at δ 30.4, besides 20 aromatic and olefinic carbons at 102.5–157.0 (Table 1). The above spectral data indicate that structure of **1** consists of an isorhapontigenin

* Corresponding author. Tel.: +86-10-63165326; fax: +86-10-63017757.

E-mail address: linmao@imm.ac.cn (M. Lin).

0031-9422/01/$ - see front matter © 2001 Elsevier Science Ltd. All rights reserved.
PII: S0031-9422(01)00269-2

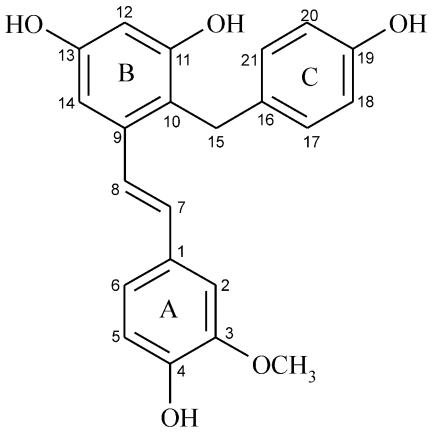

1

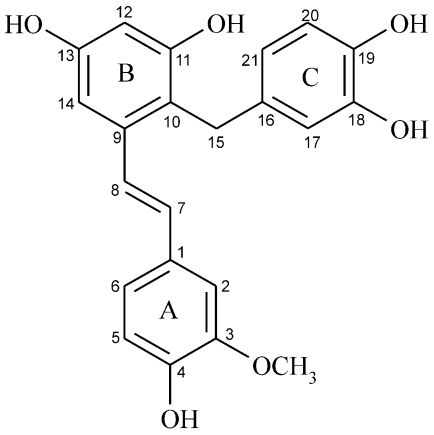

2

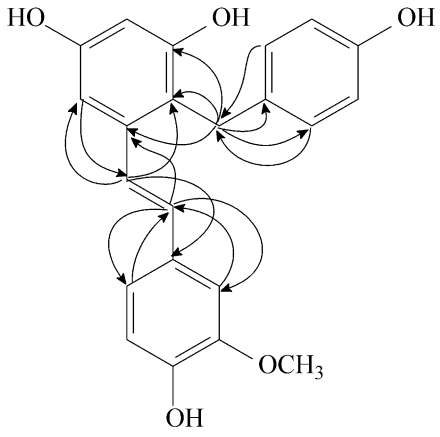

Fig. 1. Important ^{13}C–^{1}H long-range correlations for compound **1**.

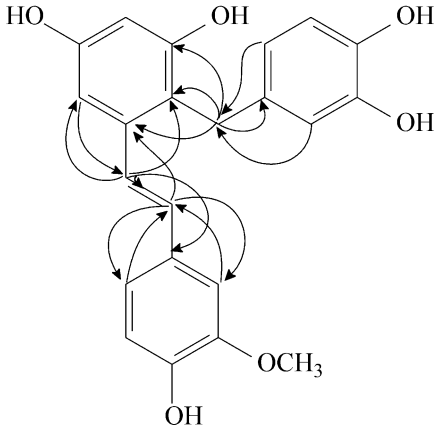

Fig. 2. Important ^{13}C–^{1}H long-range correlations for compound **2**.

(or a rhapontigenin) unit and a 4-hydroxybenzyl group. The location of the benzyl group was determined by HMBC spectral analyses of **1** (Fig. 1) and was confirmed by the following cross peaks: H-15/C-9, 10, 11, 16, 17(21) and H-17(21)/C-15. The correlations between H(C-4-OH) /C-3, 4, 5, H-6/C-4 and H(-OCH_3)/C-3 confirmed that the stilbene unit was isorhapontigenin. Thus, the structure of **1** was characterized as 10-(4-hydroxybenzyl)-isorhapontigenin.

Gnetupendin B (**2**) was obtained as a brown solid, exhibiting strong blue violet fluorescence under UV light at 254 nm. The high resolution EIMS *m/z* 380.1279 agreed with a molecular formula of $C_{22}H_{20}O_6$ (requires 380.1260) with 13 degrees of unsaturation. The ^{1}H NMR spectrum (Table 1) of **2** displayed similar patterns to those of **1**. However, the ^{1}H NMR spectrum of **2** (Fig. 2) showed ten aromatic and olefinic protons, including two ABX systems which appeared at δ 7.07 (1H, *d*, $J=2.1$ Hz, H-2), 6.86 (1H, *d*, $J=8.1$ Hz, H-5), 6.91 (1H, *dd*, $J=2.1$ and 8.1 Hz, H-6) for ring A and δ 6.64 (1H, *d*, $J=1.8$ Hz, H-17), 6.67 (1H, *d*, $J=7.5$ Hz, H-20), 6.69 (1H, *d*, $J=1.8$ and 7.5 Hz, H-21) for ring C; two *meta*-coupled doublets at δ 6.41 (1H, *d*, $J=2.1$ Hz, H-12) and 6.68 (1H, *d*, $J=2.1$ Hz, H-14) in ring B and two *trans* olefinic protons at δ 6.85 (1H, *d*, $J=16.2$ Hz, H-7) and 7.23 (1H, *d*, $J=16.2$ Hz, H-8). The ^{1}H NMR spectrum also showed the presence of one methoxy singlet at δ 3.88 (3H, *s*, OCH_3) and one benzyl methylene singlet at δ 3.98 (2H, *s*, H-15). The ^{13}C NMR and DEPT spectra of **2** revealed the presence of one methoxy group at δ 56.1 and one benzylic methene group at δ 30.5 in addition to 20 aromatic and olefinic carbons at 102.5–157.0 (Table 1). Thus, **2** was similar to **1**, its structure was composed of an isorhapontigenin unit and a 3, 4-dihydroxybenzyl group. The connectivity of the two units were determined by the correlations between H-15/C-9,

Table 1
^1H and ^{13}C NMR spectral data for compounds **1**–**2**[a]

No. position	**1**			**2**		
	^1H	^{13}C	HMBC	^1H	^{13}C	HMBC
1		130.7			130.7	
2	7.07 *br s*	109.8	C-4, 6, 7	7.07 *d* (2.1)	109.7	C-4, 6, 7
3		148.4			148.4	
4		147.4			147.3	
5	6.78 *d* (8.4)	115.8	C-1, 3	6.86 *d* (8.1)	115.8	C-1, 3
6	6.93 *dd* (1.8, 8.4)	121.0	C-2, 4, 7	6.91 *d* (2.1, 8.1)	121.1	C-2, 4, 7
7	6.85 *d* (16.2)	130.2	C-2, 6, 9	6.85 *d* (16.2)	130.1	C-2, 6, 9
8	7.24 *d* (16.2)	125.0	C-1, 10, 14	7.23 *d* (16.2)	125.1	C-1, 10, 14
9		139.4			139.5	
10	6.68 *d* (2.1)	104.2		6.68 *d* (2.1)	104.1	
11		157.0			157.0	
12	6.41 *d* (2.1)	102.5	C-10, 13, 14	6.41 *d* (2.1)	102.5	C-10, 13, 14
13		157.0			157.0	
14		118.3	C-8, 10, 12, 13		118.3	C-8, 10, 12, 13
15	4.02 *s*	30.4	C-9, 10, 11, 16, 17(21)	3.98 *s*	30.5	C-9, 10, 11, 16
16		133.9			134.9	
17	7.08 *d* (8.7)	130.0	C-15, 19	6.64 *d* (1.8)	120.3	C-15, 19, 21
18	6.68 *d* (8.7)	115.7	C-16		145.6	
19		155.9			143.5	
20	6.68 *d* (8.7)	115.7	C-16	6.67 *d* (7.5)	115.7	C-16, 18
21	7.08 *d* (8.7)	130.0	C-15, 19	6.69 *dd* (1.8, 5)	116.2	C-15, 19
OCH3	3.87 *s*	56.1	C-3	3.87 *s*	56.1	C-3
OH	7.72 *s* (C-4)		C-3, 5	8.20*[b]		
	8.08 *s* (C-11)		C-13, 14	8.02*		
	8.28 *s* (C-13)		C-10, 11, 12	7.66*		
	8.02 *s* (C-19)		C-18(20), 19	7.58*		

[a] Measured in CD_3COCD_3 at 300 MHz for ^1H and 75 MHz for ^{13}C, respectively, with assignments confirmed by ^1H-^1H COSY, HMQC, HMBC and NOESY spectra.
[b] *Each was a broad singlet, and the signals cannot be assigned unambiguously; hence, they are interchangeable.

10, 11, 16; H-17/C-15 and H-21/C-15. Thus, **2** was characterized as 10-(3,4-dihydroxybenzyl)-isorhapontigenin.

The inhibitory effect of compound **2** on prostaglandin E_2 (PGE_2) production in mouse peritoneal macrophages stimulated with lipopolysaccharide (LPS) was tested (Hu and Cheng, 2000). The inhibitory rate of compound **2** was 24.4% ($P < 0.05$) at the concentration of 10^{-7} mol/l, with meloxicam used as a positive control with IC_{50} of 2.86×10^{-8} mol/l. It suggested that compound **2** may has cyclo-oxygenase-2 inhibitory activity.

3. Experimental

3.1. General experimental procedures

UV spectra were recorded on a Shimadzu UV-3000 spectrophotometer. IR spectra were recorded on a Perkin-Elmer 683 infrared spectrometer as KBr pellets. NMR spectra were recorded on a Varian Mercury-300 NMR spectrometer using TMS as internal standard. EIMS and HREIMS were obtained using an Autospec-UltimaTof mass spectrometer. HPLC was performed on a Waters Model 510 instrument equipped with a Waters 2487 Dual λ Absorbance UV Detector.

3.2. Plant material

The lianas of *G. pendulum* C. Y. Cheng (Gnetaceae) were collected at Menghai in Xishuangbanna County of Yunnan Province, People's Republic of China in July 1999, and were identified by Professor W.Z. Song, Institute of Materia Medica, Chinese Academy of Medical Sciences and Peking Union Medial College. A voucher specimen has been deposited in the herbarium of this Institute.

3.3. Extraction and isolation

The dried and powdered lianas of *G. pendulum* (10 kg) were extracted with 60% aq EtOH under conditions of refluxing, and the crude extract (1.5 kg) obtained after removing solvent in vacuo was further extracted with EtOAc to provide a EtOAc soluble residue (90 g) after evaporating to dryness. The residue was next subjected to silica gel column chromatography (140–180 mesh, 10 $\times$150 cm) eluted with $CHCl_3$–MeOH–H_2O (8:2.5:1) to provide five fractions (A-E). Isorhapontigenin (4.5 g, 0.045%) and resveratrol (100 mg, 0.001%) were obtained from fraction A by additional silica gel column chromatography (40 μm, 5×100 cm) with $CHCl_3$–

MeOH (9:1). Fraction B (12 g) was subjected to ODS column chromatography (RP-18, 35–75 μm, 4×35 cm) eluted with a MeOH–H_2O gradient of increasing MeOH to provide fractions B_1–B_3. Fraction B_3 (5.9 g) was subjected to ODS column chromatography (RP-18, 35–75 μm, 4×35 cm) eluted with MeOH–H_2O (4.5:5.5) and then purified by medium-pressure liquid chromatography (Lobar column, RP-18, 43–63 μm, 2.5×31 cm, MeOH–H_2O of 3.5:6.5) to provide shegansu B (570 mg, 0.0057%). Fraction B_2 (60 mg) was subjected to preparative HPLC (10 μm, 300×7.8 mm) with MeOH–H_2O (1:1) to provide **1** (24 mg, 0.00024%). Fraction B_1 (0.7 g) was subjected to medium-pressure liquid chromatography (Lobar column, RP-18, 43–63 μm, 2.5×31 cm, MeOH–H_2O of 3.5:6.5) to provide **2** (144 mg, 0.0014%).

3.4. Gnetupendin A (*1*)

Pale yellow solid; UV ($c = 0.02$, MeOH) λ_{max} (log ε): 228 (4.5), 291 (*sh*), 306 (*sh*), 325 (4.6) nm; IR (KBr) ν_{max} cm^{-1}: 3410, 1604, 1599, 1514, 1466, 1344, 1267, 1159, 1020, 1007, 953, 849, 833, 800, 781; ^1H (300 MHz) and ^{13}C (75 MHz) NMR spectral data: see Table 1; FABMS *m/z*: 364.1; HR–EIMS *m/z*: 364.1316 $[M]^+$ (calc. for $C_{22}H_{20}O_5$, 364.1311).

3.5. Gnetupendin B (*2*)

Brown solid; UV ($c = 0.02$, MeOH) λ_{max} (log ε): 224 (4.5), 296 (*sh*), 305 (*sh*), 325 (4.4) nm; IR (KBr) ν_{max}: 3321, 1606, 1516, 1464, 1344, 1275, 1155, 1016, 953, 845, 814, 789; ^1H (300 MHz) and ^{13}C (75 MHz) NMR spectral data: see Table 1; EIMS *m/z* (%): 380 $[M]^+$ (25), 258 (M–$C_6H_6O_2$) (100), 243 (258-15) (15); HR–EIMS *m/z* 380.1279 $[M]^+$ (calc. for $C_{22}H_{20}O_6$, 380.1260).

Acknowledgements

This research program was supported by the National Nature Science Foundation of the People's Republic of China (No. 30,070,889). The authors thank the Department of Instrumental Analysis, Institute of Materia Medica, Chinese Academy of Medical Sciences and Peking Union Medial College, for the measurement of UV, IR, NMR and MS spectra, the authors also thank Professor G.F. Cheng for biological testing.

References

Chen, H., Lin, M., 1998. A pair of dimeric stilbene epimers from *Gnetum montanum*. Chin. Chem. Lett. 9, 1013–1015.

Chen, H., Lin, M., 1999a. Gnetifolins L and O, two dimeric stilbenes from *Gnetum montanum*. Chin. Chem. Lett. 10, 579–582.

Chen, H., Lin, M., 1999b. Studies on the chemical constituents of *Gnetum montanum*. Chin. Trad. Herb. Drugs 30, 571–573.

Cichewicz, R.H., Kouzi, S.A., Hamann, M.T., 2000. Dimerization of resveratrol by the grapevine pathogen *Botrytis cinerea*. J. Nat. Prod. 63, 29–33.

Dai, J.R., Hallock, Y.F., Cardellina, II, J.H., Boyd, M.R., 1998. HIV-Inhibitory and cytotoxic oligostilbenes from the leaves of *Hopea malibato*. J. Nat. Prod. 61, 351–353.

Ducrot, P.H., Kollmann, A., Balla, A.E., Majira, A., Kerhoas, L., Delorne, R., Einhorn, J., 1998. Cyphostemmins A-B, two new antifungal oligostilbenes from *Cyphostemma crotalarioides* (Vitaceae). Tetrahedron Lett. 39, 9655–9658.

Hu, Y.F., Cheng, G.F., 2000. Establishment of screening models for selective cyclo-oxygenase-2 inhibitors. Acta Pharm. Sin. 35, 343–346.

Huang, K.S., Wang, Y.H., Li, R.L., Lin, M., 2000a. Five new stilbene dimers from the lianas of *Gnetum hainanense*. J. Nat. Prod. 63, 86–89.

Huang, K.S., Wang, Y.H., Li, R.L., Lin, M., 2000b. Stilbene dimers from the lianas of *Gnetum hainanense*. Phytochemistry 54, 875–881.

Ingham, J.L., 1976. Trihydroxystilbene as phytoalexin from groundnuts (*Arachis Hypogaea*). Phytochemistry 15, 1791–1793.

Kulanthaivel, P., Janzen, W.P., Ballas, L.M., Jiang, J.B., Hu, C.Q., Darges, J.W., Seldin, J.C., Cofield, D.J., Adams, L.M., 1995. Naturally occurring protein kinase inhibitors; II. Isolation of oligomeric stilbenes from *Caragana sinica*. Planta Med. 61, 41–44.

Langcake, P., Pryce, R.J., 1977. A new class of phytoalexins from grapevines. Experienta 33 (2), 151–152.

Li, J.B., Lin, M., Li, S.Z., Song, W.Z., 1991. Studies on structure of gnetifolin A from *Gnetum parvifolium*. Acta Pharm. Sin. 26, 437–441.

Lin, M., Li, J.B., Wu, B., Zheng, Q.T., 1991. A stilbene derivative from *Gnetum parvifolium*. Phytochemistry 30, 4201–4203.

Lin, M., Li, J.B., Li, S.Z., Yu, D.Q., Liang, X.T., 1992. A dimeric stilbene from *Gnetum parvifolium*. Phytochemistry 31, 633–638.

Oshima, Y., Namao, K., Kamijou, A., Matsuoka, S., Nakano, M., Terao, K., Ohizumi, Y., 1995. Powerful hepatoprotective and hepatotoxic plant oligostilbenes, isolated from the Oriental medicinal plant *Vitis coignetiae* (Vitaceae). Experientia 51, 63–66.

Wang, Y. H., Huang, K. S., Lin, M., 2001. Four new stilbene dimers from the lianas of *Gnetum hainanense*. J. Asian Nat. Prod., in press.

Xu, Q., Lin, M., 1997. Gnetifolin K, a new stilbene diglucoside from *Gnetum parvifolium*. Chin. Chem. Lett. 8, 509–510.

Zhou, L.X., Lin, M., 2000. A new stilbene dimer-shegansu B from *Belamcanda chinensis*. J. Asian Nat. Prod. 2, 169–175.

PERGAMON

Phytochemistry 58 (2001) 595–598

PHYTOCHEMISTRY

www.elsevier.com/locate/phytochem

Flavonoids from *Glycyrrhiza pallidiflora* hairy root cultures

Wei Li[a], Yoshihisa Asada[b,*], Kazuo Koike[a], Masao Hirotani[b], Hekai Rui[b], Takafumi Yoshikawa[b], Tamotsu Nikaido[a]

[a]*School of Pharmaceutical Sciences, Toho University, 2-2-1 Miyama, Funabashi-city, Chiba 274-8510, Japan*
[b]*School of Pharmaceutical Sciences, Kitasato University, 5-9-1 Shirokane, Minato-ku, Tokyo 108-8641, Japan*

Received 3 January 2001; received in revised form 8 May 2001

Abstract

Glycyrrhiza pallidiflora hairy roots were induced from axenic young plants by direct infection with *Agrobacterium rhizogenes*. The chemical constituents were then investigated after mass culture. The isoflavone, licoagroisoflavone and the coumestan, licoagroside C, were isolated along with seven known flavonoids. Their structures were determined on the basis of spectroscopic evidence.
© 2001 Elsevier Science Ltd. All rights reserved.

Keywords: Licorice; *Glycyrrhiza pallidiflora*; Leguminosae; Hairy root; Flavonoids; Licoagroisoflavone; Licoagroside C; Coumestan

1. Introduction

The roots of *Glycyrrhiza* species are one of the most important crude drugs in China and Europe. In our studies on hairy root cultures to produce useful compounds, we have established several hairy root culture lines of *Glycyrrhiza* species, including *G. glabra*, *G. ularensis*, *G. eurycarpa*, *G. aspera* and *G. pallidiflora*. The chemical constituents of *G. glabra* have been reported previously (Asada et al., 1998, 1999; Li et al., 1998, 2000). In the analysis of the flavonoid constituents of these hairy root cultures, *G. pallidiflora* hairy root cultures showed a very different HPLC pattern than *G. glabra* hairy root cultures. We report here the isolation and structure determination of chemical constituents from *G. pallidiflora* hairy root cultures.

2. Results and discussion

Hairy roots of *G. pallidiflora* were induced from axenic young plants by direct infection with *Agrobacterium rhizogenes* pRi 15834; pGSGlu1 (GUS) as described previously (Yoshikawa and Furuya, 1987). The opines, agropine and mannopine, were detected from the hairy roots by paper electrophoresis.

Mass culture was carried out on Gamborg's B5 plant medium. After 4 weeks of culture, the hairy roots were harvested. The dried roots were extracted with methanol and the extract was partitioned between ethyl acetate and water. The ethyl acetate extract was applied to a silica gel column and further purified by normal-phase and reversed-phase HPLC to give two new flavonoids, named licoagroisoflavone (**1**) and licoagroside C (**2**), together with seven known flavonoids, calycosin (**3**), erythrinin (**4**), isoliquiritigenin (**5**), echinatin (**6**), maackiain (**7**), trifolirhizin (**8**) and ononin (**9**) (Fig. 1).

Licoagroisoflavone (**1**) was obtained as a pale yellow powder. In the EI mass spectrum, **1** exhibited a molecular ion peak at m/z 336, which is smaller by 18 mass units than that of erythrinin (**4**). Its molecular formula, $C_{20}H_{16}O_5$, was established based on its the HR–EI mass spectrum. The ^{1}H NMR spectrum of **1** was similar to that of **4,** except for proton signals due to a prenyl group. The ^{1}H NMR spectrum of **1** showed a singlet at δ 8.17, which is characteristic of the olefinic proton of isoflavones (Markham and Geiger, 1994). The spectrum also showed the presence of AA′XX′-type aromatic proton signals at δ 7.30 (2H, *d*, $J=8.5$ Hz) and 7.75 (2H, *d*, $J=8.5$ Hz) due to B ring protons and a singlet aromatic proton signal at δ 6.55 (1H, *s*) due to an A ring proton. Proton signals due to a prenyl moiety were observed at δ 1.75 (3H, *br s*, H_3-8″), 3.07 (1H, *dd*, $J=15.0$, 7.5 Hz, H_a-4″), 3.39 (1H, *dd*, $J=15.0$, 9.5 Hz, H_b-4″), 4.95 (1H, *br s*, H_a-7″), 5.17 (1H, *br s*, H_b-7″),

* Corresponding author. Fax: +81-3-3444-6192.
E-mail address: asaday@pharm.kitasato-u.ac.jp (Y. Asada).

0031-9422/01/$ - see front matter © 2001 Elsevier Science Ltd. All rights reserved.
PII: S0031-9422(01)00268-0

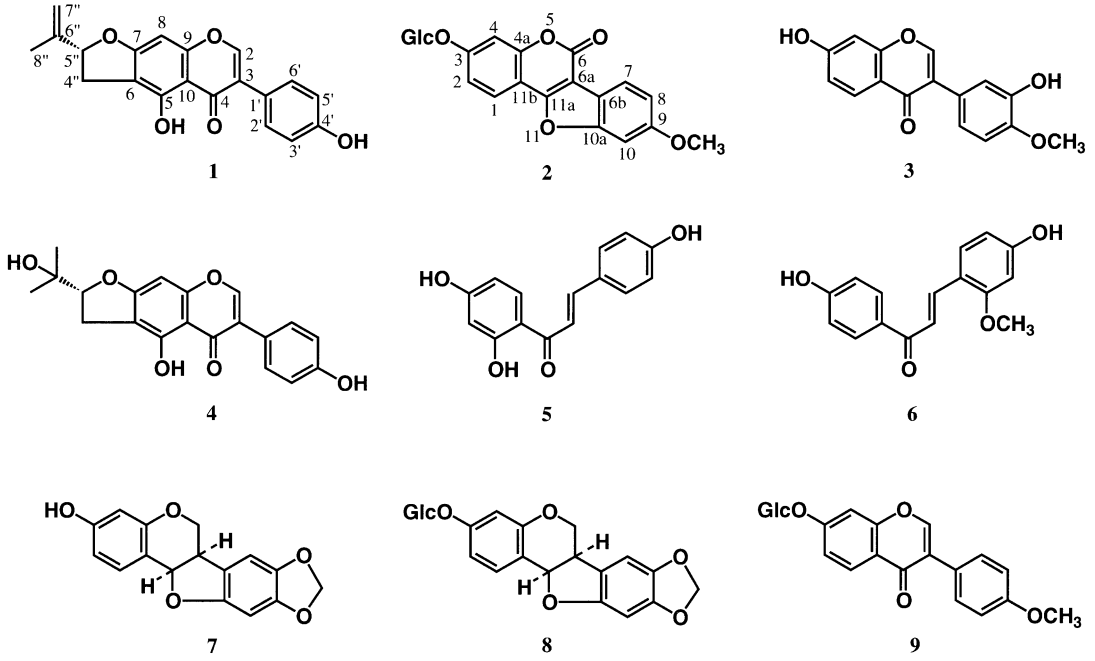

Fig. 1. Flavonoids from *Glycyrrhiza pallidiflora* hairy root cultures.

and 5.40 (1H, *br dd*, $J=9.5$, 7.5 Hz, H-5″), indicating the presence of an isopropenyl-dihydrofuran group (Tahara et al., 1984). The position of the isopropenyl-dihydrofuran side chain was assigned to be located at C-6 based on HMBC experiments (Fig. 2). The absolute configuration of C-5″ was determined by CD spectrum analysis of the osmate ester/pyridine complex. A negative Cotton effect at 470 nm indicated that **1** had an *S*-configuration at C-5″ (Tahara, Ingham, Mizutani, 1987). Thus, the structure of licoagroisoflavone (**1**) was determined as 5″-(*S*)-5, 4′-dihydroxy-5″-isopropenyl-4″, 5″-dihydrofurano [2″, 3″: 6, 7] isoflavone.

Licoagroside C (**2**) was obtained as colorless needles. The FAB mass spectrum of **2** showed a pseudo-molecular ion peak at m/z 445 $[M+H]^+$, which is larger by 14 mass units than that of ononin (**9**). Its molecular formula, $C_{22}H_{20}O_{10}$, was established based on its HR–FAB mass spectrum. The IR spectrum of **2** showed a band at 1731 cm^{-1}, indicating the presence of an unsaturated δ-lactone group (Abe et al., 1987). The ^1H NMR spectrum of **2** showed two ABX-type aromatic proton signals at δ 7.17 (1H, *dd*, $J=8.5$, 2.0 Hz), 7.36 (1H, *d*, $J=2.0$ Hz), 8.11 (1H, *d*, $J=8.5$ Hz) and δ 7.38 (1H, *dd*, $J=8.5$, 2.0 Hz), 7.48 (1H, *d*, $J=2.0$ Hz), 7.88 (1H, *d*, $J=8.5$ Hz), as well as a methoxy proton signal at δ 3.79 and an anomeric proton signal at 5.81(1H, *d*, $J=7.0$ Hz). The coupling constants of the sugar moiety protons suggested the presence of a β-D-glucopyranose. Comparison of the ^1H NMR spectrum of **2** with that of **9** showed that the olefinic proton disappeared in **2** and the AA′XX′-type aromatic proton signals in **9** changed to ABX-type aromatic proton signals in **2**. By reference to published ^1H NMR data of coumestans (Ohshima et al., 1988), the signal at δ 8.11 was assigned to the proton at C-7, which is shifted downfield by the effect of the neighboring carbonyl. Based on analyses of the HMQC and HMBC spectra of **2**, the carbons on the two aromatic rings were assigned as shown in the Experimental section, and the remaining three carbon signals (δ 104.3, 158.2, 160.0) in the aglycone moiety also suggested that **2** is a coumestan-like compound (Fukai et al., 1989). The positions of the methoxy and glucopyranosyloxy groups in **2** were determined from the HMBC spectrum, as shown in Fig. 3. The H-7 and methoxy protons were correlated to C-9 at δ 160.0. On the other hand, correlation peaks between the anomeric and H-1 protons and C-3 at δ 161.4 were observed. Thus, **2** was identified as 3-β-D-glucopyranosyl-9-methoxycoumestan, named as licoagroside C.

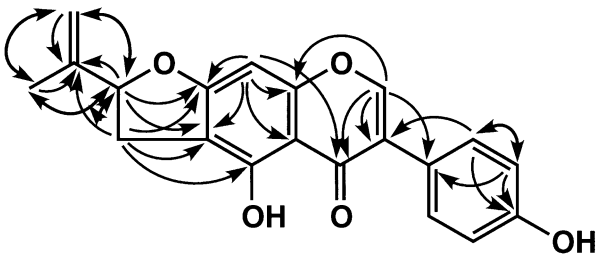

Fig. 2. ^1H–^{13}C long-range correlations (HMBC) of compound **1**.

In conclusion, we isolated two new flavonoids and seven known flavonoids from the hairy roots of *G. pallidiflora*. The known flavonoids calycosin (**3**), isoliquiritigenin (**5**), echinatin (**6**) and ononin (**9**) were previously

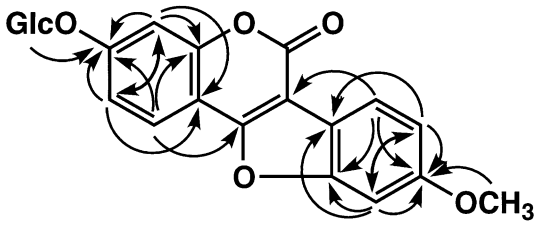

Fig. 3. ^{1}H–^{13}C long-range correlations (HMBC) of compound **2**.

obtained from the roots of *G. pallidiflora* (Nomura and Fukai, 1998). Echinatin (**6**) and ononin (**9**) were obtained from hairy root cultures of *G. glabra* in our previous studies (Li et al., 2000). The flavonoid constituents of *G. pallidiflora* hairy roots were rich in prenylated isoflavones, compared to those of *G. glabra*. *G. pallidiflora* hairy root cultures may have greater prenylation ability than *G. pallidiflora* roots, and thus give new compound **1**.

3. Experimental

3.1. General experimental procedures

Melting points were measured on a Yanaco micro melting point apparatus. The UV spectra were obtained with a Shimadzu UV-160 spectrophotometer, whereas the IR spectra were measured with a JASCO FT/IR-300E (by a KBr disk method) spectrometer. The optical rotations were measured with a JASCO DIP-370 digital polarimeter in a 0.5 dm-long cell, while the CD spectra were recorded on a JASCO J-720 W spectropolarimeter. EI–MS, FAB–MS, HR–EI–MS and HR–FAB–MS were taken on a Jeol JMS-AX505HA. ^{1}H and ^{13}C NMR spectra were measured with a Varian XL-400 spectrometer. For HPLC, a Waters model 510 HPLC system was used. Column chromatography was carried out using Wako-gel C-200. TLC was conducted on Kieselgel 60 F_{254} plates (Merck).

3.2. Mass culture of G. pallidiflora hairy root

The methods used to induce hairy root cultures of *G. pallidiflora* have been described previously (Yoshikawa and Furuya, 1987). The opines of hairy roots were detected by paper electrophoresis. Mass culture was carried out on Gamborg's B5 medium (Gamborg et al., 1968) containing 2% sucrose at 25 °C in the dark, at 50 rpm on a rotary shaker, using 500 ml Erlenmeyer flasks each containing 200 ml of medium.

3.3. Extraction and separation of flavonoids

After 4 weeks of culture, the hairy roots were harvested. The freeze-dried hairy roots (134.97 g) were extracted with MeOH. Evaporation of the solvent under reduced pressure from the combined extract gave the MeOH extract (43.85 g). The extract was then partitioned between EtOAc and H_2O. Removal of the solvent from the EtOAc phase under reduced pressure below 40 °C yielded the EtOAc extract (5.01 g). The EtOAc extract was subjected to silica gel chromatography (Wako gel C-200, ca 250 g) and eluted by $CHCl_3$:MeOH at ratios from 100:0 to 0:100 to give 11 fractions, fr. 1 (432.5 mg), fr. 2 (127.6 mg), fr. 3 (211.9 mg), fr. 4 (107.6 mg), fr. 5 (231.3 mg), fr. 6 (175.7 mg), fr. 7 (176.0 mg), fr. 8 (149.6 mg), fr. 9 (500.4 mg), fr. 10 (513.1 mg) and fr. 11 (95.8 mg). Further purification of fractions 2–10 was achieved by repeated NP–HPLC (μ-Bondasphere, 5 μm Si–100 Å, 19×150 mm) and RP–HPLC (μ-Bondasphere, 5 μm C18–100 Å, 19×150 mm) to give **1** (61.6 mg), **2** (4.4 mg), **3** (1.7 mg), **4** (1.7 mg), **5** (0.4 mg), **6** (1.0 mg), **7** (10.1 mg), **8** (25.0 mg) and **9** (13.0 mg).

3.4. Licoagroisoflavone (*1*)

Pale yellow powder, mp 196–198 °C, $[\alpha]_D$ −68.1° ($c=0.81$, MeOH, 24 °C). UV λ nm (log ε): 214 (4.57), 264 (4.67). IR υ cm^{-1}: 3403, 1673, 1619, 1571. EI–MS *m/z* (%): 336 (M^+, 100), 321 (100), 319 (43), 295 (43), 149 (54). HR–EI–MS: Found: 336.0996; Calcd for $C_{20}H_{16}O_5$ (M^+): 336.0998. ^{1}H NMR (400 MHz, pyridine-d_5): δ 1.75 (3H, *br s*, H_3-8″), 3.07 (1H, *dd*, $J=15.0$, 7.5Hz, H_a-4″), 3.39 (1H, *dd*, $J=15.0$, 9.5 Hz, H_b-4″), 4.95 (1H, *br s*, H_a-7″), 5.17 (1H, *br s*, H_b-7″), 5.40 (1H, *br dd*, $J=9.5$, 7.5 Hz, H-5″), 6.55 (1H, *s*, H-8), 7.30 (2H, *d*, $J=8.5$Hz, H-3′ and 5′), 7.75 (2H, *d*, $J=8.5$ Hz, H-2′ and 6′), 8.17 (1H, *s*, H-2). ^{13}C NMR (100 MHz, pyridine-d_5): δ 17.2 (C-8″), 31.0 (C-4″), 88.5 (C-5″), 89.3 (C-8), 107.1 (C-10), 109.1 (C-6), 112.7 (C-7″), 116.5 (C-3′ and 5′), 122.3 (C-1′), 123.7 (C-3), 131.2 (C-2′ and 6′), 144.0 (C-6″), 153.6 (C-2), 157.9 (C-5), 158.7 (C-9), 159.5 (C-4′), 166.7 (C-7), 181.6 (C-4).

3.5. Licoagroside C (*2*)

Colorless needles (MeOH), mp 245–247 °C, $[\alpha]_D$ −23.1° ($c=0.40$, MeOH, 24 °C). UV λ nm (log ε): 211 (4.21), 242 (4.20), 337 (4.26). IR υ cm^{-1}: 3411, 1731, 1630. FAB–MS (positive) *m/z*: 445 [$(M+H)^+$]. HR–FAB–MS (positive) *m/z*: Found: 445.1130; Calc. for $C_{22}H_{21}O_{10}$ [$(M+H)^+$]: 445.1135. ^{1}H NMR (400 MHz, pyridine-d_5): δ 3.79 (3H. s. OCH_3), 4.25 (1H, *ddd*, $J=8.0$, 5.0, 2.0 Hz, Glc-H-5), 4.36–4.48 (4H, m, Glc-H-2, 3, 4 and Glc-H_a-6), 4.62 (1H, *dd*, $J=12.0$, 2.0 Hz, Glc-H_b-6), 5.81 (1H, d, $J=7.0$ Hz, Glc-H-1), 7.17 (1H, *dd*, $J=8.5$, 2.0 Hz, H-8), 7.36 (1H, *d*, $J=2.0$ Hz, H-10), 7.38 (1H, *dd*, $J=8.5$, 2.0 Hz, H-2), 7.48 (1H, *d*, $J=2.0$ Hz, H-4), 7.88 (1H, *d*, $J=8.5$ Hz, H-1), 8.11 (1H, *d*, $J=8.5$ Hz, H-7). ^{13}C NMR (100 MHz, pyridine-d_5):

δ 56.0 (OCH_3), 62.5 (Glc-C-6), 71.3 (Glc-C-4), 75.0 (Glc-C-2), 78.6 (Glc-C-3), 79.4 (Glc-C-5), 97.6 (C-10), 102.2 (Glc-C-1), 104.3 (C-6a), 105.2 (C-4), 107.4 (C-11b), 114.1 (C-8), 114.7 (C-2), 117.1 (C-6b), 121.8 (C-1), 123.0 (C-7), 155.3 (C-4a), 157.0 (C-10a), 158.2 (C-6), 160.0 (C-9 and 11a), 161.4 (C-3).

*3.6. Preparation and CD measurements of osmate ester-pyridine complex of **1***

A solution of **1** (0.40 mg, 1.2 μmol) in CH_2Cl_2 (65 μl) containing 25 μmol of pyridine was treated with OsO_4 (1.4 μmol in 10 μl CH_2Cl_2) for about 30 min at room temperature. The mixture was diluted with CH_2Cl_2 to a final volume of 2.8 ml. The CD spectrum of this solution was recorded over the range 400–600 nm. CD (23 °C): $[\theta]_{470}$ −11178.7.

Acknowledgements

This work was supported by a ''High-tech Research Center'' grant from the Ministry of Education, Science, Sports and Culture of Japan. The authors wish to thank Ms. Michiko Sato at the Analytical Center of Kitasato University for NMR measurements.

References

Abe, N., Sato, H., Sakamura, S., 1987. Antifungal stress compounds from Adzuki been, *Vigna angularis*, treated with *Cephalosporium gregatum*. Agricultural and Biological Chemistry 52 (2), 349–353.

Asada, Y., Li, W., Yoshikawa, T., 1998. Isoprenylated flavonoids from hairy root cultures of *Glycyrrhiza glabra*. Phytochemistry 47 (3), 389–392.

Asada, Y., Li, W., Yoshikawa, T., 1999. The first prenylated biaurone, licoagrone from hairy root cultures of *Glycyrrhiza glabra*. Phytochemistry 50 (6), 1015–1019.

Fukai, T., Wang, Q., Kitakawa, T., Kusano, K., Nomura, T., Iitaka, Y., 1989. Structures of six isoprenoid-substitutents, gancaonins F, G, H, I, glycyrol, and isoglycyrol from xibei licorice (*Glycyrrhiza* sp.). Heterocycles 29 (9), 1761–1772.

Gamborg, O., Miller, R., Ojima, K., 1968. Nutrient requirements of suspension cultures of soybean root cells. Experimental Cell Research 50, 151–158.

Li, W., Asada, Y., Yoshikawa, T., 1998. Antimicrobial flavonoids from *Glycyrrhiza glabra* hairy root cultures. Planta Medica 64 (8), 746–747.

Li, W., Asada, Y., Yoshikawa, T., 2000. Flavonoid constituents from *Glycyrrhiza glabra* hairy root cultures. Phytochemistry 55 (5), 447–456.

Markham, K.R., Geiger, H., 1994. ^{1}H nuclear magnetic resonance spectroscopy of flavonoids and their glycosides in hexadeuterodimethylsulfoxide. In: Harborne, J.B. (Ed.), The Flavonoids. Advances in Research Since 1986. Chapman and Hall, London, pp. 441–497.

Nomura, T., Fukai, T., 1998. Phenolic constituents of licorice (*Glycyrrhiza species*). In: Herz, W., Kirby, G.W., Moore, R.E., Steglich, W., Tamm, C. (Eds.), Fortschritte der Chemie Organischer Naturstoffe, Vol. 73. Springer, New York, pp. 1–140.

Ohshima, Y., Okuyama, T., Takahashi, K., Takizawa, T., Shibata, S., 1988. Isolation and high performance liquid chromatography (HPLC) of isoflavonoids from the *Pueraria* root. Planta Medica 250–254.

Tahara, S., Ingham, J.L., Nakahara, S., Mizutani, J., Harborne, J.B., 1984. Fungitoxic dihydrofuranoisoflavones and related compounds in white lupin, *Lupinus albus*. Phytochemistry 23 (9), 1889–1900.

Tahara, S., Ingham, J.L., Mizutani, J., 1987. Stereochemical studies on dihydrofurano-isoflavones. Agricultural and Biological Chemistry 51 (1), 211–216.

Yoshikawa, T., Furuya, T., 1987. Saponin production by cultures of *Panax ginseng* transformed with *Agrobacterium rhizogenes*. Plant Cell Reports 6, 449–453.

PERGAMON

Phytochemistry 58 (2001) 599–602

PHYTOCHEMISTRY

www.elsevier.com/locate/phytochem

A weakly antimalarial biflavanone from *Rhus retinorrhoea*

Mohamed S. Ahmed[a], Ahmed M. Galal[b,*], Samir A. Ross[b,c], Daneel Ferreira[b], Mahmoud A. ElSohly[b,d], Abdel-Rahim S. Ibrahim[e], Jaber S. Mossa[a], Farouk S. El-Feraly[a]

[a]*Department of Pharmacognosy, College of Pharmacy, King Saud University, Riyadh, Saudi Arabia*
[b]*National Center for Natural Products Research, University of Mississippi, PO Box 1848, University, MS 38677, USA*
[c]*Department of Pharmacognosy, University of Mississippi, PO Box 1848, University, MS 38677, USA*
[d]*Department of Pharmaceutics, School of Pharmacy, University of Mississippi, University, MS 38677, USA*
[e]*Department of Pharmacognosy, College of Pharmacy, Tanta University, Tanta, Egypt*

Received 28 December 2000; received in revised form 24 April 2001

Abstract

The biflavanone (2*S*,2″*S*)-7,7″-di-*O*-methyltetrahydroamentoflavone and five known flavonoids, 7-*O*-methylnaringenin, 7,3′-*O*-dimethylquercetin, 7-*O*-methylapigenin, 7-*O*-methylluteolin, and eriodictyol were isolated from the leaves of *Rhus retinorrhoea* Steud, Ex Olive. The biflavanone exhibited moderate antimalarial activity with IC_{50} 0.98 μg/ml against *Plasmodium falciparum* (W2 Clone) and weak activity against *P. falciparum* (D6 Clone) with IC_{50} 2.8 μg/ml. Nevertheless, it did not display any cytotoxicity. 7-*O*-Methylnaringenin showed weak antimicrobial activity against *Candida albicans, C. krusei, Staphylococcus aureus, Mycobacterium smegmatis, M. intracellulare, and M. xenopi* with MIC∼ 100 μg/ml. Characterization of each compound was based on spectral analysis and comparison with reported data. © 2001 Elsevier Science Ltd. All rights reserved.

Keywords: *Rhus retinorrhoea*; Anacardiaceae; Biflavonoids; Biflavanone; Tetrahydroamentoflavone; Antimicrobial activity; Antimalarial activity

1. Introduction

Rhus retinorrhoea (Anacardiaceae) is a tree growing in the southern parts of Saudi Arabia. In a previous publication dealing with its first phytochemical investigation, we reported the isolation of four flavonoids from the leaves (Mossa et al., 1996). Some species of the genus *Rhus* are used in traditional medicine either as antimicrobial concoctions (Saxena et al., 1994) or for their cytotoxic properties (Lin et al., 1989), while others display insecticidal activities against aphids (Bestman et al., 1988). Biflavonoids have been isolated from a number of *Rhus* species (Lin and Chen, 1973; Chen et al., 1974; Young, 1979; Bestman et al., 1988). Here we report the structure of a new biflavanone **4** and the known flavonoids **1**–**3**, **5**, **6** that were purified from the dichloromethane extract of the dried leaves of *R. retinorrhoea*.

2. Results and discussion

The positive ion HRESIFTMS of compound **4** displayed a peak at *m/z* 571 $[M+H]^+$ which was consistent with a molecular formula $C_{32}H_{26}O_{10}$. The IR spectrum of **4** indicated broad OH absorption bands at 3550 and 3400 cm^{-1}, while the UV spectrum showed absorption maxima at 287 and 330 nm, characteristic of a flavanone derivative (Mabry et al., 1970). The ^1H and ^{13}C NMR spectra of biflavanoid **4** at 300 K showed the typical adverse effects of restricted rotation about the interflavanyl bond. At this temperature all the proton resonances are duplicated, hence indicating the presence of two distinct rotamers. Intramolecular NOE effects between protons of the constituent flavanyl units in the vicinity of the bond axis, represent a powerful tool to identify the rotamers in such a mixture (Brandt et al., 1987). The close proximity of e.g. the 7″-OMe (D-ring) and 2-H (C-ring) resonances of the rotamers of compound **4**, however, precluded rotamer differentiation. The biflavanone skeleton of **4** was evident from the presence of two benzylic methine carbon signals [δ 78.3 (C-2″) and 79.3, 79.2 (C-2), two methylene carbon signals [δ

* Corresponding author. Tel.: +1-662-915-1005; fax: +1-662-915-1006.
E-mail address: amgalalv@yahoo.com (A.M. Galal).

0031-9422/01/$ - see front matter © 2001 Elsevier Science Ltd. All rights reserved.
PII: S0031-9422(01)00244-8

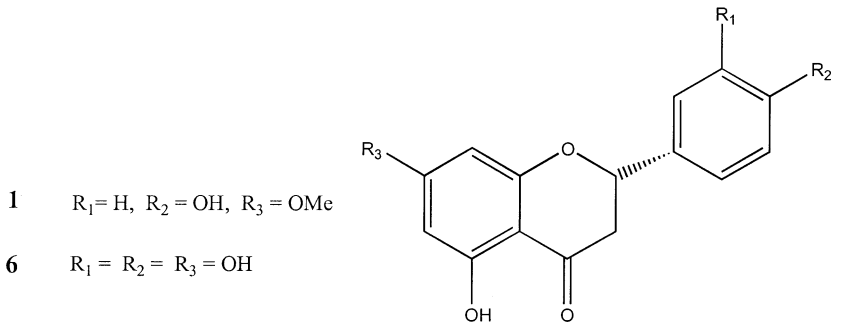

1 R_1= H, R_2 = OH, R_3 = OMe

6 R_1 = R_2 = R_3 = OH

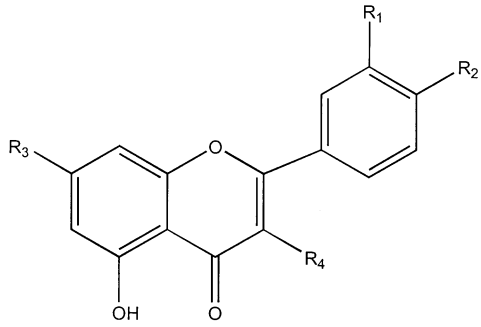

2 R_1 = R_3 =OMe, R_2 = R_4 = OH

3 R_1 = R_4 =H, R_2 =OH, R_3 = OMe

5 R_1 = R_2 = OH, R_3 = OMe, R_4 = H

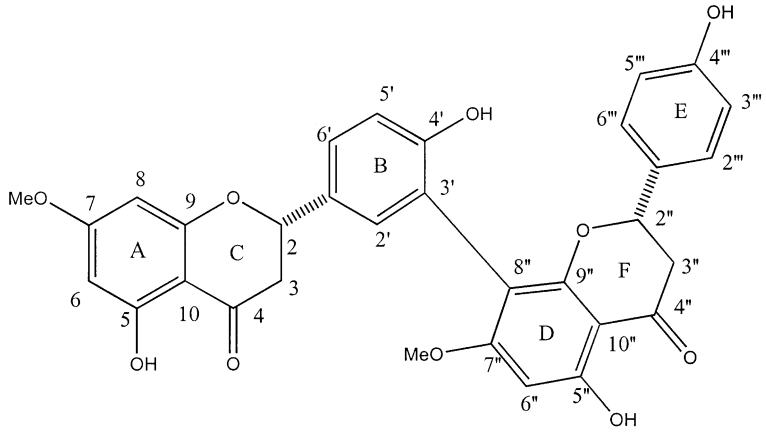

4

42.8, 42.5 (C-3) 42.1, 41.8 (C-3″) and two carbonyl carbon signals [δ 197.5, 197.4 (C-4), 198.0, 197.9, (C-4″)]. The ^{1}H NMR spectrum of **4** showed four hydroxyl signals, two are hydrogen bonded and resonate at δ 12.12, 12.10 (1H, *s*, OH-5) and 12.39, 12.37 (1H, *s*, OH-5″) and the other two non hydrogen bonded hydroxyl groups are located at δ 9.32, 9.28 (1H, *s*, OH-4′) and 9.52, 9.50 (1H, *s*, OH-4‴). The ^{1}H NMR spectrum also exhibited two methoxyl signals resonating at δ 3.77, 3.76 (3H, *s*, OMe-7), and 3.73, 3.72 (3H, *s*, OMe-7″). The location of the hydroxyl groups was defined on the basis of HMBC and ROESY correlation studies. The ^{13}C NMR spectrum exhibited two methoxyl signals at δ 56.32 (OMe-7) and 56.62 (OMe-7″), their location being assessed by the ROESY correlations. Such ROESY correlation between OMe-7, H-8 and H-6 and between OMe-7″ and H-6″ as shown in Fig. 1 strongly suggested C-8″(D-ring) as bonding site on the lower DEF flavanone unit. The carbon–carbon bond between the two flavanone moieties linking C-3′ of ring B to C-8″ of ring D was established via the following considerations; ^{1}H NMR showed a signal at δ 6.27 (1H, *s*) attributed to H-6″ which indicated the absence of proton H-8″ which in turn supported the involvement of C-8″ in the suggested linkage. The ROESY correlation between H-2 and OMe-7″ was an additional support of involvement of C-8″ in the linkage. The presence of a signal at δ 6.84 (1H, *d*, J= 8.4 Hz) attributed to H-5′ and indicated the absence of H-3′

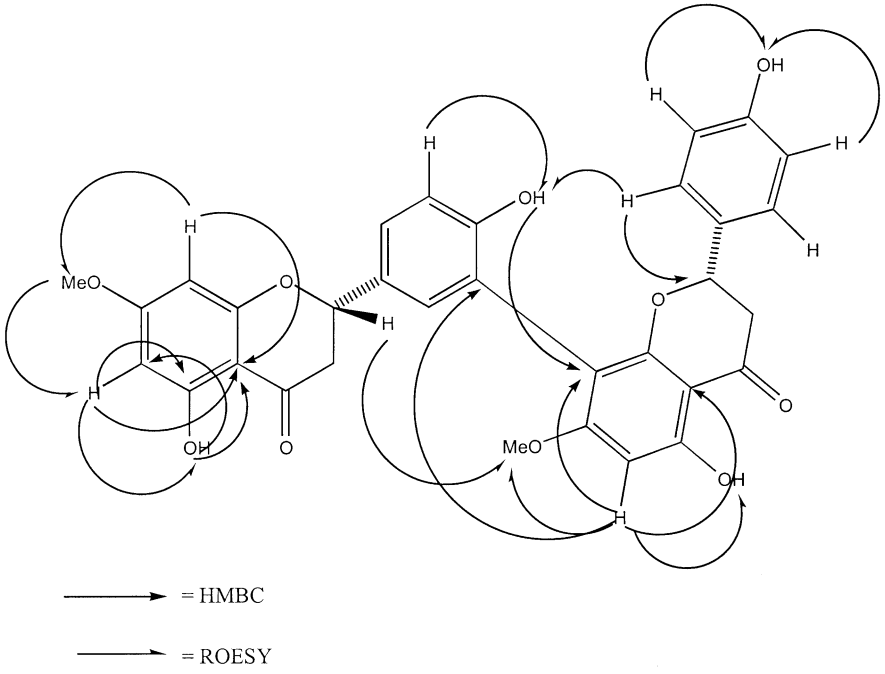

Fig. 1. Important HMBC and ROESY correlations of **4**.

and consequently suggested involvement of C-3′ in the interflavonoid linkage. The location of the linkage was confirmed by the presence of ^{2}J-HMBC correlation between H-6″ and both C-5″ and C-7″, and ^{3}J-HMBC correlation between C-6″ and both C-8″ and C-10″. In addition, there was also important ^{4}J-HMBC correlation between H-6″ and C-3′ and another between C-8″ and OH-4′.

The CD spectrum of **4** showed sequential positive and negative Cotton effects at 332 and 291 nm, respectively, which established a 2*S*, 2″*S* absolute configuration (Gaffield, 1970). Thus, on the basis of spectral analysis and comparison with published NMR spectroscopic data of closely related compounds (Markham et al., 1987), the structure of **4** was established as (2*S*,2″*S*)- 7,7″-di-*O*-methyltetrahydroamentoflavone. The identities of compounds **1**, **2**, **3, 5**, and **6** were based on comparison of their spectral data with reported values (Wagner et al., 1976; Calvert et al., 1979; Noro et al., 1983; Agrawal, 1989).

All isolated new and known compounds were tested for antimicrobial and antimalarial activity. For the antimicrobial testing, a modified microtiter-plate assay was used (National Committee for Clinical Laboratory Standards, 1997). For antimalarial testing, the method conducted is described elsewhere (Khalid A. El Sayed et al., 1996). Compound **1** showed weak antimicrobial activity against *Candida albicans, C. krusei, Staphylococcus aureus, Mycobacterium smegmatis, M. intracellulare,* and *M. xenopi* with MIC ~100 μg/ml (positive controls; nystatin for *Candida* with MIC 2.0 μg/ml, chloramphenicol for *S. aureus* with MIC 4.0 μg/ml and isoniazide for *Mycobacterium* with MIC 10.0 μg/ml). Compound **4** exhibited moderate antimalarial activity against *Plasmodium falciparum* (W2 Clone) with IC_{50} 0.98 μg/ml and weak activity against *P. falciparum* (D6 Clone) with IC_{50} 2.8 μg/ml (positive control; chloroquine with IC_{50} 0.026 and 0.238 μg/ml against D6 Clone and W2 Clone, respectively). Nevertheless, compound **4** did not display any cytotoxicity.

3. Experimental

3.1. General

IR spectra were recorded with an ATI Mattson genesis series Fourier transform (FT–IR) spectrophotometer. UV spectra were obtained on a Hewlett Packard 8452A diode array spectrophotometer. Optical rotations were recorded at ambient temperature using a JASCO DIP-370 digital polarimeter. CD spectra were recorded in MeOH at ambient temperature on a Jasco J715 spectropolarimeter. 1D and 2D NMR spectra were obtained on a Brüker Avance DRX 500 spectrometer. HRESIFTMS was obtained using a Bruker Bioapex FT–MS in ESI mode. For TLC, glass supported silica gel plates (0.25 mm layer, F_{250}, E. Merck) were used and Silica gel 60 (230–400 mesh, E. Merck) was employed for column chromatography.

3.2. Plant material

R. retinorrhoea was collected during 1993 from the southern region of Saudi Arabia. The plant was identi-

fied by Dr. Sultan-ul-Abdeen, College of Pharmacy, King Saud University. A voucher specimen is deposited at the herbarium of the College of Pharmacy, King Saud University, Riyadh, 11451, Saudi Arabia.

3.3. Extraction and isolation

Dried and ground leaves of *R. retinorrhoea* (1.4 kg) were extracted with CH_2Cl_2 in a Soxhlet apparatus. The CH_2Cl_2 extract (133 g) was partitioned between hexane and MeCN (1:1, 6 L). A portion of the MeCN extract (30 g) was applied to a Si gel column (900 g) using gradients of C_6H_6 and EtOAc(0→50%). This column yielded **1** (2.6 g), **2** (59.0 mg), **3** (342 mg), **4** (40 mg), respectively, and a mixture of two compounds (7.0 g) which was subjected to a Si gel column (360 g) chromatography using gradients of EtOAc in hexane (25→75%) then gradients of MeOH in EtOAc (5→10%) to afford compounds **5** (33 mg), and **6** (31 mg).

Compound **4** : yellow powder, amorphous. $[\alpha]_D$ −25.4 (*c* 0.024, DMSO). CD (MeOH, *c* 0.00012) $[\theta]_{332}$ 15517, $[\theta]_{291}$ 44114.4; UV λ_{max} MeOH nm (logϵ): 287 (4.68), 330 (3.20). IR ν_{max} (KBr) cm^{-1} 3350 (OH), 3400 (OH), 1660 (C=O), 1600, 1520, 1460, 1380, 1325, 1230, 1180, 1125. ^{1}H NMR (500 MHz, DMSO) δ 12.39, 12.37 (1H, *s*, OH-5″), 12.12, 12.10 (1H, *s*, OH-5), 9.52, 9.50 (1H, *s*, OH-4‴), 9.32, 9.28 (1H, *s*, OH-4′), 7.23–7.13 (4H, *m*, H-2′, H-2‴, H-6′, H-6‴), 6.84–6.81 (1H, *d*, *J*= 8.4 Hz, H-5′), 6.69–6.67 (2H, both *d*, *J*=8.4 and 8.3 Hz, H-3‴, H-5‴), 6.68 (1H, *d*, *J*= 8.3 Hz, 6.27 (1H, *s*, H-6″), 6.06–6.04 (2H, both *d*, *J*= 2.2 Hz, H-6, H-8), 5.46–5.39 (2H, *m*, H-2, H-2″), 3.77, 3.76 (3H, *s*, OMe-7), 3.73, 3.72 (3H, *s,* OMe-7″), 3.26–3.12 (2H, *m*, H-3_{ax}, H-3_{ax}″), 2.86–2.57 (2H, *m*, H-3_{eq}, H-3_{eq}), 2.65 (1H, *dd*, *J*= 17.2, 2.7 Hz, ^{13}C NMR (125 MHz, DMSO) δ 198.0, 197.9 (C-4″), 197.5, 197.4 (C-4), 167.9 (C-7), 165.8 (C-7″), 163.7 (C-5), 163.5 (C-5″), 159.4 (C-9), 158.0 (C-4‴)156.7 (C-9″), 131.9 (C-2‴), 129.4 (C-2′), 128.6 (C-1‴), 128.3 (C-1′), 127.5 (C-6′), 120 (C-3′), 115.6 (C-5‴), 115.6 (C-3‴), 115.5 (C-5′), 107 (C-8″), 103 (C-10, C-10″), 95.1 (C-6), 94.2 (C-8), 92.8 (C-6″), 79.3, 79.2 (C-2), 78.3 (C-2″), 42.8, 42.5 (C-3), 42.1, 41.8 (C-3″), 56.6 (OMe-7″), 56.3 (OMe-7). HRESIFTMS *m*/*z* $[M+1]^+$ 571.1602 (calc. 571.1604).

Acknowledgements

The authors acknowledge the United States Department of Agriculture, Agriculture Research Service Specific Cooperative Agreement No. 58-6408-7-012 for partial support of this work. The authors are also grateful to Frank T. Wiggers and Chuck Dunbar for the NMR and the HRESIFTMS analyses and John Trott for conducting the antimalarial bioassay.

References

Agrawal, P.K., 1989. Carbon-13 NMR of Flavonoids. Elsevier Science, New York.

Bestman, H.-J., Classen, B., Kobold, U., Vostrowsky, O., Klingauf. Stein, U., 1988. Steam volatile constituents from leaves of *Rhus typhina*. Phytochemistry 27, 85–90.

Brandt, E.V., Young, D.A., Young, E., Ferreira, D., 1987. Absolute configuration of atropisomeric *m*-terphenyl type flavan-3-ols. Journal of the Chemical Society, Perkin Transaction 2, 1365–1368.

Calvert, D.J., Cambie, R.C., Davis, B.R., 1979. Carbon-13 spectra polymethoxy- and methylene dioxyflavonols. Organic Magnetic Resonance 12, 583–586.

Chen, F.C., Lin, Y.M., Wu, J.C., 1974. Rhusflavone: a new flavanoflavone from *Rhus succedenea*. Phytochemistry 13, 1571–1574.

Gaffield, W., 1970. Circular dichroism, optical rotatory dispersion and absolute configuration of flavanones, 3-hydroxyflavanones and their glucosides. Determination of aglycone chirality in flavanone glycosides. Tetrahedron 26, 4093–4108.

Khalid, A. El Sayed D., Dunbar, C., Goins, D.K., Cordova, C.R., Perry, T.L., Wesson, K.J., Sanders, S.C., Janus, S.A., Hamman, M., 1996. The marine environment: a resource for prototype antimalarial agents. Journal of Natural Toxins 5, 261–285.

Lin, Y.M., Chen, F.C., 1973. Rhusflavanone, a new biflavanone from *Rhus succedanea*. Tetrahedron Letters 48, 4747–4750.

Lin, Y.M., Cheng, F.C., Lee, K.H., 1989. Hinokiflavone, a cytotoxic principle from *Rhus succedana* and the cytotoxicity of the related biflavonoids. Planta Medica 55, 166–168.

Mabry, T.J., Markham, K.R., Thomas, M.B., 1970. The Systematic Identification of Flavonoids. Springer, New York. p. 267.

Markham, K.R., Sheppard, C., Geiger, H., 1987. ^{13}C NMR studies on some naturally occurring amentoflavone and hinokiflavone biflavonoids. Phytochemistry 26, 3335–3337.

Mossa, J.S., Abdel Sattar, E., Abou-Shoer, M., Galal, A.M., 1996. Free flavonoids from *Rhus retinorrhoea* Steud, ex Olive. International Journal of Pharmacognosy 34, 198–201.

National Committee for Clinical Laboratory Standards, 1997. Methods for dilution. Antimicrobial susceptibility test for bacteria that grow aerobically. Approved Standard M7-A. National Committee for Clinical Laboratory Standards, Wayne, PA, 4th Edition.

Noro, T., Oda, Y., Miyase, T., Ueno, A., Fukushima, S., 1983. Inhibitors of xanthine oxidase from the flowers and buds of *Daphne genkwa*. Chemical and Pharmaceutical Bulletin 31, 3984–3987.

Saxena, G., McCutcheon, A.R., Farmer, S., Towers, G.H.N., Hancock, R.E.W., 1994. Antimicrobial constituents from *Rhus glabra*. Journal of Ethnopharmacology 42, 95–99.

Wagner, H., Chari, V.M., Sounenbichler, J., 1976. Carbon-13 NMR spectra of naturally occurring flavonoids. Tetrahedron Letters 21, 1799–1802.

Young, D.A., 1979. Heartwood flavonoids and the infrageneric relationships of *Rhus* (Anacardiaceae). American Journal of Botany 66, 502–510.

PERGAMON

Phytochemistry 58 (2001) 603–605

PHYTOCHEMISTRY

www.elsevier.com/locate/phytochem

Phenanthropyran derivatives from *Phalaenopsis equestris*

Yoshihiro Manako[a], Hitoshi Wake[b], Takashi Tanaka[c], Koichiro Shimomura[d], Kanji Ishimaru[a,*]

[a]*Department of Applied Biological Sciences, Faculty of Agriculture, Saga University, 1 Honjo, Saga 840-8502, Japan*
[b]*Central Research Laboratory, Pentel Co. Ltd., 4-1-8 Yoshi-cho, Soka-city, Saitama 340-0017, Japan*
[c]*Faculty of Pharmaceutical Sciences, Nagasaki University, 1-14 Bunkyo-chou, Nagasaki, 852-8521, Japan*
[d]*Tsukuba Medicinal Plant Research Station, National Institute of Health Sciences, 1 Hachimandai, Tsukuba, Ibaraki 305-0843, Japan*

Received 30 November 2000; received in revised form 19 April 2001

Abstract

Two phenanthropyran derivatives, 3-methoxy-2,7-dihydroxy-5H-phenanthro[4,5-*bcd*]pyran and 2,3,7-trihydroxy-5H-phenanthro[4,5-*bcd*]pyran were isolated from the orchid *Phalaenopsis equestri*. Their chemical structures were elucidated from spectroscopic (NMR, MS etc.) analyses. © 2001 Elsevier Science Ltd. All rights reserved.

Keywords: *Phalaenopsis equestris*; Orchidaceae; Phenanthropyran

1. Introduction

The secondary metabolites of the Orchidaceae plants have been intensively investigated and various constituents, such as bibenzyl (Majumder and Basak, 1991a; Majumder and Pal, 1993; Majumder et al., 1997; Leong et al., 1997), stilbenoid (Majumder and Basak, 1991b; Majumder and Ghosal, 1993, 1994; Majumder et al., 1996), phenanthrene (Majumder and Sen, 1991; Majumder and Maiti, 1989; Leong et al., 1997), dihydrophenanthrene (Leong et al., 1997) and phenanthropyran (Majumder and Sabzabadi, 1988) derivatives have been reported. The orchid plants are worldwide popular ornamentals indoors and some genera such as *Vanilla, Gastrodia, Bletilla, Dendrobium* etc. are also used as important medicinal resources (e.g. Kimura and Kimura, 1991). In the present study, the secondary metabolites of *Phalaenopsis equestris*, a most popular potting orchid in Japan, were investigated and two new phenanthropyran derivatives were isolated. Their chemical structures were established following spectroscopic analyses.

2. Results and discussion

The methanol extract of the lyophilized leaves of *Phalaenopsis equestris* was subjected to column chromatography with Sephadex LH-20 and preparative C_{18} gel to afford compounds **1** and **2**.

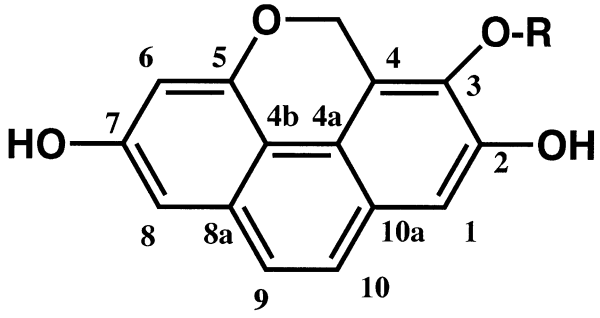

1 : R=Me
2 : R=H

Compound **1** was obtained as an off-yellow amorphous powder. The positive-ion fast atom bombardment mass spectroscopy (FAB–MS) of **1** gave a quasi-molecular ion peak at m/z 269 $[M+H]^+$, which corresponding to the molecular formula of $C_{16}H_{12}O_4$. The ^1H NMR

* Corresponding author. Fax: +81-952-28-8753.

0031-9422/01/$ - see front matter © 2001 Elsevier Science Ltd. All rights reserved.
PII: S0031-9422(01)00249-7

spectrum of **1** showed five aromatic protons; meta-coupled doublets at δ 6.61 ($J=2$ Hz) and δ 6.85 ($J=2$ Hz), ortho-coupled doublets at δ 7.50 ($J=9$ Hz) and δ 7.55 ($J=9$ Hz) and one-proton non-coupled singlet at δ 7.23 (*s*) (Table 1). Together with one low-field methylene proton signal at δ 5.62 (*d*, $J=0.7$ Hz), The ^{1}H NMR spectrum of **1** suggested the existence of 2,3,7-substituted phenanthropyran structure (Majumder and Sabzabadi, 1988). The ^{13}C NMR spectrum of **1** exhibited 14 signals (Table 2, C-1–C-10 and C-4a, C-4b, C-8a and C-10a) whose chemical shifts supported the presence of 2,3,7-substituted phenanthropyran (Majumder and Sabzabadi, 1988). The ^{1}H and ^{13}C NMR spectra of **1** also indicated the existence of one methoxyl moiety (δ 3.93 in ^{1}H NMR spectrum and δ 61.3 in the ^{13}C NMR spectrum). The carbon atoms of the aromatic methoxyl groups having at least one *ortho*-hydrogen atom appear at the expected positions (δ 54–56), while those of such groups flanked by two *ortho*-substituents were shifted downfield by 5–6 ppm (Majumder and Sabzabadi, 1988). Therefore, the methoxyl signal at δ 61.3 in ^{13}C NMR spectrum of **1** corresponded to a methoxyl group at C-3 position. The position (C-3) of the methoxyl moiety was also supported by having no observable NOE correlation cross peak between the methoxyl proton signal (δ 3.93 in ^{1}H NMR spectrum) and three aromatic proton signals (H-1, 6 and 8). From the data mentioned above, **1** was characterized as 3-methoxy-2,7-dihydroxy-5H-phenanthro[4,5-*bcd*]pyran.

Compound **2**, an off-yellow amorphous powder, exhibited $[M+H]^+$ ion peak at *m/z* 255 ($C_{15}H_{10}O_4$) in the positive-ion FAB–MS. The ^{1}H (Table 1) and ^{13}C (Table 2) NMR spectra of **2** were almost identical to those of **1**, except for the disappearance of the methoxyl signal which was observed in **1**. Therefore, **2** was concluded to be as 2,3,7-trihydroxy-5H-phenanthro[4,5-*bcd*]pyran. Both compounds are the first examples of phenanthropyrans isolated from the genus *Phalaenopsis*.

Table 1
^{1}H NMR spectral data of compounds **1** and **2** (in acetone-d_6[a], δ values)

H	1	2
1	7.23 (*s*)	7.20 (*s*)
6	6.61 (*d*, 2)	6.58 (*d*, 2)
8	6.85 (*d*, 2)	6.81 (*d*, 2)
9	7.50 (*d*, 9)	7.38 (*d*, 9)
10	7.55 (*d*, 9)	7.48 (*d*, 9)
–O–CH_2–	5.62 (*d*, 0.7)	5.58 (*br. s*)
–OMe	3.93 (*s*)	–

[a] TMS was used as the internal standard. Coupling constants (*J* in Hz) in parentheses.

Table 2
^{13}C NMR spectral data of compounds **1** and **2** (in acetone-d_6, δ values)

C	1	2
1	111.8	110.6
2	150.2	146.0
3	144.1	141.9
4	120.4	123.0
4a	118.9	120.3
4b	112.2	112.6
5	153.7	153.9
6	102.7	102.3
7	157.6	157.5
8	104.5	104.2
8a	132.2	132.4
9	126.0	124.0
10	126.5	126.6
10a	126.1	125.3
–O–CH_2–	64.8	64.8
–OMe	61.3	–

3. Experimental

3.1. General

^{1}H and ^{13}C NNR spectra were measured at 500 and 125 MHz, respectively. Column chromatography was performed on Sephadex LH-20 (Pharmacia Fine Chemical) and preparative C_{18} 125 Å (Waters) column-gels. TLC analyses was employed silica-gel plates (Merck, Kieselgel 60F254), with the mobile solvent of $CHCl_3$–MeOH (5:1). Spots of compounds on TLC plates were visualized by exposure to UV (254 nm).

3.2. Extraction and isolation

Lyophilized leaves (4.1 g) of *Phalaenopsis equestri* were mashed by a pestle and extracted with MeOH (2×200 ml, each for 2 h) at room temperature. The extract was concentrated in vacuo at 40 °C and was subjected to Sephadex LH-20 column chromatography eluted with 60% aqueous MeOH to afford three fractions (Fr. 1–3). Fr. 1 was applied to preparative C_{18} 125 Å using H_2O–MeOH (1:0–2:3) elution solvent to afford compound **1** (3.8 mg). Fr. 3 was also purified by Sephadex LH-20 (EtOH–90% aqueous EtOH) to afford compound **2** (4.6 mg).

3.2.1. Compound *1*

An off-yellow amorphous powder, ^{1}H and ^{13}C NMR spectral data of **1**, see Tables 1 and 2. Positive FABMS *m/z* (rel. int.); 269 $[M+H]^+$ (60), (Found: C, 71.32; H, 4.29. $C_{16}H_{12}O_4$ requires: C, 71.64; H, 4.48%).

3.2.2. Compound *2*

An off-yellow amorphous powder, ^{1}H and ^{13}C NMR spectral data of **2**, see Tables 1 and 2. Positive FABMS *m/z* (rel. int.); 255 $[M+H]^+$ (12), (found: C, 70.55; H, 3.88. $C_{15}H_{10}O_4$ requires: C, 70.87; H, 3.94%).

Acknowledgements

This work was supported, in part, by a subsidy from the Ministry of Health and Welfare, Science Research Fund Subsidy granted to the Japan Health Sciences Foundation.

References

Kimura, K., Kimura, T., 1991. Medicinal Plants of Japan in Color (5th printing). Hoikusha Publishing Co. Ltd., pp. 277-280.

Leong, Y.W., Kang, C.C., Harrison, L.J., Powell, A.D., 1997. Phenanthrenes, dihydrophenanthrenes and bibenzyls from the orchid *Bulbophyllum vaginatum*. Phytochemistry 44 (1), 157–165.

Majumder, P.L., Basak, M., 1991a. Two bibenzyl derivatives from the orchid *Cirrhopetalum andersonii*. Phytochemistry 30 (1), 321–324.

Majumder, P.L., Basak, M., 1991b. Two stilbenoids from the orchid *Cirrhopetalum andersonii*. Phytochemistry 30 (10), 3429–3432.

Majumder, P.L., Ghosal, S., 1993. Two stilbenoids from the orchid *Arundina bambusifolia*. Phytochemistry 32 (2), 439–444.

Majumder, P.L., Ghosal, S., 1994. Two stilbenoids from the orchid *Arundina bambusifolia*. Phytochemistry 35 (1), 205–208.

Majumder, P.L., Maiti, D.C., 1989. Flaccidinin and oxoflaccidin, two phenanthrene derivatives of the orchid *Coelogyne flaccida*. Phytochemistry 28 (3), 887–890.

Majumder, P.L., Pal, S., 1993. Cumulatin and tristin, two bibenzyl derivatives from the orchids *Dendrobium cumulatum* and *Bulbophyllum triste*. Phytochemistry 32 (6), 1561–1565.

Majumder, P.L., Sabzabadi, E., 1988. Agrostophyllin, a naturally occurring phenanthropyran derivative from *Agrostophyllum khasiyanum*. Phytochemistry 27 (6), 1899–1901.

Majumder, P.L., Sen, R.C., 1991. Pendulin, a polyoxygenated phenanthrene derivative from the orchid *Cymbidium pendulum*. Phytochemistry 30 (7), 2432–2434.

Majumder, P.L., Lahiri, S., Mukhoti, N., 1996. Four stilbenoids from the orchid *Agrostophyllum khasiyanum*. Phytochemistry 42 (4), 1157–1161.

Majumder, P.L., Roychowdhury, M., Chakraborty, S., 1997. Bibenzyl derivatives from the orchid *Bulbophyllum protractum*. Phytochemistry 44 (1), 167–172.

PERGAMON

Phytochemistry 58 (2001) 607–610

PHYTOCHEMISTRY

www.elsevier.com/locate/phytochem

Flavone C-glycosides from *Scleranthus uncinatus*

Nurettin Yayli*, Hasan Seymen, Cemalettin Baltaci

Karadeniz Technical University, Faculty of Science, Department of Chemistry, 61080 Trabzon, Turkey

Received 15 November 2000; received in revised form 14 March 2001

Abstract

Two flavone C-glycosides, 5,7,4′-trihydroxy-3′-methoxyflavone-8-C-β-D-xylopyranoside-2″-*O*-glucoside, 5,7-dihydroxy-3′-methoxy-4′-acetoxyflavone-8-C-β-D- xylopyranoside-2″-*O*-glucoside and one known maltol β-D-glucopyranoside were isolated for the first time from the *Scleranthus uncinatus* and their structures deduced by high field 1D and 2D 400 MHz NMR and (+) FAB–MS spectra. © 2001 Elsevier Science Ltd. All rights reserved.

Keywords: *Scleranthus uncinatus*; Illecebraceae; Flavone C-glycosides; Chrysoeriol 8-C-D-xyloside-2″-*O*-glucoside; 5,7-Dihydroxy-3′-methoxy-4′-acetoxyflavone-8-C-xyloside-2″-*O*-glucoside

1. Introduction

The genus *Scleranthus* comprises three species of the Illecebraceae family (Davis, 1967). One species, *S. uncinatus* Schur., which is naturalized in northern Turkey (Davis, 1967) where it has been used in traditional medicine against uterine bleeding by women. The active principles of this plant are unknown but as many flavonoids are biologically active (Agrawal, 1989), it is possible that the flavonoid constituents in this plant may contribute to its therapeutic properties. As part of a phytochemical investigation of a methanolic extract of *S. uncinatus,* two new flavone C-glycosides (**1**, **2**), isomer of scoparin 2″-*O*-xyloside (Gluchoff-Fiasson et al., 1989; Chopin and Dellamonica, 1988; Harborne, 1988) and one known maltol β-D-glucopyranoside (**3**) (Tanaka et al., 1986; Numata et al., 1990) were isolated for the first time from this plant. This paper describes the isolation and identification of two new and one known compounds, **1**–**3** through spectral analyses.

2. Results and discussion

Compound **1** showed $[M+H]^+$ at *m/z* 595 (100%) in its (+)-FABMS corresponding to the molecular formula $C_{27}H_{30}O_{15}$. This was corroborated by the ^{13}C NMR spectrum, which showed signals for all the 27 carbons of the molecule. The UV spectrum, exhibited absorption maxima at 272, 305 and 338 nm, was typical of flavones with 5,7,3′,4′-tetraoxygenation (Kuo at al., 1996). A free C_5 hydroxyl was confirmed by a bathochromic shift of 42 nm in the presence of $AlCl_3$ and a free 7-hydroxyl group was indicated by a bathochromic shift (ring A) of 11 nm upon the addition of sodium acetate (Merghem et al., 1995; Kuo et al., 1996).

The ^1H NMR spectrum showed one proton singlet at δ 6.22 indicating that ring A was trisubstituted. The absence of an aromatic methine carbon signal in the range 90.0–96.0 ppm indicated that C_8 was substituted. The clear differentiation between a 5,6,7- and 5,7,8-substition-pattern on the basis of the chemical shift of the A ring methine resonance has been previously described (Markham and Chari, 1982). From HMBC data, this proton (δ 6.22) showed correlations with carbons 5 and 8 rather than with 6 and 9 and, therefore, was assigned to position 6 (Merghem et al., 1995; Pauli and Junior, 1995). Ring B showed a pattern of three one-proton signals at δ 7.50 (1H, *d*, $J=1.2$ Hz), 6.88 (1H, *d*, $J=7.2$ Hz) and 7.42 (1H, *dd*, $J=1.2$, 7.2 Hz), the multiplicity of which showed one proton coupled to the remaining two which were, in turn, not coupled to each other. The size of the coupling constants (1.2 and 7.2 Hz) is characteristic of *meta* and *ortho* couplings as found in a 3′, 4′-oxygenated flavonoids (Venturella et al., 1995; Kuo et al., 1996). In addition, signals in the ^{13}C NMR spectrum at δ 149.30 and 151.73 indicated that the oxygenated carbons are adjacent due to the shielding effect (>10) each oxygen exerts on its neighbouring ortho carbons (Agrawal, 1989,

* Corresponding author. Tel.: +462-377-2486; fax: +462-325-3195.

E-mail address: yayli@ktu.edu.tr (N. Yayli).

0031-9422/01/$ - see front matter © 2001 Elsevier Science Ltd. All rights reserved.
PII: S0031-9422(01)00289-8

Venturella et al., 1995). The presence of one methoxyl group in the molecule was indicated by a peak in the ^{1}H NMR spectrum at δ 3.96 appearing as a singlet and integrating for 3 protons and in the ^{13}C NMR spectrum as one signal at δ 56.60. This one methoxyl group was placed on carbon 3′ (149.30) based on HMBC correlations of the methoxyl group with carbon 3′ (Fig. 2). In addition, from long-range COSY connectivities (Fig.2) the positions of the methoxyl group on ring B was confirmed since cross-peaks from $H_{2'}$ to OMe and a cross NOE correlation were seen to $H_{2'}$ to the methoxyl group in the NOESY spectrum. In the ^{1}H NMR spectrum of 1, the characteristic H_3 signal of a flavone was exhibited at δ 6.53 (1H, s) and in its the ^{13}C NMR spectrum (Table 1), the presence of signals at δ 184.12 agreed with α,β-unsaturated carbonyl group in ring C (Chopin et al., 1988; Gluchoff-Fiasson et al., 1989; Pauli, and Junior, 1995; Ventutella et al., 1995; Kuo et al., 1996).

In the ^{1}H NMR, spectrum of **1** two anomeric protons appeared at δ 4.27 (1H, *d*, J= 6.0 Hz) and 5.02 (1H, *d*, J= 10.0 Hz) indicating the presence of two sugars with a β-configuration. In the ^{13}C NMR, anomeric carbons of the sugar moieties appeared at δ 105.89 and 76.04 (HMQC, HMBC) (Table 1) (Pauli and Junior, 1995). Using 1D (^{1}H, ^{13}C, DEPT) and 2D NMR (H-COSY, TOCSY, HMQC, HMBC and NOESY) data individual sugar chemical shifts were assigned as in Table 1. Therefore, it is found that one of the sugars was β-D-glucose and the other was β-D-xylose in the pyranose form. The ^{13}C NMR spectrum showed signals for xylose at δ 76.04 (C_1), 81.34 (C_2), 77.04 (C_3), 70.17 (C_4) and 72.10 (C_5) characteristic of a C-glucoside (Chopin et al., 1988; Gluchoff-Fiasson at al., 1989; Nunes at al., 1989; Pauli and Junior, 1995; Wu et al., 1997). The xylose residue was assigned to position 8 based on HMBC correlations. The ^{1}H and ^{13}C NMR data are presented in Table 1. The sugar was also analyzed on TLC after acid hydrolysis of compound **1** and was identified as glucose.

The sequence and the linkage sites of the sugar chain were subsequently confirmed by the observation of

Table 1
^{1}H and ^{13}C NMR spectral data of the flavone compounds **1** and **2** in CD_3OD

	1[a,b]		**2**[a,b]	
C No.	^{13}C, δ	^{1}H, δ	^{13}C, δ	^{1}H, δ
2	166.00		166.22	
3	104.11	6.53, *s*	104.23	6.54, *s*
4	184.12		184.15	
5	162.69		162.61	
6	100.75	6.22, *s*	100.88	6.18
7	164.66		164.66	
8	104.04		105.41	
9	156.84		156.80	
10	105.43		105.60	
1′	123.97		124.26	
2′	110.81	7.50, *d*, J=1.2 Hz	111.19	7.62, *d*, J=1.4 Hz
3′	149.30		149.41	
4′	151.73		151.79	
5′	116.72	6.88, *d*, J=7.2 Hz	116.73	6.92, *d*, J=8.4 Hz
6′	121.78	7.42, *dd*, J=1.2, 7.2 Hz	121.81	7.47, *dd*, J=1.4, 8.4 Hz
–OCH_3	56.60	3.96, s	56.70	4.00, *s*
–OAc		–	172.92	
			20.73	1.94, *s*
Xylose				
1	76.04	5.02, *d*, J=10 Hz	76.11	5.10, *d*, J=9.6 Hz
2	81.34	4.32	82.33	4.18
3	77.04	3.90	75.85	3.87
4	70.17	4.08	70.03	4.02
5	72.10	4.28	71.98	4.06
		3.88		3.82
Glucose				
1	105.89	4.27, *d*, J=6 Hz	106.13	4.27, *d*, J=7.6 Hz
2	76.04	2.90	76.11	2.90
3	77.92	3.18	77.87	3.16
4	71.74	2.92	70.61	2.92
5	75.85	3.24	74.99	3.01
6	63.05	3.38	64.57	3.72

[a] Spectra recorded in CD_3OD.
[b] Assignments based on ^{1}H, ^{13}C, DEPT, 2D-COSY, HMQC, HMBC and NOESY spectra.

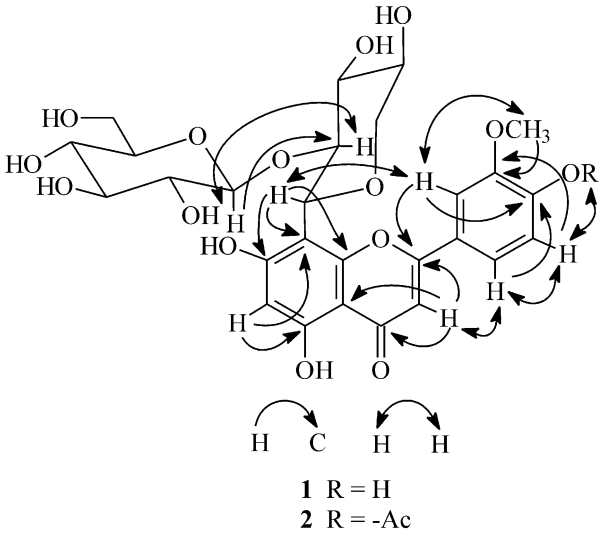

Fig. 1. Important HMBC and NOESY correlations of compounds **1** and **2**.

interresidue NOE's in NOESY between Glc H_1 with Xyl H_2 and by HMBC correlations (Fig. 1) between Glc H_1 with Xyl C_2 and Xyl H_1 with C_8 suggesting that the sacccharide chain had the structure: Glc (1→2) Xyl and this chain was attached to the C_8 of aglycone through a C-glycosidic linkage (HMBC, HMQC) (Fig. 1). Also, in the positive FAB mass spectra, the fragment at *m*/*z* 433 $[M\text{-Glucose}+H]^+$ correspond to the subsequent loss of hexose moiety at the terminal position of 1.

Based upon the above observations, the structure of the major compound **1** was established as 5,7,4′-trihydroxy-3′-methoxyflavone-8-C-β-D-xylopyranoside-2″-*O*-glucoside, which is a novel natural product and an isomer of scoparin 2″-*O*-xyloside (Chopin et al., 1988; Gluchoff-Fiasson et al., 1989).

Compound **2** showed $[M+H]^+$ at *m*/*z* 637 (100%) in its (+)-FAB–MS corresponding to the molecular formula $C_{29}H_{32}O_{16}$. Compound **2** exhibited similar NMR spectra (^1H, ^{13}C, DEPT, H-COSY, HMQC, HMBC and NOESY) (Table 1) to **1** indicating the presence of an identical flavone skeleton with a similar sugar side chain to that of **1** except for the presence of the signal for an acetyl group at the $C_{4'}$ position in ring B. In the ^1H NMR spectrum, the chemical shift for $-CH_3$ of the acetyl (δ 1.97, *s*, 3H) was indicative of acylation at $C_{4'}$. The ^{13}C NMR spectrum (Table 1) showed signals for an acetyl carbonyl carbon at δ 172.92 and methyl carbon resonance at δ 20.73, which were assigned to the $C_{4'}$ position. The site of acylation was further supported by a strong NOE observed for $H_{5'}$ with acetyl methyl protons (δ 1.97) in its NOESY spectrum (Fig. 1). Therefore, the structure of **2** was established as 5,7-dihydroxy-3′-methoxy-4′-acetoxyflavone-8-C-β-D-xylopyranoside-2″-*O*-glucoside, which is a new natural product.

The occurrence of **1**, **2** and **3** constitutes the first report of flavone C-glycosides and a maltol glycoside in the genus *Scleranthus uncinatus*.

3. Experimental

3.1. General

NMR spectra were recorded on a Varian NMR at 400 MHz instrument in CD_3OD. (+) FAB was recorded on a Zabspec MS instrument using NOBA and Glycerol matrix. UV spectra were recorded on a Shimadzu 1201. Mps were uncorr. Flash CC was performed on silica gel (230–400 mesh), PTLC was performed with precoated normal and reversed-phase silica gel RP-18 $F_{254}S$.

3.2. Plant material

Whole plants of *S. uncinatus* Schur. were collected in July 1996 at Artvin Hills (~1800 m), Turkey. A voucher specimen has been deposited in the Department of Chemistry at Karadeniz Technical University. The identification of this specious was according to Flora of Turkey (Davis, 1967).

3.3. Extraction and isolation

Dried and powdered whole plants (980 g) were successively extracted with MeOH (1 l, ×3, 24 h each). The MeOH extract was concentrated in vacuo at 30–35 °C to give a brown viscous residue (8.2 g, wet). Crude mixture (2.2 g) was subjected to flash CC on silica gel (100 g, 230–400 mesh). The column was eluted with *n*-hexane (100 ml) followed by l.c. a discontinuous gradient with *n*-hexane-$CHCl_3$ (9:1, 100 ml; 8:2, 100 ml; 7:3, 100 ml; 6:4, 100 ml), $CHCl_3$ (300 ml), $CHCl_3$–MeOH (7:1, 200 ml; 7:3, 200 ml), MeOH (200 ml) and finally with MeOH–H_2O (5:1, 200 ml) to give 13 fractions (~ 125 ml each). After TLC analysis, fractions 1–4 (fatty acid mixture called SU1), 5–8 (sugars mixture called SU2) and 9–13 (flavonoids called SU3, 220 mg) were combined. Fraction SU3 was purified by Silica gel prep. TLC using $CHCl_3$–MeOH (3:2) to give three bands (SU3A, 27 mg, $R_f=0.72$; SU3B, 147 mg, $R_f=0.48$ and SU3C, 35 mg, $R_f=0.15$, mixture). SU3A and SU3B were rechecked by reverse-phase-18 TLC in MeOH–H_2O (1:1) solvent system and found to be mixture. SU3B was rechromatographed by RP-18 PTLC using MeOH–H_2O (1:1) to give four bands; SU3BA: **3**, 7.2 mg, $R_f=0.75$; SU3BB and SU3BC contained minor unidentified compounds, $R_f=0.52$, $R_f=0.40$; SU3BD: **1**, 74 mg, $R_f=0.22$. SU3A was rechromatographed by RP-18 PTLC using MeOH–H_2O (1:1) to give two bands, SU3AA (7.8 mg, $R_f=0.35$ unidentified) and SU3AB: **2**, 17.2 mg, $R_f=0.23$.

*3.3.1. 5,7,4′-Trihydroxy-3′-methoxyflavone-8-C-β-D-xylopyranoside-2″-O-glucoside (**1**)*

Yellow amorphous crystals, mp 152–155° (dec); $[\alpha]_D$ + 71.60 °C (CH_3OH; *c* 5.14); UV λ_{max}^{MeOH} nm: 272, 305, 338; + NaOAc: 283, 299, 380; + $AlCl_3$: 280, 306, 352, 380; ^1H NMR (CD_3OD, 400 MHz) and ^{13}C NMR (CD_3OD, 100 MHz) δ (ppm) see Table 1; positive FAB–MS (NOBA) *m/z* (%); *m/z* = 595 (100) $[M+H]^+$, 565 (8), 433 (12) [M-Gluc(163) + H]$^+$, 343 (13), 313 (13), 193 (9), 179 (10).

*3.3.2. 5,7-Dihydroxy-3′-methoxy-4′-acetoxyflavone-8-C-β-D- xylopyranoside-2″-O-glucoside (**2**)*

Yellow amorphous crystals, mp 142–144° (dec); $[\alpha]_D$ + 63.04 °C (CH_3OH; *c* 0.94); UV λ_{max}^{MeOH} nm: 250, 372, 315; + NaOAc: 264, 315, 365; + $AlCl_3$: 263, 272, 280, 361; ^1H NMR (CD_3OD, 400 MHz) and ^{13}C NMR (CD_3OD, 100 MHz) δ (ppm) see Table 1; positive FAB–MS (NOBA) *m/z* (%); *m/z* = 637(100) $[M+H]^+$, 459 (8) [M-O-Gluc (179) + H]$^+$, 431 (6), 343 (7), 329 (9), 193 (6), 176 (8), 155 (14), 136 (38).

*3.3.3. Maltol β-D-glucopyranoside (**3**)*

Colorless powder, mp 106–108° (dec); identified by comparison (^1H, ^{13}C, DEPT, COSY, HMQC, HMBC and NOESY) with lit. data (Tanaka et al., 1986; Numata et al., 1990); $[\alpha]_D$ −50.0° (CH_3OH–H_2O (5 drops), 5 ml; *c* 0.36); ^1H NMR (CD_3OD, 400 MHz) δ (ppm); 6.47(H_5, *d, J* = 5.6 Hz), 7.81(H_6, *d, J* = 5.6 Hz), 2.38 (–CH_3, *s*), 5.41 ($H_{1'}$, *d, J* = 7.6 Hz), 4.18 ($H_{2'}$), 4.24 ($H_{3'}$), 4.16 ($H_{4'}$), 3.94 ($H_{5'}$), 4.32 ($H_{6'}$), 4.48 ($H_{6'}$) and ^{13}C NMR (CD_3OD, 100 MHz) δ (ppm); 161.71 (C_2), 143.04 (C_3), 175.24 (C_4), 116.65 (C_5), 155.15 (C_6), 15.26 (CH_3), 105.68 ($C_{1'}$), 75.33 ($C_{2'}$), 70.23 ($C_{3'}$), 77.95 ($C_{4'}$), 78.82 ($C_{5'}$), 62.19 ($C_{6'}$); positive FAB–MS (glycerol) *m/z* (%); *m/z* = 289 (12) $[M+H]^+$.

*3.3.4. Acid hydrolysis of **1***

Compound **1** (9 mg) was refluxed with 2 N HCl in aq. MeOH (4 ml) for 6 h. The reaction mixture was then concentrated under reduced pressure to remove MeOH. It was then diluted with H_2O (3 ml) and the aqueous layer was adjusted to pH 7 with Ag_2CO_3 and filtered. The supernatant was concentrated and compared with reference sugars on TLC (Silica gel, H_2O:MeOH:AcOH:EtOAc, 15:15:20:65). The sugars were detected by spraying the plate with a solution of aniline phthalate in BuOH which showed that the sugar in **1** was glucose.

Acknowledgements

This study was supported by a grant from Karadeniz Technical University of Türkiye and TUBİTAK NATO-B2. Thanks to Dr. J.A. Findlay, Department of Chemistry, University of New Brunswick, Fredericton, Canada for both accepting the first author as a visiting scientist and providing laboratory facilities to conduct the research. Our thanks also go to Mr. Gökhan (TUBITAK-MAM) for recording the (+) -FAB–MS spectrum.

References

Agrawal, P.K., 1989. Carbon-13 NMR of Flavonoids. Elsevier Science, Amsterdam.

Chopin, J., Dellamonica, G., 1988. In: Harborne, J.B. (Ed.), The Flavonoids. Chapman and Hall, London, pp. 63–98.

Davis, P.H., 1967. Flora of Turkey and the East Aegean Islands, Vol. 2. University Press, Edinburgh.

Gluchoff-Fiasson, K., Jay, M., Viricel, M.R., 1989. Flavone *O*- and C-glycoside from *Setaria italica*. Phytochemistry 28, 2471–2475.

Harborne, J.B., 1988. The Flavonoids. Chapman and Hall, London.

Kuo, S.H., Yen, M.H., Chung, M.I., Lin, C.N., 1996. A flavone C-glycoside and an aromatic glucoside from *Gentiana species*. Phytochemistry 41, 309–312.

Markham, K.R., Chari, V.M., 1982. In: Harborne, J.B., Marbry, T.J. (Eds.). Recent Advances in Flavonoid Research. Chapman and Hall, London, pp. 40–134.

Merghem, R., Jay, M., Viricel, M.R., Bayet, C., Voirin, B., 1995. Five 8-C-benzylated flavonoids from *Thymus hirtus* (Labiateae). Phytochemistry 38, 637–640.

Numata, A., Takahashi, C., Fujiki, R., Kitano, E., Kitajima, A., Takemura, T., 1990. Plant constituents biologically active to insects. VI. Antifeedants for larvae of the yellow butterfly, *Eurema hecabe mandarina*, in *Osmunda japonica*. Chem. Pharm. Bull. 38, 2862–2865.

Nunes, D.S., Haag, A., Bestmann, H.J., 1989. Components from the stem bark of *Dalbergia monetaria* L. Liebigs Annalen der Chemie 4, 331–335.

Pauli, G.F., Junior, P., 1995. Phenolic glycosides from *Adonis aleppica*. Phytochemistry 38, 1245–1250.

Tanaka, N., Sakai, H., Murakami, T., Saiki, Y., Chen, C.M., Iitaka, Y., 1986. Chemische und chemotaxonomische untersuchungen der Pterophyten, LXII. Chemische Untersuchungen der Inhaltsstoffe von *Arochniodes maximowiczii* OHWI. Chem. Pharm. Bull. 34, 1015–1022.

Venturella, P., Bellino, A., Marino, M.L., 1995. Three acylated flavone glycosides *Sideritis syriaca*. Phytochemistry 38, 527–530.

Wu, J.B., Cheng, Y.D., Su, L.L., Kuo, C.W., Kuo, S.C., 1997. A flavonol C-glycoside from *Moghania macrophylla*. Phytochemistry 45, 1727–1728.

PERGAMON

Phytochemistry 58 (2001) 611–613

PHYTOCHEMISTRY

www.elsevier.com/locate/phytochem

Polyphenols from *Cornulaca monacantha*

Fayez E. Kandil[a], Mary H. Grace[b,*]

[a]*Chemistry of Tanning Materials and Proteins Department, National Research Centre, Cairo, Egypt*
[b]*Chemistry of Natural and Microbial Products Department, National Research Centre, Cairo, Egypt*

Received 6 November 2000; received in revised form 28 March 2001

Abstract

The aerial parts of the Egyptian herb *Cornulaca monacantha* have yielded two new galloyltannin analogs (named monacanthin A and monacanthin B) characterized by protoctechuoyl moiety at C-6, and also a new flavonol glycoside, quercetin-4′-*O*-β-D-galactoside. The structures of the new compounds were established by conventional analytical methods and confirmed by spectral analyses. Two known flavonoids, luteolin-7-*O*-rhamnoside, luteolin-7-*O*-glucoside, and two known gallotannins, penta-*O*-galloyl-β-D-glucose and 1,2,3,6-tetra-*O*-galloyl-β-D-glucose were also isolated. © 2001 Elsevier Science Ltd. All rights reserved.

Keywords: *Cornulaca monacantha*; Chenopodiaceae; Quercetin-4′-*O*-β-D-galactoside; Gallotannins; Monacanthin A and B; Tannins

1. Introduction

Cornulaca monacantha Del. (Chenopodiaceae) is an annual herb growing wild in Egypt (Tackholm, 1974). Decoction of the leaves is used in folk medicine for treatment of jaundice (Boulos, 1983). Previous investigation of the plant revealed the presence of triterpenoid saponins (Amer et al., 1974; Dawidar et al., 1979; Kamel, et al., 2000) and the flavonoids luteolin-8-*O*-glucoside-3′-*O*-rutinoside, quercetin-3-*O*-rutinoside and quercetin-3-*O*-galactoside (Kandil and Husseiny, 1998). In the present study one new flavonol glycoside **1** and two new gallotannin compounds **4** and **5** were isolated, in addition to two known flavonoid compounds and two known gallotannins. The structures of the new compounds are elucidated in this paper.

2. Results and discussion

Three flavonoid compounds **1**–**3** and four gallotannins **4**–**7** were isolated from the ethyl acetate fraction of a 80% alcoholic extract of the aerial parts of *C. monacantha* by column chromatography on silica gel. Compound **1** was obtained as an amorphous yellow powder, which produced quercetin and galactose on acid hydrolysis. Its UV spectra with different shift reagents, before and after acid hydrolysis, suggested a flavonol glycoside with free hydroxyl groups at the 3, 5 and 7 positions and a substituted 4′ position (Mabry et al., 1970). ^{1}H NMR spectrum showed C-2′ proton signals at higher field (δ 7.50 ppm, *d*, $J = 2.5$ Hz) than C-6′ proton (δ 7.65 ppm, *dd*, $J = 8$, 2,5 Hz), indicating substitution at 4′ position. The spectrum showed also a doublet ($J = 8.5$ Hz) at δ 6.81 for H-5′. The anomeric proton of the sugar galactose appeared at δ 5.35ppm (*d*, $J = 7.5$ Hz). ^{13}C NMR confirmed the sugar as galactose and the aglycone as quercetin, except for position 4′, which showed a slight upfield shift (~0.5 ppm) compared to quercetin aglycone (Agrawal and Bansal, 1989). These results suggested that compound **1** is quercetin-4′-*O*-β-D-galactoside, a previously unreported compound. Quercetin-4′-*O*-glucoside and quercetin-4′-*O*-glucouronide have, however, been previously reported (Harborne, 1994; Kandil et al., 1997).

Compounds **2** and **3** were identified as luteolin-7-*O*-rhamnoside and luteolin-7-*O*-glucoside respectively, by acid hydrolysis, UV spectral analysis in presence of customary shift reagents and chromatography with authentic samples and spectral analysis.

Compounds **4** and **5** were both obtained as off-white amorphous powders, which gave dark blue colour with ferric chloride reagent. Both compounds produced protocatechuic acid, gallic acid and glucose on acid hydrolysis.

* Corresponding author. Fax: +202-3582253.
E-mail address: mary_grace11431@yahoo.com (M.H. Grace).

0031-9422/01/$ - see front matter © 2001 Elsevier Science Ltd. All rights reserved.
PII: S0031-9422(01)00265-5

Negative FAB mass spectrometry of compound **4** showed a molecular ion peak at *m/z* 923 [M-1] which indicated a pentagalloylglucose lacking an oxygen atom compared to penta-*O*-galloyl-D-glucose (compound **6**), which gave *m/z* 939 [M-1]. ^{1}H NMR spectrum of **4** showed spectra resembling those of penta-*O*-galloyl-D-glucose **6** (Yoshida, et al., 1984; Haslam, 1989) except for the presence of signals due to the protocatechuoyl moiety which appeared at δ 6.8 ppm (*d*, *J* = 8.5 Hz, H-5) and 7.3 ppm (*m*, H-2, 6). Based on the better resolved ^{13}C NMR spectrum of **4** (Table 1), all carbon signals of the glucose core appeared at the same position as in 1,2,3,4,6- penta-*O*-galloyl-D-glucose **6**, except for C-6, which showed a slight but significant downfield shift (0.5 ppm) indicating that the protocatechuoyl moiety is located at this position. In addition, signals due to C-5 and C-6 of the protocatechuoyl moiety appeared at 114.8 and 117.8 ppm respectively. Accordingly compound **4** has the structure of 1,2,3,4-tetra-*O*-galloyl-6-*O*-protocatechuoyl-β-D-glucose and was named monacanthin A as an unreported natural product.

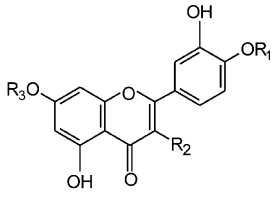

Compound **1**: R_1 = Galactose, R_2 = OH, R_3= H
Compound **2**: R_1 = H, R_2 = H, R_3 = Rhamnose
Compound **3**: R_1 = H, R_2 = H, R_3 = Glucose

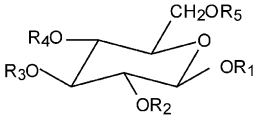

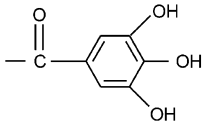

Galloyl moiety (G)

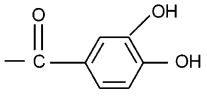

Protocatechuoyl moiety(P)

Compound **4** : R1= R2= R3= R4= G, R5= P
Compound **5** : R1= R2= R3= G, R4= H, R5 = P
Compound **6**: R_1= R_2= R_3= R_4= R_5= G
Compound **7**: R_1= R_2= R_3= R_5= G, R_4= H

Negative FAB mass spectrometry of compound **5** showed a molecular ion peak at *m/z* 771 [M-1] corresponding to a tetragalloylglucose lacking one oxygen atom (tetra-*O*-galloyl-D-glucose **7** isolated from this plant showed *m/z* 787 [M-1]). The well resolved ^{13}C NMR spectrum (Table 1) was very close to those of 1,2,3,6-tetra-*O*-galloyl-D-glucose **7** except for the presence of signals due to protocatechuoyl moiety. Signals for C-3 and C-5 of the glucose appeared at δ 76.1, together with the signal at δ 69.5 are typical for a free hydroxyl group at C-4 (Kandil et al., 1996). ^{13}C NMR showed a downfield shift (0.4 ppm) of the C-6 signal of the sugar moiety, which indicated the occupation of the protocatechuoyl moiety at this position. Accordingly compound **5** was characterized as 1,2,3-tri-*O*-galloyl-6-*O*-protocatechuoyl-β-D-glucose and is named monacanthin B as a new natural compound.

Table 1
^{13}C NMR data of compounds **4**–**7** (125 MHz, Me_2CO-d_6, TMS)

C	4	5	6	7
1	93.4	93.4	93.4	93.6
2	72.0	72.1	71.9	71.9
3	73.5	76.1	73.5	76.1
4	69.5	69.5	69.5	69.5
5	74.1	76.2	74.1	76.1
6	63.4	63.8	62.9	63.4
Galloyl				
−COO	165.0–167.0	165.0–167.0	165.0–167.0	165.0–167.0
C-2, 6	110.1	110.1	110.1	110.1
C-3, 5	146.0	146.0	146.0	146.0
C-1	121.0	121.0	121.0	121.0
C-4	139.4	139.4	139.4	139.4
Protocatechuoyl moiety				
−COO	166.0	166.0	–	–
1	121.0	121.0	–	–
2	110.1	110.1	–	–
3	146.0	146.0	–	–
4	151.5	151.5	–	–
5	114.8	114.8	–	–
6	117.8	117.8	–	–

Compounds **6** and **7** were identified as penta-*O*-galloyl-β-D-glucose and 1,2,3,6-tetra-*O*-galloyl-β-D-glucose respectively, through acid hydrolysis, chromatography with authentic samples, ^{1}H and ^{13}C NMR analysis.

3. Experimental

3.1. Plant material

Aerial parts of *Cornulaca monacantha* Del. were collected from desert areas around Cairo during December 1997. A voucher specimen of the plant was kindly identified by Dr. Loutfy Boulos, Professor of Botany, National Research Center, Cairo.

3.2. Extraction and isolation

Fresh aerial parts (1 kg) were extracted with 80% ethanol. After evaporation, the remaining aq. sol. was extracted with ether, then with ethyl acetate. The ethyl acetate soluble fraction was fractionated applying vacuum liquid

chromatography technique using column 8 cm height×12 cm i.d. packed with silica gel (40–63 μm Merck). Elution was performed using ethyl acetate and increasing amounts of a mixture of MeOH–H_2O (1:1). Twenty fractions were collected dried and subjected to repeated purification on columns of Sephadex LH-20 to give compounds: **1** (15 mg), **2** (30 mg), **3** (25 mg), **4** (25 mg), **5** (15 mg), **6** (30 mg) and **7** (15 mg).

3.3. Quercetin-4′-O-D-galactoside *1*

Yellow powder, R_f PC: 0.55 (*n*-BuOH–HOAc–H_2O 4:1:5), 0.35 (15% HOAc). UV λ_{max} (MeOH) 257, 356, (NaOMe) 268, 390 (decrease in intensity), (NaOAc) 270, 369, ($AlCl_3$) 270, 425, ($AlCl_3$ + HCl) 260, 356. ^{1}H NMR (360 Hz, DMSO-d_6), δ: 7.65 (*dd*, J=8.5, 2.5 Hz, H-6′), 7.5 (*d*, J=2.5 Hz, H-2′), 6.81 (*d*, J=8.5 Hz, H-5′), 6.40 (*d*, J=2.5 Hz, H-8), 6.20 (*d*, J=2.5 Hz, H-6), 5.35 (*d*, J=7.5, H-1″-gal.), 3.65 (*d*, J=5Hz, H-2″-gal.). ^{13}C NMR 177.5 (C-4), 164.2 (C-7), 161.0 (C-5), 156.2 (C-2, 9), 148.5 (C-4′), 144.5 (C-3′), 133.5 (C-3), 121.9 (C-6′), 121.2 (C-1′), 116.0 (C-5′), 115.5 (C-2′), 104.0 (C-10), 102.0 (C-1″), 98.2 (C-6), 93.7 (C-8), 76.0 (C-5″), 73.3 (C-3″), 71.5 (C-2″), 68.0 (C-4″), 60.0 (C-6″).

3.4. Monacanthin A *4*

1,2,3,4-Tetra-O-galloyl-6-*O*-protocatechuoyl-β-D-glucose. Negative FAB–MS *m*/*z* 923 [M-1] calc. for $C_{41}H_{31}O_{25}$. ^{1}H NMR (360 Hz, Me_2CO-d_6), glucose moiety: δ 6.4 (1H, *d*, J=7.5 Hz, H-1), 6.10 (1H, *t*, J=7.5 Hz, H-3), 5.7 (2H, *m*, H-2, 4), 4.55 (1H, *m*, H-5), 4.40(1H, *m*, H-6), galloyl moieties: δ 7.00–7.2 (*m*, H-2, 6), protocatechuoyl moiety: δ 6.8 ppm (*d*, J=8.5 Hz, H-5) and 7.3 ppm (*m*, H-2, 6).

3.5. Monacanthin B *5*

1,2,3-Tri-*O*-galloyl-6-*O*-protocatechuoyl-β-D-glucose. Negative FAB–MS *m*/*z* 771 [M-1] calc. for $C_{34}H_{27}O_{21}$. ^{1}H NMR (360 Hz, Me_2CO-d_6), glucose moiety: δ 6.25 (1H, *d*, J=8 Hz, H-1), 5.7 (1H, *t*, J=8 Hz, H-3), 5.5 (1H, *t*, J=8, H-2), 4.66 (1H, *m*, H-6), 4.20 (2H, *m*, H-4, 5), galloyl moieties: δ 7.00–7.2 (*m*, H-2, 6), protocatechuoyl moiety: δ 6.8 ppm (*d*, J=8.5 Hz, H-5) and 7.3 ppm (*m*, H-2, 6).

References

Agrawal, P.K., Bansal, M.C., 1989. C-13 NMR of flavonoids. In: Agrawal, P.K. (Ed.), Studies in Organic Chemistry. Vol. 39. Elsevier, Amsterdam.

Amer, M.A., Dawidar, A.M., Fayez, M.B., 1974. Constituents of local plants. XVII. The triterpenoid constituents of *Cornulaca monacantha*. Planta Med. 26 (3), 289.

Boulos, L., 1983. Medicinal Plants of North Africa. Reference Publications, Algonac, MI.

Dawidar, A.M., Reisch, J., Amer, M.H., 1979. Structure of manevalic and azizic acids, two new triterpenes from *Cornulaca monacantha*. Chem. Pharm. Bull. 27, 2938.

Harborne, J.B., 1994. The Flavonoids. Advances in Research Since 1986. Chapman & Hall, London.

Haslam, E., 1989. Plant Polyphenols. Cambridge University Press, Cambridge.

Kamel, M.S., Othani, K., Hassanean, H.A., Khalifa, A.A., Kasai, R., Yamaskaki, K.K., 2000. Triterpenoidal saponins from *Cornulaca monacantha*. Pharmazie 55, 460.

Kandil, F.E., Husseiny, H.A., 1998. A new flavonoid from *Cornulaca monacantha*. Oriental J. Chem. 14 (2), 215.

Kandil, F.E., El-Sayed, N.H., Micheal, H.N., Ishak, M.S., Mabry, T.J., 1996. Gallotannins and flavonoids from *Haematoxylon campechianum*. Phytochemistry 42, 1243.

Kandil, F.E., El-Sayed, N.H., Micheal, N.N., Ishak, M.S., Mabry, T.J., 1997. New flavonoids from *Psidium guava* leaves. Asian J. Chem. 9 (4), 871.

Mabry, T.J., Markham, K.R., Thomas, M.B., 1970. he Systematic Identification of Flavonoids. Springer, Berlin.

Tackholm, V., 1974. Student Flora of Egypt. Cairo University Press, Cairo, Egypt.

Yoshida, T., Hatano, T., Okuda, T., Usman-Memon, U., Shingu, T., Inoue, K., 1984. Spectral and chromatographic analysis of tannins. 1. ^{13}C NMR spectra of hydrolysable tannins. Chem. Pharm. Bull. 32, 1790.

PERGAMON

Phytochemistry 58 (2001) 615–618

PHYTOCHEMISTRY

www.elsevier.com/locate/phytochem

Phenylpropanoid glucosides from *Chrozophora obliqua*

Khaled M. Mohamed

Department of Pharmacognosy, Faculty of Pharmacy, Assiut University, Assiut 71526, Egypt

Received 10 October 2000; received in revised form 15 May 2001

Abstract

From the aerial parts of *Chrozophora obliqua*, two phenylpropanoid glucosides: 4-*O*-methyl guaiacylglycerol 9-*O*-β-glucopyranoside (**1**) and 4-*O*-methyl guaiacylglycerol 8-*O*-β-glucopyranoside (**2**) together with syringin, benzyl alcohol glucoside, isorhamnetin-3-*O*-β-glucopyranoside-7-*O*-α-rhamnopyranoside and quercetin-3-*O*-β-glucopyranoside-7-*O*-α-rhamnopyranoside have been isolated. The structures of the isolated compounds were verified by means of MS and NMR spectral analyses. © 2001 Elsevier Science Ltd. All rights reserved.

Keywords: Chrozophora obliqua Vahl.; Euphorbiaceae; Phenylpropanoid glucosides

1. Introduction

It was reported that *Chrozophora obliqua* is a potent hypoglycemic agent (Kamel, 1991). From the genus *Chrozophora*, the coumarin scopoletin, the alkaloid ricinine (Abdel-Sattar, 1985), flavonoids (Abdel-Sattar, 1985; Hashim et al., 1990), xanthones and chromones (Agrawal and Singh, 1988) were reported. From *C. obliqua*, dolabellane diterpenes have been isolated (Mohamed et al., 1994, 1995). The present study deals with the isolation and structure elucidation of two new phenylpropanoid glucosides (**1**) and (**2**) in addition to the known compounds syringin (**3**), benzyl alcohol glucoside (**4**), isorhamnetin-3-*O*-β-glucopyranoside-7-*O*-α-rhamnopyranoside (**5**) and quercetin-3-*O*-β-glucopyranoside-7-*O*-α-rhamnopyranoside (**6**).

2. Results and discussion

The dried methanolic extract of the aerial parts of *C. obliqua* was suspended in water and partitioned with ethyl acetate. The aqueous layer was subjected to column chromatography on Diaion HP-20 and the 50% methanolic eluate was repeatedly chromatographed on columns of silica gel, reversed phase RP-18 and finally on HPLC to afford six glycosides.

The molecular formula $C_{17}H_{26}O_{10}$ of compound **1** was deduced from HR FAB–MS spectrometry (see Experimental section). The ^{13}C NMR including DEPT mode measurements and ^{1}H NMR spectra of **1** (Tables 1 and 2) displayed signals at δ_C 104.1 with δ_H 4.08 (1H, *d*, $J=7.9$ Hz) corresponding to the anomeric carbon and proton of a β-glucopyranosyl unit (Bradbury and Jenkins, 1984). Enzymatic hydrolysis of **1** with β-glucosidase enzyme afforded glucose and an aglycone **1a**. The ^{1}H NMR spectrum of **1a** (Table 2) showed the presence of signals corresponding to two oxygenated methines at δ_H 4.40 (1H, *d*, $J=5.3$ Hz, H-7) and 3.44 (1H, *m*, H-8), two protons of a hydroxymethyl at δ_H 3.13 and 3.29 (each 1H, *m*, H-9), three ABX aromatic protons at δ_H 6.87 (1H, *d*, $J=1.7$ Hz, H-2), 6.84 (1H, *d*, $J=8.1$ Hz, H-5) and 6.79 (1H, *dd*, $J=1.7$, 8.1 Hz, H-6) and two methoxyl groups at δ_H 3.67 and 3.68 (each 3H, *s*). The ^{13}C NMR spectral data of **1a** (Table 1) including DEPT mode measurements exhibited eleven carbon signals comprising three signals at δ_C 73.5 (*d*), 76.3 (*d*) and 63.1 (*t*) attributable to α-substituted glycerol moiety (Otsuka et al., 1989; Sugiyama et al., 1993), two signals at δ_C 56.1 (*q*) and 56.2 (*q*) for two methoxyl groups, three signals assigned for aromatic quaternary carbons; two of them are *ortho*-oxygenated at δ_C 148.4 (*s*) and 148.9 (*s*) and the third one at δ_C 136.0 (*s*) was assigned for C-1 and three aromatic C-H signals at δ_C 111.1 (*d*), 112.0 (*d*) and 119.7 (*d*). The above mentioned NMR data indicated clearly that **1a** is a phenylpropanoid having two methoxyl groups at C-3 and C-4. Comparison of the aforementioned data with those reported earlier (Ishimaru et al., 1987; Sugiyama et al., 1993) revealed that **1a** is 4-*O*-methyl guaiacylglycerol which is a new compound.

0031-9422/01/$ - see front matter © 2001 Elsevier Science Ltd. All rights reserved.
PII: S0031-9422(01)00262-X

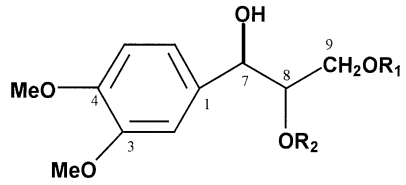

(1) R_1 = Glc, R_2 = H

(1a) R_1, R_2 = H

(2) R_1 = H, R_2 = Glc

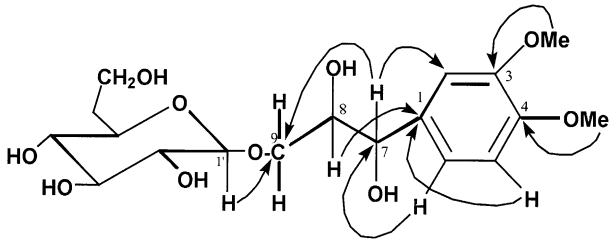

Fig. 1. Important HMBC correlations of (**1**).

Table 1
^{13}C NMR spectral data of compounds **1**, **1a** and **2** (100 MHz, DMSO-d_6)

C	1	1a	2
1	136.0, *s*[a]	136.0, *s*	134.6, *s*
2	111.3, *d*	111.1, *d*	111.2, *d*
3	148.2, *s*	148.4, *s*	148.3, *s*
4	148.7, *s*	148.9, *s*	148.8, *s*
5	111.8, *d*	112.0, *d*	111.7, *d*
6	119.2, *d*	119.7, *d*	119.2, *d*
7	72.9, *d*	73.5, *d*	72.5, *d*
8	74.1, *d*	76.3, *d*	86.9, *d*
9	71.3, *t*	63.1, *t*	61.7, *t*
MeO-(×2)	55.9, *q*, 56.0, *q*	56.1, *q*, 56.2, *q*	55.8, *q*, 55.9, *q*
1′	104.1, *d*		104.4, *d*
2′	74.4, *d*		74.3, *d*
3′	76.9, *d*		76.8, *d*
4′	70.5, *d*		70.5, *d*
5′	77.3, *d*		77.3, *d*
6′	61.5, *t*		61.5, *t*

[a] *s*: singlet, *d*: doublet, *t*: triplet, *q*: quartet.

1a was suggested to be an *erythro*-isomer on the basis of the coupling constant value 5.3 Hz of the benzylic proton H-7 signal at δ_H 4.40 (Braga et al., 1984; Hattori et al., 1987; Ishimaru et al., 1987; Miyase et al., 1987b; Hada et al., 1988). The downfield shift of the hydroxymethyl C-9 (+ 8.2 ppm) in **1** compared with its aglycone **1a** indicated clearly the attachment of the glucose moiety at C-9. The HMQC spectral analysis of **1** assigned significantly the correlations between each carbon and its directly attached protons while the interpretation of the proton–proton couplings were established by measurements of H–H COSY. The results of HMBC spectral analysis (Fig. 1) displayed correlation peaks between H-5 and C-1, H-6 and C-7, H-7 with both C-2 and C-9, H-8 and C-1 and the anomeric proton of the glucose moiety (H-1′) and C-9. From the above mentioned data, compound **1** was identified as 4-*O*-methyl guaiacylglycerol 9-*O*-β-glucopyranoside.

Table 2
^{1}H NMR spectral data of compounds **1**, **1a** and **2** (400 MHz, DMSO-d_6)

H	1	1a	2
2	6.97, *d* (1.7)[a]	6.87, *d* (1.7)	6.99, *d* (1.7)
5	6.87, *d* (8.1)	6.84, *d* (8.1)	6.86, *d* (8.1)
6	6.86, *dd* (1.7, 8.1)	6.79, *dd* (1.7, 8.1)	6.85, *dd* (1.7, 8.1)
7	4.64, *d* (4.6)	4.40, *d* (5.3)	4.47, *d* (5.6)
8	3.65, *m*	3.44, *m*	4.18, *m*
9	3.15, 3.40, *m*	3.13, 3.29, *m*	3.17, 3.39, *m*
2 x-OMe	3.72, 3.73, *s*	3.67, 3.68, *s*	3.72, 3.74, *s*
1′	4.08, *d* (7.9)		4.25, *d* (7.9)

[a] Chemical shifts in ppm, *J* values in parentheses are recorded in Hz.

The HR FAB–MS of compound **2** (see Experimental section) exhibited a molecular formula $C_{17}H_{26}O_{10}$ which is the same as that of **1**. The ^{13}C NMR spectral data of **2** (Table 1) were almost similar to those of **1** except the downfield shift of C-8 of **2** to δ_C 86.9 (+12.8 ppm) with upfield shifts of C-7 to δ_C 72.5 (−0.4 ppm) and C-9 to δ_C 61.7 (−9.6 ppm) when compared with the corresponding shifts of **1**. These data indicated that the glucose moiety of **2** should be linked to the hydroxyl group of C-8. From the ^{1}H NMR spectral data of **2** (Table 2), the coupling constant value 5.6 Hz of the H-7 signal at δ_H 4.47 suggested **2** to be an *erythro*-isomer as **1** and **1a** (Braga et al., 1984; Hattori et al., 1987; Ishimaru et al., 1987; Miyase et al., 1987b; Hada et al., 1988). Enzymatic hydrolysis of **2** with β-glucosidase enzyme provided glucose and the aglycone **1a**. Consequently, compound **2** was characterized as 4-*O*-methyl guaiacylglycerol 8-*O*-β-glucopyranoside.

Compounds **3** and **4** were identified as syringin (Sugiyama et al., 1993) and benzyl alcohol glucoside (Miyase et al., 1987a) respectively by comparison of their physical properties, ^{13}C and ^{1}H NMR spectral data with those reported earlier. The structures of compounds **5** and **6** were determined as isorhamnetin-3-*O*-β-glucopyranoside-7-*O*-α-rhamno-pyranoside and quercetin-3-*O*-β-glucopyranoside-7-*O*-α-rhamno-pyranoside respectively from the results of their FAB–MS, ^{13}C and ^{1}H NMR spectral analyses and by comparison with previously reported data (Mabry et al., 1970; Markham et al., 1978; Harborne and Mabry, 1982; Agrawal, 1989; Nakano et al., 1989).

Compounds **1** and **2** are new natural products while compounds **3**–**6** are isolated for the first time from the genus *Chrozophora*.

3. Experimental

^{1}H and ^{13}C NMR (TMS as int. standard) : 400 and 100 MHz, respectively were recorded on a Jeol JNM α-400 spectrometer. FAB MS were taken on a Jeol JMS-SX 102 spectrometer by direct inlet method at an ionizing voltage of 70 eV. Optical rotations were measured with a Union PM-1 digital polarimeter. HPLC: D-ODS-5 column (20 mm i.d.×25 cm, YMC) with UV detector; flow rate of mobile phase 6 ml/min, injection vol. 0.8–1.0 ml. CC: Kieselgel 60 (70–230 mesh, Merck) and Diaion HP-20 (Mitsubishi). TLC: silica gel 60 precoated plates, F-254 and HPTLC using RP-18 precoated plates, F-254 s (Merck).

3.1. Plant material

Aerial parts of *Chrozophora obliqua* Vahl. (Tackholm, 1974) were collected from North Sinai, Egypt, in April 1998. The plant was identified by Prof. A. Fayed, Dept. of Botany, Fac. of Science, Assiut Univ., Assiut, Egypt. A voucher specimen was deposited at the Herbarium of Dept. of Pharmacognosy, Fac. of Pharmacy, Assiut Univ., Assiut, Egypt.

3.2. Extraction and isolation of compounds (*1*–*6*)

Air-dried and powdered aerial parts (800 g) were extracted three times by maceration with MeOH at room temp. The solvent free residue (120 g) was suspended in H_2O and partitioned with EtOAc. The aq. fr. (48 g) was applied to a column of Diaion HP 20 and eluted with H_2O, 50% MeOH and MeOH successively. The 50% MeOH eluate (6.2 g) was chromatographed on silica gel column using $CHCl_3$–MeOH (7:3) and $CHCl_3$–MeOH–H_2O (7:3:1, lower layer), (13:7:1) and (6:4:1) successively to give 7 fractions. Fraction 2 (620 mg) eluted with $CHCl_3$–MeOH (7:3) was subjected to RP-18 CC using 40% MeOH to give compounds **5** (453 mg) and **6** (16 mg). Fraction 3 (82 mg) eluted with $CHCl_3$–MeOH–H_2O (7:3:1, lower layer) was applied on RP-18 CC using 35% MeOH to afford compounds **3** (30 mg) and **4** (38 mg). Fraction 4 (39 mg) eluted with $CHCl_3$–MeOH–H_2O (13:7:1) was separated by HPLC using ODS column and 30% MeOH as a solvent system to afford compounds **1** (21 mg) and **2** (6 mg).

3.2.1. Compound (*1*)

4-*O*-Methyl guaiacylglycerol 9-*O*-β-glucopyranoside, white amorphous powder, $[\alpha]_D^{21}$ −48.8°C (MeOH; *c* 0.8), R_t 33 min (ODS, 30% MeOH). HR FAB–MS (negative) *m/z*:389.1481 [M–H]$^-$ $C_{17}H_{25}O_{10}$ (req. 389.1448). ^{13}C and ^{1}H NMR (DMSO-d_6): Tables 1 and 2.

3.2.2. Compound (*2*)

4-*O*-Methyl guaiacylglycerol 8-*O*-β-glucopyranoside, white amorphous powder, $[\alpha]_D^{21}$ −42.5 °C (MeOH; *c* 0.4), R_t 35 min (ODS, 30% MeOH). HR FAB–MS (negative) *m/z*:389.1432 [M–H]$^-$ $C_{17}H_{25}O_{10}$ (req. 389.1448). ^{13}C and ^{1}H NMR (DMSO-d_6): Tables 1 and 2.

3.3. Enzymatic hydrolysis of *1* and *2*

Compound **1** (10 mg) was mixed with a soln of β-glucosidase (50 mg) in 5 ml acetate buffer (pH 5.0) and the mixture was incubated with stirring at 37 °C for 48 h. The reaction mixt. was then extracted with Et_2O (4×20 ml). The combined Et_2O layers were evapd and the residue was repeatedly crystallized from MeOH to yield aglycone **1a** (4.3 mg) as colourless crystals, mp 171–172°, $[\alpha]_D^{21}$ −32.1°C (MeOH; *c* 0.28). ^{13}C and ^{1}H NMR (DMSO-d_6 Tables 1 and 2). In the aq. phase, glucose was identified by TLC comparison with authentic substance. A sample of compound **2** (4 mg) was hydrolysed by β-glucosidase in the same way as **1** to give **1a** (1.4 mg).

References

Abdel-Sattar, E.A., 1985. A Pharmacognostical Study of *Chrozophora plicata* (Vahl.) Growing in Egypt. MSc thesis, Faculty of Pharmacy, Cairo University, Cairo, Egypt.

Agrawal, A., Singh, J., 1988. Glycosides of two xanthones and a chromone from roots of *Chrozophora prostrata*. Phytochemistry 27, 3692–3964.

Agrawal, P.K., 1989. Carbon-13 NMR of Flavonoids. Elsevier, Amsterdam, Oxford, New York, Tokyo.

Bradbury, J.H., Jenkins, G.A., 1984. Determination of the structures of trisaccharides by ^{13}C-NMR spectroscopy. J. Carbohydr. Res. 126, 125–156.

Braga, A.C.H., Zacchino, S., Badano, H., Sierra, M.G., Ruveda, E.A., 1984. ^{13}C NMR spectral and conformational analysis of 8-*O*-4′ neolignans. Phytochemistry 23, 2025–2028.

Hada, S., Hattori, M., Tezuka, Y., Kikuchi, T., Namba, T., 1988. New neolignans and lignans from the aril of *Myristica fragrans*. Phytochemistry 27, 563–568.

Harborne, J.B., Mabry, T.J., 1982. The Flavonoids Advances in Research. Chapman & Hall, London, New York.

Hashim, O.K., Abou-Zaid, M.M., Abdel-Galil, F.M., Saleh, N.A.M., 1990. The flavonoids of Egyptian *Chrozophora* species. Biochem. Syst. Ecol. 18, 151–152.

Hattori, M., Hada, S., Shu, Y., Kakiuchi, N., Namba, T., 1987. New acyclic bis-phenylpropanoids from the aril of *Myristica fragrans*. Chem. Pharm. Bull. 35, 668–674.

Ishimaru, K., Nonaka, G., Nishioka, I., 1987. Phenolic glucoside gallates from *Quercus mongolica* and *Q. acutissima*. Phytochemistry 26, 1147–1152.

Kamel, M.S., 1991. Study of *Balanites aegyptiaca* Del. and *Salvadora persica* L. Reputed to have Hypoglycemic Effects. PhD thesis, Faculty of Pharmacy, Assiut University, Assiut, Egypt.

Mabry, T.J., Markham, K.R., Thomas, M.B., 1970. The Systemic Identification of Flavonoids. Springer, New York.

Markham, K.R., Ternai, B., Stanley, R., Geiger, H., Mabry, T.J., 1978. Carbon-13 NMR studies of flavonoids-III. Tetrahedron 34, 1389–1397.

Miyase, T., Ueno, A., Takizawa, N., Kobayashi, H., Karasawa, H., 1987a. Studies on the glycosides of *Epimedium grandiflorum* Morr. var. *thunbergianum* (MIQ.) NAKAI. I. Chem. Pharm. Bull. 35, 1109–1117.

Miyase, T., Ueno, A., Takizawa, N., Kobayashi, H., Oguchi, H., 1987b. Studies on the glycosides of *Epimedium grandiflorum* Morr. var. *thunbergianum* (MIQ.) NAKAI. II. Chem. Pharm. Bull. 35, 3713–3719.

Mohamed, K.M., Ohtani, K., Kasai, R., Yamasaki, K., 1994. Dolabellane diterpene glucosides from *Chrozophora obliqua*. Phytochemistry 37, 495–500.

Mohamed, K.M., Ohtani, K., Kasai, R., Yamasaki, K., 1995. 3-Hydroxy-3-methylglutaryl dolabellane diterpenes from *Chrozophora obliqua*. Phytochemistry 39, 151–161.

Nakano, K., Nishizawa, K., Takemoto, I., Murakami, K., Takaishi, Y., Tomimatsu, T., 1989. Flavonol and phenylpropanoid glycosides from *Lilium cordatum*. Phytochemistry 28, 301–303.

Otsuka, H., Takeuchi, M., Inoshiri, S., Sato, T., Yamasaki, K., 1989. Phenolic compounds from *Coix lachryma*-Jobi var. *mayuen*. Phytochemistry 28, 883–886.

Sugiyama, M., Nagayama, E., Kikuchi, M., 1993. Lignan and phenylpropanoid glycosides from *Osmanthus asiaticus*. Phytochemistry 33, 1215–1219.

Tackholm, V., 1974. Student's Flora of Egypt, 2nd Editon. Cairo University Press, Cairo.

PERGAMON

Phytochemistry 58 (2001) 619–626

PHYTOCHEMISTRY

www.elsevier.com/locate/phytochem

5′,6′-Dehydroguiachrysine and 5′,6′-dehydroguiaflavine, two curarizing quaternary indole alkaloids from the stem bark of *Strychnos guianensis*

Jacques Penelle[a,*], Philippe Christen[b], Jordi Molgó[c], Monique Tits[a], Viviane Brandt[a], Michel Frédérich[a], Luc Angenot[a]

[a]*Université de Liège, Institut de Pharmacie, Service de Pharmacognosie, CHU, Tour 4, Avenue de l'Hôpital 1, B 4000 Liège, Belgium*
[b]*Université de Genève, Laboratoire de Chimie Analytique Pharmaceutique, 20 Bd d'Yvoy, CH-1211 Geneva 4, Switzerland*
[c]*Laboratoire de Neurobiologie Cellulaire et Moléculaire, UPR 9040, C.N.R.S., 1 Avenue de la Terrasse, Bâtiments 32-33, 91198 Gif sur Yvette cedex, France*

Received 2 January 2001; received in revised form 14 May 2001

Abstract

Two new quaternary indole alkaloids 5′,6′-dehydroguiachrysine (**1**) and 5′,6′-dehydroguiaflavine (**2**) were isolated from *Strychnos guianensis* stem bark. Their structures were determined by analysis of spectral data. Their inhibitory effects on neuromuscular transmission are also reported and compared to that of other quaternary alkaloids. © 2001 Elsevier Science Ltd. All rights reserved.

Keywords: *Strychnos guianensis* (Aubl.) Mart.; Loganiaceae; Quaternary indole alkaloids; Loganiaceae; 5′,6′-Dehydroguiachrysine; 5′,6′-Dehydroguiaflavine; 2D NMR; Curare

1. Introduction

In the course of our study on phytochemical investigations of the stembark of *Strychnos guianensis* (Penelle et al., 1999, 2000) the first botanically identified plant of South American curare (Bisset, 1992), we describe the isolation and structural determination of two new quaternary indole alkaloids: 5′,6′-dehydroguiachrysine (**1**) and 5′,6′-dehydroguiaflavine (**2**). Furthermore, we present the inhibitory effect of these new compounds and known compounds such as guiachrysine (**3**), guiaflavine (**4**), 9-methoxy-N_b-methylgeissoschizol (**5**) and C-alkaloid O (**6**) on neuromuscular transmission.

2. Results and discussion

After elimination of the tertiary alkaloidal fractions, the crude quaternary extract, precipitated with Mayer's reagent and converted to the chloride form, was separated by MPLC on a Lichrospher RP select B column using a gradient of MeCN (B) in an aq. soln. of heptanesulfonic acid (sodium salt) (A) adjusted to pH 2 with phosphoric acid. The initial fractions when the gradient was 25% B in A contained 5′,6′-dehydroguiachrysine (**1**) while the next fractions when the gradient was 30–35% B in A yielded 5′,6′-dehydroguiaflavine (**2**). These fractions, also containing guiachrysine (**3**) and guiaflavine (**4**), respectively, were submitted to column chromatography on cellulose and eluted with the system C of Karrer and Schmid (methyl ethyl ketone saturated with water and 1–3% MeOH) (Schmid et al., 1952) to afford pure products.

5′,6′-Dehydroguiachrysine (**1**) is an asymmetrical bisindole quaternary alkaloid that gave a blue-green color with ceric sulfate-sulfuric acid reagent, as for guiachrysine (**3**), guiaflavine (**4**), guianensine (Quetin-Leclercq et al., 1995). The orange color of **1** is consistent with its UV-visible spectrum showing maxima at 205, 258, 279, 328 and 421 nm. This highly conjugated chromophore is similar to that of **3**, but differs from it by bathochromic shifts observed in alkali. These bathochromic shifts

* Corresponding author. Tel.: +32-4-366-43-31; fax: +32-4-366-43-32.
E-mail address: jacques.penelle@ulg.ac.be (J. Penelle).

0031-9422/01/$ - see front matter © 2001 Elsevier Science Ltd. All rights reserved.
PII: S0031-9422(01)00255-2

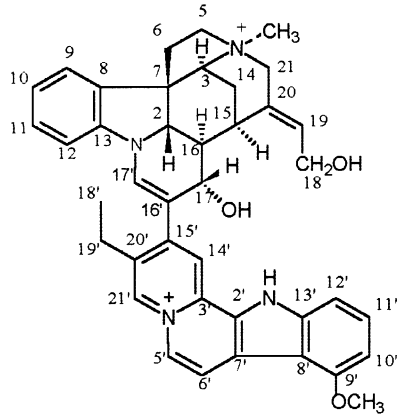

(1)

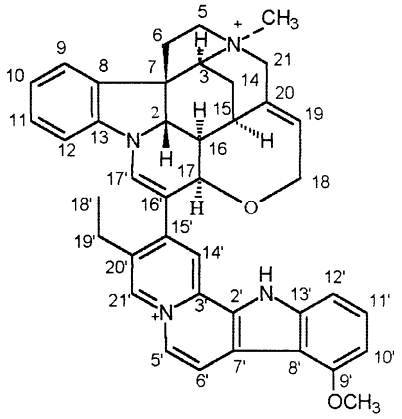

(2)

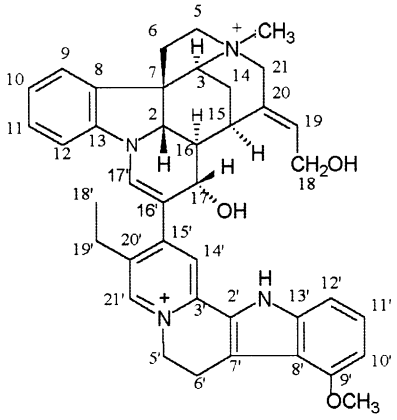

(3)

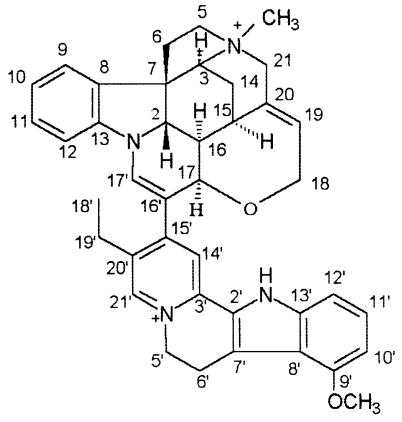

(4)

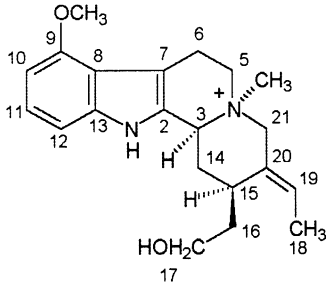

(5)

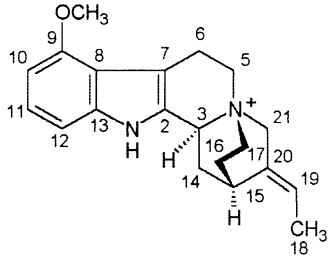

(6)

suggested an anhydronium (β-carbolinium) moiety (Gribble, 1988) as for guianensine (Quetin-Leclercq et al., 1995).

The presence of a flavopereirine-type moiety in the molecule as suggested by the UV spectra, was confirmed by ^{1}H NMR spectra. Indeed, four deshielded protons at $\delta > 8$ (two singlets and two doublets) could correspond to the pyridinium protons of rings C and D of a flavopereirine moiety (Giri et al., 1984). So, in the aromatic region of the ^{1}H NMR spectrum of **1**, two deshielded pyridine protons at δ 8.7 and 8.99, due to H-14′ and H-21′, were observed, and therefore, the shifts of C-14′ and C-21′ could be established from the HSQC spectrum at δ 121.6 and 134.8, respectively. Two other deshielded protons at δ 8.49 and 8.75 due to H-6′ and H-5′ were observed. The shifts of C-5′ and C-6′ could be established from the HSQC at δ 127.5 and 118.6, respectively. In the ^{1}H–^{1}H COSY spectrum of the aromatic region, one set of four aromatic protons was observed from an unsubstituted indole and another set of three protons from a

C-9 substituted indole nucleus was also apparent. The protons at δ 7.61 (*t*), 7.34 (*d*) and 6.91 (*d*) could be attributed to a corynanium portion of **1**. Indeed, comparison with the spectra of **3** and **4** indicated that the methoxyl group, corresponding to the three-proton singlet appearing at δ 4.14 ppm, could be at C-9 of this corynanium unit (Verpoorte et al., 1984). Consequently, the four remaining aromatic protons at δ 7.51 (*d*), 7.38 (*t*), 7.18 (*d*) and 7.04 (*t*) were assigned to a strychnan ring as for **3**. The protonated aromatic carbons were deduced by their direct correlations observed in the HSQC spectra (Table 1). In addition, the HMBC spectrum allowed the assignments made for the quaternary carbons. The H-11′ signal correlated to C-9′ and C-13′ (δ 158.0 and 144.3), while H-10′ correlated to C-8′, C-9′ and C-12′ (δ 112.8, 158.0 and 106.1). H-12′ was coupled to C-8′ and C-10′ (δ 112.8 and 102.9). Similar correlations were observed for the indoline ring: H-2, H-9 and H-11 correlated to C-13

Table 1
^{1}H and ^{13}C NMR spectral data of compound **1** (recorded in 400/100 MHz in CD_3OD)

Position	^{1}H[a]	Homonuclear correlations (H/H)	^{13}C (by HSQC and CPD)[b]	HMBC (H/C correlations)[c]
2	4.46 (*d*, 11)	16	70.2 (CH)	C-8, C-13, C-17
3	4.47	14A	73.1 (CH)	C-2, C-8
5	3.93 (*m*)	6A, 6B	65.5 (CH_2)	–
6A	2.8 (*m*)	5, 6B	39.3 (CH_2)	–
6B	2.31 (*m*)	5, 6A		–
7	–		55.8 (C)	–
8	–		132.3 (C)	–
9	7.51 (*d*)	10	124.6 (CH)	C-11, C-13
10	7.04 (*t*)	9, 11	123 (CH)	C-8, C-12
11	7.38 (*t*)	10, 12	131.2 (CH)	C-9, C-13
12	7.18 (*d*)	11	111.4 (CH)	C-8, C-10
13			146.4 (C)	–
14A	2.52	3, 14B, 15	26.1 (CH_2)	–
14B	1.95	14A		–
15	3.35 (*s*)	14A	27.5 (CH)	C-3, C-21
16	2.05 (*m*)	2, 17	49.8 (CH)	–
17	4.74 (*d*, 9.9)	16	70.3 (CH)	C-16′, C-17′, C-16
18	4.28 (*d*, 6.4)	19	58 (CH_2)	C-19, C-20
19	6.1 (*t*)	18	136.0 (CH)	C-15
20			129.7 (C)	–
21A	4.49 (*d*)	21B	65.5 (CH_2)	–
21B	4.09 (*d*, 15.8)	21A		
2′			130.9 (C)	–
3′			132.1 (C)	–
5′	8.75 (*d*, 6.7)	6′	127.5 (CH)	C-3′, C-6′, C-7′, C-21′
6′	8.49 (*d*, 6.7)	5′	118.6 (CH)	C-2′, C-5′
7′			123.6 (C)	–
8′			112.8 (C)	–
9′			158.0 (C)	–
10′	6.91 (*d*)	11′	102.9 (CH)	C-8′, C-9′, C-12′
11′	7.61 (*t*)	10′, 12′	132.1 (CH)	C-9′, C-13′
12′	7.34 (*d*)	11′	106.1 (CH)	C-8′, C-10′
13′			144.3 (C)	–
14′	8.70 (*s*)	–	121.6 (CH)	C-3′, C-16′, C-20′, C-21′
15′			149.5 (C)	–
16′			123.1 (C)	–
17′	7.38 (*s*)	–	132.7 (CH)	C-2, C-13, C-17, C-15′
18′	1.49 (*t*)	19′A, 19′B	13.6 (CH_3)	C-19′, C-20′
19′A	3.16 (*m*)	18′, 19′B	25.6 (CH_2)	C-20′
19′B	3.05 (*m*)	18′, 19′A		C-20′
20′			139.1 (C)	–
21′	8.99 (*s*)	–	134.8 (CH)	C-3′, C-5′, C-15′ C-19′, C-20′
N-CH_3	3.37	–	49.5 (CH_3)	
OCH_3	4.14	–	56.4 (CH_3)	C-9′

[a] Chemical shift (δ) in ppm from TMS, multiplicities and coupling constants in Hz are in parentheses, overlapped signal *J* unresolved.
[b] Chemical shift (δ) in ppm from TMS.
[c] Correlations from H to the indicated carbon.

(δ 146.4), while H-10 and H-12 correlated to C-8 (δ 132.3), as shown in Table 1.

Examination of its NMR spectra revealed for the corynanium portion of **1**, one methylene group at δ 25.6 corresponding to C-19′. In the ^{1}H NMR spectrum, one three-proton singlet observed at δ 3.37 corresponded to N_b-CH_3. The methylene unit H_2-19′ was clearly coupled to the methyl protons H_3-18′ (δ 1.49). In the HMBC spectrum, H_3-18′ correlated to C-19′ and C-20′ (δ 25.6 and 139.1). The other half of the structure was also deduced from NMR data. The chemical shifts of the protons and the carbons (Table 1) support the structure of a strychnan skeleton with four methylene groups (C-5, C-6, C-14 and C-21) and five methine groups (C-2, C-3, C-15 and C-17). The chemical shifts of C-18, C-19 and C-20 (δ 58, 136.0, and 129.7) were in agreement with an 18-hydroxy group and N_b-methyl as for **3**. The assignments of H-17 at δ 4.74 and C-17 at δ 70.3 were consistent with a 17-hydroxy group (Macomber, 1998). The linkage between the two moieties of 1 was deduced from the presence of a low field singlet at δ 7.38 corresponding to H-17′ (Massiot et al., 1983a). H-17′ correlated not only to C-15′ (δ 149.5) but also to C-2 (δ 70.2), C-13 (δ 146.4) and C-17 (δ 70.3). The deshielding of the isolated H-17′ enamine signal could be explained by the presence of a highly conjugated chromophore (Caprasse et al., 1984). As compared with the spectrum of strychnochrysine (Gadi-Biala et al., 1998) and **3** (Penelle et al., 2000), the C-17 signal (δ 70.3) is similar but quite different from the signal of C-17 observed for **4** (δ 79.3). This fact confirms the opening of the seven-membered ring which is observed in longicaudatine (Massiot et al., 1983b) and in **4** (Penelle et al., 1999). The signal for C-16 is shifted downfield (δ 49.8). The stereostructure still must be considered. The positive Cotton effect in the 240–250 nm region of the CD spectrum suggests the configurations of C-2β (2*S*) and C-7β (7*R*) (Klyne et al., 1966). The 15α-H (15*R*) and 3α-H (3*S*) configurations are strictly dependent on that of C-7 (Klyne et al., 1968; Klyne and Buckingham, 1974). Moreover, examination of molecular stereomodels Dreiding confirms that hypothesis. Furthermore, N_b-methyl is deduced to be α by interpretation of NOESY spectra. Indeed, a connection between the N_b-methyl and H-3 is observed. The establishment of the C-16 configuration of **1** is critical, because the influence of the tetrahydropyridinic linkage ring is difficult to determine. The large coupling constant observed between H-16 and H-2 (11 Hz) as well as the absence of connection between these protons in NOESY spectra are consistent with the configuration 16α as in isoretuline (Tavernier et al., 1978). The configuration of H-17 relative to H-16 was deduced as *trans* from the presence of a large coupling constant (10 Hz) between H-16 and H-17 in the 2D-homonuclear correlation NMR spectrum and the lack of connection in NOESY spectrum. This fact indicated an antiperiplanar position of both protons. This H-17β (17*R*) configuration is similar to that of longicaudatine Y (Massiot et al., 1983a), guianensine (Quetin-Leclercq et al., 1995), strychnochrysine (Gadi-Biala et al., 1998), 3′,4′,5′,6′-tetradehydrolongicaudatine Y (Frédérich et al., 1998) and **3** (Penelle et al., 2000) but opposite to strychnine (Blechta et al., 1994) and **4** (Penelle et al., 1999). The orientation of the side-chain is proposed to be *E*, because of the absence of connection in the NOESY spectrum between H-18 and H-21A and H-21B.

5′,6′-Dehydroguiaflavine (**2**) is also an asymmetrical bisindole quaternary alkaloid that gave a blue green color with the ceric sulfate-sulfuric acid reagent. The orange-brown color of **2** is consistent with its UV-visible spectrum showing maxima at 207, 257 and 432 nm. This highly conjugated chromophore is similar to that of **4**, but differs from it by bathochromic shifts observed in alkali. These bathochromic shifts suggested an anhydronium (β-carbolinium moiety) as for compound **1**. The presence of a 9-methoxy-flavopereirine-type moiety in the molecule, as suggested by the UV spectra was confirmed by ^{1}H and ^{13}C NMR spectra, as for compound **1** (see Table 2). The ^{1}H–^{1}H COSY spectrum of the aromatic region led us to detect one set of four benzenic protons from an unsubstituted indole and another set of three protons from 9 substituted indole nucleus. The protons at δ 7.55 (*t*), 7.3 (*m*) and 6.85 (*d*) can be attributed to the corynanium part. The four remaining aromatic protons at δ 7.53 (*d*), 7.29 (*t*), 7.08 (*d*) and 7.02 (*t*) belong to the strychnan ring. The protonated aromatic carbons were assigned by their direct correlations observed in the HSQC spectra. The HMBC spectrum confirms these attributions and allows the assignments of the quaternary carbons. Examination of NMR spectra reveals for the corynanium part, one methylene group at δ 25.3 assigned to C-19′. The methylene unit H_2-19′ was clearly coupled to the methyl protons H_3-18′ (δ 1.44). The HMBC spectrum showed H_3-18′ correlated to C-19′ and C-20′ (δ 25.3 and 138.8). The other half of the structure was also deduced from NMR data. The chemical shifts of the protons and the carbons (Table 2) support the structure of a strychnan skeleton with a N_b-methyl group (δ 55.4), four methylene groups (C-5, C-6, C-14, C-18 and C-21) and five methine groups (C-2, C-3, C-15, C-16 and C-17). The chemical shifts of the C-19–C-20 double bond (δ 137.1 and 135.1) were similar to those of strychnine methiodide (Wenkert et al., 1978) and **4** (Penelle et al., 1999). The chemical shift of H-17 at δ 5.1 is consistent with a linkage to an oxygen atom (Macomber, 1998). Moreover, H_2-18 showed long-range correlations in the HMBC spectrum to C-19, C-20 and C-17 and confirmed the presence of a seven-membered ring in **2**. The linkage between the two moieties of **2** was deduced from the presence of a lowfield singlet at δ 7.4 (Massiot et al., 1983a) which correlated to C-15′ and C-16′ (δ 149.8 and 116.4), and also to C-2 and C-17

Table 2
^1H and ^{13}C NMR spectral data of compound **2** (recorded in 500/125 MHz in CD_3OD)

Position	^1H[a]	Homonuclear correlations (H/H)	^{13}C (by HSQC and CPD)[b]	HMBC (H/C correlations)[c]
2	4.26 (*d*, 11)	16	60.6 (CH)	C6, C7, C8, C13, C16, C17
3	4.48 (*s*)	14A, 14B	76.1 (CH)	C2
5	3.9 (*m*)	6	63.6 (CH_2)	–
6A	2.35 (*m*)	5	38.6 (CH_2)	C5
6B				
7	–		54.1 (C)	
8	–		130.3 (C)	
9	7.53 (*d*)	10	124.5 (CH)	C7, C11, C13
10	7.02 (*t*)	9	123.2 (CH)	C8, C9, C12
11	7.29 (*t*)	12	131.3 (CH)	C9, C12, C13
12	7.08 (*d*)	10	111.6 (CH)	C8, C10, C13
13	–		146.5 (C)	
14A	2.77 (*d*, 15.5)	3, 14B, 15	25.7 (CH_2)	
14B	1.86 (*d*, 15.5)	3, 14A		
15	3.71 (*s*)	14A, 16, 19	31.2 (CH)	
16	1.99 (*d*, 11)	2, 15, 17	44 (CH)	
17	5.1 (*s*)	16	80.0 (CH)	
18 A	4.35 (*dd*, 7, 13.5)	18B, 19	65.4 (CH_2)	
18 B	4.15	18A, 19		C17, C19, C20
19	6.48 (*br s*)	15, 18A, 18B	137.1 (CH)	
20			135.1 (C)	
21A	4.26 (*d*, 13.4)	21 B	65.8 (CH_2)	
21B	3.98 (*d*, 13.4)	21A		C3, C5, C15
2′			130.8 (C)	
3′			131.8 (C)	
5′	8.67 (*d*, 6.6)	6′	127.3 (CH)	
6′	8.4 (*d*, 6.6)	5′	118.4 (CH)	
7′			123.4 (C)	
8′			112.7 (C)	
9′	–	–	157.9 (C)	
10′	6.85 (*d*)	11′	102.8 (CH)	C7′, C8′, C9′, C12′
11′	7.55 (*t*)	10′, 12′	132 (CH)	C9′, C13′
12′	7.3 (*d*)	11′	106.1 (CH)	C7′, C10′
13′			144.1 (C)	
14′	8.8 (*s*)		120.6 (CH)	
15′			149.8 (C)	
16′			116.4 (C)	
17′ (s)	7.4 (*s*)		134.6 (CH)	C2, C17, C15′, C16′
18′	1.44 (*t*)	19′A, 19′B	14.4 (CH_3)	C19′, C20′
19′A	3.17 (*m*)	18′	25.3 (CH_2)	C18′, C20′, C21′
19′B	3.06 (*m*)	18′		C15′, C18′, C20′, C21′
20′			138.8 (C)	
21′	8.99 (*s*)		135.6 (CH)	C3′, C5′, C15′, C19′, C20′
N-CH_3	3.49		55.4 (CH_3)	C3, C5, C21
OCH_3	4.12		56.4 (CH_3)	C9′

[a] Chemical shift (δ) in ppm from TMS, multiplicities and coupling constants in Hz are in parentheses, overlapped signal *J* unresolved.
[b] Chemical shift (δ) in ppm from TMS.
[c] Correlations from H to the indicated carbon.

(δ 60.6 and 80.0). The stereostructure still must be considered. The configuration of H-2β- (2*S*) and C-7β- (7*R*) are deduced from positive CD in the spectral region of 240–250 nm (Klyne et al., 1966). As shown by the examination of molecular stereomodels Dreiding, the H-3α (3*S*) and H-15α (15*R*) configuration are strictly dependent on the configuration of C-7 (Klyne and Buckingham, 1974). Furthermore, N_b-methyl is deduced to be α by interpretation of NOESY spectra. Indeed, a connection between the N_b-methyl and H-3 is observed. H-16α (16*R*) configuration has been deduced from the same experiments as those depicted for **1**. On the other hand, the configuration of H-17 was deduced from the presence of a very weak coupling between H-17 and H-16 in the 2D homonuclear correlation. The dihedral angle ca. 90°, observed in the dreiding stereomodel between H-16 and H-17, was in good agreement with a H-17α (17*R*) configuration as in longicaudatine (Massiot et al.,

1983b; Mukherjee et al., 1997) and **4** (Penelle et al., 1999). Moreover, a connection between these two protons is observed in NOESY spectra.

The close structural relationship of **1** and **2** to **3** and **4**, respectively, makes it necessary to suggest the possibility that **1** and **2** could be artifacts formed by dehydrogenation during work up and isolation. Little is known about the impact of storage and laboratory processing on the stability of *Strychnos guianensis* alkaloids. However, there are indications that samples of stem bark of at least some other American *Strychnos* species dried immediately after the collection retain the alkaloids well in long storage (Krukoff, 1965). In the framework of our studies, an HPLC chromatography carried out on these quaternary alkaloids indicated the same chromatographic behavior as the crude quaternary alkaloids isolated 13 years earlier (see HPLC analysis). Nevertheless, newer trials are required to fully determine the place of auto-oxidation and/or degradation of alkaloids initially present in freshly collected material, and to rule eventually out the possibility of artifact formation.

We have compared the effects of a crude quaternary extract of *Strychnos guianensis* with isolated compounds **1**–**6** as well as with a Venezuelan calabash curare (based on *Strychnos toxifera*) on neuromuscular transmission from isolated mouse hemidiaphragm preparations. Briefly, twitch height evoked by phrenic nerve stimulation (see Experimental) was evaluated before and after the addition to the medium of different concentrations of the compounds.

Although all the compounds tested induced a dose-dependent decrease in twitch height, marked differences were evident in their respective potency. The inhibitory concentration that reduced in 50% indirectly-elicited muscle contraction (IC_{50}) was calculated from the dose–response curves. Thus, Compound **3** with an IC_{50} of about 12.5 μM was found to be the most potent of the pure quaternary alkaloids isolated from *Strychnos guianensis*. The Venezuelan calabash curare was the most potent; its IC_{50} was about 6.5 μM. Compound **4** (~25.5 μM), compound **1** (~21.5 μM) and compound **2** (~24 μM) had an IC_{50} close to the IC_{50} of a crude quaternary extract of *Strychnos guianensis* (~22.5 μM). On the other hand, the monomeric alkaloids as 9-methoxy-N_b-methylgeissoschizol (**5**) and C-alkaloid O (**6**) clearly display a weaker activity than the dimeric alkaloids. Indeed, the IC_{50} of compounds **5** and **6** were near 120 and 290 μM, respectively. So the ethnobotanical use of *S. guianensis* in the preparation of arrow poisons could be partially explained by the presence of dimeric alkaloids as compounds **1**–**4**. Interestingly, 3,4-diaminopyridine (40–50 μM), after a latency of about 10–30 min, greatly augmented indirectly elicited twitches and completely reversed the neuromuscular blockade caused by the various compounds. Because 3,4-diaminopyridine is known to increase quantal acetylcholine release from motor nerve terminals (Molgo, 1982) it is deduced that the various compounds tested are competitive inhibitors of post-synaptic nicotinic acetylcholine receptors.

3. Experimental

3.1. Instruments

UV and visible spectra were recorded on a Kontron Uvikon 922 spectrophotometer. The CD spectra were measured with a Jobin Yvon CD6 dichrograph. The IR spectra were recorded as a KBr pellet on a Perkin-Elmer 1750 FTIR spectrometer. 1D and 2D NMR, ^{13}C, ^{1}H–^{13}C short- and long-range correlation HSQC, and HMBC spectra were obtained at 400/100 and 500/125 MHz on a Bruker AMX-400 and Bruker AMX-500 spectrometers. The chemical shifts are recorded in δ (ppm) based on δ TMS = 0, and the coupling constants (J) are in Hertz. The ESIMS were recorded on LC MS/MS VG Quattro 2 micromass tandem quadrupole (VG analytical, Manchester). The HRESIMS were recorded on a Q-TOF II micromass spectrometer (Manchester).

Analytical TLC was performed in precoated Si gel F_{254} (Art. 1.05735, E. Merck) plates. After development, the dried plates were examined under short-wave (254 nm) or long-wave (366 nm) UV light and sprayed with 1% ceric sulfate in 10% H_2SO_4. LiChrospher 60 RP-select B, 12 μm (Art. 1.19655.0100, E. Merck) was selected as stationnary support for the first purification, while Whatman CC31 Cellulose was used for the last purification. All solvents used were analytical grade (E. Merck).

3.2. Plant material

Stem bark of *Strychnos guianensis* (Aubl.) Mart. was collected in April, 1988 by one of us (L. A.) at Manaus, near Rio Taruma in Brazilian Amazonia. The stem bark was immediately air-dried in Brazil before being stored in Belgium at a temperature of 15 °C. Dr. A.J.M. Leeuwenberg (Wageningen) confirmed identification of the plant; voucher specimens (INPA herb. No. 150,295) are deposited at the INPA (Instituto Nacional de Pesquisas da Amazônia) at Manaus, at the Pharmaceutical Institute at Liège (Belgium), and at the Agricultural University at Wageningen (The Netherlands). Moreover, some preliminary chromatographic experiments have shown that the quaternary alkaloids gave similar and striking color reactions with respect to crude alkaloids described in the early work of Marini-Bettolo (Marini-Bettolo and Iorio, 1956).

3.3. Extraction and isolation

The powdered stem bark (600 g) was macerated for 24 h with MeOH–HOAc (99:1) and percolated with the

same mixture. After concentration of the extract under reduced pressure, precipitation by addition of H_2O and filtration, the aq. soln. was then extracted with $CHCl_3$. After separation of $CHCl_3$, the aq. soln. was basified to pH 10–11 and again extracted with $CHCl_3$. During this last operation, a ppt. was obtained. The $CHCl_3$ extracts contained tertiary alkaloids and the terminal aq. soln. quaternary alkaloids. This last soln was acidified with 5 N HCl to pH 5 and precipitated by Mayer's reagent (Evans, 1996). The ppt. was then dissolved in $Me_2CO-EtOH-H_2O$ (6:2:1) and the alkaloids converted to the chlorides by passage through an Amberlite® IRA-420 column and concentration under reduced pressure to give 6.7 g residue. A part of this residue (2 g) was chromatographed over a Lichrospher® RP-select B Merck column. The mobile phase was a mixture of two solvents; solvent A was an aq. soln. of heptanesulfonic acid (sodium salt) (1 g in 420 ml) adjusted to pH 2 with phosphoric acid, and solvent B was MeCN (Gadi-Biala et al., 1996). Because of the complexity of this extract, a linear gradient system of elution was selected: from 15 to 35% B in A. After TLC controls, using the solvent system: MeOH–25% aq. MeCOONa soln.–Me_2CO (65:35:20) (Paesen et al., 1994), the eluates of similar profiles were combined and precipitated by Mayer's reagent. Each ppt. was dissolved in $Me_2CO-EtOH-H_2O$ (6:2:1) and the alkaloids converted to the chlorides by passage through an Amberlite® IRA-420 column. Fractions containing 5′,6′-dehydroguiachrysine (12 mg) (detected when the gradient was 25% B in A) were pooled and submitted to column chromatography on cellulose, eluted with system C of Karrer and Schmid (methyl ethyl ketone saturated with water and 1–3% MeOH) (Schmid et al., 1952). This purification led to the isolation of 12 mg of pure compound **1**. Fractions containing 5′,6′-dehydroguiaflavine (**2**) (detected when the gradient was 30–35% B in A) were pooled and submitted to column chromatography on cellulose. This last purification afforded the pure compound **2** (20 mg).

3.4. Identification of compound *1*

Compound **1**: orange-brown colored amorphous powder, on TLC immediately gives a blue-green color with $Ce(SO_4)_2/H_2SO_4$; UV (MeOH) λ_{max} (nm) (log ε) 205 (4.38), 258 (4.29), 279 (4.07), 328 (3.87), 421 (3.98); (MeONa) 208 (4.33), 281 (4.21), 384 (3.92), 455 (3.72); CD_{MeOH} ($\Delta\varepsilon_{nm}$) $\Delta\varepsilon_{200}$ −7.115; $\Delta\varepsilon_{210}$ −9.59; $\Delta\varepsilon_{228}$ 0.10; $\Delta\varepsilon_{239}$ −0.85; $\Delta\varepsilon_{272}$ 4.01; $\Delta\varepsilon_{286}$ 0.40; $\Delta\varepsilon_{318}$ 8.44; $\Delta\varepsilon_{436}$ −3.06; $\Delta\varepsilon_{500}$ −0.41;IR (KBr) ν_{max} 3416, 2924, 2853, 1633, 1587, 1481, 1462, 1405, 1385, 1363, 1321, 1283, 1249, 1203, 1163, 1100, 1060, 897, 874 and 736 cm^{-1}; ^1H and ^{13}C NMR in Table 1; ESIMS m/z 626 (45) $[M]^+$ corresponding to $C_{40}H_{42}N_4O_3$, 625 (100) $[M-H]^+$, 607 (50) $[M-H-H_2O]^+$, 313 (80) $[M]^{2+}$. HRESIMS m/z 625.3179 (calc. for $C_{40}H_{41}N_4O_3$, 625.3178).

3.5. Identification of compound *2*

Compound **2**: orange-brown colored amorphous powder which gives an intense green fluorescence in MeOH at 366 nm, on TLC gives a blue–green color with $Ce(SO_4)_2/H_2SO_4$; UV (MeOH) λ_{max} (nm) (log ε) 207 (4.49), 257 (4.35), 432 (4.11); (MeONa) 207 (4.58), 259 (4.21), 284 (4.22), 392 (4.01), 454 (3.86); CD_{MeOH} ($\Delta\varepsilon_{nm}$) $\Delta\varepsilon_{200}$ −1.22; $\Delta\varepsilon_{211}$ −0.16; $\Delta\varepsilon_{216}$ −0.43; $\Delta\varepsilon_{221}$ −0.17; $\Delta\varepsilon_{225}$ −0.26; $\Delta\varepsilon_{234}$ −0.036; $\Delta\varepsilon_{248}$ −0.40; $\Delta\varepsilon_{265}$ 0.30; $\Delta\varepsilon_{289}$ −0.02; $\Delta\varepsilon_{318}$ 0.47; $\Delta\varepsilon_{351}$ 0.10; $\Delta\varepsilon_{420}$ 0.36; $\Delta\varepsilon_{500}$ 0.043; IR (KBr) ν_{max} 3409, 2965, 2927, 1641, 1583, 1481, 1461, 1402, 1351, 1258, 1201, 1100, 1030, 964, 898, 754 cm^{-1}; ^1H and ^{13}C NMR in Table 2; ESIMS m/z 608 (45) $[M]^+$ corresponding to $C_{40}H_{40}N_4O_2$, 607 (100) $[M-H]^+$, 304 $[M]^{2+}$ (18). HRESIMS m/z 607.2849 (calc. for $C_{40}H_{39}N_4O_2$, 607.3073).

3.6. Biological material

Left and right hemidiaphragm muscles with their associated phrenic nerves were isolated from Swiss–Webster mice (20–25 g) killed by dislocation of the cervical vertebrae followed by immediate exsanguination. The two hemidiaphragms were separated and each was mounted horizontally in a Rhodorsil®-lined Perspex chamber (5 ml volume). For twitch tension recordings, one of the tendons was tied with a silk thread via an adjustable stainless steel hook to an isometric transducer (FT03 Grass Instrument Division, West Warnick, RI, USA), and the other end of the hemidiaphragm muscle was pinned to the Rhodorsil-lined chamber. The phrenic nerve was stimulated at 0.1 Hz via a suction microelectrode, adapted to the diameter of the nerve, with supramaximal current pulses of 0.1 ms duration delivered through an isolation unit of a S48K Grass stimulator. The resting tension was adjusted to about 2 g for each preparation tested to obtain a maximal contractile response upon supramaximal nerve stimulation.

Nerve-evoked muscle twitch signals recorded with the isometric transducer were amplified, collected and digitized with the aid of a computer equipped with an analogue and digital I/O interface board (DT2821, Data Translation MA, USA) at a sampling rate of 2.5 kHz. Computerized data acquisition and analysis was performed with a program kindly provided by Dr. John Dempster (University of Strathclyde, Scotland).

The phrenic-nerve hemidiaphragm muscle preparation was superfused with a physiological solution of the following composition (mM) : NaCl, 154; KCl, 5; $CaCl_2$, 2; $MgCl_2$, 1; Hepes buffer, 5; glucose, 11. The solution gassed with pure O_2 had a pH = 7.4. Drugs to be tested were applied directly to the organ bath at concentrations indicated in the Results section. Usually, 10 min were allowed for drug equilibration between the different concentrations of a given compound tested.

3.7. HPLC analysis

The stationary phase was an ALTIMA C8 column (5 μm, 250×4.6) and sodium laurylsulfonate (2.18 g) in a mixture of methanol/acetonitrile/aq. soln. of potassium dihydrogen phosphate (6.82 g/l) (2:4:4) at a flow rate of 1 ml/min was used as eluent. Alkaloids were detected at 250 and 420 nm by a diode-array detector. Retentions times (in min) of alkaloids **1**–**4** appeared, respectively, at 45, 54, 39 and 46 min. The HPLC of a crude quaternary extract of *Strychnos guianensis*, obtained in 1988 and stored in a cool place, protected from light and oxygen, indicated that it contained these alkaloids because, as they were identified at each retention time, respectively.

Acknowledgements

We are indebted to Professor Burger, Dr. D. Jeannerat and Mr. A. Pinto (Department of Organic Chemistry, University of Geneva, Switzerland) for recording the NMR spectra. The allocation of time in the regional high-field NMR facilities in Lausanne-Dorigny is also gratefully acknowledged. The authors thank Professor E. De Pauw, Professor J. De Graeve, Mr. J.-C. Van Heugen (University of Liège) for providing the mass spectra and Professor P. Colson (Macromolecular Chemistry, University of Liège) for measuring the CD. This work was supported by the "Fondation Léon Frédéricq" and by the Belgian Fund for Scientific Research.

References

Bisset, N.G., 1992. Curare. In: Pelletier, S.W. (Ed.), Alkaloids: Chemical and Biological Perspectives, Vol. 8. Springer, New York, pp. 1–150.

Blechta, V., del Rio-Portilla, F., Freeman, R., 1994. Long-range carbon–proton couplings in strychnine. Magnetic Resonance in Chemistry 32, 134–137.

Caprasse, M., Angenot, L., Tavernier, D., Anteunis, M.J.O., 1984. Isolement et détermination de structure de l'afrocurarine. Planta Medica 50, 131–133.

Evans, W.C., 1996. Trease and Evans' Pharmacognosy, 14th Edition. W. B. Saunders, London, p. 573.

Frédérich, M., Quetin-Leclercq, J., Gadi Biala, R., Brandt, V., Penelle, J., Tits, M., Angenot, L., 1998. 3′,4′,5′,6′-Tetradehydrolongicaudatine Y, an anhydronium base from *Strychnos usambarensis*. Phytochemistry 48, 1263–1266.

Gadi Biala, R., Tits, M., Penelle, J., Frédérich, M., Brandt, V., Prospéri, C., Llabrès, G., Angenot, L., 1998. Strychnochrysine, a new bisindole alkaloid from the roots of *Strychnos nux-vomica*. Journal of Natural Products 61, 139–141.

Gadi Biala, R., Tits, M., Wauters, J.N., Angenot, L., 1996. A new HPLC method for the assay of alkaloids in *Strychnos nux-vomica* and *Strychnos ignatii*. Fitoterapia 62, 163–165.

Giri, V.S., Maiti, B.C., Pakrashi, C., 1984. Convenient synthesis of 6,7-dihydroflavopereirine and flavopereirine. Heterocycles 22, 233–236.

Gribble, C.W., 1988. Synthesis of zwitterionic indolo(2,3-*a*)quinolizine alkaloids. In: Atta-ur-Rahman (Ed.), Studies in Natural Products Chemistry, Vol. 1. Elsevier, Amsterdam, pp. 123–162.

Klyne, W., Buckingham, J., 1974. Absolute configurations of organic molecules. In: Atlas of Stereochemistry. Chapman and Hall, London, pp. 150–151.

Klyne, W., Swan, R.J., Bycroft, B.W., Schmid, H., 1966. Ermittlung der absoluten Konfiguration von Indolinalkaloiden durch Vergleiche der optischen Rotationsdispersionen ihrer N(*a*)-Acylderivative. Helvetica Chimica Acta 49, 833–841.

Klyne, W., Swan, R.J., Gorman, A.A., Guggisberg, A., Schmid, H., 1968. Optische Rotationdispersion von Indolinalkaloiden mit Ketogruppen. Helvetica Chimica Acta 51, 1168–1184.

Krukoff, B.A., 1965. Notes on the American species of *Strychnos* VII. Memoirs of the New York Botanical Garden 12, 11 and 43.

Macomber, R.S., 1998. Correlating proton chemical shifts with molecular structure. In: A Complete Introduction to Modern NMR Spectroscopy. John Wiley & Sons, New York, p. 68.

Marini-Bettolo, G.B., Iorio, M.A., 1956. Ricerche sugli alcaloidi curarizzanti di varie specie di Strychnos del Brasile-Nota IX. Gli alcaloidi della *S. guianensis* (Aubl.) Mart. Gazzetta Chimica Italiana 86, 1305–1323.

Massiot, G., Thepenier, P., Jacquier, M.-J., Lounkokobi, J., Mirand, C., Zèches, M., Le Men-Olivier, L., Delaude, C., 1983a. Further alkaloids from *Strychnos longicaudata* and *Strychnos ngouniensis*. Tetrahedron 39, 3645–3656.

Massiot, G., Zèches, M., Mirand, C., Le Men-Oÿivier, L., Delaude, C., Baser, K.H.C., Bavovada, R., Bisset, N.G., Hylands, P.J., Strömbom, J., Verpoorte, R., 1983b. Occurrence of longicaudatine, a new type of bis-indole base and bisor-C-alkaloid H in *Strychnos* species. Journal of Organic Chemistry 48, 1869–1872.

Molgo, J., 1982. Effects of aminopyridines on neuromuscular transmission. In: Aminopyridines and similarly drugs: effects on nerves, muscles and synapses. Advances in the Biosciences 35, 95–116.

Mukherjee, R., da Silva, T.M.S., Guiamarães, J.B.L., Oliveira, E., Keifer, P.A., Shoolery, J.N., 1997. Tertiary alkaloid fraction of *Strychnos atlantica*: confirmation of the identity and structures of indole alkaloids by high field nuclear magnetic resonance spectroscopy. Phytochemical Analysis 8, 115–119.

Paesen, J., Quintens, I., Thoithi, G., Roets, E., Reybrouck, G., Hoogmartens, J., 1994. Quantitative analysis of quaternary ammonium antiseptics using thin layer densitometry. Journal of Chromatography A 677, 377–384.

Penelle, J., Tits, M., Christen, P., Brandt, V., Frédérich, M., Angenot, L., 1999. Guiaflavine, a new bisindole quaternary alkaloid from the stem bark of *Strychnos guianensis*. Journal of Natural Products 62, 898–900.

Penelle, J., Tits, M., Christen, P., Molgo, J., Brandt, V., Frédérich, M., Angenot, L., 2000. Quaternary indole alkaloids from the stem bark of *Strychnos guianensis*. Phytochemistry 53, 1057–1066.

Quetin-Leclercq, J., Llabrès, G., Warin, R., Belem-Pinheiro, M.-L., Mavar-Manga, H., Angenot, L., 1995. Guianensine, a zwitterionic alkaloid from *Strychnos guianensis*. Phytochemistry 40, 1557–1559.

Schmid, H., Kebrle, J., Karrer, P., 1952. Über Curare-Alkaloide aus Kalebassen. Helvetica Chimica Acta 35, 1864–1879.

Tavernier, D., Anteunis, M.J.O., Tits, M., Angenot, L., 1978. The ^{1}H NMR spectra of the *Strychnos* alkaloids retuline isoretuline, and their *N*-deacetyl compounds. Bulletin de la Société de Chimie de Belgique 87, 595–607.

Verpoorte, R., van Beek, T.A., Riegman, R.L.H., Hylands, P.J., Bisset, N.G., 1984. Aromatic chemical shifts in *ar*-hydroxy- and-methoxy-substituted indole alkaloids; reference data and substituent-induced chemical shifts for ten different chromophoric groups. Organic Magnetic Resonance 22, 328–335.

Wenkert, E., Cheung, H.T.A., Gottlieb, H.E., 1978. Carbon-13 nuclear magnetic resonance spectroscopy of naturally occurring substances. 56. Strychnos alkaloids. Journal of Organic Chemistry 43, 1099–1105.

PERGAMON

Phytochemistry 58 (2001) 627–629

PHYTOCHEMISTRY

www.elsevier.com/locate/phytochem

Indolopyridoquinazoline alkaloid from *Leptothyrsa sprucei*

Xing-Cong Li[a], D. Chuck Dunbar[a], Hala N. ElSohly[a], Larry A. Walker[a,b], Alice M. Clark[c,*]

[a]*National Center for Natural Products Research, Research Institute of Pharmaceutical Sciences, School of Pharmacy, The University of Mississippi, University, MS, USA*

[b]*Department of Pharmacology, School of Pharmacy, The University of Mississippi, University, MS, USA*

[c]*Department of Pharmacognosy, School of Pharmacy, The University of Mississippi, University, MS, USA*

Received 26 September 2000; received in revised form 23 March 2001

Abstract

The indolopyridoquinazoline alkaloid, 3-hydoxyrutaecarpine, was isolated from *Leptothyrsa sprucei*, along with 8-methoxypsoralen, 5-methoxypsoralen, imperatorin, isoimperatorin, kaempferol 3-*O*-α-L-rhamnopyranoside, clematine and cnidioside B. The usefulness of the gradient ^{1}H–^{15}N HMBC NMR spectroscopy in the structure elucidation of 3-hydroxyrutaecarpine is noted.
© 2001 Elsevier Science Ltd. All rights reserved.

Keywords: *Leptothyrsa sprucei*; Rutaceae; Alkaloids; 3-Hydoxyrutaecarpine; ^{15}N NMR

1. Introduction

Leptothyrsa sprucei Hooker f. is a monotypic genus plant belonging to the family Rutaceae. A phytochemical investigation of its twigs and leaves has resulted in the isolation of a new indolopyridoquinazoline alkaloid, 3-hydoxyrutaecarpine (**1**), along with known compounds that were identified by their spectral data as 8-methoxypsoralen (Duddeck and Kasier, 1982), 5-methoxypsoralen (Duddeck and Kasier, 1982), imperatorin (Lee and Soine, 1969), isoimperatorin (Lee and Soine, 1969), kaempferol 3-*O*-α-L-rhamnopyranoside (afzelin) (Matthes et al., 1980; Fossen et al., 1999), clematine (Chen et al., 1993) and cnidioside B (Yahara et al., 1993). The structure elucidation of **1** was facilitated by the powerful gradient ^{1}H–^{15}N HMBC NMR spectroscopy (Farley et al., 1997).

2. Results and discussion

Compound **1** was obtained as colorless needles, mp 280–282°. Its molecular formula was established as $C_{18}H_{13}N_3O_2$ by a combination of high resolution ESIMS and ^{13}C NMR spectra. The presence of three nitrogens in **1** was confirmed by the ^{1}H–^{15}N HMBC experiment (Farley et al., 1997), which indirectly detected three nitrogen signals at δ 124.8, 155.0 and 224.9. The IR spectrum of **1** showed absorption of a conjugated carbonyl group at 1652 cm^{-1}. The ^{1}H NMR spectrum, supported by a DQF-COSY experiment, indicated the presence of one 1,2-substituted aromatic ring, two coupled methylenes, one 1,2,4-substituted aromatic ring and two phenolic hydroxy or amino groups (Table 1). The nine carbon signals bearing protons were determined by the HMQC experiment, which establishes one bond correlations (Table 1). The remaining nine quaternary carbon signals were assigned based on long range H/C correlations from a ^{1}H–^{13}C HMBC experiment ($J_{CH}=10$ Hz) (Table 1). With the aid of a ^{1}H–^{15}N HMBC experiment ($J_{NH}=5$ Hz), which provided one, two and three bond H/N correlations, partial structures A–C of **1** were readily constructed, as shown in Fig. 1. Further analysis of the HMBC correlations between the methylene proton at δ 3.14 (*t*, $J=6.8$ Hz, H-8) and the two quaternary carbons at δ 116.6 (C-8a) and 125.0 (C-9a) indicated that the junction of partial structures A/B was C-8→C-8a and C-14a→C-13a. The HMBC correlation between the methylene proton at δ 4.41 (*t*, $J=6.8$ Hz, H-7) and the carbonyl carbon at δ 160.3 (C-5) confirmed that the junction of partial structures B/C should be C-5→N-6 and N-14→C-14a.

* Corresponding author. Tel.: +1-662-915-1005; fax: +1-662-915-1006.

E-mail address: pgclark@olemiss.edu (A.M. Clark).

0031-9422/01/$ - see front matter © 2001 Elsevier Science Ltd. All rights reserved.
PII: S0031-9422(01)00248-5

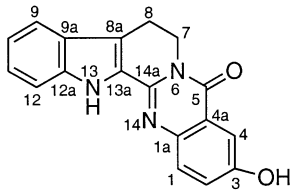

Table 1
NMR spectral data of compound **1** in $CDCl_3$

Position	Chemical shifts		HMBC correlation	
	$\delta_{C(N)}$	δ_H	H/C	H/N
1	128.2	7.56, *d* (8.8)	C-1a, 3, 4a	N-14
1a	140.5			
2	123.9	7.27, *dd* (8.8, 2.7)	C-1a, 3, 4	
3	155.0			
4	109.7	7.48, *d* (2.7)	C-1a, 2, 3, 5	
4a	121.7			
5	160.3			
6 (N)	155.0			
7	40.9	4.41, *t* (6.8)	C-5, 8, 8a, 14a	N-6
8	19.0	3.14 *t* (6.8)	C-7, 8a, 9a, 13a	N-6
8a	116.6			
9	119.7	7.59, *d* (7.4)	C-8a, 11, 12a	
9a	125.0			
10	119.6	7.05, *t* (7.4)	C-9a, 12	
11	124.3	7.22, *t* (7.4)	C-9, 12a	
12	112.3	7.46, *d* (7.4)	C-9a, 10	N-13
12a	138.4			
13 (N)	124.8			
13a	127.3			
14 (N)	224.9			
14a	142.6			
HO-3		10.1, *br s*		
NH-13		11.7, *s*	C-8a, 9a, 12a, 13a	N-13

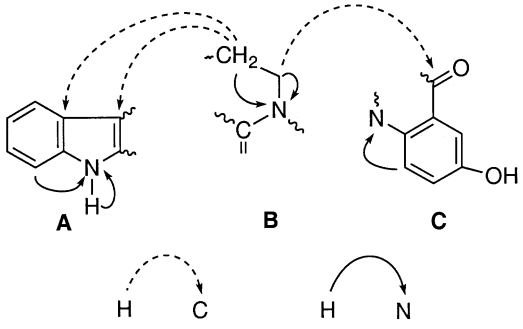

Fig. 1. Partial structures **A**–**C** of **1** based on HMBC experiments.

Based on the above evidence, the structure of **1** was established as 3-hydroxy-8,13-dihydro-indolo[2′,3′:3,4] pyrido[2,1-b]quinazolin-5(7*H*)-one, which has been given the trivial name of 3-hydroxyrutaecarpine. Compound **1** and the seven known compounds that were isolated were tested for antifungal and antibacterial activity by methods previously described (Li et al., 1999) and were found to be inactive.

The ^1H–^{15}N HMBC experiment employed in this study has been demonstrated to be powerful in the structure elucidation of **1**. It not only clearly indicates the number of nitrogens in **1**, but also gives C/N connectivity information as well. For compounds containing several nitrogen atoms, the ^1H–^{15}N HMBC experiment can significantly complement the conventional ^1H–^{13}C HMBC experiment to construct molecular skeletons.

It is interesting to note that rutaecarpine and similar indolopyridoquinazoline alkaloids only occur in rutaceous plants (Mester, 1983). The isolation of 3-hydroxyrutaecarpine, coumarins, flavonoids, and benzofuran derivatives from this key monotypic genus plant might be of significance regarding the chemotaxonomy of the family Rutaceae.

3. Experimental

3.1. General

Melting points: uncorr. Spectra were recorded on the following apparatus: UV, Hewlett Packard 8453 spectrometer; IR, ATI Mattson Genesis Series FTIR; ESI–FTMS, Brüker-Magnex BioAPEX 30es ion cyclotron high resolution HPLC-FT spectrometer; NMR, Brüker Avance DRX-400 (400 MHz) or DRX-500 (500 MHz). Proton and carbon chemical shifts are relative to the internal standard TMS. Nitrogen (^{15}N) chemical shifts are reported relative to liquid ammonia using a nitromethane chemical shift of δ 380.2. DQF-COSY, HMQC, gradient ^1H–^{13}C HMBC ($J=10$ Hz) and gradient ^1H–^{15}N HMBC ($J_{NH}=5$ Hz) were performed with standard pulse programs on DRX-500. Column chromatography was carried out using normal phase silica gel (40 μm, J. T. Baker) or reversed-phase silica gel (RP-18, 40 μm, J. T. Baker). TLC was performed on silica gel sheets (Alugram® Sil G/UV_{254}, Macherey-Nagel, Germany) and reversed-phase plates (RP-18 F_{254S}, Merck, Germany).

3.2. Plant material

The twigs and leaves of *Leptothyrsa sprucei* Hooker f. were collected in Peru in June, 1995. A voucher specimen of this plant is deposited at the National Center for Natural Products Research (Voucher No. IBE 11340).

3.3. Extraction and isolation

Dried twigs and leaves (180 g) were ground and the powdered material was percolated with 95% EtOH (3 l × 3). Removal of the solvent by evaporation under vacuum at 45 °C yielded an EtOH extract (8.5 g), which was dissolved in MeOH–H_2O (9:1, 500 ml) and defatted with hexane (500 ml × 4). To the MeOH–H_2O layer was added 100 ml of H_2O and the resulting solution was

further partitioned with $CHCl_3$ (500 ml). The $CHCl_3$ layer was evaporated to dryness under vacuum at 45 °C to give a residue (2.1 g) that was applied to a silica gel (40 g) using a stepwise gradient solvent system consisting of $CHCl_3$–MeOH (0–100%, a total of 3 l) to yield pooled fractions A–K. Fraction A (430 mg) was loaded onto to a Supelco Discovery RP-18 tube (2 g) and washed with aqueous MeOH. The 80% MeOH eluate (50 ml) was evaporated to give a residue (272 mg), which was further subjected to RP-18 (30 g) chromatography using 70–80% MeOH (2 l) to yield 8-methoxypsoralen (43.8 mg), 5-methoxypsoralen (20.1 mg), imperatorin (8.3 mg) and isoimperatorin (16.0 mg). Fraction B (21.1 mg) was crystallized with MeOH to afford **1** (7.8 mg). Fraction G (80 mg) was applied to a RP-18 column (20 g), using 50% MeOH (500 ml) to yield kaempferol 3-*O*-α-L-rhamnopyranoside (8.8 mg). Fraction I (170 mg) was subjected to RP-18 chromatography (20 g) using an aqueous MeOH gradient (0–100%, a total of 2.7 l) to give clematine (7.5 mg) and cnidioside B (3.8 mg).

3.4. 3-Hydroxyrutaecarpine (*1*)

Colorless needles (MeOH), mp 280–282°; UV λ_{max}^{MeOH} nm (log ε): 220 (4.62), 230 (4.61), 340 (4.66); IR ν_{max}^{KBr} cm^{-1}: 3319, 1652, 1601, 1487, 1314, 989, 828; NMR data: see Table 1; ESI–MS *m*/*z*: 304.1069 {calcd for [M($C_{18}H_{13}N_3O_2$)•H], 304.1086}.

Acknowledgements

The authors thank Dr. Melissa Jacob, Ms. Marinda Logan, Ms. Sharon Sanders and Ms. Belynda Smiley for biological testing and technical assistance. This work was supported by the United States Department of Agriculture, Agricultural Service Specific Cooperative Agreement No. 58-6408-7-012 and the National Institutes of Health, National Institute of Allergy and Infectious Diseases, Division of AIDS, Grant No. AI 27094.

References

Chen, Y., Liu, J., Davidson, R.S., Howarth, O.W., 1993. Isolation and structure of clematine, a new flavanone glycoside from *Clematis armandii* Franch. Tetrahedron 49, 5169–5176.

Duddeck, H., Kasier, M., 1982. ^{13}C NMR spectroscopy of coumarin derivatives. Organic and Magnetic Resonance 20, 55–72.

Farley, K.A., Walker, G.S., Martin, G.E., 1997. Long-range two-dimensional ^{1}H–^{15}N heteronuclear shift correlation at natural abundance using GHNMQC. A study of the reverse transcriptase inhibitor delavirdine. Magnetic Resonance in Chemistry 35, 671–679.

Fossen, T., Larsen, A., Kiremire, B.T., Anderson, Ø.M., 1999. Flavonoids from blue flowers of *Nymphaea caerulea*. Phytochemistry 51, 1133–1137.

Lee, K.-H., Soine, T.O., 1969. Coumarins X: Spectral studies on some linear furanocoumarins. Journal of Pharmaceutical Sciences 58, 681–683.

Li, X.-C., ElSohly, H.N., Nimrod, A.C., Clark, A.M., 1999. Two auronols from *Pseudolarix amabilis*. Journal of Natural Products 62, 767–769.

Matthes, H.W.D., Luu, B., Ourisson, G., 1980. Cytotoxic components of *Zingiber zerumbet*, *Curcuma zedoaria* and *C. domestica*. Phytochemistry 19, 2643–2650.

Mester, I., 1983. In: Waterman, P. G., Grundon, M. F. (Eds.), Chemistry and Chemical Taxonomy of the Rutales. Academic Press, London, pp. 31–96.

Yahara, S., Sugimura, C., Nohara, T., Niiho, Y., Nakajima, Y., Ito, H., 1993. Studies on the constituents of *Cnidii monnieri* Fructus. Shoyakugaku Zasshi 47, 74–78.

PERGAMON

Phytochemistry 58 (2001) 631–635

PHYTOCHEMISTRY

www.elsevier.com/locate/phytochem

Quinones from *Heliotropium ovalifolium*

Alain Guntern[a], Jean-Robert Ioset[a], Emerson F. Queiroz[a], Chris M. Foggin[b], Kurt Hostettmann[a,*]

[a]*Institut de Pharmacognosie et Phytochimie, Université de Lausanne, BEP, CH-1015 Lausanne, Switzerland*
[b]*Central Veterinary Research Laboratory, PO Box CY 551, Causeway, Harare, Zimbabwe*

Received 7 May 2001; received in revised form 19 June 2001

Abstract

Two new benzoquinones, heliotropinones A and B, have been isolated from the aerial parts of *Heliotropium ovalifolium*. Their structures were elucidated by spectrometric methods including high resolution electrospray ionization (ESI-HR), EI mass spectrometry, ^{1}H, ^{13}C and 2D NMR experiments. The two quinones demonstrated antifungal activities against *Cladosporium cucumerinum* and *Candida albicans* as well as antibacterial activity against *Bacillus subtilis*. © 2001 Elsevier Science Ltd. All rights reserved.

Keywords: *Heliotropium ovalifolium*; Boraginaceae; Quinones; Heliotropinone A-B; *Cladosporium cucumerinum*; *Candida albicans*; *Bacillus subtilis*

1. Introduction

Since the hypothesis of a plant intoxication was suggested to explain the flaccid trunk paralysis occurring in free-ranging elephants on the southern shore of Lake Kariba in Zimbabwe (Kock et al., 1994), we have focused our investigations on the flora of Fothergill Island.

After observation of the elephant feeding habit,*Heliotropium ovalifolium* Forsk. (Boraginaceae) was suspected to be possibly responsible for the floppy trunk syndrome. This herbaceous plant is known to contain pyrrolizidine alkaloids (Tiwari and Masood, 1977; Mohanraj et al., 1981; Rizk et al., 1991), and has already been reported to be responsible for intoxications of horses, goats and sheep (Abu et al., 1982; Creeper et al., 1999). As there was no evidence of liver injuries in culled elephants (Kock et al., 1994), investigations were not focused primarily on pyrrolizidine alkaloids.

Methanol and dichloromethane extracts from the aerial parts of *H. ovalifolium* have thus been tested for their neurotoxic properties on rat neuronal cell lines, (P. Jenner, Neurodegenerative Diseases Research Center, King's College London, personal communication) and multidimensional neuropharmacological tests concerning behavioral, neurological, and autonomic patterns (P. Gómez-Serranillos, Departamento de Farmacologia, Universidad Complutense, Madrid personal communication), but no evidence of toxicity could be attributed to these extracts.

Besides these assays, the same extracts were also tested in routine screening against different microorganisms. The dichloromethane extract of *H. ovalifolium* showed activities against the phytopathogenic fungus *Cladosporium cucumerinum* (Homans and Fuchs, 1970). As no further chemical nor biological studies have previously been reported on this plant, the investigation of the active extract of *H. ovalifolium* was undertaken.

2. Results and discussion

The active dichloromethane extract was separated by column chroatography on silica gel into fractions A–L. The antifungal activity against *C. cucumerinum* was found to be concentrated in fraction J. A HPLC/DAD analysis of this fraction showed the presence of compounds whose UV spectra appeared to be characteristic of quinone derivatives (Thomson, 1971). Successive purification of fraction J by reversed phase medium pressure chromatography and semi-preparative chromatography using a C-18 radial compression column led to the isolation of the active compounds **1** and **2** (Fig. 1).

On the basis of the high resolution electrospray ionization mass (HR–ESI–MS) analyses, a molecular formula

* Corresponding author. Tel.: +41-21-692-4561; fax: +41-21-692-4565.
E-mail address: kurt.hostettmann@ipp.unil.ch (K. Hostettmann).

0031-9422/01/$ - see front matter © 2001 Elsevier Science Ltd. All rights reserved.
PII: S0031-9422(01)00302-8

Table 1
^{1}H NMR data of compounds **1** and **2** (500 MHz, $CDCl_3$)

	1	**2**
5	2.36 (1H, *m*, H-5), 2.47 (1H, *m*, H-5)	2.10 (1H, *m*, H-9), 2.54 (1H, *m*, H-5)
7	2.21 (1H, *dd*, J = 5.9 Hz, 7.8 Hz, H-7)	2.00 (1H, *t*, H-7)
8	2.48 (1H, *m*, H-8), 2.56 (1H, *m*, H-8)	2.24 (1H, *m*, H-8), 2.66 (1H, *m*, H-8)
9	–	1.42 (1H, *m*, H-9),1.72 (1H, *m*, H-9)
10	4.91 (1H, *brs*, H-10), 4.71 (1H, *brs*, H-10)	1.52 (1H, *m*, H-10),1.64 (1H,m, H-10)
11	1.74 (3H, *s*, H-11)	2.02 (1H, *m*, H-11), 2.40 (1H, *m*, H-11)
12	0.98 (3H, *s*, H-12)	–
13	5.78 (1H, *dd*, J = 10.7 Hz, 16.6 Hz, H-13)	4.71 (1H, *s*, H-13),4.87 (1H, *s*, H-13)
14	4.98 (1H, *dd*, J = 10.7 Hz, 1 Hz, H-14), 4.96 (1H, *d*, J = 16.6Hz, H-14)	0.66 (3H, *s*, H-11)
15, 16	4.00 (6H, *s*, H-15 and H-16)	4.00 (6H, *s*, H-13 and H-14)

of C_{18} H_{22} O_4 was established for compounds **1** and **2**. In both cases, the existence of a quinonic moiety suggested by the UV spectra was confirmed by the presence of two ketonic functions located around δ 184.0 (C-1 and C-4) and of two quaternary carbons around δ 144.5 (C-2 and C-3) in the ^{13}C NMR Spectrum (Table 2). Long-range correlations observed in the HMBC spectra of **1** and **2** between these two latter signals and the ^{1}H NMR resonance seen at δ 4.00 (6H), indicated a substitution of C-2 and C-3 by methoxyl groups. This symmetric pattern was confirmed by observation of a typical overlapped signal at δ 61.2 (2 carbons) in the ^{13}C NMR spectra of both products (Table 2).

For compound **1**, aliphatic and olefinic methyl groups were identified by the presence of ^{1}H NMR signals at δ 0.98 and 1.74, both integrating for three protons. The latter resonance was determined as a part of a vinylidene group through HMBC correlation with the ^{13}C NMR signal at δ 112.6 geminally linked to protons at δ 4.71 (*brs*) and 4.91 (*brs*) (H-10). An ABX system observed in the ^{1}H NMR spectrum at δ 4.96 (*d*, J = 17 Hz, H-14), 4.98 (*dd*, J = 1 Hz, J = 11 Hz, H-14) and 5.78 (*dd*, J = 11 Hz, J = 17 Hz, H-13) indicated the presence of a vinyl group. The location of the vinyl, vinylidene and methyl groups on the benzoquinone skeleton was carried out by HMBC experiments. The methyl group at δ 0.98 (CH_3-12) was found to be attached to C-6 after observation of long-range heteronuclear correlations with δ 34.4 (C-5), δ 38.1 (C-6), δ 47.5 (C-7), δ 146.3 (C-13). The vinyl group was also positioned on C-6 through HMBC correlations between the ^{13}C NMR signal at 38.1 (C-6) and the methylene group protons located at δ 4.96 and 4.98 (H-14). Observation of a HMBC cross-peak between the ^{13}C NMR resonance at δ 47.5 (C-7) and the ^{1}H NMR signal at δ 1.74 enabled assignment of the position of the vinylidene moiety at C-7. The structure of the non-quinonic part of the molecule was confirmed by comparison of its spectroscopic data

Table 2
^{13}C NMR and DEPT data and HMBC connectivities of compounds **1** and **2** (125 MHz, $CDCl_3$)

	1			**2**		
	13C[a]	DEPT	HMBC	13C[a]	DEPT	HMBC
1	184.0a	C		184.4a	C	
2	144.6b	C		144.5b	C	
3	144.5b	C		144.6b	C	
4	183.7a	C		184.1a	C	
4a	138.8	C		138.8	C	
5	34.4	CH_2	C-4a, C-6, C-7, C-8a, C-12, C-13	38.6	CH_2	C-4a, C-6, C-7, C-8a, C-9, C-14
6	38.1	C		34.2	C	
7	47.5	CH	C-5, C-6, C-8, C-8a, C-9, C-10, C-11, C-12, C-13	43.7	CH	C-5, C-6, C-8, C-8a, C-9, C-11, C-12, C-13, C-14
8	26.3	CH_2	C-4a, C-6, C-7, C-8a, C-9	22.7	CH_2	C-4a, C-6, C-7, C-8a, C-12
8a	139.5	C		139.3	C	
9	145.8	C		41.0	CH_2	C-5, C-6, C-7, C-10, C-11, C-14
10	113.3	CH_2	C-7, C-9, C-11	23.2	CH_2	C-6, C-9, C-11, C-12
11	24.5	CH_3	C-7, C-9, C-10	36.8	CH_2	C-7, C-9, C-10, C-12, C-13
12	20.0	CH_3	C-5, C-6, C-7, C-13	148.1	C	
13	146.3	CH	C-5, C-6, C-7, C-12, C-14	107.6	CH_2	C-7, C-11, C-12
14	111.6	CH_2	C-6, C-13	17.3	CH_3	C-5, C-6, C-7, C-9
15,16	61.2	CH_3	C-2, C-3	61.2	CH_3	C-2, C-3

[a] Values with the same letter may be interchanged.

with those from lobane derivatives isolated from a soft coral of *Lobophytum* sp. (Alcyonidae) (Raju and Subbaraju, 1993). Correct assignment of C-8a is supported by the HMBC connectivity between δ 2.21 (H-7) and δ 139.5 (C-8a). Complete DEPT data and HMBC connectivities for compound **1** are shown in Table 2. Compound **1** was finally identified as 7-isopropenyl-2,3-dimethoxy-6-methyl-6-vinyl-5,6,7,8-tetrahydronaphthalene-1,4-dione named heliotropinone A (Fig. 1).

The UV spectrum of compound **2** was very similar to that of **1**, suggesting also the presence of a benzoquinone structure. The ^{1}H NMR spectrum exhibited two protons at δ 4.71 and 4.87. These signals were attached to the sp^2 hybridized carbon at δ 107.6, as shown by a HSQC experiment, suggesting the presence of a terminal methylene moiety. The ^{1}H NMR spectrum showed also a singlet integrating for three protons at δ 0.66 (CH_3-14) that was attributed to a methyl group. The terminal methylene was attached at C-12 after analysis of the long-range correlations with the carbons δ 43.7 (C-7), 36.8 (C-11) and 148.1 (C-12). The position of the tertiary methyl group (δ 0.66) on C-6 was deduced from the correlations observed in the HMBC spectrum with the carbons δ 34.2 (C-6), 38.6 (C-5), 41.0 (C-9) and 43.7 (C-7). Correct assignment of C-8a is supported by the HMBC connectivity between δ 2.00 (H-7) and δ 139.3 (C-8a). Complete DEPT data and HMBC connectivities for compound **2** are shown in Table 2. Compound **2** was thus identified as 2,3-dimethoxy-8a-methyl-5-methylene-5,6,7,8,8a,9,10,10a-octahydroanthracene-1,4-dione and named heliotropinone B (Fig. 1).

From a biogenetic point of view, it appears important to mention that several terpenoid benzoquinone derivatives (cordiachromes) presenting a closely related structure to those of heliotropinones A and B have already been described from *Cordia* ssp., a genus also belonging to the Boraginaceae family (Moir and Thomson, 1973).

A closely related compound with a structure similar to heliotropinone A was also found in *Arnebia euchroma* (Boraginaceae), with inhibitory effects against prostaglandin biosynthesis (Xin-Sheng et al., 1983).

To our knowledge heliotropinones A and B are the first benzoquinone derivatives to be reported in a plant belonging to the genus *Heliotropium*. This gives further proof of the chemotaxonomic unity of the Boraginaceae family.

Heliotropinones A and B were found to be equally active against *C. cucumerinum* and *Candida albicans* in bioautographic assays on TLC plates (Rahalison et al., 1994) but were less potent than nystatin, a commercially available antifungal agent. Dilution tests on TLC were also performed with *Bacillus subtilis* (Rahalison et al., 1991), showing similar antibacterial effects for both compounds, with lower activities than those of chloramphenicol, used as reference compound. The results of the bioassays are reported in Table 3.

At the moment, a lack of suitable bioassays does not allow any conclusion on the involvement of *H. ovalifolium* in elephant flaccid trunk paralysis. Further investigations will be focused on finding assays convenient to target neurotoxicity in crude plant extracts.

3. Experimental

3.1. General

^{1}H and ^{13}C NMR: Varian Unity Inova NMR instrument. ^{1}H and ^{13}C NMR spectra were recorded in $CHCl_3$ at 500.00 and 125 MHz, respectively. TMS: int.

Table 3
Antifungal and antibacterial activities for compounds **1** and **2**

Compound	*Cladosporium cucumerinum*[a]	*Candida albicans*[a]	*Bacillus subtilis*[a]
1	2	4	0.2
2	2	2	0.2
Nystatin	1	1	–
Chloramphenicol	i[b]	i	0.01

[a] Minimal amount (μg) of compound to inhibit growth on a silica gel TLC plate.
[b] i, inactive at 10 μg.

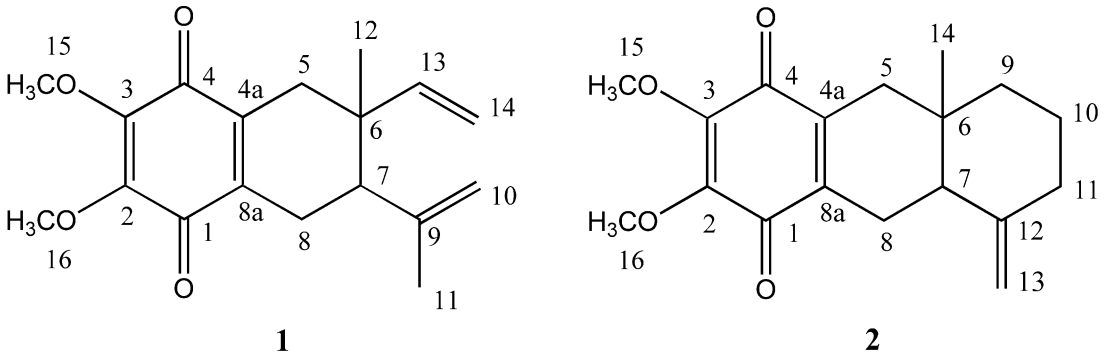

Fig. 1. Heliotropinones A (**1**) and B (**2**).

standard. UV: Varian DMS 100S UV–vis spectrophotometer. UV spectra were recorded in MeOH. $[\alpha]_D$: Perkin-Elmer-241 polarimeter. TLC: silica gel 60 F_{254} Al sheets (Merck) using petrol ether–EtOAc 1 :1. CC: silica gel (63–200 μm; 750×65 mm i.d. and 63×200 μm; 400×20 mm i.d., Merck), MPLC: RP-18 Lichroprep (40-63 μm; 270×25 mm i.d.; Merck). EI–MS and D/CI–MS: Finnigan MAT TSQ-700 triple stage quadrupole instrument. HPLC/UV/DAD with a Nova-Pak RP-18 column (4 μm; 250×3.9 mm i.d.; Waters) using a CH_3CN-water gradient (20:80→100:0) in 25 min. The detection was performed at 210 and 254 nm. Semi-preparative HPLC was performed with a Shimadzu LC-8 pump equipped with a Knauer UV detector using a μBondapak® C_{18} prepacked radial-compression column (10 μm, 25×100 mm; Waters).

3.2. Plant material

The aerial parts of *H. ovalifolium* were collected in March 1999 at Fothergill Island, Zimbabwe. A voucher is deposited at the Institut de Pharmacognosie et Phytochimie, Lausannne, Switzerland (No. 99034).

3.3. Extraction and isolation

The air-dried powdered aerial parts (1.3 kg) of *H. ovalifolium* were extracted at room temperature with dichloromethane to afford 49 g of extract. This extract was first fractionated by column chromatography on silica gel with a petrol ether–EtOAc gradient (9:1→1:4) giving fractions A–L. Fr. J (2.3 g) was separated by medium pressure liquid chromatography (MPLC) with CH_3CN–H_2O (70:30). Further purification by semi-preparative chromatography using a μBondapak® C_{18} (10 μm, 25×100 mm) radial compression column with CH_3CN–H_2O (70-30) as the mobile phase led to the isolation of compounds **1** (8 mg) and **2** (11 mg).

3.4. Biological assays

3.4.1. Sample preparation for bioautographic assays

Geometric dilutions were obtained from freshly prepared stock solutions of the isolated and reference compounds at a concentration of 1 mg/ml in an appropriate solvent. Ten microliters of these solutions were applied on the TLC plates using graduated capillaries.

3.4.2. Bioautographic assays

Direct bioautography with *C. cucumerinum*: after application of the samples on a silica gel 60 F_{254} Al sheet (Merck), the TLC plate was developed in petrol ether–EtOAc (1:1) solvent system and thoroughly dried for complete removal of solvent. The plate was then sprayed with a suspension of *C. cucumerinum* in a nutritive medium and incubated for 2–3 days in polystyrene boxes with a moist atmosphere. Clear inhibition zones appeared against a dark gray background. Nystatin (Sigma) was used as reference compound.

3.4.2.1. Agar overlay bioautography with C. albicans. After application of the samples on a silica gel 60 F_{254} glass plate (Merck), this was developed using a petrol ether–EtOAc (1:1) solvent system and thoroughly dried for complete removal of solvents. An inoculum of yeast (approx. 10^7 cells/ml) in molten malt agar (Biokar Diagnostics) was distributed over the plates. The medium solidified as a thin layer (approx. 1 mm) and the plates were then incubated overnight at 30 °C in polystyrene boxes with a moist atmosphere. Inhibition zones were visible after spraying with an aqueous solution of methylthiazolyltetrazolium bromide (MTT) (2.5 mg/ml). Active compounds appeared as clear spots against a purple background. Nystatin (Sigma) was used as reference compound.

3.4.2.2. Agar overlay bioautography with B. subtilis. The same method was used as for *C. albicans*. Concentration of the inoculum, approx. 10^8 cells/ml. Chloramphenicol (Sigma) was used as reference compound.

3.5. Heliotropinone A (*1*)

7-Isopropenyl-2,3-dimethoxy-6-methyl-6-vinyl-5,6,7,8-tetrahydronaphthalene-1,4-dione; dark yellow oil $[\alpha]_D$ 0° (MeOH, *c* 0.05); UV λ_{max}^{MeOH}nm (log ε): 222 (*sh,* 5.64), 279 (5.54), 406 (3.94); ^{1}H NMR (500 MHz, $CDCl_3$): see Table 1. ^{13}C NMR (125 MHz, $CDCl_3$): see Table 2. HR-ESI–MS: (positive mode) *m/z* 303.159 ($C_{18}H_{23}O_4$ $[M+H]^+$, requires 303.152). EI–MS *m/z* (rel. int.): 302 $[M]^+$ (52), 287 (100), 255 (22), 247 (18), 219 (18), 93 (22), 91 (24).

3.6. Heliotropinone B (*2*)

2,3-Dimethoxy-8a-methyl-5-methylene-5,6,7,8,8a,9,10,10a-octahydroanthracene-1,4-dione; dark yellow oil; $[\alpha]_D$ +4, (MeOH, *c* 0.05); UV λ_{max}^{MeOH}nm (log ε): 213 (5.14), 279 (5.39), 412 (3.98); ^{1}H NMR (500 MHz, $CDCl_3$): see Table 1. ^{13}C NMR (125 MHz, $CDCl_3$): see Table 2; HR-ESI–MS: (positive mode) *m/z* 303.158 ($C_{18}H_{23}O_4$ $[M+H]^+$, requires 303.152) EI–MS *m/z* (rel. int.): 302 $[M]^+$ (100), 287 (16), 255 (18), 93 (10), 91 (14).

Acknowledgements

The authors would like to thank the Swiss National Science Foundation for financial support of this work (grant No. 2000-063670.00, to K. Hostettmann). Thanks are also due to Professor T. A. Jenny-Beyer and Mr. F. Nydegger, Institut de Chimie Organique, University of

Fribourg, Switzerland, for the HR-MS measurements. We also express our gratitude to Martha Schauss and Henry Coletto, Gilroy, CA, USA for all their fieldwork at Fothergill Island, Zimbabwe.

References

Abu, D.H., Adam, S.E., Tartour, G., 1982. The effects of *Heliotropium ovalifolium* on goats and sheep. British Veterinary Journal 138, 463–472.

Creeper, J.H., Mitchell, A.A., Jubb, T.F., Colegate, S.M., 1999. Pyrrolizidine alkaloid poisoning of horses grazing a native heliotrope (*Heliotropium ovalifolium*). Australian Veterinary Journal 77, 401–402.

Homans, A.L., Fuchs, A., 1970. Direct bioautography on thin-layer chromatograms as a method for detecting fungitoxic substances. Journal of Chromatography 51, 327–329.

Kock, N.D., Goedegebuure, S.A., Lane, E.P., Lucke, V., Tyrrell, D., Kock, M.D., 1994. Flaccid trunk paralysis in free-ranging elephants (*Loxodonta africana*) in Zimbabwe. Journal of Wildlife Diseases 30, 432–435.

Mohanraj, S., Kulanthaivel, P., Subramanian, P., Herz, W., 1981. Helifoline, a pyrrolizidine alkaloid from *Heliotropium ovalifolium*. Phytochemistry 20, 1991–1995.

Moir, M., Thomson, R.H., 1973. Naturally occurring quinones. Part XXII. Terpenoid quinones in *Cordia ssp*. Journal of the Chemical Society Perkin I, 1352–1356.

Rahalison, L., Hamburger, M., Monod, M., Frenk, E., Hostettmann, K., 1991. A bioautographic agar overlay method for the detection of antifungal compounds from higher plants. Phytochemical Analysis 2, 199–203.

Rahalison, L., Hamburger, M., Monod, M., Frenk, E., Hostettmann, K., 1994. Antifungal tests in phytochemical investigations: comparison of bioautographic methods using phytopathogenic and human pathogenic fungi. Planta Medica 60, 41–44.

Raju, B.L., Subbaraju, G.V., 1993. Two new oxygenated lobanes from a soft coral of *Lobophytum* species of the Andaman and Nicobar Coasts. Journal of Natural Products 56, 961–966.

Rizk, A.M., Hammouda, F.M., Hassan, N.M., 1991. Pyrrolizidine alkaloids from *Heliotropium arabinense* and *H. ovalifolium*. Qatar University Science Journal 11, 113–119.

Thomson, R.H., 1971. Naturally Occurring Quinones. Academic, London.

Tiwari, K.P., Masood, M., 1977. Chemical constituents of *Heliotropium ovalifolium*. Proceedings of the National Academy of Science (India), Sect. A 47, 72.

Xin-Sheng, Y., Ebizuka, Y., Noguchi, H., Kiuchi, F., Sankawa, U., 1983. Structure of arnebinone, a novel monoterpenylbenzoquinone with inhibitory effect to prostaglandin biosynthesis. Tetrahedron Letters 24, 3247–3250.

PERGAMON

Phytochemistry 58 (2001) 637–640

PHYTOCHEMISTRY

www.elsevier.com/locate/phytochem

Benzoxazinoid glucosides from *Acanthus ilicifolius*

Tripetch Kanchanapoom[a,b], Mohamed Salah Kamel[c], Ryoji Kasai[a], Chayan Picheansoonthon[b], Yoshikazu Hiraga[d], Kazuo Yamasaki[a,*]

[a]*Institute of Pharmaceutical Sciences, Faculty of Medicine, Hiroshima University, 1-2-3 Kasumi, Minami-ku, Hiroshima 734-8551, Japan*
[b]*Department of Pharmaceutical Botany and Pharmacognosy, Faculty of Pharmaceutical Sciences, Khon Kaen University, Khon Kaen, Thailand*
[c]*Department of Pharmacognosy, Faculty of Pharmacy, Assiut University, Assiut, Egypt*
[d]*Department of Chemistry, Graduate School of Science, Hiroshima University 1-3-1, Kagamiyama, Higashi-Hiroshima 739-8526, Japan*

Received 2 February 2001; received in revised form 8 May 2001

Abstract

From the aerial parts of *Acanthus ilicifolius*, two benzoxazinoid glucosides, 7-chloro-(*2R*)-2-*O*-β-D-glucopyranosyl-2*H*-1,4-benzoxazin-3(4*H*)-one and (*2R*)-2-*O*-β-D-glucopyranosyl-5-hydroxy-2*H*-1,4-benzoxazin-3(4*H*)-one have been isolated, together with six known compounds. The structural elucidations were based on the analyses of spectroscopic data. © 2001 Elsevier Science Ltd. All rights reserved.

Keywords: Acanthus ilicifolius; Acanthaceae; Aerial parts; Benzoxazinoid glucoside

1. Introduction

Acanthus ilicifolius L. (Acanthaceae, Thai name: Ngueak-Plaa-Moo) is a spiny herb distributed in the mangroves of southern Thailand. In Thai traditional medicine, the plant is used as a purgative and an anti-inflammatory, as well as the leaves dispensed with pepper (*Piper nigrum* L.) as tonic pills for longevity. In a previous paper (Kanchanapoom et al., 2001), we reported the isolation and structural elucidation of lignan glucosides. Further investigation of the aerial part of the same plant affords two new benzoxazinoid glucosides (**4, 5**) together with six known compounds (**1–3, 6–8**). Benzoxazinoids have been found to occur as allo chemicals from monocotelydonous plants in the family Gramineae (Hofman and Hofmanova, 1969; Nagao et al., 1985), as well as reported from dicotyledonous plants in the family Acanthaceae (Wolf et al., 1985; Pratt et al., 1995), Ranunculaceae (Ozden et al., 1992) and Scrophulariaceae (Pratt et al., 1995). The present paper deals with the structural determination of these compounds. Also the usage of this plant in Thai traditional medicines are discussed.

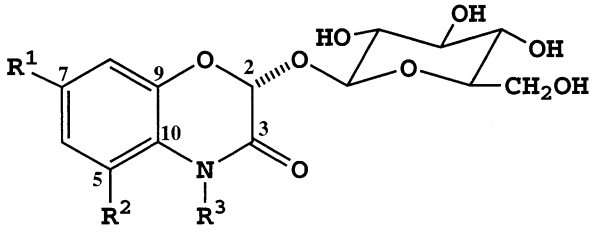

	R^1	R^2	R^3
1	H	H	H
2	H	H	OH
3	OH	H	H
4	Cl	H	H
5	H	OH	H

2. Results and discussion

From the methanolic extract of the aerial part of *A. ilicifolius*, eight compounds (**1–8**) were isolated. Six were identified as known compounds; (*2R*)-2-*O*-β-D-gluco-

* Corresponding author. Tel.: +81-82-257-5285; fax: +81-82-257-5289.
E-mail address: yamasaki@pharm.hiroshima-u.ac.jp (K. Yamasaki).

0031-9422/01/$ - see front matter © 2001 Elsevier Science Ltd. All rights reserved.
PII: S0031-9422(01)00267-9

pyranosyl-2*H*-1,4-benzoxazin-3(4*H*)-one (HBOA-Glc, blepharin) (**1**) (Tietze et al., 1991), (*2R*)-2-*O*-β-D-glucopyranosyl-4-hydroxy-2*H*-1,4-benzoxazin-3(4*H*)-one (DIBOA-Glc) (**2**) (Hartenstein and Sicker, 1994), (*2R*)-2-*O*-β-D-glucopyranosyl-7-hydroxy-2*H*-1,4-benzoxazin-3(4*H*)-one (DHBOA-Glc) (**3**) (Nagao et al., 1985), adenosine (**6**) (Otsuka et al., 1989), syringic acid β-glucopyranosyl ester (**7**) (Inoshiri et al., 1987) and 2,6-dimethoxy-*p*-hydroquinone 1-*O*-β-glucopyranoside (**8**) (Otsuka et al., 1989) by comparison of physical data with literature values and from spectroscopic evidence.

Compound **4** (Fig. 1) exhibited the characteristic pattern of a substance having a chlorine atom from negative FAB–MS. The molecular formula was determined by HR–FAB mass spectrometry as $C_{14}H_{16}O_8NCl$. The ^1H and ^{13}C NMR spectral data were similar to those of **1**. However, the ^1H NMR spectrum showed the presence of an ABX system at δ 6.91 (1H, *d*, $J=8.4$ Hz,), δ 7.05 (1H, *dd*, $J=8.4$, 2.5 Hz) and δ 7.23 (1H, *d*, $J=2.5$ Hz), indicating that the chlorine atom was attached to the aromatic ring. The position of the chlorine atom was assigned to C-7 by irridiation of N–H at δ 11.10 which induced a 7% NOE at δ 6.91 ($J=8.4$ Hz, H-5). Moreover, all carbon signals were established by using COSY, HSQC and HMBC. The (*2R*)-stereochemistry of the linkage at the anomeric carbon of the aglycone part could be deduced from the positive values, $[\alpha]_D^{26}$ +198.0°, of the opitical rotation. Such positive values are a typical feature for (*2R*)-configuration. On the basis of these spectral data, the structure of compound **4** was elucidated to be 7-chloro-(*2R*)-2-*O*-β-D-glucopyranosyl-2*H*-1,4-benzoxazin-3(4*H*)-one. This chlorinated compound is a natural product, and was not found as an artifact since the process of extraction and isolation did not involve acidic media. Furthermore, since this plant was collected from the mangrove forest, the source of chlorine atom might come from a mineral source (NaCl).

The molecular formula of compound **5** was determined as $C_{14}H_{17}O_9N$ by HR–FAB mass spectrometry. The ^1H and ^{13}C NMR spectra suggested it to be a benzoxazinoid glucoside. Inspection of the FAB mass spectrometry revealed a molecular ion 16 mass units larger than **1**, and the ABB′ system at δ 6.53 (2H, *brd*, $J=8.3$ Hz) and δ 6.75 (1H, *dd*, $J=8.3$, 8.1 Hz) was observed from the ^1H NMR spectrum, indicating the presence of a hydroxyl group on the aromatic ring. The hydroxyl group was assigned to attach at C-5 due to the downfield shift of C-5 (+29.5 ppm) together with the upfield shift of C-6 (−14.7 ppm), C-8 (−8.2 ppm) and C-10 (−11.5 ppm), compared to **1**. Besides, irradation of the N–H signal at δ 12.20, the NOE enhancement was not observed from the spectrum. The (*2R*)-stereochemistry could be determined from the positive values, $[\alpha]_D^{26}$ +95.0°, of the opitical rotation. Consequently, the structure of compound **5** was concluded as (*2R*)-2-*O*-β-D-glucopyranosyl-5-hydroxy-2*H*-1,4-benzoxazin-3(4*H*)-one.

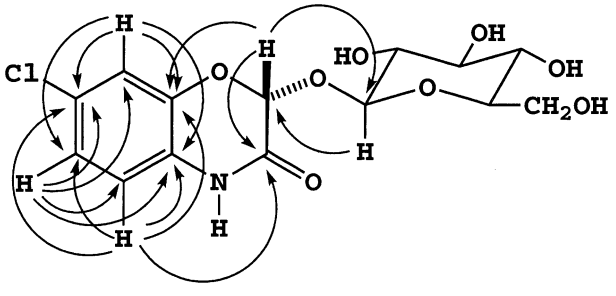

Fig. 1. HMBC correlations of compound **4**.

The biological activities of the isolated benzoxazinoids have not been investigated. The presence of benzoxazinoids (**1, 2**) as the major constituents are in agreement with Thai traditional usage as an anti-inflammatory (Otsuka et al., 1988). However, the toxicological and pharmacological properties of benzoxazinoids have been reported as the chemical resistance factors against insects, fungi, bacteria and virus in many crop plants of the family Gramineae (Niemeyer, 1988; Sicker et al., 2000), as well as mutagenic activities (Hashimoto and Shudo, 1996). In addition, the aglycone of **2** (DIBOA) was shown to be mutagenic in a test with *Salmonella typhimurium* TA 100 and TA 98 (Hashimoto and Shudo, 1996). On the basis of these results, the internal use of this species for treatments in Thai traditional medicine should be considered.

3. Experimental

3.1. General

NMR spectra were recorded in DMSO-d_6 or methanol-d_4 using a JEOL JNM A-400 spectrometer (400 MHz for ^1H NMR and 100 MHz for ^{13}C NMR) and JNM-ECP 500 (500 MHz for ^1H NMR and 125 MHz for ^{13}C NMR) with tetramethylsilane (TMS) as internal standard. MS were recorded on a JEOL JMS-SX 102 spectrometer. Optical rotations were measured with a Union PM-1 digital polarimeter. Preparative HPLC was carried out on columns of ODS (150×20 mm i.d., YMC) with a Tosoh refraction index (RI-8) detector. For CC, silica gel G 60 (Merck), NH-silica gel (Fuji Silysia Chemical, Ltd.), YMC-gel ODS (50 μm, YMC), polyamide C-200 (Wako) and highly porous copolymer of styrene and divinylbenzene (Mitsubishi Chem. Ind. Co., Ltd.) were used. The solvent systems were: (I) EtOAc–EtOH–H_2O (4:1:0.1), (II) EtOAc–EtOH–H_2O (7:3:0.3), (III) EtOAc–EtOH–H_2O (6:4:1), (IV) 14% MeCN, (V) 90–50% MeCN, (VI) 10% MeCN, (VII) 90% MeCN, (VIII) EtOAc–MeOH–H_2O (4:1:0.1), (IX) EtOAc–MeOH–H_2O (7:3:0.3), (X) EtOAc–EtOH–H_2O (6:4:1) and 15% MeCN. The spray reagent used for TLC was 10% H_2SO_4 in 50% EtOH.

3.2. Plant material

Acanthus ilicifolius L. was collected in April 1997 from Satun Province, Southern of Thailand. The identification of the plant was confirmed by Professor Vichiara Jirawongse, Department of Pharmaceutical Botany and Pharmacognosy, Faculty of Pharmaceutical Sciences, Khon Kaen University. A voucher sample (KKU-0001) is kept in the Herbarium of the Faculty of Pharmaceutical Sciences, Khon Kaen University, Thailand.

3.3. Extraction and isolation

The dried aerial part (2.5 kg) of *A. ilicifolius* was extracted with hot MeOH. After removal of the solvent by evaporation, the residue (380.0 g) was defatted with Et_2O. The aqueous layer was subjected to a column of highly porous copolymer of styrene and divinylbenzene (Mitsubishi Chem. Ind.) and eluted with H_2O, 30% MeOH, 60% MeOH, MeOH and Me_2CO, successively. The fraction eluted with 30% MeOH (9.2 g) was applied to a column of silica gel (system I, II and III, respectively) affording four fractions. Fraction 2 (3.3 g) was further separated on columns of RP-18 (system IV) and NH-silica gel (system V) to provide compounds **1** (1.0 g), **3** (15 mg), **5** (7 mg), **7** (15 mg) and **8** (10 mg). Fraction 2 (2.2 g) was purified by using RP-18 (system VI) and polyamide (system VII) columns to give compounds **2** (840 mg) and **6** (49 mg). The fraction eluted with 60% MeOH was subjected to a column of silica gel (system VIII, IX and X, respectively) to give five fractions. A portion of fraction 2 was purified by ODS–HPLC (system XI) to provide compound **4** (15 mg).

3.4. 7-Chloro-(2R)-2-O-β-D-glucopyranosyl-2H-1,4-benzoxazin-3(4H)-one

White amorphous powder, $[\alpha]_D^{26}$ +198.0° (DMSO, *c* 0.33); ^{1}H NMR (DMSO-d_6): δ 2.91 (1H, *dd*, *J* = 8.5, 8.3 Hz, H-2 Glc), δ 3.00 (1H, *dd*, *J* = 9.3, 9.0 Hz, H-4 Glc), δ 3.13 (1H, *dd*, *J* = 8.9, 8.8 Hz, H-3 Glc), δ 3.17 (1H, *m*, H-5 Glc), δ 3.41 (1H, *dd*, *J* = 11.7, 5.7 Hz, H-6 Glc), δ 3.69 (1H, *brd*, *J* = 11.7 Hz, H-6 Glc), δ 4.54 (1H, *d*, *J* = 8.1 Hz, H-1 Glc), δ 5.70 (1H, *s*, H-2), δ 6.91 (1H, *d*, *J* = 8.4 Hz, H-5), δ 7.05 (1H, *dd*, *J* = 8.4, 2.5 Hz, H-6), δ 7.23 (1H, *d*, *J* = 2.5 Hz, H-8), δ 11.10 (1H, *brs*, N–H); ^{13}C NMR (DMSO-d_6): Table 1; negative HR–FAB–MS, *m*/*z*: 360.0486 ($C_{14}H_{15}O_8NCl$ requires 360.0486).

3.5. (2R)-2-O-β-D-Glucopyranosyl-5-hydroxy-2H-1,4-benzoxazin-3(4H)-one

Amorphous powder, $[\alpha]_D^{26}$ +95.0° (DMSO, *c* 0.40); ^{1}H NMR (DMSO-d_6): δ 2.89 (1H, *dd*, *J* = 8.3, 8.1 Hz, H-2 Glc), δ 3.02 (1H, *dd*, *J* = 9.3, 9.0 Hz, H-4 Glc), δ 3.13 (1H, *dd*, *J* = 9.3, 8.8 Hz, H-3 Glc), δ 3.14 (1H, *m*, H-5 Glc), δ 3.43 (1H, *dd*, *J* = 11.0, 4.6 Hz, H-6 Glc), δ 3.66 (1H, *brd*, *J* = 11.5 Hz, H-6 Glc), δ 4.53 (1H, *d*, *J* = 7.8 Hz, H-1 Glc), δ 5.62 (1H, *s*, H-2), δ 6.53 (2H, *brd*, *J* = 8.3 Hz, H-6,8), δ 6.75 (1H, *dd*, *J* = 8.3, 8.1 Hz, H-7), δ 12.20 (1H, *brs*, N–H); ^{13}C NMR ((DMSO-d_6): Table 1; negative HR–FAB–MS, *m*/*z*: 342.0820 ($C_{14}H_{16}O_9N$ requires 342.0825).

Table 1
^{13}C NMR spectral data of compounds **1**–**5** (DMSO-d_6, 100 MHz)

C	1	2	3	4	5
2	94.5	96.2	94.6	94.5	94.6
3	160.4	155.4	159.7	160.0	159.9
5	115.5	112.8	115.9	117.1	145.0
6	123.2	123.9	109.5	123.4	108.5[a]
7	122.8	122.9	153.5	126.1	122.6
8	117.7	117.5	104.8	118.7	109.5[a]
9	140.2	140.3	141.0	141.6	141.3
10	126.2	128.3	118.2	127.1	114.7
G-1	102.5	102.5	102.5	102.7	102.4
G-2	73.2	73.2	73.3	73.2	73.3
G-3	77.4	77.3	77.3	77.5	77.3
G-4	69.7	69.6	69.7	69.7	69.6
G-5	76.6	76.6	76.7	76.7	76.7
G-6	61.0	60.9	61.0	61.0	61.0

[a] Assignments may be interchanged.

Acknowledgements

We would like to thank the Research Center for Molecular Medicine, Hiroshima University for the used of its NMR facilities.

References

Hartenstein, H., Sicker, D., 1994. (2*R*)-2-β-Glucopyranosyloxy-4-hydroxy-2H-1,4-benzoxazin-3(*4H*)-one from *Secale cereale*. Phytochemistry 35, 827–828.

Hashimoto, Y., Shudo, K., 1996. Chemistry of biologically active benzoxazinoids. Phytochemistry 43, 551–559.

Hofman, J., Hofmanova, O., 1969. 1,4-Benzoxazine derivatives in plants. European Journal of Biochemistry 8, 109–112.

Inoshiri, S., Sasaki, M., Kohda, H., Otsuka, H., Yamasaki, K., 1987. Aromatic glycosides from *Berchemia racemosa*. Phytochemistry 26, 2811–2814.

Kanchanapoom, T., Kamel, M.S., Kasai, K., Yamasaki, K., Picheansoonthon, C., Hiraga, Y., 2001. Lignan glucosides from *Acanthus ilicifolius*. Phytochemistry 56, 369–372.

Nagao, T., Otsuka, H., Kohda, H., Sato, T., Yamasaki, K., 1985. Benzoxazinones from *Coix lachryma-jobi* var. *ma-yuen*. Phytochemistry 24, 2959–2962.

Niemeyer, H.M., 1988. Hydroxamic acids (4-hydroxy-1,4-benzoxazin-3-ones), defence chemicals in the Gramineae. Phytochemistry 27, 3349–3358.

Otsuka, H., Hirai, Y., Nagao, T., Yamasaki, K., 1988. Anti-inflammatory activity of benzoxazinoids from roots of *Coix lachryma-jobi* var. *ma-yuen*. Journal of Natural Products 51, 74–79.

Otsuka, H., Takeuchi, M., Inoshiri, S., Sato, T., Yamasaki, K., 1989. Phenolic compounds from *Coix lachryma-jobi* var. *ma-yuen*. Phytochemistry 28, 883–886.

Ozden, S., Ozden, T., Attila, I., Kucukislamoglu, M., Okatan, A., 1992. Isolation and identification via high-performance liquid chromatography and thin-layer chromatography of benzoxazolinone precursors from *Consolida orientalis* flowers. Journal of Chromatography 609, 402–406.

Pratt, K., Kumar, P., Chilton, W.S., 1995. Cyclic hydroxamic acids in dicotyledonnous plants. Biochemical Systematics and Ecology 23, 781–785.

Sicker, D., Frey, M., Schulz, M., Gierl, A., 2000. Role of natural benzoxazinones in the survival strategy of plants. In: Jeon, K.W. (Ed.), International Review of Cytology: A Survey of Cell Biology. Academic, NY, 198, pp. 319–346.

Tietze, L., Beller, M., Terfort, A., Dolle, A., 1991. First synthesis and structural determination of blepharin and 1-′epiblepharin. Synthesis 1118–1120.

Wolf, R.B., Spencer, G., Plattner, R.D., 1985. Benzoxazolinone, 2,4-dihydroxy-1,4-benzoxazin-3-one, and its glucoside from *Acanthus mollis* seeds inhibit velvetleaf germination and growth. Journal of Natural Products 48, 59–63.

PERGAMON

Phytochemistry 58 (2001) 641–644

PHYTOCHEMISTRY

www.elsevier.com/locate/phytochem

Glucides of *Cnidium monnieri* fruit

Junichi Kitajima*, Toru Ishikawa, Yoshie Aoki

Showa Pharmaceutical University, Higashi-Tamagawagakuen 3, Machida, Tokyo 194-8543, Japan

Received 31 January 2001; received in revised form 19 April 2001

Abstract

From the fruit of *Cnidium monnieri* Cusson (Umbelliferae), two glucides were isolated together with other known glucides. Their structures were clarified as glycerol 2-*O*-α-L-fucopyranoside and D-quinovitol (6-deoxy-D-glucitol), respectively. © 2001 Elsevier Science Ltd. All rights reserved.

Keywords: *Cnidium monnieri*; Umbelliferae; Glycerol 2-*O*-α-L-fucopyranoside; D-Quinovitol; Glucide

1. Introduction

In previous papers, we reported the separation and characterization of a hemiterpenoid (2*S*,3*R*)-2-methylbutane-1,2,3,4-tetrol (**1**), seven monoterpenoid polyols (3,7-dimethyloct-3(10)-ene-1,2,6,7-tetrols, 3,7-dimethyloctane-1,2,6,7-tetrols, 3,7-dimethyloct-3(10)-ene-1,2,6,7,8-pentols and *trans*-*p*-menthane-1β,2α,8,9-tetrol), five monoterpenoid glucosides and five aromatic compound glucosides as the constituents of the water-soluble portion of a Chinese herbal medicine She chuang zi, the fruit of *Cnidium monnieri* Cusson (Umbelliferae) (Kitajima et al., 1998a, 1999a). The present study was carried out to isolate and characterise glucide fraction.

2. Results and discussion

The methanolic extract of the fruit of *C. monnieri* was partitioned between ethyl acetate and water, and the aqueous layer was subjected to Amberlite XAD-II chromotography to give water and methanol fractions. These fractions were subjected to Sephadex LH-20, silica gel, Lobar RP-8, octadecyl silica (ODS), carbohydrate analysis and polymer type column chromatographies to give eight glucides (**2**–**9**) and a sugar mixture. Glucides **2–5** were identified as erythritol, D-threitol, D-mannitol and 2-deoxy-D-ribono-1,4-lactone (Kitajima et al., 1999b), respectively. The sugar mixture was analyzed by HPLC using a carbohydrate analysis column, and the mixture was found to contain lactose (**10a**), maltose (**10b**), sucrose (**10c**), glucose (**10d**) and fructose (**10e**) in the ratio of 3:5:4:11:1. Glucide **5** is the second example of its isolation from natural sources.

Glucide **6** ($C_9H_{18}O_7$, a colorless syrup, $[\alpha]_D^{23}$ −127°) showed the $[M+H]^+$ ion peak at *m*/*z* 239 in the positive FAB–MS and its formula was determined from the accurate mass number of $[M+H]^+$. Acid hydrolysis of **6** gave fucose, and the ^1H, ^{13}C and ^{13}C-^1H correlation spectroscopy (COSY) NMR spectral data revealed the presence of 1 mol of α-fucopyranose and 1 mol of glycerol. The fucose should be in the L-form as $[M]_D$ of **6** showed a minus value (−302°) same as the methyl α-fucopyranoside (−350°) (Hough and Richardson, 1967). Furthermore, the heteronuclear multiple-bond correlation (HMBC) spectrum showed a H–C long-range correlation between the anomeric proton of fucose and C-2 carbon of glycerol indicating that **6** was glycerol 2-*O*-α-L-fucopyranoside.

Glucide **7** ($C_6H_{12}O_5$, a colorless syrup, $[\alpha]_D^{24}$ −11°) was a diastereoisomeric compound of **8** which was identified as 1-deoxy-D-glucitol (Kitajima et al., 1999b); these diastereomers could be separated by HPLC using polymer type column (Wakobeads T-100S). By comparison of NMR spectral data and optical rotation value with those of deoxyhexitols (L-rhamnitol (**7a**), L-fucitol (**7b**) and D-quinovitol ($[\alpha]_D^{24}$ −8°; Table 1) which were obtained by $NaBH_4$ reduction of the corresponding methylpentoses, **7** was identified as quinovitol (6-deoxy-D-glucitol).

* Corresponding author.

0031-9422/01/$ - see front matter © 2001 Elsevier Science Ltd. All rights reserved.
PII: S0031-9422(01)00238-2

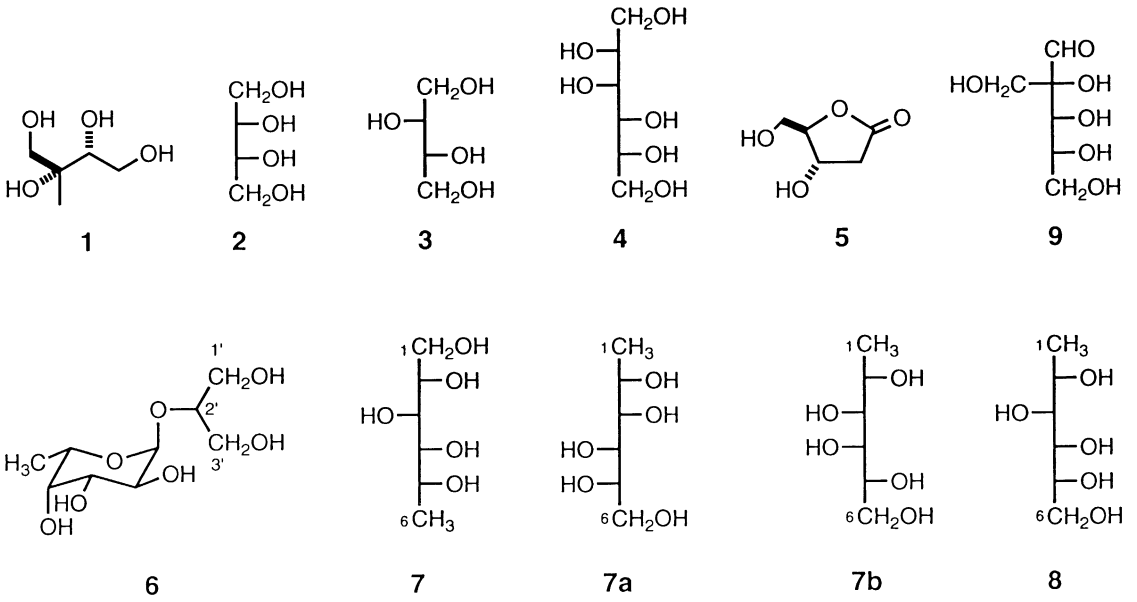

Fig. 1. Structures of compounds **1**–**9**, **7a** and **7b**.

Table 1
^{13}C NMR chemical shifts of **6**, **7**, **7a**, **7b** and **8** (in pyridine-d_5, 125 MHz)[a]

	6	7	7a[c]	7b	8
C-1	63.07				
C-2	82.02				
C-3	62.49				
C-1	101.13	64.46	21.36	20.80	20.32
C-2	70.42	71.06	68.71	67.47	70.01
C-3	71.66	75.41	75.14[b]	75.01	74.03
C-4	73.36	77.75	73.39[b]	72.27	74.86
C-5	67.61	68.49	71.68	72.43	73.21
C-6	17.22	21.07	65.30	65.24	65.23

[a] δ In ppm from TMS.
[b] Assignments may be interchanged in each column.
[c] Measured at 67.5 MHz.

Though **6** and **7** are very simple compounds, they are both new.

Glucide **9** ($C_6H_{12}O_6$, an amorphous powder, $[\alpha]_D^{22}$ -15°), which is one of the main components of the water-soluble portion, was identified as D-hamamelose by comparison of its NMR spectral data and optical rotation value with those published (Szarek et al., 1983; Nonaka et al., 1984).

Recently, a biosynthetic route leading to an isoprene which did not involve the mevalonate route was defined (Rohmer et al., 1996). In this route, hemiterpenoid **1**, which leaded from the rearrangement of deoxyxylulose phosphate (DXP) followed by a concomitant reduction, was considered as the first putative precursor of isopentenyl diphosphate (IPP). Besides, DXP results from the condensation of glyceraldehyde 3-phosphate (GAP) and pyruvic acid. (Duvold et al., 1997a,b; Kuzuzama et al., 2000). We also reported the possibility of the biosynthetic relationship between **1** and branched sugar D-apiose (Kitajima et al., 1998b). As co-existence of **1** and branched sugar D-hamamelose occurs in this fruit, and hamamelose is biosynthesized from two moles of GAP (Vickery and Vickery, 1981), a biosynthetic relationship between these two branched sugars might be suggested.

3. Experimental

Melting points were determined on a Yanagimoto micro melting point apparatus and are uncorrected. Optical rotations were measured on a JASCO DIP-370 digital polarimeter. FAB–MS were recorded with a Jeol HX-110 spectrometer using glycerol as matrix. ^1H and ^{13}C NMR spectra were taken on Jeol JNM GX-270 and A-500 spectrometers with tetramethylsilane as an internal standard, and chemical shifts were recorded in δ value. ^1H–^{13}C COSY, HMBC and NOESY spectra were obtained with the usual pulse sequence and data processing was performed with standard Jeol software. Column chromatography was carried out under TLC monitoring using Kieselgel 60 (70–230 mesh, Merck), Sephadex LH-20 (25–100 mm, Pharmacia), Lobar RP-8 column (Merck) and Amberlite XAD-II (Organo). TLC was performed on silica gel (Merck 5721) and spots were detected with *p*-anisaldehyde-H_2SO_4 reagent. HPLC separations were carried out on a JASCO chromatograph (980-system) with a JASCO RI-930 detector, and Symmetry Prep$^{TM}C_{18}$ 7 μm [waters; column size, 7.8×300 mm], Carbohydrate Analysis [Waters; column size, 3.9×300 mm] and Wakobeads T-100s [Wako; column size, 6.0×150 mm] were used as columns.

4. Extraction and separation of glucides

As reported in the previous paper (Kitajima et al., 1998a, 1999a), commercial fruit of *C. monnieri* Cusson (1 kg, purchased from Kinokuniya Chinese Medicine Pharmacy, Ltd., Japan, Lot. No. MU961715Y) was extracted with MeOH (5l). The aqueous portion of the MeOH extract was extracted with hot MeOH and the hot MeOH soluble portion was subjected to column chromatography on Amberlite XAD-II ($H_2O \rightarrow$MeOH) to afford water and MeOH eluent (21.2 g and 10.6 g), respectively. The MeOH eluate fraction was applied to a Sephadex LH-20 (MeOH) column which furnished six fractions (frs. 1 to 6). Fr. 2 (8.4 g) was purified by silica gel [$CHCl_3$–MeOH–H_2O (9:1:0.1→17:3:0.3→4:1:0.1→7:3:0.5)→MeOH] column chromatography to afford 14 fractions (frs. 2-1 to 2-14). From fr. 2-4 (465 mg), **5** (24 mg) was isolated by Lobar RP-8 [CH_3CN–H_2O (3:17)] and Sephadex LH-20 (MeOH) column chromatographic steps. The water eluent (21.2 g) was subjected to Sephadex LH-20 (MeOH) column chromatography to afford five fractions (frs. 1′ to 5′). Fr. 2′ (15.3 g) was purified by silica gel [$CHCl_3$–MeOH–H_2O (17:3:0.3→4:1:0.1→7:3:0.5)→MeOH] column chromatography to afford nine fractions. Fr. 2′-6 (369 mg) was subjected to a Lobar RP-8 column [CH_3CN–H_2O (1:99)] and HPLC [Carbohydrate Analysis, CH_3CN–H_2O (19:1)] to give **6** (10 mg), a mixture of **7** and **8** (40 mg) and a mixture of **2** and **3**. A mixture of **2** and **3** was acetylated with Ac_2O and pyridine, and the acetylated fraction was subjected to HPLC [Symmetryprep C_{18}, MeOH–H_2O (1:1)] to give **2**-acetate and **3**-acetate. They were deacetylated by heating with 5% NH_4OH–MeOH for 2 h in a water bath to give **2** (28 mg) and **3** (10 mg), respectively. A mixture of **7** and **8** was subjected to HPLC [Wakobeads T-100S ×2; CH_3CN–H_2O (17:3)] to give **7** (4 mg) and **8** (25 mg). The fr. 2′-7 (2.17 g) was subjected to Lobar RP-8 column [CH_3CN–H_2O (1:99)] and silica gel [$CHCl_3$–MeOH–H_2O (17:3:0.3→4:1:0.1→7:3:0.5)→MeOH] column chromatograpies, and purified by HPLC [Symmetryprep C_{18}, MeOH–H_2O (1:1)] to give **9** (403 mg). Fr. 2′-8 (565 mg) was treated with hot MeOH to give a residue (following solvent removal) and precipitate **4** (520 mg). The residue was applied to a silica gel column, eluted with $CHCl_3$–MeOH–H_2O (3:2:0.5) to afford a sugar fraction which was analyzed by HPLC [Carbohydrate analysis, CH_3CN–H_2O (17:3); flow rate 1.5 ml/min] to show the presence of lactose (**10a**, 11.8 min), maltose (**10b**, 11.4 min), sucrose (**10c**, 8.4 min), glucose (**10d**, 5.7 min) and fructose (**10e**, 5.1 min) in the ratio of 3:5:4:1:11.

The following compounds were identified by comparison with either authentic compounds or by analyses of NMR spectral and $[\alpha]_D$ data.

Erythritol (**2**), D-threitol (**3**), D-mannitol (**4**), 2-deoxy-D-ribono-1,4-lactone (**5**), 1-deoxy-D-glucitol (**8**) and D-hamamelose (**9**).

4.1. Glycerol 2-O-α-L-fucopyranoside (6)

A colorless syrup, $[\alpha]_D^{23}$ −127° ($c = 0.9$, MeOH). Positive FAB–MS m/z: 277 $[M+K]^+$, 261 $[M+Na]^+$, 239.1152 $[M+H]^+$ (base, calc. for $C_9H_{19}O_7$: 239.1131). ^{1}H NMR (pyridine-d_5) δ: 5.63 (1H, *d*, $J = 4.0$ Hz, H-1), 4.64 (1H, *dd*, $J = 4.0$, 10.0 Hz, H-2), 4.53 (1H, *dd*, $J = 3.0$, 10.0 Hz, H-3), 4.14 (1H, *br d*, $J = 3.0$ Hz, H-4), 4.61 (1H, *br d*, $J = 6.5$ Hz, H-5), 1.53 (3H, *d*, $J = 6.5$ Hz, H_3-6), 4.21 (1H, *dd*, $J = 4.0$, 11.5 Hz, H-1′a), 4.23 (1H, *dd*, $J = 6.0$, 11.5 Hz, H-1′b), 4.32 (1H, m, H-2′), 4.20 (1H, *dd*, $J = 6.0$, 11.5 Hz, H-3′a), 4.27 (1H, *dd*, $J = 4.0$, 11.5 Hz, H-3′b).

4.2. Acid hydrolysis of 6

Glucide **6** (5 mg) was dissolved in aq. 2 N H_2SO_4 and heated in a water bath for 3 h. The hydrolysate was neutralized with $NaHCO_3$ and the salt filtered off, and the filtrate was performed on TLC [silica gel, solv.; $CHCl_3$–MeOH–H_2O (7:3:0.5)] to show the presence of fucose [R_f 0.33, rhamnose: 0.41, quinovose: 0.37).

4.3. D-Quinovitol (7)

A colorless syrup, $[\alpha]_D^{24}$ −11° ($c = 0.2$, MeOH). Positive FAB–MS m/z: 189.0733 $[M+Na]^+$ (base, calc. for $C_6H_{14}O_5Na$: 189.0739). ^{1}H NMR (pyridine-d_5) δ: 1.68 (3H, *d*, $J = 6.0$ Hz, H_3-6), 4.50 (1H, *m*, H-5), 4.22 (1H, *br d*, $J = 6.5$ Hz, H-4), 4.56 (1H, *br d*, $J = 6.5$ Hz, H-3), 4.83 (1H, *m*, H-2), 4.35 (1H, *dd*, $J = 6.5$, 11.5 Hz, H-1a), 4.44 (1H, *dd*, $J = 6.5$, 11.5 Hz, H-1b).

4.4. $NaBH_4$ reduction of D-quinovose, L-rhamnose and L-fucose

Commercial L-rhamnose, L-fucose and D-quinovose (each 50 mg) were dissolved in MeOH (10 ml) and stirred with $NaBH_4$ (10 mg) for 5 h at room temperature, respectively. After work-up, the residues were purified by Sephadex LH-20 (MeOH) to give L-rhamnitol (**7a**), L-fucitol (**7b**) and D-quinovitol ($[\alpha]_D^{24}$ −8° ($c = 4.0$, MeOH), each 40 mg), respectively. The ^{1}H and ^{13}C NMR spectral data, and optical rotation value of **7** were identical with those of D-quinovitol.

Acknowledgements

The authors thank Messrs. Y. Takase and H. Suzuki of the Central Analytical Department of this University for NMR and MS measurements.

References

Duvold, T., Bravo, J.M., Pale-Grosdemange, C., Rohmer, M., 1997. Biosynthesis of 2-*C*-methyl-D-erythritol, a putative C_5 intermediate

in the mevalonate independent pathway for isoprenoid biosynthesis. Tetrahedron Lett. 38, 4769–4777.

Duvold, T., Cali, P., Bravo, J.M., Rohmer, M., 1997. Incorporation of 2-*C*-methyl-D-erythritol, a putative isoprenoid precursor in the mevalonate-independent pathway, into ubiquinone and menaquinone of *Escherichia coli*. Tetrahedron Lett. 38, 6181–6184.

Hough L., Richardson A.C., 1967. In: Coffey, S. (Ed.), Rodd's Chemistry of Carbon Compounds. Vol. 1^{F}. Elsevier Publishing, Barking, p. 520.

Kitajima, J., Aoki, Y., Ishikawa, T., Tanaka, Y., 1998a. Monoterpenoid polyols in fruit of *Cnidium monnieri*. Chem. Pharm. Bull. 46, 1580–1582.

Kitajima, J., Aoki, Y., Ishikawa, T., Tanaka, Y., 1999a. Monoterpenoid glucosides of *Cnidium monnieri* fruit. Chem. Pharm. Bull. 47, 639–642.

Kitajima, J., Ishikawa, T., Tanaka, Y., Ida, Y., 1999b. Water-soluble constituents of fennel. IX. Glucides and nucleosides. Chem. Pharm. Bull. 47, 988–992.

Kitajima, J., Suzuki, N., Ishikawa, T., Tanaka, Y., 1998b. New hemiterpenoid pentol and monoterpenoid glycoside of torillis japonica fruit, and consideration of the origin of apiose. Chem. Pharm. Bull. 46, 1583–1586.

Kuzuyama, T., Takahashi, S., Takagi, M., Seto, H., 2000. Characterization of 1-deoxy-D-xylulose 5-phosphate reductoisomerase, an enzyme involved in isopentenyl diphosphate biosynthesis, and identification of its catalytic amino acid residues. J. Biol. Chem. 275, 19928–19932.

Nonaka, G., Ishimaru, K., Tanaka, T., Nishioka, I., 1984. Tannins and related compounds. XVII. Gallohamameloses from *Castanea crenata* L. and *Sanguisorba officinalis* L. Chem. Pharm. Bull. 32, 483–489.

Rohmer, M., Seemann, M., Horbach, S., Bringer-Meyer, S., Sahm, H., 1996. Glyceraldehyde 3-phosphate and pyruvate as precursors of isoprenic units in an alternative non-mevalonate pathway for terpenoid. J. Am. Chem. Soc. 118, 2564–2566.

Szarek, W.A., Pinto, B.M., Grindley, T.B., 1983. A highly stereoselective intramolecular aldol condensation. Part II. Synthesis of D, L-hamamelose from 2,2′-*O*-methylene-bis-D-glycerose. Can. J. Chem. 61, 461–469.

Vickery, M.L., Vickery, B., 1981. Secondary Plant Metabolism. Macmillan, London. p. 27.

PERGAMON

Phytochemistry 58 (2001) 645–651

PHYTOCHEMISTRY

www.elsevier.com/locate/phytochem

Glycosides and xanthine oxidase inhibitors from *Conyza bonariensis*

L.D. Kong[a], Z. Abliz[b], C.X. Zhou[a], L.J. Li[b], C.H.K. Cheng[c], R.X. Tan[a,*]

[a]*Institute of Functional Biomolecule, State Key Laboratory of Pharmaceutical Biotechnology, School of Life Science, Nanjing University, Nanjing 210093, People's Republic of China*

[b]*Department of Instrumental Analysis for Determination of Chemical Structures, Institute of Materia Medica, Chinese Academy of Medical Sciences and Peking Union Medical College, Beijing 100050, People's Republic of China*

[c]*Department of Biochemistry, The Chinese University of Hong Kong, Shatin, N. T., Hong Kong*

Received in revised form 12 December 2000

Abstract

Fractionation of the xanthine oxidase inhibitory methanol extract of *Conyza bonariensis* afforded three glycosides, in addition to nine known compounds including amyrin, β-sitostero1 daucosterol, syringic acid 3-hydroxy-5-methoxybenzoic acid, eugenol 4-*O*-glucopyranoside, and luteolin, apigenin and takakin 8-*O*-glucuronide. The structures of the glycosides were established by a combination of spectroscopic methods (IR, MS, ^{1}H and ^{13}C NMR, DEPT, COSY, HMQC and HMBC) as 4-hydroxypyridin-3-carboxylic acid 4-*O*-glucopyranoside, 8-hydroxy-6,7-dihydrolinalool 8-*O*-glucopyranoside and bonaroside [viz. 1,3,4,12-tetrahydroxy-2-(9-hexadecenoylamino)octadecane 1-*O*-glucopyranoside]. The in vitro enzyme assay showed that syringic acid and takakin 8-*O*-glucuronide displayed weak inhibitory activity against xanthine oxidase with IC_{50} values of 500 ± 41 μM and 170 ± 12 μM, respectively. © 2001 Elsevier Science Ltd. All rights reserved.

Keywords: *Conyza bonariensis*; Asteraceae; 4-Hydroxypyridin-3-carboxylic acid 4-*O*-glucopyranoside; 8-Hydroxy-6,7-dihydrolinalool 8-*O*-glucopyranoside; Bonaroside; Syringic acid; Takakin 8-*O*-glucuronide

1. Introduction

Conyza bonariensis (L.) Crong (Asteraceae) has been phytochemically investigated (El-Karemy et al., 1986; Rizk et al., 1986; Ferraro et al., 1988; Sanz and Marco, 1991). However, the species growing in China has not been examined to date. In continuation of our investigations of plant-derived xanthine oxidase inhibitors (Li et al., 1999; Zhou et al., 1999), the methanol extract was found to be active against the enzyme which is closely related to the hyperuricemia and gout (Tsutomu et al., 1991; Cos et al., 1998). We therefore analyzed the extract in detail in order to characterize the xanthine oxidase inhibitor(s).

2. Results and discussion

Repeated chromatography of the methanol extract of *C. bonariensis* on silica gel and Sephadex LH-20 afforded three new glycosides (**1**–**3**), in addition to the known constituents amyrin, β-sitosterol, daucosterol, apigenin, luteolin, takakin 8-*O*-glucuronide, syringic acid and 3-hydroxy-5-methoxybenzoic acid. The in vitro evaluation of these isolates demonstrated that the enzyme inhibitors present in the title species were syringic acid and the three flavonoids.

The identification of amyrin, β-sitosterol and daucosterol was accomplished by direct comparisons (co-TLC, IR and EIMS) with authentic samples available in our laboratory. The spectral data (IR, EIMS, ^{1}H and ^{13}C NMR) of the two acids revealed that they were syringic acid (Cuenca et al., 1992) and 3-hydroxy-5-methoxybenzoic acid (Majumder et al., 1996), respectively. Syringic acid was previously found to have antioxidant (Yoshiki et al., 1995), antibacterial (Fernandez et al., 1996), antifungal (Lattanzio et al., 1994), properties, as well as being protective against cell damage induced by superoxide anion radicals in murine dermal fibroblasts (Masaki et al., 1995). The structures of apigenin and luteolin were ascertained by their IR, EIMS, ^{1}H and ^{13}C NMR spectra (Markham et al., 1978; Noro et al., 1983; Tosun and Akyuz, 1997). Both flavones were previously

* Corresponding author. Tel./fax: +86-25-359-3201.
E-mail address: rxtan@netra.nju.edu.cn (R.X. Tan).

0031-9422/01/$ - see front matter © 2001 Elsevier Science Ltd. All rights reserved.
PII: S0031-9422(01)00176-5

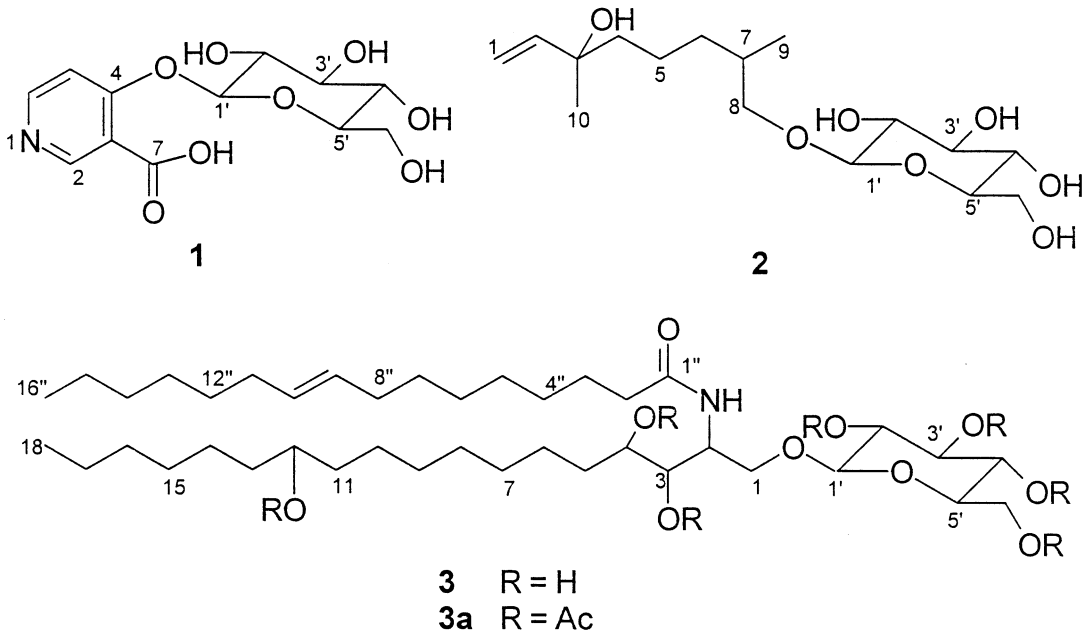

investigated biologically and reported to be antioxidant and anti-inflammatory (Maokn et al., 1996; Silvan et al., 1996; Yokozawa et al., 1997). Furthermore, apigenin was found to inhibit tumor necrosis factor-induced intercellular adhesion molecule-1 upregulation in vivo (Panes et al., 1996), and to have anti-TPA-induced transformation, anti-protein kinase C activation and anti-TPA-induced c-jun expression activities (Lee and Lin, 1997), whereas luteolin had cancer chemopreventive and antiplatelet effects (Cai et al., 1997; Lin et al., 1997). Furthermore, luteolin and apigenin have been reported to be xanthine oxidase inhibitors (Cos et al. 1998, Kasai et al., 1999). The flavone glycoside was identified as takakin 8-O-glucuronide by the IR, EIMS, ^{1}H and ^{13}C NMR spectral data (Chen et al., 1994). The second glycoside was demonstrated to be eugenol 4-*O*-glucopyranoside by its spectral data (FABMS, IR, ^{1}H and ^{13}C NMR), characterized previously as the corresponding peracetate from *Artemisia dracunculus* (Jakupovic et al., 1991).

In the ^{1}H NMR spectrum of compound **1**, a broadened singlet at δ 8.34 and a pair of mutually coupled doublets ($J=5.6$ Hz) at δ 8.15 and 6.61 indicated that it was most likely a pyridine derivative carrying presumably 3-carbonyl and 4-hydroxyl (or amino) groups (Rasala, 1993). This hypothesis was subsequently confirmed by the ^{13}C NMR spectrum of **1**, which exhibited a total of twelve carbon resonance lines consisting of one methylene, eight methine and three quaternary carbons. Subtracting a set of carbon signals due to a glucopyranosyl group, the rest was ascribable to the 4-hydroxypyridin-3-carboxylic acid nucleus (Yu et al., 1989). As to the attachment of the glucopyranosyl group, the chemical shift of the anomeric proton doublet ($J=7.8$ Hz) at δ 4.91 supported the formulated glycosidation pattern if compared with that of carboxylic (δ ~6.20) and phenolic (δ~4.90) glucosides described previously (Jakupovic et al., 1991; Tan et al., 1993). Finally, the structure of glycoside **1** was reinforced by its FABMS spectrum which gave an intense protonated molecular ion at m/z 302, accompanied by a strong fragment at m/z 140 produced through the elimination of the glucosyl moiety from the quasimolecular ion.

The structure of glycoside **2** followed from its spectral data. The El mass spectrum of **2** was not informative. However, an intense quasimolecular ion was observed at m/z 335 ($[M+H]^{+}$) in its FABMS spectrum. Besides a set of proton resonances attributable to a glucopyranosyl moiety, the ^{1}H NMR spectrum of glycoside **2** exhibited a methyl singlet at δ 1.20, a three-proton doublet ($J=6.7$ Hz) at δ 0.91, a pair of double doublets at δ 3.82 and 3.66 due to an oxygenated methylene group, and a set of signals at δ 5.88 (1 H, *dd*, $J=17.4$, 10.8 Hz), 5.15 (IH, *dd*, $J=17.4$, 1.5 Hz) and 4.98 (1H, *dd*, $J=10.8$, 1.5 Hz) arising from a vinyl function. These ^{1}H NMR spectroscopic data showed that compound **2** was most probably a 8-hydroxy-6,7-dihydrolinalool glucoside (Tan et al., 1991; Schulz et al., 1997). This proposal was substantiated by its ^{13}C NMR and DEPT spectra. All carbon signals could be assigned by comparing them with those of 6,7-dihydrolinalool analogs (Yu et al., 1989). The glucopyranosyloxy group was shown to be at C-8 by the glycosidation induced downfield shift (δ 76.2) of the 8-oxygenated methylene carbon

signal. In conclusion, glycoside **2** was 8-hydroxy-6,7-dihydrolinalool 8-*O*-glucopyranoside.

The molecular formula of compound **3** was found to be $C_{40}H_{77}NO_{10}$ by its FABMS, ^1H and ^{13}C NMR, and DEPT data and the HREIMS spectrum of the corresponding peracetate (**3a**). The ^1H and ^{13}C NMR spectra of **3** indicated that it was also a glucopyranoside (Table 1). Furthermore, a carbonyl IR absorption at 1720 cm^{-1}, and the six-proton triplet ($J = 7.0$ Hz) at δ 0.86 and a pair of olefinic proton signals at δ 5.34 and 5.42 in its ^1H NMR spectrum demonstrated that it possessed presumably two aliphatic chains, one of which carried a double bond. Thus, the three unsaturations of the molecular formula could be readily assigned to a double bond, a carbonyl and a glucopyranosyl group. This hypothesis was subsequently confirmed by the ^{13}C NMR spectrum and FABMS of **3**. In addition to the quasimolecular ion at m/z 754 $[M+Na]^+$, the FABMS spectrum of **3** exhibited an intense fragment peak at m/z 570 which was produced by elimination of the glucosyl residue from the protonated molecular ion. The loss of hexadecenamide from the molecular ion gave rise to the fragment at m/z 316. The 9,10-double bond was assigned to the hexa decenoyl group on the basis of the typical fragment ion at m/z 500 which was formed by elimination of pentene from that at m/z 570 through McLafferty rearrangement (Fig. 1). Obviously, the other aliphatic chain should consist of eighteen carbons. Moreover, the presence of a total of seven hydroxyl groups in the molecule was deduced by comparison between the molecular ions appearing in the FABMS spectra of **3** and **3a**. Accordingly, after subtraction of the four hydroxyls involved in the glucopyranosyl group, the other three had to be positioned in the C_{18} chain. The ^1H–^1H COSY spectrum of **3** showed that a pair of double doublets of an oxygenated methylene at δ 4.01 (*dd*, $J = 10.5$, 6.2 Hz) and 3.76 (*dd*, $J = 10.5$, 3.5 Hz) coupled to the oxygen-bearing methine signal at δ 4.24 (*ddd*, $J = 6.5$, 6.2, 3.5 Hz). This resonance showed a correlation with the double doublet ($J = 6.5$, 6.0 Hz) at δ 3.56 which coupled further to the signal at δ 3.48 (*ddd*, $J = 6.2$, 6.5, 3.5 Hz). In the HMQC spectrum of **3**, the signal at δ 4.24 correlated to the methine carbon at δ 51.6. These observations required the given 1,3,4-trioxygenated and 2-nitrigenated pattern. The glycosidation at C-1 was indicated by the downfield shifted signal of C-1 at δ 70.0 (Kasai et al., 1999). The 9-hexadecenoylamino group was found to be at C-2 by the resonance of H-2 at δ 4.24 which was shifted remarkably downfield owing to acylation. In addition to the 3,4-diol system, the final hydroxyl group was found to be at C-12 by diagnostic fragment ions in FABMS spectrum of **3a**. The characteristic fragment at m/z 157, which yielded the peak at m/z 115 due to the loss of ketene, was produced through the cleavage of the C_{11}–C_{12} bond (Fig. 2). In conclusion, glycoside **3** was 1, 3,4,1 2-tetrahydroxy-2-(9-hexadecenoylamino)octadecane 1-*O*-glucopyranoside. The configuration at the chiral centers could not be established without chemical transformations that would require much more material. We have named this glycoside bonaroside.

Table 1
^1H and ^{13}C NMR spectral data of glycoside **3**[a]

Position	δ_C[b] (DEPT)	δ_H[b], multiplicity J (Hz)
1	70.0 (CH_2)	4.01 *dd* (10.5, 6.2), 3.76 *dd* (10.5, 3.5)
2	51.6 (CH)	4.24 *ddd* (6.5, 6.2, 3.5)
3	75.5 (CH)	3.56 *dd* (6.5, 6.0)
4	72.8 (CH)	3.48 *ddd* (6.2, 6.0, 3.5)
5	32.7 (CH_2)	1.48 *m* (2H)
6, 10, 14	30.5 ($2CH_2$), 30.3 (CH_2) *d*	
16	33.1 (CH_2)	1.25 *m* (2H)
17	23.7 (CH_2)	1.25 *m* (2H)
18	14.5 (CH_3)	0.86 *t* (7.0)
1′	104.7 (CH)	4.24 *d* (7.8)
2′	75.0 (CH)	3.13 *dd* (9.0,7.8)
3′	77.8 (CH)	3.33 *dd* (9.l, 9.0)
4′	71.5 (CH)	3.26 *m*
5′	78.0 (CH)	3.26 *m*
6′	62.6 (CH_2)	3.83 *dd* (11.9, 2.7), 3.63 *dd* (11.9, 4.8)
1″	177.1 (C)	
2″	35.7 (CH_2)	1.58–1.62 *m* (2H)
3″	26.1 (CH_2)	1.26 *m* (2H)
8″, 11″	27.1 (CH_2), 26.1 (CH_2)	1.95–2.01 *m* (4H)
9″	131.4 (CH)	5.36 *br dt* (16.8, 6.5)
10″	131.5 (CH)	5.42 *br dt* (16.8, 6.5)
14″	33.1 (CH_2)	1.25 *m* (2H)
15″	23.7 (CH_2)	1.25 *m* (2H)
16″	14.5 (CH_3)	0.86 *t* (7.0)

[a] Assigned by spin decoupling, ^1H–^1H COSY and HMQC experiments.

[b] The chemical shifts of C-7–C-9, C–15, C-4″–C-7″, C-12″ and C-13″: 30.9–30.6 (10 CH_2), and those of protons thereon: 1.25–1.32 m (20 H).

All isolates were tested for the xanthine oxidase inhibitory activity as described elsewhere (Li et al., 1999; Zhou et al., 1999). The xanthine oxidase inhibitors present in the methanol extract of *C. bonariensis* were revealed to be syringic acid, luteolin, apigenin and takakin 8-*O*-β-D-glucuronide. In addition to the known xanthine oxidase inhibitory flavone luteolin and apigenin (Kasai et al., 1999; Cos et al., 1998), syringic acid and takakin 8-O-glucuronide were displayed for the first time to be active against the enzyme with IC_{50} values of 500 ± 41 and 170 ± 12 μM, respectively. The IC_{50} value of allopurinol co-assayed in the study as positive control was shown to be 10.

The present phytochemical investigation of *C. bonariensis* growing widely in China has led to the characterization of three new glycosides and four xanthine oxidase inhibitory natural products. However, except widespread compounds such as amyrin, β-sitosterol,

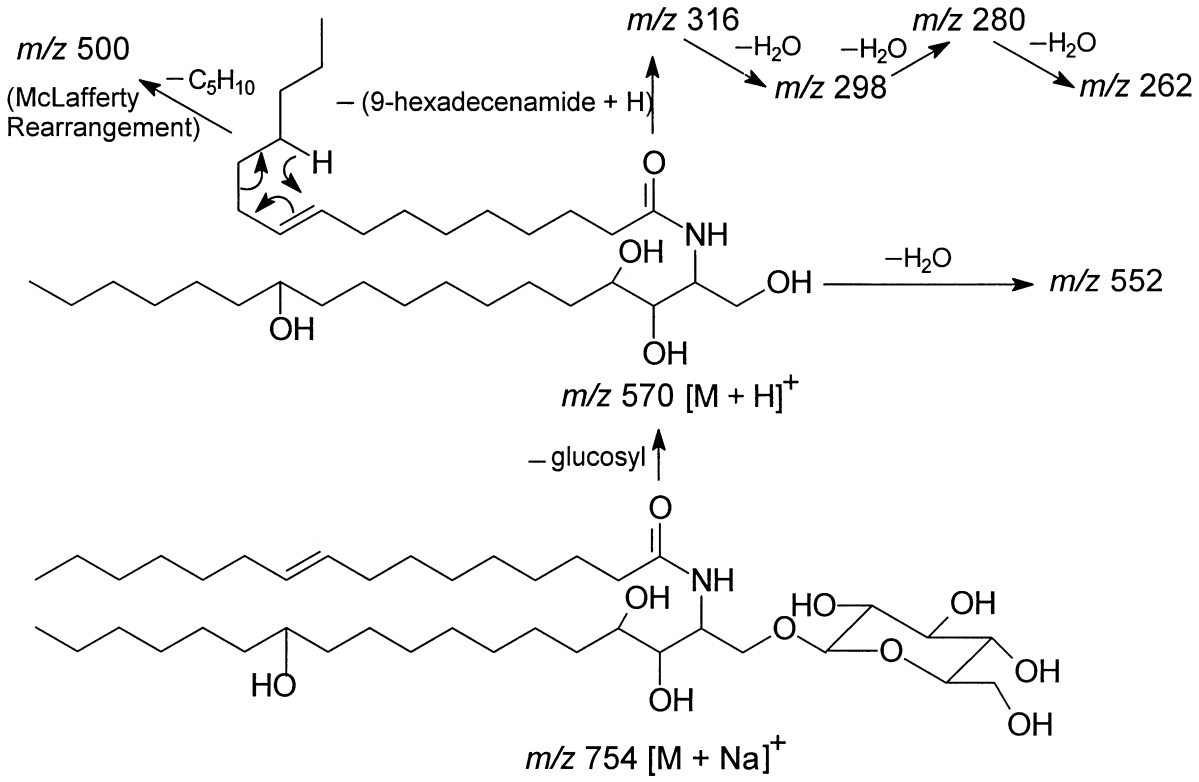

Fig. 1. Diagnostic fragments of glycoside **3**.

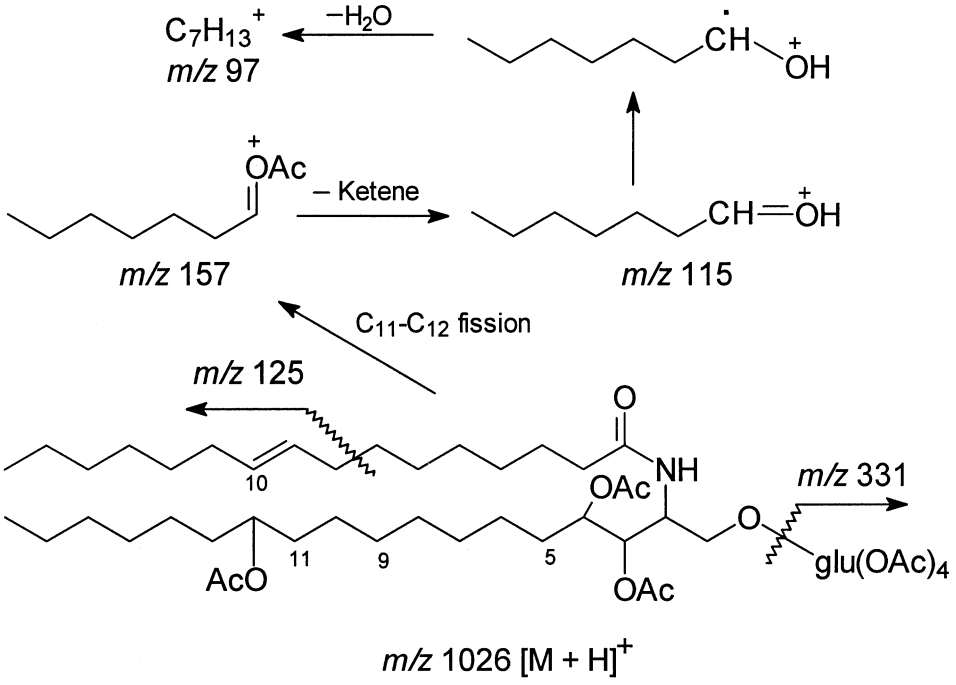

Fig. 2. Diagnostic FABMS fragmentions of **3a**.

daucosterol, luteolin and apigenin, the constituents of *C. bonariensis* growing in China are quite different from those of the same species collected abroad (El-Karemy et at., 1986; Rizk et al., 1986; Ferraro et al., 1988; Sanz and Marco, 1991). This is presumably due to different phytochemical strategies and/or geographical deviation, the latter affecting putatively the biosynthesis and accumulation of plant secondary metabolites.

3. Experimental

3.1. General

Optical rotations were measured on a DXP-118 instrument. IR spectra were recorded in KBr disks on a Perkin-Elmer 577 instrument. All NMR experiments were performed on a Jeol JNM-A 500 FT–NMR spectrometer using TMS as the internal standard. El and FABMS experiments were run on either VG-ZAB-HS or Jeol JMX-HX110 mass spectrometers, respectively. Silica gel (200–300 mesh) for column chromatography and GF_{254} (30–40 μ) for TLC were produced by Qingdao Marine Chemical Factory, Qingdao, China. Sephadex LH-20 was from Pharmacia Biotech, Sweden. Other chemicals used in this study were of analytical grade.

3.2. Plant material

The aerial parts of *C. bonariensis* was collected on 19 June 1996 from the Xuanwu Lake Park, and identified by Professor Z.P. Wang, School of Life Science, Nanjing University, Nanjing 210093, China. A voucher specimen, registered under the number Y 96619B, was preserved in the Herbarium of Nanjing University, Nanjing, China.

3.3. Extraction and isolation

The powdered air-dried plant material (900 g) was extracted twice (24 h each) with MeOH at room temperature. Evaporation of solvent from the combined extracts in vacuo at 55°C gave a dark residue (57 g) which was dissolved in MeOH followed by filtration. The filtrate was concentrated to a black gum (32 g) under reduced pressure and subsequently separated by CC (silica gel, 900 g, 200–300 mesh). Elution with petrol–acetone gradient (9:1→10:1) was followed by acetone and acetone-MeOH mixtures (100:5→1:10). According to TLC monitoring and xanthine oxidase assay, seven fractions were collected (F-1: 3.2 g, F-2: 2.1 g, F-3: 3.4 g, F-4: 2.6 g, F-5: 4.6 g, F-6: 3.5 g and F-7: 2.5 g). F-1 and F-3 contained nothing of interest. F-4 and F-5 showed significant inhibitory activity against xanthine oxidase. CC of F-2 over silica gel (200 g, 200–300 mesh) with a gradient of petrol-acetone mixtures (25:1→1:9) gave β-sitosterol (96 mg) and amyrin (39 mg). CC of F-4 on silica gel with a $CHCl_3$–MeOH gradient (100:1→+2:1) yielded 2 fractions (F-4-1 and F-4-2). Gel filtration of F-4-1 on Sephadex LH-20 with $CHCl_3$–MeOH (1:1) yielded syringic acid (28 mg) and pigments. Luteolin (35 mg) and apigenin (26 mg) were obtained from F-4-2 by column chromatography on silica gel (50 g) using $CHCl_3$–MeOH mixtures of a growing polarity. F-5 was applied to a silica gel column (800 g) eluted with $CHCl_3$–MeOH gradient to afford 3 fractions (F-5-l, F-5-2 and F-5-3). Repeated gel filtration of F-5-1 on Sephadex LH-20 with $CHCl_3$–MeOH (1:1) afforded **2** (18 mg) and **3** (15 mg). Gel filtration of F-5-2 over Sephadex LH-20 with $CHCl_3$–MeOH (1:9) yielded again **3** (7 mg) and takakin 8-*O*-glucuronide (34 mg). CC of F-5-3 over silica gel with $CHCl_3$–MeOH gradient (50:1→2:1) gave daucosterol (120 mg) and eugenol 4-*O*-glucopyranoside (26 mg). Separation of F-6 and F-7 following the same procedure gave again eugenol 4-*O*-glucopyranoside (16 mg), glycoside **1** (220 mg) and 3-hydroxy-5-methoxybenzoic acid (38 mg).

3.4. Xanthine oxidase assay

The xanthine oxidase inhibitory activity was measured according to a slight modification of the previously reported method (Li et al., 1999; Zhou et al., 1999). Xanthine oxidase from cow milk, xanthine and the standard inhibitor allopurinol were purchased from Sigma Chemical Co. (St. Louis, MO, USA). The reaction mixture contains 80 mM sodium pyrophosphate buffer (pH = 8.5), 120 μM xanthine and 0.1 unit of xanthine oxidase. The absorption at 295 nm indicating the formation of uric acid at 25°C was monitored and the initial rate was calculated. The test materials, initially dissolved in DMSO and then diluted with the same buffer, were incorporated in the enzyme assay to assess the inhibitory activity. Extracts, fractions and isolates were tested at 100 μg/ml, and those inhibiting the enzyme >50% were further tested to determine IC_{50} values.

3.5. 4-Hydroxypyridyl-3-oic acid 4-O-glucopyranoside (*1*)

Colourless needles, mp 203–205°C, $[\alpha]_D^{25}$ −250.4° (MeOH; *c* 1.35). FABMS *m/z:* 302.0889 $[M+H]^+$ ($[C_{12}H_{15}NO_8+H]^+$ requires 302.0878), 40 $[M+H-glucosyl]^+$. ^1H NMR (D_2O, 500 MHz): δ 8.34 (1H, *brs*, H-2), 8.15 (1H, *br d*, *J* = 5.6 Hz, H-6), 6.61 (1H, *d*, *J* = 5.6 Hz, H-5), 4.91 (1H, *d*, *J* = 7.8 Hz, H-1′), 3.45–3.60 (4H, *m*, H-2′–H-5′), 3.93 (1H, *dd*, *J* = 12.2, 0.3 Hz, H-6′a), 3.75 (1H, *dd*, *J* = 12.2, 5.0 Hz, H-6′b). ^{13}C NMR (D_2O, 125 MHz) (multiplicities by the DEPT pulse sequences): δ 146.7 (*d*, C-2), 126.5 (*s*, C-3), 147.2 (*s*, C-4), 116.6 (*d*, C-5), 158.6 (*d*, C-6), 176.6 (*s*, C-7), 102.3 (*d*, C-1′), 73.8 (*d*, C-2′), 76.2 (*d*, C-3′), 70.2 (*d*, C-4′), 77.4 (*d*, C-5′), 61.4 (*t*, C-6′).

3.6. 8-Hydroxy-6,7-dihydrolinalool 8-O-glucopyranoside (*2*)

Gum. IR (KBr) ν_{max} cm^{-1}: 3300 (OH), 1650 (C=C). FABMS *m/z:* 335.2101 $[M+H]^+$ ($[C_{16}H_{30}O_7+H]^+$ requires 335.2072). ^1H NMR (CD_3OD, 500 MHz): δ5.8 8 (1H, *dd*, *J* = 17.4, 10.8 Hz, H-2), 5.15 (1H, *dd*, *J* = 17.4, 1.5 Hz, H-1a), 4.98 (1H, *dd*, *J* = 10.8, 1.5 Hz,

H-1b), 3.82 (1H, *dd*, $J=12.1$, 3.3 Hz, H-8a), 3.66 (1H, *dd*, $J=12.1$, 6.9 Hz, H-8b), 1.72 (1H, *m*, H-7), 1.44–1.30 (2H, *m*, H-4), 1.20 (3H, *s*, H-10), 1.18–0.88 (4H, *m*, H-5–H-6), 0.91 (3H, *d*, $J=6.7$ Hz, H-9), 4.20 (1H, *d*, $J=7.8$ Hz, H-1′), 3.14 (1H, *dd*, $J=9.0$, 7.8 Hz, H-2′), 3.21–3.37 (3H, *m*, H-3′–H-5′), 3.84 (1H, *dd*, $J=12.2$, 2.1 Hz, H-6′a), 3.64 (1H, *dd*, $J=12.2$, 5.0 Hz, H-6′b). ^{13}C NMR (CD_3OD, 125 MHz) (multiplicities by the DEPT pulse sequences): δ 110.4 (t, C-1), 145.1 (*d*, C-2), 72.5 (*s*, C-3), 42.2 (*t*, C-4), 21.3 (*t*, C-5), 34.1 (*t*, C-6), 33.1 (*d*, C-7), 76.2 (*t*, C-8), 16.0 (*q*, C-9), 26.2 (*q*, C-10), 103.1 (*d*, C-1′), 73.7 (*d*, C-2′), 76.5 (*d*, C-3′), 70.2 (*d*, C-4′), 76.7 (*d*, C-5′), 61.4 (*t*, C-6′).

3.7. Bonaroside (*3*)

White powder, mp 172–174°C, $[\alpha]_D^{25}+178.6°$ (MeOH; *c* 0.14). IR (KBr) ν_{max} 3350 (OH), 1720 (C=O). FABMS data and fragmentation were illustrated in Fig. 1. ^{1}H and ^{13}C NMR, see Table 1. Treatment of compound **3** with Ac_2O–pyridine (1:1) at room temperature for 36 h followed by preparative TLC with $CHCl_3$–MeOH (25:1), gave the corresponding peracetate **3a**. FABMS *m/z:* 1026.6380 $[M+H]^+$ ($[C_{54}H_{91}NO_{17}+H]^+$ requires 1026.6367), 984 $[M+H–ketene]^+$, 966 $[M+H–AcOH]^+$, 772 [M–9-hexadecenamide]$^+$, 331 $[glu(OAc)_4]^+$, 157 $[CH_3CH_2CH_2CH_2CH_2CH_2–CH=O^+Ac]$, 115 $[CH_3CH_2CH_2CH_2CH_2CH_2–C=O^+H]$. Other spectral measurements were not permitted due to very limited amount of the derivative.

Acknowledgements

Grants to L.D.K. from China Postdoctoral Science Foundation (No. 9615) and R.X.T. from the National Natural Science Foundation (Nos. 39725033 and 39970083) and from the fund from the Doctoral Program of Higher Education (No. 1999028419) are gratefully acknowledged.

References

Cal, Q.Y., Rahn, R.O., Zhang, R.W., 1997. Dietary flavonoids, quercetin, luteolin and genistein, reduced oxidative DNA damage and lipid peroxidation and quench free radicals. Cancer Letters 119, 99–107.

Chen, Z.T., Lee, S.T., Chen, C.M., 1994. New flavanoid glycosides of *Helicteres angustica*. Heterocycles 38, 1399–1406.

Cos, P., Ying, L., Calomme, M., Hu, J.P., Cimanga, K., Van Poel, B., Pieters, L., Vlietinck, A.J., Vanden Berghe, D., 1998. Structure–activity relationship and classification of flavonoide as inhibitors of xanthine oxidase and superoxide scavengers. Journal of Natural Products 61, 71–76.

Cuenca, M.D.R., Borkosky, S., Catalan, C.A.N., Diaz, J.G., Herz, W. A cadinanolide and other sesquiterpene lactones from *Mikania haenkeana*. Phytochemistry 31, 3521–3525, and related references cited therein.

El-Karemy, Z.A.R., Mansour, R.M.A., Frayed, A.A., Saleh, N.A.M., 1986. The flavonoids of local members of Astereae (Compositae). Biochemical Systematics and Ecology 15, 53–55.

Fernandez, M.A., Garcia, M.D., Saenz, M.T., 1996. Antibacterial activity of phenolic acid fractions of *Scrophulariafrutescens* and *S. sambucifolia*. Journal of Ethnopharmacology 53, 11–14.

Ferraro, G.E., Broussalis, A.M., Van Baaren, C.M., Muschietti, L.V., Coussio, J.D., 1988. Polyphenolic compounds isolated from *Conyza bonariensis* (Compositae). Rev. Latinoam. Quim. 19, 141–143.

Jakupovic, J., Tan, R.X., Bohlmann, F., Jia, Z.J., Huneck, S., 1991. Acetylenes and other constituents from *Artemisia dracunlus*. Planta Medica 57, 450–453.

Kasai, R., Sasaki, A., Hashimoto, T., Kaneko, T., Ohtani, K., Yamasaki, K., 1999. Cycloartane glycosides from *Trichosanthes tricuspidata*. Phytochemistry 51, 803–808.

Lattanzio, V., De Cicco, V., Di Venere, D., Lima, G., Salerno, M., 1994. Antifungal activity of phenolics against fungi commonly encountered during storage. Italian Journal of Food Sciences 6, 23–30.

Lee, S.F., Lin, J.-K., 1997. Inhibitory effects of phytopolyphenols on TPA-induced transformation, PKC activation, and c-jun expression in mouse fibroblast cells. Nutrition and Cancer 28, 177–183.

Li, H., Meng, J.C., Cheng, C.H.K., Higa, T., Tanaka, J., Tan, R.X., 1999. New guaianolides and xanthine oxidase inhibitory flavonols from *Ajania fruticulosa*. Journal of Natural Products 62, 1053–1055.

Lin, C.N., Kuo, S.H., Chung, M.I., Ko, F.N., Teng, C.M., 1997. A new flavone C-glycoside and antiplatelet and vasorelaxing flavones from *Gentiana arisanensis*. Journal of Natural Products 60, 851–853.

Majumder, P.L., Banerjee, S., Sen, S., 1996. Three stilbenoids from the orchid *Agrostophyllum callosum*. Phytochemistry 42, 847–852, and related references cited therein.

Maokn, T., Sakushima, A., Coskun, M., Ito, Y., 1996. Antioxidant activity of phenolic compounds of *Boreava orientalis*. Nihon Yukagakkaishi 45, 671–673.

Markham, K.R., Ternai, B., Stanley, R., Geiger, H., Mabry, T.J., 1978. Carbon-13 NMR studies of flavonoids–III naturally occurring flavonoid glycosides and their acylated derivatives. Tetrahedron 34, 1389–1397.

Masaki, H., Atsumi, T., Sakurai, H., 1995. Protective activity of hamamelitannin on cell damage induced by superoxide anion radicals in murine dermal fibroblasts. Biological Pharmaceutical Bulletin 18, 59–63.

Noro, T., Oda, Y., Miyase, T., Ueno, A., Fukushima, S., 1983. Inhibitors of xanthine oxidase from the flowers and buds of *Daphne genkwa*. Chemical Pharmaceutical Bulletin (Tokyo) 31, 3984–3987.

Panes, J., Gerritsen, M.E., Anderson, D.C., Miyasaka, M., Granger, D., 1996. Apigenin inhibits tumor necrosis factor-induced intercellular adhesion molecule — 1 upregulation in vivo. Neil Microcirculation (Philadelphia) 3, 279–286.

Rasala, D., 1993. H-1 NMR spectra of substituted aminopyridines. Spectroscopy Letters 26, 227–235.

Rizk, A.M., Heiba, H.I., Ma'Ayergi, H.A., Batanoury, K.H., 1986. Constituents of plants growing in Qatar. Fitoterapia 57, 3–9.

Sanz, J.F., Marco, J.A., 1991. A new butenolide from *Conyza bonariensis*.. Liebigs Annalen Chemie (4), 399–400.

Schulz, S., Gross, J., Hilker, M., 1997. Origin of the defensive secretion of the leaf beetle *Chrysomela lapponica*. Tetrahedron 53, 9203–9212.

Silvan, A.M., Abad, M.J., Bemiejo, P., Villar, A., Sollhuber, M., 1996. Anti-inflammatory activity of three flavonoids from *Santolina oblongifolia*. Phytotherapy Research 10 (Suppl. 1), S65–S66.

Tan, R.X., Hu, Y.H., Liu, Z.L., Pan, X., 1993. New kaurane diterpenoids from *Aster tongolensis*. Journal of Natural Products 56, 1917–1922.

Tan, R.X., Jakupovic, J., Bohlmann, F., Jia, Z.J., Huneck, S., 1991. Sesquiterpene lactones and other constituents from *Artemisia xerophytica*. Phytochemistry 30, 583–587.

Tosun, F., Akyuz, C., 1997. Flavonoids of *Gonocytisus angulatus*. Pharm. Sci. 3, 377–378.

Tsutomu, H., Taeko, Y., Rieko, Y., Yukihiko, I., Muneto, M., Kazufumi, Y., Isao, A., Sansei, N., Tadaka, N., Masao, Y., Takuo, O., 1991. Inhibitory effects of galloylated flavonoids on xanthine oxidase. Planta Medica 57, 83–84.

Yokozawa, T., Dong, E., Liu, S.M., Shimizu, M., 1997. Antioxidative activity of flavones and flavonols in vitro. Phytotherapy Research 11, 446–449.

Yoshiki, Y., Okubo, K., Onuma, M., Igrashi, K., 1995. Chemiluminescence of benzoic and cinnamic acids, and flavonoids in the presence of aldehyde and hydrogen peroxide or hydroxyl radical by fenton reaction. Phytochemistry 39, 225–229.

Yu, D.Q., Yang, J.S., Xie, J.Y., 1989. Handbook of Analytical Chemistry. Beijing, Chemical Industry Press (Book 5, NMR Analysis, (a) pp. 526–527, (b) pp. 675–676).

Zhou, C.X., Tanaka, J., Cheng, C.H.K., Higa, T., Tan, R.X., 1999. Steroidal alkaloids and stilbenoids from *Veratrum taliense*. Planta Medica 65, 480–482.

PERGAMON

Phytochemistry 58 (2001) 653–656

PHYTOCHEMISTRY

www.elsevier.com/locate/phytochem

Sesquiterpenes and alkaloids from *Scorodocarpus borneensis*

Christophe Wiart[a], Marie-Thérèse Martin[b], Khalijah Awang[c], Nathalie Hue[b], Laurent Serani[b], Olivier Laprévote[b,*], Mary Païs[b], Mawardi Rhamani[a]

[a]*Department of Chemistry, Universiti Pertanian Malaysia, 43400 Serdang, Malaysia*
[b]*Institut de Chimie des Substances Naturelles, C.N.R.S., 91198 Gif-sur-Yvette Cedex, France*
[c]*Department of Chemistry, University of Malaya, 59100 Kuala Lumpur, Malaysia*

Received 4 December 2000; received in revised form 26 February 2001

Abstract

A new sesquiterpene, scodopin, and a mixture of three tryptamine-type alkaloids, scorodocarpines A–C, were isolated from the fruits of *Scorodocarpus borneensis*, together with a known hemisynthetic sesquiterpene, cadalene-β-carboxylic acid, which was isolated from the bark. The structures of the new compounds were elucidated by interpretation of spectral data, especially tandem mass spectrometry for the alkaloid mixture. © 2001 Elsevier Science Ltd. All rights reserved.

Keywords: *Scorodocarpus borneensis*; Olacaceae; Sesquiterpenes; Tryptamine-type alkaloids; Tandem mass spectrometry

1. Introduction

From the fruits of *Scorodocarpus borneensis* (Baill.) Becc. (Olacaceae) collected in Malaysia, we have isolated a new sesquiterpene scodopin **1** and a mixture of three tryptamine-type alkaloids named scorodocarpines A–C (**2**–**4**). In addition, a sesquiterpene **5** of the cadalene group was isolated from the bark. Compound **5** has been synthesized previously, but was not known as a natural product (Parasmeswara Reddy and Khrisna Rao, 1982). The structures of the new compounds were established especially by 2D NMR along with tandem mass spectrosmetry (LSIMS/MS) for compounds **2**–**4**.

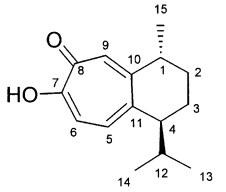

1

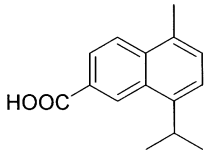

5

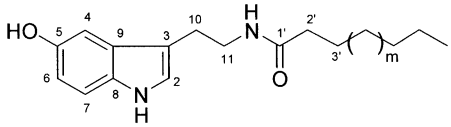

2 m = 16

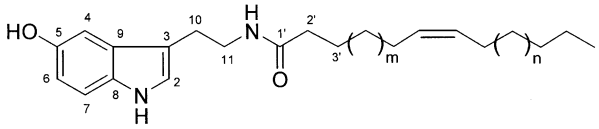

3 m = 8, n = 4
4 m = 6, n = 4

2. Results and discussion

Scodopin (**1**) gave a MH^+ peak in the HRCIMS at *m*/*z* 233.1545 which matched the molecular formula $C_{15}H_{20}O_2$ (Δ 0.0004 u). The UV spectrum (λ_{max} 251 and 333 nm) together with the IR spectrum (ν 1619 and 1603 cm^{-1}) suggested a highly conjugated keto derivative. In the ^{13}C NMR spectrum, the carbonyl resonated at δ 174.7 and a peak at δ 163.5 could be assigned to a phenolic

* Corresponding author. Tel.: +33-1-69823032; fax: +33-1-690 77247.
E-mail address: laprevote@icsn.cnrs-gif.fr (O. Laprévote).

0031-9422/01/$ - see front matter © 2001 Elsevier Science Ltd. All rights reserved.
PII: S0031-9422(01)00103-0

carbon. Only three signals appeared in the aromatic region of the ^{1}H NMR spectrum, a singlet (1H) at δ 7.23 and two doublets (1H each, $J=11$ Hz) of two vicinal protons at δ 7.12 and 7.25. The aliphatic region showed the resonances of a methyl group at δ 1.22 (3H, *d*, $J=6.5$ Hz). The signals of an isopropyl moiety appeared at δ 0.78 (3H, *d*, $J=6.5$ Hz), 0.87 (3H, *d*, $J=6.5$ Hz) and 1.87 (1H, *m*). The spectrum also showed five other signals, which with the aid of the HMQC spectrum were identified as two methine and four methylene protons (Table 1). The connections between the aliphatic carbons were deduced from the spin system H_{15}–H_1–H_2–H_3–H_4–H_{12}–Me_{13}–Me_{14} revealed in the COSY experiment and were confirmed by the HMBC spectrum (Table 1). The latter was used to establish the linkage with the aromatic seven membered A ring (diagnostic cross peaks Me-15/C-10 and H-4/C-10,C-11), as well as the final structure of this ring, which was deduced together with the ^{1}H and the ^{13}C resonance data from the correlations H-6/C-7,C-8,C-11 and H-9/C-1,C-7,C-8,C-10,C-11. The relative stereochemistry at C-1 and C-4 was determined using the NOESY experiment measured at −40°C (Table 1). In these conditions, scodopin (**1**) adopts the usual half chair conformation for ring B. The correlations H-2βax/Me-13 and H-3αax/Me-15 indicated H-1β and H-4α configurations, respectively.

Scorodocarpines A–C (**2**–**4**),were isolated as a mixture. The EIMS showed three $[M]^{+\cdot}$ peaks at *m/z* 498, 496 and 468 corresponding to the molecular formulas of $C_{32}H_{54}O_2N_2$, $C_{32}H_{52}O_2N_2$ and $C_{30}H_{48}O_2N_2$, respectively. The UV spectrum exhibited maxima at 223, 278 and 304 nm suggesting an indole residue and the IR showed a band at 1636 cm^{-1} assignable to an amide carbonyl group. These data, along with peaks at *m/z* 160 and 146 observed in the mass spectrum (Maeda et al., 1993), were in accordance with the structure of *N*-acyl-5-hydroxytryptamines. The acyl residues were saturated (22 carbons) for compound **2**, and monounsaturated with 22 and 20 carbons for compounds **3** and **4,** respectively. The *N*-acyl-5-hydroxytryptamine type structure was confirmed by the NMR spectra ($CDCl_3$–CD_3OD 9:1, Table 2). The presence of the 5-hydroxyindole moiety

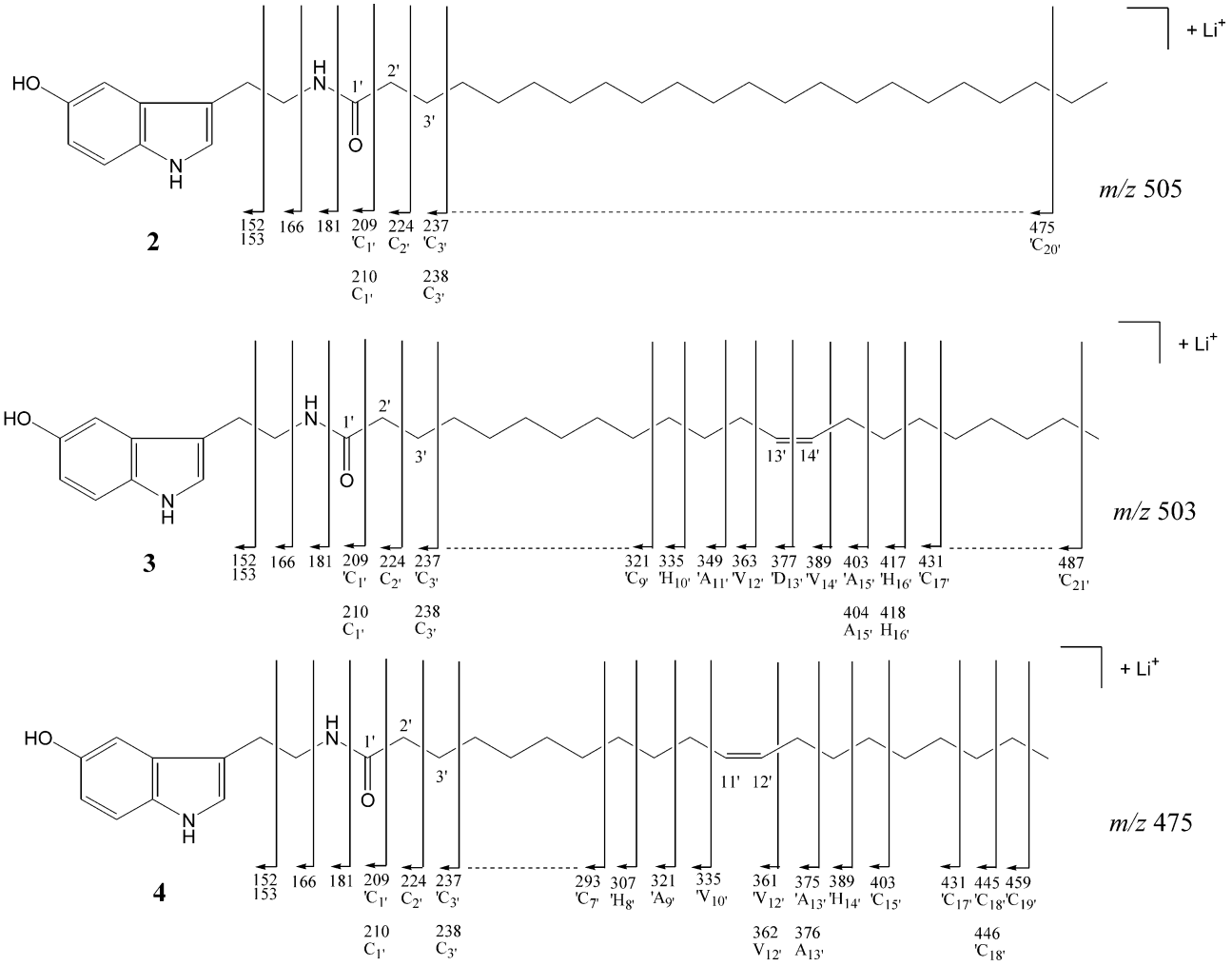

Scheme 1.

Table 1
^{13}C NMR (75 MHz) and ^{1}H NMR (400 MHz) data for scodopin (**1**) in $CDCl_3$[a]

Position	δ_C	δ_H (*J* Hz)	HMBC	NOESY[b]
1	36.9	2.86 *q* (6)	2,9,10,11,15	2α,β,9,15
2	26.9	β 1.96 *m* α1.43 *m*	1,4,15	2β,3
			1,4,15	3, 13
3	19.5	1.78 *m*	1,2,4,12	4,15
4	48.0	2.48 *m*	2,5,10,11,12,13,14	5,12,13,14
5	142.8	7.25 *d* (11)	4,6,8,10	12,14
6	126.3	7.12 *d* (11)	5,7,8,11	
7	163.5			
8	174.7			
9	122.1	7.23 *s*	1,7,8,10,11	15
10	152.3			
11	141.4			
12	33.7	1.87 *m*	4,13	13,14
13	19.8	0.78 *d* (6.5)	4,12,14	
14	21.8	0.87 *d* (6.5)	4,12,13	
15	23.7	1.22 *d* (6.5)	1,2,10	

[a] Assignments based on 2D experiments.
[b] Measured at −40°C.

Table 2
^{13}C NMR (75 MHz) and ^{1}H NMR (400 MHz) data for scorodocarpines (**2–4**) ($CDCl_3$–CD_4O 9:1)[a]

Position	δ_C	δ_H (*J* Hz)	HMBC
1		8.40 *br s*	
2	123.2	6.93	3,8,9
3	112.4		
4	103.1	6.99 *d* (2)	5,6,8
5	150.2		
6	112.6	6.75 *dd* (8.5, 2)	
7	112.1	7.17 *d* (8.5)	5,9
8	131.7		
9	128.3		
10	25.7	2.85 *t* (7)	2,3,9,11
11	40.0	3.48 *t* (7)	3,10,1′
1′	173.8		
2′	37.2	2.08 *t* (7)	1′,3′
3′	26.0	1.53 *m*	
(CH_2)m or n	29.8	1.23 *br s*	
$\underline{CH_2}$-CH=CH	27.4	1.98 *m*	
$\underline{CH}$=CH	130.1	5.32 *dd* (5, 5)	
CH_3-CH_2-$\underline{CH_2}$	32.1	1.23 *m*	
CH_3-$\underline{CH_2}$-CH_2	22.9	1.25 *m*	
CH_3	14.3	0.85 *t* (7)	α- and β-CH_2
$\underline{NH}$-CO		6.05 *t* (7)	

[a] Assignments based on 2D experiments.

was deduced from the coupling pattern of H-7 (δ 7.17, *d*, *J* = 8.5 Hz), H-6 (δ 6.75, *dd*, *J* = 8.5 and 2) and H-4 (δ 6.99, *d*, *J* = 2), while H-2 gave a singulet at δ 6.93, and was further supported by the typical ^{13}C NMR signals of the indole nucleus (Kamano et al., 1999) and the correlations observed in the HMBC experiment (Table 2). The latter also displayed a correlation between C-9 and H-10 of the tryptamine chain (CH_2-10, δ_H 2.85 and δ_C 25.7; CH_2-11, δ_H 3.48, δ_C 40.0). The signals of the amide NH appeared at δ 6.05 (*t*, *J* = 7) and the indole NH at δ 8.40 with small intensities due to partial deuterium exchange. The characteristic resonances of the acyl chains are given in Table 2. The geometry of the double bonds (δ_H 5.32, δ_C 130.1) is *Z*, which is deduced from the chemical shift of the α-CH_2 group (δ_C 27.4). The chains are linear owing to the presence of an unique signal for a terminal methyl at δ 14.3.

The structures of the tryptamine side chains were confirmed by an LSIMS/MS experiment which in addition allowed to determine the position of the double bond inside the chains. The LSIMS spectrum recorded in the presence of lithium iodide showed three peaks at *m/z* 505, 503 and 475 corresponding to ions $[\mathbf{2}+Li]^+$, $[\mathbf{3}+Li]^+$ and $[\mathbf{4}+Li]^+$, respectively.

The CID spectra of the precursor ion $[\mathbf{2}+Li]^+$ at *m/z* 505 displayed a series of peaks separated by 14 mass units in the *m/z* range 475–209. These fragments are generated by charge-remote fragmentation processes leading to losses of C_nH_{2n+2} neutral species from the precursor ion. They can be attributed to $'C_m$-type ions ($m = 1', 2', \ldots, 20'$) in agreement with the nomenclature proposed by Griffiths et al. (1996) and completed by Claeys et al. (1996). The fatty acyl moiety of compound **2** was thus easily identified as a docosanoate chain (Scheme 1).

The CID spectra of the precursor ion $[\mathbf{3}+Li]^+$ at *m/z* 503 showed fragment ion peaks identical to some of those observed on the corresponding spectrum of $[\mathbf{2}+Li]^+$, in particular the signals at *m/z* 209/210, 224, 237/238, 251 and 265. Two other ion peaks at *m/z* 349 and 403 were characteristic of allylic cleavages on both sides of a double bond located at position $C_{13'}$-$C_{14'}$ (Scheme 1). The fragments at *m/z* 335 ($'H_{10'}$) and 417/418 ($'H/_{16'}/H_{16'}$) corresponded to homoallylic cleavages and the ions $'V_{12'}$ and $'V_{14'}$ (*m/z* 363 and 389, respectively) were attributed to the vinylic fragmentations. The 13-docosenoate fatty acyl chain was thus unambiguously recognized by these mass spectrometric data.

The $[\mathbf{4}+Li]^+$ ion at *m/z* 475 showed a very similar behavior under high-energy collisional activation. The abundant fragment ion at *m/z* 321 assigned to the $'A_{9'}$ ion and the ions at *m/z* 375/376 (ions $'A_{13'}/A_{13'}$) indicated the presence of a double bond at position $C_{11'}$–$C_{12'}$. The other signals at *m/z* 293 ($'C_{7'}$), 307 ($'H_{8'}$), 335 ($'V_{10'}$), 361/362 ($'V_{12'}/V_{12'}$) and 389 ($'H_{14'}$) were in agreement with the structure. Thus, compound **4** corresponded to the product of *N*-acylation of serotonine by 11-eicosenoic acid.

Acyl tryptamines were known to exist in other plants, having various side chains (Maeda et al., 1993; Kamano et al., 1999), but unsaturated side chains were found for the first time in this study. They correspond to known acids isolated from several plants species. However,

these acids have not been found in the Olacaceae family whose chemical study is still scarce.

3. Experimental

3.1. General

Optical rotation at 20° were taken on a Perkin-Elmer 241 polarimeter. Spectra were recorded as follow: UV: MeOH, Varian CARY 100; IR: $CHCl_3$ or KBr, Perkin-Elmer SPECTRUM BX; NMR: Bruker AM 300 (^{13}C NMR spectra) and Bruker AMX 400 (^1H NMR and 2D NMR spectra); EIMS: Thermoquest Automass Multi; HRCIMS: Kratos MS-80 RF, MS/MS: see Section 3.4.

3.2. Plant material

Fruits and bark of *Scorodocarpus borneensis* (Baill.) Becc. (Olacaceae) were collected from Kuala Kangsar, Perak (Malaysia). The plant was identified by one of us (C.W). Voucher specimens (K1) are deposited at the Chemistry Department, Universiti Pertanian Malaysia.

3.3. Extraction and isolation

Dried fruits (200 g) of *S. borneensis* were extracted exhaustively with EtOH at room temperature. The extract (5.2 g) was repeatedly chromatographied on silica gel yielding scodopin **1** (12 mg, 1. $CHCl_3$–MeOH 99:1, 2. $CHCl_3$–MeOH 99.5:0.5) and the mixture of scorodocarpines A–C (**2**–**4**) (15 mg, 1. $CHCl_3$–MeOH 99.1, 2. $CHCl_3$–MeOH 98:2, 3. $CHCl_3$–MeOH 98:2).

Dried ground bark (300 g) of *S. borneensis* was extracted in the same way with EtOH. The extract (10.3 g) was again repeatedly chromatographied on silica gel affording compound **5** (20 mg, 1. petroleum ether, 2. petroleum ether–$CHCl_3$ 99:1).

3.4. Tandem mass spectrometry

The MS/MS spectra were obtained using a ZabSpec-T five sector tandem mass spectrometer (Micromass, Manchester, UK) with $E_1B_1E_2$-B_2E_3 geometry (E: electrostatic analyzers, B: magnets). The sample was dissolved in a liquid matrix (*m*-nitrobenzyl alcohol–glycerol–trifluoroacetic acid 50:50:1, saturated with lithium iodide). $[M+Li]^+$ precursor ions were generated by cesium ion bombardment at 30 keV. The precursor ions submitted to MS/MS experiments were selected by MS1 set at appropriate E and B values and then focused in a collision cell located in the fourth field-free region (between E_2 and B_2). Argon was introduced at a pressure leading to an almost 70% attenuation of the precursor ion beam. The collision cell was floated at 4 kilovolts so as to attain a collision energy of 4 keV. Further experimental details are given elsewhere (Gleye et al., 1999).

3.5. Scodopin (*1*)

Amorphous gum. $[\alpha]_D$ 0° ($CHCl_3$, *c* 0.5) UV λ_{max} nm (log ε) 251 (3.94), 330 (3.75), IR ($CHCl_3$) ν cm^{-1} 3388, 1619, 1603. HRCIMS *m/z* 233.1545 $[M+H]^+$ ($C_{15}H_{21}O_2$, Δ 0.0004 u). ^1H and ^{13}C NMR, see Table 1.

3.6. Mixture of scorodocarpines A, B and C (*2*–*4*)

Amorphous gum. UV λ_{max} nm (log ε) 223 (4.55), 278 (4.02), 304 (3.90). IR (KBr) ν cm^{-1} 3502, 3416, 3405, 1636 1543, 1489, 1470, 800, 730. EIMS *m/z* 498 $[M]^{+\cdot}$, *m/z* 496 $[M]^{+\cdot}$, *m/z* 468 $[M]^{+\cdot}$, 160, 146. ^1H and ^{13}C NMR, see Table 2.

3.7. Cadalene-β-carboxylic acid (*5*)

^1H NMR ($CDCl_3$) : 7.46 (1H, *d*, *J* = 6.5 Hz, H-2), 7.44 (1H, *d*, *J* = 6.5 Hz, H-3), 9.08 (1H, *d*, *J* = 2.5 Hz, H-5), 8.18 (1H, *dd*, *J* = 8.5, 2.5 Hz, H-7), 8.12 (1H, *d*, *J* = 8.5 Hz, H-8), 3.88 (1H, *sept*, *J* = 7 Hz, H-11), 1.46 (6H, *d*, *J* = 7 Hz, Me-12, Me-13), 2.72 (3H, *s*, Me-14); ^{13}C NMR ($CDCl_3$): 132.1 (C-1), 129.3 (C-2), 122.4 (C-3), 144.7 (C-4), 128.0 (C-5), 125.8 (C-6), 124.6 (C-7), 125.4 (C-8), 135.7 (C-8), 130.7 (C-10), 28.5 (C-11), 23.8 (C-12, C-13), 19.5 (C-14), 172.7 (C-15).

References

Claeys, M., Nizigiyimana, L., Van den Heuvel, H., Derrick, P.J., 1996. Mechanistic aspects of charge-remote fragmentation in saturated and mono-unsaturated fatty acid derivatives. Evidence for homolytic cleavage. Rapid Communications in Mass Spectrometry 10, 770–774.

Gleye, C., Laurens, A., Laprévote, O., Serani, L., Hocquemiller, R., 1999. Isolation and structure elucidation of sabadelin, an acetogenin from roots of *Annona muricata*. Phytochemistry 52, 1403–1408.

Griffiths, W.J., Yang, Y., Lindgren, J.Å., Sjövall, J., 1996. Charge remote fragmentation of fatty acid anions in 400 eV collisions with xenon atoms. Rapid Communications in Mass Spectrometry 10, 21–28.

Kamano, Y., Morita, H., Takano, R., Kotake, A., Nogawa, T., Hashima, H., Takeya, K., Pettit, G.R., 1999. Bufobutanoic acid and bufopyramide, two new indole alkaloids from the chinese traditional drug ch'an su. Heterocycles 50, 499–503.

Maeda, U., Hara, N., Fujimoto, Y., Srivastava, A., Gupta, Y.K., Sahai, M., 1993. *N*-Fatty acyl tryptamines from *Annona reticulata*. Phytochemistry 34, 1633–1635.

Parasmeswara Reddy, M., Khrisna Rao, G.S., 1982. Synthesis of *ar*-γ-muurolen-15-oic acid (cadalene-β-carboxylic acid) and 7-hydroxycadalenal. Indian Journal of Chemistry 21B, 885–886.

PERGAMON

Phytochemistry 58 (2001) 657–661

PHYTOCHEMISTRY

www.elsevier.com/locate/phytochem

Gallotannin biosynthesis: β-glucogallin: hexagalloyl 3-*O*-galloyltransferase from *Rhus typhina* leaves

Ruth Niemetz, Georg G. Gross*

Molekulare Botanik, Universität Ulm, D-89069 Ulm, Germany

Received 11 May 2001; received in revised form 22 June 2001

Abstract

Leaves of staghorn sumac (*Rhus typhina*) contain several galloyltransferases that catalyze the β-glucogallin dependent transformation of 1,2,3,4,6-pentagalloylglucose to gallotannins. Among these, an enzyme has been isolated that preferentially acylates the 3-position of the hexagalloylglucose, 3-*O*-digalloyl-1,2,3,4,6-tetra-*O*-galloylglucose, to afford the corresponding heptagalloylglucose being characterized by a 3-*O*-*meta*-trigalloyl side-chain. The enzyme, for which a M_r of ca. 260,000 was determined, was purified to apparent homogeneity. SDS-PAGE suggested an $\alpha_4\beta_4$-conformation of the native enzyme. It had a pH-optimum and an isolelectric point at pH 5.6, was most stable at pH 4.0–4.3, and displayed excellent heat-stability and in particular an extreme cold-tolerance. We propose the systematic name "β-glucogallin: hexagalloylglucose 3-*O*-galloyltransferase" for this new enzyme. © 2001 Elsevier Science Ltd. All rights reserved.

Keywords: *Rhus typhina*; Anacardiaceae; Staghorn sumac; Biosynthesis; Gallotannins; Galloyltransferase

1. Introduction

Gallotannins, a subclass of hydrolyzable plant tannins, are receiving increasing attention as interesting chemotherapeuticals, a function that emerged from ethnopharmacological traditions, in particular of the Far East. For example, their antioxidant and radical scavenging activities have been investigated in relation to tumor prevention (Okuda, 1993); other potential applications regard vasodilatory effects (Goto et al., 1996) or use as diuretica and ailments of bladder and urinary tract (Haslam, 1996). The chemical structure of gallotannins is derived from a central polyphenolic unit, 1,2,3,4,6-penta-*O*-galloyl-β-D-glucose (Fig. 1; **2**). The phenolic hydroxyls of this key compound undergo substitution with additional galloyl residues to yield characteristic *meta*-depsidically linked diaryl or oligoaryl side-chains, like the *m*-digalloyl group (**3**) depicted in Fig. 1. Complex structures containing up to 12 galloyl residues can result from such processes. In the genus *Rhus*, these transitions are confined to positions 2, 3 and 4 of the glucose core (Nishizawa et al., 1982), while gallotannins from *Quercus* or *Paeonia* can bear *meta*-depside bonds also at C-6 (Nishizawa et al., 1980, 1983a, b). Biosynthesis studies with cell-free extracts from leaves of *Rhus typhina* (staghorn sumac) have shown that β-glucogallin (1-*O*-galloyl-β-D-glucose, **1**) is utilized not only as principal galloyl donor in the formation of pentagalloylglucose, but also in the subsequent acylation of this precursor to gallotannins (Hofmann and Gross, 1990). Two enzymes have been recently described that preferentially catalyzed the galloylation of 1,2,3,4,6-pentagalloylglucose (**2**) to hexa- and heptagalloylglucoses (Niemetz and Gross, 1998, 1999). A third enzyme activity encountered in these investigations, in contrast, displayed significant affinity against hexagalloylgucose substrates, in particular towards 3-*O*-digalloyl-1,2,4,6-tetra-*O*-galloyl-β-D-glucose (Fig. 3; **6**). The properties of this latter enzyme are described here .

2. Results and discussion

2.1. Enzyme purification

The transferase was isolated from homogenates of sumac leaves in the presence of PVP and borate, i.e.

* Corresponding author. Tel.: +49-731-50-22624; fax: +49-731-50-22809.

E-mail address: georg.gross@biologie.uni-ulm.de (G.G. Gross).

0031-9422/01/$ - see front matter © 2001 Elsevier Science Ltd. All rights reserved.
PII: S0031-9422(01)00300-4

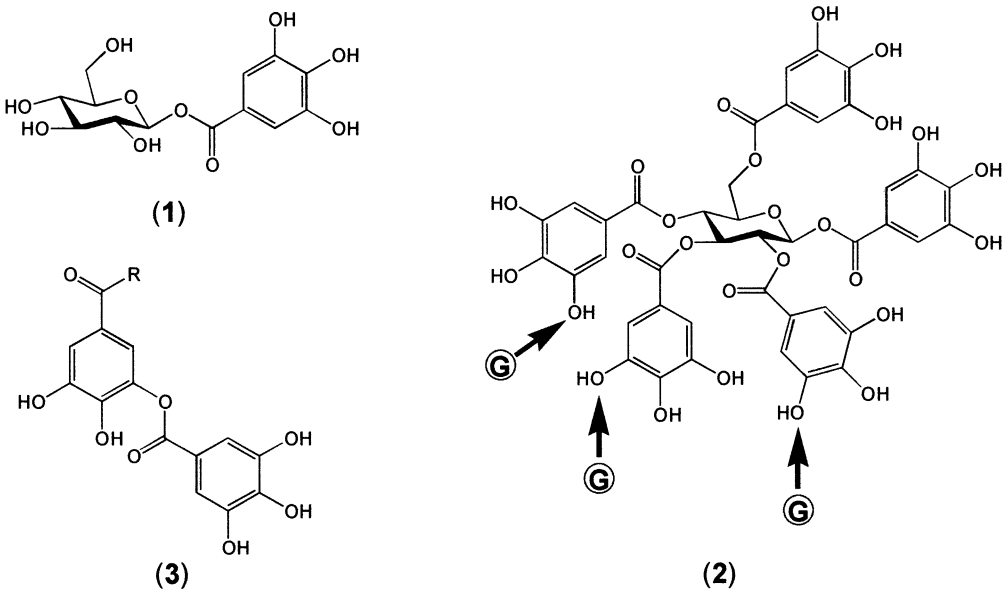

Fig. 1. Important compounds related to the structure and biosynthesis of gallotannins in *Rhus typhina*: (**1**) β-Glucogallin (1-*O*-galloyl-β-D-glucose), the principal galloyl donor; (**2**) 1,2,3,4,6-penta-*O*-galloyl-β-D-glucose, the basic galloyl acceptor in the biosynthesis of gallotannins. Arrows indicate positions for the attachment of additional galloyl groups (Ⓖ) in these transformations to yield *m*-digalloyl residues (**3**) and higher analogs.

agents that effectively form complexes with inhibitory endogenous plant phenolics. Residual contaminants were removed by stirring with Dowex anion-exchange resin, followed by ammonium sulfate fractionation of the crude extract. The enzyme solution was further purified by two gel-filtration steps. A first conventional step on Sephacryl S-300 efficiently removed a gallotannin degrading esterase ("plant tannase"; Niehaus and Gross, 1997), and also revealed the existence of several galloyltransferase activities (Fig. 2). Two of these (peaks A and C in Fig. 2) were ascribed to previously published pentagalloylglucose acylating galloyltransferases with M_r values of 360,000 and 170,000, respectively (Niemetz and Gross, 1998, 1999), while the third enzyme fraction (B in Fig. 2) obviously represented a novel galloyltransferase that preferentially acylated hexagalloylglucose substrates. This fraction was subjected to a second gel-filtration step by HPLC gel-permeation on a Merck GPC-diol column. Final purification was achieved by hydrophobic-interaction chromatography on butyl-sepharose. The transferase had thus been purified 625-fold with 3.2% yield to apparent homogeneity, as shown by PAGE under non-denaturing conditions. The results of a representative purification protocol with the hexagalloylglucose, 3-*O*-digalloyl-1,2,4,6-tetra-*O*-galloyl-β-D-glucose (**6**), as standard substrate are summarized in Table 1. The pure enzyme could be stored at 0–4 °C for several weeks without significant loss of activity.

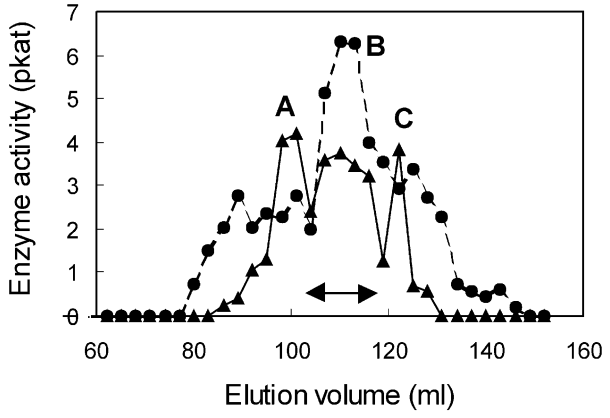

Fig. 2. Separation of gallotannin-synthesizing galloyltransferases from sumac leaves by gel-filtration on Sephacryl S-300. Enzyme activities were assayed with (▲) 1,2,3,4,6-penta-*O*-galloyl-β-D-glucose (**2**) and with (●) the hexagalloylglucose, 3-*O*-digalloyl-1,2,4,6-tetra-*O*-galloyl-β-D-glucose (**6**), respectively. Fractions representing peak B were pooled as indicated by the inserted double-arrow and further purified. Characteristics of the transferases constituting peaks A and C have been reported earlier (Niemetz and Gross, 1998, 1999).

2.2. General properties of the enzyme

The galloyltransferase reaction proceeded linearly between 2 and 18 μg protein under standard assay conditions (up to ca. 4 pkat, depending on the progress of the purification sequence), except for a slight lag-phase at 0–2 μg protein. No reaction occurred with protein denatured by heat or acid. Linearity of the reaction was maintained for ca. 60 min under standard conditions. The enzyme was inactive below pH 3.2 and above pH 7.5, with a maximum at pH 5.6 (citrate buffer); half-maximal activities were at pH 4.2 and 6.2. After pre-incubation at 30 °C for 3 or 24 h, respectively, the transferase was found most stable at pH 4.0–4.3 (half-

maxima at pH 3.2 and 4.7); rapid inactivation occurred below pH 2.5 and above pH 7 (pH 6 after 24 h duration of pH exposure). An isoelectric point of 5.6 was determined for the protein by chromatofocussing on a Pharmacia Mono P-column. The enzyme reaction proceeded optimally at 45 °C, with half-maximal activities at 32 and 55 °C. No reaction occurred above 70 °C, while a relative activity of 50% was observed even at 0 °C. After preincubation at pH 4 for 2 h at different temperatures, the transferase was stable at 0–20 °C (half-maximal at 35 °C) and was inactivated above 50 °C. The enzyme was thus characterized by an extreme cold-tolerance exceeding that of related galloylglucose synthesizing transferases. Its excellent heat-stability is similar to that of the earlier described transferase A (Fig. 2; Niemetz and Gross, 1998), but in clear contrast to the

Table 1
Purification of galloyltransferase from *Rhus typhina* leaves[a]

Step	Total protein (mg)	Total activity (pkat)	Specific activity (pkat mg^{-1})	Purification (-fold)	Recovery (%)
Dowex filtrate	2630	328	0.12	–	100
$(NH_4)_2SO_4$, 30–70% ppt.	168	262	1.56	13	80
Sephacryl S-300	13.9	180	13.0	108	55
GPC-diol[b]	4.0	84.8	21.2	177	26
Butyl-sepharose[c]	0.14	10.5	75.0	625	3.2

[a] Crude extracts were not assayed because of excess contaminants preventing HPLC analysis of reaction products. 3-*O*-Digalloyl-1,2,4,6-tetra-*O*-galloyl-β-D-glucose (**6**) was used as standard acceptor substrate.
[b] Enzyme from this step was used to determine its general properties.
[c] Substrate specificities and K_m values were determined with the pure enzyme.

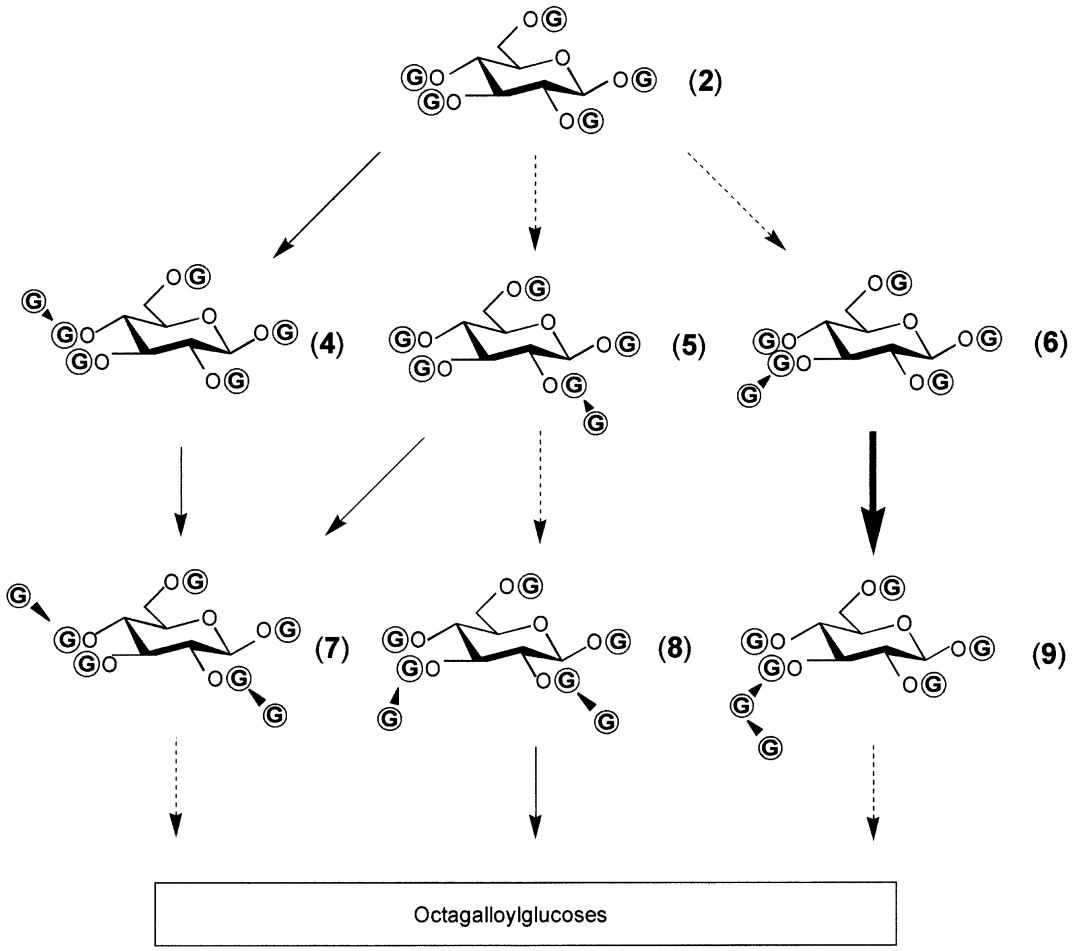

Fig. 3. Transformation of pentagalloylglucose (**2**) to hexagalloylglucoses (**4–6**), heptagalloylglucoses (**7–9**) and octagalloylglucoses, catalyzed by β-glucogallin: hexagalloylglucose 3-*O*-galloyltransferase from sumac (*Rhus typhina*) leaves. The main reaction is marked by a bold arrow, minor reactions by thin arrows; dashed arrows symbolize trace reactivities. Ⓖ, Galloyl; Ⓖ▶Ⓖ, *m*-digalloyl (**3**) residue.

pronounced heat-sensitivity of transferase C (Fig. 2; Niemetz and Gross, 1999). From the above temperature dependence data, an average activation energy of 47 kJ mol^{-1} was calculated that corresponds to a Q_{10} value of 1.9. Gel-filtration experiments with a calibrated Sephacryl S-300 column revealed an apparent M_r of 260,000 ± 20,000 for the enzyme. After denaturing SDS-PAGE of the pure enzyme, the existence of two protein bands of ca. M_r 36,000 and 24,000 was observed which would suggest that the native transferase exist in an $\alpha_4\beta_4$-configuration.

2.3. Substrate specificity and reaction products

The enzyme exhibited normal Michaelis–Menten kinetics with the donor, β-glucogallin (**1**), between 1 and 4 μM concentration (with a lag-phase, i.e. subproportional reactivity, at 0–1 μM) and with the standard acceptor substrate, 3-*O*-digalloyl-1,2,4,6-tetra-*O*-galloyl-β-D-glucose (**6**), at ca. 100–300 μM concentration (lag-phase 0–100 μM). Increasing substrate inhibition ocurred above these values. As summarized in Table 2, numerous galloylglucoses were acylated by the transferase, but it is evident that hexagalloylglucoses were the preferred substrates. Among these, compound (**6**) must be considered as the most prominent substrate according to the criteria of both relative enzyme activities and v_{max} K_m^{-1} values and was therefore chosen as standard enzyme assay substrate. Heptagalloylglucoses (**7–9**) and mixtures of octa- and nonagalloylglucose isomers (compounds with defined structure were not available) were utilized as substrates with reaction rates that were at least equal to that of pentagalloylglucose (**2**).

Analysis of reaction products by reversed-phase HPLC showed that pentagalloylglucose (**2**) was transformed to hexagalloylglucoses (**4**), (**5**) and (**6**) in a ratio of 2:1:1. Upon utilization of hexagalloylglucoses as enzyme substrates, compound (**4**) was predominantly acylated to heptagalloylglucose (**7**), while (**5**) afforded (**7**) and (**8**) in a ratio of 2:1. The standard enzyme assay substrate, hexagalloylglucose (**6**), was exclusively galloylated to yield the heptagalloylglucose, 3-*O*-trigalloyl-1,2,4,6-tetra-*O*-galloyl-β-D-glucose (**9**). In accordance with earlier analyses of the components of Chinese gallotannin from *R. semialata* (Nishizawa et al., 1982) and also with our previous enzyme studies with *R. typhina* (Niemetz and Gross, 1998, 1999), no evidence for the formation of *m*-digalloyl residues in positions 1 or 6 of pentagalloylglucose has been obtained.

In summary, the reported kinetic data and metabolic transformations suggest that this enzyme is primarily involved in acylating the 3-*O*-*meta*-digalloyl group of hexagalloylglucose (**6**) to form the 3-*O*-*meta*-trigalloyl residue of heptagalloylglucose (**9**) (Fig. 3). This reaction was also catalyzed by an earlier reported acyltransferase (Niemetz and Gross, 1998) which, however, was most active in the conversion of pentagalloylglucose to hexagalloylglucose (**6**). Its other properties were also significantly different, like those of an acyltransferase with particular affinity towards the 2- and 4-positions of pentagalloylglucose (Niemetz and Gross, 1999). It is thus evident that the transferase described here is a new enzyme, for which the systematic name "β-glucogallin: hexagalloylglucose 3-*O*-galloyltransferase" is proposed.

3. Experimental

3.1. General experimental procedures

The origin of chemicals used in this investigation has been reported recently, as well as the techniques employed for native and SDS-PAGE, protein determinations and analysis of enzyme reaction products (Niemetz and Gross, 1998). Standard enzyme activitiy assays (70 μl vol.) were composed of 25 mM citrate buffer (pH 5.0), 3.6 mM β-glucogallin (**1**), 265 μM hexagalloylglucose (**6**) and 50 μl enzyme (ca. 7 μg–0.5 mg protein, depending on the purification degree). Acid-denatured enzyme was used for blanks. After incubation at 30 °C for 1 h, reactions were terminated by adding 10 μl 1 N HCl; extraction and HPLC-analysis of reaction products

Table 2
Substrate specificity of sumac leaf galloyltransferase[a]

Substrate	Relative activity (%)	v_{max} (nkat)	K_m (μM)	v_{max} K_m^{-1} ($\times 10^{-3}$)
1-*O*-Galloyl-β-D-glucose (β-glucogallin) (**1**)	–	–	2000	–
1,2,3,6-Tetra-*O*-galloyl-β-D-glucose	3.4	3.7	220	17
1,2,3,4,6-Penta-*O*-galloyl-β-D-glucose (**2**)	34	12	135	88
Hexagalloyl-β-D-glucose (**4**)	68	31.1	105	300
Hexagalloyl-β-D-glucose (**5**)	57	18.3	160	110
Hexagalloyl-β-D-glucose (**6**)	100	34.0	100	340
Heptagalloyl-β-D-glucose (**7**)	38	7.7	125	62
Heptagalloyl-β-D-glucose (**8**)	34	13.8	175	78
Heptagalloyl-β-D-glucose (**9**)	38	11.3	130	87

[a] Determinations were performed under standard assay conditions. Relative activities are compared to the reaction rate observed with 3-*O*-digalloyl-1,2,4,6-tetra-*O*-galloyl-β-D-glucose (**6**) equal to 100%.

have been described in detail by Niemetz and Gross (1998). The IEP of the enzyme was determined by chromatofocussing on a 200×5 mm i.d. Mono P column (Pharmacia). As buffers were employed: A = 0.025 M bis-Tris (2[bis(2-hydroxyethyl)imino]-2-(hydroxymethyl)-1,3-propanediol; Serva, Heidelberg), adjusted to pH 7.1 with iminodiacetic acid (Sigma); B = Polybuffer 74 (Pharmacia), diluted 1:10 with redistilled H_2O and adjusted to pH 4.0 with iminodiacetic acid. After equilibration with buffer A, elution of applied protein samples (100 μl vol.) was achieved by a linear gradient (0–45 min) of 0–100% B in A (flow rate 0.5 ml min^{-1}). Proteins and pH values of column eluates were monitored by spectrophotometry (UV 280 nm) and with a flow-through pH-electrode.

3.2. Plant material

Young leaves (2–4 months old) of staghorn sumac (*R. typhina*) were collected from trees in the surroundings of the university or plucked from greenhouse-grown plants. After washing with dist. H_2O, they were either immediately used as enzyme source, or frozen in liquid N_2 and stored at −20 °C in evacuated plastic bags where they could be stored for more than 6 months without apparent loss of enzyme activity.

3.3. Enzyme purification

All steps were carried out at 0–4 °C, and 2-mercaptoethanol (5 mM final conc) was added to all buffers. *R. typhina* leaves (80 g) were homogenized, extracted with Tris-borate buffer in the presence of PVP, and treated with Dowex 1X4 (50–100 mesh, borate form) as described previously (Niemetz and Gross, 1998). The filtrate was fractionated with solid $(NH_4)_2SO_4$. The 30–70% ppt. was redissolved in a minimal vol. of 50 mM phosphate buffer (pH 7.5, containing 0.1 M NaCl) and subjected to gel-filtration on Sephacryl S-300 (Pharmacia; column 400×2.4 mm i.d.) equilibrated in the same buffer. The active fractions were concentrated by ultrafiltration (Filtron Macrosep; exclusion limit 10,000 dalton) and subjected to HPLC by gel-permeation chromatography (GPC) on a diol-substituted column (Bio GPC-diol 'Superformance' glass column system; Merck, Darmstadt; 300×10 mm i.d.; 5 μm particle size; eluent 10 mM NaH_3PO_4 plus 300 mM NaCl, pH 7.2; flow rate 0.5 ml min^{-1}). The active frs were combined, adjusted to pH 5.0, supplemented with 1.25 M ammonium sulfate and subjected to HIC on butyl-sepharose (Merck; column 10×18 mm i.d.) equilibrated with 50 mM phosphate buffer (pH 5.0) plus 1.25 M ammonium sulfate. The column was successively washed with decreasing concns of ammonium sulfate (1.25, 0.625 and 0 M) in phosphate buffer (pH 5.0), followed by elution of the enzyme with redistilled H_2O.

Acknowledgements

We thank Mrs. A. Müller for perfect technical assistance, and the Deutsche Forschungsgemeinschaft (Bonn) and the Fonds der Chemischen Industrie (Frankfurt/M.) for generous financial support.

References

Goto, H., Shimada, Y., Akechi, K., Kohta, M., Hattori, M., Terasawa, K., 1996. Endothelium vasodilator effect of extract prepared from the roots of *Paeonia lactiflora* on isolated rat aorta. Planta Medica 62, 436–439.

Haslam, E., 1996. Natural polyphenols (vegetable tannins) as drugs: possible modes of action. Journal of Natural Products 59, 205–215.

Hofmann, A.S., Gross, G.G., 1990. Biosynthesis of gallotannins: Formation of polygalloylglucoses by enzymatic acylation of 1,2,3,4,6-penta-*O*-galloylglucose. Archives of Biochemistry and Biophysics 283, 530–532.

Niehaus, J.U., Gross, G.G., 1997. A gallotannin degrading esterase from leaves of pedunculate oak. Phytochemistry 45, 1555–1560.

Niemetz, R., Gross, G.G., 1998. Gallotannin biosynthesis: purification of β-glucogallin: 1,2,3,4,6-pentagalloyl-β-D-glucose galloyltransferase from sumac leaves. Phytochemistry 49, 327–332.

Niemetz, R., Gross, G.G., 1999. Gallotannin biosynthesis: a new β-glucogallin-dependent galloyltransferase from sumac leaves acylating gallotannins at positions 2 and 4. Journal of Plant Physiology 155, 441–446.

Nishizawa, M., Yamagishi, T., Nonaka, G., Nishioka, I., 1980. Structure of gallotannins in *Paeoniae radix*. Chemical and Pharmaceutical Bulletin (Tokyo) 28, 2850–2852.

Nishizawa, M., Yamagishi, T., Nonaka, G., Nishioka, I., 1982. Tannins and related compounds. Part 5. Isolation and characterization of polygalloylglucoses from Chinese gallotannin. Journal of the Chemical Society Perkin Transactions 1, 2963–2968.

Nishizawa, M., Yamagishi, T., Nonaka, G., Nishioka, I., 1983a. Tannins and related compounds. Part 9. Characterization of polygalloylglucoses from Turkish galls. Journal of the Chemical Society Perkin Transactions 1, 961–965.

Nishizawa, M., Yamagishi, T., Nonaka, G., Nishioka, I., Nagasawa, T., Oura, H., 1983b. Tannins and related compounds. XII. Isolation and characterization of galloylglucoses from *Paeoniae radix* and their effect on urea-nitrogen concentration in rat serum. Chemical and Pharmaceutical Bulletin (Tokyo) 31, 2593–2600.

Okuda, T., 1993. Natural polyphenols as antioxidants and their potential use in cancer prevention. In: Scalbert, A. (Ed.), Polyphenolic Phenomena. INRA Editions, Paris, pp. 221–235.

PERGAMON

Phytochemistry 58 (2001) 663–669

PHYTOCHEMISTRY

www.elsevier.com/locate/phytochem

Phospholipids modulate the substrate specificity of soluble UDP-glucose:steroid glucosyltransferase from eggplant leaves

Cezary Pązkowski, Małgorzata Kalinowska, Zdzisław A. Wojciechowski*

Department of Biochemistry, Warsaw University, ul. Miecznikowa 1, 02-096, Warsaw, Poland

Received 5 April 2001; received in revised form 14 June 2001

Abstract

UDP-glucose-dependent glucosylation of solasodine and diosgenin by a soluble, partially purified enzyme fraction from eggplant leaves is affected in a markedly different way by some phospholipids. While glucosylation of diosgenin and some closely related spirostanols, e.g. tigogenin or yamogenin, is strongly inhibited by relatively low concentrations of several phospholipids, the glucosylation of solasodine is unaffected or even slightly stimulated. These effects depend both on the structure of the polar head group and the nature of the acyl chains present in the phospholipid. The most potent inhibitors of diosgenin glucosylation are choline-containing lipids: phosphatidylcholine (PC) and sphingomyelin (SM) but the removal of phosphocholine moiety from these phospholipids by treatment with phospholipase C results in an almost complete recovery of the diosgenin glucoside formation by the enzyme. Significant inhibition of diosgenin glucoside synthesis and stimulation of solasodine glucosylation was found only with PC molecular species containing fatty acids with chain length of 12–18 carbon atoms. PC with shorter or longer acyl chains had little effect on glucosylation of either diosgenin or solasodine. Our results indicate that interaction between the investigated glucosyltransferase and lipids are quite specific and suggest that modulation of the enzyme activity by the nature of the lipid environment may be of importance for regulation of in vivo synthesis of steroidal saponins and glycoalkaloids in eggplant. © 2001 Elsevier Science Ltd. All rights reserved.

Keywords: *Solanum melongena*; Solanaceae; Eggplant; Steroidal saponins; Glycoalkaloids; UDP-glucose; Glucosyltransferase; Lipid modulation

1. Introduction

Solanum melongena L. (garden eggplant) is an interesting model plant for studies on the biosynthesis of steroidal glycoalkaloids and saponins and its regulation since this plant is known for the ability to synthesize both these types of steroid oligosides. Eggplant glycoalkaloids, solamargine and solasonine, which are derivatives of solasodine (a steroidal alkaloid of the spirosolane type) occur mainly in leaves and unripe fruits (Bajak et al., 1979; Vohora et al., 1984; Aubert et al., 1989; Blankemeyer et al., 1998) while saponins, so-called melongosides, which are derivatives of diosgenin and tigogenin (steroidal sapogenins of the spirostane type) accumulate mainly in seeds (Kintia and Shvets, 1985; Kintia, 1996).

Several years ago we reported (Pączkowski and Wojciechowski, 1993, 1994) that crude fraction of soluble proteins (105 000 *g* supernatant) obtained from eggplant leaves efficiently catalyzed glucosylation of diosgenin and tigogenin as well as solasodine in the presence of UDP-glucose (UDPGlc) as the sugar source. The reaction products which were identified as 3β-D-monoglucosides of diosgenin, tigogenin or solasodine, respectively, may be regarded as intermediates in the biosynthesis of melongosides and solamargine. More recently the enzyme (enzymes ?) responsible for UDPGlc-dependent glucosylation of the above mentioned steroids has been partially purified (ca. 50-fold) and characterized (Pączkowski et al., 1997, 1998). Co-purification of UDPGlc:diosgenin GlcTase and UDPGlc:-solasodine GlcTase activities during the purification procedure, identical native M_r values (55 kDa) and very similar sensitivities of these two GlcTase activities to a number of different chemicals indicated that glucosylation of solasodine and diosgenin was catalyzed by a

Abbreviations: PC, phosphatidylcholine; PE, phosphatidylethanolamine; PG, phosphatidylglycerol; PA, phosphatidic acid; PS, phosphatidylserine; PI, phosphatidylinositol; SM, sphingomyelin; DAG, diacylglycerol; PLC, phospholipase C; GlcTase, glucosyltransferase

* Corresponding author. Tel.: +48-22-5543305; fax: +48-22-5543221.

E-mail address: zawoj@biol.uw.edu.pl (Z.A. Wojciechowski).

0031-9422/01/$ - see front matter © 2001 Elsevier Science Ltd. All rights reserved.
PII: S0031-9422(01)00292-8

single enzyme protein exhibiting a relatively broad specificity with respect to the sugar acceptor. On the other hand, some data suggested a possibility that these enzyme activities might reside in two related but separate enzyme proteins. First, the activity ratio of UDPGlc:diosgenin to UDPGlc:solasodine GlcTase activity was significantly different in individual organs of eggplant. Second, these two enzyme activities were affected by several non-ionic detergents in a completely different manner strongly inhibiting glucosylation of diosgenin or tigogenin but having no effect or even slightly stimulating glucosylation of solasodine.

In the present paper we would like to report that several natural phospholipids can act on UDPGlc:diosgenin and UDPGlc:solasodine GlcTase activities in a similar way as demonstrated earlier for non-ionic detergents. It cannot be ruled out that these effects may be of importance for in vivo regulation of steroidal saponin and glycoalkaloid biosynthesis in eggplant.

2. Results

2.1. Effect of membrane lipids on diosgenin, tigogenin and solasodine glucosylation

The influence of several natural or synthetic lipids on activities of soluble, partially purified GlcTase from eggplant leaves is shown in Table 1. GlcTase activities were measured simultaneously with the use of all natural for eggplant steroidal substrates, i.e. diosgenin, tigogenin and solasodine, as acceptors of sugar moiety from UDPGlc. The data summarized in Table 1 demonstrate that glucosylation of steroidal sapogenins characteristic for eggplant, i.e. diosgenin and tigogenin is more or less strongly inhibited by several phospholipids. In contrast, glucosylation of eggplant steroidal alkaloid-solasodine was affected much less or, in some instances, it was even significantly stimulated. Among tested lipids the most pronounced inhibitory effect on sapogenin glucosylation was exerted by phospholipids containing phosphocholine moiety, i.e. by PC and SM. With these two lipids, strong inhibition (70–90%) of diosgenin or tigogenin glucosylation was observed at relatively low concentration 37.5 μM. At the same concentration PC and SM significantly increased glucosylation of solasodine–by 55 or 24% using egg yolk PC or bovine brain SM, respectively. It is worth of mentioning that some acidic glycerophospholipid tested, i.e. PI or PS, exerted much less pronounced inhibitory effect on glucosylation of eggplant steroidal sapogenins as compared to PC but they stimulated glucosylation of solasodine to a similar extent.

Results shown in Table 1 clearly indicate that phosphocholine moiety is essential for inhibition of diosgenin or tigogenin and stimulation of solasodine glucosylation by PC and SM. Neither DAG nor ceramide which are derivatives of PC and SM deprived of phosphocholine moiety had a significant effect on glucosylation of all tested steroid substrates.

Data shown in Fig. 1 demonstrate that inhibitory effects of PC and SM on glucosylation of steroidal sapogenins and stimulatory effects of these lipids on glucosylation of solasodine are concentration-dependent. Significant inhibition of diosgenin and tigogenin glucosylation was found at PC or SM concentrations as low as 4 μM, i.e. at concentrations only *ca.* 10-times higher than those of steroids used as the enzyme substrates.

The kinetic analysis indicated (data not shown) that addition of 10 μM di-$C_{16:0}$ PC had a negligible effect on apparent K_m values for diosgenin (0.33 μM) or UDPGlc (2.1 μM) but decreased the V_{max} of the enzyme ca. 2-fold,

Table 1
Effect of various lipids on glucosylation of diosgenin, tigogenin and solasodine by delipidated and partly purified UDPGlc-glucosyltransferase from eggplant leaves

Lipid added (37.5 μM)	Glucosylation rate (nmol/mg protein/h)					
	Diosgenin		Tigogenin		Solasodine	
	(25*R*-spirost-5-en-3β-ol)		(25*R*-5α-spirostan-3β-ol)		(22*R*,25*S*-tomat-5-enin-3β-ol)	
None	5.20±0.28	(100.0)[a]	3.13±0.16	(100.0)[a]	2.90±0.12	(100.0)[a]
PC (egg yolk)	1.41±0.35	(27.1)	0.99±0.08	(31.6)	4.51±0.24	(155.5)
PC (di-$C_{16:0}$)	1.09±0.02	(20.9)	0.72±0.02	(23.0)	3.59±0.44	(123.7)
PE (di-$C_{16:0}$)	3.81±0.04	(73.3)	1.83±0.03	(58.6)	2.29±0.22	(79.0)
PG (di-$C_{16:0}$)	3.03±0.12	(58.2)	1.17±0.10	(37.4)	1.77±0.57	(60.9)
PA (di-$C_{16:0}$)	2.89±0.16	(55.6)	0.93±0.03	(29.7)	2.94±0.31	(101.4)
PS (di-$C_{16:0}$)	4.15±0.29	(79.9)	1.69±0.11	(54.1)	4.21±0.51	(145.0)
PI (bovine liver)	3.16±0.37	(60.7)	1.20±0.03	(38.4)	4.73±0.06	(163.2)
SM (bovine brain)	0.59±0.04	(12.2)	0.27±0.08	(8.7)	3.61±0.31	(124.4)
Ceramide (bovine brain)	4.67±0.11	(89.8)	nd[b]		2.60±0.31	(89.5)
DAG (di-$C_{16:0}$)	5.57±0.12	(107.2)	nd[b]		2.83±0.05	(97.6)

[a] Relative glucosylation rate (%).
[b] Not determined.

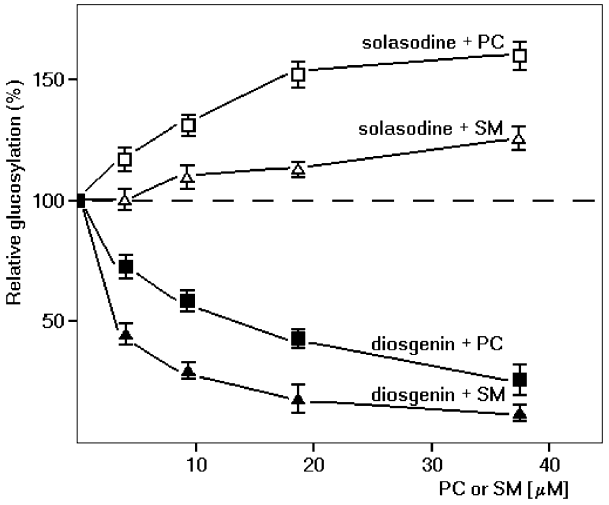

Fig. 1. Inhibition of UDPGlc:diosgenin (closed symbols) and stimulation of UDPGlc:solasodine GlcTase (open symbols) by increasing concentrations of PC (from egg yolk) or SM (from bovine brain).

i.e. from 18.0 to 9.8 nmol×mg protein^{-1} x h^{-1}. We were unable to determine how PC or SM affects kinetic constants for solasodine because in the presence of di-$C_{16:0}$ PC a non-hiperbolic enzyme kinetics was observed – in contrast to a typical Michaelis-Menten kinetics observed in the absence of lipid activator (Pączkowski et al., 1997).

Our earlier work (Pączkowski and Wojciechowski, 1994) has shown that crude fractions of soluble proteins (105 000 *g* supernatant from eggplant seedlings homogenate) can efficiently glycosylate, besides of steroids native to eggplant, several other steroidal sapogenins, e.g. yamogenin, hecogenin or nuatigenin, and steroidal alkaloids, e.g. tomatidine. We have also found (Pączkowski et al., 1998) that several non-ionic detergents, including Tween 80, are potent inhibitors of diosgenin and tigogenin glucosylation but they have little effect on glucosylation of solasodine, i.e. these detergents act in a similar manner to that described in the present paper for PC or SM.

Effects exerted by Tween 80, PC and SM on glucosylation of the above listed structural analogues of eggplant steroids are compared in Table 2. With yamogenin (25 *S*-epimer of diosgenin) the inhibitory effects of PC and SM were quite similar to those found for diosgenin and tigogenin (compare with data presented in Table 1). Tween 80, at 0.1% concentration, reduced glucosylation of yamogenin by more than 95%, similarly as in the case of diosgenin or tigogenin. It is of interest, however, that using other steroidal sapogenins inhibition by Tween 80 was much lower and there was no clear inhibition in the presence of PC or SM. It should be noted that hecogenin differs from tigogenin only by the occurrence of an additional oxo group in the ring C and nuatigenin is a pseudo-spirostane sapogenin containing an additional hydroxyl group in the ring F. Glucosylation of tomatidine, in contrast to that of solasodine, was significantly inhibited by Tween 80 but SM and PC stimulated its glucosylation to a similar extent as in the case of solasodine.

2.2. Influence of acyl moieties present in PC on glucosylation of diosgenin and solasodine

In order to establish whether the above described effects depend on acyl composition of phospholipid molecules we tested several PC species containing saturated fatty acids of different chain length. Results of this experiment demonstrated (see Fig. 2) that marked inhibition of diosgenin glucoside formation as well as significant stimulation of solasodine glucosylation could be found only using PC species containing fatty acids with chain length of 12–18 carbon atoms. PC species containing shorter or longer acyl components were much less effective or even inactive. It should be noted, however, that comparing effects of distearoyl- (di-$C_{18:0}$), dioleoyl- (di-$C_{18:1}$) and dilinoleoyl- (di-$C_{18:3}$) PC's no clear differences could be found in their effects on GlcTase activities studied (data not shown). Using dimyristoyl- (di-$C_{14:0}$) PC, which is, according to data presented in Fig. 2, the most efficient effector, we found that its effects on inhibition of diosgenin glucosylation and stimulation of solasodine glucosylation were temperature-independent. Relative degree of inhibition/stimulation was almost the same regardless incubations

Table 2
Comparison of effects of non-ionic detergent Tween 80, dipalmitoyl-PC or SM (from bovine brain) on glucosylation rates of some steroids structurally related to eggplant sapogenins or alkaloid

Steroidal acceptor added (0.75 μM)	Relative glucosylation rate (%)[a]		
	+ Tween 80[b]	+ PC[c]	+ SM[c]
Yamogenin (25*S*-spirost-5-en-3β-ol)	< 5	23	7
Hecogenin (25*R*-5α-spirostan-3β-ol-12-one)	35	103	74
Nuatigenin (22*S*,25*S*-epoxy-furost-5-ene-3β,26-diol)	48	107	108
Tomatidine (*22S*,25*S*-5α-tomatanin-3β-ol)	60	136	129

[a] Glucosylation rate in the absence of detergent or lipid is taken as 100%.
[b] A final concentration of Tween 80 in the assay mixture was 0.1%.
[c] Final concentrations of PC and SM were 37.5 μM.

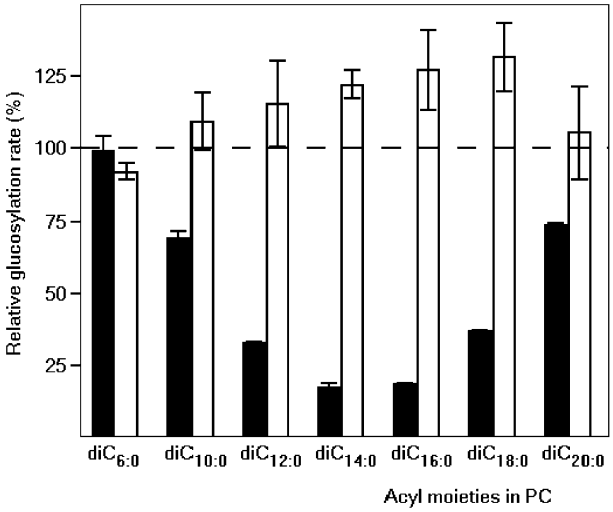

Fig. 2. Effect of phosphatidylcholines with different acyl chains on glucosylation of diosgenin (black bars) or solasodine (empty bars). Broken line shows the relative glucosylation rate in the absence of any PC.

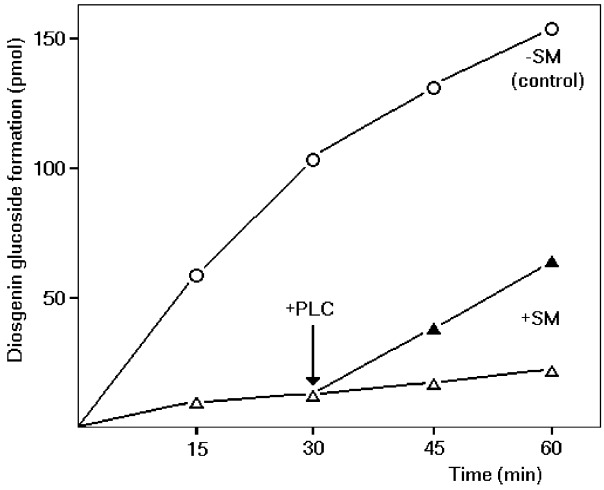

Fig. 3. Reversal of the inhibitory effect of bovine brain sphingomyelin (SM) on diosgenin glucosylation by treatment with phospholipase C from *Clostridium perfringens* (PLC). After 30 min incubation in the presence of 37.5 μM SM (open triangles), PLC (0.1 unit per incubated sample) was added. Black triangles show glucosylation of diosgenin in samples treated with PLC. In a control experiment incubations were carried out in absence of SM (open circles).

were carried out above (30 °C) or below (16 °C) the point of transition from gel to liquid-crystalline phase (22–24 °C) characteristic for dimyristoyl-PC (data not shown). These results clearly suggest that the above described effects of phospholipids on the activity of GlcTase studied are independent on their physical state.

2.3. Reversibility of phospholipid effects on GlcTase activity

It was an interesting question whether strong inhibition of steroidal sapogenin glucosylation by phosphocholine-containing lipids is an irreversible phenomenon. In order to elucidate this question, after 30-min-long incubation of eggplant GlcTase with diosgenin, labelled UDPGlc and bovine brain SM, incubated samples were treated with phospholipase C from *Clostridium perfringens* (type I, Sigma) which is known to remove phosphocholine moiety from both SM and PC.

Data summarized in Fig. 3 clearly demonstrate that hydrolysis of SM into phosphocholine and ceramide resulted in an almost complete recovery of diosgenin glucosylation rate which can be observed in the absence of SM. A similar experiment with the use of di-$C_{16:0}$ PC instead of SM gave in principle the same results (data not shown). Therefore, inhibition of diosgenin glucosylation by PC and SM is entirely reversible after hydrolytic removal of phosphocholine moiety from these lipids.

2.4. Effects of unlabelled diosgenin, tigogenin and solasodine on glucosylation of [3-^{3}H]tigogenin

Fig. 4 shows results of an experiment in which the influence of excess amounts (up to 5-fold) of unlabelled steroidal sapogenins native to eggplant as well as of solasodine was studied on glucosylation rate of tritium labelled tigogenin. As it could be predicted both unlabelled tigogenin and diosgenin decreased amounts of labelled tigogenin glucoside formed. Even a higher decrease of glucosylation of radioactive tigogenin, however, was found in the presence of unlabelled solasodine. This means that solasodine evidently can compete for steroid-substrate binding site in the enzyme responsible for glucosylation of tigogenin. It should be mentioned that in the experiment shown in Fig. 4 a very high concentration of cold UDPGlc were used. Therefore, decrease of [3-^{3}H]tigogenin glucosylation in the presence of unlabelled solasodine cannot be explained simply by competition for donor nucleotide sugar. In this experiment consumption of UDPGlc during the incubation never exceeded 1.5% of the amount added to the assay medium.

3. Discussion

The in vitro influence of lipids on activities of enzymes solubilized from membranous structures is a well-known phenomenon (Sandermann, 1978; Carruthers and Melchior, 1986). Stimulation or inhibition by some specific lipids has been also reported for a number of membrane-bound glycosyltransferases of plant origin (see e.g. Kaushal and Elbein, 1987; Coves et al., 1988; Saugy et al. 1988; Ullmann et al., 1993). The above-mentioned effects are not surprising since lipids constitute a natural environment for all membrane-bound enzymes. Reports on modulation by lipids of typical

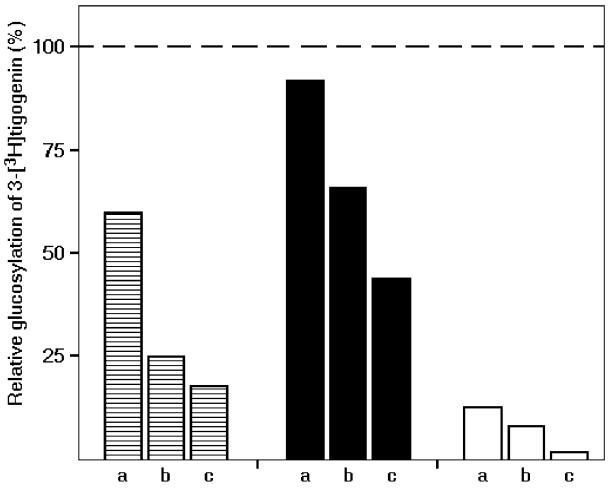

Fig. 4. Effect of excess amounts of unlabelled tigogenin (hatched bars), diosgenin (black bars) or solasodine (empty bars) on glucosylation of 3-[^{3}H]tigogenin. Labelled tigogenin (0.95 μM, sp. act. 11.67 GBq/mmol) and unlabelled UDPGlc (56.6 μM) were incubated in the presence of unlabelled tigogenin, diosgenin or solasodine (0.95, 1.90 or 4.75 μM for a, b and c, respectively). Broken line shows the glucosylation rate of labelled tigogenin in the absence of any unlabelled steroid.

cytosolic enzymes are scarce. In latter cases it has been postulated a subtle regulation of the activity of "cytosolic" enzymes by their binding to the cellular membranes, at least in a temporary way (Żydowo, 1993; Sims et al., 1999). Although steroid-specific GlcTase from eggplant leaves was found in 105 000 *g* supernatant obtained from the crude homogenate and, therefore, it has been initially described as a cytosolic enzyme (Pączkowski and Wojciechowski, 1994; Pączkowski et al., 1997, 1998), it seems quite possible that in vivo this enzyme is weakly membrane-bound or, at least, it can transiently interact with cellular membranes. The well-marked hydrophobic nature of its steroidal substrates as well as its evident sensitivity to some natural lipids, reported in the present study, are serious arguments for such a hypothesis. It is noteworthy that "cytosolic", flavonol-specific GlcTase from *Chrysosplenium americanum* leaves has been found to be associated with vesicle-like structures by immunolocalization (Latchinian-Sadek and Ibrahim, 1991).

In our previous paper (Pączkowski et al., 1998) we have suggested the presence in eggplant leaves of two separate UDPGlc-dependent GlcTases specific for spirostane sapogenins, i.e. diosgenin and tigogenin, and for solasodine, respectively. This suggestion based mainly on two findings: First, the ratios of UDPGlc:diosgenin GlcTase activity to UDPGlc:solasodine GlcTase activity were significantly different in crude cytosolic fractions obtained from various organs of eggplants of different age, ranging from 0.7 (ripening seeds) to 1.9 (stems). Second, several non-ionic detergents including Tween 20, Tween 80, Triton X-100 and Tyloxapol used at very low concentrations (0.05–0.1%) strongly reduced the rate of diosgenin glucosylation but had little effect on the formation of solasodine glucoside or were in the latter case even slightly stimulatory. At first sight the results of our present work support the above suggestion furnishing evidence that some natural lipids, particularly these containing phosphocholine moiety such as PC or SM, exert completely different effects on glucosylation rates of spirostane sapogenins occurring in eggplant, i.e. diosgenin and tigogenin, and glucosylation rate of eggplant steroidal alkaloid–solasodine. However, with some other steroids tested, which have been shown earlier (Pączkowski and Wojciechowski, 1994) to be good substrates for cytosolic GlcTase from eggplant leaves, both non-ionic detergent Tween 80 and choline containing phospholipids had intermediary effects as compared to the effects on glucosylation of diosgenin/tigogenin and solasodine. This is particularly evident for hecogenin which is steroidal sapogenin differing from tigogenin only by the presence of an additional oxo group at C-12. These results suggest rather a possibility that glucosylation of both steroidal sapogenins and alkaloids is catalyzed by a single enzyme but the specificity of this enzyme can be modulated in the presence of some amphipathic molecules such as detergents or phospholipids. Modulatory effects of lipid-enzyme interactions on substrate specificities of some enzymes have been well-documented in several cases (see e.g. Inagaki et al., 1986; Woscholski et al., 1995; Pappan et al., 1998; Frank et al., 1999). Such effects have been also reported by Magdalou et al., (1982) for UDP-glucuronosyltransferase isolated in a pure form from pig liver. The latter enzyme showed variable activity with several phenolic compounds used as substrates depending on the chemical nature of lipid effectors present in assay mixtures and these authors concluded that the ratio of glycosylation rate of various phenolics is not a static property of the enzyme, but can be modulated by the structure of the phospholipid present in the enzyme environment.

An additional evidence for glucosylation of solasodine as well as diosgenin and tigogenin by a single GlcTase furnished experiments in which effects of cold tigogenin, diosgenin and solasodine on glucosylation rate of [3-^{3}H]tigogenin were studied. The results of these experiments clearly indicate that cold solasodine can efficiently compete with labelled tigogenin for a binding site in the enzyme. In fact, cold solasodine decreased the rate of [3-^{3}H]tigogenin glucosylation even more strongly that cold tigogenin or diosgenin– this is, however, in accordance with the results presented in our previous paper (Pączkowski et al., 1998) indicating that K_m value of partially purified eggplant GlcTase for solasodine (0.04 μM) was several-fold lower than that for diosgenin (0.33 μM). In the present study K_m of 0.26 μM was measured for the third natural substrate of eggplant GlcTase, i.e. tigogenin.

Different ratios of glucosylation rates of solasodine and diosgenin reported by us earlier (Pączkowski et al., 1998) for crude cytosolic preparations obtained from various organs of eggplants may be explained by variable quantity and quality of lipids present in these preparations.

4. Experimental

4.1. Enzyme preparations

Crude lipid-depleted enzyme preparations (''acetone powders'') were obtained from crude cytosol fraction (105 000 *g* supernatant) of 8-week-old eggplant, cv. Black Beauty, leaves exactly as previously described (Pączkowski and Wojciechowski, 1994). These ''acetone powders'', when kept dry at −20 °C, retained almost all of the GlcTase activity for several months and were used as a source of partially purified enzyme according to Pączkowski et al. (1998). In contrast to crude ''acetone powders'', partially purified GlcTase preparations were quite unstable and lost ca. 60% activity during 24-h-long storage at 4 °C.

4.2. Glucosyltransferase assays with labelled UDPGlc

GlcTase activities were assayed essentially as previously described (Pączkowski et al., 1998) by measuring the transfer of labelled glucose from UDP-[^{3}H]glucose or UDP-[^{14}C]glucose to a steroid acceptor at saturating concentrations of both substrates. Unless otherwise stated, the standard assay mixture contained in a final volume of 0.53 ml: 30 or 0.6 μg protein, for crude or partially purified enzyme, respectively, in 0.50 ml 0.05 M HEPES buffer, pH 7.3 containing 10 mM 2-mercaptoethanol; diosgenin or solasodine (0.4 nmol) in 0.01 ml EtOH; UDP-[^{3}H]Glc or UDP-[^{14}C]Glc (1.5 nmol, 2×10^5 dpm) in 0.01 ml 50% EtOH, and varying amount of a lipid effector solution in 0.01 ml EtOH. In some experiments a steroid substrate and a lipid effector were added to the assay mixture as a clear dispersion in 0.02 ml water prepared by sonication according to Jensen and Schutzbach (1985). The effects of lipids on the GlcTase activities studied were, however, virtually the same, regardless of the method of their introduction into the incubation medium. Incubations were carried out at least in triplicate, usually at 30 °C, for 45 min. The reaction was terminated and the labelled glucoside product was separated from the labelled substrate and/or its degradation products by extraction with *n*-butanol as described earlier (Pączkowski and Wojciechowski, 1994). Aliquots of the organic phases were transferred to scintillation vials, evaporated to dryness and counted for radioactivity in a toluene-based scintillation fluid.

4.3. Glucosyltransferase assays with labelled tigogenin

The incubation conditions were similar to the above described for enzyme assays with labelled UDPGlc but [3-^{3}H]tigogenin (0.5 nmol, 3.5×10^5 dpm) and unlabelled UDPGlc (30 nmol) were used as the substrates. After extraction with *n*-butanol labelled tigogenin glucoside was separated from labelled tigogenin by TLC as described below, eluted from silica gel with MeOH and counted for radioactivity. Labelled [^{3}H]tigogenin was prepared as previously stated (Pączkowski et al., 1998).

4.4. Identification of the reaction products

For identification of products of the enzymic reaction, the *n*-butanol extracts were evaporated to dryness. Dry residues were dissolved in a small volume of $CHCl_3$–MeOH (2:1) and then subjected to TLC on silica-gel plates (DC Plastikfolien, Kieselgel 60, Merck) developed with $CHCl_3$–MeOH (17:3). Labelled glycosides were localized on the plates by autoradiography. For partially purified enzyme, incubations with all tested steroids afforded a single radioactive product with $R_f = 0.51$ (diosgenin, tigogenin, yamogenin and hecogenin); $R_f = 0.46$ (nuatigenin); $R_f = 0.36$ (tomatidine) and $R_f = 0.20$ (solasodine).

Acknowledgements

This work was supported by research grant BW 1455/2/1999 awarded to C.P. from the Faculty of Biology, Warsaw University.

References

Aubert, S., Daunay, M.C., Pochard, E., 1989. Saponosides steroidiques de l'aubergine (*Solanum melongena* L.). Agronomie 9, 641–651.

Bajak, K.L., Kaur, G., Chadha, M.L., 1979. Glycoalkaloid content and other chemical constituents of the fruits of some egg plants (*Solanum melongena* L.) varieties. J. Plant Foods 3, 163–168.

Blankemeyer, J.T., McWilliams, M.L., Rayburn, J.R., Weissenberg, M., Friedman, M., 1998. Developmental toxicity of solamargine and solasonine glycoalkaloids in frog embryos. Food Chem. Toxicol. 36, 383–389.

Carruthers, A., Melchior, D.L., 1986. How bilayer lipids affect membrane protein activity. TIBS 11, 331–335.

Coves, J., Joyard, J., Douce, R., 1988. Lipid requirement and kinetic studies of solubilized UDP-galactose:diacylglycerol galactosyltransferase activity from spinach chloroplast envelope. Proc. Natl. Acad. Sci., USA 85, 4966–4970.

Frank, C., Keilhack, H., Opitz, F., Zschornig, O., Bohner, F.D., 1999. Binding of phosphatidic acid to the protein-tyrosine phosphatase SHP-1 as a basis for activity modulation. Biochemistry 38, 11993–20002.

Inagaki, T., Rao, N.A., Yagi, K., 1986. Modulation by phospholipid of the activity of monoamine oxidase purified from pig liver. J. Biochem. (Tokyo) 100, 597–603.

Jensen, J.W., Schutzbach, J.S., 1985. Activation of dolichyl-phospho-mannose synthase by phospholipids. Eur. J. Biochem. 153, 41–48.

Kaushal, G.P., Elbein, A.D., 1987. Partial purification and characterization of β-mannosyltransferase from suspension-cultured soybean cells. Biochemistry 26, 7953–7960.

Kintia, P.K., 1996. Chemistry and biological activity of steroid saponins from Moldovian plants. Adv. Exp. Med. Biol. 404, 309–334.

Kintia, P.K., Shvets, S.A., 1985. Melongosides N, O and P: steroidal saponins from seeds of *Solanum melongena*. Phytochemistry 24, 1567–1569.

Latchinian-Sadek, L., Ibrahim, R.K., 1991. Flavonol ring B-specific *O*-glucosyltransferase; purification, production of polyclonal antibodies and immmunolocalization. Arch. Biochem. Biophys. 289, 230–236.

Magdalou, J., Hochman, Y., Zakim, D., 1982. Factors modulating the catalytic specificity of a pure form of UDP-glucuronosyltransferase. J. Biol. Chem. 257, 13624–13629.

Pączkowski, C., Kalinowska, M., Wojciechowski, Z.A., 1997. UDP-glucose:solasodine glucosyltransferase from eggplant (*Solanum melongena* L.) leaves:partial purification and characterization. Acta Biochim. Polon. 44, 43–54.

Pączkowski, C., Kalinowska, M., Wojciechowski, Z.A., 1998. The 3-*O*-glucosylation of steroidal sapogenins and alkaloids in eggplant (*Solanum melongena*): evidence for two separate glucosyltransferases. Phytochemistry 48, 1151–1159.

Pączkowski, C., Wojciechowski, Z.A., 1993. The *in vitro* synthesis of diosgenin mono- and diglucoside by enzyme preparation from *Solanum melongena* leaves. Acta Biochim. Polon. 40, 141–143.

Pączkowski, C., Wojciechowski, Z.A., 1994. Glucosylation and galactosylation of diosgenin and solasodine by soluble glucosyltransferase(s) from *Solanum melongena* leaves. Phytochemistry 35, 1429–1434.

Pappan, K., Austin-Brown, S., Chapman, K.D., Wang, X., 1998. Substrate selectivity and lipid modulation of plant phospholipase D: alpha-, beta-, and gamma. Arch. Biochem. Biophys. 253, 131–140.

Sandermann, H., 1978. Regulation of membrane enzymes by lipids. Biochim. Biophys. Acta 515, 209–237.

Saugy, M., Farkas, V., MacLachlan, G., 1988. Phosphatases and phosphodiesterases interfere with 1,3-β-D-glucan synthase activity in pea epicotyl membrane preparations. Eur. J. Biochem. 117, 135–138.

Sims, B., Mahnke-Zizelman, D.K., Profit, A.A., Prestwich, G.D., Sabina, R.L., Theibert, A.B., 1999. Regulation of AMP deaminase by phosphoinositides. J. Biol. Chem. 274, 25701–25707.

Ullmann, P., Ury, A., Rimmele, D., Benveniste, P., Bouvier-Nave, P., 1993. UDP-glucose sterol β-D-glucosyltransferase, a plasma membrane-bound enzyme of plants: enzymatic properties and lipid dependence. Biochemie 75, 713–723.

Vohora, S.B., Kumar, I., Khan, M.S.Y., 1984. Effect of alkaloids of *Solanum melongena* on the central nervous system. J. Ethnopharmacol. 11, 331–336.

Woscholski, R., Kodaki, T., Palmer, R.H., Waterfield, M.D., Parker, P.J., 1995. Modulation of the substrate specificity of the mammalian phosphatidylinositol 3-kinase by cholesterol sulfate and sulfatide. Biochemistry 34, 11489–11493.

Żydowo, M.M., 1993. Regulatory effects of the lipid-cytosolic enzyme interaction: AMP-deaminase. Acta Biochim. Polon. 40, 429–432.

PERGAMON

Phytochemistry 58 (2001) 671–676

PHYTOCHEMISTRY

www.elsevier.com/locate/phytochem

8-Dimethylallylnaringenin 2′-hydroxylase, the crucial cytochrome P450 mono-oxygenase for lavandulylated flavanone formation in *Sophora flavescens* cultured cells

Hirobumi Yamamoto[a], Atsushi Yatou[b], Kenichiro Inoue[b,*]

[a]*Medicinal Plant Garden, School of Pharmaceutical Sciences, Nagasaki University, 1-14 Bunkyo-machi, Nagasaki 852-8521, Japan*
[b]*Department of Pharmacognosy, Gifu Pharmaceutical University, 6-1 Mitahora-higashi 5 chome, Gifu 502-8585, Japan*

Received 9 March 2001; received in revised form 18 May 2001

Abstract

8-Dimethylallylnaringenin (8-DMAN) 2′-hydroxylase, which is indispensable for the formation of a lavandulylated flavanone, sophoraflavanone G, was detected in cell suspension cultures of *Sophora flavescens*. The enzyme catalyzes the 2′-hydroxylation of 8-DMAN to leachianone G, and is tightly bound to the membrane. It required NADPH and molecular oxygen as cofactors, and was inhibited by several cytochrome P450 inhibitors such as carbon monoxide and cytochrome c, indicating that the reaction is mediated by a cytochrome P450 monooxygenase. The optimum pH of 8-DMAN 2′-hydroxylase was 8.5, and the enzyme hydroxylated only 8-DMAN. Apparent K*m* values for 8-DMAN and NADPH of the enzyme were 55 and 34 μM, respectively. © 2001 Elsevier Science Ltd. All rights reserved.

Keywords: *Sophora flavescens*; Leguminosae; Cell suspension cultures; Biosynthesis; Cytochrome P450 mono-oxygenase; Prenylated flavanones; 8-Dimethylallylnaringenin; Leachianone G; Sophoraflavanone G

1. Introduction

Prenylated flavonoids are widely distributed in leguminous, moraceous, berberidaceous and iridaceous plants (Barron and Ibrahim, 1996). In most cases, one or two dimethylallyl moieties are bound to the A or B rings of flavonoids, and sometimes cyclization of a double bond of this side chain with a neighboring phenolic OH function forms a chromene ring as seen in euchrestaflavanone c and osajin in *Euchresta japonica* (Shirataki et al., 1982). Furthermore, it is characteristic of prenylated flavonoids in *Sophora flavescens*, a leguminous plant, to possess a lavandulyl group, an irregular monoterpenoid unit, at the C-6 or C-8 position of 2′-hydroxyflavanone (Hatayama and Komatsu, 1971; Wu et al., 1985a,b,c, 1986). For elucidation of the formation mechanism of this unique prenyl group, we have established cell suspension cultures of *S. flavescens* which produced sophoraflavanone G (SFG), one of the main lavandulylated flavanones in the intact plant (Yamamoto et al., 1991). We have also found that the production of SFG in the cultured cells was stimulated by the addition of some elicitors (Yamamoto et al., 1995) as well as cork tissues (Yamamoto et al., 1996, 1999). Recently, we reported naringenin 8-dimethylallyltransferase in the microsomal fraction from *S. flavescens* cultured cells that prenylated C-8 of (−)-(2*S*)-naringenin to afford (−)-(2*S*)-8-dimethylallylnaringenin (8-DMAN; sophoraflavanone B) as the sole prenylated product (Yamamoto et al., 2000a). The enzyme prenylated naringenin more effectively compared to other flavanone derivatives. Interestingly, when 2′-hydroxynaringenin was used as a prenyl acceptor, the formation of SFG, a lavandulylated flavanone, together with that of 2′-hydroxy-8-dimethylallylnaringenin (leachianone G, LG) was observed. At that time, any naringenin 2′-hydroxylation activity could not be detected in *S. flavescens* cells. These data suggest that the 2′-hydroxy group of flavanone plays an important role for the formation of a lavandulyl group in *S. flavescens* cells, and that a lavandulyl group is formed by two-step dimethylallylations, between which 2′-hydroxylation is inserted (Fig. 1).

* Corresponding author. Tel.: +81-58-237-3931; fax: +81-58-237-5979.
E-mail address: inoueken@gifu-pu.ac.jp (K. Inoue).

0031-9422/01/$ - see front matter © 2001 Elsevier Science Ltd. All rights reserved.
PII: S0031-9422(01)00270-9

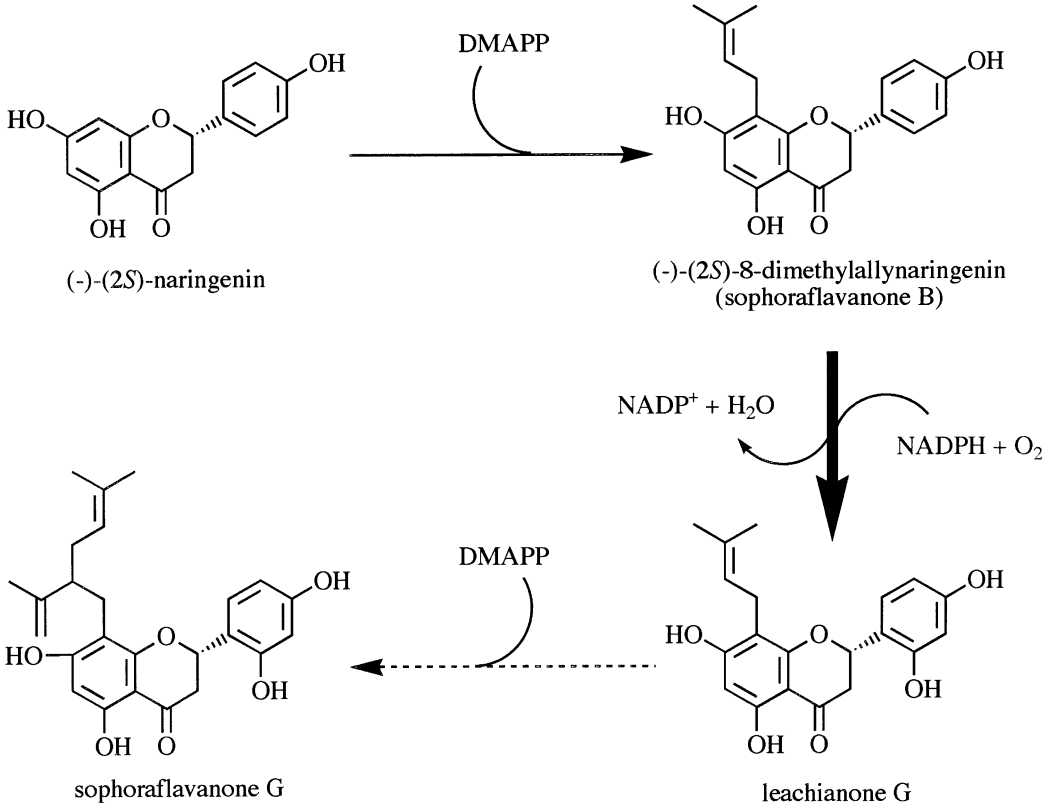

Fig. 1. Proposed biosynthetic route to sophoraflavanone G from naringenin in *Sophora flavescens* cultured cells. DMAPP: dimethylallyl diphosphate.

In the present paper, we report the detection and characterization of 8-DMAN 2′-hydroxylase, essential for the formation of lavandulylated flavanones, in *S. flavescens* cultured cells.

2. Results and discussion

2.1. Detection of 8-DMAN 2′-hydroxylase activity

When crude cell-free extracts or the microsomal fraction from *S. flavescens* cell suspension cultures were incubated with (−)-(2*S*)-8-DMAN and NADPH, the formation of a new compound whose retention time and UV absorption pattern were completely identical to those of leachianone G (LG) was observed in HPLC-photodiode array analysis. The reaction product was isolated on a preparative scale, and was identified as LG by the direct comparison of its EI-MS spectrum with that of authentic LG. More than 90% of the hydroxylation activity still remained in the twice-washed 100,000×*g* pellets, indicating that the hydroxylase was tightly bound to the membrane fraction of the cells (data not shown). The activity depended on the presence of the active enzyme, 8-DMAN and NADPH, and the latter could not be replaced by NADH, FAD or FMN (Table 1).

Table 1
Activity and cofactor requirement of 8-DMAN 2′-hydroxylase from cultured cells of *Sophora flavescens*[a]

Conditions	Relative activity (%)
Complete assay	100.0
Heat-denatured enzyme	0.0
- 8-DMAN	0.0
- Protein	0.0
- NADPH	0.0
- 1 mM NADPH + 1 mM NADH	16.2
- 1 mM NADPH + 1 mM FAD	7.3
- 1 mM NADPH + 1 mM FMN	9.5

[a] The complete assay contained microsomal protein (430 μg), 1 mM (S)-8-DMAN, and 1 mM NADPH. Incubations were carried out as described in Experimental (incubation time: 120 min). 8-DMAN 2′-hydroxylase activity in the complete assay was 13.3 pkat/mg protein.

2.2. Biochemical properties of 8-DMAN 2′-hydroxylase

The pH optimum of 2′-hydroxylase activity was 8.5 in Tris–HCl buffer. The activity in glycine-NaOH buffer at pH 8.5 was only 60% of that observed in Tris–HCl-buffer (data not shown). The hydroxylation of 8-DMAN was linear with time up to 60 min and with protein concentration from 0.06 mg to 0.6 mg in the standard assay. The substrate specificity of 8-DMAN 2′-hydroxylase for

several flavonoids including chemically synthesized dimethylallylated naringenins (Tahara et al., 1994) was investigated. Among these, only 8-DMAN was hydroxylated, but other flavonoids examined, kaempferol, quercetin, apigenin, genistein, naringenin, 6-dimethylallylnaringenin, 3′-dimethylallylnaringenin, 3′,6-di-(dimethylallyl)naringenin, 6″,6″-dimethyl-4″,5″-dihydropyrano-[2″,3″:6,7]naringenin and 6″,6″-dimethyl-4″,5″-dihydropyrano-[2″,3″:7,8]naringenin were not hydroxylated (data not shown). The optimal concentrations of (−)-(2*S*)-8-DMAN and NADPH for enzymatic hydroxylation were between 0.5 and 1 mM, and the apparent K_m values for 8-DMAN and NADPH were calculated as 55 and 34 μM, respectively (Figs. 2 and 3).

2.3. Involvement of cytochrome P450 in 8-DMAN 2′-hydroxylation

In addition to NADPH, 8-DMAN 2′-hydroxylase required molecular oxygen (Table 2). Replacement of O_2 in the reaction mixture by N_2 prior to the incubation led to a significant decrease in the activity. When O_2 in the reaction mixture was completely removed by the addition of an excess of glucose, glucose oxidase and catalase (Kochs and Grisebach, 1987), the formation of LG was hardly detectable (Table 2). These findings suggested the participation of cytochrome P450 haemoprotein in the hydroxylation of 8-DMAN. To confirm this hypothesis, the effects of several cytochrome P450 inhibitors were examined (Table 3). Carbon monoxide, a well-known inhibitor of cytochrome P450 (Ortiz de Montellano and Correia, 1995), strongly inhibited the

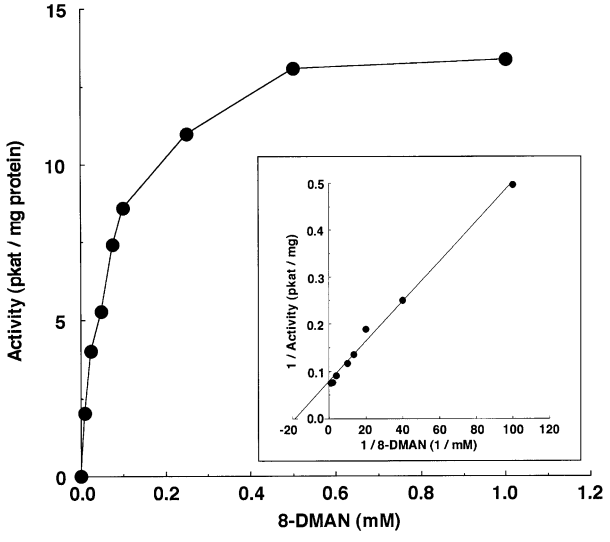

Fig. 2. Dependence of 8-DMAN 2′-hydroxylase on the concentration of (−)-(2*S*)-8-dimethylallylnaringenin (DMAN) measured with the microsomal fraction of *Sophora flavescens*. Insert: Lineweaver-Burk plot with varying concentrations (0.01–1 mM) to calculate the apparent K_m value for (−)-(2*S*)-8-DMAN.

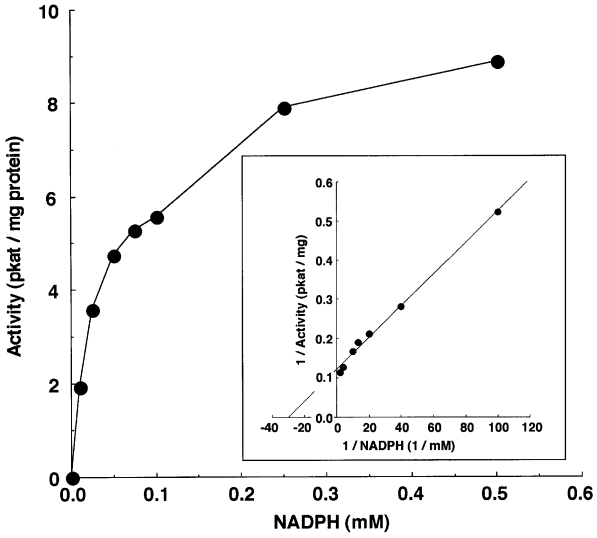

Fig. 3. Dependence of 8-DMAN 2′-hydroxylase on the concentration of NADPH measured with the microsomal fraction of *Sophora flavescens*. Insert: Lineweaver–Burk plot with varying concentrations (0.01–0.5 mM) to calculate the apparent K_m value for NADPH.

Table 2
Oxygen dependence of 8-DMAN 2′-hydroxylase activity[a]

Conditions	Relative activity (%)
Air bubbled	100.0
N_2 bubbled	13.7
+ Glucose + glucose oxidase + catalase	8.8
+ Glucose + heat-denatured glucose oxidase + catalase	89.4

[a] Incubations were carried out as described in Experimental. 8-DMAN 2′-hydroxylase activity in air bubbled control was 12.6 pkat/mg protein

Table 3
Effects of cytochrome P450 inhibitors on 8-DMAN 2′-hydroxylase activity[a]

Inhibitor	Relative activity (%)
Air (dark)	100.0
CO/O_2 (9:1, dark)	14.5
CO/O_2 (9:1, light)	77.0
None	100.0
Ancymidol 1 mM	94.7
Metyrapone 1 mM	76.0
Miconazole 1 mM	63.7
Tropolon 1 mM	69.9
Cytochrome 10 mM	29.1
KCN 1 mM	109.0

[a] Incubations were carried out as described in Experimental. White light (20,000 lx) was used for the reversion experiment. 8-DMAN 2′-hydroxylase activity in the control assay (Air, Dark) was 15.5 pkat/mg protein.

hydroxylation in the dark, and this inhibition was partially reversible by the illumination. Cytochrome c, which competitively removes electrons from the NADPH-cytochrome c reductase complex (Ortiz de Montellano and Correia 1995), was the strongest inhibitor tested. Even at 10 μM cytochrome c, the activity was inhibited by about 70%. Other inhibitors, ancymidol (Graebe 1987), metyrapone and miconazole (Ortiz de Montellano and Correia 1995) and tropolone (Rueffer and Zenk, 1994) showed less pronounced inhibition of 8-DMAN 2′-hydroxylation similar to their effects on other plant cytochrome P450 mono-oxygenases (Tang and Suga 1994; Petersen, 1997; Yamamoto et al., 2000b). Potassium cyanide, an inhibitor of peroxidase, hardly affected the activity (Saunders et al., 1964). These results indicate that 8-DMAN 2′-hydroxylase belongs to the group of cytochrome P450 monooxygenases.

Several studies have been done on the flavonoid hydroxlases, most of which are cytochome P450-dependent. 2′- and 3′-Hydroxylases from *Cicer arietinum* were specific solely for 4′-methoxyisoflavones but the substrate specificity for flavanones was not described (Clemens et al., 1993; Overkamp et al., 2000). Heterologous expression in yeast demonstrated that CYP81E1, a cytochrome P450 cDNA cloned from *Glycyrrhiza echinata,* is isoflavone 2′-hydroxylase, which catalyzed the hydroxylation of isoflavones such as daidzein and formononetin but did not that of flavanones (Akashi et al., 1998). Furthermore, up to the present time, nothing has been reported about flavanone 2′-hydroxylase. The cytochrome P450-dependent hydroxylase investigated in this paper, which catalyzes the hydroxylation of 8-dimethylallynaringenin alone, accordingly, is the first example of the 2′-hydroxylase of prenylated flavanones.

Recently we demonstrated that the presence of 2′-OH function of naringenin is indispensable for the formation of SFG in *S. flavescens* cultured cells (Yamamoto et al., 2000a). We also speculated that a lavandulyl group at C-8 of naringenin is formed by phased dimethylallylations, between which the hydroxylation at C-2′ intervenes, since naringenin 2′-hydroxylase activity was hardly detectable in *Sophora* cells. In this paper, we demonstrated that 8-DMAN was converted to LG by membrane-bound 8-DMAN 2′-hydroxylase from *S. flavescens* cultured cells and that 8-DMAN 2′-hydroxylase is a member of the cytochrome P450 mono-oxygenase family. It follows from these results that SFG is biosynthesized from naringenin via 8-DMAN and LG, successively, by naringenin 8-dimethylallyltransferase, 8-DMAN 2′-hydroxylase and an uncharacterized membrane-bound lavandulyl moiety synthase (Yamamoto et al., 2000a) in *S. flavescens* cells (Fig. 1).

In leguminous plants, prenylation of flavonoids is known to take place in the plastids (Biggs et al., 1990). Furthermore, their dimethylallyl groups are found to be derived from the non-mevalonate pathway (Hano et al., 1994; Asada et al., 2000) which is operative in the formation of isoprenoids biosynthesized in the plastids such as monoterpenoids (Eisenreich et al., 1997; Adam et al., 1998; Turner et al., 1999), as well as β-carotene and prenyl chains of chlorophylls (Lichtenthaler et al., 1997; Disch et al., 1998). In contrast, in *Lithospermum erythrorhizon* cultured cells, geranyl pyrophosphate supplied from the mevalonate pathway in the endoplasmic reticulum/cytosol (Sommer et al., 1995; Li et al., 1998) was utilized for the prenylation of *p*-hydroxybenzoic acid which took place in the endoplasmic reticulum (Yamaga et al., 1993). In SFG biosynthesis, 2′-hydroxylation catalyzed by a cytochrome P450 monooxygenase occurred between two prenylations, and most of cytochrome P450 enzymes were associated with the endoplasmic reticulum (von Wachenfeldt and Johnson, 1995). Thus, in *Sophora* cells, the reaction site of the two prenylations in relation to the source of two dimethylallyl moieties might be different. For the complete elucidation of the lavandulyl moiety formation in *Sophora* cells, it will be necessary to clarify the subcellular localization of the three membrane-bound enzymes including 8-DMAN 2′-hydroxylase and two prenyltransferases as well as the origin of dimethylallyl diphosphate.

3. Experimental

3.1. Chemicals

(−)-(*2S*)-8-Dimethylallylnaringenin was enzymatically synthesized using naringenin 8-dimethylallyltransferase from *Sophora flavescens* cultured cells (Yamamoto et al., 2000a). 6-Dimethylallylnaringenin, 3′-dimethylallylnaringenin, 3′,6-di-(dimethylallyl)naringenin, 6″,6″-dimethyl-4″,5″-dihydropyrano-[2″,3″:6,7]naringenin and 6″,6″-dimethyl-4″,5″-dihydropyrano-[2″,3″:7,8]naringenin were chemically synthesized from naringenin and 2-methyl-3-buten-2-ol in the presence of boron trifluoride/etherate according to the method of Tahara et al. (1994). Apigenin, genistein, kaempferol, naringenin and quercetin were purchased from Funakoshi, Japan.

3.2. Plant material and culture method

The origin and subculturing of callus cultures (Yamamoto et al., 1991) and the establishment of cell suspension cultures (Yamamoto et al., 1996) of *Sophora flavescens* were described in the previous papers.

3.3. Enzyme preparation

For enzyme preparation, all procedures were carried out at 4 °C. Thirty grams of *S. flavescens* cells cultured for 8–10 days were homogenized by a Teflon homogenizer in 100 mM K-Pi buffer (pH 6.5, 60 ml) containing 10 mM

DTT and 3 g PVPP. The homogenate was centrifuged at 12,000×*g* for 20 min, and the supernatant was further ultracentrifuged at 100,000×*g* for 20 min. The pellet was washed twice with 100 mM Tris–HCl buffer (pH 8.5) containing 10 mM DTT and then resuspended in 5 ml of the same buffer.

3.4. Protein content

Protein content was determined according to the method of Bradford (1976).

3.5. Enzyme reaction

The incubation mixture contained 150 nmol 8-dimethylallylnaringenin dissolved in 15 μl EtOH, 150 nmol NADPH and 60 μl of the microsomal fraction (ca. 0.5 mg of microsomal protein) in a total vol. of 150 μl. The reaction was initiated by the addition of NADPH to the mixture and, after incubation for 60 min at 30 °C, was terminated by the addition of 30 μl of 6 M HCl. The reaction mixture was extracted with 150 μl of EtOAc containing 50 nmol 1-naphthaleneacetic acid as an internal standard. The EtOAc extract was evaporated, dissolved in 70 μl MeOH and analyzed by HPLC.

For the investigation of the effects of different gaseous environments, test tubes (10 ml) containing all the reaction components except NADPH were sealed with septum caps in ice-water bath, and 200 ml of N_2, CO/O_2 (9:1) mixture or air was slowly bubbled into the mixture, respectively. The reaction was initiated by the addition of 150 nmol NADPH in the 15 μl of the same buffer. In the System Biotron, incubation was carried out for 60 min at 30 °C in the dark (tubes covered with aluminum foil) and under 20,000 lx of fluorescent lights for examining the effect of the light on the inhibition by CO. The reaction was stopped, treated and analyzed as described above.

For the oxygen consuming experiments, 40 mM glucose, 50 units glucose oxidase (Nacalai Tesque, Japan) and 105 units catalase (Sigma, USA) were added to the enzyme solution containing 150 nmol 8-DMAN and, after preincubation for 30 min at 30 °C, the reactions were initiated by addition of 150 nmol NADPH.

3.6. HPLC analysis

The amount of leachianone G formed was determined by HPLC using Capcellpak C18 AG-120 column (4.6×250 mm, Shiseido, Japan) in an oven at 40 °C, with CH_3CN/H_2O linear gradient solvent system containing 1% AcOH, from 20% to 60% CH_3CN in 40 min, at a flow rate of 0.9 ml/min, monitoring the absorption at 294 nm or using a photodiode-array SPDM-6A system (Shimadzu, Japan). The quantities were calculated from the peak area at 294 nm recorded by Chromatopac C-R4A (Shimadzu, Japan).

3.7. Isolation and identification of the reaction product

The microsomal fraction obtained from 30 g of the fresh cells was incubated with 750 nmol 8-DMAN and 750 nmol NADPH in 100 mM Tris–HCl buffer (pH 8.5, total vol. 7.5 ml) at 30 °C for 2 h. The reaction was terminated by the addition of 1.5 ml of 6 M HCl, and the products were extracted with EtOAc (3×7.5 ml). The organic layers were combined and concd in vacuo. The residue was dissolved in MeOH and purified by HPLC using the following conditions: column, Hikarisil C18 (4.6×250 mm, Asahi Chemical Ind. Co., Ltd., Japan); solvent, CH_3CN/H_2O linear gradient solvent system, from 20% CH_3CN to 50% CH_3CN in 60 min; flow rate, 1 ml/min; oven temp., 40 °C; detection, 294 nm. The fraction around Rt 50 min was collected and evaporated in vacuo.

EI–MS. *m*/*z*; 356 (M^+), 338, 323, 295, 283, 270, 205, 192, 177, 165, 136.

References

Adam, K.P., Theil, R., Zapp, J., Becker, H., 1998. Involvement of the mevalonic acid pathway and the glyceraldehyde-pyruvate pathway in terpenoid biosynthesis of the liverworts *Ricciocarpos matans*, and *Conocephalum conicum*. Archives of Biochemistry and Biophysics 354, 181–187.

Akashi, T., Aoki, T., Ayabe, S., 1998. CYP81E1, a cytochrome P450 cDNA of licorice (*Glycyrrhiza echinata* L.), encodes isoflavanone 2′-hydroxylase. Biochemical Biophysical Research Communications 251, 67–70.

Asada, Y., Li, W., Yoshikawa, T., 2000. Biosynthesis of the dimethylallyl moiety of glabrol in *Glycyrrhiza glabra* hairy root cultures via a non-mevalonate pathway. Phytochemistry 55, 323–326.

Barron, D., Ibrahim, R.K., 1996. Isoprenylated flavonoids—a survay. Phytochemistry 43, 921–982.

Biggs, D.R., Welle, R., Grisebach, H., 1990. Intercellular localization of prenyltransferases of isoflavonoid phytoalexin biosynthesis in bean and soybean. Planta 181, 244–248.

Bradford, M.M., 1976. A rapid and sensitive method for the quantitation of microgram quantities of protein utilizing the principle of protein-dye binding. Analytical Biochemistry 72, 248–254.

Clemens, S., Hinderer, W., Wittkampf, U., Barz, W., 1993. Characterization of cytochrome P450-dependent isoflavone hydroxylases from chickpea. Phytochemistry 32, 653–657.

Disch, A., Hemmerlin, A., Bach, T.J., Rohmer, M., 1998. Mevalonate-derived isopentenyl diphosphate is the biosynthetic precursor of ubiquinone prenyl side chain in tobacco BY-2 cells. Biochemical Journal 331, 615–621.

Eisenreich, W., Sanger, S., Zenk, M.H., Bacher, A., 1997. Monoterpenoid essential oils are not of mevalonate origin. Tetrahedron Letters 38, 3389–3892.

Graebe, J.E., 1987. Gibberellin biosynthesis and control. Annual Review of Plant Physiology 38, 419–465.

Hano, Y., Ayukawa, A., Nomura, T., Ueda, S., 1994. Origin of the acetate units composing the hemiterpene moieties of chalcomoracin in *Morus alba* cell cultures. Journal of the American Chemical Society 116, 4189–4193.

Hatayama, K., Komatsu, M., 1971. Studies on the constituents of *Sophora* species. V. Constituents of the root of *Sophora angustifolia* Sieb. Et Zucc. (2). Chemical Pharmaceutical Bulletin 19, 2126–2131.

Kochs, G., Grisebach, H., 1987. Induction and characterization of a NADPH-dependent flavone synthase from cell cultures of soybean. Zeitschrift für Naturforschung 42c, 343–348.

Li, S.M, Hennig, S., Heide, L., 1998. Shikonin: a geranyl diphosphate-derived plant hemiterpenoid formed via the mevalonate pathway. Tetrahedron Letters 39, 2721–2724.

Lichtenthaler, H.K., Schwender, J., Disch, A., Rohmer, M., 1997. Biosynthesis of isoprenoids in higher plant chloroplasts proceeds via a mevalonate-independent pathway. FEBS Letters 400, 271–274.

Ortiz de Montellano, P.R., Correia, M.A., 1995. Inhibition of cytochrome P450 enzymes. In: Ortiz de Montellano, P.R. (Ed.), Cytochrome P450: Structure, mechanism and biochemistry, 2nd edition. Plenum, New York, pp. 305–364.

Overkamp, S., Hein, F., Barz, W., 2000. Cloning and characterization of eight cytochrome P450 cDNAs from chickpea (*Cicer arietinum* L.) cell suspension cultures. Plant Sciences 155, 101–108.

Petersen, M., 1997. Cytochrome P450-dependent hydroxylation in the biosynthesis of rosmarinic acid in *Coleus*. Phytochemistry 45, 1165–1172.

Rueffer, M., Zenk, M.H., 1994. Canadine synthase from *Thalictrum tuberosum* cell cultures catalyses the formation of the methylenedioxy bridge in berberine synthesis. Phytochemistry 36, 1219–1223.

Saunders, B.C., Holmes-Siedle, A.G., Stark, B.D., 1964. Peroxidase. Butterworth, London.

Shirataki, Y., Manaka, A., Yokoe, I., Komatsu, M., 1982. Two prenylflavanones from *Euchresta japonica*. Phytochemistry 21, 2959–2963.

Sommer, S., Severin, K., Camara, B., Heide, L., 1995. Intracellular localization of geranylpyrophosphate synthase from cell cultures of *Lithospermum erythrorhizon*. Phytochemistry 38, 623–627.

Tahara, S., Katagiri, Y., Ingham, J.L., Mizutani, J., 1994. Prenylated flavonoids in the roots of yellow lupin. Phytochemistry 36, 1261–1271.

Tang, Y.X., Suga, T., 1994. Evidence for the involvement of cytochrome P-450-dependent monooxygenases in the allylic hydroxylation of terpineols by *Nicotiana tabacum* cell cultures. Phytochemistry 37, 731–735.

Turner, G., Gershenzon, J., Nielson, E.E., Froehlich, J.E., Croteau, R., 1999. Limonene synthase, the enzyme responsible for monoterpene biosynthesis in peppermint, is localized to leucoplasts of oil gland secretory cells. Plant Physiology 120, 879–886.

von Wachenfeldt, C., Johnson, E.F., 1995. Structures of eucaryotic cytochrome P-450 enzymes. In: Ortiz de Montellano, P.R. (Ed.), Cytochrome P450: Structure, Mechanism, and Biochemistry, 2nd Edition. Plenum, New York, pp. 183–223.

Wu, L.J., Miyase, T., Ueno, A., Kuroyanagi, M., Noro, T., Fukushima, S., 1985a. Studies on the constituents of *Sophora flavescens*. Aiton. II. Chemical Pharmaceutical Bulletin 33, 3231–3236.

Wu, L.J., Miyase, T., Ueno, A., Kuroyanagi, M., Noro, T., Fukushima, S., 1985b. Studies on the constituents of *Sophora flavescens*. Ait. III.. Yakugaku Zasshi 105, 736–741.

Wu, L.J., Miyase, T., Ueno, A., Kuroyanagi, M., Noro, T., Fukushima, S., Sasaki, S., 1985c. Studies on the constituents of *Sophora flavescens*. Ait. IV.. Yakugaku Zasshi 105, 1034–1039.

Wu, L.J., Miyase, T., Ueno, A., Kuroyanagi, M., Noro, T., Fukushima, S., Sasaki, S., 1986. Studies on the constituents of *Sophora flavescens*.. Ait. V. Yakugaku Zasshi 106, 22–26.

Yamaga, Y., Nakanishi, K., Fukui, H., Tabata, M., 1993. Intracellular localization of *p*-hydroxybenzoate geranyltransferase, a key enzyme involved in shikonin biosynthesis. Phytochemistry 32, 633–636.

Yamamoto, H., Kawai, S., Mayumi, J., Tanaka, T., Iinuma, M., Mizuno, M., 1991. Prenylated flavanone production in callus cultures of *Sophora flavescens* var. *angustifolia*. Zeitschrift für Naturforschung 46c, 172–176.

Yamamoto, H., Ichimura, M., Inoue, K., 1995. Stimulation of prenylated flavanone production by mannans and acidic polysaccharides in callus culture of *Sophora flavescens*. Phytochemistry 40, 77–81.

Yamamoto, H., Yamaguchi, M., Inoue, K., 1996. Absorption and increase in the production of prenylated flavanones in *Sophora flavescens* cell suspension cultures by cork pieces. Phytochemistry 43, 603–608.

Yamamoto, H., Yazaki, K., Hayashi, H., Taguchi, G., Inoue, K., 1999. Effects of cork tissues on the production of secondary metabolites in various plant cell cultures. In: Pandalai, S.G. (Ed.), Recent Research Developments in Biotechnology and Bioengineering, Vol. 2, Part II. Research Signpost, India, pp. 273–281.

Yamamoto, H., Senda, M., Inoue, K., 2000a. Flavanone 8-dimethylallyltransferase in *Sophora flavescens* cell suspension cultures. Phytochemistry 54, 649–655.

Yamamoto, H., Inoue, K., Li, S.M., Heide, L., 2000b. Geranylhydroquinone 3″-hydroxylase, a cytochrome P-450 monooxygenase from *Lithospermum erythrorhizon* cell suspension cultures. Planta 210, 312–317.

PERGAMON

Phytochemistry 58 (2001) 677–682

PHYTOCHEMISTRY

www.elsevier.com/locate/phytochem

A serine endopeptidase from cucumber leaves is inhibited by L-arginine, guanidino compounds and divalent cations

Yasuo Yamauchi[a,*], Toshio Sugimoto[b], Kuni Sueyoshi[b,1], Yoshikiyo Oji[b], Kiyoshi Tanaka[a]

[a]*Laboratory of Plant Biotechnology, Faculty of Agriculture, Tottori University, Koyama, Tottori 680-8553, Japan*
[b]*Department of Biological and Environmental Sciences, Faculty of Agriculture, Kobe University, Rokkodai 1-1, Nada-ku, Kobe 657-8501, Japan*

Received 15 February 2001; received in revised form 5 June 2001

Abstract

An endopeptidase was purified and characterized from green leaves of cucumber (*Cucumis sativus* L. suyo). The purified enzyme, a basic amino acid-specific endopeptidase with a pI of 5.0, was a monomeric protein of 80 kDa whose pH optimum was 9.5. Inhibitor analysis suggested that it was a serine endopeptidase and contained sulfhydryl groups essential for catalytic activity. Analysis of internal amino acid sequences of the endopeptidase showed no significant similarity to other proteins. Its activity was inhibited by L-Arg and guanidino compounds having high hydrophobicity, as well as divalent cations such as Mg^{2+} and Ca^{2+}. The K_i values of L-Arg and Mg^{2+}, which are also likely in vivo inhibitors, were 3.5 and 10 mM, respectively. Inhibition by L-Arg and Mg^{2+} was additive, and more than 70% of the activity was reversibly inhibited under their physiologically significant concentrations. These results suggest that the enzyme is possibly regulated by L-Arg and/or guanidino compounds, and by divalent cations in vivo. © 2001 Elsevier Science Ltd. All rights reserved.

Keywords: *Cucumis sativus*; Cucurbitaceae; Serine endopeptidase; Trypsin-like; Inhibition; Arginine; Guanidino compound; Magnesium

1. Introduction

In all organisms, protein turnover is a highly regulated, selective process. It is well known that the mammalian cell contains highly regulated protein degradation systems such as ubiquitin-proteasome in the cytosol (Hershko and Ciechanover, 1992) and the Ca^{2+}, calpain, and calpastatin systems (Sorimachi and Suzuki, 1998). Many reports also imply the existence of highly regulated proteolytic systems in plants, but only a few have described the role played by plant endopeptidases in regulation of protein turnover (Vierstra, 1993; von Kampen et al., 1996).

It is difficult to investigate endopeptidases since they are both present at low levels and occur in multiple isoforms. To overcome this problem, we have developed both polyacrylamide gel electrophoretic and activity staining methods to separate and detect low proteolytic activities, as well as a method for detection of measurable endopeptidase activities using artificial substrates (Yamauchi et al., 1995). These techniques were used to detect two major endopeptidases that degraded benzoyl (Bz)-Arg-naphthylamide (NA) and carbobenzoxy (CBZ)-Leu-Leu-Glu-NA, respectively (Yamauchi et al., 1996). This report describes the purification and characterization of the Bz-Arg-NA degrading endopeptidase (CEP 5.0). The enzyme was a basic amino acid-specific endopeptidase that is plausibly regulated by L-Arg and/or guanidino compounds and divalent cations whose cellular concentrations may change with environmental conditions.

2. Results and discussion

The Bz-Arg-NA degrading endopeptidase was purified to apparent homogenets by successive chromatography on DEAE-Toyopearl, hydroxyapatite, phenyl-

Abbreviations: Bz, benzoyl; CBZ, carbobenzoxy; CEP, cucumber endopeptidase; 2-ME, 2-mercaptoethanol; PB, phosphate buffer; NA, naphthylamide

* Corresponding author. Tel.: +81-857-31-6702; fax: +81-857-31-6702.

E-mail address: yamauchi@muses.tottori-u.ac.jp (Y. Yamauchi).

[1] Present address: Department of Applied Biological Chemistry, Faculty of Agriculture, Niigata University, Niigata 950-2181, Japan.

0031-9422/01/$ - see front matter © 2001 Elsevier Science Ltd. All rights reserved.
PII: S0031-9422(01)00309-0

sepharose, Arg-sepharose, and mono Q columns (Table 1). The endopeptidase was named CEP 5.0 because the purified enzyme migrated as a single band (pI = 5.0) when submitted to nondenaturing isoelectric focusing (Fig. 1A). The molecular mass of CEP 5.0 was 80 kDa as estimated by both SDS-PAGE and gel filtration (Fig. 1B and C), suggesting that CEP 5.0 was an 80 kDa monomeric protein. The enzyme, with an optimum pH of around 9.5, showed half-maximal activities at pH7.4 and 10.5. CEP 5.0 was most active at 50 °C and was completely denatured when incubated at 70 °C (data not shown).

As shown in Table 2, diisopropyl fluorophosphate and phenylmethylsulfonyl fluoride reduced the activity of CEP 5.0 as did leupeptin, suggesting that CEP 5.0 is a serine endopeptidase. Enzyme inhibitors such as *p*-chloromercuribenzoic acid and *N*-ethylmaleimide also inhibited CEP 5.0. This suggests that CEP 5.0 contained sulfhydryl groups essential to its catalytic activity.

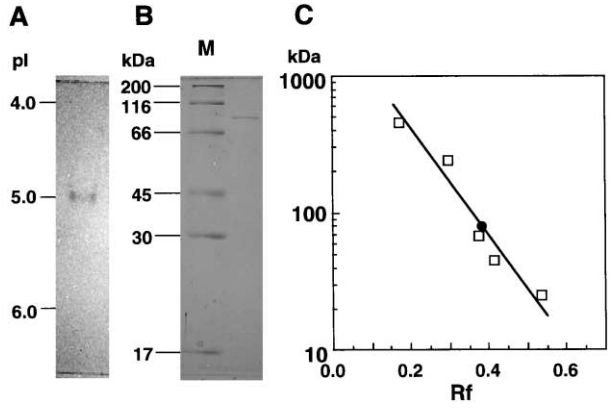

Fig. 1. Estimation of pI and molecular mass of CEP 5.0: (A) 1 μg of purified CEP 5.0 was subjected to isoelectric focusing on a 7.5% (w/v) acrylamide, 2% SERVALYT (pH 4.0–6.0) gel; (B) 1 μg of purified CEP 5.0 was subjected to SDS-PAGE on a 13% (w/v) acrylamide gel under reducing conditions. The molecular mass of protein markers are given in the lane M. (C) Plot of the R_f values against log molecular mass for CEP 5.0 (●) and marker proteins (□) on Superose 12 column. Marker proteins were ferritin (450 kDa), catalase (240 kDa), bovine serum albumin (67 kDa), egg albumin (45 kDa), and chymotrypsinogen A (25 kDa).

The substrate specificity of CEP 5.0 was determined to be trypsin-like by using various artificial substrates. The enzyme cleaved artificial substrates such as Bz-Arg-NA and Bz-Lys-*p*-nitroanilide, but did not cleave those diagnostic for aminopeptidase, caspase, cathepsin D, chymotrypsin, elastase, glutamyl endopeptidase and subtilisin (data not shown). Plant serine endopeptidases of 80–82 kDa whose pH optimum are at alkaline pH, have been isolated from ragweed, *Euphorbia supina* and bamboo (Bagarozzi et al., 1996; Arima et al., 2000a,b); however, their substrate specificities are quite different from CEP 5.0, i.e. they have chymotyrpsin-like or subtilisin-like activities. CEP 5.0 degraded gelatin, but did not degrade azocasein, carboxymethyl-BSA, acid-denatured haemoglobin and Rubisco (data not shown).

Since amino acid sequencing of the N-terminus of CEP 5.0 showed that it was blocked, internal amino acid sequences were analyzed after CNBr cleavage treatment of purified CEP 5.0 and separation of the cleaved peptides by SDS-PAGE. The N-terminal amino acids sequences of a 25 and a 20 kDa polypeptide were "FSLDLEAQE" and "PTGPQAQQE", respectively. Homology search of the Swissplot and translated EMBL databases revealed

Table 2
Effects of inhibitors on CEP 5.0 activity

Inhibitor	Concentration	Relative activity (%)
Control	–	100[a]
Diisopropyl fluorophosphate	1 mM	6.8
	10 mM	0
Phenylmethylsulfonyl fluoride	1 mM	79.3
	10 mM	22.4
p-Chloromercuri benzoic acid	0.5 mM	42.9
	2.5 mM	25.3
N-Ethylmaleimide	1 mM	21.3
	10 mM	11.6
Leupeptin	10 μM	0.9
Pepstatin A	10 μM	78.4
Soybean trypsin inhibitor	0.1%	127
SDS	0.1%	0

[a] Activity in the absence of inhibitor is defined as 100% (0.28 units of Bz-Arg-NA cleaving activity).

Table 1
Summary of purification of CEP 5.0

Step	Total protein (mg)	Total activity (Units)[a]	Specific activity (Units/mg)	Purification-fold	Yield (%)
Crude extract	4430	89 090	22.15	1.0	100
45–55% Ammonium sulfate	653.6	82 600	130	5.87	84.2
DEAE-Toyopearl	20.16	25 980	1289	58.2	26.5
Hydroxyapatite	7.26	21 500	2960	133.7	21.9
Phenyl-sepharose	1.46	10 600	7274	328.5	10.8
Arg-sepharose	0.917	12 880	14 050	634.6	13.1
MonoQ	0.0245	1627	66 400	2998	1.66

[a] Bz-Arg-NA was used as a substrate, and one unit was defined as the formation of 1 nmol of naphthylamine per minute.

no significant similarity of these sequences to other proteins.

Although substrate inhibition at low substrate levels (Fig. 2A) prevented the determination of the Km for Bz-Arg-NA, the Km for Bz-Lys-*p*-nitroanilide was 50 μM. Thus, Bz-Lys-*p*-nitroanilide was used as the substrate in subsequent kinetic experiments. To determine what portion of Bz-Arg-NA inhibited CEP 5.0, we first examined the effects of amino acids on CEP 5.0 activity. Only L-Arg significantly inhibited CEP 5.0 (Fig. 2B), whereas other amino acids, Ala, Asn, Glu, Gln, His, Ile, Lys, Met, L-ornithine, Phe, Pro, Ser, Val, Tyr showed little or no inhibitory effects. The Ki value of L-Arg was 3.5 mM and about 90% of activity was inhibited in the presence of 20 mM L-Arg (Fig. 2B).

The increased inhibition with Bz-Arg-NA compared to L-Arg (Fig. 2A and B) suggests that modification of L-Arg caused the increased inhibition. The effect of modification of L-Arg on inhibitory activity using various L-Arg-derivatives was further examined (Fig. 3A and Table 3). N^{α}-amino group modified L-Arg-derivatives such as acetyl-L-Arg slightly changed its inhibitory activity, compared with the large inhibition observed with Bz-L-Arg (Fig. 2B). Modification of the carboxyl group of L-Arg increased inhibitory activity drastically (Fig. 2C). Methylester and ethylester derivatives became stronger inhibitors, and L-Arg modified by naphthylamine and nitroaniline almost completely inhibited CEP 5.0 at much lower range. N^{γ}-methyl-L-Arg which is a guanidino group-methylated L-Arg-derivative, showed an increase of inhibition. These results indicate that strong inhibition is due to hydrophobicity of L-Arg-derivatives, and that Bz-Arg-NA showed substrate-inhibition because it had hydrophobic bases on both the amino- and carboxyl-groups of L-Arg. Inhibition by L-Arg-derivatives

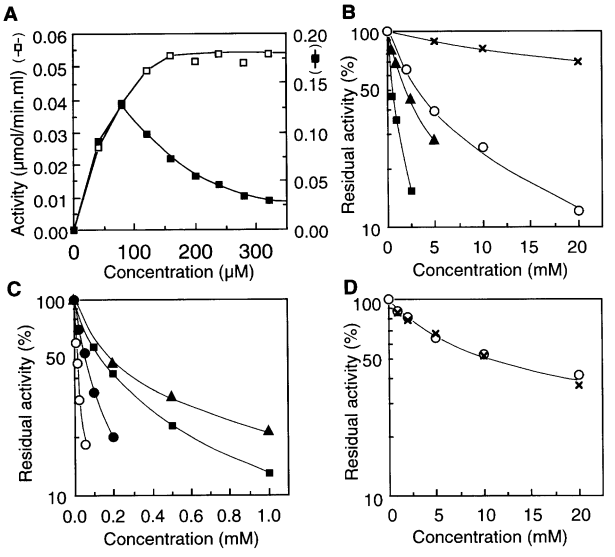

Fig. 2. Inhibition of CEP 5.0 by various Arg-derivatives and divalent cations: (A) CEP 5.0 was incubated with various concentrations of Bz-Lys-*p*-nitroanilide (□) or Bz-Arg-NA (■) as the substrates; (B) CEP 5.0 activity was measured with various concentrations of L-Arg (○), L-Lys (x) or N^{α}-modified L-Arg-derivatives; acetyl-L-Arg (▲) or Bz-L-Arg (■). (C) CEP 5.0 activity was measured with various concentrations of C-modified L-Arg-derivatives; L-arginine methylester (▲), L-arginine ethylester (■), L-Arg-*p*-nitroanilide (●) or L-Arg-NA (○). (D) CEP 5.0 activity was measured with various concentrations of Mg^{2+} (x) or Ca^{2+} (○). Activity in the absence of effector was defined as 100%. The values represent the average of at least three independent measurements using 0.27 units of Bz-Lys-*p*-nitroanilide cleaving activity of CEP 5.0 and the range of the experimental error was within ±3%.

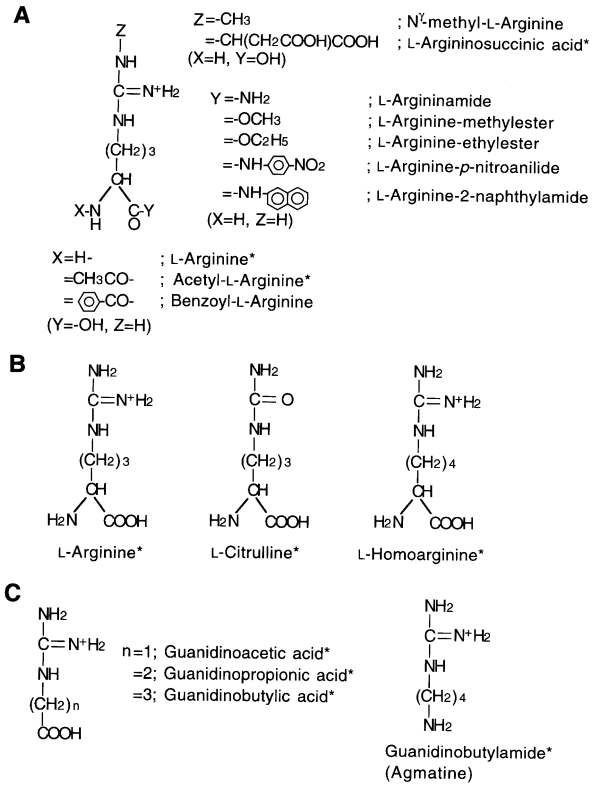

Fig. 3. Structures of L-Arg-derivatives and guanidino compounds using in this study: (A) L-Arg-derivatives modified by various chemical groups; (B) L-Arg and amino acids whose structures are similar to L-Arg; (C) guanidino compounds observed in plants. Asterisk shows substance observed in plants.

Table 3
Summary of kinetic analysis of L-Arg-derivatives against CEP 5.0 activity

Site modified	L-Arg-derivatives	K_i (mM)	Inhibitory fashion
Intact	L-Arg	3.5	Competitive
N^{α}-modified	Acetyl-L-Arg	2.5	Competitive
	Bz-L-Arg	0.39	Competitive
C-modified	L-Argininamide	0.19	Competitive
	L-Arginine-methylester	94×10^{-3}	Competitive
	L-Arginine-ethylester	66×10^{-3}	Competitive
	L-Arg-*p*-nitroanilide	58×10^{-3}	Non-competitive
	L-Arg-NA	14×10^{-3}	Non-competitive
N^{γ}-modified	N^{γ}-Methyl-L-Arg	1.5	Competitive

0.27 units of Bz-Lys-*p*-nitroanilide cleaving activity was used.

was competitive except for non-competitive inhibition by L-Arg-*p*-nitroanilide and L-Arg-NA (Fig. 4).

Neither L-citrulline, which lacks a positively charged guanidino group (structure is referred to in Fig. 3B), nor L-Lys and L-ornithine that have a positive charge at physiological pH, inhibited the reaction (data not shown). L-Argininosuccinic acid, in spite of having positively charged guanidino group, also did not inhibit activity, indicating steric hindrance by the large succinic group. These results suggest that an intact positively charged guanidino group at physiological pH is essential for inhibition.

We examined whether other guanidino compounds observed in plant tissues also inhibit CEP 5.0 (structures are referred to Fig. 3B and C, Table 4). Guanidino butylic acid showed almost equal inhibition to L-Arg; however, guanidino propionic acid showed less inhibition and guanidino acetic acid showed no inhibitory activity, suggesting that shortening of the hydrocarbon chains of guanidino compounds decreased inhibitory activity. Homoarginine, which has a longer hydrocarbon chain than L-Arg, and guanidinobutylamine (agmatine) showed strong inhibition at much lower range than L-Arg. Although these highly hydrophobic guanidino compounds only occur at low levels (Kato et al., 1986), it is possible that they and other unidentified guanidino compounds might regulate CEP 5.0 activity in vivo.

Arg is thought to be an endogenous inhibitor of CEP 5.0 because plants can contain Arg up to 5 mM (Winter et al., 1993). As Arg is the most economic utilizer of nitrogen because of its high N/C ratio (4N:6C), plants usually use Arg for storage and transport of N. Generally Arg contents in plants are affected by nutrient conditions and aging. For example, Arg content in leaves of young tulips cultivated in a medium containing nitrogen was over 70 times higher than those in leaves

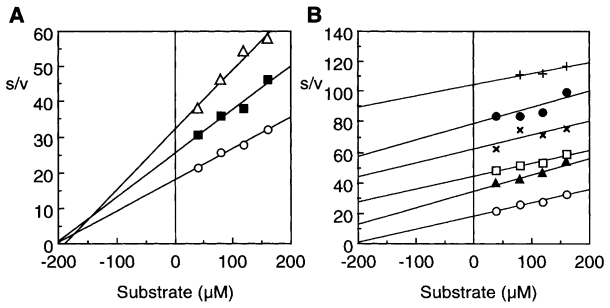

Fig. 4. Kinetic analysis of the inhibition of CEP 5.0 on Hanes–Woolf plots: (A) CEP 5.0 was incubated without (○) or with 5 μM (■) or 10 μM (△) L-Arg-NA; (B) CEP 5.0 was incubated without (○) or with L-Arg-derivatives. Symbols are 10 mM Bz-L-Arg (+), 0.2 mM N^{γ}-methyl-L-Arg (●), 4 mM L-Arg (**x**), 0.1 mM L-arginine methylester (□), or 5 mM Mg^{2+} (▲), respectively. The values represent the average of at least three independent measurements using 0.27 units of Bz-Lys-*p*-nitroanilide cleaving activity of CEP 5.0 and the range of the experimental error was within ±3%.

Table 4
Summary of kinetic analysis of guanidino compounds detected in plants against CEP 5.0 activity

Guanidino compounds	K_i (mM)	Inhibitory fashion
Guanidinoacetic acid	–[a]	–
Guanidinopropionic acid	>20	Competitive
Guanidinobutyric acid	2.8	Competitive
Guanidinobutylamide (agmatine)	0.5	Competitive
Homoarginine	30×10^{-3}	Competitive

0.27 units of Bz-Lys-*p*-nitroanilide cleaving activity was used.
[a] Not inhibited.

after flowering and in nitrogen starved conditions (Ohyama et al., 1985). Therefore, CEP 5.0 may be regulated in response to nutrient and developmental changes in Arg content. A few endopeptidases inhibited by L-Arg have been reported in animals; however, the inhibition was less effective than the case for CEP 5.0 (Hatton, 1973; Polakoski and McRorie, 1973), and no plant endopeptidase regulated by Arg has been reported.

CEP 5.0 was also competitively inhibited by divalent cations such as Mg^{2+} and Ca^{2+} (Figs. 2D and 4B). This indicates that Mg^{2+} and Ca^{2+} interferes with binding of the substrate, either due to binding of themselves to the catalytic site or to a closely related site. The K_i value of inhibition by divalent cations was about 10 mM.

Divalent cations such as Ca^{2+} and Mg^{2+} are well known regulators of plant endopeptidases (Liu and Jagendorf, 1986; Bushnell et al., 1993; Anastassiou and Argyroudi-Akoyunoglou, 1995), and may play important roles in protein degradation of plants. The most likely divalent cation for regulation of CEP 5.0 in vivo is Mg^{2+} because it is the most abundant soluble divalent cation while intracellular free Ca^{2+} is usually kept to low levels (Kreimer et al., 1988). The concentration of Mg^{2+} is assumed to be 13–17 mM in the vacuole and 2–10 mM in cytosol and chloroplasts (Leigh and Wyn Jones, 1986; Stelzer et al., 1990; Marschner, 1995). These concentrations are high enough to inhibit CEP 5.0.

Moreover, we examined the inhibition of CEP 5.0 in the presence of various physiological concentration of L-Arg and Mg^{2+}, which are the most likely inhibitors in vivo (Fig. 5). Inhibition by L-Arg and Mg^{2+} was additive and reversible (data not shown), and 5 mM of L-Arg and Mg^{2+} inhibited the enzyme activity more than 70% compared to the control activity. This suggests the plausible regulation of CEP 5.0 by physiological concentration of L-Arg and Mg^{2+} in vivo.

In conclusion, CEP 5.0 is possibly regulated by L-Arg and/or guanidino compounds and Mg^{2+} whose cellular concentrations may change with environmental conditions. To clarify the physiological role of CEP 5.0, we will investigate in future the native substrate and localization of CEP 5.0.

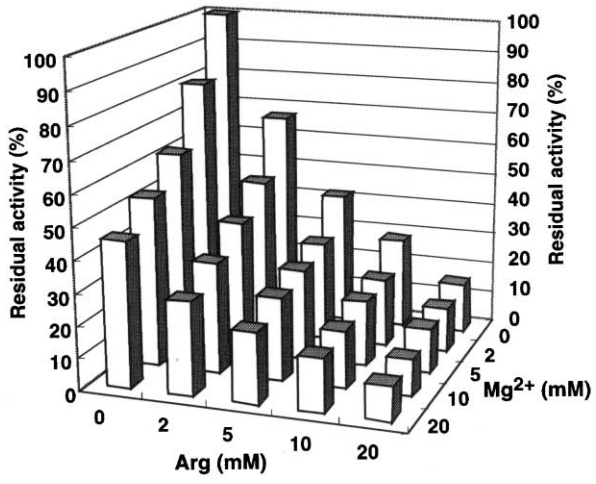

Fig. 5. Inhibition of CEP 5.0 by L-Arg and Mg^{2+} is additive. CEP 5.0 (0.27 units of Bz-Lys-*p*-nitroanilide cleaving activity) was incubated with various combination of L-Arg and Mg^{2+} concentration. Activity in the absence both of L-Arg and Mg^{2+} was defined as 100%.

3. Experimental

3.1. Materials

All of the Arg-derivatives and Fast Garnet GBC were purchased from Sigma Co. Ltd. (St. Louis, MO, USA). Leupeptin and pepstatin A were purchased from Peptide Institute, Inc. (Osaka, Japan). All other reagents were purchased from Wako Pure Chemical Co. Ltd. (Osaka, Japan). Cucumber seeds (*Cucumis sativus* L. suyo) purchased from Takii Seed Co. Ltd. (Kyoto, Japan), were germinated in the dark at 25 °C for 6 days then transferred to a greenhouse. Harvested leaves were frozen in liquid N_2 and stored below −20 °C until use.

3.2. Enzyme activities

To monitor benzoyl (Bz)-Arg-naphthylamide (NA) degrading activity, assays using 60 μM of Bz-Arg-NA as a substrate by the method described previously were employed (Yamauchi et al., 1996). For kinetic analysis of the endopeptidase, 160 μM of Bz-Lys-*p*-nitroanilide was used as a substrate in 50 mM Hepes-KOH, pH 8.0, to a final volume of 1 ml. After incubation at 37 °C, the reaction was stopped by addition of 0.5 ml of 30% (v/v) acetic acid and absorbance at 410 nm measured. One unit was defined as the formation of 1 nmol of nitroaniline or naphthylamine per minute.

3.3. Purification of cucumber endopeptidase with a pI of 5.0 (CEP 5.0)

Leaves (300 g) were extracted with 5 volumes of 50 mM potassium phosphate buffer (K-PB), pH 7.0, containing 2 mM 2-mercaptoethanol (2-ME) and 0.1 mM EDTA. Debris was removed by filtration using two layers of cheesecloth. After centrifugation at 20,000 *g* for 20 min, the supernatant was fractionated by the addition of solid ammonium sulfate. The fraction precipitating between 45 and 55% ammonium sulfate saturation was dissolved in a minimum volume of 25 mM K-PB, pH 7.0, containing 1 mM 2-ME (buffer A) and dialyzed against buffer A. The dialysate was applied to a DEAE-Toyopearl column (4×20 cm, Tosoh Corp., Japan) equilibrated with buffer A, and a linear gradient of 0–0.2 M NaCl (total 1.2 l) was applied to elute the enzymes. Active fractions of CEP 5.0 after DEAE-Toyopearl chromatography were combined and dialyzed against 10 mM Na-PB, pH 6.8, containing 1 mM 2-ME. The dialysate was applied to a hydroxyapatite column (2×15 cm, Bio-Rad, CA, USA) and eluted by a linear gradient of 0–0.2 M Na-PB (total 200 ml). After active fractions were combined, an equal volume of 60% saturated ammonium sulfate in 50 mM K-PB, pH 7.0, containing 1 mM 2-ME was added. This solution was applied to a Phenyl-Sepharose column (1.5×8 cm, Amersham Pharmacia Biotech, Sweden) equilibrated with 30% ammonium sulfate saturated in 50 mM K-PB, pH 7.0, containing 1 mM 2-ME and the proteins were eluted by a linear gradient of 30–0% ammonium sulfate (total 100 ml). Active fractions were concentrated by a DEAE-mini column (1 ml), then applied to an Arg-Sepharose (1.5×8 cm, Amersham Pharmacia Biotech, Sweden) column equilibrated with buffer A containing 0.1 mM EDTA. A linear gradient of 0–0.1 M NaCl was applied to elute the enzyme (total 100 ml). The active fractions were dialyzed against buffer A, then applied to a Mono Q column (0.32×3 cm, SMART system, Amersham Pharmacia Biotech, Sweden). The column was eluted with a linear gradient of 0–0.3 M NaCl in buffer A (total 8 ml). All (purification) steps were performed at temperatures from 0 to 4 °C.

3.4. Characterization of CEP 5.0

To investigate the effect of inhibitors, CEP 5.0 was preincubated with each inhibitor in the reaction mixture without substrate for 30 min at 4 °C. The substrate was then added to the mixture and residual activity was measured. Native molecular weights were estimated on the basis of comparison of the retention time of marker proteins on a Superose 12 column (0.32×30 cm, SMART system, Amersham Pharmacia Biotech, Sweden) equilibrated with 25 mM K-PB, pH 7.0, containing 0.1 M NaCl and 1 mM 2-ME. In the experiment on the effect of L-Arg-derivatives on CEP 5.0, L-Arg-derivatives were used as inhibitors because CEP 5.0 could not cleave them even though their structure resemble the Bz-Arg-NA substrate.

3.5. Protein analysis

Isoelectric focusing was performed with a 7.5% (w/v) polyacrylamide gel containing SERVALYT of pH

range 4.0–6.0 (Serva Electrophoresis GmbH, Germany) under non-denaturing conditions. Cathode and anode buffers were 40 mM Glu and 0.2 M His, respectively. SDS-PAGE and Tricine/SDS-PAGE were performed by the method of Laemmli (1970) and Schägger and von Jagow (1987), respectively. Gels were stained for proteins with Coomassie Brilliant Blue R-250. Protein concentration was determined by the method of Bradford with bovine serum albumin as the standard (Bradford, 1976).

3.6. Sequencing of internal peptides of CEP 5.0

CEP 5.0 (2 μg) was dissolved in 1 ml of 70% formic acid containing 1 mg of CNBr, and allowed to stand overnight in the dark. After evaporation using a SpeedVac concentrator (model A160, SAVANT Instruments Inc., NY, USA), the cleaved peptides were dissolved in 50 μl of SDS sample buffer and separated by Tricine/SDS-PAGE using a 15% polyacrylamide gel. After electroblotting to a poly (vinylidene difluoride) membrane, peptides were stained by CBB R-250 and portions of major bands were excised and sequenced by an automated pulsed liquid protein sequencer (model 491, Applied Biosystems, Foster City, CA, USA).

References

Arima, K., Uchikoba, T., Yonezawa, H., Shimada, M., Kaneda, M., 2000a. Cucumisin-like protease from the latex of *Euphorbia supina*. Phytochemistry 53, 639–644.

Arima, K., Uchikoba, T., Yonezawa, H., Shimada, M., Kaneda, M., 2000b. Isolation and characterization of a serine protease from the sprouts of *Pleioblastus hindsii* Nakai. Phytochemistry 54, 559–565.

Anastassiou, R., Argyroudi-Akoyunoglou, J.H., 1995. Thylakoid-bound proteolytic activity against LHCII apoprotein in bean. Photosyn. Res. 43, 241–250.

Bagarozzi, D.A., Pike Jr, R., Potempa, J., Travis, J., 1996. Purification and characterization of a novel endopeptidase in ragweed (*Ambrosia artemisiifolia*) pollen. J. Biol. Chem. 271, 26227–26232.

Bradford, M.M., 1976. A rapid and sensitive method for the quantitation of microgram quantities of protein utilizing the principle of protein-dye binding. Anal. Biochem. 72, 248–254.

Bushnell, T.P., Bushnell, D., Jagendorf, A.T., 1993. A purified zinc protease of pea chloroplasts, EP1, degrades the large subunit of ribulose-1,5-bisphosphate carboxylase/oxygenase. Plant Physiol. 103, 585–591.

Hatton, M.W.C., 1973. Studies on the coagulant enzyme from *Agkistrodon rhodostoma* venom. Biochem. J. 131, 799–807.

Hershko, A., Ciechanover, A., 1992. The ubiquitin system for protein degradation. Ann. Rev. Biochem. 61, 761–807.

Kato, T., Kondo, T., Mizuno, K., 1986. Occurrence of guanidino compounds in several plants. Soil Sci. Plant Nutr. 32, 487–491.

Kreimer, G., Melkonian, M., Holtum, J.A.M., Latzko, E., 1988. Stromal free calcium concentration and light-mediated activation of chloroplast fructose-1,6 bisphosphatase. Plant Physiol. 86, 423–428.

Laemmli, U.K., 1970. Cleavage of structural proteins during the assembly of the head of bacteriophage T4. Nature 227, 680–685.

Leigh, R.A., Wyn Jones, R.G., 1986. Cellular compartmentation in plant nutrition. In: Tinker, B., Läuchli, A. (Eds.), Advances in Plant Nutrition 2. Praeger Scientific, New York, pp. 249–279.

Liu, X.Q., Jagendorf, A.T., 1986. Neutral peptidases in the stroma of pea chloroplasts. Plant Physiol. 81, 603–608.

Marschner, H., 1995. Mineral Nutrition of Higher Plants. Academic Press, San Diego, CA, pp. 277–285.

Ohyama, T., Ikarashi, T., Baba, A., 1985. Nitrogen accumulation in the roots of tulip plants (*Tulipa gesneriana*). Soil Sci. Plant Nutr. 31, 581–588.

Polakoski, K.L., McRorie, R.A., 1973. Boar acrosin: II: classification, inhibition, and specificity studies of a proteinase from sperm acrosomes. J. Biol. Chem. 248, 8183–8188.

Schägger, H., von Jagow, G., 1987. Tricine-sodium dodecyl sulfate-polyacrylamide gel electrophoresis for the separation of proteins in the range from 1 to 100 kDa. Anal. Biochem. 166, 368–379.

Sorimachi, H., Suzuki, K., 1998. μ- and m-Calpain. In: Barrett, A.J., Rawlings, N.D., Woessner Jr, F. F. (Eds.), Handbook of Proteolytic Enzymes. Academic Press, San Diego, CA, pp. 643–654.

Stelzer, R., Lehmann, H., Kramer, D., Lüttge, U., 1990. X-ray microprobe analysis of vacuoles of spruce needle mesophyll, endodermis and trasfusion parenchyma cells at different seasons of the year. Bot. Acta 103, 415–423.

Vierstra, R.D., 1993. Protein degradation in plants. Ann. Rev. Plant Physiol. Plant Mol. Biol. 44, 385–410.

von Kampen, J., Wettern, M., Schulz, M., 1996. The ubiquitin system in plants. Physiol. Plant. 97, 618–624.

Winter, H., Robinson, D.G., Heldt, H.W., 1993. Subcellular volumes and metabolite concentrations in barley leaves. Planta 191, 180–190.

Yamauchi, Y., Sugimoto, T., Oji, Y., 1995. A method for the separation and detection of proteases using substrate-containing gel isoelectric focusing electrophoresis. Biosci. Biotech. Biochem. 59, 767–768.

Yamauchi, Y., Sugimoto, T., Sueyoshi, K., Oji, Y., 1996. Emergence of proteases in germinating cucumber cotyledons and their roles in the two-step degradation of storage protein. Plant Cell Physiol. 37, 279–284.

PERGAMON

Phytochemistry 58 (2001) 683–692

PHYTOCHEMISTRY

www.elsevier.com/locate/phytochem

Physiological function of bromoperoxidase in the red marine alga, *Corallina pilulifera*: production of bromoform as an allelochemical and the simultaneous elimination of hydrogen peroxide

Noboru Ohsawa[a], Yasuhiro Ogata[b], Noriyuki Okada[b], Nobuya Itoh[a,*]

[a]*Biotechnology Research Center, Toyama Prefectural University, Kurokawa 5180, Kosugi, Toyama 939-0398, Japan*
[b]*Applied Chemistry and Biotechnology, Faculty of Engineering, Fukui University, Bunkyo 3-9-1, Fukui 910-8507, Japan*

Received 30 August 2000; received in revised form 19 April 2001

Abstract

The physiological function of vanadium-bromoperoxidase (BPO) in the marine red alga, *Corallina pilulifera*, has been characterized from the viewpoint of allelochemical formation. The algae emit bromoform ($CHBr_3$) depending on the enzyme activity level in vivo (Itoh, N., Shinya, M., 1994. Seasonal evolution of bromomethanes from coralline algae and its effect on atmospheric ozone. Marine Chemistry 45, 95–103). We demonstrated that bromoform produced by *C. pilulifera* played an important role in eliminating epiphytic organisms, especially microalgae on the surface. Such data suggest a strong relationship between the coralline algae and the coralline flat (deforested area in the marine environment: called isoyake in Japanese). *Lithophyllum yessoense*, the main inhabitant of coralline flats in Japan, produced a lower level of $CHBr_3$ than *C. pilulifera*, and showed BPO activity. On the other hand, the seasonal change of BPO activity in *C. pilulifera* in vivo was in proportion to superoxide dismutase (SOD) activity and in inverse proportion to catalase activity. The phenomenon implies that BPO could be a potential substitute for catalase, because the enzyme catalyzes an efficient Br^--dependent catalase reaction. © 2001 Elsevier Science Ltd. All rights reserved.

Keywords: *Corallina pilulifera*; *Lithophyllum yessoense*; Bromoperoxidase; Allelochemical; Bromoform; Active oxygen

1. Introduction

Volatile halogenated compounds in ocean water and the atmosphere are divided into two groups: anthropogenic compounds such as chlorofluorocarbons (CFC), $CHCl_3$, CCl_4, CH_3Br and trichloroethylene ($ClCH=CCl_2$), and natural volatile halomethanes including CH_3Cl, CH_3Br, CH_3I, $CHBr_3$, CH_2Br_2 and $CHClBr_2$ (Lovelock, 1975; Moore, 1977; Geshwend et al., 1985; Harper, 1994; Itoh, 1997; Butler, 2000). The evaluation of natural halogenated compounds in the atmosphere and ocean water is important to assess the effect of these compounds on the atmosphere (Rasmussen et al., 1982; Class and Ballschmiter, 1988; Harper, 1994; Itoh, 1997; Butler, 2000) and the marine environment. Although natural halogenated compounds in ocean water have been reported (Lovelock, 1975; Geshwend et al., 1985; Harper, 1994; Itoh, 1997), the specific origin, formation and physiological function of these natural compounds is not well understood.

Natural tri- and dihalomethanes are formed by haloperoxidase-catalyzed reactions with organic compounds, especially β-ketoacids including 3-oxo-octanoic acid (Beissner et al., 1981), oxalacetate, phospho-enol-pyruvate, pyruvate etc. (Itoh and Shinya, 1994), which are very common in biological metabolic pathways. In contrast, biogenic monohalomethanes are synthesized by *S*-adenosylmethionine (SAM):halide ion methyltransferase reactions, which have been reported in marine microalga (Itoh et al., 1997), macroalgae (Wuosmaa and Hager, 1990) and terrestrial plants (Attieh et al., 1995; Ni and Hager, 1998) and fungus (Harper, 1985, Saxena et al., 1998).

Haloperoxidases generally oxidize a halide anion (X^-) into a halonium cation (X^+) with H_2O_2, and the produced X^+ acts on many organic substrates as an electrophile

* Corresponding author. Tel.: +81-766-56-7500; fax: +81-766-56-2498.
E-mail address: itoh@pu-toyama.ac.jp (N. Itoh).

0031-9422/01/$ - see front matter © 2001 Elsevier Science Ltd. All rights reserved.
PII: S0031-9422(01)00259-X

(Itoh et al., 1988). They are divided into three groups: heme types, eukaryotic heme types, and bacterial types containing protoporphyrin IX as a prosthetic group (Morris and Hager, 1966); bacterial non-metal enzymes (Wiesner et al., 1988); and eukaryotic vanadium-containing enzymes (Vilter, 1984, Butler, 1998). Vanadium-haloperoxidases have been found in marine algae (Krenn et al., 1989), fungi (Messerschmidt, et al., 1997), and lichen (Plat et al., 1987). Marine algae containing vanadium-haloperoxidases are widespread and the source of diverse halogenated compounds observed in the marine environment (Neidleman and Geigert, 1986). However, the physiological functions of the enzyme and the halogenated compounds produced by the enzyme are unclear.

We and others have reported on the vanadium-containing bromoperoxidases (BPO) from red algae, *C. pilulifera* (Itoh et al., 1986, 1987c; 1996; Shimonishi et al., 1998) and *C. officinalis* (Yu and Whittaker, 1989; Sheffield et al., 1993), which are immunologically the same enzymes (Itoh, et al., 1987a). BPO of *C. pilulifera* was first characterized as a non-heme iron enzyme because of its high iron content. However, it was found to contain another essential metal, vanadium, for halogenation activity (Krenn et al., 1989a, Itoh et al., 1996). The present study reveals the physiological function of the enzyme as a bromoform producer and hydrogen oxide eliminator. From the data, we also discuss the relationship between bromoform emission from coralline algae and the continuation of coralline flat (isoyake area) in the marine environment.

2. Results and discussion

2.1. Effect of bromoform on supressing surface epiphytes

Fig. 1 shows a scanning electron micrograph (SEM) of the surfaces of living and dead *C. pilulifera* samples which had been incubated for 2 weeks in clean sea water. The surface of the dead algae was completely covered with various types of diatoms. By contrast, the surfaces of living algae, which were releasing bromoform (0.9 ng/min/g wet algae:0.026 ng/min/cm^2 surface area), dibromomethane and chlorodibromomethane (approximately 85:10:5 by weight) (Itoh and Shinya, 1994), were quite clean, with few epiphytic diatoms. As described below, the surface of intact *Lithophyllum yessoense*, which emitted bromoform, was also clean. Although the dead algae had completely lost the ability

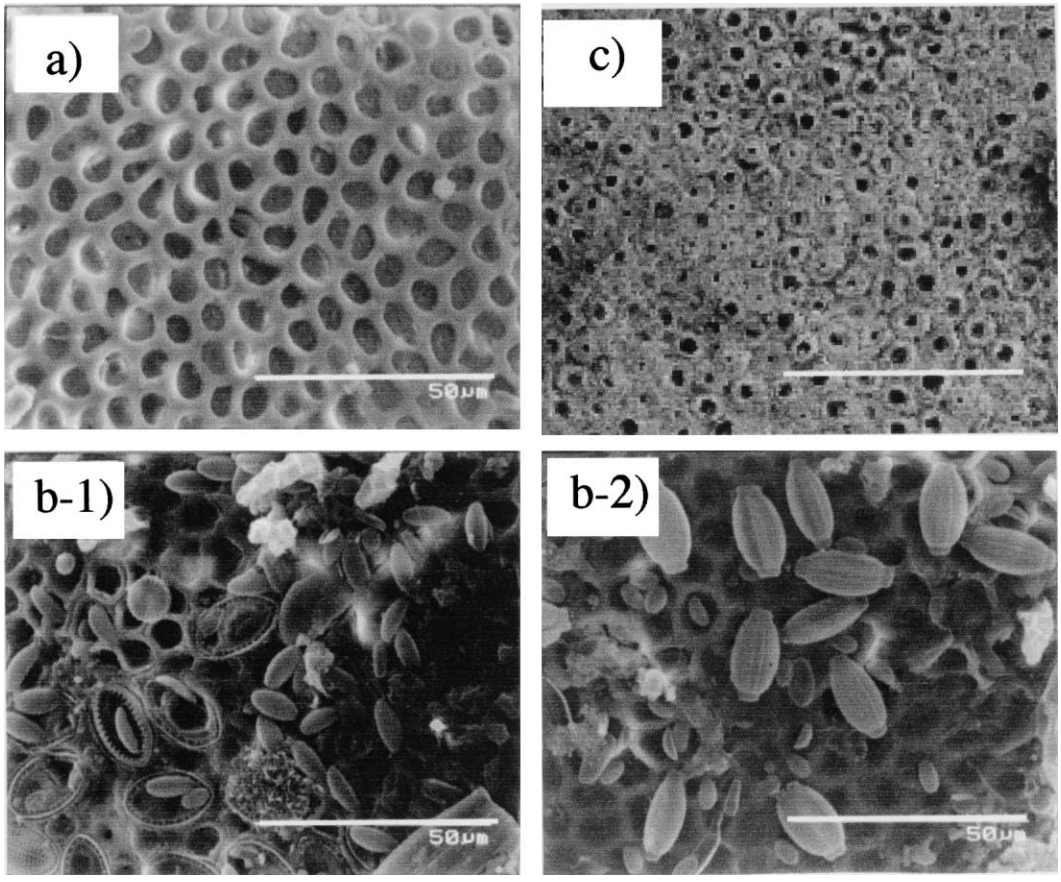

Fig. 1. Photographs of scanning electron microscopy (SEM) of coralline algae. Living (a) and dead (b1 and b2) incubated in natural sea water for 2 weeks in a mesh container with a glass cap. Living *Litophyllum yessoense* (c). The bar indicates 50 μm.

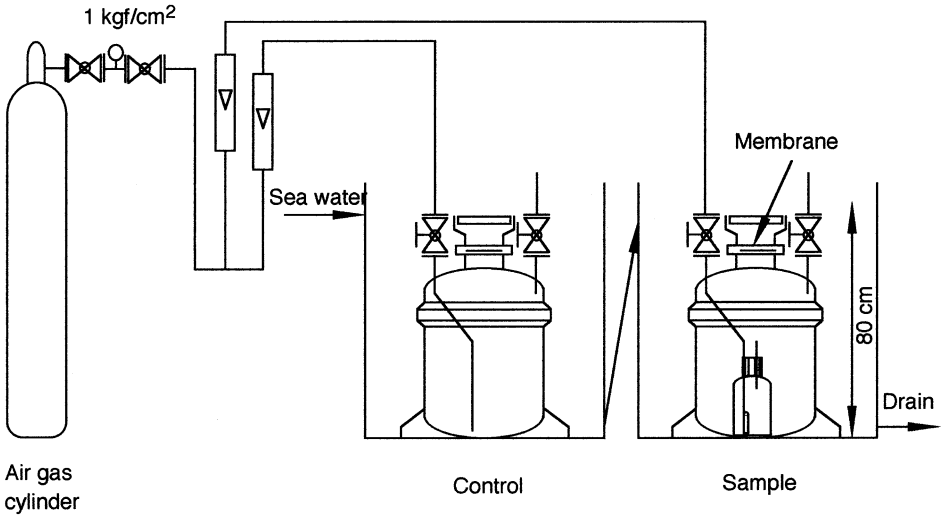

Fig. 2. Schematic of air-pressurized bromoform vaporizer.

to resist epiphyte invasion, bromoform production was speculated to be one of these systems. Therefore, we focused on the physiological function of bromoform, which was the main volatile halogenated product from *C. pilulifera* and *L. yessoense*, to confirm its effect on eliminating epiphytic microalgae. The bromoform vaporizer apparatus (Fig. 2) emitted bromoform with air across a hydrophobic membrane interface (10 cm^2) into natural seawater, and the emission rate was controlled from 0.02 to 0.4 ng/min/cm^2 according to the rate of living *C. pilulifera*. The effect of bromoform on eliminating epiphytic microalgae was observed above the emission rate of 0.09 ng/min/cm^2 of bromoform (Fig. 3). Various microalgae were observed on the control membrane surfaces. At the emission rate of 0.02 ng/min/cm^2 of bromoform, much microalgae was detected on the membrane. Therefore, the lower limit range of bromoform emission for inhibiting the adhesion of microalgae was concluded to be above 0.02 ng/min/cm^2. Although the value was a little high, it almost coincided with the emission rates of *C. pilulifera*, which range from 0.19 to 2.1 ng/min/g wet algae of bromoform (0.005 and 0.06 ng/min/cm^2 of algal surface). Some researchers have speculated that volatile halogenated compounds are involved in the algal control of the surface epiphytes or that Br^+OH^- released by algae is part of a host defense system (Wever et al., 1991), however, there had been no confirmation concerning the physiological aspect of these substances. This is the first report to elucidate the function of bromoform to inhibit the growth of surface epiphytes.

2.2. Emission of bromoform from a major inhabitant, Lithophyllum yessoense, of the coralline flat

Coralline flats (deforested areas in the marine environment:the phenomenon known as isoyake in Japanese) are a serious problem for fisheries. In this region, many algal species disappear and crustose coralline algae such as *L. yessoens* remain to become the prominent species in the subtidal zone. Once isoyake occurs, it continues for a long time. Consequently, it causes severe damage to inshore fisheries. To elucidate the relationship between bromoform emission from coralline algae and isoyake, we measured the emission of bromoform from *L. yessoense*, a major inhabitant of isoyake areas in Japan. The data showed that the alga also produced bromoform and its derivatives at a rate of 0.007 ng/min/cm^2 of algal surface (0.017 ng/min/g wet algae; the apparent value was low because of the large amount of calcium carbonate skeleton in crustose coralline algae), which was the same emission rate level of *C. pilulifera*. Similarly with *C. pilulifera*, *L. yessoense* emits not only bromoform but also dibromomethane and chlorodibromomethane (approximately 6:3:1 by weight) (Fig. 4). The data supported that these compounds are produced by BPO, widely distributed in coralline algae (Yamada et al., 1985). We first reported that a major isoyake inhabitant produces bromoform and its derivatives. Interestingly, *L. yessoense* BPO was not recoverd in the supernatant solution (soluble cytosol fraction) following the disruption of algae with sea-sand and centrifugation, suggesting that BPO exists as a membrane-bound form in *L. yessoense*. Therefore, we used the cell-debris fraction as a crude enzyme preparation. BPO of *L. yessoense* required H_2O_2, KBr and oxalacetate, a suitable substrate, for bromoform production. Furthermore, the enzyme appeared to be a member of the vanadium-haloperoxidases of coralline algae (Yamada et al., 1985; Itoh et al., 1986). The bromoform-producing activity of the BPO of *L. yessoense* was estimated to be equivalent to 1.0 unit/g wet algae by the monochlorodimedone assay method.

Taniguchi et al. (1994) reported that dibromomethane is a chemical inducer of larval settlement and

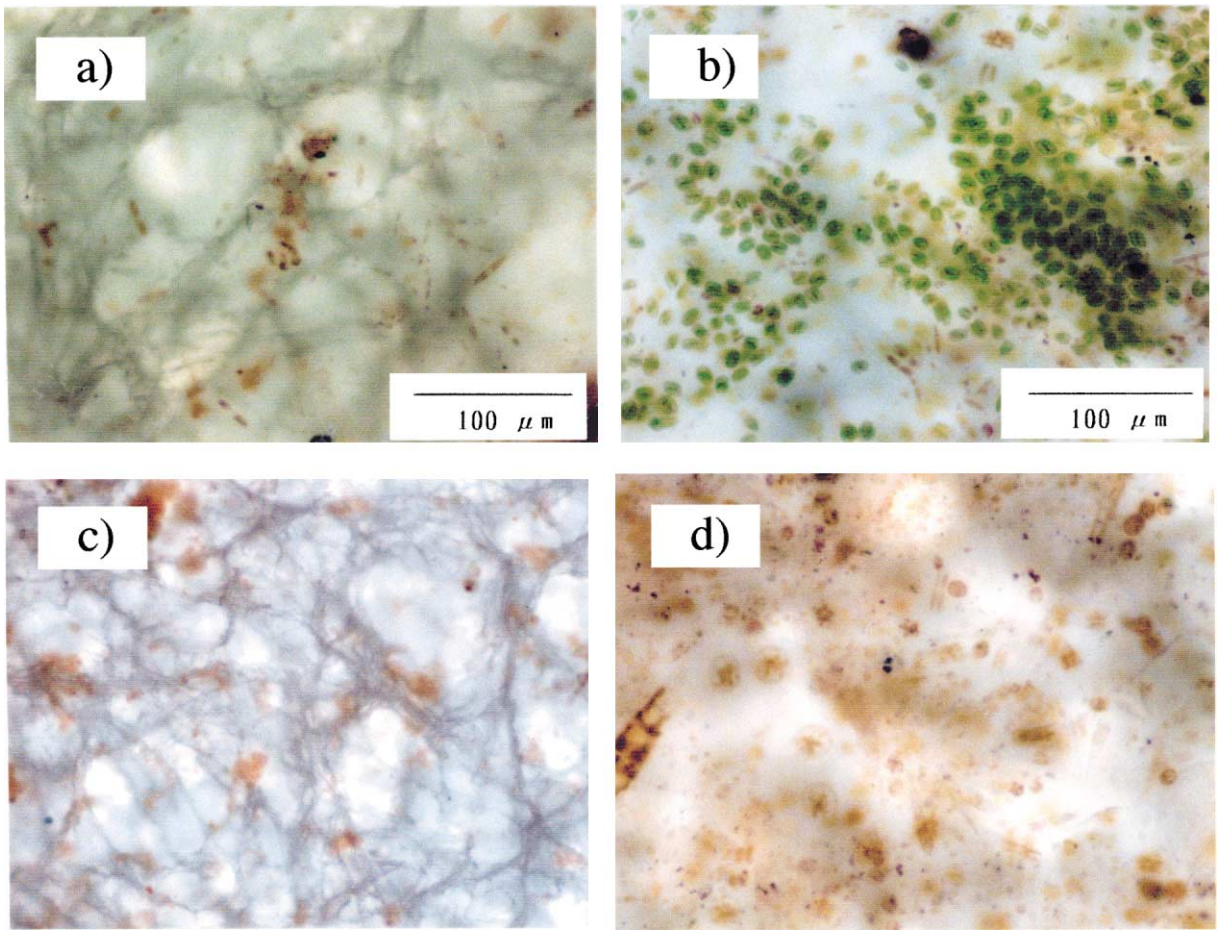

Fig. 3. Photographs by phase contrast microscopy of membranes in an air- pressurized bromoform vaporizer in the presence of $CHBr_3$ and in the absence of $CHBr_3$ after the incubation with natural seawater. The mean emission rate of bromoform was 0.26 ng/min/cm^2 membrane and seawater temperature was 19 °C from 22 May to 19 June (a). Control (b). The rate was 0.09 ng/min/cm^2 membrane and seawater temperature was 25 °C from 10 July to 7 August (c). Control (d).

metamorphosis of the sea urchin *Strongylocentrotus nudus*, and bromoform only induces settlement. Denboh et al. (1997) demonstrated that bromoform at a concentration as low as 3 ppm reduced the normal sporophyte formation of *Laminaria*, but they assumed unknown compounds to be true allelochemicals. The data presented here show that coralline algae, such as *C. pilulifera* and *L. yessoens*, suppress the growth of microalgae and other algae on their surface by releasing bromoform. By this mechanism the algae could obtain a sufficient supply of sunlight and nutrition, making it easy for them to be the dominant algae on shoreline rocks. *C. pilulifera* grows quite close together and appears to attain a high bromoform concentration as a whole. Because of bromoform's low melting point of 7.5 °C and low solubility in water, it would remain on the algal surface for some time in cold sea water. The features of bromoform appear to be suitable as an allelochemical for coralline algae. The high content of BPO (1–2%) in *C. pilulifera* (Itoh et al., 1996) suggests that the enzyme is essential for it to become the dominant algal species. Our results, together with those of Taniguchi et al. (1994) and Denboh et al. (1997), suggest a strong relationship between isoyake and bromoform produced by coralline algae. It is generally agreed that isoyake is caused by heavy grazing pressures of herbivores such as sea urchins. Coralline algae products, especially bromoform, induce larval settlement of sea urchins. We speculate that coralline algae not only induce some kinds of invertebrates but also inhibit growth of other algae; therefore, once isoyake is caused by a disturbance of the ecological balance such as temperature, nutrition and grazing by invertebrates, then the situation continues for a long time depending on the bromoform from coralline algae.

2.3. Acceleration of bromoform production by exogenous substrates

Some marine algae containing BPO are known to be accessible to substrates and are able to brominate organic compounds such as phenol red (Wever et al., 1991). We measured the acceleration of bromoform formation caused by substrates in intact *C. pilulifera*

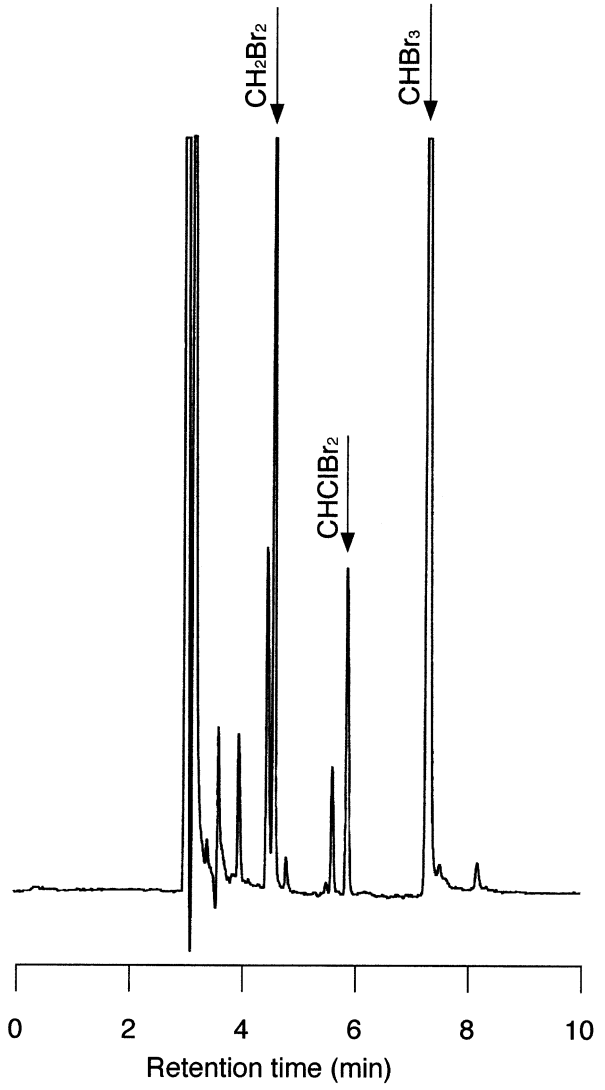

Fig. 4. Gas chromatogram (ECD) of halomethanes released by *Litophyllum yessoense*. Main peaks were identified by standard compounds, but minor peaks could not be identified.

and *L. yessoense* algae using head-space analyses. For *C. pilulifera*, the addition of exogenous substrates accelerated the emission of bromoform (Fig. 5a). The effect of adding H_2O_2 to the seawater was especially prominent, increasing the rate of emission about 10 times relative to the control. For *L. yessoense*, only H_2O_2 was effective (Fig. 5b). The results indicated that both algae are able to utilize the exogenous H_2O_2 to produce bromoform, and that the supply of H_2O_2 to the BPO reaction is the rate-determining step of bromoform formation. The effect of KBr was rather inhibitory for both algae. Therefore, the BPOs appeared to be saturated with bromide ions in vivo for both algae. Considering the high K_m value of the BPO of *C. pilulifera* toward Br^- ions (1.1×10^{-2} M) (Itoh et al., 1986) and the low concentration of Br^- ions in natural sea water (0.85 mM), the alga must concentrate Br^- ions in its body. Itoh and Shinya (1994) reported as endogenous substrates for bromoform formation by BPO,β-keto acids such as oxalacetate, pyruvate etc. Although oxalacetate addition increased the bromoform emission rate about 2.5-fold for *C. pilulifera*, it was inhibitory for *L. yessoense*. Wever et al.(1991) suggested that free Br^+OH^- released in sea water by brown algae directly reacted with dissolved organic acids in the water to produce bromoform. If this hypothesis is correct, bromoform formation must be promoted by the addition of oxalacetate. Because the oxalacetate addition was ineffective, this theory could not be adapted for *L. yessoense*.

To discover a possible natural exogenous substrate, we examined fluvic acid, which is a complex organic acid having keto and carboxylic groups made from humus soil, as a bromoform-producing substrate. As shown in Fig. 6, both molecular weight fractions of fluvic acid (see experimental) proved a good substrate for production of bromoform in *C. pilulifera*, coinciding with oxalacetate. However, the BPO in *C. pilulifera* does not liberate free Br^+OH^- through its reaction (Itoh et al., 1987c), suggesting that BPOs in the algae are located where the exogenous organic compounds can be easily accessed. A portion of the enzymes maybe localized at the calcified cell-wall. That both fulvic acid fractions were inert for *L. yessoense* clearly showed that free Br^+OH^- was not released in sea water by the alga, because free Br^+OH^- efficiently produced bromoform with fluvic acid.

2.4. Seasonal change of active oxygen-eliminating enzymes in C. pilulifera

The BPO activity in *C. pilulifera* is known to vary seasonally depending on its specific activity in vivo (Itoh et al., 1996). To elucidate its function, we compared its variation with other active oxygen-eliminating enzymes such as a catalase, peroxidase (POD) and super oxide dismutase (SOD). As shown in Table 1, we could not detect glutathion peroxidase (GPO) and ascorbate peroxidase (APO) activities in the cell-free extracts of *C.*

Table 1
The activities of active oxygen-eliminating enzymes in *Corallina pulifera*

Sample	BPO	Catalase	SOD	POD	APO	GPO
	(U/g wet algae)					
Crude extract	3.5	1.8	348	7.1	0	0
After dialysis[a]	3.1	0.8	N.T.	1.3	N.T.[b]	N.T.

[a] Dialysis was necessary to avoid the influence of Br^- -dependent catalase and peroxidase activities of BPO.
[b] N.T.: not tested.

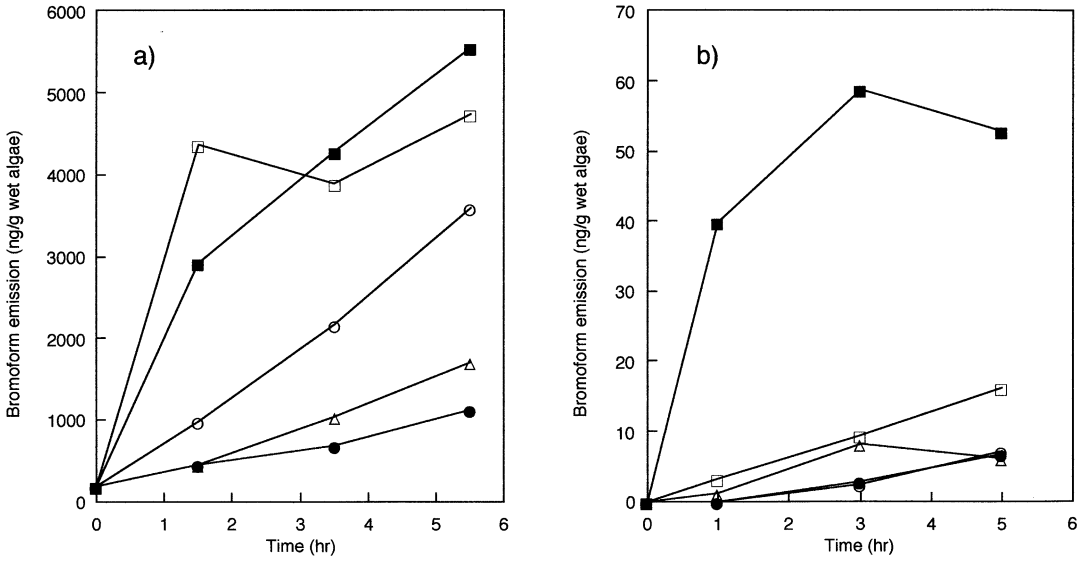

Fig. 5. The effect of addition of endogenous substrates on bromoform emission from *Corallina pilulifera* (a) and *Lithophyllum yessoense* (b): (△) control; (●) 20 mM KBr; (○) 1 mM oxalacetate; (■) 2 mM H_2O_2; (□) 1 mM oxalacetate plus 2 mM H_2O_2. Each point was the mean value of two analyses.

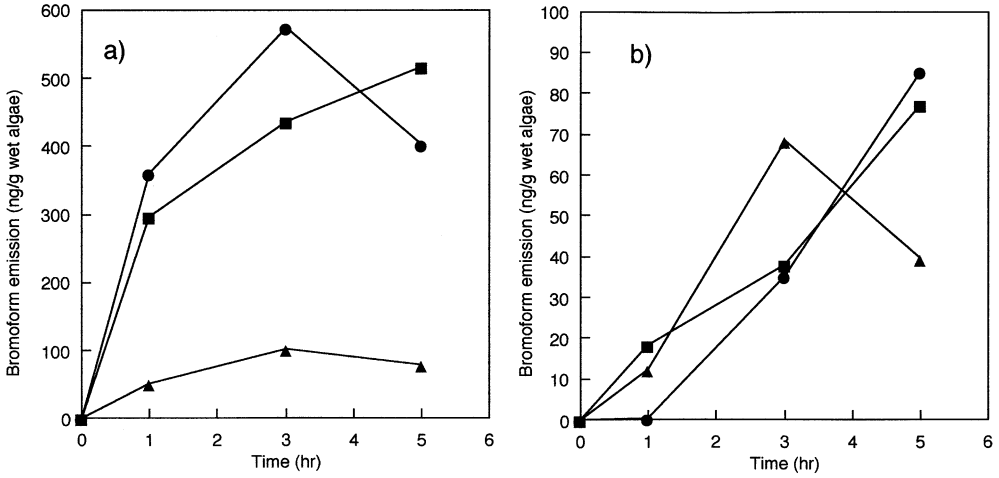

Fig. 6. The effect of addition of exogenous substrates on bromoform emission from *Corallina pilulifera* (a) and *Lithophyllum yessoense* (b): (▲) control; (■) 3 ppm of low molecular weight fraction of fulvic acid; (●) 3 ppm of high molecular weight fraction of fulvic acid. Each point was the mean value of two analyses.

pilulifera. The algae showed catalase and strong super oxide dismutase (SOD) activities and weak peroxidase activity. Therefore, the seasonal change in catalase and SOD activity was measured comparing with BPO activity throughout the year and plotted in Fig. 7. The BPO activity increased during winter and spring and peaked in late spring with the SOD activity. However, it was not synchronized with the catalase activity. The level of catalase activity was high in mid-winter and dropped in an early spring when the BPO and SOD activities were high. The results suggested that the catalase activity was repressed at low level when BPO could be used as a substitute for H_2O_2 elimination. The results suggested that BPO in *C. pilulifera* functions to eliminate H_2O_2 compensating for catalase.

2.5. Characterization of the BPO with regard to active oxygen elimination

The specific activity of BPO in *C. pilulifea* is regulated by the vanadium content of the enzyme (Itoh et al., 1996). *C. pilulifera* BPO also contains a large amount of iron whose function has been unclear. BPO oxidizes Br^- with H_2O_2 to the Br^+OH^- intermediate, and the Br^+OH^- can decompose another H_2O_2 when a suitable organic substrate is absent Eq. (1).

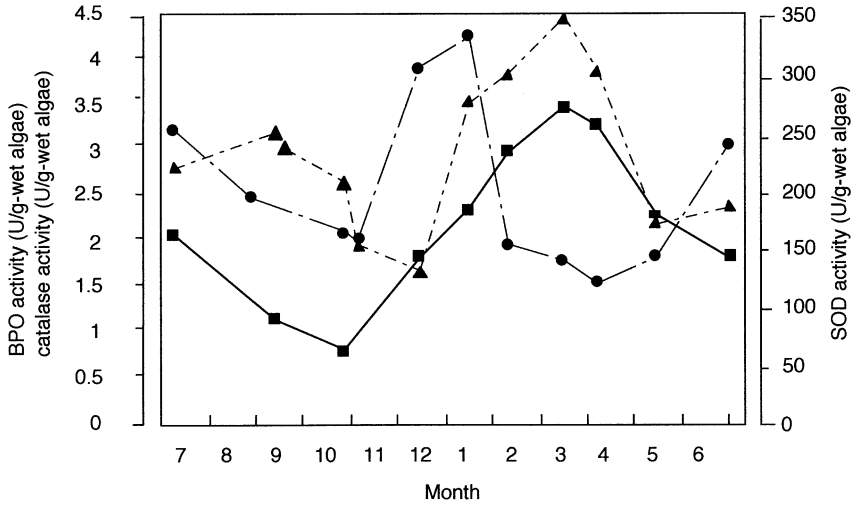

Fig. 7. Seasonal change of BPO activity (■), catalase activity (●) and SOD activity (▲) in *Corallina pilulifera* from May 1998 to April 1999 at the same spot of Himi, Toyama, Japan. Each point was the mean value of triplicate samples.

$$\begin{aligned} &\text{Enz.}+H^+X^-+H_2O_2 \rightarrow X^+OH^-(\text{or Enz}-X^+OH^-)+H_2O \\ &X^+OH^-+H_2O_2 \rightarrow H^+X^-+H_2O+O_2. \end{aligned} \quad (1)$$

This is a characteristic property of vanadium-BPO, which can catalyze an efficient Br^--dependent catalase reaction (Itoh, 1987b; Butler, 1998). The chemical reaction of Br^+OH^- with H_2O_2 is known to produce singlet oxygen. To elucidate the relationship between the enzymatic singlet oxygen formation and the vanadate and iron contents of the enzyme, we used the reconstituted enzyme after treatment of the native purified enzyme as shown in Table 2. The vanadate-treated enzyme showed high BPO activity depending on the vanadate content. However, the relationship between the activity and vanadate content of the enzyme was not linear. The results implied that there are different vanadate-binding mechanisms in the reconstituted enzyme. Although we first speculated that ferric iron co-existing with vanadate plays a role in depleting singlet oxygen, the reconstituted BPO which lost iron had a high production of singlet oxygen from KBr and H_2O_2. The emission rate of singlet oxygen coincided with the BPO activity, and has no relation with iron content. Therefore, a role for iron in eliminating the singlet oxygen produced by the enzyme was ruled out. Vanadium-BPO from *C. pilulifera* certainly followed the reaction described in Eq. (1) to decompose H_2O_2 and yield singlet oxygen.

3. Experimental

3.1. Collection of algae and crude enzyme preparation

Algal samples of *C. pilulifera* were collected at an intertidal area of Himi (N 37°, E 137°, Toyama Prefecture, Japan) on the Sea of Japan between June 1998 and May 1999, unless otherwise indicated. *Lithophyllum yessoense* samples from Taisei, Kudou-gun (N 42°, E 140°, Hokkaido, Japan) were supplied by Dr. Daisuke Fujita of The Toyama Prefectural Fisheries Experimental Station. The samples were kept in sea water and brought to our laboratory within 2 days. Apparently clean algae samples were used for the experiments. Each sample of alga (0.5 g) was disrupted with sea sand (40–80 mesh) in a chilled mortar with a pestle and extracted with 4 ml of 50 mM potassium phosphate buffer (pH 6.5). Unless otherwise indicated, this buffer was used throughout the experiments. After centrifugation ($8000\times g$, 20 min), the supernatant was used as a crude enzyme solution.

Table 2
Relationship among BPO activity, metal content and singlet oxygen forming tare of the reconstituted enzymes

Enzyme sample[a]	BPO activity (U/mg)	Vanadium content (mol/mol-enzyme)	Iron content (mol/mol-enzyme)	$^1O_2$ forming rate (μmol/min/mg)
Purified BPO	23.7	1.1	38.4	37.3
Vanadate-treated BPO	71.6	9.1	9.1	85.3
Reconstituted BPO	23.5	1.3	1.4	44.8

[a] The enzyme was purified from the stock of algae at −20 °C collected at Mikuni, Fukui 1995.

3.2. Enzyme purification

The enzyme was purified from the crude extracts of *C. pilulifera* and shown to be homogeneous on SDS–PAGE as described in the previous paper (Itoh et al., 1985).

3.3. Halomethanes analysis

Detection of halomethanes was performed by headspace analysis (Itoh and Shinya, 1994). A 0.5–2 g wet weight of *C. pilulifera or L. yessoense* sample, which had been well washed with autoclaved seawater and dried between paper towels for 2 min, was transferred into 50 ml of membrane-filtered seawater in a 50-ml vial (20 ml headspace), sealed with a silicon rubber septum and an aluminum-cap, and incubated at 20 °C, for 1–6 h. After incubation, the vial was kept at 60 °C for 15 min to insure the transfer of volatile halomethanes to the gas phase; then the gas (100 μl) was drawn and analyzed by gas chromatography (GC). A control run was done without incubation of the algal sample at 20 °C. GC analysis was performed with a Shimadzu GC-14B system equipped with a DB-624 capillary column (0.3 mm×30 m, 3 μm film, J & W Scientific, CA) under the following conditions: electron capture detector (ECD), injection and detection temp. 180 °C, column temp. 130 °C, flow rate 0.75 ml/min of N_2, split ratio 15. In vitro formation of bromoform was measured in a reaction mixture consisting of 5 mmol of buffer (pH 6.0), 0.5 mmol potassium bromide, 50 μmol of oxalacetate or fulvic acid (3 ppm), 50 μmol of hydrogen peroxide, and an appropriate amount of bromoperoxidase (ca. 1 unit) in a total volume of 50 ml using a 50-ml headspace vial in the same manner described above. The reactions were carried out for 2 h at 25 °C then treated at 60 °C. A control run was done without the enzyme or hydrogen peroxide.

3.4. Enzyme assay

The bromoperoxidase (BPO) activity was measured as described in previous papers based on the conversion of monochlorodimedone to bromochlorodimedone at 290 nm (Yamada et al., 1985). One unit of enzyme activity was defined as the amount of the enzyme that catalyzed the conversion of 1 μmol of monochlorodimedone ($\varepsilon = 19{,}900\ M^{-1}\ cm^{-1}$) in 1 min at 25 °C.

Super oxide dismutase (SOD) activity was assayed according to the methods of McCord and Fridovich (1978). The reaction mixture contained 75 μmol of the buffer (pH 7.8), 150 nmol EDTA, 15 nmol cytochrome *c*, 75 nmol xanthine, 0.04 U xanthine oxidasae and a suitable amount of enzyme solution in a total volume of 1.5 ml. The activity was monitored at 550 nm at 25 °C, and one unit of enzyme activity was defined as the amount of enzyme that inhibited 50% of the reduction of cytochrome *c*.

Catalase activity was assayed by measuring the decrease at 240 nm (the absorption maximum of hydrogen peroxide, $\varepsilon = 43.6\ M^{-1}\ cm^{-1}$) in a total volume of 1.5 ml as described previously (Itoh et al., 1986).

Glutathion peroxidase (GPO) activity was measured according to the method of Flohe and Gunzler (1984). The reaction mixture contained 75 μmol of the buffer (pH 6.0), 3 μmol EDTA, 1.5 μmol reduced glutathione, 0.3 μmol hydrogen peroxide, 0.24 μmol NADPH, 3 μmol NaN_3, 0.11 U oxidized glutathione reductase and a suitable amount of enzyme solution in a total volume of 1.5 ml. Ascorbate peroxidase (APO) activity was assayed by the decrease in absorption at 290 nm due to ascorbate ($\varepsilon = 2{,}800\ M^{-1}cm^{-1}$) oxidation (Ishikawa et al., 1995). The reaction mixture contained 75 μmol of the buffer (pH 7.0), 0.75 μmol ascorbate, 45 nmol hydrogen peroxide, and a suitable amount of enzyme solution in a total volume of 1.5 ml.

General peroxidase (POD) activity was measured with *o*-dianisidine at 25 °C. The appearance of the oxidized compound ($\varepsilon = 11{,}300\ M^{-1}\ cm^{-1}$) was measured at 460 nm in the reaction mixture consisting of 15 μmol of the buffer (pH 6.0), 0.008% (w/v) *o*-dianisidine, 0.2 μmol hydrogen peroxide, and a suitable amount of enzyme solution in a total volume of 1.5 ml (Anon, 1972).

The protein concentration was estimated by measuring the absorbance at 280 nm or by using the Bio-Rad Protein Assay kit with bovine serum albumin as a standard protein according to the manufacturer's protocol.

3.5. Reconstitution of the enzyme and metal analysis

The purified BPO was dialyzed against 50 mM citrate buffer (pH 3.7) with 1 mM EDTA to remove the prosthetic group, then incubated with 0.5 mM Na_2VO_3 in 0.1 M Tris–HCl buffer (pH 7.0) to reconstitute the enzyme, and dialyzed against Tris–HCl buffer (pH 7.0) plus 1 mM EDTA (reconstituted enzyme); or the enzyme was first incubated with 5 mM Na_2VO_3 and then dialyzed against 0.1 M Tris–HCl buffer(pH 7.0) plus 1 mM EDTA (vanadate-treated enzyme). Quantitative analysis of the vanadium and iron content of the enzyme was done by HPLC-spectrometry of chelated complexes of an azo dye with metal ions as described previously (Miura and Itoh, 1997).

3.6. Singlet oxygen analysis

Generation of singlet oxygen ($^1O_2$) in the BPO-catalyzed reaction was determined by measuring the chemiluminesecence from 2-methyl-6-(4-methoxyphenyl)-3,7-dihydroimidazo[1,2-a]pyrazin-3-one hydrochloride (MC LA) with an ALOKA Luminescence reader BLR-201

(ALOKA, Tokyo, Japan) (Nakano, 1990). The reaction mixture comprised 2 μmol sodium acetate buffer (pH 4.5), 1.0 nmol MCLA, 2 μmol H_2O_2, 2 μmol KBr and 2.8 units of BPO in a total volume of 1.0 ml. The reaction was started by addition of the enzyme. Chemiluminesecence counts per min were determined from the calibration curve, which had been made by chemical reaction of MCLA with NaOBr solution. One micromole of NaOBr produced 22,000 kcounts/min of chemiluminesence.

3.7. Bromoform vaporizer

As shown in Fig. 2, we constructed an air-pressurized bromoform vaporizer system to mimic the emission of bromoform from *C. pilulifera* in vivo. This apparatus was made of stainless steel, and could emit bromoform across a hydrophobic polytetrafluoroethylene (PTFE) membrane interface with air into seawater. The system was placed into a stainless tank (0.8 meter in depth), and clean natural sea water flowed in and out of the tank at 5 l/min for four weeks. Bromoform emission was controlled by the flow rate of air and sea water temperature. A control was done without bromoform.

3.8. Microscopic analysis

Scanning electron microscopy (SEM) observation of the surfaces of living or dead *C. pilulifera* was performed with a Hitachi S-2400 scanning electron microscope. Coralline algae is quite useful for SEM observation, because it has a solid calcium carbonate skeleton. A collected living alga sample releasing bromoform was placed into a stainless mesh cylindrical container (diameter:5 cm, height:9 cm) with a glass cap to prevent predation by benthonic invertebrates, in which the algae could freely receive fresh sea water and sunlight, and laid in a solid clean sea spot (90±30 cm depth). After two weeks incubation under natural conditions, the specimen and a control (dead algae incubated under the same conditions) were briefly washed with fresh water and dried under vacuum. The specimens were coated with gold by an ion spattering apparatus, and measured by SEM at 15 kV.

The surface of the PTFE membranes settled on the bromoform vaporizer was removed and observed using an Olympus BX-50 phase-contrast microscope (Tokyo, Japan).

3.9. Chemicals

Xanthine oxidase was obtained from Oriental Yeast, Tokyo, Japan, and ferricytochrome *c* from Wako Pure Chemical Industries, Japan. MCLA was supplied by Tokyo Kasei Co., Ltd., Japan, and fulvic acid by the Japanese Society of Humic Substances, Kobe, Japan. The fulvic acid was separated into low molecular weight (lower than Mr:1330) and high molecular weight (higher than Mr:1330) fractions by Sephadex G-25 gel filtration chromatography with water as an eluent using cyanocobalamin as a marker compound (Mr:1330), and the two fractions evaporated and dried under vacuum. All other reagents used in this study were of analytical grade.

Acknowledgements

We are indebted to Dr. D. Fujita of Toyama Prefectural Fisheries Experimental Station, Toyama, Japan, for collection of the *L. yessoense* sample. The study was supported in part by a Grant-in-Aid for Scientific Research from the Ministry of Education, Science, Sports and Culture of Japan.

References

Anon., 1972. Worthington Enzymes Worthington Biochemical Corp., Lakewood, NJ, pp. 43–45.

Attieh, J.M., Hanson, A.D., Saini, H.S., 1995. Purification and characterization of a novel methyl transferase responsible for biosynthesis of halomethanes and methanethiol in *Brassica oleracea*. Journal of Biological Chemistry 270, 9250–9257.

Beissner, R.S., Guilford, W.J., Coates, R.M., Hager, L.P., 1981. Synthesis of brominated heptanones and bromoform by a bromoperoxidase of marine origin. Biochemistry 20, 3724–3731.

Butler, A., 1998. Vanadium bromoperoxidase. Current Opinion in Chemical Biology 2, 279–285.

Butler, J.M., 2000. Better budgets for methyl halides? Nature 403, 260–261.

Class, T.H., Ballschmiter, K., 1988. Chemistry of organic traces in air. Journal of Atmospheric Chemistry 6, 35–46.

Denboh, T., Suzuki, M., Mizuno, Y., Ichimura, T., 1997. Suppression of Laminaria sporelings by allelochemicals from coralline red algae. Botanica Marina 40, 249–256.

Flohe, L., Gunzler, W.A., 1984. Assay of glutathione peroxidase. Methods in Enzymology 105, 114–121.

Gschwend, P.M., MacFarlane, J.K., Newman, K.A., 1985. Volatile halogenated organic compounds released to seawater from temperate marine macroalgae. Science 227, 1033–1035.

Harper, D.B., 1985. Halomethane from halide ion-a highly efficient fungal conversion of environmental significance. Nature 315, 55–57.

Harper, D.B., 1994. Biochemistry of atmospheric gas production and consumption. Biochemical Society Transactions 22, 1007–1011.

Ishikawa, T., Sasaki, K., Takeda, T., Shigeoka, S., 1995. Cloning and expression of cDNA encoding a new type of ascorbate peroxide from spinach. FEBS Letters 367, 28–32.

Itoh, N., 1995. Volatile halogenated compounds from marine algae; their formation mechanisms and geochemical aspects. Recent Research Development in Phytochemistry 1, 309–327.

Itoh, N., Hasan, A.K.M.Q., Izumi, Y., Yamada, H., 1987. Immunological properties of bromoperoxidases in coralline algae. Biochemistry International 15, 27–33.

Itoh, N., Hasan, A.K.M.Q., Izumi, Y., Yamada, H., 1988. Substrate specificity, regiospecificity and stereospecificity of halogenation reactions catalyzed by non-heme-type bromoperoxidase of *Corallina pilulifera*. European Journal of Biochemistry 172, 477–484.

Itoh, N., Izumi, Y., Yamada, H., 1985. Purification of bromoperoxidase from *Corallina pilulifera*. Biochemical and Biophysical Research Communications 131, 428–435.

Itoh, N., Izumi, Y., Yamada, H., 1986. Characterization of nonheme type bromoperoxidase in *Corallina pilulifera*. Journal of Biological Chemistry 261, 5149–5200.

Itoh, N., Izumi, Y., Yamada, H., 1987a. Characterization of nonheme iron and reaction mechanism of bromoperoxidase in *Corallina pilulifera*. Journal of Biological Chemistry 262, 11982–11987.

Itoh, N., Izumi, Y., Yamada, H., 1987b. Haloperoxidase-catalyzed halogenation of nitrogen-containing aromatic heterocycles represented by nucleic bases. Biochemistry 26, 282–289.

Itoh, N., Shinya, M., 1994. Seasonal evolution of bromomethanes from coralline algae and its effect on atmospheric ozone. Marine Chemistry 45, 95–103.

Itoh, N., Sasaki, H., Ohsawa, N., Shibata, M.S., Miura, J., 1996. Bromoperoxidase in *Corallina pilulifera* is regulated by its vanadate content. Phytochemistry 42, 277–281.

Itoh, N., Tujita, M., Ando, T., Hisatomi, G., Higashi, T., 1997. Formation and emission of monohalomethanes from marine algae. Phytochemistry 45, 67–73.

Krenn, B.E., Izumi, Y., Yamada, H., Wever, R., 1989. A comparison of different (vanadium)-bromoperoxidases;the bromoperoxidase from *Corallina pilulifera* is also a vanadium enzyme. Biochimica et Biophysica Acta. 998, 98–106.

Krenn, B.E., Tromp, M.G.M., Wever, R., 1989. The brown algae *Ascophyllum nodosum* contains two different vanadium bromoperoxidases. Journal of Biological Chemistry 264, 19287–19292.

Lovelock, J.E., 1975. Natural halocarbons in the air and in the sea. Nature 256, 193–194.

McCord, J.M., Fridovich, I., 1978. Preparation and assay of super oxide dismutase. Methods in Enzymology 53, 382–393.

Messerschmidt, A., Prade, L., Wever, R., 1997. Implications for the catalytic mechanism of the vanadium-containing enzyme chloroperoxidase from the fungus *Ceuvularia inaequalis* by X-ray structures of the native and peroxide form. Biological Chemistry 378, 309–315.

Miura, J., Itoh, N., 1997. Detection of vanadium, cobalt, nickel and iron in bromoperoxidases from *Pseudomonas* and *Corallina pilulifera* by high performance liquid chromatography. Journal of Liquid Chromatography & Related Technologies 20, 2367–2376.

Moore, R.E., 1977. Volatile compounds from marine algae. Accounts of Chemical Research 10, 40–47.

Morris, D.R., Hager, L.P., 1966. Chloroperoxidase I. Isolation and properties of the crystalline glycoprotein. Journal of Biological Chemistry 241, 1763–1768.

Nakano, M., 1990. Determination of superoxide radical and singlet oxygen based on chemiluminescence of luciferin analogs. Methods in Enzymology 186, 585–591.

Neidleman, S.L., Geigert, J., 1986. Biohalogenation. Ellis Horwood, Chichester, UK.

Ni, X., Hager, L.P., 1998. cDNA cloning of *Batis maritima* methyl chloride transferase and purification of the enzyme. Proceedings of National Academy of Science of USA 95, 12866–12871.

Plat, H., Krenn, B.E., Wever, R., 1987. The bromoperoxidase from the lichen *Xanthoria parietina* is a novel vanadium enzyme. Biochemical Journal 248, 277–279.

Rasmussen, R.A., Khalil, M.A.K., Gunawardena, R., Hoyt, S.D., 1982. Atmospheric methyl iodide (CH_3I). Journal of Geophysical Research 87, 3086–3090.

Saxena, D., Aouad, S., Attieh, J., Saini, H.S., 1998. Biochemical characterization of chloromethane emission from the wood-rotting fungus *Phellinus pomaceus*. Applied and Environmental Microbiolohy 64, 2831–2835.

Sheffield, D.J., Harry, T., Smith, A.J., Rogers, L.J., 1993. Purification and characterization of the vanadium bromoperoxidase from the macroalga *Corallina officinalis*. Phytochemistry 32, 21–26.

Shimonishi, M., Kuwamoto, S., Inoue, H., Wever, R., Ohshiro, T., Izumi, Y., Inoue, T., 1988. Cloning and expression of the gene for a vanadium-dependent bromoperoxidase from a marine macro-alga, *Corallina pilulifera*. FEBS Letters 428, 105–110.

Taniguchi, K., Kurata, K., Maruzoi, T., Suzuki, M., 1994. Dibromomethane, a chemical inducer of larval settlement and metamorphosis of the sea urchin *Strongylocentrotus nudus*. Fisheries Science 60, 795–796.

Vilter, H., 1984. Peroxidases from phaeophyceae: a vanadium(V)-dependent peroxidase from *Ascophyllum nodosum*. Phytochemistry 23, 1387–1390.

Wever, R., Tromp, M.G.M., Krenn, B.E., Marjani, A., Tol, M.V., 1991. Brominating activity of the sea weed *Ascophyllum nodosum*: Impact on the biosphere. Environmental Science and Technology 25, 446–449.

Wiesner, W., van Pee K.-H., Lingens, F., 1988. Purification and characterization of a novel bacterial non-heme chloroperoxidase from *Pseudomonas pyrrocinia*. Journal of Biological Chemistry 263, 13725–13732.

Wuosmaa, A.M., Hager, L.P., 1990. Methyl chloride transferase: a carbocation route for biosynthesis of halometabolites. Science 249, 160–162.

Yamada, H., Itoh, N., Murakami, S., Izumi, Y., 1985. New bromoperoxidase from coralline algae that brominates phenol compounds. Agricultural and Biological Chemistry 49, 2961–2967.

Yu, H., Whittaker, J.W., 1989. Vanadate activation of bromoperoxidase from *Corallina officinalis*. Biochemical and Biophysical Research Communications 160, 87–92.

PERGAMON

Phytochemistry 58 (2001) 693–701

PHYTOCHEMISTRY

www.elsevier.com/locate/phytochem

Involvement of pectin methyl-esterase during the ripening of grape berries: partial cDNA isolation, transcript expression and changes in the degree of methyl-esterification of cell wall pectins

Laurent Barnavon[a,*,1], Thierry Doco[a], Nancy Terrier[b], Agnès Ageorges[b], Charles Romieu[b], Patrice Pellerin[a]

[a]*Unité de Recherches Biopolymères et Arômes, IPV-INRA, 2 Place Viala, 34 060 Montpellier, France*
[b]*Unité de Recherches de Biochimie Métabolique et Technologie, IPV-INRA, 2 Place Viala, 34 060 Montpellier, France*

Received 12 December 2000; received in revised form 14 May 2001

Abstract

Grape berries (*Vitis vinifera* L., cv Ugni blanc) were harvested at 12 different weeks of development in 1996 and 1997. Ripening was induced at *veraison*, the crucial stage of berry softening, and was followed by a rapid accumulation of glucose and fructose and an increase of pH. Total RNAs, crude proteins and cell wall material were isolated from each developmental stage. A partial length cDNA (*pme*1, accession number AF159122, GenBank™) encoding a pectin methyl-esterase (PME, EC 3.1.1.11) was cloned by RT–PCR with degenerate primers. Northern blots revealed that mRNAs coding for PME accumulate from one week before the onset of ripening until complete maturity, indicating that this transcript represents an early marker of *veraison* and could be involved in berry softening. However, PME activity was detected during all developmental stages. Total activity per berry increased, whereas "specific" activity, on a fresh weight basis, decreased during development. The amount of cell wall material (per berry and per g of berry) followed the same pattern as that of PME activity (total and "specific" respectively), indicating they were tightly correlated and that PME levels varied very little in the cell walls. Nevertheless, the degree of methyl-esterification of insoluble pectins decreased throughout the development from 68% in green stages to less than 20% for the ripe berries, and this observation is consistent with the induction of PME mRNAs during ripening. Relations between transcript expression, PME activity, the DE of insoluble pectic polysaccharides and their involvement in grape berry ripening are discussed. © 2001 Elsevier Science Ltd. All rights reserved.

Keywords: Cell wall; Development; Grape berry; Pectin methyl-esterase; softening

1. Introduction

Plant cell walls consist of complex networks of polysaccharides and proteins surrounding the plasma membrane. The cell wall is involved in the mechanical resistance of the plant cell but must also allow for growth. Primary cell walls in fruit parenchyma are composed of pectic polysaccharides, cellulose and hemicellulose, and minor components such as structural proteins (Carpita and Gibeaut, 1993).

Plant cell growth involves the enlargement of these networks, of which the composition and elasticity is controlled by a complex set of cell wall modifying enzymes. Rapid softening is also frequently encountered during fruit ripening (Fischer and Bennett, 1991). The release and depolymerization of polygalacturonans play a major role in fruit softening. Pectin methyl esterase (PME, EC 3.1.1.11), a ubiquitous cell wall-bound enzyme, catalyses the hydrolysis of methyl-ester groups from galacturonosyl residues. PMEs may play important roles in determining the extent to which demethylated

Abbreviations: cv, cultivar; CWM, cell wall material; DE, degree of esterification; GC–EIMS, gas chromatography–electronic impact mass spectrometry; HEPES, *N*-[2-hydroxyethyl]piperazine-*N*′[2-ethane sulfonic acid]; HGs, homogalacturonans; PG, polygalacturonase; PME, pectin methylesterase; RG-I, rhamnogalacturonan I; RG-II, rhamnogalacturonan II; RT–PCR, reverse transcription–polymerase chain reaction; SDS, sodium dodecylsulfate, UA uronic acid content.

[1] Present address: Université de Neuchâtel, Laboratoire de Biochimie, Rue Emile Argand, 11 2007 Neuchâtel, Switzerland.

* Corresponding author at present address. Fax: +33-4-99-61-26-83.

E-mail addresses: laurent.barnavon@unine.ch (L. Barnavon), doco@ensam.inra.fr (T. Doco).

0031-9422/01/$ - see front matter © 2001 Elsevier Science Ltd. All rights reserved.
PII: S0031-9422(01)00274-6

polygalacturonans are accessible to degradation by polygalacturonases (Fischer and Bennett, 1991), releasing galacturonic acid (exo-PG, EC 3.2.1.67) or oligogalacturonate (endo-PG, EC 3.2.1.15), and the availability of homogalacturonan carboxylic groups for Ca^{2+} binding. Increasing the number of carboxylic groups in pectins should lead to an increase in the number of Ca^{2+} bridges between homogalacturonan chains but also to an increase in their accessibility to cell wall hydrolases (Fischer and Bennett, 1991; Seymour and Gross, 1996). These two factors may have an opposing effect on cell wall deformability.

Usually, several PME isoforms with different pH and temperature optima, pI and molecular masses are present in the same plant species (Warrilow and Jones, 1995; Micheli et al., 2000), but their respective functions and action patterns have not been elucidated. In tomato plant, multiple isoforms of PME were present in different tissues, and both tissue-specific and ubiquitously expressed isoforms of PME have been reported (Gaffé et al., 1994). A specific isoform has been described as involved in cell wall metabolism during fruit growth and development prior to ripening (Ray et al., 1988), whereas another isozyme could be specific to ripening. The expression in tomatoes of an antisense PME gene resulted in a higher degree of methyl-esterification of pectins, thereby decreasing their sensivity to PG and resulting in higher molecular mass pectins in transgenic fruit juice (Thakur et al., 1996). However, transgenic tomatoes with reduced PME activity ripened normally (Tieman et al., 1992).

Nevertheless, the exact roles of PME during the softening of fruits is still only partially understood, and several authors have described contradictory changes of PME activity during fruit-ripening (Seymour et al., 1991; Christensen et al., 1998).

The cell walls of grape berries, especially from the epidermal cells of the skin, form a barrier to the diffusion of components such as aromas and polyphenols which are important for the quality of wines. Grape primary cell walls are also the source of wine pectic polysaccharides. The structural properties of cell walls determine the mechanical resistance, the texture, and the ease of processing berries. Grape berries are non-climacteric fruits. The earliest signal of the induction of ripening is an abrupt increase in fruit deformability which occurs within 24 h (Kanellis and Roubelakis-Angelakis, 1993). Berries undergo dramatic changes (acceleration of growth, rapid softening) at the stage called *veraison* which corresponds to the onset of ripening, and occurs 5–8 weeks before maturity (Kanellis and Roubelakis-Angelakis, 1993). *Veraison* is also characterized by the end of organic acid accumulation and the onset of glucose and fructose storage. As for other fruits, softening is possibly due to enzymic mechanisms whose identity and expression regulation remain very partially understood. It can be expected that enzymes involved in cell wall metabolism should be particularly active during the softening period, typical of *veraison*.

The understanding of changes during the development and softening of grape berries may have considerable importance in enology. The primary cell walls of grape berries have a common set of structural polysaccharides with their distribution varying among cultivars. The main glycosyl residues of grape cell walls are cellulosic glucose and galacturonans (Lecas and Brillouet, 1994). The degree of methyl-esterification of grape HGs can vary from 40 to 80% (Lecas and Brillouet, 1994) according to the cultivar, the development stage and the tissue. In grapes, PME displays maximum activity at pH 7.0–7.5 (Lee et al., 1979), although earlier studies (Marteau et al., 1961) reported a maximum activity at pH 5.6.

The aim of this study was to elucidate the role of PME and the consequences of its action on cell walls during the maturation of grape berries. Molecular biology tools have been used to elucidate the possible involvement of PMEs in grape (*Vitis vinifera* L., cultivar Ugni blanc) ripening and softening. A cDNA coding for PME has been isolated and the expression patterns of the corresponding mRNA were followed during ripening, in parallel with PME activity and the degree of homogalacturonan esterification.

2. Results

2.1. Grape berry development

Veraison, previously described by viticulturists as the onset of color change, has been defined in this study as the beginning of berry softening and of the accumulation of glucose and fructose. Both events happened at week 7 (*veraison*) in the present study. The changes of berry fresh and dry weights, pH and sugar content are typical for grapes (upper panel Fig. 1). The average weight of berries increased steadily (phase I or herbaceous period, weeks 1 to 6) until *veraison*, before growth slowed (phase II or lag phase, weeks 7 and 8) and then increased again up to maturity (phase III or maturation period, weeks 9 to 12, Fig. 1A). The growth of berries followed a typical double sigmoid curve (Kanellis and Roubelakis-Angelakis, 1993) and *veraison* corresponded to the inception of the slow growth phase. Dry weight, pH, and °Brix (Fig. 1B) were stable until week 6, and increased markedly from *veraison*. The pH value remained between 2.45 and 2.55 during the first phase (herbaceous period) marked by the accumulation of organic acids. The pH increased from *veraison* to reach a maximum of 3.2–3.3 at maturity. Total soluble solids remained in the range 4.8–6°Brix during the early phase of organic acid accumulation until week 6, and

increased notably from week 7 due to the massive accumulation of sugars and water (Kanellis and Roubelakis-Angelakis, 1993).

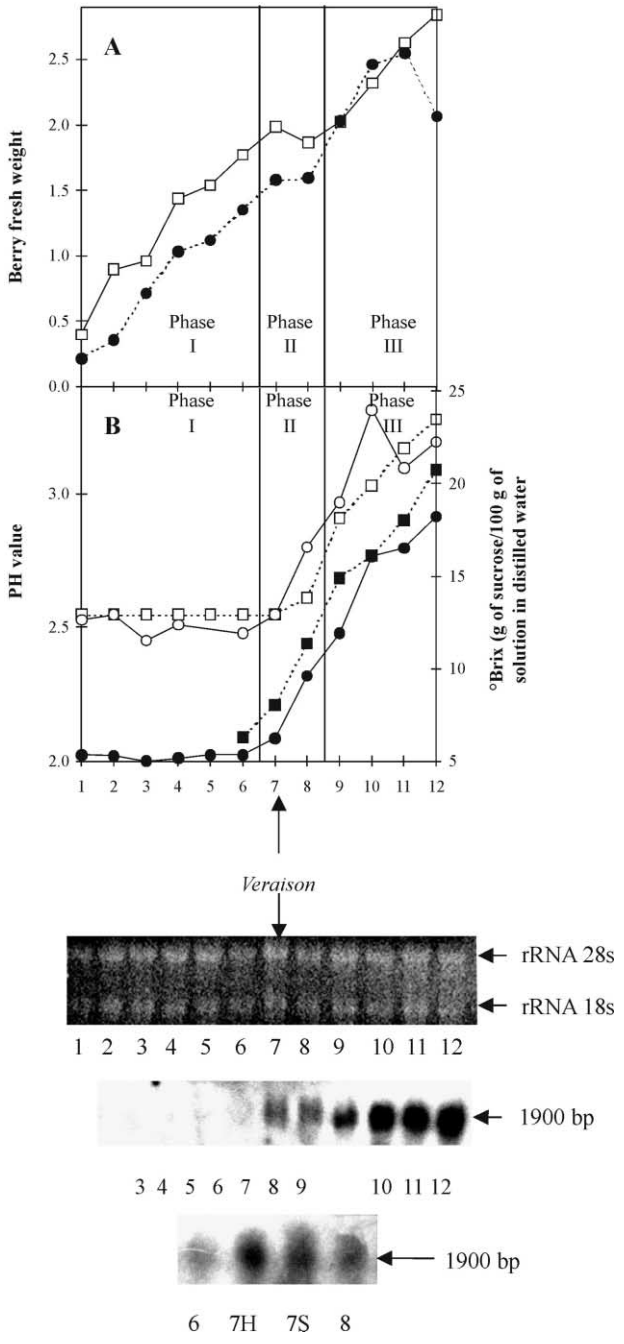

Fig. 1. Upper panel, the development of Ugni blanc berries. A, average berry fresh weight (□, 1996 and ●,1997). B, pH (□, 1996 and ○, 1997) and °Brix (■, 1996 and ●, 1997) of the resulting must. Lower panel, expression pattern of mRNA coding for *pme*1. Fifteen micrograms of total RNA were separated on 1.2% denaturing agarose-formaldehyde gel electrophoresis and transferred onto a nylon membrane. C, total RNA blots were stained with ethydium bromide as a loading control; northern blots were hybridized with the *pme*1 probe (^{32}P labelled cDNA); D, total RNA from harvest 1997, week 7 (*veraison*) corresponding to a mix of ~ 50% hard and soft berries from veraison stage; E, northern blot differentiating hard (7H) and soft (7S) berries from the *veraison* stage (week 7).

2.2. Isolation of a cDNA clone for pectin methylesterase

PCR allowed the amplification of a 290 base long fragment *pme*1 from first strand cDNA. Sequence alignment using ClustalV indicated that the corresponding sequence obtained by RT-PCR showed significant similarities with PMEs in data banks (Fig. 2). The amino acid sequence deduced for *pme*1 showed 82% identity and 90% similarity with a PME (AA 333 to 428, on a full length alignment basis) from *Prunus persica* (Glover et al., 1996).

2.3. Expression pattern of mRNAs coding for PME

Total RNA loadings were controlled by staining the ribonucleic acids with ethydium bromide (Fig. 1C). The expression of mRNAs coding for PME in grape berries at several developmental stages was followed by Northern-blot with *pme*1 clone as probe. Only one mRNA band (Fig. 1D) was detectable (between 1.9 kb in length ± 0.1 kb, according to the membrane considered). No transcripts could be detected during phase I (green stages). PME mRNAs accumulated from one week before *veraison* (week 6) to week 12 (Fig. 1D), and a similar pattern of mRNA expression was observed for the 1996 harvest (data not shown). A third Northern-blot, in which total RNAs of hard and soft berries from *veraison* stage were separated (data not shown), revealed that PME mRNAs accumulated prior to softening (Fig. 1E).

2.4. PME activity

Crude protein extracts from grape berries at all developmental stages (1996 and 1997) were analyzed for PME activity and determination were performed in triplicates. PME activity was detected at all stages of development, even during phase I, although mRNA transcripts had not been previously detected. The activity patterns were similar between the two vintages (data not shown). The values of PME activity are expressed either as total (in nkat/berry), as "specific" activity (in nkat/g of berry fresh weight), or as nkat per mg of CWM (Fig. 3).

Total PME activity per berry (Fig. 3A) increased almost linearly during the green stages to reach a maximum one week before *veraison* (ca. 39 nkat/berry). The enzymic activity decreased between weeks 6 and 8, before increasing again to reach a maximum of ca. 53 nkat/berry (week 11) at maturity. This substantial increase in PME activity as ripening progresses, is consistent with pattern previously described for non-climacteric fruits such as raspberry (Iannetta et al., 1999).

The general patterns of "specific" activity (nkat/g of berry fresh weight, Fig. 3A) were also very similar for the two years studied. PME "specific" activity reached a

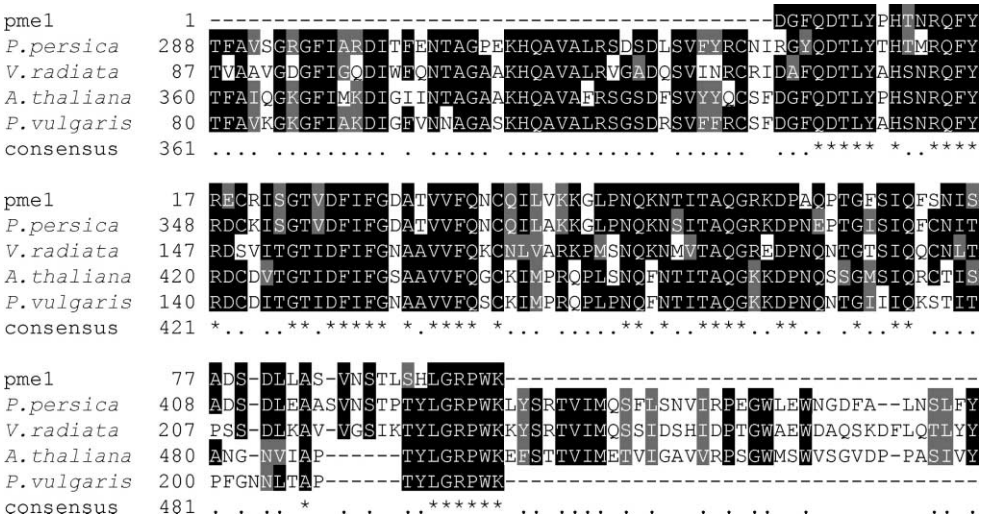

Fig. 2. Alignments of the deduced amino acid sequences of *pme*1 clone with several plant PMEs (accession numbers are X95991 for *P. persica*, X94443 for *V. radiata*, X81585 for *A. thaliana* and S25171 for *P. vulgaris*). (*) Identity, (.) similarity. Authors thank BOXSHADE for shading sequence alignments.

maximum during week 1 (ca. 46 nkat), decreased steadily until week 4 (ca. 26 nkat), and then remained steady up to week 6 (ca. 26–28 nkat). The lag phase around *veraison* was also characterized by a decrease in PME "specific" activity which remained constant during phase III (ca. 18 nkat at week 12).

When expressed on per mg of CWM, PME activity is still detectable but to a lower extent and the pattern remains to a steady state level all along the berry development (Fig. 3B).

2.5. Isolation and quantification of cell wall material

Cell walls were isolated from each developmental stage in 1997. Grape cell wall quantities (Fig. 4) have been expressed either as total (mg per berry) or on a fresh weight basis (mg per g of berry fresh weight). These curves showed similar patterns to those of total and "specific" PME activity. As PMEs are cell wall-bound enzymes, it is also interesting to express results as nkat per mg of dry cell wall. This calculation showed that on a per mg of CWM basis (Fig. 3B), PME activity remained similar throughout development (in the range of 1.2–1.5 nkat) although activity tended to increase between weeks 7 and 8.

2.6. Concentration and degree of methyl-esterification of cell wall homogalacturonans

The cell wall isolation procedure leads to the recovery of primary cell walls devoid of water-soluble pectins after endogenous hydrolases had been inactivated during the phenol extraction procedure (Huber, 1991). Uronic acid (UA) contents were determined as anhydromoles of galacturonic acid by the colorimetric *m*-hydroxydiphenyl assay (Blumenkrantz and Absoe-Hansen, 1973) (Fig. 5). Uronic acids, mainly galacturonic acids (at least 94.6% checked by methanolysis and trimethylsilylation, detection was performed by GC–EIMS, data not shown), accumulated during the green stages (phase I, week 1 to 5) and their relative cell wall content increased from 4 to 10% (Fig. 5A). Both phases II and III were characterized by a slow increase to reach 12.5% at complete maturity. Together with the accumulation of total cell wall material per berry, these data indicate that the whole period of ripening is marked by homogalacturonan biosynthesis. On a per berry basis (Fig. 5A), the accumulation of UA followed the same general pattern as the percentage in cell wall material, which increased from 0.5 (week 1) to 4 mg at maturity (week 12).

The percentage of esterification (DE) of cell wall homogalacturonans (Fig. 5B) decreased rapidly during green stages until week 3 (from 68 to ca. 40%) underwent a 3 week steady-state period until week 6, and finally decreased from *veraison* (week 7) to reach less than 20% in the last stages of ripening (maturation period).

3. Discussion

Samples of grape berries (*Vitis vinifera* L., cv Ugni blanc) were harvested during two vintages (1996 and 1997). Even in a single-cultivar vineyard, variations in timing, developmental kinetics and the extent of ripening occur between berries on a cluster, between clusters on a vine and between different vines. Therefore, sampling allowed us to discard unsynchronized berries in order to minimize variation within samples.

The development of berries, cv Ugni blanc, was characterized by physical and biochemical analysis (upper

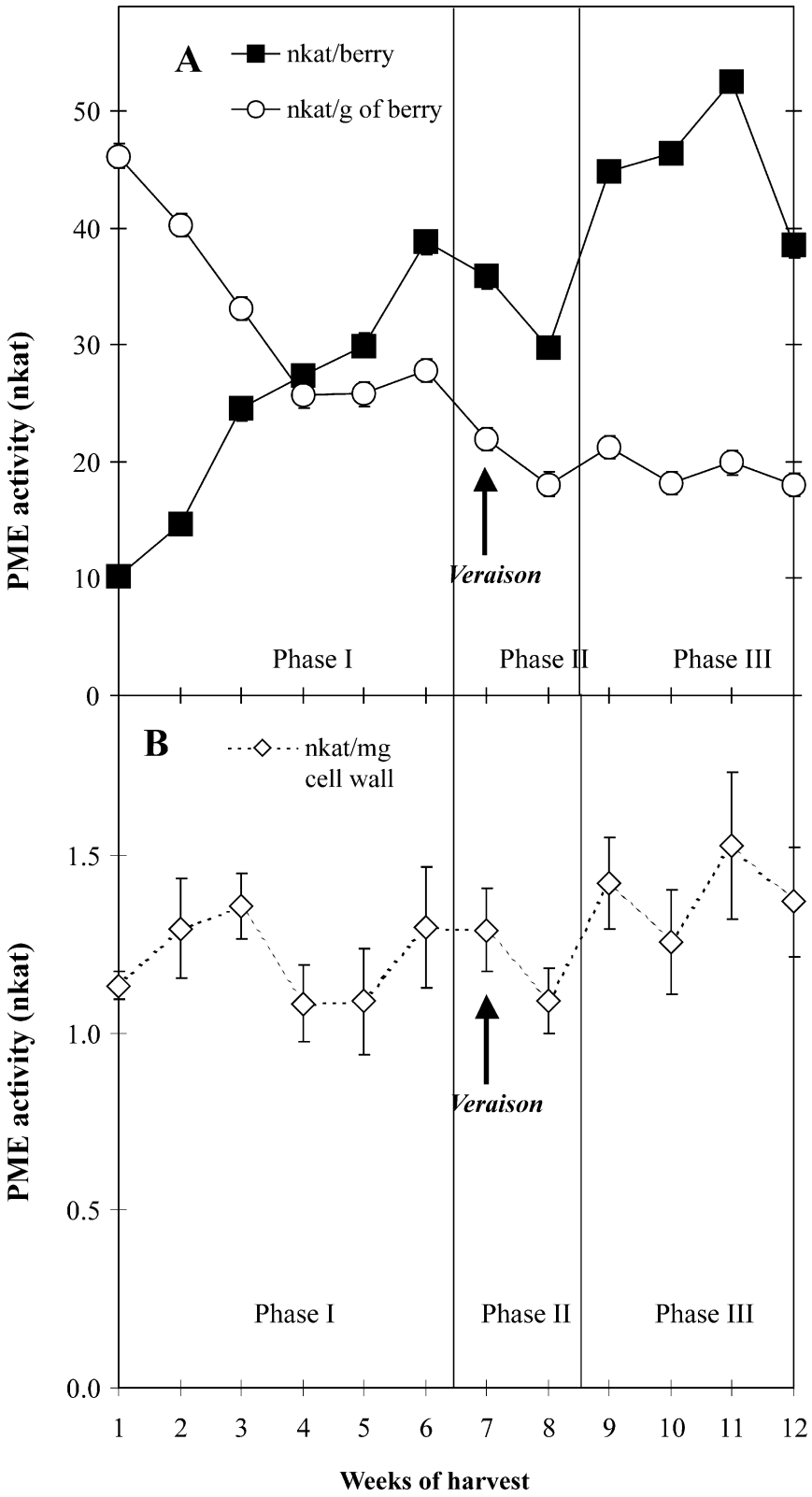

Fig. 3. PME activity during the ripening of grape berries in 1997. A, total activity in nkat per berry (■) and "specific" activity in nkat per g of berry fresh weight (○); B, activity in nkat per mg of dried cell wall material (◇). Bars represent standard error ($n = 3$).

panel, Fig. 1). The growth of grape berries is divided into 3 phases, and follows a typical double sigmoid curve (Kanellis and Roubelakis-Angelakis, 1993). Phase I (green stages) is characterized by a rapid accumulation of organic acids. Acidity reaches its highest level during phase II, a slow growth (lag) phase. *Veraison* (week 7) is

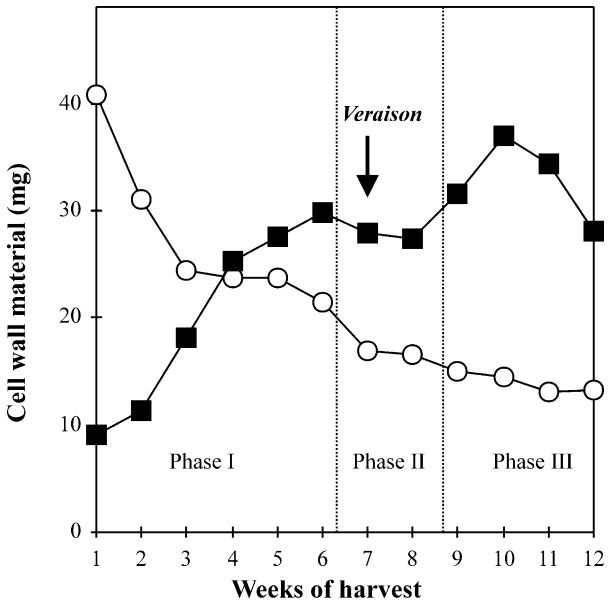

Fig. 4. Amount of cell wall material (CWM) of Ugni blanc grape berries during ripening in 1997, expressed as mg of dried cell wall per berry (■) and per g of fresh weight (○).

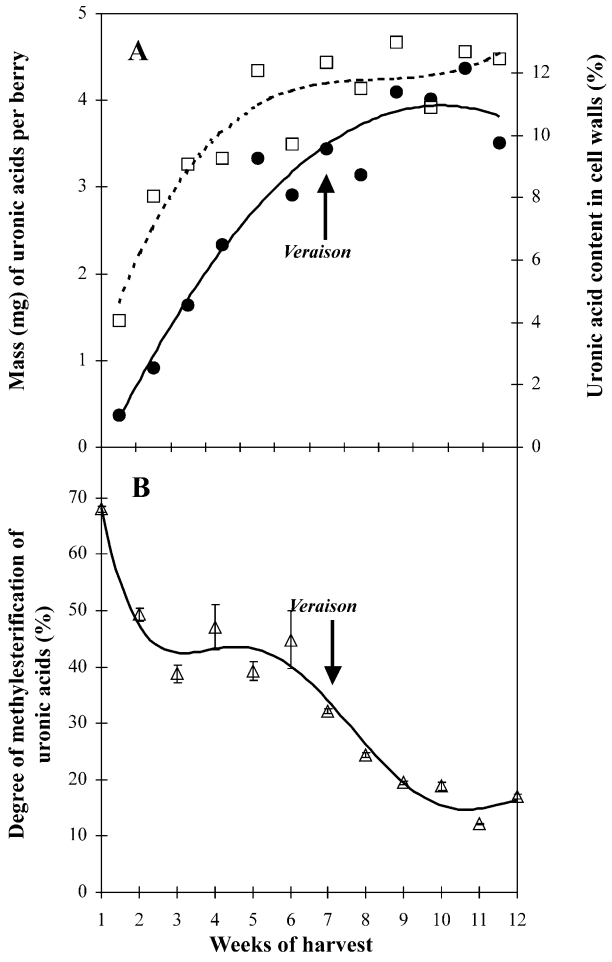

Fig. 5. Amount of cell wall uronic acids during the ripening of grape berries in 1997. A, relative content as a percentage of cell walls (□), mass (mg) of uronic acids per berry (●), data are means ($n=3$) and the variation was lower than 10% of the reported data; B, degree of methyl esterification (△), bars represent standard error ($n=3$).

characterized by several marked changes affecting berries: initial softening and an increase in deformability followed by a second acceleration of growth linked to the accumulation of glucose, fructose and water, and a decrease of organic acid content (Kanellis and Roubelakis-Angelakis, 1993). These last phenomena continue during ripening (phase III, ripening or maturation period). For both vintages 1996 and 1997, *veraison* was clearly indicated by the sudden softening of berries, associated with the increase in °Brix (corresponding to glucose and fructose accumulation) and the concomitant increase in pH (Fig. 1B).

Results presented here clearly show that major changes occuring at the beginning of ripening (i.e. softening, the onset of the second growth period, sugar accumulation, acid breakdown) are associated with the expression of the *pme*1 gene. Moreover, the *pme*1 mRNAs detected here were induced about one week before softening (week 6) and Fig. 1E revealed that the inception of mRNA accumulation occurred prior to softening. The existence of early molecular events associated with the triggering of ripening constitutes a key for the study of signal events responsible for the induction of ripening in non-climacteric (ethylene insensitive) fruits like grape berries. This rapid increase in *pme*1 transcripts is consistent with the accumulation of a large number of cDNAs in Shiraz grape (Davies and Robinson, 2000) occurring at the onset of ripening, including a putative N-terminal domain of some pectin methylesterases.

The *pme*1 deduced amino acid sequences shared significant similarity with other plant PMEs (Fig. 2). The size of the *pme*1 transcript (1.9 ± 0.1 kb) is consistent with previous data (Ray et al., 1988; Nairn et al., 1998). The clone had been isolated from grapes harvested at a post-*veraison* stage (one week later) and may be specific for this period of ripeness. Therefore, the presence of other PME isoforms exhibiting a different expression pattern during grape berry development cannot be excluded. This hypothesis is reinforced by the failure to detect mRNAs during green phase I, a period marked by a high PME "specific" activity in grapes. Therefore other PME genes, with no cross-reactivity with *pme*1, may be expressed before ripening (phase I).

Different kinetic properties of PME isoforms can reflect different physiological functions. For instance, the PE-C form of tomato PME is more effective on pectins with low DE than other isoforms (Warrilow and Jones; 1995). In the present study, the lack of *pme*1 mRNAs in green stages may be explained by similar mechanisms. Nevertheless, according to the expression pattern of mRNAs obtained, the partial length cDNA isolated in the present study can be considered as an early marker of *veraison*. In order to elucidate the presence of several

PME isoforms, lower stringency conditions and/or Southern blots will be necessary.

During phase I, the thickening, and expansion of cell walls was accompanied by a marked increase of newly synthesized homogalacturonans. The growth of berries after the onset of ripening is mainly due to the accumulation of sugars and to water influx but is also due to the synthesis of wall material (Nunan et al., 1998). During phase II and III, CWM and homogalacturonans accumulated more slowly, corresponding with slower cell enlargement and thinning of walls to accommodate fruit expansion (Fougère-Rifot et al., 1996). However, biosynthesis in phase I and II is not sufficient to offset thickening and enlargement of walls.

The total amount of uronic acids per berry increased rapidly during phase I and more slowly during phases II and III. The continuous accumulation of uronic acids throughout berry development can be explained by the bio synthesis of highly methyl-esterified homogalacturonans (Liners and VanCutsem, 1992).

Total pectins from Muscat Gordo grapes (Nunan et al., 1998) decline from 58%, two weeks before *veraison*, to reach 47% four weeks after *veraison*. The large decrease observed during the development of Ugni blanc grapes may be cultivar-specific.

Immunocytochemical studies of carrot cells revealed that pectins of different DE can be located separately inside primary walls and middle lamellae (Liners and VanCutsem, 1992). In the present study, DE values are averages calculated for total pectins which are in fact a mixture of "old" de-esterified and de novo synthesized, highly methylated pectins (Liners and VanCutsem, 1992). The average DE value decreased in two steps during berry development and was not strictly correlated with the pattern of PME activity (expressed either as total or as "specific" activity). This might suggest the presence of other PME isoforms and a precise regulation mechanism of the activity of these isoenzymes. As the activity of PME in the cell wall was constant and DE decreased throughout maturation, different isoforms of PME could be expressed at specific stages of development. However, in vitro determination of PME activity does not necessarily reflect the in vivo regulation of the enzyme. Even though PME activity was not strictly correlated with DE values of the cell wall, the observed decrease of DE indicates that PME(s) play(s) a major role in the development of grape berries, possibly by allowing the action of depolymerases such as polygalacturonase.

Further analysis of polysaccharides present in these HEPES extracts and the determination of the molecular size distribution of pectic polysaccharides (CWM and extracts) could be a key to understanding the mechanism of solubilization and depolymerization of pectins during grape berry ripening. Further work needs to be done in order to elucidate the substrate and product specificity, and conditions for optimal activity of the different PME isoenzymes that may be involved in important cell wall changes associated with grape berry development.

4. Experimental

4.1. Plant material

Grape berries (*Vitis vinifera* L., cv. Ugni blanc) were harvested (Domaine du Chapître, INRA, Villeneuve-Les-Maguelone, France) weekly from June to September during 1996 and 1997. Berries were immediately cooled to 4 °C and separated according to their diameter until *veraison* (week 7) and according to their density (determined by flotation in several sucrose solutions) after softening occurred. A randomly chosen sample (30 berries) was kept aside for further characterization as described below. Whole berries were frozen in liquid nitrogen (less than 2 h after harvest), deseeded and powdered with a ball blender (Dangoumau). The resulting ground berries were stored at −80 °C and further used for total RNA, protein and cell wall extractions.

4.2. Berry measurements

For each sample, the average diameter, fresh and dry (by lyophilisation) weight of berries were determined. The musts from squeezed berries were used to measure pH and total soluble solids (degrees Brix determined by using an ATAGO N1 hand refractometer).

4.3. Isolation of total RNA

Total RNA isolation was performed on 5 g aliquots of ground berries. Total RNA concentration and purity were estimated by measurement of absorbance at 230, 260 and 280 nm. The quality of the RNA was checked with 1% agarose gel electrophoresis (Tesnière and Vayda, 1991).

4.4. Isolation of partial cDNA clones

Total RNAs (15 μg) extracted from pre-mature berries (week 8) were used as a template for reverse-transcription (RT) reactions according to the supplier's protocol (SuperScript™ II, Gibco BRL, Life Technologies). Degenerate PCR primers obtained by sequence alignments were kindly supplied by Dr B. Fils-Lycaon (Unité de Technologie des Produits Végétaux, INRA Avignon, France). The primers used in the RT-PCR were originally discribed to amplify a PME fragment of apricot fruit (*Prunus armeniaca*). The sequences were obtained by sequence alignment with other fruit PMEs in conserved regions, corresponding to the COOH

terminal region (AA 333–428) of a peach (*Prunus persica*) sequence.

Deduced degenerate oligonucleotides were synthesized with the sequences 5′-GA(C/T)G(G/C)IT(A/T)(C/T)CA(A/G)GA(C/T)ACICTIT-3′ (upstream primer, corresponding to DGFQDTLY) and 5′-TTCCAIGGIC(G/T)ICCNAG(A/G)TA-3′ (downstream primer, corresponding to YLGRPWK of the amino acid sequences) respectively, where I is inosine, an analogue to G, and N is all 4 nucleotides. Cycles (40 repeats) of specific amplification by PCR (MiniCycler™ MJ Research) were performed as follows: 94 °C 1 min, 42 °C 1 min and 72 °C 1 min. PCR products were separated on a 1.2% agarose gel electrophoresis (Nusieve® GTG®, FMC®) and purified using a gel extraction kit (JETsorb, Genomed). The purified PCR fragments were cloned in pGEM®-T Easy vector (Promega). DNA sequences were performed with the Taq DyeDeoxy™ Terminator Cycle Sequencing Kit (Applied Biosystems, Inc) using SP6 and T7 primers, and were analysed with an ABI (model 373A, Applied Biosystems, Inc) sequencer. Analysis of the cloned sequences was performed by a similarity search using the BLASTX + BEAUTY Web site.

4.5. Northern blot analyses

For northern blot analyses, 15 μg of total RNAs were loaded onto a 1.2% denaturing agarose-formaldehyde gel electrophoresis, running for 3 h (80 mV) and transferred onto a nylon membrane (Hybond™-N, Amersham) during 20 h. cDNA probes used were obtained by *Eco* RI digestion (5 u/μg DNA, 2 h at 37 °C). ^{32}P labelled probes were obtained from 50 ng cDNA according to the Megaprime DNA labelling system (random priming, Amersham). ^{32}P dCTP and non-labelled nucleotides were discarded by NICK™ Columns (Pharmacia Biotech) purification. Membranes were pre-hybridized in 5×SSC, 5× Denhardt's solution, 0.5% SDS and 300 μg/ml of denatured salmon sperm DNA during 4 h at 65 °C. Labelled probes were added to the pre-hybridization buffer (1.10^6 cpm/ml buffer), and hybridization occurred at 65 °C for 20 h. Northern blots were washed stringently at 65 °C in 2×SSC, 0.1% SDS for 20 min (twice); 1×SSC, 0.1% SDS for 20 min and a rapid final wash in 0.1×SSC at room temperature. Autoradiography was performed with Blue XB-1 imaging film (18×24 cm, Kodak) at −80 °C. Signals on the hybridized membranes were quantified by SigmaGel (Jandel Scientific).

4.6. Extraction of total proteins

All steps were performed at 4 °C. Aliquots of ground berries (5 g each) were homogenised for 15 h in 10 ml of 0.5 M Tris-HCl pH 8.5, containing 1% Triton X-100 (w/v), 20% glycerol (v/v), 5% polyvinylpyrrolydone (w/v), 2 M NaCl and 20 mM ß-mercaptoethanol. The suspension was then centrifuged at 17,000×*g* for 30 min. The whole extraction procedure was repeated on the pellets. Supernatants (ca. 25 ml) were pooled and ammonium sulphate was slowly added up to 100% saturation, the suspension was then stirred for 2 h and left to stand for 12 h at 4 °C. The precipitated proteins were removed and redissolved in 5 ml of 0.1 M sodium phosphate pH 7.5 to give the crude extract used for the determination of PME activity.

4.7. Determination of PME activity

The PME activity in crude protein extracts was determined by following the release of methanol (Klavons and Bennett, 1986) from citrus pectin (Fluka AG, M_r ca. 25,000–50,000), all assays being performed in triplicate for the 2 harvests 1996 and 1997. Aliquots of crude protein extracts (10 μl each) were diluted 10-fold in 0.1 M sodium phosphate, pH 7.5 to which was added 1 ml 0.05% (w/v) citrus pectin in the same buffer and transferred into screw-cap tubes. The reaction rates of methyl hydrolysis were checked at several time points. Finally, the mixture was incubated 30 min at 30 °C and the reaction was stopped by boiling for 10 min. Alcohol oxidase (1 unit/ml, Sigma A-2404) was added and incubated 15 min at 25 °C. A 2 ml solution of 20 mM 2,4-pentanedione in 2 M ammonium acetate 50 mM acetic acid was added and the reaction mixture was incubated at 60 °C for 15 min (Klavons and Bennett, 1986). The absorbance was then measured at 412 nm against the same reaction mixture incubated with a boiled crude extract. The amount of methanol released allowed the determination of PME activity expressed in nkat.

4.8. Purification of grape berry cell walls

The procedure of purification was adapted from Huber (1991). All steps prior to phenol extraction were performed at 4 °C. The ground "powder" (5 g) obtained by milling whole deseeded grape berries in liquid nitrogen was thawed for 2 h in 25 ml of 40 mM HEPES pH 7.0 and centrifuged at 10,000×*g* for 30 min. Extraction was repeated twice with 25 ml HEPES. Lipids and bound proteins were extracted from insoluble pellets with 25 ml of buffered phenol in 0.5 M Tris–HCl pH 7.5 under agitation (20 °C, 60 min). Supernatants were eliminated by centrifugation (23,000×*g*, 30 min, 20 °C). This procedure was repeated once. Phenol was then removed by treatment with chloroform followed by filtration (filters Sartorius, Teflon®, 47 mm, 0,45 μm) under vacuum. Cell wall material (CWM) was freeze-dried and stored overnight in a vacuum oven at 55 °C in the presence of P_2O_5 and weighed. Finally, CWM was finely milled in liquid nitrogen with a Spex 6700 Freezer-mill for 5 min (top impact frequency), stored under vacuum at 55 °C in the presence of P_2O_5 and weighed.

4.9. Analysis of cell walls

All procedures were carried out on ca. 5 mg of dried CWM. Uronic acids were measured in triplicate by the *m*-hydroxydiphenyl method (Blumenkrantz and Absoe-Hansen, 1973) using polygalacturonic acid (sodium-salt 85–90%, Sigma) as a standard (0 to 20 μg range), with a preliminary dissolution of the CWM in concentrated sulphuric acid 98%. The degree of methyl-esterification of HGs was determined by saponification of CWM and enzymic oxidation of methanol released by alcohol oxidase, as described earlier.

Acknowledgements

The authors wish to thank Dr. Fils-Lycaon (Unité de Technologie des Produits Végétaux, INRA Avignon, France) for supplying PCR primers. We also gratefully thank C. Tesnière (Unité de Recherches de Biochimie Métabolique et Technologie, INRA-IPV, France) and P. Williams (Unité de Recherches Biopolymères et Arômes, INRA-IPV, France) for their technical assistance.

References

Blumenkrantz, N., Asboe-Hansen, G., 1973. New method for quantitative determination of uronic acids. Analytical Biochemistry 54, 484–489.

Carpita, N.C., Gibeaut, D.M., 1993. Structural models of primary cell walls in flowering plants: consistency of molecular structure with the physical properties of the walls during growth. Plant Journal 3, 1–30.

Christensen, T.M.I.E., Nielsen, J., Kreiberg, J., Rasmussen, P., Mikkelsen, J.D., 1998. Pectin methyl esterase from orange fruit: characterization and localization by in-situ hybridization and immunochemistry. Planta 206, 493–503.

Davies, C., Robinson, S.P., 2000. Differential screening indicates a dramatic change in mRNA profiles during grape berry ripening. Cloning and characterization of cDNAs encoding putative cell wall and stress response proteins. Plant Physiology 122, 803–812.

Fischer, R.L., Bennett, A.B., 1991. Role of cell wall hydrolases in fruit ripening. Annual Review of Plant Physiology and Plant Molecular Biology 42, 675–703.

Fougère-Rifot, M., Cholet, C., Bouard, J., 1996. Evolution des parois des cellules de l'hypoderme de la baie de raisin lors de leur transformation en cellules de pulpe. Journal International Scientifique de la Vigne et du Vin 30, 47–51.

Gaffé, J., Tieman, D.M., Handa, A.K., 1994. Pectin methylesterase isoforms in tomato (*Lycopersicon esculentum*) tissues: effect of expression of a pectin methylesterase antisense gene. Plant Physiology 105, 199–203.

Glover, H., Brady, C.J., Lee, E., Speirs, J., 1996. Multiple pectin esterase genes are expressed in ripening peach fruit: nucleotide sequence of a cDNA encoding peach pectin esterase. Plant Physiology 112, 864.

Huber, D.J., 1991. Acidified phenol alters tomato cell wall pectin solubility and calcium content. Phytochemistry 30, 2523–2527.

Iannetta, P.P.M., Van den Berg, J., Wheatley, R.E., McNicol, R.J., Davies, H.V., 1999. The role of ethylene and cell wall modifying enzymes in raspberry (*Rubus idaeus*) fruit ripening. Physiologia Plantarum 105, 338–347.

Kanellis, A.K., Roubelakis-Angelakis, K.A., 1993. Grape. In: Seymour, G.B., Taylor, J.E., Tucker, G.A. (Eds.), Biochemistry of Fruit Ripening. Chapman & Hall, London, pp. 189–234.

Klavons, J.A., Bennett, R.D., 1986. Determination of methanol using alcohol oxydase and its application to methyl ester content of pectins. Journal of Agricultural and Food Chemistry 34, 597–599.

Lecas, M., Brillouet, J.-M., 1994. Cell wall composition of grape berry skins. Phytochemistry 35, 1241–1243.

Lee, C.Y., Smith, N.L., Nelson, R.R., 1979. Relationship between pectin methylesterase activity and the formation of methanol in Concord grape juice and wine. Food Chemistry 4, 143–148.

Liners, F., VanCutsem, P., 1992. Distribution of pectic polysaccharides throughout walls of suspension-cultured carrot cells. An immunocytochemical study. Protoplasma 170, 10–21.

Marteau, G., Scheur, J., Olivieri, C., 1961. Cinétique de la libération enzymatique du méthanol au cours des transformations pectolytiques du raisin. Annales de Technologie Agricole 10, 161–183.

Micheli, A., Sundberg, B., Goldberg, R., Richard, L., 2000. Radial distribution pattern of pectin methylesterases across the cambial region of hybrid aspen at activity and dormancy. Plant Physiology 124, 191–199.

Nairn, C.J., Lewandowski, D.J., Burns, J.K., 1998. Genetics and expression of two pectinesterase genes in Valencia orange. Physiologia Plantarum 102, 226–235.

Nunan, K.J., Sims, I.M., Bacic, A., Robinson, S.P., Fincher, G.B., 1998. Changes in cell wall composition during ripening of grape berries. Plant Physiology 118, 783–792.

Ray, J., Knapp, J., Grierson, D., Bird, C., Schuch, W., 1988. Identification and sequence determination of a cDNA clone for tomato pectin esterase. European Journal of Biochemistry 174, 119–124.

Seymour, G.B., Gross, K.C., 1996. Cell wall disassembly and fruit softening. Postharvest News and Information 7, 45N–52N.

Seymour, T.A., Preston, J.F., Wicker, L., Lindsay, J.A., Marshall, M.R., 1991. Purification and properties of pectinesterases of Marsh white grapefruit pulp. Journal of Agricultural and Food Chemistry 39, 1080–1085.

Tesnière, C., Vayda, M.E., 1991. Method for the isolation of high-quality RNA from grape berry tissues without contaminating tannins or carbohydrates. Plant Molecular Biology Report 9, 242–251.

Thakur, B.R., Singh, R.K., Handa, A.K., 1996. Effect of a antisense pectin methylesterase gene on the chemistry of pectin in tomato (*Lycopersicon esculentum*) juice. Journal of Agricultural and Food Chemistry 44, 628–630.

Tieman, D.M., Harriman, R.W., Ramamohan, G., Handa, A.K., 1992. An antisense pectin methylesterase gene alters pectin chemistry and soluble solids in tomato fruit. Plant Cell 4, 667–679.

Warrilow, A., Jones, M., 1995. Different forms of tomato pectinesterase have different kinetic properties. Phytochemistry 39, 277–282.

PERGAMON

Phytochemistry 58 (2001) 703–707

PHYTOCHEMISTRY

www.elsevier.com/locate/phytochem

Effect of *Mentha* × *piperita* essential oil and monoterpenes on cucumber root membrane potential

Massimo Maffei*, Wanda Camusso, Silvano Sacco

Department of Plant Biology, University of Turin, Viale P.A. Mattioli 25, I-10125 Torino, Italy

Received 12 February 2001; received in revised form 2 July 2001

Abstract

Peppermint (*Mentha piperita* L.) essential oil and its main components were assessed for their ability to interfere with plant plasma membrane potentials. Tests were conducted on root segments isolated from etiolated seedlings of cucumber (*Cucumis sativus* L.). Increasing the concentration of peppermint essential oil from 5 to 50 ppm caused a decrease in membrane potential (V_m) hyperpolarization of 10–3 mV, whereas concentrations from 100 up to 900 ppm caused an increasing depolarization of V_m (from 5 to 110 mV). When tested at 300 ppm, (+)-menthyl acetate, (−)-limonene and 1,8-cineole did not exert any significant effect on V_m, whereas (+)-menthofuran (73 mV), (+)-pulegone (85 mV), (+)-neomenthol (96 mV), (−)-menthol (105 mV) and (−)-menthone (111 mV) showed increased ability to depolarize V_m. A plot of log of octanol–water partition coefficient (K_{ow}) against their depolarizing effect showed a significant negative correlation, suggesting that among all monoterpenoids increased membrane depolarization depends on lower K_{ow}. However, among monoterpene ketones, alcohols and furans, increased membrane depolarization is associated with a decline in water solubility. The possible effect of monoterpenoids on membrane ion fluxes is also discussed, since changes in the bioelectric potential of cells imply changes in the flux of ions across the plasma membrane © 2001 Published by Elsevier Science Ltd.

Keywords: *Mentha* × *piperita*; Labiatae; Peppermint; *Cucumis sativus*; Cucumber; Root membrane potentials; Monoterpene water solubility; Membrane depolarization; Essential oils; (+)-Pulegone; (−)-Menthol; (−)-Menthone; (+)-Neomenthol

1. Introduction

Membrane potential (V_m) results from an imbalance in the number of cations and anions across biological membranes. However, the binding of many plant natural products to membranes causes conformational changes in the ion channels and membrane-bound proteins, increasing or decreasing ion flow (Warber, 1998). Higher plants synthesize a great variety of terpenoid natural products, which can be involved in plant-plant, plant-pathogen and plant-herbivore interactions. Monoterpenoids are the major components of some essential oils: they have toxic effects on seed germination (Robinson, 1983; Rice, 1984), growth of some bacterial strains (Knobloch et al., 1989; Economou and Nahrstedt, 1991), development and growth of some insects (Lee et al., 1999), growth of pathogenic fungi (Adam et al., 1998), and interact at the cell level with cytosolic Ca^{2+}, probably through an intracellular Ca^{2+} store release (Takeuchi et al., 1994) and Ca^{2+} channel blocking (Taylor et al., 1985; Hills and Aaroson, 1991). Due to the relative hydrophobicity of most monoterpenoids, it is postulated that these compounds would accumulate in biological membranes (Griffin et al., 2000), and thus could affect ion flow.

Previous studies have demonstrated that peppermint (*Mentha piperita* L.) essential oil and its main monoterpenoid components are able to interfere with cucumber (*Cucumis sativus* L.) root respiratory functions (Mucciarelli et al., 2001). In particular, (+)-pulegone was found to be the most toxic compound for root and mitochondrial respiration. (−)-Menthone had less inhibiting action than (+)-pulegone, whereas (−)-menthol was the least inhibitory compound tested. In the same study it was noted that terpenoids had a greater inhibition on the respiration of intact cucumber root segments than on isolated root mitochondria, suggesting that inhibition was probably due to terpenoid interaction

* Corresponding author. Tel.: +39-011-658387; fax.: +39-011-6707459.

E-mail address: massimo.maffei@unito.it (M. Maffei).

0031-9422/01/$ - see front matter © 2001 Published by Elsevier Science Ltd.
PII: S0031-9422(01)00313-2

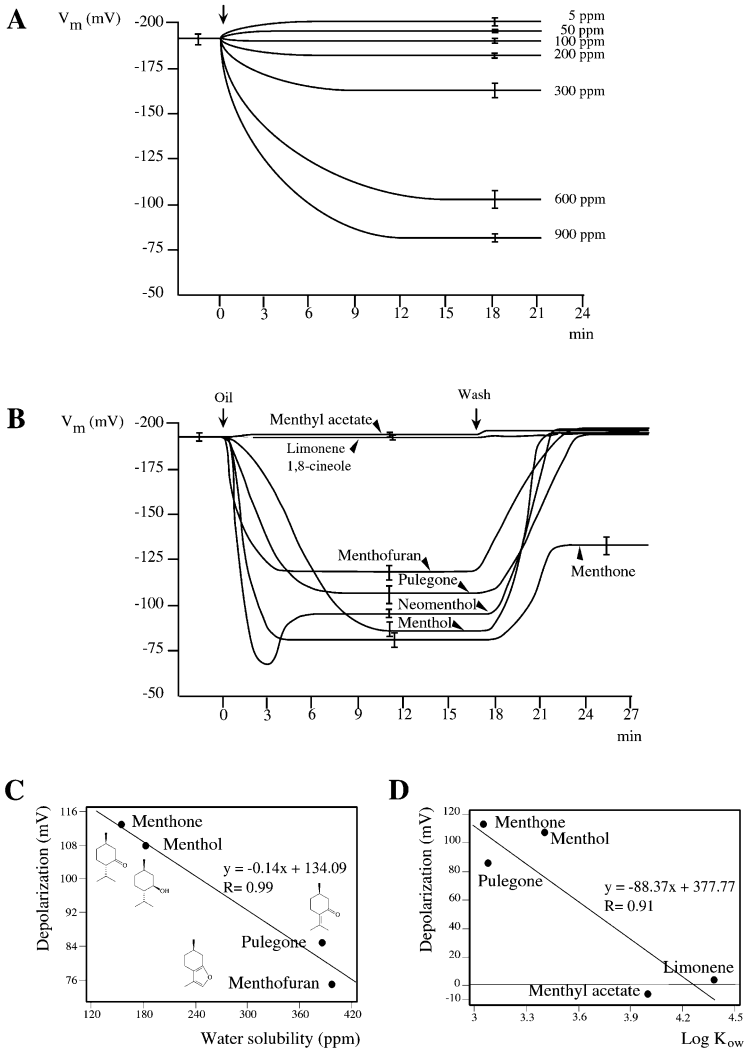

Fig. 1. A. Effect of increasing peppermint oil concentrations on transmembrane potential (V_m). Essential oil concentrations up to 50 ppm induce a slight hyperpolarization, whereas concentrations greater than 100 ppm cause a drastic membrane depolarization. Arrow indicates the starting time of essential oil perfusion. B. Effect of some essential oil components used at 300 ppm on V_m. (−)-Limonene and 1,8-cieneole do not exert any significant effect, wherease menthyl acetate caused a slight hyperpolarization. (+)-Neomenthol perfusion caused a rapid and transient depolarization of V_m which reaches a steady depolarized value after a few minutes. The depolarizing effect of all compounds, except (−)-menthone, is annulled by washing root segments with a fresh buffer solution. Arrows indicate the starting time of component perfusion (oil) and the starting time when a fresh buffer solution was perfused (Wash). C. Plot of the depolarizing value of some oxygenated monoterpenes tested against their water solubility. A negative correlation was found between depolarizing effect and water solubility of compounds. D. Plot of the depolarizing value of some monoterpene tested against log of octanol–water partition coefficient (K_{ow}) as reported by Griffin et al. (1999). Even in this case a significant negative correlation was found between depolarizing effect and log K_{ow} of compounds. For all plots, bars indicate standard deviation.

with cell walls and plasma membranes (Mucciarelli et al., 2001). A interaction of terpenoids with the plasma membrane could trigger the initiation of a series of physiological responses via intracellular transduction pathways (Kombrink and Somssich, 1995). Besides, interaction of terpenes may alter ion permeability and fluxes across the plasma membrane, possibly triggering an oxidative burst as observed in some plant cell systems after elicitor treatments (Nürnberger et al., 1994).

The aim of the present work was the evaluation of the effect of peppermint essential oil and individual oil components on transmembrane potential in root cells of *Cucumis sativus*.

2. Results and discussion

The essential oil of the peppermint plants used in this study was characterized by the presence of the oxygenated monoterpene compounds, (−)-menthol (40.53%), (−)-menthone (14.63%), (+)-menthofuran (4.32%), (+)-menthyl acetate (4.07%) (+)-pulegone (0.80%) and (+)-neomenthol (2.02%) along with substantial percentages of the monoterpene oxide 1,8-cineole (6.53%) and the olefin (−)-limonene (2.57%). Minor mono- and sesquiterpenes as reported earlier (Maffei and Sacco, 1987) made up the remainder of the oil composition.

Perfusion of cucumber root segments with increasing concentrations of peppermint essential oil caused a significant change in the V_m (Fig. 1A). Perfusion with peppermint oil at 5 and 50 ppm prompted a significant membrane hyperpolarization, whereas increased depolarization was observed with oil concentrations from 100 up to 900 ppm. Depolarizing and hyperpolarizing effects were fully reversible by washing root segments with a fresh buffered solution (data not shown). These results parallel previous studies in which there was a positive correlation between peppermint oil concentration and inhibition of cucumber root and mitochondrial respiration for concentrations ranging from 50 to 900 ppm (Mucciarelli et al., 2001).

In order to understand which of the oil components was responsible for the depolarizing effects, (+)-pulegone and some other oil components were perfused at 300 ppm on root membranes and the V_m measured (Fig. 1B). Perfusion with 300 ppm (−)-menthyl acetate, caused a slight and not significant membrane hyperpolarization, whereas 300 ppm (−)-limonene and 300 ppm 1,8-cineole did not cause any significant V_m variation. Increasing root membrane V_m depolarization was observed when (+)-menthofuran, (+)-pulegone, (+)-neomenthol, (−)-menthol and (−)-menthone were applied at 300 ppm (Fig. 1B). Washing out of all compounds with fresh buffer prompted a membrane hyperpolarization with full recovery of the original V_m for all compounds except (−)-menthone, for which root membrane V_m remained depolarized even after washing. In particular, (+)-neomenthol and (−)-menthone induced a very rapid membrane depolarization, with (+)-neomenthol showing a transient depolarization of at least 130 mV (S.E. ± 1.7), followed by a slight hyperpolarization, to end up at a net depolarized V_m. This observation suggests that monoterpenoids interact reversibly with the plasma membrane [except (−)-menthone, for which recovery of V_m was only partial], probably by affecting ion channels or acting as pore-forming molecules, as demonstrated in artificial lipid bilayers (Griffin et al., 2000). These data are also in agreement with previous data on cucumber root respiration inhibition, where washing of cucumber root and mitochondria with a fresh solution recovered initial respiratory levels (Mucciarelli et al., 2001).

Assuming that V_m depolarization caused by 600 ppm of essential oil was additive and dependent on the relative percentage of each component in the total oil (Fig. 1A), and assuming the oil composition is as stated above, it is possible to extrapolate that when tested at 300 ppm (Fig. 1B) (−)-menthol was tested 1.23 times (40.53% of 600 ppm total oil = 243 ppm menthol; 300 ppm /243 ppm = 1.23), (−)-menthone 3.41 times, (+)-menthofuran 26.09 times, (+)-pulegone 75 times, (+)-neomenthol 25 times, (−)-menthyl acetate 12.5 times, (−)-limonene 18.75 times and 1,8-cineole 7.5 times greater than the concentration expected in 600 ppm of the total essential oil. Thus, (−)-menthol appears to be the main component responsible for depolarization of V_m by the total essential oil, followed by (−)-menthone. (+)-Pulegone, used at 75 times the normal concentrations expected in a 600 ppm oil solution does not exceed (−)-menthol and/or (−)-menthone V_m depolarization.

The plot of V_m depolarization against the water solubility (WS, expressed in ppm) (Fischer, 1991; Weidenhamer et al., 1993) of some oil components (Fig. 1C) showed a significant negative correlation, with a direct correlation between V_m depolarization and lipophily of oxygenated monoterpenes. Fig. 1D shows the plot of V_m depolarization against the log of octanol–water partition coefficient (K_{ow}) for some of the monoterpenoids tested, as reported by Griffin et al. (1999). Also in this case a significant negative correlation was observed, with decreasing V_m depolarization values with increasing log K_{ow}. Recent findings have shown that monoterpenes affect biological membranes by damaging their structure and changing their lipid packing density which increases ion permeability and perturbs membrane-bound enzyme function (Griffin et al., 2000). Our results suggest that decreasing water solubility of monoterpenes increases the possibility for terpenoids to interact with and disrupt membrane integrity, thus causing a rapid and reversible membrane V_m depolarization. These data parallel previous investigations done on antimicrobial activity (Knobloch et al., 1989), toxicity in plant cell cultures (Brown et al., 1987), and inhibition of tissue (Fisher, 1986; 1991) and mitochondria respiration (Mucciarelli et al., 2001).

Changes in the bioelectric potential of cells imply changes in the flux of ions across the plasma membrane. Changes in membrane potential initiate several signal transduction pathways (Sanders and Bethke, 2000). Preliminary data on (−)-menthol-induced increase of cucumber root cytosolic free calcium ions, $(Ca^{2+})_i$, (Maffei and Camusso, 2000) suggest that (−)-menthol could play an important role in early events in the signal transduction pathway. Ca^{2+} channels are activated by membrane depolarization; by implication, signals that elicit membrane depolarization, such as the action on some monoterpenes, could trigger entry of Ca^{2+} from the external medium (Sanders and Bethke, 2000). Moreover, opening of anion channels not only results in a loss of Cl^- from the cytosol but also in membrane depolarization (see also Swandulla et al., 1986; Hawthorn et al., 1988; Hills and Aaronson, 1991; Chiyotani et al., 1994; Dierkes et al., 1997). Anion channel opening appears to be an early event in many signal transduction pathways and probably leads to the activation of voltage-gated Ca^{2+} channels (Sanders and Bethke, 2000).

A direct comparison of the present data with our previous results (Mucciarelli et al., 2001) indicates that

(+)-pulegone, which acts as a possible uncoupling agent of cucumber root and mitochondria respiration, has little effect on membrane potential, whereas (−)-menthol shows an almost 100-fold V_m depolarizing action with respect to (+)-pulegone, although (−)-menthol has less inhibitory action on root respiration. The fact that (−)-menthol is more disruptive to membrane potential, while (+)-pulegone inhibits root respiration more readily could be an explanation why plants make mixtures of monoterpenes; perhaps they can have different modes of action. For allelopathic purposes, it may be useful for a plant to have more than one kind of weapon at its disposal.

Since monoterpenes can cause such extensive membrane depolarization, they are clearly toxic to plant cells. Perhaps this is why they are often found to be sequestered in secretory structures (Gershenzon et al., 2000).

Further studies are under way to understand better the effect of monoterpenes on membrane ion equilibrium and their direct and indirect involvement in the signal transduction pathway.

3. Experimental

3.1. Plant material and seed germination

Cucumber (*Cucumis sativus* L. var. ''Piccolo di Parigi'') seeds were purchased from Franchi Sementi, Bergamo, Italy. Seeds were washed with tap water for 4 h and then placed for 48 h in the dark (20 °C isothermal) on 9 cm Petri dishes containing 2 paper filters saturated with 5 ml of 5 mM MES-Na (2-[*N*′-morpholino] ethanesulfonic acid sodium salt) buffer, pH 6.0, with the addition of 0.5 mM $CaSO_4$. Peppermint (*Mentha* × *piperita* L.) plants were grown in experimental plots of the Botanical Garden of the University of Torino, and were distilled when in full bloom.

3.2. Essential oil distillation and chemicals

Peppermint oil was steam distilled by using a modified Clevenger apparatus as reported earlier (Mucciarelli et al., 2001). Essential oil GC analyses and compound identification were performed as reported elsewhere (Maffei et al., 1999). (−)-Menthol, (−)-menthyl acetate, (+)-neomenthol, (−)-menthone, (+)-pulegone, (−)-limonene, 1,8-cineole and (+)-menthofuran (purity > 99%) were purchased from Sigma-Aldrich (Milano, Italy).

3.3. Root segment membrane potential determination

For treatments and controls, 15 seeds per each of 10 Petri dishes were incubated in the dark at 28 °C. Three days after germination, roots of seedlings were used for membrane potential determination. Membrane potentials were determined in root segments. The transmembrane potential (V_m) was determined in the root elongating zone with glass micropipettes with a tip resistance of 4–10 MΩ and filled with 1 M KCl. Micropipettes were used as micro-salt bridges to Ag/AgCl electrodes and inserted vertically in the tissue by means of a Narishige micromanipulator (Sacco and Maffei, 1997). Cucumber roots were always equilibrated for 60 min in 5 mM MES-Na (pH 6.0).

3.4. Effect of essential oil and essential oil component upon membrane potential

V_m from root segments of control seedlings germinated for three days in the dark were measured for ca. 30 min, then perfusion was carried on with the addition of increasing concentrations of total essential oil (from 5 to 900 ppm). Root segments were also perfused with 300 ppm of (+)-pulegone and other oil components. Total essential oil and oil components were dissolved in methanol ($\leqslant 0.4\%$) which was present in both treatments and controls. Water solubility values were obtained from Smyrl and Le Maguer (1980) and Weidenhamer et al. (1993), whereas values of Log octanol-water partition coefficient (K_{ow}) were obtained from Griffin et al. (1999).

3.5. Statistics

At least five replicates were performed for each experiment. The data obtained were analyzed by standard ANOVA using Systat 5.2 software for Macintosh. Significant differences are intended at $P < 0.05$.

Acknowledgements

The authors wish to thank Elena Condini for technical support during V_m measurements. This work was supported by a grant from M.U.R.S.T. to M. Maffei

References

Adam, K., Sivropoulou, A., Kokkini, S., Lanaras, T., Arsenakis, M., 1998. Antifungal activities of *Origanum vulgare* subsp. Hirtum, *Mentha spicata*, *Lavandula angustifolia* and *Salvia fruticosa* essential oils against human pathogenic fungi. J. Agric. Food Chem. 46, 1739–1745.

Brown, J.T., Hegarty, P.K., Charlwood, B.V., 1987. Mono- and sesquiterpene biosynthesis in plant cells in culture. Part 4. The toxicity of monoterpenes to plant cell cultures. Plant Sci. 48, 195–201.

Chiyotani, A., Tamaoki, J., Takeuchi, S., Kondo, M., Isono, K., Konno, K., 1994. Stimulation by menthol of Cl secretion via a Ca^{2+}-dependent mechanism in canine airway epithelium. Br. J. Pharmacol. 112, 571–575.

Dierkes, P.W., Hochstrate, P., Schlue, W.R., 1997. Voltage-dependent Ca^{2+} influx into idenified leech neurones. Brain Res. 746, 285–293.

Economou, D., Nahrstedt, A., 1991. Chemical, physiological, and toxicological aspects of the essential oil of some species of the genus *Bystropogon*. Planta Med. 57, 347–351.

Fischer, N.H., 1986. The function of mono and sesquiterpenes as plant germination and growth regulators. In: Putnam, A.R., Tang, C.-S. (Eds.), The Science of Allelopathy. Whiley-Interscience, New York, pp. 203–218.

Fischer, N.H., 1991. Plant terpenoids as allelopathic agents. In: Harborne, J.B., Tomas-Barberan, F.A. (Eds.), Ecological Chemistry and Biochemistry of Plant Terpenoids. Oxford Science Publications, Oxford, pp. 377–398.

Gershenzon, J., McConkey, M.E., Croteau, R., 2000. Regulation of monoterpene accumulation in leaves of peppermint. Plant Physiol. 122, 205–213.

Griffin, S., Grant Wyllie, S., Markham, J.L., 1999. Determination of octanol-water partition coefficient for terpenoids using reversed-phase high performance liquid chromatography. J. Chromatog. A 864, 221–228.

Griffin, S., Markham, J.L., Dennis, G., Grant Wyllie, S., 2000. Using atomic force microscopy to view the effects of terpenoids on the stability and packing of phosphatidylcholine supported lipid bilayers. Proceedings 31st International Symposium on Essential Oils, Hamburg, 10–13 September.

Hawthorn, M., Ferrante, J., Luchowski, E., Rutledge, A., Wei, X.Y., Triggle, D.J., 1988. The actions of peppermint oil and menthol on calcium channel dependent processes in intestinal, neuronal and cardiac preparations. Aliment. Pharmacol. Ther. 2, 101–118.

Hills, J.M., Aaronson, P.I., 1991. The mechanism of action of peppermint oil on gastrointestinal smooth muscle. An analysis using patch clamp electrophysiology and isolated tissue pharmacology in rabbit and guinea pig. Gastroenterology 101, 55–65.

Knobloch, K., Pauli, A., Iberl, B., Weigand, H., Weis, N., 1989. Antibacterial and antifungal properties of essential oil components. J. Essent. Oil Res. 1, 119–128.

Kombrink, E., Somssich, I.E., 1995. Defense responses of plants to pathogens. Adv. Bot. Res. 21, 1–34.

Lee, S., Tsao, R., Coats, J.R., 1999. Insecticidal activity of monoterpenoids to western corn rootworm (Coleoptera: Chrisomelidae), twospotted spider mite (Acari: Tetranychidae) and house fly (Diptera: Muscidae). J. Econ. Entomol. 92, 56–67.

Maffei, M., Sacco, T., 1987. Chemical and morphometrical comparison between two peppermint notomorphs. Planta Med. 2, 214–216.

Maffei, M., Camusso, W., 2000, Allelopathic effects of peppermint essential oil in higher plants: intracellular calcium variations. Proceedings 31st International Symposium on Essential Oils, Hamburg, 10–13 September.

Maffei, M., Canova, D., Bertea, C.M., Scannerini, S., 1999. UV-A effects on photomorphogenesis and essential-oil composition in *Mentha piperita*. J. Photochem. Photobiol. 52, 105–110.

Mucciarelli, M., Camusso, W., Bertea, C.M., Bossi, S., Maffei, M., 2001. Effect of (+)-pulegone and other oil components of *Mentha* x *piperita* on cucumber respiration. Phytochemistry 57, 91–98.

Nürnberger, T., Nennstiel, D., Jabs, T., Sacks, W.R., Hahlbrock, K., Scheel, D., 1994. High affinity binding of a fungal oligopeptide elicitor to parsley plasma membranes triggers multiple defense responses. Cell 78, 449–460.

Rice, E.L., 1984. Allelopathy, 2nd Edition. Academic, Orlando.

Robinson, T., 1983. The Organic Constituents of Higher Plants, 5th Edition. Cordus Press, North Amherst, MA.

Sacco, S., Maffei, M., 1997. The effect of isosakuranetin (5,7-dihydroxy 4′-methoxy flavanone) on potassium uptake in wheat root segments. Phytochemistry 46, 245–248.

Sanders, D., Bethke, P., 2000. Membrane transport. In: Buchanan, B., Gruissem, W., Jones, R. (Eds.), Biochemistry & Molecular Biology of Plants. American Society of Plant Physiologists, Rockville, MD, pp. 110–159.

Smyrl, T.G., Le Maguer, M., 1980. Solubilities of terpenic essential oil components in aqueous solutions. J. Chem. Eng. Data 25, 150–152.

Swandulla, D., Schafer, K., Lux, H.D., 1986. Calcium channel current inactivation is selectively modulated by menthol. Neurosci. Lett. 68, 23–28.

Takeuchi, S., Tamaoki, L., Kondo, M., Konno, K., 1994. Effect of menthol on cytosolic Ca^{2+} levels in canine airway epithelium in culture. Biochem. Biophys. Res. Commun. 201, 1333–1338.

Taylor, B.A., Duthie, H.L., Luscombe, D.K., 1985. Calcium antagonist activity of menthol on gastrointestinal smooth muscle. Br. J. Clin. Pharm. 20, 293–294.

Warber, S., 1998. Modes of action at target sites. In: Kaufman, P.B., Leland, J.C., Warber, S., Duke, J.A., Brielmann, H.L. (Eds.), Natural Products from Plants. CRC Press, Boca Raton, pp. 157–182.

Weidenhamer, J.D., Macias, F.A., Fischer, N.H., Williamson, G.B., 1993. Just how insoluble are monoterpenes. J. Chem. Ecol. 19, 1799–1807.

PERGAMON

Phytochemistry 58 (2001) 709–716

PHYTOCHEMISTRY

www.elsevier.com/locate/phytochem

Biosynthesis of ochratoxins by *Aspergillus ochraceus*

Jonathan P. Harris, Peter G. Mantle*

Biochemistry Department, Imperial College of Science, Technology and Medicine, London, SW7 2AY, UK

Received 19 January 2001; received in revised form 5 July 2001

Abstract

Shaken liquid fermentation of an isolate of *Aspergillus ochraceus* showed growth-associated production of ochratoxins A and B, followed by production of a related polyketide diaporthin. Later, between 150 and 250 h, mellein accumulated transitorily. In contrast, shaken solid substrate (shredded wheat) fermentation over 14 days produced mainly ochratoxins A and B (ratio ca. 5:1) in very high yield (up to 10 mg/g). In these systems experiments with ^{14}C-labelled precursors and putative intermediates revealed temporal separation of early and late stages of the ochratoxin biosynthetic pathway, but did not support an intermediary role for mellein. The pentaketide intermediate ochratoxin β was biotransformed very efficiently into both ochratoxins A and B, 14 and 19%, respectively. The already chlorinated ochratoxin α was only biotransformed significantly (4.85%) into ochratoxin A, indicating that chlorination is mainly a penultimate biosynthetic step in the biosynthesis of ochratoxin A. This was supported by poor (1.5%) conversion of radiolabelled ochratoxin B into ochratoxin A. Experiments implied that some ochratoxin B may arise by dechlorination of ochratoxin A. © 2001 Elsevier Science Ltd. All rights reserved.

Keywords: *Aspergillus ochraceus*; Pulse-radiolabeling; Shaken solid substrate fermentation; Ochratoxin A; Ochratoxin B; Ochratoxin α; Ochratoxin β; Mellein; Ethionine

1. Introduction

The mycotoxin ochratoxin A (OTA, **1**) (Fig. 1), first obtained from a South African *Aspergillus ochraceus* isolate (van der Merwe et al., 1965a), consists of a dihydroisocoumarin moiety (the pentaketide-derived ochratoxin α, **3**; Fig. 2) linked through the carboxyl group to phenylalanine. Corresponding des-chloro analogues are ochratoxins B (OTB, **2**) and β (**4**). Unlike ochratoxin α, ochratoxin β and mellein (**5**) have both been isolated from ochratoxinogenic *A. ochraceus* fermentations (Moore et al., 1972; Delgadillo, 1986).

^{14}C-labelled precursor feeding experiments and subsequent chemical degradation showed that phenylalanine was incorporated into OTA, whereas ochratoxin α was constructed from five acetate units with a one carbon addition at C-7 from methionine (Ferriera and Pitout, 1969; Searcy et al., 1969; Steyn et al., 1970). A crude cell-free enzyme preparation (OTA synthetase, requiring ATP and Mg^{++} ions) catalysed the linking of ochratoxin α with phenylalanine (Ferriera and Pitout, 1969). Wei et al. (1971) demonstrated incorporation of ^{36}Cl into OTA. The methylation inhibitor ethionine completely inhibited OTA production (Yamazaki et al. 1971).

The ^{13}C NMR spectrum of OTA was fully assigned by de Jesus et al. (1980); ochratoxinogenic fungal cultures fed [1-^{13}C] or [1, 2-$^{13}C_2$]acetate showed enhanced signals and ^{13}C–^{13}C coupling evidence supporting a pentaketide folding pattern similar to that in the biosynthesis of citrinin and mellein.

Huff and Hamilton (1979), recognising the lack of research in the pathway of OTA biosynthesis, proposed a scheme, although this unfortunately ignored the ubiquitous OTB. Subsequently, the ochratoxin polyketide synthase was reported to produce mellein; Abell et al., (1982) showed that there was no keto-enol tautomerism, but an unfunctionalised double-bond between C-6 and C-7 in the mellein pentaketide chain. Also, the carbonyl at C-3 may have been reduced to a hydroxyl prior to folding (Abell et al., 1983). The requisite methylation step was thought to occur after the production of mellein although the subsequent putative intermediates 7-methylmellein, 7-methoxymellein and 7-formylmellein

* Corresponding author. Tel.: +44-207-594-5245; fAx: +44-207-225-0960.

E-mail address: p.mantle@ic.ac.uk (P.G. Mantle).

0031-9422/01/$ - see front matter © 2001 Elsevier Science Ltd. All rights reserved.
PII: S0031-9422(01)00316-8

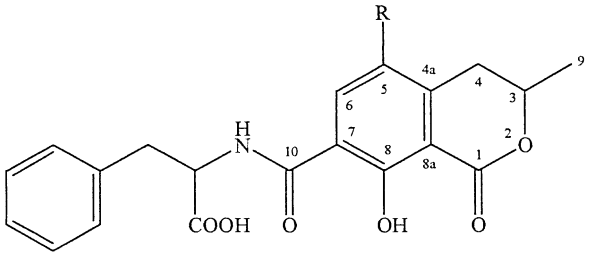

Ochratoxin A (**1**): R = Cl

Ochratoxin B (**2**): R = H

Fig. 1. Structures of the *Aspergillus ochraceus* mycotoxins ochratoxins A and B.

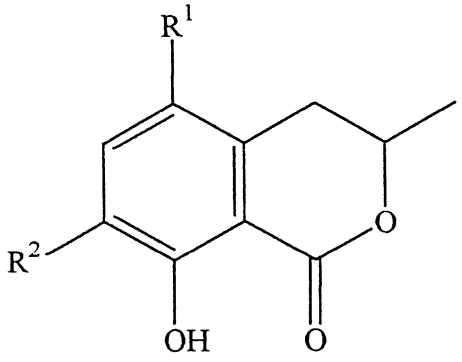

Ochratoxin α (**3**): $R^1 = Cl$; $R^2 = CO_2H$

Ochratoxin β (**4**): $R^1 = H$; $R^2 = CO_2H$

Mellein (**5**): $R^1 = R^2 = H$

Fig. 2. Structures of the dihydroisocoumarins ochratoxins α and β and mellein.

have not been isolated from fungal fermentation producing ochratoxins.

Chlorination of ochratoxin β by a chloroperoxidase was reasoned as occurring prior to joining the aromatic nucleus to phenylalanine via an acyl activated phosphoochratoxin α reacting with phenylalanine with its carboxy group protected by ethyl esterification. This reaction would result in ochratoxin C which could be transesterified to the OTA methyl ester, both of which OTA derivatives have been isolated from *A. ochraceus* cultures (van der Merwe et al. 1965b; Steyn and Holzapfel, 1967). Alternatively, ochratoxin C might be hydrolysed directly to OTA.

OTA, as a nephrotoxin and a carcinogen, is currently the subject of proposed EC legislation to place an upper limit of 5 μg/kg (5 ppb) in commodities for human food. It is timely, therefore, to contribute to the understanding of some fermentation dynamics of *A. ochraceus*, as one of the fungi involved in commodity spoilage, and of some later steps in the biosynthesis of ochratoxins.

2. Results and discussion

2.1. Experiments in shaken liquid fermentation

2.1.1. Culture dynamics

In potato dextrose broth, accumulation of biomass was complete within 3–4 days and was closely associated with production of ochratoxins (Fig. 3) (also noted by Steyn et al., 1970; Wei et al., 1971). There were also second and third temporal phases of secondary metabolite occurrence measured concerning the polyketides diaporthin (**6**; Fig. 4) and mellein.

Throughout the phase of ochratoxin occurrence there was a ratio of A:B of approximately 3:1. Diaporthin was also accompanied by approximately half the amount of orthosporin (de-*O*-methyl diaporthin; Harris and Mantle, 2001). The transitory appearance of mellein might plausibly be interpreted as reflecting cessation of involvement of this putative intermediate in ochratoxin biosynthesis after growth-associated production of the phenylalanine moiety declined. Alternatively, the observed temporal sequence of metabolites simply reflected progressive decline in biosynthetic complexity from ochratoxins (requiring phenylalanine, methionine, acetate and chlorine) to mellein which is solely derived from acetate.

2.1.2. Effect of ethionine

The only marked effect of the methylation inhibitor ethionine on accumulation of ochratoxins in submerged fermentation was on yield of OTA when added during early idiophase at 32 h (Table 1). This is consistent with methylation of the pentaketide occurring early in biosynthesis. The less obvious or nil effect on excreted OTB would be consistent with some of this arising by dechlorination of OTA.

2.1.3. Radioactivity experiment

Radiolabel from [1-^{14}C]acetate was incorporated into OTA when added as early as only 8 h into the fermentation; the finding demonstrated the close association of ochratoxin biosynthesis with replicatory growth (Table 2). The optimum time of addition of the polyketide precursor to achieve maximum specific radioactivity in OTA was at 22.5 h, consistent with a principle of maximum rate of isocoumarin biosynthesis preceding prominent occurrence of OTA in broth (Fig. 3). Reinterpretation of the data of Lillehoj et al.

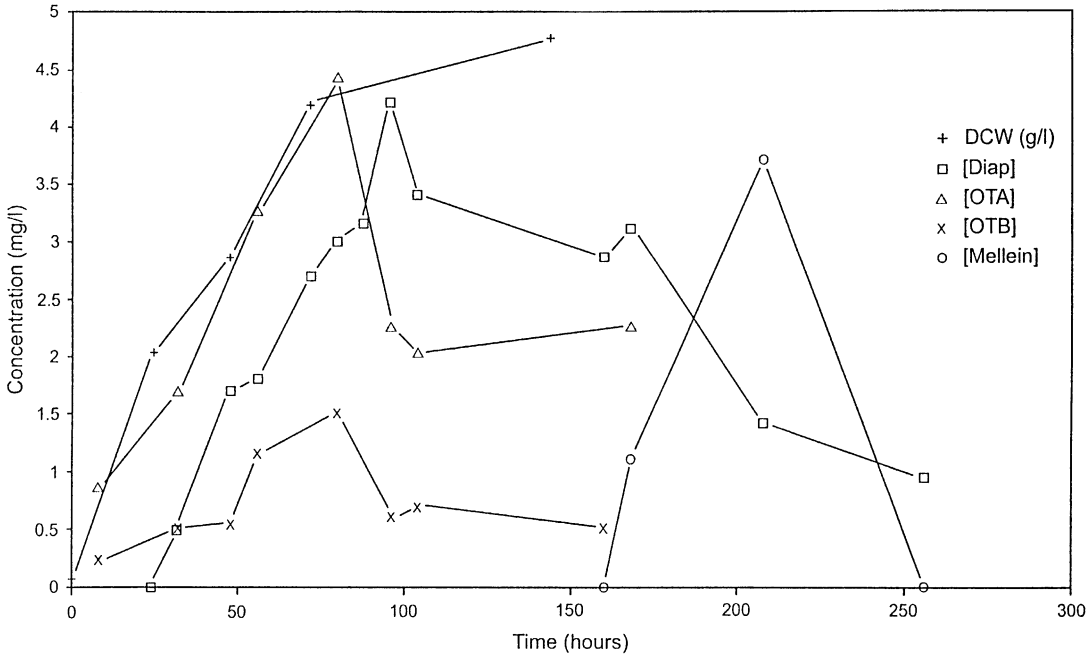

Fig. 3. Dry cell weight (DCW), diaporthin ([Diap]), ochratoxin A ([OTA]), ochratoxin B ([OTB]) and mellein ([Mellein]) concentration versus time for an A. ochraceus fermentation in potato dextrose broth.

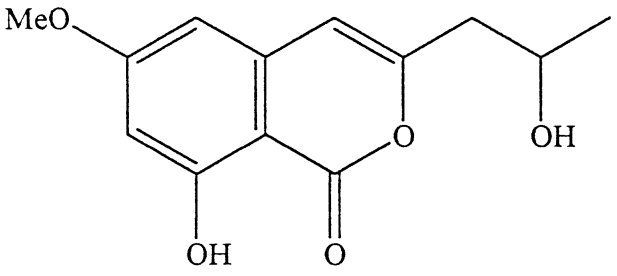

Fig. 4. Structure of diaporthin (**6**).

Table 1
Effect of adding ethionine (50 mg) at different fermentation stages in potato dextrose broth on the concentrations of ochratoxins A and B measured 80 h after inoculation

Ethionine addition times (h)	[Ochratoxin A] (mg/l)	[Ochratoxin B] (mg/l)
32	2.1	1.2
50	4.2	1.3
56	3.7	1.3
72	4.5	1.3
Control	4.8	1.4

Table 2
Effect of adding [1-^{14}C]acetate (5 μCi) to potato dextrose broth fermentations at different stages on the amount and specific radioactivity of [^{14}C]ochratoxin A recovered and analysed 80 h after inoculation

Addition time (h)	Ochratoxin A (μg)	Specific radioactivity (dpm/μg)
8	23	6
22.5	143	37
32	143	18
50	152	15

(1978) reveals evidence of a similar temporal separation of steps in ochratoxin biosynthesis.

2.2. Experiments in shaken solid substrate fermentation

2.2.1. Culture dynamics

Ergosterol, as a measure of fungal mycelium in the substrate, increased linearly through days 4–8 of *A. ochraceus* growth in shaken shredded wheat substrate (Fig. 5). Accumulation of OTA and OTB closely followed fungal growth and was near maximum after 2 weeks; a 5:1 ratio up to day 9 diverged later in favour of OTB, possibly reflecting limitation of substrate chlorine ions for OTA formation (Stander et al., 2000). Yields of 10 mg OTA/g substrate have been achieved. If ergosterol were even as much as 1% of *A. ochraceus* mycelial biomass, OTA would become 1/10th of fungal biomass; this is probably a conservative estimate. Mellein, diaporthin and orthosporin were absent or barely detected throughout this two-week fermentation. Contentious aspects of ochratoxin biosynthesis were therefore explored in this unusual medium in which secondary metabolism in *A. ochraceus* was highly focused on the ochratoxin pathway.

2.2.2. Radioactivity experiments

The magnitude of the relative incorporations of the three radioactive biosynthetic precursors into OTA and

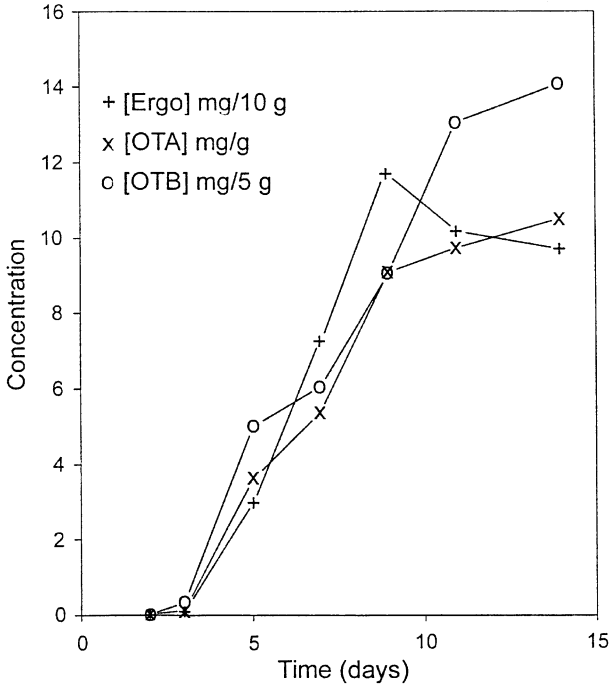

Fig. 5. Changes in ergosterol ([Ergo]), ochratoxin A ([OTA]) and ocratoxin B ([OTB]) concentraion during 2 weeks of an *Aspergillus ochraceus* solid substrate fermentation.

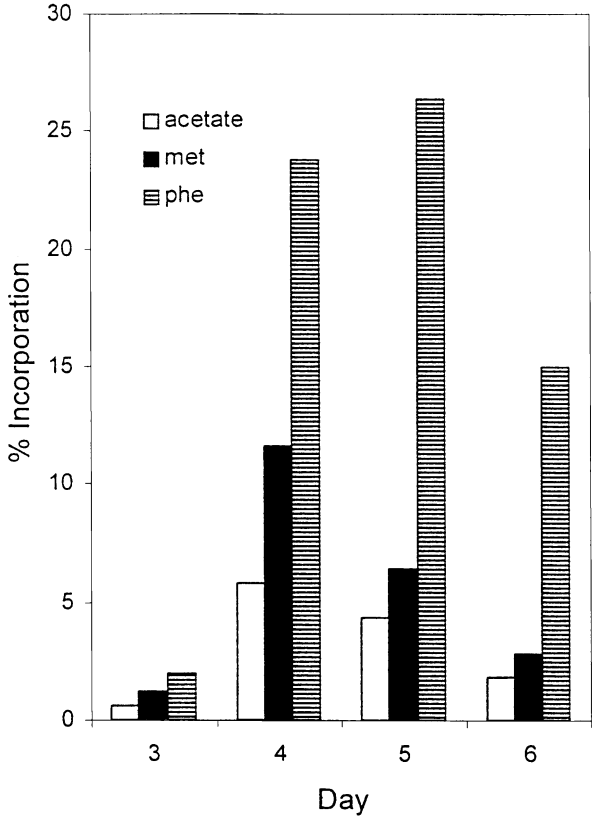

Fig. 6. The % incorporation of 5 μCi of either [1-^{14}C]acetate, [methyl-^{14}C]methionine or [U-^{14}C]phenylalanine into [^{14}C]ochratoxin A during 5 h after adding to *Aspergillus ochraceus* solid substrate fermentations on days 3, 4, 5 and 6.

OTB, when added to fermentations on days 3, 4, 5 or 6 (Figs. 6 and 7), showed that the experimental system was well suited to biosynthetic study. The data also demonstrated temporal separation of optima for isocoumarin biosynthesis (day 4 for OTA; days 4–5 for OTB) and addition of the phenylalanine moiety (day 5 for OTA; days 5–6 for OTB). Notably, 50% of the L-[U-^{14}C]phenylalanine added at 5 days was incorporated into OTA and OTB.

Relative incorporations of the putative intermediates ochratoxins α and β and mellein (Table 3) indicated a strong preferential role of α into A, but similar strong involvement of β into both A and B as subsequently isolated. ^{14}C from mellein occurred in much smaller amount in ochratoxins, which may only reflect indirect incorporation of the radiolabel from mellein catabolism. To suggest that the rather negative experimental result arose from poor uptake of added mellein seems weak when added ochratoxins α and β, both only having an additional carboxyl group, were incorporated so extensively into OTA and OTB. Mellein was only a transitory product in shaken liquid culture (Fig. 3) and therefore *A. ochraceus* is well able to degrade it; no trace of mellein was found in the fermentation fed [^{14}C]mellein. Indeed, the same putative indirect incorporation may explain the small amount of radiolabel in OTB after feeding with ochratoxin α.

Autoradiography of chromatograms of neutral and acidic components of extracts of cultures fed ochratoxin α showed some ^{14}C in neutral non-polar components, in addition to qualitative confirmation of incorporation into ochratoxins. This supports the interpretation of only indirect incorporation from ochratoxin α to OTB. Conversely, there was no autoradiographic evidence of biotransformations in the fermentation given ochratoxin β other than into OTA and OTB. In the fermentation given [^{14}C]mellein there were no particular locations of radiolabel in any fraction of extract, supporting the notion of its rather rapid and extensive catabolism.

In following the fate of dual-labeled OTA and OTB in shaken shredded wheat culture, more than 40% of the added OTA was recovered in the form as added (Table 4). However, an amount equivalent to ca.10% was present as OTB although with the ^{3}H:^{14}C ratio being slightly different. If this is a real change it might imply that the phenylalanine moiety can be transferred to OTB more readily than can the dihydroisocoumarin moiety, which would have to be dechlorinated. Very little (approx. 6.5%) of the added dual-labeled OTB was recovered as such with a similar ^{3}H:^{14}C ratio and even less was incorporated into OTA. Thus, experimental change of doubly-labelled OTA into OTB 5 h after it was added to a fermentation in early idiophase (Table 4) was the most significant interconversion observed. Generally maintained

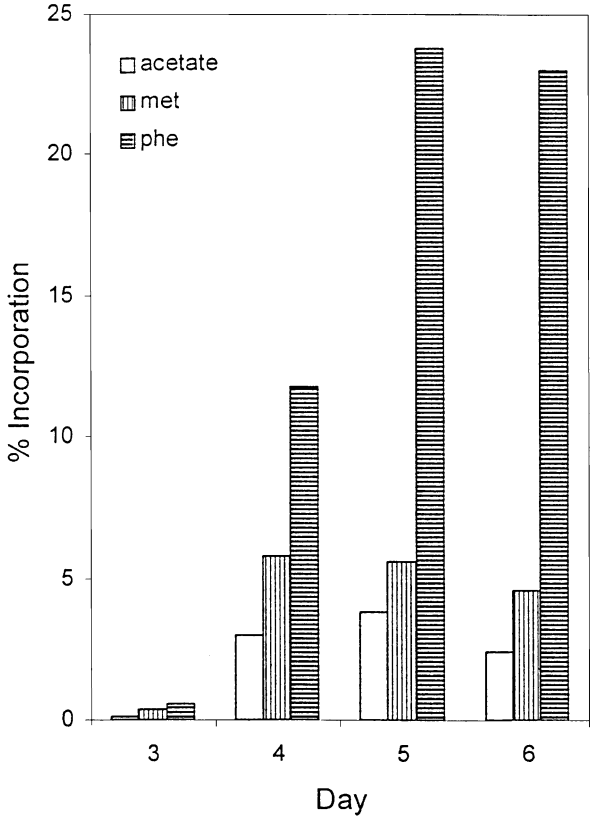

Fig. 7. The % incorporation of 5 μCi of either [1-^{14}C]acetate, [methyl-^{14}C]methionine or [U-^{14}C]phenylalanine into [^{14}C]ochratoxin B during 5 h after adding to *Aspergillus ochraceus* solid substrate fermentations on days 3, 4, 5 and 6.

Table 3
The % incorporation of 0.13 μCi [^{14}C]ochratoxin α, 0.1 μCi [^{14}C] ochratoxin β or 0.096 μCi [^{14}C]mellein into [^{14}C]ochratoxins A and B during 5 h of solid substrate fermentation at the 4 day stage

	[^{14}C]ochratoxin α	[^{14}C]ochratoxin β	[^{14}C]mellein
Ochratoxin A	4.85	14.32	0.56
Ochratoxin B	0.47	18.98	0.68

^{3}H:^{14}C ratios confirmed the validity of most of the transformations observed. Correct interpretation of the findings depends on the extent of cellular uptake of the compounds administered; conversion of OTA to OTB as a catabolic step could be extracellular, but chlorination of OTB to OTA probably requires cellular uptake. If there is not an uptake mechanism for OTB, this could impose a limit on experimentation. It is concluded from all the experiments that chlorination of both ochratoxin β and OTB can give rise to OTA. However, there was no evidence for the intermediate role of the ester ochratoxin C proposed by Huff and Hamilton (1979), presumably interpreted as having a role in protecting the phenylalanine carboxyl during the last biosynthetic steps. These results suggest that one, possibly dominant, biosynthetic pathway involves ochratoxins β→α→A, with also a branch for ochratoxins β→B. An alternative pathway might be ochratoxins β→B→A but, if ochratoxin α is not directly involved, it is difficult to explain the present demonstration that it can occur naturally. However, mellein seems not to be involved as a precursor of either pathway. The discovery of 5-methyl-, 5-formyl- and 5-carboxymellein in culture broth of *Nummulariella marginata* (Whalley and Edwards, 1985) provides a precedent for an oxidation system for a substituted methyl group, yet if such compounds are stable enough to be isolated from fermentation broth it is questioned why 7-methyl- and 7-formylmellein have not, so far, been discovered. Results of the second dual-labeling experiment complemented the first (Table 4). Over half the added OTA was recovered and only 3% was incorporated into OTB although with a slightly different radionuclide ratio. Autoradiography of culture extract chromatograms showed no ^{14}C in neutral fractions, in contrast to results from experiments with [^{14}C] ochratoxins α and β and mellein. Where [^{14}C] OTA or OTB was added, radioactivity was only obvious in the unchanged ochratoxin corresponding to what had been added. Thus, although it was shown that OTA can be converted into OTB nonspecifically, there was no convincing evidence whether or not specific biotransformation of OTB into OTA had occurred.

Since the dual-labelled experiments did not achieve the high percentage incorporations of the experiments in which ochratoxins α and β were administered, it could be argued that the inter-conversion of OTA and OTB, although shown to occur, is not as important in the biosynthetic pathway as the reactions involving ochratoxins α and β.

3. Experimental

3.1. Fungi

Two isolates of A. ochraceus were used; D2306 for its high yield of ochratoxins (Connole et al. 1981; as also used since by Tapia and Seawright, 1984, Stander et al., 2000; Stoev et al., 2000) and KBf for its production of mellein (though not producing ochratoxins; Mantle and McHugh, 1993). The fungi were maintained on potato dextrose agar (Difco).

3.2. Culture conditions

Submerged liquid culture was in potato dextrose broth (Difco), 100 ml in 500 ml Erlenmeyer flasks, inoculated with spores to give 2–4×10^{6} spores ml^{-1} and incubated on an orbital shaker (200 rpm, 10 cm eccentric throw), at 28 °C for isolate D2306 and 22 °C for isolate KBf.

Table 4
The % incorporation and ^{3}H:^{14}C ratio of ochratoxins A and B recovered after adding dual-labelled ochratoxins A and B to solid substrate fermentations

Experiment	Isotope	% Incorporation	^{3}H:^{14}C
Ochratoxin A added for 5 h on day 5			
Ochratoxin A	^{3}H	43.2	1:0.47
	^{14}C	41.5	
Ochratoxin B	^{3}H	12.1	1:0.33
	^{14}C	8.2	
Ochratoxin B added for 5 h on day 5			
Ohratoxin A	^{3}H	1.4	1:0.43
	^{14}C	1.5	
Ochratoxin B	^{3}H	6.7	1:0.37
	^{14}C	6.4	
Ochratoxin A added on day 6 and incubated overnight			
Ochratoxin A	^{3}H	58.3	1:0.48
	^{14}C	57.5	
Ochratoxin B	^{3}H	3.3	1:0.29
	^{14}C	2	

Shaken solid substrate fermentation in Erlenmeyer flasks was developed from the principle first devised for aflatoxins (Shotwell et al., 1966), then applied to OTA (Hesseltine, 1972) and scaled up to rotating barrel fermenters (Lindenfelser and Ciegler, 1975). Shredded wheat breakfast cereal (Cereal Partners UK, Welwyn Garden City), 40 g per flask, was autoclaved, moistened to an initial moisture content of approximately 35% with sterile water (16 ml) and incubated on the orbital shaker at 28 °C. Sterile water was also added at 24 and 48 h (4 and 2 ml, respectively). Water evaporation and metabolic dissimilation of substrate during the subsequent 2 weeks of shaken fermentation resulted in approximately 35 g of moist chocolate-coloured granules in each flask. Some small-scale fermentations were performed as 2 g of shredded wheat in 50 ml flasks for radiochemical experiments.

3.3. Biosynthetic preparation of dual-labeled OTA and OTB

After 4 days in standard shredded wheat culture, 2 g material was transferred to a 50 ml flask and given 5 μCi each of [methyl-^{14}C]methionine and L-[2, 3, 4, 5, 6-^{3}H]phenylalanine. Shaken incubation continued for 5 h and the culture was extracted for OTA (3.4 mg, 0.15 μCi ^{3}H:0.07 μCi ^{14}C, ratio ^{3}H:^{14}C 1: 0.47) and OTB (1.5 mg, 0.29 μCi ^{3}H:0.11 μCi ^{14}C, ratio ^{3}H:^{14}C 1: 0.38). Radioactivity from phenylalanine was incorporated about twice as efficiently as that from methionine.

3.4. Preparation of ^{14}C labeled ochratoxins α and β

OTA (1.16 mg, 0.21 μCi) and OTB (1.44 mg, 0.14 μCi), from cultures fed [methyl-^{14}C]methionine for 5 h on day 4, were each hydrolysed in 50 ml 6 M HCl by reflux for 18 h. The cooled mixture was extracted with EtOAc and ochratoxins α and β were purified by HPLC (see below) detected at 323 nm (retention time, Rt, 10 and 6 min, respectively, at 8.4 ml min^{-1}).

3.5. Biosynthetic preparation of [^{14}C]mellein

Sodium [1-^{14}C]acetate (10 μCi) was added to a 37 h liquid fermentation flask culture of isolate KBf and the fermentation continued for 1 h. [^{14}C] Mellein (2.22 mg) was obtained by extraction of culture filtrate with EtOAc followed by C18 SepPak and HPLC purification (see below). The measured radioactivity (1.67 μCi) represented 16.7% incorporation of radiolabel from [1-^{14}C]acetate.

3.6. Source of authentic compounds

OTA and OTB were isolated from solid substrates (2 g) by extraction in 100 ml EtOAc:0.01 M H_3PO_4, 9:1 (v:v), partition into aqueous $NaHCO_3$ (3%), acidified and back extracted into EtOAc. Residues were taken up in MeOH. OTA and OTB were purified by preparative HPLC (see later).

Ochratoxins α and β were synthesized by the acid hydrolysis of 1 mg OTA or OTB, respectively, followed by preparative HPLC (see later).

Mellein was obtained from 1 week potato dextrose broth culture of isolate KBf. The filtered broth, adjusted to pH 3, was extracted with EtOAc (100 ml) and the organic phase partitioned against a 3% aqueous $NaHCO_3$ solution to remove acidic metabolites. The organic extract was taken to dryness. The solutes, dissolved in MeOH, were processed by HPLC (below; detection at 239 nm, Rt 30 min). Combined eluates corresponding to mellein were mixed with an equal volume of H_2O and passed through a C18 SepPak classic cartridge pre-conditioned first with MeOH (20 ml) and then with H_2O (20 ml). Mellein was eluted in EtOH in the 2nd and 3rd 0.5 ml fraction. Diaporthin and orthosporin were available from other studies (Harris and Mantle, 2001).

All compounds were investigated by HR-MS, and linked scan EIMS (B/E and B^2/E) to interpret fragmentation. The EI mass spectra of OTA and OTB differ by the chlorine or proton substituent at C5, respectively. Molecular ions are very weak, as are those corresponding to losses of H_2O or CO_2. Therefore, use of EIMS for confirming OTA relies on the two important fragment ions, in this case m/z 255 and 239 (base peak). These represent, respectively, the isocoumarin moiety still with the amino nitrogen of phenylalanine and the isocoumarin alone. Principles of further EI fragmentation of the latter, with a carboxyl group reconstituted at C10, are illustrated by ochratoxin α. It is helpful to have a rationale for occurrence of fragment ions in EIMS at

least for diagnostic purposes and this has not been available before. From accurate mass measurements and linked-scan analysis of ochratoxins α and β, and of mellein, rationalised MS fragmentation [Scheme 1, extending the data of Delgadillo (1986)] showed considerable homology between ochratoxins α and β. Also, the composition of ion *m/z* 149 in ochratoxin β was identical to that of mellein. However, there was much less homology between the fragmentation patterns of the ochratoxins and mellein. Notably in ochratoxin β, absence of a B^2/E relationship between the fragment ion *m/z* 204 and the molecular ion implies that the loss of water was a thermal effect. In ochratoxin α two distinct ions of *m/z* 194 were recognised, arising via different fragmentations of the molecular ion, the minor route being via the base peak (*m/z* 212). There are also two forms of the corresponding fragment ion (*m/z* 160), with different elemental composition, in ochratoxin β. All major fragmentation losses of mellein occur in ochratoxins α and/or β. Composition of the prominent fragment ion *m/z* 134 in mellein is the same as that in ochratoxin β, but there its origin was not clear.

3.7. Analytical

The preparative HPLC system used a C18 column (30 × 2.5 cm), detection by fluorescence (excitation 340 nm, emission 400 nm) and UV absorbance (332 nm) in sequence, isocratic mobile phase H_2O:CH_3COOH:acetonitrile, 59.5:1:39.5 (v:v:v), at 5.6 ml min^{-1} (Rt ochratoxins A and B, 20 and 15 min, respectively). Ochratoxins A and B were purified further in MeOH:H_2O, 7:3 (v:v), Rt 21 and 16 min, respectively.

Analytical HPLC of 20 μl samples in MeOH used a C18 column (15 × 0.5 cm), a diode array detector and solvent flow at 1 ml min^{-1}: Rt ochratoxins A and B, 7.8 and 4.5 min, respectively. Neutral metabolites (mellein, diaporthin and orthosporin), monitored at 239 nm, had Rt of 4.5, 3.5 and 1.8 min, respectively.

TLC of portions of acidic and neutral extracts from radiolabelling experiments was performed on 10 × 10 cm TLC plates (SIL G, UV_{254} Camlab, Cambridge) in toluene–EtOAc–HCOOH, 5:4:1 (v:v:v). Dried plates were autoradiographed at −70 °C for 1 week. Ochratoxins were recognised by fluorescence. Mellein was visualised by spraying with 3% $FeCl_3$ in butan-1-ol whereby mellein is stained red (van der Merwe et al., 1965b).

3.7.1. Assay of ergosterol

One gram sample of shredded wheat culture was refluxed in MeOH (100 ml) for 2 h. 4% KOH in 95% aqueous EtOH (20 ml) was added and neutral lipids were partitioned into pentane (3×40 ml). Solutes were dissolved in MeOH for analytical HPLC in 95% aqueous MeOH, detection at 282 nm, Rt 8 min (after Newell et al., 1988).

3.8. Treatment with ethionine

Ethionine (10 ml of a 5 mg ml^{-1} sterile solution) was added to potato dextrose broth cultures 32, 50, 56 or 72 h post-inoculation. Sterile water (10 ml) was added to a control culture. After 80 h, ochratoxins were extracted from the broth and quantified.

3.9. Relative dynamics of secondary metabolite production in submerged and solid substrate fermentations

At intervals, 10 ml samples were taken from triplicate liquid cultures. Broth was filtered through a weighed sintered 10 ml glass syringe and the retained biomass

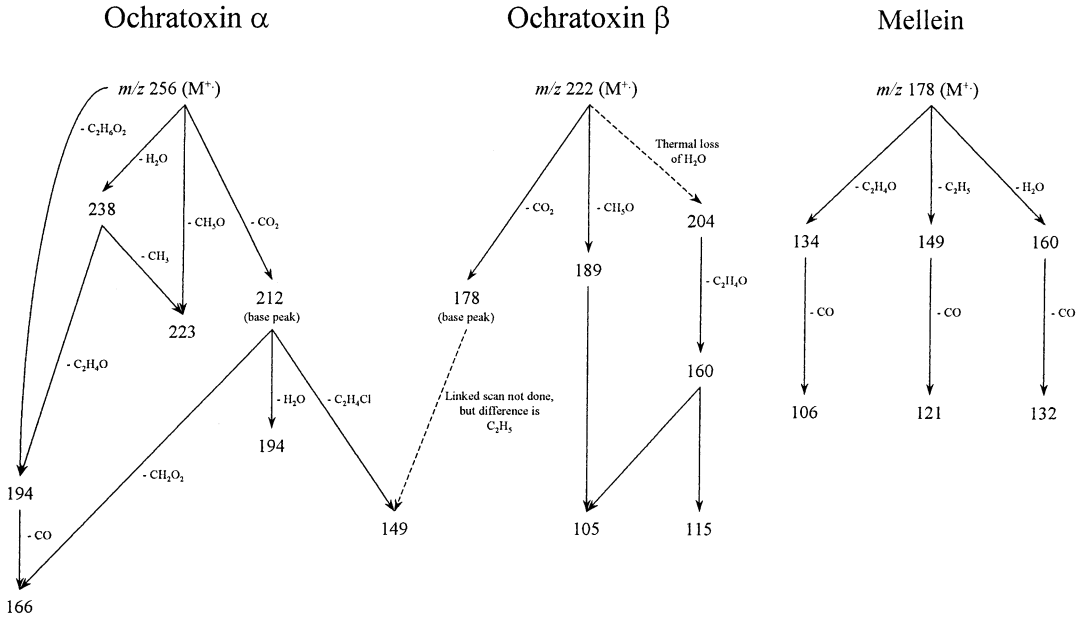

Scheme 1. EIMS fragmentation of ochratoxins α and β and mellein deduced from mass measurements and linked scan experiments.

was lyophilised to constant weight. Acidified filtrate was extracted with EtOAc which was partitioned against bicarbonate. Ensuing acidic or neutral solutes were dissolved in MeOH for HPLC quantitation. Similarly, l g solid culture was taken at intervals and acidic and neutral metabolites analysed.

3.10. Experiments with radiolabelled precursors on isolate D2306

[1-^{14}C]acetate (5 μCi) was added to a liquid fermentation at 8, 22.5, 32 or 50 h post inoculation to determine the time of optimal incorporation into OTA, as assessed at 80 h. A portion (8–25%) of extracts was analysed by HPLC and radioactivity in eluates corresponding to specific quantified metabolites was measured by scintillation counting. 2 g aliquots of fermenting shredded wheat were transferred to groups of three 50 ml flasks from standard flask fermentations after 3, 4, 5 and 6 days. To each was added 200 μl of sterile water containing 5 μCi of either [1-^{14}C]acetate, L-[U-^{14}C]phenylalanine or L-[methyl-^{14}C]methionine. Each solution was applied to the substrate as very small drops. Incubation was continued for a further 5 h before extraction of ochratoxins to compare efficiencies of incorporation of precursors.

Similarly, three 2 g amounts of 4 day culture were given 200 μl sterile water containing 0.1 μCi of either [^{14}C]ochratoxin α, [^{14}C]ochratoxin β or [^{14}C]mellein and incubated for 5 h before extraction to measure fates of the radiolabeled probes. Similar fermentation material, though at the 5 day stage, was treated with dual-labeled OTA (231 μg) or OTB (1.02 mg) to explore their fate during 5 h. Again, dual-labeled OTA (1.28 mg in 3% $NaHCO_3$) was given to 6 day culture and incubated for longer (overnight).

Acknowledgements

We thank J. Barton, Chemistry Department, Imperial College for obtaining EIMS data (Micromass Autospec Q). J.P.H. acknowledges a Research Studentship from the AFRC.

References

Abell, C., Garson, M.J., Leeper, F.J., Staunton, J., 1982. Biosynthesis of the fungal metabolites alternariol, mellein, rubrofusarin, and 6-methylsalicylic acid from CD_3CO_2H. Journal of the Chemical Society, Chemical Communications, 1011–1013.

Abell, C., Doddrell, D.M., Garson, M.J., Laue, E.D., Staunton, J., 1983. Biosynthesis of the polyketide mellein from CD_3CO_2H and $^{13}CD_3CO_2H$ in *Aspergillus melleus*: detection of deuterium by ^{2}H N.M.R. and edited ^{13}C N.M.R. spectra. Journal of the Chemical Society Chemical Communications, 694–696.

Connole, M.D., Blaney, B.J., McEwan, T., 1981. Mycotoxins in animal feeds and toxic fungi in Queensland 1971–1980. Australian Veterinary Journal 57, 314–318.

de Jesus, A.E., Steyn, P.S., Vleggaar, R., Wessels, P.L., 1980. Carbon-13 nuclear magnetic resonance assignments and biosynthesis of the mycotoxin ochratoxin A. Journal of the Chemical Society, Perkin Transactions 1, 52–54.

Delgadillo, I., 1986. Isolation of secondary metabolites of *Aspergillus ochraceus* by HPLC. Mycotoxin Research 2, 9–17.

Ferreira, N.P., Pitout, M.J., 1969. The biosynthesis of ochratoxin. Journal of the South African Chemical Institute 22, S1.

Harris, J.P., Mantle, P.G., 2001. Biosynthesis of diaporthin and orthosporin by *Aspergillus ochraceus*. Phytochemistry 57, 165–169.

Hesseltine, C.W., 1972. Solid state fermentations. Biotechnology and Bioengineering 14, 517–532.

Huff, W.E., Hamilton, P.B., 1979. Mycotoxins—their biosynthesis in fungi: ochratoxins—metabolites of combined pathways. Journal of Food Protection 42, 815–820.

Lillehoj, E.B., Aalund, O., Hald, B., 1978. Bioproduction of [^{14}C] ochratoxin A in submerged culture. Applied and Environmental Microbiology 36, 720–723.

Lindenfelser, L.A., Ciegler, A., 1975. Solid-substrate fermentor for ochratoxin A production. Applied Microbiology 29, 323–327.

Mantle, P.G., McHugh, K.M., 1993. Nephrotoxic fungi in foods from nephropathy households in Bulgaria. Mycological Research 97, 205–212.

Moore, J.H., Davis, N.D., Diener, U.L., 1972. Mellein and 4-hydroxymellein production by *Aspergillus ochraceus* Wilhelm. Applied Microbiology 23, 1067–1072.

Newell, S.Y., Arsuffi, T.L., Fallon, R.D., 1988. Fundamental procedures for determining ergosterol content of decaying plant material by liquid chromatography. Applied and Environmental Microbiology 54, 1876–1879.

Searcy, J.W., Davis, N.D., Diener, U.L., 1969. Biosynthesis of ochratoxin A. Applied Microbiology 18, 622–627.

Shotwell, O.L., Hesseltine, C.W., Stubblefield, R.D., Sorenson, W.G., 1966. Applied Microbiology 14, 425.

Stander, M.A., Steyn, P.S., Lubben, A., Miljkovic, A., Mantle, P.G., Marais, G.J., 2000. Influence of halogen salts on the production of the ochratoxins by *Aspergillus ochraceus* Wilh. Journal of Agricultural and Food Chemistry 48, 1865–1871.

Steyn, P.S., Holzapfel, C.W., 1967. The isolation of the methyl and ethyl esters of ochratoxins A and B, metabolites of *Aspergillus ochraceus* Wilh. Journal of the South African Chemical Institute 20, 186–189.

Steyn, P.S., Holzapfel, C.W., Ferreira, N.P., 1970. The biosynthesis of ochratoxins, metabolites of *Aspergillus ochraceus*. Phytochemistry 9, 1977–1983.

Stoev, S.D., Goundasheva, D., Mirtcheva, T., Mantle, P.G., 2000. Susceptibility to secondary bacterial infections in growing pigs as an early response in ochratoxicosis. Experimental and Toxicologic Pathology 52, 287–296.

Tapia, M.O., Seawright, A.A., 1984. Experimental ochratoxicosis A in pigs. Australian Veterinary Journal 61, 219–222.

van der Merwe, K.J., Steyn, P.S., Fourie, L., de Scott, B., Theron, J.J., 1965a. Ochratoxin A, a toxic metabolite produced by *Aspergillus ochraceus* Wilh. Nature 205, 1112–1113.

van der Merwe, K.J., Steyn, P.S., Fourie, L., 1965b. Mycotoxins. Part 2. The constitution of ochratoxin A, B, and C, metabolites of *Aspergillus ochraceus* Wilh. Journal of the Chemical Society, 7083–7088.

Whalley, A.J.S., Edwards, R.L., 1985. *Nummulariella marginata*: its conidial state, secondary metabolites and taxonomic relationships. Transactions of the British Mycological Society 85, 385–390.

Wei, R.-D., Strong, F.M., Smalley, E.B., 1971. Incorporation of chlorine-36 into ochratoxin A. Applied Microbiology 22, 276–277.

Yamazaki, M., Maebayashi, Y., Miyaki, K., 1971. Biosynthesis of ochratoxin A. Tetrahedron Letters 25, 2301–2303.

PERGAMON

Phytochemistry 58 (2001) 717–728

PHYTOCHEMISTRY

www.elsevier.com/locate/phytochem

Factors influencing the distributions of polyunsaturated terpenoids in the diatom, *Rhizosolenia setigera*

S.J. Rowland[a,*], W.G. Allard[a], S.T. Belt[a], G. Massé[a,b], J.-M. Robert[b], S. Blackburn[c], D. Frampton[c], A.T. Revill[c], J.K. Volkman[c]

[a]*Petroleum and Environmental Geochemistry Group, Department of Environmental Sciences, Plymouth Environmental Research Centre, University of Plymouth, Drake Circus, Plymouth PL4 8AA, UK*

[b]*ISOMer, Faculté des Sciences et des Techniques, Université de Nantes, 2 rue de la Houssinière, 44027 Nantes, Cedex 03, France*

[c]*CSIRO Division of Marine Research, Castray Esplanade, Hobart, Tasmania, Australia*

Received 17 May 2001; received in revised form 10 July 2001

Abstract

Polyunsaturated highly branched isoprenoid (HBI) hydrocarbon distributions of laboratory cultures of five strains of the planktonic diatom *Rhizosolenia setigera* (Brightwell) are shown herein to be highly variable. Some strains produced both haslenes with from three to five double bonds and rhizenes. The haslenes comprised not only Δ5 alkenes but also those with C7(20) unsaturation, including hasla-7(20),9*E*,*Z*, 23-trienes and hasla-7(20),9*E*,*Z*-13, 23-tetraenes. The rhizenes contained C7(25) unsaturation and the vinyl moiety common to all algal haslenes so far characterised. The effects of temperature and salinity on HBI composition, along with isotopic content, were determined in strain CS 389/A. Increase in growth temperature from 18 to 25 °C increased the degree of unsaturation in the haslenes and *E* to *Z* isomerisation in the triene. There was also an increase in unsaturation in the rhizenes at the highest growth temperature, with hexaenes dominant over the pentaenes but in the rhizenes, *Z* to *E* isomerisation increased. Increased salinity from 15 to 35 psu increased cell growth and rhizene production but decreased haslene production. Unsaturation in haslenes was not changed by increased salinity but unsaturation in the rhizenes decreased. These may reflect growth rate differences. The carbon isotopic compositions of the haslenes and rhizenes were similar to that of the major sterol at 18 °C, but the major HBI isomers were 3–4 per mil depleted relative to phytol released by saponification from chlorophyll a. This suggests biosynthesis of HBIs from a different isotopic pool of isopentenyl biphosphate to that from which phytol is biosynthesised. At 25 °C, further isotopic differences were observed. The variables controlling HBI distributions in *R. setigera* are still not fully understood and rationalisation of the environmental controls on the sedimentary distributions of the HBIs from *R. setigera* may only be possible once such factors are established. © 2001 Elsevier Science Ltd. All rights reserved.

Keywords: *Rhizosolenia setigera*; Bacillariophyceae; Microalgae; Diatoms; Isoprenoid alkenes; Highly branched isoprenoids; C_{30} alkenes; Rhizenes; Haslenes

1. Introduction

The only highly branched isoprenoid (HBI) hydrocarbons reported to date in the diatom *Rhizosolenia setigera* (Brightwell) are either a C_{25} pentaene (I) or C_{30} alkenes (Volkman et al., 1994, 1998; Sinninghe Damsté et al., 1999a). We have proposed the name 'haslenes' for the HBI C_{25} alkenes (Rowland et al., 2001), because they were first reported (Volkman et al., 1994) from the diatom *Haslea ostrearia* (Simonsen). We now suggest the name 'rhizenes' for the corresponding C_{30} HBIs, as they were first reported from *R. setigera* (Volkman et al., 1994).

The single haslapentaene (**I**) identified thus far in *R. setigera*, has been characterised by NMR spectroscopy and comparison with data for the same compound in *H. ostrearia* (Wraige et al., 1997; Sinninghe Damsté et al., 1999b) and the double bond positions of four rhizenes have recently been established (Belt et al., 2001). However, the factors controlling the distributions of HBIs in *R. setigera* are at present unknown. These are important since HBIs are quite commonly reported in oceanic sedimenting particles (reviewed in Belt et al., 2000a) where they may be useful indicators of specific diatom inputs. Whilst a number of benthic diatoms are known to produce haslenes (e.g. several *Haslea* spp. and

* Corresponding author. Tel.: +44-1752-233013; fax: +44-1752-233035.

E-mail address: s.rowland@plym.ac.edu (S.J. Rowland).

0031-9422/01/$ - see front matter © 2001 Elsevier Science Ltd. All rights reserved.
PII: S0031-9422(01)00318-1

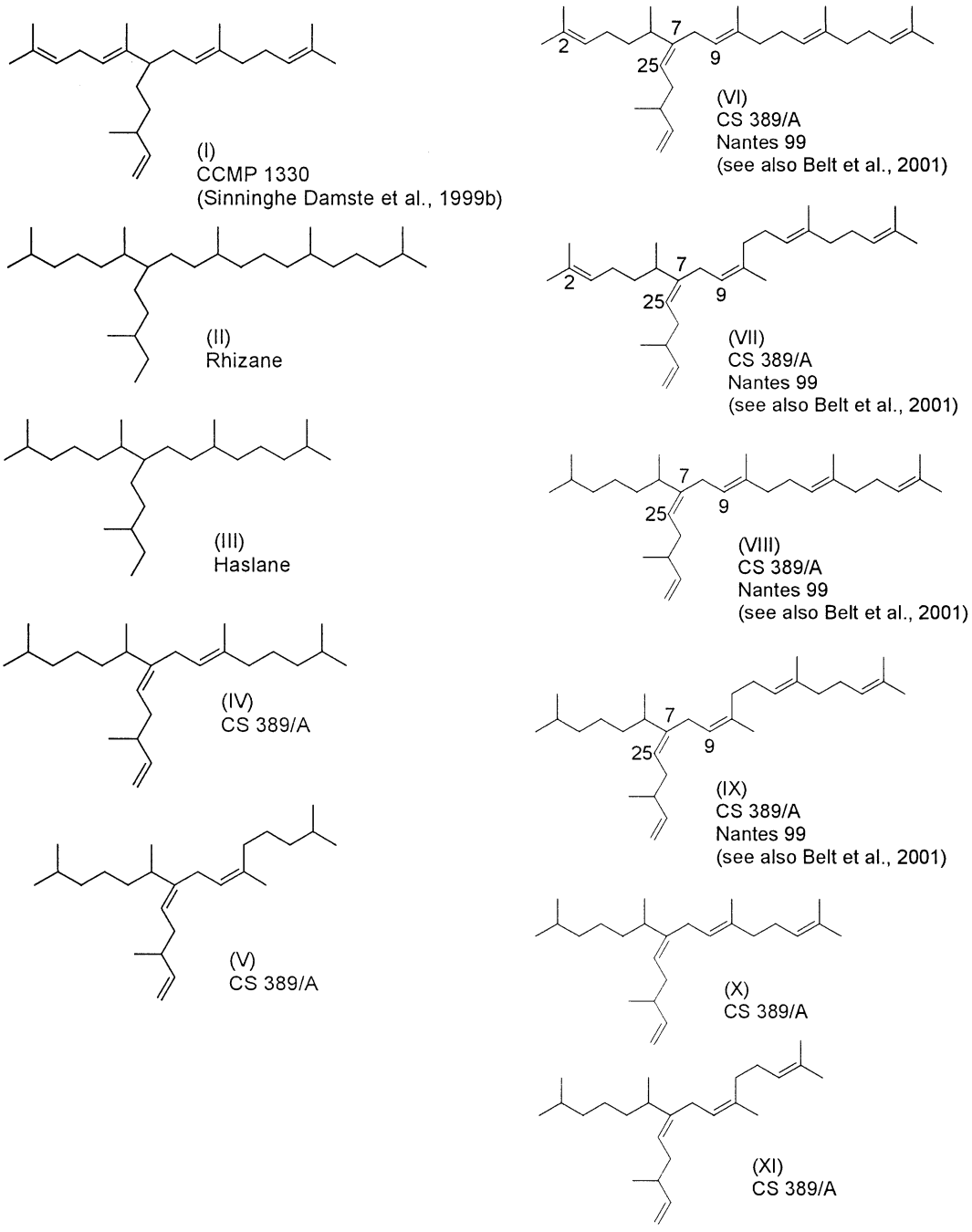

Pleurosigma intermedium; Belt et al., 2000a), *R. setigera* is to date the only marine planktonic diatom known to produce either haslene or rhizene HBIs.

The haslenes in estuarine sediments appear to allow resolution of the contributions of the benthic species to the total diatom flux (Cooke et al., 1998) and some haslenes also appear to possess cytostatic effects against human lung cancer cells in vitro (Rowland et al., 2001). It would therefore be interesting to know whether the rhizenes are equally geochemically specific and/or bioactive. Here, we report the haslenes and rhizenes of five strains of *R. setigera* and investigate the effects of growth temperature and salinity on haslene and rhizene production in one strain. Furthermore, we have investigated the effects of these variables on the carbon isotopic composition of the haslenes and rhizenes in this strain. Such data may eventually help to allow the environmental distributions of HBIs in sediments and sedimenting particles to be understood.

2. Results and discussion

R. setigera (Brightwell) is a common diatom often found in the plankton of coastal and marine waters

(Round et al., 1990). The taxonomy of the genus is however, somewhat uncertain (Round et al., 1990; Volkman et al., 1994, and references therein) and has been revised by Sundström (1986) and also been subject to several other modifications, including the transfer of the only two freshwater *Rhizosolenia* species to a new genus *Urosolenia* (Round et al., 1990).

The HBIs of three strains of *R. setigera* have been reported previously (Volkman et al., 1994, 1998; Sinninghe Damsté et al., 1999a) and, in contrast to the production of haslenes only in the benthic diatom *H. ostrearia*, the HBIs of *R. setigera* varied from rhizenes characterised by GCMS and hydrogenation to the parent rhizane (**II**) in two Australian strains CS-62 and CS-389/1 grown at 20 and 18.5 °C and 70–80 μE m^{-2} s^{-1} white light and 28 psu salinity (Volkman et al., 1994, 1998), to haslapentaene (**I**) only, in strain CCMP1330 grown at 4, 12 and 20 °C in North Atlantic seawater (Sinninghe Damsté et al., 1999a). Since the distributions in the previous reports were rather different from one another, we decided to examine further the hydrocarbons of strain CCMP 1330 and four other strains of *R. setigera*.

2.1. *R. setigera CS strain 389/A*

2.1.1. *HBI identifications and partial structural characterisation of rhizenes*

A 10 l culture of *R. setigera* was grown from an inoculum obtained from the Huon estuary, Tasmania, Australia. The wet paste obtained after centrifugation was extracted by allowing it to stand in chloroform (24 h). This yielded 220 mg of total chloroform extractable lipids. Microscale hydrogenation (Adam's catalyst) of a small aliquot of the total lipids of a culture grown at 18 °C (35 psu salinity) produced rhizane (**II**) and haslane (**III**) as the only HBIs, identified by GCMS and GC retention indices compared to the synthetic alkanes (Robson and Rowland, 1986, 1988). A small amount of an unidentified C_{30} alkane (RI $2543_{HP\text{-}5}$) with two degrees of unsaturation (ca. 10% relative to **II**) was also present (cf Prahl et al., 1980).

The total chloroform extract was further fractionated by open column chromatography on silica and fractions containing respectively, two C_{25} trienes, three C_{30} pentaenes, and three C_{30} hexaenes (identified by GCMS) obtained by elution with successive volumes of pentane. GCMS, ^{1}H and ^{13}C NMR spectroscopy revealed that the C_{25} trienes were identical to those recently identified in *Pleurosigma intermedium* (Belt et al., 2000a) viz. hasla-7(20),9*E*/*Z*,23-trienes (**IV** and **V**). Both *E* (major) and *Z* isomers were present. These Δ7(20) haslenes are therefore different to those of *H. ostrearia* and indeed of *R. setigera* strain CCMP 1330 (Sinninghe Damsté et al., 1999a) which contained a Δ5 double bond (**I**).

The presence of inseparable mixtures of three C_{30} alkenes in each of the pentaene and hexaene fractions precluded full structural characterisations by NMR, but a number of features were nonetheless clear. Namely, the rhizenes all contained a vinyl moiety (Δ28)—present in all haslenes and rhizenes identified in diatoms thus far—a number of trisubstituted double bonds and, consistent with the presence of the haslatrienes (**IV** and **V**), Δ7(25) unsaturation (^{1}H NMR: δ 5.71, 1H, *ddd*, H-28; 4.9, 2H, *m*, H-29; ^{13}C NMR DEPT,COSY,COLOC; δ 144.6, C-28; 112, C-29;142, C-7). Full structural characterisation of four of the six alkenes (**VI**–**IX**) was possible upon isolation of two pairs of isomers from a further strain of *R. setigera,* Nantes 99 (vide infra; Belt et al., 2001).

Thus, this study has shown that *R. setigera* is able to biosynthesise simultaneously, haslenes *and* rhizenes, whereas previously only one or the other was reported, and that whilst *H. ostrearia* produces haslenes with Δ5 and Δ6(17) double bonds, *P. intermedium* and *R. setigera* apparently produce haslenes with Δ7(20) unsaturation. Interestingly, haslenes and rhizenes have been reported to co-occur in some marine sediments and the present findings raise the possibility that in such cases both may have derived from *R. setigera*.

2.1.2. *Effects of salinity and temperature on HBI distributions*

To investigate the controls on the concentrations and the apparent variability of haslene and rhizene distributions in *R. setigera,* small scale cultures of strain CS 389/A were grown at two salinities (18 °C; 15 and 35 psu) and three temperatures (10,18, 25 °C; 35 psu). Each culture was grown for three growth cycles then a single sample taken from each after the third growth cycle (i.e. four samples) before culturing and harvesting in triplicate after a fourth cycle (i.e. a further 12 samples). This multiple cycle culturing was designed to allow the algae to acclimate somewhat to each set of new culture conditions. Cell concentrations in the fourth growth cycle were monitored by a calibrated fluorescence method (days 0, 2, 4, 6, 7; Fig. 1) and by microscopy (days 0, 7: mean cell counts). Cells were harvested at day 7. Cultures were filtered and filters extracted with chloroform with ultrasonication after addition of *n*-docosane as internal standard for quantification by GCMS. Recovery of the internal standard was 137±17% ($n=12$). Extracts were also saponified, re-extracted into hexane and after silylation the non-saponifiable lipids were examined by GCMS and by GC-isotope ratio monitoring-MS (GC-irm-MS). The absolute concentrations of HBIs ranged from about 5 to 20 pg $cell^{-1}$. The cell concentrations in the day 7 samples were used to estimate these concentrations.

Cell growth was faster at 35 psu salinity than at 15 psu (Fig. 1) and at 35 psu total HBI production (mean 19.4±

0.6 pg cell^{-1}) was twice that at 15 psu (10.23±0.57 pg cell^{-1}; Fig. 2a). In contrast, haslene production was greatest at the lower salinity (Fig. 2b).

The ratio of rhizenes to haslenes was, however, much higher at 35 psu (Fig. 2c) due to the higher absolute concentrations of rhizenes. Whilst unsaturation in the *E,Z* Δ7(20) haslatrienes (**IV**, **V**) was unchanged by salinity (Fig. 3a and b)—as was also the case for the Δ6(17) triene in *H. ostrearia* (Wraige et al., 1998)—unsaturation within the rhizenes was changed and was higher at the lower salinity (Figs. 2d and 3a). Whether these variations can be attributed directly to the differences in salinity, or actually reflect the difference in growth rates, will require further investigation at further, intermediate, salinities.

At 35 psu salinity, *R. setigera* did not grow well after 4 days at 10 °C (Fig. 1) but at 18 and 25 °C growth was good to 7 days (Fig. 1). Variation of growth temperature from 10 to 18 to 25 °C produced a change in the total HBI production, which maximised at 18 °C (19.4± 0.6 pg cell^{-1}; Fig. 2e). [The mean value at 10 °C (Fig. 2e) should be treated as a maximum since the measurement was based on cell counts determined at 7 days where growth had decreased (Fig. 1).] Thus maximum HBI production in *R. setigera* occurred at 35 psu, 18 °C. This may reflect the conditions to which the strain had become best acclimated in culture previously.

Within the HBIs, maximum haslene production was observed at 25 °C, and there was a steady increase in haslene production with increasing temperature (Fig. 2f). In contrast, rhizene production maximised at 18 °C, leading to a maximum in the rhizene/haslene ratio at this temperature (Fig. 2g).

Unsaturation in the haslenes also varied with temperature; haslatrienes (**IV** and **V**) were accompanied by haslatetraenes (**X**, **XI**) at 25 °C (Fig. 4c). This variation of the degree of unsaturation in the haslenes of *R. setigera* with growth temperature in strain CS 389/A contrasts with the previous observation of the invariance in the single haslapentaene (**I**) produced by *R. setigera* strain CCMP 1330 with variation of temperature between 4 and 20 °C (Sinninghe Damste et al., 1999a). However, the degree of unsaturation in the two strains CCMP 1330 vs CS 389/A was quite different (viz. 5 vs 3 and 4 double bonds, respectively) and furthermore, haslenes in the CCMP 1330 strain had a Δ5 double bond whereas those of strain CS 389/A had 7(20) unsaturation. The variation of unsaturation with temperature in this strain is similar to, though less pronounced than, that observed in the Δ5 and Δ6(17) haslenes of *H. ostrearia* which varied from diene production at 5 °C to tetraene and pentaene production at 25 °C (Rowland et al., 2001). Isomerisation of the *E* to *Z* haslene isomers also increased with increasing temperature (Fig. 4).

Strain CS 389/A cultured herein, produced both the haslenes and rhizenes at all temperatures. In contrast, strain CS 389/1 cultured at 18.5 °C, produced only rhizenes (Volkman et al., 1994), suggesting that co-production of haslenes and rhizenes is not a general phenomenon even in *R. setigera* strains from the same

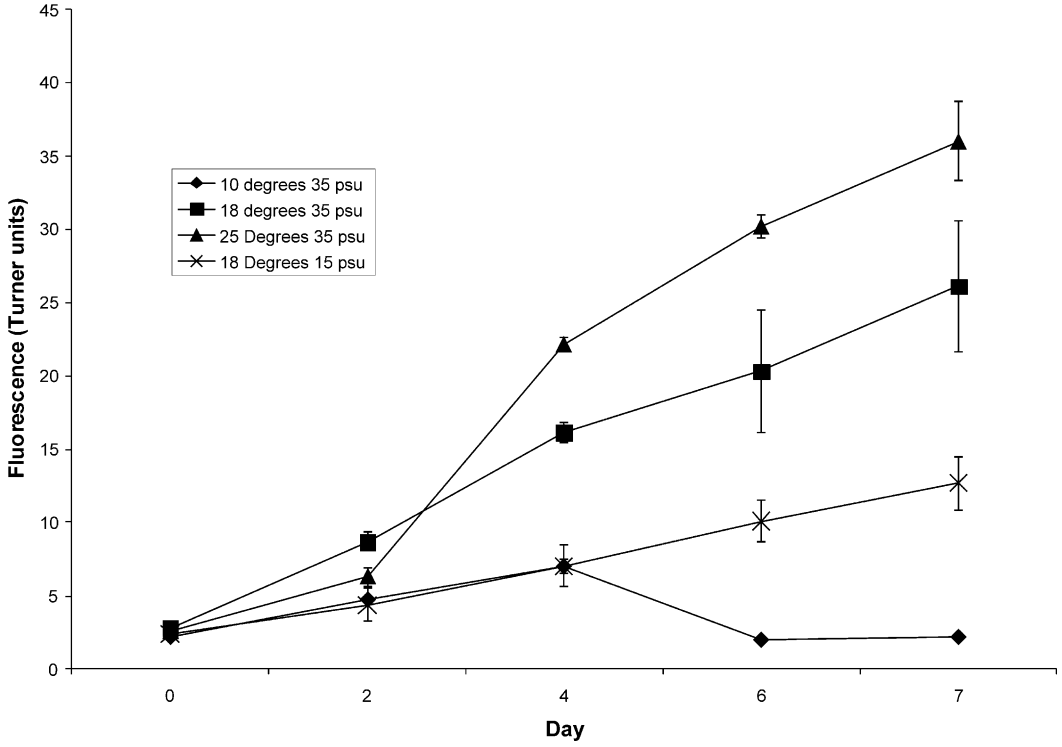

Fig. 1. Growth curves of *Rhizosolenia setigera* strain CS 389/A at 15 and 35 psu, 10, 18 and 25 °C ($n=3\pm1$ standard deviation).

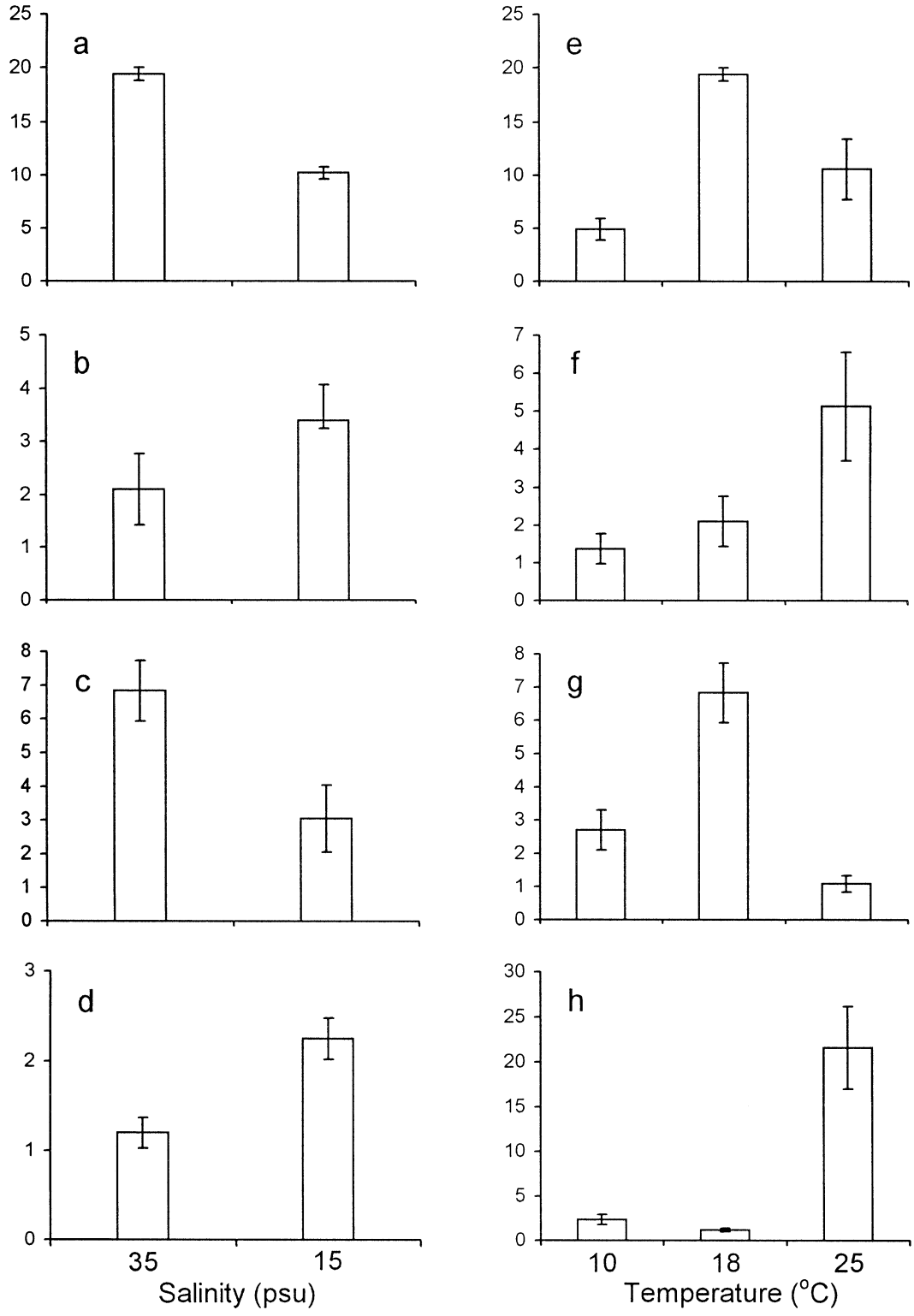

Fig. 2. Histograms illustrating variations of haslene and rhizene production (pg cell^{-1}) at different salinities and growth temperatures. Error bars indicate standard deviations of means of triplicate culturing experiments: a and e: total HBI concentrations; b and f: total haslene concentrations; c and g: rhizenes:haslenes ratio; d and h: rhizahexaenes:rhizapentaenes ratio.

general location. Nonetheless, 18 °C was the optimum temperature for rhizene production in strain CS 389/A (Fig. 2g). As with the haslene distributions, the degree of unsaturation in the rhizenes of strain CS 389/A changed reproducibly with temperature; the proportion of hexaenes to pentaenes increasing markedly with an

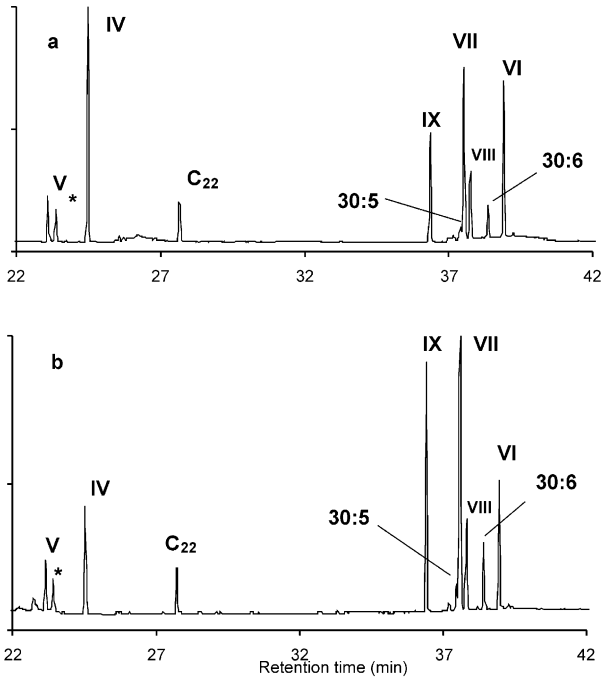

Fig. 3. GCMS total ion current chromatograms of total chloroform extracts of *Rhizosolenia setigera* strain CS 389/A at (a) 15 psu and (b) 35 psu salinity, 18 °C. Roman numerals refer to HBI structures shown in text. C_{22} = *n*-docosane internal standard. * = *n*-Henicosahexaene. 30:5, 30:6 = unknown C_{30} pentaene and hexaene, respectively.

increase in temperature from 18 to 25 °C (Figs. 2h and 4a–c). Again, this is somewhat similar to the change observed in the Δ5 and Δ6(17) haslenes of *H. ostrearia* (Rowland et al., 2001). However, opposite to the haslenes, Z to E isomerisation occurred in the rhizenes (Fig. 4).

2.1.3. Effects of temperature on the isotopic compositions of HBIs

The $^{13}C/^{12}C$ isotope ratios (in the δ notation relative to PDB standard) of phytol, haslene (**IV**), five of the six rhizenes and cholest-5, 24-dienol (Barrett et al., 1995) in *R. setigera* CS 389/A grown at 18 and 25 °C were measured by GC-irm-MS. Certified reference materials [*n*-hexadecane (*n*-C_{16}), *n*-icosane (*n*-C_{20}), *n*-tetracosane (*n*-C_{24}) and *n*-dotriacontane (*n*-C_{32})] each of known isotopic composition, were co-chromatographed with each sample during each GC-irm-MS analysis. The isotope value of the *Z*-haslatriene (**V**) could not be obtained due to insufficient GC resolution from *n*-henicosahexaene. The δ per mil value of each analyte was measured. Then, to allow for within-run instrument drift, differences between the measured and certified values of the nearest eluting *n*-alkane reference were added to the measured value of each analyte to give a range. The means and standard deviations for the ranges obtained in replicate experiments were then calculated and are shown as box and whisker diagrams in Figs. 5 and 6.

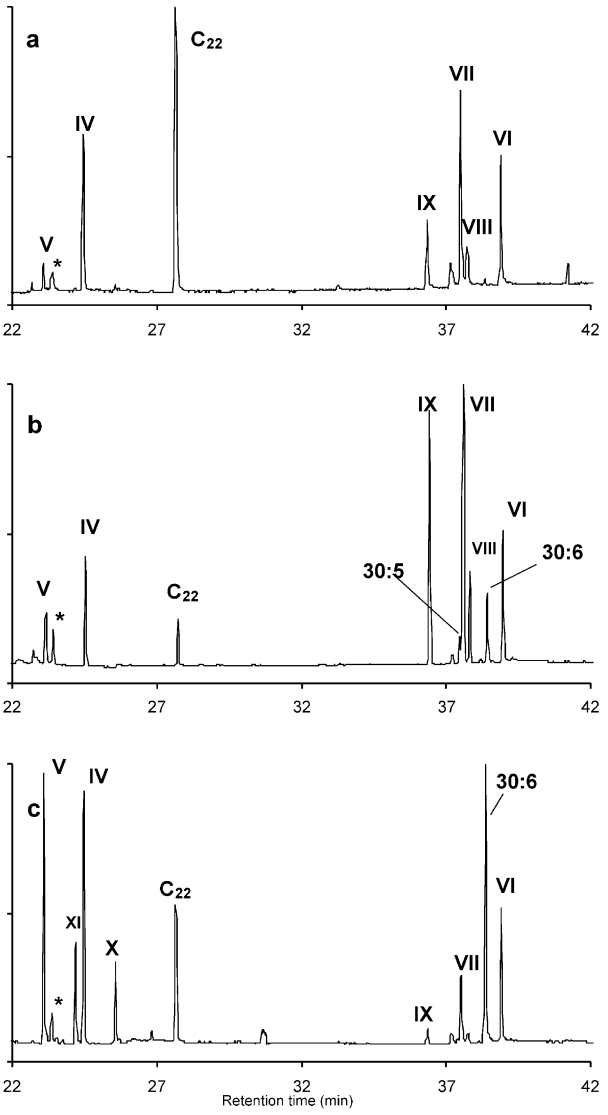

Fig. 4. GCMS total ion current chromatograms of total chloroform extracts of *Rhizosolenia setigera* strain CS 389/A at 35 psu salinity, (a) 10 (b) 18 and (c) 25 °C. Roman numerals refer to HBI structures shown in text. C_{22} = *n*-docosane internal standard. * = *n*-Henicosahexaene. 30:5, 30:6 = unknown C_{30} pentaene and hexaene, respectively.

Thus, any major differences in δ between the individual lipids which emerge are unlikely to be artefactual. The mean within-run variations from the certified values were: [($n = 10$) *n*-C_{20}, 0.4 ± 0.3 per mil; *n*-C_{24}, 0.3 ± 0.3 per mil; *n*-C_{32}, 0.4 ± 0.2 per mil].

At 18 °C, the *E*-haslatriene (**IV**) was about 3–4 per mil depleted in ^{13}C compared to phytol. This applied to both the algae cultured for three generations (Fig. 5a) and the final fourth generation samples (Fig. 5b). At 25 °C the result was the same (Fig. 5a). A previous study showed that haslapentaene (**I**) in *R. setigera* strain CCMP 1330 grown at 12 °C was 4.5 per mil depleted compared with phytol (Schouten et al., 1998). This is probably not significantly different from the 3–4 per mil determined in the present study.

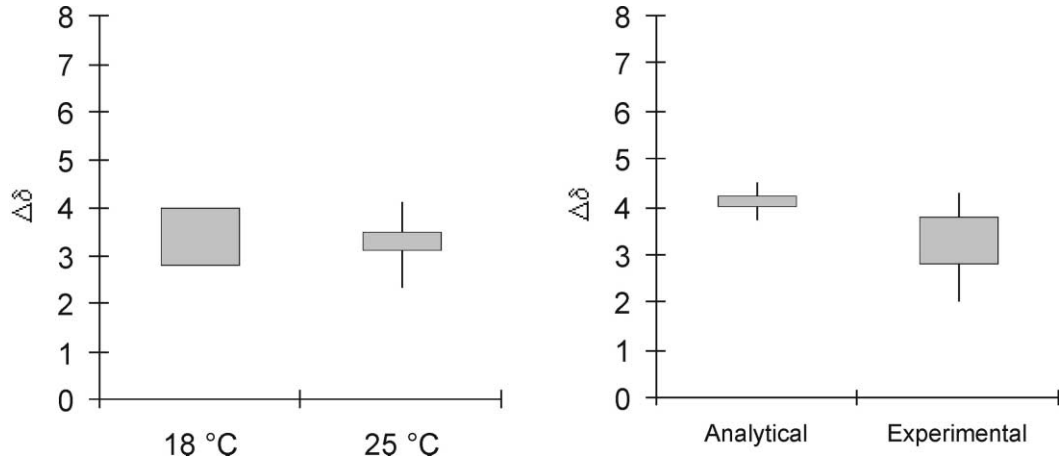

Fig. 5. Bar and whisker diagrams illustrating the influence of growth temperature on the Δδ ^{13}C isotope values of hasla −7(20), 9*E*,23-triene (**IV**) compared with phytol TMSi ether (isotopically corrected) in *Rhizosolenia setigera* CS 389/A. (a). Culture grown for three growth cycles at 18 and 25 °C. Analyses made in duplicate (18 °C) and triplicate (25 °C). (b). Culture grown for four growth cycles at 18 °C in triplicate. The results of triplicate analysis of a single sample ('Analytical') and full experimental triplicate ('Experimental') are shown. The data indicate a 3–4 per mil depletion in ^{13}C in **IV** compared with phytol.

The isotopic compositions of the haslene (Fig. 5) and cholest-5,24-dienol (desmosterol) in the present strain grown at 18 °C, were about equal (Fig. 6f), again as found previously (Schouten et al., 1998). Schouten et al. concluded from these similarities, that (**I**) was biosynthesised, like the sterol, in the cytosol of the diatom cell and not in the plastid. Our data support the contention that the haslene and the sterol in *R. setigera* CS 389/A were biosynthesised from a similar isotopic pool of isopentenyl diphosphate in the culture grown at 18 °C; perhaps in the cytosol.

At 25 °C, however, the Δδ values of the haslene (ca. 3–4 per mil; Fig. 5a) and the sterol (1–2 per mil; Fig. 6f) were somewhat different; certainly in the 4th generation samples for which the most comprehensive data set was obtained (Figs. 5a and 6f). In fact, the Δδ value of the sterol at both 18 and 25 °C, closely matched the value of the dominant alkene at each temperature (Fig. 6a, d, and f). Thus, at 18 °C, the dominant rhizenes were the *E*-pentaene (Figs. 4b and 6a; **IX**) and hexaene (Figs. 4b and 6c; **VII**) and the Δδ values of both these (and the *E*-haslatriene) and the sterol were about 3–4 per mil in the 3rd generation and in the 4th generation samples (Figs. 5a,b and 6a, c, and f). At 25 °C, the dominant alkene was an unknown hexaene (30:6 Figs. 4c and 6d), and whilst there was some spread in the data, the mean range of Δδ values of both this and the sterol were lower than those of the haslene (Fig. 5a) and the other rhizenes.

These data suggest that the biosynthesis of the dominant alkenes and sterol are coupled at both temperatures, probably from an isotopically similar pool of isopentenyl diphosphate.

Interestingly, the Δδ values of some of the individual alkenes varied quite considerably. Thus whilst the values for the C_{30} rhizapentaene (**VIII**; Fig. 6b) and rhizahexaenes (**VII**; Fig. 6c; **VI**; Fig. 6e) were similar to that of the haslenes (ca. 3–4 per mil) at both temperatures, these varied somewhat from those of the unknown hexaene 30:6 (Fig. 6d) . (Although there also appeared to be a difference in the Δδ values of the pentaene (**IX**; Fig. 5a) between 18 and 25 °C (Fig. 6a) this probably reflected the very low abundance of the pentaene at the higher temperature (0.15 ± 0.07 pg cell^{-1}; Fig. 4c), which made measurement much less accurate and prone to influences from co-eluting compounds such as bis(2-ethylhexyl)phthalate, a contaminant which was present in the procedural blank and had a similar retention index to the alkene).

Clearly, the isotope studies support our earlier conclusion that biosynthesis of the HBIs in *R. setigera* strain CS 389/A is complex. The following interpretations must therefore be viewed as speculative. Overall the isotopic measurements suggest:

1. Biosynthesis of phytol from an isotopically different pool of IPP to the haslenes, rhizenes and sterol at 18 °C, in the plastid, in agreement with a previous report for a Δ5 haslene in a different *R. setigera* strain.
2. Particularly close coupling of the biosynthesis of the major alkenes and the sterol at both temperatures, but some differences in isotopic fractionation of carbon even within the different C_{30} alkenes, especially between VI,VII and the unknown $C_{30:6}$ (Fig. 5c, d and e) at the highest growth temperature.

We propose, at both 18 and 25 °C, biosynthesis of phytol in the chloroplast from geranyl diphosphate probably via a non-mevalonate route from CO_2 as is true of phytol production in some other diatoms (Cvejic and Rohmer, 2000).

At 18 and 25 °C, we envisage biosynthesis of haslenes probably outwith the plastid, either via a mevalonate

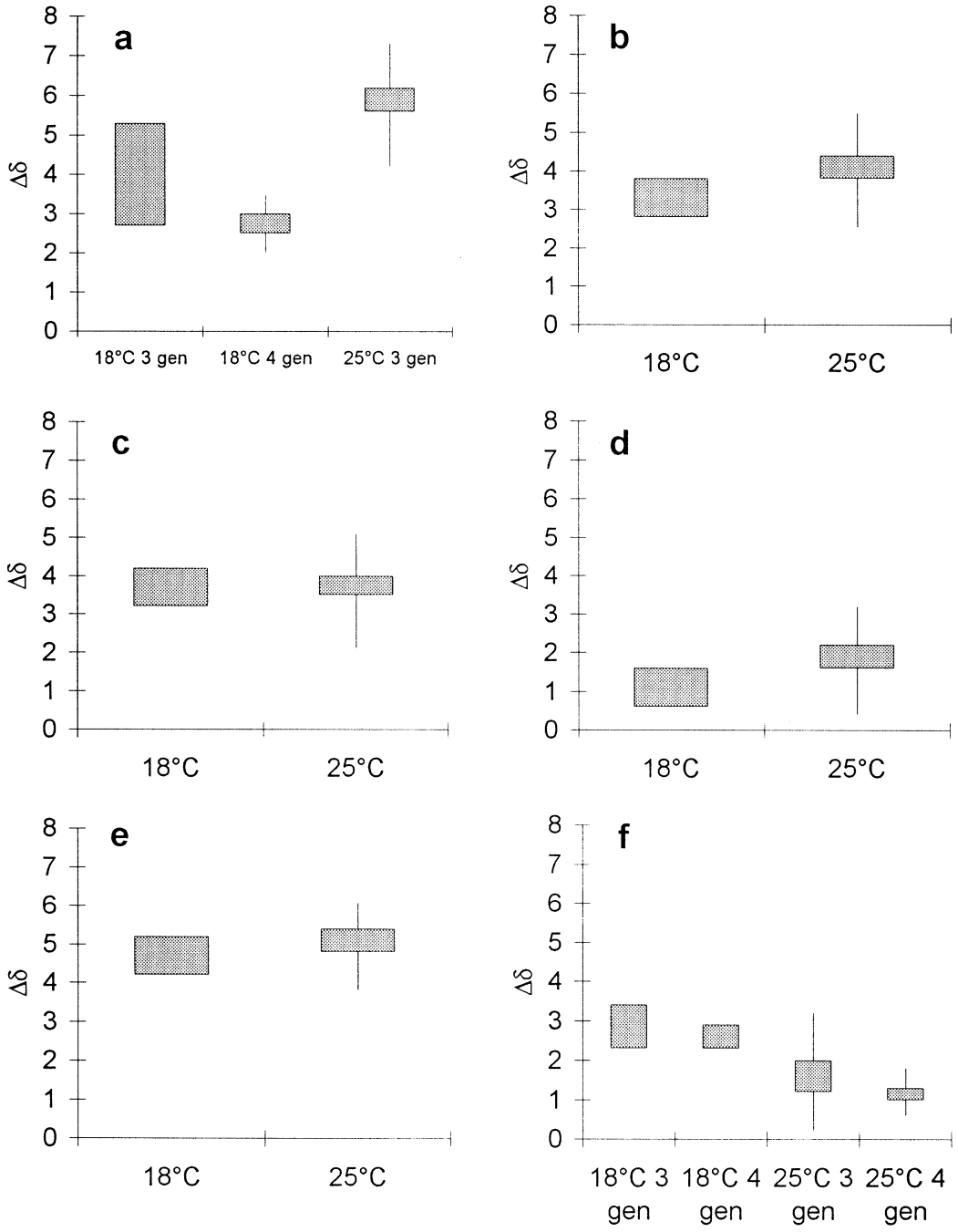

Fig. 6. Bar and whisker diagrams illustrating the influence of growth temperature on the $\Delta\delta$ ^{13}C isotope values of alkenes (**VII**–**IX**, Unknown 30:6) and cholesta-5,24,-dienol (TMSi ether, isotopically corrected) compared with phytol TMSi ether (isotopically corrected) for *Rhizosolenia setigera* CS 389/A cultures grown for three (3 gen) and four (4 gen) generations at 18 and 25 °C. (a) Rhizapentaene **IX**; (b) Rhizapentaene **VIII**; (c) Rhizahexaene **VII**; (d) unknown C_{30} hexaene 30:6; (e) Rhizahexaene **VI**; (f) cholest-5,24-dienol.

route leading to isotopic differences in the IPP compared with that used in phytol biosynthesis, or via a non-mevalonate route using an IPP pool which is isotopically distinct from that used in phytol production (cf. Cvejic and Rohmer, 2000). This might involve condensation of geranyl diphosphate (GPP) and a C_{15} isoprenyl moiety (possibly peruviyl diphosphate, PPP). The involvement of PPP rather than farnesyl diphosphate (FPP) might explain coupling to give the C-7 branched HBI structure, rather than coupling of GPP and FPP which would probably lead to a squalene-type structure.

Biosynthesis of many of the rhizenes at 18 and 25 °C (**VI**, **VII**, **VIII**, **IX**) might be from the same pool of IPP (and hence PPP) as that used for haslene biosynthesis at 18 and 25 °C, but biosynthesis of some C_{30} alkenes (e.g. unknown $C_{30:6}$)—and the sterol at 25 °C, must be from

a somewhat isotopically distinct IPP pool. Given the similarities in the isotopic values of the dominant alkenes and the sterol at both temperatures, we assume alkene synthesis from these IPP pools takes place out with the plastid, even though some terpene secondary metabolites are also believed to be produced in the chloroplast (e.g Cvejic and Rohmer, 2000, and references therein). Production in the cytoplasm is consistent with previous findings that diatoms are able to use different carbon sources in different cell compartments (Cvejic and Rohmer, 2000) and our unpublished findings which indicate that haslenes in *H. ostrearia* are not associated with the fatty acid storage lipids (which are found in the chloroplast).

Whilst more definitive studies of the biosynthetic pathways to the HBIs in *R. setigera* will also require growth of the diatom with isotopically enriched substrates, such as with $^{13}CO_2$ and also studies of the sites of ^{13}C incorporation by ^{13}C NMR, the GC-irm-MS approach used herein provided useful complementary information and did not require perturbation of algal growth with artificially high substrate concentrations or mixotrophic growth conditions. The results of our studies with isotopically enriched substrates will be published separately.

2.2. R. setigera strain CCMP 1330

When North Atlantic (off Massachusetts, USA), strain CCMP 1330 was cultured at 4–20 °C previously, it was shown to produce haslapentaene (**I**) as the only HBI, even when growth temperature was varied. (**I**) was also the only HBI produced when the same strain was cultured at 15 °C in the present study (Fig. 7a). The HBI was identified by comparison of GC and MS data with authenticated samples from *H. ostrearia* (Wraige et al., 1997) and an aliquot of the previous sample isolated from *R. setigera* (Sinninghe Damsté et al., 1999b). The *n*-alkenes reported previously were also present (Fig. 7a).

2.3. R. setigera strain CCMP 1820

The HBIs of this strain have not been reported previously but were found herein (Fig. 7b) to comprise haslapentaene (**I**) as the only HBI in a culture grown at 15 °C . Again, *n*-alkenes were also present (Fig. 7b).

2.4. R. setigera Nantes 1999 and Nantes 2000

Strains of *R. setigera* isolated from the North Atlantic (off southern Brittany, France) contained, like the Tasmanian strain CS 389/A, both haslenes and rhizenes (Fig. 7c and d) and similar to that strain, the haslenes included trienes (**IV** and **V**) with C7(20) unsaturation. The corresponding tetraene [viz. hasla-7(20),9*E*,13, 23-tetraene; **X**] and traces of the corresponding Δ2 pentaene (cf. Belt et al., 2000b) were also present in this strain grown at 15 °C. All compounds were identified by GCMS retention time and mass spectral comparison with previously authenticated compounds from *P. intermedium* (Belt et al., 2000a,b). The rhizenes present comprised two pentaenes and two hexaenes, both with C7(25) unsaturation (**VI**–**IX**) as determined by NMR for strain CS 389/A above. The relative proportions of HBIs, which were very similar in two samples, collected and cultured one year apart, are shown in Fig. 7c and d.

3. Experimental

3.1. Algal cultures

R. setigera strain CS 389/A isolated from the Huon estuary, Tasmania, Australia, was grown at 10, 18 or 25 °C, 35 psu, under white light at 80 μE m^{-2} s^{-1} in fE or fE/2-1 medium as described previously for other strains (Volkman et al., 1994, 1998). Both small scale (250 ml Erlenmeyer flasks) and larger scale samples (10 l, 18 °C) were cultured.

R. setigera strains isolated from France (Nantes 99 and Nantes 00) were isolated from Le Croisic, France and cultured in 4×60 l tanks containing underground saltwater enriched with $NaNO_3$ (8 mg ml^{-1}) and Guillard's medium (f/2, 0.2 ml l^{-1}) at 16–18°C and on the smaller scale at 15°C. Samples for hydrocarbon analysis were obtained by centrifugation. Strains CCMP 1330 and 1820 were purchased from the Guillard Collection USA and grown under the same conditions as the French strains above.

3.2. Lipid extraction and alkene isolation

Alkenes were isolated by extraction of the centrifuged algal paste with chloroform (strain CS 389/A) or hexane, aided by ultrasonication (45 min, Kerry Pulsatron HB172) followed by column chromatogaphy on silica and elution with hexane. Selected samples were saponified by heating (60 °C, 1 h) in methanolic KOH (e.g. Volkman et al., 1998) and derivatised with BSTFA/TMCS (60 °C, 30 min) prior to analyses by GC-MS and GC-irm-MS.

3.3. NMR spectroscopy

NMR spectroscopy was conducted on a JEOL EX 270 multinuclear (^1H, ^{13}C) 270 MHz spectrometer. Data were recorded on the delta scale (ppm) using the resonances of $CDCl_3$ (7.25 ppm ^1H, 77.0 ppm ^{13}C) as internal references.

3.4. Gas chromatography–mass spectrometry

Derivatised total chloroform extracts (Figs. 3 and 4), non-saponifiable lipids (Fig. 7) or alkene fractions (for

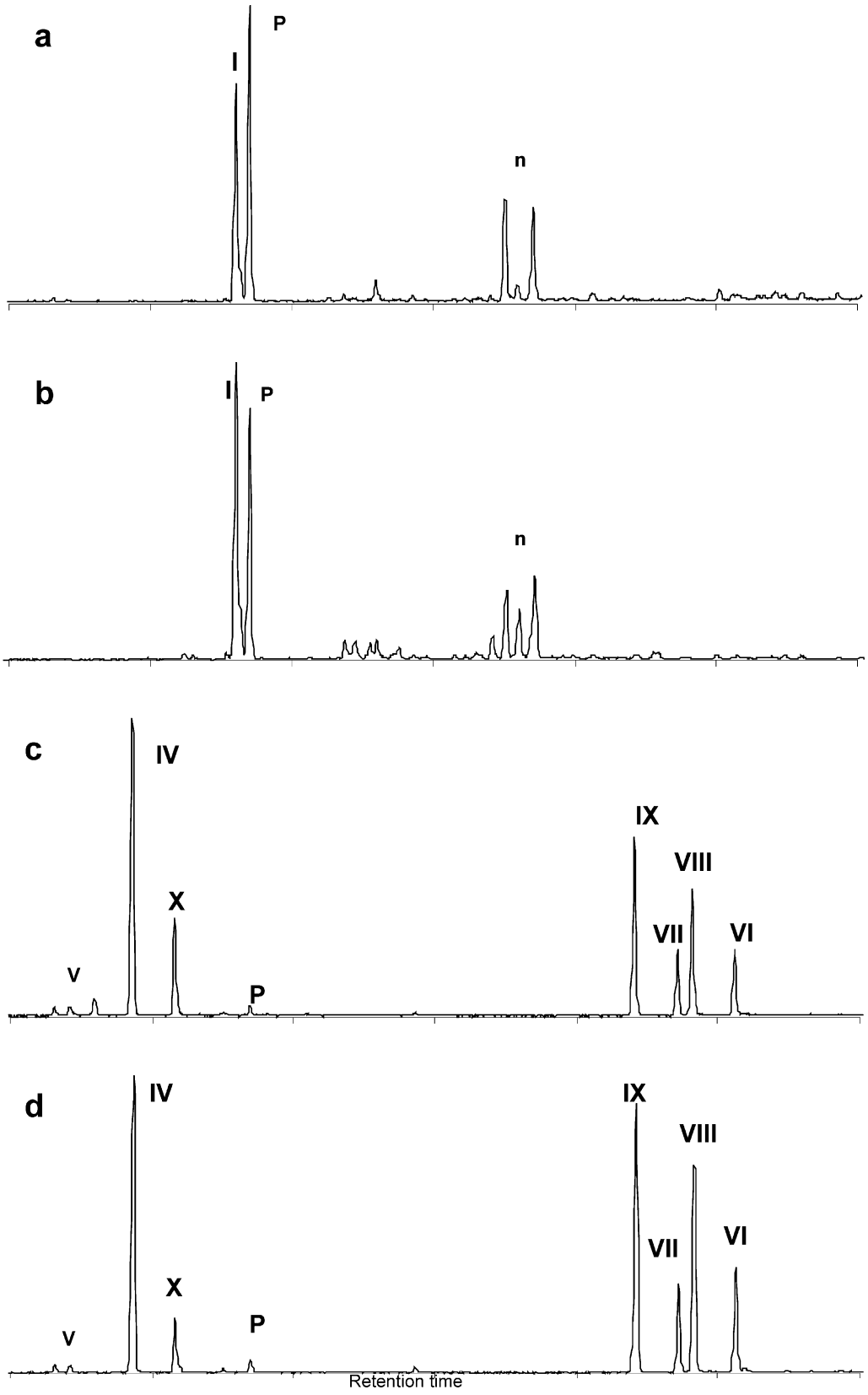

Fig. 7. GCMS total ion current chromatograms of non-saponifiable lipids (TMSi ethers) of *R. setigera* strains CCMP 1330, CCMP 1820, Nantes 99 and Nantes 00. P = phytol, TMSi ether; n = *n*-alkenes. Roman numerals refer to HBI structures shown. (a) *Rhizosolenia setigera* CCMP 1330; (b). *Rhizosolenia setigera* CCMP 1820; (c) *Rhizosolenia setigera* Nantes 1999; (d) *Rhizosolenia setigera* Nantes 2000.

NMR) from strain CS 389/A were examined by gas chromatography–mass spectrometry (GC-MS) performed using a Fisons Instruments MD800 equipped with a Carlo Erba on-column injector. The gas chromatograph was fitted with a 12 m (0.2 mm i.d.) fused silica capillary column (HP-5 Ultra stationary phase). Helium carrier gas was used. The gas chromatograph oven temperature was programmed from 40 to 300 °C at 5 °C min^{-1} and held at the final temperature for 10 min. Mass spectrometer operating conditions were; ion source temperature 250 °C and 70 eV ionisation energy. Spectra (40–650 Daltons) were collected using Fisons Masslab™ software. Alkene fractions from all other strains were examined by gas chromatography-mass spectrometry (GC-MS) performed using a Hewlett Packard 5890 series II gas chromatograph coupled to a Hewlett Packard 5970 mass selective detector fitted with a 12 m (0.2 mm i.d.) fused silica capillary column (HP-1 Ultra stationary phase). Auto-splitless injection and helium carrier gas were used. The gas chromatograph oven temperature was programmed from 40 to 300 °C at 5 °C min^{-1} and held at the final temperature for 10 min. Mass spectrometer operating conditions were; ion source temperature 250 °C and 70 eV ionisation energy. Spectra (35–500 Daltons) were collected using Hewlett Packard Chemstation™ software.

3.5. Gas chromatography–isotope ratio monitoring–mass spectrometry

GC-irm-MS was performed with a Finnigan Delta S mass spectrometer essentially as described previously (Merrit et al., 1995). GC conditions were: oven temperature 40–135 °C at 30 °C min^{-1}, 135–300 °C at 4 °C min^{-1}; 60 m DB-1, helium carrier gas. Isotopic values were determined by integration of the ion currents of m/z 44–46 produced by combustion of chromatographically separated compounds and comparison with CO_2 reference gas. Certified reference materials comprising *n*-hexadecane, *n*-icosane, *n*-tetracosane, *n*-dotriacontane and *n*-hexatriacontane of known isotopic composition were co-chromatographed with the algal lipids derivatised with BSTFA/TMCS. Determinations of the haslene were made in full procedural triplicate, including culturing conditions and in analytical triplicate (Fig. 5b). To correct for the isotopic effect of the derivatisation of phytol and cholest-5,24-dienol with BSTFA/TMCS, both free phytol (Aldrich, 97% mixture of *E* and *Z* isomers; *E*-phytol, −28.02 per mil delta notation relative to PDB standard) and a sample of phytol derivatised with each batch of BSTFA/TMCS were examined by GC-irm-MS. The difference in values was used to calculate the isotopic composition of the TMS group using a published method (Jones et al., 1991).

Acknowledgements

We thank the British Council in Australia and the Royal Society of London for travel awards (S.J.R.) and the British Council for ALLIANCE travel awards (S.T.B., J.-M.R.). We are grateful to Dr. J. Sinninghe Damsté (NIOZ, The Netherlands) for a sample of pentaene (I) isolated previously from *R. setigera* CCMP 1330 (Sinninghe Damsté et al., 1999a,b).

References

Barrett, S.M., Volkman, J.K., Dunstan, G.A., LeRoi, J.-M., 1995. Sterols of 14 species of marine diatoms (*Bacillariophyta*). J. Phycol. 31, 360–369.

Belt, S.T., Allard, W.G., Massé, G., Robert, J.-M., Rowland, S.J., 2001. Structural characterisation of C_{30} highly branched isoprenoid alkenes (rhizenes) in the marine diatom *Rhizosolenia setigera*. Tetrahedron Lett. 42, 5583–5585.

Belt, S.T., Allard, W.G., Massé, G., Robert, J.-M., Rowland, S.J., 2000a. Highly branched isoprenoids (HBIs): identification of the most common and abundant sedimentary isomers. Geochim. Cosmochim. Acta 64, 3839–3851.

Belt, S.T., Allard, W.G., Rintatalo, J., Johns, L.A., van Duin, A.C.T., Rowland, S.J., 2000b. Clay and acid catalysed isomerisation and cyclisation reactions of highly branched isoprenoid alkenes: implications for sedimentary reactions and distributions. Geochim. Cosmochim. Acta 64, 3337–3345.

Cooke, D.A., Barlow, R., Green, J., Belt, S.T., Rowland, S.J., 1998. Seasonal variations of highly branched isoprenoid hydrocarbons and pigment biomarkers in intertidal sediments of the Tamar estuary, U.K. Mar. Environ. Res. 45, 309–324.

Cvejic, J.H., Rohmer, M., 2000. CO_2 as main carbon source for isoprenoid biosynthesis via the mevalonate-independent methylerythritol 4-phosphate route in the marine diatoms *Phaeodactylum tricornutum* and *Nitzschia ovalis*. Phytochemistry 53, 21–28.

Jones, D.M., Carter, J.F., Eglinton, G., Jumeau, E.J., Fenwick, C.S., 1991. Determination of $\delta^{13}C$ values of sedimentary straight chain and cyclic alcohols by gas chromatography/isotope ratio mass spectrometry. Biol. Mass Spectrom. 20, 641–646.

Merrit, D.A., Freeman, K.H., Ricci, M.P., Studley, S.A., Hayes, J.M., 1995. Performance and optimisation of a combustion interface for isotope ratio monitoring gas chromatography/mass spectrometry. Anal. Chem. 67, 2461–2473.

Prahl, F.G., Bennet, J.T., Carpenter, R., 1980. The early diagenesis of aliphatic hydrocarbons and organic matter in sedimentary particles from Dabob Bay, Washington. Geochim. Cosmochim. Acta 44, 1967–1976.

Robson, J.N., Rowland, S.J., 1986. Identification of novel, widely-occurring sedimentary sesterterpenoids. Nature 324, 561–563.

Robson, J.N., Rowland, S.J., 1988. Synthesis of a novel, highly branched, C_{30} sedimentary hydrocarbon. Tetrahedron Lett. 29, 3837–3840.

Round, F.E., Crawford, R.M., Mann, D.G., 1990. The Diatoms. Cambridge University Press, Cambridge, UK.

Rowland, S.J., Belt, S.T., Wraige, E.J., Massé, G., Roussakis, C., Robert, J-M., 2001. Effects of temperature on polyunsaturation in cytostatic lipids of *Haslea ostrearia*. Phytochemistry 56, 597–602.

Schouten, S., Klein Breteler, W.C.M., Blokker, P., Schogt, N., Rijpstra, W.I., Grice, K., Baas, M., Sinninghe Damsté, J.S., 1998. Biosynthetic effects on the stable carbon isotope compositions of algal lipids: implications for deciphering the carbon isotope biomarker record. Geochim. Cosmochim. Acta 62, 1397–1406.

Sinninghe Damsté, J.S., Rijpstra, W.I.C., Schouten, S., Peletier, H., van der Maarel, M.J.E.C., Gieskes, W.W.C., 1999a. A C_{25} highly

branched isoprenoid alkene and C_{25} and C_{27} *n*-alkenes in the marine diatom, *Rhizosolenia setigera*. Org. Geochem. 30, 95–100.

Sinninghe Damsté, J.S., Schouten, S., Rijpstra, W.I.C., Hopmans, E.C., Peletier, H., Gieskes, W.W.C., Geenevasen, J.A.J., 1999b. Structural identification of the C_{25} highly branched isoprenoid pentaene in the marine diatom, *Rhizosolenia setigera*. Org. Geochem. 30, 1581–1583.

Sundström, B.G., 1986. The Marine Genus *Rhizosolenia*. A New Approach to Taxonomy. PhD dissertation, Lund University, Lund, Sweden.

Volkman, J.K., Barrett, S.M., Dunstan, G.A., 1994. C_{25} and C_{30} highly branched isoprenoid alkenes in laboratory cultures of two marine diatoms. Org. Geochem. 21, 407–414.

Volkman, J.K., Barrett, S.M., Blackburn, S.I., Mansour, M.P., Sikes, E.L., Gelin, F., 1998. Microalgal biomarkers: a review of recent research developments. Org. Geochem. 29, 1163–1179.

Wraige, E.J., Belt, S.T., Lewis, C.A., Cooke, D.A., Robert, J.-M., Massé, G., Rowland, S.J., 1997. Variations in structures and distributions of the C_{25} highly branched isoprenoid (HBI) alkenes in cultures of the diatom, *Haslea ostrearia* (Simonsen). Org. Geochem. 27, 97–505.

Wraige, E.J., Belt, S.T., Johns, L., Massé, G., Robert, J.-M., Rowland, S.J., 1998. Variations in structures and distributions of the C_{25} highly branched isoprenoid (HBI) alkenes in cultures of the diatom, *Haslea ostrearia*: influence of salinity. Org. Geochem. 28, 855–859.

PERGAMON

Phytochemistry 58 (2001) 729–738

PHYTOCHEMISTRY

www.elsevier.com/locate/phytochem

Herbivore-induced allene oxide synthase transcripts and jasmonic acid in *Nicotiana attenuata*

Jörg Ziegler[1], Markku Keinänen[2], Ian T. Baldwin*

Department of Molecular Ecology, Max-Planck Institute for Chemical Ecology, Carl-Zeiss-Promenade 10, D-07745 Jena, Germany

Received 9 May 2001; received in revised form 8 June 2001

Abstract

Exogenous jasmonate treatment of *Nicotiana attenuata* Torr. ex Wats. plants elicits durable resistance against herbivores and attack from its specialist herbivore, *Manduca sexta,* results in an amplification of the transient wound-induced increase in endogenous jasmonic acid levels (JA). To understand whether this ''JA burst'' is under transcriptional control, we cloned allene oxide synthase (AOS; EC 4.2.1.92), the enzyme that catalyzes the dehydration of 13(*S*)-hydroperoxy octadecatrienoic acid to an allene oxide, the first specific reaction in JA biosynthesis. An AOS cDNA coding for a 520 aa protein (58.6 kDa) with an isoelectric point of 8.74 was overexpressed in bacteria and determined to be a functional AOS. Southern blot analysis indicated the presence of more than one gene and AOS transcripts were detected in all organs, with the highest levels in stems, stem leaves and flowers. Attack by *M. sexta* larvae resulted in a sustained JA burst producing an endogenous JA amount 9-fold above control levels and 3-fold above maximum wound-induced levels, a response which could be mimicked by the addition of *Manduca* oral secretion and regurgitant to puncture wounds. *M. sexta* attack, wounding and regurgitant treatment transiently increased AOS transcript in the wounded leaf, but increases were not proportional to the JA response. Moreover, transcript accumulation lagged behind JA accumulation. Systemic wound-induced increases in AOS transcript, AOS activity or JA accumulation could not be detected. We conclude that increase in AOS transcript does not contribute to the initial increase in endogenous JA, but may contribute to sustaining the JA burst. © 2001 Elsevier Science Ltd. All rights reserved.

Keywords: Herbivory; Jasmonic acid; Allene oxide synthase; Induced defense; *Nicotiana*

1. Introduction

Research into the molecular basis of herbivore resistance (Korth and Dixon, 1997; Reymond et al., 2000; Hermsmeier et al., 2001) has revealed that a plant's wound response is involved and that the octadecanoid pathway plays a central role in resistance in three plant–insect systems (Howe et al., 1996; McConn et al., 1997; Baldwin, 1998). This is not surprising given that herbivores force their way past their host plant's protective barriers and cause wounding when they feed. It is, however, now clear that plants respond differentially to mechanical damage as compared to damage caused by herbivores (Baldwin, 1990; Korth and Dixon, 1997; Reymond et al., 2000; Schittko et al., 2001). How herbivore feeding modifies a plant's wound responses has been studied in the model plant-herbivore system: *Nicotiana attenuata–Manduca sexta*.

In *Nicotiana* species, both herbivory and mechanical wounding of leaves leads to a strong accumulation in nicotine biosynthesis that can result in amounts lethal to many herbivores (Baldwin et al., 1994a; Baldwin, 1999). After wounding, a signal is transported from the leaves to the roots where putrescine methyltransferase transcript is induced followed by nicotine synthesis (Winz and Baldwin, 2001) and the newly synthesized nicotine is translocated back to the leaves (Baldwin, 1989). Additionally, a suite of growth and defense related genes show an altered expression (Hermsmeier et al., 2001). These responses can be mimicked by the application of jasmonates to leaves or roots (Baldwin et al., 1996; Winz and Baldwin, 2001) and the wound response is strictly dependent on the plant's ability to increase endogenous

* Corresponding author. Tel.: +49-3641-643659; fax: +49-3641-643653.

E-mail address: baldwin@ice.mpg.de (I.T. Baldwin).

[1] Present address: Institute of Plant Biochemistry, Department of Natural Product Biotechnology, Weinberg 3, D-6120 Halle, Germany.

[2] Present address: Institute of Biotechnology, University of Helsinki, POB 56 (Viikingaari 5D), FIN-00014, Helsinki, Finland.

0031-9422/01/$ - see front matter © 2001 Elsevier Science Ltd. All rights reserved.
PII: S0031-9422(01)00284-9

jasmonic acid (JA) levels (Baldwin et al., 1997). The strong positive relationships between the amount of wounding, the amount of JA and the strength of the responses are disrupted, however, when *M. sexta* larvae cause the damage (Baldwin et al., 1997; Schittko et al., 2001; Winz and Baldwin, 2001). After larval attack, a further elevation in the transient, wound-induced increase in JA can be accompanied by a suppression as well as an elevation of wound-induced responses (McCloud and Baldwin, 1997; Kahl et al., 2000; Schittko et al., 2000). These effects can also be elicited by placing minute amounts of oral secretion and regurgitant, consisting of a suite of fatty acid–amino acid conjugates, into puncture wounds on a leaf (McCloud and Baldwin, 1997; Schittko et al., 2000; Halitschke et al., 2001). The differential correlation between wound- and larval- induced responses and JA accumulation led us to consider the regulation of jasmonate biosynthesis in *N. attenuata*.

Allene oxide synthase (AOS) catalyzes the first step after the branch point 13(*S*)-hydroperoxy 9(*Z*)11(*E*)15(*Z*) octadecatrienoic acid (13(*S*)-HPOT) in the oxylipin pathway that leads to jasmonate biosynthesis (Hamberg and Gardner, 1992). This pathway starts with the lipoxygenase (LOX)-catalyzed insertion of molecular oxygen into position 9 or 13 of linolenic or linoleic acid, resulting in fatty acid hydroperoxides which can serve as substrates for several enzymes such as divinylether synthase, peroxygenase or hydroperoxide lyase. Only the dehydration of one specific linolenic acid hydroperoxide, 13(*S*)-HPOT, by AOS forms the intermediate allene oxide for JA biosynthesis (Fig. 1). This allene oxide is highly unstable and is either chemically hydrolyzed to α- and γ-ketol and racemic 12-oxo-phytodienoic acid (PDA) or is cyclized by allene oxide cyclase to enantiomeric PDA, which subsequently undergoes reduction and β-oxidation to yield JA.

AOS was first purified and the cDNA cloned from flax (*Linum usitatissimum* L.). It was shown to be a cytochrome P450-dependent oxidase of the CYP74A family (Chapple, 1998; Song and Brash, 1991; Song et al., 1993). The expression of the AOS gene has been strongly correlated with increased JA contents in many study systems. Tissues with high JA levels have high levels of AOS transcripts (Maucher et al., 2000). Treatments known to lead to increased JA levels, such as wounding or treatment with sorbitol or glucose, also increase AOS transcript levels (Harms et al., 1998; Laudert et al., 1998; Howe et al., 2000; Maucher et al., 2000; Sivasankar et al., 2000) or lead to high AOS promoter activity (Kubigsteltig et al., 1999). These results suggest an important regulatory role for AOS in the biosynthesis of JA and led us to examine the correlation between AOS transcript accumulation and JA accumulation in *N. attenuata*. We report herein the cloning[1], characterization and expression patterns of AOS after mechanical wounding, regurgitant treatment, and feeding by *M. sexta* larvae.

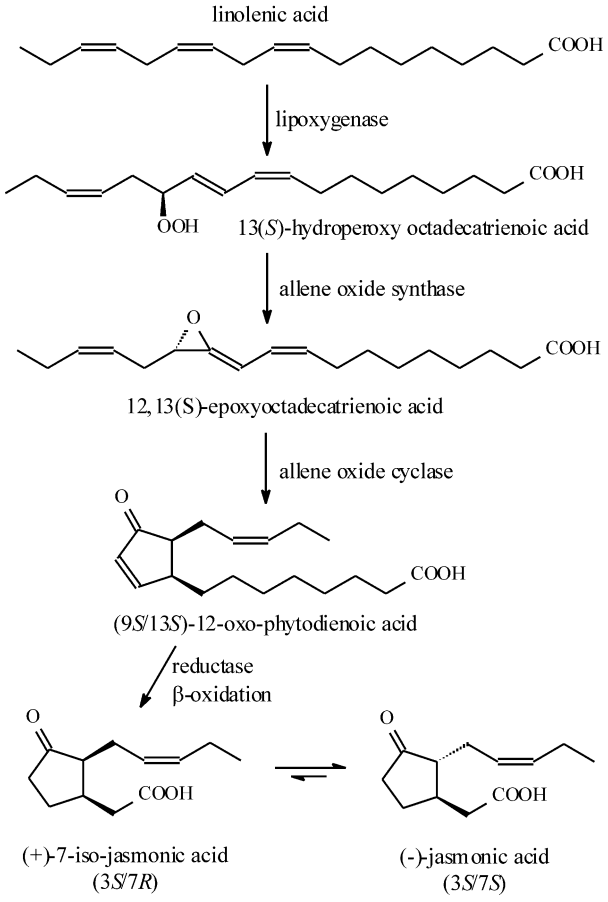

Fig. 1. Biosynthesis of jasmonic acid.

2. Results and discussion

2.1. Cloning and characterization of Nicotiana attenuata AOS

A cDNA library prepared from *N. attenuata* shoots subjected to larval feeding for 24 h was screened with the *Arabidopsis thaliana* AOS cDNA (Laudert et al., 1996). One clone of 1649 bp with strong sequence homology to other AOS cDNAs was obtained, but this clone did not encompass the whole coding region as indicated by the absence of a start codon. The missing upstream sequence was, therefore, generated by 5'RACE using mRNA isolated from leaves treated with MeJA. The full length sequence of 1761 bp contained an open reading frame of 1560 bp coding for a protein with 520 amino acids with a calculated molecular mass of 58.6 kDa and an isoelectric point of 8.74. On the protein level, the NaAOS was 79.4 and 71.3%, identical to both tomato AOS's (Sivasankar et al., 2000; Howe et al., 2000; accession numbers AJ271093, AF230371), 62.8% to the guayule AOS (Pan et al., 1995; X78166), 61.7% to the

[1] The cDNA sequence reported herein has been deposited in the GenBank database under the GenBank Accession Number AJ295274.

flax AOS (Song et al., 1993; U00428) and 60.3% to the *Arabidopsis* AOS (Laudert et al., 1996; X92510), but only 53.6% to the two AOSs of barley (Maucher et al., 2000; AJ250864, AJ251304). The heme binding consensus sequence P-V-NKQCAG of the CYP74A family of enzymes as well as the -G-KIL conserved motif, which is a CYP74-specific variation of the I helix forming the oxygen binding pocket in P450 enzymes (Brash and Song, 1995; von Wachenfeldt and Johnson, 1995) are largely preserved in the *N. attenuata* sequence (Fig. 2), but their contribution to AOS catalysis is yet unknown. It will be interesting to establish the importance of both motifs and their species-specific variations on the catalytic properties of AOS, especially considering that an allene oxide forming enzyme from corals exists that is not a member of the cytochrome P450-dependent enzymes but rather an enzyme with catalase-like properties (Koljak et al., 1997).

With the exception of guayule (*Parthenium argentatum*), where AOS represents the major protein in rubber particles and where the function is unknown (Pan et al., 1995), all AOS's implicated in JA biosynthesis have associated with chloroplasts. Arguments for this have either been the presence of an N-terminal chloroplast transit peptide on the protein (von Heijne et al., 1989; Song et al., 1993; Laudert et al., 1996; Howe et al., 2000; Sivasankar et al., 2000) or biochemical and immunocytological detection (Harms et al., 1995; Blée and Joyard, 1996; Maucher et al., 2000; Froehlich et al., 2001). The 5′ end of the NaAOS also codes for a chloroplast signal peptide as determined by the enrichment of hydroxylated amino acid residues (10% T and 18% S within the first 49 residues), the presence of an A at position 2, and the absence of charged amino acids at the N-terminal 20 amino acids (Fig. 2). Computer analysis of the first 100 amino acids using the Chlorop V1.1 program (http://www.cbs.dtu.dk/services/ChloroP/) also predicted a chloroplastidial localization with a putative cleavage site between positions 44 and 45. This indicates that the NaAOS probably also resides within the chloroplasts.

A truncated clone from the cDNA library screen that lacks 13 N-terminal residues was cloned in the expression vector pQE31 and transformed into *Escherichia coli* SG13009 host cells. Measurements of the decrease in absorbance at 235 nm revealed that bacteria harboring the vector including the insert showed a 13(*S*)-HPOT decomposing activity of 5.1 nkat/mg of protein, which was absent either in uninduced bacteria or bacteria transformed with the vector lacking the insert. GC–MS analysis of the reaction products showed the presence of two peaks with mass spectra identical to α-ketol and PDA, indicating that the recombinant *N. attenuata* protein is able to catalyze the AOS reaction.

2.2. Genomic organizsation and tissue specificity

Southern blot analysis of genomic DNA digested with endonuclease *EcoRI* or *EcoRV*, for which there are no recognition site within the *aos* reading frame, revealed in both cases a very strong, broad hybridizing band, which might be composed of two closely migrating

A

```
1    CAGTCCCATCTCCCACTACTTAAAGTTCCTCTTACCTTTTTATCAAAAAATCACACTTCATTTTCTTACAACA  73

74   ATGGCAGTAGCAACAGCAACAGCAACATTATCTTCATCTTCTTCACTTCCCTTCCATTCTCTTCATCAACAGT 146
 1    M  A  V  A  T  A  T  A  T  L  S  S  S  S  S  L  P  F  H  S  L  H  Q  Q    24

147  TTCCTTCAAAATACTTCACTGTTCGTCCCATTACAGTCTCTTTATCCGAAAAAATACCAGCAGTAACACAG   220
25   F  P  S  K  Y  F  T  V  R  P  I  T  V  S  L  S  E  K  I  P  A  V  T  Q    49
```

B

```
                heme binding              I-helix

N.a.    467 P T V E N K Q C A G    327 G G M K I F F P
L.u     482 P S V A N K Q C A G    342 G G F K I L F P
P.a.    419 P T V E N K Q C A G    279 G G V K I L F P
A.t     463 P T V G N K Q C A G    323 G G M K I L F P
H.v.1   427 P S V H N K Q C P G    286 G G L K V L L P
H.v.2   421 P S V D N K Q C P G    281 G G L K V M L P
L.e.1   480 A S I N N K Q C A G    340 G G I K I F F P
L.e.2   458 P T V G N K Q C A G    318 G G M K I F F P
consensus   P - V - N K Q C A G        - G - K I L - -
```

Fig. 2. A, N-terminal sequence of *N. attenuata* AOS; underlined: sequence obtained by 5′RACE; double underlined: putative chloroplast transit peptide cleavage site as predicted by the Chlorop V1.1 program (http://www.cbs.dtu.dk/services/ChloroP/). B, comparison of the heme binding domain and the oxygen binding I-helix of all AOS cloned thus far. N.a., *Nicotiana attenuata*; L.u., *Linum usitatissimum* (accession number: U00428); P.a., *Parthenium argentatum* (X78166), A.t., *Arabidopsis thaliana* (X92510); H.v. *Hordeum vulgare* (AJ250864 and AJ251304 for 1 and 2, respectively); L.e. *Lycopersicon esculentum* (AJ271093 and AF230371 for 1 and 2, respectively).

fragments (Fig. 3). Restriction with endonuclease *HindIII* or *XbaI*, for which one recognition site is present within the *aos* reading frame, gave a more complex banding pattern, suggesting the existence of at least two genes coding for AOS in the *N. attenuata* genome. The expression level of AOS transcript was almost undetectable in roots and rosette leaves, but was clearly visible in stem leaves and flowers (Fig. 4). Consistent with the AOS promoter activity in *Arabidopsis* (Kubigsteltig et al., 1999) and the AOS transcript level in *Lycopersicon esculentum* (Howe et al., 2000), *N. attenuata* AOS was highly expressed in stems.

2.3. AOS mRNA, activity and JA levels after M. sexta attack, wounding, regurgitant and MeJA treatment

Leaf damage could be observed within minutes after *M. sexta* larvae had been placed on the leaf and within 1 h of feeding, JA levels were significantly elevated and continued to increase up to 6 h, followed by a plateau until 12 h with amounts up to 1.8 μg/g fr., an approximate 9-fold increase above unwounded levels and a 3-fold increase above maximum wound-induced levels (Fig. 5A). As judged by the leaf damage, the larvae slowed down feeding after 12 to 14 h and JA levels strongly decreased until even uninduced levels at 18 h are attained.

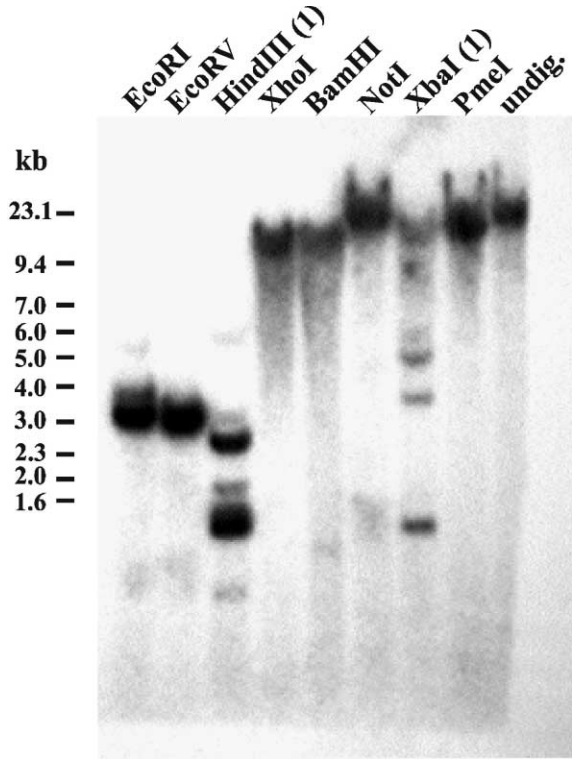

Fig. 3. Southern blot analysis of *Nicotonia attenuata* AOS. Genomic DNA was digested with the indicated restriction endonucleases. Numbers in parenthesis refer to the number of restriction endonucleases recognition within the cDNA used for hybridization. Undig., undigested genomic DNA.

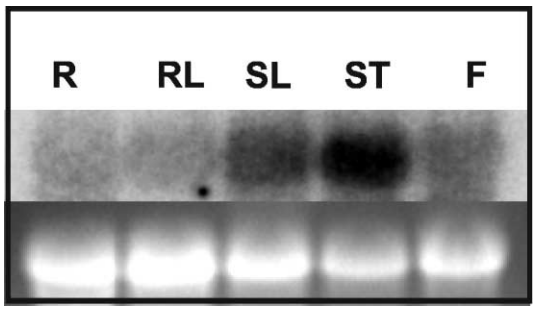

Fig. 4. Tissue specific expression of *Nicotonia attenuata* AOS. R, roots; RL, rosette leaves; SL, stem leaves; ST, stems; F, flowers. Ethidium bromide stain of 28S rRNA serves as loading control.

JA levels increased again when larvae started to feed again during the next light phase. The strong association of JA induction with feeding activity was observed in all three replicates and was found to be independent of light conditions. Concomitant with the increase in JA values, AOS transcript started to accumulate after 1 h and remained elevated for the entire time period, although at a lower level during the last 12 h (Fig. 5B). Quantification of the AOS transcript level and regression against leaf JA contents showed no significant correlation ($r^2 = 0.143$; $t_{slope} = 1.634$; $P = 0.122$). Increases in AOS transcript or JA levels in the systemic leaves were not observed.

Measurements of the metabolism of 13(*S*)-HPOT in crude extracts, which includes several enzyme activities in addition to AOS, revealed no significant change throughout the feeding experiment (data not shown). An enzyme assay with ^{14}C-labeled substrate failed to identify any AOS-specific reaction products. Instead, only substances co-migrating on reversed-phase HPLC with those observed after incubation of the substrate with recombinant hydroperoxide lyase could be detected (M. Keinänen, J. Ziegler and I.T. Baldwin, unpublished data). AOS enzyme activity could be recovered from many plant species as well as in preparations from the bacterial-expressed *N. attenuata* AOS. The same extraction method and co-incubation with plant extracts did not change the activity of recombinant AOS. Active AOS enzyme is, therefore, likely present in leaf extracts but at a very low level, that could be masked by strong hydroperoxide lyase activity. Although the constant hydroperoxide decomposing activity observed throughout the experiment may have resulted from changes in relative contributions of enzymes to this reaction, we did not observe changes in the profiles of the reaction products, which suggests that no significant changes occurred in AOS activity.

To control the onset and duration of wounding more precisely, *Nicotiana* plants were wounded with a fabric pattern wheel and either water or regurgitant was immediately applied to these wounds. A sharp JA burst starting already after 5 min that reaches a maximum at 45 min was observed, after which the JA level returned

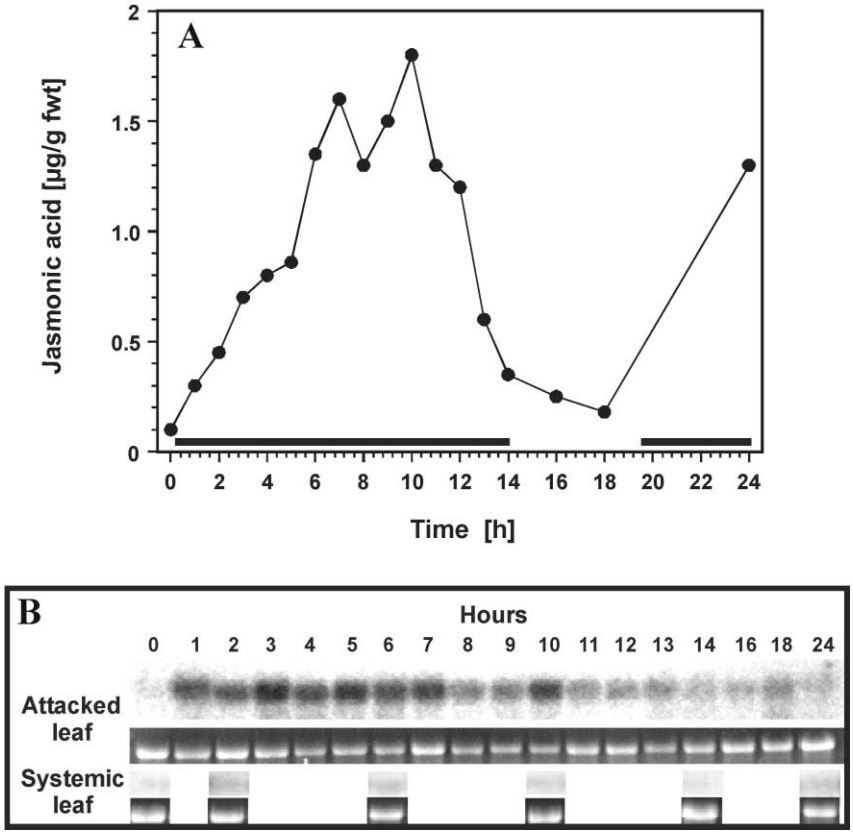

Fig. 5. Jasmonic acid levels (A) and AOS transcript accumulation (B) in attacked and adjacent, unattacked (systemic) leaves. Three first instar *Manduca sexta* larvae were placed on a mature leaf and allowed to feed for the times indicated. An individual plant was harvested at each time point and JA and northern analyses were performed on the attacked leaf tissue, while only northern analysis was performed on the unattacked leaf tissue because JA levels are known not to increase in adjacent unattacked leaves after *Manduca sexta* attack (Baldwin et al., 1997). The black bar in A denotes the time when larvae were actively feeding. Ethidium bromide stained 28S rRNA is shown as loading control.

to and remained at the basal level throughout the time course (Fig. 6A; Kahl et al., 2000; Schittko et al., 2000). Such a burst of JA also occurred during the wound response in *Macaranga tanarius* (Heil et al., 2001), but in tomato, *Arabidopsis* and *Nicotiana tabacum*, the wound-induced increase in JA persists for several hours after the initial increase or is biphasic (Laudert et al., 1996, 2000; Laudert and Weiler, 1998; Reymond et al., 2000). Although one can not exclude species specific variations, the differences in the JA response might be explained by the different types of mechanical wounding, since long lasting JA accumulations were induced by wounding larger leaf areas with a hemostat, whereas the JA bursts were induced by punching small wholes into the leaves, either with a needle or with a fabric pattern wheel.

The application of oral secretion and regurgitant from larvae reared on *N. attenuata* leaves to the puncture wounds amplified the wound-induced JA response approximately 2-fold (Fig. 6A; Kahl et al., 2000; Schittko et al., 2000). Elevated levels of AOS transcript were observed in *N. attenuata* for 3 to 4 h after wounding and were clearly preceded by the rapid increase in JA (Fig. 6B). This differs from flax, tomato and *Arabidopsis*, where AOS transcript remains elevated for more than 10 h (Harms et al., 1998; Howe et al., 2000; Sivasankar et al., 2000) or has been shown to be biphasic with a depression at 2 h (Laudert et al., 1996; Laudert and Weiler, 1998, but see Reymond et al., 2000) and where the induction of AOS gene expression accompanied or preceded JA accumulation.

Interestingly, while regurgitant treatment doubled the JA response, significant differences in neither the magnitude nor the kinetics of AOS transcript accumulation in the two treatments were detected (t_{13}s < 0.5; Ps > 0.62; Fig. 6B). In addition, the changes in AOS transcript accumulation after caterpillar attack (Fig. 5B) are not dramatically different from those resulting from mechanical wounds (Fig. 6B), despite the 9-fold differences in the amount of JA (Figs. 5A and 6A). Comparison of transcript accumulations between blots should, however, be interpreted with caution.

A second wounding event between 1–4 h after the first elicited a new burst of JA accumulation that was comparable in magnitude and timing to the first JA burst (Fig. 7A). Even an additional wounding event after 1 h, at a time when the JA content had started to decrease, led to second increase in JA, albeit slightly attenuated. This suggests a rapidly-regulated mechanism of JA generation

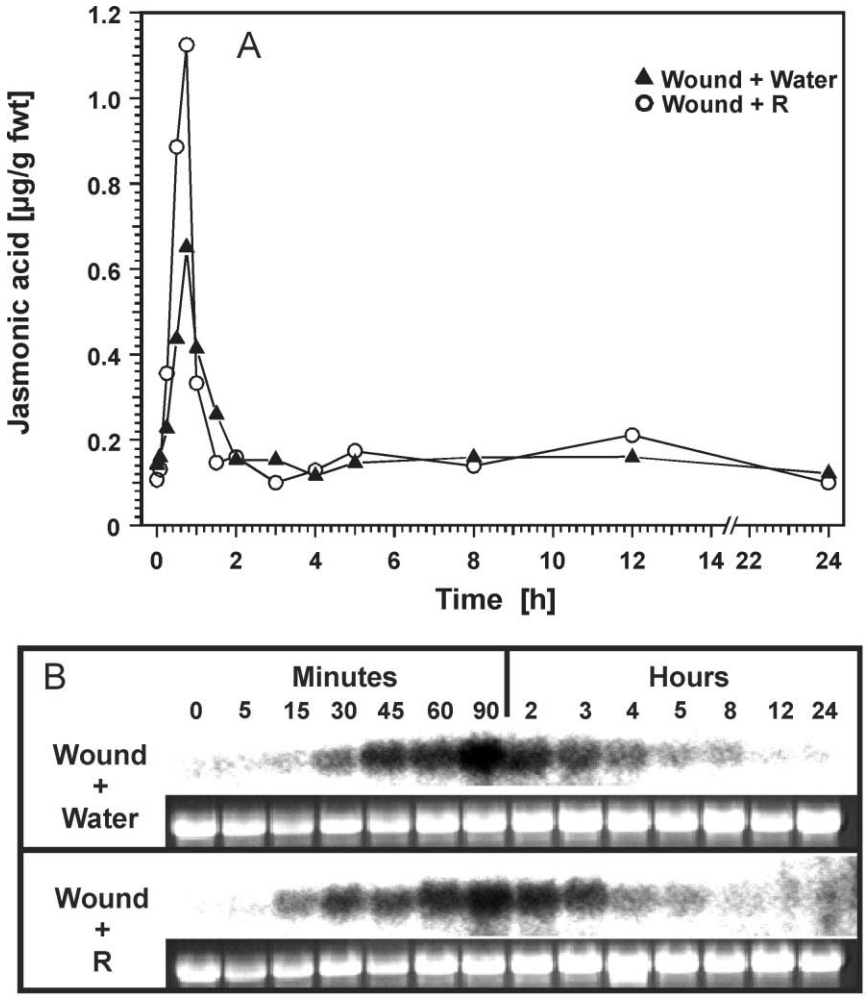

Fig. 6. Jasmonic acid levels (A) and AOS transcript accumulation (B) after wounding and water treatment or treatment with oral secretion and regurgitant (R) from *Manduca sexta* larvae. Leaves were wounded once at time zero using a fabric pattern wheel. Treated leaves from separate plants were harvested at the times indicated. Regurgitant was collected from 4th to 5th instar *Manduca sexta* larvae, diluted 1:5 with water and applied immediately after leaves were wounded. Ethidium bromide visualized 28S rRNA serves as loading control.

and degradation. If transcriptionally regulated de novo synthesis and degradation of AOS were responsible for these rapid changes, comparably rapid changes in transcripts should also occur. But the accumulation of AOS transcript after two wounding events (Fig. 7B) was not substantially different from those observed after a single wounding event (Fig. 6B). The higher basal AOS transcript level in this experiment was occasionally observed and was depending on the age and the growth of the plants.

There was only a tendency for a sustained increase the longer the second wound event was delayed (Fig 7B). The data on the kinetics and correlation of JA accumulation, AOS transcript and enzyme activity after a single wounding event raises the question whether the induction of JA in *N. attenuata* is caused by transcriptional activation of AOS. Although one cannot exclude that in *N. attenuata* other biosynthetic enzymes show an induction pattern on the transcriptional level concomitant with the JA levels, comparison with other systems suggest that neither transcripts of AOS (Fig. 5B; Laudert et al., 1996; Harms et al., 1998; Laudert and Weiler, 1998; Howe et al., 2000; Sivasankar et al., 2000), LOX (Bell et al., 1993; Heitz et al., 1997), 12-oxo-phytodienoic acid reductase (Costa et al., 2000) and allene oxide cyclase (Ziegler et al., 2000) nor their respective protein or enzyme activities change as rapidly as observed in wound-induced JA levels. Thus, other mechanisms other than transcriptional activation of JA biosynthetic genes are likely to account for wound-induced JA accumulation.

One possible explanation is post-translational activation. Although there is no report on post-translational activation of JA biosynthetic enzymes, the observation that tobacco plants compromised in the expression of a wound-inducible protein kinase (Seo et al., 1995) failed to accumulate JA after wounding as well as that the incubation of barley leaves with ursolic acid, a selective inhibitor of cyclic AMP-dependent protein kinases (Wasternack at al., 1994; Wang and Polya, 1996) failed to accumulate JA after sorbitol stress, indicates that

protein phosphorylation/dephosphorylation might play a role in the regulation of JA accumulation. In animal systems, for example, phosphorylation activates a phospholipase A2, which leads to the release of arachidonic acid needed for the biosynthesis of prostaglandins and leukotrienes. Whether a similar scenario also occurs in plant cells remains to be established, although free linolenic acid content after wounding (Conconi et al., 1996) and sorbitol stress increases simultaneously with the JA level. This suggests that substrate availability may have a role in the regulation of JA biosynthesis.

Although there are at least two lipoxygenase isoforms in *Arabidopsis*, co-suppression of only one specific chloroplast lipoxygenase gene resulted in the inability to induce JA biosynthesis (Bell et al., 1995). In contrast to this, antisense mediated depletion of one of two 13(*S*)-HPOT specific, wound-inducible lipoxygenase genes in potato did not affect JA levels, but reduced downstream events such as the induction of proteinase inhibitors (Royo et al., 1999). Thus, apart from enzymatic properties

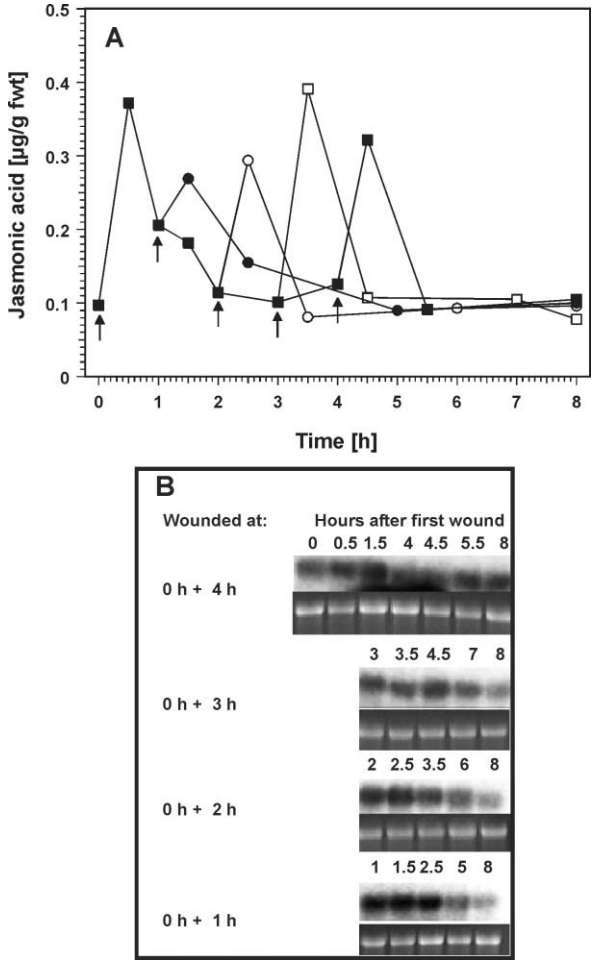

Fig. 7. Jasmonic acid levels (A) and AOS expression (B) after repetitive mechanical wounding. Leaves were wounded with a fabric pattern wheel at time zero (closed squares) and a second time (→) at either 4 h (■), 3 h (□), 2 h (○) or 1 h (●) after the initial wounding event. Leaves from an individual plant were harvested at each sampling time.

and the induction pattern, other factors must be decisive for the control of JA biosynthesis. One of these factors might be the compartmentation of biosynthetic enzymes. This is supported by the recently reported spatial distribution of enzymes for JA biosynthesis and competing reactions, which suggests that substrate flow through the different pathways might regulate JA accumulation (Froehlich et al., 2001). Laudert and Weiler (1998) recently suggested that the transport of precursors might regulate JA biosynthesis, reasoning that the decrease in JA biosynthesis by salicylic acid treatment might be due to the inhibition of the export of the JA precursor PDA out of the chloroplast. While these are plausible models, the available data on the rate-limiting steps of stress-induced JA accumulation are still too preliminary to favor support any one distinct particular mechanism.

AOS expression was strongly and transiently induced in leaves after MeJA treatment (Fig. 8) and, with a delay of 8 h, was accompanied by a steady increase in hydroperoxide metabolizing activity. But again, this activity could only be ascribed to hydroperoxide lyase activity (M. Keinänen, J. Ziegler and I.T. Baldwin, unpublished results). MeJA-induced AOS transcript level is also observed in flax (Harms et al., 1998), *Arabidopsis* (Laudert and Weiler, 1998), barley (Maucher et al., 2000) and tomato (Sivasankar et al., 2000). This can be interpreted as feedback activation of AOS leading to an increased capacity of the octadecanoid pathway (Laudert and Weiler, 1998). Recent experiments in barley have demonstrated that exogenous application of MeJA or JA does not lead to de novo biosynthesis of JA (Kramell et al., 2000), although the level of AOS transcript (Maucher et al., 2000) and enzyme activity (Ziegler, unpublished) are induced. The biological significance and the role of the induction of AOS gene transcription by exogenous MeJA remains unclear.

3. Materials and methods

3.1. Plant growth and treatments

Seeds from an inbred line (DI92) of *N. attenuata* originating from a natural population in Utah (Baldwin, 1998) were germinated in peat soil soaked with 1:50 dilution of liquid smoke (House of Herbs, Passaic, NY, USA) to synchronize germination (Baldwin et al., 1994b). After two weeks, seedlings were transferred to individual pots. After growth for an additional 10–14 days, plants had reached the rosette stage with 6–8 leaves and were ca. 2–3 days before bolting. The experiments were then conducted. Plants were grown in a 32 °C/16 h light, 26 °C/8 h dark regime with a constant air humidity of 65%. The same conditions were used during the experiments. In a phyllotactically consecutive leaf sequence, the leaf one leaf position older than the source/sink

transition leaf was assigned as the treated, local leaf, and the leaf one position younger was assigned as the systemic, untreated leaf.

Manduca sexta larvae were hatched from eggs (Carolina Biological Supply, Burlington, NC, USA) as described (Hermsmeier et al., 2001). Regurgitant was collected from the oral cavity of 4th and 5th instar larvae fed *N. attenuata* foliage according to (Schittko et al., 2001). Leaves were wounded by rolling a fabric pattern wheel six times parallel to the midvein over the upper leaf surface. In treatments with regurgitant, 20 μl of the diluted regurgitant were applied to the fresh puncture wounds of the leaf. In feeding experiments, three first instar *M. sexta* larvae were placed on a leaf and were allowed to feed for the times indicated in Fig. 5. MeJA was applied to the upper surface of the treated leaf in a lanolin paste. Each individual leaf was harvested as follows: one incision was made along the midvein taking care to leave one section without the midvein and two parallel incisions were made in the middle of the leaf lamina across the midvein, resulting in six leaf sections, which were weighed, flash frozen in liquid nitrogen and stored at −80 °C until used. The basal and apical parts without the midrib were used for the analysis of JA, the corresponding parts with the midrib were used for the extraction of RNA, and the central two parts were used for the extraction of enzymes.

3.2. Analysis of JA

JA was extracted and quantified with [1,2-^{13}C] JA as an internal standard by GC–MS as described in Baldwin et al. (1997).

3.3. Preparation of protein extracts

Leaf tissue was ground under liquid nitrogen and the resulting powder was extracted with 50 mM Na-phosphate buffer pH 7 containing 2% (w/v) PVPP and 0.1% (v/v) Triton X-100. The homogenate was centrifuged at 12,000 *g* for 10 min and the supernatant was used as the enzyme extract.

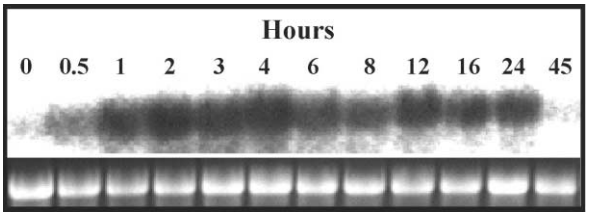

Fig. 8. AOS expression after treatment with methyl jasmonate. Fifty micrograms MeJA was applied to the upper surface of the leaf in 20 μl of lanolin paste. Ethidium bromide stain of 28S rRNA serves as loading control.

3.4. Enzyme assays

The substrate, 13(*S*)-HPOT, was prepared by incubation of linolenic acid with soybean lipoxygenase as described (Hamberg and Gotthammar, 1973). Hydroperoxide decomposing activity was measured in 50 mM sodium phosphate pH 7 in a total volume of 1 ml. The enzyme assay was started by the addition of 13(*S*)-HPOT to a final concentration of 100 μM and the reaction was followed photometrically by the decrease in the absorbance at 235 nm. To differentiate between the various hydroperoxide decomposing activities, the enzyme assay was performed with 1-[^{14}C]-13(*S*)-HPOT, the products extracted with ether and separated and quantified by RP–HPLC as described (Ziegler et al., 1997). For product identification by GC–MS, unlabelled 13(*S*)-HPOT was used as the substrate and the methylated and trimethylsilylated products were subjected to GC–MS analysis (HP 5890 Series II, Hewlett-Packard, St Louis, MO, USA) on a DB-5MS column (30 m length, 0.25 mm. i.d., 0.25 μm film thickness; J&W Scientific, Folsom, CA, USA) with a helium flow rate of 1 ml/min, and detected by MS (HP 5971) in SIM mode.

3.5. Isolation of AOS cDNA and overexpression in Escherichia coli

A cDNA library in λ-ZAPII (Stratagene) prepared from *N. attenuata* shoots after 24 h of feeding by *M. sexta* larvae was used. 5×10^5 phages of this cDNA library were screened with the 5′-*EcoRI*/*XhoI* (700 bp) fragment of the *Arabidopsis thaliana* AOS cDNA (Laudert et al., 1996). Prehybridization was performed at 55 °C in 5×SSC, 5×Denhardt's reagent, 0.5% SDS, 125 μg ml^{-1} salmon sperm DNA for 3 h, followed by hybridization at 55 °C overnight with the ^{32}P-labelled *Arabidopsis thaliana* AOS fragment in the prehybridization solution. Filters were washed 3 times for 15 min at 55 °C in 2×SSC and 0.1% SDS. Putative positive phages were checked for the presence of an AOS insert by PCR with the following primers: upstream 5′-TTC AC(CT) GG(AT) ACT TA(CT) ATG CC-3′, downstream: 5′-GTT GC(AGC) AAC GGT TG(AG) TA(GCT) CC-3′. The temperature program was 4 min at 94 °C followed by 25 cycles 1 min at 94 °C, 2 min 50 °C, 2 min at 72 °C and a final extension time for 10 min at 72 °C. A PCR fragment of 850 bp was identified as AOS by dideoxy cycle sequencing and was used for further screening under same conditions as described above, but the hybridization and washing temperatures were raised to 65 °C. The positive plaques were converted into phagemids by in vivo excision. 5′RACE was performed using the 5′RACE Kit (Gibco, Gaithersburg, MD) according to the instructions of the manufacturer. Purified mRNA (Oligotex-mRNA purification Kit, Qiagen, Hilden, Germany) from leaves treated for 4 h with MeJA was

used as a template. The gene specific primers were 5′-GTC GCA AAA CGG TTG GTA CCC-3′ for the reverse transcription and 5′-GAA ACG TCG AAG AGG GTG GG-3′ for the PCR amplification at an annealing temperature of 60 °C. The PCR fragment was cloned into the TOPO-TA cloning vector (Invitrogen San Diego, CA, USA) and sequenced.

For overexpression, the AOS cDNA was cut from the plasmid with SmaI and XhoI and cloned into the *SmaI*/*SalI* sites of the His-tag vector pQE31 (Qiagen, Hilden, Germany). *E. coli* SG13009 served as the host strain. Expression was induced by the addition of 1 mM IPTG for 4 h and the bacteria were extracted by sonication in 50 mM sodium phosphate pH 7, 300 mM NaCl, 7% glycerol, 0.1% Triton X-100 and 10 mM imidazole. After centrifugation at 12,000 *g* for 20 min the supernatant was used for tests of activity.

3.6. Northern and Southern blots

The extraction and blotting of RNA and genomic DNA was performed using standard methods (Maniatis et al., 1989). For Southern blot analysis 10 μg of genomic DNA was digested with the restriction endonucleases indicated and resolved in a 0.8 % agarose gel. For both, Northern and Southern, blots prehybridization was performed at 65 °C in 5×SSC, 5×Denhardt's reagent, 0.5% SDS, 125 μg/ml salmon sperm DNA for 3 h, followed by hybridization at 65 °C overnight with the ^{32}P-labelled 850 bp *N. attenuata* AOS fragment. Membranes were washed 3 times for 15 min at 65 °C in 2×SSC and 0.1% SDS. Autoradiograhy of the membranes on X-ray films was performed at −80 °C in the presence of intensifying screen. After scanning, the blots were quantified using the ImageQuaNT™ program (Molecular Dynamics, Krefeld, Germany).

Acknowledgements

We are grateful to Professors Elmar Weiler and Dietmar Laudert (Ruhr-University Bochum, Germany) for providing the *Arabidopsis thaliana* AOS cDNA clone. We thank Natalia Sandoval for preparing the *N. attenuata* cDNA library and Domenica Schnabelrauch for the nucleotide sequence analysis. Funded by the Max Planck Gesellschaft.

References

Baldwin, I.T., 1989. The mechanism of damaged-induced alkaloids in wild tobacco. J. Chem. Ecol. 15, 1661–1680.

Baldwin, I.T., 1989. Herbivory simulations in ecological research. Trends Ecol. Evol. 5, 91–93.

Baldwin, I.T., 1998. Jasmonate-induced responses are costly but benefit plants under attack in native populations. Proc. Natl. Acad. Sci. USA 95, 8113–8118.

Baldwin, I.T., 1999. Inducible nicotine production in native *Nicotiana* as an example of adaptive phenotypic plasticity. J. Chem. Ecol. 25, 3–30.

Baldwin, I.T., Schmelz, E.A., Ohnmeiss, T.E., 1994a. Wound-induced changes in root and shoot jasmonic acid pools correlate with induced nicotine synthesis in *Nicotiana sylvestris* Spegazzini and Comes. J. Chem. Ecol. 20, 2139–2157.

Baldwin, I.T., Schmelz, E.A., Zhang, Z.P., 1996. Effects of octadecanoid metabolites and inhibitors on induced nicotine accumulation in *Nicotiana sylvestris*.. J. Chem. Ecol. 22, 61–74.

Baldwin, I.T., Staszak-Kozinski, L., Davidson, R., 1994b. Up in smoke: I. Smoke-derived germination cues for postfire annual, *Nicotiana attenuata* Torr. Ex. Watson. J. Chem. Ecol. 20, 2345–2371.

Baldwin, I.T., Zhang, Z.P., Diab, N., Ohnmeiss, T.E., McCloud, E.S., Lynds, G.Y., Schmelz, E.A., 1997. Quantification, correlation and manipulations of wound-induced changes in jasmonic acid and nicotine in *Nicotiana sylvestris*. Planta 201, 397–404.

Bell, E., Creelman, R.A., Mullet, J.E., 1995. A chloroplast lipoxygenase is required for wound-induced jasmonic acid accumulation in *Arabidopsis*. Proc. Natl. Acad. Sci. 92, 8657–8679.

Bell, E., Mullet, J.E., 1993. Characterization of an *Arabidopsis* lipoxygenase gene responsive to methyl jasmonate and wounding. Plant Physiol 103, 113–1137.

Blée, E., Joyard, J., 1996. Envelope membranes from spinach chloroplasts are a site of metabolism of fatty acid hydroperoxides. Plant Physiol. 110, 445–454.

Brash, A.R., Song, W.C., 1995. Structure-function features of flaxseed allene oxide synthase. J. Lipid Mediators Cell Signalling 12, 275–282.

Chapple, C., 1998. Molecular-genetic analysis of plant cytochrome P450-dependent monooxygenases. Annu. Rev. Plant. Phys. Plant Mol. Biol. 49, 311–343.

Conconi, A., Miquel, M., Browse, J.A., Ryan, C.A., 1996. Intracellular levels of free linolenic and linoleic acids increase in tomato leaves in response to wounding 7. Plant Physiol 111, 797–803.

Costa, L.C., Arruda, P., Benedetti, C.E., 2000. An *Arabidopsis* gene induced by wounding functionally homologues to flavoprotein oxidoreductases. Plant Mol. Biol. 44, 61–71.

Froehlich, J.E., Itoh, A., Howe, G.A., 2001. Tomato allene oxide synthase and fatty acid hydroperoxide lyase, two cytochrome P450s involved in oxylipin metabolism, are targeted to different membranes of chloroplast envelope. Plant Physiol 125, 306–317.

Hamberg, M., Gardner, H.W., 1992. Oxylipin pathway to jasmonates: biochemistry and biological significance. Biochim. Biophys. Acta 1156, 1–18.

Hamberg, M., Gotthammar, B., 1973. A new reaction of unsaturated fatty acid hydroperoxides: formation of 11-hydroxy-12,13-epoxy-9-octadecenoic acid from 13-hydroperoxy-9,11-octadecadienoic acid. Lipids 8, 737–744.

Halitschke, R., Schittko, U., Pohnert, G., Boland, W., Baldwin, I.T., 2001. Molecular interactions between the specialist herbivore *Manduca sexta* (Lepidoptera, Sphingidae) and its natural host *Nicotiana attenuata*. III. Fatty acid-amino acid conjugates in herbivore oral secretions are necessary and sufficient for herbivore-specific plant responses. Plant Physiol. 125, 711–717.

Harms, K., Atzorn, R., Brash, A., Kühn, H., Wasternack, C., Willmitzer, L., Peña-Cortés, H., 1995. Expression of a flax allene oxide synthase cDNA leads to increased endogenous jasmonic acid (JA) levels in transgenic potato plants but not to a corresponding activation of JA-responding genes. Plant Cell 7, 1645–1654.

Harms, K., Ramirez, I., Peña-Cortés, H., 1998. Inhibition of wound-induced accumulation of allene oxide synthase transcripts in flax leaves by aspirin and salicylic acid. Plant Physiol. 118, 1057–1065.

Heil, M., Koch, T., Hilpert, A., Fiala, B., Boland, W., Linsenmair, K.E., 2001. Extrafloral nectar production of the ant-associated plant, *Macaranga tanarius*, is an induced, indirect, defensive

response elicited by jasmonic acid. Proc. Natl. Acad. Sci. 98, 1083–1088.

Heitz, T., Bergey, D.R., Ryan, C.A., 1997. A gene encoding a chloroplast-targeted lipoxygenase in tomato leaves is transiently induced by wounding, systemin, and methyl jasmonate. Plant Physiol. 114, 1085–1093.

Hermsmeier, D., Schittko, U., Baldwin, I.T., 2000. Molecular interactions between the specialist herbivore *Manduca sexta* (Lepidoptera, Sphingidae) and its natural host *Nicotiana attenuata*. I. Large-scale changes in the accumulation of growth- and defense-related plant mRNAs. Plant Physiol. 125, 683–700.

Howe, G.A., Lightner, J., Browse, J., Ryan, C.A., 1996. An octadecanoid pathway mutant (JL5) of tomato is compromised in signaling for defense against insect attack. Plant Cell 8, 2067–2077.

Howe, G.A., Lee, G.I., Itoh, A., Li, L., DeRocher, A.E., 2000. Cytochrome P450-dependent metabolism of oxylipins in tomato. Cloning and expression of allene oxide synthase and fatty acid hydroperoxide lyase. Plant Physiol. 123, 711–724.

Kahl, J., Siemens, D., Aerts, R.J., Gäbler, R., Kühnemann, F., Preston, C.A., Baldwin, I.T., 2000. Herbivore-induced ethylene suppresses a direct defense but not a putative indirect defense against an adapted herbivore. Planta 210, 336–342.

Koljak, R., Boutaud, O., Shieh, B.H., Samel, N., Brash, A.R., 1997. Identification of a naturally occurring peroxidase-lipoxygenase fusion protein. Science 277, 1994–1996.

Korth, K.L., Dixon, R.A., 1997. Evidence for chewing insect-specific molecular events distinct from a general wound response in leaves. Plant Physiol. 115, 1299–1305.

Kramell, R., Miersch, O., Atzorn, R., Parthier, B., Wasternack, C., 2000. Octadecanoid-derived alteration of gene expression and the "oxylipin signature" in stressed barely leaves. Implications for different signaling pathways. Plant Physiol. 123, 177–187.

Kubigsteltig, I., Laudert, D., Weiler, E.W., 1999. Structure and regulation of the *Arabidopsis thaliana* allene oxide synthase gene. Planta 208, 463–471.

Laudert, D., Pfannschmidt, U., Lottspeich, F., Holländer-Czytko, H., Weiler, E.W., 1996. Cloning, molecular and functional characterization of *Arabidopsis thaliana* allene oxide synthase (CYP 74), the first enzyme of the octadecanoid pathway to jasmonates. Plant. Mol. Biol. 31, 323–335.

Laudert, D., Schaller, F., Weiler, E.W., 2000. Transgenic *Nicotiana tabacum* and *Arabidopsis thaliana* plants overexpressing allene oxide synthase. Planta 211, 163–165.

Laudert, D., Weiler, E.W., 1998. Allene oxide synthase-a major control point in *Arabidopsis thaliana* octadecanoid signalling. Plant J. 15, 675–684.

Maniatis, T., Fritsch, E.F., Sambrook, J., 1989. Molecular Cloning: A Laboratory Manual. Cold Spring Harbor Laboratory Press, NY.

Maucher, H., Hause, B., Feussner, I., Ziegler, J., Wasternack, C., 2000. Allene oxide synthase of barley (*Hordeum vulgare* cv. Salome): tissue specific regulation in seedling development. Plant J. 21, 199–213.

McCloud, E.S., Baldwin, I.T., 1997. Herbivory and caterpillar regurgitants amplify the wound-induced increase in jasmonic acid but not nicotine in *Nicotiana sylvestris*. Planta 203, 430–435.

McConn, M., Creelman, R.A., Bell, E., Mullet, J.E., Browse, J., 197. Jasmonate is essential for insect defense *Arabidopsis*. Proc. Natl. Acad. Sci. USA 94, 5473–5477.

Pan, Z., Durst, F., Werck-Reichhart, D., Gardner, H.W., Camara, B., Cornish, K., Backhaus, R.A., 1995. The major protein of guayule rubber particles is a cytochrome P450. J. Biol. Chem. 270, 8487–8494.

Reymond, R., Weber, H., Damond, M., Farmer, E.E., 2000. Differential gene expression in response to mechanical wounding and insect feeding in *Arabidopsis*. Plant Cell 12, 707–719.

Schittko, U., Preston, C.A., Baldwin, I.T., 2000. Eating the evidence? *Manduca sexta* larvae can not disrupt specific jasmonate induction in *Nicotiana attenuata* by rapid consumption. Planta 210, 343–346.

Schittko, U., Hermsmeier, D., Baldwin, I.T., 2001. Molecular interactions between the specialist herbivore *Manduca sexta* (Lepidoptera, Sphingidae) and its natural host *Nicotiana attenuata*. II. Accumulation of plant mRNAs in response to insect-derived cues. Plant Physiol. 125, 701–710.

Seo, S., Okamoto, M., Seto, H., Ishizuka, K., Sano, H., Ohashi, Y., 1995. Tobacco MAP kinase: a possible mediator in wound signal transduction pathways. Science 270, 1988–1992.

Sivasankar, S., Sheldrick, B., Rothstein, S.J., 2000. Expression of allene oxide synthase determines defense gene activation in tomato. Plant Physiol 122, 1335–1342.

Song, W.C., Brash, A.R., 1991. Purification of an allene oxide synthase and identification of the enzyme as a cytochrome P-450. Science 253, 781–784.

Song, W.C., Funk, C.D., Brash, A.R., 1993. Molecular cloning of an allene oxide synthase: a cytochrome P450 specialized for the metabolism of fatty acid hydroperoxides. Proc. Natl. Acad. Sci. USA 90, 8519–8523.

von Heijne, G., Steppuhn, J., Herrmann, R.G., 1989. Domain structure of mitochondrial and chloroplast targeting peptides. Eur. J. Biochem. 180, 535–545.

von Wachenfeldt, C., Johnson, E.F., 1995. Structures of eucaryotic cytochrome P450 enzymes. In: Ortiz de Montanello, P.R. (Ed.), Cytochrome P450: Structure Mechanism, and Biochemistry, 2nd Edition. Plenum Press, New York, pp. 183–223.

Wang, B.H., Polya, G.M., 1996. Selective inhibition of cyclic AMP-dependent protein kinase by amphiphilic triterpenoids and related compounds. Phytochemistry 41, 55–63.

Wasternack, C., Atzorn, R., Blume, B., Leopold, J., Parthier, B., 1994. Ursolic acid inhibits synthesis of jasmonate-induced proteins in barley leaves. Phytochemistry 35, 49–54.

Winz, R., Baldwin, I.T., 2001. Molecular interactions between the specialist herbivore *Manduca sexta* (Lepidoptera, Sphingidae) and its natural host *Nicotiana attenuata*. IV. Insect-induced ethylene reduces jasmonate-induced nicotine accumulation by regulating putrescine *N*-methyltransferase transcripts. Plant Physiol 125, 2189–2202.

Ziegler, J., Hamberg, M., Miersch, O., Parthier, B., 1997. Purification and characterization of allene oxide cyclase from dry corn seeds. Plant Physiol 114, 565–573.

Ziegler, J., Stenzel, I., Hause, B., Maucher, H., Hamberg, M., Grimm, R., Ganal, M., Wasternack, C., 2000. Molecular cloning of allene oxide cyclase: The enzyme establishing the stereochemistry of octadecanoids and jasmonates. J. Biol. Chem. 275, 19132–19138.

PERGAMON

Phytochemistry 58 (2001) 739–742

PHYTOCHEMISTRY

www.elsevier.com/locate/phytochem

Excretion of miserotoxin and detoxification of the aglycone by grasshoppers (Orthoptera: Acrididae)☆

Dan L. Johnson[a,*], Walter Majak[b], Michael H. Benn[c]

[a]*Agriculture and Agri-Food Canada, Research Centre, Lethbridge, Alta, Canada TIJ 4B1*
[b]*AAFC, Range Research Unit, Kamloops, BC, Canada V2B 8A9*
[c]*Department of Chemistry, University of Calgary, Calgary, Alta, Canada T2N 1N4*

Received 19 February 2001; received in revised form 5 June 2001

Abstract

Two species of grasshoppers (*Melanoplus bivittatus* and *M. sanguinipes*) tolerated high levels of miserotoxin (3-nitro-1-propyl-β-D-glucopyranoside) in their diet. Miserotoxin is a causative agent in cattle poisoning when timber milkvetch (*Astragalus miser*) is consumed. Toxic effects were averted by grasshoppers in part by excretion of the intact glycoside. When the aglycone was administered, detoxification was achieved by two routes: by oxidation of the aglycone to 3-nitropropionic acid which was then conjugated with glycine, and by glucosylation of the aglycone to miserotoxin, in each case followed by excretion. Crown Copyright © 2001 Published by Elsevier Science Ltd. All rights reserved.

Keywords: *Astragalus miser*; Fabaceae; Timber milkvetch; Chemical defense; Conjugation; Aliphatic nitro compounds; Amino acids; Melanoplus; Acrididae

1. Introduction

Miserotoxin (3-nitro-1-propyl-β-D-glucopyranoside), a causative agent in cattle poisoning on rangelands in the western USA, was originally isolated from *Astragalus miser* var. *oblongifolius* (Leguminosae) (Stermitz et al., 1969). The glycoside was subsequently isolated from *A. miser* var. *serotinus* (timber milkvetch), which occurs in the Southern Interior of British Columbia, Canada (Majak and Bose, 1974). Other glycosides of 3-nitropropanol (NPOH) were also identified in timber milkvetch (Long et al., 1992). Miserotoxin is rapidly hydrolyzed by microbial enzymes of the rumen, and the aglycone is absorbed and converted to 3-nitropropionic acid (Muir et al., 1984), a potent inhibitor of mitochondrial enzymes essential to respiration (Alston et al., 1977). 3-Nitropropionic acid (NPA) is also implicated as a causative agent of neuronal degeneration in mammals (Alexi et al., 1998).

Previously we reported on the lack of NPA toxicity to melanopline grasshoppers (*Melanoplus bivittatus* and *M. sanguinipes*; Orthoptera: Acrididae), and their metabolic ability to detoxify NPA by way of conjugation with amino acids. The NPA was excreted in the frass (dry fecal pellets) as amides of glycine, L-serine and L-glutamate (Majak et al., 1998). Karakin, a glucose triester of NPA, was also detoxified after hydrolysis in vivo and conjugation of the NPA to the same amino acids (Majak et al., 1998). In feeding trials with the same species of grasshoppers using freeze-dried timber milkvetch, none of the grasshoppers died, nor did they show any sign of altered behavior or disability after subsisting on *A. miser* for 96 h at room temperature (D.L. Johnson, unpublished data). The objectives of this study were to further explore the resistance of grasshoppers to miserotoxin, and to determine the metabolic fate of the aglycone.

2. Results and discussion

2.1. Experiment 1

The concentration of miserotoxin in the timber milkvetch was found to be 4.5–5.2% on a dry-matter basis.

☆ This work was completed by D.L. Johnson et al., for the Department of Agriculture and Agri-Food, Government of Canada © Minister of Public Works and Government Service Canada 2001.

* Corresponding author. Tel.: +1-403-317-2214; fax: +1-403-382-3156.

E-mail address: johnsondl@em.agr.ca (D.L. Johnson).

0031-9422/01/$ - see front matter. Crown Copyright © 2001 Published by Elsevier Science Ltd. All rights reserved.
PII: S0031-9422(01)00310-7

The individual consumption rate of the milkvetch was approximately 40 mg/day, per grasshopper, which is a typical rate of feeding on finely ground dried plant material at room temperature. The rate of intake of miserotoxin was equivalent to approximately 2 mg of the glycoside per grasshopper per day. There was no mortality in treated or untreated groups, and there was no other signs of toxicity.

2.2. Experiment 2

Typically, more than 90% of the food that was treated with the purified glycoside and provided in feeding trays was consumed by the two-striped grasshoppers during the assessment period. The average intake of miserotoxin was estimated at approximately 4.5–4.8 mg per grasshopper per day. There was no mortality or other sign of toxicity. The frass was extracted and miserotoxin was detected on silica gel TLC.

2.3. Experiment 3

No grasshoppers died in the treated groups (a total of one grasshopper in the control groups died), and no other changes in behavior that would indicate possible toxicity were observed. The average amount of the glycoside provided was 11.5 mg per grasshopper, per day, but because of losses (estimated at ca. 20%) in tumble-treatment of the lettuce, and quantities remaining on unconsumed food, the amount of glycoside was estimated to be 6–7 mg per grasshopper. By far, the major component in the frass giving a colour test specific for aliphatic nitro compounds (Majak and Bose, 1974) was miserotoxin, as evidenced by co-chromatography with an authentic standard. The identity of the glycoside as a nitro alkyl excretion product (3.5% of the frass on a dry-matter basis) was confirmed by ^{1}H and ^{13}C NMR spectroscopy. Only a small portion ($<10\%$) of the administered miserotoxin was recovered from the frass, which suggested other pathways of elimination or reductive detoxification (although this feeding experiment was not intended to provide quantitative analysis of fate of all products). Some anaerobic bacteria can reduce the nitro alkyl moiety to the amino group (Anderson et al., 1993), and sequestration of the intact glycoside could also be possible (Duffey, 1980). However, extraction of the grasshopper cadavers and TLC screening did not reveal endogenous accumulation of ninhydrin-positive or nitro alkyl-positive products.

There was no evidence of the aglycone on TLC, suggesting the absence of β-glucosidase activity in *M. bivittatus*, and a possible avoidance of toxicity, through the elimination of the intact glycoside. The low level of β-glucosidase activity agrees with earlier tests that indicated the absence of cyanide formation when homogenates of *M. bivittatus* were incubated with amygdalin (W. Majak, unpublished data). However, a second, minor spot was observed on the TLC that was also visualized with the reagent for nitro compounds. Its R_f was consistent with that of an amino acid conjugate of NPA. This result suggested partial hydrolysis of the glycoside by the insect, or possibly by microflora of the gut, and then oxidation of the aglycone to NPA before conjugation.

2.4. Experiment 4

The average intake of the aglycone was approximately 0.5 mg per grasshopper per day. There was no mortality or other sign of toxicity, and no behaviour indicating disorientation or loss of appetite. When the frass was extracted and fractionated, an amino acid conjugate of NPA was isolated, which was identified by NMR as the glycyl amide of NPA. Clearly, it was demonstrated that *M. bivittatus* had the capacity to oxidize the aglycone, and to detoxify the NPA through conjugation with glycine. There was no evidence of excess NPOH in the frass.

However, the more common method of NPOH detoxification by *M. bivittatus* appeared to be through glucosylation to form the β-D-glucoside, which, in effect, is miserotoxin. Based on colour intensity on TLC, the ratio of the glycoside to the amino acid conjugate appeared to be approximately 2:1. On a molar basis, the yield of the glycoside (25 mg) accounted for approximately 10% of the administered aglycone. This type of glucosylation reaction has long been recognized in higher plants. When simple phenols, such as phloroglucinol or phenol itself, are administered to higher plants, they are detoxified by conversion to the corresponding glucosides (Towers, 1964). Thus, there are now three methods for the metabolic detoxification of the miserotoxin aglycone: (1) conjugation after oxidation; (2) glucosylation and (3) reduction of the nitro group to the much less toxic amino group which is effected by rumen bacteria (Anderson et al., 1993).

3. Experimental

3.1. General experimental procedures

NMR spectra were measured with a Bruker AM-400 spectrometer at 400 MHZ (^{1}H) and 100 MHZ (^{13}C) of samples dissolved in D_2O or MeOH-d4. The TLC solvent system on silica gel was chloroform–methanol (3:1) with 0.2% HCOOH and the R_f's were 0.32 for miserotoxin and 0.30 for the glycyl conjugate. The ^{1}H and ^{13}C NMR spectra of these compounds were as reported (Majak et al., 1998; Benn and Majak, 1989).

3.2. Biological materials

The grasshoppers used were the first captive generation produced from eggs laid by field-collected adult grasshoppers. [The grasshoppers we used were not from

the widely used non-diapause *Melanoplus sanguinipes* laboratory strain (Pickford and Randell, 1969), which have been shown to have enhanced detoxicative enzyme activity: Isman et al., 1996]. Grasshoppers used in toxicity assessments and feeding trials were confined in cages constructed of screen, glass and wood and supplied with adequate air flow and lighting (photoperiod 15 h light, 9 h dark; measured temp. 27–29 °C day, 22–24 °C night). Methods of rearing and handling of grasshoppers, and of assessment of grasshopper feeding, were similar to those described by Johnson and Pavlikova (1986) and Lactin and Johnson (1995). *A. miser* var. *serotinus* specimens were field collected in the Southern Interior of British Columbia. Specimens were freeze dried and ground prior to grasshopper feeding.

3.3. Experiments

3.3.1. Experiment 1: consumption and gross toxicity

Groups of 12 grasshoppers (repeated separately for *M. bivittatus* and *M. sanguinipes*, two complete replications for each species) were each confined with 1 g of freeze-dried *A. miser* var. *serotinus*, which they consumed within 48 h. Feeding behavior and frequency was observed in order to confirm that all individuals were consuming the plant material. At the end of 48 h, a second gram of freeze-dried *A. miser* var. *serotinus* was added to each cage and again it was consumed within 48 h. The concentration of miserotoxin in the timber milkvetch was determined by HPLC (Quinton et al., 1989). The experiment was subsequently repeated in four complete replications to confirm results regarding gross toxicity.

3.3.2. Experiment 2: intake and toxicity of the purified glycoside

A total of 40 fifth-instar *M. bivittatus* were confined in cages with wheat bran that was treated with (or without) purified miserotoxin, which was dissolved in water. (Treatment identifiers were coded, and unknown to handlers and observers during the assessments.) The grasshoppers were confined with measured quantities of the wheat bran provided in feeding trays each day for 8 days. The administered miserotoxin was isolated from timber milkvetch by conventional procedures (Majak and Bose, 1974; Majak et al., 1992), but continuous ethyl acetate extraction was used before column chromatography. To detect the glycoside in the frass, 1 g of it was extracted with hot ethanol and the concentrate was fractionated on silica gel column chromatography (25×2 cm) and centrifugally accelerated radial TLC (Chromatotron) as described previously (Majak et al., 1998).

3.3.3. Experiment 3: assessment of intake, excretion and fate of the glycoside

In the third experiment, the purified glycoside was applied to a mixture of lettuce leaves (streaking with pipette), and to wheat bran (stirred and mixed by tumbling until evenly absorbed). A total of 80 two-striped grasshopers (*M. bivittatus*) were confined with the treated feed in cages for 4 days. The grasshoppers were kept alive for an additional 7 days after that time, to observe any possible delayed mortality. The collected frass was extracted and fractionated by conventional procedures (Majak et al., 1998). Individual fractions were screened by TLC.

3.3.4. Experiment 4: intake of the aglycone and fate of NPOH

In a fourth experiment, the aglycone was fed to grasshoppers to determine the metabolic fate of NPOH. A total of 50 two-striped grasshoppers (*M. bivittatus*) were confined in feeding cages and fed aglycone for 6 days. 3-Nitropropanol was synthesized from 3-bromopropanol by Gary Yost, University of Utah. Frass from the grasshoppers (0.93 g) was extracted as described above.

References

Alexi, T., Hughes, P.E., Faull, R.L.M., Williams, C.E., 1998. 3-Nitropropionic acid's lethal triplet: cooperative pathways of neurodegeneration. NeuroReport 9, R57–R64.

Alston, T.A., Mela, L., Bright, H.J., 1977. 3-Nitropropionate, the toxic substance of Indigofera, is a suicide inactivator of succinate dehydrogenase. Proceedings of the National Academy of Science USA 74, 3767–3771.

Anderson, R.C., Rasmussen, M.A., Allison, M.J., 1993. Metabolism of the plant toxins nitropropionic acid nitropropanol by ruminal microorganisms. Applied and Environmental Microbiology 59, 3056–3061.

Benn, M.H., Majak, W., 1989. 3-Nitro-1-propyl-beta-D-laminariboside from *Astragalus miser* var. *serotinus*. Phytochemistry 28, 2369–2371.

Duffey, S.S., 1980. Sequestration of plant natural products by insects. Annual Review of Entomology 25, 447–477.

Isman, M.B., Feng, R., Johnson, D.L., 1996. Detoxicative enzyme activities in five species of field-collected melanopline grasshoppers (Orthoptera: Acrididae). Canadian Entomologist 128, 353–354.

Johnson, D.L., Pavlikova, E., 1986. Reduction of consumption by grasshoppers (Orthoptera: Acrididae) infected with *Nosema locustae* Canning (Microsporida: Nosematidae). Journal of Invertebrate Pathology 48, 232–238.

Lactin, D.J., Johnson, D.L., 1995. Temperature-dependent feeding rates of *Melanoplus sanguinipes* nymphs (Orthoptera: Acrididae) in laboratory trials. Environmental Entomology 24, 1291–1296.

Long, M., Benn, M., Majak, W., McDiarmid, R., 1992. 3-Nitropropyl glycosides of *Astragalus miser* var. *serotinus*. Phytochemistry 31, 321–323.

Majak, W., Benn, M., McEwan, D., Pass, M.A., 1992. Three nitropropanoyl esters of glucose from *Indigofera linnaei*. Phytochemistry 31, 2393–2395.

Majak, W., Bose, R.J., 1974. Chromatographic methods for the isolation of miserotoxin and detection of aliphatic nitro compounds. Phytochemistry 13, 1005–1010.

Majak, W., Johnson, D.L., Benn, M.H., 1998. Detoxification of 3-nitropropionic acid and karakin by melanopline grasshoppers. Phytochemistry 49, 419–422.

Muir, A.D., Majak, W., Pass, M.A., Yost, G.S., 1984. Conversion of 3-nitropropanol (miserotoxin aglycone) to 3-nitropropionic acid in cattle and sheep. Toxicology Letters 20, 137–141.

Pickford, R., Randell, R.L., 1969. A non-diapause strain of the migratory grasshopper *Melanoplus sanguinipes* (Orthoptera: Acrididae). The Canadian Entomologist 101, 894–896.

Quinton, D.A., Majak, W., Hall, J.W., 1989. The effect of cattle grazing on the growth and miserotoxin content of Columbia milkvetch. Journal of Range Management 42, 368–371.

Stermitz, F.R., Norris, F.A., Williams, M.C., 1969. Miserotoxin, a new naturally occurring nitro compound. Journal of the American Chemical Society 91, 4599–4600.

Towers, G.H.N., 1964. Metabolism of phenolics in higher plants and micro-organisms. In: Harborne, J.B. (Ed.), Biochemistry of Phenolic Compounds. Academic Press, London.

PERGAMON

Phytochemistry 58 (2001) 743–750

PHYTOCHEMISTRY

www.elsevier.com/locate/phytochem

A basic peroxidase from wheat kernel with antifungal activity

Carla Caruso[a,*], Gabriele Chilosi[b], Luca Leonardi[a], Laura Bertini[a], Paolo Magro[b], Vincenzo Buonocore[a], Carlo Caporale[a]

[a]*Dipartimento di Agrobiologia e Agrochimica Università della Tuscia, Via S. Camillo De Lellis, I-01100 Viterbo, Italy*
[b]*Dipartimento di Protezione delle Piante, Università della Tuscia, Viterbo, Via S. Camillo De Lellis, I-01100 Viterbo, Italy*

Received 6 February 2001; received in revised form 3 May 2001

Abstract

A basic heme-peroxidase (WP1) was purified to homogeneity from wheat (*Triticum aestivum*) kernels. The protein was not glycosylated and exhibited a molecular mass of 36 kDa and a pI of 8.0. The N-terminal amino acid sequence revealed a very high similarity with a wheat flour peroxidase allergen associated with baker's asthma. WPI showed indole-3-acetic acid oxidase activity in the presence of Mn^{2+} and phenolic cofactors. Antifungal assays performed in vitro towards phytopathogenic fungi indicated that WP1 was active in inhibiting germ tube elongation. This first report on antifungal properties of a heme-peroxidase gives experimental support to the idea that peroxidases play a defensive role against invading pathogens. © 2001 Elsevier Science Ltd. All rights reserved.

Keywords: Gramineae; *Triticum aestivum*; Wheat seeds; Antifungal activity; Amino acid sequence; Basic peroxidase

1. Introduction

Plant peroxidases (EC 1.11.1.7) are heme-proteins that use H_2O_2 to oxidise a large variety of hydrogen donors such as phenolic substances, amines, ascorbic acid, indole and certain inorganic ions (Van Huystee, 1987). These proteins are widespread in the plant kingdom and peroxidase isoenzymes are known to occur in a variety of plant tissues. The pattern of expression of each isoform varies in the different tissues of healthy plants and is developmentally regulated and influenced by environmental factors (Lagrimini and Rothstein, 1987); however, the role of each isoform is not fully understood. Various experiments suggest the involvement of plant peroxidases not only in biosynthetic processes related to wall development such as lignification (Lagrimini et al., 1987), suberification (Roberts and Kolattukudy, 1989) and polymerisation of hydroxyproline-rich glycoproteins (Bradley et al., 1992), but also in the regulation of cell wall elongation (Greppin et al., 1986), wound healing (Espelie and Kolattukudy, 1985; Lagrimini and Rothstein, 1987) and resistance against infection by pathogens (Flott et al., 1989; Graham and Graham, 1991; Reimers et al., 1992; Young et al., 1995; Chittoor et al., 1997). Such a wide spectrum of functions is consistent with the presence of several isoforms suggesting that different peroxidase isoenzymes might be involved in distinct processes. Moreover, peroxidases can be considered useful markers for environmental stresses since their activity is affected by low temperature, air pollution, ozone, heavy metals, wounding, salts, pathogen attack and UV radiation (Penel et al., 1992).

A better understanding of the physiological roles of peroxidases can be obtained through the isolation and structural-functional characterisation of new proteins and the identification of their targets. The major cationic peroxidases from horseradish and turnip have been intensively studied and their amino acid sequences have been determined (Welinder, 1979; Mazza and Welinder, 1980). Isolation and characterization of peroxidase isoenzymes have been reported also from several dicots such as potato, tomato, tobacco (Roberts and Kolattukudy, 1989; Roberts et al., 1988; Lagrimini et al., 1987a), and to a lesser extent from monocots. Less information is available on wheat peroxidases, probably because the isolation of a single protein is complicated by the presence of several different isoforms encoded by the hexaploid genome (Liu et al., 1990). The characterisation of

* Corresponding author. Tel.: +390-761357330; fax: +0390-761357242.
E-mail address: caruso@unitus.it (C. Caruso).

0031-9422/01/$ - see front matter © 2001 Elsevier Science Ltd. All rights reserved.
PII: S0031-9422(01)00226-6

three full length and one truncated wheat peroxidase genes has been reported, as well as the tissue-specific pattern of expression (Baga et al., 1995). These genes were found to be closely related to wheat peroxidases previously characterised from different cultivars suggesting that they represent variants of the same genes (Hertig et al., 1991; Rebmann et al., 1991). Recently, the purification and partial characterisation of a wheat peroxidase associated with baker's asthma and highly homologous with the previously characterised barley peroxidase BP1 (Rasmussen et al., 1991) has been reported (Sanchez-Monge et al., 1997).

In this paper we report the isolation and purification from wheat seeds of a cationic peroxidase (coded WP1) that also displays indole-3-acetic acid (IAA) oxidase activity in the presence of Mn^{2+} and phenolic cofactors. Antifungal experiments in vitro using different pathogenic and non-pathogenic fungi show that WP1 exhibits a weak inhibitory activity exerted on germ tube elongation, whereas it has no effect on spore germination.

2. Results and discussion

2.1. Protein purification and characterisation

Salt-soluble proteins extracted from wheat kernels and fractionated by precipitation with ammonium sulfate were subjected to cation exchange chromatography on a CM-Sepharose column (Fig. 1). The three pooled fractions with peroxidase activity (peaks I, II and III) exhibited a large number of isoenzymatic forms by isoelectric focusing. The full characterization of peak I, containing anionic isoperoxidases, is currently in progress; peak III has not been studied at the moment due to the very low amount of protein despite its high peroxidase activity. Peak II, which showed the lowest number of isoforms, was further purified by two different procedures to obtain either the heme-depleted peroxidase (apoWP1) or the enzymatically active hemeprotein (holoWP1). The complete purification of the holoenzyme was achieved submitting peak II to IE-chromatography on a Resource S column (Fig. 2A); the active peak II-2, showing only one peroxidase band on IEF, was finally loaded on an UltroPac TSK CM-3SW column and purified to homogeneity by IE-HPLC (Fig. 2B). Peak II-1, characterised by the presence of two isoforms, is still under investigation. The purification of apoenzyme was achieved in homogeneous form submitting the peak II to RP-HPLC (Fig. 3). The purified holoWP1 was homogeneous upon analysis by

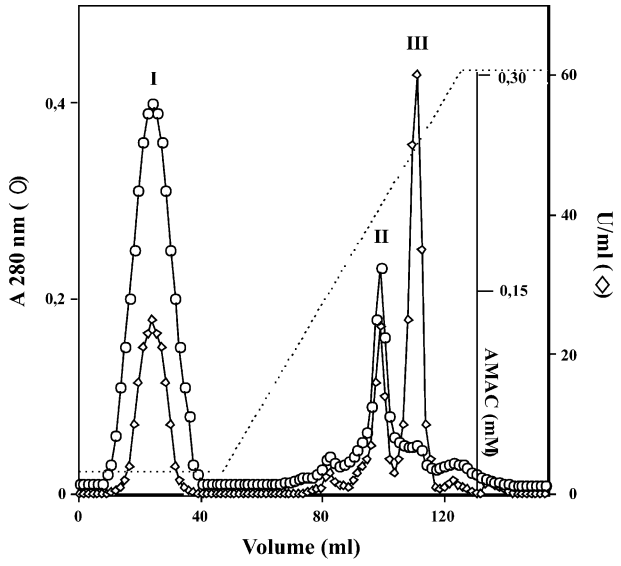

Fig. 1. CM-Sepharose fast flow chromatography of protein extract from wheat seeds. (O) Absorbance at 280 nm; (◇) peroxidase activity units; (····) ammonium acetate (AMAC) concentration.

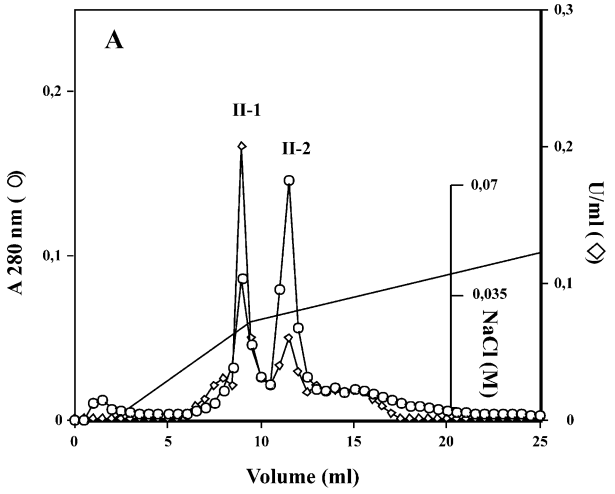

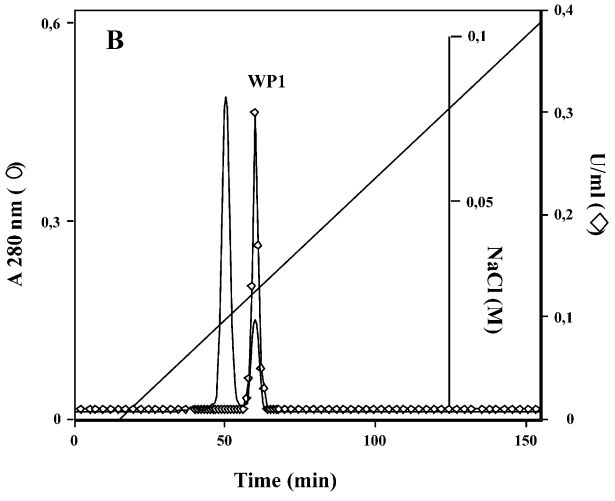

Fig. 2. Panel A: resource S chromatography of peak II from the CM-Sepharose fast flow chromatography (Fig. 1). Panel B: UltroPac TSK CM-3SW HPLC of the peak II-2 from the Resource S chromatography (panel A). (O) Absorbance at 280 nm; (◇) Peroxidase activity units; (····) NaCl concentration.

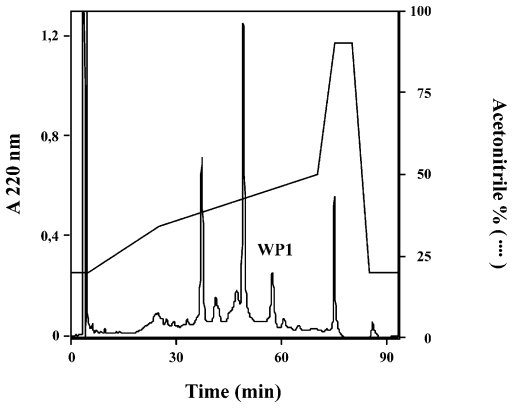

Fig. 3. RP-HPLC of peak II from CM-Sepharose fast flow chromatography (Fig. 1). (—) Absorbance at 220 nm; (····) acetonitrile concentration.

SDS–PAGE, showing a molecular weight of 36 kDa. Isoelectric focusing on purified holoWP1 stained by both Coomassie Blue and peroxidase activity confirmed the homogeneity of the sample and showed an isoelectric point of 8.0 (data not shown). Since it has been reported that several plant peroxidases are glycoproteins, holoWP1 was digested with endo-β-*N*-acetyl glucosaminidase F from *Flavobacterium meningosepticum* (Endo F) to determine the presence of sugar components. The digestion was also carried out on a standard glycoprotein (chicken ovalbumin) in order to evaluate the efficiency of the treatment. SDS-PAGE analysis of digested and untreated holoWP1 showed a single protein band with the same electrophoretic mobility indicating that WP1 was not a glycoprotein. On the contrary, a shift in the electrophoretic mobility of digested ovalbumin with respect to the control protein was detected indicating that the Endo-F treatment used for both proteins was efficient (data not shown). Moreover, analysis of both holoWP1 and ovalbumin was also performed after non denaturing-PAGE using the periodic acid-Schiff procedure that allows the detection of about 0.2 μg protein-associated carbohydrate (Doerner and White, 1990). The electrophoresis was carried out using both chicken ovalbumin (20 μg) which approximately contains 4% mannose residues by weight (0.8 μg carbohydrate) and holoWP1 (40 μg). The analysis confirmed the absence of oligosaccharide chains linked to the peroxidase whereas a detectable band was evidenced only for ovalbumin (data not shown).

The Reinheitszahl (RZ) value (A_{403}/A_{280}) for WP1 was 2.8–3, in good agreement with the values reported for other heme-peroxidases (Van Huystee, 1987). The cationic isoperoxidase we isolated displays low specific activity for guaiacol (3.0 U/mg), whereas it shows high affinity for indole-3-acetic acid (1680 U/mg). It is well known that the main natural auxin (indole-3-acetic acid) is oxidised by peroxidases and that this degradation may regulate the auxin levels in plant tissues (Gaspar et al., 1991). Moreover, it is widely reported that phenolic substances could play an important role in the regulation of IAA oxidation although the ability of some peroxidases to catalyze the oxidation of IAA in the absence of these cofactors has been reported (Gazaryan et al., 1999). The ability of wheat leaf peroxidases to catalyze the IAA oxidation in the presence of Mn^{2+} and phenolic cofactors is known from many years (Machackova et al., 1975) and our results are in agreement with these findings. However, holoWP1 ability of catalysing the aerobic oxidation of IAA in the absence of such substances was also verified. In such conditions, the enzyme was unable to degrade IAA, suggesting that it cannot be considered as a functional auxin oxidase involved in the IAA catabolism.

2.2. Sequence analysis and homology studies

The N-terminal sequence of reduced and pyridylethylated apoWP1 was determined using an automated apparatus. The sequence of the first 24 amino acid residues of WP1 aligned with the corresponding regions of a wheat peroxidase associated with baker's asthma (wheat allergen) (Sanchez-Monge et al., 1997), the two cloned peroxidases from wheat POX1 (Hertig et al., 1991) and pPOX381 (Rebmann et al., 1991), the two cloned peroxidases from barley BP1 (Johansson et al., 1992) and BP2 (Theilade and Rasmussen, 1992), and two mature proteins from horseradish (Welinder, 1979) and turnip (Mazza and Welinder, 1980) is shown in Fig. 4. Unlike other plant peroxidases the N-terminal of WP1 was accessible to the Edman degradation according to what reported also for the barley peroxidases BP1 and BP2. WP1 is less than 40% identical to the wheat peroxidase POX1 and POX381, whereas it exhibits a higher degree of identity toward the two peroxidases isolated from barley, a species closely related to wheat. A low degree of identity is observed between WP1 and two well-known peroxidases (HRP C and TP 7) from the dicot species horseradish and turnip. WP1 is highly

```
WP1                AEPPVARGLSFDFYRRTCPRAMSI
36kDa allergen     AEPPVARGLSFDFYRRTCPRAESI
HRP                      ZLRPDFYDNSCPNVSNI
POX1                     QLSSTFYDTSCPRALVA
pPOX381                  QLSSTFYDTSCPRALVI
BP1                AEPPVAPGLSFDFYRRTCPRAESI
BP2                 QPPITRGLSFDFYHGRCPGAESI
TP 7                     ZLTTNFYSTSCPNLLST
```

Fig. 4. Sequence comparison of the N-terminal region of wheat WP1 aligned with the corresponding regions of peroxidases from 36 kDa allergen, HRPC, POX1, pPOX381, BP1, BP2 and TP 7. Amino acids are shown in the one-letter code. N-terminal Z indicates pyroglutamate. The sequences are aligned to maximise homology. Residues common to six out of eight sequences are in bold face. The conserved region of IAA oxidases is boxed.

identical (23 N-terminal invariant residues out of 24) to a 36 kDa allergen purified from wheat by Sanchez-Monge et al. (1997); anyhow, it is worth noting that, unlike the wheat allergen, WP1 was found to be not glycosylated. This allergen has been indicated as a peroxidase on the basis of its enzymatic activity and sequence homology with the barley peroxidase BP1. These results may indicate that variations in the molecular structures of peroxidases are more role-specific rather than species-specific. During evolution peroxidase isoforms may have conserved large portions of their structure when they participate in similar biological functions, or have diverged to carry out different functional roles.

Very recently the presence of a binding site for IAA distinct from that involved in the binding and cleavage of hydrogen peroxide has been reported for plant peroxidase (Savitsky et al., 1999). In particular, five structurally similar fragments (helices A, B, D-D′ and C) were identified between some plant peroxidases and several auxin-binding proteins and one of this is located at the N-terminus of peroxidases (helix A) (Savitsky et al., 1999). The relevant IAA oxidase activity described in the present paper for holoWP1 prompted us to look for structural elements related to this feature. The presence at the N-terminus of a region similar to helix A (Savitsky et al., 1999) is noted in Fig. 4, confirming this close structure/function relationship of IAA oxidases.

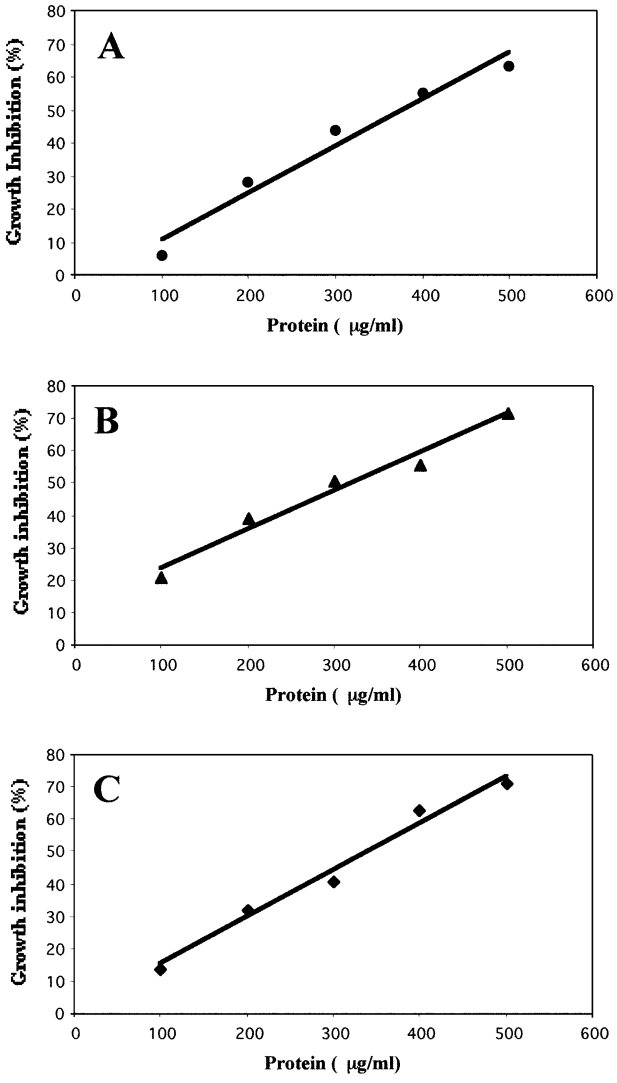

Fig. 5. Antifungal activity of holoWP1 towards *Botrytis cinerea* (A), *Trichoderma viride* (B) and *Fusarium culmorum* (C). Relative hyphal growth is expressed as percentage of hyphal growth of control cultures and data are means of two independent experiments.

2.3. Antifungal activity

In order to investigate the biological role of the heme-peroxidase WP1, the antifungal activity was tested utilizing the wide host range pathogen *Botrytis cinerea*, the wheat pathogen *Fusarium culmorum* and the non pathogenic *Trichoderma viride*. The concentration of holoWP1 required for 50% growth inhibition (IC_{50} value) of the tested fungi was determined from the dose–response curves (% growth inhibition versus protein concentration) shown in Fig. 5. HoloWP1 inhibited germ tube elongation of all the tested fungi showing IC_{50} values of 315, 336 and 377 μg/ml for *F. culmorum, T. viride* and *B. cinerea*, respectively. IC_{50} values of wheat PR-4 proteins wheatwin1 and wheatwin2 on *B. cinerea* and *F. culmorum*, assessed by the same assay, were 20–25 fold lower (Caruso et al., 1996), showing that the peroxidase was less effective than PR-4 proteins in inhibiting fungal hyphal growth. Anyway, WP1 antifungal activity, although less strong, is significant and correlated to its tridimensional structure. In fact, control experiments with heat-inactivated holoWP1 confirmed that the

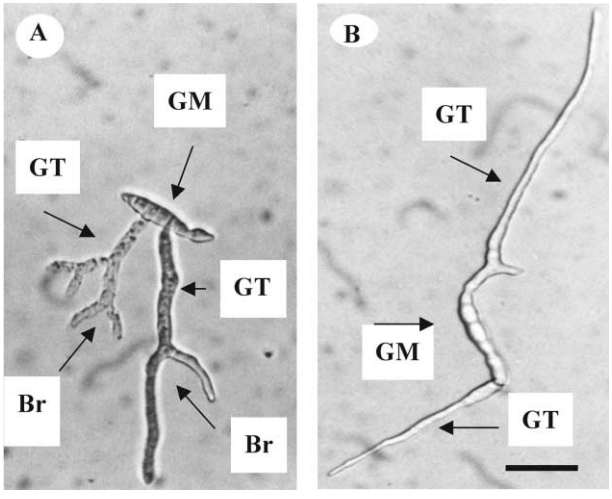

Fig. 6. *F. culmorum* growth in the presence (A) and in the absence (B) of holoWP1 (300 μg/ml). Br = branching; GM = germinating macroconidium; GT = germinating tube. Bar = 30 μm.

observed inhibition pattern was not due to a general effect on cell growth found for some basic proteins, but depends on a specific action of the native protein. To confirm the importance of the native tridimensional structure of the holoWP1, antifungal activity was also tested on the heme-depleted apoWP1 showing that the growth of the tested fungi was not affected. In any case, the antifungal activity was directed only to the inhibition of hyphal growth since the spore germination was not influenced at all in the tested concentration range.

Hyphal growth inhibition was also accompanied by a diffuse hyphal branching for all the fungi tested. *F. culmorum* growth in the presence and in the absence of WP1 is shown in Fig. 6. No accumulation of exudates was observed around hyphae, thus suggesting that the biological effect of WP1 is not directed on the modification of fungal cell wall or membranes.

3. Conclusions

The functional significance of the antifungal activity of holoWP1 is not fully understood, but the existence of a protein with antifungal activity in wheat seeds might represent a selective advantage towards a wide range of potential pathogens activity even if the toxic effect is less effective than that reported for other proteins. Anyhow, its expression together with other antifungal proteins, such as those belonging to the PR group, could indicate a protective role during seed germination and may be considered as part of the defence mechanisms that the plant activates against pathogens. This is the first report describing a weak but direct antifungal activity of a peroxidase from wheat seeds. This unique feature has never been observed before suggesting that this peroxidase could play a role in defence against invading hosts.

4. Experimental

4.1. General experimental procedures

CM-Sepharose fast flow, Resource S and isoelectric focusing reagents were from Pharmacia Biotech (Uppsala, Sweden); a μ-Bondapak C_{18} reverse-phase column (0.39×30 cm) was from Waters-Millipore (Milford, MA, USA); an UltroPac TSK CM-3SW ion-exchange column (7.5×150 mm) was from LKB-Pharmacia Biotech (Uppsala, Sweden). SDS-PAGE reagents, including low molecular weight markers, were from Bio-Rad (Italy). Bovine serum albumin, chicken ovalbumin, trifluoroacetic acid, IAA, dithiothreitol and 4-vinylpyridine were from Sigma Chemical Co. (St. Louis, MO, USA); guaiacol (*o*-methoxyphenol), 2,4-dichlorophenol (DCP) and hydrogen peroxide were from BDH (UK). All the reagents were of the highest purity commercially available.

4.2. Plant and fungal materials

Triticum aestivum, pure variety San Pastore, was kindly supplied from Istituto Sperimentale per la Cerealicoltura (S. Angelo Lodigiano, Italy). The following fungal isolates were used: *Fusarium culmorum* (isolate ISPAVE 485), *Botrytis cinerea* (isolate Bc 91/3) and *Trichoderma viride* (isolate Tv56). Sporulating cultures were obtained by growing the isolates on potato dextrose agar (PDA) (Oxoid, Hampshire, UK) at 24 °C for 14 days.

4.3. Enzyme purification

Finely ground flour from wheat seeds was extracted overnight with 0.15 M NaCl (4 ml/g) under stirring at 4 °C. The suspension was centrifuged at 18,000 *g* for 20 min at 4 °C and the clear supernatant was fractionated by ammonium sulfate; the 10–80% precipitate was collected by centrifugation at 18,000 *g* for 20 min at 4 °C and extensively dialysed against 20 mM ammonium acetate buffer (pH 7.8) at 4 °C (buffer A). The clear dialysed sample was fractionated on a CM-Sepharose fast flow column (1.6×10 cm) equilibrated with buffer A; the bound proteins were eluted with a linear gradient from 20 to 100% of 300 mM ammonium acetate buffer (pH 7.8) (buffer B) at a flow rate of 1.5 ml/min; the eluate was monitored measuring the absorbance at 280 nm and the enzymatically active fractions were pooled, concentrated by ultrafiltration and equilibrated in 20 mM ammonium acetate buffer (pH 7.4) (buffer C). Peroxidase activity was distributed into three fractions, coded peaks I, II and III in order of elution. Peak II was further purified by two different procedures to obtain either the heme-depleted peroxidase (apoenzyme) or the enzymatically active hemeprotein (holoenzyme).

4.3.1. Apoenzyme purification (apoWP1)

Peak II was resolved on a reverse phase μ-Bondapak C_{18} column using an HPLC System GOLD® (Beckman, USA) equipped with a 126 Solvent Module and a 166 UV/Vis detector interfaced with a personal computer. Eluant A was aqueous 0.07% trifluoroacetic acid and eluant B was 0.05% trifluoroacetic acid in acetonitrile. Elution was accomplished at a flow rate of 1 ml/min according to the following program: isocratic elution for 5 min at 25% B, followed by linear gradient from 25 to 34% B in 20 min, and from 34 to 44% B in 45 min. Eluate was monitored measuring the absorbance at 220 nm. Fractions were manually collected and freeze-dried.

4.3.2. Holoenzyme purification (holoWP1)

Peak II was loaded onto a Resource S column equilibrated in 20 mM ammonium acetate buffer (pH 7.4) (buffer C); the column was washed with 2 ml of buffer C

and the bound proteins were eluted with a liner gradient of NaCl (0–30 mM in 7.5 min and 30–70 mM in 30 min) in buffer C at 1.0 ml/min, the absorbance being monitored at 280 nm. The fractions containing peroxidase activity (Peaks II-1 and II-2) were concentrated by ultrafiltration and equilibrated in buffer C. Peak II-2 was further purified by IE-HPLC on a TSK-3SW high performance column equilibrated in buffer C; elution was accomplished at a flow rate of 0.6 ml/min monitoring the absorbance at 220 nm and using the following program: linear gradient from 0 to 100% of 100 mM NaCl in buffer C in 140 min, then isocratic elution for 15 min with buffer C. The eluate was monitored by measuring the absorbance at 220 nm; the enzymatically active fractions were pooled and freeze-dried on a speed-vac concentrator.

4.4. Enzyme and protein assay

The protein concentration was determined by the Bio-Rad assay, following the manufacturer's instructions and using bovine serum albumin as a standard. Peroxidase activity was measured at 30 °C in a reaction mixture (3 ml final volume) containing 13 mM H_2O_2 and 124 μM guaiacol in 50 mM Tris, pH 7.0; the reaction was started by adding the enzyme and the absorbance increase at 470 nm due to the formation of tetraguaiacol (ε 26.6 mM^{-1} cm^{-1}) was measured. One unit of enzymatic activity is defined as the amount of enzyme required for the production of 1 μmol of tetraguaiacol per minute in the above assay conditions. The oxidation of IAA was followed at 30 °C by measuring the absorbance at 247 nm; the reaction mixture (1 ml final volume) contained 1 mM $MnCl_2$, 0.23 mM IAA, 1 mM DCP in 20 mM KH_2PO_4, pH 4.7. One enzyme unit (EU) is arbitrarily defined as the amount of enzyme which produces a 0.01 absorbance change at 247 nm per min. The aerobic oxidation of IAA in the absence of phenolic compounds was performed using an O_2 micro electrode fitted with a glass tube (Hansatech instruments LTD, England). The reaction was followed at 30 °C using 2 mM IAA and 0.05, 0.1, 0.2 μM peroxidase in 50 mM sodium acetate buffer, pH 4.5 and KH_2PO_4, pH 6.0.

4.5. Electrophoresis and isoelectric focusing

SDS-PAGE was carried out in 15% polyacrylamide gel with a mini-Protean apparatus (Bio-Rad) using the discontinuous system described by Laemmli (1970); both Coomassie Blue and silver staining procedures were used following the instruction of the manufacturer. Periodic acid-Schiff staining (PAS) was performed according to Doerner and White (1990) following non-denaturing PAGE. IEF was performed in the pH range 3.5–10 using both an LKB apparatus (Pharmacia) and a mini-IEF apparatus from Bio-Rad. Proteins in the IEF gels were fixed with 20% TCA; the gels were then washed with a mixture containing 30% methanol and 10% acetic acid and stained and destained as reported for SDS–PAGE. IEF gels were also stained for peroxidase activity; the gels were soaked for 10 min in 50 mM Tris buffer (pH 7.0), and then incubated with 0.46 % (v/v) guaiacol and 13 mM H_2O_2 in the same buffer at room temperature until red bands appeared. The gels were then fixed in water/methanol/acetic acid (6.5:2.5:1, v/v).

4.6. Endo-F digestion

HoloWP1 (10 μg) and ovalbumin (10 μg) were digested with endoglycosidase F (Endo-F) (Boehringer, Mannheim) from *Flavobacterium meningosepticum* according to Elder and Alexander (1982). The proteins were incubated with 0.2 enzyme units at 37 °C for 18 h in acetate buffer 20 mM, pH 5.4, containing Triton X-100 0.2% (v/v), 0.1 mM β-mercaptoethanol and 20 mM EDTA. Both treated and untreated proteins were then analysed by SDS–PAGE.

4.7. Sequence analysis

Purified apoWP1 (apoenzyme) from RP-HPLC was reduced and pyridylethylated before sequence analysis. Protein (5 nmol) was treated with 1.5 μmol of dithiothreitol in 0.1 ml 0.25 M Tris buffer (pH 8.0), 2 mM EDTA, 6 M guanidine–HCl, for 2 h at 37 °C under nitrogen atmosphere. Alkylation was performed with 4-vinylpyridine (45 μmol) for 2 h at room temperature in the dark under nitrogen atmosphere. The reaction was stopped by freezing and excess reagents were removed by RP-HPLC on a μ-Bondapak C_{18} column. Eluents A and B and the elution program were those described above. The S-pyridylethylated apoWP1 was manually collected, freeze-dried then dissolved in aqueous 0.1% trifluoroacetic acid and subjected to automated sequence analysis using a pulsed liquid-phase automatic sequencer (Perkin Elmer-Applied Biosystems model 477A) equipped on-line with a phenylthiohydantoin amino acid derivative analyser (Perkin Elmer-Applied Biosystems model 120A). The sample was loaded onto a trifluoroacetic acid-treated glass-fiber filter, coated with polybrene and washed according to manufacturer's instructions. The sequence reagents were from Perkin Elmer-Applied Biosystems.

4.8. Antifungal activity

The antifungal activity of WP1 was tested in vitro against the following fungal isolates: *Botrytis cinerea* (isolate BC91/3), *Fusarium culmorum* (isolate ISPAVE485) and *Trichoderma viride* (isolate Tv56). Sporulating cultures were obtained by growing the isolates on Potato Dextrose Agar (PDA) (Oxoid-Unipath)

at 24 °C for 14 days. Conidia were collected by scraping a sterile inoculating loop across the surface of the plate in presence of 2× potato dextrose broth (PDB) (Sigma - Aldrich), counted with a hemocytometer and diluted to give a concentration of 106 conidia/ml. Antifungal activity assay was performed as previously reported (Chilosi et al., 2000) at WP1 concentrations from 100 to 500 μg/ml. In the controls, sterile distilled water or hot-denaturated holoWP1 replaced the native protein. The mixtures were placed on microscope slides and incubated for approximately 16 h at 21 °C in the dark in a moist environment; after incubation, germ tube elongation was evaluated by observing microscopically 100 germinating spores for each of three replicates. Hyphal growth inhibition was expressed as IC50 (protein concentration required for 50% growth inhibition) determined by regression from the dose–response curves.

Acknowledgements

We greatly acknowledge Dr. Monica Nobile for skilful assistance in sequence analysis experiments. This research was supported by a grant from Ministero per le Politiche Agricole (MIPA, former MIRAAF), Piano Nazionale Biotecnologie Vegetali, Progr. N. 152.

References

Baga, M., Chibbar, R.N., Kartha, K.K., 1995. Molecular cloning and expression analysis of peroxidase genes from wheat. Plant Mol. Biol. 29, 647–662.

Bradley, D.J., Kjellbom, P., Lamb, C.J., 1992. Elicitor- and wound-induced oxidative cross-linking of a proline-rich plant wall protein: a novel, rapid defense response. Cell 70, 21–30.

Caruso, C., Caporale, C., Chilosi, G., Vacca, F., Bertini, L., Magro, P., Poerio, E., Buonocore, V., 1996. Structural and antifungal properties of a pathogenesis-related protein from wheat. J. Prot. Chem. 15, 35–44.

Chilosi, G., Caruso, C., Caporale, C., Leonardi, L., Bertini, L., Buzi, A., Nobile, M., Magro, P., Buonocore, V., 2000. Antifungal activity of a Bowman-Birk trypsin inhibitor from wheat kernel. J. Phytopathol. 148, 477–481.

Chittoor, J.M., Leach, J.E., White, F., 1997. Differential induction of a peroxidase gene family during infection of rice by *Xanthomonas oryzae* pv. *Oryzae*. Mol. Plant-Microbe Interact 10, 861–871.

Doerner, K.C., White, B.A., 1990. Detection of glycoproteins separated by nondenaturing polyacrylamide gel electrophoresis using the periodic acid-Schiff stain. Anal. Biochem. 187, 147–150.

Elder, J.H., Alexander, S., 1982. Endo-B-N-acetylglucosaminidase F: Endoglycosydase from *Flavobacterium meningosepticum* that cleaves both high-mannose and complex glycoproteins. Proc. Natl Acad. Sci. USA 79, 4540–4544.

Espelie, K.E., Kolattukudy, P.E., 1985. Purification and characterization of an abscissic acid-inducible anion peroxidase associated with suberization in potato (*Solanum tuberosum)*. Arch. Biochem. Biophys. 240, 539–545.

Flott, B.E., Moerschbacher, B.M., Reisner, H., 1989. Peroxidase isoenzyme patterns of resistant and susceptible wheat leaves following stem rust infection. New Phytol. 111, 413–421.

Gaspar, T., Penel, C., Hagege, D., Greppin, H., 1991. Peroxidases in plant growth, differentiation, and development processes. In: Lobarzewski, J., Greppin, H., Penel, C., Gaspar, Th. (Eds.), Biochemical, Molecular, and Physiological Aspects of Plant Peroxidases. University of Geneva Press, Switzerland, pp. 249–280.

Gazaryan, I.G., Chubar, T.A., Mareeva, E.A., Lagrimini, L.M., Van Huystee, R.B., Thorneley, R.N.F., 1999. Aerobic oxidation of indole-3-acetic acid catalysed by anionic and cationic peanut peroxidase. Phytochemistry 51, 175–186.

Graham, M.Y., Graham, T.L., 1991. Rapid accumulation of anionic peroxidases and phenolic polymers in soyabean cotyledon tissues following treatment with *Phytophthora megasperma* f. sp. *glycinea* wall glucan. Plant Physiol. 97, 1445–1455.

Greppin, H., Penel, C., Gaspar, T., 1986. Molecular and Physiological Aspects of Plant Peroxidases. University of Geneva Press, Switzerland.

Hertig, C., Rebmann, G., Bull, J., Mauch, F., Dudler, R., 1991. Sequence and tissue-specific expression of a putative peroxidase gene from wheat (*Triticum aestivum* L.). Plant Mol. Biol. 16, 171–174.

Johansson, A., Rasmussen, S.K, Harthill, J.E., Welinder, K.G., 1992. cDNA, amino acid and carbohydrate sequence of barley seed-specific peroxidase BP1. Plant Mol. Biol. 18, 1151–1161.

Laemmli, U.K., 1970. Cleavage of structural proteins during assembly of the head of bacteriophage T4. Nature 227, 680–685.

Lagrimini, L.M., Burkhart, W., Moyer, M., Rothstein, S., 1987. Molecular cloning of complementary DNA encoding the lignin-forming peroxidase from tobacco: molecular analysis and tissue-specific expression. Proc. Natl. Acad. Sci. USA 84, 7542–7546.

Lagrimini, L.M., Rothstein, S., 1987. Tissue specificity of tobacco peroxidase isozymes and their induction by wounding and tobacco mosaic virus infection. Plant Physiol. 84, 438–442.

Liu, C.J, Chao, S., Gale, M.D., 1990. The genetical control of tissue-specific peroxidases, Per-1, Per-2, Per-3, Per-4, and Per-5 in wheat. Theor. Appl. Genet. 79, 305–313.

Machackova, I., Ganceva, K., Zmrhal, Z., 1975. The role of peroxidase in the metabolism of indole-3-acetic acid and phenols in wheat. Phytochemistry 14, 1251–1254.

Mazza, G., Welinder, K.G., 1980. Covalent structure of turnip peroxidase 7. Cyanogen bromide fragments, completestructure and comparison to horseradish peroxidase C. Eur. J. Biochem. 108, 481–489.

Penel, C., Gaspar, T., Greppin, H., 1992. Plant Peroxidases 1980–1990: Topics and Detailed Literature on Molecular, Biochemical and Physiological Aspects. University of Geneva Press, Switzerland.

Rasmussen, S.K., Welinder, K.G., Hejgaard, J., 1991. cDNA cloning, characterization and expression of an endosperm-specific barley peroxidase. Plant Mol. Biol. 16, 317–327.

Rebmann, G., Hertig, C., Bull, J., Mauch, F., Dudler, R., 1991. Cloning and sequencing of cDNAs encoding a pathogen-induced putative peroxidase of wheat (*Triticum aesticum* L.). Plant Mol. Biol. 16, 329–331.

Reimers, P.J., Guo, A., Leach, J.E., 1992. Increased activity of a cationic peroxidase associated with an incompatible interaction between *Xanthomonas oryzae* pv. *oryzae* and rice (O*ryza sativa*). Plant Physiol 99, 1044–1050.

Roberts, E., Kolattukudy, P.E., 1989. Molecular cloning, nucleotide sequence, and abscissic acid induction of a suberization-associated higlhy anionic peroxidase. Mol. Gen. Genet. 217, 223–232.

Roberts, E., Kutchan, T., Kolattukudy, P.E., 1988. Cloning and sequencing of cDNA for a highly anionic peroxidase from potato and the induction of its RNA in suberizing potato fruits. Plant Mol. Biol. 11, 15–31.

Sanchez-Monge, R., Garcia-Casado, G., Lopez-Otin, C., Armentia, A., Salcedo, G., 1997. Wheat flour peroxidase is a prominent allergen associated with baker's asthma. Clin. Exp. Allergy 27, 1130–1137.

Savitsky, P.A., Gazaryan, I.G., Tishkov, V.I., Lagrimini, L.M., Ruzgas, T., Gorton, L., 1999. Oxidation of indole-3-acetic acid by dioxygen catalysed by plant peroxidases: specificity for the enzyme structure. Biochem. J. 340, 579–583.

Theilade, B., Rasmussen, S.K., 1992. Structure and chromosomal localization of the gene encoding barley seed peroxidase BP 2A. Gene 118, 261–266.

Van Huystee, R.B., 1987. Some molecular aspects of plant peroxidase biosynthetic studies. Ann. Rev. Plant Physiol. 38, 205–219.

Welinder, K.G., 1979. Amino acid sequence studies of horseradish peroxidase. Amino and carboxyl termini, cyanogen bromide and tryptic fragments, the complete sequence, and some structural characteristics of horseradish peroxidase c. Eur. J. Biochem. 96, 483–502.

Young, S.A., Guo, A., Guikema, J.A., White, F.F., Leach, J.E., 1995. Rice cationic peroxidase accumu lates in xylem vessels during incompatible interactions with *Xanthomonas oryzae* pv. *Oryzae*. Plant Physiol. 107, 1333–1341.

PERGAMON

Phytochemistry 58 (2001) 751–758

PHYTOCHEMISTRY

www.elsevier.com/locate/phytochem

Phytotoxic naphthopyranone derivatives from the coprophilous fungus *Guanomyces polythrix*☆

Martha Macías[a], Alicia Gamboa[b], Miguel Ulloa[c], Rubén A. Toscano[d], Rachel Mata[a,*]

[a]*Departamento de Farmacia, Facultad de Química, Universidad Nacional Autónoma de México, D.F. 04510, Mexico*
[b]*Instituto de Ecología, Universidad Nacional Autónoma de México, D.F. 04510, Mexico*
[c]*Departamento de Botánica, Instituto de Biología, Universidad Nacional Autónoma de México, D.F. 04510, Mexico*
[d]*Laboratorio de Rayos X, Instituto de Química, Universidad Nacional Autónoma de México, D.F. 04510, Mexico*

Received 16 January 2001; received in revised form 8 May 2001

Abstract

Reinvestigation of the fermentation broth and mycelium of the coprophilous fungus *Guanomyces polythrix*, grown in static conditions, led to the isolation of several phytotoxic compounds, including two new naphthopyranone derivatives, namely (2*S*, 3*R*)-5-hydroxy-6,8-dimethoxy-2,3-dimethyl-2,3-dihydro-4*H*-naphtho[2,3-b]-pyran-4-one and (2*S*, 3*R*)-5-hydroxy-6,8,10-trimethoxy-2,3-dimethyl-2,3-dihydro-4*H*-naphtho[2,3-b]-pyran-4-one. The structures of the new compounds were established by spectral and chiroptical methods. In addition, the structure of 8-hydroxy-6-methyl-9-oxo-9*H*-xanthene-1-carboxylic acid methyl ester was unambiguously determined by X-ray analysis. The isolates caused significant inhibition of radicle growth of two weed seedlings (*Amaranthus hypochondriacus* and *Echinochloa crusgalli*) and interacted with both spinach and bovine brain calmodulins. © 2001 Elsevier Science Ltd. All rights reserved.

Keywords: *Guanomyces polythrix*; *Amaranthus hypochondriacus*; *Echinochloa crusgalli*; Calmodulin; Affinity chromatography; (2*S*, 3*R*)-5-Hydroxy-6,8-dimethoxy-2,3-dimethyl-2,3-dihydro-4*H*-naphtho[2,3-b]-pyran-4-one; (2*S*, 3*R*)-5-Hydroxy-6,8,10-trimethoxy-2,3-dimethyl-2,3-dihydro-4*H*-naphtho[2,3-b]-pyran-4-one; 8-Hydroxy-6-methyl-9-oxo-9*H*-xanthene-1-carboxylic acid methyl ester; Ergosta-4,6,8(14),22-tetraen-3-one; 4-Hydroxybenzoic acid

1. Introduction

As part of our systematic search for new herbicidal lead structures from natural sources, we have recently reported the isolation and structure elucidation of several phytotoxins from the mycelium and culture broth of the coprophilous fungus *Guanomyces polythrix* grown in agitation conditions. Fourteen compounds (**1**–**14**) were isolated, of which the phytotoxic compounds included the five new dihydronaphtopyrones derivatives (**1**–**5**), rubrofusarin B (**11**), emodin (**12**), citrinin (**13**) and 4-hydroxy-benzoic acid methyl ester (**14**). The isolates caused noted inhibition of radicle growth of two weed seedlings [*Amaranthus hypochondriacus* L. and *Echinochloa crusgalli* (L.) Beauv.] and behaved as plant calmodulin (CaM) interactors (Macías et al., 2000). For this reason, we have undertaken the further chemical investigation of *G. polythrix* grown in static conditions. Herein, we report the isolation and structure elucidation of two additional novel naphthopyranone derivatives (**6** and **7**) along with several known compounds. In addition, the phytotoxic properties of the isolates and the potential role of CaM as molecular target of the phytotoxic action are described.

2. Results and discussion

2.1. Bioactivity-guided isolation

G. polythrix was grown in liquid-substrate fermentation on PDB (potato dextrose broth). The mycelium and fermentation broth were extracted with CH_2Cl_2. The combined extract exhibited significant phytotoxic activity on seedlings of *A. hypochondriacus* and *E. crusgalli* (Table 1). Bioassay-guided fractionation of the active

☆ Taken in part from the PhD thesis of Martha Macías.

* Corresponding author. Tel.: +52-5-622-5289; fax: +52-5-622-5329.

E-mail address: rachel@servidor.unam.mx (R. Mata).

0031-9422/01/$ - see front matter © 2001 Elsevier Science Ltd. All rights reserved.
PII: S0031-9422(01)00278-3

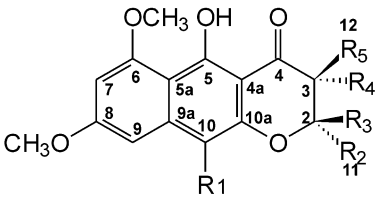

(**1**) R_1= H, R_2= CH_3, R_3= H, R_4= H, R_5= CH_3
(**2**) R_1= CH_3O, R_2= CH_3, R3= H, R_4= H, R_5= CH_3
(**3**) R_1= H, R_2= CH_3, R_3= H, R_4= H, R_5= H
(**4**) R_1= CH_3O, R_2= CH_3, R_3= H, R_4= H, R_5= H
(**6**) R_1= H, R_2= CH_3, R_3= H, R_4= CH_3, R_5= H
(**7**) R_1= CH_3O, R_2= CH_3, R_3= H, R_4= CH_3, R_5= H

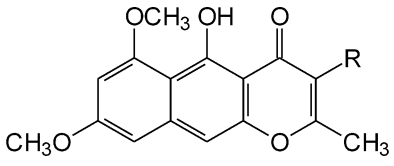

(**5**) R= CH_3
(**11**) R= H

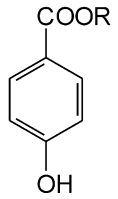

(**8**) R= H
(**14**) R= CH_3

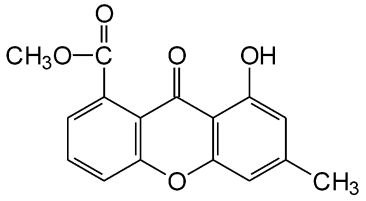

(**9**)

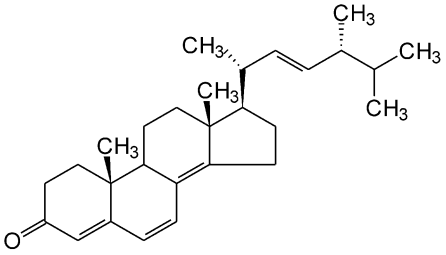

(**10**)

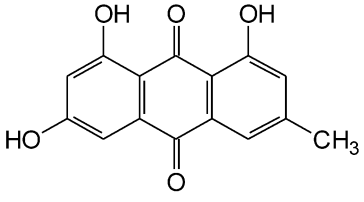

(**12**)

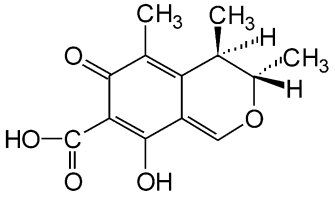

(**13**)

extract led to the isolation of two new naphtophyranone derivatives identified as (2*S*, 3*R*)-5-hydroxy-6,8-dimethoxy-2,3-dimethyl-2,3-dihydro-4*H*-naphtho[2,3-b]-pyran-4-one (**6**), and (2*S*, 3*R*)-5-hydroxy-6,8,10-trimethoxy-2,3-dimethyl-2,3-dihydro-4*H*-naphtho[2,3-b]-pyran-4-one (**7**). In addition, compounds **1-5**, rubrofusarin B (**11**), emodin (**12**), citrinin (**13**), *p*-hydoxybenzoic acid methyl ester (**14**), *p*-hydroxybenzoic acid (**8**) 8-hydroxy-6-methyl-9-oxo-9*H*-xanthene-1-carboxylic acid methyl ester (**9**) and ergosta-4,6,8(14),22-tetraen-3-one (**10**) were obtained. Compounds **8**–**10** are new to this species. Compounds **1**–**5** were identified by comparison with authentic samples (Macías et al., 2000) and compounds **8** and **10** were identified from their IR and ^{1}H NMR spectroscopic data, which were identical to those previously described in the literature (Porter et al., 1975; Seitz and Paukstelis, 1977).

2.2. Structure elucidation of compounds **6** and **7**

The molecular formulae of compounds **6** and **7** were established as $C_{17}H_{18}O_5$ and $C_{18}H_{20}O_6$, respectively, by HREIMS and were identical to those of compounds **1** and **2**, respectively, suggesting that each set of compounds were isomers. The uni and bidimensional NMR (Table 2) spectra of compounds **6** and **7** were almost identical to those of **1** and **2**, respectively (Macías et al., 2000) indicating that the new natural products have the same 2,3-dimethyl-2,3-dihydro-4*H*-naphtho[2,3-b]-pyran-4-one skeleton and that the position of the hydroxy and

Table 1
Phytogrowth-inhibitory activity of the CH_2Cl_2 extract and isolated compounds from *Guanomyces polythrix* on radicle elongation (IC_{50} M) of *A. hypochondriacus* and *E. crusgalli*

Compound	*Amaranthus hypochondriacus*	*Echinochloa crusgalli*
Extract	54.3[a]	384.3[a]
6	1.1×10^{-4}	1.3×10^{-4}
7	7.5×10^{-5}	7.0×10^{-5}
8	1.7×10^{-5}	2.3×10^{-4}
9	1.5×10^{-5}	9.8×10^{-6}
10	8.0×10^{-5}	1.7×10^{-4}
2,4-D[b]	1.8×10^{-4}	8.8×10^{-4}

[a] Expressed in μg/ml.
[b] Positive standard control.

methoxyl groups along the dihydronaphtopyrone core was the same. The most obvious differences between the NMR spectra of **6** and **7** and those of **1** and **2** were: (i) the chemical shifts and coupling constants of the methines attributable to H-2/C-2 [δ_H/δ_C 4.59 (*dq*, $J=6.5$, 3.5 Hz)/75.26 in **6** and 4.66 (*dq*, $J=3.5$, 10 Hz)/75.73 in **7** vs 4.20 (*dq*, $J=6.5$, 10 Hz)/78.0 in **1** and 4.28 (*dq*, $J=6.5$, 10 Hz)/78.3 in **2**]; and (ii) the chemical shift values of the methyl groups at C-2 and C-3 [δ_H/δ_C 1.40/16.38 (C-11), 1.22/9.6 (C-12) in **6** and 1.45/16.4 (C-11), 1.24/9.6 (C-12) in **7** vs 1.50/19.8 (C-11), 1.26/10.4 (C-12) in **1** and 1.57/19.8 (C-11), 1.28/10.8 (C-12) in **2**]. The small $J_{2\text{-}3}$ value (3 Hz) clearly indicated that the methyl groups at C-2 and C-3 in **6** and **7** were *cis* rather than *trans* as in **1** and **2**. The CD spectra of **6** and **7** showed a negative Cotton effect around 314 nm, supporting the depicted 2*S* absolute configuration (Gaffield, 1970; Macías et al., 2000). Automatically the configuration at C-3 was established as *R* due to the *cis* relationship of the methyl groups. Altogether, these observations revealed that compounds **6** and **7** were the corresponding epimers at C-3 of compounds **1** and **2,** respectively. Consequently compounds **6** and **7** were identified as (2*S*, 3*R*)-5-hydroxy-6,8-dimethoxy-2,3-dimethyl-2,3-dihydro-4*H*-naphtho[2,3-b]-pyran-4-one, and (2*S*, 3*R*)-5-hydroxy-6,8,10-trimethoxy-2,3-dimethyl-2,3-dihydro-4*H*-naphtho[2,3-b]-pyran-4-one.

2.3. X-ray crystallographic analysis of compound 9

The structure of compound **9** was unequivocally established as 8-hydroxy-6-methyl-9-oxo-9H-xanthene-1-carboxylic acid methyl ester by X-ray crystallography. The ORTEP-like view as obtained by the single-crystal X-ray analysis is shown in Fig. 1. Except for the ester group, the compound is planar (root-mean-square-deviation 0.048 Å). The mean plane defined by the atoms of the methyl ester is almost perpendicular (77.9°) to the plane of the tricyclic moiety. The hydroxyl group at C-8 is intramolecularly hydrogen bonded [O1-H1... O2 1.83(3) Å]. In the crystal, molecules of **9** stack into columns along the ***c*** axes in an anti-parallel fashion with an adjacent molecule, while the main molecule axis makes an angle of 65.8° in the opposite direction. Both types of stacking are almost perfect, as judging the

Table 2
NMR spectral data for (2*S*, 3*R*)-5-hydroxy-6,8-dimethoxy-2,3-dimethyl-2,3-dihydro-4*H*-naphtho[2,3-b]-pyran-4-one (6), and (2*S*, 3*R*)-5-hydroxy-6,8,10-trimethoxy-2,3-dimethyl-2,3-dihydro-4*H*-naphtho[2,3-b]-pyran-4-one (7)[a]

	6				7			
Position	^{13}C (δ)	δ_H (J_{HH} in Hz)	NOESY	HMBC	^{13}C (δ)	δ_H (J_{HH} in Hz)	NOESY	HMBC
1								
2	75.26	4.59 *dq*, (6.5, 3.5)	CH_3-11, H-3, CH_3-12	3, CH_3-11,	75.73	4.66 *dq*, (3.5, 6.5)	CH_3-11, H-3, CH_3-12	3, CH_3-11,
3	44.93	2.69 *dq*, (7.5, 3.5)	CH_3-12, H-2, CH_3-11	2, CH_3-12	44.96	2.75 *dq*, (3.5, 7.0)	CH_3-12, H-2, CH_3-11	2, CH_3-12
4	201.84			2, 3, CH_3-12	201.69			2, 3, CH_3-12
4a	103.50		1	3, OH-5,10	102.84			3, OH-5
5	165.49			OH-5	161.68			OH-5
5a	107.71			OH-5, 7, 9, 10	107.12			OH-5, 7, 9
6	161.27			7, OCH_3-6	161.54			7, OCH_3-6
7	96.41	6.29 *d*, (2.5)	9, OCH_3-6	9	92.59	6.34 *d*, (2.0)	9, OCH_3-9	9
8	162.38			7, OCH_3-8, 9	162.75		—	7, OCH_3-8, 9
9	98.27	6.55 *d*, (2.5)	7, 10, OCH_3-8	7, 10	96.79	6.91 *d*, (2.0)	7, 10, OCH_3-8, OCH3-10	7
9a	143.31			9, 10	131.99			9
10	101.30	6.50 *s*	9	9	162.75			9
10a	155.81			2, 10	138.3			2
CH_3-11	16.38	1.40 *d*, (6.5)	H-2, H-3, CH_3-12	2, 3	16.44	1.45 *d*, (6.5)	H-2, H-3, CH_3-12	2, 3
CH_3-12	9.58	1.22 *d*, (7.5)	H-3, H-2, CH_3-11, OH-5	3, 2	9.62	1.24 *d*, (7.0)	H-3, H-2, CH_3-11, OH-5	3, 2
OCH_3-6	55.99	3.96 *s*	7		56.14	3.97 *s*	7	
OCH_3-8	55.36	3.89 *s*	9		55.51	3.95 *s*	9	
OCH_3-10			CH_3-12		60.64	3.88 *s*	9	
OH-5		14.41 *s*				14.23 *s*	CH_3-12	

[a] Spectra were recorded in $CDCl_3$ (^1H, 500 MHz and ^{13}C, 125 MHz).

angles among the mean planes of 0.0 and 3.6°, and mean planes separations of 3.44 and 3.32 Å, respectively. It is important to point out that this compound was previously isolated from the fungus *Monilinia fructicola* (Hideaki and Takeshi, 1996). In that occasion only UV, MS and ^{1}H NMR spectroscopic data were described.

2.4. Phytogrowth-inhibitory activity of the phytochemicals

Natural products **6–10** were evaluated for their ability to inhibit the seed germination and seedling growth of *A. hypochondriacus* and *E. crusgalli*. Table 1 summarizes the phytotoxic effect of the isolates compounds at three different concentrations. The results in Table 1 are expressed as IC_{50} values (50% inhibitory concentration). As in the case of compounds **1–5** and **11–14** (Macías et al., 2000), the phytotoxins **6–10** were more potent as radical growth inhibitors than as germination inhibitors. Compound **9** was the most active against *E. crusgalli* (IC_{50} was 9.8×10^{-6} M), being more potent than the positive control 2,4-dichlorophenoxyacetic acid (2,4-D, $IC_{50}=8.8\times10^{-4}$ M). However, *A. hypochondriacus* was more sensitive to compounds **7–10**.

2.5. Interaction of phytotoxic compounds with spinach and bovine brain calmodulins

Calmodulin (CaM) is an intracellular receptor for Ca^{2+} in eukaryotes which modulates enzymatic response to calcium. This protein plays a leading role in plant signal

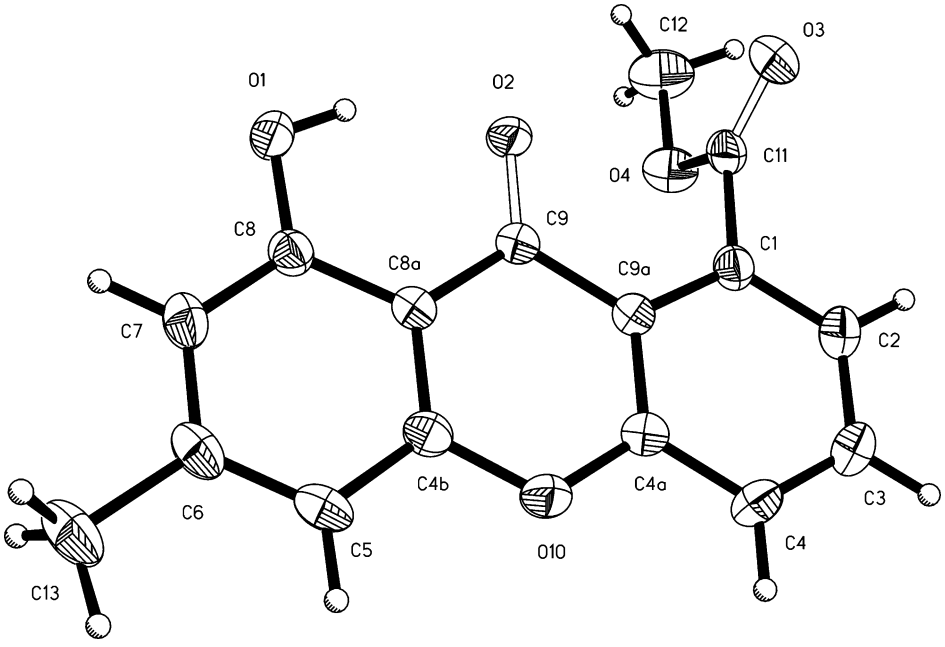

Fig. 1. ORTEP-like view of the molecular structure of 8-hydroxy-6-methyl-9-oxo-9*H*-xanthene-1-carboxylic acid methyl ester (**9**). Thermal ellipsoids at 30% probability level.

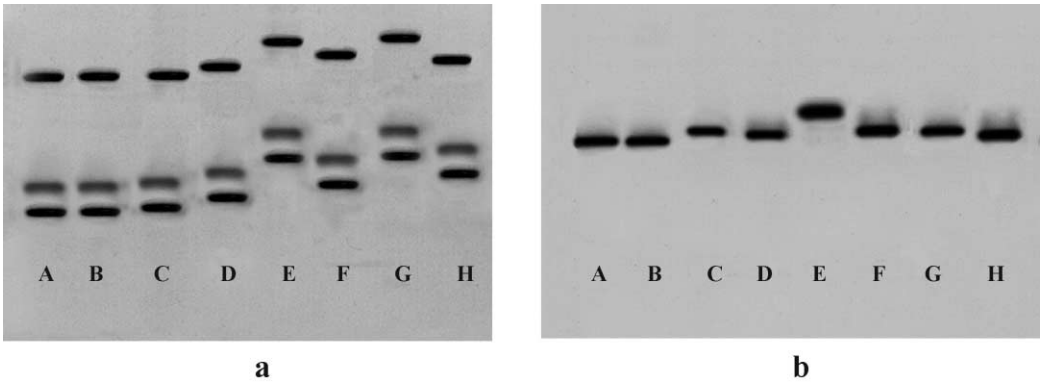

Fig. 2. SDS-PAGE of spinach (a) and bovine (b) calmodulins after treatment with compounds **6–10**. Electrophoresis of 2 μg samples of calmodulins in the presence of 1 mM $CaCl_2$. Pretreatments of the calmodulin samples: 1.5 h at 30 °C in the presence of $CaCl_2$ (A) control; B, DMSO; C, 0.033 μg/ml quercetin in DMSO; (D) **6**; (E) **7**; (F) **9**; (G) **10**; (H) **8**. In all cases were applied 0.033 μg/ml of compounds (**6–10**) in DMSO.

Table 3
Retention of phytotoxic compounds (**1**–**14**) from *Guanomyces polythrix* in a calmodulin-agarose column

Compound	μg the compound retained in the agarose column				
	Tris–HCl 20 mM 1 mM $CaCl_2$ pH = 7.0	Tris–HCl 20 mM 1 mM EGTA pH = 7.0	Tris–HCl 20 mM 1 mM $CaCl_2$ pH = 8.0	NaCl 1 M	Urea 6 M
1	10.0±0.0056	10.0±0.0021	10.0±0.0045	10.0±0.0014	10.0±0.0041
2	10.0±0.0089	10.0±0.0033	10.0±0.0074	10.0±0.0022	10.0±0.0021
3	10.0±0.0026	10.0±0.0054	10.0±0.0042	10.0±0.0021	10.0±0.0024
4	10.0±0.0051	10.0±0.0048	10.0±0.0041	10.0±0.0081	10.0±0.0021
5	10.0±0.0056	10.0±0.0074	10.0±0.0023	10.0±0.0045	10.0±0.0052
6	10.0±0.0045	10.0±0.0024	10.0±0.0030	10.0±0.0040	10.0±0.0075
7	10.0±0.0058	10.0±0.0016	10.0±0.0025	10.0±0.0078	10.0±0.0028
8	10.0±0.0046	6.9±0.0024	6.9±0.0021	6.9±0.0033	0.0±0.0038
9	10.0±0.0059	2.8±0.0058	2.8±0.0019	0.0±0.0021	0.0±0.0045
10	10.0±0.0023	10.0±0.0056	10.0±0.0080	10.0±0.0054	10.0±0.0021
11	10.0±0.0019	10.0±0.0089	10.0±0.0049	10.0±0.0047	10.0±0.0084
12	10.0±0.0027	10.0±0.0026	10.0±0.0026	10.0±0.0087	10.0±0.0012
13	6.0±0.0074	6.0±0.0052	6.0±0.0074	6.0±0.0045	6.0±0.0027
14	10.0±0.0088	7.1±0.0018	7.1±0.0022	7.1±0.0038	0.0±0.0050
Quercetin	10.0±0.0051	6.2±0.0038	6.2±0.0058	6.2±0.0074	0.0±0.0022

transduction during germination and plant growth modulating the activity of several important plant enzymes (Snedden and Fromm, 1998). Thus, continuing with our search of potential herbicides agents that could interact with CaM, the phytotoxic compounds were further evaluated for their ability to bind spinach and bovine brain Ca^{2+}–CaM complex. The interaction of any compound with Ca^{2+}–CaM complex alters its conformation and changes its electrophoretic mobility as detected in a SDS-PAGE electrophoresis (Leung et al., 1984, 1985). Fig. 2 shows that spinach CaM treated with Ca^{2+} (1 mM) and the isolates (0.033 μg/ml) had a lower electrophoretic mobility than untreated calmodulin. The strongest effect was observed with compound **7**. The mobility shift of bovine brain CaM (Fig. 2) in the presence of compounds **6**–**10** was similar to that of spinach CaM. Once more compound **7** exerted the strongest effect.

According to the results shown in Fig. 2 and those previously reported for compounds **1**–**5** and **11**–**14** (Macías et al., 2000), the interaction of compounds **1**–**14** with both spinach and bovine-brain CaMs could be irreversible (covalent), although the denaturing conditions in the SDS-PAGE electrophoresis would release any phytotoxin bound non-covalently. Thus, to obtain more information about the nature (covalent vs noncovalent) of the interaction of compounds **1**–**14** with CaM, an affinity-based chromatographic procedure employing a bovine brain CaM-agarose column was used (Bonza et al., 1998). After application of the phytotoxic compounds, the CaM-agarose column was eluted under non-denaturing (buffers I and II) and denaturing conditions (buffers III, NaCl and urea). In all cases, the eluents were analyzed spectrophotometrically to detect quantitatively the amount of bound compound (Table 3). According to the results summarized in Table 3, the interaction of compounds **1--7** and **10**–**12** with bovine brain CaM is irreversible (covalent). These phytotoxins remained attached to the CaM-agarose complex after extensive washing in non-denaturing and denaturing conditions. Compounds **8**, **9**, **14** and quercetin, however, were initially absorbed by the CaM–agarose conjugate, subsequently partially eluted with EGTA [ethylene glycol-bis(β-aminoethyl ether)-*N*,*N*,*N*′,*N*′-tetraacetic acid] containing buffer II and then totally removed on addition of urea 6M. The last set of results indicated that the interaction of **8**, **9**, **14** and quercetin with bovine brain CaM requires calcium and that the nature of the binding is non covalent. Finally, compound **13** showed a different elution profile and almost half of the phytotoxin remains attached to the CaM-agarose matrix after eluting in different conditions.

The aromatic compounds from *G. polythrix* interact directly with bovine brain and spinach CaM suggesting that these compounds may exert their phytotoxic action by inhibiting CaM-dependent process, although they could also interfere with other cellular metabolic phenomena. Affinity chromatography on CaM–agarose beads indicated that in most cases the interaction is covalent. Apparently the phytotoxins interact with the protein at different binding sites. Further work with calmodulin dependent enzymes will provide new insight about the interaction sites.

3. Experimental

3.1. General

Melting points were determined on a Fisher-Johns apparatus and are uncorrected. IR spectra were obtained

using KBr disks on a Perkin-Elmer FT 1605 spectrophotometer. UV spectra were obtained on a Lambda II UV spectrometer in MeOH solution. Optical rotations were taken on a Perkin-Elmer 241 polarimeter. CD spectra were performed on a JASCO 720 spectropolarimeter at 25 °C in MeOH solution. NMR spectra including COSY spectra, NOESY, HMBC and HMQC experiments were recorded on a Bruker DMX500, in $CDCl_3$, either at 500 (^1H) or 125 (^{13}C) MHz, using tetramethylsilane (TMS) as an internal standard. EI mass spectra were performed using a JEOL SX 102 mass spectrometer. X-ray analysis of compound **9** was accomplished on a Siemens P4/PC diffractometer equipped with graphite-monochromated radiation. Open column chromatography: silica gel 60 (70–230 mesh, Merck). Analytical and preparative TLC were performed on precoated silica gel 60 F254 plates (Merck).

3.2. Fungal material

The fungus *G. polythrix* was isolated from bat guano in Tepozotlán, Morelos, México. Voucher specimens (24486) have been deposited in the National Herbarium (MEXU), Instituto de Biología, Universidad Nacional Autónoma de México, México D.F and in the mycological collection of the Department of Plant Pathology (GAM 5803) University of Georgia, Athens, GA, USA.

Ten 2-l Erlenmeyer flasks, each containing 1000 ml of potato dextrose broth (PDB, Difco), were individually inoculated with one 1-cm^2 agar plug taken from a stock culture of *G. polythrix* maintained at 4 °C on potato dextrose agar (Difco). Flask cultures were incubated in static conditions at 28 °C for 30 days.

3.3. Extraction and isolation

After incubation, the flask contents were combined and filtered. The culture filtrate (10 l) was extracted exhaustively with CH_2Cl_2 (3×10 l). The combined organic phase was filtered over anhydrous Na_2SO_4 and concentrated in vacuo to give a green solid (615.6 mg). In addition, the mycelium was extracted with CH_2Cl_2 (3×2 l). The combined mycelial extract was evaporated to yield 1.9 g of a green solid. The extracts (culture and mycelial) were combined (2.5 g) and subjected to column chromatography on silica gel (50 g) eluting with a gradient of hexane–CH_2Cl_2 (5:5→0:10) and CH_2Cl_2–MeOH (9.9:0.1→0:10). Four hundered and fifty Fractions (30 ml each) were collected and pooled on the basis of their TLC profiles to yield 12 major fractions (FI–FXII). Bioactivity in the phytogrowth bioautographic bioassay (BPIB) showed five active pools: FIV (38.1 mg), FV (95.7 mg), FVI (105.4 mg), FVII (49.8 mg) and FVIII (77.6 mg). Active fraction FIV, eluted with hexane–CH_2Cl_2 (2:8), was resolved by preparative TLC (CH_2Cl_2) to yield **9** (5.2 mg). Phytotoxic fraction FV, eluted with hexane–CH_2Cl_2 (1:9), was applied to a on silica gel (10 g) column which was eluted with a gradient of hexane–CH_2Cl_2 (5:5→0:10) and CH_2Cl_2–MeOH (9.9:0.1→5:5). Ten secondary fractions were obtained (FV-1–FV-10). According to the BPIB, the phytotoxic activity was concentrated in secondary FV-5, eluted with CH_2Cl_2. Extensive TLC (CH_2Cl_2) of fraction FV-5 yielded **6** (5.2 mg) and **7** (4.6 mg), **1** (9.8 mg), **2** (5.1 mg), **3** (4.1 mg) and **4** (3.2 mg). Primary fraction FVI, eluted with CH_2Cl_2, was further resolved on another silica gel (15 g) column using the same elution system as for fraction FV to yield eight secondary fractions (FVI-1–FVI-8). The phytotoxic activity was found in secondary fraction FVI-6, eluted with CH_2Cl_2–MeOH (99:1). Further purification of this fraction by successive preparative TLC (CH_2Cl_2) yielded **10** (13.5 mg), **5** (3.5 mg), **11** (3.8 mg) and **14** (4.0 mg). From active fraction FVII, eluted with CH_2Cl_2–CH_3OH (99:1), spontaneously crystallized **12** (5.2 mg). Finally, fraction FVIII, eluted with CH_2Cl_2–CH_3OH (97:3), was resolved by preparative TLC [CH_2Cl_2–CH_3OH (97:3)] to render compounds **8** (5.3 mg) and **13** (15.2 mg).

3.4. Spectral data of compounds

Compound **6** [(2*S*, 3*R*)-5-hydroxy-6,8-dimethoxy-2,3-dimethyl-2,3-dihydro-4*H*-naphtho[2,3-b]-pyran-4-one]. Yellow crystalline needles, mp 165–166 °C; $[\alpha]_D + 128°$ (MeOH; *c* 1); UV (MeOH) λ_{max} nm (log ε) 409.5 (3.85), 320 (3.97), 277.5 (4.54), 252 (4.19), 235 (4.43), 214 (4.26), 209 (4.27); CD (MeOH) $\Delta\varepsilon$ (nm) -1.5×10^4 (314); IR ν_{max} (KBr) cm^{-1}: 3500, 1638, 1610; EIMS *m*/*z* 302 [M^+ (100)], 246 (90), 218 (12), 203 (6), 190 (19); HRMS *m*/*z* 302.330 (calcd for $C_{17}H_{18}O_5$, 302.322); ^1H and ^{13}C NMR (Table 2).

Compound **7** [(2*S*, 3*R*)-5-hydroxy-6,8,10-trimethoxy-2,3-dimethyl-2,3-dihydro-4*H*-naphtho-[2,3-b]-pyran-4-one]. Yellow solid, mp 154–156 °C; $[\alpha]_D + 150°$ (MeOH; *c* 1); UV (MeOH) λ_{max} nm (log ε) 411 (3.34), 320 (3.46), 277.5 (4.07), 252 (3.71), 235 (3.96), 214 (4.28), 209 (4.29); CD (MeOH) $\Delta\varepsilon$ (nm) -1.6×10^4 (314); IR ν_{max} (KBr) cm^{-1}; 3500, 1638, 1610; EIMS *m*/*z* 332 [M^+ (98)], 317 (90), 261 (100), 233 (66), 218 (14); HRMS *m*/*z* 332.351 (calc. for $C_{18}H_{20}O_6$, 332.348). ^1H and ^{13}C NMR (Table 3).

Compound **9** [8-hydroxy-6-methyl-9-oxo-9*H*-xanthene-1-carboxylic acid methyl ester]. Pale yellow needles, mp 197–198 °C; UV (MeOH) λ_{max} nm 233, 256, 289, 300, and 360; IR ν_{max} (KBr) cm^{-1} 3148, 1732 and 1650; EIMS *m*/*z* (rel. int.): 284 [M^+ (48)], 252 (100), 223 (14), 139 (8), 127 (8), 77 (9); ^{13}C NMR NMR ($CHCl_3$, 125 MHz) δ 180.44 (C-9), 169.66 ($CH_3O\underline{O}\underline{C}$-8), 161.45 (C-1), 156.02 (C-8), 155.69 (C-4a), 149.39 (C-3), 134.75, 133.61 (C-10a), 122.50 (C-7), 119.40 (C-5), 117.57 (C-8), 111.73 (C-2), 107.38 (C-4), 106.99 (C-9a), 133.61 (C-10a), 53.09 ($\underline{CH_3}OOC$-8), 22.62 (CH_3-3).

3.5. X-ray crystallographic analysis of compound **9**

Suitable crystal of **9** was obtained from EtOAc by slow evaporation. The crystal belongs to the monoclinic system, space group C2/c with $a=21.014(1)$ Å, $b=10.4145(3)$ Å, $c=13.5140(4)$ Å, $\beta=114.57(5)$ °, $Z=8$, $V=2689.75(17)$ Å^3, $D_c=1.404$ g cm^{-3}, and $\mu(CuK_\alpha)=0.882$ mm^{-1}. Of the 3733 reflections collected, only 1809 were used for structural analysis. The structure was solved by direct methods (SIR92) (Altomare et al., 1994) and refined by the full matrix-least squares methods using SHELXTL97 (Sheldrick, 1997) based on F^2 to a final $R=0.046$ and $Rw=0.134$ with $w^{-1}=[\sigma^2(Fo^2)+(0.0779P)^2+1.1731P]$ where $P=(Fo^2+2Fc^2)/3$. The hydrogen atoms attached to carbon atoms were included at idealized positions following a riding model, the hydrogen atom of the hydroxyl group was identified by difference Fourier methods and its positional parameters refined.

Crystallographic data for the structure reported in this paper have been deposited at the Cambridge Crystallographic Data Center. Copies of the data can be obtained, free of charge, on application to the Director, CCDC, 12 Union Road, Cambridge CB2 1EZ, UK (Fax: +44-1223-336033; e-mail: deposit@ccdc.cam.ac.uk).

3.6. Bioassays

3.6.1. Phytogrowth-inhibitory bioassays

The phytogrowth inhibitory activity of the extract and pure compounds was evaluated on seeds of *Amaranthus hypochondriacus* L. and *Echinochloa crusgalli* (L.) Beauv by using a Petri dish bioassay (Mata et al., 1998). In addition, a direct bioautographic bioassay system was employed to guide secondary fractionation and speed up the isolation of active compounds. The direct bioautographic assay was carried out as previously described. The results were analyzed by ANOVA ($P<0.05$), and IC_{50} values were calculated by Probit analysis based on percent of radicle growth or germination inhibition. The extract was evaluated at 10, 100 and 1000 μg ml^{-1}. The pure compounds were tested at 1, 10 and 100 μg ml^{-1}. 2,4-D was used as the positive control. The bioassays were performed at 28 °C.

3.6.2. SDS-PAGE of compounds **1–5** with spinach and bovine brain calmodulins

The interaction of the isolated compounds with both spinach and brain calmodulins (Sigma) was performed using SDS gel electrophoresis (SDS-PAGE). SDS-PAGE was done according to previously described procedures using 15% polyacrylamide gels (Leung, et al., 1984, 1985; Liao et al., 1996). The interaction of the phytotoxins with both calmodulins was determined by observing the difference in electrophoretic mobility in the presence of Ca^{2+}. In each case the electrophoresis run was done in triplicate. Quercetin was used as the positive control (Nishino et al., 1984).

3.6.3. CaM affinity chromatography

The non-reversible effect of the compounds was determined by affinity chomatography employing a bovine brain calmodulin-agarose (SIGMA) column (Bonza et al., 1998). One milligram of each compound was dissolved in 1 ml of DMSO and 10 μl of this mixture was loaded to 200 μl bed volume of calmodulin–agarose previously equilibrated with buffer I (20 mM Tris–HCl, pH 7.0, 1 mM $CaCl_2$). The column was eluted consecutively with five volumes of buffer I, five volumes of buffer II (20 mM Tris–HCl, pH 7.0, 1 mM EGTA), five volumes of buffer III (20 mM Tris–HCl, pH 8.0, 1 mM $CaCl_2$), five volumes of NaCl 1 M and five volumes of urea (6M). In each case aliquots of 200 μl were collected, concentrated in vacuo and analyzed spectrophotometrically to determine the retention of each compound. 3,4′-Dihydroxy-5,5′-dimethoxybibenzyl, obtained from *Scaphyglottis livida* (Estrada et al., 1999), was used as a negative control since this compound was not retained in the column after eluting with buffer I.

Acknowledgements

This work was supported by grants from CONACyT (27978N) and DGAPA IN207300. We wish to thank the following people: Isabel Chávez, Beatriz Quiroz, Luis Velasco-Ibarra, Javier Pérez Flores and Rocio Patiño (Instituto de Química, UNAM) for recording MS and CD spectra Marisela Gutiérrez and Graciela Chávez for registration of Irand UV spectra. The technical assistance of Samuel Aguilar Ogarrio, Isabel Rivero-Cruz and Laura Acevedo is also acknowledged. M. Macías acknowledges the fellowship awarded by CONACyT to carry out graduate studies.

References

Altomare, A., Cascarano, G., Giacovazzo, C., Guagliardi, A., Burla, M.C., Polidori, G., Camalli, M., 1994. SIR92- A Program for automatic solution of crystal structures by direct methods. J. Appl. Cryst. 27, 435.

Bonza, C., Carnelli, A., De Michelis, M.I., Rasi-Caldogno, F., 1998. Purification of the plasma membrane Ca^{2+}-ATPase from radish seedlings by calmodulin-agarose affinity chromatography. Plant Physiol. 116, 845–851.

Estrada, S., Rojas, A., Mathison, Y., Israel, A., Mata, R., 1999. Nitric oxide/cGMP mediates the spasmolytic action of 3,4′-dihydroxy-5,5′-dimethoxybibenzyl from *Scaphyglottis livida*. Planta Med. 65, 109–114.

Gaffield, W., 1990. Circular dichroism, optical rotatory dispersion and absolute configuration of flavanones, 3-hydroxyflavanones and their glycosides. Tetrahedron 26, 4093–4108.

Hideaki, K., Takeshi, S., 1986. Isolation of moniliphenone, a key intermediate in xanthone biosynthesis from *Monilinia fructicola*. J. Agric. Food Chem. 50 (6), 1671–1699.

Leung, P.C., Taylor, W.A., Wang, J.H., Tripton, C.L., 1984. Ophiobolin A a natural product inhibitor of calmodulin. J. Biol. Chem. 259, 2742–2747.

Leung, P.C., Taylor, W.A., Wang, J.H., Tripton, C.L., 1985. Role of calmodulin inhibition in the mode of action of ophiobolin A. Plant Physiol 77, 303–308.

Liao, B., Gawienowski, M.C., Zielinski, R.E, 1996. Differential stimulation of NAD kinase and binding of peptide substrates by wild-type and mutant plant calmodulin isoforms. Arch. Biochem. Biophys. 327, 53–60.

Macías, M., Ulloa, M., Gamboa, A., Mata, R., 2000. Phytotoxic compounds from the new coprophilous fungus *Guanomyces polythrix*. J. Nat. Prod. 63, 757–761.

Mata, R., Macías, M., Rojas, S., Lotina-Hennsen, B., Toscano, R., Anaya, A., 1998. Phytotoxic compounds from *Esenbeckia yaxhoob*. Phytochemistry 49, 441–449.

Nishino, H., Naitoh, E., Iwashima, A., Umezawa, K., 1984. Quercetin interacts with calmodulin, a calcium regulatory protein. Experientia 40, 184–185.

Porter, K., Bacon, C., Robinson, J., Higman, H., 1975. A Field indicator in plants associated with ergot-type toxicities in cattle. J. Agric. Food Chem. 23, 771–775.

Seitz, L., Paukstelis, J., 1977. Metabolites of *Alternaria alternata*: Ergosterol and ergosta-4,6,8(14),22-tetraen-3-one. J. Agric. Food Chem. 25, 838–841.

Sheldrick, G.M., 1997. SHELXTL97: Program for Refinement of Crystal Structures. University of Göttingen, Germany.

Snedden, W.A., Fromm, H., 1998. Calmodulin, calmodulin-related proteins and plant responses to the enviroment. Trends Plant Sci. 3, 299–304.

PERGAMON

Phytochemistry 58 (2001) 759–762

PHYTOCHEMISTRY

www.elsevier.com/locate/phytochem

Hydroxyl radical scavenging activity of β-*N*-oxalyl-L-α, β-diaminopropionic acid

Zhou Gongke[a], Kong Yingzhen[a], Cui Kairong[a], Li Zhixiao[b], Wang Yafu[a,*]

[a]*The State Key Laboratory of Arid Agroecology, Lanzhou University, Lanzhou 730000, PR China*
[b]*The State Key Laboratory of Applied Organic Chemistry, Lanzhou University, Lanzhou 730000, PR China*

Received 2 January 2001; received in revised form 19 April 2001

Abstract

Exogenous hydroxyl radical treatments increased the levels of β-*N*-oxalyl-L-α, β-diaminopropionic acid (ODAP) in grass pea seedlings. Lipid peroxidation initiated by hydroxyl radicals can be alleviated when grass pea seedlings were pretreated with exogenous ODAP, suggesting that ODAP might act as an hydroxyl radical scavenger in vivo. Competing with salicylate for hydroxyl radicals in the hydroxyl radical generating/detecting system, ODAP's in vitro hydroxyl radicals scavenging activity was assessed to confirm this result, and the role of ODAP as an effective hydroxyl radical scavenger is discussed. © 2001 Elsevier Science Ltd. All rights reserved.

Keywords: *Lathyrus sativus*; Leguminosae; Legume; Grass pea; β-*N*-Oxalyl-L-α, β-diaminopropionic acid; Hydroxyl radicals

1. Introduction

Grass pea (*Lathyrus sativus* L.), a grain legume rich in protein, is cultivated as a drought tolerant food crop requiring minimal care in semi-arid areas of Africa, Asia and Europe. It is very popular since it can give acceptable yields in dry seasons, under conditions when lentils or chickpeas fail (Praveen et al., 1994). In spite of its extreme drought tolerance, grass pea has no morphological characteristics indicative of this tolerance. Under drought conditions, the production of active oxygen species increases significantly (Smirnoff and Colombé, 1988), and many plants react to osmotic stress by increasing the concentration of proline or other amino acids to scavenge active oxygen species, including hydroxyl radical (•OH) (Smirnoff and Cumbes, 1989). It has been reported that grass pea contains a nonprotein amino acid, called β-*N*-oxalyl-L-α, β-diaminopropionic acid (ODAP), that causes animal lathyrism (Malathi et al., 1970). Our previous studies have shown that ODAP accumulated gradually in grass pea when it is subjected to polyethylene glycol stress (Xing et al., 2000). So it is important and of interest to assess whether ODAP might play a role in drought stress (Lambein et al., 1990). In the present investigation, we tested the ability of ODAP to scavenge hydroxyl radicals (•OH), one of the most reactive and toxic active oxygen species.

2. Results and discussion

2.1. The effects of •OH on the contents of ODAP and malondialdehyde in grass pea seedlings

Among the active oxygen species, •OH may be responsible for most of the oxidative damage during drought stress (Shen et al., 1997). It is highly reactive and, therefore, potentially damaging to cells, in particular by initiating lipid peroxidation (Smirnoff and Cumbes, 1989). In the present paper, the effects of •OH stress on the levels of ODAP and malondialdehyde (MDA) in grass pea seedlings were examined. •OH radical species were generated by Fenton reaction ($Fe^{2+} + H_2O_2 \rightarrow {}^{\bullet}OH + Fe^{3+} + OH^-$) and the "•OH concentration" in this paper was represented by the concentrations of the reagents, i.e. Fe^{2+} and H_2O_2 in the generation system. As shown in Fig. 1, the levels of ODAP and MDA increased with increases of •OH radical forming capacity. At lower concentrations

* Corresponding author. Tel.: +86-0931-8912891; fax: +86-0931-8912023.
E-mail address: gkzhou@263.net (Z. Gongke).

0031-9422/01/$ - see front matter © 2001 Elsevier Science Ltd. All rights reserved.
PII: S0031-9422(01)00250-3

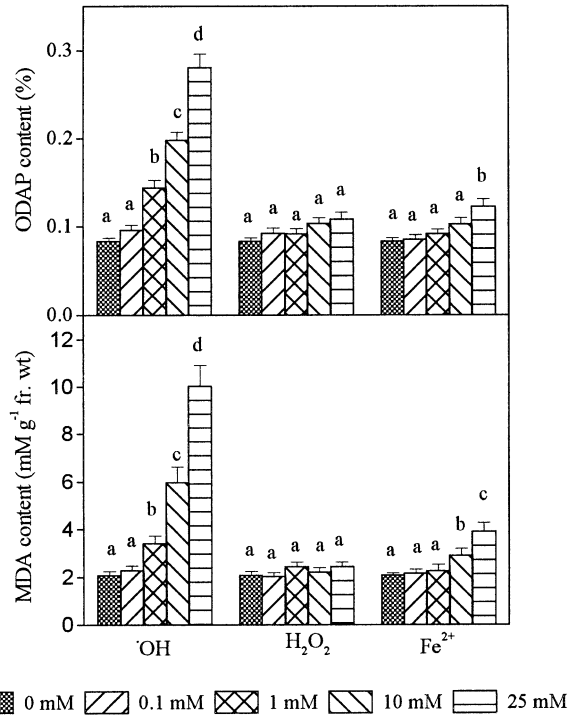

Fig. 1. The effect of ·OH, H_2O_2 and Fe^{2+} on the contents of ODAP and MDA in grass pea seedlings. Values denoted by the same letter do not significantly differ at $P<0.05$.

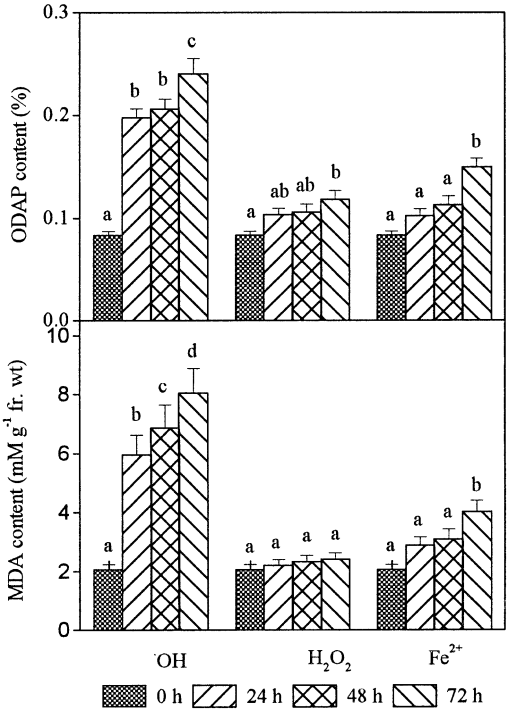

Fig. 2. Time courses of the effect of ·OH (10 mM), H_2O_2 (10 mM) and Fe^{2+} (10 mM) on the contents of ODAP and MDA in grass pea seedlings. The illustrations and significance of the letters are the same as in Fig. 1.

(0.1 mM), ODAP and MDA changed little in grass pea foliage. But at 1, 10 and 25 mM Fe^{2+} + H_2O_2 concentrations, the contents of ODAP were about 173, 237 and 336% of the control and the contents of MDA were about 164, 287 and 484% of the control, respectively. When grass pea foliage was stressed in 10 mM Fe^{2+} + H_2O_2 for 24, 48 and 72 h, the contents of ODAP and MDA increased rapidly and the former amounted to 237, 247 and 288% of the control, the later 287, 331 and 388% of the control, respectively (Fig. 2). These results indicate that with increasing levels of ·OH stress or over time at the same concentration (10 mM) of stress, an increase in lipid peroxidation appeared, along with ODAP accumulation in grass pea seedlings.

In order to make sure that the increase of ODAP and MDA resulted from the effect of ·OH, but not that of Fe^{2+} and H_2O_2, the main reagents in the Fenton reaction mixture, grass pea leaves were treated with Fe^{2+} and H_2O_2 individually. No significant changes in the levels of ODAP and MDA were observed by the presence of H_2O_2 alone at different concentrations up to 25 mM or with different treatment times (Figs. 1 and 2). This result indicated that H_2O_2 could not induce enhancement of ODAP levels or stimulate the increase of MDA. ODAP content amounted to 123 and 146% of the control when Fe^{2+} increased to 10 and 25 mM, respectively, but the levels had not been affected by the lower concentrations of Fe^{2+} (Fig. 1). When grass pea seedlings were treated with 10 mM Fe^{2+} for 24, 48 and 72 h, ODAP content increased gradually to 123, 135 and 179% of control (Fig. 2). Compared with ·OH, however, ODAP and MDA induced by Fe^{2+} were much less. Taken together, the results of the individual treatments of H_2O_2 and Fe^{2+} suggest that it is the ·OH generated by the Fenton reaction that causes the enhancement of ODAP and MDA levels in grass pea seedlings exposed to $Fe^{2+} + H_2O_2$. Statistical analysis revealed that lipidoxidation and accumulation of ODAP induced by Fe^{2+} only occurred under higher concentrations (above 10 mM indicated by MDA and 25 mM indicated by ODAP) or long-term treatment (72 h) when exposed to Fe^{2+} stress. Although iron is an essential mineral nutrient required for normal growth and development of plants at low concentrations, excess iron leads to oxidative stress. It has been reported that genes coded for both iron uptake and oxidative stress response are regulated by the same transcription factor in *E.coli* and yeast (Kampfenkel et al., 1995).

2.2. The effect of pretreatment with ODAP and DMSO on lipid peroxidation initiated by ·OH or Fe^{2+} in grass pea seedlings

The above results showed that ODAP could accumulate under oxidative stress. It has been proposed that the oxidation of membrane lipids, which may occur in plant cells exposed to adverse conditions, is a reliable indication of oxidative stress (Moran et al., 1994). In order to

determine whether the accumulated ODAP plays a role in moderating oxidative stress, grass pea seedlings pretreated with ODAP or DMSO were exposed to Fe^{2+} + H_2O_2 or Fe^{2+} stress and then MDA, the product of lipid oxidation, was measured. As shown in Fig. 3, both ODAP and DMSO pretreatments inhibited the formation of MDA initiated by •OH or Fe^{2+}, which indicated that ODAP could act as an effective scavenger of •OH in vivo. It is noteworthy that pretreatment with ODAP could significantly suppress the increase of MDA induced by higher concentrations of Fe^{2+} in grass pea seedlings. Minotti and Aust (1987) have indicated that oxidative stress induced by Fe^{2+} at high concentration is mainly due to the formation of •OH in superoxide-driven Fenton reaction catalyzed by iron. Therefore, the alleviation of Fe^{2+} stress after ODAP pretreatment might be owed to the ability of ODAP to scavenge •OH.

2.3. In vitro •OH scavenging activity of ODAP

The •OH scavenging activity of ODAP in vitro was assessed by allowing it to compete with salicylate for •OH in the •OH generating/detecting system (Smirnoff and Cumbes, 1989). A reduction in hydroxylation indicates an effective competition for •OH. Our results showed that the •OH scavenging activity of ODAP and DMSO increased as their concentrations increased (Fig. 4), this suggested that ODAP was able to scavenge •OH, which was in accordance with the result obtained in vivo that ODAP could inhibit the formation of MDA.

In conclusion, the results presented in this paper prove that ODAP could protect cells against internally generated •OH or supplement endogenous radical scavenging mechanisms. Since oxidative stress is a major damaging factor in plants exposed to drought stress, the accumulation of ODAP in grass pea under drought stress may share the same mechanism with that under •OH stress. Further experiments are needed to determine the extent to which ODAP could play this role in vivo in grass pea and to explore the mechanisms of the ODAP accumulation response to oxidative stress.

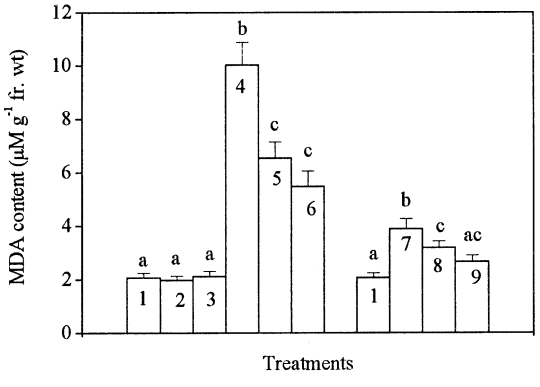

Fig. 3. The effect of pretreatment with ODAP or DMSO on the content of MDA in grass pea seedlings exposed to •OH or Fe^{2+} stress. The set of bars on the left refer to •OH stress and the set on the right refer to Fe^{2+} stress. 1—control, 2—ODAP(30 mM), 3—DMSO(30 mM), 4—•OH (25 mM), 5—ODAP + •OH, 6—DMSO + •OH, 7—Fe^{2+}(25 mM), 8—ODAP + Fe^{2+}, 9—DMSO + Fe^{2+}. The illustrations and significance of the letters are the same as in Fig. 1.

3. Experimental

3.1. Plant materials and growth conditions

Grass pea seeds were surface-sterilized with 0.2% (w/v) $HgCl_2$ for 10 min and rinsed with running water, then were soaked in water and germinated in the dark at 4 °C for 3–4 days. The seeds were grown in a Hoagland nutrient solution in a growth cabinet (PGV36, Canada) at 23/10 °C with a photoperiod of 16/8 h light/dark. Foliage excised from 15-day-old seedlings were used for all investigations.

3.2. Treatments of hydroxyl radicals and antioxidants

•OH was generated by Fenton reaction (Fe^{2+} + $H_2O_2 \rightarrow$ •OH + Fe^{3+} + OH^-). The final concentrations of each Fenton reagent were 0.1, 1, 10 and 25 mM. Foliage excised from seedlings was floated in the system used to produce •OH for 24 h with the photoperiod as described above. •OH takes effect in plant cells since it can be formed intracellularly after uptake of Fe^{2+} and H_2O_2. Another group was treated with 10 mM Fenton reagents for 24, 48 and 72 h, respectively. The •OH generating solution was refreshed every 12 h. To examine the effect of ODAP on lipid peroxidation initiated by •OH, the foliage was pretreated with 30 mM ODAP or 30 mM dimethylsulfoxide (DMSO), a specific scavenger of •OH, for 12 h in darkness and then exposed to Fe^{2+} + H_2O_2 treatment for 24 h. Foliage treated with distilled water was used as controls.

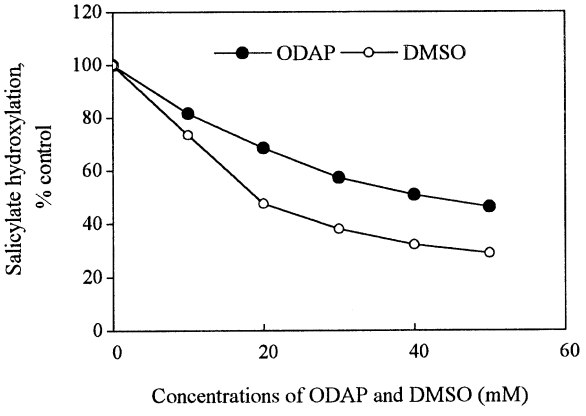

Fig. 4. The effect of ODAP or DMSO on salicylate hydroxylation initiated by •OH generated by ferrous and hydrogen peroxide.

3.3. Assessment of ODAP on •OH scavenging activity in vitro

•OH was generated by the Fenton reaction and detected by its ability to hydroxylate salicylic acid as described by Smirnoff and Cumbes (1989). The reaction mixture, total volume of 3 ml, contained 150 mM potassium phosphate buffer (pH 7.4), 0.26 mM ascorbic acid, 0.15 mM $FeSO_4$, 0.6 mM H_2O_2, 2 mM Na salicylate and varying concentrations of ODAP. The •OH scavenging activity of ODAP was assessed according to its ability to compete with salicylate for •OH. To ascertain the effect of ODAP, the specific •OH scavenger DMSO was also added to the •OH generating / detecting system and served as the reference.

3.4. Determination of ODAP content and lipid peroxidation

ODAP contents were measured as described by Wang et al. (2000): about 20 mg of dried foliage was accurately weighed and added to 2 ml of ethanol–water (3:7, v/v), shaken briefly and sonicated for 30 min (with ice added and water temperature kept at about 8 °C), then agitated with a magnetic stirrer for 2 h, centrifuged for 15 min at 15,000 *g* and filtered. A known amount of sample extract was dried under vacuum. The residue was dissolved in 100 μl $NaHCO_3$ solution (0.5 M), then 100 μl of the derivatizing reagent (100 mg of 1-fluoro-2,4-dinitrobenzene in 10 ml of acetonitrile) was added and the solution was thoroughly mixed. The derivatization was completed in 30 min at 60 °C. After cooling to room temperature, the reaction mixture was added to 0.8 ml KH_2PO_4 solution (0.01 M), vortexed for several seconds and 20 μl of the product was taken for HPLC analysis. The HPLC system consisted of a Waters Model 600E pump, a Cartridge C_{18} (5 μm) column 3.9×150 mm, a column heater and a Model 2487 dual wavelength absorbance detector set at 360 nm (all from Waters). Millenium 32 software, from Waters, was used to control system operation and collect and analyse data. The mobile phase A consisted of 0.03 M K_2HPO_4 and 1% dimethyl formamide in water (v/v) and was adjusted to pH 5.6 with glacial acetic acid, whereas the mobile phase B was acetonitrile. The mobile phase solutions were filtered through a 0.45 μm membrane filter and degassed before use. The column was thermostated at 26 °C and operated at a flow rate of 1.0 ml/min.

Determination of lipid peroxidation involved measuring the amount of MDA, a product of lipid peroxidation, in the grass pea foliage (0.5g fr. wt) by the thiobarbituric acid reaction (Stewart and Bewley, 1980). The crude extract was mixed with the same volume of a 0.5% (w/v) thiobarbituric acid solution containing 20% (w/v) tricloroacetic acid. The mixture was heated at 95 °C for 30 min and the reaction was stopped by quickly placing in an ice-bath. The cooled mixture was centrifuged at 10,000 *g* for 10 min, and the absorbance of the supernatant at 532 and 600 nm was read. After subtracting the non-specific absorbance at 600 nm, the MDA concentration was determined by its extinction coefficient of 155 mM^{-1} cm^{-1}.

3.5. Statistical analysis

The results presented here were the mean of five replicates. Means were compared by one way analysis of variance and Duncan's multiple range test at the 5% level of significance.

Acknowledgements

We wish to thank Dr. Wang Fei for his kind help for the determination of ODAP. The work was supported with the NKBRSF project of china (G200018603) and Science Foundation of Gansu Province (YS01-A25-004).

References

Kampfenkel, K., Van Montagu, M., Inze, D., 1995. Effects of iron excess on *Nicotiona plumbaginifolia* plants: implications to oxidative stress. Plant Physiol. 107, 725–735.

Lambein, F., Kuo, Y.H., Ikegami, F., Murakoshi, I., 1990. Toxic and non-toxic nonprotein amino acids in the Vicieae. In: Lubec, G., Rosenthal, G.A. (Eds.), Amino Acids: Chemistry, Biology and Medicine. ESCOM, Leiden, pp. 21–28.

Malathi, K., Padmanaban, G., Sarma, P.S., 1970. Biosynthesis of β-*N*-oxalyl-L-α, β-diaminopropionate acid, the *Lathyrus sativus* neurotoxin. Phytochemistry 9, 1603–1610.

Minotti, G., Aust, S.D., 1987. The requirement for iron (III) in the initiation of lipid peroxidation by iron (II) and hydrogen peroxide. J. Biol. Chem. 262, 1098–1103.

Moran, J.F., Becana, M., Iturbe-Ormaetxe, I., Frechilla, S., Klucas, R.V., Aparicio-Tejo, P., 1994. Drought induces oxidative stress in pea plants. Planta 194, 346–352.

Praveen, S., Joharl, R.P., Mehta, S.L., 1994. Cloning and expression of OX-DAPRO degrading genes from soil microbe. J. Plant Biochem. Biotechnol. 3, 25–29.

Shen, B., Jensen, R.G., Bohnert, H.J., 1997. Mannitol protects against oxidation by hydroxyl radicals. Plant Physiol. 115, 527–532.

Stewart, R.C., Bewley, J.D., 1980. Lipid peroxidation associated with accelerated aging of soybean axes. Plant Physiol. 65, 245–248.

Smirnoff, N., Colombé, S.V., 1988. Drought influences the activity of enzymes of the chloroplast hydrogen peroxide scavenging system. J. Exp. Bot. 39, 1097–1108.

Smirnoff, N., Cumbes, Q.J., 1989. Hydroxyl radical scavenging activity of compatible solutes. Phytochemistry 28, 1057–1060.

Wang, F., Chen, X., Chen, Q., Qin, X., Li, Z., 2000. Determination of neurotoxin ODAP and non-protein amino acids in *Lathyrus sativus* by precolumn derivatization with 1-fluoro-2,4-dinitrobenzene. J. Chromatography A 883, 113–118.

Xing, G.S., Zhou, G.K., Li, Z.X., Cui, K.R., 2000. Studies of polyamine metabolism and β-*N*-oxalyl-L-α, β-diaminopropionate acid accumulation in grass pea (*Lathyrus sativus*) under water stress. Acta Bot. Sin. 42, 1039–1044.

PERGAMON

Phytochemistry 58 (2001) 763–767

PHYTOCHEMISTRY

www.elsevier.com/locate/phytochem

Sesquiterpenoids from the fruits of *Ferula kuhistanica* and antibacterial activity of the constituents of *F. kuhistanica*

Kimiko Tamemoto[a], Yoshihisa Takaishi[a,*], Bei Chen[a], Kazuyoshi Kawazoe[a], Hirofumi Shibata[a], Tomihiko Higuti[a], Gisho Honda[b], Michiho Ito[b], Yoshio Takeda[c], Olimjon K. Kodzhimatov[d], Ozodbek Ashurmetov[d]

[a]*Faculty of Pharmaceutical Sciences, University of Tokushima, Shomachi 1-78, Tokushima 770-8505, Japan*
[b]*Faculty of Pharmaceutical Sciences, Kyoto University, Yoshida sakyoku, Kyoto 606-8501, Japan*
[c]*Faculty of Integrated Arts and Sciences, University of Tokushima, Minamijyousanjima, Tokushima 770-8502, Japan*
[d]*Academy of Sciences, Uzbekistan Institute of Botany and Botanical Garden, F. Khodzhaev, St.32, 700143 Tashkent, Uzbekistan*

Received in revised form 5 June 2001

Abstract

Ethyl acetate extracts of the air-dried fruits of *Ferula kuhistanica* afforded three daucane esters: kuhistanicaol H, I and J, together with nine other known compounds. Their structures were established on the basis of spectroscopic evidence. Isolated compounds in this paper and previously reported compounds from the roots and stems of *F. kuhistanica* were tested for antibacterial activity. Some of them were selectively toxic against Gram-positive bacteria, including methicillin-sensitive and methicillin-resistant *Staphylococcus aureus* (MSSA and MRSA). © 2001 Elsevier Science Ltd. All rights reserved.

Keywords: *Ferula kuhistanica*; Umbelliferae; Sesquiterpenes; Daucane esters; Kuhistanicaol H, I, J; Antibacterial activity; MSSA; MRSA

1. Introduction

The exclusively Old World genus *Ferula* belongs to the family Umbelliferae, and has about 130 species distributed throughout the Mediterranean to Central Asia. The chemical constituents of this genus have been studied by many groups. Several species of this genus have been used in folk medicine as tranquilizers and for the treatment of digestive disorders, rheumatism, headache, arthritis, dizziness, toothache, etc. (Gonzalez and Barrera, 1995). *Ferula kuhistanica* has been used in Uzbekistan folk medicine to treat skin diseases and wounds. In previous studies, we investigated the constituents of the roots and stems of *F. kuhistanica* (Chen et al., 2000a,b). We report here the structural elucidation of three new daucane-type sesquiterpene, kuhisutanicaols H-J (**1**–**3**) and nine known compounds from the fruits of *F. kuhistanica*. To confirm the evidence of this folk medicine for the treatment of skin diseases and wounds, we tested the antibacterial activities of some isolated compounds from the roots, stems, and fruits of *F. kuhistanica* against several bacterial species, including methicillin-resistant *Staphylococcus aureus* (MRSA).

2. Results and discussion

Ethyl acetate extracts of the air-dried fruits of *F. kuhistanica* were separated by repeated column chromatography to give three new compounds; kuhistanicaol H (**1**), I (**2**) and J (**3**), together with nine known compounds; jaeschkeanadiol *p*-hydroxybenzoate (ferutinin) (**4**), jaeschkeanadiol vanillate (**5**) (Miski et al., 1983), lancerotriol 9α-(*p*-hydroxybenzoate) (**6**) (Fraga et al., 1985), lancerotriol 9β-(*p*-hydroxybenzoate) (El-Sayed, 1990), lancerodiol *p*-hydroxybenzoate, 4β,8β-dihydroxy-6α-vanilloxdauc-9-ene, isolancerotriol 6-vanillate (Miski and Jakupovic, 1990), ferutriol 5α-(*p*-hydroxybenzoate) (Ahmed, 1990), isolancerotriol 2-*epi*-5-*p*-hydroxybenzoate (Ahmed, 1991).

Kuhistanicaol H (**1**) showed absorption bands for hydroxy (3285 cm^{-1}), ester (1698 cm^{-1}), and benzene

* Corresponding author. Tel.: +81-88-633-7275; fax: +81-88-633-9501.
E-mail address: takaishi@ph.tokushima-u.ac.jp (Y. Takaishi).

0031-9422/01/$ - see front matter © 2001 Elsevier Science Ltd. All rights reserved.
PII: S0031-9422(01)00307-7

(1609 cm^{-1}) groups in the IR spectrum. The UV spectrum of **1** showed the presence of an aromatic ring (258 nm). The ^1H NMR spectrum exhibited the presence of an angular methyl [δ_H 1.15 (3H, *s*)], an isopropyl group [δ_H 0.74, 0.90 (each 3H, *d*, $J=6.8$ Hz), 2.10 (1H, *m*)] and a *p*-hydroxy benzoic acid [δ_H 6.73 (2H, *d*, $J=8.7$ Hz), 7.81 (2H, *d*, $J=8.7$ Hz)] (Table 1). The ^{13}C NMR spectrum of **1** revealed the presence of an ester carbonyl (δ_C 168.4), a benzene ring (δ_C 116.1×2, 123.0, 133.0×2, 163.5), three oxygenated methines (δ_C 62.4, 74.4, and 75.2), two oxygenated quaternary carbons (δ_C 58.8, 87.6), one quaternary carbon, four methyls, three methylenes and two methines (Table 2). These facts were consistent with a molecular formula of $C_{22}H_{30}O_6$, which was supported by HR–FAB–MS data (*m/z* 413.1937 $[M+Na]^+$).

Except for the presence of an oxygenated carbon signal at δ_C 62.4 in **1**, the ^{13}C NMR spectrum of compound **1** was very similar to that of jaeskeanin (Razdan et al., 1989). The ^1H–^1H COSY spectrum of **1** showed proton correlations of δ_H 2.48 (5-H) with δ_H 5.37 (6-H); δ_H 2.89 (9-H) with δ_H 1.45 (10-Hα) and δ_H 1.99 (10-Hβ); δ_H 7.81 (2′-H) with δ_H 6.73 (3′-H). In the HMBC spectrum of **1**, the correlations of δ_H 3.94 (7-H) with δ_C 51.0

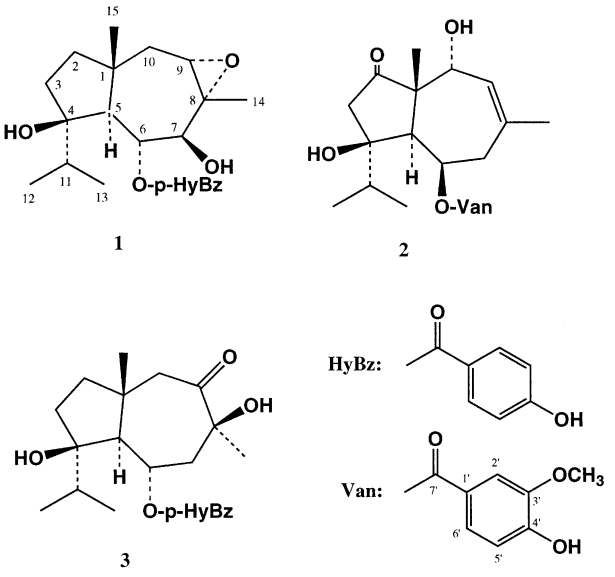

Fig. 1. Daucane esters from fruits of *F. kuhistanica*.

Table 1
^1H NMR spectral data for compounds **1**–**3** (400 MHz)

H	1	2	3
2	1.22 *m*	–	1.37 *m*
	1.52 *m*	–	1.51 *m*
3	1.55 *m*	2.10 *ABq* (15.0)	1.46 *m*
	1.94 *m*		1.93 *m*
5	2.48 *d* (11.3)	3.44 *d* (5.3)	2.40 *d* (11.1)
6	5.37 *d* (11.3)	5.47 *ddd* (2.3, 5.3, 11.4)	5.47 *ddd* (2.1, 5.0, 11.1)
7	3.94 *s*	2.34 *dd* (2.3, 15.5)	2.15 *dd* (2.1, 16.5)
		2.62 *dd* (11.4, 15.5)	2.36 *dd* (5.0,16.5)
9	2.89 *t* (7.2)	5.36 *d* (5.0)	
10	1.45 *m*	2.87 *d* (5.0)	2.54 *ABq* (12.2)
	1.99 *m*		
11	2.10 *m*	2.14 *m*	1.82 *m*
12	0.74 *d* (6.8)	0.95 *d* (6.8)	0.73 *d* (6.8)
13	0.90 *d* (6.8)	0.98 *d* (6.8)	0.83 *d* (6.8)
14	1.37 *s*	1.86 *s*	1.16 *s*
15	1.15 *s*	1.39 *s*	1.14 *s*
2′	7.81 *d* (8.7)	7.50 *d* (1.4)	7.79 *d* (8.7)
3′	6.73 *d* (8.7)	–	6.71 *d* (8.7)
5′	6.73 *d* (8.7)	6.93 *d* (8.3)	6.71 *d* (8.7)
6′	7.81 *d* (8.7)	7.59 *dd* (1.4, 8.3)	7.79 *d* (8.7)
OMe	–	3.94 *s*	

Compounds **1** and **3** were measured in CD_3OD; compound **2** was measured in $CDCl_3$, and values in parentheses represent coupling constants in Hz.

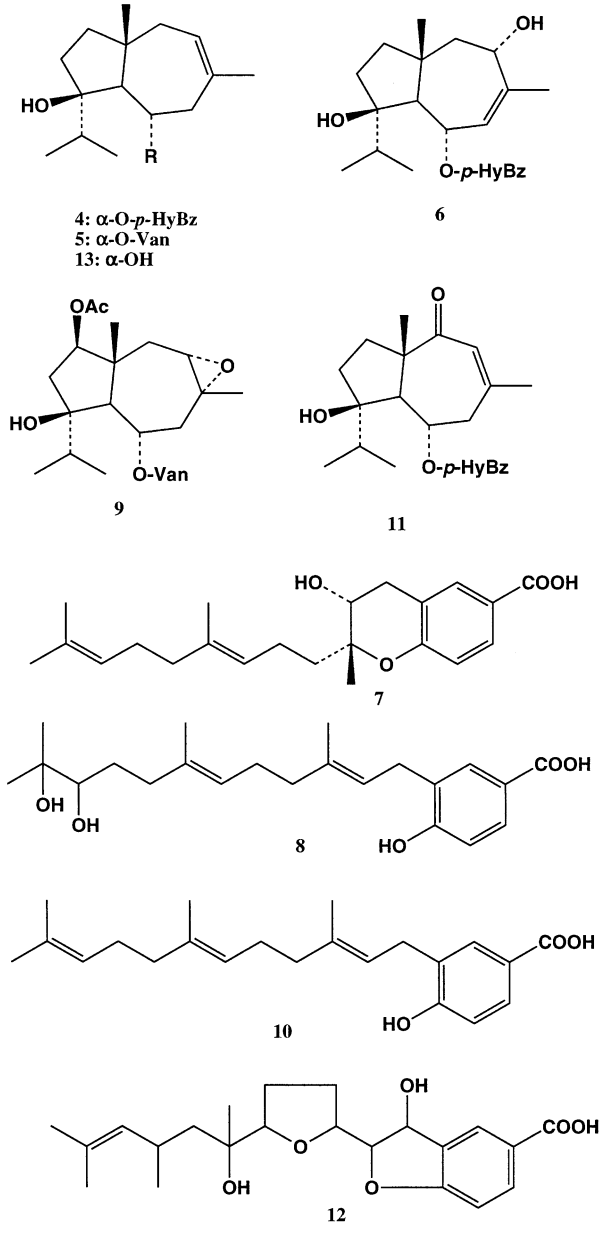

Fig. 2. Tested compounds of antibacterial activity.

Table 2
^{13}C NMR spectral data for compounds **1**–**3** (100 MHz)

C	1	2	3
1	45.6	60.5	43.0
2	40.0	210.5	42.2
3	33.2	36.3	33.2
4	87.6	74.9	85.9
5	51.0	63.7	53.1
6	74.4	70.2	71.9
7	62.4	39.6	43.2
8	58.8	135.5	78.3
9	75.2	120.4	215.0
10	41.7	64.8	51.9
11	37.8	33.6	37.6
12	17.8	16.3	17.8
13	18.8	17.6	18.8
14	22.0	28.0	27.7
15	19.8	29.6	22.6
1′	123.0	122.2	123.3
2′	133.0	118.8	133.0
3′	116.1	146.3	116.1
4′	163.5	150.4	163.4
5′	116.1	114.2	116.1
6′	133.0	124.4	133.0
7′	168.4	165.7	168.1
OCH_3	–	56.2	

Compounds **1** and **3** were measured in CD_3OD; compound **2** was measured in $CDCl_3$.

(C-5), δ_C 74.4 (C-6) and δ_C 58.8 (C-8); δ_H 0.74 (12-H_3) with δ_C 87.6 (C-4); δ_H 1.37 (14-H_3) with δ_C 62.4 (C-7), δ_C 58.8 (C-8) and δ_C 75.2 (C-9); δ_H 1.15 (15-H_3) with δ_C 45.6 (C-1), δ_C 40.0 (C-2), δ_C 51.0 (C-5) and δ_C 41.7 (C-10) were observed. Based on these findings, compound **1** was deduced to be a daucane-type sesquiterpene (Gonzalez and Barrera, 1995). In addition, the correlations of 5-H with 13-H_3 and 7-H in the NOESY spectrum showed that the configuration of the isopropyl group is α while that of 7-OH is β. Furthermore, the correlations of 6-H with 15-H_3 and 14-H_3, and correlations of 9-H with 14-H_3 and 15-H_3 showed that the configuration of the ester moiety and epoxide is α. Therefore, the structure of **1** was determined to be as shown in Fig. 1.

The ^{13}C NMR spectrum of kuhistanicaol I (**2**) was very similar to that of kuhistanicaol D (Chen et al., 2000b), except that **2** had a ketone group (δ_C 210.5). The negative HR–FAB–MS of **2** gave a molecular formula of $C_{23}H_{30}O_7$. In the ^1H–^1H COSY spectrum of **2**, correlations of δ_H 5.47 (6-H) with δ_H 3.44 (5-H), δ_H 2.34 (7-Hα) and δ_H 2.62 (7-Hβ); δ_H 5.36 (9-H) with δ_H 2.87 (10-H) were observed. The carbon chemical shift of C-1 (δ_C 60.5) of **2** showed a significant downfield shift compared with those for other daucane-type sesquiterpenoids (δ_C 40–45) (Chen et al., 2000b), and the signal due to 3-H_2 of **2** appeared to be of the AB type. Consequently, the ketone group could be placed at C-2. Correlations of 6-H with 5H and 11-H, and 15-H_3 with 10-H were observed in the NOESY spectrum. Therefore, the configuration of the isopropyl group and 10-OH is α, while that of the ester moiety is β. Thus, the structure of **2** was determined to be as shown. Many Daucane-type sesquiterpene esters were isolated from the natural source and these compounds have the ester at C-6. The configuration of this ester is almost α position but compound **2** has rare β position.

The ^{13}C NMR spectral data of kuhistanicaol J (**3**) were very similar to those of 4β, 8β, 9α-trihydroxy-6α-*p*-hydroxybenzoyloxydaucane (Ahmed, 1990), except for a methine carbon with a hydroxy group at δ_C 76.4 instead of a ketone at δ_C 215.0 in **3**, as well as the downfield shift of C-8 (δ_C 78.3) and C-10 (δ_C 51.6). In addition, the ^1H NMR spectrum of 10-H_2 of **3** appeared to be of the AB type. In the ^1H–^1H COSY spectrum of **3**, correlations of δ_H 5.47 (6-H) with δ_H 2.40 (H-5), δ_H 2.15 (7-Hα) and δ_H 2.36 (7-Hβ) were observed. Thus, the ketone could be placed at C-9. This assignment was in agreement with the NOESY spectrum, in which 15-H_3 was correlated with 6-H. Also, 5-H was correlated with 7-Hα, and 7-Hα was correlated with 14-H_3. Therefore, the configuration of the isopropyl group and the ester moiety is α, and that of 8-OH is β. Hence, the structure of **3** was determined to be as shown in Fig. 1.

To confirm the evidence for this folk medicine, three compounds (**4**–**6**) isolated from the fruits and former reported six compounds (Fig. 2); kuhistanol D (**7**), kuhistanol A (**8**), kuhistanicaol A (**9**), 3-farnesyl-*p*-hydroxybenzoic acid (**10**), 5α-*p*-hydroxybenzoyloxydauc-2-ene-1-one (**11**), kuhistanol E (**12**) (Chen et al., 2000a,b, 2001) from the roots and stems of *F. kuhistanica* were tested for antibacterial activity by the disc-diffusion test for methicillin-sensitive *S. aureus* (MSSA) and methicillin-resistant *S. aureus* (MRSA). Compounds **4**, **5**, **7**, and **8** showed significant activity by the disc-diffusion test. These compounds were measured for minimum inhibitory concentration (MIC) values against eight species of Gram-positive and Gram-negative bacteria: *S. aureus* (MSSA, MRSA), *Staphylococcus epidermidis*, *Enterococcus faecalis*, *Bacillus subtilis*, *Salmonella typhimurium, Proteus mirabilis*, and *Escherichia coli* (Table 3). Compared with other natural compounds, compounds **4** and **5** showed significant activity against the Gram-positive bacteria; *S. aureus* (MSSA, MRSA), *S. epidermidis, E. faecalis*, and *B. subtilis* (Sato et al., 1997) similar to those of standard antibiotics (ampisillin and chloramphenicol).

To study the relationship between bioactivity and structure, compound **4** was hydrolyzed under acidic conditions to give compound **13** and *p*-hydroxybenzoic acid. The MIC values of both compounds were measured. Compound **13** showed an MIC value of 125 μg/ml, while *p*-hydroxybenzoic acid was inactive (Table 3). These results showed that the bioactivity of compound **4** depends on both the sesquiterpene unit and the *p*-hydroxybenzoic acid substituent.

F. kuhistanica has been used in Uzbekistan folk medicine to treat skin diseases and wounds. Our findings

Table 3
Antibacterial activities of compounds **4**, **5**, **7**, **8**, **13**, ampicillin, chloramphenicol, *p*-hydroxybenzoic acid and salicylic acid

Organism	MIC (μg/ml)								
	Ampicillin	Chloramphenicol	**4**	**5**	**7**	**8**	**13**	*p*-Hydroxybenzoic acid	Salicylic acid
Gram-positive									
Staphylococcus aureus No. 1023[a]	1	4	8	16	31	63	125	500	500
Staphylococcus aureus No. 0024[b]	2	16	16	16	63	63	250	>1000	>1000
Staphylococcus epidermidis IFO 3762	<0.125	2	16	31	125	>250	–	–	–
Enterococcus faecalis ATCC 21212	1	2	31	31	125	>250	–	–	–
Bacillus subtilis IFO 3134	<0.125	2	16	31	63	>250	–	–	–
Gram-negative									
Salmonella typhimurium IFO 13245	1	2	>250	>250	>250	>250	–	–	–
Proteus mirabilis IFO 3849	2	16	>250	>250	>250	>250	–	–	–
Escherichia coli NIHJ JC-2	4	8	>250	>250	>250	>250	–	–	–

[a] Methicillin-sensitive *Staphylococcus aureus*.
[b] Methicillin-resistant *Staphylococcus aureus*.

regarding the antibacterial activity of isolated compounds from *F. kuhistanica* confirmed the value of this plant in the folk medicine of Uzbekistan.

3. Experimental

3.1. General

^{1}H NMR 400 MHz, ^{13}C NMR 100 MHz with TMS as an int. standard; MS: JEOL JMS SX102A instrument; CC: silica gel, Sephadex LH-20 (Pharmacia); HPLC: silica gel (Si60, Hibar RT 250-25, Merck).

3.2. Plant material

The fruits of *F. kuhistanica* were collected in July 1998 from Uzbekistan. Herbarium specimens were deposited in the herbarium of the Institute of Botany and Botanical Garten, Academy of Sciences, Uzbekistan. The plant material was identified by Professor Ozodbek Ashurmetov.

3.3. Extraction and isolation

The fruits of *F. kuhistanica* (600 g) were crushed and extracted with hexane. The residue was extracted with OEtAc. The OEtAc extracts were concd in vacuo to give a residue (60 g), which was subjected to CC on a silica gel column eluted with solvents of increasing polarity (Hex–OEtAc) to give 16 frs. Fr. 9 (5.4 g) was subjected to CC on silica gel with $CHCl_3$–MeOH to give 4 frs. (9.1–9.4). Fr. 9.1 (179.6 mg) was separated by HPLC (silica, hexane–OEtAc = 1:1) to give **2** (2.5 mg), **3** (4.3 mg), ferutriol 5α-(*p*-hydroxybenzoate) (5.3 mg) and isolancerotriol (5.9 mg). Fr 9.2 (485.5 mg) was separated by HPLC (silica, hexane–OEtAc = 1:1) to give lancerotriol 9α-(*p*-hydroxybenzoate) (74.1 mg) and isolancerotriol 2-*epi*-5-*p*-hydroxybenzoate (9.1 mg). Fr. 9.3 (512.1 mg) was subjected to CC on silica gel and separated by HPLC (silica, hexane–OEtAc = 1:1) to give 4β, 8β-dihydroxy-6α-vanilloxdauc-9-ene (12.5 mg). Fr. 9.4 (3.0 g) and fr. 11 (2.5 g) were subjected to CC on Sephadex LH-20 with MeOH and CC on silica gel with $CHCl_3$–MeOH, and then separated by HPLC (silica, hexane–OEtAc = 1:2) and preparative TLC (Hex–OEtAc = 1:2) to give **5** (2.5 mg). Fr. 3 (3.3 g) was subjected to CC on silica gel with hexane–OEtAc to give **4** (2.3 mg) and fr. 3.2. Fr. 3.2 (353.9 mg) was subjected to CC on silica gel and separated by HPLC (silica, hexane–OEtAc = 1:1, $CHCl_3$–MeOH = 95:5) to give **1** (4.8 mg), lancerotriol 9β-(*p*-hydroxybenzoate) (5.3 mg) and lancerodiol *p*-hydroxybenzoate (73.1 mg).

3.4. Kuhistanicaol H (*1*)

$[\alpha]_D^{25}$ +115.6°(MeOH *c* 0.30); IRν_{max}^{KBr} cm^{-1}: 3285, 1698, 1609, 1594, 1271, 1165, 1096, 1041; UVλ_{max}^{MeOH} nm (log ε): 258 (4.3); ^{1}H NMR δ_H(CD_3OD): Table 1; ^{13}C NMR (CD_3OD): Table 2; HR–FAB–MS *m/z* 413.1937 $[M+Na]^+$, $C_{22}H_{30}O_6Na$, requires 413.1940.

3.5. Kuhistanicaol I (*2*)

$[\alpha]_D^{25}$ +44.3°(MeOH *c* 0.50); IRν_{max}^{KBr} cm^{-1}: 3529, 1706, 1601, 1513, 1281, 1100; UVλ_{max}^{MeOH} nm (log ε): 261 (4.2); ^{1}H NMR δ_H($CDCl_3$): Table 1; ^{13}C NMR ($CDCl_3$): Table 2; HR–FAB–MS *m/z* 417.1878 $[M-H]^-$, $C_{23}H_{29}O_7$, requires 417.1913.

3.6. Kuhistanicaol J (*3*)

$[\alpha]_D^{25}$ +41.6°(MeOH *c* 0.30); IRν_{max}^{KBr} cm^{-1}: 3734, 1703, 1609, 1508, 1278; UVλ_{max}^{MeOH} nm (log ε): 258 (4.0); ^{1}H NMR δ_H (CD_3OD): Table 1; ^{13}C NMR (CD_3OD): Table 2; HR–FAB–MS *m/z* 389.1937 $[M-H]^-$, $C_{22}H_{29}O_6$, requires 389.1964.

3.7. Antibacterial activity

3.7.1. Preparation of bacterial cells

MRSA, methicillin-sensitive *S. aureus* (MSSA) strains (Sato et al., 2000) and other bacterial strains listed in Table 3 were from laboratory stock cultures. After culturing all strains on Muller–Hinton agar (Difco, Detroit, MI, USA), the cells were resuspended in Muller–Hinton broth (Difco) to give 10^8 colony-forming units/ml; the resuspended cells were then incubated.

3.7.2. Determination of antibacterial activity

During the extraction and purification procedure, disc-diffusion tests were performed with Whatman AA discs (13.0 mm) containing various concentrations of extract and DMSO as a control. The discs were placed on Mueller–Hinton agar inoculated with 10^5 colony-forming units/ml of MSSA and MRSA. The zone of inhibition was determined after incubation at 37 °C for 24 h. The disc containing DMSO showed no zone of inhibition. To estimate the antibacterial activity of the purified isolates, the minimum inhibitory concentration (MIC) was determined using Muller–Hinton agar according to the method described by the Japanese Society for Antimicrobial Chemotherapy (1981). Cell suspensions (1×10^6 colony-forming units/ml) of the examined bacteria were inoculated onto agar plates using a replicating device. Plates were read after 24 h of incubation at 37°. Ampicillin and chloramphenicol were performed by similar method.

References

Ahmed, A.A., 1990. New sesquiterpenes from *Ferula sinaica*. J. Nat. Prod. 53 (2), 483–486.

Ahmed, A.A., 1991. Daucanes and other constituents from *Ferula sinaica*. Phytochemistry 30 (4), 1207–1210.

Chen, B., Kawazoe, K., Takaishi, Y., Honda, G., Itoh, M., Takeda, Y., Kodzhimatov, O.K., Ashurmetov, O., 2000a. Prenylated benzoic acid derivatives from *Ferula kuhistanica*. J. Nat. Prod. 63 (3), 362–365.

Chen, B., Teranishi, R., Kawazoe, K., Takaishi, Y., Honda, G., Itoh, M., Takeda, Y., Kodzhimatov, O.K., 2000b. Sesquiterpenoids from *Ferula kuhistanica*. Phytochemistry 54 (7), 717–722.

Chen, B., Takaishi, Y., Kawazoe, K., Tamemoto, K., Honda, G., Itoh, M., Takeda, Y., Kodzhimatov, O.K., Ashurmetov O., 2001. Farnesyl hydroxybenzoic acid derivatives from *Ferula kuhistanica*. Chem. Pharm. Bull. 49 (6), 707–710.

El-sayed, N.H., 1990. Carotane sesquiterpene from *Ferula sinaica*. Pharmazie 45 (H. 7), 538.

Fraga, B.M., Gonzalez, A.G., Gonzalez, P., Hernandez, M.G., Larruga, C.L., 1985. Carotane sesquiterpenes from *Ferula lancerottensis*. Phytochemistry 24 (3), 501–504.

Gonzalez, A.G., Barrera, J.B., 1995. Chemistry and sources of mono- and bicyclic sesquiterpenes from *Ferula* species. Prog. Chem. Org. Nat. Prod. 64, 1–92.

Miski, M., Ulubelen, A., Mabry, T.J., 1983. Six sesquiterpene alcohol esters from *Ferula elaeochytris*. Phytochemistry 22 (10), 1983–2231.

Miski, M., Jakupovic, J., 1990. Daucane esters from *Ferula rigidula*. Phytochemistry 29 (1), 173–178.

Japanese Society for Antimicrobial Chemotherapy, 1981. Revised method for measuring minimum inhibitory concentration. Chemotherapy (Tokyo), 29, 76–79.

Razdan, T.K., Qadri, B., Qurishi, M.A., Khuroo, M.A., Kachroo, P.K., 1989. Sesquiterpene esters and sesquiterpene-coumarin ethers from *Ferula jaeskeana*. Phytochemistry 28 (12), 3389–3393.

Sato, Y., Suzaki, S., Nishikawa, T., Kihara, M., Shibata, H., Higuti, T., 2000. Phytochemical flavones isolated from *Scutellaria barbata* and antibacterial activity against methicillin-resistant *Staphylococcus aureus*. J. Ethnopharmacol. 72, 483–488.

Sato, Y., Oketani, H., Yamada, T., Singyouchi, K., Ohtsubo, T., Kihara, M., Shibata, H., Higuti, T., 1997. A xanthanolide with potent antibacterial activity against methicillin-resistant *Staphylococcus aureus*. J. Pharm. Pharmacol. 49, 1042–1044.

PERGAMON

Phytochemistry 58 (2001) 769–774

PHYTOCHEMISTRY

www.elsevier.com/locate/phytochem

Andinermals A–C, antiplasmodial constituents from *Andira inermis*☆

Carola Kraft[a], Kristina Jenett-Siems[a,*], Karsten Siems[b], Pablo N. Solis[c], Mahabir P. Gupta[c], Ulrich Bienzle[d], Eckart Eich[a]

[a]*Institut für Pharmazie (Pharmazeutische Biologie), Freie Universität Berlin, Königin-Luise-Str. 2-4, D-14195 Berlin, Germany*
[b]*AnalytiCon Discovery, D-14437 Potsdam, Germany*
[c]*Centro de Investigationes Farmacognosticas de la Flora Panameña (CIFLORPAN), Facultad de Farmacia, Universidad de Panama, and Smithsonian Tropical Research Institute, Panamá, Republica de Panama*
[d]*Institut für Tropenmedizin, Medizinische Fakultät Charité, Humboldt Universität zu Berlin, Berlin, Germany*

Received 23 April 2001; received in revised form 18 June 2001

Abstract

Bioassay-guided fractionation of the leaves from *Andira inermis* was undertaken as part of a screening program to verify the traditional use of herbal remedies against malaria. Among the isolated phenolic compounds three novel 2-arylbenzofuran-3-carbaldehydes, andinermal A–C, were obtained together with a new flavanonol glycoside, taxifolin-3-*O*-(3″-*O*-*trans*-cinnamoyl)-α-L-rhamnopyranoside. © 2001 Elsevier Science Ltd. All rights reserved.

Keywords: *Andira inermis*; Fabaceae; Antiplasmodial activity; *Plasmodium falciparum*; 2-Arylbenzofuran-3-carbaldehydes; Andinermal A–C; Flavonoids; Isoflavones

1. Introduction

During a screening program on antimalarial compounds from plant sources we investigated *Andira inermis* (W. Wright) H.B.K., Fabaceae, a tall tree characterised by a thick trunk and redpurple flowers, native from southern Mexico to northern South America. From the phytochemical point of view *A. inermis* is known to contain several isoflavones and related compounds as well as β-sitosterol and stigmasterol (Cocker et al., 1962; Lock de Ugaz et al., 1991). Recently, we demonstrated that the crude lipophilic extracts of stems and leaves showed moderate in vitro activity against *Plasmodium falciparum*; further investigation of the stems led to the isolation of active isoflavones (Kraft et al., 2000). In the present study we report the isolation and structural elucidation of three novel 2-arylbenzofuran-3-carbaldehydes as well as a new flavanonol glycoside from the active fractions of the leaves. In vitro antiplasmodial effects of the compounds were assessed.

2. Results and discussion

Bioassay-guided fractionation of the extracts from the leaves of *A. inermis* led to the isolation of the isoflavones afformosin (**1**; Caballero and Smith, 1986), calycosin (**2**; Kobayashi et al., 1985), formononetin, and prunetin (**3**, **4**; Kraft et al., 2000). Furthermore **5** and **6** turned out to be the flavanonol 3-*O*-α-L-rhamnosides astilbin (Tschesche et al., 1979) and engelitin (Reisch et al., 1984), respectively. Whereas **2**, **3**, and **4** had already been reported as constituents of the stems (Kraft et al., 2000), **1**, **5** and **6** could be isolated for the first time from *A. inermis*. Additionally four novel compounds could be obtained which turned out to be three 2-arylbenzofuran-3-carbaldehydes (**7**–**9**) and a *trans*-cinnamic acid ester of the taxifolin glycoside astilbin (**10**). Their structural elucidation was carried out by EIMS, FAB–MS, and HR–EIMS, ^{1}H NMR, ^{13}C NMR, HMBC, and COSY as well as NOE experiments.

☆ Part 5 in the series. 'Herbal remedies traditionally used against malaria'.

* Corresponding author. Tel.: +49-30-83853720; fax: +49-30-83853729.

E-mail address: kjsiems@zedat.fu-berlin.de (K. Jenett-Siems).

0031-9422/01/$ - see front matter © 2001 Elsevier Science Ltd. All rights reserved.
PII: S0031-9422(01)00295-3

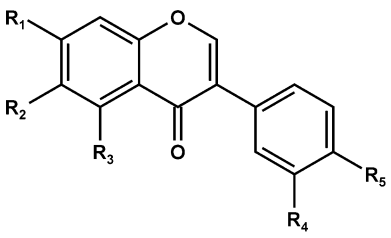

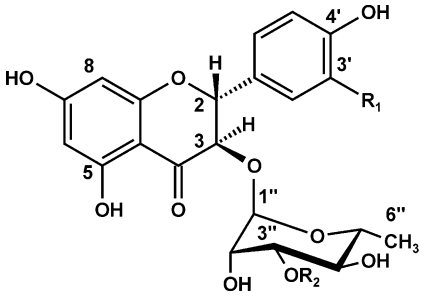

1: $R_1 = OH$; $R_2 = R_5 = OCH_3$; $R_3 = R_4 = H$
2: $R_1 = R_4 = OH$; $R_2 = R_3 = H$; $R_5 = OCH_3$
3: $R_1 = OH$; $R_2 = R_3 = R_4 = H$; $R_5 = OCH_3$
4: $R_1 = R_3 = OH$; $R_2 = R_4 = H$; $R_5 = OCH_3$

5: $R_1 = OH$; $R_2 = H$
6: $R_1 = H$; $R_2 = H$
10: $R_1 = OH$;

$R_2 =$ 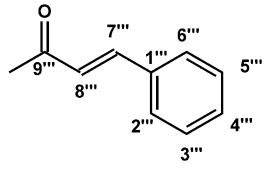

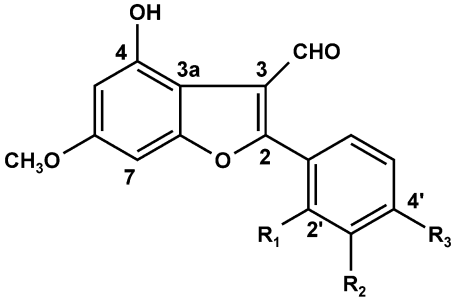

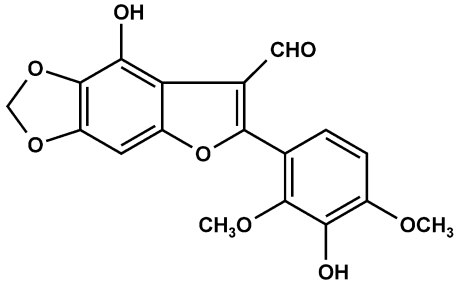

7: $R_1 = R_3 = OCH_3$; $R_2 = OH$
9: $R_1 = OCH_3$; $R_2 = R_3 = OH$

8

The EIMS of **7** exhibited an ion peak at m/z 344 $[M]^+$, its molecular formula was determined as $C_{18}H_{16}O_7$ by HR–EIMS. The signals of the ^{13}C NMR (Table 1) indicated the presence of three methoxy groups, one carbonyl group and fourteen additional carbon atoms. They were similar to published data of 2-arylbenzofuran-3-carbaldehydes (ebenfuran II and ebenfuran III) from *Onobrychis ebenoides* Bioss & Spuner, Fabaceae (Halabalaki et al., 2000). The signal for a carbonyl group at 192 ppm could be correlated to the signal at 9.81 ppm (1H, *s*) in the ^1H NMR spectrum (Table 1), thus hinting to a carbaldehyde. Additionally the ^1H NMR spectrum revealed a signal at 10.15 ppm (1H, *s*) corresponding to a chelated hydroxy group. Furthermore the ^1H NMR displayed characteristic signals of a pair of *meta*-coupled protons at 6.36 ppm (1H, *d*, $J = 1.9$ Hz, H-5) and 6.72 ppm (1H, *d*, $J = 1.9$ Hz, H-7), as well as of *ortho*-coupled protons at 6.99 ppm (1H, *d*, $J = 8.6$ Hz, H-5′) and 7.22 ppm (1H, *d*, $J = 8.6$ Hz, H-6′). In the HMBC the chelated hydroxy proton, the carbaldehyde, and both *meta*-coupled protons showed correlation to a carbon at 108 ppm corresponding to C-3a of 2-arylbenzofuran-3-carbaldehydes (Fig. 1; Table 1). The positions of the three methoxy groups (3.82, 3.85, and 3.97 ppm) were established by NOESY and HMBC experiments. Between the methoxy singlett at 3.85 ppm and the signals for H-5 and H-7 NOESY crosspeaks could be observed, as well as between the singlett at 3.92 ppm and the doublett of H-5′. The position of the third

Table 1
NMR spectral data [400 MHz or 500 MHz, acetone d_6, δ (ppm)] of compounds **7**–**9** isolated from the leaves of *Andira inermis*

Position	**7**				**8**	**9**
	δ_H[a]	δ_C[b]	HMBC correlations	NOESY correlations	δ_H[a]	δ_H[a]
2		164				
3		119				
3a		108				
4		153				
5	6.36 (1H, *d*, 1.9)	98	3a, 4, 6, 7, 5[c]	OCH_3-6		6.36 (1H, *d*, 2)
6		162	OCH_3-6			
7	6.72 (1H, *d*, 1.9)	88	3a, 5, 6, 7a	OCH_3-6	6.76 (1H, *s*)	6.72 (1H, *d*, 2)
7a		157				
1′		115				
2′		146				
3′		141				
4′		152				
5′	6.99 (1H, *d*, 8.6)	108	1′, 3′, 4′, 6′, 5′[c]	OCH_3-4′	6.99 (1H, *d*, 8.6)	6.86 (1H, *d*, 8.4)
6′	7.22 (1H, *d*, 8.6)	122	2, 2′, 4′, 6′[c]		7.21 (1H, *d*, 8.6)	7.13 (1H, *d*, 8.4)
CHO	9.81 (1H, *s*)	192	3, 3a, CHO[c]	OH-4	9.78 (1H, *s*)	9.82 (1H, *s*)
OCH_3-6	3.85 (3H, *s*)	56	6	5, 7		3.85 (3H, *s*)
OCH_3-2′	3.82 (3H, *s*)	61	2′		3.81 (3H, *s*)	3.74 (3H, *s*)
OCH_3-4′	3.97 (3H, *s*)	56	4′	5′	3.97 (3H, *s*)	
OH-4	10.15 (1H, *s*)		3a, 4, 5, 6	CHO	10.24 (1H, *s*)	10.16 (1H, *s*)
$-CH_2O_2-$					6.03 (2H, *s*)	

[a] Intensities, multiplicities and *J* values (Hz) shown in parentheses.
[b] Deduced from HMBC.
[c] ^1J-correlation.

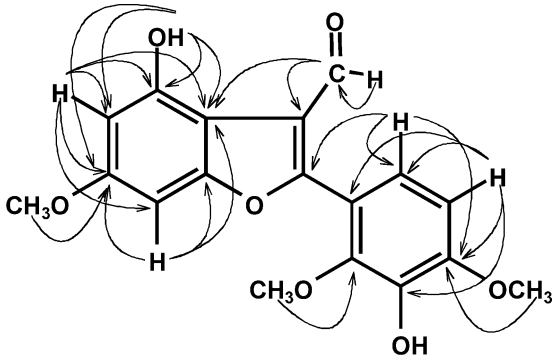

Fig. 1. HMBC correlations of compound **7**.

methoxy group could be deduced from the HMBC spectrum (Fig. 1; Table 1). Thus, **7** is 2-(2′, 4′-dimethoxy-3′-hydroxyphenyl) - 4 - hydroxy - 6 - methoxy-benzofuran-3-carbaldehyde. Compounds **8** and **9** showed again the characteristic signals at 9.78 and 9.82 ppm for the carbaldehyde moiety and at 10.24 and 10.16 ppm for the C-4 hydroxy group, respectively, in their ^{1}H NMR spectra.

The molecular formula of **8** was determined as $C_{18}H_{14}O_8$. The ^{1}H NMR spectrum indicated the presence of a methylendioxy group (6.03 ppm, 2H, *s*) and one isolated aromatic proton at 6.76 ppm. The shift of this proton, which is quite similar to that of H-7 in **7** and **9**, is a hint to a 5,6- instead of a 6,7-methylendioxy moiety. The shift and coupling patterns of the aromatic protons and methoxy groups were nearly identical with those of **7**, thus suggesting the same substitution pattern in ring B.

The EIMS of **9** showed a molecular ion peak at *m*/*z* 330, its molecular formula was calculated as $C_{17}H_{14}O_7$. Whereas the proton signals from ring A of **9** were identical with the ^{1}H NMR spectral data of **7**, the *ortho*-coupled signals in ring B are significantly highfield shifted compared to those of **7**. The position of the methoxy group at C-6 was established by NOE experiments. Irradiation of the methoxy singlett at 3.85 ppm led to the enhancement of the H-5 (6.36 ppm) and H-7 (6.72 ppm) signals; whereas the position of the second methoxy group (3.74 ppm) at C-2′ could be deduced from the shifts of the aromatic protons and the lack of NOE from H-5′ to the methoxy signal. Additionally, the fragmentation pattern in the EIMS of **9** differs from those of **7** and **8**. Dehydration of the molecule yielded the ion peak at *m*/*z* 312 $[M–H_2O]^+$, thus suggesting an *ortho*-position of the two hydroxy groups at C-3′ and C-4′. In the EIMS of **7** and **8** no dehydration could be observed. In conclusion, due to the NOE results and the observed fractionation pattern in the EIMS methylation of the hydroxy groups at C-3′ and C-4′ could be excluded. Compounds **7**–**9** represent novel 2-arylbenzofuran-3-carbaldehydes, for which we propose the names andinermal A (**7**), andinermal B (**8**), and andinermal C (**9**). Whereas isoflavones are common in the Fabaceae, the occurrence of 2-arylbenzofuran-3-carbaldehydes seems to be very rare throughout the

plant kingdom (Ferreira et al., 1975; Halabalaki et al., 2000); 2-aryl-benzofurans typically co-occur with structurally related isoflavonoids (Harborne, 1994). From the biosynthetical point of view, it is not yet clear if the benzofuran-3-carbaldehyde moiety is related to isoflavones via pterocarpanes (Ferreira et al., 1975) or if it is built directly from flavonoid precursors. The substitution pattern of ring A in this case might hint to the second possibility.

The FAB–MS spectrum of compound **10** (negative mode) showed a characteristic ion peak at *m/z* 579 $[M-H]^-$ suggesting a molecular formula of $C_{30}H_{28}O_{12}$. The ^1H NMR spectrum (Table 2) showed characteristic signals for a flavanonol moiety with a *trans*-configuration of the two protons at C-2 and C-3 ($J = 10.7$ Hz), which could be identified as taxifolin. Furthermore, signals for a α-L-rhamnosyl moiety and a *trans*-cinnamoyl moiety could be observed. The attachment of the rhamnopyranoside at C-3 was deduced from the HMBC spectrum (Table 2). The double doublet signal (5.12 ppm, $J = 3$, 9.7 Hz) of the 3″-proton of the sugar moiety was shifted lowfield and hinted to an ester bonding with *trans*-cinnamic acid. Thus **10** could be established as 3″-*O*-*trans*-cinnamoyl-astilbin, a novel flavanonol glycoside.

In the in vitro antiplasmodial assay against *Plasmodium falciparum* the lipophilic crude extract of the leaves from *A. inermis* showed moderate activity (IC_{50} values: 56 μg/ml [poW], 58.6 μg/ml [Dd2]; Kraft et al., 2000); by fractionation we found an enhanced activity for fraction 6 (IC_{50} value: 16.3 μg/ml [Dd2]), from which we isolated formononetin (**3**) and andinermal B (**8**). As **3** showed no inhibitory effects at all (Kraft et al., 2000) we suggest **8** as one active principle, which unfortunately could not be tested due to the lack of sufficient amount and additional plant material. Whereas the crude hydrophilic extract and three fractions yielded after liquid-liquid-partition (petrol, EtOAc, and H_2O) proved to be inactive, the $CHCl_3$-fraction exhibited an IC_{50} value of 20.3 μg/ml against Dd2. Antiplasmodial activities of isolated compounds from this fraction are shown in Table 3. Andinermal A (**7**) exhibited the strongest antiplasmodial activity with IC_{50} values of 2.3 μg/ml against poW and 3.9 μg/ml against Dd2; andirnermal C was slightly less active (5.9 μg/ml [poW], 6.3 μg/ml [Dd2]). Whereas the 3-*O*-rhamnosides **5** and **6** proved to be inactive, 3″-*O*-*trans*-cinnamoyl-astilbin (**10**) showed a 50% growth inhibition at 10.4 μg/ml (poW) and 4.2 μg/ml (Dd2). Taxifolin, not yet isolated from active fractions, but mentioned for A. *inermis* (Lock de Ugaz et al., 1991), was tested as a control and was slightly less active against poW (15.8 μg/ml) as well as inactive against Dd2 (38.4 μg/ml). Obviously the *trans*-cinnamoyl residue could enhance the antiplasmodial activity of the unsubstituted rhamnoside **5**. The group of the isoflavones did not show homogenous

Table 2
^1H NMR [400 MHz, acetone d_6, δ (ppm)] and ^{13}C NMR, HMBC [500 MHz, CD_3OD, δ (ppm)] spectral data of compound **10** isolated from the leaves of *Andira inermis*

Position	**10**		
	δ_H[a]	δ_C	HMBC correlations
2	5.24 (1H, *d*, 10.7)	83	1′,3, 4, 6′
3	4.72 (1H, *d*, 10.7)	78	1′, 1″, 2, 4,
4		195	
4a		102	
5		162	
6	5.97 (1H, *d*, 2)	96	4a, 5, 7
7		164	
8	5.99 (1H, *d*, 2)	97	5, 7,
8a		162	
1′		127	
2′	7.10 (1H, *d*, 1.9)	115	4′, 6′
3′		146	
4′		147	
5′	6.85 (1H, *d*, 8.1)	116	1′, 3′
6′	6.92 (1H, *dd*, 1.9, 8.1)	119	4′
1″	4.12 (1H, *d*, 1.3)	101	3, 3″ 5″
2″	3.84 (1H, *dd*, 1.3, 3)	69	
3″	5.12 (1H, *dd*, 3, 9.7)	74	
4″	3.71 (1H, *t*, 9.7)	70	
5″	4.41 (1H, *dq*, 6.2, 9.7)	69.5	
6″	1.22 (3H, *d*, 6.2)	30	5″
1‴		134	
2‴ and 6‴	7.67 (2H, *m*)	128	3‴, 4‴, 5‴
3‴, 4‴, and 5‴	7.44 (3H, *m*)	129	1‴, 2‴, 6‴
7‴	7.71 (1H, *d*, 16)	145	2‴, 6‴,9‴
8‴	6.53 (1H, *d*, 16)	118	1‴
9‴		168	
OH-5	11.94 (1H, *s*)		

[a] Intensities, multiplicities and *J* values (Hz) shown in parentheses.

Table 3
Antiplasmodial activity of isolated compounds from the leaves of *Andira inermis* against *Plasmodium falciparum*

Compound		Mean *IC* $_{50}$ values (μg/ml)±S.D.[a]	
		PoW	Dd2
Isoflavones			
Afformosin	(**1**)	36.6±3.3	38.5±7.3
Calycosin[b]	(**2**)	4.3±0.9	9.9±1.5
Formononetin[b]	(**3**)	>50	>50
Prunetin[b]	(**4**)	30.1±3.6	>50
Flavanonol glycosides			
Astilbin	(**5**)	~50	>50
Engelitin	(**6**)	>50	>50
3″-*O*-*trans*-Cinnamoyl-astilbin	(**10**)	10.4±1.3	4.2±1.3
2-Arylbenzofuran-3-carbaldehydes			
Andinermal A	(**7**)	2.3±0.4	3.9±0.2
Andinermal C	(**9**)	5.9±0.5	6.3±1.0
Controls			
Chloroquine ×2 H_3PO_4		0.006±0.002	0.063±0.01
Taxifolin		15.8±1.1	38.4±1.0

[a] Performed in triplicates.
[b] Kraft et al., 2000.

activity against *P. falciparum* at all and it is not clear which substitution patterns are necessary for the activity, nevertheless isoflavones could be detected in all active fractions and some of them, e.g. calycosin (**2**), proved to be active (Kraft et al., 2000). Additionally the 2-arylbenzofuran-3-carbaldehydes are responsible for the activity and it might be interesting, to find out the contribution of the carbaldehyde moiety to this activity.

3. Experimental

3.1. General

For fractionation silica gel 60 (70-230 mesh) was utilised. Preparative high performance liquid chromatography (HPLC) was performed on a Knauer Eurochrom 2000 equipped with a Nucleosil P 300 C-18 (10 μm) column or a Eurospher 100-C 18 (10 μm). EIMS were recorded on a Finnigan MAT CH7A (70 eV); FAB–MS and HR–EIMS on a Finnigan MAT 711 (80 eV). ^{1}H NMR, ^{13}C NMR, COSY, and NOE spectra were obtained on a Bruker AVANCE DPX 400 MHz or a Bruker DRX 500 MHz spectrometer (TMS as int. standard; acetone-d_6 as solvent).

3.2. Plant material

Leaves of *A. inermis* were collected in the area of Panama City (at the road El Llano-Carti), Republic of Panama, during March 1997. Voucher specimens (FLORPAN 2758) were identified by Professor M.D. Correa A. and deposited at the Herbarium of the University of Panama.

3.3. Extraction and isolation

Ground leaves (200 g) were extracted three times with 1.5 l of petrol–EtOAc (1:1, v/v) for 24 h at room temperature to gain a lipophilic extract. The solvents were evaporated under reduced pressure and the plant material was treated again three times with 1 l MeOH–H_2O (8:2, v/v). The MeOH was evaporated and the remaining aqueous phase was successively extracted with petrol, $CHCl_3$, and EtOAc.

The oily residue of the lipophilic extract (5 g) was subjected to column chromatography on silica gel 60 (75 g) and eluted with cyclohexane, cyclohexane–EtOAc mixtures, and MeOH to yield eight fractions. Due to the results of the bioassay, fraction 6 (30 mg, eluted with cyclohexane–EtOAc 7:3 [v/v]) was further purified by preparative HPLC (RP-18) at a 1.5 ml/min flow rate of MeOH–H_2O 4:6 (v/v) and yielded **3** (6.5 mg) and **8** (< 1 mg).

The dried $CHCl_3$ fraction (2 g) of the hydrophilic extract was chromatographed over a silica gel column (20 g) using $CHCl_3$–MeOH mixtures as eluent. The six obtained fractions were tested for their antiplasmodial activity, and fractions 2–4 were further investigated. Fractions 2 and 3 (eluted with $CHCl_3$–MeOH 9:1and 8:2 [v/v], respectively) were separated by preparative HPLC (RP-18) at a flow rate of 5.5 ml/min using a gradient H_2O–MeOH 60:40 to 0:100 (v/v) in 60 min. From 2 we gained compounds **1** (1.5 mg), **2** (1.5 mg), **3** (8 mg), **4** (1.5 mg), **7** (7 mg), and **9** (1 mg); fraction 3 afforded **10** (22 mg). Fraction 4 (eluted with $CHCl_3$–MeOH 7:3 [v/v]) was purified with H_2O–MeOH 55:45 (v/v) to afford **5** (6.7 mg) and **6** (9.2 mg).

3.4. Andinermal A (7; 2-[2′, 4′-dimethoxy-3′-hydroxyphenyl]-4-hydroxy-6-methoxy-benzofuran-3-carbaldehyde)

^{1}H NMR and ^{13}C NMR (400 MHz; acetone-d_6) see Table 1. HMBC (500 MHz; acetone-d_6) correlations: see Fig. 1; Table 1. EIMS *m*/*z*: $[M]^+$ 344 (100), $[M–CH_3]^+$ 329 (5), $[M–OCH_3]^+$ 313 (68). (+) FAB *m*/*z*: $[M+H]^+$ 345, (–) FAB *m*/*z*: $[M–H]^-$ 343. HR-EIMS *m*/*z*: 344.089480 (calc. for $C_{18}H_{16}O_7$, 344.08961).

3.5. Andinermal B (8; 2-[2′, 4′-dimethoxy-3′-hydroxyphenyl]-4-hydroxy-5,6-methylendioxy-benzofuran-3-carbaldehyde)

^{1}H NMR (400 MHz; acetone-d_6) see Table 1. EIMS *m*/*z*: $[M]^+$ 358 (96), $[M–OCH_3]^+$ 327 (100), $[M–OCH_3/-CH_3]^+$ 312 (19). HR–EIMS *m*/*z*: 358.0690 (calc. for $C_{18}H_{14}O_8$, 358.06887).

3.6. Andinermal C (9; 2-[3′, 4′-dihydroxy-2′-methoxyphenyl]-4-hydroxy-6-methoxy-benzofuran-3-carbaldehyde)

^{1}H NMR (400 MHz; acetone-d_6) see Table 1. EIMS *m*/*z*: $[M]^+$ 330 (100), $[M–CH_3]^+$ 315 (9), $[M–H_2O]^+$ 312 (10), $[M\text{-}OCH_3]^+$ 299 (57), $[M–CH_3OH]^+$ 298 (24). HR–EIMS *m*/*z*: 330.07531 (calc. for $C_{17}H_{14}O_7$ 330.073953).

3.7. 3′-O-trans-Cinnamoyl-astilbin (10)

$[\alpha]_D^{20}+1.29$ (acetone; *c* 0.22). ^{1}H NMR (400 MHz; acetone-d_6), ^{13}C NMR (500 MHz, CD_3OD) and HMBC (500 MHz; CD_3OD) correlations see Table 2. (–) FAB *m*/*z*: $[M\text{-}H]^-$ 579.

3.8. In vitro bioassay

The bioassay was performed as described earlier (Kraft et al., 2000). The chloroquine-sensitive strain poW (IC_{50} for chloroquine ×2 H_3PO_4 = 0.011 μM) and the chloroquine-resistant clone Dd2 (IC_{50} for chloroquine ×2 H_3PO_4 = 0.12 μM) of *Plasmodium falciparum*

were maintained in continuous culture according to Trager and Jensen (1976). The antiplasmodial assay was carried out according to the method described by Desjardins et al. (1979) and activities were determined by a ^{3}H-hypoxanthine-incorporation assay.

Acknowledgements

The authors are indebted to Mrs. U. Ostwald and Dr. G. Holzmann (Institut für Organische Chemie der FU Berlin) for recording the FAB and HR–EIMS spectra, to Dr. J. Klein (AnalytiCon Discovery) for performing the NOE spectra, to Mr. C. Guerra, for his support in collecting the plant material, and to Professor M.D. Correa A., Herbarium of the University of Panama, Republic of Panama, for her identification of the species.

This study was supported by a grant of the Deutsche Pharmazeutische Gesellschaft to K.J-S. CIFLORPAN acknowledges the Fundation Natura and the Organization of American States (OAS) for financial support.

References

Caballero, P., Smith, C.M., 1986. Isoflavones from an insect-resistant variety of soybean and the molecular structure of afrormosin. Journal of Natural Products 49, 1126–1129.

Cocker, W., Dahl, T., Dempsey, C., McMurry, T.B.H., 1962. Extractives from woods. Part I. Extractives from *Andira inermis* (Wright) H.B.K. Journal of the Chemical Society Perkin Transactions 1, 4906–4909.

Desjardins, R.E., Canfield, C.J., Haynes, J.D., Chulay, J.D., 1979. Quantitative assessment of antimalarial activity in vitro by a semi-automated microdilution technique. Antimicrobial Agents and Chemotherapy 16, 710–718.

Ferreira, M.A., Moir, M., Thomson, R.H., 1975. Naturally occurring quinones. Part XXV. Pterocarpenequinones (6H-benzofuro [3,2-c] [1] benzopyranquinones) from *Brya ebenus*. Journal of the Chemical Society Perkin Transactions 1, 1113–1115.

Halabalaki, M., Aligiannis, N., Papoutsi, Z., Mitakou, S., Moutsatsou, P., Sekeris, C., Skaltsounis, A.L., 2000. Three new arylbenzofurans from *Onobrychis ebenoides* and evaluation of their binding affinity for the estrogen receptor. Journal of Natural Products 63, 1672–1674.

Harborne, J.B., 1994. The Flavonoids: Advances in Research Since 1986. Chapman & Hall, London.

Kobayashi, M., Noguchi, H., Sankawa, U., 1985. Formation of isoflavones by callus culture of *Glycyrrhiza uralensis* with different production pattern. Chemical and Pharmaceutical Bulletin 33, 3811–3816.

Kraft, C., Jenett-Siems, K., Siems, K., Gupta, M.P., Bienzle, U., Eich, E., 2000. Antiplasmodial activity of isoflavones from *Andira inermis*. Journal of Ethnopharmacology 73, 131–135.

Lock de Ugaz, O., Costa, J., Sanchez, L., Ubillas Sanchez, R.P., Tempesta, M.S., 1991. Flavonoids from *Andira inermis*. Fitoterapia 62, 89–90.

Reisch, J., Hussain, R.A., Mester, I., 1984. Flavonoids from *Flindersia australis*. Phytochemistry 23, 2114–2115.

Trager, W., Jensen, J.B., 1976. Human malaria parasites in continuous culture. Science 193, 673–675.

Tschesche, R., Delhvi, S., Sepúlveda, S., Breitmaier, E., 1979. Eucryphin, a new chromone rhamnoside from the bark of *Eucryphia cordifolia*. Phytochemistry 18, 867–869.

PERGAMON

Phytochemistry 58 (2001) 775–787

PHYTOCHEMISTRY

www.elsevier.com/locate/phytochem

Synthesis and antifeedant properties of *N*-benzoylphenylisoserinates of *Lactarius* sesquiterpenoid alcohols

Piotr Kopczacki[a], Maria Gumułka[a], Marek Masnyk[a], Halina Grabarczyk[b], Gerard Nowak[b], Włodzimierz M. Daniewski[a,*]

[a]*Institute of Organic Chemistry, Polish Academy of Sciences, Kasprzaka 44/52, 01-224 Warsaw, Poland*
[b]*Department of Medicinal Plants, Academy of Medicine, Mazowiecka 33, 60-623 Poznañ, Poland*

Received 5 February 2001; received in revised form 18 June 2001

Abstract

The esterification of various sesquiterpenoid alcohols of *Lactarius* origin with *N*-benzoyl-[2*R*,3*S*]-phenylisoserine (side chain of Taxol®) produced compounds whose antifeedant properties against storage pests *Tribolium confusum, Trogoderma granarium* and *Sitophylus granarius* were measured. The introduction of the taxol side chain in these molecules, in comparison to original compounds, moderately enhanced their antifeedant activities, as well as changed their selectivity of activity towards the test insects.
© 2001 Elsevier Science Ltd. All rights reserved.

Keywords: *N*-Benzoylphenylisoserinates; *Lactarius* sesquiterpenes; Paclitaxel; Antifeedant activity; Storage pests; *Tribolium confusum*; *Trogoderma granarium*; *Sitophilus granarius*; *Rhizopertha dominica*

1. Introduction

In our recent paper (Daniewski et al., 1998) we have identified a group of compounds responsible for the resistance of *Taxus baccata* to the attack of insects. It appeared that the taxanes 10-deacetylbaccatin III (**1**) and its 7α isomer (**2**), contained in the needles of *T. baccata* and possessing a very strong antifeedant activity, protect them from the attack of insects (Fig. 1).

This fact prompted us to investigate the antifeedant activity against the storage pests, of paclitaxel (**3**), the very important anticancer compound isolated from *Taxus brevifolia*. The antifeedant activity tests of paclitaxel (**3**) revealed its very potent activity, and perhaps, its role in the bark of *T. brevifolia* in defence against insects. In our previous papers (Daniewski et al., 1993, 1995) we studied the antifeedant properties of sesquiterpenoid alcohols from *Lactarius* species. The sesquiterpenes, as in the case of 10-deacetylbaccatin III (**1**) or paclitaxel (**3**), are responsible for chemical defence of the mushrooms against several predators. Since paclitaxel (**3**) is the 10-acetyl-13-*N*-benzoylphenylisoserine ester of 10-deacetylbaccatin III, we decided to attach the paclitaxel side chain to a series of sesquiterpenoid alcohols to produce *N*-benzoylphenylisoserine esters and to investigate their biological properties.

2. Results and discussion

There are many methods of attachment of *N*-benzoylphenylisoserine to the baccatin core to produce Taxol® (Farina, 1995); among them, a very simple one, involves the synthesis of the oxazoline derivative (**5**) of *RS* (natural) phenylisoserine (**4**) (Scheme 1):

Originally the synthesis of oxazoline (**5**) required as starting material the phenylisoserine with unnatural configuration at asymmetric center 2. In order to simplify the procedure and to use the phenylisoserine with natural configuration, which is commercially available, we decided to use trimethyl *ortho*-benzoate for the cyclisation, as recently described (Kamata et al., 1998). The hydrolysis of the ester **5** to the free acid **6** as well as its esterification with properly protected baccatin III was described by Kingston et al. (1994) in the semisynthesis of paclitaxel (**3**). The same esterification procedure was applied for the acid **6** and sesquiterpenoid alcohols and it is exemplified by the following scheme where lactarorufin A (**31**) was used as sesquiterpenoid alcohol (Scheme 2).

* Corresponding author. Tel.: +48-22-6323221 x. 2330; fax: +48-22-6326681.
E-mail address: daniewsk@icho.edu.pl (W.M. Daniewski).

0031-9422/01/$ - see front matter © 2001 Elsevier Science Ltd. All rights reserved.
PII: S0031-9422(01)00294-1

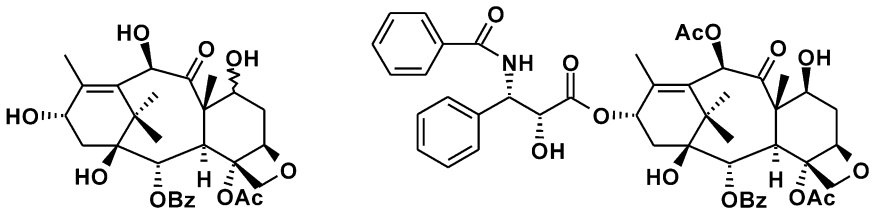

Fig. 1. **1**, R = β-OH (10-deacetylbaccatin III); **2**, R = α-OH (7-*epi*-10-deacetylbaccatin III).

The esterification reaction went smoothly to give the cyclic ester **32**. The hydrolysis of the cyclic ester to form the *N*-benzoylphenylisoserinate (**33**) required different conditions from those used for the synthesis of paclitaxel. To avoid elimination of the side chain low temperature and methanol as solvent had to be used.

Using the above general method described in the experimental part a series of *N*-benzoylphenylisoserinates of various *Lactarius* sesquiterpenoid alcohols was prepared. (Scheme 2). The series included esters of marasmane, isolactarane and lactarane sesquiterpenes. The structures of all the compounds were substantiated by their ^{1}H NMR and ^{13}C NMR spectra which are included in the experimental part. The marasmane esters (**8**, **9**) possess very characteristic signals which allow their identification. The geminal cyclopropane protons at C-4 give rise to a pair of doublets with $J = 4$–5 Hz. The geminal methyl groups at C-11 appear as singlets at ca. δ 0.90–1.1, while the C-12 methyl resonates at lower field (ca. δ 1.15–1.5). Similarly isolactarane esters (**11, 12, 14, 15**) exhibited ^{1}H NMR spectra showing three methyl group singlets, one of them (C-12) resonating at lower field. The cyclopropane protons at C-5, as in the case of marasmane sesquiterpenes produced a pair of doublets (gem. coupling $J = 5.5$ Hz). An important and characteristic ^{1}H NMR spectral feature of isolactarane esters is involving the ABq system with $J = 10$ Hz, typical of saturated γ-lactone ring, In case of ^{1}H NMR spectra of lactarane esters, signals of methyl groups appear as in the previously discussed groups. Depending on heterocyclic rings (furans or lactones), characteristic signals are exhibited. The C-13 or C-5 methylene protons of lactones form an ABq system with a large coupling constant (15–20 Hz). The value of H-8, H-9

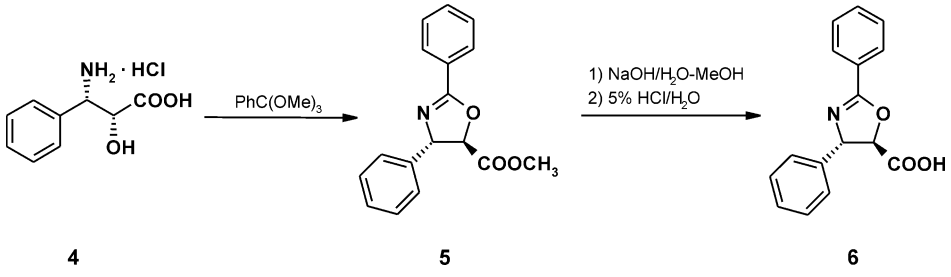

Scheme 1.

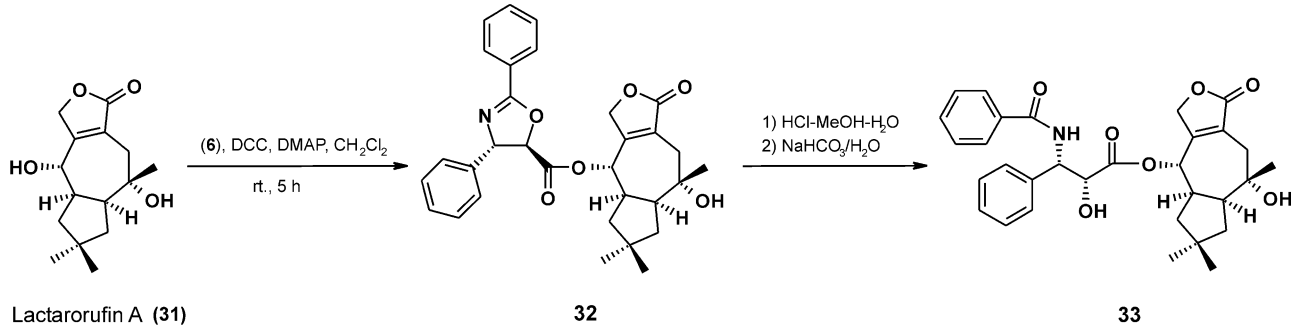

Scheme 2.

coupling constants are indicative of the *cis* or *trans* stereochemistry. As general feature the signals of protons on carbons bearing the ester groups, in the ^{1}H NMR spectra, are down field shifted in comparison with those of free alcohols (Fig. 2).

The ^{13}C NMR spectra of all the phenylisoserinates confirmed their structures and are included in the experimental part.

3. Antifeedant properties

As it was already mentioned in the introduction, we wanted to check the antifeedant properties of the synthesised compounds in order to find the influence of introduction of paclitaxel side chain into their molecules. First we checked paclitaxel (**3**) (Item 1, R = c, R' = Ac) that has a very potent antifeedant activity to the storage pests mentioned in Table 1. Therefore one can assume that its role in *Taxus brevifolia* is to protect the plant against insects. 10-Deacetyl baccatin III (**1**) (Item 1, R = H, R' = H), which is a good antifeedant, demonstrated lower activity than paclitaxel, especially against *Trogoderma granarium* and *Sitophylus granarius*. The bonding of paclitaxel side chain to the molecule of isovellerol (Item 2) decreased its activity. Introduction of paclitaxel side chain into the molecule of isolactarorufin (**10**) (Item 3, R = H) (which is an attractant) enhanced its antifeedant properties. Change of stereochemistry at C-8 (Item 4) did not influence activity. Similarly esterification of furanol (Item 5) did not have important effect on antifeedant activity. In case of furandiol (**19**) (Item 6), the esterification gave a compound **21** with twice as high activity. Introduction of the paclitaxel side chain into "artifact" (Item 7) as well as into lactarorufin A (Item 8) influenced only the selectivities of antifeedant activity. Esterification of 8-*epi*-lactarorufin A (**34**) (Item 9), which is inactive, caused some activity. Introduction of the side chain into 5-deoxy-lactarolid B (Item 10) did not increase its activity but changed its selectivity towards storage pests. Our procedure was verified with azadirachtin (Item 11) test.

4. Experimental

4.1. General

All melting points were measured on a Koffler hot plate and are uncorrected. ^{1}H and ^{13}C NMR spectra were run at 500 and 125 MHz respectively (Bruker 500 MHz spectrometer) in $CDCl_3$ as otherwise noted, using TMS as internal standard. Column chromatography (CC) was carried out using silica gel, and the TLC were conducted on silica gel or RP-18.

The phenylisoserinates were prepared from sesquiterpenoid alcohols isolated from mushrooms (*Lactarius rufus, Lactarius vellereus,* voucher numbers 33550, and 32260 respectively, specimen deposited at the Department of Systematics and Geography of Plants of the University of Warsaw) or synthesized by transformation of natural products. The references on the procedures of isolation or preparation of all the sesquiterpenes (**7**, **10**, **13**, **16**, **19**, **22**, **25**, **28**, **31**, **34**, **37**, **40**) can be found in the recent review (Daniewski and Vidari, 1999).

4.2. Preparation of oxazoline methyl ester (*5*)

Phenylisoserine (*R*,*S*) (2.87 g, 0.013 mol) was suspensed in dry toluene (50 ml) in round bottom flask (200 ml) equipped with magnetic stirrer and a still head. The reaction was heated to boiling and 15 ml of toluene was distilled off. Subsequently trimethylorthobenzoate (5 ml, 0.029 mol) was added and the volatile components were removed slowly by distillation during 8 h. Residual solids were filtered off and the filtrate evaporated in rotavap. The resulting oil was purified by chromatography over silica-gel in hexane–ethyl acetate gradient solvent system. Proper fractions were collected and gave pure ester **5** (1.5 g, 41% theoretical yield). $[\alpha]_D = +14.2^\circ$ (EtOH, *c* 1.0); ^{1}H NMR (200 MHz): δ_H 3.90 (3H *s*), 4.96 (1H, *d*, J = 6.5 Hz,), 5.50 (1H, *d*, J = 6.5 Hz,), 7.30–7.62 (8H, *m*), 8.10–8.20 (2H,*m*); ^{13}C NMR ($CDCl_3$, 50 MHz): δ_C 52.68, 74.59, 83.07, 126.39, 126.72, 127.97, 128.15, 128.22, 128.39, 128.64, 128.79, 131.86, 141.04, 163.89, 170.55.

The unidentified residual solids, by treatment with another portion of trimethyl ortho benzoate in presence of *p*-toluenesulphonic acid in toluene, can be converted into the desired ester **5**. In this way overall yield can be improved up to 66%.

4.3. (4S,5R) 2,4-Diphenyl-4,5-dihydro-oxazol-5-carboxylic acid (*6*)

Compound **5** (1.52 g, 0.0054 mol) dissolved in methanol (8 ml) was treated with sodium hydroxide (0.33 g, 0.00835 mol) dissolved in methanol (20 ml) and water (0.5 ml) at room temperature. The reaction was followed by TLC and when no starting material was detected (5 h), hydrochloric acid (6 ml, 5%) was added to the reaction mixture to obtain the pH value equal 6. Precipitated solid was filtered, washed with water and dried to give 1.23 g of the desired product with 86% yield. mp. = 207–211 °C, $[\alpha]_D = -9.97^\circ$ (0.05 *N* NaOH aq., c 1.01),^{1}H NMR (200 MHz, DMSO-d_6,): δ_H 5.00 (1H, *d*, J = 6.4 Hz,), 5.41 (1H *d*, J = 6.4 Hz,), 7.20–7.70 (8H,*m*), 7.90–8.10 (2H,*m*); ^{13}C NMR (DMSO-d_6, 50 MHz) δ_C 73.78, 82.42, 126 53, 126.64, 127.79, 128.18, 128.71, 128.80, 132.09, 141.54, 162.86, 171.45.

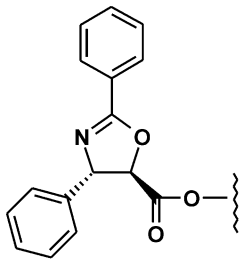

a

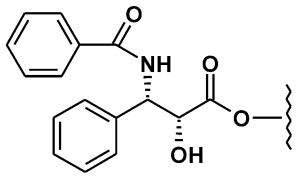

b

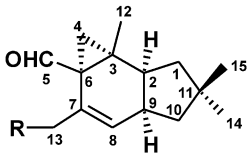

7 R = H
8 R = a
9 R = b

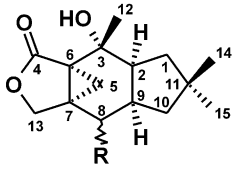

10 R = α-H
11 R = α-a
12 R = α-b
13 R = β-H
14 R = β-a
15 R = β-b

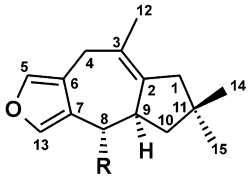

16 R = H
17 R = a
18 R = b

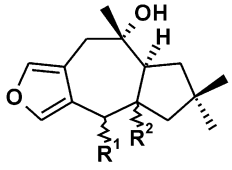

19 R^1 = α-H, R^2 = α-H
20 R^1 = α-a, R^2 = α-H
21 R^1 = α-b, R^2 = α-H
22 R^1 = β-H, R^2 = β-H
23 R^1 = β-a, R^2 = β-H
24 R^1 = β-b, R^2 = β-H

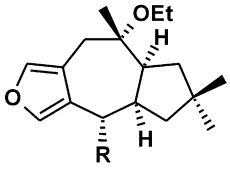

25 R = H
26 R = a
27 R = b

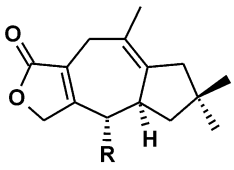

28 R = H
29 R = a
30 R = b

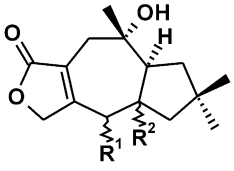

31 R^1 = α-H, R^2 = α-H
32 R^1 = α-a, R^2 = α-H
33 R^1 = α-b, R^2 = α-H
34 R^1 = β-H, R^2 = α-H
35 R^1 = β-a, R^2 = α-H
36 R^1 = β-b, R^2 = α-H
37 R^1 = β-H, R^2 = β-H
38 R^1 = β-a, R^2 = β-H
39 R^1 = β-b, R^2 = β-H

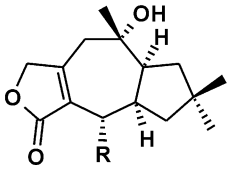

40 R = H
41 R = a
42 R = b

Fig. 2. *N*-benzoylphenyllsoserinates of *Lactarius* sesquiterpenoid alcohols and their oxazdine synthatic intermediates.

Table 1
Antifeedant activity of 10-deacetyl baccatin III (**1**) and Taxol® (**3**) and *N*-benzoyl phenylisoserinates of several sesquiterpenoid alcohols of *Lactarius* origin

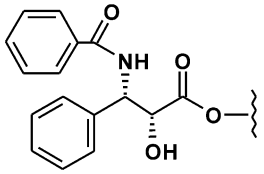

Compound		*Trogoderma granarium*, larvae	*Sitophilus granarius*, adults	*Tribolium confusum*, larvae	*Rhizopertha dominica*, adults	Average activity class[a]
Item 1 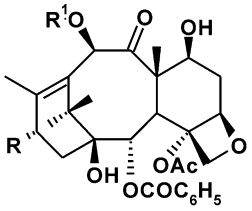	R = H R^1 = H (1)	115.5	185.0	149.4	–	150.0 III
	R = b R^1 = Ac (3)	178.9	190.8	122.6	131.5	156.0 IV
Item 2 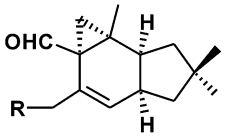	R = H (7)	200	176	161.9	–	179.3 IV
	R = b (9)	99.2	165.5	95.1	132.7	123.1 III
Item 3 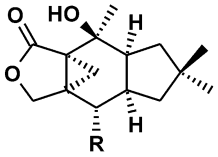	R = H (10)	−50.4	−7.0	15.3	–	-42.1 atr.
	R = b (12)	70.1	122.4	164.9	70.0	106.9 III
Item 4 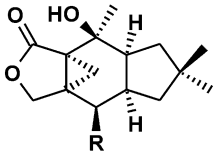	R = H (13)	42.6	35.3	−22.8	–	18.4 I
	R = b (15)	92.9	111.1	67.9	−23.0	62.2 II
Item 5 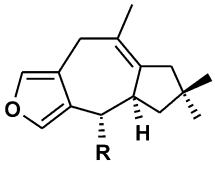	R = H (16)	21.0	137.0	152.7	–	103.6 III
	R = b (18)	43.5	102.3	103.6	141.2	97.7 II
Item 6 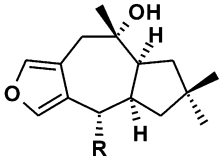	R = H (19)	9.2	60.0	95.7	–	55.0 II
	R = b (21)	78.1	118.5	84.1	125.1	101.5 III
Item 7 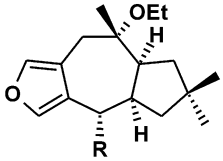	R = H (25)	41.6	173.7	163.8	–	126.4 III
	R = b (27)	119.6	115.9	91.0	172.3	124.7 III

(*continued on next page*)

Table 1 (*continued*)

Compound		*Trogoderma granarium*, larvae	*Sitophilus granarius*, adults	*Tribolium confusum*, larvae	*Rhizopertha dominica*, adults	Average activity class[a]
Item 8 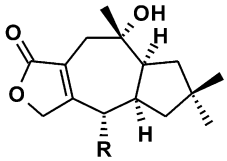	R = H (31)	148.6	88.6	144.9	–	127.4 III
	R = b (33)	118.9	162.9	11.7	51.2	86.2 II
Item 9 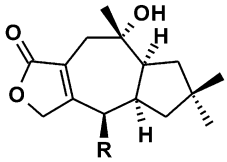	R = H (34)	−17.4	−11.9	59.3	–	10.0 I
	R = b (36)	79.9	94.6	42.7	-46.6	42.7 I
Item 10 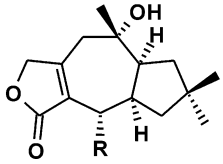	R = H (40)	93.3	73.4	150.0	–	105.6 III
	R = b (42)	123.0	129.3	66.4	133.8	113.1 III
Item 11 Azadirachtin		190.0	170.0	185.0	–	181.7 IV

[a] Below "0", attractant; class I (0–50), poor antifeedant; class II (51–100), medium antifeedant; class III (101–150), good antifeedant; class IV (151–200), very good antifeedant.

4.4. General method for the synthesis of esters of (4S,5R)-2,4-diphenyl-4,5-dihydro-oxazol-5-carboxylic acid and sesquiterpenoid alcohols of Lactarius origin

A sesquiterpenoid alcohol (1 mmol), the acid (**6**) (1.1 mmol), DMAP (18.3 mg, 0.15 mmol) and DCC (247.2 mg, 1.2 mmol) were dissolved in methylene chloride (25 ml) in a round bottom flask. The reaction was carried out at room temperature and was monitored by TLC. When the reaction was completed (3–12 h) the content of the flask was fitered, the solution evaporated in vacuo and the residue purified by chromatography to give the desired esters.

*4.4.1. Compound **8***

TLC $R_f = 0.72$ (CH_2Cl_2–Me_2CO 96:4); Oil; $[\alpha]_D^{20} = +2.62^\circ$ ($CHCl_3$, *c* 1.0); UV λ_{max} (EtOH) nm: 204 (ε 9664); IR ν_{max} ($CHCl_3$) cm^{-1}: 2955, 1753, 1702,1654; ^1H NMR: δ 0.97 (3H, *s*, H-15), 1.00 (3H, *s*, H-14), 1.23 (3H, *s*, H-12), 1.25 (1H, *d*, $J_{10\beta,10\alpha} = 12.2$ Hz, H-10β), 1.27 (1H, *d*, $J_{4\beta,4\alpha} = 4.4$ Hz, H-4β), 1.35 (1H, *dd*, $J_{1\beta,1\alpha} = 13.3$ Hz and $J_{1\beta,2\alpha} = 7.9$ Hz, H-1β), 1.60 (1H, *dd*, $J_{10\alpha,10\beta} = 12.2$ Hz and $J = 7.4$ Hz, H-10α), 1.68 (1H, *d*, $J_{4\alpha,4\beta} = 4.4$ Hz, H-4α), 1.77 (1H, *dd*, $J_{1\alpha,1\beta} = 13.3$ Hz and $J_{1\alpha,2\alpha} = 1.1$ Hz, H-1α), 2.46–2.52 (2H, *m*, H-2α and H-9α), 4.86–4.89 (1H, *m*, H-13β and H-2′), 5.28 (1H, *d*, $J_{13\alpha,13\beta} = 12.2$ Hz, H-13α), 5.39 (1H, *br s*, H-8), 5.40 (1H, *d*, $J_{2',3'} = 6.0$ Hz, H-3′), 7.28–7.55 (8H, *m*, H-Ph) 8.08–8.11 (2H, *m*, H-Ph), 9.45 (1H, *s*, H-5); ^{13}C NMR: δ 19.9 (*q*, C-12), 30.7 (*t*, C-4), 31.6 (*q*, C-15), 31.7 (*q*, C-14), 35.5 (*s*, C-11), 36.8 (*s*, C-3), 37.4 (*s*, C-6), 38.2 (*d*, C-2), 42.5 (*d*, C-9), 44.8 (*t*, C-10), 47.5 (*t*, C-1), 67.8 (*t*, C-13), 74.5 (*d*, C-3′), 83.0 (*d*, C-2′), 126.4 (*d*, C-Ph), 126.8 (*s*, C-Ph), 127.9 (*d*, C-Ph), 128.4 (*d*, C-Ph), 128.7 (*d*, C-Ph), 128.8 (*d*, C-Ph), 130.2 (*s*, C-7), 131.2 (*d*, C-8), 131.8 (*d*, C-Ph), 141.1 (*s*, C-Ph), 164.0 (*s*, NCO), 169.6 (*s*, C-1′), 200.1 (*s*, C-5); EIMS 70 eV, *m*/*z* (rel. int.): 483 $[M]^+$ (19.3), 269 (17.7), 268 (100.0), 22 (6), 193 (11), 173 (2.4), 165 (2.5), 146 (2), 120 (6), 119 (8), 105 (22), 91 (17), 90 (7), 89 (4), 77 (5), 69 (2), 55 (2), 43 (1) 41 (4); HR EIMS *m*/*z*: $[M]^+$ calc. for $C_{31}H_{33}O_4N$: 483.24096, found: 483.23978.

*4.4.2. Compound **11***

TLC $R_f = 0.24$, (hexane–EtOAc 77:23); mp 170–172 °C; $[\alpha]_D^{20} = -43.7^\circ$ ($CHCl_3$ *c* 1.1); UV λ_{max} (EtOH) nm: 243 (ε 20541); IR ν_{max} (KBr) cm^{-1}: 3475, 2957, 1957, 1895, 1769, 1740, 1656; ^1H NMR: δ 0.95 (3H, *s*, H-15), 1.10 (3H, *s*, H-14), 1.11 (1H, *d*, $J_{5\beta,5\alpha} = 6.2$ Hz, H-5β), 1.36 (1H, *t*, $J_{10\beta,10\alpha} = 11.3$ Hz, H-10β), 1.50 (1H, *dd*, $J_{1\beta,1\alpha} = 12.4$ Hz and $J_{1\beta,2\alpha} = 7.8$ Hz, H-1β), 1.64 (1H, *d*, $J_{5\alpha,5\beta} = 6.2$ Hz, H-5α), 1.68–1.74 (2H, *m*, H-1α and H-10α), 2.08–2.19 (2H, *m*, H-2α and H-9α), 4.16 (1H, *d*, $J_{13\beta,13\alpha} = 9.4$ Hz, H-13β), 4.41 (1H, *d*, $J_{13\alpha,13\beta} = 9.4$ Hz, H-13α), 4.90 (1H, *d*, $J_{2',3'} = 6.6$ Hz, H-2′), 5.37 (1H, *d*, $J_{3',2'} = 6.6$ Hz, H-3′), 5.66 (1H, *d*, $J_{8\beta,9\alpha} = 8.0$ Hz, H-8β), 7.30–7.65 (8H, *m*, H-Ph), 8.07–8.12 (2H, *m* H-Ph); ^{13}C NMR: δ 18.3 (*t*, C-5), 24.6 (*q*, C-12), 26.8 (*q*, C-15), 28.7 (*q*, C-14), 31.6 (*s*, C-11), 38.5 (*s*, C-6), 38.9 (*s*, C-7), 39.9

(*t*, C-1), 40.7 (*d*, C-2), 45.9 (*d*, C-9), 47.3 (*t*, C-10), 71.0 (*s*, C-3), 71.4 (*t*, C-13), 75.0 (*d*, C-8), 79.4 (*d*, C-3′), 83,1 (*d*, C-2′), 126.5 (*d*, C-Ph), 126.7 (*s*, C-Ph), 128.2 (*d*, C-Ph), 128.5 (*d*, C-Ph), 128.7 (*d*, C-Ph), 128.9 (*d*, C-Ph), 132.1 (*d*, C-Ph), 140.9 (*s*, C-Ph), 164.2 (*s*, NCO), 170.1 (*s*, C-1′), 175.1 (*s*, C-4); LSIMS *m*/*z* (rel. int.): 516 $[M+H]^+$ (38), 498 (15), 460 (4), 307 (29), 268 (29), 231 (6), 222 (6), 154 (100); HR LSIMS *m*/*z*: $[M+H]^+$ calc. for $C_{31}H_{34}O_6N$: 516.23859, found: 516.23813.

4.4.3. Compound **14**

TLC $R_f = 0.25$ (hexane–EtOAc 8:2); mp 86–91 °C; $[\alpha]_D^{20} = +35.24°$ ($CHCl_3$, *c* 1.0); UV λ_{max} (EtOH) nm: 243 (ε 16937); IR ν_{max} ($CHCl_3$) cm^{-1}: 3555, 3434, 2957, 1772, 1746,1655; ^1H NMR: δ 0.67 (3H, *s*, H-15), 0.85 (3H, *s*, H-14), 0.95 (1H, *t*, $J_{10\beta,10\alpha} = 11.8$ Hz, H-10β), 1.18 (1H, *d*, $J_{5\beta,5\alpha} = 6.3$ Hz, H-5β), 1.30–1.42 (3H, *m*, H-1α, H-1β and H-10α), 1.60 (3H, *s*, H-12), 1.61 (1H, *d*, $J_{5\alpha,5\beta} = 6.3$ Hz, H-5α), 1.99–2.05 (1H, *m*, H-2α), 2.25-2.32 (1H, *m*, H-9α), 4.08 (1H, *d*, $J_{13\beta,13\alpha} = 9.4$ Hz, H-13β), 4.21 (1H, *d*, $J_{13\alpha,13\beta} = 9.4$ Hz, H-13α), 5.02 (1H, *d*, $J_{2',3'} = 5.9$ Hz, H-2′), 5.56 (1H, *d*, $J_{3',2'} = 5.9$ Hz, H-3′), 5.83 (1H, *d*, $J_{8\alpha,9\alpha} = 4.5$ Hz, H-8α), 7.30–7.56 (8H, *m*, H-Ph), 8.11–8.13 (2H, *m*, H-Ph); ^{13}C NMR: δ 19.5 (*t*, C-5), 24.7 (*q*, C-12), 26.5 (*q*, C-14), 28.1 (*q*, C-15), 32.0 (*s*, C-11), 35.2 (*s*, C-6), 37.6 (*d*, C-9), 37.6 (*s*, C-7), 39.6 (*t*, C-1), 42.1 (*t*, C-10), 44.3 (*d*, C-2), 68.0 (*t*, C-13), 69.3 (*s*, C-3), 71.2 (*d*, C-8), 74.7 (*d*, C-3′), 82.9 (*d*, C-2′), 125.9 (*s*, C-Ph), 126.4 (*d*, C-Ph), 128.2 (*d*, C-Ph), 128.5 (*d*, C-Ph), 128.9 (*d*, C-Ph), 129.0 (*d*, C-Ph), 132.2 (*d*, C-Ph), 140.6 (*s*, C-Ph), 163.4 (*s*, NCO), 170.1 (*s*, C-1′), 173.6 (*s*, C-4); LSIMS *m*/*z* (rel. int.): 516 $[M+H]^+$ (100), 498 (26), 474 (2), 403 (2), 307 (12), 289 (7), 268 (100), 225 (52), 193 (8), 154 (92); HR LSIMS *m*/*z*: $[M+H]^+$ calc. for $C_{31}H_{34}O_6N$: 516.23861, found: 516.23963.

4.4.4. Compound **17**

TLC $R_f = 0.62$ (hexane–EtOAc 8:2); mp 127–131 °C; $[\alpha]_D^{20} = -57.83°$ ($CHCl_3$, *c* 1.0); UV λ_{max} (EtOH) nm: 241 (ε 15984); IR ν_{max} ($CHCl_3$) cm^{-1}: 3066, 2955, 2867, 1960, 1748, 1654; ^1H NMR: δ 0.90 (3H, *s*, H-15), 1.12 (3H, *s*, H-14), 1.46 (1H, *dd*, $J_{10\beta,10\alpha} = 12.6$ Hz, $J_{10\beta,9\alpha} = 8.3$ Hz, H-10β), 1.75 (3H, *s*, H-12), 1.91 (1H, *ddd*, $J_{10\alpha,10\beta} = 12.6$ Hz, $J_{10\alpha,9\alpha} = 7.9$ Hz and $J = 2.0$ Hz, H-10α), 2.07 (1H, *d*, $J_{1\beta,1\alpha} = 15.0$ Hz, H-1β), 2.20 (1H, *d*, $J_{1\alpha,1\beta} = 15.0$ Hz, H-1α), 2.91 (1H, *d*, $J_{4\beta,4\alpha} = 16.1$ Hz, H-4β), 3.25–3.31 (1H, *m*, H-9α), 3.40 (1H, *d*, $J_{4\alpha,4\beta} = 16.1$ Hz, H-4α), 4.94 (1H, *d*, $J_{2',3'} = 6.3$ Hz, H-2′), 5.47 (1H, *d*, $J_{3',2'} = 6.3$ Hz, H-3′), 5.82 (1H, *d*, $J_{8\beta,9\alpha} = 11.4$ Hz, H-8β), 7.13 (1H, *t*, $J = 1.5$ Hz, H-5α), 7.28–7.55 (9H, *m*, H-13 and H-Ph), 8.07–8.12 (2H, *m*, H-Ph); ^{13}C NMR: δ 21.5 (*q*, C-12), 27.5 (*q*, C-14), 28.7 (*q*, C-15), 29.4 (*t*, C-4), 37.6 (*s*, C-11), 44.6 (*d*, C-9), 45.8 (*t*, C-10), 46.5 (*t*, C-1), 73.6 (*d*, C-8), 74.7 (*d*, C-3′), 83,2 (*d*, C-2′), 121.3 (*s*, C-6), 124.2 (*s*, C-7), 126.4 (*d*, C-Ph), 128.0 (*d*, C-Ph), 128.4 (*d*, C-Ph), 128.7 (*d*, C-Ph), 128.8 (*d*, C-Ph), 130.0 (*s*, C-3), 131.9 (*d*, C-Ph), 135.7 (*s*, C-2), 135.7 (*s*, C-Ph), 137.8 (*d*, C-13), 141.1 (*s*, C-Ph), 141.8 (*d*, C-5), 164.1 (*s*, NCO), 170.1 (*s*, C-1′); EIMS 70 eV, m/z (rel. int.): 481 $[M]^+$ (6), 268 (100), 223 (8), 222 (42), 215 (14), 214 (72), 199 (41), 193 (33), 158 (28), 145 (5), 143 (7), 119 (10), 105 (23), 91 (17), 77 (8); HR EIMS *m*/*z*: $[M]^+$ calc. for $C_{31}H_{31}O_4N$: 481.22531, found: 481.22887.

4.4.5. Compound **20**

TLC $R_f = 0.63$ (C_6H_6–Me_2CO 8:2); mp 58–63 °C; $[\alpha]_D^{20} = -31.38°$ ($CHCl_3$, *c* 1.0); UV λ_{max} (EtOH) nm: 242 (ε 24950); IR ν_{max} (KBr) cm^{-1}: 3439, 3063, 2952, 2869, 1758, 1655; ^1H NMR: δ 1.09 (3H, *s*, H-15), 1.15 (3H, *s*, H-14), 1.29 (3H, *s*, H-12), 1.58–1.59 (2H, *m*, H-10), 1.63 (2H, *dd*, $J_{1\alpha,1\beta} = 13.5$ Hz and $J = 5.9$ Hz, H-1), 2.35–2.41 (1H, *m*, H-2α), 2.49–2.55 (1H, *m*, 9α), 2.56 (1H, *d*, $J_{4\beta,4\alpha} = 15.0$ Hz, H-4β), 2.82 (1H, *d*, $J_{4\alpha,4\beta} = 15.0$ Hz, H-4α), 5.00 (1H, *d*, $J_{2',3'} = 6.2$ Hz, H-2′), 5.52 (1H, *d*, $J_{3',2'} = 6.2$ Hz, H-3′), 6.06 (1H, *d*, $J_{8\beta,9\alpha} = 10.8$ Hz, H-8β), 7.13 (1H, *br s*, H-5), 7.24 (1H, *br s*, H-13), 7.28–7.57 (8H, *m*, H-Ph), 8.08–8.13 (2H, *m*, H-Ph); ^{13}C NMR: δ 30.6 (*q*, C-12), 31.8 (*q*, C-14), 32.1 (*q*, C-15), 32.5 (*t*, C-4), 35.3 (*s*, C-11), 42.6 (*t*, C-1), 43.6 (*t*, C-10), 44.8 (*d*, C-9), 53.9 (*d*, C-2), 70.7 (*d*, C-8), 71.3 (*s*, C-3), 74.7 (*d*, C-3′), 83,1 (*d*, C-2′), 118.1 (*s*, C-6), 125.1 (*s*, C-7), 126.4 (*d*, C-Ph), 126.6 (*s*, C-Ph), 128.1 (*d*, C-Ph), 128.5 (*d*, C-Ph), 128.7 (*d*, C-Ph), 128.9 (*d*, C-Ph), 132.0 (*d*, C-Ph), 138.9 (*d*, C-5), 140.9 (*s*, C-Ph), 141.9 (*d*, C-13), 164.1 (*s*, NCO), 169.1 (*s*, C-1′); EIMS 70 eV, *m*/*z* (rel. int.): 499 $[M]^+$ (3), 481 (6), 464 (7), 446 (5), 268 (16), 232 (32), 223 (16), 222 (100), 217 (14), 199 (7), 193 (58), 189 (13), 165 (6), 145 (2), 137 (3), 119 (4), 105 (15), 91 (9), 77 (6), 43 (4); HR LSIMS *m*/*z*: $[M+H]^+$ calc. for $C_{31}H_{34}O_5N$: 500.24371, found: 500.24270.

4.4.6. Compound **23**

TLC $R_f = 0.27$, (hexane–EtOAc 7:3); mp 64–68 °C; $[\alpha]_D^{20} = -21.2°$ ($CHCl_3$, *c* 1.0); UV λ_{max} (EtOH) nm: 242 (ε 16768); IR ν_{max} ($CHCl_3$) cm^{-1}: 3066, 2955, 2867, 1960, 1748, 1654; ^1H NMR: δ 0.95 (3H, *s*, H-15), 1.00 (3H, *s*, H-14), 1.05 (3H, *s*, H-12), 1.41 (1H, *dd*, $J_{10\alpha,10\beta} = 12.6$ Hz and $J_{10\alpha,9\beta} = 10.6$ Hz, H-10α), 1.50 (1H, *dd*, $J_{1\beta,1\alpha} = 12.9$ Hz and $J_{1\beta,2\alpha} = 10.8$ Hz, H-1β), 1.70 (1H, *dd*, $J_{10\beta,10\alpha} = 12.6$ Hz and $J_{10\beta,9\beta} = 7.0$ Hz, H-10β), 1.80 (1H, *dd*, $J_{1\alpha,1\beta} = 12.9$ Hz and $J_{1\alpha,2\alpha} = 8.1$ Hz, H-1α), 2.02–2.10 (1H, *m*, H-9β), 2.13–2.19 (1H, *m*, H-2α), 2.59 (1H, *d*, $J_{4\beta,4\alpha} = 14.1$ Hz, H-4β), 2.69 (1H, *d*, $J_{4\alpha,4\beta} = 14.1$ Hz, H-4α), 4.98 (1H, *d*, $J_{2',3'} = 6.4$ Hz, H-2′), 5.49 (1H, *d*, $J_{3',2'} = 6.4$ Hz, H-3′), 5.86 (1H, *d*, $J_{8\alpha,9\beta} = 10.3$ Hz, H-8α), 7.16 (1H, *s*, H-5), 7.20 (1H, *s*, H-13), 7.30–7.57 (8H, *m*, H-Ph), 8.09–8.14 (2H, *m*, H-Ph); ^{13}C NMR: δ 20.7 (*q*, C-12), 31.0 (*q*, C-15), 31.2 (*q*, C-14), 34.7 (*s*, C-11), 40.1 (*t*, C-4), 43.2 (*t*, C-1), 46.1 (*t*, C-10), 46.5 (*d*, C-9), 55.1 (*d*, C-2), 73.3 (*s*, C-3), 74.8 (*d*, C-3′), 75.7 (*d*, C-8), 83.3 (*d*, C-2′), 119.1 (*s*, C-6), 124.9 (*s*, C-7), 126.5 (*d*, C-Ph), 126.7 (*s*, C-Ph), 128.2 (*d*, C-Ph), 128.5 (*d*, C-Ph),

128.7 (*d*, C-Ph), 128.9 (*d*, C-Ph), 132.0 (*d*, C-Ph), 138.2 (*d*, C-5), 140.8 (*s*, C-Ph), 140.9 (*d*, C-13), 164.0 (*s*, NCO), 169.3 (*s*, C-1′); EIMS 70 eV, *m*/*z* (rel. int.): 499 $[M]^+$ (1.5), 269 (17), 268 (98), 266 (20), 234 (51), 222 (40), 217 (10), 194 (12), 193 (71), 189 (28),165 (19), 145 (7), 143 (4), 137 (10), 119 (35), 105 (56), 91 (100), 77 (40), 43 (97); HR EIMS *m*/*z*: $[M]^+$ calc. for $C_{31}H_{33}O_5N$: 499.23587, found: 499.23743.

4.4.7. Compound **26**

TLC $R_f = 0.46$ (hexane–EtOAc 8:2); mp 50–53 °C; $[\alpha]_D^{20} = -46.43°$ ($CHCl_3$, *c* 1.0); UV λ_{max} (EtOH) nm: 242 (ε 10297); IR ν_{max} ($CHCl_3$) cm^{-1}: 2955, 2872, 1755, 1654; ^1H NMR: δ 0.90 (3H, *t*, $J_{CH_2CH_3} = 6.9$ Hz, $-OCH_2CH_3$), 1.08 (3H, *s*, H-15), 1.16 (3H, *s*, H-14), 1.20 (3H, *s*, H-12), 1.57–1.61 (3H, *m*, H-1α, H-10α and H-10β), 1.69 (1H, *t*, $J_{1\beta,1\alpha} = 12.8$ Hz, H-1β), 2.37-2.42 (1H, *m*, H-2α), 2.58 (1H, *dd*, $J_{4\beta,4\alpha} = 15.2$ Hz and $J = 1.2$ Hz, H-4β), 2.59–2.64 (1H, *m*, H-9α), 2.75 (1H, *d*, $J_{4\alpha,4\beta} = 15.2$ Hz, H-4α), 3.28 (1H, *qn*, $J_{CH_2CH_3} = 6.9$ Hz, $-OCH_2CH_3$), 3.36 (1H, *qn*, $J_{CH_2CH_3} = 6.9$ Hz, $-OCH_2CH_3$), 5.00 (1H, *d*, $J_{2',3'} = 6.4$ Hz, H-2′), 5.54 (1H, *d*, $J_{3',2'} = 6.4$ Hz, H-3′), 6.06 (1H, *d*, $J_{8\beta,9\alpha} = 11.4$ Hz, H-8β), 7.05 (1H, *s*, H-5), 7.13 (1H, *t*, $J = 1.3$ Hz, H-13), 7.29–7.57 (8H, *m*, H-Ph), 8.09–8.13 (2H, *m*, H-Ph); ^{13}C NMR: δ 15.7 (*q*, $-CH_2CH_3$), 25.5 (*q*, C-12), 28.9 (*t*, C-4), 32.2 (*q*, C-14), 32.7 (*q*, C-15), 34.9 (*s*, C-11), 41.7 (*t*, C-1), 43.5 (*t*, C-10), 44.5 (*d*, C-9), 52.5 (*d*, C-2), 55.6 (*t*, $-CH_2CH_3$), 75.4 (*s*, C-3), 74.8 (*d*, C-3′), 77.2 (*d*, C-8), 83.2 (*d*, C-2′), 119.3 (*s*, C-6), 125.6 (*s*, C-7), 126.4 (*d*, C-Ph), 126.7 (*s*, C-Ph), 128.0 (*d*, C-Ph), 128.4 (*d*, C-Ph), 128.7 (*d*, C-Ph), 128.9 (*d*, C-Ph), 131.9 (*d*, C-Ph), 137.7 (*d*, C-5), 140.3 (*d*, C-13), 141.1 (*s*, C-Ph), 164.1 (*s*, NCO), 169.3 (*s*, C-1′); EIMS 70 eV, *m*/*z* (rel. int.): 527 $[M]^+$ (4), 512 $[M\text{-}CH_3]^+$ (2), 498 $[M\text{-}C_2H_5]^+$ (2), 269 (18), 268 (100), 260 (12), 223 (11), 222 (40), 215 (20), 193 (32), 165 (6), 137 (6), 105 (20), 91 (26) 77 (11), 43 (16); HR EIMS *m*/*z*: $[M-C_2H_5]^+$ calc. for $C_{31}H_{32}O_5N$: 498.22805, found: 498.22811.

4.4.8. Compound **29**

TLC $R_f = 0.57$ (hexane–EtOAc 7:3); mp 62–64 °C; $[\alpha]_D^{20} = -47.90°$ ($CHCl_3$, *c* 1.0); UV λ_{max} (EtOH) nm: 196 (ε 76709); 242 (ε 20511); IR ν_{max} (KBr) cm^{-1}: 3448, 2952, 2866, 1758, 1655; ^1H NMR: δ 0.92 (3H, *s*, H-15), 1.13 (3H, *s*, H-14), 1.44 (1H, *dd*, $J_{10\beta,10\alpha} = 12.5$ Hz and $J_{10\beta,9\alpha} = 9.0$ Hz, H-10β), 1.86 (1H, *dd*, $J_{10\alpha,10\beta} = 12.5$ Hz and $J_{10\alpha,9\alpha} = 4.7$ Hz, H-10α), 1.77 (3H, *s*, H-12), 2.13 (1H, *d*, $J_{1\beta,1\alpha} = 15.8$ Hz, H-1β), 2.28 (1H, *d*, $J_{1\alpha,1\beta} = 15.8$ Hz, H-1α), 2.97 (1H, *d*, $J_{4\beta,4\alpha} = 20.3$ Hz, H-4β), 3.18 (1H, *d*, $J_{4\alpha,4\beta} = 20.3$ Hz, H-4α), 3.15-3.28 (1H, *m*, H-9α), 4.64 (2H, *ABq*, $J_{AB} = 17.0$ Hz, H-13α and H-13β), 4.96 (1H, *d*, $J_{2',3'} = 6.1$ Hz, H-2′), 5.47 (1H, *d*, $J_{3',2'} = 6.1$ Hz, H-3′), 5.69 (1H, *d*, $J_{8\beta,9\alpha} = 10.9$ Hz, H-8β), 7.31–7.58 (8H, *m*, H-Ph), 8.08–8.11 (2H, *m*, H-Ph); ^{13}C NMR: δ 22.6 (*q*, C-12), 27.1 (*q*, C-15), 28.5 (*q*, C-14), 30.3 (*t*, C-4), 37.2 (*s*, C-11), 45.0 (*d*, C-9), 45.4 (*t*, C-1), 46.5 (*t*, C-10), 69.6 (*t*, C-13), 73.3 (*d*, C-8), 74.8 (*d*, C-3′), 82.8 (*d*, C-2′), 126.4 (*s*, C-2), 126.4 (*s*, C-3), 127.0 (*s*, C-6), 128.3 (*d*, C-Ph), 128.6 (*d*, C-Ph), 128.7 (*d*, C-Ph), 128.8 (*d*, C-Ph), 129.0 (*d*, C-Ph), 132.2 (*d*, C-Ph), 135.5 (*s*, C-Ph), 140.6 (*s*, C-Ph), 155.9 (*s*, C-7), 163.9 (*s*, NCO), 169.8 (*s*, C-5), 173.6 (*s*, C-1′); LSIMS *m*/*z* (rel. int.): 498 $[M+H]^+$ (60), 460 (2), 313 (2), 307 (23), 289 (11), 268 (67), 231 (6), 229 (6), 166 (6), 154 (100), 137 (76), 120 (18), 105 (26); HR LSIMS *m*/*z*: $[M+H]^+$ calc. for $C_{31}H_{32}O_5N$: 498.22806, found: 498.23098.

4.4.9. Compound **32**

TLC $R_f = 0.41$ (C_6H_6-Me_2CO 8:2); mp 83–86 °C; $[\alpha]_D^{20} = -20.45°$ ($CHCl_3$, *c* 1.0,); IR ν_{max} ($CHCl_3$) cm^{-1}: 3592, 3507, 2958, 2871, 1756, 1655; ^1H NMR: δ 1.05 (3H, *s*, H-15), 1.14 (3H, *s*, H-14), 1.28 (3H, *s*, H-12), 1.39 (1H, *dd*, $J_{10\beta,10\alpha} = 13.3$ Hz and $J_{10\beta,9\alpha} = 7.1$ Hz, H-10β), 1.55 (1H, *t*, $J = 12.9$ Hz, H-1β), 1.66 (1H, *dd*, $J_{10\alpha,10\beta} = 13.3$ Hz and $J_{10\alpha,9\alpha} = 6.0$ Hz, H-10α), 1.70 (1H, *dd*, $J_{1\alpha,1\beta} = 12.9$ Hz and $J_{1\alpha,2\alpha} = 6.9$ Hz, H-1α), 2.49-2.55 (1H, *m*, H-2α), 2.62 (2H, *ABq*, $J = 17.3$ Hz, H-4α and H-4β), 2.73-2.80 (1H, *m*, H-9α), 4.56 (1H, *d*, $J_{13\beta,13\alpha} = 17.3$ Hz, H-13β), 4.70 (1H, *d*, $J_{13\alpha,13\beta} = 17.3$ Hz, H-13α), 4.96 (1H, *d*, $J_{2',3'} = 6.2$ Hz, H-2′), 5.47 (1H, *d*, $J_{3',2'} = 6.2$ Hz, H-3′), 6.00 (1H, *d*, $J_{8\beta,9\alpha} = 10.3$ Hz, H-8β), 7.30–7.57 (8H, *m*, H-Ph), 8.06–8.10 (2H, *m*, H-Ph); ^{13}C NMR: δ 28.6 (*q*, C-14), 29.5 (*q*, C-12), 30.7 (*q*, C-15), 35.8 (*t*, C-4), 35.9 (*s*, C-11), 42.6 (*d*, C-9), 42.7 (*t*, C-10), 47.7 (*t*, C-1), 52.1 (*d*, C-2), 69.5 (*t*, C-13), 71.5 (*s*, C-3), 72.5 (*d*, C-8), 74.7 (*d*, C-3′), 82.8 (*d*, C-2′), 125.7 (*s*, C-6), 126.3 (*s*, C-Ph), 126.4 (*d*, C-Ph), 128.3 (*d*, C-Ph), 128.6 (*d*, C-Ph), 128.7 (*d*, C-Ph), 129.0 (*d*, C-Ph), 132.2 (*d*, C-Ph), 140.5 (*s*, C-Ph), 157.1 (*s*, C-7), 163.9 (*s*, NCO), 169.5 (*s*, C-5), 173.9 (*s*, C-1′); LSIMS *m*/*z* (rel. int.): 516 $[M+H]^+$ (60), 498 (4), 307 (14), 289 (8), 268 (77), 225 (15), 154 (100), 136 (77), 105 (44); HR LSIMS *m*/*z*: $[M+H]^+$ calc. for $C_{31}H_{34}O_6N$: 516.23859, found: 516.23648.

4.4.10. Compound **35**

TLC $R_f = 0.28$ (hexane–EtOAc 6:4); mp 83–87 °C; $[\alpha]_D^{20} = -66.59°$ ($CHCl_3$, *c* 1.0); UV λ_{max} (EtOH) nm: 194 (ε 52202); IR ν_{max} ($CHCl_3$) cm^{-1}: 3593, 3030, 2958, 2868, 1751, 1655; ^1H NMR: δ 0.91 (3H, *s*, H-15), 0.97 (3H, *s*, H-14), 1.04 (1H, *t*, $J_{1\beta,1\alpha} = 12.7$ Hz, H-1β), 1.12 (1H, *t*, $J = 12.2$ Hz, H-10β), 1.28 (3H, *s*, H-12), 1.43 (1H, *dd*, $J_{10\alpha,10\beta} = 12.2$ Hz and $J_{10\alpha,9\alpha} = 7.0$ Hz, H-10α), 1.55 (1H, *dd*, $J_{1\alpha,1\beta} = 12.7$ Hz and $J_{1\alpha,2\alpha} = 7.9$ Hz, H-1α), 2.47 (1H, *d*, $J_{4\beta,4\alpha} = 19.2$ Hz, H-4β), 2.57–2.63 (1H, *m*, H-2α), 2.64 (1H, *dq*, $J_{4\alpha,4\beta} = 19.2$ Hz and $J = 3.0$ Hz, H-4α), 2.93–3.01 (1H, *m*, H-9α), 4.65 (2H, *br s*, H-13), 4.93 (1H, *d*, $J_{2',3'} = 6.0$ Hz, H-2′), 5.39 (1H, *d*, $J_{3',2'} = 6.0$ Hz, H-3′) 6.96 (1H, *br s*, H-8α), 7.30–7.57 (8H, *m*, H-Ph), 8.06–8.09 (2H, *m*, H-Ph); ^{13}C NMR: δ 26.2 (*q*, C-15), 28.9 (*q*, C-14), 32.4 (*q*, C-12), 34.9 (*t*, C-4), 37.7 (*s*, C-11), 43.9 (*d*, C-9), 42.2 (*t*, C-10), 44.6 (*t*, C-1), 49.1 (*d*, C-2), 70.4 (*t*, C-13), 73.8 (*s*, C-3), 74.0 (*d*, C-8), 75.0 (*d*, C-

3′), 83.1 (*d*, C-2′), 122.6 (*s*, C-6), 126.4 (*d*, C-Ph), 126.4 (*s*, C-Ph), 128.3 (*d*, C-Ph), 128.6 (*d*, C-Ph), 128.6 (*d*, C-Ph), 129.0 (*d*, C-Ph), 132.2 (*d*, C-Ph), 140.4 (*s*, C-Ph), 157.9 (*s*, C-7), 163.9 (*s*, NCO), 174.3 (*s*, C-5), 174.3 (*s*, C-1′); LSIMS *m/z* (rel. int.): 516 $[M+H]^+$ (24), 369 (3), 307 (16), 268 (25), 222 (4), 154 (100), 137 (76); HR LSIMS *m/z*: $[M+H]^+$ calc. for $C_{31}H_{34}O_6N$: 516.23861, found: 516.23900.

4.4.11. Compound **38**

TLC $R_f = 0.26$ (hexane–Me_2CO 7:3); mp 90–92 °C; $[\alpha]_D^{20} = -41.2°$ ($CHCl_3$, *c* 1.0); UV no peaks found; IR ν_{max} (KBr) cm^{-1}: 3448, 3064, 2953, 2866, 1758, 1655; ^1H NMR: δ 0.96 (3H, *s*, H-15), 1.06 (3H, *s*, H-14), 1.09 (3H, *s*, H-12), 1.38 (1H, *dd*, $J_{10\alpha,10\beta} = 12.6$ Hz and $J_{10\alpha,9\beta} = 10.7$ Hz, H-10α), 1.53 (1H, *dd*, $J_{1\beta,1\alpha} = 13.3$ Hz and $J_{1\beta,2\alpha} = 10.5$ Hz, H-1β), 1.66 (1H, *dd*, $J_{10\beta,10\alpha} = 12.6$ Hz and $J_{10\beta,9\beta} = 6.9$ Hz, H-10β), 1.86 (1H, *dd*, $J_{1\alpha,1\beta} = 13.3$ Hz and $J_{1\alpha,2\alpha} = 8.3$ Hz, H-1α), 2.13–2.21 (1H, *m*, H-9), 2.24–2.31 (1H, *m*, H-2α), 2.36 (1H, *dq*, $J_{4\beta,4\alpha} = 15.1$ Hz and $J = 3.0$ Hz, H-4β), 2.81 (1H, *d*, $J_{4\alpha,4\beta} = 15.1$ Hz, H-4α), 4.63 (1H, *ddd*, $J_{13\beta,13\alpha} = 17.6$ Hz, $J = 3.1$ Hz and $J = 1.3$ Hz, H-13β), 4.75 (1H, *dq*, $J_{13\alpha,13\beta} = 17.6$ Hz and $J = 1.6$ Hz, H-13α), 4.98 (1H, *d*, $J_{2',3'} = 6.2$ Hz, H-2′), 5.44 (1H, *d*, $J_{3',2'} = 6.2$ Hz, H-3′), 5.89 (1H, *dd*, $J_{8\alpha,9\beta} = 10.7$ Hz and $J = 1.9$ Hz, H-8α), 7.31–7.59 (8H, *m*, H-Ph), 8.08–8.10 (2H, *m*, H-Ph); ^{13}C NMR: δ 20.7 (*q*, C-12), 30.8 (*q*, C-15), 31.2 (*q*, C-14), 34.3 (*s*, C-11), 39.5 (*t*, C-4), 43.4 (*t*, C-10), 44.0 (*d*, C-9), 46.2 (*t*, C-1), 54.4 (*d*, C-2), 68.9 (*t*, C-13), 72.1 (*s*, C-3), 75.0 (*d*, C-3′), 76.7 (*d*, C-8), 83.0 (*d*, C-2′), 124.5 (*s*, C-6), 126.3 (*s*, C-Ph), 126.4 (*d*, C-Ph), 128.4 (*d*, C-Ph), 128.6 (*d*, C-Ph), 128.6 (*d*, C-Ph), 129.0 (*d*, C-Ph), 132.2 (*d*, C-Ph), 140.3 (*s*, C-Ph), 159.1 (*s*, C-7), 163.8 (*s*, NCO), 169.4 (*s*, C-1′), 173.6 (*s*, C-5); LSIMS *m/z* (rel. int.): 1031 $[2M+H]^+$ (3), 516 $[M+H]^+$ (95), 499 (18), 307 (11), 268 (100), 222 (18), 193 (5), 154 (77), 137 (53), 105 (45); HR LSIMS *m/z*: $[M+H]^+$ calc. for $C_{31}H_{34}O_6N$: 516.23861, found: 516.23779.

4.4.12. Compound **41**

TLC $R_f = 0.26$ (hexane–EtOAc 4:6); mp 76–80 °C; $[\alpha]_D^{20} = -36.29°$ ($CHCl_3$, *c* 1.0); UV λ_{max} (EtOH) nm: 194 (ε 57717); IR ν_{max} ($CHCl_3$) cm^{-1}: 3566, 2958, 2869, 1764, 1654; ^1H NMR: δ 0.99 (3H, *s*, H-15), 1.06 (3H, *s*, H-14), 1.16 (1H, *t*, $J_{10\beta,10\alpha} = 11.9$ Hz, H-10β), 1.23 (3H, *s*, H-12), 1.25 (1H, *t*, $J_{1\beta,1\alpha} = 7.2$ Hz, H-1β), 1.62 (1H, *t*, $J_{10\alpha,10\beta} = 11.9$ Hz, H-10α), 1.67–1.74 (1H, *m*, H-1α), 2.56 (1H, *d*, $J_{4\beta,4\alpha} = 18.8$ Hz, H-4β), 2.62–2.69 (1H, *m*, H-2α), 2.80 (1H, *d*, $J_{4\alpha,4\beta} = 18.8$ Hz, H-4α), 2.85–2.91 (1H, *m*, H-9α), 4.61 (2H, *ABq*, $J_{AB} = 17.0$ Hz, H-5α and H-5β), 4.97 (1H, *d*, $J_{2',3'} = 6.5$ Hz, H-2′), 5.50 (1H, *d*, $J_{3',2'} = 6.5$ Hz, H-3′), 5.96 (1H, *d*, $J_{8\beta,9\alpha} = 5.2$ Hz, H-8β), 7.26–7.55 (8H, *m*, H-Ph), 8.08–8.11 (2H, *m*, H-Ph); ^{13}C NMR: δ 26.9 (*q*, C-15), 29.4 (*q*, C-14), 29.6 (*q*, C-12), 36.5 (*s*, C-11), 38.6 (*t*, C-4), 42.5 (*d*, C-9), 45.1 (*t*, C-10), 45.2 (*t*, C-1), 50.6 (*d*, C-2), 73.1 (*s*, C-3), 69.6 (*d*, C-8), 71.9 (*t*, C-5), 74.3 (*d*, C-3′), 83.1 (*d*, C-2′), 122.9 (*s*, C-7), 126.6 (*d*, C-Ph), 126.6 (*s*, C-Ph), 128.0 (*d*, C-Ph), 128.3 (*d*, C-Ph), 128.7 (*d*, C-Ph), 128.8 (*d*, C-Ph), 131.9 (*d*, C-Ph), 140.7 (*s*, C-Ph), 151.9 (*s*, C-6), 163.9 (*s*, NCO), 168.4 (*s*, C-13), 172.5 (*s*, C-1′); LSIMS *m/z* (rel. int.): 516 $[M+H]^+$ (58), 403 (1), 379 (1), 359 (1), 337 (1), 307 (3), 268 (85), 249 (11), 222 (12), 154 (42), 136 (38), 105 (73), 81 (100); HR LSIMS *m/z*: $[M+H]^+$ calc. for $C_{31}H_{34}O_6N$: 516.23861, found: 516.23737.

4.5. General method for the hydrolysis of esters of (4S,5R)-2,4-diphenyl-4,5-dihydro-oxazol-5-carboxylic acid and sesquiterpenoid alcohols of Lactarius origin into (2S,3R)-phenyl-isoserinates

A sesquiterpenoid alcohol (4*S*,5*R*)-2,4-diphenyl-oxazol-5-carboxylate (0.2 mmol) dissolved in methanol (25 ml) was chilled to 0 °C and treated with 0.5 N aq. HCl solution (2.5 ml). The reaction must be carried out at 0 °C. After completion of the reaction the solution was neutralised with saturated aq. sodium hydrogen carbonate solution (pH = 7) and left for 15 min. Subsequently the solution was diluted with water (75 ml) and extracted with chloroform (3×40 ml). The chloroform extract was dried over magnesium sulphate, filtered and evaporated to dryness leaving a residue, which was purified by chromatography in proper solvent system and gave the desired *N*-benzoylphenylisoserinate.

4.5.1. Compound **9**

TLC $R_f = 0.21$ (hexane–EtOAc 7:3); mp 60–63 °C; $[\alpha]_D^{20} = +15.83°$ ($CHCl_3$, *c* 1.0); UV λ_{max} (EtOH) nm: 226 (ε 17509); IR ν_{max} ($CHCl_3$) cm^{-1}: 3683, 3519, 3440, 2955, 2866, 1731, 1702, 1664, 1511; ^1H NMR: δ 0.95 (3H, *s*, H-15), 0.98 (3H, *s*, H-14), 1.23 (1H, *t*, $J_{10\beta,10\alpha} = 13.0$ Hz, H-10β), 1.26 (3H, *s*, H-12), 1.29 (1H, *d*, $J_{4\beta,4\alpha} = 4.5$ Hz, H-4β), 1.30 (1H, *dd*, $J_{1\alpha,1\beta} = 13.3$ Hz and $J_{1\alpha,2\alpha} = 1.8$ Hz, H-1α), 1.59 (1H, *dd*, $J_{10\alpha,10\beta} = 13.0$ Hz and $J_{10\alpha,9\alpha} = 7.6$ Hz, H-10α), 1.72 (1H, *dd*, $J_{1\beta,1\alpha} = 13.3$ Hz and $J_{1\beta,2\alpha} = 8.0$ Hz, H-1β), 1.80 (1H, *d*, $J_{4\alpha,4\beta} = 4.5$ Hz, H-4α), 2.42–2.50 (2H, *m*, H-2α and H-9α), 4.58 (1H, *d*, $J_{2',3'} = 2.2$ Hz, H-2′), 4.84 (1H, *d*, $J_{13\beta,13\alpha} = 12.1$ Hz, H-13β), 5.29 (1H, *d*, $J_{13\alpha,13\beta} = 12.1$ Hz, H-13α), 5.33 (1H, br *s*, H-8), 5.63 (1H, *dd*, $J_{3',NH} = 8.9$ Hz and $J_{3',2'} = 2.2$ Hz, H-3′), 7.05 (1H, *d*, $J_{NH,3'} = 8.9$ Hz, NH), 7.26–7.52 (8H, *m*, H-Ph), 7.74–7.77 (2H, *m*, H-Ph), 9.40 (1H, *s*, H-5); ^{13}C NMR: δ 20.0 (*q*, C-12), 31.0 (*t*, C-4), 31.6 (*q*, C-14), 31.7 (*q*, C-15), 35.5 (*s*, C-11), 36.9 (*s*, C-3), 37.3 (*s*, C-6), 38.3 (*d*, C-2), 42.5 (*d*, C-9), 44.8 (*t*, C-10), 47.5 (*t*, C-1), 54.5 (*d*, C-3′), 68.5 (*t*, C-13), 73.2 (*d*, C-2′), 126.9 (*d*, C-Ph), 127.0 (*s*, C-Ph), 127.9 (*d*, C-Ph), 128.5 (*d*, C-Ph), 128.6 (*d*, C-Ph), 129.9 (*s*, C-7), 131.7 (*d*, C-Ph), 131.8 (*s*, C-8), 134.1 (*s*, C-Ph), 138.8 (*s*, C-Ph), 166.7 (*s*, NCO), 172.6 (*s*, C-1′), 200.6 (*s*, C-5); LSIMS *m/z* (rel. int.): 524 $[M+Na]^+$ (9), 484 (4), 446 (12), 330 (5), 308 (28), 286 (14), 231

(28), 215 (16), 154 (20), 111 (21), 105 (100); HR LSIMS *m/z*: $[M+Na]^+$ calcd for $C_{31}H_{33}O_5NNa$: 524.24129, found: 524.24127.

4.5.2. Compound ***12***

TLC $R_f = 0.21$ (hexane–EtOAc 1:1); mp 104–108 °C; $[\alpha]_D^{20} = -9.82°$ ($CHCl_3$, *c* 1.0); UV λ_{max} (EtOH) nm: 223 (ε 16399); IR ν_{max} (KBr) cm^{-1}: 3431, 2953, 2865, 1768, 1745,1651; ^1H NMR: δ 0.68 (3H, *s*, H-15), 0.80 (3H, *s*, H-14), 1.07–1.12 (2H, *m*, H-5β and H-10β), 1.36–1.45 (2H, *m*, H-1β and H-10α), 1.56 (1H, *dd*, $J = 11.9$ Hz and $J = 2.5$ Hz, H-1α), 1.58 (3H, *s*, H-12), 1.69 (1H, *d*, $J_{5\alpha,5\beta} = 6.2$ Hz, H-5α), 2.03–2.12 (2H, *m*, H-2α and H-9α), 4.10 (1H, *d*, $J_{13\beta,13\alpha} = 9.3$ Hz, H-13β), 4.23 (1H, *d*, $J_{13\alpha,13\beta} = 9.3$ Hz, H-13α), 4.65 (1H, *d*, $J_{2',3'} = 2.0$ Hz, H-2′), 5.67 (1H, *d*, $J_{8\beta,9\alpha} = 8.0$ Hz, H-8β), 5.77 (1H, *dd*, $J_{3',NH} = 9.1$ Hz, $J_{3',2'} = 2.0$ Hz, H-3′), 7.15 (1H, *d*, $J_{NH,3'} = 9.1$, NH), 7.25–7.53 (8H, *m*, H-Ph), 7.76–7.80 (2H, *m*, H-Ph); ^{13}C NMR: δ 18.4 (*t*, C-5), 24.4 (q, C-12), 26.2 (*q*, C-15), 28.4 (*q*, C-14), 31.3 (*s*, C-11), 38.1 (*s*, C-6), 38.7 (*s*, C-7), 39.9 (*t*, C-1), 40.0 (*d*, C-2), 46.1 (*d*, C-9), 46.6 (*t*, C-10), 54.6 (*d*, C-3′), 71.0 (*s*, C-3), 71.2 (*t*, C-13), 73.5 (*d*, C-8), 80,2 (*d*, C-2′), 126.9 (*d*, C-Ph), 127.1 (*d*, C-Ph), 127.8 (*d*, C-Ph), 128.6 (*d*, C-Ph), 128.6 (*d*, C-Ph), 131.9 (*d*, C-Ph), 133.7 (*s*, C-Ph), 138.6 (*s*, C-Ph), 166.4 (*s*, NCO), 172.6 (*s*, C-1′), 175.1 (*s*, C-4); LSIMS m/z (rel. int.): 534 $[M+H]^+$ (4), 516 (3), 307 (8), 286 (100), 249 (3), 231 (12), 210 (20), 176 (2), 154 (56), 137 (46), 123 (24), 105 (60); HR LSIMS *m/z*: $[M+Na]^+$ calc. for $C_{31}H_{35}O_7NNa$: 556.23114, found: 556.23308.

4.5.3. Compound ***15***

TLC $R_f = 0.25$ (hexane–EtOAc 55:45); mp 176–183 °C; $[\alpha]_D^{20} = +49.6°$ ($CHCl_3$, *c* 1.0); UV λ_{max} (EtOH) nm: 228 (ε 14420); IR ν_{max} ($CHCl_3$) cm^{-1}: 3555, 3436, 2935, 2858, 1769, 1730,1657; ^1H NMR: δ 0.73 (3H, *s*, H-15), 0.80 (3H, *s*, H-14), 0.91 (1H, *t*, $J_{10\beta,10\alpha} = 11.7$ Hz, H-10β), 1.05 (1H, *d*, $J_{5\beta,5\alpha} = 6.2$ Hz, H-5β), 1.20–1.30 (2H, *m*, H-1α and H-10α), 1.31 (3H, *s*, H-12), 1.41 (1H, *t*, $J_{1\beta,2\alpha} = 12.1$ Hz, H-1β), 1.48 (1H, *d*, $J_{5\alpha,5\beta} = 6.2$ Hz, H-5α), 1.86–1.92 (1H, *m*, H-2α), 2.14–2.21 (1H, *m*, H-9α), 3.87 (1H, *d*, $J_{13\beta,13\alpha} = 9.3$ Hz, H-13β), 4.02 (1H, *d*, $J_{13\alpha,13\beta} = 9.3$ Hz, H-13α), 4.86 (1H, *d*, $J_{2',3'} = 2.1$ Hz, H-2′), 5.65 (1H, *d*, $J_{8\alpha,9\alpha} = 4.5$ Hz, H-8α), 5.83 (1H, *dd*, $J_{3',NH} = 9.3$ Hz, $J_{3',2'} = 2.1$ Hz, H-3′), 7.23–7.51 (9H, *m*, NH and H-Ph), 7.80–7.84 (2H, *m*, H-Ph); ^{13}C NMR: δ 19.4 (*t*, C-5), 24.9 (*q*, C-12), 26.3 (*q*, C-14), 28.6 (*q*, C-15), 32.0 (*s*, C-7), 32.1 (*s*, C-6), 34.6 (*s*, C-11), 37.5 (*d*, C-9), 39.5 (*t*, C-1), 41.9 (*t*, C-10), 44.2 (*d*, C-2), 54.8 (*d*, C-3′), 68.2 (*t*, C-13), 69.7 (*s*, C-3), 70.4 (*d*, C-8), 73,8 (*d*, C-2′), 127.0 (*d*, C-Ph), 127.3 (*d*, C-Ph), 127.8 (*d*, C-Ph), 128.5 (*d*, C-Ph), 128.6 (*d*, C-Ph), 131.6 (*d*, C-Ph), 134.2 (*s*, C-Ph), 138.7 (*s*, C-Ph), 166.9 (*s*, NCO), 172.0 (*s*, C-1′), 174.2 (*s*, C-4); LSIMS m/z (rel. int.): 556 $[M+Na]^+$ (22), 534 $[M+H]^+$ (4), 516 (3), 338 (8), 312 (16), 286 (20), 240 (3), 225 (18), 210 (5), 154 (16), 136 (17), 105 (100); HR LSIMS *m/z*: $[M+Na]^+$ calc. for $C_{31}H_{35}O_7NNa$: 556.23114, found: 556.23175.

4.5.4. Compound ***18***

TLC $R_f = 0.23$ (hexane–EtOAc 8:2); mp 68–70 °C; $[\alpha]_D^{20} = -4.55°$ ($CHCl_3$, c 1.0); UV λ_{max} (EtOH) nm: no peaks found above threshold; IR ν_{max} ($CHCl_3$) cm^{-1}: 3423, 2952, 2864, 1736, 1645; ^1H NMR: δ 0.78 (6H, *s*, H-14 and H-15), 1.16 (1H, *dd*, $J_{10\beta,10\alpha} = 12.9$ Hz and $J_{10\beta,9\alpha} = 8.1$ Hz, H-10β), 1.73 (3H, *s*, H-12), 1.83 (1H, *dd*, $J_{10\alpha,10\beta} = 12.9$ Hz and $J_{10\alpha,9\alpha} = 7.9$ Hz, H-10α), 1.94 (1H, *d*, $J_{1\beta,1\alpha} = 15.0$ Hz, H-1β), 2.11 (1H, *d*, $J_{1\alpha,1\beta} = 15.0$ Hz, H-1α), 2.89 (1H, *d*, $J_{4\beta,4\alpha} = 15.9$ Hz, H-4β), 3.25–3.31 (1H, *m*, H-9α), 3.42 (1H, *d*, $J_{4\alpha,4\beta} = 15.9$ Hz, H-4α), 4.60 (1H, *d*, $J_{2',3'} = 2.0$ Hz, H-2′), 5.73 (1H, *dd*, $J_{3',NH} = 8.8$ Hz and $J_{3',2'} = 2.0$ Hz, H-3′), 5.81 (1H, *d*, $J_{8\beta,9\alpha} = 11.1$ Hz, H-8β), 7.12 (1H, *d*, $J_{NH,3'} = 8.8$ Hz, NH), 7.13 (1H, br *s*, H-5), 7.23 (1H, *s*, H-13), 7.26–7.53 (8H, *m*, H-Ph), 7.79–7.81 (2H, *m*, H-Ph); ^{13}C NMR: δ 21.5 (*q*, C-12), 27.2 (*q*, C-14), 28.2 (*q*, C-15), 29.3 (*t*, C-4), 37.5 (*s*, C-11), 44.4 (*d*, C-9), 45.8 (*t*, C-10), 45.8 (*t*, C-1), 54.7 (*d*, C-3′), 73.8 (*d*, C-8), 74.9 (*d*, C-2′), 121.6 (*s*, C-6), 124.8 (*s*, C-7), 126.8 (*d*, C-Ph), 127.1 (*d*, C-Ph), 127.8 (*d*, C-Ph), 128.5 (*d*, C-Ph), 128.6 (*d*, C-Ph), 130.1 (*s*, C-3), 131.7 (*d*, C-Ph), 134.0 (*s*, C-2), 136.0 (*s*, C-Ph), 137.8 (*d*, C-5), 138.9 (*s*, C-13), 141.8 (*d*, C-13), 166.4 (*s*, NCO), 172.8 (*s*, C-1′); LSIMS *m/z* (rel. int.): 522 $[M+Na]^+$ (14), 338 (5), 329 (26), 308 (43), 286 (48), 258 (4), 240 (4), 215 (44), 199 (6), 187 (4), 176 (100), 154 (78), 136 (56), 120 (12), 105 (37); HR LSIMS *m/z*: $[M+Na]^+$ calc. for $C_{31}H_{33}O_5NNa$: 522.22565, found: 522.22465.

4.5.5. Compound ***21***

TLC $R_f = 0.31$ (C_6H_6–Me_2CO 8:2); mp 72–75 °C; $[\alpha]_D^{20} = -5.67°$ ($CHCl_3$, *c* 1.0); UV λ_{max} (EtOH) nm: 193 (ε 64656); IR ν_{max} (KBr) cm^{-1}: 3401, 3065, 2929, 2856, 1757, 1646; ^1H NMR (CD_3OD): δ 0.80 (3H, *s*, H-15), 0.87 (3H, *s*, H-14), 1.21 (3H, *s*, H-12), 1.28–1.38 (2H, *m*, H-10), 1.51 (1H, *dd*, $J_{1\beta,1\alpha} = 13.0$ Hz and $J_{1\beta,2\alpha} = 7.4$ Hz, H-1β), 1.58 (1H, *dd*, $J_{1\alpha,1\beta} = 13.0$ Hz and $J_{1\alpha,2\alpha} = 1.3$ Hz, H-1α), 2.28–2.33 (1H, *m*, H-2α), 2.46–2.51 (1H, *m*, H-9α), 2.57 (1H, *d*, $J_{4\beta,4\alpha} = 15.0$ Hz, H-4β), 2.73 (1H, *d*, $J_{4\alpha,4\beta} = 15.0$ Hz, H-4α), 4.73 (1H, *d*, $J_{2',3'} = 3.4$ Hz, H-2′), 5.65 (1H, *d*, $J_{3',2'} = 3.4$ Hz, H-3′), 5.96 (1H, *dd*, $J_{8\beta,9\alpha} = 11.0$ Hz and $J = 1.2$ Hz, H-8β), 7.19 (1H, *br s*, H-5), 7.22 (1H, *br s*, H-13), 7.25–7.57 (8H, *m*, H-Ph), 7.85–7.92 (2H, *m*, H-Ph); ^{13}C NMR: δ 31.1 (*q*, C-12), 32.0 (*q*, C-15), 32.4 (*q*, C-14), 33.6 (*t*, C-4), 35.8 (*s*, C-11), 43.3 (*t*, C-1), 44.4 (*t*, C-10), 45.9 (*d*, C-9), 54.7 (*d*, C-2), 54.7 (*d*, C-3′), 72.1 (*d*, C-8), 72.5 (*s*, C-3), 74.9 (*d*, C-2′), 120.5 (*s*, C-6), 126.6 (*s*, C-7), 128.2 (*d*, C-Ph), 128.5 (*d*, C-Ph), 128.6 (*d*, C-Ph), 129.5 (*d*, C-Ph), 129.6 (*d*, C-Ph), 133.0 (*d*, C-Ph), 135.2 (*s*, C-Ph), 139.9 (*d*, C-13), 140.6 (*s*, C-Ph), 142.3 (*d*, C-5), 169.4 (*s*, NCO), 172.9 (*s*, C-1′); LSIMS *m/z* (rel. int.): 1057 $[2M+Na]^+$ (1), 540 $[M+Na]^+$ (24), 413 (5), 391 (3), 330 (22), 308 (100), 286

(95), 240 (8), 215 (24), 176 (95), 136 (60), 158 (28), 105 (98); HR LSIMS *m/z*: $[M+Na]^+$ calc. for $C_{31}H_{35}O_6NNa$: 540.23621, found: 540.23982.

4.5.6. Compound ***24***

TLC $R_f = 0.29$ (hexane–EtOAc 1:1); mp 95–98 °C; $[\alpha]_D^{20} = -17.80°$ ($CHCl_3$, *c* 1.0); UV λ_{max} (EtOH) nm: 195 (ε 51825); IR ν_{max} ($CHCl_3$) cm^{-1}: 3597, 3516, 3438, 2955, 2867, 1733, 1664; ^1H NMR: δ 0.98 (3H, *s*, H-15), 1.01 (3H, *s*, H-14), 1.02 (3H, *s*, H-12), 1.28 (1H, *dd*, $J_{10\alpha,10\beta} = 12.7$ Hz and $J_{10\alpha,9\beta} = 9.9$ Hz, H-10α), 1.50 (1H, *dd*, $J_{1\beta,1\alpha} = 13.0$ Hz and $J_{1\beta,2\alpha} = 10.5$ Hz, H-1β), 1.63 (1H, *dd*, $J_{10\beta,10\alpha} = 12.7$ Hz and $J_{10\beta,9\beta} = 6.4$ Hz, H-10β), 1.80 (1H, *dd*, $J_{1\alpha,1\beta} = 13.0$ Hz and $J_{1\alpha,2\alpha} = 7.6$ Hz, H-1α), 2.07–2.14 (2H, *m*, H-2α and H-9β), 2.53 (1H, *d*, $J_{4\beta,4\alpha} = 14.0$ Hz, H-4β), 2.67 (1H, *d*, $J_{4\alpha,4\beta} = 14.0$ Hz, H-4α), 4.68 (1H, *dd*, $J_{2',3'} = 3.6$ Hz and $J_{2',OH} = 2.3$ Hz, H-2′), 5.81 (1H, *d*, $J_{8\alpha,9\beta} = 10.0$ Hz, H-8α), 5.82 (1H, *dd*, $J_{3',NH} = 9.1$ Hz and $J_{3',2'} = 3.6$ Hz, H-3′), 7.12 (1H, *t*, $J = 1.5$ Hz, H-5), 7.19 (1H, *d*, $J_{NH,3'} = 9.1$ Hz, N*H*), 7.22 (1H, *t*, $J = 1.0$ Hz, H-13), 7.28–7.51 (8H, *m*, H-Ph), 7.74–7.79 (2H, *m*, H-Ph); ^{13}C NMR: δ 20.7 (*q*, C-12), 31.0 (*q*, C-15), 31.1 (*q*, C-14), 34.7 (*s*, C-11), 40.1 (*t*, C-4), 43.2 (*t*, C-1), 46.2 (*t*, C-10), 46.4 (*d*, C-9), 54.6 (*d*, C-3′), 54.9 (*d*, C-2), 73.3 (*s*, C-3), 73.6 (*d*, C-2′), 77.1 (*d*, C-8), 118.8 (*s*, C-6), 123.9 (*s*, C-7), 126.9 (*d*, C-Ph), 127.0 (*d*, C-Ph), 127.9 (*d*, C-Ph), 128.6 (*d*, C-Ph), 128.7 (*d*, C-Ph), 131.8 (*d*, C-Ph), 133.9 (*s*, C-Ph), 138.9 (*s*, C-Ph), 139.2 (*d*, C-13), 140.7 (*d*, C-5), 166.9 (*s*, NCO), 172.1 (*s*, C-1′); LSIMS *m/z* (rel. int.): 540 $[M+Na]^+$ (18), 481 (3), 425 (6), 329 (18), 308 (19), 286 (40), 225 (19), 176 (100), 154 (55), 136 (42), 105 (40), 91 (81); HR LSIMS *m/z*: $[M+Na]^+$ calc. for $C_{31}H_{35}O_6NNa$: 540.23621, found: 540.23494.

4.5.7. Compound ***27***

TLC $R_f = 0.31$ (hexane–EtOAc 7:3); mp 69–74 °C; $[\alpha]_D^{20} = -21.16°$ ($CHCl_3$, *c* 1.0); UV λ_{max} (EtOH) nm: 196 (ε 60975); 218 (ε 21513); IR ν_{max} ($CHCl_3$) cm^{-1}: 3517, 3440, 2956, 2871, 1731, 1667; ^1H NMR: δ 0.84 (3H, *s*, H-15), 0.87 (3H, *s*, H-14), 0.90 (3H, *t*, $J = 6.9$ Hz, -OCH_2CH_3), 1.17 (3H, *s*, H-12), 1.32 (1H, *dd*, $J_{10\alpha,10\beta} = 14.0$ Hz and $J_{10\alpha,9\alpha} = 2.5$ Hz, H-10α), 1.43 (1H, *dd*, $J_{10\beta,10\alpha} = 14.0$ Hz and $J_{10\beta,9\alpha} = 6.8$ Hz, H-10β), 1.49 (1H, *dd*, $J_{1\alpha,1\beta} = 12.6$ and $J_{1\alpha,2\alpha} = 6.6$ Hz, H-1α), 1.55 (1H, *t*, $J = 12.6$ Hz, H-1β), 2.34–2.40 (1H, *m*, H-2α), 2.56 (1H, *d*, $J_{4\beta,4\alpha} = 15.4$ Hz, H-4β), 2.58-2.63 (1H, *m*, H-9α), 2.74 (1H, *d*, $J_{4\alpha,4\beta} = 15.4$ Hz, H-4α), 3.27 (1H, *qn*, $J = 6.9$ Hz, -OCH_2CH_3), 3.36 (1H, *qn*, $J = 6.9$ Hz, -OCH_2CH_3), 4.68 (1H, *d*, $J_{2',3'} = 2.2$ Hz, H-2′), 5.79 (1H, *dd*, $J_{3',NH} = 8.9$ Hz and $J_{3',2'} = 2.2$ Hz, H-3′), 6.01 (1H, *d*, $J_{8\beta,9\alpha} = 11.2$ Hz, H-8β), 6.93 (1H, *s*, H-5), 7.13 (1H, *t*, $J = 2.0$ Hz, H-13), 7.23 (1H, *d*, $J_{NH,3'} = 8.9$ Hz, N*H*), 7.26-7.53 (8H, *m*, H-Ph), 7.78-7.83 (2H, *m*, H-Ph); ^{13}C NMR: δ 15.7 (*q*, -CH_2CH_3), 25.5 (*q*, C-12), 29.1 (*t*, C-4), 31.6 (*q*, C-15), 32.1 (*q*, C-14), 34.7 (*s*, C-11), 41.8 (*t*, C-1), 43.8 (*t*, C-10), 44.2 (*d*, C-9), 51.9 (*d*, C-2), 54.7 (*d*, C-3′), 55.6 (*t*, -CH_2CH_3), 72.6 (*d*, C-8), 73.6 (*d*, C-2′), 75.4 (*s*, C-3), 119.4 (*s*, C-6), 125.2 (*s*, C-7), 126.9 (*d*, C-Ph), 127.1 (*d*, C-Ph), 127.8 (*d*, C-Ph), 128.5 (*d*, C-Ph), 128.6 (*d*, C-Ph), 131.7 (*d*, C-Ph), 133.9 (*s*, C-Ph), 138.0 (*d*, C-5), 138.8 (*s*, C-Ph), 140.4 (*d*, C-13), 166.3 (*s*, NCO), 172.1 (*s*, C-1′); LSIMS *m/z* (rel. int.): 568 $[M+Na]^+$ (18), 413 (2), 338 (2), 330 (18), 308 (95), 286 (26), 261 (19), 240 (6), 215 (100), 176 (46), 154 (23), 136 (21), 105 (66), 95 (17); HR LSIMS *m/z*: $[M+Na]^+$ calc. for $C_{33}H_{39}O_6NNa$: 568.26751, found: 568.26825.

4.5.8. Compound ***30***

TLC $R_f = 0.11$ (hexane–EtOAc 7:3); mp 80–83 °C; $[\alpha]_D^{20} = +5.23°$ ($CHCl_3$, *c* 1.0); UV λ_{max} (EtOH) nm: 204 (ε 53790); 220 (ε 41181); IR ν_{max} ($CHCl_3$) cm^{-1}: 3528, 3440, 2956, 2867, 1752, 1667; ^1H NMR: δ 0.75 (3H, *s*, H-15), 0.77 (3H, *s*, H-14), 1.12 (1H, *dd*, $J_{10\beta,10\alpha} = 12.8$ Hz and $J_{10\beta,9\alpha} = 8.8$ Hz, H-10β), 1.64 (1H, *ddd*, $J_{10\alpha,10\beta} = 12.8$ Hz, $J_{10\alpha,9\alpha} = 7.8$ Hz and $J = 1.8$ Hz, H-10α), 1.74 (3H, *br s*, H-12), 2.01 (1H, *d*, $J_{1\beta,1\alpha} = 15.0$ Hz, H-1β), 2.29 (1H, *d*, $J_{1\alpha,1\beta} = 15.0$ Hz, H-1α), 2.89 (1H, *d*, $J_{4\beta,4\alpha} = 19.9$ Hz, H-4β), 3.13–3.24 (2H, *m*, H-4α and H-9α), 4.59 (1H, *d*, $J_{13\beta,13\alpha} = 17.3$ Hz, H-13β), 4.69 (1H, *d*, $J_{2',3'} = 3.8$ Hz, H-2′), 4.70 (1H, *dd*, $J_{13\alpha,13\beta} = 17.3$ Hz and $J = 3.6$ Hz, H-13α), 5.60 (1H, *dd*, $J_{3',NH} = 11.2$ Hz and $J_{3',2'} = 3.8$ Hz, H-3′), 5.61 (1H, *d*, $J_{8\beta,9\alpha} = 11.2$ Hz, H-8β), 7.25–7.88 (9H, m, N*H* and H-Ph), 8.10–8.15 (2H, *m*, H-Ph); ^{13}C NMR: δ 22.6 (*q*, C-12), 27.2 (*q*, C-14), 28.6 (*q*, C-15), 30.9 (*t*, C-4), 36.2 (*s*, C-11), 46.1 (*d*, C-9), 45.9 (*t*, C-10), 47.5 (*t*, C-1), 57.5 (*d*, C-8), 57.5 (*d*, C-3′), 71.4 (*t*, C-13), 74.8 (*d*, C-2′), 127.2 (*s*, C-2), 128.3 (*d*, C-Ph), 128.6 (*d*, C-Ph), 128.7 (*d*, C-Ph), 129.4 (*s*, C-6), 129.5 (*d*, C-Ph), 129.6 (*d*, C-Ph), 133.0 (*d*, C-Ph), 135.2 (*s*, C-Ph), 137.4 (*s*, C-Ph), 140.4 (*s*, C-3), 159.0 (*s*, C-7), 169.4 (*s*, NCO), 173.3 (*s*, C-1′), 175.9 (*s*, C-5); LSIMS *m/z* (rel. int.): 538 $[M+Na]^+$ (18), 516 $[M+H]^+$ (8), 443 (2), 338 (5), 308 (29), 286 (100), 253 (5), 231 (15), 210 (8), 176 (70), 154 (59), 136 (42), 105 (83); HR LSIMS *m/z*: $[M+Na]^+$ calc. for $C_{31}H_{33}O_6NNa$: 538.22056, found: 538.22162.

4.5.9. Compound ***33***

TLC $R_f = 0.33$, (C_6H_6–Me_2CO 8:2); mp 101–103 °C; $[\alpha]_D^{20} = -18.40°$ ($CHCl_3$, *c* 1.0); UV λ_{max} (EtOH) nm: 218 (ε 26218); IR ν_{max} (KBr) cm^{-1}: 3428, 2955, 2867, 1746, 1649; ^1H NMR: δ 0.71 (3H, *s*, H-15), 0.90 (3H, *s*, H-14), 1.06 (1H, *dd*, $J_{10\beta,10\alpha} = 12.6$ Hz and $J_{10\beta,9\alpha} = 10.0$ Hz, H-10β), 1.22 (3H, *s*, H-12), 1.20–1.27 (1H, *m*, H-1β), 1.48 (1H, *dd*, $J_{10\alpha,10\beta} = 12.6$ Hz and $J_{10\alpha,9\alpha} = 6.8$ Hz, H-10α), 1.54 (1H, *dd*, $J_{1\alpha,1\beta} = 11.8$ Hz and $J_{1\alpha,2\alpha} = 7.2$ Hz, H-1α), 2.44–2.50 (1H, *m*, H-2α), 2.53-2.62 (3H, *m*, H-4α, 4-β and H-9α), 4.41 (1H, *br d*, $J_{13\beta,13\alpha} = 17.3$ Hz, H-13β), 4.65 (1H, *dt*, $J_{13\alpha,13\beta} = 17.3$ Hz and $J = 2.5$ Hz, H-13α), 4.71 (1H, *d*, $J_{2',3'} = 2.3$ Hz, H-2′), 5.64 (1H, *d*, $J = 5.9$ Hz, H-8β), 5.78 (1H, *dd*, $J_{3',NH} = 9.3$ Hz and $J_{3',2'} = 2.3$ Hz, H-3′), 7.25–7.54 (9H, *m*, N*H* and H-Ph), 7.78-7.81 (2H, *m*, H-Ph); ^{13}C NMR: δ 22.6 (*q*, C-15), 27.1 (*q*, C-14), 29.4 (*q*, C-12),

34.7 (*t*, C-4), 36.0 (*s*, C-11), 42.4 (*d*, C-9), 44.6 (*t*, C-1), 45.0 (*t*, C-10), 50.2 (*d*, C-2), 54.7 (*d*, C-3′), 70.6 (*t*, C-13), 71.7 (*d*, C-8), 72.3 (*s*, C-3), 73.2 (*d*, C-2′), 126.9 (*d*, C-Ph), 127.1 (*d*, C-Ph), 127.8 (*s*, C-6), 127.9 (*d*, C-Ph), 128.6 (*d*, C-Ph), 128.7 (*d*, C-Ph), 132.1 (*d*, C-Ph), 133.3 (*s*, C-Ph), 138.0 (*s*, C-Ph), 154.0 (*s*, C-7), 167.0 (*s*, NCO), 172.2 (*s*, C-1′), 174.3 (*s*, C-5); LSIMS *m/z* (rel. int.): 534 $[M+H]^+$ (10), 391 (3), 369 (5), 307 (19), 286 (24), 225 (10), 215 (8), 176 (5), 154 (100), 137 (71), 105 (39); HR LSIMS *m/z*: $[M+H]^+$ calc. for $C_{31}H_{36}O_7N$: 534.24921, found: 534.25325.

4.5.10. Compound **36**

LC $R_f = 0.16$ (hexane–Me_2CO 7:3); mp 114–117 °C; $[\alpha]_D^{20} = -11.63°$ ($CHCl_3$, *c* 1.0); UV λ_{max} (EtOH) nm: 194 (ε 59567), 220 (ε 25610); IR ν_{max} ($CHCl_3$) cm^{-1}: 3593, 3440, 2958, 2868, 1738, 1662; ^1H NMR: δ 0.88 (3H, *s*, H-15), 0.99 (3H, *s*, H-14), 1.03 (1H, *t*, $J = 12.2$ Hz, H-1β), 1.19 (1H, *t*, $J = 12.3$ Hz, H-10β), 1.21 (3H, *s*, H-12), 1.46 (1H, *dd*, $J_{10\alpha,10\beta} = 12.3$ Hz and $J_{10\alpha,9\alpha} = 8.9$ Hz, H-10α), 1.51 (1H, *dd*, $J_{1\alpha,1\beta} = 12.2$ Hz and $J_{1\alpha,2\alpha} = 7.8$ Hz, H-1α), 2.43 (1H, *d*, $J_{4\beta,4\alpha} = 19.2$ Hz, H-4β), 2.53–2.60 (1H, *m*, H-2α), 2.60 (1H, *dq*, $J_{4\alpha,4\beta} = 19.2$ Hz and $J = 2.9$ Hz, H-4α), 2.83–2.91 (1H, *m*, H-9α), 4.61 (1H, *d*, $J_{2',3'} = 2.2$ Hz, H-2′), 4.77 (2H, *br s*, H-13), 5.65 (1H, *dd*, $J_{3',NH} = 9.0$ Hz and $J_{3',2'} = 2.2$ Hz, H-3′), 6.88 (1H, *br s*, H-8α), 7.15 (1H, *d*, $J_{NH,3'} = 9.0$ Hz, N*H*), 7.28–7.48 (8H, *m*, H-Ph), 7.72–7.75 (2H, *m*, H-Ph); ^{13}C NMR: δ 26.2 (*q*, C-15), 28.9 (*q*, C-14), 29.4 (*q*, C-12), 34.8 (*t*, C-4), 37.7 (*s*, C-11), 42.3 (*t*, C-10), 43.8 (*d*, C-9), 44.6 (*t*, C-1), 48.9 (*d*, C-2), 55.0 (*d*, C-3′), 70.8 (*t*, C-13), 73.3 (*d*, C-2′), 73.6 (*s*, C-3), 74.8 (*d*, C-8), 122.2 (*s*, C-6), 127.0 (*d*, C-Ph), 127.0 (*d*, C-Ph), 128.0 (*d*, C-Ph), 128.6 (*d*, C-Ph), 128.8 (*d*, C-Ph), 131.9 (*d*, C-Ph), 133.6 (*s*, C-Ph), 138.5 (*s*, C-Ph), 158.5 (*s*, C-7), 167.5 (*s*, NCO), 174.8 (*s*, C-5), 174.8 (*s*, C-1′); LSIMS *m/z* (rel. int.): 534 $[M+H]^+$ (2), 524 (1), 460 (1), 391 (2), 369 (1), 338 (3), 307 (14), 286 (12), 231 (2), 154 (100), 136 (77), 120 (14), 105 (42); HR LSIMS *m/z*: $[M+Na]^+$ calc. for $C_{31}H_{35}O_7NNa$: 556.23112, found: 556.23110.

4.5.11. Compound **39**

TLC $R_f = 0.31$ (hexane–Me_2CO 6:4); mp 116–120 °C; $[\alpha]_D^{20} = -47.20°$ ($CHCl_3$, *c* 1.0); UV λ_{max} (EtOH) nm: 221 (ε 24542); IR ν_{max} (KBr) cm^{-1}: 3423, 2952, 2865, 1747, 1649; ^1H NMR: δ 0.97 (3H, *s*, H-15), 1.01 (3H, *s*, H-14), 1.07 (3H, *s*, H-12), 1.28 (1H, *dd*, $J_{10\alpha,10\beta} = 12.6$ Hz and $J_{10\alpha,9\beta} = 10.3$ Hz, H-10α), 1.51 (1H, *dd*, $J_{1\beta,1\alpha} = 13.2$ Hz and $J_{1\beta,2\alpha} = 10.1$ Hz, H-1β), 1.60 (1H, *dd*, $J_{10\beta,10\alpha} = 12.6$ Hz and $J_{10\beta,9\beta} = 6.4$ Hz, H-10β), 1.83 (1H, *dd*, $J_{1\alpha,1\beta} = 13.2$ Hz and $J_{1\alpha,2\alpha} = 7.8$ Hz, H-1α), 2.14-2.25 (2H, *m*, H-2α and H-9β), 2.28 (1H, *dd*, $J_{4\beta,4\alpha} = 15.1$ Hz and $J = 2.3$ Hz, H-4β), 2.75 (1H, *d*, $J_{4\alpha,4\beta} = 15.1$ Hz, H-4α), 4.56 (1H, *dd*, $J_{13\beta,13\alpha} = 18.1$ Hz and $J = 2.9$ Hz, H-13β), 4.66 (1H, *d*, $J_{2',3'} = 2.4$ Hz, H-2′), 4.78 (1H, *br d*, $J_{13\alpha,13\beta} = 18.1$ Hz, H-13α), 5.71 (1H, *dd*, $J_{3',NH} = 9.0$ Hz and $J_{3',2'} = 2.4$ Hz, H-3′), 5.79 (1H, *br d*, $J_{8\alpha,9\alpha} = 8.7$ Hz, H-8α), 7.21 (1H, *d*, $J_{NH,3'} = 9.0$ Hz, N*H*), 7.29–7.52 (8H, *m*, H-Ph), 7.75–7.78 (2H, *m*, H-Ph); ^{13}C NMR: δ 20.6 (*q*, C-12), 30.8 (*q*, C-15), 31.1 (*q*, C-14), 34.2 (*s*, C-11), 39.3 (*t*, C-4), 43.4 (*t*, C-1), 44.0 (*d*, C-9), 46.2 (*t*, C-10), 54.4 (*d*, C-2), 54.9 (*d*, C-3′), 69.3 (*t*, C-13), 72.1 (*s*, C-3), 73.5 (*d*, C-2′), 77.5 (*d*, C-8), 124.1 (*s*, C-6), 127.0 (*d*, C-Ph), 127.0 (*d*, C-Ph), 128.2 (*d*, C-Ph), 128.7 (*d*, C-Ph), 128.8 (*d*, C-Ph), 132.1 (*d*, C-Ph), 133.4 (*s*, C-Ph), 138.4 (*s*, C-Ph), 159.7 (*s*, C-7), 167.2 (*s*, NCO), 172.0 (*s*, C-1′), 174.1 (*s*, C-5); ESI-MS *m/z* (rel. int.): 1623.7016 $[3M+Na]^+$ (20), 1089.4559 $[2M+Na]^+$ (100), 556.2276 $[M+Na]^+$ (95); HR ESI-MS *m/z*: $[M+Na]^+$ calc. for $C_{31}H_{35}O_7NNa$: 556.23112, found: 556.23060.

4.5.12. Compound **42**

TLC $R_f = 0.34$ (hexane–Me_2CO 6:4); mp 102–105 °C; $[\alpha]_D^{20} = -3.80°$ ($CHCl_3$, *c* 1.0); UV λ_{max} (EtOH) nm: 194 (ε 64173), 217 (ε 23025); IR ν_{max} ($CHCl_3$) cm^{-1}: 3429, 2958, 2868, 1757, 1727, 1650; ^1H NMR: δ 0.52 (3H, *s*, H-15), 0.78 (3H, *s*, H-14), 1.06 (1H, *t*, $J = 12.4$ Hz, H-1β), 1.31 (3H, *s*, H-12), 1.51 (1H, *ddd*, $J_{1\alpha,1\beta} = 12.4$ Hz, $J_{1\alpha,2\alpha} = 7.8$ Hz and $J = 2.1$ Hz, H-1α), 1.54 (1H, *ddd*, $J_{10\alpha,10\beta} = 12.3$ Hz, $J_{10\alpha,9\alpha} = 6.8$ Hz and $J = 2.2$ Hz, H-10α), 2.48-2.58 (2H, *m*, H-2α and H-9α), 2.56 (1H, *d*, $J_{4\beta,4\alpha} = 19.4$ Hz, H-4β), 2.76 (1H, *d*, $J_{4\alpha,4\beta} = 19.4$ Hz, H-4α), 4.68 (2H, *br s*, H-5α and H-5β), 4.76 (1H, *d*, $J_{2',3'} = 1.9$ Hz, H-2′), 5.83 (1H, *d*, $J_{8\beta,9\alpha} = 2.3$ Hz, H-8β), 5.86 (1H, *dd*, $J_{3',NH} = 9.9$ Hz, $J_{3',2'} = 2.3$ Hz, H-3′), 7.21 (1H, *d*, $J_{3',NH} = 9.9$ Hz, N*H*), 7.24–7.55 (8H, *m*, H-Ph), 7.81–7.83 (2H, *m*, H-Ph); ^{13}C NMR: δ 25.3 (*q*, C-15), 28.9 (*q*, C-14), 32.2 (*q*, C-12), 36.2 (*s*, C-11), 36.8 (*t*, C-4), 42.3 (*d*, C-9), 45.8 (*t*, C-10), 46.3 (*t*, C-1), 48.8 (*d*, C-2), 54.0 (*d*, C-3′), 70.1 (*d*, C-8), 72.3 (*t*, C-5), 72.7 (*d*, C-2′), 73.0 (*s*, C-3), 122.5 (*s*, C-7), 126.9 (*d*, C-Ph), 127.1 (*d*, C-Ph), 127.7 (*d*, C-Ph), 128.6 (*d*, C-Ph), 128.8 (*d*, C-Ph), 132.3 (*d*, C-Ph), 133.3 (*s*, C-Ph), 137.9 (*s*, C-Ph), 164.2 (*s*, C-6), 167.3 (*s*, NCO), 172.5 (*s*, C-1′), 173.9 (*s*, C-13); LSIMS *m/z* (rel. int.): 1067 $[2M+H]^+$ (1), 534 $[M+H]^+$ (26), 460 (1), 286 (100), 240 (8), 210 (20), 167 (7), 154 (76), 136 (56), 105 (76); HR LSIMS *m/z*: $[M+H]^+$ calc. for $C_{31}H_{36}O_7N$: 534.24918, found: 534.24918.

4.6. Antifeedant activity test

The test is described in detail in Błoszyk et al. (1995). Insects (adults and larvae) used for the test were reared under laboratory conditions at temp. of 26 °C and 75% humidity. All compounds investigated were dissolved in EtOH at concentration of 10 mg ml^{-1}. Air dry wheat wafer discs were used as test food. The discs (1 cm in diameter) were saturated with EtOH solutions of pure compounds to produce 0.5% (by weight) contamination of the wafer in every test. Feeding of insects was recorded under three conditions: (1) on pure food (control); (2) on food with possibility of choice (choice test); on food with the compounds tested (no choice test). The wafer discs were weighed after saturation and drying in

air for 30 min before the experiments and again after 7 days of feeding by beetles or larvae. On the basis of eaten food, the index of activity of the compounds tested was calculated in the following way: three values of the food eaten were obtained in the control KK, in the no-choice test EE, and in the choice test K, E.

Thus, the relative coefficient of antifeedancy:

$$R = \frac{K - E}{K + E} \times 100$$

The total coefficient of antifeedancy is equal to $T = A + R$, and the maximum value of the coefficient can reach 200 for a perfect antifeedant.

References

Błoszyk, E., Szafrański, F., Drożdż, B., Al-Shameri, A., 1995. African plants as antifeedants against stored-product insect pests. Journal of Herbs, Spices and Medicinal Plants 3, 25–36.

Daniewski, W.M., Gumułka, M., Ptaszyñska, K., Skibicki, P., Błoszyk, E., Drożdż, B., Stromberg, S., Norin, T., Holub, M., 1993. Antifeedant activity of some sesquiterpenoids of the genus *Lactarius*. European Journal of Entomology 90, 65–70.

Daniewski, W.M., Gumułka, M., Przesmycka, D., Ptaszyńska, K., Błoszyk, E., Drożdż, B., 1995. Sesquiterpenes of *Lactarius* origin, antifeedant structure-activity relationship. Phytochemistry 38, 1161–1168.

Daniewski, W.M., Gumułka, M., Anczewski, W., Masnyk, M., Błoszyk, E., Gupta, K.K., 1998. Why the yew tree (*Taxus baccata*) is not attacked by insects. Phytochemistry 49, 1279–1282.

Daniewski, W.M., Vidari, G., 1999. Constituents of *Lactarius* (mushrooms). Progress in the Chemistry of Organic Natural Products 77, 69–171.

Farina, V., 1995. The Chemistry and Pharmacology of Taxol and its Derivatives. Elsevier Science B.V., Amsterdam. The Netherlands.

Kamata, K., Agata, I., Meyers, A.I., 1998. An efficient and versatile method for the synthesis of optically active 2-oxazolines: an acid-catalyzed condensation of ortho esters with amino alcohols. Journal of Organic Chemistry 63, 3113–3116.

Kingston, D.G.I., Chaudhary, A.G., Gunatilaka, A.A.L., Middleton, M.L., 1994. Synthesis of taxol from baccatin III via oxazoline intermediate. Tetrahedron Letters 35, 4483–4484.

PERGAMON

Phytochemistry 58 (2001) 789–798

PHYTOCHEMISTRY

www.elsevier.com/locate/phytochem

Sesquiterpenoid constituents of the liverworts *Lepidozia fauriana* and *Lepidozia vitrea*

Claudia Paul[a], Wilfried A. König[a,*], Chia-Li Wu[b]

[a]*Institut für Organische Chemie, Universität Hamburg, Martin-Luther-King-Platz 6, D-20146 Hamburg, Germany*
[b]*Tamkang University, Tamsui, Taiwan*

Received 23 April 2001; received in revised form 20 June 2001

Dedicated to Professor Yoshinori Asakawa on the occasion of his 60th birthday

Abstract

The sesquiterpene constituents of the essential oils of the Taiwanese liverworts *Lepidozia fauriana* and *L. vitrea* were investigated. 11,12-Dihydrochiloscyphone and 7,10-anhydro-11,12-dihydrochiloscypholone were isolated from *L. fauriana* and spectroscopically characterised together with their hydrogenation products. From the same species three amorphane derivatives amorpha-4,9-dien-14-al, amorpha-4,9-dien-2-ol and 7,14-anhydroamorpha-4,9-diene, and from *L. vitrea* two oxygenated elemanes, namely 7-acetoxy-elema-1,3-dien-8-ol and elema-1,3-dien-7-ol, were isolated and identified. Structure elucidation was carried out by NMR spectroscopy and chemical correlations in conjunction with enantioselective gas chromatography were utilized to establish absolute configurations. © 2001 Elsevier Science Ltd. All rights reserved.

Keywords: *Lepidozia fauriana*; *L. vitrea*; Hepaticae; Essential oil; Structure elucidation; Amorphane; Chiloscyphane; Elemane; Sesquiterpene

1. Introduction

Liverworts are a rich source of terpenoid compounds with a variety of biological activities (Asakawa, 1995). In the present work the leafy liverworts *Lepidozia fauriana* and *L. vitrea* (Lepidoziaceae) of Taiwanese origin were investigated. In the Japanese liverwort *L. vitrea* vitrenal, isobicyclogermacrenal (Matsuo et al., 1980, 1984), eudesm-3-ene-6β,7α-diol and eudesm-4(15)-ene-6β,7α-diol (Toyota et al., 1996) and in Taiwanese *L. vitrea* and *L. fauriana* lepidozenolide, 5α-hydroperoxylepidozenolide and 6β-acetoxyvitranoxide have been identified (Shu et al., 1994). These relatively polar compounds were not detected in the hydrodistillation products of our samples, but other compounds bearing these sesquiterpene backbones and some of those reported for this liverwort family were identified. Essential oil samples were analysed by GC–MS. Individual components, including a number of new oxygenated sesquiterpenes, were isolated by preparative GC and investigated by NMR (^{1}H, ^{13}C, ^{1}H–^{1}H COSY, HMQC, HMBC, TOCSY, NOESY). The absolute configuration of the new compounds was derived by dehydration of the related alcohols, polarimetric measurements, total hydrogenation and enantioselective gas chromatography using cyclodextrin stationary phases.

2. Results and discussion

The following sesquiterpenoids in the order of their elution from a capillary column with polydimethylsiloxane (CPSil-5) were identified as constituents of the essential oil of *L. fauriana* (YYF-9904-42 and YY-9803-11; relative concentrations of major compounds are given in parentheses, all other compounds are below 3% relative abundance, only identified compounds are given): δ-elemene, α-ylangene, α-copaene, β-elemene, (+)-7,10-anhydro-11,12-dihydrochiloscypholone (**3,** 10%), (−)-bicyclogermacrene (18%), (+)-11,12-dihydrochiloscyphone (**2,** 3%), 4-eudesm-7α-ol (**11,** 4%) (Barrero et al., 1997), (+)-dihydrochiloscypholone (**1**) (Nagashima et al., 1996) (19%), (−)-lepidozenal (**14**) (Matsuo et al., 1984). In the essential oil of plant sample YY-9904-30 isoledene, β-longipinene, isosativene, β-caryophyllene,

* Corresponding author. Tel.: +49-40-42838-2824; fax: +49-40-42838-2893.
E-mail address: wkoenig@chemie.uni-hamburg.de (W.A. König).

0031-9422/01/$ - see front matter © 2001 Elsevier Science Ltd. All rights reserved.
PII: S0031-9422(01)00322-3

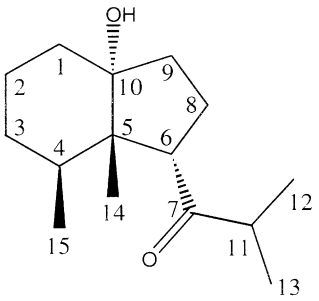

(1)

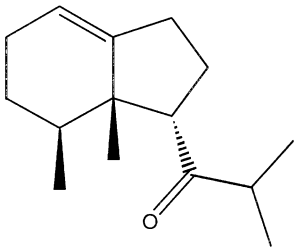

(2)

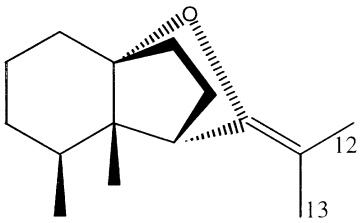

(3)

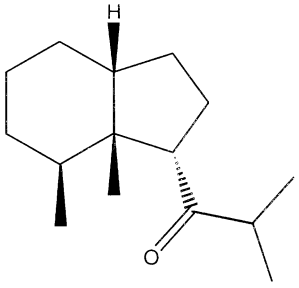

(4)

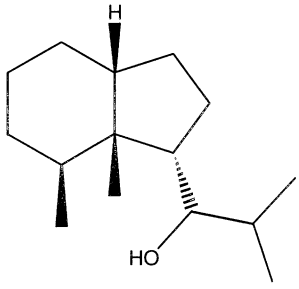

(5)

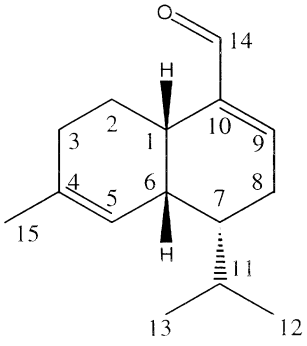

(6)

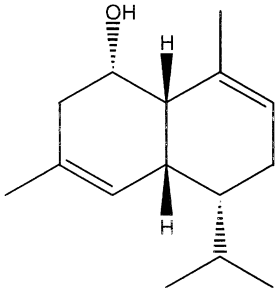

(7)

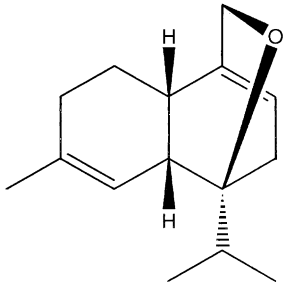

(8)

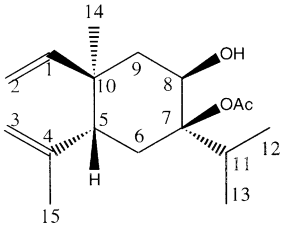

(9)

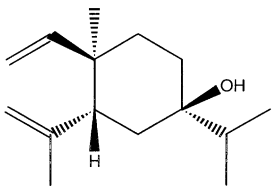

(10)

β-cedrene, thujopsene, aromadendrene, β-barbatene, **3**, *allo*-aromadendrene, α-amorphene (8%), (−)-bicyclogermacrene (23%), β-bazzanene, δ-cuprenene, **2**, maaliol, globulol, viridiflorol, cedrol, **11**, (−)-isospathulenol (**16**) (Maurer and Hauser, 1983), (+)-amorpha-4,9-dien-2-ol (**7**), (+)-amorpha-4,9-dien-14-al (**6**, 5%), **1**, (+)-7,14-anhydroamorpha-4,9-diene (**8**), and **14** (4%) were found.

In the essential oil of *L. vitrea* the following sesquiterpenoids were identified: δ-elemene, α-ylangene, β-bourbonene, β-elemene, α-barbatene, γ-maaliene, isobazzanene, β-barbatene (13%), δ-selinene, ledene (4%), cuparene, α-cuprenene, δ-cadinene, (+)-elema-1,3-dien-7-ol (**10**) (13%), germacrene B, maaliol, spathulenol, rosifoliol, (−)-eudesm-4-en-7α-ol (**11**) (10%), guai-5-en-11-ol, eudesm-4(15)-en-7-ol (**13**, 8%) (Toyota et al., 1999), (+)-eudesm-3-en-7-ol (**12**, 7%) (Toyota et al., 1999), **14,** vetivazulene (**15**) (Hayashi et al., 1969; Bellesia et al., 1976), and (+)-7-acetoxy-elema-1,3-diene-8-ol (**9**). All previously known compounds were identified by mass spectrometry in conjunction with their gas chromatographic retention indices by comparison with a spectral library established under identical experimental conditions (Joulain and König, 1998).

The mass spectrum of the new tricyclic sesquiterpene enolether 7,10-anhydro-11,12-dihydrochiloscypholone (**3**) exhibits a molecular ion signal at *m/z* 220 and an elemental composition of $C_{15}H_{24}O$. The proton NMR spectrum shows one singlet and one doublet for methyl groups (δ 0.56, 0.74) and two downfield shifted methyl singlets (δ 1.67, 1.85) indicating that these methyl groups are attached to a double bond. As the ^{13}C NMR reveals, three downfield shifted quaternary carbons (δ 152.9, 95.1, 89.1), only one double bond and another quaternary carbon bearing an oxygen function fits to this pattern. The chemical shifts of these carbons clearly indicate the presence of an enolether structure which results in a tricyclic system for the molecule. In the ^{13}C NMR four primary carbon atoms (δ 10.9, 16.5, 17.9, 19.2), five secondary carbons (δ 22.5, 25.9, 27.1, 29.9, 34.5), two tertiary (δ 32.1, 47.2) and four quaternary carbons (δ 50.7, 89.1, 95.1, 152.9) are found. The connectivity of the different groups for the chiloscyphanes **1**, **2**, **3**, **4** and **5** was established through $^1H^1$-H-COSY and HMBC experiments. The NOE-couplings of **3** and **4** are shown in Fig. 1.

To verify the structure of **3,** compound **1** was isolated and characterised by NMR. During acidic treatment (Amberlyst) of **1** compound **3** was generated which itself was converted to **2** during this process. As a result of the dehydration in 10-position the 1(10)-ene- (**2**) and 9-ene- (**2a**, not shown) double bond isomers are expected. From the ^1H NMR and TOCSY experiment conducted with **2**, it was evident that **2** was formed in a 10:1 ratio over **2a** and that the two isomers coeluted on the GC column. Hydrogenation with H_2-Pd/C of the isolated compounds **1**, **2** and **3** yielded **4** as a common product. Further reduction of **4** to the alcohol **5** was achieved with $LiAlH_4$.

Because of the lability of **1,** it can not be excluded that **2** and **3** may be generated by the sample preparation method and not be originally present in the plant.

The mass spectrum of the new sesquiterpene aldehyde amorpha-4,9-diene-14-al (**6**) exhibits a molecular ion signal at *m/z* 218 and an elemental composition of $C_{15}H_{22}O$. The proton NMR spectrum shows two doublets for methyl groups (δ 0.76, 0.82) and one methyl singlet with a downfield shift (δ 1.54) indicating that this methyl group is attached to a double bond. The one-proton-signal at δ 9.37 clearly indicates an aldehydic proton. The HSQC spectrum reveals the presence of three primary (δ 21.3, 21.8, 24.1), three secondary (δ 24.6, 27.0, 28.4) and seven methine carbons (δ 29.4, 34.8, 36.3, 44.2, 119.4, 153.5, 193.5). From the HMBC spectrum the presence of two quaternary carbons is derived (δ 137.0, 142.4). This information together with the data of the two dimensional measurements results in an amorphane skeleton.

The identification of **7** and **8** was facilitated by the analogies to **6**: The methyl doublets and the downfield

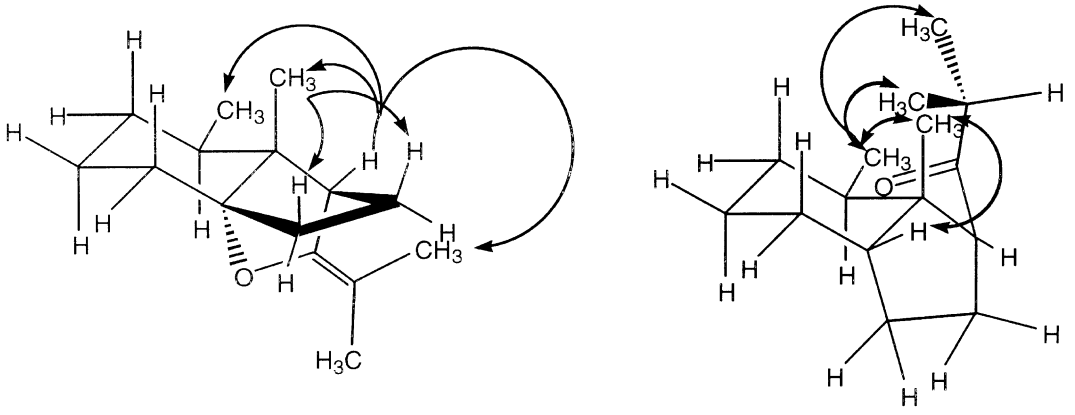

Fig. 1. Important observed NOE contacts of the chiloscyphanes **3** and **4**.

shifted singlet of a methyl attached to a double bond were present in both compounds (**7**: δ 0.87, 0.91, 1.57; **8**: δ 0.89, 0.93, 1.61). For **7** an additional methyl singlet instead of the aldehyde signal in **6** appears at δ 2.01 while in **8** the aldehyde group of **6** is reduced to an ether giving signals at δ 3.81 and 3.99, each with the integral of one proton. It is remarkable that for the ring junction protons H-1 and H-6 in all three compounds broad singlets (**6**: δ 2.60, 2.71; **7**: δ 2.30, 2.62; **8**: δ 2.48, 2.68) are observed. Complete NMR investigation of **7** together with the observed spectral analogies confirmed structure **7**. For **8** the ^{1}H-^{1}H-COSY yielded the fragment depicted in Fig. 3 which was correlated with the amorphane structure due to the obvious spectral homologies to compounds **6** and **7**. Fig. 2 gives an interpretation of the NOESY data for compounds **6** and **7**.

The absolute configuration of the amorphane derivatives was determined by correlation with (+)-α-amorphene (Bülow and König, 2000). Partial hydrogenation of **6**, **7** and **8** with H_2-Pd/C in hexane/benzene 70:30 among other products yielded differing amounts of α-amorphene which was identified by enantioselective GC on heptakis(6-*O*-tert-butyldimethylsilyl-2,3-di-*O*-methyl)-β-cyclodextrin to be the (+)-enantiomer (König et al., 1999). The hydrogenation was repeated with **8** to check its reproducibility: under the same conditions again (+)-α-amorphene was obtained together with some side products which were also obtained in the hydrogenation reaction of an α-amorphene standard.

For the oxygenated elemadienes **9** and **10** complete NMR investigations were carried out (NOESY interpretation illustrated in Fig. 4). The relative configuration at chiral center C-7 carrying the acetoxy group was not assigned beyond doubt due to lack of coupling correlations with neighbouring protons in the NOESY spectrum. The assumed configuration is the more likely one, as the methyl group H-12 shows close spatial relationship to H-6a, which itself must be in the equatorial position giving NOE-contacts with H-5 and O*H*. Dehydration of **10** yielded (5*R*,10*R*)-elema-1,3,6-triene (δ-elemene) as a single enantiomer, (5*R*,10*R*)-elema-1,3,7-triene (Ohloff et al., 1959), and (−)-γ-elemene which revealed the opposite absolute configuration of the chiral centers C-5 and C-10 when compared with the product obtained from the dehydration reaction of the reference compound (−)-elemol (Toyooka et al., 1997).

As a philogenetic peculiarity of liverworts both groups of newly identified amorphane and elemane ses-

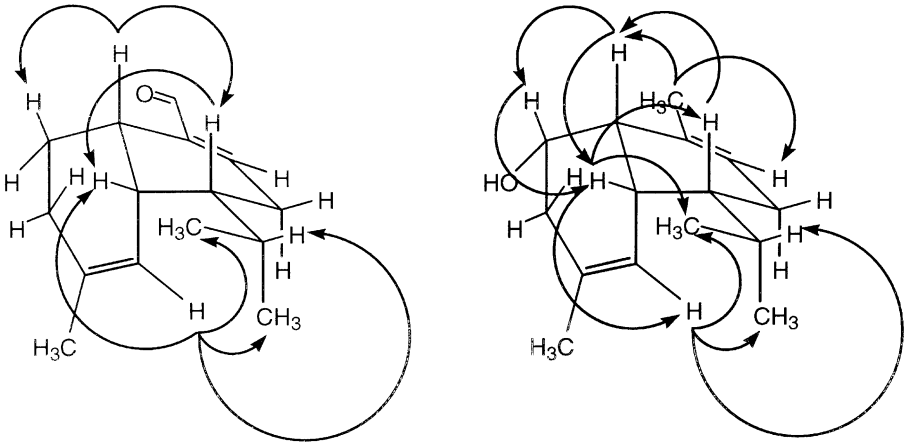
H
O
H
H
H

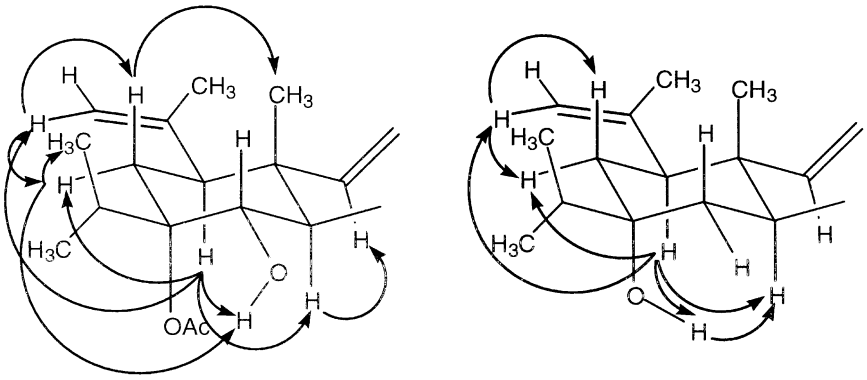

Fig. 4. Important NOE contacts of the elemanes **9** and **10**.

quiterpenes display opposite configuration as compared to higher plants. Again enantioselective GC proved as a sensitive technique in stereochemical analysis as long as reference compounds with known absolute configuration are available (König et al., 1999).

3. Experimental

3.1. General experimental procedures

3.1.1. Gas chromatography

Orion Micromat 412 double column instrument with 25 m fused silica capillaries with polysiloxane CPSil-5 and polysiloxane CPSil-19 (Chrompack); Carlo Erba Fractovap 2150 or 4160 gas chromatographs with 25 m fused silica capillaries with octakis(2,6-di-*O*-methyl-3-*O*-pentyl)-γ-cyclodextrin, heptakis(2,6-di-*O*-methyl-3-*O*-pentyl)-β-cyclodextrin or heptakis(6-*O*-tert-butyldimethylsilyl-2,3-di-*O*-methyl)-β-cyclodextrin in OV 1701 (50%, w/w), split injection; split ratio approx. 1:30; FID; carrier gas 0.5 bar H_2; injector and detector temperatures 200 and 250 °C, respectively.

3.1.2. Preparative GC

Modified Varian 1400 and 2800 instruments, equipped with a stainless steel column (1.85 m× 4.3 mm) with 10% polydimethylsiloxane SE-30 on Chromosorb W-HP or with 2.5% octakis(2,6-di-*O*-methyl-3-*O*-pentyl)-γ-cyclodextrin in OV-1701 (50 %, w/w) on Chromosorb G-HP or with 6 % heptakis(6-*O*-tert-butyldimethylsilyl-2,3-di-*O*-methyl)-β-cyclodextrin in SE-52 (50 %, w/w) on Chromosorb W-HP; FID; helium as carrier gas at a flow rate of 240 ml/min; injector and detector temperatures were 200 and 250 °C, respectively.

3.1.3. GC-MS

GC-MS measurements (EI, 70 eV) were carried out with a Hewlett Packard HP 5890 gas chromatograph coupled to a VG Analytical 70-250S mass spectrometer. Ion source temperature: 200° C.

3.1.4. NMR-spectroscopy

NMR measurements were carried out with a Bruker WM 400 or a Bruker WM 500 instrument using TMS as internal standard.

3.1.5. Polarimetry

Measurements were performed with a Polarimeter 341 (Perkin Elmer) at 589 nm at 20 °C. Due to the very small amounts of isolated compounds only the sense of optical rotation is given to avoid inaccuracies.

All microreactions were carried out with approx. 50 μg of sample; in cases where NMR investigation followed the transformation up to 0.5 mg of sample was used.

Dehydration of **1** was carried out by addition of phosphoryl chloride to a solution of the compound in benzene at 0 °C. After 0.5 h of stirring water was added and the workup was performed with aq. $NaHCO_3$ solution and benzene extraction. For (−)-elemol and **10,** the same conditions were applied with pyridine as the solvent.

Hydrogenation of **1**, **2, 3** and **8** was executed by bubbling hydrogen gas through the sample dissolved in hexane with an addition of palladium-charcoal for 1 min and additional stirring of the reaction mixture under slight positive hydrogen pressure for 3 h. Partial reduction of **6**, **7** and **8** was performed with H_2-Pd/C (1 min bubbling H_2 through the solution) in hexane/benzene 70:30 and additional stirring under hydrogen atmosphere for 30 min. Further hydrogenation of **4** was achieved by addition of an ether solution of $LiAlH_4$ to the cooled sample of **4** in ether. The reaction was quenched with water after 40 min and extracted twice with ether, and the ether phase dried over $MgSO_4$. After removal of the solvent the sample was taken up in benzene.

Rearrangement reaction of (+)-**1** was performed at room temperature in benzene with an addition of Amberlyst®. Samples were taken after 30 and 105 min respectively, and analysed by GC-MS.

3.2. Plant material and essential oils

L. fauriana was collected at Yuanyang Lake, alt. 1700 m, Hsinchu Hsien, Taiwan, in March 1998 (voucher no. YY-9803-11), and twice in April 1999 (voucher nos. YY-9904-30, YYF-9904-42). The essential oils of the liverworts were obtained by hydrodistillation (2 h) of ca. 70 g of air dried liverworts using *ca.* 1 ml of *n*-hexane as collection solvent. *L. vitrea* (voucher no. SP-9709-60) was collected in Sheipa National Park, Hsinchu Hsien, at 2000 m alt. in September 1997. 35 g of the plant material was ground and hydrodistilled yielding ca. 0.6 ml of a purple oil. Specimens of all collections are deposited at Tamkang University, Tamsui, Taiwan.

3.3. Isolation of single constituents of essential oils

The isolation was carried out using preparative GC: The oil of *L. fauriana* YYF-9904-42 was fractionated using SE-30 at 120 °C with a heating rate of 2 °C/min and yielded **1**, **2**, **3** and **11** as pure fractions. A prefractionation of oil from sample YY-9904-30 was conducted with SE-30 (120 °C; 2 °C/min) and **6**, **7**, **8** and **14** were obtained with impurities, that were removed by further gas chromatographic fractionation on octakis(2,6-di-*O*-methyl-3-*O*-pentyl)-γ-cyclodextrin. Prefractionation of *L. vitrea* oil SP-9709-60 (SE-30; 120 °C; 2 °C/min) yielded **11** and further purification using octakis(2,6-di-*O*-methyl-3-*O*-pentyl)-γ-cyclodextrin (170 °C/ 20 min; 175 °C/10 min) gave **10**. Compounds **12** and **13** were obtained using heptakis(6-*O*-tert-butyldimethylsilyl-2,3-di-*O*-methyl)-β-cyclodextrin (140 °C isothermal) and **9** and **15** could be separated from each other using heptakis(6-*O*-*tert*-butyldimethylsilyl-2,3-di-*O*-methyl)-β-cyclodextrin (160 °C isothermal) and octakis(2,6-di-*O*-methyl-3-*O*-pentyl)-γ-cyclodextrin, consecutively (Fig. 5).

3.4. Dihydrochiloscypholone (*1*)

(+)-(1*S*,3a*R*,7*S*,7a*S*)-2,3,3a,4,5,6,7,7a-Octahydro-3a-hydroxyl-7,7a-dimethyl-1-(2-methylpropanonyl)-1*H*-indene, colourless oil; RI_{CPSil5}: 1718; sense of optical rotation (benzene): +; ^{1}H NMR (500.1 MHz, C_6D_6): δ 0.57 (3H, *d*, H-15, *J* = 6.6 Hz), 0.63 (3H, *s*, H-14), 0.80 (3H, *d*, H-12, *J* = 7.9 Hz), 0.94 (3H, *d*, H-13, J = 7.6 Hz), 1.04–1.13 (1H, *m*, H-3a), 1.32–1.49 (3H, *m*, H-1a, H-2a, H-3b), 1.56–1.72 (3H, *m*, H-8a,b, H-9a), 1.85-1.89 (1H, *m*, H-9b), 1.91 (1H, *dd*, H-1b, *J* = 5.1, 12.9 Hz), 2.25–2.33 (2H, *m*, H-2b, H-11), 2.37–2.41 (1H, *m*, H-4), 2.60–2.63 (1H, *m*, H-6), 5.62 (1H, *d*, O*H*, *J* = 3.5 Hz); ^{13}C NMR (125.8 MHz, C_6D_6): δ 17.41 (*q*, C-12), 17.88 (*q*, C-15), 18.64 (*q*, C-13), 20.39 (*q*, C-14), 21.19 (*t*, C-2), 27.61 (*t*, C-8), 29.82 (*d*, C-4), 29.84 (*t*, C-3), 30.50 (*t*, C-1), 38.63 (*t*, C-9), 43.02 (*d*, C-11), 53.82 (*s*, C-5), 57.48 (*d*, C-6), 81.17 (*s*, C-10), 221.20 (*s*, C-7); MS (EI, 70 eV), *m*/*z* (rel. int.): 238 $[M]^+$(3), 149 (100), 139 (29), 122 (16), 107 (18), 93 (24), 81 (15), 79 (11), 71 (15), 69 (15), 55 (24), 43 (71), 41 (36).

3.5. 11,12-Dihydrochiloscyphone (*2*)

(+)-(1*S*,7*S*,7a*S*)-2,3,5,6,7,7a-Hexahydro-7,7a-dimethyl-1-(2-methylpropanonyl)-1*H*-indene, colourless oil; RI_{CPSil5}: 1561; sense of optical rotation (benzene): +; ^{1}H NMR (400.1 MHz, C_6D_6): δ 0.81 (3H, *s*, H-14), 0.83 (3H, *d*, H-15, *J* = 6.9 Hz), 0.91 (3H, *d*, H-13, *J* = 6.9 Hz), 0.99 (3H, *d*, H-12, *J* = 6.9 Hz), 1.30∼.36 (2H, *m*, H-3a,b), 1.55–1.70 (3H, *m*, H-4, H-8a,b), 1.86–1.97 (1H, *m*, H-2a), 2.00–2.10 (1H, *m*, H-2b), 2.40–2.49 (2H, *m*, H-9a, H-11), 2.56–2.64 (1H, *m*, H-9b), 2.75 (1H, *dd*, H-6, *J* = 1.3 ; 7.25 Hz), 5.44 (1H, *d*, H-1, *J* = 2.2 Hz); ^{13}C NMR (125.8 MHz, C_6D_6): δ 17.94 (*q*, C-15), 18.23 (*q*, C-12), 19.40 (*q*, C-13), 21.05 (*q*, C-14), 26.19 (*t*, C-2), 26.46 (*t*, C-8), 27.81 (*t*, C-3), 29.76 (*t*, C-9), 33.67 (*d*, C-4), 42.27 (*d*, C-11), 49.65 (*s*, C-5), 58.76 (*d*, C-6), 117.98 (*d*, C-1), 146.70 (*s*, C-10), 226.02 (*s*, C-7); MS (EI, 70 eV), *m*/*z* (rel. int.): 220 $[M]^+$(12), 149 (97), 122 (57), 107 (55), 93 (36), 91 (29), 79 (25), 71 (23), 55 (24), 43 (100), 41 (41).

3.6. 7,10-Anhydro-11,12-dihydrochiloscypholone (*3*)

(+)-(1*R*,5*S*,6*S*,7*S*)-5,6-Dimethyl-9-oxo-8-isopropylidene-tricyclo[5.2.2.0^{1,6}]undecane, colourless oil; RI_{CPSil5}: 1452; sense of optical rotation (benzene): +; ^{1}H NMR (500.1 MHz, C_6D_6): δ 0.56 (3H, *s*, H-14), 0.74 (3H, *d*, H-15, *J* = 7.9 Hz), 0.92–1.00 (1H, *m*, H-3a), 1.12 (1H, *m*, H-1a), 1.24–1.32 (1H, *m*, H-3b), 1.39–1.52 (3H, *m*, H-2a, H-8a, H-9a), 1.67 (3H, *s*, H-13), 1.58–1.66 (1H, *m*, H-8b), 1.65–1.73 (1H, *m*, H-9b), 1.79–1.89 (2H, *m*, H-1b, H-2b), 1.85 (3H, *s*, H-12), 1.93–2.10 (1H, *m*, H-4), 2.58 (1H, *d*, H-6, *J* = 3.8 Hz); ^{13}C NMR (125.8 MHz, C_6D_6): δ 10.85 (*q*, C-14), 16.45 (*q*, C-12), 17.91 (*q*, C-15), 19.18 (*q*, C-13), 22.50 (*t*, C-2), 25.89 (*t*, C-8), 27.10 (*t*, C-1), 29.93 (*t*, C-3), 32.08 (*d*, C-4), 34.48 (*t*, C-9), 47.17 (*d*, C-6), 50.72 (*s*, C-5), 89.10 (*s*, C-10), 95.05 (*s*, C-11), 152.90 (*s*, C-7); MS (EI, 70 eV), *m*/*z* (rel. int.): 220 $[M]^+$(49), 150 (49), 149 (64), 135 (100) 107 (58), 94 (50), 93 (55), 79 (40), 70 (50), 41 (60).

3.7. (+)-(1S,3aR,7S,7aR)-2,3,3a,4,5,6,7,7a-Octahydro-7,7a-dimethyl-1-(2-methylpropanonyl)-1H-indene (*4*)

Colourless oil; RI_{CPSil5}: 1601; sense of optical rotation (benzene): +; ^{1}H NMR (500.1 MHz, C_6D_6): δ 0.62 (3H, *d*, H-12/13, *J* = 7 Hz), 0.84–0.95 (1H, *m*, H-3a), 0.91 (3H, *d*, H-15, *J* = 7 Hz), 0.97 (3H, *s*, H-14), 1.11 (3H, *d*,

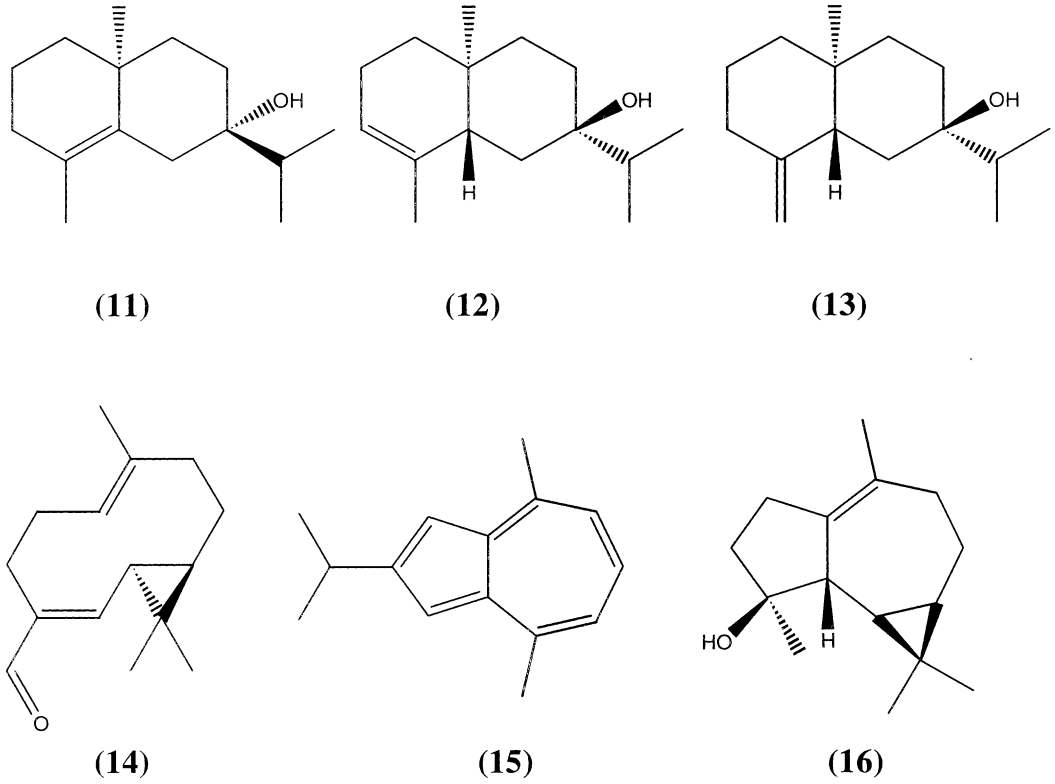

Fig. 5. Additional compounds identified from *L. fauriana* (**11**, **14**, **16**) and *L. vitrea* (**11**, **12**, **13**, **14**, **15**).

H-12/13, $J=7$ Hz), 1.23–1.46 (6H, *m*, H-1a,b, H-2a,b, H-3b, H-9a), 1.48–1.59 (2H, *m*, H-8a, H-10), 1.62–1.74 (2H, *m*, H-4, H-9b), 2.40–2.49 (1H, *m*, H-8b), 2.49–2.56 (2H, *m*, H-6, H-11); ^{13}C (100.6 MHz, C_6D_6); 1×C missing: δ 17.6 (*q*, C-12/13), 19.0 (*q*, C-15), 20.0 (*q*, C-14), 20.1 (*q*, C-12/13), 20.6 (*t*, C-2), 24.6, 24.9, 25.4 (each *t*, C-1, C-8, C-9), 29.2 (*d*, C-4), 32.2 (*t*, C-3), 42.4 (*d*, C-11), 48.9 (*s*, C-5), 49.5 (*d*, C-10), 61.7 (*d*, C-6); MS (EI, 70 eV), *m*/*z* (rel. int.): 222 $[M]^+$ (7), 151 (25), 136 (55), 109 (88), 95 (100), 81 (55), 67 (30), 55 (34), 43 (97), 41 (64).

3.8. (+)-(1S,3aR,7S,7aR)-2,3,3a,4,5,6,7,7a-Octahydro-7,7a-dimethyl-1-(2-methylpropanolyl)-1H-indene (5)

Colourless oil; RI_{CPSil5}: 1645; sense of optical rotation (benzene): +; ^{1}H NMR (500.1 MHz, C_6D_6): δ 0.75, 0.88 (each 3H, 2×*d*, H-12, H-13, 2×$J=7$ Hz), 1.07 (3H, *d*, H-15, $J=6$ Hz), 1.17 (3H, *s*, H-14), 1.28–1.59 (13H, *m*, H-1a,b, H-2a,b, H-3a,b, H-4, H-6, H-8a,b, H-9a,b, H-10, H-11), 3.45–3.51 (1H, *m*, H-7); ^{13}C (125.8 MHz, HSQC-experiment, C_6D_6): δ 12.5 (*q*), 2× 21.0 (*q*), 23.0 (*t*), 24.7 (*q*/*d*), 24.9 (*q*/*d*), 25.3 (*t*), 30.0 (*d*), 48.9 (*d*), 57.2 (*d*), 77.4 (*d*); MS (EI, 70 eV), *m*/*z* (rel. int.): 224 $[M]^+$ (0), 206 (5), 163 (100), 109 (59), 95 (52), 81 (71), 69 (43), 55 (60), 43 (58), 41 (68).

3.9. Amorpha-4,9-dien-14-al (6)

(+)-(4*R*,4a*R*,8a*S*)-3,4,4a,7,8,8a-Hexahydro-6-methyl-4-(1-methylethyl)-naphthalene-1-carbaldehyde; colourless oil; RI_{CPSil5}: 1692; sense of optical rotation (benzene): +; ^{1}H NMR (500.1 MHz, C_6D_6): δ 0.76 and 0.82 (each 3H, 2×*d*, H-12, H-13, $J=7$ Hz), 0.79–0.86 (1H, *m*, H-7), 1.39 (1H, 2*q*, H-11, $J=7$ Hz), 1.54 (3H, *s*, H-15), 1.58–1.70 (3H, *m*, H-2a, H-3a, H-8a), 1.70–1.77 (1H, *m*, H-3b), 1.83–1.89 (1H, *m*, H-8b), 2.60 (1H, *br. s*, H-6), 2.71 (1H, br. *s*, H-1), 2.98–3.03 (1H, *m*, H-2b), 5.06 (1H, *s*, H-5), 6.15 (1H, *d*, H-9, $J=6$ Hz), 9.37 (1H, *s*, H-14); ^{13}C [data taken from HMBC/HSQC (500.13 MHz)]: δ 21.3, 21.8 (2×*q*, C-12, C-13), 24.1 (*q*, C-15), 24.6 (*t*, C-2), 27.0 (*t*, C-3), 28.4 (*t*, C-8), 29.4 (*d*, C-11), 34.8 (*d*, C-1), 36.3 (*d*, C-6), 44.2 (*d*, C-7), 119.4 (*d*, C-5), 137.0 (*s*, C-4), 142.4 (*s*, C-10), 153.5 (*d*, C-9), 193.5 (*d*, C-14); MS (EI, 70 eV), *m*/*z* (rel. int.): 218 $[M]^+$ (13), 175 (39), 162 (31), 149 (22), 117 (22), 107 (70), 105 (31), 91 (100), 81 (22), 79 (34), 77 (32), 59 (21), 55 (22), 43 (27), 41 (64), 39 (27).

3.10. Amorpha-4,9-dien-2-ol (7)

(+)-(1*S*,4a*S*,5*R*,8a*S*)-1,2,4a,5,6,8a-Hexahydro-3,8-dimethyl-5-(1-methylethyl)-naphthalenol; colourless oil;

RI_{CPSil5}: 1687; sense of optical rotation (benzene): +; ^{1}H NMR (500.1 MHz, C_6D_6): δ 0.87 and 0.91 (each 3H, 2×*d*, H-12, H-13, J=7 Hz), 1.05-1.12 (1H, *m*, H-7), 1.49 (1H, 2*q*, H-11, J=7 Hz), 1.57 (3H, *s*, H-15), 1.57–1.66 (1H, *m*, H-8a), 1.85 (1H, *dd*, H-3a, J=5, 16 Hz), 1.93–2.00 (1H, *m*, H-8b), 2.01 (3H, *s*, H-14), 2.12–2.18 (1H, *m*, H-3b), 2.30 (1H, br. *s*, H-1), 2.62 (1H, br. *s*, H-6), 3.82–3.85 (1H, *m*, H-2), 5.14 (1H, *s*, H-5), 5.49 (1H, *d*, H-9, J=4 Hz); ^{13}C [data taken from HMBC/HSQC (500.13 MHz), 1×CH_2 missing]: δ 21.0, 21.7 (2×*q*, C-12, C-13), 2×24.1 (2×*q*, C-14, C-15), 29.4 (*d*, C-11), 36.4 (*t*, C-3), 38.6 (*d*, C-6), 45.3 (*d*, C-7), 46.3 (*d*, C-1), 72.6 (*t*, C-2), 120.2 (*d*, C-5), 126.0 (*d*, C-9), 133.5 (*s*, C-10), 134.4 (*s*, C-4); MS (EI, 70 eV), *m*/*z* (rel. int.): 220 $[M]^+$ (22), 159 (100), 133 (25), 119 (22), 109 (33), 107 (25), 105 (53), 95 (22), 93 (65), 91 (46), 81 (21), 79 (24), 77 (30), 55 (33), 43 (54), 41 (71), 39 (24).

3.11. 7,14-Anhydro-amorpha-4,9-diene (**8**)

(+)-(2*S*,7*R*,8*S*)-5-Methyl-8-(1-methylethyl)-9-oxa-tricyclo[6.2.2.0^{2,7}]dodeca-1(11),5-diene; colourless oil; RI_{CPSil5}: 1735; sense of optical rotation (benzene): +; ^{1}H NMR (500.1 MHz, C_6D_6): δ 0.89 and 0.93 (each 3H, *d*, H-12, H-13, J=7 Hz), 1.25–2.10 (6H, *m*), 1.52–1.62 (1H, *m*, H-11, J=7 Hz), 1.61 (3H, *s*, H-15), 2.48 (1H, br. *s*, H-1), 2.68 (1H, br. *s*, H-6), 3.81 and 3.99 (2×1H, 2×*d*, H-14a,b, J=13 Hz), 5.26 (1H, *s*, H-5), 5.61 (1H, *d*, H-9, J=3 Hz); ^{13}C [data taken from HSQC (500.13 MHz), 6×*C* missing]: δ 21.1, 21.9 (2×*q*, C-12, C-13), 24.4 (*q*, C-14), 27.7 (*d*, C-11), 30.8 (*t*), 35.7 (*d*, C-6/1), 52.3 (*t*, C-15), 120.3 (*d*, C-5), 126.0 (*d*, C-9); MS (EI, 70 eV), *m*/*z* (rel. int.): 218 $[M]^+$ (1), 202 (28), 187 (27), 159 (50), 146 (53), 131 (28), 117 (27), 105 (41), 93 (37), 92 (31), 91 (100), 81 (32), 79 (47), 77 (30), 55 (27), 43 (32), 41 (50).

3.12. 7-Acetoxy-elema-1,3-dien-8-ol (**9**)

(+)-(1*R*,2*R*,4*R*,5*R*)-4-Ethenyl-2-hydroxy-4-methyl-5-(1-methylethenyl)-1-(1-methylethyl)-cyclohexylacetate; colourless oil; RI_{CPSil5}: 1793; sense of optical rotation (benzene): +; ^{1}H NMR (500.1 MHz, C_6D_6): δ 0.55 (1H, *s*, O*H*-8), 0.73 and 0.74 (each 3H, *d*, H-12, H-13, J=9 Hz), 1.07 (3H, *s*, H-14), 1.59 (1H, br.*d*, H-6a, J=14 Hz), 1.68 (3H, *s*, OOC-CH_3), 1.69–1.72 (2H, *m*, H-9a, H-11), 1.73 (3H, *s*, H-15), 1.81 (1H, *dd*, H-6b, J=2× ~14 Hz), 2.03 (1H, *dd*, H-9b, J=3, 15 Hz), 2.50 (1H, *dd*, H-5, J=3, 13 Hz), 4.73 (1H, *s*, H-3a), .90 (1H, *d*, H-2a, J=18 Hz), 4.91 (1H, *d*, H-2b, J=10 Hz), 4.94 (1H, *dd*, H-8, J=2, 5 Hz), 4.95 (1H, *m*, H-3b), 5.77 (1H, *dd*, H-1, J=10, 18 Hz); ^{13}C [125.77 MHz, C_6D_6 and data taken from HMBC (500.13 MHz)]: δ 2×16.0 (2×*q*, C-12, C-13), 18.8 (*q*, C-14), 20.9 (*q*, OOC-*C*H_3), 25.2 (*q*, C-15), 33.8 (*d*, C-11), 34.5 (*t*, C-6), 2×38.7 (*t*, *s*,C-9, C-10), 46.0 (*d*, C-5), 72.2 (*d*, C-8), 73.5 (*s*, C-7), 110.7 (*t*, C-2), 113.0 (*t*, C-3), 147.2 (*s*, C-4), 150.3 (*d*, C-1), 169.3 (*s*, OO*C*-CH_3); MS (EI, 70 eV), *m*/*z* (rel. int.): 280 $[M]^+$ (0), 237 (3), 177 (74), 159 (50), 139 (45), 109 (29), 107 (20), 93 (22), 81 (29), 71 (32), 69 (22), 43 (100), 41 (27).

3.13. Elema-1,3-dien-7-ol (**10**)

(+)-(1*R*,3*R*,4*R*)-4-Ethenyl-4-methyl-3-(1-methylethenyl)-1-(1-methylethyl)-cyclohexanol; colourless oil; RI_{CPSil5}: 1531; sense of optical rotation (benzene): +; ^{1}H NMR (500.1 MHz, C_6D_6): δ 0.42 (1H, *s*, O*H*-7), 0.82 (6H, 2*d*, H-12, H-13, each J=7 Hz), 0.94 (3H, *s*, H-14), 1.17 (1H, br. *d*, H-9a, J=13 Hz), 1.23–1.35 (3H, *m*, H-8a,b, H-11), 1.39 (1H, br. *d*, H-6a, J=14 Hz), 1.56 (1H, *dd*, H-6b, J=13, 14 Hz), 1.74 (3H, *s*, H-15), 1.89 (1H, *dt*, H-9b, J=5, 13 Hz), 2.49 (1H, *dd*, H-5, J=3, Hz), 4.69 (1H, br. *s*, H-3a), 4.93–4.96 (2H, *m*, H-2a, H-3b), 4.98 (1H, *d*, H-2b, J=17 Hz), 5.90 (1H, *dd*, H-1, J=11 Hz, 17 Hz); ^{13}C (125.77 MHz, C_6D_6): δ 15.7 (*q*, C-14), 2×16.9 (2×*q*, C-12, C-13), 25.4 (*q*, C-15), 29.7 (*t*, C-8), 35.3 (*t*, C-9), 36.1 (*t*, C-6), 39.2 (*d*, C-11), 40.0 (*s*, C-10), 47.2 (*d*, C-5), 72.9 (*s*, C-7), 110.1 (*t*, C-2), 112.5 (*t*, C-3), 147.8 (*s*, C-4), 150.4 (*d*, C-1); MS (EI, 70 eV), *m*/*z* (rel. int.): 222 $[M]^+$ (2), 204 (4), 161 (32), 121 (27), 105 (18), 93 (46), 81 (34), 71 (58), 69 (30), 67 (26), 55 (22), 53 (21), 43 (100), 41 (57).

3.14. Eudesm-4-en-7α-ol (**11**)

(−)-1,2,3,4,4a,5,6,7-Octahydro-4a,8-dimethyl-2-(1-methylethyl)-naphthalen-2-ol; colourless oil; RI_{CPSil5}: 1606; sense of optical rotation (benzene): −; ^{1}H NMR (500.1 MHz, C_6D_6): δ 0.97 (3H, *s*, H-14), 1.01 and 1.04 (2× 3H, 2× *d*, H-12, H-13, each J=7 Hz), 1.27–1.31 (2H, *m*, H-1a, H-9a), 1.43 (1H, *s*, O*H*-7), 1.43–1.55 (6H, *m*, H-1b, H-6a,b, H-8a,b, H-9b), 1.55 (3H, *s*, CH_3-4), 1.66 (1H, 2*q*, H-11, J=7 Hz), 1.73-1.90 (2H, *m*, H-2a,b), 1.95 (1H, br.*d*, H-3a, J=14 Hz), 2.48 (1H, *dd*, H-3b, J=3, 14 Hz); ^{13}C (125.77 MHz, C_6D_6): δ 16.0, 16.2 (2×*q*, C-12, C-13), 18.2 (*q*, C-15), 18.2 (*t*, C-6), 22.9 (*q*, C-14), 28.6 (*d*, C-8), 32.2 (*t*, C-2), 33.4 (*t*, C-3), 33.5 (*s*, C-10), 36.7 (*t*, C-9), 36.7 (*d*, C-11), 39.1 (*t*, C-1), 73.2 (*s*, C-7), 127.9 (*s*, C-4), 131.1 (*s*, C-5); MS (EI, 70 eV), *m*/*z* (rel. int.): 222 $[M]^+$ (3), 179 (6), 124 (11), 123 (100), 121 (6), 105 (6), 93 (6), 91 (9), 81 (13), 79 (7), 67 (6), 55 (8), 43 (22), 41 (16).

3.15. Eudesm-3-en-7-ol (**12**)

(+)-(2*R*,4a*S*,8a*R*)-1,2,3,4,4a,5,6,8a-Octahydro-4a,8-dimethyl-2-(1-methylethyl)-2-naphthalenol; colourless oil; RI_{CPSil5}: 1650; sense of optical rotation (benzene): +; ^{1}H NMR (500.1 MHz, C_6D_6): δ 0.48 (1H, *s*, O*H*), 0.77 (3H, *s*, H-14), 0.86 and 0.88 (2×3H, 2×*d*, H-12, H-13), 1.14–1.23 (2H, *m*, H-6a, H-8a), 1.23–1.28 (1H, *m*, H-9a), 1.30–1.46 (3H, *m*, H-1a,b, H-11), 1.49 (1H, *s*, H-9b), 1.50 (1H, *s*, H-8b), 1.57–1.62 (4H, *m*, H-15, H-6b), 1.94–2.02 (1H, *m*, H-2a), 2.08–2.18 (1H, *m*, H-2b), 2.42

(1H, *d*, H-5, $J=14$ Hz), 5.39 (1H, *s*, H-3); ^{13}C (100.6 MHz, C_6D_6): δ 14.8 (q, C-14), 2× 17.0 (2×*q*, C-12, C-13), 21.3 (*q*, C-15), 23.4 (*t*, C-2), 29.7 (*t*, C-9), 2×32.8 (*s*+*t*, C-10, C-6), 36.1 (*t*, C-8), 38.1 (*t*, C-1), 39.8 (*d*, C-11), 41.3 (*d*, C-5), 73.8 (*s*, C-7), 121.5 (*d*, C-3), 135.8 (*s*, C-4); MS (EI, 70 eV), *m*/*z* (rel. int.): 222 $[M]^+$ (0), 204 (17), 162 (14), 161 (100), 121 (14), 119 (15), 107 (10), 105 (20), 95 (16), 93 (16), 91 (16), 81 (26), 79 (13), 67 (12), 55 (13), 43 (34), 41 (24).

3.16. Eudesm-4(15)-en-7-ol (**13**)

(−)-(2*R*,4a*S*,8a*R*)-Decahydro-4a-methyl-8-methylene-2-(1-methylethyl)-2-naphthalenol; colourless oil; RICPSil5: 1643; sense of optical rotation (benzene): −, (+)-enantiomer present in *L. vitrea*: ca. 7% of both enantiomers; ^{1}H NMR (500.1 MHz, C_6D_6): δ 0.69 (3H, *s*, H-14), 0.84 (6H, *d*, H-12, H-13, $J=7$ Hz), 1.14–1.20 (1H, *m*, H-9a), 1.24–1.44 (7H, *m*, H-1a,b, H-6a,b, H-8a,b, H-11), 1.46–1.55 (1H, *m*, H-2a), 1.55–1.68 (2H, *m*, H-2b, H-9b), 2.00 (1H, *ddd*, H-3a), 2.20–2.33 (2H, *m*, H-3b, H-5), 4.52 (1H, *d*, H-15a, $J=2$ Hz), 4.82 (1H, *d*, H-15b, $J=1$ Hz); ^{13}C [data taken from HSQC/HMBC (500.1 MHz, C_6D_6)]: δ 15.6 (q, C-14), 2×17.2 (2×*q*, C-12, C-13), 24.1 (*t*, C-2), 30.2 (*t*, C-8), 32.9 (*t*, C-6), 36.5 (*s*, C-10), 37.0 (*t*, C-9), 37.5 (*t*, C-3), 39.6 (*d*, C-11), 42.1 (*t*, C-1), 44.4 (*d*, C-5), 73.5 (*s*, C-7), 105.4 (*t*, C-15), 151.4 (*s*, C-4); MS (EI, 70 eV), *m*/*z* (rel. int.): 222 $[M]^+$ (0), 204 (33), 189 (10), 179 (52), 161 (100), 133 (31), 119 (30), 105 (40), 93 (30), 91 (34), 81 (34), 43 (79), 41 (51).

3.17. Lepidozenal (**14**)

NMR data in complete accordance to Zheng et al. (1990); MS data identical to that of Matsuo et al. (1984).

3.18. Vetivazulene (**15**)

4,8-Dimethyl-2-(1-methylethyl)-azulene; violett oil; RI_{CPSil5}: 1787; ^{1}H NMR (500.1 MHz, C_6D_6): δ 1.46 (6H, *d*, CH(C*H*$_3$)$_2$, $J=7$ Hz), 2.65 (6H, *s*, C*H*$_3$-4, C*H*$_3$-8), 3.30 (1H, *septett*, C*H*(CH$_3$)$_2$, $J=7$ Hz), 6.85 (2H, *d*, H-5, H-7, $J=10$ Hz), 7.12 (1H, *t*, H-6, $J=10$ Hz), 7.33 (2H, *s*, H-1, H-3); ^{1}H NMR (500.1 MHz, CCl_4): δ 1.40 (6H, *d*, CH(C*H*$_3$)$_2$, $J=7$ Hz), 2.65 (6H, *s*, C*H*$_3$-4, C*H*$_3$-8), 3.24 (1H, *septett*, C*H*(CH$_3$)$_2$, $J=7$ Hz), 6.97 (2H, *d*, H-5, H-7, $J=10$ Hz), 7.10 (2H, *s*, H-1, H-3), 7.26 (1H, *t*, H-6, $J=10$ Hz); ^{13}C data taken from HMBC (500.13 MHz, C_6D_6): δ 24.6 (2×*q*, CH(*C*H$_3$)$_2$), 24.7 (2×*q*, *C*H$_3$-4, *C*H$_3$-8), 31.0 (*d*, *C*H(CH$_3$)$_2$), 114.2 (2×*d*, C-1, C-3), 125.8 (2×*d*, C-5, C-7), 135.0 (*d*, C-6), 138.7 (2×*s*, C-4, C-8 tentative), 144.6 (2×*s*, C-3a, C-8a tentative), 158.4 (*s*, C-2); MS (EI, 70 eV), *m*/*z* (rel. int.): 198 $[M]^+$ (38), 183 (40), 177 (17), 168 (13), 159 (13), 139 (14), 81 (15), 71 (20), 69 (14), 43 (100), 41 (30).

3.19. Isospathulenol (**16**)

(−)-1,2,3,3a,4,5,6,7-Octahydro-3-hydroxyl-3,8-dimethyl-(1′,1′-dimethyl-cyclopropyl)[e]azulene; colourless oil; RI_{CPSil5}: 1630; sense of optical rotation (benzene): −; ^{1}H NMR (500.1 MHz, C_6D_6): δ 0.48–0.54 (2H, *m*, H-6, H-7), 0.97 (3H, *s*, H-12), 1.09 (3H, *s*, H-13), 1.16 (3H, *s*, H-15), 1.40–1.67 (4H, *m*, H-3a,b, H-8a,b), 1.60 (3H, br *s*, H-14), 2.13-2.18 (2H, *m*, H-9a,b), 2.24–2.30 (1H, *m*, H-2a), 2.38–2.44 (2H, *m*, H-2b, H-5); ^{13}C [data taken from HSQC/HMBC (500.13 MHz) 2×CH_2 missing]: δ 16.3 (*q*, C-13), 19.4 (*d*, C-7/6), 22.0 (*q*, C-14), 24.8 (*q*, C-15), 26.1 (*d*, C-6/7), 29.0 (*q*, C-12), 32.7 (*s*, C-11), 36.9 (*t*, C-9), 39.3 (*t*, C-3), 49.6 (*d*, C-5), 81.1 (*s*, C-4), 125.9 (*s*, C-10/1), 138.3 (*s*, C-1/10); MS (EI, 70 eV), *m*/*z* (rel. Int.): 220 $[M]^+$ (12), 205 (12), 202 (16), 159 (37), 133 (31), 119 (55), 105 (51), 93 (50), 91 (57), 79 (31), 77 (32), 43 (100), 41 (76).

Tables containing two-dimensional correlations for **1** and all new compounds (**2**–**10**) can be obtained upon request from the authors.

Acknowledgements

We thank Dr. Volker Sinnwell, University of Hamburg, for helpful comments in the course of NMR interpretations. The financial support of the DAAD (DAAD-NSC Project Based Personnel Exchange Programme) and of the Fonds der Chemischen Industrie is gratefully acknowledged.

References

Asakawa, Y., 1995. Chemical constituents of the bryophytes. In: Herz, W., Kirby, G.W., Moore, R.E., Steglich, W., Tamm, C. (Eds.), Progress in the Chemistry of Organic Natural Compounds, Vol. 65. Springer, Vienna, New York.

Barrero, A.F., Artega, P., Quilez, J.F., Rodriguez, I., Herrador, M.M., 1997. Sesquiterpene glycosides and phenylpropanoid esters from *Phonus arborescens* (*Carthamus arborescens*). Journal of Natural Products 60, 1026–1030.

Bellesia, F., Pagnoni, U.M., Trave, R., 1976. Stereospecific cyclisation of agerol to an isovetivane carbon framework. Journal of the Chemical Society Chemical Communications, 34–35.

Bülow, N., König, W.A., 2000. The role of germacrene D as a precursor in sesquiterpene biosynthesis: investigations of acid catalyzed, photochemically and thermally induced rearrangements. Phytochemistry 55, 141–168.

Hayashi, A., Kurokawa, S., Matsuura, T., 1969. Reaction of vetivazulene with sulfur. 3,5,9-Trimethylazuleno[1,2-b]thiophene. Bulletin of the Chemical Society of Japan 42, 1404–1407.

Joulain, D., König, W.A., 1998. The Atlas of Spectral Data of Sesquiterpene Hydrocarbons. E.B.-Verlag, Hamburg.

König, W.A., Bülow, N., Saritas, Y., 1999. Identification of sesquiterpene hydrocarbons by gas phase analytical methods. Flavour and Fragrance Journal 14, 367–378.

Maurer, B., Hauser, A., 1983. New sesquiterpenoids from clary sage oil (*Salvia sclarea* L.). Helvetica Chimica Acta 66, 2223–2235.

Matsuo, A., Uto, S., Nozaki, H., Nakayama, M., Hayashi, S., 1980. X-Ray crystal structure of (+)-vitrenal, a sesquiterpenoid plant-

growth inhibitor containing a novel carbon skeleton isolated from the liverwort *Lepidozia vitrea*. Journal of the Chemical Society Chemical Communications, 1220–1222.

Matsuo, A., Nozaki, H., Kubota, N., Uto, S., Nakayama, M., 1984. Structure and conformations of (−)-isobicyclogermacrenal and (−)-lepidozenal, two key sesquiterpenoids of the *cis*- and *trans*-10,3-bicyclic ring systems, from the liverwort *Lepidozia vitrea*: X-ray crystal stucture and analysis of the hydroxy derivative of (−)-isobicyclogermacrenal. Journal of the Chemical Society Perkin Transactions 1, 203–214.

Nagashima, F., Tanaka, H., Asakawa, Y., 1996. Sesqui- and diterpenoids from the liverwort *Jungermannia vulcanicola*. Phytochemistry 42, 93–96.

Ohloff, G., Farnow, H., Philipp, W., Schade, G., 1959. Über Germacron und seine pyrolytische Umwandlung. Justus Liebigs Annalen der Chemie 625, 206–229.

Shu, Y.-F., Wei, H.-C., Wu, C.-L., 1994. Sesquiterpenoids from the liverworts *Lepidozia vitrea* and *L. fauriana*. Phytochemistry 37, 773–776.

Toyooka, N., Nishino, A., Momose, T., 1997. Enantiodivergent synthesis of a decalin type of chiral building blocks and their application to terpenoid synthesis. Tetrahedron 53, 6313–6326.

Toyota, M., Nakaishi, E., Asakawa, Y., 1996. Eudesmane-type sesquiterpenoids from the liverwort *Lepidozia vitrea*. Phytochemistry 41, 833–836.

Toyota, M., Saito, T., Asakawa, Y., 1999. The absolute configuration of eudesmane-type sesquiterpenoids found in the Japanese liverwort *Chiloscyphus polyanthos*. Phytochemistry 51, 913–920.

Zheng, G.-C., Ichikawa, A., Ishitsuka, M.O., Kusumi, T., Yamamoto, H., Kakisawa, H., 1990. Cytotoxic hydroperoxylepidozenes from the actinia *Anthopleura pacifica* Uchida. Journal of Organic Chemistry 55, 3677–3679.

PERGAMON

Phytochemistry 58 (2001) 799–810

PHYTOCHEMISTRY

www.elsevier.com/locate/phytochem

Chemical study of the essential oil of *Cyperus rotundus*

Mesmin Mekem Sonwa, Wilfried A. König*

Institut für Organische Chemie, Universität Hamburg, D-20146 Hamburg Germany

Received 4 April 2001; received in revised form 25 June 2001

Abstract

Minor constituents of the essential oil of *Cyperus rotundus* have been investigated. The three new sesquiterpene hydrocarbons (−)-isorotundene, (−)-cypera-2,4(15)-diene, (−)-norrotundene and the ketone (+)-cyperadione were isolated and their structures elucidated. The absolute configuration of (−)-rotundene was derived by chemical correlation and enantioselective gas chromatography. © 2001 Elsevier Science Ltd. All rights reserved.

Keywords: *Cyperus rotundus*; Cyperaceae; Sesquiterpenes; Norsesquiterpene; (−)-Isorotundene; (−)-Cypera-2,4(15)-diene; (−)-Norrotundene; (+)-Cyperadione

1. Introduction

Cyperus rotundus is a cosmopolitan sedge belonging to the family of the Cyperaceae. It is encountered in tropical, subtropical and temperate regions. *C. rotundus* is a traditional medicinal plant appearing among Indian, Chinese and Japanese natural drugs used against spasms and stomach disorders (Dassanayake and Fosberg, 1985). The essential oil as well as solvent extracts of the rhizomes of *C. rotundus* have been subject to numerous studies (Ohira et al., 1998 and cited literature) resulting in the isolation of many terpenoids. Here we describe the isolation and structure elucidation of new patchoulane and rotundane sesquiterpenes from the essential oil of this plant.

2. Results and discussion

The analysis of the essential oil of *Cyperus rotundus* by GC and GC–MS allowed the identification of cyprotene (**1**), cypera-2,4-diene (**2**), α-copaene (**3**), cyperene (**4**), α-selinene (**5**), rotundene (**6**), valencene (**7**), ylanga-2,4-diene (**8**), γ-gurjunene (**9**), *trans*-calamenene (**10**), δ-cadinene (**11**), γ-calacorene (**12**), *epi*-α-selinene (**13**), α-muurolene (**14**), γ-muurolene (**15**), cadalene (**16**), nootkatene (**17**) by comparison with a spectral library established under identical experimental conditions (Joulain and König, 1998), cyperotundone (**18**) (Hikino et al., 1966), mustakone (**19**) (Nyasse et al., 1988), cyperol (**20**) (Hikino et al., 1967), isocyperol (**21**) (Hikino et al., 1967) and α-cyperone (**22**) (Howe and McQuillin, 1955; Haaksma et al., 1992) (Fig. 1). However, several minor compounds could not be identified by their mass spectra and had to be isolated for further investigations. Consequently, the essential oil was first separated by silica chromatography into a hydrocarbon fraction and a more polar oxygenated fraction. The hydrocarbon fraction was further separated by column chromatography, TLC over silver nitrate precoated silica and preparative GC. This resulted in the isolation and characterization of isorotundene (**23**), cypera-2,4(15)-diene (**24**) and norrotundene (**25**). From the oxygenated fraction cyperadione (**26**), a patchoulane type sesquiterpene, was isolated.

2.1. (−)-Isorotundene (*23*)

The unknown compound **23** was assigned the molecular formula $C_{15}H_{24}$ ($[M]^+$ at $m/z = 204$). The ^{13}C NMR spectrum showed 15 carbon signals, two of which were olefinic (δ 107.9 and 151.08). Through the DEPT technique two methyl groups, seven methylene groups, four methine and two quaternary carbon atoms were identified. The compound has four unsaturations and only one double bond, therefore the presence of three rings

* Corresponding author. Tel.: +49-40-42838-2824; fax: +49-40-42838-2893.

E-mail address: wkoenig@chemie.uni-hamburg.de (W.A. König).

0031-9422/01/$ - see front matter © 2001 Elsevier Science Ltd. All rights reserved.
PII: S0031-9422(01)00301-6

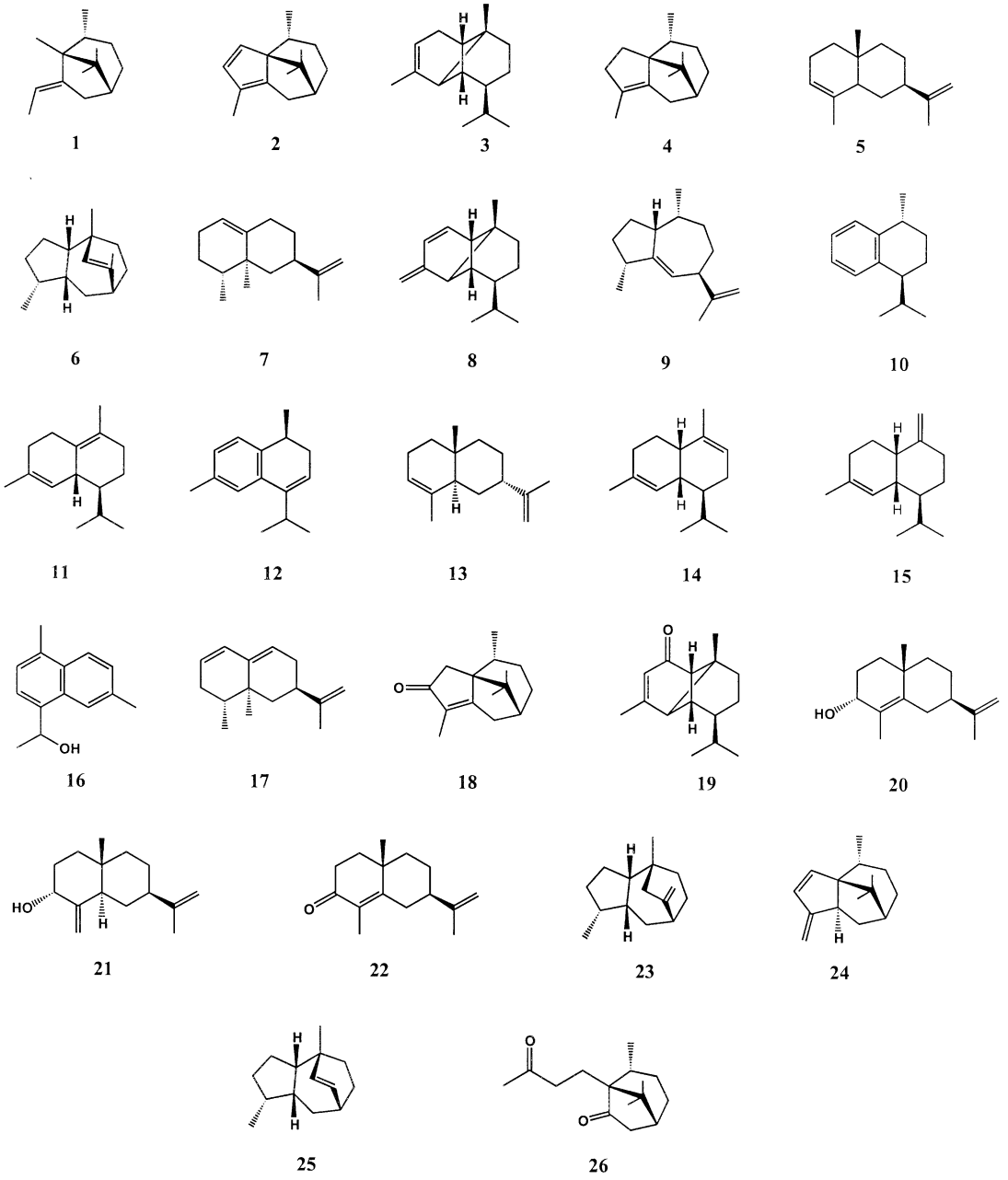

Fig. 1. Sesquiterpenes from the essential oil of *Cyperus rotundus*.

was concluded. The ^{1}H NMR and ^{13}C NMR signal assignments, achieved by ^{1}H–^{1}H-COSY and HMQC, correlations, afforded three substructures. The methine proton CH-5 (δ 1.99) couples with the methine proton CH-4 (δ 1.90) which is vicinal to methyl group CH_3-15 (δ 0.86). The latter methine proton also couples with the methylene group CH_2-3 (δ 1.22 and 1.68) itself coupled to another methylene group CH_2-2 (δ 1.46 and 1.52) which further couples with the methine proton CH-1 (δ 1.81) giving the partial structure–CH–CH(CH_3)–CH_2–CH_2–CH–. The methine proton δ 1.99 also couples with a methylene group CH_2-6 (δ 1.00 and 1.70) itself coupled to the methine proton CH-7 (δ 2.52). The proton H-7 also couples with the methylene group CH_2-8 (δ 1.05 and 1.71) which again couples with CH_2-9 (δ 1.44 and 1.72) to give the second substructure–CH–CH_2–CH–CH_2–CH_2–. The methylene group CH_2-11 (δ 2.14 and δ 2.27) and the olefinic proton at δ 5.85 couple with each other and give the third substructure–CH_2–C=CH_2. The proton-carbon long-range coupling correlations derived from the HMBC spectrum allowed to identify the skeleton of the compound. Long-range coupling correlations were found between the protons H-11, H-13 and carbon C-7 as well as between the methine proton H-7 and the carbons C-11, C-12 and C-13, indicating a bond connecting C-7 and C-12. The

proton H-11 also correlated with the carbons C-1, C-9, C-10 and C-14 while the methyl group H-14 correlates with the carbons C-1, C-9, C-10 and C-11. From these observations it was deduced that C-10 is connected to C-11, C-14 to C-10, and C-10 to C-1. Long-range correlations were observed between the protons H-6, H-5, H-4 and carbon C-1 as well as between H-1 and the carbons C-2, C-4, C-5, C-6 and C-10 indicating a bond between C-1 and C-5. The combination of all these informations led to a rotundane skeleton with an exocyclic double bond. The relative configuration at the chiral centres C-1, C-4, C-5, C-7 and C-10 was concluded from the NOESY diagram. The correlations observed between protons H-1, H-4 and H-5 indicate that these protons are on the same side of the molecule. Furthermore, the protons H-1 and H-5 show spatial interactions with the proton H-11a, which is only possible if H-1 and H-5 are located at the same side as the C-11-C-12 bridge. Therefore, compound **23**, which was named isorotundene, has the relative configuration as shown in Fig. 2.

To verify the rotundane skeleton a partial synthesis of **23** by oxymercuration-demercuration (Brown and Geoghegam, 1970) of rotundene (**6**) to isorotundenol (**27**) and subsequent dehydration (Greenwood et al., 1968) to isorotundene (**23**) and rotundene (**6**) was performed (Fig. 3). The synthesized and the isolated compounds **23** have identical spectroscopic data. Although rotundene (**6**) has been known for a long time its stereochemistry was not known as yet. The relative configuration of rotundene could not be derived from its NOESY diagram because of the overlapping of all the important signals. However, the fact that isorotundene (**23**) could be obtained from rotundene as shown in Fig. 3, proves that rotundene and isorotundene have the same relative configuration.

The identity of the relative configuration of rotundene (**6**) and isorotundene (**23**) still leaves the question about the absolute configuration open. In order to determine the absolute configuration of the two compounds, a chemical transformation of rotundene was performed in order to correlate it with (+)-γ-gurjunene (**9**). Rotundene (**6**) was submitted to ozonolysis followed by reduction with dimethyl sulfide under nitrogen (McMurry and Bosch, 1987). The desired aldehyde was not stable and was oxydised directly the to ketoacid **28** which could be isolated. The acid **28** was then decarboxylated (Fristad et al., 1983) to give ketone **29**. Subsequently **29** was allowed to react with methylenetriphenylphosphine in dimethyl sulfoxide (Greenwald et al., 1963) to yield the hydrocarbon **30** which was hydrogenated (Harmon et al., 1969) to give compound **31** (Fig. 4). Compound **31** was finally compared by enantioselective gas chromatography with the fully hydrogenated products of (+)-γ-gurjunene (**5**) and proved to have the same retention time with the major hydrogenation product (Fig. 5). The co-injection was made in a column which separates (+)- and (−)-γ-gurjunene (Fig. 6). Unfortunately, the small quantity of (−)-γ-gurjunene (which we isolated from the liverwort *Marchantia polymorpha*) was insufficient for hydrogenation and comparison with **31**. However, it is very probable that the used column also would have separated the hydrogenation products of the two enantiomers. Therefore, it is very likely that rotundene has the absolute configuration as shown for **23**.

2.2. (−)-Cypera-2,4(15)-diene (24)

The isolation of cypera-2,4(15)-diene (**24**) was achieved by a combination of column chromatography and preparative GC. The compound was assigned the molecular formula $C_{15}H_{22}$ ($[M]^+$ at $m/z = 202$). The ^{13}C NMR spectrum combined with the DEPT technique revealed three methyl groups, four methylene groups, one being olefinic (δ 102.84), five methine groups, two of which are olefinic (δ 133.26 and 139.17) and three quaternary carbon atoms, one of which is olefinic (δ 148.94).

The proton NMRspectrum displayed some signals common to patchoulane sesquiterpenes, namely the two

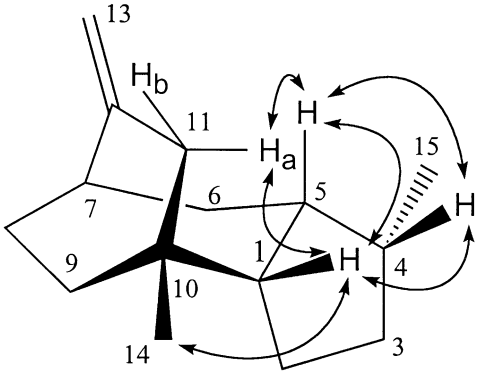

Fig. 2. Relative configuration of isorotundene with relevant NOEs.

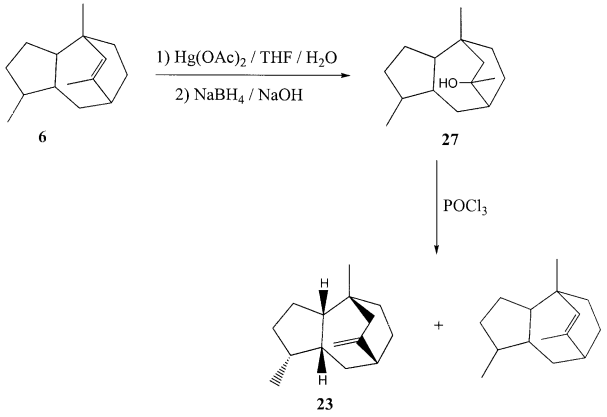

Fig. 3. Preparation of isorotundene (**23**) from rotundene (**6**).

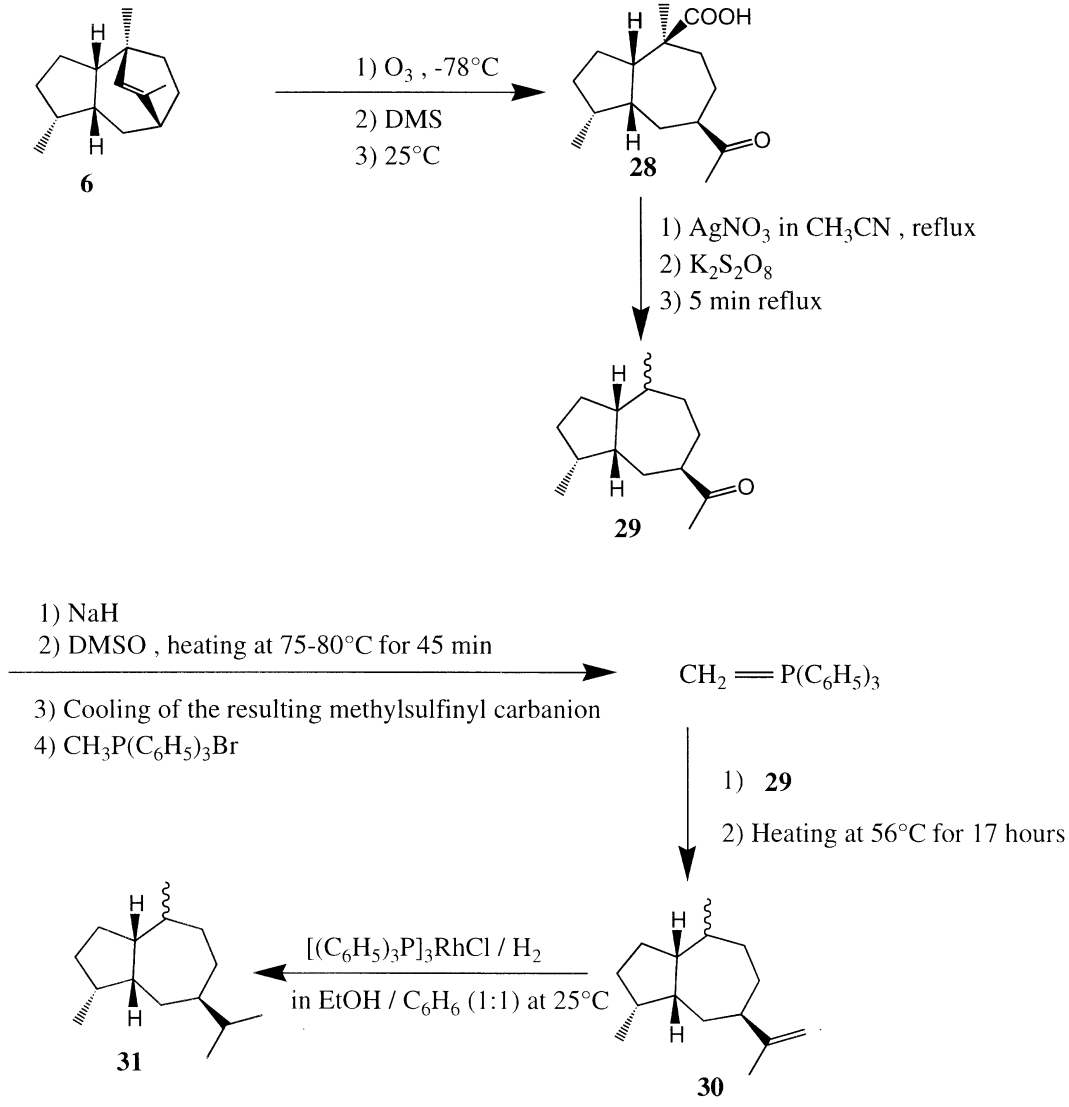

Fig. 4. Chemical conversion of the rotundane to a guaiane skeleton.

geminal methyl groups H-12 and H-13 (δ 0.99 and 1.01) which are coupled to each other (W-coupling), the methyl group at δ 0.77, appearing as a doublet and coupling with the methine proton H-10 (δ 2.12). The vinylic proton H-2 (δ 6.17) couples with another vinylic proton H-3 (δ 5.69), itself coupled to the olefinic methylene group H-15 (δ 4.98) and also to the methine proton H-5 (δ 3.03) giving the substructure –CH=CH–C(CH)=CH_2. Moreover, the coupling constant between H-2 and H-3 ($J = 5.60$ Hz) indicates that they belong to a five-membered ring. The methine proton H-5 also couples with the methylene group CH_2-6 (δ 1.68 and 2.10) which further couples with the methine proton H-7 (δ 1.85) itself coupled to the methylene group CH_2-8 (δ 1.51 and 1.86) which again couples with the methylene group CH_2-9 (δ 1.03 and 1.29) itself coupled to the methine proton CH-10 (δ 2.12). From these informations the substructure CH–CH_2–CH–CH_2–CH_2–CH– is derived.

All these informations from the ^{13}C NMR and DEPT as well as the ^1H–^1H-COSY led us to propose structure **24** for the compound. Its relative configuration resulted from the NOESY diagram which shows NOE correlations between H-5, H-9 and H-14 at one side and between H-13 and H-10 at the other. The observed correlations indicate that the methine proton H-10 is on the same side with the bridge C-1–C-7, while H-5, H-9 and H-14 are located at the opposite side of the molecule (Fig. 7). **24** was before found as a minor product during the reduction of cyperotundone (**18**) to the corresponding alcohol and subsequent dehydration to **2** (Fig. 8) (Mekem Sonwa et al., 1997).

2.3. (−)-Norrotundene (25)

The isolation of **25** was performed by the combination of many separation methods including CC at low temperature (−20° C), CC over silver nitrate precoated

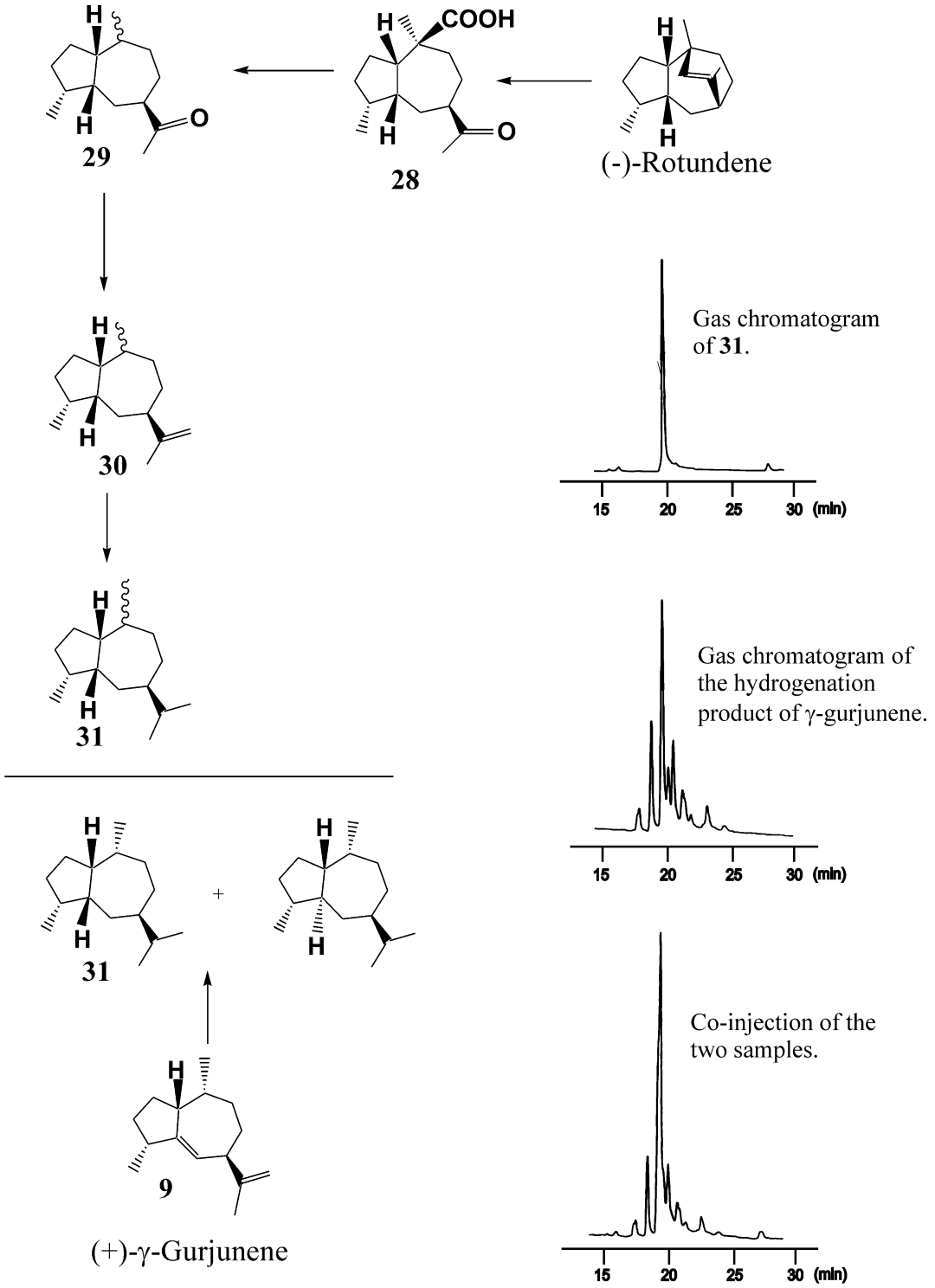

Fig. 5. Chemical transformation of rotundene and GC comparison with the hydrogenation product of (+)-γ-gurjunene.

silica, preparative TLC and GC. The compound has the molecular formula $C_{14}H_{22}$ in agreement with its mass spectrum ($[M]^+$ at m/z =190). The ^{13}C NMR and DEPT spectra revealed 14 carbon atoms, two methyl groups, five methylene groups, six methine groups from which two are olefinic (δ 129.15 and 139.10) and one quaternary carbon atom. Therefore the compound should consist of three rings since it has a total of four unsaturations, one being a double bond. The constitution of **25** was derived from interpretation of the ^1H NMR spectrum and the phase-sensitive ^1H–^1H-COSY spectrum together with the HMQC and the HMBC diagrams.The methine proton CH-1 (δ 2.20) couples with the methylene group CH_2-2 (δ 1.61 and 1.54) which

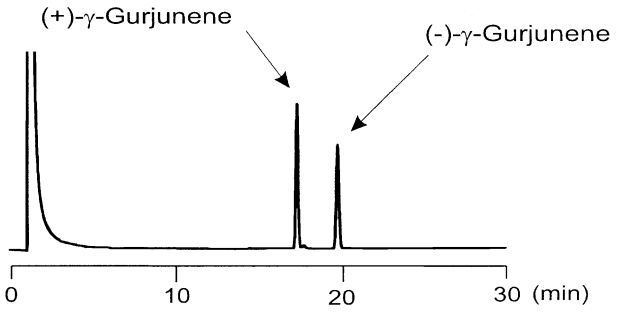

Fig. 6. Separation of (−)- and (+)-γ-gurjunene by capillary gas chromatography on a 25 m capillary column with heptakis(6-*O*-*t*.butyldimethylsilyl-2,3-di-*O*-methyl)-β-cyclodextrin (50% in OV 1701, w/w) at 100 °C.

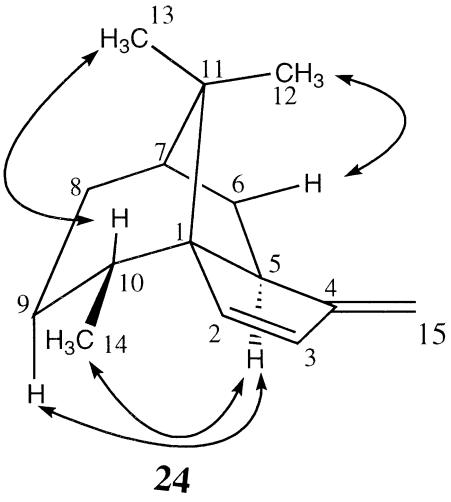

Fig. 7. Stereostructure of cypera-2,4(15)-diene (**24**) and important NOEs.

further couples with another methylene group CH_2-3 (δ 1.42 and 1.87) which couples again with the methine proton H-4 (δ 2.10) itself coupled to the methyl group CH_3-14 (δ 0.90) and the methine proton CH-5 (δ 1.80) which further couples with the methine proton H-1 (δ 2.20) and gives rise to a five-ring partial structure *a*: C_1H–CH_2–CH_2–$CH(CH_3)$–CH–C_1H–.

The methine proton H-5 also couples with methylene group CH_2-6 (δ 0.95 and 1.66) which further couples with the methine proton H-7 (δ 2.56), itself coupled to the methylene group H-8 (δ 1.12 and 1.91) which couples again with the methylene group H-9 (δ 1.52 and 1.83) to give the substructure *b*: CH–CH_2–CH–CH_2–CH_2–. Moreover, the vinylic protons H-11 and H-12 (δ 6.02) are coupled to the methine proton H-7, indicating a partial structure *c*: –CH=CH–CH–. Observing that the substructures *a* and *b* have C-5 in common and that *b* and *c* have C-7 in common, the three partial structures can be connected to give a new substructure A (Fig. 9). It may be assumed that the only tertiary methyl group of the molecule CH_3-13 is linked to the only quaternary carbon and thus yielding substructure B: CH_3–C. This assumption is confirmed by the HMBC diagram which shows long-range correlations between the protons H-13 and C-1, C-10 and C-11. Proton H-1 shows long-range connectivities to C-2, C-5, C-10 and C-11. The protons of methylene group CH_2-9 show connectivities to C-1, C-8, C-10 and C-11, while the olefinic proton H-11 is long-range coupled to C-1, C-7, C-9, C-10, C-12 and C-13. All these observations imply the two carbon-carbon connections between C-10–C-1 and C-10–C-11, leading to a rotundane skeleton for **25** (Fig. 9).

The relative stereochemistry at the chiral centres of the molecule could not be derived from the NOESY spectrum. The signals of the two methine protons H-1 and H-4 overlap and hence it is not possible to know which one of them is responsible for the NOE with the proton H-5. However, using the phase-sensitive COSY technique as well as the gradient selected HMQC method, it was possible to calculate the scalar coupling constant between H-4 and H-5 ($J = 5.85$ Hz). This value of the coupling constant corresponds (Karplus curve) to an angle of $\Phi = 35°$ between the two protons, which means that they are on the same side of the molecule. Accordingly, both of them have spatial interactions with H-1. It remains to investigate the stereochemistry at C-7 and C-10. To solve this problem the NOESY diagram was of no help because the protons H-1 and H-5 are too far from the vinylic protons H-11 and H-12. The solution came from the ^{1}H–^{1}H-COSY diagram where a long-range coupling correlation is found between proton H-1 and one of the H-9 protons. This is a case of ^4J coupling through a σ-bond which requires a particular geometry (W arrangement of the two protons) for the molecule, and this is only possible if the H-1 proton and the C-11–C12 bridge are on the same side of the molecule. Moreover, the axial–axial coupling between H-5 and H-6a is only possible for this stereochemistry of the molecule (Fig. 10). Norrotundene is probably biogenetically related to rotundene and should have the same absolute configuration.

2.4. Cyperadione (*26*)

Cyperadione (**26**) was isolated from the oxygenated fraction of *C. rotundus* oil by preparative GC. The compound has the molecular formula $C_{15}H_{24}O_2$ ($[M]^+$ at $m/z = 236$). The ^{13}C NMR- and the DEPTspectrum indicate that it has four methyl groups, two methine protons and four quaternary carbon atoms, two of which being carbonyl carbons (δ 208.50 and 220.25). From the ^{1}H NMR and the ^{1}H ^{1}H-COSY spectra, three substructures were assigned which helped to derive the full structure of the product. The methyl group CH_3-14 (δ 0.78) couples with the methine proton CH-10 (δ 2.10) which also couples with the methylene group CH_2-9 (δ 1.10 and 1.68) itself coupled to the methylene group CH_2-8 (δ 1.45 and 2.01) which further couples with the

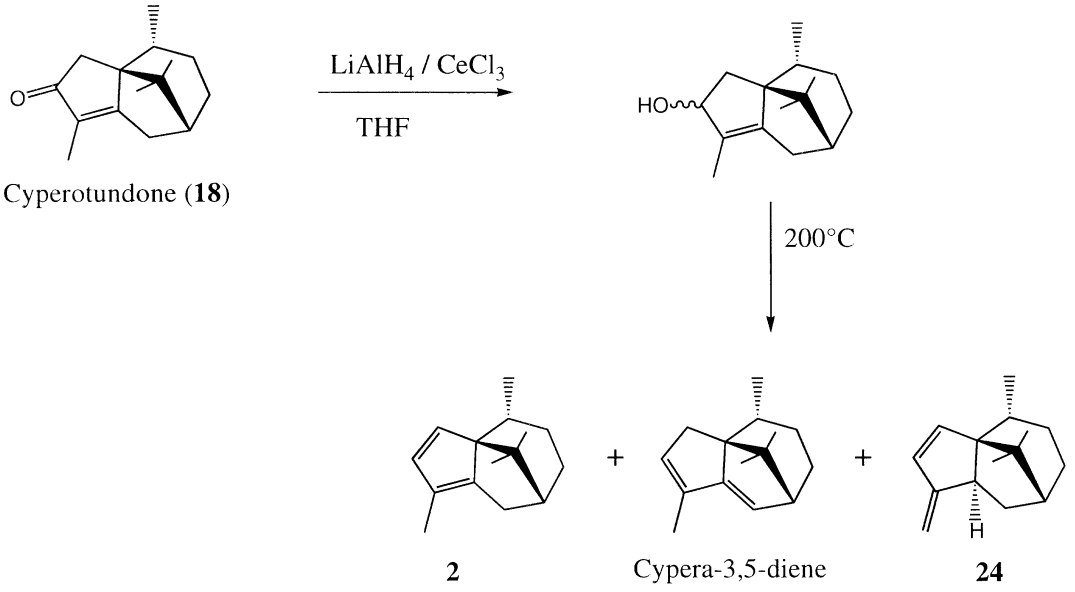

Fig. 8. Formation of cypera-2,4(15)-diene (**24**) form cyperotundone (**18**).

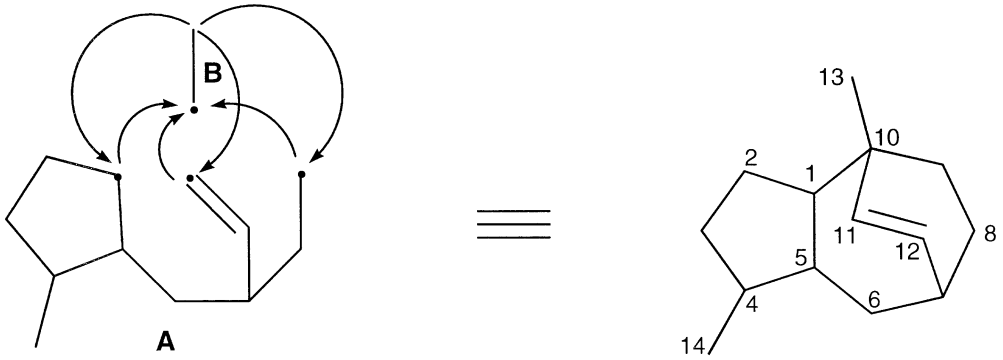

Fig. 9. Important proton-carbon long-range correlations in the HMBC spectrum of norrotundene (**25**).

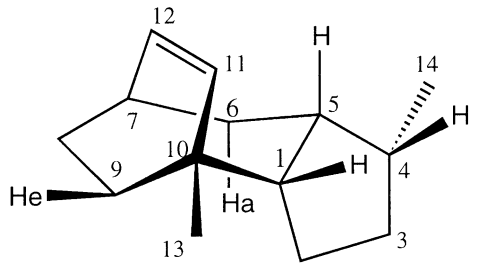

Fig. 10. Relative configuration of norrotundene (**25**). Note the W-arrangement between H-1 and H-9e, and the axial-axial disposition between H-5 and H-6a. These two geometrical patterns which are supported by the observed coupling correlations are only possible for the given stereostructure of the molecule.

methine proton CH-7 (δ 1.90) itself coupled to the methylene group CH_2-6 (δ 1.96 and 2.48). It should be pointed out that the signals of this methylene group appearing at lower field and showing no other coupling correlation to a proton may be adjacent to a carbonyl group. This is confirmed by the HMBC diagram where correlations are observed between the protons H-6 and carbonyl carbon C-7. From all this information substructure CH_3–CH–CH_2–CH_2–CH–CH_2–CO can be derived. The two methyl groups at δ 0.98 and 1.28 appearing as singlets are coupled to each other (W coupling), what indicates that they are linked to the same quaternary carbon atom giving the substructure CH_3–C–CH_3. The deshielded methyl group CH_3-15 at δ 2.18 is probably adjacent to a carbonyl function (this is also confirmed by the HMBC spectrum) and shows a long-range coupling correlation to the methylene group CH_2-3 (δ 2.35 and 2.44) which further couples with the methylene group CH_2-2 (δ 1.50 and 2.11) to give the partial structure CH_3–CO–CH_2–CH_2–. Additional structural informations were drawn from the HMBC diagram. The methylene protons H-2 are long-range correlated to carbons C-1, C-3, C-4, C-5, C-10 and C-11 while the methine proton H-10 shows connectivities to C-1, C-2, C-5, C-9, C-11 and C-14. From these observations the

three carbon–carbon connections C-1–C-2, C-1–C-10 and C-1–C-5 were deduced. Moreover, the methyl protons H-12 and H-13 are long-range correlated to C-1, C-7 and C-11, establishing the two connections C-11–C-1 and C-11–C-7. All these considerations led to structure **26** (Fig. 11), with a skeleton related to the patchoulane skeleton of cyperene (**4**). To confirm structure **26** we performed an ozonolysis of cyperene (**4**) (Fig. 12). The reaction product displayed the same spectral data as the isolated compound.

2.5. Biogenesis of patchoulane and rotundane type sesquiterpenes

Patchoulane and rotundane sesquiterpenes are characteristic for the genus *Cyperus*. Cyperene (**4**) is always the major hydrocarbon component in *Cyperus* species. Rotundene (**6**) also is always present as a major sesquiterpene hydrocarbon component. These two compounds appear to be of some chemotaxonomic importance. We have previously reported the isolation of cyprotene (**1**), a norsesquiterpene biogenetically related to cyperene from the essential oil of *Cyperus alopecuroides*. Here, we described a new norsesquiterpene, norrotundene (**25**), which most likely has a biogenetic relationship to rotundene. Besides **1** compound **25** was also identified in *C. papyrus*. It, therefore, seems to be a peculiarity of *Cyperus* species to produce norsesquiterpenes.

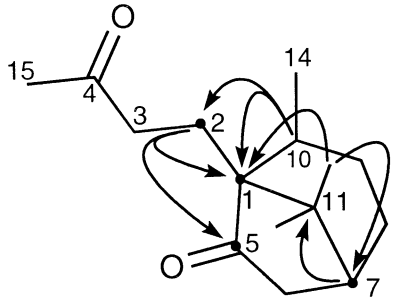

Fig. 11. Long-range correlations from the HMBC spectrum of cyperadione (**26**).

The biosynthesis of cyperene and rotundene may involve two successive cyclisation steps of farnesyl diphosphate FDP leading via a cyclodecadienyl to a cationic azulane type intermediate. At this stage two pathways *a* and *b* may take place: Path *a* proceeds by a 1,2- proton shift followed by a deprotonation leading to α-guaiene from which cyperene is formed by subsequent protonation, cyclisation and deprotonation. Path *b* proceeds by ring formation followed by a deprotonation yielding rotundene or isorotundene (Fig. 13).

3. Experimental

3.1. GC-MS

Electron impact (70 eV) GC–MS measurements were carried out on a Hewlett-Packard HP 5890 gas chromatograph equipped with a 25 m polydimethylsiloxane (Chrompack CP Sil 5 CB) capillary column and coupled to a VG Analytical VG 70-250S mass spectrometer. Helium was used as carrier gas.

3.2. NMR spectroscopy

NMR spectra were recorded using a Bruker DRX 500 (^{1}H: 500 MHz, ^{13}C: 125 MHz) and a Bruker DRX 400 (^{1}H: 400 MHz, ^{13}C: 100 MHz). Tetramethylsilane (TMS) was used as reference signal ($\delta = 0.00$).

3.3. Capillary GC

Orion Micromat 412 double column instrument with 25 m fused silica capillaries with CPSil 5 and CPSil 19 (Chrompack); Carlo Erba Fractovap 2150, 4160 instruments with 25 m fused silica capillaries with heptakis(2,6-di-*O*-methyl-3-*O*-pentyl)-β- (2,6-Me-3-Pe-β-CD) and - γ - cyclodextrin, respectively, and heptakis(6 - *O* - t.butyldimethylsilyl-2,3-di-*O*-methyl)-β-cyclodextrin (6T-2,3-Me-β-CD), all in polysiloxane OV1701 (50 wt%); split injection, flame ionization detection; carrier gas 0.5 bar hydrogen.

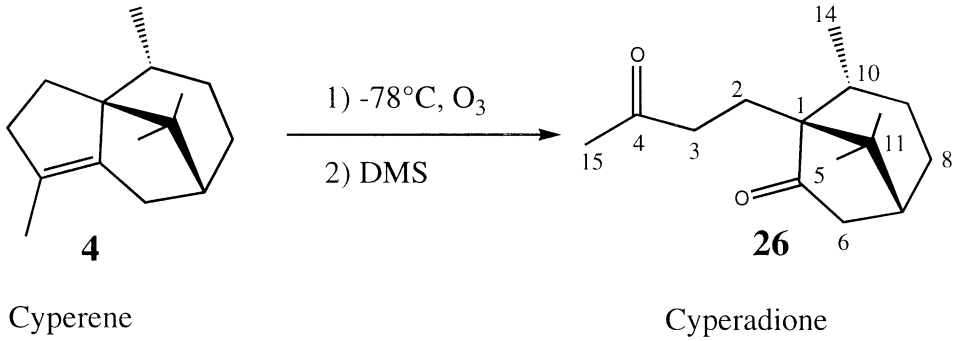

Fig. 12. Preparation of cyperadione by ozonolysis of cyperene.

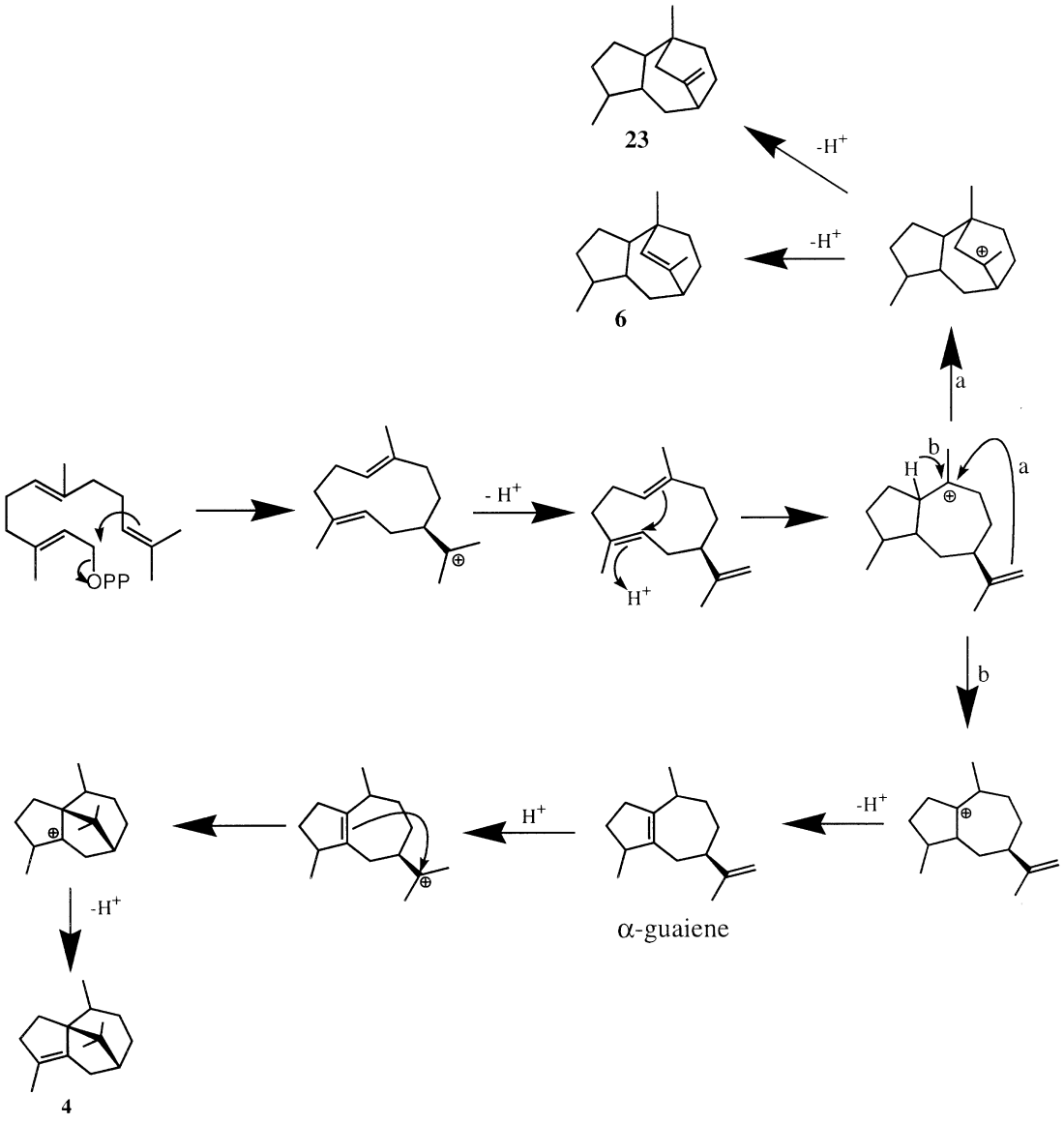

Fig. 13. Proposed biogenetic pathway for cyperene, rotundene and isorotundene.

3.4. Column chromatography at low temperature

Prefractionations of essential oils were performed on a silica gel column equipped with a condenser and connected to a Kryoflex KF 40 cooling system from Messgeräte-Werk Lauda at −20 °C. Ethanol was used as cooling liquid.

3.5. Thin layer chromatography

Thin layer chromatography was effected using glass and aluminum plates of silica 60 F_{254} (Merck). Silver nitrate coated plates were prepared by immersing the plates into an ethanol–water (4:1) solution of silver nitrate (5 mg $AgNO_3$ in 50 ml of solvent). After 30 min the plates were removed from the solution and dried in an oven. An ethanolic solution of sulfuric acid (10%) was used as a spray reagent.

3.6. Essential oil

The essential oil of *C. rotundus* was a gift of K.-D. Protzen, Paul Kaders GmbH, Hamburg.

3.7. Isolation of compound **23**

A preliminary separation of the essential oil was performed by column chromatography at low temperature (−20 °C). This resulted in a fractionation of the oil into a hydrocarbon and an oygenated fraction. One gram of the hydrocarbon fraction was then separated by TLC using petroleum ether as eluting solvent. The aim of this

separation was to eliminate the major hydrocarbon (cyperene) from the sample before any other operation. Three bands were obtained, the first two containing mainly cyperene and α-copaene. Only the third fraction ($R_f = 0.45$) was interesting because it contained the unknown products. This fraction was further separated by preparative GC (column 6T-2,3-Me-β-CD, temperature programme: from 110 to 180 °C, heating rate 2°/min). Fraction 5 of the chromatogram contained (+)-ylanga-2,4(15)-diene (**8**). Fraction 8 was analysed by GC–MS and three major products were present: α-selinene (**5**), valencene (**7**), and an unknown product. This sample was further separated by preparative TLC on silver nitrate precoated plates, using petroleum ether as eluting solvent. Two bands were obtained, the second of which ($R_f = 0.35$) was taken up in petroleum ether and purified by preparative GC. Spectroscopic analysis resulted in the structure of isorotundene **23**.

3.8. (−)- Isorotundene (*23*)

^{1}H NMR (500 MHz, C_6D_6): see Table 1. ^{13}C NMR (100 MHz, C_6D_6): δ 16.10 (*q*, C-15), 25.20 (*t*, C-2), 27.53 (*t*, C-8), 29.28 (*t*, C-9), 31.48 (*t*, C-3), 32.28 (*q*, C-14), 33.15 (*t*, C-6), 34.38 (*s*, C-10), 38.25 (*d*, C-4), 38.64 (*d*, C-7), 41.52 (*d*, C-5), 44.36 (*t*, C-11), 56.19 (*t*, C-1), 107.98 (*t*, C-13), 151.08 (*s*, C-12). MS (EI, 70 eV), *m*/*z* (rel. int.) : 204 (33) $[M]^+$, 189 (84), 175 (25), 161 (64), 144 (45), 133 (41), 119 (54), 108 (100), 93 (91), 79 (71), 67 (46), 55 (51), 41 (82).

Table 1
^{1}H NMR spectral data for compounds **23** and **25**[a]

H	23	25
1	1.81 *ddd* (9.5, 9.5, 5.9)	2.20 *dddd* (13.5, 6.6, 6.4, 7.0)
2	1.46 *dd* (9.5, 3.2)	1.54 *m*
	1.52 *m*	1.61 *m*
3	1.22 *dddd* (13.6, 11.4, 11.4, 6.7)	1.42 *dddd* (13.5, 11.0, 11.0, 6.7)
	1.68 *m*	1.87 *m*
4	1.90 *dddd* (13.6, 6.9, 6.6, 6.4)	2.10 *m*
5	1.99 *dddd* (13.2, 6.4, 6.4, 5.9)	1.80 *dddd* (13.2, 6.4, 6.4, 6.4)
6	1.00 *t* (13.2)	0.95 *dd* (13.2, 13.2)
	1.70 *m*	1.66 *ddd* (13.2, 9.1, 6.4)
7	2.52 *m*	2.56 *m*
8	1.05 *dd* (12.9, 9.5)	1.12 *ddd* (13.8, 11.7, 5.1)
	1.71 *m*	1.91 *ddd* (13.8, 9.4, 5.0)
9	1.44 *m*	1.52 *ddd* (11.7, 9.4, 6.1)
	1.72 *m*	1.83 *m*
11	2.14 *dt* (17.0, 2.5, 2.5)	6.02 *m*
	2.27 *dd* (17.0, 2.2)	
12		6.02 *m*
13	5.85 *m*	1.13 *s*
	5.85 *m*	
14	0.80 *s*	0.99 *d* (6.6)
15	0.86 *d* (6.6)	

[a] All the measurements were done in C_6D_6. The assignments were established by ^{13}C–^{1}H HMBC and HMQC

3.9. Preparation of isorotudene (*23*) from rotundene (*6*)

3.9.1. Hydration of rotundene by oxymercuration-demercuration

In a 50 ml flask, fitted with a magnetic stirrer, 48 mg of mercuric acetate were placed. To this, 3 ml of water were added followed by 3 ml of THF. After addition of 30 mg (0.148 mmol) of rotundene the reaction mixture was stirred for 15 min at room temp. to complete the oxymercuration. 3 ml of 3.0 M sodium hydroxyde were added followed by 3 ml of a solution of 0.50 M sodium borohydride in 3.0 M sodium hydroxide. Reduction of the mercurial complex is almost instantaneous. The mercury is allowed to precipitate. Sodium chloride was added to saturate the water layer. The upper layer of THF was removed and purified by preparative GC, yielding 26 mg (80%) of isorotundenol (**27**).

3.9.2. Isorotundenol $C_{15}H_{25}OH$ (*27*)

^{1}H NMR (500 MHz, C_6D_6): δ 0.75 (3H, *d*, $J = 6.61$ Hz), 0.76 (3H, *s*), 1.02 (3H, *s*), 1.08-1.54 (12H, *m*), 1.57–1.65 (2H, *m*), 1.75 (1H, *m*), 2.15 (1H, *m*). MS (EI, 70 eV), *m*/*z* (rel. int.) : 222 (5), 204 (19), 189 (27), 175 (7), 161 (14), 147 (12), 133 (13), 121 (33), 108 (100), 93 (57), 81 (39), 67 (24), 55 27), 41 (35).

3.9.3. Dehydration of isorotundenol

Phosphoryl chloride (0.5 ml) was added to a pyridine solution (1 ml) of isorotundenol (10 mg). The mixture was stirred for 10 h and pyridine was then removed by distillation at low pressure. The remaining residue was taken up in hexane and separation by prep. GC yielded 3 mg of isorotundene and 3 mg of rotundene.

3.10. Ozonolysis of rotundene

A solution of rotundene (50 mg) in dichloromethane (20 ml) was treated at −78° C with a stream of ozone until a persistant blue colour was observed. The solution was then purged with nitrogen for 5 min. After addition of dimethylsulfide (3 ml) the solution was washed with ice-cold sodium bicarbonate solution (25 ml), water and brine. The organic layer was dried ($NaSO_4$) and the solvent was evaporated. Purification of the residue by prep. GC gave the keto-acid **28** (45 mg).

^{1}H NMR (400 MHz, $CDCl_3$): δ 1.10 (3H, *d*, $J = 6.61$ Hz), 1.30 (1H, *m*), 1.35 (3H, *s*), 1.65–1.92 (9H, *m*), 2.11 (1H, *m*), 2.20 (1H, *m*), 2.29 (3H, *s*), 2.58–2.85 (2H,*m*). ^{13}C NMR (100 MHz, $CDCl_3$): 16.73, 25.10, 25.66, 27.47, 28.30, 30.07, 31.09, 31.60, 39.64, 41.70, 48.56, 48.64, 50.55, 184.59, 212.01. MS (EI, 70 eV) *m*/*z* (rel. int): 252 (13) $[M]^+$, 234 (7), 206 (15), 191 (11), 163 (36), 149 (7), 133 (10), 121 (18), 107 (25), 95 (68), 81 (43), 67 (22), 55 (28), 43 (100).

3.11. Decarboxylation of keto-acid **28**

The keto-acid (40 mg, 0.16 mol) and silver nitrate (1 mg) were dissolved in acetonitrile (6 ml) and water (2 ml) and heated to reflux. To this solution potassium peroxosulfate ($K_2S_2O_8$) (0.32 mg) in water (5 ml) was slowly added. Refluxing was continued for another 5 min before the reaction mixture was cooled and extracted with a saturated sodium bicarbonate solution (10 ml, three times), dried ($MgSO_4$) and purified by prep. GC to give 14 mg of ketone **28**.

^{1}H NMR (500 MHz, $CDCl_3$): 0.96 (3H, *dd*, $J=6.62$ Hz), 1.06 (3H, *s*), 1.40 (1H, *m*), 1.60–1.84 (7 H, *m*), 1.97–2.1 (2H, *m*), 2.13–2.24 (3H, *m*), 2.27 (3H,*s*), 2.44 (1 H, *m*), 2.69 (1H, *dd*, $J_1=13.87$ Hz, $J_2=6.94$ Hz). ^{13}C NMR (100 MHz, $CDCl_3$): 15.10 (*q*), 21.52 (*q*), 26.09 (*t*), 26.80 (*t*), 27.85 (*q*), 30.26 (*t*), 33.25 (*t*), 37.46 (*t*), 37.99 (*d*), 38.04 (*d*), 46.82 (*d*), 56.70 (*d*), 61.65 (*d*), 207.93 (*s*). MS, (EI, 70 eV), *m*/*z* (rel. int): 208 (5) $[M]^+$, 190 (7), 175 (6), 161 (5), 150(8), 135 (9), 123 (27), 109 (23), 95 (100), 81 (31), 67 (25), 55 (29), 43 (52).

3.12. Reduction of ketone **29**

In a three-necked flask sodium hydride (0.45 mmol) was washed with several portions of pentane to remove the mineral oil. The flask was then equipped with rubber stopper, a reflux condenser and a magnetic stirrer. The system was alternately evacuated and filled with nitrogen; 3 ml of dimethyl sulfoxide was introduced via a syringe and the mixture was heated at 75–80° C for 45 min. The resulting solution of methylsulfinyl carbanion was cooled in an ice-water bath, and 108 mg of methyltriphenylphosphonium bromide in 100 ml of warm dimethyl sulfoxide were added. The resulting dark red solution of the ylide was stirred at room temperature for 10 min before 7 mg of the ketone **29** in two ml of dimethyl sulfoxide were added. The reaction mixture was then heated at 56°C for 16 h after which the solution was allowed to cool and 10 ml of water were added. The two phases were extracted three times with *n*-pentane (40 ml). The *n*-pentane fractions were combined and washed with 10 ml of a (1/1) water/dimethyl sulfoxide solution and then with 30 ml of 50% saturated sodium chloride solution. The pentane layer was then dried over anhydrous sodium sulfate and purification by preparative GC gave 2 mg of the alkene **30**.

MS (EI, 70 eV), *m*/*z* (rel. int): 206 (12) $[M]^+$, 191 (18), 177 (6), 163 (51), 149 (25), 122 (39), 107 (56), 95 (60), 81 (100), 67 (57), 55 (66), 41 (79).

3.13. Hydrocarbon 31

a. **30** (1 mg) was dissolved in a mixture of ethanol (1 ml) and benzene (1 ml). The catalyst $[(Ph)_3P]_3RhCl$ (1 mg) was added and the solution turned orange. A gentle stream of hydrogen was then passed through the solution under normal pressure for 15 min. The solvent was removed under reduced pressure and petroleum ether was added, since most of the catalyst remains undissolved. Filtration through a column of alumina afforded the pure alkane **31**. MS (EI, 70 eV), $[M]^+$ $m/z=208$.

b. The hydrogenation of (+)-γ-gurjunene (**9**) followed the same procedure as that of the alkene **30** except the catalyst was replaced by nickel on charcoal.

3.14. Isolation of cypera-2,4(15)-diene and norrotundene

For the above described chemical transformation, a relatively large amount of rotundene had to be isolated from the essential oil of *C. rotundus*. For the isolation 5 g of the hydrocarbon fraction of the oil were separated by column chromatography over silver nitrate precoated silica using a petroleum ether–chloroform gradient for elution. The eluent from the column was monitored by capillary GC and 16 fractions were collected. Fractions 1–6 obtained by elution with petroleum ether contained only known hydrocarbons. Fractions 7–10 were obtained by elution with petroleum ether–chloroform (7/3) and contained the rotundene. It could be proved by GC–MS of fraction eighth that the sample also contained an unknown minor component. The separation of this fraction was performed by prep. GC (column: 2,6-Me-3Pe-β-CD; temp. programme: 100–140 °C, heating rate 2 °C/min). The chromatogram displayed five peaks the fifth containing the pure unknown product which was characterized as cypera-2,4(15)-diene (**24**). Fractions 11–15 were eluted with petroleum ether–chloroform (1/1). GC–MS revealed the presence of an unknown product of molecular weight 190 among many known sesquiterpene hydrocarbons. In order to isolate the unknown compound, the joined fractions 14 and 15 were first separated by prep. TLC over silver nitrate precoated plates, using petroleum ether–chloroform (7/3) as eluting solvent. Three bands were obtained and the third one, which contained the norsesquiterpene as major product was separated by preparative GC (column: SE 30, temp. 125 °C). Spectroscopic data permitted the characterization of the compound as norrotundene (**25**).

3.14.1. (−)-Cypera-2,4(15)-diene (**24**)

^{1}H NMR (400 MHz, C6D6): see Table 2. ^{13}C NMR (400 MHz, C6D6) : 17.32 (*q*), 19.61 (*q*), 26.36 (*q*), 26.64 (*q*), 27.70 (*t*), 28.48 (*s*), 30.16 (*t*), 32.58 (*t*), 44.96 (*d*), 47.66 (*d*), 61.93 (*s*), 102.84 (*t*), 133.26 (*d*), 139.17 (*d*), 148.94 (*s*). MS (EI, 70 eV) *m*/*z* (rel. int.): 202 (83) $[M]^+$, 187 (24), 173 (6), 173 (6), 159 (46), 145 (24), 131 (37), 118 (85), 106 (100), 91 (78), 77 (33), 69 (17), 65 (18), 55 (26), 41 (61).

3.14.2. (−)-Norrotundene (**25**)

^{1}H NMR (500 MHz, C6D6):see Table 1. ^{13}C NMR (125 MHz, C6D6) : 14.73 (*q*), 22.95 (*t*), 28.00 (*t*), 28.67

Table 2
^{1}H NMR spectral data for compounds **24** and **26**[a]

H	**24**	**26**
2	6.17 *d* (5.6) 2.11 *m*	1.50 *ddd* (15.4, 11.7, 5.7)
3	5.69 *dd* (5.6, 1.0) 2.44 *ddd* (16.4, 12.3, 5.7)	2.35 *ddd* (16.4, 11.7, 4.4)
5	3.03 *m*	
6	1.68 *m* 2.10 *m*	1.96 *d* (19.0) 2.48 *dd* (19.0, 7.3)
7	1.85 *m*	1.90 *ddd* (6.6, 3.3, 3.3)
8	1.51 *dt* (14.8, 6.1) 1.86 *m*	1.45 *dq* (13.6, 3.2) 2.01 *dddd* (13.6, 12.9, 6.0, 2.7)
9	1.03 *m* 1.29 *m*	1.10 *dddd* (14.5, 12.9, 12.9, 6.6) 1.68 *ddd* 14.5, 6.0, 6.0)
10	2.12 *dddd* (13.2, 6.1, 6.1, 6.1)	
12	0.99 *s*	1.22 *s*
13	1.01 *s*	0.98 *s*
14	0.77 *d* (6.6)	0.78 *d* (6.6)
15	4.98 *m* 4.98 *m*	2.18 *s*

[a] All the measurements were done in C_6D_6 for **24** and in $CDCI_3$ for **26**. The assignments were established by ^{13}C–^1H HMBC and HMQC

(*t*), 29.36 (*q*), 30.35 (*d*), 30.54 (*t*), 31.97 (*t*), 35.72 (*s*), 36.32 (*d*), 42.18 (*d*), 50.74 (*d*), 129.15 (*d*), 139.10 (*d*). MS (EI, 70 eV) *m*/*z* (rel. int.) : 190 (10) [M]+, 175 (15), 161 (20), 148 (7), 133 (9), 119 (7), 107 (14), 94 (100), 79 (50), 67(12), 55 (14), 41 (23).

3.15. Isolation of cyperadione (*26*)

The fraction of oxygenated sesquiterpenes was submitted to prep. TLC using petroleum ether–ethyl acetate (8/2) as eluting solvent. The second band (R_f=0.35) was then taken up in diethyl ether and submitted to further separation by prep. GC (column: 6T-2,3-Me-β-CD, 120–180 °C, 2 °C/min).

3.15.1. Cyperadione (*26*)

^{1}H NMR (400 MHz, CDCl3): see Table 2. ^{13}C NMR (100 MHz, CDCl3) : δ 16.76 (*q*), 21.87 (*t*), 22.18 (*q*), 26.42 (*t*), 27.05 (*q*), 28.10 (*t*), 30.03 (*q*), 31.32 (*d*), 38.71 (*t*), 41.79 (*d*), 41.84 (*t*), 42.96 (*s*), 58. 21 (*s*), 208.50 (*s*), 220.25 (*s*). MS (EI, 70 eV), *m*/*z* (rel. int.): 236 (66) $[M]^+$, 221 (89), 207 (7), 193 (25), 179 (63), 161 (17), 150 (20), 135 (22), 123 (22), 107 (25), 95 (19), 81 (20), 67 (23), 55 (27), 43 (100).

3.16. Ozonolosis of cyperene (*4*)

Three mg of cyperene in dichloromethane (20 ml) were treated at −78 °C with a stream of ozone until a persistant blue colour was observed. The solution was then purged with nitrogen for 5 mins. 1 ml of dimethylsulfide was then added, and washed with 10 ml of an ice-cold sodium bicarbonate solution, water and brine. The organic layer was dried over $MgSO_4$ and the solvent evaporated. The residue was then purified by prep. GC to give 3 mg of cyperadione (**26**).

Acknowledgements

The financial support of DAAD (scholarship for M. Mekem Sonwa) and of the Fonds der Chemischen Industrie is gratefully acknowledged. We also thank Dr. V. Sinnwell, University of Hamburg, for his support in obtaining the NMR spectra and to A. Meiners and M. Preusse for recording the mass spectra.

References

Brown, H.C., Geoghegam jr, P.J., 1970. Solvomercuration-demercuration. I. The oxymercuration-demercuration of representative olefins in aqueous system. A convenient mild procedure for the Markownikov hydration of the carbon–carbon double bond. Journal of Organic Chemistry 35, 1844–1850.

Dassanayake, M., Fosberg, F.R., 1985. A Revised Handbook of the Flora of Ceylon, part V. A. A. Balkema, Rotterdam, p. 181.

Fristad, W.E., Fry, M.A., Klang, J.A., 1983. Persulfate/silver ion decarboxylation of carboxylic acids. Preparation of alkanes, alkenes, and alkohols. Journal of Organic Chemistry 48, 3575–3577.

Greenwald, R., Chaykovsky, M., Corey, E.J., 1963. The Wittig reaction using methylsulfinyl carbanion-dimethyl sulfoxide. Journal of the American Chemical Society 28, 1128–1129.

Greenwood, J.M., Solomon, M.D., Sutherland, J.K., Torre, A., 1968. A cyclisation of humulene. Journal of the Chemical Society (C), 3004–3008.

Haaksma, A.A., Jansen, B.J.M., de Groot, A., 1992. Lewis acid catalysed Diels-Alder reactions of *S*-(+)-carvone with silyloxy dienes. Total synthesis of (+)-α-cyperone. Tetrahedron 48, 3121–3130.

Harmon, R.E., Parsins, J.L., Cooke, D.W., Gupta, S.K., Schoolenberg, J., 1969. Homogeneous homocatalytic hydrogenation of unsaturated organic compounds. The Journal of Organic Chemistry 34, 3684–3685.

Hikino, H., Ito, K., Aota, K., 1966. Structure and absolute configuration of cyperotundone. Chemical and Pharmaceutical Bulletin 14, 890–899.

Hikino, H., Takemoto, T., 1967. Structure and absolute configuration of cyperol and isocyperol. Chemical and Pharmaceutical Bulletin 1929–1933.

Howe, R., McQuillin, F.J., 1955. The structutre of cyperone. Part IV. The synthesis of natural (+)-α-cyperone, its enantiomorph and epimer. Journal of the Chemical Society, 2423–2428.

Joulain, D., König, W.A., 1998. The Atlas of Spectral Data of Sesquiterpene Hydrocarbons. E. B.-Verlag, Hamburg.

McMurry, J.E., Bosch, G.K., 1987. Synthesis of macrocyclic terpenoid hydrocarbons by intramolecular carbonyl coupling: bicyclogermacrene, lepidozene and casbene. Journal of Organic Chemistry 52, 4885–4893.

Mekem Sonwa, M., König, W.A., Kubeczka, K.-H., Motl, O., 1997. Sesquiterpenes from the essential oil of *Cyperus alopecuroides*. Phytochemistry 45, 1435–1439.

Nyasse, B., Ghogumu Tih, R., Sodengam, B.L., Martin, M.T., Bodo, B., 1988. Mandassidione and other sesquiterpenic ketones from *Cyperus articulatus*. Phytochemistry 27, 3319–3321.

Ohira, S., Hasegawa, T., Hyashi, K.-I., Hoshino, T., Takaoka, D., Nozaki, H., 1998. Sesquiterpenoids from *Cyperus rotundus*. Phytochemistry 47, 1577–1581.

PERGAMON

Phytochemistry 58 (2001) 811–817

PHYTOCHEMISTRY

www.elsevier.com/locate/phytochem

Megastigmane, aliphatic alcohol and benzoxazinoid glycosides from *Acanthus ebracteatus*

Tripetch Kanchanapoom[a,b], Ryoji Kasai[a], Chayan Picheansoonthon[b], Kazuo Yamasaki[a,*]

[a]*Institute of Pharmaceutical Sciences, Faculty of Medicine, Hiroshima University, 1-2-3 Kasumi, Minami-ku, Hiroshima 734-8551, Japan*
[b]*Department of Pharmaceutical Botany and Pharmacognosy, Faculty of Pharmaceutical Sciences, Khon Kaen University, Khon Kaen, Thailand*

Received 19 March 2001; received in revised form 5 June 2001

Abstract

From the aerial part of *Acanthus ebracteatus*, a megastigmane glycoside (ebracteatoside A), three aliphatic alcohol glycosides (ebracteatosides B–D), as well as 7-chloro-(2*R*)-2-*O*-β-D-glucopyranosyl-4-hydroxy-2*H*-1,4-benzoxazin-3(4*H*)-one (7-Cl-DIBOA-Glc) were isolated together with 22 known compounds. Structural elucidations were based on analyses of spectroscopic data.
© 2001 Elsevier Science Ltd. All rights reserved.

Keywords: *Acanthus ebracteatus*; Acanthaceae; Megastigmane glycoside; Aliphatic alcohol glycoside; Benzoxazinoid glucoside; Ebracteatosides A–D

1. Introduction

As part of our ongoing study on Thai medicinal plants in the genus *Acanthus* (Kanchanapoom et al., 2001a,b), we investigated the constituents of *Acanthus ebracteatus* Vahl (Acanthaceae, Thai name: Ngueak-Pla-Mo, Nam-Mo) collected from Pattani province. *A. ebracteatus* is a spiny herb distributed in the mangroves of southern Thailand. In Thai traditional medicine, the plant is widely used as a purgative and an anti-inflammatory, as well as the leaves dispensed with pepper (*Piper nigrum* L.) as tonic pills for longevity. In the preliminary studies, anti-mutagenicities of the organic extracts have been reported (Rojanapo et al., 1990). The present study deals with the isolation and structural elucidation of one new megastigmane glycoside (**3**), three new aliphatic alcohol glycosides (**5**–**7**) and one new benzoxazinoid glucoside (**10**), along with 22 known compounds from the aerial part of this plant. Also, the usage in Thai traditional medicines is discussed.

2. Results and discussion

The methanolic extract of the aerial part of *A. ebracteatus* was suspended in H_2O and defatted with Et_2O. The aqueous layer was subjected to a column of highly porous copolymer resin of styrene and divinylbenzene, using H_2O, 30% MeOH, 60% MeOH, MeOH and Me_2CO, successively. The fractions eluted with 30% and 60% MeOH were repeatedly subjected to silica gel column chromatography, as well as other RP-18 or prep. HPLC to afford 27 compounds. Twenty two were identified as known compounds; plucheoside B (**1**), alangionoside C (**2**) (Otsuka et al., 1995), premnaionoside (**4**) (Sudo et al., 2000), (2*R*)-2-*O*-β-D-glucopyranosyl-2*H*-1,4-benzoxazin-3(4*H*)-one (HBOA-Glc, **8**) (Tietze et al., 1991), (2*R*)-2-*O*-β-D-glucopyranosyl-4-hydroxy-2*H*-1,4-benzoxazin-3(4*H*)-one (DIBOA-Glc, **9**) (Hartenstein and Sicker, 1994), phenethyl alcohol 8-*O*-β-D-glucopyranosyl-(1→2)-*O*-β-D-glucopyranoside (**11**) (Ono et al., 1999), benzyl alcohol 7-*O*-β-D-glucopyranosyl-(1→2)-*O*-β-D-glucopyranoside (zizybeoside I, **12**) (Okamura et al., 1981), adenosine (**13**) (Otsuka et al., 1989), verbascoside (**14**), isoverbascoside (**15**), leucosceptoside A (**16**) (Miyase et al., 1982), martynoside (**17**) (Sasaki et al., 1978), β-hydroxyacteoside (**18**) (Kitakawa et al., 1984), vecenin-2 (**19**), schaftoside (**20**) (Markham and Chari, 1982), luteolin-7-*O*-β-D-glucuronide (**21**), apigenin-7-*O*-β-D-glucuronide (**22**) (Hase et al., 1995), (+)-lyoniresinol 3α-*O*-β-D-glucopyranoside (**23**), (−)-lyoniresinol 3α-*O*-β-D-glucopyranoside (**24**) (Achenbach et al., 1992), (8*R*, 7′*S*, 8′*R*)-5,5′-dimethoxylariciresinol 4′-*O*-β-D-glucopyranoside (**25**) (Ida et al., 1994), magnolenin C (**26**) (Rao and Wu, 1978), and (+)-syringaresinol-4-*O*-β-D-apiofuranosyl-(1→2)-*O*-β-D-glucopyranoside (**27**) (Kinjo et al., 1991)

* Corresponding author. Tel.: +81-82-257-5285; fax: +81-82-257-5289.
E-mail address: yamasaki@pharm.hiroshima-u.ac.jp (K. Yamasaki).

0031-9422/01/$ - see front matter © 2001 Elsevier Science Ltd. All rights reserved.
PII: S0031-9422(01)00306-5

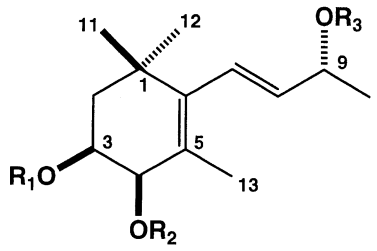

	R_1	R_2	R_3
1	Glc	H	H
2	H	Glc	H
3	H	H	Glc (2'-1") Api
1a	H	H	H

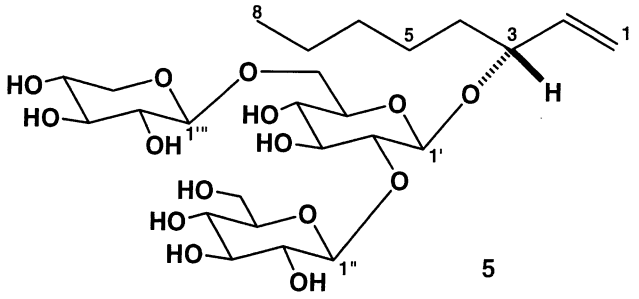

5

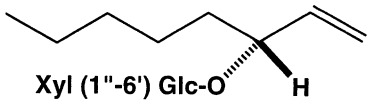

5a

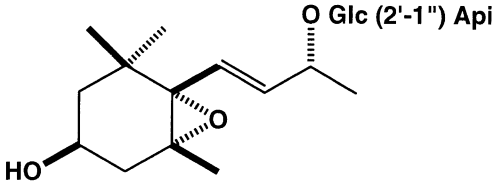

4

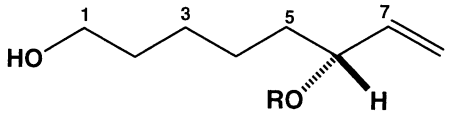

R

6 Glc (2'-1") Glc

7 Glc (6'-1") Xyl

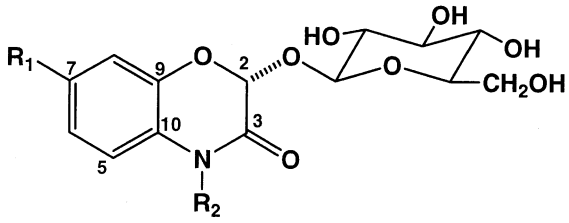

	R_1	R_2
8	H	H
9	H	OH
10	Cl	OH

by comparison of physical data with literature values and from spectroscopic evidence.

The molecular formula of compound **3** was determined as $C_{24}H_{40}O_{12}$ by HR-FAB mass spectrometry. The ^1H NMR spectrum revealed the presence of three singlet methyls, one methyl doublet, two olefinic protons, and two anomeric protons of sugar moieties. The ^{13}C NMR spectrum indicated the presence of the β-D-apiofuranosyl-(1→2)-*O*-β-D-glucopyranose unit, compared to compound **4**. The stereochemistry of an apiose could assign as D-form by the coupling of H-5″ at δ 3.61, which showed the magnetically equivalent (Snyder and Serianni, 1987). The remaining 13 carbon signals were suggested to present a megastigmane skeleton. The aglycone moiety of compound **3** was expected to be the same as that of plucheoside B (**1**) and alangionoside C (**2**). On enzymatic hydrolysis of **1**, **2** and **3** gave the same compound **1a**, identified by spectral analyses and comparing the HPLC retention time (R_f 3.38). Comparison of the ^{13}C NMR spectrum of **3** with those of **1a** showed

a significant downfield shift of C-9 (+7.9 ppm) together with the upfield shifts of C-8 (−2.1 ppm) and C-10 (−2.8 ppm), indicating that the sugar moiety is located at C-9. The absolute configuration at C-9 of **3** was assigned to be *R* from the chemical shifts at C-9 and C-10 (77.4 and 21.0, respectively) (Pabst et al., 1992; Takeda et al., 1997). Also, the absolute configurations at C-9 of **1** and **2**, which could not be determined from the previous reports (Uchiyama et al., 1989; Otsuka et al., 1995), were concluded to be *R*. Consequently, the structure of compound **3** was elucidated as shown, named ebracteatoside A.

The molecular formula of compound **5** was determined as $C_{25}H_{44}O_{15}$ by HR-FAB mass spectrometry. The ^{13}C NMR spectrum showed the presence of three sugar moities, which were identified to be a terminal β-D-glucopyranose, a terminal β-D-xylopyranose connected to a core β-D-glucopyranose unit, in addition to eight carbon signals for the aglycone. Acid hydrolysis gave D-xylose and D-glucose which were identified by TLC and comparison of the optical rotation with authentic samples. DEPT experiments indicated the presence of one methyl (δ 14.5), five methylenes (δ 23.6, 25.5, 32.9, 35.7 and 116.9) as well as two methines (δ 82.3 and 140.5) in the aglycone moiety. The chemical shifts of **5** were almost the same as those of (3*R*)-1-octen-3-ol-3-*O*-β-D-xylopyranosyl-(1→6)-*O*-β-D-glucopyranoside (**5a**), previously isolated from *Mentha spicata* (Yamamura et al., 1998), except for the additional signals of a β-D-glucopyranosyl unit. The downfield shift of C-2′ (+8.5 ppm) together with the upfield shift of C-1′ (-1.7) and C-3′ (−0.7 ppm) of the substituted sugar established the attachment of an additional unit to C-2′. Also, the HMBC correlations confirmed the positions of the sugar moieties as shown in Fig 1. Moreover, the EI–MS of its trimethylsilyl ethers exhibited the fragment ion characteristic of the 1,6-linked biose unit at *m*/*z* 481, due to TMSi-hexose-(6→1)-TMSi-pentose (Kasai et al., 1977), indicating the position of β-D-xylopyranose to C-6′. Therefore, the structure of compound **5** was assigned as (3*R*)-1-octen-3-ol-3-*O*-β-D-xylopyranosyl-(1‴→6′)-*O*-[β-D-glucopyranosyl-(1″→2′)]-*O*-β-D-glucopyranoside, named ebracteatoside B.

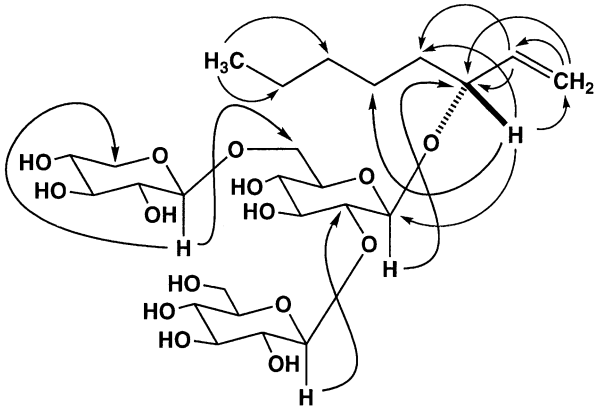

Fig. 1. The HMBC correlations of compound **5**.

Compound **6** had the molecular formula $C_{20}H_{36}O_{12}$, determined from HR-FAB mass spectrometry. The ^{13}C NMR spectrum revealed the presence of two β-D-glucopyranosyl units, one of which was attached at C-2′ due to the downfield shift (δ 83.6) of this carbon signal, in addition to eight signals for the aglycone moiety. Acid hydrolysis afforded D-glucose, identical by TLC and comparison of the optical rotation with authentic sample. The chemical shifts of the aglycone carbons were similar to those of **5**. However, the absence of the methyl signal at δ 14.5 together with the presence of one more methylene carbon at δ 62.9 were observed in **6**, indicating that the terminal methyl was substituted by a hydroxyl group. The absolute configuration at C-6 was suggested to be in the *R*-form by comparing the ^{13}C NMR spectral data with those of **5**. From these results, the structure of compound **6** was identified as (6*R*)-7-octene-1,6-diol 6-*O*-β-D-glucopyranosyl-(1→2)-*O*-β-D-glucopyranoside, named ebracteatoside C.

Compound **7** had the molecular formula $C_{19}H_{34}O_{11}$, deduced from HR-FAB mass spectrometry. The chemical shifts were very similar to those of **6**, except for the difference signals of the terminal sugar which was identified as a β-D-xylopyranose. The terminal sugar was assigned to attach at C-6′ (δ 69.5) of β-D-glucopyranose, due to the downfield shift of this signal. Consequently, the structure of compound **7** was elucidated to be (6*R*)-7-octene-1,6-diol 6-*O*-β-D-xylopyranosyl-(1→6)-*O*-β-D-glucopyranoside, named ebracteatoside D.

Compound **10** showed the characteristic pattern due to have a chlorine atom from negative FAB–MS. The molecular formula was determined by HR–FAB mass spectrometry as $C_{14}H_{16}ClNO_9$. The ^1H and ^{13}C NMR spectral data were similar to those of DIBOA-Glc (**9**). However, the ^1H NMR spectrum revealed the presence of an ABX system at δ 7.16 (1H, $J=8.5$, 2.2 Hz), δ 7.24 (1H, $J=8.5$ Hz) and δ 7.30 (1H, $J=2.2$ Hz), indicating that the chlorine atom was attached to an aromatic ring. The position of the chlorine atom was assigned to C-7 by comparing the calculation of the chemical shifts effect from the Cl atom and the observed chemical shifts from ^{13}C NMR spectrum. The chemical shift differences of the aromatic ring between **9** and **10** as to the *ipso* (C-7), *ortho* (C-6), *ortho* (C-8), *meta* (C-5), *meta* (C-9) and *para* (C-10) were +4.6, −1.0, +0.5, +1.3, +0.9 and −0.5, respectively, which agreed with those for the chlorine substituted at C-7 of the aromatic ring (Silverstein et al., 1981). The configuration at C-2 was suggested to be *R* since the optical rotation measured has a positive value as **9**. Therefore, the structure of compound **10** was identified as 7-chloro-(2*R*)-2-*O*-β-D-glucopyranosyl-4-hydroxy-2*H*-1,4-benzoxazin-3(4*H*)-one (7-Cl-DIBOA-Glc).

The biological activities of the isolated compounds have not been investigated. The presence of benzoxazinoids (**8**–

9) and phenylpropanoids (**14**–**15**) as the major constituents are in agreement with Thai traditional usage as an anti-inflammatory preparation (Otsuka et al., 1988; Cometa et al., 1993). Furthermore, the toxicological and pharmacological properties of benzoxazinoids have been reported as the chemical resistance factors against insects, fungi, bacteria and viruses in many crop plants of the family Gramineae (Niemeyer, 1988; Sicker et al., 2000), as well as having mutagenic activities (Hashimoto and Shudo, 1996). Also, the aglycone of **9** (DIBOA) was shown to be mutagenic in a test with *Salmonella typhimurium* TA 100 and TA 98 (Hashimoto and Shudo, 1996). The results on the mutagenicities of benzoxazinoids contrasted with the reported as anti-mutagenicities of the organic extracts of this plants by Rojanapo and co-workers (1990), which could be explained by the structural requirements for biological activities of benzoxazinoids. The 2-hydroxyl group of benzoxazinoids has been considered to be important for biological activities more than glucoside forms (Niemeyer, 1988). From these reports, the usage of this species for internal treatments in Thai traditional medicine should be considered.

3. Experimental

3.1. General

NMR spectra were recorded in methanol-d_4 or DMSO-d_6 using a JEOL JNM A-400 spectrometer (400 MHz for ^{1}H NMR and 100 MHz for ^{13}C NMR) with tetramethylsilane (TMS) as internal standard. MS were recorded on a Jeol JMS-SX 102 spectrometer. Optical rotations were measured with a Union PM-1 digital polarimeter. Preparative HPLC was carried out on columns of ODS (150×20 mm i.d., YMC) and polyamine II (250×20 mm i.d., YMC) with a Tosoh refraction index (RI-8) detector. Analytical HPLC was carried out on a column of ODS (100×4.6 mm i.d., YMC). For CC, silica gel G 60 (Merck), YMC-gel ODS (50 μm, YMC), and highly porous copolymer resin of styrene and divinylbenzene (Mitsubishi Chem. Ind. Co. Ltd) were used. The solvent systems were: (I) EtOAc–EtOH–H_2O (4:1:0.1), (II) EtOAc–EtOH–H_2O (7:3:0.3), (III) EtOAc–EtOH–H_2O (6:4:1), (IV) 10% MeCN, (V) 80% MeCN, (VI) 75% MeCN, (VII) EtOAc–MeOH-H_2O (4:1:0.1), (VIII) EtOAc–MeOH–H_2O (7:3:0.3), (IX) EtOAc–EtOH–H_2O (6:4:1), (X) 15% MeCN, (XI) 20% MeCN, (XII) 25% MeCN and (XIII) 40% MeOH. The spray reagent used for TLC was 10% H_2SO_4 in 50% EtOH.

3.2. Plant material

A. ebracteatus Vahl was collected in May 1997 from Pattani Province, Southern Thailand. The identification of the plant was confirmed by Professor Vichiara Jirawongse, Department of Pharmaceutical Botany and Pharmacognosy, Faculty of Pharmaceutical Sciences, Khon Kaen University. A voucher sample (KKU-0002) is kept in the Herbarium of the Faculty of Pharmaceutical Sciences, Khon Kaen University, Thailand.

3.3. Extraction and isolation

The dried aerial part (2.8 kg) of *A. ebracteatus* was extracted with hot MeOH. After removal of the solvent by evaporation, the residue (513.0 g) was defatted with Et_2O. The aqueous layer was subjected to a column of highly porous copolymer resin of styrene and divinylbenzene and eluted with H_2O, 30% MeOH, 60% MeOH, MeOH and Me_2CO, successively. The fraction eluted with 30% MeOH (21.0 g) was subjected to a column of silica gel (systems I, II and III, respectively) affording six fractions. Fraction 2 (4.0 g) was separated on RP-18 (system IV) to provide compound **8** (2.2 g). Fraction 3 (5.6 g) was purified by using RP-18 (system IV) and HPLC-polyamine II (system V) to give compounds **1** (30 mg), **3** (30 mg), **4** (36 mg), **9** (3.8 g) and **11** (42 mg). Fraction 4 (2.1 g) was subjected to RP-18 (system IV), then followed by HPLC-polyamine II (system VI) to afford compounds **6** (78 mg), **7** (5 mg) **12** (18 mg) and **13** (22 mg). Fraction 6 (2.5 g) was further purified by using RP-18 (system V) to provide compound **19** (190 mg).

The fraction eluted with 60% MeOH (48.0 g) was subjected to a column of silica gel (systems VII, VIII and IX, respectively) to give seven fractions. Fraction 2 (10.0 g) was subjected to a column of RP-18 (system X), the followed by HPLC-ODS (system XI or XII) to afford compounds **14** (3.0 g), **15** (325 mg), **16** (38 mg) and **17** (30 mg). Fraction 4 (3.7 g) was purified by using RP-18 (system X) and HPLC-ODS (system XIII) to give compounds **2** (11 mg), **18** (20 mg), **23** (112 mg) and **24** (50 mg). Fraction 5 (3.9 g) was separated on RP-18 (system X) to give nine fractions. Fractions 5-5 and 5-6 were purified by HPLC-ODS (system XIII) to provide compounds **10** (12 mg), **25** (33 mg) and **26** (36 mg). Fractions 5-8 and 5-9 were similarly purified by HPLC-ODS (system XII) to afford compounds **5** (142 mg) and **27** (34 mg). Fraction 6 (2.5 g) was subjected to RP-18 (system X) to provide six fractions. Compound **20** (75 mg) was crystallized from fraction 6-3. Finally, fraction 7 (9.9 g) was purified by RP-18 (system X), then followed by HPLC-ODS (system X) to give compounds **21** (98 mg) and **22** (66 mg).

3.4. Ebracteatoside A (*3*)

Amorphous powder, $[\alpha]_D^{17}$ −52.2° (MeOH, *c* 2.0); ^{1}H NMR (methanol-d_4): δ 1.77 (1H, *dd*, J = 12.7, 12.5 Hz, H-2ax), δ 1.43 (1H, *ddd*, J = 12.2, 3.4, 1.2 Hz, H-2eq), δ 3.74 (1H, *dt*, J = 12.0, 3.9 Hz, H-3), δ 6.07 (1H, *d*, J = 16.1 Hz, H-7), δ 5.56 (1H, *dd*, J = 16.1, 7.0 Hz, H-8),

δ 4.42 (1H, *qd*, *J*=6.6, 1.0 Hz, H-9), δ 3.82 (1H, *brd*, *J*=3.4 Hz, H-4), δ 1.30 (3H, *d*, *J*=6.4 Hz, H-10), δ 1.07 (3H, *s*, H-11), δ 1.03 (3H, *s*, H-12), δ 1.83 (3H, *s*, H-13), δ 4.44 (1H, *d*, *J*=7.8 Hz, H-1′ Glc), δ 3.51 (1H, *dd*, *J*=9.3, 7.8 Hz, H-2′ Glc), δ 3.46 (1H, *dd*, *J*=9.0, 9.0 Hz, H-3′ Glc), δ 3.33 (1H, *dd*, *J*=9.5, 8.5 Hz, H-4′ Glc), δ 3.18 (1H, *ddd*, *J*=9.5, 4.6, 2.2 Hz, H-5′ Glc), δ 3.78 (1H, *dd*, *J*=11.7, 2.4 Hz, H-6′ Glc), δ 3.66 (1H, *dd*, *J*=11.9, 4.9 Hz, H-6′ Glc), δ 5.38 (1H, *d*, *J*=1.7 Hz, H-1″ Api), δ 3.94 (1H, *d*, *J*=1.7 Hz, H-2″ Api), δ 4.06 (1H, *d*, *J*=9.5 Hz, H-4″ Api), δ 3.71 (1H, *d*, *J*=9.5 Hz, H-4″ Api), δ 3.61 (2H, *s*, H-5″ Api); ^{13}C NMR (methanol-d_4): Table 1; negative HR–FAB–MS, *m*/*z* 519.2449 ($C_{24}H_{39}O_{12}$ requires 519.2441)

3.5. Enzymatic hydrolysis of plucheoside B (*1*), alangionoside C (*2*), and ebracteatoside A (*3*)

Each sample of plucheoside B (**1**) (17 mg), alangionoside C (**2**) (9 mg) and ebracteatoside A (**3**) (15 mg) was dissolved in 0.5 ml of MeOH. A solution of crude hesperidinase (100 mg in 20 ml of H_2O) was added in each experiment. After stirring at 37 °C for 5 days, the mixtures were extracted with EtOAc, and concentrated to dryness, affording **1a** (7, 2 and 4 mg, respectively). The structure was identified by spectral analyses and comparing the HPLC retention time (R_f 3.38, solvent system: 50% MeOH)

Table 1
^{13}C NMR spectral data of compounds **1**, **1a**, **2** and **3** (methanol-d_4, 100 MHz)

C	1	1a	2	3
1	37.8	37.7	37.9	37.7
2	40.0	41.7	42.9	41.6
3	76.1	67.9	67.4	67.9
4	70.1	72.6	84.3	72.5
5	127.9	128.9	127.6	129.1
6	143.0	142.4	140.8	142.2
7	126.7	126.8	126.5	128.6
8	140.6	140.5	140.7	138.4
9	69.4	69.5	69.4	77.4
10	23.8	23.8	23.8	21.0
11	27.7	27.7	27.4	27.8
12	30.3	30.3	30.2	30.3
13	19.9	19.8	19.8	19.9
Glc-1′	102.6		106.1	100.8
2′	75.3		75.1	79.3
3′	78.1		78.0	77.9
4′	71.6		71.4	71.3
5′	78.1		78.2	77.7
6′	62.7		62.5	62.4
Api-1″				110.8
2″				78.6
3″				80.6
4″				75.3
5″				66.0

3.6. Aglycone of plucheoside B, alangionoside C and ebracteatoside A (*1a*)

Amorphous powder, $[\alpha]_D^{22}$ −65.4° (MeOH, *c* 0.52); ^{1}H NMR (methanol-d_4): δ 1.78 (1H, *dd*, *J*=12.7, 12.5 Hz, H-2ax), δ 1.42 (1H, *ddd*, *J*=12.0, 3.4, 1.2 Hz, H-2eq), δ 3.74 (1H, *dt*, *J*=12.9, 3.9 Hz, H-3), δ 3.82 (1H, *brd*, *J*=3.7 Hz, H-4), δ 6.02 (1H, *d*, *J*=16.1 Hz, H-7), δ 5.50 (1H, *dd*, *J*=16.1, 6.1 Hz, H-8), δ (1H, *qd*, *J*=6.3, 1.0 Hz, H-9), δ 1.27 (3H, *d*, *J*=6.4 Hz, H-10), δ 1.06 (3H, *s*, H-11), δ 1.03 (3H, *s*, H-12), δ 1.82 (3H, *s*, H-13); ^{13}C NMR (methanol-d_4): Table 1; negative HR–FAB–MS, *m*/*z* 225.1456 ($C_{13}H_{21}O_3$ requires 225.1490).

3.7. Ebracteatoside B(*5*)

Amorphous powder, $[\alpha]_D^{22}$ −45.0° (MeOH, *c* 2.11); ^{1}H NMR (methanol-d_4): δ 5.21 (1H, *brd*, *J*=17.3 Hz, H-1), δ 5.13 (1H, *brd*, *J*=10.5 Hz, H-1), δ 5.85 (1H, *ddd*, *J*=17.3, 10.3, 7.3 Hz, H-2), δ 4.12 (1H, *dd*, *J*=12.9, 6.6 Hz, H-3), δ 1.66 (1H, *m*, H-4), δ 1.49 (1H, *m*, H-4), δ 1.24–1.38 (6H, *m*, H-5,6,7), δ 0.89 (3H, *t*, *J*=6.8 Hz, H-8), δ 4.63 (1H, *d*, *J*=7.6 Hz, H-1″ Xyl), δ 4.42 (1H, *d*, *J*=7.6 Hz, H-1′ Glc), δ 4.32 (1H, *d*, *J*=7.3 Hz, H-1″ Glc); ^{13}C NMR (methanol-d_4): Table 2; negative HR–FAB–MS, *m*/*z* 583.2555 ($C_{25}H_{43}O_{15}$ requires 583.2601).

Table 2
^{13}C NMR spectral data of compounds **5**–**7** (methanol-d_4, 100 MHz)

C	5	C	6	7
1	116.9	8	116.6	116.2
2	140.5	7	140.8	140.8
3	83.8	6	83.6	82.5
4	35.7	5	35.7	35.7
5	25.5	4	25.7	25.8
6	32.9	3	33.6	33.6
7	23.6	2	26.9	26.9
8	14.5	1	62.9	62.9
Glc-1′	101.7	Glc-1′	101.7	103.3
2′	82.3	2′	82.6	75.3
3′	77.5[a]	3′	77.7[a]	78.1[a]
4′	71.0	4′	71.3	71.2
5′	77.5[a]	5′	78.0[a]	77.6[a]
6′	69.3	6′	62.8	69.5
Glc-1″	104.8	Glc-1″	105.0	
2″	75.9	2″	76.1	
3″	77.8[a]	3″	77.7[a]	
4″	71.4	4″	71.5	
5″	78.0[a]	5″	78.2[a]	
6″	62.7	6″	62.6	
Xyl-1‴	105.1	Xyl-1″		105.3
2‴	74.7	2″		74.9
3‴	77.5[a]	3″		77.0
4‴	71.4	4″		71.5
5‴	66.7	5″		66.9

[a] Assignments may be interchanged in each column.

3.8. Trimethylsilylation of ebracteatoside B (**5**)

Ebracteatoside B (ca. 2 mg) was heated with trimethylsilylimidazole (three drops) in a stoppered microtube at 90 °C for 1 h. After dilution with H_2O, the reaction mixture was extracted with *n*-hexane. The *n*-hexane layer was concentrated to dryness by blowing N_2 gas at room temperature. The residue was subjected to determination of EI–MS.

3.9. Ebracteatoside C (**6**)

Amorphous powder, $[\alpha]_D^{22}$ −19.8° (MeOH, *c* 2.62); ^{1}H NMR (methanol-d_4): δ 3.54 (2H, *t*, *J* = 6.1 Hz, H-1), δ 1.35–1.44 (4H, *m*, H-2, 4), δ 1.54 (2H, *m*, H-3), δ 1.72 (1H, *m*, H-5), δ 1.56 (1H, *m*, H-5), δ 4.15 (1H, *dd*, *J* = 12.9, 6.6 Hz, H-6), δ 5.89 (1H, *ddd*, *J* = 17.8, 10.0, 7.6 Hz, H-7), δ 5.22 (1H, *brd*, *J* = 17.3 Hz, H-8), δ 5.12 (1H, *brd*, *J* = 10.5 Hz, H-8), δ 4.44 (1H, *d*, *J* = 7.6 Hz, H-1′ Glc), δ 4.63 (1H, *d*, *J* = 7.8 Hz, H-1″ Glc); ^{13}C NMR (methanol-d_4): Table 2; negative HR–FAB–MS, *m*/*z* 467.2093 ($C_{20}H_{35}O_{12}$ requires 467.2128)

3.10. Acid hydrolysis of ebracteatoside B (**5**) and ebractestoside C (**6**)

Ebracteatoside B (50 mg) was dissolved in 5% HCl and heated at 90 °C for 2 h. After cooling, the reaction mixture was extracted with Et_2O. The aqueous layer was neutralized with $NaHCO_3$, concentrated to dryness. The residue was then applied to a silica gel column (system VII), affording D-xylose (6 mg, R_f 0.29, $[\alpha]_D^{24}$ +20.0°) and D-glucose (8 mg, R_f 0.16. $[\alpha]_D^{24}$ +49.5°), comparing with authentic samples. By the same method, ebracteatoside C (30 mg) provided D-glucose (5 mg, $[\alpha]_D^{24}$ +47.4°).

3.11. Ebracteatoside D (**7**)

Amorphous powder, $[\alpha]_D^{22}$ −57.7° (MeOH, *c* 0.35); ^{1}H NMR (methanol-d_4): δ 3.53 (2H, *t*, *J* = 6.6 Hz, H-1), δ 1.35–1.44 (4H, *m*, H-2, 4), δ 1.55 (2H, *m*, H-3), δ 1.68 (1H, *m*, H-5), δ 1.56 (1H, *m*, H-5), δ 4.14 (1H, *dd*, *J* = 12.9, 6.6 Hz, H-6), δ 5.87 (1H, *ddd*, *J* = 17.3, 10.5, 6.8 Hz, H-7), δ 5.22 (1H, *brd*, *J* = 17.3 Hz, H-8), δ 5.10 (1H, *brd*, *J* = 10.3 Hz, H-8), δ 4.31 (1H, *d*, *J* = 8.0 Hz, H-1′ Glc), δ 4.33 (1H, *d*, *J* = 7.3 Hz, H-1″ Xyl); ^{13}C NMR (methanol-d_4): Table 2; negative HR–FAB–MS, *m*/*z* 437.2015 ($C_{19}H_{33}O_{11}$ requires 437.2022).

3.12. 7-Chloro-(2R)-2-O-β-D-glucopyranosyl-4-hydroxy-2H-1,4-benzoxazin-3(4H)-one(7-Cl-DIBOA-Glc, **10**)

Amorphous powder, $[\alpha]_D^{22}$ +18.6° (DMSO, *c* 0.86); ^{1}H NMR (DMSO-d_6): δ 5.94 (1H, *s*, H-2), δ 7.24 (1H, *d*, *J* = 8.5 Hz, H-5),δ 7.16 (1H, *dd*, *J* = 8.5, 2.2 Hz, H-6), δ 7.30 (1H, *d*, *J* = 2.2 Hz, H-8), δ 4.56 (1H, *d*, *J* = 7.8 Hz, H-1 Glc), δ 2.91 (1H, *dd*, *J* = 8.6, 8.0 Hz, H-2 Glc), δ 3.13 (1H, *dd*, *J* = 9.3, 9.0 Hz, H-3 Glc), δ 2.99 (1H, *dd*, *J* = 9.5, 9.3 Hz, H-4 Glc), δ 3.17 (1H, *m*, H-5 Glc), δ 3.40 (1H, *dd*, *J* = 12.0, 5.9 Hz, H-6 Glc), δ 3.70 (1H, *brd*, *J* = 12.0 Hz, H-6 Glc), δ 11.10; ^{13}C NMR (DMSO-d_6): Table 3; negative HR–FAB–MS, *m*/*z*: 376.0403 ($C_{14}H_{15}O_9NCl$ requires 376.0435).

Table 3
^{13}C NMR spectral data of compounds **9** and **10** (DMSO-d_6, 100 MHz)

C	9	10
2	96.2	96.4
3	155.4	155.3
5	112.8	114.1
6	123.9	122.9
7	122.9	127.5
8	117.5	118.0
9	140.3	141.2
10	128.3	127.8
1′	102.5	102.8
2′	73.2	73.1
3′	77.3	77.6
4′	69.6	69.7
5′	76.6	76.7
6′	60.9	61.1

Acknowledgements

We would like to thank the Research Center for Molecular Medicine, Hiroshima University for the use of its NMR facilities.

References

Achenbach, H., Lowel, M., Waibel, R., Gupta, M., Solis, P., 1992. New lignan glucosides from *Stemmadenia minima*. Planta Medica 58, 270–272.

Cometa, F., Tomassini, L., Nicoletti, M., 1993. Phenylpropanoid glycosides: distribution and pharmacological activity. Fitoterapia 64, 195–217.

Hartenstein, H., Sicker, D., 1994. (2*R*)-2-β-D-Glucopyranosyloxy-4-hydroxy-2*H*-1,4-benzoxazin-3(4*H*)-one from *Secale cereale*. Phytochemistry 35, 827–828.

Hase, T., Ohtani, K., Kasai, R., Yamasaki, K., Picheansoonthon, C., 1995. Revised structure for hortensin, a flavonoid from *Millingtonia hortensis*. Phytochemistry 40, 287–290.

Hashimoto, Y., Shudo, K., 1996. Chemistry of biologically active benzoxazinoids. Phytochemistry 43, 551–559.

Ida, Y., Satoh, Y., Ohtsuka, M., Nagasao, M., Shoji, J., 1994. Phenolic constituents of *Phellodendron amurense* bark. Phytochemistry 35, 209–215.

Kanchanapoom, T., Kamel, M.S., Kasai, K., Yamasaki, K., Picheansoonthon, C., Hiraga, Y., 2001a. Lignan glucosides from *Acanthus ilicifolius*. Phytochemistry 56, 369–372.

Kanchanapoom, T., Kamel, M. S., Kasai, K., Picheansoonthon, C., Hiraga, Y., Yamasaki, K., 2001. Benzoxazinoid glucosides from *Acanthus ilicifolius*. Phytochemistry 58, 637–640.

Kasai, R., Marsuura, K., Tanakaa, O., Sanada, S., Shoji, J., 1977. Mass spectra of trimethylsilyl ethers of dammarane-type ginsengsapogenins and their related compounds. Chemical & Pharmaceutical Bulletin 25, 3277–3282.

Kinjo, J., Fukui, K., Higuchi, H., Nohara, T., 1991. The first isolation of lignan tri- and tetra-glycosides. Chemical & Pharmaceutical Bulletin 39, 1623–1625.

Kitakawa, S., Tsukamoto, H., Hisada, S., Nishibe, S., 1984. Studies on the Chinese crude drug "Forsythiae fructus." VII. A new caffeoyl glycoside from *Forsythia viridissima*. Chemical & Pharmaceutical Bulletin 32, 1209–1213.

Markham, K.R., Chari, V.M., 1982. Carbon-13 NMR spectroscopy of flavonoids. In: Harborne, J.B., Mabry, T.J (Eds.), The Flavonoids: Advances in Research. Chapman and Hall, Cambridge. pp. 19–134.

Miyase, T., Koizumi, A., Ueno, A., Noro, T., Kuroyanagi, M., Fukushima, S., Akiyama, Y., Takemoto, T., 1982. Studies on the acyl glycosides from *Leucoseptrum japonicum* (MiQ.) Kitamura *et* Murata. Chemical & Pharmaceutical Bulletin 30, 2732–2737.

Niemeyer, H.M., 1988. Hydroxamic acids (4-hydroxy-1,4-benzoxazin-3-ones), defence chemicals in the Gramineae. Phytochemistry 27, 3349–3358.

Okamura, N., Yagi, A., Nishioka, I., 1981. Studies on the constituents of *Zizyphi fructus*. V. Structures of glycosides of benzyl alcohol, vomifoliol and naringenin. Chemical & Pharmaceutical Bulletin 29, 3507–3514.

Ono, M., Yoshida, A., Ito, Y., Nohara, T., 1999. Phenethyl alcohol glycosides and isopentenol glycoside from fruit of *Bupleurum flacatum*. Phytochemistry 51, 819–823.

Otsuka, H., Hirai, Y., Nagao, T., Yamasaki, K., 1988. Anti-inflammatory activity of benzoxazinoids from roots of *Coix lachryma-jobi* var. *ma-yuen*. Journal of Natural Products 51, 74–79.

Otsuka, H., Kamada, K., Yao, M., Yuasa, K., Kida, I., Takeda, Y., 1995. Alangionoside C-F, megastigmane glycosides from *Alangium premnifolium*. Phytochemistry 38, 1431–1435.

Otsuka, H., Takeuchi, M., Inoshiri, S., Sato, T., Yamasaki, K., 1989. Phenolic compounds from *Coix lachryma-jobi* var. *ma-yuen*. Phytochemistry 28, 883–886.

Pabst, A., Barron, D., Semon, E., Schreier, P., 1992. Two diastereomeric 3- oxo-α-ionol β-D-glucosides from raspberry fruit. Phytochemistry 31, 1649–1652.

Rao, K.V., Wu, W.-N., 1978. Glycosides of Magnolia III: structural elucidation of magnolenin C. Journal of Natural Products 41, 56–62.

Rojanapo, W., Tepsuwan, A., Siripong, P., 1990. Mutagenicity and antimutagenicity of Thai medicinal plants. Basic Life Sciences 52, 447–452.

Sasaki, H., Taguchi, H., Endo, T., Yosioka, I., Higashiyama, K., Otomasu, H., 1978. The glycosides of *Martynia louisiana* Mill. A new phenylpropanoid glycoside, martynoside. Chemical & Pharmaceutical Bulletin 26, 2111–2121.

Sicker, D., Frey, M., Schulz, M., Gierl, A. 2000. Role of natural benzoxazinones in the survival strategy of plants. In: Jeon, K.W. (Ed.), International Review of Cytology: A Survey of Cell Biology. Academic, New York, pp. 198, 319–346.

Silverstein, R.M., Bassler, G.C., Morrill, T.C., 1981. Spectrometric Identification of Organic Compounds, 4th Edition. John Wiley & Son, New York.

Snyder, J.R., Serianni, A.S., 1987. DL-Apiose substitited with stable isotopes: synthesis, NMR spectral analysis, and furanose anomerization. Carbohydrate Research 166, 85–99.

Sudo, K., Ide, T., Otsuka, H., Hirata, E., Takushi, A., Shinzato, T., Takeda, Y., 2000. Megastigmane, benzyl and phenethyl alcohol glycosides, and 4,4′-dimethoxy-β-truxinic acid catapol diester from the leaves of *Premna subscandens* Merr. Chemical & Pharmaceutical Bulletin 48, 542–546.

Takeda, Y., Zhang, H., Matsumoto, T., Otsuka, H., Oosio, Y., Honda, G., Tabata, M., Fujita, T., Sun, H., Sezik, E., Yesilada, E., 1997. Megastigmane glycosides from *Salvia nemorosa*. Phytochemistry 44, 117–120.

Tietze, L., Beller, M., Terfort, A., Dolle, A., 1991. First synthesis and structural determination of blepharin and 1-′epiblepharin. Synthesis 1118–1120.

Uchiyama, T., Miyase, T., Ueno, A., Usmanghani, K., 1989. Terpenic glycosides from *Pluchea indica*. Phytochemistry 28, 3369–3372.

Yamamura, S., Ozawa, K., Ohtani, K., Kasai, R., Yamasaki, K., 1998. Antihistaminic flavones and aliphatic alcohol glycosides from *Mentha spicata*. Phytochemistry 48, 131–136.

PERGAMON

Phytochemistry 58 (2001) 819–825

PHYTOCHEMISTRY

www.elsevier.com/locate/phytochem

Glycoside carbamates from benzoxazolin-2(3*H*)-one detoxification in extracts and exudates of corn roots

Dieter Sicker[a], Bernd Schneider[b], Lothar Hennig[a], Mona Knop[c], Margot Schulz[c,*]

[a]*Institut für Organische Chemie, Universität Leipzig, Johannisallee 29, D-04103 Leipzig, Germany*
[b]*Max-Planck-Institut für Chemische Ökologie, Carl-Zeiss-Promenade 10, D-07745 Jena, Germany*
[c]*Institut für Landwirtschaftliche Botanik, Universität Bonn, Karlrobert-Kreiten-Str. 13, D-53115 Bonn, Germany*

Received 9 March 2001; received in revised form 20 June 2001

Dedicated to Professor Siegfried Hauptmann on the occasion of his 70th birthday

Abstract

Zea mays was incubated with the natural phytotoxin benzoxazolin-2(3*H*)-one (BOA) to investigate the detoxification process. A hitherto unknown detoxification product, 1-(2-hydroxyphenylamino)-1-deoxy-β-gentiobioside 1,2-carbamate (**3**), was isolated and identified. A reinvestigation of known BOA detoxification products by NMR methods led to the finding that the structure of benzoxazolin-2(3*H*)-one-*N*-β-glucoside (**1**) first reported from *Avena sativa* has to be revised. In fact, the correct structure is that of the isomeric 1-(2-hydroxyphenylamino)-1-deoxy-β-glucoside 1,2-carbamate **2**, which is structurally related to **3**. It was now shown with a synthetic mixture of **1** and **2** that **1** underwent spontaneous isomerization to form **2** in solution. Thus, *N*-glucosylation of BOA in the plant led finally to the carbamate **2**. In contrast to BOA-6-*O*-glucosylation, BOA-induced *N*-glucosylation appears first after 6–8 h of incubation. As soon as *N*-glucosylation is possible, BOA-6-*O*-glucoside is not further accumulated, whereas the amount of glucoside carbamate increases continuously during the next 40 h. Synthesis of gentiobioside carbamate seems to be a late event in BOA detoxification. All detoxification products are released into the environment via root exudation. © 2001 Elsevier Science Ltd. All rights reserved.

Keywords: *Zea mays*; Poaceae; Allelopathy; Rearrangement; Benzoxazolin-2(3*H*)-one-*N*-β-glucoside; 1-(2-Hydroxyphenylamino)-1-deoxy-β-glucoside 1,2-carbamate; 1-(2-Hydroxyphenylamino)-1-deoxy-β-gentiobioside 1,2-carbamate

1. Introduction

Plants show different, species dependent sensitivities when treated with phytotoxic allelochemicals. This well known phenomenon was observed, for instance, after application of benzoxazinones, such as DIBOA and its degradation product benzoxazolin-2(3*H*)-one (BOA) (Barnes and Putnam, 1987; Barnes et al., 1986; Sicker et al., 2000; Sicker and Schulz, 2001). One reason for the species dependent differences should be more or less developed strategies and capacities of BOA detoxification as it was recently found for diverse plant species belonging to European grain field or hoed vegetable communities (Schulz and Wieland, 1999). Species well equipped for BOA metabolization detoxify the compound via *N*-glucosylation (Wieland et al., 1998) and, to a lower degree, BOA is hydroxylated in position 6 and immediately glucosylated resulting in BOA-6-*O*-glucoside (Wieland et al., 1999). Since the Poaceae tested produced more BOA-*N*-glucoside they exhibited a more efficient BOA detoxification than dicots investigated. Most of these species contained BOA-6-*O*-glucoside as the major detoxification product. Among the monocots, corn has the best detoxification capacity as *N*-glucosylation was performed mainly whereas *O*-glucosylation was a minor detoxification product. In BOA-incubated corn roots an additional, hitherto not identified product was detected. The structure of the new disaccharidic carbamate will be presented together with the results of a reinvestigation of the detoxification pathway based on BOA-*N*-β-D-glucoside.

2. Results and discussion

2.1. Isomerization of BOA-N-β-glucoside 1 reported as a plant detoxification product of BOA

Surprisingly, on repeating our own BOA-*N*-glycosidation described we have obtained not a single compound

* Corresponding author. Tel.: +49-228-732151; fax: +49-228-731696.
E-mail address: ulp509@uni-bonn.de (M. Schulz).

0031-9422/01/$ - see front matter © 2001 Elsevier Science Ltd. All rights reserved.
PII: S0031-9422(01)00299-0

as in the first run but a ca. 1:3 mixture of two very similar compounds. This finding prompted a reinvestigation of both the natural detoxification products and the synthetic material described earlier (Wieland et al., 1998). The spectrometrical analyses show clearly that 3-β-glucopyranosyl-benzoxazolin-2(3*H*)-one **1** (BOA-*N*-β-D-glucoside) dissolved in methanol is not a stable compound, but the molecule is subjected to ring transformation yielding the constitutional isomer 1-(2-hydroxyphenylamino)-1-deoxy-β-glucopyranoside 1,2-carbamate (**2**) (Fig. 1), which represents a yet unknown natural product.

Therefore, the structure of our detoxification product assigned initially as BOA-*N*-β-glucoside (**1**) (Wieland et al., 1998) has to be revised and the compound reported there has to be described as the carbamate **2**, correctly. The structures of glucoside **1** and its isomeric carbamate **2** were determined by ^{1}H NMR, $^{1}H,^{1}H$ COSY, heteronuclear direct $^{1}H,^{13}C$ (HMQC), and long-range $^{1}H,^{13}C$ (HMBC) 2D NMR shift correlation. First spectra of the real BOA-*N*-β-glucoside (**1**) only could be obtained from an approximately 1:3 mixture together with the rearranged product **2**. The signals of **1** appeared slightly broadened but with typical coupling pattern and expected COSY cross peaks. The doublet of the anomeric proton at δ 5.45 showed a coupling constant of 8.9 Hz, indicating β-configuration. Due to the shielding effect of the aryl ring of the heterocycle, the double doublets of H-4′ (δ 3.05) and H-2′ (δ 2.92) appeared at unusual high field. Similar high field shift already has been observed by Hennig et al. (1998) for such protons (H-2 and H-4) in the D-ring of the antibiotic moenomycin A. 2D NMR spectra of the carbamate **2** were recorded after complete transformation under the same conditions. The β-glucopyranosyl configuration of the sugar unit was identified by chemical shifts, coupling constants (around 9 Hz, showing that all protons are axial) and COSY-correlation peaks. Protons H-4′ and H-2′ of this compound appeared now at unusual low field positions (δ 3.52 and 4.06, respectively). Characteristic HMBC correlations were observed between H-1′ (δ 5.30) and C-2′ (δ 70.0), C-3′ (δ 77.8), C-5′ (δ 80.2) (glucopyranosyl moiety), C=O (δ 154.5) (carbamate moiety), and C-1 (δ 129.5) [*N*-(hydroxyphenylamino) moiety] as well. In positive mode HR–ESI–MS experiments, both the pure carbamate **2** and the 1:3 mixture of **1** and **2** gave rise to the same spectrum with a $[M+H]^{+}$ peak at m/z 298.0919 which confirmed the conclusion that **1** and **2** are isomers with the elemental composition $C_{13}H_{15}NO_7$.

Hitherto, only two representatives of this class of carbohydrate carbamates are known which result from synthetic approaches, exclusively. Thus, the *N*-unsubstituted 1-deoxy-β-glucopyranoside 1,2-carbamate was prepared from D-glucopyranosylamine and phosgene in alkaline solution (Steyermark, 1962) as well as from *N*-(β-D-glucopyranosyl)triphenyl-phosphine imide and carbon dioxide in DMF (Kovacs et al., 1985). The *N*-isobutylamino derivative has been obtained by the cyclization of 1-(2-chloroethyl)-3-isobutyl-3-β-D-glucopyranosyl-1-nitrosourea (Tsujihara et al., 1981). In no case a biological activity has been reported for the compounds mentioned. In conclusion, the rearrangement observed is not described yet. An assumption for the driving force of the isomerization may be derived from the circumstance that the alcoholic 2-OH group of the glucoside **1** is more nucleophilic than the phenolic OH-group of the carbamate **2**.

The isomerization is found to be favored in alkaline solution. At pH 8, 90% of BOA-*N*-glucoside present in the 1:3 mixture is rearranged to carbamate, at pH 7

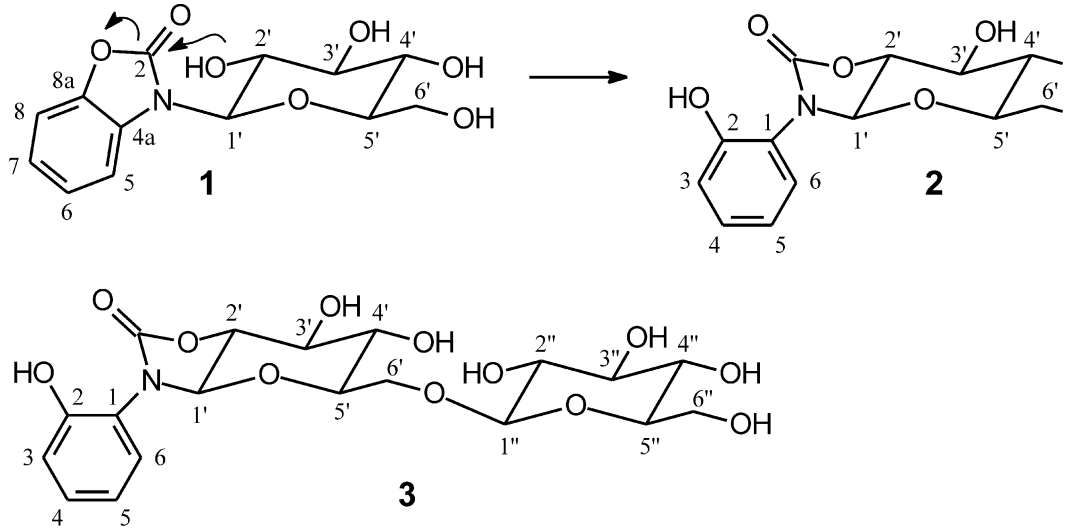

Fig. 1. Rearrangement of BOA-*N*-β-glucoside (**1**) to carbamate **2**; structure of 1-(2-hydroxyphenylamino)-1-deoxy-β-gentiobiose-1,2-carbamate (**3**).

60%, and at pH 6 only 40% when treated at 30°C for 65 min. Boiling accelerated the reaction also at pH 6.

2.2. Detection of **2** and 1-(2-hydroxyphenylamino)-1-deoxy-β-gentiobioside 1,2-carbamate **3** in extracts and exudates of corn roots

Re-investigation of a methanolic solution of synthetic BOA-*N*-glucoside that had been stored for several months at −20 °C revealed an additional, slightly more hydrophilic compound in addition to BOA-*N*-glucoside. The more hydrophilic peak was identical to the major detoxification product **2** first assumed to present BOA-*N*-glucoside and now identified as 1-(2-hydroxyphenylamino)-1-deoxy-β-glucopyranoside 1,2-carbamate **2**. Therefore, it must be concluded that in all extracts of plant species found to be able to detoxify BOA via *N*-glucosylation the glucoside carbamate should be the final product (Wieland et al., 1998; Schulz and Wieland, 1999).

In root extracts obtained from corn plants that have been incubated for 48 h, an additional compound (**3**) appeared. This compound was collected and treated with β-D-glucosidase. HPLC analysis of the enzyme assay revealed unequivocally that the treatment resulted in glucoside carbamate **2** as the only UV active product. Therefore, the additional product was assumed to present compound **2** conjugated with an additional β-D-glucose moiety. Spectroscopical analysis led to the assignation of 1-(2-hydroxyphenylamino)-1-deoxy-β-D-gentiobioside 1,2-carbamate for the structure of **3**. Thus, the ^{1}H and ^{13}C NMR spectra of carbamate **3** clearly exhibit signals of the aglycon moiety and two carbohydrate units. The chemical shift values and proton coupling pattern of the hydroxyphenylamino moiety resemble those of the corresponding unit in compound **2**. The coupling constants of H-1′ (δ 5.28, $J = 9.4$ Hz) and H-1″ (δ 4.30, $J = 7.8$ Hz) proved β-configuration at both anomeric centres. 2D Homo- and heterocorrelation experiments were used to assign all proton and carbon signals unambiguously. An HMBC cross signal between H-1′ and C-1 (δ 130.3) indicated attachment of the disaccharide to the aglycon through the nitrogen atom. The interglycosidic linkage between both glucose units was detected by means of a ^{1}H–^{13}C long-range heteronuclear correlation signal between H-1″ and C-6′ (δ 70.1), indicating the disaccharide to be gentiobiose. A positive mode HR–ESI–MS revealed an elemental composition of $C_{19}H_{25}NO_{12}$ for the neutral carbamate **3** and confirmed the findings of NMR.

With the purpose to get more insight in the course of BOA detoxification, corn seedlings were incubated, roots harvested and extracted after increasing incubation times (Fig. 2).

HPLC analyses revealed that during the first 6–8 h only BOA-6-*O*-glucoside was produced. Glucoside carbamate first appeared after 8 h. Thus, BOA-6-*O*-glucoside is not further accumulated as soon as *N*-glucosylation is possible. As gentiobioside carbamate was detectable for the first time after 18 h, this step is obviously a late event in BOA detoxification.

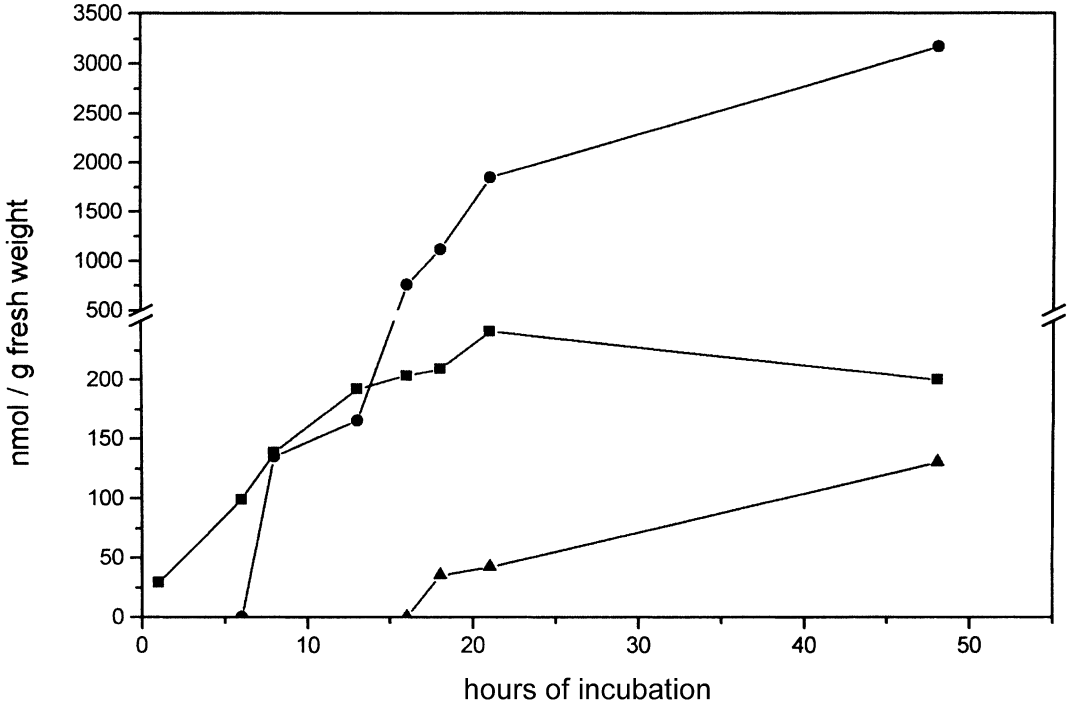

Fig. 2. Accumulation of BOA-6-*O*-glucoside (squares), gentiobioside carbamate (triangles) and glucoside carbamate (circles) in corn roots (average values from three experiments).

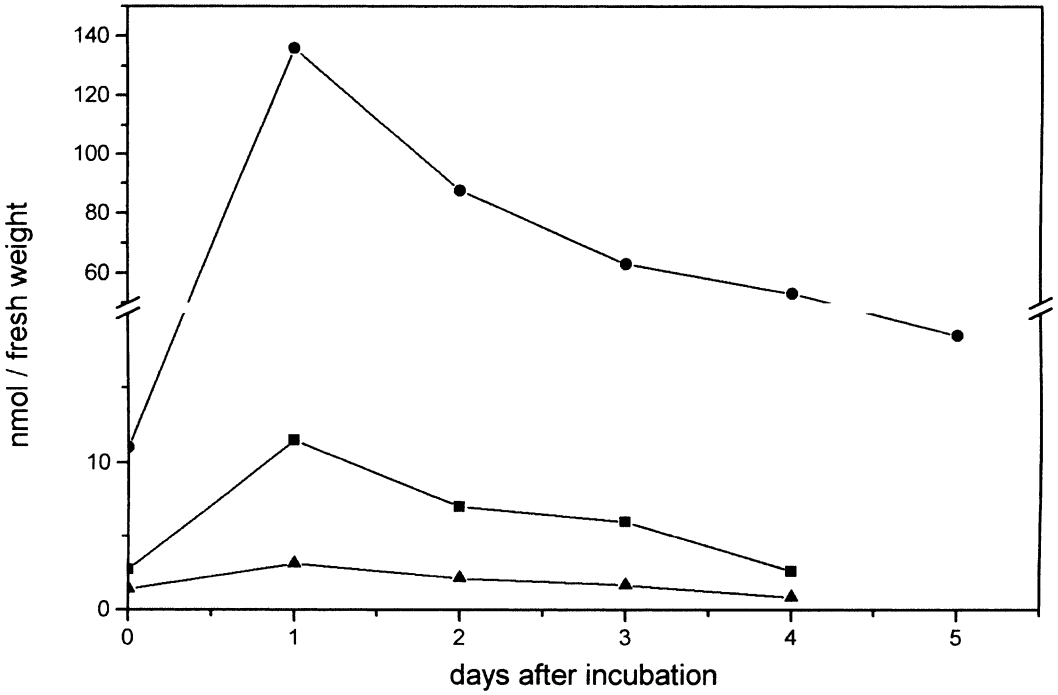

Fig. 3. Decrease of glucoside carbamate **2** (circles), of 1-(2-hydroxyphenylamino)-1-deoxy-β-gentiobioside1,2-carbamate (**3**) (triangles) and BOA-6-*O*-β-glucoside (squares) in roots of BOA incubated corn seedlings (average values of three experiments).

Since BOA metabolites were detected occasionally in the incubation medium (Wieland et al., 1999) a stable accumulation of those products in treated species was questionable. However, occurrence of the metabolites could be due to wounding as cut roots were used for incubations. Subsequent experiments gave rise of the assumption, that the compounds are released into the environment by root exudation. When corn seedlings transferred to pots after BOA incubation were checked for metabolites over a period of 4–5 days, none of the compounds was preserved at a stable level. During the first 24 h after incubation, the concentration of the metabolites still increased, reaching a maximum within the plant one day after incubation. The next days all metabolites decreased continuously: glucoside carbamate **2** was released most rapidly (5th day: 15–20% left), followed by gentiobioside carbamate **3** (4th day: 25% left) and less rapidly, the small amount of BOA-*O*-glucoside was diminished to 35% (Fig. 3).

Decrease of BOA metabolites is not restricted only to corn roots, but could be observed with BOA-incubated *Coriandrum sativum* and *Galinsoga ciliata* as well. Seedlings of the two species lost their main detoxification product BOA-6-*O*-β-D-glucoside within 5 days up to 40% (*C. sativum*) or almost completely (*G. ciliata*), (Fig. 4). It is not yet clear whether the compounds are exuded or not.

Recovery of 1-(2-hydroxyphenylamino)-1-deoxy-β-glucopyranoside 1,2-carbamate (**2**) and traces of 1-(2-hydroxyphenylamino)-1-deoxy-β-gentiobioside 1,2-carbamate (**3**) probably exuded by corn roots succeeded after concentration of the tap water where plants were placed after BOA incubation. The occurrence of 1-(2-hydroxyphenylamino)-1-deoxy-β-glucopyranoside 1,2-carbamate (**2**) in the concentrate reflected the increase and decrease of the compound in the roots (Figs. 3 and 5).

The gentiobioside carbamate **3** was detected only in traces. It is the question what happen to the exuded compounds under natural conditions. Rather likely, microbial activities might cleave one glucose moiety from compound **3** very easily resulting in glucoside carbamate **2**, the same may be true for BOA-*O*-glucoside which was not detectable in the concentrate. The further fate of the glucoside carbamate and BOA-6-OH is still unknown, but metabolization by soil microorganisms seems feasible.

3. Experimental

*3.1. Isolation of 1-(2-hydroxyphenylamino)-1-deoxy-β-gentiobioside 1,2-carbamate (**3**)*

Incubations of *Zea mays, C. sativum* and *G. ciliata* seedlings with BOA were performed as described in Schulz and Wieland (1999). For kinetics of BOA detoxification products, corn roots were incubated for 1, 2, 3, 4, 5, 6, 8, 13, 16, 18, 21, and 48 h. Corn roots were homogenized in presence of quartz sand and 30% methanol. The extract was filtered through miracloth and centrifuged for 20 min at 20 000 *g*. The supernatant was evaporated to dryness and dissolved in 2 ml 15%

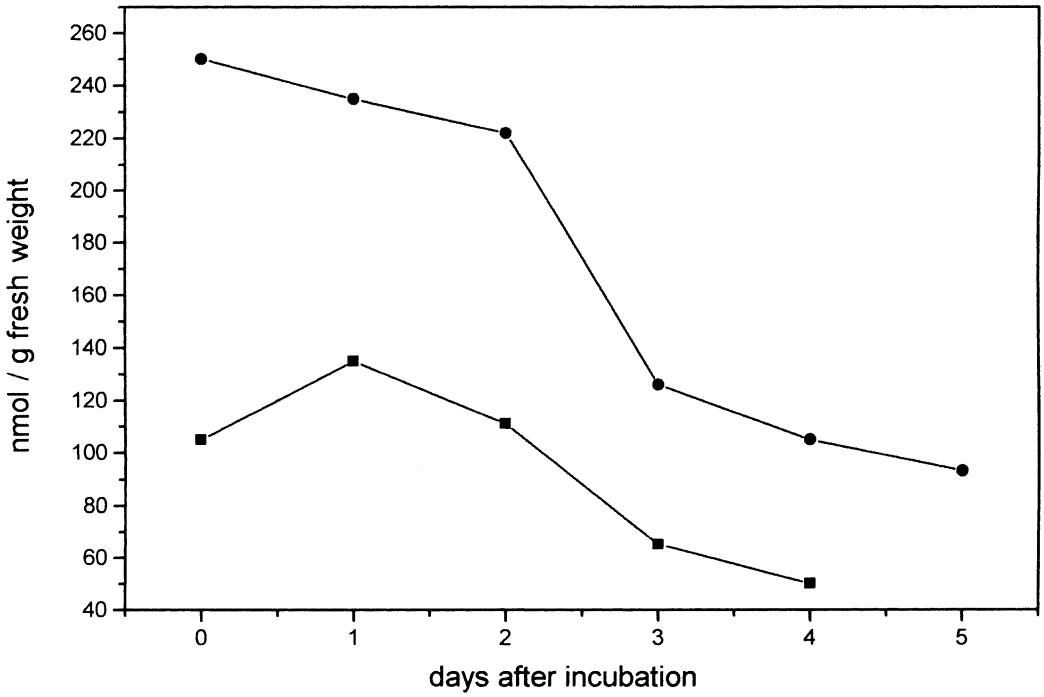

Fig. 4. Decrease of BOA-6-*O*-β-glucoside in seedlings of *Coriandrum sativum* (circles) and *Galinsoga ciliata* (squares) (average values from two experiments).

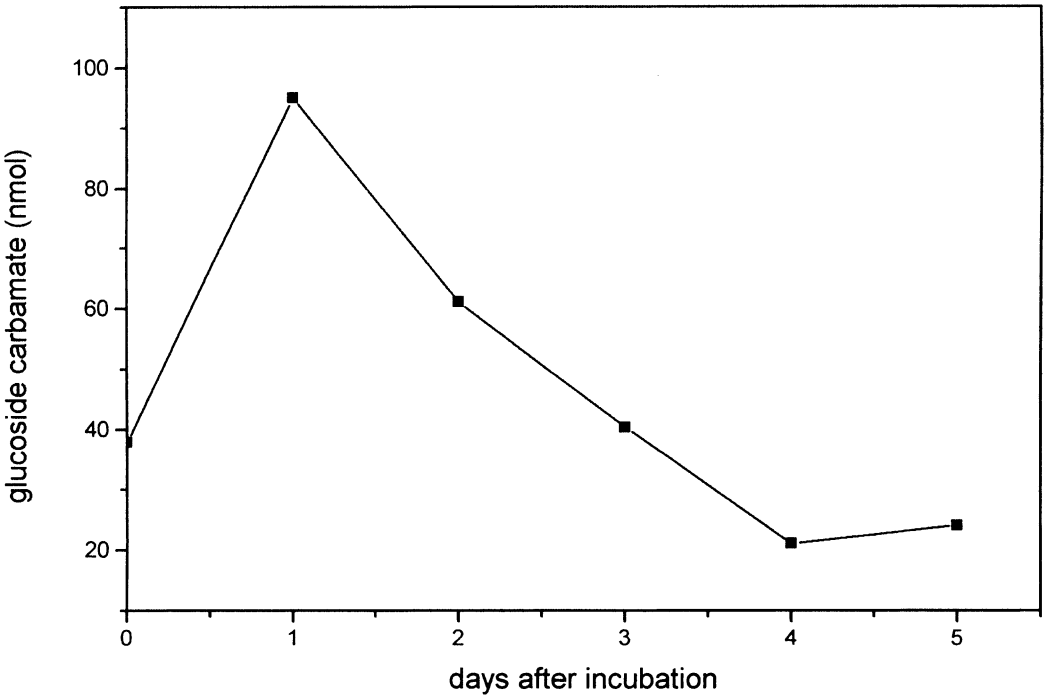

Fig. 5. Appearance of glucoside carbamate **2** in tap water (1 l per 10 g seedlings) with corn seedlings previously incubated with BOA (average values from **3** experiments).

methanol. After centrifugation at 10 000 *g* for 4 min the solution was analyzed by HPLC using the same equipment and gradient as described by Wieland et al. (1998). Quantification of detoxification products was performed using external standards (Wieland et al., 1998). The compound of interest eluting with a retention time of 16–17 min was collected, the fractions combined and evaporated in a speed vacuum centrifuge at 4 °C and

500 *g* overnight. The residues were dissolved in 500 μl 15% methanol, 10 μl of the solution was assayed with β-D-glucosidase from almonds at pH 5.5 for 10 min at 30 °C. The assay mixture was boiled for 10 min and centrifuged at 10 000 *g* for 5 min to pellet coagulated protein. The remaining part of the concentrate was purified via HPLC using first the following gradient: 20% B to 80% B in 7 min; 100% B in 1 min, the detection wavelength was 280 nm. The gradient mentioned above was used as a second step of purification. The compound was manually collected, evaporated to dryness and used for NMR studies.

3.2. BOA metabolite exudation studies

Seedlings of corn, *C. sativum* and *G. ciliata* were incubated with 500 μM BOA for 48 h and placed subsequently in soil filled pots (corn: five pots with 30 seedlings each, *G. ciliata* and *C. sativa*: 100 seedlings per pot). 30 seedlings of corn and 100 of the two other species were directly extracted and analyzed for detoxification products. Over a period of 4–5 days seedlings from one pot each day and each species were removed, cleaned from soil and either totally (*G. ciliata, C. sativa*) or only the roots were extracted. The extracts were analyzed for BOA metabolites.

For exudate collecting, aeroponically grown corn seedlings (100) were incubated with 500 μM BOA for 48 h and transferred to basins filled with aerated tap water (1 l) after washing. The tap water was collected every day and replaced over a period of 5 days. The five collected water samples were evaporated to dryness, the residues dissolved in 2 ml 15% methanol each and used for HPLC analysis after clearing by centrifugation at 10 000 *g* for 4 min.

For identification of the traces of the new compound in stored extracts, a 1:3 synthetic mixture of **1** and **2** obtained according to Wieland et al. (1998) was used for analytical comparisons.

3.3. Structural determinations

NMR analyses of the BOA-*N*-β-glucoside (1) and of carbamate 2 were carried out on a Bruker DRX 600 spectrometer [600.13 MHz (^{1}H) and 150.92 MHz (^{13}C)] and of carbamate 3 on a Bruker DRX 500 spectrometer [500.13 MHz (^{1}H) and 125.76 MHz (^{13}C)] in MeOD_4. ^{1}H NMR, ^{1}H–^{1}H COSY, HMBC, and HMQC experiments were recorded in a 5 mm TBI probe head (600 MHz) and in a 2.5 mm inverse detection microprobe head (500 MHz), respectively. Broadband decoupled ^{13}C spectra were run using a 2.5 mm broadband microprobe head (500 MHz). Tetramethylsilane (TMS) was used as an internal reference. Chemical shifts are given in δ values. High resolution mass spectra were recorded on a Bruker Daltonics 7T APEX II FT-ICR masspectrometer with electron spray ionsation (positive mode).

3.3.1. 3-β-Glucopyranosyl-benzoxazolin-2(3H)-one (*1*)

^{1}H NMR spectral data (600.13 MHz, CD_3OD): δ 7.33 (1H, *d*), 7.23 (1H, *dd*), 6.93 (1H, *d*), 6.66 (1H, *dd*), 5.45 (1H, *d*, $J_{H\text{-}1'\text{-}H\text{-}2'} = 8.9$ Hz, H-1′), 3.90 (1H, *dd*, Ha-6′), 3.62 (1H, *dd*, Hb-6′), 3.45 (1H, H-3′), 3.44 (1H, *m*, H-5′), 3.05 (1H, *dd*, H-4′), 2.92 (1H, *dd*, H-2′). ^{13}C NMR spectral data (150.92 MHz, CD_3OD): δ 132.1 (C-H), 123.1 (C-H), 120.4 (C-H), 116.2 (C-H), 86.2 (C-1′), 79.5 (C-5′), 77.3 (C-3′), 71.3 (C-2′), 70.7 (C-4′), 62.1 (C-6′) (signals detected from HMQC).

3.3.2. 1-(2-Hydroxyphenylamino)-1-deoxy-β-glucoside 1,2-carbamate (*2*)

^{1}H NMR spectral data (600.13 MHz, CD_3OD): *N*-(hydroxyphenylamino) moiety: δ 7.37 (1H, *dd*, $J_{H\text{-}6\text{-}H\text{-}5} = 7.8$ Hz, $J_{H\text{-}6\text{-}H\text{-}4} = 1.0$ Hz, H-6), 7.28 (1H, *dd*, $J_{H\text{-}3\text{-}H\text{-}4} = 7.8$ Hz, $J_{H\text{-}3\text{-}H\text{-}5} = 1.0$ Hz, H-3), 7.23 (1H, *ddd*, $J_{H\text{-}5\text{-}H\text{-}4} = 7.3$ Hz, $J_{H\text{-}5\text{-}H\text{-}6} = 7.8$ Hz, $J_{H\text{-}5\text{-}H\text{-}3} = 1.0$ Hz, H-5), 7.19 (1H, *ddd*, $J_{H\text{-}4\text{-}H\text{-}5} = 7.3$ Hz, $J_{H\text{-}4\text{-}H\text{-}3} = 7.8$ Hz, $J_{H\text{-}4\text{-}H\text{-}6} = 1.0$ Hz, H-4), glucose moiety: δ 5.30 (1H, *d*, $J_{H\text{-}1'\text{-}H\text{-}2'} = 9.4$ Hz, H-1′), 4.06 (1H, *dd*, $J_{H\text{-}2'\text{-}H\text{-}1'} = 9.4$ Hz, $J_{H\text{-}2'\text{-}H\text{-}3'} = 8.9$ Hz, H-2′), 3.93 (1H, *dd*, $J_{Ha\text{-}6'\text{-}Hb\text{-}6'} = 12.2$ Hz, $J_{Ha\text{-}6'\text{-}H\text{-}5'} = 2.1$ Hz, Ha-6′), 3.75 (1H, *dd*, $J_{Hb\text{-}6'\text{-}H\text{-}5'} = 5.7$ Hz, Hb-6′), 3.56 (1H, *dd*, $J_{H\text{-}3'\text{-}H\text{-}2'} = 8.9$ Hz, $J_{H\text{-}3'\text{-}H\text{-}4'} = 8.9$ Hz, H-3′), 3.55 (1H, *m*, H-5′), 3.52 (1H, *dd*, $J_{H\text{-}4'\text{-}H\text{-}3'} = 8.9$ Hz, $J_{H\text{-}4'\text{-}H\text{-}5'} = 9.4$ Hz, H-4′). ^{13}C NMR spectral data (150.92 MHz, CD_3OD): *N*-(hydroxyphenylamino) moiety: δ 143.2 (C-2), 129.5 (C-1), 124.1 (C-5), 123.1 (C-4), 111.5 (C-6), 109.8 (C-3), carbamate moiety: δ 154.5 (C=O, detected by HMBC), glucopyranosyl moiety: δ 84.7 (C-1′), 80.2 (C-5′), 77.8 (C-3′), 70.2 (C-4′), 70.0 (C-2′), 61.7 (C-6′). HR–ESI–MS *m/z*: 298.0919 (calc. for $C_{13}H_{16}NO_7^+$ $[M+H]^+$ 298.0921).

3.3.3. 1-(2-Hydroxyphenylamino)-1-deoxy-β-gentiobioside 1,2-carbamate (*3*)

^{1}H NMR spectral data (500.13 MHz, CD_3OD): *N*-(hydroxyphenylamino) moiety: δ 7.35 (1H, *dd*, $J_{H\text{-}6\text{-}H\text{-}5} = 7.6$ Hz, $J_{H\text{-}6\text{-}H\text{-}4} = 1.3$ Hz, H-6), 7.26 (1H, *dd*, $J_{H\text{-}3\text{-}H\text{-}4} = 7.6$ Hz, $J_{H\text{-}3\text{-}H\text{-}5} = 1.3$ Hz, H-3), 7.21 (1H, *ddd*, $J_{H\text{-}5\text{-}H\text{-}4} = 8.1$ Hz, $J_{H\text{-}5\text{-}H\text{-}6} = 7.6$ Hz, $J_{H\text{-}5\text{-}H\text{-}3} = 1.3$ Hz, H-5), 7.17 (1H, *ddd*, $J_{H\text{-}4\text{-}H\text{-}5} = 8.1$ Hz, $J_{H\text{-}4\text{-}H\text{-}3} = 7.6$ Hz, $J_{H\text{-}4\text{-}H\text{-}6} = 1.3$ Hz, H-4), gentiobiose moiety: δ 5.28 (1H, *d*, $J_{H\text{-}1'\text{-}H\text{-}2'} = 9.4$ Hz, H-1′), 4.30 (1H, *d*, $J_{H\text{-}1''\text{-}H\text{-}2''} = 7.8$ Hz, H-1″), 4.23 (1H, *dd*, $J_{Ha\text{-}6'\text{-}Hb\text{-}6'} = 11.3$ Hz, $J_{Ha\text{-}6'\text{-}H\text{-}5'} = 1.8$ Hz, Ha-6′), 4.03 (1H, H-2′), 3.82 (1H, *dd*, $J_{Ha\text{-}6''\text{-}Hb\text{-}6''} = 12.0$ Hz, $J_{Ha\text{-}6''\text{-}H\text{-}5H} = 2.1$ Hz, Ha-6″), 3.80 (1H, *dd*, $J_{Hb\text{-}6'\text{-}Ha\text{-}6'} = 11.3$ Hz, $J_{Hb\text{-}6'\text{-}H\text{-}5'} = 5.3$ Hz, Hb-6′), 3.74 (H-5″), 3.61 (1H, *dd*, $J_{Hb\text{-}6''\text{-}Ha\text{-}6} = 12.0$ Hz, $J_{Hb\text{-}6''\text{-}H\text{-}5''} = 5.4$ Hz, Hb-6″), 3.55 (H-4′), 3.54 (H-3′), 3.31 (H-3″), 3.25 (H-4″), 3.22 (H-5′), 3.19 (H-2″), ^{13}C NMR spectral data (125.76 MHz, CD_3OD): *N*-(hydroxyphenylamino) moiety: δ 144.1 (C-2), 130.3 (C-1), 125.2 (C-5), 124.1 (C-4), 112.5 (C-6), 110.9 (C-3), carbamate moiety: δ 155.3 (C=O, detected from HMBC), gentiobiose moiety: δ 104.7 (C-1), 85.5 (C-1′), 79.9 (C-5″), 78.4 (C-3′), 78.0 (C-

5′ and C-3″), 75.1 (C-2″), 71.5 (C-4″), 71.2 (C-4′), 71.0 (C-2′), 70.1 (C-6′), 62.7 (C-6″). HR–ESI–MS *m/z*: 460.1449 (calcd for $C_{19}H_{26}NO_{12}^{+}$ $[M+H]^{+}$ 460.1452).

Acknowledgements

M.S. thanks the DFG for the personal loan of a DA detector. D.S. and B.S. thank the Fonds der Chemischen Industrie for financial support of this work. We thank Dr. S. Giesa for HR–MS measurements.

References

Barnes, P., Putnam, A.R., Burke, B.A., 1986. Allelopathy activity of rye (*Secale cereale* L.). In: Putnam, A.R., Tang, C.S. (Eds.), The Science of Allelopathy. Wiley-Interscience, New York, pp. 271–286.

Barnes, P., Putnam, A.R., 1987. Role of benzoxazinones in allelopathy of rye (*Secale cereale* L.). J. Chem. Ecol. 13, 886–906.

Hennig, L., Findeisen, M., Welzel, P., Haessner, R., 1998. ^{1}H NMR studies of the moenomycins. Magn. Reson. Chem. 36, 615–620.

Kovacs, J., Pinter, I., Messmer, A., Toth, G., 1985. Unprotected sugar phosphinimines: a facile route to cyclic carbamates of amino sugars. Carbohydr. Res. 141, 57–65.

Schulz, M., Wieland, I., 1999. Variation in metabolism of BOA among species in various field communities—biochemical evidence for co-evolutionary process in plant communities? Chemoecology 9, 133–141.

Sicker, D., Frey, M., Schulz, M., Gierl, A., 2000. Role of natural benzoxazinones in the survival strategy of plants. Intern. Rev. Cytol 198, 319–346.

Sicker, D., Schulz, M., 2001. Benzoxazinones in plants: occurrence, synthetic access and biological activities. Studies in Natural Product Chemistry (review), in press.

Steyermark, P.R., 1962. Reaction of D-glucopyranosylamine with phosgene. J. Org. Chem. 27, 1058–1059.

Tsujihara, K., Ozeki, M., Morikawa, T., Taga, N., Miyazaki, M., 1981. A new class of nitrosoureas. II. Synthesis and antitumor activity of 1-(2-chloroethyl)-3,3-disubstituted-1-nitrosoureas having a glucopyranosyl, mannopyranosyl or galactopyranosyl moiety. Chem. Pharm. Bull. 29, 3262–3273.

Wieland, I., Friebe, A., Kluge, M., Sicker, D., Schulz, M., 1999. Detoxification of benzoxazolinone in higher plants. In: Macias, F.A., Galindo, J.C.G., Molinillo, J.M.G., Cutler, H.G. (Eds.), Recent Advances in Allelopathy. A Science for the Future, Vol. 1. S.A.I. Universidad de Cadiz, pp. 47–56.

Wieland, I., Kluge, M., Schneider, B., Schmidt, J., Sicker, D., Schulz, M., 1998. 3-β-D-Glucopyranosyl-benzoxazolin-2(3H)-one—a detoxification product of benzoxazolinone in oat roots. Phytochemistry 49, 719–722.

PERGAMON

Phytochemistry 58 (2001) 827–829

PHYTOCHEMISTRY

www.elsevier.com/locate/phytochem

Book reviews

Black Pepper, *Piper nigrum*. Medicinal and Aromatic Plants—Industrial Profiles
P.A. Ravindran (Ed.) Vol. 13; Harwood Academic Publishers, The Netherlands, 2000. ISBN 90-5702-453-5, $125, £86

In his Introduction to this scholarly and well-written book, P.A. Ravindran describes black pepper as the 'King of Spices' and this theme is carried through the entire work. The history of the pepper industry from Biblical times to the present is well researched, and gives an insight into the true importance of this spice. Kerela State in India was the original source of black pepper, but nowadays it is grown extensively (95% of Indian production) in this State as well as Indonesia, the second most ancient pepper growing country, Brazil, Malaysia, Sri Lanka, Malagasy Republic, several South East Asian countries, South Pacific Islands, Latin America and a number of African countries. Although India is the largest producer in terms of tonnage per annum (average 191,000 tonnes), Thailand has the highest productivity in terms of kg per ha (3595). The International Trade Centre in Geneva has estimated the current trade in spices to be 400,000–450,000 metric tonnes valued at US$1.5–2.0 billion per annum: pepper contributes 34% of the total trade in spices.

Bearing in mind the value of the plant, substantial efforts have been made to investigate and improve its crop management. Chapter 2 describes the historical recordings of the plant since Linnaeus in 1753 and the current status of over 100 cultivars. Detailed botanical descriptions of the plant parts are also given wherein the pepper fruit is described as a drupe, but more often referred to as a berry. The breeding program instigated in India over many years has produced a number of useful hybrids which are assessed for their oleoresin content, volatile (essential) oil yield and composition. Piperine is an alkaloid that contributes towards the pungency of the pepper and varies from 2 to 7.4% among the cultivars with the volatile levels being within the range 0.4–7.0%. Biotechnology has also played an important part in the improvement of the crop with in vitro culture methods for cloning from explants such as shoot tips, nodal segments and apical meristems from both juvenile and mature plants being used. *Agrobacterium tumefaciens*-mediated gene transfer has been employed to transform pepper with disease resistance to *Phytophthora* foot rot. RFLP/PCR studies and RAPD profiles have been used to establish genetic similarities and differences between different species of pepper.

In Chapter 3, details are given of the phytochemistry of the spice. Several studies into the analyses of pepper volatile oil are cited, indicating a range of concentrations for the major constituents. In summary, 15 monoterpenes have been identified with α- and β-pinenes, sabinene and limonene as the major compounds along with some 43 oxygenated compounds of monoterpenoid nature. β-Caryophyllene is the major sesquiterpene hydrocarbon found in the pepper oil, with another 24 having been identified together with around 20 oxygenated sesquiterpenes. A number of miscellaneous compounds may also be present including eugenol, myristicin and safrole. Attempts have been made to correlate phytochemical analyses with sensory evaluation.

Agronomical and nutritional aspects of pepper production are covered in detail in the next two Chapters, the latter giving specific attention to production in Indonesia. Following logically from this, there are chapters on disease conditions caused by fungi, bacteria, virus, mycoplasma, nematodes and insects. Biological control through antagonistic micro-organisms has shown some promising results. A number of shorter chapters deals with various aspects of industrial processing. Further chapters deal in some detail with the world pepper economy giving numerous graphical presentations of trends within the market.

One of the most interesting chapters in the book was that dedicated to pharmacological, toxicological and clinical applications of *Piper nigrum*. Pepper is described as a drug which increases digestive power, improves appetite, cures cold, cough, dyspnoea, diseases of the throat, intermittent fever, colic, dysentery, worms and piles. As with many spices, it also possesses a broad spectrum antimicrobial activity. Analgesic, antipyretic and anti-inflammatory actions are also described, with piperine having been shown to be one of the active

compounds in such cases. Neither pepper nor piperine produces any hepatotoxicity. In contrast, a protective impact upon key liver enzymes has been noted. In terms of mutagenic and carcinogenic properties, pepper gave favourable results, based on the Ames test. The antioxidant capacity of pepper phenolic amides was shown to be superior to the synthetic moieties BHT and BHA.

The book rounds off with considerations of end uses of pepper, listing a large number of traditional and modern uses of the spice. The chapters on the future of pepper usage considers the main obstacles to further cultivation of the plant and how best these may be overcome.

Overall, this is an exhaustive treatise on an economically important spice that is well written, enthusiastic for the subject and comprehensively covers every aspect of usage of black pepper. The book is an important addition to the literature on plant science. It will be of particular interest to students and researchers in botany, ethnobotany, biotechnology, phytochemistry, pharmacology/pharmacognosy, tropical agriculture and food technology/processing.

Stanley G. Deans
Aromatic and Medicinal Plant Group
SAC Auchincruive
South Ayrshire KA6 5HW, Scotland, UK
E-mail address: s.deans@au.sac.ac.uk

PII: S0031-9422(01)00241-2

Cell and Developmental Biology of Arabinogalactan-Proteins

E.A. Nothnagel, A. Bacic and A.E. Clarke (Eds.); Kluwer Academic/Plenum, New York, 2000, 301 pp., ISBN 0-306-46469-1, $139, £96

The book *Cell and Developmental Biology of Arabinogalactan-Proteins* edited by Nothnagel, Bacic and Clarke contains reviews of different aspects related to Arabinogalactan-Proteins (AGPs), from the definition of this group of proteins itself to the applications that they have or they may have. Data regarding the possible function of AGPs in relation to plant development are especially considered. The articles are essentially reviews but in some cases they contain also original results and they are presented in 23 chapters divided into six sections and a final section containing 16 short papers and abstracts. The six sections are devoted to specific subjects: Structure and Biosynthesis of AGPs, Localization and Action of AGPs at the Subcellular and Cellular Levels, AGPs in Somatic Embryogenesis, AGPs in Reproductive Development, AGPs in Vegetative Development and Medically and Industrially Important AGPs and Related Macromolecules. The importance and the evolving state of the subject deserves for sure a book although the reader is left with the feeling that basic questions still remain to be answered. It is remarkable, for instance, that the first chapter devotes16 lines to AGP function including a comment regarding the proposal that AGPs may be ''the garbage bin of plant metabolism''. I am sure that the authors and editors of the book would not share this opinion.

The book is based on the Proceedings of the Twentieth Symposium in Plant Physiology (Riverside, January 1999) and it is one of the rare books that may be found entirely devoted to AGPs with a special emphasis in plant development. Arabinogalactan-proteins have been a subject of interest both due to the use of arabic gum for a number of industrial applications and since it was shown that they may be useful markers for plant development. The applications of AGPs have led to the analysis of the fractions and to the finding of the complex glycoprotein nature of this family of proteins. The molecular analysis has been possible only when recombinant DNA approaches were used as it is the general case for glycoproteins in plants where these fractions are very difficult to define and characterize. The recent cloning of cDNAs corresponding to the protein component of AGPs has allowed the first analysis of their polypeptide backbone. In the book some of these results are summarized but, as references stop in 1998, the reader will find only a partial view for such a recently initiated subject.

In general terms the analysis of the protein components of the plant cell wall and the genes coding for these proteins provides interesting tools to study plant development mechanisms but the picture is still far from satisfactory. For this reason it is useful to have in a single book the various aspects related to a group of still intriguing and important protein components of the wall. The book will be useful for readers interested in the structure of the plant cell wall and its relation to plant development, in the methods to analyse complex mixtures of plant glycoproteins and in the

compounds in such cases. Neither pepper nor piperine produces any hepatotoxicity. In contrast, a protective impact upon key liver enzymes has been noted. In terms of mutagenic and carcinogenic properties, pepper gave favourable results, based on the Ames test. The antioxidant capacity of pepper phenolic amides was shown to be superior to the synthetic moieties BHT and BHA.

The book rounds off with considerations of end uses of pepper, listing a large number of traditional and modern uses of the spice. The chapters on the future of pepper usage considers the main obstacles to further cultivation of the plant and how best these may be overcome.

Overall, this is an exhaustive treatise on an economically important spice that is well written, enthusiastic for the subject and comprehensively covers every aspect of usage of black pepper. The book is an important addition to the literature on plant science. It will be of particular interest to students and researchers in botany, ethnobotany, biotechnology, phytochemistry, pharmacology/pharmacognosy, tropical agriculture and food technology/processing.

Stanley G. Deans
Aromatic and Medicinal Plant Group
SAC Auchincruive
South Ayrshire KA6 5HW, Scotland, UK
E-mail address: s.deans@au.sac.ac.uk

PII: S0031-9422(01)00241-2

Cell and Developmental Biology of Arabinogalactan-Proteins

E.A. Nothnagel, A. Bacic and A.E. Clarke (Eds.); Kluwer Academic/Plenum, New York, 2000, 301 pp., ISBN 0-306-46469-1, $139, £96

The book *Cell and Developmental Biology of Arabinogalactan-Proteins* edited by Nothnagel, Bacic and Clarke contains reviews of different aspects related to Arabinogalactan-Proteins (AGPs), from the definition of this group of proteins itself to the applications that they have or they may have. Data regarding the possible function of AGPs in relation to plant development are especially considered. The articles are essentially reviews but in some cases they contain also original results and they are presented in 23 chapters divided into six sections and a final section containing 16 short papers and abstracts. The six sections are devoted to specific subjects: Structure and Biosynthesis of AGPs, Localization and Action of AGPs at the Subcellular and Cellular Levels, AGPs in Somatic Embryogenesis, AGPs in Reproductive Development, AGPs in Vegetative Development and Medically and Industrially Important AGPs and Related Macromolecules. The importance and the evolving state of the subject deserves for sure a book although the reader is left with the feeling that basic questions still remain to be answered. It is remarkable, for instance, that the first chapter devotes16 lines to AGP function including a comment regarding the proposal that AGPs may be ''the garbage bin of plant metabolism''. I am sure that the authors and editors of the book would not share this opinion.

The book is based on the Proceedings of the Twentieth Symposium in Plant Physiology (Riverside, January 1999) and it is one of the rare books that may be found entirely devoted to AGPs with a special emphasis in plant development. Arabinogalactan-proteins have been a subject of interest both due to the use of arabic gum for a number of industrial applications and since it was shown that they may be useful markers for plant development. The applications of AGPs have led to the analysis of the fractions and to the finding of the complex glycoprotein nature of this family of proteins. The molecular analysis has been possible only when recombinant DNA approaches were used as it is the general case for glycoproteins in plants where these fractions are very difficult to define and characterize. The recent cloning of cDNAs corresponding to the protein component of AGPs has allowed the first analysis of their polypeptide backbone. In the book some of these results are summarized but, as references stop in 1998, the reader will find only a partial view for such a recently initiated subject.

In general terms the analysis of the protein components of the plant cell wall and the genes coding for these proteins provides interesting tools to study plant development mechanisms but the picture is still far from satisfactory. For this reason it is useful to have in a single book the various aspects related to a group of still intriguing and important protein components of the wall. The book will be useful for readers interested in the structure of the plant cell wall and its relation to plant development, in the methods to analyse complex mixtures of plant glycoproteins and in the

characterization and uses of arabic gum. It may be interesting to begin considering the preface by Adrianne Clarke, one of the editors of the book, that states the questions that remain still to be addressed. The field is wide open and to be pursued it needs the kind of work outlined in the book.

Pere Puigdomenech
Institut de Biologia Molecular de Barcelona
CID-CSIC
Jordi Girona 18
08034 Barcelona, Spain
E-mail address: pprgmp@cid.csic.es

PII: S0031-9422(01)00230-8

PERGAMON

Phytochemistry 58 (2001) 831

PHYTOCHEMISTRY

www.elsevier.com/locate/phytochem

Announcement

PSE Symposium: Dietary Phytochemicals and Human Health

Salamanca, Spain,
18–20 April 2002

The meeting aims to review the present knowledge on the implications on health of natural, non-nutrient phytochemicals. Important topics are the structure–activity relationships, bioavailability and mechanisms of uptake and transport, biomarkers of exposure and effects, and the effects of dietary phytochemicals and their metabolites on gene expression, apoptosis and cell proliferation. Furthermore the impact of recent developments in genomics and proteomics technology on phytochemical research will be dealt with. The date of the meeting invites one to consider new research proposals with respect to the coming European FrameWork 6 programme.

Major topics of the symposium:

Bioavailability of phytochemicals
Epidemiology and effects
Biomakers of exposure and effect
Genomics and proteomics in phytochemical research

Registration fees

Before 15 March 2002:

- PSE members, students unemployed and retired people: 240 euro
- Rest of participants: 350 euro

After 5 March 2002:

- PSE members, students unemployed and retired people: 300 euro
- Rest of participants: 410 euro
- Accompanying people: 100 euro

Symposium web site: http://www.usal.es/phytochem/netsymposium.html
More information can be obtained at: phytochem@gugu.usal.es

0031-9422/01/$ - see front matter © 2001 Elsevier Science Ltd. All rights reserved.
PII: S0031-9422(01)00398-3

PERGAMON

Phytochemistry 58 (2001) 833–840

PHYTOCHEMISTRY

www.elsevier.com/locate/phytochem

Preparation of antibody against agatharesinol, a norlignan, using a hapten-carrier conjugate

Takeshi Nagasaki[a], Seiichi Yasuda[b], Takanori Imai[a,*]

[a]*Laboratory of Biomass Resources Utilization, Graduate School of Bioagricultural Sciences, Nagoya University, Nagoya 464-8601, Japan*
[b]*Laboratory of Forest Chemistry, Graduate School of Bioagricultural Sciences, Nagoya University, Nagoya 464-8601, Japan*

Received in revised form 3 July 2001

Abstract

In order to immunolabel heartwood extractives in Japanese cedar (Sugi, *Cryptomeria japonica*), we attempted to prepare antibodies against agatharesinol, a major norlignan of these heartwood extractives. Agatharesinol by itself is not antigenic due to its low-M_r, and thus was covalently bound to bovine serum albumin in order to synthesize an antigenic hapten-carrier conjugate (artificial antigen). The number of agatharesinol molecules per artificial antigen molecule was estimated as 27–28 by quantifying Lys in an acid hydrolysate of the artificial antigen by HPLC. Reaction between the artificial antigen and serum obtained from a rabbit immunized with the artificial antigen was competitively inhibited by agatharesinol, indicating the successful production of anti-agatharesinol antibodies. Inhibition by sequirin C, another major norlignan in Sugi, was weaker than that by agatharesinol. Furthermore, an EtOAc soluble fraction, which contains mainly norlignans, inhibited the reaction more strongly than any of the other fractions of Sugi heartwood extractives. Thus, the antiserum we have produced reacts most strongly with agatharesinol and recognizes norlignans almost selectively among Sugi heartwood extractives. © 2001 Elsevier Science Ltd. All rights reserved.

Keywords: *Cryptomeria japonica*; Taxodiaceae; Artificial antigen; Antibody; Heartwood extractives; Agatharesinol; Norlignan

1. Introduction

When heartwood is treated with various kinds of organic solvents, low-M_r substances called "heartwood extractives" are extracted. The formation of heartwood extractives has been studied from both biochemical (Hillis and Inoue, 1966) and cytological (Wardrop and Cronshaw, 1962; Nobuchi and Harada, 1985) perspectives.

In cytological studies, reagents that react with chemically unsaturated structures, such as potassium permanganate or osmium tetraoxide, are used to examine the heartwood extractives (Wardrop and Cronshaw, 1962; Nobuchi and Harada, 1985). Nobuchi and Harada, (1985) reported that in the inner white zone of Sugi, cytoplasmic matrices in ray parenchyma cells and accumulations over the inner surfaces of tracheid cell walls adjacent to parenchyma cells were strongly stained with the dye-reagent. This observation suggests that the stained substances, which were believed to be heartwood extractives, were biosynthesized in parenchyma cells and then transferred to tracheids, where they accumulated. However, to determine the precise chemical structure of such stained substances is impossible, and no irrefutable proof exists that these substances were heartwood extractives. Consequently, questions concerning the biosynthesis, transfer, accumulation and distribution of heartwood extractives are still open to investigation.

In immunological studies, a particular compound can be surveyed and characterized according to the selectivity of an antigen–antibody reaction. By applying immunolabeling to microscopic sections of plant tissues, various kinds of plant polymers such as proteins (Moukha et al., 1993; Nakashima et al., 1997), polysaccharides (Moore et al., 1986; Awano et al., 1998) and lignin (Joseleau and Ruel, 1997; Ruel et al., 1999) have been localized in situ, and their formation examined.

Substances with a M_r of less than 1000 are not ordinarily antigenic, which include most heartwood extractives. However, antibodies can be raised to low-M_r substances using antigenic hapten-carrier conjugates (artificial antigens) in which low-M_r substances (haptens) are covalently bound to proteins or synthetic

* Corresponding author. Fax: +81-52-789-4012.
E-mail address: takaimai@agr.nagoya-u.ac.jp (T. Imai).

0031-9422/01/$ - see front matter © 2001 Elsevier Science Ltd. All rights reserved.
PII: S0031-9422(01)00323-5

polypeptides (hapten-carriers). This strategy has been applied to various kinds of low-M_r substances such as plant hormones (Atzorn and Weiler, 1983; Moctezuma and Feldman, 1999), flavonol glucoside (Lamoureux et al., 1986), steroids (Africa and Haber, 1971) and cinnamyl alcohols (Lewis and Davin, 1992). Therefore, immunolabeling may be an effective method by which to study the formation of heartwood extractives in situ.

Japanese cedar (*Cryptomeria japonica* D. Don, Sugi) is one of the species in which heartwood extractives have been well studied. Its major extractives are classified as norlignans, with agatharesinol being one of the most abundant norlignans (Ogiyama et al., 1983). Although agatharesinol is not present in normal sapwood, it can be detected in sapwood wounded mechanically (Ohashi et al., 1990) or damaged by insects (Takahashi et al., 1983), indicating that the biosynthesis of agatharesinol can be induced artificially in sapwood. Thus, agatharesinol is the most suitable substance with which to dynamically investigate the formation of heartwood extractives in Sugi.

In the present study, we attempted to immunolabel heartwood extractives from Japanese cedar by preparing antibodies against agatharesinol. Agatharesinol was covalently bound to bovine serum albumin (BSA) in order to produce an artificial antigen. The number of haptens in the artificial antigen (epitope density) was determined. A rabbit was then immunized with the artificial antigen, and production of anti-agatharesinol antibodies and recognition selectivity of the serum examined.

2. Results and discussion

2.1. Determination of the epitope density of the agatharesinol artificial antigen

Epitope density affects an antibody titer to the hapten (Erlanger, 1980). Fig. 1 shows the supposed structure of our artificial antigen. To synthesize this artificial antigen, *p*-aminohippuric acid (*p*AHA) was bound to BSA in order to provide an aromatic amino group, and then agatharesinol was diazocoupled. Agatharesinol is assumed to be bound to the ε-amino group of the Lys residue in BSA via the interposing *p*AHA. Therefore, epitope density can be estimated by determining the number of free ε-amino groups of Lys residues that remain unsubstituted by *p*AHA coupled with agatharesinol. To distinguish the substituted Lys residues from the unsubstituted ones, the artificial antigen was reacted with 2,4-dinitrofluorobenzene (DNFB). Because DNFB easily reacts with amino groups, the unsubstituted Lys residues are converted to dinitrophenyl Lys (DNP-Lys) residues by dinitrophenylation. The artificial antigen and the dinitrophenylated artificial antigen (DNP-artificial antigen) were then hydrolized with 6N HCl. *p*AHA coupled with agatharesinol is bound to BSA via an amide linkage, and the linkage is easily hydrolyzed by the acid treatment. Therefore, during acid hydrolysis of the artificial antigen, Lys is generated from both the substituted and unsubstituted Lys residues. On the other hand, because DNP-Lys is never converted to Lys by treatment with acid, the hydrolysis of the DNP-artificial antigen gives Lys only from the substituted Lys residues. The proportion of the amount of Lys generated from the DNP-artificial antigen to that from the artificial antigen indicates the degree of substitution of Lys residues with haptens. Lys in the hydrolysates was quantified by HPLC employing Phe in the hydrolysates as an internal standard because Phe is stable during acid hydrolysis and dinitrophenylation. Using this procedure, the degree of substitution was determined to be 46.1%. The number of Lys residues per BSA, as indicated in the Entrez datebase, is 59. Thus, 27–28 Lys residues per artificial antigen molecule are assumed to be substituted with the hapten.

2.2. Confirmation of production of anti-agatharesinol antibody

To confirm the production of antibodies against the artificial antigen, dot-blot immunoassays and enzyme-linked immunosorbent assays (ELISAs) were used. In the dot-blot immunoassay, varying amounts of the artificial antigen and serum concentrations were tested, with coloration decreasing as both the amount of artificial antigen and serum concentration decreased. Thus, coloration depends on both the amount of the artificial antigen and the concentration of the serum (Fig. 2). Coloration was not observed when the dots were incubated with preimmune serum, nor was any coloration seen in dots that had not absorbed the artificial antigen (Fig. 2). These results indicate that anti-artificial antigen antibodies had been produced. In ELISA, coloration increased with an increase in both the amount of artificial antigen and serum concentration. This assay also demonstrated production of anti-artificial antigen antibodies (Fig. 3).

Production of antibodies against agatharesinol was examined by dot-blot immunoassay and ELISA. In dot-blot immunoassay using the artificial antigen, *p*AHA-substituted BSA and BSA, coloration was observed only for the artificial antigen, but was very faint for both BSA and *p*AHA-substituted BSA (Fig. 4). This indicates that antibodies which recognize the agatharesinol moiety in the artificial antigen have been produced. In an ELISA using a competitive inhibition reaction in which antiserum preincubated with agatharesinol was used, coloration decreased with an increase in the concentration of agatharesinol (Fig. 5). This decrease was proportional to the concentration of agatharesinol ranging from 10^{-3} to 10^{-5} M when the assay was carried out using serum diluted 20,000 fold. The inhibition of col-

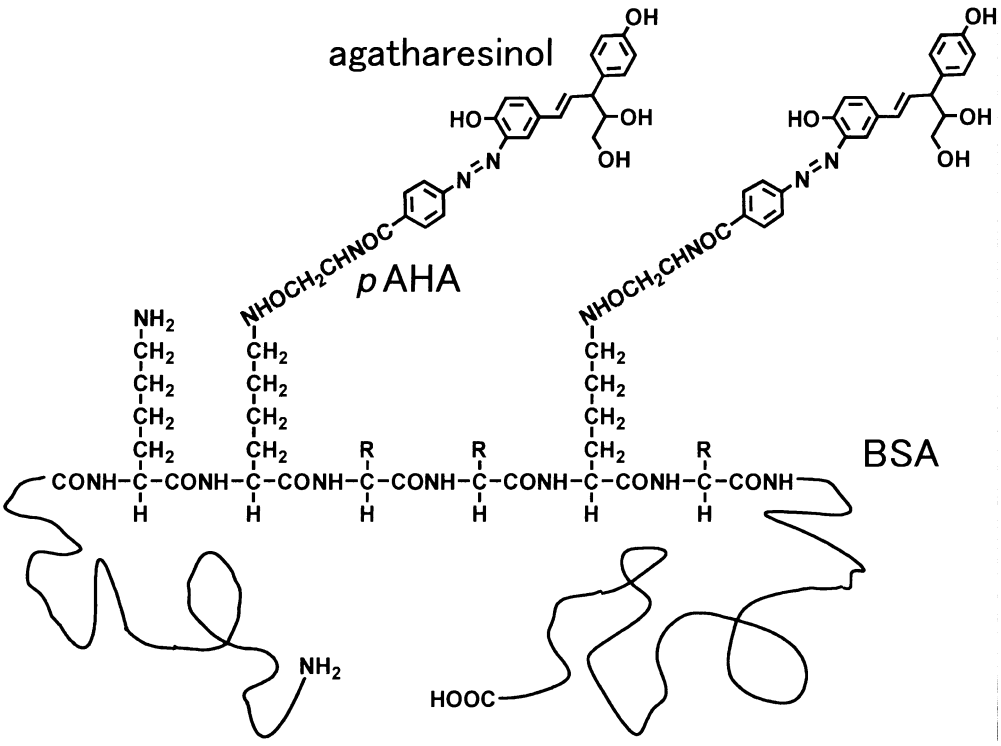

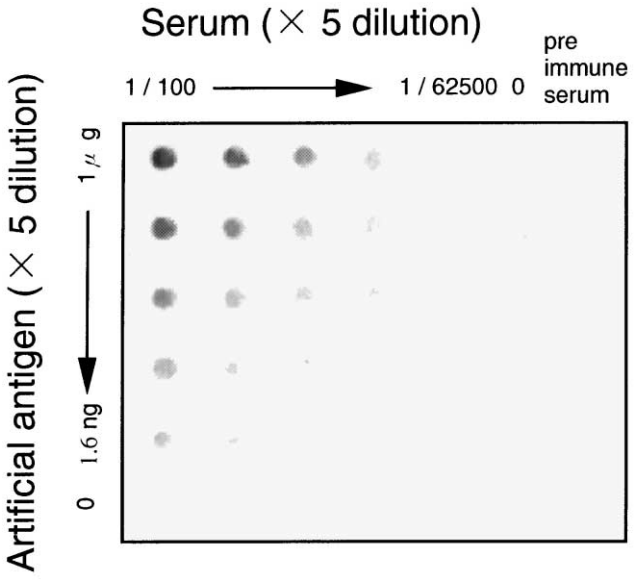

Fig. 2. Dot blot immunoassay using various amounts of artificial antigen and various concentrations of serum. Preimmune serum is serum obtained from the rabbit before injection of the artificial antigen.

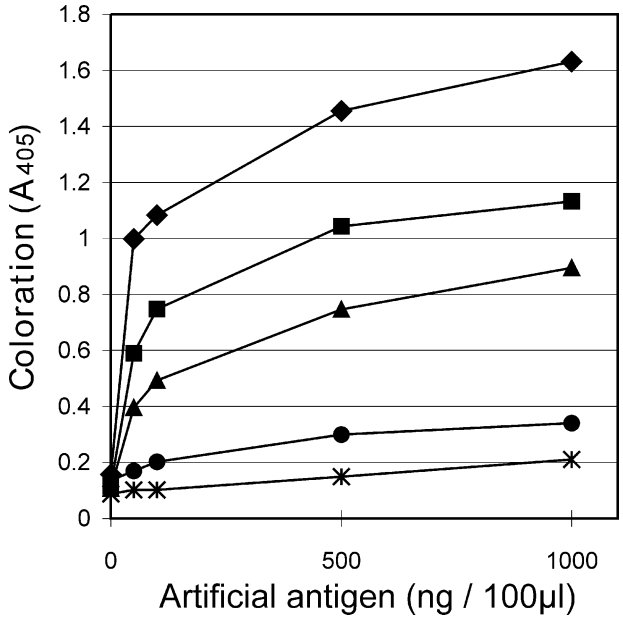

Fig. 3. Checkerboard titration of the artificial antigen against the following dilutions of antiserum: 1/1000 (◆), 1/5000 (■), 1/10,000 (▲), 1/50,000 (●), 1/100,000 (∗).

oration was due to the fact that some antibodies had already reacted with agatharesinol during the pre-incubation, resulting in a decrease in anti-agatharesinol antibodies available for the following reaction between the artificial antigen and the antiserum. Therefore, the competitive inhibition-ELISA definitively demonstrated that anti-agatharesinol antibodies had been produced.

2.3. Recognition selectivity of the antiserum

In the antiserum, antibodies against hapten-carrier (*p*AHA-substituted BSA) moiety of the artificial antigen were also supposed to present, and they must reduce the sensitivity in competitive inhibition-ELISA for determining

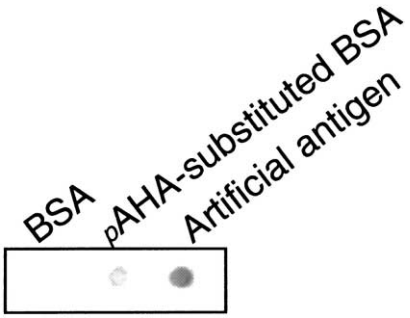

Fig. 4. Dot-blot immunoassay using BSA, *p*AHA-substituted BSA and artificial antigen.

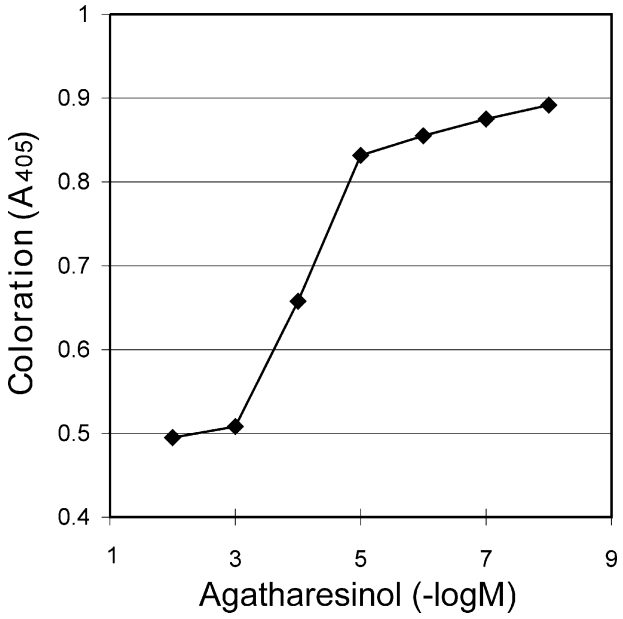

Fig. 5. Inhibition of reaction between artificial antigen and antiserum by agatharesinol.

the recognition selectivity of the antiserum. Then, to remove these antibodies, the antiserum was submitted to the affinity purification using gel to which *p*AHA-substituted BSA had been covalently bound. Reactivities of our antiserum with other Sugi heartwood norlignans (sequirin C, sugiresinol, hydroxysugiresinol and hinokiresinol) were compared with that of agatharesinol by competitive inhibition-ELISA to examine the recognition selectivity (Table 1, their structural formulae shown in Fig. 6). The reactivity of our antiserum with the norlignans showed a similar tendency before and after purification. The inhibition ability of sugiresinol, an isomer of agatharesinol of which dihydroxypentene structure so-called side chain is cyclized, was lower than that of agatharesinol, that is, our antiserum is less reactive with sugiresinol than with agatharesinol. Our antiserum was also reactive with hinokiresinol, an analogue of agatharesinol of which dihydroxyethane structure in the side chain is substituted with an ethene structure, while the

Table 1
Reactivities of the antiserum with norligans and other phenylpropanoids[a]

Class	Substance	% Reactivity	
		Before purification	After purification
Norlignan	Agatharesinol	100[b]	100[b]
	Sequirin C	66.6	62.3
	Sugiresinol	77.9	64.1
	Hydroxysugiresinol	66.5	65.8
	Hinokiresinol	110.0	206.9
Cinnamyl alcohol	Coniferyl alcohol	55.5	33.6
Cinnamic acid	*p*-Coumaric acid	60.4	34.2
Lignan	Hinokinin	59.5	44.2
Lignin model compound	Guaiacylglycerol-β-guaiacyl ether	72.2	25.1

[a] Data represent means for three independent measurements.
[b] Reactivity of agatharesinol with each antiserum was defined to be 100%.

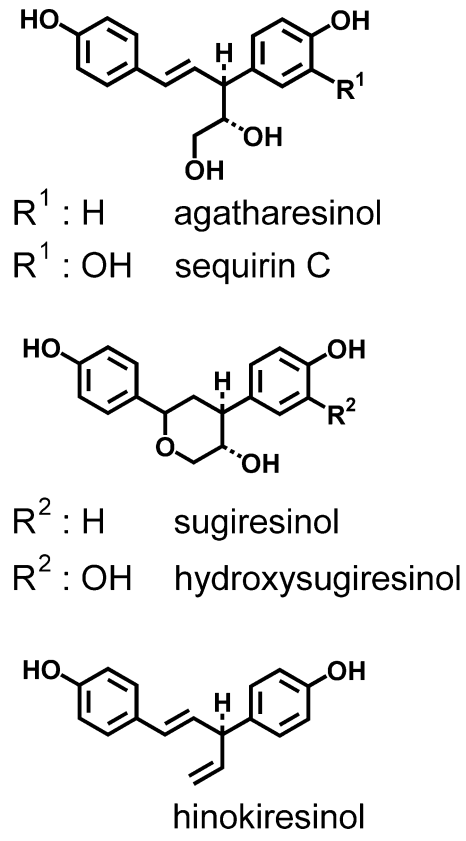

Fig. 6. Structural formulae of Sugi heartwood norlignans.

propene structure remains. These results indicate that the propene structural unit in the side chain participates in the reaction between the antiserum and norlignan. The inhibition ability of sequirin C, a derivatives of agatharesinol of which aromatic ring is mono-hydroxylated, was lower than that of agatharesinol, indicating

that *p*-hydroxy substitution pattern on the aromatic ring also participates in the antigen-antibody reaction. The difference in the reactivities among norlignans could lead to proposal of the chemical structure required as antigenic determinant, that is, 1,3-bis-(*p*-hydroxy phenyl) propene structural unit. Thus, the antiserum is able to recognize a slight difference in chemical structure and differentiate between the norlignans.

Phenylpropanoids classified other than norlignan such as cinnamyl alcohol (coniferyl alcohol), cinnamic acid (*p*-coumaric acid), lignan (hinokinin) and guaiacylglycerol-*β*-guaiacyl ether (model compound for lignin *β*-O-4 structural unit) were also used as competitors to examine the cross reactivity (Table 1). Their inhibition abilities were lower than those of the norlignans both before and after the purification, indicating that the antiserum is less reactive with phenylpropanoids other than norlignan. The partially purified antiserum, especially, was much less reactive with coniferyl alcohol, *p*-coumaric acid and guaiacylglycerol-*β*-guaiacyl ether (approximately 30% of that of agatharesinol). Thus, the recognition selectivity of the antiserum was improved by the affinity purification, and the purified antiserum is able to differentiate norlignans among other phenylpropanoids with the highest reactivity to one of the norlignans, namely, agatharesinol.

Competitive inhibition-ELISAs using MeOH extract (whole extracts before successive fractionation) of Sugi heartwood, and its *n*-hexane, C_6H_6 and EtOAc soluble fractions as competitors, were performed to examine the reactivity of the antiserum among Sugi heartwood extractives (Table 2). The MeOH extract and the EtOAc extract strongly inhibited the antigen–antibody reaction, but inhibition by the *n*-hexane extract and the C_6H_6 extract was much smaller. The EtOAc extract had the strongest inhibition ability. These results indicate that the antiserum reacts preferentially with the EtOAc extractives in Sugi heartwood. The EtOAc extract contains mainly norlignans which consist exclusively of agatharesinol and sequirin-C, while the amount other norlignans present, such as sugiresinol and hydroxysugiresinol, is markedly less (Ogiyama et al., 1983). As previously mentioned, the reactivity of the antiserum with sequirin C was lower than that with agatharesinol. Thus, our antiserum reacts strongest with agatharesinol and recognizes norlignans almost selectively among Sugi heartwood extractives.

Table 2
Inhibition of reaction between artificial antigen and antiserum by Sugi heartwood extracts[a]

Fraction	% Inhibition
MeOH[b]	47.2
n-Hexane[c]	29.2
C_6H_6[c]	26.5
EtOAc[c]	100[d]

[a] Data represent means for three independent measurements.
[b] MeOH extract of Sugi heartwood.
[c] MeOH extract successively fractionated by *n*-hexane, C_6H_6 and EtOAc.
[d] Inhibition by the EtOAc extract was defined to be 100%.

3. Experimental

3.1. Isolation of heartwood extractives from Sugi

Sugi wood meal (ca. 2 kg) was extracted with MeOH at room temp. for 5 days. The MeOH extract was successively fractionated with *n*-hexane, C_6H_6 and EtOAc. The EtOAc soluble part was further fractionated by silica gel column chromatography (Me_2CO–*n*-hexane (4 : 3)). Agatharesinol (ca. 2 g) and sequirin-C (ca. 5.7 g) were isolated and then identified by ^1H, and ^{13}C NMR spectroscopic analyses.

3.2. Preparation of the agatharesinol artificial antigen

The artificial antigen was prepared according to the method of Weiler (1980). The procedure consisted of the following steps.

3.2.1. Binding of pAHA to BSA

BSA (200 mg), *p*AHA (200 mg) and 1-ethyl-3-(3-dimethylamino propyl)-carbodiimide (EDC) (200 mg) were dissolved in water (120 ml). The soln. was adjusted to pH 6.4 and stirred in the dark at room temp. for 20 h, during which time more EDC (100 mg) was added. The reaction soln. was then dialyzed against water and lyophilized to produce *p*AHA-substituted BSA.

3.2.2. Diazotization of pAHA-substituted BSA

Substituted BSA (120 mg) was dissolved in water (20 ml) and the pH adjusted to 1.5 with 1 M HCl. The soln. was cooled on an ice bath, and $NaNO_2$ (240 mg) in water (2 ml) and ammonium sulfamate (120 mg) in water (2 ml) added successively.

3.2.3. Coupling of the diazotized pAHA-substituted BSA to agatharesinol

The soln. of diazotized *p*AHA-substituted BSA was added dropwise to a soln. of agatharesinol (10 mg) in MeOH (0.5 ml) and borate buffer (0.1 M, pH 9.0) (10 ml). The soln. was allowed to stand in an ice bath for 30 min and the reaction soln. then dialyzed against water and lyophilized to produce the artificial antigen.

3.3. Determination of epitope density

Epitope density was determined by measuring the number of free amino groups of Lys residues in the

artificial antigen. The procedure for the determination consisted of the following steps.

3.3.1. Dinitrophenylation

The artificial antigen (1 mg) was dissolved in 5% (w/v) aqueous sodium hydrogencarbonate containing 6 M guanidine (500 μl), and the soln. stirred in the dark at room temp. for 1 h. Next, 10% (v/v) DNFB in EtOH (1 ml) was added and the mixture stirred in the dark at room temp. for 2 h. The reaction mixture was centrifuged and the ppt. washed successively in water, EtOH and Et_2O, and dried at room temp. over calcium chloride under reduced pressure.

3.3.2. Acid hydrolysis

The artificial antigen (1 mg) or the dinitrophenylated artificial antigen (1 mg) were hydrolyzed with 6 N HCl at 110 °C in sealed glass tubes for 20 h. The reaction solns. were then evaporated to dryness under reduced pressure.

3.3.3. HPLC analysis

The hydrolysates obtained above were analyzed by HPLC according to the method of Kuwano et al., (1987). The hydrolysate was dissolved in EtOH–water–TEA (triethylamine) (2:2:1) (20 μl), then the solvent was removed under reduced pressure. The residue was dissolved in EtOH–water–TEA–PITC (phenylisothiocyanate) (7:1:1:1) (50 μl), and the soln. was allowed to stand at room temp. for 20 min. The reaction solns. were then evaporated to dryness under reduced pressure. The phenylthiocarbamyl (PTC) amino acids were separated by HPLC using a Wakopack WS-PTC column (ϕ 4×200 mm), and (A) CH_3CN–0.1 M CH_3COONH_4 (5:95) and (B) CH_3CN–0.1 M CH_3COONH_4 (60:40) as the mobile phase at a flow rate of 1.0 ml/min. The gradient elution program was as follows; 0% B to 70% B for 15 min on a linear gradient and 70% B for next 5 min. The separated PTC-amino acids were detected at 254 nm.

3.4. Immunization

A New Zealand White, 11-week-old rabbit was immunized. The initial injection was carried out with a mixture of the artificial antigen (1 mg) dissolved in phosphate buffered saline (PBS) (0.5 ml) and Freund's complete adjuvant (0.5 ml). Injection was repeated 4 times at 10-day intervals in the same way using Freund's incomplete adjuvant instead of the complete adjuvant. One week after the last injection, blood was collected and allowed to stand at room temp. for 1 h, then centrifuged to separate out the serum.

3.5. Purification of the antiserum

The antiserum was submitted to partial affinity purification to remove antibodies against *p*AHA-substituted BSA (hapten-carrier) moiety of the artificial antigen. The procedure consisted of the following steps.

3.5.1. Preparation of affinity gel

*p*AHA-substituted BSA (40 mg) dissolved in water (1 ml) were mixed with Affi-Gel 102 (Bio-rad) (1 ml), followed by addition of EDC (5 mg). The soln. was adjusted to pH 4.9 and gently stirred by inversion in the dark at room temp. for 3 h, during which time more EDC (5 mg) was added. The reaction soln. was then centrifuged to give the affinity gel (ca. 1 ml).

3.5.2. Affinity purification

The antiserum was diluted with the equal volume of Tris buffered saline (TBS; 25 mM Tris–HCl (pH 7.6), 150 mM NaCl). The antiserum solution (6 ml) was mixed with the affinity gel (ca. 1 ml) and gently stirred by inversion at 4 °C for 20 h. The reaction soln. was then centrifuged to give the purified antiserum.

3.6. Dot-blot immunoassay

All procedures described below were performed at room temp. A sheet of Hybond-P membrane (Amersham) was soaked in MeOH for 10 min and PBS for 15 min, successively. The sheet was then placed in a dot-blot manifold and artificial antigen (1 μg, 200 ng, 40 ng, 8 ng, 1.6 ng) in PBS (10 μl) or PBS alone (10 μl, as a control) was added to the wells. The solns. were aspirated, the wells washed with PBS (100 μl) and then the wells were blocked with PBS-milk (3% (w/v) skim milk in PBS) (300 μl). After the wells were washed three times with PBS-T (PBS containing 0.5% (v/v) Tween 20), rabbit sera (1/100, 1/500, 1/2500, 1/12500, 1/62500) diluted in PBS (100 μl), preimmune serum (1/100) diluted in PBS (100 μl), or PBS alone (100 μl, as a control) was added to the wells. After 1 h, the wells were washed thoroughly with PBS-T, then goat: anti-rabbit IgG-alkaline phosphatase conjugate (Bio-Rad) (1/3000) diluted in PBS-milk (100 μl) was added to the wells. After 1 h, the wells were washed thoroughly with PBS-T.

The membrane was then removed from the manifold and washed again with PBS. Coloration was performed using an alkaline phosphatase conjugate substrate kit (Bio-Rad) containing 5-bromo-4-chloro-3-indolylphosphate toluidinium as the substrate and nitroblue tetrazolium as the enhancer, according to the manufacturer's instructions.

In other dot-blot immunoassays, the artificial antigen, *p*AHA-substituted BSA and BSA (each 1 μg) in PBS were absorbed onto a membrane, and this membrane assayed using the serum diluted (1/2000) in PBS (100 μl) according to the procedure described above.

3.7. ELISA

ELISA was carried out according to the method of Hassan et al. (1988) with slight modifications. All

procedures described below were performed at room temp. Artificial antigen (1 μg, 500 ng, 100 ng, 50 ng) in PBS (100 μl) or PBS alone (100 μl, as a control) was added to the wells of a 96-well microtitration plate (Iwaki), and the plate allowed to stand for 2 h. All solns. were then removed and the wells were washed three times with PBS (400 μl). Wells were blocked with PBS-OA (5% (w/v) ovalbumin and 5% (w/v) sucrose in PBS) (400 μl), washed three times with PBS and rabbit sera (1/1000, 1/5000, 1/10,000, 1/50,000, 1/100,000) diluted in PBS (100 μl) added to the wells. After 2 h, the wells were washed thoroughly with PBS, then goat: anti-rabbit IgG-alkaline phosphatase conjugate (1/3000) diluted in PBS (100 μl) was added to the wells. After 1 h, the wells were washed thoroughly with PBS. Coloration was performed using an alkaline phosphatase substrate kit (Bio-Rad) containing *p*-nitrophenylphosphate as the substrate, according to the manufacturer's instructions.

3.8. Competitive inhibition-ELISA

The amount of artificial antigen for plate coating and the concentration of the rabbit serum to be used in the competitive inhibition-ELISA were determined using the checkerboard titration described above (Fig. 3) (Hassan et al., 1988). The inhibition reaction was performed using 300 ng/100 μl of the artificial antigen soln. for the coating and rabbit serum diluted 1/20,000.

When using agatharesinol as the competitor, rabbit antiserum was preincubated with agatharesinol in MeOH (10^{-2}, 10^{-3}, 10^{-4}, 10^{-5}, 10^{-6}, 10^{-7}, 10^{-8} M) at room temp. for 2 h, and ELISA using the preincubated antisera was performed according to the procedure described above.

When comparing the reactivity of the serum to agatharesinol and those to other phenylpropanoids (sequirin C, sugiresinol, hydroxysugiresinol, hinokiresinol, coniferyl alcohol, *p*-coumaric acid, hinokinin and guaiacylglycerol-β-guaiacyl ether), the optimal concentration of competitors (10^{-4} M) was chosen from the results of an agatharesinol inhibition ELISA (Fig. 5), since a linear relationship was observed between coloration and competitor concentration. The reactivities of the purified antiserum with the phenylpropanoids were also examined using 2000 ng/100 μl of the artificial antigen soln. for the coating, purified antiserum diluted 1/5000 and 10^{-3} M of the competitor concentration.

When using Sugi heartwood extracts as the competitors, the rabbit antiserum was first incubated with an equal concentration (5 ng/μl) of extract dissolved in MeOH at room temp. for 2 h, and the preincubated antisera then used for the ELISA.

Acknowledgements

We are grateful to Nichiha corporation for providing the Sugi chips.

References

Africa, B., Haber, E., 1971. The production and characterization of specific antibodies to aldosterone. Immunochemistry 8, 479–486.

Atzorn, R., Weiler, E.W., 1983. The immunoassay of gibberellins. I. Radioimmunoassays for the gibberellins A_1, A_3, A_4, A_7, A_9 and A_{20}. Planta 159, 1–6.

Awano, T., Takabe, K., Fujita, M., 1998. Localization of glucuronoxylans in Japanese beech visualized by immunogold labeling. Protoplasma 202, 213–222.

Erlanger, B.F., 1980. The preparation of antigenic hapten-carrier conjugates: a survey. In: Helen, V.V. (Ed.), Methods in Enzymology, Vol. 70. Academic, London, pp. 85–104.

Hillis, W.E., Inoue, T., 1966. The formation of polyphenols in trees-III. The effect of enzyme inhibitors. Phytochemistry 5, 483–490.

Hassan, F., Rothnie, N.E., Yeung, S.P., Palmer, M.V., 1988. Enzyme-linked immunosorbent assays for alkenyl glucosinolates. J. Agric. Food Chem. 36, 398–403.

Joseleau, J.-P., Ruel, K., 1997. Study of lignification by noninvasive techniques in growing maize internodes: an investigation by Fourier transform infrared cross-polarization-magic angle spinning ^{13}C-nuclear magnetic resonance spectroscopy and immunocytochemical transmission electron microscopy. Plant Physiol. 114, 1123–1133.

Kuwano, K., Sakamaki, C., Mitamura, T., 1987. Rapid analysis of amino acids by HPLC using pre-column derivatization with PITC. Nippon Nogeikagaku Kaishi 61, 53–55.

Lamoureux, S.W., Vacha, W.E.K., Ibrahim, R.K., 1986. Localization of partially methylated flavonol glucosides in *Chrysosplenium americanum*. I. Preparation and some properties of a trimethyl flavonol glucoside antibody. Plant Science 44, 169–173.

Lewis, N.G., Davin, L.B., 1992. Stereoselectivity in polyphenol biosynthesis. In: Hemingway, R.W., Laks, P.E. (Eds.), Plant Polyphenols. Plenum Press, New York, pp. 73–95.

Moctezuma, E., Feldman, L.J., 1999. Auxin redistributes upwards in graviresponding gynophores of the peanut plant. Planta 209, 180–186.

Moore, P.J., Darvill, A.G., Albersheim, P., Staehelin, L.A., 1986. Immunogold localization of xyloglucan and rhamnogalacturonan I in the cell walls of suspension-cultured sycamore cells. Plant Physiol. 82, 787–794.

Moukha, S.M., Wosten, H.A.B., Asther, M., Wessels, J.G.H., 1993. In situ localization of the secretion of lignin peroxidases in colonies of *Phanerochaete chrysosporium* using a sandwiched mode of culture. J. Gen. Microbiol. 139, 969–978.

Nakashima, J.M., Awano, T., Takabe, K., Fujita, M., Sakaki, H., 1997. Immunocytochemical localization of phenylalanine ammonia-lyase and cinnamyl alcohol dehydrogenase in differentiating tracheary elements derived from *Zinnia* mesophyll cells. Plant Cell Physiol. 38, 113–123.

Nobuchi, T., Harada, H., 1985. Ultrastructural changes in parenchyma cells of Sugi (*Cryptomeria japonica* D. Don) associated with heartwood formation. Mokuzai Gakkaishi 31, 965–973.

Ogiyama, K., Yasue, M., Takahashi, K., 1983. Proceedings, 1st. International Symposium on Wood and Pulping Chemistry II, Tukuba, pp. 101–106.

Ohashi, H., Imai, T., Yoshida, K., Yasue, M., 1990. Characterization of physiological functions of sapwood fluctuation of extractives in the withering process of Japanese cedar sapwood. Holzforschung 44, 79–86.

Ruel, K., Burlat, V., Joseleau, J.-P., 1999. Relationship between ultrastructural topochemistry of lignin and wood properties. IAWA J. 20, 203–211.

Takahashi, K., Yasue, M., Ogiyama, K., 1983. Phenols of "Tobigusare" wood, discolored Sugi (*Cryptomeria japonica* D. Don) sapwood. Mokuzai Gakkaishi 29, 806–809.

Wardrop, A.B., Cronshaw, J., 1962. Formation of phenolic substances in the ray parenchyma of angiosperms. Nature 193, 90–92.

Weiler, E.W., 1980. Radioimmunoassays for the differential and direct analysis of free and conjugated abscisic acid in plant extracts. Planta 148, 262–272.

PERGAMON

Phytochemistry 58 (2001) 841–847

PHYTOCHEMISTRY

www.elsevier.com/locate/phytochem

Characterization of native and yeast-expressed tomato fruit fructokinase enzymes

Marina Petreikov, Nir Dai, David Granot, Arthur A. Schaffer*

Department of Vegetable Crops, Agricultural Research Organization, Volcani Center, Bet Dagan, 50250, Israel

Received 8 April 2001; received in revised form 16 July 2001

Abstract

Three fructokinase isozymes (FKI, FKII, FKIII) were separated from both immature and ripe tomato fruit pericarp. All three isozymes were specific for fructose with undetectable activity towards glucose or mannose. The three isozymes could be distinguished from one another with respect to response to fructose, Mg and nucleotide donor concentrations and this allowed the comparison of the fruit enzymes with the gene products of the two known cloned tomato fructokinase genes, *LeFRK1* and *LeFRK2*. FKI was characterized by both substrate (fructose), as well as Mg, inhibition; FKII was inhibited by neither fructose nor Mg; and FKIII was inhibited by fructose but not by Mg. ATP was the preferred nucleotide donor for all three FKs and FKI showed inhibition by CTP and GTP above 1 mM. All three FKs showed competitive inhibition by ADP. During the maturation of the tomato fruit total FK activity decreased dramatically. There were decreases in activity of all three FKs, nevertheless, all were still observed in the ripe fruit. The two tomato *LeFRK* genes were expressed in yeast and the gene products were characterized with respect to the distinguishing characteristics of fructose, Mg and nucleotide inhibition. Our results indicate that FKI is the gene product of *LeFRK2* and FKII is probably the gene product of *LeFRK1*. © 2001 Elsevier Science Ltd. All rights reserved.

Keywords: *Lycopersicon esculentum* Mill.; Hexokinase; Substrate inhibition; Gene product

1. Introduction

The developing tomato fruit sink metabolizes translocated suc via either invertase or suc synthase. The path of sucrose catabolism is developmentally regulated: the sucrose synthase pathway is associated with the young fruit which transiently accumulates starch, while the invertase pathway is associated with the later stages of fruit development (Ruan and Patrick, 1995; Ho, 1996; Schaffer and Petreikov, 1997a). In addition to changes in the biochemical pathway, the transition between the two developmental stages is accompanied by changes in the translocation pathway, from a symplastic to an apoplastic one, as well (Ruan and Patrick, 1995; Ho, 1996).

Irrespective of the initial enzyme in the pathway, free fru accounts for one half of the imported suc and its phosphorylation is requisite for its further metabolism. Fru phosphorylation may be carried out either by hexokinases (EC 2.7.1.1), which can phosphorylate both glucose and fructose, or by specific fructokinases (EC 2.7.1.4). The irreversible fructokinase reaction is likely to play an important role in determining carbon flux in sink tissue (Viola, 1996). The activity pattern of fructokinase in developing tomato fruit, but not hexokinase, parallels the transient starch content in the fruit (Schaffer and Petreikov, 1997a).

Fructokinases have been characterized from a number of plant tissues (see recent review by Pego and Smeekens, 2000). It is not uncommon to find two or three isoforms upon separation by ion-exchange chromatography (i.e. potato tuber, Gardner et al., 1992; Renz and Stitt 1993) which may also show tissue and developmental specifity (Renz et al., 1993). Some fructokinases show substrate inhibition by fructose (i.e. tomato, Schaffer and Petreikov, 1997b; potato, Gardner et al. 1992; Renz and Stitt, 1993) which may be physiologically significant in the case of tomato fruit which contains high fructose levels (Schaffer and Petreikov, 1997b). Fructokinases can also be characterized by their nucleotide specificity; Huber and Akazawa (1985) reported a fructokinase utilizing UTP while most other

* Corresponding author. Tel.: +972-3-9683646; fax: +972-3-9669642.

E-mail address: arnoamya@netvision.net.il (A.A. Schaffer).

0031-9422/01/$ - see front matter © 2001 Elsevier Science Ltd. All rights reserved.
PII: S0031-9422(01)00331-4

reported fructokinases show relative specificity to ATP. FKs can also be distinguished by the characteristic of inhibition by excess Mg ions. The fructokinase from pollen grains (Nakamura et al., 1991) and from soybean nodules (Copeland and Morell, 1985) was inhibited by Mg concentrations above 1–2 mM while that of pea seeds was not (Turner et al., 1977). A fructokinase from tomato fruit similarly showed the phenomenon of Mg inhibition (Schaffer and Petreikov, 1997b).

Tomato fruit fructokinases have recently attracted increasing attention due to their possible role in transient starch accumulation (Schaffer and Petreikov, 1997a; Kanayama et al., 1997, 1998), in addition to possible physiological roles in hexose accumulation and sugar sensing (Pego and Smeekens, 2000). Martinez-Barajas and Randall (1996) separated two isoforms of fructokinase from tomato fruit, which showed similar sensitivity to inhibition by fructose and similar nucleotide specificity. However, Kanayama et al. (1997) cloned two fructokinase genes from tomato with different expression patterns, as well as different kinetic characteristics of the expressed protein. One of the genes (*LeFRK2*) which is expressed primarily in the early stages of fruit development yields a gene product which, when expressed in yeast shows inhibition by fructose (Kanayama et al., 1998). The other gene (*LeFRK1*) is expressed throughout fruit development (Kanayama et al 1997) and its yeast-expressed gene product is not inhibited by fructose (Kanayama et al., 1998). The *LeFRK2* gene was hypothesized to be responsible for the fructokinase activity associated with transient starch accumulation (Kanayama et al., 1998) while the *LeFRK1* gene was suggested to play a housekeeping role in carbohydrate metabolism throughout the plant, supplying fru6P for glycolysis.

In light of these recent data we reinvestigated fructokinase activity in developing tomato fruit. We report here three FK isoforms, which can be distinguished one from the other on the basis of fru and Mg inhibition and nucleotide specificity. Furthermore, we attempt to relate the two known *LeFRK* gene products to the FK isoforms present in the tomato fruit.

2. Results

2.1. Fructokinase isoenzymes during fruit development

2.1.1. Separation on HPLC-ion exchange

Hexose phosphorylation activity from young tomato fruit were separated by HPLC-ion exchange chromatography (Fig. 1). We observed three peaks of activity with fructose as substrate, as well as two additional peaks of activity with glucose (termed HKI and HKII). The three fructose phosphorylating peaks (termed FKI, FKII and FKIII, according to the order of elution) were observed using two assay methods. One assay contained low fru (1.0 mM) and low Mg (0.5 mM), with which the FKI enzyme showed maximal activity. The second assay contained high fru (10 mM) and high Mg (3 mM), which gave maximal activities for FKII. The FKIII enzyme, which eluted only under high ionic concentration, showed approximately equal activities with both assays.

2.1.2. Activity during development

The total FK activity in crude extracts of immature (15 DAA) and ripe fruit pericarp is presented in Table 1. Recovery experiments indicated that differences in extractable activity between the different stage fruit were not artifactually due to inhibitory substances in the mature fruit. Similar recovery of a known amount of purified FKI (from the MonoQ fractions, as described further on) was obtained from both fruit developmental stages (not shown). Activity with both assay systems is higher in the young fruit and sharply declines in the more mature fruit. At both stages of fruit development activity is higher with the low fru/low Mg assay system, indicating that even in the mature fruit the major activity is inhibited by excess fructose and Mg.

A comparison of the chromatograms of the pericarp fructokinase enzymes from immature (15 DAA) and ripe fruit stages (Fig. 2) indicates that the three peaks of fructose phosphorylation activity were observed in both stages. The enzyme first eluted (FKI), assayed under low substrate conditions, remained the dominant peak of activity even in the ripe fruit. The FKII enzyme was present in the ripe fruit but generally was the least active of the three FKs.

2.2. Characterization of the three tomato fruit FK enzymes and comparison with the two yeast-expressed LeFRK (LeFRK-Y) gene products

In order to determine the relationships between the native FK enzymes and the products of the two *LeFRK* genes, enzyme extracts from mutant yeast lacking endogenous hexose kinase activity and expressing each of the two described *LeFRK* genes were separated on

Table 1
Fructokinase activity in immature and mature tomato fruit pericarp

Maturity stage	Fructokinase activity (nmol g^{-1} fw min^{-1})	
	Assay 1[a]	Assay 2[b]
Immature	184 + 25	85 + 8
Mature	63 + 8	27 + 1

[a] Assay 1 contained low fru (1.0 mM) and low Mg (0.5 mM).
[b] Assay 2 contained high fru (10 mM) and high Mg (3 mM). Data are averages + S.E. of 4 (immature) and 7 (mature) separate extractions from individual fruit.

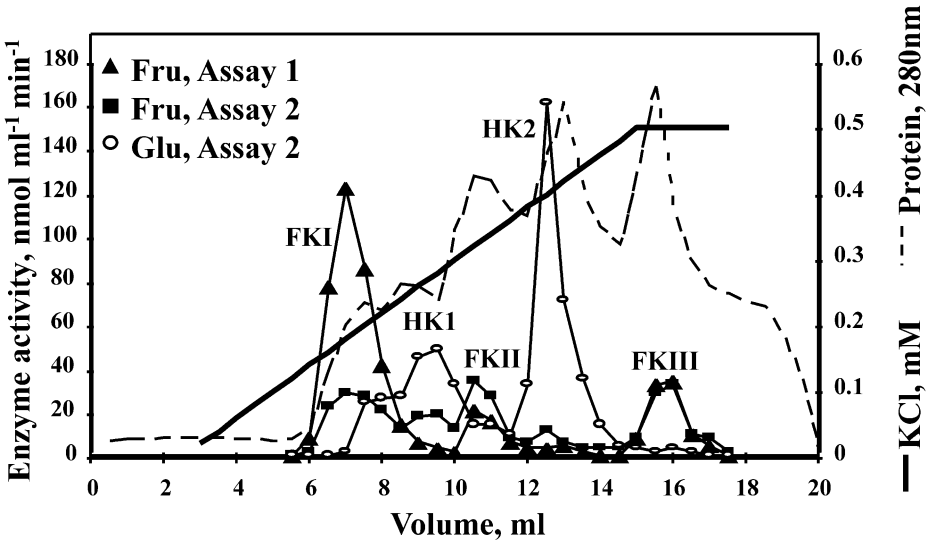

Fig. 1. HPLC-ion exchange (MonoP) separation of hexose kinase activity in immature tomato fruit pericarp. Assay 1 contained low fru (1.0 mM) and low Mg (0.5 mM). Assay 2 contained high fru or glu (10 mM) and high Mg (3 mM).

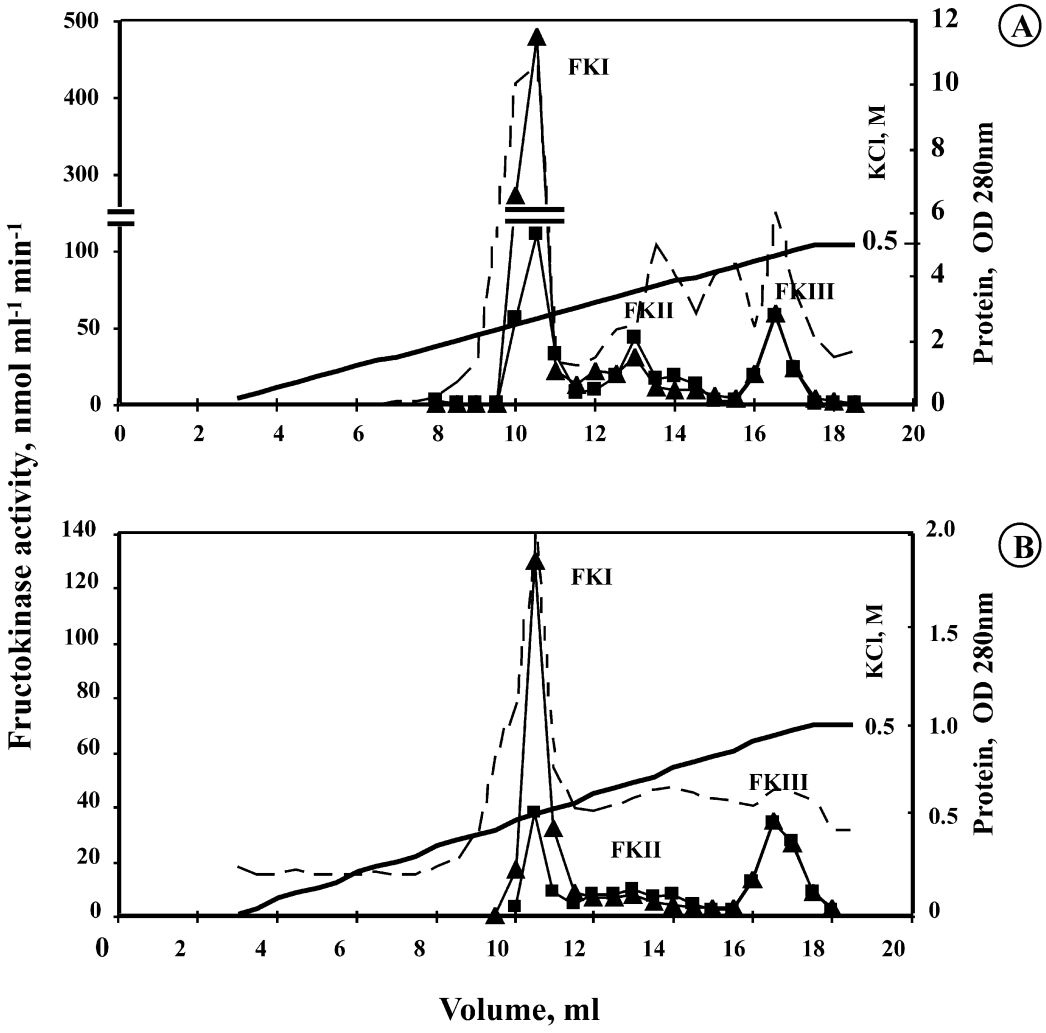

Fig. 2. HPLC-ion exchange (MonoQ) separation of fructokinase activity in immature (A) and mature (B) tomato fruit pericarp. Assays are as in Fig. 1. Note the different scales in the two chromatograms.

MonoQ ion chromatography under the same conditions as the tomato extract (not shown). The partially purified native FK enzymes and the yeast-expressed enzymes were partially characterized and compared as described below.

2.2.1. Hexose specificity and inhibition by fru

All three native fruit enzymes were specific for fru, with no discernible activity with glu or mannose (not shown). Of the three enzymes FKII had the lowest affinity for the substrate (Fig. 3a). Both yeast-expressed enzymes were also specific for fru, with no discernible activity with glucose or mannose. The *LeFRK1*-Y enzyme has an affinity pattern for fru analogous to FKII (Fig. 3b). Both FKI and FKIII from tomato fruit show the characteristic of substrate inhibition by high levels of fructose, while FKII shows Michaelis-Menten kinetics with fru concentrations up to 10mM (Fig. 3a). The yeast-expressed *LeFRK1*-Y similarly shows Michaelis-Menten kinetics with fru concentrations up to 10mM, while *LeFRK2*-Y shows the characteristic of substrate inhibition by high levels of fructose (Fig. 3b).

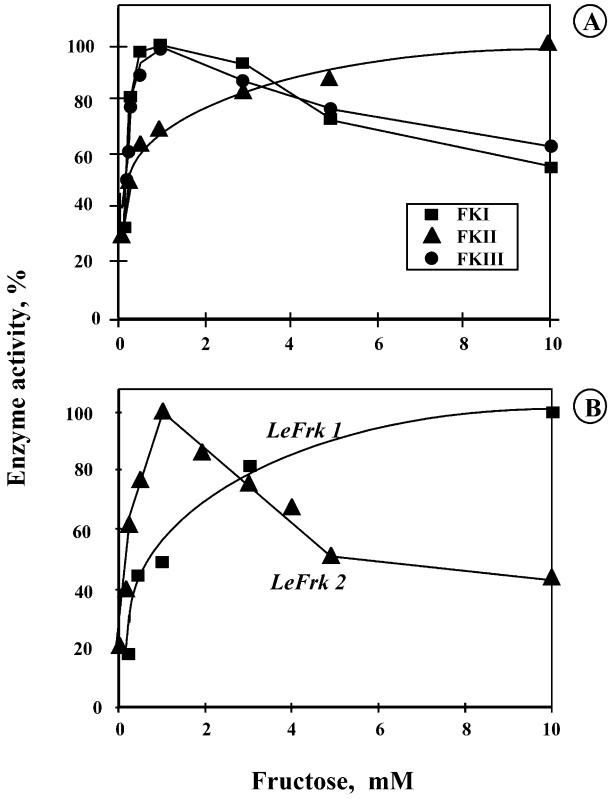

Fig. 3. Effect of fru concentration on the activity of the three fructokinase isoforms from (A) immature fruit pericarp and from (B) yeast-expressed *LeFRK* genes. Data are expressed as percentage of maximal activity for each enzyme in order to emphasize the similar and distinct patterns of activity. Maximal activities were, nmol g^{-1} fw min^{-1}: FK1, 710; FKII, 38; FKIII, 71; *LeFRK1-Y,* 148; *LeFRK2-Y,* 238.

2.2.2. Inhibition by Mg

Of the fruit enzymes only FKI shows the characteristic of inhibition by Mg concentrations above 1 mM (Fig. 4a). FKII shows no inhibition by Mg while FKIII shows little, if any, inhibition. Of the yeast-expressed enzymes only *LeFRK2*-Y is inhibited by Mg concentrations above 1 mM, while *LeFRK1*-Y is not (Fig. 4b).

2.2.3. Nucleotide specificity

The three fruit enzymes responded differently to the four nucleotide substrates (Fig. 5 a–c). FKI had highest activity with ATP and GTP at concentrations up to 0.5 mM. However, above 0.5 mM this enzyme showed inhibition by GTP and CTP. FKII and FKIII showed preferred activity with ATP with no indication of inhibition by high NTP concentrations. All three enzymes also showed product inhibition by ADP (not shown).

The two yeast-expressed enzymes also responded differently to the four nucleotide substrates (Fig. 6a and b). *LeFRK2*-Y responded in a similar fashion as the tomato fruit FKI, with highest activity with ATP and GTP at concentrations up to 0.5 mM, together with inhibition by GTP and CTP at concentrations above 0.5 mM. *LeFRK1*-Y showed preferred activity with ATP alone. Both enzymes also showed product inhibition by ADP.

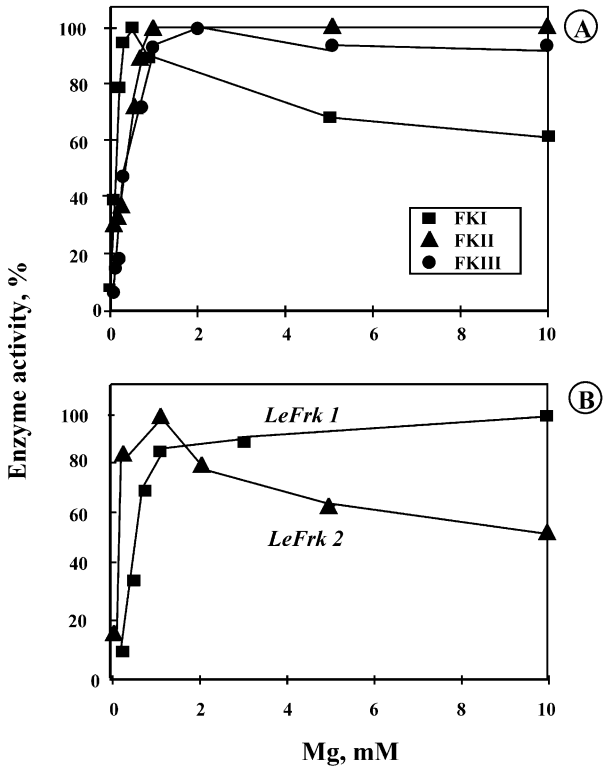

Fig. 4. Effect of Mg concentration on the activity of the three fructokinase isoforms from (A) immature fruit pericarp and from (B) yeast-expressed *LeFRK* genes. Data are expressed as percentage of maximal activity for each enzyme. Maximal activities were, in nmol ml^{-1} min^{-1}: FK1, 840; FKII, 52; FKIII, 161; *LeFRK1-Y,* 150; *LeFRK2-Y,* 226.

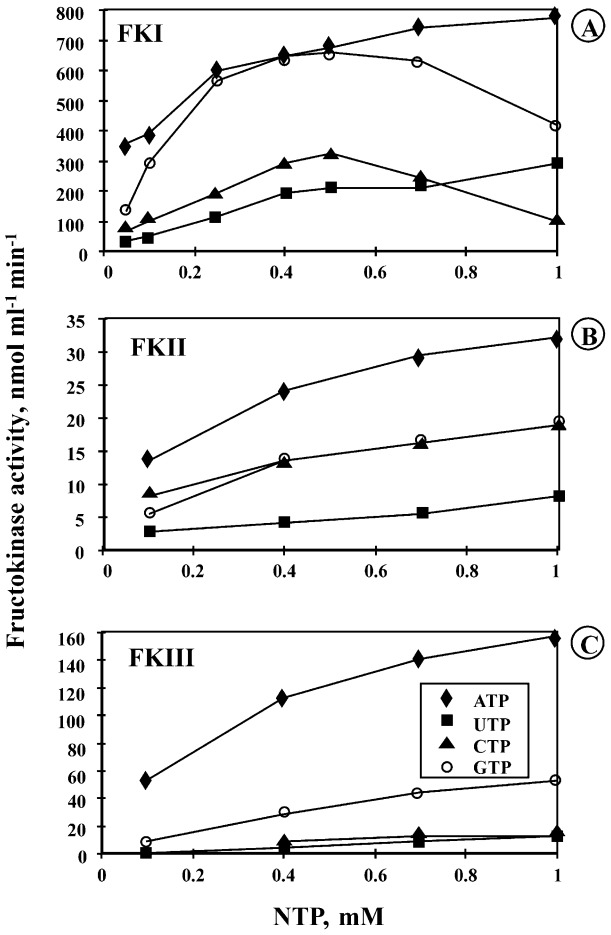

Fig. 5. Effect of nucleotide concentrations on the activity of the three fructokinase isoforms from immature tomato fruit pericarp. (A), FKI; (B), FKII; (C) FKIII.

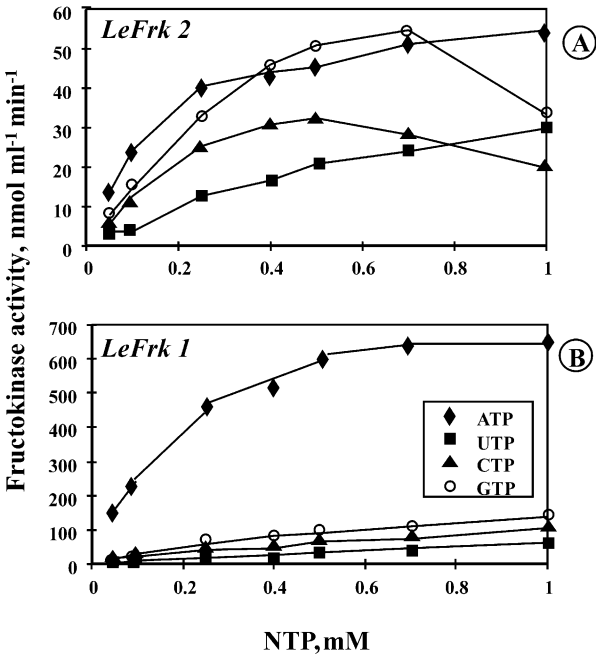

Fig. 6. Effect of nucleotide concentrations on the activity of the two yeast expressed fructokinase enzymes. (A), *LeFRKI*; (B), *LeFRKII*.

2.2.4. Coelution of yeast-expressed and tomato fruit fructokinase

Each of the *LeFkr-Y* gene products were chromatographed individually, and also together with the enzyme extract from tomato pericarp, in order to determine whether they coelute with any of the tomato enzymes. *LeFRK2*-Y coeluted with the tomato FKI under the same conditions used for the separation of the fruit enzymes. The *LeFRK1*-Y protein eluted slightly after FKII, coeluting with the second hexokinase enzyme, HK2 (not shown).

3. Discussion

We report here three distinct forms of fructokinase in tomato fruit, which can be distinguished one from the other on the basis of their responses to fructose, Mg and NTP concentrations. The first enzyme which eluted from ion-exchange chromatography, FKI, was inhibited by both high fru and high Mg. It also showed a characteristic and unique response to NTP concentration, with inhibition at high concentrations of GTP and CTP. The second eluted enzyme, FKII, had lowest affinity for fru and was inhibited by neither fru nor Mg, while the third enzyme, FKIII, was inhibited by fru but not by Mg.

These distinguishing characterisitics allowed us to compare the gene products for the two known *LeFRK* genes and to attempt to assign gene–product relationships between the genes and the native enzymes. The *LeFRK2* gene encodes for the FK1 protein, based on the similarities in fru inhibition, Mg inhibition and, especially, the unique response to NTPs, together with the coelution of the two proteins. To further prove this identity we have recently shown that antisense *FRK2* tomato fruit show a complete knockout of the FKI protein specifically, while the other two peaks of activity are unmodified (unpublished).

The gene product of *LeFRK1* appears likely to be the FKII protein, based on their similar low affinity for fructose and the absence of inhibition by either fru or Mg. Although the *LeFRK1*-Y protein product eluted slightly after the native FKII protein, this may be due to different post-translational modifications in plants and yeast, as previously suggested (Dai et al., 1997; Veramendi et al., 1999). The FKIII protein may be either be a distinct gene product or a post-translationally modified product of either of the two known genes. However, considering the distinguishing characterisitics of fru and Mg inhibition, together with the large difference in ionic strength required to elute the protein, it is reasonable to suggest that it is, in fact, a product of a third gene. Pego and Smeekens (2000) reported a third FK

gene in Arabidopsis and we have found an additional FK gene in tomato which is exclusively expressed in anthers, and is presently under study (unpublished).

Multiple fructokinases have been reported in other plant tissues. In potato tuber three enzymes were separated by ion-exchange chromatography (Gardner et al., 1992; Renz and Stitt, 1993) but in one study all three forms were inhibited by high fructose concentrations (Renz and Stitt, 1993) while in the other report only the first two eluted proteins were inhibited (Gardner et al., 1992). Similarly, Martinez-Barajas and Randall (1996) reported two tomato fruit isoforms and considering their relatively similar kinetic characterisitics they are possibly due to minor modifications of the *LeFRK2* gene product (Martinez-Barajas et al., 1997). Regretfully, much of the enzyme data for FKs available in the literature cannot be directly compared, due to the different techniques used in separation and enzyme characterization. Pego and Smeekens (2000) recently attempted to clarify the confusion regarding the different fructokinases in plants and suggested that the reported fructokinase isoforms may be attributed to only two different enzymes. Considering that so few genes for fructokinases have so far been characterized, the classification of the fructokinases will undoubtedly become clearer with additional gene cloning, which will allow for classification based on homologies between a large population of sequences from numerous plant species.

Fructokinase activity in tomato fruit has been associated with the transient accumulation of starch (Schaffer and Petreikov, 1997a). Kanayama et al. (1997, 1998) showed that the temporal and spatial expression of the *LeFRK2* gene in tomato fruit coincides with, although is not limited to, this transient starch accumulation and suggested that the *LeFRK2* gene product was particularly important for starch synthesis. We therefore hypothesized that since the FKI protein is the *LeFRK2* gene product, its activity would most likely be absent or relatively low, in comparison to the other FK enzymes in the mature fruit. The results of the present study show that the *LeFRK2* gene product remains the major native FK in the ripe fruit. It does not undergo any particular loss of activity, compared to the other fructokinases and its suggested specific role in transient starch synthesis is not certain.

The distinguishing characteristics of the three enzymes (inhibition by fru and Mg and response to nucleotides) may be of physiological significance, perhaps related to distinct localization and compartmentation of the isoforms. The trait of fructose inhibition has been proposed as a possible classifying characterisitc of fructokinase enzymes (Pego and Smeekens, 2000) and its physiological significance may be related to a parallel fructose inhibition of the sucrose synthase enzyme at physiological levels of fructose found in tomato fruit (Schaffer and Petreikov, 1997b) leading to a 'double brake' mechanism which may control sucrose metabolism flux (Kanayama et al., 1997, 1998; Schaffer and Petreikov, 1997b; Pego and Smeekens, 2000). Based on the similar characteristic of the yeast-expressed enzyme, the trait of Mg inhibition appears to be inherent to the enzyme and not artifactual, although we do not posit physiological significance. Similarly the unique trait of CTP and GTP inhibition of the FKI enzyme is also characteristic of the protein and not artifactual since the heterologous yeast-expressed protein has the identical trait.

This study paves the way for the analysis of the physiological significance of the individual tomato fruit fructokinases using plants with genetically modified activities of the individual fructokinases. These studies are in progress.

4. Experimental

4.1. Plant materials and yeast strains

Plants of tomato (*Lycopersicon esculentum* Mill (cv. 7844 and F144) were grown under standard conditions in a greenhouse in Bet Dagan, Israel. Flowers were allowed to self-pollinate. Chemicals and enzymes were purchased from Sigma or Boehringer Mannheim. Yeast strains and transformation methods were as described previously (Kanayama et al., 1998).

4.2. Enzyme extractions and assays

Fructokinase (EC 2.7.1.4) and hexokinase (EC 2.7.1.1) activities were extracted from pericarp tissue (4.5 g) of immature green (approximately 15 days after flowering) or red tomato fruit as described in Schaffer and Petreikov (1997a) with the addition of 1 mM PMSF to the extraction buffer. The 25–80% ammonium sulfate precipitate was collected, resuspended in extraction buffer, desalted on Sephadex G-25 and filtered through a 0.2 μm polysulfone membrane (Whatman International Ltd., Maidstone, England). The protein separation was performed on a Shimadzu HPLC system. For the separation of the fructokinase enzymes in young and mature fruit, as well as the yeast-expressed enzymes, the protein extract was applied (flow rate 0.5 ml/min) to a Mono-Q column HR 5/5 (Pharmacia Biotech AB, Uppsala, Sweden) prequilibrated with buffer containing 20 mM HEPES (pH 7.0) and 2.5 mM DTT. Unbound protein was eluted with the same buffer, followed by a 0–0.5 M KCl salt gradient. Protein was monitored at 280 nm. Fractions of 0.5 ml were collected and both fructose and glucose phosphorylating activities were measured. The fractions containing peak activities of the individual isoenzymes were bulked for further characterization.

The yeast-expressed enzymes were extracted as described previously (Kanayama et al., 1998). Enzyme extracts were separated on Mono-Q ion-exchange chromatography under identical conditions as for the fruit pericarp enzyme extracts. For the results presented in Fig. 1 a Mono-P column was used under identical elution and buffer conditions as described for the Mono-Q column.

Two different assays were used for measuring fructokinase activity. Assay 1 was conducted with low fructose and magnesium concentrations and the reaction mixture (1 ml) contained 30 mM HEPES (pH 7.6), 9 mM KCl, 0.5 mM $MgCl_2$, 1 mM ATP, 1 mM NAD, 1 unit PGI (type III), 1 unit NAD-dependent G-6-P DH (from *Leuconostoc*) and the reaction was initiated with 1 mM fructose. Assay 2 for fructokinase activity was conducted with high fructose (10 mM) and magnesium (3 mM) concentrations. For determining hexokinase activity glucose (10 mM) served as substrate, magnesium levels were 3 mM $MgCl_2$ and PGI was excluded from the reaction mixture. All the enzymatic reactions were carried out at 37 °C and $A_{340\ nm}$ was monitored continuously, as previously described (Petreikov and Schaffer, 1997a). Optimum conditions for each isoenzyme were used in enzyme assays for characterization of the three FK isoforms. For FKI assay 1 (low fru and Mg), while for FKII and FKIII, assay 2 (high fru and M) were used. ADP inhibition studies were carried out using the same enzyme extract with ADP concentrations ranging up to 5.0 mM.

Acknowledgements

The assistance of Dr. Lena Yeselson and Shmuel Shen is gratefully acknowledged.

References

Dai, N., Schaffer, A., Petreikov, M., Granot, D., 1997. Potato (*Solanum tuberosum* L.) fructokinase expressed in yeast exhibits inhibition by fructose of both in vitro enzyme activity and rate of cell proliferation. Plant Sci. 128, 191–197.

Copeland, L., Morell, M., 1985. Hexose kinases from the plant cytosolic fraction of soybean nodules. Plant Physiol. 79, 114–117.

Gardner, A., Davies, H.V., Burch, L.R., 1992. Purification and properties of fructokinase from developing tubers of potato (*Solanum tuberosum* L.). Plant Physiol. 100, 178–183.

Huber, S.C., Akazawa, T., 1985. A novel sucrose synthase pathway for sucrose degradation in cultured sycamore cells. Plant Physiol 81, 1008–1011.

Kanayama, Y., Dai, N., Granot, D., Petreikov, M., Schaffer, A., Bennett, A.B., 1997. Divergent fructokinase genes are differnetially expressed in tomato (*Lycopersicon esculentum* Mill.). Plant Physiol. 113, 1379–1384.

Kanayama, Y., Granot, D., Dai, N., Petreikov, M., Schaffer, A., Powell, A., Bennett, A.B., 1998. Tomato fructokinases exhibit differential expression and substrate regulation. Plant Physiol. 117, 85–90.

Martinez-Barajas, E., Randall, D.D., 1996. Purification and characterization of fructokinase from developing tomato (*Lycopersicon esculentum* Mill.) fruits. Planta 199, 451–458.

Martinez-Barajas, E., Luethy, M.H., Randall, D.D., 1997. Molecular cloning and analysis of fructokinase exoression in tomato (*Lycopersicon esculentum* Mill.). Plant Sci. 125, 13–20.

Nakamura, N., Shimizu, M., Suzuki, H., 1991. Characterization of hexose kinases from camellia and lily pollen grains. Physiol. Plant. 81, 215–220.

Renz, A., Merlo, L., Stitt, M., 1993. Partial purification from potato tubers of three fructokinases and three hexokinases which show different organ and developmental specificity. Planta 190, 156–165.

Renz, A., Stitt, M., 1993. Substrate specificity and product inhibition of different forms of fructokinases and hexokinases in developing potato tubers. Planta 190, 166–175.

Ruan, Y.-L., Patrick, J.W., 1995. The cellular pathway of postphloem sugar transport in developing tomato fruit. Planta 196, 434–444.

Schaffer, A.A., Petreikov, M., 1997a. Sucrose-to-starch metabolism in tomato fruit undergoing transient starch accumulation. Plant Physiol. 113, 739–746.

Schaffer, A.A., Petreikov, M., 1997b. Inhibition of fructokinase and sucrose synthase by physiological levels of fructose in young tomato fruit undergoing transient starch accumulation. Physiol. Plant. 110, 800–806.

Turner, J.F., Garrison, D.D., Copeland, L., 1977. Fructokinase (fraction IV) of pea seeds. Plant Physiol. 60, 666–669.

Veramendi, J., Roessner, U., Renz, A., Willmitzer, L., Trethwey, R.N., 1999. Antisense repression of hexokinase 1 leads to an overaccumulation of starch in leaves of transgenic potato plants but not to significant changes in tuber carbolydrate metabolism. Plant Physiol. 121, 123–133.

Viola, R., 1996. Hexose metabolism in discs excised from developing potato (*Solanum tuberosum*) tubers. II. Estimations of fluxes in vivo and evidence that fructokinase catalyses a near rate-limiting reaction. Planta 198, 186–196.

PERGAMON

Phytochemistry 58 (2001) 849–857

PHYTOCHEMISTRY

www.elsevier.com/locate/phytochem

Induction of phenylalanine ammonia-lyase activity by tryptophan in *Ustilago maydis*

Seong Hwan Kim[a], James W. Kronstad[b,c], Brian E. Ellis[b,*]

[a]*Forest Products Biotechnology, Department of Wood Science, University of British Columbia, 2424 Main Mall, Vancouver, BC, V6T 1Z4, Canada*
[b]*Biotechnology Laboratory, Faculty of Agricultural Sciences, University of British Columbia, 2424 Main Mall, Vancouver, BC, V6T 1Z4, Canada*
[c]*Department of Microbiology and Immunology, University of British Columbia, 2424 Main Mall, Vancouver, BC, V6T 1Z4, Canada*

Received 4 April 2001; received in revised form 20 June 2001

Abstract

To understand the regulation of phenylalanine ammonia-lyase (PAL) activity in the corn smut fungus, *Ustilago maydis*, we examined the effects of different media, metabolic effectors (including aromatic amino acids), and environmental factors on induction and repression of PAL activity. PAL was detected only in cell extracts and not in the culture medium. *U. maydis* PAL is constitutively produced at a low level in all media tested but its regulation can be influenced by aromatic amino acids. L-Tryptophan (0.3 mM) induces PAL activity 3- to 5-fold but tryptophan analogs and tryptophan-related metabolites do not. The enzyme is most readily induced during the early stationary phase of growth and the induced activity remains relatively constant during stationary stage. No induction or inhibition of PAL activity was observed as a function of culture temperature, pH or light. PAL induction was repressed by glucose but not by its reaction product, *t*-cinnamic acid. Induction did not require de novo protein synthesis, suggesting that some form of post-translational protein modification or a metabolic effect may be involved. This study shows that the regulation of *U. maydis* PAL is very different from the patterns known for plants and other fungi. © 2001 Elsevier Science Ltd. All rights reserved.

Keywords: *Ustilago maydis*; Basidiomycetes; Corn smut; Phenylalanine ammonia-lyase; Tryptophan; enhancement; Enzyme regulation; Metabolic effector

1. Introduction

Phenylalanine ammonia-lyase (PAL; EC 4.3.1.5) catalyzes the nonoxidative deamination of L-phenylalanine to form *trans*-cinnamic acid and a free ammonium ion. The enzyme occurs in plants (Camm and Towers, 1973), fungi (Vance et al., 1975), and actinomycetes (Emes and Vining,1970), but not in animals. The properties and genetic control of PAL in both plants and fungi are important factors in our general understanding of the metabolic processes that yield phenylpropanoid secondary metabolites and energy. Substrate inducibility of PAL activity is observed in some fungi, but not in plants, which raises the question of how the mechanisms underlying the regulation of PAL differ among fungi, and between plants and fungi.

In plants, PAL is the entrypoint enzyme into phenylpropanoid metabolism and it regulates the biosynthesis of a wide range of secondary compounds, including lignin, flavonoids, furanocoumarin and isoflavonoid phytoalexins, and wound protectant hydroxycinnamic acid esters (Jones, 1984). Plant PAL activity can be induced by pathogen attack, and by environmental stresses such as wounding and light (Hahlbrock and Scheel, 1989). In gherkin and mustard, PAL induction is reported to result from the activation of a constitutive pool of inactive enzyme (Attridge et al., 1974), but in other plant species, PAL induction is the result of de novo synthesis of the enzyme (Hahlbrock and Schröder, 1975), or of a decrease in the rate of degradation of the enzyme (Zucker, 1971). Plant PAL activity appears to be regulated largely at the level of transcription (Lawton and Lamb, 1987) but it can also be modulated by the protein components of a system that inactivates the enzyme (Ritenour and Saltveit, 1996).

While PAL has been extensively studied in plants, relatively little is known about the fungal enzyme.

* Corresponding author. Tel.: +1-604-822-3451; fax: +1-604-822-8640.
E-mail address: bee@interchg.ubc.ca (B.E. Ellis).

0031-9422/01/$ - see front matter © 2001 Elsevier Science Ltd. All rights reserved.
PII: S0031-9422(01)00327-2

Studies on fungal PAL induction and regulation have been limited to *Rhodosporidium toruloides* (formerly *Rhodotorula glutinis*) (Gilbert and Tully, 1982; Kane and Fiske, 1984) and *Neurospora crassa* (Sikora and Marzluf, 1982) although phenylalanine catabolism has been observed in many microbial species. In *R. toruloides*, the enzyme is induced by L-phenylanine or L-tyrosine, while growth with glucose or ammonium salts represses enzyme synthesis. This regulation has been shown to occur at the level of transcription (Kane and Fiske, 1984; Gilbert et al., 1983)]. *R. toruloides* PAL is also inducible in response to signals of nitrogen deprivation or carbon limitation (Marusich et al., 1981). In *N. crassa*, PAL synthesis requires specific induction by L-phenylalanine and nitrogen derepression (Gilbert et al., 1983). This pattern of responses suggests that deamination by PAL could be the initial step in phenylalanine catabolism in these fungi, but this has not been systematically examined.

The corn smut fungus, *U. maydis*, is a pathogenic basidiomycete that can cause significant economic losses in corn production (Agrios, 1988). The infection of corn by this fungus is characterized by distinct galls (plant tumors) on stems, leaves, ears, and tassels. The disease symptoms also include stunting, and chlorosis, and accumulation of anthocyanins in stems and leaves, especially in the areas with developing tumors. In a previous study, we purified and characterized the PAL protein from *U. maydis* (Kim et al., 1996). Compared to yeast and plant PALs, *U. maydis* PAL has some unique protein properties such as high substrate specificity for L-phenylalanine, high pI value (pH 6.3), and marked thermal stability (Kim et al., 1996), but these traits provide little insight into the physiological role of the enzyme. In order to gain a better understanding of the function of PAL in pathogenic *Ustilago* species, we have investigated the nature of induction of PAL activity in the corn pathogen, *U. maydis*. Our results reveal a pattern of regulation of *Ustilago* PAL that is very different from the patterns known for plants and other fungi.

2. Results

2.1. Induction experiments

In order to determine whether PAL activity is detectable in *U. maydis* cells grown in standard microbial culture media, we tested seven different nutrient sources. Minimal medium containing 2% (w/v) ammonium nitrate, beef extract, casamino acid, potato dextrose broth, peptone or yeast extract were employed. PAL activity was present in cells grown with each of the nutrient sources tested, although the level varied. In all cases, PAL activity was detected only in cell extracts and not in the growth medium. Based on these results, regulation of PAL was investigated in two media: a nutrient-rich (complete) medium and a minimal medium. Depending on inoculum density, the PAL specific activity levels measured at the early stationary phase of cell growth ranged from 4 to 16 pkatal/mg protein in minimal medium, and from 14 to 22 pkatal/mg protein in complete medium.

Since aromatic amino acids have been shown to function as inducers of PAL in some fungi (Kalghatgi and Subba Rao, 1976; Gilbert and Tully, 1982; Sikora and Marzluf, 1982), L-phenylalanine, L-tyrosine, and L-tryptophan were tested for their ability to induce PAL in *U. maydis* strain 518. The PAL activity levels obtained from fungal cells grown in minimal medium (pH 7.0) supplemented with these amino acids (1 mM each) are presented in Fig. 1. The highest PAL activity was obtained in cells grown in L-tryptophan-supplemented medium, whereas L-tyrosine or L-phenylalanine supplementation had very little effect. Interestingly, PAL induction by L-tryptophan was strongly reduced by co-supplementation with L-phenylalanine.

U. maydis was able to grow slowly on either tryptophan or phenylalanine (2% w/v) as a sole carbon and nitrogen source. In this case, culture growth was better in the tryptophan medium, but PAL activity was higher in the phenylalanine medium. In absolute terms, however, these culture conditions did not result in any marked enhancement of PAL specific activity as compared to the results shown in Fig. 1.

To determine whether PAL induction by tryptophan is concentration-dependent, different amounts (0.03, 0.1, 0.3, 1.0, and 3.0 mM) of L-tryptophan were used to supplement minimal medium cultures. The increase in PAL activity responded linearly to the increase in L-tryptophan

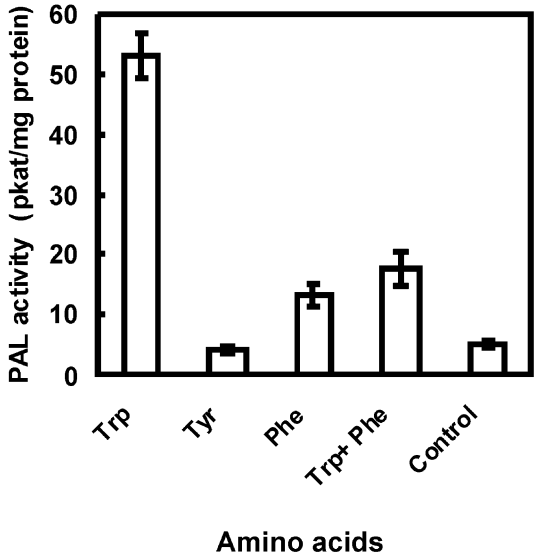

Fig. 1. Effect of aromatic amino acids on induction of PAL activity in *Ustilago maydis*. Each amino acid (1 mM) was added to minimal medium and the fugal cells were grown for 36 h, harvested and assayed for PAL activity. Trp, L-tryptophan; Tyr, L-tyrosine; Phe, L-phenlalanine; control, H_2O.

concentration up to 0.3 mM amino acid, and then declined (data not shown). Based on these results, 0.3 mM L-tryptophan was used for the subsequent studies of PAL regulation.

2.2. PAL induction period

In order to define the time-point of highest PAL inducibility during the culture cycle, *U. maydis* cultures were supplemented with 0.3 mM L-tryptophan at various time points in the growth cycle, incubated for two hours, harvested and assayed for PAL activity. Enhancement of PAL activity by these additions of exogenous L-tryptophan was only observed in cultures that had entered stationary phase (Fig. 2). This pattern was also observed when tryptophan was provided to the cells at the beginning of the culture growth, and cultures were subsequently harvested at various time points in the growth cycle and assayed for PAL activity (data not shown). In this case, the elevated PAL levels were stable for at least twelve hours during the stationary phase of culture growth (data not shown).

2.3. PAL inducibility by tryptophan isomers, precursors, and metabolites

An array of tryptophan optical isomers, precursors, and metabolites was tested for their ability to induce PAL. Both isomeric forms of tryptophan tested were able to induce increased PAL activity, and to a similar degree (Table 1). On the other hand, PAL activity failed to increase in response to any of the tryptophan precursors and metabolites tested, although indole-3-pyruvic acid gave a slight positive response. Therefore, PAL induction appears to be tryptophan-specific. Indole-3-acetic acid (IAA), which has been reported to occur naturally in *U. maydis* cultures (Navarre, 1990), reduced PAL activity almost 50% below control levels, while indole (0.3 mM) itself was too inhibitory to fungal cell growth to test for PAL induction.

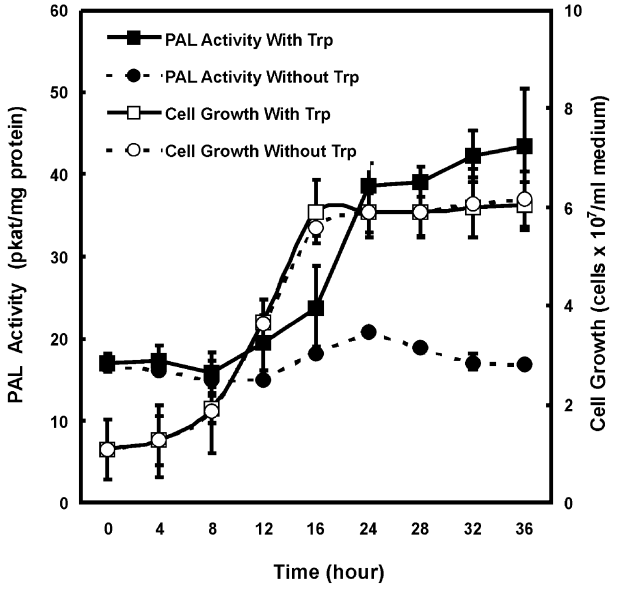

Fig. 2. Effect of L-tryptophan (Trp) addition on cell growth and extractable PAL activity in *Ustilago maydis*. L-Trypophan (0.3 mM) was added at different times in the cell cycle. Cells were harvested 2 h later and assayed for PAL activity.

2.4. Tryptophan effect on PAL induction in other U. maydis strains and Ustilago species

The observation that PAL induction was tryptophan-specific prompted us to investigate whether PAL induction by L-tryptophan is a general phenomenon in *Ustilago* species. For this purpose, several *U. maydis* strains and other smut species were tested (Table 2). PAL

Table 1
Effect of tryptophan analogs and tryptophan-related metabolites on PAL induction in *Ustilago maydis*[a]

Compounds	Relative PAL activity (%)[b]
No supplement	100
Anthranilic acid	110±10
Indole-3-acetamide	82±9
Indole-3-acetic acid	55±6
Indole-3-acetonitrile	107±11
Indole-3-butyric acid	114±12
Indole-3-carbinol	116±9
Indole-3-carboxylic acid	101±10
DL-Indole-3-lactic acid	88±7
Indole-3-pyruvic acid	135±5
Kynurenic acid	76±9
Tryptamine	98±10
Tryptophol	86±8
D-Tryptophan	318±14
L-Tryptophan	340±12

[a] Cells were grown in minimal medium for 16 h before addition of the exogenous compounds (0.3 mM each), harvested after 2 h further incubation, and used for PAL assay.

[b] Relative PAL activity is presented as the percentage of the value of PAL activity in the control which has no supplement. Control PAL activity was12 pkatal/mg protein.

Table 2
Ustilago species and *U. maydis* strains used in this study

Species/strain	Relevant genotype	Source or Ref.
U. maydis 518	*a2b2*	Gold et al. (1994)
U. maydis 521	*a1b1*	Gold et al. (1994)
U. maydis UM031	*a1b2*	This study
U. maydis UM032	*a2b1*	This study
U. maydis D132	*a1/a2 b1/b2*	This study
U. maydis D132-9	*a1/a2 b2/b1:: HygB*^{r}	This study
U. hordei	*MAT1*	Bakkeren et al. (1992)
U. nigra	Wild type field isolate	Bakkeren et al. (1992)
U. aegilopsidis	Wild type field isolate	Bakkeren et al. (1992)
Sporisorium reilianum	Wild type field isolate	Bakkeren et al. (1992)

induction (4- to 7-fold) by L-tryptophan was observed in all six *U. maydis* strains tested (data not shown). However, among other *Ustilago* species, only *U. nigra* displayed PAL induction by L-tryptophan (Fig. 3). All the *Ustilago* species tested did possess PAL, and its expression was detectable even without L-tryptophan supplementation. These results show that although PAL is widespread within the *Ustilago* genus, its induction by L-tryptophan is confined to certain species.

2.5. Effect of carbon and nitrogen sources on PAL activity induction

Various carbon and nitrogen sources were tested for their effect on PAL activity. Different levels of PAL activity and cell growth were obtained from the cells grown with the carbon sources tested (Fig. 4). Among these carbon sources, lactose and galactose resulted in the highest PAL activity, even though they proved to be the poorest sources for cell growth. In general, *U. maydis* cultures displayed higher PAL activity when they were grown on carbon sources that supported poorer growth, and lower activity when grown on more readily metabolized sugars such as glucose, mannose and sucrose.

To understand how carbon sources influence PAL activity under tryptophan-induction conditions, glucose was selected as a representative carbon source and its effect on PAL induction in *U. maydis* was investigated. Glucose supplementation repressed PAL production both in the presence and absence of L-tryptophan, and in both the nutrient-rich (complete) and minimal (glutamine only) media (Fig. 5). The repressive effect of glucose was observed under tryptophan-induced conditions

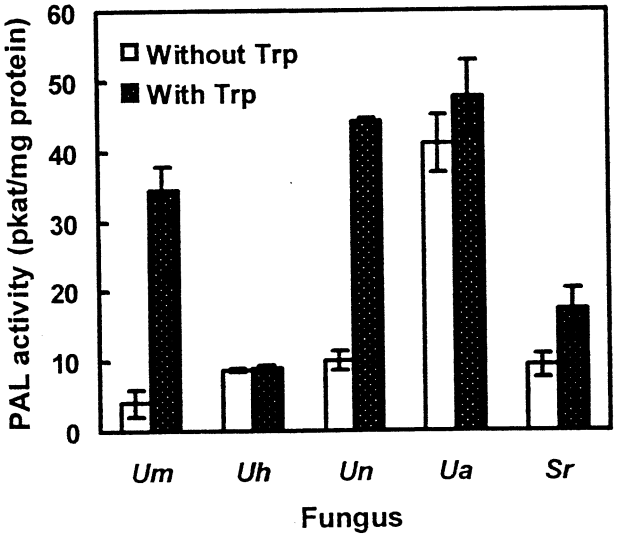

Fig. 3. Effect of L-trytophan (Trp) supplement on PAL activity in different *Ustilago* and related species. The fungal cells were grown in minimal media for 36 h with or without 0.3 mM L-trytophan, harvested, and assayed for activity. *Um, U. maydis; Uh, U. hordei; Un, U. nigra; Ua, U. aegliopsidis; Sr, Sporisorium reilianum.*

if the glucose was present from the beginning of the culture cycle, but not if the extra glucose was added later (16 h) in the culture cycle (data not shown). These results indicate that glucose repression can modulate *Ustilago* PAL expression, but that the repressive effect is limited to the early growth stage.

The effects of nitrogen source on *U. maydis* cell growth and PAL activity level are shown in Fig. 6. Provision of nitrogen in the form of inorganic salts, or asparagine, reduced PAL activity far below the levels obtained when L-tryptophan or L-phenylalanine was provided as the sole nitrogen source for cultures. Varying the ratio of ammonium nitrogen to nitrate nitrogen from 1:10 to 10:1 in the non-amino acid media did influence the level of PAL in the cultures after 24 h growth (data not shown), but the pattern of change did not suggest a strong preference for one form of inorganic nitrogen.

2.6. Effect of inhibitors on PAL activity in vivo

It had previously been determined that purified *U. maydis* PAL could be partially inhibited by the reaction product, *t*-cinnamic acid (Kim, 1997). When *t*-cinnamate (0.3 mM) was added to the L-tryptophan-supplemented culture medium, it substantially inhibited culture growth (60% of control), but had only a modest effect on the levels of PAL induced by 0.3 mM L-tryptophan supplementation (80% of control). Inhibition of PAL activity by addition of the potent and specific PAL inhibitor, 2-aminoindane-2-phosphonate (Zon and Amrhein, 1992) (0.1 mM), had no effect on fungal growth during the subsequent 24 h (data not shown).

2.7. Influence of physical environment

In order to examine the effect of environmental factors on PAL regulation, *U. maydis* cultures were grown in complete medium under various light, pH, and temperature regimes. No PAL induction or inhibition was observed when the cultures were incubated in light or dark, or at different medium pH values (pH 4, 5, 6, 7, 8), and/or at different temperatures (18, 24, 30°) (data not shown).

2.8. De novo synthesis versus activation in PAL induction

Induction of PAL activity in most plants and some fungi results from de novo synthesis of the enzyme. The origins of induced PAL activity in *U. maydis* were investigated by the use of inhibitors of translation and transcription, and with radiotracers and immunoprecipitation. In both the L-tryptophan-induced and-uninduced conditions, PAL activity was reduced slightly (to 70–80% of control) when *U. maydis* cells were incubated in the presence of

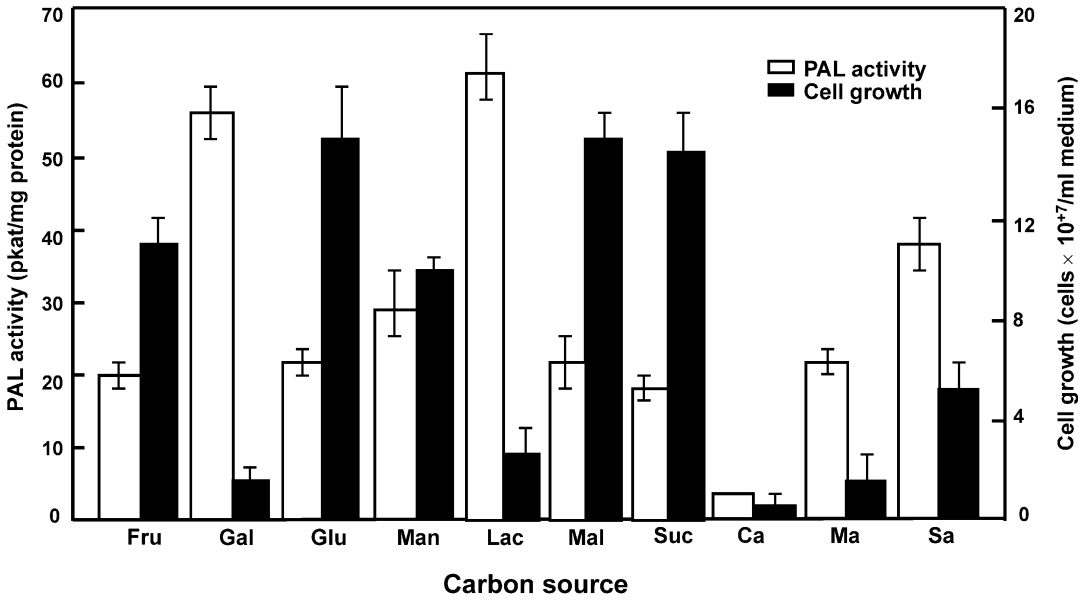

Fig. 4. Effect of various carbon sources on *Ustilago maydis* cell growth and PAL activity. Fru, fructose; Gal, galatose; Glu, glucose; Man, Mannose; Lac, lactose; Mal, maltose; Suc, sucrose; CA, citric acid; MA, malic acid; SA, succinic acid. Cells were grown for 36 h in minimal medium composed of 20 mM NH_4NO_3 and basal salt solution with each carbon source (2%) and harvested for PAL assay and cell count.

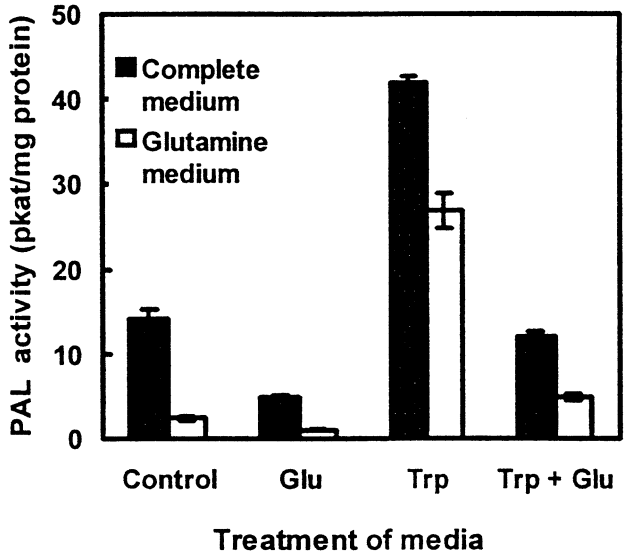

Fig. 5. Effect of glucose addition on *Ustilago maydis* PAL induction by L-trytophan. For the effect of glucose (Glu) addition, complete medium and glutamine (20 mM)-only medium were each supplemented with 2% glucose or 0.3 mM L-trytophan (Trp), or both. The fungal cells were grown in these media for 36 h and harvested for PAL assay.

actinomycin-D, a transcriptional inhibitor, or cycloheximide, an inhibitor of translation (Table 3). This implies that gene transcription and protein synthesis are needed to maintain PAL levels during the log phase of culture growth. However, radiolabeling of newly synthesized proteins showed that there was no difference in PAL protein labeling between the cells grown in L-tryptophan-induced and-uninduced conditions (Table 4). Taken together, these observations suggest that the induction of PAL activity by L-tryptophan supplementation is not primarily the result of de novo synthesis of PAL, but may instead reflect activation of PAL enzyme produced during the log phase of culture growth. The fact that the greatest enhancement of PAL activity by exogenous L-tryptophan is obtained in the stationary phase of culture growth (Fig. 2), when most protein synthesis has ceased, is consistent with this interpretation.

3. Discussion

3.1. PAL induction by L-tryptophan

The influence of aromatic amino acids on fungal PAL regulation has been studied in only a few species. In the red yeast (Marusich et al., 1981), *R. toruloides*, L-phenylalanine and L-tyrosine acted as PAL inducers, while in *N. crassa* (Sikora and Marzluf, 1982), L-phenylalanine and in *R. solani* (Kalghatgi and Subba Rao, 1976) L-phenylalanine, L-tyrosine, and L-tryptophan all served as PAL inducers. In all of these cases, the best PAL inducer was its substrate, L-phenylalanine. In contrast, the most effective inducer of PAL activity in *U. maydis* was L-tryptophan (Fig. 1), although L-phenylalanine had some effect. The response to tryptophan is also quite sensitive, since the level of L-tryptophan (0.3 mM) giving the highest PAL induction in *U. maydis* is substantially lower than the level of L-phenylalanine supplementation (6 mM) required for PAL induction in *R. toruloides* (Marusich et al., 1981; Wick and Willis, 1982).

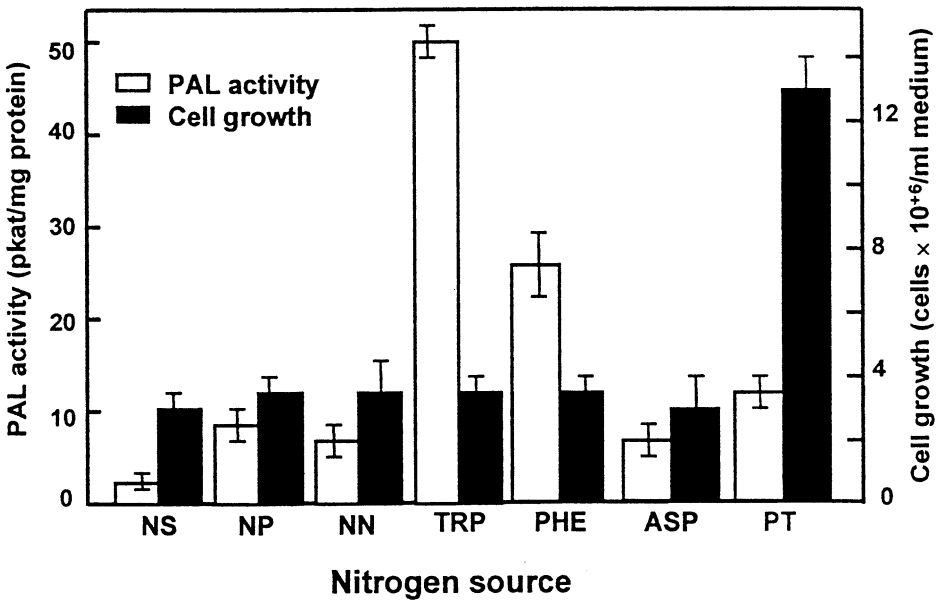

Fig. 6. Effect of nitrogen source on *U. maydis* cell growth and PAL acitivity. Each nitrogen source (3 mM) was added to minimal medium and the fungal cells were for 36 h and harvested for PAL assay and cell count. NS, $(NH_4)_2SO_4$; NP, $NH_4H_2PO_4$; NN, NH_4NO_3; TRP, L-tryptophan; PHE, L-phenylalanine; ASP, L-asparagine, and PT, peptone.

Table 3
Effect of actinomycin D and cycloheximide on *Ustilago maydis* PAL activity

Treatment[a]	PAL activity (pkatal/mg protein)			
	Induced[b]		Uninduced	
	12 h	16 h	12 h	16 h
No addition	19.6±1.8	32.8±2.2	13.3±1.6	20.5±2.1
Actinomycin D	13.9±1.9	23.3±0.8	9.2±1.2	15.1±0.6
Cycloheximide	16.2±1.7	26.4±1.3	11.3±1.0	16.8±1.2

[a] Actinomycin D (100 μg ml^{-1}) and cycloheximide (10 μg ml^{-1}) were added at mid (12 h) or late (16 h) log phase in the cell growth cycle, and cells were harvested 4 h later and used for the PAL assay.

[b] Induced: L-tryptophan (0.3 mM) was added to minimal medium at the time of inoculation; uninduced: no L-tryptophan supplement was added.

Table 4
PAL protein synthesis in L-tryptophan-induced and-uninduced conditions[a]

Cell harvest time	Newly synthesized PAL (dpm) [b]	
	Induced	Uninduced
16 h	382±36	388±47
20 h	461±56	473±62

[a] Induced: L-tryptophan (0.3 mM) was supplemented to minimal medium at the time of inoculation; uninduced: no L-tryptophan supplement was added.

[b] Proteins of *Ustilago maydis* were radiolabeled in vivo with L-^{3}H-amino acid mixture. The labeled PAL proteins were immunoprecipitated with anti-PAL antibodies and counted. The reported dpm values were obtained by subtracting the values of control proteins immunoprecipitated with pre-immune-serum.

However, induction of PAL in *Ustilago* cultures by L-tryptophan does not appear to be a typical microbial catabolic system directed at nutrient scavenging. First, a significant basal level of PAL is always detectable in the cultures, unlike in the three fungal species mentioned above, in which PAL activity is detectable only when the fungi are grown in media supplemented with aromatic amino acids which induce PAL. Second, in contrast to other fungi like *R. toruloides* and *N. crassa*, the inducer does not appear to have a logical metabolic connection with the reaction catalyzed by the induced enzyme. L-Phenylalanine, the obvious induction candidate, is much less effective in this role than L-tryptophan. Finally, the L-tryptophan effect on PAL induction is not operative in all the *Ustilago* species tested.

Since PAL induction in *U. maydis* results only from tryptophan supplementation and not from tryptophan precursors or metabolites, it is worth asking whether the endogenous level of tryptophan in the host plants is sufficient for *U. maydis* PAL induction. There are no data for corn, but the level of free tryptophan in tobacco leaves and carrot cell cultures has been reported as 16.7 μM (Widholm, 1974) and 81 μM (Widholm, 1972), respectively. In this study, *U. maydis* PAL was measurably induced by 30 μM tryptophan supplementation, suggesting that the enzyme might be inducible by either the endogenous level of free tryptophan, or enhanced levels of tryptophan resulting from proteolytic degradation of host proteins during biotrophic growth of the fungus in corn tissues.

3.2. Regulatory features of PAL

The production of many inducible enzymes by microorganisms is subject to catabolic repression when the organisms are grown in the presence of a potential carbon and energy source. In addition to carbon catabolic enzymes, many proteins, including those involved in bioluminescence, photosynthesis, sporulation, antibiotic biosynthesis, pigment biosynthesis, and extracellular macromolecular degradation, have been shown to be subject to catabolic repression (Saier, 1991). Glucose repression was observed with *U. maydis* in the present study. Both basal PAL levels and the induction of PAL by L-tryptophan were reduced by glucose addition to the medium (Fig. 5). A similar phenomenon was reported in *R. toruloides*, where PAL induction by L-phenylalanine was repressed by glucose (Gilbert and Tully,1982). We found that glucose repression of *U. maydis* PAL induction took place only at the early growth stage, but there are no corresponding data for *R. toruloides*. It thus remains unclear whether glucose repression of PAL at the early growth stage is a common feature in PAL-producing fungi.

The induction of PAL in *U. maydis* by tryptophan is not primarily the result of de novo synthesis of the protein, as shown by immunoprecipitation (Table 3) and Western blot assay results (data not shown). Alternative mechanisms could be some form of post-translational protein modification such as phosphorylation of the enzyme (Bolwell, 1992; Allwood et al., 1999), or a metabolic (non-covalent) influence on the *Ustilago* PAL activity. The behavior of the *Ustilago* enzyme is thus very different from that seen in *Rhodosporidium* (Wick and Willis, 1982; Gilbert et al., 1985) and *Neurospora* (Sikora and Marzluf, 1982), where induction of elevated PAL activity by phenylalanine is controlled primarily at the transcriptional level.

Some aspects of the results obtained in this study are reminiscent of classic microbial secondary metabolism. For example, the tryptophan inducibility of PAL is invoked only during the stationary phase of culture growth, and the induction appears to require tryptophan itself, rather than tryptophan metabolites or precursors. The pattern of highest inducibility and longer stability of *U. maydis* PAL during the stationary phase of growth differs from that seen with *R. toruloides*, where PAL was highly induced by L-phenylalanine during mid- to late-log phase of growth and showed variation in stability during the stationary phase of growth (Gilbert et al., 1983; Marusich et al., 1981)

It is noteworthy that IAA is also most actively produced at the stationary phase in the culture cycle of *U. maydis* (Navarre, 1990). Considering that tryptophan is the major precursor for IAA production in this fungus, the induction and suppression of PAL by tryptophan and IAA, respectively, suggests that a metabolic control mechanism links phenylalanine metabolism to tryptophan metabolism during the late growing period of *U. maydis*. It has been clearly established in both prokaryotes and eukaryotes that the synthesis of these two aromatic amino acids, phenylalanine and tryptophan, is derived from chorismate through the shikimate pathway (Braus, 1991; Hrazdina and Jensen, 1992). Logically, the synthesis and catabolism of each amino acid will be regulated to reflect their demands and their levels. From this perspective, it is conceivable that *U. maydis* PAL regulation is indirectly under the influence of tryptophan levels through metabolic feedback mechanisms that control synthesis and catabolism of all the aromatic amino acids. The suppressive effect of L-phenylalanine on tryptophan's ability to induce *U. maydis* PAL (Fig. 1) may reflect such an interaction. Studies on the effect of tryptophan on the synthesis of the PAL substrate, phenylalanine, could provide further insight into potential metabolic connections between tryptophan metabolism and PAL regulation.

t-Cinnamic acid, the product of the PAL reaction, is moderately inhibitory to *U. maydis* cell growth. Toxicity of *t*-cinnamic acid was also observed in *R. toruloides* cultures (Kane and Fiske, 1984; Marusich, Jensen and Zamir, 1981). In some plant systems like bean (Bolwell et al., 1988) and alfalfa (Orr. Edwards and Dixon, 1993) cell suspension cultures, addition of exogenous *t*-cinnamic acid was shown to suppress PAL induction. This has led to the suggestion that feedback inhibition by *t*-cinnamic acid could help control diversion of L-phenylalanine from primary metabolism to secondary metabolism and thereby avoid the accumulation of *t*-cinnamic acid to levels that might become toxic to cells. However such a mechanism does not appear to operate in *U. maydis*.

In conclusion, the work described in this paper has provided new information concerning fungal PAL regulation. When compared to higher plants and the fungal saprophytes, *R. toruloides* and *N. crassa*, regulation of PAL in *U. maydis* presents several novel features. However, it remains to be established whether or how this novelty is related to the biotrophic life-style of this organism. We are currently exploring that question by isolation and manipulation of the gene encoding PAL in *U. maydis*.

4. Experimental

4.1. Fungal strains and cultures

The Ustilago strains used in this study are listed in Table 1. Cultures were grown on potato dextrose agar (PDA, Difco) and on complete or minimal medium (2% glucose, 20 mM NH_4NO_3, and salt solution, pH 7.0) (Kim et al., 1996). A sporidial suspension (1 ml) (about

10^7 cells) was inoculated into 50 ml complete or minimal medium in 250 ml Erlenmeyer flasks and grown for 24–48 h at 30° with shaking (250 rpm). Alternatively, 100 μl sporidial suspension was inoculated into 5 ml complete or minimal medium in 15 ml culture tubes and grown for 16–36 h. Unless otherwise indicated, *U. maydis* strain 518 and minimal medium were used for the experiments on PAL regulation. Fungal cell growth was measured by counting the number of sporidia using a haemocytometer, with five replicates. Measurements for cell growth are illustrated in the figures with columns (mean value) and vertical bars (±S.D.). The experiments were repeated three times with essentially identical results. S.D. values calculated from the means of these independent experiments were less than 10%.

4.2. Chemicals

L-^{3}H-amino acid mixture was purchased from ICN Biomedical Pharmaceuticals, Inc. L-[U-^{14}C]-phenylalanine (474 mCi/mmol) was purchased from Amersham International. 2-Aminoindan-2-phosphonic acid (AIP) (Zon and Amrhein, 1992) was provided by J. Zon (Technical University Wroclaw, Poland). Diethyl pyrocarbonate (DEPC), cycloheximide, actinomycin D, Protein A-Sepharose beads, bovine serum albumin, L-phenylalanine, L-tyrosine, L- or D-tryptophan, t-cinnamic acid, indole, and indolic derivatives were obtained from Sigma (St. Louis, Mo.). Westran membrane was purchased from Schleicher & Schuell; Zeta-Probe membrane from Bio-Rad, and microbial media from Difco. All other chemicals (analytical reagent grade) were obtained from Sigma or Aldrich.

4.3. Enzyme extraction and assay

Cultures were harvested in a 1.5 ml microfuge tube and the fungal cells were washed two times with sterile distilled water. The cell pellet was homogenized for 20 s at 4 °C with alumina and a mini-pestle (Mandel Scientific Co.). The homogenate was suspended in 200 μl ice-cold 0.5 M sodium phosphate buffer, pH 8.0, vortexed for 5 min with frequent cooling in ice and then centrifuged at 14,000 g for 15 min at 4 °C. The supernatant was desalted through a PD-10 column (Pharmacia) and used for PAL assays and other experimental analyses. PAL activity (three replicates per protein extract) was measured by a radiometric method as described by Campbell and Ellis (1992) using L-[U-^{14}C]-phenylalanine as substrate. Protein was determined by a dye-binding method (Bradford, 1976) with bovine serum albumin as a standard. Unless otherwise described, all experiments were repeated at least twice with three or five replicates. Values presented in Tables are the mean and SD of all activity measurements for three cultures, while in figures, the PAL activity column indicates the mean and the vertical bar indicates S.D. S.D. values calculated from the means of these independent experiments were less than 10%.

4.4. Immunoprecipitation of radio-labeled PAL protein

U. maydis cells were grown in minimal medium (50 ml) for 12 or 16 h with or without L-tryptophan (0.3 mM). After addition of 50 μCi ^{3}H-labeled amino acid mixture, the cultures were further incubated for 4 h. Following harvest by centrifugation at 6000 g for 10 min at 4 °C, the cells were washed three times with sterile distilled water and frozen in liquid nitrogen. Protein crude extracts were prepared by grinding the cells with alumina as described above. Radiolabeled PAL proteins were immunoprecipitated with U. maydis PAL antiserum (or preimmune serum) and protein A-Sepharose 4B beads, using a protocol described in 'Antibodies: A Laboratory Manual' (Harlow and Lane, 1988). After heating in SDS sample buffer at 85 °C for 10 min, immunoprecipitated proteins were separated from the beads by centrifugation and the radioactivity in the supernatant was measured using a Beckman LS-5000TA scintillation counter.

Acknowledgements

The financial support of the Natural Sciences and Engineering Research Council of Canada is gratefully acknowledged. S.H. K. was the holder of a University Graduate Fellowship from the University of British Columbia.

References

Agrios, G.N., 1988. The Smuts. In: Plant Pathology. Academic Press, San Diego, pp. 474-486.

Allwood, E.G., Davies, D.R., Gerrish, C., Ellis, B.E., Bolwell, G.P., 1999. Phosphorylation of phenylalanine ammonia-lyase: evidence for a novel protein kinase and identification of the phosphorylated residue. FEBS Letters 457, 47–52.

Attridge, T.H., Johnson, C.B., Smith, H., 1974. Density labelling evidence for the phytochrome-mediated activation of phenylalanine ammonia-lyase in mustard cotyledons. Biochim. Biophys. Acta 343, 440–451.

Bakkeren, G., Gibbard, B., Yee, A., Froeliger, E., Leong, S., Kronstad, J., 1992. The *a* and *b* loci of *Ustilago maydis* hybridize with DNA sequences from other smut fungi. Mol. Plant-Microbe Interact. 5, 347–355.

Bolwell, G.P., Mavandad, M., Millar, D.J., Edwards, K.J., Schuch, W., Dixon, R.A., 1988. Inhibition of RNA levels and activities by *trans*-cinnamic acid in elicitor-induced bean cells. Phytochemistry 27, 2109–2117.

Bolwell, G.P., 1992. A role for phosphorylation in the down-regulation of phenylalanine ammonia-lyase in suspension-cultured cells of french bean. Phytochemistry 31, 4081–4086.

Bradford, M.M., 1976. A rapid and sensitive method for the quantification

of microgram quantities of protein utilizing the principle of dye-binding. Anal. Biochem. 72, 248–254.

Braus, C.H., 1991. Aromatic amino acid biosynthesis in the yeast *Saccharomyces cerevisiae*: a model system for the regulation of a eukaryotic biosynthetic pathway. Microbiol. Rev. 55, 349–370.

Camm, E.L., Towers, G.H.N., 1973. Phenylalanine ammonia-lyase. Phytochemistry 12, 961–973.

Campbell, M.M., Ellis, B.E., 1992. Fungal elicitor-mediated responses in pine cell cultures: III. Purification and characterization of phenylalanine ammonia-lyase. Plant Physiol. 98, 62–70.

Emes, A.V., Vining, L.C., 1970. Partial purification and properties of L-phenylalanine ammonia-lyase from *Streptomyces verticillatus*.. Can. J. Biochem. 48, 613–622.

Gilbert, H.J., Tully, M., 1982. Synthesis and degradation of phenylalanine ammonia-lyase of *Rhodosporidium toruloides*. J. Bacteriol. 150, 498–505.

Gilbert, H.J., Stephenson, J.R., Tully, M.J., 1983. Control of synthesis of functional mRNA coding for phenylalanine ammonia-lyase from *Rhodosporidium toruloides*. J. Bacteriol. 153, 1147–1154.

Gilbert, H.J., Clarke, I.N., Gibson, R.K., Stephenson, J.R., Tully, M.J., 1985. Molecular cloning of the phenylalanine ammonia-lyase gene from *Rhodosporidium toruloides* in *Escherichia coli* K-12. J. Bacteriol. 161, 314–320.

Gold, S., Duncan, G., Barrett, K., Kronstad, J., 1994. cAMP regulates morphogenesis in the fungal pathogen *Ustilago maydis*. Proc. Natl. Acad. Sci. USA 98, 5684–5688.

Hahlbrock, K., Scheel, D., 1989. Physiology and molecular biology of phenylpropanoid metabolism. Annu. Rev. Plant. Physiol. Plant. Mol. Biol. 40, 347–369.

Hahlbrock, K., Schröder, J., 1975. Light-induced changes of enzyme activities in parsley cell suspension cultures. Increased rate of synthesis of phenylalanine ammonia-lyase. Arch. Biochem. Biophys. 166, 47–53.

Harlow, E., Lane, D., 1988. Antibodies, a laboratory manual. Cold Spring Harbor Laboratory, New York, p. 468.

Hrazdina, G., Jensen, R.A., 1992. Spatial organization of enzymes in plant metabolic pathways. Annu. Rev. Plant. Physiol. Plant. Mol. Biol. 43, 241–267.

Jones, D.H., 1984. Phenylalanine ammonia-lyase: regulation of its induction and its role in plant development. Phytochemistry 23, 1349–1359.

Kalghatgi, K.K., Subba Rao, P.V., 1976. Regulation of L-phenylalanine ammonia-lyase from *Rhizoctonia solani*. J. Bacteriol. 126, 568–578.

Kane, J.F., Fiske, M.J., 1984. Regulation of phenylalanine ammonia-lyase in *Rhodotorula glutinis*. J. Bacteriol. 160, 963–966.

Kim, S.H., Kronstad, J.W., Ellis, B.E., 1996. Purification and characterization of phenylalanine ammonia-lyase from *Ustilago maydis*. Phytochemistry 43, 351–357.

Kim, S.H., 1997. Biochemical and Molecular Studies on Phenylalanine Ammonia-lyase in the Phytopathogenic Fungus *Ustilago maydis*. PhD thesis, University of British Columbia, Vancouver.

Lawton, M.A., Lamb, C.J., 1987. Transcriptional activation of plant defense genes by fungal elicitor, wounding and infection. Mol. Cell. Biol. 7, 335–341.

Marusich, W.C., Jensen, R.A., Zamir, L.O., 1981. Induction of L-phenylalanine ammonia-lyase during utilization of phenylalanine as a carbon or nitrogen source. J. Bacteriol. 146, 1013–1019.

Navarre, D.A., 1990. Phytohormone Production, Auxin Biosynthesis and Electrophoretic Karyotypes for *Ustilago maydis* and other Smuts. MSc thesis, Louisiana State University, Baton Rouge.

Orr, J.D., Edwards, R., Dixon, R.A., 1993. Stress responses in alfalfa (*Medicago sativa* L.) XIV. Changes in the levels of phenylpropanoid pathway intermediates in relation to regulation of L-phenylalanine ammonia-lyase in elicitor-treated cell-suspension cultures. Plant Physiol. 101, 847–856.

Ritenour, M.A., Saltveit, M.E., 1996. Identification of a phenylalanine ammonia-lyase inactivating factor in harvested head lettuce (*Lactuca sativa*). Physiol. Plant 97, 327–331.

Saier Jr, M.H., 1991. A multiplicity of potential carbon catabolite repression mechanisms in prokaryotic and eukaryotic microorganisms. New Biologist 3, 1137–1147.

Sikora, L.A., Marzluf, G.A., 1982. Regulation of L-phenylalanine ammonia-lyase by phenylalanine and nitrogen in *Neurospora crassa*. J. Bacteriol 150, 1287–1291.

Vance, C.P., Bandoni, R.J., Towers, G.H.N., 1975. Further observations on phenylalanine ammonia-lyase in fungi. Phytochemistry 14, 1513–1514.

Wick, J.F., Willis, J.E., 1982. Phenylalanine-dependent *de novo* synthesis of phenylalanine ammonia-lyase from *Rhodotorula glutinis*. Arch. Biochem. Biophys. 216, 385–391.

Widholm, J.M., 1972. Anthranilate synthetase from 5-methyltryptophan-susceptible and -resistant cultured *Daucus carota* cells. Biochim. Biophys. Acta 297, 48–57.

Widholm, J.M., 1974. Control of aromatic amino acid biosynthesis in cultured plant tissues: Effect of intermediates and aromatic amino acids on free levels. Physiol. Plant. 30, 13–18.

Zon, J., Amrhein, N., 1992. Inhibitor of phenylalanine ammonia-lyase: 2-aminoindane-2-phosphonic acid and related compounds. Liebigs Ann. Chem. 625-628.

Zucker, M., 1971. Induction of phenylalanine ammonia-lyase in *Xanthium* leaf discs. Plant Physiol. 47, 442–444.

PERGAMON

Phytochemistry 58 (2001) 859–864

PHYTOCHEMISTRY

www.elsevier.com/locate/phytochem

Purification and characterization of a cationic isoperoxidase from scented-geranium

Seok Hyun Lee[a], Eun Soo Kim[b], Mi Young Lee[a,*]

[a]*Department of Life Science, College of Science, Soonchunhyang University, Asan, Choongnam 336-745, South Korea*
[b]*Department of Biological Science, Konkuk University, Hwayang, Kwangjin, Seoul, 143-701, South Korea*

Received 9 March 2001; received in revised form 19 June 2001

Abstract

A strongly cationic isoperoxidase named PC3 was purified to homogeneity from scented-geranium (*Pelargonium graveolens*) callus by using DEAE-Sephacel chromatography, CM–cellulose chromatography and Sephacryl S-200 gel filtration, respectively. The enzyme was a glycoprotein with M_r of ca. 58 kDa estimated by SDS–PAGE and Sephadex G-150 gel filtration. The pI value of the enzyme was 9.1. Kinetic studies revealed that PC3 had a very low K_m value for scopoletin of 0.01 mM and could use ascorbate as a substrate. Interestingly, PC3 could not oxidize ferulic acid as a substrate. Chemical modification of the enzyme showed that PC3 was rapidly inactivated by His, Cys, Trp and Lys-specific reagents. The second order rate constants and reaction orders with respect to these inactivations were determined. Notably, ca. 4–7-fold activity boosting of PC3 occurred by adenine and imidazole when anilino substrates, such as *o*-dianisidine and *o*-phenylenediamine were oxidized, whereas this activity boosting did not occur when several phenolic substrates were used. © 2001 Published by Elsevier Science Ltd.

Keywords: *Pelargonium graveolens*; Geraniaceae; Purification; Characterization; Cationic isoperoxidase

1. Introduction

Multiple forms of plant peroxidases (EC 1.11.1.7) are widely distributed in all higher plants (van Huystee and Cairns, 1982). Peroxidases have been implicated in a wide range of cellular reactions such as phenolic compound oxidation, indole-3-acetic acid oxidation, lignification and polysaccharide cross-linking. Obviously they play a key role in plant growth and development (van Huystee, 1987). Moreover, they are known to be related with the defense mechanisms toward pathogens and various stresses including metal ion (Antje et al., 1996), salt (Bakardjieva et al., 1996) and air pollution damage (Castillo et al., 1987).

According to the classification by Welinder (Dunford, 1999; Hiraga et al., 2001), classical secretory plant peroxidases such as horseradish peroxidase (HRP), peanut peroxidase and barley peroxidase belonged to the class III peroxidase superfamily. They have two conserved calcium ions, an N-terminal signal peptide, four conserved disulfide bridges and 0–25% carbohydrate content. All the enzymes in class III have an imidazole side chain of His as their proximal ligands, and conserved Arg and His residues on the distal side of the heme. However, distinct differences in physicochemical and catalytic properties have been reported among peroxidase isozymes even within one plant family (Lee and Kim, 1994). Therefore, more detailed catalytic and molecular studies of individual isoperoxidases are desirable. There are at least eight distinguishable isoperoxidases in Korean radish, and six of them were purified to near homogeneity (Yoo and Kim, 1988; Lee and Kim, 1990, 1993, 1998a,b; Lee et al., 1994; Kim and Kim, 1996). The physicochemical, catalytic and immunological properties of Korean radish peroxidases (KRP) were studied in detail (Yoo and Kim, 1988; Lee and Kim, 1990, 1993, 1998a,b; Lee et al., 1994; Kim and Kim, 1996), indicating that different isoperoxidases might have different specificities toward physiological substrates in vivo. Studies on the gene structure, overexpression and promoter function of individual isoperoxidase have been intensively studied in various plants such as tobacco (Dowd et al., 2000), Arabidopsis (Tognolli et al., 2000), rice (Hiraga et al., 2000), sweet potato (Kim et al., 2000) as well as Korean

* Corresponding author. Tel.: +82-41-530-1355; fax: +82-41-530-1355.

E-mail address: miyoung@sch.ac.kr (M. Young Lee).

0031-9422/01/$ - see front matter © 2001 Published by Elsevier Science Ltd.
PII: S0031-9422(01)00325-9

radish (Park and Kim, 1996a, b; Lee and Kim, 1998; Lee et al., 1999).

Pelargonium graveolense, referred to as scented-geranium, is an important ornamental plant worldwide, and has been studied extensively with respect to its conventional horticultural traits (Raj et al., 1997). However, only few reports have so far focused on the isolation and characterization of catalytic and kinetic properties of enzymes from this plant.

In the present investigation, a strongly cationic isoperoxidase PC3 was purified to homogeneity from scented-geranium callus and some of its physicochemical, kinetic and catalytic properties examined in detail.

2. Results and discussion

2.1. Enzyme purification

Scented-geranium (*P. graveolense*) callus was induced as previously reported (Lee and Lee, 2000). The crude extracts of geranium callus contained three cationic isoperoxidases, PC1, PC2 and PC3, and three anionic isoperoxidases, PA1, PA2 and PA3, when subjected to starch gel electrophoresis at pH 7. In this nomenclature system, the suffix numbers denote which isoperoxidase migrates the greater distance to either anode (letter "A") or cathode (letter "C"). The lower the number the less the migration. Among the cationic isoforms, a strongly cationic isoperoxidase, PC3, was purified 56-fold to an electrophoretically homogeneous form by chromatographic sepn methods of DEAE–Sephacel chromatography, CM–cellulose chromatography and Sephacryl S-200 gel filtration (Tables 1 and 2).

2.2. Physicochemical properties

The M_r of PC3 was determined to be ca. 58 K by SDS–PAGE (Fig. 1) and Sephadex G-150 gel filtration, showing that PC3 is a monomeric protein. These results suggest that the M_r for PC3 falls within the range of other isoperoxidases such as KRP (Lee and Kim, 1994), HRP (Shannon et al., 1966), JRP (Morita et al., 1971) and peanut peroxidase (van Huystee, 1987). The isoelectric point of PC3 was determined to be 9.1, and the enzyme was shown to contain carbohydrate (Grossman and Neville, 1971). The enzymes in class II secreted fungal peroxidase and class III classical secretory plant peroxidase are glycosylated (Dunford, 1999). Potential *N*-glycosylation sites and carbohydrate contents have been determined for KRP (Kim and Kim, 1996), HRP (Shannon et al., 1966) and peanut peroxidase (Shaw et al., 2000; Lege et al., 2001) by deglycosylation, *N*-glycan profiling or NMR spectroscopy.

2.3. Kinetic studies

Substrate utilities of isoperoxidase PC3 have been investigated in terms of optimal pH and K_m values in order to infer the physiological functions of the enzyme. Geranium isoperoxidase PC3 had a pH optimum around 6.0 when guaiacol and H_2O_2 were used as the substrates. The optimum pHs with respect to various substrates such as *o*-dianisidine, *o*-phenylenediamine, caffeic acid, esculetin, scopoletin, chlorogenic acid, and ascorbic acid were also determined to be in the range of 4.0–6.0 (Table 3). These ranges were similar to those of six isoperoxidases from Korean radish (Lee and Kim, 1994).

Geranium PC3 had K_m values of 7.3 mM for guaiacol and 3.0 mM for H_2O_2. The K_m values of six Korean radish isoperoxidases against guaiacol ranged within 5.6–19.4 mM, and the K_m values against H_2O_2 ranged within 0.19–2.5 mM (Lee and Kim, 1994). PC3 showed high affinities for scopoletin among various substrates tested with the K_m value of 0.01 mM, and showed sigmoidal saturation mode for scopoletin oxidation in spite of its monomeric structure. Similar sigmoidal saturation curve for scopoletin oxidation was also shown in C_1 and A_3 from Korean radish (Lee and Kim, 1990; Park et al., 1994). The K_m values of five Korean radish isoperoxidases toward scopoletin ranged between 0.18 and 5.6 mM, and only A_{3n} could not use scopoletin as a substrate (Lee and Kim, 1998a). Interestingly, geranium PC3 could not utilize ferulic acid, the intermediate of lignin biosynthesis in the cell, as a substrate. Furthermore, ascorbate was peroxidized by PC3 with the low K_m value of 0.03 mM, indicating that PC3 has good ascorbate peroxidase activity as well. However, six isoperoxidases from Korean radish could not utilize

Table 1
Purification of isoperoxidase PC3 from scented-geranium callus

Purification step	Total protein (mg)	Total activity (unit)	Specific activity (unit/mg)	Yield (%)	Purification fold	RZ value (A_{403}/A_{280})
Crude extract	413.2	10.5	0.03	100	1	–[a]
DEAE–Sephacel	30.3	4.6	0.15	43	5	–
CM–cellulose	10.9	3.8	0.36	37	12	–
Sephacryl S-200	1.3	2.2	1.69	20	56	1.95

[a] Not determined.

Table 2
Physicochemical properties of isoperoxidase PC3 from scented-geranium callus

	Molecular weight		Presence of carbohydrate	pI
	SDS–PAGE	Gel filtration		
PC3	58,000	58,000	Yes	9.1
KRP C_3[a]	44,000	44,000	Yes	9.0
KRP C_1[a]	45,000	45,000	Yes	8.6

[a] Data were supplied from Lee and Kim (1994).

Table 3
Summary of optimum pH and K_m values for various substrates of isoperoxidase PC3 from scented-geranium callus

Substrates	Optimum pH	K_m (mM)
Guaiacol	6.0	7.3
H_2O_2	6.0	3.0
o-Dianisidine	4.5	0.31
o-Phenylenediamine	6.0	0.25
Caffeic acid	5.0	0.12
Esculetin	5.0	0.17
Scopoletin	5.5	0.01
Chlorogenic acid	4.0	0.45
Ascorbic acid	6.0	0.03
Ferulic acid	–[a]	–

[a] Not reactive.

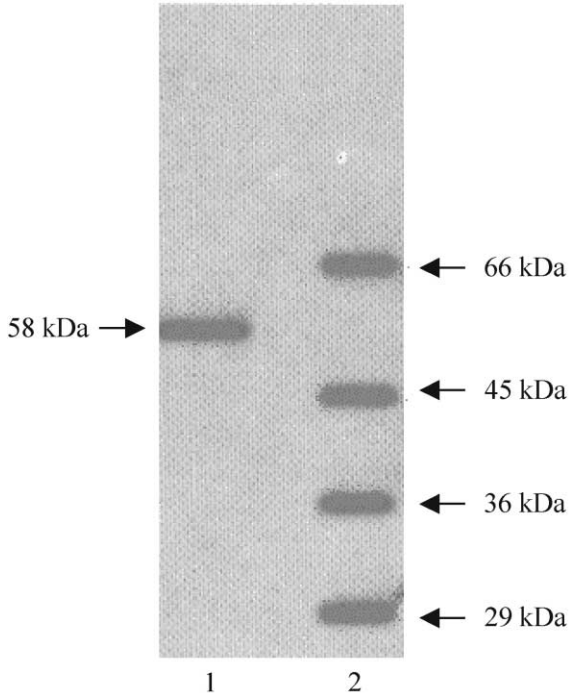

Fig. 1. SDS-polyacrylamide gel electrophoregram of a cationic isoperoxidase PC3 from scented-geranium callus: lane 1, purified isoperoxidase PC3 from scented-geranium callus; lane 2, standard molecular weight markers.

ascorbate as the substrate (Lee and Kim, 1994). Ascorbate peroxidase from Japanese radish utilized mainly ascorbate as the substrate with the K_m value of 0.77 mM, while it did not utilize guaiacol at all (Ohya et al., 1997). In contrast, ascorbate peroxidase from soybean utilized both guaiacol and ascorbate very much (Dalton et al., 1987) like our geranium PC3.

2.4. Chemical modification

In order to find out which amino acid residues might be involved in the catalysis of substrates at or near the active site of geranium PC3, chemical modification of the enzyme was performed using various modifying reagents (Table 4). PC3 was rapidly inactivated by the His specific reagent DEP, when the time dependent inactivation of the enzyme in the presence of DEP was examined. The time course for the inactivation was dependent on the reagent concentration, and the slopes of the inactivation plots obtained at different concentrations of DEP were linearly related to the DP concentration (data not shown).

From this plot, the second-order rate constant for inactivation was determined to be 2.0×10^3 M^{-1} min^{-1}. A double-logarithmic plot of the reciprocal of the half-time of inactivation against reagent concentration yielded a reaction order of 1.04 with respect to DEP, indicating that there might be one essential His residue per active site. The inactivation by DEP was completely protected in the presence of substrate guaiacol (data not shown), suggesting that the His residue modified by DEP might be located at or near the guaiacol binding site. In the case of KRP, DEP did not significantly inactivate the enzyme (Yoo and Kim, 1988), although highly conserved His-containing sequences were expected to be in the region of active site (Park and Kim, 1996a). Geranium PC3 was also rapidly inactivated by the Trp specific reagent NBS and the Lys specific reagent PLP with second order rate constants of $1.7\times$

Table 4
Summary of second-order rate constants and reaction orders for isoperoxidase PC3 inactivation by various chemical modification reagents

Modification reagents	Second-order rate constants (M^{-1} min^{-1})	Reaction orders
PHMB	1.0×10^5	0.95
Iodoacetamide	9.3×10^2	1.01
DTNB	1.2×10^3	1.08
NBS	1.7×10^4	0.92
DEP	2.0×10^3	1.04
PLP	2.1×10^3	1.02

PHMB, *p*-hydroxymercuribenzoic acid; DTNB, 5,5′-dithiobis-2-nitrobenzoic acid; NBS, *N*-bromosuccinimide; DEP, diethylpyrocarbonate; PLP, pyridoxal-5-phosphate.

10^4 and 2.1×10^3 M^{-1} min^{-1}, respectively. Reaction orders with respect to NBS and PLP were 0.92 and 1.02, respectively, again indicating that one essential Trp and one essential Lys residue were present. Notably, the thiol specific reagents PHMB, iodoacetamide and DTNB inactivated the enzyme rapidly with second order rate constants of 1×10^5, 9.3×10^2 and 1.2×10^3 M^{-1} min^{-1}, respectively. PC3 inactivation by PHMB was much stronger than by DTNB and iodoacetamide. Class III secretory plant peroxidases are reported to have four conserved disulfide bridges and thus there seemed to be no free Cys residue (Dunford, 1999). However, isoperoxidase A_1 from Korean radish (Lee and Kim, 1993) and ascorbate peroxidase from Japanese radish (Ohya et al., 1997) were reported to be inactivated by PHMB and DTNB, implying that free Cys participate in the active center or maintenance of the conformation of the enzyme. Moreover, *Arabidopsis thaliana* peroxidase N (Mirza et al., 2000) also has a free Cys residue at the substrate-binding site, unlike other class III secretory plant peroxidases.

2.5. Activity boosting by various nitrogenous compounds

Effects of various nitrogenous compounds on the peroxidative activity of geranium PC3 were examined (Table 5). Oxidation of the anilino substrate *o*-dianisidine was stimulated by adenine and imidazole at pH 8 as much as 4- and 7-fold, respectively. Stimulations by adenine and imidazole did not occur at lower pH values. Moreover, activity boostings by adenine and imidazole also occurred in the *o*-phenylenediamine oxidation by PC3. However, the oxidation of phenolic substrates such as guaiacol, chlorogenic acid, caffeic acid, scopoletin and esculetin was not stimulated by any of the nitrogenous compounds such as adenine, imidazole, cytosine, guanine, histidine, nicotinate, tryptophan and uracil (Table 5).

In particular, ammonium salt, which has been reported to be an excellent stimulator of dianisidine oxidation in HRP (Kuo and Fridovich, 1988), had no effect on the PC3. A similar boosting effect of imidazole on dianisidine oxidation was found in KRP (Lee et al., 2000), whereas a boosting effect did not occur in myeloperoxidase, chloroperoxidase, *Escherichia coli* hydroperoxidase and methemoglobin peroxidase (Kuo and Fridovich, 1988). More detailed kinetics of these boosting reactions and active site structure determination will be needed in order to understand the mechanism of adenine and imidazole action on anilino substrate oxidation.

3. Experimental

3.1. Experimental plant and callus induction

The plant material used in this investigation, *P. graveolens* or scented-geranium, was purchased from a local market near Asan, Korea. Scented-geranium callus induction was performed as previously reported (Lee and Lee, 2000).

3.2. Peroxidase activity assays with various substrates

Peroxidase activity was assayed by a modified procedure of Lee and Kim (1994). Briefly, the assay mixture contained 15 mM substrate, 5 mM H_2O_2, 40 mM Na–Pi buffer (pH 6.5) and 50 ul of enzyme solution in a total volume of 1 ml. The reaction was initiated by the addition of H_2O_2. Substrates for the enzyme included guaiacol, *o*-dianisidine, *o*-phenylenediamine, caffeic acid, esculetin, scopoletin, chlorogenic acid, ascorbic acid, ferulic acid and H_2O_2. Kinetic data were obtained from triple replications of activity assays.

3.3. Gel electrophoresis

Starch gel electrophoresis was performed as described (Lee and Kim, 1994). Isoperoxidase bands were visualized by placing the gel in a solution of 100 mg of 3-amino-9-ethyl carbazole in 10 ml of DMF, 184 ml of 50

Table 5
Effect of various nitrogenous compounds on the peroxidative activity of isoperoxidase PC3 from scented-geranium callus[a]

Effector	Adenine	Ammonium ion	Cytosine	Guanine	Histidine	Imidazole	Nicotinate	Tryptophan	Uracil
Amino substrate									
o-Dianisidine	4	1.1	0.9	1.1	0.94	7	1.2	0.68	0.85
o-Phenylene diamine	3.8	1.25	1.05	1.18	1.15	7.5	1.08	0.8	0.97
Phenolic substrate									
Guaiacol	1.13	0.99	1.09	1.07	0.88	1.5	1.15	0.98	0.85
Chlorogenic acid	1.25	1.2	0.9	0.89	0.96	0.85	0.93	0.7	0.9
Caffeic acid	0.96	1.96	0.97	0.78	0.92	0.82	0.9	0.8	0.75
Esculetin	1.06	0.79	0.98	0.95	0.97	0.79	1.11	0.74	0.7
Scopoletin	1.5	1.1	0.85	1.07	1.2	1.2	0.97	0.9	0.8

[a] The values presented here have been shown relative to the peroxidative activity without booster which was given a value of 1. All experiments were repeated four times.

mM NaOAc buffer (pH 5.0), 10 ml of 100 mM $CaCl_2$ and 0.2 ml of 30% H_2O_2. SDS–PAGE was carried out as described by Laemmli (1970).

3.4. Enzyme purification

Scented-geranium callus was homogenized with 50 mM Na–Pi buffer (pH 6.5) containing sea sand. The homogenate was centrifuged at 12,000 ***g*** for 20 min and the supernatant was saturated with $(NH_4)_2SO_4$ up to 90% and centrifuged at 13,000 ***g*** for 30 min. The precipitate was then dialyzed twice against 5 mM Na–Pi buffer (pH 6) and used as the enzyme extract. The enzyme preparation was loaded on a DEAE–Sephacel ion exchange column (3.5×12 cm) pre-equilibrated with 5 mM Na–Pi buffer (pH 6). Initial elution of the DEAE–Sephacel column with 5 mM Na–Pi buffer (pH 6) yielded largely a mixt. of all cationic isoperoxidases. The eluant was applied on a CM–cellulose ion exchange column (2.5×4 cm) pre-equilibrated with 10 mM Na–Pi buffer (pH 6). Isoperoxidase PC3 was eluted with 50 mM Na–Pi buffer (pH 6) following the elution of PC1 and PC2 with 30 mM Na–Pi buffer (pH 6). Sephacryl S-200 gel filtration chromatography with CM–cellulose fractions which contain PC3 activity was also performed. This procedure removed minor contaminating proteins and provided a single polypeptide band as evidenced by SDS–PAGE analysis.

3.5. Molecular weight and glycosylation determination

M_r of isoperoxidase PC3 was estimated by gel filtration chromatography on Sephadex G-150 column (1.5×78 cm). The subunit M_r of the enzyme was determined by SDS-PAGE. Glycosylation was determined by the procedure described by Grossman and Neville (1971).

3.6. Chemical modification

The purified PC3, kept at a final concentration of 40 nM, was incubated with several modifying reagents such as *p*-hydroxymercuribenzoic acid (PHMB) in 50 mM NaOAc buffer (pH 4.5), *N*-bromosuccinimide (NBS) in 50 mM NaOAc buffer (pH 4.0), iodoacetamide in 50 mM Na–Pi buffer (pH 6.5), 5,5′-dithiobis-2-nitrobenzoic acid (DTNB) and diethylpyrocarbonate (DEP) in 50 mM Na–Pi buffer (pH 7.2) and pyridoxal-5-phosphate (PLP) in 50 mM Na–Pi buffer (pH 7.0) at 30 °C. The chemical modification reagents were added at different final concentrations (0.1–10 mM), and the residual enzyme activity was measured at predetermined time intervals. The second order rate constants and reaction orders with respect to the inactivation with these modifying reagents were also determined as described by Lee and Kim (1993).

3.7. Effects of nitrogenous compounds on the peroxidation of various substrates

The stimulatory effects of nitrogenous compounds on the peroxidation of several substrates were examined as described (Lee et al., 2000). The reaction mixtures contained 0.18 mM nitrogenous compounds, 0.36 mM H_2O_2, and 50 ul of 5 nM enzyme in a total volume of 1 ml. The buffer systems were 50 mM NaOAc buffer, 50 mM Na–Pi buffer and 50 mM Tris–HCl buffer depending upon the pH ranges studied. The nitrogenous compounds tested included adenine, guanine, cytosine, ammonium ion, histidine, imidazole, nicotinic acid, tryptophan and uracil.

Acknowledgements

This work was supported by a grant from the Korea Research Foundation (1997-011-D-00020).

References

Antje, B., Ahmed, A., Marina, A., Andreas, B., Karl-Josef, D., 1996. Heavy metal-induced changes in peroxidase activity in leaves, roots and cell suspension cultures of *Hordeum vulgare* L. In: Obinger, C., Burner, U., Ebermann, R., Penel, C., Greppin, H. (Eds.), Plant Peroxidases: Biochemistry and Physiology. University of Agriculture, Vienna, University of Geneva, Geneva, pp. 374–379.

Bakardjieva, N.T., Christova, N.V., Christov, K., 1996. Reaction of peroxidase from different plant species to increased temperatures and the effect of calcium and zinc ions. In: Obinger, C., Burner, U., Ebermann, R., Penel, C., Greppin, H. (Eds.), Plant Peroxidases: Biochemistry and Physiology. University of Agriculture, Vienna, University of Geneva, Geneva, pp. 345–351.

Castillo, F.J., Miller, P.R., Greppin, H., 1987. Extracellular biochemical markers of photochemical oxidant air pollution damage to Norway spruce. Experientia 43, 111–115.

Dalton, D.A., Hanus, F.J., Rusell, S.A., Evans, H.J., 1987. Purification, properties and distribution of ascorbate peroxidase in legume root nodules. Plant Physiol. 83, 789–794.

Dowd, P.F., Herms, D.A., Berhow, M.A., Lagrimini, L.M., 2000. Mechanisms of insect resistance in transgenic plants (over)-expressing a tobacco anionic peroxidase. In: Penel, C., Gaspar, T., Greppin, H. (Eds.), Plant Peroxidase Newsletter: Plant Biochemistry and Physiology. University of Geneva, Geneva, pp. 93–101.

Dunford, H.B., 1999. Heme peroxidase nomenclature. In: Penel, C., Gaspar, T., Greppin, H. (Eds.), Plant Peroxidase Newsletter: Plant Biochemistry and Physiology. University of Geneva, Geneva, pp. 65–71.

Grossman, H., Neville, D.N., 1971. Glycoproteins of cell surfaces. J. Biol. Chem. 246, 6339–6346.

Hiraga, S., Sasaki, K., Ito, H., Ohashi, Y., Matsui, H., 2001. A large family of class III plant peroxidases. Plant Cell Physiology 15, 462–468.

Hiraga, S., Yamamoto, K., Ito, H., Sasaki, K., Matsui, H., Honma, M., Nagamura, Y., Sasaki, T., Ohashi, Y., 2000. Diverse expression profiles of 21 rice peroxidase genes. FEBS Lett. 14 (471), 245–250.

Kim, S.H., Kim, S.S., 1996. Carbohydrate moieties of three radish peroxidases. Phytochemistry 42, 287–290.

Kim, K.Y., Kwon, H.K., Kwon, S.Y., Lee, H.S., Hur, Y., Bang, J.W.,

Choi, K.S., Kwak, S.S., 2000. Differential expression of four sweet potato peroxidase genes in response to abscisic acid and ethephon. Phytochemistry 54, 19–22.

Kuo, C., Fridovich, I., 1988. Stimulation of the activity of horseradish peroxidase by nitrogenous compounds. J. Biol. Chem. 263, 3811–3817.

Laemmli, U.K., 1970. Cleavage of structural proteins during the assembly of the head of bacteriophage T4. Nature 227, 680–685.

Lee, D.J., Kim, S.S., 1998. The regulation of 5′ upstream regions of a Korean radish cationic peroxidase gene by gibberellic acid and abscisic acid. Plant Science 139, 105–115.

Lee, D.J., Kim, S.S., Kim, S.S., 1999. Regulation of the Korean radish cationic peroxidase promoter by phytohormones and other reagents. J. Biochem. Mol. Biol. 32, 51–59.

Lee, D.J., Kim, S.S., Lee, M.Y., 2000. Peroxidase activity boosting by various nitrogenous compounds. J. Biochem. Mol. Biol. 33, 312–316. (formerly Korean Biochem. J.).

Lee, M.Y., Choi, Y., Kim, S.S., 1994. Purification and immunological relationships of six radish isoperoxidases. Plant Physiol. Biochem. 32, 259–265.

Lee, M.Y., Kim, S.S., 1990. Purification and characterization of the far migrating anionic isoperoxidase A_3 from Korean-radish root. Korean Biochem. J. 23, 440–446. (presently J. Biochem. Mol. Biol.).

Lee, M.Y., Kim, S.S., 1993. Essential sulfhydryl residue in radish peroxidase isozyme. Korean Biochem. J. 26, 151–156. (presently J. Biochem. Mol. Biol.).

Lee, M.Y., Kim, S.S., 1994. Characteristics of six isoperoxidases from Korean radish root. Phytochemistry 35, 276–290.

Lee, M.Y., Kim, S.S., 1998a. Characteristics of a low molecular weight minor anionic isoperoxidase A_{3n} from radish. J. Biochem. Mol. Biol. 31, 548–553.

Lee, M.Y., Kim, S.S., 1998b. Inactivation and cleavage of radish peroxidase by various reducing agents. Phytochemistry 49, 23–27.

Lee, S.H., Lee, M.Y., 2000. Plant regeneration of geranium (*Pelargonium graveolense*) callus and changes of peroxidase isozyme pattern. J. Korean. Soc. Agric. Chem. Biotechnol. 43, 184–189.

Lege, B., Ma, S., van Huystee, R.B., 2001. The effects of the site-directed removal of N-glycosylation from cationic peanut peroxidase on its function. Arch. Biochem. Biophys. 1, 17–24.

Mirza, O., Henriksen, A., Ostergaard, L., Welinder, K.G., Gajhede, M., 2000. *Arabidopsis thaliana* peroxidase N: structure of a novel neutral peroxidase. Acta Crystallogr. D Biol. Crystallogr. 56, 372–375.

Morita, Y., Yoshhida, C., Maeda, Y., 1971. Properties and structures of peroxidase isozymes of Japanese radish. Agric. Biol. Chem. 35, 1074–1083.

Ohya, T., Morimura, Y., Saji, H., Mihara, T., Ikawa, T., 1997. Purification and characterization of ascorbate peroxidase in roots of Japanese radish. Plant Science 125, 137–145.

Park, J.H., Kim, S.S., 1996a. Isolation, restriction mapping, and promoter sequence analysis of an isoperoxidase gene from Korean radish, *Raphanus sativus*. J. Biochem. Mol. Biol. 29, 52–57.

Park, J.H., Kim, S.S., 1996b. cDNA cloning and overexpression of an isoperoxidase gene from Korean radish, *Raphanus sativus*. J. Biochem. Mol. Biol. 29, 137–141.

Park, J.H., Lee, S.J., Kim, S.S., 1994. Catalytic and immunological comparison of two cationic isoperoxidases from Korean radish root. Korean Biochem. J. 27, 211–216. (presently J. Biochem. Mol. Biol.).

Raj, S.K., Bi, Y.M., Saxena, P.K., 1997. Somatic embryogenesis and Agrobacterium-mediated transformation system for scented geranium (Pelargonium sp. Frensharm). Planta 201, 434–440.

Shannon, L.M., Kay, E., Lew, J.Y., 1966. Peroxidase isozymes from horseradish roots: 1. Isolation and physical properties. J. Biol. Chem. 241, 2166–2172.

Shaw, G.S., Sun, Y., Barber, K.R., van Huystee, R.B., 2000. Sequence specific analysis of the heterogeneous glycan chain from peanut peroxidase by ^{1}H-NMR spectroscopy. Phytochemistry 53, 135–144.

Tognolli, M., Overney, S., Penel, C., Greppin, H., Simon, P., 2000. A genetic and enzymatic survey of *Arabidopsis thaliana* peroxidases. In: Penel, C., Gaspar, T., Greppin, H. (Eds.), Plant Peroxidase Newsletter: Plant Biochemistry and Physiology. University of Geneva, Geneva, pp. 3–12.

van Huystee, R.B., Cairns, W.L., 1982. Progress and prospects in the use of peroxidase to study cell development. Phytochemistry 21, 1843–1847.

van Huystee, R.B., 1987. Some molecular aspects of plant peroxidase biosynthetic studies. Annu. Rev. Plant Physiol. 38, 205–219.

Yoo, W.I., Kim, S.S., 1988. Purification and characterization of an anionic isoperoxidase from Korean-radish root. Korean Biochem. J. 21, 207–213. (presently J. Biochem. Mol. Biol.).

PERGAMON

Phytochemistry 58 (2001) 865–874

PHYTOCHEMISTRY

www.elsevier.com/locate/phytochem

Ethnopharmacology and bioinformatic combination for leads discovery: application to phospholipase A_2 inhibitors

Philippe Bernard[a,*], Thomas Scior[b], Bruno Didier[c], Marcel Hibert[b], Jean-Yves Berthon[c]

[a]*GREENPHARMA S. A., 1 rue de Chartres, B.P. 6759, 45067 Orléans Cedex 2, France*
[b]*Universidad de las Americas Puebla, 72820 Cholula, Puebla, Mexico*
[c]*Laboratoire de Pharmacochimie de la Communication Cellulaire, UMR CNRS/ULP 7081 Faculté de Pharmacie, 74 route du Rhin, 67400 Illkirch-Graffenstaden, France*

Received 13 November 2000; received in revised form 8 June 2001

Abstract

A program combining ethnopharmacology and bioinformatic approaches has successfully been applied on anti-inflammatory activity. (i) An ethnobotanical study allowed the identification of several plants associated with putative anti-inflammatory properties as potential leads. (ii) On the other hand, it is well known that phospholipase A_2 is a target implicated in the pro-inflammatory process. Thus, (iii) some selected plant extracts were experimentally tested on phospholipase A_2. Finally, (iv) these experimental results combined with bioinformatic tools, such as database exploitation and molecular modeling, allowed to suggest that one compound, betulin and its oxidative form betulinic acid, might be responsible of the anti-PLA_2 activity. This suggestion was confirmed experimentally. © 2001 Elsevier Science Ltd. All rights reserved.

Keywords: Ethnopharmacology; Bioinformatic; Anti-inflammatory; Phospholipase A_2

1. Introduction

A research program aiming at the discovery of 'new leads' (Bernard et al., 1999a), combining ethnopharmacology studies with bioinformatic ones, was initiated to find new molecules implicated in the modulation of inflammation processes. The first step of this program was to define the biomolecular target (enzyme, receptor...). The criteria for the selection of this target were (i) implication of the target in the inflammatory process, (ii) the feasibility of an assay (availability of enzyme sources, completion of the enzymatic tests...) and (iii) the quantity of experimental data available for the bioinformatic treatment. Since the phospholipase A_2 (PLA_2) plays a crucial role in modulating both the cyclooxygenase and the 5-lipoxygenase pathways which are simultaneous pathways of the inflammation process, PLA_2 was found to be the best target.

PLA_2 corresponds to a class of enzymes which catalyze the hydrolysis of membrane glycerophospholipids at the sn-2 position to release fatty acids and lysophospholipids. When the fatty acid is the arachidonic acid, a complementary metabolism leads to pro-inflammatory mediators such as prostaglandins, leukotrienes, thromboxanes and platelet activating factors (PAF) (Irvine, 1982). Thus, modulating pro-inflammatory lipid mediator production by inhibiting PLA_2 activity remains a potential strategy for the development of new drugs for the treatment of inflammatory diseases (Mayer and Marshall, 1993; Posadas et al., 2000; Seno et al., 2001). Nevertheless, the evidence now exists that more than one form of PLA_2 might be found (Mayer and Marshall, 1993; Friess et al., 2001). The first one which corresponds to the low molecular weight (14 kDa) is a Ca^{2+}-dependent extracellular PLA_2. It is found in mammalian pancreases, several snake venoms, human platelets, human placentas, and rheumatoid synovial fluids (Dennis et al., 1991). The second form is represented by a high molecular weight (85 kDa) cytosolic PLA_2 (Clark et al., 1990). The latter, a less known form, will not be used in this bioinformatic study, even if some authors suggested that both the 14 kDa and 85 kDa PLA_2 may be potential targets for the modulation of inflammatory diseases (Mayer and Marshall, 1993).

Since several PLA_2 inhibitors are known, we used them in a recent study, to propose a pharmacophore of

* Corresponding author. Tel.: +33-2-38-49-49-17; fax: +33-2-38-49-49-18.
E-mail address: philippe.bernard@greenpharma.com (P. Bernard).

0031-9422/01/$ - see front matter © 2001 Elsevier Science Ltd. All rights reserved.
PII: S0031-9422(01)00312-0

Table 1
Plant extracts screening on PLA_2 activity

Number	Scientific name	Family	Origin	Part used	Activity of PLA_2 (%)
1	*Abuta grandifolia*	Menispermaceae	South America	Stem	−50
2	*Althaea officinalis*	Malvaceae	Europe	Leaf	0
3	*Astrocaryum vulgare*	Arecaceae	South America	Fruits	30
4	*Baccharis triptera*	Asteraceae	South America	Leaf	−50
5	*Bactris gasipaes*	Arecaceae	South America	Fruits	30
6	*Bowdichia major*	Fabaceae	South America	Seeds	30
7	*Bryophyllum calicinum*	Crassulaceae	South America	Leaf	30
8	*Caraipa minor*	Clusiaceae	South America	Bark	−70
9	*Cariniana brasiliensis*	Lecythidaceae	South America	Bark	0
10	*Cassia hirsuta*	Fabaceae	South America	Leaf	50
11	*Cassia hirsuta*	Fabaceae	South America	Root	50
12	*Cecropia palmata*	Cecropiaceae	South America	Leaf	30
13	*Chenopodium ambrosioides*	Chenopodiaceae	Central America	Leaf	60
14	*Cissus sicyoides*	Vitaceae	South America	Creeper	−20
15	*Costus spicatus*	Zingiberaceae	South America	Leaf	−20
16	*Croton cajucara*	Euphorbiaceae	South America	Bark	30
17	*Detarium microcarpum*	Mimosaceae	Africa	Fruits	0
18	*Dorstenia reniformis*	Moraceae	South America	Plant	−50
19	*Duguetia riparia*	Annonaceae	South America	Bark	0
20	*Entada africana*	Mimosaceae	Africa	Bark	−60
21	*Genipa americana*	Rubiaceae	South America	Bark	−100
22	*Glycoxylon huberi*	Sapotaceae	South America	Bark	−50
23	*Gomphrena macrocephala*	Amaranthaceae	South America	Bark	−10
24	*Himathantus sucuuba*	Apocynaceae	South America	Bark	0
25	*Himathantus sucuuba*	Apocynaceae	South America	Sap	−30
26	*Hura crepitans*	Euphorbiaceae	South America	Bark	−20
27	*Hyptis suaveolens*	Lamiaceae	South America	Plant	0
28	*Jatropha curcas*	Euphorbiaceae	South America	Seeds	30
29	*Leopoldinia imperialis*	Arecaceae	South America	Bark	−70
30	*Leopoldinia imperialis*	Arecaceae	South America	Sap	−80
31	*Luffa operculata*	Cucurbitaceae	South America	Fruits	−20
32	*Macairea viscosa*	Melastomataceae	South America	Sap	−30
33	*Mammea americana*	Clusiaceae	South America	Fruits	−10
34	*Mauritia flexuora*	Arecaceae	South America	Fruits	−30
35	*Maytenus ilicifolia*	Celestraceae	South America	Leaf	−50
36	*Mikania lindleyana*	Asteraceae	South America	Leaf	0
37	*Momordica charantia*	Cucurbitaceae	South America	Plant	−30
38	*Morus alba*	Moraceae	Asia	Leaf	−70
39	*Myrcia sphaerocarpa*	Myrtaceae	South America	Leaf	0
40	*Nymphaea rudgeana*	Nymphaeaceae	South America	Leaf	−50
41	*Ocimum basilicum*	Lamiaceae	South America	Leaf	−50
42	*Ocimum gratissimum*	Lamiaceae	South America	Leaf	0
43	*Orbignya speciosa*	Arecaceae	South America	Seeds	−20
44	*Orbignya speciosa*	Arecaceae	South America	Fruits	−20
45	*Parahancornia fasciculata*	Apocynaceae	South America	Sap	−30
46	*Petiveria alliacea*	Phytolaccaceae	South America	Leaf	−30
47	*Physalis edulis*	Solanaceae	South America	Root	0
48	*Pilocarpus microphyllus*	Rutaceae	South America	Root	30
49	*Piper arboreum*	Piperaceae	South America	Leaf	0
50	*Piper callosum*	Piperaceae	South America	Leaf	0
51	*Platonia insignis*	Clusiaceae	South America	Seeds	−30
52	*Portulaca pilosa*	Portulaceae	South America	Leaf	−20
53	*Prosopis africana*	Mimosaceae	Africa	Bark	−30
54	*Scoparia dulcis*	Scrophulariaceae	South America	Plant	−100
55	*Sesamum indicum*	Pedaliaceae	South America	Seeds	0
56	*Smilax papiracea*	Smilacaceae	South America	Root	70
57	*Struthanthus flexicaulis*	Loranthaceae	South America	Stem	−50
58	*Stryphnodendron barbatimao*	Fabaceae	South America	Seeds	0
59	*Stryphnodendron barbatimao*	Fabaceae	South America	Bark	−30
60	*Terminalia macroptera*	Combretaceae	Africa	Bark	−30
61	*Tynanthus elegans*	Bignonaceae	South America	Stem	−20
62	*Uncaria tomentosa*	Rubiaceae	South America	Leaf	30
63	*Uncaria tomentosa*	Rubiaceae	South America	Bark	30
64	*Vatairea guianensis*	Fabaceae	South America	Seeds	50
65	*Virola surinamensis*	Myristicaceae	South America	Bark	60
66	*Vismia latifolia*	Clusiaceae	South America	Leaf	0
67	*Vitex agnus-castus*	Verbenaceae	Europe	Leaf	−30
68	*Zizyphus joazeiro*	Rhamnaceae	South America	Bark	−70

the human non-pancreatic PLA_2 (Bernard et al., 2001). In this study, we confirmed that an anionic group, such as a carboxylate group, is highly desirable in ligands interacting with this enzyme. We also demonstrated that this anionic group is necessary in both human and bovine pancreatic PLA_2 inhibitors (Pintore et al., 2001). In addition, the analysis of the different crystallized PLA_2/ligand complexes available in the Protein Brookhaven Data Bank (PDB) (http://www.rcsb.org/pdb/) revealed the importance of the phosphate or carboxylate groups in PLA_2 ligands. Indeed, such groups are found to be in interaction with the calcium ion present in the PLA_2 structures.

Among all the PLA_2, one subtype was selected and used as reference in this study: the bovine pancreatic phospholipase A_2 (bp-PLA_2). Indeed, this enzyme presents the double advantage to be crystallized (the three dimensional structure is available and can be used in a bioinformatic study) and to be commercially available to realize enzymatic tests. In addition, the homology between the different phospholipasesA_2 is relatively high and the catalytic site of the different PLA_2 remains similar. Thus, even if some ligands are specific of some PLA_2, the same lead structure can be used for every PLA_2; only pharmaco-modulations will give the specificity. For example, the indole substructure has been used to design PLA_2 inhibitors in both human non-pancreatic PLA_2 and cytosolic PLA_2 (Draheim et al., 1995; Dillard et al., 1996; Lehr, 1997).

We describe the combination between experimental data and bioinformatic data to rationalize a phytochemical lead discovery. The use of our database (Bernard et al., 1999a) containing ethnopharmacological experimental information will allow it to identify the chemical compound responsible for the PLA_2 inhibition, from a plant extract where anti-PLA_2 activity was detected.

2. Results and discussion

2.1. Plants selection and extracts screening on PLA_2 activity

An ethnobotanical study realized in South America (Santarem, Brasilia) allowed the identification of 56 plants used as anti-inflammatory remedies, often used to cure snake and dog bites or rheumatic pains. Six plants from other regions were also selected with the same ethnobotanical properties. Starting from this plant material, 68 extracts were obtained as described in the experimental section and tested for PLA_2 inhibition. The results are listed in Table 1. In this table, the lower the activity value, the better is the inhibitory potency of the corresponding extract. Positive values seem to indicate an activation of the PLA_2 activity. In Table 1, seven plants were found to inhibit more than 50% of the PLA_2 activity. These

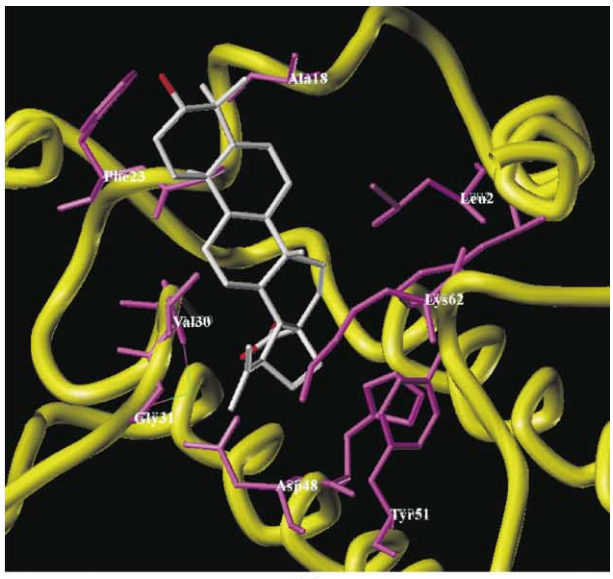

(a)

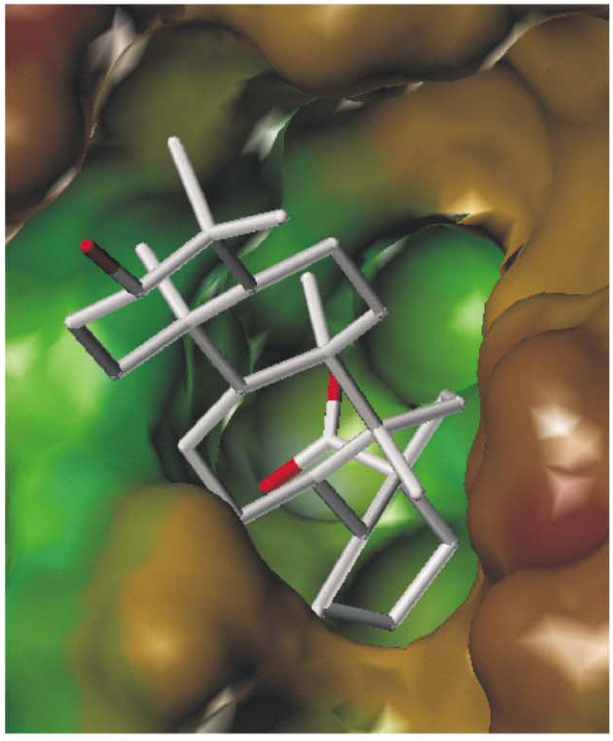

(b)

Fig. 1. Docking of betulinic acid into the binding site of bovine PLA_2. (a) View of the calcium binding site. (b) Representation of betulinic acid inserted into the binding site, described by the lipophilic volume contour. The close define a large lipophilic domains. The carboxylate group, located in the bottom of the cavity, interacts with the calcium atom, not visible in this view.

plants are *Genipa americana* (100% of inhibition), *Scoparia dulcis* (100%), *Leopoldinia imperialis* (70-80%), *Caraipa minor* (70%), *Morus alba* (70%), *Zizyphus joazeiro* (70%) and *Entada africana* (60%).

There is no qualitative and quantitative correlation between the anti-PLA_2 activity of the plant extracts and

the anti-inflammatory ethnopharmacological properties. Two reasons can explain this observation. First, the traditional uses can include some non-appropriate applications. Second, several other biological targets might be responsible for the anti-inflammatory properties of these plants.

2.2. Chemical identification of the anti-PLA_2 activity compound from the selected plant extracts

Different ethnobotanical databases, such as our database (Bernard et al., 1999a), the NAPRALERT database (available from STN International, c/o Chemical Abstracts Service, PO Box 3012, Columbus, OH 43210, USA) and the combined chemical library database (available from CRC Press UK, Pocock House, 235 Southwark Bridge Road, London, SE1 6LY, UK), were used to analyze the known chemical composition of each selected plant. The bibliographic chemical analysis revealed a variable number of chemicals according to each plant; no chemical components are described for *Leopoldinia* whereas more than 60 chemicals are described for *Morus alba*. Interestingly, although all phytochemicals have not yet been identified, the chemical comparison of these selected plants indicates that only one compound, betulinic acid, was present in four plants among the seven: *Scoparia dulcis*, *Caraipa minor*, *Morus alba* and *Zizyphus joazeiro*. Three 'inactive' plants were also described to possess betulinic acid: *Bowdichia*, *Cassia* and *Vismia*, but in bark and not in leave or seeds. These observations suggest that betulinic acid might be responsible of the activity. Moreover, two arguments could be in agreement with this suggestion. First, triterpens have already been described as anti-inflammatory compounds (Recio et al., 1995). Betulinic acid has also been described for numerous biological activities, such as antitumor, antiviral, antimalarial, antiplasmodial activities (Combined chemical library

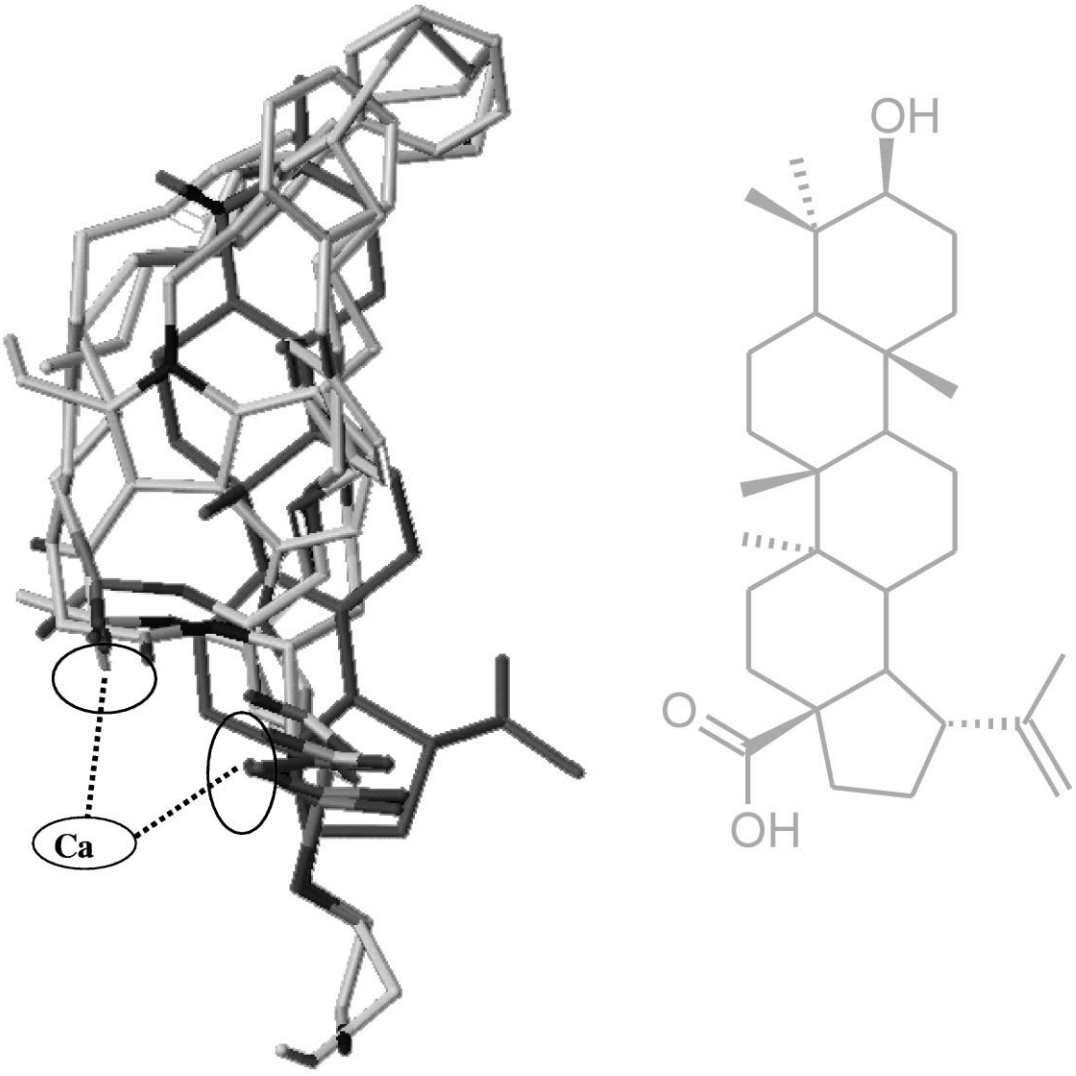

Fig. 2. Protein-based alignment of betulinic acid, in magenta, compared to the other ligands extracted from the crystallographic data. The interactions with the calcium atom are visualized.

database). Second, as mentioned in the experimental section, this compound possesses a carboxylate group as defined by our pharmacophore model of PLA_2.

In order to verify if betulinic acid corresponded to a candidate implicated in the PLA_2 inhibition, this compound was docked into the PLA_2 crystal structure. The docking, presented in Fig. 1, confirms that betulinic acid can be inserted into the PLA_2 binding site with correct energy values. Indeed, the binding energy of betulinic acid into the enzyme binding site is about −90 kcal/mol. This binding energy is in the same order as the binding energies found for the ligand-enzyme complexes extracted from the crystallographic databank PDB and minimized in the same conditions than betulinic acid-PLA_2 complex. For example, the binding energies for the GEL-PLA2 complex and the GLE-PLA2 complex are -85 kcal/mol (backbone rms = 0.17 Å) and −70 kcal/mol (backbone rms = 0.23 Å), respectively. Moreover, Fig. 2 presents the proteine-based alignment of the betulinic acid compared to the four other ligands, described in the experimental section and extracted from their crystal structure PLA_2 complexes. This figure is in agreement with the fact that betulinic acid, well fits to the others ligand structures and occupies the same volume. For indication, betulinic acid represents a cylinder, of about 13 Å long with a diameter of 5 Å, which occupies the place of the natural substrates, the phospholipids.

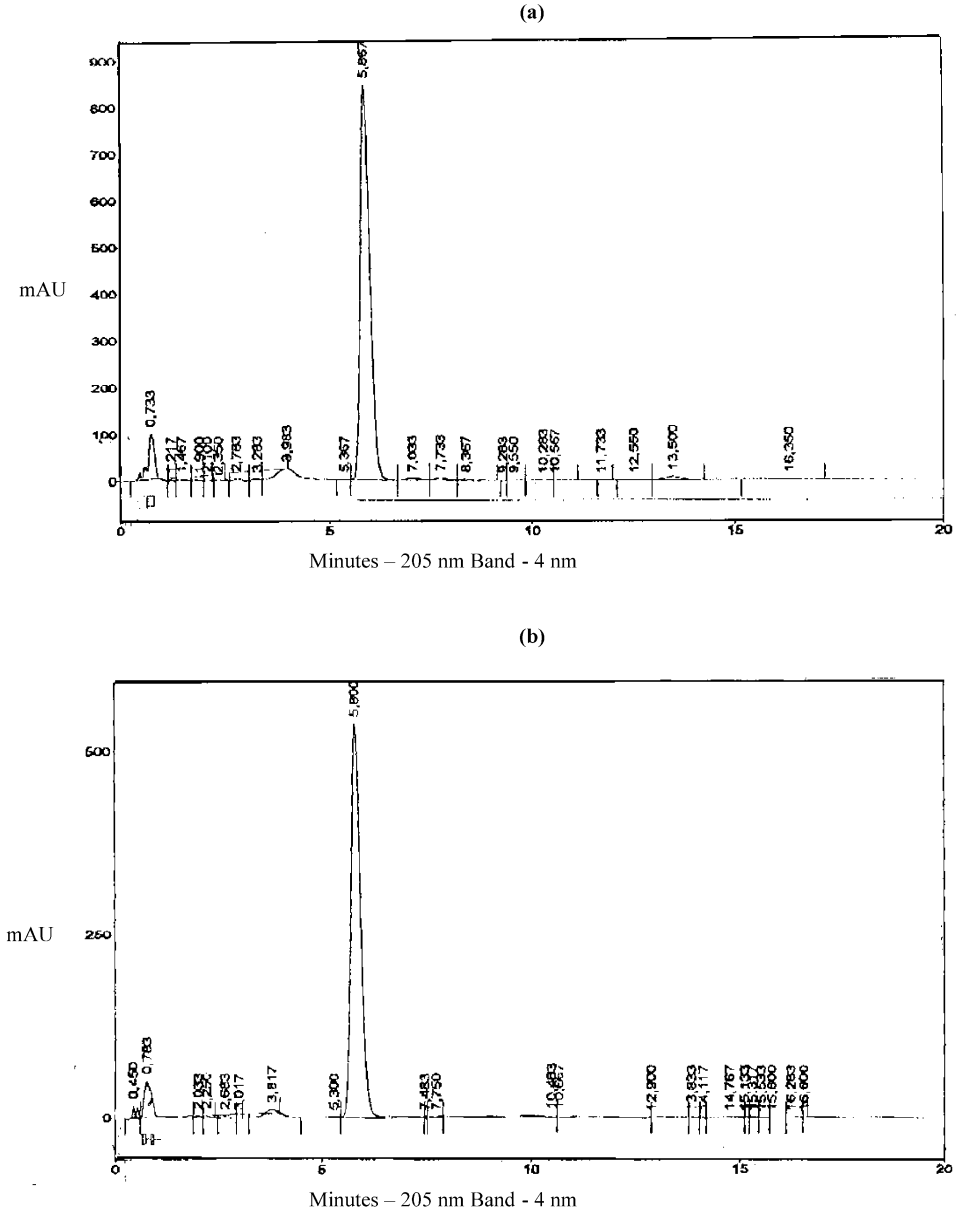

Fig. 3. Comparison of the HPLC profiles of (a) betulin and (b) *Betula alba* triterpenic extract.

Following the bibliographical chemical analysis, three plant extracts, active on anti-PLA_2 activity, were found without betulinic acid. These results suggest that either the presence of betulinic acid was not confirm in these plants, or another chemical is responsible for the biological activity. Nevertheless, among the other described chemicals, no compound was able to be correctly docked into the enzyme binding site. The anti-PLA_2 activity of these plants still remains not elucidated.

2.3. Experimental confirmation that betulinic acid is implicated in the anti-PLA_2 activity

In order to experimentally confirm that betulinic acid is implicated in the anti-PLA_2 activity, we realized an extract of *Betula alba* L. (Betulaceae), which is known to be among the plants richer in betulin and betulinic acid (Bruneton, 1993). The extract, realized as described in the experimental section, was developed to obtain a

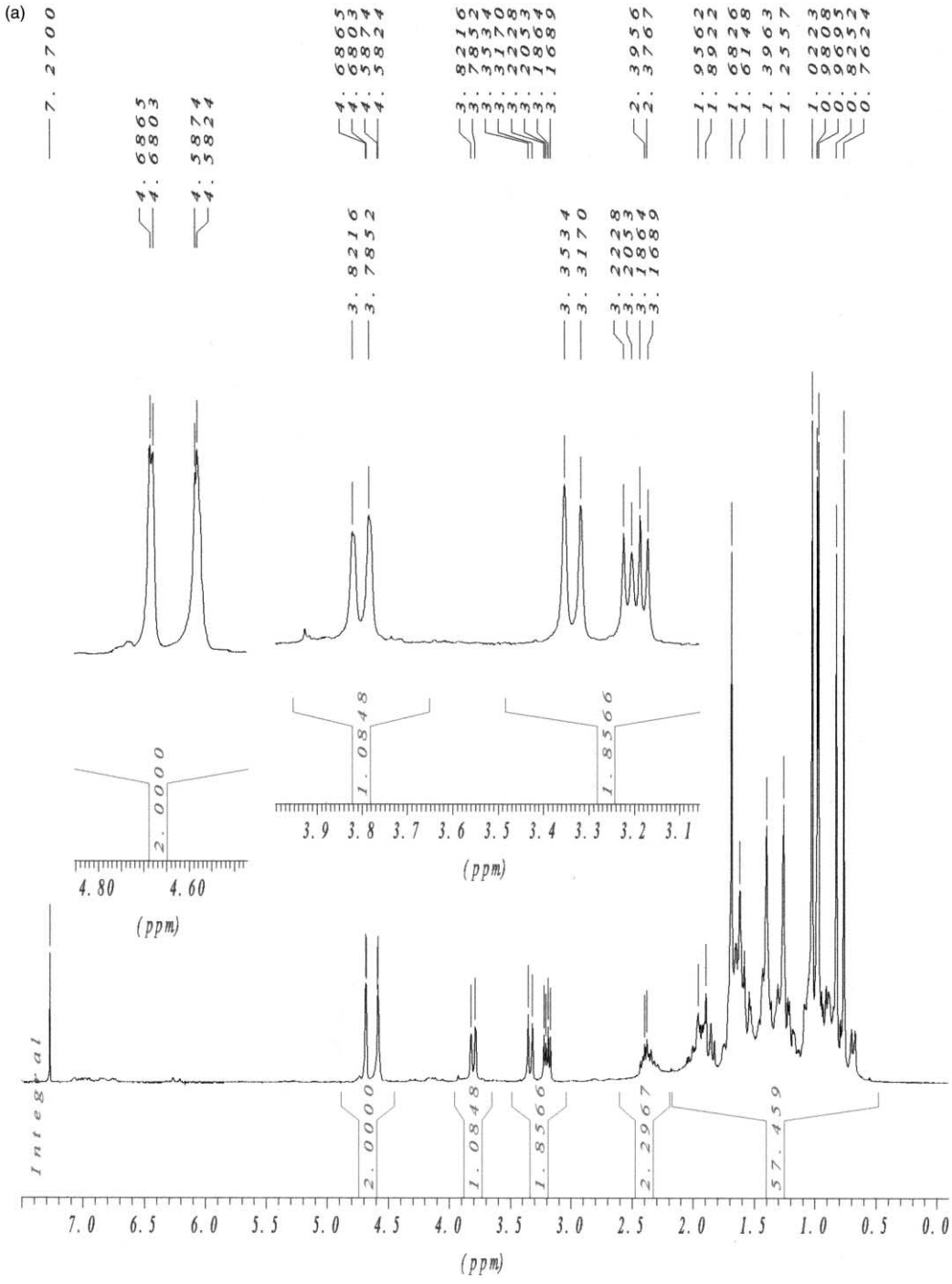

Fig. 4. NMR spectra of *Betula alba* triterpenic extract: (a) [^{1}H] NMR and (b) [^{13}C] NMR.

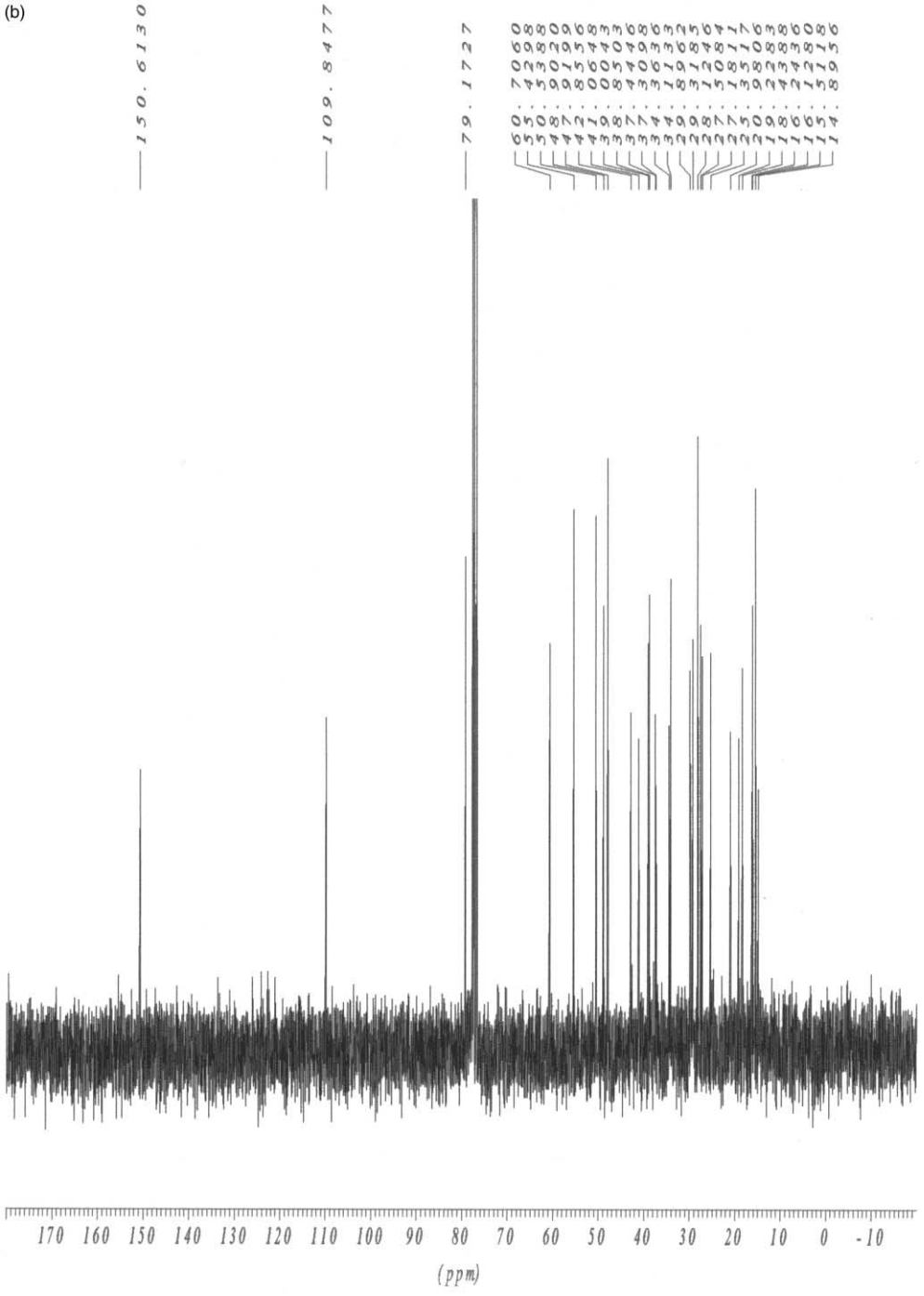

Fig. 4 (*continued*).

larger quantity of triterpens. Interestingly, the characterization by mean of HPLC and NMR analyses revealed that this extract contains essentially betulin, the reduced form of betulinic acid. Then, this extract, betulin and betulinic acid were tested on the PLA_2. The biological results are presented in Table 2. This table confirms that *Betula alba* extract, betulin and betulinic acid have an anti-PLA_2 activity. Moreover, betulinic acid is found to be the better inhibitor of PLA_2. This result is in agreement with our pharmacophore model which describes the importance of a carboxylate group for the inhibition of the PLA_2.

2.4. Conclusion

This study allowed to validate the approach which consists in the combination of the ethnopharmacological domain with the bioinformatic one. Indeed, the experimental data in one hand, combined with the database exploitation and molecular modeling in another hand,

Table 2
PLA_2 inhibitory activity of betulinic acid, betulin and *Betula alba* extract. These standards were dissolved to a concentration of 0.5% (w/v) in 96% (v/v) ethanol. The values indicate the percent of inhibition at a given concentration

Final volume and corresponding concentration added in the anti-PLA_2 assay	Inhibition of PLA_2 (%)		
	Betulinic acid	Betulin	*Betula alba* extract
200 µl (~2.5 µM)	30	15	10
400 µl (~5 µM)	40	30	30

allowed to identify one compound implicated in the anti-PLA_2 activity.

This approach will be more and more efficient and precise with the growing number of phytochemical data.

3. Experimental

3.1. Plant materials

All plants and their ethnobotanical information were obtained from the Greentech company via its network, which has a permit (permission No: 1/41/94/0084-0, Health Ministry: 101656-2) for collecting and exporting plant materials from Brazil. A collection of voucher specimens is available within the Greentech company.

3.2. Plant extracts

All plant extracts were realized in the same conditions: each plant extract, listed in Table 1, was prepared with 10% of dried plant organs mixed during 20 min in a solution of propylene glycol/deionized water 50 °C. Then, the final plant extracts were obtained after filtration.

3.3. Extraction purification and characterization methods

Triterpens were extracted from *Betula alba* as described hereafter (patent in record). The dried bark of *Betula alba* (3 kg) was crushed and mixed at room temperature (12 h) with toluene (1/1). After impregnation, the bark was mixed with toluene (1:5) at 111 °C during 8 h. The solution was filtrate and after evaporation, a second extraction in the same condition was realized. The obtained dry extract was now mixed at 40 °C with an ethanol solution 99° (1:10). The triterpenic extract was finally obtained by filtration and concentration under vacuum to give a residue (90 g) which was subjected to chemical analyses.

Twenty microlitres of a solution 1.5 mg/ml of the triterpenic extract was submitted to isocratic HPLC analysis, acetonitrile/water: 78/22. A column purospher RP 18 and 5 µm 125×4 mm was used. The detection at 205 nm reveals a major peak at 5.80 mn (Fig. 3). Since betulin possesses the same HPLC profile is these conditions, the peak was identified as being betulin.

To confirm this hypothesis, a NMR study of the triterpenic extract was realized. [^{1}H] and [^{13}C] NMR spectra were performed as following. Each reference substance (10 mg), betulin and betulinic acid, purchased by Sigma-Aldrich was dissolved in 0.7 ml of $CDCl_3$. Spectra were recorded on a DPX Avance 300 Bruker using standard parameters. Spectra analyses of the *Betula alba* extract are shown in Fig. 4: (a) [^{1}H] NMR in $CDCl_3$ of the *Betula alba* extract shows typical peaks of betulin at $\delta = 4.68$ and 4.58 ppm (*d*, 1H, $J = 1.7$ Hz, $=CH_2$), 3.80 and 3.33 ppm (*d* 1H, $J = 10.9$ Hz, CH_2OH), 3.19 ppm (*dd*, 1H $J = 5.3$, 10.9 Hz, C*H*OH) and no signals after 7.00 ppm, sign of the lack of acidic proton, as in case of betulinic acid. (b) This is confirmed with the [^{13}C] NMR in $CDCl_3$. Indeed, no acid carbon were detected but an alcoholic carbon is recorded at 60.7 ppm. Thus, the [^{1}H] NMR and the [^{13}C] NMR, in agreement with the chromatographic data, clearly demonstrate the presence of pure betulin in this *Betula alba* extract.

3.4. Compounds

Betulin and betulinic acid were purchased from Sigma-Aldrich. These molecules were used as reference compounds. The standards were dissolved to a concentration of 0.5% (w/v) in 96% (v/v) ethanol.

3.5. Enzymatic tests on PLA_2

Bovine pancreatic PLA_2 and lecithin were purchased from Sigma Chemical Co. PLA_2 activity was determined by titrimetric method according to the Sigma procedure. Briefly, a mixture, which contains 10 ml of a lecithin solution 2% prepared according to the Sigma procedure, is maintained at pH = 8 by addition of a solution 10 mM NaOH until pH stabilization (pH variation does not exceed 0.01 pH unit/mn). 200 µl of a bp-PLA_2 solution 2,5 units/ml, with or without 400 µl of a solution containing either plant extract or inhibitor compound, is added to the mixture. The inhibitory effect is recorded by measuring the quantity of NaOH added to the total mixture to maintain the pH = 8.

The percent inhibition of PLA_2 activity is calculated as follows:

$$\% \text{ Inhibition} = [(A - B)/A] \times 100$$

where A = [NaOH] added in the sample without plant extract or inhibitor and B = [NaOH] added in the sample with plant extract or inhibitor.

3.6. Bioinformatic section

3.6.1. Enzyme

Since the inhibitory activities used in the experimental section were measured on the bovine pancreatic PLA_2, crystal structure of bovine pancreatic PLA_2 were used in the modeling section.

Many bovine pancreatic PLA_2 have been crystallized and are available in the PDB. Nevertheless, only bp-PLA_2-ligand complexes were selected because they include a 'pocket', near the site active, able to receive more easily the inhibitor ligands. Thus, only four structures were selected: PDB code: 1BP2 (Dijkstra et al., 1981), 1FDK (Sekar et al., 1997), 1MKV (Sekar et al., 1998) and 3BP2 (Dijkstra et al., 1984). The four ligands associated to bovine structures are respectively, (i) 2-methyl-2,4-pentanediol (MPD) (PDB code: 1BP2), (ii) 1-decyl-3-trifluoro ethyl-*sn*-glycero-2-phosphomethanol (GLE) (PDB code: 1FDK), (iii) L-1-*o*-octyl-2-heptylphosphonyl-*sn*-glycero-3-phosphoethanolamine (GEL) (PDB code: 1MKV) and (iv) pyruvoil group (PVL) (PDB code: 3BP2). Amidst the bp-PLA_2 complexed structures, the 1MKV complex was chosen because the GEL is the biggest ligand of the series. Thus, the opening of the binding site is maximal with this ligand. Furthermore, it binds the Ca^{2+} ion of the active site as a bidentante ligand, with a mechanism similar to the other ligands-PLA_2 complexes (Schevitz et al., 1995). Moreover, it has been demonstrated that this binding region is a pharmacophore element of different types of PLA_2 (Bernard et al., 2001; Pintore et al., 2001).

To make the selected structure suitable for further modeling, water molecules were removed and hydrogen atoms were added to the original PDB structures using the BIOPOLYMER module of Sybyl/Tripos (Sybyl is available from Tripos Associates, 1699 South Hanley Road, St Louis, MO 63144). Then the geometry of the protein was optimized using the Tripos Force Field with a gradient convergence of 0.01 kcal/mol and with the Kollman charges, implemented in the Sybyl package, as electrostatic component.

3.6.2. Ligands

The ligands were modeled using Sybyl 6.5 on a Silicon Graphics O_2 R10000 station. The starting conformations were optimized by molecular mechanics algorithm using the Tripos Force Field. The lowest energy conformations were found by means of the SYBYL/SEARCH option and then used as initial conformations for docking. The charges were calculated by the MOPAC AM1 semi-empirical method.

3.6.3. Ligand-enzyme docking

In our previous papers (Bernard et al., 2001; Pintore et al., 2001), we had identified the importance of an acidic region on the pharmacophore of the PLA_2 inhibitors. Indeed, this pharmacophoric element interacts with the calcium atom inserted in the enzyme structure. Therefore, the priority, for the identification of new natural inhibitors of PLA_2, was the presence of this carboxylate group. Then, the FIT ATOMS option of Sybyl allowed to place the carboxyl group of the selected ligands into the enzyme, prepared as mentioned above, at the position corresponding to the GEL phosphoryl group. Since GEL bounds the calcium atom by means of two oxygen atoms, the two GEL oxygen atoms were successively used as the anchor point. The molecule was then rotated around the three coordinate axis as previously described (Bernard et al., 1999b) with a step of 30°. For each orientation a complete conformational search was made using the SYBYL/SYSTEMATIC SEARCH option. All rotatable bonds were relaxed and the rotation step was also fixed at 30°. The total energy of the enzyme-ligand complex was calculated for each conformation generated. The geometry of the lowest energy conformations found for the enzyme-ligand complexes was then refined by further spatial rotations and conformational search with a step of 5° in the interval of ±30° around the torsion values obtained. These refined enzyme-ligand complexes were optimized using the Tripos Force Field with a gradient convergence of 0.01 kcal/mol. An approximation of the binding energy E_{int} resulting from the ligands binding into the enzyme active site is calculated as follow:

$$E_{int} = E_{complex} - (E_{enzyme} + E_{inhibitor})$$

where $E_{complex}$, E_{enzyme} and $E_{inhibitor}$ are the energies of the minimized complex, the enzyme of the complex and the inhibitor extracted from the complex, respectively.

References

Bernard, P., Berthon, J.-Y., Chretien, J.R., 1999a. Computer-aided molecular selection and design of natural bioactive molecules. Curr. Opin. Drug Disc. Develop. 2, 213–223.

Bernard, P., Kireev, D.B., Chretien, J.R., Fortier, P.-L., Coppet, L., 1999b. Automated docking of 82 *N*-benzylpiperidine derivatives to mouse acetylcholinesterase and comparative molecular field analysis with 'natural' alignment. J. Comput.-Aided Mol. Des. 13, 355–371.

Bernard, P., Pintore, M., Berthon, J.-Y., Chretien, J.R., 2001. A molecular modeling and 3D QSAR study of a large series of indole inhibitors of human non-pancreatic secretory phospholipase A_2. Eur. J. Med. Chem. 36, 1–19.

Bruneton, J., 1993. Pharmacognosie, Phytochimie-Plantes Médicinales, 2nd Edition. Technique et Documentation, Lavoisier.

Clark, J.D., Milona, N., Knopf, J.L., 1990. Purification of a 110-kilodalton cytosolic phospholipase A_2 from the human monocytic cell line U937. Proc. Nat. Acad. Sci. USA 87, 7708–7712.

Dennis, E.A., Rhee, S.G., Billah, M.M., Hannun, Y.A., 1991. Role of phospholipase in generating lipid second messengers in signal transduction. FASEB J. 5, 2068–2077.

Dijkstra, B.V., Kalk, K.H., Hol, H.W.J., Drenth, J., 1981. Structure of bovine pancreatic phospholipase A_2 at 17. A resolution. J. Mol. Biol. 147, 97–123.

Dijkstra, B.V., Kalk, K.H., Hol, H.W.J., Drenth, J., de Haas, G.H., Egmond, M.R., Slotboom, A.J., 1984. Role of the N-terminus in the interaction of pancreatic phospholipase A_2 with aggregated substrates. Properties and crystal structure of transaminated phospholipase A_2. Biochemistry 23, 2759–2766.

Dillard, R.D., Bach, N.J., Draheim, S.E., Berry, D.R., Carlson, D.G., Chirgadze, N.Y., Clawson, D.K., Hartley, L.W., Johnson, L.M., Jones, N.D., McKinney, E.R., Mihelich, E.D., Olkowski, J.L., Schevitz, R.W., Smith, A.C., Snyder, D.W., Sommers, C.D., Wery, J.-P., 1996. Indole inhibitors of human nonpancreatic secretory phospholipase A_2. 1. Indole-3-acetamides. J. Med. Chem. 39, 5119–5136.

Draheim, S.E., Hartley, L.W., Jones, N.D., Mihelich, E.D., Olkowski, J.L., Snyder, D.W., Sommers, C., Wery, J.-P., 1995. Structure-based design of the first potent and selective inhibitor of human non-pancreatic secretory phospholipase A_2. Nat. Struct. Biol. 2, 458–465.

Friess, H., Shrikhande, S., Riesle, E., Kashiwagi, M., Baczako, K., Zimmermann, A., Uhl, W., Buchler, M.W., 2001. Phospholipase A_2 isoforms in acute pancreatitis. Ann. Surg 233, 204–212.

Irvine, R.F., 1982. How is the level of free arachidonic acid controlled in mammalian cells? Biochem. J. 204, 3–16.

Lehr, M., 1997. Synthesis, biological evaluation, and structure-activity relationships of 3-acylindole-2-carboxylic acids as inhibitors of the cytosolic phospholipase A_2. J. Med. Chem. 40, 2694–2705.

Mayer, R.J., Marshall, L.A., 1993. New insights on mammalian phospholipase A_2(s); comparison of arachidonoyl-selective and-nonselective enzymes. FASEB J. 7, 339–348.

Pintore, M., Bernard, P., Berthon, J.-Y., Chretien, J.R., 2001. Protein-based alignment in 3D QSAR of 26 indole inhibitors of human pancreatic phospholipase A_2. Eur. J. Med. Chem. 36, 21–30.

Posadas, I., Terencio, M.C., De Rosa, S., Paya, M., 2000. Cavernolide: a new inhibitor of human $sPLA_2$ sharing unusual chemical features. Life Sci. 67, 3007–3014.

Recio, M., Giner, R.M., Manez, S., Gueho, J., Julien, H.R., Hostettmann, K., Rios, J.L., 1995. Investigations on the steroidal anti-inflammatory activity of triterpenoids from *Diospyros leucomelas*. Planta Med. 61, 9–12.

Schevitz, R.W., Bach, N.J., Carlson, D.G., Chirgadze, N.Y., Clawson, D.K., Dillard, R.D., Draheim, S.E., Hartley, L.W., Jones, N.D., Mihelich, E.D., Olkowski, J.L., Snyder, D.W., Sommers, C., Wery, J.-P., 1995. Structure-based design of the first potent and selective inhibitor of human non-pancreatic secretory phospholipase A_2. Nat. Struct. Biol. 2, 458–465.

Sekar, K., Eswaramoorthy, S., Jain, M.K., Sundaralingam, M., 1997. Crystal structure of the complex of bovine pancreatic phospholipase A_2 with the inhibitor 1-hexadecyl-3-(trifluoroethyl)-sn-glycero-2-phosphomethanol. Biochemistry 36, 14186–14191.

Sekar, K., Kumar, A., Liu, X., Tsai, M.D., Gelb, M.H., Sundarilingam, M., 1998. Structure of the complex of bovine pancreatic phospholipase A_2 with a transition-state analogue. Acta Crystallogr. D Biol. Crystallogr. 54, 334–341.

Seno, K., Okuno, T., Nishi, K., Murakami, Y., Yamada, K., Nakamoto, S., Ono, T., 2001. Pyrrolidine inhibitors of human cytosolic phospholipase A_2. Part 2: synthesis of potent and crystallized 4-triphenylmethylthio derivative 'pyrrophenone'. Bioorg. Med. Chem. Lett. 26, 587–590.

PERGAMON

Phytochemistry 58 (2001) 875–881

PHYTOCHEMISTRY

www.elsevier.com/locate/phytochem

Biosynthesis of thiophenes in *Tagetes patula*

Lilla Margl[a,b,1], Wolfgang Eisenreich[c,*], Petra Adam[c], Adelbert Bacher[c], Meinhart H. Zenk[a]

[a]*Biozentrum-Pharmazie, Universität Halle, Weinbergweg 22, D-06120 Halle/Saale, Germany*
[b]*Department of Plant Anatomy, Eotvos Lorand University of Sciences, Puskinstv. 11-13, H-1088 Budapest, Hungary*
[c]*Lehrstuhl für Organische Chemie und Biochemie, Technische Universität München, Lichtenbergstr. 4, D-85747 Garching, Germany*

Received 16 July 2001; received in revised form 3 August 2001

Abstract

The biosynthesis of 5-(3-buten-1-ynyl)-2,2′-bithiophene was studied in root cultures of *Tagetes patula*. Organ cultures were grown with [U-$^{13}C_6$]glucose or [1-^{13}C]glucose. The bithiopene and amino acids from cell protein were isolated and analysed by quantitative NMR spectroscopy. Retrobiosynthetic analysis establish acetyl-CoA or a closely related compound (e.g. malonyl-CoA) as building blocks and their orientations in the bithiophene. The data confirm a previously suggested biosynthetic route via long-chain fatty acids and polyacetylenes. However, a polyketide-like biosynthesis via a carbocyclic intermediate cannot be excluded. © 2001 Elsevier Science Ltd. All rights reserved.

Keywords: Thiophene; Biosynthesis; Retrobiosynthetic analysis; NMR spectroscopy; Metabolic network; *Tagetes*

1. Introduction

A naturally occurring thiophene derivative, α-terthiophene, was isolated in 1947 from *Tagetes erecta* (Zehmeister and Sease, 1947). In the meantime, more than 150 thiophene-type natural products comprising one, two, or three thiophene rings and side chains with a variable number of double or triple bonds (Bohlmann and Zdero, 1985; Kagan, 1991) have been characterized from Asteraceae and fungi (Sörensen, 1977; Bohlmann, 1988).

In *Tagetes* species, bi- or trithiophenes with 12 carbon atoms are predominant (Bohlmann et al., 1973). Oleic acid has been proposed to serve as precursor in thiophene biosynthesis via acetylene intermediates; cysteine has been proposed to serve as sulphur source (Bohlmann et al., 1973; Jente et al., 1981, 1988; Bohlmann, 1988; Menelaou et al., 1991; Arroo et al., 1995). Labelling experiments were hampered by low isotope incorporation rates ($<1\%$).

Isotope incorporation studies are commonly interpreted as if metabolism proceeded in a linear and unidirectional fashion. Based on this implicit assumption, the diversion of isotope from a given precursor to a given target compound is accepted as evidence for direct metabolic relatedness between the respective molecular species. In reality, however, metabolism is a complex network, and metabolic flux can occur from any node in the network to virtually any other node. As a consequence, isotope incorporation studies have repeatedly resulted in remarkable errors of interpretation, especially in the case of low incorporation rates.

Recently, relatively fail-safe alternatives using general ^{13}C labelled precursors, such as glucose or acetate, have been developed for the quantitative assessment of carbon flux in bacteria and suspension cultures of plant cells (for review, see Eisenreich and Bacher, 2000). Briefly, the isotopomer composition of metabolites in biosynthetic sinks (e.g., amino acids) can be used to reconstruct the isotopomer pattern of central metabolic intermediates (e.g., acetyl-CoA, phosphoenolpyruvate, pyruvate, hydroxyethyl-TPP) on a retrobiosynthetic basis. These labelling patterns can then be used to predict labelling patterns of secondary metabolites via hypothetical biosynthetic pathways. Predictions can be verified or falsified by comparison with the observed labelling patterns of secondary metabolites. Moreover,

* Corresponding author. Tel.: +49-89-289-13043; fax: +49-89-289-13363.
E-mail address: wolfgang.eisenreich@ch.tum.de (W. Eisenreich).
[1] Present address: Research Institute for Medicinal Plants, Lupaszigetistr. 4, H-2011 Budakalász, Hungary.

0031-9422/01/$ - see front matter © 2001 Elsevier Science Ltd. All rights reserved.
PII: S0031-9422(01)00360-0

the labelling patterns reveal quantitative aspects of carbon flux and transport in the metabolic network of the organism under investigation.

This paper describes the incorporation of [U-$^{13}C_6$]- and [1-^{13}C]glucose by root cultures of *Tagetes patula*. Retrobiosynthetic analysis of amino acids is used to quantitatively establish the flux of carbon from glucose into 5-(3-buten-1-ynyl)-2,2′-bithiophene (BBT, **1**, Fig. 1).

2. Results and discussion

2.1. NMR signal assignments

Since retrobiosynthetic NMR studies are dependent on correct NMR signal assignments, the reported ^{13}C NMR signal assignments of [5-(3-buten-1-ynyl)-2,2′-bithiophene (BBT, **1**, Fig. 1) (Menelaou et al., 1991) were confirmed by INADEQUATE spectroscopy of multiply ^{13}C-labeled samples (from the incorporation experiment with totally ^{13}C-labeled glucose) (Table 1).

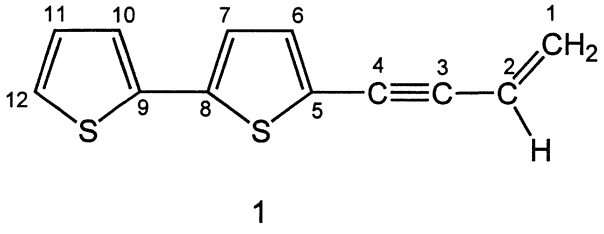

1

Fig. 1. Structure of 5-(3-buten-1-ynuyl)-2,2′-bithiophene (BBT, **1**).

2.2. Incorporation experiments

Root cultures of *Tagetes patula* described in this study produced [5-(3-buten-1-ynyl)-2,2′-bithiophene (BBT, **1**, Fig. 1) at 8.5 mg per g of dry cell mass.

Preliminary incorporation experiments using isotope labelled acetate samples as precursors revealed incorporation rates into BBT well below 1% (data not shown) in accordance with published data (Menelaou et al., 1991). The low enrichments might reflect poor uptake rates of the proffered potential precursors, or poor utilization of exogenous acetate for cell metabolism in root cells of *Tagetes*.

In order to quantitatively establish the carbon flux from a general carbon source into thiophenes, we decided to use ^{13}C-labelled glucose as precursor. The organ culture could be grown in medium containing glucose instead of sucrose without loss of viability or thiophene production. The root cells were, therefore, grown in medium containing a mixture of [U-$^{13}C_6$]glucose or [1-^{13}C]glucose and natural abundance glucose at ratios of 1:10 or 1:2, respectively (w/w). After 13 days, the cells were harvested. BBT was isolated and analysed by quantitative NMR spectroscopy as described in the Experimental Section.

All ^{13}C NMR signals of BBT from the experiment with [U-$^{13}C_6$]glucose are shown in Fig. 2. Quaternary atoms show low intensities due to their relaxation behaviour. The average ^{13}C abundance of all carbon atoms determined as described under Experimental was 12.1±0.9% ^{13}C (Table 1). With the exception of C-1 and C-12, carbon signals showed relatively intense satellites indicative of ^{13}C–^{13}C coupling via one bond (coupling constants, 50–110 Hz, Table 1). The relative

Table 1
NMR data of BBT isolated from root cultures of *T. patula*

Position	Chemical shifts, ppm		Coupling constants, Hz		Precursors			
	δ^{13}C	δ^{1}H	J_{HH}	J_{CC}	[1-^{13}C]glucose		[U-$^{13}C_6$]glucose	
					% ^{13}C[a]	%^{13}C	%^{13}C^{13}C[b]	INADEQUATE
1	126.96	5.71, 5.53	17.5, 2.0, 11.2, 2.0	71.9	9.2	12.6	10.0	
2	116.81	6.01	17.5,11.3	89.0	1.6	11.1	73.6	3
3	92.94			89.0	7.9	10.9	76.9	2
4	83.21			106.8	1.0	11.8	76.9	5
5	121.77			106.8	10.0	13.4	75.5	4
6	132.81	7.08	3.8	59.1	1.4	11.7	74.8	7
7	123.51	7.01	3.8	59.0	9.1	12.1	73.7	6
8	138.99			71.4	1.1	11.8	71.2	9
9	136.69			71.4	11.6	14.3	77.6	8
10	124.24	7.16	3.8	57.4	1.5	11.8	74.3	11
11	127.92	7.00	3.7,5.0	57.4	9.5	11.4	75.4	10
12	125.00	7.21	5.1	61.9	1.5	12.1	11.1	

[a] ^{13}C abundance.

[b] Relative fractions of ^{13}C-coupled satellites in the overall signal intensity of a given atom.

fractions of satellite signals in the global ^{13}C NMR signal intensities of all atoms except for C-1 and C-12 was 75.0±1.9%. The signals of C-1 and C-12 showed satellites of much lower relative intensities (10.0 resp. 11.1%) reflecting ^{13}C–^{13}C coupling caused by statistical recombination of ^{13}C labelled precursor units.

BBT isotopomers derived from the analysis of carbon–carbon coupling constants (Table 1) as well as from a two-dimensional INADEQUATE experiments (Table 1, Fig. 3) are summarized in Fig. 4A. The figure represents a superposition of five $^{13}C_2$-isotopomers. The numbers in Fig. 4A indicate the relative fractions of each respective isotopomer. No isotopomers with more than two adjacent ^{13}C atoms were detected at significant abundance. It follows that the $^{13}C_6$-labelled glucose precursor had been converted into $^{13}C_2$-fragments prior to incorporation into the thiophene.

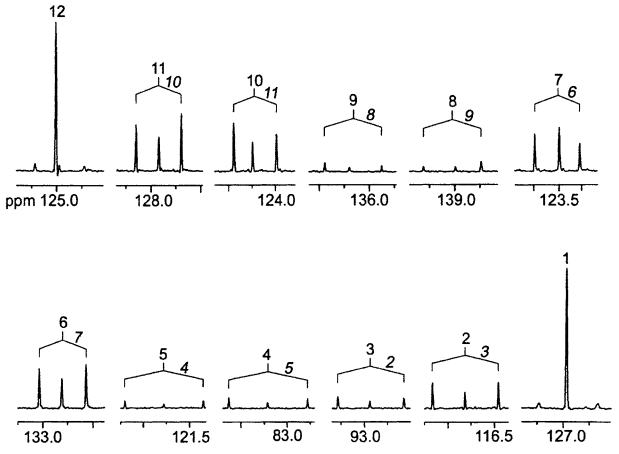

Fig. 2. ^{13}C NMR signals of BBT from the experiment with [U-$^{13}C_6$]glucose. ^{13}C-coupling patterns are indicated. Numbers in italics indicate carbon atoms ^{13}C-coupled to the respective index atoms.

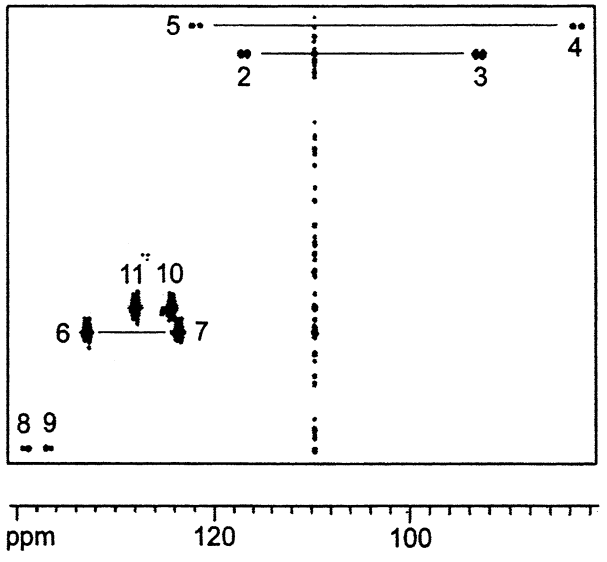

Fig. 3. Two-dimensional INADEQUATE spectrum of BBT from the experiment with [U-$^{13}C_6$]glucose.

The experimentally determined isotope distribution of BBT from the experiment with [1-^{13}C]glucose as precursor is summarized in Table 1 and Fig. 4B. From [1-^{13}C]glucose, six carbon atoms of BBT acquired ^{13}C enrichment with an average ^{13}C abundance of 9.6±1.2% ^{13}C, whereas six positions had ^{13}C abundances of 1.3±0.3% ^{13}C, i.e. in the natural abundance range (Table 1, Fig. 4B).

2.3. Analysis of labelling patterns by the retrobiosynthetic approach

Biosynthetic hypotheses can be subjected to a rigorous test via prediction of BBT labelling patterns from labelling patterns of putative biosynthetic precursors. These can be derived in turn from experimentally determined labelling patterns of amino acids by retrobiosynthetic analysis which has been reviewed recently (Eisenreich and Bacher, 2000).

The labelling patterns of phenylalanine (**2**), leucine (**4**), and valine (**6**) obtained by hydrolysis of cell mass from the experiment with [U-$^{13}C_6$]glucose are shown in Fig. 5. The side chain of phenylalanine reflects the labelling pattern of phosphoenol pyruvate (**3**) from which it is biosynthetically obtained via the shikimate pathway of aromatic amino acid biosynthesis. As a result, phosphoenol pyruvate (**3**) acquired contiguous ^{13}C-labelling from [U-$^{13}C_6$]glucose via glycolytic degradation. Notably, the presence of a significant fraction of [2,3-$^{13}C_2$]phosphoenol pyruvate signalled its biosynthetic origin (approximately 25% of phosphoenol pyruvate biosynthesized during the feeding period) via a

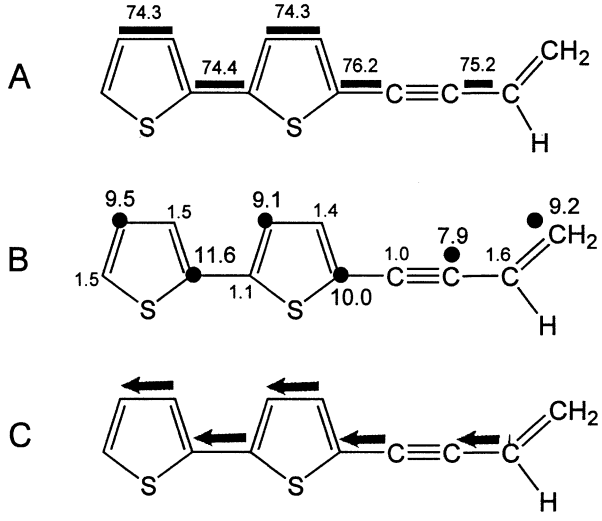

Fig. 4. (A) ^{13}C-labelling patterns of BBT from the experiment with [U-$^{13}C_6$]glucose. Bold lines indicate $^{13}C_2$-labelled isotopomers and numbers indicate their relative abundance (see Experimental). (B) ^{13}C-labelling patterns of BBT from the experiment with [1-^{13}C]glucose. Filled circles indicate significantly ^{13}C-enriched atoms. Numbers indicate ^{13}C abundance in%. (C) Orientation of the acetate precursor units is symbolised by bold arrows directed from C-1 to C-2.

triose phosphate processed in the reductive branch of the pentose phosphate cycle.

The labelling pattern of plastidic acetyl-CoA (**5**), and that of hydroxyethyl-TPP (''activated acetaldehyde'', **7**) can be extracted from the labelling patterns of leucine (**4**) and valine (**6**) on basis of the unique leucine and valine biosynthetic pathways which are assumed to proceed in the plastidic compartment of the plant cell. As a result, significant fractions of [U-$^{13}C_2$]acetyl-CoA and [U-$^{13}C_2$]hydroxyethyl-TPP were detected (Fig. 5). There is no evidence for the formation of singly ^{13}C-labelled isotopomers of acetyl-CoA or hydroxyethyl-TPP from [U-$^{13}C_6$]glucose. Obviously, the doubly ^{13}C-labeled isotopomers in **5** and **7** were generated from a plastidic triose phosphate pool via decarboxylation of pyruvate. In keeping with this hypothesis, the ''bond labelling'' between C-1 and C-2 of acetyl-CoA (**5**) and hydroxyethyl-TPP (**7**) closely resembles the ^{13}C-connectivity between C-2 and C-3 of phosphoenolpyruvate (**3**, Fig. 5).

The observed labelling pattern in BBT implies biosynthetic precursors with only two contiguous ^{13}C atoms (Fig. 4A). The labelling pattern of the two-carbon building block can be reconstructed accurately from the labelling pattern of BBT as shown by the standard deviations (Fig. 6A). The reconstructed labelling pattern of acetyl-CoA from leucine closely matches the labelling pattern of the two-carbon building block in the thiophene derivative indicating its biosynthetic origin via plastidic acetyl-CoA. This result clearly suggests a polyketide origin of BBT (**1**) either anabolically from acetate units or catabolically from a preformed fatty acid such as oleic acid by partial degradation.

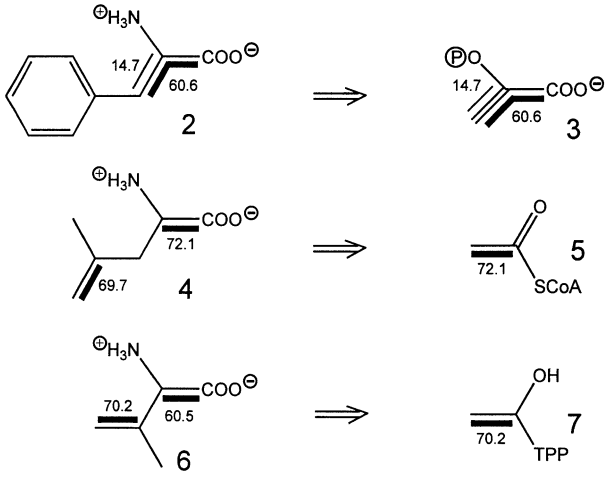

Fig. 5. Incorporation experiment with [U-$^{13}C_6$]glucose. Reconstruction of the labelling patterns of phosphoenol pyruvate (**3**), acetyl-CoA (**5**), and hydroxyethyl-TPP (**7**) from the labelling patterns of phenylalanine (**2**), leucine (**4**), and valine (**6**), respectively. Bold lines indicate multiple ^{13}C-labelled isotopomers and numbers indicate their relative abundance. The isotopomer composition of the aromatic ring of phenylalanine could not be determined due to signal overlapping.

The same retrodictive/predictive approach can be applied for the experiment with [1-^{13}C]glucose. The labelling patterns of phenylalanine, leucine, valine, and their precursors phosphoenol pyruvate, acetyl-CoA, and hydroxyethyl-TPP (obtained by retrobiosynthetic analysis) are shown in Fig. 7. Briefly, [1-^{13}C]glucose is converted into [3-^{13}C]phosphoenol pyruvate, [2-^{13}C]acetyl-CoA, and [2-^{13}C]hydroxyethyl-TPP by the mechanisms described above. Similar labelling patterns were observed in incorporation experiments using [1-^{13}C]glucose in various plants and plant cell cultures (Eichinger et al., 1999; Eisenreich et al., 1999; Goese et al., 1999; Werner et al., 1999; Wang et al., 2001).

The reconstructed labelling patterns of the two-carbon building block from BBT and acetyl-CoA (Fig. 6B) were identical within the experimental limits of quantitative NMR spectroscopy confirming the biosynthetic origin of BBT from acetyl-CoA or a closely related compound (i.e. malonyl-CoA). In addition to the information obtained from the experiment with [U-$^{13}C_6$]glucose, the orientation of the C_2 building blocks can now be determined (Fig. 4C).

The low incorporation rates of isotope-labelled acetate into BBT (see above) show that only a minor fraction of plastidic acetyl-CoA can be assembled from exogenous acetate in root cultures of *Tagetes* under the conditions of cultivation. On the other hand, high enrichment values were found with ^{13}C-labelled glucose as a precursor. Obviously, exogenous glucose is channelled efficiently into plastidic acetyl-CoA.

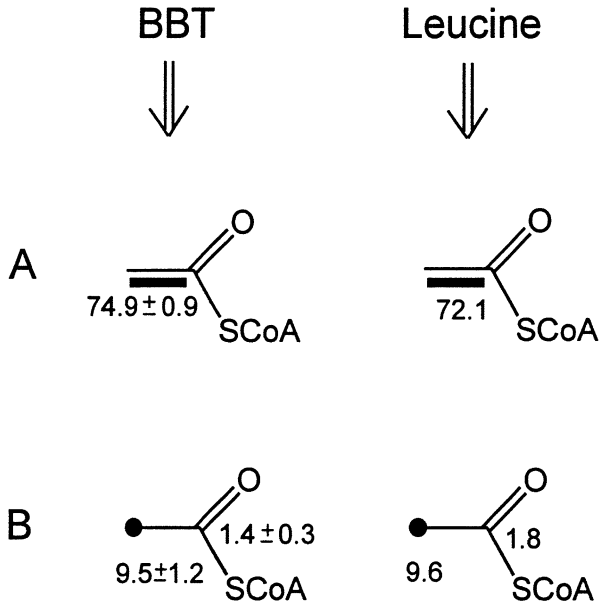

Fig. 6. Comparison of the labelling patterns of acetyl-CoA reconstructed from leucine (cf. Fig. 5) with the labelling patterns of the C_2 building blocks in the bithiophene BBT, (A) in the experiment with [U-$^{13}C_6$]glucose and (B) in the experiment with [1-^{13}C]glucose. For more details, see Fig. 4.

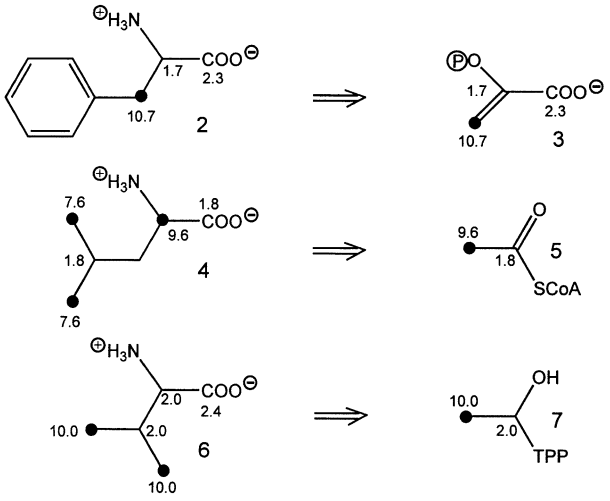

Fig. 7. Incorporation experiment with [1-^{13}C]glucose. Reconstruction of the labelling patterns of phosphoenol pyruvate (**3**), acetyl-CoA (**5**), and hydroxyethyl-TPP (**7**) from the labelling patterns of phenylalanine (**2**), leucine (**4**), and valine (**6**), respectively. Filled circles indicate significantly ^{13}C-enriched atoms. Numbers indicate ^{13}C abundance in%. The labelling pattern of the aromatic ring of phenylalanine could not be determined due to signal overlapping.

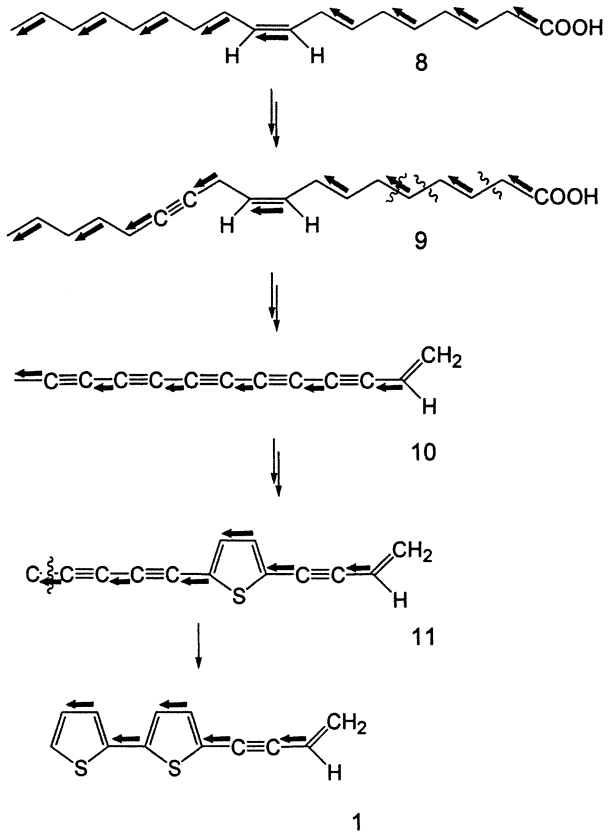

Fig. 8. Orientation of acetate units in BBT (**1**) biosynthesized from oleic acid (**8**) via crepenynic acid (**9**), **10** and **11** (see also text). The orientation of the acetate precursor units is symbolised by bold arrows directed from C-1 to C-2 (cf. Fig 4C).

Mainly based on the co-existence of thiophenes, oleic acid and polyacetylenes in Asteraceae, biosynthesis of **1** has been proposed to proceed via crepenynic acid (**9**), **10** and **11** (Fig. 8) (Sörensen et al., 1954; Gunstone et al., 1967; Bohlmann et al., 1976; Jacobs et al., 1995). Plant enzymes catalysing triple bond formation in C_{18} fatty acids were characterized recently (Lee et al., 1998). The reaction of long-chain polyines and H_2S leading to thiophenes is a well-known reaction in vitro (Bohlmann and Zdero, 1985).

The labelling patterns found in our study are well in line with that earlier proposal (Fig. 8). However, it must be emphasised that our data do not exclude a biosynthetic route in which a thiophene precursor could be obtained by ring opening of a cyclic polyketide intermediate.

3. Experimental

3.1. Materials

[U-$^{13}C_6$]Glucose (99% ^{13}C) and [1-^{13}C]glucose (99% ^{13}C) were obtained from Omicron (South Bend, IN). [1,2-$^{13}C_2$]Acetate (sodium salt) was from Isotec (Miamisburg, OH).

3.2. Plant cell cultures

Commercially available seeds of *Tagetes patula* (L.) cv. Carmen were sterilized with 70% (v/v) EtOH and 10% (v/v) household bleach (HYPO), rinsed twice with sterile water, and placed on hormone-free Nitsch medium (Nitsch and Nitsch, 1969). After one week in darkness, the approximately 1 cm-long roots of the seedlings were cut and transferred into 10 ml of MS medium, pH 6, (Murashige and Skoog, 1962) containing 100 mg of myo-inositol, 100 mg of NZ-amine, and 30 g of sucrose per liter (medium A). After 10 days, 10 ml of medium A were added to the growing cultures. After three weeks, the root cultures were transferred into 300 ml shake flasks containing 100 ml of medium A and incubated for 14 days.

3.3. Labelling experiments

Roots of *T. patula* (35 g of wet cells) grown on MS medium were transferred into a 300 ml Erlenmeyer flasks with 100 ml of autoclaved medium A containing 27 g of unlabelled glucose and 3 g of [U-$^{13}C_6$]glucose or 20 g of unlabelled glucose and 10 g of [1-^{13}C]glucose per litre as sole carbon source. The cultures were grown for 8 days in darkness at 23 °C under shaking (100 rpm). A sterile solution of 100 mM methyljasmonate (50 μl) was added, and the cultures were incubated for 5 days. The root cell material was harvested by suction and washed

with a small amount of water. The yield was 63 g (wet weight).

3.4. Isolation of BBT

The plant material was extracted three times with 200 ml of 70% (v/v) methanol. The extract was filtered. The solution was extracted twice with 600 ml of a hexane/*tert*-butylmethylether mixture (1:1, v/v). The organic phase was concentrated to dryness under reduced pressure. The residue was dissolved in 3 ml of hexane. Aliquots of 600 μl were spotted onto TLC plates (Polygram, SIL/UV 254, Macherey-Nagel). The plates were developed with a mixture of hexane, dioxane and butanol (75:25:1, v/v). The plates were dried and illuminated at 360 nm. The R_f value was 0.79 for BBT (dark blue fluorescent). Zones containing BBT were scraped off and were eluted with freshly distilled diethylether. The solution was concentrated to dryness under reduced pressure. Crude BBT was dissolved in 300 μl of hexane and placed on a column of silica gel 60 (0.032–0.063 mm, Merck, 6×0.5 cm) which had been equilibrated with hexane. The column was subsequently developed with 4 ml of hexane, 4 ml of hexane containing 1% (v/v) diethylether, 4 ml of hexane containing 3% diethylether, 4 ml of hexane containing 5% diethylether, and finally with 4 ml of hexane containing 10% diethylether. Fractions of 1 ml were collected and concentrated to dryness under reduced pressure. BBT eluted with hexane containing 1% (v/v) diethylether. All steps were carried out under dim light.

3.5. Isolation of amino acids

Amino acids were isolated from residual cell mass as described elsewhere (Eisenreich et al., 1991).

3.6. Gas chromatography

The purity of BBT was >95% as estimated by GC analysis (Perkin Elmer 8500; fused silica coated with PERMABOND OV-1 DF, Macherey-Nagel, 25 m×0.25 mm; temperature gradient, 120–300 °C, 5 °C min^{-1}; flow, 1.5 ml min^{-1}; retention times, BBT, 12.41 min).

3.7. NMR spectroscopy

^1H and ^{13}C NMR spectra were recorded at 500.13 and 125.6 MHz, respectively, using a DRX 500 spectrometer from Bruker Instruments, Karlsruhe, Germany. Two-dimensional INADEQUATE experiments were performed according to standard Bruker software (XWINNMR 1.3). BBT was measured in deuterated chloroform as solvent. Tyrosine was measured in D_2O (pH 13), and leucine and valine were measured in D_2O (pH 1). Signals were referenced to solvent peaks or external trimethylsilylpropane sulfonate.

3.8. Determination of ^{13}C enrichment

Determination of ^{13}C enrichment has been described earlier. Briefly, ^{13}C NMR spectra of the isotope labeled compound under study and of natural abundance material were recorded under the same experimental conditions. Integrals were determined for every ^{13}C NMR signal, and the signal integral for each respective carbon atom in the labeled compound was referenced to that of the natural abundance material, thus affording relative ^{13}C abundances for each position in the labeled molecular species.

In certain cases, these relative abundances can be converted to approximate absolute enrichment by assigning a value of 1.1% to the carbon atom with the lowest ^{13}C enrichment and referencing all other carbons to that position. In other cases, absolute ^{13}C enrichment can be obtained for certain atoms from ^{13}C coupling satellites in ^1H NMR spectra provided that any hydrogen atom of the compound under study is a singlet or a doublet where the coupling satellites can be determined to relatively high accuracy.

In NMR spectra of multiple-labeled samples displaying ^{13}C–^{13}C coupling, each satellite in the ^1H-decoupled spectra is integrated separately. The integral of each respective satellite pair is then referenced to the global signal intensity of a given carbon atom.

Acknowledgements

This work was supported by grants from the Deutsche Forschungsgemeinschaft (SFB 369) and the Fonds der Chemischen Industrie. We thank Professor Dr. Nyiredy (Budakalsz) for helpful discussions. We thank Angelika Werner and Fritz Wendling for expert help with the preparation of the manuscript.

References

Arroo, R.R.J., Jacobs, J.J.M., de Koning, E.A.H., de Waard, M., van de Westerlo, E., van Gallen, P.M., Swolfs, A.E.M., Klunder, A.J.H., Croes, A.F., Wullems, G.J., 1995. Thiophene interconversions in *Tagetes patula* hairy-root cultures. Phytochemistry 38, 1193–1197.

Bohlmann, F., 1988. Naturally-occurring acetylenes. In: Lam, J., Breteler, H., Arnason, T., Hansen, L. (Eds.), Naturally Occurring Acetylenes and Related Compounds. Elsevier, Amsterdam, Oxford New York, Tokyo, pp. 1–20.

Bohlmann, F., Zdero, C., 1985. Naturally occurring thiophenes. In: Weissberger, A., Taylor, E.C. (Eds.), Thiophene and its Derivates. John Wiley & Sons, New York, pp. 261–323.

Bohlmann, F., Zdero, C., Grenz, M., 1976. Polyacetylene compounds. Part 241. Constituents of some genera of the tribes Heleniaea and Senecioneae. Phytochemistry 15, 1309–1310.

Bohlmann, F., Burkhardt, T., Zdero, C., 1973. Distribution of acetylenes. 1. Compositae. In: Naturally Occuring Acetylenes. Academic Press, London, New York, pp. 340–464.

Eichinger, D., Bacher, A., Zenk, M.H., Eisenreich, W., 1999. Analysis of metabolic pathways via quantitative prediction of isotope labeling patterns: a retrobiosynthetic ^{13}C NMR study on the monoterpene loganin. Phytochemistry 51, 223–236.

Eisenreich, W., Schwarzkopf, B., Bacher, A., 1991. Biosynthesis of nucleotides, flavins, and deazaflavins in *Methanobacterium thermoautotrophicum*. J. Biol. Chem. 266, 9622–9631.

Eisenreich, W., Rieder, C., Grammes, C., Hessler, G., Adam, K.-P., Becker, H., Arigoni, D., Bacher, A., 1999. Biosynthesis of a neo-epiverrucosane diterpene in the liverwort *Fossombronia alaskana*. A retrobiosynthetic NMR study. J. Biol. Chem. 274, 12–20.

Eisenreich, W., Bacher, A., 2000. Elucidation of biosynthetic pathways by retrodictive/predictive comparison of isotopomer patterns determined by NMR spectroscopy. In: Setlow, J.K. (Ed.), Genetic Engineering, Principles and Methods, Vol. 22. Kluwer Academic/Plenum Publishers, New York, pp. 121–151.

Goese, M., Kammhuber, K., Bacher, A., Zenk, M.H., Eisenreich, W., 1999. Biosynthesis of bitter acids in hops. A ^{13}C-NMR and ^{2}H-NMR study on the building blocks of humulone. Eur. J. Biochem. 263, 447–454.

Gunstone, F.D., Kilgast, D., Powell, R.G., Taylor, G.M., 1967. *Afzelia cuanzensis* seed oil: a source of crepenynic and 14,15-dehydrocrepenynic acid. Chem. Commun., 295–296.

Jacobs, J.J., Arroo, R.R., de Koning, E.A., Klunder, A.J., Croers, A.F., Wullems, G.J., 1995. Isolation and characterization of mutants of thiophene synthesis in *Tagetes erecta*. Plant Physiol. 107, 807–814.

Jente, R., Olatunji, G.A., Bosold, F., 1981. Formation of natural thiophene derivatives from acetylenes by *Tagetes patula*. Phytochemistry 20, 2169–2175.

Jente, R., Richter, E., Bosold, F., Olatunji, G.A., 1988. Experiments on biosynthesis and metabolism of acetylenes and thiophenes. In: Lam, J., Breteler, H., Arnason, T., Hansen, L. (Eds.), Naturally Occurring Acetylenes and Related Compounds. Elsevier, Tokio, Amsterdam, Oxford, New York, pp. 187–199.

Kagan, J., 1991. Naturally occurring di- and trithiophenes. Prog. Chem. Org. Nat. Prod 56, 87–169.

Lee, M., Lenman, M., Banas, A., Bafor, M., Singh, S., Schweizer, M., Nilsson, R., Liljenberg, C., Dahlqvist, A., Gummeson, P.O., Sjödahl, S., Green, A., Stymne, S., 1998. Identification of non-heme diiron proteins that catalyze triple bond and epoxy group formation. Science 280, 915–918.

Menelaou, M.A., Vargas, D., Fischer, N.H., Foroozesh, M., Thibodeaux, T.M., 1991. Biosynthetic studies of bithiophenes in hairy root cultures of *Tagetes patula* using carbon-13 labeled acetates. Spectrosc. Lett. 24, 353–370.

Murashige, T., Skoog, F., 1962. Revised medium for rapid growth and bioassays with tobacco tissue cultures. Physiol. Plantarum 15, 473–497.

Nitsch, J.P., Nitsch, C., 1969. Haploid plants from pollen grains. Science 163, 85–87.

Sörensen, J.S., Holme, D., Borlaug, E.T., Sorensen, N.A., 1954. Studies related to naturally occurring acetylene compounds. XX. A preliminary communication on some polyacetylenic pigments from Compositae plants. Acta Chem. Scand. 8, 1769–1778.

Sörensen, N.A., 1977. Polyacetylenes and conservatism of chemical characters in the Compositae. In: Heywood, V.H., Harborne, J.B., Turner, B.L. (Eds.), The Biology and Chemistry of the Compositae I. Academic Press, London, pp. 385–409.

Wang, C.-Z., Maier, U.H., Eisenreich, W., Adam, P., Obersteiner, I., Keil, M., Bacher, A., Zenk, M.H., 2001. Unexpected biosynthetic precursors of amarogentin—a retrobiosynthetic ^{13}C NMR study. Eur. J. Org. Chem., 1459–1465.

Werner, I., Bacher, A., Eisenreich, W., 1999. Analysis of gallic acid biosynthesis via quantitative prediction of isotope labeling patterns. In: Gross, G.G., Hemingway, R.W., Yoshida, T. (Eds.), Plant Polyphenols 2. Plenum Press, New York, pp. 43–61.

Zehmeister, L., Sease, J.W., 1947. A blue-fluorescing compound, terthienyl, isolated from marigold. J. Amer. Chem. Soc. 69, 273.

PERGAMON

Phytochemistry 58 (2001) 883–889

PHYTOCHEMISTRY

www.elsevier.com/locate/phytochem

Calystegines in *Calystegia sepium* derive from the tropane alkaloid pathway

Yvonne Scholl, Dirk Höke, Birgit Dräger*

Institut für Pharmazeutische Biologie, Martin-Luther-Universität Halle-Wittenberg, Hoher Weg 8, 06120 Halle/Saale, Germany

Received 5 July 2001; received in revised form 2 August 2001

Abstract

Calystegines were measured in roots and aerial parts of *Calystegia sepium*. The accumulation appears developmentally regulated. Calystegine accumulation in hairy root cultures follows growth and reaches maximal values of 1,5 mg/g dry mass. ^{15}N-Labelled tropinone was fed to root cultures and the incorporation of label into calystegines and further metabolites of the tropane alkaloid pathway was measured after 2, 4 and 6 days. Pseudotropine was completely labelled after 2 days, and calystegine A_3 was labelled faster than the calystegines of the B-group. 2,7-Dihydroxynortropane also incorporated ^{15}N from tropinone and is suggested to be a by-product of the tropane alkaloid pathway leading to calystegines. © 2001 Elsevier Science Ltd. All rights reserved.

Keywords: *Calystegia sepium*; Convolvulaceae; Root culture; Calystegine; Tropane alkaloid; Biosynthesis; ^{15}N-Tropinone

1. Introduction

Calystegines, hydroxylated nortropane derivatives, were first identified in transformed root cultures of *Calystegia sepium* (Convolvulaceae) (Goldmann et al., 1990). Due to their resemblance to monosaccharides calystegines show specific glycosidase inhibitory activity and have a high therapeutic potential like other alkaloidal glycosidase inhibitors (Asano et al., 2000). Initially, 105 different plant species from 26 families were screened, and calystegines were shown to be restricted to roots of *Calystegia sepium*, *Convolvulus arvensis* and *Atropa belladonna* (Solanaceae), they were not found in aerial parts (Tepfer et al., 1988). Later, Schimming et al. (1998) described a wide-spread distribution of calystegines in the family of Convolvulaceae. Their occurrence varies in both, quantity and composition, in different plants and plant organs. Calystegines were shown in aerial parts of many Convolvulaceae as well as in roots.

Convolvulaceae are closely related to Solanaceae for which tropane alkaloids are typical metabolites, and Convolvulaceae also contain tropane alkaloids or metabolites of their biosynthesis, e.g. cuscohygrin was reported for several Convolvulaceae (Evans and Somanbandhu, 1973). Tropine esters as well as pseudotropine esters were isolated from Convolvulaceae (Jenett-Siems et al., 1998). Tropine and pseudotropine derivatives in *Convolvulus arvensis* have been suspected to be responsible for animal intoxication (Todd et al., 1995).

It is proposed that calystegines are biosynthesised by the tropane alkaloid pathway which has been elucidated in a number of Solanaceae (Fig. 1). The tropane ring in tropinone is formed starting from putrescine. Tropinone is reduced by two different enzymes, which catalyse the formation of either tropine or pseudotropine (Dräger et al., 1988; Portsteffen et al., 1992; Hashimoto et al., 1993; Dräger and Schaal, 1994). Tropine is incorporated into the medicinally important tropane alkaloid hyoscyamine (racemic mixture: atropine), while pseudotropine was postulated to be the first specific precursor for calystegines in Solanaceae (Dräger et al., 1994). Tropinone reductases were characterised from roots of several Solanaceae, but they have not been reported for Convolvulaceae so far. Thus, the hypothesis of calystegine biosynthesis by a specific branch of the tropane alkaloid pathway is supported by the co-occurrence with tropane alkaloids and by the structural similarity, but evidence by labelled precursor feeding is scarce. Application of ^{14}C-putrescine, an early metabolite

* Corresponding author. Tel.: +49-345-55-25-765; fax: +49-345-55-25-021.

E-mail address: draeger@pharmazie.uni-halle.de (B. Dräger).

0031-9422/01/$ - see front matter © 2001 Elsevier Science Ltd. All rights reserved.
PII: S0031-9422(01)00362-4

in the tropane pathway, resulted in labelled calystegines in *Calystegia sepium* root cultures (Goldmann et al., 1990). After feeding of ^{15}N-tropinone to root cultures of *Atropa belladonna* (Solanaceae), labelled calystegine A_3 could be isolated (Dräger et al., 1994).

Recently, dihydroxy nortropane alkaloids were isolated from root cultures of *Calystegia sepium* (Asano et al., 2001). These compounds carry hydroxyl functions in positions 2 and 7, 2 and 3, or 3 and 7 on the nortropane skeleton. Their origin from tropinone and pseudotropine is difficult to explain for those structures that do not carry a hydroxyl group in position 3. We were interested whether these compounds as well as the calystegines in *Calystegia sepium* could be put into one biosynthetic line starting from tropinone.

We show here a detailed kinetic analysis of ^{15}N-tropinone incorporation into pseudotropine and into the major calystegines in root cultures of *Calystegia sepium*. For clarification of calystegine accumulation in the plant, aerial parts and roots of the intact *Calystegia sepium* plants were analysed at different developmental stages.

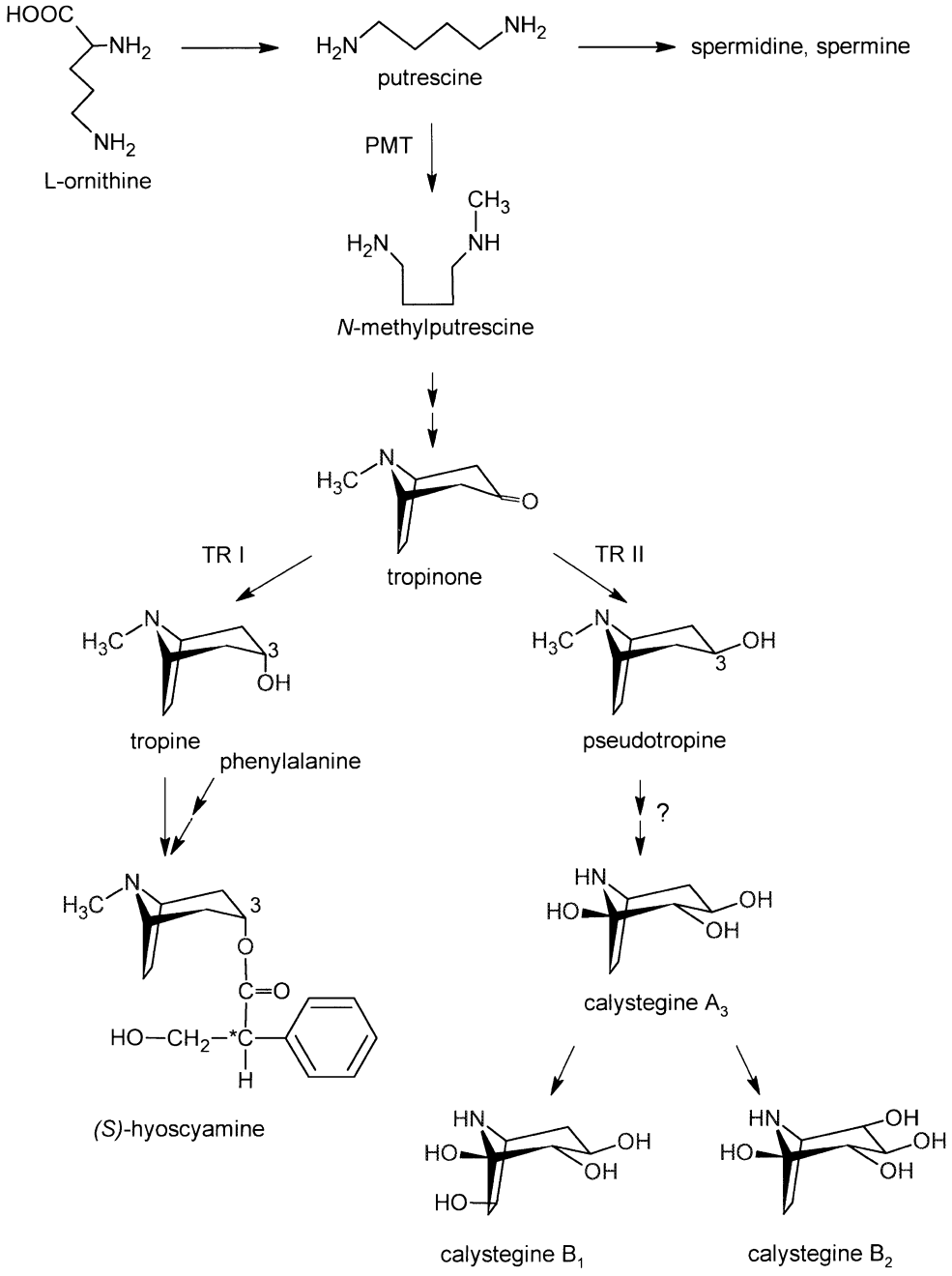

Fig. 1. Tropane alkaloid metabolism. Dotted arrows may indicate more than one biosynthetic step; PMT = putrescine methyltransferase; TR I = tropine forming tropinone reductase; TR II = pseudotropine forming tropinone reductase.

2. Results and discussion

2.1. Distribution of calystegines in Calystegia sepium plants

Seedlings 4–5 days after germination show highest concentrations in total calystegines (5.7 mg/g dry mass, Fig. 2). After 1 week in the climate chamber plants had grown up to 10 cm (ca. 40 mg total dry mass) and were separated in roots and aerial parts. The total calystegine concentration in roots was in the same range as in seedlings, while calystegines in aerial parts were less concentrated. The level of calystegines in roots decreased during further plant growth. In 3 week-old plants young leaves were the tissues with highest calystegine levels (2.3 mg/g dry mass). A similar accumulation pattern was shown for several species of Solanaceae before, where young aerial parts of the plants accumulated maximal calystegine concentrations, e.g. ca. 7 mg/g dry mass in young leaves of *Atropa belladonna* (Dräger, 1995). In *Calystegia sepium*, only low amounts of calystegines (ca. 500 μg/g dry mass) were measured in flowers.

Calystegines A_3 and B_2 were the major compounds, and the ratio of calystegines B_2 to A_3 was rather constant (1:2–3) in all tissues, except for flowers which contain similar concentrations of calystegines A_3, B_1 and B_2. In most samples calystegines A_5 and B_1 could be detected in comparison with authentic compounds by GC–MS, but they were not quantified. Further calystegines cannot be excluded, but dihydroxynortropanes were not found in aerial parts of plants. The non-uniform distribution of calystegines, especially the low concentration (less than 100 μg/g dry mass) in fully developed leaves, may be a reason why calystegines were not detected in the above-ground organs of *Calystegia sepium* in earlier investigations (Tepfer et al., 1988).

2.2. Accumulation of calystegines in Calystegia sepium root culture

Calystegine accumulation (Fig. 3) paralleled growth of the hairy root culture and was maximal (total 1.5 mg/g dry mass) in the late culture stage. Root cultures of *Atropa belladonna* showed a similar accumulation pattern and concentration (total 2 mg/g dry mass) for calystegines (Rothe et al., 2001). In addition to the calystegine mixture in intact *C. sepium* plants, calystegine B_1 appeared in root cultures in the same concentration range as calystegines A_3 and B_2. Further calystegines, e.g. calystegine A_5 and 2,7-dihydroxynortropane were identified in roots older than 16 days, but they appeared too dilute (< 10 μg/g dry mass) to be quantified reliably. Calystegine production (μg accumulation per flask and day) was calculated to be best at day 18, thus 16-day-old cultures were chosen for feeding labelled precursors.

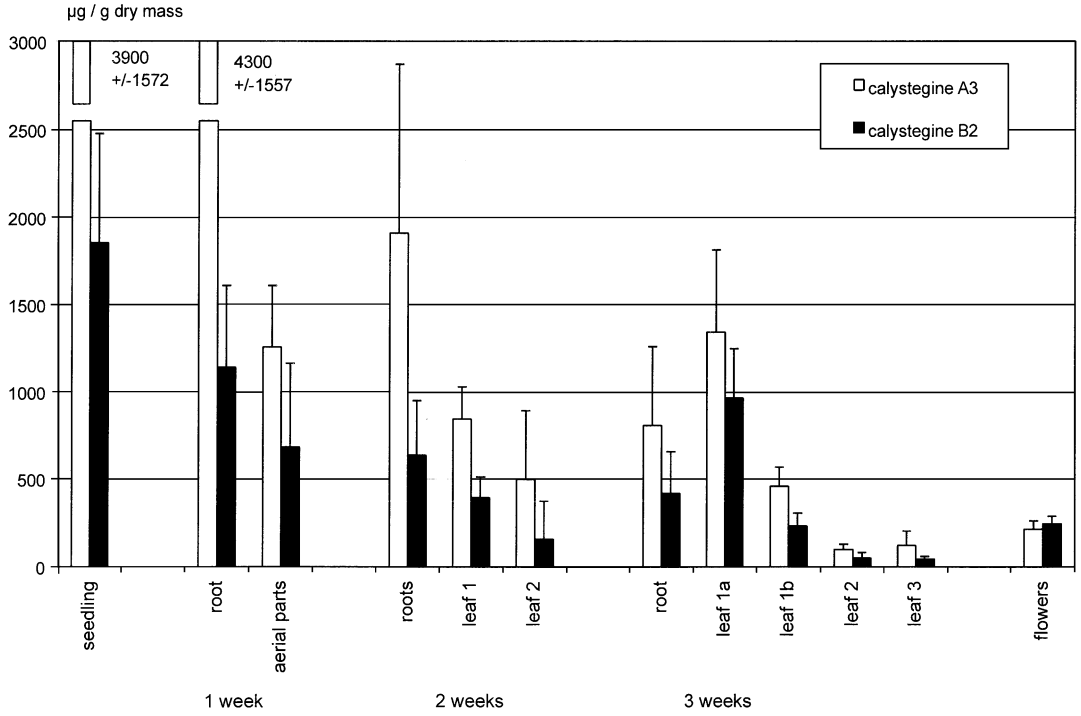

Fig. 2. Accumulation of calystegines in plants of *Calystegia sepium* (bars represent standard deviation). Leaf 1 and leaf 1b = 1-week-old leaves; leaf 1a = developing leaves including the shoot top within 1-week-old leaves; leaf 2 = 2-week-old leaves; leaf 3 = 3-week-old leaves.

2.3. Feeding of ^{15}N-tropinone

^{15}N-Tropinone was applied in a final concentration of 1 mM to *Calystegia sepium* root cultures for 2, 4 and 6 days. Pseudotropine, the calystegines A_3, B_1 and B_2 and 2,7-dihydroxynortropane were identified by their typical fragmentation pattern in GC–MS (Table 1). For the calystegines a molecular ion could not be detected in the GC–MS-spectrum. A continuous increase in the ratio of labelled to non-labelled nitrogen-containing fragments was observed for all calystegines during the period of 6 days.

The incorporation of label by ^{15}N into one representative fragment of each of the calystegines A_3, B_1 ad B_2 and into the molecular ion of 2,7-dihydroxynortropane and pseudotropine was followed quantitatively at 3 points of time (Fig. 4). The N-containing major fragment of calystegine A_3 (156) was almost completely replaced by the m/z +1-fragment (157) after 6 days (Fig. 4A). For calystegine B_1 the increase in fragment m/z 244 + 1 in relation to fragment m/z 244 is illustrated (Fig. 4B). The major fragment of calystegine B_2 [m/z 217, putative $(CH)_3$-$(O\text{-}TMS)_2^+$ (Dräger, 1995)] does

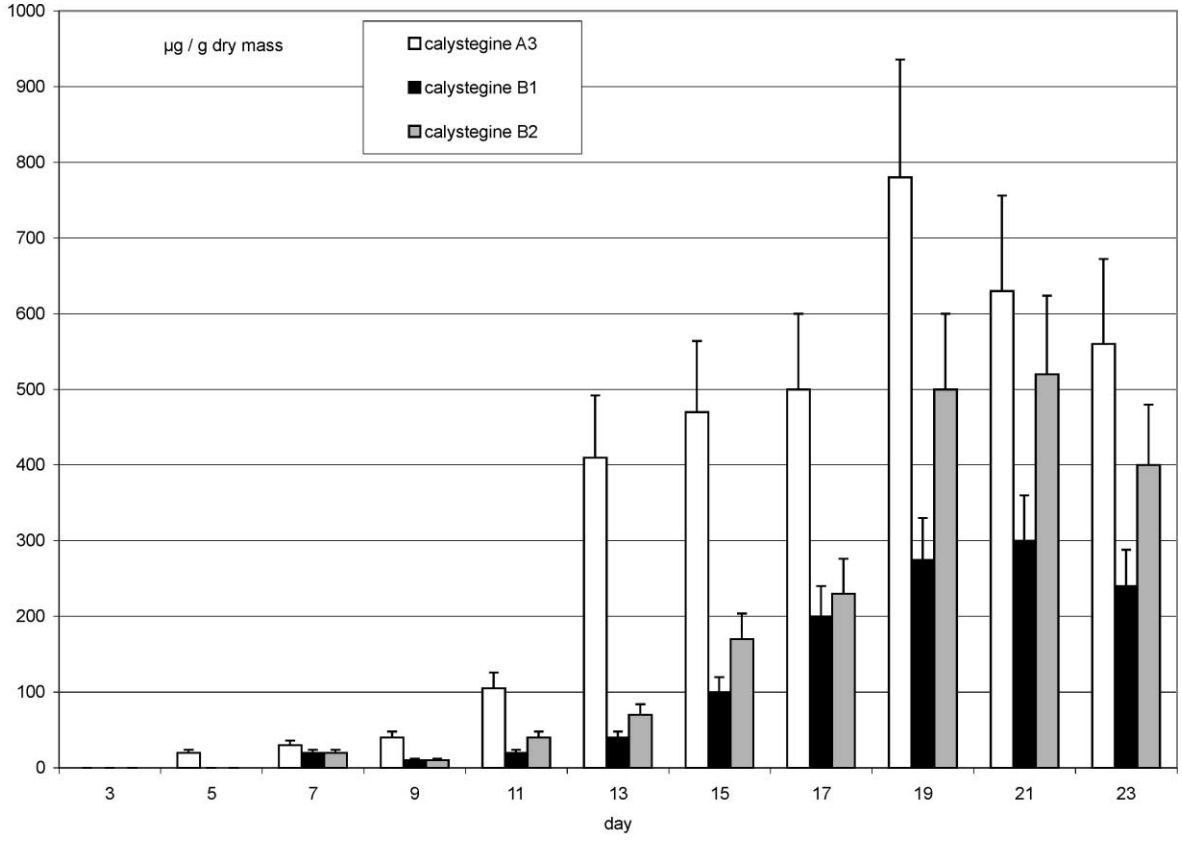

Fig. 3. Accumulation of calystegines in root cultures of *Calystegia sepium*.

Table 1
MS-fragmentation of pseudotropine and nortropane alkaloids as TMSi-derivates

Compound	Retention time in min	Characteristic ions (abundance %)[b]					
Pseudotropine	5.60	83 (100)[a]	96 (55)	124 (13)	184 (15)	198 (10)	213 (8)[d]
2,7-Dihydroxy- nortropane	10.36	80 (68)	81 (71)	156 (18)	171 (36)	272 (2)	**287** (10)[d]
Calystegine A_3	14.91	101 (1)[b]	116 (1)[b]	**156** (100)	244 (8)	285 (3)	
Calystegine B_1	18.40	101 (2)[b]	129 (16)[b]	**244** (46)	373 (8)		
Calystegine B_2	20.04	**156** (7)[c]	217 (100)[b]	244 (7)	373 (2)		

[a] Values in brackets indicate relative abundance.
[b] No nitrogen contained; all fragments except those labelled with [b] increased +1 in mass after ^{15}N-tropinone feeding.
[c] Fragments in which the incorporation of label is followed quantitatively (Fig. 5) are printed in bold.
[d] Molecular ion.

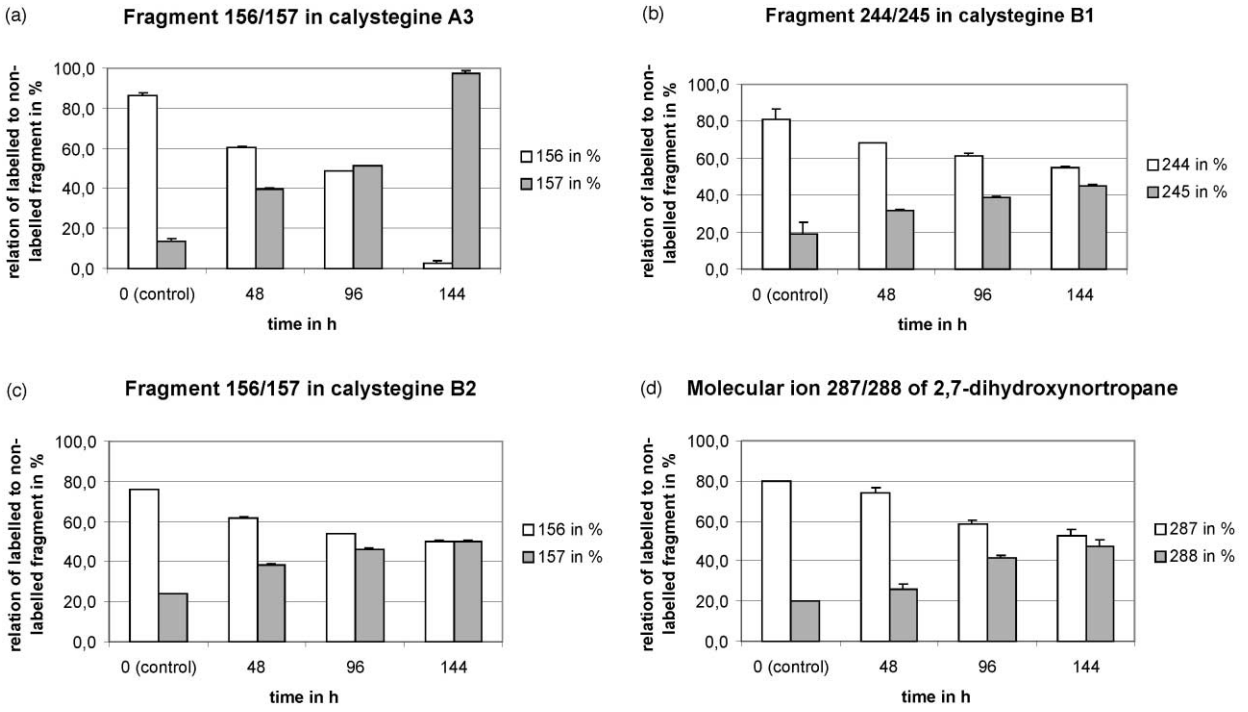

Fig. 4. Incorporation of ^{15}N into fragments of calystegines A_3, B_1, B_2 and 2,7-dihydroxynortropane. Data are average of 3 determinations. Standard deviation is given in bars.

not contain nitrogen, thus the fragment m/z 156/157 was monitored. Although the relative abundance of the fragment is low, an increase of the m/z 156 + 1-fragment can be seen here as well (Fig. 4C).

Incorporation of ^{15}N-tropinone into 2,7-dihydroxynortropane is evident by the increase of +1 in the molecular ion (Fig. 4D). The other fragments increased in the m/z +1 proportion in a similar manner. A possible fragmentation route for the silylated 2,7-dihydroxynortropane is suggested in Fig. 5. The label in 2,7-dihydroxynortropane indicates the origin of the compound in the tropane pathway, however, the direct lineage from tropinone is improbable because of the lack of an hydroxyl group in position 3.

Regarding the velocity of incorporation of ^{15}N, pseudotropine was labelled first and appeared as almost 100% m + 1 in the molecular ion after 2 days (data not shown). The ratio of labelled fragments in the calystegine A_3 rises faster than in the calystegine B pool. This may be taken as a hint that calystegines of the A-group are synthesised first and followed by tetra-hydroxylated nortropanes. For 2,7-dihydroxynortropane an ^{15}N-incorporation velocity similar to that of calystegines B_1 and B_2 was measured. 2,7-Dihydroxynortropane rather is a by-product of the biosynthetic pathway. The positions of the two hydroxyl groups and the relatively low labelling impair the idea that the dihydroxylated compound might be a metabolite on the way to the tri- and tetrahydroxylated calystegines.

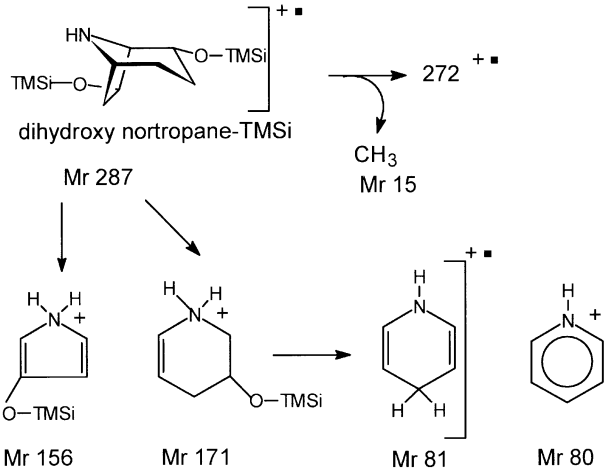

Fig. 5. Suggested fragmentation of 2,7-dihydroxynortropane after silylation in GC–MS analysis.

The incorporation of ^{15}N-tropinone into the calystegines that is shown here is consistent with the biosynthetic Scheme first proposed by Dräger et al. (1994).

3. Conclusions

Calystegines are accumulated in the whole plant of *Calystegia sepium* in a development-related pattern. Calystegines are products of the tropane alkaloid

pathway. 2,7-Dihydroxynortropane also appears as metabolite of that pathway, the loss of the hydroxyl group at C3 requires further investigations. The biological role of calystegines may relate to their interaction with carbohydrate accepting enzymes and remains to be elucidated.

4. Experimental

4.1. Plant material

Seeds and flowers of *Calystegia sepium* were collected from wild grown plants at the bank of the river Saale in Halle/ Germany. The seeds were shaken in conc. H_2SO_4 for 1 h, thereafter in 6% NaOCl for 15 min followed by 15 min in 10% H_2O_2. The surface-sterilised seeds were carefully slit with a scalpel to enable fast soaking and a simultaneous germination. They were laid out on petri dishes containing water agar (1,5% agar in distilled water) and kept dark. After 4 days, 3–4 cm long roots were formed and the cotyledons were unfolded. Twelve hours incubation under artificial light promoted the greening of the cotyledons. The seedlings were planted into pots containing sterilised soil (compost soil mixed with sand) and cultivated in climate chambers (HERAEUS HB 1014; 14 h light, 10 h darkness; 23 °C in light, 18 °C in darkness; 80% humidity). Plants were harvested after 1, 2 and 3 weeks after transfer into the climate chamber. The plant material was separated into roots and aerial parts. Leaves of 2-week-old plants and 3-week-old plants were further separated according to their age. In 3-week-old plants, the youngest leaves were separated into leaves (1b) and developing leaves including the shoot top (1a). Side stems (runners) were separated accordingly. Fresh mass and dry mass after lyophilisation were determined of all samples.

4.2. Root cultures

Hairy root cultures (transformed by *Agrobacterium rhizogenes* 15834) of *Calystegia sepium* were obtained from the Institute of Pharmaceutical Biology, TU Braunschweig, Germany, in 1996 and continuously cultivated in Gamborg's B5 medium with 3% sucrose in 300 ml flasks containing 70 ml medium on a gyratory shaker at 100 rpm. Approx. 50 mg fresh mass were subcultured into fresh medium every 3 weeks. For analysis roots were separated from the medium, blotted dry on filter paper, weighed and lyophilised. Dry mass was determined of all growth stages.

4.3. ^{15}N-Tropinone feeding

Sixteen-day-old cultures were fed with a sterile aq. soln. of ^{15}N-tropinone (98 at.% ^{15}N, measured by MS), 50 mM, buffered with HCl to pH 7.0, and with non-labelled tropinone, 50 mM sterile buffered aq. soln. as control. Final concentrations were always 1 mM in the culture medium. Roots were harvested after 48, 96 and 144 h, weighed and lyophilised.

4.4. Extract preparation

Fresh or freeze-dried tissues (typically 1–3 g fresh mass) were homogenized twice with an Ultra Thurrax in 20 ml 50% MeOH and centrifuged at 4500 *g*. The combined supernatants were reduced under vacuum to 1.5–2.0 ml aq. soln. in a rotary vaporizer.

For leaf tissue analysis this extract (0.5 or 1 ml) was directly lyophilised and the residue was derivatised by silylation with 30 μl pyridine, 40 μl HMDS and 10 μl TMCS. Dissolution was completed if necessary by an ultrasonic bath (1 min). Gentle heating, ca. 70 °C for 30 min ensured complete derivatisation. Fifty microliters of a stock soln. of azobenzene (1 mg/ml in *n*-hexane) were added as internal standard. 370 μl *n*-hexane filled up the volume to 500 μl.

For root tissues the crude extract was purified by strong acidic cation exchange resin I LAB (Merck, Darmstadt, Germany) as described (Keiner and Dräger, 2000).

An aliquot of the purified extract was lyophilised and derivatised as described above.

Plant tissues were extracted and analysed as 8 individual samples from at least 4 different plants, results are given as average. Calystegines in root cultures were determined in 8 different flasks and are expressed as average.

Concentrations of metabolites are expressed on dry mass basis. Typical relations of fresh mass to dry mass for above ground organs are 8–12% dry mass and for roots 12.5–14.3% dry mass. Roots cultures had 8–12% dry mass depending on their growth stage.

4.5. GC

Instrumentation: gas chromatograph HP 6890; simultaneous detection by FID and PND, column HP5 (30 m×0.25 mm i.d., 0.25 μm film thickness), split injection 20:1, carrier gas helium (1 ml min^{-1} constant flow), injection temp. 250 °C, detector temp. 310 °C, temp. programme 160 °C, 5°/min up to 240 °C.

4.6. GC–MS

Instrumentation: Gas chromatograph HP 5890, detector HP 5972, column DB5 (30 m x 0.32 mm i.d., 0.25 μm film thickness), splitless injection, carrier gas helium (1 ml min^{-1} constant flow), injection temp. 250 °C, detector temp. 250 °C, EIMS 70eV, temp. programme 100 °C, 2 min hold, 5°/min up to 240 °C.

Acknowledgements

We thank Henry D. Boswell and David J. Robins, Glasgow University, for synthesis of ^{15}N-tropinone and Richard J. Robins, Nantes, France, for providing it. Isolated 2,7-dihdyroxynortropane was a generous gift from Naoki Asano, Kanazawa, Japan. We thank Ines Böttcher in our laboratory for establishment and initial characterisation of the *C. sepium* root culture. Y. Scholl is grateful for a grant from the Landesgraduiertenförderung Sachsen-Anhalt.

References

Asano, N., Nash, R.J., Molyneux, R.J., Fleet, G.W.J., 2000. Sugar-mimic glycosidase inhibitors: natural occurence, biological activity and prospects for therapeutic application. Tetrahedron 11, 1645–1680.

Asano, N., Yokoyama, K., Sakurai, M., Ikeda, K., Kizu, H., Kato, A., Arisawa, M., Höke, D., Dräger, B., Watson, A.A., Nash, R.J., 2001. Dihydroxynortropane alkaloids from calystegine-producing plants. Phytochemistry 57, 721–726.

Dräger, B., 1995. Identification and quantification of calystegines, polyhydroxyl nortropane alkaloids. Phytochem. Anal. 6, 31–37.

Dräger, B., Funck, C., Hoehler, A., Mrachatz, G., Nahrstedt, A., Portsteffen, A., Schaal, A., Schmidt, R., 1994. Calystegines as a new group tropane alkaloids in Solanaceae. Plant Cell Tissue and Organ Culture 38, 235–240.

Dräger, B., Hashimoto, T., Yamada, Y., 1988. Purification and characterization of pseudotropine forming tropinone reductase from *Hyascyamus niger* root cultures. Agric. Biol. Chem. 52, 2663–2667.

Dräger, B., Schaal, A., 1994. Tropinone reduction in *Atropa belladonna* root cultures. Phytochemistry 35, 1441–1447.

Dräger, B., Van Almssick, A., Mrachatz, G., 1995. Distribution of calystegines in several Solanaceae. Planta Medica 61, 577–579.

Evans, W.C., Somanbandhu, A.-O., 1973. Cuschohygrine: A constituent of the roots of some British Convolvulaceae. Phytochemistry 13, 519–520.

Goldmann, A., Milat, M.L., Ducrot, P.H., Lallemand, J.Y., Maille, M., Lepingle, A., Charpin, I., Tepfer, D., 1990. Tropane derivatives from *Calystegia sepium*. Phytochemistry 29, 2125–2128.

Hashimoto, T., Yun, D.J., Yamada, Y., 1993. Production of tropane alkaloids in genetically engineered root cultures. Phytochemistry 32, 713–718.

Jenett-Siems, K., Mann, P., Kaloga, M., Siems, K., Jakupovic, J., Witte, L., Eich, E., 1998. Tropane alkaloids with a unique type of acyl moiety from two *Convolvulus* species. Phytochemistry 49, 1449–1451.

Keiner, R., Dräger, B., 2000. Calystegine distribution in potato (*Solanum tuberosum*) tubers and plants. Plant-Science 150, 171–179.

Portsteffen, A., Dräger, B., Nahrstedt, A., 1992. Two tropinone reducing enzymes from *Datura stramonium* transformed root cultures. Phytochemistry 31, 1135–1138.

Rothe, G., Garske, U., Dräger, B., 2001. Calystegines in root cultures of *Atropa belladonna* respond to sucrose, not to elicitation. Plant-Science 160, 1043–1053.

Schimming, T., Tofern, B., Mann, P., Richter, A., Jenett-Siems, K., Dräger, B., Asano, N., Gupta, M.P., Correa, M.D., Eich, E., 1998. Distribution and taxonomic significance of calystegines in the Convolvulaceae. Phytochemistry 49, 1989–1995.

Tepfer, D., Goldmann, A., Pamboukdjian, N., Maille, M., Lepingle, A., Chevalier, D., Denarie, J., Rosenberg, C., 1988. A plasmid of *Rhizobium meliloti* 41 encodes catabolism of two compounds from root exudate of *Calystegia sepium*. J. Bacteriol. 170, 1153–1161.

Todd, F.S., Stermitz, F.R., Schultheis, P., Knight, A.P., Traub-Dargatz, J., 1995. Tropane alkaloids and toxicity of *Convolvulus arvensis*. Phytochemistry 39, 301–303.

PERGAMON

Phytochemistry 58 (2001) 891–895

PHYTOCHEMISTRY

www.elsevier.com/locate/phytochem

Biotransformation of 4β-hydroxyeudesmane-1,6-dione by *Gliocladium roseum* and *Exserohilum halodes*

Andrés García-Granados[a,*], María C. Gutiérrez[a], Francisco Rivas[a], José M. Arias[b]

[a]*Departamento de Química Orgánica, Facultad de Ciencias, Universidad de Granada, 18071 Granada, Spain*
[b]*Departamento de Microbiología, Facultad de Ciencias, Universidad de Granada, 18071 Granada, Spain*

Received 8 June 2001; received in revised form 24 July 2001

Abstract

Biotransformation of sesquiterpene 4β-hydroxyeudesmane-1,6-dione by the filamentous fungi *Gliocladium roseum* and *Exserohilum halodes* was achieved. With *Exserohilum halodes*, only one metabolite was obtained, as a result of the regio- and stereoselective reduction of the keto group at C-1, which is difficult to achieve by chemical means. Five metabolites were produced with *Gliocladium roseum*, three of which, the 7α-hydroxylated, the 7α,11- and the 1α,8α-dihydroxylated derivatives, have not previously been reported. The hydroxylation at C-11 is the main action of this microorganism. These 11-hydroxylated compounds can be chemically transformed into 6β,12-eudesmanolides. © 2001 Published by Elsevier Science Ltd.

Keywords: Biotransformation; Sesquiterpene; Eudesmane; Hydroxylation; *Gliocladium roseum*; *Exserohilum halodes*

1. Introduction

Gliocladium roseum (CECT 2733), the anamorphic form of *Nectria ochroleuca* (IMI 40022), is a filamentous fungus that had been used previously to hydroxylate the sesquiterpene patchoulol (Becher et al., 1978) as well as to biotransform a derivative of the diterpene varodiol in order to produce an *ent*-ambrox® derivative (García-Granados et al., 1999). *Exserohilum halodes* (CECT 2716) is a synonym of *Exserohilum rostratum*, the anamorphic form of *Setosphaeria rostrata* (IMI 76563).

Eudesmane sesquiterpenes are common in nature (Fischer et al., 1979; Fraga, 2000) and they possess significant biological properties (Rodríguez et al., 1976; Picman, 1986; Robles et al., 1995; Marles et al., 1995; Fraga, 1997; Schmidt, 1999). Several biotransformations of eudesmane compounds have been accomplished in the last decade (Amate et al., 1991; Atta-ur-Rahman et al., 1994; Shimizu et al., 1994; García et al., 1995; El-Sharkawy et al., 1996; Miyazawa et al., 1997; García-Granados et al., 1998, 2000a,b).

In previous papers (García-Granados et al., 1991, 1993) we reported the incubations of several 4β-hydroxyeudesmane compounds by the filamentous fungi *Curvularia lunata* (ATCC 12017) and *Rhizopus nigricans* (ATCC 10404). The action of these microorganisms was directed mainly to the isopropyl moiety, *Curvularia lunata* to C-12 and *Rhizopus nigricans* to C-11. In both cases, the best results were obtained on the 1,6-diketo derivative. Consequently, we have chosen this substrate to carry out several biotransformations with the microorganisms *Exserohilum halodes* and *Gliocladium roseum*.

2. Results and discussion

4β-Hydroxyeudesmane-1,6-dione **(1)** was obtained from a natural compound **(2)** isolated from *Sideritis varoi* subsp. *cuatrecasasii* (García-Granados et al., 1985), a synonym of *Sideritis leucantha* Cav. subsp. *meridionalis* (Font Quer) O. Socorro (Socorro, 2001). Deacetylation of **2** gave the trihydroxyl derivative **3**, which was oxidized to give the 1,6-diketo derivative **1**.

The incubation of **1** with *Exserohilum halodes* for 13 days produced only a limited quantity (15%) of meta-

* Corresponding author. Tel./Fax: +34-958-243364.
E-mail address: agarcia@ugr.es (A. García-Granados).

0031-9422/01/$ - see front matter © 2001 Published by Elsevier Science Ltd.
PII: S0031-9422(01)00340-5

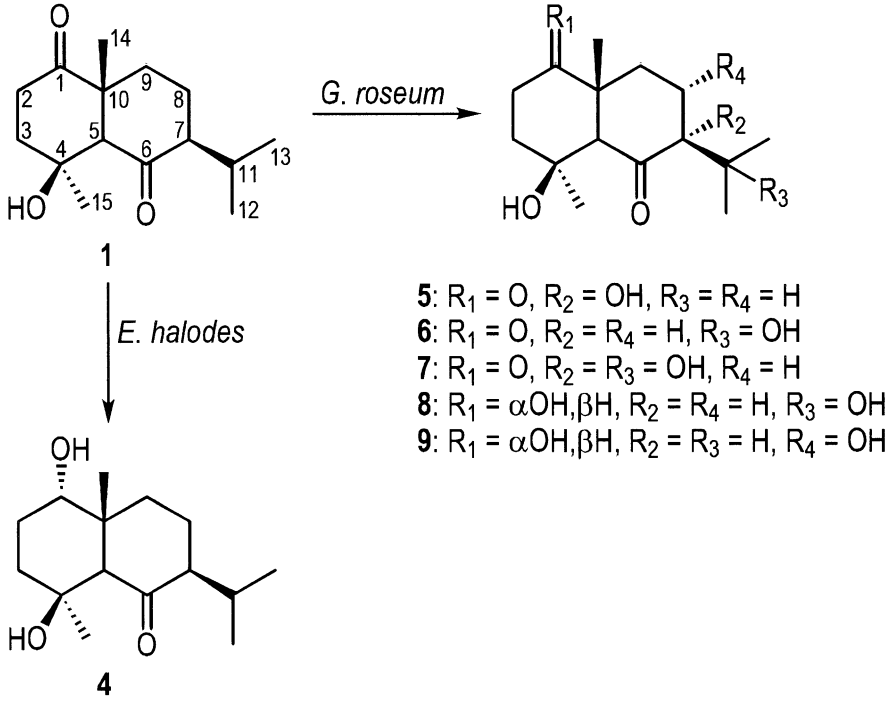

Fig. 1. Bioconversion of sesquiterpene 4β-hydroxyeudesmane-1,6-dione by *Gliocladium roseum* and *Exserohilum halodes*.

bolite **4**. This metabolite (**4**) was the result of the regio- and stereoselective reduction of the keto group at C-1 of substrate **1** from the β face giving a (1*S*)-hydroxyl derivative, which, due to the steric hindrance, is difficult to achieve by chemical means. The *S* configuration at C-1 could easily be deduced from the signal in the ^{1}H NMR spectrum (δ 3.52, 1H, *dd*, $J_{1,2\beta} = J_{1,2\alpha} = 3.0$ Hz), with coupling constants corresponding to an equatorial proton. This metabolite previously appeared in the incubation of substrate **1** with the microorganism *Curvularia lunata* (García-Granados et al., 1991).

Substrate **1** was more efficiently biotransformed by *Gliocladium roseum*. Incubation of this compound for 5 days yielded the metabolites **5** (2%), **6** (27%), **7** (3%), **8** (58%) and **9** (5%).

Metabolite **5** had a molecular formula of $C_{15}H_{24}O_4$, which indicated the presence of an additional hydroxyl group in the molecule. The ^{13}C NMR spectrum revealed β-effects on C-8 and C-11 and γ-effects on C-5, C-9, C-12 and C-13, positioning the new hydroxyl group at C-7. Consequently, metabolite **5** was 4β,7α-dihydroxyeudesmane-1,6-dione.

Metabolite **6** had the same molecular formula as the above metabolite (**5**), and its spectral data suggested a new hydroxyl group at C-11. This metabolite (**6**) was previously obtained in the incubation of substrate **1** with *Rhizopus nigricans* (García-Granados et al., 1993).

The molecular formula ($C_{15}H_{24}O_5$) of the third metabolite (**7**) was in agreement with the presence of two new hydroxyl groups. These functional groups were positioned at C-7 and C-11, by comparison of the spectral data of this metabolite (**7**) with those of metabolites **5** and **6**. Hence, metabolite **7** was 4β,7α,11-trihydroxyeudesmane-1,6-dione.

The main metabolite isolated (**8**) showed spectral data that, by comparison with those of metabolites **4** and **6**, indicated that *Gliocladium roseum*, besides the introduction of a hydroxyl group at C-11, also had reduced the carbonyl group at C-1 of the molecule, producing an *S*-alcohol. This metabolite (**8**) also resulted from the incubation of substrate **1** with *Rhizopus nigricans* (García-Granados et al., 1993).

The last metabolite isolated (**9**) had the same molecular formula ($C_{15}H_{26}O_4$) as metabolite **8**. Its ^{1}H NMR spectrum revealed two signals of geminal protons to hydroxyl groups at δ 3.55 (1H, *dd*, $J_{1,2\beta} = J_{1,2\alpha} = 2.9$ Hz), characteristic of a 1α-hydroxyl group, and at δ 4.04 (1H, *ddd*, $J_{8,9\alpha} = 10.8$, $J_{8,7} = 10.1$, $J_{8,9\beta} = 5.0$ Hz) due to an axial proton. The position of the new function was determined by the β-effects found on the adjacent carbons (C-7 and C-9). Therefore, metabolite **9** was 1α,4β,8α-trihydroxyeudesman-6-one.

3. Conclusions

Several conclusions can be drawn from the above biotransformation results. On the one hand, bioconversion of substrate (**1**) by *Exserohilum halodes* is more limited, reducing only the carbonyl group at C-1, producing an *S*-alcohol, as is usual in enzymatic reductions (Sih and Rosazza, 1976). On the other hand, *Gliocladium*

roseum achieved the complete bioconversion of substrate (**1**), producing mainly 11-hydroxyl derivatives (88%). These 11-hydroxylated compounds can be chemically transformed into 12-hydroxyl derivatives, precursors of 6β,12-eudesmanolides (García-Granados et al., 1993). The main action achieved on the substrate (**1**) by *Gliocladium roseum* is similar to the carried out by *Rhizopus nigricans* (García-Granados et al., 1993), although the first one, also produced 7α- and 8α-hydroxylated derivatives. All the microorganisms tested on the substrate (**1**) have reduced only the carbonyl group at C-1, while the one situated at C-6 remained unaltered (García-Granados et al., 1991, 1993).

In summary *Exserohilum halodes* produced only one known compound of difficult access by chemical means while *Gliocladium roseum* originated five compounds, three of which, have not previously been reported.

4. Experimental

Measurements of NMR spectra (300.13 MHz ^{1}H and 75.47 MHz ^{13}C) were made in $CDCl_3$ (which also provided the lock signal) in a Bruker AM-300 spectrometer. The assignments of ^{13}C chemical shifts (Table 1) were made with the aid of distortionless enhancement by polarization transfer (DEPT) using a flip angle of 135°. IR spectra were recorded on a Nicolet 20SX FT–IR spectrometer. High-resolution mass spectra were made by LSIMS (FAB) ionization mode in a MICROMASS AUTOSPEC-Q spectrometer (EBE geometry). Melting points (uncorr.) were determined using a Kofler (Reichter) apparatus. Optical rotations were measured on a Perkin-Elmer 241 polarimeter at 25°. Silica gel Scharlau 60 (40–60 μm) was used for flash chromatography. CH_2Cl_2 or $CHCl_3$ containing increasing amounts of Me_2CO were used as eluents. Analytical plates (silica gel, Merck 60 G) were rendered visible by spraying with H_2SO_4–AcOH, followed by heating to 120°. The identity of compound **2** was confirmed by direct comparison with an authentic sample (IR, MS, NMR, etc.).

4.1. Isolation of 6β-acetoxy-1β,4β-dihydroxyeudesmane (*2*)

6β-Acetoxy-1β,4β-dihydroxyeudesmane was isolated from *Sideritis varoi* subsp. *cuatrecasasii* (García-Granados et al., 1985), a synonym of *Sideritis leucantha* Cav. subsp. *meridionalis* (Font Quer) O. Socorro (Socorro, 2001).

4.2. Deacetylation of *2*

6β-Acetoxy-1β,4β-dihydroxyeudesmane (**2**, 1.20 g) was dissolved in MeOH/H_2O (70%) (70 ml) containing KOH (5%) (3.5 g) and refluxed for 1 h. The reaction mixture was extracted with CH_2Cl_2, dried over Na_2SO_4 and evaporated to dryness. Chromatography on a silica gel column yielded 1β,4β,6β-trihydroxyeudesmane (**3**, 952 mg, 92%) (García-Granados et al., 1991).

4.3. Oxidation of *3*

Jones' reagent was added dropwise to a stirred solution of 1β,4β,6β-trihydroxyeudesmane (**3**, 905 mg) in acetone at room temp. until an orange-brown colour persisted (30 min), following the oxidation by TLC. Methanol was then added and the reaction mixture was diluted with water and extracted with CH_2Cl_2. The organic layer was dried over anhydrous Na_2SO_4 and evaporated to dryness. Chromatography on a silica gel column yielded 4β-hydroxyeudesmane-1,6-dione (**1**, 815 mg, 91%) (García-Granados et al., 1991). Syrup; $[\alpha]_D = +67°$ ($CHCl_3$, *c* 1); IR ν_{max} ($CHCl_3$): 3527, 1712 and 1705 cm^{-1}, ^{1}H NMR ($CDCl_3$): δ 0.87 and 0.91 (3H each, *d*, $J = 6.6$ Hz, 3H-12 and 3H-13), 1.24 and 1.25 (3H each, *s*, 3H-14 and 3H-15), 2.58 (1H, *s*, H-5) and 3.07 (1H, *ddd*, $J_{2\beta,2\alpha} = J_{2\beta,3\alpha} = 14.2$, $J_{2\beta,3\beta} = 6.0$ Hz, H-2β).

4.4. Organism, media and culture conditions

Gliocladium roseum CECT 2733 and *Exserohilum halodes* CECT 2716 were obtained from the Colección Española de Cultivos Tipo, Departamento de Microbiología, Facultad de Ciencias, Universidad de Valencia, Spain, and was kept in YEPGA medium containing yeast extract (1%), peptone (1%), glucose (2%) and agar (2%) in H_2O at pH 5. In all transformation experiments a medium of peptone (0.1%), yeast extract (0.1%), beef extract (0.1%) and glucose (0.5%) in H_2O at pH 5.7 was used. Erlenmeyer flasks (250 ml) containing 80 ml of medium were inoculated with a dense suspension of the corresponding microorganism. The cultures were incubated by shaking (150 rpm) at 28° for 6 days, after which, substrate 1 (5–10%) in EtOH was added.

4.5. Biotransformation of substrate *1* with Exserohilum halodes

Substrate **1** (124 mg) was dissolved in EtOH (2 ml), distributed between 2 Erlenmeyer flask cultures and incubated for 13 days, after which the cultures were filtered and pooled; the cells were washed thoroughly with water and the liquid was satd. with NaCl and extracted twice with CH_2Cl_2. Both extracts were pooled, dried with anhydrous Na_2SO_4, and evaporated at 40° in vacuum to give a mixture of compounds (102 mg). This mixture was chromatographed on a silica gel column to obtain 83 mg of starting material **1** and 19 mg (15%) of 1α,4β-dihydroxyeudesman-1-one (**4**) (García-Granados

et al., 1991). Syrup; $[\alpha]_D = +21$ ($CHCl_3$, *c* 1); IR ν_{max} ($CHCl_3$): 3444 and 1690 cm^{-1}; ^1H NMR ($CDCl_3$): δ 0.85 and 0.88 (3H each, *d*, $J = 6.6$ Hz, 3H-12 and 3H-13), 0.98 (3H, *s*, 3H-14), 1.18 (3H, *s*, 3H-15), 2.64 (1H, *s*, H-5) and 3.52 (1H, *dd*, $J_{1,2\beta} = J_{1,2\alpha} = 3.0$ Hz, H-1).

4.6. Biotransformation of substrate *1* with Gliocladium roseum

670 mg of substrate **1** were dissolved in EtOH (9 ml), distributed between 9 Erlenmeyer flask cultures and incubated for 5 days, after which the cultures were processed as indicated above for the biotransformation of substrate **1** with *Exserohilum halodes*. The resulting mixture (667 mg) was chromatographed on a silica gel column to obtain 11 mg (2%) of 4β,7α-dihydroxyeudesmane-1,6-dione (**5**); syrup; $[\alpha]_D = +91^\circ$ ($CHCl_3$, *c* 1); IR ν_{max} ($CHCl_3$): 3514 and 1701 cm^{-1}; ^1H NMR ($CDCl_3$): δ 0.92 and 0.94 (3H each, *d*, $J = 6.8$ Hz, 3H-12 and 3H-13), 1.24 and 1.25 (3H each, s, 3H-14 and 3H-15), 3.08 (1H, *ddd*, $J_{2\beta,2\alpha} = J_{2\beta,3\alpha} = 14,3$, $J_{2\beta,3\beta} = 6.1$ Hz, H-2β) and 3.54 (1H, *s*, H-5); HRLSIMS, m/z: $[M+Na]^+$ 291.1565, ($C_{15}H_{24}O_4Na$, 291.1572, PPM +2.4); 190 mg (27%) of 4β,11-dihydroxyeudesmane-1,6-dione (**6**) (García-Granados et al., 1993); syrup; $[\alpha]_D = +61^\circ$ ($CHCl_3$, *c* 1); IR ν_{max} ($CHCl_3$): 3527 and 1700 cm^{-1}; ^1H NMR ($CDCl_3$): δ 1.18 and 1.21 (3H each, *s*, 3H-12 and 3H-13), 1.23 and 1.24 (3H each, *s*, 3H-14 and 3H-15), 2.39 (1H, *dd*, $J_{7,8\beta} = 12.2$, $J_{7,8\alpha} = 7.3$ Hz, H-7), 2.55 (1H, *s*, H-5) and 3.03 (1H, *ddd*, $J_{2\beta,2\alpha} = J_{2\beta,3\alpha} = 14.2$, $J_{2\beta,3\beta} = 6.0$ Hz, H-2β); 20 mg (3%) of 4β,7α,11-trihydroxyeudesmane-1,6-dione (**7**); syrup; $[\alpha]_D = +89^\circ$ ($CHCl_3$, *c* 1); IR ν_{max} ($CHCl_3$): 3498 and 1700 cm^{-1}; ^1H NMR ($CDCl_3$): δ 1.22 and 1.26 (3H each, *s*, 3H-14 and 3H-15), 1.30 and 1.44 (3H each, *s*, 3H-12 and 3H-13), 1.70 (1H, *ddd*, $J_{3\alpha,3\beta} = J_{3\alpha,2\beta} = 14.3$, $J_{3\alpha,2\alpha} = 4.5$ Hz, H-3α), 2.04 (1H, *ddd*, $J_{3\beta,3\alpha} = 14.3$, $J_{3\beta,2\beta} = 5.9$, $J_{3\beta,2\alpha} = 2.8$ Hz, H-3β), 2.15 (1H, *ddd*, $J_{2\alpha,2\beta} = 14.3$, $J_{2\alpha,3\alpha} = 4.5$, $J_{2\alpha,3\beta} = 2.8$ Hz, H-2α), 3.07 (1H, *ddd*, $J_{2\beta,2\alpha} = J_{2\beta,3\alpha} = 14.3$, $J_{2\beta,3\beta} = 5.9$ Hz, H-2β) and 3.45 (1H, *s*, H-5); HRLSIMS, m/z: $[M+Na]^+$ 307.1527, ($C_{15}H_{24}O_5Na$, 307.1521, PPM-1.9); 414 mg (58%) of 1α,4β,11-trihydroxyeudesman-6-one (**8**) (García-Granados et al., 1993); syrup; $[\alpha]_D = +50^\circ$ ($CHCl_3$, *c* 1); IR ν_{max} ($CHCl_3$): 3443 and 1684 cm^{-1}; ^1H NMR ($CDCl_3$): δ 1.00 (3H, *s*, 3H-14), 1.19 (3H, *s*, 3H-15), 1.18 and 1.23 (3H each, *s*, 3H-12 and 3H-13), 2.41 (1H, *ddd*, $J_{7,8\beta} = 12.7$, $J_{7,8\alpha} = 6.3$, $J_{7,5} = 1.1$ Hz, H-7), 2.64 (1H, *bs*, H-5) and 3.51 (1H, *dd*, $J_{1,2\beta} = J_{1,2\alpha} = 2.8$ Hz, H-1); and 32 mg (5%) of 1α,4β,8α-trihydroxyeudesman-6-one (**9**); syrup; $[\alpha]_D = +100^\circ$ ($CHCl_3$, *c* 1); IR ν_{max} ($CHCl_3$): 3412 and 1690 cm^{-1}; ^1H NMR ($CDCl_3$): δ 0.96 (3H, *s*, 3H-14), 1.06 and 1.10 (3H each, *d*, $J = 7.1$ Hz, 3H-12 and 3H-13), 1.22 (3H, *s*, 3H-15), 2.62 (1H, *s*, H-5), 3.55 (1H, *dd*, $J_{1,2\beta} = J_{1,2\alpha} = 2.9$ Hz, H-1β), and 4.04 (1H, *ddd*, $J_{8,9\alpha} = 10.8$, $J_{8,7} = 10.1$, $J_{8,9\beta} = 5.0$ Hz, H-8); HRLSIMS, *m/z*: $[M+Na]^+$ 293.1727, ($C_{15}H_{26}O_4Na$, 293.1729, PPM +0.7).

Table 1
^{13}C NMR chemical shifts for compounds **1**, **4**, **5**, **6**, **7**, **8** and **9**

	Compounds						
	1	**4**	**5**	**6**	**7**	**8**	**9**
C-1	213.8	73.6	213.5	213.1	213.0	73.3	73.2
C-2	33.1	25.3	33.9	32.7	33.8	25.3	24.9
C-3	39.6	33.8	39.7	39.5	39.5	32.5	32.5
C-4	69.6	70.1	69.9	69.5	69.8	70.1	69.9
C-5	63.3	57.1	57.2	63.5	58.1	57.7	56.3
C-6	215.0	218.5	214.2	217.2	216.4	221.2	214.1
C-7	57.7	58.1	80.2	60.0	79.8	60.3	64.5
C-8	25.7	26.5	32.2	24.9	29.0	25.7	69.9
C-9	33.9	35.1	28.9	33.7	29.3	34.7	45.4
C-10	53.8	45.9	53.7	53.7	52.6	46.2	40.5
C-11	26.2	26.1	31.5	71.0	74.9	71.1	25.0
C-12	21.4	21.6	17.0	28.5	25.1	28.7	20.4
C-13	18.7	18.8	16.6	26.0	24.0	26.1	19.6
C-14	19.7	19.5	19.1	19.5	19.2	19.4	19.5
C-15	29.3	30.4	29.1	29.2	29.1	30.3	30.2

Acknowledgements

This work was financially supported by grants from the Comisión Interministerial de Ciencia y Tecnología (PM98-0213) and the Consejería de Educación y Ciencia de la Junta de Andalucía (FQM 0139). We thank Laura López (CECT) for her assistance with the taxonomy of the microorganisms used in this work and David Nesbitt for improving the use of English in the manuscript.

References

Amate, Y., García-Granados, A., Martínez, A., Sáenz de Buruaga, A., Bretón, J.L., Onorato, M.E., Arias, J.M., 1991. Biotransformation of 6β-eudesmanolides functionalized at C-3 with *Curvularia lunata* and *Rhizopus nigricans* cultures. Tetrahedron 47, 5811–5818.

Atta-ur-Rahman, Choudhary, M.I., Ata, A., Alam, M., Farooq, A., Perveen, S., Shekhani, M.S., 1994. Microbial transformations of 7α-hydroxyfrullanolide. J. Nat. Prod. 57, 1251–1255.

Becher, E., Schuep, W., Matzinger, P.K., Ehret, C., Teissiere, P.J., Maruyama, H., Suhara, Y., Ito, S., Ogawa, M., 1978. Hydroxypatchoulol and its derivatives. Ger. Offen. 2,739,449 (Cl. C07C35/22) 23 March 1978, Brit. Appl. 76/36,397, 02 Sept 1976; pp. 67.

El-Sharkawy, S., Zaghloul, A.M., Badria, F.A., Matooq, G.T., 1996. Biotransformation of α-santonin. Mansoura J. Pharm. 12, 99–109.

Fischer, N.H., Olivier, E.J., Fischer, H.D., 1979. The biogenesis and chemistry of sesquiterpene lactones. In: Herz, W., Grisebach, H., Kirby, G.W. (Eds.), Fortschritt der Chemie organischer Naturstoffe, Vol. 38. Springer-Verlag, New York, pp. 47–390.

Fraga, B.M., 1997. Natural sesquiterpenoids. Nat. Prod. Rep. 14, 145–162.

Fraga, B.M., 2000. Natural sesquiterpenoids. Nat. Prod. Rep. 17, 483–504.

García, Y., García-Granados, A., Martínez, A., Parra, A., Rivas, F., Arias, J.M., 1995. Microbial transformations of 6α- and 6β-eudesmanolides by *Rhizopus nigricans* cultures. J. Nat. Prod. 58, 1498–1507.

García-Granados, A., Molina, A., Sáenz de Buruaga, A., Sáenz de Buruaga, J.M., 1985. Sesquiterpenes from two subspecies of *Sideritis varoi*. Phytochemistry 24, 97–101.

García-Granados, A., Martínez, A., Onorato, M.E., Rivas, F., Arias, J.M., 1991. Chemical-microbiological synthesis of 6β-eudesmanolides by *Curvularia lunata* cultures from eudesmanes with functions at C-1 and C-6. Tetrahedron 47, 91–102.

García-Granados, A., Martínez, A., Parra, A., Rivas, F., Onorato, M.E., Arias, J.M., 1993. Chemical-microbiological synthesis of 6β-eudesmanolides from 11-hydroxyl derivatives obtained by *Rhizopus nigricans* cultures: synthesis of 6β-dendroserins. Tetrahedron 49, 1091–1102.

García-Granados, A., Parra, A., Simeó, Y., Extremera, A.L., 1998. Chemical, enzymatic and microbiological synthesis of 8,12-eudesmanolides: synthesis of sivasinolide and yomogin analogs. Tetrahedron 54, 14421–14436.

García-Granados, A., Martínez, A., Quirós, R., Extremera, A.L., 1999. Chemical-microbiological semisynthesis of enantio-Ambrox® derivatives. Tetrahedron 55, 8567–8578.

García-Granados, A., Melguizo, E., Parra, A., Pérez, F.L., Simeó, Y., Viseras, B., Arias, J.M., 2000a. Chemical semisynthesis and biotransformation with *Rhizopus nigricans* of several sesquiterpenes: obtention of new 1α- and 2α-hydroxyselinane derivatives. Tetrahedron 56, 6517–6526.

García-Granados, A., Melguizo, E., Parra, A., Simeó, Y., Viseras, B., Dobado, J.A., Molina, J., Arias, J.M., 2000b. Regioselective enzymatic acylations of polyhydroxylated eudesmanes: semisynthesis, theoretical calculations, and biotransformation of cyclic sulfites. J. Org. Chem. 65, 8214–8223.

Marles, R.J., Pazos-Sanou, L., Compadre, C.M., Pezzuto, J.M., Boszyk, E., Arnason, J.T., 1995. Sesquiterpene lactones revisited: recent developments in the assessment of biological activities and structure relationships. In: Arnason, J.T., Mata, R., Romeo, J.T., (Eds.), Phytochemistry of Medicinal Plants, Vol. 29. Plenum Press, New York, pp. 333–356.

Miyazawa, M., Honjo, Y., Kameoka, H., 1997. Biotransformation of the sesquiterpenoid β-selinene using the plant-pathogenic fungus *Glomerella cingulata* as a biocatalyst. Phytochemistry 44, 433–436.

Picman, A.K., 1986. Biological activities of sesquiterpene lactones. Biochem. Sys. Ecol 14, 255–281.

Robles, M., Aregullin, M., West, J., Rodríguez, E., 1995. Recent studies on the zoopharmacognosy, pharmacology and neurotoxicology of sesquiterpene lactones. Planta Med. 61, 199–203.

Rodríguez, E., Towers, G.H.N., Mitchell, J.C., 1976. Biological activities of sesquiterpene lactones. Phytochemistry 15, 1573–1580.

Schmidt, T.J., 1999. Toxic activities of sesquiterpene lactones: structural and biochemical aspects. Current Org. Chem. 3, 577–608.

Shimizu, N., Akita, H., Inamaya, S., Oishi, T., 1994. A formal synthesis of (–)-α-santonin from chiral α,β-epoxyeudesmanolide via enzyme-catalyzed hydrolysis. Chem. Pharm. Bull. 42, 1160–1162.

Sih, C.J., Rosazza, J.P.N., 1976. Microbial transformations in organic synthesis. In: Jones, J.B., Sih, C.J., Perlman, D. (Eds.), Applications of biochemical Systems in Organic Chemistry, Part 1. John Wiley and Sons Inc., New York, p. 69.

Socorro, O., 2001. Estudio de las Zahareñas, Rabos de Gato o Garranchuelos de la Provincia de Granada.

PERGAMON

Phytochemistry 58 (2001) 897–904

PHYTOCHEMISTRY

www.elsevier.com/locate/phytochem

Identification of an indigo precursor from leaves of *Isatis tinctoria* (Woad)

Thierry Maugard[a,*], Estelle Enaud[a], Patrick Choisy[b], Marie Dominique Legoy[a]

[a]*Laboratoire de Génie Protéique et Cellulaire, EA3169, Université de La Rochelle, Avenue Michel Crépeau, 17042 La Rochelle cedex 1, France*
[b]*CRITT Horticole 18, rue de l'Arsenal, 17300 Rochefort, France*

Received 23 April 2001; received in revised form 24 July 2001

Abstract

Indole is presumably a product of indole-3-glycerol phosphate catabolism in *Isatis tinctoria*. It is oxidized into indoxyl and stored in young leaves as indigo precursor. Further oxidation and dimerization of indoxyl produces indigoid pigments. In this work, we describe an HPLC method dedicated to the identification and quantification of indigoid pigments (indigo, indirubin, isoindigo and isoindirubin) and indigo precursors produced in *I. tinctoria* (Woad). This work, carried out with two cultivars of *I. tinctoria*, has confirmed that the quantity of indigo precursors is dependent on the species and the harvest period. In addition we have shown for the first time that young leaves of *I. tinctoria*, harvested in June contained a new indigo precursor in addition to isatan B (indoxyl-5-ketogluconate) and indican (indoxyl-β-D-glucoside). We suggest the name "isatan C" for this new indigo precursor in *I. tinctoria*. Its chemical characteristics point to an dioxindole ester with PM of 395. We have shown that isatan C reacts with isatan B increasing the red pigment production. © 2001 Elsevier Science Ltd. All rights reserved.

Keywords: Woad; *Isatis tinctoria*; Brassicaceae; Indigo; Indirubin; Isoindirubin; Isatan; Indican

1. Introduction

The blue dye indigo (indigotin) is one of the oldest natural dyestuffs known to human beings (Ensley et al., 1983). Indigo has, for centuries, been obtained from a variety of plant sources such as *Indigofera* (tropical species, Africa, Asia, East Indies, South America), *Polygonum tinctorium* (Far East, China, Korea) and *Isatis tinctoria* (Woad) (Europe). Indigo is an artefact of secondary metabolism. *Indigofera tinctoria* and *P. tinctoriuni* contain indican (indoxyl-β-D-glucoside) which serves as a starting material for indigo production, whereas *I. tinctoria* (Woad) contains isatan B (indoxyl-β-ketogluconate), as a major indigo precursor and indican as minor a indigo precursor (Epstein et al., 1967; Maier et al., 1990). In old leaves, precursors are broken down by hydrolases when the leaves are damaged and exposed to the air. The liberated indoxyl is spontaneously oxidized by oxygen yielding indigo. Isatin is generated from indoxyl in an oxygen-rich environment as a side reaction. The condensation of indoxyl with isatin produces indirubin which is a by-product of biosynthetic indigo production. It is well known that plants contain, in addition to *trans*-indigo (indigotin, blue) and *trans*-indirubin (isoindigotin, red), certain impurities such as *cis*-indigo (blue), *cis*-indirubin (isoindirubin, red), indigo brown (isoindigo), indigo gluten, indigo yellow and traces of flavonoids that makes natural indigo a more pleasing tinge than synthetic indigo (Perkin and Bloxam, 1907; Perkin, 1907).

In the present work, a qualitative and quantitative HPLC method is described for the identification and the separation of indigoid pigments and precursors present in *I. tinctoria* leaves. We show for the first time, that *I. tinctoria* produces three indigo precursors, isatan B as a major precursor, indican as a minor precursor and an other precursor that we named "isatan C". Eventually, this work describes the possible effect of isatan C on the red pigments production.

* Corresponding author. Tel.: +33-5-46-45-82-77; fax: +33-5-46-45-82-47.
E-mail address: tmaugard@univ-lr.fr (T. Maugard).

0031-9422/01/$ - see front matter © 2001 Elsevier Science Ltd. All rights reserved.
PII: S0031-9422(01)00335-1

2. Results and discussion

2.1. Extraction and identification of compounds from Isatis tinctoria

An extract of *I. tinctoria* (IT BM) harvested on 27th June 2000 is displayed in Fig. 1.

Extraction and HPLC analyses were performed as described in Experimental. The major compounds produced in *I. tinctoria* were identified by their UV and mass spectra:

Compound **1**: *Indican*. HPLC t_R 7.6 min, UV λ_{max} 218, 280. MS: *m/z* 296 (MH^+). HPLC t_R, mass spectrum and UV spectrum were identical to those of commercially available indican (Sigma).

Compound **2**: *Isatan B*. HPLC t_R 9.2 min, UV λ_{max} 218, 280. MS: *m/z* 310 (MH^+). No standard was available for isatan B. Consequently, it was necessary to produce pure isatan B and characterize it using NMR. ^1H NMR (D_2O) δ (ppm) 3.42 (*s*, 2H, H-1), 3.71 (*d*, 1H, H-4 or H-7), 3.73 (*d*, 1H, H-4 or H-7), 4.85 (*d*, 1H, H-4 or H-7), 6.98 (d, 1H, H-4 or H-7), 7.00 (*d*, 1H, H), 7.12 (*t*, 1H, H-4 or H-7), 7.31 (*d*, 1H, H-5 or H-6), 7.58 (d, 1H, H-5 or H-6).

Compound **3**: *Isatin*. HPLC t_R 11.9 min, UV λ_{max} 210, 244, 305. MS: *m/z* 148 (MH^+). HPLC t_R, mass spectrum and UV spectrum were identical to those of commercially available isatin (Sigma).

Compound **5**: *Indoxyl*. HPLC t_R 18.3 min, UV λ_{max} 240 nm. MS: *m/z* 134 (MH^+). HPLC t_R, mass spectrum and UV spectrum were identical to those of product generated by the hydrolysis of commercial 3-acetoxindole (indoxyl acetate) by the lipase of *Rhizomucor miehei*.

Compounds **6**, **7** and **8**: HPLC t_R 19.3, 21.6 and 22.2 min respectively. UV spectra of these three compounds correspond to flavonoid spectra.

Compound **4**: HPLC t_R 14.9 min. The mass spectrum indicated 396, assigned as MH^+, 398, assigned as MH_3^+ and 378, assigned as $MH^+–H_2O$. High resolution–mass spectrometry indicated 777 assigned as $[2(M–H_2O)+Na]^+$. A possible molecular formula is $C_{20}H_{13}O_8N_1$ (M, 395). The UV spectrum (UV λ_{max} 218, 280, Fig. 3) was similar to isatan B, indican and indoxyl acetate spectra. The amount of material isolated has not permitted the acquisition of a ^1H NMR spectrum. Alkaline media, in presence of oxygen, induce the synthesis of indigoid pigments out of isatan B and indoxylacetate, whereas indican remains unhydrolysed. This instability in alkaline media is consistent with the ester bound of isatan B, indoxyl acetate and compound **4**. On the basis of these results, we conclude that compound **4** is a new indigo precursor present in young leaves of *I. tinctoria*. Indeed, compound **4** is probably composed of dioxindole moiety (UV λ_{max} 218, 280) which binds an organic acid through ester bound. This new indigo precursor was named isatan C.

Acetone extract of young leaves of *I. tinctoria* (harvested June 27 2000), plated on TLC were developed by fuming ammonia vapour (pH > 13). One band developed a red/brown colour at R_f 0.7, one band developed a blue color at R_f 0.6 and one band developed a brown colour at R_f 0.2. These three compounds are three indigo precursors of woad, indican (R_f 0.2), isatan B (R_f 0.6) and isatan C (R_f 0.7).

Compounds **9**, **10**, **11**, **12** and **13**: the indigoid pigments produced in *I. tinctoria* were separated into five

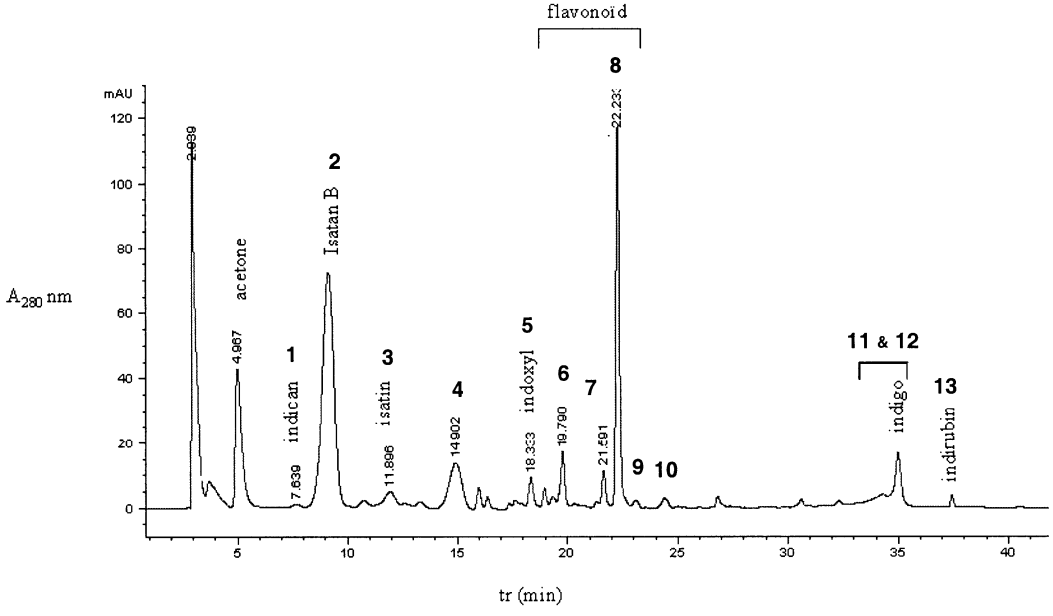

Fig. 1. HPLC analysis of an extract of *Isatis tinctoria* leaves harvested on 27 June 2000. Chromatograms were recorded at 280 nm. HPLC analysis was performed as described in Experimental.

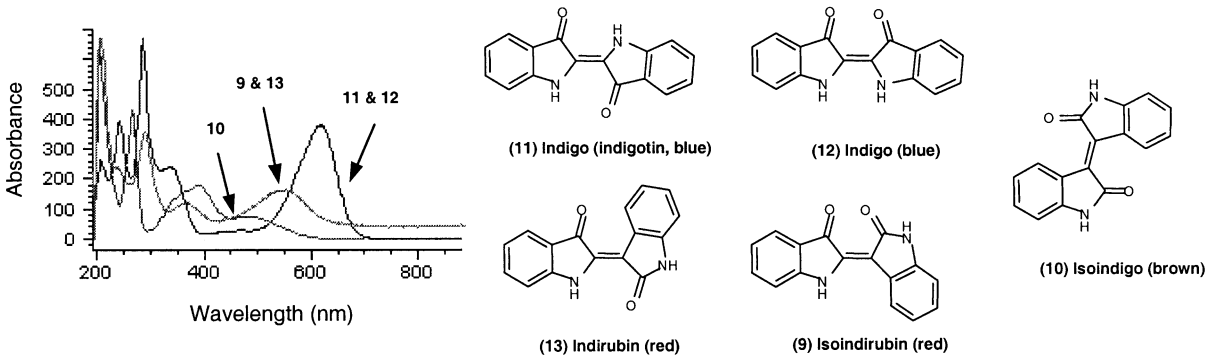

Fig. 2. UV/visible spectrocopy of pigments **9**, **10**, **11**, **12** and **13** formed in *Isatis tinctoria*. The pigments were seperated by HPLC, and UV/visible spectra were recorded. The spectrum of pigment **9** is typical of isoindirubin, pigment **10** corresponds to isoindigo, **11** and **12** are two isomers of indigo and **13** corresponds to indirubin.

compounds, of which two were blue (**11** and **12**, HPLC t_R: 34–36 min), two were red/purple (**9**, HPLC t_R: 23 min, **13**, HPLC t_R: 37.5 mm) and one was brown (10, HPLC t_R: 24.5 min). Pigments **11** and **13** were much more predominant. The UV/visible spectra of compounds **11** and **13** (UV 603 and 552 nm λ_{max} respectively) match the literature for *trans*-indigo (indigotin) and *trans*-indirubin (isoindigotin), respectively (Fearon and Boggust, 1950; Friedmann et al., 1950). The UV/visible spectra of compounds **9**, **10** and **12** (Fig 2, UV λ_{max} 552 nm, 500 nm and 603 nm respectively) correspond to *cis*-indirubin (isoindirubin), isoindigo (indigo brown) and *cis*-indigo, respectively. Mass spectrum yielded an apparent MH^+ ion at *m*/*z* 263 for compounds 9, 10, 11, 12 and 13, indicating a molecular mass of 262. Fragmentation of the *m*/*z* 263 ion in each case yielded *m*/*z* 235 (−CO) and 219 (−CO−NH_2). The same ions were seen when standard indigo (Sigma) was fragmented in the same way. We noted that *cis*-indirubin and *cis*-indigo had exactly the same UV/visible spectrum and mass spectrum (MS: *m*/*z* 263, MH^+) as *trans*-indirubin and *trans*-indigo, respectively. Isoindirubin (*cis*) is an isomer of indirubin (*trans*), as *cis*-indigo is an isomer of *trans*-indigo (indigotin) (Fig. 2).

2.2. Quantification of indigo precursors from Isatis tinctoria

The amount of indigo precursors present in old leaves and young leaves of two cultivars of *I. tinctoria* (IT BM and IT MC) was estimated at A_{280} (Fig. 4). The concentrations were evaluated with leaves harvested on 9, 15 and 30 May 2000 and 27 June 2000. The two cultivars of *I. tinctoria* contain similar but not identical concentrations of indigo precursors. We may notice that indigo precursors' quantity present in the young leaves, increased during time. Moreover, the amount of precursors present in IT MC young leaves is higher than the amount present in IT BM young leaves. Finally, young leaves contain higher concentrations of indigo precursors than older ones. This study confirms that the quantity of indigo precursors is dependent of the cultivars and of the period of harvest. It is important to notice that isatan B was observed in *I. tinctoria* leaves, from the harvest of April, whereas indican and compound **4** (isatan C) were observed and consequently quantified only from the harvest of the end of June.

2.3. Transformation of indigo precursors in alkaline media

The conversion of indigo precursors into indigo was followed by HPLC. Products were detected using a UV detector at 280, 550 (red pigments) and 603 nm (blue pigments) (Fig. 5, Table 1, Scheme 1). HPLC analysis was performed as described in Experimental.

Pure isatan B treated with an alkaline medium (NaOH solution 0.05 M, in water/CH_3CN 90/10, v/v. pH 13), produces indoxyl since the ester bond spontaneously brakes down. Indoxyl is then oxidized by air yielding indigo (**11**) (HPLC t_R: 32 min, blue).

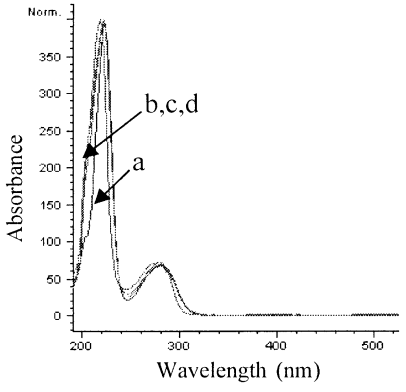

Fig. 3. Spectral characterization of compound **4**. UV spectrum online from HPLC: (a) indican, (b) indoxyl acetate, (c) isatan B, (d) compound **4**.

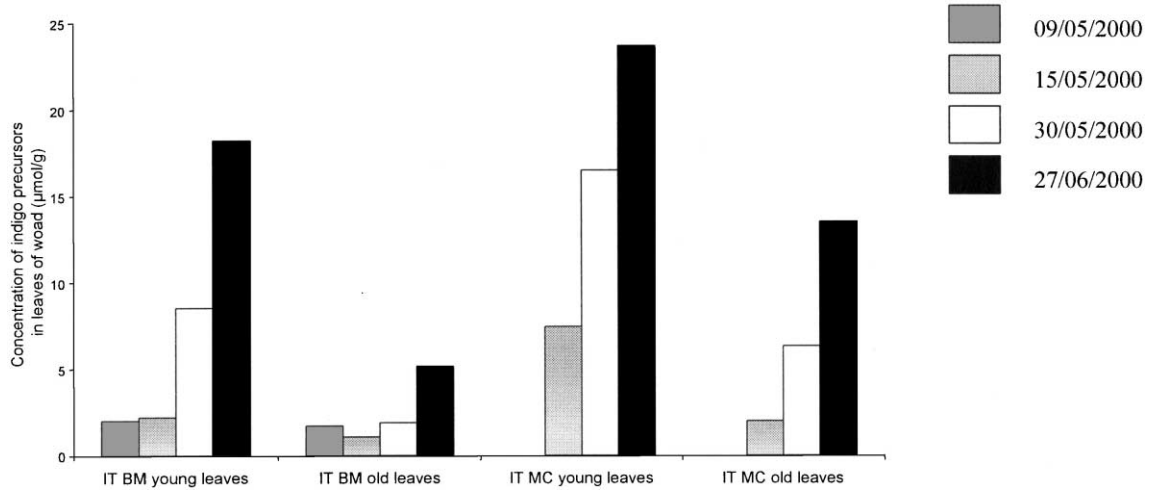

Fig. 4. Concentration of indigo precursors present in old leaves and young leaves of two cultivars of *Isatis tinctoria*. We consider young leaves as those located on the apex and old leaves those located underneath. Young leaves may be easily differentiated from old ones since they are light green and smaller than old leaves which are dark green. The concentrations were measured on leaves harvested on 9, 15 and 30 May 2000 and, finally, on 27 June 2000. Extraction and quantification were performed as described in Experimental.

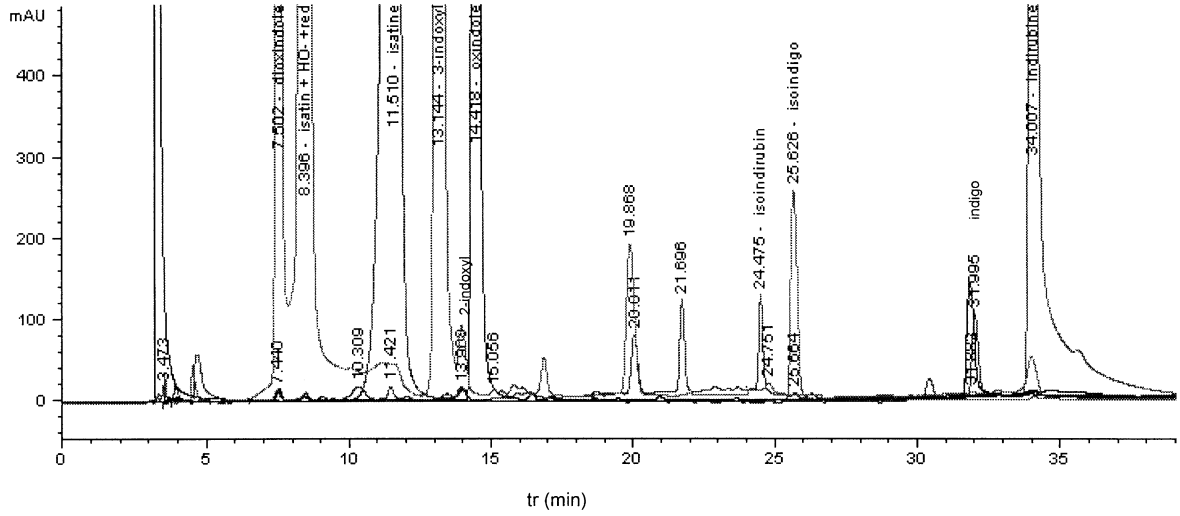

Fig. 5. HPLC analysis of the transformation of indigo precursors. Chromatograms were recorded at 280 nm. HPLC analysis was performed as described in Experimental.

Table 1
Alkaline formation of indigoid pigments

	Indigo (**11**) A_{603}, area units	Indirubin (**13**) A_{552}, area units	Isoindirubin (**9**) A_{552},area units
Isatan B	8000	5	–
Isatan C	300	200	5000
Isatan B and Isatan C	5000	200	100
Isatan B and Isatin	6800	3000	–
Isatan C and Isatin	870	1000	50

Indigo precursors were incubated with NaOH solution 0.05 M, in water/CH_3CN 90/10, v/v, pH 13. After 30 min, mixtures were analysed by HPLC. HPLC analysis was performed as described in Experimental. Dye production was analysed by recording A_{603} for blue pigments and A_{552} for red pigments.

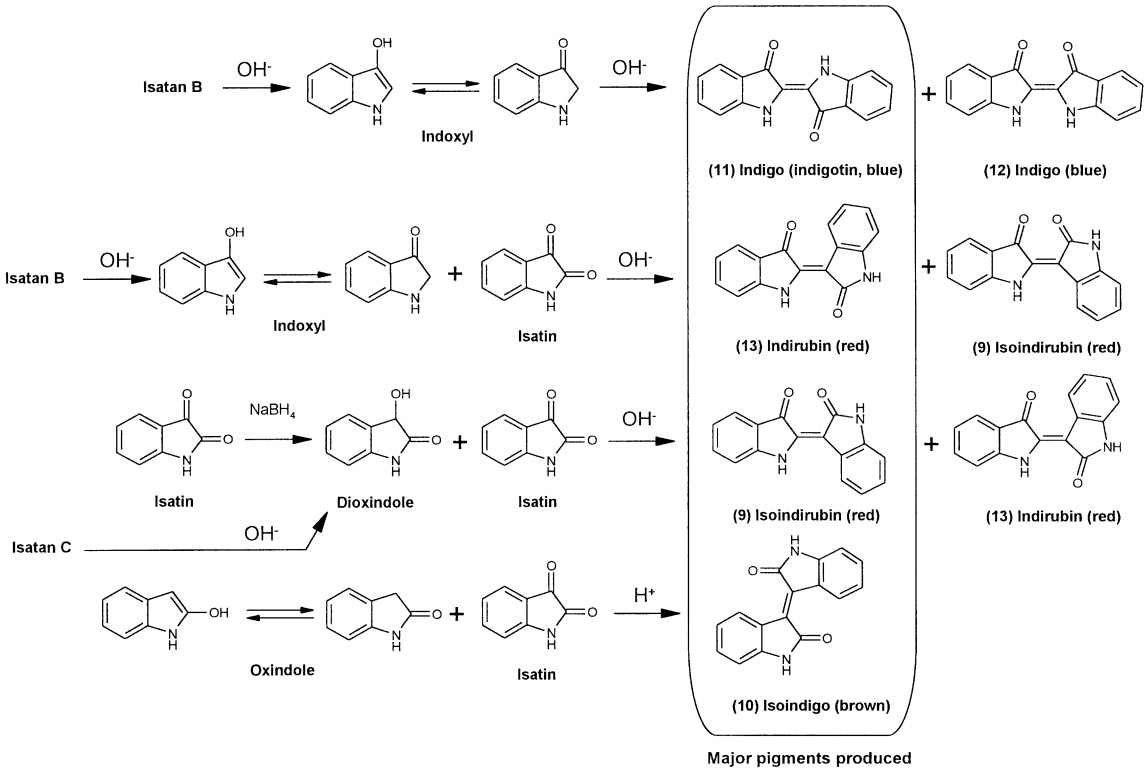

Scheme 1. Chemical pigments formation.

Isatan B added to isatin solution in 0.05 M NaOH, produces indoxyl which is oxidized yielding indigo. In addition, indoxyl reacts with isatin yielding indirubin (**13**) (HPLC t_R: 34 min, red). We noticed that indigo appeared to be the major pigment produced. When higher concentrations of isatin were used, pigment production decreased. Under these conditions, isatin appeared to be an inhibitor of the pigments production.

Isatan C in alkaline solution (0.05 M NaOH) produces dioxindole since the ester bond brakes down. Dioxindole is then oxidized by air yielding three pigments, indigo (**11**) and indirubin (**13**) (HPLC t_R: 34 min) as minor pigments, and another major red pigment, isoindirubin (**9**) (HPLC t_R: 24.5 min). The same result is obtained with a solution of isatin reduced by $NaBH_4$ in alkaline medium. Indeed, the product generated by $NaBH_4$ reduction of isatin is dioxindole (HPLC t_R: 7.5 min) as confirmed by HPLC t_R and UV spectra. Dioxindole may react with isatin in alkaline medium yielding isoindirubin and indirubin.

The reaction of isatan B and isatan C in alkaline medium produces indoxyl and dioxindole, which may be oxidized by air yielding indigo (**11**), indirubin (**13**) and isoindirubin (**9**).

A solution of oxindole and isatin in an alkaline medium do not produce any pigment. The condensation of oxindole with isatin may only be achieved in acidic media. In these conditions, the solution produces isoindigo, a brown pigment (**10**) (HPLC t_R: 25.6 min, λ_{max} 500 nm).

These results confirm that isatan C hydrolysis produces dioxindole that may react with isatin yielding isoindirubin (**9**) and indirubin (**13**). Isatan C is an indigo precursor and more specifically a precursor of red pigments present in *I. tinctoria*, and its chemical nature was established as dioxindole ester.

2.4. Discussion

The metabolism of indigo precursors is still under study. It is likely that indole is a product of indole-3-glycerol phosphate (Xia and Zenk, 1992) but not of tryptophan catabolism in vegetables. The indole ring could be oxidised by cytochrome P450 enzyme producing indoxyl and dioxindole. P450s are monooxygenases that catalyze the oxidation of a remarkably broad range of endogenous and exogenous chemicals. In plants they play important roles in biosynthetic pathways, including those of sterols, isoprenoids, alkaloids, oxygenated fatty acids, and phenylpropanoids (Bolwell et al., 1994; Durst and O'Keefe, 1995; Schuler, 1996). Indeed there is not yet evidence for the existence in plants of naphtalene dioxygenase or xylene mono-oxygenase (Ensley et al., 1983; Mermod et al., 1986), enzymes which are known to oxidize indole to indoxyl in some bacteria. In young leaves plants protect indoxyl, a highly unstable intermediate, from spontaneous oxidation to indigo by glycosylation to yield indican or by addition of 5-ketogluconate to yield isatan B. Further oxydation transforms

indoxyl to dioxindole. As indoxyl, plants may protect dioxindole by addition of an organic acid to yield isatan C. In the case of indican, this pathway has been located in vacuoles in which indican is synthesized from UDP-glucose and indoxyl (Minami et al., 2000; Marcinek et al., 2000). These indigo precursors are broken down by hydrolases when the leaves are old or damaged. Indoxyl liberated from isatan B and indican in old leaves is oxidized spontaneously by air yielding indigo. Isatin is generated from indoxyl and/or dioxindole in an oxygen-rich environment as a side reaction. Dioxindole is liberated from isatan C. The condensation of indoxyl with isatin produces indirubin, whereas the condensation of dioxindole with isatine yields isoindirubin and indirubin, which are by-products of the biosynthesis of indigo (Scheme 2).

3. Conclusion

In this work, an HPLC method is described to identify and quantify the pigments (indigo, indirubin and isoindirubin) and the indigo precursors produced in *I. tinctoria*. Our work with two cultivars of *I. tinctoria* has

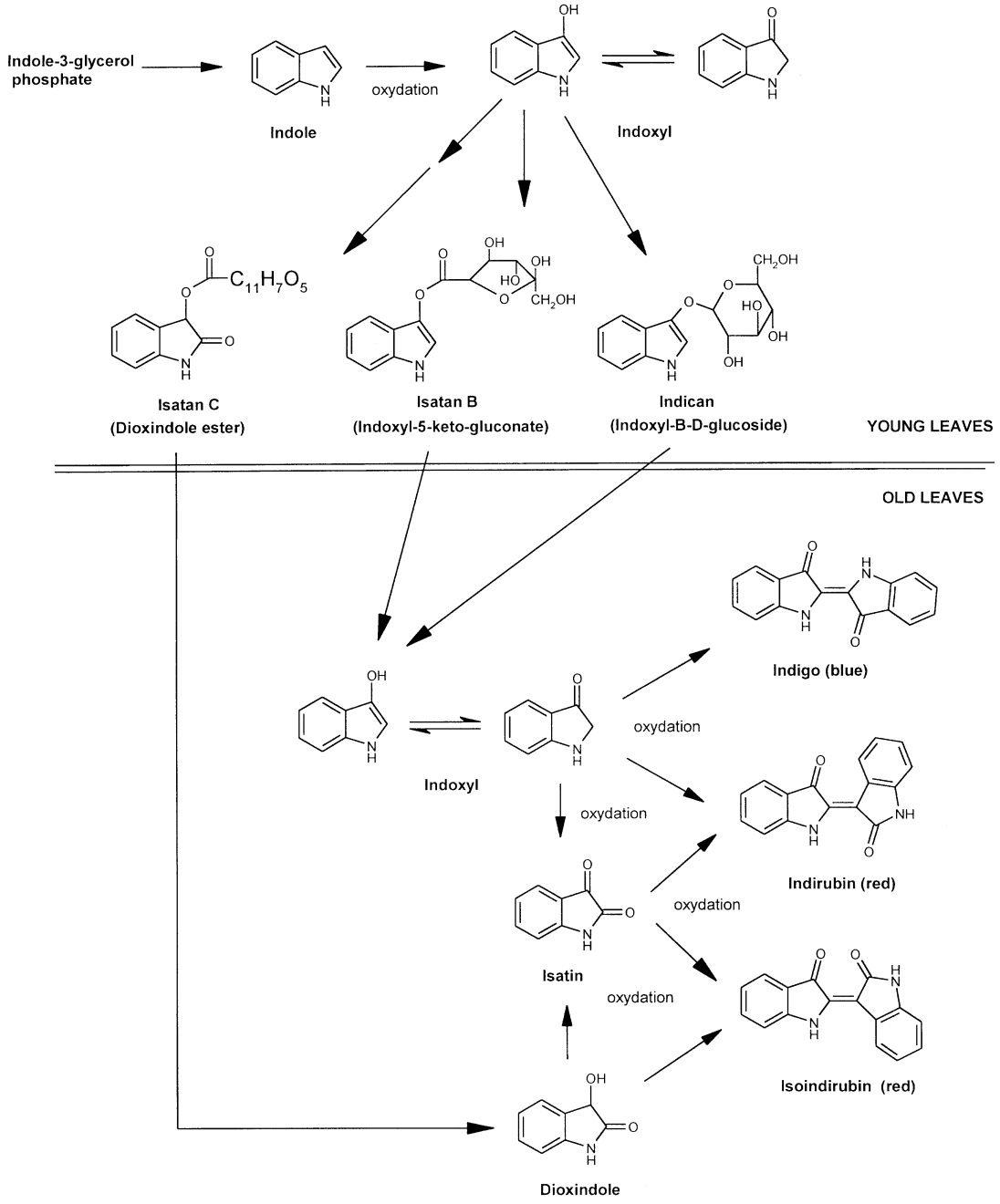

Scheme 2. Pigment formation in *Isatis tinctoria*.

confirmed that the quantity of indigo precursors is dependent of the cultivars and harvest period. We have shown for the first time that young leaves of *I. tinctoria*, harvested from June, produced a new indigo precursor in addition to isatan B and indican. The name "isatan C" is proposed to describe this new indigo precursor in woad. Its chemical nature was tentatively established as dioxindole ester with PM of 395 and possible molecular formula $C_{20}H_{13}O_8N$. However its structure is not completely specified due to low amounts of the precursor and to higher instability. Finally, we have shown that isatan C increases the pigments production and especially isoindirubin. These results confirm that *I. tinctoria* harvested in June produced isatan C as indigo precursor which favours the production of red pigments, indirubin and isoindirubin.

4. Experimental

4.1. Biological and chemical material

Indigo, indican, isatin, oxindole and 3-acetoxy-indole (indoxyl acetate), were obtained from Sigma Chemical Co. (USA). Isatan B and isatan C were obtained from an extract of woad. The extraction procedure is described below.

4.2. Chemical pigment synthesis

Indirubin was prepared by reaction of isatin with 3-acetoxy-indole in alkaline media. Under argon, isatin (1 mmol) and sodium carbonate (2.4 mmol) were added to a solution of indoxyl acetate (1 mmol) in methanol (5 ml) (Hoessel et al., 1999; Russel and Kaup, 1969). The mixture was stirred for 1 h at room temperature and filtered off after 24 h hold. The residue was washed with methanol and cold water until neutral reaction of the filtrate. The product (dark violet crystals) was dried over potassium hydroxide in the dessicator. Indirubin was identified by ^{1}H NMR, UV spectrum and mass analysis (coupled to HPLC). Indirubin: yield 85%, UV λ_{max} 552 nm, M: m/z 263 (MH^+).

Isoindirubin was prepared by reaction of isatin with $NaBH_4$ in alkaline media. Isatin (1 mmol) and $NaBH_4$ (0.5 mmol) were stirred at 25 °C in methanol (3 ml). After 1 h, isatine (1 mmol) and 1 ml of NaOH 0.1 M were added. The mixture was stirred at room temperature and was filtered after 12 h hold, The residue was washed with methanol and cold water. Products (two dark violet crystals) were dried over potassium hydroxide in a dessicator. Pigments were identified according to the UV spectrum and mass analysis (coupled to HPLC). Indirubin: yields 85%, UV λ_{max} 552 nm, MS: m/z 263 (MH^+); Isoindirubin: yield 10%, UV λ_{max} 552 nm, MS: m/z 263 (MH^+).

Isoindigo was prepared by reaction of isatin with oxindole in acid media and identified by ^{1}H NMR, UV spectrum and mass analysis (coupled to HPLC) (Hoessel et al., 1999; Russel and Kaup, 1969). Oxindole (1 mmol) and isatin (1 mmol) were stirred at 95 °C in a mixture of glacial acetic acid (3 ml) and concentrated hydrochloric acid (50 μl). After 3 h, the precipitate (dark brown crystals) was filtered off and washed with methanol and diethyl ether. Yield: 90%, UV λ_{max} 550, MS: m/z 263 (MH^+).

4.3. Plant material

Two cultivars of *I. tinctoria* (IT BM and IT MC) were grown in a field of CRITT Horticole (St Savin, France). The date of seeding was 23 March 2000. In this paper, we consider young leaves as those located on the apex and old leaves those located underneath. Young leaves may be easily differentiated from old ones since they are light green and smaller than old leaves which are dark green. Leaves were harvested from June to September. The leaves were weekly for indigo quantification. Four overall harvests were carried out monthly.

4.4. Extraction

Reactions were conducted in screw-cap glass vials. In standard procedure, fresh leaves were ground in a mortar and suspended in acetone/acetic acid 1% v/v (10 ml/g of fresh leaves) and stirred at 24 °C for 4 h. After filtration, acetone was evaporated under reduced pressure. The residue was dissolved in a small volume of methanol and analyzed by TLC and HPLC or HPLC–MS.

Pigment concentrations and yields of indigo precursors produced from *I. tinctoria* were quantified by HPLC analysis with reference to a standard curve of products dissolved in methanol.

4.5. TLC analysis

TLC was used for qualitative analysis on silica gel 60 F plates (Merck). Elution was carried out with the mixture: ethyl acetate/acetone (1/1, v/v). Conversion of the indoxyl glycosides (indigo precursors) into indigo and indirubin on TLC plates were achieved by fuming with NH_3 vapor from a concentrated solution (pH >13).

4.6. Separation and identification of Indigo precursors and pigments from Isatis tinctoria by HPLC

Separation and identification of indigo precursors and pigments was conducted using an HPLC system from Hewlett Packard (processor, pump, UV detector and injector model 1100). Analyses were carried out with an Ultrasep C18 (250×4 mm, 6 μ) reverse phase column from ICS (France), at 50 °C with a flow rate of 0.85 ml/

min using a gradient made of solvent A (CH_3OH/TFA 0.2%) and solvent B (H_2O/TFA 0.2%). Programme: 0–10 min: 85% B/ 15% A to 75% B/ 25% A; 10–30 min: 75 to 30% B; 30–40 min: hold at 30% B; 40–45 min: 30 to 85% B. Products were detected and quantified using a diode array detector at 280 nm. During the chromatographic analysis, UV/visible spectra of each individual peak were acquired online using a diode array detector. Further characterisation of purified peaks was achieved by HPLC–MS analyses, with comparisons to the A_{280} traces (online) obtained with rapid-scanning UV analysis.

4.7. Hydrolysis of indigo precursors

To identify products (indoxyl, dioxindole, isatin, indigo, indirubin, isoindirubin) formed from indigo precursors, pure indigo precursors or extracts of *I. tinctoria* leaves were incubated with (i) a NaOH solution (0.05 M) in H_2O/CH_3CN, 90/10, v/v, pH 13, or (ii) with Lipozyme® (lipase from *R. miehei*) in an appropriate medium (*tert*-amyl alcohol/water, 95/5, v/v). Aliquots (200 μl) were taken at different time and methanol (200 μl) was added. The mixture was analysed by HPLC and TLC.

4.8. Purification of indigo precursors and study of isatan C transformation

The purification of indigo precursors and the transformation of isatan C in alkaline media were followed by preparative HPLC. We used an Ultrasep C18 (250×8 mm, 6 μ) reverse phase column from ICS (France), at 50 °C with a flow rate of 2.3 ml/min and with a gradient composed of solvent A (CH_3CN/TFA 0.2%) and solvent B (H_2O/TFA 0.2%). Programme: 0–10 min: 85% B/ 15% A to 75% B/ 25% A; 10–30 min: 75 to 30% B; 30–40 min: hold at 30% B; 40–45 min: 30 to 85% B. Products were detected using a UV detector at 280, 550 and 603 nm.

4.9. Structural analysis

^{1}H NMR were recorded on a Jeol-JNM LA400 (400 MHz) spectrometer (Laboratoire Commun d'Analyse, Université de La Rochelle), with an internal reference of tetramethylsilane. HPLC–MS analysis was carried out in the Centre Régional de Mesure Physiques de L'Ouest (CRMPO), Université de Rennes, France. HPLC–MS analyses were recorded using an HPLC coupled to an API III+ (Sciex, Thornhillm, L3T 1P2, ON. Canada). We have used the same column and gradient system as described above.

Acknowledgements

This project was financially supported by the CRITT Horticole, France.

References

Bolwell, G.P., Bozak, K., Zimmerlin, A., 1994. Plant cytochrome P450. Phytochemistry 37, 1491–1506.

Durst, F., O'Keefe, D., 1995. Plant cytochromes P450s: an overview. Drug Metab. Drug Interact. 12, 171–187.

Ensley, B.D., Ratzkin, B.J., Osslund, T.D., Simon, M.J., Wackett, L.P., Gibson, D.T., 1983. Expression of naphthalene oxidation genes in *Escherichia coli* results in the biosynthesis of indigo. Science 222, 167–169.

Epstein, E., Nabors, M.W., Stowe, B.B., 1967. Origin of indigo of woad. Nature 216, 547–549.

Fearon, W.R., Boggust, W.A., 1950. Pigments derived from tryptophan: urosein, tryptochrome. Biochem. J. 46, 62–67.

Friedmann, E., Marrian, D.H., Perutz, M.F., 1950. Contribution to the chemistry of leucaemic urine. Biochim. Biophys. Acta 5, 45–52.

Hoessel, R., Leclerc, S., Endicott, J.A., Nobel, M.E., Lawrie, A., Tunnah, P., Leost, M., Damiens, E., Marie, D., Marko, D., Niederberger, E., Tang, W., Eisenbrand, G., Meijer, L., 1999. Indirubin, the active constituent of a Chinese antileukaemia medicine, inhibits cyclin-dependant kinases. Nat. Cell. Biol. 1, 60–67.

Maier, W., Schumann, B., Gröger, D., 1990. Biosynthesis of indoxyl derivatives in *Isatis tinctoria* and *Polygonum tinctorium*. Phytochemistry 29, 817–819.

Marcinek, H., Weyler, W., Deus-Neumann, B., Zenk, M.H., 2000. Indoxyl-UDPG-glucosyltransferase from *Baphicacanthus cusia*. Phytochemistry 53, 201–208.

Mermod, N., Harayama, S., Timmis, K.N., 1986. New route to bacterial production of indigo. BioTechnology 4, 321–326.

Minami, Y., Nishimura, O., Hara-Nishimura, I., Nishimura, M., Matsubara, H., 2000. Tissue and intracellular localization of indican and the purification and characterization of indican synthase from indigo plants. Plant Cell Physiol. 41, 218–225.

Perkin, A.G., 1907. Constituents of natural indigo. Part II. J. Chem. Soc., 435–440.

Perkin, A.G., Bloxam, P., 1907. Some constituents of natural indigo. Part I. J. Chem. Soc., 279–288.

Russel, G.A., Kaupp, G., 1969. Oxidation of carbanions. IV. Oxidation of indoxyl to indigo in basic solution. J. Am. Chem. Soc. 91, 3851–3859.

Schuler, M.A., 1996. Plant cytochrome P450 monooxygenases. Crit. Rev. Plant Sci. 15, 235–284.

Xia, Z.K., Zenk, M.H., 1992. Biosynthesis of indigo precursors in higher plants. Phytochemistry 31, 2695–2697.

PERGAMON

Phytochemistry 58 (2001) 905–909

PHYTOCHEMISTRY

www.elsevier.com/locate/phytochem

Isolation, structure determination, and phytotoxicity of unusual dioxopiperazines from the phytopathogenic fungus *Phoma lingam*

M. Soledade C. Pedras*, Corinne J. Biesenthal

Department of Chemistry, University of Saskatchewan, 110 Science Place, Saskatoon SK S7N 5C9, Canada

Received 24 May 2001; received in revised form 16 July 2001

Abstract

The isolation, chemical structure elucidation, and bioactivity of polanrazines B–F, five new dioxopiperazines produced by isolates of the blackleg fungus [*Phoma lingam,* perfect stage *Leptosphaeria maculans* (Desm.) Ces. et de Not.] originating from Poland, are reported. Polanrazines C and E showed moderate but selective toxicity, causing necrotic and chlorotic lesions (1–3 mm diameter) on brown mustard leaves. © 2001 Elsevier Science Ltd. All rights reserved.

Keywords: Blackleg disease; Crucifer; Dioxopiperazines; *Leptosphaeria maculans*; *Phoma lingam*

1. Introduction

Blackleg of cruciferous plants is a devastating fungal disease caused by the phytopathogen *Leptosphaeria maculans* (Desm.) Ces. et de Not., asexual stage *Phoma lingam* (Tode ex Fr.) Desm. Virulent isolates of the fungus have caused enormous yield losses in rapeseed (*Brassica napus* L. and *B. rapa* L.) and canola (*B. napus* L. and *B. rapa* L.) in Canada and worldwide (Gugel and Petrie, 1992). To develop appropriate control practices that prevent blackleg disease outbreaks and a rapid breakdown of plant resistance, it is essential to characterize and differentiate the various fungal isolate types. Initially, two different groups of *P. lingam* (originally called "strains") were characterized in Canada on the basis of virulence, host range, and cultural tests: a highly virulent type (V) causing leaf spots and severe stem cankers on rapeseed and cabbage (*B. oleracea* L.) and a weakly virulent type (W) causing only superficial leaf and stem lesions on rapeseed and cabbage (McGee and Petrie, 1978). Subsequently, due to the broad variability of fungal isolates causing blackleg, additional subgroups within each of the V and W groups were proposed (Williams and Fitt, 1999; Howlett et al., 2001). Thus far, isolates belonging to the V group, also known as A group or aggressive, appear to be responsible for the largest yield losses in Canada, UK, France, Germany, and Australia, whereas in Poland the W isolates appear to cause significant crop damage as well (Williams and Fitt, 1999). Current evidence indicates that isolates of the blackleg fungus occurring in Canada and previously characterized as W isolates, also known as avirulent, B group, or nonaggressive, are likely *P. wasabiae* Yokogi, and not *P. lingam* (Pedras et al., 1995, 1996; Taylor et al., 1995; Pedras, 1998; Reddy et al., 1998); however, since no formal reclassification has occurred yet, these isolates will be hereon referred to as W group. Moreover, we have also reported on isolates Laird 2 and Mayfair 2, thus far two unique W Canadian isolates classified as *P. lingam*, whose metabolite profile is rather different from those of either V or W isolates (Pedras et al., 1998, 1999).

Recent studies of isolates of the species *P. lingam* collected in different countries suggested that there are at least three distinct groups which may constitute three different *Phoma* species (Pedras and Biesenthal, 2000). Chemical analysis of the secondary metabolites of such isolates indicated that isolates of *P. lingam* originating from Poland were clearly different from Canadian, French, German, or Australian isolates (Pedras and Biesenthal, 1998, 2000). To characterize and clarify the relationship among diverse blackleg isolates, we have analyzed fungal isolates from Poland and here wish to report their secondary metabolites, compounds **1**–**7**.

* Corresponding author. Tel.: +1-306-966-4772; fax: +1-306-966-4730.

E-mail address: soledade.pedras@usask.ca (M.S.C. Pedras).

0031-9422/01/$ - see front matter © 2001 Elsevier Science Ltd. All rights reserved.
PII: S0031-9422(01)00348-X

Dioxopiperazines **3**–**7** represent new metabolites which we named polanrazines B, C, D, E and F. Discussion of the implications of our findings and suggestions for isolate grouping are also provided.

2. Results and discussion

Initially, eight Polish isolates (IBCN 19–26) of *P. lingam* were grown in liquid cultures, the culture broths extracted with EtOAc, and the extracts analyzed by TLC, HPLC, and ^{1}H NMR spectroscopic analyses. Both the HPLC chromatograms and ^{1}H NMR spectra of each extract were similar and suggested the presence of aromatic compounds not available in our library containing *P. lingam* metabolites isolated to date (Pedras, 1998). Furthermore, bioassay of those extracts (as reported in the Experimental) on leaves of canola, brown mustard (*B. juncea*), and white mustard (*Sinapis alba*) suggested that these extracts were more phytotoxic to brown mustard than to canola or white mustard. Subsequently, Polish isolate IBCN 19 was selected to grow on a larger scale for metabolite isolation and chemical structure determination. The EtOAc extract of the culture broth was fractionated by FCC followed by multiple fractionation by prep. TLC, as described in the experimental, to yield phomapyrone A (**1**) and compounds **2**–**7**. The structures of phomapyrone A (**1**) (Pedras et al., 1994) and L-valyl-L-tryptophan anhydride (**2**) (Pedras et al., 1998) were readily established by comparison of their chromatographic and spectroscopic data with that of authentic samples available in our compound library (Pedras and Biesenthal, 2000). Phomapyrone (**1**) was previously isolated from W Canadian isolates (Pedras et al. 1994), isolates Mayfair 2 and Laird 2 (Pedras et al., 1998, 1999) whereas **2** was only isolated from isolates Mayfair 2 and Laird 2 (Pedras et al., 1998, 1999).

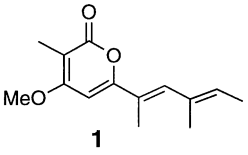

1

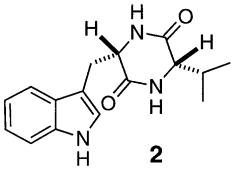

2

The remaining constituents appeared to be structurally related to dioxopiperazine **2**, as their ^{1}H and ^{13}C NMR spectra showed the expected signals of a 2,5-dioxopiperazine ring containing 3-methyleneindolyl and isopropyl substituents (Table 1). Compared to L-valyl-L-tryptophan anhydride (**2**), the least polar of the dioxopiperazines (**3**) showed two methyl singlets instead of the methine protons at C2′ and C5′. That these methyl groups were likely attached to sulfur atoms was suggested by their chemical shifts, and confirmed by HRMS (for $C_{18}H_{23}N_3O_2S_2$). Because no trivial name was assigned to L-valyl-L-tryptophan anhydride (**2**) we propose that it be named polanrazine A and that compound **3** be named polanrazine B. Similarly, the structures of **4**–**7** were assigned from analysis of NMR (Table 1) and HRMS data. The regiochemistry of the substituents at C2′ and C5′ was assigned based on HMBC correlations of the methyl protons to C5′, in compounds **4** and **6**, or to C2′, in compound **5**. Compound **6** was readily distinguished from **4** based on the chemical shifts of the methyl group (δ_H 3.18, δ_C 51.5 in **6** vs. δ_H 0.81, δ_C 9.7 in **4**). The unusually low proton and carbon chemical shifts of the SMe group of **4** might be due to a shielding effect of the indole ring (Lambert et al., 1998). The relative configurations were established by NOE experiments between the methylene protons at C1′ and methyne proton at C8′. The absolute configuration of compounds **3**–**7** was not established; however in previous work we established by total synthesis that the stereogenic centers of **2** (2′ and 5′) had *S,S* configuration, and are now suggesting a similar assignment for the corresponding stereogenic centers of **3**–**7**. Similar to trivial names of **2** and **3,** we propose that **4**–**7** be named polanrazines C–E.

Dioxopiperazines are common secondary metabolites produced by a variety of microorganisms of both marine and terrestrial origin; in fact V isolates of *P. lingam* produce a variety of epithiodioxopiperazines including the phytotoxins sirodesmins (Pedras, 1998). On the other hand, dioxopiperazines such as polanrazines C-E having OH/OR groups at the α-carbon of the amino acid residues appear to be rather unusual (e.g. Nozawa et al., 1989; King et al., 1992).

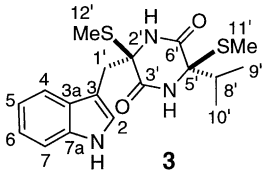

3

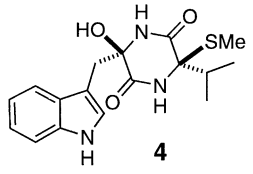

4

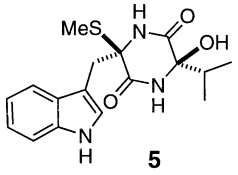

5

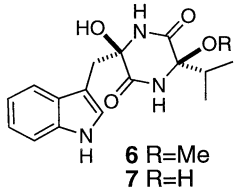

6 R=Me
7 R=H

The phytotoxicity assays of polanrazines A–E (**2**–**7**) on plants resistant and susceptible to *P. lingam* indicated that both **4** and **6** had moderate but selective toxicity, causing necrotic and chlorotic lesions (1–3 mm diameter) on brown mustard leaves (5×10^{-4} M), whereas no damage was observed on canola or white mustard leaves. Lower concentration of these metabolites (**2**–**7**) caused no macroscopic effects. Furthermore,

preliminary inoculations of canola and brown mustard with spores of isolate IBCN 19 have shown that brown mustard is more susceptible to Polish isolates than canola, whereas the W isolates from Canada cause low to no disease symptoms on either species (Gugel and Petrie, 1992).

The present studies indicate that blackleg W isolates originating from Poland produce metabolites similar to those obtained from Canadian isolates Laird 2 and Mayfair 2 (Pedras et al., 1998, 1999). It may be that Mayfair 2 and Laird 2 isolates have not originated in Canada but got to North America through seed brought in from European countries (Pedras and Biesenthal, 2000). Further studies to establish the secondary metabolite profiles of blackleg fungal isolates will be of great assistance in the chemotaxonomic classification of the "complex species" presently known as *P. lingam*/*L. maculans*. Polanrazines A–E will be useful chemotaxonomic markers for grouping new isolates in the appropriate "W group" as they do not appear to be produced by other blackleg isolate types. Nonetheless, this statement does not imply that the virulence of the Polish fungal isolates is related with the production of polanrazines A–E, such a conclusion will require additional investigations. Moreover, the metabolite profile obtained for Polish isolates suggest that this group is distinct from the W Canadian group (*P. wasabiae*). Because brown mustard, a crop traditionally resistant to blackleg disease, was shown to be more susceptible to these "W Polish" isolates, there is a possibility that such isolates will cause new blackleg epidemics. Thus, to prevent additional disease outbreaks, systematic screening of blackleg isolates must be carried out in areas where brown mustard is widely grown.

3. Experimental

3.1. General

All chemicals were purchased from Sigma-Aldrich Canada Ltd., Oakville, ON. All solvents were HPLC grade and used as such, except for CH_2Cl_2 and $CHCl_3$ which were redistilled. Preparative (prep.) TLC: (Merck, Kieselgel 60 F_{254}), 20 × 20 cm × 0.25 mm; analytical TLC (Merck, Kieselgel 60 F_{254}, aluminum sheets) 5 × 2 cm × 0.2 mm; compounds were visualized by exposure to UV light and by dipping the plates in a 5% aq (w/v) phosphomolybdic acid solution containing a trace of ceric sulfate and 4% (v/v) H_2SO_4, followed by heating at 200 °C. Flash column chromatography (FCC): silica gel Merck, grade 60, mesh size 230–400, 60 Å.

High pressure liquid chromatography (HPLC) analysis was carried out with a high performance liquid chromatograph equipped with quaternary pump, automatic injector, and diode-array detector (wavelength

Table 1
^1H and ^{13}C NMR chemical shifts (ppm) and ^1H multiplicities (*J* in Hz) for compounds **3**–**7** (solvent)

C/H #	Polanrazine B **3** (CD_2Cl_2)		Polanrazine C **4** (CD_3OD)		Polanrazine D **5** (CD_3OD)		Polanrazine E **6** (CD_3CN)		Polanrazine F **7** (CD_3OD)	
	δ_H	δ_C	δ_H	δ_C	δ_H	δ_C	δ_H	δ_C	δ_H	δ_C
2	7.20 *s*	125.4	7.15 *s*	125.5	7.11 *s*	125.5	7.10 *s*	125.9	7.09 *s*	125.2
3	–	108.3	–	108.0	–	108.1	–	108.1	–	107.6
3a	–	128.3	–	128.5	–	128.4	–	128.6	–	128.4
4	7.39 *d*, 8.0	111.5	7.29 *d*, 8	111.0	7.27 *d*, 8	111.0	7.33 *d*, 7.5	111.7	7.28 *d*, 7.5	110.9
5	7.16 *dd*, 7.5, 7.5	120.3	7.01 *dd*, 8, 8	119.0	7.00 *dd*, 8, 8	119.0	7.08 *dd*. 7	119.5	6.99 *dd*. 8	118.9
6	7.21 *dd*, 7.5, 7.5	122.5	7.07 *dd*, 7, 7	121.3	7.05 *dd*, 7, 7	121.2	7.05 *dd*, 7	121.9,	7.05 *dd*, 7.5	121.2,
7	7.64 *d*, 7.8	119.1	7.76 *d*, 8	119.2	7.71 *d*, 8	119.1	7.65 *d*, 7.5	119.5	7.70 *d*, 8	119.1
7a	–	136.4	–	136.8	–	136.7	–	136.8	–	136.8
1′	3.28 *d*, 14.5	36.1	3.13 *d*, 14	35.5	3.17 *d*, 14	35.2	3.14 *d*, 14	36.1	3.13 *d*, 14	35.2
1′	3.78 *d*, 14.5	36.1	3.74 *d*, 14	35.5	3.72 *d*, 14	35.2	3.57 *d*, 14	36.1	3.66 *d*, 14	35.2
2′	–	67.4	–	83.2	–	69.4	–	83.3	–	83.3
3′	–	166.1	–	168.5	–	168.4	–	168.9	–	169.4
5′	–	69.2	–	72.8	–	84.1	–	89.9	–	84.1
6′	–	166.7	–	169.2	–	169.0	–	165.6	–	168.7
8′	2.22 *m*	33.1	2.23 *m*	37.0	2.28 *m*	35.2	1.97 *m*	35.7	1.82 *m*	35.1
9′/10′	0.14 *d*, 7	16.0	1.0 *d*, 7	17.5	−0.25 *d*, 7	15.1	−0.04 *d*, 7	15.6	−0.15 *d*, 7	15.0
10′/9′	0.92 *d*, 7	15.0	1.04 *d*, 7	15.5	0.62 *d*, 7	13.2	0.62 *d*, 7	14.1	0.64 *d*, 7	13.3
11′ SMe	2.23 *s*	14.5	0.81 *s*	9.7	2.28 *s*	12.1	–	–	–	–
12′ SMe	2.44 *s*	14.7	–	–	–	–	–	–	–	–
11′ OMe	–	–	–	–	–	–	3.18 s	51.5	–	–
OH	–	–	–	–	–	–	4.75 *br s*	–	–	–
NH	5.71 *br s*	–	–	–	–	–	6.31 *br s*	–	–	–
NH	6.09 *br s*	–	–	–	–	–	7.21 *br s*	–	–	–
NH	8.33 *br s*	–	–	–	–	–	9.17 *br s*	–	–	–

range 190–600 nm), degasser, and a Hypersil ODS column (5 μm particle size silica, 4.6 i.d. × 200 mm), equipped with a low-dispersion column-inlet filter. Two different elution methods were employed; method A: linear gradient from 75% H_2O–25% CH_3CN to 100% CH_3CN, at a flow rate 1.0 ml/min over 35 min; method B: isocratic elution 80% H_2O–20% CH_3CN for 10 min, followed by gradient elutions, 80% H_2O–20% CH_3CN to 60% H_2O–40% CH_3CN for 10 min, and 60% H_2O–40% CH_3CN to 25% H_2O–75% CH_3CN for 10 min, at a flow rate 1.0 ml/min.

NMR spectra were recorded on a Bruker AMX 300 or 500 spectrometer; for ^1H (300 or 500 MHz), δ values were referenced to CD_3OD (CD_2HOD at 3.31 ppm), CD_2Cl_2 ($CDHCl_2$ at 5.32 ppm), or CD_3CN (CHD_2CN at 1.94 ppm), and for ^{13}C (75.5 or 125.8 MHz) referenced to CD_3OD (49.15 ppm), CD_2Cl_2 (54.00 ppm), or CD_3CN (118.69 ppm). The list of coupling constants (J, reported to the nearest 0.5 Hz) corresponds to the order of the multiplicity assignment.

Mass spectra (MS) [high resolution (HR), electron impact (EI), or fast atom bombardment (FAB)] were obtained on a VG 70 SE mass spectrometer, employing a solids probe. Specific rotations, $[\alpha]_D$ were determined at ambient temperature on a Perkin-Elmer 141 polarimeter using a 1 ml, 10 cm path length cell; the units are 10^{-1} deg cm^2 g^{-1} and the concentrations are reported in g/100 ml. Infrared spectra were recorded on a Bio-Rad FTS-40 spectrometer. Spectra were measured by the diffuse reflectance method on samples dispersed in KBr; only diagnostic peaks are reported.

3.2. Fungal cultures and bioassays

The eight Polish isolates of *P. lingam*, IBCN 19-26, were obtained from the IBCN blackleg collection at Agriculture and Agri-Food Canada, Saskatoon. Liquid cultures of these isolates were grown as previously reported (Pedras and Biesenthal, 2000). For isolation of metabolites, isolate IBCN 19 was grown in 250 ml Erlenmeyer flasks containing 100 ml minimal medium (total 4 l) inoculated with fungal spores at 2×10^9 per flask were incubated on a shaker at 150 rpm, at 24±2 °C for 6 days, and worked up as described below.

Plants were grown in a growth chamber for 3 weeks, with 16 h light (fluorescent and incandescent, 450–530 μmol s^{-1} m^{-2})/8 h dark, at 24±2 °C. Three different species of known resistance to V isolates of *Phoma lingam* were employed in the bioassays: *Brassica napus*, cv. Westar (susceptible) and *B. juncea*, cv. Cutlass (resistant), *Sinapis alba*, cv. Ochre (resistant). EtOAc extracts (2 mg/ml) or pure compounds (5×10^{-4}, 1×10^{-4}, 2×10^{-5}M) where dissolved in MeOH–H_20 (1:1). Leaves were punctured with a needle (6 punctures per leaf) and 10 μl droplets (6 droplets per leaf) were applied on punctured sites. Control leaves were treated similarly employing a 1:1 MeOH–H_20 solution. Plants were incubated in a growth chamber as reported above (16 h light/8 h dark, at 24±2 °C); leaves were observed over a 1-week period and the diameter of each lesion was measured after 7 days.

3.3. Isolation of compounds 3–7

The broth and mycelium were separated by gravity filtration, the broth (3 l) was concentrated (400 ml) and extracted with EtOAc (220 mg). Flash column chromatography (FCC) (eluted with CH_2Cl_2–MeOH, 95:5, 250 ml; 90:10, 250 ml of the EtOAc extract yielded the following fractions: F1 containing compounds **1** and **3**, F2 containing compounds **2**–**4**, F3–F4 containing compounds **2** and **5**, F6–F9 containing compounds **6** and **7**. Prep. TLC separation (CH_2Cl_2–MeOH, 97:3, double elution) of F1 (20 mg) yielded phomapyrone A (**1**, 4 mg) and polanrazine B (**3**), which was combined with a prep. TLC fraction eluted from F2 and further separated to yield chromatographically homogeneous material (**3**, 3.5 mg). Prep. TLC separation (CH_2Cl_2–MeOH, 96:4, double elution) of F2 (30 mg) yielded polanrazine B (**3**) which was combined with a prep. TLC band obtained from F1, and a mixture (20 mg) containing polanrazines C and D (**4**, **5**). Separation of this mixture using multiple prep. TLC (CH_2Cl_2–MeOH, 96:4, multiple development) yielded chromatographically homogeneous materials **4** (6.5 mg) and **5** (2.5 mg). Finally prep. TLC separation (CH_2Cl_2–MeOH, 96:4, double elution) of F6-9 (6 mg) yielded polanrazine E (**6**, 1 mg) and F (**7**, 1.5 mg).

3.4. Polanrazine B (3)

HPLC $t_R = 22.4$ min (solvent system B); $[\alpha]_D -60°$ (c 0.2 $CHCl_3$); HR–EI–MS m/z (% relative abundance) measured: 377.1230 (377.1232 calc. for $C_{18}H_{23}N_3O_2S_2$); FTIR υ_{max}: 3388, 3190, 2926,1665, 1452, 1413, 1075 cm^{-1}; λ_{max} (log ε) 218 (4.5) nm.

3.5. Polanrazine C (4)

HPLC $t_R = 10.6$ min (solvent system B); $[\alpha]_D$ 16° (c 0.18 MeOH); HR–EI–MS m/z (% relative abundance) measured: 347.1306 (347.1304 calcd. for $C_{17}H_{21}N_3O_3S_1$); FTIR ν_{max}: 3335 3220, 2956, 2926, 1673, 1435, 1075 cm^{-1}; λ_{max} (log ε) 219 (4.3) nm.

3.6. Polanrazine D (5)

HPLC $t_R = 11.3$ min (solvent system B); $[\alpha]_D -8.2$ ° (c 0.18 MeOH); HREIMS m/z (% relative abundance) measured: 347.1306 (347.1303 calc. for $C_{17}H_{21}N_3O_3S_1$. FTIR ν_{max}: 3444, 3347, 2968, 2926, 1677, 1625, 1465, 1427, 1058 cm^{-1}; λ_{max}(log ε) 219 nm (4.0).

3.7. Polanrazine E (6)

HPLC $t_R = 9.6$ min (solvent system B); $[\alpha]_D - 6$ ° (*c* 0.07 MeOH); HREIMS *m/z* (% relative abundance) measured: 331.1531 (331.1532 calc. for $C_{17}H_{21}N_3O_4$). FTIR v_{max}: 3342, 3223, 2962, 2927, 2857, 1682, 1429, 1094 cm_{-1}; λ_{max} (log ε) 222 (4.3), 282 (3.7) nm.

3.8. Polanrazine F (7)

HPLC $t_R = 7.0$ min (solvent system B); $[\alpha]_D - 10$ ° (*c* 0.26 MeOH); HR–EI–MS *m/z* (% relative abundance) measured: 317.1377 (317.1376 calcd. for $C_{16}H_{19}N_3O_4$); FTIR v_{max}: 3319, 2970, 2931, 1680, 1426, 1086, 1043 cm_{-1}; λ_{max} (log ε) 219 (4.2), 281 (3.5) nm.

Acknowledgements

We would like to thank G. Séguin-Swartz and R. Gugel, Agriculture and Agri-Food Canada, Saskatoon Research Station, Saskatchewan, for kindly providing isolates from the International Blackleg of Crucifers Network (IBCN) collection available in Saskatoon, and K. Brown, Department of Chemistry, University of Saskatchewan, for NMR spectral measurements. Financial support from the Natural Sciences and Engineering Research Council (Canada) and the University of Saskatchewan is gratefully acknowledged.

References

Gugel, R.K., Petrie, G.A., 1992. History, occurrence, impact, and control of blackleg of rapeseed. Canadian Journal of Plant Pathology 14, 36–45.

Howlett, B.J., Idnurm, A., Pedras, M.S.C., 2001. *Leptosphaeria maculans* the causal agent of blackleg disease of Brassicas. Fungal Genetics and Biology 33, 1–14.

King, R.R., Lawrence, C.H., Calhoun, L.A., 1992. Chemistry of phytotoxins associated with *Streptomyces scabies*, the causal organism of potato common scab. Journal of Agriculture and Food Chemistry 40, 834–837.

Lambert, J.B., Shurvell, H.F., Lightner, D.A., Cooks, R.G., 1998. Organic Structural Spectroscopy. Prentice-Hall, New Jersey.

McGee, D.C., Petrie, G.A., 1978. Variability of *Leptosphaeria maculans* in relation to blackleg of oilseed rape. Phytopathology 68, 625–630.

Nozawa, K., Udagawa, S-I., Nakajima, S., Kawai, K-I., 1989. A dioxopiperazine derivative from *Penicillium megasporum*. Phytochemistry 28, 929–931.

Pedras, M.S.C., 1998. Towards an understanding and control of plant fungal diseases in Brassicaceae. Recent Research Developments in Agricultural and Food Chemistry 2, 513–532.

Pedras, M.S.C., Biesenthal, C.J., 1998. Production of the host-selective toxin phomalide by isolates of *Leptosphaeria maculans* and its correlation with sirodesmin PL production. Canadian Journal of Microbiology 44, 547–553.

Pedras, M.S.C., Biesenthal, C.J., 2000. HPLC analyses of cultures of *Phoma* spp.: differentiation among groups and species through secondary metabolite profiles. Canadian Journal of Microbiology 46, 685–691.

Pedras, M.S.C., Erosa-López, C.C., Quail, J.W., Taylor, J.L., 1999. Phomalairdenone: a new host-selective phytotoxin from a virulent type of the blackleg fungus *Phoma lingam*. Bioorganic and Medicinal Chemistry Letters 9, 3291–3294.

Pedras, M.S.C., Morales, V.M., Taylor, J.L., 1994. Phomapyrones: three metabolites from the blackleg fungus. Phytochemistry 36, 1315–1318.

Pedras, M.S.C., Smith, K.C., Taylor, J.L., 1998. Production of a 2,5-dioxopiperazine by a new isolate type of the blackleg fungus *Phoma lingam*. Phytochemistry 49, 1575–1577.

Pedras, M.S.C., Taylor, J.L., Morales, V.M., 1995. Phomaligin A and other yellow pigments in *Phoma lingam* and *P. wasabiae*. Phytochemistry 38, 1215–1222.

Pedras, M.S.C., Taylor, J.L., Morales, V.M., 1996. The blackleg fungus of rapeseed: how many species? Acta Horticulturae 407, 441–446.

Reddy, P.V., Patel, R., White Jr., J.F., 1998. Phylogenetic and developmental evidence supporting reclassification of cruciferous pathogens *Phoma lingam* and *Phoma wasabiae* in *Plenodomus*. Canadian Journal of Botany 76, 1916–1922.

Taylor, J.L., Pedras, M.S.C., Morales, V.M., 1995. Horizontal transfer in the phytopathogenic fungal genus *Leptosphaeria* and host-range expansion. Trends in Microbiology 3, 202–206.

Williams, R.H., Fitt, B.D., 1999. Differentiating A and B groups of *Leptosphaeria maculans*, causal agent of stem canker (blackleg) of oilseed rape. Plant Pathology 48, 161–175.

PERGAMON

Phytochemistry 58 (2001) 911–921

PHYTOCHEMISTRY

www.elsevier.com/locate/phytochem

Apical dominance in *Pssu-ipt*-transformed tobacco

Jan M.C. Geuns[a,*], Rafaël Smets[b], Tom Struyf[a], Els Prinsen[b], Roland Valcke[c], Harry Van Onckelen[b]

[a]*Laboratory of Plant Physiology, Kasteelpark Arenberg 31, B-3001 Leuven, Belgium*
[b]*Department of Biology, UA, Universiteitsplein 1, B-2610 Antwerp, Belgium*
[c]*Laboratory of Plant Physiology, Limburgs Universitair Centrum Department SBG, Universitaire Campus, B-3590 Diepenbeek, Belgium*

Received 21 May 2001; received in revised form 23 July 2001

Abstract

In *Pssu-ipt*-transformed tobacco, apical dominance was released by defoliation of the upper nodes, while the apex remained intact. After defoliation, the concentration of cytokinins (CKs) increased whereas IAA remained constant, evoking an increase in the CK/IAA ratio in the buds. Moreover, defoliation resulted in a tremendous increase in the concentrations of aromatic amines (AAs): tyramine (TYR), phenethylamine (PEA) and an as yet unidentified compound. Although the total aliphatic monoamine and polyamine (PA) concentration remained constant, putrescine (PUT) and spermidine (SPD) concentrations in the axillary buds decreased, whereas the concentration of spermine (SPM) increased. Similar changes in PAs and AAs could be observed in the buds of untransformed SR1 plants after decapitation, whereas defoliation without removal of the apex had no effect. This is the first report on the possible involvement of PAs and AAs in apical dominance. © 2001 Elsevier Science Ltd. All rights reserved.

Keywords: *Nicotiana tabacum* L.; Solanaceae; Tobacco; Apical dominance by defoliation; *Ipt*; Polyamines; Aromatic amines; Cytokinins; IAA

1. Introduction

By its correlative control the shoot apex exerts a central coordinating influence on plant development (eg. axillary bud growth, the orientation of laterals, the growth of rhizomes and stolons, and leaf abscission) (Phillips, 1975; Cline, 1991, 1997; Tamas, 1995; Beveridge, 2000). Tamas (1995) discussed the up-to-date knowledge of the hormonal regulation of apical dominance and this for shoot apex dominance as well as for reproductive dominance. Most important conclusions concerning the expression of the dominance exerted by the shoot apex were (Tamas, 1995).

(1) The apex produces IAA and may be substituted for by applied IAA (references in Hillman, 1984; Tamas, 1995). The expression of dominance by the shoot apex requires basipetal IAA transport in the subapical part of the stem, as evidenced by the release of axillary buds from inhibition by application of TIBA in lanolin below the shoot apex (Tucker, 1978). The weak apical dominance in tomato line "Craigella" may be explained by a lack of IAA transport from the shoot apex (Brenner et al., 1987).

(2) Exogenous cytokinin application to axillary buds stimulates bud outgrowth. Axillary bud growth potential is generally well correlated with the level of naturally occurring cytokinins in the bud. This may be under the control of the shoot apex (auxin gradient). Repressed lateral buds do not synthesize cytokinins. Axillary bud growth might be triggered either by a redirection of the cytokinin supply from the roots, necessary to initiate axillary bud growth, or by a decline in auxin supply from the apex, enabling the axillary buds to start cytokinin synthesis or by the conversion of an inactive precursor to an active cytokinin (references in Tamas, 1995).

(3) Exogenously applied gibberellins do not release axillary buds from apical dominance, but are able to cause rapid elongation in released buds.

(4) The inhibition of axillary bud growth is closely related to the abscisic acid content of the buds. In *Phaseolus vulgaris*, bud outgrowth is preceded by several hours by a decline in ABA level (Gocal et al., 1991). In nonbranching mutants of tomato (Blind, Cls) the ABA content of the axillary buds is much higher than in the

* Corresponding author. Tel.: +32-16-321510; fax: +32-16-321509.
E-mail address: jan.geuns@bio.kuleuven.ac.be (J.M.C. Geuns).

0031-9422/01/$ - see front matter © 2001 Elsevier Science Ltd. All rights reserved.
PII: S0031-9422(01)00338-7

branching parental line *Craigella* (Tucker, 1978). The ABA accumulated in inhibited buds is either and most probably transported from the leaves or synthesized within the buds. ABA is probably not the correlative signal released by a dominant shoot apex, but its level is regulated by basipetal transport of IAA. This way ABA acts in the suppressed bud as a second factor under control of a dominant shoot apex. In *Phaseolus*, decapitation lowers the ABA level in axillary buds, but this is prevented by the application of IAA to the cut stump (Knox and Wareing, 1984). The function of ABA might be the inhibition of the cell cycle (Nougarede et al., 1990).

(5) In spite of some reports on the involvement of ethylene in apical dominance, recent evidence shows a general lack of correlation between axillary bud growth inhibition and ethylene levels in bud tissue (references in Tamas, 1995).

Although much information is available on hormonal effects on apical dominance, the basic mechanism of apical dominance remains unresolved. IAA seems to be the best candidate as correlative signal. Cytokinin might

Table 1
Growth of axillary buds and leaves of intact *ipt*-plants, and of plants defoliated at the upper 6 nodes (1–6) or at the lower ones (7–12). The more + the more swelling was seen. Negative sign means no effect. 0 = no axillary shoot outgrowth. Lengths are given in mm. Remnants are the remnants of the winged petioles. Apical leaves and apical buds are the leaves and buds above the upper defoliated node (+1: just above, +3 more to the apex). Axillary shoots: lengths in mm of the shoots that developed from the buds. Axillary shoots + leaf: total length of axillary shoot + longest leaf (in mm)

		3 Days	6 Days	10 Days	15 Days		21 Days	
Intact:		–	–	–	–		–	
Upper 6 nodes defoliated								
Buds:					Ax. shoots	Shoots + leaf	Ax. shoots	Shoots + leaf
	1	+	+ +	+ + +	55±20	162±43	80±26	226±53
	2	+	+ +	+ + +	27±14	119±52	42±13	157±47
	3	+	+ +	+ + +	12±6	76±42	23±18	128±51
	4	+	+ +	+ + +	13±3	102±18	27±12	132±14
	5	+	+ +	+ + +	0	18±10	4±1.8	55±14
	6	+	+ +	+ + +	0	14±3.5	0	15±2.5
	7	+	+ +	+ +	0	22±4.6	0	24±5.2
	8	+	+ +	+ +	0	10±2.2	0	13±1.5
	9	+	+ +	+ +	0	37±17	0	40±17.7
	10	+	+ +	+ +	0	26±13.5	0	28±13.6
	11	+	+ +	+ +	0	29±13.4	0	30±13.4
	12	+	+ +	+ +	0	37±14.6	0	40±14.9
Remnants		–	+ +	+ +	+ + +		+ + +	
Apical leaves		–	+	+ +	+1: 277±14 +2: 238±26 +3: 187±14		+1: 297±8.8 +2: 255±23 +3: 195±13	
Apical buds		–	+	+ +	+1: 10±3 +2: swollen +3: swollen		+1: 27±3.3 +2: 10±4 +3: swollen	
Lower 6 nodes defoliated								
Buds:	1–6:	–	–	–	–	–	–	–
	7:	+	+	+	0	5±2.8	0	
	8:	+	+	+	0	7±2.6	0	
	9:	+	+	+	0	9±2.9	0	
	10:	+	+	+	0	6±2.3	0	
	11:	+	+	+	0	6±2.1	0	
	12:	–	–	–	0	–	0	–
Remnants		–	–	–	–		–	
Apical leaves		–	+	+ +	+1: 55±9.5 +2: 35±13 +3: 21±9		+1: 60±14 +2: 40±15 +3: 30±11	
Apical buds		–	+	+ +	+1: – +2: – +3: –		+1: – +2: – +3: –	

be the key factor in promoting axillary bud growth (Tamas, 1995).

In a previous study with *ipt* (isopentenyl transferase)-transformed tobacco plants we analysed the polyamine and sterol composition in leaves of different physiological age (Geuns et al., 1997). In these plants the chimeric *Pssu-ipt* gene consisted of gene 4 (*ipt*) from *Agrobacterium tumefaciens* coupled to the light-inducible ssu-promotor (*Pssu*) from the gene encoding for the small subunit of Rubisco of *Pisum sativum* L. The *ipt* gene encodes an isopentenyl transferase that catalyses the conversion of 5′-AMP and isopentenyl pyrophosphate into isopentenyl-adenosine-5′-monophosphate, the first and rate-limiting step in the biosynthesis of CKs. Transformed *ipt*-plants are generally known to have a low apical dominance, but our untreated *ipt*-transformed tobacco plants did not show release from apical dominance at the age used. After cutting the leaves, we observed an enhanced outgrowth of the axillary buds. Polyamines are essential in plant growth and differentiation and are involved in cell elongation and division (Galston and Kaur-Sawhney, 1995). Therefore, we studied polyamines, amines and hormones during the development of axillary buds of *ipt* transformed plants after cutting off the leaves.

2. Results and discussion

In preliminary experiments it was shown that removal of all the leaves of *ipt*-transformed tobacco plants provoked the swelling of all the axillary buds after 3 days (upper, middle and lower ones). However, 6 days after defoliation, only the upper buds continued swelling and growing and the lower buds became repressed again. Removal of only one leaf at the top (leaf 1, see Fig. 5), in the middle (leaf 8) or at the bottom (leaf 15) did not influence the swelling of the axillary buds (results not shown). Removal of all the leaves of control SR1 plants had no influence on the outgrowth of the axillary buds (results not shown).

In intact *ipt*-plants all the axillary buds remained small and repressed for the whole duration of the experiment (Table 1, intact). Removal of the upper 6 leaves provoked swelling of the upper axillary buds (1–6) as well as of the lower ones (7–12) after 3 days (Table 1, 3 days). The upper buds continued swelling and developed side shoots and even the leaves of the side shoots expanded (Table 1, days 15 and 21). After 6 days the lower axillary buds arrested swelling and obviously became repressed again. The remnants of the winged petioles of the upper leaves were also enlarged and continued expanding till day 15. It has to be emphasised that in all these experiments the apex remained attached to the plants. The apex leaves started growing out and also their axillary buds were swelling. After 21 days the apex leaves became very large and the axillary buds of the apex leaves just above the first defoliated node developed shoots (Table 1, Fig. 5). This enhanced growth of the apex leaves and the remnants of the winged petioles may be explained by an enhanced availability of nutrients as the sink by the upper leaves was removed. Removal of the lower 6 leaves provoked a minor swelling of the lower axillary buds after 3 days, whereas the upper buds were not influenced. After 6 days the lower buds did not continue swelling and obviously became repressed again. The remnants of the winged petioles did not grow out. The apex leaves grew out but at 21 days their length was only a fraction of the length of the apex leaves grown on plants with the upper leaves removed, and their axillary buds did not swell (Table 1). Defoliation of untransformed SR1 plants did not influence swelling or outgrowth of axillary buds (results not shown). To the best of our knowledge this is the first report that in *ipt*-plants removal of the upper leaves evokes the release from apical dominance at an early stage of development.

From the above observations it was obvious that removal of the upper leaves provoked the most pronounced physiological effects on release of apical dominance. Therefore, we studied the influence of the removal of the upper 5 leaves on the swelling and polyamine content of the upper 5, the middle 5 and the lower 5 axillary buds. For each treatment the buds of 11 plants were combined giving sufficient material for biochemical analyses. The upper and middle buds doubled their fresh and dry weights between days 1 and 2 after defoliation, the lower buds doubling in size between days 2 and 3 (results not shown).

In the axillary buds the following AAs and PAs were identified by co-chromatography and LC–MS data obtained with authentic standards: PUT, SPD, SPM, TYR and PEA (results not given). A compound eluting in the HPLC chromatograms before PEA could not be positively identified, but it was certainly not identical to diaminopropane. For convenience, it was given the same calibration value as that of PEA and therefore expressed as μmolU or nmolU.

In untreated *ipt*-plants the concentrations of the PAs and AAs did not change significantly during the duration of the experiment (results not shown).

After defoliation of the upper 5 nodes, the PUT concentration decreased in upper buds 1 day after defoliation (Fig. 1A), and was partly restored from day 2 on. The PUT concentration at day 1 was lower due to a decrease of the PUT amount per bud and not due to a sudden increase in weight. The PUT concentration started to increase between days 1 and 2. This means that its rate of biosynthesis was much higher than the growth rate as the buds doubled in weight between days 1 and 2 and its concentration still increased. Consequently the absolute amounts of PUT per bud significantly increased (Fig. 1A). The SPD concentration gradually

decreased between days 0 and 3 (Fig. 1B). At day 1 the SPD concentration was lower due to less SPD per bud. As the concentration of SPD remained more or less constant between days 1 and 2 it can be deduced that its rate of biosynthesis paralleled the growth rate as both the weight of the buds and their SPD content doubled (Fig. 1B). The SPM concentration increased at day 1 and decreased when the growth of the buds proceeded (Fig. 1C). The rate of SPM biosynthesis was higher than the growth rate as its concentration increased between 0 and 1 days, paralleled growth rate between days 1 and 2 and levelled off between days 2 and 3. Possibly the increase in SPM is partly due to a rapid conversion of PUT and SPD into SPM as the absolute amounts of PUT and SPD significantly decreased at day 1 and that of SPM significantly increased.

In middle buds the changes of PUT, SPD and SPM showed the same trend as in upper buds, however, they were less pronounced whereas in the lower buds hardly any changes were observed (results not shown).

In the upper buds of defoliated plants the concentration of TYR, PEA and the unknown increased very significantly already 1 day after defoliation and continued increasing until day 3 after defoliation (Fig. 2 A–C). The amount of TYR per bud increased from 0.43 nmol/bud to 19.3 at day 3, i.e. ca. 45 ×, that of PEA from 0.1 nmol/bud to 0.91 (9×) and of the unknown from 0.13 to 1.68 nmolU/bud (ca. 13×).

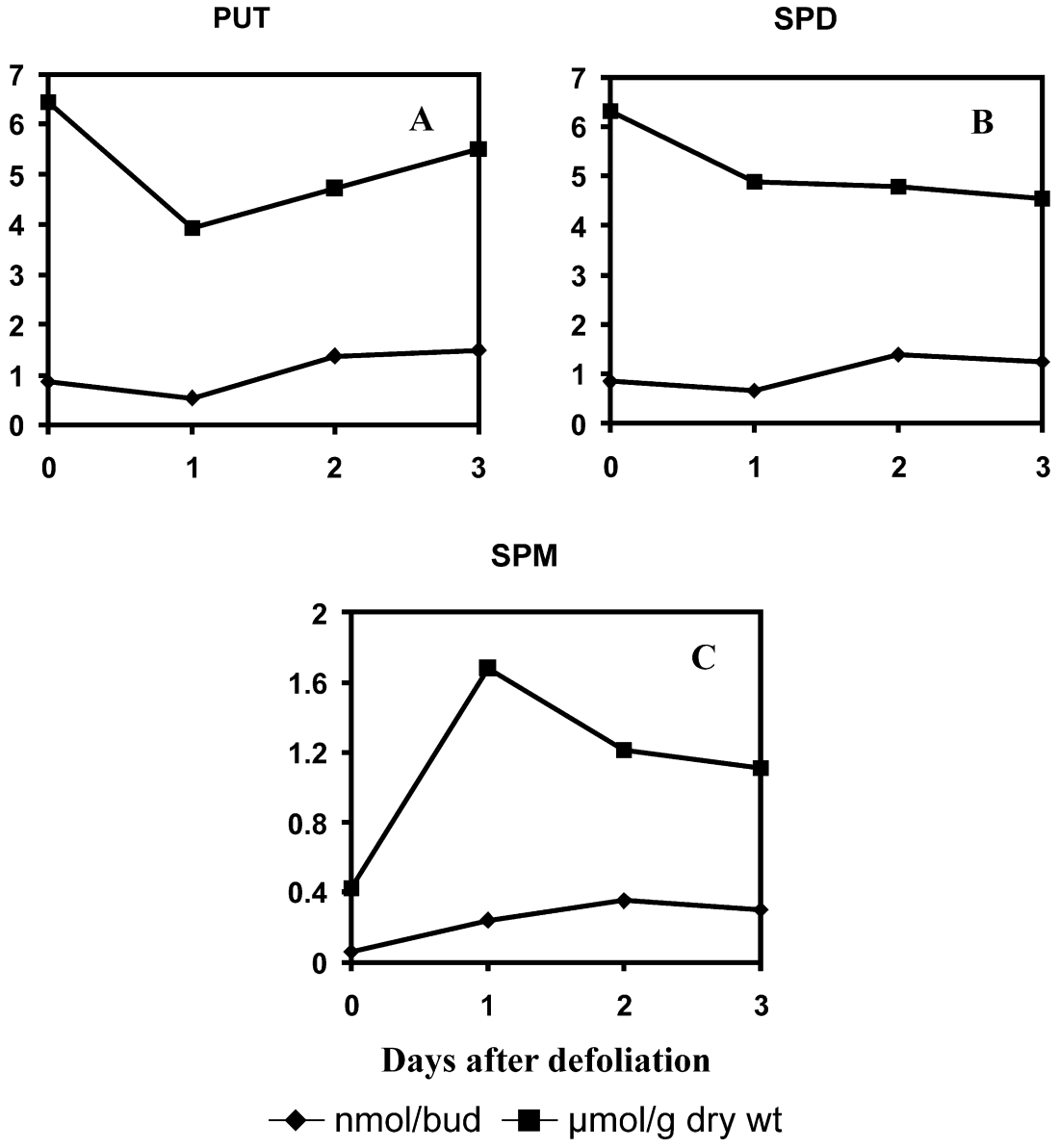

Fig. 1. Put (A), Spd (B) and Spm (C) in upper axillary buds after defoliation of the upper 5 nodes of *ipt*-plants. The concentration is in µmol/g dry wt, the amounts in nmol/bud; s.e. between 5 and 10%, not given in the figure as error bars have the same size as the data labels.

In the middle and lower buds the same trend of changes of amines occurred as in upper buds, but much more attenuated and with a tendency to decrease at day 3, as these buds became repressed again (results not shown).

In untransformed SR1 tobacco plants, no effects of defoliation on axillary bud growth were observed. Release of apical dominance was only induced by decapitation. In order to investigate whether the same phenomena could be observed by decapitation of SR1 plants as by defoliation of *ipt*-plants, SR1 plants were decapitated above the first leaf having a length of ca. 20 mm.

The fresh and dry weights of the upper axillary buds of intact SR1 plants did not change significantly. The fresh and dry weights of upper axillary buds from decapitated plants gradually increased with time starting from 6 h after decapitation. As expected application of 1% IAA to the cut surfaces nearly abolished the weight increases of the buds (results not shown). The effects of decapitation decreased from the first to the fifth nodes, the upper 3 buds showing the most pronounced effects that furthermore occurred earlier than in lower buds. However, to reduce the information only the mean values of buds 1–3 are discussed.

In intact SR1 plants the concentration of PUT, SPD, TYR and PEA did not change significantly, nor the amounts per bud. SPM was present only in trace amounts (results not shown).

In decapitated SR1 plants the PUT and SPD concentration remained constant in upper buds, because growth increase was compensated for by higher PUT

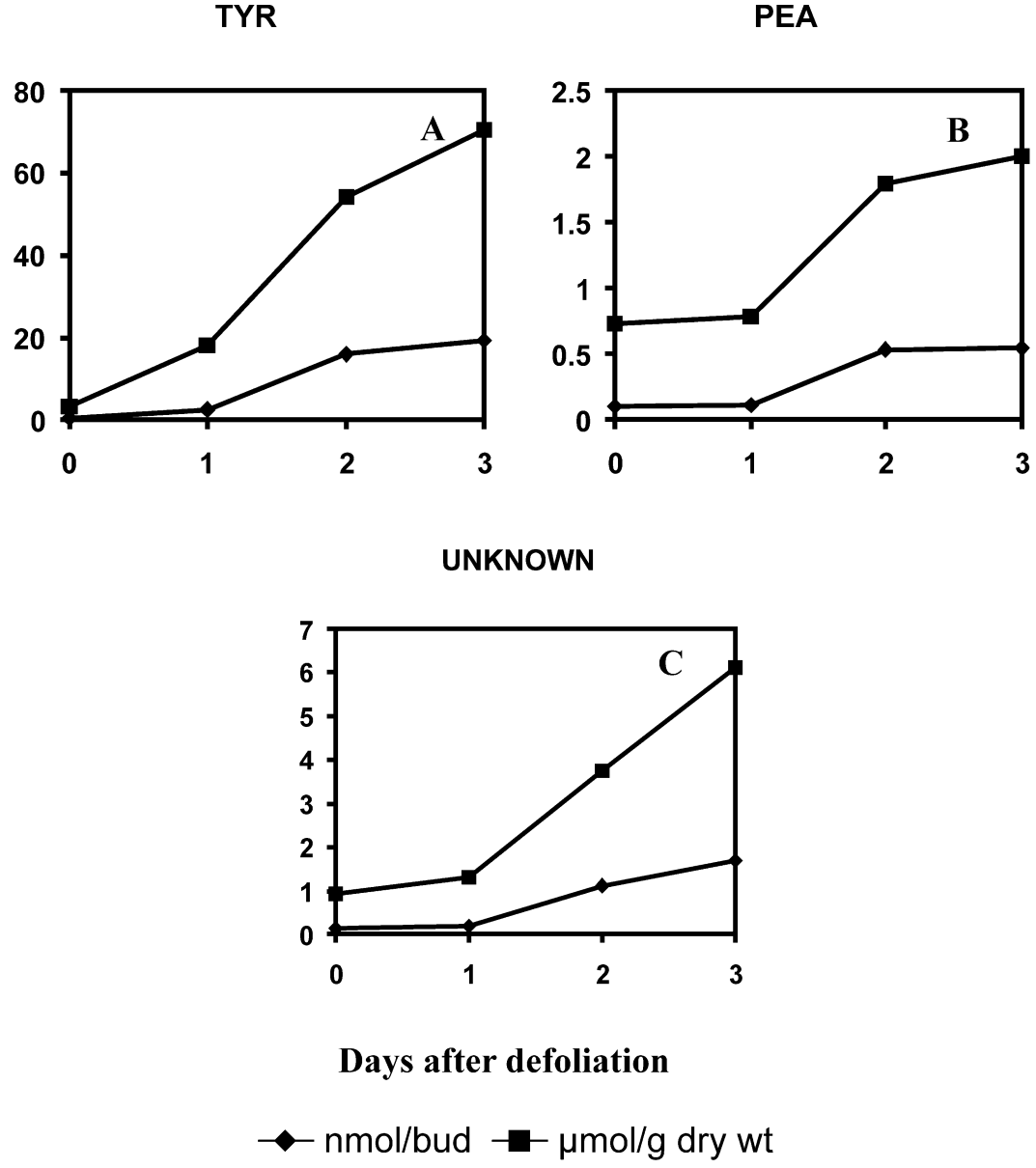

Fig. 2. Tyr (A), Pea (B) and unknown (C) in upper axillary buds after defoliation of the upper 5 nodes of *ipt*-plants. The concentration is in µmol/g dry wt, the amounts in nmol/bud; s.e. between 5 and 10%, not given in the figure as error bars have the same size as the data labels.

and SPD amounts per bud (results not shown). The concentration of TYR started to increase from 6 h on to reach a concentration of 28 μmol/g dry wt (Fig. 3A), due to a huge accumulation per bud (change from 0.12 to 46.7 nmol/bud (389 ×) at day 3). The PEA concentration started increasing after 12 h (Fig. 3B), the accumulation in the bud at 6 h already changing from 0.04 to 30.9 nmol/bud (772 ×) at day 3. The fifth bud showed only a small increase in weight and a small increase in AA concentration (results not shown).

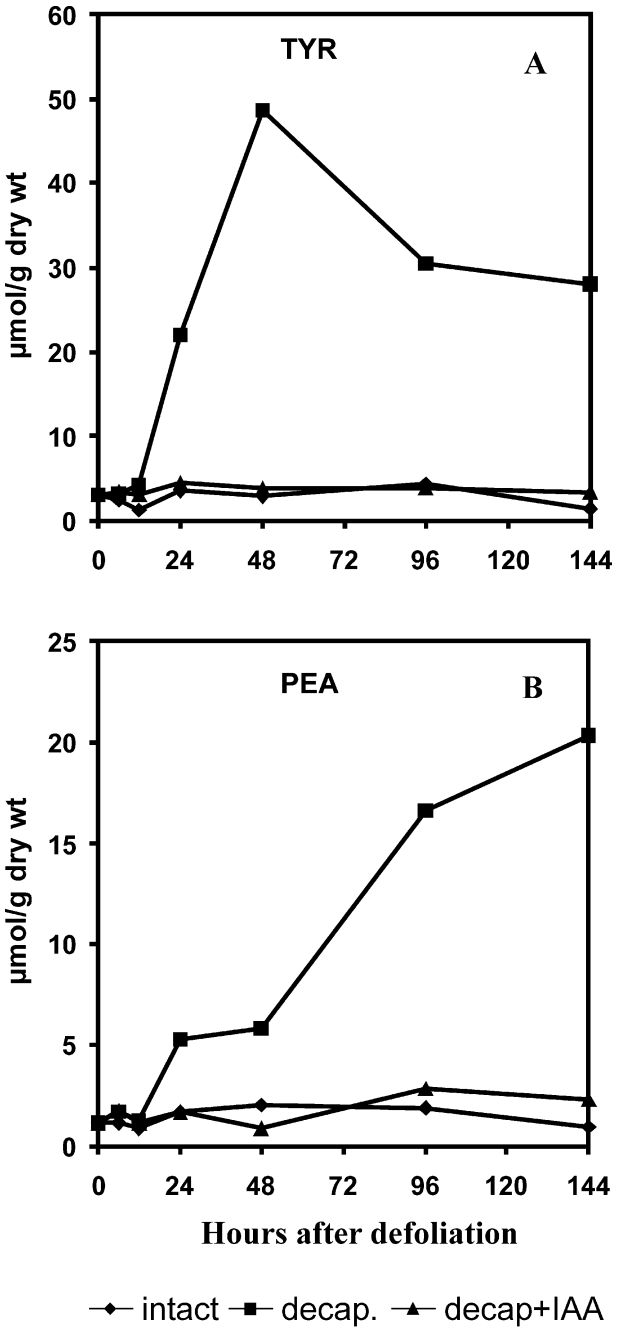

Fig. 3. Tyr (A) and Pea (B) concentration in μg/g dry wt in upper axillary buds of decapitated SR1 plants and in decapitated plants that received 1% IAA in lanolin; s.e. between 5 and 10%, not given in the figure as error bars have the same size as the data labels.

Application of IAA to the stumps of decapitated SR1 plants completely prevented the increases in concentration and in accumulation of PAs (results not shown) and AAs (Fig. 3A and B) as well as release from apical dominance.

As far as we know no studies have been published on the changes of AAs in the axillary buds in relation with apical dominance. The huge increases in AA concentration during release from apical dominance as well as the inhibition of both AAs and growth when IAA is applied to decapitated SR1 plants, suggest that AAs may have a fundamental function in the release from apical dominance or in the subsequent development and growth of the axillary shoots. From our results it is not clear whether these compounds mediate the action of plant hormones or whether they are part of their signal response pathways. Further research should be done to unravel their exact function.

High PA concentrations have often been correlated with cell division and rapidly growing tissues (Serafini-Fracassini, 1991) but the function of AAs is far from being understood. One of the first indications for a physiological function of TYR and PEA in tobacco was reported by Perdrizet and Prevost (1981). PEA was the main amine of green vegetative tissue, but TYR was the main amine in the stem and it accumulated in the flowers. Béranger-Novat et al. (1994) showed that dormancy break of spindle tree embryos by GA3 was accompanied with an increase in aliphatic amines and ADC activity, whereas TYR decreased. Aziz et al. (1998) found that the effects of salt stress on proline accumulation were correlated with the changing levels of PAs and TYR in leaf discs of tomato. Low concentrations of applied TYR stimulated the proline accumulation. In leaf explants of *Medicago sativa* the early cellular events were correlated with the endogenous contents of PAs and AAs. Proembryogenic cell mass formation was positively correlated with free TYR and negatively correlated with free PEA contents (Cvikrová et al., 1999). Martin-Tanguy (1997) found a relationship of PAs and AAs in relation with flowering in tobacco. SPD as well as TYR availability (in conjugated forms) could be limiting factor(s) in sexual development in tobacco.

Christou and Barton (1989) found that various substituted phenethylamines were extremely toxic towards wild-type callus tissue cultures of tobacco, soybean, corn and sunflower. In calli from plants transformed with genes encoding enzymes of CK biosynthesis, the toxicity was inversely correlated with the CK content. Exogenous applied CKs reduced the toxicity. Tobacco crown gall cultures with a high CK content were resistent. Phenethylethanol and PEA were weakly inhibitory. Structures with an additional aromatic hydoxyl (TYR, octapamine) showed a severe toxicity. A second hydroxyl

group on the aromatic ring (dopamine) enhanced toxicity and even calli containing the *ipt*-gene became inhibited. Epinephrine with two aromatic hydroxyls and a methyl group on the amine, was lethal to all types of tissues tested, including crown gall. It is a very interesting point that PEA, TYR and an unknown very strongly accumulated in axillary buds together with the CKs (see below). It is not known whether these AAs have any antagonistic activity with CKs in the axillary buds of defoliated *ipt*-plants or decapitated SR1-plants. Further research should be done to unravel these problems.

As the effects of defoliation of upper nodes of transgene *ipt*-lines were most pronounced in upper axillary buds, cytokinins (CKs) and IAA levels in these organs were determined. IAA, iPMP, iPA, iP, iPG, ZRP, DHZP, ZR, DHZR, Z, DHZ, Z-N9-G, DHZ-N9-G were the compounds analysed in three independent series of sampling.

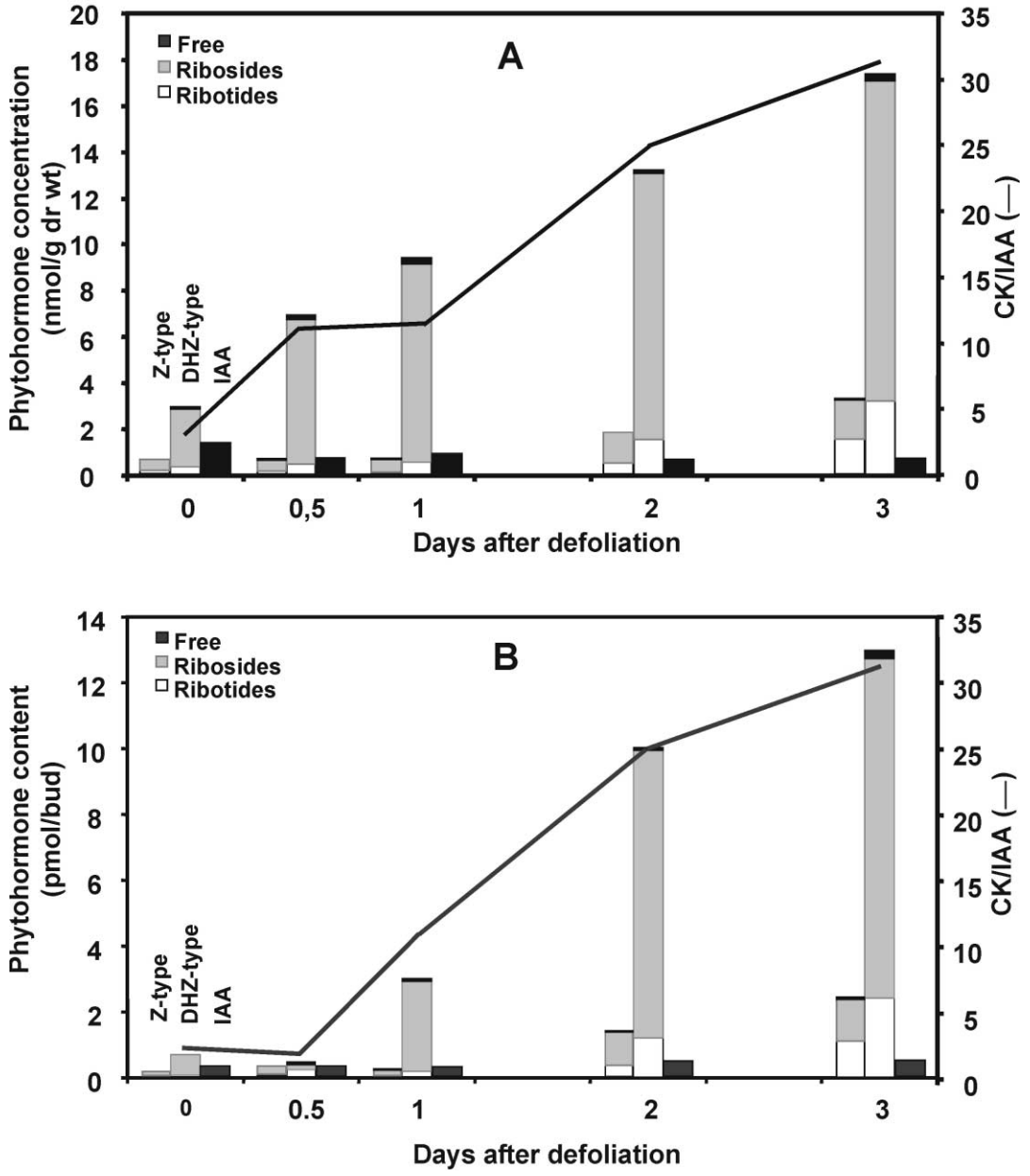

Fig. 4. CKs and IAA in upper axillary buds of *ipt*-plants after defoliation of the upper 5 nodes. A: CKs (in nmol/g dry wt) in function of time after defoliation. DHZ: dihydrozeatin (black zone, DHZ-type bars); DHZR: dihydrozeatin riboside (grey zone, DHZ-type bars); DHZRP: dihydrozeatin-5′-phosphate (white zone, DHZ-type bars); Z: zeatin (black zone, Z-type bars); ZR: zeatin riboside (grey zone, Z-type bars); ZRP: zeatin riboside-5′-phosphate (White zone, Z-type bars); IAA: indolyl-3-acetic acid; CK/IAA: ratio of CKs over IAA concentration (curve). B: CKs in pmol/bud. Although between different experiments the CK changes followed the same trend, the absolute amounts found differed among the individual experiments. Therefore, a typical analysis is given.

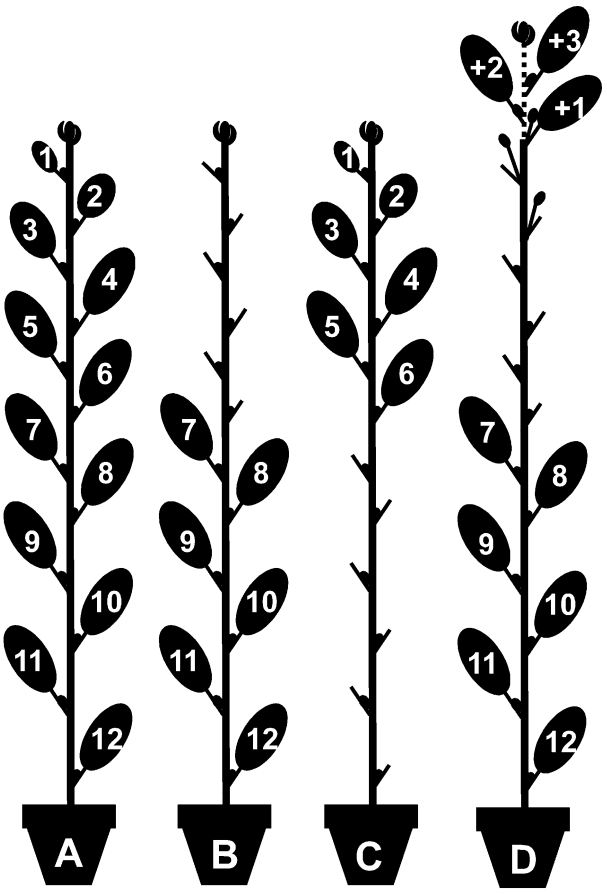

Fig. 5. A. Numbering of leaves and axillary buds of SR1 and *ipt*-plants. B. Defoliation of the six top leaves. C. Defoliation of the six lower leaves. D shows a defoliated plant (upper nodes) after a 3 weeks growth period. The apex leaves and axillary buds have been growing and are numbered +1–+3 (see Table 1).

An initial increase in the total amount of CKs, caused by the dihydrozeatin derivates, was observed 12 h after defoliation (Fig. 4). As the bud dry weights remained constant, an increased CK concentration occurred. A 3-fold increase in the levels of cytokinins occurred at day 2 in comparison to day 1. Although this increase coincided with a doubling in fresh and dry weights, still an enhanced concentration was observed meaning that their rate of accumulation in the bud surpassed the growth rate of the buds. This phenomenon was due to a dramatic increase in the dihydrozeatin type CKs and to a lesser extent the zeatin type CKs. For both types of CKs, mainly the ribosides accumulated after defoliation. Also their ribotide precursors showed a strong increase in concentrations. The initially relative low ZRP level was probably caused by its high turn-over rate into ZR, DHZP and Z. The free bases zeatin and dihydrozeatin demonstrated a steady state level during the first day and a slight increase from day 2 on. The concentration of zeatin, probably the physiologically active component (Dewitte et al., 1999; Laureys et al., 1998) seems to be strictly regulated as no huge accumulation was observed. The glucosides and iP-components were present only in small amounts and their concentrations were not significantly influenced by defoliation (results not shown).

Analysis of upper axillary buds of intact control SR1 plants revealed only trace amounts of the CKs found in buds of untreated *ipt*-plants (results not shown). From these analyses it may be concluded that the upper axillary buds of untreated *ipt*-plants contained CKs in amounts far above those in control SR1 tobacco, proving that the *ipt*-gene was active before defoliation.

Buds showed no significant difference in levels of IAA (Fig. 4B) during the experiment, resulting in a slight decrease of its concentration (Fig. 4A). This seems to point out that IAA in the buds acts independently from the physiological changes. As after defoliation, the total amount of CKs increased whereas the IAA levels remained constant, the CK/ IAA balance in the upper axillary buds shifted in favor of release from apical dominance. After passing a certain threshold, not being reached by WT or intact *ipt*-plants, buds started to grow. In pea, decapitation and partial defoliation led to slightly decreased levels of ABA, unchanged levels of GAs, lowered levels of IAA (2-fold) and significantly enhanced levels of Z and ZR (up to 5-fold) in the internodes. The release of apical dominance corresponded well with the (Z + ZR)/IAA ratio (Kotov and Kotova, 2000). Emery et al. (1998) found that in lupin, a plant not adhering to classical apical dominance, the best relationship between the level of growth factors in apical buds and branching pattern was the ratio CK/IAA, implying that a high CK/IAA at a given bud would promote growth.

In the buds, mainly DZR and ZR were found to accumulate after triggering. As shown by Werbrouck et al. (1995), these compounds are the dominant CK derivates being transported through the xylem out of the roots towards the upper organs. Therefore, defoliation might shift the xylem transpiration stream from the leaves to the buds causing an increase in CK levels. However, as buds were released from apical dominance only after defoliation of five but not of a single leaf, a relocation of CK transport alone does not seem to explain the complete process. In *Ipomoea nil*, Cline et al. (1997) decapitated the shoots and defoliated the upper nodes. IAA applied to the cut surfaces of the stems and to all the petioles but one prevented the release of the axillary buds, except the bud of the petiole stump without IAA. Cambridge and Morrid (1996) showed a transfer of IAA from the leaf by the phloem to the polar auxin transport pathway in pea. These results support the idea that the IAA supply from the leaf is important in the maintenance of apical dominance. After decapitation in bean (Bangerth, 1994) and in pea (Li et al., 1995), strong increases in CK levels in the xylem were observed. Feeding NAA to the top of the plant could

reduce these amounts. Defoliating the 5 upper nodes of *ipt* transformed plants might therefore cause a drop in the basipetal IAA transport, resulting in an increased release of mainly DZR and ZR from the roots into the xylem. According to Lomax et al. (1995), the velocity of basipetal IAA transport varied from 5 to 20 mm/h depending on the species and the place of measurement across the stem. Plants used in our experiment were treated at a height of about 25 cm. This implies that the reduced IAA signal would reach the roots after at least 12 h. Therefore, the initial increase in CK amount and concentration after 12 h might be due to a relocation of the CK transport from the leaf to the bud. The strong increase in CK levels and dry weight between days 1 and 2 however, could be the result of a response of the roots after a decline in IAA transported out of the leaves. The removal of only one leaf causes probably a minor reduction in IAA transport that is not sufficient to induce enhanced CK levels in the xylem. Swelling of the lower buds, which took place at the same time as for the upper buds is then also caused by these elevated CK concentrations in the xylem. However, because the upper buds act as a stronger sink, they will become dominant over the lower ones. Why lower buds stop swelling after defoliation of their nodes is however unclear. Differences in age of leaves and/ or buds in comparison to the upper organs, causing a differential response, might explain the reason lower buds being prevented to grow out.

Faiss et al. (1997) proposed the concept that CKs have paracrine, i.e. locally restricted, functions in tobacco. Also Rupp et al. (1999) suggested that cytokinins present in *ipt*-transformed *Arabidopsis* shoot meristems are synthesised locally. These data however do not really conflict ours. The already high cytokinin concentrations in the axillary buds of the transgene lines before the onset of our experiment are probably derived from local production. The fact that we worked with a light sensitive *Pssu* promoter supports the idea that these cytokinins are not root derived. As the *ipt*-gene is already active, defoliation probably causes non *ipt*-related CKs to be transported out of other plant organs, plausibly the root, into the buds. Thereby, a certain threshold in the CK/IAA balance is passed, which causes buds to form axillary shoots. The model we propose therefore supports the idea that CK's playing a role in apical dominance of *ipt*-tranformed plants, are locally as well as root derived.

2.1. General conclusion

From our results it may be deduced that defoliation of upper nodes of *ipt*-plants leads to an enhanced CK concentration in the axillary buds, the basal level of CK being already high in *ipt*-transformed plants. As a result the CK/IAA ratio quickly exceeds a threshold value releasing the axillary buds from apical dominance. It might be possible that by a reduced IAA gradient more CKs are transported upwards from the roots to the buds. This releases both upper and lower buds from apical dominance, the lower buds becoming repressed again by the developing upper buds. Axillary bud release is accompanied by a change in PA composition (decrease of PUT and SPD, increase in SPM), their total concentration remaining constant. The release of apical dominance is also accompanied by a tremendous increase in the concentrations of TYR, PEA and a yet unknown compound. This might indicate that these compounds have a fundamental function in the subsequent growth and development of axillary buds into shoots. This study seems to be the first report on a possible function of PAs and AAs in apical dominance. However, additional studies are required to determine the exact function of these amines in relation with hormone effects.

3. Experimental

3.1. Plant material and treatment

Seeds of *Pssu-ipt*-transformed tobacco (*Nicotiana tabacum* L. cv. Petit Havana SR1) were of the same progeny and were grown as described (Geuns et al., 1997). Plants with a shoot length of ca. 30 cm and having at least 15 leaves were selected and used in the study. These plants are further named *ipt* plants. Numbering of leaves was from upper (=1) to lower leaves (see Fig 5A for numbering).

At day 0, the treatment consisted in removing different numbers of leaves (Fig. 5B and C). Care was taken not to remove or damage the axillary buds. In all cases the apex remained attached to the stems. The defoliated plants were visually inspected after 3, 6, 10, 15 and 21 days.

For the experiments using *ipt* plants, the buds of ca. 30 cm high plants were collected at different time intervals after defoliation. The upper axillary buds (1–5), the middle (6–10) and the lower ones (11–15) of the different plants were combined to obtain sufficient material for analyses. After registration of the fresh weight, the buds were frozen in liquid nitrogen and freeze dried.

Non-transformed tobacco seedlings (SR1) with a shoot length of ca. 30 cm were selected. The apex consisted of the apical meristem and the smallest leaves. The uppermost leaf of ca. 20 mm length was named the first leaf. Control SR1-plants were decapitated above the first leaf. Thirty plants were taken per treatment and all the axillary buds of the first till the fifth nodes were collected separately. One series of decapitated plants was treated with 1% IAA in lanolin to inverse the release from apical dominance.

3.2. Polyamine analysis

PAs and AAs were analysed after dansylation as described in Geuns et al. (1997).

3.3. Hormone analyses

For cytokinin and IAA determinations, buds of tobacco plants grown in a greenhouse were harvested. Samples were immediately frozen in liquid nitrogen, lyophylized and stored at −70 °C until extraction. Frozen plant samples were ground in liquid nitrogen, transferred into Bieleski solution (Bieleski, 1964) and extracted overnight at −20 °C. For respectively IAA and each cytokinin compound determined, 250 pmol of [phenyl-$^{13}C_6$]-IAA (Cambridge Isotope Laboratories Inc., Andover, MA, USA) and 10 pmol of the corresponding deuterated cytokinin standard ([$^2H_5$] DHZ, [$^2H_5$]DHZR, [$^2H_5$]DHZ-N9-G, [$^2H_5$]DHZMP, [$^2H_6$]iP, [$^2H_6$]iPA, [$^2H_6$]iPG, [$^2H_6$]iPMP from APEX Int., Honiton, Devon, UK) were added to the sample before centrifugation (24,000 *g*, 15′, 4 °C). The pellet was resuspended for 1 h at 4 °C in 80% MeOH and centrifuged once more. The supernatants of both fractions were pooled and dried. After dissolving in water, cytokinins were purified by a combination of solid phase and immunoaffinity chromatography as previously described by Redig et al. (1996). IAA is concentrated on a consecutive C18 cartridge (Prinsen et al., 1995) underneath the immunoaffinity column and methylated prior to analysis (Prinsen et al., 1995, 1997). Hormones were quantified by microLC-(ES+)MS/MS in MRM mode (Prinsen et al., 1998). The chromatograms obtained were processed by means of Masslynx software (Micromass). Concentrations were calculated following the principles of isotope dilution and expressed in nmol per gram dry wt.

Acknowledgements

The authors acknowledge the skilful technical support of Jan Daenen, Hilde Verlinden and Colette Wellens. The authors also acknowledge financial support from the Belgian FWO (J.M.C.G.: grant No. G.0111.01) and the FWO-WOG-plantengroeiregulatoren.

References

Aziz, A., Martin-Tanguy, J., Larher, F., 1998. Stress-induced changes in polyamines and tyramine levels can regulate proline accumulation in tomato leaf discs treated with sodium chloride. Physiol. Plant 104, 195–202.

Bangerth, F., 1994. Response of cytokinin concentration in the xylem exudate of bean (*Phaseolus vulgaris* L.) plants to decapitation and auxin treatment, and relationship to apical dominance. Planta 194, 439–442.

Béranger-Novat, H., Monin, J., Martin-Tanguy, J., 1994. Polyamines and their biosynthetic enzymes in dormant embryos of the spindle tree (*Euonymus europaeus* L.) and in dormancy break obtained after treatment with gibberellic acid. Plant Sc. 102, 139–145.

Beveridge, C.A., 2000. Long-distance signalling and a mutational analysis of branching in pea. Plant Growth Regulation 32, 193–203.

Bieleski, R.L., 1964. The problem of halting enzyme action when extracting plant tissues, Anal. Biochem. 9, 431–442.

Brenner, M.L., Wolley, D.J., Sjut, V., Salerno, D., 1987. Analysis of apical dominance in relation to IAA transport. Hort. Sci. 22, 833–835.

Cambridge, A.P., Morris, D.A., 1996. Transfer of exogenous auxin from the phloem to the polar auxin transport pathway in pea (*Pisum sativum* L.). Planta 199, 583–588.

Christou, P., Barton, K.A., 1989. Cytokinin antagonist activity of substituted phenethylamines in plant cell culture. Plant Physiol. 89, 564–568.

Cline, M.J., 1991. Apical dominance. Bot. Rev. 57, 318–358.

Cline, M.J., 1997. Concepts and terminology of apical dominance. Am. J. Bot. 84, 1064–1069.

Cline, M.J., Wessel, T., Iwamura, H., 1997. Cytokinin/auxin control of apical dominance. Plant Cell Physiol 38, 659–667.

Cvikrová, M., Binarová, P., Cenklová, V., Eder, J., Macháčková, I., 1999. Reinitiation of cell division and polyamine and aromatic monoamine levels in alfalfa explants during the induction of somatic embryogenesis. Physiol. Plant 105, 330–337.

Dewitte, W., Chiappetta, A., Azmi, A., Witters, E., Strnad, M., Rembur, J., Noin, M., Chriqui, D., Van Onckelen, H., 1999. Dynamics of cytokinins in apical shoot meristems of a day-neutral tobacco during floral transition and flower formation. Plant Physiol. 119, 111–121.

Emery, R.J., 1998. N, Longnecker, N. E., Atkins, C.A., Branch development in *Lupinus angustifolius* L. II. Relationship with endogenous ABA, IAA and cytokinins in axillary and main stem buds. J. Exp. Bot 49, 555–562.

Faiss, M., Zalubilova, J., Strnad, M., Schmülling, T., 1997. Conditional transgenic expression of the *ipt* gene indicates a function for cytokinins in paracrine signaling in whole tobacco plants. Plant J. 12, 401–415.

Galston, A.W., Kaur-Sawhney, R., 1995. Polyamines as endogenous growth regulators. In: Davies, P.J. (Ed.), Plant Hormones. Kluwer Academic Publishers, The Netherlands, pp. 158–178.

Geuns, J.M.C., Van Loenhout, H.E.M., Valcke, R.L.M., Van Loven, K., 1997. Redig, Pascale, Veselov, S. Y., Kudoyarova, G.R., Van Onckelen, H.A., Vendrig, J.C., Sterols and polyamines in *ipt*-transformed tobacco plants. Phytochemistry 44, 797–804.

Gocal, G.F.W., Pharis, R.P., Yeung, E.C., Pearce, D., 1991. Changes after decapitation in concentrations of indole-3-acetic acid and abscisic acid in the larger axillary bud of *Phaseolus vulgaris* L. cv Tender Green. Plant Physiol. 95, 344–350.

Hillman, J.R., 1984. Apical dominance. In: Wilkins, M.B. (Ed.), Advanced Plant Physiology. Pitman, London, pp. 127–148.

Knox, J.P., Wareing, P.F., 1984. Apical dominance in *Phaseolus vulgaris* L: the possible roles of abscisic and indole–3-acetic acid. J. Exp. Bot. 35, 239–244.

Kotov, A.A., Kotova, L.M., 2000. The contents of auxins and cytokinins in pea internodes as related to the growth of lateral buds. J. Plant Physiol. 156, 438–448.

Laureys, F., Dewitte, W., Witters, E., Van Montagu, M., Inzé, D., Van Onckelen, H., 1998. Zeatin is indispensable for the G2-M transition in tobacco BY–2 cells. FEBS Letters 426, 29–32.

Li, C.-J., Guevara, E., Herrera, J., Bangerth, F., 1995. Effect of apex excision and replacement by 1-naphthylacetic acid on cytokinin concentration and apical dominance in pea. Physiol. Plant. 94, 465–469.

Lomax, T.L., Muday, G.K., Rubery, P.H., 1995. In: Davies, P.J. (Ed.), Plant Hormones: Physiology, Biochemistry, and Molecular Biology. Kluwer Academic Publishers, The Netherlands, pp. 509–530.

Martin-Tanguy, J., 1997. Conjugated polyamines and reproductive development: Biochemical, molecular and physiological approaches. Physiol. Plant 100, 675–688.

Nougarede, A., Landre, P., Jennane, A., 1990. Intranucleolar visualization of nucleic acids and acidic proteins in inhibited and reactivated pea cotyledonary buds. Protoplasma 156, 183–191.

Perdrizet, E., Prevost, J., 1981. Aliphatic and aromatic amines during development of *Nicotiana tabacum*. Phytochemistry 20, 2131–2134.

Phillips, I.D.J., 1975. Apical dominance. Ann. Rev. Plant Physiol. 26, 341–367.

Prinsen, E., Redig, P., Strnad, M., Galis, I., Van Dongen, W., Van Onckelen, H., 1995. Quantifying phytohormones in transformed plants. In: Gartland, K., Davey, M. (Eds.), Methods in Molecular Biology, Vol. 44, *Agrobacterium* protocols. Humana Press, Totowa, NJ, pp. 245–261.

Prinsen, E., Van Dongen, W., Esmans, E.L., Van Onckelen, H.A., 1997. HPLC linked electrospray tandem mass spectrometry: a rapid and reliable method to analyse indole-3-acetic acid metabolism in bacteria. J. Mass Spectrom. 32, 12–22.

Prinsen, E., Van Dongen, W., Esmans, E., Van Onckelen, H., 1998. Micro and capillary liquid chromatography-tandem mass spectrometry: a new dimension in phytohormone research. J. Chromatogr. A 826, 25–37.

Redig, P., Schmülling, T., Van Onckelen, H., 1996. Analysis of cytokinin metabolism in *ipt* transgenic tobacco by liquid chromatography-tandem mass spectrometry. Plant Physiol. 112, 141–148.

Rupp, H.-M., Frank, M., Werner, T., Strnad, M., Schmülling, T., 1999. Increased steady state mRNA levels of the STM and KNAT1 homeobox genes in cytokinin overproducing *Arabidopsis thaliana* indicate a role for cytokinins in the shoot apical meristem. Plant J. 18, 557–563.

Serafini-Fracassini, D., 1991. Cell cycle-dependent changes in plant polyamine metabolism. In: Slocum, R.D., Fores, H.E. (Eds.), Biochemistry and Physiology of Polyamines in Plants. CRC press, Boca Raton, pp. 160–171.

Tamas, I.A., 1995. Hormonal regulation of apical dominance. In: Davies, P.J. (Ed.), Plant Hormones. Kluwer Academic Publishers, The Netherlands, pp. 572–597.

Tucker, D.J., 1978. Apical dominance in tomato: the possible roles of auxin and abscisic acid. Plant Sci. Lett. 12, 273–278.

Werbrouck, S.P.O., Van der Jeugt, B., Dewitte, W., Prinsen, E., Van Onckelen, H.A., Debergh, P.C., 1995. The metabolism of benzyladenine in *Spathiphyllum floribundum* "Schott Petite" in relation to acclimatization problems. Plant Cell Rep. 14, 662–665.

PERGAMON

Phytochemistry 58 (2001) 923–927

PHYTOCHEMISTRY

www.elsevier.com/locate/phytochem

Deep blue anthocyanins from blue *Dianella* berries

Stephen J. Bloor

Industrial Research Ltd, PO Box 31-310, Lower Hutt, New Zealand

Received 17 May 2001; accepted 3 August 2001

Abstract

Three anthocyanins, all acylated delphinidin 3,7,3′,5′-tetraglucosides, and a naphthalene glycoside, 2-acetyl-1,5-dihydroxy-3 methyl-8-*O*(xylosyl-(1→6)-glucosyl) naphthalene, have been isolated from the berries of two *Dianella* species, *D. nigra* and *D. tasmanica*. The anthocyanins show exceptional blueness at in vivo pH values due to effective intramolecular copigmentation involving *p*-coumaroyl-glucose units (GC) at the 7, 3′ and 5′ of the delphinidin anthocyanidin. Evidence is presented to show that the effectiveness of the copigmentation can be ranked; 3′,5′ GC > 7 GC > 3 GC. © 2001 Elsevier Science Ltd. All rights reserved.

Keywords: Liliaceae; *Dianella nigra*; *Dianella tasmanica*; Acylated anthocyanin; Blue berries; Delphinidin

1. Introduction

Anthocyanins with acylated sugar residues have been the subject of much study both for their contribution to natural flower colour and their potential as colourants for food or cosmetics. Many of the anthocyanins responsible for blue flower colour belong to this class. Typically, the most effective blue anthocyanins are those with two aromatic acyl groups attached to sugar groups which are directly attached to the anthocyanidin chromophore, e.g. ternatins (Saito et al., 1985; Terahara et al.,1996), the blue pigments of *Ceanothus* (Bloor, 1997), and cinerarin (Goto et al., 1984). Recently, evidence has also been presented to show that placement of such groups at the 3, 7 and 3′ positions is especially advantageous in terms of colour stability (Figueiredo et al., 1999).

A search for anthocyanin pigments with even greater blueness and stability has led to a study of the pigments present in the blue berries of two *Dianella* species. For the first time, delphinidin anthocyanins substituted with glucose at the 3, 7, 3′ and 5′ positions are reported. The four delphinidin tetraglucosides, **1**–**4**, described in this work bear *p*-coumaroyl groups on two, three, all four, or none of the sugars respectively.

Dianella species (Blue flax lily, blueberry lily) are rhizomatorous herbs characterised by blue or blue-violet berries. The major New Zealand species is *Dianella nigra* Colenso featuring small, intensely blue, round berries. Of the more numerous Australian species, *Dianella tasmanica* Hook. f. is remarkable for its larger and more elongated blue-violet fruits. Previous chemical studies of the genus have focused on the naphthoquinone compounds (in roots of *D. nigra* and *D. revoluta* R. Br.) which are also found in other members of the Liliaceae (Cooke and Sparrow, 1965; Briggs et al., 1975). Some of these quinones have been shown to be associated with the toxic effects of various Liliaceae species when ingested by livestock (Colegate et al., 1986).

2. Results and discussion

Preliminary analysis by HPLC of the berry juice and extract from *D. nigra* and *D. tasmanica* showed the presence of three anthocyanins (**1**–**3**). Both species contained **2** as the major pigment but *D. nigra* had **3** as a minor pigment while in *D. tasmanica* the minor pigment was **1**.

The three anthocyanins were purified from acidic water and alcoholic extracts of the berries using RP CC, cyanopropyl CC, and Sephadex LH20 CC. From ^{1}H NMR data, the predominant anthocyanin **2** comprised a delphinidin anthocyanin unit, four β-glucose sugars and three *trans*-*p*-coumaroyl groups. This was supported by the clear ESMS molecular ion at m/z 1389. Two of the glucoses and two of the *p*-coumaroyl groups were identical in the NMR spectra and were characterised by broad signals in the ^{1}H NMR spectrum. Long range H–C

E-mail address: s.bloor@irl.cri.nz

0031-9422/01/$ - see front matter © 2001 Elsevier Science Ltd. All rights reserved.
PII: S0031-9422(01)00343-0

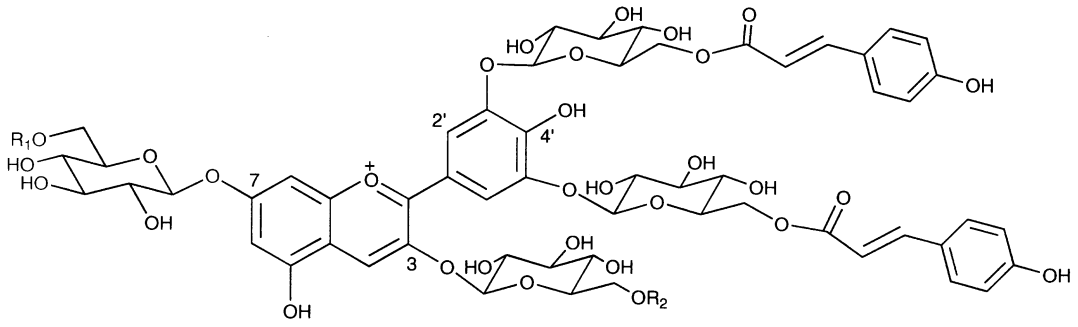

1 $R_1 = R_2 = H$

2 R_1 = *p-coumaroyl*, $R_2 = H$

3 $R_1 = R_2$ = *p-coumaroyl*

4 deacyl **1**

coupling identified the anomeric protons of the sugars at C-3 and C-7 of the delphinidin unit and connections evident from a TOCSY experiment showed the 6 position of the C-3 sugar was not acylated while the 6 position of the 7 sugar was shifted downfield by acylation. An HMBC correlation showed that the one of the *p*-coumaroyl groups was attached at this latter site. The remaining set of equivalent glucose 6-*O*-*p*-coumaroyl moieties could be assigned to the 3′ and 5′ positions of the delphinidin. A long range coupling between the anomeric protons of these latter groups and a carbon signal at 148 ppm confirmed this. The diagnostic singlet signal for H-2′ and H-6′ of the delphinidin (broad at 7.9 ppm in spectra run at 25 °C but sharper at 45 °C) was further evidence for the symmetrical 3′,5′ disubstitution. Thus, **2** is delphinidin 3-glucoside-7,3′,5′-tri(6-*O*-*p*-coumaroyl-β-glucoside).

The *D. nigra* minor anthocyanin, **3**, eluted later on HPLC suggesting the possibility of extra acylation. An ESMS ion at 1535 and additional peaks in the NMR spectra indicated **3** had yet another *p*-coumaric acid group. Assignment of this acyl group to the last logical site, the C-6 position of the 3-sugar was confirmed by the downfield ^{1}H NMR shift of this signal relative to that seen in **2**. Most of the other signals were very similar to those for **2** showing **3** was delphinidin 3,7,3′,5′-tetra (6-*O*-*p*-coumaroyl-β-glucoside).

The third anthocyanin, **1**, was lacking one of the *p*-coumaroyl groups of **2**. The remaining two *p*-coumaroyl groups had identical NMR data showing these were the substituents on the 3′ and 5′ glucoses. The remaining NMR data were consistent with delphinidin 3,7-diglucoside-3′, 5′-di(6-*O*-*p*-coumaroyl-β-glucoside).

Alkaline hydrolysis of the major anthocyanin **2** yielded delphinidin 3,7,3′,5′-tetraglucoside (**4**). Partial alkaline hydrolysis gave **1** as well as a number of other products that, from their on-line spectra, were clearly the other various possible mono- and di-acylated anthocyanins.

This is the first time that an anthocyanin has been described with glycosylation at these four sites. As glycosylation of anthocyanins is known to occur almost always at the 3 position, often at either the 5- or 7-positions (but not both), sometimes at the 3′, or 3′ and 5′, and never at the 4′ position then these *Dianella* compounds could be said to be maximally glycosylated. The substitution of the sugars by aromatic acyl groups is known to be a major factor in the in vivo stabilisation of these pigments. Formation of folded conformations whereby the acyl groups are stacked above and below the plane of the anthocyanidin protect the molecule from hydration. Pigments **1**–**3** demonstrate this effect and offer an opportunity to assess the relative stacking capability of the variously situated acyl groups.

Recently Yoshida et al. (2000) have demonstrated, using ^{1}H NMR spectral data, that in acidic methanol conditions a caffeoyl residue on the 5 sugar makes little contribution to stacking while that on the 3′ sugar has a significant stacking ability. Work with other pigments show that *p*-coumaroyl groups attached to sugars at the 7 and 3′ (e.g. *Ceanothus*) or 3′ and 5′ positions (e.g. ternatins) are especially well sited to doubly stack to the delphinidin pyrilium chromophore. Using similar arguments the stacking ability of the various *p*-coumaroyl groups in **1**–**3** can be assessed. Firstly, the ^{1}H NMR chemical shifts of the delphinidin H-4 and those of the *p*-coumaroyl groups are shifted upfield by the shielding effect of ring currents due to stacking. The relative upfield shift as the number of *p*-coumaroyl groups increases from 2 to 4 (8.33 in **1**, 8.18 in **2** and 8.08 in **3**) suggests that all four *p*-coumaroyl groups have some

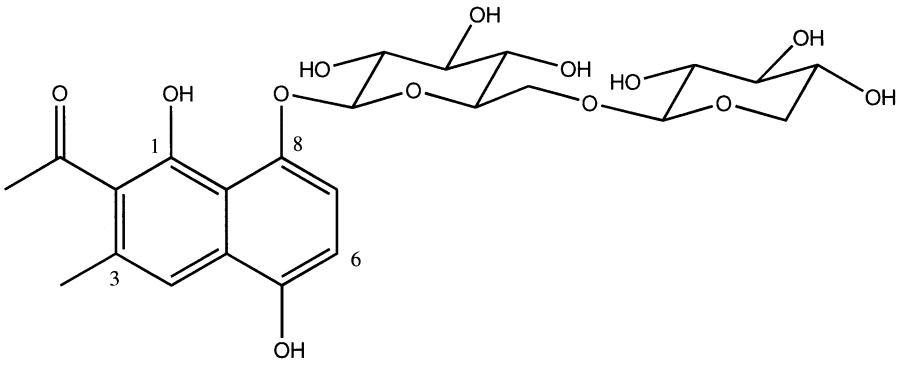

5

contribution. The chemical shifts of the *p*-coumaroyl protons in **2** are very similar to those found for the *p*-coumaroyl groups on the 7 and 3′ sugars in the *Ceanothus* anthocyanins, which are known to be involved in stacking. The relative upfield shifts are most pronounced for the 3′ and 5′ *p*-coumaroyl groups followed by the 7 and then the 3. This data suggests the 3′ and 5′ *p*-coumaroyl groups stack more tightly with the anthocyanidin than the 7 group, which in turn is more tightly stacked than the *p*-coumaroyl group on the 3 sugar. This observation is similar to that seen in the ternatins. In those members of the ternatin series of pigments, which have linear chains of *p*-coumaroyl-glucose groups attached at the 3′ and 5′ positions, the inner *p*-coumaroyl groups appear to stack more tightly than the more distant groups.

The coupling constants between H-5 and H-6 of the glucose units can also be used to assess the degree of folding. In **2** and **3** the 7 sugar has a large J_{5-6b} indicating a high ratio of the folded rotamer. In compound **3** the 3 sugar has a more normal rotamer distribution. The analogous data for the 3′ and 5′ sugars is not accessible since the signals for these groups in the ^{1}H NMR spectrum of **1**–**3** are too broad. This agrees with the chemical shift data above in that the *p*-coumaroyl group at position 3 is the least tightly stacked of the four groups. Further confirmation of this ranking of copigmentation ability is seen in the visible spectra of **1**–**3**. The bathochromic shift of the visible maximum relative to the parent glycoside has been shown to be a convenient guide to the degree of copigmentation. In this case the visible spectral maxima for **2** and **3** are the same, whereas the maximum for **1** is lower, supporting a more effective copigmentation role for the 7 *p*-coumaroyl group than the 3 *p*-coumaroyl group.

The juice expressed from the *Dianella nigra* berries is deeply blue. Microscopic examination shows this colour is due to a combination of soluble blue pigment and appreciable quantity of deep blue particles. Analysis of the supernatant and a methanolic solution of the pellet from centrifugation of the juice showed the water-soluble pigment was mainly **2** while the pigment in the particles was almost pure **3**. The tetra-acylated anthocyanin **3** is almost insoluble in water and the intensely blue particles are most probably made up of self-associated aggregates of this pigment. Pigment **2** is intensely blue in mildly acidic buffer solutions above pH 4. The pH of the berry juice is 5.4.

The extracts from the berries also contained a yellow, non-anthocyanic pigment, **5** (ESMS 526 amu). This compound was clearly a diglycoside and comparison of NMR data with known constituents of *Dianella* species indicated 5 had not been previously reported but was closely related to dianellin, a naphthalene rhamnoglucoside (Briggs et al., 1975). The sugar groups of **5** were identified as xylose and glucose from their NMR data. The xylose is linked to the 6 position of the glucose based on NOE data and the shift of the glucose C-6. Compound **5** also features an acetyl group at C-2 and a methyl group at C-3 attached to the napthalene nucleus, that are characteristic of most of the *Dianella* compounds. An H-bonded hydroxy group at 9.6 ppm was assigned to the C-1 position adjacent to the acetyl group and a NOE between the glucose anomeric proton and this hydroxy proton placed the disaccharide chain at C-8. The other hydroxyl group could be assigned to C-5 based on the observed coupling pattern of the aromatic protons. Thus **5** is 2-acetyl-1,5-dihydroxy-3-methyl-8-*O* (xylosyl(1→6)glucosyl) naphthalene.

Despite their attractive appearance the berries of *Dianella* appear to have attracted limited attention as a food or colourant. This may be due to the presence of quinones or quinone precursors such as **5**. Upon acid hydrolysis **5** yields stypandrone, a known toxin (Colegate et al., 1986).

3. Experimental

3.1. General procedures

NMR experiments were run at 500 MHz or at 300 MHz (75 MHz for ^{13}C). Anthocyanin samples **1**–**3** were

dissolved in 2% CF_3COOD in CD_3OD. Compound **5** was run in DMSO-d_6. MS were obtained using a VG Quattro (Electrospray) or VG ZAB (FAB) instrument. RP HPLC analyses were performed as described previously (Bloor, 1997) using a Waters 600 solvent delivery system with a Merck Lichrospher (5 μm, 119×4 mm) 100 RP-18 endcapped column (column temperature 24 °C) and a Waters 996 PDA detector.

3.2. Isolation of pigments

Berries were collected in summer from cultivated plants at the Gracefield Science Centre, Lower Hutt, N.Z. (*D. nigra*) and Commonwealth Park, Canberra, ACT, Australia (*D. tasmanica*). Fresh or frozen berries were extracted by crushing with 0.2% TFA in H_2O. After standing for 1 h the mixture was centrifuged. The aqueous supernatant was lyophilised. The remaining berry residue was further extracted by grinding with 0.2% TFA in MeOH and again centrifuged. H_2O was added to the MeOH extract and the MeOH was evaporated and the extract lyophilised. The solid aqueous extract was subjected to RP CC eluted with a 0.1% TFA in H_2O to MeOH gradient. Pigment fractions were further purified using Sephadex LH20 CC or Lobar CN LPCC (both using 1:1 MeOH: H_2O with 0.1% TFA) to yield pigments **1**, **2** and **5**. Compound **3** was purified from the solid MeOH extract using a Lobar CN column (3:1 MeOH:H_2O with 0.1% TFA).

3.3. Hydrolysis of pigments

Alkaline hydrolysis was performed on **2** by adding 1 N NaOH to a methanolic solution of **2** at 0 °C under nitrogen. Complete hydrolysis was achieved in 30 mins., (for partial hydrolysis the reaction was stopped after 10 mins) and the reaction was halted by the addition of 2N HCl. Compound **4** was purified from the hydrolysis mixture by RP CC (3:97 MeOH:H_2O with 0.1% TFA).

3.3.1. Delphinidin 3,7-Di-O-β-glucopyranoside-3′, 5′-di-O- (6-O-p-coumaroyl-β-glucopyranoside) (*1*)

UV-vis (0.01% HCl–MeOH) λ_{max} nm: 300 (br), 541. ^{1}H NMR data: see Table 1.

3.3.2. Delphinidin 3-O-β-D-glucopyranoside-7,3′,5′-tri-O-(6-O-p-coumaroyl-β- glucopyranoside) (*2*)

UV-Vis (0.01% HCl–MeOH) λ_{max} nm: 300 (br), 546. ^{1}H and ^{13}C NMR data: see Tables 1 and 2.

3.3.3. Delphinidin 3,7,3′,5′-tetra-O-(6-O-p-coumaroyl-β-glucopyranoside) (*3*)

UV-vis (0.01% HCl–MeOH) λ_{max} nm: 300 (br), 546. ^{1}H and ^{13}C NMR data: see Tables 1 and 2.

Table 1
^{1}H NMR spectral data for pigments **1**–**3**

		1	**2**	**3**
Delphinidin	4	8.33 *s*	8.18 *s*	8.08 *s*
	6	6.86 *d* 1.5	6.73 *d* (1.5)	6.75 *d* (1.5)
	8	6.7 *m*	6.69 *d*	6.67 *d* (1.5)
	2′,6′	7.9 *br s* (2H)[b]	7.9 *br s* (2H)[b]	7.9 *br s* (2H)[b]
3-Glucose	1	4.74 *d* 7.5	4.66 *d* (7.6)	4.65 *d* (7.5)
	6a	4.04 *dd* (12,2)	4.02 *dd* (12.2, 2.4)	4.61 *dd* (12.5, 2.5)
	6b	3.84 *m*	3.96 *dd* (12.2, 5.1)	4.55 *dd* (12.5, 7)
7-Glucose	1	5.35 *d* (8)	5.44 *d* (8)	5.45 *d* (8)
	6a	4.07 *d* (9.5)	4.9 obsc[a]	4.85 *dd* (11.5, 3)
	6b	3.78 *m*	4.30 *dd* (11.7, 10.2)	4.34 *dd* (12, 9.5)
3′,5′-Glucose	1	5.29 (2H) *m*	5.29 (2H) *m*	5.31 (2H) *m*
	6a	4.83 obsc	5.0 obsc	obsc
	6b	4.12 *br m*	4.11 *br m*	obsc
3-*p*-Cou	α			6.39 *d* (16)
	β			7.65 *d* (16)
	2,6			7.37 *d* (2H, 9)
	3,5			6.80 *d* (2H, 9)
7-*p*-Cou	α		6.15 *d* (15.6)	6.15 *d* (16)
	β		7.47 *d* (15.6)	7.46 *d* (16)
	2,6		6.70 *d* (8.5)	6.70 *d* (9)
	3,5		6.49 *d* (8.5)	6.49 *d* (9)
3′,5′-*p*-Cou	α	5.89 *br d* (2H, 16)	5.80 *br d* (2H)	5.74 *br d* (2H)
	β	7.30 *d* (2H, 16)	7.00 *d* (2H, 16.1)	6.94 *d* (2H, 16)
	2,6	6.7 *m* (4H)	6.70 *d* (4H, 8.5)	6.60 *d* (4H, 9)
	3,5	6.47 *br d* (4H)	6.49 *d* (4H, 8.5)	6.4 *br* (4H)[b]

[a] obsc—Signal obscured by HOD resonance.
[b] Signal broad but sharpens at 45 °C.

Table 2
^{13}C NMR spectral data for compounds **2**–**4**, 125 MHz in CD_3OD/CF_3COOD (98:2), δ in ppm[a]

		2	3	4
Delphinidin	2	162.0	161.9	165.1
	3	146.9	146.7	147.0
	4	134.8	134.2	138.1
	5	155.7	155.7	158.5
	6	105.2	105.3	103.8
	7	168.2	168.1	167.9
	8	95.3	95.6	97.7
	9	158.2	157.8	157.3
	10	115.5	115.5	115.5
	1′	120.5	119.4	120.6
	2′,6′	117.0	117.0	118.2
	3′,5′	147.9	147.9	147.7
	4′	147.6	147.6	147.4
3-Glc	1	104.0	103.7	103.8
	6	62.2	64.5	62.5
7-Glc	1	102.1	102.1	101.4
	6	65.0	64.9	62.5
3′,5′-Glc	1	102.0	101.7	103.8
	6	65.9	65.9	62.5

[a] Signals for *p*-coumaric acid groups in **2** and **3**; 169 (C=O), 114 (C-α), 145–148 (C-β), 126–127 (C-1), 130–131 (C-2,6), 117–118 (C-3,5) and 160–161 (C-4).

3.3.4. Delphinidin 3,7,3′,5′-tetra-O-(β-glucopyranoside) (**4**)

UV-Vis (0.01% HCl–MeOH) λ_{max} nm: 280, 521. FAB MS *m*/*z*: 951 [M^+], 790, 629. ^1H NMR spectral data (300 MHz, D_2O:TFA-*d*, 95:5): δ 8.80 (1H, *s*, H-4), 7.80 (2H, *s*, H-2′,6′), 6.98 (1H, *s*, H-6), 6.62 (1H, *s*, H-8), 5.14 (1H, *d*, 7.5 Hz, glc H-1), 5.07 (1H, *d*, 7.2 Hz, glc H-1), 4.8–4.9 (2 remaining Glc anomeric signals obscured by HOD resonance). ^{13}C NMR data: see Table 2.

3.3.5. 2-Acetyl-1,5-dihydroxy-3 methyl-8-O(β-xylopyranosyl-(16)-O-(β-glucopyranosyl)) naphthalene (**5**)

UV λ_{max}^{MeOH} nm: 219, 315, 346; ^1H NMR spectral data (500 MHz, DMSO-d_6): δ 2.24 (3H, *s*, 3-Me), 2.51 (3H, *s*, 2-Ac), 3.0–3.6 (7H, sugar signals), 3.69(1H, *dd*, $J=11.5$, 5.5, H-5 xyl), 4.02 (1H, *d*, $J=10.5$, H-6a glc), 4.23 (1H, *d*, $J=7.5$ Hz, H-1 xyl), 4.86 (1H, *d*, $J=7.5$, H-1 glc), 6.77(1H, *d*, $J=8$ Hz, H-6), 7.27 (1H, *d*, $J=8$ Hz , H-7), 7.41 (1H, *s*, H-4). ^{13}C NMR spectral data (125 MHz, DMSO-d_6): δ 19.5 (C-3 Me), 32.1 ($\underline{C}H_3CO$), 65.7 (xyl C-5), 68.7 (glc C-6), 69.8 (xyl C-4), 70.0 (glc C-4), 73.5 (glc C-2), 73.5 (xyl C-2), 76.3 (glc C-3), 76.3 (glc C-5), 76.6 (xyl C-3), 103.5 (glc C-1), 104.3 (xyl C-1), 109.1 (C-6), 112.2 (C-7), 114.0 (C-4), 114.1 (C-9), 125.7 (C-2), 126.4 (C-10), 131.5 (C-3), 147.0 (C-8), 148.3 (C-5), 150.3 (C-1), 205.2 ($CH_3\underline{C}O$).

Acknowledgements

The author thanks the Department of Chemistry, Australian National University, ACT, Australia for a visiting fellowship, Herbert Wong (Ind. Res.) for NMR spectroscopy and Rosemary Webby for initial plant collection. This work was funded by the New Zealand Foundation for Research Science and Technology (Contract CO-8804).

References

Bloor, S.J., 1997. Blue flower colour derived from flavonol-anthocyanin co-pigmentation in *Ceanothus papillosus*. Phytochemistry 45, 1399–1405.

Briggs, L.H., Briggs, L.R., King, A.W., 1975. New Zealand phytochemical survey. 14. Constituents of *Dianella nigra* Col. N. Z. J. Sci. 18, 559–563.

Colegate, S.M., Dorling, P.R., Huxtable, C.R., 1986. Dianellidin, stypandrol and dianellinone: an oxidation-related series from *Dianella revoluta*. Phytochemistry 25, 1245–1247.

Cooke, R.G., Sparrow, L.G., 1965. Colouring matters of Australian plants. XII. Quinones from *Dianella nigra* and *Stypandra grandis*. Aust. J. Chem. 18, 218–225.

Figueiredo, P., George, F., Tatsuzawa, F., Toki, K. Saito, Brouillard, R., 1999. New features of intramolecular copigmentation by acylated anthocyanins. Phytochemistry 51, 125–132.

Goto, T., Kondo, T., Kawai, T., Tamura, H., 1984. Structure of cinerarin, a tetra-acylated anthocyanin isolated from the blue garden cineraria, *Senecio cruentus*. Tetrahedron Lett. 25, 6021–6024.

Saito, N., Abe, K., Honda, T., Timberlake, C.F., Bridle, P., 1985. Acylated delphindin glucosides and flavonols from *Clitoria ternatea*. Phytochemistry 24, 1583–1586.

Terahara, N., Oda, M., Matsui, T., Osajima, Y., Saito, N., Toki, K., Honda, T., 1996. Five new anthocyanins, ternatins A3, B4, B3, and D2, from *Clitoria ternatea*. J. Nat. Prod. 59, 139–144.

Yoshida, K., Toyama, Y., Kameda, K., Kondo, T., 2000. Contribution of each caffeoyl residue of the pigment molecule of gentiodelphin to blue colour development. Phytochemistry 54, 85–92.

PERGAMON

Phytochemistry 58 (2001) 929–933

PHYTOCHEMISTRY

www.elsevier.com/locate/phytochem

Biocatalytic chlorination of aromatic hydrocarbons by chloroperoxidase of *Caldariomyces fumago*

Rafael Vázquez-Duhalt[a,*], Marcela Ayala[a], Facundo J. Márquez-Rocha[b]

[a]*Biotechnology Institute UNAM, AP 510-3, Cuernavaca, Morelos 62271, Mexico*
[b]*Marine Bioprocess Enginering Laboratory, CICESE, Baja California, 22860, Mexico*

Received 19 March 2001; received in revised form 5 July 2001

Abstract

Chloroperoxidase from *Caldariomyces fumago* was able to chlorinate 17 of 20 aromatic hydrocarbons assayed in the presence of hydrogen peroxide and chloride ions. Reaction rates varied from 0.6 min^{-1} for naphthalene to 758 min^{-1} for 9-methylanthracene. Mono-, di- and tri-chlorinated compounds were obtained from the chloroperoxidase-mediated reaction on aromatic compounds. Dichloroacenaphthene, trichloroacenaphthene, 9,10-dichloroanthracene, chloropyrene, dichloropyrene, dichlorobiphenylene and trichlorobiphenylene were identified by mass spectral analyses as products from acenaphthene, anthracene, pyrene and biophenylene respectively. Polycyclic aromatic hydrocarbons with 5 and 6 aromatic rings were also substrates for the chloroperoxidase reaction. The importance of the microbial chlorination of aromatic pollutants and its potential environmental impact are discussed.
© 2001 Elsevier Science Ltd. All rights reserved.

Keywords: Fungal chloroperoxidase; Enzymatic chlorination; Polycyclic aromatic hydrocarbons

1. Introduction

Organochlorine industrial compounds, chlorinated pesticides and polychlorinated biphenyls (PCBs) are considered among the most important pollutant xenobiotics. Their toxic effects have been extensively studied (Evangelista de Duffard and Duffard, 1996; Giesy and Kannan 1998; Tilson and Kodavanti, 1998). Because of their potential public health risk, some organochlorine compounds, such as PCBs, have been banned in western countries, but many are still manufactured and used as pesticides, plasticizers, paint and printing-ink components, adhesives, flame retardants, hydraulic and heat transfer fluids, refrigerants, solvents, additives for cutting oils, and textile auxiliaries. Thus, contamination with organochlorine compounds still occurs and this is of great public concern due to potential toxicity to humans and wildlife. Microbiological studies have been almost entirely focused on the degradation of these toxic compounds (Robinson, 1998; Wiegel and Wu, 2000; Chaudhry and Chapalamadugu, 1991).

In spite of the microbial capacity to produce halogenated compounds (Neidleman, 1975; de Jong and Field, 1997), information is scarce on the microbial production of toxic organochlorine compounds. In addition to de novo synthesis of chlorinated compounds, microorganisms transform some non-halogenated xenobiotics into organochlorine compounds with a possible increase in their toxicity. In this work, we show the capacity of chloroperoxidase from the fungus *Caldariomyces fumago* to chlorinate aromatic hydrocarbons, including polycyclic aromatic hydrocarbons (PAHs). PAHs are widely dispersed in the environment, and they are considered to be a potential health risk because of their possible carcinogenic and mutagenic activities. Chloroperoxidase (CPO) is a 42,000 Da extracellular heme glycoenzyme containing ferriprotoporphyrin IX as the prosthetic group (Sundaramoorthy et al., 1995). CPO exhibits a broad spectrum of chemical reactivities, it is a peroxide-dependent chlorinating enzyme and it also catalyzes peroxidase-, catalase- and cytochrome P450-type reactions of dehydrogenation, H_2O_2 decomposition and oxygen insertion, respectively (Yi et al., 1999). CPO is only one of a variety of halogenase enzymes that can be found in nature, other enzymes such as vanadium and non-heme halogenases (van Pee et al., 2000; Vollenbroek et al., 1995) are also potentially able to chlorinate organic pollutants.

* Corresponding author at: Instituto de Biotecnologıa UNAM, Aparto Postal 510-3, Cuernavaca, Morelos 62250, Mexico. Tel.: +52-5622-7655; fax: +52-7317-2388.
E-mail address: vazqduh@ibt.unam.mx (R. Vázquez-Duhalt).

0031-9422/01/$ - see front matter © 2001 Elsevier Science Ltd. All rights reserved.
PII: S0031-9422(01)00326-0

2. Results and discussion

Chloroperoxidase was able to utilize 17 of the 20 aromatic hydrocarbons assayed as substrate (Table 1). Only biphenyl, and the oxygen-containing dibenzofuran and anthrone, were not substrates for CPO under our reaction conditions. The specific activity values were from 0.6 min^{-1} for naphthalene to 758 min^{-1} for 9-methylanthracene. Interestingly, recalcitrant and carcinogenic 5- and 6-aromatic rings PAHs were substrates for chloroperoxidase in the presence of hydrogen peroxide and chloride ions. Chloroperoxidase is able to perform a broad range of reactions, like the enantioselective epoxidation of alkenes (Zaks and Dodds, 1995), oxidation of phenolic pollutants (Aitken et al., 1994; Carmichael et al., 1983), oxygenation of sulfides (Colonna et al., 1990), oxidation of organophosphorus pesticides (Hernandez et al., 1998), and the PAH–DNA adduct formation (Marquez-Rocha et al., 1997), to give only a few examples. In addition, CPO is able to oxidize very complex molecules, such as asphaltenes (Fedorak et al., 1993) and complex mixtures such as petroleum distillates (Ayala et al., 1998). Thus this halogenating enzyme is the most versatile enzymatic hemoprotein. Other halogenases are also able to perform halogenations, mainly chlorination, on a variety of substrates (Neidleman, 1975; Vollenbroek et al., 1995).

Table 1
Specific activity of chloroperoxidase from *Caldariomyces fumago* against aromatic compounds

Aromatic compound	Specific activity (min^{-1})
9-Methylanthracene	758 (±27)
Azulene	676 (±34)
Anthracene	134 (±14)
2-Methylanthracene	107 (±8)
7,12-Dimethylbenzanthracene	87 (±8)
Benzo[a]pyrene	84 (±6)
7-Methylbenzo[a]pyrene	81 (±7)
Acenaphthene	65 (±8)
Pyrene	53 (±6)
Benzo[ghi]perylene	45 (±7)
Perylene	25 (±10)
Biphenylene	10 (±0.5)
Phenanthrene	7 (±0.1)
Fluoranthene	3 (±0.2)
Fluorene	1.9 (±0.13)
Triphenylene	0.8 (±0.09)
Naphthalene	0.6 (±0.01)
Biphenyl	NR[a]
Dibenzofuran	NR[a]
Anthrone	NR[a]

[a] NR, no reaction detected.

The chemical nature of the reaction products was determined by gas chromatography–mass spectrometry (GC–MS). The mass spectra of the products from the enzymatic reaction with acenaphthene, anthracene, biphenylene, fluorene, phenanthrene, pyrene, and triphenylene are shown in Table 2. Monochlorinated, dichlorinated and trichlorinated compounds were found (Fig. 1), and they showed major ions at $m/z = [M^+]$-35, $m/z = [M^+]$-70, and $m/z = [M^+]$-105, respectively. No oxygen incorporation was detected in any of the products from the CPO-mediated reactions. In addition, no reaction could be detected with any PAH tested under peroxidase activity conditions (pH 5.0 and in the absence of chlorine ions). Significant information is available on the toxicity of chlorinated aromatic compounds, such as polychlorophenols (International

Table 2
Mass spectral data of the products from the chloroperoxidase-mediated reaction on aromatic compounds

Substrate	Product	Mass spectral ions (m/z)[a,b]
Acenaphthene	Dichloroacenaphthene	224 (39), 222 (64) [M^+], 187 (100), 152 (95), 93 (17), 75 (24).
	Trichloroacenaphthene	258 (57), 256 (81) (M^+], 221 (66), 186 (100), 150 (50), 110 (27), 98 (18), 75 (23).
Anthracene	9,10-Dichloroanthracene	248 (68), 246 (100) [M^+], 176 (43), 87 (10).
Biphenylene	Dichlorobiphenylene	222 (64), 220 (100) [M^+], 185 (17), 150 (45), 75 (11).
	Trichlorobiphenylene	258 (30), 256 (93), 254 (100) [M^+], 219 (13), 184 (49), 149 (14), 74 (10).
Fluorene	Dichlorofluorene	238 (25), 237 (7), 236 (40) [M^+], 201 (31), 199 (18), 166 (63), 165 (100), 164 (17), 163 (24), 100 (11), 82 (35).
Phenanthrene	Chlorophenanthrene	214 (32), 213 (16) [M^+], 212 (100), 177 (20), 176 (55), 175 (11), 174 (10), 151 (14), 150 (14), 106 (17), 88 (33), 87 (11), 75 (13).
Pyrene	Chloropyrene	238 (31), 236 (100) [M^+], 200 (34), 100 (12).
	Dichloropyrene	272 (62), 270 (100) [M^+], 235 (11), 200 (53), 135 (12), 100 (23).
Triphenylene	Chlorotriphenylene	265 (7), 264 (34), 263 (21) [M^+], 262 (100), 227 (14), 226 (63), 225 (16), 224 (23), 200 (11), 132 (9), 131 (20), 113 (56), 112 (43), 100 (21), 99 (12), 87 (9).

[a] Values in parentheses are relative abundances.
[b] [M^+] molecular ion.

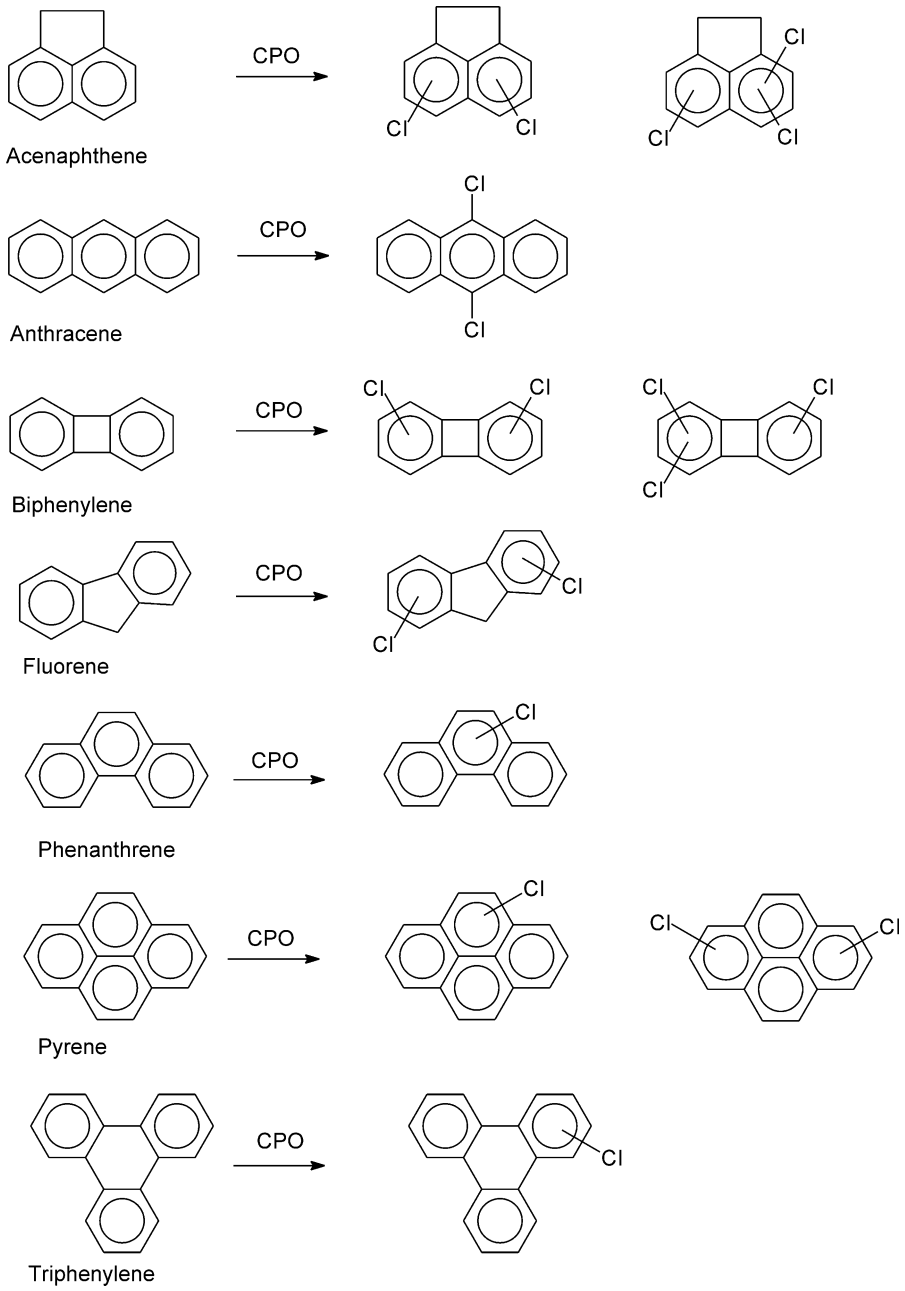

Fig 1. Chlorinated products from the enzymatic halogenation of aromatic compounds by chloroperoxidase in the presence of hydrogen peroxide and chloride ions.

Agency for Research on Cancer, 1999) and PCBs (Robinson, 1998; Wiegel and Wu, 2000), and to a less extent, on the toxicity of chlorinated derivatives of polycyclic aromatic hydrocarbons. Chlorinated PAHs have been tested for mutagenic activity by the Ames test on *Salmonella typhimurium* (Colmsjo et al., 1984; Johnsen et al., 1989). Chlorinated fluorene, flouranthene and benzo(a)pyrene acted as strong mutagens both in the presence and in the absence of metabolic activation, while only benzo(a)pyrene showed mutagenic activity as parent hydrocarbon. Mono- and di-chloropyrene isomers showed from 40 to 4000 times higher mutagenic activity than 1-nitropyrene and pyrenoquinones, respectively. On the other hand, a mixture of chlorinated chrysene isomers was considerably more potent than the parent hydrocarbon in terms of embryolethality and cytochrome P450 induction (7-ethoxyresorufin-*O*-deethylase and aryl hydrocarbon hydroxylase) (Gustafsson et al., 1994). The chlorinated chrysene caused anomalies, including edema and beak defects, similar to those reported after treatment of chick embryos with coplanar PCBs. These effects of the chlorinated mixture were mainly accounted for by 6-chlorochrysene and 6,12-dichlorochrysene. Chloronaphthalene was 5000-times

more potent than naphthalene for the inhibition of mitochondrial respiration in molar basis (Beach and Harmon, 1992). Monochloronaphthalene represent a risk for human health (Tsunenar et al., 1982) and for aquatic organisms (Ward et al., 1981).

3. Conclusions

Chloroperoxidase from the imperfect fungus *Caldariomyces fumago* is the most versatile enzyme in the hemoprotein family (Yi et al., 1999). CPO performs halogenase, peroxidase, catalase and cytochrome P450-like reactions. However, under our reaction conditions and with PAHs as substrates, CPO only acts as halogenase and no oxygenated products could be detected. In contrast, peroxidase activity on aromatic compounds produces mainly quinones, such as in the case of lignin peroxidase (Hammel et al., 1986; Vazquez-Duhalt et al., 1994) and manganese peroxidase (Bogan et al., 1996).

Caldariomyces fumago has been isolated from damp sites and also has been reported as a marine fungus (Dawson and Sono, 1987; Colonna et al., 1999). Chloroperoxidase, as other halogenases, is an extracellular enzyme that can react with a variety of substrates in the microbial environment. This enzyme is able to catalyze PAH-DNA adduct formation in vitro (Marquez-Rocha et al., 1997), suggesting the production of genotoxic aromatic intermediates. The present work shows that the transformation of aromatic pollutants into chlorinated derivatives by microbial enzymes may occur in polluted sites. This biocatalytic process should be considered because the toxicity and environmental impact of aromatic compounds may be increased.

4. Experimental

4.1. Chemicals

Purified CPO [EC 1.11.1.10] from *C. fumago* 89362 (Commonwealth Mycological Institute, Kew, Surrey, UK) was produced in a fructose medium and purified according to Pickard et al. (1991); all preparations used in this study had an $Rz = 1.36$, which corresponds to 95% purity. Hydrogen peroxide and buffer salts were obtained from J.T. Baker (Phillisburg, NJ). Polycyclic aromatic hydrocarbons were purchased from Aldrich Chemical (Milwaukee, WI). HPLC-grade acetonitrile and methylene chloride were purchased from Fisher Scientific (Springfield, NJ).

4.2. Reaction rate measurements

Reactions were carried out in a 1-ml reaction mixture containing 20 μM substrate and 15% acetonitrile in a 60 mM acetate buffer, pH 3.0, with 20 mM KCl at room temperature. From 0.4 pmol to 0.2 nmol of the purified enzyme were used in the mixtures. Reactions were started by addition of 1 mM H_2O_2 and monitored by HPLC. Reaction rates were measured from the differences in peak area after 10 min and referred to the purified protein concentration for specific activity calculations. Reported values are the mean of three replicates. Specific reaction rates are given as mol of substrate converted per mol of enzyme per minute or simply in min^{-1}. Reactions for 5 and 6 aromatic rings PAHs 7,12-dimethylbenzanthracene, benzo[a]pyrene, 7-methylbenzo[a]pyrene, benzo[ghi]perylene and perylene were also monitored by fluorescence spectrum, with an excitation at 300 nm, in a Luminescence spectrometer, Perkin-Elmer, Model LS 50, during 2 min at 25 °C. The CPO activity was measured as the disappearance of the respective maximum emission peak for each PAH over a two minute reaction.

4.3. Analytical methods

Substrate concentration was measured in a Perkin-Elmer (series 200) HPLC system, using a C_{18} Hypersyl 5 μm Hewlett-Packard column eluted with an acetonitrile–water (70:30 v/v) solvent mixture. Substrate and product detection was carried out using a diode array detector coupled to the HPLC system. Product identification was performed in a Hewlett-Packard GC (model 6890)-MS (model 5972) equipped with a SPB-20 column (30 m×0.25 mm, Supelco). The temperature program started at 100 °C for 2 min; the temperature was raised to 290 °C at a rate of 8 °C/min and kept at 290 °C for 10 min.

Acknowledgements

This work was supported by The National Council of Science and Technology of Mexico (CONACYT grant 33611-U) and by The Mexican Oil Institute (grant FIES 98-110-VI).

References

Aitken, M.D., Massey, I.J., Chen, T., Heck, P.E., 1994. Characterization of reaction products from the enzyme catalyzed oxidation of phenolic pollutants. Wat. Res. 28, 1879.

Ayala, M., Tinoco, R., Hernandez, V., Bremauntz, P., Vazquez-Duhalt, R., 1998. Biocatalytic oxidation of fuel as an alternative to biodesulfurization. Fuel Processing Technol. 57, 101–111.

Beach, A.C., Harmon, H.J., 1992. Additive effects and potential inhibitory mechanism of some common aromatic pollutants on in vitro mitochondrial respiration. J. Biochem. Toxicol. 7, 155–161.

Bogan, B.W., Lamar, R.T., Hammel, K.E., 1996. Fluorene oxidation in vivo by Phanerochaete chrysosporium and in vitro during manganese peroxidase-dependant lipid peroxidation. Appl. Environ. Microbiol. 62, 1788–1792.

Carmichael, R., Fedorak, P.M., Pickard, M.A., 1983. Oxidation of phenols by chloroperoxidase. Biotechnol. Lett. 7, 284–294.

Chaudhry, G.R., Chapalamadugu, S., 1991. Biodegradation of halogenated organic compounds. Microbiol Rev. 55, 59. –79.

Colmsjo, A., Rannug, A., Rannug, U., 1984. Some chloro derivatives of polycyclic aromatic hydrocarbons are potent mutagens in *Salmonella typhimurium*. Mutat. Res. 135, 21. –29.

Colonna, S., Gaggero, N., Richelmi, C., Pasta, P., 1999. Recent biotechnological developments in the use of peroxidases. Trends Biotechnol. 17, 163–168.

Colonna, S., Gaggero, N., Manfredi, A., Casella, L., Gullotti, M., Carrea, G., Pasta, P., 1990. Enantioselective oxidations of sulfides catalyzed by chloroperoxidase. Biochemistry 29, 10465. –10468.

Dawson, J.H., Sono, M., 1987. Cytochrome P-450 and chloroperoxidase: thiolate-ligand heme enzymes. Spectroscopic detemination of their active site structures and mechanistic implications of thiolate ligand. Chem. Rev. 87, 1255–1270.

de Jong, E., Field, J.A., 1997. Sulfur tuft and turkey tail: biosynthesis and biodegradation of organohalogens by Basidiomycetes. Annu. Rev. Microbiol. 51, 375–414.

Evangelista de Duffard, A.M., Duffard, R., 1996. Behavioral toxicology, risk assessment, and chlorinated hydrocarbons. Environ Health Perspect. 104 (2), 353–360.

Fedorak, P.M., Semple, K.M., Vazquez-Duhalt, R., Westlake, D.W.S., 1993. Chloroperoxidase-mediated modifications of petroporphyrins and asphaltenes. Enzyme Microb. Technol. 15, 429–437.

Giesy, J.P., Kannan, K., 1998. Dioxin-like and non-dioxin-like toxic effects of polychlorinated biphenyls (PCBs): implications for risk assessment. Crit. Rev. Toxicol. 28, 511–569.

Gustafsson, E., Brunstrom, B., Nilsson, U., 1994. Lethality and EROD-inducing potency of chlorinated chrysene in chick embryos. Chemosphere 29, 2301–2308.

Hammel, K.E., Kalyanaraman, B., Kirk, T.K., 1986. Oxidation of polycyclic aromatic hydrocarbons and dibenzo(p)dioxins by *Phanerochaete chrysosporium* ligninase. J. Biol. Chem. 261, 16948–16952.

Hernandez, J., Robledo, N.R., Velasco, L., Quintero, R., Pickard, M.A., Vazquez-Duhalt, R., 1998. Chloroperoxidase-mediated oxidation of organophosphorus pesticides. Pest. Biochem. Physiol. 61, 87–94.

International Agency for Research on Cancer, 1999. Polychlorophenols and their sodium salts. IARC Monographs on the Evaluation of the Carcinogenic Risks of Chemicals on Humans. 71 (2), 769–816.

Johnsen, S., Gribbestad, I.S., Johansen, S., 1989. Formation of chlorinated PAH: a possible health hazard from water chlorination. Sci. Total Environ. 81–82, 231–238.

Marquez-Rocha, F.J., Pica-Granados, Y., Sandoval-Villasana, A.M., Vazquez-Duhalt, R., 1997. Determination of genotoxicity using a chloroperoxidase-mediated model of PAH-DNA adduct formation. Bull. Environ. Contam. Toxicol. 59, 788–795.

Neidleman, S.L., 1975. Microbial halogenation. CRC Crit. Rev. Microbiol. 3, 333–358.

Pickard, M.A., Kadima, T.A., Carmichael, R.D.J., 1991. Chloroperoxidase a peroxidase with potential. Ind. Microb. 7, 235–242.

Robinson, G.K., 1998. (Bio)remediation of polychlorinated biphenyls (PCBs): problems, perspectives and solutions. Biochem. Soc. Trans. 26, 686–690.

Sundaramoorthy, M., Terner, J., Poulos, T.L., 1995. The crystal structure of chloroperoxidase: a heme peroxidase-cytochrome P450 functional hybrid. Structure 3, 1367–1377.

Tilson, H.A., Kodavanti, P.R., 1998. The neurotoxicity of polychlorinated biphenyls. Neurotoxicology 19, 517–525.

Tsunenar, S., Yonemitsu, K., Uchimura, Y., Takaesu, H., Kamisato, M., 1982. A rare fetal case of wood preservative, monochloronaphthalene (MCN), poisoning. Forensic Sci. Int. 20, 173–178.

van Pee, K.H., Keller, S., Wage, T., Wynands, I., Schnerr, H., Zehner, S., 2000. Enzymatic halogenation catalyzed via a catalytic triad and by oxidoreductases. Biol. Chem. 381, 1–5.

Vazquez-Duhalt, R., Westlake, D.W.S., Fedorak, P.M., 1994. Lignin peroxidase oxidation of aromatic compounds in systems containing organic solvents. Appl. Environ. Microbiol. 60, 459–466.

Vollenbroek, E.G., Simons, L.H., van Schijndel, J.W., Barnett, P., Balzar, M., Dekker, H., van der Linden, C., Wever, R., 1995. Vanadium chloroperoxidases occur widely in nature. Biochem. Soc. Trans. 23, 267–271.

Ward, G.S., Parrish, P.R., Rigby, R.A., 1981. Early life stage toxicity test with a saltwater fish: effects of eight chemicals on survival growth, and development of sheepshead minnows (*Cyprinodon variegatus*). J. Toxicol. Environ. Health 8, 225–240.

Wiegel, J., Wu, Q., 2000. Microbial reductive dehalogenation of polychlorinated biphenyls. FEMS Microbiol. Ecol. 32, 1–15.

Yi, X., Mroczko, M., Manjol, K.M., Wang, X., Hager, L.P., 1999. Replacement of the proximal heme thiolate ligand in chloroperoxidase with a histidine residue. Proc. Nat. Acad. Sci. 96, 12412–12417.

Zaks, A., Dodds, D.R., 1995. Chloroperoxidase asymmetric oxidations: Substrate specificity and mechanistic study. J. Am. Chem. Soc. 117, 10419–10424.

PERGAMON

Phytochemistry 58 (2001) 935–941

PHYTOCHEMISTRY

www.elsevier.com/locate/phytochem

Volatile compounds of endophyte-free and infected tall fescue (*Festuca arundinacea* Schreb.)

Qin Yue, Chunlin Wang, Thomas J. Gianfagna*, William A. Meyer

Plant Science Department, Rutgers University, 59 Dudley Road, New Brunswick, NJ 08901-8520, USA

Received 9 March 2001; received in revised form 17 July 2001

Abstract

Volatile compounds produced by intact plants and ground leaf tissue from endophyte-infected (E+) and endophyte-free (E−) tall fescue (*Festuca arundinacea* Schreb.) were collected by a purge-and-trap procedure and analyzed by gas chromatography/mass spectrometry The volatile compound profile from ground leaf tissue was similar between E+ and E− clonal plants; however, the sheaths of E+ clonal plants produced higher levels of 1-octen-3-ol, a characteristic volatile compound derived from lipid peroxidation in fungi, which was absent in E− clonal plants. Intact plants produced fewer volatiles than macerated leaves. At 25 °C, (*Z*)-3-hexen-1-ol acetate was the most abundant compound, accounting for 77 and 89% of the total volatile emission from E+ and E− plants, respectively. Higher temperature (32 °C) significantly reduced the production of (*Z*)-3-hexen-1-ol acetate. Nonanal was the most abundant compound at 32 °C accounting for 52 and 45% of the total volatile emission from E+ and E− plants. Treatment of E+ and E− plants with jasmonic acid (JA) dramatically altered the volatile compound profile. The levels of (*E*)-β-ocimene increased more than 200-fold and accounted for at least 43% of the total volatile emission. Although the presence of endophyte resulted in some qualitative and quantitative differences in the production of volatile compounds, they are unlikely to account for the differences in insect resistance between E+ and E− plants. Nevertheless, the production of a unique spectrum of volatiles after JA treatment may represent a significant plant-based defense response in tall fescue that is independent of endophyte. © 2001 Elsevier Science Ltd. All rights reserved.

Keywords: *Festuca arundinacea* Schreb.; Gramineae; Endophyte; 1-Octen-3-ol,3-hexen-1-ol acetate; β-Ocimene; Jasmonic acid

1. Introduction

Tall fescue *Festuca arundinacea* Schreb., one of the most widespread agricultural grass species, is often asymptotically infected by the fungal endophyte *Neotyphodium coenophialum*, which resides in the intercellular spaces of the leaf sheath. The benefit of the symbiotic endophyte–grass association has been widely demonstrated both in the laboratory and in field trials (Bacon et al., 1997). It is well documented that endophyte-infected (E+) turfgrasses often exhibit superior resistance to insects and diseases, and may even be more tolerant of drought and other abiotic environmental stresses, compared to their endophyte-free (E−) counterparts (Clay, 1988, 1992; Clay and Cheplick, 1989; Breen, 1994; Siegel and Bush, 1996; Bush et al., 1997; Leuchtmann and Clay, 1997). The enhanced resistance of E+ grasses towards insects and diseases is generally considered to result from the production of defense compounds by the endophyte–grass interaction. The most thoroughly described compounds to date are alkaloids including the ergot alkaloids, lolitrems, peramine, and lolines, which are toxic agents to grazing animals and/or insect feeding deterrents (Siegel and Bush, 1996). However, there are other defense mechanisms that may well operate in endophyte–grass associations. It is known that volatile compounds emanating from plants play an important role in plant–insect interactions, and may allow insect pests to find suitable plant hosts on which to feed, or may be used by insect predators in search of prey (Berney and Chapman, 1994). Knowledge of volatiles in E+ grasses may, therefore, be useful in understanding the chemical basis for the benefits of endophyte–grass associations. Recently, volatiles of E− tall fescue cultivars have been studied in relation to animal feed palatability (Tava et al., 1991; 1995; Mayland et

* Corresponding author. Tel.: +1-732-932-9711x252; fax: +1-732-932-9441.

E-mail address: gianfagna@aesop.rutgers.edu (T.J. Gianfagna).

0031-9422/01/$ - see front matter © 2001 Elsevier Science Ltd. All rights reserved.
PII: S0031-9422(01)00353-3

al., 1997). Little is known, however, about the volatile profile of E+ grasses. The present study examined the spectrum of volatile compounds from E+ and E− tall fescues to determine whether the presence of *Neotyphodium* endophyte affects the production of volatile compounds.

2. Results and discussion

2.1. Macerated tissue

Macerated tissue may provide information concerning the production of volatiles from tissue either damaged mechanically or by herbivory. The majority of the identified volatiles from macerated tissue are lipid degradation products classified as hydrocarbons, aldehydes, ketones, alcohols, esters, and furans. Most of these compounds have previously been reported to occur in the essential oil and/or fresh tissues of tall fescue (Tava et al., 1991; 1995; Mayland et al., 1997). There are more individual volatiles present in the E+ and E− FD4N clones (Table 1) than in selections 161, 230, 246 and 259 (Table 2). In addition to lipid peroxidation products, there are, however, several carotenoid breakdown products, such as β-cyclocitral, β-homocyclocitral, β-ionone, detected in selections 161, 230, 246 and 259.

Among the listed compounds in Table 1 are a variety of 6-carbon aldehydes [(*Z*)-3-hexenal, (*E*)-2-hexenal] and alcohols [hexanol, (*Z*)-3-hexen-1-ol, (*Z*)-3-hexen-1-ol acetate], which are commonly described as "green leaf volatiles" (GLVs). These are the major components of E+ and E− FD4N plants, representing 60–80% of the total volatile emission. In E+ FD4N plants, GLVs represent 62% of total volatiles in the sheaths and 80% in the blades. The blades of E+ FD4N plants produced much higher levels of (*Z*)-3-hexen-1-ol acetate than the sheaths. There are, however, no significant differences in GLVs between the sheaths and blades in E− FD4N plants. The blades of E− FD4N produced much higher levels of (*E*,*Z*)-2,6-nonadienal and 2-nonenal than the sheaths, whereas the levels of these compounds were similar in sheaths and blades of E+ clones. The results indicate that volatile production depends upon the tissue type, and the presence of endophyte. E+ FD4N plants produced lower levels of 1,3-heptadienal, 2,4-heptadienal, nonanal, (*E*,*Z*)-2,6-nonadienal, 2-nonenal, and 5-ethyl-2(5H) furanone, than E− FD4N plants. 1-octen-3-ol, a major component which accounted for 16.3% of total volatiles in the sheaths of E+ FD4N tall fescue, was not found in the sheaths and blades of E− FD4N plants, and was also absent in the blades of E+ FD4N plants, where only a few endophytes are present. The endophyte may be responsible for the emission of this compound from E+ plants.

Table 1
Volatile compounds of macerated leaf sheaths and blades from endophyte-free (E−) and endophyte-infected (E+) clonal FD4N tall fescue plants

Volatile compounds	Leaf sheath (ng/g/3 h)		Leaf blade (ng/g/3 h)		Significance[a] ($LSD_{0.05}$)
	E+	E−	E+	E−	
Hydrocarbons					
Pentane	4	10	6	7	NS
Hexane	13	20	33	17	NS
2,3-Dimethyl-1-pentene[b]	nd[c]	2	3	2	NS
Octane	1	14	3	3	NS
Nonane	2	10	1	6	NS
Decane	2	5	nd	2	NS
Dodecane	1	6	1	12	*
Tetradecane	1	9	1	1	*
Aldehydes and ketones					
1-Pentanal[b]	8	4	2	6	NS
4-Pentenal[b]	3	6	2	6	NS
1-Penten-3-one	10	11	7	18	NS
3-Pentanone	1	29	1	19	*
(*Z*)-3-Hexenal	306	492	195	548	*
(*E*)-2-Hexenal	165	478	110	548	*
(*E*,*E*)-2,4 Hexadienal	16	81	7	71	NS
Cyclohexanone	2	nd	nd	nd	NS
4-Methylcyclohexanone	3	17	1	18	NS
(*E*)-2-Heptenal	2	5	1	12	*
1,3-Heptadienal[b]	nd	5	nd	5	*
2,4-Heptadienal	1	11	1	13	*
Nonanal	4	60	7	55	*
6-Nonenal[b]	1	10	1	32	*
(*E*,*Z*)-2,6-Nonadienal	26	31	20	231	*
2-Nonenal[b]	14	6	7	121	*
Decanal	1	6	2	15	*
Alcohols and ester					
1-Penten-3-ol	16	24	24	17	NS
3-Methyl-1- butanol	2	2	1	2	NS
2-Penten-1-ol[b]	3	4	3	3	NS
Hexanol	113	90	21	251	NS
(*Z*)-3-Hexen-1-ol	55	187	32	213	*
(*Z*)-3-Hexen-1-ol acetate	14	166	254	76	*
2-Butoxyethanol	4	nd	nd	nd	*
2-Ethyl-1-hexanol	4	9	1	7	*
1-Octen-3-ol	171	nd	nd	nd	*
2-Octen-1-ol[b]	2	nd	nd	nd	*
2,6-Nonadien-1-ol[b]	1	<1	1	6	*
2-Nonen-1-ol[b]	<1	<1	<1	10	*
1-Nonanol	1	<1	1	1	NS
Monoterpenes and others					
Limonene	7	12	2	6	NS
2-Ethyl furan	5	9	2	10	NS
2-Ethyl thiophene	nd	19	nd	20	*
5-Ethyl-2(5*H*) furanone[b]	71	234	13	346	*
Total	1057	2087	767	2736	*

[a] Means for amount of volatiles compared by LSD test, $P \leqslant 0.05$, $n = 3$. NS or *, nonsignficant or significant, respectively.

[b] Tentative identification based upon mass spectra comparison with NIST library.

[c] nd, not detected.

Table 2
Volatile compounds of macerated leaves from four genetically related selections of tall fescue. Selections 161 and 259 are endophyte-free (E−) and selections 230 and 246 are endophyte-infected (E+)

Volatile compounds	Tall fescue selections (ng/g/3 h)				Significance[a] ($LSD_{0.05}$)
	E−		E+		
	161	259	230	246	
Hydrocarbons					
Octane	80	57	175	59	*
Nonane	2	tr[c]	1	1	NS
Decane	1	1	tr	1	NS
Undecane	<1	tr	tr	<1	NS
Dodecane	1	<1	1	<1	NS
Aldehydes and ketones					
Hexanal	118	138	244	151	*
(*E*)-2-Hexenal	213	260	410	266	NS
Heptanal	95	105	392	84	*
Octanedione[b]	4	2	3	1	NS
2,4-Heptadienal	1	1	12	<1	*
2,2,6-Trimethyl cyclohexanone	1	1	2	1	NS
Octanal	54	53	181	53	*
Nonanal	546	660	2401	590	*
(*E*,*Z*)-2,6-Nonadienal	9	12	86	8	*
(*E*)-2-Nonenal[b]	3	4	22	4	*
Decanal	16	7	22	8	*
Undecanal	1	<1	4	1	NS
Alcohols and ester					
Hexanol	6	2	5	1	NS
(*Z*)-3-Hexen-1-ol	61	33	112	21	*
(*Z*)-3-Hexen-1-ol acetate	183	205	44	30	*
Heptanol	<1	tr	1	<1	NS
1-Octen-3-ol	2	1	6	2	NS
Octanol	125	48	49	36	*
Terpenes and others					NS
Limonene	1	<1	1	<1	NS
(*E*)-β-ocimene	1	<1	<1	tr	NS
(*Z*)-β-ocimene/(*E*)-α-ocimene[b]	1	tr	tr	tr	NS
β-Cyclocitral[b]	5	3	6	2	NS
β-Homocyclocitral[b]	1	<1	1	<1	NS
β-Ionone	6	3	8	1	NS
2-Pentyl furan[b]	5	4	10	4	NS
Total	1544	1605	4200	1331	*

[a] Means for amount of volatiles compared by LSD test, $P \leqslant 0.05$, $n = 3$. NS or *, nonsignficant or significant, respectively.
[b] Tentative identification based upon mass spectra comparison with NIST library.
[c] tr (trace) = <0.1.

Nonetheless, 1-octen-3-ol was present in all four E+ and E− natural plant selections (Table 2), although it was at much lower levels than in the FD4N E+ clone. Previous studies have also shown that 1-octen-3-ol was detectable in E− tall fescues (Tava et al., 1995; Mayland et al., 1997). It is not clear how endophytes affect the production of 1-octen-3-ol in E+ plants. It has been demonstrated that 1-octen-3-ol is a major volatile in mushroom (*Agaricus campestris*) (Tressl et al., 1982), in other filamentous fungi including *Laetisaria arvalis* and *Pleurotus pulmonarius* (Brodowsky and Oliw, 1993), and also bracket fungi (*Fomitopsis pinicola* and *Fomes fomentarius*) (Faldt et al., 1999). If endophytes can indeed enhance the production of 1-octen-3-ol in E+ plants, the lower levels of this compound found in E+ cultivars 230 and 246, as compared to the E+ FD4N plant sheaths, may reflect either lower levels of endophyte infection or the influences of plant genotype.

In the genetically related E+ and E− selections, nonanal was the most abundant component, representing 35–56% of total volatiles (Table 2), whereas it was less than 3% of total volatiles in the clonal FD4N plants. GLVs, which were major volatiles in FD4N plants, were 19–39% of total volatiles in E+ and E− selections. It has been documented that nonanal is primarily produced from auto-oxidation of oleic acid (Hwang et al., 1994) and GLVs are formed by enzymatic oxidative degradation of unsaturated fatty acids, particularly of linoleic and linolenic acid (Hatanaka, 1983). The higher ratio of nonanal to GLVs in the selections 161, 259, 246 and 230 suggest that these plants may have higher ratios of oleic acid to linoleic or linolenic acid.

The four genetically related E+ and E− selections exhibited a similar volatile profile, and they only differed in a few trace components. Nevertheless, quantitative differences in both relative amounts of individual components within a selection and total amount of volatile emission collected from each selection were observed. Among the four genetically related E+ and E− selections, 230 produced the highest levels of total volatiles.

(*Z*)-3-hexen-1-ol acetate was the only volatile produced at lower levels in E+ plants (both FD4N clones and the genetically related plant selections) compared to E− plants. E− selections 161 and 259 produced (*Z*)-3-hexen-1-ol acetate at the levels of 183 and 205 ng/g/3 h, respectively. In E+ plants 230 and 246, the level of this compound was 44 and 30 ng/g/3 h, respectively. The sheaths of the E− FD4N plant produced (*Z*)-3-hexen-1-ol acetate at 166 ng/g/3 h, while it was only 14 ng/g/3 h in the sheaths of the E+ FD4N plant. Further investigations are warranted to determine if endophytes can inhibit the synthesis of (*Z*)-3-hexen-1-ol acetate in E+ tall fescues.

Volatiles are known to mediate insect-plant interactions and may be attractants or repellents (Berney and Chapman, 1994). 1-Octen-3-ol has been reported as a strong attractant to the moth *Epinotia tedella* (Faldt et al., 1999), tabanid flies (French and Kline, 1989), tsetse flies (Vale et al., 1988), and mosquitoes (Van Essen et al., 1994). 1-Octen-3-ol, (*E*)-2-hexenal and 1-octen-3-one, are known to enhance the aggregation of red legged earth mites (*Halotydeus destructor*) at low concentrations

and reduce the aggregation at higher concentration (Jiang et al., 1997). (*Z*)-3-hexen-1-ol acetate, which is present at lower levels in E+ plants than in E− plants, has been found to be attractive to adult Colorado potato beetles (*Leptinotasa decemlineata*) (Lwande et al., 1988) and cabbage root flies (Wallbank and Wheatley, 1979).

2.2. Intact plants

Intact E+ and E− plants produced a smaller number of volatile compounds than macerated leaf tissue (Table 3). Most notably was a decline in GLVs, particularly the 6-carbon aldehydes and alcohols. The predominant volatiles were 7–10 carbon aldehydes, (*Z*)-3-hexen-1-ol acetate and several monoterpenes. A dramatic change in the volatile profile of intact E+ and E− plants occurred with a change in temperature. At 25 °C, (*Z*)-3-hexen-1-ol acetate was the most abundant compound, accounting for 77 and 89% of the total volatile emission from E+ and E− plants, respectively. Higher temperature (32 °C) significantly reduced the production of (*Z*)-3-hexen-1-ol acetate. Nonanal was the most abundant compound at 32 °C accounting for 52 and 45% of the total volatile emission from E+ and E− plants. The monoterpenes accounted for a higher percentage of the total volatile emission profile at the higher temperature, although there were no differences in the amounts of monoterpenes or nonanal at 32 °C compared to 25 °C (data not shown). Since insects often respond to a mixture of volatile compounds rather than one compound in itself, this change in composition may affect plant–insect interactions. In fruit tissue, volatile esters are synthesized by an alcohol acyltransferase from 4 to 6 carbon alcohols and acetyl CoA (Perez et al., 1993). If a similar enzyme exists in tall fescue leaves, it may be much less active at 32 °C than at 25 °C.

Jasmonic acid (JA) is a hormone produced from linolenic acid especially after membrane lipids in the leaf are damaged by herbivory. JA treatment of E+ and E− plants significantly affected the volatile compound emission profile (Table 4). JA induced the synthesis of the monoterpene (*E*)-β-ocimene more than 200-fold in FD4N E+ and E− clonal plants, and accounted for more than 43% of the total volatile emissions. Another compound, whose spectrum matched closely with both (*Z*)-β-ocimene and (*E*)-α-ocimene, but which we could not conclusively identify, accounted for 31% of the total volatile emission. There were also significant increases in other monoterpenes such as (*E*,*Z*)-allo-ocimene, limonene, myrcene and linalool. Methyl salicylate, indole and nonanal also increased after JA treatment. Similar results were found for the four genetically related tall fescue selections (data not shown). β-Ocimene is produced in cotton and other plants in response to herbivore damage (Pare and Tumlinson, 1997). β-Ocimene is a powerful attractant of predatory mites (Takabayashi et al., 1994; Gols et al., 1999), aphid parasitoids (Du Yongjun et al., 1998) and the generalist parasitoid *Cotesia marginiventris* (Rose et al., 1998). In gerbera daisy leaves (*Gerbera jamesonii*), JA treatment induced the production of a complex odor blend comprised largely of terpenoids, including (*E*)-β-ocimene, which attracted the predatory mite, *Phytoseuilus persimilis* (Gols et al., 1999). The induction of β-ocimene by JA may, therefore, be a component of the defense response of tall fescue to phytophagous insect attack.

Although there were some qualitative and quantitative differences in the production of volatile compounds between plant genotypes and the presence of endophyte, they are unlikely to account for the differences in insect resistance between E+ and E− plants. Nevertheless, the production of volatiles after JA treatment may represent a significant plant-based defense response of tall fescue that is independent of the presence of endophyte.

Table 3
Volatile compounds from intact clonal FD4N endophyte-free (E−) and endophyte-infected (E+) tall fescue plants at 25 and 32 °C. Data are expressed as a percentage of the total amount of volatile compounds

Volatile compounds	Temperature				Significance[a] ($LSD_{0.05}$)
	25 °C		32 °C		
	E−	E+	E−	E+	
	(% total volatile compounds)				
Aldehydes and ketones					
Heptanal	1.0	0.3	4.4	3.6	NS
Octanal	1.8	0.6	7.2	6.0	NS
Nonanal	10.3	4.0	52.3	44.7	*
Decanal	2.3	0.8	8.5	10.1	NS
2-Butanone	0.7	–	–	–	NS
6-Methyl-5-hepten-2-one	0.3	0.1	0.7	0.5	NS
2-Octanone	0.4	<0.1	2.6	0.5	NS
Alcohols					
(*Z*)-3-Hexen-1-ol	0.7	0.7	–	–	NS
Heptanol	0.1	–	–	0.2	NS
(*Z*)-3-Hexen-1-ol acetate	76.6	89.1	3.2	1.9	*
2-Ethyl-1-hexanol	0.1	–	0.7	0.5	NS
1-Octanol	0.1	–	0.6	0.4	NS
Monoterpenes					
Unknown monoterpene	–	–	0.6	0.4	NS
Myrcene	0.4	0.2	3.5	4.0	NS
Limonene	0.3	0.2	1.9	0.2	NS
(*E*)-β-Ocimene	0.6	0.4	3.8	9.3	*
Unknown monoterpene	0.7	0.5	4.2	8.3	*
Unknown monoterpene	–	<0.1	–	0.5	NS
(*E*,*Z*)-allo-ocimene	0.4	0.4	2.9	4.3	NS

[a] Means for amount of volatiles compared by LSD test, $P \leqslant 0.05$, $n = 3$. NS or *, nonsignficant or significant, respectively. Data were transformed to the arcsin$\sqrt{}$% prior to analysis.

Table 4
The effect of jasmonic acid on the production of volatile compounds by intact, clonal, endophyte-infected (E+) and endophyte-free (E−) tall fescue plants

Compound	Treatment				Significance[a] ($LSD_{0.05}$)
	Control		+Jasmonic acid		
	(ng/g/3h)	(% total)	(ng/g/3h)	(% total)	
E−					
(*E*)-β-ocimene	4	2	3318	45	*
(*Z*)-β-ocimene/(*E*)-α-ocimene[b]	4	2	2453	33	*
(*E*,*Z*)-allo-ocimene	2	1	998	14	*
Linalool	11	5	32	<1	*
Limonene	5	2	27	<1	*
Myrcene	6	3	22	<1	*
3-Hexen-1-ol acetate	83	39	82	1	NS
Methyl salicylate	10	5	58	4	*
Indole	nd[c]	–	1	<1	*
Nonanal	3	2	12	<1	*
E+					
(*E*)-β-ocimene	6	2	1380	43	*
(*Z*)-β-ocimene/(*E*)-α-ocimene[b]	4	2	998	31	*
(*E*,*Z*)-allo-ocimene	tr[d]	–	364	11	*
Linalool	9	5	22	<1	NS
Limonene	8	4	27	<1	*
Myrcene	7	4	13	<1	NS
3-Hexen-1-ol acetate	105	54	163	5	NS
Methyl salicylate	7	4	27	<1	*
Indole	1	<1	5	<1	*
Nonanal	5	2	7	<1	NS

[a] Means for amount of volatiles compared by LSD test, $P \leqslant 0.05$, $n = 3$. NS or *, nonsignficant or significant, respectively.
[b] Tentative identification based upon mass spectra comparison with NIST library.
[c] nd, not detected.
[d] tr, trace.

3. Materials and methods

3.1. Plant materials

Five tall fescue selections (FD4N E+ and E− clonal plants, two naturally occurring E− plants designated as selections 161 and 259, and two naturally occurring E+ plants designated as selections 230 and 246) were used in this study. FD4N E− clones were generated from FD4N E+ plants by fungicidal treatment. Selections 161, 230, 246 and 259 are genetically related having the same pollen parent. The presence of *Neotyphodium coenophialum* endophyte was tested by rose bengal staining (Saha et al., 1988). All grasses were maintained in 15-cm containers at 25 °C day and 20 °C night temperatures in the greenhouse.

3.2. Method of collecting volatiles from the macerated plants

To analyze volatiles in macerated tissues, 10 g of sample was quickly homogenized in liquid nitrogen with a mortar and pestle, and tissue homogenates were poured into a purge-and-trap apparatus fitted with a Tenax-Carbo trap tube and purged with ultra-pure nitrogen gas. Ten μl of 100 ppm toulene-d_8 in methylene chloride (Baker Chemicals) was added as an internal standard. Trapping was undertaken at 50 °C for 60 min with nitrogen gas at a flow rate of 40 ml/min.

3.3. Method of collecting volatiles from intact plants

Intact plant volatiles were collected by dynamic headspace analysis based upon a modification of the methods previously described (Robertson et al., 1993). Greenhouse-grown plants were placed in a growth chamber at 25 °C, with a 12 h photoperiod, for 1 day before trapping volatile compounds. Generally, the plant being examined was removed from its container and the roots washed free of soil mix with tap water followed by distilled water. The plant was placed in a 400-ml beaker with 200 ml of distilled water, and then placed into a 3-l glass chamber equipped with air inlet, flowmeter and Tenax-Carbo trap tube. Air, filtered through traps containing molecular sieve 5 Å and activated charcoal, was purged at a rate of 35 ml/min and then drawn over the plant for 3 h by a small diaphragm vacuum pump at a rate 150 ml/min. The apparatus was

set up in a growth chamber at 25 °C with a light level of 250 μmol/m^2/s. Volatile compounds were trapped approximately 6 h after the beginning of the photoperiod.

3.4. JA treatment

From a stock solution of JA (200 μmol/ml), 50 μl was diluted into 5 ml of water and then sprayed onto the whole plant. After 24 h, the volatiles were collected as described above.

3.5. Experimental design

For each experiment there were three samples per plant or treatment. Data were analyzed by an analysis of variance and means separated by LSD test, $P \leqslant 0.05$. Each experiment was repeated once with similar results.

3.6. Gas chromatography-mass spectrometry (GC-MS)

The Tenax-Carbo trap tube was purged with nitrogen for 30 min at a rate of 25 ml/min to remove moisture. Volatiles trapped on the adsorbent tube were directly and thermally desorbed into the GC injector by using the Short Path Thermal Desorption System II (SIS, Ringoes, NJ) at 250 °C for 5 min. A Varian 3400 GC was fitted with DB-I capillary column (30 m, I.D. = 0.25 mm, film thickness = 0.15 μm, J&W Scientific, Folsom, CA). Injector temperature was 250 °C. The initial oven temperature was −20 °C, and it was raised to 40 °C at a rate of 5 °C/min, then to 150 °C at a rate of 3 °C/min and finally up to 280 °C at a rate of 15 °C/min. Split ratio was 5:1. A Finnigan magnetic sector mass detector (MAT 8230) was connected to the GC with an interface tube at 280 °C. The electron ionization voltage was 70 eV and the mass range scanned was 35–350. Peak identification was based on co-chromatography and mass spectral comparisons with authentic standards, or when not available, tentative identifications were determined using a NIST or Wiley mass spectral library.

Acknowledgements

The authors thank Drs. Rongqi Sun, M.D. Richardson, J.M. Johnson-Cicalese, and Y. Ju for their help and advice during the preliminary stages of this project.

References

Bacon, C.W., Richardson, M.D., White, J.F., 1997. Modification and uses of endophyte-enhanced turfgrasses: a role for molecular technology. Crop Sci. 37, 1415–1425.

Berney, E.A., Chapman, R.F., 1994. Host-Plant Selection by Phytophagous Insects. Chapman & Hall, New York, London.

Breen, J.P., 1994. Acremonium endophyte interactions with enhanced plant resistance to insects. Annu. Rev. Entomol. 39, 401–423.

Brodowsky, I.D., Oliw, E.H., 1993. Biosynthesis of 8*R*-hydroxylinoeic acid by the fungus *Laetisaria arvalis*. Biochim. Biophys. Acta 1168, 68–72.

Bush, L.P., Wilkinson, H.W., Schardl, C.L., 1997. Bioprotective alkaloids of grass-fungal endophyte symbioses. Plant Physiol. 114, 1–7.

Clay, K., 1988. Fungal endophytes of grasses: a defensive mutualism between plants and fungi. Ecology 69, 10–16.

Clay, K., 1992. Fungal endophytes of plants: biological and chemical diversity. Nat. Toxins 1, 147–149.

Clay, K., Cheplick, G.P., 1989. Effect of alkaloids from fungi-endophyte-infected grasses on fall armyworm (*Spodoptera frugiperda*). J. Chem. Ecol. 15, 169–182.

Du Yongjun, Poppy G. M., Powell, W., Pickett, J.A., Wadhams, L.J., Woodcock, C.M., 1998. Identification of semiochemicals released during aphid feeding that attract parasitoid *Aphidius ervi*. J. Chem. Ecol. 24, 1355–1368.

Faldt, J., Jonsell, M., Nordlander, G., Borg-Karlson, A., 1999. Volatiles of bracket fungi *Formitopsis pinicola* and *Fomes fomentarius* and their functions as insect attractants. J. Chem. Ecol. 25, 567–590.

French, F.E., Kline, D.L., 1989. 1-Octen-3-ol, an effective attractant for *Tabanidae* (Diptera). J. Med. Entomol. 26, 459–461.

Gols, R., Posthumus, M.A., Dicke, M., 1999. Jasmonic acid induces the production of gerbera volatiles that attract the biological control agent netherlands. Entomol. Exp. Appl. 93, 77–86.

Hatanaka, A., 1983. Biosynthesis of leaf alcohol. Bull. Inst. Chem. Res. (Kyoto Univ.) 61, 180–192.

Hwang, H., Hatman, T.G., Karwe, M.V., Izzo, H.V., Ho, C., 1994. Aroma generation in extruded and heated wheat flour. ACS Symposium Series 558, 144–157.

Jiang, Y., Ridsdill-Smith, T.J., Ghisalberti, E.L., 1997. The effect of volatile metabolites of lipid peroxidation on the aggregation of red-legged earth mites *Halotydeus destructor* (Acarina: Penthaleidae) on damaged cotyledons of subterranean clover. J. Chem. Ecol. 23, 163–174.

Leuchtmann, A., Clay, K., 1997. The population biology of grass endophytes. In: Carroll, G.C., Tudzynski, P. (Eds.), The Mycota. V. Plant Relationships, Part B. Springer, Berlin, Heidelberg, New York, pp. 185–204.

Lwande, W., McDowell, P.G., Amiani, H., Amoke, P., 1988. Analysis of airborne volatiles of cowpea. Phytochemistry 28, 421–423.

Mayland, H.P., Flath, R.A., Shewmaker, G.E., 1997. Volatiles from fresh and air-dried vegetative tissues of tall fescue (*Festuca arundinacea* Schreb.): relationship to cattle preference. J. Agric. Food Chem. 45, 2204–2210.

Pare, P.W., Tumlinson, J.H., 1997. De novo biosynthesis of volatiles induced by insect herbivory in cotton plants. Plant Physiol. 114, 1161–1167.

Perez, A.G., Sanz, C., Olias, J.M., 1993. Partial purification and some properties of alcohol acyltransferase from strawberry fruits. J. Agric. Food Chem. 41, 1462–1466.

Robertson, G.W., Griffiths, D.W., Smith, W.M., Butcher, R.D., 1993. The application of thermal desorption-gas chromatography-mass spectrometry to the analysis of flower volatiles from five varieties of oilseed rape (*Brasssica napus* spp. *oleifera*). Phytochem. Analysis 4, 152–157.

Rose, U.S.R., Lewis, W.J., Tumlinson, J.H., 1998. Specificity of systemically released cotton volatiles as attractants for specialist and generalist parasitic wasps. J. Chem. Ecol. 24, 303–319.

Saha, D.C., Jackson, M.A., Johnson-Cicalese, J.M., 1988. A rapid staining method for detection of endophytic fungi in turf and forage grasses. Phytopath. 78, 237–239.

Siegel, M.R., Bush, L.P., 1996. Defensive chemicals in grass-fungal endophyte associations. Recent Adv. Phytochem. 30, 81–118.

Takabayashi, J., Dicke, M., Takahashi, S., Posthumus, M.A., van Beek, T.A., 1994. Leaf age affects composition of herbivore-induced synomones and attraction of predatory mites. J. Chem. Ecol. 20, 373–386.

Tava, A., Berardo, N., Odoardi, M., 1991. Composition of essential oil of tall fescue. Phytochemistry 30, 1455.

Tava, A., Berardo, N., Cunico, C., Romani, M., Odoardi, M., 1995. Cultivar differences and seasonal changes of primary metabolites and flavor constituents in tall fescue in relation to palatability. J. Agric. Food Chem. 43, 98–101.

Tressl, R., Bahri, D., Engel, K.H., 1982. Formation of eight-carbon and ten-carbon components in mushrooms (*Agaricus campestris*). J. Agric. Food Chem. 30, 89–93.

Vale, G.A., Lovemore, D.F., Flint, S., Cockbill, G.F., 1988. Odour-baited targets to control tsetse flies, *Glossina spp*. (Diptera: Glossinidae), in Zimbabwe. Bull. Entomol. Res. 78, 293–300.

Van Essen, P.H.A., Kemme, J.A., Ritchie, S.A., Kay, B.H., 1994. Differential responses of *Aedes* and *Culex* mosquitoes to octenol or light in combination with carbon dioxide in Queensland. Med. Vet. Entomol. 8, 673–676.

Wallbank, B.E., Wheatley, G.A., 1979. Some responses of cabbage root fly (*Delia brassicae*) to allyl isothiocyanate and other volatile constituents of crucifers. Ann. Appl. Biol. 91, 1–12.

PERGAMON

Phytochemistry 58 (2001) 943–947

PHYTOCHEMISTRY

www.elsevier.com/locate/phytochem

Acacetin glycosides as taxonomic markers in *Calamintha* and *Micromeria*

Petar D. Marin[a,1], Renée J. Grayer[a,*], Nigel C. Veitch[a], Geoffrey C. Kite[a], Jeffrey B. Harborne[b]

[a]*Jodrell Laboratory, Royal Botanic Gardens, Kew, Richmond, Surrey, TW9 3DS, UK*
[b]*Department of Botany, The University of Reading, Whiteknights, PO Box 221, Reading, RG6 6AS, UK*

Received 20 June 2001; received in revised form 10 August 2001

Abstract

A new acetylated flavone glycoside, acacetin 7-*O*-[6‴″-*O*-acetylglucosyl(1‴″→2″)]rhamnosyl(1‴→6″)glucoside, has been isolated from the leaves of *Calamintha glandulosa* together with the known compound acacetin 7-*O*-rhamnosyl(1‴→6″)glucoside. The occurrence of these flavonoids in the closely related genera *Satureja, Micromeria, Acinos* and *Clinopodium* indicates that their distribution may be of taxonomic significance. © 2001 Elsevier Science Ltd. All rights reserved.

Keywords: *Calamintha glandulosa*; *Micromeria*; Lamiaceae; Acacetin 7-*O*-[6‴″-*O*-acetylglucosyl(1‴″→2″)]rhamnosyl(1‴→6″)glucoside; Acacetin 7-*O*-rhamnosyl(1‴→6″)glucoside (linarin); Chemosystematics

1. Introduction

Calamintha Miller, *Micromeria* Benth., *Satureja* L., *Clinopodium* L. and *Acinos* Miller are five closely related genera of aromatic plants belonging to the family Lamiaceae, subfamily Nepetoideae and tribe Saturejeae. Many species grow in open habitats in the Mediterranean area, and some are endemic to local regions of the Balkan Peninsula. The boundaries among the genera are poorly defined, and their taxonomic treatment has changed many times. For example, Briquet (1896) treated them as only one genus, *Satureja sensu lato*, whereas Bentham (1848) and Boissier (1879) recognised *Micromeria, Satureja* and *Calamintha* (*Acinos* and *Clinopodium* being included in *Calamintha*). They are treated as five separate genera in Flora Europaea (Ball and Getliffe, 1972; Chater and Guinea, 1972) and by Silic (1979). In contrast, Stace (1991) again merged *Acinos* and *Calamintha* with *Clinopodium* in his treatment for the Flora of the British Isles. These different conclusions suggest that more characters are needed to define the generic boundaries in this group of plants.

Chemical characters can often provide additional information to complement data from morphological and other studies. For this reason a number of species representing each genus was surveyed for flavonoids. During this investigation, which was carried out using both HPLC coupled to diode array detection and liquid chromatography–mass spectrometry (LC–MS), a new acetylated acacetin glycoside (**1**) was detected in the leaf extracts of several species. The compound always co-occurred with another acacetin glycoside (**2**). This communication describes the isolation of **1** and **2** from *Calamintha glandulosa* (Req.) Benth. [Syn. *C. nepeta* (L.) Savi ssp. *glandulosa* (Req.) P.W. Ball], the identification of the compounds by means of spectroscopic techniques, and their distribution among the five genera.

2. Results and discussion

2.1. Identification of flavone glycosides *1* and *2*

Compounds **1** and **2** were obtained from a methanolic extract of *C. glandulosa* leaves by preparative PC and

* Corresponding author. Tel.: +44-20-8332-5312; fax: +44-20-8332-5310.
E-mail address: r.grayer@rbgkew.org.uk (R.J. Grayer).
[1] Present address: Faculty of Biology, Botanical Institute and Garden, University of Belgrade, Studentski trg 16, 11000 Belgrade, Yugoslavia.

0031-9422/01/$ - see front matter © 2001 Elsevier Science Ltd. All rights reserved.
PII: S0031-9422(01)00352-1

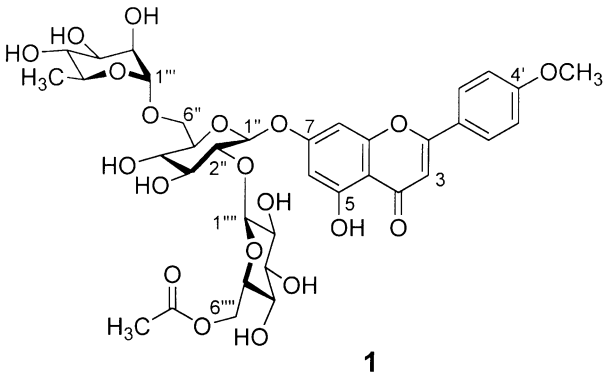

1

semi-preparative HPLC. Their UV spectra were identical ($\lambda_{max} = 268$ and 333 nm) and typical of those of flavone 7-*O*-glycosides (Markham, 1982). First-order APCI–MS (positive mode) of **1** and **2** gave $[M+H]^+$ ions at *m*/*z* 797 and 593, respectively, with both showing a protonated aglycone $[A+H]^+$ at *m*/*z* 285. These data suggested that **1** and **2** were glycosylated derivatives of the same flavonoid aglycone.

The ^{1}H NMR spectrum of **1** contained resonances characteristic for an $ArOCH_3$ group (δ 3.87), three anomeric sugar protons (δ 5.22, 4.57 and 4.52) and an acetyl group (δ 1.95), as well as those for aromatic and other glycosidic protons. Analysis of the aromatic proton resonances, their corresponding ^{13}C NMR chemical shifts (HSQC) and their long range ^{1}H–^{13}C connectivities (HMBC) indicated that the aglycone was a derivative of apigenin (5,7,4′-trihydroxyflavone) (Markham et al., 1982; Markham and Geiger, 1994). The downfield shift of the H-3′,5′ protons at δ 7.15 compared to apigenin (δ 6.98) indicated that the 4′-hydroxyl group of **1** was substituted. The nature of this substitution was determined by 1D ROESY experiments using the XSROESY pulse sequence (Gradwell et al., 1997). A strong ROE connectivity detected between H-3′,5′ and the methoxyl group at δ 3.87 confirmed that the aglycone was apigenin 4′-methyl ether (acacetin). This was consistent with the prominent ion observed at *m*/*z* 285 in APCI-MS of **1**, corresponding to $[A+H]^+$.

ROE connectivities were also detected between the anomeric proton at δ 5.22 and both H-6 and H-8 of the aglycone, indicating that the site of glycosylation was at C-7. Assignment of the ^{1}H and ^{13}C NMR resonances of the primary sugar was achieved using DQF–COSY and HSQC data acquired in DMSO-d_6 (Table 1). Use of this solvent allowed the exchangeable sugar hydroxyl resonances to be retained in the ^{1}H NMR spectrum. These were assigned from $^3J(^1H, ^1H)$ connectivities observed in DQF–COSY spectra with the corresponding non-exchangeable sugar protons (Veitch et al., 1998). The $^3J_{H\text{-}1'',H\text{-}2''}$ coupling constant of 7.1 Hz and the ROE connectivities detected between H-1″ and both H-3″ and H-5″ confirmed that the primary sugar was β-glucopyranose. The DQF–COSY data indicated that free

Table 1
^{1}H and ^{13}C NMR chemical shift data for the acetylated flavone *O*-glycoside **1** (δ in DMSO-d_6 at 37 °C)

		Assignment		
	Atom	δ ^{1}H	δ ^{1}H (OH)	δ ^{13}C
	2			163.9
	3	6.92 *s*		103.8
	4			181.9
	5		12.88 *br s*	161.1
	6	6.47 *d* (2.1)		99.7
	7			162.8
	8	6.74 *d* (2.1)		94.7
	9			156.8
	10			105.4
	1′			122.6
	2′, 6′	8.04 *d* (8.9)		128.3
	3′, 5′	7.15 *d* (8.9)		114.6
	4′			162.4
	OCH_3	3.87 *s*		55.5
Glc	1″	5.22 *d* (7.1)		98.3
	2″	3.53 *br m*		82.8
	3″	3.54 *m*	5.46 *br d*	75.5
	4″	3.24 *m*	5.32 *m*	69.1
	5″	3.67 *m*		75.4
	6″	3.88 *m*		65.8
		3.47 *m*		
Rha	1‴	4.57 *br s*		100.4
	2‴	3.69 *m*	4.55 *d* (4.4)	70.3
	3‴	3.48 *m*	4.38 *d* (6.0)	70.7
	4‴	3.17 *m*	4.64 *d* (5.5)	72.0
	5‴	3.43 *m*		68.2
	6‴	1.08 *d* (6.1)		17.7
Glc	1⁗	4.52 *d* (7.9)		104.6
	2⁗	3.03 *m*	5.33 *m*	74.5
	3⁗	3.23 *m*	5.01 *d* (5.0)	75.9
	4⁗	3.10 *m*	5.12 *d* (5.5)	69.7
	5⁗	3.43 *m*		73.7
	6⁗	4.18 *dd* (11.8, 1.7)		63.5
		4.01 *dd* (11.8, 5.5)		
	OAc	1.95 *s*		20.4
				170.1

hydroxyl groups were absent from both C-2″ and C-6″ of the primary Glc residue. A weak ROE connectivity detected between the 6″-CH_2 proton of the primary Glc residue at δ 3.88 and the anomeric proton at δ 4.57 indicated that a second sugar residue was attached at C-6″. Assignment of the ^{1}H and ^{13}C NMR resonances of this residue (DQF–COSY, HSQC and HMBC data) identified it as α-rhamnopyranose (Table 1). Further analysis of the DQF–COSY data indicated that resonances corresponding to 2‴-OH, 3‴-OH and 4‴-OH were present in the ^{1}H NMR spectrum. This confirmed that no additional groups were linked to the Rha residue.

A ROE connectivity detected between H-1″ of the primary Glc residue and the remaining anomeric proton at δ 4.52 confirmed that a third sugar residue was linked

at the 2″ position. This was also evident from the characteristic downfield shift of the C-2″ resonance to δ_C 82.8. The (1‴→2″)-linked sugar was identified as β-glucopyranose by complete assignment of its ^1H and ^{13}C NMR resonances, and the $^3J_{H\text{-}1''',H\text{-}2'''}$ coupling constant of 7.9 Hz (Table 1). The ^1H and ^{13}C resonances of the 6‴-CH_2 group of this Glc residue were also downfield shifted. DQF–COSY data indicated that only resonances for 2‴-OH, 3‴-OH and 4‴-OH were present in the ^1H NMR spectrum. This confirmed that 6‴-CH_2 was the site of substitution of the acetyl group of **1** (δ_H 1.95; δ_C 20.4, 170.1). Further evidence was provided by the series of ions noted in the first order APCI–MS (positive mode) of **1** at *m*/*z* 651, 447 and 285, which corresponded to successive losses of Rha (146 amu), acetylGlc (204 amu) and Glc (162 amu) from the pseudomolecular ion at *m*/*z* 797. High resolution MS of **1** gave a molecular formula of $C_{36}H_{44}O_{20}$. Compound **1** was therefore identified as acacetin 7-*O*-[6‴-*O*-acetylglucosyl (1‴→2″)]rhamnosyl(1‴→6″)glucoside, a new acylated flavone triglycoside.

The ^1H NMR spectrum of **2** was similar to that of **1** but lacked the resonances of the acetylglucosyl residue. Comparison of the NMR data with spectra obtained for an authentic sample confirmed **2** to be the known compound, acacetin 7-*O*-rhamnosyl(1‴→6″)glucoside (acacetin 7-*O*-rutinoside or linarin).

2.2. Occurrence of compounds 1 and 2 in Acinos, Calamintha, Clinopodium, Micromeria and Satureja species

The distribution and relative amounts of leaf flavonoids **1** and **2** in species of the above five genera are summarised in Table 2. *Calamintha glandulosa* and all the species of *Micromeria* investigated contained both compounds. They were the most abundant flavonoids in *C. glandulosa* and *M. dalmatica*, and among the major flavonoids in *M. thymifolia* and *M. albanica*. However, in *M. juliana* and *M. cristata*, **1** and **2** were only minor compounds. All four *Satureja* species, *Acinos arvensis* and *A. hungaricus* contained **2**, but lacked **1**. The compounds were not detected in either *A. majoranifolius* or *Clinopodium vulgare*.

Several acacetin glycosides have been reported previously from *Calamintha nepeta* (Souleles and Shammas, 1985) including **2**, which has also been isolated from *Micromeria* spp. (Tomás-Barberán et al., 1991). In addition, the flavanone glycoside corresponding to **2**, isosakuranetin 7-*O*-rutinoside (neoponcirin), has been reported from five species of *Micromeria* (*M. graeca*, *M. fruticulosa*, *M. juliana*, *M. montana*, *M. thymifolia*) and from *Calamintha nepeta* (Bellino et al., 1980).

Bentham (1848), Boissier (1879) and Stace (1991) considered *Calamintha* to be so closely related to *Acinos* and *Clinopodium* that they combined the three genera into one. However, the distribution of the unusual acetylated acacetin glycoside **1** suggests that the genus *Calamintha*, or at least *C. glandulosa*, is more closely related to the genus *Micromeria* than to *Acinos* or *Clinopodium*. The quantitative differences in the content of acacetin glycosides among species of *Micromeria* are also of systematic interest. *Micromeria albanica, M. thymifolia* and *M. dalmatica*, which have higher relative levels of **1** and **2,** are placed in section *Pseudomelissa* Benth., whereas *M. juliana* and *M. cristata*, with lower relative levels of these compounds, are placed in section *Eumicromeria*. These flavonoid glycoside characters correlate well with results obtained from other studies, in which the two sections were distinguished by differences in the flavone aglycone profiles of their leaf surfaces (Tomás-Barberán et al., 1991) and micromorphological features (Husain et al., 1990).

Table 2
Distribution of acacetin 7-*O*-[6‴-*O*-acetylglucosyl(1‴→2″)]rhamnosyl (1‴→6″)glucoside (**1**) and acacetin 7-*O*-rhamnosyl(1‴→6″)glucoside (**2**) in *Calamintha* and related taxa and relative amounts present in the plants

Taxon	Relative amount[a]	
	1	**2**
Calamintha glandulosa	++	++
Micromeria albanica	+	++
M. cristata	+/-	+/-
M. dalmatica	++	++
M. juliana	+/-	+/-
M. thymifolia	+	++
Satureja cuneifolia	–	+/-
S. kitaibelii	–	+
S. montana ssp. *montana*	–	+
S. montana ssp. *variegata*	–	t
Acinos arvensis ssp. *villosus*	–	+
A. hungaricus	–	+
A. majoranifolius	–	–
Clinopodium vulgare	–	–

[a] UV absorbance in absorbance units [AU] on HPLC chromatograms for 10 μl injections containing the compounds extracted from 5 mg of dried leaf. Key: ++, >1.0 AU; +, 0.1–1.0 AU; +/- 0.01–0.1 AU; t, trace (<0.01 AU); –, not detected.

3. Materials and methods

3.1. General

^1H NMR (500 and 400 MHz) and ^{13}C NMR (125 and 100 MHz) spectra were recorded in DMSO-d_6, with the residual solvent resonances used as internal references at δ 2.50 and 39.5, respectively. High-resolution ESIMS (negative mode) were obtained on a Bruker Apex II instrument (calibrant masses 307, 514, 611 and 784). Positive ion first-order APCI–MS were obtained with a quadrupole ion-trap instrument (Finnigan LCQ) using

Table 3
Taxa investigated with collection locality and accession number

Taxon	Place and date of collection	Collector and accession No.	Kew accession No.
Acinos arvensis (Lam.) Dandy ssp. *villosus* (Gaud.) Soják	Klinje (BiH); 27.6.1976	C. Silic AA 0676	BI 8746
A. hungaricus (Simonkai) Silic	Stol (Yu); 10.7.1994	P.D. Marin AH 0794	BI 8732
A. majoranifolius (Mill.) Silic	Rumija (Yu); 28.8.1982	C. Silic AM 0882	BI 8733
Calamintha glandulosa (Req.) Benth.	Kotor (Yu); 25.5.1997	P.D.Marin CG 0697	BI 7898
Clinopodium vulgare L.	Samcekinci (Yu); 10.8.1998	P.D. Marin CV 0898	BI 8734
Micromeria albanica (Gris. ex K. Maly) Silic	Bistrica (Yu); 4.9.1997	P.D. Marin MA 0997	BI 8704
M. cristata (Hampe) Grisebach	Sicevo (Yu); 15.7.1998	P.D. Marin MC 0798	BI 8707
M. dalmatica Benth.	Lovcen (Yu); 26.6.1997	P.D. Marin MD 0697	BI 8705
M. juliana (L.) Benth. ex Reich.	Kotor (Yu); 25.6.1997	P.D. Marin MJ 0697	BI 8706
M. thymifolia (Scop.) Fritsch	Priboj (Yu); 26.6.1998	P.D. Marin MT 0698	BI 8731
Satureja cuneifolia Ten.	Peljesac (Cro); 15.8.70	C. Silic SC0870	BI 8730
S. kitaibelii Wierzb. ex Heuff.	Sicevo (Yu); 15.7.1998	P.D. Marin SK 0798	BI 7899
S. montana L. ssp. *montana*	Benkovac (Cro); 1.8.1989	P.D. Marin SM 0889	BI 8728
S. montana L. ssp. *variegata* (Host) P.W. Ball	Mosor (BiH); 1.7.1990	P.D. Marin SV 0790	BI 8729

a vaporiser temperature of 550 °C, sheath and auxiliary nitrogen gas pressures of 80 and 20 psi, a needle current of 5 μA, and a heated capillary temp. of 150 °C. Samples were introduced by direct infusion, or via an HPLC fitted with a Merck (Darmstadt, Germany) LiChrospher 100RP-18 (250×4.0 mm i.d.; 5 μm particle size) column using a 20 min linear gradient of 25–100% MeOH in 1% aq. HOAc at 1 ml/min. The system for analytical and semipreparative HPLC consisted of a Waters LC600 pump and a 996 photodiode array detector. For analytical HPLC, the same column and gradient were used as for LC–MS described above, but the eluting solvents were 2% aq. HOAc and MeOH, HOAc, H_2O (18:1:1). An identical LiChrospher column but with 10 mm i.d. was used used for semipreparative HPLC, and the eluting solvents consisted of H_2O (A) and MeOH (B). Elution was with a linear gradient, starting with 50% B and changing to 60% B over 15 min, followed by isocratic elution with 100% B for 5 min. The column temperature was 30 °C for both analytical and semi-preparative HPLC.

3.2. Plant material

The origin and accession numbers of *Calamintha glandulosa* and species from other genera studied are given in Table 3. The samples were identified and authenticated by the first author. Voucher specimens have been deposited at the Herbarium of the Botanical Institute and Garden, Faculty of Biology, University of Belgrade.

3.3. Extraction and isolation

Air dried leaves (0.5 g) of the 13 accessions of *Acinos*, *Calamintha*, *Clinopodium*, *Micromeria*, and *Satureja* were crushed and boiled for ca. 2 min in 10 ml of 80% aq. MeOH (H_2O:MeOH, 20:80), and then extracted at room temperature for 24 h. After filtration and solvent removal by rotary evapn, each of the extracts was dissolved in 1 ml of 80% aq. MeOH. The crude extracts were analysed by HPLC with diode array detection and then separated into several fractions by means of preparative paper chromatography to remove rosmarinic acid from the flavonoids. These fractions were analysed by both HPLC and LC–MS. Compounds **1** and **2** were found in the fractions with an R_f-value of 0.50 in solvent BAW (*n*-BuOH, HOAc, H_2O, 4:1:5, v/v, upper layer). To isolate the flavonoids, an extract of *Calamintha glandulosa* was prepared by the same method described above, but with 20 g of dried leaves and 250 ml of 80% aq. MeOH. A preliminary purification was carried out with preparative paper chromatography using BAW and 15% aq. HOAc as solvents and the fractions containing **1** and **2** were further separated by semi-preparative HPLC to obtain pure samples of each flavonoid for spectroscopic analysis. An authentic sample of acacetin 7-*O*-rhamnosyl(1‴→6″)glucoside (acacetin 7-*O*-rutinoside or linarin) (**2**) was obtained from Apin Chemicals Ltd.

3.4. Acacetin 7-O-[6‴-O-acetyl-β-glucopyranosyl (1‴→2″)]α-rhamnopyranosyl(1‴→6″)β-glucopyranoside (*1*)

Pale yellow solid. UV (MeOH) λ_{max} (nm): 268, 333. ^1H and ^{13}C NMR: see Table 1. APCI–MS *m*/*z*: 797 $[M+H]^+$, 651, 447, 285 $[A+H]^+$. HR–ESIMS *m*/*z*: 795.2347 $[M-H]^+$ (calc. for $C_{36}H_{43}O_{20}$, 795.2342).

Acknowledgements

P.D.M. is grateful to The Royal Society for financial support. Access to high field NMR facilities were kindly provided by the Medical Research Council Biomedical NMR Centre, National Institute for Medical Research, Mill Hill, London, UK. We thank chemiSPEC (North of England Business and Innovation Centre, Sunderland Enterprise Park East, Sunderland, UK) for high-resolution MS data.

References

Ball, P.W., Getliffe, F., 1972. *Clinopodium* L. In: Tutin, T.G., Heywood, V.H., Burges, N.A., Moore, D.M., Valentine, D.H., Walters, S.M., Webb, D.A. (Eds.), Flora Europaea. Cambridge University Press, Cambridge, pp. 166–167.

Bellino, A., Venturella, P., Marcenò, C., 1980. Naringenin and neoponcirin from *Micromeria* species and *Calamintha nepeta*. Fitoterapia 51, 163–165.

Bentham, G., 1848. *Satureja* L., *Micromeria* Benth. et *Calamintha* Moench. In: De Candole, A.P. (Ed.), Prodromus Systematis Naturalis Regni Vegetabilis, Vol. 12. Treuttel and Wurz, Paris, pp. 208–234.

Boissier, P.E., 1879. Flora Orientalis, 4. H. Georg, Basel, Geneva, 562–583.

Briquet, J.I., 1896. In: Engler, H.G.A., Prantl, K.A.E. (Eds.), Die natürlichen Pflanzenfamilien, Teil 4, Abt. 3a. Ed. Engelmann, Leipzig.

Chater, A.O., Guinea, E., 1972. *Micromeria* Bentham. In: Tutin, T.G., Heywood, V.H., Burges, N.A., Moore, D.M., Valentine, D.H., Walters, S.M., Webb, D.A. (Eds.), Flora Europaea. Cambridge University Press, Cambridge, pp. 167–170.

Gradwell, M.J., Kogelberg, H., Frenkiel, T.A., 1997. Applying excitation sculpting to construct singly and doubly selective 1D NMR experiments. Journal of Magnetic Resonance 124, 267–270.

Husain, S.Z., Marin, P.D., Silic, C., Quaiser, M., Petcovic, B., 1990. A micromorphological study of some representative genera in the tribe Saturejeae (Lamiaceae). Botanical Journal of the Linnaean Society 103, 59–80.

Markham, K.R., 1982. Techniques of Flavonoid Identification. Academic Press, London.

Markham, K.R., Chari, V.M., Mabry, T.J., 1982. Carbon-13 NMR spectroscopy of flavonoids. In: Harborne, J.B., Mabry, T.J. (Eds.), The Flavonoids. Advances in Research. Chapman and Hall, London, pp. 19–134.

Markham, K.R., Geiger, H., 1994. ^{1}H NMR spectroscopy of flavonoids and their glycosides in DMSO-d_6. In: Harborne, J.B. (Ed.), The Flavonoids. Advances in Research since 1986. Chapman and Hall, London, pp. 441–497.

Silic, C., 1979. Monografija rodova *Satureja* L., *Calamintha* Miller, *Micromeria* Bentham, *Acinos* Miller i *Clinopodium* L. u flori Jugoslavije. Zemaljski Muzej BiH, Sarajevo.

Souleles, C., Shammas, G., 1985. Leaf and flower constituents of *Calamintha nepeta* (L.) Savi. Plantes Médicinales et Phytothérapie 19, 286–290.

Stace, C.A., 1991. New Flora of the British Isles. Cambridge University Press, Cambridge.

Tomás-Barberán, F.A., Gil, M.I., Marin, P.D., Tomás-Lorente, F., 1991. Flavonoids from some Yugoslavian *Micromeria* species: chemotaxonomical aspects. Biochemical Systematics and Ecology 19, 697–698.

Veitch, N.C., Grayer, R.J., Irwin, J.L., Takeda, K., 1998. Flavonoid cellobiosides from *Salvia uliginosa*. Phytochemistry 48, 389–393.

PERGAMON

Phytochemistry 58 (2001) 949–958

PHYTOCHEMISTRY

www.elsevier.com/locate/phytochem

High molecular compounds (polysaccharides and proanthocyanidins) from *Hamamelis virginiana* bark: influence on human skin keratinocyte proliferation and differentiation and influence on irritated skin

Alexandra Deters[a], Andreas Dauer[a], Esther Schnetz[b], Manige Fartasch[b], Andreas Hensel[a,*]

[a]*Hochschule Wädenswil, University of Applied Sciences, Pharmaceutical Biotechnology, Glycopharmacy Research Group, Gruental, CH-8820 Wädenswil, Switzerland*

[b]*Department of Dermatology, Glycopharmacy Research Group, University of Erlangen-Nürnberg, Hartmannstr. 43, D-91052 Erlangen, Germany*

Received 17 July 2001; received in revised form 10 August 2001

Abstract

Although extracts from *Hamamelis* bark have long been used in therapy of skin diseases and in cosmetic formulas there are only few pharmacological investigations verifying the activity of distinct *Hamamelis* bark constituents. Therefore two major classes of constituents, namely polymeric proanthocyanidins and polysaccharides were isolated from *Hamamelis* bark and tested concerning their influence on proliferation and differentiation of cultured human keratinocytes. While the polysaccharide fraction, consisting mainly of arabans and arabinogalactans, did not effect human keratinozytes, the proanthocyanidins strongly increased the proliferation of the cells, while the differentiation was not influenced significantly. Within a preliminary cumulative in vivo study on SLS-irritated skin, proanthocyanidins (ProcyanoPlus) were proven to reduce transepidermal water loss and erythema formation. Furthermore, a clinical scoring indicated that procyanidins can influence irritative processes significantly. © 2001 Elsevier Science Ltd. All rights reserved.

Keywords: *Hamamelis virginiana* L.; Polysaccharides; Araban; Arabinogalactan; Polysaccharides; Proanthocyanidins; Skin; Keratinocytes; Proliferation; Differentiation; Clinical study

1. Introduction

Extracts and destillates from *Hamamelis* bark and leaves are widely used as part of skin care products and in dermatological treatment of sun burn, irritated skin, atopic eczema (Korting et al., 1995) and to promote wound healing via anti-inflammatory effects (Korting et al., 1993). Several reports from traditional medicine indicate the efficacy of *Hamamelis* preparations in dermatology (Laux and Oschmann, 1993; Swoboda and Meurer, 1991). On the other side the clinical effects of this herbal drug in dermatology are proven only by very preliminary studies (Erdelmeier et al., 1996) while no information is available on pharmacological in vitro activities of *Hamamelis* ingredients on relevant skin cells to get a positive in vivo–in vitro correlation. However, the compounds responsible for the dermatological activity, are not identified clearly yet. It is assumed that the tannin fraction, consisting of hydrolysable and condensed tannins, which acounts up to 12% for *Hamamelis* bark (Hoffmann-Bohm et al., 1993) may contribute to the efficacy. Nevertheless, this was not proven unambigiously up to now.

During aqueous extraction of the plant material the presence of higher amounts of polysaccharides gets obvious. As some high-molecular carbohydrates are known to influence skin physiology in some cases quite extensively (Kitamura et al., 1997; Yagi et al., 1997; Chithra et al., 1998; Strickland et al., 1999; Eskelinin and Santalahti, 1992) the polysaccharide fraction of *Hamamelis* also may contribute to the dermatological activity.

* Corresponding author. Tel.: +41-1789-9670; fax: +41-1789-9950.

E-mail address: a.hensel@hswzfh.ch (A. Hensel).

0031-9422/01/$ - see front matter © 2001 Elsevier Science Ltd. All rights reserved.
PII: S0031-9422(01)00361-2

The aim of the present study was first to investigate the structural features of the *Hamamelis* bark polysaccharides and secondly to evaluate the dermatological potential of these polysaccharides and of high-molecular proanthocyanidin fraction on in vivo and in vitro skin proliferation and skin differentiation in keratinozyte in vitro culture.

A widely used pharmacological test system for such investigations are in vitro submerged cell cultures of human keratinocytes as a dynamic proliferating and differentiating system. This in vitro system represents the complex differentiation process of epidermal skin, leading to the anuclear cells filled with fibrous keratin and getting plasticized by hydration (Ponec and Kempenaar, 1995; Gibbs et al., 1997; van der Sandt et al., 1999). Beside toxic effects, different reaction patterns of keratinocytes towards exogenous test compounds can be detected using this system: compounds inducing cell differentiation can be separated from substances promoting the differentiation by increased formation of keratins K1 and K10. Therefore submerged keratinocytes allow detailed statements of potential mode of action of the test compounds.

2. Results

2.1. Isolation, fractionation and characterization of Hamamelis polysaccharides

Raw polysaccharides (RPS) with a carbohydrate content >99% and residual protein impurities of 0.4% were isolated from *Hamamelis* bark in a yield of 0.4%. A 1% solution of RPS showed kinematic viscosity of 1080 mPa s^{-1}, indicating that the mucilage consists of polymers with a low degree of polymerisation.

Fractionation of RPS by IEC resulted in one neutral and three acidic polymer fractions (Table 1). Each fraction was further separated by GPC on Sephacryl S-300 to yield, finally, 10 subfractions which were characterized concerning average molecular weight, uronic acid content, monosaccharide composition and linkage types of the respective monomers.

Neutral fractions H I.2 and H I.3 with quite low molecular weights between 4 and 13 kDa consisted mainly of arabinose. Linkage analysis of these fractions and GC–MS identification of the partially methylated alditol acetates indicated the presence of highly branched arabans with 1,3- and 1,3,5-linked arabinose residues (Table 2). This linkage pattern can be correlated to

Table 2
Linkage analysis of polysaccharide fractions H I and carboxyl-reduced fractions H II and III. Data indicate the respective molar composition

Carbohydrate	Linkage type	H I.1	H I.2	H I.3	H II.1	H III.1
Arabinose	1-		18	14	18	20
	1,2-	27	47	45	14	14
	1,3,5	15	31	33	4	3
0.5						
Xylose	1-	2				
	1,2-	2				
0.5						
Rhamnose	1,2,3-					2
	1,2,4-					7
0.5						
Glucose	1,4-	18	2	7	6	6
	1,4,6-	6	1	3		
0.5						
Galactose	1-				1	2
	1,3-	7			101	17
	1,6-				2	1
	1,3,6-	21			25	8
0.5						
Mannose	1,4-					
0.5						
Galacturonic acid[a]		2	1	1	18	20

[a] Determined as (1→4)-galactose.

Table 1
Fractionation of *Hamamelis* raw polysaccharides (RPS)

RPS									
Neutral fraction H I (13%)			0.1 M Eluate H II (41%)		0.25 M Eluate H III (26%)			0.5 M Eluate H IV (20%)	
H I.1	H I.2	H I.3	H II.1	H II.2	H III.1	H III.2	H III.3	H IV.1	H IV.1
6% of H I	38% of H I	56% of H I	62% of H II	38% of H II	55% of H III	29% of H III	16% of H III	15% of H IV	85% of H IV
126 kDa	13 kDa	4 kDa	158 kDa	50 kDa	79 kDa	16 kDa	5 kDa	126 kDa	4 kDa
			2% Rha	39% Rha	9% Rha	45% Rha		12% Rha	31% Rha
35% Ara	96% Ara	93% Ara	39% Ara	15% Ara	33% Ara	20% Ara	3% Ara	30% Ara	19% Ara
3% Xyl			tr.[b] Xyl	11% Xyl	tr. Xyl				
9% Man			4% Man				11% Man		
26% Gal			37% Gal	15% Gal	27% Gal	19% Gal		22% Gal	13% Gal
21% Glc	tr. Glc	4% Glc	6% Glc		8% Glc		45% Glc		
6% UA[a]	3% UA	3% UA	22% UA	20% UA	23% UA	16% UA	41% UA	36% UA	37% UA

[a] UA, uronic acids.
[b] tr., traces.

an araban with 1,3-backbone and side chains of 1,2-arabinose units, attached to the backbone via O-5 (Fig. 1).

The high molecular fraction H I.1 consisted mainly of arabinose and galactose in the ratio of about 3 to 2. The respective linkage pattern showed the existence of a typical neutral type II arabinogalactan with a 1,3-galactose backbone and branched arabinose side chains attached via O-6. The proportion of 1,2- and 1,4,6-linked glucose was determined to origin from starch.

All neutral fractions were contaminated with minor amounts of a glucan with 1,4- and 1,4,6-linked glucose. These carbohydrates may derive from α-linked starch, as the respective β-linked glucans would not be soluble by the aqueous extraction.

Acidic fractions consisted of a variety of heterogenous acidic arabinorhamnogalacturonans: the main chain of these polymers is build up by 1,3-linked galacturonic acid units; inserted 1,2-linked rhamnose units bear more or less branched arabinose-galactose side chains which are attched to the backbone via three-fold linked rhamnose units. These acidic polymers are the main compounds of fractions H II.2, H III.1, H III. 2, and H IV.1 and 2.

Fractions H II.1 and H III.3 additionally were composed by mannoglucans, typical reserve polysaccharides with β-1,4-mannose-glucose blocks, similar to that found in several *Digitalis* species (Hensel et al., 1998).

2.2. Influence of Hamamelis polysaccharides on keratinocytes

Raw polysaccharides (RPS) from *Hamamelis* bark were tested in concentrations of 0.1, 1, 10 and 50 μg/mL. After about three days of incubation it was obvious by mircroscopic observation that cells treated with 10 and 50 μg RPS showed nearly the same proliferation and differentiation behaviour as the untreated control groups.

Evaluation of proliferation rates by BrdU-incorporation indicated no significant influence of RPS after 10 days of incubation (Fig. 2A). The keratin K1 and K10

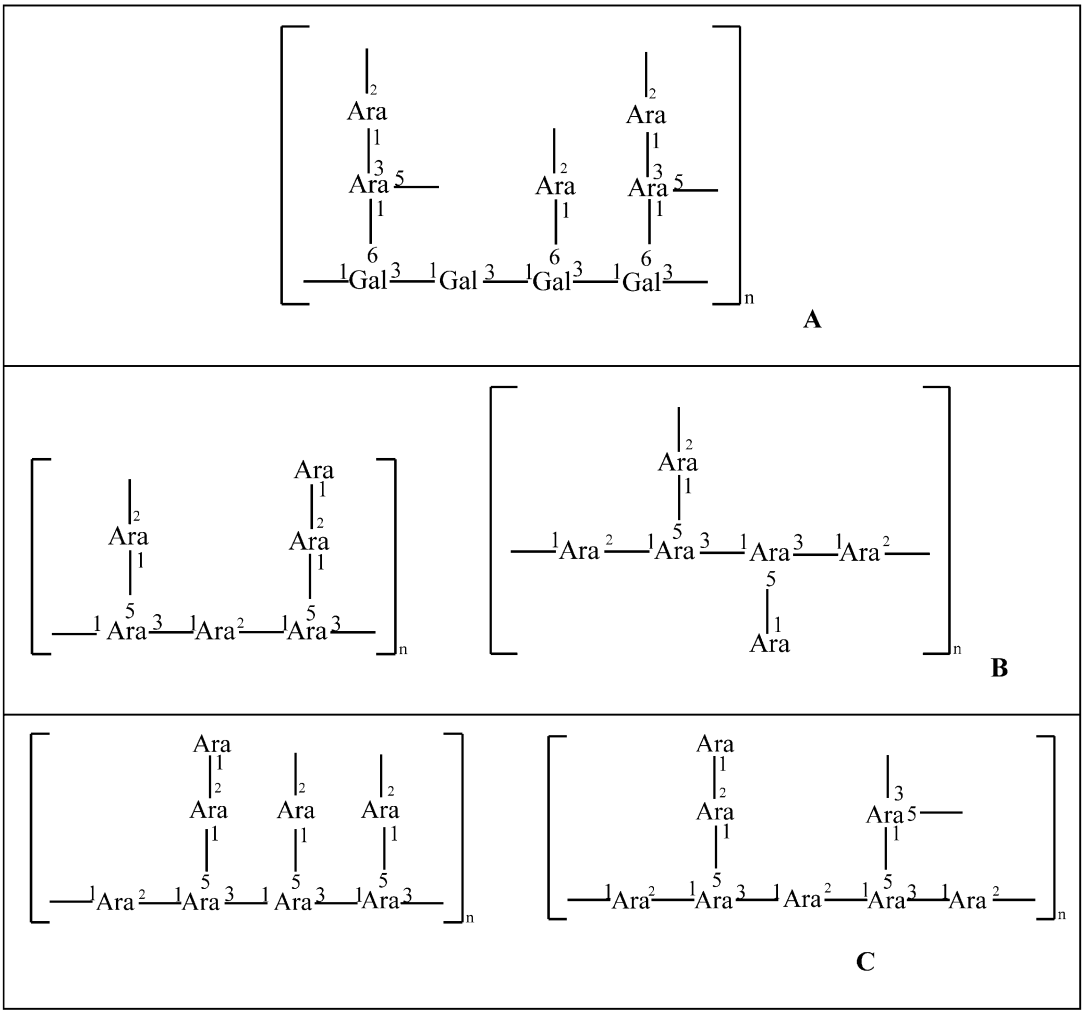

Fig. 1. Proposed structures of polysaccharides from *Hamamelis virginiana*: general structure of type II arabinogalactan H I.1 (A), neutral araban H I.2 (B), neutral araban H I.3 (C). The degree of substitution and length of side chains may vary among the polymers by heterodispersity.

formation also was not influenced significantly by RPS (Fig. 2B).

Mitochondrial activity of RPS-treated keratinocytes was significant lower for the cells treated with 10 and 50 μg polysaccharides compared to the untreated control. This phenomenon may be attributed to an adhesive polymer layer on the outer cell surface with an inhibited energy flux into the cells.

LDH values were on control levels for all groups, indicating RPS to be non-toxic.

Summarizing *Hamamelis* polysaccharides have no influence on proliferation, differentiation and metabolic activity of human keratinocytes.

2.3. Influence of polymeric proanthocyanidins on human keratinocytes

Two fractions, B and C, of polymeric proanthocyanidins have been isolated from *Hamamelis* bark and characterized according to methods described in a recent study (Dauer et al., 1998; Dauer, 2000). These fractions with a high purity (>95% calculated as catechin) were characterized as proanthocyanidins consisting of 3-*O*-galloylated catechin- and 3-*O*-galloylated epicatechin units with 4⇒8-interflavan linkage. Galloylation occurred only at the *O*-3 position while all other positions were not esterified. The respective polymers showed average molecular weights of about 1500 Da (fraction B) and 3400 Da (fraction C) determined by GPC and thiolytic degradation.

Toxic effects of both tannin fractions against human keratinocytes were not observed in the dose range from 1 to 100 μg/ml as evaluated by the respective lactatdehydrogenase titers, which were on control level (<5 U/ml) over the complete time of incubation.

Treatment of keratinocytes with both fractions B and C for 9 days resulted in the formation of typical cell monolayers which differed from the untreated control groups by the degree of confluence: while the procyanidin-treated groups formed complete monolayers, the control groups showed only about 40 to 50% confluence at the same time.

As expected from these observations, a signficant increase of cell proliferation was found for the procyanidin-treated groups, as determined by bromo-deoxyuridine (BrdU)-incorporation into the keratinocyte DNA and subsequent quantification by anti-BrdU-antibodies (Fig. 3). After 9 days of incubation fraction B enhanced the cell proliferation rates in doses of 1 and 10 μg/ml significantly, while fraction C had no effects at 1 μg level, but exceeded significant proliferation rates at 10 μg/ml. All further studies were performed with fraction C because of the limited availability of fraction B.

When monitoring the cell proliferation rates during incubation procyanidin fraction C significant differences to the control groups occured after 6 days of incubation: a time-dependent increase of cell growth compared to the control group was observed. Differences were significant after an incubation period of 6 days (Fig. 4). This indicates that the procyanidins do not act when added to the incubation medium as an punctuell stimulus, but have to be applied continously over longer time periods to stimulate growth processes.

Mitochondrial activity of the keratinocytes was determined by MTT-test by feeding fraction C in doses

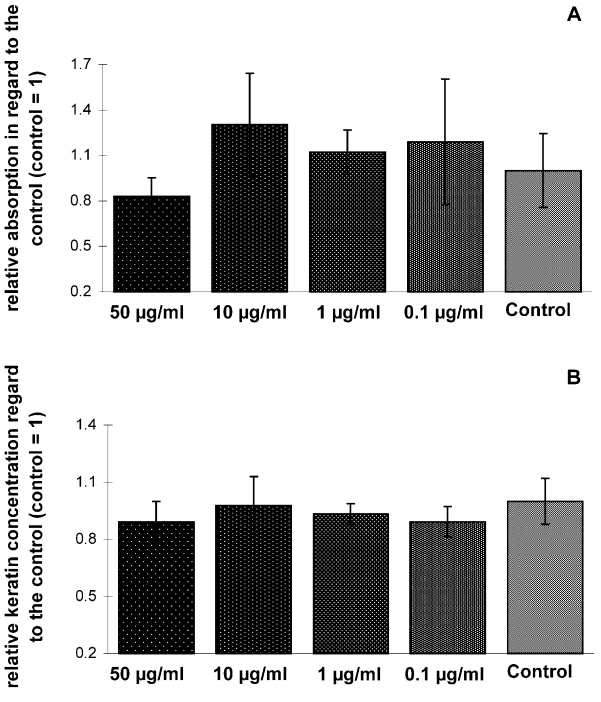

Fig. 2. Effects of raw polysaccharides from *Hamamelis virginiana* on cell proliferation (A) and differentiation (B) of normal human keratinocytes in different concentrations after 9 days of incubation. Results, determined by BrdU-incorporation in cell DNA and keratin K1/K10 determination (ELISA) are the mean±SD ($n=5$) and are not significant to the untreated control groups.

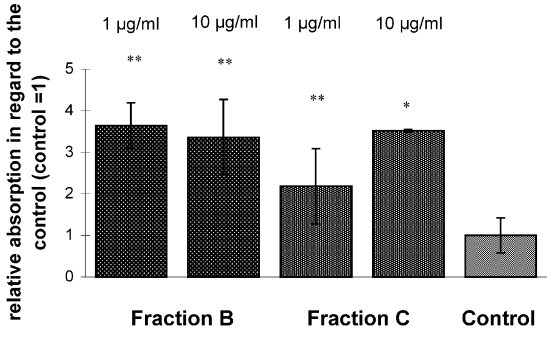

Fig. 3. Effects of oligomeric procyanidin fractions B and C (ProcyanoPlus) from *Hamamelis virginiana* on cell proliferation of normal human keratinocytes in concentrations of 1 and 10 μg/ml after 9 days of incubation. Results, determined by BrdU-incorporation in cell DNA, are the mean±SD ($n=10$) with $*P>0.1$ and $**P>0.05$ in comparison to the untreated control groups.

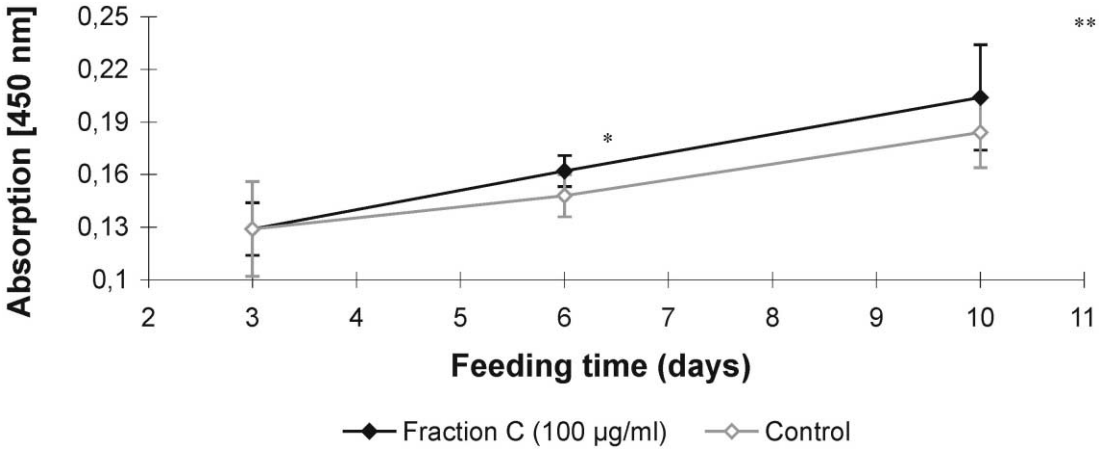

Fig. 4. Effect of oligomeric procyanidin fraction C (ProcyanoPlus) on cell proliferation of normal human keratinozytes over a 10 days incubation period as dertermined by BrdU-incorporation test (*$P > 0.1$ and **$P > 0.05$ in comparison to the untreated control groups).

of 1 and 10 µg/ml (Fig. 5). Significant increase of mitochondrial activity were observed with both concentrations and indicated an induction of metabolic activity by contact of the cells with fraction C.

In addition to these parameters, typical differentiation-specific keratins K1 and K10 (Muzarelli et al., 1999; Lane et al., 1985) were surveyed in the cells treated with fractions B and C with high-dose calcium as positive control. At doses of 1 and 10 µg/ml no significant increase of keratin formation was observed in procyanidin-treated groups (Fig. 6). This clearly indicates that the condensed tannins only induce keratinocyte proliferation, but do not act on the differentiation towards cornified cells.

2.4. Influence of procyanidins on irritated skin

For preliminary in vivo evaluation of *Hamamelis* procyanidins on irritated skin a semi-solid formulation containing 1% of *Hamamelis* procyanidin (ProcyanoPlus) was tested on its efficacy in preventing an sodium lauryl sulfate (SLS) induced irritant contact dermatitis in a standardized repeated short-time occlusive irritation test (ROIT) (Fartasch et al., 1999; Schnetz et al., 2000).

Over a three day period, defined skin areas of healthy volunteers were irritated using 0.5% SLS and with procyanidins in aqueous Eucerin®. To evaluate the influence of the pure cream formulation aqueous "placebo" Eucerin® without procyanidins was used additionally. One test site (positive control) received the irritant alone, two further test sites served as control (remained untreated or water).

The results of the TEWL correlated well with the results of the clinical score and the colorimetry. In all cases an irritation with SLS—with or without test product—had led to an increase of the TEWL values in comparison to the untreated area. This shows clearly that a local barrier disruption had occurred. By the pretreatment with ProcyanoPlus in aqueous eucerine and by pretreatment with eucerine alone the intensity of

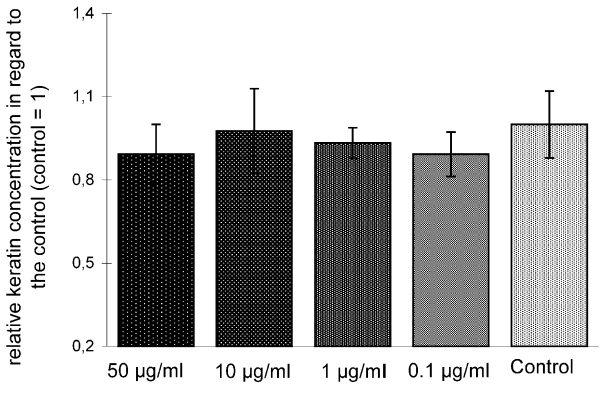

Fig. 5. Effects of oligomeric procyanidin fractions B and C (ProcyanoPlus) from *Hamamelis virginiana* on cell differentiation of normal human keratinocytes in concentrations of 1 and 10 µg/ml after 9 days of incubation. Results, determined by quantification of keratin K1, K10 concentrations (ELISA), are not significant to the untreated control groups.

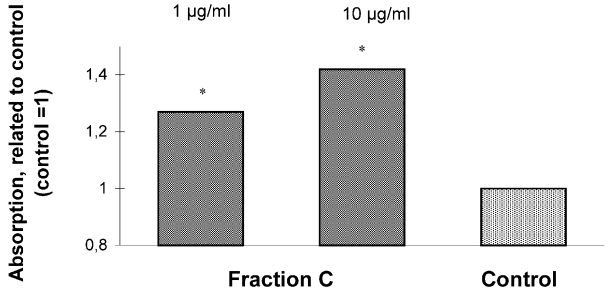

Fig. 6. Effects of oligomeric procyanidin fraction C (ProcyanoPlus) from *Hamamelis virginiana* on mitochondrial activity of natural human keratinocytes in concentrations at 1 and 10 µg/ml level after 9 days of incubation. Results, determined by MTT-test, are the mean ± SD ($n = 10$) with *$P > 0.1$ in comparison to the untreated control groups.

the reaction was diminished (Fig. 7). This effect was clearly more pronounced when ProcyanoPlus was applied. Treatment of the SLS-irritated skin areas with "placebo" aqueous Eucerin® reduced TEWL-increase for 45%, in comparison to SLS induced TEWL enhancement. Treatment with the procyanidin-containing formulation decreased TEWL significantly by 53%.

2.4.1. Clinical score

Treatment with 0.5% SLS caused an increase in the clinical scoring as a measure of dermal inflammation (Fig. 8). The clinical signs of an inflammation were clearly reduced by treatment with either aqueous Eucerine of ProcyanoPlus. But the effect of ProcyanoPlus was significantly better compared to pure eucerine.

Similar results were obtained by colorimetry measurements (Fig. 9), assessing skin color as a sign for erythema formation: irritation with SLS leads to strongly increased values, which are reduced when the irritated skin areas are treated with procyanidins.

3. Discussion

Information on pharmacological effects of high molecular compounds from *Hamamelis* bark is limited to only few reports due to the complexicity of the chemical structures of these compounds. Erdelmeier et al. (1996) reported on antiviral and antiphlogistic activities of high molecular weight proanthocyanidins from *Hamamelis* bark.

Up to now, no information is available about effects of *Hamamelis* plant metabolites on normal human keratinocytes. Furthermore, to our knowledge this is the first time that structural data about polysaccharides

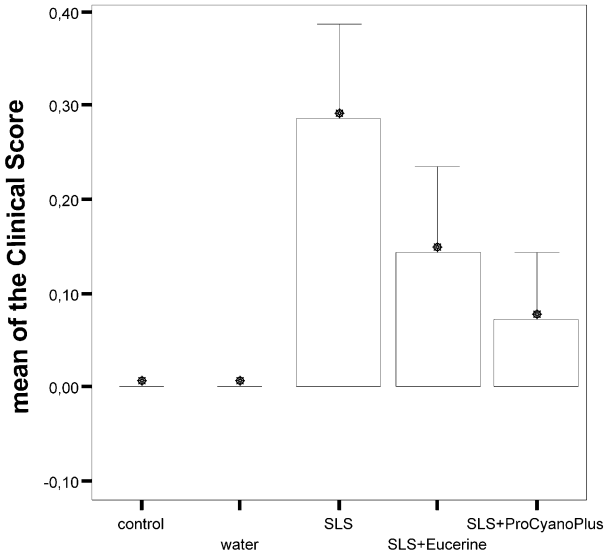

Fig. 8. Clinical scoring after 3 days cumulative irritation of skin by SLS 0.5% and treatment with aqueous Eucerin® or aqueous Eucerin® containing 1% fraction C (ProcyanoPlus). Bars represent the mean of the clinical score, error bars represent the standard error of the mean.

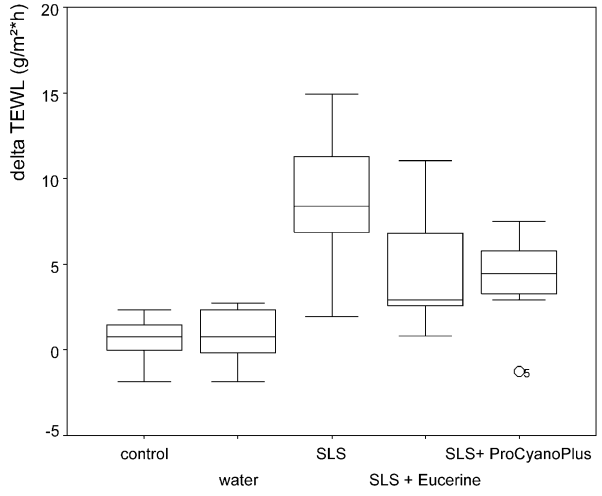

Fig. 7. Transepidermal water loss (TEWL) after a three days cumulative irritation of the skin by SLS 0.5% and treatment with aqueous Eucerin® or aqueous Eucerin® containing 1% fraction C (ProcyanoPlus). The distribution of data are presented as box plots. Box plots show the median, the 25th percentile, the 75th percentile, and values that are far removed from the rest. The lower boundary of the box is the 25th percentile, the upper boundary the 75th percentile; the line inside the box represents the median. Lines are drawn from the ends of the box to the largest and smallest observed values that are not outliers. Cases with values that are between 1.5 and 3 box lengths from the upper or lower edge of the box are called outliers (designated with the letter o.

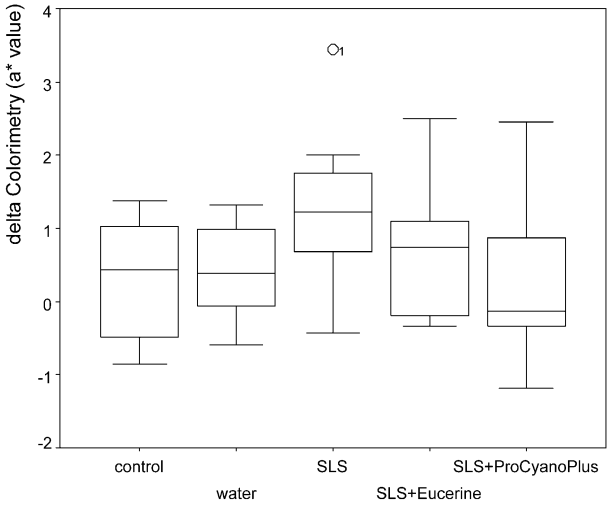

Fig. 9. Colorimetric data after a 3 day cumulative irritation of skin by SLS 0.5% and treatment with aqueous Eucerin® or aqueous Eucerin® containing 1% fraction C (ProcyanoPlus). The distribution of data are presented as box plots. Box plots show the median, the 25th percentile, the 75th percentile, and values that are far removed from the rest. The lower boundary of the box is the 25th percentile, the upper boundary the 75th percentile; the line inside the box represents the median. Lines are drawn from the ends of the box to the largest and smallest observed values that are not outliers. Cases with values that are between 1.5 and 3 box lengths from the upper or lower edge of the box are called outliers (designated with the letter o).

occurring in the bark of *Hamamelis virginiana* L. are provided.

This study focused on the effects of polymeric proanthocyanidins and polysaccharides isolated from the bark of *Hamamelis virginiana* on normal human keratinocytes.

Additionally, polysaccharides were included in this study, due to the fact that carbohydrates—also polysaccharides—are getting more and more into the focus of skin research because of antiphlogistic and proliferation enhancing effects as well as for stimulation of skin immune response (Berthod et al., 1994; Kitamura et al., 1997; Muzarelli et al., 1999).

For this reason, water-soluble polysaccharides were isolated in good yields from *Hamamelis* bark, fractionated and structurally characterized. Molecular weights, monomer composition and linkage types were determined. Principally, three different types of polysaccharides were identified: low molecular 1,3-linked arabans were the major polymers of the neutral fraction. While arabans are commonly 1,5-linked polymers the *Hamamelis* arabans represent quite unusual structures. Minor amounts of type II arabinogalactans, commonly occuring as cell structural components, were found additionally to the arabans in the neutral fraction of the mucilage. The heterogeneous acidic fractions consisted almost exclusively of rhamnogalacturonans with a high portion of neutral pentoses, mainly arabinose.

Testing of these polysaccharides on a dynamic keratinocyte cell system with the specific properties of forming differentiated, cornified cells after adequate stimuli did not indicate any positive carbohydate-mediated activity. Thus, polysaccharides cannot significantly contribute to the skin activity of *Hamamelis* bark.

In contrast, two different polymeric procyanidin fractions exhibited strong and dose-dependent induction of cell proliferation and mitochondrial activity of keratinocytes. Interestingly, these compounds did not influence the state of differentiation of keratinocytes. These results indicate, that *Hamamelis* proanthocyanidins only stimulate cell growth extensively, but do not influence the formation of cross-linked cornified envelopes (Thatcher and Rice, 1985). Thus, polymeric proanthocyanidins act as good proliferation stimulants for skin cells, leading probably to enhanced cell growth. As the effects were observed at low doses, likely to be reached under in vivo conditions in the skin epidermis the results may be of relevance for the respective in vivo situation. Similar inductors of cell proliferation, without induction to keratinized, differentiated cells are part of classical skin care products, as for example *Aloe vera* gel. From our point of view, it is promising that the tannins tested are not toxic towards the cells. The adstringent properties of the tannins do not have any negative influence on the cells within the dose-range tested.

In a preliminary clinical pilot study the procyanidins were tested within a cumulative irritation model on skin of healthy volunteers. All test parameters, including clinical scoring, transepidermal water loss and measurement of the skin colour, indicated clearly that the procyanidins positively influenced SLS induced irritation and skin barrier disruption.

Summarizing, high-molecular proanthocyanidins from the bark of *Hamamelis virginiana* L. can be assessed to be at least partly responsible for the medicinal use of this plant in dermatology and cosmetics. If and to what extent the hydrolysable and low-molecular condensed tannins, which are also present in the material contribute to the skin activity has to be evaluated in further studies.

Summarizing also, the results of this study demonstrate that polymeric proanthocyanidins from *Hamamelis virginiana* can be assessed to be at least partly responsible for the medicinal use of tannin-containing *Hamamelis*-preparations in dermatology and cosmetics by influencing keratinocyte proliferation.

4. Experimental

4.1. General

Heat-sterilization was performed either at 121 °C/1 h in an autoclave or at 175 °C/2 h in an oven. Statistical analysis was done using an unpaired student *t*-test.

Hamamelis polysaccharides were extracted from a batch of *Hamamelis viriginiana* bark, obtained in 1998 from Abtswinder Naturheilmittel, Abtswind, Germany. A voucher specimen is retained in the documentation center of the Institute of Pharmaceutical Biology, University of Erlangen.

Proanthocyanidins (patent pending) were obtained under the trade name ProcyanoPlus by DermoPlus-Hensel (Schlossbergstrasse 53, CH-8820 Wädenswil, Switzerland).

4.2. Isolation and fractionation of polysaccharides and procyanidins

Polysaccharide isolation: 200 g of powdered material were pre-extracted for 20 h in a Soxhlet system with acetone and subsequently for 30 h with methanol. The eluates were discarded. The residue was dried at 40 °C (154 g) and after addition of 30 g polyvinylpyrrolidone extracted three times with 770 ml of water. The combined extracts were concentrated to a 150 ml volume and slowly added into 600 ml 2-propanol. The precipitated raw polysaccharides (RPS) were centrifuged at 3600 *g*, dialysed and lyophilized to yield a nearly white powder (0.51% related to the dried starting material).

Fractionation of RPS was performed by IEC on DEAE-Sephacel (Pharmacia, Freiburg). Conditions: gel in the phosphate form, column dimension 20×2 cm, flow rate 80 ml/h, fraction size 5 ml, mobile phases: water, then step gradient with sodium phosphate buffers pH 6.0 with ion strength 0.1 mol/l, 0.25 mol/l, 0.5 mol/l. Carbohydrate-containing fractions were pooled, dialysed and lyophilized.

All fractions obtained from IEC were further fractionated by GPC on Sephacryl HR S-300 (Pharmacia, Freiburg). Conditions: column dimensions 1.9×77 cm, flow rate 25 ml/h, fraction size 2 ml, mobile phase: water. Carbohydrate-containing fractions were pooled, dialysed and lyophilized.

Isolation of proanthocyanidins (Dauer et al., 1998): the powdered *Hamamelis* bark (400 g) was percolated using acetone–water mixture in the ratio 7:3. The acetone was removed from the extract in vacuo and the aqueous residue was first extracted extensively with petroleum ether (rejected) and following with ethyl acetate (5×300 ml, rejected). The aqueous phase was freeze-dried to yield 47 g solid, brownish product. Of this 6.0 g were chromatographed on a Sephadex LH-20 column (Amersham-Pharmacia, Upsala) with ethanol (fraction A, yield 46%), methanol (fraction B, yield 26%) and acetone–water mixture (fraction C, yield 11%).

4.3. Polysaccharide analysis

Total carbohydrates were assayed with the phenol–sulphuric test (Dubois et al., 1956) and by resorcinol-test (Monsigny et al., 1988). Determination of uronic acids was performed using m-hydroxydiphenyl and galacturonic acid as reference material (Blumenkrantz and Asboe-Hansen, 1973). Carbohydrate-containing solutions were concentrated under reduced pressure at temperatures below 40 °C. Cellulose membranes with cut-off of 3500 Da were used for dialysis. The molecular weight distribution of polysaccharides was determined by GPC using standard dextrans (Sigma, Steinheim, Germany). Polysaccharides were hydrolysed with trifluoracetic acid 2 mol at 121 °C for 60 min. Alditol acetates of neutral sugars were prepared according to Blakeney et al. (1983). GLC was performed on a Hewlett-Packard HP 6890 system with mass selective detector at 220 °C with helium as carrier gas (pressure 1.3 bar) on a HP-225 fused silica capillary column (30 m×0.25 mm i.d., film thickness 0.25 μm).

Reduction of acidic polysaccharides to the carboxyl-reduced polymers was accomplished in the presence of carbodiimide and $NaBD_4$ as described by Taylor and Conrad (1972). Methylation analysis was performed according to the Hakamori method, modified by Harris et al. (1984).

4.4. Submerged keratinocyte culture

Keratinocytes were obtained either from commercial available cultures (Cell Systems, St Katharinen) or isolated from human skin, obtained by operative resection. Therefore the skin was decontaminated using a solution of fungizone (0.2%), gentamycin (5.9 μg/ml), sodium hydrogen carbonate (7.5%) in DMEM medium (Gibco, Karlsruhe). Tissue was dissected mechanically and after incubation of the tissue in dispase solution, dermis and epidermis were separated. The epidermis was trypsinated for 15 min at 34 °C with trypsin 0.05% and sodium edetate 0.53 mM. Reaction was stopped by the addition of TNS (Cell Systems, St Katharinen). Keratinocytes were centrifuged at 463 *g* for 5 min, resuspended in PBS, centrifuged again and resuspended in KGM-2 incubation medium in 96-well-tissue plates. Incubation was perfomed at 34 °C in a humidified 5% carbon dioxide atmosphere.

Secondary cultures were obtained at 60 to 70% confluence after trypsinisation. All cultures were free from contaminants of fibroblasts or melanocytes and were confluent after about 9 to 14 days of culture.

Feeding of the test substances to the keratinocytes was done after dissolving the compounds in KGM–2/DMSO mixtures. Positive controls were obtained from high-calcium media (Ca^{2+}, 1.5 mM), negative controls incubated in medium with no supplements.

4.5. Characterization of keratinocyte physiology

Growth rates were determined after trypsinisation using trypan-blue, mitochondrial activity by the MTT-test according to Mosmann (1983).

Lactat dehydrogenase (Amador et al., 1963) was quantified from the incubation supernatant using LDH-assay kit (Sigma, Steinheim).

Cell proliferation was determined by BrdU-kit (Boehringer, Mannheim) according to Porstmann et al., 1985.

For quantification of keratins K1 and K10 the cells were washed with PBS and keratins solubilized by adding 150 μl urea 8 M, β-mercaptoethanol 0.2 M and Tris 1.5 mM. Fifty microlitres of the solubilisate was transferred to a 96-well microtiter plate with 100 μl sodium carbonate buffer 0.05 M. The mixture was incubated for 18 h at 4 °C. After removal of excess of the keratin antigen and 1 h incubation with block medium (milk powder 7% in PBS with Tween 20, 0.05%) 100 μl of a monoclonal mouse-anti-human-keratin-antibody (Dako, Hamburg, diluted 1:400 in block medium) was added. The mixture was incubated at 37 °C for 60 min. After washing three times with 150 μl PBS containing Tween 20 0.05%, 150 μl POD-conjugated goat-anti mouse-IgG-antibody (Sigma, Steinheim, 1:2000 in block medium) was added and the mixture incubated at 37 °C for 60 min. After 3 washing steps, 100 μl of substrate solution (phenylendiamine 0.4 mg/ml in sodium

phosphate buffer 0.2 M, pH 5.0 and 11 μl hydrogen peroxide 30%) was added, the mixture reacted 10 min at room temperature and the reaction stopped by addition of 100 μl sulfuric acid 2.5 M. The absorbance was determined in an ELISA-reader at 492 nm. Calibration was performed using standard keratins.

4.6. Clinical testing

4.6.1. Test protocol (ROIT)

Fifty microliters of the irritant (aqueous SLS, 0.5%, purity of SLS >99%, Merck, Darmstadt, Germany) was applied twice daily under patch occlusion for 30 min, with an interval of 3–3.5 h. This schedule was followed for 3 consecutive days. Application was performed by means of a flat aluminum chamber (Large Finn Chambers®, inner diameter: 12 mm) with filter paper discs, fixed on Scanpor® tape. The middle part of both volar forearms was used as the test site with a total of 2 patches on each arm. One test site received the irritant alone, two other test sites were pretreated with the test products (ProcyanoPlus and aqueous Eucerine, 0.05 ml/2 cm^2 skin) 10 min before the irritant was applied. Two further test sites served as control sites (remained untreated or water). The procedure was repeated every day during the experiment. The placing of the products was changed from person to person according to a system of rotation (randomization).

4.6.2. Evaluation

All measurements were carried out in air-conditioned rooms (room temperature 20–22 °C, relative humidity between 30–45%, room temperature and humidity data being recorded during the measurements, applying the guidelines of the Standardization Group of the European Society of Contact Dermatitis (Pinnagoda et al., 1990; Fullerton et al., 1996). All measurements were performed after a rest of 30 min for equilibration. Measurements were performed in the morning of day 1 and in the afternoon of day 3.

4.6.3. Transepidermal water loss (TEWL) measurements

The quantitative measurements of TEWL were carried out using the Tewameter TM 210 (Courage and Khazaka, Cologne, Germany). The TEWL was calculated automatically and expressed in g/m^2 h. The Tewameter probe was used in a holding device to avoid heating of the probe. The probe was rested on the skin and TEWL was continuously recorded for a period of 3 min. Mean values were obtained from two successive recordings for every test site.

4.6.4. Skin temperature

Skin temperature was measured prior to TEWL measurements using a Digimed H11S device (ttw, Waldkirch, Germany) and had to range between 28–32 °C (Mathias et al., 1981).

4.6.5. Clinical examination

Visual scoring was performed according to the following scale: 0, no reaction; 0.5, slight scaling or very weak erythema; smooth surface; 1, weak erythema, possibly slight infiltration, slight roughness, slight scaling, mild edema, fine fissures; 2, erythema, more roughness, scaling and edema, fissures; 3, pronounced erythema, extensive scaling, pronounced edema, possibly vesicles, bullae, pustules and/ or pronounced crusting.

4.6.6. Colorimetry

For colorimetry, the measuring head of a Chroma-Meter CR 300 (Minolta, Ahrensburg, Germany) was applied to the skin avoiding pressure. Measurements were conducted in triplicate. For the measurements the L^* a^* b^* system was chosen, for this coordinates most closely reflects the color of human skin (Ale et al., 1996); a^* represents the green ($-a^*$)–red ($+a^*$) axis, therefore we used this coordinate for evaluation.

4.6.7. Volunteers

Seven healthy caucasian subjects (2 male, 5 female; age 22 to 38 years, mean age 29.8 years) with no history of atopic eczema or other skin diseases. Written informed consent was obtained from all of them. The study was approved by the ethical committee.

References

Ale, I., Laugier, J.P.K., Maibach, H.I., 1996. Spacial variability of basal skin chromametry on the ventral forearm of healthy volunteers. Arch. Derm. Res. 288, 774–777.

Amador, E., Dorfman, L.E., Wacker, W.E.C., 1963. Serum lactic dehydrogenase, an analytical assessment of current assays. Clin. Chem. 9, 391–395.

Berthod, F., Saintigny, F., Chretioen, D., Hayek, C., Collombel, C., Damou, O., 1944. Optimization of thickness, pore size and mechanical properties of a biomaterial designed for deep burn coverage. Clinical Mater. 15, 259–265.

Blakeney, A.B., Harris, P.J., Henry, R.J., Stone, B.A., 1983. A simple and rapid preparation of alditol acetats for monosaccharid analysis. Carbohydr. Res. 113, 291–299.

Blumenkrantz, N., Asboe-Hansen, G., 1973. New method for quantitative determination of uronic acids. Anal. Biochem. 54, 484–489.

Chithra, P., Sajithal, G.B., Chandrakasan, G., 1998. Influence of *Aloe vera* on the glucosaminoglycans in the matrix of healing dermal wounds in rats. J. Ethnopharmacol 59, 179–186.

Dauer, A., Metzner, P., Schimmer, O., 1998. Proanthocyanidines from the bark of *Hamamelis virginiana* exhibit antimutagenic properties against nitroaromatic componds. Planta Medica 64, 324–327.

Dauer, A., 2001. Untersuchungen zur antimutagenen Wirkung von Gerbstoffen aus der Rinde von *Hamamelis virginiana* L. in *Salmonella typhimurium* und menschlichen Hepatomzellen (HepG2). Dissertation, Universität Erlangen-Nürnberg.

Dubois, M., Gilles, K.A., Hamilton, J.K., Rebers, P.A., Smith, F., 1956. Colorimetric method for determination of sugars and related substances. Anal. Chem. 28, 350–355.

Erdelmeier, C.A., Cinatl, J. Jr., Rabenau, H., Doerr, H.W., Biber, A., Koch, E., 1996. Antiviral and antiphlogistic activities of *Hamamelis virginiana* bark. Planta Medica 62, 241–245.

Eskelinin, A., Santalahti, J., 1992. Special natural cartilage polysaccharides for the treatment of sun-damaged skin in femals. J. Int. Med. Res. 20, 99–105.

Fartasch, M., Schnetz, E., Ennen, J., Lanzendörfer, G., Diepgen, T.L., 1999. Characterization of barrier alteration by repetitve irritation—effect of barrier cream. Zeitschrift für Hautkrankheiten 74, 1–6.

Fullerton, A., Fischer, T., Lauti, A., Wilhelm, K.P., Takiwaki, H., Serup, J., 1996. Guidelines for the measurement of skin colour and erythema. Contact Dermatitis 35, 1–10.

Gibbs, S., Vicanová, J., Bouwstra, J., Valstar, D., Kempenaar, J., Ponec, M., 1997. Culture of reconstructed epidermis in a defined medium at 33 °C shows a delayed epidermal maturation, prolonged lifespan and improved stratum corneum. Arch. Derm. Res. 289, 585–595.

Harris, P.J., Henry, R.J., Blakeney, A.B., Stone, A.B., 1984. A simple and rapid preparation of alditol acetats for monosaccharide analysis. Carbohydr. Res. 127, 59–73.

Hensel, A., Schmidgall, J., Kreis, W., 1998. The plant cell wall- a potential source for pharmacologically active polysaccharides. Helv. Chim. Acta 73, 37.

Hoffmann-Bohm, K., Ferstel, W., Aye, R.D., 1993. *Hamamelis*. In: Hänsel, R., Keller, G., Rimpler, H., Schneider, G. (Eds.), Hagers Handbuch der Pharmazeutischen Praxis, Vol. 5. Springer Verlag, Berlin, New York, pp. 368–384.

Kitamura, N., Ota, Y., Haratake, A., Ikemoto, T., Tanno, O., Horikoshi, T., 1997. Effects of ethyl-a-D-glycosid on skin barrier disruption. Skin Pharmacol. 10, 153–159.

Korting, H.C., Schäfer-Korting, M., Hart, H., Laux, P., Schmid, M., 1993. Anti-inflammatory activity of *Hamamelis* distillate applied topically to the skin. Influence of vehicle and dose. Eur. J. Clin. Pharmacol. 44, 315–318.

Korting, H.C., Schäfer-Korting, M., Klovekorn, W., Klovekorn, G., Martin, C., Laux, P., 1995. Comperative efficiacy of *Hamamelis* distillate and hydrocortisone cream in atopic eczema. Eur. J. Clin. Pharmacol. 48, 461–465.

Lane, E.B., Bartek, J., Purlcis, P.-F., Leigh, I.M., 1985. Keratin antigens in differentiating skin. Ann. NY Acad. Sci. 455, 241–258.

Laux, P., Oschmann, R., 1993. Die Zaubernuss *Hamamelis virginiana* L. Zeitschrift für Phytotherapie 14, 155–166.

Mathias, T., Wilson, D., Maibach, H.I., 1981. Transepidermal water loss as a function of skin temperature. J. Invest. Dermatol 77, 219–220.

Monsigny, M., Petit, C., Roche, A.-C., 1988. Colorimetric determination of neutral sugars by a resorcinol sulfuric acid mikromethod. Anal. Biochem. 175, 525–530.

Mosmann, M., 1983. Rapid colorimetric assay for cellular growth and survival: applications to proliferation and cytotoxicity assays. J. Immun. Methods 65, 55–163.

Muzarelli, R.A., Mattioli-Belmonte, M., Pugnaloni, A., Biagini, G., 1999. Biochemistry, histology and clinical uses of chitins and chitosans in wound healing. EXS 87, 251–264.

Pinnagoda, J., Tupker, R.A., Agner, T., Serup, J., 1990. Guidelines for transepidermal water loss (TEWL) measurement. Contact Dermatitis 22, 164–178.

Ponec, M., Kempenaar, J., 1995. Use of human skin rekombinants as an in vitro model for testing the irritation potential of cutanous irritants. Skin Pharmacol. 8, 49–59.

Porstmann, T., Ternyck, T., Avrameas, S., 1985. Quantitation of 5-bromo-2-deoxyuridine into DNA an enzyme immunoassay for the assesment of the lymphoid cell proliferative response. J. Immunol. Methods 82, 169–179.

Schnetz, E., Diepgen, T.L., Elsner, P., Frosch, P.J., Klotz, A.J., Kresken, J., Kuss, O., Merk, H., Schwanitz, H.J., Wigger-Alberti, W., Fartasch, M., 2000. Multicentre study for the development of an in vivo model to evaluate the influence of topical formulations on irritation. Contact Dermatitis 42, 336–343.

Strickland, F.M., Darvill, A., Albersheim, P., Eberhard, S., Pauly, M., Pelley, R.P., 1999. Inhibition of UV-induced immun suppression and interleukin-10 production by plant oligosaccharides and polysaccharides. Photochem. hotobiol 69, 141–147.

Swoboda, M., Meurer, J., 1991. Therapie von Neurodermitis mit *Hamamelis virginiana*-Destillat in Salbenform. Zeitschrift für Phytotherapie 12, 114–117.

Taylor, R.T., Conrad, H.E., 1972. Stochiometric depolymerization of polyuronides and glycosaminoglycans to monosaccharids following reduction of their carbodiimid-activated carboxyl groups. Biochem. 11, 1383–1388.

Thatcher, S.M., Rice, R.H., 1985. Keratinocyte-specific transglutaminase of cultured human epidermal cells: Relation to cross-linked envelope formation and terminal differentiation. Cell 40, 685–695.

van der Sandt, J., Roguet, R., Cohen, C., Esdaile, D., Ponec, M., Cosini, E., Barker, C., Fusenig, N., Liebsch, M., Benford, D., de Brugerolle de Fraissinette, A., Fartasch, M., 1999. The use of keratinocytes and human skin models for predicting skin irritations. ATLA—Alternatives to laboratory animal 27, 723–755.

Yagi, A., Egusa, T., Arase, M., Tanabe, M., Tsuji, H., 1997. Isolation and characterization of the glycoprotein fraction with a proliferation-promoting activity on human and hamster cells in vitro from Aloe vera gel. Planta Med. 63, 18–21.

PERGAMON

Phytochemistry 58 (2001) 959–962

PHYTOCHEMISTRY

www.elsevier.com/locate/phytochem

Quassinoids from *Eurycoma longifolia* as plant growth inhibitors

Suratwadee Jiwajinda[a,*], Vilai Santisopasri[b], Akira Murakami[c], Nobuhiro Hirai[d], Hajime Ohigashi[d]

[a]*Central Laboratory and Greenhouse Complex, Kasetsart University, Kamphaengsaen Campus, Nakhon-Pathom 73140, Thailand*
[b]*Department of Biochemistry, Faculty of Science, Kasetsart University, Chatuchak, Bangkok 10900, Thailand*
[c]*Department of Biotechnological Science, Faculty of Biology-Oriented Science and Technology, Kinki University, Iwade-Uchita, Wakayama 649-6493, Japan*
[d]*Division of Applied Life Sciences, Graduate School of Agriculture, Kyoto University, Kyoto 606-8502, Japan*

Received in revised form 19 June 2001

Abstract

Seven quassinoids including a new 12-*epi*-11-dehydroklaineanone were isolated from the leaves of *Eurycoma longifolia* (Simaroubaceae) as plant growth inhibitors or related compounds. The strongest activity was found in 14,15β-dihydroxyklaineanone.
© 2001 Elsevier Science Ltd. All rights reserved.

Keywords: *Eurycoma longifolia*; Simaroubaceae; Plant-growth inhibitor; Quassinoid

1. Introduction

Eurycoma longifolia (Simaroubaceae) is one of the most well known folk medicines for intermittent fever (malaria) in Southeast Asia (Chan et al., 1986). This plant has been reported to contain various bioactive quassinoids and squalene- or tirucallane-type tritertpenoids (Morita et al., 1993a,b; Itokawa et al., 1992). In our continuing investigation on plant growth regulators from Thai plants, we found plant growth inhibitory potentials in this plant. This report deals with the isolation and identification of the active principles and their plant growth inhibitory activities against cucumber seedlings, i.e. compounds **1**–**7**.

2. Results and discussion

Bioassay guided purification gave two major active fractions, A and B. Seven compounds were isolated by further chromatography including preparative HPLC of these two fractions. The spectral data of **1** and **2** were identical with those of C_{19}-quassinoids (Fig. 1), longilactone and 6-dehydrolongilactone, respectively (Morita et al., 1993a,b). Compounds **3**, **5**, **6** and **7** were identified as klaineanone-type C_{20}-quassinoids, 11-dehydroklaineanone, 15β-hydroxyklaineanone, 14,15β-dihydroxyklaineanone, and 15-β-*O*-acetyl-14-hydroxyklaineanone (Fig. 1), respectively, by comparison of the spectral data with those of known compounds previously reported (Itokawa et al., 1992; Morita et al., 1993b; Polonsky and Baskevitch, 1995). This is the first finding that compound **6** occurs in *E. longifolia*, while its occurrence in *Perriera orientalis* has been previously reported (Polonsky and Baskevitch, 1995).

A new compound (**4**) was obtained as a glassy resin ($[\alpha]_D^{25}$ −11.2° ($c=0.1$, MeOH); UV λ_{max} (MeOH) nm (log ε): 238 (4.2); IR ν_{max} (KBr) cm^{-1}: 3400, 1720, 1660). The HR–EIMS spectrum of **4** exhibited a molecular ion peak at m/z 362.1727 ($C_{20}H_{26}O_6$ calc. for 362.1729). The ^1H NMR spectrum (Table 1) resembled that of **3** except for signals corresponding to H-9, H-12, H-13, H-14, H-15β and H-15α. The resonances corresponding to H-9, H-13 and H-15α were shifted upfield to 3.08, 2.07 and 2.93 ppm in **4** from 3.74, 2.25 and 3.67 in **3**, respectively. Also the signals of H-12, H-14 and H-15β appearing at 3.72, 1.93 and 2.64 ppm in **3** were shifted downfield to 4.02, 2.07 and 2.75 ppm in **4**, respectively.

Furthermore, the coupling constant of H-12 of **4** ($J=10.9$ Hz) was larger than that ($J=2.9$ Hz) of **3**, suggesting that **4** is an epimer of **3** at C-12. In support of

* Corresponding author. Tel.: +66-34-351399; fax: +66-34-351392.
E-mail address: rdiswj@nontri.ku.ac.th (S. Jiwajinda).

0031-9422/01/$ - see front matter © 2001 Elsevier Science Ltd. All rights reserved.
PII: S0031-9422(01)00333-8

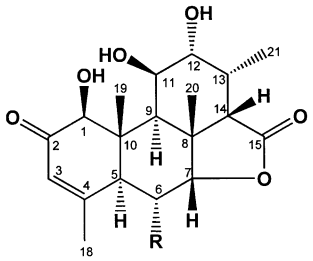

	R
1 : longilactone	−OH
2 : 6-dehydrolongilactone	−H

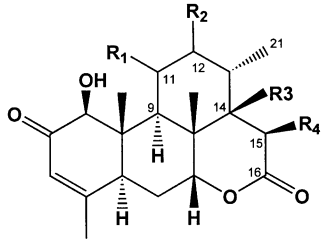

	R_1	R_2	R_3	R_4
3 : 11-dehydroklaineanone	=O	···OH	−H	−H
4 : 12-*epi*-11-dehydroklaineanone	=O	◄OH	−H	−H
5 : 15β-hydroxyklaineanone	◄OH	···OH	−H	−OH
6 : 14,15β-dihydroxyklaineanone	◄OH	···OH	−OH	−OH
7 : 15β-*O* -acetyl-14-hydroxyklaineanone	◄OH	···OH	−OH	−OAc

Fig. 1. Structures of quassinoids isolated from *Eurycoma longifolia*.

Table 1
The ^{1}H NMR spectral data of compounds **3** and **4**

	Compound **3**		Compound **4**		Δδ (ppm)	NOEs observed in **4**
Position	δ (ppm)	*J* (Hz)	δ (ppm)	*J* (Hz)		
H-1	4.03 (*s*)	–	4.00 (*s*)	–	0.03	
H-3	5.98 (*br*, *s*)	1.28, 2.7	5.98 (*br*, *s*)	1.3	0.00	
H-5	2.90 (*br*, *d*)	10.9	2.82 (*br*, *d*)	12.7	0.08	
H-6	2.15 (*m*)	–	2.15 (*m*)	–	0.00	
H-7	4.50 (*t*)	2.8	4.53 (*t*)	2.7	−0.03	
H-9	3.74 (*s*)	–	3.08 (*s*)	–	0.66	[a]
H-12	3.72 (*d*)	2.9	4.02 (*d*)	10.9	−0.30	
H-13	2.25 (*m*)	–	2.07 (*m*)	–	0.18	[a]
H-14	1.93 (*m*)	–	2.07 (*m*)	–	−0.14	
H-15 β	2.64 (*dd*)	6.7, 19.3	2.75 (*dd*)	6.3, 19.0	−0.11	
H-15 α	3.67 (*dd*)	12.4, 19.4	2.93 (*dd*)	12.6, 19.0	0.74	
H-18	1.98 (*s*)	–	1.98 (*s*)	–	0.00	
H-19	1.26 (*s*)	–	1.28 (*s*)	–	−0.02	
H-20	1.13 (*s*)	–	1.13 (*s*)	–	0.00	
H-21	1.11 (*d*)	7.06	1.12 (*d*)	6.3	−0.01	[a]

[a] NOEs to H-12 were observed.

this, NOEs were observed between Hα-9 and H-12, H-12 and H-13, and H-12 and H-21. Hence, the structure of **4** was determined to be the epimer of **3** at C-12 named 12-*epi*-11-dehydroklaineanone (Fig. 1).

The plant-growth inhibitory activities of **1**–**7** against cucumber seedlings were tested as described in the previous report (Jiwajinda et al., 2000). Of the compounds tested, the activities of **5** and **6** were significantly higher than the others. In particular, the activity of **6** against root growth is remarkable (Table 2). Interestingly, while **3** showed slight activity to inhibit growth of cucumber (IC_{50} = 55.6 μM on shoot growth and 77.3 μM on root growth, compound **4** was inactive at a concentration less than 200 μM. It is notable that **7** showed an effective inhibitory activity (IC_{50} = 17.6 μM) towards root growth but was inactive against shoot growth. Compounds **1**–**7** showed no inhibitory activity against rice seedlings (IC_{50} > 200 μM). Based on these results, the following conclusions may be provisionaly presented for plant growth inhibition of quassinoids. (1) C-20 quassinoids with a hydroxyl group at C-15 may possess more significant plant growth inhibitory activity than C-19 quassinoids. (2) The absolute configuration of the C-12 hydroxyl group may be one important factor for activity. (3) Masking of the hydroxyl group at C-15 with an acyl group may be a factor to give selectivity in plant growth inhibition.

So far, quassinoids have been reported to exhibit a wide range of bioactivities to animals on both in vitro

Table 2
Inhibitory activities of quassinoids (**1**–**7**) against the growth of cucumber and rice seedling[a]

Compound	Cucumber seedling		Rice seedling	
	IC_{50} (μM) root growth	IC_{50} (μM) shoot growth	IC_{50} (μM) root growth	IC_{50} (μM) shoot growth
1	65.6±10	95.0±1.0	>200	>200
2	25.7±0.5	48.6±0.5	>200	>200
3	55.6±1.0	77.3±1.0	>200	>200
4	>200	>200	>200	>200
5	10.5±0.5	23.7±0.5	>200	>200
6	2.5±0.5	22.7±0.5	>200	>200
7	17.6±0.5	>200	>200	>200

[a] IC_{50}s were graphically determined by the plot between log (concentration) and % inhibition in the length of roots or shoots to that of the controls (without test compound). Inhibitions (%) were calculated by {[average length in the control—average length with test compound]/average length in the control}×100.

and in vivo (Morita et al., 1993b; Itokawa et al., 1992; Okano et al., 1990). Thus, plant growth inhibitory activity may be useful as a preliminary screening method for finding valuable quassinoids with medicinal activities. Further investigation on other bioactivities to the animal cells of these isolated quassinoids is now in process.

3. Experimental

3.1. General

Melting point were determined by a micro melting point apparatus (Yanaco Seisakusho Co., Ltd., Japan) and were uncorrected. Optical rotation dispersion measurements employed a Jasco J-5 polarimeter. Infrared and UV absorption spectra were recorded on Shimadzu model 435 and Shimadzu UV-200 spectrophotometers, respectively. Proton NMR spectra were obtained on a Jeol JX 400 NMR spectrometer, 400 MHz, in $CDCl_3$ and TMS as an internal standard. High resolution mass spectra were recorded on a Jeol-DX 300 Mass spectrometer. High performance liquid chromatography was carried out on a Hitachi 665-A HPLC.

3.2. Plant materials

Leaves of *Eurycoma longifolia* were collected at Surajthani, Thailand. A voucher specimen (Specimen No. BK 4316 collecter PUT No.2724) is kept in Bangkok Herbarium, Department of Agriculture, Ministry of Agriculture and Co-operation, Bangkok, Thailand.

3.3. Bioassay

The assays were tested in triplicate. The control experiments were conducted in distilled water (without test compound). The maximum concentration of test compound in the assay was 200 μM.

Cucumber seedling test: the seeds of *Curcumis sativas* were sterilized by soaking in sodium hypochlorite solution (1% active chloride content) for 15 min, and washed under running tap water for 2 h. Ten sterile seeds were sown on filter paper containing a definite concentration of test compound in a petri dish (9 cm id.). Distilled water (3 ml) was added to the Petri dish and incubation was carried out at 30 °C under continuous light for 5 days. The elongation of roots and shoots were measured compared to those of the controls.

Rice seedling test: seeds of rice *Oryza sativa*, cv. Nipponbare were sterilized as well as cucumber seeds. Sterile seeds were dipped in distilled water and incubated at 30 °C for 3–5 days until the seeds were germinated (about 2 mm hypocotyl), with changes of the water twice a day. Seven germinated seeds were transferred to a glass tube (3 cm id.×2 cm height) containing a definite concentration of test compound in distilled water (1 ml) and incubated at 30 °C under continuous light for 7 days. The elongation of second leaf sheath and dry weight of root were measured compared to those of the controls.

3.4. Extraction and isolation

Separation of the active principles was guided by a bioassay using cucumber seedlings. The ethanol extract (9 g) from the dried leaves (500 g) of *Eurycoma longifolia* was partitioned between EtOAc (300×2 ml) and H_2O (500 ml). The active EtOAc part (2.5 g) was applied to silica gel column (25×500 mm) eluted stepwise with 20% increasingly EtOAc in hexane, 100% EtOAC and then MeOH. Two active fractions, A (100% EtOAc eluate, 90 mg) and B (100% MeOH eluate, 146 mg), were derived. Both fractions were further purified on silica gel and ODS gel, and finally by preparative HPLC on μ-Bondasphere C_{18} (19×150 mm) eluted with 35% MeOH in water (7 ml/min) to give compound **1** (5.6 mg, t_R 12.5 min), **4** (3.0 mg, t_R 13.5 min) and **6** (6.2 mg, t_R 19.5 min) from fraction A. Also, **2** (8.0 mg, t_R 22 min), **3** (6.9 mg,

t_R 26.2 min), **5** (23 mg, t_R 28.5 min), and **7** (18.0 mg, t_R 20.5 min) were obtained from fraction B.

Compound **4**: 12-*epi*-11-dehydroklaineanone, a colorless glassy resin, $[\alpha]_D^{25}$ −11.2 ° ($c = 0.1$, MeOH); EI–MS at 70 ev, m/z (% rel. int.) 362 [M^+] (36), 344 (10), 333 (18), 315 (12), 283 (11), 239 (14), 213 (15), 187 (20), 159 (31), 135 (32), 119 (28), 109 (34), 95 (82), 77 (44), 67 (62), 55 (68), 41 (100); HR–EIMS (probe): 70 ev). [M^+] m/z 362.1727 ($C_{20}H_{26}O_6$, requires 362.1729); UV λ_{max} (MeOH) nm (log ε): 238 (4.2); IR ν_{max} (KBr) cm^{-1}: 3400, 1720, 1660; ^1H NMR (see Table 1).

Acknowledgements

We wish to thank Dr. Vichai Korpraditsakul of Kasetsart University, Thailand, for supplying the plant materials and Mr. Winai Somprasong of Bangkok Herbarium, Department of Agriculture, Ministry of Agriculture and Co-operation, Bangkok, Thailand, for helpful identified plant specimen. S.J. gives grateful thanks for a research fellowship from the Japan Society for the Promotion of Science (JSPS).

References

Chan, K.L., O'Neill, M.J., Phillipson, J.D., Warhurst, D.C., 1986. Plants as sources of antimalarial drugs. Part 3. *Eurycoma longifolia*. Planta Medica 52, 105–107.

Itokawa, H., Kishi, E., Morita, H., Takeya, K., 1992. Cytotoxic quassinoids and tirucallane-type triterpenes from the wood of *Eurycoma longifolia*. Chemical and Pharmaceutical Bulletin 40, 1053.

Jiwajinda, S., Santisopasri, V., Ohigashi, H., 2000. Coumarin-related compound as plant growth inhibitors from two Rutaceous plants in Thailand. Bioscience, Biotechnology, and Biochemistry 64, 420–423.

Morita, H., Kishi, E., Takeya, K., Itokawa, H., Iitaka, Y., 1993a. New quassinoids from the root of *Eurycoma longifolia*. Chemistry Letters, 749–752.

Morita, H., Kishi, E., Takeya, K., Itokawa, H., Iitaka, Y., 1993b. Highly oxygenated quassinoids from *Eurycoma longifolia*. Phytochemistry 33, 691–696.

Polonsky, J., Baskevitch, Z., 1995. Carbon-13 nuclear magnetic resonance spectral analysis of quassinoid bitter principles. Journal of Organic Chemistry 40, 2499–2504.

Okano, M., Fukamiya, N., Lee, K.H., 1990. Biologically active compounds from Simaroubaceous Plants. Biological active compounds from Simaroubaceous plants. In: Atta-ur-Rahman et al. (Eds.), Studies in Natural Products Chemistry, Vol. 7. Elsevier Science Publishers BV, Amsterdam, pp. 369–404.

PERGAMON

Phytochemistry 58 (2001) 963–968

PHYTOCHEMISTRY

www.elsevier.com/locate/phytochem

Acetyl and butyrylcholinesterase-inhibiting triterpenoid alkaloids from *Buxus papillosa*

Atta-ur-Rahman[1], Shehnaz Parveen, Asaad Khalid, Afgan Farooq, M. Iqbal Choudhary*

H.E.J. Research Institute of Chemistry, International Center for Chemical Sciences, University of Karachi, Karachi-75270, Pakistan

Received 19 March 2001; received in revised form 20 June 2001

Abstract

Three triterpenoid alkaloids, buxakashmiramine [(20*S*)-20-dimethylamino-4′,6′-dimethoxy-5′-hydroxybenzoylamino-3β-methyl-buxan-31-ol] (**1**), buxakarachiamine [(20*S*)-20-dimethylamino-2′-hydroxy-3β-methyl-3′-methyl-butanoylamino-9,10-*seco*-buxa-9(11), 10(19)-dien-31-ol] (**2**) and buxahejramine [(20*S*)-20-dimethylamino-2′-hydroxy-3β-methyl-3′-methyl-pentanoylamino-9,10-*seco*-buxa-9(11), 10(19)-dien-31-ol] (**3**) were isolated from the leaves of *Buxus papillosa*. Four known bases, cycloprotobuxine-C (**4**), cyclovirobuxeine-A (**5**), cyclomicrophylline-A (**6**) and sempervіraminol (**7**) were isolated for the first time from this species. Their structures were established through extensive spectroscopic studies. Most of these compounds exhibited anticholinesterase activity.
© 2001 Published by Elsevier Science Ltd.

Keywords: *Buxus papillosa*; Buxaceae; Triterpenoid alkaloids; Buxakashmiramine; Buxakarachiamine; Buxahejramine; Anticholinesterase activity

1. Introduction

Buxus papillosa C.K. Schneider (Buxaceae) is widely distributed in the North West frontier province of Pakistan. *Buxus* species find extensive use in the treatment of various ailments, such as rheumatism, skin disorders and venereal diseases in the indigenous system of medicine (Cordell, 1981). *B. papillosa* is the most extensively investigated species of the genus *Buxus* and has so far afforded more than 50 triterpenoidal and steroidal alkaloids (Atta-ur-Rahman, 1990; Naz, 1995). As a consequence of continuing phytochemical investigations on this plant, we report on the isolation and characterization of three new bases buxakashmiramine (**1**), buxakarachiamine (**2**) and buxahejramine (**3**), along with four known triterpenoidal bases cycloprotobuxine-C (**4**), cyclovirobuxeine-A (**5**), cyclomicrophylline-A (**6**) and sempervіraminol (**7**). The structure elucidation studies were carried out through extensive spectroscopic studies.

2. Results and discussion

The ethanolic extract of the air-dried leaves of *B. papillosa* was evaporated to a gum and dissolved in water. After defatting with hexane, the aqueous layer was extracted with $CHCl_3$ at different pH values. The fraction obtained at pH 9.0 afforded compounds **1–3**.

Buxakashmiramine (**1**), $C_{36}H_{56}N_2O_5$, showed UV absorptions at 211 and 260 nm, attributable to a substituted secondary benzamidic chromophore (Silverstein et al., 1981). The IR spectrum displayed bands at 3352 (OH), 2854 (CH), and 1578 (C=C) cm^{-1}. The HREI MS displayed the M^+ at m/z 596.4238 corresponding to the molecular formula $C_{36}H_{56}N_2O_5$ (calc. 596.4188) indicating 10 degrees of unsaturation in the molecule. Cleavage of the substituted benzoyl moiety yielded a peak at m/z 181. The base peak at m/z 72 represented the trimethyliminium ion cleaved from the C-17 of main skeleton (Budzikiewicz, 1972). The overall mass fragmentation pattern of alkaloid **1** was very similar to *Buxus* alkaloids bearing an *N,N*-dimethyl amino group at C-20 and a benzamide group at C-3 (Atta-ur-Rahman, 1990).

Three 3H singlets at δ 0.78, 0.92, and 0.93 in the ^1H NMR spectrum of **1** were assigned to the tertiary C-30, C-18 and C-32 methyl group protons. A doublet at δ 0.98 ($J_{21,\ 20} = 6.5$ Hz) was due to the C-21 secondary methyl protons, while the vicinal C-20 methine proton appeared as a multiplet at δ 2.04. A set of AB doublets at δ 3.18 and 3.35 ($J_{31\alpha,\ 31\beta} = 12.5$ Hz) was due to the C-31 hydroxymethylene protons. The C-19 methylene protons of the cyclopropane ring also appeared as AB

[1] Also corresponding author.
* Corresponding author. Fax: +92-21-924-3235.
E-mail address: zainraa@digicom.net.pk (M.I. Choudhary).

0031-9422/01/$ - see front matter © 2001 Published by Elsevier Science Ltd.
PII: S0031-9422(01)00332-6

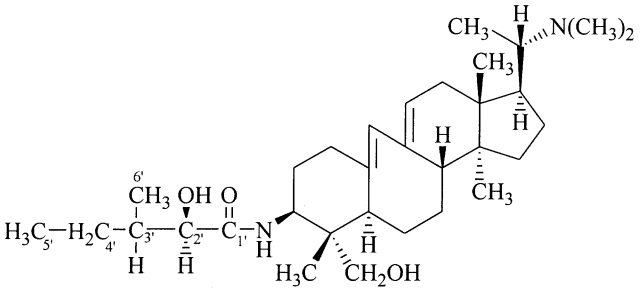

3

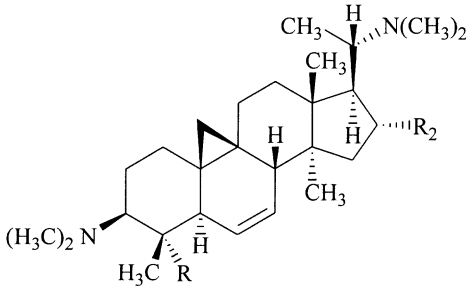

4 R = CH_3, R_2 = H
5 R = CH_3, R_2 = OH
6 R = CH_2OH, R_2 = OH

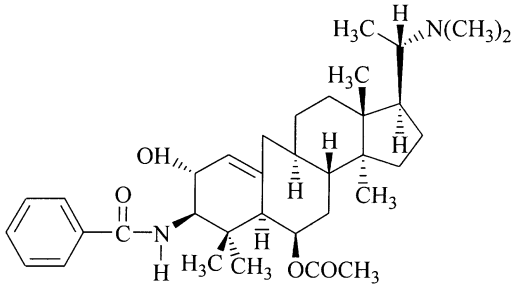

7

doublets at δ 0.37 and 0.56 ($J_{19\alpha,\ 19\beta}$ = 4.1 Hz). A 3H singlet at δ 2.90 and a broad 6H singlet at δ 2.31 were due to the N_a-methyl at C-3 and the N_b-dimethyl protons at C-20, respectively. The C-3H appeared as a double doublet at δ 4.69 ($J_{3,\ 2\alpha}$ = 3.7 Hz, $J_{3,2\beta}$ = 10.8 Hz). The axial disposition (α-orientation) of C-3H is consistent with the *trans* diaxial coupling of 10.8 Hz observed between C-3αH and the C-2βH. The α-stereochemistry of the C-31 hydroxymethylene protons is based on X-ray diffraction studies done by Guilhem (1975) and the ^{13}C NMR studies by Sangare et al. (1975) in which it was shown that of the two methyl substituents at C-4, it is the α (C-31) methyl which undergoes preferential oxidation. As the *Buxus* alkaloids are biogenetically related to cycloartenol, the configuration at six of its asymmetric centres is predicted as 5α, 8β, 9β, 10β, 13β and 14α. Similarly the assignment of α-configuration to the 20-methyl amino group is again on the basis of biogenetic precedents, where it is known that all reported 20-amino steroids possess the α-configuration at that centre (Brown and Kupchan, 1962). An interesting 6H singlet at δ 3.87 was assigned with the help of various NMR techniques such as HMBC and HMQC to the two methoxy groups substituted at C-4′ and C-6′ of the benzoyl ring, while a downfield 2H singlet at δ 6.56 was due to the two aromatic protons at C-3′ and C-7′ of the benzoyl group.

The broad-band decoupled ^{13}C NMR spectra of **1** indicated the presence of 9 methyl, 10 methylene, 7 methine, and 10 quaternary carbons. The C-19 methylene appeared at δ 29.8, while the C-3 methine appeared at δ 56.7. The two methoxy carbons resonated at δ 56.6. Five downfield signals at δ 173.4, 127.7, 104.3 and 136.4 were assigned to the amidic carbonyl, C-4′/C-6′ bearing the methoxy groups, C-5′ bearing the hydroxyl, the aromatic C-3′/C-7′ and the C-2′, respectively. One-bond ^{1}H/^{13}C chemical shift correlations were determined by the HMQC (Atta-ur-Rahman and Choudhary, 1996). Complete assignments of ^{1}H and ^{13}C NMR spectra, multiplicities and one-bond ^{1}H/^{13}C connectivities are shown in Table 1.

The dimethoxy benzoyl fragment, has very rarely been observed in *Buxus* alkaloids. It was established by the long-range ^{1}H/^{13}C correlations as determined by the HMBC spectrum (Fig. 1). The C-4′/C-6′ methoxy protons at δ 3.87 were found to be correlated with the C-4′/C-6′ (δ 147.4) and the C-5′ (δ 127.7) in the HMBC spectrum. The aromatic protons resonating at δ 6.56 (H-3′/H-7′) showed long-range heteronuclear correlation with the C-1′ carbonyl (δ 173.8) and with C-2′ (δ 136.4) and C-4′ (δ 147.4) of the benzoyl ring. The N_a-CH_3 protons (δ 2.90) and H-3α (δ 4.69) also showed long-range interactions with the C-1′ carbonyl. The COSY-45° couplings observed between H-3α (δ 4.69)/H_2-2 (δ 2.08, 1.72), H_2-2/H_2-1 (δ 1.37, 1.78), H-5 (δ 2.10)/H_2-6 (δ 1.75), H_2-6/H_2-7 (δ 1.39), H_2-7/H-8 (δ 1.49), H_2-11 (δ 1.72)/H_2-12 (δ 1.38), H_2-15 (δ 1.60, 1.65)/H_2-16 (δ 1.17), H-31α (δ 3.18)/H-31β (δ 3.35) and H-19α (δ 0.37)/H-19β (δ 0.56) helped in unraveling the spin systems involved and in assigning structure **1** to this new alkaloid.

Table 1
^{13}C NMR chemical shift assignments and $^{1}H/^{13}C$ one-bond shift correlations of each protonated carbon of **1** and **2** as determined from the HMQC spectra

C. No.	δ C (m[a])	δ H (*J* in Hz)	δ C (m[a])	δ H (*J* in Hz)
	1		**2**	
1	32.2 (CH_2)	137 *m*, 1.78 *m*	40.3 (CH_2)	2.30 *m*, 2.32 *m*
2	27.4 (CH_2)	2.08 *m*, 1.72 *m*	27.6 (CH_2)	1.63 *m*, 2.06 *m*
3	56.7 (CH)	4.69 *dd* (3.7, 10.8)	57.6 (CH)	4.54 *dd* (3.0., 12.7)
4	45.9 (C)		46.0 (C)	
5	41.6 (CH)	2.10 *m*	45.0 (CH)	2.29 *m*
6	26.3 (CH_2)	1.75 *m*	27.0 (CH_2)	1.92 *m*, 2.27 *m*
7	25.7 (CH_2)	1.39 *m*	28.7 (CH_2)	1.30 *m*, 1.33 *m*
8	48.3 (CH)	1.49 *m*	49.5 (CH)	2.08 *m*
9	20.2 (C)		138.6 (C)	
10	39.8 (C)		135.3 (C)	
11	20.5 (CH_2)	1.72 *m*	128.3 (CH)	5.50 *br s*
12	35.6 (CH_2)	1.38 *m*	38.5 (CH_2)	1.99 *m*, 2.20 *m*
13	45.1 (C)		44.2 (C)	
14	49.0 (C)		48.5 (C)	
15	32.8 (CH_2)	1.60 *m*, 1.65 *m*	33.3 (CH_2)	1.55 *m*
16	25.8 (CH_2)	1.17 *m*	25.2 (CH_2)	1.32 *m*, 1.50 *m*
17	50.2 (CH)	1.28 *m*	32.1 (CH)	1.51 *m*
18	18.5 (CH_3)	0.93 *s*	7.7 (CH_3)	0.71 *s*
19	29.8 (CH_2)	0.37*d,* (4.1), 0.56 *d* (4.1)	129.7 (CH)	5.99 *s*
20	63.1 (CH)	2.04 *m*	48.0 (CH)	1.93 *m*
21	10.5 (CH_3)	0.98 *d*, (6.5)	11.8 (CH_3)	1.31 *d* (5.8)
30	13.5 (CH_3)	0.78 *s*	12.5 (CH_3)	0.65 *s*
31	64.7 (CH_2)	3.18 *d*, (12.5), 3.35 *d* (12.5)	64.0(CH_2)	3.30 *d*, (12.8), 3.10 *d* (12.8)
32	19.5 (CH_3)	0.93 *s*	15.8 (CH_3)	0.77 *s*
N_a-CH_3	35.0 (CH_3)	2.90 *s*	32.0 (CH_3)	2.89 *s*
$N_b(CH_3)_2$	39.4 (CH_3)	2.31 *s*	38.0, 42.0 (CH_3)	2.64 *s*
1′	173.8 (C)		177.0 (C)	
2′	136.4 (C)		72.8(CH)	4.92 *d* (3.3)
3′	104.3 (CH)	6.56 *s*	31.0 (CH)	1.88 *m*
4′	147.4 (C)		19.8 (CH_3)	1.05 *d* (6.8)
5′	127.7 (C)		15.3 (CH_3)	0.82 *d* (6.7)
6′	147.4 (C)			
7′	104.3 (CH)	6.56 *s*		
OCH_3	56.6 (CH_3)	3.87 *s*		

[a] m = Multiplicity as determined by DEPT.

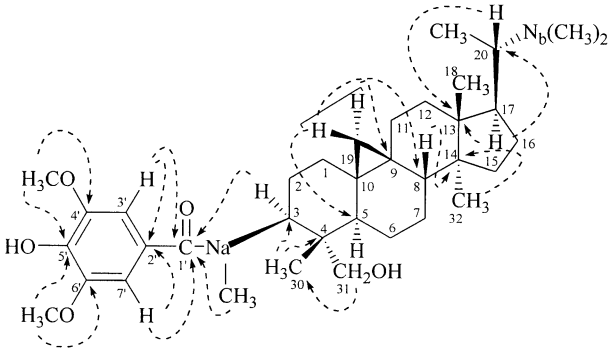

Fig. 1. Important HMBC interactions observed for compound **1**.

Compound **2** (*m*/*z* 514.4149, $C_{32}H_{54}N_2O_3$) which was isolated as white amorphous powder, showed UV absorption maxima at 238 and 245 nm characteristic of a 9(10→19) *abeo*-diene system (Atta-ur-Rahman et al., 1991). The IR spectrum displayed bands at 3358 (OH), 2855 (CH), 1645 (amide carbonyl) and 1602 (C=C) cm^{-1}. The HREI MS of alkaloid **2** displayed the M^+ at *m*/*z* 514.4149, $C_{32}H_{54}N_2O_3$ (calc. 514.4134) indicating seven double bond equivalents in the molecule. The M^+ was further confirmed by FD MS. A peak at *m*/*z* 499 arose due to the loss of a methyl group from the M^+. The base peak at *m*/*z* 72 was due to the trimethyliminium cation.

The ^1H NMR spectrum ($CDCl_3$, 400 MHz) of alkaloid **2** featured three singlets for the three tertiary methyl groups at δ 0.65, 0.71 and 0.77 assigned to C-30, C-18 and C-32, respectively, while a doublet at δ 1.31 ($J_{20,\ 21} = 5.8$ Hz) was due to the C-21 secondary methyl protons. Two other 3H doublets, resonating at δ 0.82 ($J_{5',\ 3'} = 6.7$ Hz) and 1.05 ($J_{4',\ 3'} = 6.8$ Hz), were assigned to the C-5′ and C-4′ methyl protons of the isobutanol group attached to the C-3 amidic carbonyl, respectively.

A 6H singlet at δ 2.64 was assigned to the *N,N*-dimethyl protons at C-20, while a 3H singlet at δ 2.89 was due to the N_a-methyl protons at C-3. A set of AB doublets resonating at δ 3.10 and 3.30 ($J_{31\alpha,31\beta}=12.8$ Hz) was due to the C-31α and C-31β methylenic protons geminal to the hydroxyl group. A broad singlet at δ 5.50 was assigned to the vinylic H-11, while a singlet at δ 5.99 was due to the isolated vinylic H-19. The C–3H appeared as a double doublet at δ 4.54 ($J_{3\alpha,2\alpha}=3.0$ Hz, $J_{3\alpha,2\beta}=12.7$ Hz). The *trans* diaxial coupling of 12.7 Hz established its stereochemistry to be axial (α-orientation). A doublet resonating at δ 4.29 ($J_{2',3'}=3.3$ Hz) was ascribed to the C-2′ methine proton geminal to the hydroxyl group in the C-3 amidic side chain. The vicinal C-3′ H appeared as a multiplet at δ 1.88. The configuration at C-2′ was determined by Horeau's method for secondary alcohols (Horeau, 1962) and was determined to be *S*.

The COSY-45° spectrum displayed cross-peaks between H-3α (δ 4.54)/H_2-2 (δ 1.63, 2.06), H-31α (δ 3.10) /H-31β (δ 3.30) and H-17 (δ 1.51)/H_2-16 (δ 1.32, 1.50). The H-2′ (δ 4.29) geminal to a hydroxyl group was found to be coupled with the vicinal H-3′ (δ 1.88) which was further coupled with the two methyls (H_3-4′ and H_3-5′) resonating at δ 1.05 and 0.82, respectively. The HMBC spectrum served to confirm the disposition of the different groups in the C-3 side chain (Fig. 2). In the HMBC spectrum, H_3-4′ and H_3-5′ showed correlations with the C-3′ (δ 31.0) and C-2′ (δ 72.8), while the H-1′ was correlated with C-3′ (δ 31.0), C-4′ (δ 19.8), and C-5′ (δ 15.3), and with the carbonyl carbon (δ 177.0). The N_a–CH_3 protons were found to be correlated with the carbonyl carbon and with C-3 (δ 57.6). Complete ^{1}H and ^{13}C NMR assignments, multiplicties along with one-bond ^{1}H/^{13}C connectivities are presented in Table 1.

Alkaloid **3** (*m*/*z* 528.4293, $C_{33}H_{56}N_2O_3$, calc. 528.4291) was also isolated as white amorphous powder. It closely resembled alkaloid **2** in its spectral behavior, as the only difference between them is the presence of an additional CH_2 in the side chain of **3**. This was manifested in the ^{1}H NMR spectra in the appearance in **3** of a doublet at δ 0.76 ($J_{6',3'}=6.5$ Hz) and of a triplet at δ 0.95 ($J_{5',4'}=7.0$ Hz), both integrating for three protons each. In the COSY-45° spectrum the H_3-6′ doublet at δ 0.76 was found to be coupled with H-3′ (multiplet at δ 1.60), which was further coupled with H-2′ at δ 4.45. The 3H triplet of H_3-5′ (δ 0.95) showed cross-peaks with the two 1H multiplets of H_2-4′ at δ 1.45 and 1.55, thus establishing the C-3 amidic side chain of alkaloid **3**. It was apparent from these data that **3** differed in its structure from alkaloid **2** only in the nature of the C-3 side chain, there being a 1-hydroxy-2-methyl butyl moiety in **3**, instead of 1-hydroxy-2-methyl propyl group as in alkaloid **2**. The ^{13}C NMR spectra (BB, DEPT, $CDCl_3$, 500 MHz) of **3** were in good accord with the established structure, displaying nine CH_3, nine CH_2, nine CH and six quaternary carbon centers. The complete ^{13}C NMR data are presented in the experimental section.

In addition to these new natural products, four known triterpenoid alkaloids cycloprotobuxine-C (**4**) (Kuchkova et al., 1976), cyclovirobuxeine-A (**5**) (Khoung-Huu et al., 1966), cylomicrophylline-A (**6**) (Nakano and Terao, 1965), and sempervirаminol (**7**) (Atta-ur-Rahman et al., 1999) were also isolated for the first time from this species of the genus *Buxus*. The isolates were characterized by comparison of their UV, IR, ^{1}HNMR, and MS spectral data with those reported in the literature.

These alkaloids were tested for acetylcholinesterase and butyrylcholinesterase inhibitory activity because buxaminol-E, a steroidal alkaloid from *B. sempervirens* was reported as a good inhibitor of the enzyme (Kvaltinova et al., 1991). Inhibition of acetylcholinesterase is considered as a promising approach for the treatment of Alzheimer's disease (AD) and for possible therapeutic applications in the treatment of Parkinson's disease, ageing, and myasthenia gravis (Quinn, 1987; Nochi et al., 1995). Meanwhile, BChE has been considered to be directly associated with the side effects of the AChE inhibitors and the existing drugs of Alzheimer's disease (Tong et al., 1996). More recent studies have shown that BChE is found in significantly higher quantities in AD plaques than in the plaques of age related non-demented brains. Other recent studies have also reported that the unfavorable side effects profile of AChE inhibitors are

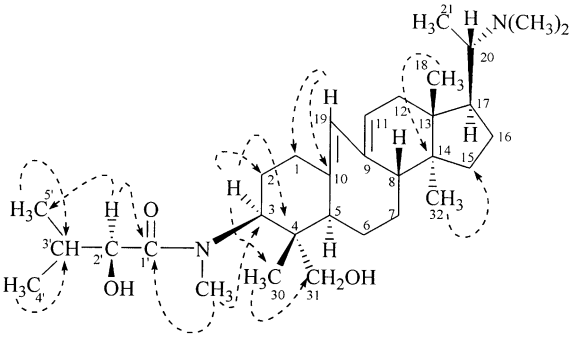

Fig. 2. Important HMBC interactions observed for **2**.

Table 2
In vitro inhibition of cholinesterases by alkaloids **1–7**

Compound	IC_{50} (μM)±SEM[a]	
	AChE	BChE
1	25.4±1.1	0.74±0.03
2	143±1.3	*n.t*[b]
3	162±4.9	*n.t*
4	38.8±2.2	2.73±0.07
5	105.7±5.6	2.05±0.05
6	235±2.7	2.43±0.05
7	inactive	*n.t*
Physostigmine (Control)	0.04 1±0.001	0.875±0.008

[a] IC_{50} are the mean±standard mean error of five assays.
[b] *n.t* not tested due to insufficient amount.

not associated with their poor selectivity towards AChE (Yu et al., 1999). Thus, new cholinesterase inhibitors, in addition to their potential clinical importance if followed by proper pharmacological-investigations, would help in defining the role of BChE in brain development, health and ageing and would in the meantime reveal the value of BChE inhibition as a novel strategy for the treatment of AD. The concentration of alkaloids that inhibited the enzyme activity by 50% (IC_{50}) are presented in Table 2. Eserine ((−)-physostigmine) was used as a positive control.

3. Experimental

3.1. General experimental procedure

Optical rotations were measured on a Jasco DIP-360 digital polarimeter. UV and IR spectra were recorded in MeOH on Shimadzu UV-240 and in $CHCl_3$ on Shimadzu IR-2240 spectrophotometers, respectively. ^{1}HNMR spectra were recorded in $CDCl_3$ at 400 MHz and 500 MHz on Bruker AM-400 and AMX-500 NMR spectrometers, respectively. ^{13}CNMR were recorded at 100 and 125 MHz on the same instruments. HREI MS were recorded on a Jeol-JMS HX 110 mass spectrometer. Column chromatography was carried out using silica gel (70–230 mesh, ASTM, Merck) and preparative TLC was done with silica GF-254 plates (20×20 cm, 0.25 mm thick).

3.2. Materials and methods

The leaves of *Buxus papillosa* C.K. Schneider (100 kg) were collected from the Northern regions of Pakistan in December 1994. The plant was identified by Dr. Tahir Ali, Plant Taxonomist and a specimen voucher (KUH 66486) was deposited in the herbarium of the Department of Botany, University of Karachi. The EtOH extract of the leaves was concentrated to a gum (3.5 kg). Water (5 l) was added and the mixture was defatted with hexane (20 l). The defatted aqueous extract was extracted with $CHCl_3$ (20 l) at different pH values (3.0, 7.0, 9.0). The $CHCl_3$ fraction obtained at pH 9.0 (88.5 g) was subjected to column chromatography using silica gel (70–230 mesh, ASTM, Merck, 2 kg) and eluted with increasing polarities of pet. ether–$CHCl_3$ and $CHCl_3$–MeOH mixtures. The fraction obtained on elution with $CHCl_3$–MeOH (95:5) was repeatedly washed with acetone and then with MeOH to yield **1** as a white powdery mass (30 mg, 8.5×10^{-4}% yield).

Elution of the column with $CHCl_3$–MeOH (96:4) afforded a fraction (4.0 g) which showed several alkaloidal spots on TLC. This was loaded onto a silica gel column (120 g) using pet. ether:acetone:diethylamine (95:4:1) as eluant. A fraction thus obtained (50 mg) was subjected to prep. TLC using the same solvent system to afford **2** (R_f=0.14, 15 mg, 4.3×10^{-4}% yield) and **3** (R_f=0.12, 12 mg, 3.4×10^{-4}% yield) as white amorphous solids.

3.2.1. (−)-Buxakashmiramine (*1*)

$[\alpha]_D^{25}$: −3° ($CHCl_3$, *c* 0.62): UV λ_{max}^{MeOH} nm (log ε): 211(4.46), 260 (3.8); IR $\nu_{max}^{CHCl_3}$ cm^{-1}: 3352 (OH), 2854 (CH), 1578 (C=C), 1110 (C–O–C);: ^{1}HNMR (400 MHz, $CDCl_3$) δ: see Table 1; ^{13}CNMR (100 MHz, $CDCl_3$) δ see Table 1. HREI MS *m*/*z* (rel. int. %): 596.4238 ($C_{36}H_{56}N_2O_5$, 50), 581.3888 ($C_{35}H_{53}N_2O_5$,14), 181.0512 ($C_9H_9O_4$, 33), 72.0812 ($C_4H_{10}N$, 100).

3.2.2. (−)-Buxakarachiamine (*2*)

$[\alpha]_D^{25}$: −9° ($CHCl_3$, *c* 0.22); UV λ_{max}^{MeOH} nm (log ε): 245 (4.2), 238 (4.2); IR $\nu_{max}^{CHCl_3}$ cm^{-1}: 3358 (OH), 2855 (CH), 1645 (amide carbonyl), 1602 (C=C); ^{1}HNMR ($CDCI_3$, 400 MHz) δ: see Table 1; ^{13}CNMR (100 MHz, $CDCI_3$) δ: see Table 1. HREI MS *m*/*z* (rel. int. %): 514.4149 ($C_{32}H_{54}N_2O_3$,6), 499.3893 ($C_{31}H_{51}N_2O_3$,1), 72.0822 ($C_4H_{10}N$, 100).

3.2.3. (−)-Buxahejramine (*3*)

$[\alpha]_D^{25}$: −7° ($CHCl_3$, *c* 0.14); UV λ_{max}^{MeOH} nm (log ε): 245 (4.2), 239 (4.18); IR $\nu_{max}^{CHCI_3}$ cm^{-1}: 3274 (OH), 2845 (CH), 1603 (C=C); ^{1}HNMR (500 MHz, $CDCl_3$) δ: 0.64 (3H, *s*, CH_3), 0.69 (3H, *s*, CH_3), 0.74 (3H, *s*, CH_3), 0.77 (3H, *d*, $J_{6',3'}$=6.5 Hz, H-6′), 0.95 (3H, *t*, $J_{5'4'}$=7.5 Hz, CH_3-5′), 1.01 (3H, *d*, $J_{21,20}$=6.0 Hz, 21-CH_3), 2.41 (6H, *br s*, N_b $(CH_3)_2$), 2.87 (3H,*s*, N_a–CH_3), 3.05 and 3.28 (2H, AB *d*, $J_{31\alpha,31\beta}$=12.5 Hz, H-31α, H-31β), 4.45 (1H, *d*, $J_{2',3'}$=2.5 Hz, H-2′), 4.52 (1H, *dd*, $J_{3\alpha,2\alpha}$=4.0 Hz, $J_{3\alpha,2\beta}$=13.0 Hz, H-3α), 5.51 (1H, *brs*, H-11), 5.99 (1H, *s*, H-19). ^{13}CNMR (125 MHz, $CDCl_3$) δ: 11.2 (C-2l), 11.9 (C-5′), 12.4 (C-18), 12.6 (C-30), 12.7 (C-32),17.3 (C-6′), 25.2 (C-16), 26.8 (C-4′), 27.1 (C-6), 27.5 (C-2), 28.7 (C-7), 29.7 (C-3′), 31.9 (C-17), 32.0 (N_a-CH_3), 33.3 (C-15), 38.4 (C-12), 40.3 (C-1), 40.8 (C-N_b $(CH_3)_2$), 44.5 (C-13), 44.9 (C-5), 46.0 (C-4), 48.4 (C-14), 49.4 (C-8), 57.5 (C-3), 64.0 (C-31), 65.7 (C-20), 70.6 (C-2′), 127.8 (C-11), 129.5 (C-19), 135.6 (C-10), 138.6 (C-9), 177.2 (C-1′). HREI MS *m*/*z* (rel. int. %): 528.4239 ($C_{33}H_{56}N_2O_3$, 15), 513.4026 ($C_{32}H_{53}N_2O_3$, 3), 72.0800 ($C_4H_{10}N$, 100).

3.2.4. AChE and BChE inhibition assay

Electric eel acetylcholineesterase, horse serum butyrylcholinesterase, acetylthiocholine iodide, butyrylthiocholine chloride, 5-5′-thiobis-2-nitrobenzoic acid (DTNB) and eserine were purchased from Sigma (St. Louis, MO). Buffers and other chemicals were of analytical grade. Acetylcholinesterase inhibition was determined spectrophotometrically using acetylthiocholine as substrate by modifying the method of Ellman et al. (1961). The reaction was carried in 100 mM sodium phosphate buffer (pH 8.0) at 25 °C. In a typical assay

140 μl buffer, 20 μl enzyme preparation and 20 μl test compound solution were mixed and incubated for 30 min. 10 μl of DTNB was added and the reaction was then started by adding 10 μl of acetylthiocholine. The butyrylthiocholine chloride was used as a substrate to assay BChE with all the other reagents and conditions being same. The hydrolysis of acetylthiocholine/butyrylthiocholine was determined by monitoring the formation of yellow 5-thio-2-nitrobenzoate anion (as a result of the reaction of 5,5′-dithiobis-2-nitrobenzoic acid with thiocholine released by the enzymatic hydrolysis of acetylthiocholine/butyrylthiocholine) at a wavelength of 412 nm on microtitre plate spectrophotometer (Molecular Devise, USA).

Acknowledgements

We gratefully acknowledge Dr. Sultan Ahmed for collection of the plant.

References

Atta-ur-Rahman, Choudhary, M.I., 1996. Solving Problems with NMR Spectroscopy. Academic Press, San Diego.

Atta-ur-Rahman, Ahmed, D., Asif, E., Ahmad, S., 1991. Chemical constituents of *Buxus sempervirens*. Journal of Natural Products 54, 79–82.

Atta-ur-Rahman, Choudhary, M.I., Ata, A., Naz, S., Sener, B., Turkoz, S., 1999. New steroidal alkaloids from the roots of *Buxus sempervirens*. Journal of Natural Products 62, 665–669.

Atta-ur-Rahman, 1990. Handbook of Natural Product Data: Diterpenoid and Steroidal Alkaloids, Vol. 1. Elsevier Science, Amsterdam.

Brown, K.S., Kupchan, S.M., 1962. The configuration of cyclobuxine and its interelation with cycloeucalenol. Journal of American Chemical Society 84, 4592–4594.

Budzikiewicz, H., 1972. Steroids. In: Wailer, G.R. (Ed.), Biochemical Application of Mass Spectrometry. Wiley-Interscience, New York, p. 251.

Cordell, G.A., 1981. Introduction to Alkaloids: A Biogenetic Approach. Wiley-Interscience, New York.

Ellman, G.L., Courtney, K.D., Andres, V., Featherstone, R.M., 1961. A new and rapid colorimetric determination of acetylcholinesterase activity. Biochemical Pharmacology 7, 88–90.

Guilhem, J., 1975. The configuration at C-4 of steroidal alkaloids from *Buxus*: an X-ray structure determination. Tetrahedron Letters, 2937–2938.

Horeau, A., 1962. Determination des configurations par "Dedoublement Partiel"—II. Precisions et Complements. Tetrahedron Letters 965–969.

Khuong-Huu-Laine, F., Magdeleine, M.J., Bisset, N.G., Goutarel, R., 1966. Alcaloides steroidiques .45. Famille des Buxacees (4e Communication) alcaloides du *Buxus malayana* Ridl. - cyclovirobuxine D, cyclovirobuxeines A et B, cycloprotobuxine A, cyclomicrophylline B Et cyclomalayanine B. Bulletin De La Societe Chimique De France, 758–762.

Kuchkova, K.I., Voticky, Z., Paulik, V., 1976. *Buxus* Alkaloids. 13. Alkaloids from *Buxus sempervirens* var. *Argentea* Hort ex Steud. Chemicke Zvesti 30, 174–178.

Kvaltinova, Z., Lukovic, L., Machova, J., Fatranska, M., 1991. Effect of the steroidal alkaloid buxaminol-E on blood pressure, acetylcholinesterase activity and (^{3}H) quinuclidinyl benzilate binding in cerebral cortex. Pharmacology 43, 20–25.

Nakano, T., Terao, S., 1965. *Buxus* alkaloids. Part IV. Isolation and structure elucidation of eight new alkaloids, cyclomicrophyllines-A, -B, and -C, dihydrocyclomicrophylline-A and -F, cyclomicrophyllidine-A, dihydrocyclomicrophyllidine-A and cyclomicrobuxine from *Buxus microphylla* Sieb. et Zucc. var *suffruticosa* Makino. Journal of Chemical Society 4512–4537.

Naz, S., 1995. Phytochemical and structural studies on the chemical constituents of *Buxus sempervirens* and *Buxus papillosa*. PhD dissertation, H.E.J. Research Institute of Chemistry, University of Karachi, Karachi, Pakistan.

Nochi, S., Asakawa, N., Sato, T., 1995. Kinetic study on the inhibition of acetylcholinesterase by 1-benzyl-4-[(5,6-dimethoxy-1-indanon)-2-yl] methylpiperidine hydrochloride (E2020). Biological and Pharmaceutical Bulletin 18, 1145–1147.

Quinn, D.M., 1987. Acetylcholinesterase: enzyme structure, reaction dynamics and virtual transition states. Chemical Reviews 87, 955–979.

Sangare, M., Khuong-Huu, F., Herlem, D., Milliet, A., Septe, B., Berenger, G., Lukacs, G., 1975. Revision of the configuration of the C-4 hydroxymethylene group in *Buxus* alkaloids by ^{13}C-NMR spectroscopy. Tetrahedron Letters, 1791–1794.

Silverstein, R.M., Bassler, G.C., Morrill, T.C., 1981. Spectrometric Identification of Organic Compounds. John Wiley and Sons, New York.

Tong, W., Collantes, E.R., Chen, Y., Welsh, W.J., 1996. A comparative molecular field analysis study of *N*-benzylpiperidines as acetylcholinesterase innhibitors. Journal of Medicinal Chemistry 39, 380–387.

Yu, Q., Holloway, H.W., Utsuki, T., Brossi, A., Greig, N.H., 1999. Synthesis of novel phenserine-based selective inhibitors of butyrylcholinesterase for Alzheimer's disease. Journal of Medicinal Chemistry 42, 1855–1861.

PERGAMON

Phytochemistry 58 (2001) 969–972

PHYTOCHEMISTRY

www.elsevier.com/locate/phytochem

ent-Daucane and acorane sesquiterpenes from ×*Cupressocyparis leylandii* foliage

Laurence G. Cool*

University of California Forest Products Laboratory, 1301 S. 46th St., Richmond, CA 94804, USA

Received 24 April 2001; received in revised form 10 July 2001

Abstract

One new *ent*-daucadiene and enantiomers of four previously reported daucadienes or acoradienes were identified in foliage of the hybrid cypress species ×*Cupressocyparis leylandii*. The major compound is (+)-dauca-5,8-diene; minor congeners are (−)-dauca-4,8-diene, (−)-dauca-8,11-diene, (−)-acora-3,7(14)-diene and 1*S*-dauca-4(11),8-diene. None of these compounds is observed in foliage of either of the parent species, *Cupressus macrocarpa* and *Chamaecyparis nootkatensis*. However, we have subsequently found them in some specimens of *Cupressus macnabiana*. © 2001 Elsevier Science Ltd. All rights reserved.

Keywords: *Cupressocyparis leylandii*; *Cupressus macnabiana*; Cupressaceae; Foliage; Sesquiterpenes; Enantiomers; Daucane; Acorane

1. Introduction

×*Cupressocyparis leylandii* (Jacks. et Dall.) Dall. is an intergeneric artificial hybrid of *Cupressus macrocarpa* Hartw. ex Gord. and *Chamaecyparis nootkatensis* (D. Don) Spach. (Dallimore and Jackson, 1948). It is a rapid-growing and rather popular horticultural plant.

Gas chromatographic–mass spectral (GC–MS) analysis of the foliage volatiles showed that the sesquiterpenes were unlike those of any other member of the Cupressaceae thus far studied. Moreover, the major hydrocarbon and several of the minor ones do not appear in published spectral libraries, nor were they in our extensive collection of terpenoid GC–MS data. A recent paper (Mardarowicz et al., 1999) on the foliar essential oil of *C. leylandii* was unhelpful, since most of the sesquiterpenes were unidentified. The structure of these sesquiterpene hydrocarbons is the subject of this report.

2. Results and discussion

The major sesquiterpene from ×*Cupressocyparis leylandii* foliage oil was purified and identified as (+)-dauca-5,8-diene **1**. The NMR data of the *C. leylandii* material was identical to that given by Hashidoko et al. (1992) for (−)-dauca-5,8-diene from glandular trichomes of *Rosa rugosa* leaves, but the optical rotation was +100° vs. −121° for the *R. rugosa*-derived material. Enantioselective capillary GC of the hydrocarbons from both sources resolved the enantiomers very well (Table 1) and showed that dauca-5,8-diene from each source was of high (>95%) optical purity. The only other report of **1** is as a minor constituent in *Daucus carota* seed oil (Mazzoni et al., 1999), where its co-occurrence with other 1*R* dauc-8-enes implies it is the same (−) enantiomer as in *R. rugosa*.

Mass spectral data given by Hashidoko et al. (1992) for congeners of dauca-5,8-diene matched two other unknowns in *C. leylandii*, and GC–MS analysis of the sesquiterpenes from both sources under identical conditions confirmed the presence of dauca-8,11-diene (isodaucene) **2** and acora-3,7(14)-diene **3**. Sufficient **2** was obtained from *C. leylandii* for ^{1}H NMR confirmation of its identity. Both compounds have been reported by Castro et al. (1984) from *Calea prunifolia* foliage, with the same absolute stereochemistry [i.e., (+)] as in *R. rugosa*. (+)-Isodaucene apparently occurs in *Vernonia galpinii* foliage (Bohlmann and Zdero, 1982; structure revised by Cassidy and Ghisalberti, 1993) and *Daucus carota* seed oil (Mazzoni et al., 1999).

* Tel.: +1-510-215-4216; fax: +1-510-215-4299.
E-mail address: larry.cool@ucop.edu

0031-9422/01/$ - see front matter © 2001 Elsevier Science Ltd. All rights reserved.
PII: S0031-9422(01)00342-9

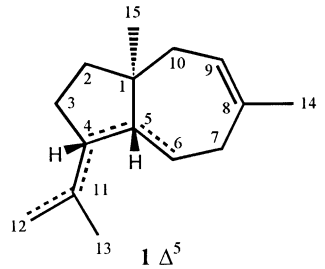

1 Δ^5
2 Δ^{11}
4 Δ^4
5 $\Delta^{4(11)}$

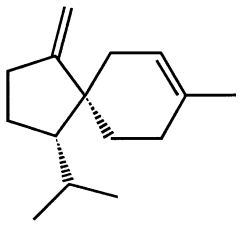

3

Table 1
GC retention indices of *Cupressocyparis leylandii* sesquiterpenes and enantiomers on permethylated β-cyclodextrin column

Compound and source	Kovats Retention Index
(+)-daucene ex *Daucus carota* seed oil	1399
(–)-daucene ex *Cupressocyparis leylandii* foliage	1408
(+)-acora-3,7(14)-diene ex *Rosa rugosa* foliage	1484
(–)-acora-3,7(14)-diene ex *C. leylandii* foliage	1486
(+)-dauca-5,8-diene ex *C. leylandii* foliage	1499
(–)-dauca-5,8-diene ex *R. rugosa* foliage	1506
(–)-dauca-8,11-diene ex *C. leylandii* foliage	1538
(+)-dauca-8,11-diene ex *R. rugosa* foliage	1539
(+)-dauca-4(11),8-diene ex *C. leylandii* foliage	1557

A minor *C. leylandii* component was dauca-4,8-diene (daucene) **4**, identified by GC–MS comparison with carrot seed oil.

Since **1** is enantiomeric to dauca-5,8-diene from *R. rugosa*, it was expected that the biosynthetically-related compounds **2**–**4** would also occur as the (heretofore unreported) antipodes in *C. leylandii*. Enantioselective GC proved that this is indeed the case. The Kovats indices for the relevant enantiomers are given in Table 1.

A late-eluting unknown sesquiterpene had a distinctive mass spectrum with a base peak of 136. Its structure was determined by 1D and 2D NMR spectroscopy to be dauca-4(11),8-diene **5**. Proton-carbon assignments were by HMQC; three-bond ^1H–^1H connectivites were determined by DQCOSY and HMQC–TOCSY experiments. The HMBC spectrum verified key heteronuclear three-bond linkages: H-15 to C-2,-5 and -10; and H-14 to C-7. A *trans* ring fusion is indicated by the δ 19.0 value for C-15, compared to $\delta \sim 25$ expected for a *cis*-fused daucadiene (Seto et al., 1985; Marcos et al., 1995). There was insufficient material for accurate measurement of the optical rotation, but the sign appears to be (+).

Dauca-4(11),8-diene was recently reported from the liverwort *Bazzania trilobata* (Warmers and König, 1999) but the MS and NMR spectral data of the liverwort-derived material do not agree with that from *C. leylandii*. There are problems with some of the NMR assignments in the *B. trilobata* study that make the identity of this component questionable. In the following discussion, the C_6D_6 (rather than $CDCl_3$) data of Warmers and König (1999) are used, and the δ-ranges for ^1H multiplets have been abbreviated to their approximate midpoints.

The data presented by Warmers and König (1999) for C-3 (^{13}C: δ 41.2; ^1H: δ∼1.36, ∼1.48) are not consistent with an allylic methylene in this position; values closer to ^{13}C: δ∼30 and ^1H: δ∼2.3 would be expected (Bohlmann et al., 1983). More significantly, the data assigned to C-10 are ^{13}C: δ 31.0 (^1H: δ∼2.02 and ∼2.23), while other dauc-8-enes typically have a ^{13}C signal at $\delta \sim 42$ (^1H: δ∼2) for C-10 (Bohlmann and Zdero, 1982; Bohlmann et al., 1983; Hashidoko et al. 1992; Ghisalberti, 1994; Mazzoni et al., 1999). In fact, there is no methylene group in the *B. trilobata* sesquiterpene that is a candidate for this allylic C-10 methylene.

An alternative identification of this *B. trilobata* sesquiterpene as *trans*-dauca-4(11),7-diene is proposed. This appears to be consistent with the 1D NMR spectroscopic data (including NOEs) of Warmers and König (1999) if the ring carbon signals are assigned as follows (C_6D_6 solvent data; changed assignments in bold type): δ 44.7 (C-1), 41.2 (**C-2/10**), 31.0 (**C-3**), 139.0 (C-4), 52.4 (C-5), 30.2 (**C-6**), 124.1 (**C-7**), 136.1 (C-8), 30.0 (**C-9**), 40.2 (**C-10/2**). Examination of the ^{13}C NMR spectral data of Marcos et al. (1995) on several analogs of dauc-7- and dauc-8-enes shows that these reassignments are in good accord with the proposed structure. It is particularly significant that all *trans*-dauc-8-enes have a C-6 signal around $\delta \sim 24$, while the two *trans*-dauc-7-ene analogs have $\delta \sim 30$, very close to the value for the *B. trilobata* sesquiterpene.

To substantiate the assumed 1*S* absolute stereochemistry of **5** from *C. leylandii*, the hydrocarbon was hydrogenated over Pd/C using the conditions of Warmers and König (1999) and the products compared with the hydrogenation products of authentic (−)-isodaucene **2**. Two monounsaturated and two saturated compounds were produced from each starting material, and the mixtures were qualitatively identical by GC–MS and enantioselective GC.

GC–MS examination of the foliar terpenes of a number of specimens of the *C. leylandii* parent species *C. macrocarpa* and *C. nootkatensis* showed no trace of **1**–**5**. This implies that although the relevant cyclase gene must be carried by one of the parents, it is apparently silent. Why this is so and how the biosynthetic pathway is activated in the hybrid are intriguing questions that remain to be answered.

Sesquiterpenes **1**–**5** are also absent from 17 other *Cupressus* species we have examined, but our recent work on the California endemic *C. macnabiana* A. Murr.—a tree supposedly rather distantly related to *C. macrocarpa* within the genus—has revealed the same compounds, in similar proportions, in some individuals (K. Jiang et al., unpublished data).

3. Experimental

3.1. Plant material

Foliage of ×*Cupressocyparis leylandii* was collected from several horticultural specimens in Pismo Beach, CA (December 1997). *Rosa rugosa* leaves were collected from a horticultural specimen in Berkeley, CA in March 2000.

3.2. Sesquiterpene isolation and purification

Hydrodistillation (from satd NaCl with $NaHCO_3$) of the LN_2-ground *C. leylandii* foliage (ca. 2 kg); LC of the oil (silica gel; hexane–EtOAc eluents); prep. GC and FTIR of purified **1** were as described before (Kim et al., 1994). Before LC most of the monoterpenes were removed by evaporation under N_2 flow at ca. 100 °C. The hydrocarbon fraction from LC was then separated by repeated complexation LC on 20% $AgNO_3/SiO_2$ using hexane–EtOAc or hexane–benzene gradients. Final purification of **1**–**4** was by prep. GC on a Carbowax 20M column, 160 °C; **5** required an additional purification step on an SE-30 column (185 °C).

Fresh *R. rugosa* leaves were extracted whole with *n*-pentane. The extract was passed through silica gel to isolate a hydrocarbon fraction for GC–MS and enantioselective GC analysis.

Enantioselective GC was by splitless (0.7 min) injection of the relevant compound or fraction, with *n*-hexadecane as internal retention time standard, on a 10% permethyl-β-cyclodextrin/90% OV-1701 WCOT capillary column, 0.25 mm i.d. × 30 m. Injector 180 °C, column temperature program: 60 °C (0.7 min), 30 °C min^{-1} to 90 °C, 1 °C min^{-1} to 135 °C. Kovats indices were determined by r.t. comparison with *n*-alkanes analysed with the same temperature program.

3.2.1. (+)-Dauca-5,8-diene (*1*)

Oil; $[\alpha]_D^{22}$ +100 °C (*n*-hexane; *c* 1.6). IR ν_{max}^{KBr} cm^{-1}: 2956, 2874, 1463, 1449, 1414, 1383, 1374, 1366, 1136, 1057, 929, 766, 715.

3.2.2. (+?)-Dauca-4(11),8-diene, (3aS,8aS)-3-isopropylidene-6,8a-dimethyl-1,2,3,3a,4,5,8,8a-octahydroazulene (*5*)

Oil; $[\alpha]_D^{22} > +40$ °C (*n*-hexane; $c < 0.1$); EIHRMS: $[M]^+$ *m/z* 204.18769 (calcd for $C_{15}H_{24}$, 204.18780); GC–MS 70 eV, *m/z* (rel.int.): 204 $[M]^+$ (22), 189 $[M–Me]^+$ (2), 161 (18), 148 (3), 136 (100), 133 (10), 121 (60), 119 (10), 107 (17), 105 (15), 93 (19), 91 (18), 79 (12), 77 (11), 55 (10), 41 (22); ^1H NMR (499.9 MHz, C_6D_6, δ from TMS): 0.98 (3H, *s*, H-15), 1.42 (1H, *ddd*, *J* = 11.6, 11.3, 9.0 Hz, H-2b), 1.53 (1H, *ddd*, *J* = 11.6, 7.5, ~1 Hz, H-2a), 1.58 (1H, *dddd*, *J* = 13.7, 12.1, 11.7, 2.6 Hz, H-6a), 1.77 (3H, *br s*, H-12), 1.85 (3H, *br q*, *J* = 1.7 Hz, H-13), 1.88 (3H, *br s*, H-14), 2.11 (1H, *ddd*, *J* = 14.7, 5.2, 2.6 Hz, H-7a), 2.15 (1H, *br d*, *J* ~ 15 Hz, H-10a), 2.20 (1H, *dd*, *J* = 15.1, 8.1 Hz, H-10b), 2.18–2.25 (1H, *br m*, H-7b), 2.25–2.32 (1H, *br m*, H-5), 2.28–2.35 (1H, *br m*, H-3a), 2.33–2.36 (1H, *m*, H-6b), 2.39–2.47 (1H, *br m*, H-3b), 5.59 (1H, *br m*, H-9). ^{13}C NMR (125.7 MHz, C_6D_6, δ from TMS): 19.0 (*q*, C-15), 20.4 (*q*, C-13), 23.2 (*q*, C-12), 25.1 (*t*, C-6), 27.1 (*q*, C-14), 29.6 (*t*, C-3), 34.4 (*t*, C-7), 40.3 (*t*, C-2), 41.4 (*t*, C-10), 42.5 (*s*, C-1), 57.5 (*d*, C-5), 121.9 (*s*, C-11), 122.7 (*d*, C-9), 138.0 (*s*, C-4/8), 138.1 (s, C-8/4); multiplicities by DEPT and HMQC.

Acknowledgements

Thanks to Dr. Clayton Heathcock for helpful discussions of NMR spectroscopic data and for reviewing the manuscript, and to Dr. Robert P. Adams and M. Joseph Casanova for sending samples of carrot seed oil and components. Special thanks to Dr. Donald J. Bowler for invaluable help with the 2D NMR experiments. *Deo gratias*.

References

Bohlmann, F., Zdero, C., 1982. Glaucolides and other constituents from South African *Vernonia* species. Phytochemistry 21, 2263–2267.

Bohlmann, F., Ludwig, G.W., Jakupovic, J., King, R.M., Robinson, H., 1983. A daucanolide from *Ageratum fastigiatum*. Phytochemistry 22, 983–986.

Cassidy, M.P., Ghisalberti, E.L., 1993. New terpene hydrocarbons from the sponge *Higginsia* sp. J. Nat. Prod 56, 1190–1193.

Castro, V., Jakupovic, J., Bohlmann, F., 1984. A new type of sesquiterpene and acorane derivative from *Calea prunifolia*. J. Nat. Prod 47, 802–808.

Dallimore, W., Jackson, A.B., 1948. A Handbook of Coniferae Including Gingkoaceae. Edward Arnold Ltd, London.

Ghisalberti, E.L., 1994. The daucane (carotane) class of sesquiterpenes. Phytochemistry 37, 597–623.

Hashidoko, Y., Tahara, S., Mizutani, J., 1992. Sesquiterpene hydrocarbons in glandular trichome exudate of *Rosa rugosa* leaves. Z. Naturforsch 47c, 353–359.

Kim, Y.-K., Cool, L.G., Zavarin, E., 1994. *cis*-Calamenene-related sesquiterpenoids from *Cupressus bakeri* foliage. Phytochemistry 36, 961–965.

Marcos, I.S., Oliva, I.M., Díez, P.B., Lithgow, A.M., Moro, R.F., Narciso, M.G., Urones, J.G., 1995. Approach to the synthesis of diterpenes with the bicyclo[5. 3.0]decane system: (±) 10-*epi*-tormesol. Tetrahedron 51, 12403–12416.

Mardarowicz, M., Cisowski, W., Krauze-Baranowska, M., Migas, P., 1999. Chemical composition of Leyland cypress essential oil. J. Essent. Oil Res. 11, 9–12.

Mazzoni, V., Tomi, F., Casanova, J., 1999. A daucane-type sesquiterpene from *Daucus carota* seed oil. Flavour Fragr. J. 14, 268–272.
Seto, H., Fujimoto, Y., Tatsuno, T., Yoshioka, H., 1985. Synthetic studies on carotane and dolastane type terpenes: a new entry to the total synthesis of (±)-daucene via intramolecular [2 + 2] photocycloaddition. Synth. Comm. 15, 1217–1224.
Warmers, U., König, W.A., 1999. Sesquiterpene constituents of the liverwort *Bazzania trilobata*. Phytochemistry 52, 99–104.

PERGAMON

Phytochemistry 58 (2001) 973–980

PHYTOCHEMISTRY

www.elsevier.com/locate/phytochem

Synthesis and bioactivity of natural and C-3 fluorinated biosynthetic precursors of 28-homobrassinolide

Lydia R. Galagovsky*, Eduardo G. Gros, Javier A. Ramírez

Departamento de Química Orgánica, Facultad de Ciencias Exactas y Naturales, Universidad de Buenos Aires, Pabellón 2, Ciudad Universitaria, 1428 Buenos Aires, Argentina

Received 24 April 2001; received in revised form 3 August 2001

Abstract

In this paper we describe the synthesis of two new fluorinated brassinosteroids: (22*R*,23*R*)-22,23-dihydroxy-3α-fluorostigmastan-6-one and (22*R*,23*R*)-22,23-dihydroxy-3β-fluorostigmastan-6-one. Their bioactivities were evaluated in the rice lamina inclination test and compared with that of 28-homocastasterone, 28-homotyphasterol and 28-homoteasterone, possible biosynthetic precursors of 28-homobrassinolide. Results confirmed expected similarities between the biosynthesis of 24-ethylbrassinosteroids (named as the 28-homo series) and that described for 24-methylbrassinosteroids, and also indicated that these precursors might exhibit per se activities. © 2001 Published by Elsevier Science Ltd.

Keywords: Brassinosteroids; Biosynthesis; C-3 Fluorinated analogs; Bioactivity; 28-Homobrassinolide

1. Introduction

Brassinosteroids have attracted considerable interest since 1979, when the isolation and structure determination of brassinolide (**1**) (see Fig. 1) was reported (Grove et al., 1979). Some brassinosteroids, including **1** and castasterone (**2**), display powerful plant growth-regulating activity at doses as low as 1 ng per individual plant (Grove et al., 1979; Cutler et al., 1991). Brassinosteroids are able to increase yield and stress resistance of a number of important crops (Sakurai et al., 1999; Khripach et al., 1999). Numerous studies of the chemistry and biology of brassinosteroids, as well as of their potential commercial applications, have been reported (Arteca, 1995). Some structural variations of active brassinosteroids involving the presence of a 24-ethyl group have also been reported. This 28-homo family of brassinosteroids is basically formed by 28-homobrassinolide (**3**), 28-homocastasterone (**4**), 28-homotyphasterol (**5**) and 28-homoteasterone (**6**) (see Fig. 1) which possess substantial bioactivity (Takatsuto and Ikekawa, 1984; Schmidt et al., 1993; Abe et al., 1995) and have been widely employed in field trials (Cutler et al., 1991) because of their greater synthetic accessibility compared to **1**.

Many studies have been devoted in establishing the biosynthetic pathway to natural brassinosteroids. The most important features of this pathway were deduced from biochemical studies using cultured cells administered labelled compounds (Fujioka and Sakurai, 1997; Sakurai and Fujioka, 1997), but the discovery of brassinosteroid-deficient mutants provided new experimental methodologies. Genetic, molecular and biochemical studies on these mutants confirmed the proposed pathways, and also gave the molecular basis for this biosynthesis (Sakurai et al., 1999). Fig. 2 shows the last steps of the well established early C6-oxidation pathway (Fujioka et al., 1995). 3-Dehydroteasterone (**7**) (see Fig. 2) was found to be an intermediate in the reversible conversion between teasterone and typhasterol (Suzuki et al., 1995). This is a rather unusual equilibrium because it involves the transformation from a more stable equatorial 3β-alcohol into the axial less stable 3α-alcohol in typhasterol (Khripach et al., 1999). The bioactivity displayed in several bioassays by the biosynthetic intermediates shown in Fig. 2 was found to increase according to the position on the biosynthetic pathway (Fujioka et al., 1995). These results were explained by assuming that the precursors are transformed into the more active compounds in plant tissues during the bioassay; the closer the intermediate in the pathway to brassinolide, the greater is the exhibited activity (Suzuki et al., 1995).

* Corresponding author. Tel.: +54-11-4576-3346; fax: +54-11-4576-3385.

E-mail address: lyrgala@qo.fcen.uba.ar (L.R. Galagovsky).

0031-9422/01/$ - see front matter © 2001 Published by Elsevier Science Ltd.
PII: S0031-9422(01)00379-X

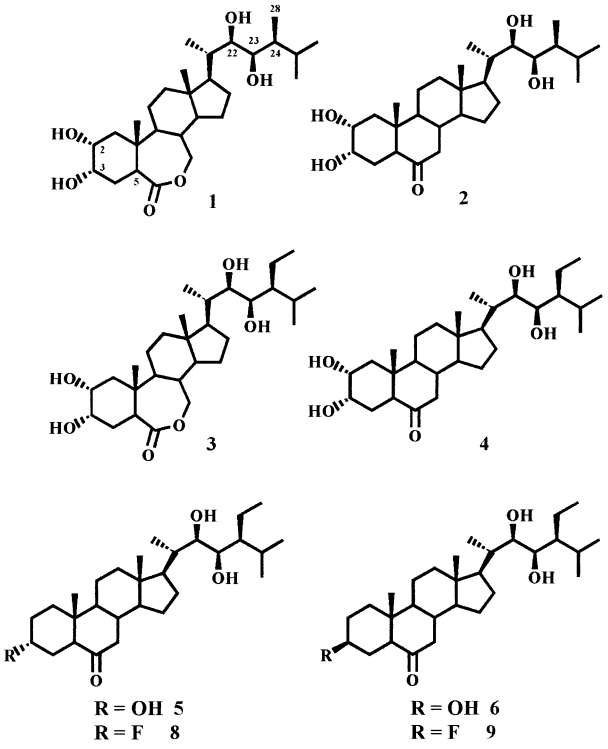

Fig. 1. Structures of various brassinosteroids.

28-Homobrassinosteroids may be biosynthesized from the corresponding plant steroid (sitosterol) through similar pathways to those of brassinolide, although no evidence for this has yet been reported (Sakurai, 1999). The presence of a C-3 fluorine in the A ring replacing the C-3 hydroxy group may alter its ability to go through the biosynthetic pathway, particularly in the case of a C-3β fluorine.

Our aim was to perform studies on the biosynthesis of 28-homobrassinosteroids. Thus, we have synthesized known compounds **3**–**6**, and two new analogs (22*R*,23*R*)-22,23-dihydroxy-3α-fluorostigmastan-6-one (**8**) and (22*R*, 23*R*)-22,23-dihydroxy-3β-fluorostigmastan-6-one (**9**), in which a fluorine atom replaces the 3-hydroxy group of the related natural compounds 28-homotyphasterol (**5**) and 28-homoteasterone (**6**), respectively (see Fig. 1).

Bioactivities were tested by the rice lamina inclination assay (Takeno and Pharis, 1982), using *Oriza sativa* L. cv Chui, a local rice cultivar.

2. Results and discussion

Syntheses of compounds **3**–**6** were performed as reported (Takatsuto and Ikekawa, 1984; Voigt et al., 1996; Teme Centurión et al., 1998).

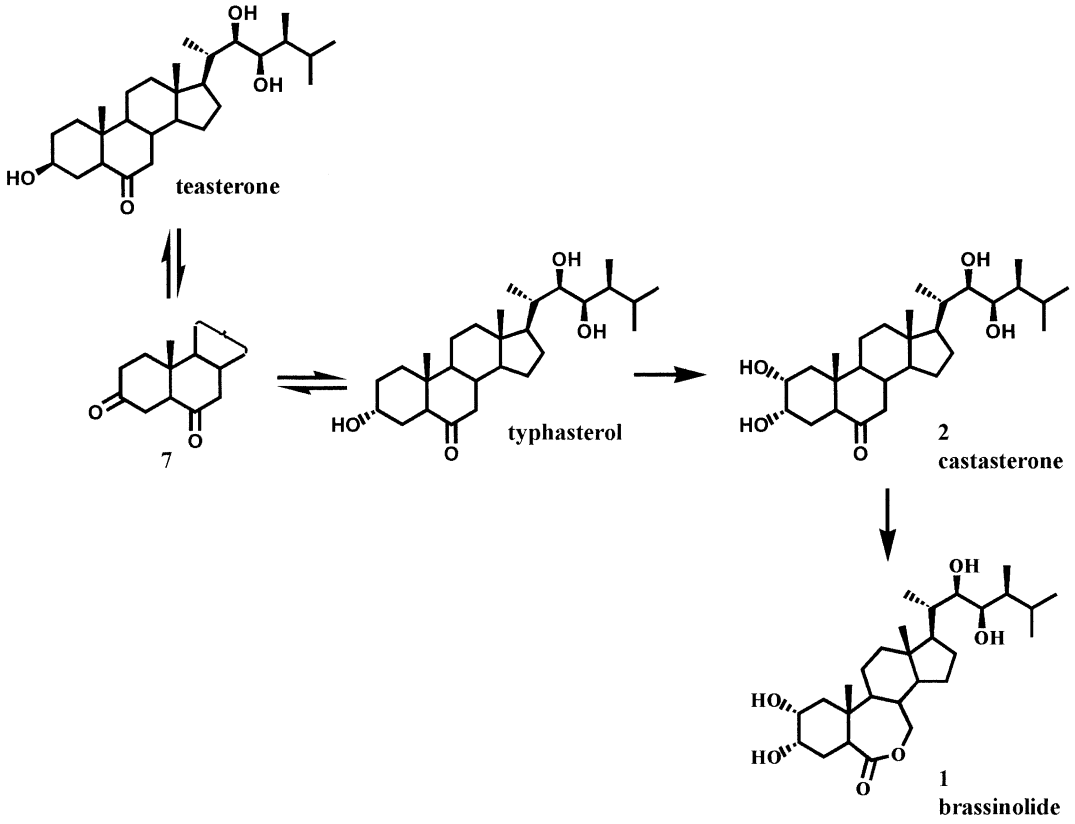

Fig. 2. Brassinosteroid biosynthesis: the early C6-oxidation pathway.

Reasons for replacing the hydroxyl groups of biological molecules by fluorine have been reviewed (Welch, 1987). Due to its high electronegativity, a fluorine atom should exert a similar polar effect as oxygen does and could act as an hydrogen bond acceptor as well. Furthermore, the van der Waals' radius of fluorine does not introduce any disturbance on the molecular geometry. Thus, compounds **8** and **9** might mimic 28-homotyphasterol (**5**) and 28-homoteasterone (**6**), respectively. However, the strong C–F bond usually prevents chemical reactions of the carbon attached to fluorine. Thus compound **9** would not be expected to produce downstream metabolites in the biosynthetic pathway considering that it cannot be dehydrogenated to a 28-homo analog of **7** (see Fig. 2). Selection of C-3 fluorinated analogs was also made on the basis of recent reports concerning interesting changes in bioactivity due to the introduction of fluorine in brassinosteroids analogs (Back et al., 1999; Ramírez et al., 2000).

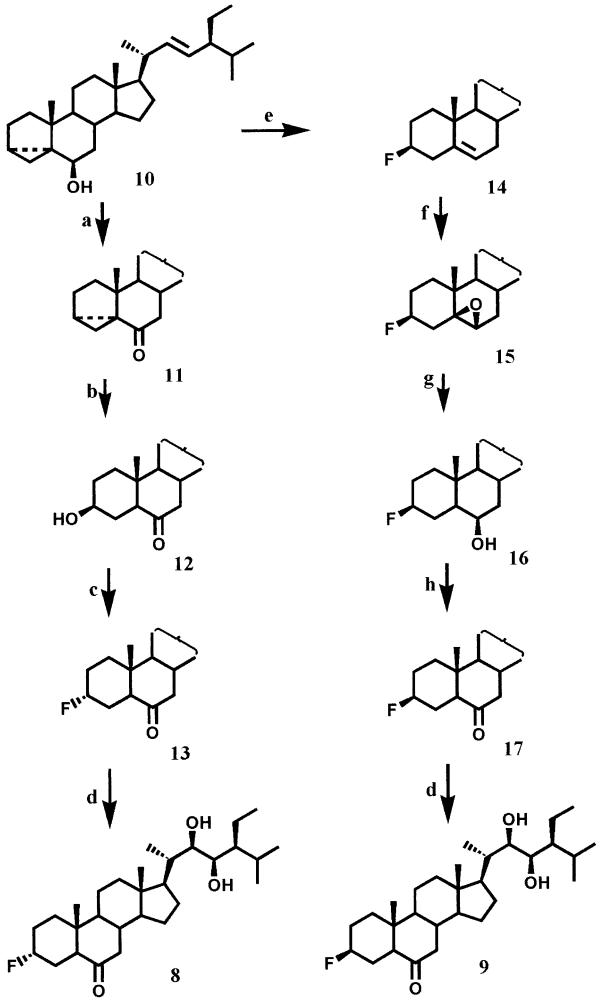

Scheme 1. Synthetic strategy to obtain fluorinated analogs **8** and **9**. Reagents and conditions: *a*: Jones reagent, acetone, 0 °C, 15 min. *b*: $HClO_4$, dioxane, H_2O, reflux, 1 h. *c*: DAST, CH_2Cl_2, −78 °C, 10 min. *d*: K_2OsO_4, $K_3Fe(CN)_6$, $(DHQD)_2Phal$, K_2CO_3, *t*-BuOH, H_2O, $CH_3SO_3NH_2$, r.t., 9 days. *e*: HF 48% aq, toluene, r.t., 1 h. *f*: $KMnO_4$, $Fe(NO_3)_3$, *t*-BuOH, H_2O, CH_2Cl_2, r.t., 2h. *g*: $NaBH_3CN$, $BF_3.Et_2O$, THF, reflux, 1 h. *h*: PCC, $HPy^+CF^3COO^-$, CH_2Cl_2, r.t., 15 min.

Synthesis of the fluorinated brassinosteroid analogs **8** and **9** is summarized in Scheme 1. Compound **11** was obtained in three steps following the described procedure by Wada and Marumo (1981). Hydrolytic cleavage of this 3α,5-cyclo-6-keto steroid with perchloric acid yielded compound **12**, which was subsequently fluorinated with diethylaminosulfurtrifluoride (DAST) (Rozen et al., 1979) to give compound **13**. The substitution of the 3β-hydroxy group, by a fluoride, proceeded with inversion of configuration according to the multiplicity pattern of the resulting 3β-H geminal to the fluoro group is evidencec assessed by ^1H NMR special analysis (see Table 1).

Osmium-catalyzed asymmetric dihydroxylation (Sharpless et al., 1992) (CAD) of the Δ^{22} double bond of **13** using $K_3Fe(CN)_6$ as cooxidant and hydroquinidine-1,4-phthalazinediyl diether [$(DHQD)_2$-PHAL] as chiral ligand gave, after purification, 38% yield of compound **8** (9% total yield from stigmasterol). CAD yields the diasteromeric 22S,23S isomer in a minor proportion (ratio 3:1), and more than 30% of the starting material, that could be recycled.

(22*E*)-3β-Fluorostigmasta-5,22-diene (**14**) was obtained as described (Ponce et al., 2000). Stereo and regioselective epoxidation of **14** with $KMnO_4/Fe(NO_3)_3$/*t*-BuOH gave compound **15** and reductive opening of the resulting 5β,6β epoxide with sodium cyanoborohydride gave compound **16**. Activation of the epoxide by complexion with boron trifluoride etherate as a Lewis acid (Hutchins et al., 1981) was required to ensure the attack of the hydride at the more substituted position. Subsequent oxidation of **16** with PCC to **17** followed by CAD gave compound **9** in 8% yield (from stigmasterol). Configurations at C-22 and C-23 were established by comparison with chemical shifts and coupling constants of closely related known compounds (Ando et al., 1993). The correct stereochemistry at C-5 in both compounds **8** and **9** was determined on the basis of coupling constants between the 5α-H and both 4α- and 4β-H in their ^1H NMR spectra.

All the proposed structures were verified by MS and NMR spectroscopic analyses. The presence of a fluorine in the A ring introduces additional complexity in both the ^1H and ^{13}C NMR spectra due to long-range coupling; these effects are a valuable source for structural information. Considering that an assignment of 3-fluoro steroids has not been previously reported, a complete analysis with DEPT-135, COSY-45, and HETCOR experiments was performed on these new analogs.

Table 1 details the NMR spectral description of the main positions of the 3-fluoro analogs **8** and **9**. Dose dependent bioactivities of compounds **3**, **4**, **5**, **6**, **8** and **9** were evaluated using the highly sensitive modified rice lamina inclination test (Table 2). Data are presented as

Table 1
^{1}H and ^{13}C NMR spectroscopic data for fluorinated brassinosteroid analogs[a]

Position	Compound **8**		Compound **9**	
	^{13}C shift	^{1}H shift	^{13}C shift	^{1}H shift
1	31.9	1α: 1.58 1β ≈1.60	36.0 $J_{C\text{-}F}=10.8$	1α: 1.22 1β : 1.82
2	26.3 $J_{C\text{-}F}=21.7$	2α: 1.93 2β: 1.60 $J_{H\text{-}F}$ ≈45	28.0 $J_{C\text{-}F}=17.9$	2α: 1.97 2β: 1.60
3	88.5 $J_{C\text{-}F}=167.1$	3β: 4.90 $J_{H\text{-}F}=47.8$	92.3 $J_{C\text{-}F}=174.1$	3α: 4.45 $J_{H\text{-}F}=48.9$
4	25.9 $J_{C\text{-}F}=21.4$	4α: 1.97 4β: 1.68 $J_{H\text{-}F}$ ≈45	27.2 $J_{C\text{-}F}=19.7$	4α: 2.05 $J_{H\text{-}F}$ ≈13 4β: 1.67
5	51.9	5α: 2.63 $J=12.8$ and 3.0	56.0 $J_{C\text{-}F}=10.8$	5α: 2.17 $J=12.6$
6	211.8	–	209.7	–
7	46.8	7α: 2.31 $J=13.0$ and 4.5 7β: 2.00	46.6	7α: 2.33 $J=13.2$ and 4.4 7β: 1.95
8	38.0	8β: 1.80	37.8	8β: 1.80
9	53.8	9α: 1.35	56.8	9α: 1.25
10	41.2	–	40.9	–
11	21.1	11α: 1.34 11β: 1.06	21.1	11α: 1.36 11β: 1.02
12	39.4	12α: 1.25 12β: 2.03	39.4	12α: 1.22 12β: 2.02
13	42.9	–	42.9	–
14	56.9	14α: 1.27	56.8	14α: 1.24
15	24.0	1.06 and 1.52	24.0	1.06 and 1.50
16	28.7	1.29 and 1.72	28.7	1.29 and 1.73
17	55.9	17α: 1.20	55.9	17α: 1.19
18	12.2	0.68	12.2	0.68
19	12.3	0.74	13.1	0.78

[a] ^{13}C and ^{1}H shifts are in ppm relative to TMS. J are in Hz.

Table 2
Rice lamina inclination test[a]

	Compounds					
Dose (ng/plant)	**3**	**4**	**5**	**6**	**8**	**9**
5	35±3[b]	30±2	24±4	10±2	10±1	11±1
50	90±4	84±5	72±8	25±6	34±8	23±4
500	101±4	97±4	77±8	60±6	86±6	38±8

[a] Values are angles (degrees) between the lamina and sheath, representing the means of 15–25 replicates.
[b] ± Standard error. Average angle of control: 11±2.

mean values with standard errors. Results showed, as expected, decreasing values when the upstream biosynthetic precursor was tested (see Fig. 1). Compounds **3** and **4** showed highest bioactivity at all doses tested. Biosynthetic precursors **5** and **6** were 20–40% less active than **3** and **4**, respectively, at the highest dose tested. This characteristic diminished for compound **5** and was maintained for compound **6**, at lower doses. Compounds **6**, **8** and **9** gave no significant response at 5 ng/plant.

Fluorinated compounds exhibited different behavior. Compound **8** showed a similar response to that of its naturally related compound **5**, at the highest dose, but was 50% less active at 50 ng/plant.

Compound **9** showed similarly low response at 50 ng/plant, but was 40% less active relative to its natural analog **6** at, the highest dose.

Visual inspection of the plant seedlings treated with the natural precursors **5** and **6** showed that in spite of the lower average response (Table 2) a significant number of seedlings exhibited a large response, typical for that of the most active compounds. This fact suggested that the statistical distribution of responses could be analyzed.

Fig. 3a–c shows the histogram for the pairs of compounds **3**–**4**, **5**–**8** and **6**–**9** at the highest tested dose, respectively. Top values of the bars of each histogram have been linked for clearer observation of the distribution profiles.

Fig. 3a shows the distribution displayed—which proved to be normal—for the more active compounds **3** and **4**. Highest frequency of angle values falls into the 91–120° interval. Fig. 3b shows the comparative profile of the distribution obtained for the natural compound **5** and its fluorinated analog **8**. Profiles elicit clear bimodal distributions. The most frequent angle values for compound **5** fall into the 61–90 and 121–150 ranges, and for the fluorinated analog **8**, the most frequent angles fall into the 31–60 and 91–120 ranges. This bimodal distribution may be interpreted as a partially overlapped two-phase response.

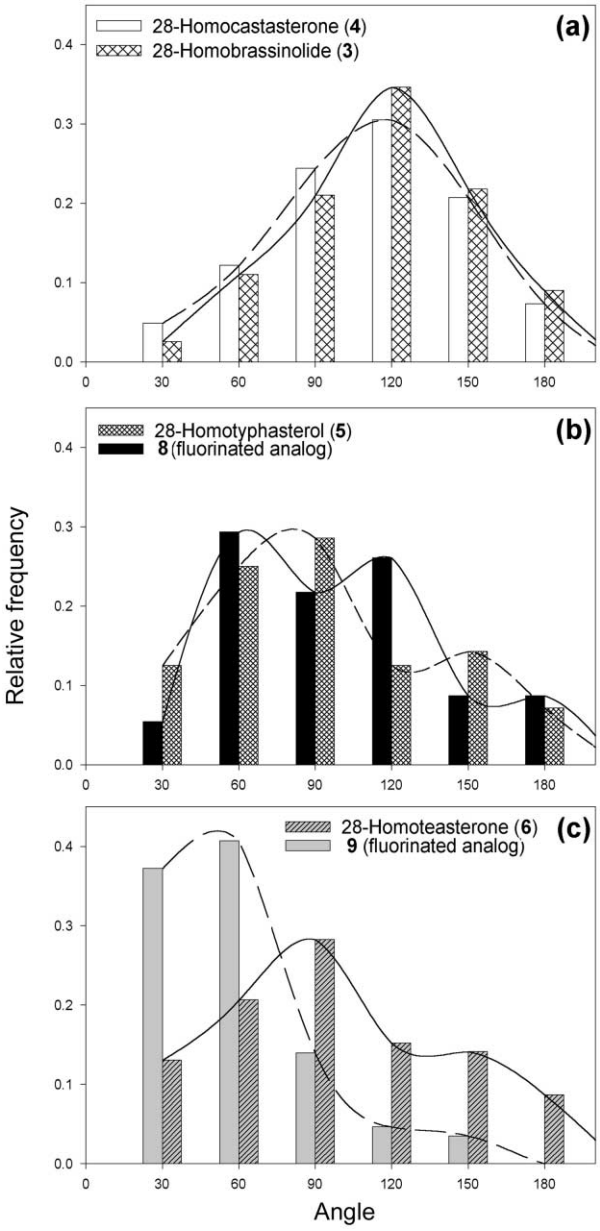

Fig. 3. Number of seedlings (relative to total number) vs. angle in the rice lamina inclination test.

Responses shown in Fig. 3c indicate a clear bimodal profile for the natural compound **6** with the most frequent angle values in the 61–90 and 121–150 ranges. On the other hand, fluorinated analog **9** shows a skewed distribution profile with the most frequent angle values in the 31–60 range. The presence of a fluorine atom in position 3β of compound **9** could have blocked its further biosynthetic transformation into a 3-keto intermediate, so that the bioactivity elicited could be assumed as a per se response and not due to downstream metabolites. This type of per se activity has been recently reported for non fluorinated analogs (Sung et al., 2000). On the other hand, the presence of a α-fluorine at C-3 in compound **8** seems not to interfere with further biotransformations. Considering these facts, it seems reasonable to assume that compounds **5**, **6** and **8** show a bimodal distribution due to an intrinsic bioactivity, partially overlapped with that due to further biosynthetic metabolites.

3. Conclusions

Along with the synthesis of known compounds **3**–**6**, two new C-3 fluorinated analogs of the natural 28-homobrassinosteroids, named (22*R*,23*R*)-22,23-dihydroxy-3α-fluorostigmastan-6-one (**8**) and (22*R*,23*R*)-22,23-dihydroxy-3β-fluorostigmastan-6-one (**9**) were prepared. Evaluation of the relative bioactivities of compounds **3**–**6** seems to indicate a similar biosynthetic pattern between the C-24 ethyl and the more abundant C-24 methyl brassinosteroids. Responses showed that the closer the intermediate in the biosynthetic pathway to 28-homobrassinolide, the more active it is.

Considering that compound **9** is not able to undergo further biosynthetic transformation during the bioassay, then the exhibited bioactivity indicates a per se activity which has an average value 60% lower than that of the most active compound. On the other hand, compounds **5**, **6** and **8**, elicite a larger average bioactivity due to intrinsic activity coupled with those of greater activity coming from more downstream biosynthetic metabolites produced during the bioassay.

Finally, the rice lamina inclination test, the most commonly used bioassay for evaluating the bioactivity of brassinosteroids, can mask information when the mean and the standard error is reported for compounds which do not show a normal response distribution.

4. Experimental

Melting points (mp) were determined on a Fisher Johns apparatus and are uncorrected. ^{1}H NMR and ^{13}C NMR spectra were recorded on a Brüker AM-500 at 500 MHz and at 125.1 MHz, respectively, chemical shifts (δ) are given in ppm downfield from TMS as the internal standard. ^{19}F-NMR spectra were recorded on a Bruker AM-500 at 470.4 MHz., chemical shifts (δ) are given in ppm upfield from CFCl3 as the internal standard. Coupling constant (J) values are in Hz. High-resolution mass spectra (EI and FAB) were obtained for all new compounds on a ZAB BEqQ instrument (VG-Micromass). FAB were obtained using NBA-Li as matrix. Low resolution mass spectra were recorded on a Shimadzu QP-5000 at 70 eV. Unless otherwise indicated, all solvents and reagents used were of commercial grade. Reactions were monitored by TLC on precoated plates with silica gel F254 0.2 mm (Merck). Column

chromatography was carried out on silica gel 60, 0.04–0.063 mm (Merck).

4.1. Rice lamina inclination test

Rice seedlings (*Oryza sativa*, cv Chui) were washed with ethanol (1 min) and water and were then left in water at 30 °C for two days (with a 16 h photoperiod). Germinated seeds were cultivated on agar under the same growing conditions for four days. Intact seedlings (4–5 cm long) were inoculated with 0.5 μl of the test compound solution (in ethanol) just under the 2nd leaf joint. After 48 h in the dark (at 30 °C), the magnitude of the induced angle between the leaf and the sheath was measured by using Bersoft Image Measurement™ (http://bersoft.com/bimagem/index.html).

4.2. Synthesis

4.2.1. (22E)-3α-Fluorostigmast-22-en-6-one (**13**)

A solution of (22*E*)-3β-hydroxystigmast-22-en-6-one (Wada and Marumo, 1981) (**12**) (430 mg, 1.00 mmol) in 18 ml of CH_2Cl_2 was slowly added to a solution of DAST (0.49 g, 3.04 mmol) in 3 ml of CH_2Cl_2 cooled to −78 °C. After 10 min the mixture was warmed to room temperature and poured into water, washed with $NaHCO_3$ and treated in the usual manner. Purification of the crude product by column chromatography (hexane/EtOAc 98:2) yielded 57% of **13**. Mp 156–157 °C. ^{1}H NMR: 0.68 (H-18, 3H, s), 0.73 (H-19, 3H, *s*), 0.79 (H-27, 3H, *d*, $J=6.5$ Hz), 0.81 (H-29, 3H, *t*, $J=7.4$ Hz), 0.85 (H-26, 3H, *d*, $J=6.3$ Hz), 1.02 (H-21, 3H, *d*, $J=6.7$ Hz), 2.31 (H-7α, 1H, *dd*, $J=13.0$ Hz, 4.5 Hz), 2.63 (H-5α, 1H, *dd*, $J=12.8$ Hz, 3.0 Hz), 5.02 (23-H, 1H, *dd*, $J=15.1$ Hz, 8.6 Hz), 4.90 (H-3β, 1H, double *m*, $J_{H,F}=48.3$ Hz), 5.15 (22-H, 1H, *dd*, $J=15.1$ Hz, 8.6 Hz). ^{13}C NMR: 12.2 (*q*, C-18), 12.2 (*q*, C-29), 12.3 (*q*, C-19), 18.9 (*q*, C-26), 21.1 (*t*, C-11), 21.1 (*q*, C-27), 21.2 (*q*, C-21), 24.0 (*t*, C-15), 25.4 (*t*, C-28), 25.9 (*dt*, C-4, $J_{C,F}=21.4$ Hz), 26.3 (*dt*, C-2, $J_{C,F}=21.7$ Hz), 28.7 (*t*, C-16), 31.7 (*d*, C-25), 31.9 (*t*, C-1), 38.0 (*d*, C-8), 39.4 (*t*, C-12), 40.4 (*d*, C-20), 41.2 (*s*, C-10), 42.9 (*s*, C-13), 46.8 (*t*, C-7), 51.2 (*d*, C-24), 51.9 (*d*, C-5), 53.8 (*d*, C-9), 55.9 (*d*, C-17), 56.9 (*d*, C-14), 88.5 (*dd*, C-3, $J_{C,F}=167.1$ Hz), 129.6 (*d*, C-23), 138.0 (*d*, C-22), 211.8 (*s*, C-6). ^{19}F NMR: −184.0 (m). MS (EI) *m*/*z* (rel. int.): 430 (M+, 8.1), 415 (1.0), 387 (6.3), 289 (13.3), 149 (40.9), 55 (100). HRMS (EI): calc. for $C_{29}H_{47}OF$: 430.3611, found: 430.3608.

4.2.2. (22R,23R)-22,23-Dihydroxy-3α-fluorostigmastan-6-one (**8**)

A mixture of **13** (180 mg, 0.42 mmol), *t*-butanol/water (1:1) (40 ml), $(DHQD)_2$–PHAL (390 mg, 0.21 mmol), methansulfonamide (190 mg, 0.84 mmol), potassium ferricyanide (1.9 g, 2.51 mmol), potassium carbonate (828 mg, 42 mmol), and potassium osmate dihydrate (15 mg, 0.04 mmol) was stirred at room temperature for 9 days. An excess of $NaHSO_3$ was added until no evolution of bubbles was observed. Layers were separated and the aqueous phase was thoroughly extracted with CH_2Cl_2/MeOH (95:5). Combined organic layers were washed with 0.25 M H_2SO_4 and 2% NaOH. Purification by column chromatography (CH_2Cl_2/acetonitrile gradient) separated (22*R*,23*R*)-22,23-dihydroxy-3α-fluorostigmastan-6-one from its 22S, 23*S* diasteromer, with 38% yield. Mp 201–202 °C. ^{1}H NMR: 0.68 (H-18, 3H, *s*), 0.73 (H-19, 3H, *s*), 0.91 (H-21, 3H, *d*, $J=6.8$ Hz), 0.92–0.99 (H-26, H-27 and H-29, 9H, m), 2.31 (H-7α, 1H, *dd*, $J=12.9$ Hz, 4.4 Hz), 2.63 (H-5α, 1H, *dd*, $J=12.9$ Hz, 3.0 Hz), 3.58 (H-22, 1H, *dd*, $J=8.4$ Hz, 1.3 Hz), 3.71 (H-23, 1H, *dd*, $J=8.4$ Hz, 1.3 Hz), 4.90 (H-3β, 1H, *double m*, $J_{H,F}=48.3$ Hz). ^{13}C NMR: 12.0 (*q*, C-21), 12.2 (*q*, C-18), 12.3 (*q*, C-19), 13.8 (*q*, C-29), 19.1 (*t*, C-28), 19.6 (*q*, C-26), 21.1 (*t*, C-11), 21.3 (*q*, C-27), 24.0 (*t*, C-15), 25.9 (*dt*, C-4, $J_{C,F}=21.5$ Hz), 26.3 (*dt*, C-2, $J_{C,F}=21.6$ Hz), 28.7 (*t*, C-16), 29.2 (*d*, C-25), 31.9 (*t*, C-1), 37.2 (*d*, C-20), 38.0 (*d*, C-8), 39.4 (*t*, C-12), 41.2 (*s*, C-10), 42.9 (*s*, C-13), 46.7 (*d*, C-24), 46.8 (*t*, C-7), 51.9 (*d*, C-5), 53.8 (*d*, C-9), 55.9 (*d*, C-17), 56.9 (*d*, C-14), 72.6 (*d*, C-23), 74.5 (*d*, C-22), 88.5 (*dd*, C-3, $J_{C,F}=167.2$ Hz), 211.8 (*s*, C-6). ^{19}F NMR: −184.0 (*m*). MS (FAB) *m*/*z* (rel. int.): 471.3 (87) $[M+Li]^+$, 294.0 (19). HRMS (FAB): calc. for $C_{29}H_{47}OFLi$ $(M+Li)^+$: 471.3826, found: 471.3811.

4.2.3. (22E)-5β,6β-Epoxy-3β-fluorostigmast-22-ene (**15**)

A mixture of potassium permanganate (1.1 g, 6.96 mmol) and ferric nitrate nonahydrate (0.55 g, 1.36 mmol) was ground to a fine powder and water (0.4 ml) was added. To a stirred suspension of this mixture in CH_2Cl_2 (20 ml), (22*E*)-3β-fluorostigmasta-5,22-diene (**14**) (Ponce et al., 2000) (0.9 g, 2.17 mmol) and *t*-butanol (2 ml) were added. After 2 h at room temperature the reaction was completed and the product was separated from the inorganic residue by adding Et_2O (20 ml), stirring for 5 min and filtering through Celite. After evaporation of the solvent, the crude product was purified by column chromatography (hexane/EtOAc 97:3) yielding **15** (72%). Mp 130 °C. ^{1}H NMR: 0.66 (H-18, 3H, *s*), 0.79 (H-27, 3H, *d*, $J=6.5$ Hz), 0.81 (H-29, 3H, *t*, $J=7.4$ Hz), 0.85 (H-26, 3H, *d*, $J=6.3$ Hz), 1.01 (H-19, 3H, *s*), 1.02 (H-21, 3H, *d*, $J=6.7$ Hz), 3.03 (H-6α, 1H, *d*, $J=2.1$ Hz), 4.57 (H-3α, 1H, *double m*, $J_{H,F}=49.5$ Hz), 5.02 (H-23, 1H, *dd*, $J=15.1$ Hz, 8.6 Hz), 5.15 (H-22, 1H, *dd*, $J=15.1$ Hz, 8.6 Hz). ^{13}C NMR: 11.9 (*q*, C-18), 12.2 (*q*, C-29), 17.0 (*q*, C-19), 18.8 (*q*, C-26), 21.1 (*t*, C-11), 21.1 (*q*, C-21), 21.1 (*q*, C-27), 24.2 (*t*, C-15), 25.4 (*t*, C-28), 27.8 (*dt*, C-2, $J_{C,F}=21.0$ Hz), 28.8 (*t*, C-16), 29.6 (*d*, C-8), 31.6 (*d*, C-25), 32.4 (*t*, C-7), 34.7 (*dt*, C-4, $J_{C,F}=21.1$ Hz), 35.4 (*s*, C-10), 38.7 (*dt*, C-1, $J_{C,F}=10.1$

Hz), 39.6 (*t*, C-12), 40.3 (*d*, C-20), 41.9 (*s*, C-13), 50.6 (*d*, C-9), 51.2 (*d*, C-24), 56.0 (*d*, C-17), 56.3 (*d*, C-14), 62.0 (*d*, C-5, $J_{C,F}=15.0$ Hz, 63.1 (*d*, C-6), 90.0 (*dd*, C-3, $J_{C,F}=170.1$ Hz), 129.7 (*d*, C-23), 138.0 (*d*, C-22). ^{19}F NMR: −171.3 (m). MS (EI) *m/z* (rel. int.): 430 (M+, 7.6), 413 (4.3), 387 (4.0), 369 (12.3), 289 (15.1), 43 (100). HRMS (EI): calc. $C_{29}H_{47}OF$: 430.3611, found: 430.3611.

4.2.4. (22E)-3β-Fluoro-6β-hydroxystigmast-22-ene (16)

A solution of the epoxide **15** (170 mg, 0.39 mmol), $NaBH_3CN$ (85 mg, 1.35 mmol), and a small quantity of bromocresol green indicator in 10 ml of dry THF was stirred, while BF_3–OEt_2 in a few ml of THF was added dropwise until a color change to yellow was noted, and stirring was continued under N_2 atmosphere at reflux for 1 h. Upon completion, the reaction was diluted with NaCl (satd. soln.) and extracted with ether. After the solution was dried (Na_2SO_4), the solvent was removed under reduced pressure. The residue was purified by column chromatography (hexane/EtOAc 95:5) to yield **16** in 80%. Mp 136 °C. ^1H NMR: 0.71 (H-18, 3H, *s*), 0.79 (H-27, 3H, *d*, $J=6.5$ Hz), 0.81 (H-29, 3H, *t*, $J=7.4$ Hz), 0.85 (H-26, 3H, *d*, $J=6.3$ Hz), 1.01 (H-19, 3H, *s*), 1.02 (H-21, 3H, *d*, $J=6.7$ Hz), 3.80 (H-6α, 1H, *d*, $J=2.5$ Hz), 4.52 (H-3α, 1H, *double* m, $J_{H,F}=49.3$ Hz), 5.02 (H-23, 1H, *dd*, $J=15.1$ Hz, 8.6 Hz), 5.15 (H-22, 1H, *dd*, $J=15.1$ Hz, 8.6 Hz). ^{13}C NMR: 12.1 (*q*, C-29), 12.3 (*q*, C-18), 15.7 (*q*, C-19), 18.9 (*q*, C-26), 21.0 (*q*, C-27), 21.2 (*t*, C-11), 21.2 (*q*, C-21), 24.3 (*t*, C-15), 25.4 (*t*, C-28), 28.9 (*t*, C-16), 31.7 (*d*, C-25), 31.8 (*d*, C-8), 28.5 (*dt*, C-2, $J_{C,F}=19.0$ Hz), 35.4 (*s*, C-10), 32.4 (*dt*, C-4, $J_{C,F}=18.0$ Hz), 37.8 (*dt*, C-1, $J_{C,F}=12.0$ Hz), 39.6 (*t*, C-7), 39.8 (*t*, C-12), 40.4 (*d*, C-20), 42.6 (*s*, C-13), 46.7 (*dt*, C-5, $J_{C,F}=9.5$ Hz), 51.2 (*d*, C-24), 54.1 (*d*, C-9), 56.0 (*d*, C-17), 56.8 (*d*, C-14), 71.8 (*d*, C-6), 93.1 (*dd*, C-3, $J_{C,F}=172.5$ Hz), 129.6 (*d*, C-23), 138.0 (*d*, C-22). ^{19}F NMR: −169.5 (m). MS (EI) *m/z* (rel. int.): 432 (M^+, 29.7), 417 (2.8), 371 (21.3), 275 (30.0), 55 (100). HRMS (EI): calc. for $C_{29}H_{49}OF$: 432.3767, found: 432.3761.

4.2.5. (22E)-3β-Fluorostigmast-22-en-6-one (17)

A solution of compound **16** (210 mg, 0.49 mmol) in CH_2Cl_2 (25 ml) was treated with pyridinium chlorochromate (109 mg, 0.51 mmol) and pyridinium trifluoroacetate (30 mg, 0.155 mmol). The mixture was stirred for 15 min at room temperature and then filtered through Celite, and the solution evaporated under reduced pressure. After chromatographic purification of the crude product (hexane/EtOAc 97:3), compound **17** was isolated in 92% yield. Mp 146–147 °C. ^1H NMR: 0.71 (H-18, 3H, *s*), 0.78 (H-19, 3H, *s*), 0.79 (H-27, 3H, *d*, $J=6.5$ Hz), 0.81 (H-29, 3H, *t*, $J=7.4$ Hz), 0.85 (H-26, 3H, *d*, $J=6.3$ Hz), 1.02 (H-21, 3H, *d*, $J=6.5$ Hz), 2.17 (H-5α, 1H, *d*, $J=12.6$, Hz), 2.33 (H-7α, 1H, *dd*, $J=13.2$, 4.4 Hz), 4.46 (H-3α, 1H, double *m*, $J_{H,F}=48.5$ Hz), 5.02 (H-23, 1H, *dd*, $J=15.1$ Hz, 8.6 Hz), 5.15 (H-22, 1H, *dd*, $J=15.1$ Hz, 8.6 Hz). ^{13}C NMR: 12.1 (*q*, C-29), 12.2 (*q*, C-18), 13.1 (*q*, C-19), 18.8 (*q*, C-26), 21.1 (*t*, C-11), 21.1 (*q*, C-27), 21.2 (*q*, C-21), 24.0 (*t*, C-15), 25.4 (*t*, C-28), 27.2 (*dt*, C-4, $J_{C,F}=19.7$ Hz), 28.0 (*t*, C-2, $J_{C,F}=17.9$ Hz), 28.7 (*t*, C-16), 31.7 (*d*, C-25), 36.0 (*t*, C-1, $J_{C,F}=10.8$ Hz), 37.8 (*t*, C-8), 39.4 (*t*, C-12), 40.4 (*d*, C-20), 40.9 (*s*, C-10), 42.9 (*s*, C-13), 46.6 (*t*, C-7), 51.2 (*d*, C-24), 55.9 (*d*, C-17), 56.0 (*dd*, C-5, $J_{C,F}=10.8$ Hz), 56.8 (*d*, C-9), 56.8 (*d*, C-14), 92.3 (*dd*, C-3, $J_{C,F}=174.1$ Hz), 129.7 (*d*, C-23), 138.1 (*d*, C-22), 209.7 (*s*, C-6). ^{19}F NMR: −172.6 (m). MS (EI) *m/z* (rel. int.):430 (M^+, 3.2), 415 (0.6), 387 (2.4), 318 (4.5), 289 (5.5), 44 (100). HRMS (EI): calc. for $C_{29}H_{47}OF$: 430.3611, found: 430.3605.

4.2.6. (22R,23R)-22,23-Dihydroxy-3β-fluorostigmastan-6-one (9)

Compound **17** (180 mg, 0.42 mmol) was treated similarly to compound **13**. After chromatographic purification of the crude product (hexane/EtOAc 85:15), compound **9** was isolated in 31% yield. Mp 198 °C. ^1H NMR: 0.68 (H-18, 3H, *s*), 0.78 (H-19, 3H, *s*), 0.91 (H-21, 3H, *d*, $J=6.8$ Hz), 0.92–0.99 (H-26, H-27 and H-29, 9H, *m*), 2.17 (H-5α, 1H, *d*, $J=12.6$ Hz), 2.33 (H-7α, 1H, *dd*, $J=13.2$, 4.4 Hz), 3.58 (H-22, 1H, *dd*, $J=8.4$ Hz, 1.3 Hz), 3.71 (H-23, 1H, *dd*, $J=8.4$ Hz, 1.3 Hz), 4.45 (H-3α, 1H, double m, $J_{H,F}=48.9$ Hz). ^{13}C NMR: 12.0 (*q*, C-21), 12.2 (*q*, C-18), 13.1 (*q*, C-19), 13.8 (*q*, C-29), 19.1 (*t*, C-28), 19.6 (*q*, C-26), 21.1 (*t*, C-11), 21.3 (*q*, C-27), 24.0 (*t*, C-15), 27.2 (*dt*, C-4, $J_{C,F}=19.7$ Hz), 28.0 (*dt*, C-2, $J_{C,F}=18.0$ Hz), 28.7 (*t*, C-16), 29.3 (*d*, C-25), 36.1 (*t*, C-1, $J_{C,F}=10.5$ Hz), 37.2 (*d*, C-20), 37.8 (*d*, C-8), 39.4 (*t*, C-12), 40.8 (*s*, C-10), 42.9 (*s*, C-13), 46.7 (*t*, C-7), 46.7 (*d*, C-24), 55.8 (*d*, C-17), 56.1 (*dd*, C-5, $J_{C,F}=10.9$ Hz), 56.8 (*d*, C-9), 56.9 (*d*, C-14), 72.5 (*d*, C-23), 74.4 (*d*, C-22), 92.2 (*dd*, C-3, $J_{C,F}=174.0$ Hz), 209.6 (*s*, C-6). ^{19}F NMR: −172.6 (m). MS (FAB) *m/z* (rel. int.): 471.3 (100) M+Li, 397.3 (29), 294.0 (20). HRMS (FAB): calc. for $C_{29}H_{47}OFLi$ $(M+Li)^+$: 471.3826, found: 471.3816.

Acknowledgements

We thank the University of Buenos Aires for financial support and UMYMFOR (CONICET-FCEN) for spectroscopic determinations. High resolution and FAB mass spectrometry was provided by the Washington University Mass Spectrometry Resource, an NIH Research Resource (Grant No. P41RR00954).

References

Abe, H., Takatsuto, S., Nakayama, M., Yokota, T., 1995. 28-Homotyphasterol, a new natural brassinosteroid from rice (*Oryza sativa* L.) bran. Biosci. Biotech. Biochem. 52 (2), 176–178.

Ando, T., Aburatani, M., Koseki, N., Asakawa, S., Mouri, T., Abe, H., 1993. ^{13}C NMR assignment of brassinosteroids by two-dimensional techniques. Magn. Reson. Chem. 31, 94–99.

Arteca, R.N., 1995. Brassinosteroids. In: Davies, P.J. (Ed.), Plant Hormones. Kluwer Academic, The Netherlands, pp. 206–213.

Back, T.G., Janzen, L., Nakajima, S.K., Pharis, R.P., 1999. Synthesis and biological activity of 25-methoxy-, 25-fluoro-, and 25-azabrassinolide and 25-fluorocastasterone: surprising effects of heteroatom substituents at C-25. J. Org. Chem. 64 (15), 5494–5498.

Cutler, H.G., Yokota, T., Adam, G., (Eds.), 1991. Brassinosteroids: Chemistry, Bioactivity and Applications. ACS Symp. Series 474. American Chemical Society, Washington, DC.

Fujioka, S., Inoue, T., Takatsuto, S., Yanagisawa, T., Yokota, T., Sakurai, A., 1995. Biological activity of biosynthetical-related congeners of brassinolide. Biosci. Biotech. Biochem. 59 (10), 1973–1975.

Fujioka, S., Sakurai, A., 1997. Biosynthesis and metabolism of brassinosteroids. Physiol. Plant 100, 710–715.

Grove, M.D., Spencer, G.F., Rohwedder, W.K., Mandava, N., Worley, J.F., Warthen Jr., J.D., Steffens, G.L., Flippen-Anderson, J.L., Cook Jr., J.C., 1979. Brassinolide, a plant growth-promoting steroid isolated from *Brassica napus* pollen. Nature 281, 216.

Hutchins, R.O., Taffer, I.M., Burgoyne, W., 1981. Regio and stereoselective cleavage of epoxides with cyanoborohydride and boron trifluoride etherate. J. Org. Chem. 46, 5214–5215.

Khripach, V.A., Zhabinskii, V.N., de Groot, A.E. (Eds.), 1999. Brassinosteroids: A New Class of Plant Hormones. Academic Press, San Diego.

Ponce, M.A., Ramírez, J.A., Galagovsky, L.R., Gros, E.G., Erra-Balsells, R., 2000. Singlet-oxygen ene reaction with 3β-substituted stigmastanes. An alternative pathway for the classical Schenck rearrangement. J. Chem. Soc. Perkin Trans. 2, 2351–2357.

Ramirez, J.A., Gros, E.G., Galagovsky, L.R., 2000. Effects on bioactivity due to C-5 heteroatom substituents on synthetic 28-homobrassinosteroid analogs. Tetrahedron 56, 6171–6180.

Rozen, S., Faust, Y., Ben-Yakov, H., 1979. A new method for fluorination of steroids. Tetrahedron Lett. 20, 1823–1826.

Sakurai, A., Fujioka, S., 1997. Studies on biosynthesis of brassinosteroids. Biosci. Biotech. Biochem. 61, 757–762.

Sakurai, A., 1999. Brassinosteroid biosynthesis. Plant Physiol. Biochem. 37 (5), 351–361.

Sakurai, A., Yokota, T., Clouse, S. D. (Eds.), 1999. Brassinosteroids: Steroidal Plant Hormones. Springler, Tokyo.

Schmidt, J., Yokota, T., Spengler, B., Adam, G., 1993. 28-Homoteasterone, a naturally occurring brassinosteroid from seeds of *Raphanus sativus*. Phytochemistry 34 (2), 391–392.

Sharpless, K.B., Amberg, W., Bennani, Y.L., 1992. The osmium-catalyzed asymmetric dihydroxilation: a new ligand class and a process improvement. J. Org. Chem. 57, 2768–2771.

Sung, C.Y., Janzen, L., Pharis, R.P., Back, T.G., 2000. Synthesis and bioactivity of 6α- and 6β-hydroxy analogues of castasterone. Phytochemistry 55, 121–126.

Suzuki, H., Fujioka, S., Takatsuto, S., Yokota, T., Murofushi, N., Sakurai, A., 1995. Biosynthesis of brassinosteroids in seedlings of *Catharantus roseus*, *Nicotiana tabacum*, and *Oryza sativa*. Biosci. Biotech. Biochem. 59 (10), 168–172.

Takatsuto, S., Ikekawa, N., 1984. Synthesis and activity of plant growth-promoting steroids, (22*R*,23*R*,24*S*)-28-homobrassinosteroids, with modifications in rings A and B. J. Chem. Soc. Perkin Trans. 1, 439–447.

Takeno, K., Pharis, R.P., 1982. Brassinosteroid-induced bending of the leaf lamina of dwarf rice seedlings: an auxin-mediated phenomenon. Plant Cell Physiol 23, 1275–1281.

Teme Centurión, O.M., Galagovsky, L.R., 1998. Alternative synthesis of (24S)-homoethylcastasterone from stigmasterol. An. Assoc. Quím. Argent. 86 (3–6), 104–109.

Voigt, B., Schmidt, J., Adam, G., 1996. Synthesis of 24-epiteasterone, 24-epityphasterol and their B-homo-6a-oxalactones from ergosterol. Tetrahedron 52, 1997–2004.

Wada, K., Marumo, S., 1981. Synthesis and plant-promoting activity of brassinolide analogs. Agric. Biol. Chem. 45 (11), 2579–2585.

Welch, J.T., 1987. Advances in the preparation of biologically active organofluorine compounds. Tetrahedron 43, 3123–3197.

PERGAMON

Phytochemistry 58 (2001) 981–985

PHYTOCHEMISTRY

www.elsevier.com/locate/phytochem

Cysteine sulfoxide derivatives in *Petiveria alliacea*

Roman Kubec, Rabi A. Musah*

Department of Chemistry, State University of New York at Albany, Albany, NY, 12222, USA

Received 9 March 2001; received in revised form 19 June 2001

Abstract

Two diastereomers of *S*-benzyl-L-cysteine sulfoxide have been isolated from fresh roots of *Petiveria alliacea*. Their structures and absolute configurations have been determined by NMR, MALDI-HRMS, IR and CD spectroscopy and confirmed by comparison with authentic compounds. Both the R_S and S_S diastereomers of the sulfoxide are present in all parts of the plant (root, stem, and leaves) with the latter diastereomer being predominant. Their total content greatly varied in different parts of the plant between 0.07 and 2.97 mg g^{-1} fr. wt, being by far the highest in the root. *S*-Benzylcysteine has also been detected in trace amounts (<10 μg g^{-1} fr. wt) in all parts of the plant. This represents the first report of the presence of *S*-benzylcysteine derivatives in nature. © 2001 Elsevier Science Ltd. All rights reserved.

Keywords: *Petiveria alliacea*; Phytolaccaceae, *S*-Benzylcysteine sulfoxide; Petiveriin; *S*-Benzylcysteine; Flavor precursor

1. Introduction

Petiveria alliacea L. (family Phytolaccaceae) is a perennial shrub indigenous to the Amazon Rainforest and widely distributed in other areas including tropical America, the Caribbean, Africa, Sri Lanka, and the southeastern Unites States. It is known by many names among which "anamu", "apacin", "guiné", "pipi", "tipi", and "garlic guinea henweed" are noteworthy. It has commonly been used in folk medicine and various preparations made from this plant are considered to have antiinflammatory, antimicrobial, antispasmodic, diuretic, and stimulant effects, among others.

The presence in *P. alliacea* of several volatile compounds, most of them containing a benzyl or phenyl moiety has been reported. Whereas Szczepanski et al. (1972) identified benzyl-2-hydroxyethyl trisulfide, Adegosan (1974) found *cis*-3,5-diphenyl-1,2,4-trithiolan (trithiolaniacin), benzaldehyde, benzoic acid, elemental sulfur, and *trans*-stilbene. Sousa et al. (1990) isolated dibenzyl trisulfide and Ayedoun et al. (1998) observed benzaldehyde, benzyl alcohol, *cis*- and *trans*-stilbenes, benzyl benzoate, dibenzyl disulfide, and dibenzyl trisulfide in the root oil.

The present paper describes our investigations on isolation and identification of non-volatile precursors of the above mentioned compounds.

2. Results and discussion

Two abundant constituents of an amino acid fraction from the roots of *Petiveria alliacea* were isolated by ion-exchange chromatography and prep. HPLC as white crystalline solids. Their NMR, IR, and UV spectra as well as their chromatographic behavior were very similar. The ^1H and ^{13}C NMR spectra revealed that both compounds are α-amino acids containing an unsubstituted benzyl moiety and two pairs of heterosteric methylene protons. The IR spectra contained a very strong absorption band near 1020 cm^{-1}, indicating the presence of a sulfoxide group. The MALDI-HRMS data showed m/z $[M]^+$ of 227.0616 and 227.0626, respectively, corresponding to a molecular formula of $C_{10}H_{13}NO_3S$ for both compounds (req. 227.0616). In accordance with the above data, the two amino acids were identified as diastereomers of *S*-benzylcysteine sulfoxide.

There are two chiral centers in *S*-benzylcysteine sulfoxide (the sulfur and α-carbon atoms) and thus four stereoisomers exist. All of them were synthesized and their absolute configurations were determined by NMR and CD spectrometry. The CD spectra of corresponding

* Corresponding author. Tel.: +1-518-437-3740; fax: +1-518-437-3741.

E-mail address: musah@csc.albany.edu (R.A. Musah).

0031-9422/01/$ - see front matter © 2001 Elsevier Science Ltd. All rights reserved.
PII: S0031-9422(01)00304-1

diastereomers were almost mirror images, consisting of a single maximum around 224 nm (Fig. 1). Unfortunately, when strongly perturbing groups are present around the sulfur atom (e.g. alkylthio, allyl, benzyl), CD spectrometry cannot be used to directly determine the absolute configuration of sulfoxides (Axelrod et al., 1968; Ottenheijm et al., 1981). However, the diastereomers of all *S*-substituted cysteine sulfoxides display ^{1}H NMR spectra with a characteristic ABX pattern for the S(O)CH_2CH(NH_2) methylene protons. The isomers with both the amino group and the oxygen atom on the same side of the molecule show two distinct doublets of doublets at $\sim\delta$ 3.25 ($J_{AX} = \sim 7$–8.5 Hz) and δ 3.50 ($J_{BX} = \sim 5.5$–7 Hz), respectively. On the other hand, the methylene protons of derivatives with the opposite configuration typically resonate in the much narrower region of $\sim\delta$ 3.30–3.45 with the coupling constants of $J_{AX} = \sim 3.5$–4 Hz and $J_{BX} = \sim 8.5$–10.5 Hz. The coupling constants J_{AB} are similar for both diastereomers ($\sim$13.5–14 Hz) (Kuttan et al., 1974; Broek et al., 1987; Kubota et al., 1998). Employing this rule, the absolute configuration of all synthesized derivatives was unambiguously determined. Furthermore, the specific rotation values of the corresponding antipodes were nearly opposite, confirming the correct structural assignment. Along with NMR, CD spectrometry and polarimetry were also employed to determine the absolute configuration of the compounds isolated from the root of *P. alliacea*. The CD spectrum of the first eluting isomer showed a positive sign of the Cotton effect ($\Delta\varepsilon_{max}$ +12.7 at 222 nm) and a specific rotation of $[\alpha]_D^{22}$ +31°. The second isomer gave a CD spectrum with a negative sign of the Cotton effect ($\Delta\varepsilon_{max}$−14.6 at 224 nm) and a specific rotation of $[\alpha]_D^{22}$ −55°. On the basis of the above data and together with their other spectroscopic and chromatographic characteristics, the absolute configuration of the isolated amino acids were determined as (R_CR_S)-*S*-benzyl-L-cysteine sulfoxide (**1a**) and (R_CS_S)-*S*-benzyl-L-cysteine sulfoxide (**1b**), respectively. In close analogy to alliin (*S*-allylcysteine sulfoxide) and other related *S*-alk(en)ylcysteine sulfoxides, the new amino acids have trivially been named petiveriin A (the dextrorotary R_CR_S isomer, **1a**) and petiveriin B (the levorotary R_CS_S isomer, **1b**).

Aliphatic *S*-substituted cysteine sulfoxides have been isolated from various plants, fungi, and algae. They occur almost exclusively in the R_CS_S configuration (e.g. in *Allium* and *Brassica* species). So far, there are only two known *S*-substituted cysteine derivatives in which both diastereomeric forms have been found to occur in nature. (R_CR_S)-*S*-(*trans*-1-Propenyl)cysteine sulfoxide is widely distributed in onion and other alliaceous species, whereas its (R_CS_S) diastereomer was identified in *Santalum album* L. (in the form of a γ-glutamyl dipeptide; Kuttan et al., 1974). Similarly, (R_CS_S)-*S*-(methylthiomethyl) cysteine sulfoxide was found in *Marasmius* species (Gmelin et al., 1976; Broek et al., 1987) and the corresponding (R_CR_S) diastereomer has recently been isolated from *Scorodocarpus borneensis* Becc. (Kubota et al., 1998). However, the presence in a plant of both diastereomers has not been reported thus far. Using pure synthetic diastereomers, we have observed that the cysteine sulfoxides are not interconvertible under the conditions

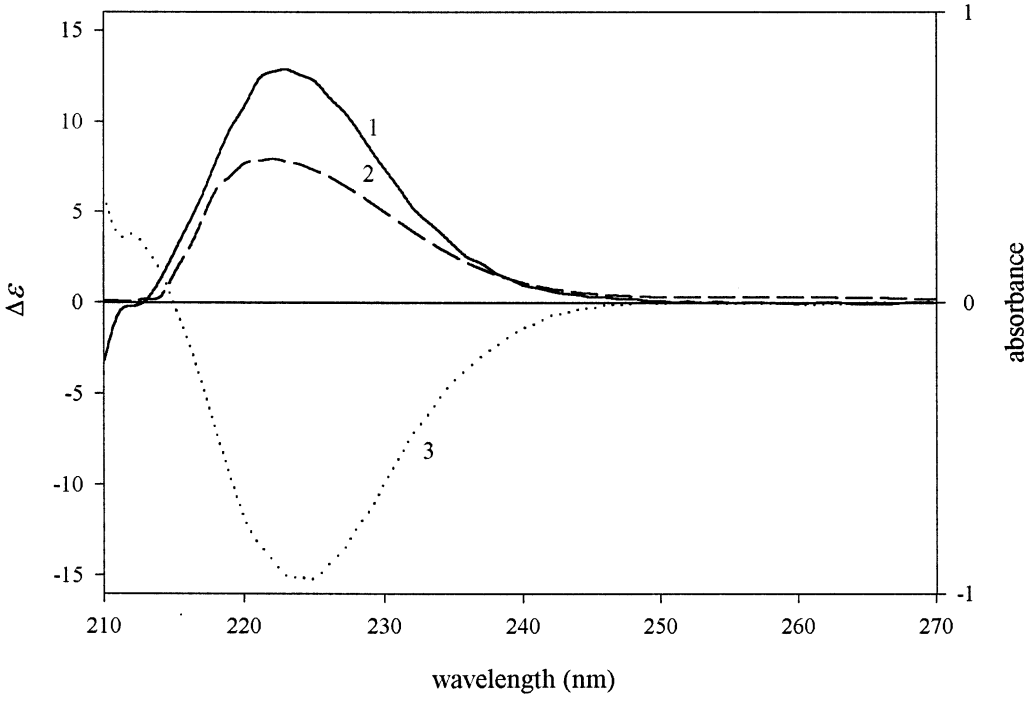

Fig. 1. The CD and UV spectra of petiveriin A (1 and 2, respectively) and the CD spectrum of petiveriin B (3).

used during extraction and isolation of the compounds (e.g. refluxing in MeOH for 20 min). Thus, they are not artifacts arising during isolation and they are naturally present in the tissue. To our knowledge, **1a** and **1b** are the first naturally occurring *S*-benzyl cysteine derivatives to be observed and the first naturally occurring aromatic *S*-substituted cysteines to be reported. In view of the presence of these aromatic cysteine derivatives, it appears likely that some aliphatic cysteine sulfoxide derivatives analogous to those observed in garlic, onion and other alliaceous plants may also be present in the *P. alliacea*.

S-Benzyl-L-cysteine, a presumable biochemical precursor of petiveriin, has also been detected in all parts of the plant. However, due to its very low content (<10 μg g^{-1} fr. wt) it could not be isolated in sufficient quantity to confirm its structure by spectroscopic methods. Identification was made by comparing its chromatographic behavior (TLC and HPLC) with that observed for *S*-benzyl-L-cysteine obtained from laboratory synthesis (Fig. 2).

The total content of both *S*-benzylcysteine sulfoxide diastereomers has been determined in different parts of the plant (root, stem, and leaves) by HPLC. As shown in Table 1, the content ranges between 0.07 and 2.97 mg g^{-1} fr. wt, being the highest in the root. Interestingly, it was observed that not only the total content but also the relative amounts of petiveriin A and B vary significantly from 40:60 in the root to 22:78 in the leaves and 12:88 in the stem. However, the content of *S*-substituted cysteine derivatives depends on many factors including soil composition, climate, harvest date etc. (Fenwick and Hanley, 1985; Block, 1992). Thus, it can be assumed that the content of petiveriin is dependent on such factors and may vary considerably in plants growing in different areas.

Further research on *P. alliacea* is still being conducted in our laboratory. Our preliminary data indicate that both petiveriin A and B serve as non-volatile precursors of the phenyl/benzyl-containing volatile compounds

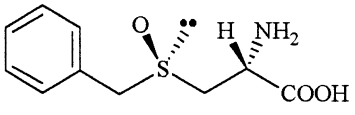

1a, petiveriin A

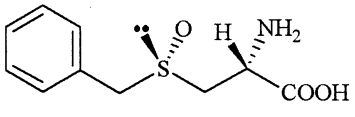

1b, petiveriin B

Fig. 2. The structure of petiveriin A and petiveriin B.

Table 1
The total content and relative ratios of *S*-benzylcysteine sulfoxides in different parts of *P. alliacea*

Tissue analyzed	mg g^{-1} fr. wt	**1a:1b**
Root	2.97±0.16	40:60
Stem	0.29±0.03	12:88
Leaves	0.07±0.01	22:78

previously found in this plant. We propose that these amino acids are enzymatically cleaved to give *S*-benzyl phenylmethanethiosulfinate in a fashion similar to that observed in the formation of allicin (diallyl thiosulfinate) and other thiosulfinates in *Allium* species (Stoll and Seebeck, 1949; Block, 1992). Our results also indicate that the vast majority of the volatiles that have so far been identified in extracts of *P. alliacea* are not present in a fresh tissue. They are, in fact, only degradation products generated during isolation procedures from labile *S*-benzyl phenylmethanethiosulfinate (Kice et al., 1960; Furukawa et al., 1973; White and Dellinger, 1985; Block, 1992).

3. Experimental

3.1. General experimental procedures

^{1}H and ^{13}C NMR spectra were recorded on a Varian Gemini 300 HC spectrometer, and IR spectra were recorded using a Perkin Elmer RX I FTIR spectrometer. UV spectra were measured on a Shimadzu UV-1601PC spectrophotometer and CD spectra on an Aviv 62DS circular dichroism spectrometer. Specific rotation values were determined by means of a Perkin-Elmer 243B polarimeter. HPLC separations were performed on a Dynamax SD-200 binary pump system, employing a Varian PDA 330 detector, a C-18 reverse phase column (Rainin Microsorb-MV 100 Å, 250×4.6 mm, 5 μm), using 10 mM KH_2PO_4 buffer (solv. A, pH 7.0) with MeCN (solv. B) as the mobile phase, with a flow rate of 1 ml min^{-1}. The gradient was as follows: A/B 100/0 (0 min), 95/5 (in 20 min), 60/40 (in 30 min) held for 15 min. Alternatively, a preparative C-18 reverse phase column (Rainin Dynamax-100 Å, 250×21.4 mm, 8 μm) was used. TLC was performed on precoated Aldrich plastic plates (silica gel polyester) with *n*-BuOH–H_2O–HOAc (4:1:1 v/v/v) or *n*-PrOH–H_2O (7:3 v/v/v) as the mobile phase. Ninhydrin (0.2% soln. in ethanol) was used for detection. Melting points (uncorr.) were determined using a Köfler hot stage.

3.2. Plant material

Whole fresh plants of *Petiveria alliacea* were obtained from Native Habitat Landscaping, FL, USA. They were

collected in Vero Beach, Indian River County, FL, USA in October 2000, immediately shipped, and stored in the freezer at −30 °C until analysis. A voucher specimen is deposited in the herbarium PIHG at the Florida Department of Agriculture and Consumer Services, Division of Plant Industry, Gainesville, FL, USA under the number 7801.

3.3. Extraction and purification

Fresh roots (69.0 g) were carefully cleaned and homogenized in MeOH using a blender, and extracted with boiling MeOH (2×600 ml). The extracts were combined, concentrated to ca. 400 ml by vacuum evaporation (40 °C), and adjusted to 500 ml by addition of 3% HCl. The precipitate that appeared on acidification was filtered off and the filtrate was passed through a cation-exchange column (19×2.1 cm; Amberlite 200, H^+ form, 20–50 mesh). After washing the column with 3% HCl (300 ml) and H_2O (300 ml), the amino acid fraction was eluted with 500 ml of 1 M NH_4OH. The yellow eluent obtained was concentrated to ca. 20 ml and subjected to prep. HPLC. The fractions eluting at 18.1 and 18.9 min were collected, evaporated, and the residues re-crystallized from boiling H_2O to yield 24 and 29 mg of white crystalline **1a** and **1b**, respectively.

3.4. Quantitative determination

Extracts were prepared from each part of the plant (leaves, stem, and root) as described above. These were analyzed by HPLC without derivatization. *S*-(4-Chlorobenzyl)cysteine, added to the samples before extraction, was used as an internal standard. At least three analyses of each extract were done. Calibration curves were computed using solutions prepared from the synthetic diastereomers of *S*-benzyl-L-cysteine sulfoxide (**1a** and **1b**).

3.5. Reference compounds

S-Benzylcysteine, *S*-(4-chlorobenzyl)cysteine (internal standard) and *S*-benzylcysteine sulfoxide were synthesized as described by Stoll and Seebeck (1949). Pure diastereomers of *S*-benzylcysteine sulfoxide were obtained by repeated fractional re-crystallization (H_2O–Me_2CO–HOAc 70:30:1 v/v/v) and by prep. HPLC.

(R$_C$R$_S$)-S-Benzyl-L-cysteine sulfoxide (**1a**, petiveriin A): small white plates; mp 172–173 °C; $[\alpha]_D^{22}$ +34° (1 M NaOH; *c* 1.0); CD $\Delta\varepsilon_{max}$ (0.1 M NaOH; *c* 0.2; 22 °C): +12.9 (223 nm); UV λ_{max} (0.1 M NaOH) nm (log ε): 220 (4.05), 259 (2.65); IR (KBr) ν_{max} cm^{-1}: 3463 (*w, br*), 3040–2900 (*s, br*), 1633 (*vs*), 1594 (*vs*), 1424 (*s*), 1359 (*s*), 1307 (*m*), 1071 (*s*), 1019 (*vs*), 696 (*s*); ^{1}H NMR (300 MHz; CD_3OD/DCl; DSS): δ 3.36 (1H, *dd*, *J* = 3.6, 14.4 Hz, H-3a), 3.46 (1H, *dd*, *J* = 8.4, 14.4 Hz, H-3b), 4.25 (1H, *d*, *J* = 13.2 Hz, H-5a), 4.37 (1H, *d*, *J* = 13.2 Hz, H-5b), 4.57 (1H, *dd*, *J* = 3.6, 8.4 Hz, H-2), 7.367.43 (5H, *m*, H_{arom}); ^{13}C NMR (75 MHz; CD_3OD/DCl; DSS): δ 49.6 (C-2), 49.7 (C-3), 58.9 (C-5), 129.8 (C-9), 130.0 (C-8), 130.8 (C-6), 131.6 (C-7), 169.7 (C-1); TLC R_f 0.50 (*n*-BuOH–H_2O–HOAc, 4:1:1), R_f 0.69 (*n*-PrOH–H_2O, 7:3). *ms* (M+)m/t: 227.0616 calc. for C_{10} H_{13} NO_3S: 227.0616.

(R$_C$S$_S$)-S-Benzyl-L-cysteine sulfoxide (**1b**, petiveriin B): long tiny white needles; mp 166–168 °C): $[\alpha]_D^{22}$ −59° (1 M NaOH; *c* 1.0); CD $\Delta\varepsilon_{max}$ (0.1 M NaOH; *c* 0.2; 22 °C): −15.1 (225 nm); UV λ_{max} (0.1 M NaOH) nm (log ε): 220 (3.98), 259 (2.60); IR (KBr) ν_{max} cm^{-1}: 3423 (*s, br*), 3040–2900 (*m, br*), 1664 (*vs*), 1590 (*s*), 1521 (*s*), 1425 (*m*), 1351 (*m*), 1299 (*m*), 1273 (*m*), 1071 (*m*), 1017 (vs), 696 (*m*); ^{1}H NMR (300 MHz; CD_3OD/DCl; DSS): δ 3.22 (1H, *dd*, *J* = 6.9, 13.5 Hz, H-3a), 3.51 (1H, *dd*, *J* = 6.7, 13.5 Hz, H-3b), 4.18 (1H, *d*, *J* = 13.2 Hz, H-5a), 4.38 (1H, *d*, *J* = 13.2 Hz, H-5b), 4.52 (1H, *t*, *J* = 6.8 Hz, H-2), 7.377.43 (5H, *m*, H_{arom}); ^{13}C NMR (75 MHz; CD_3OD/DCl; DSS): δ 50.5 (C-2), 50.7 (C-3), 59.6 (C-5), 129.7 (C-9), 130.0 (C-8), 130.8 (C-6), 131.6 (C-7), 169.5 (C-1); TLC: identical with **1a**. *ms*(M^+) *m*/*z*: 227.0626. Calc. for C_{16} H_{13} NO_3S: 227.0616

(S$_C$S$_S$)-S-Benzyl-D-cysteine sulfoxide (**1c**): small white plates; mp 173–174 °C; $[\alpha]_D^{22}$: −33° (1 M NaOH; *c* 1.0); CD $\Delta\varepsilon_{max}$ (0.1 M NaOH; *c* 0.2; 22 °C): −12.7 (223 nm); UV λ_{max} (0.1 M NaOH) nm (log ε): 220 (4.06), 259 (2.58); IR (KBr): identical with 1a; ^{1}H NMR (300 MHz; CD_3OD/DCl; DSS): δ 3.35 (1H, *dd*, *J* = 3.9, 14.7 Hz, H-3a), 3.42 (1H, *dd*, *J* = 8.1, 14.7 Hz, H-3b), 4.24 (1H, *d*, *J* = 12.9 Hz, H-5a), 4.35 (1H, *d*, *J* = 12.9 Hz, H-5b), 4.56 (1H, *dd*, *J* = 3.9, 8.1 Hz, H-2), 7.37–7.43 (5H, *m*, H_{arom}); ^{13}C NMR (75 MHz; CD_3OD/DCl; DSS): δ 49.6 (C-2), 49.7 (C-3), 58.9 (C-5), 129.8 (C-9), 130.1 (C-8), 130.8 (C-6), 131.6 (C-7), 169.7 (C-1); TLC: identical with **1a**.

(S$_C$R$_S$)-S-Benzyl-D-cysteine sulfoxide (**1d**): long tiny white needles; mp 165–167 °C; $[\alpha]_D^{22}$: +54° (1 M NaOH; *c* 1.0); CD $\Delta\varepsilon_{max}$ (0.1 M NaOH; *c* 0.2; 22 °C): +11.2 (224 nm); UV λ_{max} (0.1 M NaOH) nm (log ε): 220 (3.98), 259 (2.60); IR (KBr): identical with **1b**; ^{1}H NMR (300 MHz; CD_3OD/DCl; DSS): δ 3.20 (1H, *dd*, *J* = 6.9, 13.5 Hz, H-3a), 3.51 (1H, *dd*, *J* = 6.7, 13.5 Hz, H-3b), 4.17 (1H, *d*, *J* = 13.1 Hz, H-5a), 4.38 (1H, *d*, *J* = 13.1 Hz, H-5b), 4.52 (1H, *t*, *J* = 6.8 Hz, H-2), 7.36–7.42 (5H, *m*, H_{arom}); ^{13}C NMR (75 MHz; CD_3OD/DCl; DSS): δ 50.4 (C-2), 50.7 (C-3), 59.6 (C-5), 129.7 (C-9), 130.0 (C-8), 130.9 (C-6), 131.7 (C-7), 169.5 (C-1); TLC: identical with **1a**.

Acknowledgements

The authors would like to thank Dr. Eric Block for helpful discussions and critical reading of the manuscript. Support for this work was provided by the State University of New York at Albany.

References

Adesogan, E.K., 1974. Trithiolaniacin, a novel trithiolan from *Petiveria alliacea*. J. Chem. Soc. Chem. Commun. 21, 906–907.

Axelrod, M., Bickart, P., Goldstein, M.L., Green, M.M., Kjær, A., Mislow, K., 1968. Absolute configuration and optical rotatory dispersion of methyl alkyl sulfoxides. Tetrahedron Lett. 29, 3249–3252.

Ayedoun, M.A., Moudachirou, M., Sossou, P.V., Garneau, F.-X., Gagnon, H., Jean, F.-I., 1998. Volatile constituents of the root oil of *Petiveria alliacea* L. from Benin. J. Essent. Oil Res. 10, 645–646.

Block, E., 1992. The organosulfur chemistry of the genus *Allium*-implications for the organic chemistry of sulfur. Angew. Chem., Int. Ed. Engl. 31, 1135–1178.

Broek, L.A.G.M., Breuer, M.L., Liskamp, R.M.J., Ottenheijm, H.C.J., 1987. Total synthesis and absolute configuration of the natural dipeptide γ-glutamylmarasmine. J. Org. Chem. 52, 1511–1517.

Fenwick, G.R., Hanley, A.B., 1985. The genus *Allium*—part 2. Crit. Rev. Food Sci. Nutr. 22, 273–377.

Furukawa, M., Tsuiji, S., Kojima, Y., Hayashi, S., 1973. The reaction of benzyl phenylmethanethiosulfinate with amines. Chem. Pharm. Bull. 21, 2391–2395.

Gmelin, R., Luxa, H.-H., Roth, K., Höfle, G., 1976. Dipeptide precursor of garlic odour in *Marasmius* species. Phytochemistry 15, 1717–1721.

Kice, J.L., Parham, F.M., Simons, R.M., 1960. The thermal decomposition of thiosulfonates. J. Am. Chem. Soc. 82, 834–842.

Kubota, K., Hirayama, H., Sato, Y., Kobayashi, A., Sugawara, F., 1998. Amino acid precursors of the garlic-like odour in *Scorodocarpus borneensis*. Phytochemistry 49, 99–102.

Kuttan, R., Nair, F.G., Radhakrishnan, A.N., Spande, T.F., Yeh, H.J., Witkop, B., 1974. The isolation and characterization of γ-glutamyl-*S*-(*trans*-1-propenyl)-L-cysteine sulfoxide from sandal (*Santalum album* L). An interesting occurrence of sulfoxide diastereoisomers in nature. Biochemistry 13, 4394–4400.

Ottenheijm, H.C.J., Liskamp, R.M.J., Helquist, P., Lauher, J.W., Shekhani, M.S., 1981. Absolute configuration of sparsomycin. A chiroptical study of sulfoxides. J. Am. Chem. Soc. 103, 1720–1723.

Sousa, J.R., Demuner, A.J., Pinheiro, J.A., Breitmaier, E., Cassels, B.K., 1990. Dibenzyl trisulphide and *trans*-*N*-methyl-4-methoxyproline from *Petiveria alliacea*. Phytochemistry 29, 3653–3655.

Stoll, A., Seebeck, E., 1949. Über die Spezifität der Alliinase und die Synthese mehrerer dem Alliin verwandter Verbindungen. Helv. Chim. Acta 32, 866–876.

Szczepanski, C., Zgorzelak, P., Hoyer, G.-A., 1972. Isolierung, Strukturaufklärung und Synthese einer antimikrobiell wirksamen Substanz aus *Petiveria alliacea* L. Arzneim.-Forsch. 22, 1975–1976.

White, R.C., Dellinger, D., 1985. Photolysis of benzyl toluene-α-thiosulphonate. J. Chem. Res. S 64–65.

PERGAMON

Phytochemistry 58 (2001) 987–988

PHYTOCHEMISTRY

www.elsevier.com/locate/phytochem

Book reviews

Sage: The Genus *Salvia*

S.E. Kintzios (Ed.); Harwood Academic Publishers, Amsterdam, 2000, 296 pp., ISBN 90-5823-005-8, £73

This multi-author book is volume 14 of the series *Medicinal and Aromatic Plants—Industrial Profiles*. This is a very timely and interesting wide ranging review of the genus *Salvia*. The genus has been attracting a lot of renewed interest with several companies and academic groups trying to show therapeutic effects to support claims for benefits in, for example, treating CNS disorders.

The volume is divided into sections covering the botany, chemical constituents, cultivation and breeding, pharmacology, biotechnology, commercial aspects and bibliographic information sources. There are 20 chapters with nearly half concerned primarily with aspects of the chemistry, folklore and therapeutic activity.

Chapter 1 starts with a list of the approximately 400 species. Although, for some reason, authorities are used sporadically in the list, nonetheless it contains interesting information on folk uses of certain species and in particular cosmetic uses. The chapters in general have a lot of detail for the specialist, e.g. Li on the chemistry of salvianolic acids and Korousou et al. on the botany of Greek sage species.

The review of the pharmacology by Baricevic and Bartol is particularly good, covering a wide range of activities and modes of action and is very well referenced and written in a manner suitable for both the specialist and non-specialist. Research on the anti-hypertensive properties of Dan-Shen and the active chemical is described in some detail.

The section on biotechnology includes a chapter by Isabelle Hippolyte on cell culture as a way of producing rosmarinic acid which can be obtained in 36% dry weight yields.

All in all, this is a good reference book on Sage knowledge to date and will be a good introduction to new workers on the genus or people interested in herbal medicines in general who want to understand the modes of action and biology of the plants.

Robert J. Nash
Institute of Grassland and Environmental Research
Plas Gogerddan, Aberystwyth
Ceredigion, Wales, 5723 3EB, UK

PII: S0031-9422(01)00339-9

Ginkgo biloba

T.A. van Beek (Ed.), Vol. 12 in the series Medicinal and Aromatic Plants—Industrial Profiles; Harwood Academic Publishers, Amsterdam, The Netherlands, 2000, 548 pp., ISBN 90-5702-488-8, £79 or $126

Several books have already appeared on this fascinating tree of Chinese origin which has become over the last 10 years one of the most widely used herbal medicines. The interest in Ginkgo and in its constituents is still growing after several studies and clinical trials demonstrated its potential in the treatment of Alzheimer's disease. The publication of the present book is timely as it covers really all aspects of *Ginkgo biloba* and the phytopharmaceuticals derived from its leaves. The book is divided into 28 different chapters, all of them are written by scientists actively involved in one way or another in the study of Ginkgo. The first five chapters deal with botanical and ecological aspects as well as with the large-scale cultivation of the tree and plant cell biotechnology. Chapters 6–12, and chapter 14 are of prime importance as they are devoted to the constituents of Ginkgo, their isolation and their analysis. Very useful information on all analytical problems

involving the four main classes of Ginkgo constituents, namely the ginkgolides and other terpenoids, the flavonoids, the alkyl phenols and the polyprenols, is provided. Of special historical interest is Chapter 8 by K. Nakanishi who established the structures of the ginkgolides in 1966. At this time, no biological activity was known for these important compounds. Chapters 15–22 deal with the pharmacology of Ginkgo constituents and extracts, with the mode of action as well as with adverse effects. Very important for all phytopharmaceuticals are clinical trials. Fortunately, they are not missing in the present book where accounts of randomised clinical trials are reported.

The Editor of this book has done an outstanding work by selecting the appropriate topics and contributors in order to provide a full coverage of a plant which is becoming a major phytopharmaceutical worldwide. The three aspects of any herbal remedy, namely safety, efficacy and quality, are particularly well, and also critically, treated. This masterly work is a must for all people interested in medicinal plants. It will be useful for every teacher in the field of pharmacognosy, for pharmacists who sell drugs of plant origin, for medical doctors who have to answer questions of their patients, for scientists involved in plant analysis, for biologists and agronomists and finally for researchers in industry who are involved in the development of phytopharmaceuticals.

The book is well presented with some illustrations and with numerous and accurate literature references. It can be warmly recommended and should find its place in all scientific libraries in academia as well as in industry. The affordable price will also convince many individuals to purchase it.

Kurt Hostettmann
Institute of Pharmacognosy and Phytochemistry
University of Lausanne, CH-1015 Lausanne-Dorigny
Switzerland
E-mail address: kurt.hostettmann@ipp.unil.ch

PII: S0031-9422(01)00282-5

PERGAMON

Phytochemistry 58 (2001) 987–988

PHYTOCHEMISTRY

www.elsevier.com/locate/phytochem

Book reviews

Sage: The Genus *Salvia*

S.E. Kintzios (Ed.); Harwood Academic Publishers, Amsterdam, 2000, 296 pp., ISBN 90-5823-005-8, £73

This multi-author book is volume 14 of the series *Medicinal and Aromatic Plants—Industrial Profiles*. This is a very timely and interesting wide ranging review of the genus *Salvia*. The genus has been attracting a lot of renewed interest with several companies and academic groups trying to show therapeutic effects to support claims for benefits in, for example, treating CNS disorders.

The volume is divided into sections covering the botany, chemical constituents, cultivation and breeding, pharmacology, biotechnology, commercial aspects and bibliographic information sources. There are 20 chapters with nearly half concerned primarily with aspects of the chemistry, folklore and therapeutic activity.

Chapter 1 starts with a list of the approximately 400 species. Although, for some reason, authorities are used sporadically in the list, nonetheless it contains interesting information on folk uses of certain species and in particular cosmetic uses. The chapters in general have a lot of detail for the specialist, e.g. Li on the chemistry of salvianolic acids and Korousou et al. on the botany of Greek sage species.

The review of the pharmacology by Baricevic and Bartol is particularly good, covering a wide range of activities and modes of action and is very well referenced and written in a manner suitable for both the specialist and non-specialist. Research on the anti-hypertensive properties of Dan-Shen and the active chemical is described in some detail.

The section on biotechnology includes a chapter by Isabelle Hippolyte on cell culture as a way of producing rosmarinic acid which can be obtained in 36% dry weight yields.

All in all, this is a good reference book on Sage knowledge to date and will be a good introduction to new workers on the genus or people interested in herbal medicines in general who want to understand the modes of action and biology of the plants.

Robert J. Nash
Institute of Grassland and Environmental Research
Plas Gogerddan, Aberystwyth
Ceredigion, Wales, 5723 3EB, UK

PII: S0031-9422(01)00339-9

Ginkgo biloba

T.A. van Beek (Ed.), Vol. 12 in the series Medicinal and Aromatic Plants—Industrial Profiles; Harwood Academic Publishers, Amsterdam, The Netherlands, 2000, 548 pp., ISBN 90-5702-488-8, £79 or $126

Several books have already appeared on this fascinating tree of Chinese origin which has become over the last 10 years one of the most widely used herbal medicines. The interest in Ginkgo and in its constituents is still growing after several studies and clinical trials demonstrated its potential in the treatment of Alzheimer's disease. The publication of the present book is timely as it covers really all aspects of *Ginkgo biloba* and the phytopharmaceuticals derived from its leaves. The book is divided into 28 different chapters, all of them are written by scientists actively involved in one way or another in the study of Ginkgo. The first five chapters deal with botanical and ecological aspects as well as with the large-scale cultivation of the tree and plant cell biotechnology. Chapters 6–12, and chapter 14 are of prime importance as they are devoted to the constituents of Ginkgo, their isolation and their analysis. Very useful information on all analytical problems

PERGAMON

Phytochemistry 58 (2001) 989–994

PHYTOCHEMISTRY

www.elsevier.com/locate/phytochem

3β-Brassinosteroid dehydrogenase activity in *Arabidopsis* and tomato

Ute Stündl[1], Bernd Schneider*

Max-Planck-Institut für Chemische Ökologie, Carl-Zeiss-Promenade 10, D-07745 Jena, Germany

Received 14 May 2001; received in revised form 6 August 2001

Abstract

Enzymatic conversion of 24-epiteasterone to 3-dehydro-24-epiteasterone, representing a reversible step in the biosynthesis of 24*R*-methyl brassinosteroids, was monitored in vitro in *Arabidopsis thaliana* and *Lycopersicon esculentum* using fluorescent tagging and HPLC analysis. In both species 24-epiteasterone was metabolized by the cytosolic fraction of induced root-callus suspension cultures in a NAD dependent manner. This 3β-dehydrogenation was only slightly inhibited by 12-fold excess of other 3β-hydroxy intermediates of the early (cathasterone) and late C-6 oxidation pathway (6-deoxo-cathasterone, 6-deoxo-teasterone), indicating a rather specific protein. 3-Dehydro-6-deoxoteasterone and 3α-hydroxy intermediates of brassinosteroid biosynthesis did not reduce conversion of 24-epiteasterone to 3-dehydro-24-epiteasterone. In contrast to light-grown cultures the reaction was clearly inhibited in the dark. © 2001 Elsevier Science Ltd. All rights reserved.

Keywords: *Arabidopsis thaliana*; *Lycopersicon esculentum*; Biosynthesis; Brassinosteroids; 3-Dehydro-24-epiteasterone; 24-Epiteasterone; 3β-Steroid dehydrogenase

1. Introduction

Brassinosteroids represent the only known steroidal group of plant growth regulators. Their biosynthetic pathways and biological activity have been elaborated during the last decades. However, only by means of recent molecular characterization of brassinosteroid-deficient mutants these compounds have gained acceptance as a new class of plant hormones. Several mutants are known, which are blocked in biosynthetic steps in the phytosterol part of the pathway or in steps of the brassinosteroid-specific part of the biosynthetic sequence downstream campesterol (Altmann, 1999). Molecular characterization of these mutants indicated sequence homologies of highly conserved domains with known enzymes. These experiments provided evidence for involvement of cytochrome P450s (Szekeres et al., 1996; Choe et al., 1998; Bishop et al., 1999), steroid reductase (Fujioka et al., 1997; Li et al., 1997), desaturase (Choe et al., 1999b), and multifunctional enzymes (Choe et al., 1999a) in brassinosteroid biosynthesis, for example, although functional expression of cloned proteins was achieved in only a few cases. There are, however, also a number of biosynthetic steps for which mutants are not yet available. In the brassinosteroid specific downstream part of the pathway, this is true for inversion of configuration at C-3, 2α-hydroxylation, and conversion of castasterone to brassinolide by Baeyer-Villiger oxidation.

Inversion of stereochemistry at C-3 from 3β- to 3α-hydroxyl represents a biosynthetic feature common for many steroids, e.g. ecdysteroids (Milner and Rees, 1985), cardenolides (Kawaguchi et al., 1993), and pregnanes (Finsterbusch et al., 1999). It has been reported that inversion of 3β-hydroxy function to 3α-hydroxy of brassinosteroids may also operate in the opposite direction and, therefore, has to be considered reversible. Moreover, the equilibrium between 3α- and 3β-epimers is strongly influenced by regio- and stereoselective 3β-glycosidation (Kolbe et al., 1998). Involvement of 3-dehydro intermediates in the epimerization of plant (Suzuki et al., 1994; Hai et al. 1996) and mammalian steroids (Huang and Luu-The, 2000; Chetyrkin et al., 2001) has been demonstrated several times. This finding raises the question of whether this reversible inversion process is catalyzed by one protein, an ''epimerase'', or by a set of up to four enzymes, which probably catalyze

* Corresponding author. Tel.: +49-3641-643634; fax: +49-3641-643665.

E-mail address: schneider@ice.mpg.de (B. Schneider).

[1] Present address: Institut für Molekulare Biotechnologie, Beutenbergstr. 11, D-07745 Jena, Germany.

0031-9422/01/$ - see front matter © 2001 Elsevier Science Ltd. All rights reserved.
PII: S0031-9422(01)00387-9

individual oxidative and reductive reactions. Three of four possible reactions were demonstrated with enzyme preparations from cultured tomato cells (Winter et al., 1999). When 3-dehydro-24-epiteasterone was incubated with a microsomal fraction, 24-epiteasterone was formed in a NADPH dependent reaction. Formation of 24-epityphasterol from the same substrate was achieved by means of a cytosolic fraction preferring NADH as a cofactor. The same cytosolic fraction was able to convert 24-epityphasterol to 3-dehydro-24-epiteasterone in the presence of NAD. These results suggest that at least two enzymes are involved in inversion of C-3 stereochemistry in *Lycopersicon esculentum*. However, the conversion of 24-epiteasterone to 3-dehydro-24-epiteasterone could not be demonstrated in these experiments. Here we report the latter conversion in *Arabidopsis* and tomato, and characterization of the enzyme in some detail.

2. Results and discussion

2.1. Optimization of assay conditions

Cytosolic and microsomal fractions of *A. thaliana* root-callus suspension cultures were prepared and incubated with 24-epiteasterone (**1**) to demonstrate conversion to 3-dehydro-24-epiteasterone (**2**) (Fig. 1). In preliminary experiments, assay conditions were similar to those previously used successfully with preparations from tomato cell suspensions (10 mM Na-K-phosphate buffer, pH 7.0; 250 mM sucrose; 400 mM sodium ascorbate; 1 mM NAD; 3 h, 30 °C) (Winter et al., 1999) to convert 24-epityphasterol (**3**) to **2**. Incubation of the cytosolic fraction with the substrate 24-epiteasterone (**1**) resulted in the dehydrogenated product, 3-dehydro-24-epiteasterone (**2**), while experiments using the microsomal fraction failed to give any product. Both substrate **1** and product **2**, after derivatization with dansylaminophenylboronic acid, were analyzed by reversed-phase HPLC and fluorescence detection. Under the chromatographic conditions used, **1** was detectable at 20.3 min in the HPLC trace, and 3-dehydro-24-epiteasterone (**2**) appeared at 17.4 min.

To identify optimal assay conditions for conversion of 24-epiteasterone, different buffer systems were tested within the pH range of 6.0 to 9.0. Maximum formation of 3-dehydro-24-epiteasterone (**2**) was measured in 20 mM phosphate buffer at pH 7.5 with NAD as a cofactor, 15% glycerol, and 1 mM EDTA for 19 h at 30 °C (Fig. 2). For optimum product formation, the root-callus cultures have been induced with 1 μM 24-epiteasterone. Preparations from non-induced *Arabidopsis* cultures exhibited neglectable activity only.

These general conditions, therefore, were used in all further experiments. In comparison with phosphate buffer, for example, the pH optimum in 20 mM Tris–HCl buffer was shifted to 8.0 and the reaction was significantly inhibited. Only the cytosolic fraction was able to convert 24-epiteasterone (**1**) to 3-dehydro-24-epiteasterone (**2**). No product formation was observed after incubation using the optimized conditions with the microsomal fraction.

The results presented here and earlier (Winter et al., 1999) reveal that at least two enzymes are involved in the reversible inversion of configuration of 3-hydroxy function in brassinosteroid biosynthesis. Both 3β- and 3α-dehydrogenase activities of *Arabidopsis* are localized in the cytosol, respectively. Stereospecific reduction of 3-dehydro-24-epiteasterone as a substrate was found separately in cytosolic (reduction to 3α-OH) and microsomal fractions (reduction to 3β-OH) (Winter et al., 1999). Together with regio- and substrate-specific glycosidations (Kolbe et al., 1998), this reversible part of brassinosteroid biosynthesis suggests the possibility of back conversion and temporarily removes intermediates from the main stream of biosynthesis. This mechanism might be considered an important instrument regulating endogenous levels of brassinosteroids in specific stages of plant development.

Interestingly, a cytosolic fraction of cultured cells of the liverwort *Marchantia polymorpha* (Park et al., 1999) has been used to convert teasterone to typhasterol without the presence of any cofactor. This is in contrast to the 3β-dehydrogenase from *Arabidopsis* described here, whose activity was clearly enhanced by application of an electron acceptor and preferred NAD over NADP.

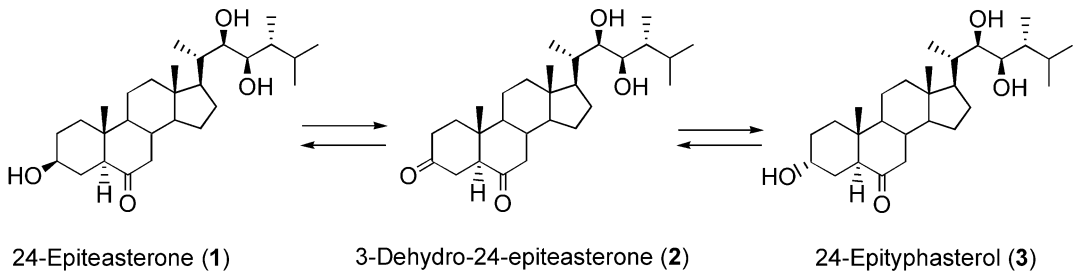

Fig. 1. Reversible conversion of 24-epiteasterone (**1**) to 24-epityphasterol (**2**) via 3-dehydro-24-epiteasterone (**2**) in *Arabidodpsis thaliana* and *Lycopersicon esculentum*.

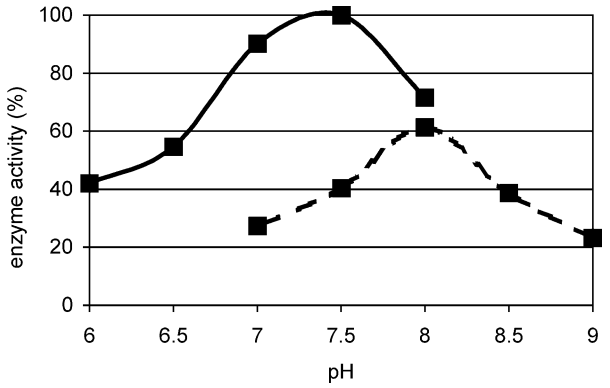

Fig. 2. pH Optimum of 3β-brassinosteroid dehydrogenase activity from *Arabidopsis thaliana* in 20 mM phosphate buffer (solid line) and 20 mM Tris–HCl buffer (dotted line) (NAD, 15% glycerol, 1 mM EDTA, 19 h, 30 °C).

2.2. 3β-Dehydrogenase activity in light- and dark-grown Arabidopsis suspension cultures

The detection of parallel early and late C-6 oxidation route of brassinosteroid biosynthesis in *Catharanthus roseus* (Choi et al., 1997) and *Arabidopsis thaliana* (Noguchi et al., 2000) raises the question of the function of these pathways. It has been suggested that brassinosteroid biosynthesis is regulated by light (Li et al., 1996) and that the early C-6 oxidation predominates in dark-grown *Arabidopsis* seedlings and the late C-6 oxidation pathway occurs mainly in light-grown plants (Fujioka et al., 1997; Choe et al., 1998). Although the biosynthesis of 24*R*-configured brassinosteroids has not been studied in detail, it is expected to proceed in a manner analogous to the established biosynthetic sequence of 24*S*-configured brassinosteroids to brassinolide. In our experiments, the 24*R* configured substrate, 24-epiteasterone, was used. Reversible steps in the biosynthesis as, for example, C-3 epimerization, which occur within both the 24*S* and 24*R* series, are considered possible mechanisms to regulate the level of endogenous plant growth regulators. Therefore we studied the activity of dehydrogenase activity in the cytosolic fractions of light-and dark-grown *A. thaliana* root-callus suspension cultures. The results shown in Table 1. indicate that in contrast to light-grown cultures the reaction is clearly inhibited in dark-grown cells.

Table 1
3β-Dehydrogenase activity in the cytosolic fraction of *Arabidopsis thaliana* root-callus suspension cultures derived from light-and dark-grown seedlings. Average enzyme activities of experiments carried out in triplicate are shown

Culture conditions	Assay conditions	Enzyme activity	
		μmol min^{-1}	%
Light-grown	1 mM NAD	1.200	100.0
Light-grown	–	0.085	7.1
Dark-grown	1 mM NAD	0.563	46.9
Dark-grown	–	0.035	2.9

This finding disagrees to some extent with the hypothesis mentioned above, which emphasizes that the early C-6 pathway operates in the dark and the late C-6 pathway is predominant in the light (Fujioka et al., 1997; Choe et al., 1998). However, since only an individual non-rate-limiting reaction has been studied here, conclusions about the total pathway with respect to regulation by light are not possible.

2.3. Substrate specificity of 3β-dehydrogenase

24*R*- and 24*S*-methyl brassinosteroids, co-occurring in *Arabidopsis* (Schmidt et al., 1997) and many other plants, probably are derived from the two epimeric precursors campesterol and 22,23-dihydrobrassicasterol. Further branching into the early and late C-6-oxidation pathway takes place from campestanol, during which routes 6-oxo- and 6-deoxobrassinosteroids are formed. Several compounds of either type have been found (Fujioka et al., 1998; Noguchi et al., 1999) and determined quantitatively (Nomura et al., 2001). These different brassinosteroids might be specifically involved in various growth and developmental processes, which are controlled by that class of plant hormones.

It has been suggested that brassinosteroid biosynthetic enzymes might have dual functions in parallel early and late C-6 oxidation pathways, e.g. 22α-hydroxylation of campestanol and 6-oxocampestanol is catalyzed by CYP90B (Bishop et al., 1999). Dual or even multiple functions of brassinosteroid biosynthetic enzymes might be true also for other steps which neccessarily have to be passed through in each of established or hypothetical subpathways. Inversion of configuration, including 3β-dehydrogenation, occurs both in the early and late C-6 oxidation pathways and is also suggested for further parallel routes to brassinosteroids possessing different side chain alkylation pattern or stereochemistry, as, for example 24*R*- or 24*S*-methyl substituents. Hitherto it has not been clear whether the enzymes involved in epimerization are specific to a special substrate or are able to accept intermediates of parallel pathways. To characterize the substrate specificity of the enzyme under investigation, we tested the inhibitory effect of the hypothetical 3β-intermediates cathasterone (early C-6 oxidation pathway to brassinolide), 6-deoxocathasterone, and 6-deoxoteasterone (late C-6 oxidation pathway to brassinolide). These three substances showed a slight inhibitory effect on dehydrogenation rate of 24-epiteasterone when used in 12-fold concentration in comparison with the substrate (Table 2). Teasterone (early C-6 oxidation pathway) was also tested but unfortunately interfered with 24-epiteasterone in HPLC and GC–MS analyses. 3α-Epimeric compounds, 6-deoxotyphasterol and 6-deoxocastasterone, and a 3-

Table 2
Effect of brassinosteroid biosynthetic intermediates on the conversion of 24-epiteasterone (**1**) to 3-dehydro-24-epiteasterone (**2**) by the cytosolic fraction of *Arabidopsis thaliana* root-callus suspension cultures. The experiment without intermediates was used as control. Average enzyme activities of experiments carried out in triplicate are shown

Compound	Substituent at C-3	Enzyme activity	
		μmol min^{-1}	%
Control		1.200	100.0
Cathasterone	3β-OH	1.134	94.5
6-Deoxocathasterone	3β-OH	1.164	97.0
6-Deoxoteasterone	3β-OH	1.122	93.5
3-Dehydro-6-deoxoteasterone	Keto	1.214	101.2
6-Deoxotyphasterol	3α-OH	1.198	99.8
6-Deoxocastasterone	3α-OH	1.182	98.5

Table 3
Conversion of 24-epiteasterone (**1**) to 3-dehydro-24-epiteasterone (**2**) by the cytosolic fraction of *Lycopersicon esculentum* (var. 'Harzfeuer') root-callus suspension cultures. Average enzyme activities of experiments carried out in triplicate are shown

Electron acceptor (1 mM)	Enzyme activity	
	μmol min^{-1}	%
–	0.061	6.3
NAD[a]	0.044	4.5
NAD	0.970	100.0
NADP	0.543	56.0
FAD	0.035	3.6
FMN	0.049	5.0

[a] Control experiment without substrate.

keto intermediate, 3-dehydro-6-deoxoteasterone, were also used in these experiments because 3α-dehydrogenase acitivity and reductive conversion of 3-dehydro intermediates have been observed earlier in a cytosolic fraction of tomato (Winter et al., 1999). However, no significant inhibition of 3α-dehydrogenation of 24-epiteasterone could be observed by these competing substrates.

In conclusion, the protein studied here seems to be rather specific for 3β-dehydrogenation of 24-epiteasterone. Other 3β-configured substrates compete only slightly with the substrate.

2.4. Conversion of 24-epiteasterone in tomato

It has been reported that intermediates of the early C-6 oxidation pathway in tomato have been depleted (Bishop et al., 1999). This depletion might be connected to reduced activity of one or more enzymes in that branch of the pathway. With respect to the finding that 3β-dehydrogenase activity from *Arabidopsis* seems to be rather specific for dehydrogenation of 24-epiteasterone, representing a member of the hypothetical early C-6 oxidation route to 24*R* brassinosteroids, non-detection of this activity in tomato (Winter et al., 1999) seems to confirm Bishop's hypothesis. Therefore, it is useful to know if there is generally any 24-epiteasterone 3β-dehydrogenase activity in tomato or if gene activity has been lost due to utilization of long-term subcultured tomato cell suspension cultures in previous experiments (Winter et al., 1999). Thus, root-callus suspension cultures of two different tomato varieties have been freshly established for each feeding experiment and their 24-epiteasterone metabolizing activity has been tested in an analogous manner as described for *Arabidopsis* cultures. Whereas tomato root-callus suspension cultures of the variety 'Harzfeuer', induced with 1 μM 24-epiteasterone, showed 3β-dehydrogenase activity of 0.97 μmol min^{-1} (Table 3) comparable to those of *Arabidopsis* (1.20 μmol min^{-1}, Table 1), we could not detect any 24-epiteasterone metabolizing activity in cultures of the variety Tamina. Only neglectable activity was found in non-induced cultures of 'Harzfeuer'.

As summarized in Table 3, the cytosolic fraction of tomato variety 'Harzfeuer' converted 24-epiteasterone (**1**) to 3-dehydro-24-epiteasterone (**2**) in a NAD-dependent manner. NADP was also active as an electron acceptor. These findings suggest that there may be some species specificity in *Lycopersicon* with respect to 3β-dehydrogenase activity. Consequently, in 'Tamina', which is not able to form 3-dehydro-24-epiteasterone (**2**) from 24-epiteasterone (**1**), an alternative pathway to produce active brassinosteroids may operate.

3. Experimental

3.1. Plant material and culture conditions.

Arabidopsis thaliana cv. *C24* and *Lycopersicon esculentum* cv. Harzfeuer and cv. Tamina were used. Sterile seeds were germinated on auxin- and cytokinin-free B5 medium (Gamborg et al., 1968) containing sucrose (20 g l^{-1}) at 23 °C on a rotary shaker at 85 rpm for two weeks under permanent illumination (15 μmol m^{-2} s^{-1}). The roots were separated from the seedlings, minced under sterile conditions, and placed into 100 ml of RM 28 medium (Ecker, 1990) in 250 ml conical flasks. The cultures were maintained for three weeks under the same conditions as the seedlings, with weekly replacement of the nutrient medium. The *Arabidopsis* cultures used for probing enzyme activity in the dark were kept in complete darkness by wrapping with alumina foil. During the three-week culture period, root-callus suspension cultures developed, which were used for further investigations. Cultures have been freshly established from seeds of *A. thaliana* and *L. esculentum*, respectively, for every experiment.

3.2. Enzyme preparation and assay conditions

Twelve hours before extraction the root-callus suspension cultures of *Arabidopsis* and tomato were induced by application of 100 nmol 24-epiteasterone (1 μM final concentration). Preparations from non-induced cells were used as controls. Freshly harvested callus tissue (about 5 g fr. wt.) was frozen with liquid N_2. After mechanical disruption with mortar and pestle, the homogenate was dissolved in 20 mM phosphate buffer (pH 7.5, 15% glycerol, 1.0 mM EDTA, 0.1 mM DTE) and centrifuged twice at 5000 *g* for 10 min and at 25,000 *g* for 30 min. Separation of the cytosolic and microsomal fraction was performed twice by ultracentrifugation at 100,000 *g* for 1 h. For enzymatic studies the 25,000 *g* and 100,000 *g* pellets were washed with buffer before use. All experiments have been carried out in triplicate.

If not otherwise mentioned in the text, assays were carried out in a total volume of 1.0 ml containing 2.5 μM brassinosteroid, 1 mM electron acceptor, and 250 μg protein in phosphate buffer. After incubating the assay mixtures for 19 h at 30 °C, we extracted the brassinosteroids with $CHCl_3$. The organic phase was separated by centrifugation, removed from the upper phase, and evaporated with a SpeedVac. 50% aliquots of the samples were analyzed by HPLC with fluorescence detection. Protein quantification was performed according to Bradford (1976). The enzyme activity was measured as the relative peak area of substrate and product.

3.3. HPLC and derivatization

Aliquots from enzyme assays were treated with 100 μl of dansylaminophenylboronic acid (1 mg in 1 ml MeCN–pyridine 99:1) for 20 min at 75 °C to convert brassinosteroids to boronates. Chromatographic analysis of dansyl derivatives was carried out on LiChrospher 100 RP18; 5 μm; 2504 mm; 0.8 ml min^{-1}. An excitation wavelength of 230 nm and emission wavelength of 520 nm were used in all cases. Separations were carried out using MeCN–H_2O (17:3, v:v) under isocratic conditions.

Acknowledgements

We thank Takao Yokota (Utsunomiya, Japan) for kind gifts of cathasterone, 6-deoxocathasterone, 6-deoxoteasterone, teasterone, 6-deoxotyphasterol, 6-deoxocastasterone, and 3-dehydro-6-deoxoteasterone, and Thomas Altmann (Golm, Germany) for a gift of *Arabidopsis* seeds and his advice in establishing root-callus cultures. Emily Wheeler (Jena, Germany) is gratefully acknowledged for linguistic support in the preparation of this manuscript. This investigation was financially supported by the Deutsche Forschungsgemeinschaft (Bonn, Germany) and the Fonds der Chemischen Industrie (Frankfurt/Main, Germany).

References

Altmann, T., 1999. Molecular physiology of brassinosteroids revealed by the analysis of mutants. Planta 208, 1–11.

Bishop, G.J., Nomura, T., Yokota, T., Harrison, K., Noguchi, T., Fujioka, S., Takatsuto, S., Jones, J.D.G., Kamiya, Y., 1999. The tomato dwarf enzyme catalyses C-6 oxidation in brassinosteroid biosynthesis. Proc. Natl. Acad. Sci. USA 96, 1761–1766.

Bradford, M.M., 1976. Rapid and sensitive method for quantitation of microgram quantities of protein utilizing principle of protein-dye binding. Anal. Biochem. 72, 248–254.

Chetyrkin, S.V., Hu, J., Gough, W.H., Dumaual, N., Kedishvili, N.Y., 2001. Further characterization of human microsomal 3-hydroxysteroid dehydrogenase. Arch. Biochem. Biophys. 386, 1–10.

Choe, S., Dilkes, B.D., Fujioka, S., Takatsuto, S., Sakurai, A., Feldman, K.A., 1998. The *DWF4* gene of *Arabidopsis* encodes a cytochrome P450 that mediates multiple 22α-hydroxylation steps in brassinosteroid biosynthesis. Plant Cell 10, 231–243.

Choe, S., Dilkes, B.P., Gregory, B.D., Ross, A.S., Yuan, H., Noguchi, T., Fujioka, S., Takatsuto, S., Tanaka, A., Yoshida, S., Tax, F.E., Feldmann, K.A., 1999a. The *Arabidopsis dwarf1* mutant is defective in the conversion of 24-methylenecholesterol to campesterol in brassinosteroid biosynthesis. Plant Physiol. 119, 897–907.

Choe, S., Noguchi, T., Fujioka, S., Takatsuto, S., Tissier, C.P., Gregory, B.D., Ross, A.S., Tanaka, A., Yoshida, S., Tax, F.E., Feldmann, K.A., 1999b. The *Arabidopsis dwf7/ste1* mutant is defective in the Δ^7 sterol C-5 desaturation step leading to brassinosteroid biosynthesis. Plant Cell 11, 207–221.

Choi, Y.H., Fujioka, S., Nomura, T., Harada, A., Yokota, T., Takatsuto, S., Sakurai, A., 1997. An alternative brassinolide biosynthetic pathway via late C-6 oxidation. Phytochemistry 44, 609–613.

Ecker, J., 1990. PFGE and YAC analysis of the *Arabidopsis* genome. Methods 1, 186–194.

Finsterbusch, A., Lindemann, P., Grimm, R., Eckerskorn, C., Luckner, M., 1999. Δ^5-3β-Hydroxysteroid dehydrogenase from *Digitalis lanata* Ehrh.—a multifunctional enzyme in steroid metabolism? Planta 209, 478–486.

Fujioka, S., Li, J.M., Choi, Y.H., Seto, H., Takatsuto, S., Noguchi, T., Watanabe, T., Kuriyama, H., Yokota, T., Chory, J., Sakurai, A., 1997. The *Arabidopsis deetiolated2* mutant is blocked in early brassinosteroid biosynthesis. Plant Cell 11, 1951–1962.

Fujioka, S., Noguchi, T., Yokota, T., Takatsuto, S., Yoshida, S., 1998. Brassinosteroids in *Arabidopsis thaliana*. Phytochemistry 48, 595–599.

Gamborg, O.L., Miller, R.A., Ojima, K., 1968. Nutrient requirements of suspension cultures of soybean root cells. Exp. Cell Res. 50, 151–158.

Hai, T., Schneider, B., Porzel, A., Adam, G., 1996. Metabolism of 24-epicastasterone in cell suspension cultures of *Lycopersicon esculentum*. Phytochemistry 41, 197–201.

Huang, X.F., Luu-The, V., 2000. Molecular characterization of a first human 3(α→β)-hydroxysteroid epimerase. J. Biol. Chem. 275, 29452–29457.

Kawaguchi, K., Hirotani, M., Furuya, T., 1993. *Strophanthus* species (members of the dogbane family): in vitro culture and the production of cardenolides. In: Bajaj, Y.P.S. (Ed.), Biotechnology in Agriculture and Forestry, Vol. 21: Medicinal and Aromatic Plants. Springer, Berlin, pp. 371–386.

Kolbe, A., Schneider, B., Porzel, A., Adam, G., 1998. Metabolic inversion of the 3-hydroxy function in brassinosteroids. Phytochemistry 48, 467–470.

Li, J.M., Nagpal, P., Vitart, V., McMorris, T.C., Chory, J., 1996. A role for brassinosteroids in light-dependent development of *Arabidopsis*. Science 272, 398–401.

Li, J.M., Biswas, M.G., Chao, A., Russell, D.W., Chory, J., 1997. Conservation of function between mammalian and plant steroid 5α-reductases. Proc. Natl. Acad. Sci. USA 94, 3554–3559.

Milner, N.P., Rees, H.H., 1985. Involvement of 3-dehydroecdysone in the 3-epimerization of ecdysone. Biochem. J. 231, 369–374.

Noguchi, T., Fujioka, S., Choe, S., Takatsuto, S., Yoshida, S., Yuan, H., Feldman, K.A., Tax, F.E., 1999. Brassinosteroid-insensitive dwarf mutants of *Arabidopsis* accumulate brassinosteroids. Plant Physiol. 121, 743–752.

Noguchi, T., Fujioka, S., Choe, S., Takatsuto, S., Tax, F.E., Yoshida, S., Feldman, K.A., 2000. Biosynthetic pathway of brassinolide in *Arabidopsis*. Plant Physiol. 124, 201–209.

Nomura, T., Sato, T., Bishop, G.J., Kamiya, Y., Takatsuto, S., Yokota, T., 2001. Accumulation of 6-deoxocathasterone and 6-deoxocastasterone in *Arabidopsis*, pea and tomato is suggestive of common rate-limiting steps in brassinosteroid biosynthesis. Phytochemistry 57, 171–178.

Park, S.-H., Han, K.-S., Kim, T.-W., Shim, J.-K., Takatsuto, S., Yokota, T., Kim, S.-K., 1999. In vivo and in vitro conversion of teasterone to typhasterol in cultured cells of *Marchantia polymorpha*. Plant Cell Physiol. 40, 955–960.

Schmidt, J., Altmann, T., Adam, G., 1997. Brassinosteroids from seeds of *Arabidopsis thaliana*. Phytochemistry 45, 1325–1327.

Suzuki, H., Inoue, T., Fujioka, S., Takatsuto, S., Yanagisawa, T., Yokota, T., Murofushi, N., Sakurai, A., 1994. Possible involvement of 3-dehydroteasterone in the conversion of teasterone to typhasterol in cultured cells of *Catharanthus roseus*. Biosci. Biotech. Biochem. 58, 1186–1188.

Szekeres, M., Nemeth, K., Koncz-Kalman, Z., Mathur, J., Kauschmann, A., Altmann, T., Redei, G.P., Nagy, F., Schell, J., Koncz, C., 1996. Brassinosteroids rescue the deficiency of CYP90, a cytochrome P450, controlling cell elongation and de-etiolation in *Arabidopsis*. Cell 85, 171–182.

Winter, J., Schneider, B., Meyenburg, S., Strack, D., Adam, G., 1999. Monitoring brassinosteroid biosynthetic enzymes by fluorescent tagging and HPLC analysis of their substrates and products. Phytochemistry 51, 237–242.

PERGAMON

Phytochemistry 58 (2001) 995–1005

PHYTOCHEMISTRY

www.elsevier.com/locate/phytochem

Partial purification and characterization of a soybean β-glucosidase with high specific activity towards isoflavone conjugates

Ming-Ching Hsieh[1], Terrence L. Graham*

Department of Plant Pathology, The Ohio State University, Columbus, OH 43210, USA

Received 4 May 2001; received in revised form 6 August 2001

Abstract

A β-glucosidase with high specific activity towards isoflavone conjugates was purified from soybean [*Glycine max*] roots by high salt extraction from a low speed centrifugal pellet and subsequent anion and cation exchange chromatography. Purification required stabilization throughout fractionation in 10% glycerol. The enzyme is most likely a dimer (approximate M_r 165 kDa) with potential subunits of M_r 80 and/or 75 kDa. The pH and temperature optima are pH 6 and 30 °C, respectively. The enzyme was highly heat-stable. Of the various potential effectors examined, silver and mercury ions were the most inhibitory. The IC_{50} of silver ions was increased from 140 μM to 14 mM in the presence of 250 μM β-mercaptoethanol. Glucono-δ-lactone was not strongly inhibitory (IC_{50} 24 mM). The activity was highly active against isoflavone conjugates, with a specificity constant 160–1000 fold higher for isoflavone conjugates over the generic chromogenic substrate, *p*-nitrophenyl β-glucoside. The enzyme was inactive against the flavonol glycosides tested. The partially purified enzyme had similar K_m and k_{cat} towards 7-*O*-glucosyl- and 7-*O*-glucosyl-6″-malonyl-isoflavones, suggesting that it may be able to cleave the esterified glucosyl conjugate. We hypothesize that the enzyme is involved in the release of daidzein and genistein, both of which play central roles in soybean defense. © 2001 Elsevier Science Ltd. All rights reserved.

Keywords: Glycine max; Leguminosae; Soybean; Phenylpropanoid; Isoflavone; Genistein; Daidzein; β-Glucosidase; Partial purification

1. Introduction

β-Glucosidases (β-D-glucoside glucohydrolase, EC 3.2.1.21) comprise a heterogeneous group of enzymes that are able to cleave the β-glucosidic linkages of di- and/or oligo-saccharides, or other glucose conjugates. β-Glucosidases are widely distributed in the living world and play pivotal roles in many biological processes, such as degradation of cellulosic biomass, hydrolysis of glycolipids, cyanogenesis, and modification of secondary metabolites (Esen, 1993). In plants, β-glucosidase activity is involved in processes such as the compartmentalization and activity of phytohormones (Kleczkowski and Schell, 1995), defense mechanisms against microbes, insects, or parasitic plants (Bell, 1981; Poulton, 1990; Phillips and Streit, 1996), floral development and pigmentation (Harborne and Mabry, 1982; Koes et al., 1994), and they are also thought to have roles in lignification and cell wall decomposition (Hösel et al., 1978; Leah et al., 1995). Several β-glucosidases of plant origin are highly substrate-specific, such as those having selective specificity toward sapinin (Inoue and Ebizuka, 1996), hydrojuglone (Duroux et al., 1998), cinnamyl alcohols (Dharmawardhana et al., 1995), cyanogenic glycosides (Conn, 1993), flavones (Maier et al., 1993) and isoflavones (Hösel and Barz, 1975). Despite the availability of crystal structures for several plant β-glucosidases, the aglycone-binding site is still poorly understood. In a recent study, the active site of the maize β-glucosidase for the substrate DIMBOA-glucoside and its interaction with the cyanogenic glucoside dhurrin was examined (Czjzek et al., 2000).

Isoflavone conjugates are sometimes constitutively present in large quantities in legumes (see e.g. Graham,

* Corresponding author. Tel.: +614-292-1375; fax: +1-614-292-4455.

E-mail address: graham.1@osu.edu (T.L. Graham).

[1] Current address: Department of Chemistry, University of Pennsylvania, Philadelphia, PA 19104-6323, USA.

0031-9422/01/$ - see front matter © 2001 Elsevier Science Ltd. All rights reserved.
PII: S0031-9422(01)00380-6

1991b). These isoflavone conjugates, including isoflavone 7-*O*-glucosides and isoflavone 7-*O*-glucoside-6″-*O*-malonates, may serve as pools for the release of free aglycones, which in turn may play important roles in plant-microbe interactions and defensive mechanisms against pathogen infection (Graham et al., 1990; Kessmann et al., 1990; Mackenbrock and Barz, 1991; Dakora and Phillips, 1996). Released isoflavones, for instance, can be either incorporated into the biosynthetic pathway of phytoalexins (Ebel, 1986; Barz and Welle, 1992; Kleczkowski and Schell, 1995) or act as preformed toxins, termed phytoanticipins (Johnson et al., 1976; Kramer et al., 1984; Weidenborner et al., 1990; Rivera-Vargas et al., 1993). Free isoflavones may also function as chemoattractants for both pathogens (Morris and Ward, 1992) and symbionts (Phillips et al., 1992) or as regulators of gene expression in Rhizobium spp. (Hungria and Stacey, 1997). More recently, the isoflavone genistein has been hypothesized to play a regulatory role in the activation of a soybean Type II NADH oxidase thought to participate in the establishment of competency for response to pathogen elicitors (see Graham and Graham, 1996a,b and reviews Graham and Graham, 1999, 2000).

In plants, the accumulation of isoflavone conjugates may be mediated by several enzymes (Fig. 1). The hydrolytic enzymes, isoflavone 7-*O*-glucoside-6″-*O*-malonate malonylesterase and isoflavone 7-*O*-glucoside β-glucosidase, from chickpea have been purified and characterized (Hösel and Barz, 1975; Hinderer et. al., 1986). Although non-specific β-glucosidase activities hydrolyzing isoflavone glucosides in the process of miso preparation and a lactase phlorizin hydrolase have been reported in soybean (Matsuura and Obata, 1993; Matsuura et al., 1995; Day et al., 2000), we know of no reports of characterization of β-glucosidases in soybean with preferential activity towards isoflavone conjugates. Because of the critical roles daidzein and genistein may play in soybean defense, we undertook the characterization of some of the enzymes involved in the turnover of their conjugates. In this report, a soybean isoflavone conjugate-hydrolyzing β-glucosidase (ICHG) was partially purified and characterized. The enzyme has high specific activity towards genistein/daidzein 7-*O*-glucoside (genistin and daidzin) and genistein/daidzein 7-*O*-glucosyl 6″-*O*-malonate (MGD and MGG), with very low K_m and high k_{cat} values. The specificity constant (k_{cat}/K_m) is 160–1000 fold higher for the isoflavone

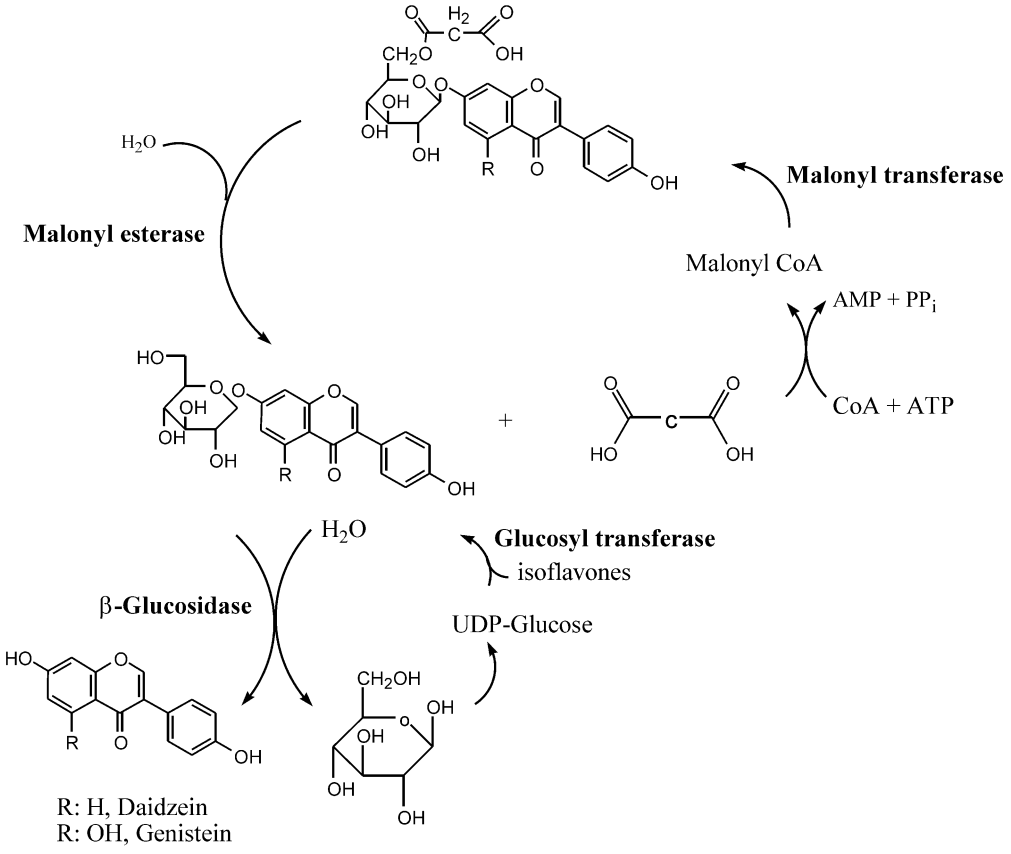

Fig. 1. Enzymatic regulation of the isoflavone conjugate pools. The scheme is based on the four purified enzymes from chickpea where malonylesterase and β-glucosidase hydrolyze isoflavone 7-*O*-glucoside-6″-*O*-malonates and isoflavone 7-*O*-glucosides, respectively, and glucosyltransferase and malonyltransferase transfer glucose and malonate sequentially to the isoflavone moiety.

conjugates over the chromogenic substrate *p*-nitrophenyl β-glucoside. Isoflavone conjugate hydrolysis in soybean may differ from that of chickpeas in that we found no evidence for an esterase active on MGG or MGD. Although we cannot preclude the existence of such an esterase, the partially purified glucosidase characterized in this report was able to hydrolyze both the glucosyl and malonyl glucosyl isoflavones directly with similar kinetics.

2. Results and discussion

2.1. Purification of the isoflavone conjugate-hydrolyzing β-glucosidase

Many studies were performed with various soybean organs to develop the optimal purification protocol. For example, vacuum infiltration of soybean cotyledons with 0.2 M phosphate buffer, pH. 6, containing 200–500 uM NaCl and subsequent isolation of the intercellular washing fluids by centrifugation led to a preparation highly enriched for the glucosidase, suggesting a possible apoplastic localization. These intercellular washing fluids contain no cytoplasmic marker enzymes (T.L. Graham, unpublished). However, due to the relatively low level of the ICHG in cotyledons and the difficulty in preparing large amounts of the intercellular fluids, we chose to work with roots. Roots contained the highest specific activity of ICHG in the soybean seedling. For example, a crude preparation from roots was about 800-fold more enriched for the enzyme than a crude preparation from cotyledons (data not shown). In roots, activity was found to be associated with the low speed centrifugal pellet.

Enzyme activity was solubilized from the pellet with 0.2 M phosphate buffer, pH 6, containing 0.5 M NaCl and fractionated by 40–60% ammonium sulfate saturation. Due to empirical results regarding the instability of the enzyme, a desalting column (Sephadex G-25) was chosen over dialysis for salt removal, and 10% glycerol was always present in the buffer from this step onward. When the desalted protein solution was passed through a DEAE-Sephadex A-50 column at pH 6.0, nearly all of the enzyme activity was in the unbound fractions (Fig. 2A). The active fractions were pooled and 5 mM final concentration of sodium ascorbate was introduced to maximize stability. The protein sample was then loaded onto a CM-Sephadex C-50 column and eluted with a linear gradient of buffer F in buffer E. The activity peak was eluted at 0.56 M NaCl (Fig. 2B). SDS polyacrylamide gel electrophoresis (PAGE) of various fractions under reducing conditions is shown in Fig. 3. Although the banding patterns for the fractions from the DEAE and CM-Sephadex columns are qualitatively similar, the analysis of the gel with ImageQuant software (Molecular Dynamics) determined that the pixel volume of the 80 kD band was three to four fold enriched in comparison to the other minor bands. This is consistent with the separation from a majority of other proteins for this fraction as shown in Fig. 2B. At this point, the ICHG was purified approximately 20-fold with a 20% recovery rate (Table 1). The most active fractions were pooled and lyophilized until almost only glycerol was left. Aliquots of this glycerol solution of ICHG were stored at −20 °C for further study. Under these conditions, the enzyme aliquots did not freeze solid and activity was stable for at least six months.

2.2. Properties of the isoflavone conjugate-hydrolyzing β-glucosidase

The molecular mass of ICHG upon SDS PAGE under non-reducing conditions was judged to be approximately 165 kDa (data not shown), while under reducing conditions a major band of mass 80 kDa and a less intensely staining band of 75 kDa were seen (Fig. 3). Though both of these bands were reproducibly associated with activity throughout purification, it is not clear whether the two bands represent different polypeptides or different post-translational modifications of a single polypeptide. Thus, while it is likely that the enzyme is a dimer, with monomers linked through a disulfide bond, its precise subunit composition will require further clarification. The ICHG tolerates very high concentrations of β-mercaptoethanol, with 50% inhibition of enzyme activity (IC_{50}) at 1.1 M, suggesting that the monomer form may also be catalytically active. Many β-glucosidases contain either identical or non-identical subunits. The number of subunits varies from 2 to 10 (or more) depending on the enzyme. For instance, a 60 kDa coniferin-hydrolyzing β-glucosidase from lodgepole pine has two non-identical subunits with M_r of 28 and 24 kDa (Dharmawardhana et al., 1995). The furostanol glycoside 26-*O*-β-glucosidase from *Costus speciosus* is a 110 kDa protein with two subunits with M_r of 54 and 58 kDa (Inoue and Ebizuka, 1996). Furthermore, the isoflavone hydrolyzing β-glucosidase from chickpea has apparent M_r of 125–135 kDa with two identical subunits of 68 kDa (Hösel and Barz, 1975).

The ICHG showed a pH optimum at approximately pH 6 at 30 °C. The optimum temperature was 30 °C. Both are typical for β-glucosidases (Esen, 1993). The enzyme is highly heat stable and remains substantially active (87%) after 45 min at 50 °C.

Several chemicals reported to be effectors of β-glucosidases were examined. Of all the chemicals tested for the inhibition of enzyme activity, only silver and mercury ions were inhibitory at the 1 mM level (Table 2), suggesting that sulfhydryl groups may play an essential role in enzyme activity. However, other sulfhydryl

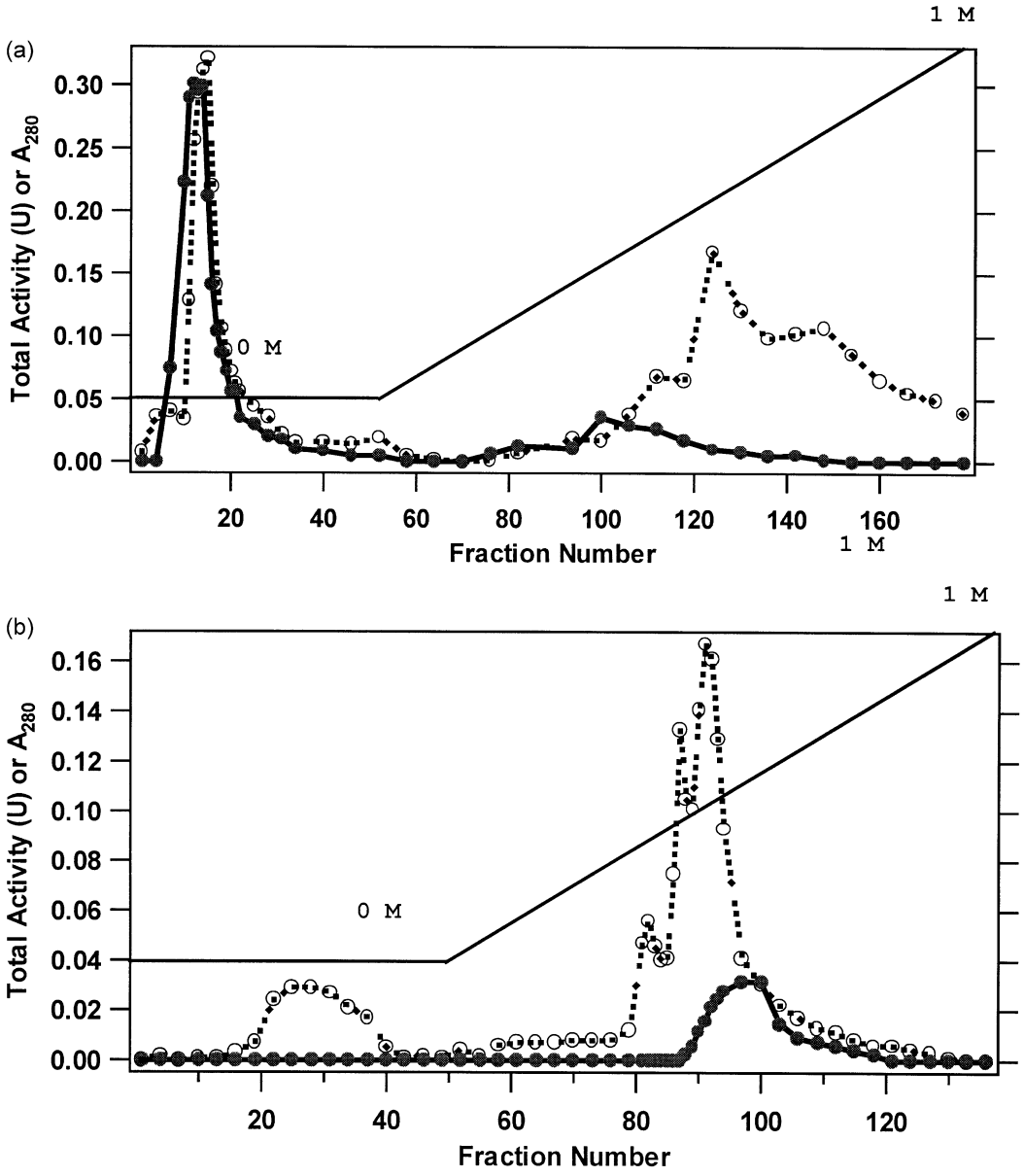

Fig. 2. The purification of the isoflavone-specific β-glucosidase. The chromatograms for anion exchange on DEAE-Sephadex (a), and cation exchange on CM-Sephadex (b). Symbols: open circle and dashed line, A280; closed circle and solid line, total activity. The linear salt gradients are shown.

Table 1
The purification scheme for the isoflavone conjugate-hydrolyzing β-glucosidase from soybean roots

Purification step	Total activity[a] (mU)	Total protein (mg)	Specific activity (mU/mg protein)	Yield (%)	Purity (fold)
Root cell wall wash	8780	124	70	100	1
Ammonium sulfate (40–60%)	10,540	50	220	120	3
DEAE-Sephadex	2960	12	240	34	3.4
CM-Sephadex	1740	1.3	1340	20	20

[a] The enzyme activity was measured by an HPLC method using a natural isoflavone conjugate mixture as substrate. The activity was calculated from the concentration of the released daidzein.

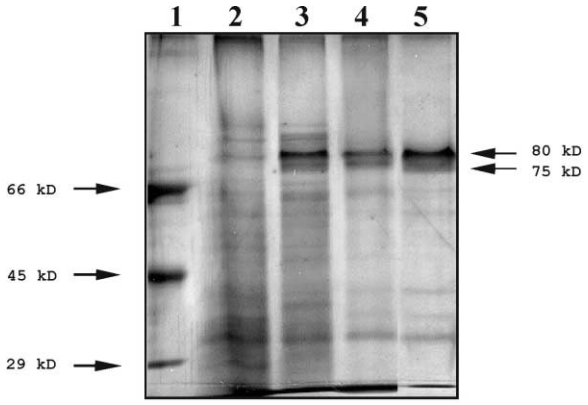

Fig. 3. SDS-PAGE analysis. Protein samples from each step of purification were subjected to SDS-PAGE (7.5% acrylamide) under reducing conditions. lane 1, protein markers; lane 2, crude root pellet extract; lane 3, 40–60% ammonium sulfate fraction; lane 4, activity peak from DEAE-Sephadex; lane 5, activity peak from CM-Sephadex.

group modifiers such as iodoacetate and *p*-chloromercuribenzoate (PCMB) had little or no effect (Table 2), possibly due either to the different accessibility of the protein SH groups to these compounds (Esen, 1992) or to their different redox potentials (Jocelyn, 1972). Consistent with the presence of critical sulfhydryl groups, inhibition by silver ions was prevented in the presence of β-mercaptoethanol. In the presence of 250 mM β-mercaptoethanol, the IC_{50} for Ag^{+} inhibition increased 100 fold from 140 μM (without β-mercaptoethanol) to 14 mM (data not shown). The importance of SH groups in ICHG is consistent with the fact that cysteine residues are involved in stability and enzyme activity of β-glucosidases (Rotrekl et al., 1999; Hakulinen et al., 2000), although most β-glucosidases in Family 1 (Henrissat, 1991) require two essential carboxylates for their catalytic activity, contributing to the general acid/base and nucleophilic catalysis (Zechel and Withers, 2000). The transition state analogue inhibitor, glucono-δ-lactone, was not very effective. The IC_{50} with this inhibitor was 24 mM (data not shown), while the counterpart in chickpea was more sensitive to this inhibitor, with an IC_{50} of 1 mM (Hösel and Barz, 1975).

The activity of the ICHG on a variety of glycoside substrates is summarized in Table 3. This enzyme is able to hydrolyze a range of synthetic glucosides, but generally only with relatively low specificity constant (k_{cat}/K_m). Although the enzyme has moderate affinity with several other natural glucosides, the specificity constant for those tested is far lower than that of the isoflavone conjugates (Table 3). Interestingly, the enzyme showed no measurable activity with several flavonol glycosides, although we did not test the 7-*O*-substituted flavones or flavonols. In contrast, commercial almond emulsin β-glucosidase has much higher specificity toward the synthetic substrate, *p*-nitrophenyl β-glucoside than toward the isoflavone conjugates (Table 3). While almond emulsin β-glucosidase does not hydrolyze the malonylglucosyl isoflavone conjugates, consistent with the fact that most β-glucosidases only cleave non-modified terminal glucose residues, the partially purified ICHG apparently hydrolyzes malonyl isoflavone glucosides as well as isoflavone glucosides with similar kinetics (Table 3). The breakdown of isoflavone conjugates is mediated by two distinct enzymes in chickpea, a malonylesterase and a β-glucosidase, which successively

Table 2
The effect of inorganic and organic chemicals on the activity of the isoflavone-conjugate hydrolyzing β-glucosidase

Inorganic chemicals		Relative activity[a] (%)	Organic chemicals[b]		Relative activity[a]
$AgNO_3$	1 mM	35	Iodoacetate	1 mM	97
	10 mM	0		10 mM	74
$HgCl_2$	1 mM	62	PCMB	0.1 mM	102
	10 mM	23		1 mM	103
$CaCl_2$	1 mM	99	Glucono-δ-lactone	1 mM	99
	10 mM	94		10 mM	93
$MgCl_2$	1 mM	92	PMSF (in 95% EtOH)	1 mM	89
	10 mM	82		control	97
$CoCl_2$	1 mM	97		10 mM	41
	10 mM	102		Control	37
$MnCl_2$	1 mM	99	Eserine	1 mM	87
	10 mM	74	DMSO	5%	117
$CuSO_4$	1 mM	99	EGMME	5%	109
	10 mM	115	EGDME	5%	120
$ZnSO_4$	1 mM	104			
	10 mM	77			

[a] Values are the means of two determinations in two independent experiments.
[b] Chemical abbreviations: PCMB, *p*-chrolomercuribenzoate; DMSO, dimethyl sulfoxide; PMSF, phenylmethylsulfonyl fluoride; EGGME, ethylene glycol monomethyl ether; EGDME, ethylene glycol dimethyl ether.

Table 3
Reaction parameters and substrate specificity of the isoflavone conjugate-hydrolyzing glucosidase (ICHG) compared with that of the glucosidase from almond emulsin (AEG)

Substrates	Structures	ICHG			AEG		
		K_m[a] (M)	k_{cat}[a] (s^{-1})	k_{cat}/K_m (M^{-1} s^{-1})	K_m[a] (M)	k_{cat}[a] (s^{-1})	k_{cat}/K_m (M^{-1} s^{-1})
p-Nitrophenyl β-glucoside	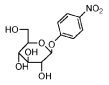	1.3×10^{-3}	0.11	8.1×10^{1}	2.2×10^{-3}	1.2×10^{2}	5.2×10^{4}
p-Nitrophenyl β-galactoside	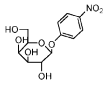	1.3×10^{-2}	0.93	7.2×10^{1}	2.6×10^{-3}	6.8	2.6×10^{3}
p-Nitrophenyl β-mannoside	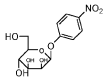	N.R.[b]	–	–	N.R.	–	–
p-Nitrophenyl α-glucoside	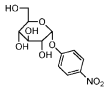	N.R.	–	–	N.R.	–	–
p-Nitrophenyl α-galactoside	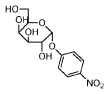	8.4×10^{-4}	0.49	5.8×10^{2}	N.R.	–	–
p-Nitrophenyl α-mannoside	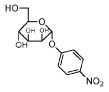	9.9×10^{-3}	0.10	1.0×10^{1}	[c]	–	–
o-Nitrophenyl β-glucoside	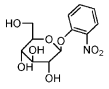	1.4×10^{-3}	1.4	1.0×10^{3}	3.9×10^{-3}	5.0	1.3×10^{3}
4-Methylumbelliferyl β-glucoside	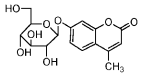	2.3×10^{-4}	0.05	2.3×10^{2}	2.3×10^{-3}	4.7×10^{1}	2.0×10^{4}
Salicin	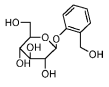	3.5×10^{-3}	0.21	6.0×10^{1}	1.1×10^{-2}	0.83	7.6×10^{1}
Esculin	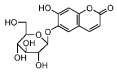	8.8×10^{-3}	0.02	2.8			
Arbutin	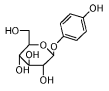	6.1×10^{-3}	0.15	2.4×10^{1}			
Genistein 7-*O*-glucoside (genistin)	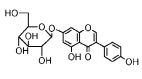	3.3×10^{-4}	4.45	1.3×10^{4}	1.1×10^{-2}	0.65	5.9×10^{1}
Genistein 7-*O*-glucosyl 6-*O*-malonate (MGG)	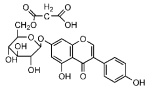	5.4×10^{-5}	4.38	8.1×10^{4}	[c]	–	–
Daidzein 7-*O*-glucoside (daidzin)	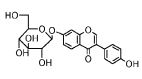	9.1×10^{-5}	3.07	3.4×10^{4}			

(*continued on next page*)

Table 3 (*continued*)

Substrates	Structures	ICHG			AEG		
		K_m[a] (M)	k_{cat}[a] (s^{-1})	k_{cat}/K_m (M^{-1} s^{-1})	K_m[a] (M)	k_{cat}[a] (s^{-1})	k_{cat}/K_m (M^{-1} s^{-1})
Daidzein 7-*O*-glucosyl 6"-*O*-malonate (MDG)	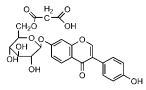	1.2×10^{-4}	4.34	3.6×10^{4}			
Rutin	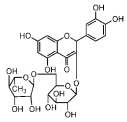	N.R.	–	–			
Isoquercitrin	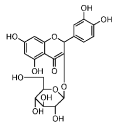	N.R.	–	–			
Phloridzin	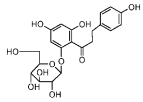	N.R.	–	–			
Amygdalin	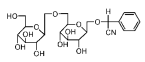	[c]	–	–			

[a] Values are means of determinations in three independent experiments.
[b] N.R.: no reaction at 40 °C for 30 min.
[c] The products were too small to measure or difficult to calculate K_m and V_{max}.

remove the malonyl and glucose moieties, respectively (Fig. 1). By using the isoflavone conjugate mixture coupled with the HPLC assay, we are able to examine these two enzyme activities simultaneously. However, a separate malonylesterase activity was never observed in any soybean tissue extract or at any stage of purification. Moreover, the lack of esterase activity in the partially purified IGHG preparation was also demonstrated when malonylated isoflavone glucosides were the sole substrates in the assay system with an excess of the glucosidase inhibitor, glucono-δ-lactone, over its IC_{50} value (data not shown). While the current data certainly do not preclude the existence of a separate isoflavone malonyl esterase in soybean and do not unequivocally support the existence of both activities in ICHG, it is possible that the soybean system may differ in this regard from the chickpea system. In the literature, only one other β-glucosidase, the flavone 7-*O*-glucoside-specific β-glucosidase from ligulate florets of *Chamomilla recutita*, can also use apigenin 7-*O*-acetylglucoside as a substrate, but the V_{max} was reduced dramatically when the glucose is esterified (Maier et al., 1993). Ultimately, more detailed characterization of the various enzymes will be needed to resolve these issues.

3. Conclusions

The hydrolysis of glucosyl and malonylglucosyl isoflavone conjugates is biologically relevant. A relatively high percentage of the total malonylated isoflavone glucosides is found in the apoplast in soybean (T. L. Graham, unpublished observation) and in chickpea. The genistein aglycone is toxic to fungal pathogens, such as *Phytophthora sojae* (Rivera-Vargas et al., 1993), and genistein also may function to activate an extracellular NADH oxidase that functions in defense potentiation (Graham and Graham, 1999). The quick release of genistein during pathogen attack by the apoplastic isoflavone conjugate-hydrolyzing β-glucosidase may thus be critically important for several aspects of disease resistance.

Although previous non-specific β-glucosidases were reported to hydrolyze isoflavone glucosides in soybean (Matsuura and Obata, 1993; Matsuura et al., 1995), the currently purified soybean ICHG has higher specific activity towards isoflavone conjugates with substrate specificity constants 160-fold to 1000-fold over *p*-nitrophenyl β-glucoside (Table 3). The β-glucosidase B and C isolated from soybean cotyledons had a relatively low

reaction rates (79 and 38%, respectively) with isoflavone glucosides compared to *p*-nitrophenyl β-glucoside (100%) (Matsuura and Obata, 1993; Matsuura et al., 1995). The substrate binding affinities of ICGH towards isoflavone conjugates are comparable to the chickpea isoflavone-specific β-glucosidase and flavone-glucoside-cleaving β-glucosidase from *Charmomilla recutita* (in the submillimolar range), suggesting favored binding to their natural substrates (Hösel and Barz, 1975; Maier et al., 1993). However, chickpea isoflavone-specific β-glucosidase has apparently higher specificity constants toward formononetin and biochanin A glucosides ($\sim 10^6$ M^{-1} s^{-1}) than that of ICHG. Furthermore, Hg^+, Ag^+ and glucono-δ-lactone are all inhibitory to ICGH, consistent with other plant β-glucosidases, although ICGH is less sensitive to Hg^+ and glucono-δ-lactone compared to the chickpea enzyme. Although further characterization will be required to firmly determine this, the ICHG may hydrolyze isoflavone malonylglucosides directly. This may distinguish it from the chickpea β-glucosidase. Taken together, we conclude that the β-glucosidase purified from soybean roots is a novel β-glucosidase with high specificity toward isoflavone conjugates.

4. Experimental

4.1. Plant material

Soybean (*Glycine max* L.) cv. Williams was obtained from Dr. A. F. Schmitthnner (Department of Plant Pathology, The Ohio State University and the Ohio Agricultural Research and Development Center, Wooster, OH). Seedlings were grown as described previously (Graham, 1991a). Soybean roots from 7–9 day-old seedlings were washed with tap water to remove planting media and blotted with paper towels. The roots were frozen at −20 °C until used.

4.2. Isolation and purification of isoflavone conjugates

Isoflavone conjugate substrates were prepared as follows. Soybean cv. Williams seeds (50 g) were ground to a fine powder with a coffee grinder and the powder was extracted with 100 ml chloroform for 30 min with stirring. The slurry was filtered through Whatman No. 1 filter paper with suction and washed two more times with chloroform. The defatted soybean flour was extracted twice with 50 ml distilled water. The aqueous extract (100 ml) was clarified by low speed centrifugation (International Equipment Co., Needham, MA). The isoflavone conjugates of genistein and daidzein were partially purified using a C18 PrepSep column (Fisher Scientific, Springfield, NJ). The crude aqueous substrate preparation was passed through the column, and the column was washed successively with water and 1 ml of 10% acetonitrile (HPLC grade, Sigma Chemical Co., MO). The 10% eluent was discarded. Washing with 1 ml of 20% acetonitrile released bound daidzin, genistin, MGD and MGG. This provided a preparation of the isoflavone conjugates free of aglycones (which remained bound to the column and are eluted only at higher acetonitrile concentrations). For measurement of enzyme activity in initial protein fractionations, this isoflavone conjugate fraction was brought to dryness and dissolved in an appropriate amount of 100 mM phosphate–50 mM citrate buffer, pH 5.0 to make the concentrations of each isoflavone conjugate greater than 2.5 mM as judged by HPLC (Graham, 1991a). For final purification and characterization of the glucosidase, individual isoflavone conjugates were isolated by semi-preparative HPLC using a Merck Lichrosorb RP-18 10 mm C18 column (Alltech Associates, Deerfield, IL) with non-acidic water and acetonitrile as described by Graham (1991a).

4.3. Buffers

Buffer A, 200 mM sodium phosphate buffer, pH 6.0; buffer B, 200 mM sodium phosphate buffer, pH 6.0, containing 0.5 M NaCl; buffer C, 20 mM sodium phosphate buffer, pH 6.0, containing 3 mM DTT and 10% glycerol; buffer D, buffer C containing 1 M NaCl; buffer E, buffer C containing 5 mM sodium ascorbate; and buffer F, buffer D containing 5 mM sodium ascorbate.

4.4. Enzyme extraction and purification

Frozen roots were ground almost to a powder in a mortar and pestle pre-chilled to 0 °C and extracted three times with cold buffer A (1 ml buffer/ 1 g tissue). The combined extracts were centrifuged at 10,000×*g* for 10 min. The pellet was extracted with buffer B (1 ml buffer/ g tissue) overnight at 4 °C. The root residue was further extracted one more time with an equal volume of buffer B for another 3 h. The crude extracts were pooled and 1% (w/v) insoluble polyvinylpolypyrolidone (PVPP) was added to remove phenolics. This mixture was stirred for 3 h on ice. The extract was then filtered through four-layers of cheesecloth, and clarified by centrifugation at 10,000×*g* for 20 min. The resulting solution was slowly brought to 40–60% saturation with solid ammonium sulfate at 4 °C followed by gentle stirring overnight. The pellet was collected by centrifugation at 10,000×*g* for 20 min, and then dissolved in a minimum volume of buffer C. The protein solution was clarified by centrifugation and desalted using a Sephadex G-25 column (1.7×20 cm) equilibrated with buffer C. The desalted protein solution was applied to a DEAE-Sephadex A-50 column (2.8×35 cm) equilibrated with the same buffer system and washed with buffer C. The enzyme was found in the unbound fractions. Sodium

ascorbate was added to the protein solution to a final concentration of 5 mM, and the solution was then loaded onto a column of CM-Sephadex C-50 (2.8×19 cm), equilibrated with buffer E. The elution was carried out with a 400 ml linear gradient of buffer F in buffer E. Chromatographic fractions having ICHG activity were pooled and lyophilized. The concentrated enzyme was stored at −20 °C for further study.

4.5. Enzyme and protein assays

Protein concentration was determined by the Bradford (1976) method with BSA as standard. During purification and unless otherwise noted, ICHG activity was determined in 0.2 M phosphate–0.1 M citrate buffer, pH 5.0 at 40 °C in a total reaction volume of 10 μl containing 5 μl of isoflavone conjugate mixture. The reaction was stopped at 30 min by adding 90 μl of methanol and activity was measured by quantifying the release of aglycones by HPLC (Graham, 1991a). This enzyme assay allowed us to simultaneously examine the relative release of aglycones from both daidzein and genistein conjugates, and also allowed us to measure the possible esterase activities in fractions leading to the formation of daidzin and genistin from MGD and MGG, respectively. During the course of the fractionation, the glucosidic activities towards daidzein and genistein conjugates were always comparable and thus results are expressed in terms of total aglycone release. One unit of enzyme activity was defined as the amount of enzyme that produced 1 mmol of product per minute. Specific activity was expressed as enzyme units per mg protein. No apparent conversion of MGD or MGG to daidzin or genistin was observed in any extract or during any fractionation step; that is, we never observed an isoflavone-specific malonylesterase activity as reported in chickpea (Hösel and Barz, 1975).

In the study of substrate specificity, the concentration of substrate was 2 mM unless otherwise noted. Daidzein 7-*O*-glucoside, daidzein 7-*O*-glucoside-6″-*O*-malate, genistein 7-*O*-glucoside, and genistein 7-*O*-glucoside-6″-*O*-malate were assayed at 0.2, 0.18, 0.79 and 1.15 mM, respectively. The appropriate concentration of the ICHG used for each substrate was determined graphically from the linear portions of initial reaction velocity. All substrates were dissolved in 0.2 M phosphate–0.1 M citrate buffer, pH 5.0, except that *p*-nitrophenyl α-glucoside, 4-methylumbelliferyl β-glucoside, and genistein 7-*O*-glucoside were dissolved in ethylene glycol monoethyl ether at 50 mM and then diluted to final concentration in the same buffer.

Depending on the substrate, activity was measured either spectrophotometrically or by HPLC. For those substrates releasing an aglycone with known molar coefficient (ϵ), the assay solution containing the enzyme (10 μl) and substrate (90 μl) in 0.2 M phosphate–0.1 M citrate buffer, pH 5.0, was incubated at 40 °C for various time courses. The reaction was stopped by alkalization of the assay mixture with 100 μl of sodium carbonate, and the mix was then diluted to 1 ml with distilled water for measurement of absorbance. For quantitative calculations, the following wavelengths and ε values (mM^{-1} cm^{-1}) were used: *p*-nitrophenol, 400 nm, $\varepsilon = 19.3$; *o*-nitrophenol, 420 nm, $\varepsilon = 4.55$; 4-methylumbelliferone, 360 nm, $\varepsilon = 18.25$; and salicyl alcohol, 295 nm, $\varepsilon = 3.3$. For the substrates, esculin and arbutin, without known ε values, the following method was developed. The UV spectrum of esculin showed a peak at 374 nm and the absorbance intensity decreased over time with enzymatic activity. The activity assay was conducted as described above, and the absorbance change was converted to concentration by a linear standard curve made from various concentrations of esculin in 100 μl Na_2CO_3 and 900 μl water. The enzyme activity against arbutin was determined similarly at 267 nm.

Activity against several natural substrates was assayed by the HPLC method for isoflavone conjugates as described above for enzyme purification, except that the total reaction volume was 15 μl and the reaction was stopped at various times by adding 85 μl of methanol. The substrates assayed by HPLC included the four isoflavone conjugates, two flavonol glycosides (rutin and isoquercitrin), phloridzin (a chalcone glucoside), and amygdalin (a cyanogenic di-glucoside). Commercial almond emulsin β-glucosidase, a classic non-specific β-glucosidase, was also examined to compare substrate specificity. All K_m and V_{max} values were calculated based on Lineweaver-Burk plots, and the k_{cat} value is equal to V_{max} divided by the total enzyme concentration (in molarity) which was calculated using M_r of 165 kDa for ICHG and 135 kDa for almond emulsin β-glucosidase. The kinetic parameters reported are the mean values of two or three independent determinations.

The temperature optimum of the ICHG was resolved by incubating the enzyme solution with isoflavone conjugates over a temperature range from 0 to 90 °C for 30 min. Enzyme activity was monitored by the standard HPLC method. To determine the pH optimum, 4-methylumbelliferyl β-glucoside was used in various buffers varying in pH values from 2.6 to 10.6. Enzyme activity was determined spectrophotometrically as described above.

4.6. SDS-polyacrylamide gel electrophoresis (PAGE)

SDS-PAGE was performed as described by Laemmli (1970) using a Mini-Protein II electrophoresis system (Bio-Rad). Analyses were carried out under non-reducing or reducing (mercaptoethanol) conditions as specified. The molecular markers used were bovine serum albumin (66 kD), ovalbumin (45 kD), and carbonic

anhydrase (29 kD) all from Sigma Chemical Co. Protein gels were stained with silver stain (Bio-Rad).

4.7. Inhibition assays

Several inorganic and organic compounds and solvents were examined for their inhibitory effects. The reaction mixture was in 0.2 M phosphate–0.1 M citrate buffer, pH 5.0 using a total reaction volume of 15 μl incubated at 40 °C for 30 min; the reaction was stopped by adding 85 μl of methanol. The enzyme activity was measured by HPLC and designated as 100% in the absence of added chemicals. The activity reported is the average from two independent measurements. A series of concentrations of Ag^+, β-mercaptoethanol and glucono-δ-lactone, respectively, were further inspected to determine the concentration for 50% inhibition (IC_{50}). For prevention of inhibition of activity by silver ions, 250 mM of β-mercaptoethanol was incubated with 5 μl of isoflavone-conjugate substrate and 5 μl of various concentrations of Ag^+ for 20 min before the enzyme was introduced. IC_{50} values are obtained from the least square fit to the Langmuir isotherm equation, $v_i/v_0 = 1/(1 + [I]/IC_{50})$, using Igor Pro software (WaveMetrics, Inc., OR), where v_i is the velocity in the presence of inhibitor at concentration [I] and v_0 is the velocity in the absence of inhibitor.

Acknowledgements

We would like to acknowledge frequent stimulating conversations with and useful suggestions for the work from Dr. Madge Graham. Funding for this project was provided by grants from the USDA-NRI and the North Central Biotechnical Consortium. Salaries and research support were also provided by State and Federal Funds appropriated to the Ohio Agricultural Research and Development Center, the Ohio State University.

References

Barz, W., Welle, R., 1992. Biosynthesis and metabolism of isoflavones and pterocarpan phytoalexins in chickpea, soybean, and phytopathogenic fungi. Recent Adv. Phytochem. 26, 139–164.

Bell, E.A., 1981. The physiological role(s) of secondary (natural) products. In: Stumpf, P.K., Conn, E.E. (Eds.), The Biochemistry of Plants, Secondary Plant Products, Vol. 7. Academic Press, New York, pp. 1–19.

Bradford, M.M., 1976. A rapid and sensitive method for quantitation of microgram quantities of protein utilizing the principle of protein-dye binding. Anal. Biochem. 72, 248–254.

Conn, E.E., 1993. β-Glucosidases in plants. In: Esen, A. (Ed.), β-Glucosidase: Biochemistry and Molecular Biology. American Chemical Society, Washington, DC, pp. 14–26.

Czjzek, M., Cicek, M., Zamboni, V., Bevan, D.R., Henrissat, B., Esen, A., 2000. The mechanism of substrate (aglycone) specificity in β-glucosidases is revealed by crystal structures of mutant maize β-glucosidase-DIMBOA, -DIMBOAGlc, and -dhurrin complexes. Proc. Natl. Acad. Sci. 97, 13555–13560.

Dakora, F.D., Phillips, D.A., 1996. Diverse functions of isoflavonoids in legumes transcend antimicrobial definitions of phytoalexins. Physiol. Mol. Plant Pathol. 49, 1–20.

Day, A.J., Cañada, F.J., Díaz, J.C., Kroon, P.A., Mclauchlan, R., Faulds, C.B., Plumb, G.W., Morgan, M.R.A., Williamson, G., 2000. Dietary flavonoids and isoflavone glycosides are hydrolysed by the lactase site of lactase phlorizin dydrolase. FEBS Lett. 468, 166–170.

Dharmawardhana, D.P., Ellis, B.E., Carlson, J.E., 1995. A β-glucosidase from lodgepole pine xylem specific for the lignin precursor coniferin. Plant Physiol. 107, 331–339.

Duroux, L., Delmotte, F.M., Lancelin, J.-M., Kéravis, G., Jay-Allemand, C., 1998. Insight into naphthoquinone metabolism: β-glucosidase-catalysed hydrolysis of hydrojuglone β-D-glucopyranoside. Biochem. J. 333, 275–283.

Ebel, J., 1986. Phytoalexin synthesis: the biochemical analysis of the induction process. Annu. Rev. Phytopathol. 24, 235–264.

Esen, A., 1992. Purification and partial characterization of maize (*Zea mays* L.) β-glucosidase. Plant Physiol. 98, 174–182.

Esen, A., 1993. β-Glucosidases, overview. In: Esen, A. (Ed.), β-Glucosidase: Biochemistry and Molecular Biology. American Chemical Society, Washington, DC, pp. 1–13.

Graham, T.L., 1991a. A rapid, high resolution HPLC profiling procedure for plant and microbial aromatic secondary metabolites. Plant Physiol. 95, 584–593.

Graham, T.L., 1991b. Flavonoid and isoflavonoid distribution in developing soybean seedling tissues and in seed and root exudates. Plant Physiol. 95, 594–603.

Graham, T.L., Graham, M.Y., 1996a. Signaling in soybean phenylpropanoid responses. Dissection of primary, secondary, and conditioning effects of light, wounding, and elicitor treatments. Plant Physiol. 110, 1123–1133.

Graham, T. L., Graham, M. Y., 1996b. Cell surface reduction of tetrazolium dyes induces elicitation competency in soybean. In: 8th International Congress Molecular Plant–Microbe Interactions, Knoxville, TN, 14-19 July 1996.

Graham, T.L., Graham, M.Y., 1999. Role of hypersensitive cell death in conditioning elicitation competency and defense potentiation. Physiol. Mol. Plant Pathol. 55, 13–20.

Graham, T.L., Graham, M.Y., 2000. Defense potentiation and elicitation competency: redox conditioning effects of salicylic acid and genistein. In: Stacey, G., Keen, N.T. (Eds.), Plant Microbe Interactions, Vol. 5. APS Press, St. Paul, MN, pp. 181–220.

Graham, T.L., Kim, J.E., Graham, M.Y., 1990. Role of constitutive isoflavone conjugates in the accumulation of glyceollin in soybean infected with *Phytophthora megasperma*. Mol. Plant–Microbe Interactions 3, 157–166.

Hakulinen, N., Paavilainen, S., Korpela, T., Rouvinen, J., 2000. The crystal structure of β-glucosidase from *Bacillus circulans* sp. *alkalophilus*: Ability to form long polymeric assemblies. J. Struct. Biol. 129, 69–79.

Harborne, J.B., Mabry, T.J., 1982. The Flavonoids: Advances in Research. Chapman and Hall, London.

Henrissat, B., 1991. A classification of glycosyl hydrolases based on amino acid sequence similarities. Biochem. J. 280, 309–316.

Hinderer, W., Köster, J., Barz, W., 1986. Purification and properties of a specific isoflavone 7-*O*-glucoside-6″-malonate malonylesterase from roots of chickpea (*Cicer arietinum* L.). Arch. Biochem. Biophys. 248, 570–578.

Hösel, W., Barz, W., 1975. β-Glucosidases from *Cicer arietinum* L.: purification and properties of isoflavone-7-*O*-glucoside-specific-β-glucosidases. Eur. J. Biochem. 57, 607–616.

Hösel, W., Surholt, E., Borgmann, E., 1978. Characterization of β-glucosidase isoenzymes possibly involved in lignification from chickpea (*Cicer arietinum* L.) cell suspension cultures. Eur. J. Biochem. 84, 487–492.

Hungria, M., Stacey, G., 1997. Molecular signals exchanged between host plants and rhizobia: basic aspects and potential application in agriculture. Soil Biol. Biochem. 29, 819–830.

Inoue, K., Ebizuka, Y., 1996. Purification and characterization of furostanol glycoside 26-O-β-glucosidase from *Costus speciosus* rhizomes. FEBS Lett. 378, 157–160.

Johnson, G., Maag, D.D., Johnson, D.K., Thomas, R.D., 1976. The role of phytoalexins in the resistance of sugarbeet (*Beta vulgaris*) to *Cercospora beticola*. Physiol. Plant Pathol. 8, 225–230.

Jocelyn, P.C., 1972. Biochemistry of the SH group. The Occurrence, Chemical Properties, Metabolism and Biological Function of Thiols and Disulphides. Academic Press, New York, pp. 404.

Kessmann, H., Edwards, R., Geno, P.W., Dixon, R.A., 1990. Stress responses in alfalfa (*Medicago sativa* L.). V. Constitutive and elicitor-induced accumulation of isoflavonoid conjugates in cell suspension cultures. Plant Physiol. 94, 227–232.

Kleczkowski, K., Schell, J., 1995. Phytohormone conjugates: nature and function. Crit. Rev. Plant Sci. 14, 283–298.

Koes, R.E., Quattrocchino, F., Mol, J.N.M., 1994. The flavonoid biosynthetic pathway in plants: function and evolution. BioEssays 16, 123–132.

Kramer, R.P., Hindorf, H., Jha, H.C., Kallage, J., Zilliken, F., 1984. Antifungal activity of soybean and chickpea isoflavones and their reduced derivatives. Phytochemistry 23, 2203–2205.

Laemmli, U.K., 1970. Cleavage of structural proteins during the assembly of the head of the bacteriophage T4. Nature 227, 680–685.

Leah, R., Kigel, J., Svendsen, I., Mundy, J., 1995. Biochemical and molecular characterization of a barley seed β-glucosidase. J. Biol. Chem. 270, 15789–15797.

Mackenbrock, U., Barz, W., 1991. Elicitor-induced formation of pterocarpan phytoalexins in chickpea (*Cicer arietinum* L.) cell suspension cultures from constitutive isoflavone conjugates upon inhibition of phenylalanine ammonia lyase. Z. Naturforsch. 46c, 43–50.

Maier, R., Carle, R., Kreis, W., Reinhard, E., 1993. Purification and characterization of a flavone 7-O-glucoside-specific glucosidase from ligulate florets of *Chamomilla recutita*. Planta Med. 59, 436–441.

Matsuura, M., Obata, A., 1993. β-Glucosidases from soybeans hydrolyze daidzin and genistin. J. Food Sci. 58, 144–147.

Matsuura, M., Sasaki, J., Murao, S., 1995. Studies on β-glucosidases from soybeans that hydrolyze daidzin and genistin: isolation and characterization of an isozyme. Biosci. Biotech. Biochem. 59, 1623–1627.

Morris, P.F., Ward, E.W.B., 1992. Chemoattraction of zoospores of the soybean pathogen, *Phytophthora sojae*, by isoflavones. Physiol. Plant Pathol. 40, 17–22.

Phillips, D. A., Streit, W., 1996. Legume signals to rhizobial symbionts: a new approach for defining rhizosphere colonization. In: Stacey, G., Keen, N. (Eds.), Plant–Microbe Interactions, Vol. 1. pp. 236–271.

Phillips, D.A., Stafford, H.A., Ibrahim, R.K., 1992. Flavonoids: plant signals to soil microbes. Recent Adv. Phytochem. 26, 201–231.

Poulton, J.E., 1990. Cyanogenesis in plants. Plant Physiol 94, 401–405.

Rivera-Vargas, L.I., Schmitthenner, A.F., Graham, T.L., 1993. Soybean flavonoid effects on and metabolism by *Phytophthora sojae*. Phytochemistry 32, 851–857.

Rotrekl, V., Nejedla, E., Kucera, I., Abdallah, F., Palme, K., Brzobohaty, B., 1999. The role of cysteine residues in structure and enzyme activity of a maize β-glucosidase. Eur. J. Biochem. 266, 1056–1065.

Weidenborner, M., Hindorf, H., Jha, H.C., Tsotsonos, P., Egge, H., 1990. Antifungal activity of isoflavonoids in different reduced stages on *Rhizoctonia solani* and *Sclerotium rolfsii*. Phytochemistry 29, 801–803.

Zechel, D.L., Withers, S.G., 2000. Glycosidase mechanisms: anatomy of a finely tuned catalyst. Acc. Chem. Res. 33, 11–18.

PERGAMON

Phytochemistry 58 (2001) 1007–1013

PHYTOCHEMISTRY

www.elsevier.com/locate/phytochem

Phospho*enol*pyruvate carboxylase from cherimoya fruit: properties, kinetics and effects of high CO_2

Teresa Muñoz, María Isabel Escribano, Carmen Merodio*

Departamento de Ciencia y Tecnología de Productos Vegetales, Instituto del Frío, Consejo Superior de Investigaciones Científicas, Ciudad Universitaria, 28040-Madrid, Spain

Received 23 February 2001; received in revised form 30 July 2001

Abstract

Phospho*enol*pyruvate carboxylase (PEPC, EC 4.1.1.31) regulatory properties were studied in non-photosynthetic (mesocarp) and photosynthetic (peel) tissues from cherimoya (*Annona cherimola* Mill.) fruit stored in air, in order to gain a better understanding of in vivo enzyme regulation. Analyses were also performed with fruit treated with 20% CO_2–20% O_2 to define the role of PEPC as part of an adaptive mechanism to high external carbon dioxide levels. The results revealed that the special kinetic characteristics of the enzyme from mesocarp—high V_{max} and low sensibility to L-malate inhibition - are related to the active acid metabolism of these fruits and point to a high rate of reassimilation of respired CO_2 into keto-acids. With respect to fruit stored in air, PEPC in crude extracts from CO_2-treated cherimoyas gave a similar V_{max} (1.12 ± 0.03 μkat·mg^{-1} protein), a lower apparent K_m (68 ± 9 μM for PEP) and a higher I_{50} of L-malate (5.95 ± 0.3 mM). These kinetic values showed the increase in the affinity of this enzyme toward one of its substrate, PEP, by elevated external CO_2 concentrations. The lower K_m value and lower sensitivity to L-malate are consistent with higher in vivo carboxylation reaction efficiency in CO_2-treated cherimoyas, while pointing to an additional enzyme regulation system via CO_2. © 2001 Elsevier Science Ltd. All rights reserved.

Keywords: Annona cherimola; Annonaceae; Cherimoya; High CO_2 levels; Kinetic properties; L-Malate; Non-photosynthetic tissues; Phospho*enol*pyruvate carboxylase; Pyruvate

1. Introduction

Phospho*enol*pyruvate carboxylase (PEPC, EC 4.1.1.31) catalyses irreversible carboxylation of phosphoenolpyruvate (PEP) in the presence of Mg^{2+} and/or Mn^{2+} and bicarbonate to yield oxaloacetate and Pi under physiological conditions. PEPC, with a relatively low K_m for the bicarbonate substrate, plays a general role in the carbon economy of fruits by recapturing atmospheric or respiratory CO_2 in C_4-dicarboxylic acid metabolism (Blanke, 1991). Several functions have been described for the PEPC enzyme in non-photosynthetic tissues: replenishment of tricarboxylic acid cycle intermediates, NADPH generation, recapture of respired CO_2, malate fermentation, pH stability and maintenance of electroneutrality (Andreo et al., 1987).

PEPC enzyme is present in all fruits so far examined (Blanke et al., 1986; Blanke and Notton, 1991) and has been characterised in several kinds of fruit (Lakso and Kliewer, 1975; Blanke et al., 1988; Notton and Blanke, 1993; Law and Plaxton, 1995). PEPC has been reported to refix some of the CO_2 produced during respiration in climacteric fruit (Blanke et al., 1987). With respect to the effect of high external CO_2 concentrations on PEPC activity, Blanke and Notton (1991) observed no inhibition of this activity in vitro up to 125 mM CO_2 (equivalent to 87% CO_2) in avocado fruit. Thus, there was no inhibition of enzyme activity at the intercellular CO_2 concentration of 2–3% at harvest, which rose to 20% CO_2 during the respiratory climacteric in this fruit.

Ripening cherimoya fruit have been found to exhibit a high respiration rate (with two maxima of up to 200 mg CO_2 kg^{-1} h^{-1}) and high acidity (Merodio and De La Plaza, 1997). Also, we have observed that pretreatments with high concentrations of CO_2 (20%) improved fruit chilling tolerance during storage at low temperatures (Merodio et al., 1998) and delayed the ripening process during storage at ambient temperature (Muñoz et al., 1999). Bearing in mind these specific characteristics of cherimoya fruit, the aims of the present study were 1) to

* Corresponding author:Tel.: +34-91-5445607; fax: +34-91-5493627.

E-mail address: merodio@if.csic.es (C. Merodio).

0031-9422/01/$ - see front matter © 2001 Elsevier Science Ltd. All rights reserved.
PII: S0031-9422(01)00385-5

examine the activity and kinetic properties of crude PEPC extracts from cherimoya fruit extracted from mesocarp, a non-photosynthetic tissue, and from green photosynthetic peel tissues, as a first step towards the formulation of a model for *in vivo* regulation of PEPC in *Annonas*; and 2) to analyse the effect of treatment with 20% CO_2 on properties of PEPC and its metabolic implications in ripening cherimoya fruit.

2. Results and discussion

2.1. Kinetic characterisation of PEPC in crude extracts from cherimoya fruit mesocarp and peel

PEPC activity (0.39 ± 0.02 μkat mg^{-1} protein) in cherimoya fruit was extremely high (two or three orders higher) as compared to those described for kiwi, avocado and grape (Lakso and Kliewer, 1975; Blanke et al., 1988; Blanke and Notton, 1991) and similar to the values of 0.54 μkat mg^{-1} protein obtained from purified enzyme of banana (Law and Plaxon, 1995). The PEPC was extracted from cherimoya fruit as a soluble enzyme. Enzyme extraction was aided by the inclusion of DTT and PVPP in the extraction medium. When the crude extract was filtered through a deslating column (Econo-Pac 10DG, 10×30 cm, Sigma, 1 ml/min) the PEPC activity decreased more than six-fold. The enzyme required a divalent cation (Mg^{2+} or Mn^{2+}) for its activity, but the addition of 10 units of malate dehydrogenase (MDH) to the standard assay medium did not change the rate of NADH oxidation of the crude cherimoya enzyme extract. Moreover, because in crude cherimoya fruit extracts the MDH activity is one order of magnitude higher than PEPC activity (data not shown), the former was not a limiting factor in the assay of PEPC activity following the method previously described by Blanke et al. (1986). Thus, the assay of PEPC activity in crude cherimoya fruit extract was carried out without the addition of exogenous MDH enzyme. This result is consistent with the notion that both PEPC and MDH enzymes could be physiologically bound.

The properties and kinetic data for cherimoya fruit PEPCs were evaluated after 4 days of storage at 20 °C, when maximum PEPC activity was reached. An optimum pH of 7.8 was found for PEPC extracted from mesocarp in the pH range 6–9 (Fig. 1), determined in the presence of either 50 mM Tris–HCl or 50 mM MOPS–KOH and using saturating substrate concentrations (4 mM PEP and 12 mM bicarbonate) with 460–480 ppm CO_2 present in the laboratory. This optimum pH value was similar to those reported for PEPC in avocado (Blanke and Notton, 1991), apple (Blanke et al., 1986) and banana (Law and Plaxton, 1995).

The PEPC crude extract extracted from mesocarp and peel was used to compare kinetic properties for the substrate PEP, in the presence of saturating bicarbonate

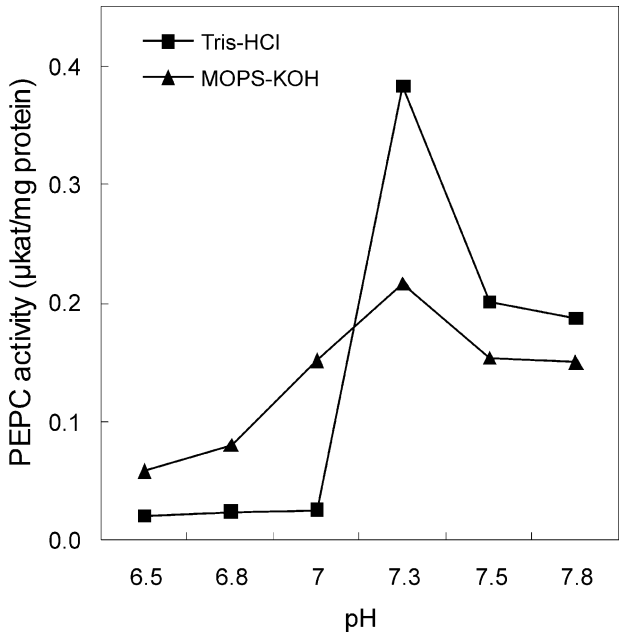

Fig. 1. Effect of pH on cherimoya PEPC activity measured in the presence of specified buffers (50 mM) and using a saturating PEP and bicarbonate concentrations.

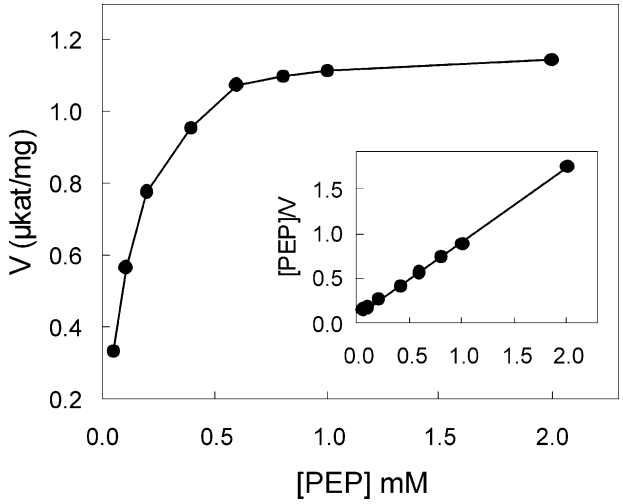

Fig. 2. Dependence on PEP concentration of the PEPC activity extracted from mesocarp tissues. The insert shows the Hanes–Woolf plot.

concentration. As Fig. 2 shows, PEPC from mesocarp followed a hyperbolic Michaelis–Menten kinetics in a substrate (PEP) concentration ranging from 0.05 to 2 mM, being saturated from 1 mM. Estimation of the kinetics parameters by different fitting approaches (Table 1) yielded similar apparent K_m (120 ± 8 μM for PEP) and V_{max} values (1.26 ± 0.02 μ kat mg^{-1} protein).

The enzyme extracted from cherimoya peel had a similar apparent K_m value (140 ± 6 μM) to PEPC from mesocarp, but the V_{max} was 0.57 ± 0.01μ kat·mg^{-1} protein (Fig. 3 and Table 1), that is 2.2 times lower than

Table 1
Kinetics parameters (PEP) for PEPC extracted from different tissues of cherimoyas stored in air or in 20% CO_2 at pH 7.8, estimated by different fitting approaches. Data are means of V_{max} (μKat/mg protein) and K_m (μM) values ± S.E.

Treatment	Tissue	Michaelis–Menten	Hanes–Woolf	Lineweaver–Burk
Air	Mesocarp	$V_{max}=1.26\pm0.02$ $K_m=120\pm8$	$V_{max}=1.24\pm0.01$ $K_m=110\pm5$	$V_{max}=1.32\pm0.05$ $K_m=150\pm5$
20% CO_2	Mesocarp	$V_{max}=1.12\pm0.03$ $K_m=68\pm9$	$V_{max}=1.12\pm0.03$ $K_m=70\pm6$	$V_{max}=1.13\pm0.05$ $K_m=70\pm5$
Air	Peel	$V_{max}=0.57\pm0.01$ $K_m=140\pm6$	$V_{max}=0.56\pm0.01$ $K_m=134\pm6$	$V_{max}=0.56\pm0.03$ $K_m=134\pm5$

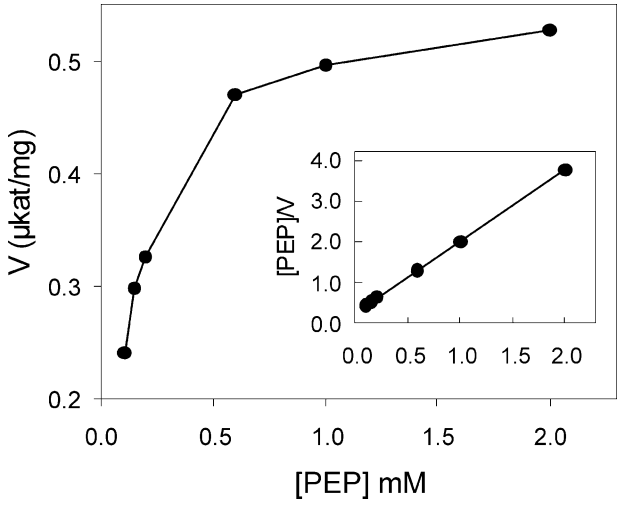

Fig. 3. Dependence on PEP concentration of the PEPC activity extracted from peel tissues. The insert shows the Hanes–Woolf plot.

the value obtained for non-photosynthetic tissues (Fig. 2 and Table 1).

PEPCs extracted from cherimoya fruit yielded higher V_{max} values for PEP than those previously reported in other fruits and plant sources and a K_m value which was comparable to those described in apple fruit, higher than in other fruits like avocado or banana, and lower than in maize leaf (a C_4-species) (Blanke et al., 1986 and references therein; Blanke and Notton, 1991; Law and Plaxton, 1995).

2.2. Effect of inhibitors on PEPC activity

Malate and pyruvate are known inhibitors of PEPC. Fig. 4 shows a semi-logarithmic representation of the dose-response curve of mesocarp PEPC activity in the presence of L-malate in a concentration range 1–12 mM. Malate inhibited enzyme activity, and the concentration required to produce 50% inhibition (I_{50} value) at pH 7.8 was 3.84±0.2 mM. PEPC from cherimoya mesocarp was more resistant to the inhibition of pyruvate, the I_{50} value being 9.5±0.5 mM, (Table 2). The L-malate and pyruvate I_{50} values for PEPC from peel were 2.01±0.1 and 8.15±0.3 mM respectively (Table 2). PEPC enzyme extracted from photosynthetic

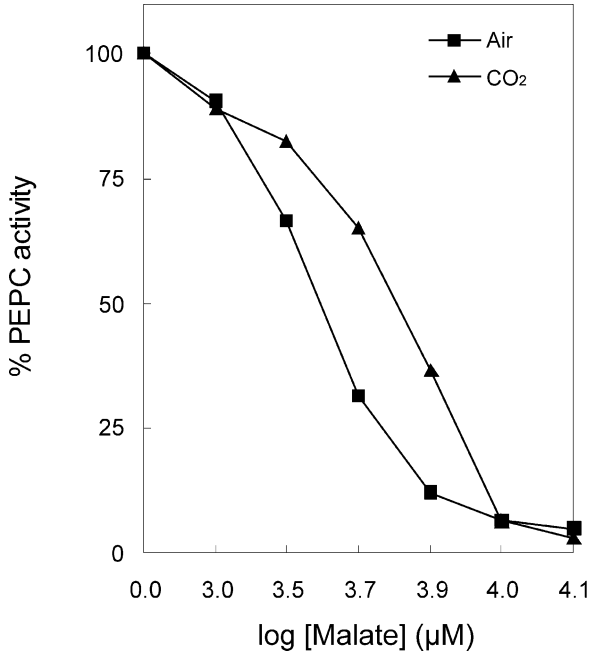

Fig. 4. Semilogarithmic plots of the dose-response curves used to determine I_{50} value for L-malate on PEPC activity extracted from mesocarp of air and 20% CO_2-treated fruit.

Table 2
I_{50} values for PEPC activity extracted from different tissues of cherimoyas stored in air or in 20% CO_2 at pH 7.8. Data are means ±S.E.

Treatment	Tissue	L-Malate (mM)	Pyruvate (mM)
Air	Mesocarp	3.84±0.2 a[a]	9.50±0.5 a
20% CO_2	Mesocarp	5.95±0.3 b	9.70±0.6 a
Air	Peel	2.01±0.1 c	8.15±0.3 b

[a] Mean separation within columns (by LSD test) at $P\leqslant 0.05$.

cherimoya tissues showed higher sensitivity to L-malate and pyruvate inhibition than enzyme from non-photosynthetic tissues.

For avocado, the inhibitory effect of malate on PEPC was pH dependent; the value of I_{50} was 150 μM at pH 7.0 and 46 mM at pH 8.0 (Blanke and Notton, 1991). The latter concentration was comparable to that reported

for the I_{50} of grape berry (35 mM) at pH 7.4 (Lakso and Kliewer, 1975). For cherimoya fruit PEPC, a value of I_{50} 3.84 mM at pH 7.8 was found, that is comparable to the concentrations reported for maize leaf PEPC (10 mM at pH 8.0, Gonzalez et al., 1984) or banana fruit PEPC (8 mM at pH 8.0, Law and Plaxton, 1995).

2.3. Changes in the regulatory and kinetic properties of PEPC enzyme from CO_2-treated cherimoyas

Calculation of the endogenous bicarbonate in the bulter using Henderson-Hasselbach equatation yielded 0.41 mM HCO_3 at pH 7.8 and 470 ppm CO_2 at room temperature. The effect of L-malate and pyruvate inhibitors was studied in PEPC extracted from mesocarp tissues of cherimoyas treated with 20% CO_2 (Fig. 4 and Table 2). As regards malate inhibition, the I_{50} value of CO_2-treated cherimoyas was 5.95 ± 0.3 mM, that is 1.5-time higher than in air-treated ones. Although significant differences were achieved in susceptibility to L-malate inhibition, the value of I_{50} for pyruvate was similar in air and CO_2-treated fruit (9.5 ± 0.5 mM and 9.7 ± 0.6 mM, respectively).

PEPC from CO_2-treated fruit exhibited a hyperbolic Michaelis–Menten curve with substrate (PEP) concentration ranging from 0.05 to 2 mM. The estimation of kinetic parameters yielded a similar V_{max} (1.12 ± 0.03 μkat mg^{-1} protein) but a lower apparent K_m value (68 ± 9 μM) for PEP (Fig. 5 and Table 1) than air-treated fruits. These kinetic values revealed increased affinity of this enzyme toward its substrate, PEP, caused by high external CO_2 concentrations. The lower K_m value, together with lower sensitivity to L-malate supports the notion of higher *in vivo* carboxylation reaction efficiency in CO_2-treated cherimoyas, while revealing an additional enzyme regulation system via CO_2.

2.4. Physiological implications of PEPC activity and effect of high levels of external CO_2

PEPC in cherimoya fruit has some of the kinetic properties (high V_{max} and intermediate K_m values) and the degree of L-malate and pyruvate inhibitions characteristic of the PEPC from C_4 and CAM species (Huber and Edwards, 1975; Osmond, 1978). The differences in the regulatory properties of PEPC from mesocarp and peel tissues (similar K_m, higher V_{max} and I_{50} values) may be related to different physiological functions. In non-photosynthetic tissues, due to its high respiration rate and where it has been previously confirmed by inmunodetection assays the absence of RuBPCase (Del Cura et al., 1996), PEPC could be involved in the re-assimilation of the CO_2 released during the climacteric respiration, as has been proposed in the case of other climacteric fruits (Blanke et al., 1986; Law and Plaxton, 1995). The high value of V_{max} and low sensitivity towards L-malate inhibition are consistent with the high concentrations of

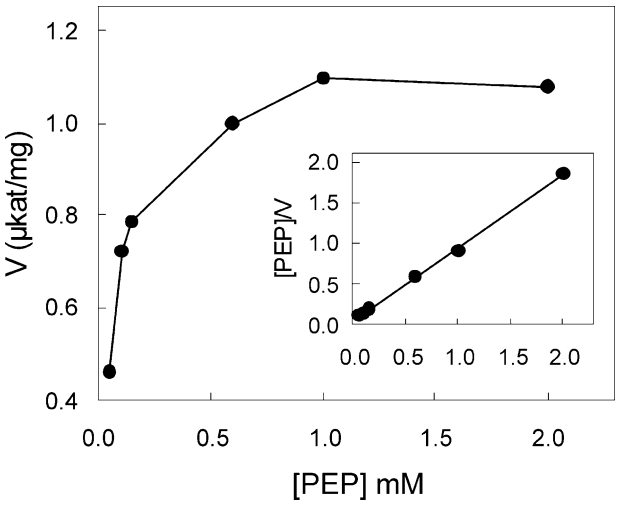

Fig. 5. Dependence on PEP concentration of the PEPC activity extracted from mesocarp of 20% CO_2-treated cherimoyas. The insert shows the Hanes–Woolf plot.

organic acids, mainly malate, in cherimoya fruit (Merodio and De La Plaza, 1997). Moreover, in the large vacuoles present in these non-photosynthetic tissues, PEPC-derived keto-acids (or malate) may be accumulated for osmoregulation and/or as storage molecules for carbon and reducing power to be used later for the metabolism of cherimoya fruits, or may have a more general role in furnishing substrate to the mitochondria, functioning anaplerotically (Bihzad and El-Shora, 1996). The consumption of these TCA-intermediates during ripening in different biosynthetic reactions, serving particularly in this fruit for massive accumulation of nitrogenous compounds (Escribano and Merodio, 1994; Escribano et al., 1996), supports the necessity of an active PEPC for the synthesis of carbon skeletons.

Moreover, the differences found in PEPC kinetical properties (similar K_m, higher V_{max} and lower L-malate sensitivity), suggest that in non-photosynthetic tissues PEPC may be subject to a different regulatory mechanism in vivo. This regulation is in good agreement with the requirement of an active PEPC in cherimoya fruit. Although changes in the cytosolic levels of opposing allosteric effectors and H^+ probably contribute to the overall regulation of PEPC activity in vivo, research over the past decade has focused primarily on the reversible phosphorylation of the enzyme (Wedding et al., 1989; Jiao and Chollet, 1991; Echevarria et al., 1994). It was recently proposed that a protein phosphorylation cycle imposes an additional but related level of regulation on different PEPC isoforms and is a general regulatory mechanism affecting higher plant PEPC in vivo (Chollet et al., 1996 and references therein; Law and Plaxton, 1997). Enzyme phosphorylation results in an increase of catalytic activity (an approximately twofold increase in the V_{max} or decrease in the K_m for PEP) and more notably, a

two- to threefold decrease in L-malate sensitivity (Osuna et al., 1996; Law and Plaxton, 1997; Vidal and Chollet, 1997). Moreover, some evidences suggest that the activation of PEPC kinase activity/PEPC phosphorylation state depends on the prior alkalinisation of the cytosol (Pierre et al., 1992). Time-course kinetic studies suggest that PEPC in banana fruit exists mainly in the dephosphorylated form, but its kinase is expressed throughout ripening (Law and Plaxton, 1997).

The fine tuning of carboxylating activity may be the result of a delicate balance between positive and negative effectors whose influence would be further modulated by the regulatory phosphorylation process and cytoplasmic pH. These regulatory process may prove essential for the functioning of PEPC (and to continue to fix respiratory carbon dioxide) in the highly acidic environment in cherimoya cell metabolism as measured by ^{31}P MNR experiments (Muñoz et al., 2001).

Analysing the overall effect of CO_2 treatment on PEPC, we observed that while the V_{max} value did not change, the enzyme was less sensitive to feedback inhibition by L-malate and showed a higher affinity (lower K_m) for PEP. These results suggest higher in vivo PEPC efficiency under increasing external CO_2 levels where substrate (PEP) availability is low due to utilisation by nonimpaired aerobic respiration, phenylpropanoid and CO_2-activated fermentative pathways (Muñoz et al., 1997; Assis et al., 2001). These results further indicate that another level of enzyme regulation takes place under the CO_2 treatment. It has been reported that positive effectors (e.g., hexose–phosphates) increase the apparent affinity of PEPC for PEP, so that by lowering the K_m value for this substrate, the positive effector enhances the enzyme's ability to compete with L-malate (Raghavendra et al., 1993; Moraes and Plaxton, 2000). Moreover, the putative positive effectors could act directly on in vivo PEPC activity while also modulating the degree of enzyme phosphorylation (Jiao and Chollet, 1992; Echevarria et al., 1994; Zhang et al., 1995). This particular PEPC regulation, which increases enzyme affinity for PEP and reduces its sensitivity to inhibition by L-malate, will allow the PEPC to continue carboxylating PEP at high rates under low substrate availability and to cope with the high malate concentration in CO_2-treated mesocarp cells. These regulatory properties are consistent with increased synthesis of nitrogen-derived compounds such as polyamines (mainly spermidine and spermine) in cherimoya fruit treated with high CO_2 levels (Muñoz et al., 1999). As in other systems, in cherimoya fruit this enzyme may discharge an additional vital function in co-ordinating carbon and nitrogen metabolisms by replenishing the dicarboxylic acids consumed (Huppe and Turpin, 1994), regulated by the increase of some metabolic positive effector(s) such as sugar-P, ammonium or glutamine (Vanlerberghe et al., 1990; Thi Manh et al., 1993).

It has been reported that PEPC in ripening bananas is regulated by metabolites involved in carbohydrate and nitrogen metabolism in a pH-dependent fashion (Law and Plaxton, 1995, 1997). The enzyme activation in CO_2-treated fruit may not only protect cherimoya PEPC against L-malate, but may also adjust its catalytic activity to the demand of carbon skeletons (e.g. oxaloacetate and 2-oxoglutarate) required for ammonium assimilation and transamination reactions in tissues active in the synthesis of nitrogen compounds, to replenish TCA cycle intermediates consumed in biosynthesis (unpublished results).

3. Concluding remarks

Our results demonstrate that PEPC of cherimoya fruit is highly regulated in order to adapt its activity to the demand of C_4-carbon skeletons deriving from the cellular metabolic changes imposed by different postharvest conditions. Through changes in the kinetic constant (K_m for PEP) and sensitivity to malate, the PEPC regulatory mechanism may play a fundamental role in adapting cherimoya tissues to high CO_2 levels. In this mechanism, pH may play a fundamental role in vivo, as an overall regulator of kinetic properties, covalent modifications and allosteric effects of this enzyme in cherimoyas. The pH as an environmental signal is of particular relevance in these fruits, which store parts of their carbon reserves as organic acids. Further study is now in progress on the in vivo relationship between cytoplasmic and vacuolar pH, the levels of related metabolites and the activity of PEPC-kinase, during cherimoya ripening at atmospheric and 20% CO_2.

4. Experimental

4.1. Plant material

Cherimoya (*Annona cherimola* Mill., cv. 'Fino de Jete') fruits harvested in Almuñecar (Granada, Spain) were selected for freedom of physical and pathological defects. At the Instituto del Frío (Madrid), fruits classified uniformly by colour, size and weight were randomly divided into two groups of 20 cherimoyas each and stored in the dark at 20 °C. Each group was placed in separate respiration chambers (20 l) in a continuous flow (100 ml min^{-1}) of air or a gas mixture containing 20% CO_2 + 20% O_2 + 60% N_2. After three days under CO_2 treatment, the fruits were transferred to air for two additional days. To detemine the maximum PEPC activity, for futher characterization studies, fruit were sampled after 1, 2, 3, 4 and 5 days of storage at 20 °C. Peel and mesocarp tissues from three cherimoyas were frozen in liquid nitrogen and stored at −80 °C.

4.2. Enzyme extraction

Frozen tissue (2.5 g) was ground in a precooled pestle and mortar with clean sand (0.5 g) and was homogenised using a buffer:tissue ratio of 3:1. Extraction buffer was 50 mM Tris–HCl (pH 7.8), 10 mM $MgCl_2$, 5 mM $NaHCO_3$, 2 mM DTT, 0.25 mM EDTA and 2% (w/v) PVPP. The homogenate was filtered through two layers of muslin and centrifuged at 20,000 *g* for 30 min. All steps were carried out at 4 °C. The clear supernatant was used for enzyme assay.

4.3. Assay of PEPC activity

Activity of PEPC was determined spectrophotometrically as described by Blanke et al. (1986) at 340 nm by coupling the reaction to the oxidation of NADH in the presence of malate dehydrogenase (MDH). Enzyme activity was expressed as μkat of PEP consumed per mg of protein. The rate of PEP carboxylation declined during the course of the reaction. An approximation to linearity was obtained over the initial period of about 10 min. The standard assay medium contained 0.2 ml of crude enzyme extract (which contained endogenous MDH activity), 0.14 mM NADH, 10 mM $MgCl_2$, 12 mM $NaHCO_3$, 10 mM DTT, 0.25 mM EDTA and 50 mM Tris–HCl buffer (pH 7.8). The reaction was started by the addition of PEP at 4 mM final concentration in the spectrophotometer cuvette containing the assay mixture at 27 °C. The rate of oxidation of NADH was measured in the linear range (1 min).

4.4. Kinetics studies

For the determination of pH optimun and buffer dependence of PEPC activity, 50 mM of Tris–HCl or MOPS–KOH was used in the pH range 6.5–9.

Kinetic parameters and their standard errors were calculated using the curve-fitting facilities of the software package SigmaPlot 6.0 (SPSS Inc., Chicago, IL). V_{max} and apparent K_m values were determined from the plot of initial velocities vs. substrate concentration fitted by non-linear regression to the standard Michaelis–Menten equation, and from linear regression equations using the Hanes–Woolf and Lineweaver–Burk models (all the r^2 values were higher than 0.98).

The L-malate and pyruvate concentrations required for 50% inhibition of PEPC activity under the above assay conditions were determined graphically from semilogarithmic plots of the dose–response curves and defined as malate or pyruvate I_{50} values.

4.5. Protein estimation

Protein concentration was measured by the Bradford (1976) method using a protein-dye reagent (Bio-Rad) and BSA as a standard.

4.6. Statistical analyses

Data from at least three replicates per sample were subjected to analysis of variance (Statgraphics program, STSC, Rockville, Md.). Multiple variance analysis was employed to determine the significance of the data at $P \leqslant 0.05$. The results presented here represent data from three or more experiments performed in succession.

Acknowledgements

This work was supported by Spain Comisión Interministerial de Ciencia y Tecnología (CICYT) grant (ALI99-0954-C03-01). The authors are grateful to Dr. Jesús Pérez-Gil for kinetic parameter adjustments.

References

Andreo, C.S., Gonzalez, D.H., Iglesias, A.A., 1987. Higher plant phosphoenolpyruvate carboxylase. Structure and regulation. FEBS Letters 213, 1–8.

Assis, J.S., Maldonado, R., Muñoz, T., Escribano, M.I., Merodio, C., 2001. Effect of high carbon dioxide concentration on PAL activity and phenolic contents in ripening cherimoya fruit. Postharvest Biology and Technology 23, 33–39.

Bihzad, M.A., El-Shora, H.M., 1996. Phosphoenolpyruvate carboxylase from *Rumex dentatus* a C_3-plant. Journal of Plant Physiology 149, 669–676.

Blanke, M.M., 1991. Respiration of apple and avocado fruits. Postharvest, News and Information 2, 429–436.

Blanke, M.M., Hucklesby, D.P., Notton, B.A., 1987. Distribution and physiological significance of photosynthetic phospho*enol*pyruvate carboxylase in developing apple fruit. Journal of Plant Physiology 129, 319–325.

Blanke, M.M., Hucklesby, D.P., Notton, B.A., 1988. Phospho*enol*pyruvate carboxykinase in aubergine, kiwi and apple fruit. Gartenbauwissenschaft 53, 65–70.

Blanke, M.M., Notton, B.A., 1991. Kinetics and physiological significance of photosynthetic phosphoenolpyruvate carboxylase in avocado fruit. Journal of Plant Physiology 137, 553–558.

Blanke, M.M., Notton, B.A., Hucklesby, D.P., 1986. Physical and kinetic properties of photosynthetic phospho*enol*pyruvate carboxylase in developing apple fruit. Phytochemistry 25, 601–606.

Bradford, M.M., 1976. A rapid and sensitive method for the quantitation of microgram quantities of protein utilizing the principle of protein-dye binding. Analytical Biochemistry 72, 248–254.

Chollet, R., Vidal, J., O'Leary, M.H., 1996. Phospho*enol*pyruvate carboxylase: a ubiquitous, highly regulated enzyme in plants. Annual Review of Plant Physiology and Plant Molecular Biology 47, 273–298.

Del Cura, B., Escribano, M.I., Zamorano, J.P., Merodio, C., 1996. High carbon dioxide delays postharvest changes in RuBPCase and polygalacturonase-related protein in cherimoya peel. Journal of the American Society for Horticultural Science 121, 735–739.

Echevarria, C., Pacquit, V., Bakrim, N., Osuna, L., Delgado, B., Arrio-Dupont, M., Vidal, J., 1994. The effect of pH on the covalent and metabolic control of C_4 phospho*enol*pyruvate carboxylase from *Sorghum* leaf. Archives of Biochemistry and Biophysics 315, 425–430.

Escribano, M.I., Aguado, P., Reguera, R.M., Merodio, C., 1996. Conjugated polyamine levels and putrescine synthesis in cherimoya

fruit during storage at different temperatures. Journal of Plant Physiology 147, 736–742.

Escribano, M.I., Merodio, C., 1994. The relevance of polyamine levels in cherimoya (*Annona cherimola* Mill.) fruit ripening. Journal of Plant Physiology 143, 207–212.

González, D.H., Iglesias, A.A., Andreo, C.S., 1984. On the regulation of phosphoenolpyruvate carboxylase activity from maize leaves by L-malate. Effect of pH. Journal of Plant Physiology 116, 425–434.

Huber, S.C., Edwards, G.E., 1975. Inhibition of phospho*enol*pyruvate carboxylase from C_4-plants by malate and aspartate. Canadian Journal of Botany 53, 1925–1933.

Huppe, H.C., Turpin, D.H., 1994. Integration of carbon and nitrogen metabolism in plant and algal cells. Annual Review of Plant Physiology and Molecular Biology 45, 577–607.

Jiao, J., Chollet, R., 1991. Posttranslational regulation of phospho*enol*pyruvate carboxylase in C_4 and Crassulacean acid metabolism plants. Plant Physiology 95, 981–985.

Jiao, J., Chollet, R., 1992. Light activation of maize phospho*enol*pyruvate carboxylase protein-serine kinase activity is inhibited by mesophyll and bundle sheath-directed photosynthesis inhibitors. Plant Physiology 98, 152–156.

Lakso, A.N., Kliewer, W.M., 1975. Physical properties of phospho*enol*pyruvate carboxylase and malic enzyme in grape berries. The American Journal of Enology and Viticulture 26, 75–78.

Law, R.D., Plaxton, W.C., 1995. Purification and characterization of a novel phospho*enol*pyruvate carboxylase from banana fruit. Biochemical Journal 307, 807–816.

Law, R.D., Plaxton, W.C., 1997. Regulatory phosphorylation of banana fruit phospho*enol*pyruvate carboxylase by a copurifying phospho*enol*pyruvate carboxylase-kinase. European Journal of Biochemistry 247, 642–651.

Merodio, C., De La Plaza, J.L., 1997. Cherimoya. In: Mitra, S.K. (Ed.), Postharvest Physiology and Storage of Tropical and Subtropical Fruits. CAB International, Wallingford, pp. 269–293.

Merodio, C., Muñoz, M.T., Del Cura, B., Buitrago, D., Escribano, M.I., 1998. Effect of high CO_2 level on the titres of γ-aminobutyric acid, total polyamines and some pathogenesis-related proteins in cherimoya fruit stored at low temperature. Journal of Experimental Botany 49, 1339–1347.

Moraes, T.F., Plaxton, W.C., 2000. Purification and characterization of phospho*enol*pyruvate carboxylase from *Brassica napus* (rapeseed) suspension cell cultures. Implications for phospho*enol*pyruvate carboxylase regulation during phosphate starvation, and the integration of glycolysis with nitrogen assimilation. European Journal of Biochemistry 267, 4465–4476.

Muñoz, M.T., Aguado, P., Ortega, N., Escribano, M.I., Merodio, C., 1999. Regulation of ethylene and polyamine synthesis by elevated carbon dioxide in cherimoya fruit stored at ripening and chilling temperatures. Australian Journal of Plant Physiology 26, 201–209.

Muñoz, M.T., Escribano, M.I., Merodio, C., 1997. Ethanolic metabolism in cherimoya fruit during storage at ambient and under high CO_2 atmospheres. Journal of Horticultural Science 72, 363–370.

Muñoz, T., Ruíz-Cabello, J., Molina-García, A.D., Escribano, M.I., Merodio, C., 2001. Chilling temperature storage changes the inorganic phosphate pool distribution in cherimoya (*Annona cherimola*) fruit. Journal of the American Society for Horticultural Science 126, 122–127.

Notton, B.A., Blanke, M.M., 1993. Phospho*enol*pyruvate carboxylase in avocado fruit: purification and properties. Phytochemistry 33, 1333–1337.

Osmond, C.B., 1978. Crassulacean acid metabolism: a curiosity in context. Annual Review of Plant Physiology 29, 379–414.

Osuna, L., González, C., Cejudo, F.J., Vidal, J., Echevarria, C., 1996. In vivo and in vitro phosphorylation of the phospho*enol*pyruvate carboxylase from wheat seeds during germination. Plant Physiology 111, 551–558.

Pierre, J.N., Pacquit, V., Vidal, J., Gadal, P., 1992. Regulatory phosphorylation of phospho*enol*pyruvate carboxylase in protoplats from *Sorghum* mesophyll cells: pH and Ca^{2+} as possible components of the light transduction pathway. European Journal of Biochemistry 210, 531–537.

Raghavendra, A.S., Yin, Z., Heber, U., 1993. Light-dependent pH changes in leaves of C_4 plants. Planta 189, 278–287.

Thi Manh, C., Bismuth, E., Boutin, J.P., Provot, M., Champigny, M.L., 1993. Metabolite effectors for short-term nitrogen-dependent enhancement of phospho*enol*pyruvate carboxylase activity and decrease of net sucrose synthesis in wheat leaves. Physiologia Plantarum 89, 460–466.

Vanlerberghe, G.C., Schuller, K.A., Smith, R.G., Feil, R., Plaxton, W.C., Turpin, D.H., 1990. Relationship between NH_4^+ assimilation rate and *in vivo* phospho*enol*pyruvate carboxylase activity. Regulation of anaplerotic carbon flux in the green alga *Selenastrum minutum*. Plant Physiology 94, 284–290.

Vidal, J., Chollet, R., 1997. Regulatory phosphorylation of C_4 PEP carboxylase. Trends in Plant Science 2, 231–237.

Wedding, R.T., Black, M.K., Meyer, C.R., 1989. Activation of higher plant phospho*enol*pyruvate carboxylase by glucose-6-phosphate. Plant Physiology 90, 648–652.

Zhang, X.Q., Li, B., Chollet, R., 1995. In vivo regulatory phosphorylation of soybean nodule phospho*enol*pyruvate carboxylase. Plant Physiology 108, 1561–1568.

PERGAMON

Phytochemistry 58 (2001) 1015–1024

PHYTOCHEMISTRY

www.elsevier.com/locate/phytochem

Isolation and properties of arginase from a shade plant, ginseng (*Panax ginseng* C.A. Meyer) roots

Hye Jin Hwang, Eun Hee Kim, Young Dong Cho*

Department of Biochemistry, College of Science, Yonsei University, Seoul 120-749, South Korea

Received 15 February 2001; received in revised form 2 August 2001

Abstract

Arginase (EC 3.5.3.1) was purified to homogeneity from root tissues of three-year-old ginseng (*Panax ginseng* C.A. Meyer), shade plant, and was found to be an extraordinarily large molecule relatively stable to heat. The enzyme was decameric having a molecular mass of 352,000 Da, with an optimal temperature and pH of 60 °C and 9.5, respectively. Analogues of arginine could not replace it as substrate, and a cysteine residue is at or near the active site. Maximum activity was obtained with Mn^{2+} and Co^{2+} also activated the proteins, whereas, both agmatine and 5′-deoxy-methylthioadenosine were inhibitors. Specific activities of the enzyme in sliced ginseng roots were increased by plant hormones such as GA_3, IAA, kinetin and putrescine, whereas the activities of the purified enzyme were unaffected by putrescine. Increases in arginase activities by these plant hormones could affect metabolism of polyamine intracellularly. © 2001 Elsevier Science Ltd. All rights reserved.

Keywords: Ginseng (*Panax ginseng* C.A. Meyer); Araliaceae; Arginase; Plant hormones; Heat stability

1. Introduction

An important feature of arginine metabolism is the degradation of arginine to ornithine and urea by arginase (EC 3.5.3.1) since both free arginine and bound protein arginine constitute a large part of the nitrogen reserves in storage organs in many plant species (Polacco and Holland, 1993; Nordin and Naesholm, 1997). Ornithine is a precursor of proline and/or polyamines and arginine nitrogen in urea is recycled by urease-catalyzed hydrolysis to ammonia (Polacco and Holland, 1993). For utilization of arginine, arginase activity increases sharply during germination in several species such as pumpkin (Splittstoesser, 1969), broad bean (Kollöffel and Van Dijke, 1975), soybean (Kang and Cho, 1990), *Arabidopsis thaliana* (Zonia et al., 1995), and loblolly pine (King and Gifford, 1997).

There are several reports of plant arginase cDNAs from *Arabidopsis thaliana* (Krumpelman et al., 1995) and soybean (Goldraij et al., 1998), as well as hormonal effects in tomato ovaries (Alabadí et al., 1996), and arginase purification and characterization from soybean axes (Kang and Cho, 1990), iris bulbs (Boutin, 1982), *Arachis hypogea* L. seedlings (Desai, 1983), and the lichen, *Evernia prunastri* (Martín-Falquina and Legaz, 1984). However, little is yet understood about properties of plant arginases versus those of animals and bacteria, in part because the plant enzymes have not been extensively purified to provide information on their properties. Although information on plant arginases is available, it is almost always obtained from annual plant sources; little has been published on perennial plant arginases.

Ginseng (*Panax ginseng* C.A. Meyer), a perennial shade plant, has been used as herbal medicine in the Orient, especially in China, Japan and Korea for thousands of years. However, 10 years ago, arginine was reported to be a major nitrogenous compound, representing approximately 60.6% of the free amino acid

Abbreviations: dcSAM, decarboxylated *S*-adenosylmethionine; DTNB, 5,5′-dithiobis-2-nitrobenzoic acid; EDAC, 1-ethyl-3-(3-dimethyl) aminopropylcarbodiimide; GA_3, gibberellic acid 3; IAA, indole-3-acetic acid; MGBG, methyl glyoxal bis-(guanylhydrazone); MTA, 5′-deoxy-5′-methylthioadenosine; PCMB, *ρ*-chloromercuribenzoate; PLP, pyridoxal-5′-phosphate

* Corresponding author. Tel.: +82-2-2123-2697; fax: +82-2-313-1608.

E-mail address: cyd516@yonsei.ac.kr (Y.D. Cho).

0031-9422/01/$ - see front matter © 2001 Elsevier Science Ltd. All rights reserved.
PII: S0031-9422(01)00392-2

nitrogen and 13.6% of the total nitrogen in three-year-old ginseng roots (Park et al., 1990). Since there have been no reports on properties of arginase in a shade plant being rich in arginine, we have chosen ginseng as a representative shade plant for the present study. Here we describe the first purification of arginase from ginseng roots to apparent homogeneity and properties of the purified enzyme.

2. Results and discussion

Although arginases have been purified and characterized from such non-shade plants as soybean (Kang and Cho, 1990), iris bulbs (Boutin, 1982), *Arachis hypogea* L. seedlings (Desai, 1983), and *Evernia prunastri* (Martín-Falquina and Legaz, 1984), there are no descriptions of the properties of shade plant arginases. Hence, we focused upon the shade plant, ginseng, where it was found that the specific activity of its ginseng arginase increased steadily after germination and reached its highest level in 3-year-old roots (data not included). Beyond 3 years growth, the specific activity of the arginase gradually decreased. Additionally, very low activities were detected in leaves from 1 to 5-year-old ginsengs as compared to that of roots. Accordingly, 3-year-old ginseng roots were used in the present studies.

2.1. Arginase purification and heat stability

The purification of arginase to apparent homogeneity is summarized in Table 1, whose final specific activity was 18,090 units/mg, i.e. with a 1055 fold enrichment and a 0.5% recovery with respect to the total activity of the crude extract toward L-arginine. Since the method employed for iris bulb enzyme (Boutin, 1982) was not suitable, we used two different columns such as phenyl sepharose and arginine sepharose 4B. Heat treatment was also conducted since heat application removed large amounts of unwanted proteins which were not removed or fractionated using various column chromatographic procedures. To ensure the conditions used in heat treatment were innocuous for arginase, experiments were carried out at various temperatures and pH 7.5 (Fig. 1a). Even for longer incubation times from 15 min to 1 h, there was no decrease in enzyme activity at 50 °C. Therefore, heat treatment was effective in removing non-arginase proteins with no effect on arginase activity.

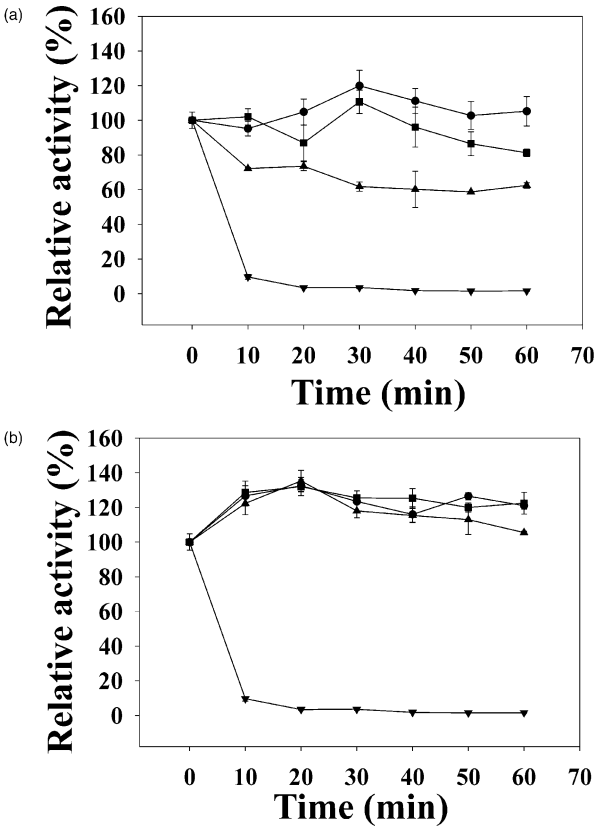

Fig. 1. Heat stability of arginase activities. The enzyme was incubated in 10 mM Tris–HCl [pH 7.5 (a) and pH 9.5 (b)] buffer containing 1 mM $MnCl_2$ and 400 mM L-arginine at 40 °C (●), 50 °C (■), 60 °C (▲), and 70 °C (▼) for various time intervals. After the indicated time, residual activities of the enzyme were determined as described in Experimantal. Arginase activity is presented as a percentage of initial activity. Each value represents the mean ±S.D. of three replicates.

2.2. Molecular weight determination

Coomassie blue staining following SDS–PAGE revealed that there was only one polypeptide (Fig. 2a), and silver staining gave comparable results as well (data not included). To our knowledge, however, this is the

Table 1
Purification table of arginase from ginseng (*Panax ginseng* C.A. Meyer) roots

Step	Total protein (mg)	Total activity (units)	Specific activity (units/mg)	Purification fold (fold)	Yield (%)
Crude extract	3151	54040	17.15	–	100
45–60% $(NH_4)_2SO_4$	360.9	27850	77.18	4.500	51.54
Heat treatment	113.6	17860	157.2	9.17	33.05
DEAE-sepharose	8.29	11430	1379	80.41	21.15
Phenyl-sepharose	0.22	3936	17770	1036	7.28
Arginine sepharose 4B	0.015	271.4	18090	1055	0.50

Prepared from 300 g of fresh ginseng roots.

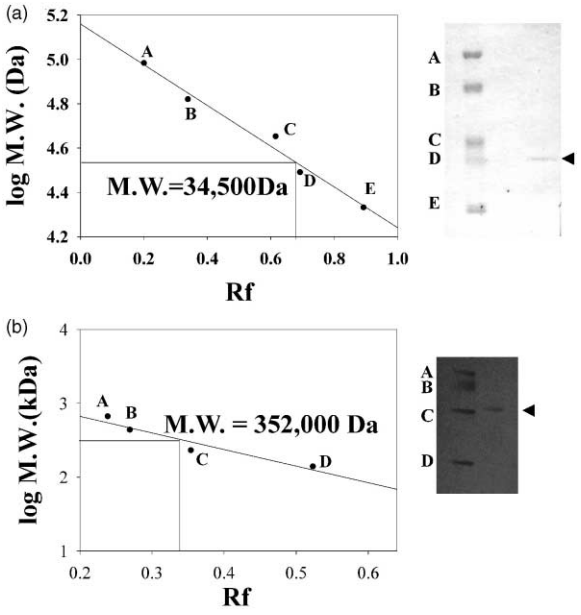

Fig. 2. Molecular weight of purified ginseng arginase as estimated by SDS–PAGE (a) and 4–20% gradient gel electrophoresis (b). (a) Molecular standard markers and an aliquot of purified arginase were electro-phoresed on 10% SDS-polyacrylamide gel and stained by Coomassie brilliant blue. The protein markers used were: A, phosphorylase *b* (96,400 Da); B, serum albumin (66,200 Da); C, ovalbumin (45,000 Da); D, carbonic anhydrase (31,000 Da) and E, trypsin inhibitor (21,500 Da). The subunit of arginase is indicated in the symbol (◀) (b) 4–20% polyacrylamide gel was used and the protein markers are: A, thyroglo-bulin (669,000 Da); B, ferritin (440,000 Da); C, catalase (232,000 Da) and D, lactate dehydrogenase (140,000 Da). The native arginase is indicated in the symbol (◀).

first reported homogeneity of arginase from a shade plant, whose analysis by SDS–PAGE showed one band with a molecular mass of approximately 34,500 Da (Fig. 2a). On the other hand, results of gradient gel electrophoresis gave a single band corresponding to a molecular mass of 352,000 Da (Fig. 2b). We did not, however, observe any dissociation of the enzyme into subunits or oligomers during electrophoresis and other manipulations. Analysis of the UV spectra of the ginseng enzyme revealed that there was identical conformation before and after heat treatment (data not included), and such results suggest that there is no dissociation of the decameric enzyme into subunits or oligomers and no effect on the subunit itself. The gel-based subunit and native sizes indicate that ginseng root arginase is decameric. With respect to molecular mass and number of subunits, ginseng arginase differs markedly from other arginases reported thus far, since the molecular masses of those from animals and micro-organisms are in the range of 98,000 (Brusdeilins et al., 1983) to 278,000 (Reddy and Campbell, 1968). Additionally, the number of subunits reported ranges from three to six i.e. a trimer from *Saccharomyces cerevisiae* (Green et al., 1990), a tetramer from mouse liver (Spolarics and Bond, 1988), and hexamers from iris bulbs (Boutin, 1982) and *Bacillus brevis* Nagano (Kanda et al., 1997). There have been reports on the presence of decameric enzymes, such as carbonic anhydrase from *Vicia canencens* leaves (Demir et al., 1999) and arginine decarboxylase form *E. coli* B (Boecker, 1978), but, no decameric arginase has been reported from a plant source.

2.3. Substrate specificity

Substrate specificity studies (Table 2) showed that purified arginase is highly specific for L-arginine since analogs such as L-homoarginine, agmatine, and canavanine did not replace it as a substrate. However, other arginases differ in their substrate specifities: arginase from rat liver (Reczkowski and Ash, 1994) can use argininamide, L-canavanine, and homoarginine as substrates, in addition to L-arginine. Whereas, the arginases from *Helicobacter pylori* (Mendz et al, 1998), rat small intestine (Fujimoto et al., 1976), and iris bulb (Boutin, 1982) are specific for only *L*-arginine.

2.4. Chemical modifications

Chemical modifications were carried out for the purpose of identifying amino acids located in the binding/catalytic site of ginseng arginase. Among the chemical modification reagents employed, treatment of the enzyme with sulfhydryl-specific reagents, DTNB and PCMB, resulted in loss of activity (Table 3), these following pseudo first order kinetics (data not included). DTNB-treated enzyme activity was restored to more than 96% of the control after 10 min treatment with 0.1 mM DTT, indicating that its inactivation is due, not to a change in conformation of the enzyme, but to modification of a cysteine residue in the active center. Furthermore, the presence of the substrate, arginine, reduced the rate of modification (Table 3), which also suggested that the cysteine residue is directly involved in enzyme activity. This finding thus explains the difference between mammalian and plant arginases, since treatment of rat liver arginase with *N*-bromosuccinimide demonstrated that a histidine residue is catalytically essential (Daghigh et al.,

Table 2
Substrate specificity of ginseng arginase

Substrate (100 mM)	Relative activity (%)
L-Arginine	100±3.8
Agmatine	N.D.
Canavanine	N.D.
γ-Guanidinobutyrate	N.D.
L-Homoarginine	5.57 ±0.031
MGBG	N.D.

Enzyme (5 μg) was incubated with analogues of arginine and then activities were assayed as described in Experimental. Arginase activity is presented as a percentage of control activity with L-arginine. MGBG and N.D. stand for 'methyl glyoxal bis-(guanylhydrazone)' and 'not detected', repectively.

Table 3
Inhibitory effects of chemical modification reagents on purified ginseng arginase activity

Reagents	Concentration (mM)	Relative activity (%)	Substrate protection
None	–	100±0.03	–[a]
DTNB	0.1	98.3±0.045	100±0.016
	1	74.6±0.056	96.4±0.038
EDAC	0.1	95.0±0.13	–
	1	100±0.25	–
Hydroxylamine	0.1	88.7±0.35	–
	1	96.3±0.57	–
PCMB	0.1	96.8±0.46	99.1±0.15
	1	2.95±0.45	84.9±0.25
Phenylglyoxal	0.1	112±0.87	–
	1	119±2.3	–
PLP	0.1	114±1.5	–
	1	133±1.25	–
Succinyl anhydride	0.1	88.5±0.24	–
	1	101±1.25	–

Enzyme (5 μg) was incubated with the chemical reagents (0.1 and 1 mM, respectively), with activities assayed as described in Experimental. Arginase activity is presented as a percentage of control activity without any chemical reagents. When sulfhydryl group inhibitors were tested, β-mercaptoethanol was removed from the enzyme solution before incubation. DTNB, 5,5-dithiobis-2-nitrobenzoic acid; EDAC, 1-ethyl-3-(3-dimethyl) aminopropylcarbodiimide; PCMB, ρ-chloromercuribenzoate; PLP, pyridoxal-5-phosphate. Arginine was used as a substrate in substrate protection experiments.

[a] Substrate protection experiments were not carried out.

1996) and the X-ray diffraction study of rat liver arginase provided the result that His, Asp, Glu, and Arg residues are related to arginine binding and catalysis (Kanyo et al., 1996). Thus, our results are in accordance with reports of Ber et al. (1978) and Muszyńska et al. (1972) that the SH group of cysteine is essential for the catalytic activity of arginases from non-shade plants. It is thus tentatively proposed that either arginases from a non-shade plant or a shade plant need the SH group of cysteine for catalytic activity.

2.5. Effects of metal ions on arginase

A common feature of all arginases so far studied is a requirement for divalent cation activators although metal activation seems to be species dependent. That is, while Co^{2+}, Ni^{2+}, Cd^{2+}, and Zn^{2+} activate arginase from some sources (Hellerman and Perkins, 1935; Harrell and Sokolovsky, 1972; Green et al., 1991), one general property is the requirement for metal ions, especially Mn^{2+}, for full catalytic activity (Carvajal et al., 1971; Hirsch-Kolb et al., 1971; Green et al., 1991; Kuhn et al., 1995; Kanyo et al., 1996). Among the cations examined, Mn^{2+} was the most effective as expected and Co^{2+} could replace Mn^{2+} as a metal activator, especially at 1 mM (Table 4). The arginase from *Helicobacter pylori* (Mendz et al., 1998) is activated fourfold by cobalt and twofold by nickel rather than manganese. Activity of arginase with Co^{2+} is an important observation since we could not exclude the possibility that the enzyme with Co^{2+} might maintain activity to some extent in case of deficiency in Mn^{2+} in vivo.

Table 4
Effects of metal ions on purified ginseng arginase activity

Metal ion added	Concentration (mM)	Relative activity (%)
$CaCl_2$	0.01	N.D.
	0.1	N.D.
	1	N.D.
$CoCl_2$	0.01	2.412±0.02
	0.1	44.08±1.5
	1	67.54±2.1
$FeCl_2$	0.01	2.851±0.01
	0.1	N.D.
	1	N.D.
$FeCl_3$	0.01	2.851±0.03
	0.1	4.605±0.02
	1	6.798±0.15
$MgCl_2$	0.01	1.316±0.02
	0.1	N.D.
	1	N.D.
$MnCl_2$	0.01	87.6±0.15
	0.1	100±0.058
	1	63.4±0.85

Arginase (5 μg) was incubated with L-arginine and several metal ions and then activities were assayed as described in Experimental. Arginase activity is summarized as a percentage of control activity in the presence of 0.1 mM $MnCl_2$. N.D. stands for 'not detected'.

2.6. Effects of polyamines, agmatine and MTA on arginase

We have previously shown that agmatine produced by arginase from arginine and MTA formed by spermine synthase from dcSAM inhibited soybean arginase and spermine synthase, respectively (Park and Cho, 1992; Kim and Cho, 2000). To determine if polyamines and

their intermediates affect purified ginseng arginase, we assayed its activity after incubation of arginase with them. Among those examined, agmatine and MTA were found to have inhibitory effects (Table 5), suggesting that they could reduce levels of putrescine through reducing ornithine. However, the amounts of these compounds in a shade plant are not known even though physiological and biochemical roles of ingredients such as saponin have been extensively studied. Therefore, the in vivo physiological and biochemical role of agmatine and MTA in ginseng roots are as yet unclear.

2.7. Kinetic properties

The K_m of the purified ginseng arginase was determined by a Lineweaver–Burk plot to be 82.7 mM (Fig. 3). To further confirm this value, Hanes–Woolf and Eadie–Hofstee plots were also employed giving the same value. The ginseng arginase K_m for arginine is similar to that reported for soybean (83 mM) (Kang and Cho, 1990), but differs somewhat from those reported for the embryo axis of *Arachis hypogea* L. seedlings (5.6 mM) (Desai, 1983), *Bacillus brevis* Nagano (12.8 mM) (Kanda et al., 1997), *Saccharomyces cerevisiae* (15.7 mM) (Green et al., 1990), and rat small intestine (19 mM) (Fujimoto et al., 1976). To determine the optimum pH for arginase, we assayed its activity in buffers from pH 6.0 to 10.5, using each buffer in its effective range. The activity was highest at pH 9.5 (Fig. 4a), this being similar to that of arginases from iris bulbs (pH 9.0) (Boutin, 1982), *Bacillus brevis* Nagano (pH 9.0) (Kanda et al., 1997), soybean (pH 9.5) (Kang and Cho, 1990) and rat small intestine (pH 9.5) (Fujimoto et al., 1976), but this was

Table 5
Effects of polyamines and their analogues on purified arginase activity

Substances	Concentration (mM)	Relative activity (%)
None	–	100±0.05
Putrescine	0.01	98.5±0.24
	0.1	100±0.15
	1	120±0.13
Spermidine	0.01	120±0.015
	0.1	122±0.02
	1	122±0.078
Spermine	0.01	125±0.087
	0.1	113±0.089
	1	108±0.075
Cadaverine	0.01	116±0.15
	0.1	123±0.25
	1	101±0.34
Agmatine	0.01	110±0.021
	0.1	103±0.32
	1	67.7±0.78
MTA	0.01	101±2.4
	0.1	84±1.4
	1	67±0.24

Arginase (5 μg) was incubated at 37 °C for 20 min in 10 mM Tris–HCl (pH 7.5) buffer in the presence of the indicated concentrations of these compounds and then assayed for enzyme activity. Arginase activity is presented as a percentage of that of enzyme incubated in the absence of any compound.

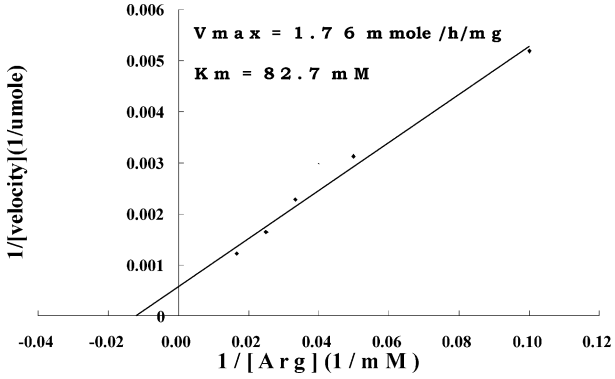

Fig. 3. Lineweaver–Burk plot of initial reaction velocities (mmole urea formed per 1 h) for arginase measured at various concentrations of L-arginine.

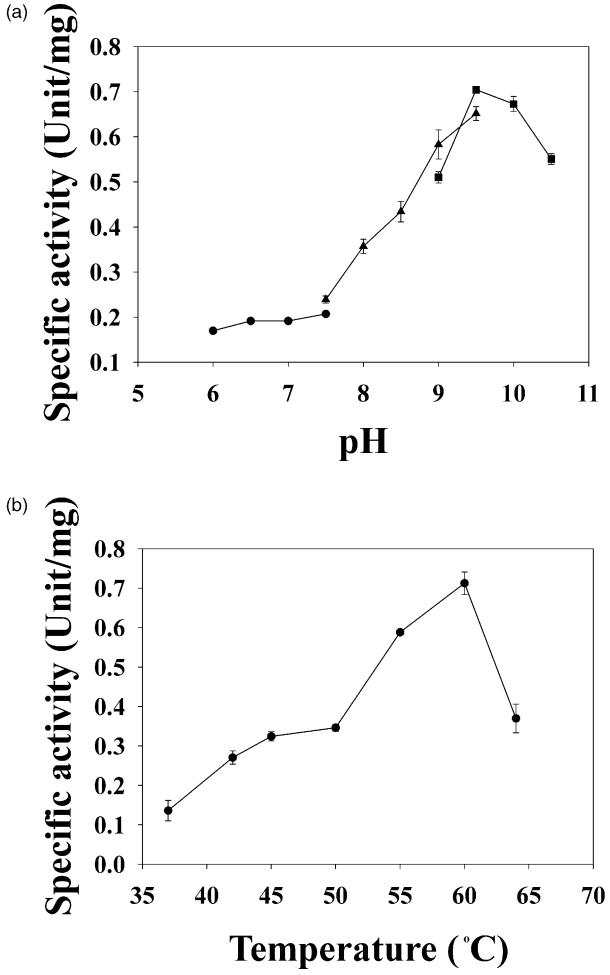

Fig. 4. Determination of optimum pH (a) and optimum temperature (b) for purified ginseng arginase. (a) The reaction buffers used were potassium phosphate for pH 6.0–7.5 (●), Tris–HCl for pH 7.5–9.5 (▲), and glycine/NaOH for pH 9.0–10.5 (■). (b) The reaction temperature was 37, 42, 45, 50, 55, 60 and 65 °C. Each value represents the mean ±s.d. of the results from three replicates.

dissimilar to that of mouse liver arginase (pH 7.4) (Spolarics and Bond, 1998). An optimum temperature for arginase from soybean (Kang and Cho, 1990), iris bulbs (Boutin, 1982), *Bacillus brevis* Nagano (Kanda et al., 1997), rat small intestine (Fujimoto et al., 1976), *Saccharomyces cerevisiae* (Green et al., 1990), and human liver (Kuhn et al., 1995) is in the range of 30 to 37 °C. However, the optimum temperature for ginseng arginase was 60 °C (Fig. 4b), which is high compared to those reported so far. Although there is no report on arginase having such a high optimum temperature, that of a decameric carbonic anhydrase from *Vicia canencens* leaves is 70 °C (Demir et al., 1999). Since both optimum pH and temperature were relatively high, we carried out enzymatic kinetic analyses at 60 °C and pH 9.5 for 1 h (enzyme assay conditions) to determine if any decrease in enzymatic activity occurs during the incubation period (Fig. 1b), but none was observed. Since freezing and thawing caused about 15% loss in enzyme activity in buffer B, we did not freeze the enzyme solution and it was routinely stored at temperatures ranging from 0 to 4 °C in this buffer. Under these conditions, the enzyme activity was reduced by about ca. 8% of the original activity one day after storage. Further, since glycerol, dimethyl sulfoxide, and dimethylformamide in buffer were not effective in preventing this loss of activity, the enzyme should be used immediately after purification.

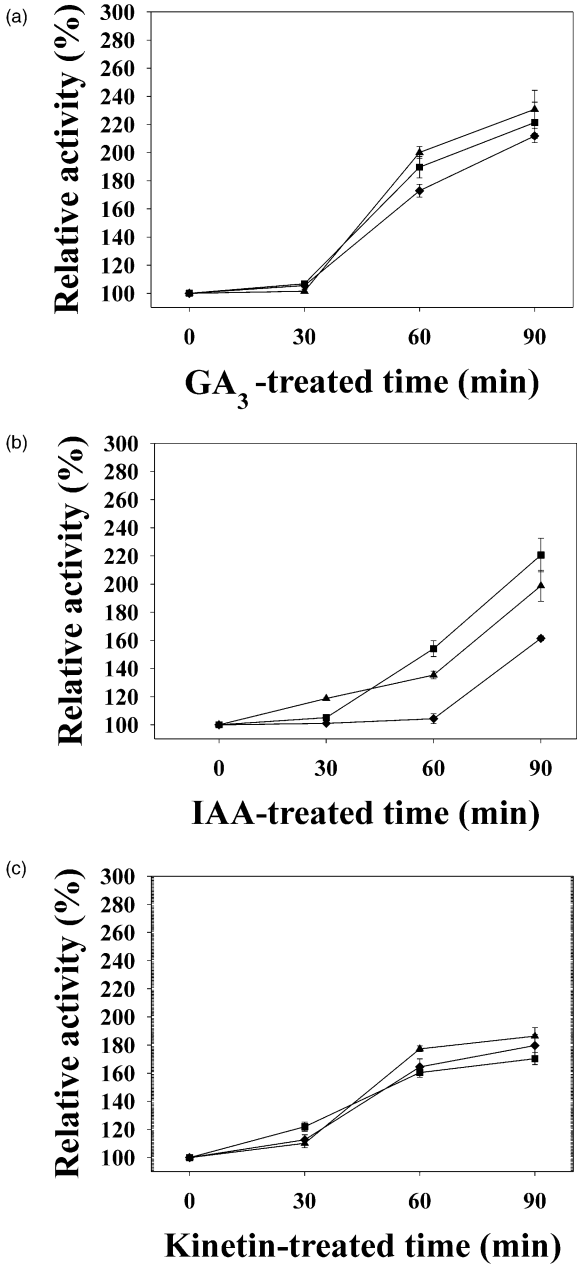

Fig. 5. Time course of arginase activities in GA_3-treated (a), IAA-treated (b), and kinetin-treated (c) slices. Sliced ginseng roots were cultured in Petri dishes containing each plant hormone at the concentrations of 1 nM (■), 10 nM (▲), and 100 nM (◆) at 25 °C for indicated time intervals. For details, see Experimental. Arginase activity is presented as a percentage of each control activity in the absence of each hormone. Each value represents the mean ±S.D. of the results from three replicates.

2.8. Effects of various compounds on arginase activity in sliced ginseng roots

Little has been published on an increase in specific activity of a shade plant arginase in the presence of plant hormones, substrate and polyamines. Indeed, while attempts to induce arginase activity by arginine in soybean (Yu and Cho, 1998) were unsuccessful, other attempts to increase the specific activity by addition GA_3 and IAA in tomato ovaries (Alabadí et al., 1996) were successful (Fig. 5). That is, 30 min after addition of GA_3, arginase specific activity started to increase steadily up to about 230% until 90 min, compared to the control specific activity. Similar results were observed for IAA (about 220% increase) and kinetin (about 180% increase) (Fig. 5). Putrescine at 100 μM increased arginase specific activity up to about 180% after 120 min incubation, compared to that of the control specific activity (Fig. 6). However, the other polyamines seemed to have no effect on arginase specific activity. Further work is thus necessary to verify how they increase the specific activity of a shade plant arginase, since they appear to effect polyamine metabolism.

3. Experimental

3.1. Plant materials and chemicals

Three-year-old ginseng (*Panax ginseng* C.A. Meyer) roots were purchased from a ginseng farm. Trizma base, GA_3, IAA, kinetin, agmatine, ornithine, putrescine, spermidine, spermine, canavanine, cadaverine, L-homoarginine, MGBG, MTA, EDAC, DTNB, PCMB, PLP, agar and Coomassie brilliant blue R-250 were purchased from Sigma (USA). DEAE-sepharose fast flow

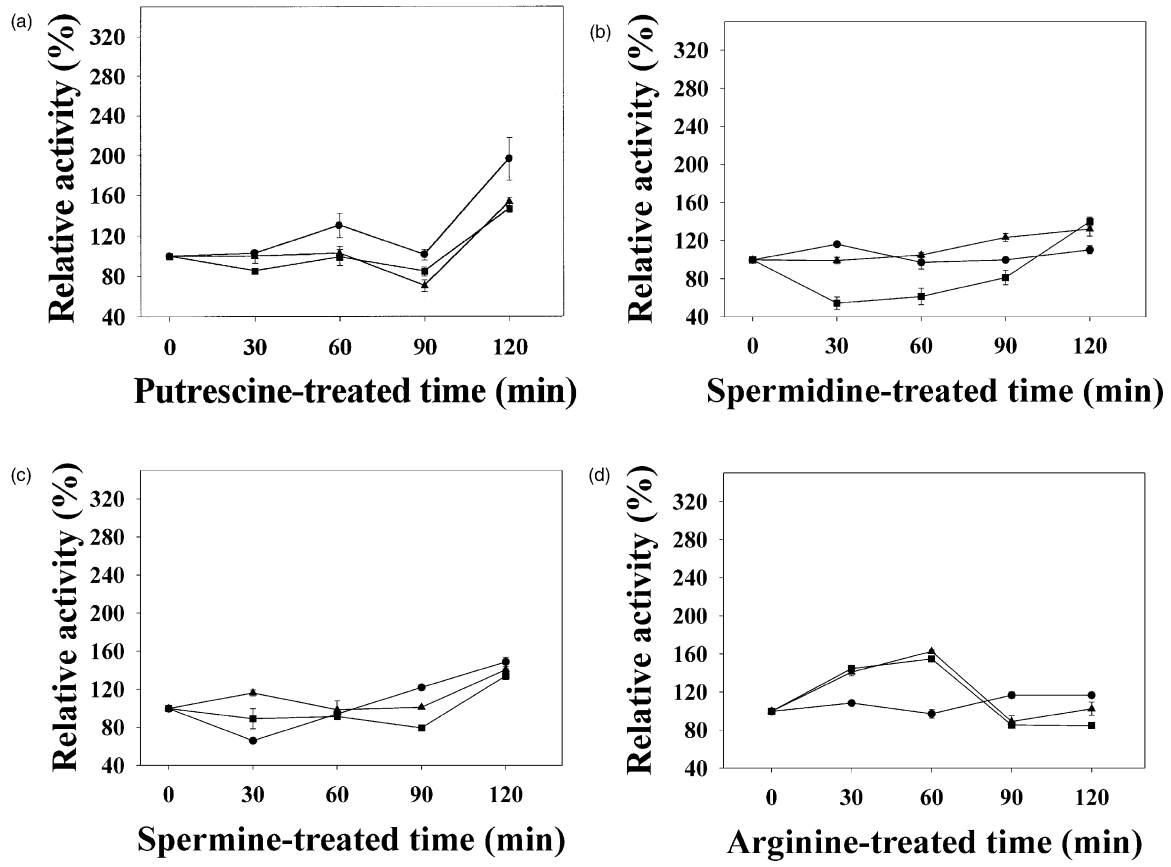

Fig. 6. Time course of arginase activities in putrescine-treated (a), spermidine-treated (b), spermine-treated (c), and arginine-treated (d) slices. Sliced ginseng roots were cultured in Petri dishes containing each compound at the concentrations of 1 μM (▲), 10 μM (■), and 100 μM (●) at 25 °C for indicated time intervals. For details, see Experimental. Arginase activity is presented as a percentage of the control activity in the absence of any substance. Each value represents the mean ±S.D. of the results from three replicates.

resin, Phenyl-sepharose 6B fast flow resin, arginine-sepharose 4B resin, high molecular weight calibration kit, acrylamide, *N*,*N*-methylene-bisacrylamide, *L*-arginine, bovine serum albumin, and ammonium sulfate were purchased from Amersham-Pharmacia Biotech (UK). Other chemicals used were of the highest quality commercially available.

3.2. Arginase assay

The reaction mixture contained 25 mM Tris–HCl (pH 9.5), 1 mM $MnCl_2$, 100 mM L-arginine and enzyme solution in a total volume of 200 μl. The reaction was conducted at 60 °C for 1 h and was terminated by addition of 20 μl of 70% a perchloric acid. Precipitated proteins were removed by centrifugation at 12,000×*g* for 10 min and urea in the supernatant was spectrophotometrically measured by the modified method of Archibald (Archibald, 1945). One unit is defined as the amount of enzyme producing 1 μmol per 1 h. The arginase activity was a linear function of both enzyme concentration and incubation time up to at least 1 h under these conditions. All enzyme assays were made in triplicate, and generally reproduced within ±5%.

3.3. Protein determination

Protein concentration was determined by the method of Bradford (Walker, 1996) with bovine serum albumin as the standard protein.

3.4. Arginase purification

All purification procedures were performed at 0–4 °C, unless otherwise stated. Fresh ginseng roots (300 g) were homogenized in a chilled electric mixer with two volumes of buffer A [50 mM Tris–HCl (pH 7.5) buffer containing 1 mM $MnCl_2$, 0.1% β-mercaptoethanol, and 10% glycerol]. The homogenate was filtered through four layers of gauze and clarified by centrifugation at 14,000×*g* for 20 min. The supernatant was pooled as a crude extract, which was adjusted to 45% (w/v) saturation with solid $(NH_4)_2SO_4$ and stirred at 4 °C for 1 h. The resulting solution was centrifuged at 13,000×*g* for 20 min and the pellet was discarded. The supernatant was brought to 60% (w/v) saturation with solid $(NH_4)_2SO_4$ and treated as above, except that the pellet was retained. The pellet was dissolved in a minimal volume of buffer B [10 mM Tris–HCl (pH 7.5) buffer containing 0.1% β-

mercaptoethanol] and then dialyzed with the same buffer overnight. The dialyzed solution with 400 mM L-arginine (pH 7.5) and 1 mM $MnCl_2$ was rapidly brought to 50 °C in a hot-water bath, maintained at this temperature by swirling for 15 min, and then cooled in an ice bath. After the precipitate was removed by centrifugation at 12,000×*g* for 20 min, the supernatant was dialyzed with buffer B overnight. The dialysate was applied to a DEAE-sepharose fast flow anion exchange column previously equilibrated with buffer B. The column was washed with 600 ml of the same buffer and an equal volume of buffer containing 0.1 M NaCl. The arginase was eluted with a 300 ml linear gradient of 0.1–0.3 M NaCl in buffer B at a flow rate of 46 ml/h. Active fractions were collected and dialyzed with 10 mM Tris–HCl (pH 7.5) buffer. This protein solution was applied to a phenyl-sepharose 6B fast flow hydrophobic column previously equilibrated with 10 mM Tris–HCl (pH 7.5) buffer containing 30 mM $(NH_4)_2SO_4$. The column was washed with a 50 ml of the same buffer. The arginase was eluted with 40 ml of 10 mM Tris–HCl (pH 7.5) buffer at a flow rate of 30 ml/h. Active fractions were collected and concentrated. This protein solution was applied to an arginine-sepharose 4B affinity column previously equilibrated with 10 mM Tris–HCl (pH 7.5) buffer. The column was washed with 20 ml of the same buffer and eluted with a 10 ml linear gradient of 0–0.4 M arginine in 10 mM Tris–HCl (pH 7.5) buffer at a flow rate 5 ml/h. Active fractions were collected and dialyzed with buffer B.

3.5. Molecular weight determination

The molecular weight of the native purified enzyme was estimated by 4–20% native pore gradient gel electrophoresis by the method of Davis (Walker, 1996); thyroglobulin (669,000 Da), ferritin (440,000 Da), catalase (232,000 Da), and lactate dehydrogenase (140,000 Da) served as molecular standard markers. The molecular weight of subunits was obtained by SDS–PAGE. SDS–PAGE was performed by the method of Laemmli (Walker, 1996) using a 10% separating gel and phosphorylase B (96,400 Da), serum albumin (66,200 Da), ovalbumin (45,000 Da), carbonic anhydrase (31,000 Da), and trypsin inhibitor (21,500 Da) served as molecular markers. The gels were stained with Coomassie brilliant blue R-250.

3.6. Heat stability

The enzyme solution containing 1 mM $MnCl_2$ and 400 mM L-arginine was incubated at various temperature and pH for various time intervals to find the temperature at which heat treatment could be carried out and to find stability of enzyme during incubation time. After incubation, the enzyme solution was centrifuged at 12,000×*g* for 20 min to remove denatured proteins and the supernatant was dialyzed with buffer B for 2 h to remove remaining arginine and urea formed. The remaining arginase activity was assayed as described elsewhere. The enzyme solution not treated with heat was used as the control and the enzyme activities were expressed as a percentage of the control activity.

3.7. Substrate specificity

Several compounds with a guanidino group were used to determine the substrate specificity for the arginase of ginseng roots. Each compound was added to a reaction mixture instead of arginine and the enzyme assay was performed as described before. The reaction mixture containing arginine used as the control and the enzyme activities were expressed as a percentage of the control activity.

3.8. Chemical modification

The enzyme solution was incubated with modification reagents such as EDAC, DTNB, hydroxylamine, PCMB, phenylglyoxal, PLP, and succinyl anhydride under appropriately different conditions (Walker, 1996). After incubation, the enzyme activity was assayed as described. The reaction mixture containing the enzyme solution not treated was used as the control and the enzyme activities are expressed as a percentage of the control activity.

3.9. Effects of metal ions on arginase

The chloride salts of divalent cations (Ca^{2+}, Co^{2+}, Fe^{2+}, Mg^{2+} and Mn^{2+}) were used. The concentrations of ions were varied in the reaction mixture over a range from 0.01 to 1 mM, with the enzyme activity assayed as before. The reaction mixture containing 0.1 mM $MnCl_2$ was used as the control and the enzyme activities were expressed as a percentage of the control activity.

3.10. Effects of polyamines, agmatine and MTA on arginase

Various concentrations of cadaverine, agmatine, MTA, putrescine, spermidine and spermine were added to the enzyme solution and the mixtures were incubated at 37 °C for 20 min, with the enzyme assay being performed as described aforehand. The enzyme solution not treated with any compounds was used as the control and the enzyme activities were expressed as a percentage of the control activity.

3.11. Effects of plant hormones on arginase activity in sliced ginseng roots

Three-year-old ginseng roots were treated with various concentrations of GA_3, IAA and kinetin. Ginseng roots were sterilized in 95% ethanol for 5 s and rinsed with autoclaved distilled water. These roots were re-sterilized

in 3% sodium hyperchlorite for 10 min and rinsed with autoclaved distilled water. Sterilized roots were sliced to 0.7–1.0 mm thick, 1 g of sliced ginseng roots was incubated with Murashige and Skoog salt medium (pH 5.0) containing 3% sucrose (w/v) and various concentrations of plant hormones in Petri dishes at 25 °C. After incubation for a given time (0, 30, 60 and 90 min), sliced ginseng roots were transferred on new Murashige and Skoog salt medium (pH 5.7) containing 8 g/l of agar and cultured at 25 °C for 40 h. After that, samples were immediately frozen in liquid nitrogen and stored at −70 °C. Samples were homogenized with 2 ml of buffer A. The homogenate was centrifuged at 14,000×*g* for 20 min and the supernatant was used as enzyme solution. The enzyme assay was performed as described in Experimental. Solutions of plant hormones were prepared as 1000-fold stock solutions. Stock solutions of IAA and GA_3 were dissolved in 100% ethanol and that of kinetin was dissolved in 1 N NaOH.

3.12. Effects of polyamines and arginine on arginase activity in sliced ginseng roots

Three-year-old ginseng roots were treated with various concentrations of polyamines and arginine. Sliced ginseng roots were prepared and used as described above, except that polyamines and arginine were used instead of plant hormones.

3.13. General methods

Optimum pH, optimum temperature, K_m and V_{max} of purified enzyme were determined as described previously (Kamio and Terawa, 1983).

Acknowledgements

This work was supported by the Korean Ministry of Education (1998-015-D00235).

References

Alabadí, D., Agüero, M.S., Péreg-Amador, M.A., Carbonell, J., 1996. Arginase, arginine decarboxylase, ornithine decarboxylase, and polyamines in tomato ovaries. Plant Physiol. 112, 1237–1244.

Archibald, R.M., 1945. Colorimetric determination of urea. J. Biol. Chem. 157, 507–518.

Ber, E., Muszyńska, G., Čechová, D, 1978. The lack of free SH groups in rat liver arginase. Bull Acad. Polon. Sci. Ser. Sci. Biol. 26, 665–668.

Boecker, E.A., 1978. Arginine decarboxylase from *Escherichia coli* B: Mechanism of dissociation from the decamer to the dimer. Biochemistry 17, 258–263.

Boutin, J.P., 1982. Purification, properties and subunit structure of arginase from iris bulbs. Eur. J. Biochem. 127, 237–243.

Brusdeilins, M., Hapke, C., Huberts, H.H., Schumacher, K., 1983. Identification of the apparently lymphocyte-specific human liver-derived inhibitory protein (LIP) as cytoplasmic liver L-arginase. J. Immunol. 131, 2427–2431.

Carvajal, N., Venegas, A., Oestreicher, G., Plaza, M., 1971. Effect of manganese on the quaternary structure of human liver arginase. Biochim. Biophys. Acta 250, 437–442.

Daghigh, F., Cavalli, R.C., Soprano, D.R., Ash, D.E., 1996. Chemical modification and inactivation of rat liver arginase by *N*-bromosuccinimide: reaction with His141. Arch. Biochem. Biophys. 327, 107–112.

Demir, Y., Demir, N., Kufrevioglu, O., 1999. Carbonic anhydrase from *Vicia canencens* leaves. Prep. Biochem. Biotechnol 29, 235–244.

Desai, H.V., 1983. Purification and properties of arginase from *Arachis hypogea* L. seedlings. Indian J. Biochem. Biophys. 20, 236–237.

Fujimoto, M., Kameji, T., Kanaya, A., Hagihira, H., 1976. Purification and properties of rat small intestinal arginase. J. Biochem. 79, 441–449.

Goldraij, A., Coello, P., Polacco, J.C., 1998. Arginase is inoperative in developing soybean embryos. Plant Physiol 116, 867.

Green, S.M., Eisenstein, E., Mcphie, P., Hensley, P., 1990. The purification and characterization of arginase from *Saccharomyces cerevisiae*. J. Biol. Chem. 265, 1601–1607.

Green, S.M., Ginsburg, A., Lewis, M.S., Hensley, P., 1991. Roles of metal ions in the maintenance of the tertiary and quaternary structure of arginase from *Saccharomyces cerevisiae*. J. Biol. Chem. 266, 21474–21481.

Harrell, D., Sokolovsky, M., 1972. Beef-liver arginase: isolation and molecular properties. Eur. J. Biochem. 25, 102–108.

Hellerman, L., Perkins, M.E., 1935. Activation of enzyme: III. The role of metal ions in the activation of arginase. The hydrolysis of arginine induced by certain metal ions with urease. J. Biol. Chem. 112, 175–194.

Hirsch-Kolb, H., Kolb, H.J., Greenberg, D.M., 1971. Nuclear magnetic resonance studies of manganese binding of rat liver arginase. J Biol. Chem. 246, 395–401.

Kamio, Y., Terawa, Y., 1983. Purification and properties of *Selenomonas ruminantium* lysine decarboxylase. J. Bacteriol 153, 658–664.

Kanda, M., Ohgishi, K., Hanawa, T., Saito, Y., 1997. Arginase of *Bacillus brevis* Nagano: purification, properties, and implication in gramicidin S biosynthesis. Arch. Biochem. Biophys. 344, 37–42.

Kang, J.H., Cho, Y.D., 1990. Purification and properties of arginase from soybean, *Glycine max*, axes. Plant Physiol 93, 1230–1234.

Kanyo, Z.F., Scolnick, L.R., Ash, D.E., Christianson, D.W., 1996. Structure of a unique binuclear manganese cluster in arginase. Nature 383, 554–557.

Kim, Y.O., Cho, Y.D., 2000. Growth inhibition in suspension-cultured soybean cells in the presence of ferulic acid is mediated through spermine accumulation. J. Plant Physiol. 156, 133–136.

King, J.E., Gifford, D.J., 1997. Amino acid utilization in seeds of loblolly pine during germination and early seedling growth. Plant Physiol. 113, 1125–1135.

Kollöffel, C., Van Dijke, H.D., 1975. Mitochondrial arginase activity from cotyledons of developing and germinating seeds of *Vicia faba* L. Plant Physiol. 55, 507–510.

Krumpelman, P.M., Freyermuth, S.K., Cannon, J.F., Fink, G.R., Polacco, J.C., 1995. Nucleotide sequence of *Arabidopsis thaliana* arginase expressed in yeast. Plant Physiol. 107, 1479–1480.

Kuhn, N.J., Ward, S., Piponski, M., Young, T.W., 1995. Purification of human hepatic arginase and its manganese (II)-dependent and pH-dependent interconversion between active and inactive forms: a possible pH-sensing function of the enzyme on the ornithine cycle. Arch. Biochem. Biophys. 320, 24–34.

Martín-Falquina, A., Legaz, M.E., 1984. Purification and properties of the constitutive arginase of *Evernia prunastri*. Plant Physiol. 76, 1065–1069.

Mendz, G.L., Holmes, E.M., Ferrero, R.L., 1998. In situ characterization of *Helicobacter pylori* arginase. Biochim. Biophys. Acta 1388, 465–477.

Muszyńska, G., Severina, L.O., Lobyreva, L.W., 1972. Characteristics of arginases from plant, ureotelic and uricotelic organisms. Acta Biochim. Pol. 19, 109–116.

Nordin, A., Naesholm, T., 1997. Nitrogen storage forms in nine boreal understorey plant species. Oecologia 110, 487–492.

Park, H., Cho, B.G., Lee, M.K., 1990. Nitrogen compounds of Korea ginseng and their physiological significance. Korean J. Ginseng Science 14, 317–331.

Park, Y.C., Cho, Y.D., 1992. Purification of arginine decarboxylase from soybean. Korean J. Biochem. Mol. Biol. 25, 618–623.

Polacco, J.C., Holland, M.A., 1993. Roles of urease in plant cells. Int. Rev. Cytol 145, 65–103.

Reczkowski, R.S., Ash, D.E., 1994. Rat liver arginase: kinetic mechanism, alternate substrates, and inhibitors. Arch. Biochem. Biophys. 312, 31–37.

Reddy, S.R., Campbell, J.W., 1968. A low molecular weight arginase in the earthworm. Biochim. Biophys. Acta 159, 557–560.

Splittstoesser, W.E., 1969. The appearance of arginine and arginase in pumpkin cotyledons. Characterization of arginase. Phytochemistry 8, 753–758.

Spolarics, Z., Bond, J.S., 1988. Multiple molecular forms of mouse liver arginase. Arch. Biochem. Biophys. 260, 469–479.

Walker, J.M., 1996. The Protein Potocols Handbook. Humana Press Inc, Totowa, NJ.

Yu, K.H., Cho, Y.D., 1998. Relationship between induced arginase activity and the level of free amino acids and polyamines in the excised embryonic axes of germinating soybean seeds. J. Plant Physiol. 153, 226–229.

Zonia, L.E., Stebbins, N.E., Palacco, J.C., 1995. Essential role of urease in germination of nitrogen-limited *Arabidopsis thaliana* seeds. Plant Physiol. 107, 1097–1103.

PERGAMON

Phytochemistry 58 (2001) 1025–1034

PHYTOCHEMISTRY

www.elsevier.com/locate/phytochem

Failed expression of an *endo*-β-1,4-glucanhydrolase (cellulase) in a non-abscinding mutant of *Lupinus angustifolius* cv Danja

Janice Henderson, Linden Lyne, Daphne J. Osborne*

Oxford Research Unit, Open University, Foxcombe Hall, Boars Hill, Oxford, OX1 5HR, UK

Received 17 May 2001; received in revised form 24 August 2001

Abstract

Cellulase expressions in a normal shedding wild-type and a non-abscinding single gene mutant of *Lupinus angustifolius* have been studied during ethylene treatments of leaf abscission zone explants. Of the range of different glycohydrolases investigated only the abscission cell-specific β-1,4-glucanhydrolase (cellulase) was not produced in the non-abscinding mutant. An *endo*-polygalacturonase was induced equally in both wild-type and mutant and other glycohydrolases were equally up-regulated. The abscission cell-specific cellulase induced at shedding of wild-type is antigenically similar to the *Phaseolus vulgaris* induced leaf abscission pI 9.5 cellulase but with a higher molecular mass (50 kD compared with 48 kD) and like the bean abscission-specific cellulase that of lupin is not glycosylated. Causes of the loss of function of cellulase expression in the non-shedding mutant are discussed. © 2001 Elsevier Science Ltd. All rights reserved.

Keywords: Cellulase; β-1,4-Glucanhydrolase; Abscission; Mutant gene; *Lupinus angustifolius*; Glycohydrolases, Polygalacturonase

1. Introduction

Modification of abscission zone formation or suppression of abscission cell separation has long been a goal in agronomics because of the potential this offers for improving yield or facilitating harvesting. Mutants with reduced flower bud abscission can provide advantages for beans, tomatoes and cotton where early pod or fruit shedding is common during transient stress conditions. Reduced abscission of all parts is valuable for fodder crops where total vegetative yield is the objective. For certain special crops, such as the plantation oil palm, the absence of abscission in ripe fruit can abolish shedding losses before and during bunch harvesting and hence permit extended lipid synthesis (Henderson and Osborne, 1999).

In Australia, a spontaneous single gene mutant was discovered in the early 1990s amongst plants of *Lupinus angustifolius* cv Danja. This mutant does not shed any organ despite an apparently normal pattern of growth and senescence (Atkins and Pigeaire, 1993). The wild-type of this cultivar is a narrow-leafed variety grown commercially for compound animal feed. The seeds of other white lupins are important sources of protein for livestock (Edwards and van Barneveld, 1998). Since abscission normally occurs primarily among fertilised flowers and small pods (Pigeaire et al., 1992) a non-abscinding mutant offers benefits with respect to yield from assimilates filling pods that might otherwise abscind prematurely. Also, the absence of abscission of leaves under stress conditions permits the retention of all nutrients taken up and the continued mobilisation of metabolites to the reproductive structures. It is to the biochemistry of organ shedding in the wild-type and the single gene non-abscinding mutant (*Abs*$^{-}$) of this lupin that the current paper is directed.

A common feature of the biochemistry of abscission is the synthesis of tissue-specific ethylene-induced hydrolases which degrade the polysaccharide and protein complex of the middle lamella and loosen the primary walls of cells in the separation layer (Osborne, 1989). In the leaf pulvinus-petiolar or pulvinus-stem abscission zones of bean (*Phaseolus vulgaris*) a specific cell wall loosening pI 9.5 cellulase is induced (Horton and Osborne, 1967; Reid et al., 1974) and in tomato flower abscission, multiple cellulase mRNAs are newly expressed at the separating zone in the pedicel (Lashbrook et

* Corresponding author. Tel.: +44-1865-487690; fax: +44-1865-326322.

E-mail address: d.j.osborne@open.ac.uk (D.J. Osborne).

0031-9422/01/$ - see front matter © 2001 Elsevier Science Ltd. All rights reserved.
PII: S0031-9422(01)00384-3

al., 1994; del Campillo and Bennett, 1996). In addition to cellulase, a polygalacturonase increases during cell separation in tomato leaf and flower abscission zones (Kalaitzis et al., 1997) and is induced with very high levels of activity in oil palm fruit abscission zones (Henderson et al., 2001). Activities of β-galactosidase and other glycosidases can also rise during abscission but these are generally up-regulated rather than induced (Henderson and Osborne, 1999). Although polygalacturonase and other cell wall hydrolase activities in the leaves of lupin change during abscission in the wild-type zone and in the zone of the non-abscinding mutant, we report here that a specific difference in the abscission-linked cellulase expression alone could account for the loss of shedding competence in the *Abs*$^-$ mutant.

2. Results

2.1. Cellulase

After 72 h in ethylene leaflet abscission of the wild-type explants is complete. Enzyme assays for total *exo*- and *endo*-β-1,4-glucanhydrolase in wild-type and the non-abscinding *Abs*$^-$ mutant showed an increase in cellulase activity at abscission only in the zone tissue of the wild-type. Cellulase activity remains low in the adjacent non-zone tissue of both wild-type and *Abs*$^-$ (Table 1).

The cellulase present in intact 0 h zones of both wild-type and *Abs*$^-$ has an optimal activity between pH 4.3 to 5.8 (Fig. 1A) and this, we believe, represents the consititutive cellulase present both in zone and non-zone cells of both genetic lines (compare Figs. 1A and 2A). In wild-type 72 h ethylene-treated tissue (100% abscission) cellulase activity occurs over a wide range of pHs including pH 6.3–7.8 (Fig. 1B) indicating that, in addition to a constitutive cellulase, a new isoenzyme activity is induced at abscission that extends to a higher pH range. Whereas, in the 72 h ethylene-treated *Abs*$^-$ tissue in which no abscission occurs (0%) the pH dependency and optimum for this cellulase remains at pH 4.3–5.8 with a similar pH profile to that of the 0 h intact zones. Final viscosity readings even after 24 h incubations showed no decrease at higher pH (pH 7.3 and 7.8) in extracts from *Abs*$^-$ material.

Table 1
Comparison of cellulase activity at pH 7.8 in extracts of wild-type (WT) and *Abs*$^-$ lupin explants at 0 h and after incubation in ethylene (2.5 μl l^{-1}) for 72 h[a]

	Cellulase activity (% decrease in viscosity)			
	WT		*Abs*$^-$	
	0 h	72 h	0 h	72 h
Zone	4.0±5.6	41.4±5.5	9.0±2.5	3.8±1.3
Non-zone	14.7±2.5	9.0±0.3	9.9±3.2	7.4±4.8
Abscission	0%	100%	0%	0%

[a] Change in viscosity was measured over 3 h ($n=3\pm$s.d.)

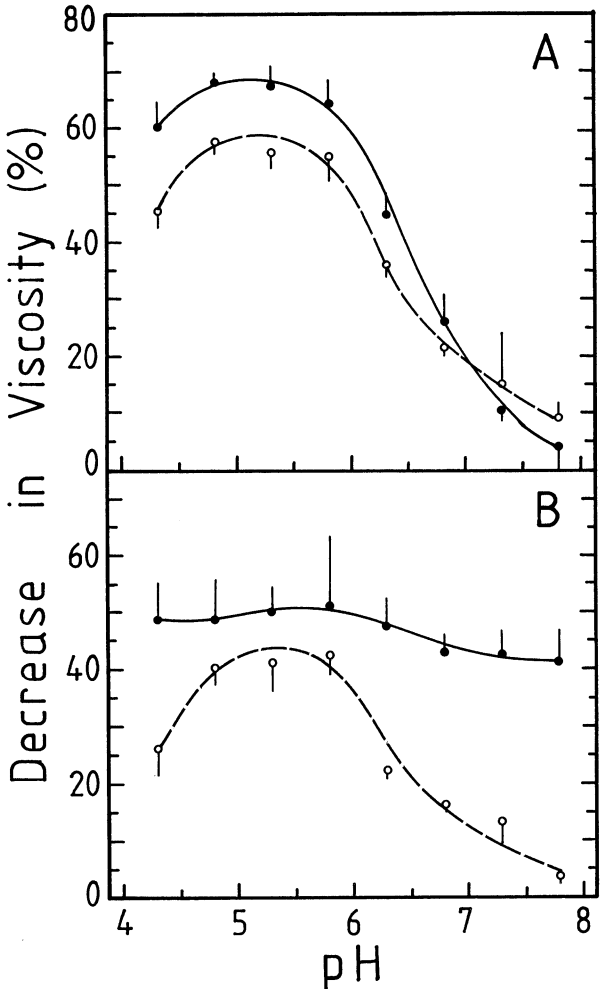

Fig. 1. pH activity profiles of cellulase from extracts of freshly cut (0 h) intact abscission zone cells (A) and after 72 h in ethylene, 2.5 μl l^{-1} (B). Change in viscosity was measured over 3 h ($n=3\pm s.d.$). Wild-type (100% abscission) ●; *Abs*$^-$ (0% abscission) ○ (See Section 4.4.1.).

Coomassie staining of IEF gels (Fig. 3) shows inducible or up-regulated protein bands in 72 h zones of both wild-type and *Abs*$^-$ at pIs 8.4–8.6 and 9.3 (calibrated using the IEF standard protein mix (Sigma, Novex) and from the known pI of tomato PG1). Viscometric assays of gel segments containing these bands excised from IEF gels run in parallel with those for protein staining confirm the presence of an *endo*-cellulase activity induced at pI 8.4–8.5 in the wild-type but no activity above background in this induced band in *Abs*$^-$ (Table 2). Another cellulase activity present in both wild-type and *Abs*$^-$ includes pIs 4.6–5.1, and is detectable at 0 and 72 h but with slightly higher activity in wild-type.

Activity gels (IEF) to visualise enzymic production of reducing groups at 72 h after coating the gel with CMC solution, incubation and development with TTC/NaOH show an *endo*-cellulase activity present at the point of

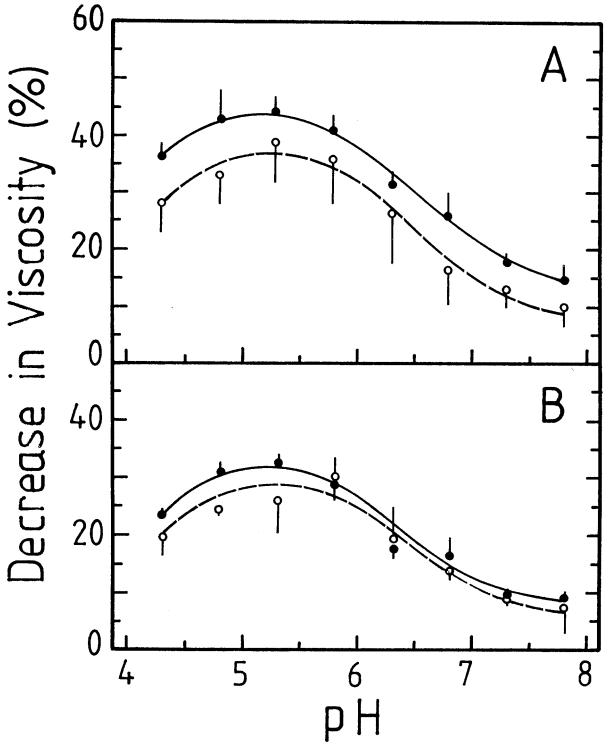

Fig. 2. pH activity profiles of cellulase from extracts of freshly cut (0 h) petiole (non-zone) tissue (A) and after 72 h in ethylene, 2.5 μl l^{-1} (B). Change in viscosity was measured over 3 h ($n=2\pm s.d.$). Wild-type ●; *Abs*$^-$ ○ (See Section 4.4.1.).

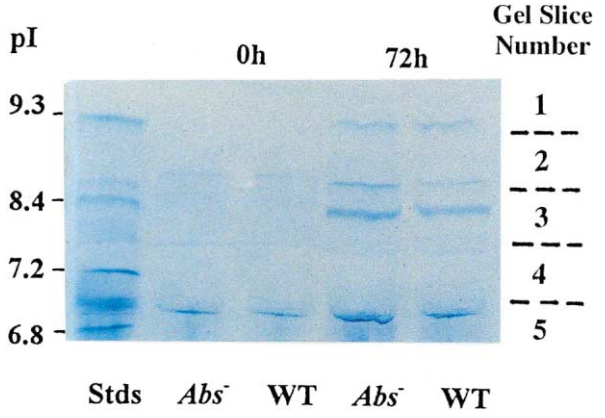

Fig. 3. Isoelectrophoretic fractionation of protein extracts from 0 and 72 h ethylene-treated explants (2.5 μl l^{-1}). Wild-type, WT (100% abscission at 72 h) and *Abs*$^-$ (0% abscission). Stained with Coomassie Blue to show inducible or up-regulated protein bands at pI 8.4–8.6 and 9.3.

application (ca pI 7.0, gel slice 5, Table 2) and at ca pI 5.1 (gel slice 8, Table 2) in both wild-type and *Abs*$^-$. Only in wild-type were reducing groups detectable at pI 8.4–8.5 (corresponding to gel slice 3, Table 2) indicating an increase in the presence of reducing end groups resulting from an *endo*-cellulase activity at this pI (activity gel not shown).

Abscission cellulase in extracts of the abscinded wild-type lupin at 72 h is recognised in Western blotting by

Table 2
Cellulase activity in 1 cm slices cut from IEF gels of wild-type (WT) and *Abs*$^-$ lupin abscission zone extracts fractionated at 0 h and after 72 h in ethylene (2.5 μl l^{-1})[a]

		Cellulase activity (% decrease in viscosity)			
		0 h		72 h	
pI	Gel slice number	WT	*Abs*$^-$	WT	*Abs*$^-$
9.5	1	0	0	11.7	8.0
	2	0	0	16.5	7.8
8.4–8.5	3	0	0	65.9	9.5
	4	0	2.6	46.3	14.0
6.8	5	3.5	6.0	29.3	2.9
	6	2.9	0	9.5	0
	7	12.8	2.1	16.7	10.2
5.1	8	20.3	10.9	35.8	19.6
	9	13.0	9.3	28.0	21.0
3.5	10	17.8	1.1	9.7	1.7
Abscission		0%	0%	100%	0%

[a] Sample application was at ca. pI 7.0; the pI of each slice was determined by calibration against an IEF standard protein mix (gel slices 1–5 shown in Fig. 3). Each slice was added to a 2% solution of CMC and incubated as described in Section 4.4.1. Final measurements of viscosity were made at 24 h. Representative set of experiments repeated 3 times.

two cellulase pI 9.5 antisera (LL and MM) raised against bean (Fig. 4). Immunorecognition of the bean abscission cellulase on SDS–PAGE gels indicated a molecular mass ca 48 kD which is in agreement with the data of others (Brummell et al., 1994). Run on the same gels as bean, the lupin abscission cellulase of wild-type has a molecular mass that is slightly higher than bean at about 50 kD. No abscission cellulase can be recognised in Western blots of extracts of *Abs*$^-$ at 72 h.

In immunoprecipitation experiments the addition of the pI 9.5 antisera solution (MT) to bean or lupin cellulase extracts reduced activity of the cellulase in viscosity assays by ca 92% (bean) or ca 88% (lupin). Addition of PG antisera or of the YZ 2.23 monoclonal antibody had no inhibitory effects upon cellulase activity measured by CMC loss in viscosity. This lack of reduction in enzyme activity following the addition of YZ 2.23 confirms also that neither bean nor lupin cellulases possess the *N*-linked xylose-fucose heptasaccharide sequence common to many plant proteins (McManus et al., 1988).

Further evidence for the absence of glycosylation comes from experiments in which lupin extracts of 72 h wild-type fractionated by SDS–PAGE directly or were first fractionated on IEF gels and the IEF gel slices at pI 8.4 to 8.5 then re-fractionated on SDS–PAGE gels before staining for glycoprotein. No glycosylated bands were evident above 42 kD. Western blots of SDS–PAGE gels of proteins extracted from abscinded bean domes, or from 72 h wild-type and *Abs*$^-$ abscission zones probed with the monoclonal YZ 2.23 also showed no recognition between 42 kD and 58 kD, again indicating the absence

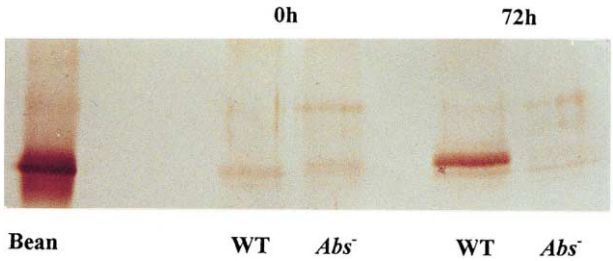

Fig. 4. Western blot of SDS–PAGE fractionation of lupin abscission zone proteins at 0 h and after 72 h in ethylene (2.5 μl l^{-1}); wild-type (WT, 100% abscission) and *Abs*$^{-}$ (0% abscission) together with bean (100% abscission) as control. All probed with the pI 9.5 antiserum (LL) to abscission zone-specific cellulase of bean (48 kD). Each lane 4 μg protein.

Table 3
(A) β-Glucosidase activity in lupin extracts of abscission zone and non-zone wild-type (WT) and *Abs*$^{-}$ tissue at 0 h and after 72 h in ethylene (2.5 μl l^{-1}). Activity measured over 2 h as *p*-nitrophenol release from *p*-nitrophenol-β-glucopyranoside as described in Section 4.4.3. ($n=3\pm s.d.$). (B) Polygalacturonase activity in the same extracts measured over 20 h by liberation of reducing sugar from a polygalacturonic acid substrate as described in Section 4.4.2. ($n=3\pm s.d.$)

	WT		*Abs*$^{-}$	
	0 h	72 h	0 h	72 h
(A) β-Glucosidase activity (nmol p-nitrophenol g^{-1} min^{-1})				
Zone	129.1±14.3	715.6±24.3	135.0±5.4	745.2±18.5
Non-zone	60.4±9.7	192.9±64.0	46.6±13.6	211.1±57.9
Abscission	0%	100%	0%	0%
(B) Polygalacturonase activity (nmol reducing groups g^{-1} min^{-1})				
Zone	7.7±3.2	37.8±10.0	7.8±3.6	35.1±6.3
Non-zone	8.4±1.5	14.6±2.0	6.2±1.7	15.4±3.1
Abscission	0%	100%	0%	0%

of glycosylation of a cellulase protein in either bean or lupin between these kD values.

In a direct comparison of the extent of cellulase induction in bean and wild-type lupin, under similar conditions of ethylene treatment, the activity of *endo*-cellulase in abscinded lupin was always approximately half that extractable from the same fresh weight of abscinded bean abscission zones.

2.2. β-Glucosidase

There is a low level of constitutive activity in both lupin lines at 0 h and an up-regulation (ca 5×) in both after 72 h in ethylene (Table 3A). Non-zone tissue shows a similar low level of activity at 0 h with a 3–4 times increase at 72 h (Table 3A).

Although total enzyme assays for β-glucosidase indicate similar levels of increased activity after 72 h in ethylene in both wild-type and mutant, when extracts of zone tissue of both are fractionated on IEF gels and the gel slices assayed with *p*-nitrophenyl-β-glucopyranoside, three β-glucosidase isoenzymes are detected at pIs ca 8.5, 7.0 and 5.5 (Fig. 5). Of particular interest is the isoform at pI ca 8.5 which is not present at 0 h and is induced in 72 h zone tissue of both wild-type and *Abs*$^{-}$. The large increase in the activity of the pI 7.0 isoform and the smaller contribution of the induced pI ca 8.5 isoform probably together represent the induction of the total glucosidase activity observed by Osborne and Thompson (1992). As in their experiments, there is no quantitative difference between the two genetic lines (wild-type and *Abs*$^{-}$).

The induced pI ca 8.5 glucosidase isoform has a similar pI to that of cellulase but the two activities have been separated by re-fractionation on SDS–PAGE. For this the location of the active β-glucosidase in 72 h zone tissue at pI 8.4 to 8.5 in both wild-type and *Abs*$^{-}$ was first confirmed by assay of gel slices following electrofocussing. The wild-type and *Abs*$^{-}$ 0 h and 72 h IEF gel slices from pI 8.4–8.5 and control IEF gel slices were then re-fractionated, together with protein standards, by SDS–PAGE. After silver-staining, a protein band, not present in either 0h tissue or in the control IEF gel slices, was observed at ca 63 kD (Fig. 6). Since Western blots confirm the induced lupin abscission cellulase to be antigenically similar to bean but with a slightly higher molecular mass (ca 50 kD compared with 48 kD), the 63 kD band may well correspond with the induced pI ca 8.5 β-glucosidase.

2.3. Other glycosidases

β-Galactosidase is also up-regulated to a very high level of activity after 72 h incubation in ethylene but,

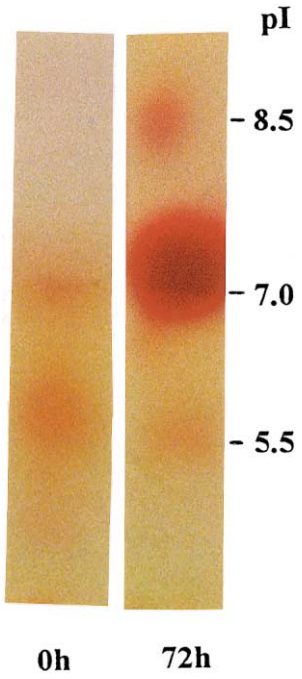

Fig. 5. β-Glucosidase activity in gel slices (IEF) of wild-type zones at 0 and 72 h of ethylene treatment (2.5 μl l^{-1}). At 72 h a new β-glucosidase activity is induced at pI ca 8.5 with up-regulation of activity at pI ca 7.0. A third activity resides at pI ca 5.5. Each gel slice assayed with *p*-nitrophenyl-β-glucopyranoside as substrate.

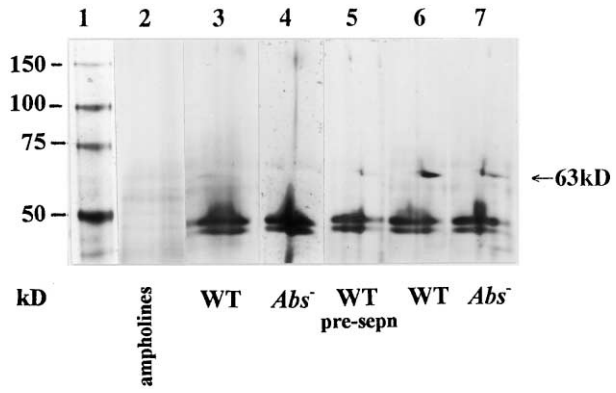

Fig. 6. Location of the pI 8.5 induced β-glucosidase activity excised from an IEF gel and re-fractionated on SDS-PAGE show the induced protein at 63 kD with the progression of abscission in wild-type (WT) and similar protein at 72 h in the non-abscinded *Abs*$^{-}$. (1) MW markers; (2) IEF control gel slice; (3 and 4) WT and *Abs*$^{-}$ at 0 h; (5) WT, 72 h pre-separation; (6) WT (100% abscission) at 72 h; (7) *Abs*$^{-}$ (0% abscission) at 72 h.

again, no differences were detected in either the intact or abscinded abscission zones or in the non-zone tissues between the two genetic lines.

Five other *exo*-cleaving enzymes that could play a minor, though possibly still critical, role in lupin leaf abscission, either show low levels of up-regulation at 72 h in both wild-type and mutant (β-cellobioside, β-xylosidase and α-arabinofuranosidase) or remain essentially unchanged in both (α-glucosidase, α-galactosidase) (Table 4).

2.4. Polygalacturonase

In tomato fruit ripening both *exo*- and *endo*- isoforms are induced (Pressey and Avants, 1973; Pressey, 1987). When lupin abscission zone extracts were fractionated on IEF gels in parallel with tomato fruit extracts, Western blots showed recognition with tomato *endo*-PG antiserum for both wild-type and *Abs*$^{-}$ zones at both 0 h and 72 h (Fig. 7A) with a greater intensity in both at 72 h. The pI of lupin PG is ca 9.0, higher than that for tomato *endo*-PG1 (pI 8.6) (Ali and Brady, 1982). Western blots of SDS–PAGE gels (Fig 7B) run in parallel with an extract of ripe tomato fruit give a molecular mass for the lupin PG of 40 to 44 kD, slightly lower than that for tomato *endo*-PG (43 to 46 kD) reported by Tucker et al. (1980) and Ali and Brady (1982).

Direct assays for PG activity in extracts of abscission zone and non-zone tissue at 0 h show no differences

Table 4
Glycosidase activities in lupin extracts of abscission zone wild-type (WT) and *Abs*$^{-}$ tissue at 0 h and after 72 h in ethylene (2.5 μl l^{-1})[a]

	Glycosidase activity (nmol *p*-nitrophenol g^{-1} min^{-1})			
	WT		*Abs*$^{-}$	
	0 h	72 h	0 h	72 h
α-Glucosidase[d]	8.3±4.9	11.1±0.8	9.7±1.8	8.8±0.5
β-Galactosidase[b]	777.5±31.6	1801.9±160.7	749.2±62.2	1876.9±263.7
β-Cellobiosidase[d]	6.2±1.4	17.7±1.8	5.8±1.0	17.3±3.5
β-Xylosidase[d]	17.0±0.8	49.1±2.0	24.3±1.0	59.4±1.6
α-Galactosidase[c]	192.2±40.6	234.0±20.6	224.3±22.2	291.9±34.5
α-Arabinofuranosidase[c]	123.8±42.4	203.4±68.3	104.2±45.9	145.5±18.7
Abscission	0%	100%	0%	0%

[a] Activity measured as *p*-nitrophenol release from *p*-nitrophenol-β-glycoside substrates as described in Section 4.4.3. ($n=3\pm s.d.$).
[b] Assayed over 0.5 h.
[c] Assayed over 2 h.
[d] Assayed over 6 h.

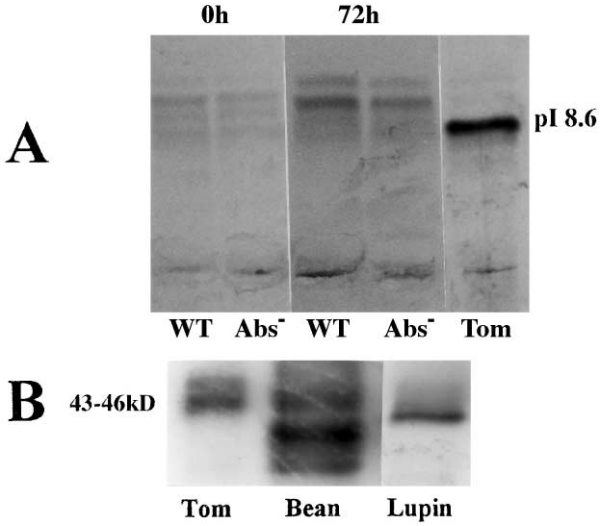

Fig. 7. Western blots probed with tomato fruit *endo*-PG antiserum: A. IEF fractionation of proteins from abscission zones at 0 h and after 72 h in ethylene (2.5 μl l^{-1}). Wild-type (WT, 100% abscission) and *Abs*$^{-}$ (0% abscission) compared with an extract of ripe tomato fruit expressing tomato *endo*-PG1 (pI 8.6). Both wild-type and *Abs*$^{-}$ are equally induced but have a higher pI than tomato PG. Each lane 27 μg protein. B. SDS-PAGE fractionation of proteins from lupin abscission zones of wild-type (100% abscission) after 72 h ethylene treatment (2.5 μl l^{-1}) in comparison with protein extracts of tomato fruit (43–46 kD) and abscinded bean abscission zones. Each lane 9 μg protein.

between the two lupin lines, and by 72 h in ethylene that in wild-type and *Abs*$^{-}$ is up-regulated to the same extent, abscission zone tissue (ca ×4) and non-zone tissue (ca ×2) (Table 3B).

2.5. Laminarinase (β-1,3-glucanhydrolase)

Of potential interest in abscission is β-1,3-glucanhydrolase. Both Abeles and Forrence (1970) and Felix and Meins (1985) have recorded large increases in this enzyme in plants and in excised leaf sections of bean and tobacco respectively, in response to ethylene. In the lupin, using reducing group assays with laminarin as substrate, β-1,3-glucanhydrolase activity rose four-fold in zone tissue after 72 h in ethylene, but no differences were found between the extracts of the abscinded tissue of wild-type and those of *Abs*$^{-}$ (data not shown).

3. Discussion

Whilst the mutant non-abscinding *Abs*$^{-}$ plants develop normally in every respect and initially are indistinguishable from wild-type, no abscission of the leaflets (nor of any other organ) occurs. Furthermore, the leaflets are not induced to abscind by incubation under ethylene at levels as high as 100 μl l^{-1} for 120 h (Clements and Atkins, 2001). However, the leaflet explants do release ethylene, and they do show a normal level of ACC-enhanced ethylene production (Thompson, unpublished data). Ethylene applied to etiolated wild-type and mutant lupin seedlings inhibits shoot elongation in both, causes lateral swelling of the shoots and the typical 'triple response' (Osborne and Thompson, 1992). The *Abs*$^{-}$ mutant, therefore, can perceive and respond to ethylene so a general insensitivity to ethylene (as in an ETR mutant) is not the reason for the absence of abscission. Also, at 0 h there are no obvious anatomical differences between the abscission zone regions of wild-type and the *Abs*$^{-}$ mutant (Clements and Atkins, 2001)

The pH profiles for cellulases (including the abscission pI 9.5 cellulase) reported for the petiole-leaf abscission zone of the bean, by del Campillo et al. (1988) show that they are very similar to those we find induced in the abscinded zone of the wild-type lupin.

Fractionation of extracts of the lupin abscission-site proteins at 0 and 72 h run in parallel with similar extracts from bean have shown that on IEF gels, there is an induced protein band in wild-type with cellulase activity at a lower pI than that induced at bean abscission (pI 8.4–8.5 compared with pI 9.5). In addition, in the *Abs*$^{-}$ mutant, a protein band that also fractionates at pI 8.4–8.5 is induced at 72 h, but this has no *endo*-cellulase activity; nor does this fraction liberate reducing sugars when incubated with CMC—unlike the corresponding fraction from wild-type. When fractionated on SDS-gels and silver-stained, a protein band is seen to be induced by 72 h in ethylene in both wild-type and *Abs*$^{-}$ with a molecular mass (calculated from marker standards) of ca 50 kD compared with ca 48 kD for the bean abscission cellulase. Western blots (using both the original L.Lewis bean pI 9.5 and a new antibody raised against a bean cellulase protein amplified from a bean abscission cellulase cDNA transformed into *E. coli*) both confirmed similar antigenic recognition at ca 48 and 50 kD for the bean and wild-type lupin cellulase, respectively. This is not unexpected since lupin and bean are both members of the Leguminosae. However, there was no recognition by pI 9.5 cellulase antiserum of any protein band (including that at 50 kD) in *Abs*$^{-}$ blots.

The cellulases as a group of enzymes show a high level of heterogeneity between species (Brummell et al., 1994) and between different tissues in the same plant, as in peach (Bonghi et al, 1992). Some isoforms are glycosylated as in ripening avocado (Bennett and Christoffersen, 1986) and in leaves and fruits of pepper plants (Ferrarese et al., 1995), whilst the basic form of cellulase in the bean leaf, the pI 9.5 abscission-induced cellulase, is reported as not glycosylated (Bennett and Christoffersen, 1986). The difference in mobility that we find between lupin and bean abscission cellulase appears not to be the result of differential addition of sugar residues as neither lupin nor bean abscission cellulase is positive in our glycosylation tests. Also, neither bean nor lupin

cellulase bands are recognised on Western blots by the monoclonal YZ 2.23 indicating an absence of the abscission cell-linked, but common *N*-xylose-fucose oligosaccharide protein terminus (McManus et al., 1988).

Polygalacturonase is another much studied and important enzyme in fruit ripening and in some species also in abscission (Roberts et al., 1997; Henderson and Osborne, 1999). The increase in PG activity observed in lupin in both the abscinding and non-abscinding genetic lines appears not to be directly linked to abscission but rather to a response to ethylene. Although PG has been reported as an *exo*-acting enzyme in bean abscission zones (Berger and Reid, 1979) in our experiments, the recognition by the tomato *endo*-PG antiserum of a protein in the abscinded bean dome shows it to possess *endo*-PG activity (Fig. 7B). This *endo*-PG activity is induced to the same extent in both wild-type and *Abs*$^-$ lupin even though *Abs*$^-$ does not shed, so failure of *Abs*$^-$ to abscind is unlikely to be due to failures in PG.

β-Glucosidase is of special interest as this enzyme was considered to be equally induced by ethylene in both wild-type and *Abs*$^-$ abscission zones by Osborne and Thompson (1992) using a less sensitive assay procedure. They found that ethylene led to a similar rise in the level of expressed activity by wild-type and *Abs*$^-$ at 72 h despite the lack of abscission in *Abs*$^-$. Present results indicate that the rise includes the expression of a new β-glucosidase isoenzyme and the up-regulation of at least one other isoform as part of the ethylene-inducible response.

Another enzyme, β-1,3-glucanhydrolase, is also equally enhanced in the abscinding zone cells of wild-type and the non-abscinding zone cells of *Abs*$^-$ when the tissues are exposed to ethylene. One may conclude that even if β-glucosidase and β-1,3-glucanhydrolase are important components of the enzyme cohort that is responsible for abscission cell separation, neither determines the difference in shedding between wild-type and *Abs*$^-$. Although it seems evident that a critical threshold level of ethylene is an essential requirement for triggering abscission, ethylene induces in both abscission cells and in neighbour non-abscission cells an array of different new or up-regulated gene expressions and suppressions that are not directly related to the shedding response, but instead are linked to an accumulation of pathogenesis-related proteins or stress-related proteins (del Campillo and Lewis, 1992). A comparison of such accelerations or repressions between an abscinding wild-type and a non-abscinding mutant provides the opportunity to discriminate between those expressions directly essential to abscission and those that are "fellow travellers" of a wider array of ethylene controlled responses.

Although not all potential wall-modifying glyco- and glucan-hydrolases were investigated in relation to the non-abscission of *Abs*$^-$ only the absence of an inducible abscission-specific cellulase is recognisable as the enzymic expression lacking in the non-separating *Abs*$^-$. As a single gene mutant (Atkins and Pigeaire, 1993) this could be the only gene activity that has been lost or suppressed in *Abs*$^-$.

Taken together, the results suggest that there could be the production, in the *Abs*$^-$ mutant, of a protein with a disabled cellulase function. This situation could arise from a mutant cellulase gene or alternatively from failures in the subsequent transcription, translational or post-translational events of a normal gene.

4. Experimental

4.1. Plant material

Seeds of *L. angustifolius* cv Danja and *Abs*$^-$ were sown in 30 cm diameter pots in multipurpose compost in an unheated greenhouse under natural light conditions during the months of May–November. Plants were harvested at an average of 44 days (39 days min, 50 days max) when they were about 8–10 inches tall and when each plant had 6–8 fully expanded leaves.

For the bean (*Phasolus vulgaris* L. var. Masterpiece) plants were grown in seed boxes under the same conditions as for lupin and the primary leaves harvested when plants were ca 21 days old (20 days min; 30 days max).

4.2. Preparation of explants

For the lupin, the compound leaves, including the petiole, were first cut from the plant. Explants containing the leaflet abscission zones were prepared by removing the lower part of the petiole to leave a length ca 2 cm and shortening the blades of the leaflets so that only a 1 to 2 mm base of each leaflet and its pulvinule remained where each leaflet abscission zone joined the petiole. Explants were placed on glass in a glass dish over 2% (w/v) agar. Each dish (ca 1 l) was sealed with a glass lid fitted with a Suba-Seal. Ethylene was injected to give a concentration of 2.5 μl l^{-1}, and the dishes were held in an unlit incubator at 25 °C for 72 h with daily aeration. For the wild-type material a thin slice of tissue was removed from the petiole surface of the abscission zone after the zone cells had separated (72 h). For the *Abs*$^-$ material an equivalent amount of tissue was excised to include the whole of the region of the non-separated zone. For 0 h samples, the unseparated abscission zones were excised directly from the freshly collected leaves. For non-zone material, 5 mm segments of petiole tissue were cut from 3 to 4 mm below the attachment of the pinnules.

For the bean, the pulvinus-petiole abscission zone of the primary leaf was excised as a 1.5 cm segment to include the whole of the pulvinus, the abscission zone and ca. 1 cm of the subtending petiole. The explants

were held in glass containers on perspex racks over 2% agar and, as for the lupin explants, ethylene was injected to give a final concentration of 2.5 μl l^{-1}. All explants had completed abscission by 48 h and a narrow slice of tissue (< 1 mm) was removed from the exposed surface of the petiole dome at the pulvinar/petiolar junction. For 0 h samples, a thin slice (to include all the abscission zone cells) was excised directly from the leaf pulvinus-petiole junction.

4.3. Extraction of tissue

The amount of zone tissue obtained from ca 30 lupin plants was 200–300 mg. Freshly collected tissue (200 mg) was ground in a cooled mortar with 200 μl 50 mM sodium acetate pH 5.5 containing protease inhibitors leupeptin (1μg ml^{-1}), amidinophenylmethane sulfonyl fluoride (APMSF, 40 μg ml^{-1}), 200 mM NaCl and a little acid-washed sand. After centrifugation in a benchtop microfuge (Beckman) at 9000 g_{max} for 1 min, the pellet was re-extracted in de-ionised (MilliQ) water (200 μl) and centrifuged. The two supernatants were combined and assayed directly. Extracts of non-zone tissue were prepared in the same way. Extraction procedures for the bean were similar to those for lupin and experiments were carried out in parallel.

The presence of NaCl did not interfere with any of the enzyme assays (viscosity, reducing sugar, *p*-nitrophenol release). Partial purification of enzyme extracts (gel filtration/ultrafiltration) always resulted in some loss of each enzyme activity. Heterologous mixtures of wild-type and *Abs*$^-$ extracts indicated no inhibition or activation of any enzyme assayed. Protein determinations were made by the method of Bradford (1976) with BSA as the standard.

4.4. Enzyme assays

4.4.1. Viscosity measurements

Cellulase (EC 3.2.1.4) activity was measured by a decrease in viscosity of a solution of carboxymethyl cellulose (CMC, Hercules, USA, Type 7HF). Enzyme extract (50 μl) was added to 400 μl of a 2% (w/v) aqueous solution of CMC with 50 μl 1 M buffer (acetate or phosphate) at the appropriate pH. Viscosity readings were started after a 5 min equilibration period in the water bath (30 °C) and taken thereafter at regular intervals. The pH-dependent activity was determined for cellulase with acetate (pH 3.8–5.8) and phosphate (pH 6.3–7.8) buffers.

4.4.2. Reducing sugar assays

Polygalacturonase (PG, EC 3.2.1.15) and β-1,3-glucanhydrolase (laminarinase, EC 3.2.1.39) activities were measured by the cyanoacetamide method for reducing sugars (Gross, 1982). Enzyme extract (20 μl) was added to each substrate (50 μl) in 50 mM acetate buffer (130 μl); for PG activity, polygalacturonic acid (10 mg ml^{-1}, Sigma) at pH 5.5; for laminarinase activity, laminarin (30 mg ml^{-1}, Sigma) at pH 4.7, and cellulase, CMC (10 mg ml^{-1}) at pH 5.5 and 7.8. Galacturonic acid was used as the standard for PG and glucose for laminarinase and cellulase.

4.4.3. p-Nitrophenol release

Exo-glycosidase activities were determined with *p*-nitrophenylglycoside substrates (Sigma). Enzyme extract (20 μl) was added to substrate (200 μl, 2 mg ml^{-1}) in 50 mM acetate buffer (30 μl). Activities of α- and β-glucosidase, β-cellobiosidase and α-galactosidase were measured at pH 5.3; β-galactosidase, α-arabinofuranosidase and β-xylosidase at pH 4.3. Assays were terminated with 1.25 ml 200 mM sodium carbonate and the release of *p*-nitrophenol assessed at 400 nm. Activity was calculated by reference to standard curves of *p*-nitrophenol.

4.5. Electrophoresis

4.5.1. Isoelectricfocusing

Zone tissue was extracted in 50 mM sodium acetate pH 5.5 (without NaCl) for isoelectric focusing. Pre-cast IEF gels on a plastic backing (pI 3.5–9.5, Pharmacia Ampholine PAGplates) were used with an Ultrophor Electrofocusing Unit (LKB 2217) and electrofocusing constant power supply (LKB 2197). The Ultrophor unit was connected to a MultiTemp II thermostatic circulator (LKB) with the temperature set at 5 °C and pre-cooled 1 h before electrophoresis. Gels (7–14 cm wide) were run at 5 to 7.5 W power with starting voltage of ~250 V for 1.5 h. The voltage at the end of the gel run never exceeded 1500 V. Each sample was loaded onto a 1×0.5 cm applicator strip (2 application pieces were placed on top of each other for 30–50 μl samples). A standard IEF protein mix (Sigma, Novex) with pIs between 3.6 and 9.3 and a tomato PG1 (pI 8.6) enzyme preparation were used to calibrate the pI of the cellulase isoenzyme induced at lupin abscission.

After electrophoresis, the cellulase protein activity at each pI was confirmed by direct enzyme assay. For this, each sample lane of the gel (10 cm in length) was cut into 1 cm horizontal slices and each slice was added to 700 μl 1.5% CMC in 50 mM sodium acetate pH 5.8 and viscosity changes measured over time. The tubes were covered in parafilm and a final viscosity reading was taken after 24 h.

4.5.2. Activity gels

In parallel with viscosity assays for cellulase activity, the formation of reducing sugars from CMC was located visually on other similar sample gels by the addition of triphenyltetrazolium chloride (TTC) in 1 N NaOH

which, on heating, forms a pink precipitate with reducing groups. For this, it was necessary first to remove all the ampholytes from the IEF gels by thorough washing (3×5 min in 50 ml 100 mM acetate pH 5.8) with gentle rotation. Each gel was then blotted and overlaid with ca 1 ml substrate solution (1% CMC in 50 mM sodium acetate pH 5.8), covered with transparent film, placed in a sealed plastic box and incubated at 30 °C (18 h). Gels were then rinsed briefly in distilled water, placed in a hot TTC/NaOH solution [0.15% (w/v) TCC in 1 N NaOH] and heated in a microwave oven, 20 s full power, once or twice until pink bands representing reducing sugars appeared, and the gel background was not too dark (Pan et al., 1989). The activity of β-glucosidase was located also on IEF gels by the liberation of reducing sugar from a 0.002% solution of *p*-nitrophenyl-β-glucopyranoside in 50 mM sodium acetate pH 5.3 for 3 h (with development as for cellulase location). A control IEF gel of the fractionated sample was routinely overlaid with deionised water alone; on development with TTC/NaOH, this consistently showed a pink spot of activity only at pI 3.5 which represented negatively-charged reducing sugars present in the original extracts.

4.5.3. SDS–PAGE

For these gels, the discontinuous SDS–PAGE method of Laemmli (1970) was used. Enzyme extracts (100 mg fresh weight) were extracted in the presence of NaCl (0.5 M) and concentrated to 100 μl under nitrogen gas by ultrafiltration (Flowgen, 3 K) to remove buffer salts and NaCl. Aliquots (30 μl) were denatured in sample buffer (60 mM 2-amino-2-(hydroxymethyl)-1,3-propanediol (Tris)–HCl, pH 6.8 containing 10% (v/v) glycerol, 2.5% (w/v) 2-mercaptoethanol, 2% (w/v) SDS and 0.005% (w/v) bromophenol blue) by heating at 100 °C for 3 min. Samples were fractionated by electrophoresis through 10% (v/v) acrylamide gel (Pro-Sieve, Flowgen) at constant voltage (130 V) at room temperature.

4.5.4. Western blotting

Proteins fractionated by SDS–PAGE were electroblotted (Multiphor, Pharmacia) onto nitrocellulose membrane (Schleicher and Schull, 0.45 μm) using the semi-dry method (Bjerrum and Schafer-Nielson, 1986). After transfer, membranes were first blocked with a solution containing BSA (2%, Sigma) and dried milk powder (2%, Marvel). Blots were then exposed to solutions of antisera of primary antigens: (i) bean pI 9.5 cellulase antiserum (Koehler et al., 1981) from Dr. L. Lewis (LL) via Dr. R. Sexton, University of Stirling; (ii) a new pI 9.5 bean cellulase antiserum from Dr. M.T. McManus (MM) (Massey University, New Zealand) produced from the full-length pBAC10 cDNA (Tucker and Milligan, 1991) cloned into expression vector pPROEX-1 (Life Technologies Inc. Gathersbury, MD, USA) and transformed into *E. coli* strain DH5α. Induction and purification of the expressed protein and production of antibodies in laboratory rabbits was as described in Hunter et al. (1999); (iii) tomato *endo*-polygalacturonase antiserum (Tucker and Grierson, 1982) from Dr. G. Tucker, University of Nottingham, Sutton Bonington; (iv) the monoclonal YZ2.23 raised against an abscission zone-specific protein of *Sambucus nigra* that recognises a xylose-fucose heptasaccharide antigenic glyco-grouping of sequence Manα3(Manα6)(Xylβ2)Manβ4GlcNAcβ4(Fucα3)GlcNAc (McManus et al., 1988).

The washed blots were exposed to either a solution of HRP-conjugated rabbit (cellulase, polygalacturonase) or rat (YZ 2.23) second antibody (Sigma, 1:1000) in PBS/1% blocking buffer and developed with 2 mM 3,3′-diaminobenzidine (Sigma) in 50 mM Tris/HCl pH 7.4 and 2% H_2O_2.

4.5.5. Immunoprecipitation

For these experiments another Dr. L. Lewis pI 9.5 antiserum sample was used from Dr. M. Tucker, USDA, Maryland, USA. Extracts of abscinded wild-type lupin (72 h) and bean (48 h) abscission zones were incubated with either 20 μl of the pI 9.5 abscission cellulase antiserum to a final dilution of 1:3 at pH 8.5 or pH 5.5; or 20 μl of distilled water. The mixtures were first held on ice for 15 min, then centrifuged (16,900 g_{max}, 10 min, 4 °C). Each sample was adjusted to pH 5.8 with 1M sodium acetate (50 μl) and finally incubated with similarly buffered CMC. Viscosity was measured over time as described for cellulase.

Other immunoprecipitations with the antisera to tomato PG or with the monoclonal YZ 2.23 to the *Sambucus nigra* abscission-cell derived *N*-linked xylose-fucose heptasaccharide were carried out as controls.

4.5.6. Direct staining for glycoprotein

Enzyme extracts of wild-type 72 h abscinded abscission zones of lupin were first fractionated by isoelectric focusing and the protein band containing cellulase activity (pI 8.4–8.5) excised from the IEF gel. Duplicate gel pieces were then inserted into wells of SDS–PAGE gels and the pI 8.4–8.5 proteins were re-fractionated together with lanes containing purified tomato polygalacturonase (43–46 kD) and horseradish peroxidase (40 kD) which are both glycosylated. Soybean trypsin inhibitor was run as the unglycosylated protein control lane. The SDS gels were then either silver-stained for protein (GelCode SilverSNAP stain kit) or stained with a GelCode glycoprotein staining kit (both from Pierce and Warriner, UK). Gels were also transferred to membranes and the blots probed with the monoclonal YZ 2.23 for recognition of *N*-acetyl xylose-fucose heptasaccharide glycosylation.

Acknowledgements

We are indebted to Professor Craig Atkins and Dr. Jon Clements for providing their seed of wild-type and *Abs*$^{-}$ *Lupinus angustifolius*. A BBSRC ROPA Award funding is acknowledged. This work was carried out during the tenure by D.J.O. of a Leverhulme Fellowship.

References

Abeles, F.B., Forrence, L.E., 1970. Temporal and hormonal control of β-1,3-glucanase in *Phaseolus vulgaris* L. Plant Physiol. 45, 395–400.

Ali, Z.M., Brady, C.J., 1982. Purification and characterization of the polygalacturonases of tomato fruits. Aust. J. Plant Physiol. 9, 155–169.

Atkins, C.A., Pigeaire, A., 1993. Application of cytokinins to flowers increase pod set in *Lupinus angustifolius* L. Aust. J. Agric. Res. 44, 1799–1819.

Bennett, A.B., Christoffersen, R.E., 1986. Synthesis and processing of cellulase from ripening avocado fruit. Plant Physiol. 81, 830–835.

Berger, R.K., Reid, P.D., 1979. Role of polygalacturonase in bean leaf abscission. Plant Physiol. 63, 1133–1137.

Bjerrum, O.J., Schafer-Nielsen, C., 1986. Buffer systems and transfer parameters for semi-dry electroblotting with a horizontal apparatus. In: Dunn, M. (Ed.), Electrophoresis '86. VCH, Weinheim, Germany, pp. 315–327.

Bonghi, C., Rascio, N., Ramina, A., Cassadoro, G., 1992. Cellulase and polygalacturonase involvement in the abscission of lead and fruit explants of peach. Plant Mol. Biol. 20, 839–848.

Bradford, M.M., 1976. A rapid and sensitive method for the quantitation of microgram quantities of protein utilising the principle of protein dye binding. Anal. Biochem. 72, 248–254.

Brummell, D.A., Lashbrook, C.C., Bennett, A.B., 1994. Plant endo-1,4-β-D-glucanases. Am. Chem. Soc. Symp. Ser. 566, 100–129.

Clements, J., Atkins, C., 2001. Characterization of a non-abscission mutant in *Lupinus angustifolius* L. I. Genetic and structural aspects. Am. J. Bot. 88, 31–42.

del Campillo, E., Bennett, A., 1996. Pedicel breakstrength and cellulase gene expression during tomato flower abscission. Plant Physiol. 111, 813–820.

del Campillo, E., Durbin, M., Lewis, L.N., 1988. Changes in two forms of membrane-associated cellulase during ethylene-induced abscission. Plant Physiol. 88, 904–909.

del Campillo, E., Lewis, L.N., 1992. Identification and kinetics of accumulation of proteins induced by ethylene in bean abscission zones. Plant Physiol. 98, 955–961.

Edwards, A.C., van Barneveld, R.J., 1998. Lupins for livestock, fish. In: Gladstones, J.S., Atkins, C., Hamblin, J. (Eds.), Lupins as Crop Plants. Biology, Production and Utilization. CAB International, UK, pp. 385–409.

Felix, G., Meins Jr, F., 1985. Purification, immunoassay and characterization of an abundant cytokinin-regulated polypeptide in cultured tobacco tissues. Planta 164, 423–428.

Ferrarese, L., Trainotti, L., Moretto, P., Polverino de Laureto, P., Rascio, N., Casadoro, G., 1995. Differential ethylene-inducible expression of cellulase in pepper plants. Plant Mol. Biol. 29, 735–747.

Gross, K.C., 1982. A rapid and sensitive spectrophotometric method for assaying polygalacturonase using 2-cyanoacetamide. HortScience 17, 933–934.

Henderson, J., Davies, H.A., Heyes, S.J., Osborne, D.J., 2001. The study of a monocotyledon abscission zone using microscopic, chemical, enzymatic and solid state ^{13}C CP/MAS NMR analyses. Phytochemistry 56, 131–139.

Henderson, J., Osborne, D.J., 1999. Ethylene as the initiator of the inter-tissue signalling and gene expression cascades in ripening and abscission of oil palm fruit. In: Kanellis, A.K., Chang, C., Klee, H., Bleecker, A.B., Pech, J.C., Grierson, D. (Eds.), Biology and Biotechnology of the Plant Hormone Ethylene II. Kluwer Academic Publishers, Dordrecht, pp. 129–136.

Horton, R.F., Osborne, D.J., 1967. Senescence, abscission and cellulase activity in *Phaseolus vulgaris*. Nature (London) 214, 1086–1088.

Hunter, D.A., Yoo, S.D., Butcher, S.M., McManus, M.T., 1999. Expression of 1-aminocyclopropane-1-carboxylate oxidase during leaf ontogeny in white clover. Plant Physiol. 120, 131–141.

Kalaitzis, P., Solomos, T., Tucker, M.L., 1997. Three different polygalacturonases are expressed in tomato leaf and flower abscission, each with a different temporal expression pattern. Plant Physiol. 113, 1303–1308.

Koehler, D.E., Lewis, L.L., Shannon, L.M., Durbin, M.L., 1981. Purification of a cellulase from kidney bean abscission zones. Phytochemistry 20, 409–412.

Laemmli, E.K., 1981. Cleavage of structural proteins during the assembly of the head of bacteriophage T4. Nature 227, 680–685.

Lashbrook, C.C., Gonzalez-Bosch, C., Bennett, A.B., 1994. Two divergent *endo*-β1,4-glucanase genes exhibit overlapping expression in ripening fruit and abscising flowers. Plant Cell 6, 1485–1493.

McManus, M.T., McKeating, J., Secher, D.S., Osborne, D.J., Ashford, D., Dwek, R.A., Rademacher, T.W., 1988. Identification of a monoclonal antibody to abscission tissue that recognises xylose/fucose-containing *N*-linked oligosaccharides from higher plants. Planta 175, 506–512.

Osborne, D.J., 1989. Abscission. Crit. Rev. Plant Sci. 8, 103–129.

Osborne, D.J., Thompson, D.S., 1992. Target or non-target: hormonal signal perception and response in the determination of cell performance. In: Karssen, C.M., van Loon, L.C., Vreugdenhil, D. (Eds.), Progress in Plant Growth Regulation. Kluwer Academic Publishers, Dordrecht, pp. 237–247.

Pan, S.-Q., Ye, X.-S., Kuc, J., 1989. Direct detection of β-1,3-glucanase isozymes on polyacrylamide electrophoresis and isoelectric focusing gels. Anal. Biochem. 182, 136–140.

Pigeaire, A., Seymour, M., Delane, R., Atkins, C.A., 1992. Predominance of flowers and newly-formed pods in reproductive abscission of *Lupinus angustifolius* L. Aust. J. Agric. Res. 43, 117–1129.

Pressey, R., 1987. *Exo*-polygalacturonase in tomato fruit. Phytochemistry 26, 1867–1870.

Pressey, R., Avants, J.K., 1973. Two forms of polygalacturonase in tomatoes. Biochim. Biophys. Acta 309, 363–369.

Reid, P.D., Strong, H.G., Lew, F., Lewis, L.N., 1974. Cellulase and abscission in the red kidney bean (*Phaseolus vulgaris*). Plant Physiol. 53, 732–737.

Roberts, J.A., Coupe, S.A., Whitelaw, C.A., Taylor, J.E., 1997. Spatial and temporal expression of abscission-related genes during ethylene-promoted organ shedding. In: Kanellis, A.K., Chang, C., Kende, H., Grierson, D. (Eds.), Biology and Biotechnology of the Plant Hormone Ethylene, NATO-ASI Series 3, Vol 34. Kluwer Academic Press, Dordrecht, pp. 185–190.

Tucker, G.A., Grierson, D., 1982. Synthesis of polygalacturonase during tomato fruit ripening. Planta 155, 64–67.

Tucker, M.L., Milligan, S.B., 1991. Sequence analysis and comparison of avocado fruit and bean abscission cellulases. Plant Physiol. 95, 928–933.

Tucker, G.A., Robertson, N.G., Grierson, D., 1980. Changes in polygalacturonase isoenzymes during the "ripening" of normal and mutant tomato fruit. Eur. J. Biochem. 112, 119–124.

PERGAMON

Phytochemistry 58 (2001) 1035–1042

PHYTOCHEMISTRY

www.elsevier.com/locate/phytochem

Chemical syntheses of caffeoyl and 5-OH coniferyl aldehydes and alcohols and determination of lignin *O*-methyltransferase activities in dicot and monocot species

Fang Chen, Parvathi Kota, Jack W. Blount, Richard A. Dixon*

Plant Biology Division, Samuel Roberts Noble Foundation, 2510 Sam Noble Parkway, Ardmore, OK 73401, USA

Received 3 July 2001; accepted 27 July 2001

Abstract

To investigate the substrate preferences of *O*-methyltransferases in the monolignol biosynthetic pathways, caffeoyl and 5-hydroxy coniferyl aldehydes were synthesized by a new procedure involving a Wittig reaction with the corresponding hydroxybenzaldehydes. The same procedure can also be used to synthesize caffeoyl and 5-hydroxyconiferyl alcohols. Relative *O*-methyltransferase activities against these substrates were determined using crude extracts and recombinant caffeic acid *O*-methyltransferase from alfalfa (*Medicago sativa*), and crude extracts from the model legume *Medicago truncatula*, tobacco, wheat and tall fescue. Extracts from all these species catalyzed methylation of the various monolignol aldehydes and alcohols more effectively than the corresponding hydroxycinnamic acids. © 2001 Elsevier Science Ltd. All rights reserved.

Keywords: *Medicago sativa*; *Medicago truncatula*; *Nicotiana tabacum*; *Triticum aestivum*; *Festuca arundinacea*; Leguminosae; Solanaceae; Gramineae; Syntheses; Caffeoyl aldehyde; 5-Hydroxyconiferaldehyde; *O*-Methyltransferase; Lignin

1. Introduction

The current concept of monolignol biosynthesis is a metabolic grid, through which side chain reduction and ring hydroxylation/methylation can occur at several different levels (reviewed in Lewis and Yamamoto 1990, Whetten and Sederoff 1995, Dixon et al., 2001). This concept was first proposed following the discovery of apparently independent pathways for monolignol *O*-methylation at the levels of hydroxycinnamic acids and their coenzyme A esters, catalyzed by caffeic acid *O*-methyltransferase (COMT) and caffeoyl CoA *O*-methyltransferase (CCoAOMT), respectively (Ye et al., 1994; Higuchi 1996). However, in recent years, increasing evidence has pointed to the hydroxylation/methylation of cinnamyl aldehydes or cinnamyl alcohols in lignin biosynthesis (Chen et al., 1999; Osakabe et al., 1999; Li et al., 2000).

Our recent studies (Guo et al., 2001) have centered on genetic manipulation of the *O*-methylation reactions of guaiacyl (G) and syringyl (S) lignin biosynthesis in alfalfa (*Medicago sativa*). Alfalfa is the world's major forage legume and a species in which lignification has important implications for forage digestibility and therefore utilization efficiency (Jung et al., 1997). To fully understand the opportunities for, and consequences of, genetically modifying lignin *O*-methyltransferases (OMTs), it is important to determine relative OMT activities against all potential substrates in the monolignol pathway. Unfortunately, caffeoyl- and 5-hydroxyconiferyl aldehydes and alcohols are not commercially available, and present some challenges in synthesis due to their *o*-dihydroxy ring substitution. In the past, 4-hydroxycinnamyl alcohol was synthesized by reducing 4-hydroxycinnamic acid esters with lithium aluminum hydride or diisobutylaluminum hydride (DIBALH) (Quideau and Ralph, 1992; Terashima et al., 1995). 4-Hydroxycinnamaldehyde was obtained by reduction of cinnamic acid ester or chloride followed by oxidation of the alcohol by manganese dioxide. These protocols involve many reaction steps and separations, leading to poor yields and difficulties with purification. Daubresse et al. (1994) developed a mild protocol to synthesize coumaryl, coniferyl, and sinapyl aldehydes and alcohols, performed under phase-transfer conditions.

* Corresponding author. Fax: +1-580-221-7380.
E-mail address: radixon@noble.org (R.A. Dixon).

0031-9422/01/$ - see front matter © 2001 Elsevier Science Ltd. All rights reserved.
PII: S0031-9422(01)00391-0

We tried to use this procedure for synthesis of caffeoyl aldehyde and 5-hydroxyconiferaldehyde but without success. Nevertheless, the idea of using a Wittig reaction (McMurry, 2000) with (1,3 - dioxolan - 2 - yl) - methyltriphenylphosphonium bromide inspired us to develop a new procedure for synthesis of these compounds. We have found that 18-crown-6 can effectively catalyze the Wittig reaction and give good yields for synthesis of monolignol precursors. We here describe the synthetic procedures, and the use of caffeoyl and 5-hydroxyconiferyl aldehydes and alcohols to determine substrate preferences for OMTs in extracts from several plant species.

2. Results and discussion

2.1. New synthetic approaches for hydroxycinnamyl aldehydes and alcohols

To investigate fully the monolignol biosynthetic pathway, it is a prerequisite to obtain all potential substrates in the pathway. Caffeoyl aldehyde, caffeoyl alcohol, 5-hydroxyconiferaldehyde and 5-hydroxyconiferyl alcohol are all potential substrates for monolignol *O*-methyltransferase but are not commercially available at this time. In recent reports, 5-hydroxyconiferaldehyde was prepared from 5-hydroxyvanillin (Osakabe et al., 1999). This protocol demands several steps of reaction and purification (Fig. 1), and gives only moderate overall yield (reported to be around 25%). Daubresse et al. (1994) have described mild syntheses of cinnamyl aldehydes and alcohols from 4-acetoxybenzaldehyde. The key step for this procedure is a Wittig reaction with (1,3-dioxolan-2-yl-methyl)-triphenylphosphonium bromide catalyzed by tris-[2-(2-methoxyethoxy)-ethyl]amine (TDA-1). We therefore attempted to prepare caffeoyl aldehyde and 5-hydroxyconiferaldehyde using this procedure. However, in our hands, the yields of dioxolanes obtained from 3,4-diacetoxybenzaldehyde and 3,4-diacetoxy-5 methoxybenzaldehyde were too low and the predominant products of the reaction were the corresponding piperonals even if the phenolic groups were already acetylated. To exploit the convenience of synthesis of cinnamyl aldehydes and alcohols with (1,3-dioxolan-2-yl-methyl)-triphenylphosphonium bromide, we tried two alternative catalysts for Wittig reactions, 18-crown-6 (1,4,7,10,13,16-hexaoxacyclooctadecane) and tetrabutylammonium bromide, and found that 18-crown-6 most efficiently catalyzed the reactions with 3,4-diacetoxy-5-methoxybenzaldehyde and 3,4-diacetoxybenzaldehyde. The new procedure (Fig. 2) described here requires fewer steps than previous methods, can be

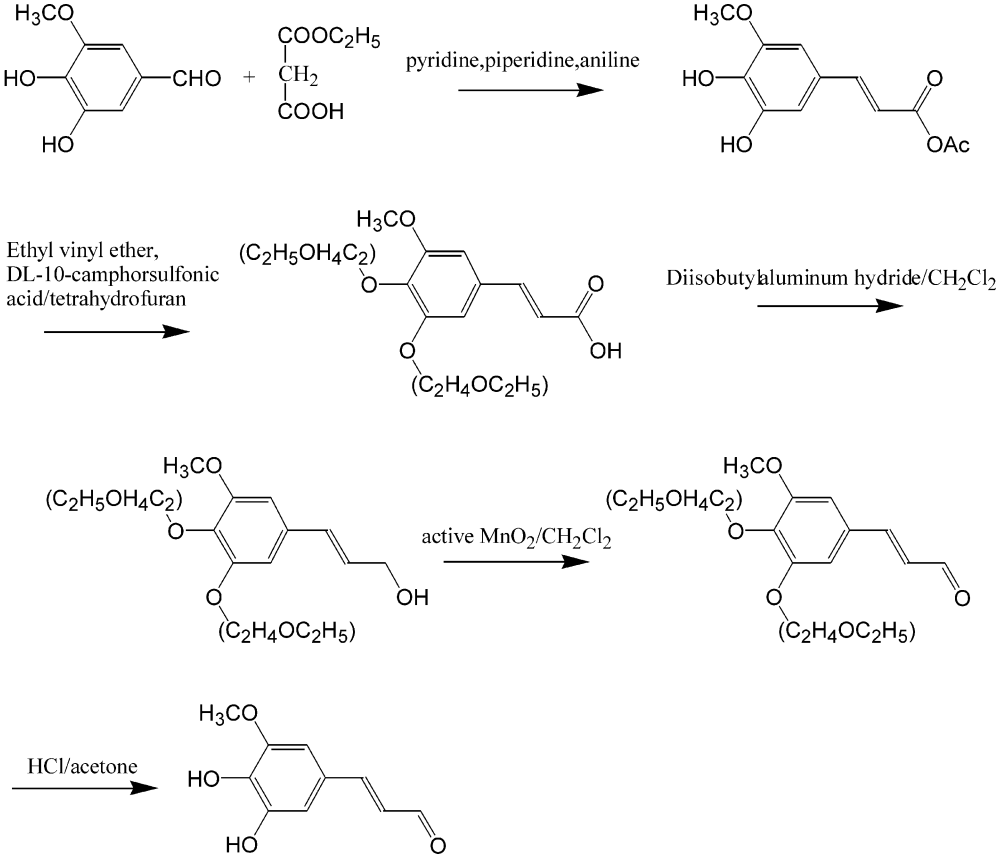

Fig. 1. Synthesis of 5-hydroxyconiferaldehyde from 5-hydroxyvanillin and monoethyl malonate.

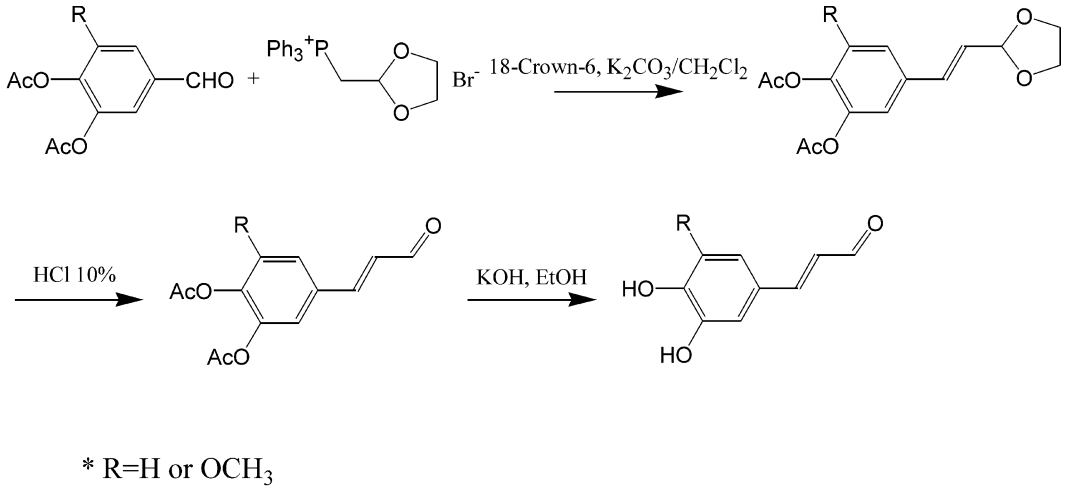

Fig. 2. Synthesis of caffeoyl and 5-hydroxyconiferyl aldehydes by a Wittig reaction with the corresponding hydroxybenzaldehydes and (1,3-dioxolan-2-yl-methyl)- triphenylphosphonium bromide.

performed in ambient atmosphere, and gives higher yields than previous methods (50–60% being routine in our hands).

3,4 - Dihydroxybenzaldehyde and 3,4 - dihydroxy - 5 - methoxybenzaldehyde can be acetylated at both phenolic hydroxyls using acetic anhydride under alkaline conditions. The acetylated products were then mixed with (1,3-dioxolan-2-yl-methyl)- triphenylphosphonium bromide, 18-crown-6 and solid K_2CO_3 in dry dichloromethane to produce the corresponding dioxolanes. The process can easily be monitored by GC/MS in one-hour intervals to ensure the maximum yield. Dioxolanes are obtained as isomers with a Z/E ratio of about 60/40, as described by Daubresse et al. (1994). After removal of the solid phase by filtration, the mixture can be hydrolyzed without further purification. Acid hydrolysis of the dioxolanes leads to nearly pure (E)-acetylated aldehydes as revealed by GC/MS. After purification of the 3,4-diacetoxyconiferyl aldehyde by column chromatography, the acetyl groups can be removed by transesterification in absolute EtOH. Fig. 3 shows the mass spectra of the resulting caffeoyl aldehyde and 5-hydroxyconiferaldehyde after trimethylsilylation. Methoxime derivatization of the products was also conducted to confirm the presence of the aldehyde groups. Fig. 4 shows the mass spectra of caffeoyl aldehyde and 5-hydroxyconiferaldehyde after methoximation and trimethylsilylation.

Caffeoyl alcohol and 5-hydroxyconiferyl alcohol can be obtained by condensation of 3,4-dihydroxybenzaldehyde or 5-hydroxyvanillin, respectively, with monoethyl malonate according to the method of Umezawa et al. (1991). However, the yield for these compounds (around 20%) is much lower than that reported for the synthesis of coniferyl alcohol (around 50%). With the procedure described by Daubresse et al. (1994), we were able to synthesize caffeoyl alcohol and 5-hydroxyconiferyl alcohol from 3,4-diacetoxycaffeoyl aldehyde and 3,4-diacetoxyconiferaldehyde with a yield of approximately 70%. Fig. 5 shows the mass spectra of the obtained products. The results reported here show that a Wittig reaction with (1,3-dioxolan-2-yl-methyl)-triphenylphosphonium bromide is a relatively straightforward method for synthesis of caffeoyl and 5-hydroxyconiferyl aldehydes and alcohols in good yield. The method can be performed with limited demands on synthetic expertise.

2.2. Substrate preferences of O-methyltransferases in dicots and monocots

To determine if the various hydroxycinnamyl aldehydes and alcohols were effective substrates for alfalfa COMT, the alfalfa COMT cDNA (Inoue et al., 1998) was cloned into the pET15b vector and expressed in *E. coli*. The His-tagged recombinant COMT enzyme was purified to homogeneity from the soluble protein using nickel affinity chromatography. Enzyme assays were conducted with the usual substrates, caffeic acid, 5-hydroxyferulic acid, and caffeoyl and 5-hydroxy-coniferyl aldehydes and alcohols. HPLC/diode-array analyses with parallel radio-detection showed that all these compounds acted as substrates for recombinant alfalfa COMT and gave the predicted products (Parvathi et al., 2001). The relative activites are summarized in Table 1. These results provide in vitro evidence for a potential alternative pathway to monolignols involving methylation of hydroxycinnamyl aldehydes and alcohols.

To determine whether OMT activity against all the hydroxycinnamyl aldehydes and alcohols was also found in other plant species, we assayed crude extracts from alfalfa, *Medicago truncatula* (a close relative of alfalfa), tobacco, wheat and tall fescue. The results (Table 1) indicate that, in each case, all substrates were effectively methylated, and, in each case, caffeic acid was

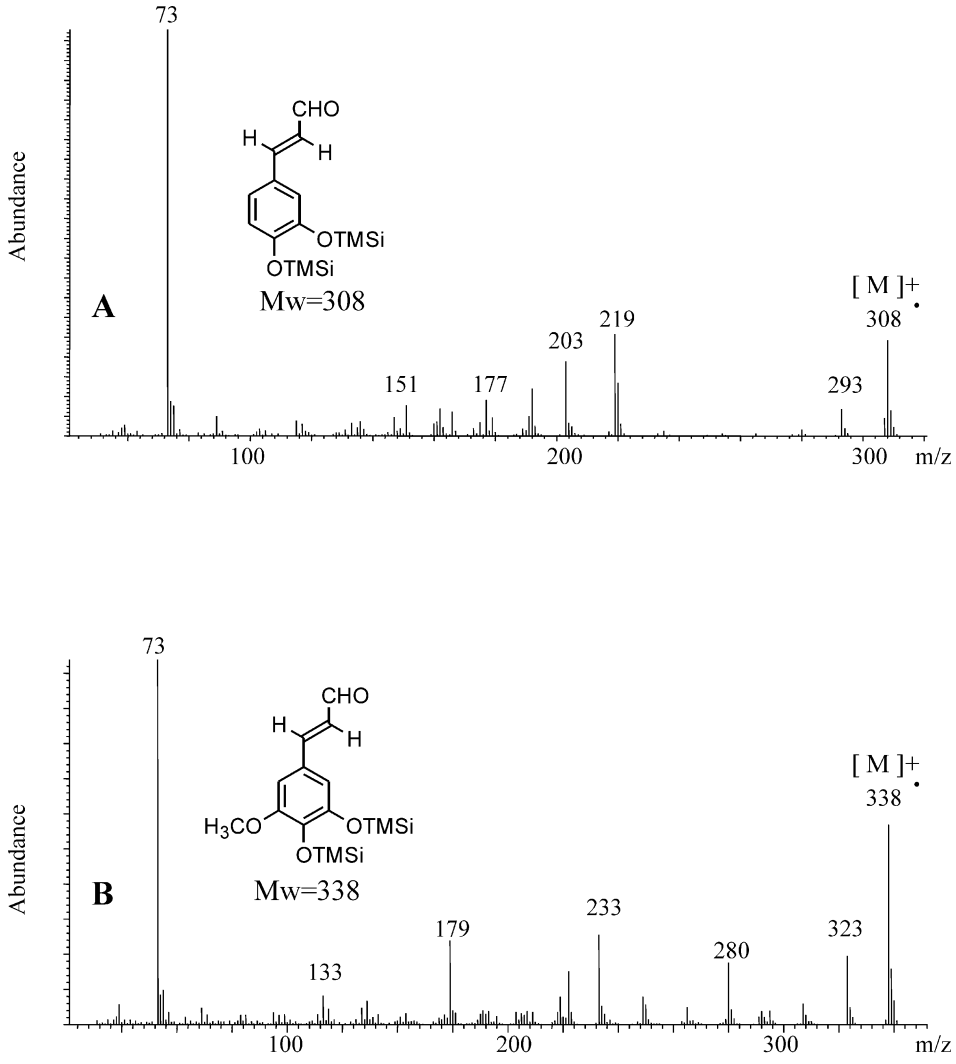

Fig. 3. Mass spectra of caffeoyl aldehyde (**A**) and 5-hydroxyconiferaldehyde (**B**) after TMSi derivatization.

the poorest substrate. In alfalfa, *M. truncatula*, tobacco and fescue, 5-hydroxyferulic acid, caffeoyl aldehyde, caffeoyl alcohol and 5-hydroxyconiferyl alcohol were methylated much more effectively than caffeic acid. In contrast, 5-hydroxyconiferaldehyde was methylated with about the same efficiency as caffeic acid in extracts from alfalfa and *M. truncatula*, whereas this compound was as good a substrate as the other aldehydes and alcohols in extracts from wheat. There were no obvious differences in substrate preferences between monocots and dicots in this experiment (compare alfalfa and tall fescue).

Recently, some OMTs have been found to have an unexpectedly broad range of substrates and even to exhibit functional overlap between different biosynthetic pathways. For example, a series of 38 potential substrates have been tested with four recombinant OMTs of *Thalictrum tuberosum* (Frick and Kutchan, 1999; Frick et al., 2001). Some of the enzymes showed similar catalytic activity with catechol, caffeic acid and the alkaloid norcoclaurine. It is not clear whether these enzymes are also active with caffeoyl aldehyde or 5-hydroxyconiferaldehyde, although this would not appear unlikely. To fully address OMT substrate preferences in vivo, or the potential activities of the large number of OMTs now appearing in plant gene EST databases or being identified from proteomic analyses (Van der Mijnsbrugge et al., 2000; Bell et al., 2001), even broader ranges of substrates will be needed. The relatively facile synthetic procedure reported here will make such substrates more widely available.

3. Experimental

3.1. Plant material, enzymes and chemicals

All plants used in this study were grown under standard greenhouse conditions. Stem tissues were collected and ground under liquid N_2. The powdered tissues were

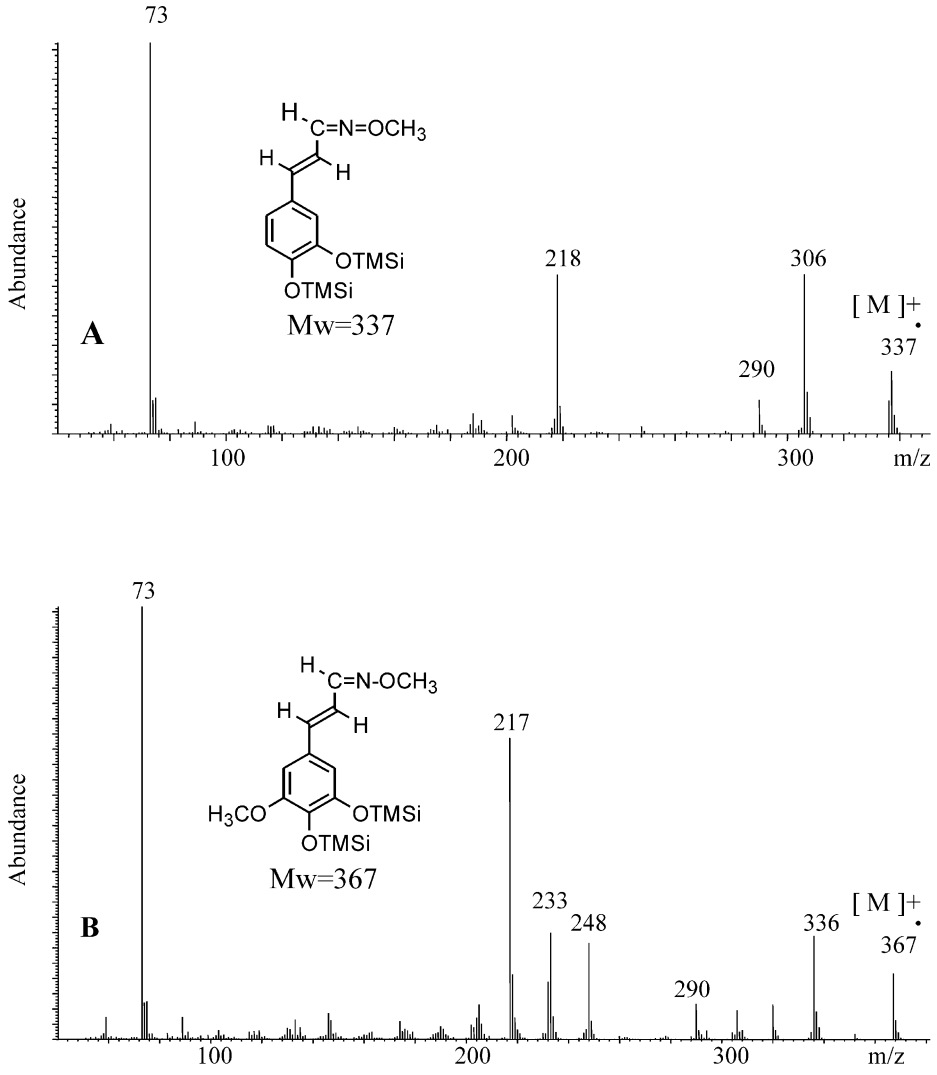

Fig. 4. Mass spectra of caffeoyl aldehyde (**A**) and 5-hydroxyconiferaldehyde (**B**) after methoxime derivatization and TMSi derivatization.

extracted and the soluble proteins were used for enzyme assay (Parvathi et al., 2001). Expression of alfalfa COMT in *E. coli* was performed as described previously (Parvathi et al., 2001). The enzyme was extracted from the *E. coli* cells by sonication and purified from the soluble fraction using His.bind resin (Novagen, Madison, WI, USA) according to the manufacturer's protocol. 3,4-Dihydroxybenzaldehyde, 5-hydroxy vanillin, (1,3-dixoxolan-2-yl-methyl)-triphenylphosphosphonium bromide, 18-crown-6, acetic anhydride, and ethyl acetate were purchased from Aldrich-Sigma Co (St. Louis, MO, USA) and used without further purification.

3.2. Synthesis procedures

3,4-Diacetoxy-3-methoxybenzaldehyde (5 mmol) and (1,3-dioxolan-2-yl-methyl)-triphenylphosphosphonium bromide (5 mmol) were dissolved in CH_2Cl_2 (80 ml) with vigorous stirring. Solid K_2CO_3 (5 mmol) and 18-crown-6 (0.05 mmol) were added. The reaction mixture was kept at room temperature for 8 h. The organic phase was separated from the solid phase by filtration. Aqueous HCl (10%, 50 ml) was added to the organic portion and the mixture stirred at room temperature for a further 6 h. During this period, a small amount of organic phase was taken and subjected to GC/MS analysis. After 2 h, 3,4-diacetoxyconiferaldehyde could be detected (MS *m*/*z*: 278, 236, 194, 177, 166, 151). At the end of the reaction, the mixture was diluted with 50 ml H_2O and extracted three times with 100 ml CH_2Cl_2. The combined organic layers were washed with saturated $NaHCO_3$ and saturated aqueous NaCl solution successively, dried over $MgSO_4$ and evaporated under vacuum. The residue was dissolved in a small amount of CH_2Cl_2 and passed through a silica gel column (eluted with CH_2Cl_2: EtOAc, 90:10, v/v). The eluate was monitored by TLC and the portions containing 3,4-diacetoxyconiferaldehyde were pooled. After evaporation of

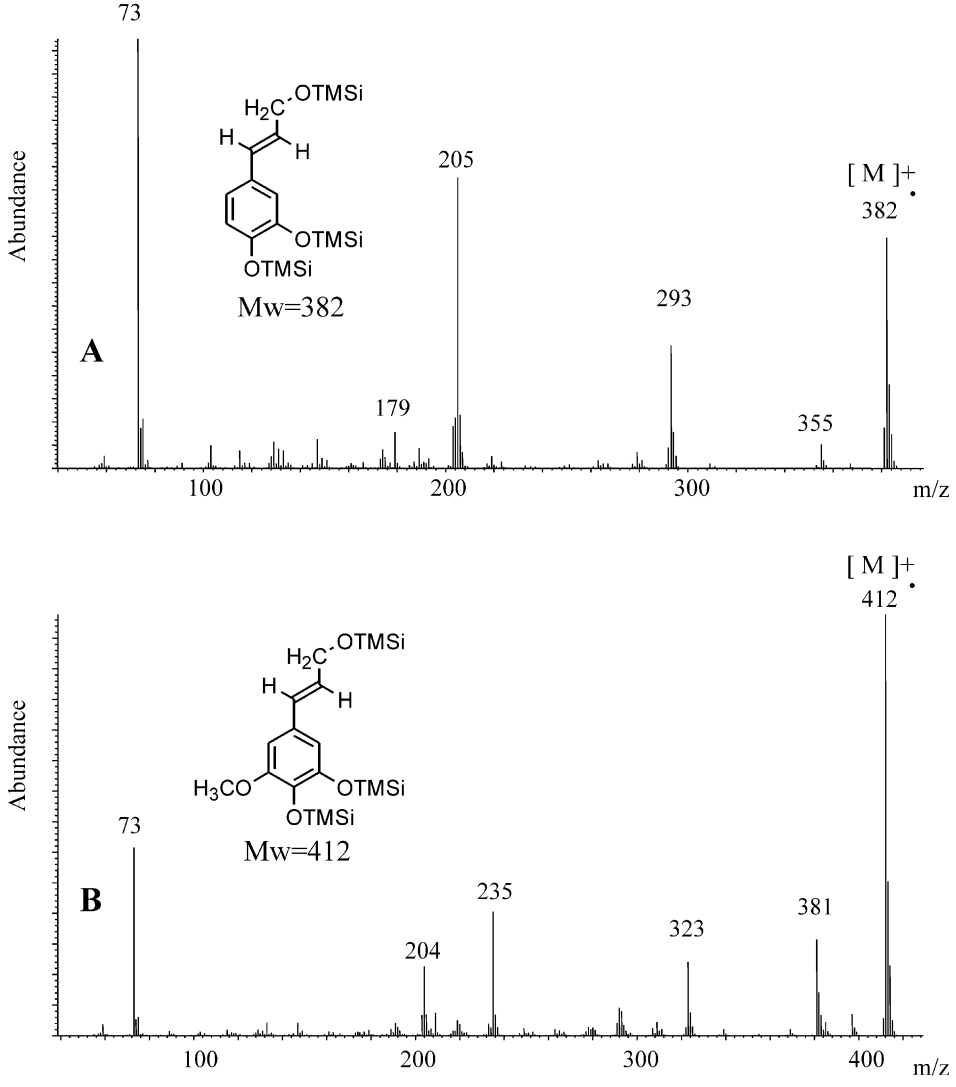

Fig. 5. Mass spectra of caffeoyl alcohol (**A**) and 5-hydroxyconiferyl alcohol (**B**) after TMSi derivatization.

Table 1
Methylation of a range of potential monolignol precursors by purified recombinant alfalfa COMT and crude preparations from alfalfa and four other species[a]

Substrate (50 μM)	OMT activity (pkat mg^{-1} protein)					
	Recombinant alfalfa COMT	Alfalfa	*M. truncatula*	Tobacco	Wheat	Tall fescue
Caffeic acid	2989±105	4.9±0.3	6.4±0.1	1.6±0.1	0.7±0.04	2.6±0.3
5-OH Ferulic acid	9235±110	15.0±0.9	14.7 ±1.5	20.3±1.3	5.8±0.3	31.3±1.3
Caffeoyl aldehyde	11408±725	14.4±0.9	13.3±0.7	20.1±0.4	5.9±0.1	24.0±0.5
Caffeoyl alcohol	17286±364	24.1±0.4	19.1±0.6	23.8±1.7	4.6±0.3	28.4±1.1
5-OH Coniferaldehyde	1655±138	5.2±0.3	6.9±0.5	5.9±0.1	5.7±0.1	9.4±0.9
5-OH Coniferyl alcohol	5965±624	13.0±0.8	16.0±0.7	7.6±0.2	4.2±0.1	26.3±2.0

Data represent the mean and spread of values for two replicate assays.

[a] Crude enzyme extracts from alfalfa, *M. truncatula* and tobacco were prepared from the 6–9th internodes, the extract from wheat was from the pseudo stem and leaf sheath, and the extract from tall fescue was from the 1st–4th stem internodes.

the solvent, 3,4-diacetoxyconiferaldehyde was obtained as a white solid (1.05 g, 72% yield). The 3,4-diacetoxyconiferaldehyde (0.56 g) was dissolved in 100 ml of 0.2 M KOH in 95% EtOH, and stirred for 8 h under N_2. The solvent was removed under vacuum, and the mixture diluted with 50 ml H_2O and extracted with ethyl

acetate (50 ml ×3). The combined organic layers were dried over Na_2SO_4 and evaporated to give 5-OH coniferaldehyde (0.29 g).

5-Hydroxyconiferyl alcohol was synthesized from 3,4-diacetoxyconiferaldehyde (70% yield) according to the procedure described by Daubresse et al. (1994). Caffeoyl aldehyde and alcohol were synthesized using the same procedure starting from 3,4-diacetoxybenzaldehyde with overall yield of 49–53%.

3.3. Derivatization for GC/MS analysis

Methoxime derivatization of the carbonyl groups of caffeoyl aldehyde and 5-hydroxyconiferaldehyde was performed using 0.5 ml MOX reagent (Pierce, Rockford, IL, USA) at 60 °C for 3 h, followed by evaporation to dryness with N_2. TMSi derivatization of the synthesized products and methoxime derivatives was performed using 250 μl MSTFA reagent (Pierce, Rockford, IL, USA) at 30 °C for 2 h.

3.4. Gas chromatography/ mass spectrometry

The synthesized products were identified by GC/MS. The GC/MS was performed on a Hewlett Packard 5890 series II gas chromatograph with a 5971 series mass selective detector (column: HP-1, 60 m×0.25 mm×0.25 μm film thickness). The mass spectra were obtained using electron ionization (70 eV) with a 60 to 650 m/z scanning range.

3.5. Enzyme extraction and assay

Stem internodes from alfalfa were collected and ground under liquid N_2. The powdered tissue was extracted for 1 h at 4 °C in extraction buffer (100 mM Tris–HCl, pH 7.5, 0.2 mM $MgCl_2$, 2mM DTT and 10% glycerol). The samples were then centrifuged at 12,000 g for 10 min at 4 °C and the extracts desalted on PD-10 columns (Pharmacia). The soluble protein fractions were used for COMT enzyme assay. The protein concentration was measured using Bradford's reagent (Bio-Rad) with BSA as standard (Bradford, 1976). COMT activity was assayed as described previously (Gowri et al., 1991, Inoue et al., 1998).

Acknowledgements

We thank Drs. Kazuhiko Fukushima and Seiichi Yasuda (Nagoya University, Nagoya, Japan) for valuable discussions and suggestions, David Huhman and Dr. Lloyd Sumner for assistance with mass spectrometry, and Drs. Lloyd Sumner and Hideyuki Suzuki for critical reading of the manuscript. This work was supported by The Samuel Roberts Noble Foundation.

References

Bell, C.J., Dixon, R.A., Farmer, A.D., Flores, R., Inman, J., Gonzales, R.A., Harrison, M.J., Paiva, N.L., Scott, A.D., Weller, J.W., May, G.D., 2001. The Medicago Genome initiative: a model legume database. Nucleic Acids Res. 29, 114–117.

Bradford, M.M., 1976. A rapid and sensitive method for the quatitation of microgram quatities of protein utilizing the principle of protein-dye binding. Anal. Biochem. 72, 248–254.

Chen, F., Yasuda, S., Fukushima, K., 1999. Evidence for a novel biosynthetic pathway that regulates the ratio of syringyl to guaiacyl residues in lignin in the differentiating xylem of *Magnolia kobus* DC. Planta 207, 597–603.

Dixon, R.A., Chen, F., Guo, D., Parvathi, K., 2001. The biosynthesis of monolignols: a "metabolic grid," or independent pathways to guaiacyl and syringyl units? Phytochemistry 57, 1069–1084.

Daubresse, N., Francesch, C., Mhamdi F., Rolando, C., 1994. A mild synthesis of coumaryl, coniferyl, sinapyl aldehydes and alcohol. Synthesis, 369–371.

Frick, S., Kutchan, T.M., 1999. Molecular cloning and functional expression of *O*-methyltransferase common to isoquinoline alkaloid and phenylpropanoid biosynthesis. Plant J. 17, 329–339.

Frick, S., Ounaroon, A., Kutchan, T.M., 2001. Combinatorial biochemistry in plants: the case of *O*-methyltransferases. Phytochemistry 56, 1–4.

Gowri, G., Bugos, R.C., Campbell, W.H., Maxwell, C.A., Dixon, R.A., 1991. Stress responses in alfalfa (*Medicago sativa* L.) X. Molecular cloning and expression of *S*-adenosyl-L-methionine:-caffeic acid 3-*O*-methyltransferase, a key enzyme of lignin biosynthesis. Plant Physiol. 97, 7–14.

Guo, D., Chen, F., Inoue, K., Blount, J.W., Dixon, R.A., 2001. Downregulation of caffeic acid 3-*O*-methyltransferase and caffeoyl CoA 3-*O*-methyltransferase in transgenic alfalfa: impacts on lignin structure and implications for the biosynthesis of G and S lignin. Plant Cell 13, 73–88.

Higuchi, T., 1996. Biosynthesis of wood components. In: Timell, T.E. (Ed.), Biochemistry and Molecular Biology of Wood. Heidelberg, Springer, Berlin, New York, pp. 156–168.

Inoue, K., Sewalt, V.J.H., Ballance, G.M., Ni, W., Sturzer, C., Dixon, R.A., 1998. Developmental expression and substrate specificities of alfalfa caffeic acid 3-*O*-methyltransferase and caffeoyl CoA 3-*O*-methyltranserase in relation to lignification. Plant Physiol 117, 761–770.

Jung, H.G., Sheaffer, C.C., Barnes, D.K., Halgerson, J.L., 1997. Forage quality variation in the US alfalfa core collection. Crop Sci. 37, 1361–1366.

Lewis, N.G., Yamamoto, E., 1990. Lignin: occurrence, biogenesis and biodegradation. Annu. Rev. Plant Physiol. Plant Mol. Biol. 41, 455–496.

Li, L., Popko, J., Umezawa, T., Chiang, L.V., 2000. 5-Hydroxyconiferyl aldehyde modulates enzymatic methylation for syringyl monolignol formation, a new view of monolignol biosynthesis in angiosperms. J. Biol. Chem. 275, 6537–6545.

McMurry, J., 2000. Organic Chemistry. Fifth ed. Brooks/Cole, Pacific Grove, CA, USA.

Osakabe, K., Tsao, C.C., Li, L., Popko, J., Umezawa, T., Carraway, D.T., Smeltzer, R.H., Joshi, C.T., Chiang, V.L., 1999. Coniferyl aldehyde 5-hydroxylation and methylation direct syringyl lignin biosynthesis in angiosperms. Proc. Natl. Acad. Sci. USA 96, 8955–8960.

Parvathi, K., Chen, F., Guo, D., Blount, J.W., Dixon, R.A., 2001. Substrate preferences of *O*-methyltransferases in alfalfa suggest new pathway for 3-*O*-methylation of monolignols. Plant J. 25, 193–202.

Quideau, S., Ralph, J., 1992. Facile large-scale synthesis of coniferyl, sinapyl, and *p*-coumaryl alcohol. J. Agric. Food Chem. 40, 1108–1110.

Terashima, N., Ralph, S.A., Landucci, L.L., 1995. New facile synthesis of monolignol glucosides; *p*-glucocoumaryl alcohol, coniferin and syringin. Holzforschung 50, 151–155.

Umezawa, T., Davin, L.B., Lewis, N.G., 1991. Formation of lignans (−)-secoisolariciresinol and (−)-matairesinol with *Forsythia intermedia* cell-free extracts. J. Biol. Chem. 266, 10210–10217.

Van der Mijnsbrugge, K., Meyermans, H., Van Montagu, M., Bauw, G., Boerjan, W., 2000. Wood formation in poplar: identification, characterization, and seasonal variation of xylem proteins. Planta 210, 589–598.

Whetten, R., Sederoff, R., 1995. Lignin biosynthesis. Plant Cell 7, 1001–1013.

Ye, Z., Kneusel, R.E., Matern, U., Varner, J.E., 1994. An alternative methylation pathway in lignin biosynthesis in *Zinnia*. Plant Cell 6, 1427–1439.

PERGAMON

Phytochemistry 58 (2001) 1043–1047

PHYTOCHEMISTRY

www.elsevier.com/locate/phytochem

Bioactivity of 25-hydroxy-, 26-hydroxy, 25,26-dihydroxy- and 25,26-epoxybrassinolide

Richard P. Pharis[a,1], Loeke Janzen[a], Suanne K. Nakajima[b], Jialiang Zhu[b], Thomas G. Back[b,*,1]

[a]*Department of Biological Sciences, University of Calgary, Calgary, AB, Canada T2N 1N4*
[b]*Department of Chemistry, University of Calgary, Calgary, AB, Canada T2N 1N4*

Received 18 May 2001; received in revised form 3 August 2001

Abstract

The bioactivity of 25-hydroxybrassinolide, (25*S*)- and (25*R*)-26-hydroxybrassinolide, (25*S*)- and (25*R*)-25,26-dihydroxybrassinolide, and of (25*R*)-25,26-epoxybrassinolide was tested in the rice leaf lamina inclination assay. The 25- and (25*S*)-26-hydroxy derivatives are known metabolites of the naturally-occurring phytohormone brassinolide, whereas the other compounds are novel, but closely related, congeners. When tested alone, all showed either no activity or only weak activity at relatively high doses. When coapplied with indole-3-acetic acid (IAA), an auxin that synergizes the effects of brassinosteroids, enhanced bioactivity was observed for each compound. However, even when applied together with IAA, none of the compounds proved more bioactive than brassinolide with or without IAA. We conclude from these results that enzymatic hydroxylation of endogenous brassinolide at C-25 and/or C-26 does not enhance brassinosteroid activity, and so does not comprise an activation pathway in brassinolide biosynthesis. Instead, these hydroxylations result in modest to appreciable metabolic deactivation. © 2001 Elsevier Science Ltd. All rights reserved.

Keywords: Rice leaf lamina inclination assay; Brassinolide; Metabolites; 25- and 26-hydroxylated brassinolide derivatives

1. Introduction

Brassinolide (**1**) is a powerful steroidal phytohormone whose structure was first determined by Grove et al. (1979). The chemistry and biology of **1** and of related brassinosteroids such as 24-epibrassinolide (**2**) and castasterone (**3**) has recently been reviewed (Cutler et al., 1991; Khripach et al., 1999; Sakurai et al., 1999). Structures **1**–**3** are shown in Fig. 1. The metabolism of brassinosteroids such as **1**–**3** is of considerable current interest and has been studied both in cell cultures and intact plants (Adam et al., 1996; Adam and Schneider, 1999; Khripach et al., 1999). For example, the metabolism of exogenously applied 24-epibrassinolide (**2**) in cell cultures of *Lycopersicon esculentum* resulted in enzymatic hydroxylation at C-25 and C-26, followed by glucosylation of these sites (Schneider et al., 1994; Hai et al., 1995) (Fig. 2). The glucosylated conjugates have low activity in bioassays and thus appear to constitute metabolic deactivation products. However, the hydroxylated aglycones **4** and **5** were described as having varying degrees of bioactivity (Hai et al., 1995; Adam et al., 1996; Voigt et al., 1996). Thus, the role of the hydroxylated aglycones, as either activation or deactivation products, is currently less clear. The question of metabolic activation vs. deactivation of exogenously applied brassinosteroids is also of practical importance for commercial applications, since it affects both their efficacy and persistence.

The metabolism of brassinolide (**1**), which is generally recognized as the most active of the naturally-occurring brassinosteroids, has also been studied. Voigt et al. (1996) reported that 25-hydroxybrassinolide (**6**) displays comparable bioactivity to **1** in the rice leaf lamina inclination bioassay. In contrast, Seto et al. (1999) found relatively low activity for **6** and for (25*S*)-26-hydroxybrassinolide (**7**). Moreover, we recently reported that 25-fluorobrassinolide (**8**) and 25-azabrassinolide (**9**), where enzymatic hydroxylation at C-25 is expected to be

[1] Senior authors.

* Corresponding author. Tel.: +1-403-220-6256; fax: +1-403-289-9488.

E-mail address: tgback@ucalgary.ca (T.G. Back).

0031-9422/01/$ - see front matter © 2001 Elsevier Science Ltd. All rights reserved.
PII: S0031-9422(01)00381-8

blocked, show no bioactivity in the rice leaf lamina inclination bioassay (Back et al., 1999). This suggested the possibility that enzymatic hydroxylation at this position is required for biological activity of brassinosteroids such as **1**, and that the hydroxylated metabolites are the true phytohormone 'effectors'. The latter hypothesis is also consistent with an earlier report that hydroxylation at C-25 is an activating step in the 24-epibrassinolide series, since 25-hydroxy-24-epibrassinolide (**4**) was found to be ca. ten times more active than **2** in the rice leaf lamina inclination test (Hai et al., 1995; Adam et al., 1996). On the other hand, strong activity was found for the 25-methoxy (Back et al., 1999) and 25-methyl (Mori and Takeuchi, 1988; Back et al., 2000a) analogues **10** and **11**, respectively, indicating that strong bioactivity is possible even in the absence of a 25-hydroxyl group. Neff et al. (1999) reported an *Arabidopsis bas1-D* mutant that accumulates 26-hydroxybrassinolide, but has reduced levels of **1** and other endogenous brassinosteroids. This was attributed to enhanced expression of a cytochrome P450 that results in the hydroxylation of brassinosteroids at C-26. The authors concluded that *BAS1* is a key control point in the brassinolide signal transduction process. A precise measurement of the relative biological activities of brassinosteroids and their hydroxylated metabolites is therefore of importance in attempts to better understand and control brassinosteroid-regulated effects. While it is generally agreed that metabolic glucosylation of brassinosteroids results in deactivation, there have been conflicting reports regarding whether enzymatic hydroxylation at C-25 and C-26 represents an activation or deactivation step. Moreover, the effect of the C-25 configuration of 26-hydroxylated brassinosteroids (where C-25 is a stereocenter) upon their biological activity has not yet been studied.

In order to shed further light on the bioactivity of C-25 and C-26-hydroxylated derivatives of **1**, we recently developed new synthetic routes to the known compounds **6** and **7**, as well as to a series of novel but related analogues. The latter include (*25R*)-26-hydroxybrassinolide (**12**), both C-25 epimers **13** and **14** of 25-26-dihydroxybrassinolide and the 25,26-epoxide **15** (Back et al., 2000b). The structures of compounds **6**–**15** are shown in Fig. 3. We now report the biological activity of the known metabolites **6** and **7** and of the novel congeners **12**–**15**, as determined in the rice leaf lamina inclination bioassay (Takeno and Pharis, 1982).

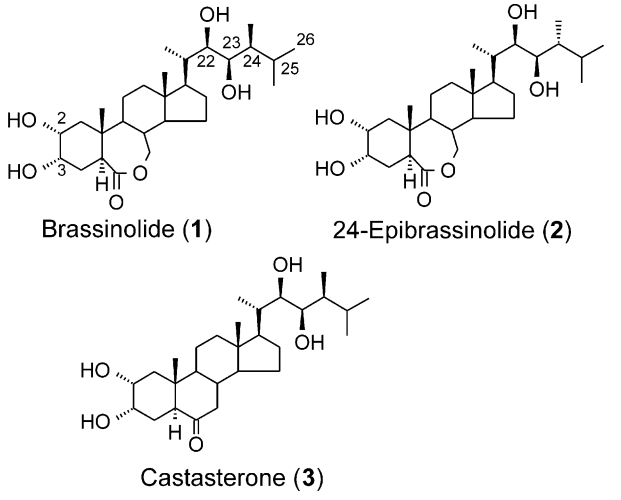

Fig. 1. Structures of some naturally-occurring brassinosteroids.

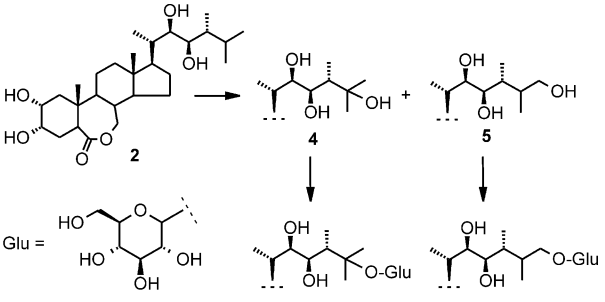

Fig. 2. Hydroxylation and glucosylation of 24-epibrassinolide.

2. Results and discussion

The biological activity of compounds **6**, **7** and **12**–**15** is shown in Figs. 4–9, respectively, with **1** included as a standard for comparison. Since it is known that the effects of brassinosteroids are synergized by auxins such as indole-3-acetic acid (IAA) (Takeno and Pharis, 1982;

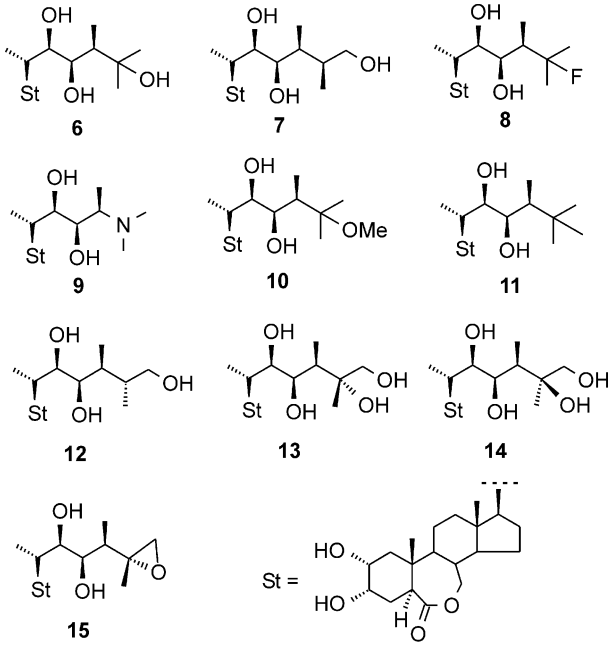

Fig. 3. Structures of side-chain metabolites and congeners of brassinolide.

Mandava, 1988; Sasse, 1991), the bioassays were also repeated in the presence of 1000 ng of IAA. The coapplication of IAA has been observed to enhance the activity of **1** by a factor of 10–100, thus dropping the threshold activity from ca. 1 ng to ca. 0.1 ng–0.01 ng (Baron et al., 1998 and Figs. 4–9).

Of the known brassinolide metabolites **6** and **7**, when assayed alone, the 25-hydroxy analogue **6** showed stronger bioactivity than the (25*S*)-26-hydroxy derivative **7** (Figs. 4 and 5, respectively), but this activity was only observed at relatively high doses ($\geqslant$100 ng). However, when **6** and **7** were coapplied with IAA, the bioactivity of both metabolites was appreciably and comparably enhanced (Figs. 4 and 5), but in neither case did it approach that of brassinolide with IAA. The (25*R*)-26-hydroxy epimer **12** was similar to **7** in the absence of IAA, but showed a slightly greater enhancement of bioactivity than **7** when each was coapplied with IAA (Fig. 6). The low activity of both epimers **7** and **12**, when applied alone, contrasts sharply with their relatively high bioactivity when coapplied with IAA. As such, they may prove useful tools in studying the mechanism of auxin synergism in brassinosteroid induced cell expansion. The diminished bioactivity seen

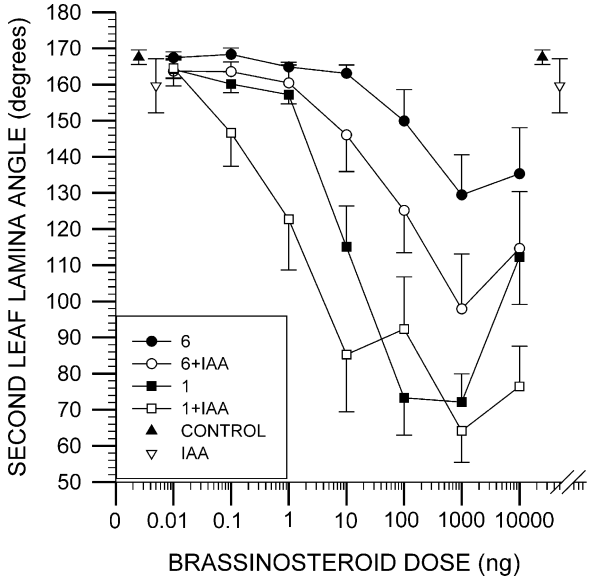

Fig. 4. Rice leaf lamina inclination bioassay of **6**, compared to brassinolide (**1**), with and without coapplication of 1000 ng of IAA. Error bars represent 95% confidence limits.

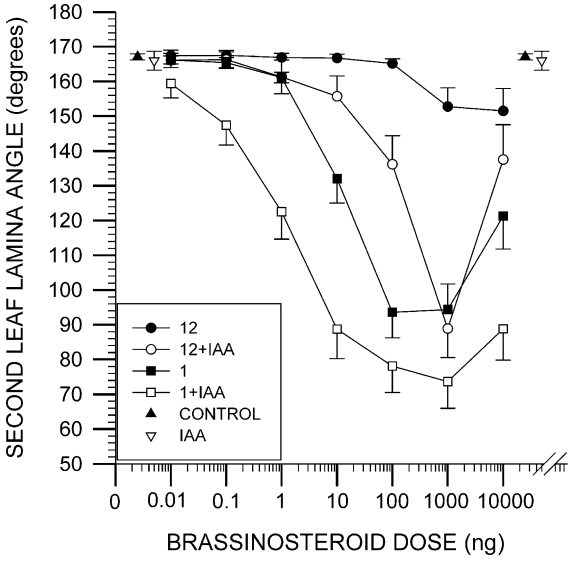

Fig. 6. Rice leaf lamina inclination bioassay of **12**, compared to brassinolide (**1**), with and without coapplication of 1000 ng of IAA. Error bars represent 95% confidence limits.

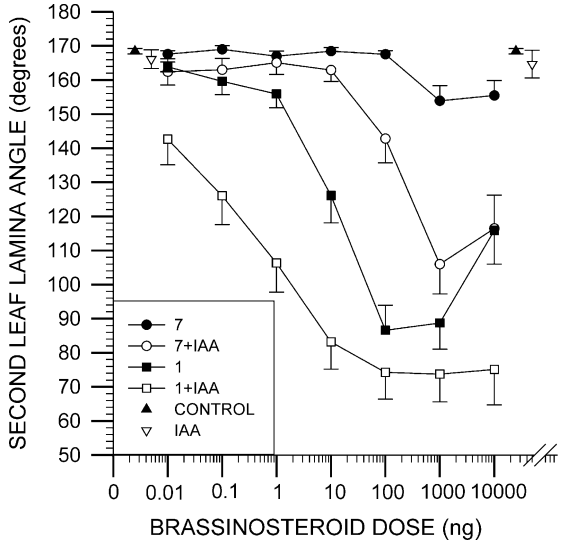

Fig. 5. Rice leaf lamina inclination bioassay of **7**, compared to brassinolide (**1**), with and without coapplication of 1000 ng of IAA. Error bars represent 95% confidence limits.

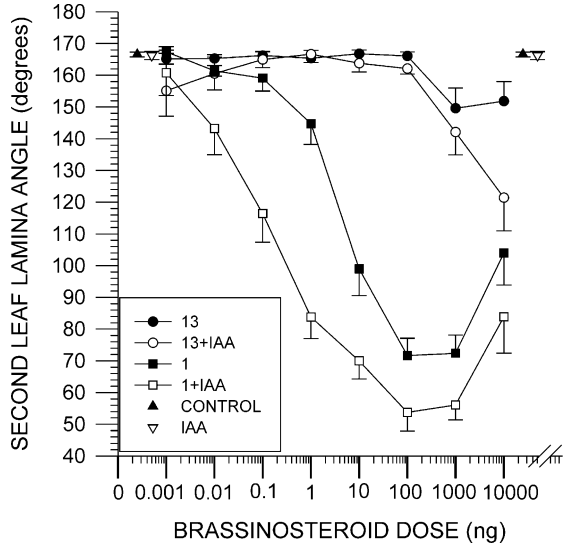

Fig. 7. Rice leaf lamina inclination bioassay of **13**, compared to brassinolide (**1**), with and without coapplication of 1000 ng of IAA. Error bars represent 95% confidence limits.

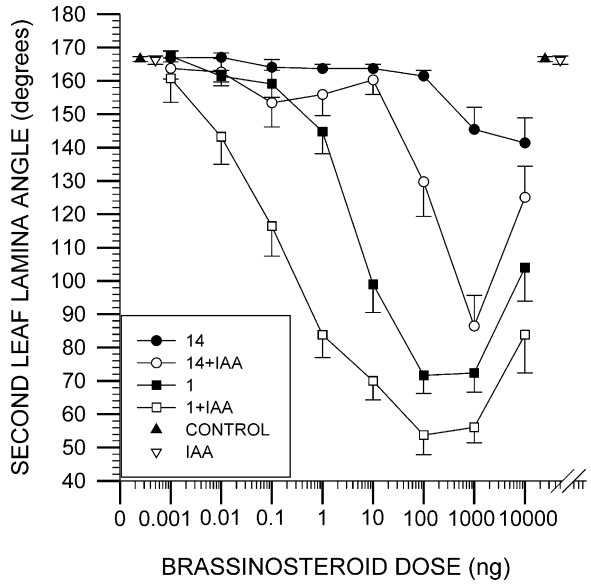

Fig. 8. Rice leaf lamina inclination bioassay of **14**, compared to brassinolide (**1**), with and without coapplication of 1000 ng of IAA. Error bars represent 95% confidence limits.

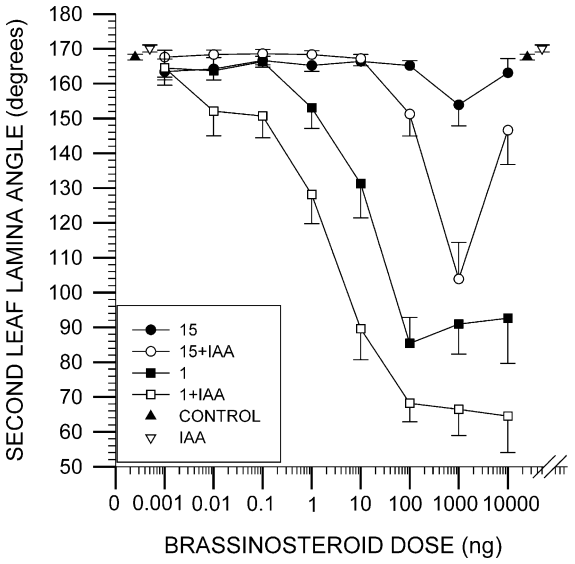

Fig. 9. Rice leaf lamina inclination bioassay of **15**, compared to brassinolide (**1**), with and without coapplication of 1000 ng of IAA. Error bars represent 95% confidence limits.

at the highest doses (10,000 ng) of brassinolide (**1**) or derivatives **6**, **7** and **12**, particularly in the presence of IAA, is not clearly understood. We tentatively attribute it to saturation and/or toxicity effects.

The bioactivity of the two 25,26-dihydroxy analogues **13** and **14** is shown in Figs. 7 and 8, respectively. Both epimers displayed only weak activity, and only at the highest doses of 1000 and 10,000 ng when applied on their own. However, when coapplied with IAA, the activity of **13** showed only slight enhancement (Fig. 7), while the 25-*S* epimer **14** gave a much stronger response when coapplied with IAA (Fig. 8). In this respect, the dihydroxylated epimers **13** and **14** differ from the monohydroxylated epimeric pair **7** and **12**, in which **12** was enhanced only slightly more than **7** by coapplied IAA. Thus, 25,26-dihydroxylation results in greater epimeric discrimination with respect to the C-25 stereocentre than does 26-monohydroxylation in the expression of IAA synergy. Epoxide **15** showed similar behaviour to **14** when coapplied with IAA, but displayed only weak activity at the 1000 ng dose on its own (Fig. 9). The loss of biological activity at the 10,000 ng dose was especially noticeable for **14** and **15**, but not **13**, when they were coapplied with IAA (Figs. 7–9). It is possible that the activity of epoxide **15** stems from its hydrolysis to **13** and/or **14** in vivo.

Our results indicate that neither the known brassinolide metabolites **6** and **7**, nor the novel, but structurally related analogues **12**–**15**, approach the bioactivity of brassinolide in the rice leaf lamination inclination assay. All of compounds **6**, **7** and **12**–**15**, when assayed alone, proved only weakly active, and only at the highest doses. While the activity of all of these compounds was appreciably and significantly increased by the coapplication of IAA, even then bioactivity did not exceed that of brassinolide (**1**) without coapplied auxin, and was substantially lower than that of **1** plus IAA. The considerably lower bioactivity of the hydroxylated and epoxy derivatives **6**, **7** and **12**–**15**, compared to **1** itself, thus indicates that hydroxylation at C-25 and/or C-26 does not comprise an activation pathway in brassinolide biosynthesis in rice, regardless of the configuration at C-25 stereocenters. Instead, it strongly suggests that enzymatic hydroxylation at these positions is part of an overall metabolic deactivation process.

3. Experimental

3.1. Preparation

The known hydroxylated metabolites **6** and **7**, the novel hydroxylated analogues **12**–**14**, and the epoxide **15** were prepared as reported earlier (Back et al., 2000b).

3.2. Bioassays

Compounds **6**, **7** and **12**–**15** were tested for biological activity by means of the rice leaf lamina assay, using a dwarf cv., Tan-ginbozu, as described by Takeno and Pharis (1982). Brassinolide (**1**) was included in the bioassays as a standard. The compounds were dissolved in 95% ethanol and applied as 0.5 μl microdrops to the rice plants 48 h after planting the germinated seeds on 0.8% water agar. At high doses, several rounds of application of the 0.5 μl microdrops were required to attain the desired dose per plant. Where IAA was a co-treatment, 1,000 ng of IAA was similarly applied per plant ca. 2 h prior to the application of the brassinosteroids.

The resultant leaf lamina angle was measured 60–65 h later. For an individual bioassay, each data point is the mean of the leaf angles from ca. 36 plants for doses up to 100 ng and from ca. 24 plants for the 1000 and 10,000 ng doses. Parallel applications of ethanol alone (control) and IAA alone (1000 ng) were carried out for each bioassay (see Figs. 4–9). In each of Figs. 4–9, error bars represent 95% confidence limits.

Acknowledgements

We thank Agritope Inc. (now Exelixis Plant Sciences Inc.) and the Natural Sciences and Engineering Research Council of Canada (NSERC) for financial support. We thank Mrs. S. Horácek for assistance with the rice leaf lamina assay, and Dr. R. Yamdagni, Ms. D. Fox and Ms. Q. Wu for mass spectra.

References

Adam, G., Porzel, A., Schmidt, J., Schneider, B., Voigt, B., 1996. New developments in brassinosteroid research. In: Atta-ur-Rahman, (Ed.), Studies in Natural Products Chemistry, Vol. 18. Elsevier, Amsterdam, pp. 495–549.

Adam, G., Schneider, B. 1999. In: Sakurai, A., Yokota, T., Clouse, S.D. (Eds.). Brassinosteroids: Steroidal Plant Hormones. Springer-Verlag, Tokyo.

Back, T.G., Janzen, L., Nakajima, S.K., Pharis, R.P., 1999. Synthesis and biological activity of 25-methoxy-, 25-fluoro- and 25-azabrassinolide and 25-fluorocastasterone: surprising effects of heteroatom substituents at C-25. J. Org. Chem. 64, 5494–5498.

Back, T.G., Janzen, L., Nakajima, S.K., Pharis, R.P., 2000a. Effect of chain length and ring size of alkyl and cycloalkyl side-chain substituents upon the biological activity of brassinosteroids. Preparation of novel analogues with activity exceeding that of brassinolide. J. Org. Chem. 65, 3047–3052.

Back, T.G., Nakajima, S.K., Zhu, J., 2000b. Synthesis of 25-hydroxy, 26-hydroxy- and 25,26-dihydroxybrassinolide. Synlett, 1649–1651.

Baron, D.L., Luo, W., Janzen, L., Pharis, R.P., Back, T.G., 1998. Structure-activity studies of brassinolide B-ring analogues. Phytochemistry 49, 1849–1858.

Cutler, H.G., Yokota, T., Adam, G. (Eds.), 1991. Brassinosteroids: Chemistry, Bioactivity and Applications ACS Symposium Series 474. American Chemical Society, Washington, DC.

Grove, M.D., Spencer, G.F., Rohwedder, W.K., Mandava, N., Worley, J.F., Warthen Jr., J.D., Steffens, G.L., Flippen-Anderson, J.L., Cook Jr., J.C., 1979. Brassinolide, a plant growth-promoting steroid isolated from *Brassica napus* pollen. Nature 281, 216–217.

Hai, T., Schneider, B., Adam, G., 1995. Metabolic conversion of 24-Epi-brassinolide into pentahydroxylated brassinosteroid glucosides in tomato cell cultures. Phytochemistry 40, 443–448.

Khripach, V.A., Zhabinskii, V.N., de Groot, A.E., 1999. Brassinosteroids: a new class of plant hormones. Academic Press, San Diego.

Mandava, N.B., 1988. Plant growth-promoting brassinosteroids. Annual Review of Plant Physiology and Plant Molecular Biology 39, 23–52.

Mori, K., Takeuchi, T., 1988. Synthesis of 25-methyldolichosterone, 25-methyl-2,3-diepidolichosterone, 25-methylcastasterone and 25-methylbrassinolide. Liebigs Ann. Chem. 815-818.

Neff, M.M., Nguyen, S.M., Malancharuvil, E.J., Fujioka, S., Noguchi, T., Seto, H., Tsubuki, M., Honda, T., Takatsuto, S., Yoshida, S., Chory, J., 1999. *BAS*1: a gene regulating brassinosteroid levels and light responsiveness in *arabidopsis*. Proc. Natl. Acad. Sci. U.S.A 96, 15316–15323.

Sakurai, A., Yokota, T., Clouse, S.D. (Eds.), 1999. Brassinosteroids: Steroidal Plant Hormones. Springer-Verlag, Tokyo.

Sasse, J.M., 1991. The case for brassinosteroids as endogenous plant hormones. In: Cutler, H.G., Yokota, T., Adam, G. (Eds.), Brassinosteroids: Chemistry, Bioactivity and Applications. ACS Symposium Series 474. American Chemical Society, Washington, DC, pp. 158–166.

Schneider, B., Kolbe, A., Porzel, A., Adam, G., 1994. A metabolite of 24-epibrassinolide in cell suspension cultures of *Lycopersicon esculentum*. Phytochemistry 36, 319–321.

Seto, H., Fujioka, S., Koshino, H., Yoshida, S., Tsubuki, M., Honda, T., 1999. Synthesis and biological evaluation of extra-hydroxylated brassinolide analogs. Tetrahedron 55, 8341–8352.

Takeno, K., Pharis, R.P., 1982. Brassinosteroid-induced bending of the leaf lamina of dwarf rice seedlings: an auxin-mediated phenomenon. Plant and Cell Physiology 23, 1275–1281.

Voigt, B., Porzel, A., Golsch, D., Adam, W., Adam, G., 1996. Regioselective oxyfunctionalization of brassinosteroids by methyl(trifluoromethyl)dioxirane: synthesis of 25-hydroxybrassinolide and 25-hydroxy-24-epibrassinolide by direct C-H insertion. Tetrahedron 52, 10653–10658.

PERGAMON

Phytochemistry 58 (2001) 1049–1054

PHYTOCHEMISTRY

www.elsevier.com/locate/phytochem

Biosynthesis of a hopane triterpene and three diterpenes in the liverwort *Fossombronia alaskana*

Ursula Hertewich, Josef Zapp, Hans Becker, Klaus Peter Adam*

FR 8.7, Pharmakognosie und Analytische Phytochemie der Universität des Saarlandes, 66041 Saarbrücken, Germany

Received 16 May 2001; received in revised form 10 July 2001

Abstract

The biosynthesis of the triterpene 22-(30)-hopene-29-acid and the diterpenes 7,17-sacculatadiene-11,12-dial (sacculatal), *trans*-phytol and a new neoverrucosane-type diterpenoid (5-oxo-neoverrucos-(13)-ene) was studied by incorporation of [1-^{13}C]-labelled glucose into axenic cultures of the artic liverwort *Fossombronia alaskana*. Quantitative ^{13}C NMR spectroscopic analysis of the resulting labelling patterns showed that the isoprene units of the triterpene are derived from the mevalonic acid pathway, whereas the isoprene units of the diterpenes are built up via the methylerythritol phosphate pathway. © 2001 Elsevier Science Ltd. All rights reserved.

Keywords: *Fossombronia alaskana*; Isopentenyl diphosphate; Mevalonic acid pathway; Methylerythritol phosphate pathway; Isoprenoids; Triterpene; Diterpene; ^{13}C labelling; Liverwort; Quantitative ^{13}C NMR spectroscopy; Neoverrucosane

1. Introduction

Isoprenoids are the largest group of secondary metabolites with over 30,000 known compounds, including the steroids (Dictonary of Natural Products, 2000). Their common building block, the isoprene unit, is derived from isopentenyl diphosphate (IPP). Whereas in the past, the mevalonic acid (MVA) pathway has been accepted as the only biosynthetic route leading to IPP, the existence of the methylerythritol phosphate (MEP) pathway as an alternative route for IPP has only been known for a few years (Rohmer et al., 1993; Schwarz, 1994). The reaction sequence of this alternative pathway is established up to the formation of the cyclic diphosphate intermediate 2-C-methylerythritol-2,4-cyclodiphosphate (Rohmer et al., 1993; Sprenger et al., 1997; Lois et al., 1998; Takahashi et al., 1998; Rohdich et al., 1999; Herz et al., 2000; Lüttgen et al., 2000); several subsequent so far unknown steps finally lead to IPP.

This methylerythritol phosphate pathway can be distinguished from the mevalonic acid pathway on the basis of different labelling patterns of the isoprene units resulting after incorporation of [1-^{13}C]glucose into isoprenoids (Rohmer et al., 1993; Schwarz, 1994; Schwender et al., 1996).

The general understanding of isoprenoid biosynthesis has extensively changed by the discovery of the methylerythritol phosphate (MEP) pathway. Whereas vertebrates and archaebacteria appear to use only the mevalonate pathway for the biosynthesis of isoprenoids, different eubacteria have been found to use either the mevalonate or the MEP pathway.

Several algae (with the exception of chlorophytes), bryophytes and higher plants have been found to use the MVA pathway for the biosynthesis of steroids, and the MEP pathway for the biosynthesis of hemiterpenoids, monoterpenoids, carotenoids, phytol and other diterpenes (for review, see Lichtenthaler et al., 1997a; Eisenreich et al., 1998, Lichtenthaler, 1999; Rohmer, 1999). Whereas the deoxyxylulose pathway seems to be limited to the plastid compartment, the mevalonate pathway appears to be operative in the cytoplasm of plant cells. However, segregation of the two pathways is not necessarily complete, and exchange of metabolites between the two pools has been observed in plants and plant cell cultures (Schwarz, 1994; Nabeta et al., 1995; Arigoni et al., 1997; Adam and Zapp, 1998; Piel et al., 1998; Adam et al., 1999).

* Corresponding author. Tel.: +49-681-302-2220; fax: +49-681-302-2476.

E-mail address: k.adam@juno.com (K.P. Adam).

0031-9422/01/$ - see front matter © 2001 Elsevier Science Ltd. All rights reserved.
PII: S0031-9422(01)00359-4

In continuation of our previous work on IPP biosynthesis in liverworts (Thiel et al., 1997; Adam et al., 1998; Eisenreich et al., 1999; Barlow et al., 2001) that covered hemi-, mono- sesqui- and diterpene formation in this plant taxon, this study was initiated to elucidate triterpene biosynthesis in liverworts. Until now, no information on the IPP biosynthesis of triterpenes in liverworts has been available. For this study we have chosen axenic cultures of the arctic liverwort *Fossombronia alaskana* as an experimental system. This liverwort appeared to be a useful candidate since we demonstrated previously that this plant forms larger amounts of triterpenes of the hopane series (Grammes et al., 1994).

In this paper, we describe the incorporation of [1-^{13}C]glucose into the triterpene 22-(30)-hopene-29-acid as well as three structurally different diterpenes (**1**–**3**) in *F. alaskana*. The biosynthesis of their isoprene units has been studied based on the NMR spectroscopic analysis of their ^{13}C labelling patterns.

2. Results and discussion

The triterpene 22-(30)-hopene-29-acid (**4**) and the diterpenes 7,17-sacculatadiene-11,12-dial (**1**), 5-oxo-neoverrucos-(13)-ene (**2**) and *trans*-phytol (**3**) were isolated with standard chromatographic procedures. Assignments of the ^{13}C NMR spectroscopic signals of the purified compounds were obtained from the literature (Grammes et al., 1994, (**4**); Asakawa et al., 1980 (**1**); Adam et al., 1998 (**3**) and by 2D NMR spectroscopic experiments (**2**). Labelling patterns and absolute ^{13}C enrichments of the compounds were individually determined by quantitative ^{13}C NMR spectroscopy using Cr(III)-acetylacetonate as a relaxation reagent for the carbon nuclei (Braun et al., 1996). The absolute enrichment has been calculated from the integrals of ^{13}C NMR signals on the basis of ^{13}C satellite analysis of the well separated proton signals in the respective ^{1}H NMR spectra.

22-(30)-Hopene-29-acid (**4**) shows three labelled carbons per isoprene unit with an average ^{13}C abundance of 6.68±0.45 (Table 1). The labelling positions correspond to the MVA pathway (Fig. 1). The remaining carbon atoms also display an increased ^{13}C abundance (3.61–4.45%), compared to the expected natural abundance of 1.11%. This general background labelling might be explained by complex metabolic turnover of [1-^{13}C]glucose during the growth period with subsequent statistical distribution of the labelled carbon atoms in various positions of intermediates of carbohydrate metabolism (e.g. metabolism of glucose to carbon dioxide and subsequent assimilation via the Calvin cycle).

7,17-Sacculatadiene-11,12-dial (**1**) and 5-oxo-neoverrucos-(13)-ene (**2**) both showed an enrichment pattern typical for the alternative MEP pathway, with an average ^{13}C abundance of 8.16±0.62% and 8.04±0.29%, respectively (Table 2). The isolated compounds also show a ^{13}C enrichment (3.15±0.26% and 2.98±0.20%, respectively) of the unlabelled positions as already discussed above. The rearrangement reaction during formation of the *neoverrucosane* skeleton has been demonstrated in an earlier study on the biosynthesis of 8α-acetoxy-13α-hydroxy-5-oxo-13-*epi*-neoverrucosane biosynthesis in *F. alaskana* (Eisenreich et al., 1999).

The labelling pattern of *trans*-phytol (**3**) from *F. alaskana* proves the formation of the isoprene units via the MEP pathway (average abundance of enriched ^{13}C: 8.21±0.21%, Table 2). Again, an increased ^{13}C background labelling could be observed (4.23±0.15%, Table 2).

The analysis of the labelling patterns demonstrates that both pathways of IPP biosynthesis operate in *F. alaskana*. The investigated compounds could be assigned to two groups formed independently from each other: firstly the triterpene, biosynthesised via the MVA pathway, and secondly the diterpenes, derived from the MEP pathway. In all compounds we observed a strict separa-

Table 1
^{13}C abundances of 22-(30)-hopene-29-acid (**4**)

Carbon atom in IPP units[a]	Carbon atom[b]	% ^{13}C[c]
1^{I}	2	4.10
2^{I}	3	**6.78**
3^{I}	4	3.71
4^{I}	23	**6.26**
5^{I}	24	**6.85**
1^{II}	6	4.10
2^{II}	5	**7.16**
3^{II}	10	3.91
4^{II}	1	**6.50**
5^{II}	25	**6.88**
1^{III}	11	3.61
2^{III}	9	**7.09**
3^{III}	8	3.71
4^{III}	7	**6.90**
5^{III}	26	**6.88**
1^{IV}	12	4.03
2^{IV}	13	**6.83**
3^{IV}	14	3.75
4^{IV}	15	**6.90**
5^{IV}	27	**6.88**
1^{V}	16	3.64
2^{V}	17	**6.91**
3^{V}	18	3.91
4^{V}	19	**6.82**
5^{V}	28	**6.85**
1^{VI}	20	4.45
2^{VI}	21	**5.62**
3^{VI}	22	3.71
4^{VI}	29	**5.64**
5^{VI}	30	**6.85**

[a] I, II, III, IV, V, VI denote individual C_5 units.
[b] Bold type: labelled positions.
[c] ^{13}C abundances obtained from the ^{13}C satellite analysis of H-21.

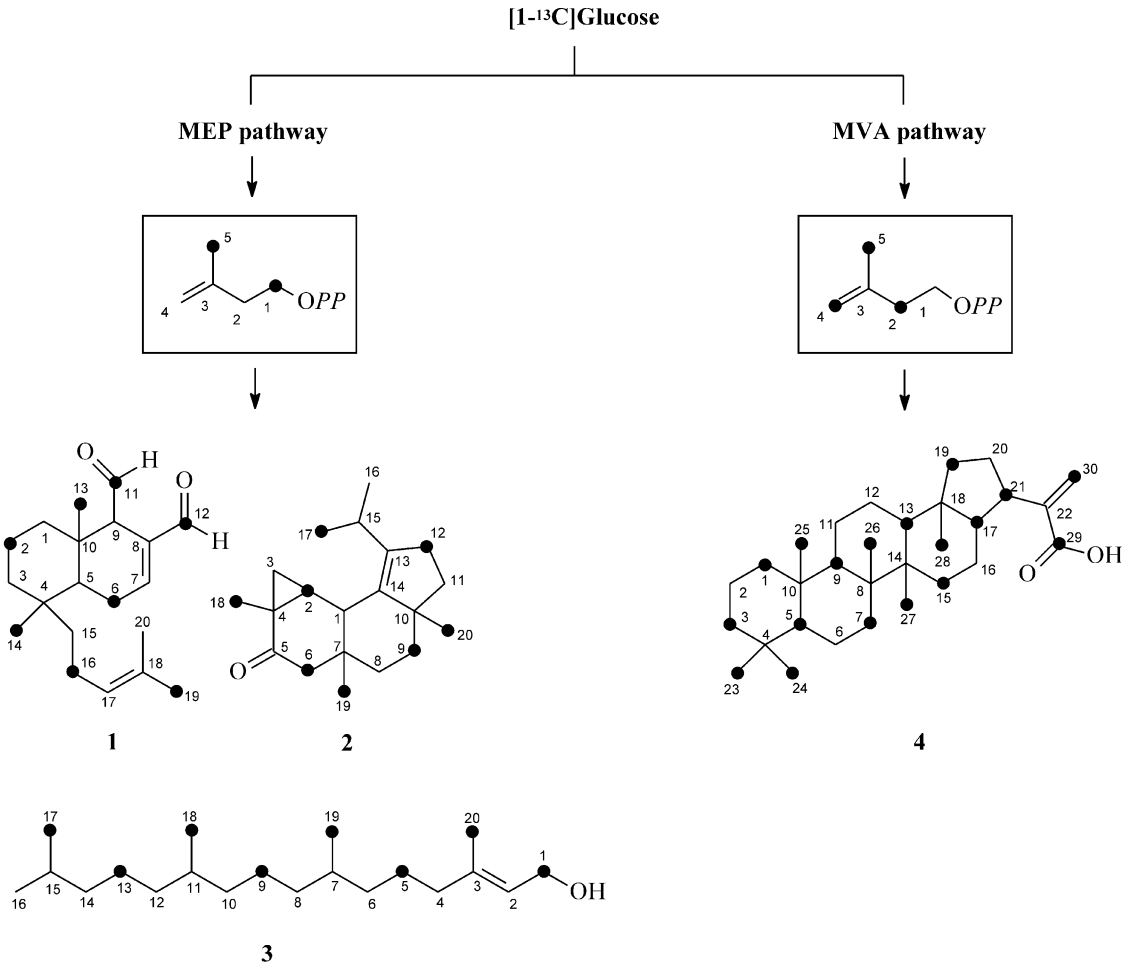

Fig. 1. Incorporation of [1-^{13}C]glucose into IPP via MVA pathway and MEP pathway and the resulting labelling patterns of compounds **1**, **2**, **3** and **4**. *PP* = diphosphate residue, ● = ^{13}C labelled position.

tion of the two pathway specific labelling patterns. A significant mixing of both IPP biosynthesis pathways in any of the isoprene units could not be deduced from the data. However, a minor incorporation of both IPP species in an isoprene unit could not be excluded, since the respective labelling could have been masked by the variation of the ^{13}C abundance data.

These results are in agreement with our earlier findings from the liverworts *R. natans*, *C. conicum* and *Trichocolea tomentella* (Adam et al., 1998; Barlow et al., 2001). They confirm the assumption that at least two well separated types of cellular compartments exist in liverworts, with different IPP biosynthesis machineries creating either C_5-units, mono- and diterpenes (MEP pathway) or sesquiterpenes and sterols and—as demonstrated in this study—also triterpenes (MVA pathway).

The results also support the current hypothesis of localization of the biosynthesis of the different isoprenoid classes assuming that the MEP pathway is located in the cytoplasm while the MEP pathway is segregated in plastids (Lichtenthaler et al., 1997b; Rohdich et al., 1999).

The quantitative analysis of the labelling patterns (Table 3) leads to an even more detailed view of the biosynthesis of the diterpenes. The average ^{13}C abundances of the background-labelled carbons of the sacculatane (**1**) (3.15±0.26% ^{13}C) and the neoverrucosane (**2**) (2.98±0.20% ^{13}C) are similar but much lower than the corresponding data of phytol (**4**) (4.23±0.15% ^{13}C). These differences possibly indicate the presence of two independent compartments in *F. alaskana* that both synthesize diterpenes via the MEP pathway. Since phytol is part of the chlorophyll molecule it could be assumed that its biosynthesis is localized in the chloroplasts whereas the diterpenes **1** and **2** are formed in a different plastidial compartment.

5-Oxo-neoverrucos-(13)-ene (**2**) is a previously unreported neoverrucosane type diterpenoid. Both the ^{1}H and ^{13}C NMR spectra were very similar to the related compound 13-hydroxy-5-oxo-*epi*-neoverrucosane (Grammes et al., 1997). In contrast to 13-hydroxy-5-oxo-*epi*-neoverrucosane, the ^{13}C NMR spectrum showed the presence of one double bond instead of the hydroxy group in position 13 (δ_C 136.1 and 139.1, both *s*). The structure

Table 2
^{13}C abundances of labelled 7,17- sacculatadiene-11,12-dial (**1**), 5-oxo-neoverrucos-(13)-ene (**2**) and *trans*-phytol (**3**)

Carbon atom in IPP units[a,b]	Carbon atom	% ^{13}C[c] (**1**)	Carbon atom	% ^{13}C[d] (**2**)	Carbon atom	% ^{13}C[e] (**3**)
1^{I}	16	**9.19**	6	**7.78**	1	**8.04**
2^{I}	17	3.38	5	2.50	2	4.15
3^{I}	18	3.71	4	3.10	3	4.32
4^{I}	20	3.41	3	2.98	4	4.04
5^{I}	19	**8.73**	18	**7.86**	20	**7.90**
1^{II}	2	**7.30**	2	**7.95**	5	**8.16**
2^{II}	3	3.14	1	2.80	6	3.95
3^{II}	4	3.06	7	2.97	7	4.45
4^{II}	15	3.09	8	3.07	8	4.24
5^{II}	14	**8.58**	19	**7.90**	19	**8.51**
1^{III}	6	**7.89**	9	**7.87**	9	**8.28**
2^{III}	5	2.69	14	3.20	10	4.24
3^{III}	10	3.00	10	3.31	11	4.50
4^{III}	1	2.81	11	3.09	12[f]	4.24
5^{III}	13	**7.35**	20	**8.36**	18	**8.51**
1^{IV}	11	**7.99**	12	**8.69**	13	**8.03**
2^{IV}	9	3.18	13	2.84	14[f]	4.07
3^{IV}	8	3.20	15	3.04	15	4.28
4^{IV}	7	3.09	16	2.86	16	4.37
5^{IV}	12	**8.37**	17	**7.90**	17	**8.32**

[a] Bold type: labelled positions.
[b] I, II, III, IV denote individual C_5 units.
[c] ^{13}C abundances obtained from the ^{13}C satellite analysis of H-12.
[d] ^{13}C abundances obtained from the ^{13}C satellite analysis of H-19.
[e] ^{13}C abundances obtained from the ^{13}C satellite analysis of H-1.
[f] Signals may be interchanged.

Table 3
Comparison of ^{13}C enrichments in isoprenoids from *Fossombronia alaskana*

Compound	% ^{13}C labelled carbons	% ^{13}C unlabelled carbons	Ratio labelled/unlabelled
7,17-Sacculatadiene-11,12-dial (**1**)	8.16±0.62	3.15±0.26	2.59
13-α-Hydroxy-5-oxo-epineoverrucosane (**2**)	8.04±0.29	2.98±0.20	2.70
22-(30)-Hopene-29-acid (**3**)	6.68±0.45	3.94±0.25	1.69
trans-Phytol (**4**)	8.21±0.21	4.23±0.15	1.94

of compound **2** was established from analysing DEPT, COSY, HSQC and HMBC NMR spectral data.

3. Experimental

3.1. Spectroscopy and spectrometry

NMR spectra were recorded in $CDCl_3$ [^1H NMR (500 MHz), ^{13}C NMR (125 MHz)] relative to $CDCl_3$ at δ_H 7.24, δ_C 77.0. ^{13}C multiplicities were determined using the DEPT pulse sequence. 2D spectra were recorded as COSY, HSQC and HMBC experiments. Quantitative ^{13}C NMR measurements were recorded with the inverse gated decoupling pulse sequence in the presence of 0.1 M $Cr(acac)_3$ (Braun et al., 1996). For integration, the signal-to-noise ratio of the ^{13}C-signals was at least 40:1. In case of overlapping signals, ^{13}C abundance data were either obtained by doubling the integral of the non-overlapped half of the signal or by averaging integrals.

3.2. Plant material and labelling procedure

The axenic culture of *F. alaskana* Steere & Inoue was provided by Professor Basile, New York Botanical Garden. The liverwort was grown in 200 ml Erlenmeyer flasks under continuous incandescent light (60 μmol photons m^{-2} s^{-1} photosynthetically active radiation) at 22 °C on 75 ml of Gamborg B5 medium (Gamborg et al., 1968) solidified with 0.9% agar and supplemented with 1% glucose. For labelling 20% of the glucose was substituted by [1-^{13}C]glucose. Cultures were grown for 12 weeks.

3.3. Extraction and isolation

The extraction and isolation scheme followed standard procedures of our group (Adam et al., 1998). Dried ^{13}C labelled plant material (25 g) was ground and extracted in a Soxhlet apparatus using diethyl ether. After removal of the solvent, the crude extract was subjected to silica gel chromatography (vacuum liquid chromatography, VLC) employing a *n*-hexane–EtOAc gradient. The VLC fraction containing crude 7,17- sacculatadiene-11,12-dial and 22-(30)-hopene-29-acid (9–10% EtOAc) was further purified via HPLC (250 × 4 mm, Si 60 Lichrospher Merck, 5 μm, *n*-hexane–EtOAc, 91:9), yielding 7 mg of (**1**) and 15 mg of (**4**). VLC fractions (15–20% EtOAc) were purified by HPLC (250×4 mm, Si 60 Lichrospher, Merck, *n*-hexane-TBME 93:7) yielding 4 mg of (**2**) as a colourless oil.

The chlorophyll-containing fractions were combined and saponified by reaction overnight at room temperature with 6% (w/v) KOH in methanol. Following hydrolysis, the mixture was extracted 5×with CH_2Cl_2. After removal of the solvent, the mixture was separated by VLC on silica gel with *n*-hexane–EtOAc (3.8% EtOAc) yielding 20 mg of *trans*-phytol (**3**).

3.3.1. 5-Oxo-neoverrucos-(13)-ene (2)

TLC (*n*-hexane–EtOAc 50:50), $R_f = 0.66$, purple with anisaldehyde/H_2SO_4. $[\alpha]_D^{20} = 72.5^\circ$ ($c = 0.05$). GC–MS (EI): *m/z* 55; 69 (base peak); 91; 105; 121; 135; 145; 187; 203; 243; 271; 286 ($[M]^+$). IR ν_{max}^{KBr}: cm^{-1}: 2905, 1675, 1565, 1510, 1370. ^1H NMR: δ_H 0.73 (3H, *s*, H-19); 0.98 (1H, *m*, H-3); 0.98 (3H, *d*, $J = 6$ Hz, H-16); 0.99 (3H, *d*, $J = 6$ Hz, H-17); 1.03 (3H, *s*, H-20); 1.16 (1H, *m*, H-8); 1.18 (1H, *m*, H-3); 1.24 (3H, *s*, H-18); 1.35 (1H, *m*, H-9); 1.49 (1H, *m*, H-11); 1.51 (1H, *m*, H-8); 1.53 (1H, *m*, H-9); 1.60 (1H, *m*, H-11); 1.91 (1H, *m*, H-2); 1.95 (1H, *d*, $J = 14$ Hz, H-6); 2.06 (1H, *d*, $J = 14$ Hz, H-6); 2.30 (2H, *m*, H-12); 2.40 (1H, *br s*, H-1), 3.01 (1H, *m*, H-15). ^{13}C NMR: δ_C 17.6 (*q*, C-19); 19.8 (*q*, C-18); 21.7 (*q*, C-16); 21.9 (*q*, C-17); 24.3 (*q*, C-20); 27.3 (*d*, C-15); 28.7 (*t*, C-3); 28.8 (*d*, C-2); 29.1 (*t*, C-12); 30.2 (*s*, C-4); 35.7 (*t*, C-9); 36.9 (*t*, C-8); 38.0 (*t*, C-11); 44.0 (*s*, C-7); 47.2 (*d*, C-1); 49.6 (*s*, C-10); 51.8 (*t*, C-6); 136.4 (*s*, C-13); 139.1 (*s*, C-14); 210.6 (*s*, C-5).

Acknowledgements

Publication No. 157 of "Arbeitskreis Chemie und Biologie der Moose". We are grateful to the "Saarländische Landesgraduiertenförderung" for providing financial support to U.H.

References

Adam, K.P., Thiel, R., Zapp, J., 1999. Incorporation of 1-[1-^{13}C]deoxy-D-xylulose in chamomile sesquiterpenes. Archives of Biochemistry and Biophysics 369, 127–132.

Adam, K.P., Thiel, R., Zapp, J., Becker, H., 1998. Involvement of the mevalonic acid pathway and the glyceraldehyde-pyruvate pathway in terpenoid biosynthesis of the liverworts *Conocephalum conicum* and *Ricciocarpos natans*. Archives of Biochemistry and Biophysics 354, 181–187.

Adam, K.P., Zapp, J., 1998. Biosynthesis of the isoprene units of chamomile sesquiterpenes. Phytochemistry 48, 953–959.

Arigoni, D., Sagner, S., Latzel, C., Eisenreich, W., Bacher, A., Zenk, M.H., 1997. Terpenoid biosynthesis from 1-deoxy-D-xylulose in higher plants by intramolecular skeletal rearrangement. Proceedings of the National Academy of Sciences of the USA 94, 10600–10605.

Asakawa, Y., Toyota, M., Takemoto, T., 1980. Four new sacculatane-type diterpenoids from *Trichocoleopsis sacculata* and *Pellia endiviaefolia*. Phytochemistry 19, 1799–1803.

Barlow, A.J., Becker, H., Adam, K.P., 2001. Biosynthesis of the hemi- and monoterpene moieties of isoprenyl phenyl ethers from the liverwort *Trichocolea tomentella*. Phytochemistry 57, 7–14.

Braun, S., Kalinowski, H.O., Berger, S., 1996. 100 and more basic NMR experiments. VCH-Wiley, Weinheim, New York.

Dictionary of Natural Products, 2000. Version 9.1 (CD-ROM). Chapman and Hall/CRC Press, London, New York.

Eisenreich, W., Rieder, C., Grammes, C., Heßler, G., Adam, K.-P., Becker, H., Arigoni, D., Bacher, A., 1999. Biosynthesis of a neo-*epi*-verrucosane diterpene in the liverwort *Fossombronia alaskana*. A retrobiosynthetic NMR study. Journal of Biological Chemistry 274, 36312–36320.

Eisenreich, W., Schwarz, M., Cartayrade, A., Arigoni, D., Zenk, M.H., Bacher, A., 1998. The deoxyxylulose phosphate pathway of terpenoid biosynthesis in plants and microorganisms. Chemistry and Biology 5, R221–R233.

Gamborg, O.L., Miller, R.A., Ojiama, K., 1968. Plant cell cultures. I. Nutrient requirements of suspension cultures of soybean root cells. Experimental Cell Research 50, 151–158.

Grammes, C., Burkhardt, G., Becker, H., 1994. Triterpenes from *Fossombronia liverworts*. Phytochemistry 35, 1293–1296.

Grammes, C., Burkhardt, G., Veith, M., Huch, V., Becker, H., 1997. *Neoverrucosane* and *epi*-homoverrucosane-type diterpenoids from *Fossombronia alaskana*. Phytochemistry 44, 1495–1502.

Herz, S., Wungsintaweekul, J., Schuhr, C.A., Hecht, S., Lüttgen, H., Sagner, S., Fellermeier, M., Eisenreich, W., Zenk, M.H., Bacher, A., Rohdich, F., 2000. Biosynthesis of terpenoids: YgbB protein of *Escherichia coli* phosphorylates the 2-hydroxy group of 4-diphosphocytidyl-2-*C*-methylerythritol. Proceedings of the National Academy of Sciences of the USA 97, 2486–2490.

Lichtenthaler, H.K., 1999. The 1-deoxy-D-xylulose-5-phosphate pathway of isoprenoid biosynthesis in plants. Annual Review of Plant Physiology and Plant Molecular Biology 50, 47–65.

Lichtenthaler, H.K., Rohmer, M., Schwender, J., 1997a. Two independent biochemical pathways for isopentenyl diphosphate and isoprenoid biosynthesis in higher plants. Physiologica Plantarum 101, 643–652.

Lichtenthaler, H.K., Schwender, J., Disch, A., Rohmer, M., 1997b. Biosynthesis of isoprenoids in higher plant chloroplasts proceeds via a mevalonate-independent pathway. FEBS Letters 400, 271–274.

Lois, L.M., Campos, N., Putra, S.R., Danielsen, K., Rohmer, M., Boronat, A., 1998. Cloning and characterization of a gene from *Escherichia coli* encoding a transketolase-like enzyme that catalyses the synthesis of D-1-deoxyxylulose-5-phosphate, a common precursor for isoprenoid, thiamin, and pyridoxol biosynthesis. Proceedings of the National Academy of Sciences of the USA 95, 2105–2110.

Lüttgen, H., Rohdich, F., Herz, S., Wungsintaweekul, J., Hecht, S., Schuhr, C.A., Fellermeier, M., Sagner, S., Zenk, M.H., Bacher, A., Eisenreich, W., 2000. Biosynthesis of terpenoids: YgbB protein converts 4-diphosphocytidyl-2-*C*-methylerythritol 2-phosphate to 2-*C*-methylerythritol 2,4-cyclodiphosphate. Proceedings of the National Academy of Sciences of the USA 97, 1062–1067.

Nabeta, K., Ishikawa, T., Kawae, T., Okuyama, H., 1995. Biosynthesis of heteroscyphic acid A in cell cultures of *Heteroscyphus planus*: nonequivalent labelling of C-5 units in diterpene biosynthesis. Journal of the Chemical Society, Chemical Communications 681.

Piel, J., Donath, J., Bandemer, K., Boland, W., 1998. Mevalonate-independent biosynthesis of terpenoid volatiles in plants: Induced and constitutive emission of volatiles. Angewandte Chemie 37, 2478–2481.

Rohdich, F., Wungsintaweekul, J., Fellermeier, M., Sagner, S., Herz, S., Kis, K., Eisenreich, W., Bacher, A., Zenk, M.H., 1999. Cytidine 5′-triphosphate-dependent biosynthesis of isoprenoids: YgbP protein of *Escherichia coli* catalyzes the formation of 4-diphosphocytidyl-2-*C*-methylerythritol. Proceedings of the National Academy of Sciences of the USA 96, 11758–11763.

Rohmer, M., 1999. The discovery of a mevalonate-independent pathway for isoprenoid biosynthesis in bacteria, algae and higher plants. Natural Product Reports 16, 565–574.

Rohmer, M., Knani, M., Simonin, P., Sutter, B., Sahm, H., 1993. Isoprenoid biosynthesis in bacteria: a novel pathway for the early steps leading to isopentenyl diphosphate. Biochemical Journal 295, 517–524.

Schwarz, M.K., 1994. Terpen-Biosynthese in *Ginkgo biloba*: Eine überraschende Geschichte. PhD Thesis No. 10951, Eidgenössische Technische Hochschule, Zürich.

Schwender, J., Seemann, M., Lichtenthaler, H.K., Rohmer, M., 1996. Biosynthesis of isoprenoids (carotenoids, sterols, prenyl side-chains of chlorophylls and plastochinone) via a novel pyruvate/glyceraldehyde 3-phosphate non-mevalonate pathway in the green alga *Scenedesmus obliquus*. Biochemical Journal 316, 73–80.

Sprenger, G.A., Schörgen, U., Wiegert, T., Grolle, S., De Graaf, A.A., Taylor, S.V., Begley, T.P., Bringer-Meyer, S., Sahm, H., 1997. Identification of a thiamin-dependent synthase in *Escherichia coli* required for the formation of the 1-deoxy-D-xylulose 5-phosphate precursor to isoprenoids, thiamin, and pyridoxol. Proceedings of the National Academy of Sciences of the USA 94, 12857–12862.

Takahashi, S., Kuzuyama, T., Watanabe, H., Seto, H., 1998. A 1-deoxy-D-xylulose 5-phosphate reductoisomerase catalyzing the formation of 2-C-methyl-D-erythritol 4-phosphate in an alternative nonmevalonate pathway for terpenoid biosynthesis. Proceedings of the National Academy of Sciences of the USA 95, 9879–9884.

Thiel, R., Adam, K.P., Zapp, J., Becker, H., 1997. Isopentenyl diphosphate biosynthesis in liverworts. Pharmaceutical and Pharmacological Letters 2/3, 103–105.

PERGAMON

Phytochemistry 58 (2001) 1055–1065

PHYTOCHEMISTRY

www.elsevier.com/locate/phytochem

Trichloroethylene oxidative metabolism in plants: the trichloroethanol pathway

Tanya Q. Shang[a], Sharon L. Doty[a], Angela M. Wilson[a], William N. Howald[b], Milton P. Gordon[b,*]

[a]*Department of Biochemistry, University of Washington, Seattle, WA 98195, USA*
[b]*Mass Spectrometry Center, Department of Medicinal Chemistry, University of Washington, Seattle, WA 98195, USA*

Received 24 April 2001; received in revised form 14 August 2001

Abstract

Trichloroethylene (TCE) is a widespread and persistent environmental contaminant. Recently, plants, poplar trees in particular, have been investigated as a tool to remove TCE from soil and groundwater. The metabolism of TCE in plants is being investigated for two reasons: one, plant uptake and metabolism represent an important aspect of the environmental fate of the contaminant; two, metabolism pattern and metabolite identification will help assess the applicability of phytoremediation. It was previously shown that TCE metabolites in plants are similar to ones that result from cytochrome P450-mediated oxidation in mammals: trichloroethanol, trichloroacetate and dichloroacetate. Our measurements indicate that one of these metabolites, trichloroethanol, is further glycosylated in tobacco and poplar. The glycoside was detected in all tissues (roots, stems and leaves) in comparable levels, and was at least 10 fold more abundant than free trichloroethanol. The glycoside in tobacco was identified as the ß-D-glucoside of trichloroethanol by comparison of the mass spectra and the chromatographic retention time of its acetylation product to that of the synthesized standard. Trichloroethanol and its glucoside did not persist in plant tissue once plants are removed from TCE contaminated water, indicating further metabolism. © 2001 Elsevier Science Ltd. All rights reserved.

Keywords: *Nicotiana tabacum*; Solanceae; *Populus*; Trichocarpa; Salicaceae; Xenobiotic metabolism; Glycosides; Trichloroethylene; Trichloroethanol glucoside; Phytoremediation; GC–MS

1. Introduction

Trichloroethylene (TCE) is one of the most common environmental pollutants in the industrialized world. It has been used for decades in military, industrial, medical and household settings (Ensley, 1991), in a wide range of applications including as a metal degreaser, dry cleaning agent, and anaesthetic. TCE is relatively stable in the environment, and has persisted in some aquifers for decades. Trichloroethylene is a hepatotoxin, mutagen and suspected carcinogen (Lash et al., 2000; Moore and Harrington-Brock, 2000). The prevalence of this contaminant, coupled with the limited biodegradability, presents a difficult and expensive remediation problem.

Recently, phytoremediation, or the use of plants for environmental cleanup, has been studied as a potential tool for the inexpensive and efficient removal of TCE from the environment. Laboratory studies showed that a number of plant species are capable of taking up and metabolizing TCE (Anderson and Walton, 1995; Narayanan et al., 1995; Newman et al., 1997; Orchard et al., 2000), and a controlled field study showed that poplar trees in an artificially constructed aquifer contributed to the removal of 99% of TCE injected to simulated ground water (Newman et al., 1999).

Though phytoremediation has shown initial promise, further research needs to be undertaken to gain a better understanding of its biochemical and ecological implications. One of the most important areas that requires more research is the fate of TCE in plants.

In mammals, TCE is metabolized via two pathways: the oxidative pathway mediated by cytochrome P450 monooxygenases (primarily 2E1), and the glutathione conjugation pathway catalyzed by glutathione-*S*-transferase. The oxidative pathway is the predominant one, resulting in

Abbreviations: GC–MS: gas chromatography–mass spectrometry; TCE: trichloroethylene; TCOH: trichloroethanol; TCAA: trichloroacetic acid; DCAA: dichloroacetic acid; BSA: bovine serum albumin; ECNCI: electron capture negative chemical ionization; EI: electron ionization

* Corresponding author. Tel.: +1-206-543-1769; fax: +1-206-685-8279.

E-mail address: miltong@u.washington.edu (M.P. Gordon).

0031-9422/01/$ - see front matter © 2001 Elsevier Science Ltd. All rights reserved.
PII: S0031-9422(01)00369-7

metabolites such as trichloroethanol (TCOH), trichloroacetate (TCAA), and dichloroacetate (DCAA). These metabolites can be dechlorinated to oxalic acid. Trichloroethanol is conjugated to glucuronic acid (for review of mammalian metabolism of TCE see Lash et al., 2000).

In previous studies, TCOH, TCAA and DCAA were found in plants exposed to TCE, both in controlled exposures and in field conditions (Newman et al., 1997, 1999; Doucette et al., 1998; Orchard et al., 2000). The concentrations of these metabolites are low, the highest level reported being 40 ppm (fresh weight basis) for TCAA in poplar trees exposed to TCE in a controlled field situation for 3 seasons (Newman et al., 1999). Experiments utilizing [^{14}C] TCE to trace the fate of TCE carbon in plants showed that most of the radioactivity incorporated in plant tissue can not be extracted by organic solvents (Schroll et al., 1994; Schnabel et al., 1997; Orchard et al., 2000). Since TCE and the aforementioned metabolites are analyzed by solvent extraction, the majority of plant TCE metabolites have not been identified.

Miller (1941a,b) found that tomato and gourd plants take up TCOH and metabolize it to its corresponding glycoside. Being very polar, TCOH glycosides would not be extractable by organic solvents, and are, therefore, good candidates for the unidentified TCE metabolites.

This study investigates the metabolism of TCOH as a part of the overall TCE metabolism in plants. In particular, the identification and characterization of the TCOH glycoside as a TCE metabolite is reported.

2. Results and discussion

Among the previously identified TCE plant metabolites, TCOH is the primary metabolite in tobacco (Doty et al., 2000). Although other TCE metabolites, such as TCAA and DCAA, have been reported (Newman et al., 1997; Orchard et al., 2000), the concentrations of these metabolites were often below the level of detection in our experiments. Since TCOH was the most prevalent metabolite in several plant species, we chose to study the fate of this metabolite. The release of free TCOH upon-glucosidase hydrolysis was used as an assay for the existence of TCOH glycosides.

2.1. TCOH is conjugated to sugars in tobacco plants exposed to TCE or TCOH

Tobacco plants were treated with TCE, and the tissues (leaf, stem and root) were harvested and extracted for free and glycosylated TCOH. Fig. 1 is a typical pair of GC chromatographs from the glycoside assay. Upon hydrolysis with ß-glucosidase, a much higher level of trichloroethanol was released, in comparison to the free trichloroethanol in the BSA (bovine serum albumin) control.

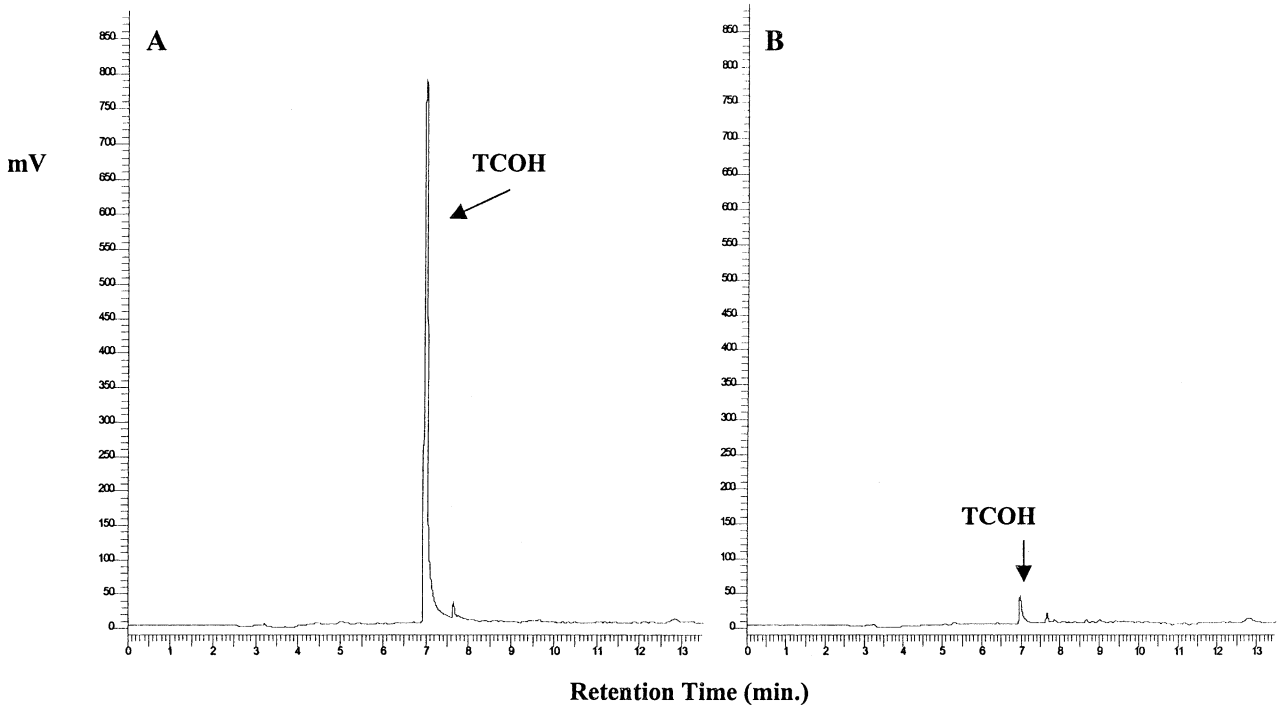

Fig. 1. A sample gas chromatograph (GC–ECD) of the trichloroethanol glycoside assay. Tobacco leaves dose with TCE were extracted. A, extract incubated with β-glucosidase. B, extract incubated with BSA.

When exposed to TCOH, tobacco plants took up TCOH and transported it to the shoots (discussed in Section 2.3.). Similar to TCE treated plants, ß-glucosidase hydrolysis released a high level of TCOH in these plant tissues.

Table 1 lists the percentage of trichloroethanol that is glycosylated in tobacco under various treatments. In all tissues tested, most of the TCOH exists in some kind of glycoside form. The percentage of glycosylation was not influenced by whether the plant was dosed with TCE or TCOH, nor was it influenced by the expression of a TCE-metabolizing transgene, the human P450 2E1.

2.2. Identity of the TCOH-glycoside in tobacco

The identity of the glycoside was investigated with GC–MS. Hydroponic tobacco plants (both transgenic and wild-type) were treated with trichloroethanol, and the leaves were extracted and acetylated. The acetylated extract was subjected to GC using electron capture negative chemical ionization (ECNCI) and electron ionization (EI) mass spectrometry (MS) in comparison to the synthesized TCOH-ß-glucoside tetra-acetate standard (Fig. 2). In both ionization modes, the spectra of the acetylated tobacco glycoside were identical to those of the standard (Figs. 3 and 4, respectively). In addition, when the standard and the acetylated tobacco extracts were mixed and subjected to chromatography as before, the synthesized glucoside and the tobacco glycoside co-eluted as one peak (not shown). The ECNCI mass spectrum of the acetylated glucoside

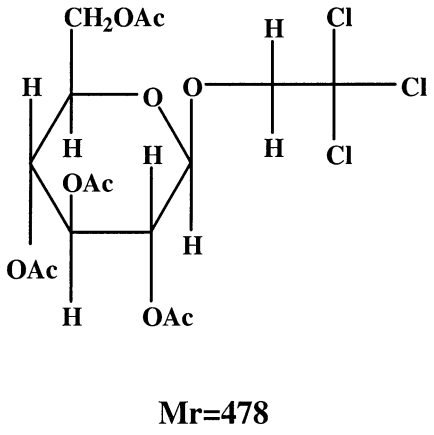

Fig. 2. The structure of the acetylated TCOH β-glucoside. The molecular formula is $C_{16}H_{21}Cl_3O_{10}$.

(Fig. 3) yielded the molecular ion (M^-) at m/z 478 as well as its chloride adduct $[M+l]^-$ at m/z 513 exhibiting isotopic envelopes characteristic for three and four chlorine atoms, respectively. The molecular ion of the glucoside was not observed in the EI spectra (Fig. 4). While mass spectra do not establish whether the acetylated glucoside was in the α- or β-conformation, the glucoside only releases significant amounts of trichloroethanol upon β-glucosidase hydrolysis, but not α-glucosidase (data not shown).

Miller (1941a,b) found that chloral hydrate and trichloroethanol were both converted to β-glycosides in plants. The sugar component, however, varied with species. In *Lagenaria leucantha* Rusby (gourd), a β-glucoside

Table 1
Formation and glycosylation of trichloroethanol in tobacco plants and cultures treated with TCE or TCOH[a]

Plant	Dosed with	Tissue	Range of total TCOH concentration (μg/g fresh wt)	% Glycosylation of total TCOH
Transgenic tobacco [b]	TCE	Leaf	4–31	97±1 ($n=8$)[d]
		Stem	3–1.5	87±7 ($n=8$)
		Root	0.7–6.8	75±15 ($n=8$)
	TCOH	Leaf	12–27	95±1 ($n=4$)
		Stem	4–13	82±4 ($n=4$)
		Root	14–50	95±3 ($n=4$)
Tobacco (wild-type)	TCE[c]	Leaf	0.3–0.5	89±1 ($n=4$)
	TCOH	Leaf	4–22	97±1 ($n=3$)
		Stem	10–15	88±2 ($n=3$)
		Root	20–35	88±7 ($n=3$)
Tobacco hairy roots (wild-type)[e]	TCE		1.7–6.4	82±3 ($n=3$)
	TCOH		140–188	96±0 ($n=3$)
Tobacco leaf suspensions (wild-type)	TCE		0–0.01	0% ($n=3$)
	TCOH		6.5–9	41±34 ($n=3$)

[a] All plants were hydroponic and were dosed with 10g/ml TCE or TCOH in root solutions for 5 days. TCOH concentrations listed were combined values of free and glycosylated TCOH.

[b] Transgenic tobacco plants express human cytochrome P450 2E1 as described in Doty et al., 2000.

[c] In TCE dosed wild-type tobacco, TCOH was detected in leaves only.

[d] n, Number of replicates.

[e] Hairy roots were generated from wild-type tobacco transformed by wild-type *Agrobacterium rhizogenes* as described in Experimental.

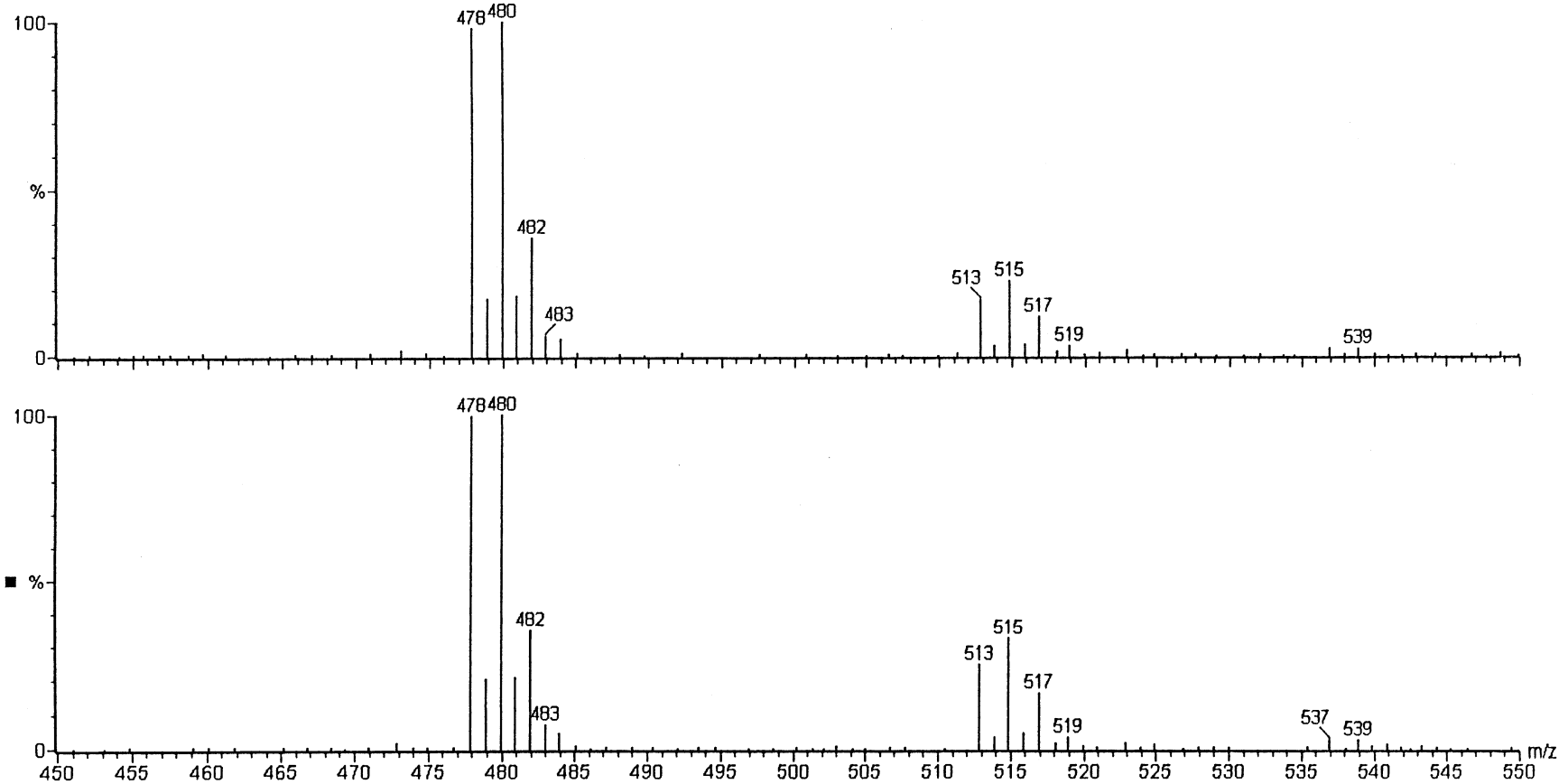

Fig. 3. Elcetron capture negative chemical ionization mass spectra of synthesized tricholoroethyl-β-D-glucopyranose tetra-acetate standard (top) and the acetylated glycoside extracted from tobacco leaves (bottom).

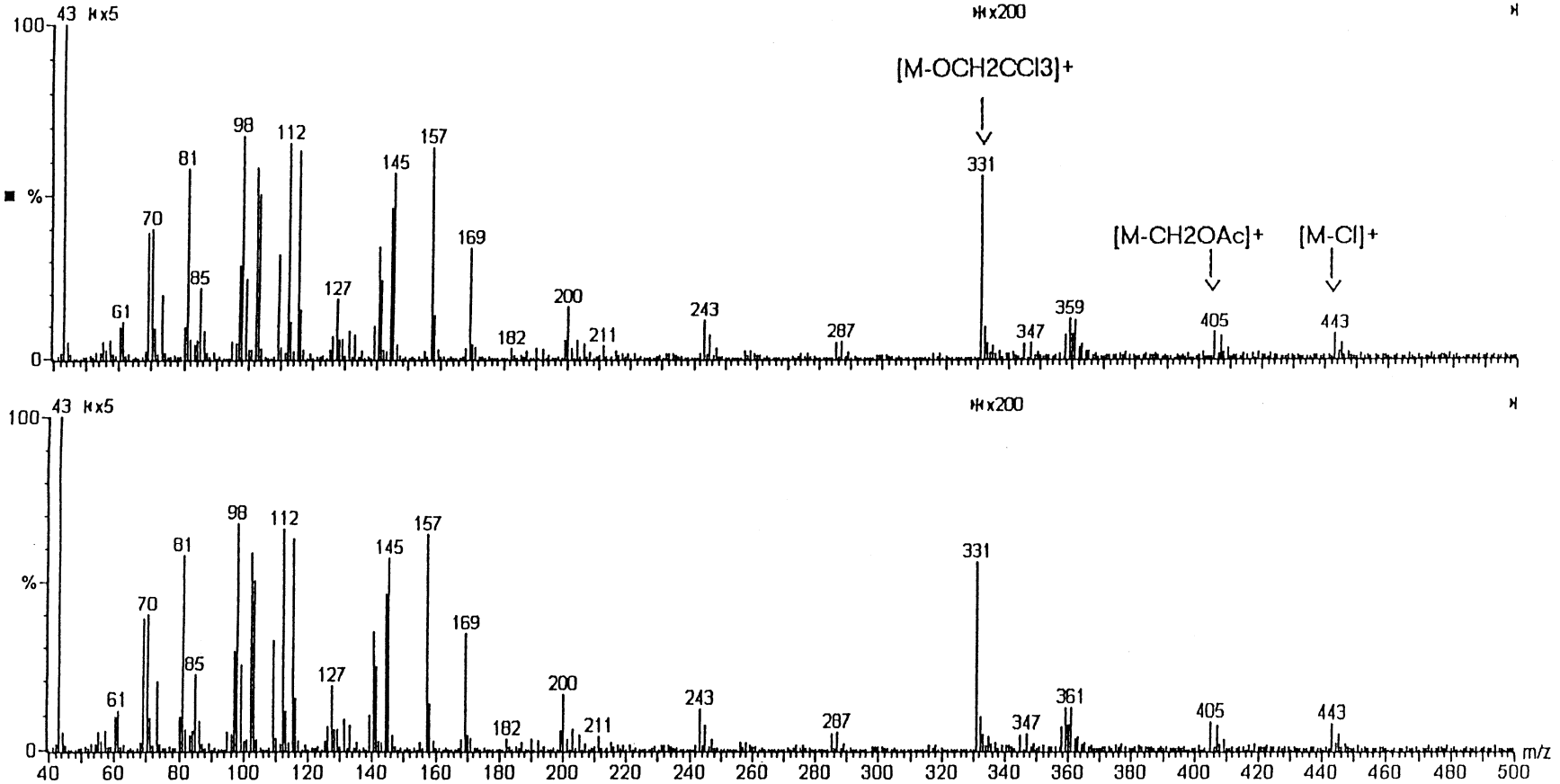

Fig. 4. Electron impact mass spectra of synthesized trichloroethyl-β-D-glucopyranose tetra-acetate standard (top) and the acetylated glycoside extracted from tobacco leaves (bottom).

was formed, while in tomato it was a β-gentiobioside. We propose that in tobacco, glucose is the sugar moiety, given the identical behavior of the glycoside and the synthesized glucoside both in terms of mass spectra and chromatographic retention time, as described above. However, we can not rule out the possibility of another hexose, such as galactose or mannose, as the conjugant, since such glycosides would produce similar mass spectra as a glucoside would. It is not known whether the GC system used in this study can distinguish between various monosaccharide conjugates, but the alditol acetates of the free monosaccharides, including glucose, fructose, and galactose, have been separated by Dormaar and Willms (1990) using the same typeof GC column. Therefore, the co-elution of the acetylation products of the glycoside and the authentic glucoside strongly supports the identification assignment.

Though only the monosaccharide conjugate was detected in TCE treated tobacco plants, conjugates with oligosaccharides can not be ruled out, since the acetylation products of such conjugates can not be detected with the instrumentation used in this study.

2.3. The fate of trichloroethanol in tobacco

Tobacco plants (both transgenic and wild-type) were treated with 10 mg l^{-1} trichloroethanol for 5 days. At the end of 5 days, 94±11% of total TCOH was recovered as either unaltered or glycosylated (including in growth media or in tissue). Twenty-two ±7% of the TCOH dose was recovered in plant tissue, mostly in glycosylated form (85–96% glycosylated, depending on tissue type). Table 2 shows that a significant amount of trichloroethanol can be taken up from roots and transported to leaves.

In plants dosed with TCE, leaves usually accumulate higher concentrations of oxidative metabolites such as TCOH than do roots (Newman et al., 1997, 1999). It was previously postulated that oxidation of TCE occurs primarily in leaves after TCE is transported from the roots (Newman et al., 1997). The results here showed that this is not necessarily the case, since plants can transport trichloroethanol into leaves, sometimes resulting in concentrations higher than those in roots.

There is additional evidence suggesting that TCE oxidation can occur in roots, and the resulting TCOH is glycosylated in the roots and transported to the shoots. When tobacco hairy root culture (see experimental) was treated with TCE or trichloroethanol, TCOH-glycoside was produced in both treatments (Table 1), showing that roots are capable of both TCE oxidation and TCOH glycosylation in the absence of the rest of the plant. Therefore, at least some of the TCOH and its glycoside are formed prior to transport to leaves. In addition, hairy roots accumulate much higher concentrations of total TCOH than do roots of whole plants (Table 1), whether upon TCE or TCOH treatment. In contrast, when tobacco leaves were excised and suspended in

Table 2
Trichloroethanol concentration (μg/g) taken up in hydroponic tobacco plants exposed to trichloroethanol in root solutions after 5 days

Plant number	Leaf	Stem	Root
1	27	4.4	14
2	27	13	30
3	21	10	49
4	18	12	36
5	22	13	32

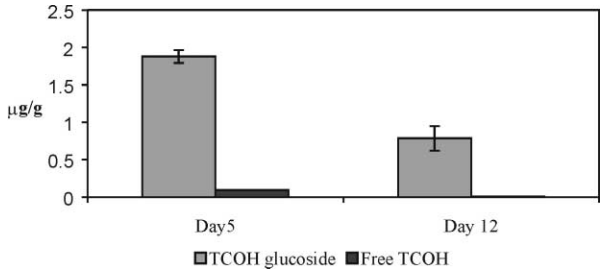

Fig. 5. Disappearance of trichloroethanol and its glucoside in hydroponic tobacco plants (average of two experiments). Plants were treated with TCE in the root solution for 5 days, then moved to uncontaminated media for 7 more days.

Table 3
Formation and glycosylation of trichloroethanol in various plants and cultures treated with TCE [a]

Plant	Tissue	Range of TCOH concentration (μg/g)	% Glycosylation of total TCOH
Poplar H11-11 [b]	Leaf	0.06–0.4	96±6 (n=3)[c]
	Stem	0.05–0.06	
Leuceana leucocephala	Leaf	0.6–5.8	88±14 (n=10)
	Stem	0.2–13	92±9 (n=8)
	Root	0.1–6	91±10 (n=5)
Belladonna hairy roots		0.7–1.2	85±1 (n=3)

[a] All plants were hydroponic and were dosed with 10 g /mL TCE or TCOH in root solutions for 5 days. TCOH concentrations listed were combined values of free and glycosylated TCOH.

[b] In hydroponic poplar dosed with TCE, free TCOH was detected in leaves only, and no TCOH, free or glycosylated, was detected in roots.

[c] n = number of replicates.

media containing TCE or TCOH, the concentrations of trichloroethanol accumulation in leaf tissue were much lower than in hairy roots, with no or low glycosylation (Table 1).

We propose, therefore, that glycosylation occurs in the roots, and the glycoside is transported to the shoots. On the other hand, the transport of the glycoside does not preclude the possibility that some glycosylation also occurs to free TCOH after it moves up to the shoots.

2.4. Trichloroethanol and its glucoside do not persist in tobacco

Fig. 5 shows that neither trichloroethanol nor its glucoside accumulates in tobacco plants after the plants are removed from TCE. The glucoside disappears at a slower rate (58% reduction over 5 days) than the free trichloroethanol (86%).

The decline of TCOH and TCOH-glycoside after removal of TCE source indicates further metabolism of TCOH, which is slower than the rate of TCE oxidation, since TCOH accumulates in the presence of a continuous supply of TCE. As discussed earlier, TCOH may oxidize to TCAA, which may be dechlorinated to such products as oxalic acid. The glycosides can be hydrolyzed when plants become injured or undergo other physiological changes (Lamoureux and Rusness, 1986). The glycosides may also become incorporated into polymers such as polysaccharides, and eventually be incorporated as cell wall components (for review see Colemann et al. 1997). All these pathways may contribute to the disappearance of TCOH in tobacco, and further research is needed to ascertain the final fate of TCOH and its glycoside.

The toxicity of trichloroethanol has not been clearly established, though other metabolites of TCE, such as TCAA and DCAA, are considered toxic (Lash et al., 2000). This study shows that in plants, trichloroethanol is stabilized by glycosylation. The toxicity of the glycoside is not known, but it is likely that once ingested, the glycoside will be hydrolyzed to release free trichloroethanol. The concentrations of trichloroethanol and its glycoside in all plants tested have been low (Tables 1 and 3). Nevertheless, it is a factor to be considered where phytoremediation is used.

2.5. Trichloroethanol and the glycoside as TCE metabolites in other plant species

In addition to tobacco, the oxidation of TCE to trichloroethanol and its corresponding glycosides also occurs in poplar, *L. leucocephala* (a tropical legume) and *Atropa belladonna* hairy roots (Table 3). Poplar and *leucocephala* are both candidates for phytoremediation of halogenated hydrocarbons. *A. Belladonna* is a medicinal plant used as a model system for *Agrobacterium rhizogenes*-mediated transformation of plants with mammalian genes of xenobiotic detoxification properties (Banerjee et al., unpublished). In all tissues tested, at least 85% of total TCOH was sugar conjugated. The only exception is suspension callus cells of poplar (Fig. 6). Though TCOH is readily taken up by the cells, only about $22 \pm 7\%$ was in the glycoside form. This suggests that full glycosylation of TCOH may be tissue dependent, as the callus cell culture is undifferentiated.

Doucette et al. (1997) found TCOH in saw palmetto, oak and castor bean plants on TCE contaminated sites, at up to 0.3 g/g dry weight basis. Assuming approximately 50–90% water content, this corresponds to about 0.03–0.15 μg/g fresh weight. Newman et al. (1999) found up to 0.56 μg/g free TCOH in poplar leaves in a controlled field study where poplar trees were treated with TCE in simulated groundwater. The concentrations reported here are

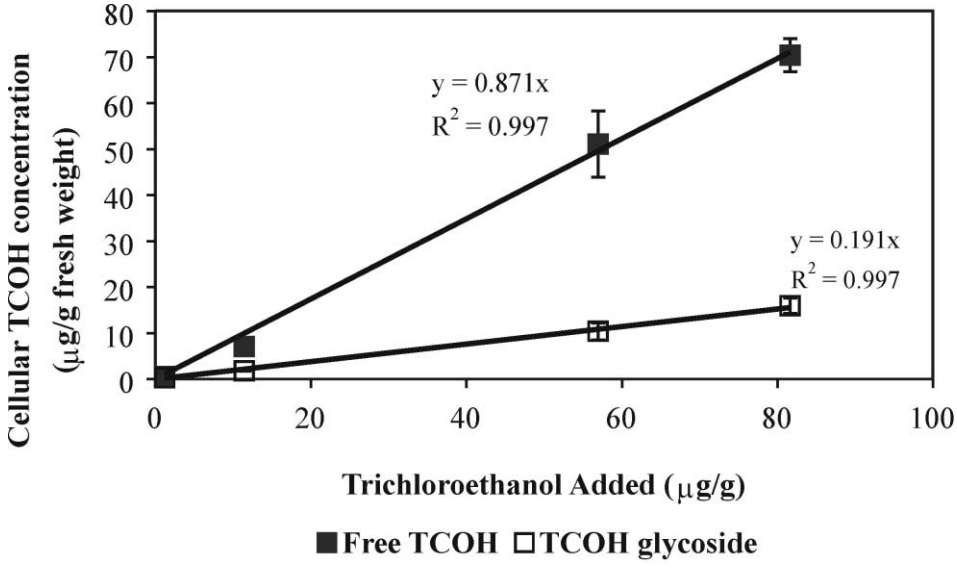

Fig. 6. Trichloroethanol uptake and glycoslation in poplar suspension cell culture. Every datum point is the average of triplicates.

in agreement with the overall range of concentrations reported elsewhere.

3. Concluding remarks

Fig. 7 shows an integrated scheme of the proposed TCE metabolism pathway in plants.

In mammals, detoxification of a xenobiotic substance is described as a three-phase process: oxidation (phase I), conjugation (phase II) and excretion (phase III) (Sandermann, 1994). Sandermann proposed the "green liver" concept to describe the similarity between plant and mammalian detoxification of xenobiotics. Previously, it has been shown that oxidation of TCE leads to similar metabolites in plants to those in mammals. This study

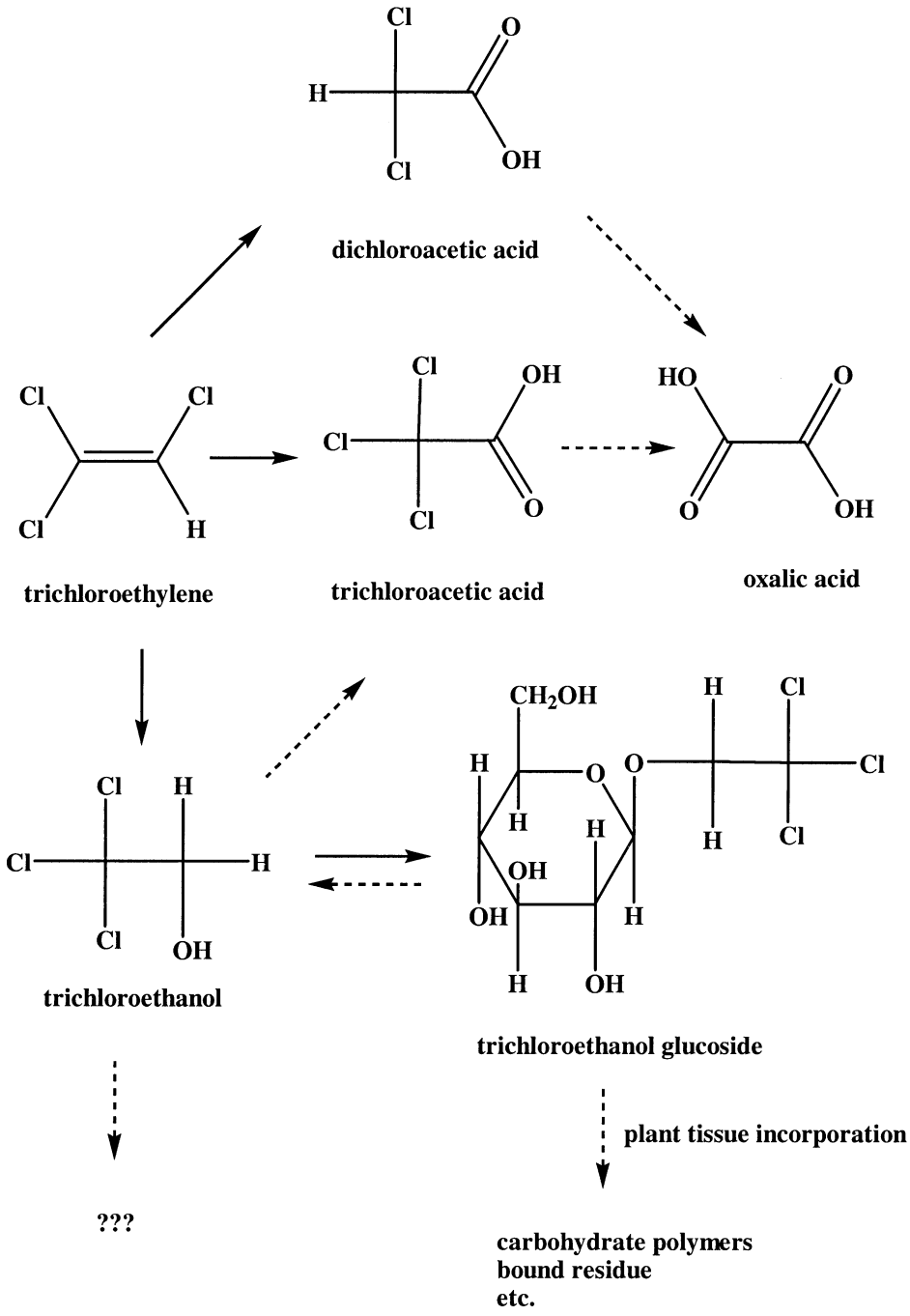

Fig. 7. Proposed scheme of TCE metabolism in higher plants. Solid arrows represent pathways that have been experimentally observed, and dotted arrows represent pathways that are speculated.

shows that one of the oxidation products, trichloroethanol, is conjugated to glucose, a process paralleled in mammals by conjugation to glucuronic acid (Lash et al., 2000). Radiolabel tracer studies showed that some of the radiolabels are transformed to bound residue, possibly incorporated to structural components of the plant. Thus, mammalian metabolism of TCE is closely mirrored in higher plants, adding to a growing body of evidence that support the green liver concept.

4. Experimental

Chemicals and enzymes were purchased from Sigma, St. Louis, MO, unless otherwise noted.

4.1. Plants, cell and tissue culture

Plant species used in this study were tobacco (*Nicotiana tabacum* cv. Xanthii), poplar (*Populus trichocarpa* x *Populus deltoides*), *Atropa belladonna* and *Leuceana leucocephala*.

Poplar suspension cells were prepared by transformation of H11-11 hybrid poplar (P. *trichocarpa* x P. *deltoides*) with *Agrobacterium tumefacien*s strain A281. The resulting callus cells were grown on hormone-free media, and the Agrobacteria were eliminated with antibiotics. Suspension cells were prepared from the callus, and maintained in media containing Murashige and Skoog (MS) basal salts, MS vitamins and 3% sucrose, pH 5.7–5.9. Cells were shaken on an orbital shaker at room temperature at 100 rpm, and were diluted weekly with fresh media.

Tobacco hairy root culture was prepared by inoculating surface sterilized tobacco leaves with 2-day culture of *Agrobacterium rhizogenes* strain R1000. The resulting hairy roots were excised and grown in liquid MS media containing 500 μg/ml cefotaxime to eliminate the Agrobacteria. One root tip was used to establish a clone of hairy root culture, which was maintained in MS media with 3% sucrose without hormones and antibiotics.

4.2. Assay for TCE metabolism

Hydroponic plants were generated by surface-sterilizing the stems in 10% bleach for 12 min and 10% iodophore for 2 min, and rinsing several times in sterile water. Plants were grown in sterile hydroponic solution and treated with TCE. as described in Doty et al. (2000).

Poplar suspension cell cultures were axenic as verified by microscopy and by plating samples of the cells periodically on non-selective media. The cells were grown to at least 0.2 g/ml, and diluted with fresh MS media to approximately 0.06 g/ml. Aliquots of the diluted cells (50 ml) were distributed into 125-ml glass 2-armed Erlenmeyer flasks. The two arms of each flask were sealed with a screw cap with Teflon-lined septum and a screw cap with Teflon mini-nert valve (Pierce, Rockford, IL), respectively. TCE saturated water (~1000 ppm) was chilled on ice to minimize evaporation, and injected with a glass gastight syringe (Hamilton, Reno, NV) through the mini-nert valve. The flasks were shaken at 100 rpm at room temperature for 5 days. Cell suspensions were vacuum filtered, and the cells collected on filter paper were weighed and flash frozen in liquid nitrogen, and stored at −80 °C until analysis.

Hairy roots were grown to a dense stage and transferred to 2-armed Erlenmeyer flasks. TCE treatment was carried out as described above in the case of cell culture. At the end of the 5-day incubation, roots were removed from media and briefly blotted dry on filter paper, weighed and flash frozen in liquid nitrogen, and stored at −80 °C until analysis.

4.3. Assay for TCOH uptake and metabolism

Hydroponic plants, cells and hairy roots were treated with TCOH the same way as in the case of TCE, except the flasks were not air-tight. Loosely fitted screw caps or aluminum foil-covered cotton plugs were used to keep the solutions sterile.

4.4. Determination of TCOH and TCOH-glycoside in plant tissue

The procedures described below were modified from Miller (1941a,b) and Mortimer and Shields (1995). Plant tissue or filtered suspension cells were ground to a powder in liquid nitrogen, then extracted twice with five to ten volumes of acetone. The mixture of plant tissue and acetone was vacuum filtered with a Büchner funnel and Whatman No. 1 filters. The filtrate was reduced in a rotary evaporator at room temperature. After all the acetone was removed, the aqueous extract was clarified by centrifugation at 12,000 rpm for 5 min. The supernatant was divided into two equal aliquots. One aliquot was hydrolyzed with an equal volume of almond ß-glucosidase (1 mg/ml in potassium phosphate buffer at pH 5.0). The other aliquot received an equal volume of the same concentration of BSA as control. The reactions were carried out at 37 °C for 2 h. The reaction mixtures were then transferred to glass centrifuge tubes, and a half volume of 1 N H_2SO_4/10% NaCl solution was added to each tube. The mixture was vortexed for 1 min, and 10 ml methyl-*tert*-butyl ether (MTBE) was added, followed by vortexing (1 min) and centrifugation (6000 rpm, 5 min). The MTBE layer was transferred to a glass vial containing 2 g Na_2SO_4 and dried for 1 h. The MTBE extract was transferred to an autosampler vial and analyzed on GC–ECD. BSA treatments give free TCOH concentrations, and glucosidase treatments lead to total TCOH concentrations (free plus sugar conjugated). Percentage glycosylation values were calculated

as follows: % glycosylation = ([TCOH]$_{total}$–[TCOH]$_{free}$)/([TCOH]$_{total}$)*100.

4.5. Isolation and acetylation of trichloroethanol-glycoside from plant tissue

Plant tissue was ground to a powder in liquid nitrogen, then extracted as described above. After rotary evaporation and centrifugation, the aqueous extract was transferred to a glass flask and washed with MTBE and hexane in a separatory funnel. The washed extract was purged with a gentle stream of nitrogen to remove traces of organic solvents, and lyophilized to a powder. Approximately 50 mg of the powder was weighed into a 10-ml glass vial with a conical bottom and a magnetic stirrer (Reacti-vial, Pierce). Pyridine (1 ml) was added to dissolve the powder, followed with the addition of 0.5 ml acetic anhydride (Fisher Scientific, Houston, TX). The mixture was stirred at room temperature for 2 h. The acetylated glycoside was precipitated by addition of 10 ml ice cold water and centrifugation (8000 rpm, 10 min). After removal of the supernatant, the pellet was dissolved in 1 ml acetone, dried with anhydrous Na_2SO_4, and analyzed with GC-MS.

4.6. Synthesis of trichloroethanol-glucoside tetra-acetate

The synthesis was modified from Miller (1941b). In a 125-ml glass flask, 6.4 ml 2,2,2-trichloroethanol was dissolved in 30 ml benzene and cooled on ice. 5 g 2,3,4,6-Tetra-*O*-acetyl-D-glucopyranosyl bromide (Arcos, Fisher Scientific) and 4.5 g silver carbonate was added, and the mixture was allowed to stand on ice for 3 h, and was shaken frequently. The mixture was then allowed to stand at room temperature overnight. The remaining solids were removed by filtration, and washed with benzene. The filtrate was evaporated in vacuo. After the removal of benzene, the resulting syrup was washed with water, and dissolved in absolute ethanol for GC–MS analysis.

4.7. Gas chromatography–mass spectrometry (GC-MS)

ECNCI–MS and EI–MS were performed on Finnigan Trio 1000 (ThermoQuest Corp., San Jose, CA) and Micromass Trio 2000 (Micromass Ltd, Manchester, UK) quadrupole mass spectrometers, respectively. Each instrument was directly interfaced to an Hewlett-Packard 5890 gas chromatograph (Agilent Technologies, Palo Alto, CA) fitted with a J&W DB-5 (J&W Scientific, Rancho Cordova, CA) fused-silica capillary gas chromatographic column (30 m×0.32 mm I.D., 0.25 m film thickness) and operated with helium as carrier gas (head pressure, 5 psi).

The ionization conditions for the respective instruments were as follows: ECNCI using methane as a moderating gas (~1 mbar), with a filament emission current and electron energy of 100 μA and 75 eV respectively; and EI with an emission and energy of 200 μA and 70 eV, respectively. The ion source temperatures in both cases were 200 °C with the GC/MS interfaces held at 250 °C.

4.8. Gas chromatography–electron capture detection (GC–ECD)

Routine GC–ECD analysis of trichloroethanol and other chlorinated metabolites was performed with a Perkin Elmer autosystem gas chromatograph (Perkin Elmer, Norwalk, CT) with a Restek (Restek Corp., Bellefonte, PA) XTI-5 column (30 m×0.25 mm I.D.,1 m film thickness).

Acknowledgements

This publication was made possible by grant No. P42ES04696 from the National Institute of Environmental Health, NIH with funding provided by EPA.

References

Anderson, T.A., Walton, B.T., 1994. Comparative fate of [^{14}C] trichloroethylene in the root zone of plants from a former solvent disposal site. Eniviron. Toxicol. Chem. 14 (12), 2041–2047.

Colemann, J.D., Blake-Klaff, M.M.A., Davis, T.G.E., 1997. Detoxification of xenobiotics by plants: chemical modification and vacuolar compartmentation. Trends Plant Sci. 2 (4), 144–151.

Dormaar, J.F., Willms, W.D., 1990. Effect of grazing and cultivation on some chemcial properties of soils in the mixed prairie. J. Range Manage. 43 (5), 456–460.

Doty, S.L., Shang, T.Q., Wilson, A.M., Tangen, J., Westergreen, A.D., Newman, L.A., Strand, S.E., Gordon, M.P., 2000. Enhanced metabolism of halogenated hydrocarbons in transgenic plants containing mammalian cytochrome P450 2E1. Proc. Nat. Acad. Sci. 97 (12), 6287–6291.

Doucette, W.J., Bugbee, B., Hayhurst, S., Plaehn, W.A., Downey, D.C., Taffinder, S.A., Edwards, R., 1998. Phytoremediation of dissolved-phase trichloroethylene using mature vegetation. In: Wickramanayake, G.B., Hinchee, R.E. (Eds.), Bioremediation and Phytoremediation: Chlorinated and Recalcitrant Compounds. Battelle Press, Columbus.

Ensley, B.D., 1991. Biochemical diversity of trichloroethylene metabolism. Annu. Rev. Microbiol. 45, 283–299.

Lamoureux, G.L., Rusness, D.G., 1986. Xenobiotic conjugation in higher plants. In: Paulson, G.D., Caldwell, J., Huston, D.H., Menn, J.J. (Eds.), ACS Symposium Series 299. American Chemical Society, Washington, DC.

Lash, L.H., Fisher, J.W., Lipscomb, J.C., Parker, J.C., 2000. Metabolism of Trichloroethylene. Environ. Health perspect. 108 (supplement 2), 177–200.

Miller, L.P., 1941a. Formation of β-2,2,2-trichloroethyl-gentiobioside in tomato plants grown in media containing chloral hydrate, trichloroethyl alcohol, or chloral cyanohydrin. Contrib. Boyce Thompson Inst. 12, 15–23.

Miller, L.P., 1941b. Fate of chloral hydrate absorbed by growing plants of lagenaria leucantha. Contrib. Boyce Thompson Inst. 12, 167–169.

Moore, M.M., Harrington-Brock, K.H., 2000. Mutagenicity of trichloroethylene and its metabolites: implications for the risk assessment of trichloroethylene. Envrion. Health Perspect 108 (supplement 2), 215–233.

Mortimer, R.D., Shields, J.B., 1995. Total, free and glucose-conjugated acid metabolites from permethrin and cypermethrin in foods by gas chromatography-electron capture detection. J. AOAC Intl. 78 (5), 1302–1307.

Narayanan, M., Davis, L.C., Erickson, L.E., 1995. Fate of volatile chlorinated organic compounds in a laboratory chamber with alfalfa plants. Environ. Sci. Technol. 29 (9), 2437–2444.

Newman, L.A., Strand, S.E., Choe, N., Duffy, J., Ekuan, G., Ruszaj, M., Shurtleff, B.B., Wilmoth, J., Heilman, P., Gordon, M.P., 1997. Uptake and biotransformation of trichloroethylene by hybrid poplars. Environ. Sci. Technol. 31 (4), 1062–1067.

Newman, L.A., Wang, X., Muiznieks, I.A., Ekuan, G., Ruszaj, M., Cortellucci, R., Domroes, D., Karscig, G., Newman, T., Crampton, R.S., Hashmonay, R.A., Yost, M.G., Heilman, P.E., Duffy, J., Gordon, M.P., Strand, S.E., 1999. Remediation of TCE in an artificial aquifer with trees: a controlled field study. Environ. Sci. Technol. 33 (13), 2257–2265.

Orchard, B.J., Doucette, W.J., Chard, J.K., Bugbee, B., 2000. Uptake of TCE by hybrid poplar trees grown hydroponically in flow through plant growth chambers. Environ. Toxicol. Chem. 19 (4), 895–903.

Sandermann, H., 1994. Higher plant metabolism of xenobiotics: the 'green liver' concept. Pharmacogenetics 4, 225–241.

Schnabel, W.E., Dietz, A.C., Burken, J.G., Schnoor, J.L., Alvarez, P.J., 1997. Uptake and transformation of trichloroethylene by edible garden plants. Wat. Res. 31 (4), 816–824.

Schroll, R., Bierling, B., Cao, G., Dorfler, U., Lahaniati, M., Langenbach, T., Scheunert, I., Winkler, R., 1994. Uptake pathways of organic chemicals from soil by agricultural plants. Chemosphere 28 (2), 297–303.

PERGAMON

Phytochemistry 58 (2001) 1067–1072

PHYTOCHEMISTRY

www.elsevier.com/locate/phytochem

Response of prostaglandin content in the red alga *Gracilaria verrucosa* to season and solar irradiance

Andrey B. Imbs*, Anna V. Vologodskaya, Natalia V. Nevshupova, Svetlana V. Khotimchenko, Edouard A. Titlyanov

Institute of Marine Biology, Far East Branch, Russian Academy of Sciences, 690041 Vladivostok, Russia

Received 9 April 2001; received in revised form 13 July 2001

Abstract

The influence of solar irradiance and seasons on prostaglandin (PG) and arachidonic acid (AA) content in the marine red alga *Gracilaria verrucosa* (Huds.) Papenf. (unattached form) was investigated. PGA_2, PGE_2, PGF_2, and 15-keto-PGE_2 were isolated from the alga, quantitatively analyzed as 4-methyl-7-methoxycoumarin esters by high-performance liquid chromatography, and their chemical structures were confirmed by ^1H NMR. In June–September, the PG content in the alga was relatively stable (420 μg/g of dry wt. of $PGE_2 + PGF_2$; 40 μg/g of PGA_2) and it increased 1.5 times in October. The highest level of PGs was detected in November (2500 μg/g of $PGE_2 + PGF_2$; 74 μg/g of PGA_2) when water temperature was fairly low (5–10 °C). Algae grown for five months at 50% of incident photosynthetic active radiation (PAR_0) contained two times less PGE_2 and PGF_2 than algae grown under natural conditions, but the amount of these PG in algae grown at 5% of PAR_0 was close to the normal level. On the contrary, when algae were grown at 5% of PAR_0 the content of PGA_2 increased up to 4 times compared to algae cultivated at 100% PAR_0. In June–November, the amount of AA in total algal lipids slightly varied from 48.9 to 56.7% and did not virtually depend on the light intensity. The probable reasons of the PG content variation in response to environmental factors are discussed. © 2001 Elsevier Science Ltd. All rights reserved.

Keywords: *Gracilaria verrucosa*; Solar irradiance; Environmental conditions; High-performance liquid chromatography; Gas chromatography; NMR; Prostaglandins; Arachidonic acid; 4-Bromomethyl-7-methoxycoumarin

1. Introduction

Red algae are rich in polyunsaturated fatty acids (PUFA) with 20 carbon atoms, mainly arachidonic (AA) and eicosapentaenoic acids, which are precursors of prostaglandins (PG). It has been demonstrated that marine plants are capable of metabolizing C_{20} PUFA to eicosanoids via various oxidative pathways. Oxidized fatty acid derivatives were isolated from fairly many species of Rhodophyta (Gerwick and Bernart, 1993). Algae of the genus *Gracilaria*, as well as *Gracilariopsis*, are of particular interest because they contain eicosanoids characteristic of the higher plants and human. Acyclic eicosanoids such as 12-HETE and 12-HEPE were found in *Gracilariopsis lemeneiformis* (Jiang and Gerwick, 1991). Two isomers of LTB_4 (6-*trans*-LTB_4 and 6-*trans*-12-*epi*-LTB_4,) as well as 8-HETE were detected in *Gracilaria asiatica* (Sajiki and Kakimi, 1998; Sajiki, 1999). However, members of the genus *Gracilaria* are distinguished from other red algae by that they contain PG. Thus, PGE_2 and PGF_2 were isolated from *Gracilaria lichenoids* (Gregson et al., 1979); PGE_2 and 15-keto-PGE_2 were found in *G. asiatica* (Sajiki, 1999). *Gracilaria verrucosa* was found to contain PGA_2 in addition to PGE_2; however, its presence in the alga may be a consequence of partial non-enzymatic dehydration of PGE_2 (Fusetani and Hashimoto, 1984). These PG from Japanese *G. verrucosa* appear to be responsible for a gastro-intestinal disorder, known as ''ogonori'' poisoning, which is associated with ingestion of the popular edible seaweeds in Japan (Fusetani and Hashimoto, 1984).

The most widespread *G. verrucosa* in the Sea of Japan is the attached form of alga growing on a rocky substrate. However, there is an unattached form of the same species found in lagoons, which differs from the

* Corresponding author. Tel.: +7-4232-310905; fax: +7-4232-310900.

E-mail address: andreyimbs@hotmail.com (A.B. Imbs).

0031-9422/01/$ - see front matter © 2001 Elsevier Science Ltd. All rights reserved.
PII: S0031-9422(01)00321-1

attached form by that it reproduces asexually, by fragmentation (Tityanova et al., 1990). The unattached form contains much more agar and twice as much lipids as the attached one (Lapshina et al., 1993; Khotimchenko and Levchenko, 1997).

The aim of the present study was to determine the PG composition and the influence of environmental factors such as season and solar irradiance on the PG content in the unattached form of *G. verrucosa*. In addition, we have investigated the relation between contents of AA and PG in this alga.

2. Results and discussion

2.1. Identification of PG in the alga and optimization of HPLC analytical method

We identified prostaglandins PGA_2, PGE_2, PGF_2, and 15-keto-PGE_2 as major eicosanoids in the unattached form of red alga *G. verrucosa*. The presence of these compounds in the form of methyl esters was confirmed by co-chromatography with the authentic PG standards using TLC and HPLC. It was shown that at least 25 mg PGE_2 methyl ester, 8 mg 15-keto-PGE_2 methyl ester, and 20 mg PGF_2 methyl ester can be isolated from 1 kg of fresh *G. verrucosa* using a combination of chromatographic methods (Nevshupova and Imbs, 1999). The structure of PGE_2, PGF_2, and 15-keto-PGE_2 was unequivocally proved by analysis of their ^{1}H NMR spectra which were identical to those of authentic PG methyl esters and the spectra reported previously (Schneider et al., 1977; Fusetani and Hashimoto, 1984). Unfortunately, the quantity of obtained PGA_2 methyl ester was not sufficient for correct NMR analysis. The presence of PGF_2 in the attached form of *G. verrucosa* has not been reported in recent works (Sajiki and Kakimi, 1998; Sajiki, 1999).

To determine the quantity of PG in *G. verrucosa* samples, we applied the HPLC analysis of their 4-bromomethyl-7-methoxycoumarin (BrMMC) derivatives. Firstly, a semi-preparative amount of BrMMC derivatives of individual PGB_2, PGD_2, PGA_2, PGE_2, and $PGF_{2\alpha}$ was synthesized with a yield more than 80%. We applied the reaction between organic acid salt and BrMMC in the presence of a phase-transfer catalyst in non-aquiver solvent as described earlier (Tsuchiya et al., 1982; Berger and Petz, 1991) with some variances. Acetonitrile usually used as the solvent was partly replaced with chloroform to increase the solubility of BrMMC and the lipid extract of *G. verrucosa*. The optimum temperature was 50–55 °C and time 50–60 min. The structure of the synthesized compounds was confirmed by the ^{1}H NMR analysis. As an example, the structure of (4′-methylene-7′-methoxycoumarin)-PGA_2 ester (**1**) and selected ^{1}H NMR signal assignments (Table 1) are presented. The spectrum showed a terminal methyl signal at δ 0.89 (*t*), one carbinol methine at δ 4.09 (*m*), three sets of double bound at δ 5.40, 5.43, 5.61, 5.70, and a methylene adjacent to a carboxyl group at δ 2.32. The values of 5, 6, and 16 Hz coupling constants are typical of the $\Delta5(Z)$ and $\Delta13(E)$ olefin functionalities. A set of double bound at δ 6.18, 7.50 suggested the presence of α,β-unsaturated cyclopentenone. These features were quite similar to those of PGA_2 ester. The spectrum also showed signals of four coumarin protons at δ 6.33, 6.84, 6.99, 7.42 and a methoxy group at δ 3.66 (*s*) (Table 1). The ^{1}H NMR spectra of other synthesized compounds contained the described signals of the methylmethoxycoumarin group and signals similar to ^{1}H NMR shifts of PG esters published elsewhere (Schneider et al., 1977; Chen and Janda, 1997, 1998; Mikolajczyk et al., 2000).

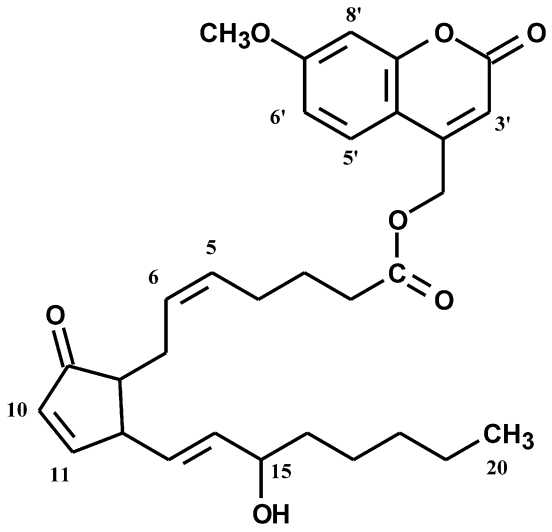

1

An isocratic reversed-phase HPLC separation of the BrMMC derivatives of the five synthesized PG was achieved within 30 min in a single run. The peaks of esters were completely resolved when a 25-cm column was used. With a 15-cm column, the resolution of PGE_2 and PGF_2 was poorer, but the analysis time was reduced to 16 min. As a rule, we determined the sum of PGE_2 and PGF_2 because many tests on a 25-cm column showed that the amount of PGE_2 related to that of PGF_2 as 25:10 and this value was quite stable in all experiments.

Fusetani and Hashimoto (1984) successfully used hot methanol to extract PG from *G. verrucosa*. Our experiments showed that the heating time strongly influences the content of PG in the prepared extract. The maximum content of PG was isolated from alga after 5 min heating, but the PG level fell drastically after 1 h heating (Table 2). A temporary increase in the amount of PGA_2 in 30 min was most likely caused by non-enzymatic

Table 1
Selected ^{1}H NMR spectra assignments for (4′-methylene-7′-methoxycoumarin)PGA_2 ester (**1**) (250 MHz, $CDCl_3$)

H	δ (ppm/TMS)	J (Hz)
3	6.33 *t*	1.5
5	7.42 *d*	9.5
6	6.99 *d*	2.5
8	6.84 *s*	
2	2.32 *t*	7
3	1.87 *m*	
4	2.09 *m*	
5	5.40 *t*	5
6	5.43 *t*	5
10	7.50 *dd*	6, 2
11	6.18 *dd*	6, 2
13	5.61 *dd*	16, 6
14	5.70 *dd*	16, 6
15	4.09 *m*	
OMe	3.66 *s*	
17,18,19	1.20–1.35 *m*	
20	0.89 *t*	6

Table 2
Changes in the prostaglandins content in methanol extract of *G. verrucosa* (unattached form) at heating (55 °C)

Heating time (min)	Content of prostaglandins in algal extract (μg/g dry wt.)		
	15-keto-PGE_2	$PGE_2 + PGF_2$	PGA_2
5	90	398	40
30	47	307	78
60	14	115	22

dehydratation of PGE_2. A long-period soaking of *G. verrucosa* (up to 48 h) in methanol at room temperature recovered PG with a very low yield. The classic method of total lipids extraction with chloroform–methanol was not suitable because of chromatographic difficulties in detecting extremely low levels of PG in algal total lipid extract.

It should be noted that our attempts at the direct HPLC analysis of crude reaction mixture after derivatization with BrMMC were unsuccessful. To remove an excess of BrMMC and non-polar substances, we purified BrMMC derivatives on a solid-phase extraction tube with silica gel. All PG esters were quantitatively recovered from the tube without appreciable losses.

Thus, high-performance liquid chromatography of the BrMMC derivatives of PG has proven to be a powerful method for the analysis of eicosanoids in marine algae. Using this method, we obtained new data on the variation of *G. verrucosa* PG content in relation to season and light intensity.

2.2. Changes of PG and AA content related with seasons and solar irradiance

In the lagoons of southern Primorye, the unattached form of *G. verrucosa* begins to grow in May. Growth is highest in July–August; in September–October it is markedly retarded, and fragmentation of the thalli commences. In December–March, alive alga winters frozen into the ice (Tityanova et al., 1990).

In June–September 1999, the unattached form of *G. verrucosa* did not show significant differences in the levels of 15-keto-PGE_2, PGE_2, and PGF_2 but there were higher levels of the PG in algae collected in October (Table 3). The highest level of the above PG was detected in November when water temperature is relatively low (5–10 °C). In contrast, no significant difference ($P > 0.05$) in the PGA_2 content of *G. verrucosa* was found in June-November (Table 3). Measurements of the levels of PG in *G. verrucosa* were repeated at the next year (2000) and the results did not differ significantly ($P < 0.05$, data not shown). Recently, an appreciable increase in the PGF_2 level in February compared to July was described for the attached form of *G. asiatica* growing in the Bay of Tokyo, Sea of Japan (Sajiki, 1997).

A variety of factors can be responsible for the accumulation of PG in the cold season: environmental conditions (solar irradiance, seawater temperature, contents of dissolved components, etc.), level of the PG biosynthesis substrate (arachidonic acid) in algal tissues, activity of enzymes of eicosanoid synthesis, stage of life cycle, and others.

We found that the level of PG in the unattached form of *G. verrucosa* depends on solar irradiation. The content of PG in algae cultivated during 5 months under

Table 3
Changes in the content of prostaglandins (μg/g dry wt.) in *G. verrucosa* (unattached form) during June–November

Prostaglandin	Collection time				
	June	July	September	October	November
15-keto-PGE_2	90 ± 6^a	86 ± 18^a	120 ± 42^a	$231 \pm ^b$	306 ± 18^c
$PGE_2 + PGF_2$	398 ± 21^a	413 ± 45^a	429 ± 64^a	640 ± 43^b	2468 ± 112^c
PGA_2	40 ± 4^a	47 ± 14^a	46 ± 12^a	67 ± 17^a	74 ± 4^a

Data are mean ± S.D. of triplicates. Different superscript letters in the same measurements are significantly different ($P < 0.01$) among the same prostaglandin.

Table 4
Changes in the content of prostaglandins (μg/g dry wt.) in *G. verrucosa* (unattached form) grown during June-October at various levels of photosynthetic active radiation (PAR_0)

Prostaglandin	PAR_0		
	95%	50%	5%
15-keto-PGE_2	231 ± 3^a	113 ± 12^b	213 ± 15^a
PGE_2+PGF_2	640 ± 43^a	332 ± 52^b	496 ± 1^c
PGA_2	67 ± 17^a	122 ± 20^b	226 ± 27^c

Data are mean ± S.D. of triplicates. Different superscript letters in the same measurements are significantly different ($P<0.05$) among the same prostaglandin.

different light intensity are shown in Table 4. The amount of 15-keto-PGE_2, PGE_2, and PGF_2 in algae exposed to 50% of incident photosynthetic active radiation (PAR_0) was about half that of the control sample ($P<0.01$), but the quantity of 15-keto-PGE_2 was relatively stable and the level of PGE_2 and PGF_2 were slightly lower ($P<0.05$) in algae grown under extremely low illumination conditions (5% PAR_0). On the contrary, the decreasing light intensity led to a consistent increase in PGA_2 in the algae ($P<0.05$). Hence, it is highly improbable that the reduced solar irradiance in October-November can cause the observed high level of main PG (except for PGA_2) in *G. verrucosa* in the cold period. Conceivably, the mechanism of formation of PGA_2 in *G. verrucosa* differs from that of the other PG, and part of PGA_2 originated from PGE_2 by a non-enzymatic process which intensified under adverse environmental conditions.

The changes in the fatty acid composition of a number of *Gracilaria* species cultivated under different environmental conditions were previously investigated, and it was shown that the arachidonic acid is the dominant fatty acid (Khotimchenko and Levchenko, 1997). Our data on *G. verrucosa* are indicative only of a slight increase in AA content (Table 5) in total algal lipids in the cold period, as well as under reduced solar irradiance (data not shown), and confirm the conclusion that the increase in AA content due to low temperature and low light intensity, which has been demonstrated in higher plants, is not consistent in *G. verrucosa* (Dawes et al., 1993).

Table 5
Content of arachidonic and eicosapentaenoic acids (% of total fatty acids) in *G. verrucosa* (unattached form) in June–November

Collection time	Content of fatty acids (%)		Seawater temperature (°C)
	Arachidonic	Eicosapentaenoic	
June	48.9	0.9	17
July	49.2	1.1	20
August	46.6	0.5	22
September	49.6	0.5	18
October	45.9	5.5	10
November	56.7	1.6	5

There was only a slight increase in AA content in November which did not correlate with a 6-fold rise in PG amount in the alga. On the other hand, the inhibition of PG synthesis in *G. verrucosa* by a high level of AA was postulated earlier (Sajiki, 1997). Thus, it is improbable that the seasonal changes in PG content in the unattached form of *G. verrucosa* were regulated by the AA level in algae lipids.

It is also unlikely that the total level of PG in *G. verrucosa* is dependent on the mode of reproduction because both the attached form, which reproduces sexually, and the unattached form, which reproduces vegetatively way, have markedly higher PG content in the summer than in the winter.

It should be noted that the PG content in the attached form of *G. verrucosa* collected at the same site was twice lower (207 ± 14 μg/g dry wt. of PGE_2+PGF_2, July sample) compared to the unattached one. This difference in PG content can be attributed to that the unattached form of the alga synthesized and accumulated twice as much lipids as the attached one, 5.6 and 2.8 mg/g, respectively (Khotimchenko and Levchenko, 1997).

The major lipid classes of *Gracilaria* that contain AA are monogalactosyldiacylglycerol (75% of AA), and phosphatidylcholine (73% of AA) (Araki et al., 1990). Since neither phospholipase A_1 nor A_2 activity was detected in raw alga (Sajiki, 1997), the splitting-off of arachidonic acid by acylhydrolases from monogalactosyldiacyl glycerol can be considered as a probable source of the substrate for PG synthesis in *G. verrucosa*. In this event, the PG level in *G. verrucosa* can be modulated through regulation of the activity of acylhydrolases or enzymes of the AA oxidation cascade.

It is most likely that the increased PG level in *G. verrucosa* is a response to decreased water temperature in the fall-winter period and it is not related to reduced solar irradiance. *G. verrucosa* is the rare algal species that contains PG and the level of PUFA in this alga is little dependent on water temperature, so we can postulate that PG may be involved in processes allow the algal tissue to survive in cold water and ice.

3. Experimental

3.1. Study site and sampling

Samples of *G. verrucosa* (unattached form) were collected during June–November 1999 in lagoons of southern Primorye (Peter the Great Bay, the Sea of Japan). Algae were grown in lagoons by the method of "rope culture" (Titlyanov et al., 1995) from June through October under natural light at 95% of incident

photosynthetic active radiation (PAR_0). Irradiance level was maintained using neutral density filters (50 and 5% PAR_0) and determined with an LI-190SA flat quantum sensor (LI-Cor, Lincoln, Nebraska). All samples were immediately frozen and stored at −20 °C not more than 1 week before analysis.

3.2. Isolation of PG methyl esters from G. verrucosa

Frozen alga (347 g) was extracted with $CHCl_3$–MeOH (1:2), the total lipid extract (730 mg) was redissolved in 10 ml of Et_2O, and 20 ml of saturated solution of diazamethane in Et_2O at 0 °C was added to obtain carboxylic acid methyl esters. After 1 h, the solution was evaporated and the residue was separated by low pressure silica gel column chromatography with gradient from $CHCl_3$ to MeOH. Fractions containing total PG methyl esters were additionally separated using a gradient of C_6H_6–EtOAc. Finally, pure PGE_2 methyl ester (9 mg), 15-keto-PGE_2 methyl ester (3 mg) and PGF_2 methyl ester (7 mg) were isolated by preparative HPLC with MeOH–H_2O (4.5 ml min^{-1}) on a Zorbax ODS column (25 cm×9.4 mm i.d.) with a refractive index detector. TLC of the obtained PG methyl esters was carried out on silica gel plates with C_6H_6–EtOAc (1:1); analytical HPLC was performed on a Zorbax ODS column (25 cm×4.6 mm i.d.) with UV detectors (200 nm) in MeOH–H_2O (65:35) at a flow rate of 1 ml min^{-1}. ^1H NMR spectra of PG esters were recorded at 250 MHz in $CDCl_3$.

3.3. Synthesis of 4′-methylen-7′-methoxycoumarin esters of PG

The work solutions of 21 mg dicyclohexyl-18-crown-6 (DCHC) in 0.2 ml CH_3CN and 15 mg 4-bromomethyl-7-methoxycumarin (BrMMC) in a mixture of 0.1 ml CH_3CN and 0.9 ml $CHCl_3$ were prepared. 1 mg PG was transferred with 0.1 ml $CHCl_3$ into a 1 ml reaction vial with a screw cap. After adding 0.05 ml of the DCHC solution, 0.2 ml of the BrMMC solution, and 0.1 g K_2CO_3, the PG reacted for 1 h at 55 °C. The reaction mixture was filtered, evaporated, and the PG ester was purified by TLC in $CHCl_3$–MeOH (9:1). BrMMC derivatives of PGB_2, PGD_2, PGA_2, PGE_2, and $PGF_{2\alpha}$ were synthesized. ^1H NMR spectra of PG derivatives were recorded at 250 MHz in $CDCl_3$.

3.4. Analysis of the PG content in G. verrucosa

About 120 g of freshly frozen alga were homogenized with 200 ml of MeOH, heated to 60C, and after 5 min filtered under vacuum. The solution was evaporated to a volume of 50 ml, acidified to pH 2, and extracted twice with 50 ml of EtOAc. Evaporation to dryness of combined extracts resulted in 97 mg of polar lipids. About 30 mg of the polar lipids were transferred with 0.2 ml $CHCl_3$ into a 1 ml reaction vial with a screw cap. After adding 0.1 ml CH_3CN, 0.05 ml of the DCHC solution, 0.2 ml of the BrMMC solution, and 0.2 g of K_2CO_3, the mixture was heated at 55 °C for 1 h. The reaction mixture was filtered, dried, dissolved in C_6H_6–EtOAc (85:15), and placed on a 3 ml solid-phase extraction tube with silica gel. The tube was washed with 2 ml of the same system, then the crude PG esters were eluted with 3 ml $CHCl_3$–MeOH (1:1). The last fraction was evaporated, solved in 0.2 ml MeOH and a 10 μl portion was analyzed by HPLC on a Zorbax ODS column (15 cm×4.6 mm i.d.) with a UV detector at 313 nm. An isocratic system of MeOH–H_2O (70:30) at a flow rate of 1.5 ml min^{-1} was used. The quantity of PG esters was calculated using calibration graphs of peak areas of PG esters standards synthesized previously.

3.5. Fatty acid (FA) analysis

Lipids were extracted according to Bligh and Dyer (1959). Fatty acid methyl esters (FAME) of total lipids were prepared according to Carreau and Dubacq (1979) and purified by TLC in C_6H_6. Analysis of FAME was carried out on a GC equipped with a flame-ionization detector, a fused quartz capillary column (30 m×0.25 mm i.d.) with Supelcowax 10M; split ratio 1:30, carrier gas He (1 ml min^{-1}). The column and detector temp was 210°, the injector temp was 240°. Identification of FAME was confirmed by chromatographic comparison with authentic standards and calculation of ECL (Christie, 1988).

3.6. Statistical analysis

Statistical analysis of the data was carried out as described elsewhere (Friedlander et al., 1993). Significant differences were located using Duncan's new multiple range test (one-way ANOVA's) and Student's *t*-test.

Acknowledgements

This work was supported by the Russian Foundation for Basic Research, project 98-03-32892. The authors want to thank T.N. Koznova for her translating of the manuscript.

References

Araki, S., Sakurai, T., Oohusa, T., Kayama, M., Nisizawa, K., 1990. Content of arachidonic and eicosapentaenoic acids in polar lipids from *Gracilaria* (Gracilariales, Rhodophyta). Hydrobiologia 204, 513–519.

Berger, K., Petz, M., 1991. Fluorescence HPLC determination of penicillins using 4-bromomethyl-7-methoxycoumarin as pre-column labelling agent. Deutsche Lebensmittel-Rundschau 87, 137–141.

Bligh, E.G., Dyer, W.J., 1959. A rapid method of total lipid extraction and purification. Can. J. Biochem. Physiol. 37, 911–917.

Carreau, J.P., Dubacq, J.P., 1979. Adaptation of macro-scale method to the micro-scale for fatty acid methyl transesterification of biological lipid extracts. J. Chromatogr. 151, 384–390.

Chen, S.Q., Janda, K.D., 1997. Synthesis of prostaglandin E-2 methyl ester on a soluble- polymer support for the construction of prostanoid libraries. J. Am. Chem. Soc. 119, 8724–8725.

Chen, S.Q., Janda, K.D., 1998. Total synthesis of naturally occurring prostaglandin F-2 alpha on a non-cross-linked polystyrene support. Tetrahedron Lett. 39, 3943–3946.

Christie, W.W., 1988. Equivalent chain-lengths of methyl ester derivatives of fatty acids on gas chromatography. J. Chromatogr. 447, 305–314.

Dawes, C.J., Kovach, C., Friedlander, M., 1993. Exposure of *Gracilaria* to various environmental conditions. II. The effect on fatty acid composition. Botanica Marina 36, 289–296.

Friedlander, M., Dawes, C., Levy, I., 1993. Exposure of *Gracilaria* to various environmental conditions. II. The effect of growth. Botanica Marina 36, 283–288.

Fusetani, N., Hashimoto, K., 1984. Prostaglandin E_2 — a candidate for causative agent of ogonori poisoning. Bull. Jpn. Soc. Sci. 50, 465–469.

Gerwick, W.H., Bernart, M.W., 1993. Eicosanoids and related compounds from marine algae. Marine Biotechnology 1, 102–152.

Gregson, R.P., Marwood, J.F., Quinn, R.J., 1979. The occurrence of prostaglandins PGE2 and PGF2-alfa in a plant—the red alga *Gracilaria lichenoides*. Tetrahedron Lett. 46, 4505–4506.

Jiang, Z.D., Gerwick, W.H., 1991. Eicosanoids and other hydroxylated fatty acids from the marine alga *Gracilariopsis lemaneiformis*. Phytochemistry 30, 1187–1190.

Khotimchenko, S.V., Levchenko, E.V., 1997. Lipids of the red alga *Gracilaria verrucosa* (Huds.) Papenf. Botanica Marina 40, 541–545.

Lapshina, A.A., Belokopytov, S.V., Ivanova, E.G., Tityanov, E.A., 1993. Agar concentration and properties in the unattached form of *Gracilaria verrucosa* depending on thalli growth intensity and habitat conditions. Russian J. Marine Biology 5-6, 107–117.

Mikolajczyk, M., Mikina, M., Jankowiak, A., 2000. A novel synthesis of racemic and enantiomeric forms of prostaglandin B-1 methyl ester. Journal of Organic Chemistry 65, 5127–5130.

Nevshupova, N.V., Imbs, A.B., 1999. Prostaglandin composition of red alga *Gracilaria verrucosa*. Russian J. Marine Biology 25, 142–143.

Sajiki, J., 1997. Effects of acetic acid treatment on the concentrations of arachidonic acid and prostaglandin E2 in the red algae, *Gracilaria asiatica* and *G. rhodocaudata*. Fisheries Sci. 63, 128–131.

Sajiki, J., Kakimi, H., 1998. Identification of eicosanoids in the red algae, *Gracilaria asiatica*, using high-performance liquid chromatography and electrospray ionization mass spectrometry. J. Chromatogr. 795, 227–237.

Sajiki, J., 1999. Acid treatment increased leukotriene B4 in the red alga, *Gracilaria asiatica* (= *verrucosa*). Fisheries Sci. 65, 914–918.

Schneider, W.P., Bundy, G.L., Lincoln, F.H., Daniels, E.G., Pike, J.E., 1977. Isolation and chemical convertions of prostaglandins from *Plexaura homomalla*: preparation of prostaglandin E_2, prostaglandin $F_2\alpha$, and their 5,6-*trans* isomers. J. Am. Chem. Soc. 99, 1222–1232.

Tityanova, T.V., Titlyanov, E.A., Kozmenko, V.B., 1990. Unattached form of *Gracilaria verrucosa* in lagoons of the southern Primorye. Russian J. Marine Biology 15, 45–50.

Titlyanov, E.A., Tityanova, T.V., Skriptsova, A.V., 1995. First experimental cultivation of unattached form of an agariferous alga *Gracilaria* in Russia. Russian J. Marine Biology 21, 146–156.

Tsuchiya, H., Hayashi, T., Naruse, H., Takagi, N., 1982. Sensitive high-performance liquid chromatographic method for prostaglandins using a fluorescence reagent, 4-bromomethyl-7- acetoxycoumarin. J. Chromatogr. 231, 247–254.

PERGAMON

Phytochemistry 58 (2001) 1073–1081

PHYTOCHEMISTRY

www.elsevier.com/locate/phytochem

Potential allelochemicals from *Sambucus nigra*

Brigida D'Abrosca[a], Marina DellaGreca[b], Antonio Fiorentino[a,*], Pietro Monaco[b], Lucio Previtera[b], Ana M. Simonet[c], Armando Zarrelli[b]

[a]*Dipartimento di Scienze della Vita, II Università di Napoli, via Vivaldi 43, I-81100, Caserta, Italy*
[b]*Dipartimento di Chimica Organica e Biochimica, Università Federico II, Complesso Universitario Monte S. Angelo, via Cinthia, I-80126 Napoli, Italy*
[c]*Departamento de Química Orgánica, Facultad de Ciencias, Universidad de Cádiz, Apdo. 40, 11510 Puerto Real, Cádiz, Spain*

Received 11 June 2001; received in revised form 5 September 2001

Abstract

Twenty-four aromatic metabolites belonging to cyanogenins, lignans, flavonoids, and phenolic glycosides were obtained from *Sambucus nigra*. Structures were determined on the basis of their spectroscopic features. Two compounds have been isolated and identified as (2*S*)-2-*O*-β-D-glucopyranosyl-2-hydroxyphenylacetic acid and benzyl 2-*O*-β-D-glucopyranosyl-2,6-dihydroxybenzoate. All the compounds have been assayed on dicotyledons *Lactuca sativa* (lettuce) and *Raphanus sativus* (radish) and monocotyledon *Allium cepa* (onion) to test their stimulatory or inhibitory effects on seed germination and radicle elongation. Cyanogenins have a mainly inhibiting effect while lignans stimulate the growth. Some compounds show different effects on dicotyledons and monocotyledons.
© 2001 Elsevier Science Ltd. All rights reserved.

Keywords: *Sambucus nigra*; Adoxaceae; Cyanogenins; Lignans; Flavonoids; Phenolic glycosides; Allelopathic activity

1. Introduction

Weed interference, which consists of the effects of competition and/or allelopathy, represents a serious threat to several crops. *Sambucus nigra* L., a shrub widely found throughout Italy, causes large crops losses, and, in a previous study Jensen and Nielsen (1973) reported the presence of cyanogenic glycosides. These compounds are considered highly phytotoxic since the action of microbes in the rhizosphere produces HCN and benzaldehydes (Conn, 1981). In a study of the detrimental effects of weeds on crops, we have reinvestigated *S. nigra* and, together with the cyanogenic glycosides **1**–**5** (Della Greca et al., 2000a) and three related compounds **6**–**8** (Della Greca et al., 2000b), we have isolated the phenolic glycosides **9**–**13** besides the lignans **14**–**19** and the flavonoids **20**–**24**. All the compounds have been tested for their effects on the seed germination and growth of *Lactuca sativa* L., *Raphanus sativus* L., and *Allium cepa* L.

2. Results and discussion

The air dried leaves of *S. nigra* were sequentially extracted with petrol, EtOAc, and MeOH. A preliminary seed germination test on *R. sativus* evidenced a strong inhibitory activity only of the MeOH extract, which was distributed between water and EtOAc (Scheme 1). The organic fraction was chromatographed on silica gel column to give fractions A–C. Chromatography on Sephadex LH-20 of fraction A, eluted with $CHCl_3$, gave the degraded cyanogenins **6**–**8** (Della Greca et al., 2000b) along with the neolignan (2*R-trans*) 2,3-dihydro-2-(4-hydroxy-3-methoxyphenyl)-3-(hydroxymethyl)-7-methoxy-5-benzofuranpropanol acetate (**14**) (Popoff and Theander, 1975) and the lignans (+) pinoresinol (**17**) (Pelter et al., 1982), (+) medioresinol (**18**) (Zhuang et al., 1982) and (+) lariciresinol (**19**) (Katayama et al., 1992). Fraction B, eluted with EtOAc, was re-chromatographed on Sephadex LH-20 to give the glucoside **13**, besides a further two neolignans, identified as (2*R-trans*)-2,3-dihydro-2-(4-hydroxy-3-methoxyphenyl)-3-(hydroxymethyl)-7-methoxy-5-benzofuran-propanol (**15**) (Toshio et al., 1989) and (2*R-trans*)-2,3-dihydro-2-(4-hydroxy-3-methoxyphenyl)-3-(hydroxymethyl)-7-

* Corresponding author. Tel.: +39-0823-274576; fax +39-0823-274571.
E-mail address: antonio.fiorentino@unina2.it (A. Fiorentino).

0031-9422/01/$ - see front matter © 2001 Elsevier Science Ltd. All rights reserved.
PII: S0031-9422(01)00401-0

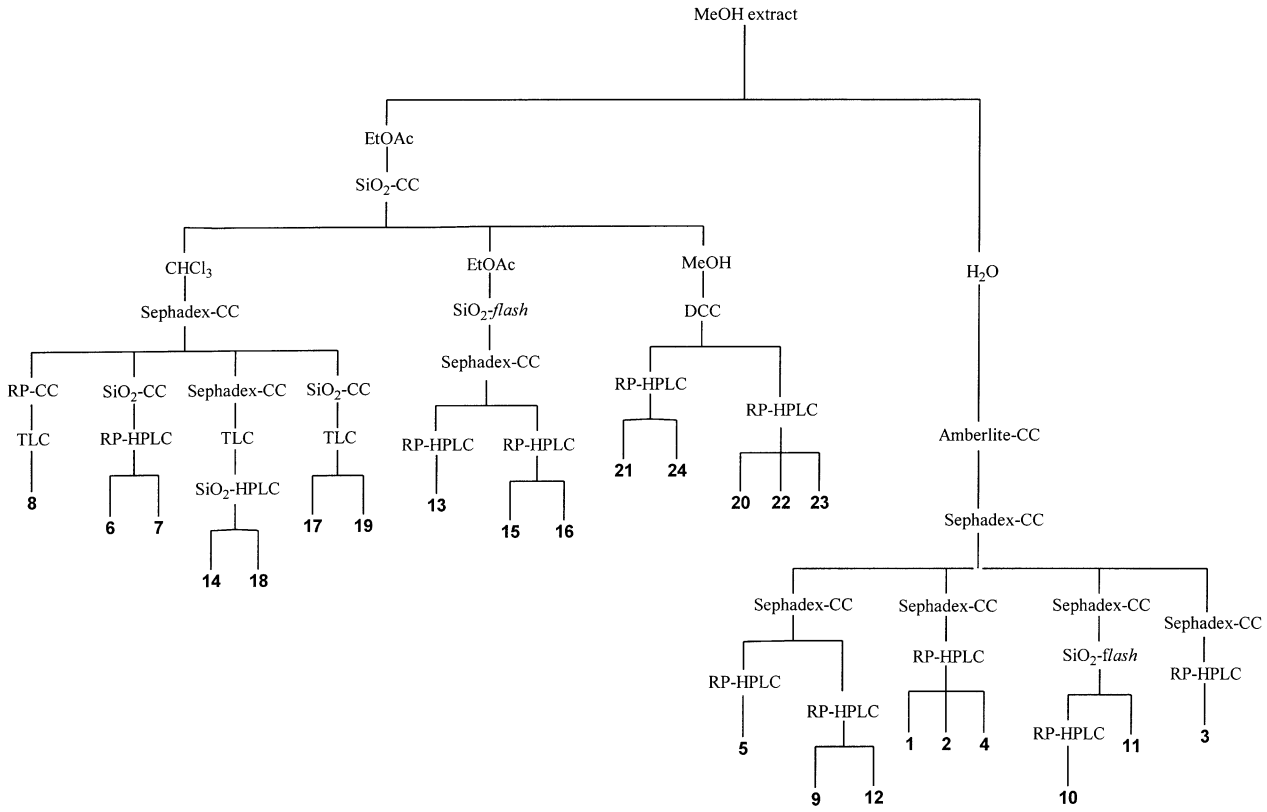

Scheme 1.

hydroxy-5-benzofuran-propanol (**16**) (Popoff and Theander, 1975).

The new compound **13** had the molecular formula $C_{20}H_{22}O_9$ according to the elemental analysis and the ^{13}C NMR data. The EIMS spectrum showed a peak at *m/z* 244 due to the loss of the glucose, besides other peaks at *m/z* 137, 107, 91 and 77. The ^1H NMR spectrum showed three aromatic protons as two double doublets at δ 6.73 and 6.59 and a triplet at δ 7.26, besides five further aromatic protons in the 7.55–7.32 ppm range. A singlet at δ 5.37, two double doublets at δ 3.86 and 3.65, and four overlapping protons in the 3.45–3.35 ppm range were also present in the spectrum. Also on the basis of HMQC and HMBC experiments structure of benzyl 2-*O*-β-D-glucopyranosyl-2,6-dihydroxybenzoate structure. Accordingly enzymatic hydrolysis with β-glucosidase gave verimol K (Sy and Brown, 1998). Fraction C, eluted with MeOH, was chromatographed by DCCC to give the flavone glycosides quercitin 3-glucoside (**20**) and quercitin 3-*O*-neohesperidoside (**24**) (Markham et al., 1978), kampferol 3-*O*-neohesperidoside (**21**) and kampferol 3-glucoside (**22**) (Harborne and Williams, 1988) and rhamnetin 3-glucoside (**23**).

The aqueous fraction was chromatographed on Amberlite XAD-4 and the fraction eluted with MeOH was partitioned on Sephadex LH-20 into fractions A–D. Fraction A, eluted with water, gave the cyanogenin (2*S*)-[β-D-apiofuranosyl-(1→2)]-β-D-glucopyranosyl-mandelonitrile (**5**) (Della Greca et al., 2000a) and the glycosides **9** and **12**. The first, $[\alpha]_D$ +6°, has been isolated for the first time and identified as (2*S*)-2-*O*-β-D-glucopyranosyl-2-hydroxy-phenylacetic acid. It had the molecular peak at *m/z* 314 in the EIMS spectrum and showed 14 carbon signals in the ^{13}C NMR spectrum in accordance to the molecular formula $C_{14}H_{18}O_8$. All its physical data were identical to those reported by Kitajima and Tanaka (1993) for (2*R*)-2-*O*-β-D-glucopyranosyl-2-hydroxy-phenylacetic acid, isolated from *Prunus zippeliana*, except for its rotation, thus justifying the *S* configuration at C-2. Accordingly, acid hydrolysis of **9** gave *l*-mandelic acid. We have identified compound **12** as icariside F_2 [benzyl alcohol β-D-apiofuranosyl-(1→6)-β-D-glucopyranoside] by comparison with the NMR data given by Miyase et al. (1989). Fraction B, eluted with MeOH–H_2O (1:3), consisted of the cyanogenins sambunigrin (**1**), prunasin (**2**) and 6-acetyl holocalin (**4**) (Della Greca et al., 2000a). Fraction C, eluted with MeOH–H_2O (1:2), afforded the glucosides **10** and **11**. The first glucoside was obtained by enzymatic synthesis by Trincone et al. (1994) while the latter was reported as a tobacco fragrance-improving agent by Keniji et al. (2000). Fraction D, eluted with MeOH–H_2O (1:1), afforded the cyanogenin holocalin (**3**) (Della Greca et al., 2000a).

All the compounds have been tested on *L. sativa* (lettuce), *R. sativus* (radish), and *A. cepa* (onion) to evalu-

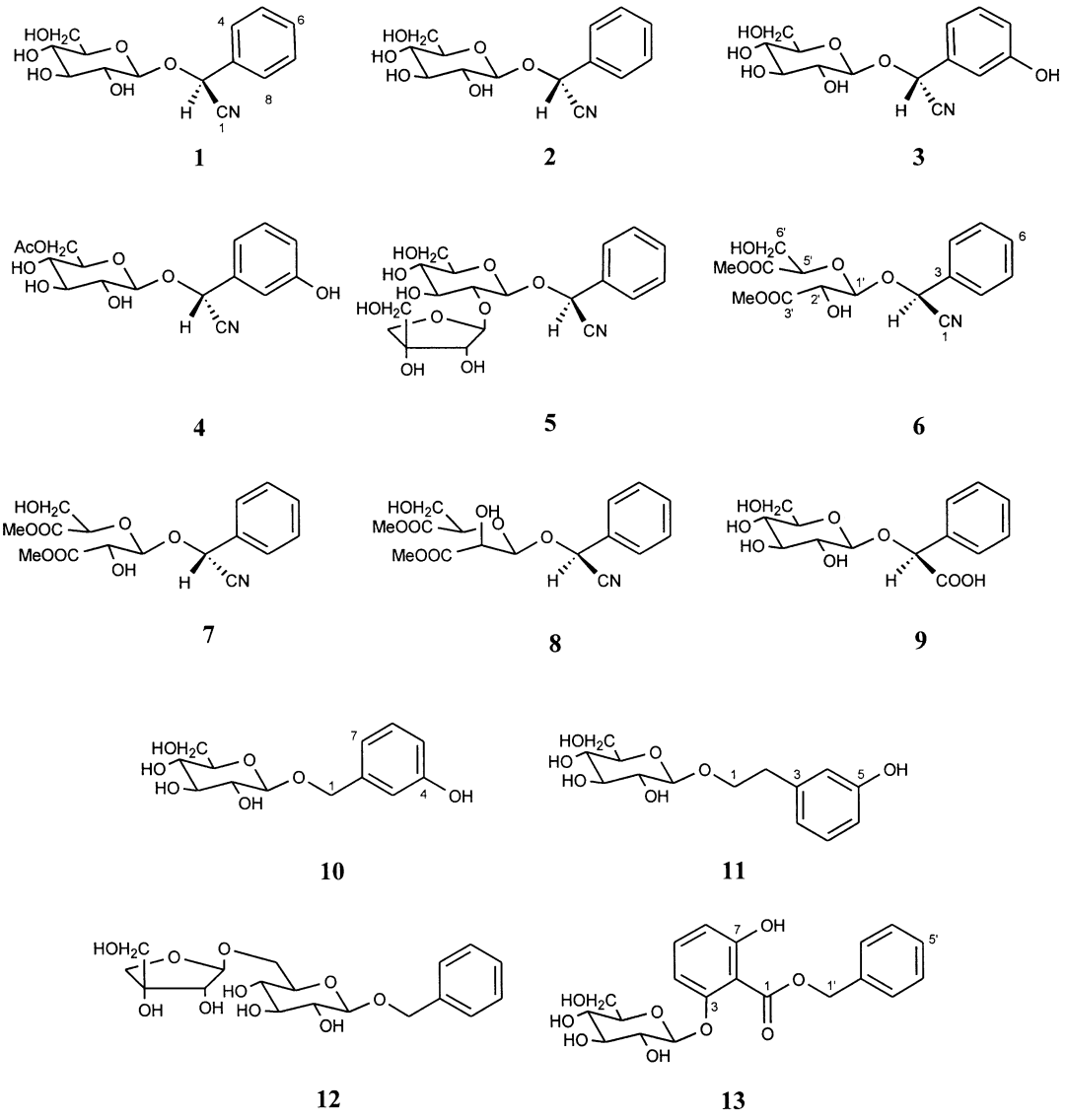

ate their influence on the seed germination and the radicle elongation. The assays have been run according to the procedures optimised by Macías et al. (2000). Flavonoids **20**–**24** show no significant activity, while the effects of the active compounds, presented as percentage differences from the control, are reported in Tables 1 and 2 and in Figs. 1 and 2.

Cyanogenins **1**–**3** inhibit the germination of the test species at the highest concentration. The effects are stronger on dicotyledons *R. sativus* and *L. sativa* than on monocotyledon *A. cepa*. The inhibition decreases with dilution and at 10^{-5} M concentration only the most active holocalin (**3**) conserves its activity while sambunigrin (**1**), and prunasin (**2**) have a slight stimulant effect. A chemical comparison between sambunigrin (**1**) and prunasin (**2**) shows that the different configuration at the C-2 stereocentre is non-influent, while the introduction of the hydroxyl group at the *meta* position of prunasin (**2**) to give holocalin (**3**) enhances the activity. All the modifications of cyanogenins, such as acetylation of holocalin (**3**) to **4**, glycosylation of sambunigrin (**1**) to **5** as well as glucose oxidation, which transforms **1** and **2** into **6** and **7**, reduce the inhibitory activity, and the overall germination effects of the compounds show less than 10% difference from the control. The effects on the radicle elongation of the three species are rather similar to those observed for germination. Cyanogenins **1**–**3** have strong activity at the highest concentrations and an almost total inhibition is observed at 10^{-3} M concentration on *R. sativus*. At the lowest concentrations sambunigrin (**1**) and prunasin (**2**) stimulate the radicle growth of *R. sativus* slightly. The effect of the modification of cyanogenins is less strong on the radicle length. Only acetyl-holocalin (**4**) is practically inactive, while the other cyanohydrins are moderately inhibiting.

Among glycosides **9**–**13**, **9** and **10** may be considered to derive respectively from sambunigrin (**1**) and holocalin (**3**) by hydrolysis of nitrile or from hydrolysis and subsequent decarboxylation. Both of them affect the

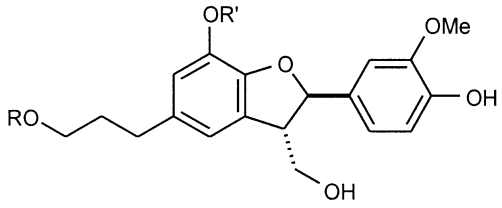

14 R = Ac R' = Me
15 R = H R' = Me
16 R = H R' = H

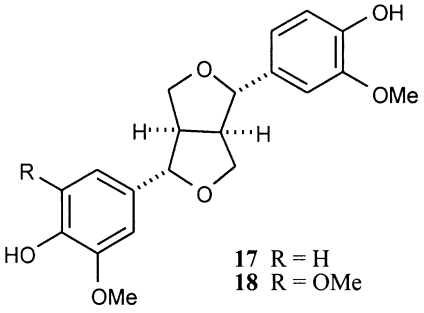

17 R = H
18 R = OMe

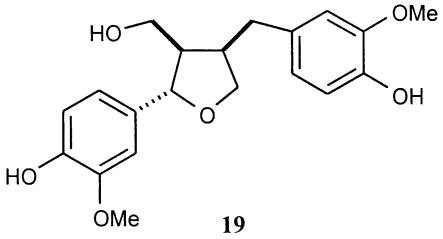

19

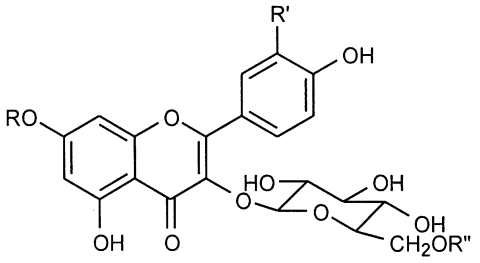

20 R = H R' = OH R" = H
21 R = H R' = H R" = rha
22 R = H R' = H R" = H
23 R = Me R' = OH R" = H
24 R = H R' = OH R" = rha

Table 1
Bioactivity data of compounds **1–19** on the radicle length of *Lactuca sativa*, *Raphanus sativum* and *Allium cepa*[a]

		1	**2**	**3**	**4**	**5**	**6**	**7**	**8**	**9**	**10**	**11**	**12**	**13**	**14**	**15**	**16**	**17**	**18**	**19**
Lactuca sativa	10^{-3} M	[–]	[–]	[–]	–	–	(–)	(–)	(–)	0	0	(+)	0	+	[+]	[–]	+	[+]	[+]	+
	10^{-4} M	(–)	(–)	(–)	0	–	(–)	(–)	(–)	0	0	(+)	0	+	(+)	0	(+)	[+]	[+]	0
	10^{-5} M	–	–	(–)	0	–	–	(–)	(–)	0	+	0	0	+	(+)	(+)	+	(+)	[+]	(+)
	10^{-6} M	0	0	(–)	0	–	–	–	–	0	+	0	0	0	+	(+)	(+)	[+]	(+)	(+)
Raphanus sativus	10^{-3} M	[–]	[–]	[–]	0	0	–	–	–	–	–	–	0	(–)	–	(+)	–	[+]	+	–
	10^{-4} M	0	–	(–)	0	0	–	–	–	–	–	–	0	–	+	(+)	+	[+]	(+)	–
	10^{-5} M	+	+	–	0	0	–	–	–	–	0	–	0	(+)	[+]	(+)	(+)	[+]	(+)	0
	10^{-6} M	+	+	–	0	0	0	0	0	–	0	0	0	(+)	(+)	[+]	(+)	[+]	+	[+]
Allium cepa	10^{-3} M	(–)	(–)	(–)	0	0	(–)	(–)	–	(–)	–	–	–	–	+	(–)	[–]	+	–	+
	10^{-4} M	(–)	–	0	0	0	(–)	(–)	(–)	–	0	–	–	0	+	+	+	+	0	0
	10^{-5} M	–	(–)	0	–	+	(–)	(–)	(–)	–	0	0	+	(+)	(+)	+	0	0	0	(+)
	10^{-6} M	0	0	0	0	+	0	–	–	–	0	–	+	+	+	(+)	(+)	(+)	–	(+)

[a] 0, Stimulatory or inhibitory values $<10\%$; + and –, stimulatory or inhibitory values between 10 and 30%; (+) and (–), stimulatory or inhibitory values between 31 and 60%; [+] and [–], stimulatory or inhibitory values $>61\%$.

germination of the three species slightly. It is worth noting that the effect is inhibiting on dicotyledons and stimulating on monocotyledon. Further effects are observed on the radicle elongation and a reduction of the length occurs in the test species. The other glycosides **11**–**13** have an analogous behaviour.

The neolignans **14**–**16** have little effect on the germination of the three species, while they stimulate the radicle elongation of lettuce and radish quite well. *A. cepa* is inhibited at its highest concentration. Furofuran lignans **17** and **18** have no effect on the germination of dicotyledons, whereas they do influence onion. It is interesting that compound **17** is stimulating but **18** is inhibiting. The chemical difference between the compounds is the presence of a further methoxyl group in **18**. The radicle elongation test shows that the compounds have strong effects on dicotyledons, while they influence monocotyledon only slightly. The effect is that of a strong increase of the radicle length which is higher with compound **17**. Lignan **19** has little effect on the germination but a good stimulating effect on the radicle elongation.

Table 2
Bioactivity of compounds **1**–**19** on the germination of *Lactuca sativa*, *Raphanus sativum* and *Allium cepa*[a]

		1	**2**	**3**	**4**	**5**	**6**	**7**	**8**	**9**	**10**	**11**	**12**	**13**	**14**	**15**	**16**	**17**	**18**	**19**
Lactuca sativa	10^{-3} M	(−)	(−)	[−]	0	0	0	0	0	−	0	−	−	0	0	−	0	0	0	0
	10^{-4} M	0	0	(−)	0	0	0	0	0	−	0	−	−	0	0	−	0	0	0	0
	10^{-5} M	0	0	−	0	0	0	0	0	0	0	−	0	0	0	−	0	0	0	0
	10^{-6} M	0	0	0	0	0	0	0	0	0	0	0	0	0	0	−	0	0	0	0
Raphanus sativus	10^{-3} M	−	−	[−]	0	−	0	0	0	−	0	0	−	0	0	0	0	0	+	0
	10^{-4} M	−	−	−	0	−	0	0	0	−	0	0	−	0	0	0	0	0	+	0
	10^{-5} M	0	0	(−)	0	0	0	0	0	−	0	0	0	0	0	0	0	0	+	0
	10^{-6} M	0	0	0	0	0	0	0	0	0	0	0	0	0	0	0	0	0	(+)	0
Allium cepa	10^{-3} M	−	−	−	0	0	0	0	0	+	+	0	+	+	+	+	0	(+)	(−)	0
	10^{-4} M	−	−	−	0	0	0	0	0	+	+	0	+	(+)	+	+	0	(+)	(−)	+
	10^{-5} M	0	+	0	0	0	0	0	0	0	+	+	+	+	+	0	0	(+)	+	+
	10^{-6} M	0	0	−	0	0	0	0	0	0	+	+	+	(+)	+	0	0	(+)	0	+

[a] 0, Stimulatory or inhibitory values <10%; + and −, stimulatory or inhibitory values between 10 and 30%; (+) and (−), stimulatory or inhibitory values between 31 and 60%; [+] and [−], stimulatory or inhibitory values >61%.

In conclusion, *S. nigra* produces phytostimulating and phytoinhibiting metabolites. Lignans belong to the first group, while the cyanogenins and their derivatives belong to the latter.

3. Experimental

3.1. General experimental procedures

NMR spectra were recorded at 400 MHz for ^{1}H and 100 MHz for ^{13}C on a Bruker AC400 spectrometer with 0.05 solns. in $CDCl_3$ or CD_3OD at 37 °C. Proton-detected heteronuclear correlations were measured using HMQC (optimised for $^1J_{HC} = 145$ Hz) and HMBC (optimised for $^1J_{HC} = 7$ Hz). Optical rotations were measured on a Perkin–Elmer 343 polarimeter. IR spectra were determined in $CHCl_3$ solns on a FT–IR Perkin–Elmer 1740 spectrometer. UV spectra were obtained on a Perkin–Elmer Lambda 7 spectrophotometer in EtOH solns. EI mass spectra were obtained with a Kratos MS 80 apparatus. FAB mass spectra were recorded on a VG ZAB 2SE apparatus. HPLC UV apparatus consisted of a Beckman pump—System Gold 127, a Beckman System Gold 166 UV detector, and a Shimadzu Chromatopac C-R6A recorder. Preparative HPLC were performed using SiO_2 (Maxsil Silica 10 μm, 250×10 mm i.d., Phenomenex), RP-18 (Luna 10 μm, 250×10 mm i.d., Phenomenex), or RP-8 (Luna 10 μm, 250×10 mm i.d., Phenomenex) columns. Analytical TLC was performed on Merck Kieselgel 60 F_{254} or RP-18 F_{254} plates with 0.2 mm film thickness. Spots were visualised by UV light or by spraying with H_2SO_4–AcOH–H_2O (1:20:4) followed by heating for 5 min at 110 °C. Preparative TLC was performed on Merck Kieselgel 60 F_{254} plates, with 0.5 or 1 mm film thickness. Flash column chromatography was performed on Merck Kieselgel 60 (230–400 mesh) at a medium pressure. Column chromatography (CC) was performed on Merck Kieselgel 60 (70–240 mesh), on Sephadex LH-20® (Pharmacia) or on Amberlite XAD-4 (20-60 mesh, Fluka). DCCC was performed on a D.C.C.-A Tokyo Rikakikai LTD (300 columns, 400×2 mm).

3.2. Plant material

Plants of *S. nigra* L. were collected in Agerola (Naples) in July and identified by professor G. Aliotta. A voucher specimen (HERBNAPG074) was deposited at the Dipartimento di Biologia Vegetale of University Federico II of Naples.

3.3. Extraction and isolation

The air-dried and powdered plant material (4.1 kg) was sequentially and exhaustively extracted with petrol, EtOAc and MeOH. The MeOH extract (370 g) was partitioned between H_2O (2 l) and EtOAc (1 l).

The organic fraction (92.9 g) was chromatographed on SiO_2 to give fractions A–C. Fraction A (57 g), eluted with $CHCl_3$, was chromatographed on Sephadex LH-20 eluting with hexane –$CHCl_3$–MeOH (3:1:1) and collecting volumes of 10 ml. Fractions 15-19 were chromatographed on TLC [$CHCl_3$–AcOEt (4:1)] and purified on RP-8 eluting with MeOH–MeCN–H_2O (3:2:5) to give compound **8** (18 mg). Silica gel chromatography of fractions 20–23 gave the epimeric mixture of **6** and **7** that was resolved on RP-18 HPLC by eluting with MeOH–MeCN–H_2O (1:1:3) (5 and 3 mg, respectively). Fractions 24–30 were re-chromatographed on TLC [$CHCl_3$–MeOH (99:1)] and SiO_2 HPLC [hexane–acetone (13:7)] to give the lignans **14** (15 mg) and **18** (8 mg). Finally, fractions 31–37 were purified first by flash chromatography [$CHCl_3$–MeOH (49:1)] and then by TLC [benzene–MeOH (9:1)], to give the compounds **17** (21 mg) and **19** (19 mg). Fraction B (11 g), eluted with EtOAc, was chromatographed on SiO_2. The fractions so

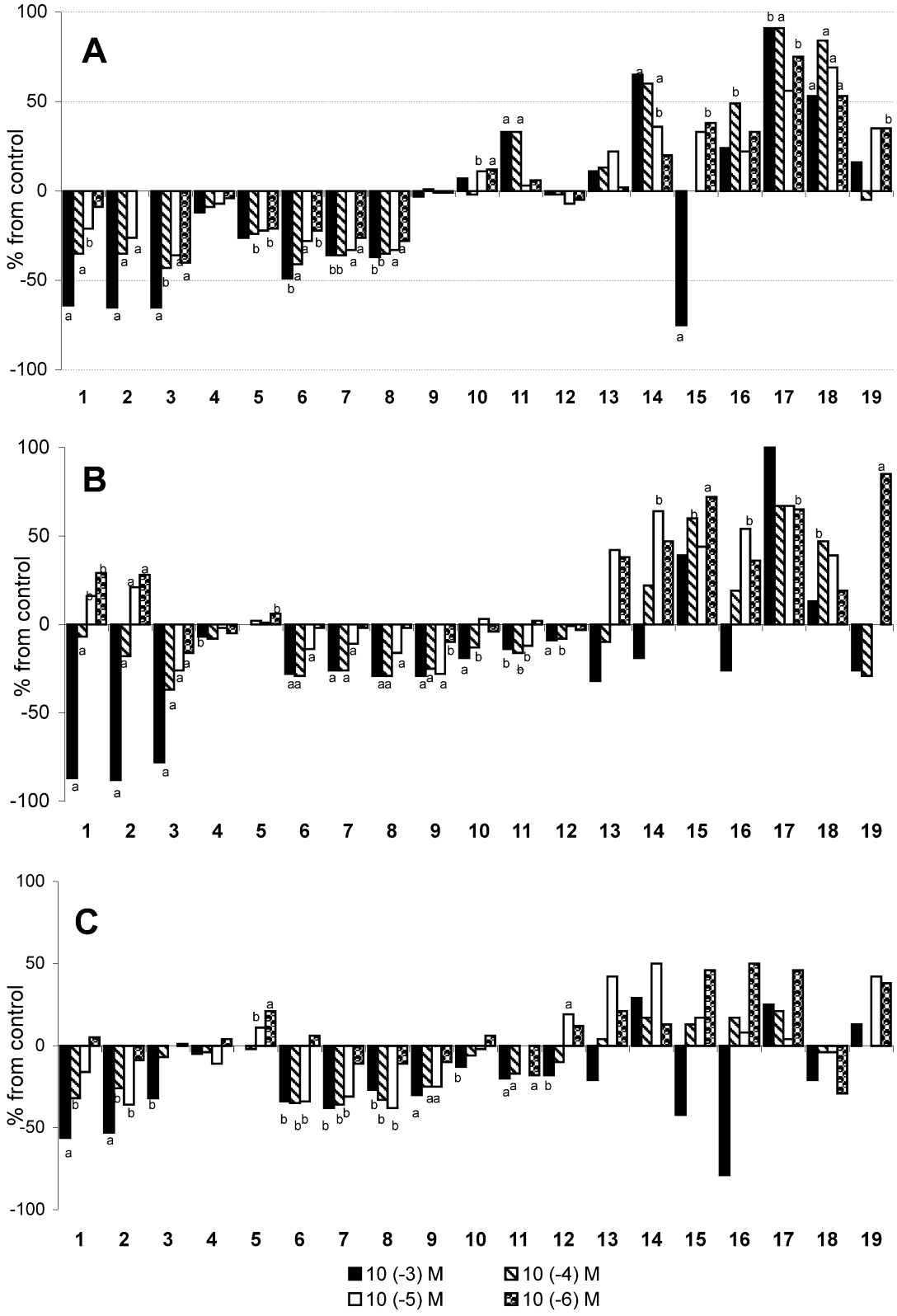

Fig. 1. Effect of compounds **1**–**19** on radical length of *Lactuca sativa* (A), *Raphanus sativus* (B) and *Allium cepa* (C). Values presented as percentage differences from control; $P > 0.05$ for the Welch's test. A, $P < 0.01$; B, $0.01 < P < 0.05$.

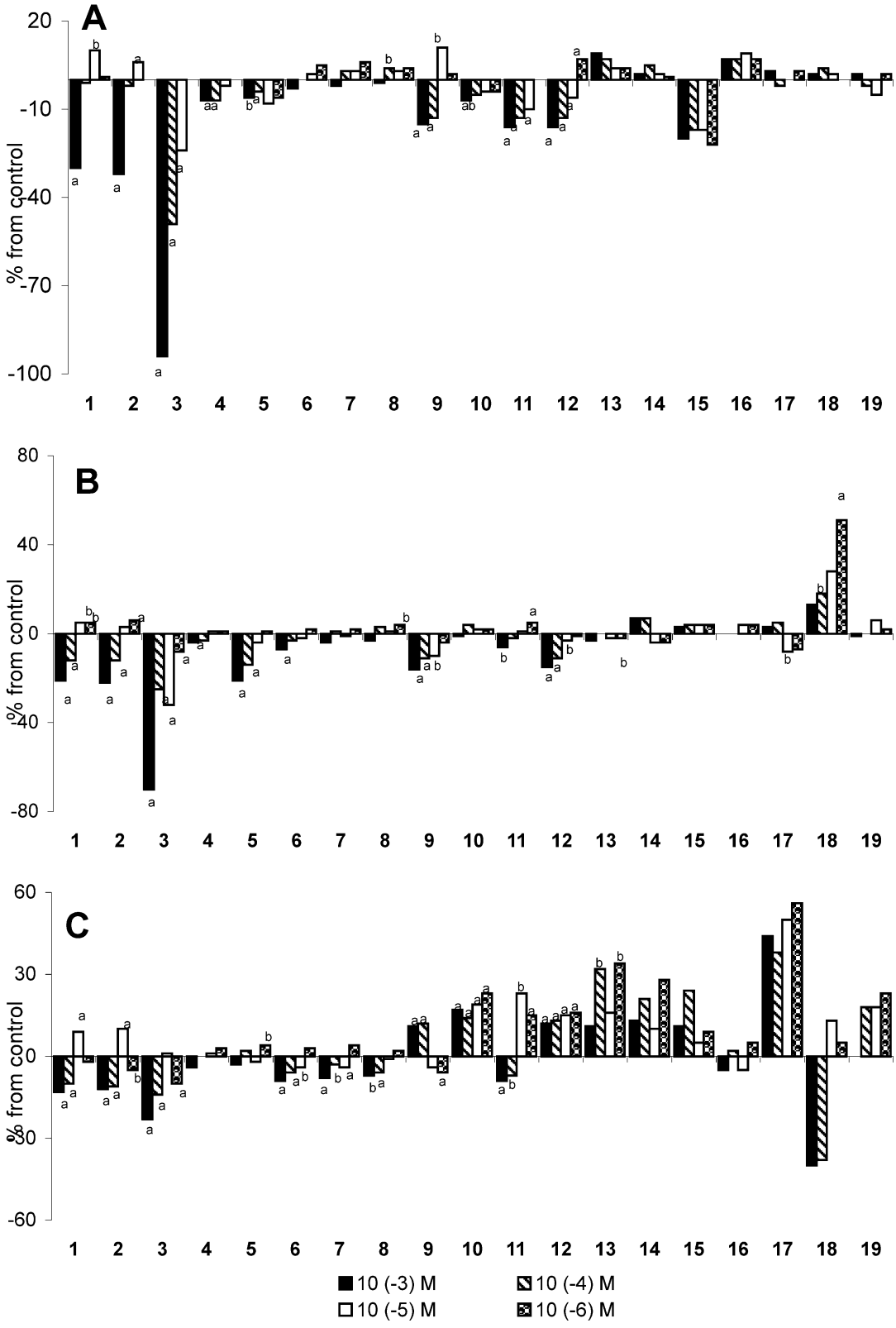

Fig. 2. Effect of compounds **1**–**19** on seed germination of *Lactuca sativa* (A), *Raphanus sativus* (B) and *Allium cepa* (C). Values presented as percentage differences from control; $P > 0.05$ for the Welch's test. A, $P < 0.01$; B, $0.01 < P < 0.05$.

obtained, eluted with $CHCl_3$–MeOH–H_2O (14:5:1), were re-chromatographed by Sephadex LH-20 with MeOH-H_2O (7:3) as eluent; fractions 43–48 were purified by RP-18 HPLC [MeOH–MeCN–H_2O (37:2:11)] to give glucoside **13** (21 mg), while fractions 51-58 were purified by RP-18 HPLC [MeOH–MeCN–H_2O (9:2:9)] to give compounds **15** (11 mg) and **16** (7 mg). Fraction C (10.2 g), eluted with MeOH, was chromatographed on a DCCC apparatus with $CHCl_3$–MeOH–H_2O (13:7:5) in ascending mode, using the upper layer as mobile phase. RP-18 HPLC of the fractions 17–22 [A: 2% AcOH, B: MeOH-2% AcOH (8:2); gradient A:B from 19:1 to 3:2 in 30 min] gave the disaccharide flavonoids **21** (25 mg) and **24** (19 mg); RP-18 HPLC purification of the fractions 75–96 [A: 2% AcOH, B: MeOH-2% AcOH (8:2); gradient A:B from 3:1 to 9:11 in 30 min] gave the flavone glucosides **20** (18 mg), **22** (14 mg) and **23** (6 mg).

The aqueous layer, conc. at 500 ml, was chromatographed on Amberlite XAD-4 and, using chromatography on Sephadex LH-20, the MeOH elute (5.9 g) was partitioned into the fractions A–D. Fraction A (1.9 g), eluted with H_2O, was re-chromatographed on Sephadex LH-20 using MeOH-$CHCl_3$–hexane (4:2:1) as eluent to give crude **5**, which was purified by RP-18 HPLC [MeOH–MeCN–H_2O (17:3:30), 6 mg)] and a mixture of glycosides **9** and **12** that was resolved by RP-18 HPLC (13 and 11 mg, respectively). Fraction B (345 mg), eluted with H_2O–MeOH (3:1) was re-chromatographed on Sephadex LH-20, using MeOH–$CHCl_3$–hexane (4:2:1) as eluent to give a mixture of cyanogenic glycosides **1**, **2** and **4** which was resolved by RP-18 HPLC [A: 2% AcOH, B: MeOH-2% AcOH (8:2); gradient A:B from 17:3 to 7:3 in 25 min; **1**, **2** and **4**: 45, 68 and 8 mg, respectively]. Subsequent purification of fraction C (684 mg), eluted with MeOH–H_2O (2:1), on Sephadex LH-20 and then by flash chromatography [$CHCl_3$–MeOH–H_2O (13:7:3), lower layer] gave the compound **11** (9 mg) and a fraction that, purified by RP-18 HPLC [MeOH–MeCN–H_2O (7:2:4)], gave the glucoside **10** (13 mg). Fraction D (2.0 g), eluted with H_2O–MeOH (1:1) was chromatographed on Sephadex LH-20, using MeOH–$CHCl_3$–hexane (4:2:1) as eluent to give crude **3** (220 mg). An aliquot of the crude product was purified by RP-18 HPLC [A: 2% AcOH, B: MeOH-2% AcOH (8:2); gradient A:B from 4:1 to 3:1 in 10 min].

3.4. Compound characterisation

3.4.1. (2S)-2-O-β-D-Glucopyranosyl-2-hydroxyphenylacetic acid (9)

Colorless oil; $[\alpha]_D$ +6°; UV (EtOH) λ_{max} nm: 279; ^{1}H NMR (CD_3OD) δ 7.50 (2H, *m*, H-4 and H-8), 7.32 (3H, *m*, H-5–H-7), 5.27 (1H, *s*, H-2), 4.51 (1H, *d*, J = 8.0 Hz, glc-1), 3.86 (1H, *dd*, J = 11.8 and 1.1 Hz, glc-6), 3.68 (1H, *dd*, J = 11.8 and 5.6 Hz, glc-6), 3.50–3.30 (4H, *m*, glc-2–glc-5). EIMS *m*/*z*: 314 $[M]^+$, 152 $[M-glucose]^+$. (Found: C, 53.3; H, 5.9. $C_{14}H_{18}O_8$ requires: C, 53.5; H, 5.8%.)

3.4.2. 3-Hydroxybenzyl 1-O-β-D-glucopyranoside (10)

Colorless oil; UV λ_{max} (EtOH) nm 280; ^{1}H NMR (CD_3OD) δ 7.14 (1H, *dt*, J = 7.7 and 1.0 Hz, H-6), 6.87 (1H, *dd*, J = 7.7 and 1.9 Hz, H-7), 6.86 (1H, *d*, J = 1.8 Hz, H-3), 6.71 (1H, *ddd*, J = 7.7, 1.9 and 1.0 Hz, H-5), 4.85 (1H, *d*, J = 11.8 Hz, H-1), 4.59 (1H, *d*, J = 11.8 Hz, H-1), 4.35 (1H, *d*, J = 7.7 Hz, glc-1), 3.89 (1H, *dd*, J = 12.0 and 2.2 Hz, glc-6), 3.69 (1H, *dd*, J = 12.0 and 5.5 Hz, glc-6), 3.35–3.20 (4H, H-2′–H5′). EIMS *m*/*z*: 286 $[M]^+$, 124 $[M-glucose]^+$, 107 $[M-OH-glucose]^+$. (Found: C, 54.4; H, 6.5. $C_{13}H_{18}O_7$ requires: C, 54.5; H, 6.3%.)

3.4.3. 1-O-β-D-Glucopyranosyl-2-(3-hydroxyphenyl)-ethanol (11)

Colorless oil; UV λ_{max} (EtOH) nm: 280; ^{1}H NMR (CD_3OD) δ 7.09–6.78 (4H, *m*, H-4, H-6–H-8), 4.75 (1H, *d*, J = 8.0 Hz, glc-1), 3.92 (1H, *dd*, J = 11.8 and 1.1 Hz, glc-6), 3.73 (1H, overlapped, glc-6), 3.72 (2H, *t*, J = 7.0 Hz, H-1), 3.50–3.30 (4H, *m*, glc-2–glc-5), 2.71 (2H, *t*, J = 7.0 Hz, H-2). EIMS *m*/*z*: 300 $[M]^+$, 138 $[M-glucose]^+$. (Found: C, 59.9; H, 6.8. $C_{14}H_{20}O_7$ requires: C, 56.0, H, 6.7%.)

3.4.4. Benzyl alcohol β-D-apiofuranosyl-(1→6)-β-D-glucopyranoside (12)

Colorless oil; UV λ_{max} (EtOH) nm: 280. ^{1}H NMR (CD_3OD) δ 7.42–7.25 (5H, *m*, H-3–H-7), 5.07 (1H, *d*, J = 2.0 Hz, api-1), 4.91 (1H, *d*, J = 11.9 Hz, H-1), 4.66 (1H, *d*, J = 11.9 Hz, H-1), 4.33 (1H, *d*, J = 7.8 Hz, glc-1), 4.05–3.30 (11H, glc-2–glc-6 and api-2–api-5). FABMS (negative) *m*/*z*: 401 $[M-H]^-$, 269 $[M-api-H]^-$, 107 $[M-api-glc-H]^-$. (Found: C, 53.8; H, 6.4. $C_{18}H_{26}O_{10}$ requires: C, 53.7, H, 6.5%.)

3.4.5. Benzyl 2-O-β-D-glucopyranosyl-2,6-dihydroxybenzoate (13)

Colorless oil; IR ν_{max} ($CHCl_3$) cm^{-1}: 1715, 1605. ^{1}H NMR (CD_3OD) δ 7.55–7.32 (5H, *m*, H-3′–H-7′), 7.26 (1H, *t*, J = 8.4 Hz, H-5), 6.73 (1H, *dd*, J = 8.4 and 1.0 Hz, H-4), 6.59 (1H, *dd*, J = 8.4 and 1.0 Hz, H-6), 5.37 (2H, *s*, H-1), 4.93 (1H, *d*, J = 7.2 Hz, glc-1), 3.86 (1H, *dd*, J = 12.0 and 1.2 Hz, glc-6), 3.65 (1H, *dd*, J = 12.0 and 5.9 Hz, glc-6), 3.45–3.35 (4H, *m*, glc-2–glc-5); ^{13}C NMR (CD_3OD) δ 170.3 (C-1), 160.1 (C-3), 158.5 (C-7), 137.6 (C-2′), 134.3 (C-5), 129.8 (C-4′, C-6′), 129.5 (C-3′, C-5′, C-7′), 111.9 (C-6), 108.1 (C-2), 108.0 (C-4), 103.0 (glc-1), 78.6 (glc-5), 78.2 (glc-3), 75.2 (glc-2), 71.5 (glc-4), 68.4 (C-1′), 62.8 (glc-6). EIMS *m*/*z*: 244, 137, 107, 91, 77. (Found: C, 59.0; H, 5.4. $C_{20}H_{22}O_9$ requires C, 59.1, H, 5.5%.)

3.5. Bioassays

Seeds of *R. sativus* L. "Saxa", collected during 2000, were purchased from Improta Co., Naples. Seeds of *L. sativa* and *A. cepa,* collected during 2000, were obtained from Blumen® (Milan, Italy). All undersized or damaged

seeds were discarded and the assay seeds were selected for uniformity.

For the bioassays we used Petri dishes in two sizes (90 and 50 mm diameter) with one sheet of Whatman No. 1 filter paper as support. In three replicate experiments, germination and growth were conducted in aqueous solutions at controlled pH. Test solns. (10^{-3} M) were prepared using MES (2-[*N*-morpholino]ethanesulfonic acid, 10 mM, pH 6) and the rest (10^{-4} –10^{-6} M) were obtained by dilution. Parallel controls were performed. After adding 30 seeds and aqueous solns., Petri dishes were sealed with Parafilm® to ensure closed-system models. Seeds were placed in a growth chamber KBW Binder 240 at 25 °C, with 60% relative humidity, and a 12 h photoperiod, 10,000 lux. Germination percentage was determined daily for four days for radish and five days for onion and lettuce (no more germination occurred after this time). After growth, plants were frozen at −20 °C to avoid subsequent growth until the measurement process.

Data are reported as percentage differences from control in the graphics and tables. Thus, zero represents the control; positive values represent stimulation of the control; positive values represent stimulation of the parameter studied and negative values represent inhibition.

3.5.1. Statistical treatment

Comparison was made between the two blocks assayed by applying Welch's test, a variant of Student's *t* test (Zar, 1984; Martin and Luna, 1990), calculating mean values for every parameter (germination average, and radicle elongation) and their population variance within a Petri dish.

Coefficient of variation (CV) was used to compare dispersion from different populations. This parameter is expressed as a percentage and represents the ratio between the standard deviation and the sample mean.

Acknowledgements

The authors thank one of the referees for the helpful discussion for the compound **13** identification.

References

Conn, E.E., 1981. Cyanogenic glycosides. Biochem. Plants 7, 479–500.

DellaGreca, M., Fiorentino, A., Monaco, P., Previtera, L., Simonet, A.M., 2000a. Cyanogenic glycosides from *Sambucus nigra*. Nat. Prod. Lett. 14, 175–182.

DellaGreca, M., Fiorentino, A., Monaco, P., Previtera, L., Simonet, A.M., 2000b. Degraded cyanogenic glucosides from *Sambucus nigra*. Tetrahedron Lett. 41, 6507–6510.

Harborne, J.B., Williams, C.A., 1988. Flavone and flavonol glycosides. In: Harborne, J.B. (Ed.), The Flavonoids. Chapman and Hall, London, pp. 304–328.

Jensen, S.R., Nielsen, B.J., 1973. Cyanogenic glucosides in *Sambucus nigra* L.. Acta Chem. Scand. 27, 2661–2662.

Katayama, T., Davin, L.B., Lewis, N.G., 1992. An extraordinary accumulation of (−)-pinoresinol in cell-free extracts of *Forsythia intermedia*: evidence for enantiospecific reduction of (+)-pinoresinol. Phytochemistry 31, 3875–3879.

Kenji, I., Yoko, T., Hiroshi, S., Masataka, M., 2000. The Tobacco Fragrance Improving Agents. Patent: Jpn. Kokai Tokkyo Koho.

Kitajima, J., Tanaka, Y., 1993. Constituents of *Prunus zippeliana* leaves and branches. Chem. Pharm. Bull. 41, 2007–2009.

Macías, F.A., Castellano, D., Molinillo, J.M.G., 2000. Search for a standard phytotoxic bioassay for allelochemicals. Selection of standard target species. J. Agric. Food Chem. 48, 2512–2521.

Markham, K.R., Tennai, B., Stanley, R., Geiger, H., Mabry, T.J., 1978. Carbon-13 NMR studies of flavonoids. Tetrahedron 34, 1389–1397.

Martin, A.A., Luna del Castillo, J.de D., 1990. Bioestadistica Para las Ciencias de la Salud. Ed. Norma, Madrid.

Miyase, T., Ueno, A., Takizawa, N., Kobayashi, H., Oguchi, H., 1989. Ionone and lignan glycosides from *Epimedium diphyllum*. Phytochemistry 28, 3483–3485.

Pelter, A., Ward, E.S., Watson, D.J., Collins, P., Kai, I.T., 1982. Synthesis of 2,6-diaryl-4,8-dihydroxy-3,7-dioxobicyclo[3.3.0]octanes. J. Chem. Soc. Perkin 1, 175–181.

Popoff, T., Theander, O., 1975. Two glycosides of a new dilignol from *Pinus silvestris*. Phyto. 14, 2065–2066.

Sy, L.K., Brown, G.D., 1998. Novel phenylpropanoids and lignans from *Illicium verum*. J. Nat. Prod. 61, 987–992.

Toshio, M., Akira, U., Nobuo, T., Hiromi, K., Hiroko, O., 1989. Ionone and lignan glycosides from *Epimedium diphyllum*. Phytochemistry 28, 3483–3485.

Trincone, A., Improta, R., Nucci, R., Rossi, M., Gambacorta, A., 1994. Enzymic synthesis of carbohydrate derivatives using β-glycosidase of *Solfolobus solfataricus*. Biocatalysis 10, 195–210.

Zar, J.H., 1994. Statistical Analysis. Prentice-Hall, Englewood Cliffs, NJ.

Zhuang, L., Seligmann, O., Jurcic, K., Wagner, H., 1982. Constituents of *Daphne tangutica*. Planta Med. 45, 172–176.

PERGAMON

Phytochemistry 58 (2001) 1083–1086

PHYTOCHEMISTRY

www.elsevier.com/locate/phytochem

Alkamides from *Artemisia dracunculus*

Bouchra Saadali[a], Driss Boriky[a], Mohamed Blaghen[b], Maurice Vanhaelen[c], Mohammed Talbi[a,*]

[a]*Laboratoire de Chimie Analytique et Structurale, associé au CNRSTP, Faculté des Sciences, Ben M'Sik BP7960, Casablanca, Morocco*
[b]*Laboratoire de Microbiologie, Biotechnologie et Environnement, Faculté des Sciences Aïn Chock, Mâarif BP5366, Casablanca, Morocco*
[c]*Laboratoire de Pharmacognosie et Bromatologie, Institut de Pharmacie de l'Université Libre de Bruxelles, U.L.B. CP205/4, Bd du Triomphe, B-1050 Bruxelles, Belgium*

Received 30 May 2001; accepted 6 August 2001

Abstract

From the aerial parts of *Artemisia dracunculus*, one known alkamide, pellitorine, two new alkamides neopellitorine A and neopellitorine B, and one known coumarin herniarine were isolated. Structures were elucidated by means of UV, IR, MS, ^{1}H and ^{13}C NMR. These compounds showed insecticidal activity against *Sitophilus oryzae* and *Rhyzopertha dominica* at 200 μg/ml concentrations. © 2001 Elsevier Science Ltd. All rights reserved.

Keywords: *Artemisia dracunculus*; Asteraceae; Anthemideae; *N*-Isobutyl amides; Insecticidal activity; *Sitophilus oryzae*; *Rhyzopertha dominica*

1. Introduction

The large genus *Artemisia*, from the tribe Anthemideae, has been the subject of numerous chemical and biological studies (Tan et al., 1998). The species give sesquiterpene lactones, coumarins and acetylenes as the main metabolites (Marco and Barbera, 1990). Preparations from *Artemisia* plants have a long tradition in adjuvant therapy. In previous papers we reported eudesmanolides from the aerial parts of *Artemisia herba alba* (Boriky et al., 1996). This paper describes the isolation and structural elucidation of three alkamides and one know coumarin from the aerial parts of *A. dracunculus*, and their insecticidal effect against the rice wevil (*Sitophilus oryzae*) and grain borer (*Rhyzopertha dominica*). These stored products pests are characterized by their bioecology and the nature of their damage. In fact, these two harmful insects cause the most damage in stocks of corn and barley in Morocco and through out the world.

2. Results and discussion

The petroleum ether extract of aerial parts afforded, after silica gel chromatography pure amide compounds **1**–**3**. Pellitorine **1** is reported for the first time in an *Anacyclus* species (Dunstan and Garnett, 1895). The IR spectrum of these compounds indicated the presence of amide group (bands at 3300, 3070, 1650 and 1540 cm^{-1}) as well as olefinic double bands (1630 and 950 cm^{-1}). This together with the absorption maximum at 257 nm suggested a chromophore of conjugated dienoic acid amides for **1**–**3**. The amide moiety was established by the mass spectrum. The peaks matching $[M-15]^{+}$, $[M-43]^{+}$, $[M-57]^{+}$, $[M-72]^{+}$ and $[M-100]^{+}$ were assigned to a piperidide moiety for **3**.

The ^{1}H NMR spectra of compounds **1**–**2** showed characteristic signals at δ 3.18 (H-1′), δ 1.80 (H-2′), and δ 0.92 (H-3′,4′) indicating the isobutylamide moiety (Su and Horvart, 1981; Greger and Hofer, 1987; Bauer et al., 1988, 1989). In addition, the signals of a conjugated diene moiety were apparent (δ 5.82 (H-2), δ 7.21 (H-3), δ 6.24 (H-4) and δ 6.12 (H-5)) in a *trans–cis* configuration as indicated by the coupling constants of 15 and 11 Hz for each pair of olefinic protons (Greger and Hofer, 1987; Bauer et al., 1988, 1989). The structure of **2** differed from the **1** in the hydrocarbon chain attached to a carbon bearing the conjugated diene moiety, which could be observed from the ^{1}H and ^{13}C NMR spectra (Tables 1 and 2). Compound **3** showed different signals in ^{1}H NMR spectrum caused by the amine part, three multiplets at δ 1.57, δ 1.64 and δ 1.62 that were characteristic to the cyclic methylenes and two typical multiplets at δ 3.49 and δ 3.61 attached to protons in α

* Corresponding author. Tel.: +212-270-4671; fax: +212-270-4675.
E-mail address: acsl@caramail.com (M. Talbi).

0031-9422/01/$ - see front matter © 2001 Elsevier Science Ltd. All rights reserved.
PII: S0031-9422(01)00347-8

position of nitrogen (Greger et al., 1982). Also the presence of an piperidide moiety was supported by the ^{13}C NMR signals at δ 25.6 (C-2′), δ 24.7 (C-3′), δ 26.7 (C-4′), δ 46.9 (C-1′) and δ 43.2 (C-5′). The structure of **3** differed from the **1** in the amine moiety, which could be deduced from the MS-fragmentation pattern $[M-84]^+$ instead of $[M-72]^+$ and the ^1H, ^{13}C NMR spectra (Tables 1 and 2).

Compounds **1**–**3** have never been identified as constituents of *Artemisia*. Compounds **2** and **3** have been isolated for the first time, while compound **1** has previously been found in *Anacyclus pyrethrum* (Dunstan and Garnett, 1895). According to previous reports (Jacobson, 1954; Bohlmann and Hoffmann, 1983) unsaturated isobutylamides are well-known from the Asteraceae and for their insecticidal activities (Greger, 1984). They have also been reported from other genera such as *Spilanthes* (Ramscwak et al., 1999), *Echinacea* (Bauer et al., 1989), Achillea (Greger et al., 1982; Greger and Hofer, 1989) and *Acmella* (Martin and Becker, 1985).

Table 1
^1H NMR data of compounds **2** and **3** (600 MHz, $CDCl_3$, TMS as int. standard; chemical shifts in δ values (ppm); coupling constants in Hz in parentheses)

H	**2**	**3**
2	5.81 *d* (15)	6.25 *d* (15)
3	7.18 *dd* (15; 11)	7.23 *dd* (15; 11)
4	6.20 *m*	6.17 *dd* (11; 11)
5	6.06 *m*	6.05 *m*
6	2.40 *d* (3)	2.14 *q* (7)
7	–	1.42 *m*
8	–	1.29 *m*
9	–	1.29 *m*
10	–	0.89 *t* (7)
11	1.98 *s*	–
NH	5.55 *br s*	–
1′	3.17 *t* (6.6)	3.49 *m*
2′	1.80 *m*	1.57 *m*
3′	0.92 *d* (6.6)	1.64 *m*
4′	0.92 *d* (6.6)	1.62 *m*
5′	–	3.61 *m*

Table 2
^{13}C NMR data of compounds **2** and **3** [150 MHz, $CDCl_3$, TMS as int. standard; chemical shifts in δ values (ppm)]

C	**2**[a]	**3**[a]
1	166.1	165.8
2	123.2	118.5
3	138.9a	142.9
4	129.7	128.8
5	140.2a	142.6
6	31.2	32.9
7	68.2b	28.5
8	64.9	31.4
9	64.9	22.5
10	65.4b	14.0
11	18.7	–
1′	46.9	46.9b
2′	28.5	25.6a
3′	19.9	24.7a
4′	19.9	26.7a
5′	–	43.2b

[a] a,b, interchangeable signals.

Insecticidal tests on *Sitophilus oryzae* and *Rhyzopertha dominica* revealed that compounds **1**–**3** were very active, as shown in Fig. 1. Indeed compound **2** showed 100% mortality at a concentration of 200 μg/ml after 3 days on the two insects tested, however, compounds **1** and **3** showed a mortality of about 50 and 80%, respectively, toward *R. dominica* and *S. oryzae* at the same concentration after 3 days.

This investigation yielded two purely olefinic alkamides and an acetylenic alkamide. Two of the three compounds possessed an isobutyl side chain. The difference in insecticidal activity of these compounds could be attributed to their structural difference, especially the acetylenic group contained in compound **2** which showed the best insecticidal activity.

3. Experimental

3.1. General

^1H and ^{13}C NMR spectra were recorded in $CDCl_3$ on Varian Unity 600 instrument at 600 and 150 MHz, respectively; the chemical shifts are reported in δ units (ppm) values relative to TMS. IR spectra were recorded as films on a Nicolet 205-FTIR spectrometer. UV spectra were determined in MeOH with Shimadzu 265FS spectrophotometer. HR-EI-MS and ES-MS measurements were carried out on a Fisons VG Autospec. TLC were carried out on Silica gel F_{254} precoated plates (0.25

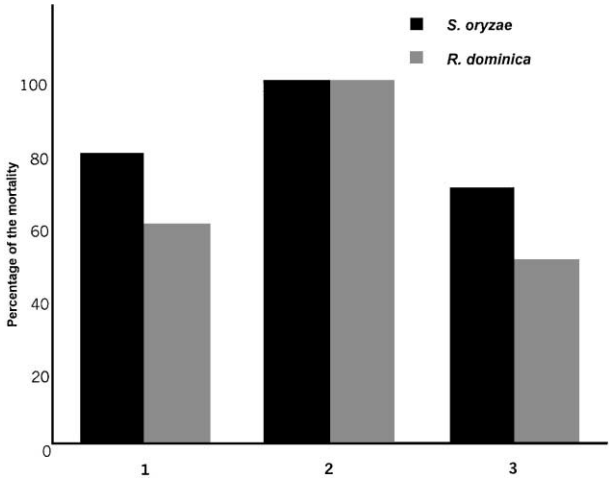

Fig. 1. Toxicity of compounds **1**–**3** on *S. oryzae* and *R. dominica* at 200 μg/ml concentration after 3 days. Statistical analysis was done using ANOVA ($P < 10^{-3}$).

mm). C.C were also performed on Silica gel (Merck Silica gel 60, 70–230 mesh).

3.2. Plant material

Aerial parts of plants *A. dracunculus* were collected at Salé, Morocco, in September 1997. Identification of the plant was confirmed by Dr. A. Ouyahya. A voucher specimen is deposited in the herbarium of the DBEV (Département de Botanique et Ecologie Végétal, Institut Scientifique) in Rabat (Morocco).

3.3. Extraction and isolation

The plant material was air-dried at room temp., finely ground and extracted (100 g), successively with petroleum ether (pb 40–60°) and CH_2Cl_2. The extracts were filtered, and the solvent was concentrated under reduced pressure. One portion (6 g) of the crude petroleum ether extract was fractionated by column chromatography on silica gel [A: hexane–EtOAc (9:1), B: hexane–EtOAc (7:3) and C: hexane–EtOAc (4:6)]. Fraction A (1.06 g) was fractionated by column chromatography on silica gel (hexane–EtOAc, 2:3) to give **1** (36 mg), **2** (17 mg) and **3** (9 mg). Crystallization of the fraction B from CH_2Cl_2 afforded 476 mg of herniarine **4**. This compound was isolated from *A. dracunculus* and identified as described previously (Ahmad and Misra., 1997).

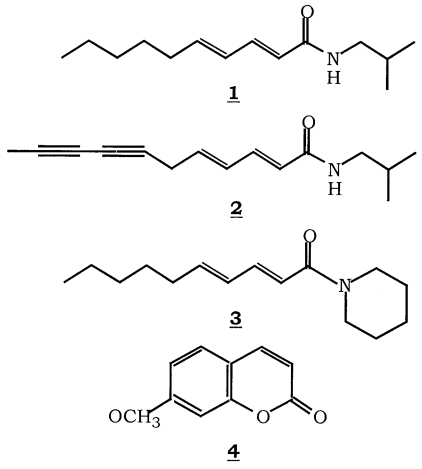

3.4. Deca-2E, 4Z-diynoic acid isobutylamide *1*

Yellow oil; UV λ_{max} nm: 257; IR $\surd_{max}$ cm^{-1}: 3300, 3070, 1650, 1540 (–CO–NH–); 2950 (CH–); 1650, 950 (–C=C–); HR-EI-MS: *m/z* (%, rel. int.) $[M]^+$ 223.1939 (26.5) (calc. for 223.1936), 208.1706 (5.8), 180.1391 (5.7), 166.1236 (6), 151.1123 (100), 124.0763 (2.1), 100.0402 (4.3); ES-MS: *m/z* (%) $[2M]^+$ 447.65 (14), 226.42 (4), 225.37 (13), $[M+1]^+$ 224.36 (100), 196.18 (4), 177.09 (11), 156.16 (11).

3.5. Undeca-2E, 4Z-dien-7,9-diynoic acid isobutylamide *2*

Yellow oil; UV λ_{max} nm: 257; IR $\surd_{max}$ cm^{-1}: 3300, 3070, 1660, 1520 (–CO–NH–); 2960 (CH–); 1620, 990 (–C=C–); EI-MS: *m/z* (%, rel. int.) $[M]^+$ 229 (33), 214 (10), 186 (7), 172 (12), 157 (100), 129 (31), 127 (38), 57 (43.5); ES-MS: *m/z* (%) $[M]^+$ 459.56 (5), $[M+2]^+$ 231.36 (18), $[M+1]^+$ 230.31 (100), 226.30 (5), 196.25 (24), 158.18 (12), 156.17 (41); ^1H and ^{13}C NMR data are presented in Tables 1 and 2.

3.6. Deca-2E, 4Z-dienoic acid piperidide *3*

Yellow oil; UV λ_{max} nm: 257; IR $\surd_{max}$ cm^{-1}: 3280, 3080, 1670, 1638 (–CO–N<); 2940 (CH–); 1630, 970 (–C=C–); EI-MS: *m/z* (%, re. int.) $[M+1]^+$ 236 (4.5), $[M]^+$ 235 (17.5), 192 (25.5), 178 (12), 164 (31), 151 (24), 138 (25), 127 (34), 112 (46), 84 (100), 57 (38.5); ^1H and ^{13}C NMR data are presented in Tables 1 and 2.

3.7. Insecticidal test

The procedure was similar to the one described by Regnaut–Roger (Hamraoui and Regnault, 1997).

The isolated compounds (each sample at a concentration 5 mg/ml) were tested for their insecticidal activity, using paper discs (Whatman, Ø = 9 mm) impregnated with 30, 40 and 50 µl of the samples from which the solvent was allowed to evaporate at room temperature. Then, the paper disc was introduced into the experimental chamber containing 10 g of wheat and 20 adults insects (each species was tested separately). The tests were conducted in semi-aerated medium at 25 °C and a relative humidity of 70%.

Three replicates were employed for each sample and the mortality was recorded at 24 h, 2, 3 and 4 days.

Acknowledgements

We are grateful to Mr. C. Moulard, to Dr. M. Luhmer for MS and NMR measurements and, to the "Département des Relations Internationales" of U.L.B. for their financial support.

References

Ahmad, A., Misra, L.N., 1997. Isolation of herniarin and other constituents from *Matricaria chamomilla* flowers. Int. J. Pharmacognosy 35, 121–125.

Bohlmann, F., Hoffmann, H., 1983. Further amides from *Echinacea purpurea* isolated rom the areal parts, chemotaxonomic relevance. Phytochemistry 22, 1173–1175.

Bauer, R., Remiger, P., Wagner, H., 1988. Alkamides from the roots of *Echinacea purpurea*. Phytochemistry 27, 2339–2342.

Bauer, R., Remiger, P., Wagner, H., 1989. Alkamides from the roots of *Echinacea angustifolia*. Phytochemistry 28, 505–508.

Boriky, D., Berrada, M., Talbi, M., Keravis, G., Rouessac, F., 1996. Eudesmanolides from *Artemisia herba-alba*. Phytochemistry 43, 309–311.

Dunstan, W.R., Garnett, H., 1895. Note on the active constituent of the pellitory of medicine. Chem. Soc. 67, 100–102.

Greger, H., Grenz, M., Bohlmann, F., 1982. Piperides and other amides from *Achillea* species. Phytochemistry 21, 1071–1074.

Greger, H., 1984. Alkamides: structural relationships, distribution and biological activity. Planta Med. 50, 366–375.

Greger, H., Hofer, O., 1987. Highly unsaturated isopentyl amides from *Achillea wilhelmsii*. J. Nat. Prod. 50, 1100–1107.

Greger, H., Hofer, O., 1989. Polyenoic acid piperidides and other alkamides from *Achillea millefolium*. Phytochemistry 28, 2363–2368.

Hamraoui, A., Regnault-Roger, C., 1997. Comparaison des activités insecticides des monoterpènes sur deux espèces d'insectes ravageurs des cultures: *Ceratitis capitata* et *Rhopalosiphum padi*. Acta Bot. Gallica 144, 413–417.

Jacobson, M., 1954. Occurrence of a pungent insecticial principle in *American coneflower* roots. Science 120, 1028.

Martin, R., Becker, H., 1985. Amides and other constituents from *Acmella ciliata*. Phytochemistry 24, 2295–2300.

Marco, J.A., Barbera, O., 1990. Natural products from the genus *Artemisia*. In: Atta-ur-Rahman, X. (Ed.), Studies in Natural Products Chemistry, Vol. 7A. Elsevier Science, Amsterdam, p. 201.

Ramsewak, R.S., Erickson, A.J., Nair, M.G., 1999. Bioactive *N*-isobutylamides from the flower buds of *Spilanthes acmella*. Phytochemistry 51, 729–732.

Su, H.C.F., Horvart, R., 1981. Isolation, identification and insecticidal properties of *Piper nigrum* amides. J. Agric. Food. Chem. 29, 115–118.

Tan, R.X., Zheng, W.F., Tang, H.Q., 1998. Biologically active substances from the genus *Artemisia*. Planta Med. 64, 295–302.

PERGAMON

Phytochemistry 58 (2001) 1087–1095

PHYTOCHEMISTRY

www.elsevier.com/locate/phytochem

Scyptolin A and B, cyclic depsipeptides from axenic cultures of *Scytonema hofmanni* PCC 7110

Ute Matern[a,*], Lukas Oberer[b], Rocco A. Falchetto[b], Marcel Erhard[c], Wilfried A. König[d], Michael Herdman[e], Jürgen Weckesser[a]

[a]*Institut für Biologie II (Mikrobiologie), Albert-Ludwigs-Universität, Schänzlestraße 1, D-79104 Freiburg i. Br., Germany*
[b]*Novartis Pharma AG, Preclinical Research, CH-4002 Basel, Switzerland*
[c]*AnagnosTec GmbH, Im Biotechnologiepark, D-14943 Luckenwalde, Germany*
[d]*Institut für Organische Chemie, Universität Hamburg, Martin-Luther-King-Platz 6, D-20146 Hamburg, Germany*
[e]*Unité de Physiologie Microbienne (CNRS URA 2172), Département de Biochimie et Génétique Moleculaire, Institut Pasteur, 28 Rue du Dr. Roux, 75724, Paris Cedex 15, France*

Received 15 May 2001; received in revised form 3 September 2001

Abstract

Two novel cyclic depsipeptides were isolated from axenic cultures of the terrestrial cyanobacterium *Scytonema hofmanni* PCC 7110 and designated scyptolin A and B. Amino acid analyses in context with mass and $^{1}H/^{13}C$ NMR spectroscopies revealed a composition typical for heterologous cyanopeptolins but containing the uncommon residue 3′-chloro-*N*-methyl-Tyr (cmTyr) and a unique sidechain. Scyptolin A and B both consist of the *N*-acylated peptide But[1]-Ala[2]-Thr[3]-Thr[4]-Leu[5]-Ahp[6] (3-amino-6-hydroxy-2-oxo-1-piperidine)-Thr[7]-cmTyr[8]-Val[9], which forms a 19-membered ring by esterification of the carboxyl of Val[9] with the hydroxyl of Thr[4]. In scyptolin B, the hydroxyl of the Thr[3] residue is additionally esterified with *N*-butyroyl-Ala. Both scyptolin A and B exhibit selective inhibition of porcine pancreatic elastase *in vitro* with IC_{50} values of 3.1 μg/ml. © 2001 Elsevier Science Ltd. All rights reserved.

Keywords: *Scytonema hofmanni*; Cyanobacteria; Cyanopeptolins; Cyclic depsipeptides; Scyptolin

1. Introduction

Cyanobacteria are a rich source of secondary metabolites, such as alkaloids, phenolic dilactones, polyketides and macrolides or peptides, which biosynthetically originate from widely different pathways and show a broad spectrum of biological activities (Namikoshi and Rinehart, 1996). Some of these metabolites are potent toxins (Beasley et al., 2000), a phenomenon which initially caught the attention of the food and health industries (Humpage et al., 2000). Selective pharmacological activities have also been observed, e. g. antiviral (Mundt et al., 1997), antitumor (Trimurtulu et al., 1994), or immunosuppressive (Zhang et al., 1997) effects were reported for various of these compounds, and some cyanobacterial metabolites were even introduced as molecular tools in protein phosphatase research (Toivola, 1998).

Whereas the toxic cyclic heptapeptides (microcystins) were studied intensively and more than 60 structural variations have been reported so far, much less is known about the related non-toxic metabolites produced by different strains of cyanobacteria. As a consequence, the attention has recently shifted to these unusual cyanobacterial secondary metabolites, and especially to the cyanopeptolins (Martin et al., 1993), e.g. microcystilid A (Tsukamoto et al., 1993), the aeruginopeptins (Harada et al., 1993), the micropeptins (Banker and Carmeli, 1999), or the cyanopeptolins A–B (Martin et al., 1993), S (Jakobi et al., 1995) and SS (Jakobi et al., 1996).

Some cyanopeptolins are known as specific inhibitors of serine proteases including elastase. This protease appears to be a rewarding object of research, since its activity is of critical importance in a number of human diseases, e.g. lung emphysema which is mediated by the excessive action of elastase (Mal et al., 1999). Furthermore, it has been proposed that unphysiologically high levels of elastase activity are involved in myocardial damage (Zaidi et al., 1999) and may cause a particular

* Corresponding author. Tel.: +49-761-203-2615; fax: +49-761-203-2678.
E-mail address: matern@uni-freiburg.de (U. Matern).

0031-9422/01/$ - see front matter © 2001 Elsevier Science Ltd. All rights reserved.
PII: S0031-9422(01)00400-9

form of psoriasis (Orem et al., 1997). Thus, natural elastase inhibitors might serve as valuable lead structures in pharmaceutical research dedicated to the development of new and more effective drugs.

We describe here the isolation and structural elucidation of two novel compounds, scyptolin A and B from axenic cultured cells of *Scytonema hofmanni* PCC 7110. These metabolites significantly inhibited porcin pancreatic elastase in in vitro assays. Since the human elastase sequence is highly homologous to the elastase from other vertebrates (Bode et al., 1989), commercial porcine pancreatic elastase can be conveniently used for the inhibition assays.

2. Results

2.1. Isolation of scyptolin A and B

Scytonema hofmanni PCC 7110, was grown axenically for four weeks in stationary culture under continuous irradiation. The cells were collected by filtration, deep-frozen and lyophilized. The lyophilized cell mass was extracted with aq. MeOH, and the extract was fractionated by stepwise adsorption and desorption of the amphiphilic, charged components to reversed phase chromatographic materials and ion exchange matrices. Two compounds, A and B, were eventually isolated from the partially purified extract by reversed phase HPLC in acidic aq. acetonitrile. Starting from 7 to 9 g of dry cell mass in different rounds of purification, 5 and 25 mg, respectively, of pure compounds A and B, were recovered on average. Ultraviolet and NMR spectroscopies (Reshef and Carmeli, 2001) suggested that both compounds belonged to the class of depsipeptides containing aromatic residues, and, with reference to the taxonomic source, the compounds were designated scyptolin A and scyptolin B.

2.2. Structural composition of scyptolin A and B

The amino acid analyses revealed an identical qualitative pattern for both scyptolin A and B and indicated a core composition of Thr, Ala, Val and Leu. However, distinct quantitative differences were recorded with stoichiometries of 3:1:1:1 for scyptolin A vs. 3:2:1:1 for scyptolin B. While these data would be compatible with the scyptolins being regular oligopeptides, their hydrophobicity upon chromatography pointed to more uncommon features, such as a blocked *N*-terminus and/or a cyclic structure. The chirality of the amino acids was determined by GC of their trifluoroacetylated methyl esters on a chiral stationary phase (König et al., 1989) and revealed the L-configuration for all amino acids employed, as described for other cyanopeptolins (Jakobi et al., 1995).

Three prominent ions were observed on LC–MS analysis in the positive-ion mode of scyptolin A at m/z 963.3 (base peak), 1003.5 (45% rel. intensity) and 981.1 Da (15% rel. intensity). Similarly, scyptolin B yielded ions at m/z 1104.4 (base peak), 1144.5 (85% rel. intensity) and 1121.3 Da (12% rel. intensity). In both instances, the isotopic distribution of the ions indicated the presence of chlorine in the molecules. The HR–MS of scyptolin A revealed a monoisotopic mass [M + Na] of 1003.4512 corresponding to the molecular composition of $C_{45}H_{69}N_8O_{14}Cl$, and the mass of scyptolin B [M + Na] was determined at 1144.5297 revealing the composition of $C_{52}H_{80}N_9O_{16}Cl$. Furthermore, the absorption in the ultraviolet range (λ_{max} 281.54 and 281.98 nm, respectively) and the banding pattern on IR spectroscopy (identical for both compounds) with prominent signals also in the range from 660 to 720 cm^{-1} supported the identification of chlorinated, aromatic peptides.

The ^1H NMR of scyptolin A revealed at least 69 protons resonating in the range from 10.5 and 0 ppm (Table 1). HSQC correlations and integration indicated 10 methyl, six methylene and 17 methine groups, leaving 10 protons unattached to carbon. The latter protons were assigned to six NH groups (doublets in the range 8.5–7.2 ppm), one phenolic OH (10 ppm) and three alcoholic OH groups (6.04, 4.91 and 4.47 ppm). Among the methyl groups, one primary (triplet), eight secondary (doublets) and one *N*-methyl group (singlet at 2.7 ppm, resonating at 30.4 ppm on ^{13}C NMR) were distinguished. All six methylene groups are attached to carbons as indicated by their ^1H and ^{13}C shifts (Table 1). The ^{13}C correlation of the methine groups revealed that four are attached to oxygen and eight to nitrogen, three represent aromatic and two aliphatic groups. The three aromatic protons belong to a 1,3,4-trisubstituted aromatic ring with the substituents CH_2 (no. 1), chlorine (no. 3) and OH (no. 4), which is part of the amino acid 3′-chloro-*N*-methyl-Tyr present in both scyptolin A and B. The structure of this amino acid was deduced from coupling constants, ^1H and ^{13}C shifts, COSY, ROESY and HMBC correlations of scyptolin B and with reference to the literature (Ishida et al., 1997).

The following *N*-acylated amino acids were identified from the spinsystems in the TOCSY and COSY and in accordance with their H–C correlations in the HSQC spectra: Ala, Leu, Val, Thr, *O*-acylated Thr, *N*-alkylated Thr, *N*-alkylated (3′-substituted) Tyr, and the Ahp (Radau, 2000) ring system. The configuration of the Ahp residue was inferred from NOEs and corresponded to the configuration observed in other cyanopeptolins (Martin et al., 1993). The *N*-alkylation of the Thr residue was supported further by the NOE correlation (double-headed arrow in Fig. 1, Table 1). The spinsystem of a propyl chain indicated an additional butyryl group. The amino acid sequence could be deduced from sequential proton NOE's like $\alpha-N_{i,\,i+1}$, $\beta-N_{i,\,i+1}$,

Table 1
NMR data of scyptolin A and B

Amino acid	Pos.	δ ^{13}C mult.	δ ^{1}H mult., J (Hz)	LR H–C correlations[a]	NOE-correlations[a]
Scyptolin A					
But[1]	1	172.3 *s*		Ala[2]-NH, 2, But[1]-2,3	
	2	37.2 *t*	2.08 *t*, 7.2		Ala[2]-NH
	3	19.0 *t*	1.49 *m*		
	4	14.0 *q*	0.84 *t*, 7.4		
Ala[2]	1	173.1 *s*		Thr[3]-NH,2, Ala[2]-2,3	
	2	48.2 *d*	4.40 *m*		Thr[3]-NH
	3	18.0 *q*	1.21 *d,* 6.5		
	NH		8.01 *d,* 7.5	But[1]-1	But[1]-2
Thr[3]	1	171.0 *s*		Thr[4]-NH,2, Thr[3]-2,3	
	2	58.0 *d*	4.36 *m*		Thr[4]-NH
	3	66.8 *d*	3.99 *m*		Thr[4]-NH
	4	19.4	1.02 *d,* 6.4		
	NH		7.81 *d,* 8.1	Ala[2]-1	Ala[2]-2
	OH		4.91 *d,* 5.0		
Thr[4]	1	169.6 *s*		Leu[5]-NH, Thr[4]-2	
	2	55.0 *d*	4.64 *m*		Leu[5]-NH
	3	72.1 *d*	5.49 *q*, 6.7	Val[9]-1	Leu[5]-NH
	4	18.0 *q*	1.22 *d,* 7.0		
	NH		7.71 *d,* 9.2	Thr[3]-1	Thr[3]-2
Leu[5]	1	171.0 *s*		Ahp[6]-NH	
	2	51.0 *d*	4.28 *m*		Ahp[6]-NH
	3	39.6 *t*	1.83/1.38 2×*m*		
	4	24.5 *d*	1.50 *m*		
	5	23.6 *q*	0.87 *d,* 6.9		
	6	21.0 *q*	0.75 *d,* 7.5		
	NH		8.44 *d,* 8.4	Thr[4]-1	Thr[4]-2,3, Ahp[6]-NH
Ahp[6]	1	170.1 *s*		Thr[7]-2, Ahp[6]-2	
	2	49.1 *d*	4.43 *m*		
	3	22.1 *t*	2.55/1.71 2×*m*		
	4	29.6 *t*	1.95/1.66 2×*m*		
	5	75.0 *d*	5.05 *s*		Thr[7]-3,OH
	NH		7.34 *d,* 9.4	Leu[5]-1	Leu[5]-NH,2
	OH		6.04 *d,* 3.1		Val[9]-NH, Val[9]-5
Thr[7]	1	170.8 *s*		cmTyr[8]-NCH_3,Thr[7]-2	
	2	55.6 *d*	4.37 *d,* 8.2		cmTyr[8]-2
	3	64.5 *d*	3.63 *m*		Ahp[6]-5
	4	19.4 *q*	0.26 *d,* 6.0		cmTyr[8]-2′,5′,6′
	OH		4.47 *d,* 4.5		Ahp[6]-5
cmTyr[8]	1	169.5 *s*		Val[9]-NH, cmTyr[8]-2	
	2	60.6 *d*	4.97 *m*		Thr[7]-2,Val[9]-NH,cmTyr[8]-NCH_3
	3	33.0 *t*	3.13/2.72 2×*m*		cmTyr[8]-2′,6′,NCH_3
	NCH_3	30.4 *q*	2.70 *s*	Thr[7]-1	Val[9]-NH, cmTyr[8]-2,3
	1′	129.3 *s*		cmTyr[8]-3	
	2′	131.0 *d*	7.07 *s*		cmTyr[8]-3
	3′	120.1 *s*		cmTyr[8]-5′	
	4′	152.7 *s*		cmTyr[8]-2′,6′	
	5′	117.2 *d*	6.86 *d,* 8.2		
	6′	129.3 *d*	6.99 *d,* 8.2		cmTyr[8]-3
	OH		10.0 broad		
Val[9]	1	172.7 *s*		Thr[4]-3,Val[9]-2	
	2	56.3 *d*	4.64 *m*		
	3	30.8 *d*	2.04 *m*		
	4	19.5 *q*	0.86 *d,* 6.9		
	5	17.8 *q*	0.75 *d,* 7.4		
	NH		7.66 *d,* 9.4	cmTyr[8]-1	cmTyr[8]-2, NCH_3,Ahp[6]-OH

(*continued on next page*)

Table 1 (*continued*)

Amino acid	Pos.	δ ^{13}C mult.	δ ^{1}H mult., J (Hz)	LR H–C correlations[a]	NOE-correlations[a]
Scyptolin B					
But[1]	1	172.1 *s*		Ala[2]-NH, 2, But[1]-2,3	
	2	37.2 *t*	2.09 *m*		Ala[2]-NH
	3	18.9 *t*	1.50 *m*		
	4	13.9 *q*	0.85 *t*, 7.5		
Ala[2]	1	172.6 *s*		Thr[3]-NH,2, Ala[2]-2,3	
	2	48.1 *d*	4.39 *m*		Thr[3]-NH
	3	17.9 *q*	1.21 *d,* 7.0		
	NH		8.03 *d,* 7.4	But[1]-1	But[1]-2, Thr[3]-NH
Thr[3]	1	169.2 *s*		Thr[4]-NH, Thr[3]-2	
	2	55.4 *d*	4.69 *m*		Thr[4]-NH
	3	70.5 *d*	4.98 *m*	Ala[11]-1	Thr[4]-NH
	4	15.9	1.10 *d,* 6.4		
	NH		7.85 *d,* 8.4	Ala[2]-1	Ala[2]-2,NH, Thr[4]-NH
Thr[4]	1	168.9 *s*		Leu[5]-NH, Thr[4]-2	
	2	55.4 *d*	4.63 *m*		Leu[5]-NH
	3	72.0 *d*	5.49 *q*, 6.7	Val[9]-1	Leu[5]-NH
	4	17.9 *q*	1.20 *d,* 6.3		
	NH		8.08 *d,* 8.9	Thr[3]-1	Thr[3]-NH,2
Leu[5]	1	170.7 *s*		Ahp[6]-NH	
	2	50.8 *d*	4.30 *m*		Ahp[6]-NH
	3	39.5 *t*	1.83/1.36 2×*m*		
	4	24.4 *d*	1.51 *m*		
	5	21.1 *q*	0.75 *d,* 6.5		
	6	23.7 *q*	0.89 *d,* 7.6		
	NH		8.42 *d,* 8.7	Thr[4]-1	Thr[4]-2,3, Ahp[6]-NH
Ahp[6]	1	169.8 *s*		Thr[7]-2, Ahp[6]-2	
	2	49.1 *d*	4.45 *m*		
	3	22.1 *t*	2.56/1.70 2×*m*		
	4	29.5 *t*	1.95/1.65 2×*m*		
	5	74.8 *d*	5.05 *s*		Thr[7]-3,OH
	NH		7.34 *d,* 9.4	Leu[5]-1	Leu[5]-NH,2
	OH		5.99 *d,* 3.1		Val[9]-NH, Val[9]-5
Thr[7]	1	170.5 *s*		cmTyr[8]-NCH_3,Thr[7]-2	
	2	55.6 *d*	4.68 *d,* 8.2		cmTyr[8]-2
	3	64.5 *d*	3.64 *m*		Ahp[6]-5
	4	19.3 *q*	0.26 *d,* 6.1		cmTyr[8]-2′,5′,6′
	OH		4.49 *d,* 4.8		Ahp[6]-5
cmTyr[8]	1	169.1 *s*		Val[9]-NH, cmTyr[8]-2	
	2	60.7 *d*	4.98 *m*		Thr[7]-2,Val[9]-NH,cmTyr[8]-NCH_3
	3	33.1 *t*	3.11/2.74 2×*m*		cmTyr[8]-2′,6′,NCH_3
	NCH_3	30.4 *q*	2.71 *s*	Thr[7]-1	Val[9]-NH, cmTyr[8]-2,3
	1′	129.3 *s*		cmTyr[8]-3,5′	
	2′	131.0 *d*	7.09 *s*		cmTyr[8]-3,6′
	3′	120.1 *s*		cmTyr[8]-2′,5′	
	4′	152.4 *s*		cmTyr[8]-2′,6′	
	5′	117.2 *d*	6.87 *d,* 8.2		
	6′	129.3 *d*	7.00 *d,* 8.2	cmTyr[8]-3,2′	cmTyr[8]-3
	OH		9.9 broad		
Val[9]	1	172.2 *s*		Thr[4]-3,Val[9]-2	
	2	56.1 *d*	4.69 *m*		
	3	31.0 *d*	2.05 *m*		
	4	19.7 *q*	0.85 *d,* 7.6		
	5	17.6 *q*	0.73 *d,* 7.7		
	NH		7.60 *d,* 9.5	cmTyr[8]-1	cmTyr[8]-2, NCH_3,Ahp[6]-OH
But[10]	1	172.2 *s*		Ala[11]-NH, 2, But[10]-2	
	2	37.1 *t*	2.09 *m*		Ala[11]-NH
	3	18.8 *t*	1.50 *m*		

(*continued on next page*)

Table 1 (*continued*)

Amino acid	Pos.	δ ^{13}C mult.	δ ^{1}H mult., J (Hz)	LR H–C correlations[a]	NOE-correlations[a]
	4	13.9 *q*	0.85 *t*, 7.5		
Ala^{11}	1	171.8 *s*		Thr^{3}-3, Ala^{11}-2,3	
	2	48.2 *d*	4.30 *m*		
	3	18.2 *q*	1.30 *d*, 7.2		
	NH		8.14 *d*, 6.8	But^{10}-1	But^{10}-2

[a] HMBC and NOE correlations within the spin system of an amino acid are not listed.

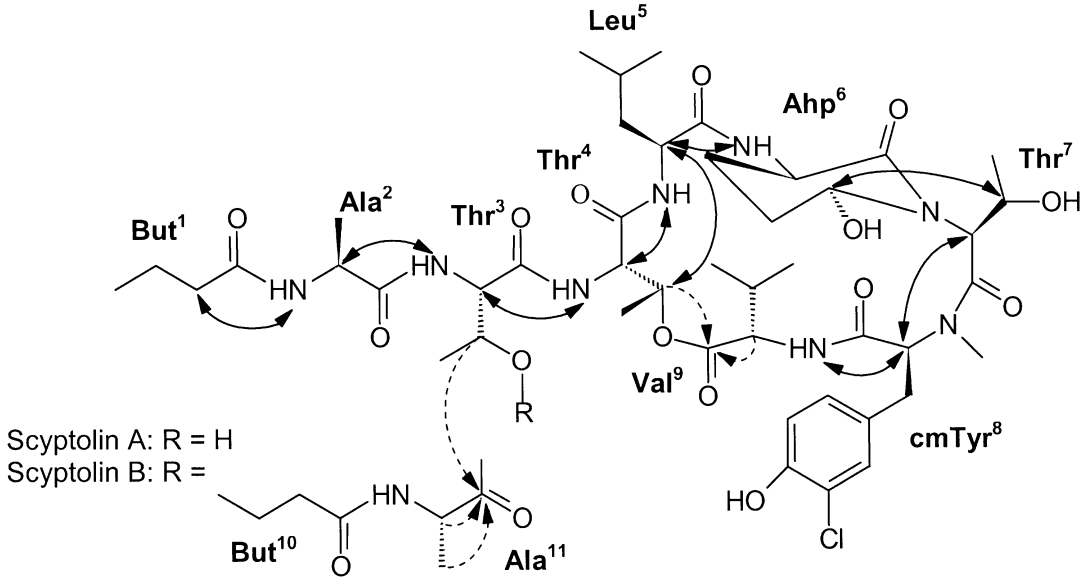

Fig. 1. Chemical composition of scyptolin A and B. Dotted arrows indicate the HMBC correlations of carbonyl groups, and double-headed arrows designate the NOE correlations. **But,** butyric acid; **Ahp,** 3-amino-6-hydroxy-2-oxo-1-piperidine; **cmTyr,** 3′-chloro-*N*-methyl-Tyr.

$\delta-\beta_{\ i,\ i+1}$ or $\alpha-\alpha_{,\ i,\ i+1}$ (Table 1). The α–α NOE between Thr^{7} and cmTyr^{8} indicate a *cis*-amide bond between these two amino acids. All other amide bonds show *trans* configuration, and the sequential NOE's (Table 1) are pointed out by double-headed arrows in Fig. 1. No NOE correlation is observed across the ester bridge between Val^{9} and Thr^{4} of scyptolin A and scyptolin B, and across the ester bridge between Ala^{11} and Thr^{3} of scyptolin B, while the HMBC correlations (dotted arrows, Fig. 1) supported the Thr^{4}-Val^{9} and Thr^{3}-Ala^{11} ester linkages.

The NMR data of scyptolin A is fully compatible with the composition of $C_{45}H_{69}ClN_8O_{14}$ derived from HR–MS and amounting to a nominal M_r of 980. Furthermore, the prominent ions observed on positive mode ESI–MS at m/z 981.2, 1003.5 and 963.3 (base peak) can be assigned to the pseudomolecular ion [MH$^+$] and the ions resulting from sodium addition [M + Na] and loss of water [MH–H_2O], respectively. Taken together, the structure of scyptolin A can be assigned as in Fig. 1.

The ^{1}H NMR of scyptolin B showed the presence of at least 80 protons resonating in the range 10.5 and 0.2 ppm and due to 12 methyl, eight methylene and 18 methine groups in addition to 10 exchangeable protons (Table 1). TOCSY and COSY spectra revealed the same amino acid composition as in scyptolin A, but indicated in addition the presence of one Ala and one butyryl residue as well as the *O*-acylation of a Thr residue (Table 1).

The ^{13}C shifts and the HMBC data (dotted arrows in Fig. 1) of the carbonyl groups are summarized in Table 1. An additional butyryl-Ala group is responsible for the elemental composition of $C_{52}H_{80}ClN_9O_{16}$ and a nominal M_r of 1121 of scyptolin B, which is again fully supported by the fragmentation pattern recorded on ESI–MS with the molecular ion [MH$^+$] at m/z 1121.4 accompanied by the signals for [M + Na] (m/z 1144.5 Da) and [MH−H_2O] forming the base peak (m/z 1104.4 Da).

2.3. Enzyme inhibition

Since some cyanopeptolins are known to inhibit protease activities, scyptolin A and B were subjected to inhibition assays with commercial proteases which are of medicinal relevance, e.g. trypsin, thrombin, plasmin,

papain and elastase. Among these proteases only elastase was inhibited to a significant extent at low concentrations, and an IC_{50} of 3.1 μg/ml was determined for both scyptolin A and B. Trypsin and papain were hardly affected ($IC_{50} > 500$ μg/ml), no inhibition at all was determined with plasmin and thrombin under the conditions employed. This result is puzzling in a sense, since the active site of serine-type proteases is proposed to be highly homologous.

3. Discussion

Terrestrial *Scytonema hofmanni*, in contrast to various related cyanobacteria, has hardly been investigated for its spectrum of secondary metabolites, and only a few compounds, e.g. the herbicidal cyanobacterin and hydroxycyanobacterin (Lee and Gleason, 1994) or the mirabimides (Carmeli et al., 1991) were characterized, none of which being a cyclic depsipeptide. This report, therefore, presents the first depsipeptide metabolites from *Scytonema* species. The core structure of scyptolin A an B is very similar to that of cyanopeptolins from other cyanobacteria (Weckesser et al., 1996), but two peculiar features distinguish these metabolites from most heterologous depsipeptides. The fifth position which is commonly held by a basic amino acid (Arg, Lys, *N*-Me-Lys, *N,N*-Di-Me-Lys) or Tyr and tetrahydrotyrosine (ThTyr), respectively, is replaced by Leu in the scyptolins, as had been reported also for nostopeptins (Okino et al., 1997). Furthermore, the *N*-methyl-Tyr residue in eighth position is 3-chlorinated in the scyptolins. This unusual amino acid has been detected before in only few heterologous cyanopeptolins (Ishida et al., 1997; Rouhiainen et al., 2000). A blocked *N*-terminus is typical for the cyanopeptolins, while the kind of acyl residue is variable ranging from aromatic (4-hydroxyphenyllactic acid) or medium chain-length aliphatic acids (hexanoic, octanoic acids) to mono and disulfated glyceric acid and even include hydrophilic amino acids (Gln, Thr, Asp; Weckesser et al., 1996). However, the *N*-terminal butyroylation detected in the scyptolins has not yet been observed in other cyanopeptolins.

Scyptolin A and B are homologous cyanopeptolins with scyptolin B representing the *N*-butyroyl-Ala-ester of scyptolin A. Thus, scyptolin A might be considered as a biogenetic precursor or as a breakdown product of scyptolin B, which even could have resulted as an artefact of purification. One step of the purification was carried out at pH 2.8, a condition that might partially hydrolyze scyptolin B. This concern was settled, however, by HPLC separation of crude *Scytonema* cell extracts which also detected scyptolin A, and the quantitative ratio of scyptolin A to B was repoduced in several runs. Moreover, incubations at pH 2.8 for up to 4 h of crude extracts did not release scyptolin A. Taking into account that *Scytonema* produces scyptolin B far in excess of scyptolin A, we propose that scyptolin A is the precursor of scyptolin B. This assumption requires further experimental support.

It is conceivable that cyanobacteria produce the unusual peptide metabolites to defend their ecological niche and to regulate their life cycle, respectively. For example, the heptapeptide microcystins were supposed to be harmful to competitors (Carmichael, 1992) and to chelate those metal ions (Humble et al., 1997) which are known to be toxic at high concentrations. Microcystins and other cyanopeptolins have also been described as more or less potent protein phosphatase inhibitors (Boland et al., 1993; Rapala, 1998), and cycles of protein phosphorylation and dephosphorylation are an integral part of metabolic regulation. Furthermore, energy-dependent proteases were proposed to play an important role in regulating cyanobacterial adaptive responses (for review see Mann, 2000), and a particular serine protease was cloned from *Anabaena* that is thought to be induced during nitrogen deficiency (Maldner et al., 1991). Signalling processes via proteases are supposedly as difficult to control as the kinase/phosphatase cycle and accordingly appear to require selective inhibitors.

The protease inhibitory capacities of depsipeptide metabolites have been tested occasionally, i.e. the nostopeptins A and B were found to be potent inhibitors of elastase and chymotrypsin (Okino et al., 1997). The scyptolins A and B also blocked elastase activity at low concentration but failed to inhibit any of the other serine-type proteases in the in vitro assays. An eventual effect on chymotrypsin activity remains to be tested, however, since the scyptolins and nostopeptins share the Leu-Ahp motif (Okino et al., 1997). Just like in other studies (Nakanishi et al., 2000), porcine pancreatic elastase was chosen for the assays, which is most similar to human leukocyte elastase (Bode et al., 1989) and allows to extrapolate the results to the human enzyme. The molecular basis for this kind of selectivity is unclear and the spatial structure of the enzyme-inhibitor complexes needs to be investigated. It appears possible that the mode of action reflects the physiological function of the scyptolins, but this aspect still remains a matter of speculation.

4. Experimental

4.1. Organism and culture conditions

Scytonema hofmanni PCC 7110 was obtained from the Pasteur Culture Collection (Institut Pasteur, Paris, France). Cells were grown photoautotrophically at 28 °C in 10-l flasks (Schott, Mainz, Germany) filled with 7 l of BG-11 growth medium (Rippka et al., 1979). These flasks were aerated at 0.5 bar and irradiated continuously with fluorescent white light (1000 Lux). After

4 weeks of culture, the cells were harvested by filtration through a net (pore size 55 μm), lyophilyzed and stored at −20 °C.

4.2. Extraction and purification

The cells (ca. 8 g dry wt.) were extracted three times with 75% (v/v) aq. MeOH. The cell debris was removed by centrifugation (Sorvall SLA-3000, 10,000 rpm, 20 min), the supernatant was diluted with water to adjust the concentration of MeOH to 10%, and Sephadex LH20 (Amersham Pharmacia Biotech, Freiburg, Germany), which had been pre-equilibrated in 50% aq. MeOH, was added. The solid material was removed by suction through a syringe equipped with a filter plate. Subsequently, Chromabond C_{18} (Macherey and Nagel, Düren, Germany), which had been pre-equilibrated in 90% aq. MeOH, was added to the filtrate and the particulate material was collected again by suction through a filter syringe. The amphiphilic components were eluted from the Chromabond C_{18} particles in 90% aq. MeOH, and the eluate was adjusted to 30% aq. MeOH, at pH 7.5. This solution was partially purified by filtration through anion exchange catridges (QMA, Waters, Eschborn, Germany). The pH was adjusted to 2.8, and the solution was applied subsequently to cation exchange catridges (SA, Waters, Eschborn, Germany), which partially resolved the depsipeptides. Elution was carried out using 0.25 mM ammonium hydrogencarbonate in 30% aq. MeOH. The fractions containing scyptolin A or B were diluted with water to 10% MeOH, and the peptide components were adsorbed to a C_{18}-cartridge. Elution was carried out with a small volume of 90% MeOH, and the solution was applied to a SP 250/21 Nucleosil 100-7 C_{18}-HPLC-column (Macherey and Nagel, Düren, Germany) using a Waters 600 multisolvent delivery system in line with a model 991 photodiode array detector (Waters, Eschborn, Germany) for final separation in acidic aq. acetonitrile under isocratic conditions at 40 °C. The depsipeptide A was separated in water/acetonitrile/0.5% TFA-acetonitrile 69/21/10, while the depsipeptide B was purified in water/acetonitrile/0.5% TFA-acetonitrile 60/30/10 at a flow rate of 10 ml/min. The fractions containing the depsipeptides were pooled and dried in a speed vac (maxi dry lyo, Heto-Holten GmbH, Wettenberg, Germany) at 35 °C for 12 h.

4.3. Amino acid analysis

The amino acid analysis was performed using a Waters kit (AccQ Tag, Waters, Eschborn, Germany). The pure depsipeptides (0.5 μg) were hydrolysed in a hydrolysis vial containing 2 mg PhOH in 200 μl 6 M HCl. The vial was sealed and heated under nitrogen to 115 °C for 22 h. The mixture was dried subsequently in a speed vac and the sample was redissolved in 20 μl 0.02 M HCl for derivatization with a fluorescence label. Reference amino acids were treated the same way, for comparison, the derivatives were separated on a Waters AccQ Tag column in Waters AccQ Tag eluent A (acetate-phosphate buffer), and the fluorescence was recorded at 250 and 395 nm exication and emission wavelength, respectively.

For the determination of absolute configuration of the amino acids, approximately 1 mg of the scyptolin sample was taken up in 1 ml of 6 N HCl and heated at 110 °C for 18 h in a screw cap glass vial with teflon liner in the cap. The hydrolyzate was then taken to dryness by a stream of nitrogen, and the residue was treated with a 2.5 molar solution of HCl gas in MeOH for esterification of the amino acids for 30 min at 100 °C. After removal of the excess of MeOH and HCl the sample was taken up in 0.2 ml of dichloromethane and 0.05 ml of trifluoroacetic anhydride and kept at room temp. for 30 min. Excess of the reagent was removed in a gentle stream of dry nitrogen and the residue was dissolved in 0.2 ml of dichloromethane for gas chromatographic analysis. The sample was injected onto a 25 m capillary column with octakis(3-*O*-butyryl-2,6-di-*O*-pentyl)-γ-cyclodextrin (60% in polysiloxane OV 1701, w/w) at 80 °C. A temp. program of 1 °C/min was used. The peak assignment was achieved by comparison and co-injection with samples of racemic amino acid derivatives which were prepared in the same way. On the chiral stationary phase used in this experiment except for proline the D-enantiomers are eluted before the L-enantiomers (König et al., 1989).

4.4. Spectrometry

For mass spectral analysis, the samples were loaded onto an Inertsil ODS-3, C18, 5 μm, 50×0.8 mm column equipped with a C18, 2×0.8 mm μ-guard column (LC Packings) using a FAMOS μ-sampling workstation (LC Packings, Amsterdam, The Netherlands). Chromatography was carried out using an HP1100 HPLC system (Hewlett-Packard, Waldbronn, Germany) running at 100 μl/min. The flow was split by an Acurate μ-flow processor (LC Packings) installed between the HPLC pump and the injector of the FAMOS workstation to yield a flow of 25 μl/min on the reversed-phase column. The HPLC solvents were: A, 0.05% TFA/water; B, 96% acetonitrile/0.05% TFA/water. Linear gradients from 10% to 80% B were run over 12 min, with an isocratic step of 3 min at 95% at the end of the gradient. The column effluent passed through a U-Z view 30 nl flow cell (LC Packings) with the detector set at 214 nm, and from there was then directed through a fused silica capillary (340 μm o.d.×50 μm i.d.) into the electrospray source of an LCQ ion trap mass spectrometer (Finnigan Corp., San Jose, CA, USA) run in the full scan mode for mass determination with the scan range set between

200 and 2000 amu. The source was operated at 4.5 kV with the heated capillary set at 220 °C and sheath nitrogen gas flow rate at 80. The ion time was set at 500 ms and the target number of ions at 5×10^7. Three microscans/spectrum were performed. The electron multiplier was set at −1000 V and spectra were collected in the positive-ion mode.

The ultraviolet absorption was measured on a Perkin Elmer Lambda 19 spectrometer (Perkin Elmer GmbH, Überlingen, Germany) employing 0.1 g/l of the sample in MeOH. The IR transmission spectra were recorded on a Perkin Elmer FT–IR Microscope i-Series coupled with a Spectrum 2000 FT–IR Spectrometer (Perkin Elmer GmbH, Überlingen, Germany).

NMR spectra were recorded on a BRUKER DMX 500 (Faellanden, Switzerland) spectrometer using a selective probe for the 1D–^{13}C spectrum and a triple inverse probe for the 1D–^{1}H and 2D spectra. The sample concentration was <2 mg/0.5 ml DMSO-d_6. ^{1}H and ^{13}C shifts are referenced to DMSO-d_6 = 2.49 ppm and 39.9 ppm respectively. The following NMR experiments were carried out: 1D–^{1}H, 1D–^{13}C, ^{1}H–^{1}H–COSY, ^{1}H–^{1}H–ROESY, ^{1}H–^{1}H–TOCSY, ^{1}H–^{13}C–COSY (HSQC), and the amino acid sequence was deduced primarily by HMBC correlations.

4.5. Enzyme inhibition

The isolated depsipeptides were dissolved in 50% aq. MeOH at 500 μg/ml, and a series of dilutions was preincubated with either one of the proteases trypsin, plasmin, thrombin, elastase and papain. Then, a *p*-nitrophenyl-labeled substrate peptide was added and the proteolytic release of *p*-nitrophenol was recorded spectrophotometrically at 405 nm (ELISA reader Dynatech MR 5000, Dynatech, Chantilly, Virginia, USA). All assays were carried out in microtiter plates and repeated in triplicate.

The following buffers were used: (A) 0.1 M Tris–HCl, pH 8.2, containing 23 mM $CaCl_2$, for trypsin (Elfant et al., 1985); (B) 0.05 M Tris–HCl, pH 8.9 for plasmin (Lottenberg et al., 1981, with modifications); (C) 0.2 M Tris–HCl, pH 8.0, for elastase (Bieth et al., 1974); (D) 0.2 M Tris–HCl, pH 8.0 for thrombin (adapted according to Lottenberg et al., 1981); (E) 0.1 M sodium phosphate, pH 6.5, containing 1 mM EDTA for papain (Barrett, 1981).

Trypsin *EC 3.4.21.4* (Sigma T 8802) was dissolved in 1 mM HCl containing 20 mM $CaCl_2$ (pH 3.1; 0.1 mg/ml). 10 μl of this solution were preincubated with the depsipeptide (10 μl) and 130 μl buffer A for 10 min at 25 °C. Subsequently, 150 μl of the substrate BAPNA (Sigma B 3133, 0.45 mg/ml in water) were added, and the incubation was continued for an additional 3 min.

Plasmin *EC 3.4.21.7* (Sigma P 8644) was dissolved in buffer B (0.5 mg/ml). 10 μl of this solution were preincubated with the depsipeptide (10 μl) and 170 μl buffer B for 10 min at 25 °C before 10 μl of the substrate *N*-*p*-tosyl-Gly-Pro-Lys-*p*-nitroanilide (Sigma T 6140, 1.1 mg/ml in water) were added and the incubation continued for 3 min.

Elastase Type IV *EC 3.4.21.36* (Sigma E 0258) was dissolved in buffer C (0.075 mg/ml). 10 μl of this solution were preincubated with the depsipeptide (10 μl) and 150 μl buffer C for 20 min at 30 °C. Then, 30 μl of the substrate *N*-succinyl-Ala-Ala-Ala-*p*-nitroanilide (Sigma S 4760, 18 mg/20 ml buffer C) were added, and the incubation was continued for an additional 3 min.

Thrombin *EC 3.4.21.5* (Sigma T 4648) was dissolved in buffer D (0.5 mg/ml). 10 μl of this solution were preincubated with the depsipeptide (10 μl) and 170 μl buffer D for 10 min at 25 °C. Thereafter, 10 μl of the substrate *N*-*p*-tosyl-Gly-Pro-Lys-*p*-nitroanilide (Sigma T 6140, 0.5 mg/ml water) were added, and the incubation was continued for an additional 3 min.

Papain *EC 3.4.22.2* (Sigma P3125) was dissolved in buffer E (100 μl in 1 ml). 10 μl of this solution were preincubated with the depsipeptide (10 μl) and 170 μl buffer E, containing additionally 2 mM cysteine (Sigma C 7755), for 10 min at 40 °C. Subsequently, 10 μl of the substrate BAPNA (Sigma B 3133, 4.2 mg/ml DMSO) were added and the incubation was continued for an additional 3 min.

4.6. Compound characterization

Scyptolin A: Colourless amorphous powder. Optical rotation $[\alpha]_D^{20}$ −66,0° (MeOH). Ultraviolet absorption λ_{max}^{MeOH} nm (log ε): 281.54 (3.29). Infrared spectrum ν_{max}^{film} cm^{-1}: 3364, 3310 (NH and OH stretching), 3063 (aromatic CH stretching), 2967, 2938, 2877 (aliphatic CH stretching), 1737 (ester C=O stretching), 1675 (amide C=O), 1530 (amide II).

Scyptolin B: Colourless amorphous powder. Optical rotation $[\alpha]_D^{20}$ −58.1° (MeOH). Ultraviolet absorption λ_{max}^{MeOH} nm (log ε): 281.98 (3.35). Infrared spectrum ν_{max}^{film} cm^{-1}: 3364, 3286 (NH and OH stretching), 3058 (aromatic CH stretching), 2965, 2938, 2876 (aliphatic CH stretching), 1738 (ester C=O stretching), 1666 (amide C=O stretching), 1534 (amide II).

Acknowledgements

We thank U. Neumann (University of Freiburg) for his introductory advice and S. Moss (Novartis, Basel) for infrared and ultraviolet analyses. The work was supported by the Deutsche Forschungsgemeinschaft and the Fonds der Chemischen Industrie.

References

Banker, R., Carmeli, S., 1999. Inhibitors of serine proteases from a waterbloom of the cyanobacterium *Microcystis* sp. Tetrahedron 55, 10835–10844.

Barrett, A.J., 1981. Cystatin, the egg white inhibitor of cysteine proteinases. Methods in Enzymology 80, 771–778.

Beasley, V.R., Lovell, R.A., Holmes, K.R., Walcott, H.E., Schaeffer, D.J., Hoffmann, W.E., Carmichael, W.W., 2000. Microcystin-LR decreases hepatic and renal perfusion, and causes circulatory shock, severe hypoglycemia, and terminal hyperkalemia in intravascularly dosed swine. Journal of Toxicology and Environmental Health 61, 281–303.

Bieth, J., Spiess, B., Wermuth, C.G., 1974. The synthesis and analytical use of a highly sensitive and convenient substrate of elastase. Biochemical Medicine 11, 350–357.

Bode, W., Meyer Jr., E., Powers, J.C., 1989. Human leukocyte and porcine pancreatic elastase X-ray crystal structures, mechanism, substrate specifity and mechanism-based inhibitors. Biochemistry 28, 1951–1963.

Boland, M.P., Taylor, F.J.R., Holmes, C.B.F., 1993. Identification and characterization of a type-1 protein phosphatase from the ocadaic acid-producing marine dinoflagellate *Prorocentrum lima*. FEBS Letters 334, 13–17.

Carmeli, S., Moore, R.E., Patterson, G.M.L., 1991. Mirabimides A-D, new *N*-acylpyrrolinones from the blue-green alga *Scytonema mirabile*. Tetrahedron 47, 2087–2096.

Carmichael, W.W., 1992. Cyanobacteria secondary metabolites—the cyanotoxins. Journal of Applied Bacteriology 72, 445–459.

Elfant, M., Bryant, L., Starcher, B., 1985. Isolation and characterization of a proteinase inhibitor from marama beans. Proceedings of the Society for Experimental Biology and Medicine 180, 329–333.

Harada, K.-I., Mayumi, T., Shimada, T., Suzuki, M., Kondo, F., Watanabe, M.F., 1993. Occurrence of four depsipeptides, aeruginopeptins, together with microcystins from toxic cyanobacteria. Tetrahedron Letters 34, 6091–6094.

Humble, A.V., Gadd, G.M., Codd, G.A., 1997. Binding of copper and zinc to three cyanobacterial microcystins quantified by differential pulse polarography. Water Research 31, 1679–1686.

Humpage, A.R., Hardy, S.J., Moore, E., Froscio, S.M., Falconer, I.R., 2000. Microcystins (cyanobacterial toxins) in drinking water enhance the growth of aberrant crypt foci in the mouse colon. Journal of Toxicology and Enviromental Health 61, 155–165.

Ishida, K., Matsuda, H., Murakami, M., Yamaguchi, K., 1997. Micropeptins 478-A and -B, plasmin inhibitors from the cyanobacterium *Microcystis aeruginosa*. Journal of Natural Products 60, 184–187.

Jakobi, C., Oberer, L., Quiquerez, C., König, W.A., Weckesser, J., 1995. Cyanopeptolin S, a sulfate-containing depsipeptide from a water bloom of *Microcystis* sp. FEMS Microbiology Letters 129, 129–133.

Jakobi, C., Rinehart, K., Neuber, R., Mez, K., Weckesser, J., 1996. Cyanopeptolin SS, a disulphated depsipeptide from a water bloom: structural elucidation and biological activities. Phycologia 35, 111–116.

König, W.A., Krebber, R., Mischnick, P., 1989. Cyclodextrins as chiral stationary phases in capillary gas chromatography, part V: octakis(3-*O*-butyryl-2,6-di-*O*-pentyl)-γ-cyclodextrin. Journal of High Resolution Chromatography 12, 732–738.

Lee, E.S.J., Gleason, F.K., 1994. A second algicidal natural product from the cyanobacterium *Scytonema hofmanni*. Plant Science 103, 155–160.

Lottenberg, R., Christensen, U., Jackson, C.M., Coleman, P.L., 1981. Assay of coagulation proteases using peptide chromogenic and fluorogenic substrates. Methods in Enzymology 80, 341–361.

Mal, H., Crestani, B., Aubier, M., Fournier, M., 1999. Emphysema: new concepts. M S-Medicine Sciences 15, 833–841.

Maldener, I., Lockau, W., Cai, Y., Wolk, C.P., 1991. Calcium-dependent protease of the cyanobacterium *Anabaena*. Molecular cloning and expression of the gene in *Escherichia coli*, sequencing and site-directed mutagenesis. Molecular and General Genetics 225, 113–120.

Mann, N.H., 2000. Detecting the environment. In: Whitton, B.A., Potts, M. (Eds.), The Ecology of the Cyanobacteria. Kluwer Academic Publishers, Dordrecht, pp. 367–395.

Martin, C., Oberer, L., Ino, T., König, W.A., Busch, M., Weckesser, J., 1993. Cyanopeptolines, new depsipeptides from the cyanobacterium *Microcystis* sp. PCC 7806. Journal of Antibiotics 46, 1550–1556.

Mundt, S., Nowotny, A., Mentel, R., Lesnau, A., Lindequist, U., 1997. Antiviral activity of the cyanobacterium *Microcystis aeruginosa* SPH 01. Pharmaceutical and Pharmacological Letters 7, 161–163.

Nakanishi, I., Kinoshita, T., Sato, A., Tada, T., 2000. Structure of porcine pancreatic elastase complexed with FR901277, a novel macrocyclic inhibitor of elastases, at 1.6 Å resolution. Biopolymers 53, 434–445.

Namikoshi, M., Rinehart, K.L., 1996. Bioactive compounds produced by cyanobacteria. Journal of Industrial Microbiology and Biotechnology 17, 373–384.

Okino, T., Qi, S., Matsuda, H., Murakami, M., Yamaguchi, K., 1997. Nostopeptins A and B, elastase inhibitors from the cyanobacterium *Nostoc minutum*. Journal of Natural Products 60, 158–161.

Orem, A., Deger, O., Cimsit, G., Bahadir, S., 1997. Plasma polymorphonuclear leukocyte elastase levels and its relation to disease activity in psoriasis. Clinica Chimica Acta 264, 49–56.

Radau, G., 2000. Serine proteases inhibiting cyanopeptides. Pharmazie 55, 555–560.

Rapala, J., 1998. Toxin Production by Freshwater Cyanobacteria: Effects of Environmental Factors. PhD thesis, University of Helsinki.

Reshef, V., Carmeli, S., 2001. Protease inhibitors from water bloom of the cyanobacterium *Microcystis aeruginosa*. Tetrahedron 57, 2885–2894.

Rippka, R., Deruelles, J., Waterbury, J.B., Herdman, M., Stanier, R.Y., 1979. Generic assignments, strain histories and properties of pure cultures of cyanobacteria. Journal of General Microbiology 111, 1–61.

Rouhiainen, L., Paulin, L., Suomalainen, S., Hyytiäinen, H., Buikema, W., Haselkorn, R., Sivonen, K., 2000. Genes encoding synthetases of cyclic depsipeptides, anabaenopeptilides, in *Anabaena* strain 90. Molecular Microbiology 37, 156–167.

Toivola, D., 1998. Microcystins: potent tools to study serine/threonine protein phosphatases and their role in cytoskeletal regulation. Acta Academiae Aboensis Ser B Mathematica et Physica Matematik Naturvetenskaper Teknik 57, 3–39.

Trimurtulu, G., Ohtani, I., Patterson, G.M.L., Moore, R.E., Corbett, T.H., Valeriote, F.A., Demchik, L., 1994. Total structures of cryptophycins, potent antitumor depsipeptides from the blue-green alga *Nostoc* sp. strain GSV 224. Journal of the American Chemical Society 116, 4729–4737.

Tsukamoto, S., Painuly, P., Young, K.A., Yang, X., Shimizu, Y., 1993. Microcystilide A: a novel cell-differentiation-promoting depsipeptide from *Microcystis aeruginosa* NO-15-1840. Journal of American Chemical Society 115, 11046–11047.

Weckesser, J., Cornel, M., Jakobi, C., 1996. Cyanopeptolins, depsipeptides from cyanobacteria. Systematic and Applied Microbiology 19, 133–138.

Zaidi, S.H.E., Hui, C.-C., Cheah, A.Y.L., You, X.-M., Husain, M., Rabinovitch, M., 1999. Targeted overexpression of elafin protects mice against cardiac dysfunction and mortality following viral myocarditis. Journal of Clinical Investigation 103, 1211–1219.

Zhang, L.-H., Longley, R.E., Koehn, F.E., 1997. Antiproliferative and immunosuppressive properties of microcolin A, a marine-derived lipopeptide. Life Sciences 60, 751–762.

PERGAMON

Phytochemistry 58 (2001) 1097–1105

PHYTOCHEMISTRY

www.elsevier.com/locate/phytochem

Antioxidant capacity of a 3-deoxyanthocyanidin from soybean

Alejandro D. Boveris[a], Andrea Galatro[a], Luis Sambrotta[b], Rafael Ricco[c], Alberto A. Gurni[c], Susana Puntarulo[a,*]

[a]*Physical Chemistry-PRALIB, School of Pharmacy and Biochemistry, University of Buenos Aires, Argentina*
[b]*LANAIS RNM F (CONICET-UBA), School of Pharmacy and Biochemistry, University of Buenos Aires, Argentina*
[c]*Pharmacobotany, School of Pharmacy and Biochemistry, University of Buenos Aires, Argentina*

Received 14 May 2001; received in revised form 3 August 2001

Abstract

Soybean cotyledons directly exposed to UV-C (190–280 nm) contained a colored pigment in those areas of the epidermis directly exposed to UV-C. Ethanolic extracts from UV-C irradiated cotyledons showed a significant peak at 532 nm at pH = 10, but not seen at pH = 6, successive changes in pH were accompanied by reversible changes in the spectra. The identity of the pigment isolated from soybean cotyledons was established as apigeninidin by comparing the features of standard of a apigeninidin (from sorghum) previously characterized by FAB–MS, UV, HPLC, ^{1}H NMR, and IR spectroscopy. To characterize antioxidant activity of this compound, its ability to scavenge radical species in vitro was tested. In the concentration range tested (up to 200 μg ml $^{-1}$), apigeninidin did not show any scavenger activity towards hydroxyl radical, quinones or NO. However, ascorbyl radical and lipid radicals were effectively quenched in a dose-dependent manner. Overall, UV-C radiation triggers molecular signals that lead in soybean cotyledons to the synthesis and accumulation of an antioxidant pigment, apigeninidin, that shows scavenger activity against ascorbyl and lipid radicals in in vitro studies. © 2001 Elsevier Science Ltd. All rights reserved.

Keywords: *Glycine max*; Fabaceae antioxidant capacity; 3-Deoxyanthocyanidin; Apigeninidin

1. Introduction

Flavonoid glycosides constitute an important group of plant secondary metabolites. Various soybean flavonoids have been identified, including coumestrol, biochanin A, genistein, naringenin, isorhamnetin, quercetin, isoquercetin, daidzein, formononetin, kaempferol, apigenin, and chrysin (Rivera-Vargas et al., 1993). An aurone (hispidol-6-glucoside) that in solution showed color changes in response to high pH reaching a peak at 478 nm, has been described in soybean cotyledons (Wong, 1966). Flavonoids play a significant role in many physiological processes. Flavonoids and other phenylpropanoids have long been thought to participate in protecting against UV radiation, because they accumulate primarily in the epidermal and hypodermal layers of leaves and stems (the most illuminated layers) (Dixon and Paiva, 1995). Recently, Kozak et al. (1999) reported that UV-B + UV-C radiation seems to be responsible for the appearance in soybean cotyledons, of a colored pigment with a strong absorption in the UV region. The increase in flavonoid accumulation occurred specifically in areas that had been exposed to UV-C radiation, in agreement with previous data from Lois (1994) on leaves of *Arabidopsis* exposed to UV radiation. Kozak et al. (1999), suggested by comparison with literature values, as the identity of observed pigment an uncommon 3-deoxyanthocyanidin, probably apigeninidin or a related compound. This finding was potentially very interesting since this compound has not been identified in legumes previously, and anthocyanidins are usually present as glycosides and not as free aglycones. In fact, soybean anthocyanidins previously identified in hypocotyls are malvidin glycosides and related compounds like delphinidin (Peters et al., 1984). Apigeninidin (3-deoxypelargonidin) was the first 3-deoxyanthocyanidin to be isolated; it was found by Robinson and Robinson (1932) in the bright scarlet corollas of *Rechsteineria cardinalis* (formerly *Gesneria cardinalis*). It occurs widely in the Gesneriaceae as a petal pigment and it is

* Corresponding author. Tel.: +54-11-4964-8244; fax: +54-11-4508-3646.
E-mail address: susanap@ffyb.uba.ar (S. Puntarulo).

0031-9422/01/$ - see front matter © 2001 Elsevier Science Ltd. All rights reserved.
PII: S0031-9422(01)00378-8

present in the fronds of several ferns (Harborne, 1967), in the leaf of *Sorghum vulgare*, (Stafford, 1965), and in the stems of *Sorghum bicolor* (Rey et al., 1993).

Regarding its physiological function, apigeninidin showed a high fungicidal activity in sorghum (Aida et al., 1996). Ratty and Das (1988) reported the effect of several flavonoids on nonenzymatic lipid peroxidation and showed that flavonoid aglycones were more potent in their antiperoxidative action than their corresponding glycosides. Moreover, the flavonoid aglycones (apigenin, luteolin, chrysoeriol, kaempferol, quercetin and isorhamnetin) from an illuminated parsley cell suspension culture change the antioxidative capacity of plasma in rats (Hempel et al., 1999).

The aim of this work was to study the nature of the colored pigment that appeared after UV irradiation in superficial layers of soybean cotyledons. Soybean plants were exposed in vivo to UV-C and the pigment was characterized by FAB–MS, UV and HPLC, and its properties were compared with the features of an standard of apigeninidin (from sorghum). The antioxidant capacity of this pigment against hydroxyl, semiquinone, nitric oxide (NO), ascorbyl and lipid radicals was also assessed by in vitro studies employing electron paramagnetic resonance (EPR) methods.

2. Results

Soybean cotyledons exposed to UV-C radiation (190–280 nm) accumulated a colored pigment in the epidermis as early as 15 h after receiving the UV irradiation, with a maximum after 24 h of irradiation. Pigmentation was observed in areas of the epidermis directly exposed to the UV-C source (Fig. 1); cotyledons from control and UV-B (280–320 nm) exposed plants did not show any change in pigmentation over the studied time period, in agreement with previous data from Kozak et al. (1999).

The spectra of ethanolic extracts of soybean cotyledons from control and UV-C irradiated plants after 24 h of a single exposure showed that absorbance in the region between 250 and 340 nm increased after irradiation (data not shown). Extraction with 0.01% (v/v) HCl in methanol gave an orange solution. This solution turned yellow after fuming with HCl, and changed back to red after exposure to ammonia. As previously reported with soybean cotyledons exposed to UV-B + UV-C, ethanolic extracts from UV-C irradiated cotyledons showed a significant peak at 532 nm at pH = 10, but not seen at pH = 6, and successive changes in pH were accompanied by reversible changes in the spectra (Kozak et al., 1999).

Kozak et al. (1999) suggested, by comparison with literature values (Harborne, 1967), that the above spectral data were consistent with the features of an uncommon 3-deoxyanthocyanidin, probably apigeninidin or a related compound. Further studies were therefore performed to establish the identity of the pigment. Apigeninidin is a natural component in sorghum (Rey et al., 1993). Apigeninidin from sorghum was purchased, characterized by FAB–MS, UV, HPLC, ^{1}H NMR and IR spectroscopy, to be employed as standard. Although apigeninidin has been prepared through total synthesis (Harborne, 1967; Sweeny, 1977, 1981) NMR spectroscopic data was not reported. The extremely low solubility of apigeninidin in different deuterated solvents made it difficult to reach an appropriate concentration to acquire NMR spectra. However, the data reported here were obtained using an acid medium, such as the mixture TFA_d–$DMSO_{d6}$–CD_3OD, 1:3:1, to acquire a ^{1}H NMR spectrum of the standard apigeninidin from sorghum. The ^{1}H NMR of sorghum apigeninidin showed the profile expected for this type of compound (3-deoxyanthocyanidin) (Mitchell et al., 1998): ^{1}H NMR δ: 9.05 (*d*, 1H, H4, $J = 8.8$ Hz), 8.34 (*d*, 2H, H2′ and H6′, $J = 9.1$ Hz), 8.15 (*d*, 1H, H3, $J = 8.8$ Hz), 7.06 (*d*, 2H, H3′ and H5′, $J = 9.1$ Hz), 6.97 (*d*, 1H, H6, $J = 1.7$ Hz), 6.70 (*d*, 1H, H8, $J = 1.7$ Hz). The ^{1}H NMR spectrum of the pigment isolated from soybean cotyledons was not of the quality of that obtained with the standard, since due to the experimental isolation procedure, a low amount of sample was obtained. However, FAB-MS studies were useful to characterize the pigment isolated from soybean. FAB-MS data shows a m/z at 255 (rel. int. 15) corresponding to $[M]^+$, and a m/z signal at 162 (rel. int. 100) corresponding to $[M]^+$–C_6H_5O. The FAB-MS of the standard (from sorghum) showed the same pattern with signals at 255 (*rel. int*. 100), and 162 (rel. int. 12). No other significant signals were found neither in experiments employing standard pigment nor in soybean samples. The standard of apigeninidin (from sorghum), was characterized by IR and UV, and the data obtained were consistent with data from the literature: IR KBr cm^{-1}: 3400, 3049, 1640, 1536, 1510, 1338, 1234, 1175, 1150, 838; and UV spectroscopy of apigeninidin in 0.01% (v/v) HCl–methanol, showed λ_{max} at 240, 276, 324 and 476 nm.

Aglycones are not usually found in living tissues. Since acid-containing solvents were used during extraction and isolation, under the experimental conditions employed in this study hydrolysis was minimized. Chromatograms were obtained on extracts within minutes of extracting the tissue with ice-cold methanol containing 0.1% (v/v) HCl to prevent hydrolysis (Harborne, 1967).

TLC studies of the extract obtained from irradiated cotyledons of soybean indicated that R_f values for the single pigment band were 0.75 and 0.63 in Forestal: HOAc:HCl:H_2O (30:3:10) and HCO_2H:HCl:H_2O (9:2:3) solvents, respectively. The UV–visible spectrum of the isolated pigment in 0.01% (v/v) HCl in methanol

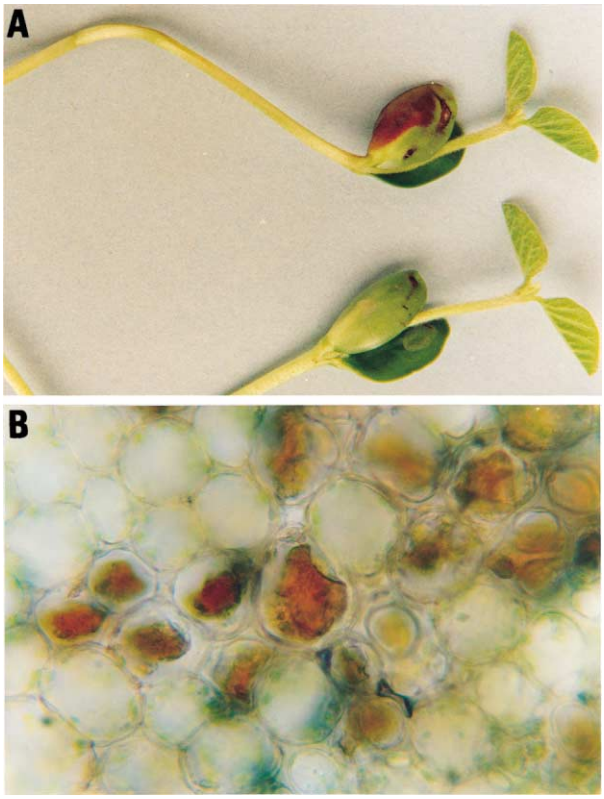

Fig. 1. Effect of UV-C (190–280 nm) on soybean cotyledons. A, UV-C irradiated seedling (top) and control seedling (bottom); B, longitudinal sections of epidermis of fresh cotyledons photographed at ×400, 24 h after UV-C exposure. A Leitz–Wetzler microscope equipped with a Canon A1 camera and regular 135-mm 100 ASA color film was used for the photograph.

showed a clearly defined maximum at 476 nm and another maximum at 276 nm (Fig. 2). The ratio $E_{440nm/474nm}$ was 0.55. No changes were detected after treatment of the pigment isolated from soybean cotyledons in 0.01% (v/v) HCl in methanol, with drops of 5% (w/v) $AlCl_3$ in methanol, suggesting that the molecule had no free *o*-dihydroxyl groups.

HPLC chromatograms of the standard of apigeninidin from sorghum and the pigment isolated from soybean were compared. Data shown in Fig. 3A using the standard apigeninidin (from sorghum) and in Fig. 3B employing the pigment extracted from soybean cotyledons, are in agreement in terms of R_t (2.85 min).

To assess the ability of apigeninidin to function as an antioxidant, in vitro studies were performed. Ascorbyl radical was generated by ascorbic acid in potassium phosphate buffer pH = 7.4. The EPR signal obtained under these conditions showed hyperfine splittings that are characteristic for ascorbyl radicals ($a^H = 1.88$ G, $g = 2.0054$) (Buettner and Jurkiewicz, 1993). The supplementation of the reaction medium with 200 μg ml^{-1} of apigeninidin significantly decreased the area of the recorded signal (Fig. 4A). The content of lipid radicals in rat liver microsomes, were detected by EPR using α-(4-pyridyl 1-oxide)-*N*-*t*-butyl nitrone (POBN) as spin trap. The characteristic signal of the POBN-lipid radical

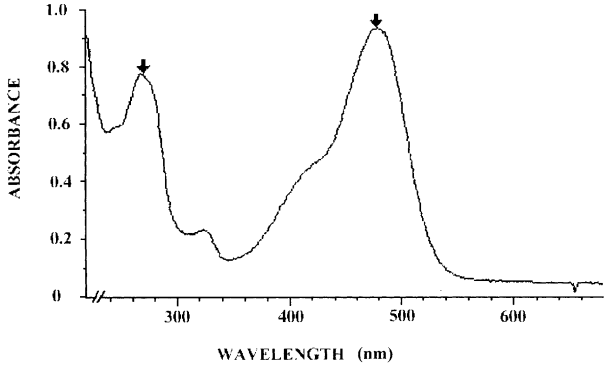

Fig. 2. UV-visible spectrum of the isolated pigment in 0.01% (v/v) HCl in methanol. Arrows indicate λ 276 and 476 nm, respectively.

adduct ($a^N = 15.8$ G, $a^H = 2.6$ G), (Jurkiewicz and Buettner, 1994) was significantly decreased in the presence of 200 μg ml^{-1} of apigeninidin (Fig. 4B). The content of thiobarbituric acid reactive substances (TBARS) is currently used as an index of lipid peroxidation (Slater, 1984). TBARS content in rat liver microsomes was significantly decreased by the addition of apigeninidin as shown in Fig. 5. The dose-dependent effect of apigeninidin on ascorbyl radical, lipid radical and TBARS content was studied (Fig. 5). Comparable

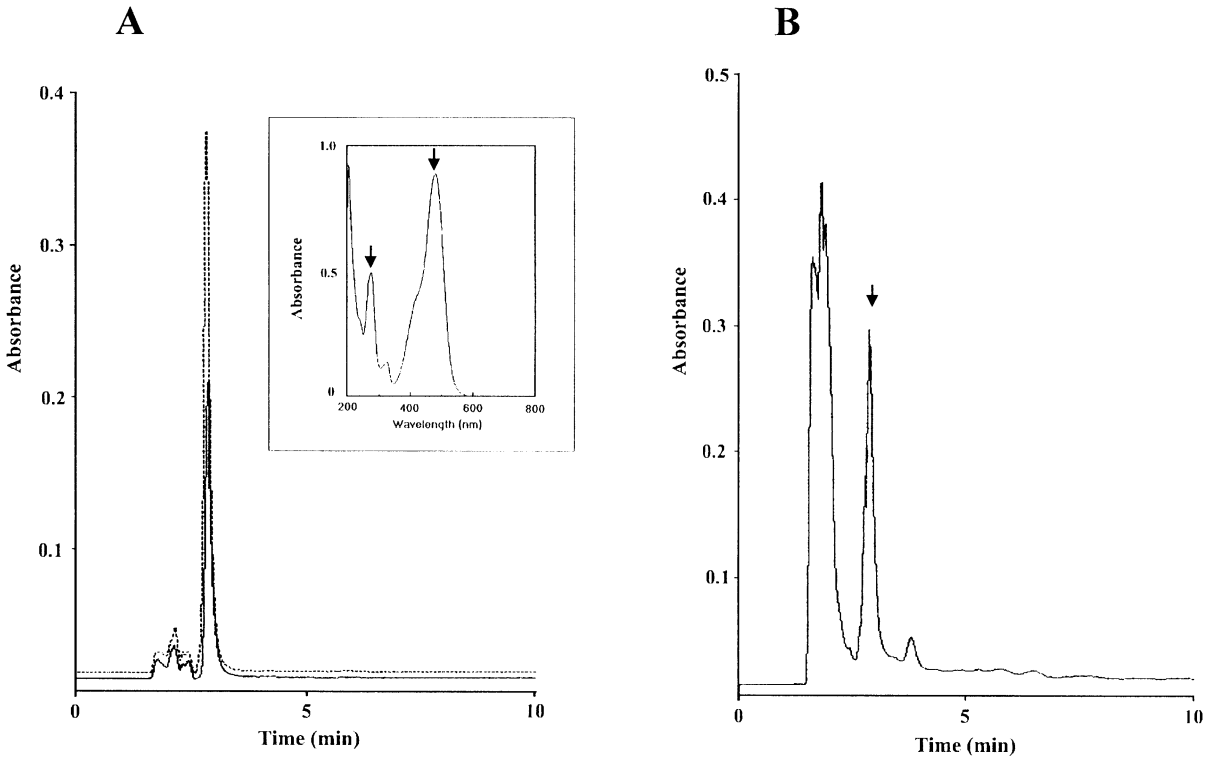

Fig. 3. Identification of apigeninidin by high performance liquid chromatography (HPLC). A, chromatogram of standard apigeninidin (from sorghum) in mobile phase (H_2O–THF–H_3PO_4 85% (v/v)-iso-PrOH (58:40:1:1) monitored to 270 (—) and 482 nm (·····) (Rt: 2.85 min). Inset, absorption spectra of the natural standard apigeninidin (from sorghum) in the same mobile phase. Arrows indicate the peaks at 270 and 482 nm; B, chromatograms obtained with the pigment isolated from soybean cotyledons exposed to UV-C (—) monitored to 270 nm. Arrow indicates R_f: 2.85 min.

results were obtained employing apigeninidin partially purified from soybean cotyledons exposed to UV-C (data not shown).

Hydroxyl radicals, semiquinone radicals and nitric oxide were generated in vitro as indicated in the Experimental section. The addition of apigeninidin (up to a concentration of 160, 200 and 200 μg ml^{-1} respectively), did not significantly affect the amount of each of the mentioned radicals detected by EPR.

3. Discussion

During the Precambrian, ultraviolet radiation reaching the Earth's surface, including UV-C wavelengths (190–280 nm), was considerably higher than at present because of the lack of absorbing gases (e.g. O_2 and O_3) in the atmosphere (Kastin et al., 1989). Although protection from UV-C radiation is not currently biologically important, high UV-C flux would have been damaging to photosynthetic organisms exposed to solar radiation in the past. Dillon and Castenholz (1999) postulated that a cyanobacterial extracellular sheath pigment may have been an important ecophysiological protective factor in cyanobacterial evolutionary history. The results presented here suggest that in soybean cotyledons, there are metabolic pathways that could be triggered by UV-C radiation. No UV-B exposure was required for the appearance of the pigment in soybean cotyledons since UV-C by itself could lead to apigeninidin accumulation. Adaptation to photooxidative stress is multifactorial, it may be also possible that UV-C irradiation activates molecular signals in common with more than one metabolic pathway. It has been shown that light-mediated responses affect the activity of the enzymes involved in flavonoid and anthocyanin biosynthesis (Lewis et al., 1998). The presence of apigeninidin in soybean has not been previously fully verified and the results presented here employing TLC, FAB-MS, and HPLC confirmed the identity of the observed pigment in soybean cotyledons exposed to UV-C as apigeninidin. The presence of this compound in soybean is an interesting finding since as it was previously indicated, aglycones are not normally found in living tissues and soybean anthocyanins previously identified in hypocotyls are malvidin glycosides and related pigments like delphinidin (Peters et al., 1984). On the other hand, since the experimental procedure employed is used to isolate glycosides, it should be discarded that the presence of the pigment could be an artifact generated by experimental isolation (Peters et al., 1984).

Flavonoids in general attract wide attention as possible useful agents for combating the pathological states

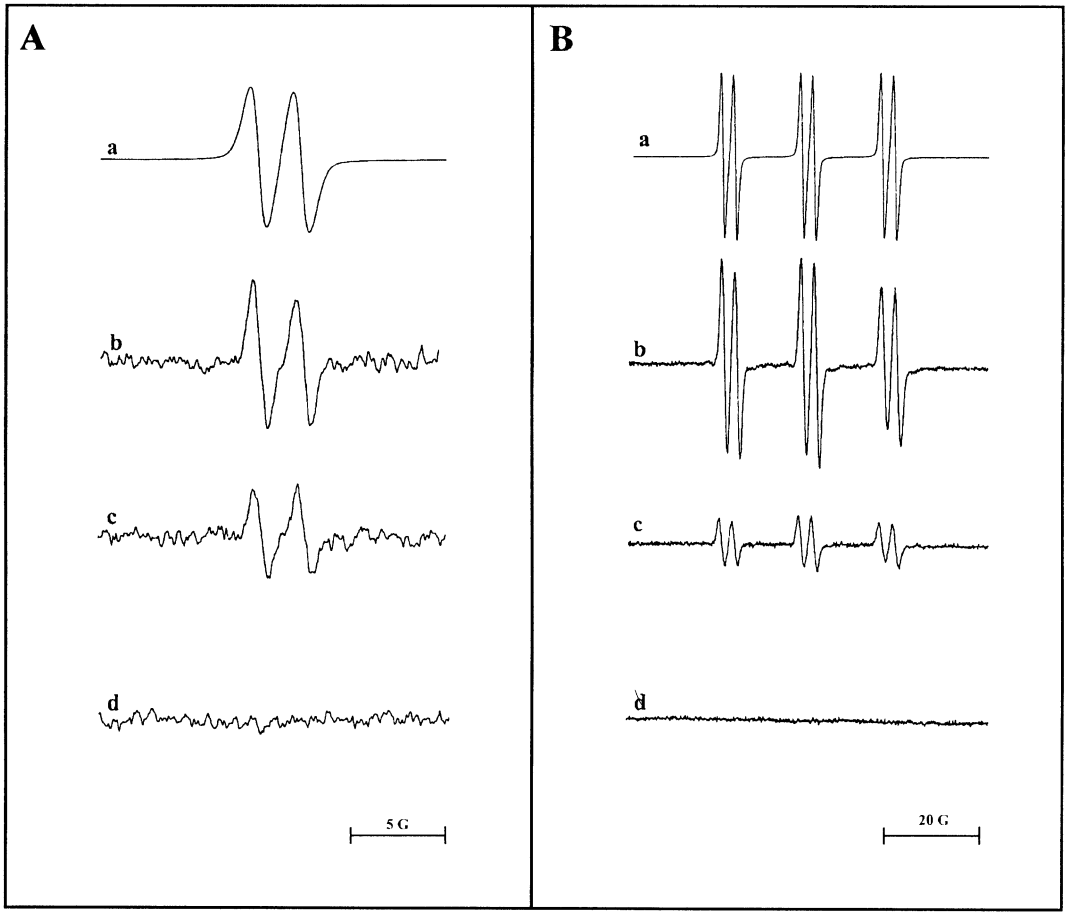

Fig. 4. Apigeninidin scavenging activity against ascorbyl radical and lipid radicals. A, electron paramagnetic resonance (EPR) spectra from ascorbyl radical generated by ascorbic acid in potassium phosphate buffer pH = 7.4. Computer simulated spectrum employing as spectral parameters $a^H = 1.88$ G and g = 2.0054 (a); ascorbic acid in 100 mM potassium phosphate buffer pH = 7.4 (b); ascorbic acid in 100 mM potassium phosphate buffer pH = 7.4 and 200 μg ml^{-1} apigeninidin (c); and basal system (in the absence of ascorbic acid)(d). B, EPR spectra of the lipid radicals-POBN (α-(4-pyridyl 1-oxide)-*N*-*t*-butyl nitrone) spin adduct. Computer simulated spectrum employing as spectral parameters $a^N = 15.8$ G and $a^H = 2.6$ G and g = 2.005 (a); lipid radicals-POBN spin adduct generated in rat liver microsomes (b); as (a), but in the presence of 200 μg ml^{-1} apigeninidin (c); and basal system (in the absence of microsomes) (d).

associated with free radical overproduction. To characterize the antioxidant activity of apigeninidin, its ability to scavenge radical species in vitro was tested. In the concentration range studied (up to 200 μg ml^{-1}), apigeninidin did not show any scavenger activity towards hydroxyl radical, semiquinones or NO. However ascorbyl radical and lipid radicals were effectively quenched.

Ascorbyl radical may be considered as a terminal product of free radical transformations in the biological antioxidant defense system. In living photosynthetic tissues both the enzymatic and non-enzymatic generation of ascorbyl radicals occur and could be substantially increased under oxidative stress conditions. For example, after exposure to UV-B the ascorbyl radical-dependent EPR signal was enhanced by 76 and 46% in algal cultures and soybean leaves, respectively (Malanga et al., 1999). The ability of apigeninidin to act as an scavenger of ascorbyl radical could have positive applications in terms of preventing the development of oxidative stress in those situations where ascorbyl radical content is increased.

In previous reports on structure-activity analysis of several flavonoids on non-enzymatic lipid peroxidation in rat brain mitochondria, it was concluded that flavonoid molecules with polyhydroxylated substitutions on rings A and B, a 2,3-double bond, a free 3-hydroxyl substitution and a 4-keto moiety, would confer upon the compound potent antioxidant properties (Ratty and Das, 1988). In that study, the flavonoid aglycones were more potent in their antiperoxidative action than their corresponding glycosides. According to the structure of apigeninidin, the lack of the ketone group (different that of the flavone), and the 3′ and 4′ hydroxy groups (different that of the catechin) that contribute to stabilize the radical formed, strong antioxidative effect was not expected, at least studying in vitro systems. It was also reported that flavonoids having fewer than four

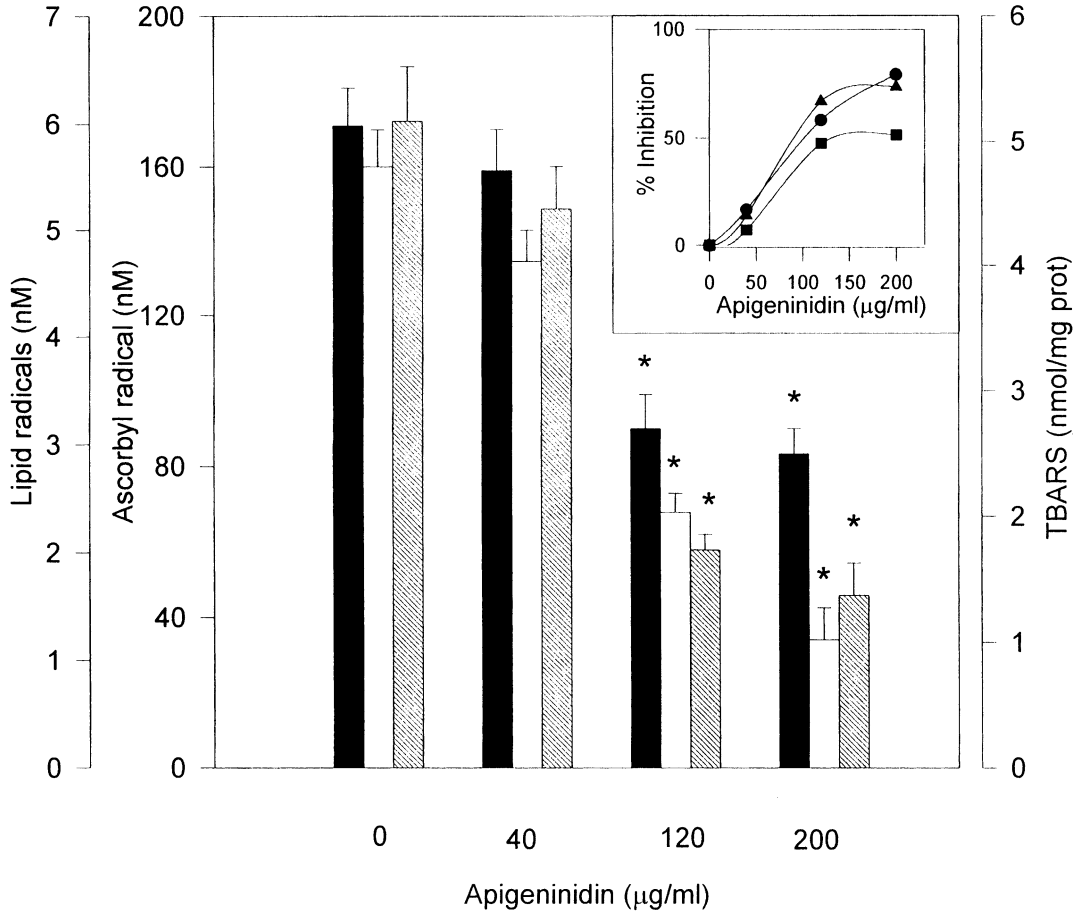

Fig. 5. Dose-dependent effect of apigeninidin on ascorbyl radical (■), thiobarbituric acid reactive substances (TBARS) (□) and lipid radical (▨) content. Lipid radical content and TBARS were assessed after 20 min incubation at 37° and ascorbyl radical was measured immediately as described in Experimental. Inset: percentages of inhibition by apigeninidin supplementation on ascorbyl radicals (■), TBARS (●) and lipid radicals (▲). * Significantly different ($P<0.05$, ANOVA) from control (without addition of apigeninidin).

hydroxyl groups show very little antioxidant efficiency (Larson, 1988). The effect of apigeninidin on lipid peroxidation was tested by measuring its quenching ability on TBARS and lipid radical content in microsomal membranes. Under the experimental conditions used here, a significant capacity of the pigment to limit lipid peroxidation was measured. It can be concluded that the antioxidant activity of the pigment depends on its posibility of accessing the membrane location where radicals are generated. Thus, the antioxidant capacity of apigininidin could be related not only to the pigment structural features but to the membrane characteristics as well.

The results presented here suggest that UV-C radiation triggers molecular signals that lead to the production of the pigment apigeninidin that exhibits antioxidant capacity. Further studies are required to assess the potential cellular function of the compound described here beside its ability of acting as scavenger of ascorbyl radical or as an inhibitor of lipid peroxidation. Moreover, since it was reported that flavonoid aglycones increased antioxidant capacity of blood plasma (Hempel et al., 1999) and soybean products are widely consumed in Western and Asian diets for health benefits, it could be of potential interest to use this cellular response to develop strategies to improve antioxidant capacity of soybean before the utilization of this products in the food and cosmetic industries.

4. Experimental

4.1. Plant material

Soybean seeds (*Glycine max* var Hood) were grown in controlled environmental conditions for 7 days at 26°, under hydroponic culture in modified Steinberg nutrient solution (Tiffin, 1966). Fe was supplemented as an Fe–EDTA (1:2) complex to a final concentration of 50 μM. The buffers and the water used to prepare all solutions were passed through columns containing Chelex 100 resin (Sigma Chemical Co.) to remove metal con-

taminants. The photo-period was approximately 12:12 h light:dark. Relative irradiance was measured using a Jarrell-Ash monochromator and an EMI 9634q5 photomultiplier for UV detection. The fluence rate at the surface was approximately 38 W m^{-2} of photosynthetically active radiation (Philips 40-W day-light-fluorescent light). A germicidal UV-C lamp (190–280 nm) with a band intensity centered at 254 nm (TUV 30 W/630 TB, Philips, The Netherlands) was used for UV-C treatments. Plants were situated 15 cm below the lamp and exposed to UV-C for 60 min. Cotyledons were excised 24 h after UV exposure.

4.2. Extraction and isolation procedures

The epidermical pigment was obtained by scraping the superficial layers of the cotyledons with ice-cold methanol containing 0.1% v/v conc. HCl to avoid hydrolysis (Harborne, 1967). Immediately after extraction, the colored solution was analyzed by TLC performed on Sigma Cell Type 100 cellulose, using HCO_2H:HCl:H_2O (9:2:3) and Forestal:HOAc:HCl:H_2O (30:3:10) as the mobile phases. A mixture of apigeninidin, pelargonidin and cyanidin was used as reference. After drying thoroughly the chromatograms under nitrogen flow, they were observed under daylight. An orange-yellow band, which turned to red after fuming with ammonia was observed. This band showed identical R_f, original color and reaction with ammonia than the standard apigeninidin. The original acid extract was employed for chromatographic assays using Forestal. Bands with the same R_f of apigeninidin from several chromatograms were eluted with ice-cold methanol containing 0.01% v/v conc. HCl, pooled and purified by chromatography using formic acid–HCl–H_2O (9:2:3). Bands were finally eluted with ice-cold methanol containing 0.01% v/v conc. HCl to perform characterization analysis.

4.3. Characterization analysis

FAB–MS studies were collected on a VG-ZAB-SEQ4F Spectrometer. Nuclear Magnetic Resonance (^{1}H NMR) was obtained on a Bruker MSL 300 spectrometer with a mixture of TFA d-DMSO d_6–CD_3OD 1:3:1 as solvent and TMS as internal standard. IR was recorded on a Bruker IFS 25 FT IR in KBr. The UV-visible spectrum of the isolated pigment in 0.01% (v/v) HCl in methanol was recorded in a Hewlett Packard 8452 A diode array spectrophotometer. HPLC analysis were performed with a reverse-phase column (Lichosorbs RP 18). The mobile phase was H_2O-THF-H_3PO_4 85% (v/v)-*iso*-PrOH (58:40:l:l) at a flow rate of 1 ml min^{-1} (Rey et al., 1993). UV detection was monitored at 270 or 482 nm with Waters 486 absorbance detector. Apigeninidin (from sorghum) was used as standard.

4.4. Electron paramagnetic resonance (EPR) measurements

The antioxidant capacity of apigeninidin was assessed studying its scavenger capacity on in vitro systems, by measuring free radical generation before and after pigment addition. Free radical measurements were performed at room temperature in a Bruker (Karlsruhe, Germany) ECS 106 EPR spectrometer with a ER 4102ST cavity.

4.4.1. Scavenging of hydroxyl radicals

Prior to use, the spin trap DMPO (5,5′-dimethyl-pyroline-*N*-oxide), was purified following the method of Green and Hill (1984), to remove contaminants that contribute to EPR background signal. In this procedure, 10 ml of 1 M DMPO in doubly distilled water were mixed with 1.25 g activated charcoal for 1 min, allowed to stand for 1 h, and then filtered. This purification procedure was repeated twice. Hydroxyl radicals were generated by a basic system consisting of 100 mM DMPO, rat liver microsomes (0.4 mg prot ml^{-1}), 0.2 mM sodium azide, 0.3 mM DTPA (diethylene-triaminepentaacetic acid), and 100 mM potassium phosphate buffer pH = 7.4, in the presence or absence of apigeninidin. Reactions were started by addition of 0.5 mM NADPH. The microsomal reaction system was incubated at 37° for 20 min and immediately transferred to a Pasteur pipette for recording. The EPR settings were: microwave power 20 mW, time constant 655.36 ms, modulation amplitude 0.490 G; field scan 100 G, sweep time 168 s, and modulation frequency 50 kHz (McCay et al., 1992). Quantification of the spin adduct was performed using an aqueous solution of 2,2,5,5-tetramethyl piperidine 1-oxyl (TEMPO) introduced into the same sample cell used for spin trapping. EPR spectra for both sample and TEMPO solutions were recorded at exactly the same spectrometer settings and the first derivative EPR spectra were double integrated to obtain the area intensity, then the concentration of spin adduct was calculated according to Kotake et al. (1996).

4.4.2. Scavenging of semiquinone radicals

The reaction system for semiquinone radical generation was: 1 mM Q_0 (2,3-dimethoxy-5-methyl-1,4-benzoquinone), 1 mM Q_0H_2, 100 mM potassium phosphate buffer pH = 7.4, and aliquots of apigeninidin. The setting of the Bruker Espectrometer ECS 106 were: microwave power 20 mW; center field 3490 G; time constant 1310.72 ms, modulation amplitude 0.979 G, sweep time 168 s, modulation frecuency 50 kHz, and sweep width 50 G. Quantification of the spin adduct was performed using an aqueous solution of TEMPO as previously indicated.

4.4.3. Scavenging of nitric oxide

NO was generated using *S*-nitroso-*N*-acetyl-penicillamine (SNAP) as NO donor. The reaction mixture

consisted of: 50 μM SNAP, *N*-methyl-D-glucamine dithiocarbamate iron (MGD:Fe (20:2 mM)) as spin trap, 100 mM potassium phosphate buffer pH = 7.4, and aliquots of apigeninidin. The EPR spectrometer settings were: microwave power 20 mW, center field 3450 G, time constant 164 ms, modulation amplitude 6.2 G, sweep time 168 s, modulation frequency 50 kHz, and sweep width 150 G (Komarov and Lai, 1995). Quantification of the spin adduct was performed using an aqueous solution of TEMPO as previously indicated.

4.4.4. Scavenging of ascorbyl radicals

The reaction mixture was: 62.5 μM ascorbic acid in 100 mM potassium phosphate buffer pH = 7.4 and aliquots of apigeninidin. The EPR spectrometer settings were: microwave power 1 mW, microwave frequency 9.75 GHz, center field 3487 G, time constant 327.68 ms, modulation amplitude 1 G and sweep width 15 G (Buettner and Jurkiewicz, 1993). Quantification of the spin adduct was performed using an aqueous solution of TEMPO as previously indicated.

4.4.5. Scavenging of lipid radicals

Rat liver microsomes prepared by differential centrifugation (0.4 mg prot ml^{-1}) were supplemented with 100 mM α-(4-pyridyl 1-oxide)-*N*-*t*-butyl nitrone (POBN), 5.5 mM ADP, 0.1 mM $FeCl_3$, 1 mM NADPH, 100 mM potassium phosphate buffer pH = 7.4, and incubated for 20 min at 37° in the presence or absence of aliquots of apigeninidin. The EPR spectrometer settings for the spin trapping experiments were: microwave power 20 mW, microwave frequency 9.75 GHz, center field 3480 G, time constant 82 ms, modulation amplitude 1.2 G and sweep width 100 G (Jurkiewicz and Buettner, 1994). Quantification of the spin adduct was performed using an aqueous solution of TEMPO as previously indicated.

4.4.6. Scavenging of thiobarbituric acid reactive substances (TBARS)

Microsomal TBARS content was measured using a modified fluorescence method (Fraga et al., 1987). Rat liver microsomes prepared by differential centrifugation (0.4 mg prot ml^{-1}) were supplemented with 5.5 mM ADP, 0.1 mM $FeCl_3$, 1 mM NADPH, 100 mM potassium phosphate buffer pH = 7.4, and incubated for 20 min at 37° in the presence or absence of aliquots of apigeninidin. To 0.5 ml of suspension, 0.05 ml of 4% (w/v) BHT and 0.5 ml of 3% (w/v) sodium dodecyl sulfate were added. After mixing, 2 ml of 0.1 N HCl, 0.3 ml 10% (w/v) phosphotungstic acid, and 1 ml of 0.7% (w/v) 2-thiobarbituric acid were added. The mixture was heated for 45 min in boiling water, and TBARS were extracted into 5 ml of *n*-butanol. After a brief centrifugation, the fluorescence of the *n*-butanol layer was measured at 515 nm excitation and 555 nm emission. The values were expressed as nmol TBARS (malondialdehyde equivalents) per mg protein. Malondialdehyde standards were prepared from 1,1,3,3-tetramethoxypropane.

4.4.7. Statistical analyses

Data are expressed as mean ± S.E. from 4 to 6 independent experiments. Statistical tests were carried out using Statview S.E.±, v 1.03 (Abacus Concepts Inc, Berkeley, CA, USA).

Acknowledgements

This study was supported by grants from the University of Buenos Aires, and Consejo Nacional de Investigaciones Científicas y Técnicas (CONICET) (PIP 0821/98). S.P. is career investigator from CONICET. A.G. and A.D.B. are fellows from CONICET.

References

Aida, Y., Tamogami, S., Kodama, O., Tsukiboshi, T., 1996. Synthesis of 7-methoxyapigeninidin and its fungicidal activity against *Gloeocercospora sorghi*. Bioscience, Biotechnology, and Biochemistry 60, 1495–1496.

Buettner, G.R., Jurkiewicz, B.A., 1993. Ascorbate free radical as a marker of oxidative stress: an EPR study. Free Radical Biology and Medicine 14, 49–55.

Dillon, J.G., Castenholz, R.W., 1999. Scytonemin, a cyanobacterial sheath pigment, protects against UVC radiation: implications for early photosynthetic life. Journal of Phycology 35, 673–681.

Dixon, R.A., Paiva, N.L., 1995. Stress-induced phenylpropanoid metabolism. Plant Cell 7, 1085–1097.

Fraga, C.G., Leibovitz, B.E., Tappel, A.L., 1987. Halogenated compounds as initiators of lipid peroxidation in tissue slices. Free Radical Biology and Medicine 3, 119–123.

Green, M.J., Hill, H.A., 1984. Chemistry of dioxygen. Methods in Enzymology 105, 3–22.

Harborne, J.B., 1967. The anthocyanin pigments. In: Harborne, J.B. (Ed.), Comparative Biochemistry of the Flavonoids. Academic Press, London and New York, pp. 1–36.

Hempel, J., Pforte, H., Raab, B., Engst, W., Bohm, H., Jacobasch, G., 1999. Flavonols and flavones of parsley cell suspension culture change the antioxidative capacity of plasma in rats. Nahrung 43, 201–204.

Jurkiewicz, B.A., Buettner, G.R., 1994. Ultraviolet light-induced free radical formation in skin: an electron paramagnetic resonance study. Photochemistry and Photobiology 59, 1–4.

Kasting, J.F., Zahnle, K.J., Pinto, J.P., Young, A.T., 1989. Sulfur, ultraviolet radiation, and the early evolution of life. Origins of Life and Evolution of the Biosphere 19, 95–108.

Komarov, A.M., Lai, C.S., 1995. Detection of nitric oxide production in mice by spin trapping electron paramagnetic resonance spectroscopy. Biochimica et Biophysica Acta 1272, 29–36.

Kotake, Y., Tanigawa, T., Tanigawa, M., Ueno, I., Allen, D.R., Lai, C., 1996. Continuos monitoring of cellular nitric oxide generation by spin trapping with an iron-dithiocarbamate complex. Biochimica et Biophysica Acta 1289, 362–368.

Kozak, R.G., Ricco, R.A., Gurni, A.A., Boveris, A.D., Puntarulo, S., 1999. Antioxidant response of soybean cotyledons (*Glycine max*) to ultraviolet irradiation. Canadian Journal of Plant Science 79, 181–189.

Larson, R.A., 1988. The antioxidants of higher plants. Phytochemistry 27, 969–978.

Lewis, C.E., Walker, J.R.L., Lancaster, J.E., Conner, A.J., 1998. Light regulation of anthocyanin, flavonoid and phenolic acid biosynthesis in potato minitubers in vitro. Australian Journal of Plant Physiology 25, 915–922.

Lois, R., 1994. Accumulation of UV-absorbing flavonoids induced by UV-B radiation in *Arabidopsis thailiana* L. Planta 194, 498–503.

Malanga, G., Kozak, R.G., Puntarulo, S., 1999. *N*-Acetylcysteine dependent protection against UV-B damage in two photosynthetic organisms. Plant Science 141, 129–137.

McCay, P.B., Reinke, L.A., Rau, J.M., 1992. Hydroxyl radicals are generated by hepatic microsomes during NADPH oxidation: relationship to ethanol metabolism. Free Radical Research Communications 15, 335–346.

Mitchell, K.M., Markham, K.R., Boase, M.R., 1998. Pigment chemistry and color of *Pelargonium* flowers. Phytochemistry 47, 355–361.

Peters, D.W., Wilcox, J.R., Vorst, J.J., Nielsen, N.C., 1984. Hypocotyl pigments in soybeans. Crop Science 24, 237–239.

Ratty, A.K., Das, N.P., 1988. Effects of flavonoids on nonenzymatic lipid peroxidation: structure–activity relationship. Biochemical Medicine and Metabolic Biology 39, 69–79.

Rey, J.P., Pousset, J.L., Levesque, J., Wanty, P., 1993. Isolation and composition of a natural dye from the stems of *Sorghum bicolor* (L.) Moench subsp. *americanum caudatum*. Cereal Chemistry 70, 759–760.

Rivera-Vargas, L.I., Schmitthenner, A.F., Graham, T.L., 1993. Soybean flavonoid effects on and metabolism by *Phytophthora sojae*. Phytochemistry 32, 851–857.

Robinson, G.M., Robinson, R., 1932. A survey of anthocyanins. Biochemical Journal 26, 1647–1664.

Slater, T.F., 1984. Overview of methods used for detecting lipid peroxidation. Methods in Enzymology 105, 283–293.

Stafford, H.A., 1965. Flavonoids and related phenolic compounds produced in the first internode of *Sorghum vulgare Pers*. in darkness and in light. Plant Physiology 40, 130–138.

Sweeny, J.G., Iacobucci, G.A., 1977. Synthesis of anthocyanidins—II. Tetrahedron 33, 2927–2932.

Sweeny, J.G., Iacobucci, G.A., 1981. Synthesis of anthocyanidins—III. Tetrahedron 37, 1481–1483.

Tiffin, L.O., 1966. Iron translocation I. Plant culture, exudate sampling, iron uptake analysis. Plant Physiology 41, 510–514.

Wong, E., 1966. Occurrence and biosynthesis of 4′,6-dihydroxy-aurone in soybean. Phytochemistry 5, 463–467.

PERGAMON

Phytochemistry 58 (2001) 1107–1111

PHYTOCHEMISTRY

www.elsevier.com/locate/phytochem

Taraxastane-type triterpenoids from *Saussurea petrovii*

Jingqiu Dai[a], Chenyang Zhao[b], Qi Zhang[b], Zhong-Li Liu[a], Rongliang Zheng[b], Li Yang[a,*]

[a]*National Laboratory of Applied Organic Chemistry, Lanzhou University, Lanzhou 730000, China*
[b]*Department of Biology, Lanzhou University, Lanzhou 730000, China*

Received 8 May 2001; received in revised form 16 August 2001

Abstract

Two taraxastane triterpenoids, i.e. taraxast-20-ene-3β,30-diol (**1**) and 20α,21α-epoxy-taraxastane-3β,22α-diol (**2**), as well as four known triterpenes taraxast-20(30)ene-3β,21α-diol (**3**), taraxast-20(30)-ene-3β-ol (**4**), taraxast-20-ene-3β-ol (**5**) and taraxastane-3β,20α-diol (**6**) were isolated from the Chinese medicinal plant *Saussurea petrovii*. Their structures were elucidated by spectroscopic methods. These compounds, especially **1** and **2**, exhibit significant antitumor and antibacterial activity.

Keywords: Saussurea petrovii Compositae; Taraxastane; Triterpenoids, Cytotoxicity; Antibiosis

1. Introduction

Saussurea petrovii (Compositae) is a perennial herbaceous plant growing mainly in North China. Its rhizome has been used as a traditional Chinese medicine for treatment of rheumatism and bleeding since ancient times (Ma et al., 1982). Its phytochemical or pharmacological properties have not been reported to date. In our effort to find biologically active components from Chinese medicinal plants (Zhu et al., 1999; Su et al., 2000; Wang et al., 2000; Zhang et al., 2000) we found two new triterpenoids, i.e. taraxast-20-ene-3β,30-diol (**1**) and 20α,21α-epoxy-taraxastane- 3β,22α-diol (**2**), as well as four known triterpenes taraxast-20(30)ene-3β,21α-diol (**3**), taraxast-20-ene-3β-ol (**4**), taraxast-20-ene-3β-ol (**5**) and taraxastane-3β,20α-diol (**6**) in the acetone extract of *Saussurea petrovii*. Compound **1** was previously reported as an oxidation product of taraxasterol (Pai and Kulkarni, 1977), but it has not been reported as a natural product. We report herein the isolation, structural elucidation and antitumor and antibacterial activities of these compounds. It was found that **1** and **2** possess strong cytotoxicity against mouse melanoma (B16) cells.

2. Results and discussion

From the acetone extract of the rhizome of *S. petrovii,* six taraxastane-type triterpenoids (**1**–**6**) were obtained and purified by repeated chromatography on silica gel. Each of the isolates was subjected to detailed spectroscopic analyses to establish their chemical structures.

Compound **1** was obtained as colorless crystals. The EIMS revealed a molecular ion peak at *m*/*z* 442. The ^{13}C NMR and DEPT spectra of **1** exhibited 30 carbon signals ($7\times CH_3$, $10\times CH_2$, $7\times CH$, $6\times C$), and the molecular composition of **1** was deduced to be $C_{30}H_{50}O_2$, which was confirmed by HR–EIMS (*m*/*z* 442.3811, calc. 442.3811). Its IR spectrum showed strong absorptions for hydroxyl groups and double bonds (3234 and 1656 cm^{-1}, respectively). The ^1H NMR spectrum demonstrated the presence of seven methyl groups, of which six were singlets (δ 0.75, 0.76, 0.85, 0.95, 0.96, 1.04) and one was a doublet (δ 1.00, *d*, *J* = 6.4 Hz), and an olefinic proton (δ 5.51, *dd*, *J* = 6.6, 1.8 Hz), two hydroxymethylene protons (δ 4.13, *d*, *J* = 12.3 Hz; δ 4.02, *d*, *J* = 12.3 Hz) and a hydroxymethine proton (δ 3.21, 1H, *dd*, *J* = 11.2, 4.9 Hz). These spectral data suggested that **1** was a pentacyclic triterpene with two hydroxyl groups and a trisubstituted double bond (Table 1). Comparison of the ^{13}C NMR spectroscopic data with those of pseudotaraxasterol (Reynolds et al., 1986) and its 22α-hydroxy derivative (Chiang and Kuo, 2000) showed that, except for the ring E carbons and C-28, the chemical shifts are almost identical. This suggested that the second

* Corresponding author. Tel.: +86-931-8912500; fax: +86-931-8625657.
E-mail address: liuzl@lzu.edu.cn (L. Yang).

0031-9422/01/$ - see front matter © 2001 Published by Elsevier Science Ltd. All rights reserved.
PII: S0031-9422(01)00397-1

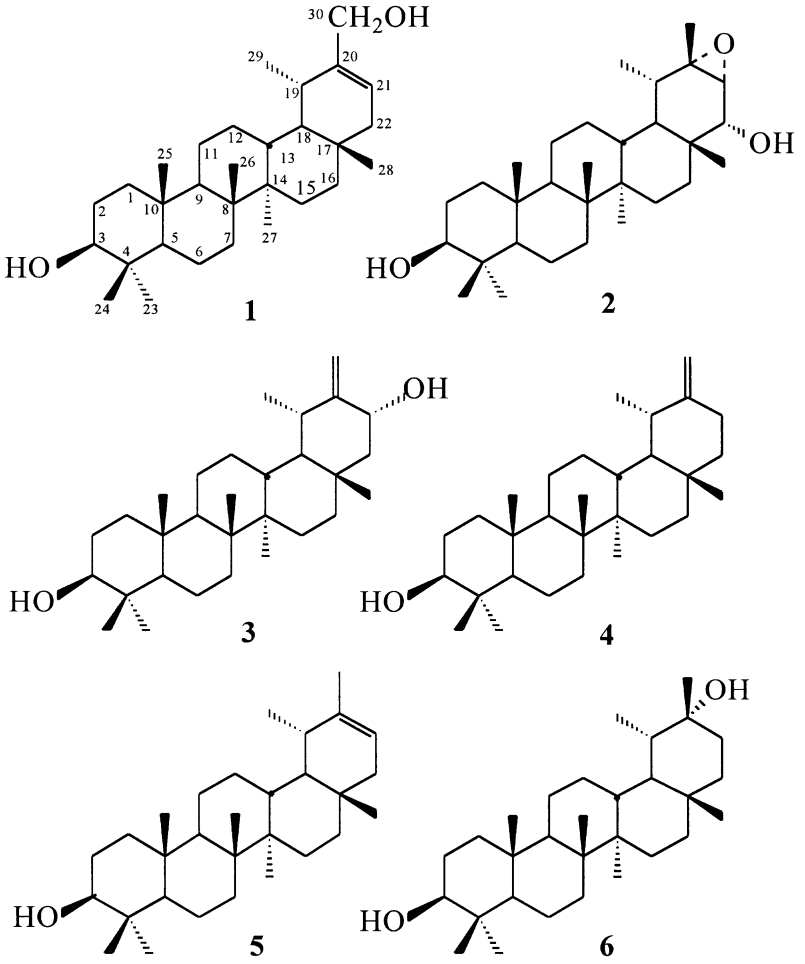

hydroxyl group must be located on ring E. Its definitive location was established by 2D NMR spectroscopic experiments. The ^{1}H–^{1}H COSY spectrum of **1** showed that the olefinic proton (δ 5.51) correlated only with H-22α (δ 1.55). In the HMBC spectrum H-16, H-18, H-22 and Me-28 correlated with C-17 (δ 34.5); H-19, H-21 and H-30 (hydroxymethyl group) correlated with C-20 (δ 143.7), indicating that the double bond is located at the C-20 (21) positions and C-30 is hydroxylated (Fig. 1). Therefore, compound **1** is deduced to be taraxast-20-ene-3β,30-diol.

Compound **2** was assigned the molecular formula $C_{30}H_{50}O_3$ by HR–EIMS (m/z 458.3746, calc. 458.3759). The IR absorption bands at 3240 cm^{-1} indicated the presence of hydroxyl groups. Comparison of the 1D (^{1}H, ^{13}C / DEPT) and 2D (^{1}H–^{1}H COSY, HMQC, HMBC) NMR spectra of **2** with those of **1** (Table 1) revealed that **2** possessed a similar structure except in ring E. Compound **2** has two more protons on oxygenated carbons at δ 3.12 (d, J=4.1 Hz) and δ 2.93 (d, J=4.1 Hz) and three oxygenated carbons at 65.7 (correlated to the ^{1}H signal at δ 2.93), 60.8 (correlated to the ^{1}H signal at δ 3.12) and δ 70.5 (a quaternary carbon), but no double bond was observed. Taking into account of the 6 double bond equivalent, compound **2** was deduced to be a taraxastane triterpenoid with an epoxy

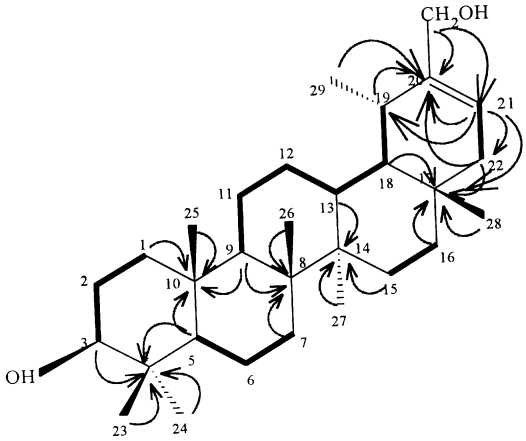

Fig. 1. ^{1}H–^{1}H COSY (—) and HMBC (H→C) correlations of compound

moiety and a hydroxyl group. ^{1}H–^{1}H COSY and HMQC (Fig. 2) showed the presence of a −CH−CH− fragment bearing an epoxide oxygen (δ 60.8) and one hydroxyl group (δ 65.7), suggesting that they are located at C-21 and C-22 respectively. This was confirmed by HMBC spectrum which showed clear correlations of H-21 with C-20, C-19 and C-30, and correlations of H-22 with C-17 and C-28 (Fig. 2). The magnitude of the coupling constant (4.1 Hz) between H-21 and H-22 suggested that

they are located at the same face of the molecule. The NOESY spectrum showed clear cross peaks between H-19β, H-21, H-22 and H-30, indicating the α-configuration of the epoxide. The COSY correlation between H-21β and H-22β and the J coupling of 4.1 Hz confirmed that H-22 must be an equatorial hydrogen, hence the 22-hydroxyl must be axial (α-configuration). In addition, the significant upfield shift of the C-18 and H-18 chemical shifts (δ 37.0 and 1.10 respectively) relative to those of **1** and related compounds without epoxy functionality (Reynolds et al., 1986; Mahato and Kundu, 1994) indicates that C-18 and H-18 are shielded by the α-epoxide. Therefore, **2** was deduced as 20α,21α-epoxy-taraxastane-3β,22α-diol which has not been reported in the literature.

Table 1
^{1}H and ^{13}C NMR spectral data for compounds **1** and **2** (400/100.58 MHz, $CDCl_3$)[a]

Compound	**1**		**2**	
Position	δ_C	δ_H (*J* in Hz)	δ_C	δ_H (*J* in Hz)
1α		0.91 *m*		0.95 *m*
1β	38.7	1.73 *m*	38.6	1.73 *m*
2α		1.55 *m*		1.55 *m*
2β	27.6	1.54 *m*	27.3	1.59 *m*
3	79.0	3.21 *dd* (11.2, 4.9)	79.0	3.22 *dd* (11.4, 4.9)
4	38.9		38.8	
5	55.3	0.76 *m*	55.2	0.71 *m*
6	18.3	1.54 *m*	18.4	1.53 *m*
7	34.2	1.36 *m*	34.1	1.38 *m*
8	41.1		41.2	
9	50.4	1.36 *dd* (11.7, 4.7)	49.9	1.35 *dd* (11.0, 4.5)
10	37.1		37.0	
11α		1.27 *m*		1.28 *m*
11β	21.6	1.59 *m*	21.3	1.54 *m*
12α		0.92 *m*		1.10 *m*
12β	27.0	1.62 *m*	26.1	1.69 *m*
13	39.2	1.55 *m*	37.0	1.75 *m*
14	42.4		43.3	
15α		1.68 *m*		1.61 *m*
15β	27.4	1.11 *m*	27.4	0.97 *m*
16	36.7	1.54 *m*	34.0	1.76 *m*
17	34.5		35.9	
18	48.5	1.25 *m*	37.4	1.28 *m*
19	32.0	2.04 *d* (7.1)	40.3	1.41 *m*
20	143.7		70.5	
21	120.7	5.59 *dd* (6.6, 1.8)	60.8	3.12 *d* (4.1)
22α		1.88 *m*		
22β	41.7	1.88 *m*	65.7	2.93 *d* (4.1)
23	15.4	0.75 *s*	15.3	0.77 *s*
24	27.9	0.96 *s*	27.9	0.97 *s*
25	16.3	0.85 *s*	16.1	0.86 *s*
26	16.0	1.04 *s*	15.9	1.02 *s*
27	14.8	0.95 *s*	15.5	0.96 *s*
28	17.7	0.76 *s*	17.7	0.97 *s*
29	22.5	1.00 *d* (6.4)	17.0	1.07 *d* (7.1)
30α		4.13 *d* (12.3)		
30β	65.5	4.02 *d* (12.3)	27.1	1.30 *s*

[a] Some ^{1}H peaks overlapped in the range of δ 1.2–1.9, hence the coupling constants could not be measured. Chemical shift assignments of those peaks were based on their ^{1}H–^{1}H COSY and HMQC spectra.

The structures of **3**, **4**, **5** and **6** were identified as taraxast-20(30)ene-3β,21α-diol, taraxast-20(30)ene-3β-ol, taraxast-20-ene-3β-ol and taraxastane-3β,20α-diol, respectively, by comparing their NMR spectral data with those reported in the literature (Anjaneyulu et al., 1985; Reynolds et al., 1986; Mahato and Kundu, 1994; Petrovic et al., 1999). Recently **3** was first isolated and identified from *Hieracium gymnocephalum* (Petrovic et al., 1999), but only 1 mg of **3** was obtained from 1.15 kg of the plant, and no melting point and optical rotation data were reported.

The cytotoxicity and antibacterial activity of compounds **1**–**6** have not been reported previously. Therefore, the antitumour activity of **1**–**6** was determined using the [3-(4,5-dimethylthiazol-2-yl)-2,5-diphenyltetrazolium bromide] (MTT) assay (Price and McMillan, 1990) with three tumor cell lines, i.e. human hepatoma cells, (SMMC-7721), human uterine cervix carcinoma cells (Hela) and mouse melanotic carcinoma cells (B16) with vincristine as a positive control (Table 2). It is seen from the table that all of these compounds exhibit moderate in vitro cytotoxic activity against these tumor cells, especially for Hela and B16 cells. The 50% inhibitory concentration (IC_{50}) values of the new compounds **1** and **2** are comparable to vincristine in the case of Hela and much smaller than vincristine in the case of B16.

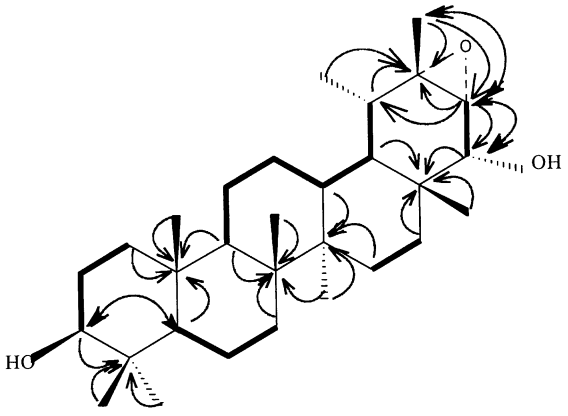

Fig. 2. ^{1}H–^{1}H COSY (—), HMBC (H→C) and NOESY (H←→H) correlations of compound **2**.

Table 2
Antitumor activity for compounds **1**–**6**[a]

Compound	SMMC-7721	B16	Hela
1	176.3±2.4	20.1±2.6	86.3±5.0
2	113.6±4.3	51.4±3.7	88.7±6.0
3	125.3±4.7	87.4±4.7	98.7±2.2
4	142.7±3.3	98.2±3.1	117.3±4.6
5	131.8±1.9	86.4±4.5	123.6±2.2
6	104.1±4.3	79.7±5.6	71.8±4.4
Vincristine	63.2±1.8	70.7±2.8	67.2±2.2

[a] Activities are expressed as IC_{50} (50% inhibitory concentration) in μg ml^{-1}. Data are expressed as mean±standard deviations of triplicate determinations.

The IC_{50} of 20 μg/ml demonstrates **1** as being an effective inhibitor of B16.

The antibacterial activity of **1**–**6** was determined against *Bacillus subtilis, Escherichia coli* and *Staphylococcus aureus* and compared with that of chloramphenicol (Table 3). It is seen that these triterpenoids, especially **1** and **6**, possess antibacterial activity close to that of the positive control, chloramphenicol.

Table 3
Antibacterial activity of compounds **1**–**6**[a]

Compound	*Bacillus subtilis*	*Escherichia coli*	*Staphylococcus aureus*
1	14.0±1.0	13.7±1.4	14.7±1.5
2	13.9±0.8	14.1±2.9	10.5±2.1
3	11.5±0.7	14.5±1.9	8.5±1.9
4	11.1±1.2	12.8±1.3	8.3±0.5
5	12.0±0.6	13.6±0.6	9.1±1.4
6	13.7 ±0.7	14.8±0.8	14.5±1.6
Chloramphenicol	14.5±1.1	14.9±1.3	15.1±1.2

[a] Activities are expressed as the diameter of the inhibitory zone in mm. Data are expressed as mean±standard deviations of triplicate determinations.

3. Experimental

3.1. General

Melting points were determined on a Yanagimoto melting point apparatus and were uncorrected. Optical rotations were measured on a Perkin-Elmer 241 polarimeter. The IR spectra were taken on a Nicolet 170SX FT-IR spectrometer. ^1H, ^{13}C NMR and 2D NMR spectra were recorded using a Bruker AM 400 NMR spectrometer at 400 and 100.58 MHz respectively with TMS as internal standard. HR–EIMS and EIMS data were obtained using a Bruker APEX II FT–MS and HP-5988 MS spectrometers respectively. Silica gel (200–300 and 300–400 mesh) was used for CC and silica GF_{254} for TLC. Spots were detected on TLC under UV or by heating after spraying with 5% H_2SO_4 in C_2H_5OH.

3.2. Plant material

The whole plants of *Saussurea petrovii* were collected in the suburb of Lanzhou city, Gansu province, China, in August 1999. A voucher specimen (No. 9901) was deposited at the National Laboratory of Applied Organic Chemistry, Lanzhou University, Lanzhou, China, and identified by Professor Yong-Hong Zhang at the Department of Chemistry, Lanzhou University.

3.3. Extraction and isolation

The chopped whole plant material (3.0 kg) was extracted repeatedly (3 times, 7 days each time) with acetone at room temperature to give a residue (80 g) after evaporation. This residue was separated by CC over 800 g silica gel (200–300 mesh) with a gradient (2000 ml each eluant) of petroleum ether-acetone (30:1, 20:1, 15:1, 10:1, 5:1, 3:1, 1:1, 0:1). From the fraction of petroleum ether-acetone (15:1), crude crystals of **4** and **5** were obtained successively. Recrystallization from AcOEt gave **4** (60 mg) and **5** (45 mg). The fraction of petroleum ether-acetone (5:1, 10 g) was separated on CC over 200 g silica gel (200–300 mesh) with $CHCl_3$-MeOH (25:1, 1000 ml, 20:1, 1000 ml) to give two subfractions A and B. Fraction A (6.0 g) was separated on CC over 60 g silica gel (200–300 mesh) with petroleum ether–AcOEt (4:1, 350 ml) to give crude **1** and **2**. Fraction B (3.5 g) was separated on CC over 40 g silica gel (200–300 mesh) with petroleum ether–EtOAc (4:1, 250 ml) to give crude **3** and **6.** Subsequently, each of them was purified by rechromatography on a silica gel column (300-400 mesh) with petroleum ether–Me_2CO (6:1) to give pure compounds **1** (35 mg), **2** (17 mg), **3** (30 mg) and **6** (15 mg).

3.4. Taraxast-20-ene-3β,30-diol (*1*)

Colorless crystals, mp 198–200 °C ($CHCl_3$–MeOH); $[\alpha]_D^{25}$ +116 (*c* 0.35, $CHCl_3$); HR–EIMS: $m/z = 442.3811$ [$C_{30}H_{50}O_2$, requires 442.3811]; IR (KBr): $\nu_{max} = 3420$ (OH), 1656 (C=C) cm^{-1}. EI–MS: m/z (rel. int.) = 442 (5) $[M]^+$, 424 (6), 391 (3), 273 (5), 229 (7), 207 (86), 189 (100), 135 (49), 121 (44), 81 (36). For ^1H and ^{13}C NMR spectral data see Table 1. For 2D NMR specral correlations see Fig. 1.

3.5. 20α,21α-Epoxy-taraxastane-3β,22α-diol (*2*)

Colorless crystals, mp 223–224 °C ($CHCl_3$–MeOH); $[\alpha]_D^{25}$ +121° (*c* 0.56, $CHCl_3$); HR–EIMS: $m/z = 458.3746$ [$C_{30}H_{50}O_3$, requires 458.3759]; IR (KBr): $\nu_{max} = 3240$ (OH) cm^{-1}. EIMS: m/z (rel. int.) = 458 (3) $[M]^+$, 440 (5), 397 (3), 247 (4), 243 (11), 207 (73), 189 (100), 175 (26), 149 (23), 95 (52). For ^1H and ^{13}C NMR spectral data see Table 1. For 2D NMR correlations see Fig. 2.

3.6. Taraxast-20(30)ene-3β,21α-diol (*3*)

Colorless crystals, mp 256–258 °C ($CHCl_3$–MeOH); $[\alpha]_D^{25}$ +225 (*c* 0.09, $CHCl_3$); HR–EIMS: $m/z = 442.3819$ [$C_{30}H_{50}O_2$, requires 442.3811]; IR (KBr): $\nu_{max} = 3234$ (OH), 1637 (C=C) cm^{-1}. The ^1H and ^{13}C NMR data are identical with those reported recently (Petrovic et al., 1999).

3.7. Cytotoxicity assay

The cytotoxicity of compounds **1**–**6** was tested in three cell lines: human hepatoma (SMMC-7721), mouse melanoma (B16) and human carcinoma of uterine cervix

(Hela). Cells were cultured at 37 °C under a humidified atmosphere of 5% CO_2 in RPMI 1640 medium supplemented with 10% fetal calf serum and dispersed in replicate 96-well plates with 1×10^4 cells/well for 24 h. Compounds **1**–**6** (10–400 μM) or vincristine (used as a positive control) were then added. After 48-h exposure to the toxins, cell viability was determined by the [3-(4,5-dimethylthiazol-2-yl)-2,5-diphenyltetrazolium bromide] (MTT) colorimetric assay (Price and McMillan, 1990) by measuring the absorbance at 595 nm with an ELISA reader. Each test was performed in triplicate.

3.8. Antibacterial assay

The paper-disk method (Xu and Bian, 1982) was used for antibacterial tests. A 10 μg portion of comounds **1**–**6** or chloramphenicol (used as a positive control) was applied onto a paper disk, and the paper disk was air-dried. Then the disks were placed on agar plates that had been seeded with *B. subtilis*, *E. coli* or *S. aureus*, respectively, and incubated at 37 °C for 24 h. The antibacterial activity was determined by measuring the diameter of the inhibitory circles. Each test was performed in triplicate.

Acknowledgements

The authors are grateful to Professor Yong-Hong Zhang, Department of Chemistry, Lanzhou University, for her help in identifying the plant material. They also thank the Department of Science and Technology of China for financial support (Grant No. G1998051113).

References

Anjaneyulu, V., Harischandra, K., Ravi, K., Connolly, J.D., 1985. Triterpenoids from *Mangifera indica*. Phytochemistry 24, 2359.

Chiang, Y.M., Kuo, Y.H., 2000. Taraxastane-type triterpenes from the aerial roots of *Ficus microcarpa*. J. Nat. Prod 63, 898.

Ma, Y.C., Fu, H.C., Chen, S., 1982. Flora Intramongolica 2nd ed., Vol. 6. Intramongolica People's Press, Huhhot.

Mahato, S.B., Kundu, A.P., 1994. ^{13}C NMR spectra of pentacyclic triterpenoids—a compilation and some salient features. Phytochemistry 37, 1517.

Pai, P.P., Kulkarni, G.H., 1977. Oxidation studies on taraxasterol, taraxasteryl acetate and taraxastenone. Indian J. Chem. 15B, 1134.

Petrovic, S.D., Gorunovic, M.S., Wray, V., Merfort, I., 1999. A taraxasterol derivative and phenolic compounds from *Hieracium gymnocephalum*. Phytochemistry 50, 293.

Price, P., McMillan, T.J., 1990. Use of the tetrazolium assay in measuring the response of human tumor cells to ionizing radiation. Cancer Res. 50, 1392.

Reynolds, W.F., McLean, S., Poplawski, J., Enriquez, R.G., Escobar, L.I., Leon, I., 1986. Total assignment of ^{13}C and ^{1}H spectra of three isomeric triterpenol derivatives by 2D NMR; An investigation of complex natural products. Tetrahedron 42, 3419.

Su, B.N., Yang, L., Gao, K., Jia, Z.J., 2000. Aquaticol, a bis-sesquiterpene and iridoid glucosides from *Yeronica anagallis-aquatica*. Planta Med. 66, 281.

Xu, S.Y., Bian, Q.L., 1982. Pharmacology Experimental Methods. People's Health Press, Beijing.

Zhang, Y.H., Yang, L., Cheng, D.L., 2000. Iridoid glucosides from *Caryopteris mongholica*. Pharmazie 55, 845.

Zhu, Y., Yang, L., Jia, Z.J., 1999. Novel highly oxygenated bisabolane sesquiterpenes from *Cremanthodium discoideum*. J. Nat. Prod 62, 1479.

PERGAMON

Phytochemistry 58 (2001) 1113–1120

PHYTOCHEMISTRY

www.elsevier.com/locate/phytochem

Cytotoxic isoflavones from *Erythrina indica*☆

Augustin E. Nkengfack[a,*], Anatole G.B. Azebaze[a], Alain K. Waffo[a], Zacharias T. Fomum[a], Michelle Meyer[b], Fanie R. van Heerden[c]

[a]*Department of Organic Chemistry, Faculty of Science University of Yaounde I, PO Box 812 Yaounde, Cameroon*
[b]*Laboratoire de Chimie des Substances Naturelles, 63 rue Buffon, 75005, Paris Cedex 05, France*
[c]*Department of Chemistry and Biochemistry, Rand Afrikaans University, PO Box 524, Johannesburg, Auckland Park 2006, South Africa*

Received 8 April 2001; received in revised form 1 August 2001

Abstract

Bioassay-directed fractionation of the CH_2Cl_2–MeOH (1:1) extract of the stem bark of *Erythrina indica,* has resulted in the isolation of two new isoflavone derivatives named indicanines D and E together with 11 known compounds including: six isoflavones (genistein, wighteone, alpinumisoflavone, dimethylalpinumisoflavone, 8-prenyl erythrinin C, and erysenegalensein E), one cinnamate (erythrinassinate B), two pentacyclic triterpenes (oleanolic acid and erythrodiol), and two phytosterols (stigmasterol and its 3-*O*-β-D-glucopyranoside). The structures of the new compounds were elucidated by means of spectroscopic analysis. The in vitro cytocidal activity against KB cells of some of the isolated compounds is also reported. © 2001 Elsevier Science Ltd. All rights reserved.

Keywords: Erythrina indica; Leguminosae; Papilionaceae; Indicanines D and E, Isoflavones; Ferulic acid ester; Pentacyclic triterpenes; Phytosterols; Cytotoxic activity

1. Introduction

The genus *Erythrina* (Leguminosae) occurs in the tropical and subtropical regions over the world and comprises about 110 species (Dyke and Quessy, 1981). Some of these species have been used in traditional medicine for the treatment of several diseases (Dalziel, 1937). *Erythrina,* species are also a rich source of bioactive alkaloids (Ghosal et al., 1971; Furukawa et al., 1976; Barakat et al., 1977; Cordell, 1981) and of many flavonoid compounds (Nakanishi et al., 1981; Fomum et al., 1986; Mitscher et al., 1988; Nkengfack et al., 1997). Recently, investigations on the root bark constituents of *Erythrina indica,* a plant used in cameroonian folk medicine for the treatment of trachoma, elephantiasis, and microbial infections (Ayensu, 1978), have resulted in the isolation and identification of eight phenolic metabolites among which there were two 3-phenyl coumarin derivatives, indicanines A and B, and one new isoflavone derivative, indicanine C, along with five known compounds including, robustic acid, 8-prenyldaidzein, daidzein, cajanin, and dimethyl alpinumisoflavone (Azebaze et al., 2000; Nkengfack et al., 2000). As part of our continuing search for biological active principles related to non-alkaloidal compounds in *Erythrina* species, now we wish to report the phytochemical analysis of the stem bark of *Erythrina indica* as well as the in vitro cytotoxic activity and potency of some of the isolated compounds.

2. Results and discussion

Dried and ground stem bark of *Erythrina indica* was extracted with a dichloromethane–methanol (1:1) and methanol, successively. These extracts were concentrated to dryness under vacuum and their cytocidal activities against KB cells were evaluated in vitro. As a result, ED_{50} values of the CH_2Cl_2–MeOH (1:1) and MeOH extracts were l0 and 36 μg/ml respectively. Since the first extract showed strong cytocidal activity, we decided to elucidate its active principle (s). Extensive column chromatography on silica gel of this residue yielded pure indicanines D (**1**) and E (**2**) together with eleven known compounds. Compounds (**3**–**8**) were characterized as isoflavones from their spectral data and identified as

☆ Part 37 in the series "*Erythrina* studies". For part 36, see Nkengfack et al., 2000.

* Corresponding author. Fax +237-22-18-73.
E-mail address: ankengf@uycdc.uninet.cm (A.E. Nkengfack).

0031-9422/01/$ - see front matter © 2001 Elsevier Science Ltd. All rights reserved.
PII: S0031-9422(01)00368-5

genistein (**3**) (Imamura et al., 1981) wighteone (**4**) (Min et al., 1991), alpinumisoflavone (**5**) (Khalid and Waterman, 1983) dimethylalpinumisoflavone (**6**) (Khalid and Waterman, 1983), 8-prenylerythrinin C (**7**) (Fomum et al., 1990), and erysenegalensein E (**8**) (Wandji et al., 1994), whereas compounds (**9**–**13**) were identified by comparison of their spectral data with literature values as erythrinassinate B (**9**) (Fomum et al., 1990), oleanolic acid (**10**) (Mahato and Kundu, 1994), erythrodiol (**11**) (David et al., 1981), stigmasterol (**12**) (Alam et al., 1996), and stigmasteiol 3-*O*-β-D glucopyranoside (**13**) (Alam et al., 1996).

Compound (**1**), obtained as yellow needles. mp 212–214 °C, reacted positively to $FeCl_3$ reagent suggesting the presence of phenolic hydroxyl group(s). Its high resolution FAB-mass spectrum gave an $[MH]^+$ ion at *m*/*z* 803.5826 (calc. 803.5825) consistent with a molecular formula $C_{51}H_{75}O_7$ corresponding to 13° of unsaturation. The IR spectrum exhibited vibration bands for free hydroxyl (3420) chelated hydroxyl (3227) conjugated carbonyl (1647), olefine (1631, 1516). and ether (1285, 1142) cm^{-1} functionalities. The ^1H NMR signal at δ 7.80 (H-2), ^{13}C NMR signal at δ 153.9, and UV absorption band at λ_{max}^{MeOH} 270 nm (log ε 4.46) were all typical of an isoflavone skeleton (Agrawal and Bansal, 1989; Mabry et al., 1970). The small bathochromic shift (Δλ = 3 and 4 nm) observed in the UV spectrum of (**1**) by adding the $AlCl_3$ and NaOAc reagents, respectively, suggested that (**1**) has chelated and free hydroxyl groups at C-5 and C-7 positions, respectively (Mabry et al., 1970). This was confirmed by the presence, in the ^1H NMR spectrum of the downfield signals at δ 13.04 and 8.89 due to intramolecular hydrogen bonded group and free hydroxyl phenolic group at C-5 and C-7 positions, respectively. Compound (**1**) has also one γ, γ-dimethylallyl group which was confirmed in the ^1H NMR spectrum by one 2H doublet at δ 3.43 (2H, *J* = 7.0 Hz, H-1″), one 1H triplet at δ 5.25 (1H, *J* = 7.0 Hz, H-2″), two 3H singlets at 1.68 (Me, *trans*) and 1.79 (Me, *cis*). The presence of an hydroxyprenylated unit linked to an aromatic ring was also indicated by two diastereotopic benzylic proton signals appearing as two double doublets at δ 2.94 (1H, *J* = 8.0, 15.0 Hz, H-1‴ and 3.19 (1H, *J* = 8.0, 15.0 Hz, H-1‴), one methine proton signal as a doublet of doublet at δ 4.36 (1H, *dd*, *J* = 2.0. 8.0 Hz, H-2‴), two olefinic *gem*-proton signals as two doublets at δ 4.88 (1H, *d*, *J* = 1.0 Hz) and 4.98 (1H, *d*, *J* = 1.0 Hz, H-4‴) and one methyl proton signal as singlet at δ 1.84 (3H, *s*). In the aromatic region, a typical AA′BB′ spin system of four aromatic protons at δ 7.37 (2H, *J* = 9.0 Hz, H-2′ and H-6′) and 6.88 (2H, *J* = 9.0 Hz, H-3′ and H-5′) was also shown suggesting the presence of a *para*-substituted ring B. Furthermore, the set of signals consisting 1H singlet at δ 5.25 due to an hydroxyl group, one methine multiplet at δ 4.20 (1H, *m*, H-1⁗), two 1H double doublets at 3.70 (1H *dd*, *J* = 12.0. 9.0 Hz) and 3.60 (1H, *dd*, *J* = 12.0. 9.0 Hz) due to diastereostopic hydroxyl methyl protons, a 46 H broad band signal at δ 1.39 corresponding to $(CH_2)_{23}$ and one 3H triplet at δ 0.85 (3H, *J* = 6.8 Hz) due to a terminal methyl group established the presence of an hydroxylmethylpentacosanyl long chain moiety.

It remained for us to establish unambiguously the positions of the long chain moiety, the free and hydroxylated prenyl groups on the isoflavone skeleton.

The presence of the two five-carbon units (prenyl and hydroxylated) in compound (**1**) was confirmed by the E1-mass spectrum which showed the highest ion peak at *m*/*z* 422 (A_1) due probably to the loss of the hydroxylhexacosanyl moiety from the molecular ion and important ion fragments at *m*/*z* 351 $[A_1–C_4H_7O]^+$ and 295 $[A_1–C_4H_7O–C_4H_8]^+$. Other important ion fragments such as ion fragments at *m*/*z* 177 and 118 were also observed. Both resulted from the Retro Diels–Alder (RDA) cleavage of the most stable ion at *m*/*z* 295 (see Scheme 1) and suggested that the two five carbon units were linked to ring A (*m*/*z* 177), notably at the C-6 and C-8 positions since the ^1H NMR did not show any signal between δ 5.90–6.10 characteristic of the protons of these positions (Agrawal and Bansal, 1989). The relative positions of these groups were determined on the basis of the long-range proton heteronuclear correlations experiment. Thus, the HMBC spectrum of compound (**1**) (Fig. 1) showed through ^2J and ^3J interactions that a ^1H signal at δ 3.19 (H-1‴) was correlated to ^{13}C signals at δ 162.1 (C-7), 154.3 (C-9), 104.6 (C-8), 77.1 (C-2′) and ^1H signal at δ 7.80 showed correlations with ^{13}C signals at δ 154.3 (C-9), indicating that the hydroxyprenylated group was located at C-8 position. Furthermore, the observed correlations between the chelated hydroxyl proton at δ 13.04 and C-5 (δ 158.9), C-6 (δ 113.1), and C-10 (105.9) and between the H-1′ protons at δ 3.43 and C-5 (δ 158.9), C-6 (δ 113.1), and C-7 (δ 162.1) indicated that the free prenyl group was linked to the C-6 position. On the other hand, the three bond correlations of the methine proton at δ 4.20 (H-1⁗) to C-4′ (δ 158.4) and hydroxymethylene carbon (δ 65.2) established that the hydroxymethylpentacosanyl long chain moiety was

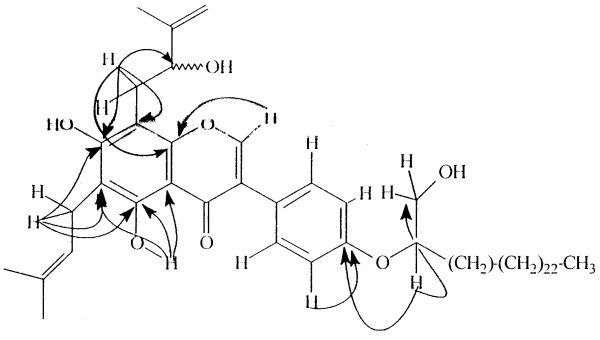

Fig. 1. Significant long-range correlations observed in $^{13}C–^1H$ HMBC spectrum of indicanine D (**1**) in $CDCl_3$.

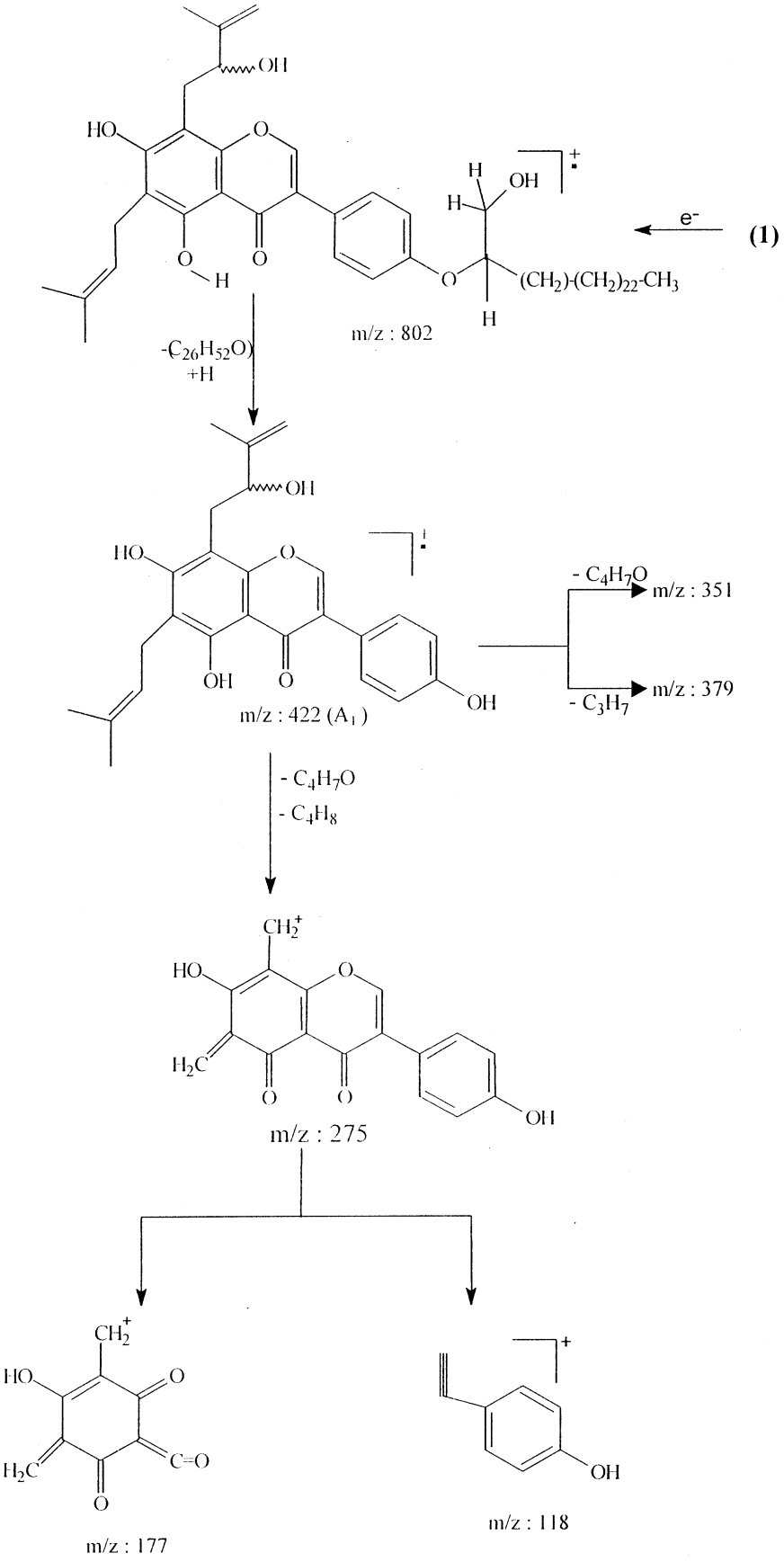

Scheme 1. Mass spectral fragmentation of indicanine D (**1**). Note: Compound **8** has an OH group at 4′ position in B ring. (*continued on next page*).

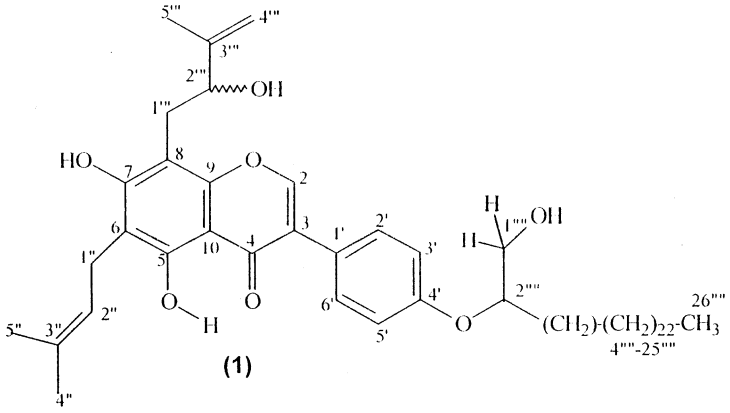

(1)

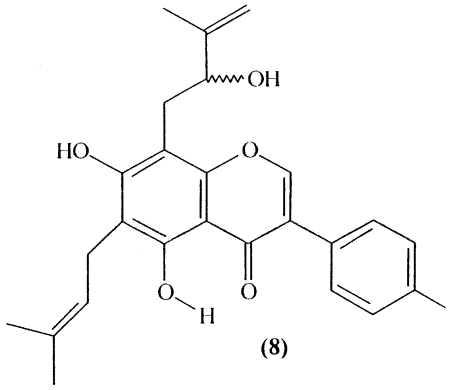

(8)

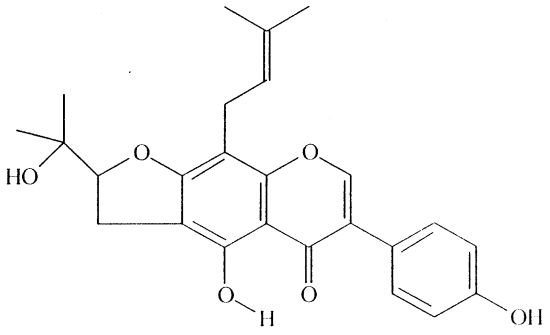

(7)

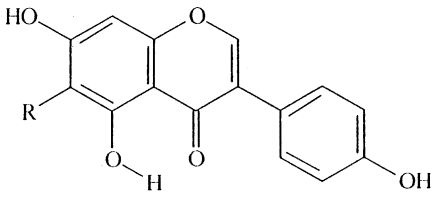

(3): R = H
(4): R = Prenyl

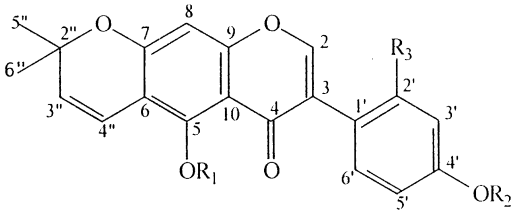

(2): R_1=CH_3, R_2=CH_3, R_3=OH
(5): R_1=H, R_2=H, R_3=H
(6): R_1=CH_3, R_2=CH_3, R_3=H

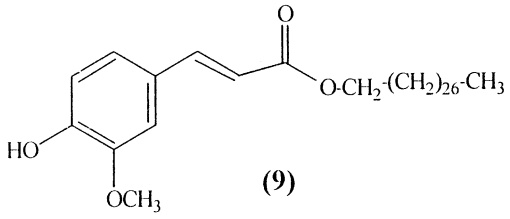

(9)

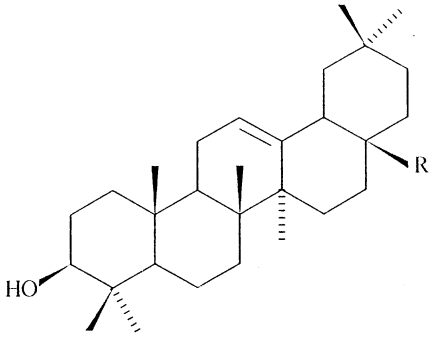

(10) : R=COOH
(11) : R=CH_2OH

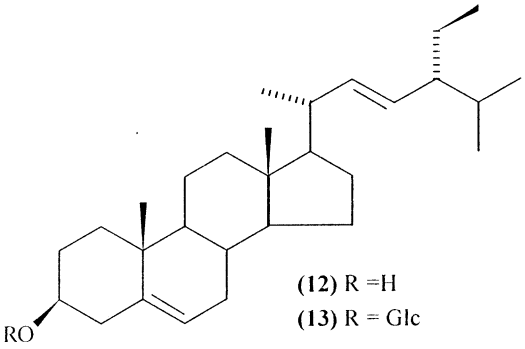

(12) R =H
(13) R = Glc

Scheme 1 (*continued*).

linked to oxygen atom at C-4′ position. Further evidence of the structure of indicanine D (**1**) was given by the analysis of the ^1H–^1H NOESY spectrum as shown in Fig. 2.

From the above spectroscopic evidence, compound (**1**) was deduced to be 5,7-dihydroxy-6-(γ, γ-dimethylallyl)-8-(2‴-hydroxy-3‴-methylbut-3‴-enyl)-4′-(1‴′-hydroxymethylpentacosanyl)isoflavone.

Compound (**2**), to which we have assigned trivial name indicanine E, was obtained as brown crystals, mp 138–139 °C, and reacted positively to the $FeCl_3$ reagent. Its high-resolution EI mass spectrum displayed a molecular ion $[M^+]$ at m/z 380.1257 in agreement with the empirical formula $C_{22}H_{70}O_6$, (380.1259) corresponding to 13° of unsaturation. Its IR spectrum showed absorption bands for free hydroxyl (3485), conjugated carbonyl (1660), olefin (1630) and ether (1275, 1178) cm^{-1} functionalities.

The broad band decoupled ^{13}C NMR spectrum of compound (**2**) showed 22 carbon signals. The analysis of this spectrum with the Jmod and DEPT techniques unequivocally indicated that four of these were methyls, seven were methines and eleven quaternary carbons (among which one carbonyl, 9 sp^2carbons, and one sp^3 carbon). The UV spectrum [λ_{max}^{MeOH} 286 nm (log ε 4.62)] of indicanine E was typical of compounds having an isoflavone skeleton (Mabry et al., l970). This was supported by the ^1H and ^{13}C NMR spectra which showed resonance signals at δ 7.98 for H-2 and δ 151.3 (C-2) characteristic of isoflavone (Agrawal and Bansal, 1989; Mabry et al., 1970).

Also, the ^1H NMR spectrum of compound (**2**) showed an AB spin system consisting of two doublets at δ 5.85 and 6.70 (J=10.0 Hz) which, together with the 6H singlet at δ 1.45, suggested the presence of 2″,2″-dimethylpyrano substituent. The base ion peak at m/z 365 $[M–Me]^+$ in the EIMS and the set of signals at δ 28.3, 78.4, 131.1, and 116.4 in the ^{13}C NMR spectrum provided further support for the presence of a *gem*-dimethyl chromene system (Mabry et al., 1970). The ^1H NMR spectrum further revealed the presence of 1H singlet at δ 6.59 which could he assigned either to a H-6 or a H-8 proton of ring A, two methoxyl groups signals at δ 3.85 (3H, *s*) and δ 3.84 (3H, *s*) and one broad hydroxyl signal at δ 3.00. In the aromatic region, the appearance of an ABX spin system at δ 7.40 (1H, *d*, J=6.6 Hz), 6.80 (1H, *d*, J=2.1 Hz), and 6.95 (1H, *dd*, J=6.6. 2.1 Hz) established the presence of three aromatic protons on ring B. The location of one methoxyl group and a *gem*-dimethylpyran moiety on ring A was determined from the mass spectral fragmentation pattern which exhibited fragment ions at m/z 217 and 148 caused by a usual (RDA) cleavage from ion $[M–Me]^+$ at m/z 365. The absence of the C-5 chelated hydroxyl signal between δ 11–13 permitted us to locate one of the methoxyl groups at C-5 position. It remained to establish whether the fusion of the γ, γ dimethylpyran moiety on ring A was linear or angular. This was deduced from 2D NOESY spectrum (Fig. 3) which shows no correlation between the single aromatic ring A proton at δ 6.59 (H-6 or H-8) and methoxyl protons at δ 3.85, but correlation contours between methoxyl protons at δ 3.85 and one (δ 6.71) of the AB spin system. This finding indicated clearly that the *gem*-dimethylpyran moiety was fused in a linear manner on ring A. On the other hand, the ion peak at m/z 148 is due to ring B carrying one hydroxyl and the second methoxyl substituent. The *meta* position of these two moieties was determined by the ^{13}C NMR spectrum which shows diagnostic signals at δ 157.4 and 156.4 due to *meta* aromatic carbons bearing an oxygen atom (Agrawal and Bansal, 1989). The 2′(OH)/4′(OMe) substitution pattern was readily deduced, once more, on the basis of the phase sensitive NOESY experiment which showed interactions between methoxyl protons at δ 3.84 and H-3 (δ 6.80) and H-5′(δ 6.95). On these grounds, compound (**2**) was characterized as 2′-hydroxyl-5, 4′-dimethoxyl-2‴, 2‴-dimethylpyran-[5‴, 6‴: 6,7]isoflavone.

Compounds (**1**), (**4**), (**5**) and (**8**) were evaluated for their cytotoxic activity and potency against KB cells using established methods (Monks et al., 1988; Boyd, 1989). As shown in Table 2, wighteone (**4**) appeared to be the most potent compound.

Alpinumisoflavone (**5**) is as potent or slightly more potent than erysenegalensein E (**8**) whereas 8-prenylerythrinin C (7) and indicanine D (**1**) displayed weak cytotoxic activity.

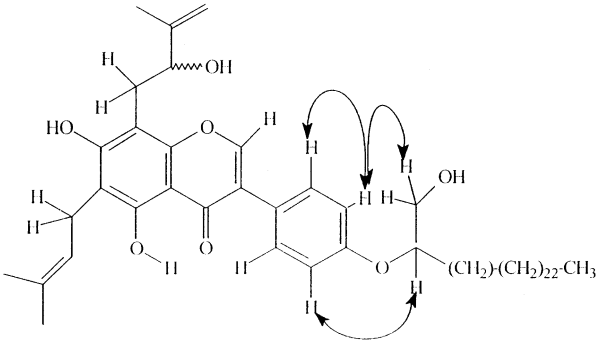

Fig. 2. Selected NOESY correlations for indicanine D (**1**).

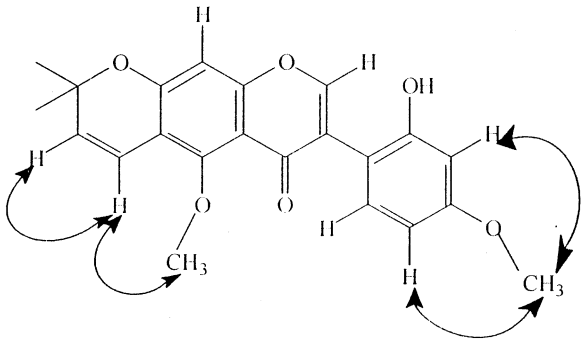

Fig. 3. Selected NOESY correlations for indicanine E (**2**).

Table 1
^1H (300 MHz) and ^{13}C (75 MHz) assignments for indicanine D (**1**) and indicanine E (**2**)

(**1**) ($CDCl_3$)			(**2**) (Acetone-d_6)		
Attribution	^{13}C	^1H[J(Hz)]	Attribution	^{13}C	^1H [J(Hz)]
2	153.9	7.80, *s*	2	151.3	7.98, *s*
3	122.3	–	3	125.0	–
4	182.0	–	4	174.5	–
5	158.9	–	5	158.4	–
6	113.1	–	6	113.8	–
7	162.1	–	7	159.2	–
8	104.6	–	8	100.9	6.59, *s*
9	154.3	–	9	151.5	–
10	105.9	–	10	113.8	–
1′	123.3	–	1′	124.1	–
2′	131.0	7.37, (*d*, *J* = 9.0)	2′	156.4	–
3′	115.9	6.88, (*d*, *J* = 9.0)	3′	119.9	6.80, (*d*, *J* = 2.1)
4′	158.4	–	4′	157.4	–
5′	115.9	6.88, (*d*, *J* = 9.0)	5′	115.6	6.95, (*dd*, *J* = 2.1; 6.6)
6′	131.0	7.37, (*d*, *J* = 9.0)	6′	131.7	7.40, (*d*, *J* = 6.6)
1″	22.4	3.43, (*d*, *J* = 9.0)	1″	–	–
2″	l23 4	5.25, (*t*, *J* = 7,0)	2″	78.4	–
3″	131.4	–	3″	131.1	5.85, (*d*, *J* = 10.0)
4″	25.8	1.68, *s*	4″	116.4	6.70, (*d*, *J* = 10.0)
5″	18.4	1.79, *s*	5″ and 6″	28.3	1.45, *s*
		2.94, (*dd*, *J* = 8.0; 15.0)			
1″	29.4	3.19 (*dd*, *J* = 8.0; 15.0)	5-OCH_3	62.7	3.85, *s*
2″	77.1	4.36 (dd J = 2.0; 8.0)	4′-OCH_3	56.2	3.84, *s*
3″	147.6	–			
		4.88 (*d*, *J* = 1.0)			
4″	1107	4.98, (d, *J* = 1.0)			
5″	17.8	1.84, *s*			
		3.60, (*dd*, *J* = 9.0;12.0)			
CH_2OH	65.1	3.70, (*dd*, *J* = 9.0;12.0)			
1‴	70.2	4.20, *m*,			
2‴ - 24‴	21.8–34.1	1.39 $(CH)_{23}$			
25‴	14.1	0.85, *t*			
5-OH	–	13.04, *s*			
7-OH	–	8.89, *s*			
CH_2OH	–	5.25, *s*			
2‴-OH	–	–			

Table 2
Cytotoxicity against human KB cells

Compounds	ED_{50} (μg/ml)
CH_2 Cl_2–MeOH extract	10
MeOH extract	36
Indicanine D (**1**)	12.5
Wighteone (**4**)	0.78
Alpinumisoflavone (**5**)	4.13
Erysenegalensein E (**8**)	6.25
8-Prenyl erythrinin C (**7**)	13

3. Experimental

3.1. General experimental procedures

Melting points were determined on a Kofler hot-stage apparatus and are uncorrected. Silica gel, 60 GF 254, was used for TLC with the mixture of *n*-hexane-ethyl acetate as eluent system. The $[\alpha]_D$ value was measured with a Perkin-Elmer 141 polarimeter. IR spectra were recorded on a SHIMADZU 408 Spectrophotomcter in KBr disks. UV spectra were obtained on a Beckman Model 25 Spectrophotometer. EIMS (ionization voltage 70 eV) were measured with LKB9000S and Nermag/Sidar U 3:1 Spectrometers. ^1H and ^{13}C NMR spectra were recorded on a Varian Gemini 2000 and Bruker spectrometers equipped with a 5 mm ^1H and ^{13}C probe operating at 300 and 75 MHz, respectively with TMS as internal standard. DEPT, Jmod, amid 2D NMR spectra were measured with the usual pulse sequence and data processing were obtained with standard software.

3.2. Plant material

Stem bark of *Erythrina indica* was collected in June 1998 at Ibadan (Nigeria). A voucher specimen (No. 49028 HNC) documenting the collection was identified

at the National Herbarium, Yaounde, Cameroon and is on deposit there.

3.3. Extraction and isolation

Air dried powdered stem bark of *E. indica* (6 kg) was extracted successively with CH_2Cl_2–MeOH (1:1) and MeOH at room temp. during 24 h. Both extracts were concentrated under vacuum to afford a viscous mass of CH_2Cl_2–MeOH (1:1) extract (150 g) and a sticky residue of methanol extract (100 g). These two extracts were assayed for their cytotoxicity against KB cell line. As a result, ED_{50} values of the CH_2Cl_2–MeOH (1:1) and MeOH extracts were l0 and 36 μg/ml, respectively. Since the first extract showed strong cytocidal activity, we decided to elucidate the active principle(s) of this extract. The crude extract was then subjected to flash column chromatography over Si gel 60 (70–230 mesh, ASTM; Merck) eluting with a *n*-hexane–EtOAc mixture with increasing polarity. A total of 30 fractions of ca. 300 ml each were collected and combined on the basis of TLC analysis leading to three main series A–C. Fractions 1–15, eluted with the mixture of *n*-hexane–EtOAc (17:3) gave series A (76 g); series B (10 g) was constituted of fractions 16–23 eluted with a mixture of *n*-hexane–EtOAc (3:2) while serie C (25 g) resulted from fractions 24–30 eluted with *n*-hexane–EtOAc (1:1).

Series A was column chromatographed over Si gel packed in *n*-hexane. Gradient elution was effected with *n*-hexane–EtOAc mixture. A total of 80 fractions of ca 300 ml each were collected and combined on the basis of TLC. The pure compounds were obtained either by direct crystallization or after further purifications by column chromatography. Crystallization of the combined fractions 1–10, eluted with *n*-hexane–EtOAc (19:1), gave erythrinassinate B (**9**) (2 g), and dimethylalpinumisofiavone (**6**) (1.5 g). The combined fractions 11–40, eluted with *n*-hexane–EtOAc (9:1), afforded stigmasterol (**12**) (300 mg), indicanine D (**1**) (25 mg), and indicanine E (**2**) (35 mg), respectively. The combined fractions 41–80, eluted with *n*-hexane–EtOAc (17:3), yielded erythrodiol (**11**) (200 mg), erysenegalesein E (**8**) (15 mg) alpinumisoflavone (**5**) (400 mg), and oleanolic acid (**10**) (50 mg).

Series B, treated in the same manner as A, yielded wighteone (**4**) (20 mg), 8-prenylerythrinin C (**7**) (20 mg), and genistein (**3**) (30 mg).

From series C, very rich in tannins, only 3-*O*-β-D glucopyranosyl stigmasterol (**13**) (150 mg) was obtained.

3.4. 5,7- Dihydroxy-6 (γ,γ-dimethylallyl)-8-(2‴-hydroxy-3‴-methylbut-3‴–enyl)-4′-(1″-hydroxymethylpenta cosanyl) isoflavone (indicanine D) (*1*)

Yellow needles, mp 212–214 °C, $[\alpha]_D^{20} + 8.5$ ° (MeOH; *c* 0.045) UV λ_{max}^{MeOh} nm (log ε): 270 (4.46), + [$AlCl_3$] 273 (4.43), + [NaOAc] 274 (4.40); IR ν_{max}^{KBr} cm^{-1}: 3420, 3227, 1647, 1631, 1516, 1285, and 1142; ^1H NMR ($CDCl_3$) see Table 1, ^{13}C NMR ($CDCl_3$) see Table 1; FABMS: *m/z* 803.5826 $[M+H]^+$ (Calc. for $C_{51}H_{79}O_7$, 803.5825); EIMS *m/z* (rel int): 422 $[M–C_{26}H_{51}O]^+$ (9), 351 $[M–C_{26}11_{51}O–C_4H_7O]^+$ (18), 295 $[M–C_{26}H_{51}O–C_4H_7O–C_3H_7]^+$ (45), 260 (33), 177 (39), 118(27), 83 (56), 69(57), 55 (35), 43 (75).

3.5. 2′-Hydroxy-5,4′-dimethoxy-2″-2″-dimethylpyran-[5″- 6″:6,7] isoflavone (Indicanine E) (*2*)

Brown crystals, mp 138–139 °C; UV λ_{max}^{MeOH} nm (log ε) 286 (4.62); IR ν_{max}^{KBr} cm^{-1}: 3485, 1660, 1630, 1275 and 1178; ^1H NMR (acetone-d_6), see Table 1; ^{13}C NMR (acetone d_6), see Table 1; HREIMS *m/z* 380.1257 (Calc. for $C_{22}H_{20}O_6$, 380.1259); EIMS *m/z* (rel. int): 380 $[M]^+$ (15), 365 (100), 336 (83), 307 (15), 217 $[M–CH_3\text{-}148]^+$ (15), 202 (22), 183 (24), 148 $[M–CH_3\text{-}217]^+$ (15), 105 (20), 55 (25), 43 (45), 28 (50).

3.6. Cytotoxicity assay

Cytotoxicity to human solid tumor cells was evaluated at Cell Culture Laboratory of "Museum National d′Histoire Naturelle", Paris, France. Each test material was added to cultivated KB cell after 24 h and the cells were further cultivated for 72 h. The ratio of the living cells was evaluated according to literature (Monks et al., 1988; Boyd, 1989) and cytocidal activity was indicated as ED_{50} values.

Acknowledgements

This investigation was supported by grant No. F/1392-3F from the International Foundation for Science (IFS), Stockholm (Sweden) and 3 months visiting fellowship from "Museum National d′Histoire Naturelle", Paris, France.

References

Agrawal, P.K., Bansal, M.C., 1989. In: Agrawal, P.K. (Ed.), Carbon-13 NM of Flavonoids. Elsevier, Amsterdam, pp. 83–235.

Alam, M.S., Chopra, N., Ali, N., Niwa, M., 1996. Oleanen and stigmasterol derivatives from *Ambroma augusta*. Phytochemistry 41, 1197–1200.

Ayensu, E.S., 1978. Medicinal Plants of West Africa. P.I.B.. Reference Publication, Algonac, MI, p. 153.

Azebaze, G.A., Waffo, A.K., Nkengfack, A.F., Fomum, Z.T., Meyer, M., Bodo, B., Van Heerden, F.R., 2000. Indicanin A, a new phenylcoumarin from root bark of *Erythrina indica*. J. Nat. Prod. 63, 855–856.

Barakal, I., Jackson, A.H., Abdulla, M.I., 1977. Further studies of *Erythrina* alkaloids. Llyodia 40, 471–475.

Boyd, M.R., 1989. Principles and Practice of Oncology Updates, Vol. 3. Lippincott, J.B, Philadelphia, p. 1.

Cordell, G.A., 1981. Introduction to Alkaloids: A. Biogenetic Approach. John Wiley & Sons, New York, pp. 450–462.

Dalziel, J.M., 1937. The Useful Plants of West Tropical Africa. Crown Agents For Colonies, London, p. 612.

David, N.W., Mabry, B., Heftamann, F., 1981. The location of the methylol group in sapogenol C and erythrodiol and its biosynthesis significance. Phytochemistry 20, 2299–2300.

Dyke, S.F., Quessy, D., 1981. The Alkaloids Chemistry and Physiology, Vol. 18. In: Rodrigo, R.G.A. (Ed.), Academic Press, New York, p. 1.

Fomum, Z.T., Ayafor, J.F., Mbafor, J.F., 1986. *Erythrina* studies part 2. Structures of three novel prenylated antibacterial flavanones. Sigmoidin A–C, from *E. sigmoidea*. J. Chem. Soc. Perkin Trans. 1, 33–37.

Fomum, Z.T., Wandji, J., Nkengfack, A.E., Ubillas, R., Kidllay, B.K., Tempesta, M.S., 1990. A new prenylated isoflavone and long chain esters from two *Erythrina* species. J. Nat. Prod. 53, 1425–1429.

Furukawa, H., Ito, K., Haruna, M., Jinno, Y., 1976. Studies on the *Erythrina* alkaloids XI. Alkaloids of *Erythrina crystagalli* Linn. Structure of new alkaloid, Crystamidine. Chem. Pharm. Bull. 24, 52–55.

Ghosal, S., Majumdar, S.K., Chakrabotti, A., 1971. *Erythrina* alkaloids. Occurence of (+) *N*-norprotosinomenine and other alkaloids in *Ery thrina lithosperma*. Austr. J. Chem. 24, 2733–2735.

Imamura, H., Hibino. Y., Ito, H., Ohashi, H., 1981. Isoflavonoids of *Erythrina cristagalli* (Leguminosae). Res. Bull. Fac. Agric., Gifu UNIV., pp. 77–79.

Khalid, S.A., Waterman, P.G., 1983. Thonningin-A and thonningin-B. Two 3-phenylcoumarins from the seeds of *Milletia thonningii*. Phytochemistry 22, 1001–1003.

Mabry, T.J., Markham, K.R., Thomas, M.B., 1970. The Systematic Identification of Flavonoids. Academic Press, New York, pp. 165–166.

Mahato, S.B., Kundu, P.A., 1994. ^{13}C NMR spectra of pentacyclic triterpenoids—a compilation and sonic salient features. Phytochemistry 31, 2199–2249.

Min, C., Si, Q.L., Jun-Hong, C., 1991. Two isoflavones from *Flemningia philippinensis*. Phytochemistry 30, 3842–3844.

Mitscher, L.A., Gollapudi, S.R., Gerlach, D.C., Drake, S.O., Veliz, E.A., Ward, J.A., 1988. Erycristin; a new antimicrobial pterocarpan from *Erythrina cristagalli*. Phytochemistry 27, 381–385.

Monks, A., Shoemaker, R.H., Alley, M.C., Scudiero, D.A., Fine, D.L, McLemore, T.L., Abbott, B.J., Paull, K.D., Mayo, J.G., Boyd, M.R., 1988. Predictions of Response to Cancer Therapy. Alan R. Liss, New York.

Nakanishi, K., Kamat, S.H., Chuo, F.Y., Kubo, I., 1981. Antimicrobial agents from East African medicinal plant: *Erythrina abyssinica*. Heterocycles 15, 1163–1170.

Nkengfack, A.F., Vouffo, W.F., Vardamides, J.C., Kouam, J., Fomum, Z.T., Meyer, M., Sterner, O., 1997. Phenolic metabolites from *Erythrina* species. Phytochemistry 46, 573–578.

Nkengfack, A.F., Waffo, A.K., Azebaze, G.A., Fomum, Z.T., Meyer, M., Bodo, B., Van Heerden, F.R., 2000. Indicanines B and C, two isoflavonoid derivatives from the root bark of *Erythrina indica*. Phytochemistry 53, 981–985.

Wandji, J., Fomum, Z.T., Tillequin, F., Seguin, F., Koch, M., 1994. Two isoflavones from *Erythrina senegalensis*. Phytochemistry 35, 245–248.

PERGAMON

Phytochemistry 58 (2001) 1121–1128

PHYTOCHEMISTRY

www.elsevier.com/locate/phytochem

A bis-sesquiterpene and sesquiterpenolides from *Inula macrophylla*

Bo Fu[a], Bao-Ning Su[a], Yoshihisa Takaishi[a,*], Gisho Honda[b], Michiho Ito[b], Yoshio Takeda[c], Olimjon K. Kodzhimatov[d], Ozodbek Ashurmetov[d]

[a]*Faculty of Pharmaceutical Sciences, University of Tokushima, Shomachi 1-78, Tokushima 770-8505, Japan*
[b]*Faculty of Pharmaceutical Sciences, Kyoto University, Yoshida Sakyoku, Kyoto 606-8501, Japan*
[c]*Faculty of Integrated Arts and Sciences, University of Tokushima, Minamijyosanjima, Tokushima 770-8502, Japan*
[d]*Academy of Sciences, Uzbekistan Institute of Botany, F. Khodzhaev St. 32, 700143 Tashkent, Uzbekistan*

Received in revised form 3 July 2001

Abstract

Macrophyllidimer C, a novel bis-sesquiterpene, in which the two sesquiterpene units are directly connected by a C–C bond, and eight other sesquiterpenolides were obtained from the bark of *Inula macrophylla*. Seven of these, macrophyllilactones A–G, are new eudesmanolide- and elemanolide-type sesquiterpenes. Their structures were determined on the basis of spectroscopic evidence and chemical reaction. © 2001 Published by Elsevier Science Ltd.

Keywords: *Inula macrophylla*; Compositae; Macrophyllidimer C; bis-Sesquiterpene; Macrophyllilactones A–G; Eudesmanolide and elemanolide sesquiterpenes

1. Introduction

The traditional Uzbekistan herb *Inula macrophylla* Kar. et Kir. (Compositae) has been used to treat many diseases, including bronchitis, diabetes, and intestinal ulcers. The characteristic components of the genus *Inula* are sesquiterpenes, especially eudesmanolides (Oksuz and Topcu, 1992; Oksuz et al., 1997), guaianolides (Topcu and Oksuz, 1990; Tan et al., 1998), and monoterpenes (Bokadia et al., 1986; Marco et al., 1993). However, the phytochemistry of *Inula macrophylla* has not yet been studied. Recently, Topcu et al. (1993) and Cantrell et al. (1999) reported on the cytotoxic and antibacterial activities of sesquiterpenoids from the genus *Inula*. These findings inspired us to investigate the chemical constituents of *I. macrophylla*. We have previously reported the structural determination of monoterpene and bis-sesquiterpenes (Su et al., 2000a,b), and rearranged eudesmane sesquiterpene acids (Su et al., 2000c) from this plant. As part of our continuing study of Uzbekistan plants, this paper reports a novel bis-sesquiterpene, macrophyllidimer C (**1**) and seven new eudesmane and elemane sesquiterpenolides, macrophyllilactones A–G (**2**–**8**), together with one known eudesmanolide **9**, which were isolated from the bark of *I. macrophylla*.

2. Results and discussion

Macrophyllidimer C (**1**) was obtained as a colorless oil. Its IR spectrum showed absorption bands of a hydroxyl (3511 cm^{-1}), the carbonyl of a γ-lactone (174 6 cm^{-1}), an α β-unsaturated lactone (1717 and 1638 cm^{-1}), and terminal olefinic bonds (919 and 868 cm^{-1}). The ^{13}C NMR and DEPT spectra (Table 1) exhibited 30 carbon signals including nine quaternary carbons, seven methines, 10 methylenes, and four methyls. FABMS showed molecular ion peaks at m/z 537 $[M+Na]^+$ and 515 $[M+H]^+$. These findings suggested that this compound was a bis-sesquiterpene similar to those isolated previously (Su et al., 2000b). Its molecular formula was established to be $C_{30}H_{42}O_7$ based on the above information, which was supported by HRFABMS of its acetylated product (**1a**), which gave molecular ion peaks at m/z 663.3151 $[M+Na]^+$ and 641.3421 $[M+H]^+$ for $C_{36}H_{48}O_{10}$ Na and $C_{36}H_{49}O_{10}$, respectively (calc. 663.3145 and 641.3326). The ^1H NMR spectrum (Table 1) of compound **1** exhibited five olefinic proton

* Corresponding author. Tel.: +81-88-6337275; fax: +81-88-6339501.
E-mail address: takaishi@ph.tokushima-u.ac.jp (Y. Takaishi).

0031-9422/01/$ - see front matter © 2001 Published by Elsevier Science Ltd.
PII: S0031-9422(01)00334-X

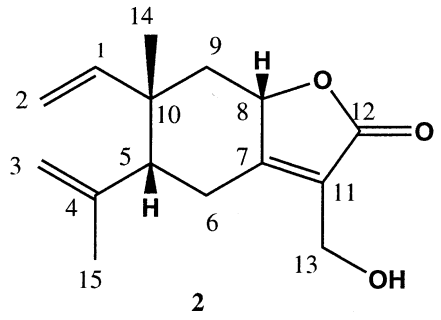

2

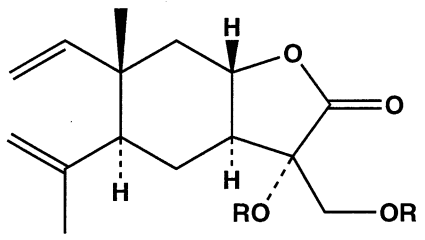

3 R=H
3a R=Ac

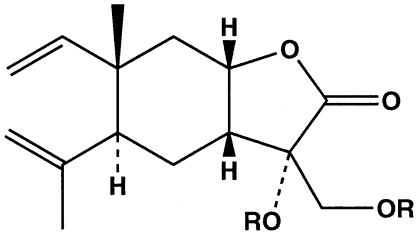

4 R=H
4a R=Ac

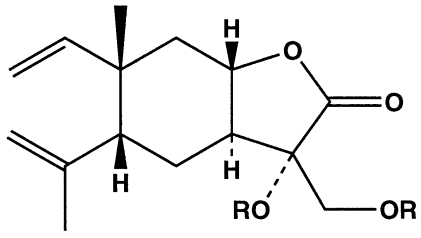

5 R=H
5a R=Ac

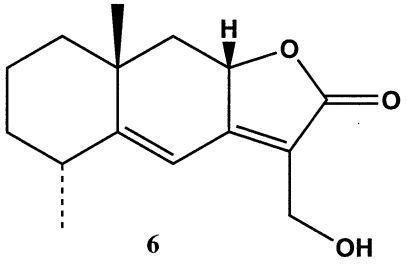

6

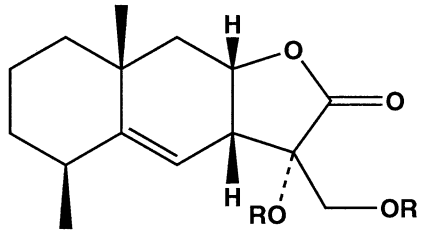

7 R=H
7a R=Ac

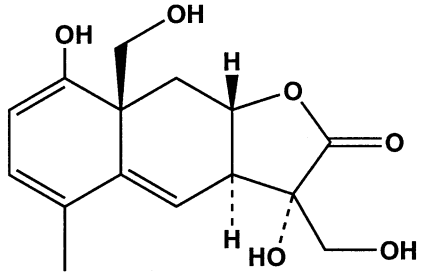

8

signals at δ_H 5.73 (1-H) , 5.02 (2a-H), 4.96 (2b-H), 5.00 (3a-H) and 4.73 (3b-H), which showed the presence of an elemanolide-type sesquiterpene unit in the structure of **1** (unit A, Fig. 1). The ^{13}C NMR spectrum also showed the corresponding carbon signals at δ_C 146.4 (C-1), 112.2 (C-2), 114.3 (C-3) and 144.7 (C-4). In the ^1H–^1H COSY spectrum, four fragments were defined through the correlations of 1-H with 2a-H and 2b-H, 3a-H with 3b-H, 8-H with 9-H, and 5-H with 6-H were observed. In the HMBC spectrum, these fragments were connected by the correlations from 8-H to C-11, C-12, C-6, C-7 and C-10, 5-H to C-1, C-3, C-14, C-15, C-9 and C-7, 14-H to C-1, C-5, C-9 and C-10, and 15-H to C-3, C-4 and C-5, which confirmed the partial structure. Apart from those signals of unit A, the remaining signals in the ^1H and ^{13}C NMR spectra were consistent with another elemanolide sesquiterpene moiety (unit B, Fig. 1). On the basis of 2D NMR spectroscopic technique,

Table 1
NMR spectral data of compounds **1** and **1a**[a]

	1		**1a**	
No.	δ_H	δ_C	δ_H	δ_C
1	5.73 *dd* (17.2, 10.8)	146.4 *d*	5.74 *dd* (17.4, 10.8)	146.3 *d*
2	5.02 *d* (17.5); 4.96, *d* (10.8)	112.2 *t*	5.04 *d* (17.4); 4.97 *d* (10.8)	112.3 *t*
3	5.00 *br s*; 4.73, *br s*	114.3 *t*	5.02 *br s*; 4.90 *br s*	114.3 *t*
4		144.7 *s*		144.6 *s*
5	2.11 *dd* (12.8, 4.0)	53.2 *d*	2.11 *m* (overlapped)	53.4 *d*
6	2.83 *dd* (β,14.4, 4.0); 2.63 *dd* (α, 14.4, 13.8)	28.5 *t*	2.94 *dd* (β, 14.4, 4.0); 2.62 *dd* (α, 14.4, 13.8)	28.9 *t*
7		165.0 *s*		166.8 *s*
8	4.89 *dd* (12.0, 6.2)	78.6 *d*	4.90 *dd* (12.2, 6.2)	78.3 *d*
9	2.25*dd* (β, 12.4, 6.2); 1.42*dd* (α, 12.4, 12.0)	45.8 *t*	2.27 *dd* (β, 12.4, 6.2); 1.41 *dd* (α, 12.4, 12.0)	46.0 *t*
10		40.8 *s*		40.8 *s*
11		123.0 *s*		119.4 *s*
12		177.8 *s*		179.2 *s*
13	4.39 *brs*	54.8 *t*	4.88 *brs*	55.2 *t*
14	1.18 *s*	17.2 *q*	1.19 *s*	17.3 *q*
15	1.81 *brdt* (14.4, 7.5), 1.42 *m* (overlapped)	16.9 *t*	1.92 *m* (overlapped), 1.47 *m* (overlapped)	16.9 *q*
1′	1.54 *m* (overlapped), 1.12 *m* (overlapped)	42.6 *t*	1.51 *q* (overlapped), 1.16 *m* (overlapped)	42.9 *t*
2′	1.22 *t* (7.2)	28.7 *q*	1.26 *t* (7.2)	28.0 *q*
3′	1.12 *d* (7.6)	23.0 *q*	1.16 *d* (7.6)	23.0 *q*
4′	2.49 *m*	38.5 *d*	2.50 *m*	38.1 *d*
5′		152.8 *s*		152.7 *s*
6′	5.05 *d* (3.5)	112.7 *d*	5.34 *d* (4.2)	119.4 *d*
7′	2.98 *dd* (5.6, 3.5)	44.9 *d*	3.23 *dd* (6.8, 4.2)	43.8 *d*
8′	5.12 *ddd* (12.8, 6.0, 5.6)	77.9 *d*	5.15 *ddd* (12.8, 6.8, 6.0)	78.3 *d*
9′	2.15 *dd* (α, 14.3, 12.8); 1.58 *dd* (β, 14.3, 6.0)	42.2 *t*	2.10 *m* (β); 1.62 *m* (α)	41.9 *t*
10′		33.0 *s*		32.8 *s*
11′		76.8 *s*		82.2 *d*
12′		174.1 *s*		178.3 *s*
13′	3.92 *d* (12.0); 3.72, *d* (12.0)	64.1 *t*	4.56 *d* (12.0); 4.26 *d* (12.0)	63.8 *t*
14′	1.76 *s*	24.8 *q*	1.79 *s*	24.8 *q*
15′	1.60–1.57 *m*	32.9 *t*	1.62 *m* (overlapped)	32.8 *t*
OH	3.81 *brs* (11-OH); 3.71 *brs* (overlapped, 13-OH)			
OAc			2.14 *s*, 2.12 *s*, 2.17 *s*	24.0 *q*; 21.5 *q*; 20.7 *q*; 170.1 *s*; 171.2 *s*; 171.8 *s*

[a] 400 MHz for ^{1}H NMR, 100 MHz for ^{13}C NMR and DEPT. Coupling constants are in parentheses in Hz.

the structure of unit B was also elucidated, especially by the correlations of 1′-H with 2′-H, and 4′-H with 3′-H, 15′-H and 6′-H (long-range coupling) in the ^{1}H–^{1}H COSY spectrum, as well as by the correlations of 3′-H to C-5′ and C-15′, 15′-H to C-5′ and C-3′, 6′-H to C-4′, C-8′, C-10′ and C-11′, 1′-H to C-5′, C-9′ and C-14′, and 2′-H to C-10′ in the HMBC spectrum. Based on a comparison of the ^{1}H and ^{13}C NMR spectral data of unit B with those of unit A, the two olefinic methylenes of unit A were replaced by two methyls at δ_H 1.22 (2′-H) and 1.12 (3′-H) in the structure of unit B. Thus, unit B possesed two single bonds instead of the two double bonds at C-1, C-2, C-3 and C-4 in unit A.

Considering the position through which the two sesquiterpene units are reportedly connected (Su et al., 2000b), the connection in compound **1** was at first thought to be between C-13 and C-13′. However, based on a careful study of the HMBC spectrum of **1**, correlations of an oxygenated methylene proton at δ_H 4.39 (13-H) with C-7 and C-12, which indicated the presence of a hydroxyl group at C-13, were observed. Acetylation of **1** gave an acetylated product **1a**. In the ^{1}H NMR spectrum of **1a**, the signals of 13-H and 13′-H were shifted downfield (Table 1) supported the above conclusion and effectively eliminated the possibility of the connection through either an ether or ester group between C-13 and C-13′. In the ^{1}H–^{1}H COSY spectra of **1a** and **1**, 15-H was correlated to 15′-H, and in the HMBC spectrum of **1**, 15-H correlated to C-15′ and C-4′; while 15′-H correlated to C-15 and C-4. Thus, the two

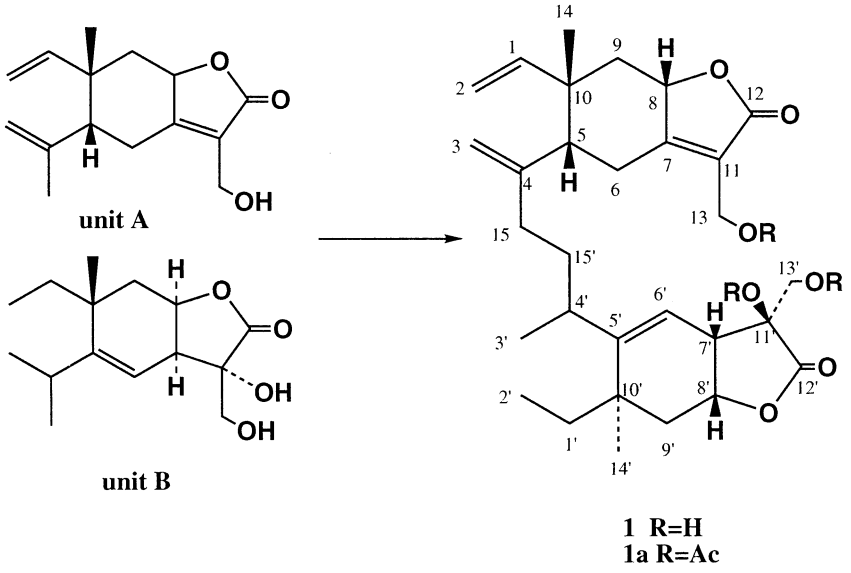

Fig. 1. Two sesquiterpene units of **1**.

units were concluded to be connected by a direct C–C bond between C-15 and C-15′.

The NOESY spectrum exhibited the correlations of 8-H with 9β-H (δ_H 2.25, *dd*, J = 12.4, 6.2 Hz) and 14-H, 5-H with 6β-H and 14-H, 3-H with 6α-H (δ_H 2.63, *dd*, J = 14.4, 13.8 Hz), 7′-H with 8′-H and 11′-OH (δ_H 3.81, *brs*), and 9′α-H (δ_H 2.15, *dd*, J = 14.3, 12.8 Hz) with 14′-H. According to these correlations and coupling constants, the relative configuration of **1** was determined to be as shown.

HRFABMS of macrophyllilactone A (**2**) gave a molecular ion peak at m/z 249.1484 $[M+H]^+$ for $C_{15}H_{21}O_3$ (calc. 249.1491), and based on a strong fragment peak at m/z 230 for the loss of water seen in the ElMS of **2**, the molecular formula of compound **2** was established to be $C_{15}H_{20}O_3$. Its ^{1}H NMR, ^{13}C NMR and DEPT spectra (Table 2) were very similar to those of unit A of **1**, and also displayed the typical double bond signals of 1-H, 2-H and 3-H of an elemanolide-type sesquiterpene. Based on the correlations in the 2D NMR spectra of **2**, its structure was confirmed to be the same as that shown for unit A of **1**.

On the basis of the FABMS of macrophyllilactone B (**3**) and the HRFABMS of its acetylated product (**3a**), the molecular formula of **3** was determined to be $C_{15}H_{22}O_4$. The ^{1}H and ^{13}C NMR spectra (Table 2) of compound **3** were similar to those of **2**, apart from a methine carbon (δ_C 44.9) and an oxygenated quaternary carbon (δ_C 78.0) instead of the double bond at C-7 and C-11 in **2**. Thus, the difference in the molecular formula of **2** and **3** was H_2O, which indicated the presence of another hydroxyl group in addition to the one at C-13. In the HMBC spectrum, the clear correlations of the corresponding methine proton at δ_H 2.34 with C-12, C-13, C-5, and C-9 confirmed that this methine proton was

Table 2
^{13}C NMR spectral data of compounds **2**–**3** and **6**–**8** in $CDCl_3$[a]

C	2	3	6	7	8
1	146.3 *d*	148.5 *d*	39.8 *t*	42.3 *t*	156.8 *s*
2	114.2 *t*	113.3 *t*	18.1 *t*	16.9 *t*	119.5 *d*
3	112.1 *t*	111.6 *t*	20.8 *t*	32.9 *t*	126.2 *d*
4	146.6 *s*	146.2 *s*	40.7 *d*	38.5 *d*	140.1 *s*
5	53.2 *d*	49.7 *d*	158.7 *s*	152.6 *s*	147.7 *s*
6	28.4 *t*	23.0 *t*	112.7 *d*	112.9 *d*	118.8 *d*
7	164.8 *s*	44.9 *d*	163.7 *s*	45.0 *d*	47.8 *d*
8	78.5 *d*	77.9 *d*	76.5 *d*	77.9 *d*	79.2 *d*
9	45.7 *t*	39.7 *t*	43.4 *t*	42.3 *t*	39.9 *t*
10	40.7 *s*	38.6 *s*	38.70 *s*	33.0 *s*	42.5 *s*
11	122.9 *s*	78.0 *s*	118.6 *s*	77.7 *s*	76.4 *s*
12	173.9 *s*	177.6 *s*	175.1 *s*	177.7 *s*	178.4 *s*
13	54.8 *t*	63.0 *t*	55.6 *t*	64.0 *t*	66.0 *t*
14	17.2 *q*	18.3 *q*	20.8 *q*	28.7 *q*	67.6 *t*
15	24.7 *q*	24.9 *q*	29.6 *q*	23.0 *q*	21.8 *q*

[a] 100 MHz for ^{13}C NMR and DEPT.

7-H. In addition, the oxygenated quaternary carbon at δ_C 78.0 correlated with 6-H and 8-H, which indicated that the quaternary carbon was C-11. The coupling constant of 8-H (δ_H 5.02, *ddd*, J = 12.8, 12.0, 1.9) implied the presence of a 7,8-*trans*-lactone in the structure of **3**. The NOESY correlations of 8-H with 6β-H and 14-H, 5-H with 7-H and 9α-H, and 6β-H with 9β-H, 3b-H, 14-H and 13b-H also supported the relative configuration of **3** as shown.

Compounds **4** and **5** were an inseparable mixture, even through attempted HPLC separation of their acetates. The ^{1}H and ^{13}C NMR spectra (Table 3) of the mixture were very similar to those of **3**. FABMS of them showed the same molecular ion peaks at m/z 289 $[M+Na]$ and 267 $[M+H]$ as for **3**. Their ^{1}H–^{1}H COSY

Table 3
^{13}C NMR spectral data of compounds **4**–**5** and **7a** in $CDCl_3$[a]

C	4	5	4a	5a	7a
1	148.2 *d*	147.8 *d*	148.1 *d*	147.5 *d*	42.9 *t*
2	112.7 *t*	113.4 *t*	113.1 *t*	113.5 *t*	16.9 *t*
3	110.9 *t*	111.5 *t*	111.4 *t*	111.4 *t*	32.8 *t*
4	146.6 *s*	145.8 *s*	146.2 *s*	145.5 *s*	38.1 *t*
5	48.1 *d*	47.9 *d*	47.1 *d*	48.4 *d*	152.5 *s*
6	24.7 *t*	23.4 *t*	23.9 *t*	24.4 *t*	114.6 *d*
7	37.9 *d*	41.2 *d*	39.4 *d*	38.2 *d*	43.8 *d*
8	75.3 *d*	75.3 *d*	76.4 *d*	75.2 *d*	77.3 *d*
9	42.5 *t*	39.8 *t*	38.8 *t*	41.7 *t*	41.9 *t*
10	40.0 *s*	38.9 *s*	38.9 *s*	38.3 *s*	32.8 *s*
11	75.2 *s*	78.2 *s*	82.2 *s*	80.1 *s*	82.2 *s*
12	178.9 *s*	178.1 *s*	180.3 *s*	181.3 *s*	171.5 *s*
13	65.4 *t*	64.1 *t*	63.5 *t*	63.4 *t*	63.8 *t*
14	17.1 *q*	20.6 *q*	17.5 *q*	20.9 *q*	28.1 *q*
15	25.3 *q*	25.5 *q*	25.5 *q*	24.5 *q*	23.0 *q*
OAc			21.3 *q*	20.9 *q*	21.0 *q*
			21.2 *q*	20.9 *q*	20.9 *q*
			170.2 *s*	170.0 *s*	170.2 *s*
			169.3 *s*	169.5 *s*	170.0 *s*

[a] 100 MHz for ^{13}C NMR and DEPT.

and HMBC spectra indicated that **4** and **5** were also 11,13-dihydroxy-1,3-elemadien-12, 8-olides like **3**. However, in the NOESY spectrum of the mixture, the 5-H of **4** correlated with 9α-H, and 9β-H correlated with 7-H, 8-H and 14-H, which clearly confirmed that compound **4** had a 5αH, 10βMe-*trans*-7βH, 8βH-*cis*-configuration. The NOESY spectrum also showed the correlations of 14-H of **5** with 5-H, 9β-H and 8-H, 7-H with 9α-H, and 13-H with 6β-H and 8-H. Consequently, it can be deduced that compound **5** had a 5βH,10βMe-*cis*-7αH, 8βH-*trans*-configuration. Hence, compounds **3**, **4** and **5** were stereoisomers.

Compound **6**, macrophyllilactone E, showed strong IR bands for a hydroxyl (3512 cm^{-1}) and an γ-unsaturated lactone (1737 and 1658 cm^{-1}). Its EIMS spectrum showed a molecular ion peak at *m*/*z* 248 and a strong fragment peak at *m*/*z* 230 due to the loss of water. HRFABMS gave a molecular ion peak at *m*/*z* 249.1502 (calc. for $C_{15}H_{21}O_3$, 249.1491), which supported a molecular formula of $C_{15}H_{20}O_3$. An eudesmanolide skeleton was deduced from the methyl signals at δ_H 1.27 (*s*) and 1.29 (*d*, $J=7.6$ Hz) in its ^1H NMR spectrum, which were similar to those of neoalantolactone from *Inula racemosa* (Ravindranath et al., 1978). The obvious difference is that another methyl signal in the structure of neoalantolactone was replaced by a hydroxymethyl at δ_H 4.45 (13-H_2) in that of **6**. The hydroxymethyl was confirmed to be 13-H_2 due to the correlations of the hydroxymethyl protons with the carbon at δ_C 163.7 (C-7) and 175.1 (C-12) in the HMBC spectrum. The stereochemistries of 8β-H and 4β-H were derived from the NOESY correlations of 8-H with 9β-H and 14-H, 4-H with 9β-H and 2β-H. Therefore, the compound **6** was determined to have the structure as shown.

The EIMS of macrophyllilactone F (**7**) gave a molecular ion peak at *m*/*z* 266 and a strong fragment peak at *m*/*z* 235 due to the loss of a hydroxymethyl group. Its ^1H NMR and ^{13}C NMR spectra were almost the same as those of 11,13-dihydroxyalantolactone, which is an oxidation product of alantolactone with OsO_4 (Cantrell et al., 1999). The NOESY spectrum and the coupling constants revealed that **7** was a stereoisomer of 11,13-dihydroxyalantolactone, showing the correlations of 9β-H with 14-H and 8-H, of 7-H with 6-H and 8-H, and of 15-H with 2β-H and 3β-H, of 14-H with 2β-H. Thus, **7** had a 7βH, 8βH-*cis*-lactone configuration. In the ^1H NMR spectrum of the acetate **7a** of **7**, 8β-H was shifted downfield to δ_H 5.25 due to the effect of the 13-acetoxy group. This supported the notion that 13-H and 8β-H were close to each other in space. Therefore, the relative configuration of the 11α-hydroxyl was determined.

The ^1H NMR spectrum of macrophyllilactone G (**8**) displayed a typical 12, 8-lactone signal like **7**. Its EIMS showed a molecular ion peak at *m*/*z* 294 and fragment peaks at *m*/*z* 263 $[M–CH_2OH]^+$, 258 $[M–2H_2O]^+$, and 245 $[M–CH_2OH–H_2O]^+$, which implied the presence of hydroxyl and hydroxylmethyl groups. The molecular formula of **8** was suggested to be $C_{15}H_{18}O_6$ by consideration of the ^{13}C NMR spectral data (Table 2). The UV spectrum of **8** showed a presence of conjugated diene unit (274 nm). The ^1H NMR spectrum of **8** was compared to that of **7**: a pair of doublets at δ_H 6.92 and 6.66 was observed in that of **8**, and the ^1H NMR spectrum of **8** also showed signals of a hydroxymethyl group at δ_H 4.56 and 4.44 and a 13-hydroxylmethyl instead of the signal of the methyl group (14-H_3) of **7**. The corresponding carbon signals were also to be found in the ^{13}C NMR spectrum, and the ^{13}C NMR spectral data revealed that the pair of doublets was attributed to two double bonds. Based on the coupling constant (8.0 Hz) between the pair of doublets, the conjugated diene was deduced to be at C-1 and C-2, as well as C-3 and C-4. In the HMBC spectrum, the key correlations of one olefinic proton (2-H) of the conjugated diene with C-4 and C-10, and the other proton (3-H) with C-1, C-5 and C-15 further confirmed the conclusion. Since the methyl group signal was shifted downfield to δ_H 2.28, it should be attached to a double bond and is attributed to 15-H. This indicated that another hydroxymethyl group was located at C-14. In addition, a sharp singlet at δ_H 8.84 inferred the presence of a hydroxyl group attached to a ring similar to an aromatic ring. Consistent with this notion, a hydroxyl group was likely at C-1. In the HMBC spectrum of **8**, the downfield olefinic quaternary carbon at δ_C 156.8 correlated with 3-H and 14-H, which supported the location of 1-hydroxyl group in the structure of **8**. In the NOESY spectrum of **8**, the correlations of 9β-H with 8-H, 14-H and 13-H as well as of 7-H with 9α-H permitted assignment of the stereochemistry.

Compound **9**, reynosin, was identified by comparison of its physical and spectral data with those in the literature (Ando and Takase, 1977).

3. Experimental

3.1. General

^{1}H NMR (400 MHz), ^{13}C NMR (100 MHz with TMS as internal standard; MS: Jeol JMS-DX-303 and JMS SX-102 A; CC: silica gel 60 (Merck), Sephadex LH-20 (Pharmacia); HPLC: GPC (general permeation chromatography, Asahipark GS-310 2G, MeOH), silica gel (Si60, HIbar, TR250-25, Merck) IR: 1720 infrared Fourier-transform spectrometer (Perkin-Elmer); UV: UV2100 UV-vis recording spectrometer (Shimadzu); Optical rotation: JASCO DIP-370 digital polarimeter.

3.2. Plant material

The bark of *Inula macrophylla* (1.6 kg) was purchased at a medicinal plant market in Uzbekistan, in August 1997, and identified by Dr. Olimjon K. Kodzhimatov. A voucher specimen (ESM4141) is preserved at the herbarium of the Academy of Sciences, Institute of Botany, and Botanical Garden Uzbekistan.

3.3. Extraction and isolation

The MeOH extract (228 g) of the powdered air-dried bark (1.6 kg,) obtained with MeOH at 60 °C three times, 6 h each) of *I. macrophylla* were partitioned between H_2O and $CHCl_3$. The $CHCl_3$-soluble fraction (115 g) was subjected to a silica gel column chromatograph (eluted with *n*-hexane–EtOAc, from 10:1 to 1:1 then with pure EtOAc) to give 11 fractions. Fraction 9 (7.5 g) was applied to a silica gel column (eluted with *n*-hexane–EtOAc, from 2:1 to 1:6, then with pure EtOAc) to give 12 fractions (9.01–9.12). Fr. 9.01 (2.7 g) was applied to a Sephadex LH-20 column (eluted with MeOH), and 8 fractions (9.01.1–9.01.8) were obtained. Fr. 9.01.4 was further separated by HPLC (silica gel, *n*-hexane–EtOAc, 2.5:1) to give compounds **8** (6.6 mg), **6** (15 mg), **2** (6.5 mg) and **9** (18 mg). Fr. 9.01.5 was purified by GPC (eluted with MeOH) to give 9 fractions (9.01.5.1–9.01.5.9). Fr. 9.01.5.4 was separated by HPLC (silica gel, *n*-hexane–EtOAc, 2:1) to give a mixture of **4** and **5** (16.3 mg) as well as **3** (4.7 mg), **7** (16.7 mg) and **1** (36.5 mg). Compounds **1** (20.6 mg), **3** (4.2 mg), **7** (12 mg), and the mixture of **4** and **5** (15 mg) were respectively acetylated by Ac_2O–pyridine and DMAP, and purified by preparative TLC (developed with *n*-hexane–EtOAc, 2:1) to give a mixture of **4a** and **5a** (12.9 mg), **7a** (10.9 mg), **1a** (15.2 mg) and **3a** (3.5 mg), respectively.

3.4. Macrophyllidimer C (*1*) and *1a*

Macrophyllidimer C (**1**): colorless oil, $[\alpha]_D^{25}$ −87.2° ($CHCl_3$; *c* 0.83); UV (MeOH) λ_{max} (log ε) nm: 219 (*br*, 4.29), 203 (4.35); IR (KBr) ν_{max} cm^{-1}: 3836, 3511, 3089, 3026., 2933, 2869, 2360, 2339, 1746, 1717, 1684, 1638, 1457, 1378, 1337, 1223, 1209, 1070, 1021, 972, 919, 903, 868; EI–MS *m*/*z* (rel. int.): 230 [M–H_2O-266]$^+$ (21), 162 [230–C_5H_7]$^+$ (61), 147 (31), 133 (22), 105 (81), 91 (100), 77 (47), 55 (52), 41 (70); FABMS (rel. int.) *m*/*z* (**1**): 537 [M + Na]$^+$ (9) 519 [M + Na–H_2O]$^+$(19), 289 [M + Na-249]$^+$ (38), 271 [266 + Na–H_2O]$^+$(100), 249 [M + H-266]$^+$(93), 231 [249-H_2O]$^+$(7); (**1a**): 663 [M + Na]$^+$(7) 641 [M + H]$^+$ (3) 603 [M + H-HOAc]$^+$ (3), 581 [M + Na]$^+$, 373 [350 + Na]$^+$(59), 313 [290 + Na]$^+$(100); HRFABMS *m*/*z* (**1a**) 663.3145 (calc. for $C_{36}H_{48}O_{10}Na$, 663.3151), 641.3326 (calc. for $C_{36}H_{49}O_{10}$, 641.3421), 603.2934 (calc. for $C_{34}H_{44}$,O_8Na, 603.2890); ^{1}H NMR, ^{13}C NMR and DEPT data of **1** and **1a**, see Table 1.

3.5. Macrophyllilactone A (*2*)

Colorless oil, $[\alpha]_D^{25}$ −60.9° ($CHCl_3$; *c* 0.97); UV (MeOH) λ_{max} (log ε) nm: 218 (*br*, 4.04), 191 (3.29); IR (KBr) ν_{max} cm^{-1}: 3650, 3391, 3020, 2928, 2331, 1718, 1678, 1629, 1462, 1385, 1331, 1220, 1201, 1021, 975, 923, 903, 859; EI–MS *m*/*z* (rel. int.): 230 [M–H_2O]$^+$(100), 217 [M–CH_2OH]$^+$ (7) 215 [M–H_2O–CH_3]$^+$ (81), 201 (37), 188 (40), 174 (29), 133 (62), 121 (99), 105 (95), 91 (90), 77 (88), 55 (46), 41 (83), 39 (72), 31(14); FABMS (rel. int.) *m*/*z* :249 [M + H]$^+$(100) 231 [M + H–H_2O]$^+$ (9), 214 (17), 152 (29), 135 (29), 91(20); HRFABMS *m*/*z* 249.1484 (calc. for $C_{15}H_{21}O_3$, 249.1491); ^{1}H NMR data δ_H ($CDCl_3$): 1.18 (3H, *s*, 14-Hβ), 1.76 (3H, *s*, 15-H), 1.42 (1H, *dd*, *J* = 12.4, 11.7, 9-Hα), 2.26 (1H, *dd*, *J* = 12.4, 6.1, 9-Hβ), 2.12 (1H, *dd*, *J* = 13.6, 4.0, 5-Hβ), 2.59 (1H, *dd*, *J* = 14.4, 13.6, 6-Hα), 2.83 (1H, *dd*, *J* = 14.4, 4.0, 6-Hβ), 4.40 (2H, *brs*, 13-H), 4.73 (1H, *brs*, 3a-H), 5.00 (1H, *brs*, 3b-H), 4.89 (1H, *dd*, *J* = 11.7, 6.1, 8-Hβ), 4.96 (1H, *d*, *J* = 10.8, 2a-H), 5.02 (1H, *d*, *J* = 17.2, 2b-H), 5.74 (1H, *dd*, *J* = 17.2, 10.8, 1-H); ^{13}C NMR and DEPT data, see Table 2.

3.6. Macrophyllilactone B (*3*) and *3a*

Colorless oil, $[\alpha]_D^{24}$ +23.4° ($CHCl_3$; *c* 0.47); UV (MeOH) γ_{max} (log ε) nm: 203 (3.54), 194 (2.77); IR (KBr) ν_{max}cm^{-1}: 3641, 3510, 3029, 2930, 2331, 1759, 1658, 1630, 1462, 1385, 1329, 1226, 1201, 1021, 998, 923, 903, 854; EI–MS *m*/*z* (rel. int.): 235 [M–CH_2OH]$^+$(17), 207 [M–CH_2OH–CO]$^+$ (10) 189 [207-H_2O]$^+$ (38) 161 (99), 145 (42), 109 (98), 105 (100), 77 (89), *55* (88), 43 (83), 41 (92), 39 (88), 31 (89); FABMS (rei. int.) *m*/*z*: 289 [M + Na]$^+$(9), 267 [M + H]$^+$(15), 249 [M + H-H_2O]$^+$(9), 214 (81), 197 (53), 181 (38), 135 (89), 91 (100); HRFABMS *m*/*z* (**3a**): 373.1581 (calc. for $C_{19}H_{26}O_6Na$,

373.1627), 351.1725 (calc. for $C_{19}H_{27}O_6$, 351.1808); ^{1}H NMR data δ_H ($CDCl_3$): (**3**) 1.03 (3H, *s*, 14-Hβ), 1.71 (3H, *s*, 15-H), 1.46 (1H, *m*, 6-Hα), 1.50 (1H, *m*, 6-Hβ), 1.42 (1H, *dd*, *J*=16.0, 12.0, 9-Hα), 2.09 (1H, *dd*, *J*=16.0, 1.9, 9-Hβ), 1.95 (1H, *dd*, *J*=13.6, 4.0, 5-Hα), 2.34 (1H, *m*, 7-Hα), 3.23 (1H, *brd*, *J*=11.4, 13-OH), 3.69 (1H, *brs*, 11-OH), 3.73 (1H, *d*, *J*=120, 13a-Hβ), 4.06 (1H, *d*, *J*=12.0, 13b-Hβ), 4.59 (1H, *brs*, 3a-H), 4.88 (1H, *brs*, 3b-H), 4.97 (1H, *d*, *J*=10.8, 2a-H), 5.00 (1H, *d*, *J*=17.6, 2b-H), 5.02 (1H, *ddd*, *J*=11.7, 12.0, 1.9, 8-Hβ), 5.72 (1H, *dd*, *J*=17.6, 10.8, 1-H); ^{13}C NMR and DEPT data, see Table 2.

3.7. Macrophyllilactone C and D (*4* and *5*)

Colorless oil, $[\alpha]_D^{20}$ +65.9° ($CHCl_3$; *c* 1.18); UV (MeOH) λ_{max} (log ε) nm: 204 (3.48), 193 (2.81); IR (KBr) ν_{max}cm^{-1}: 3670, 3531, 3084, 3024, 2969, 2360, 1761, 1698 (*sh*) 1639, 1451, 1379, 1338, 1301, 1216, 1125, 1038, 1000, 911; FABMS (rel. int.) *m*/*z* : 289 $[M+Na]^+$ (100), 267 $[M+H]^+$(9), 231(5), 163 (4), 161 (8), 105 (8), 91 (11), 77 (8), 55 (6); ^{1}H NMR data δ_H ($CDCl_3$): (**4**) 1.03 (3H, *s*, 14-Hβ), 1.72 (3H, *s*, 15-H), 1.82 (1H, *m*, 6-Hα), 1.86 (1H, *m*, 6-Hβ), 1.87 (1H, *dd*, *J*=12.2, 12.0, 9-Hα), 1.98 (1H, *dd*, *J*=12.2, 5.6, 9-Hβ), 2.55 (1H, *dd*, *J*=13.9, 4.6, 5-Hα), 2.84 (1H, *m*, 7-Hβ), 2.98 (1H, *brd*, *J*=11.2, 13-OH), 3.64 (1H, *d*, *J*=11.6, 13a-Hβ), 3.70 (1H, *d*, *J*=11.6, 13b-Hβ), 3.90 (1H, *brs*, 11-OH), 4.78 (1H, *ddd*, *J*=12.0, 6.1, 5.6, 8-Hβ), 4.66 (1H, *brs*, 3a-H), 4.94 (1H, *brs*, 3b-H), 4.89 (1H, *d*, *J*=10.9, 2a-H), 4.95 (1H, *d*, *J*=17.6, 2b-H), 5.84 (1H, *dd*, *J*=17.6, 10.9, 1-H); (**5**) 1.02 (3H, *s*, 14-Hβ), 1.75 (3H, *s*, 15-H), 1.79 (1H, *m*, 6-Hα), 1.81(1H, *m*, 6-Hβ), 1.80 (1H, *dd*, *J*=12.3, 12.1, 9-Hα), 1.94 (1H, *dd*, *J*=12.3, 6.0, 9-Hβ), 2.05(1H, *dd*, *J*=9.5, 4.6, 5-Hβ), 2.42 (1H, *m*, 7-Hα), 3.01 (1H, *brd*, *J*=11.2, 13-OH), 3.71 (1H, d, *J*=12.0, 13a-Hβ), 3.99 (1H, *d*, *J*=12.0, 13b-Hβ), 3.88 (1H, *brs*, 11-OH), 4.91 (1H, *ddd*, *J*=12.1, 10.2, 6.0, 8-Hβ), 4.69 (1H, *brs*, 3a-H), 4.92 (1H, *brs*, 3b-H), 4.97 (1H, *d*, *J*=10.7, 2a-H), 5.00 (1H, *d*, *J*=17.6, 2b H), 5.83 (1H, *dd*, *J*=17.6, 10.7, 1-H); ^{13}C NMR and DEPT data, see Table 3.

3.8. *4a* and *5a*

FABMS (rel. int.) *m*/*z*: 373 $[M+Na]^+$ (100), 313 $[M+Na–HOAc]^+$ 351 $[M+H]^+$ (87), 291 $[M+H–HOAc]^+$(66), 231 $[M+H–2HOAc]^+$ (24), 176 (27), 154 (25), 137 (45), 105 (24), 91(26), 77 (22); HRFABMS *m*/*z*: 267.1579 (calc. for $C_{15}H_{23}O_4$, 267.1596); ^{1}H NMR data δ_H ($CDCl_3$): (**4a**) 0.99 (3H, *s*, 14-Hβ), 1.71 (3H, *s*, 15-H), 1.70 (1H, *m*, 6-Hα), 1.79 (1H, *m*, 6-Hβ), 1.81 (1H, *dd*, *J*=12.4, 12.0, 9-Hα), 1.88 (1H, *dd*, *J*=12.4, 6.0, 9-Hβ), 2.10 (3H, *s*, CH_3 of OAc), 2.12 (3H, *s*, CH_3 of OAc), 2.37(1H, *dd*, *J*=13.8 4.5, 5-Hα), 3.02 (1H, *ddd*, *J*=12.2, 5.8, 5.4, 7-Hβ), 4.82 (1H, *d*, *J*=12.0, 13a-Hβ), 4.91 (1H, *d*, *J*=12.0, 13b-Hβ), 4.83 (1H, *ddd*, *J*=12.0, 6.0, 5.4, 8-Hβ), 4.60 (1H, *brs*, 3a-H), 4.89 (1H, *brs*, 3b-H), 4.95 (1H, *d*, *J*=11.1, 2a-H), 4.97 (1H, *d*, *J*=17.4, 2b-H), 5.88 (1H, *dd*, *J*=17.4, 11.1, 1-H); (**5a**) 1.01 (3H, *s*, 14-Hβ), 1.69 (3H, *s*, 15-H), 1.95 (1H, *m*, 6-Hα), 1.99(1H, *m*, 6-Hβ), 1.65 (1H, *dd*, *J*=12.4, 12.0, 9-Hα), 1.91 (1H, *dd*, *J*=12.4, 5.8, 9-Hβ), 2.11 (3H, *s*, $CH_3$of OAc), 2.13 (3H, *s*, CH_3 of OAc), 2.07 (1H, *m*, overlapped, 5-Hα), 3.41 (1H, *ddd*, *J*=11.8, 10.2, 5.0, 7-Hα), 4.32 (1H, *d*, *J*=12.1 13a-Hβ), 4.60 (1H, *d*, *J*=12.1, 13b-Hβ), 4.79 (1H, *ddd*, *J*=12.0, 10.2, 5.8, 8-Hβ), 4.62 (1H, *brs*, 3a-H), 4.94 (1H, *brs*, 3b-H), 4.90 (1H, *d*, *J*=11.1, 2a-H), 4.93 (111, *d*, *J*=17.4, 2b-H), 5.76 (111, *dd*, *J*=17.4, 11.2, 1-H); ^{13}C NMR and DEPT data, see Table 3.

3.9. Macrophyllilactone E (*6*)

Colorless oil, $[\alpha]_D^{24}$ +26.2° ($CHCl_3$; *c* 0.45); UV (MeOH) λ_{max} (log ε) nm: 275 (*br*, 3.03), 215 (*br*, 3.63) 205 (3.88); IR (KBr) ν_{max} cm^{-1}: 3512, 3010, 2930, 2331, 1737, 1658, 1630, 1462, 1385, 1329, 1226, 1201, 1021, 979, 923, 903, 854; EI–MS *m*/*z* (rel. int.): 248 $[M]^+$(67), 230 $[M-H_2O]^+$ (55), 215 (37), 159 (41) 146 (58), 131 (47), 105 (56), 91 (72), 77 (50), 55 (61), 41 (100); FABMS (rel. int.) *m*/*z*: 271 $[M+Na]^+$ (9), 249 $[M+H]^+$ (31), 231 $[M+H–H_2O]^+$ (100); HRFABMS *mlz:* 249.1502 (calc. for $C_{15}H_{21}O_3$, 249.1491); ^{1}H NMR data δ_H ($CDC1_3$): 1.27 (3H, *s*, 14-Hβ), 1.29 (3H, *d*, *J*=7.6, 15-Hα), 1.65–1.69 (2H, *m*, overlapped, 1-H), 1.52 (1H, *m*, 2-Hα), 1.95 (1H, *m*, 2-Hβ), 1.63 (1H, *m*, 3-Hα), 1.72 (1H, *m*, 3-Hβ), 1.54 (1H, *dd*, *J*=17.6, 13.4, 9-Hα), 2.18 (1H, *dd*, *J*=17.6, 5.8, 9-Hβ), 2.78 (1H, *m*, 4-Hβ), 4.45 (2H, *d*, *J*=3.8, 13-H), 4.80 (1H, *dd*, *J*=13.4, 5.8, 8-Hβ), 6.36 (1H, *brs*, 6-H); ^{13}C NMR and DEPT, data see, Table 2.

3.10. Macrophyllilactone F (7 and *7a*)

Macrophyllilactone F (**7**): colorless oil $[\alpha]_D^{20}$ +150.0° ($CHCl_3$; *c* 1.20); UV (MeOH) λ_{max} (log ε) nm: 276 (*br*, 3.41), 204 (3.56); IR (KBr) ν_{max} cm^{-1}: 3532, 3412, 3030, 3021, 3009, 2934, 1758, 1638, 1462, 1376, 1341,1294, 1215, 1109, 1074, 1023, 972 909; El–MS *mlz* (rel. int.): 266 $[M]^+$ (44), 235 $[M–CH_2OH]^+$ (31), 207 (22), 191 (65) 162 (99), 147 (100), 133 (59), 119 (80), 105 (98), 91 (99), 77 (99), 55 (82), 43 (54), 41 (98), 31 (87); FABMS (rel. int.) *m*/*z* (**7**): 289 $[M+Na]^+$(63), 267 $[M+H]^+$ (52), 231 $[M+H–2H_2O]^+$ (39), 161 (43), 147 (47), 105 (93), 91(100); (**7a**): 373 $[M+Na]^+$(22), 351 $[M+H]^+$ (100), 291 $[M+H–HOAc]^+$ (84), 231 $[M+H-2HOAc]^+$ (59), 214 (56), 197 (26), 105 (29), 91 (54); HRFABMS *m*/*z* (**7a**): 351.1779 (calc. for $C_{19}H_{27}O_6$, 351.1808); ^{1}H NMR data δ_H ($CDCl_3$): (**7**) 1.11 (3H, *d*, *J*=7.6, 15-Hβ), 1.21 (3H, *s*, 14-Hβ), 1.15 (1H, *m*, 1-Hα), 1.61 (1H, *m*, 1-Hβ), 1.44 (1H, *m*, 2-Hα), 1.80 (1H, *m*, 2-Hβ), 1.46 (1H,

m, 3-Hα), 1.53 (1H, *m*, overlapped, 3-Hβ), 1.59 (1H, *dd*, *J* = 15.0, 14.0, 9-Hα), 2.13 (1H, *dd*, *J* = 15.0, 3.0, 9-Hβ), 2.46 (1H, *m*, 4-Hα), 2.98 (1H, *dd*, *J* = 5.5, 3.4, 7-Hβ), 3.18 (1H, *d*, *J* = 11.4, 13-OH), 3.73 (1H, *d*, *J* = 12.4, 13a-Hβ), 3.91 (1H, *d*, *J* = 12.4, 13b-Hβ), 4.15 (1H, *brs*, 11-OH), 5.07 (1H, *d*, *J* = 3.4, 6-H), 5.11 (1H, *ddd*, *J* = 14.0, 5.5, 3.0, 8-Hβ); (**7a**) 1.13 (3H, *d*, *J* = 7.6, 15-Hβ), 1.26 (3H *s*, 14-Hβ), 1.17 (1H, *m*, overlapped, 1-Hα), 1.62 (1H, *m*, overlapped, 1-Hβ), 1.46 (1H, *m*, 2-Hα), 1.80 (1H, *m*, 2-Hβ), 1.54 (1H, *m*, overlapped, 3-Hα), 1.58 (1H, *m*, overlapped, 3-Hβ), 1.59 (1H, *dd*, *J* = 15.4, 14.2, 9-Hα), 2.13 (1H, *dd*, *J* = 15.4, 3.2, 9-Hβ), 2.00 (3H, *s*, CH_3 of OAc), 2.10 (311, *s*, CH_3 of OAc), 2.50 (1H, *m*, 4-Hα), 3.23 (1H, *dd*, *J* = 6.6, 4.2, 7-Hβ), 4.26 (1H, *d*, *J* = 12.1 13a-Hβ), 4.57 (1H, *d*, *J* = 12.1, 13b-Hβ), 5.25 (1H, *ddd*, *J* = 14.2, 6.6, 3.2, 8-Hβ), 5.34 (1H, *d*, *J* = 4.2, 6-H) ; ^{13}C NMR and DEPT data of **7** and **7a**, see Tables 2 and 3.

3.11. Macrophyllilactone G (*8*)

Colorless oil, $[\alpha]_D^{24}$ +121.0° ($CHCl_3$; *c* 0.40); UV (MeOH) γ_{max} (log ε) nm: 274 (*br*. 3.13), 252 (2.99), 204 (3.93), 196 (3.26), 191 (3.12); IR (KBr) ν_{max} cm^{-1}: 3590, 3480, 3358, 2976, 2937, 1761, 1633, 1570, 1457, 1379, 1344, 1230, 1221, 1210 1159, 997, 911, 896, 778, 763, 689; EI–MS *m*/*z* (rel. int.): 263 $[M–CH_2OH]^+$(11), 258 $[M–2H_2O]^+$ (20), 245 $[M–CH_2OH–H_2O]^+$(15), 215 (18), 205 (19) 187 (20), 131 (22), 105 (53), 91 (56), 55 (100), 43 (45); FABMS (rel. int.) *m*/*z*: 317 $[M+Na]^+$ (6), 295 $[M+H]^+$(7), 286 $[M+Na–CH_2OH]^+$(13), 277 $[M+H–H_2O]^+$ (6), 251 (31); HRFABMS *m*/*z*: 295.1576 (calc. for $C_{15}H_{19}0_6$, 295.1531);^1H NMR data δ_H ($CDCl_3$): 1.78 (1H, *dd*, *J* = 12.9, 5.4, 9-Ha), 1.97(1H, *dd*, *J* = 12.9, 5.6,9-1113), 2.28 (3H, *s*, 15-H), 2.86 (1H, *dd*, *J* = 11.2, 3.8, 7-Hα), 3.25 (1H, *brd*, *J* = 11.3, 13-OH), 3.69 (1H, *brs*, 11-OH), 3.79 (1H, *d*, *J* = 12.5, 13a-Hβ), 3.88 (1H, *d*, *J* = 12.5, 13b-Hβ), 4.44 (1H, *d*, *J* = 12.4, 14a-Hβ), 4.56 (1H, *J* = 12.4, 14b-Hβ), 5.00 (1H, *ddd*, *J* = 12.4, 11.2, 5.6, 8-Hβ), 6.66 (1H, *d*, *J* = 8.0, 2-H), 6.72 (1H, *d*, *J* = 3.8, 6-H), 6.92 (1H, *d*, *J* = 8.0, 3-H), 8.84 (1H, *s*, 1-OH); ^{13}C NMR and DEPT data, see Table 2.

References

Ando, M., Takase, K., 1977. Studies in the syntheses of sesquiterpene lactones—II. Tetrahedron 33, 2785–2789.

Bokadia, M.M., MacLeod, A.J., Mehta, S.C., Mehta, B.K., Patel, H., 1986. The essential oil of *Inula racemosa*. Phytochemistry 25, 2887–2888.

Cantrell, C.L., Abate, L., Fronczek, F.R., Franzblau, S.G., Quijano, L., Fischer, N.H., 1999. Antimycobacterial eudesmanolides from *Inula helenium* and *Rudbeckia subtomentosa*. Planta Medica 65, 351–355.

Marco, J.A., Sanz-Cervera, J.F., Manglano, E., 1993. Chlorinated thymol derivatives from *Inula crithmoides*. Phytochemistry 33, 875–878.

Ravindranath, K.R., Raghavan, R., Paknikar, S.K., Trivedi, G.K., Bhattacharyya, S.C., 1978. Structure and stereochemistry of inunolide, dihydroinunolide and neoalantolactone. Indian Journal of Chemistry 16B, 27–31.

Oksuz, S., Topcu, G., 1992. A eudesmanolide and other constituents from *Inula gravelens*. Phytochemistry 31, 195–197.

Oksuz, S., Topcu, G., Krawiec, M., Watson, W., 1997. Eudesmanolides and other constituents of *Inula thapsoides*. Phytochemistry 46, 1131–1134.

Su, B.-N., Takaishi, Y., Tori, M., Takaoka, S., Honda, O., Itoh, M., Takeda, Y., Kodzhimatov, O.K., Ashurmetov, O., 2000a. Macrophyllols A and B, two unusual novel sesquiterpene and monoterpene dimers from the bark of *Inula macrophylla*. Organic Letters 4, 493–496.

Su, B.-N., Takaishi, Y., Tori, M., Takaoka, S., Honda, G., Itoh, M., Takeda, Y., Kodzhimatov, O.K., Ashurmetov, O., 2000b. Macrophyllidimers A and B, two novel sesquiterpene dimers from the bark of *Inula macrophylla*. Tetrahedron Letters 41, 1475–1479.

Su, B.-N., Takaishi, Y., Yabuuchi, T., Kusumi, T., Tori, M., Takaoka, S., 2000c. The structure and absolute configurations of macrophilic acids A-E, five new rearranged eudesmane sesquiterpene acids from the bark of *Inula macrophylla*. Tetrahedron Letters 41, 2395–2400.

Tan, R.X., Tang, H.Q., Hu, J., Shuai, B., 1998. Lignans and sesquiterpene lactones from *Artemisia sieversina* and *Inula racemosa*. Phytochemistry 49, 157–161.

Topcu, T., Oksuz, S., 1990. Guaianolides from *Inula anatolica*. Phytochemistry 29, 3666–3667.

Topcu, G., Oksuz, S., Shieh, H.-L., Cordell, G.A., Pezzuto, J.M., Bozok-Johansson, C., 1993. Cytotoxic and antibacterial sesquiterpenes from *Inula graveolens*. Phytochemistry 33, 407–410.

PERGAMON

Phytochemistry 58 (2001) 1129–1134

PHYTOCHEMISTRY

www.elsevier.com/locate/phytochem

Dibenzofurans from the cultured lichen mycobionts of *Lecanora cinereocarnea*

Takao Tanahashi[a,*], Yukiko Takenaka[a], Naotaka Nagakura[a], Nobuo Hamada[b]

[a]*Kobe Pharmaceutical University, 4-19-1, Motoyamakita-machi, Higashinada-ku, Kobe 658-8558, Japan*
[b]*Osaka City Institute of Public Health and Environmental Sciences, 8-34, Tojo-cho, Tennouji-ku, Osaka 543-0026, Japan*

Received 7 June 2001; received in revised form 23 August 2001

Abstract

From the cultures of the spore-derived mycobionts of the lichen *Lecanora cinereocarnea*, five dibenzofurans, 3,7-dihydroxy-1,9-dimethyldibenzofuran, 2-chloro-3,7-dihydroxy-1,9-dimethyldibenzofuran, 2,8-dichloro-3,7-dihydroxy-1,9-dimethyldibenzofuran, 3-hydroxy-7-methoxy-1,9-dimethyldibenzofuran, and 2-chloro-7-hydroxy-3-methoxy-1,9-dimethyldibenzofuran, were isolated. Their structures were determined by spectroscopic methods. © 2001 Elsevier Science Ltd. All rights reserved.

Keywords: *Lecanora cinereocarnea*; Lichen; Isolated mycobiont; 3,7-Dihydroxy-1,9-dimethyldibenzofuran; Structure elucidation

1. Introduction

Lichens, a symbiotic association of mycobiont and photobiont partners, produce diverse secondary metabolites, some of which show a wide range of potentially useful biological activities (Yamamoto, 1991). One of the intriguing questions in lichenology is the role of mycobiont and photobiont partners in the biosynthesis of such substances. Our recent studies demonstrated that cultures of spore-derived lichen mycobionts have an ability to produce certain lichen substances or novel metabolites in large amounts under osmotically stressed conditions (Tanahashi et al., 1997, 1999, 2000; Takenaka et al., 2000). It was also pointed out that cultures of lichen mycobionts could be good systems for investigating secondary metabolism in lichens. In the course of our studies on cultured lichen mycobionts, we cultivated mycobionts of the lichen *Lecanora cinereocarnea* and isolated from their cultures five dibenzofurans, four of which are new. The isolation and structural determination of these compounds are reported.

2. Results and discussion

The polyspore-derived mycobionts of *Lecanora cinereocarnea* collected in Japan were cultured on conventional malt-yeast extract medium supplemented with 10% sucrose at 18 °C in the dark. After cultivation over 11–12 months, the colonies and agar medium were harvested and extracted with cold Et_2O and Me_2CO. The extract was separated by a combination of preparative TLC and preparative HPLC to afford five compounds, **1**–**5**.

Compound **1** was isolated as colorless needles, mp. 242 °C. Its HR–EIMS spectrum indicated a molecular formula of $C_{14}H_{12}O_3$. Its ^{1}H NMR spectrum (Table 1) exhibited a broad singlet for a methyl group and a pair of *meta*-coupled doublets. The ^{13}C NMR spectrum of **1** showed a methyl carbon, two aromatic CH carbons and four quaternary carbons, two of which were oxygenated (Table 2). These NMR spectral features together with its structural formula suggested a symmetrical dibenzofuran structure for **1**. The presence of two phenolic hydroxyl groups in **1** was indicated by its acetylation to a diacetate **1a**. The substitution pattern on the aromatic rings was demonstrated by the HMBC spectrum of **1** where an aromatic proton at δ 6.70 was coupled with two oxygenated carbons at δ 156.9 and 159.2, a methine carbon at δ 114.8 and a quaternary carbon at δ 117.6, the latter two carbons were correlated with the methyl

* Corresponding author. Tel.: +81-78-441-7546; fax: +81-78-441-7546.
E-mail address: tanahash@kobepharma-u.ac.jp (T. Tanahashi).

0031-9422/01/$ - see front matter © 2001 Elsevier Science Ltd. All rights reserved.
PII: S0031-9422(01)00394-6

protons at δ 2.76. Final confirmation was obtained by direct comparison with an authentic sample prepared from 3,5-dimethoxytoluene (Asahina and Aoki, 1941). Although this compound has already been known as a synthetic product, this constitutes the first instance of it's isolation and characterization as a natural product.

The HR–EIMS spectrum of compound **2** established the composition $C_{14}H_{11}ClO_3$. Conventional acetylation of **2** gave a diacetate **2a**, $C_{18}H_{15}ClO_5$. The ^1H NMR spectrum of **2** exhibited signals for two methyl groups atδ 2.76 and 2.86, a pair of *meta*-coupled aromatic protons at δ 6.57 and 6.70 and an aromatic proton at δ 6.86. These findings suggested the isolated compound to be a chlorinated derivative of **1**. Significant HMBC correlations between the aromatic proton at δ 6.86 and two oxygenated carbons at δ 152.5 and 156.3 showed that the chlorine atom was substituted at C-2 rather than C-4. This was further confirmed by HMBC experiments with **2a**. Thus, the structure of **2** was determined as 2-chloro-3,7-dihydroxy-1,9-dimethyldibenzofuran.

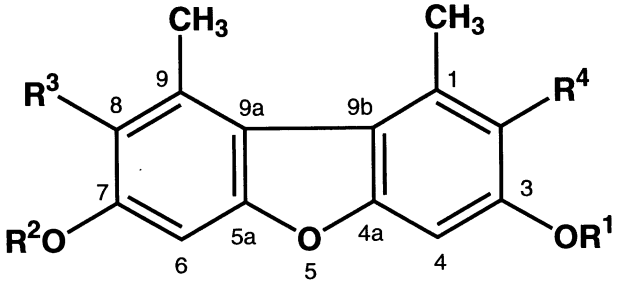

1: $R^1=R^2=R^3=R^4=H$

2: $R^1=R^2=R^3=H$, $R^4=Cl$

3: $R^1=R^2=H$, $R^3=R^4=Cl$

4: $R^1=R^3=R^4=H$, $R^2=CH_3$

5: $R^1=CH_3$, $R^2=R^3=H$, $R^4=Cl$

6: $R^1=R^2=CH_3$, $R^3=R^4=H$

1a: $R^1=R^2=Ac$, $R^3=R^4=H$

2a: $R^1=R^2=Ac$, $R^3=H$, $R^4=Cl$

3a: $R^1=R^2=Ac$, $R^3=R^4=Cl$

4a: $R^1=Ac$, $R^2=CH_3$, $R^3=R^4=H$

5a: $R^1=CH_3$, $R^2=Ac$, $R^3=H$, $R^4=Cl$

Compound **3**, $C_{14}H_{10}Cl_2O_3$, also showed NMR spectral features suggesting a symmetrical structure. The ^{13}C NMR spectral data of **3** and its acetate **3a** were in good agreement with those of chlorinated aromatic ring of **2** and **2a**, respectively, suggesting chlorination at C-2 and C-8 in **3** and **3a**. This proposal was further supported by

Table 1
^1H NMR spectral data for compounds **1**–**5** and **1a**–**5a**

H	1[b]	2[b]	3[b]	4[b]	5[b]
2	6.55 *br d* (2.0)[a]			6.57 *m*	
4	6.70 *d* (2.0)	6.86 *s*	6.82 *s*	6.72 *d* (2.0)	7.08 *s*
6	6.70 *d* (2.0)	6.70 *d* (2.5)	6.82 *s*	6.88 *d* (2.0)	6.75 *d* (2.0)
8	6.55 *br d* (2.0)	6.57 *br d* (2.5)	6.66 *m*	6.61 *m*	
1-Me	2.76 *br s*	2.86 *s*	2.75 *s*	2.79 *br s*	2.92 *s*
9-Me	2.76 *br s*	2.76 *br s*	2.75 *s*	2.81 *br s*	2.81 *br s*
3-OMe					3.93 *s*
7-OMe				3.83 *s*	
H	1a[c]	2a[c]	3a[c]	4a[c]	5a[c]
2	6.86 *br d* (2.0)		6.71 *m*		
4	7.18 *d* (2.0)	7.24 *s*	7.25 *s*	6.91 *d* (2.0)	7.00 *s*
6	7.18 *d* (2.0)	7.20 *d* (2.0)	7.25 *s*	7.14 *d* (2.0)	7.17 *d* (2.0)
8	6.86 *br d* (2.0)	6.89 *br d* (2.0)		6.82 *m*	6.86 *m*
1-Me	2.91 *br s*	2.99 *s*	2.93 *s*	2.87 *br s*	2.97 *s*
9-Me	2.91 *br s*	2.90 *br s*	2.93 *s*	2.89 *br s*	2.89 *br s*
3-OMe				3.98 *s*	
7-OMe			3.88 *s*		
3-OAc	2.34 *s*	2.40 *s*	2.41 *s*	2.41 *s*	
7-OAc	2.34 *s*	2.34 *s*	2.41 *s*		2.34 *s*

[a] Values in parentheses are coupling constants in Hz.
[b] Measured in CD_3OD.
[c] Measured in $CDCl_3$.

significant correlations between the aromatic proton signal and two oxygenated carbon signals in the HMBC spectra of **3** and **3a**. Accordingly, the isolated compound was characterized as 2,8-dichloro-3,7-dihydroxy-1,9-dimethyldibenzofuran.

A comparison of the ^1H and ^{13}C NMR spectra of the new compound **4** with those of **1** suggested a close relationship between their structures. The NMR spectral features of **4** resembled those of **1** except for the presence of an aromatic methoxyl signal [δ_H 3.83, δ_C 56.0]. The HR–EIMS of **4**, showed a molecular ion peak at *m/z* 242.0961, indicating a molecular formula of $C_{15}H_{14}O_3$, an increase of CH_2 when comparing with **1**. Conventional acetylation of **4** yielded the monoacetate **4a**. These findings suggested that a hydroxyl group of **1** was methylated in **4**, and this received further support from methylation of **1** with dimethylsulfate, which afforded **4** and the dimethyl ether **6**. Thus, **4** was also elucidated.

Compound **5** was isolated in minute amount. Its HR–EIMS spectrum indicated a molecular formula of $C_{15}H_{13}ClO_3$. Its ^1H NMR spectrum exhibited signals for two methyl groups at δ 2.81 and 2.93, a methoxyl group at δ 3.93, a pair of *meta*-coupled aromatic protons at δ 6.61 and 6.75, and an aromatic proton at δ 7.08 (s). Acetylation of **5** yielded an acetate **5a**, indicating the presence of a phenolic hydroxyl group in **5**. These findings suggested that **5** is a chlorinated derivative of **4**. The detailed 2D-NMR studies confirmed that the substitution of chlorine atom was at C-2, and not at C-4, C-5, nor C-7. The NOESY spectrum showed a through-space connectivity between the methoxyl group and a

Table 2
^{13}C NMR spectral data for compounds **1**–**5** and **1a**–**5a**

C	**1**[a]	**2**[a]	**3**[a]	**4**[a]	**5**[a]	**1a**[b]	**2a**[b]	**3a**[b]	**4a**[b]	**5a**[b]
1	132.9	130.5	130.9	133.2	130.9	133.0	131.3	131.6	132.8	131.1[i]
2	114.8	118.9[c]	119.0[d]	115.0	119.5[f]	119.3	122.9[g]	122.7[h]	118.9	117.6
3	156.9	152.5	153.1	157.2	155.0	149.1	145.6	146.1	148.2	154.5[j]
4	96.6	97.4	97.4	96.6	94.5	103.1	104.7	104.8	102.8	93.3
4a	159.2	156.3	156.6	159.1[e]	156.4	157.2	154.5	154.8	156.6	155.8[j]
5a	159.2	159.6	156.6	159.6[e]	159.7	157.2	157.5	154.8	158.5	156.8
6	96.6	96.7	97.4	94.7	96.7	103.1	103.3	104.8	93.7	103.0
7	156.9	157.4	153.1	159.4	157.7	149.1	149.5	146.1	159.0	148.5
8	114.8	115.4	119.0[d]	114.3	115.7	119.3	119.9	122.7[h]	114.0	119.6
9	132.9	133.2	130.9	133.0	133.5	133.0	133.2	131.6	131.9	132.3[i]
9a	117.6	117.2	118.4[d]	118.5	117.0	121.5	121.2	123.5[h]	116.7	121.9
9b	117.6	118.5[c]	118.4[d]	117.4	119.4[f]	121.5	123.1[g]	123.5[h]	122.1	119.0
1-Me	25.1	21.2	22.0	25.1	21.2	24.9	21.2	22.0	24.8	21.1
9-Me	25.1	25.7	22.0	25.1	25.7	24.9	25.5	22.0	24.8	25.5
3-OMe					56.9					56.5
7-OMe				56.0					55.5	
3-OAc						21.2	20.7	20.7	21.2	
						169.5	168.7	168.6	168.6	
7-OAc						21.2	21.2	20.7		21.2
						169.5	169.3	168.6		169.5

[a] Measured in CD_3OD.
[b] Measured in $CDCl_3$.
[c–j] Values with the same letters may be interchangeable.

singlet for a aromatic proton. In the HMBC spectrum of **5**, the aromatic proton signal was coupled with two oxygenated carbons at δ 155.0 and 156.4, and two quaternary carbons at δ 119.4 and 119.5; the latter two carbon resonances were correlated with the methyl singlet at δ 2.92, implying that a methoxyl group and a chlorine atom were located at C-3 and C-2, respectively, on the same benzene ring of the dibenzofuran. Further, HMBC correlations among the signals due to another benzene ring, as well as comparison of the ^1H and ^{13}C NMR spectral data of **5** and **5a** with those of **1** and **1a** suggested the same substitution pattern on a benzene ring of **1** and **5**. These observations thus allowed us to formulate the structure **5** for the isolated compound. The location of the chlorine atom at C-2 in **5** was further supported by comparative studies of the ^{13}C NMR spectral data of **1**, **2**, **4**, **5**, **1a**, **2a**, **4a** and **5a**. When a chlorine atom was introduced at C-2 in **1** and **1a**, C-2 was shifted downfield whereas C-1, C-3, C-4a and 1-Me were shifted upfield. Similar trends were observed with **4**, **5**, **4a** and **5a**. Accordingly the structure of **5** was elucidated as 2-chloro-7-hydroxy-3-methoxy-1,9-dimethyldibenzofuran.

It is noteworthy that the isolated dibenzofurans from the cultured mycobionts have no carboxyl group in the structure by contrast with dibenzofurans from natural lichens such as pannaric acid (Huneck and Yoshimura, 1996). According to Culberson and Ahamdjian, most lichen substances arise from phenolic acid precursors such as orsellinic acid. In non-lichen fungi these precursors lead to phycotoxic compounds, the biosynthesis of which includes a phenolic acid decarboxylation involving fungal decarboxylases. In lichens the algal partner may inhibit such decarboxylases to divert the phenolic acid precursors into secondary metabolites that are nontoxic to photobionts and accumulate in large quantities in the thallus (Culberson and Ahmajian, 1980). This hypothesis was consistent with our results that dibenzofurans with no carboxyl group were obtained from the cultured mycobionts. These results indicated that dormant fungal metabolism was induced in the cultures of the isolated mycobiont.

3. Experimental

3.1. General

Melting points were measured on a Yanaco micro melting point apparatus and are uncorr. The UV spectra were recorded on a Shimadzu UV-240 spectrophotometer and the IR spectra on a Shimadzu FTIR-8200 infrared spectrophotometer. HR–EIMS were obtained with a Hitachi M-4100 mass spectrometer. The NMR spectroscopic experiments were performed with Varian VXR-500, Varian Gemini-300 and Varian Gemini-200 spectrometers, with tetramethylsilane as internal standard. HPLC was performed using a Waters system (600E Multisolvent Delivery System, 486 Tunable Absorbance Detector). Thin-layer chromatography was performed on precoated Kieselgel $60F_{254}$ plates (Merck) and spots were visualized under UV light.

3.2. Plant material

Specimens of *Lecanora cinereocarnea* (Eschw.) Vain. were collected from the bark of trees in Okinawa Prefecture, Japan (27 N, ca. 100 m alt.) in 1996. The voucher specimen was identified by Dr. H. Miyawaki, Saga University, Japan and was deposited at Osaka City Institute of Public Health and Environmental Sciences with the registration No. NH96112944. Mycobionts of *L. cinereocarenea* were obtained from the spores discharged from apothecia of a thallus, and were cultivated in test tubes containing modified MY10 medium (malt extract 10 g, yeast extract 4 g, sucrose 100 g, agar 15 g, H_2O 1 l, pH 7) at 18 °C in the dark. After cultivation for 11–12 months, the colonies and slants with crystals were harvested.

3.3. Extraction and isolation

(1) The harvested colonies (101 test tubes, fresh cell weight 12.3 g) were extracted continuously with Et_2O and then with Me_2CO. The slants were collected and extracted in the same way. The Et_2O extracts were concentrated under reduced pressure to give a residue (550 mg). The extracts were repeatedly subjected to preparative TLC (toluene–acetone 9:1) and preparative HPLC (μBondasphere 5 μC18-100 Å, MeCN–H_2O, 7:13), giving **1** (1.2 mg), **2** (14.7 mg), **3** (20.3 mg), **4** (4.9 mg) and **5** (1.6 mg). The Me_2CO extracts (898 mg) were also repeatedly purified by preparative TLC and preparative HPLC to afford **2** (5.0 mg), **3** (7.5 mg), **4** (2.5 mg) and **5** (1.4 mg).

(2) The harvested colonies (37 test tubes, dry cell weight 6.86 g) and slants were extracted continuously with Et_2O and then with Me_2CO. The Et_2O extracts (380 mg from the colonies and 1.02 g from the slants) were repeatedly subjected to preparative TLC with (toluene–acetone, 19:1, Me_2CO–$CHCl_3$, 3:1), giving **1** (3.3 mg), **2** (7.9 mg) and **3** (11.4 mg). The Me_2CO extracts (898 mg from the colonies and 3.72 g from the slants) were also repeatedly purified by preparative TLC with (toluene–acetone, 19:1) to afford **1** (5.0 mg), **2** (11.6 mg) and **3** (24.5 mg).

3.3.1. 3,7-Dihydroxy-1,9-dimethyldibenzofuran (*1*)

Colorless crystalline solid, mp 242 °C (MeOH). UV λ_{max}^{MeOH} nm (log ε): 219 (4.51), 226 (4.52), 239.5 (4.35), 257 *sh* (4.09), 263 (4.12), 302 (4.23), 310 (4.23); IR ν_{max}^{KBr} cm^{-1}: 3275, 1616, 1585, 824; ^1H NMR: see Table 1; ^{13}C NMR: see Table 2; HMBC correlations: 1-CH_3/9-CH_3→C-1/C-9, C-2/C-8, C-9a/C-9b; H-2/H-8→C-3/C-7, C-4/C-6, C-9a/C-9b; H-4/H-6→C-2/C-8, C-3/C-7, C-4a/C-5a, C-9a/C-9b; HR-EIMS *m/z*: calc. for $C_{14}H_{12}O_3$ $[M]^+$: 228.0787. Found: 228.0781.

3.3.2. 2-Chloro-3,7-dihydroxy-1,9-dimethyldibenzofuran (*2*)

Colorless crystalline solid, mp 193–194 °C (MeOH). UV λ_{max}^{MeOH} nm (log ε): 205 (4.37), 223 (4.55), 228 (4.57), 243 *sh* (4.35), 263 (4.09), 306.5 (4.25), 314.5 (4.25); IR ν_{max}^{KBr} cm^{-1}: 3324, 1611, 1576, 830; ^1H NMR: see Table 1; ^{13}C NMR: see Table 2; NOESY correlation: H-8↔9-CH_3; HMBC correlations: 1-CH_3→C-1, C-2, C-9b; H-4→C-2, C-3, C-4a, C-9b; H-6→ C-5a, C-7, C-8, C-9a; H-8→C-6, C-7, C-9a; 9-CH_3→C-8, C-9, C-9a; HR-EIMS *m/z*: calcd. for $C_{14}H_{11}{}^{35}ClO_3$ $[M]^+$: 262.0397. Found: 262.0374; calc. for $C_{14}H_{11}{}^{37}ClO_3$ $[M]^+$: 264.0368. Found: 264.0357.

3.3.3. 2,8-Dichloro-3,7-dihydroxy-1,9-dimethyldibenzofuran (*3*)

Colorless crystalline solid, mp 217.5–218.5 °C (MeOH). UV λ_{max}^{MeOH} nm (log ε): 231 (4.60), 245 (4.35), 262.5 (4.02), 309 *sh* (4.27), 317.5 (4.32); IR ν_{max}^{KBr} cm^{-1}: 3422, 1607, 1583, 812; ^1H NMR: see Table 1; ^{13}C NMR: see Table 2; HMBC correlations: 1-CH_3/9-CH_3→C-1/C-9, C-2/C-8, C-9a/C-9b; H-4/H-6→C-2/C-8, C-3/C-7, C-4a/C-5a, C-9a/C-9b; HR–EIMS *m/z*: calc. for $C_{14}H_{10}{}^{35}Cl_2O_3$ $[M]^+$: 296.0007. Found: 296.0016; calc. for $C_{14}H_{10}{}^{35}Cl^{37}ClO_3$ $[M]^+$: 297.9978. Found: 297.9962; calc. for $C_{14}H_{10}{}^{37}Cl_2O_3$ $[M]^+$: 299.9948. Found: 299.9936.

3.3.4. 3-Hydroxy-7-methoxy-1,9-dimethyldibenzofuran (*4*)

Colorless crystalline solid, mp 139–139.5 °C (MeOH). UV λ_{max}^{MeOH} nm (log ε): 219 (4.45), 225.5 (4.46), 239 *sh* (4.30), 257 *sh* (4.04), 263 (4.07), 300.5 (4.19), 308.5 (4.23); IR ν_{max}^{KBr} cm^{-1}: 3368, 1612, 1582, 808; ^1H NMR: see Table 1; ^{13}C NMR: see Table 2; NOESY correlations: 1-CH_3↔H-2; OCH_3↔H-4; H-8↔9-CH_3; HMBC correlations: 1-CH_3→C-1, C-2, C-9b; H-4→C-4a; H-6→C-5a, C-6; H-8→C-7; 9-CH_3→C-8, C-9, C-9a; HR–EIMS *m/z*: calc. for $C_{15}H_{13}O_3$ $[M]^+$: 242.0944. Found: 242.0961.

3.3.5. 2-Chloro-7-hydroxy-3-methoxy-1,9-dimethyldibenzofuran (*5*)

Colorless crystalline solid, mp 198–199 °C (MeOH). UV λ_{max}^{MeOH} nm (log ε): 227 (4.26), 241 *sh* (4.18), 255 (3.88), 263 (3.91), 305 (4.07), 312.5 (4.06); IR ν_{max}^{KBr} cm^{-1}: 3110, 1638, 1609, 1589, 814; ^1H NMR: see Table 1; ^{13}C NMR: see Table 2; NOESY correlations: H-4↔OCH_3, H-8↔9-CH_3; HMBC correlations: 1-CH_3→C-1, C-2, C-9b; OCH_3→C-3; H-4→C-2, C-3, C-4a, C-9b; H-6→C-5a, C-8, C-9a; H-8→C-6, C-9a; 9-CH_3→C-8, C-9, C-9a. HR–EIMS *m/z*: calc. for $C_{15}H_{14}{}^{35}ClO_3$ $[M]^+$: 276.0554. Found: 276.0577; calc. for $C_{15}H_{14}{}^{37}ClO_3$ $[M]^+$: 278.0524. Found: 278.0503.

3.4. Acetylation of *1*–*5*

Compound **1** (3.4 mg) was acetylated with Ac_2O-pyridine (each 0.1 ml) and the crude acetate was purified by preparative TLC ($CHCl_3$) to yield **1a** (3.9 mg). Com-

pound **2** (7.7 mg) and **3** (7.8 mg) were acetylated and purified in the same as for **1** to give **2a** (8.0 mg) and **3a** (7.6 mg), respectively. A mixture (19.1 mg) of **4** and **5** was acetylated and purified by preparative HPLC (μBondasphere 5 μC18–100 Å, MeCN–H_2O, 5:3) to give **4a** (2.9 mg) and **5a** (4.6 mg).

3.4.1. 3,7-Diacetoxy-1,9-dimethyldibenzofuran (*1a*)

Colorless crystalline solid, mp. 162–162.3°C (MeOH). UV λ_{max}^{MeOH} nm (log ε): 213 (4.66), 227 (4.73), 252 (4.21), 260 (4.30), 287 (4.46), 296 *sh* (4.34); IR ν_{max}^{KBr} cm^{-1}: 1753, 1609, 1585, 1499; ^1H NMR: see Table 1; ^{13}C NMR: see Table 2; HMBC correlations: 1-CH_3/9-CH_3→C-1/C-9, C-2/C-8, C-9a/C-9b; H-2/H-8→C-1/C-9, C-3/C-7, C-4/C-6, C-9a/C-9b; H-4/H-6→C-2/C-8. EIMS *m/z* (rel. int.%): 312 (21.6) $[M]^+$, 270 (17.8), 228 (100); HR–EIMS *m/z*: calc. for $C_{18}H_{16}O_5$ $[M]^+$: 312.0998. Found: 312.1015.

3.4.2. 3,7-Diacetoxy-2-chloro-1,9-dimethyldibenzofuran (*2a*)

Colorless crystalline solid, mp 171.5–172.0 °C (MeOH). UV λ_{max}^{MeOH} nm (log ε): 216 (4.51), 230 (4.61), 253 (4.02), 261 (4.12), 289 (4.29), 299 *sh* (4.11), 312 (3.74); IR ν_{max}^{KBr} cm^{-1}: 1765, 1601, 1587; ^1H NMR: see Table 1; ^{13}C NMR: see Table 2; HMBC correlations: 1-CH_3→C-1, C-2, C-9b; H-4→C-2, C-3, C-4a, C-9b; H-6→C-7, C-8; H-8→C-6, C-7, C-9a; 9-CH_3→C-8, C-9, C-9a; EIMS *m/z*: (rel. int.%): 348 (3.5), 346 (9.8) $[M]^+$, 306 (5.5), 304 (15.4), 264 (37), 262 (100); HR-EIMS *m/z* calc. for $C_{18}H_{15}{}^{35}ClO_5$ $[M]^+$: 346.0609. Found: 346.0602; calc. for $C_{18}H_{15}{}^{37}ClO_5$ $[M]^+$: 348.0579. Found: 348.0583.

3.4.3. 3,7-Diacetoxy-2,8-dichloro-1,9-dimethyldibenzofuran (*3a*)

Colorless crystalline solid, mp 192–193 °C (MeOH). UV λ_{max}^{MeOH} nm (log ε): 218 (4.52), 233 (4.66), 253 (4.03), 261 (4.12), 293 (4.29), 304 *sh* (4.00); IR ν_{max}^{KBr} cm^{-1}: 1771, 1593; ^1H NMR: see Table 1; ^{13}C NMR: see Table 2; HMBC correlations: 1-CH_3/9-CH_3→C-1/C-9, C-2/C-8, C-9a/C-9b; H-4/H-6→C-2/C-8, C-3/C-7, C-4a/C-5a, C-9a/C-9b; EIMS *m/z*: (rel. int.%): 384 (1.1), 382 (4.9), 380 (7.9) $[M]^+$, 342 (1.4), 340 (4.9), 338 (9.3), 300 (12), 298 (67), 296 (100); HR–EIMS *m/z* calc. for $C_{18}H_{14}{}^{35}Cl_2O_5$ $[M]^+$: 380.0219. Found: 380.0203; calc. for $C_{18}H_{14}{}^{35}Cl^{37}ClO_5$ $[M]^+$: 382.0189. Found: 382.0143; calc. for $C_{18}H_{14}{}^{37}Cl_2O_5$ $[M]^+$: 384.0160. Found: 384.0108.

3.4.4. 3-Acetoxy-7-methoxy-1,9-dimethyldibenzofuran (*4a*)

Colorless crystalline solid, mp 116–117 °C (MeOH). UV λ_{max}^{MeOH} nm (log ε): 215.5 (4.35), 226 (4.49), 237 *sh* (4.35), 256 *sh* (4.01), 262 (4.09), 295 (4.26), 301 (4.26), 305.5 (4.26); IR ν_{max}^{KBr} cm^{-1}: 1759, 1607, 1578, 829; ^1H NMR: see Table 1; ^{13}C NMR: see Table 2; EIMS *m/z*: (rel. int.%): 284 (37) $[M]^+$, 242 (100). HR–EIMS *m/z*: calc. for $C_{17}H_{16}O_4$ $[M]^+$: 284.1049. Found: 284.1060.

3.4.5. 7-Acetoxy-2-chloro-3-methoxy-1,9-dimethyldibenzofuran (*5a*)

Colorless crystalline solid, mp 169 °C (MeOH). UV λ_{max}^{MeOH} nm (log ε): 229.5 (4.41), 254.5 (3.88), 262 (3.95), 291 *sh* (4.04), 301 (4.10), 313.5 (3.95); IR ν_{max}^{KBr} cm^{-1}: 1747, 1607, 1541, 810; ^1H NMR: see Table 1; ^{13}C NMR: see Table 2; EIMS *m/z*: (rel. int.%): 320 (11), 318 (30) $[M]^+$, 278 (36), 276 (100), 262 (12), 260 (35); HR–EIMS *m/z*: calc. for $C_{17}H_{15}{}^{35}ClO_4$ $[M]^+$: 318.0659. Found: 318.0675; calc. for $C_{17}H_{15}{}^{37}ClO_4$ $[M]^+$: 320.0630. Found: 320.0637.

3.5. Synthesis of *1* and *4*

Compound **1** was prepared from 3,5-dimethoxytoluene according to Asahina. (Asahina and Aoki, 1941). The physical and spectral data of the product were identical to those of the isolated compound. To a solution of **1** (19.8 mg) in acetone (20 ml) were added K_2CO_3 (600 mg) and Me_2SO_4 (20 μl), and the whole was heated under reflux for 4 h. The reaction mixture was diluted with 5% $NaHCO_3$ and extracted with $CHCl_3$. The washed and dried $CHCl_3$ layers were concentrated in vacuo and the residue was subjected to prep. TLC with (toluene–acetone 19:1) to afford a monomethyl ether (3.3 mg) and a dimethyl ether (**6**) (17.9 mg). The monomethyl ether was identified with **4**. **6**: needles, mp. 153.7–154 °C (MeOH). ^1H NMR ($CDCl_3$): δ 2.83 (6H, *s*, 1-CH_3 and 9-CH_3), 3.84 (6H, *s*, 3-OCH_3 and 7-OCH_3), 6.69 (2H, *m*, H-2 and H-8), 6.92 (2H, *m*, H-4 and H-6). EIMS *m/z* (%): 330 $[M]^+$ (35), 315 (100), 300 (7.3), 285 (28). HR–EIMS *m/z*: calc. for $C_{16}H_{16}O_3$ $[M]^+$: 256.1100. Found: 256.1095.

Acknowledgements

This research was financially supported by Grant-in-Aid for Scientific Research (C) (No. 09672179 and No. 11672129) from the Ministry of Education, Sciences, Sports and Culture of Japan and Kobe Pharmaceutical University Collaboration Fund. We are grateful to Dr. H. Miyawaki (Saga University, Japan) for identification of the voucher specimen. Thanks are also due to Dr. M. Sugiura (Kobe Pharmaceutical University) for ^1H and ^{13}C NMR spectra, and to Dr. K. Saiki (Kobe Pharmaceutical University) for mass spectra measurements.

References

Asahina, Y., Aoki, M., 1941. On oxy-diphenyleneoxide derivatives. Yakugaku Zasshi 64, 41–47.

Culberson, C.F., Ahmajian, V., 1980. Artificial reestablishment of lichens. II. Secondary products of resynthesized *Cladonia cristatella* and *Lecanora chrysoleuca*. Mycologia 72, 90–109.

Huneck, S., Yoshimura, I., 1996. Identification of Lichen Substances. Springer Verlag, Berlin, Heidelberg.

Takenaka, Y., Tanahashi, T., Nagakura, N., Hamada, N., 2000. 2,3-Dialkylchromones from mycobiont cultures of the lichen *Graphis scripta*. Heterocycles 53, 1589–1593.

Tanahashi, T., Kuroishi, M., Kuwahara, A., Nagakura, N., Hamada, N., 1997. Four phenolics from the cultured lichen mycobiont of *Graphis scripta* var. *pulverulenta*. Chem. Pharm. Bull. 45, 1183–1185.

Tanahashi, T., Takenaka, Y., Nagakura, N., Ikuta, Y., Tani, K., Hamada, N., 1999. Xanthones from the cultured lichen mycobionts of *Pyrenula japonica* and *Pyrenula pseudobufonia*. Phytochemistry 52, 401–405.

Tanahashi, T., Takenaka, Y., Nagakura, N., Hamada, N., Miyawaki, H., 2000. Two isocoumarins from the cultured lichen mycobiont of *Graphis* sp. Heterocycles 53, 723–728.

Yamamoto, Y., 1991. Production of lichen substances. In: Komamine, A., Misawa, M., DiCosmo, F. (Eds.), Plant Cell Culture in Japan. CMC, Tokyo, pp. 58–71.

PERGAMON

Phytochemistry 58 (2001) 1135–1139

PHYTOCHEMISTRY

www.elsevier.com/locate/phytochem

Diterpenoids from *Euphorbia paralias*

Samir A.M. Abdelgaleil[a], Shehata M.I. Kassem[a], Matsumi Doe[b], Masanori Baba[c], Munehiro Nakatani[d,*]

[a]*Department of Pesticide Chemistry, Faculty of Agriculture, Alexandria University, Alexandria, Egypt*
[b]*Analytical Division, Graduate School of Science, Osaka City University, 3-3-7 Sugimoto, Sumiyoshi-ku, Osaka 558-8585, Japan*
[c]*Faculty of Medicine, Kagoshima University, 8-35-1 Sakuragaoka, Kagoshima 890-8520, Japan*
[d]*Department of Chemistry and Bioscience, Faculty of Science, Kagoshima University, 1-21-35 korimoto, Kagoshima 890-0065, Japan*

Received 4 May 2001; received in revised form 14 August 2001

Abstract

Two segatane diterpenoids containing a bicyclic [4,3,1] ring system were isolated, together with 11 known diterpenoids, four segetanes, five jatrophanes and two paralianes, from the aerial parts of *Euphorbia paralias*. The structures of the new compounds were established by spectroscopic means, including by 2D NMR and CD spectroscopic analyses. The antifeedant and antiviral activities of the isolated compounds are also described. © 2001 Elsevier Science Ltd. All rights reserved.

Keywords: *Euphorbia paralias*; Euphorbiaceae; Diterpenoids; Segetanes A and B; Segetanes; Paralinones; Jatrophenes; Paralianes; Antifeeding activity; Antiviral activity

1. Introduction

Euphorbiaceae plants are well known to contain irritant and tumor-promoting constituents (Hecker, 1977). In particular, diterpenoids from the Euphorbiaceae have been found to possess interesting biological activities (Evans and Soper, 1978). *Euphorbia paralias* L. (Sea Spurge) is a hardy perennial which inhabits sandy coasts and shingle beaches and is native to the entire Mediterranean region. It is also one of the most common *Euphorbia* species growing in Egypt (Tackholm, 1974). Chemical constituents of this species have been investigated previously and the presence of irritant and cytotoxic ingenanes (Sayed et al., 1980), paralinones (Öksüz et al., 1997), segetanes, jatrophanes, paralianes and another tetracyclic diterpenoids (Jakupovic et al., 1998a,b), as well as triterpenoids and flavonoids (Rizk et al., 1974, 1976; Khafagy et al., 1976), have been reported.

In this paper, we report the isolation and structure elucidation of two new segetane diterpenoids, containing a conjugated enone system, together with 11 known diterpenoids, four segatanes, five jatrophanes and two paralianes, from the aerial parts of *Euphorbia paralias*. The antifeeding and antiviral activities of the isolated compounds against the larvae of the Japanese insect pest *Spodoptera littoralis* and HIV-1 replication are also described.

2. Results and discussion

The CH_2Cl_2 soluble part of the methanol extract of the dried aerial parts of *Euphorbia paralias* was fractionated by column chromatography on silica gel and purified by HPLC to afford two new segetane diterpenoids possessing a conjugated enone, named segetenes A (**1**) and B (**2**), and eleven known diterpenoids in the segetanes (**3–6**), jatrophanes (**7–11**) and paralianes (**12** and **13**), which had previously been isolated from the same plant collected in Turkey (Öksüz et al., 1997) and Spain (Jakupovic et al., 1998b), and from *Euphorbia segetalis* (Jakupovic et al., 1998a). The known compounds were identified by comparison of their NMR spectral data with those reported previously.

Segetene A (**1**) was obtained as a white amorphous powder of $[\alpha]_D$ −4° (*c* 0.17, MeOH). Its molecular formula $C_{37}H_{44}O_{14}$ (16 unsaturations) was determined by accurate HR–FAB–MS (*m*/*z*: 713.2802 $[M+H]^+$, Δ −0.8 mmu.). In the FAB–MS, the presence of the prominent peak at *m*/*z* 105 [C_6H_5–CO] implied the presence of a benzoyl moiety in the molecule. The UV spectrum also showed the presence of the benzoyl group together with

* Corresponding author. Tel.: +81-99-285-8114; fax: +81-99-285-8117.
E-mail address: nakat@mail.sci.kagoshima-u.ac.jp (M. Nakatani).

0031-9422/01/$ - see front matter © 2001 Elsevier Science Ltd. All rights reserved.
PII: S0031-9422(01)00393-4

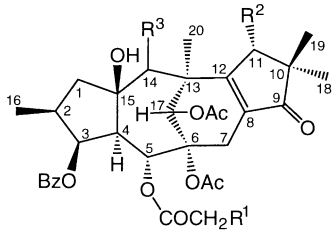

	1	2
R^1	H	OAc
R^2	OAc	H
R^3	β-OAc	α-OAc

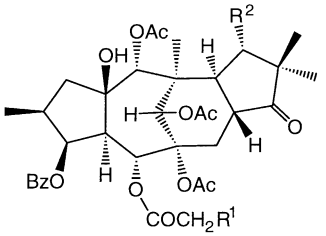

	3	4	5	6
R^1	H	OAc	OAc	OH
R^2	OAc	H	OAc	H

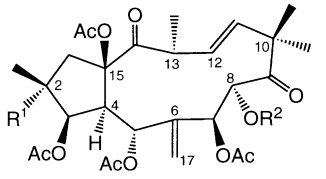

	7	8	9	10	11
R^1	OAc	OAc	H	OAc	OAc
R^2	iBu	Ang	iBu	MeBu	Bz

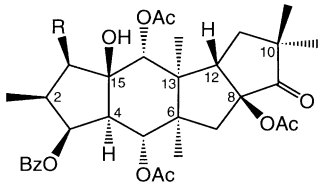

	12	13
R	OAc	H

a conjugated enone group at 231 nm (ε 25,000). The IR spectrum exhibited characteristic absorption bands for hydroxyl (3600–3400 cm^{-1}) and carbonyl (1751 and 1701 cm^{-1}) groups. From the ^1H and ^{13}C NMR spectroscopic analyses (Table 1), 11 of the unsaturation elements were present as double bonds: four carbon-carbon (one benzene ring and one tetra-substituted) and seven carbonyls (one keto and six ester). Therefore, the molecule is pentacyclic. The NMR spectra also revealed that **1** contained nine methyl groups (three tertiary, one secondary and five acetyl), two methylenes, twelve methines (5 olefinic), fourteen quaternary carbons (three olefinic and one keto and six ester carbonyls) and one tertiary hydroxyl group.

All of the proton-bearing carbons were assigned by the HMQC experiment. Extensive studies using spin decoupling and the COSY and HMBC revealed **1** to be a segetane type diterpenoid. The ^1H and ^{13}C NMR spectra resembled those of segetane **3**, isolated from the same plant collected in Spain (Jakupovic et al., 1998a,b), except for the presence of an additional tetra-substituted double bond in **1**. The conjugated enone system in **1** was apparent from the presence of a downfield shifted olefinic carbon (C-12) at δ 164.2 and a carbonyl carbon (C-9) at δ 208.4 compared with δ 214.2 in **3**. Irradiation of the H-11 triplet at δ 6.13 coalesced a pair of methylene signals at δ 2.47 (*dd*, $J = 17.0$ and 2.0 Hz, H-7α) and 2.90 (*br d*, $J = 17.0$ Hz, H-7β) to a pair of doublets. This homoallylic coupling clarified the partial structure of C_7–C_{11}.

Further information by HMBC spectrum elucidated the presence of the bicyclo[4.3.1^{6,13}]decane ring system and the location of acetoxy and benzoyloxy groups in the skeleton at the positions, 5, 6, 11, 14 and 17, and at C-3, respectively, similarly to **3** (Fig. 1).

The relative stereochemisrty of **1** was established by NOE studies (Fig. 2). The NOE correlations of H-4

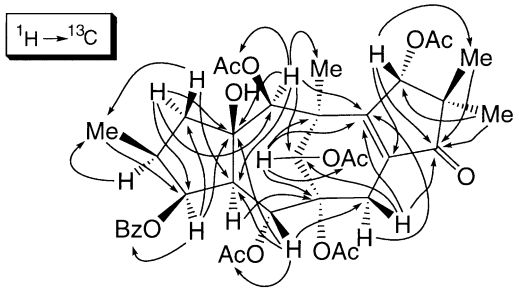

Fig. 1. Selected HMBC correlations in **1**.

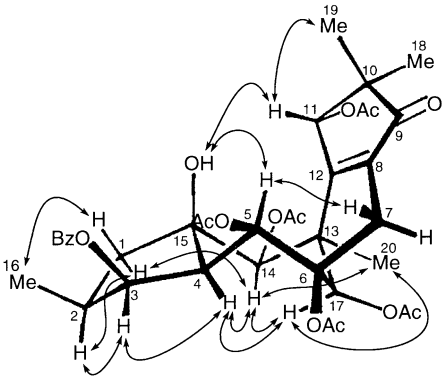

Fig. 2. Significant NOE correlations in **1**.

with H-1α, H-3 and H-17 established that the stereochemistry of **1** was virtually the same as that of the segatanes, **3**–**6** (Öksüz et al., 1997; Jakupovic et al., 1998a,b). On the other hand, the H-14 signal in **1** showed NOEs with the H-1α, H-4 and H-17 signals and the 13-Me (20) indicating it to possess an α configulation, different from that of the previously reported segatanes. Finally, the absolute stereochemistry of **1** was determined from the CD spectrum (Fig. 2), which showed a split CD curve at 242 ($\Delta\varepsilon+0.7$) and 224 nm ($\Delta\varepsilon-0.3$) due to a coupling of the π–π^* transitions of the benzoate and enone chromophores. The positive splitting suggested a positive twisting of the two chromophores to reveal the absolute stereochemistry at C-3 to be *S*. This is the first report of the occurrence of this type of segatane diterpenoid.

The segetene structure of compound **2**, having the same molecular formula $C_{37}H_{44}O_{14}$ as **1**, was readily suggested from the spectral data. Compound **2** showed similar IR and UV spectra to those of **1**. The ^1H and ^{13}C NMR spectra of **2** (Table 1) displayed the presence of eight methyls, four methylenes, eleven methines, and fourteen quaternary carbons, including one conjugated enone structure, five acetyl and one benzoyl groups. Thus, the molecule is also pentacyclic.

The spectra were similar to those of **1**, except for the lack of the isolated oxymethine signal coupling with allylic H_2-7 signals in **1**, and the presence of two addi-

Table 1
^{13}C and ^1H NMR spectral data for **1** and **2**

Compound number	**1**		**2**	
	C	H	C	H
1α	47.7 *t*	2.34 *dd* (15.1, 10.0)	47.7 *t*	2.32 *dd* (15.4, 10.0)
1β		1.52 *dd* (15.1, 10.2)		1.47 *dd* (15.4, 10.3)
2	36.7 *d*	2.15 *m*	36.8 *d*	2.14 *m*
3	81.0 *d*	5.74 *t* (3.5)	81.1 *d*	5.73 *t* (3.4)
4	47.8 *d*	3.59 *dd* (11.0, 3.0)	47.8 *d*	3.61 *dd* (11.0, 3.2)
5	67.5 *d*	5.39 *d* (11.0)	69.3 *d*	5.43 *d* (10.7)
6	82.5 *s*		82.3 *s*	
7α	29.3 *t*	2.47 *dd* (17.0, 2.0)	29.5 *t*	2.38 *br dt* (16.8, 2.9)
7β		2.90 *br d* (17,0)		2.83 *br d* (16.8)
8	136.9 *s*		131.8 *s*	
9	208.4 *s*		211.7 *s*	
10	48.0 *s*		43.9 *s*	
11α	79.6 *d*		42.1 *t*	2.32 *br d* (16.7)
11β		6.13 *t* (2)		2.73 *br dt* (16.7, 2.9)
12	164.2 *s*		169.9 *s*	
13	47.3 *s*		46.9 *s*	
14	75.7 *d*	5.38 *s*	75.8 *d*	5.31 *s*
15	82.9 *s*		82.8 *s*	
16	14.6 *q*	0.91 *d* (7.0)	14.6 *q*	0.90 *d* (6.8)
17	70.0 *d*	6.53 *s*	69.0 *d*	6.53 *s*
18	19.1 *q*	1.02 *s*	20.3 *q*	1.13 *s*
19	23.5 *q*	1.24 *s*	24.7 *q*	1.10 *s*
20	22.0 *q*	1.10 *s*	22.1 *q*	1.03 *s*
5-OR	169.9 *s*		166.8 *s*	
	21.1 *q*	1.87 *s*	60.4 *t*	4.44 *d* (15.9)
				4.48 *d* (15.9)
			169.8 *s*	
			20.8 *q*	2.04 *s*
6-OAc	169.5		170.3 *s*	
	20.4 *q*	2.00 *s*	22.1 *q*	2.02 *s*
11-OAc	170.3 *s*			
	20.6 *q*	2.11 *s*		
14-OAc	170.0 *s*		170.3 *s*	
	20.9 *q*	2.22 *s*	21.0 *q*	2.23 *s*
17-OAc	169.9 *s*		169.9 *s*	
	20.9 *q*	2.09 *s*	21.2 *s*	2.02 *s*
3-OBz				
1′	165.7 *s*		165.6 *s*	
2′	129.3 *s*		129.3 *s*	
3′,7′	128.7 *d*	7.72 *dd* (8, 1)	129.1 *d*	7.72 *dt* (8.3, 1.3)
4′,6′	129.0 *d*	7.40 *dd* (7, 1)	128.7 *d*	7.39 *t* (8.1)
5′	133.4 *d*	7.55 *tt* (8, 1)	131.8 *d*	7.54 *tt* (7.4, 1.2)
OH		2.60 *s*		2.46 *s*

Measured in $CDCl_3$ at 125 and 600 MHz. *J* values (in Hz) are presented in parentheses.

Table 2
Biological activity of compounds **1**–**13**

Compound	Antifeeding[a] (ppm)	Antiviral[b] EC_{50} (μg/ml)	Cytotoxic[c] CC_{50} (μg/ml)	Compound	Antifeeding[a] (ppm)	Antiviral[b] EC_{50} (μg/ml)	Cytotoxic[c] CC_{50} (μg/ml)
1	> 1000	> 100	> 100	**8**	500	> 100	> 100
2	> 1000	–	–	**9**	500–1000	45	45
3	1000	> 100	> 100	**10**	–	40	40
4	1000	> 100	> 100	**11**	–	79	79
5	500	51	51	**12**	500–1000	70	70
6	–	> 100	> 100	**13**	1000	14	49
7	500–1000	69	69				

[a] Against the third-instar larvae of *S. littoralis* (50 ppm: ca 1 μg/cm^2).
[b] Against HIV-1 replication based on the inhibition of virus-induced cytopathicity in MT-4 cells.
[c] Inhibition of the growth of MT-4 cells.

tional methylene signals in **2**. One of these methylenes showed a characteristic AB signal at δ 4.44 (*d*, $J = 15.9$ Hz) and 4.48 (δ, $J = 15.8$ Hz) assigned to acetoxyacetate methylene protons, $CH_3CO_2\underline{CH_2}COO$–, which were confirmed from the HMBC correlations with two ester carbonyl carbons at δ 166.8 and 169.8. These carbonyl carbons were correlated to an oxymethine proton at δ 5.43 attached to C-5 at δ 69.3 and acetyl methyl protons at δ 2.02, respectively. This acetoxyacetate group has been observed in the segatanes, **4** and **5**, from *E. paralias* (Öksüz et al., 1997; Jakupovic et al., 1998a,b). The other methylene protons at δ 2.32 (*br d*, $J = 16.7$ Hz) and 2.73 (*br dt*, $J = 16.7$ and 2.9 Hz) were assigned to H_2-11 from their homoallylic couplings with the 7-methylene protons at δ 2.38 (*br dt*, $J = 16.8$ and 2.9 Hz) and 2.83 (*br d*, $J = 16.8$ Hz). Other protons in **2**, including the acetyl and benzoyl groups, were assigned to the same positions in **1** by HMQC and HMBC studies to clarify a similar structure for **2**, except for the stereochemistry.

The stereochemistry of **2** was also determined by NOE experiments (Fig. 3), which revealed that it differed from **1** only at C-14. Thus, the H-14 singlet at δ 5.31 showed NOEs only with H-11β at δ 2.73 and the 13α-Me (20) at δ 1.03, not with the H-4 and H-7 signals. This NOE observation strongly suggested H-14 to be in a β configulation. The CD spectrum showed a similar positive split absorption at 245 nm ($\Delta\varepsilon + 0.3$) and 226 nm ($\Delta\varepsilon - 1.9$) with **1** to elucidate the absolute structure of **2**.

Insect antifeeding and antiviral activities of the isolated compounds were examined (Table 2). Antifeedant activity was tested by the conventional leaf disk method (Wada and Munakata, 1968) against the third instar larvae of *Spodoptera littoralis*. The tests were performed at 500 and 1000 ppm, with 50 ppm corresponding to a concentration of ca. 1 μg/leaf-cm^2. The most potent compounds were **5** and **8**, which were moderately active at 500 ppm. This activity was comparable to those of many limonoid antifeedants from the Meliaceae (Huang et al., 1995; Mootoo et al., 1996; Nakatani, 1999). Although compounds **3**, **4**, **7**, **9**, **12** and **13** also showed moderate activities at 500–1000 ppm, the new compounds **1** and **2** were not active at 1000 ppm. Antiviral activity against HIV-1 replication was tested on the inhibition of virus-induced cytopathicity in MT-4 cells (Pauwels et al., 1988). In the tested compounds, only one compound **13** showed a moderate activity ($EC_{50} = 14$ μg/ml). Although compounds **5**, **7**, **10**, **11** and **12** also showed the activities in the range 40–79 μg/ml, their activities were concluded to be due to their cytotoxicity.

3. Experimental

3.1. General

^{1}H and ^{13}C NMR spectra were measured at 600 and 125 MHz in $CDCl_3$ on a Jeol FX-600 spectrophotometer. IR (KBr) and UV (MeOH) spectra were recorded on JASCO FT/IR 5300 and Shimadzu UV-210A spectrophotometers. Optical rotation and CD spectra were measured at 22° on JASCO DIP-370S and JASCO J-720 spectrophotometers. HPLC were performed on a Waters μBondapak C_{18} column by using 20–45% H_2O/MeOH as solvent.

3.2. Plant material

The aerial parts of *Euphorbia paralias* were collected in January 1999 from Marsa-Matrouh, Egypt, and identified by Dr. Khaleil Darweish of Alexandria University. A voucher specimen is deposited in the Faculty of Agriculture, Alexandria University.

3.3. Extraction and isolation of compounds *1–13*

The dried and powdered aerial parts (1.2 kg) of *Euphorbia paralias* were extracted with MeOH (8 l) at room temperature for 4 weeks. The extract was concentrated under reduced pressure to give a crude extract (137 g). The MeOH extract (30 g) was dissolved in a small amount of H_2O–MeOH (1:1) and extracted with hexane and CH_2Cl_2 (500 ml×3). The CH_2Cl_2 extract (8.6 g) was applied to a silica gel column (320 g) using a

gradient hexane–EtOAc (20–100%) as eluant. Fourteen fractions (each 100 ml) were collected and monitored by TLC. Fractions 8–11 were purified through HPLC with a reversed phase μBondapak C_{18} column using 20–45% H_2O/MeOH as solvent to give **1** (9.2 mg), **2** (8.2 mg), **3** (9.2 mg), **4** (5.8 mg), **5** (35.2 mg), **6** (1.8 mg), **7** (24.9 mg), **8** (4.5 mg), **9** (3.4 mg), **10** (1.8 mg), **11** (1.6 mg), **12** (15.1 mg), and **13** (5.4 mg).

3.4. Segetene A (1); 5α,6,11α,14β,17(R)-pentaacetoxy-3β-benzoyloxy-15β-hydroxyseget-8(12)-en-9-one

A white amorphous powder, $C_{37}H_{44}O_{14}$; HRFAB–MS *m/z*: 713.2802 $[M+H]^+$, Δ −0.8 mmu.; $[\alpha]_D$ −4° (*c* 0.17); IR ν_{max} cm^{-1}: 3600–3400, 2974, 1751, 1701, 1647, 1373, 1224, 1030 and 715 ; UV λ_{max} nm (ε): 204 (8000), 231 (25,000) and 273 (2000); CD: $\Delta\varepsilon_{224}$ −0.3 and $\Delta\varepsilon_{242}$ +0.7. NMR spectral data, see Table 1.

3.5. Segetene B (2); 6,14α,17(R)-triacetoxy-5α-(2-acetoxyacetoxy)-3β-benzoyloxy-15β-hydroxyseget-8(12)-en-9-one

A white amorphous powder, $C_{37}H_{44}O_{14}$; HR–FAB–MS *m/z*: 713.3 $[M+H]^+$; $[\alpha]_D$ −51° (*c* 0.13); IR ν_{max} cm^{-1}: 3600–3300, 2966, 1751, 1726, 1373, 1244, 1033 and 715 ; UV λ_{max} nm (ε): 205 (4000) and 232 (11000); CD: $\Delta\varepsilon_{226}$ −1.9 and $\Delta\varepsilon_{242+}$0.3. NMR data, see Table 1.

3.6. Antifeedant test

The antifeedant potential of the isolated compounds was tested by a conventional leaf disk method against third-instar larvae of *Spodopetra littoralis*. Five leaf disks (diameter 1.2 cm) of Chinese cabbage (*Brassica campestris* var. *chinensis*) were immersed in an acetone solution of the sample for 2 s. The treated disks were arranged alternatively with another five control disks (immersed only in acetone) close to the wall of a Petri dish. Ten larvae were placed in the center of each Petri dish. The eaten areas of treated and untreated leaf disks were evaluated at appropriate intervals for 2–12 h. The experiment was terminated after the larvae had eaten approximately 50% of one of the disks. This choice test was done at concentrations 500 and 1000 ppm to determine the minimum antifeedant inhibitory concentration of the isolated compounds.

3.7. Antiviral assays

The activity of the compounds against HIV-1 replication was based on the inhibition of virus-induced cytopathicity in MT-4 cells. MT-4 cells (100,000 cells/ml) were infected with HIV-1 (IIIB strain) at a multiplicity of infection of 0.02 and were cultured in the presence of various concentrations of the test compounds. After a 4-day incubation at 37 °C, the number of viable MT-4 cells was measured by the MTT method (Pauwels et al., 1988). Cytotoxicity of the compounds was evaluated in parallel with their anti-HIV-1 activity. It was based on the viability of mock-infected MT-4 cells as determined by the MTT method.

Acknowledgements

We would like to thank Mr. K. Takezaki, Kagoshima Prefectural Agricultural Experiment Station, for the supply of the insects.

References

Evans, F.J., Soper, C.J., 1978. The tigliane, daphnane and ingenane diterpenes, their chemistry, distribution and biological activities. Lloydia 41, 193–233.

Hecker, E., 1977. New toxic, irritant and cocarcinogenic diterpenoids esters from Euphorbiaceae and from Thymelaeaceae. Pure and Applied Chemistry 49, 1423–1431.

Huang, R.C., Zhou, J.-B., Suenaga, H., Takezaki, K., Tadera, K., Nakatani, M., 1995. Insect antifeeding property of limonoids from Okinawan and Chinese *Melia azedarach* L., and from Chinese *Melia toosendan* (Meliaceae). Bioscience, Biotechnology and Biochemistry 59, 1755–1757.

Jakupovic, J., Jeske, F., Morgenstern, T., Tsichritzis, F., Marco, J.A., Berendsohn, W., 1998a. Diterpenes from *Euphorbia segetalis*. Phytochemistry 47, 1583–1600.

Jakupovic, J., Morgenstern, T., Marco, J.A., Berendsohn, W., 1998b. Diterpenes from *Euphorbia paralias*. Phytochemistry 47, 1611–1619.

Khafagy, S.M., Gharbo, S.A., Abdel Salam, N.A., 1976. Phytochemical study of *Euphorbia paralias*. Planta Medica 29, 301–304.

Mootoo, B.S., Ramsewak, R., Khan, A., Tinto, W.F., Reynolds, W.F., McLean, S., Yu, M., 1996. Tetranortriterpenoids from *Ruagea glabra*. Journal of Natural Products 59, 544–547.

Nakatani, M., 1999. Limonoids from *Melia toosendan* (Meliaceae) and their antifeedant activity. Heterocycles 50, 595–609.

Öksüz, S., Gurek, F., Yang, S., Lin, L., Cordell, G.A., Pezzuto, J.M., Wagner, H., Lotter, H., 1997. Palalinones A and B, novel diterpene esters from *Euphorbia paralias*. Tetrahedron 53, 3215–3222.

Pauwels, R., Balzarini, J., Baba, M., Snoeck, R., Schols, D., Herdewijn, P., Desmyter, J., De Clercq, E., 1988. Rapid and automated assay for the detection of anti-HIV compounds. Journal of Virological Methods 20, 309–321.

Rizk, A.F.M., Youssef, A.M., Diab, M.A., Salem, H.M., 1974. Constituents of Egyptian Euphorbiaceae. I. Triterpenoids and related substances of *Euphorbia palalias*. Zeitschrift fur Naturforschung C29, 529–531.

Rizk, A.F.M., Youssef, A.F.M., Diab, M.A., Salem, H.M., 1976. Constituents of Egyptian Euphorbiaceae. Part 2: Flavonoids of *Euphorbia segetalis*. Pharmazie 31, 405–407.

Sayed, M.D., Rizk, A., Hammouda, F.M., El-Missiry, M.M., Williamson, E.M., Evans, F.J., 1980. Constituents of Egyptian Euphorbiaceae. IX. Irritant and cytotoxic ingenane esters from *Euphorbia paralias* L. Experientia 36, 1206–1207.

Tackholm, V., 1974. Student Flora of Egypt, 2nd Edition. Cairo University Press, Beirrut.

Wada, K., Munakata, K., 1968. Naturally occurring insect control chemicals, isobaldine, a feeding inhibitor and cocculolidine, an insecticide in the leaves of *Cocculus trilobus*. Journal of Agriculture and Food Chemistry 16, 471–474.

PERGAMON

Phytochemistry 58 (2001) 1141–1145

PHYTOCHEMISTRY

www.elsevier.com/locate/phytochem

Antifungal highly oxygenated guaianolides and other constituents from *Ajania fruticulosa*

J.C. Meng[a,b], Y.F. Hu[c], J.H. Chen[a], R.X. Tan[a,*]

[a]*Institute of Functional Biomolecule, School of Life Sciences, Nanjing University, Nanjing 210093, PR China*
[b]*Zhuzhou Industrial & Technical College, Zhuzhou 412008, PR China*
[c]*Department of Chemistry, Nanjing University, Nanjing 210093, PR China*

Received 24 April 2001; received in revised form 17 August 2001

Abstract

Three highly oxygenated guaianolides were isolated from the aerial parts of *Ajania fruticulosa* along with 17 known phytochemicals including a triterpene (α-amyrin), two plant sterols (β-sitosterol, daucosterol), four flavonoids (axillarin, centaureidin, santin and 5,7,4′-trihydroxy-3,3′-dimethoxyflavone), and ten sesquiterpenes [1α-hydroperoxy-4β,8α,10α,13-tetrahydroxyguaia-2-en-12,6α-olide, 1α-hydroperoxy-4α,10α-dihydroxyguaia-9α-angeloyloxyguaia-2,11(13)-dien-12,6α-olide, 3β,4α-dihydroxyguaia-11(13),10(14)-dien-12,6α-olide, 1α,4α,10α-trihydroxy-9α-angeloyloxyguaia-2,11(13)-dien-12,6α-olide, 1β,2β-epoxy-3β,4α,10α-trihydroxy-guaia-11(13)-en-12,6α-olide and 2-oxo-8α-hydroxyguaia-1(10),3,11(13)-trien-12,6α-olide, ketoplenolide B, alantolactone, 9β-hydroxyeudesma-4,11(13)-dien-12-oic acid and 9β-acetoxyeudesma-4,11(13)-dien-12-oic acid]. The structures of the three guaianolides were elucidated by a combination of spectroscopic methods (EIMS, HREIMS, COSY, HMQC, HMBC and NOESY) as 1β,2β-epoxy-3β,4α,8β,10α-tetrahydroxyguaia-11(13)-en-12,6α-olide (**1**), 1β,2β-epoxy-3β,4α,9α,10α-tetrahydroxyguaia-11(13)-en-12,6α-olide (**2**) and 1β,2β-epoxy-10α-hydroperoxy-3β,4α,8β-trihydroxyguaia-11(13)-en-12,6α-olide (**3**), respectively. Antifungal bioassay of all isolates showed that guaianolides **1**, **2**, **3**, and 1β,2β-epoxy-3β,4α,10α-trihydroxyguaia-11(13)-en-12,6α-olide were inhibitory to the growth of *Candida albicans* with MICs being 20, 20, 20, and 40 μg/ml, respectively. © 2001 Published by Elsevier Science Ltd.

Keywords: *Ajania fruticulosa*; Asteraceae; Guaianolides; Flavonoids; Sesquiterpenes

1. Introduction

Ajania fruticulosa (Ledeb.) Poljak (Asteraceae), distributed mainly in the northwestern part of China, has long been used as traditional Chinese medicine in the treatment of appendicitis, tuberculosis and emphysema. Sesquiterpenes and phenolic constituents were isolated from this species in a previous phytochemical investigation (Li et al., 1999). In our continued investigation of structurally novel and/or biologically active constituents of medicinal plants (Meng et al., 2000), we reexamined the title plant phytochemically to characterize further three new highly oxygenated guaianolides (**1**–**3**) in addition to 17 known constituents, four of which were also active.

2. Results and discussion

Repeated silica gel chromatography of the crude extract of *Ajania fruticulosa* afforded a triterpene, two plant sterols, four flavonoids, three new and six known guaianolides, and other four sesquiterpene lactones. The triterpene (α-amyrin) and two plant sterols (β-sitosterol and daucosterol) were identified by direct comparisons (TLC, IR, ^{1}H NMR) with the authentic samples available in our laboratory. The ^{1}H and ^{13}C NMR data of four flavonoids revealed that they were axillarin (Al-Yahya et al., 1988), centaureidin (Martinez et al., 1997), santin (Rashid et al., 1992), and 5,7,4′-trihydroxy-3,3′-dimethoxyflavone (Dong et al., 1987). The ten known sesquiterpene lactones were shown by extensive spectroscopic analyses to be 1α-hydroperoxy-4β,8α,10α,13-tetrahydroxyguaia-2-en-12,6α-olide (Li et al., 1999), 1α-hydroperoxy-4α,10α-dihydroxyguaia-9α-angeloyloxyguaia-2,11(13)-dien-12,6α-olide (Li et al., 1999), 3β,4α-dihydroxyguaia-11(13),10(14)-dien-12,6α-olide (Sigstad

* Corresponding author. Tel./fax: +86-25-359-3201.
E-mail address: rxtan@netra.nju.edu.cn (R.X. Tan).

0031-9422/01/$ - see front matter © 2001 Published by Elsevier Science Ltd.
PII: S0031-9422(01)00389-2

et al., 1991), 1α,4α,10α-trihydroxy-9α-angeloyloxyguaia-2,11(13)-dien-12,6α-olide (Wang et al., 1994), 1β,2β-epoxy-3β,4α,10α-trihydroxyguaia-11(13)-en-12,6α-olide (Jakupovic et al., 1988), 2-oxo-8α-hydroxyguaia-1(10),3,11(13)-trien-12,6α-olide (Daniewskii et al., 1988), ketoplenolide B (Wang et al., 1994), alantolactone (Tsuda et al., 1957), 9β-hydroxyeudesma-4,11(13)-dien-12-oic acid (Tan et al., 1995a), and 9β-acetoxyeudesma-4,11(13)-dien-12-oic acid (Tan et al., 1995b), respectively.

Compound **1** was obtained as a colorless gum. The EIMS spectrum of **1** gave a molecular ion at *m*/*z* 312 $[M]^+$ accompanied by an intense fragment peak at *m*/*z* 294 produced by an elimination of H_2O from parent molecule. Its molecular formula $C_{15}H_{20}O_7$ was indicated by the exact weight (*m*/*z* 312.1217) of the molecular ion given by the HREIMS spectrum of **1**. In the ^1H NMR spectrum of **1**, it showed two methyl singlets at *δ* 1.12 (3H, *s*, H-14) and 1.31 (3H, *s*, H-15), and two exomethylene proton signals at *δ* 5.56 (1H, *br s*, H-13a) and 5.98 (1H, *d*, *J* = 3.3 Hz, H-13b). The ^{13}C NMR spectrum of **1** displayed 15 carbon resonances including two methyl, two methylene, six methine, and five quaternary carbons. In addition, the chemical shifts and coupling pattern of two oxygenated methine singlets at *δ* 3.60 and 4.04 in the ^1H NMR spectrum, along with the carbon resonance lines at *δ* 72.3 (C), 62.9 (CH), and 66.1 (CH) in the ^{13}C NMR spectrum, demonstrated the presence of an 1β,2β-epoxy-3β-hydroxyl moiety on a five-member ring (Jakupovic et al., 1988). All these observations suggested that compound **1** was a highly oxygenated guaianolide (Jakupovic et al., 1988). This hypothesis was confirmed by 2D NMR spectroscopic analyses (HMQC, HMBC and NOESY) which allowed as well the unequivocal assignment of all ^1H and ^{13}C NMR spectral data. Moreover, the 8-hydroxyl group had a broad singlet at *δ* 3.86 (H-8) which showed typically long-range correlations with C-6 and C-10 in the HMBC spectrum. Furthermore, the signals due to H-14 and H-15 were exhibited as a pair of three-proton singlets at *δ* 1.12 and 1.32 indicating the presence of 4- and 10-dihydroxyls. Relative to the biogenetically rationalized α-configuration for H-7 (Huneck et al., 1991), the stereochemistry of compound **1** was readily established by a NOESY experiment. The clear NOE correlations between any pair of H-5, H-7 and H-8 suggested that 8-OH was in a *β*-configuration. Similarly, the formulated configurations of C-1–C-4 and C-10 were deduced from the NOE correlations of H-5 with H-2 and H-3, and of H-6 with H-14 and H-15. In conclusion, the structure of compound **1** was determined to be 1β,2β-epoxy-3β,4α,8β,10α-tetrahydroxyguaia-11(13)-en-12,6α-olide.

The molecular ion at *m*/*z* 312.1215 in its HREIMS spectrum of compound **2** indicated that its molecular formula was also $C_{15}H_{20}O_7$. The ^1H and ^{13}C NMR spectra of **2** were similar to those of compound **1**. All proton and carbon data of compound **2** were assigned exactly by extensive 2D NMR spectroscopic analyses (COSY, HMQC, HMBC and NOESY). However, the 9-hydroxyl group was required by the H-9 singlet at *δ* 5.25 which, as anticipated, exhibited long-range correlations with C-7 and C-14 in the HMBC spectrum. As in the case of compound **1**, the stereochemistry of compound **2** was established by NOE correlations in its NOESY spectrum where strong cross peaks between any pair of H-14, H-6 and H-9 substantiated the *α*-orientation of the 9-hydroxyl group. In conclusion, the structure of compound **2** was determined to be 1β,2β-epoxy-3β,4α,9α,10α-tetrahydroxyguaia-11(13)-en-12,6α-olide.

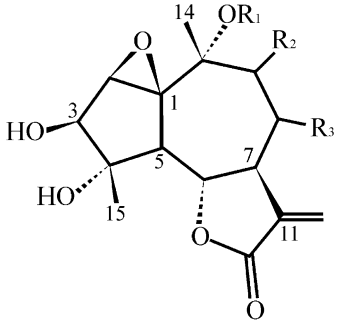

1 $R_1 = R_2 = H$, $R_3 = \beta$-OH
2 $R_1 = R_3 = H$, $R_2 = \alpha$-OH
3 $R_1 = OH$, $R_2 = H$, $R_3 = \beta$-OH

Compound **3** was obtained as a colorless gum. The molecular formula $C_{15}H_{20}O_8$, indicates an oxygen atom more than that of guaianolide **1**, could be readily deduced from the molecular ion at *m*/*z* 328.1164 in the HREIMS spectrometry. The ^1H and ^{13}C NMR spectra of compound **3** were similar to those in compound **1** in the splitting pattern and the chemical shifts suggested that it was also a highly oxygenated guaianolide with its structure very similar to that of **1**. The 2D NMR spectra (COSY, HMQC, HMBC and NOESY) confirmed this assumption with all ^1H and ^{13}C NMR spectroscopic data assigned unambiguously. The C-10 resonance of **3** at *δ* 95, shifted downfield by 24.4 ppm from that of **1**, along with a broadened singlet at *δ* 7.70 in the ^1H NMR spectrum, demonstrated the presence of a 10-hydroperoxyl group. Again, the stereochemistry of compound **3** was unequivocally assigned on the basis of NOE correlations exhibited in its NOESY spectrum. Thus, the *α*-orientation of hydroperoxyl group was required by the NOE correlations between H-14 and H-6. And the strong cross peak between any pair of H-5, H-7 and H-8 indicated the β-configuration of the 8-hydroxyl group. Accordingly, compound **3** was 1β,2β-epoxy-10α-hydroperoxy-3β,4α,8β-trihydroxyguaia-11(13)-en-12,6α-olide.

All isolates were tested for their antifungal activity against *Candida albicans*. The new guaianolides **1**, **2**, and **3** were inhibitory to the growth of *Candida albicans* with the same MIC values of 20 μg/ml, while 1β,2β-

epoxy-3β,4α,10α-trihydroxyguaia-11(13)-en-12,6α-olide was also active with a MIC of ~40 μg/ml.

3. Experimental

3.1. General

Optical rotations were measured on a DXP-118 apparatus. EIMS and HREIMS experiments were run on VG-ZAB-HS and Jeol JMX-HX110 mass spectrometers, respectively. All NMR experiments were performed on a Jeol JNM-A 500 FT–NMR spectrometer using TMS as the internal standard. Silica gel (200–300 mesh) for column chromatography and GF_{254} (30–40 μ) for TLC were produced by Qingdao Marine Chemical Factory, Qingdao, People's Republic of China. Sephadex LH-20 was from Pharmacia Biotech., Sweden. All other chemicals used in this study were of analytical grade.

3.2. Plant material

The aerial parts of *Ajania fruticulosa* was recollected in July, 1998 from Gaolan Mountain near Lanzhou Railway Station, Lanzhou, China, and identified by Professor G. L. Zhang. A voucher specimen (GLZ-92721) has been deposited in the herbarium of Lanzhou University, Lanzhou 730070, China.

3.3. Extraction and isolation

The air-dried plant material (3.2 kg) was pulverized, and then extracted three times with petroleum ether–Et_2O–MeOH (1:1:1) at room temperature. The extract was concentrated under reduced pressure to give a residue (102 g) which was dissolved completely at 50 °C in a minimum amount of MeOH. The solution was kept at −20 °C overnight to precipitate waxy substances, then filtered while chilled. In vacuo removal of the solvent from the filtrate afforded a black gum (50 g) which was applied to a silica gel column (1.2 kg) using petroleum ether with gradually increasing amounts of acetone to give α-amyrin (24 mg), β-sitosterol (102 mg), and daucosterol (88 mg) together with other five fractions (F-1, 2 g; F-2, 9 g; F-3, 15 g; F-4, 18 g; and F-5, 2 g). Column chromatography of F-2 over silica gel (240 g, 200–300 mesh) with a chloroform–acetone gradient (15:1–10:1, each 200 ml) followed by gel filtration over Sephadex LH-20 with $CHCl_3$–MeOH (1:1) afforded centaureidin (17 mg) and 5,7,4′-trihydroxy-3,3′-dimethoxyflavone (21 mg). F-3 was subjected to silica gel chromatography (500 g, 200–300 mesh) eluting with a $CHCl_3$–MeOH gradient (15:1, 13:1, 11:1, 9:1, each 300 ml) to give santin (17 mg), axillarin (21 mg), ketoplenolide B (18 mg) and alantolactone (23 mg), respectively. Column chromatography of F-4 with a $CHCl_3$–MeOH gradient gave three fractions (F-4-1, 4.5 g; F-4-2, 5.3 g; F-4-3, 7.1 g). CC of F-4-1 with $CHCl_3$ containing gradually increasing amounts of MeOH (15:1–10:1) afforded 2-oxo-8α-hydroxyguaia-1(10),3,11(13)-trien-12,6α-olide (15 mg; 15:1, 300 ml), 9β-acetoxyeudesma-4,11(13)-dien-12-oic acid (21 mg; 15:1, 500 ml), 9β-hydroxyeudesma-4,11(13)-dien-12-oic acid (18 mg; 13:1, 350 ml), and 3β,4α-dihydroxyguaia-11(13),10(14)-dien-12,6α-olide (24 mg; 11:1, 500 ml). Also by a combination of silica gel column chromatography (300 g, 200–300 mesh) eluting with a CH_2Cl_2–MeOH gradient (15:1, 13:1, 10:1, each 500 ml), F-4-2 finally yielded 1α-hydroperoxy-4β,8α,10α,13-tetrahydroxyguaia-2-en-12,6α-olide (13 mg), 1α-hydroperoxy-4α,10α-dihydroxyguaia-9α-angeloyloxyguaia-2,11(13)-dien-12,6α-olide (11 mg), and 1α,4α,10α-trihydroxy-9α-angeloyloxyguaia-2,11(13)-dien-12,6α-olide (26 mg), respectively. Repetitive gel filtrations [Sephadex LH-20, $CHCl_3$–MeOH (1:1)] of F-4-3 afforded the interesting fractions F-4-3-1 (210 mg) and F-4-3-2 (150 mg). F-4-3-1 was then subjected to silica gel column chromatography (20 g, 200–300 mesh) eluting with CH_2Cl_2–MeOH (10:1, each 200 ml) and finally gave 1β,2β-epoxy-3β,4α,10α-trihydroxyguaia-11(13)-en-12,6α-olide (20 mg), and **3** (15 mg). Preparative TLC of F-4-3-2 (CH_2Cl_2-MeOH, 9:1) yielded **1** (12 mg, R_f = 0.40), and **2** (17 mg, R_f = 0.54).

3.4. 1β,2β-Epoxy-3β,4α,8β,10α-tetrahydroxyguaia-11(13)-en-12,6α-olide (1)

Colorless gum; $[\alpha]_D^{20}$ +31 ° (MeOH; *c* 0.12); EIMS *m*/*z* (rel. int.): 312 $[M]^+$ (5), 297 $[M^+–Me]$ (12), 294 $[M^+–H_2O]$ (48), 57 (100); HREIMS *m*/*z*: 312.1217 (calc. for $C_{15}H_{20}O_7$: 312.1209); ^1H and ^{13}C NMR spectral data are given in Table 1.

Table 1
NMR spectral data for guaianolide **1** (DMSO-d_6, 500 MHz)

Position	δ_H (*J* in Hz)	δ_C (DEPT)	HMBC
1		72.3 (C)	
2	3.60 *s*	62.9 (CH)	C-4, C-5
3	4.04 *s*	66.1 (CH)	C-1, C-2, C-5, C-15
4		83.4 (C)	
5	2.46 *d* (11.0)	57.3 (CH)	C-2, C-4, C-7, C-10
6	4.38 *dd* (10.2, 10.8)	76.4 (CH)	C-8
7	3.45 *m*	51.4 (CH)	C-5, C-9
8α	3.86 br *s*	68.4 (CH)	C-6, C-10
9α	1.64 *m*	36.3 (CH_2)	C-1, C-14
9β	1.83 *m*		C-1, C-14
10		70.6 (C)	
11		139.8 (C)	
12		169.6 (C)	
13a	5.56 br *s*	119.2 (CH_2)	C-7, C-12
13b	5.98 *d* (3.3)		C-7, C-12
14	1.12 *s*	26.2 (CH_3)	C-1, C-9
15	1.31 *s*	21.6 (CH_3)	C-3, C-5

Table 2
NMR spectral data for guaianolide **2** (DMSO-d_6, 500 MHz)

Position	δ_H (*J* in Hz)	δ_C (DEPT)	HMBC
1		72.0 (C)	
2	3.86 *s*	61.8 (CH)	C-4
3	4.16 *s*	65.3 (CH)	C-1, C-2, C-5, C-15
4		78.6 (C)	
5	2.64 *d* (10.8)	49.8 (CH)	C-7, C-15
6	4.33 *t* (10.4)	78.8 (CH)	C-8
7	3.54 *dd* (6.4, 10.4)	41.4 (CH)	C-9
8α	1.89 *m*	33.6 (CH_2)	
8β	2.10 *m*		
9β	5.25 *s*	70.1 (CH)	C-7, C-14
10		73.6 (C)	
11		140.5 (C)	
12		169.6 (C)	
13a	5.53 *d* (3.2)	118.4 (CH_2)	C-7, C-12
13b	5.99 *d* (3.6)		C-7, C-12
14	1.03 *s*	22.2 (CH_3)	C-1, C-9
15	1.35 *s*	25.6 (CH_3)	C-3, C-5

3.5. 1β,2β-Epoxy-3β,4α,9α,10α-tetrahydroxyguaia-11(13)-en-12,6α-olide (**2**)

Colorless gum; $[\alpha]_D^{20}$ +18 ° (MeOH; *c* 0.10); EIMS *m*/*z* (rel. int.): 312 $[M]^+$ (3), 297 $[M^+–Me]$ (11), 294 $[M^+–H_2O]$ (22), 57 (100); HREIMS *m*/*z*: 312.1215 (calc. for $C_{15}H_{20}O_7$: 312.1209); ^1H and ^{13}C NMR spectral data are listed in Table 2.

3.6. 1β,2β-Epoxy-10α-hydroperoxy-3β,4α,8β,-trihydroxyguaia-11(13)-en-12,6α-olide (**3**)

Colorless gum; $[\alpha]_D^{20}$ +24 ° (MeOH; *c* 0.10); EIMS *m*/*z* (rel. int.): 328 $[M]^+$ (0.7), 297 $[M^+–Me]$ (22), 294 $[M^+–H_2O]$ (10), 260 $[294–H_2O_2]$ (9), 83 (70), 57 (100); HREIMS *m*/*z*: 328.1164 (calc. for $C_{15}H_{20}O_8$: 328.1158); ^1H and ^{13}C NMR spectral data are tabulated in Table 3.

Table 3
NMR spectral data for guaianolide **3** (DMSO-d_6, 500 MHz)

Position	δ_H (*J* in Hz)	δ_C (DEPT)	HMBC
1		67.5 (C)	
2	3.72 *s*	61.4 (CH)	C-4, C-5
3	4.12 *s*	65.1 (CH)	C-1, C-2, C-5, C-15
4		79.5 (C)	
5	2.70 *d* (8.8)	44.1 (CH)	C-7, C-15
6	4.33 *dd* (8.9, 9.6)	75.5 (CH)	C-8
7	3.60 *m*	51.3 (CH)	C-8, C-9
8α	4.03 br *s*	68.5 (CH)	C-6, C-10
9α	1.78 *m*	46.4 (CH_2)	C-1, C-10, C-14
9β	2.12 *m*		
10		95.0 (C)	
11		138.6 (C)	
12		169.0 (C)	
13a	6.09 *s*	123.6 (CH_2)	C-7, C-12
13b	6.18 *s*		C-7, C-12
14	1.05 *s*	27.7 (CH_3)	C-1, C-9
15	1.36 *s*	26.0 (CH_3)	C-3, C-5
–OOH	7.70 br *s*		C-14

3.7. Antifungal assays

All isolates were dissolved in DMF at concentrations of 10, 20, and 40 μg/ml, respectively. The concentration of DMF in the broth media was maintained at 1%, which did not affect the growth of the test microorganism. The minimal inhibitory concentrations (MIC) against *Candida albicans* were measured by the serial 2-fold dilution method as reported in the literature (Kubo et al., 1991). Ketoconazole was used as a positive control at concentrations of 1, 2, and 4 μg/ml, respectively.

Acknowledgements

Grants to RXT from the National Natural Science Foundation (Nos. 39725033 and 39970083) and from the Doctoral Training Programme (No. 1999028419) are gratefully acknowledged.

References

Al-Yahya, M.A., El-Sayed, A.M., Mossa, J.S., 1988. Potential cancer chemopreventive and cytotoxic agents from *Pulicarin crispa*. J. Nat. Prod. 51, 621–624.

Daniewskii, W., Skibicki, P., Gumulka, M., Drozoz, B., Grabarczyk, H., Bloszyk, E., 1988. Sesquiterpene lactones XXXV. Constituents of *Reichardia tingitana* and their antifeedant activity. Acta Soc. Bot. Pol. 57, 539–545.

Dong, X.P., Che, C.T., Farnsworth, N.R., 1987. Cytotoxic flavonols from *Gutierrezia microcephala*. J. Nat. Prod. 50, 337–338.

Huneck, S., Zdero, C., Bohlmann, F., Jia, Z.J., Huneck, S., 1991. Seco-guaianolides and other constituents from *Artemisia* species. Phytochemistry 30, 583–587.

Jakupovic, J., Boeker, R., Grenz, M., Paredes, L., Bohlmann, F., Self-El-Din, A., 1988. Highly oxygenated guaianolides from *Otanthus maritimus*. Phytochemistry 27, 1135–1140.

Kubo, T., Himejima, M., Muroi, H., 1991. Antimicrobial activity of flavor components of cardamon *Elettaria cardamomum* (Zingiberaceae). J. Agri. Food Chem. 39, 1984–1986.

Li, H., Meng, J.C., Cheng, C.H.K., Higa, T., Tanaka, J., Tan, R.X., 1999. New guaianolides and xanthine oxidase inhibitory flavonols from *Ajania fruticulosa*. J. Nat. Prod. 63, 1053–1055.

Martinez, J., Silvan, A.M., Abad, M.J., 1997. Isolation of two flavonoids from *Tanacetum microphyllum* as PMA-induced ear edema inhibitors. J. Nat. Prod. 60, 142–144.

Meng, J.C., Zhu, Q.X., Tan, R.X., 2000. New antimicrobial mono- and sesquiterpenes from *Soroseris hookeriana* subsp. *erysimoides*. Planta Med. 66, 541–544.

Rashid, M.A., Armstrong, J.A., Gray, A.I., Waterman, P.G., 1992. Alkaloids, flavonols and coumarins from *Drummondita hassellii* and *D. calida*. Phytochemistry 31, 1265–1269.

Sigstad, E.E., Catalan, C.A.N., Gutierrez, A.B., Diaz, J.G., Goedken, V.L., Herz, W., 1991. Guaianolides and germacranolides from *Stevia grisebachiana*. Phytochemistry 30, 1933–1940.

Tan, R.X., Wang, W.Z., Yang, L., Wei, J.H., 1995a. A new eudesmenoic acid from *Artemisia phaeolepis*. J. Nat. Prod. 58, 288–290.

Tan, R.X., Jia, Z.J., Yan, Z.Q., Deng, C.H., 1995b. New eudesmane acids from *Artemisia hedinii* Ostenf. Indian J. Chem. 34B, 565–568.

Tsuda, K., Tanabe, K., Iwai, I., Funakoshi, K., 1957. The structure of alantolactone. J. Am. Chem. Soc. 79, 5721–5724.

Wang, W.Z., Tan, R.X., Yao, Y.M., Wang, Q., Jiang, F.X., 1994. Sesquiterpene lactones from *Ajania fruticulosa*. Phytochemistry 37, 1347–1349.

PERGAMON

Phytochemistry 58 (2001) 1147–1148

PHYTOCHEMISTRY

www.elsevier.com/locate/phytochem

Book reviews

Chemotaxonomie der Pflanzen, Volume XIb—2: Leguminosae, Part 3
R. Hegnauer and M. Hegnauer, Birkhäuser-Verlag, Basel, 1494 pp., 2001. SFR 998. ISBN 3-7643-6269-3.

During the 1950′s Robert Hegnauer of Leiden University made the decision to devote a major part of his working life to the writing of a complete review of known phytochemistry, setting the data in a taxonomic context but not neglecting ethnobotanical, ecological, physiological and medicinal aspects. The first volume of this masterwork appeared in 1962 and dealt with the chemotaxonomy of thallophytes, bryophytes, pteridophytes and gymnosperms. Subsequent volumes, appearing every two or three years, covered the consierable richness in chemistry of angiosperms, family by family. The present volume under review is the 13th and final book in the series. It is devoted to the phytochemistry of a single subfamily, the Papilionoideae, of the Leguminosae.

What we have here is a masterly review of the chemistry of these plants, species by species, genus by genus and tribe by tribe. There are many tables and many figures with structural formulae. The work is completely up-to-date, with an Appendix recording the primary literature up to December 2000. Nothing of importance is omitted. Take the Vicieae, for example, a tribe which includes *Lathyrus*, *Lens*, *Pisum* and *Vicia*. There are 65 pages of text on the Vicieae, followed by 322 refences, and the results of surveys for 10 classes of chemical are described. The book concludes with an Appendix on recent ethnobotany and there are complete indexes to both taxonomy and chemistry.

In writing this volume, Robert Hegnauer has been joined by his wife Minie, not surprisingly considering the vast amount of data contained herein. It is undoubtedly a masterwork. The Hegnauers are to be congratulated on completing this mammoth task, particularly in the face of battle with ill-health in recent years. Legume phytochemists will rejoice greatly at this appearance of this splendid account of papilionoid phytochemistry.

Jeffery B. Harborne
University of Reading, School of Plant Sciences, Department of Botany, Whiteknights, PO Box 221, Reading RG6 6AS, UK

PII: S0031-9422(01)00367-3

Natural Terpenoids as Messengers
P. Harrawijn, A.M. van Oosten and P.G.M. Piron, Kluwer Academic, Dordrecht, The Netherlands, 2001. 440 pp. £100. ISBN 0792368916.

The contents of this novel and instructive book on terpenoids can be appreciated better from the subtitle "a multi-disciplinary study of terpenoid production, biological functions and practical applications". Some terpenoids—especially mono- and sesquiterpenoids—are indeed important messenger signals in nature, but as a class, they have many other roles as well. Many of their biological properties are discussed here with regard to their roles as messengers at the cellular level as well as acting as semiochemicals. A significant chapter in the book describes terpenoids as being beneficial to human health and the applications of terpenoids in medicine are particularly well covered.

As one might expect in a book on terpenoids, there is much information given on their biosynthesis in different organisms, from bacteria to vertebrates. Some of the key enzymes of isoprenoid biosynthesis are considered, as well as the regulation of biosynthesis via feedback mechanisms.

This attractive textbook is well illustrated with descriptive figures portraying the various interactions that are possible between insects and plants, fungi and plants, and so on. The text is clear and fully referenced. My only regret is that the authors, who are perfectly fluent in English, did not consult an Englishman to read

the text before typesetting. Nevertheless, this is a highly readable volume and the authors should be congratulated in producing this lively account of terpenoids in their natural environments.

Jeffrey B. Harborne
University of Reading, School of Plant Sciences, Department of Botany, Whiteknights, PO Box 221, Reading RG6 6AS, UK

PII: S0031-9422(01)00366-1

PERGAMON

Phytochemistry 58 (2001) 1147–1148

PHYTOCHEMISTRY

www.elsevier.com/locate/phytochem

Book reviews

Chemotaxonomie der Pflanzen, Volume XIb—2: Leguminosae, Part 3
R. Hegnauer and M. Hegnauer, Birkhäuser-Verlag, Basel, 1494 pp., 2001. SFR 998. ISBN 3-7643-6269-3.

During the 1950′s Robert Hegnauer of Leiden University made the decision to devote a major part of his working life to the writing of a complete review of known phytochemistry, setting the data in a taxonomic context but not neglecting ethnobotanical, ecological, physiological and medicinal aspects. The first volume of this masterwork appeared in 1962 and dealt with the chemotaxonomy of thallophytes, bryophytes, pteridophytes and gymnosperms. Subsequent volumes, appearing every two or three years, covered the consierable richness in chemistry of angiosperms, family by family. The present volume under review is the 13th and final book in the series. It is devoted to the phytochemistry of a single subfamily, the Papilionoideae, of the Leguminosae.

What we have here is a masterly review of the chemistry of these plants, species by species, genus by genus and tribe by tribe. There are many tables and many figures with structural formulae. The work is completely up-to-date, with an Appendix recording the primary literature up to December 2000. Nothing of importance is omitted. Take the Vicieae, for example, a tribe which includes *Lathyrus*, *Lens*, *Pisum* and *Vicia*. There are 65 pages of text on the Vicieae, followed by 322 refences, and the results of surveys for 10 classes of chemical are described. The book concludes with an Appendix on recent ethnobotany and there are complete indexes to both taxonomy and chemistry.

In writing this volume, Robert Hegnauer has been joined by his wife Minie, not surprisingly considering the vast amount of data contained herein. It is undoubtedly a masterwork. The Hegnauers are to be congratulated on completing this mammoth task, particularly in the face of battle with ill-health in recent years. Legume phytochemists will rejoice greatly at this appearance of this splendid account of papilionoid phytochemistry.

Jeffery B. Harborne
University of Reading, School of Plant Sciences, Department of Botany, Whiteknights, PO Box 221, Reading RG6 6AS, UK

PII: S0031-9422(01)00367-3

Natural Terpenoids as Messengers
P. Harrawijn, A.M. van Oosten and P.G.M. Piron, Kluwer Academic, Dordrecht, The Netherlands, 2001. 440 pp. £100. ISBN 0792368916.

The contents of this novel and instructive book on terpenoids can be appreciated better from the subtitle "a multi-disciplinary study of terpenoid production, biological functions and practical applications". Some terpenoids—especially mono- and sesquiterpenoids—are indeed important messenger signals in nature, but as a class, they have many other roles as well. Many of their biological properties are discussed here with regard to their roles as messengers at the cellular level as well as acting as semiochemicals. A significant chapter in the book describes terpenoids as being beneficial to human health and the applications of terpenoids in medicine are particularly well covered.

As one might expect in a book on terpenoids, there is much information given on their biosynthesis in different organisms, from bacteria to vertebrates. Some of the key enzymes of isoprenoid biosynthesis are considered, as well as the regulation of biosynthesis via feedback mechanisms.

This attractive textbook is well illustrated with descriptive figures portraying the various interactions that are possible between insects and plants, fungi and plants, and so on. The text is clear and fully referenced. My only regret is that the authors, who are perfectly fluent in English, did not consult an Englishman to read

PERGAMON

Phytochemistry 58 (2001) 1149–1152

PHYTOCHEMISTRY

www.elsevier.com/locate/phytochem

Monoterpene glucosides from *Origanum syriacum*

M.S. Kamel[a,*], M.H. Assaf[a], H.A. Hasanean[a], K. Ohtani[b], R. Kasai[b], K. Yamasaki[b]

[a]*Department of Pharmacognosy, Faculty of Pharmacy, Assiut University, Assiut 71526, Egypt*
[b]*Institute of Pharmaceutical Sciences, Hiroshima University School of Medicine, 1-2-3 Kasumi, Minami-Ku, Hiroshima 734, Japan*

Received 19 June 2001; received in revised form 14 August 2001

Abstract

From the aerial parts of *Origanum syriacum*, three new monoterpene glucosides thymoquinol 2,5-*O*-β-diglucopyranoside (**3**), carvacrol 2-*O*-β-glucopyranosyl-(1→2)-β-glucopyranoside (**4**) and *p*-menth-1-ene-3,4-diol 4-*O*-β-glucopyranoside (**5**) together with two known monoterpene glucosides thymoquinol 2-*O*-β-glucopyranoside (**1**), thymoquinol 5-*O*-β-glucopyranoside (**2**) have been isolated. The structures of the isolated compounds were verified by means of MS and NMR spectral analyses. © 2001 Elsevier Science Ltd. All rights reserved.

Keywords: *Origanum syriacum*; Lamiaceae; Thymoquinol glucosides; Carvacrol glucoside

1. Introduction

Origanum syriacum L. (Lamiaceae) is an aromatic, herbaceous and perennial plant growing wild in the Sinai Desert of Egypt (Tackholm, 1974). The essential oils and the constituents of many *Origanum* species have been intensively studied (Sendra et al., 1980; Ravid et al., 1983; Akgul et al., 1987; Harvala et al., 1987; Halim et al., 1991; Afsharypuor et al., 1997). In folk medicine, *Origanum* species are used as powerful disinfectants, flavouring agents, in perfumes and in scenting soaps (Gunther, 1949; Chiej, 1984; Kotb, 1985). It was reported that thymol and carvacrol represent the major constituents of the essential oils of *Origanum* species (Sarer et al., 1982). From Egyptian majorana (*Origanum vulgare*), arbutin and methyl arbutin have been already isolated and quantitatively estimated (Assaf et al., 1987). The present study deals with isolation and assignment of three new and two known monoterpene glucosides from the aerial parts of *Origanum syriacum* L.

2. Results and discussion

The ethanolic extract of the aerial parts of *O. syriacum* was deffated with CH_2Cl_2 and the aqueous layer was subjected to a column chromatography of Diaion HP-20. The methanol eluate was repeatedly chromatographed on columns of silica gel and then by MPLC and HPLC to afford 5 glycosides.

The structure of compound **1** was determined as thymoquinol 2-*O*-β-glucopyranoside while that of **2** was identified as thymoquinol 5-*O*-β-glucopyranoside previously isolated from *Schisandrae chinensis* (Yahara et al., 1993). The enzymatic hydrolysis of compounds **1** and **2** produced thymoquinol as aglycone (**1a**). In general, this is the first report for isolation of compounds **1** and **2** from family lamiaceae. The molecular formula of compound **3** was deduced as $C_{22}H_{34}O_{12}$ from HR FAB-MS spectrometry (see Experimental). The enzymatic hydrolysis of **3** gave also the aglycone **1a**. ^{13}C NMR spectrum (Table 1) and DEPT experiment of **3** displayed the presence of two unsubstituted β-glucopyranosyl units from the signals at δ 104.0 (C-1, 1′); 75.1, 75.0 (C-2, 2′); 78.6 (C-3, 3′); 71.3, 71.4 (C-4, 4′); 78.7 (C-5, 5′) and 62.4 (C-6, 6′) (Bradbury et al., 1984) together with 10 carbon signals for the aglycone as follows: 3 methyl groups (δ 16.4, 23.3 and 23.2), 3 methines (δ 119.1, 114.9 and 26.8) and 4 quaternary carbons (δ 152.3, 150.9, 137.0 and 126.2). Comparison of the ^{13}C NMR data of **3** with those of **1**, **2** and **1a** (Table 1) revealed that compound **3** is a bisdesmoside and its aglycone is 2,5-disubstituted thymoquinol. From ^{1}H NMR spectrum of **3**, the two singlets at δ 7.60 and 7.50 were assigned for H-3 and H-6, respectively (Metwally et al., 1986). The one proton

* Corresponding author. Tel.: +20-088-332-196; fax: +20-088-332-776.
E-mail address: mkamel@mailcity.com (M.S. Kamel).

0031-9422/01/$ - see front matter © 2001 Elsevier Science Ltd. All rights reserved.
PII: S0031-9422(01)00386-7

multiplet at δ 3.80 together with two methyl doublets at δ 1.26 and 1.21 were obvious for H-8, 9 and 10, respectively and the methyl singlet at δ 2.40 was assigned for H-7 (Laswell et al., 1977). The β-configuration of the glucopyranosyl units was deduced from the coupling constants (6.8, 7.3 Hz) of the anomeric proton doublets at δ 5.46 and 5.47, respectively in the ^{1}H NMR spectrum of **3**. The negative FAB-MS spectrum of 3 exhibited M^+ at m/z 489 $[M–H]^-$ as well as significant peaks at m/z 327 [M–H-glucose]$^-$ and 165 [glucose]$^-$. Consequently the structure of compound 3 was assigned as thymoquinol 2,5-*O*-β-diglucopyranoside.

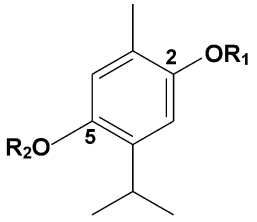

	R1	R2
(1)	Glc	H
(1a)	H	H
(2)	H	Glc
(3)	Glc	Glc

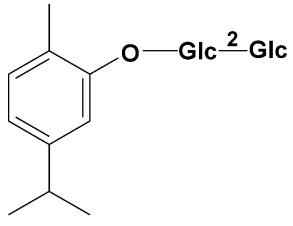

(4)

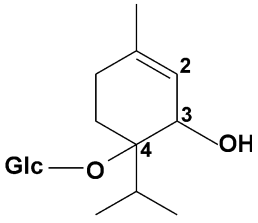

(5)

The molecular formula of compound **4** was deduced as $C_{22}H_{34}O_{11}$ from HR FAB–MS spectrometry (see Experimental). ^{13}C NMR spectrum (Table 1) and DEPT experiment of **4** displayed the presence of one unsubstituted β-glucopyranosyl unit from the signals at δ 106.5 (C-1′), 76.8 (C-2′), 78.6 (C-3′), 71.3 (C-4′) 78.7 (C-5′) and 62.4 (C-6′), one substituted β-glucopyranosyl unit from the signals at δ 100.1 (C-1), 83.4 (C-2), 78.1 (C-3), 71.1 (C-4), 78.3 (C-5) and 62.2 (C-6) (Bradbury et al., 1984) together with 10 carbon signals for the aglycone as follows: 3 methyl groups (δ 16.3, 24.3 and 24.0), 4 methines (δ 130.7, 119.8, 112.8 and 34.2) and 3 quaternary carbons (δ 156.4, 147.9 and 124.9). ^{1}H NMR spectrum of **4** revealed the presence of one methyl singlet (δ 2.5) and two methyl doublets (δ 1.15 and 1.16) assignable for Me-7, 9 and 10, respectively. Moreover, the two doublet signals at δ 5.5 and 5.6 ($J = 7.6$ and 7.2 Hz, respectively) deduced the β-configuration of the glucopyranosyl units. ^{13}C NMR signals of the aglycone were similar to those reported for carvacrol (Zechmeister, 1979). The downfield shift of C-2 (δ 83.4) of the inner glucopyranosyl residue indicated its substitution with the terminal glucopyranosyl unit at this position (Bradbury et al., 1984). The negative FAB–MS spectrum of **4** exhibited M^+ at m/z 473 $[M–H]^-$ as well as significant peaks at m/z 311 [M–H-glucose]$^-$ and 149 [M–H–2 glucose]$^-$. Consequently the structure of compound **4** was assigned as carvacrol 2-*O*-β-glucopyranosyl-(1→2)-β-glucopyranoside.

Table 1
^{13}C NMR spectral data of compounds **1–5** (100 MHz,C_5D_5N)

C	1	1a[e]	2	3	4	5
1	137.2	133.8	133.6	137.0	124.9	143.4
2	148.7	148.3	150.5	150.9	156.4	123.4
3	120.1	118.4	117.6	119.1	119.8	72.8
4	122.8	122.6	126.1	126.2	147.9	79.8
5	152.0	149.6	151.9	152.3	112.8	33.1
6	112.9	113.7	115.9	114.9	130.7	25.2
7	16.4	16.4	16.2	16.4	16.3	16.9
8	26.4	27.4	27.3	26.8	34.2	34.1
9	23.5[a]	23.2	22.9[a]	23.3[a]	24.3[a]	21.4[a]
10	23.3[a]	23.2	22.8[a]	23.2[a]	24.0[a]	21.2[a]
Glc						
1	104.5		104.3	104.0	100.1	97.9
2	75.1		75.0	75.1[b]	83.4	75.3
3	78.3[b]		78.2[b]	78.6[c]	78.1[a]	78.1[b]
4	71.4		71.3	71.3[d]	71.1[b]	71.9
5	78.6[b]		78.4[b]	78.7[c]	78.3[a]	78.5[b]
6	62.4		62.3	62.4	62.2[c]	62.7
Glc′						
1′				104.0	106.5	
2′				75.0[b]	76.8	
3′				78.6[c]	78.6[a]	
4′				71.4[d]	71.3[b]	
5′				78.7[c]	78.7[a]	
6′				62.4	62.4[c]	

[a, b, c, d] Assignments may be interchangeable in each column.
[e] Data published for the first time for thymoquinol.

The molecular formula of compound **5** was deduced as $C_{16}H_{28}O_7$ from HR FAB-MS spectrometry (see Experimental). ^{13}C NMR spectrum (Table 1) and DEPT experiment of **5** displayed the presence of one β-glucopyranosyl unit from the signals at δ 97.9 (C-1), 75.3 (C-2), 78.1 (C-3), 71.9 (C-4) 78.5 (5) and 62.7 (C-6) (Bradbury et al., 1984) together with 10 carbon signals for the aglycone as follows: 3 methyl groups (δ 16.9, 21.4 and 21.2), 2 methylene groups (δ 33.1 and 25.2), 3 methines (δ 123.4, 72.8 and 34.1) and 2 quaternary carbons (δ 143.4 and 79.8). The carbon signals at δ 72.8 and 79.8 indicated the attachment of two hydroxyl groups to these carbons (Breitmaier et al., 1987). On the other hand, ^{1}H NMR spectrum of **5** revealed the presence of one methyl singlet (δ 1.5) and two methyl doublets (δ 0.87) assignable for Me-7, 9 and 10 respectively. The broad singlets at δ 5.5 and 4.7 were assigned for H-2 and 3 respectively proving the attachment of the hydroxyl

groups to C-3 and C-4 of the aglycone together with the location of the double bond between C-1 and 2. Furthermore, comparison of ^{13}C NMR spectrum of **5** with *p*-menth-1-ene-4-ol confirmed the location of the hydroxyl group at C-3 of **5** from its downfield shift to δ 72.8 (Zechmeister, 1979). Moreover, the one proton multiplet signal at δ 3.9 in the ^1H NMR spectrum of **5** was interpreted for H-8 while the four protons multiplet at δ 1.8 – 2.2 was assigned for two methylene groups (H-5 and 6). The doublet signal at δ 5.16 ($J=8$ Hz) deduced the β-configuration of the glucopyranosyl unit. The attachment of the β-glucosyl moiety to C-4 of the aglycone was based on the downfield shift of this carbon (δ 79.8) in addition to the upfield shift of the anomeric carbon of the glucosyl unit (δ 97.9) that is characteristic for the attachment of the glucosyl moiety to a tertiary alcohol (Zhou et al., 1981; Mohamed et al., 1994). In general, the absolute configuration of the chiral center C-3 could not be determined because of the location of both a double bond and a quaternary chiral center (C-4) vicinal to it. The negative FAB-MS spectrum of **5** exhibited M^+ at *m/z* 331 $[M–H]^-$ as well as a significant peak at *m/z* 169 $[M–H\text{-glucose}]^-$. Consequently the structure of compound **5** was assigned as *p*-menth-1-ene-3, 4-diol 4-*O*-β-glucopyranoside.

3. Experimental

^1H and ^{13}C NMR (TMS as int. standard): 400 MHz and 100 MHz respectively were recorded on a Jeol JNM α-400 spectrometer. FAB MS spectra were taken on a Jeol JMS-SX 102 spectrometer by direct inlet method at an ionizing voltage of 70 eV MPLC: RP-18 column (20 mm i.d. ×40 cm); flow rate of mobile phase 3 ml/min. HPLC: D-ODS-5 and polyamine columns (each 20 mm i.d. ×25 cm, YMC) with a Toyo Soda high speed chromatograph HLC-803 D pump and a Tosoh refraction index (RI-8) detector; flow rate of mobile phase 6 ml/min, injection vol. 0.8–1.0 ml. On the ODS column, 60% MeOH (I) and 55% MeOH (II) were used while 90% MeCN (III) was used on the polyamine column. CC: Kieselgel 60 (70–230 mesh, Merck) and Diaion HP 20 (Mitsubishi). TLC: silica gel 60 precoated plates F-254 and HPTLC using RP-18 precoated plates, F-254 s (Merck).

3.1. Plant material

The aerial parts (stems and leaves) of *O. syriacum* L. (Lamiaceae) were collected from Saint Kathrine, Sinai desert, Egypt in May 1997. The plant was identified by Dr. Salah El-Naggar, Department of Botany, Faculty of Science, Assiut University, Assiut, Egypt. A voucher specimen is deposited at the Herbarium of Department of Pharmacognosy, Faculty of Pharmacy, Assiut University, Assiut, Egypt.

3.2. Extraction and isolation of compounds (*1–5*)

The air-dried powdered aerial parts of *O. syriacum* (2 kg) were extracted with 70% EtOH. The dried ethanolic extract (450 g) was suspended in H_2O and deffated with CH_2Cl_2. The aq. fr. was applied to a column of Diaion HP-20 and eluted with H_2O, MeOH and acetone successively. The MeOH eluate (30 g) was chromatographed by silica gel CC using CH_2Cl_2–MeOH–H_2O (85:15:1) and finally with (70:30:3) to give 5 fractions. Fraction 2 (500 mg) was separated by MPLC on RP-18 using 65% MeOH and HPLC using ODS column and solvent I to afford compounds **1** (white powder, 90 mg), **2** (white powder, 40 mg) and **5** (white powder, 15 mg). Fraction 3 (350 mg) was subjected to HPLC using first ODS column with solvent II and then Polyamine column with solvent III to give compounds **3 (**white powder, 60 mg) and **4** (white powder, 40 mg).

3.2.1. Compound (*1*)

Thymoquinol 2-*O*-β-glucopyranoside, HR FAB-MS (negative) *m/z*: 327.1469 $[M–H]^-$ $C_{16}H_{23}O_7$ (req. 327.1444). ^{13}C NMR (C_5D_5N, Table 1). ^1H NMR (C_5D_5N): δ 7.50 (1H, *s,* H-3), 7.10 (1H, *s*, H-6), 5.40 (1H, *d*, $J=6.8$ Hz, H-1 Glc), 3.82 (1H, *m*, H-8), 2.40 (3H, *s*, Me-7), 1.21 and 1.20 (each 3H, *d*, $J=6.1$ and 6.6 Hz, respectively, Me-9 and 10).

3.2.2. Compound (*1a*)

Thymoquinol, ^{13}C NMR (C_5D_5N, Table 1). ^1H NMR (C_5D_5N): δ 7.20 (1H, *s,* H-3), 7.10 (1H, *s*, H-6), 3.70 (1H, *m*, H-8), 2.40 (3H, *s*, Me-7), 1.30 (6H, *d*, $J=7.1$ Hz, Me-9 and 10).

3.2.3. Compound (*2*)

Thymoquinol 5-*O*-β-glucopyranoside, HR FAB-MS (negative) *m/z*: 327.1419 $[M–H]^-$ $C_{16}H_{23}O_7$ (req. 327.1444). ^{13}C NMR (C_5D_5N, Table 1). ^1H NMR (C_5D_5N): δ 7.60 (1H, *s,* H-3), 7.0 (1H, *s*, H-6), 5.40 (1H, *d*, $J=6.4$ Hz, H-1 Glc), 3.60 (1H, *m*, H-8), 2.40 (3H, *s*, Me-7), 1.32 (6H, *d*, $J=6.8$ Hz, Me-9 and 10).

3.2.4. Compound (*3*)

Thymoquinol 2,5-*O*-β-diglucopyranoside, $[\alpha]_D^{25}$ −12.5° (MeOH; c 1.20). HR FAB–MS (negative) *m/z*: 489.1955 $[M–H]^-$ $C_{22}H_{33}O_{12}$ (req. 489.1972). ^{13}C NMR (C_5D_5N, Table 1). ^1H NMR (C_5D_5N): δ 7.60 (1H, *s,* H-3), 7.50 (1H, *s*, H-6), 5.47 (1H, *d*, $J=7.3$ Hz, H-1 Glc), 5.46 (1H, *d*, $J=6.8$ Hz, H-1′ Glc), 3.80 (1H, *m*, H-8), 2.40 (3H, *s*, Me-7), 1.26 and 1.21 (each 3H, *d*, $J=7.1$ Hz, Me-9 and 10).

3.2.5. Compound (*4*)

Carvacrol 2-*O*-β-glucopyranosyl-(1→2)-β-glucopyranoside, $[\alpha]_D^{25}$ −25.1° (MeOH; c 1.60). HR FAB–MS (negative) *m/z*: 473.2058 $[M–H]^-$ $C_{22}H_{33}O_{11}$ (req. 473.2023). ^{13}C NMR (C_5D_5N, Table 1). ^1H NMR

(C_5D_5N): δ 7.40 (1H, *bs,* H-3), 7.04 (1H, *d*, $J=8$ Hz, H-6), 6.76 (1H, *bd*, $J=7.6$ Hz, H-5), 5.60 (1H, *d*, $J=7.2$ Hz, H-1 Glc), 5.50 (1H, *d*, $J=7.6$ Hz, H-1′ Glc), 2.80 (1H, *m*, H-8), 2.50 (3H, *s*, Me-7), 1.16 and 1.15 (each 3H, *d*, $J=6.8$ Hz, Me-9 and 10).

3.2.6. Compound (*5*)

p-Menth-1-ene-3,4-diol 4-*O*-β-glucopyranoside, $[\alpha]_D^{25}$ −18.9° (MeOH; *c* 1.50). HR FAB–MS (negative) *m*/*z*: 331.1758 $[M-H]^-$ $C_{16}H_{27}O_7$ (req. 331.1757). ^{13}C NMR (C_5D_5N, Table 1). ^1H NMR (C_5D_5N): δ 5.50 (1H, *bs,* H-2), 5.16 (1H, *d*, $J=8.0$ Hz, H-1 Glc), 4.70 (1H, *bs*, H-3), 3.90 (1H, *m*, H-8), 1.80–2.20 (4H, *m*, H-5 and 6), 1.50 (3H, s, H-7), 0.87 (6H, *d*, $J=6.8$ Hz, Me-9 and 10).

3.2.7. Enzymatic hydrolysis of compound *1*

Compound **1** (20 mg) was dissolved in 0.5 ml MeOH and a solution of β-glucosidase (100 mg) in 20 ml water was added. The mixture was extracted with diethyl ether (3 times ×20 ml) after stirring at 37 °C for 2 days. The combined ethereal extracts were evaporated and the residue was purified by HPLC using 95% MeCN on polyamine column to afford the aglycone **1a** (6 mg). Compounds **2** and **3** have been subjected to same procedure as **1** to afford the aglycone **1a**.

Acknowledgements

The authors are grateful to the Japan Society for Promotion of Science (JSPS) and a Grant-in-Aid, Ministry of Education and Culture, Japan for the financial support of this work. Also, we would like to thank the Research Center of Molecular Medicine of the Hiroshima University School of Medicine, Japan, for NMR measurements.

References

Afsharypuor, S., Ebrahim, S., Erfan, M., 1997. Volatile constituents of *Origanum vulgare* ssp. *Viride* (Syn. *O. heracleoticum*) from Iran. Planta Medica 63, 179–180.

Akgul, A., Bayrak, A., 1987. Constituents of essential oils from *Origanum* species growing wild in Turkey. Planta Medica 53 (4), 114.

Assaf, M.H., Ali, A.A., Makboul, A.M., Beck, J.P., Anton, R., 1987. Preliminary study of phenolic glycosides from *Origanum majorana*, quantitative estimation of arbutin, cytotoxic activity of hydroquinone. Planta Medica 53 (4), 343–345.

Bradbury, H., Jenkins, J., 1984. Determination of the structures of trisaccharides by ^{13}C-NMR spectroscopy. Carbohydr. Res. 126, 125–156.

Breitmaier, E., Voelter, W., 1987. Carbon-13 NMR spectroscopy, 3rd. Edition. Verlagsgesellschaft mbH: Weinheim, Germany, D-6940.

Chiej, R., 1984. The Macdonald Encyclopedia of Medicinal Plants. Macdonald Co. Ltd, London, pp. 212–297.

Gunther, E., 1949. The Essential Oils, Vol. 3, 535. Van Nostrand Co, New York.

Halim, A.F., Mashaly, M.M., Zaghloul, A.M., Abdel-Fattah, H., De Potter, H.L., 1991. Chemical constituents of the essential oils of *Origanum syriacum* and *Stachys aegyptiaca*. International Journal of Pharmacognosy 29 (1), 1–5.

Harvala, C., Menounos, P., Argyriadou, N., 1987. Essential oil from *Origanum dictamnus*. Planta Medica 53 (4), 107–109.

Kotb, F., 1985. Medicinal plants in Libya, 632, Arab Encyclopedia House.

Laswell, W, Hufford, C., 1977. Aromatic constituents from *Uvaria chamae*. Phytochemistry 16, 1439–1441.

Metwally, M., Dawidar, A., Metwally, S., 1986. A new thymol derivative from *Pulicaria undulata*. Chemical Pharmaceutical Bulletin 34 (1), 378–379.

Mohamed, K., Ohtani, K., Kasai, R., Yamasaki, K., 1994. Dolabellane diterpene glucosides from *Chrozophora obliqua*. Phytochemistry 37, 495–500.

Ravid, U., Putievsky, E., 1983. Essential oils of *Majorana syriaca*, *Coridothymus capitatus* and *Satureja thymbra* plants growing wild in Israel. Planta Medica 49, 248–249.

Sarer, E., Schefler, J., Baerheim, S., 1982. Monoterpenes of the essential oil of *Origanum majorana*. Planta Medica 46, 236–239.

Sendra, J.M., Cunat, P., 1980. Volatile constituents of Spanish *Origanum* (*Coriandothymus capitatis*) essential oil. Phytochemistry 19, 89–92 and 1513–1517.

Tackholm, V., 1974. Students Flora of Egypt, 2nd edn., 562. Cooperative Printing Co, Beirut.

Yahara, S., Sakamoto, C., Nohara, T., Niiho, Y., Nakajima, Y., Ito, H., 1993. Thymoquinol 5-*O*-beta-D-glucopyranoside, kaempferol 3-*O*-beta-rutinoside and protocatechuic acid from fruit of *Scisandrae chinensis*. Shoyakugaku zassi 47 (4), 420–422.

Zechmeister, L., 1979. Progress in the Chemistry of Organic Natural Products, Vol. 36, 24. Springer-Verlag, Wien, New York.

Zhou, J., Wu, M., Taniyasu, S., Besso, H., Tanaka, O., Saruwatari, Y., Fuwa, T., 1981. Dammarane saponins of Sanchi-ginseng, root of *Panax notoginseng* (Burk.) F. H. Chen (Araliaceae): structures of new saponins, notoginsenosides-R1 and -R2, and identification of ginsenosides-Rg2 and Rh-1. Chemical Pharmaceutical Bulletin 29, 2844–2850.

PERGAMON

Phytochemistry 58 (2001) 1153–1157

PHYTOCHEMISTRY

www.elsevier.com/locate/phytochem

Clerodane-type diterpenes from the seed pods of *Hymenaea courbaril* var. *stilbocarpa*

Raquel T. Nogueira[a], George J. Shepherd[b], Antonio Laverde Jr.[a], Anita J. Marsaioli[a], Paulo M. Imamura[a,*]

[a]*Instituto de Química, UNICAMP, CP 6154, Campinas, 13083-970, SP, Brazil*
[b]*Instituto de Biologia, UNICAMP, Brazil*

Received in revised form 6 June 2001

Abstract

Three known and two new diterpenes were isolated from the ethyl acetate extract of *Hymenaea courbaril* var. *stilbocarpa* seed pods. One of the compounds was elucidated as (5*R**,8*S**,9*S**,10*R**)-cleroda-3,13*E*-dien-15-oic acid and the other was elucidated, after treatment with diazomethane, as methyl (5*S**,8*S**,9*S**,10*R**)-cleroda-3,13*E*-dien-15-oate. The known diterpenes were identified as (−)-ozic acid, (−)-isoozic acid and (−)-kovalenic acid which were characterized as their methyl ester derivatives. © 2001 Elsevier Science Ltd. All rights reserved.

Keywords: *Hymenaea courbaril* var. *stilbocarpa*; Clerodane; Diterpenes

1. Introduction

Hymenaea (*Caesalpinoideae*, Ditareae) is a genus widely distributed from Central to South America, mainly in the Amazon basin (Lee and Langenheim, 1975). The trunk exudes a resin, which is locally used in folk medicine for treatment of wounds, bronchitis and stomach disorders (Marsaioli et al., 1975; Corrêa, 1984). Analgesic and anti-inflammatory activities were also reported for the hydroalcoholic extract of the bark (Neves et al., 1993). The "jatoba" fruits, a commonly used name, provides a large quantities of proteic flour containing soluble and insoluble fibers; it was recently used in the preparation of high-fiber content snacks (Chang et al., 1998). *Hymenaea* species are known to mainly contain diterpenes of the *enantio*-labdanoic type in the trunk resin and bark extract (Nakano and Djerassi, 1961; Cunningham et al., 1973,1974; Marsaioli et al., 1975; Imamura et al., 1977), and *ent*-halimane diterpenes in the seed pod resin (Khoo et al., 1973). Searching for new source of diterpenes to be used as starting material in organic synthesis (Costa et al., 1999), we have investigated the composition of the seed pod resin of *H. courbaril* var. *stilbocarpa* Hayne and have succeed in isolating three of the known diterpenes and two new clerodanes, (−)-(5*R**, 8*S**,9*S**,10*R**)-cleroda-3,13*E*-dien-15-oic acid (**4**) and (−)-(5*S**,8*S**,9*S**,10*R**)-cleroda-3,13*E*-dien-15-oic acid, the latter being characterized as a methyl ester derivative **5b**.

2. Results and discussion

The ethyl acetate extract of *H. courbaril* var. *stilbocarpa* seed pods was submitted to a combination of column chromatography (silica gel), preparative TLC on $SiO_2/AgNO_3$ (5%) and RP-HPLC to afford three known and two new diterpenoid acids **4** and **5a**. The three known diterpenes were characterized as methyl ester derivatives: methyl (−)-ozate (**1**) {$[\alpha]_D^{20}$ −39.5° (*c* 7.0, $CHCl_3$)}, (Stipanovic et al., 1979); methyl (−)-isoozate (**2**) {$[\alpha]_D^{20}$ −23.0° (*c* 1.2, $CHCl_3$)}, (Khoo et al 1973) and methyl (−)-kovalenate (**3**) {$[\alpha]_D^{20}$ −58.0° (*c* 0.7, $CHCl_3$)}, (Hara et al., 1995). (Fig. 1).

Compound **4** was obtained as a colorless oil, $[\alpha]_D^{20}$ −61.0° (*c* 0.4, $CHCl_3$) and the HREIMS gave a $[M]^+$ at *m*/*z* 304.23205 corresponding to a molecular formula $C_{20}H_{30}O_3$ (calc. 304.24023). The ^1H NMR spectra of **4** and **3** showed similar features except for the presence of a singlet at δ 3.70 assigned to the methoxyl group of **3**

* Corresponding author. Tel.: +55-19-788-3065; fax; +55-19-788-3023.

E-mail address: imam@iqm.unicamp.br (P.M. Imamura).

0031-9422/01/$ - see front matter © 2001 Elsevier Science Ltd. All rights reserved.
PII: S0031-9422(01)00303-X

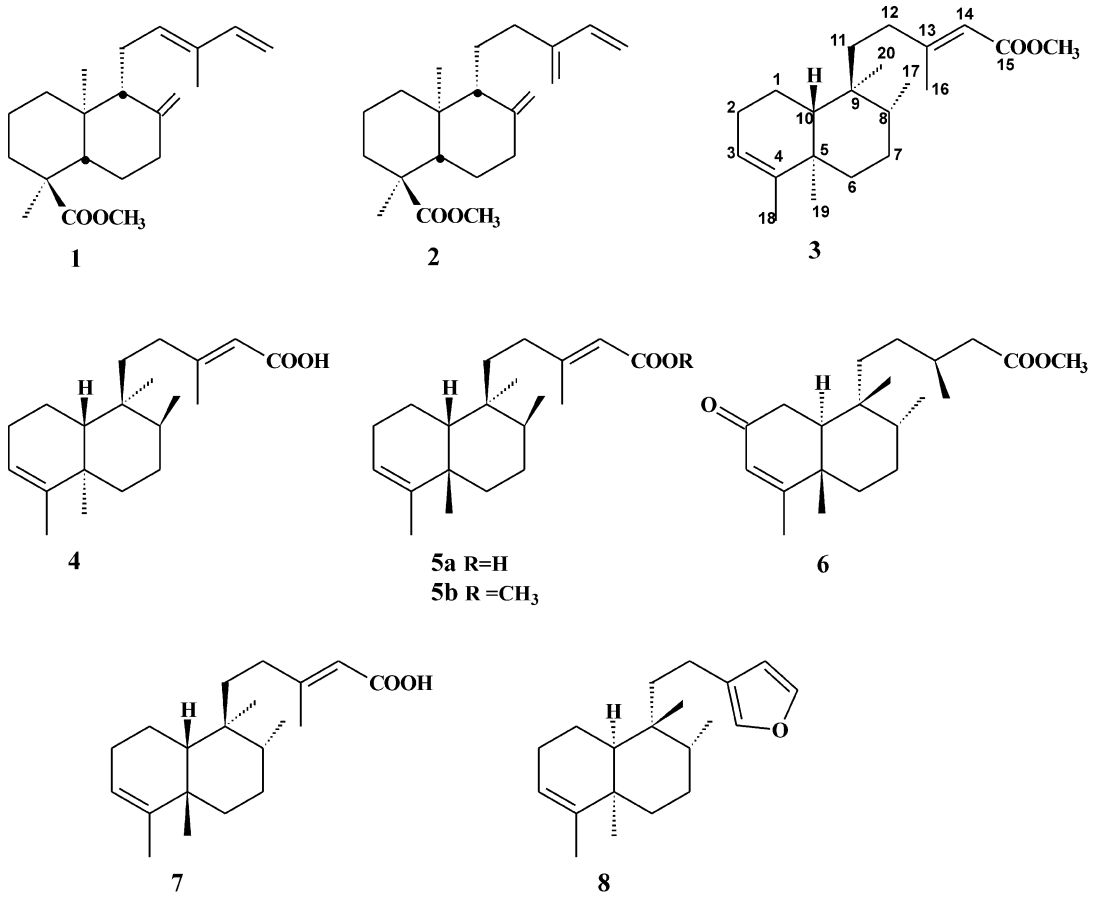

Fig. 1.

and a slight deshielding of the signals at δ 0.94 (*s*, H-20) and 0.95 (*d*, $J=6.0$ Hz, H-17) of **4** when compared with those of **3** [δ 0.73 (*s*, H-20) and δ 0.82 (*d*, $J=6.0$ Hz), H-17]. The remaining characteristic signals of **4** at δ 1.05 (*s*, H-19), 1.59 (*bd*, $J=1.5$ Hz, H-18) and 2.19 (*d*, $J=1.2$ Hz, H-16), δ 5.20 (*bs*, H-3) and 5.71 (*bd*, $J=0.9$ Hz, H-14) had similar chemical shift with those of **3**. From this first analysis we concluded that both compounds shared equal diterpene skeletons with different ring B relative configurations.

The full ^{1}H and ^{13}C NMR signal assignments were based on homonuclear and heteronuclear 2D NMR experiments (COSY-90, HETCOR, COLOC) (Table 1). The COSY-90 contour plot displayed cross peaks between H-14 at δ 5.71 and H-16 at δ 2.19 and H-12 at δ 2.13. The latter also correlates with the diastereotopic methylene hydrogens of C-11 at δ 1.16 and δ 1.55. Thus with all side chain hydrogens fully assigned, the corresponding carbon chemical shifts were easily obtained by one bond $^{1}H/^{13}C$ chemical shift correlations. (Table 1). To establish ring A ^{1}H and ^{13}C connectivities we have taken H-3 (δ 5.20) as safe entry point. The cross peaks in the COSY spectrum confirmed that hydrogen H-3 is coupled to hydrogens at δ 1.59 and δ 2.04 and according to the HETCOR spectrum, they correspond to C-18 methyl group (δ 18.0) and H-2 (δ 26.8). The COLOC plot proves the existence of a long range $^{1}H,^{13}C$ coupling between the quaternary C-4 (δ 144.4) and H-18 (δ 1.59) and H-19 (δ 1.05) which correspond to C-18 (δ 18.0) and C-19 (δ 20.6), respectively. All other signals not yet assigned were identified analogously (Table 1). The *trans* relationship at the AB ring juncture was first inferred from the chemical shift of C-19 at δ 20.6 (δ 33.2 for *cis* fusion) (Lopes et al., 1987) and the spatial proximity between H-19 and H-20 was inferred from the cross peak in the phase sensitive NOESY spectrum (Fig. 2).

A γ-gauche interaction between C-17 (axial, δ 14.8) and C-6 (δ 30.1) was invoked to explain the C-6 shielding ($\Delta\delta=-6.7$) of **4** in comparison with the corresponding carbon of **3** (δ 36.8, C-17 equatorial). There is also a good agreement between the C-6 chemical shifts of **4** (δ 30.1) and 2-oxo-3-cleroden-15-oic acid **(6)** (δ 29.1) (Urones et al., 1991), which has the same relative stereochemistry at C-5, C-8, C-9 and C-10. Therefore, the suggested structure for **4** is (5*R**,8*S**,9*S**,10*R**)-cleroda-3,13*E*-dien-15-oic acid.

Compound **5a** was obtained as colorless crystals, mp 175–178 °C, and its decomposition was prevented by methylation with diazomethane. It was therefore characterized as the methyl ester **5b**, an oil $[\alpha]_{D}^{20}$ −65.0° (*c* 1.1,

Table 1
^1H and ^{13}C NMR spectral data for **4** and **5b** in $CDCl_3$ (300 MHz)

Position	**4**		**5b**	
	δ_C (ppm)	δ_H (ppm)	δ_C (ppm)	δ_H (ppm)
1	17.9 (CH_2)	1.43 *m*	20.0 (CH_2)	1.59 *m*; 1.78 *m*
2	26.8 (CH_2)	2.04 *m*	25.8 (CH_2)	1.97 *m*
3	120.2 (CH)	5.20 *bs*	122.5 (CH)	5.34 *bs*
4	144.4 (C)		142.0 (C)	
5	37.6 (C)		38.7 (C)	
6	30.1 (CH_2)	1.43 *m*	32.2 (CH_2)	1.52 *m*; 1.64 *m*
7	25.5 (CH_2)	1.31 *m*; 1.95 *m*	27.2 (CH_2)	1.42 *m*
8	35.1 (CH)	1.65 *m*	37.5 (CH)	1.58 *m*
9	38.8 (C)		38.8 (C)	
10	45.1 (CH)	1.43 *m*	44.7 (CH)	1.42 *m*
11	37.5 (CH_2)	1.16 *m*; 1.55 *m*	35.9 (CH_2)	1.25 *m*; 1.88 *dt* (J = 13.9 and 5.9 Hz)
12	34.8 (CH_2)	2.13 *m*	35.2 (CH_2)	2.04 *dt* (J = 13.9 and 5.9 Hz); 2.18 *dt* (J = 13.9 and 5.9 Hz)
13	164.0 (C)		162.1 (C)	
14	114.3 (CH)	5.71 *bd* (J = 0.9 Hz)	114.7 (CH)	5.69 *d* (J = 1.2 Hz)
15	170.7 (C)		167.4 (C)	
16	19.5 (CH_3)	2.19 *d* (J = 1.2 Hz)	19.2 (CH_3)	2.18 *d* (J = 1.2 Hz)
17	14.8 (CH_3)	0.95 *d* (J = 6.0 Hz)	15.4 (CH_3)	0.86 *d* (J = 6.0 Hz)
18	18.0 (CH_3)	1.59 *bd* (J = 1.5 Hz)	19.4 (CH_3)	1.64 *dd* (J = 3.5 and 1.9 Hz)
19	20.6 (CH_3)	1.05 *s*	27.7 (CH_3)	1.15 *s*
20	20.4 (CH_3)	0.94 *s*	26.4 (CH_3)	1.03 *s*
OCH_3			50.8 (CH_3)	3.70 *s*

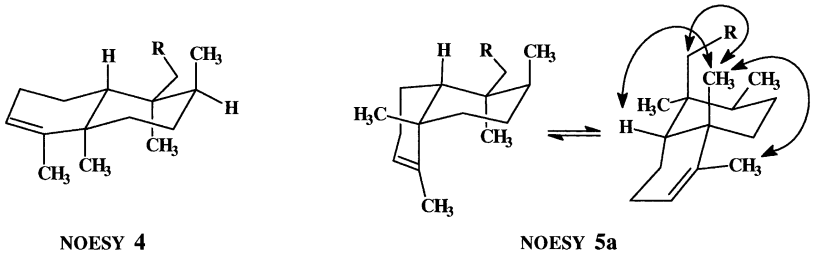

Fig. 2. Significant correlation in the NOESY spectrum of **4** and **5a**.

$CHCl_3$). The HREIMS gave a $[M]^+$ at m/z 318.25581 corresponding to a molecular formula $C_{21}H_{32}O_3$ (calc. 318.25588). The ^1H NMR spectrum of **5b** was very similar to those of **3** and **4**, except for the deshielding of H-18 (δ 1.64), H-19 (δ 1.15), H-20 (δ 1.03) and shielding of H-17 (δ 0.86) when compared with those of **4**. (Table 1).

The complete assignments of the ^1H and ^{13}C signals of **5b** were based on homonuclear and heteronuclear 2D experiments (COSY-90, HETCOR, COLOC) (Table 1), and by comparison with the ^{13}C NMR spectra of **4** which depicted major differences in the chemical shift of the carbons belonging to the decalin moiety.

Owing to the C-20 and C-17 methyl resonance differences in **5a** ($\Delta\delta_C = 11.0$) and **4** ($\Delta\delta_C = 5.6$), *cis*-decalin and *trans* decalin, respectively, we proposed that both compounds share the same *trans* methyl relationship. Moreover a literature survey revealed that compounds **3** (*trans* decalin) and **7** (*cis* decalin) possessing a *cis* relationship between C-20 and C-17 displayed a $\Delta\delta \sim 2$, therefore, corroborating the proposed C-20/C-17 *trans* relationship in compound **5b**. The *cis* relationship at the AB ring juncture was first inferred from the C-19 chemical shift (δ 27.7). The relative configuration at C-5 and C-10 was confirmed by nOe enhancements arising from the dipolar interaction between H-19 (δ 1.15) and H-10 (δ 1.42). The spatial proximity between H-19 (δ 1.15), H-10 (δ 1.42), H-11 (δ 1.88, 1.25) was confirmed by cross peaks between these signals in the NOESY experiment of the underivatized acid. The proximity of H-19 and H-11 is due to the flexibility of *cis*-decalin system for A/B rings of **5** as shown in Fig. 2. Finally, the structure of **5b** was established as methyl (−)-(5*S**,8*S**,9*S**,10*R**)-cleroda-3,13*E*-dien-15-oate. This conclusion was corroborated by comparison of ^1H NMR spectroscopic data of **5b** with those reported for **8**, a solidagoic acid derivative (Anthonsen et al., 1973) that has the same relative stereochemistry at C-5, C-8, C-9 and C-10. The chemical shifts of the methyl groups at δ 1.17 for C-19, 1.08 for C-20 and 0.92 for C-17, are in good agreement with those

observed for **5b**, which appeared, respectively, at δ 1.15, 1.03 and 0.86. As far as we know, this is the first report of clerodane diterpenes in *Hymenaea*, the co-occurrence of *cis*- and *trans*-clerodanes is also noteworthy.

Taking into consideration that the absolute configuration of **3** has already been established (Caputo and Mangoni, 1974), and that **3, 4** and **5b** have been isolated from the same extract, we tentatively propose that the absolute configuration of **4** is (−)-(5*R*,8*S*,9*S*,10*R*)-cleroda-3,13*E*-dien-15-oic acid and that of **5b** is (−)-(5S,8S,9S,10R)-cleroda-3,13*E*-dien-15-oic acid with both acids belonging to the same enantiomeric series as depicted in Fig. 1.

3. Experimental

3.1. General

^{1}H and ^{13}C NMR spectra were recorded in $CDCl_3$ solution at 300 MHz and 75.5 MHz, respectively, with a Bruker AC 300/P spectrometer (internal standard TMS). IR spectra of neat samples were measured with a Perkin-Elmer 1600 series FTIR. Mass spectra of purified compounds were recorded with a Hewlett-Packard 5890 GC equipped with a Model 5970 mass-selective detector. Elemental analyses were performed with a Perkin-Elmer 2400 CHN analyzer. Optical rotations were measured with a Carl Zeiss photoelectric polarimeter.

3.2. Isolation

The seed pods of *H. courbaril* var. *stilbocarpa* were collected in August 1993 at Fazenda Santa Elisa (IAC—Campinas). A voucher specimen was deposited in the Herbarium of IB-UEC (No. GS 01/02). Dry seed pods (668.4 g) were pulverized and soaked in EtOAc (31) for 5 days at room temperature, with occasional shaking. Filtration and solvent evaporation at reduced pressure produced a crude extract (60.0 g) as a viscous oily resin. Acid and base extraction furnished the acidic (41.0 g) and the neutral fraction (17.0 g). A sample of the acidic fraction (712 mg) was submitted to preparative TLC on SiO_2/5% $AgNO_3$ eluting four times with benzene: EtOAc (9:1; v/v) to afford two fractions which were immediately esterified with CH_2N_2 to furnish the corresponding methyl esters **1** (10 mg) and **2** (17 mg), respectively. A third fraction containing a mixture of, at least 4 compounds was also obtained. This fraction was submitted to further purification on a HPLC semi-preparative μ-Bondpack C-18 column (250 mm×10 mm×5 μm, Waters) and eluted with MeOH–H_2O (85:15) containing 1% of formic acid to furnish four fractions. The first fraction containing an oil, was esterified with diazomethane to furnish compound **3** (22 mg). Two other fractions containing compound **4** (6 mg) and **5a** (14 mg) were obtained. Due to instability observed for the latter, this acid was esterified with excess of diazomethane and characterized as a methyl ester **5b**.

3.3. (−)-(5R,8S,9S,10R)-Cleroda-3,13E-dien-15 oic acid (*4*)

$[\alpha]_D^{20}$ −61.0° (*c* 0.4, $CHCl_3$); HREIMS *m*/*z*: 304.23205 $[M]^+$ (calc. 304.24023 for $C_{20}H_{32}O_2$); IR ν_{max}^{film} cm^{-1}: 3600–3200, 1690, 1638; ^{1}H NMR: Table 1; ^{13}C NMR: Table 1.

3.4. Methyl (−)-(5S,8S,9S,10R)-cleroda-3,13E-dien-15 oate (*5b*)

$[\alpha]_D^{20}$ −65.0 (*c* 1.1, $CHCl_3$); HREIMS *m*/*z*: 318.25581 $[M]^+$ (calc. 318.25588 for $C_{21}H_{34}O_2$); IR ν_{max}^{film} cm^{-1}: 1721, 1648, 1150; ^{1}H NMR: Table 1; ^{13}C NMR: Table 1.

Acknowledgements

This work was performed with financial support of FAPESP. R.T.N. thanks CAPES and FAEP/UNICAMP for fellowship and A.L.J. for CNPq. We also thank Dr. L.H.B. Baptistella for helpful discussion.

References

Anthonsen, T., Henderson, M.S., Martin, A., Murray, R.D.H., McCrindle, R., McMaster, D., 1973. Constituents of *Solidago* species. Part IV. Solidagoic acids A and B, diterpenoids from *Solidago gigantea* var. *serotina*. Canadian Journal of Chemistry 51, 1332–1345.

Caputo, R., Mangoni, L., 1974. Diterpenes from *Araucaria bidwilli*. Phytochemistry 13, 467–470.

Chang, Y.K., Silva, M.R., Gutkoski, L.C., Sebio, L., Da Silva, M.A.A.P., 1998. Development of extruded snacks using jatobá (*Hymenaea stigonocarpa* Mart) flour and cassava starch blends. Journal of the Science of Food and Agriculture 78, 59–66.

Corrêa, M.P., 1984. Dicionário de Plantas Úteis do Brasil, Ministério da Agricultura, IBDF. Imprensa Nacional, Rio de Janeiro,. pp. 593-599.

Costa, M., Tanaka, C.M.A., Imamura, P.M., Marsaioli, A.J., 1999. Isolation and synthesis of a new clerodane from *Echinodorus grandiflorus*. Phytochemistry 50, 117–122.

Cunningham, A., Martin, S.S., Langenheim, J.H., 1973. Resin acids from two Amazonian species of *Hymenaea*. Phytochemistry 12, 633–635.

Cunningham, A., Martin, S.S., Langenheim, J.H., 1974. Labd-13-en-8-ol-15-oic acid in trunk resin of Amazonian *Hymenaea courbaril*. Phytochemistry 13, 294–295.

Hara, N., Asaki, Y., Gupta, Y.K., Singh, A.K., Sahai, M., 1995. Clerodane and *ent*-halimane diterpenes from *Polyalthia longifolia*. Phytochemistry 38, 189–194.

Imamura, P.M., Marsaioli, A.J., Barata, L.E.S., Rúveda, E.A., 1977. ^{13}C NMR spectral analysis of Eperuane diterpenes. Phytochemistry 16, 1842–1844.

Khoo, S.F., Oehlschlager, A.C., Ourisson, G., 1973. Structure and stereochemistry of the diterpenes of *Hymenaea courbaril* (Caesalpinoideae) seed pod resin. Tetrahedron 29, 3379–3388.

Lee, Y.T., Langenheim, J.H., 1975. Systematics of the genus *Hymenaea* L. (Leguminosae, Caesalpinioideae, Detarieae). Chemistry of California Press Ltd. 69, 1–109.

Lopes, L.M.X., Bolzani, V.daS., Trevisan, L.M., 1978. Clerodane diterpenes from *Aristolochia* species. Phytochemistry 26, 2781–2784.

Marsaioli, A.J., Leitão Filho, H.F., de Campello, J.P., 1975. Diterpenes in bark of *Hymenaea courbaril*. Phytochemistry 14, 1882–1883.

Nakano, T., Djerassi, C., 1961. Terpenoids. XLVI. Copalic acid. Journal of Organic Chemistry 26, 167–173.

Neves, M.C.A., Neves, P.C.A., Zanini, J.C., Medeiros, Y.S., Yunes, R.A., Calixto, J.B., 1993. Analgesic and antiinflammatory activities of the crude hydroalcoholic extract obtained from the bark of *Hymenaea martiana*. Phytotherapy Research 7, 356–362.

Stipanovic, R.D., O'Brien, D.H., Rogers, C.E., Thompson, T.E., 1979. Diterpenoid acids, (−)-*cis* and (−)-*trans*-ozic acid, in wild sunflower, *Helianthus occidentalis*. Journal Agricultural Food Chemistry 27, 458–459.

Urones, J.G., Basabe, P., Marcos, I.S., Martín, D.D., Jiménez, V., Sexmero, M.J., Gómez, B., Slawin, A.M.Z., Williams, D.J., 1991. (5*S*,8*R*,9*R*,10*S*,13*S*)-2-Oxo-3-cleroden-15-oic acid from *Cistus palinhae*. Phytochemistry 30, 3471–3473.

PERGAMON

Phytochemistry 58 (2001) 1159–1166

PHYTOCHEMISTRY

www.elsevier.com/locate/phytochem

Deoxyarteannuin B, dihydro-deoxyarteannuin B and *trans*-5-hydroxy-2-isopropenyl-5-methylhex-3-en-1-ol from *Artemisia anuua*

Lai-King Sy, Geoffrey D. Brown*

Chemistry Department, The University of Hong Kong, Pokfulam Rd., Hong Kong

Received 4 May 2001; received in revised form 16 July 2001

Abstract

The amorphane sesquiterpenes, deoxyarteannuin B and dihydro-deoxyarteannuin B, were isolated from *Artemisia annua* and their structures mainly determined by two-dimensional NMR spectoscopic analyses. The irregular monoterpene, *trans*-5-hydroxy-2-isopropenyl-5-methylhex-3-en-1-ol, was also characterized in the same way, and its structure was confirmed by synthesis from lavandulol. All of these natural products are suggested to be formed by autoxidation reactions. Full assignments of the ^{1}H and ^{13}C resonances for the known natural products *epi*-deoxyarteannuin B and isoannulide, determined by the same methodology, are also reported. © 2001 Elsevier Science Ltd. All rights reserved.

Keywords: *Artemisia annua* L.; Compositae; Sesquiterpene; Monoterpene; Deoxyarteannuin B; Dihydro-deoxyarteannuin B; *Epi*-deoxyarteannuin B; Isoannulide; *trans*-5-Hydroxy-2-isopropenyl-5-methylhex-3-en-1-ol; 2D-NMR

1. Introduction

Artemisia annua L. (Compositae) is the source of the important anti-malarial drug artemisinin (Haynes and Vonwiller, 1997). Extensive phytochemical investigation of this species has resulted in the isolation of a large number of cadinane and amorphane sesquiterpenes over the past two decades (Sy et al., 1998), in addition to artemisinin itself. Most of the natural products reported from this species have been characterized by NMR spectroscopic analyses (Agrawal et al., 1991; Marsaioli et al., 1994; Karle and Lin, 1995; Agrawal and Bishnoi, 1996). We now report the isolation and structure determination, by 2D-NMR, of three new constituents from *A. annua*, deoxyarteannuin B (**1**), dihydro-deoxyarteannuin B (**2**) and *trans*-5-hydroxy-2-isopropenyl-5-methylhex-3-en-1-ol (**11**).

2. Results and discussion

Extensive HPLC separation of a relatively non-polar fraction from the CH_2Cl_2 extract of *A. annua* yielded the new sesquiterpene **1**. The base peak in the mass spectrum of **1** occurred at m/z 232, corresponding to the molecular formula $C_{15}H_{20}O_2$ as evidenced by high-resolution mass spectrometry. The IR spectroscopic analysis was consistent with the presence of a five-membered lactone ring (ν 1751 cm^{-1}), while ^{13}C/DEPT NMR spectra confirmed the presence of fifteen carbon atoms with twenty protons directly attached (Table 1). The structure of **1**, therefore, contains six double bond equivalents, of which two are already accounted for by the lactone ring. A further two equivalents were identified as being due to carbon-carbon double bonds as indicated by the characteristic resonances observed in the ^{13}C and ^{1}H NMR spectra (δ_C 142.5, 139.9, 118.8 and 116.8 ppm and δ_H 6.10, 5.36 and 5.13 ppm). One of these double bonds in compound **1** was shown to be a γ-substitutent on the butyrolactone ring by HSQC (Tables 1 and 2), HMBC (Fig. 2) and ^{1}H–^{1}H COSY experiments (in particular by correlations observed from C-7 to H-13a/b, C-11 to H-13a and C-12 to H-13a in HMBC and by a weak correlation seen in ^{1}H–^{1}H

* Corresponding author. Tel.: +852-2859-7915; fax: +852-2857-1586.

E-mail address: gdbrown@hkucc.hku.hk (G.D. Brown).

0031-9422/01/$ - see front matter © 2001 Elsevier Science Ltd. All rights reserved.
PII: S0031-9422(01)00358-2

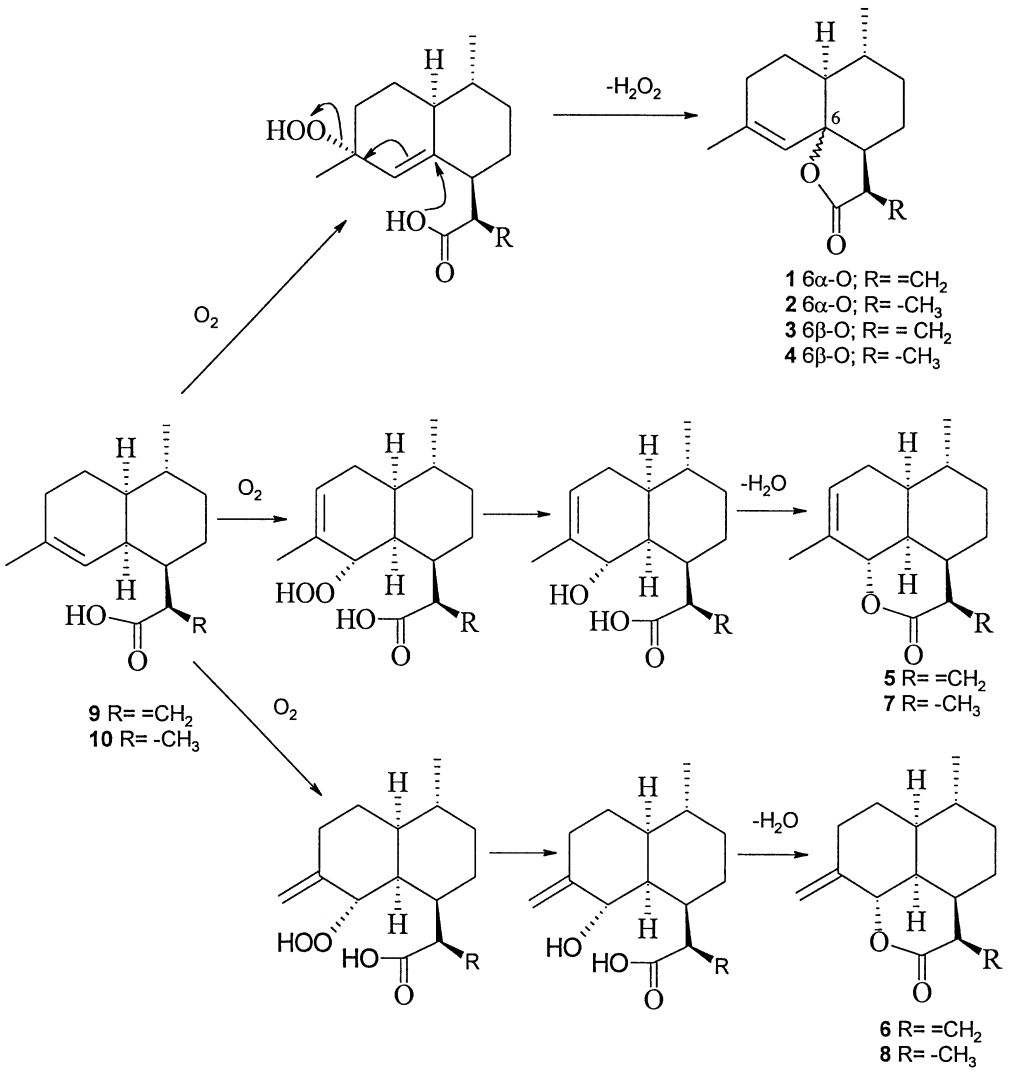

Scheme 1. Proposed biogenesis of sesquiterpenes **1–8** from autoxidation reactions of arteannuic acid (artemisinic acid) (**9**) and dihydroartemisinic acid (**10**) in *A. annua*.

COSY from H-7 to H-13a/b, which corresponds to a small allylic coupling). The second double bond was shown to be substituted by a methyl group by HMBC correlations from C-3, C-4 and C-5 to H-15, and the tri-substituted nature of this double bond was confirmed by a weak correlation observed in ^{1}H–^{1}H COSY from H-5 to H-3. The remaining two double bond equivalents required in the structure of **1** were then identified as being due to two fused six-membered rings by strong correlations observed in the ^{1}H-^{1}H COSY spectrum between successive pairs of vicinal protons around the amorphane skeleton of **1** (from H-3 "clockwise" as far as H-7). Following complete assignment of all the ^{1}H resonances for **1**, the relative stereochemistry was determined by NOESY correlations, which showed the decalin ring to be *cis*-fused.

In addition, the 11,13-dihydro analog of **1**, dihydrodeoxyarteannuin B (**2**), was isolated from the same extract, and was fully characterized by 2D-NMR spectroscopic analysis in the same way as **1**. The known compounds, *epi*-deoxyarteannuin B (**3**) and dihydro-*epi*-deoxyarteannuin B (**4**), were also obtained and are epimeric with **1** and **2** at the 6-position. Although compound **3** was reported on several occasions, both as a natural product from *A. annua* (Roth and Acton, 1987; El-Feraly et al., 1989; Brown, 1992) and through synthesis (Jung et al., 1987), full NMR spectral assignments for compound **3** are reported for the first time in Tables 1 and 2. These data support the structure proposed for **1**. Previously published 2D-NMR assignments for **4** (Brown, 1992; Sy et al., 1998) are reproduced for completeness and to allow comparison with the assignments of **2**.

Through repeated HPLC, isoannulide (**5**) was also isolated from this extract of *A. annua*. This natural product was described previously only as a mixture with annulide (**6**) (Brown, 1993), and there was some uncertainty regarding the ^{13}C and ^{1}H NMR spectral assignments for **5** as a result. Complete and unambiguous NMR spectral assignments for **5** are presented for the

first time in Tables 1 and 2. A minor revision to the previous ^{13}C assignments for the alkene carbons of annulide (**4**) is reported, based on 2D-NMR analysis. The assignments established for annulide and isoannulide (Tables 1 and 2) are consistent with those recently reported for their 11,13-dihydro analogues, arteannuins J (**7**) and I (**8**) (Sy et al., 1998).

Although deoxyarteannuin B (**1**) was not reported previously as a secondary metabolite, it is known as a synthetic product. Thus, Acton and Roth (1989) obtained **1** together with its 6-epimer, *epi*-deoxyarteannuin B (**3**), as products from the photo-oxygenation of arteannuic acid (**9**). However, Jung et al. (1987) isolated only *epi*-deoxyarteannuin B (together with

Table 1
^{13}C NMR spectroscopic assignments[a,b] for sesquiterpenes **1–6**

Position	1	2	3	4	5	6
1 (CH)	44.8	46.7	44.2	46.6	40.9	42.7
2 (CH_2)	19.9	20.1	21.6	21.0	26.9	28.7
3 (CH_2)	26.1	26.1	31.0	30.8	124.1 (CH)	29.3
4 (C)	142.5	142.3	141.3	142.2	130.5	145.3
5 (CH)	118.8	120.5	123.8	121.8	74.7	75.5
6 (C)	89.4	86.7	83.4	83.2	39.4 (CH)	43.3 (CH)
7 (CH)	52.5	49.8	44.9	42.8	38.6	40.3
8 (CH_2)	22.1	22.0	28.5	23.4	30.5	30.5
9 (CH_2)	34.3	35.3	29.9	32.4	34.9	34.8
10 (CH)	30.7	30.7	28.4	29.6	29.0	27.9
11 (C)	139.9	39.0 (CH)	142.9	39.7 (CH)	140.0	139.1
12 (C)	170.8	180.6	170.6	179.4	166.7	165.1
13 (CH_2)	116.8	13.2 (CH_3)	120.7	9.4 (CH_3)	129.2	129.1
14 (CH_3)	19.8	19.9	20.0	19.6	20.2	20.0
15 (CH_3)	23.6	24.1	23.2	23.8	18.5	106.5 (CH_2)

[a] Multiplicity of ^{13}C determined from DEPT.
[b] ^{13}C connected to ^{1}H by a single bond determined from HSQC.

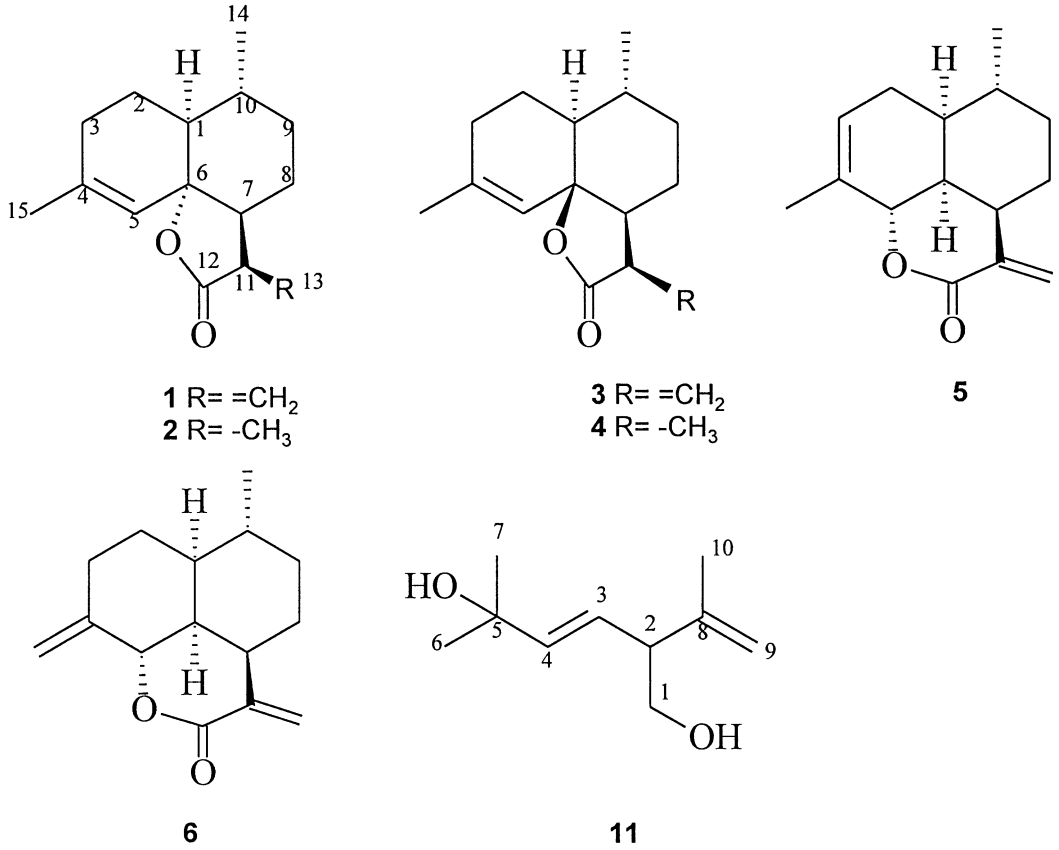

Fig. 1. Sesquiterpenes and monoterpenes isolated from *A. annua*.

arteannuin B) from this reaction, and El-Feraly et al. (1989) found that oxidation of arteannuic acid, using a variety of chemical reagents, yielded only *epi*-deoxyarteannuin B. We speculate that **1–8** may be biogenetically derived from the ene-type reactions of molecular oxygen with the tri-substituted double bond in **9/10** as shown in Scheme 1 (Roth and Acton, 1989). This hypothesis is based on our general ideas concerning the autoxidation chemistry of terpenes (Sy and Brown, 1999). More specifically, we have previously presented results regarding the biogenetic origins of several sesquiterpene metabolites of *A. annua* from hydroperoxides which are derived from autoxidation of the $\Delta^{4,5}$-double bond of dihydroartemisinic acid (**10**) (Sy et al., 1998, 1999).

In addition to the amorphane sesquiterpenes **1–6**, the irregular monoterpene **11** was also isolated from more polar fractions. *trans*-5-Hydroxy-2-isopropenyl-5-methylhex-3-en-1-ol (**11**) is apparently a new natural product, although its 1-acetate was reported previously from a *Lavandula* oil (Belsten et al., 1972). The structure of this irregular monoterpene was determined by 2D-NMR (Fig. 2; Tables 3 and 4). Thus, correlations between vicinal protons in the ^{1}H–^{1}H COSY spectrum

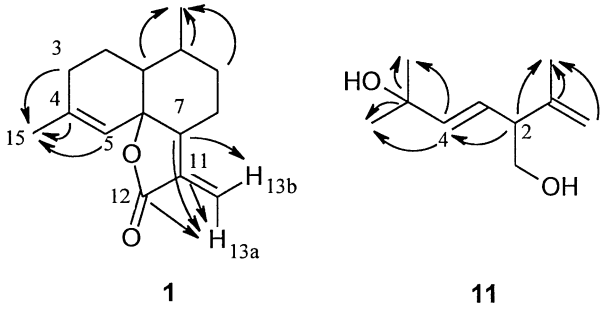

1 **11**

Fig. 2. HMBC correlations, indicated by arrows from ^{13}C to ^{1}H used in determining the planar structures of **1** and **11**.

Table 2
^{1}H NMR spectroscopic assignments[a] for sesquiterpenes **1–6**

Position	1	2	3	4	5	6
1	1.66	1.53	1.25 (*ddd*, 13.0, 10.7, 2.9)	1.26	1.52	1.56
2α	2.04 (*dddd*, 18.1, 10.2, 6.9, 2.7)	2.03	1.86	1.89	2.22	1.45
2β	1.84	1.80	1.67	1.68	2.22	2.04
3α	1.94	2.03	2.10 (*dd*, 18.1, 6.2)	2.10	5.46 (*dd*, 1.6, 1.6)	2.26 (*ddd*, 13.9, 3.4, 3.4)
3β	1.94	1.93	2.03	2.06		2.17 (*dd*, 13.9, 13.0)
5	5.13 (*t*, 1.5)	5.53 (s)	5.28 (*br* s)	5.64	4.88 (*d*, 10.5)	5.03 (*d*, 11.9)
6	–	–	–	–	2.19	2.01
7	2.66 (*dddd*,11.7, 2.7, 2.7, 1.5)	2.19 (*ddd*, 12.5, 9.0, 2.5)	2.71 (*dd*, 6.9, 6.9)	2.11	2.68 (*ddd*, 11.6, 5.1, 5.1)	2.66 (*ddd*, 11.9, 5.5, 5.5)
8α	1.93	1.68	1.89	1.73	1.79	1.69
8β	1.35 (*dddd*, 12.6, 12.6, 11.7, 3.9)	1.44	1.38	1.18	1.69	1.69
9α	1.18 (*dddd*, 12.6, 12.6, 12.6, 3.7)	1.16	1.12	1.06	1.13 (*dddd*, 12.3, 12.3, 12.3, 3.9)	1.17 (*dddd*, 12.5, 12.5, 12.5, 3.7)
9β	1.80	1.82	1.67	1.67	1.78	1.85
10	1.56	1.55	1.56	1.42	1.31	1.70
11	–	2.74 (*dq*, 9.0, 8.0)	–	3.15	–	–
13[b]	6.10 (*d*, 3.2)	1.35 (3H, *d*, 8.0)	6.17 (*d*, 1.0)	1.14	6.52 (*dd*, 1.3, 1.3)	6.51 (*s*)
13[c]	5.36 (*d*, 3.2)		5.56 (*d*, 1.0)		5.63 (*dd*, 1.3, 1.3)	5.60 (*s*)
14	1.00 (3H, *d*, 6.4 Hz)	0.96 (3H, *d*, 6.2)	0.97 (3H, *d*, 6.6)	0.93	0.88 (3H, *d*, 6.2)	0.92 (3H, *d*, 6.4)
15	1.67 (3H, *s*)	1.70 (3H, *s*)	1.67 (3H, *s*)	1.69	1.82 (3H, s)	5.20 (*ddd*, 1.8, 1.6, 1.6)[d] 4.88 (*ddd*, 1.8, 1.8, 1.8)[e]

[a] Integral (if not 1H), multiplicities and coupling constants (*J* in units of Hz) indicated in parentheses when clearly seen in 1-D ^{1}H -NMR.
[b] ^{1}H *syn* with carbonyl group.
[c] ^{1}H *anti* to carbonyl group.
[d] ^{1}H *syn* with lactone ring.
[e] ^{1}H *anti* to lactone ring.

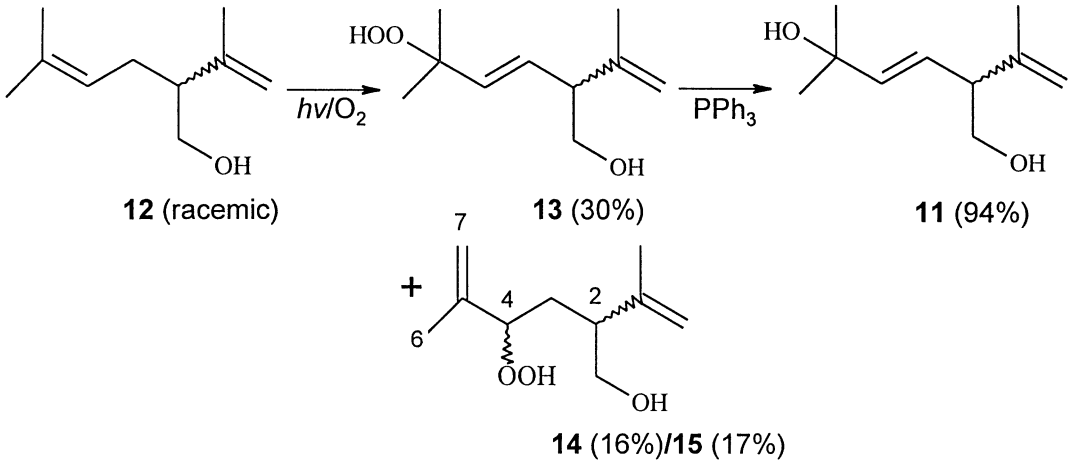

Scheme 2. Biomimetic synthesis of **11** from racemic **12** via the tertiary allylic hydroperoxide **13**.

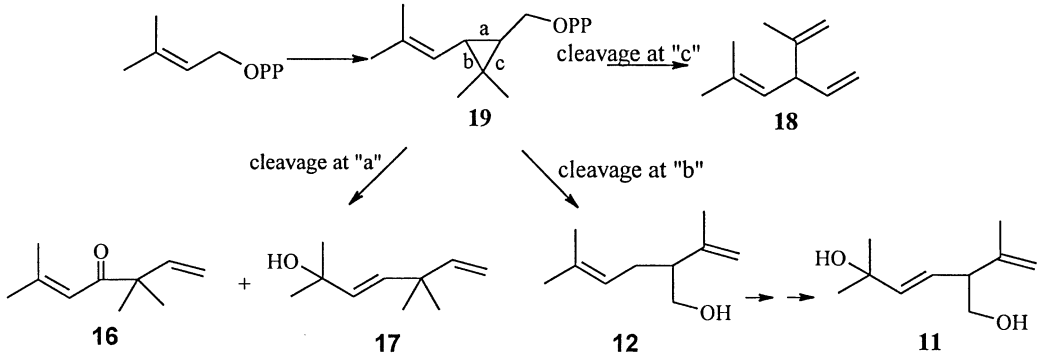

Scheme 3. Proposed biogenesis of three classes of irregular monoterpenoids from the genus *Artemisia*.

of **11** indicated that the molecule contained a "core" consisting of a (HO)CH_2–CH–CH=CH spin system, while correlations observed in the HMBC spectrum indicated the location of 2-isopropylidene and 2-isopropanol "substituents" at C-2 and C-4 respectively. It was thought that **11** was derived from the monoterpene lavandulol (**12**) (Banthorpe et al., 1977) by spontaneous autoxidation reactions occurring in the plant. In order to confirm the structure proposed for compound **11** from 2D-NMR spectral analysis, a "biomimetic synthesis", in which racemic lavandulol was first subjected to photo-oxygenation was performed. This resulted in the three allylic hydroperoxides (**13–15**) which are expected from the ene-type reaction of singlet oxygen with the trisubstituted double bond in lavandulol. Reduction of the tertiary allylic hydroperoxide **13** by triphenylphosphine (Scheme 2) afforded an allylic alcohol with identical NMR spectra to the natural product **11**.

Several other irregular monoterpenes were reported previously from the genus *Artemisia* including the artemisinanes, artemisia ketone (**16**) and yomogi alcohol (**17**), and the santolinane, santolinatriene (**18**). The occurrence of the lavandulane skeleton in *A. annua*, as exemplified by **11**, is consistent with previous proposals that all three irregular monoterpene skeletons may be derived from the common precursor, chrysanthemyl pyrophosphate (**19**) (Scheme 3), by cleavage reactions associated with each of the three carbon-carbon bonds of a cyclopropyl ring (Banthorpe et al., 1977; Charlwood and Charlwood, 1991).

Table 3
^{13}C NMR spectroscopic assignments for monoterpenes **11** and **13–15**

Position	δ_C[a]			
	11	**13**	**14**	**15**
1 (CH_2)	63.6	63.7	63.9	64.2
2 (CH)	52.2	52.3	45.7	46.4
3 (CH)	125.3	130.1	29.7 (CH_2)	31.5 (CH_2)
4 (CH)	140.7	136.4	87.5	87.2
5 (C)	70.7	81.9	143.0	144.1
6 (CH_3)	29.93[b]	24.7[b]	16.9	17.5
7 (CH_3)	29.87[b]	23.7[b]	115.2 (CH_2)	113.7 (CH_2)
8 (C)	145.0	144.4	144.4	144.6
9 (CH_2)	112.5	112.1	114.1	114.2
10 (CH_3)	20.7	21.1	19.5	19.5

[a] ^{13}C and ^{1}H connected by a single bond deduced from HSQC.
[b] Interchangeable within column.

Table 4
^{1}H NMR spectroscopic assignments for monoterpenes **11** and **13–15**

Position[a,b]	**11**	**13**	**14**	**15**
1	3.67 (*dd*, 10.7, 7.5)	3.71 (*dd*, 10.7, 5.9)	3.55	3.55
	3.59 (*dd*, 10.7, 7.1)	3.60 (*dd*, 10.7, 7.9)	3.55	3.55
2	2.90 (*ddd*, 7.5, 7.5, 7.1)	2.90 (*ddd*, 8.2, 7.9, 5.9)	2.31 (*dddd*, 8.9, 6.4, 6.4, 5.5)	2.51 (*dddd*, 8.9, 6.6, 6.6, 5.7)
3	5.58 (*dd*, 15.8, 7.5)	5.58 (*dd*, 16.5, 8.2)	1.70 (*ddd*, 14.0, 8.9, 6.2)	1.67 (*ddd*, 14.9, 9.6, 5.7)
			1.58 (*ddd*, 14.0, 7.8, 5.5)	1.54 (*ddd*, 14.9, 8.9, 3.7)
4	5.75 (*d*, 15.8)	5.68 (*d*, 16.5)	4.34 (*dd*, 7.8, 6.2)	4.33 (*dd*, 9.6, 3.7)
5	–	–	–	–
6	1.33 (3H, *s*)	1.32 (3H, *s*)[c]	1.74 (3H, *dd*, 1.6, 0.9)	1.76 (3H, *d*, 1.6)
7	1.33 (3H, *s*)	1.36 (3H, *s*)[c]	5.04 (*dq*, 1.6, 1.6)[d]	5.00 (*q*, 1.6)[d]
			5.01 (*dq*, 1.6, 0.9)[e]	5.02 (*s*)[e]
8	–	–	–	–
9	4.92 (*s*)[d]	4.88 (*dd*, 1.4, 1.4)[d]	4.97 (*dq*, 1.6, 1.6)[d]	4.99 (*q*, 1.6)[d]
	4.82 (*s*)[e]	4.78 (*s*)[e]	4.83 (*dq*, 1.6, 0.9)[e]	4.89 (*s*)[e]
10	1.73 (3H, *s*)	1.73 (3H, *s*)	1.72 (3H, *dd*, 1.6, 0.9)	1.72 (3H, *d*, 1.6)
–OH		2.65 (*br s*)		
–OOH		8.87 (*br s*)	8.27 (*br s*)	8.27 (*br s*)

[a] ^{13}C and ^{1}H connected by a single bond deduced from HSQC.
[b] Integral (if not 1H), multiplicities and coupling constants (*J* in units of Hz) indicated in parentheses when clearly seen in 1-D ^{1}H-NMR
[c] Interchangeable within column.
[d] ^{1}H *syn* with methyl group in isopropenyl substituent.
[e] ^{1}H *anti* to methyl group in isopropenyl substituent.

3. Experimental

Chemical shifts are expressed in ppm (δ) relative to TMS as internal standard. Proton chemical shifts, multiplicities, coupling constants, and integrals reported in this section are those which are clearly resolved in one-dimensional ^{1}HNMR without recourse to 2D-NMR analysis (see Tables 1 and 2 for 2D-NMR results). All NMR experiments were run on a Bruker DRX 500 instrument. HSQC and HMBC spectra were recorded with 1024 data points in F_2 and 256 data points in F_1. High-resolution MS were recorded in EI mode at 70 e.v. on a Finnigan-MAT 95 MS spectrometer. IR spectra were recorded in $CHCl_3$ on a Shimadzu FTIR-8201 PC instrument. Column chromatography was performed using silica gel 60–200 μm (Merck). HPLC separations were performed using a Varian chromatograph equipped with RI star 9040 and UV 9050 detectors and a YMC diol column, 20 mm×25 cm column, flow rate 8 ml/minute.

3.1. Plant material

A. annua plants were grown outdoors from seeds supplied by the NCCPG *Artemisia* collection (31 Smith Street, Elsworth, Cambridge, CB3 8HY, UK). Taxonomically verified specimens are held by the collection. Mature plants were harvested in April, 3–4 months after sowing, when they were just beginning to come into flower.

3.2. Extraction and isolation

The fresh aerial parts of *A. annua* (266 g) were ground to a fine powder under liquid nitrogen and then extracted with CH_2Cl_2. The organic extract was dried ($MgSO_4$) and solvent removed on a rotary evaporator to yield an aromatic dark green gum (1.77 g, 0.67% w/w) which was subjected to repeated HPLC separation. Compound **1** (1 mg) was obtained from HPLC in 18% EtOAc/*n*-hexane (R_t 12.5 min), then from

HPLC in 7% EtOAc/*n*-hexane (R_t 18.1 min); compound **2** (0.5 mg) was obtained from HPLC in 18% EtOAc/*n*-hexane (R_t 13.8 min), then from 5% EtOAc/*n*-hexane (R_t 26.6 min); compound **3** (2 mg) was obtained from HPLC in 18% EtOAc/*n*-hexane (R_t 12.5 min), then from 7% EtOAc/*n*-hexane (R_t 17.6 min); compound **4** (15 mg) was obtained from HPLC in 18% EtOAc/*n*-hexane (R_t 12.5 min), then from 7% EtOAc/*n*-hexane (R_t 18.4 min); compound **5** (1 mg) was obtained from HPLC in 18% EtOAc/*n*-hexane; (R_t 13.1 min), then from 7% EtOAc/*n*-hexane (R_t 26.6 min); compound **6** (4 mg) was obtained from HPLC in 18% EtOAc/*n*-hexane (R_t 13.1 min), then from 7% EtOAc/*n*-hexane (R_t 27.3 min); compound **11** (1 mg) was obtained from HPLC in 50% EtOAC/*n*-hexane/1%CH_3COOH (R_t 17.0 min), then from 26% EtOAc/*n*-hexane/0.7%CH_3COOH (R_t 42.0 min).

3.3. Deoxyarteannuin B (*1*)

Oil. IR ν_{max} ($CHCl_3$) cm^{-1}: 3020, 2930, 2855, 1751, 1456; ^1H NMR: see Table 2; ^{13}C NMR: see Table 1; HREIMS: *m/z* (rel. int.) 232.1466 [M^+, $C_{15}H_{20}O_2$, requires 232.1463] (100), 217 (25), 187 (70), 173 (33).

3.4. Dihydro-deoxyarteannuin B (*2*)

Oil. IR ν_{max} ($CHCl_3$) 3026, 2934, 2874, 1761, 1456 cm^{-1}; ^1H NMR: see Table 2; ^{13}C NMR: see Table 1; HREIMS: *m/z* (rel. int.) 234.1613 [M^+, $C_{15}H_{22}O_2$, requires 234.1620] (19), 219 (4), 190 (91), 161 (100).

3.5. Epi-deoxyarteannuin B (*3*)

See Brown (1992) and Roth and Acton (1987) for physical properties other than NMR spectral analyses. Full ^1H and ^{13}C NMR assignments are given in Tables 1 and 2.

3.6. Dihydro-epi-deoxyarteannuin B (*4*)

See Sy et al., 1998 for physical properties; NMR assignments in Tables 1 and 2 reproduced from this reference.

3.7. Isoannulide (*5*)

See Brown (1993) for physical properties other than NMR spectral analyses. Full ^1H and ^{13}C NMR assignments are given in Tables 1 and 2.

3.8. Annulide (*6*)

See Brown (1993) for physical properties other than NMR spectral analyses. Full ^1H and ^{13}C NMR assignments are given in Tables 1 and 2.

3.9. Trans-5-hydroxy-2-isopropenyl-5-methylhex-3-en-1-ol (*11*)

Oil. IR ν_{max} ($CHCl_3$) cm^{-1}: 3591, 3406 (*br*), 3011, 2976, 2936, 2882, 1645, 1454, 1375; ^1H NMR: see Table 4; ^{13}C NMR: see Table 3; HREIMS: *m/z* (rel. int.) 152.1173 [M^+-H_2O, $C_{10}H_{16}O$, requires 152.1201] (17), 134.1083 [M^+–$2H_2O$, $C_{10}H_{14}$ requires 134.1096] (25), 122 (70), 119 (35), 107 (100).

3.10. Photo-oxygenation of lavandulol

To a solution of (±)-lavandulol (2-isopropenyl-5-methyl-hex-4-en-1-ol, *ex*. Fluka, Cat. No. 61735) in acetone (310 mg/30 ml) was added methylene blue (5 mg) and the mixture was irradiated by a strong light source (500 W tungsten bulb) for 2 h in an ice bath. The solvent was removed on a rotary evaporator, and the residue was taken up into Et_2O, filtered to remove the photosensitizer, and solvent removed to yield a crude product (300 mg; 97% w/w) which was separated by HPLC (35% EtOAc/*n*-hexane) into compound **13** (114 mg, 30%; R_t 58.0 min); compound **14** (58 mg, 16%; R_t 41.3 min); and compound **15** (62 mg, 17%; R_t 46.7 min).

3.11. trans-5-hydroperoxy-2ξ-isopropenyl-5-methylhex-3-en-1-ol (*13*)

Oil. IR ν_{max} ($CHCl_3$) cm^{-1} 3530, 3350 (*br*), 3011, 2982, 1645, 1456, 1379; ^1H NMR: see Table 4; ^{13}C NMR: see Table 3; HREIMS: *m/z* (rel. int.) 168.1147 [M^+–H_2O, $C_{10}H_{16}O_2$, requires 168.1150] (3), 153 (12), 150 (11), 137 (54), 122 (75), 107 (100).

3.12. 4ξ-Hydroperoxy-2ξ-isopropenyl-5-methylene-hexan-1-ol (*14*)

Oil. IR ν_{max} ($CHCl_3$) cm^{-1}: 3528, 3329 (*br*), 3013, 2943, 1645, 1447, 1377; ^1H NMR: see Table 4; ^{13}C NMR: see Table 3; HREIMS: *m/z* (rel. int.) 168.1152 [M^+-H_2O, $C_{10}H_{16}O_2$ requires 168.1150] (13), 153 (30), 151 (36), 150 (100), 148 (28), 135 (35), 107 (65).

3.13. 4ξ-Hydroperoxy-2ξ-isopropenyl-5-methylene-hexan-1-ol (*15*)

Oil. IR ν_{max} ($CHCl_3$) cm^{-1}: 3524, 3310 (*br*), 3012, 2945, 1645, 1447, 1377; ^1H NMR: see Table 4; ^{13}C NMR: see Table 3; HREIMS: *m/z* (rel. int.) 186.1258 [M^+, $C_{10}H_{18}O_3$, requires 186.1256] (0.5), 150 (12), 137 (12), 122 (20), 121 (28), 107 (100).

3.14. Reduction of allylic hydroperoxide *13*

To a solution of compound **13** in MeOH (46.4 mg/10 ml) was added PPh_3 (65 mg) and the reaction mixture

was stirred for 3 h at room temperature. Solvent was removed under reduced pressure, and the crude residue subjected to CC (45% EtOAC, *n*-hexane) to yield compound **11** (40 mg, 94%), with identical spectroscopic properties to the natural product *trans*-5-hydroxy-2-isopropenyl-5-methylhex-3-en-1-ol isolated from *A. annua*.

Acknowledgements

We thank the Generic Drug Research Programme of the University of Hong Kong for providing a post-doctoral fellowship to Dr. Jaclyn Sy. Seeds of *A. annua* were kindly supplied by Dr. J. Twibel of the NCCPG *Artemisia* collection. This project was funded by a grant from the Committee on Research and Conference Grants (CRCG).

References

Acton, N., Roth, R.J., 1989. Synthesis of *epi*-deoxy- and deoxy-arteannuin B. Phytochemistry 28, 3530–3531.

Agrawal, P.K., Bishnoi, V., 1996. Sesquiterpenes from *Artemisia annua*: ^{13}C NMR shielding behaviour. J. Sci. Ind. Res. 55, 17–26.

Agrawal, P.K., Vishwakarma, R.A., Jain, D.C., Roy, R., 1991. High field NMR spectroscopic studies of arteannuin B and a reappraisal of the structure of arteannuin C. Phytochemistry 30, 3469–3471.

Banthorpe, D.V., Doonan, S., Gutowski, J.A., 1977. Biosynthesis of irregular monoterpenes in extracts from higher plants. Phytochemistry 16, 85–92.

Belsten, J.C., Bramwell, A.F., Burrell, J.W.K., Michalkiewicz, D.M., 1972. Structure and synthesis of a newly discovered terpenoid isolated from lavandin oil: *trans*-5-hydroxy-2-isopropenyl-5-methylhex-3-enyl-acetate. Tetrahedron 28, 3439–3440.

Brown, G.D., 1992. Two new compounds from *Artemisia annua*. J. Nat. Prod. 55, 1756–1760.

Brown, G.D., 1993. Annulide, a sesquiterpene lactone from *Artemisia annua*. Phytochemistry 32, 391–393.

Charlwood, B.V., Charlwood, K.A., 1991. Monoterpenoids. In: Dey, P.M., Harborne, J.B. (Eds.), Methods in Plant Biochemistry, Terpenoids. Academic Press, London.

El-Feraly, F.S., Al-Meshal, I.A., Khalifa, S.I., 1989. *epi*-Deoxyarteannuin B and 6,7-dehydroartemisinic acid from *Artemisia annua*. J. Nat. Prod. 52, 196–198.

Haynes, R.K., Vonwiller, S.C., 1997. From qinghaosu, marvelous herb of antiquity, to the antimalarial trioxane qinghaosu and some remarkable new chemistry. Acc. Chem. Res. 30, 73–79.

Jung, M., Yongyeol, Y., ElSohly, H.N., McChesney, J.D., 1987. J. Nat. Prod. 50, 972–973.

Karle, J.M., Lin, A.J., 1995. Correlation of the crystal structures of diastereoisomeric artemisinin derivatives with their proton NMR spectra in $CDCl_3$. Acta Cryst. B51, 1063–1068.

Marsaioli, A.J., Fujiwara, F.Y., Foglio, M.A., Sharapin, N., Zhang, J.-S., 1994. Proton and carbon-13 NMR and conformation in solution of some amorphanes (qinghaosu derivatives). Mag. Res. Chem. 32, 583–590.

Roth, R.J., Acton, N., 1987. Isolation of *epi*-deoxyarteannuin B from *Artemisia annua*. Planta Med. 576.

Roth, R.J., Acton, N., 1989. A simple conversion of artemisinic acid into artemisinin. J. Nat. Prod. 52, 1183–1185.

Sy, L.-K., Brown, G.D., Haynes, R., 1998. A novel endoperoxide and related sesquiterpenes from *Artemisia annua* which are possibly derived from allylic hydroperoxides. Tetrahedron 54, 4345–4356.

Sy, L.-K., Brown, G.D., 1999. Novel *seco*-cycloartanes from *Kadsura coccinea* and the assisted autoxidation of a tri-substituted alkene. Tetrahedron 55, 119–132.

Sy, L.-K., Ngo, K.-S., Brown, G.D., 1999. Biomimetic synthesis of arteannuin H and the 3,2-rearrangement of allylic hydroperoxides. Tetrahedron 55, 15127–15140.

PERGAMON

Phytochemistry 58 (2001) 1167–1170

PHYTOCHEMISTRY

www.elsevier.com/locate/phytochem

Taxines from the needles of *Taxus wallichiana*

Jeevan Kumar Prasain, Piotr Stefanowicz, Taira Kiyota, Farida Habeichi, Yasuo Konishi*

Biotechnology Research Institute, National Research Council Canada, 6100 Royalmount Avenue, Montreal, Quebec, Canada H4P 2R2

Received 9 March 2001; received in revised form 6 June 2001

Abstract

A taxine, 5α*O*-(3′-dimethylamino-3′-phenylpropionyl) taxinine M (**1**) together with two known compounds 7-*O*-acetyltaxine A (**2**) and 2α-acetoxy-2′β-deacetylaustrospicatine (**3**) were isolated from the needles of the Himalayan yew, *Taxus wallichiana* Zucc. Their structures were elucidated on the basis of the NMR spectral data, ESI–MS/MS analysis and chemical methods. Compounds **1** and **3** showed moderate cytotoxic activity against the lung cancer cell line A549 in vitro. © 2001 Elsevier Science Ltd. All rights reserved.

Keywords: *Taxus wallichiana*; Taxaceae; Taxine; Cytotoxic

1. Introduction

The emergence of paclitaxel (taxol) as one of the most useful anticancer natural products has stimulated great interest in analysis of *Taxus* species with a view to finding alternative sources of this compound. As a result, numerous taxoids have been reported from various *Taxus* species (Wani et al., 1971; Chen and Kingston, 1994; Zhang et al., 2000). The needles of the Himalayan yew (*Taxus wallichiana* Zucc., Taxaceae) is one of the valuable source of taxoids (Appendino et al., 1992; Chattopadhyay et al., 1999). Recently, a new taxane IDN5109, derived from 14β-hydroxy-10-deacetylbaccatin III, is reported to have a potent antitumor activity in ovarian carcinoma (Nicoletti et al., 2000). In course of our program to isolate bio-active taxoids from the needles of *Taxus wallichiana*, we isolated a new taxine 5α-*O*-(3′-dimethylamino-3′-phenylpropionyl) taxinine M (**1**). To the best of our knowledge, this is the first benzoate containing cytotoxic taxine belonging to taxagifine type. We report herein the structure elucidation of this minor compound together with its cytotoxic activity against the lung tumor cell line A549.

2. Results and discussion

The air-dried needles (1 kg) of *T. wallichiana* were extracted with EtOH, and the EtOH extract was dissolved in EtOAc and extracted with 10% HCl. Following an acid-base partition scheme, we isolated **1** (0.5 mg) along with two other known taxines, 7-*O*-acetyltaxine A (**2**) and 2α-acetoxy-2β-deacetylaustrospicatine (**3**). Purification of these compounds was performed by semi-preparative reversed phase HPLC.

Compound **1** was obtained as a colorless solid having $[\theta]_{308}^{25}$ 2500 (0.001 M, MeOH). The HR–FAB–MS showed an intense $[M+H]^+$ ion at *m*/*z* 862.36481 which corresponded to a molecular formula of $C_{46}H_{55}NO_{15}$. Low collision energy electrospray tandem mass spectrometric (ESI–MS/MS) analysis of this compound provided a series of product ions representing diterpene ring fragments and side chains. The product ion at *m*/*z* 194.1 corresponds to a loss of 193.1 Da from the *m*/*z* 861.8 to a product ion at *m*/*z* 668.7.

Further loss of three acetic acid molecules (3×60 Da), an acetyl group (42 Da), and a benzoic acid molecule (122 Da) produced an ion at *m*/*z* 324.9. There is an another series of product ions due the loss three molecules of acetic acid, an acetyl, and a benzoic acid molecule originating from the ion at *m*/*z* 668.7. From these fragmentation patterns, it was deduced that compound **1** has at least four acetyl groups, one benzoate, and a nitrogen containing side chain (193.2 Da).

The product ion at *m*/*z* 194.1 was further characterized by the MS/MS/MS experiment. Four product ions were observed at *m*/*z* 46, 79, 107 and 149 corresponding to $(CH_3)_2NH_2^+$, $[C_6H_7]^+$, $C_7H_6OH^+$ and $C_6H_5C_2H_2COOH_2^+$, respectively. Thus these data indicated the presence of an *N*-dimethyl phenyl propionate side chain in the molecule. Furthermore, the side chain was considered to be 3-(dimethylamino)-3-phenylpropionate

* Corresponding author. Tel.: +1-514-496-6339: Fax: +1-514-496-5143.

E-mail address: yasuo.konishi@nrc.ca (Y. Konishi).

0031-9422/01/$ - see front matter © 2001 Elsevier Science Ltd. All rights reserved.
PII: S0031-9422(01)00305-3

(Winterstein ester) in view of the biosynthesis of taxoid phenylisoserine side chain (Leete and Badem, 1966).

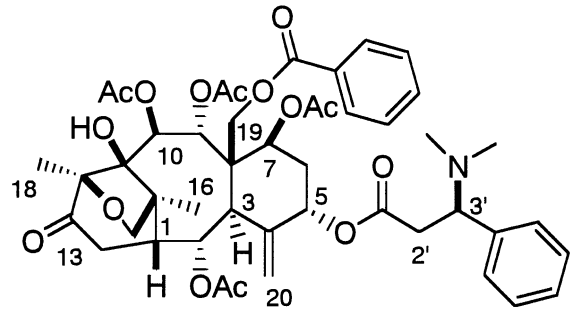

1

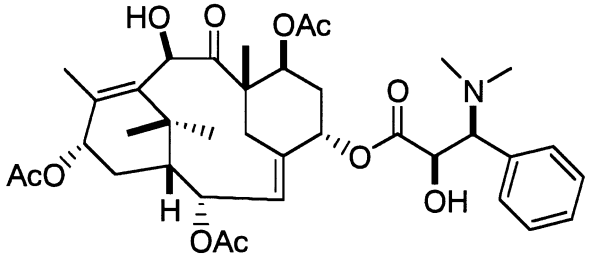

2

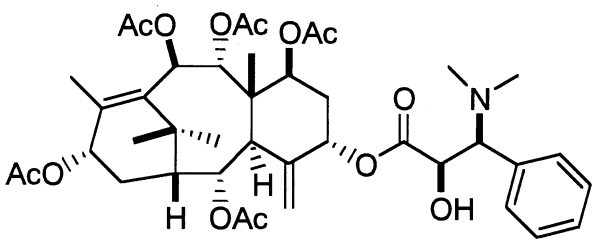

3

In order to confirm the structure of this side chain, 3-dimethylamino-3-phenylpropionic acid was synthesized by reacting 3-amino-3-phenylpropionic acid with formaldehyde and sodium borohydride. The MS/MS analysis of which produced product ions identical to those of the ion 194. Thus the presence of a Winterstein ester in **1** was concluded and remaining structure elucidation was performed by its NMR spectral analysis.

A part of the ^{1}H NMR spectrum of **1** in MeOH was similar to that of taxinine M (Beutler et al., 1991), indicating the presence of a tetracyclic structure with one isolated double bond, four acetates and one benzoate group (Table 1). The connectivities of the protons in the taxane skeleton of **1** were determined by its ^{1}H–^{1}H COSY spectrum. The ^{1}H NMR spectrum of **1** showed the presence of only two methyl groups (δ 1.15 *s* and 1.26 *s*) instead of four, which is common in many taxoids, and two oxymethylenes (δ 4.10, *d*, 7.9 Hz, 3.65, *d*, 8.0 Hz, and δ 5.19, *d*, 12.2 Hz, 4.37, *d*, 12.2 Hz).

The HMQC and HMBC spectra of **1** indicated the oxygenation at C-17, with the oxygen present as an oxido bridge to C-12. The carbonyl carbon (δ 205.7) showed a long range correlation with the methyl group (δ 1.15) which showed correlations with both C-12 and C-11 in the HMBC spectrum. Thus the carbonyl carbon was assigned at C-13. The long range correlation observed in the HMBC spectrum of **1** between H-19 and the benzoate carbonyl clearly indicated the position of benzoate group at C-19. Likewise, the H_2-20 showed correlations with both C-3 and C-5, indicating an exocyclic double bond at C-4. The presence of a Winterstein ester in **1** was supported by the signals at 2.88 (3H, *s*), 2.76 (3H, *s*), 3.78 (2H, *m*), 4.95 (1H, *m*), and 7.48 (5H, *m*) in the ^{1}H NMR spectrum. Since the compound was purified

Table 1
^{1}H and ^{13}C NMR spectroscopic data of **1**

Position	δ_C[a]	δ_H
1	48.1	2.48 *m*
2	69.5	6.11 *br d*, 10.2
3	40.0	3.42 *d*, 10.2
4	140.0	
5	76.0	5.23 *br s*
6	40.0	2.0 *m*
		1.55 *m*
7	64.0	5.34 *br d*, 6.2
8	49.7	
9	70.4	5.31 *d*, 3.0
10	64.0	5.29 *d*, 3.0
11	80.2	4.15 *br s*
12	91.4	
13	205.7	
14	34.5	3.10 *dd*, 11.5, 19.2
		2.65 *d*, 19.2
15	49.7	
16	15.4	1.26
17	82.2	4.10 *d*, 7.9
		3.65 *d*, 8.0
18	11.9	1.15 *s*
19	60.8	5.19 *d*, 12.2
		4.37 *d*, 12.2
20	116.7	5.49 *s*
		4.75 *s*
$N(Me)_2$	38.8	2.76 *s*
	42.3	2.88 *s*
19-O*CO*C6H5	167.5	
19-OBz (*ipso*)	130.1	
19-OBz (*ortho*)	130.1×2	8.12 *d*, 7.9
19-OBz (*meta*)	128.6×2	7.48 *m*
19-OBz (*para*)	133.7	7.58 *m*
1′	Ob	
2′	35.9	3.78 *m*
3′	65.9	4.95 *m*
3′-Ph (*ipso*)	141.0	
3′-Ph (*ortho*)	130.1	7.48 *m*
3′-Ph (*meta*)	128.6	7.48 *m*
3′-Ph (*para*)	128.6	7.48 *m*
Ac	168.0	
	168.0×2	
	172.2	
	21.2×2	1.97 *s*, 2.11 *s*
	20.5×2	1.97 *s*, 2.06 *s*

[a] The ^{13}C NMR data were deduced from the HMQC and HMBC spectra. Direct measurement of ^{13}C NMR was not possible due to the meager quantity of the sample. δ in ppm and *J* in Hz. Ob = obscure. 1D and 2D NMR experiments (500 MHz in $CDCl_3$).

by HPLC using acetonitrile/water/TFA system, the dimethylamino group was protonated and the ^{1}H NMR signals were found to be shifted more downfield than those of similar basic taxoids.

The stereochemistry of **1** around the diterpene skeleton was deduced by comparison with taxinine M, in view the similarity in splitting pattern (coupling constants) in the ^{1}H NMR, and NOESY correlations. As in the case of taxinine M, NOESY correlations were observed between the proton pairs H-3/H-10, H-9/Me-17, H-2/Me-17, OH-11/H*b*-16, and H*a*-16/Me-17. Moreover, transannular interactions between the pairs H-3/H-10, H-9/Me-17, H-2/Me-17 may occur because the internal space may be inadequate for all the quasi-axial hydrogen atoms to fit without interacting. In this situation, some of the carbon bonds adopt eclipsed or partially eclipsed conformations (March, 1992).

The small value (ca. 3 Hz) of $J_{9,10}$ is due to an eclipsed conformation around the C-9, C-10 bond causing H-9 and H-10 to adopt an anticlinal position (Barboni et al., 1995a,b). The conformation of ring B is in the taxagifine-type owing to the presence of the C-12, C-17 oxygen bridge and the large coupling constant between H-2 and H-3 (Table 1). The signal at δ 5.23 (1H, *br s*) was characteristic of H-5α (Shi et al., 1999). The coupling constant of H-7 (δ 5.34, *br d*, 6.2 Hz) was similar to that of taxinine M. The stereochemistry at the chiral centre C-3′ was assigned as *R* from the biosynthesis of Winterstein's acid (Leete and Badem, 1966). Based on these evidences, the sterochemistry of **1** was elucidated, and the isolate was determined to be 5α- *O*-(3′-dimethylamino-3′-phenylpropionyl) taxinine M.

Compounds **2** and **3** were identified as 7-*O*-acetyltaxine A and 2α-acetoxy-2′β-deacetylaustrospicatine, respectively by comparison of their spectral data with published ones (Ettouati et al., 1988; Barboni et al., 1995a,b). Compound **1** is a minor constituent of the needles of the Himalayan yew in which taxine's concentration might be much lower than in the European or the Japanese yew (Barboni et al., 1995a,b).

We, for the first time, have attempted to elucidate the structure of a taxine through MS/MS analyses. The MS/MS analyses revealed that compound **1** is composed of four major segments, i.e. a core diterpene ring, one benzoate, four acetate, and one Winterstein ester side chain. It is interesting to note that no taxines are reported to be of the taxagifine type and compound **1** represents the first example of the taxine with a taxagifine core structure and is the second example of a taxoid involving both a benzoate and the Winterstein ester (Kobayashi et al., 1996). This type of compound possesses a different diterpene ring conformation than those of the taxol type. The unusual conformation may be responsible for diminution in biological activity compared to taxol (Chauviére et al., 1982).

Compounds **1**–**3** were evaluated for their cytotoxicity against A549 cell line and **1** and **3** showed a cytotoxicity with ED_{50} 10.1±2.4 and 28.3±3.8 μM, respectively, while **2** was inactive.

Cytotoxicity of many taxines against cancer cells has not been fully investigated. Taxinine M is reported to show a weak toxicity in the brine shrimp assay (Beutler et al., 1991). The co-occurrence of an aromatic group and an alkaloid side chain in **1** may be responsible for its cytotoxicity against A549 cells by the fact that similar activity was observed with taxuspine N (Kobayashi et al., 1996). Further elaboration on structure–activity relationships of **1** is underway.

3. Experimental

3.1. General

CD spectra were recorded with a JASCO J-710 spectropolarimeter. Mass spectrometry measurements were performed by using a Sciex API III tandem quadrupole mass spectrometer. Full-scan mass spectra were obtained while continuously scanning from *m*/*z* 300 to 1000 with a step size of 0.1 *m*/*z* and with a dwell time of 2.0 ms. MS/MS spectrum of 3-dimethylamino-3-phenylpropionic acid was obtained by selecting the protonated ion at *m*/*z* 194 at the first quadrupole (Q1), followed by collision-induced dissociation (cid) with argon gas at the second quadrupole (Q2). The resulting fragments were analyzed by the third quadrupole (Q3).

MS/MS/MS experiment of compound **1** was performed by accelerating **1** at the orifice with a high orifice potential of 150 V and by fragmenting it at Q0. The fragment with *m*/*z* 194 was selected at Q1 and was further fragmented at Q2 with argon collision gas. The fragments were analyzed by Q3. The parent scan of compound **1** in MS/MS/MS was carried out under the same condition. After fragmenting compound **1** at Q0 using orifice potential 150, the parent fragment for the ion at *m*/*z* 445 was found in the parent scan experiment. A high resolution FAB mass spectrometry was VG Micromass ZAB 2F HS. ^{1}H and 2D NMR spectra were recorded on a Bruker AMX2 500 NMR spectrometer. HPLC was performed using a Waters Delta Prep 4000 with a semi preparative RP-Vydac C-8. The eluant was monitored by the absorbance at 254 nm. Chemicals used for the synthesis of 3-dimethylamino-3-phenylpropionic acid were purchased from Aldrich.

3.2. Plant material

The needles of *T. wallichiana* were obtained from plants grown in the garden of Trichandra college, Tribhuvan University, Nepal.

3.3. Extraction and isolation

Air-dried needles (1 kg) were extracted with EtOH (4 lit ×3) at room temperature. The EtOH solvent was

evaporated under reduced pressure to obtain a semi-solid EtOH extract (110 g). A fraction of EtOH extract (50 g) was dissolved in EtOAc and extracted with 10% HCl. The acidic phase was washed with EtOAc (2 × 200 ml) and neutralized with Na_2CO_3, followed by extraction with EtOAc. After drying (Na_2SO_4), a semi-solid residue (0.5 g) was obtained which was further fractionated by the reversed-phase HPLC [a linear gradient of acetonitrile from 0 to 40% (0.6%/min) in 0.1% TFA; flow rate, 13 ml/min)]. Compounds **1**, **2** and **3** were eluted at the 40, 36 and 29% CH_3CN in the gradient system, respectively. All collected fractions were lyophilized immediately, and tested for cytotoxic activity. Those found inactive and complicated mixture were discarded. After lyophilization, 0.9 mg of **1**, 1.0 mg of **2** and 1.5 mg of **3** were obtained.

3.4. 5α-O-(3′-Dimethylamino-3′-phenylpropionyl) taxinine M (*1*)

Colorless solid, $[\theta]_{308}^{25}$ 2500 (0.001 M, MeOH). ^1H and ^{13}C NMR data, see Table 1; HR–FAB–MS *m*/*z* 862.36481 $[M+H]^+$ (required for $C_{46}H_{55}NO_{15}$ 862.36500).

3.5. Preparation of 3-dimethylamino-3-phenylpropionic acid

To a stirred solution of *dl*-3-phenyl-3-amino-phenyl propionic acid (500 mg) in H_2O/MeOH (10 ml, v/v 1:1) and formaldehyde (1 ml, 37%), $NaBH_4$ (0.7 g) was added and the mixture was stirred at 0° C for 30 min. The reaction mixture was further incubated for 5 h to give 3-dimethylamino-3-phenylpropoinic acid that was dissolved in AcOH, lyophilized and purified by reversed-phase semi-prep (yield 30%). HPLC [linear gradient (0.5%/min) of CH_3CN from 0 to 30% in 0.1% TFA with a flow rate of 13 ml/min] was used for purification. ESI–MS *m*/*z* $[M+H]^+$ 194; ^1H NMR (500 MHz, MeOH-d_4) δ 7.51 (5H, m, H-Ph), 4.79 (1H, *t*, $J=7.0$ Hz, H-3), 3.34 (1H, *dd*, $J=17.0$, 6.0 Hz, H-2a), 3.19 (1H, *dd*, $J=17.0$, 7.0 Hz, H-2b), 2.79 (6H, *s*, NMe_2).

3.6. Cytotoxic activity

A549 cells were cultivated in Dulbecco's Eagle Modified medium supplemented with 5% bovine calf serum (Hyclin). Cellular viability in the presence and absence of test samples was determined using the standard MTT (3-[4,5-dimethylthiazol-2-yl]-2,5-diphenyltetrazolium bromide; Sigma) method (Mosmann, 1983). Briefly, 0.2 ml cell suspension containing 2000 cells was seeded to each well of a 96-well microtitre plate (Costar, Corning Inc., NY), and incubated in a CO_2 incubator at 37 ^{0}C for 24 h before test compounds were added.

New medium with or without test compound was added to each well ($n=3$). The cells were further incubated at the same condition for 48 h. The medium was removed by aspiration, and crystals of viable cells were dissolved in DMSO (100 μl/well) and the plate was read immediately on a microtitrer plate reader (SOFTmax, Molecular Device) at the wavelength of 540 nm. Absorbance taken from cell grown in the absence of test compound was considered as a negative control.

Acknowledgements

We thank Dr. Justin Powlowski (Concordia University, Montreal) for his help in recording CD spectrum.

References

Appendino, G., Gariboldi, P., Gabetta, B., Pace, R., Bombardelli, E., Viterbo, D., 1992. 14 β-Hydroxy-10-deacetyl-baccatin III, a new taxane from Himalayan yew (*Taxus wallichiana zucc*). J. Chem. Soc. Perkin Trans. 1, 2925–2929.

Barboni, L., Gariboldi, P., Torregiani, E., Appendino, G., Verese, M., Gabetta, B., Bombardelli, E., 1995a. Minor taxoids from *Taxus wallichiana*. J. Nat. Prod. 58, 934–939.

Barboni, L., Gariboldi, P., Appendino, G., Enriu, R., Gabetta, B., Bombardelli, E., 1995b. New taxoids from *Taxus baccata* L. Liebigs Ann. Chem. 345–349.

Beutler, J.A., Chmurny, G.M., Look, S.A., Witherup, K.M., 1991. Taxinine M, a new tetracyclic taxane from *Taxus brevifolia*. J. Nat. Prod. 54, 893–897.

Chauviére, G., Guénard, D., Pascard, C., Picot, F., Potier, P., Prangé, T., 1982. Taxagifine: New taxane derivative from *Taxus baccata* (Taxaceae). J. Chem. Soc. Chem. Commun., 495–496.

Chattopadhyay, S.K., Tripathi, V., Sharma, R.P., Shawl, A.S., Joshi, B.S., Roy, R., 1999. A brevifoliol analogue from the Himalayan yew *Taxus wallichiana*. Phytochemistry 50, 131–133.

Chen, R., Kingston, D.G., 1994. Isolation and structure elucidation of new taxoids from *Taxus brevifolia*. J. Nat. Prod. 57, 1017–1021.

Ettouati, L., Anond, A., Convert, O., Laurent, D., Poupat, C., Potier, P., 1988. Plants de nouvelle-caledonie, 114′Taxanes isoles des feuilles d *Austrotaxus spicata* Compton (Taxacee). Bull. Soc. Chim. France 749–755.

Kobayashi, J., Hosoyama, H., Katsui, T., Yoshida, N., Shigemori, H., 1996. Taxuspines N, O, and P, new taxoids from Japanese yew *Taxus cuspidata*. Tetrahedron 52, 5391–5396.

Leete, W., Bodem, G.B., 1966. The biosynthesis of 3-dimethylamino-3-phenylpropanoic acid in yew. Tetrahedron Lett. 33, 3925–3927.

March, J., 1992. Advanced Organic Chemistry, 4th Edition (Chapter 4). John Wiley & Sons, New York. pp. 155–156.

Nicoletti, M.I., Colombo, T., Rossi, C., Monardo, C., Stura, S., Zucchetti, M., Riva, A., Morazzoni, P., Donati, M.B., Bombardelli, E., D'Incalci, M., Giavazzi, R., 2000. IDN5109, a taxane with oral bioavailability and potent antitumor activity. Cancer Res. 60, 842–846.

Mosmann, T., 1983. Rapid colorimetric assay for cellular growth and survival: application to proliferation and cytotoxicity assays. J. Immunol. Meth. 65, 55–63.

Shi, Q.-W., Oritani, T., Sugiyama, T., Yamada, T., 1999. Two novel pseudoalkaloid taxanes from the Chinese yew, *Taxus chinensis* Var. *0mairei*. Phytochemistry 52, 1571–1575.

Wani, M.C., Taylor, H.L., Wall, M.E., Coggon, P., McPhail, A.T., 1971. Plant antitumor agents VI. The isolation and structure of taxol, a novel antileukemic and antitumor agent from *Taxus brevifolia*. J. Am. Chem. Soc. 93, 2325–2327.

Zhang, J., Sauriol, F., Mamer, O., Zamir, L.O., 2000. New taxanes from the needles of *Taxus canadensis*. J. Nat. Prod. 63, 929–933.

PERGAMON

Phytochemistry 58 (2001) 1171–1175

PHYTOCHEMISTRY

www.elsevier.com/locate/phytochem

Apianane terpenoids from *Salvia officinalis*

Kayoko Miura, Hiroe Kikuzaki, Nobuji Nakatani*

Division of Food and Health Science, Graduate School of Human Life Science, Osaka City University, 3-3-138 Sugimoto, Sumiyoshi, Osaka, 558-8585, Japan

Received 9 March 2001; received in revised form 16 July 2001

Abstract

Three apianane terpenoids, *rel*-(5*S*, 6*S*, 7*S*, 10*R*, 12*S*, 13*R*)-7-hydroxyapiana-8,14-diene-11,16-dion-(22,6)-olide, *rel*-(5*S*, 6*S*, 7*R*, 10*R*, 12*S*, 13*R*)-7-hydroxyapiana-8,14-diene-11,16-dion-(22,6)-olide and *rel*-(5*S*, 6*S*, 7*S*, 10*R*, 12*R*, 13*S*)-7-hydroxyapiana-8,14-diene-11,16-dion-(22,6)-olide were isolated from the leaves of *Salvia officinalis*, together with 15 known compounds, salvigenin, lupeol, β-sitosterol, stigmasterol, physcion, carnosol, rosmadial, rosmanol, epirosmanol, isorosmanol, columbaridione, atuntzensin A, miltirone, carnosic acid and 12-*O*-methyl carnosic acid. Their structures were established on the basis of spectral evidence.
© 2001 Published by Elsevier Science Ltd.

Keywords: *Salvia officinalis*; Labiatae; Apianane; Abietane; Diterpenoid; Sage

1. Introduction

Sage, *Salvia officinalis*, has been most commonly known not only as a culinary herb for flavoring and seasoning, but it has been also of great medicinal importance. Many components have been isolated from *S. officinalis* such as diterpenoids (Brieskorn and Fuchs, 1962; Djarmati et al. 1992; Cuvelier and Berset, 1994; Tada et al., 1994, 1997), triterpenoids (Brieskorn and Kapadia, 1980), flavonoids, (Brieskorn and Biechele, 1971; Brieskorn and Kapadia, 1979), phenolic glycosides (Wang et al., 1998a,b, 1999) and phenolic acid derivatives (Lu and Foo, 1999; Lu et al., 1999). In continuation of our chemical investigation of *S. officinalis*, we reported the isolation of antioxidative diterpenoids, flavonoids (Nakatani et al., 1989) and glycosides (Wang et al., 2000). In this paper, we describe the isolation and structural determination of C_{23} terpenoids, named apianane (Luis et al., 1996) from the methylene chloride extract of *S. officinalis*.

2. Results and discussion

Repeated chromatography of the methylene chloride extract of the leaves of *S. officinalis* afforded new compounds **1**, **2** and **3** (Fig. 1), together with 16 known compounds. The known compounds were identified with salvigenin, lupeol, β-sitosterol, stigmasterol, physcion, carnosol, rosmadial, rosmanol, epirosmanol, isorosmanol, columbaridione, atuntzensin A, miltirone, carnosic acid and 12-*O*-methyl carnosic acid by comparing with spectral data of authentic samples and the previous reports (Inatani et al., 1982; Nakatani and Inatani, 1983, 1984; Houlihan et al., 1985; Al-Hazimi et al., 1987; Wu et al., 1993; Luis et al., 1994, Richheimer et al., 1996). Lupeol, physion, columbaridione, atuntzensin A and miltirone were isolated from sage for the first time.

Compound **1** was obtained as colorless needles from benzene/ acetone, mp 245 °C, with positive optical rotation ($[\alpha]_D^{27}$ +131.3° *c* 0.420, $CHCl_3$). The molecular formula of **1** was assigned as $C_{23}H_{28}O_5$ based on HR–MS analysis. The ^{13}C NMR spectrum (Table 1) of **1** also revealed the presence of 23 carbon atoms, including three carbonyl carbons (δ 176.7, 198.2 and 200.5). The IR spectrum of **1** showed the presence of a hydroxyl group at 3465 cm^{-1}, a γ-lactone at 1774 cm^{-1}, and α,β-unsaturated ketone functions at 1718 and 1672 cm^{-1}. The ^1H NMR spectrum of **1** (Table 2) showed signals for an isopropyl group (δ 0.65 and 0.75, each 3H, *d*, *J* = 6.8 Hz and δ 2.53, *sept*, *J* = 6.8 Hz), geminal dimethyl groups (δ 0.83 and 1.00, *s*), three methylene groups (δ 1.2∼1.6 and δ 2.86), a methine proton (δ 2.14, *s*),

* Corresponding author. Fax: +81-6-6605-3086.
E-mail address: nakatani@life.osaka-cu.ac.jp (N. Nakatani).

0031-9422/01/$ - see front matter © 2001 Published by Elsevier Science Ltd.
PII: S0031-9422(01)00341-7

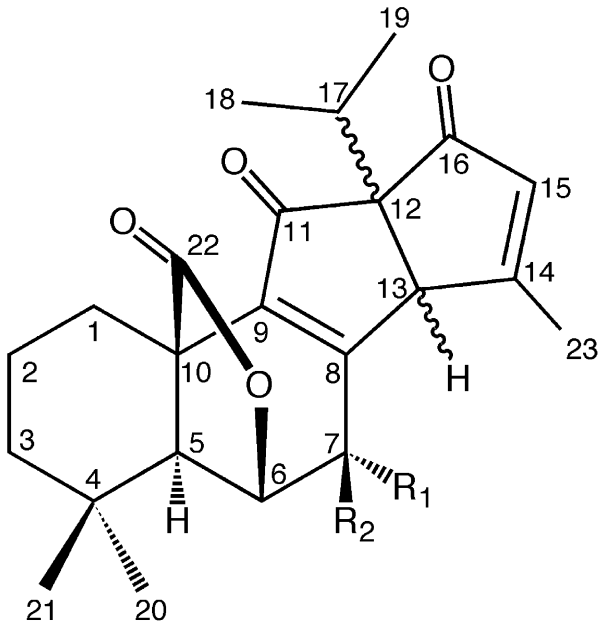

1: *rel*-(12*S*, 13*R*) R_1=OH R_2=H
2: *rel*-(12*S*, 13*R*) R_1=H R_2=OH
3: *rel*-(12*R*, 13*S*) R_1=OH R_2=H

Fig. 1. Structures of compounds **1**–**3**.

Table 1
^{13}C NMR spectral data of compounds **1**–**3** ($(CD_3)_2CO$, 125 MHz)

C	1	2	3
1	24.1	24.1	24.5
2	18.8	18.7	18.8
3	38.8	38.6	39.0
4	31.3	31.8	31.5
5	50.9	55.8	51.5
6	78.5	79.6	78.1
7	68.5	70.3	67.7
8	168.8	171.4	170.0
9	144.1	140.8	142.0
10	45.6	45.4	45.4
11	198.2	197.5	198.0
12	74.4	73.2	73.1
13	55.0	51.8	52.0
14	178.5	176.7	175.7
15	130.9	129.9	130.4
16	200.5	201.1	200.3
17	34.3	33.9	33.9
18	17.3	17.6	17.7
19	17.6	17.7	17.7
20	31.4	31.4	31.5
21	21.8	21.7	22.0
22	176.7	177.2	176.6
23	19.9	18.7	19.0

two methine protons bearing oxygen functions (δ 4.57 and δ 4.69) and a hydroxyl group (δ 5.56). Analysis the ^{1}H–^{1}H COSY spectrum revealed that the methine proton at δ 4.57 was coupled with the protons at δ 4.69 and δ 2.86, respectively. These signals suggested that the partial structure of **1** was an abietane skeleton possessing a γ-lactone (Nakatani and Inatani, 1984). Signals of a methine proton (δ 3.89), a methyl protons (δ 2.49), an olefinic proton (δ 5.76), and olefinic carbons (δ 130.9, 144.1, 168.8 and 178.5) were observed in the ^{1}H and ^{13}C NMR spectra. Based on these data, it was deduced that this compound (**1**) was a rare C_{23} terpenoid which was proposed as apianane (Luis et al., 1996). The assignment of all signals was made by ^{1}H–^{1}H COSY, HMQC and HMBC (Table 3) experiments and by comparison of the spectral data of apiananes. All signals obtained for **1** were in good agreement with those of 7α-methoxyapiana-8,14-diene-11,16-dion-(22,6)-olide, reported by Luis et al. (1996), except for the signal of a methoxyl group. The downfield shift of signals at C-6, C-8, H-7 and H-13, and the upfield shift of a signal at C-7 in the ^{1}H and ^{13}C NMR spectra of **1** showed the presence of a hydroxyl group at C-7 in **1** instead of a methoxyl group. Furthermore its relative configuration was confirmed by a NOESY experiment (Fig. 2). That is, the absence of the NOESY correlation between H-5 and H-7 suggested that H-7 had a β-configuration and the hydroxyl group at C-7 was in the α-configuration. In addition, the strong NOESY correlation between the signals of the proton pairs (H-7 and H-13, H-13 and H_3-18, 19) confirmed that the stereochemical relationship between H-13 and 12-isopropyl group was *cis* with β-configuration. Thus **1** was determined to be *rel*-(5*S*, 6*S*, 7*S*, 10*R*, 12*S*, 13*R*)-7-hydroxyapiana-8,14-diene-11,16-dion-(22,6)-olide.

Compound **2** had a molecular formula of $C_{23}H_{28}O_5$ by HR–MS, which is the same as that of **1**. The IR, UV, ^{1}H and ^{13}C NMR spectral data of **2** were very similar to those of **1**, except for the optical rotation ($[\alpha]_D^{27}$ +89.2° *c* 0.251, $CHCl_3$), suggesting that **2** had a different stereostructure from **1**. Comparing the ^{1}H and ^{13}C NMR spectra of **2** with those of **1**, some differences were observed. The signals of H-6 (δ 4.83) and H-7 (δ 4.98) were paramagnetically shifted ($\Delta\delta$+0.26 and $\Delta\delta$+0.29 ppm, respectively) in comparison with those of **1**. Moreover, the signals of C-5 (δ 55.8), C-9 (δ 140.8) and C-13 (δ 51.8) were shifted. The observed differences suggested **2** to be an isomer of **1** at C-7. A NOESY experiment of **2** (Fig. 2) showed a strong cross peak between H-5 and H-7, indicating that H-7 had an α-configuration. In addition, the absence of the NOESY correlation between the signals of H-13 and H-7 suggested H-13 had a β-configuration as for **1**. Moreover, H-13 was also correlated with the isopropyl methyl groups, which suggested the stereostructure between H-13 and the 12-isopropyl group of **2** to be in the *cis*-configuration as for **1**. Thus compound **2** was determined to be *rel*-(5*S*, 6*S*, 7*R*, 10*R*, 12*S*, 13*R*)-7-hydroxyapiana-8,14-diene-11,16-dion-(22,6)-olide.

Compound **3** had a molecular formula of $C_{23}H_{28}O_5$ by HR–MS, and was very similar to **1** and **2** in the IR,

Table 2
^{1}H NMR spectral data of compounds **1**–**3** ($(CD_3)_2CO$, 500 MHz)

H	1	2	3
1α	1.53 *ddd* (5.1, 13.5, 14.9)	1.52 *ddd* (5.1, 13.3, 14.9)	1.68 *ddd* (5.1, 13.3, 14.5)
1β	2.86 overlap	2.77 *br d* (14.9)	2.72 *br d* (14.5)
2 α	1.52 *m*	1.52 *m*	1.53 *ddddd* (2.7, 3.2, 3.6, 5.1, 13.5)
2 β	1.37 *ddddd* (2.7, 4.2, 13.5, 13.6, 13.7)	1.32 *m*	1.36 *ddddd* (2.6, 4.2, 13.0, 13.3, 13.5)
3 α	1.23 *ddd* (3.1, 13.6, 13.6)	1.15 *ddd* (2.4, 13.5, 13.5)	1.23 *ddd* (3.2, 13.0, 13.1)
3 β	1.39 *m*	1.36 *m*	1.42 *m*
5	2.14 *s*	2.11 *s*	2.02 *s*
6	4.57 *dd* (0.8, 3.3)	4.83 *dd* (0.7, 2.7)	4.62 *dd* (0.7, 3.2)
7 α	5.56 *d* (6.6, OH)	4.98 *ddd* (1.0, 2.7, 9.3)	5.77 *d* (6.8, OH)
7 β	4.69 *ddd* (1.0, 3.3, 6.6)	5.22 *d* (9.3, OH)	4.73 *dd* (3.2, 6.8)
13	3.89 *ddq* (1.0, 1.0, 1.1)	4.05 *dqd* (1.0, 1.2, 1.3)	4.04 *br s*
15	5.76 *dq* (1.0, 1.2)	5.72 *dq* (1.3, 1.5)	5.73 *dq* (1.3, 1.5)
17	2.53 *sept* (6.8)	2.55 *sept* (6.8)	2.55 *sept* (6.8)
18	0.65 *d* (6.8)	0.70 *d* (6.8)	0.81 *d* (6.8)
19	0.75 *d* (6.8)	0.77 *d* (6.8)	0.80 *d* (6.8)
20	1.00 *s*	0.98 *s*	1.00 *s*
21	0.83 *s*	0.85 *s*	0.84 *s*
23	2.49 *dd* (1.1, 1.2)	2.39 *dd* (1.2, 1.5)	2.39 *dd* (1.0, 1.5)

Table 3
HMBC correlations of compounds **1**–**3** (H→C)

H	1	2	3
1α	2, 3, 9, 10, 22	9, 10, 22	2, 3, 9, 10, 22
1β	2, 3, 10, 22	22	–
2 α	4, 10	–	–
2 β	1, 3, 4	–	1
3 α	1, 2, 4, 21	4, 21	2, 4, 21
3 β	1, 2, 4, 5	–	1, 2, 5
5	4, 7, 9, 10, 21, 22	7, 9, 10, 20, 21, 22	4, 7, 9, 10, 20, 21, 22
6	4, 7, 8, 10, 22	4, 5, 8, 10, 22	4, 8, 22
7-OH	7, 8	–	–
7 -H	5, 6, 8, 9	–	–
13	7, 8, 9, 12, 14, 15, 16, 17, 23	8, 9, 12, 14, 15, 17	8, 9, 12, 14, 15, 17, 23
15	12, 13, 14, 16, 23	12, 13, 14, 16, 23	12, 13, 14, 16, 23
17	11, 12, 13, 16, 18, 19	11, 12, 13, 16, 18, 19	12, 13, 16, 18, 19
18	12, 17, 19	12, 17, 19	12, 17, 19
19	12, 17, 18	12, 17, 18	12, 17, 18
20	3, 4, 5, 21	3, 4, 5, 21	3, 4, 5, 21
21	3, 4, 5, 20	3, 5, 20	3, 4, 5, 20
23	13, 14, 15	13, 14, 15	13, 14, 15

UV, ^{1}H NMR and ^{13}C NMR spectral data. However, **3** also exhibited a different optical rotation ($[\alpha]_D^{27}$ +18.8° *c* 0.136, $CHCl_3$) from those of **1** and **2**. This fact indicated **3** to have the different stereostructure. As shown in Fig. 2, the absence of the correlation between H-5 and H-7 in a NOESY experiment suggested a β-configuration of H-7 as for **1**. The strong cross peak between H-13 and H_3-18, 19 observed in a NOESY experiment as well as the presence of the NOESY correlation between H-5 and H_3-18, and H-1α and H_3-18 indicated an α-configuration for both H-13 and the 12-isopropyl group. Thus **3** was *rel*- (5*S*, 6*S*, 7*S*, 10*R*, 12*R*, 13*S*)-7-hydroxyapiana-8,14-diene-11,16-dion-(22,6)-olide.

3. Experimental

3.1. General

Mps were measured with a Yanagimoto micro-melting point apparatus and are uncorrected. Optical rotations were measured using a JASCO P-1030 polarimeter. UV spectra were recorded on a Shimadzu UV-2500PC spectrophotometer. IR spectra were run on a Perkin-Elmer FT–IR 1720X spectrometer. The ^{1}H, ^{13}C and 2D NMR spectra (^{1}H–^{1}H COSY, HMQC, HMBC and NOESY) were obtained on a Varian Unity plus 500 (500 MHz) spectrometer. The chemical shifts were

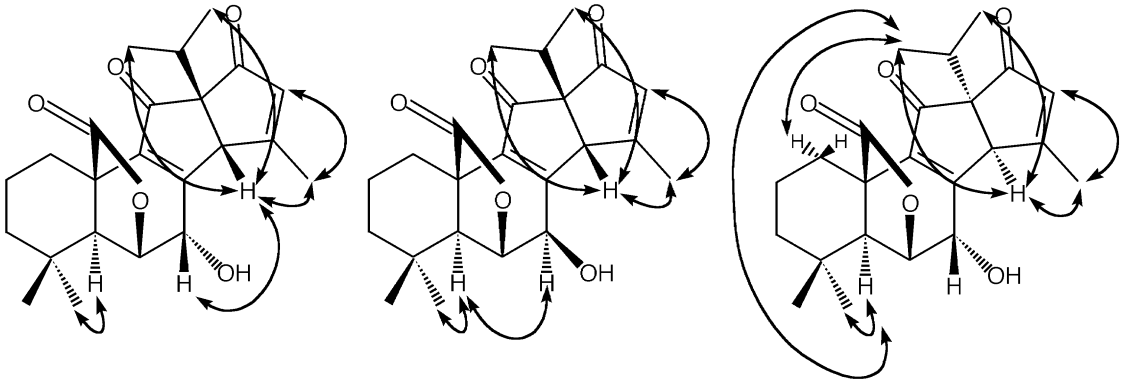

Fig. 2. Significant NOESY correlations of **1**–**3**.

relative to the TMS or solvent peak. EIMS and HR–MS (70 eV) were measured on a Hitachi M-2000 mass spectrometer. Column chromatography was performed using silica gel 60 (70–230 mesh, Merck), Sephadex LH-20 (Pharmacia) and Chromatorex ODS DM1020T (100–200 mesh, Fuji Silysia Chemical). TLC was performed on silica gel 60 F_{254} plates (Merck) and ODS plates (Merck).

3.2. Plant material

S. officinalis was kindly provided by Takasago Perfumery Co., Ltd.

3.3. Extraction and isolation

Air dried and ground leaves of *S. officinalis* (1.0 kg) were extracted 3 times with CH_2Cl_2 (4000 ml) at room temperature. Evaporation of solvent under reduced pressure gave the CH_2Cl_2 extract (129.7 g). The CH_2Cl_2 extract (22.2 g) was dissolved in *n*-hexane and the hexane soluble part (21.8 g) was subjected to column chromatography on silica gel (500 g) using *n*-hexane with increasing amounts of Me_2CO as eluent to afford 15 fractions by monitoring with TLC. (Fr. 1∼5 (eluted with *n*-hexane, 5000 ml), Fr. 6 (eluted with *n*-hexane–Me_2CO (95:5), 2600 ml), Fr. 7 (eluted with *n*-hexane–Me_2CO (90:10), 3000 ml), Fr. 8–10 (eluted with *n*-hexane-Me_2CO (85:15), 4000 ml), Fr. 11 (eluted with *n*-hexane-Me_2CO (80:20), 1600 ml), Fr. 12 (eluted with *n*-hexane-Me_2CO (75:15), 2000 ml), Fr. 13 (eluted with *n*-hexane-Me_2CO (50:50), 2800 ml), Fr.14 (eluted with Me_2CO, 2000 ml) and Fr. 15 (eluted with MeOH, 2000 ml)). Repeated chromatography of the less polar fraction (Fr. 6, 1.23 g) and recrystallization afforded known compounds, lupeol (colorless crystals, 4.7 mg), physcion (orange solid, 2.6 mg), β-sitosterol (50 mg) and stigmasterol (5 mg). Fr. 8 (0.9 g) was successively subjected to a Sephadex LH-20 column chromatography eluted with Me_2CO and a silica gel column eluted with C_6H_6–Me_2CO to give rosmadial (colourless crystals, 4.4 mg), columbaridione (orange solid, 2 mg) and miltirone (orange solid, 1.4 mg). The mixture (4.6 g) of Fr. 11 and Fr. 12 was applied to a Sephadex LH-20 column with Me_2CO to separate 9 fractions (Fr. A–I). Furthermore, Fr. C was subjected to column chromatography on silica gel eluted with C_6H_6–Me_2CO (97:3) to afford crude solid of **1**, which was triturated with C_6H_6 to separate crystals. These colorless crystals were recrystallized from a mixture of C_6H_6 and Me_2CO to afford **1** (10.1 mg). The C_6H_6 soluble part was applied to a silica gel column eluted with CH_2Cl_2–Me_2CO (97:3) to afford amorphous solids, **2** (2.5 mg) and **3** (1.5 mg). Fr. D was triturated with Me_2CO to separate the insoluble solid, which was recrystallized from Me_2CO to afford salvigenin (yellow crystals, 23 mg). Rechromatography of Me_2CO soluble part of Fr. D on Sephadex LH-20 eluting with Me_2CO and on silica gel eluting with C_6H_6–Me_2CO gave atuntzensin A (yellow solid, 3.8 mg) and 12-*O*-methyl carnosic acid (off-white solid, 400 mg). Fr. E was also triturated with Me_2CO to separate insoluble solid, which was recrystallized from Me_2CO to afford rosmanol (colorless prisms, 475 mg). The acetone soluble part of Fr. E was applied to a silica gel column with a solution of C_6H_6–Me_2CO (95:5) as an eluting solvent to afford epirosmanol (5 mg). The *n*-hexane insoluble part (0.4 g) of the CH_2Cl_2 extract was subjected to on Sephadex LH-20 chromatography with Me_2CO as an eluent to afford carnosic acid (9 mg), carnosol (40 mg) and isorosmanol (11 mg).

3.4. rel-(5S, 6S, 7S, 10R, 12S, 13R)-7-Hydroxyapiana-8, 14-diene-11,16-dion-(22,6)-olide (1)

Mp 245 °C. UV λ_{max}^{EtOH} nm (log ϵ): 211 (4.09). IR $\nu_{max}^{CHCl_3}$ cm^{-1}: 3465, 1774, 1718, 1672, 1611, 1171, 1076, 957. ^1H and ^{13}C NMR: Tables 1 and 2. EI–MS (direct inlet, 70 eV) *m/z* (rel. int.) : 384 $[M]^+$ (10), 342 (44), 340

(51), 298 (100), 296 (29), 41 (10). HR–MS *m/z:* 384.1926 ($C_{23}H_{28}O_5$ calc. for 384.1934).

*3.5. rel-(5S, 6S, 7R, 10R, 12S, 13R)-7-Hydroxyapiana-8,14-diene-11,16-dion-(22,6)-olide (**2**)*

Amorphous solid. UV λ_{max}^{EtOH} nm (log ϵ): 215 (3.99). IR ν_{max}^{CHCl3} cm^{-1} : 3449, 1775, 1719, 1686, 1619, 1217, 1174, 1099, 919. ^1H and ^{13}C NMR: Tables 1 and 2. EI–MS (direct inlet, 70 eV) *m/z* (rel. int.) : 384 $[M]^+$ (64), 342 (100), 340 (43), 298 (43), 281 (15), 69 (24), 41 (42). HR-MS *m/z*: 384.1919 ($C_{23}H_{28}O_5$ calc. for 384.1934).

*3.6. rel-(5S, 6S, 7S, 10R, 12R, 13S)-7-Hydroxyapiana-8,14-diene-11,16-dion-(22,6)-olide (**3**)*

Amorphous solid. UV λ_{max}^{EtOH} nm (log ε): 216 (4.30) IR $\nu_{max}^{CHCl_3}$ cm^{-1}: 3351, 1785, 1718, 1677, 1621, 1218, 1174, 1083, 961. ^1H and ^{13}C NMR: Tables 1 and 2. EI–MS (direct inlet, 70 eV) *m/z* (rel. int.) : 384 $[M]^+$ (53), 342 (100), 340 (17), 298 (17), 281 (13), 42 (33). HR–MS *m/z*: 384.1928 ($C_{23}H_{28}O_5$ calc. for 384.1934).

Acknowledgements

This study was performed through support from the Special Coordination Funds for Promoting Science and Technology (Leading Research Utilizing Potential of Regional Science and Technology) of the Ministry of Education, Culture, Sports, Science and Technology of the Japanese Government. The authors are grateful to Ms. T. Maekawa of Faculty of Human Life Science, Osaka City University, for measuring the NMR spectra.

References

Al-Hazimi, H.M.G., Miana, G.A., Deep, M.S.H., 1987. Terpenoids from *Salvia lanigera*. Phytochemistry 26, 1091–1093.

Brieskorn, C.H., Biechele, W., 1971. The flavones from *Salvia officinalis* L. Archiv der Pharmazie 304, 557–561.

Brieskorn, C.H., Fuchs, A., 1962. The constituents of *Salvia officinalis* XIII: The structure of picrosalvin, a diterpene-*O*-diphenollactone from sage leaf. Chemische Berichte 95, 3034–3041.

Brieskorn, C.H., Kapadia, Z., 1979. Constituents of *Salvia officinalis*, XXIII: 5-Methoxysalvigenin in leaves of *Salvia officinalis*. Planta Medica 35, 376–378.

Brieskorn, C.H., Kapadia, Z., 1980. Constituents of *Salvia officinalis*, XXIV: Triterpenes and pristan in leaves of *Salvia officinalis*. Planta Medica 38, 86–89.

Cuvelier, M.-E., Berset, C., Richard, H., 1994. Antioxidant constituents in sage (*Salvia officinalis*). Journal of Agricultural and Food Chemistry 42, 665–669.

Djarmati, Z., Jankov, R.M., Djordjevic, A., Ribar, B., Lazar, D., Engel, P., 1992. Carnosic acid 12-methyl ether-γ-lactone, a ferruginol-type diterpene from *Salvia officinalis*. Phytochemistry 31, 1307–1309.

Houlihan, C.M., Ho, C.-T., Chang, S.S., 1985. The structure of rosmariquinone—a new antioxidant isolated from *Rosmarinus officinalis* L. Journal of the American Oil Chemists' Society 62, 96–98.

Inatani, R., Nakatani, N., Fuwa, H., Seto, H., 1982. Structure of a new antioxidative phenolic diterpene isolated from rosemary (*Rosmarinus officinalis* L.). Agricultural and Biological Chemistry 46, 1661–1666.

Lu, Y., Foo, L.Y., 1999. Rosmarinic acid derivatives from *Salvia officinalis*. Phytochemistry 51, 91–94.

Lu, Y., Foo, L.Y., Wong, H., 1999. Sagecoumarin, a novel caffeic acid trimer from *Salvia officinalis*. Phytochemistry 52, 1149–1152.

Luis, J.G., Grillo, T.A., Quinones, W., Kishi, M.P., 1994. Columbaridione, a diterpenequinone from *Salvia columbariae*. Phytochemistry 36, 251–252.

Luis, J.G., Lahlou, E.H., Andres, L.S., Sood, G.H.N., Ripoll, M.M., 1996. Apiananes: C_{23} terpenoids with a new type of skeleton from *Salvia apiana*. Tetrahedron Letters 37, 4213–4216.

Nakatani, N., Inatani, R., 1983. A new diterpene lactone rosmadial, from rosemary (*Rosmarinus officinalis* L.). Agricultural and Biological Chemistry 47, 353–358.

Nakatani, N., Inatani, R., 1984. Two antioxidative diterpenes from rosemary (*Rosmarinus officinalis* L.) and a revised structure for rosmanol. Agricultural and Biological Chemistry 48, 2081–2085.

Nakatani, N., Inatani, R., Fujii, A., 1989. Food antioxidant production from sage. Japan Patent 1-44232.

Richheimer, S.L., Bernart, W., King, G.A., Kent, M.C., Bailey, D.T., 1996. Antioxidant activity of lipid-soluble phenolic diterpenes from rosemary. Journal of the American Oil Chemists' Society 73, 507–514.

Tada, M., Okuno, K., Chiba, K., Ohnishi, E., Yoshii, T., 1994. Antiviral diterpenes from *Salvia officinalis*. Phytochemistry 35, 539–541.

Tada, M., Hara, T., Hara, C., Chiba, K., 1997. A quinone methide from *Salvia officinalis*. Phytochemistry 45, 1475–1477.

Wang, M., Kikuzaki, H., Zhu, N., Sang, S., Nakatani, N., Ho, C.-T., 2000. Isolation and structural elucidation of two new glycosides from sage (*Salvia officinalis* L.). Journal of Agricultural and Food Chemistry 48, 235–238.

Wang, M., Li, J., Rangarajan, M., Shao, Y., LaVoie, E.J., Huang, T.-C., Ho, C.-T., 1998a. Antioxidative phenolic compounds from sage (*Salvia officinalis*). Journal of Agricultural and Food Chemistry 46, 4869–4873.

Wang, M., Shao, Y., Huang, T.-C., Wei, G.-J., Ho, C.-T., 1998b. Isolation and structural elucidation of aroma constituents bound as glycosides from sage (*Salvia officinalis*). Journal of Agricultural and Food Chemistry 46, 2509–2511.

Wang, M., Shao, Y., Li, J., Rangarajan, M., LaVoie, E.J., Ho, C.-T., 1999. Antioxidative phenolic glycosides from sage (*Salvia officinalis*). Journal of Natural Products 62, 454–456.

Wu, S.-H., Zhang, H.-J., Lin, Z.-W., Sun, H.-D., 1993. Terpenoids from *Isodon Grandifolia* var. *Atuntzensis*. Phytochemistry 34, 1176–1178.

PERGAMON

Phytochemistry 58 (2001) 1177–1182

PHYTOCHEMISTRY

www.elsevier.com/locate/phytochem

Triterpenoid saponins from *Mollugo spergula*

Niranjan P. Sahu[a,*], Kazuo Koike[b], Sukdeb Banerjee[a], Basudeb Achari[a], Tamotsu Nikaido[b]

[a]*Indian Institute of Chemical Biology, 4 Raja S C Mullick Road, Calcutta 700032, India*
[b]*Department of Pharmacognosy, School of Pharmaceutical Sciences, Toho University, 2-2-1 Miyama, Funabashi, Chiba 274-8510, Japan*

Received 1 March 2001; received in revised form 4 July 2001

Abstract

Two novel triterpenoid saponins belonging to a modified hopane group, spergulin A {3-*O*-(β-D-xylopyranosyl 4-sulphate)-spergulagenin A} (**1**) and spergulin B {3-*O*-[α-rhamnopyranosyl (1→2)-β-D-xylopyranosyl]-spergulatriol} (**4**) were isolated from the aerial part of *Mollugo spergula* along with spergulacin (**2**) and spergulacin A (**3**). Their structures and relative stereochemistry were determined by a combination of 2D–NMR (COSY, TOCSY, HETCOR, NOESY and HMBC) and HR-FAB–MS analysis coupled with strategic chemical and enzymatic transformations. © 2001 Elsevier Science Ltd. All rights reserved.

Keywords: *Mollugo spergula*; Molluginaceae; Triterpene saponins; Triterpene; Spergulin A; Spergulin B; 2D NMR; Rearranged hopane; Bis-nor hopane

1. Introduction

Mollugo spergula Linn. (Syn. *Glinus oppositifolia*) (Family: Molluginaceae) is an annual herb which finds application for the treatment of skin diseases in the indigenous system of medicine (Sastri, 1962). Previous chemical investigations of the plant had led to the isolation of a number of genuine and rearranged triterpenes of hopane series (Chakrabarti et al., 1966, 1968; Kitagawa et al., 1974, 1977) and two triterpenoid saponins (Barua et al., 1986a,b). In continuation of our work on chemical studies on naturally occurring saponins (Sahu and Achari, 2001) we decided to reinvestigate the saponin constituents of the plant. The present paper describes the isolation and characterization of two new triterpenoid saponins including a sulfated derivative saponin. As detailed spectral data for the two saponins reported by Barua et al. (1986a,b) are not available, those have also been presented here.

2. Results and discussion

Spergulin A (**1**) was assigned the molecular formula $C_{35}H_{58}O_{11}S$ from the negative high resolution FAB–MS, supported by elemental analysis. The presence of a sulfur atom as part of a sulfate group was also evident from the fragment ions at m/z 97 $[SO_4H]^-$ and 80 $[SO_3]^-$ in the negative low resolution FAB–MS and from the peak at 1383 cm^{-1} for a sulfate group in the IR spectrum. The compound displayed 35 signals in its ^{13}C NMR spectrum of which five could be assigned to a pentose unit. Structure elucidation for spergulin A was mainly accomplished by critical analysis of the 1D and 2D NMR results. HMBC measurement proved to be the method of choice; beginning with assignments for the methyl groups, two and three bond correlations permitted the assignment of most of the signals. The determination of atom connectivities was straightforward and unambiguous. Thus the HMBC correlation involving signals of H-3 with C-23 and C-24; H-3 and H-5 with C-4 and C-25; and 3H-25 with C-1, C-9 and C-10 identified most of the structural elements of rings A and B. This was gradually extended to cover the other rings. Thus the C-9 signal showed cross peaks with 3H-26 and H(β)-11; C-11 with H-13; and C-14 with H-13, 3H-26, 3H-27 and 3H-28. Further observation of HMBC involving C-15 and C-13 with 17-H provided a clear picture of the six membered rings A–D. The cyclopentanyl nature of ring E was ascertained from the following HMBC correlations: H-17/C-21 and C-22, H(β)-19/C-21, H-17/C-18, H(β)-19/C-18, H(α)-20/C-29, H(β)-20/C-18, 3H-29/C-20. That the ketomethyl group is attached to C-21 was established from the observed HMBC between C-22 and 3H-29, H-17, H(α)-20 as also between C-21 and 3H-30.

* Corresponding author. Fax: +91-33-473-5197/0284.
E-mail address: npsahu@iicb.res.in (N.P. Sahu).

0031-9422/01/$ - see front matter © 2001 Elsevier Science Ltd. All rights reserved.
PII: S0031-9422(01)00346-6

Regarding the substitution pattern, the downfield chemical shifts attributed to 16-H (δ 3.59) and 12-H (δ 3.67) as well as to the corresponding carbon signals suggested the presence of –OH groups at C-16 and C-12. The signals of 2H-11 and H-13 showed HMBC cross peaks with δ 67.3 (C-12) whereas the δ 64.1 (C-16) signal displayed correlations with H-17 and H-15α signals confirming the placement of hydroxy groups. The relative orientations of the aglycone hydrogens and the stereochemistry of the ring system of spergulin A (**1**) were established from identified ^{1}H–^{1}H coupling patterns and cross peaks generated from phase-sensitive NOESY. The β-orientation of the hydroxy groups was evident from the NOESY cross peaks between H(α)-12 and 3H-27, 28 as also between H(α)-16 and 3H-27, 28, 29.

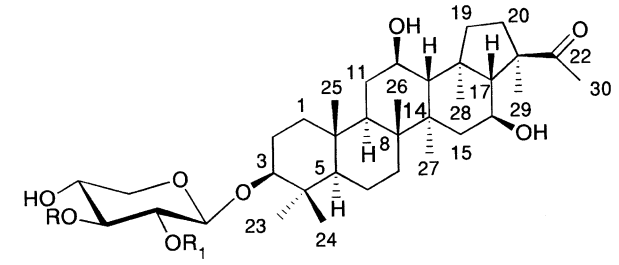

	R	R_1
1.	SO_3H	H
2.	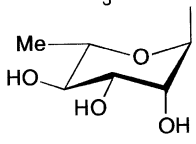	H
3.	H	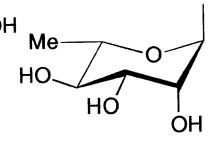

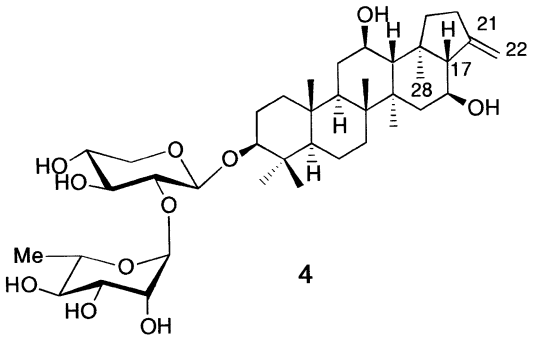

4

From ^{1}H and ^{13}C chemical shifts, ^{1}H–^{1}H coupling constants and a close examination of TOCSY spectrum, it was obvious that the sugar constituent is D-xylose (The absolute configuration of the monosaccharides were chosen in keeping with those commonly encountered among plant glycosides). Acid hydrolysis of **1** followed by GLC analysis of the hydrolysate after derivatisation gave only one peak corresponding to xylose. The anomeric proton signal appeared as a doublet at δ 4.23 ($J = 7.4$ Hz) confirming its β-configuration ($^4C_1$ conformation). That the sugar constituent was attached to C-3 (δ 87.8) of the aglycone moiety was evident from HMBC and NOESY cross peaks. Thus C-3 showed HMBC with H-1 of xylose, which in turn showed NOE correlation with that of H-3 of the aglycone. Interestingly, the C-3 chemical shift of xylose appeared significantly downfield (δ 82.6) in comparison with that (δ 77.7) of standard methyl β-D-5-xylose, indicating the presence of a substituent. Absence of any NMR signal attributable to a substituent and the IR and mass spectral evidence for a sulfate group as discussed earlier helped to identify the substituent. This was confirmed by solvolysis of the compound to yield sulfuric acid and compound (**5**), characterized mainly by 2D NMR techniques. Acid hydrolysis of **5** furnished the sapogenin spergulagenin A (**6**). Thus the structure of spergulin A is established as 3-*O*-(β-D-xylopyranosyl 4-sulphate)-spergulagenin A (**1**). The same sapogenin had been isolated earlier by Barua et al. (1986 a, b) and Chakrabarti et al. (1966), but only the melting point and some ^{1}H NMR data were reported.

Spergulacin (**2**) and spergulacin A (**3**) proved to be saponins of the same sapogenin **6** and their structures were elucidated following the same method as used for **1**. The monosaccharides for both **2** and **3** were shown to be D-xylose and L-rhamnose, present in 1:1 ratio based on GLC analysis of the acid hydrolysate. β-Configuration ($^4C_1$ conformation) for the xylopyranosyl unit and α-configuration for the rhamnopyranosyl unit were inferred from the large $J_{H1,H2}$ for the xylopyranosyl unit and the singlet like appearance of the H-1 signal for the rhamnopyranosyl unit respectively. The observed HMBC between the H-1 signals of xylose and C-3 signal of the aglycone suggested that in both the saponins xylose was linked directly to the aglycone at C-3. Interglycosidic linkages in **2** and **3** were derived from the observed HMBC of H-1 of rhamnose with C-3 of xylose in **2** and C-2 of xylose in **3**. Compounds **2** and **3** were found to be identical with spergulacin and spergulacin A respectively reported earlier by Barua et al. (1986a,b).

Spergulin B (**4**) was concluded to be a new saponin of another sapogenin spergulatriol (**8**) reported previously by Kitagawa et al. (1977). The structure elucidation was principally based on 2D NMR analysis of the genin (**8**) and the prosapogenin (**7**) obtained by enzymatic hydrolysis of **4.** The monosaccharides were identified as xylose and rhamnose by co-GLC with authentic specimens (vide experimental). Interglycosidic and sugar-aglycone linkages were deduced on the basis of the arguments as described for **2** and **3**. Further, the prosapogenin (**7**) liberated by the enzymatic hydrolysis contained only xylose, linked to C-3 of the aglycone. Thus the structure of spergulin B was established as 3-*O*-[α-rhamnopyranosyl (1→2)-β-D-xylopyranosyl]-spergulatriol (**4**).

It is noteworthy that saponins based on hopane or rearranged hopane skeletons are very few while none have been reported for nor hopane sapogenins (Mahato et al., 1988; Mahato and Nandy, 1991; Mahato and Garai, 1998).

3. Experimental

3.1. General procedures

All melting points were measured on a Yanagimoto micromelting point apparatus and are uncorrected. ^{1}H and ^{13}C NMR were recorded using a Jeol ECP-500 spectrometer (^{1}H at 500 MHz and ^{13}C at 125 MHz) in DMSO-d_6 or C_5D_5N with TMS as internal standard. LR and HR FAB–MS (negative) were done using KRATOS CONCEPT mass spectrometer with a mixture of glycerol and *m*-nitrobenzyl alcohol for LR–FAB–MS and PEG-600 for HR–FAB–MS as matrices. MALDI–TOF–MS (positive) were performed on a Perspective Biosystems Voyager DE-STR spectrometer with 2,5-dihydroxybenzoic acid as matrix. TLC was carried out on silica gel 60 F_{254} (Merck) [$CHCl_3$:MeOH:H_2O; 30:13:2] and spots were visualized by spraying with 10% H_2SO_4.

3.2. Plant material

The plant material was collected from the suburbs of Calcutta, India and identified at Indian Botanic Garden, Howrah. A voucher specimen was deposited at the Steroids and Terpenoids Chemistry Department.

3.3. Extraction and isolation

The air-dried powdered plant (1 kg) (aerial part of *Mollugo spergula*) was successively extracted with light petrol (60–80 °C), $CHCl_3$ and MeOH under reflux conditions. The residue (15 g) obtained after evaporation of the MeOH under reduced pressure was applied to a column of Diaion HP 20 (500 g) and the column washed with water followed by 30, 40, 60, 80 and 100% of MeOH. Fractions eluted with 60% MeOH showed single spot on TLC over silica gel and the residue was crystallized from methanol-water to furnish 150 mg of spergulin A (**1**) (R_f 0.41). The residue from fractions eluted with 80% methanol was rechromatographed over silica gel. Fractions eluted with $CHCl_3$–MeOH (17:3) showed three spots on TLC and the residue was subjected to fractional crystallization to obtain spergulacin (**2**) (R_f 0.59) (135 mg). The mother liquor was chromatographed repeatedly over silica gel and eluted with various mixtures of chlorform and methanol. Later fractions eluted with $CHCl_3$–MeOH (17: 3) furnished 95 mg of spergulacin A (**3**) (R_f 0.55), while fractions eluted with $CHCl_3$–MeOH (4:1) gave 65 mg of spergulin B (**4**) (R_f 0.49).

3.4. Spergulin A (*1*)

Colorless needles, mp 220–221 °C (dec.); $[\alpha]_D^{25}$ +19.1° (*c* 0.66, DMSO); IR: ν_{max} cm^{-1} (KBr): 3550, 3468, 1698, 1637, 1460, 1383, 1062, 1021, 972, 824; HR FAB–MS (negative): *m*/*z* 685.36164 [M–H]$^-$, (calc. for $C_{35}H_{57}O_{11}S$, *m*/*z* 685.36216); LR–FAB–MS (negative): *m*/*z* 685.4 [M–H]$^-$, 641.3, 459.1, 352.1, 227.0, 199.0, 97.0 [SO_4H]$^-$ and 80.0 [SO_3]$^-$; MALDI–TOF–MS (positive): 747.03 [M + Na + K–1]$^+$, 731.11 [M + 2Na–1]$^+$, 687.07 [M + H]$^+$. ^{1}H NMR (DMSO-d_6). Sugar moiety: 4.23 (*d*, *J* = 7.4 Hz, H′-1), 3.13 (*m*, H′-2), 3.91 (*t*, *J* = 9 Hz, H′-3), 3.43 (*m*, H′-4), 3.09 (*m*, H′$_a$-5), 3.71 (*dd*, *J* = 5.5, 11.4 Hz, H′$_b$-5); ^{13}C NMR (DMSO-d_6) data: Table 2. (Found: C, 57.91; H, 8.28; S, 4.26. $C_{35}H_{57}O_{11}NaS.H_2O$ requires: C, 57.83; H, 8.18; S, 4.41%.).

3.5. Solvolysis of spergulin A (*1*)

Spergulin A (18 mg) was refluxed with a mixture of pyridine and dioxane (4:1, 5 ml) for 6 h. The reaction mixture was passed through a Sep-pak cartridge (Waters), and eluted successively with water (15 ml) and MeOH (15 ml). The MeOH eluted fraction was chromatographed on silica gel using chloroform–methanol–water (50:10:1) to yield **5** (14.5 mg), crystallized from methanol–acetonitrile to furnish fine needles, mp 238–240 °C (dec.); $[\alpha]_D^{20}$ +16.30° (*c* 0.92, pyridine); IR: ν_{max} cm^{-1} (KBr): 3433, 1696, 1651, 1642, 1097, 1043 and 972; LR–FAB–MS (positive): *m*/*z* 645 [M + K]$^+$, 629 [M + Na]$^+$; ^{1}H NMR (DMSO-d_6): δ 0.74, 0.79, 0.90, 0.91, 0.95, 0.96, 1.25, 2.10 (each 3H *s*, H_3 of C-24, 25, 27, 28, 26, 23, 29, 30), 0.67 (1H, *d*, *J* = 10.7 Hz, H-5), 1.30 (1H, *d*, *J* = 10.5 Hz, H-13), 1.62 (1H, *d*, *J* = 11.4 Hz, H-17), 1.75 (1H, *dd*, *J* = 8.7, 14.0 Hz, H-20β), 2.01 (1H, *dd*, *J* = 7.1, 12.4 Hz, H-19β), 2.96 (*m*, H-3α), 3.58 (*m*, H-16α), 3.67 (*m*, H-12α), Sugar moiety: 4.11 (*d*, *J* = 7.5 Hz, H′-1), 2.95 (*m*, H′-2), 3.07 (*m*, H′-3), 3.26 (*m*, H′-4), 2.96 (*m*, H′$_a$-5), 3.64 (*dd*, *J* = 5.2, 11.2 Hz, H′$_b$-5).; ^{13}C NMR (DMSO-d_6): Table 2. (Found: C, 69.19; H, 9.51; $C_{35}H_{58}O_8$ requires: C, 69.27; H, 9.63%).

The aqueous part was examined by paper chromatography (Advantee, No. 50) employing methanol–water (1:1). Sulfuric acid was detected as a light yellow spot (R_f 0.71) after spraying the paper with a solution of potassium rhodizonate (10 mg in 50 ml of 50% methanol).

3.6. Acid hydrolysis of *5*

Compound **5** (5 mg) was heated in 1 ml of 1 M HCl (dioxane–H_2O, 1:1) at 80 °C for 2 h on a water bath. Dioxane was distilled off under reduced pressure and the solution was extracted with EtOAc (1 ml ×3). The organic layer was washed with water, dried, and the residue was crystallized from EtOAc to give fine needles (3 mg) of spergulagenin A (**6**), mp 276–277 °C; [lit. (Kitagawa

et al., 1975), mp 278–279.5 °C; $[\alpha]_D^{20}$ +35.3° (*c* 0.68, pyridine); LR–FAB–MS (positive): *m/z* 497 $[M+Na]^+$, 513 $[M+K]^+$; ^{1}H NMR (DMSO-d_6): δ 0.67, 0.78, 0.89, 0.91, 0.92, 0.96, 1.25, 2.10 (each 3H *s*, H_3 of C-24, 25, 23, 27, 28, 26, 29, 30), 0.63 (1H, *d*, *J* = 9.4 Hz, H-5), 1.30 (1H, *d*, *J* = 11 Hz, H-13), 1.62 (1H, *d*, *J* = 11.5 Hz, H-17), 1.75 (1H, *dd*, *J* = 8.5, 14 Hz, H-20β), 2.01 (1H, *dd*, *J* = 7.5, 12.5 Hz, H-19β), 2.98 (1H, *m*, H-3α), 3.68 (1H, *m*, H-12α), 3.58 (1H, *m*, H-16α); ^{13}C NMR: Table 2. (Found: C, 75.86; H, 10.65; Calc. for $C_{30}H_{50}O_4$: C, 75.90; H.10.62%).

The aqueous part was neutralized by passing through an ion-exchange resin (Amberlite MB-3) column, then dried under vacuum, and treated with 1-(trimethylsilyl) imidazole at room temperature for 2 h. Excess reagent was decomposed with water and the mixture extracted with *n*-hexane (1 ml ×2). The monosaccharide was identified as xylose (R_t 20.26) by co-GLC analysis of the TMSi derivative with standard sample (R_t 20.56).

3.7. Spergulacin (**2**)

The compound was crystallized from MeOH to yield microneedles, mp 280–282 °C (dec.); $[\alpha]_D^{20}$ −13.7° (*c* 0.76, pyridine) [lit. (Barua et al., 1986b)]; HR–FAB–MS (negative): *m/z* 751.46564 $[M-H]^-$ (calc. for $C_{41}H_{67}O_{12}$: *m/z* 751.46325); LR–FAB–MS (positive): *m/z* 753.4 $[M+H]^+$; ^{1}H NMR (DMSO-d_6): δ 0.75, 0.80, 0.91, 0.92, 0.95, 0.96, 1.26, 2.10 (each 3H, *s*, H_3 of C-24, 25, 27, 28, 23, 26, 29, 30), 0.67 (1H, *d*, *J* = 10.8 Hz, H-5), 1.30 (1H, *d*, *J* = 10.8 Hz, H-13), 1.62 (1H, *d*, *J* = 11.5 Hz, H-17), 1.76 (1H, *dd*, *J* = 9, 13.8 Hz, H-20β), 2.01 (1H, *dd*, *J* = 7.3, 12.4 Hz, H-19β), 3.02 (1H, *dd*, *J* = 4.5, 11.5 Hz, H-3α), 3.60 (*m*, H-16α), 3.67 (*m*, H-12α), Sugar moiety: 4.17 (*d*, *J* = 7.5 Hz, H′-1), 3.10 (*m*, H′-2), 3.30 (*m*, H′-3), 3.31 (*m*, H′-4), 3.10 (*m*, H′$_a$-5), 3.70 (*m*, H′$_b$-5); 5.0 (s, H″-1), 3.71 (m, H″-2), 3.48 (m, H″-3), 3.19 (m, H″-4), 3.86 (m, H″-5) and 1.10 (*d*, *J* = 6.2 Hz, CH_3); ^{13}C NMR: Table 2. (Found: C, 65.38; H, 9.15; calc. for $C_{41}H_{68}O_{12}$: C, 65.40, H, 9.10%).

3.8. Spergulacin A (**3**)

Crystallized from methanol as colorless needles, mp 260–262 °C (dec.); $[\alpha]_D^{20}$ −16.1° (*c* 0.77, pyridine); [lit., (Barua et al., 1986a)]; HR–FAB–MS (negative): *m/z* 751.46515 $[M-H]^-$ (calc. for $C_{41}H_{68}O_{12}$: *m/z* 751.46325); LR–FAB–MS (positive): 753.5 $[M+H]^+$; ^{1}H NMR (DMSO-d_6): δ 0.74, 0.79, 0.905, 0.910, 0.94, 0.95, 1.25, 2.10 (each 3H, *s*, H_3 of C-24, 25, 27, 28, 23, 26, 29, 30), 0.67 (1H, *d*, *J* = 10.8 Hz, H-5), 1.30 (1H, *d*, *J* = 10.8 Hz, H-13), 1.61 (1H, *d*, *J* = 11.5 Hz, H-17), 1.73 (1H, *dd*, *J* = 8.5, 14 Hz, H-20β), 2.01 (1H, *dd*, *J* = 7.3, 12.4 Hz, H-19β), 3.02 (*m*, H-3α), 3.59 (*m*, H-16α), 3.71 (*m*, H-12α).

Table 1
^{1}H NMR chemical shifts[a] of spergulin A (**1**)[b] and spergulatriol (**8**)[c]

H	**1** δ (ppm), *J* (Hz)	**8** δ (ppm), *J* (Hz)
1.	1.58 (+, 1α), 0.91 (+, 1β)	1.00 (*m*, 1α), 1.70 (*m*, 1β)
2.	1.68 (*m*, 2α), 1.56 (*m*, 2β)	1.84 (+, 2α and 2β)
3.	3.04 (*dd* like, 3α)	3.45 (*m*, 3α)
5.	0.68 (*d*, 11.5, 5α)	0.82 (*dd*, 2.3, 12.1, 5α)
6.	1.48 (+, 6α), 1.37 (+, 6β)	1.42 (*m*, H-6α), 1.57 (*m*, 6β)
7.	1.17 (+, 7α), 1.41 (+, 7β)	1.50 (*m*, 7α), 1.31 (*m*, 7β)
9.	1.17 (*m*, 9α)	1.42 (*m*, 9α)
11.	1.67 (*m*, 11α), 1.22 (*t*-like, 11β)	2.13 (*m*, 11α), 1.66 (*m*, 11β)
12.	3.67 (*m*, 12α)	4.22 (*m*, 12α)
13.	1.31 (*d*, 10.6, 13β)	1.80 (*d*,, 10.8, 13β)
15.	1.17 (+, 15α), 1.41 (+, 15β)	1.90 (*dd*, 4.4, 12.4, 15α), 1.76 (*m*, 15β)
16.	3.59 (*m*, 16α)	4.32 (*dt*, 4.4, 10.1, 16α)
17.	1.63 (*d*, 11.4, 17β)	2.15 (+,17β)
19.	1.33 (*m*, 19α), 2.01 (*dd*, 7.4, 12.4, H-19β)	2.54 (*ddd*, 1.7, 8.6, 12.5, H-19α), 1.80 (+, 19β)
20.	1.49 (*m*, 20α), 1.76 (*dd*, 7, 14.3, 20β)	2.43 (*m*, 20α), 2.47 (*m*, 20β)
22.	–	5.15 (*t*, 2.1, H$_a$-22), 6.07 (*t*, 2.1, H$_b$-22)
23.	0.98 (*s*, CH_3-23)	1.24 (*s*, CH_3-23)
24.	0.73 (*s*, CH_3-24)	1.04 (*s*, CH_3-24)
25.	0.80 (*s*, CH_3-25)	0.89 (*s*, CH_3-25)
26.	0.96 (*s*, CH_3-26)	1.07 (*s*, CH_3-26)
27.	0.92 (*s*, CH_3-27)	1.16 (*s*, CH_3-27)
28.	0.92 (*s*, *CH*$_3$-28)	1.09 (*s*, *CH*$_3$-28)
29.	1.26 (*s*, CH$_3$-29)	–
30.	2.10 (*s*, CH$_3$-30)	–

[a] Assignments based upon COSY, HOHAHA, TOCSY, HETCOR, HSQC, HMBC and NOESY experiments.
[b] In DMSO-d_6 (30 °C).
[c] In C_5D_5N (30 °C), + overlap.

Table 2
^{13}C NMR chemical shifts[a] [δ_c ($\pm$ 0.1)] of **1, 2**, **3**, **4, 5**, **6**, **7** and **8**

Carbon no.	**1**[b]	**2**[b]	**3**[b]	**4**[c]	**5**[b]	**6**[b]	**7**[c]	**8**[c]
1.	38.2	38.2	38.5	39.1	38.1	38.2	38.9	39.1
2.	25.7	25.8	26.0	27.0	25.8	27.0	26.9	28.3
3.	87.8	87.8	87.5	88.5	87.5	76.6	88.6	78.0
4.	38.8	38.8	38.7	39.6	38.7	38.4	39.7	39.5
5.	54.8	54.8	55.1	56.0	54.7	54.6	55.8	55.7
6.	17.9	17.8	17.9	18.66	17.8	18.0	18.7	19.0
7.	32.8	32.8	32.9	33.6	32.7	32.8	33.6	33.6
8.	44.7	44.7	44.8	45.4	44.6	44.7	45.3	45.37
9.	48.1	48.1	48.1	49.2	48.0	48.1	49.2	49.3
10.	36.2	36.1	36.2	37.0	36.1	36.4	37.0	37.3
11	31.8	31.8	31.8	33.1	31.7	31.8	33.2	33.2
12.	67.3	67.3	67.3	69.3	67.2	67.2	69.3	69.3
13.	54.5	54.5	54.56	53.9	54.4	54.5	53.9	54.0
14.	40.9	40.9	41.0	41.8	40.8	40.8	41.8	41.8
15.	44.4	44.3	44.3	45.1	44.2	44.3	45.1	45.1
16.	64.1	64.0	64.1	67.2	64.0	64.0	67.2	67.2
17.	62.7	62.8	62.9	62.2	62.8	62.8	62.2	62.2
18.	46.0	45.9	46.0	45.4	45.9	45.9	45.38	45.39
19.	44.6	44.6	44.7	43.2	45.5	44.5	43.2	43.2
20.	36.7	36.7	36.8	29.9	36.6	36.6	29.9	29.9
21.	52.2	52.2	52.2	152.0	52.1	52.1	152.2	152.2
22.	213.6	213.6	213.6	106.0	213.6	213.6	106.0	106.0
23.	27.3	27.4	27.3	28.0	27.4	28.0	28.1	28.7
24.	16.1	16.0	16.0	16.9	16.1	15.6	16.8	16.3
25.	15.5	15.5	15.8	16.2	15.5	15.5	16.1	16.1
26.	16.5	16.5	16.6	17.0	16.5	16.5	17.0	17.1
27.	18.5	18.4	18.5	19.1	18.4	18.4	19.1	19.1
28.	17.1	17.1	17.2	16.0	17.1	17.1	16.0	16.0
29.	20.1	20.1	20.1	–	20.0	20.0	–	–
30.	25.7	25.7	25.8	–	25.7	25.7	–	–
Xylose								
C-1′	105.7	105.6	104.6	106.1	106.0		107.7	
C-2′	72.3	73.8	77.8	78.0	73.7		75.6	
C-3′	82.6	81.0	76.6	79.6	76.7		78.7	
C-4′	68.4	68.2	70.0	71.5	69.5		71.3	
C-5′	65.0	65.3	65.5	66.9	65.5		67.1	
Rhamnose								
C-1″		100.5	100.1	101.9				
C-2″		70.5	70.3	72.4				
C-3″		70.6	70.4	72.6				
C-4″		72.1	72.1	74.1				
C-5″		68.0	68.01	69.7				
CH_3		17.8	17.9	18.7				

[a] Assignments based upon COSY, TOCSY, HETCOR, HSQC, HMBC and NOESY experiments.
[b] In DMSO-d_6 (30 °C).
[c] In C_5D_5N (30 °C).

Sugar moiety: 4.23 (*d*, $J=7.0$ Hz, H′-1), 3.23 (*m*, H′-2), 3.19 (*m*, H′-3), 3.27 (*m*, H′-4), 3.02 (*m*, H′$_a$-5), 3.68 (*dd*, $J=5$, 11.3 Hz, H′$_b$-5), 5.22 (*s*, H″-1), 3.71 (*m*, H″-2), 3.48 (*m*, H″-3), 3.14 (*m*, H″-4), 3.78 (*dd*, $J=6.2$, 9.2 Hz, H″-5) and 1.06 (*d*, $J=6.2$ Hz, CH_3); ^{13}C NMR: Table 2. (Found: C, 65.36; H, 9.14; calc. for $C_{41}H_{68}O_{12}$: C, 65.40; H, 9.10%).

3.9. Acid hydrolysis of *2* and *3*

Both of **2** and **3** (5 mg each) was hydrolyzed separately with 1 M HCl in a manner similar to that described for **5**. In both the cases, the genin was identified as spergulagenin A (mp, PMR, CMR and MS) and the monosaccharides were found to be xylose (R_t 13.55) and rhamnose (R_t 20.20) (co-GLC of the TMSi derivatives with standard samples).

3.10. Spergulin B (*4*)

Colorless powder, mp 271–273 °C (dec.); $[\alpha]_D^{20}$ −20.0° (*c* 0.85, pyridine); IR: ν_{max} cm^{-1} (KBr): 3414, 1654, 1454, 1040, 985, 839; HR–FAB–MS (negative): *m*/*z*

707.43757 $[M–H]^-$ (calc. for $C_{39}H_{63}O_{11}$: *m/z* 707.43734); LR–FAB–MS (positive): *m/z* 709.4 $[M+H]^+$; MALDI–TOF–MS (positive): 747.03 $[M+K]^+$, 731.11 $[M+Na]^+$; ^1H NMR (C_5D_5N): δ 0.84, 1.04, 1.07, 1.17, 1.18, 1.25 (each 3H *s*, H_3 of C-25, 26, 28, 27, 24, 23), 0.74 (1H, *d*, $J=11.5$ Hz, H-5), 1.77 (1H, *d*, $J=10.8$ Hz, H-13), 2.12 (1H, *m*, H-17), 3.30 (1H, *dd*, $J=4.1$, 11.7 Hz, H-3α), 4.18 (1H, *t*, $J=8.5$ Hz, H-12α), 4.30 (*m*, H-16α), Sugar moiety: 4.84 (*d*, $J=6.2$ Hz, H′-1), 4.23 (*m*, H′-2), 4.16 (*m*, H′-3), 4.14 (*m*, H′-4), 4.33 (*m*, H'_a-5), 3.71 (*dd*, $J=9.6$, 11.0 Hz, H'_b-5), 6.52 (*brs*, H″-1), 4.86 (*dd*, $J=1.4$, 3.2 Hz, H″-2), 4.67 (*dd*, $J=3.4$, 9.4 Hz, H″-3), 4.33 (*m*, H″-4), 4.76 (*m,* H″-5) and 1.71(*d,* $J=6.2$ Hz, CH_3); ^{13}C NMR (C_5D_5N): Table 2. (Found: C, 66.10; H, 9.05; $C_{39}H_{64}O_{11}$ requires: C, 66.07; H, 9.10%).

3.11. Enzymatic hydrolysis of spergulin B (**4**)

A solution of **4** (9 mg) in acetate buffer (pH 5.0, 1 ml) was treated with naringinase (ca 100 mg) at 37 °C for 6 days to obtain a precipitate which showed two spots on TLC. The mixture was chromatographed on a silica gel column using $CHCl_3$–MeOH–H_2O (5:1:0.1) to yield the prosapogenin **7** (3.1 mg) and the genin **8** (2.2 mg). The aqueous part was worked up as described earlier and the monosaccharides were identified to be xylose and rhamnose by co-GLC analysis of the TMS derivatives with authentic samples.

3.12. Prosapogenin (7)

Amorphous powder, $[\alpha]_D^{20}+34.8°$ (*c* 0.10, MeOH); IR ν_{max} cm^{-1} (KBr): 3428, 1657, 1461, 1042, 971, 890; MALDI–TOF–MS (positive): *m/z* 585 $[M+Na]^+$; ^1H NMR (C_5D_5N): δ 0.83, 1.00, 1.04, 1.08, 1.18, 1.31 (each 3H *s*, 6 x-CH_3), 0.78 (1H, *d*, $J=11.5$ Hz, H-5), 1.79 (1H, *d*, $J=10.8$ Hz, H-13), 2.12 (*m*, H-17), 3.36 (1H, *dd*, $J=4.3$, 11.6 Hz, H-3), 5.15 (1H, *brs*, H_a-22) and 6.07 (1H, *brs*, H_b-22), Sugar moiety: 4.85(*d*, $J=7.6$ Hz, H′-1), 4.03 (*t*, 8 Hz, H′-2), 4.17 (*t*, 9 Hz, H′-3), 4.23 (*dd*, $J=5$, 10 Hz, H′-4), 3.78 (*t*, $J=11.2$ Hz, H'_a-5), 4.39 (*dd*, $J=5.3$, 11.3 Hz, H'_b-5); ^{13}C NMR (C_5D_5N): Table 2. (Found: C, 70.38; H, 9.69; $C_{33}H_{54}O_7$ requires: C, 70.40; H, 9.67%).

3.13. Spergulatriol (**8**)

Crystallized from methanol as fine needles, mp 221–222 °C (dec.), $[\alpha]_D^{20}$ +54.8° (*c* 0.28, $CHCl_3$) [lit. (Kitagawa et al., 1977) mp 224–226 °C (dec.), $[\alpha]_D^{28}$ +60.90° (*c* 0.29, $CHCl_3$)]; IR ν_{max} cm^{-1} (KBr): 3432, 1660, 1081, 1029, 970; MALDI–TOF–MS (positive): *m/z* 453 $[M+Na]^+$, 469 $[M+K]^+$; LR FAB–MS (positive): *m/z* 431 $[M+H]^+$, 429 $[M–H]^+$, 413 $[M–H_2O+H]^+$, 395 $[M–2H_2O+H]^+$, 377 $[M–3H_2O+H]^+$; ^1H and ^{13}C NMR (C_5D_5N): Tables 1 and 2. (Found: C, 78.14; H, 10.70; calc. for $C_{28}H_{46}O_3$: C, 78.09; H, 10.77%).

Acknowledgements

We thank Shri Rajendra Mahato, IICB for collection of the plant material and some technical assistance.

References

Barua, A.K., Datta, P.K., Ray, S., Venkateswaran, R.V., 1986a. Spergulacin-A: a triterpenoid saponin from *Mollugo spergula*. Phytochemistry 25, 2577–2579.

Barua, A.K., Ray, S., Dutta, P.K., Venkateswaran, R.V., 1986b. A triterpene glycoside from *Mollugo spergula*. Phytochemistry 25, 1762–1764.

Chakrabarti, P., Mukherjee, D.K., Barua, A.K., 1966. The constitution of spergulagenic acid: a new sapogenin from *Mollugo spergula*. Tetrahedron 22, 1431–1435.

Chakrabarti, P., Mukherjee, D.K., Barua, A.K., Das, B.C., 1968. The structure and stereochemistry of spergulagenic acid. Tetrahedron 24, 1107–1111.

Kitagawa, I., Suzuki, H., Kitazawa, K., Yamao, N., Yosioka, I., 1975. Saponin and sapogenol. IX. Structure of spergulagenin A, a new migrated hopane-type sapogenol isolated from *Mollugo spergula* L. Chem. Pharm. Bull. 23, 355–364.

Kitagawa, I., Suzuki, H., Yoshioka, I., Akiyama, T., Silverton, J.V., 1974. Structure of spergulagenin A isolated from *Mollugo spergula* L. possessing a new migrated hopane skeleton. Tetrahedron Lett. 1173–1176.

Kitagawa, I., Yamanaka, H., Nakanishi, T., Yosioka, I., 1977. Saponin and sapogenol. XXII. Structure of spergulatriol, a new bisnorhopane-type genuine sapogenol of isoanhydrospergulatriol, from the root of *Mollugo spergula*. Chem. Pharm. Bull. 25, 2430–2436.

Mahato, S.B., Sarkar, S.K., Podder, G., 1988. Triterpenoid saponins. Phytochemistry 27, 3037–3067.

Mahato, S.B., Nandy, A.K., 1991. Triterpenoid saponins discovered between 1987 and 1989. Phytochemistry 30, 1357–1390.

Mahato, S.B., Garai, S., 1998. Triterpenoid saponins. In: Herz, W., Kirby, G.W., Moore, R.E., Steglich, W., Tamm, C. (Eds.), Progress in the Chemistry of Organic Natural Products. Vol. 74. Springer Wien, New York, pp. 1–195.

Sahu, N.P., Achari, B., 2001. Advances in structural determination of saponins and terpenoid glycosides. Current Organic Chemistry 5 (3), 315–334.

Sastri, B.N., 1962. The Wealth of India, Raw Materials, Vol. 6. Council of Scientific and Industrial Research, New Delhi, pp. 396–397.

PERGAMON

Phytochemistry 58 (2001) 1183–1187

PHYTOCHEMISTRY

www.elsevier.com/locate/phytochem

Insecticidal sesquiterpene polyol esters from *Celastrus angulatus*

Wu Wenjun[a,*], Wang Mingan[b], Zhou Wenming[a], Zhu Jinbo[a], Ji Zhiqing[a], Hu Zhaonong[a]

[a]*Department of Plant Protection, Northwestern Agricultural University, Yangling, Shanxi 712100, People's Republic of China*
[b]*Department of Applied Chemistry, China Agricultural University, Beijing 100094, People's Republic of China*

Received 27 February 2001; received in revised form 23 May 2001

Abstract

Three insecticidal sesquiterpene polyol esters were isolated from the root bark of *Celastrus angulatus* by bioassay-guided fractionation. Their chemical structures were elucidated as 1α,2α-diacetoxy-8β-isobutanoyloxy- 9α-benzoyloxy-13-(α-methyl)butanoyloxy-4β, 6β-dihydroxy-β-dihydroagarofuran (**1**), 1α,2α-diacetoxy-8β-(β- furancarbonyloxy)-9α-benzoyloxy-13-isobutanoyloxy-4β, 6β-dihydroxy-β-dihydroagarofuran (**2**) and 1α, 6β, 8α,13-tetraacetoxy-9α-benzoyloxy-2 α-hydroxy-β-dihydroagarofuran (**3**) mainly by analyses NMR and MS spectral data. © 2001 Published by Elsevier Science Ltd.

Keywords: *Celastrus angulatus*; Celastraceae; Insecticide; β-Dihydroagarofuran sesquiterpene

1. Introduction

The plants of the Celastraceae family produce various β-dihydroagarofuran sesquiterpene polyol esters and alkaloids, some of which exhibit insect antifeedant, insecticidal and antitumor activity (Bruning and Wagner, 1978; Tu, 1991; Takaishi et al., 1993). Many species of the Celastraceae family such as the Chinese bittersweet, *Celastrus angulatus* Max., are widely distributed and used as traditional insecticides in China (Jacobson, 1958). Results of bioactivity tests showed the plant extract exhibited antifeedant, narcotic and insecticidal activity against several insects (Wu, 1991). In our previous study, some antifeedant and insecticidal components were isolated from *C. angulatus*, *C. flagellris* and *C. orbiculatus* (Wakabayashi et al., 1988; Wu et al., 1992, 2001; Wang and Chen, 1995; 1997). Continued activity-guided fractionation has led to isolation of three new sesquiterpene polyol esters (**1**, **2** and **3**) with the β-dihydroagarofuran skeleton from the root bark of *C. angulatus*. In this paper, we present the isolation and structure elucidation of compounds **1**–**3**.

2. Results and discussion

Compound **1** was analyzed for $C_{35}H_{48}O_{13}$ by HR–FAB–MS. Its IR spectrum revealed a characteristic ester absorption at 1748 cm^{-1} and free hydroxyl absorption at 3419 cm^{-1}. The NMR spectra suggested the presence of two acetate esters [^{1}H NMR δ 1.59 *s* and 2.15 *s* (2×3H); ^{13}C NMR δ 20.5, 21.1, 169.4, 169.5 (2×Ac)], one isobutanoate ester [^{1}H NMR δ 0.95 *d*, 0.98 *d* (2×3H, J=7.0 Hz), 2.45 *m* (1H); ^{13}C NMR δ 18.5, 18.7, 34.1, 175.7], one (α-methyl) butanoate ester [^{1}H NMR δ 1.06 *t* (3H, J=7.0 Hz), 1.37 *d* (3H, J=7.2 Hz), 2.72 *m*, 1.90 *m*, 1.65 *m* (3×1H); ^{13}C NMR δ 11.7, 16.9, 26.6, 41.6, 176.2] and one benzoate ester [^{1}H NMR δ 7.90 *d* (2H, J=7.2 Hz), 7.60 *t* (1H, J=7.5 Hz), and 7.40 *dd* (2H, J=7.2, 7.5 Hz); ^{13}C NMR δ 128.2, 128.6,129.5.133.4, 165.7] and two free hydroxyl groups [^{1}H NMR δ 3.20 *s*, 5.25 *s* (2×1H, disappeared when exchange with D_2O)], which were confirmed by fragmentation ions at m/z 661 $[M–CH_3]^+$, 643 $[661–H_2O]^+$, 633 $[M–Ac]^+$, 616 $[M–HOAc]^+$, 600 $[M+H–HOAc–OH]^+$, 85 $[CH_3CH_2CHMeCO]^+$, 105 $[C_6H_5CO]^+$, 71 $[Me_2CHCO]^+$, 43 $[Ac]^+$ in the EI mass spectrum and m/z 659 $[M+H–H_2O]^+$, 641 $[M+H-2H_2O]^+$, 599 [659-HOAc]$^+$, 469 [659-2HOAc–Me_2CH CO]$^+$ and 409 in the FAB mass spectrum.

The ^{1}H NMR spectrum of compound **1** showed the presence of three tertiary methyl groups at δ 1.65 *s*, 1.76

* Corresponding author. Tel.: +86-29-7092191; fax: +86-29-7093987 or +86-10-62891384.

E-mail addresses: wenjun_wu@263.net (W. Wenjun), manwang@public3.bta.net.cn (W. Mingan).

0031-9422/01/$ - see front matter © 2001 Published by Elsevier Science Ltd.
PII: S0031-9422(01)00314-4

s and 1.80 *s*. The signals observed at δ 5.52 *d* (J = 3.1 Hz), 5.43 *m*, 5.63 *dd* (J = 10.0, 3.0 Hz) and 6.11 *d* (J = 10.0 Hz) were assigned to the four protons attached to carbon atoms bearing secondary ester groups, and signals at δ 4.63 *d*, 4.97 *d* (J = 13.4 Hz) were assigned to the two protons attached to carbon atoms bearing primary ester group. The signal observed at δ 5.25 *s* was the proton attached to carbon atom bearing hydroxy group. The ^{13}C NMR DEPT spectrum of the parent skeleton of 1 showed three methyls, two methylenes, six methines, and four quaternary carbons. Their chemical shifts were very similar to those of other 1,2,4,6,8,9,13-heptasubstituded β-dihydroagarofuran (Liu et al., 1991, 1995; Wang et al., 1991: Tu et al., 1992).

From the COSY spectrum of compound 1, the doublets at δ 4.63 and 4.97, the doublet at δ 5.52, the multiplet at δ 5.43, the double doublet at δ 5.63 and the doublet at δ 6.11 were assigned to H-13, H-1, H-2, H-8 and H-9. The singlet at δ 5.25 was assigned to H-6 because the dihedral angles of H-6 and H-7 were near 90°in similar compounds containing an ester or hydroxy group at C-6 (Liu et al., 1991; 1995; Wang et al., 1991; Tu et al., 1992). The remaining ^{1}H signals were assigned as shown in Table 1. The ^{13}C NMR signals were assigned on the basis of ^{13}C–^{1}H COSY and are given in Table 1. Generally, H-1, H-2, and H-6 in this class of compounds have axial, equatorial, and axial stereochemistry, respectively. The large coupling constant ($J_{8,9}$ = 10.0 Hz) between H-8 and H-9 suggested that both had axial stereochemistry which was confirmed by the cross peaks between H-1 and H-9, H-6 and H-8 in the NOESY spectrum of **1**.

One of the two free hydroxy groups was situated at C-4, the second at C-6 as shown by the ^{1}H NMR chemical shift, because the normal value of H-6 is generally greater than or near to δ 6.00 when OH-6 is esterified (Liu et al., 1991, 1995; Wang et al., 1991; Tu et al., 1992). Comparing the ^{1}H NMR chemical shift of **1** with known compounds **4** (Wang et al., 1991) and **5** (Liu et al., 1995) isolated from *C. angulatus*, we found only the chemical shift of one of the H-13 protons shifted downfield by 0.12 or 0.21, the other signals were very similar. This result suggested that only the ester group at C-13 was changed into an (α-methyl)butanoate ester in **1** from the isobutanoate ester in **4** or acetate ester in **5**, the other ester groups are the same as in **4** and **5**, which were confirmed by the cross peaks between H-1 and the carbonyl at δ 169.4, H-2 and the carbonyl at δ 169.5, H-8 and the carbonyl at δ 175.7, H-9 and the carbonyl at δ 165.7, H-13 and the carbonyl at δ 176.2 in COLOC spectrum (Sang et al., 1991), respectively. Therefore, the structure of **1** was elucidated to be 1α,2α-diacetoxy-8β-isobutanoyloxy-9α-benzoyloxy-13-(α-methyl)butanoyl-oxy-4β,6β-dihydroxy-β-dihydroagarofuran.

Compound **2** was analyzed for $C_{35}H_{42}O_{14}$ by HR–FAB–MS. Its ^{1}H NMR and ^{13}C NMR spectral data suggested the presence of two acetate esters, one isobutanoate ester, one benzoate ester, one β-furancarboxylate ester and two free hydroxyl groups. The ^{1}H NMR and ^{13}C NMR spectroscopic data for **2** were very similar to those of **1** and **4**, which suggested that **2** also contained the 1,2,4,6,8,9,13-heptasubstituted-β-dihydroagarofuran skeleton. Compound **2** was found to have the same stereochemistry for H-1, H-2, H-6, H-8 and H-9 as **1** and **4** because of the similar coupling patterns, coupling constants and the cross peaks in the NOESY spectrum. As with **1** and **4**, the two free hydroxyl groups were at C-4 and C-6. Comparing the ^{1}H NMR spectrum of **2** with **1** and **4**, we found only the chemical shifts of H-7, H-8 and H-9 were downfield, the other signals were very similar. These results suggested that only the ester group at C-8 should be changed into the β-furancarboxylate ester in **2** from the isobutanoate ester in **1** and **4**, the other ester groups are the same as in **4**. The ester group distributions were confirmed by the COLOC spectrum, which

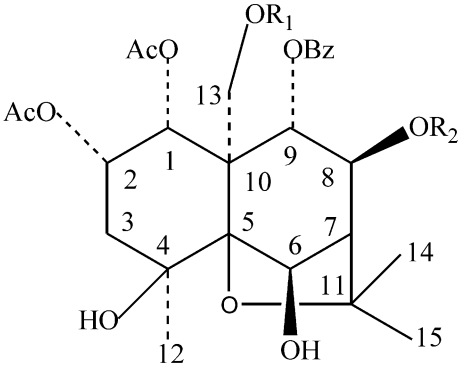

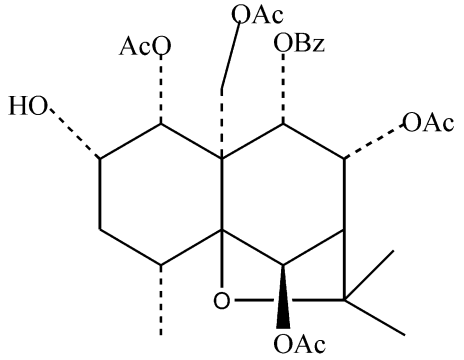

3

1 R_1 = $CH_3CH_2CHMeCO$ R_2 = Me_2CHCO

2 R_1 = Me_2CHCO R_2 = Fu

4 R_1 = R_2 = Me_2CHCO

5 R_1 = Ac R_2 = Me_2CHCO

Table 1
^1H and ^{13}C NMR chemical shifts of compounds **1**–**3** ($CDCl_3$, 300 MHz)

No.	1	2	3	1	2	3
1	5.52 *d* (3.1)	5.54 *d* (3.4)	5.21 *br.s*	75.1	75.1	73.5
2	5.43 *m*	5.41 *m*	4.37 *m*	67.4	67.4	76.8
3	2.04 *m*, 2.18 *m*	2.09 *m*, 2.20 *m*	1.92 *m*, 2.35 *m*	41.3	41.2	31.1
4			2.37 *m*	72.2	72.1	33.1
5				91.6	91.5	89.8
6	5.25 *s*	5.27 *s*	6.16 *s*	76.6	76.8	74.7
7	2.63 *d* (3.0)	2.80 *d* (3.3)	2.54 *d* (4.1)	53.6	53.4	52.8
8	5.63 *dd* (10.0, 3.0)	5.67 *dd* (9.8, 3.3)	5.60 *dd* (6.0, 4.1)	73.9	74.7	70.8
9	6.11 *d* (10.0)	6.18 *d* (9.8)	5.83 *d* (6.0)	75.3	75.1	73.5
10				50.6	50.6	50.9
11				84.6	84.5	81.3
12	1.65 *s*	1.65 *s*	1.21 *d* (7.0)	24.2	24.2	17.8
13	4.63 *d*, 4.97 *d* (13.4)	4.72 *d*, 4.90 *d* (13.4)	5.02 *d*, 5.06 *d* (12.5)	61.7	61.7	63.3
14	1.76 *s*	1.78 *s*	1.43 *s*	26.3	26.2	24.3
15	1.80 *s*	1.81 *s*	1.52 *s*	30.1	30.0	30.2
4-OH	3.20 *s*	3.19 *s*				
6-OH	5.25 *s*	5.27 *s*				
2-OH			2.89 *s*			

showed cross peaks between H-1 and the carbonyl at δ 169.4, H-2 and the carbonyl at δ 169.5, H-8 and the carbonyl at δ 161.8, H-9 at δ 6.18 and the carbonyl at δ 165.7, respectively. The ester group at C-13 would be an isobutanoate. Thus, the structure of 2 was 1α,2α-diacetoxy-8β - (β - furancarbonyloxy) - 9α - benzoyloxy - 13 - isobutanoyloxy-4β,6β-dihydroxy-β-dihydroagarofuran.

Compound **3** was analyzed for $C_{30}H_{38}O_{12}$ by HR–FAB–MS. Its ^1H NMR and ^{13}C NMR spectral data suggested the presence of four acetate esters, one benzoate ester, one free hydroxyl group, and the 1,2,6,8,9,13-hexasubstituted β-dihydroagarofuran skeleton (Rozsa and Pekzer, 1989; Rozsa et al., 1989). Based on the COSY spectrum, H-1, H-2, H-6, H-8, H-9 and the other protons were assigned and are shown in Table 1. The signals at δ 5.02 *d*, 5.06 *d* ($J = 12.5$ Hz) were assigned to H-13. The H-2 proton also showed one cross peak with free hydroxy proton at δ 2.89 (disappeared when exchanged with D_2O) in the COSY spectrum, which indicated that the substituent group at C-2 was hydroxy group. The ester group distributions were determined from the COLOC spectrum, which showed clearly cross peaks between H-9 and the carbonyl carbon at δ 165.2, H-8 and the carbonyl carbon at δ 169.6. This observation indicated one acetate ester was at C-8, the benzoate ester at C-9, and the other three acetate esters were at C-1, C-6 and C-13. As with **1** and **2**, the H-1, H-2 and H-6 had axial, equatorial and axial orientations. The coupling constant ($J_{8,9} = 6.0$ Hz) between H-8 and H-9 indicated that they had different stereochemistry. The cross peaks between H-8 and H-9, H-8 and H-14, H-9 and H-14, H-7 and H-8, H-1 and H-9 in the NOESY spectrum showed that H-8 and H-9 had the equatorial and axial orientation, respectively. Thus, the structure of **3** was 1α,6β,8α,13-tetraacetoxy-9α-benzoyloxy-2α-hydroxy-β-dihydroagarofuran.

The preliminary bioassay results (methodology described in Wu et al., 1992) showed that the KD_{50} values (the dose required to knock down 50% of the population of *Mythimna separate*) for compounds **1**–**3** were 135.3, 73.3, 388.0 μg/g, respectively. Compounds **1** and **2** exhibited stronger activity than celangulin IV (KD_{50} 260.0 μg/g), but were weaker than celangulin II (KD_{50} 46.0 μg/g); on the other hand, compound **3** was much weaker than both celangulin II and IV. These data suggest that the number and orientation of the ester groups have characteristic influence on active strength of β-dihydroagarofuran sesquiterpene polyol esters.

3. Experimental

3.1. General experimental procedures

Melting points were measured on a X_4 apparatus and are uncorrected. Optical rotations were measured on a JASCO 500C polarimeter. UV spectra were obtained on a 756MC spectrophotometer. IR spectra were determined on Equinox 55 instrument (KBr plate). ^1H NMR, ^{13}C NMR, COSY, ^{13}C–^1H COSY, NOESY and COLOC

spectra were recorded on a Bruker DPX 300 NMR spectrometer with $CDCl_3$ as solvent and TMS as internal standard. EIMS were obtained on VG ZAB–HS mass spectrometer operating at 70 eV with a direct insert system, whereas FAB–MS and HR–FAB–MS employed a Brüker Apex II mass spectrometer using nitrobenzoyl alcohol and sodium chloride as matrixes.

3.2. Plant material

The root bark of *C. angulatus* was collected in Mazhao villiage, Zhouzhi county, Shanxi Province, China, (1995) and authenticated by Professor Yang Jianqiang of the Department of Plant Protection, Northwestern Agricultural University. A voucher specimen (sample No. NWAU95-C06) was deposited at the Department of Plant Protection, Northwestern Agricultural University.

3.3. Extraction and isolation

The dried and pulverized root bark (6.6 kg) of *C. angulatus* was extracted with petroleum ether under reflux for 3 h. The extracted material was re-extracted with petroleum ether two times. The extracts obtained were combined and concentrated to give a yellow semi-solid residue (260 g). This crude extract was applied to a silica gel (200–300 mesh) column using EtOAc–petroleum ether (2:8–8:2) as eluent to give 180 fractions (each 500 ml). Fractions 116–176 were combined (40 g) and applied to a silica gel (200–300 mesh) coloumn using EtOAc–petroleum ether (4:6) to give 29 fractions (each 500 ml). Fractions 21–28 (9 g) were subjected to low-pressure LC (RP-18, MeOH–H_2O 65:35) to give 140 fractions (each 100 ml). Fractions 7–9, 98–112, 113–122 were combined respectively, and subjected to HPLC (RP-18, MeOH-H_2O 60:40) to afford compound **1** (23 mg), 2 (74 mg) and 3 (65 mg).

3.3.1. Compound *1*

Amorphous white powder; mp 95–96 °C. $[\alpha]_D^{24}$ −12.8°($CHCl_3$; *c* 0.60). UV λ_{max}^{MeOH} nm (log ε): 244 (3.4530). IR υ_{max} cm^{-1}: 3416 (OH), 2974, 1741 (C=O), 1370, 1235, 1148, 1095, 1033, 952, 712. ^1H NMR (300 MHz, $CDCl_3$): δ 1.59 and 2.15 (each 3H, *s*, 2×Ac), 0.95 and 0.98 (each 3H, *d*, *J* = 7.0 Hz), 2.45 (1H, *m*, Me_2CHCO), 1.06 (3H, *t*, *J* = 7.0 Hz), 1.37 (3H, *d*, *J* = 7.0 Hz), 2.72, 1.90, 1.65 (each 1H, *m*, $CH_3CH_2CHMeCO$), 7.90 (2H, *d*, *J* = 7.2 Hz), 7.60 (1H, *t*, *J* = 7.5 Hz), 7.40 (2H, *dd*, *J* = 7.2, 7.5 Hz, C_6H_5CO); ^{13}C NMR (75 MHz, $CDCl_3$): δ 20.5, 21.1, 169.4, 169.5 (2×Ac), 18.5, 18.7, 34.1, 175.7 (Me_2CHCO), 11.7, 16.9, 26.6, 41.6, 176.2 ($CH_3CH_2CHMeCO$), 128.2, 128.6, 129.5, 133.4, 165.7 (C_6H_5CO). ^1H NMR and ^{13}C NMR data for sesquiterpenoid portion see Table 1. FAB–MS *m/z*: 699 $[M+Na]^+$, 659 $[M+H-H_2O]^+$, 641 $[M+H-2H_2O]^+$, 599 [659-HOAc]$^+$, 469 [659-2×HOAc–Me_2CHCO]$^+$, 409; EIMS 70 eV *m/z*: 661 $[M-CH_3]^+$, 643 [661-H_2O]$^+$, 633 $[M-Ac]^+$, 616 [M–HOAc]$^+$, 600 [661 + H–HOAc]$^+$, 244, 202, 105 [C_6H_5CO]$^+$, 85 [$CH_3CH_2CHMeCO$]$^+$, 71 [Me_2CHCO]$^+$, 43 $[Ac]^+$; HR–FAB–MS *m/z*: 699.2980 $[M+Na]^+$ (calc. for $C_{35}H_{48}O_{13}Na$, 699.2987).

3.3.2. Compound *2*

Amorphous white powder, mp 248–249°C. $[\alpha]_D^{24}$ +7.6° ($CHCl_3$; *c* 0.66). UV λ_{max}^{MeOH} nm (log ε): 247 (3.3481). IR υ_{max} cm^{-1}: 3383 (OH), 2979, 1727 (C=O), 1443, 1269, 1149, 1105, 1031, 955, 756, 714. ^1H NMR (300 MHz, $CDCl_3$): δ 1.53 and 2.16 (each 3H, *s*, 2×Ac), 1.35 and 1.37 (each 3H, *d*, *J* = 7.1 Hz), 2.86 (1H, *m*, Me_2CHCO), 7.83 (2H, *d*, *J* = 7.2 Hz), 7.54 (1H, *t*, *J* = 7.5 Hz), 7.39 (2H, *dd*, *J* = 7.2, 7.5 Hz, C_6H_5CO), 6.63 (1H, *d*, *J* = 1.8 Hz), 7.35 (1H, *d*, *J* = 1.8 Hz), 7.91 (1H, *d*, *J* = 0.5 Hz, β-furancarbonyl); ^{13}C NMR (75 MHz, $CDCl_3$): δ 20.3, 21.1, 169.4, 169.5 (2×Ac), 19.0, 19.1, 34.3, 176.6 (Me_2CHCO), 128.5, 129.3, 129.4, 133.3, 165.7 (C_6H_5CO), 109.5, 118.6, 143.8, 148.2, 161.8 (β-furancarbonyl). ^1H NMR and ^{13}C NMR data for sesquiterpenoid portion see Table 1. FAB–MS *m/z*: 709 $[M+Na]^+$, 687 $[M+H]^+$, 669 $[M-OH]^+$, 577 $[M+H-CH_3-Fu]^+$; EIMS 70 eV *m/z*: 671 [M-CH_3]$^+$, 626 [M–HOAc]$^+$, 608 [626-H_2O]$^+$, 593 [608-CH_3]$^+$, 574 [M–FuOH]$^+$, 566 [M–2HOAc]$^+$, 551 [M–CH_3–2HOAc]$^+$, 514 [574–HOAc]$^+$, 244, 229, 202, 105 [C_6H_5CO]$^+$, 95 [Fu]$^+$, 71 [Me_2CHCO]$^+$, 43 $[Ac]^+$; HR–FAB–MS *m/z*: 709.2467 $[M+Na]^+$ (calc for $C_{35}H_{42}O_{14}Na$, 709.2466).

3.3.3. Compound *3*

Amorphous white powder, mp 99–100°C. $[\alpha]_D^{24}$ −19.9°($CHCl_3$, C 0.66). UV λ nm (log ε) 243 (3.4676), 274 (2.9809). IR υ_{max} cm^{-1}: 3472 (OH), 2976, 1743 (C=O), 1374, 1237, 1106, 1039, 872, 714. ^1H NMR (300 MHz, $CDCl_3$): δ 2.04, 2.13, 2.15 and 2.24 (each 3H, s, 4×Ac), 7.98 (2H, *d*, *J* = 7.2 Hz), 7.55 (1H, *t*, *J* = 7.5 Hz), 7.44 (2H, *dd*, *J* = 7.2, 7.5 Hz, C_6H_5CO); ^{13}C NMR (75 MHz, $CDCl_3$): δ 20.9, 21.2, 21.3, 21.4, 169.6, 169.8, 169.9, 170.6 (4×Ac), 128.4, 129.5, 129.9, 133.1, 165.2 (C_6H_5CO). ^1H NMR and ^{13}C NMR data for sesquiterpenoid portion see Table 1. FA–BMS *m/z*: 613 $[M+Na]^+$, 591 $[M+H]^+$, 573 $[M-OH]^+$, 531 [M + H–HOAc]$^+$, 471 [M + H–2HOAc]$^+$; EIMS 70 eV *m/z*: 548 [M + H–Ac]$^+$, 530 [M + H–HOAc]$^+$, 515 [M–CH_3–HOAc]$^+$, 505 [548–Ac]$^+$, 244, 218, 105 [C_6H_5CO]$^+$, 43 $[Ac]^+$; HR–FAB–MS *m/z*: 613.2552 $[M+Na]^+$ (calc. for $C_{30}H_{38}O_{12}Na$, 613.2555).

References

Bruning, R., Wagner, H., 1978. Übersicht über die Celastreae-Inhatsstoffe: Chemie, Chemotaxnomie, Biosynthese, Pharmakologie. Phytochemistry 17, 1821–1858.

Jacobson, M., 1958. Insecticides from plants, a review of the literature, 1941–1953. Agricultural Handbook No. 154, USDA, US Government Printing Office. Washington, DC, pp. 44.

Liu, J.K., Becker, H., Zapp, J., Wu, D.G., 1995. Four sesquiterpenes from the insecticidal plant *Celastrus angulatus*. Phytochemistry 40, 841–846.

Liu, J.K., Han, X.W., Jia, Z.J., Ju, Y., Wang, H.Q., 1991. Two sesquiterpene alkaloids from *Celastrus angulatus*. Phytochemistry 30, 3437–3440.

Rozsa, Z., Pelczer, I., 1989. New sesquiterpene esters from *Euonymus europaeus* and *E. Latifolius*. J. Chem. Soc. Perkin Trans. 1, 1089–1095.

Rozsa, Z., Perjesi, A., Pelczer, I., Argay, G., Kalman, A., 1989. New sesquiterpene esters and alkaloids from *Euonymus japonicus*: the ejap serius. X-ray molecular structures of ejap-2,-3,-4,-5,-6 and-10. J. Chem. Soc. Perkin Trans. 1, 1079–1088.

Sang, H., Wang, H.Q., Tu, Y.Q., Chen, Y.Z., 1991. New β-dihydroagarofuran sesquiterpenoids from *Celastrus paniculatus*. Magn. Reson. Chem. 29, 650–655.

Takaishi, Y., Ohshima, S., Nakano, K., Tomimatsu, T., Tokuda, H., Nishido, H., Iwashima, A., 1993. Structures of sesquiterpene polyol esters from *Celastrus stephanotiifolius* with potential tumor-promotion inhibitory activity. J. Nat. Prod. 56, 815–824.

Tu, Y.Q., 1991. Structure of two new sesquiterpenoid insect antifeedants from *Celastrus rosthornianus*. J. Chem. Soc. Perkin Trans. 1, 425–427.

Tu, Y.Q., Wu, D.G., Zhou, J., Chen, Y.Z., 1992. Sesquiterpenes from two species of Celastreace. Phytochemistry 31, 1281–1283.

Wakabayashi, N., Wu, W.J., Waters, R.M., Redfern, R.E., Mills, Jr, G.D., Demilo, A.B., Lusby, W.R., Andrzejewski, D., 1988. Celangulin: a non-alkaloidal insect antifeedant from *Celastrus angulatus*. J. Nat. Prod. 51, 537–542.

Wang, M.A., Chen, F.H., 1995. Two new sesquiterpenes from *Celastrus orbiculatus*. Chinese Chemical Letters 6, 229–230.

Wang, M.A., Chen, F.H., 1997. Sesquiterpene polyol esters from *Celastrus flagellaris*. J. Nat. Prod. 60, 602–603.

Wang, M.T., Qin, H.L., Kong, M., Li, Y.Z., 1991. Insecticidal sesquiterpene polyol ester from *Celastrus angulatus*. Phytochemistry 30, 3931–3933.

Wu, W.J., 1991. A review of the studies on insecticidal action of Chinese bittersweet, *Celastrus angulatus* Max. Plant Protection 17, 34–38.

Wu, W.J., Tu, Y.Q., Zhu, J.B., 1992. Celangulin II, III and IV: new insecticidal sesquiterpenoids from *Celastrus angulatus*. J. Nat. Prod. 55, 1294–1298.

Wu, W.J., Wang, M.A., Zhu, J.B., Zhou, W.M., Hu, Z.N., Ji, Z.Q., 2001. Five new insecticidal sesquiterpenoids from *Celastrus angulatus*. J. Nat. Prod. 64, 364–367.

PERGAMON

Phytochemistry 58 (2001) 1189–1194

PHYTOCHEMISTRY

www.elsevier.com/locate/phytochem

Highly hydroxylated guaianolides of *Achillea asiatica* and Middle European *Achillea* species

Sabine Glasl[a,*], Armin Presser[c], Disan Gunbilig[b], Ingrid Werner[a], Samdan Narantuya[b], Ernst Haslinger[c], Johann Jurenitsch[a], Wolfgang Kubelka[a]

[a]*Institute of Pharmacognosy, University of Vienna, Althanstraße 14, A-1090 Wien, Austria*
[b]*Institute of Chemistry and Chemical Technology, Mongolian Academy of Sciences, Ulaanbaatar-51, Mongolia*
[c]*Institute of Pharmaceutical Chemistry, University of Graz, Schubertstraße 1, A-8010 Graz, Austria*

Received 12 February 2001; received in revised form 29 May 2001

Dedicated to Univ. Prof. Dr. W. Fleischhacker, Vienna on the occasion of his 70th birthday

Abstract

From flower heads of *Achillea asiatica* (L.) Serg., three new guaianolides were isolated by repeated column chromatography and HPLC. The constitution and the stereochemistry of these new, labile compounds were determined by MS, one (^{1}H, ^{13}C, selective ^{1}H-TOCSY and ^{1}H-NOESY) and two-dimensional NMR experiments (^{1}H, ^{1}H-COSY, ^{1}H, ^{13}C-HSQC, ^{1}H, ^{13}C-HMBC). The substances were identified as 8α-angeloxy-2α, 4α,10β-trihydroxy-6βH,7αH, 11βH-1(5)-guaien-12,6α-olide (**1**), 8α-angeloxy-1β,2β:4β,5β-diepoxy-10β-hydroxy-6βH, 7αH, 11βH-12,6α-guaianolide (**2**) and 8α-angeloxy-4α,10β-dihydroxy-2-oxo-6βH,7αH, 11βH-1(5)-guaien-12,6α-olide (**3**). They were also detected in Middle European species (*Achillea collina, Achillea ceretanica* (2× and 4×), *Achillea roseoalba, Achillea asplenifolia*) by HPLC, TLC and off line MS and have not been described before. The possibility that these compounds might be products of an oxidation process is discussed. © 2001 Elsevier Science Ltd. All rights reserved.

Keywords: *Achillea asiatica*; *Achillea collina*; *Achillea ceretanica*; *Achillea roseoalba*; *Achillea asplenifolia*; Compositae; Guaianolides; Sesquiterpene lactones; Proazulenes

1. Introduction

The isolation and characterization of some flavonoids and sesquiterpenes of Mongolian *Achillea asiatica* have recently been reported for the first time (Narantuya et al., 1999). The sesquiterpene pattern on TLC corresponded to proazulene containing species such as *Achillea collina*. The apolar and medium polar sesquiterpenes 8α-angeloxy-artabsin, 8α-tigloxy-artabsin, achillicin, 8α-angeloxy-3-oxa-artabsin, 8α-tigloxy-3-oxa-artabsin and 3-oxa-achillicin were identified by their chromatographical (TLC, HPLC) and spectral (UV, MS) behaviour (Narantuya et al., 1999). As the drug contained considerable amounts of polar proazulenes, the isolation and structure elucidation of the respective compounds (**1–3**) was carried out. In addition their presence in Middle European *Achillea* species was shown by combination of HPLC, TLC and off line MS after extraction with dichloromethane and purification on silica gel.

2. Results and discussion

Compounds **1–3** were isolated from polar fractions and are characterized by lability under the influence of light, oxygen and room temperature. **1** and **2** are proazulenes, giving a blue colour by spraying with acetic acid–phosphoric acid reagent, whereas **3** showed brown spots with anisaldehyde reagent on TLC. Molecular weights were determined by combination of EI- and CI-MS. The fragmentation pattern of all three compounds on electron impact ionization suggested the presence of several OH– and CH_3– groups but did not clearly show the molecular weights. Therefore the more soft chemical ionization was employed using either isobutane (positive mode, protonation of the molecule by H^+ ions) or the mixture CH_4–N_2O (77 + 23, negative mode, abstraction of one proton by OH^- ions) as reactant gas. The fragment $m/z = 83$ of high intensity as well as the occurrence

* Corresponding author. Tel.: +43-1-4277-55207; fax: +43-1-4277-9552.
E-mail address: sabine.glasl@univie.ac.at (S. Glasl).

0031-9422/01/$ - see front matter © 2001 Elsevier Science Ltd. All rights reserved.
PII: S0031-9422(01)00281-3

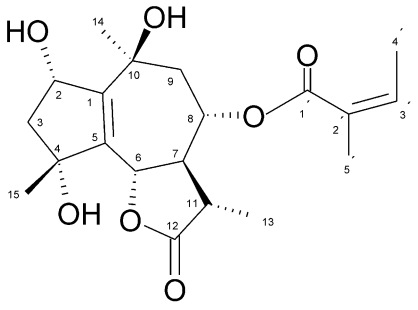

1

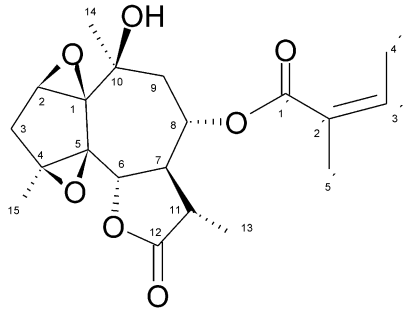

2

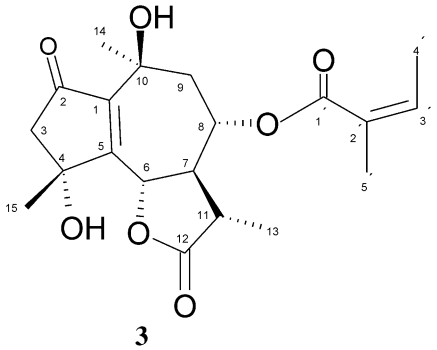

3

of another fragment resulting from a loss of 100 mass units indicated an unsaturated C-5 carboxylic acid ($M^+ - 82–18$). This was confirmed by ^{1}H-NMR spectrometry which showed the signals of an angelate for each compound. NMR spectra of **1**–**3** were recorded in deuterated acetone as in this solvent possible hydroxyl protons appear as sharp signals (see Table 1). That of **1** was additionally measured in chloroform-d, showing shifted proton signals but no deviations of the carbons compared to the spectra obtained with acetone-d_6 as solvent. The combination of the mass spectra with the information from the NMR experiments indicated the following for **1**–**3**: **1** (molecular mass $m/z = 380$, $C_{20}H_{28}O_7$, 7 double bond equivalents), **2** and **3** (molecular mass $m/z = 378$, $C_{20}H_{26}O_7$, eight double bond equivalents). The difference of one double bond equivalent must be related to a modified oxygen function as **1** showed three clearly visible OH signals (singlets at $\delta = 3.40$ and 4.04 ppm, doublet at $\delta = 3.72$ ppm) in contrast to **2** and **3**. They both exhibited a smaller number of hydroxyl groups, thus correlating well with the different chromatographical behaviour (Glasl et al., 2001).

In **1,** four spin systems were determined with the help of ^{1}H,^{1}H COSY, ^{1}H,^{13}C HSQC and selective ^{1}H-TOCSY (irradiation of H-2, H-3, H-8) experiments which could be connected with the aid of the ^{1}H,^{13}C-HMBC spectrum in addition to the carbon shifts. The largest spin system from C-6 to C-9 including the saturated lactone ring was connected via a quaternary carbon with a free hydroxyl group (C-10, $\delta = 71$ ppm) to a sp^2 carbon (C-1, $\delta = 147$ ppm). The corresponding sp^2 carbon of this double bond was represented by C-5 ($\delta = 143$ ppm) which showed cross peaks to CH_3-15, H-2β and H-2α in the ^{1}H,^{13}C HMBC. These correlations finally led to a 1(5)-guaien-12,6-olide substituted by three hydroxyl groups (positions 1, 4 and 10) and an angelate in position 8. Compound **1** as well as **2** and **3** showed substitution with angelic acid in position 8, indicated by a cross peak of H-8 to the carboxylic carbon of the acid ($\delta = 166–168$ ppm) in the ^{1}H,^{13}C HMBC on the one hand and the shift of H-8 at high frequency ($\delta = 5.60–5.66$ ppm) on the other hand. From the literature, is known that the substitution of the OH-group in position 8 with acetic acid causes reduction of the shielding (Martinez and Munoz-Zamora, 1988) and shifts the geminal proton for more than 1 ppm to deeper field, which confirms the described conditions in the present substances.

The more apolar compounds **2** and **3** had the same molecular formula but differed in the number of hydroxyl functions. Compared with **1** compound **3** had only two hydroxyl groups (singlets at $\delta = 3.94$ and 4.58 ppm) and lacked the doublet corresponding to OH-2 as well as H-2. An additional quaternary carbon at $\delta = 206$ ppm as well as a high frequency shift of H-6 ($\delta = 5.78$ ppm, $\Delta\delta = 0.3$ ppm) suggested that C-2 carried a carbonyl. Conjugation with the 1(5) double bond resulted in a shift of λ_{max} to 230 nm in contrast to **1** which had only a slight shoulder at 220 nm. Signals of H-7, H-11 and CH_3-15 were shifted to higher frequency and those of H-3β and H-3α appeared as a two proton singlet at $\delta = 2.58$ ppm. The latter seems to be typical for five-membered rings with one carbonyl function, as the same phenomenon has been described for a similar compound oxygenated in position 3 (Bordoloi et al., 1989).

The chemical shifts in the ^{1}H,^{13}C-HMBC of compound **2** suggested the presence of three additional carbons with an oxygen function besides C-4 and C-10 instead of one carbonyl and two sp^2 carbons. The one hydroxyl visible in the ^{1}H NMR as a singlet ($\delta = 4.61$ ppm) was related to position 10 due to a long range coupling with C-9. Consequently five of the seven oxygens were thus accounted for by this OH group, the lactone ring and the angelate. Thus the four remaining C–O functions formed two epoxides in positions 1, 2 and 4, 5.

Selective NOE experiments were necessary to determine the stereochemistry of **1–3**. Irradiation of the protons H-6,

Table 1
^{1}H-NMR data of compounds **1**, **2** and **3** (400 MHz, δ ppm, TMS as int. standard)

H	**1**		**1**		**2**		**3**	
	Chloroform-*d*		Acetone-d_6		Acetone-d_6		Acetone-d_6	
2	α OH n.d.[a]		α OH 3.70	*d*	α 3.53	*d*	–	
	β 4.74	*br t*	β 4.72–4.77	*m*	–			
3α	1.99	*dd*	1.85	*dd*	1.82	*dd*	2.54[b]	*d*
3β	2.38	*m*	2.22–2.29	*m*	1.90	*d*	2.59[b]	*d*
4α	n. d.	(OH)	3.39	*s*	–		3.94	*s* (OH)
6β	5.30	*dd*	5.47	*dd*	5.43	*d*	5.78	*d*
7α	2.19	*q*	2.54	*q*	2.55	*q*	2.72	*q*
8β	5.48	*m*	5.56–5.62	*m*	5.65	*td*	5.60	*m*
9α	1.93	*m*	1.93–2.00	*m*	2.05	*t*	1.95	*dd*
9β	2.30	*dd*	2.17	*dd*	2.30	*dd*	2.28	*dd*
10β (OH)	n. d.		4.04	*s*	4.64	*s*	4.57	*s*
11β	2.60	*m*	2.64–2.70	*m*	2.79–2.84	*m*	2.78–2.84	*m*
13α (CH_3)	1.21	*d*	1.21	*d*	1.23	*d*	1.23	*d*
14α (CH_3)	1.53	*s*	1.65	*s*	1.14	*s*	1.63	*s*
15 (CH_3)	1.46	*s*	1.46	*s*	1.46	*s*	1.71	*s*
3′	6.14	*qq*	6.19	*qq*	6.18	*qq*	6.22	*qq*
4′ CH_3	2.00	*dq*	2.01	*dq*	1.99	*dq*	2.02	*dq*
5′ CH_3 (s)	1.84	*m*	1.90–1.94	*m*	1.89–1.92	*m*	1.91–1.93	*m*

Multiplicities and coupling constants of overlapping signals were estimated from selective 1D-TOCSY- and NOESY experiments; *J* (Hz): compound **1**: 2α,2β = 7.6; 2β,3β = 3.5; 3α,3β = 13.8; 6,7 = 10.4; 6,8 = 1.8; 7,8 = 10.7; 8,9β = 4.8; 9α,9β = 14.2; 11,13 = 6.9; 3′,4′ = 7.2; 3′,5′ = 1.5; compound **2**: 2α,3α = 2.6; 3α,3β = 15.9; 6,7 = 10.2; 7,8 = 10.6; 8,9β = 3.8; 9α,9β = 13.9; 11,13 = 7.1; 3′,4′ = 7.2; 3′,5′ = 1.5; compound **3**: 3α,3β = 18.5; 6,7 = 10.7; 7,8 = 10.1; 8,9β = 4.9; 9α,9β = 15.3; 11,13 = 6.9; 3′,4′ = 7.2; 3′,5′ = 1.5.

[a] n.d., not detectable.

[b] Signals interchangeable.

H-7, H-8, H-11, CH_3-13 and CH_3-14 suggested a similar stereochemistry of the seven-membered ring in all three compounds. The values of the coupling constants with respect to the Dieder dihedral angles indicated axial orientation for H-6β, H-7α, H-8β and H-9α. Positive NOEs between H-6β and CH_3-15 as well as from H-2β to H-3β and OH-10β led to the relative configurations of **1** and **3**. The orientation of H-2 in compound **2** as alpha was shown by positive NOEs with H-3α (strong) and H-9α (weak). Also that H-2α showed only one cross peak with H-3α can be explained if it is α orientated, implying dihedral angles of 90° with H-3β (therefore no coupling) and of 45° with H-3α leading to a coupling constant of 3–4 Hz. If H-2 was β orientated only coupling with H-3β would be expected. Positive NOEs between CH_3-15α and H-7α, H-3α (both strong) and CH_3-13α (weak) led to the relative configuration shown.

Similar substances lacking the oxygen in position 8 have been reported from *Artemisia absinthium*: artabsinolide A (8-deangeloxy-derivative of **3**) and the 8-deangeloxy-derivative of **2** with both epoxides α-orientated (Kelsey and Shafizadeh, 1979; Beauhaire and Fourrey, 1982). Beauhaire and Fourrey (1982) showed that artabsin dissolved in methanol together with Rose Bengal was converted via an unstable 1,4-endoperoxide to several intermediates in the presence of oxygen. Similarly the compounds **1**–**3** might be formed from 8α-angeloxyartabsin, one of the main compounds in *Achillea asiatica* (Narantuya et al., 1999), by a ''photo-oxygenation'' process. This might take place during the vegetation period in the living plant or could be triggered artificially during the isolation procedure by careless handling. To minimize the latter, fractions were not heated beyond 40 °C, protected from daylight by tin foil and dried before storage over night at + 4 °C maximum. **1**–**3** were also detected in the proazulene containing Middle European species *A. collina, Achillea ceretanica* (2× and 4×), *Achillea roseoalba* and *Achillea asplenifolia*. After a drying period of three weeks at room temperature these species were extracted and analyzed within 1 day, which indicates the oxidation to take place already in the living plant.

The occurrence of guaianolides without exocyclic methylengroup in the lactone ring corresponds with the literature describing this carbon skeleton as characteristic for diploid and tetraploid taxa of the *Achillea millefolim* group (Kubelka et al., 1999). They show antiphlogistic activity in the croton oil ear test (Kastner et al., 1993) lacking any allergenic potential due to the saturated methyl group in the lactone ring, which could also be expected for the compounds presented in this paper. Considering the increased polarity of **1**–**3** compared to 8α-angeloxy- and 8α-tigloxyartabsin a higher rate of transfer into aqueous preparations might occur. Taking these facts into account, a contribution of **1–3** to the efficacy of remedies prepared from *Achillea* can be expected. Quantification analyses and pharmacological investigations are in process.

3. Experimental

3.1. Plant material, extraction, isolation

Aerial parts of *A. asiatica* (L.) Serg. were collected in Central Mongolia (Töv aimag) near the River Shavart, at the time of full flowering. The plants were identified by Dr. Ganbold (Institute of Biology and Biotechnology, Mongolian Academy of Sciences), voucher specimens were deposited at the same Institute, Ulaanbaatar, Mongolia.

One thousand grams dried above ground parts (chopped) of *A. asiatica* were extracted three times in portions with dichloromethane by ultrasonification for 10 min. The oily green residue (29.0 g) was solved again in dichloromethane and purified by addition of the same volume of methanol–water (1 + 1). Evaporation of the dichloromethane at 40 °C maximum yield an oily sticky residue which was filtered and extracted again. After extraction of the unified methanol–water (1 + 1) fractions with dichloromethane 3.9 g of a yellow oily residue resulted. Separation into eleven fractions was performed by VLC using silica gel as stationary phase and dichloromethane, dichloromethane–acetone and dichloromethane–methanol with increasing polarity as mobile phase. Repeated HPLC (RP-8) and CC (silica gel) yielded 16.0 mg of **1**, 1.6 mg of **2** and 3.0 mg of **3** (colourless oils; Glasl et al., 2001). Due to the lability of the compounds this amount does not represent the real concentrations in the plant.

For the identification of **1**–**3** in the Middleeuropean taxa dried flowerheads (2 g) of the respective drug were extracted and purified as described above. The yellow oily residue (0.1 g) was fractionated by CC on silica gel using dichloromethane and dichloromethane-acetone with increasing polarity. The polar proazulene fractions containing **1** eluted with the mixture dichloromethane-acetone (7 + 3) and were analyzed by TLC and HPLC with the pure compound as reference (Glasl et al., 2001).

3.2. Thin layer chromatography

Silica gel 60 Merck plates (0.25 mm) were used with dichloromethane–acetone (9 + 1, v/v; **1**: $R_f = 0.1$; **2**: $R_f = 0.18$; **3**: $R_f = 0.25$; matricin: $R_f = 0.4$) and dichloromethane–methanol (9 + 1, V/V; **1**: $R_f = 0.5$; matricin: $R_f = 0.8$) as mobile phase. As reference a dichloromethane extract of chamomile was prepared. After detection with acetic acid–phosphoric acid reagent (Stahl, 1967) under heat (140 °C) proazulenes **1** and **2** gave blue coloured spots, **3** was characterized by quenching of fluorescence and brown colour after spraying with anisaldehyde sulfuric acid reagent (Dequeker, 1964).

3.3. HPLC

The HPLC system consisted of a Perkin-Elmer Series 200 pump and a LC235C diode array detector (detection at 220 and 255 nm). All computations were performed using the Perkin-Elmer software Turbochrom®. Separations were carried out using a Hewlett Packard LiChrospher®100 RP-8 5 μm column (250×4.0 mm) guarded by a Hewlett Packard LiChrospher®100 RP-8 5 μm guard column (4×4 mm). The binary system employed the eluents methanol and water according to a gradient. The elution started from 20% methanol to 80% methanol in 90 min (linear; rate = 0.67%/min) with a flow-rate of 1.0 ml/min at room temperature. The identification of **1-3** in the Middle European taxa was achieved by retention times and the UV-vis spectra (DAD detection), additionally off-line TLC-MS was performed by sampling the corresponding HPLC fractions. The fractions were extracted with dichloromethane, the organic layer was removed under reduced pressure, the residue was redissolved in ≈50 μl dichloromethane and used for TLC confirmation and off-line MS (Glasl et al., 2001).

3.4. Structure elucidation

3.4.1. MS

A Shimadzu QP-1000 EX MSPAC 200 with direct inlet and two possible ionisation modi (EI-MS, CI-MS) was used. EI-mode: ion source: 250 °C, 70 eV; vacuum: 4×10^{-6} torr; scan: 40–500/2s; heating rate of sample vial: 80 °C/min; CI-mode: ion source: 180 °C, 200 eV; reactant gas: CH_4–N_2O (77 + 23) 4.8 and isobutane 4.0, pre-pressure: 1 bar; vacuum: 5×10^{-5} torr; scan: 60–400/2s; heating rate of sample vial: 80 °C/min. HRMS spectra were measured with a Finnigan MAT 8230 instrument at the Institute of Organic Chemistry, University of Vienna (70 eV, resolution 1000).

3.4.2. IR

A solution of the respective compound in dichloromethane was dropped on a silicium plate (13×1 mm, polished optically, Korth Kristalle GmbH) leaving a slight oily film. Spectra were recorded with a Perkin-Elmer System 2000GC IR (software Spectrum for Windows 1.30); resolution: 4 cm^{-1}; J-stop resolution: 7.77 cm^{-1}; apodization: strong; gain: 1; OPD velocity: 2 cm/s; interferogramm: bi-directional double sided; phase correction: self 64; number of scans: 1; scan range: 5200–370 cm^{-1}; interval: 1.0 cm^{-1}.

3.4.3. UV

The UV spectra were recorded on line in methanol–water by DAD detection during an HPLC run.

3.4.4. NMR

^1H, ^{13}C, ^1H, ^1H-COSY, ^1H, ^{13}C-HSQC, ^1H, ^{13}C-HMBC, selective ^1H-TOCSY and ^1H-NOE experiments were recorded with a Varian Unity Inova 400 NMR spectrometer at 297 K. Tubes: 5 mm diameter (Kontes). Dual probe head with shielded *z*-gradients or broadband

probe (400 MHz). Solvents: acetone-d_6, chloroform-*d*. TMS was used as internal standard. Chemical shifts were given in ppm. The HMBC experiment was optimized for a long-range coupling constant of 8 Hz. Before NOE experiments were performed, dissolved oxygen was removed by bubbling Ar through the solution.

3.4.5. 8α-Angeloxy-2α,4α,10β-trihydroxy-6βH,7αH, 11βH-1(5)-guaien-12,6α-olide (**1**)

CIMS (CH_4–N_2O, 77 + 23) *m*/*z* (% rel. int.): 379 $[M-H]^-$ (83.5), 361 $[M-H-OH]^-$ (12.9), 279 [M−H–angeloxy]$^-$ (95.7), 261 [M−H–angeloxy–OH]$^-$ (100.0), 243 [M−H–angeloxy–OH–OH]$^-$ (27.0), 233 (85.1); EI-MS *m*/*z* (% rel. int.): 380 $[M]^+$ (0.48), 365 $[M-CH_3]^+$ (48.7), 362 $[M-OH]^+$ (2.6), 347 $[M-CH_3-OH]^+$ (2.14), 265 $[M-CH_3$–angeloxy$]^+$ (4.3), 262 [M−OH–angeloxy]$^+$ (29.7), 247 $[M-CH_3$–OH-angeloxy$]^+$ (32.6), 229 $[M-CH_3$–OH-angeloxy–OH$]^+$ (8.7), 219 (17.2), 205 (14.1), 201 (15.0), 83 [ang]$^+$ (100.0); HREI–MS *m*/*z*: 365.1602 $[M-CH_3]^+$ (calc for $C_{19}H_{25}O_7$ 365.1600); IR: ν_{max} cm^{-1}: 2929 (*s*, CH), 1779 (*s*, C=O γ-lactone), 1714 (*s*, C=O angelic acid), 1233 (*m*, C–O angelic acid), 1159 (*s*, C–O γ-lactone). Optical rotation $[\alpha]_D^{20}$ + 7.4, ($CHCl_3$; *c* 0.11); UV λ_{max} = 222 nm (methanol–water). For ^1H and ^{13}C NMR data, see Tables 1 and 2.

3.4.6. 8α-Angeloxy-1β,2β:4β,5β-diepoxy-10β-hydroxy-6βH,7αH,11βH-12,6α-guaianolide (**2**)

CI-MS (isobutane) *m*/*z* (% rel. int.): 379 $[M+H]^+$ (100.0), 361 $[M+H-OH]^+$ (49.6), 279 [M + H–angeloxy]$^+$ (22.6), 261 [M + H–angeloxy–OH]$^+$ (48.7), 243 [M + H–angeloxy–OH–OH]$^+$ (24.8), 101 (59.5), 83 [ang]$^+$ (58.6); EI–MS *m*/*z* (% rel. int.): 379 (0.3), 378 $[M]^+$ (0.1), 361 (0.5), 360 $[M-OH]^+$ (0.3), 278 [M−angeloxy]$^+$ (0.6), 260 [M−angeloxy–OH]$^+$ (4.2), 245 [M−angeloxy–OH–CH_3]$^+$ (1.6), 236 (2.9), 218 (14.3), 163 (8.5), 111 (50.8), 83 [ang]$^+$ (100.0); HREI–MS *m*/*z*: 378.1685 (calc for $C_{20}H_{26}O_7$ 378.1679); IR ν_{max} cm^{-1}: 2928 (*s*, CH), 2855 (*m*, CH), 1779 (*s*, C=O γ-lactone), 1713 (*s*, C=O angelic acid), 1648 (*w*, C=H), 1232 (*m*, C–O angelic acid), 1159 (*s*, C–O γ-lactone). Optical rotation $[\alpha]_D^{20}$ + 2.7, ($CHCl_3$; *c* 0.16); UV λ_{max} = 222 nm (methanol–water). For ^1H and ^{13}C NMR data, see Tables 1 and 2.

3.4.7. 8α-Angeloxy-4α,10β-dihydroxy-2-oxo-6βH,7αH, 11βH-1(5)-guaien-12,6α-olide (**3**)

CI–MS (isobutane) *m*/*z* (% rel. int.): 379 $[M+H]^+$ (15.2), 361 $[M+H-OH]^+$ (100.0), 343 [M + H—OH–OH]$^+$ (8.2), 279 [M + H–angeloxy]$^+$ (3.0), 261 [M + H–angeloxy–OH]$^+$ (12.1), 243 [M + H–angeloxy–OH–OH]$^+$ (5.5); EI–MS *m*/*z* (% rel. int.): 379 (1.4), 378 $[M]^+$ (0.4), 363 $[M-CH_3]^+$ (1.3), 361 (19.3), 360 $[M-OH]^+$ (1.3), 344 (1.5), 343 (6.9), 263 [M−angeloxy–CH_3]$^+$ (89.4), 260 [M−angeloxy–OH]$^+$ (32.0), 246 (2.1), 243 (10.1), 221 (17.6), 205 (33.8), 83 [ang]$^+$ (100.0); HREI-MS *m*/*z*: 378.1676 (calc for $C_{20}H_{26}O_7$ 378.1679); IR ν_{max} cm^{-1}: 2927 (*s*, CH), 2855 (*m*, CH), 1788 (*s*, C=O γ-lactone), 1714, 1700 (*s*, overlapping signals: C=O angelic acid and C=O carbonyl), 1266 (*s*), 1235 (*s*, C–O angelic acid), 1147 (*s*, C–O γ-lactone). Optical rotation $[\alpha]_D^{20}$ + 9.5, ($CHCl_3$; *c* 0.44); UV λ_{max} = 230 nm (methanol–water). For ^1H and ^{13}C NMR data, see Tables 1 and 2.

Table 2
^{13}C-NMR data of compounds **1**, **2** and **3** resulting from ^1H,^{13}C-HSQC and ^1H,^{13}C-HMBC (400 MHz, δ ppm, acetone-d_6, TMS as int. standard)

C		1	2	3
1	C_q	147.7	67.7	143.1
2	CH, C_q	74.4	64.5	206.1
3	CH_2	51.0	33.1	52.8
4	C_q	82.7	74.5	76.2
5	C_q	143.8	66.7	169.9
6	C_q	76.8	74.0	76.1
7	CH	54.8	53.7	53.2
8	CH	73.7	72.5	72.7
9	CH_2	46.8	46.3	44.4
10	C_q	71.2	70.9	71.0
11	CH	41.2	40.8	41.5
12	COO	178.1	177.3	177.1
13	CH_3	15.3	15.8	14.9
14	CH_3	29.6	26.3	29.5
15	CH_3	28.2	16.8	27.1
1′	C_q	167.1	166.7	166.9
2′	C_q	128.7	128.2	128.2
3′	CH	139.7	139.1	140.0
4′	CH_3	15.9	15.7	15.9
5′	CH_3	20.7	20.4	20.5

Acknowledgements

Financial support by ÖAD is gratefully acknowledged. Collections of the Middle European plant material were carried out within a project supported financially by the "Fond zur Förderung der wissenschaftlichen Forschung" (P09341-BIO). The authors thank Dr. Ganbold from the Mongolian Academy of Sciences for the identification of *Achillea asiatica*.

References

Beauhaire, J., Fourrey, J.L., 1982. Structures of the artabsinolides. Photo-oxygenation studies on artabsin. Journal of the Chemical Society, Perkin Transactions 1, 861–864.

Bordoloi, M., Sarmah, J.C., Sharma, R.P., 1989. Biomimetic transformation of a guaianolide to a pseudoguaianolide. Tetrahedron 45, 289–302.

Dequeker, R., 1964. Over een niet gewone Handelspolygala. Pharmaceutisch Tijdschrift voor Belgie 41, 39–47.

Glasl, S., Gunbilig, D., Narantuya, S., Jurenitsch J., 2001. Combination of chromatographic and spectroscopic methods for the isolation and characterization of polar guaianolides from *Achillea asiatica*. Journal of Chromatography B, in press.

Kastner, U., Sosa, S., Tubaro, A., Della Loggia, R., Jurenitsch, J., 1993. Anti-edematous activity of sesquiterpene lactones from dif-

ferent taxa of the *Achillea millefolium* group. Planta Medica 59 (Suppl.), A669.

Kelsey, R.G., Shafizadeh, F., 1979. Sesquiterpene lactones and systematics of the genus *Artemisia*. Phytochemistry 18, 1591–1611.

Kubelka, W., Kastner, U., Glasl, S., Saukel, J., Jurenitsch, J., 1999. Chemotaxonomic relevance of sesquiterpenes within the *Achillea millefolium* group. Biochemical Systematics and Ecology 27, 437–444.

Martinez, V.M., Munoz-Zamora, A., 1988. Conformational analysis of achillin and leukodin. Journal of Natural Products 51, 221–228.

Narantuya, S., Glasl, S., Batsuren, D., Jurenitsch, J., 1999. The flavonoids and sesquiterpenes of *Achillea asiatica* (L.) Serg. Scientia Pharmaceutica 67, 69–76.

Stahl, E., 1967. Dünnschicht-Chromatographie, Reagens Nr. 65. Springer Verlag, New York, p. 825.

PERGAMON

Phytochemistry 58 (2001) 1195–1198

PHYTOCHEMISTRY

www.elsevier.com/locate/phytochem

Triterpenoids from *Lawsonia alba*

Bina. S. Siddiqui*, Muhammad Nadeem Kardar

H.E.J. Research Institute of Chemistry, University of Karachi, Pakistan

Received 11 January 2001; received in revised form 5 July 2001

Abstract

Two pentacyclic triterpenoids have been isolated from the aerial parts of *Lawsonia alba*. The structures of the new constituents, named as lawsonic acid and lawsonin have been elucidated as 3α-*E*-ferulyloxy-lup-20(29)-en-28-oic acid and 3α-*E*-ferulyloxy-urs-11-en-13β-ol respectively through spectroscopic studies. © 2001 Elsevier Science Ltd. All rights reserved.

Keywords: *Lawsonia alba*; Lythraceae; Aerial parts; Triterpenoids; 3α-*E*-Ferulyloxy-lup-20 (29)-en-28-oic acid and 3α; -*E*-Ferulyloxy-urs-11-en-13β-ol; Lawsonic acid and Lawsonin

1. Introduction

Lawsonia is a monotypic genus represented by *Lawsonia inermis* Linn (syn. *Lawsonia alba* Lam, Lythraceae), a native of North Africa and south-west Asia, widely cultivated as an ornamental hedge and dye-plant. The leaves of *L. inermis* have long been used in India and Middle East countries as a cosmetic for colouring palms of hands and dyeing of hair for personal adornment (Manjunath, 1962). The leaves also used as a prophylactic in the form of paste or decoction for the skin inflammation (Chopra et al., 1956). The essential oil obtained from the flowers finds use in perfumery due to its β-ionone content. The leaves have been reported to contain various compounds like coumarins, flavonoids, gallic acid, naphthoquinones, naphthalene derivatives, lupane type triterpenoids (Handa et al., 1997; Mebe et al., 1998), aliphatic constituents, phenolic glycosides and xanthones (Gupta et al., 1992). Recently, reports have appeared on the chemical constituents of the roots (Gupta et al., 1992) and bark (Gupta et al., 1992). However, studies on the chemical constituents of the seeds are lacking and only analysis of fatty acids, waxes and colouring matter is reported (Manjunath, 1962). In the present work, studies on the chemical constituents of the aerial parts of *Lawsonia alba,* collected from Karachi university campus were undertaken which resulted in the isolation and structure elucidation of two new triterpenoids of lupane and α-amyrin skeleton, named as lawsonic acid and lawsonin along with three known constituents, β-sitosterol, oleanaldehyde and betulinaldehyde. The structures of these constituents have been elucidated through spectral studies including 1D ^{1}H and ^{13}C NMR (broad band and DEPT) and 2D NMR (COSY-45, NOESY, *J*-resolved, HMQC and HMBC) analysis. These studies form the basis of present communication.

2. Results and discussion

The HR–EIMS of lawsonic acid (**1**) showed molecular ion peak at *m/z* 632.4076 corresponding to the formula $C_{40}H_{56}O_6$. Five methyl singlets at δ 0.86, 1.01, 0.85, 0.87 and 0.97 in the ^{1}H NMR spectrum and the molecular formula were indicative of a triterpenoidal skeleton. The ^{1}H NMR spectrum further displayed an isopropenyl side chain by signals at *δ* 1.63 (3H, *s*, H-30), 4.57 and 4.67 (each 1H, *d*, H-29a and H-29b) manifesting its relation with lupane type of triterpenoids. These protons had their connectivities with carbons at *δ* 147.8 and 110.6 respectively in the HMBC spectrum. Besides these, a quaternary carbon at *δ* 179.2 in the BB spectrum was assigned to C-28 from its connectivity with H-29 a/b and H-30 in the HMBC spectrum. The molecular formula indicated that apart from a C-30 skeleton 1 had a side chain of C-10 units. This could be decided as 6′-methoxy-7′-hydroxy-*trans*-cinnamoyloxy (*E*-ferulyloxy) group on the basis of spectral data (vide experimental).

* Corresponding author. Tel.: +92-21-4968926 and 4983591; fax: +92-21-4968926 and 496124.

E-mail address: bina@khi.comsats.net.pk (B.S. Siddiqui).

0031-9422/01/$ - see front matter © 2001 Elsevier Science Ltd. All rights reserved.
PII: S0031-9422(01)00329-6

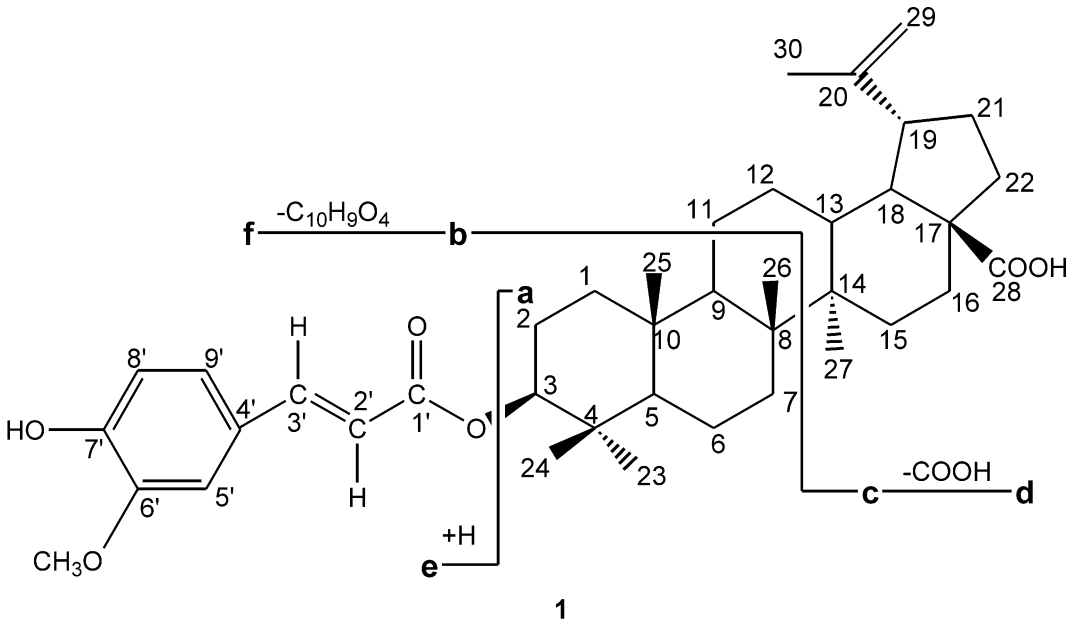

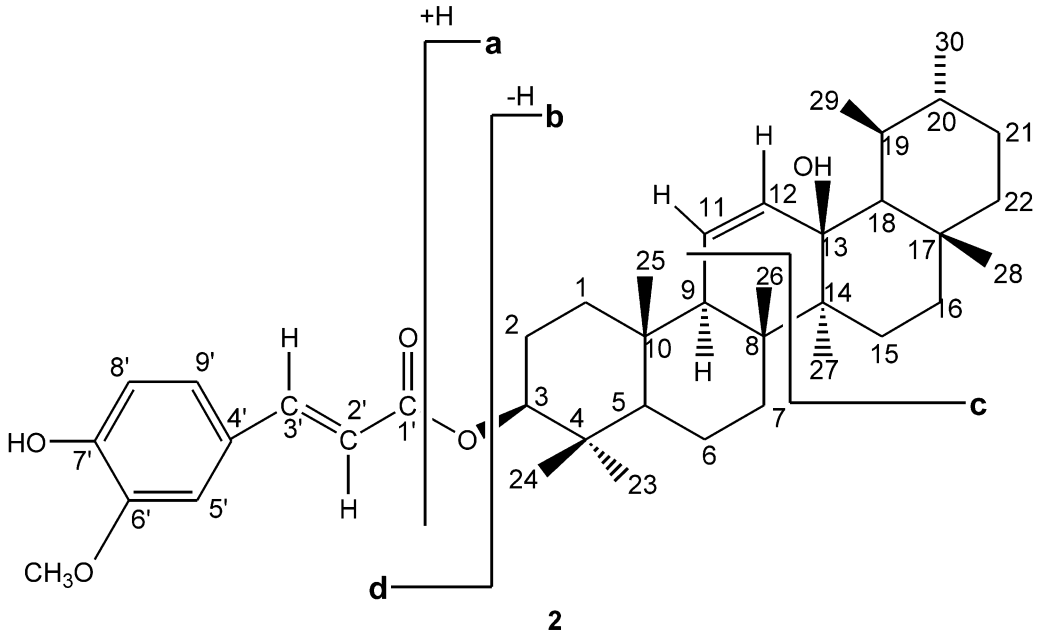

Important MS fragments of **1** and **2**

The ^{1}H NMR spectrum showed two doublets at δ 7.59 and 6.30 each with a coupling constant of 15.9 Hz (H-3′ and H-2′ respectively); two one-proton doublets at δ 7.03 (J = 1.6 Hz, H-5′) and 6.91 (J = 8.1 Hz, H-8′) and a one-proton double doublet at δ 7.06 (J = 8.1, 1.6 Hz, H-9′). The carbons connected to these protons were identified at δ 145.6 (C-3′), 115.0 (C-2′), 109.5 (C-5′), 114.6 (C-8′) and 123.0 (C-9′) respectively in the HMQC spectrum. The UV maxima at 325.2 and 299.4 nm further support this moiety. Furthermore, four downfield quaternary carbons were noted in the BB spectrum at δ 167.5, 127.0, 146.0 and 147.2 which were ascribable to C-1′, C-4′, C-6′ and C-7′ respectively through comparison of their shifts with the reported values (Kuo, et al., 1997) and interaction observed for these carbons and aromatic protons in the HMBC spectrum. A three-proton downfield signal was present at 3.90 (δ_c, 55.5) which could be placed at C-6′ as these protons had interaction

with H-5′ in the NOESY spectrum. This ester group was placed at C-3 on biogentic consideration since there was only one downfield double doublet at δ 4.89 ($J=11.6$, 4.7 Hz). These features justified 12 out of 13 unsaturations hence the remaining double bond equivalence was justified by a carboxyl group at C-17 which was supported by a significant mass fragment at m/z 248 (B.P) due to cleavage of ring C. Thus the structure of lawsonic acid was elucidated as 3α-*E*-ferulyloxy-lup-20 (29)-en-28-oic acid and substantiated by various mass fragments at m/z 438 (fragment **a**), 385 (fragment **b**), 248 (fragment **c**), 203 (fragment **d**), 194 (fragment **e**), 189 (fragment **f**) (vide structure). The skeleton was finally confirmed through hydrolysis of 1 with 2% methanolic KOH which yielded betulinic acid (vide experimental).

The HR–EIMS of lawsonin (**2**) showed a molecular ion peak at m/z 600.4178 corresponding to the formula $C_{40}H_{56}O_4$ [M^+–H_2O]. The presence of six methyl singlets at δ 0.87,0.88, 0.89, 0.99, 1.05, and 1.14 and two doublets of three-proton each at δ 0.95 ($J=6.2$ Hz) and 0.94 ($J=5.4$ Hz) in the ^{1}H-NMR spectrum were indicative of its triterpenoidal skeleton. The two doublets of methyl protons and a doublet of H-18 at δ 2.01 ($J=12.3$ Hz) manifested that it belongs to ursane series. The molecular formula, number of unsaturation, UV absorption at 323.6 nm, and the NMR data (vide infra) further suggested its relation with an α-amyrin group with a *E*-ferulyloxy substituent. Thus, the ^{1}H NMR spectrum displayed two AB doublets at δ 7.59 and 6.30 with a coupling constant of 15.9 Hz which were attributable to H-3′ and H-2′ respectively. These had connectivity with C-3′ (δ 144.4) and C-2′ (δ 116.2) respectively in the HMQC spectrum. The ^{1}H NMR spectrum further showed three downfield protons at δ 7.06 (*dd*, $J=8.1$, 1.6 Hz), 7.03 (*d*, $J=1.6$ Hz) and 6.91 (*d*, $J=8.1$ Hz) due to ortho-meta (H-9′), meta (H-5′) and ortho (H-8′) coupled protons. These protons had cross peaks at δ 123.0 (C-9′), 109.2 (C-5′) and 114.6 (C-8′) respectively in the HMQC spectrum. One of the substituents in the aromatic ring was decided as a methoxy group considering a three-proton singlet at δ 3.90 (δ_c 55.5.), while the other could be a hydroxyl group as all the carbons of the molecule were justified. Their respective positions could be decided on the basis of interactions in the NOESY spectrum which showed connectivity between H-5′ and-OCH_3 and hence the hydroxyl group was placed at C-7′ and the methoxy group at C-'6.

The ester group was placed at C-3 of the terpenoidal skeleton on biogenetic grounds and was supported by the characteristic double doublet of H-3 now present at δ 4.65 ($J=11.5$, 5.2 Hz) instead of its normal value (*ca.* δ 3.11). These features justified eleven unsaturations, five by the skeletal rings and six by the ester group and left one double bond equivalent to be decided. This could be accounted for by a double bond at C-11 due to two one-proton signals at δ 5.57 (*br. d*, $J=5.8$ Hz) and 5.50 (*dd*, $J=5.8$, 3.0 Hz). That H-12 has a larger coupling constant with H-9 as compared to that of H-11 was established on the basis of 2D NMR data including ^{1}H–^{1}H-COSY and HMBC interactions. This observation has been recorded earlier also based on 2D NMR experiments (Siddiqui et al., 1999). This left only one oxygen to be accounted for which was decided to be a hydroxyl group (δ 1.6 *br. s*, exchangeable with D_2O) located on a non-protonated carbon as no other carbinylic proton was present and the ^{13}C NMR had a non-protonated downfield carbon at δ 80.7. It was placed at C-13 as H-12 showed only one coupling with H-9. An interaction of the hydroxyl proton with H-29 (δ 0.95) and H-18β (δ 2.01, *d*, $J=12.3$ Hz) displayed the β disposition of the hydroxyl group at C-13. In the light of these considerations, the structure of lawsonin was elucidated as 3α-*E*-ferulyloxy-13β-hydroxy-urs-11-ene. Substantial evidence was also provided by the mass fragments at m/z 442 (fragment **a**), 424 (fragment **b**), 234 (fragment **c**), 193 (fragment **d**) (vide structure).

Table 1
^{13}C NMR spectral data for compounds **1** and **2**

No.	1	2	No.	1	2
1	38.3	39.0	21	29.7	25.6
2	26.2	27.2	22	37.3	37.0
3	79.7	80.4	23	28.1	28.0
4	38.8	39.7	24	16.3	17.0
5	47.8	55.9	25	16.3	17.0
6	16.9	18.3	26	16.4	16.4
7	23.2	33.2	27	14.9	25.4
8	42.9	38.6	28	179.2	23.6
9	52.2	45.5	29	110.6	20.2
10	37.2	38.1	30	19.5	23.7
11	21.2	120.7	1′	167.5	167.1
12	23.8	125..2	2′	115	116.2
13	38.5	80.7	3′	145.6	144.4
14	43	42.7	4′	127.0	127.0
15	30.3	29.7	5′	109.5	109.2
16	31.3	23.6	6′	146	146.2
17	55.8	42.8	7′	147.2	147.2
18	46.7	55.9	8′	114.6	114.6
19	49.8	32.5	9′	123.0	123.0
20	147.8	33.2	OCH_3	55.5	55.5

3. Experimental

3.1. General

The NMR spectra were recorded on Bruker AMX-500 instrument with TMS as int. standard. MS were obtained on Finnigan MAT 311A instrument. IR spectra were recorded on JASCO IR A-1 spectrophotometer, whereas UV spectra were recorded on Hitachi U-3200 spectrophotometer. Optical rotations were measured on JASCO DIP-360 digital polarimeter. The petrol used was of the boiling range 60–80 °C.

3.2. Plant material

The aerial parts (40 kg) of *Lawsonia alba* were collected from the region of University of Karachi, Pakistan in October 1998. The plant was identified by Dr. Surayya Khatoon, University of Karachi, and a voucher (specimen No. 67503) has been deposited at the Herbarium of the same University.

3.3. Extraction and isolation

The aerial parts of *Lawsonia alba* (40 kg) was extracted with dichloromethane (×5) and the marc left was repeatedly extracted with methanol (×5) at room temperature. The solvent from both these extracts was removed separately under reduced pressure. The gummy residue from dichloromethane extract was treated with petrol to give petrol soluble and insoluble fractions. The latter was treated with Et_2O to yield Et_2O soluble and Et_2O insoluble fractions. The Et_2O insoluble fraction was divided into EtOAc soluble and EtOAc insoluble fractions. The EtOAc soluble fraction was concentrated and poured into an excess of petrol and was kept in cold over night. A brownish residue (4 g) which settled down was filtered and subjected to column chromatography over silica gel GF_{254}. The column was eluted with $CHCl_3$, $CHCl_3$–MeOH and MeOH in order of increasing polarity. The fractions were combined on the basis of TLC to give 29 fractions. Out of these, fractions No 5 (15 mg), and No 9 (18 mg), were pure showing single spots on TLC. Their spectral studies revealed them to be new constituents and they were named as lawsonic acid (**1**) and lawsonin (**2**). Fraction No. 8 showed three main spots, which were separated through thick layer chromatography on silica gel (GF_{254}, E-Merck; ($CHCl_3$–MeOH, 9.8:0.2). Three pure compounds were thus obtained which were identified as β-sitosterol (9.1 mg), oleanaldehyde (6.0 mg) and betulinaldehyde (4 mg) through comparison of their spectral data, with those reported in literature (Budzikiewicz et al., 1963).

3.3.1. Lawsonic acid (*1*)

Amorphous powder (15 mg); $[\alpha]_D^{26}$ +7.8 (MeOH, *c*, 0.76); UV λ_{max} MeOH nm: 325.2, 299.4; IR ν_{max} $CHCl_3$ cm^{-1}: 3650 (OH), 2900 (C–H), 1700 (C=O), 1600–1450 (aromatic), 1350 (C–O); ^1H NMR spectral data ($CDCl_3$) δ: 0.85, 0.86, 0.87, 0.97, 1.01 (each 3H, *s*, 5×CH_3), 4.57 (1H, br.*s*, H-29a), 4.67 (1H, br.*s*, H-29b), 4.89 (1H, *dd*, *J* = 11.6, 4.7 Hz, H-3), 6.30 (1H, *d*, *J* = 15.9 Hz, H-2′), 6.91 (1H, *d*, *J* = 8.1 Hz, H-8′), 7.03 (1H, *d*, *J* = 1.6 Hz, H-5′), 7.06 (1H, *dd*, *J* = 8.1, 1.6 Hz, H-9′), 7.59 (1H, *d*, *J* = 15.9 Hz, H-3′); HR–EIMS *m*/*z*: 632.4073 (calc. $C_{40}H_{56}O_6$ 632.4076); EIMS *m*/*z* (rel. int.): 632 [M^+] (16), 438 (13), 248 (100), 233 (14), 207 (19.3), 203 (98), 194 (3.27), 189 (75), 177 (21.7), 163 (94.3), 133 (50); ^{13}C NMR: Table 1.

3.3.1.1. Hydrolysis of (1). To lawsonic acid (5 mg) 2% methanolic KOH (1 ml) was added and the reaction mixture was kept overnight at room temperature. On usual work up a whitish solid was obtained showing a single spot on TLC. It formed fine needles in MeOH. m.p. 282-285 °C (betulinic acid m.p. 282-285 °C, Ikuta et al., 1988). M^+ 456.

3.3.2. Lawsonin (*2*)

Amorphous powder (18 mg); $[\alpha]_D^{25}$ + 36.4 (MeOH, *c*, 0.245); UV λ_{max} MeOH nm: 323.6, 294.0; IR ν_{max}: $CHCl_3$ cm^{-1}: 3500 (OH), 2800 (C–H), 1700 (C=O), 1600–1450 (aromatic), 1300 (C–O); ^1H NMR spectral data ($CDCl_3$) δ: 0.87, 0.88, 0.89, 0.99, 1.05, 1.14 (each 3H, *s*, 6×CH_3), 0.94 (3H, *d*, *J* = 5.48, H-29/H-30), 0.95 (3H, *d*, *J* = 6.2, H-29/H-30), 4.65 (1H, *dd*, *J* = 11.5, 5.2 Hz, H-3), 5.50 (1H, *dd*, *J* = 5.8, 3.1 Hz, H-12), 5.57 (1H, *br*. *d*, *J* = 5.8 Hz, H-11), 6.30 (1H, *dd*, *J* = 15.9, H-2′), 6.91 (1H, *d*, *J* = 81.Hz, H-8′), 7.03 (1H, *d*, *J* = 1.6 Hz, H-5′), 7.06 (1H, *dd*, *J* = 8.1, 1.6 Hz, H-9′), 7.59 (1H, *J* = 15.9 Hz, H-3′); HR–EIMS *m*/*z*: 600.4176 (calc. $C_{40}H_{56}O_4$ 600.4178); EIMS *m*/*z* (rel. int.); 600 [M^+] (63.4), 442 (23.8), 424 (10.10), 414 (15.26), 234 (30.53), 232 (19.30), 207 (54.34), 203 (100), 193 (5.47), 189 (59.6), 177(21.7), 163 (94.6), 123 (79.3); ^{13}C NMR: Table 1.

References

Budzikiewicz, L.H., Wilson, J.M., Djerassi, C., 1963. Mass spectrometry in structural and stereochemical problems. XXXII. Pentacyclic triterpenes. J. Am. Chem. Soc. 85, 3688–3699.

Chopra, R.N., Nayar, S.L., Chopra, I.C., 1956. Glossary of Indian Medicinal Plants. Council of Scientific and Industrial Research, New Delhi, p. 151.

Gupta, S., Ali, M., Alam, M.S., Niwa, M., Sakai, T., 1992. 24β-Ethycholest-4-en-3β-ol from roots of *Lawsonia inermis*. Phytochemistry 31, 2558–2560.

Handa, G., Kapil, A., Sharma, S., Singh, J., 1997. Lawnermis acid: a new anticomlementry triterpenoid from *Lawsonia inermis*. Indian Journal of Chemistry 36B, 252–256.

Ikuta, A., Itokawa, H., 1988. Triterpenoids of *Paeonia japonica* callus tissue. Phytochemistry 27, 2813–2815.

Kuo, Y.H., Chang, C.I., Kuo, Y.H., 1997. Triterpens from *Diospyros maritima*. Phytochemistry 46, 1135–1137.

Manjunath, B.L., 1962. The Wealth of India. Council of Scientific and Industrial Research New, Delhi, pp. 47–50.

Mebe, P.P., Cordell, G.A., Pezzuto, J.M., 1998. Pentacyclic triterpenes and naphthaquinones from *Euclea divinorum*. Phytochemistry 47, 311–313.

Siddiqui, B.S., Sultana, I., Begum, S., 1999. Triterpenoidal constituents from *Eucalyptus camaldulensis* var. *obtusa* leaves. Phytochemistry 54, 861–865.

PERGAMON

Phytochemistry 58 (2001) 1199–1204

PHYTOCHEMISTRY

www.elsevier.com/locate/phytochem

Further constituents from the bark of *Holarrhena pubescens*

Bina Shaheen Siddiqui[a,*], Shahid Bader Usmani[a], S. Tahir Ali[b], Sabira Begum[a], Ghazala H. Rizwani[b]

[a]*H.E.J. Research Institute of Chemistry, International Centre for Chemical Sciences, University of Karachi, Karachi 75270, Pakistan*
[b]*Department of Pharmacognosy, University of Karachi, Karachi 75270, Pakistan*

Received 11 January 2001; received in revised form 27 June 2001

Abstract

Three compounds, pubadysone [11α-hydroxy-18,20-oxido-3-oxo-pregna-1,4,17(20)-triene] (**1**), puboestrene [3-acetoxy-17-oxo-1,3,5(10)-estratriene] (**2**) and pubamide [3,18-dioxo-11α-hydroxycona-1,4-diene] (**3**), have been isolated from the bark of *Holarrhena pubescens*. Their structures have been established through spectroscopic studies. © 2001 Elsevier Science Ltd. All rights reserved.

Keywords: Holarrhena pubescens; Apocynaceae; Bark; Steroids; Alkaloids

1. Introduction

Holarrhena pubescens (Buch. Ham) [synonym: *H. antidysenterica* L. Apocynaceae] is an Indian medicinal tree. The tree is common in the forests of India and Pakistan indigenous to tropical Himalaya and Assam (Bhutani et al., 1984). The stem bark of this plant, commercially known as kurchi, has astringent, antidysenteric, anthelmintic, stomachic, febrifugal and tonic properties. It is used in the treatment of amoebic dysentery and diarrhoea (Sastri, 1957), usually administered as an extract or decoction. A hot decoction of bark is used as a gargle in toothache (Dymock et al., 1980). Chemical studies on *H. pubescens* were undertaken as far back as 1858 when the alkaloid conessine was first isolated from the bark of the plant (Dymock et al., 1980). Since then this plant has been extensively studied for its alkaloids (Atta-ur-Rahman, 1990) due to their pharmacological significance. Studies undertaken by our group on the bark of the plant led to the isolation of several new compounds (Begum et al., 1993, 1994; Siddiqui et al., 1993, 1994, 1995). In continuation of these investigations three new compounds pubadysone, a steroid in the pregnane series, puboestrene, a steroid in the oestrone series and pubamide an alkaloid in the conanine series have now been obtained. The isolation and structure elucidation of these constituents form the basis of this report. The structural studies are based on 1D and 2D NMR experiments (COSY 45, HMQC and HMBC) and other spectral evidences.

2. Results and discussion

Pubadysone (**1**) showed a molecular ion peak in the HRMS at *m*/*z* 326.1857, corresponding to the molecular formula $C_{21}H_{26}O_3$ (calc. 326.1881). The molecular formula showed nine double bond equivalents in the molecule. Compound **1** showed one three-proton singlet for a tertiary methyl at δ 1.34 and an olefinic methyl singlet at δ 2.07 in the ^{1}H NMR spectrum (Table 1). It exhibited strong absorptions in the IR spectrum at 1650 cm^{-1} and the UV spectrum at 247 nm indicating the presence of a conjugated carbonyl moiety. The ^{1}H NMR spectrum showed three deshielded olefinic protons at *δ* 7.81 (1H, *d*, *J* = 10.3 Hz, H-1), 6.15 (1H, *dd*, *J* = 10.3, 2.0 Hz, H-2) and 6.09 (1H, *t*, *J* = 2.0 Hz, H-4), accounting for three double-bond equivalents (2 C=C and 1 C=O). The chemical shifts and coupling constants of the olefinic signals, along with a peak at *m*/*z* 121.0679, permitted the location of a 1,4-dien-3-one moiety in ring A of the molecule (Davis et al., 1970). This was further confirmed by ^{13}C NMR showing a signal at *δ*, 186.7 characteristic of an α,β-unsaturated ketone, and other peaks at δ, 158.8, 125.3, 124.7 and 167.8 for olefinic carbons (Table 1). A one-proton

* Corresponding author. Tel./fax: +92-21-4968926.
E-mail address: bina@khi.comsats.net.pk (B.S. Siddiqui).

0031-9422/01/$ - see front matter © 2001 Elsevier Science Ltd. All rights reserved.
PII: S0031-9422(01)00330-2

doublet of triplets at δ, 3.69 ($J=11.0$, 11.0, 4.7 Hz) indicated an axial proton geminal to an OH group followed by a peak at δ, 70.1 in the ^{13}C NMR spectrum. The multiplicities and coupling constants of this signal suggested the location of the OH group at either C-7 or C-11. The downfield chemical shift (δ, 7.81) of H-1 which is comparable with other 11α-OH compounds (Bhutani et al., 1988) located this group at position 11. Further support was obtained from the interactions in the HMBC spectrum. Two mutually coupled doublets at δ, 3.68 and 3.51 ($J=9.2$), a vinylic three-proton singlet at δ, 2.07 and the remaining six degrees of unsaturation indicated that a five-membered unsaturated ring with oxygen as a hetero atom is present in a pregnane-type skeleton. These observations were further confirmed by ^{13}C NMR signals at δ, 72.7, 110.1 and 158.6 assigned to C-18, C-17 and C-20, respectively. These observations led to the assignment of structure **1** to pubadysone. The structure was substantiated by various connectivities observed in COSY 45°, NOESY, HMQC and HMBC spectra and mass fragments (vide structure).

The molecular formula of **2**, $C_{20}H_{24}O_3$, was obtained through accurate mass measurement (found 312.1702, calcd. for $C_{20}H_{24}O_3$: 312.1725) of the molecular ion and showed nine double-bond equivalents. Its IR (1720, 1600, 1590, 1480 and 1450 cm^{-1}) and UV (267 nm) absorptions and the signals in the ^1H NMR spectrum at δ, 7.26 (1H, *d*, $J=8.5$ Hz, H-1), 6.84 (1H, *dd*, $J=8.5$, 2.6 Hz, H-2), 6.98 (1H, *d*, $J=2.6$ Hz, H-4) and 2.27 (3H, *s*, $COCH_3$) (Table 1) were suggestive of an aromatic ring A carrying an acetoxy function. In the HMQC spectrum, cross peaks for hydrogen and carbon connectivities were noted for C-1/H-1 (δ, 126.4/7.26), C-2/H-2 (δ, 118.8/6.84), C-4/H-4 (δ, 121.6/6.98) and $CO\underline{C}H_3/COC\underline{H}_3$ (21.1/2.27). Besides these, in the Broad Band spectrum signals were present at δ, 169.9 ($\underline{C}OCH_3$), 148.7 (C-3), 138.0 (C-5) and 137.4 (C-10). The mass fragments at *m/z* 134.0347 and 178.1397 (vide structure) confirmed this ring. The placement of the acetoxy group at C-3 was fully supported by the multiplicities of H-1, H-2 and H-3, and HMBC correlations.

The presence of a tertiary methyl signal at δ, 0.90 (3H, *s*, H-18) and absence of H-19 signal in both ^1H and ^{13}C NMR showed that **2** belongs to the estrane series of steroids. The IR spectrum further showed an absorption at 1745 cm^{-1}, characteristic of a five- membered ketone which was placed at C-17 on the basis of the connectivities of H-16a, H-16b (δ, 2.36, 2.10) and H-18 (δ, 0.90) with the carbonyl carbon (δ, 220.5) observed in the HMBC spectrum. This was further confirmed by comparison to data for other 17-keto steroids (Breitmaier and Voelter, 1978; Johnson and Jankowski, 1978). On the basis of these observations, structure **2** has been assigned to puboestrene.

The molecular formula ($C_{21}H_{27}NO_3$) of **3**, obtained through accurate mass measurement (found 341.1989, calc. for $C_{21}H_{27}NO_3$: 341.1990) of the molecular ion showed nine double-bond equivalents. Its IR (1660 cm^{-1}) and UV (245 nm) absorptions indicated the presence of 1,4-dien-3-one system in ring A. The dienone system was supported by the ^1H NMR signals at δ, 7.77 (1H, *d*, $J=10.5$ Hz), 6.10 (1H, *dd*, $J=10.5$, 2.0 Hz) and 6.09 (1H, *t*, $J=2.0$ Hz) (Table 1); the corresponding carbon signals were observed in the HMQC plot at δ, 159.1, 126.6 and 124.8, and quaternary carbons at δ, 186.9 (C-3) and 168.7 (C-5) in the broad band spectrum. This ring was substantiated by a strong peak at *m/z* 121.0727 (C_8H_9O) in the HRMS (Budzikiewicz et al., 1964). The IR spectrum also showed the presence of an OH group (3400 cm^{-1}) which was placed at C-11 with α-disposition on the basis of the evidence discussed for compound **1**. The IR spectrum (1690 cm^{-1}) and remaining degree of unsaturation revealed the presence of another carbonyl group in the molecule. The absence of a carbon-18 signal, and downfield chemical shifts of C-14 and C-20 (i.e. δ, 59.4 and 67.8) were suggestive of a carbonyl group at position 18, making a five-membered lactam ring. This was supported by a mass fragment at *m/z* 71.0371 (C_3H_5NO) in the HRMS spectrum (vide structure) and a signal at δ, 183.8 for amido carbonyl carbon in the ^{13}C NMR spectrum. Thus, pubamide has been assigned structure **3**, which was further supported by significant mass fragments (vide structure).

3. Experimental

3.1. General

Mps are uncorrected. Mass spectra were recorded on a Finnigan MAT 112 and 312 double-focusing mass spectrometer connected to a PDP 11/34 computer system; NMR spectra ($CDCl_3$ 400 MHz for ^1H and 75 MHz for ^{13}C) were recorded on a Bruker AM 400 and an AM 300 FT NMR, respectively. The chemical shifts are reported in δ, (ppm) and the coupling constants are in Hz. The ^{13}C NMR spectral assignments (Table 1) have been made partly through a comparison of the chemical shifts with the published data for similar compounds (Atta-ur-Rahman, 1990) and partly through the appearance of signals in DEPT, HMQC (Table 1) and HMBC spectra. Precoated thin-layer cards (DC-karten SiF) were used for TLC. The petroleum ether used was of the boiling range 60–70 °C. Flash column chromatography was performed on model Eyela EF-10. Si gel used was from Merck 9385 and Al_2O_3 was from Merck 90.

3.2. Plant material

The bark of *H. pubescens (H. antidysenterica)* was supplied by courtesy of Hamdard Foundation Pakistan

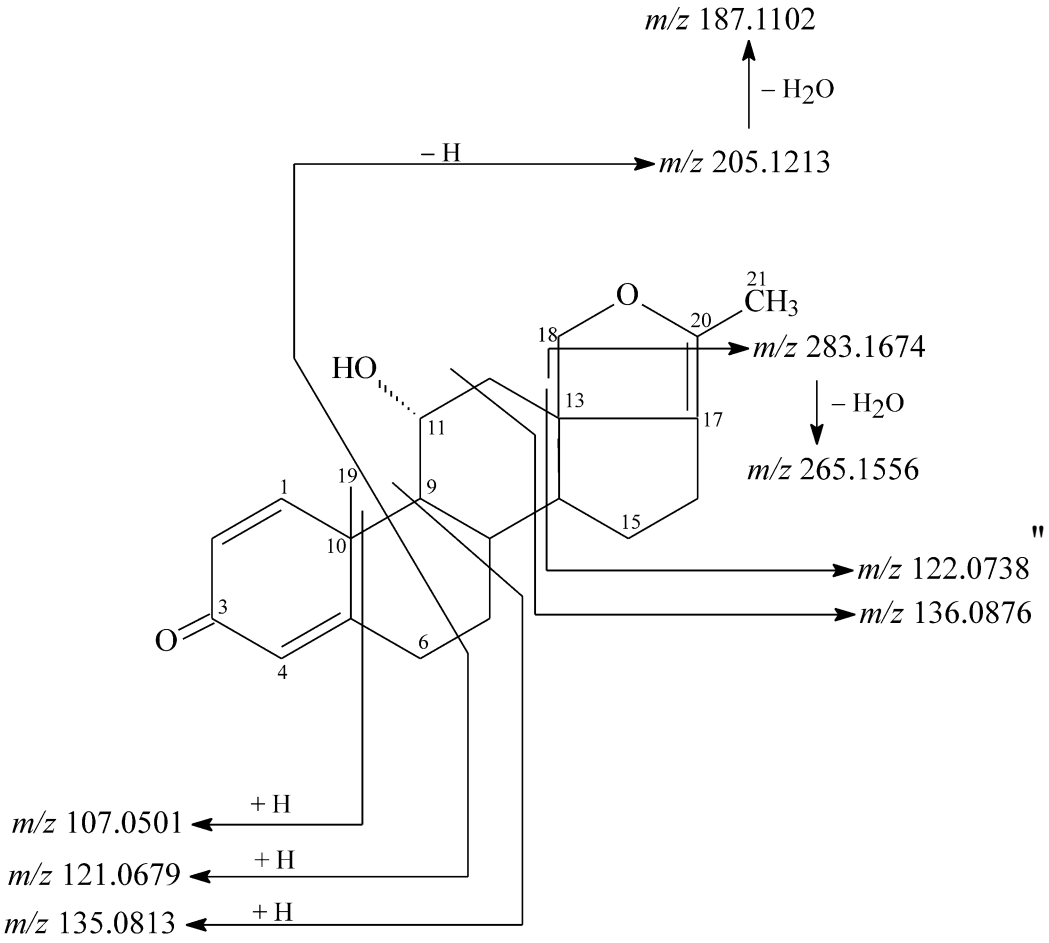

1

Ltd. It was identified by Miss. Ashreen Jahan, a botanist at Hamdard Foundation Pakistan Ltd.

3.3. Extraction and isolation

Uncrushed bark (10 kg) was macerated with 10% methanolic NaOH (10 l) for 48 h at 28 °C, and repeatedly percolated with MeOH for 48 h (five times) at the same temperature following the reported procedure (Siddiqui and Pillay, 1932) in order to hydrolyze the tannates. Each extract was neutralized with 30% aqueous HOAc. The syrupy concentrate (2 l) obtained on removal of the solvent from the combined extracts under reduced pressure was acidified by adding 10% aqueous HOAc at 28 °C and the solution was extracted with EtOAc. The aqueous phase was basified with 20% NH_3 and again shaken out with EtOAc. The EtOAc phase was treated with vigorous stream of CO_2. The precipitate containing the carbonate bases was filtered and the filtrate was dried over anhydrous Na_2SO_4 and freed of the solvent under reduced pressure. The residue (20 g) from the filtrate was divided into petroleum ether soluble and petroleum ether insoluble fractions. The petroleum ether soluble fraction yielded conessine (9 g) according to the reported isolation procedure (Siddiqui and Pillay, 1932). The petroleum ether insoluble portion (11 g), when dissolved in 10% aqueous AcOH and treated with $(NH_4)_2SO_4$, furnished a colourless precipitate of sulfates which was filtered. The sulfate mother liquor was made alkaline with 10% aqueous NaOH and extracted with EtOAc. The EtOAc phase was washed with H_2O to neutral pH, dried (Na_2SO_4) and evaporated under reduced pressure to give a colourless residue (9.5 g). This residue was subjected to flash column chromatography (Al_2O_3, Merck 90; petroleum ether, petroleum ether–EtOAc; $CHCl_3$, in order of increasing polarity). Nine fractions were ultimately obtained on combining the eluates on the basis of TLC. The major fraction eluted with $CHCl_3$ was re-chromatographed on flash column (Si gel; petroleum ether, petroleum ether–EtOAc, in order of increasing polarity). The petroleum ether–EtOAc (4:6) eluate furnished a crude fraction A (52 mg). The petro-

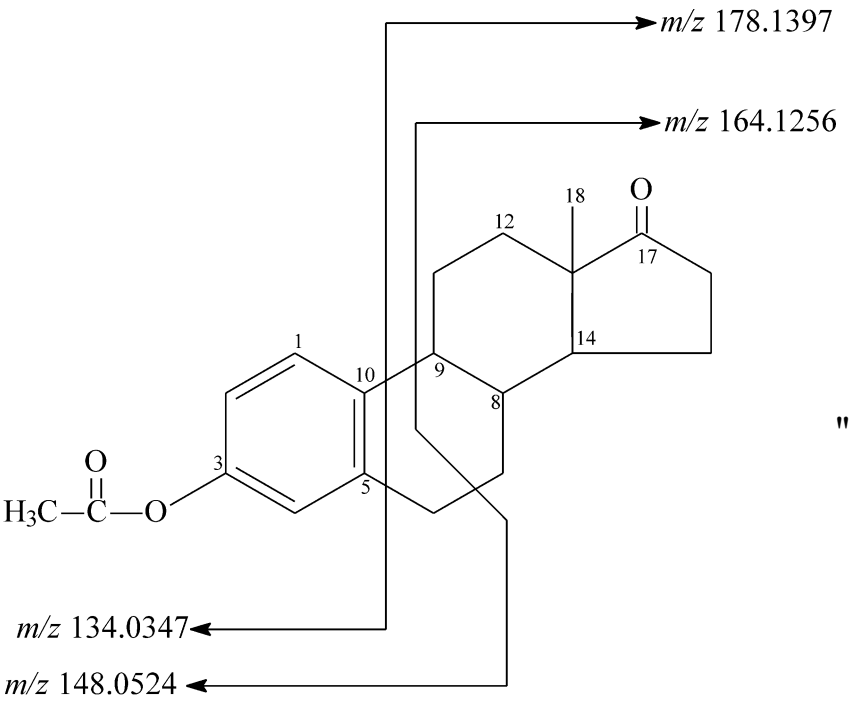
m/z 178.1397
m/z 164.1256
18
O
12
17
1
14
10
9
8
3
5
O
H3C—C—O
m/z 134.0347
m/z 148.0524

"

2

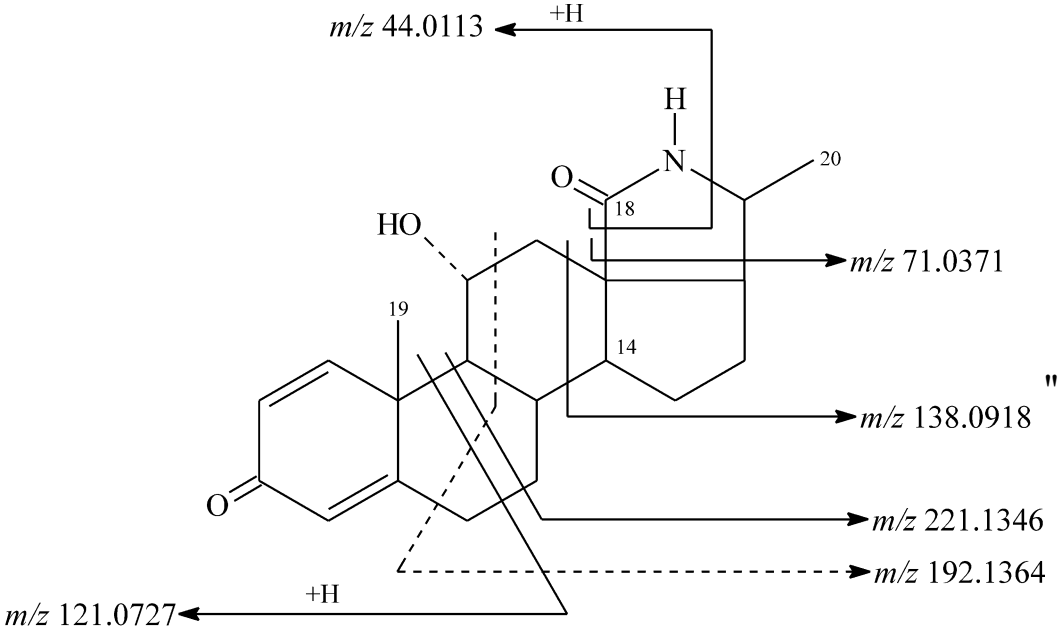
m/z 44.0113
+H
H
N
20
O
18
HO
m/z 71.0371
19
14
m/z 138.0918
O
m/z 221.1346
m/z 192.1364
+H
m/z 121.0727

"

3

Table 1
^{1}H and ^{13}C NMR spectral data for compounds **1**–**3**[a]

Position	**1**		**2**		**3**	
	δ_C	δ_H (*m*, *J* in Hz)	δ_C	δ_H (*m*, *J* in Hz)	δ_C	δ_H (*m*, *J* in Hz)
1	158.8	7.81 (*d*, 10.3)	126.4	7.26 (*d*, 8.5)	159.1	7.77 (*d*, 10.5)
2	125.3	6.15 (*dd*, 10.3,2.0)	118.8	6.84 (*dd*, 8.5, 2.6)	126.6	6.10 (*dd,* 10.5, 2.0)
3	186.7	–	148.7	–	186.9	–
4	124.7	6.09 (*t*, 2.0)	121.6	6.98 (*d*, 2.6)	124.8	6.09 (*t*, 2.0)
5	167.8	–	138.0	–	168.7	–
6	33.6	2.04 (*m*) 1.22 (*m*)	29.4	1.40 (*m*) 1.90 (*m*)	29.7	1.30 (*m*) 1.90 (*m*)
7	27.7	1.36 (*m*) 1.29 (*m*)	26.4	1.40 (*m*) 2.40 (*m*)	33.1	1.52 (*m*) 1.54 (*m*)
8	36.0	1.42 (*m*)	38.1	1.52 (*m*)	33.0	2.32 (*m*)
9	59.1	1.50 (*m*)	44.2	2.26 (*m*)	60.0	1.00 (*m*)
10	43.9	–	137.4	–	44.4	–
11	70.1	(β) 3.69 (*ddd*, 11.0, 11.0, 4.7)	25.8	1.64 (*m*) 2.04 (*m*)	77.2	(β) 4.48 (*ddd,* 10.5, 10.5, 5.0)
12	50.7	(α) 2.55 (*dd*, 11.0, 4.7) (β) 1.58 (*m*)	31.6	1.42 (*m*) 1.90 (*m*)	43.7	1.42 (*m*) 2.32 (*m*)
13	53.5	–	48.0		61.6	–
14	47.6	1.22 (*m*)	50.6	1.42 (*m*)	59.4	2.14 (*m*)
15	26.2	1.70 (*m*) 1.60 (*m*)	21.6	2.20 (*m*) 2.52 (*m*)	23.2	1.32 (*m*) 1.38 (*m*)
16	34.0	2.44 (*ddd*, 13.1, 4.9, 1.3) 2.36 (*ddd*, 13.1, 4.1, 2.6)	35.9	2.10 (*dd*, 18.8, 6.0) 2.36 (*ddd*, 18.8, 8.7)	34.1	1.12 (*m*) 2.00 (*m*)
17	110.1	–	220.5	–	53.7	1.18 (*m*)
18	72.7	3.68 (*d*, 9.2) 3.51 (*d*, 9.2)	13.9	0.90 (*s*)	183.8	–
19	18.6	1.34 (*s*)			18.8	1.37 (*s*)
20	158.6	–		–	67.8	3.90 (*m*)
21	22.2	2.07 (*s*)			16.4	1.19 (*d*, 6.5)
$COCH_3$			21.1	2.27 (*s*)	-	-
$\underline{C}OCH_3$			169.9			

[a] The assignments are based on COSY-45°, *J*-resolved, broad band, DEPT, HMQC and HMBC spectra.

leum ether–EtOAc (3:7) eluate afforded B (38 mg) and petroleum ether–EtOAc (2:8) eluate gave fraction C (46 mg). The crude fractions A, B and C afforded **1** (22 mg), **2** (17 mg) and **3** (13 mg), respectively, on purification on thin layer plates of si gel with solvent systems $CHCl_3$–MeOH (9:1; 8.8:1.2 and 8.5:1.5, respectively).

3.4. 11α-Hydroxy 18, 20-oxido-3-oxo-pregna-1,4,17 (20)-triene (*1*)

Orange red plates (MeOH); mp 108–110 °C; UV λ_{max} (MeOH) 204, 247 nm; IR ν_{max} ($CHCl_3$), 3400, 3000, 1650, 1610, 1590, 1150 cm^{-1}; EIMS (70 eV) *m*/*z* $(M)^+$ 326.1857 ($C_{21}H_{26}O_3$ requires $(M)^+$ 326.1881) (90), 283.1674 (15), 265.1556 (32), 205.1213 (45), 187.1102 (16), 136.0876 (20), 135.0813 (18), 122.0738 (100), 121.0679 (80), 107.0501 (22); ^{1}H NMR and ^{13}C NMR: Table 1.

3.5. 3-Acetoxy-17-oxo-estra-1,3,5(10)-triene (*2*)

Reddish plates (MeOH); mp 92–94 °C; UV λ_{max} (MeOH) 204, 267 and 275 nm; IR ν_{max} ($CHCl_3$), 3150, 1745, 1720, 1600, 1590, 1480, 1450, 1150 cm^{-1}; EIMS (70 eV) *m*/*z* $(M)^+$ 312.1702 ($C_{20}H_{24}O_3$ requires $(M)^+$ 312.1725) (34), 269.1529 (100), 178.1397 (22), 164.1256 (18), 148.0524 (24), 134.0347 (8); ^{1}H and ^{13}C NMR: Table 1.

3.6. 3,18-Dioxo-11α-hydroxy-cona-1,4-diene (*3*)

Orange rods (MeOH); mp 130–132 °C; UV λ_{max} (MeOH) 245, and 201 nm; IR ν_{max} ($CHCl_3$), 3400, 3000, 1690, 1660, 1610, 1595, 1150 cm^{-1}; EIMS (70 eV) *m*/*z* $(M)^+$ 341.1989 ($C_{21}H_{27}NO_3$ requires $(M)^+$ 341.1990) (21), 323.1854 (17), 221.1346 (100), 192.1364 (18), 138.0918 (24), 121.0727 (15), 71.0371 (35), 44.0113 (14); ^{1}H and ^{13}C NMR: Table 1.

References

Atta-ur-Rahman, 1990. Handbook of Natural Product Data, Diterpenoid and Steroidal Alkaloids. Elsevier, New York, pp. 452-481.
Begum, S., Usmani, S.B., Siddiqui, B.S., Siddiqui, S., 1993. Alkaloidal

constituents of the bark of *Holarrhena antidysenterica*. Heterocycles 36, 717–723.

Begum, S., Usmani, S.B., Siddiqui, B.S., Siddiqui, S., 1994. Alkaloids from the bark of *Holarrhena pubescens*. Phytochemistry 36, 1537–1541.

Bhutani, K.K., Ali, M., Sharma, S.R., Vaid, R.M., Gupta, D.K., 1988. Three new steroidal alkaloids from the bark of *Holarrhena antidysenterica*. Phytochemistry 27, 925–928.

Bhutani, K.K., Raj, S., Gupta, D.K., Kumar, S., Atal, C.K., Kaul, M.K., 1984. Profile of kurchi in India. Indian Drugs 21, 212–216.

Breitmaier, E., Voelter, W., 1978. Monographs in Modern Chemistry Vol. V. Carbon 13 NMR spectroscopy. VCH-Verlagsgesellschaft FRG 8, 227–235.

Budzikiewicz, H., Djerassi, C., Williams, D.H., 1964. Structure Elucidation of Natural Products by Mass Spectrometry. Holden Day, San Francisco, pp. 6–48.

Davis, J.B., Jewers, K., Manchanda, A.H., Wood, A.B., 1970. Maingayine: a new steroidal alkaloid from *Paravallaris maingayi*. Chemistry and Industry, 627.

Dymock, W., Warden, C.J.H., Hooper, D., 1980. Pharmacographia Indica, The Institute of Health and Tibbi Research, Vol. 2. (republished under the auspices of Hamdard National Foundation of Pakistan), pp. 391–398.

Johnson, L.F., Jankowski, W.C., 1978. Carbon-13 NMR Spectra. Robert E. Krieger Publishing Company, New York (Compound No. 481).

Sastri, B.N., 1957. The Wealth of India, Vol. 5. Council of Scientific and Industrial Research, New Dehli, pp. 103–107.

Siddiqui, S., Pillay, P.P., 1932. The alkaloids of *Holarrhena antidysenterica* Part I. Three new alkaloids from the bark of Indian *Holarrhena* and new method of isolation and further purification of conessine. Journal of Indian Chemical Society 9, 553–563.

Siddiqui, B.S., Usmani, S.B., Begum, S., Siddiqui, S., 1993. Steroidal alkaloids and an androstane derivative from the bark of *Holarrhena pubescens*. Phytochemistry 33, 925–928.

Siddiqui, B.S., Usmani, S.B., Begum, S., Siddiqui, S., 1994. Steroidal constituents of *Holarrhena pubescens*. Journal of Natural Products 57, 27–31.

Siddiqui, B.S., Usmani, S.B., Begum, S., Siddiqui, S., Gilani, A.H., Aftab, K., 1995. Hypotensive constituents from the bark of *Holarrhena pubescens* (*Holarrhena antidysenterica*). Heterocycles 41, 267–276.

PERGAMON

Phytochemistry 58 (2001) 1205–1207

PHYTOCHEMISTRY

www.elsevier.com/locate/phytochem

Sesquiterpene pyridine alkaloids from *Peritassa campestris*

Luciano M. Lião[a,*], Paulo C. Vieira[b], Edson Rodrigues-Filho[b], João B. Fernandes[b], Maria F.G.F. da Silva[b]

[a]*Instituto de Química, Universidade Federal de Goiás, C.P. 131, 74001-970 Goiânia, GO, Brazil*
[b]*Departamento de Química, Universidade Federal de São Carlos, C.P. 676, 13565-905 São Carlos, SP, Brazil*

Received 20 December 2000; received in revised form 14 May 2001

Abstract

An investigation of the methanol and ethyl acetate extracts from the roots of *Peritassa campestris* (Hippocrateaceae) afforded the sesquiterpene pyridine alkaloid, 4-hydroxy-7-epi-chuchuhuanine E-V, and nine known alkaloids, forrestine, euonimine, ebenifoline E-I, wilforine, euojaponine F, euonine, wilforjine, neowilforine, and wilforzine. The structures of the isolates were elucidated on the basis of spectral data, particularly HMQC and HMBC experiments. © 2001 Published by Elsevier Science Ltd.

Keywords: *Peritassa campestris*; Hippocrateaceae; Sesquiterpene pyridine alkaloids; 4-Hydroxy-7-epi-chuchuhuanine E-V

1. Introduction

Sesquiterpene pyridine alkaloids, based on a highly oxygenated dihydro-β-agarofuran core on a sesquiterpene moiety, and evoninoate or wilfordate esters on their alkaloid moiety, constitute a relatively small group of natural products frequently found in plants of the Celastraceae family (Brüning and Wagner, 1978). Recently, these alkaloids have also been described in plants of the Hippocrateaceae (Mata et al., 1990; Lião et al., 1997). This chemical aspect reinforces the recent botanical classification in which the two families, Celastraceae and Hippocrateaceae, appear to be grouped in the Celastraceae (Brüning and Wagner, 1978; Heywood, 1993). These alkaloids have also been of interest due to their cytotoxicity against several human tumour cell lines (Kuo et al., 1994), and their insect antifeedant, and insecticidal activities (Shirota et al., 1994). Sesquiterpene pyridine alkaloids isolated from *Tripterygium* species have also shown immunosuppressive activity (Zheng et al., 1989).

As part of our continuing search for bioactive compounds from plants, especially from the savanna, we investigated the MeOH and EtOAc soluble portions of the crude extract of the roots of *Peritassa campestris* Cambess. (Hippocrateaceae), a plant that occurs in the Brazilian savanna (Cerrado), popularly known as "bacupari do campo", and which is used in folk medicine for wound healing in the form of a decoction (Septímio, 1994). In this paper we report the isolation and structure elucidation of a new sesquiterpene pyridine alkaloid, 4-hydroxy-7-epi-chuchuhuanine E-V (**1**), and the isolation of nine known alkaloids forrestine (Chunquan et al., 1992), euonimine, ebenifoline E-I, euojaponine F, euonine (Itokawa et al., 1993), wilforine (Beroza, 1951), wilforjine (Deng et al., 1992), neowilforine (He et al., 1989), and wilforzine (He et al., 1987).

2. Results and discussion

4-Hydroxy-7-epi-chuchuhuanine E-V (**1**) was isolated as a colorless amorphous solid, in low yield, and its IR spectrum displayed absorptions at 3614, 1740, and 1583 cm^{-1}. The ^1H and ^{13}C NMR spectra suggested a dihydro-β-agarofuran sesquiterpene skeleton with an evoninic diester bridge. The sesquiterpene moiety was characterised in the ^1H NMR spectrum by tertiary methyl groups at δ 1.67 (3H, *s*, Me-14) and δ 1.58 (3H, *d*, $J=1.2$ Hz, Me-12), coupling with one hydrogen-bonded hydroxyl group at δ 4.50 (*q*, $J=1.2$ Hz, OH-4), two sets of methylene protons at δ 4.62 (*d*, $J=13.6$ Hz, H-11a), δ 5.28 (*d*, $J=13.6$ Hz, H-11b), δ 3.67 (*d*, $J=11.6$ Hz, H-15a) and δ 5.98 (*d*, $J=11.6$ Hz, H-15b), seven methine protons at δ 5.43 (*d*, $J=4.0$ Hz, H-1), 4.07 (*dd*, $J=4.0$

* Corresponding author. Tel.: +55-62-521-1008; fax: +55-62-521-1008.

E-mail address: luciano@quimica.ufg.br (L.M. Lião).

0031-9422/01/$ - see front matter © 2001 Published by Elsevier Science Ltd.
PII: S0031-9422(01)00315-6

and 2.4 Hz, H-2), 4.76 (*d*, $J=2.4$ Hz, H-3), 7.03 (*s*, H-5), 2.33 (*d*, $J=4.0$ Hz, H-6), 5.53 (*dd*, $J=6.0$ and 4.0 Hz, H-7) and 5.35 (*d*, $J=6.0$ Hz, H-8), and five acetyl groups at δ 2.31, 2.21, 2.15, 2.01 and 1.95. A further oxygenated functional group was assumed to be a hydroxyl group, based on a broad singlet at δ 3.65 (exchanged with D_2O). The evoninic acid fragment in **1** was assigned by the signals at δ 8.05 (*dd*, $J=8.0$ and 2.0 Hz, H-4′), 7.26 (*dd*, $J=8.0$ and 4.8 Hz, H-5′) and 8.69 (*dd*, $J=4.8$ and 2.0 Hz, H-6′), corresponding to a 2,3-disubstituted pyridine unit. It also contains two secondary methyl groups at δ 1.38 (*d*, $J=6.8$ Hz, Me-9′) and 1.15 (*d*, $J=7.2$ Hz, Me-10′), coupled with two methine protons at δ 4.66 (*dq*, $J=6.8$ and 1.0 Hz, H-7′) and 2.53 (*dq*, $J=7.2$ and 1.0 Hz, H-8′). This sesquiterpene pyridine alkaloid includes one macrocyclic structure formed by two ester linkages between one sesquiterpene molecule and one evoninic acid, at positions 3 and 15. In order to determine the positions of the acetate groups and consequently the hydroxyl group position, ^1H–^1H COSY, HMQC and HMBC spectra were recorded. In the former the cross-peak of H-2 (δ 4.07) with H-1 (δ 5.43) and H-3 (δ 4.76), suggested the position of the hydroxyl group at C-2, which reinforced by the observation that H-2 was at higher field than the corresponding proton in alkaloids containing a benzoyl or acetyl group, attached to this position. This proposal was confirmed by the HMBC spectrum which located the acetate groups by cross-peaks between these groups and H-1, H-5, H-7, H-8, and H-11. The ^{13}C NMR spectrum showed 36 signals, characteristic of evoninoate sesquiterpene pyridine alkaloids and showing five acetate groups. The carbon attached to the hydroxyl group appeared at δ 69.65, approximately δ 1.0 deshielded when compared with alkaloids with an acetate group at carbon 2. Additional support was obtained by a full scan ESI mass spectrum, where the molecular ion peak for this compound was detected at m/z 764 ($[M+H]^+$), reinforcing this structural proposal.

The relative stereochemistry around the dihydroagarofuran nucleus was determined from the coupling constants to be the same as other alkaloids isolated, including wilforine, wherein the stereochemistry was determined by X-ray analysis (Lião et al., 1997). The C-7 epimeric relationship between this compound and chuchuhuanine E-V (**1a**), was defined by the coupling constant between H-7 and H-8. While in **1** this coupling constant was 6.0 Hz, in **1a** it was 9.4 Hz (Shirota et al., 1994), indicating a *cis* and *trans* H-7/H-8 relationship for **1** and **1a**, respectively.

Alkaloid **1** was assayed for lethality in the brine shrimp toxicity (BST) test, and showed LC_{50} 99.0 μg/ml. This test is proposed as a simple bioassay for natural product research, which active compounds could then be subjected to more elaborate bioassays for specific pharmacological activities. Sesquiterpene pyridine alkaloids was assayed against several tumor cell lines, and emarginatine F turned out to be active against some cell lines (Kuo et al., 1994).

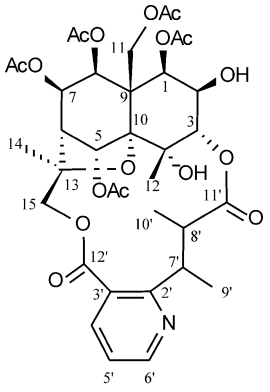

1

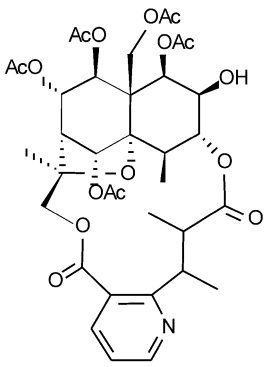

1a

3. Experimental

3.1. General experimental procedures

NMR: Bruker DRX 400, in $CDCl_3$ and TMS as int. standard; ESI-MSMS: low resolution on a triple quadrupole Micromass Quattro LC instrument, equipped with a "Z-spray" ion source; HRMS were obtained on a Fisons VG Autospec; $[\alpha]_D$: Perkin-Elmer 241 instrument; DCCC: Tokyo Rikakikai Co. with 300 columns of 40 cm×2 mm i.d.

3.2. Plant material

Roots of *P. campestris* were collected in a Savanna Reserve at Universidade Federal de São Carlos, in October 1992 and identified by Dr. Maria Helena de O. Antunes, Departamento de Botânica, Universidade Federal de São Carlos, São Paulo, Brazil, wherein a voucher specimen (no. 2845) is deposited.

3.3. Extraction and isolation

The roots were dried, powdered (2.8 kg) and successively extracted with hexane, CH_2Cl_2 and MeOH at room temperature. The combined extracts were submitted to liquid-liquid partition, resulting in hexane (5.1 g), methanol (35.84 g), ethyl acetate (5.87 g), *n*-butanol (5.21 g), and aqueous (23.80 g) extracts. The methanolic extract (3.5 g) was submitted to droplet countercurrent chromatography (DCCC), using the aqueous layer of hexane:MeOH:H_2O:EtOAc (5:4:1:2) as the stationary and the organic layer as the mobile phase, in a flow rate of 0.6 ml/min. The collected fractions were monitored by TLC and grouped in 22 fractions. Fractions 20–22 were separately filtered on Florisil (70–230 mesh) using hexane:CH_2Cl_2:MeOH (8:2:0.5). Fraction 20 was flash chromatographed on silica gel (230–400 mesh), eluting with hexane: CH_2Cl_2:MeOH (8:2:0.5), affording wilforine

(330.0 mg, 9.428%) and a mixture of sesquiterpene pyridine alkaloids. Fraction 22 was submitted to recycling HPLC using a GS-310P column (MeOH; 50.0× 2.15; 3 ml/min; UV 254 nm), affording euojaponine F (15.7 mg, 0.448%), wilforjine (5.9 mg, 0.168%), wilforzine (3.5 mg, 0.100%), and another mixture of alkaloids. The ethyl acetate extract (3.0 g) was also submitted to DCCC, using the aqueous layer of $CHCl_3$:MeOH:*n*-BuOH:H_2O (10:10:1:6) as the stationary and the organic layer as the mobile phase, in a flow rate of 0.6 ml/min, and after TLC was grouped in 12 fractions. Fractions 3, 4 and 5, after Florisil filtration, were individually submitted to recycling HPLC under the same conditions as the methanol extract, affording forrestine (186.8 mg, 6.226%), wilforine (50.1 mg, 1.670%), euojaponine F (0.4 mg, 0.013%), euonine (4.2 mg, 0.140%), neowilforine (4.3 mg, 0.143%), euonimine (6.1 mg, 0.203%), and a mixture of sesquiterpene pyridine alkaloids. The mixtures of alkaloids obtained were monitored by TLC using the Dragendorff reagent and grouped into two sets. The second set was rechromatographed on recycling HPLC using a Shim-pack column (silica 5 μ; 2.0×25 cm; hexane: CH_2Cl_2:MeOH− (8:2:0.5); 3 ml/min; UV 254 nm), affording the alkaloid **1** (1.5 mg, 0.023%) and ebenifoline E-I (2.0 mg, 0.038%).

3.4. Biological assays

The in vitro lethality assay against *Artemia salina* (BST) was carried out according to procedures described in Alkofahi et al. (1989).

3.4.1. 4-Hydroxy-7-epi-chuchuhuanine E-V (*1*)

This was obtained as a colorless amorphous solid: $[\alpha]_D^{20}$ −37.4° ($CHCl_3$; 0.002,); UV λ_{max}^{MeOH} nm (log ε): 201 (3.92), 223 (3.61), 265 (3.24) nm; IR $\nu_{max}^{CHCl_3}$ cm^{-1}: 3614, 1740, 1583, 1566, 1231 cm^{-1}; ^1H NMR (400 MHz, $CDCl_3$): see text; ^{13}C NMR (100 MHz, $CDCl_3$): δ 9.3 (*q*, C-10′), 11.8 (*q*, C-9′), 18.5 (*q*, C-14), 20.5 (*q*, $OCO\underline{C}H_3$), 20.8 (*q*, $OCO\underline{C}H_3$), 21.0 (*q*, $OCO\underline{C}H_3$), 21.4 (*q*, $OCO\underline{C}H_3$), 21.6 (*q*, $OCO\underline{C}H_3$), 22.7 (*q*, C-12), 36.3 (*d*, C-7′), 44.9 (*d*, C-8′), 50.4 (*d*, C-6), 52.5 (*s*, C-9), 60.3 (*t*, C-11), 68.9 (*d*, C-7), 69.6 (*d*, C-2), 69.9 (*t*, C-15), 70.4 (*s*, C-4), 70.9 (*d*, C-8), 73.8 (*d*, C-5), 75.3 (*d*, C-1), 77.9 (*d*, C-3), 83.9 (*s*, C-13), 94.4 (*s*, C-10), 121.1 (*d*, C-5′), 125.3 (*s*, C-3′), 137.6 (*d*, C-4′), 151.4 (*d*, C-6′), 165.1 (*s*, C-2′), 165.1 (*s*, $O\underline{C}OCH_3$), 168.5 (*s*, C-12′), 169.1 (*s*, $O\underline{C}OCH_3$), 169.3 (*s*, $O\underline{C}OCH_3$), 169.9 (*s*, $O\underline{C}OCH_3$), 170.1 (*s*, $O\underline{C}OCH_3$), 174.4 (*s*, C-11′); ESI-MSMS (probe) 30 eV, *m*/*z* (rel. int.): 764 $[M+H]^+$ (5), 746 (21), 728 92), 686 (9), 206 (100), 188 (9), 178 (33), 160 (6); HR-MS *m*/*z*: 763.2672 (calcd for $C_{36}H_{45}NO_{17}$, 763.2687).

Acknowledgements

The authors thank CNPq (Conselho Nacional de Desenvolvimento Científico e Tecnológico), FAPESP (Fundação de Amparo à Pesquisa do Estado de São Paulo), FUNAPE/UFG (Fundação de Apoio à Pesquisa da UFG), and CAPES/PICDT (Fundação Coordenação de Aperfeiçoamento de Pessoal de Nível Superior/Programa de Incentivo a Capacitação Docente e Técnica) for financial support.

References

Alkofahi, A., Rupprecht, J.K., Anderson, J.E., McLaughlin, J.L., Mikolajczak, K.L., Scott, B.A., 1989. Search for new pesticides from higher-plants. In: American Chemical Society Symposium Series, Vol. 387. Washington, pp. 25–43.

Beroza, M., 1951. Alkaloids from *Tripterygium wilfordii* Hook, wilforine and wilfordine. J. Am. Chem. Soc. 73, 3656–3659.

Brüning, R., Wagner, H., 1978. Übersicht über die Celastraceeninhaltsstoffe: Chemie, Chemotaxonomie, Biosynthese, Pharmakologie. Phytochemistry 17, 1821–1858.

Chunquan, C., Jikai, L., Dagang, W., 1992. Forrestine, an alkaloid from *Tripterygium forrestii*. Phytochemistry 31, 4391–4392.

Deng, F., Xia, Z., Xu, R., Chen, J., 1992. The structures of triptotetraolide and wilforjine. Zhiwu Xuebao 34, 618–621.

He, Z.S., Li, Y., Fang, S.D., Hong, S.H., 1987. Structures of wilforgine, wilforzine and wilformine from *Tripterygium wilfordii*. Acta Chim. Sinica 45, 510–513.

He, Z.S., Li, Y., Fang, S.D., Hong, S.H., 1989. Structures of wilfortrine and neowilforine from *Tripterygium wilfordii* Hook. F. Huaxue Xuebao 47, 178–181.

Heywood, V.H., 1993. Flowering Plants of the World. Oxford University Press, New York. pp. 178–183.

Itokawa, H., Shirota, O., Morita, H., Takeya, K., Litaka, Y., 1993. Isolation, structural elucidation and conformational analysis of sesquiterpene pyridine alkaloids from *Maytenus ebenifolia* Reiss. X-ray molecular structure of ebenifoline W-I. J. Chem. Soc. Perkin Trans. 1, 1247–1253.

Kuo, Y.H., King, M.L., Chen, C.F., Chen, H.Y., Chen, C.H., Chen, K., Lee, K.H., 1994. Two new macrolide sesquiterpene pyridine alkaloids from *Maytenus emarginata*: emarginatine G and the cytotoxic emarginatine F. J. Nat. Prod. 57, 263–269.

Lião, L.M., Caracelli, I., Vieira, P.C., Silva, M.F.G.F., Fernandes, J.B., Rodrigues-Filho, E., Zukerman-Schpector, J., 1997. Crystal structure of wilforine. A sesquiterpene pyridine alkaloid from *Salacia campestris*. Anais Assoc. Bras. Quím. 46, 184–188.

Mata, R., Calzada, F., Díaz, E., Toscano, R.A., 1990. Chemical studies on Mexican plants used in traditional medicine, XV. Sesquiterpene evoninoate alkaloids from *Hippocratea excelsa*. J. Nat. Prod. 53, 1212–1219.

Septímio, L. R., 1994. A Fitoterapia Baseada em Ervas Medicinais do Cerrado. In: Ministério da Cultura, SIPE (Secretaria de Intercâmbio e Projetos Especiais), Brasília, p. 103.

Shirota, O., Otsuka, A., Morita, H., Takeya, K., Itokawa, H., 1994. Sesquiterpene pyridine alkaloids from *Maytenus chuchuhuasca*. Heterocycles 38, 2219–2229.

Zheng, Y.L., Xu, Y., Lin, J.F., 1989. Immunosuppressive effects of wilfortrine and euonine. Acta Pharm. Sinica 24, 568–572.

PERGAMON

Phytochemistry 58 (2001) 1209–1212

PHYTOCHEMISTRY

www.elsevier.com/locate/phytochem

Betacyanins from vine cactus *Hylocereus polyrhizus*

Sławomir Wybraniec[a,*], Itzhak Platzner[b], Shimona Geresh[c], Hugo E. Gottlieb[d], Marcela Haimberg[e], Michael Mogilnitzki[e], Yosef Mizrahi[c]

[a]*Department of Chemical Engineering and Technology, Cracow University of Technology, Warszawska 24, Cracow 31-155, Poland*
[b]*Ben Gurion University of the Negev from NRCN, POB 9001, 84190 Beer-Sheva, Israel*
[c]*The Institutes for Applied Research, Ben Gurion University of the Negev, POB 653, 84105 Beer-Sheva, Israel*
[d]*Chemistry Department, Bar Ilan University, 52900 Ramat Gan, Israel*
[e]*Research and Development Division, Makteshim Ltd., 84100 Beer-Sheva, Israel*

Received 13 June 2001; received in revised form 18 July 2001

Abstract

The presence of betacyanin pigments and their isoforms has been detected in the fruit of *Hylocereus polyrhizus*, a vine cactus native to South America. Along with the known betanin and phyllocactin (6′-*O*-malonylbetanin), a new betacyanin was structurally elucidated as betanidin 5-*O*-[6′-*O*-(3″-hydroxy-3″-methyl-glutaryl)-β-D-glucopyranoside] (proposed trivial name hylocerenin) by means of electrospray MS/MS, HPLC, and NMR techniques. © 2001 Elsevier Science Ltd. All rights reserved.

Keywords: Vine cactus; *Hylocereus polyrhizus*; Cactaceae; Betacyanins; Betalains; Betanin; Phyllocactin

1. Introduction

Hylocereus polyrhizus [(F. A. C. Weber) Britton and Rose] and its related species belong to the vine cacti from the subfamily Cactoideae of the tribe Cacteae (Raveh et al., 1993). This tribe contains many species with edible fruits mostly known as pitaya, or pitahaya. The common name of these fruits is pitaya since they contain scales on the fruit skin and hence the name pitaya "the scaly fruit" (Canto, 2000).

In the last two decades efforts have been made to develop the cultivation of pitayas, vine species of the genus *Hylocereus*. Some of them contained pulp of red and/or purple colors of various hues (Mizrahi et al. 1997; Mizrahi and Nerd, 1999; Canto, 2000). In Israel, some of these cacti are already produced commercially, among them *Hylocereus polyrhizus* with glowing deep red-purple fruit flesh (Fig. 1) (Mizrahi and Nerd, 1999). The pulp of *H. polyrhizus* is already used in Israel for the production of red-violet colored ice cream. They have also the potential to be used in low temperature dairy drinks and in light drinks with or without other fruit juices. In cacti the most important fruit pigments are the betacyanins and betaxanthins (Gibson and Nobel, 1986), the betalains.

The pigments in these newly domesticated species are unknown, therefore, their structure elucidation is reported here.

2. Results and discussion

The presence of the betacyanins (**1**–**3**) and their *15R*-isoforms (**1′**–**3′**) has been detected by HPLC of fruit pulp extracts from *H. polyrhizus* by their characteristic spectral properties (Fig. 2). From the ratio of the absorbances at 540 and 320 nm (1:0.14) the presence of hydroxycinnamoyl residues as acylating moieties in **1**–**3** can be excluded (Heuer et al., 1994).

Compounds **1/1′** were assigned as betanin and isobetanin, by UV-vis spectroscopy and co-chromatography with authentic betanin from red beet. The assignment was confirmed by ESI–MS/MS giving the expected protonated molecular ion $[M+H]^+$ (m/z 551) and the prominent daughter ion at m/z 389 [betanidin + H]$^+$. Subsequent NMR analysis confirmed undoubtedly the aglycones (betanidin, isobetanidin) in the compounds **1** and **1′**, respectively. The only significant differences in

* Corresponding author. Tel.: +48-12-628-2707; fax: +48-12-633-3374.
E-mail address: swybran@chemia.pk.edu.pl (S. Wybraniec).

0031-9422/01/$ - see front matter © 2001 Elsevier Science Ltd. All rights reserved.
PII: S0031-9422(01)00336-3

Fig. 1. Fruits of *Hylocereus polyrhizus*.

chemical shifts are a small (0.03 ppm) shielding of H-15. The suggestion is that the pairs of compounds are *11Z* or *E* isomers. The small chemical shift difference between H-4 and H-7 of 0.12 ppm is characteristic of a substitution of the hydroxyl group at C-5 (Heuer et al., 1992, 1994). The signals of the ^{1}H NMR were comparable to those published recently (Strack et al., 1993).

Compounds **2** and **2′** were identified as already known phyllocactin and isophyllocactin, respectively (Fig. 3) (Minale et al., 1966). The MS and NMR data of phyllocactin has been recently discussed (Kobayashi et al., 2000). The protonated parent ion ($[M+H]^+$) for compound 2 was found at *m/z* 637 [550 (betanin) + 86 (malonyl) + H]$^+$ and the daughter ions at *m/z* 551 [betanin + H]$^+$ and 389 [betanidin + H]$^+$. Additional ions at *m/z* 619 and 593 were assigned to losses of H_2O and CO_2 (Table 1). The 1D and 2D ^{1}H NMR data of **2** and **2′** were virtually the same as published recently (Kobayashi et al., 2000). The presence of the aglycone, glucose and malonyl moieties was confirmed and the small chemical shift of 0.14 ppm

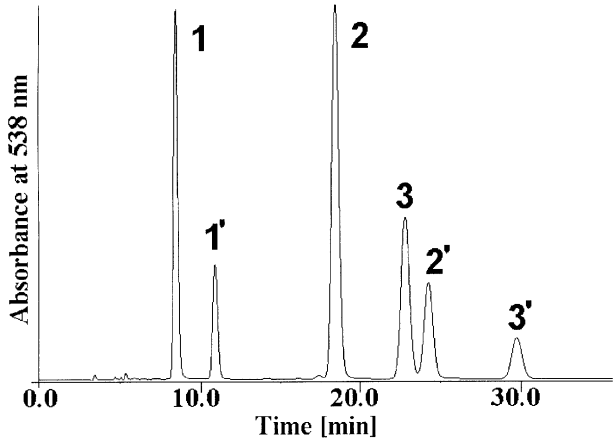

Fig. 2. HPLC pattern of betacyanins from fruit pulp of *Hylocereus polyrhizus*. For peak identification see Table 1. Peak numbers refer to Fig. 3.

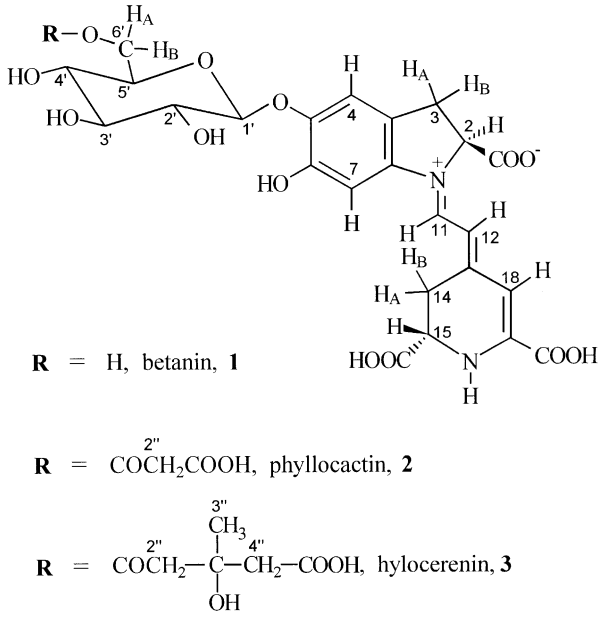

Fig. 3. Chemical structures of analyzed betacyanins in *Hylocereus polyrhizus*. Compound numbers refer to Fig. 2 and Table 1.

between H-4 and H-7 indicated the substitution at the hydroxyl group at C-5 of betanidin. Additionally the AB quartet of H-2″A/H-2″B at $\delta = 3.46$ ppm suggested a malonate moiety. The low field chemical shift of H-6′A/H-6′B (4.59 and 4.35) provides definitive evidence that the malonate moiety is bound to C-6′.

The protonated parent ion ($[M+H]^+$) for compound **3** was found at *m/z* 695 (Table 1). Characteristic ions at *m/z* 551 and 389 indicated that compound **3** is a derivative of betanin and betanidin. The mass difference (*m/z* 695–551) of 144 suggested the presence of aliphatic acyl moiety connected to the glucose of **1**. The additional ions found after fragmentation of $[M+H]^+$ for **3** and **3′** at *m/z* 677, 651 and 633 were assigned to losses of H_2O and CO_2. Compounds **3** and **3′** had ^{1}H NMR spectra which were virtually identical to those of **2** and **2′**, respectively, except of the absence of the malonate protons H_2-2″ at $\delta = 3.46$ ppm. Instead, an extra singlet of H_3-3″ (methyl group) at $\delta = 1.57$ ppm and two new methylene groups at $\delta = 2.89$ ppm (singlet of H-4″) and 2.71 ppm (AB quartet of H-2″A/H-2″B) were seen. These data are in accordance with the MS data and are indicative for the presence of a 3-hydroxy-3-methylglutaryl moiety (HMG) at C-6′ of betanin.

Hence, the combination of ESI–MS and ^{1}H NMR data identified **3** as betanidin 5-*O*-[6′-*O*-(3″-hydroxy-3″-methylglutaryl)-β-D-glucopyranoside], a new betacyanin pigment (Fig. 3). A similar compound, amaranthin acylated with 3-hydroxy-3-methyl-glutaric acid (iresinin-I) has been isolated from *Iresine herbstii* (Amaranthaceae) (Minale et al., 1966). Upon β-glucuronidase treatment iresinin-I yielded glucuronic acid and degradation products (Minale et al., 1966) containing most probably 6′-HMG-betanin, an

Table 1
Retention time, HPLC–PDA and ESI–MS/MS data of betacyanins from fruit pulp of *Hylocereus polyrhizus*

Compound[a]	R_t (min)	Relative conc. (%)	HPLC–PDA (λ_{max}, nm)	Characteristic ions from ESI–MS/MS		
				$[M+H]^+$	Other characteristic ions	Betacyanin
1	8.1	25.3	537	551	389	Betanin
1′	11.1	7.8	537	551	389	Isobetanin
2	18.2	35.7	539	637	619; 593; 551; 389	Phyllocactin
2′	24.3	7.4	538	637	619; 593; 551; 389	Isophyllocactin
3	22.6	19.8	541	695	677; 651; 633; 551; 389	Hylocerenin[b]
3′	29.8	4.0	540	695	677; 651; 633; 551; 389	Isohylocerenin[c]

[a] Compound numbers correspond to peak numbers in Fig. 2.
[b] New compound: betanidin 5-*O*-[6′-*O*-(3″-hydroxy-3″-methyl-glutaryl)-β-D-glucopyranoside].
[c] New compound: isobetanidin 5-*O*-[6′-*O*-(3″-hydroxy-3″-methyl-glutaryl)-β-D-glucopyranoside].

artificially formed compound, which is now shown to be an endogenously occurring pigment in *H. polyrhizus*.

The *15S*-forms are eluted in HPLC (ODS-type columns with acidic eluents) earlier than the *15R*-forms (the isoforms) (Bokern et al., 1991; Schliemann et al., 1996). Therefore, peaks **1**, **2** and **3** can be attributed to betanidin based forms, whereas peaks **1′**, **2′** and **3′** to isobetanidin based forms.

The contents of all pigments in purified extracts before HPLC fractionation ranged between 30 and 80 mg betanin equivalents/100 g of fresh fruit pulp, taking E_{538} (1%) = 1120 (Forni et al., 1992) for spectrophotometric calculations of betacyanins concentration in purified extracts. Fruit pulp of *H. polyrhizus* is characterized by the glowing purple-red colour, which can be attributed to the presence of **3** in the fruit. Assuming that the E_{538}(1%) of the all pigments are similar, the relative concentrations of *H. polyrhizus* pigments were calculated from the chromatogram (Fig. 2) and showed in Table 1.

In summary, the betacyanins of fruits of *H. polyrhizus* were identified as the known betanin, phyllocactin and their *iso*-forms. Additionally, a new betacyanin was identified as betanidin 5-*O*-[6′-*O*-(3″-hydroxy-3″-methyl-glutaryl)-β-D-glucopyranoside] and its isoform. The formation of the *15R*-isoforms (**1′–3′**) may occur during fruit maturation, but they could be also artefacts of isolation.

3. Experimental

3.1. Plant material

Seven-year-old plants of *Hylocereus polyrhizus* grown on trellis system under greenhouse conditions in Beer-Sheva, Israel, were used (Mizrahi and Nerd, 1999). All flowers were hand-crossed pollinated with other compatible clones and tagged (Weiss et al., 1994). Fruits were harvested for analysis when reaching full ripening stage, 35 days after pollination for *H. polyrhizus* (Nerd et al., 1999). The edible pulp was taken for analysis.

3.2. Pigment extraction

One hundred grams of the peeled fruit (of watery consistency) were shaken with 200 ml 80% aq. EtOH for few minutes, followed by fast filtration and centrifugation at 18 000 rpm and −4 °C for 20 min. After careful decantation, the extract was concentrated in vacuo at 25 °C to 3–4 ml and stored in a dark vessel at −18 °C. The roots from red beet (*Beta vulgaris*) was processed by the same procedure.

3.3. Extract purification

The concentrated betacyanin extracts were purified prior to prep. HPLC by column chromatography (40×1.2 cm, i.d.) on Sephadex G-25 (Sigma Steinheim, Germany) according to Adams and von Elbe (1977) and subsequently on LH-20-100 (Sigma Steinheim, Germany) (Schliemann et al., 1996). The betacyanin fractions were lyophilized.

3.4. HPLC

Preparative HPLC was carried out with a Waters Delta Prep 4000 prep. chromatography system (Waters, Milford MA, USA) equipped with a LiChroCART® 250-10, LiChrospher® 60 RP-select B, (10 μm) column protected by a guard column. The separation was performed isocratically using a mixture of 90% solvent A (0.5% aq. TFA) with 10% solvent B (acetonitrile) for 35 min, at a flow rate of 3.1 ml min^{-1} (injection volume: 1 ml; detection at 538 nm). **1**: R_t 14–17 min; **2**: R_t 25–29 min; **3**: R_t 41–45 min. To remove the solvent, the pooled fractions were concentrated in vacuo and subsequently lyophilised. The yields were: **2**—3.3 mg; **3**—2.1 mg. After checking the purity of the fractions by analytical HPLC the compounds were dissolved in appropriate solvents prior to analysis by UV/vis, electrospray MS/MS or ^{1}H NMR. Analytical HPLC was carried out on LC-10AT-VP chromatograph with photodiode-array SPD-M10A VP detector (Shimadzu Corp., Kyoto, Japan) equipped

with a LiChroCART® 250-4, LiChrospher® 60 RP-select B, (5 μm) column. The elution system was the same as for the prep. HPLC at a flow rate of 0.5 ml/min (injection volume: 10 μl; detection at 538 nm).

3.5. UV/vis

UV/vis absorption spectra in the range of 200–800 nm were recorded with a Jasco U-530 UV/vis spectrophotometer (JASCO Corp., Tokyo, Japan). On-line spectra in the range of 200–700 nm were obtained by HPLC-photodiode array detection.

3.6. Electrospray MS/MS and NMR

Electrospray mass spectra were obtained with LCQ Deca FINNIGAN-MAT mass spectrometer (subsidiary of ThermoQuest Corp., USA), operating in the positive ion, full scan MS/MS mode. The spectra were taken in the presence of minute quantities of formic acid promoting $[M+H]^+$ ion production (electrospray voltage 4.5 kV, heated capillary temperature 210 °C; sheath gas: nitrogen; injection: 80 μl min^{-1}).

Compound **1** (betanin), (positive ion mode) (*m*/*z*, rel. int.): 551 $[M+H]^+$ (100). Compound **2** (phyllocactin), (positive ion mode) (*m*/*z*, rel. int.): 637 $[M+H]^+$ (100); daughter ion scan mode of *m*/*z* 637: 619 $[M+H-H_2O]^+$ (20); 593 $[M+H-CO_2]^+$ (100); 551 [betanin + H]$^+$ (65); 389 [betanidin + H]$^+$ (18). Compound **3** (hylocerenin), (positive ion mode) (*m*/*z*, rel. int.): 695 $[M+H]^+$ (100); daughter ion scan mode of *m*/*z* 695: 677 $[M+H-H_2O]^+$ (5); 651 $[M+H-CO_2]^+$ (3); 633 $[M+H-CO_2-H_2O]^+$ (7); 551 [betanin + H]$^+$ (3); 389 [betanidin + H]$^+$ (100).

1D and 2D ^{1}H (COSY) NMR spectra were recorded at 300 K on a Bruker DMX-600 instrument locked to the major deuterium resonance of the solvent, CD_3OD containing traces of DCl. Chemical shifts are given in ppm relative to TMS and coupling constants in Hz.

Compound **3** {betanidin 5-*O*-[6′-*O*-(3″-hydroxy-3″-methyl-glutaryl)-β-D-glucopyranoside]} ^{1}H NMR (600.1 MHz, CD_3OD/DCl) $\delta = 8.69$ (1H, *d*, $J_{11-12} = 12.3$ Hz, H-11), 7.34 (1H, *s*, H-7), 7.22 (1H, *s*, H-4), 6.46 (1H, *s*, H-18), 6.24 (1H, *d*, H-12), 5.47 (1H, *dd*, $J_{2-3A} = 9.9$ Hz, H-2), 4.87 (1H, *d*, $J_{1'-2'} = 7.8$ Hz, H-1′), 4.64 (1H, *dd*, $J_{15-14A} = 5.3$ Hz, $J_{15-14B} = 7.3$ Hz, H-15), 4.56 (1H, *dd*, $J_{6'A-6'B} = 12.1$ Hz, H-6′A), 4.37 (1H, *dd*, H-6′B), 3.74 (1H, *m*, $J_{5'-6'A} = 2.1$ Hz, $J_{5'-6'B} = 6.5$ Hz, H-5′), 3.73 (1H, *dd*, $J_{3A-3B} = 16.4$ Hz, H-3A), 3.72 (1H, *dd*, $J_{14A-14B} = 17.4$ Hz, H-14A), 3.57 (1H, *m*, H-2′), 3.53 (1H, *m*, H-3′), 3.50 (1H, *dd*, H-3B), 3.43 (1H, *m*, H-4′), 3.31 (1H, *dd*, H-14B), 2.89 (2H, *s*, H-4″), 2.71 (2H, AB*q*, H-2″A, H-2″B), 1.57 (3H, s, H-3″).

Acknowledgements

The authors wish to express their thanks to Dr. Y. Gilboa for his dedicated assistance in the HPLC work.

References

Adams, J.P., von Elbe, J.H., 1977. Betanine separation and quantification by chromatography on gels. J. Food Sci. 42, 410–414.

Bokern, M., Heuer, S., Wray, V., Witte, L., Macek, T., Vanek, T., Strack, D., 1991. Ferulic acid conjugates and betacyanins from cell cultures of *Beta vulgaris*. Phytochemistry 30, 3261–3265.

Canto, A.R., 2000. Pitahayas. Estado mundial de su cultivo y comercializacion. Fundacion Yucatan Produce, A.C. Universidad Autonoma Chapingo, Mexico.

Forni, E., Polesello, A., Montefiori, D., Maestrelli, A., 1992. HPLC analysis of the pigments of blood-red prickly pear (*Opuntia ficus indica*). J. Chromatogr. 593, 177–183.

Gibson, A.C., Nobel, P.S., 1986. The Cactus Primer. Harvard University Press, Cambridge.

Heuer, S., Richter, S., Metzger, J.W., Wray, V., Nimtz, M., Strack, D., 1994. Betacyanins from bracts of *Bougainvillea glabra*. Phytochemistry 37, 761–767.

Heuer, S., Wray, V., Metzger, J.W., Strack, D., 1992. Betacyanins from flowers of *Gomphrena globosa*. Phytochemistry 31, 1801–1807.

Kobayashi, N., Schmidt, J., Nimtz, M., Wray, V., Schliemann, W., 2000. Betalains from Christmas cactus. Phytochemistry 54, 419–426.

Minale, L., Piattelli, M., De Stefano, S., Nicolaus, R.A., 1966. Pigments of Centrospermae-VI. Acylated betacyanins. Phytochemistry 5, 1037–1052.

Mizrahi, Y., Nerd, A., 1999. Climbing and columnar cacti: new arid land fruit crops. In: Janick, J. (Ed.), Perspectives on New Crops and New Uses. American Society for Horticultural Sciences Press, Alexandria, pp. 358–366.

Mizrahi, Y., Nerd, A., Nobel, P.S., 1997. Cacti as crops. Hort. Rev. 18, 291–320.

Nerd, A., Gutman, F., Mizrahi, Y., 1999. Ripening and postharvest be-haviour of fruits of two *Hylocereus* species (Cactaceae). Postharvest Biol. Tech. 17, 39–45.

Raveh, E., Weiss, J., Nerd, A., Mizrahi, Y., 1993. Pitayas (genus *Hylocereus*): a new fruit crop for the Negev Desert of Israel. In: Janick, J., Simon, J.E. (Eds.), New Crops. Wiley, New York, pp. 491–495.

Schliemann, W., Joy IV, R.W., Komamine, A., Metzger, J.W., Wray, V., Strack, D., 1996. Betacyanins from plants and cell cultures of *Phytolacca americana*. Phytochemistry 42, 1039–1046.

Strack, D., Steglich, W., Wray, V., 1993. Betalains. In: Watermann, P.G. (Ed.), Methods in Plant Biochemistry. Academic Press, London, pp. 421–450.

Weiss, J., Nerd, A., Mizrahi, Y., 1994. Flowering behaviour and pollination requirements in climbing cacti with fruit crop potential. Hort. Science 29, 1487–1492.

PERGAMON

Phytochemistry 58 (2001) 1213–1217

PHYTOCHEMISTRY

www.elsevier.com/locate/phytochem

The structures of antioxidant and cytotoxic agents from natural source: anthraquinones and tannins from roots of *Rumex patientia*

L. Ömür Demirezer[a,*], Ayse Kuruüzüm-Uz[a], Isabelle Bergere[b], H.-J. Schiewe[b], Axel Zeeck[b]

[a]*Faculty of Pharmacy, Department of Pharmacognosy, Hacettepe University, TR-06100 Ankara, Turkey*
[b]*Institute of Organic Chemistry, Georg-August University, D-37077 Göttingen, Germany*

Received 28 May 2001; received in revised form 23 July 2001; accepted 23 July 2001

Abstract

A new anthraquinone glycoside, emodin-6-*O*-β-D-glucopyranoside, and a new simple halogenated flavan-3-ol, 6-chlorocatechin, have been isolated from the roots of *Rumex patientia* L. together with seven known phenolic compounds. Their structures were elucidated on the basis of spectroscopic methods. Cytotoxic effects and radical scavenging properties of the isolated compounds have been demonstrated. © 2001 Elsevier Science Ltd. All rights reserved.

Keywords: *Rumex patientia*; Polygonaceae, Anthraquinones; Emodin-6-*O*-β-D-glucopyranoside; Tannins; 6-Chlorocatechin

1. Introduction

The dried roots of *Rumex patientia* L. (Polygonaceae) have been used as purgative, constipate, depurative and tonic in Turkish traditional medicine (Baytop, 1984). It was reported that *R. patientia* contains anthraquinone, tannin, naphthalene and naphthoquinone derivatives (Sharma et al., 1977; Demirezer and Kuruüzüm, 1997b; Suri et al., 1978). A literature search revealed only few information on the characterization of tannins and anthraquinone glycosides from *Rumex* species. Previously we reported that the aqueous extract of the roots of *R. patientia* exhibited a highly antiinflammatory activity (Süleyman et al., 1999). Several novel naphthalenes from this material have been also reported by our group (Kuruüzüm et al., 2001). In the course of continuous studies on this plant a new anthraquinone glycoside, emodin-6-*O*-β-D-glucopyranoside (**6**), a new simple halogenated flavan-3-ol, 6-chlorocatechin (**7**) and seven known compounds, chrysophanol (**1**), physcion (**2**), emodin (**3**), chrysophanol-8-*O*-β-D-glucopyranoside (**4**), emodin-8-*O*-β-D-glucopyranoside (**5**), catechin (**8**) and orcinol (**9**) were isolated. Cytotoxic effects and radical scavenging properties of this compounds have been investigated.

2. Results and discussion

The aqueous and methanolic extract of the roots of *R. patientia* were subjected to repeated different column chromatographies to yield compounds **1**–**9**. Known compounds were shown to be chrysophanol (1), physcion (**2**), emodin (**3**), chrysophanol-8-*O*-β-D-glucopyranoside (**4**, emodin-8-*O*-β-D-glucopyranoside (**5**), catechin (**8**) and orcinol (**9**) by comparison with authentic samples and their spectral data with those previously reported (Cohen and Towers, 1995; Coskun et al., 1990; Demirezer, 1991; Foo and Karchesy, 1989; Lin et al., 1990; Lin and Wei, 1993; Markham and Geiger, 1993; Pascual Teresa et al., 1986; Sakar et al., 1993; Van Der Nat et al., 1991).

The presence of the anthraquinone derivatives and flavan-3-ols were detected by TLC on Si gel with spraying a 5% KOH solution and 1% vanillin-H_2SO_4, respectively, according to their red spots. Colour reactions and the UV and IR spectra of the compounds (**1**–**6**) indicated that they contain a hydroxy anthraquinone chromophor. The infrared spectrum of **6** showed the presence of free hydroxyl groups (3432 cm^{-1}), non-chelated (1670 cm^{-1})

* Corresponding author. Tel.: +90-312-305-10-89; fax: +90-312-311-47-77,.
E-mail address: omurd@hacettepe.edu.tr (L.Ö.Demirezer).

0031-9422/01/$ - see front matter © 2001 Elsevier Science Ltd. All rights reserved.
PII: S0031-9422(01)00337-5

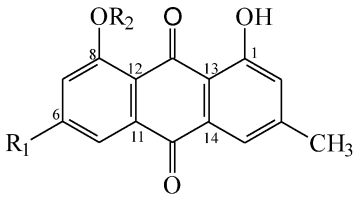

	R_1	R_2
1	H	H
2	OCH_3	H
3	OH	H
4	H	glu
5	OH	glu

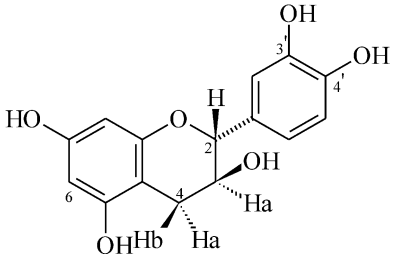

8

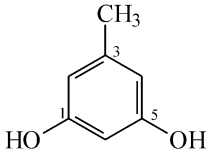

9

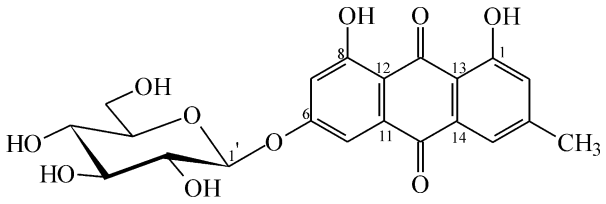

Compound 6

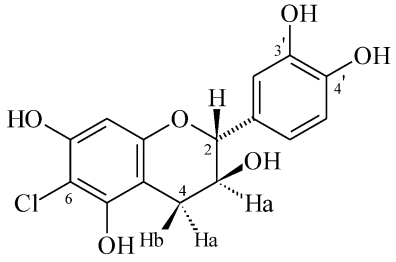

Compound 7

and chelated carbonyl groups (1633 cm^{-1}) and aromatic ring moieties (1060 cm^{-1}). In the UV spectrum of 6, absorption maxima were exhibited at 223, 264, 293 sh and 411 nm.

The structure of compound **6**, $C_{21}H_{20}O_{10}$, in DMSO-d_6 was determined from the one-dimensional ^1H and ^{13}C NMR spectra and by using 2D sequences. The ^1H NMR spectrum of compound **6** (see Table 1) exhibited two doublet signals at δ 7.33 and 7.87 (each 1H, *d*, $J = 2.1$ Hz) due to meta coupled aromatic protons at H-5 and H-7, respectively; two broad singlet signals at δ 7.17 and 7.50 (each 1H) assigned to H-2 and H-4, respectively; aromatic methyl proton signal at δ 2.42 (3H, s), a glucosyl anomeric proton at δ 5.07 (*d*, $J = 7.4$ Hz) and the other proton signals of the sugar moiety, indicating the presence of a β-glucosidic moiety attached to one of the hydroxyl groups of emodin. In the COSY experiment, cross peaks were revealed between the methyl proton signal and aromatic protons (H-2, H-4) indicating that the methyl group was next to them on the same aromatic ring.

Furthermore, in the ^{13}C NMR spectrum (see Table 1), the characteristic signals of emodin were observed. The proton bearing carbon atoms were assigned with a HMQC experiment. A HMBC experiment was used to determine the position of different carbon atoms of 6. However, the assigment of positions **6** and **8** for compounds **5** and **6** was not possible by means of HMBC experiments as the proton H-7 (δ_H 7.33) correlated with both neighboured carbon atoms (**5**: δ_C 173.9, 163.3 and **6**: δ_C 159.9, 159.7) and proton 5 (δ_H 7.87) with none of them.

Other spectroscopic experiments such NOESY delay or relay COSY have been carried out but none of them allowed an exact assigment of these two carbon atoms. For **5** and **6**, a HMBC correlation between 1′-H (**5**: δ_H 4.95 and **6**: δ_H 5.07) of the glucose unit and the aglycone (**5**: δ_C 163.3 and **6**: δ_C 159.9) can be observed. In both cases, the considered carbon atom is not at position 1. Based on a comparison with literature data (Demirezer, 1991) compound **5** was assumed to be emodin-8-glucoside and compound **6**, which exhibited remarkable differences to **5** in ^{13}C data especially at position 6 (**5**: δ_C 173.9 and 6: δ_C 159.9) and its physical data (R_f ($CHCl_3$/CH_3OH/H_2O, 80:20:2) *5*: 0.36, *6*: 0.08) was deduced to be emodin-6-*O*-β-D-glucoside.

Colour reaction and the UV and IR spectra of compound **7** suggested the presence of a flavan-3-ol skele-

Table 1
^{1}H and ^{13}C NMR spectral data for compound **6** (DMSO-d_6)

C/H	^{1}H		^{13}C	HMBC[b]
	δ_H		δ_C	
1	–	*J* (Hz)	161.71	
2	7.17 *bs*		124.09	C-4, C-13, CH_3
3	–		147.29	
4	7.50 *bs*		119.55	C-2, C-10, C-13, CH_3
5	7.87 *d*	2.1	112.13	C-10, C-12
6	–		159.91	
7	7.33 *d*	2.1	111.94	C-6, C-7, C-8, C-12
8	–		159.66	
9	–		186.78	
10	–		181.95	
11	–		135.91	
12	–		115.74	
13	–		114.57	
14	–		132.20	
CH_3	2.42 *s*		21.38	C-2, C-3, C-4
Glucose				
1′	5.07 *d*	7.4	100.67	C-6
2′	3.10–3.50[a]		73.43	
3′	3.10–3.50		76.60	
4′	3.10–3.50		69.71	
5′	3.10–3.50		77.25	
6′	3.55 *dd*	3.73*dd*	60.40*dd*	
	11.5/3	11.5/3	60.40	

[a] Signal pattern unclear due to overlapping.
[b] Correlation of the aglycone moeity only.

Table 2
^{1}H and ^{13}C NMR spectral data for compound **7** (DMSO-d_6)

C/H	^{1}H		^{13}C	HMBC
	δ_HJ (Hz)		δ_C	
2	4.75 *d*	6.7	82.90	C-3, C-4, C-8a, C-1, C-2, C-6
3	4.02 *ddd*	7.2/6.7/5.2	68.28	C-4a
4α	2.76 *dd*	16.3/5.2	27.89	C-2, C-3, C4a, C-5, C-8a
4β	2.55 *dd*	16.3/7.2		C-2, C-3, C-4a, C-5, C-8a
4a	–	–	102.02	
5	–	–	155.50	
6	–	–	100.18	
7	–	–	153.40	
8	6.07 *s*	–	96.62	C-4a, C-5, C-6, C-7
8a	-	-	152.09	
1	-	-	131.88	
2	6.81 *d*	1.8	114.86	C-2, C-3′, C′-4, C′-6
3	-	-	146.21[a]	
4	-	-	146.25[a]	
5	6.75 *d*	8.1	116.12	C-1′, C-3′, C-4′
6	6.69 *dd*	8.1/1.8	119.56	C-2, C-2′, C-4′

[a] Values for C-3′ and C-4′ can be interchanged.

ton. Its ESI MS gave ion double peaks for $[M–H]^+$ at m/z 325/323 and $[2M–H]^+$ at *m/z* 649/647 with the isotope pattern of a chloro derivative, indicating the compound **7** to be a chloro flavan-3-ol. This conclusion was supported by the 1D and 2D NMR spectral data. Based on this results, the molecular formula of **6** was determined as $C_{15}H_{13}O_6Cl$.

The ^{1}H NMR spectrum of **7** (see Table 2) in CD_3OD exhibited a singlet at δ 6.07 of an aromatic proton; two doublets at δ 6.81 ($J=1.8$ Hz) and 6.75 ($J=8.1$ Hz) and a doublet of doublet at δ 6.69 ($J=8.1/1.8$ Hz) which were assigned to H-8, H-2, H-5 and H-6, respectively. However, the proton resonances observed at δ 4.75 (H-2, *d*, $J=6.7$ Hz), δ 4.02 (H-3, dd*d*, $J=$ 7.2/6.7/5.2 Hz), δ 2.76 (H-4α, d*d*, $J=16.3/5.2$ Hz) and δ 2.55 (H-4β, d*d*, $J=16.3/7.2$ Hz). The large coupling constant ($J=6.7$ Hz) of H-2 with H-3 indicated that this unit had the 2, 3 *trans* configuration. The ^{1}H NMR data of **7** were similar to those of catechin except for the presence of signal due to H-6.

The assigments for all carbons and protons of **7** (see Table 2) were determined from 1D (^{1}H, ^{13}C) NMR and 2D (COSY, HMQC, HMBC) NMR spectra. In comparison to the ^{13}C NMR spectrum of catechin, the C-6 resonance of compound **7** was shifted almost 5 ppm downfield to δ 100.18. Therefore, the chloro group was considered to be located at position C-6. ^{1}H, ^{1}H-homonuclear COSY spectrum showed the aromatic protons in the same spin system.

Considering the coupling constant of H-2 and H-3 and the sign and the value of the optical rotation of 7 ($[\alpha]_D^{20}=+50^\circ$, c = 0.16, DMSO), it can be deduced that the absolute stereochemistry of **7** is (2*R*,3*S*)-6-chloro-5,7,3′,4′- tetrahydroxylflavan-3-ol [= 6-chlorocatechin]. This is the first report of the occurrence of a halogenated flavan-3-ol in nature.

In the present study, compounds **7** and **8** exhibited a potent DPPH radical scavenging activity while compounds **1**–**6** and **9** did not show any activity.

Cytotoxicity tests were done with MCF (human breast carcinoma), HM02 (human melanoma) and HEPG2 (Human epidermoid carcinoma) cells. Compounds **1**–**9** did not inhibit the growth of the cell lines. In our previous study, *R. patientia* was examined against brine shrimp and was found to possess potent cytotoxic activity ($LC_{50}=1.30$ μg/ml) Nevertheless purified anthraquinone aglycons from *Rumex scutatus* possesses strong cytotoxic activity but anthraquinone glycosides and catechin are inactive (Demirezer and Kuruüzüm, 1997a).

In conclusion, using either varying cell lines or cytotoxic methods may bring forth differences.

3. Experimental

UV: Shimadzu UV-160A Spectrophotometer; IR: Perkin-Elmer FTIR 1720X Infrared Spectrometer; ^{1}H NMR and ^{13}C NMR spectra: Bruker AMX-300 at 300 MHz (for proton) and 75.5 MHz (for carbon) ; EI MS: Finnigan MAT 311A (70 eV); DCI MS: Varian MAT

731; TLC: normal phase Si gel 60 F_{254} (Merck 5554, 0.2 mm) and reversed phase Si gel, RP18 F_{254} (Merck 5559,0.2 mm); CC: normal phase Si gel 60 (Merck, 0.063 - 0.200 mm), reversed phase Si gel (LiChroprep RP-18, Merck 25–40 μm), sephadex LH-20 (Fluka), polyamide (Polyamid-MN-polyamid SC 6, Macherey-Nagel, Düren). In CC, fractions were selected on the basis of TLC and pooled.

3.1. Plant material

Roots of *Rumex patientia* L. were collected from Bor/Nigde, Turkey in September 1996 at an altitude of 1050 m. A voucher specimen (no: HUEF 96003) has been deposited in the Herbarium of the Faculty of Pharmacy, Hacettepe University, Ankara, Turkey.

3.2. Extraction and isolation

As a preliminary step, dried and powdered roots of *Rumex patientia* L. (500 g) were extracted with water (2×3.5 l) at 40–60 °C. The aqueous extracts were combined and concentrated. The suspended residue was partitioned with *n*-hexane, EtOAc and *n*-BuOH, respectively. Each extract was concentrated and lyophilized in vacuo.

The *n*-hexane fraction (370 mg) was chromatographed on Si gel column with a gradient of petroleum ether and EtOAc to yield compound **1** (15 mg) and compound **2** (20 mg).

The *n*-BuOH fraction (4.6 g) was subjected to Si gel column chromatography eluted with $CHCl_3$–MeOH (90:10→20:80) to give compound **3** (14 mg).

The EtOAc fraction (1.7 g) was applied to a polyamide column using increasing amounts of MeOH in H_2O. The fractions eluted with 40 and 50% MeOH were subjected to MPLC using RP-18 material as stationary phase and a H_2O-MeOH gradient solvent system and purified by repeated sephadex LH-20 column chromatographies eluted with MeOH to afford compound **4** (23 mg), compound **7** (7 mg), compound **8** (17 mg) and compound **9** (17 mg).

As the second step, dried and powdered roots of *R. patientia* (500 g) were extracted with MeOH (3×2.5 l) at 40–60 °C and evaporated to dryness (99 g). Aqueous extract, isolated compounds and methanolic extract were compared by TLC. In addition to the presence of the isolated compounds, several non-isolated anthraquinone derivatives were found in the methanolic extract.

Forty grams of methanolic extract were fractionated on a polyamide column by a gradient elution with H_2O–MeOH mixtures. The fractions eluted with 60 and 70% MeOH were rechromatographed over Si gel (EtOAc–MeOH–H_2O, 100:17:13) and Sephadex LH-20 (MeOH) to yield compound **5** (18 mg) and compound **6** (6.4 mg).

3.3. Emodin-6-O-β-D-glucopyranoside (6)

Amorphous; ESI MS *m/z*: 453 (23) $[M+Na]^+$, 413 (29), 365 (5); UV λ_{max} (MeOH) nm: 223, 264, 293 *sh*, 411; IR ν_{max} (KBr) cm^{-1}: 3432 (OH), 2921, 2850, 1670 (free C=O), 1633 (chelated C=O), 1060 (C–O); ^1H (300 MHz; DMSO-d_6) and ^{13}C NMR (75.5 MHz; DMSO-d_6): Table 1; R_f: 0.08 ($CHCl_3$/CH_3OH/H_2O, 80:20:2).

3.4. 6-Chlorocatechin (7)

Amorphous; ESIMS *m/z*: 649 (35), 647 (100) $[2M–H]^+$, 325 (24), 323 (70) $[M–H]^+$, 287 (5) $[M–H–Cl]^+$; UV λ_{max} (MeOH) nm: 208, 233 *sh*, 281; IR ν_{max} (KBr) cm^{-1}: 3381 (OH), 2922 (CH), 1623 (C=C, arom); ^1H (300 MHz; CD_3OD) and ^{13}C NMR (75.5 MHz; CD_3OD): Table 2; $[\alpha]_D^{20} = +50°$ ($c = 0.16$, DMSO); r_f: 0.36 ($CHCl_3$/CH_3OH/H_2O, 80:20:2).

3.5. Assay for antioxidative activity (Cuendet et al., 1997)

After developing and drying, TLC plates were sprayed with a 0.2% DPPH (1,1-diphenyl-2-picrylhydrazyl) solution in MeOH. The plates were examined 30 min after spraying. Active compounds appeared as yellow spots against a purple background. Quercetin was used as reference compound.

3.6. Assay for cytotoxic activity

Cytotoxic effect of pure compounds were tested against different cell lines, i.e. MCF (human breast carcinoma), HM02 (human melanoma) and HEPG2 (human epidermoid carcinoma). This study was carried out by Professor Dr. W. Beil (Faculty of Medicine, Institute of Pharmacology, MHH-Hannover).

Acknowledgements

We thank Professor Dr. W. Beil (Medizinische Hochschule Hannover) for performing the cytotoxic activity tests.

References

Baytop, T., 1984. Therapy with Medicinal Plants (Past and Present). Nobel Tip Kitabevleri, Istanbul.

Cohen, P.A., Towers, G.H.N., 1995. The anthraquinones of *Heterodermia obscurata*. Phytochemistry 40, 911–915.

Coskun, M., Satake, T., Hori, K., Saiki, Y., Tanker, M., 1990. Anthroquinone glycosides from *Rhamnus libanoticus*. Phytochemistry 29, 2018–2020.

Cuendet, M., Hostettmann, K., Potterat, O., Dyatmiko, W., 1997. Iridoid glycosides with free radical scavenging properties from *Fagraea blumei*. Helvetica Chimica Acta 80, 1144–1152.

Demirezer, L.Ö., 1991. Glukofrangulinanthrone A/B, deren Oxidationsformen und davon abgeleitete Zuckerester aus Rhamnus-Arten: Beiträge zur chemisch-analytischen und -physiologischen Kennzeichnung. Dissertation. Johann Wolfgang Goethe Universität, Frankfurt/M., Germany.

Demirezer, L.Ö, Kuruüzüm, A., 1997a. Rapid and simple biological activity screening of some *Rumex* species; evaluation of bioguided fractions of *R. scutatus* and pure compounds. Zeitschrift für Naturforschung 52c, 665–669.

Demirezer, L.Ö, Kuruüzüm, A., 1997b. A comparative chemotaxonomic study on eleven *Rumex* species growing in Turkey. FABAD Journal of Pharmaceutical Sciences 22, 153–158.

Foo, L.Y., Karchesy, J.J., 1989. Procyanidin dimers and trimers from douglas fir inner bark. Phytochemistry 28, 1743–1747.

Kuruüzüm, A., Demirezer, L.Ö, Bergere, I., Zeeck, A., 2001. Five naphthalene glycosides from the roots of *Rumex patientia*. Phytochemistry 56, 399–402.

Lin, C.N., Chung, M.I., Lu, C.M., 1990. Anthraquinones from *Rhamnus formosana*. Phytochemistry 29, 3903–3905.

Lin, C.N., Wei, B.L., 1993. Anthraquinone and naphthalene glycosides from *Rhamnus nakaharai*. Phytochemistry 33, 905–908.

Markham, K.R., Geiger, H., 1993. In: Harborne, J.B. (Ed.), The Flavonoids: advances in research since 1986. Chapman & Hall, London, pp. 441–497.

Pascual, T.J., de Urones, J.G., Marcos, I.S., Basabe Barcala, P., Garrido, N.M., 1986. Diterpenoid and other components of *Cistus laurifolius*. Phytochemistry 25, 1185–1187.

Sakar, M.K., Petereit, F., Nahrstedt, A., 1993. Two floroglucinol glucosides, flavan gallates and flavonol glycosides from *Sedum sediforme* flowers. Phytochemistry 33, 171–174.

Sharma, M., Sharma, P., Rangaswami, S., 1977. Orientalone, a new 1,4-naphthoquinone from *Rumex orientalis*. Indian Journal of Chemistry 15B, 544–545.

Suri, J.L., Dhar, K.L., Atal, C.K., 1978. Chemical constituents of *Rumex orientalis* Bernh. Journal of Indian Chemical Society 55, 292–293.

Süleyman, H., Demirezer, L.Ö., Kuruüzüm, A., Banoglu, Z.N., Göçer, F., Özbakir, G., Gepdiremen, A., 1999. Antiinflammatory effect of the aqueous extract from *Rumex patientia* L. roots. Journal of Ethnopharmacology 65, 141–148.

Van Der Nat, J.M., Van der Sluis, W.G., Thart, L.A., Van Dijk, H., de Silva, K.T.D., Labadie, R.P., 1991. Activity-guided isolation and identification of *Azadirachta indica* bark extract constituents which specifically inhibit chemiluminescence production by activated human polymorphonuclear leukocytes. Planta Medica 57, 64–68.

PERGAMON

Phytochemistry 58 (2001) 1219–1223

PHYTOCHEMISTRY

www.elsevier.com/locate/phytochem

Lignanamides and other phenolic constituents from the bark of kenaf (*Hibiscus cannabinus*)

Ana M. L. Seca, Artur M. S. Silva*, Armando J. D. Silvestre, José. A. S. Cavaleiro*, Fernando M. J. Domingues, Carlos Pascoal-Neto

Department of Chemistry, University of Aveiro, 3810-193 Aveiro, Portugal

Received 3 May 2001; received in revised form 3 July 2001

Abstract

Two new acyclic phenylpropane lignanamides, grossamide K and *erythro*-canabisine H, and the naphthol glucoside 2,5-dimethyl-3-*O*-β-D-glucopyranosylnaphthol, along with six known compounds were isolated from the acetone extract of bark of *Hibiscus cannabinus*. All structures were established by spectroscopic methods including 2D NMR techniques, which allowed the correction of certain previously reported ^{13}C NMR assignments of grossamide. © 2001 Elsevier Science Ltd. All rights reserved.

Keywords: Kenaf (*Hibiscus cannabinus*); Malvaceae; Lignanamides; Grossamide K; *erythro*-Canabisine H; Naphthol glucoside

1. Introduction

Kenaf (*Hibiscus cannabinus*) is an annual dicotyledonous herbaceous plant, well known in Asia and Africa, which has been recently cultivated in some Mediterranean areas. This plant was used in traditional medicine (Chifundera et al., 1994) and also by pulp and paper industries since its core and bark are sources of fibres with different lengths (Pande and Roy, 1996). In previous phytochemical investigations on kenaf, we have reported the aliphatic composition of the bark and core (Seca et al., 2000) and also the identification of new lignans isolated from the core (Seca et al., 2001). In the present study we report the isolation and structural characterisation of new lignanamides, named grossamide K **1** and *erythro*-canabisine H **2**, and of the 2,5-dimethyl-3-*O*-β-D-glucopyranosylnaphthol **3**, as well as six other compounds from the acetone extract of bark of *Hibiscus cannabinus*.

2. Results and discussion

The bark of *Hibiscus cannabinus* was finely ground and extracted, successively, with light petroleum and acetone. The acetone extract was partitioned with dichloromethane, chloroform and acetone, giving three fractions. Each one of these fractions was subjected to column and preparative thin layer chromatography leading to the isolation of three new compounds **1**–**3** (two lignanamides and a naphthol glucoside) (Fig. 1) and six other compounds.

Spectral data of compounds **1** and **4** have some similarities. The NMR spectra of both compounds displayed resonances corresponding of two methine groups, which correlate each other in the COSY spectra. The connectivities found in the HMBC spectra suggest that these two methine groups belong to a furan ring of a benzodihydrofuran structure (Fig. 1). The coupling constant of these protons ($J = 6.4$ Hz) indicates that these protons have *trans* configuration. The aromatic region of the ^1H NMR spectra of both **1** and **4** shows an AB set of signals; the coupling constant ($J = 15.6/15.8$ Hz) of these vinylic systems indicates that they have a *trans* configuration. The long-range connectivities of these protons, found in the HMBC spectra, with those of the carbons at δ 166.7/167.4 and the IR absorption bands at 3301–3355 (N–H) and 1650–1652 cm^{-1} (C=O), suggest the presence of an α,β-unsaturated amide moiety in both structures.

Analysis of the ^1H, ^{13}C and COSY NMR spectra of **1** and **4** also shows the proton and carbon resonances corresponding to two vicinal methylene groups. In the HMBC spectra these proton resonances correlates with those of the amide carbons (δ 166.7/167.4) and of a *p*-substituted

* Corresponding authors. Tel.: +351-234370714; fax: +351-234370084.

E-mail addresses: arturs@dq.ua.pt (A.M.S. Silva), jcavaleiro@dq.ua.pt (J.A.S. Cavaleiro).

0031-9422/01/$ - see front matter © 2001 Elsevier Science Ltd. All rights reserved.
PII: S0031-9422(01)00311-9

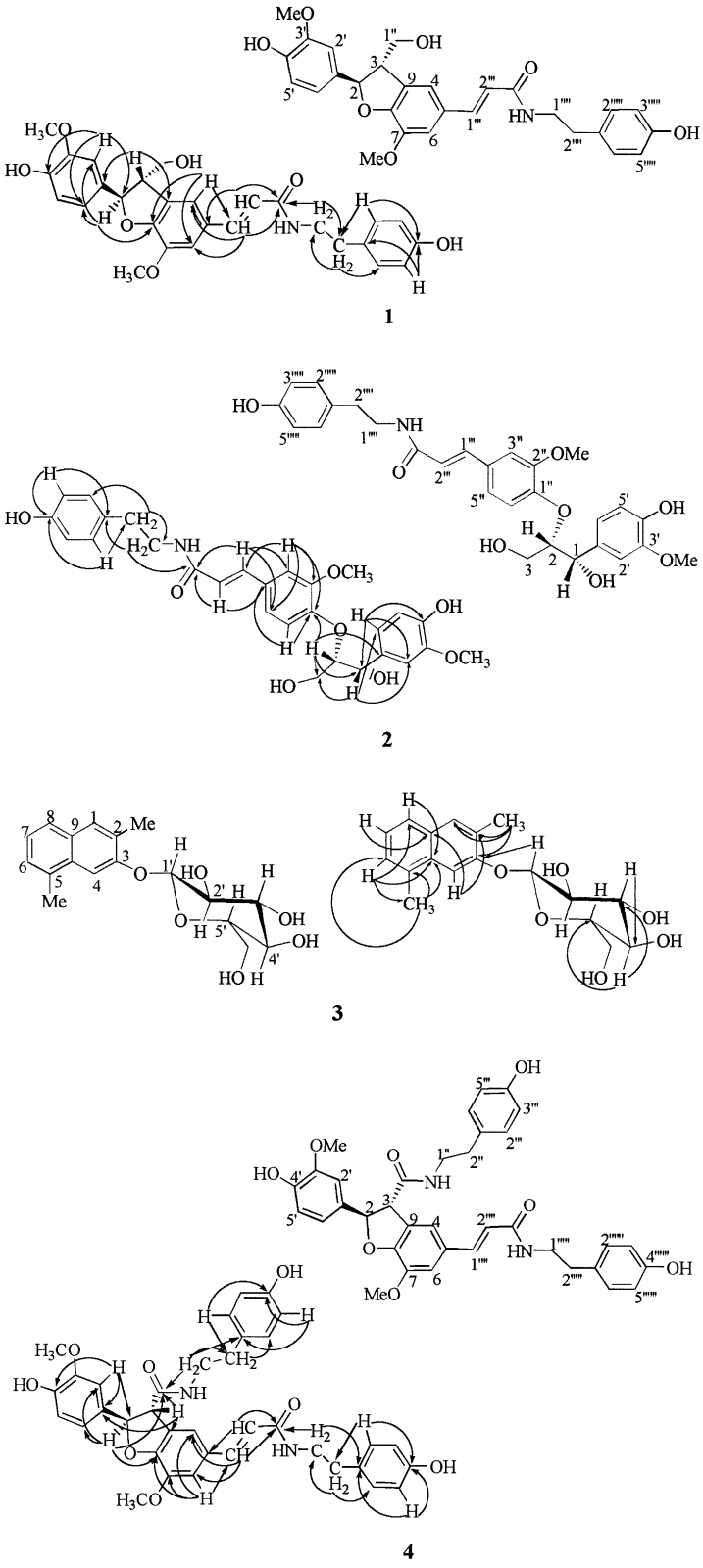

Fig. 1. Structure of compounds **1**–**4** from bark of *Hibiscus cannabinus* and major HMBC connectivities.

aromatic ring. These data, together with the presence of fragments $[M\text{-}136]^+$ and $[HOC_6H_4CH_2CH_2NH_2]^+$ (m/z 137) in the mass spectra, indicate the presence of at least one tyramine moiety in these structures.

The ^1H and ^{13}C NMR spectra of compound **1** indicate the presence of another methylene group, which are coupled with H-3 and other proton at δ_H 4.40 (1H, *s br*, which disappears after shaking its $CDCl_3$ solution with

D_2O). These data indicated the presence of a hydroxymethyl group attached to the position 3 of the benzodihydrofuran nuclei.

The spectral data of **1** are compatible with the structure of a lignanamide like grossamide K (Fig. 1), which was confirmed by the HR–FABMS spectrum, which shows a $[M+H]^+$ ion at m/z 492.2019 being consistent with the molecular formula $C_{28}H_{29}NO_7$ (calculated mass: 492.2022). The assignment of all carbon resonances supporting the assignment of the grossamide K **1** structure was done from the connectivities found in its HMBC spectrum (Fig. 1).

The presence of another tyramine moiety on structure **4** was deduced from its ^1H and ^{13}C NMR, where two additional methylene groups and another amide group were observed. These methylene proton present connectivities with the carbons of the amide group and of the *ortho* position of a *p*-substituted aromatic ring. This data was also confirmed by the molecular ion at m/z 625 $[C_{36}H_{36}N_2O_8+H]^+$ and the fragment at m/z 351 [M-2×tyr]. The discussed spectroscopic data and the analysis of the HMBC spectra (Fig. 1) support the assignment of its structure to grossamide (Lajide et al., 1995; Santos et al., 1996) and allowed the correction of the literature assignment of C-4, C-2′, C-4′, C-5′ and C-8.

The ^1H NMR spectrum of **2** showed basically the same resonances and coupling constants of grossamide K **1** (see experimental), but with a few differences. The absence of the dihydrofuran ring was suggested by the presence of a protonated aromatic carbon resonance (C-6″), instead the signal of the quaternary carbon C-9 of grossamide K **1**, and some important connectivities found in the HMBC spectrum (Fig. 3). The HR–FABMS of **2** showed a $[M+Na]^+$ ion at m/z 532.1971, consistent with the molecular formula of $C_{28}H_{31}O_8$ (calculated mass: 532.1947). Due to the skeleton similarities to canabisine E (Sakakibara et al., 1995) compound **2** was called canabisine H.

Due to the presence of two chiral carbons in the 1,2,3-trioxygenated propane moiety of canabisine H **2**, two possible diastereomers (*erythro* and *threo*) might be present. In their ^1H NMR spectrum H-1 appears as a slightly broad singlet, suggesting a small coupling constant with H-2, which indicates the presence of the *erythro* diastereomer (Shimomura et al., 1987; Abraham et al., 1991).

The FAB–HRMS spectrum of **3** exhibits the molecular ion peak at m/z 335.1490 corresponding to a molecular formula $C_{18}H_{23}O_6$ $[(M+H)^+$; calculated mass: 335.1495]. In the EI–MS spectrum the molecular ion at m/z 334 and the main fragment at m/z 172, corresponding to loss of $C_6H_{12}O_5$, have been observed. These data and analysis of the NMR spectra of **3** let us to conclude on the presence of a six-membered monosaccharide unity. Acid hydrolysis of **3** afforded only one sugar, which was identified by gas chromatography as glucose by comparison with authentic sugar sample (see Experimental). The anomeric proton of the glucose moiety appears as a doublet (δ_H 5.15, $J_{H1\text{-}H2}=7.5$ Hz), indicating the presence of this sugar in the β configuration. The spectroscopic data of **3** and the analysis of its HMBC spectrum (Fig. 1) allowed to conclude that the glucose moiety is attached to the 3 position of the naphthol unit and to fully assign this structure as 2,5-dimethyl-3-*O*-β-D-glucopyranosylnaphthol.

Additional isolated compounds were identified by comparing available literature data with their spectral features as kaempherol-3,7-rhamnoside (Mulinacci et al., 1995; Grasza et al., 1993), lariciresinol (Badawi et al., 1983; Katayama et al., 1993), pinoresinol (Tsukamoto et al., 1984; Deyama et al., 1987), syringaresinol (Ratnayake et al., 1992; Changzeng and Zhongjian, 1997) and of the most abundant compound (3.7% of extract), *N-trans*-feruloyl tyramine (Fukuda et al., 1983; Lajide et al., 1995).

3. Experimental

3.1. General

^1H and ^{13}C NMR spectra were recorded in acetone-d_6 on a Bruker AMX 300 spectrometer operating at 300.13 and 75.47 MHz, respectively; chemical shifts are expressed in δ (ppm) values relative to TMS as internal reference and the coupling constants J are expressed in Hz. ^1H Assignments were made using 2D COSY and NOESY (mixing time of 800 ms) experiments, while ^{13}C assignments were made using 2D HETCOR and HMBC experiments (long range C/H coupling constants were optimised to 4 and 7 Hz). MS were obtained at 70 eV electron impact and positive FAB (nitrobenzyl alcohol as matrix) ionisation using a VG Autospect Q mass spectrometer. IR spectra were obtained with a MATTSON 7000 FTIR spectrometer. GC analysis was performed using a Carlo Erba GC 6000 Vega Series 2 chromathograph equipped with a FID detector. Injector and detector temperatures were 220 and 250 °C respectively. Initial oven temperature was 220 °C (5 min), then 10 °C/min up to 230 °C (6 min), carrier gas hydrogen (55 cm/s), split ratio, 1:100, injections 2 μl. Fused silica capillary column DB-225 (30 m×0.25 mm×0.15 m) was used. Prep. TLC was carried out on silica gel plates (Merck silica gel 60 F_{254}); spots were detected under UV (λ 254 and/or 366 nm). Phenolic compounds were detected by the appearance of a brown colour when the TLC plates were sprayed with a (3:2) $CHCl_3$:pyridine solution of $FeCl_3$ (1%) (Browning, 1967). Column chromatography was also performed on silica gel (Merck silica gel 60, 70–230 mesh).

3.2. Plant material

Hibiscus cannabinus, variety Salvador, was harvested in Figueira da Foz, Portugal in September 1995.

3.3. Extraction and isolation

Stems of *H. cannabinus* were separated from foliage and air-dried at room temperature. The bark of *H. cannabinus* was separated from core and then finely ground (1503 g) and extracted successively with light petroleum and Me_2CO. The Me_2CO extract (12.9 g) was defatted with hexane and then fractionated by its solubility in CH_2Cl_2, $CHCl_3$ and Me_2CO. The residue obtained from the CH_2Cl_2 soluble fraction was subjected to silica gel CC. The column was eluted with $CHCl_3$–EtOAc (10:1) (fr I), $CHCl_3$–EtOAc (2:1) (fr II), and $CHCl_3$–EtOAc (1:1) (fr III). Fr I was chromatographed on prep. TLC, eluted with Et_2O-light petroleum (6:1), to give **7** (58.9 mg). Fr II on prep. TLC, eluted with CH_2Cl_2–EtOAc (2:1) yielded **8** (15.9 mg) and **9** (133.3 mg). Fr III on prep. TLC, eluted with $CHCl_3$–EtOAc (1:2) gave **2** (12.1 mg). The residue obtained from the $CHCl_3$ fraction was then subjected to prep. TLC, eluted with different mixtures of $CHCl_3$–EtOAc, to give **6** (11.8 mg), **7** (5.1 mg) and **9** (31.0 mg). The residue obtained from the fraction taken in acetone was subjected to silica gel CC. The column was eluted with $CHCl_3$–Me_2CO (1:2) (fr I), $CHCl_3$–Me_2CO (1:4) (fr II), and Me_2CO (fr III). Fr I was chromatographed by prep. TLC, eluting with $CHCl_3$–Me_2CO (2:1), to give **1** (24.3 mg), **2** (28.0 mg), **4** (11.6 mg) and **9** (315.2 mg). Fr II by prep. TLC, eluted with EtOAc yielded **2** (13.7 mg) and **3** (12.8 mg). Fr III by ppt. on Me_2CO gave **5** (31.6 mg).

3.3.1. 2-(4-Hydroxy-3-methoxyphenyl)-3-hydroxymethyl-5-[N-2-(4-hydroxyphenyl)ethyl]carbamoylethenyl-7-methoxybenzodihydrofuran (grossamide K) 1

Yellowish oil, IR ν_{max} (KBr) cm^{-1}: 3355 (N–H), 2937, 1652 (C=O), 1598, 1513 (C=C), 1207, 1145, 1029, 823. ^1H NMR: δ 2.75 (2H, *t*, *J* = 7.0 Hz, H-2‴), 3.56–3.50 (2H, *m*, H-1‴), 3.57 (1H, *q*, *J* = 6.4 Hz, H-3), 3.79–3.91 (2H, *m*, H-1″), 3.80 (3H, *s*, 3′-OCH_3), 3.85 (3H, *s*, 7-OCH_3), 4.40 (1H, *s*, 1″-OH), 5.60 (1H, *d*, *J* = 6.4 Hz, H-2), 6.54 (1H, *d*, *J* = 15.6 Hz, H-2‴), 6.76 (2H, *d*, *J* = 8.7 Hz, H-3⁗,5⁗), 6.82 (1H, *d*, *J* = 8.2 Hz, H-5′), 6.88 (1H, *dd*, *J* = 2.0 and 8.2 Hz, H-6′), 7.00 (1H, *d*, *J* = 2.0 Hz, H-2′), 7.06 (2H, *d*, *J* = 8.7 Hz, H-2⁗,6⁗), 7.07 (1H, *s*, H-6), 7.14 (1H, *s*, H-4), 7.40 (1H, *t*, *J* = 5.5 Hz, CONH), 7.49 (1H, *d*, *J* = 15.6 Hz, H-1‴), 7.78* (1H, *s*, 4′-OH), 8.32* (1H, *s*, 4⁗-OH). *They can be interchanged. ^{13}C NMR: δ 35.6 (C-2‴), 42.0 (C-1‴), 54.3 (C-3), 56.2 (3′-OCH_3), 56.3 (7-OCH_3), 64.3 (C-1″), 88.9 (C-2), 110.5 (C-2′), 112.8 (C-6), 115.7 (C-5′), 116.0 (C-3⁗,5⁗), 117.8 (C-4), 119.6 (C-6′), 119.8 (C-2‴), 129.7 (C-5), 130.5 (C-2⁗,6⁗), 130.8 (C-9), 130.9 (C-1⁗), 133.8 (C-1′), 140.7 (C-1‴), 145.2 (C-7), 147.4 (C-4′), 148.4 (C-3′), 150.7 (C-8), 156.7 (C-4⁗), 166.7 (CONR). EIMS 70eV, *m*/*z* (rel. int.): 491 $[M]^+$ (13), 473 $[M-18]^+$ (20), 461 $[M-30]^+$ (13), 355 $[M-136]^+$ (15), 137 (38), 107 (100), 77 (28). HR–FABMS *m*/*z*: 492.2019, $[M+H]^+$ (calc. for $C_{28}H_{29}NO_7$ + H: 492.2022).

3.3.2. Erythro-1-(4-hydroxy-3-methoxyphenyl)-2-{4-{2-[N-2-(4- hydroxyphenyl)ethyl]carbamoylethenyl-2-methoxyphenoxyl}}-1,3-propanodiol (erythro-canabisine H) 2

Yellowish oil, IR ν_{max} (KBr) cm^{-1}: 3291 (N–H), 1654 (C=O), 1594, 1515 (C=C), 1363, 1263, 1031, 825. ^1H NMR: δ 2.74 (2H, *t*, *J* = 7.4 Hz, H-2⁗), 3.46–3.51 (2H, *m*, H-1⁗), 3.52–3.56 (1H, *m*, H-3), 3.80 (3H, *s*, 3′-OCH_3), 3.88 (3H, *s*, 2″-OCH_3), 3.71–3.86 (1H, *m*, H-3), 4.33–4.35 (1H, *m*, H-2), 4.90 (1H, *s br*, H-1), 6.57 (1H, *d*, *J* = 15.6 Hz, H-2‴), 6.76 (2H, *d*, *J* = 8.1 Hz, H-3⁗,5⁗), 6.77 (1H, *d*, *J* = 8.3 Hz, H-5′), 6.90 (1H, *dd*, *J* = 1.4 and 8.3 Hz, H-6′), 6.98-7.07 (1H, *m*, H-5″), 7.05 (2H, *d*, *J* = 8.1 Hz, H-2⁗,6⁗), 7.10 (1H, *d*, *J* = 1.4 Hz, H-2′), 7.13 (1H, *d*, *J* = 8.7 Hz, H-6″), 7.18 (1H, *d*, *J* = 1.8 Hz, H-3″), 7.42-7.44 (1H, *m*, CONH), 7.46 (1H, *d*, *J* = 15.6 Hz, H-1‴), 8.41 (2H, *s*, 4′,4⁗-OH). ^{13}C NMR: δ 35.6 (C-2‴), 42.0 (C-1⁗), 56.1* (2″-OCH_3), 56.2* (3′-OCH_3), 61.8 (C-3), 73.6 (C-1), 87.2 (C-2), 111.3 (C-2′), 111.8 (C-3″), 115.2 (C-5′), 116.0 (C-3⁗,5⁗), 118.2 (C-6″), 120.4 (C-6′), 120.9 (C-2‴), 122.2 (C-5″), 130.1 (C-4″), 130.5 (C-2⁗,6⁗), 130.9 (C-1⁗), 133.7 (C-1′), 140.2 (C-1‴), 146.8 (C-4′), 148.0 (C-3′), 150.9 (C-1″), 151.4 (C-2″), 156.7 (C-4⁗), 166.6 (CONR). *They can be interchanged. FABMS *m*/*z* (rel. int.): 532 $[M+Na]^+$ (28), 510 $[M+H]^+$ (33), 177 (70). HR–FABMS *m*/*z*: 532.1971 $[M+Na]^+$ (calc. for $C_{28}H_{31}NO_8$ + Na: 532.1947).

3.3.3. 2,5-Dimethyl-3-O-β-D-glucopyranosylnaphthol 3

Yellowish oil, IR ν_{max} (KBr) cm^{-1}: 3322, 2931, 1511 (C=C), 1440, 1241, 1074. ^1H NMR: δ 2.40 (3H, *s*, 2-CH_3), 2.61 (3H, *s*, 5-CH_3), 3.45–3.48 (1H, *m*, H-4′), 3.58–3.63 (2H, *m*, H-2′,5′), 3.64 (1H, *dd*, *J* = 1.8 and 9.9 Hz, H-3′), 3.73 (1H, *dd*, *J* = 1.8 and 8.1 Hz, H-6′), 3.94-3.98 (1H, *m*, H-6′), 4.43 (1H, *d*, *J* = 4.2 Hz, 4′-OH), 4.51 (1H, *s*, 2′-OH), 4.72 (1H, *d*, *J* = 3.3 Hz, 3′-OH), 5.15 (1H, *d*, *J* = 7.5 Hz, H-1′), 7.18–7.22 (2H, *m*, H-6,7), 7.61 (1H, *s*, H-4), 7.63 (1H, *s*, H-1), 7.56–7.63 (1H, *m*, H-8). ^{13}C NMR: δ 16.9 (2-CH_3), 19.5 (5-CH_3), 62.8 (C-6′), 71.5 (C-4′), 74.7 (C-2′), 78.1 (C-3′), 78.2 (C-5′), 102.2 (C-1′), 107.3 (C-4), 124.5 (C-7), 125.9 (C-8), 126.7 (C-6), 128.9 (C-2), 129.9 (C-1), 130.5 (C-9), 133.3 (C-5), 134.0 (C-10), 155.6 (C-3). EIMS 70 eV, *m*/*z* (rel. int.): 334 M^+ (7), 172 $[M-162]^+$ (100), 157 (15). HR–FABMS *m*/*z*: 335.1490 $[M+H]^+$ (calc. for $C_{18}H_{23}O_6$: 335.1495).

3.3.4. 2-(4-Hydroxy-3-methoxyphenyl)-3-[N-2-(4-hydroxyphenyl)ethyl]carbamoyl-5-[N-2-(4-hydroxyphenyl)ethyl]carbamoylethenyl-7-methoxybenzodihydrofuran (grossamide) 4

Yellowish oil, IR ν_{max} (KBr) cm^{-1}: 3301 (N–H), 1650 (C=O), 1610, 1513 (C=C), 1213, 1147, 827. ^1H NMR: δ 2.77 (2H, *t*, *J* = 7.1 Hz, H-2⁗), 2.83 (2H, *t*, *J* = 6.0 Hz, H-2″), 3.50–3.57 (2H, *m*, H-1⁗), 3.75–3.75 (2H, *m*, H-1″), 3.80 (3H, *s*, 3′-OCH_3), 3.83 (3H, *s*, 7-OCH_3), 4.18 (1H, *d*, *J* = 8.6 Hz, H-3), 6.02 (1H, *d*, *J* = 8.6 Hz, H-2),

6.44 (1H, *s*, H-4), 6.46 (1H, *d*, $J=15.8$ Hz, H-2‴), 6.74 (2H, *d*, $J=8.3$ Hz, H-3⁗,5⁗), 6.77 (2H, *d*, $J=6.9$ Hz, H-2‴,6‴), 6.80 (2H, *d*, $J=6.9$ Hz, H-3‴,5‴), 6.70–6.8 1 (1H, *m*, H-6′), 6.81 (1H, *s*, H-5′), 6.96 (1H, *s*, H-2′), 7.05 (2H, *d*, $J=$ 8.3 Hz, H-2⁗,6⁗), 7.07 (1H, *s*, H-6), 7.41 (1H, *d*, $J=15.8$ Hz, H-1‴), 7.50 (1H, *t*, $J=5.2$ Hz, 3-CONH), 7.55 (1H, *t*, $J=$ 5.7 Hz, 2‴-CONH), 7.85* (1H, *s*, 4′-OH), 8.32* (1H, *s*, 4‴-OH), 8.90* (1H, *s*, 4⁗-OH). * They can be interchanged. ^{13}C NMR: δ 34.5 (C-2″), 35.4 (C-2′‴), 41.4 (C-1″), 42.0 (C-1′‴), 56.2 (7,3′-OCH_3), 57.6 (C-3), 88.8 (C-2), 110.4 (C-2′), 111.0 (C-6), 115.7 (C-5′), 115.9 (C-3⁗,5⁗), 116.7 (C-3‴,5‴), 118.8 (C-2‴), 119.0 (C-4), 119.7 (C-6′), 129.0 (C-9), 129.4 (C-5), 130.3 (C-2⁗,6⁗), 130.4 (C-1‴), 130.5 (C-2‴,6‴), 130.7 (C-1⁗), 132.3 (C-1′), 141.2 (C-1‴), 145.4 (C-7), 147.5 (C-4′), 148.3 (C-3′), 150.4 (C-8), 156.5 (C-4‴), 156.7 (C-4⁗), 167.4 (2‴-CONR), 170.3 (3-CONR). FABMS *m*/*z* (rel. int.): 625 $M+H^+$ (20), 488 $[(M+H)\text{-tyr}]^+$ (5), 451 $[(M+H)\text{-}2\times\text{tyr}]^+$ (10).

3.4. Hydrolysis of 2,5-dimethyl-3-O-β-D-glucopyranosylnaphthol **3**

The hydrolysis of compound **3** (2–3 mg) was carried out with 72% H_2SO_4 (0.1 ml) at room temperature during 3 h, followed by 3% H_2SO_4 at 100 °C during 2.5 h. One ml of the reaction mixture was neutralised with 200 μl of 25% NH_3 aqueous solution and then the monosaccharide(s) were reduced by the addition of 100 μl of 3 M NH_3 solution containing $NaBH_4$ 150 mg/ml, during 1 h at 30 °C. Excess $NaBH_4$ was decomposed by addition of HOAc (100 μl). Acetylation of alditol(s) was carried out with Ac_2O (3 ml) in the presence of 1-methylimidazole (0.45 μl), according to Blakeney et al. (1983). The obtained acetates were extracted with CH_2Cl_2; the organic layer was washed three times with water, evaporated to dryness at 30 °C under nitrogen atmosphere. The dry residue was diluted with CH_2Cl_2 and analysed by GC. The presence of glucose was identified by comparison with the sample obtained when this pure monosaccharide was submitted to the same procedure.

Acknowledgements

Thanks are due to the University of Aveiro and "Fundação para a Ciência e a Tecnologia" for funding. One of us (A.M.L.S.) is grateful to PRAXIS XXI for a PhD grant (BD/3412/94).

References

Abraham, R.J., Fisher, J., Loftus, P., 1991. Introduction to NMR Spectroscopy. John Wiley & Sons, Chichester.

Badawi, M.M., Handa, S.S., Kinghorn, A.D., Cordell, G.A., Farnsworth, N.R., 1983. Plant anticancer agents XXVII: antileukemic and cytotoxic constituents of *Dirca occidentalis* (Thymelaeaceae). Journal of Pharmaceutical Sciences 72, 1285–1287.

Blakeney, A.B., Harris, P.J., Henry, R.J., Stone, B.A., 1983. A simple and rapid preparation of alditol acetates for monosaccharide analysis. Carbohydrate Research 113, 291–299.

Browning, B.L., 1967. Methods of Wood Chemistry, Vol. I. Interscience, New York.

Changzeng, W., Zhongjian, J., 1997. Lignan, phenylpropanoid and iridoid glycosides from *Pedicularis torta*. Phytochemistry 45, 159–166.

Chifundera, K., Balagizi, K., Kizungu, B., 1994. Les empoisonnements et leurs antidotes en médecine traditionnelle au Bushi, Zaire. Fitoterapia 65, 307–313.

Deyama, T., Ikawa, T., Kitagawa, S., Nishibe, S., 1987. The constituents of *Eucommia ulmoides* Oliv. V. Isolation of dihydroxydehydrodiconiferyl alcohol isomers and phenolic compounds. Chemical Pharmaceutical Bulletin 35, 1785–1789.

Fukuda, N., Yonemitsu, M., Kimura, T., 1983. Studies on the constituents of the stems of *Tinospora tuberculata* Beumée. *N-trans*- and *N-cis*-feruloyl tyramine, and a new phenolic glucoside, tinotuberide. Chemical Pharmaceutical Bulletin 31, 156–161.

Grasza, B., Olechnowicz-Stepien, W., Królicki, Z.A., 1993. Flavonoid glycosides from the leaves of some *Euonymus* species. Fitoterapia 64, 379–380.

Katayama, T., Davin, L.B., Chu, A., Lewis, N.G., 1993. Novel benzylic ether reductions in lignan biogenesis in *Forsythia intermedia*. Phytochemistry 33, 581–591.

Lajide, L., Escoubas, P., Mizutani, J., 1995. Termite antifeedant activity in *Xylopia aethiopica*. Phytochemistry 40, 1105–1112.

Mulinacci, N., Vincieri, F.F., Baldi, A., Bambagiotti-Alberti, M., Sendl, A., Wagner, H., 1995. Flavonol glycosides from *Sedum telephium* subspecies *maximum* leaves. Phytochemistry 38, 531–533.

Pande, H., Roy, D.N., 1996. Delignification kinetics of soda pulping of kenaf. Journal of Wood Chemistry and Technology 16, 311–325.

Ratnayake, S., Fang, X.-P., Anderson, J.E., McLaughlin, J.L., 1992. Bioactive constituents from the twigs of *Asimina parviflora*. Journal of Natural Products 55, 1462–1467.

Sakakibara, I., Ikeya, Y., Hayashi, K., Okada, M., Maruno, M., 1995. Three acyclic bis-phenylpropane lignanamides from fruits of *Cannabis sativa*. Phytochemistry 38, 1003–1007.

Santos, L.P., Boaventura, M.A., Oliveira, A.B., Cassady, J.M., 1996. Grossamide and *N-trans*-caffeoyltyramine from *Annona crassiflora* seeds. Planta Medica 62, 76.

Sêca, A.M.L., Silva, A.M.S., Silvestre, A.J.D., Cavaleiro, J.A.S., Domingues, F.M.J., Pascoal-Neto, C., 2000. Chemical composition of the light petroleum extract of *Hibiscus cannabinus* bark and core. Phytochemical Analysis 11, 345.

Sêca, A.M.L., Silva, A.M.S., Silvestre, A.J.D., Cavaleiro, J.A.S., Domingues, F.M.J., Pascoal-Neto, C., 2001. Phenolic constituents from the core of *Hibiscus cannabinus*. Phytochemistry 56, 759–767.

Shimomura, H., Sashida, Y., Oohara, M., 1987. Lignans from *Machilus thunbergii*. Phytochemistry 26, 1513–1515.

Tsukamoto, H., Hisada, S., Nishibe, S., 1984. Lignans from bark of *Fraxinus mandshurica* var. *japonica* and *F. japonica*. Chemical Pharmaceutical Bulletin 32, 4482–4489.

PERGAMON

Phytochemistry 58 (2001) 1225–1228

PHYTOCHEMISTRY

www.elsevier.com/locate/phytochem

Hydroxysesamone and 2,3-epoxysesamone from roots of *Sesamum indicum*

A.F.M. Feroj Hasan, Toshio Furumoto, Setara Begum, Hiroshi Fukui*

Department of Biochemistry and Food Science, Faculty of Agriculture, Kagawa University, Kagawa 761-0795, Japan

Received 12 April 2001; received in revised form 17 July 2001

Abstract

A red naphthoquinone, named hydroxysesamone, was isolated from the roots of *Sesamum indicum* together with a known yellow naphthoxirene derivative, 2,3-epoxy-2,3-dihydro-5,8-dihydroxy-2-(3-methyl-2-butenyl)-1,4-naphthoquinone, named 2,3-epoxysesamone. The structure of the naphthoquinone was characterized as 2,5,8-trihydroxy-3-(3-methyl-2-butenyl)-1,4-naphthoquinone on the basis of spectral evidence. Full assignments of NMR resonances of 2,3-epoxysesamone were also confirmed by two-dimensional NMR spectroscopic experiments. Chlorosesamone, hydroxysesamone and 2,3-epoxysesamone all showed antifungal activities toward *Cladosporium fulvum*. © 2001 Elsevier Science Ltd. All rights reserved.

Keywords: *Sesamum indicum*; Pedaliaceae; Sesame root; Naphthoquinones; Hydroxysesamone; Chlorosesamone; 2,3-Epoxysesamone; Antifungal activity

1. Introduction

Sesamum indicum L. (Pedaliaceae) is one of the most important crops throughout the world, and its seeds have been utilized for a long time as edible oilseeds and food materials. There are many phytochemical studies on the genus *Sesamum* which have been concerned with lignans (Bedigian et al., 1985; Osawa et al., 1985), phenolic acids (Das et al., 1966; Dabrowski and Sosulski, 1984), flavonoids (Krishnaswamy et al., 1970; Sinha and Dogra, 1985), saponins (Fenwick and Oakenfull, 1983; Sinha and Dogra, 1985), alkaloids (Sinha and Dogra, 1985). However, little research has been reported on the constituents of the roots, an unutilized part of sesame. In our search for antifungal compounds among the metabolites of sesame roots, chlorosesamone (**1**) was isolated from the roots of *S. indicum* and characterized (Hasan et al., 2000).

Chlorosesamone (**1**) is a chlorinated antifungal naphthoquinone. Natural chlorine-containing compounds occurring in higher plants are of increasing interest due to their frequent occurrence and various biological activities (Engvild, 1986), but only has a limited knowledge of their biosynthetic pathways. During our further research, we found that sesame roots contain two additional antifungal metabolites. In this paper, we report the isolation and structural elucidation of a new red naphthoquinone, named hydroxysesamone (**2**), and full assignments of NMR resonances of a known yellow naphthoxirene derivative (Potterat et al., 1987; Ogasawara et al., 1993), named 2,3-epoxysesamone (**3**), which seem to be biogenetically related to chlorosesamone (**1**).

2. Results and discussion

Hydroxysesamone (**2**) was isolated as red needles from fresh roots of *S. indicum* after purification as described in the Experimental. The HR–EIMS and ^{13}C NMR spectral data (Table 1) for **2** revealed the molecular formula $C_{15}H_{14}O_5$, which corresponds to the substitution of a hydroxyl group for a chlorine atom in chlorosesamone (**1**, $C_{15}H_{13}O_4Cl$) (Hasan et al., 2000). The ^{13}C NMR spectrum of **2** showed 15 resonances, two due to methyl groups, one to methylene, three to methines and nine to quaternary carbons from its DEPT data, confirming that three of the protons in the

* Corresponding author. Tel.: +81-87-891-3084; fax: +81-87-891-3021.

E-mail address: fukui@ag.kagawa-u.ac.jp (H. Fukui).

0031-9422/01/$ - see front matter © 2001 Elsevier Science Ltd. All rights reserved.
PII: S0031-9422(01)00357-0

molecule are bound to oxygen atoms. The ^1H and ^{13}C NMR spectral data for **2** (Table 1), as well as its UV-vis and IR bands, were similar to those of **1**. These findings suggested that **2** is a trihydroxylated naphthoquinone analogue. The structure of hydroxysesamone (**2**) was unambiguously substantiated by analysis of ^1H–^1H COSY, HMQC, LR-HETCOR (HMBC and COLOC) and DIFNOE data.

A 3-substituted 2,5,8-trihydroxy-1,4-naphthoquinone ring was deduced from the ten carbon (C-1–C-8a), two aromatic methine protons (δ_H 7.26, *d*, $J=9.4$ Hz, H-6 and 7.14, *d*, $J=9.4$ Hz, H-7), one hydroxyl proton (δ_H 7.37, *br.s*, 2-OH), and two chelated hydroxyl protons (δ_H 12.82, *s*, 5-OH and 11.46, *s*, 8-OH) signals. Moreover, the chemical shifts of C-2 (δ_C 153.3), C-5 (δ_C 157.1) and C-8 (δ_C 157.5) suggested bonds between these carbon atoms and the hydroxyl groups. The HMQC and LR-HETCOR experiments supported this deduction. The 2-OH signal was correlated with the C-2 and C-3 resonances, and 5-OH and 8-OH signals respectively correlated with the C-4a, C-5 and C-6 signals and with C-7, C-8 and C-8a signals, providing further evidence for the 2,5,8-trihydroxy-3-substituted, not a 5,6,8-trihydroxy-7-substituted, ring. The NMR spectroscopic assignments of two C_3 units (C-4a–C-6 and C-7–C-8a) including two chelated hydroxyl group (5-OH and 8-OH) were presumed by comparison to the chemical shifts of chelated hydroxyl group for 5- (2,5-hydroxyl isomer, δ_H 12.45) and 8-hydroxylapachol (2,8-hydroxyl isomer, δ_H 11.00) (Khan and Mlungwana, 1999). However, these assignments in **2** may be interchanged because of no availability of LR-HETCOR correlations.

The ^1H NMR spectrum of **2** (Table 1) exhibited two methyl broad singlets at δ_H 1.67 and 1.76, one methylene broad doublet at δ_H 3.28 ($J=7.3$ Hz) and one vinylic methine signal (δ_H 5.16, *tqq*, $J=7.3$, 1.4 and 1.4 Hz). These signals closely resembled those of the side chain of **1** (Hasan et al., 2000) and lapachol derivatives (Khan and Mlungwana, 1999), suggesting the presence of a 3-methyl-2-butenyl group in **2**. The structure of the side chain was confirmed by the ^1H–^1H COSY and LR-HETCOR experiments. Furthermore, the NMR spectroscopic assignments of the two methyl groups (C-4′ and C-5′) were established by the DIFNOE data. Irradiation of the H-4′ methyl signal (δ_H 1.67) caused NOE enhancement of the H-2′ vinylic methine signal (δ_H 5.16), indicating that the C-4′ methyl group and H-2′ proton lie on the same side of the double bond. The attachment of the side chain to the naphthoquinone ring was demonstrated by the correlation of the H-1′ signal with the C-2, C-3 and C-4 observed in the LR-HETCOR experiments. Therefore, the structure for hydroxysesamone (**2**) was unambiguously established as 2,5,8-trihydroxy-3-(3-methyl-2-butenyl)-1,4-naphthoquinone.

Compound **3** was isolated as pale yellow crystals, and had the same molecular formula $C_{15}H_{14}O_5$ (HR–EIMS and ^{13}C NMR spectral data) as **2**. The ^1H and ^{13}C NMR spectra of **3** (Table 1) showed the presence of two carbonyl groups, three olefinic methines and five olefinic quaternary carbons, indicating that **3** contains three

Table 1
^1H and ^{13}C NMR spectral data for hydroxysesamone (**2**) in $CDCl_3$ and 2,3-epoxysesamone (**3**) in benzene-d_6

	2		**3**	
Position	δ_C	δ_H[a]	δ_C	δ_H[a]
1	182.5		195.3	
2	153.3		59.3	3.48 *s*
3	124.6		63.4	
4	188.5		195.9	
4a	110.8[b]		111.5	
5	157.1[b]		157.3	
6	131.5[b]	7.26 *d* (9.4)	129.2	6.68 *d* (9.4)
7	127.4[b]	7.14 *d* (9.4)	128.9	6.71 *d* (9.4)
8	157.5[b]		156.8	
8a	110.2[b]		111.6	
1′	22.1	3.28 *br.d* (7.3)	26.1	2.46 *br.dd* (15.4, 6.9) 2.74 *br.dd* (15.4, 8.2)
2′	119.2	5.16 *tqq* (7.3, 1.4, 1.4)	115.6	4.92 *ddqq* (8.2, 6.9, 1.4, 1.4)
3′	134.2		137.2	
4′	25.7	1.67 *br.s*	25.7	1.53 *br.s*
5′	17.9	1.76 *br.s*	17.9	1.44 *br.s*
2-OH		7.37 *br.s*		
5-OH		12.82[b] *s*		11.89 *s*
8-OH		11.46[b] *s*		11.71 *s*

[a] *J* values in parentheses (Hz).
[b] C_3 units determined by LR-HETCOR.

rings in its structure. Furthermore, one methine singlet at δ_H 3.48 and two oxygen-bearing carbon signals (δ_C 59.3 and 63.4), respectively, were present instead of one hydroxyl proton (δ_H 7.37) and two olefinic carbon (δ_C 153.3 and 124.6) signals observed in **2**. These facts suggested that **3** is a 2,3-epoxy analogue of **2**. The MS and NMR spectral data for **3** were identical with those for a naphthoxirene derivative previously isolated from the root bark of *S. angolense* (Potterat et al., 1987) and from the hairy roots of *S. indicum* (Ogasawara et al., 1993). Thus, compound **3** was identified as 2,3-epoxy-2,3-dihydro-5,8-dihydroxy-2-(3-methyl-2-butenyl)-1,4-naphthoquinone, and was named 2,3-epoxysesamone.

Assignments of ^1H and ^{13}C NMR spectroscopic signals of **3**, some of which were ambiguous previously, were also confirmed on the basis of DEPT, ^1H–^1H COSY, HSQC, LR-HETCOR and DIFNOE data in the same manner as in the structural elucidation of **2**, since its structure was determined mainly by X-ray diffraction analysis (Potterat et al., 1987). The LR-HETCOR experiments of **3** revealed significant long-range ^{13}C–^1H correlations as follows: H-2/C-1, C-1′ and C-8a; 5-OH/C-4a, C-5 and C-6; 8-OH/C-7, C-8 and C-8a; H-1′/C-2, C-3 and C-4. Consequently, full assignments of the NMR resonances of 2,3-epoxysesamone (**3**) were unambiguously accomplished.

The carbon skeletons of hydroxysesamone (**2**) and 2,3-epoxysesamone (**3**), a naphthoquinone ring plus a prenyl side chain, are identical with that of chlorosesamone (**1**), suggesting that these metabolites have the same biosynthetic origin. In addition, the naphthoquinone moiety of these metabolites would be biosynthesized from shikimate and 2-ketoglutarate (Inoue et al., 1984; Herbert, 1989; Haslam, 1993; Thomson, 1997). The biogenetic origin of the prenyl side chain and relationship of **1**, **2** and **3**, especially the mechanism and precursor for chlorination, are interesting topics now under investigation.

The antifungal activities toward *Cladosporium fulvum* of **1**, **2** and **3** were tested using a bioautographical assay (Fukui et al., 1999). In this assay, chlorosesamone (**1**), hydroxysesamone (**2**) and 2,3-epoxysesamone (**3**) inhibited the spore germination of the fungus at respective amounts of 0.1, 1 and 10 μg per spot, indicating that **1** having chlorine atom in the molecule is the strongest fungicide among three naphthoquinones **1**–**3**.

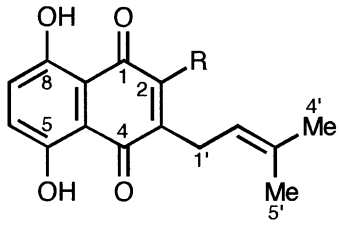

1 R = Cl
2 R = OH

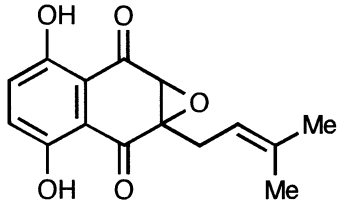

3

3. Experimental

3.1. General experimental procedures

Mps are uncorr. NMR spectra were recorded with a Jeol JNM-A400 FT NMR spectrometer at 400 MHz for ^1H and 100.4 MHz for ^{13}C. All NMR chemical shifts were referenced to the signal of the deuterated solvent used ($CDCl_3$, δ_H 7.24, δ_C 77.0; benzene-d_6, δ_H 7.15, δ_C 128.0). Mass spectra were measured with a Jeol JMS-SX102AQQ hybrid mass spectrometer. UV spectra were obtained with a HITACHI 340 recording spectrophotometer, and IR spectra with a JASCO A-302 spectrometer. Silica gel 60 (70–230 mesh, Nacalai Tesque) and Sephadex LH-20 (Amersham Pharmacia Biotech) were used for CC. TLC were done on silica gel 60 F_{254} (Merck).

3.2. Plant material

Seeds of *Sesamum inducum* L. were purchased from the seed and seedling supplier (Hashimoto Seed) in Kagawa, Japan. Sesame plants were cultivated in the field of Kagawa University in 1999, and the roots were harvested ca. three months after sowing the seeds.

3.3. Extraction and isolation of 2 and 3

Fresh roots of *S. indicum* (5 kg) were treated with MeOH, then were filtered from MeOH through filter paper. This treatment was repeated twice. The MeOH soln. obtained was evaporated in vacuo, and the aq. residue was partitioned with EtOAc (×3) to give the EtOAc-soluble fraction (10 g). This fraction was separated by silica gel CC eluted stepwise with mixtures of *n*-hexane and EtOAc. A fraction eluted with 20% EtOAc in *n*-hexane was purified by Sephadex LH-20 CC with MeOH–$CHCl_3$ (1:1) as eluent to afford compound **2** (45 mg). A fraction eluted with 15% EtOAc in *n*-hexane was subjected to a combination of silica gel CC (1% Me_2CO in $CHCl_3$), Sephadex LH-20 CC (EtOH–C_6H_6,

1:2) and prep. TLC (EtOAc–*n*-hexane–HOAc, 2:98: 0.2, triple development). A R_f 0.53 band was further purified by Sephadex LH-20 CC with EtOH–C_6H_6 (3:2) as eluent to give compound **3** (49 mg).

3.4. Hydroxysesamone (**2**)

Red needles from *n*-hexane–$CHCl_3$, mp 145–146 °C. UV-vis λ_{max} (MeOH) nm (log ϵ): 242 (4.05), 270 (3.81), 287 (3.76), 484 (3.64), 538 (3.64). IR ν_{max} ($CHCl_3$) cm^{-1}: 3415, 1605, 1570, 1455. ^1H and ^{13}C NMR spectral data ($CDCl_3$): Table 1. EIMS (probe) 70 eV, *m*/*z* (rel. int.): 274 $[M]^+$ (95), 259 (100). HR-EIMS *m*/*z*: 274.0838; $C_{15}H_{14}O_5$ requires 274.0841.

3.5. 2,3-Epoxysesamone (**3**)

Pale yellow crystals from MeOH, mp 85–86 °C. $[\alpha]_D^{25}$ −43° ($CHCl_3$; *c* 0.34). HR-EIMS *m*/*z*: 274.0845; $C_{15}H_{14}O_5$ requires 274.0841. The EIMS, UV and IR spectral data matched the lit. values (Potterat et al., 1987). ^1H and ^{13}C NMR spectral data (benzene-d_6): Table 1.

References

Bedigian, D., Seigler, D.S., Harlan, J.R., 1985. Sesamin, sesamolin and the origin of sesame. Biochemical Systematics and Ecology 13, 133–139.

Dabrowski, K.J., Sosulski, F.W., 1984. Composition of free and hydrolyzable phenolic acids in defatted flours of ten oilseeds. Journal of Agricultural and Food Chemistry 32, 128–130.

Das, V.S.R., Rao, K.N., Rao, J.V.S., 1966. Phenolic acids in some members of Pedaliaceae. Current Science 35, 160.

Engvild, K.C., 1986. Chlorine-containing natural compounds in higher plants. Phytochemistry 25, 781–791.

Fenwick, D.E., Oakenfull, D., 1983. Saponin content of food plants and some prepared foods. Journal of the Science of Food and Agriculture 34, 186–191.

Fukui, H., Hasan, A.F.M.F., Kyo, M., 1999. Formation and secretion of a unique quinone by hairy root cultures of *Lithospermum erythrorhizon*. Phytochemistry 51, 511–515.

Hasan, A.F.M.F., Begum, S., Furumoto, T., Fukui, H., 2000. A new chlorinated red naphthoquinone from roots of *Sesamum indicum*. Bioscience, Biotechnology, and Biochemistry 64, 873–874.

Haslam, H., 1993. Shikimic Acid: Metabolism and Metabolites. John Wiley & Sons, Chichester.

Herbert, R.B., 1989. The Biosynthesis of Secondary Metabolites. 2nd Edition. Chapman & Hall, London.

Inoue, K., Ueda, S., Nayeshiro, H., Moritome, N., Inouye, H., 1984. Biosynthesis of naphthoquinones and anthraquinones in *Streptocarpus dunnii* cell cultures. Phytochemistry 23, 313–318.

Khan, R.M., Mlungwana, S.M., 1999. 5-Hydroxylapachol: a cytotoxic agent from *Tectona grandis*. Phytochemistry 50, 439–442.

Krishnaswamy, N.R., Seshadri, T.R., Tahir, P.J., 1970. Flavone glucosides of *Nepeta hindustana* & *Sesamum indicum*: nepitrin and pedaliin and their aglucones. Indian Journal of Chemistry 8, 1074–1078.

Ogasawara, T., Chiba, K., Tada, M., 1993. Production in high-yield of a naphthoquinone by a hairy root culture of *Sesamum indicum*. Phytochemistry 33, 1095–1098.

Osawa, T., Nagata, M., Namiki, M., Fukuda, Y., 1985. Sesamolinol, a novel antioxidant isolated from sesame seeds. Agricultural and Biological Chemistry 49, 3351–3352.

Potterat, O., Stoeckli-Evans, H., Msonthi, J.D., Hostettmann, K., 1987. Two new antifungal naphthoxirene derivatives and their glucosides from *Sesamum angolense* WELW. Helvetica Chimica Acta 70, 1551–1557.

Sinha, S.K.P., Dogra, J.V.V., 1985. A survey of the plants of Bhagalpur and Santhal Pargana for saponin, flavonoids and alkaloids. International Journal of Crude Drug Research 23, 77–86.

Thomson, R.H., 1997. Naturally Occurring Quinones IV: Recent Advances. Blackie Academic & Professional, London.

PERGAMON

Phytochemistry 58 (2001) 1229–1233

PHYTOCHEMISTRY

www.elsevier.com/locate/phytochem

A flavonoid sulphate and other compounds from the roots of *Centaurea bracteata*

Guido Flamini*, Maria Pardini, Ivano Morelli

Dipartimento di Chimica Bioorganica e Biofarmacia,Universita di Pisa, Via Bonanno 33, 56126 Pisa, Italy

Received 6 April 2001; received in revised form 26 July 2001

Abstract

The roots of *Centaurea bracteata* Scop. (Asteraceae) have been studied for the first time. Twenty-three compounds were isolated and identified, namely a sterol glucoside, two quinic acid derivatives, one sugar, and 19 flavonoids (five sulphates), one of which, centaradixin, resulted in a new natural product. Structural elucidation was performed mainly by means of FABMS, 1D and 2D NMR spectroscopy. NMR data of some sulphate flavonoids are reported for the first time. © 2001 Elsevier Science Ltd. All rights reserved.

Keywords: *Centaurea bracteata*; Asteraceae; Flavonoids; Axillarin 7-sulphate; Centaradixin

1. Introduction

Centaurea bracteata Scop. (Asteraceae), known in Italy as "fiordaliso bratteato" is a herbaceous plant placed by Pignatti (1982) in the *C. jacea* group, together with 10 other species. The plant is not used in Italian folk medicine, although other species of the same genus (i.e. *Centaurea cyanus* and *Centaurea scabiosa*) are used against coughs and as ophthalmic drugs (Poletti, 1978) or vulneraries (Mazza, 2000). The studies on this genus deal mainly with sesquiterpene lactones, while flavonoids are less investigated; only our previous study about its aerial parts is reported in literature (Flamini et al., 2001); the roots have never been studied at all.

This paper deals with the isolation and characterisation of 23 substances belonging to various classes of compounds, in particular two quinic acid derivatives, a sterol glucoside, a monosaccharide, and 19 flavonoids, one of which is a new natural products. Moreover, NMR data of some known flavonoid sulphates are reported for the first time.

2. Results and discussion

From the *n*-hexane residue (R_H), by repeated flash and p-TLC chromatographies, four compounds were isolated, namely jaceidin, jacein, 6-hydroxyluteolin-6,4′-dimethylether and centaureidin, which were identified by comparison of their physical and spectroscopic properties with literature reports (Roitman and James, 1985; Agrawal et al., 1989). Similarly, from the chloroform extract (R_C), hispidulin, 6-hydroxykaempferol 3,6-dimethylether and β-sitosterol 3-*O*-glucoside were obtained (Agrawal et al., 1989; Reher and Budensisky, 1992).

Fractionation of the $CHCl_3$–MeOH (9:1) extract (R_{CM}) by size-exclusion chromatography, column chromatography, and preparative TLC, led to the isolation of further eight pure compounds. These were axillarin, nepetin, 6-hydroxyluteolin-6,4′-dimethylether-7-*O*-glucoside, jacesiolin, centaurein, nepetin 7-glucoside, 5-caffeoylquinic acid and fructose (Collado et al., 1985; Iwahashi et al., 1985; Barbera et al., 1986; Berghöfer and Hölzl, 1987; Wada et al., 1987; Agrawal et al., 1989), all identified by ^1H and ^{13}C NMR spectroscopy.

The R_{MAc} and R_{MBu} residues, after size-exclusion chromatography and repeated Lobar RP-8, RP-18, flash and preparative TLC chromatographies, gave 3-caffeoylquinic acid methyl ester, axillarin 7-glucoside, isokaempferide, nepetin 7-sulphate, patuletin 7-sulphate, hispidulin 7-sulphate, quercetin 3,3′-disulphate and the new flavonoid sulphate, which we named centaradixin (**1**) Table 1. Known isolates were identified by comparison with literature data (Saleh et al., 1971; Redaelli et al., 1980; Iwahashi et al., 1985; Kubo et al., 1986; Ahmed and Mabry, 1987; Barron and Ibrahim,

* Corresponding author. Tel.: +39-050-44074; fax: +39-050-43321.
E-mail address: flamini@farm.unipi.it (G. Flamini).

0031-9422/01/$ - see front matter © 2001 Elsevier Science Ltd. All rights reserved.
PII: S0031-9422(01)00345-4

Table 1
^{13}C NMR data for compound **1** and patuletin and nepetin 7-sulphates (50 MHz)[a]

Carbon	**1**[b]	**1**[c]	Patuletin 7-sulphate[b]	Nepetin 7-sulphate[b]
2	156.3 *s*	159.0 *s*	147.9 *s*	164.4 *s*
3	137.6 *s*	139.5 *s*	135.7 *s*	102.4 *d*
4	178.4 *s*	180.5 *s*	176.2 *s*	182.3 *s*
5	150.4 *s*	152.3 *s*	150.1[d] *s*	151.4[d] *s*
6	133.3 *s*	135.7 *s*	132.4 *s*	133.2 *s*
7	152.9[d] *s*	153.8[d] *s*	152.7[d] *s*	152.8[d] *s*
8	97.9 *d*	100.6 *d*	97.7 *d*	98.3 *d*
9	152.0[d] *s*	153.0[d] *s*	151.3[d] *s*	152.6[d] *s*
10	106.6 *s*	109.3 *s*	105.3 *s*	106.2 *s*
1′	120.4 *s*	122.7 *s*	121.8 *s*	120.5 *s*
2′	116.1 *d*	116.6 *d*	115.7 *d*	116.3 *d*
3′	145.6 *s*	146.4 *s*	145.2 *s*	146.4 *s*
4′	149.5 *s*	150.2 *s*	149.9[d] *s*	151.3[d] *s*
5′	115.2 *d*	116.6 *d*	114.6 *d*	113.1 *d*
6′	120.8 *d*	122.8 *d*	120.4 *d*	119.3 *d*
3-OMe	59.6 *q*	60.5 *q*	60.2 *q*	60.2 *q*
6-OMe	60.3 *q*	61.7 *q*		

[a] Multiplicities deduced by DEPT experiments.
[b] Measured in DMSO-d_6.
[c] Measured in CD_3OD.
[d] Signals may be exchanged.

1987a; Nishizawa et al., 1988; Tomas-Barberan et al., 1987; Agrawal et al., 1989).

Centaradixin (**1**) was obtained as a yellowish amorphous powder that appears on TLC as a yellow-orange arrow-shaped spot after treatment with Naturstoffereagenz A-PEG. The negative FABMS spectrum gave a quasimolecular peak $[M-H]^-$ at 425 *m/z*, corresponding to the molecular formula $C_{17}H_{14}O_{11}S$, supported also by elemental analysis (see Experimental); another significant ion at *m/z* 448 ($[M+Na-H]^-$) showed the presence of sodium in the sample. The ^{13}C NMR spectrum showed 17 resonances, sorted by DEPT experiments into 4 CH, 2 CH_3 and 11 quaternary C. In the ^{1}H NMR spectrum obtained in DMSO-d_6 a three-proton ABM system was present (δ 7.56, *d*, $J=2.0$ Hz; 7.50, *dd*, $J=8.3$, 2.0 Hz; 6.90, *d*, $J=8.3$ Hz), typical of the 3′,4′-disubstituted ring B of a flavonoid unit. Ring A showed only a resonance as one-proton singlet at δ 7.28. Moreover, two three-proton singlets were present at δ 3.73 and 3.78. The situation was very close to that of axillarin, apart from the signal of ring A that resulted deshielded. This circumstance was more evident in the ^{1}H NMR spectrum recorded in CD_3OD, where the resonance of the ring A proton appeared at very low fields (δ 7.36). Analysis of the ^{13}C NMR spectrum confirmed the 'strange' situation of ring A with respect to axillarin. Resonances of ring A carbons showed the typical shifts due to the presence of a sulphate group linked to the C-7 hydroxy group (Barron and Ibrahim, 1987b; Barron et al., 1988): 4.6 ppm upfield for the *ipso* carbon (C-7), 4.3 and 6.6 ppm downfield for the *ortho* carbons (C-6 and C-8, respectively), and 3.1 ppm downfield for the *para* carbon (C-10), in DMSO-d_6; in CD_3OD the results are very similar (−4.9, +3.1, +5.6 and +3.0 ppm, respectively). This situation is confirmed also by the large downfield shift (0.80 ppm) experienced by the proton attached to the *alpha* carbon (H-8).

The high resonance value of the two methoxyl groups (δ 59.6 and 60.3) suggested that both the *ortho* positions should be substituted, so they must be placed only at the 3 and 6 position (Agrawal et al., 1989). This situation is corroborated by the characteristic downfield shifts observed for C-2, C-3 and C-4 (ca. 10.5, 4.0 and 2.5 ppm, respectively) because the 3-OCH_3, and the shifts experienced by C-5, C-6, C-7 and C-9 (ca. −9, +31, −10, −5 ppm, respectively) due to the 6-OCH_3 with respect to quercetin (Agrawal et al., 1989) and by comparison with similar methoxy-substituted flavonoids (Barbera et al., 1986; Agrawal et al., 1989) (Fig. 1). Moreover, a cross peak was evidenced in the NOESY spectrum between the 3-OCH_3 and the H-2′ and H-6′ resonances.

Therefore, **1** is axillarin 7-sulphate sodium salt, which we named centaradixin. This structure is supported by its negative FABMS spectrum where, besides the quasimolecular peak at *m/z* 425, $[M-H]^-$, and at *m/z* 448, $[M+Na-H]^-$, there was a peak due to loss of a sulphate group at *m/z* 345, $[M-H-80]^-$. Finally, the presence of sodium was confirmed by the yellow colour obtained by the flame assay; acid hydrolysis of **1** liberated axillarin and sulphate, identified by TLC with authentic samples and precipitation with barium chloride, respectively.

Most of the known flavonoid sulphates have been characterized only by UV and MS measurements, so we report their NMR data for the first time.

Summarising, the roots of *C. bracteata* yielded 23 compounds, among which 19 were flavonoids, two caffeoylquinic derivatives, one sugar and one sterol glucoside. Most of the flavonoids, according to the pattern of this genus, were polymethoxylated and three compounds have been obtained in great amounts (centaureidin 7800 mg, nepetin-7-glucoside 455 mg, and 6-hydroxyluteolin-6,4′-dimethylether-7-glucoside 335 mg; 0.51, 0.03 and 0.02% with respect to the dry plant material). It is quite interesting to note that the main constituent of the roots was centaureidin (7800 mg),

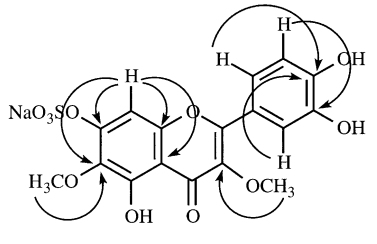

1

Fig. 1. Significant CH long range correlations observed in COLOC of compound **1**.

while in the aerial parts was its isomer jaceidin (3650 mg) (Flamini et al., 2001). Five of the flavonoids, were sulphate conjugate; these compounds are relatively rare in nature (Williams and Harborne, 1994) and, among the Asteraceae, they are produced only by four tribes: Inuleae, Eupatorieae, Senecioneae and Heliantheae (Barron et al., 1988). We have reported the identification of another flavonoid sulphate from the aerial parts of *C. bracteata* (Flamini et al., 2001). This study definitively confirms the presence of flavonoid sulphate esters in the genus *Centaurea* and that now there are five producing tribes among the Asteraceae, comprising also the Centaureinae.

Flavonoid sulphates, generally, are obtained as potassium salts, while our isolates are all the less common sodium salts. Till now only the genus *Lippia* (Verbenaceae) seems to produce sodium salts, among which nepetin and hispidulin 7-sulphates (Tomas-Barberan et al., 1987); our study is the first report, besides the new compound centaradixin (**1**), of patuletin 7-sulphate and quercetin 3,3′-disulphate sodium salts.

Normally, these compounds have been obtained from the aerial parts; Varin et al. (1986) went into detail about *Flaveria bidentis* affirming the presence of the highest amounts of flavonoids sulphates in the buds, followed by the leaves, while in the roots they were completely absent. Therefore, the presence of five flavonoid sulphates in the roots of *C. bracteata*, besides the further one isolated from the aerial parts (Flamini et al., 2001), seems to be noteworthy. Really, on the contrary with respect to *F. bidentis, C. bracteata* prefers to synthetize/store these substances in the roots.

Our findings seem to confirm the previous observations on *Brickellia* spp. and *Flaveria chloraefolia* (Barron et al., 1988) about the competition between the glucosilation and sulphation reactions for the same aglycones. In fact we have observed the concomitant presence of the 7-glucosides and 7-sulphates, of axillarin and nepetin; moreover the aerial parts (Flamini et al., 2001) contained quercetin 3-glucoside-3′-sulphate and the roots quercetin 3,3′-disulphate.

The large diffusion of flavonoid sulphates in water or hydrophyte plants (Tomas-Barberan et al., 1987; Barron et al., 1988; De Beck et al., 1998; Seabra and Correia Alves, 1988) seems to support the view that this conjugation could represent an ecological adaptation to the aquatic habitat. However our findings, both on the aerial parts (Flamini et al., 2001) and the roots, seems to contradict this hypotesis, in fact *C. bracteata* has been collected in a very arid environment, the normal habitat according to Pignatti (1982), that describes this species as a xerophytic one.

Flavonoids sulphates showed many biological activities, useful both to human health and plant physiology. They are enzymes inhibitors (Haraguchi et al., 1996), allergens (Sallusto et al., 2000), antioxidants (Yagi et al., 1994), regulators of auxin transport (Faulkner and Rubery, 1992). Moreover, rutine sulfate was demonstrated to be not carcinogenic (Habs et al., 1984).

The group of *C. jacea* to which *C. bracteata* belongs together with other ten species, was also considered as constituted by polymorphic forms of one (*C. jacea*) or two (*C. jacea* and *C. nigrescens*) species (Pignatti, 1982). Comparing the chemicals isolated from the other studied species of this group [*C. jacea*, *C. nigrescens* and *C. pannonica* (Bowie and Cameron, 1965; Bohlmann and Zdero, 1967; Wagner et al., 1969; Rosler et al., 1970; Monya, 1971; Kaïj-a-Kamb et al., 1992)], we can see some convergences but also many differences. Consequently, the separation of the species as suggested by Pignatti (1982) could be correct hypothesis.

Sesquiterpene lactones, typical compounds of this genus, are not produced at all by *C. bracteata*. The same is true for the other studied species of this group. If this finding will be confirmed for the remaining species of the group, it could be of chemotaxonomical interest.

3. Experimental

3.1. General

Melting points (uncorrected) were determined with a Kofler apparatus; optical rotations were measured on a Perkin-Elmer 241 polarimeter; FABMS were recorded, in the negative mode, with a VG ZAB instrument; ^{1}H and ^{13}C NMR spectra were obtained with a Bruker AC200 spectrometer in CD_3OD, DMSO-d_6, and $CDCl_3$, using TMS as internal standard. All 1D and 2D NMR experiments were performed using the standard Bruker library of microprograms.

The following adsorbents were used for purification: flash chromatography, Merck Kieselgel 60 (230–410 mesh); low-pressure chromatography, Merck Lobar Lichroprep RP-8 (31 × 2.5 cm); size-exclusion chromatography, Pharmacia Fine Chemicals Sephadex LH-20; analytical TLC, Merck Kieselgel 60 F_{254} precoated plates; chromatograms were visualised under UV light at 254 and 366 nm and/or sprayed with Komarowsky or Cerium Sulphate or Naturstoffereagenz A-PEG reagents.

3.2. Plant material

The roots were collected during full bloom at Montelaterone, Amiata Mount, South Tuscany, Italy, at 600 m above the sea level, in July 1999. A voucher specimen is deposited in PI (Herbarium of the University of Pisa).

3.3. Extraction and isolation

The dried and ground roots (1540 g) were extracted, successively, in a Soxhlet apparatus with *n*-hexane,

$CHCl_3$, $CHCl_3$–MeOH (9:1) (6.0 l × 35 h) and, at room temperature, with MeOH (7.0 l × 7 days × 3 times). After removal of solvents, in vacuo at up to 40 °C, the following residues were obtained: R_H (14.1 g), R_C (14.7 g), R_{CM} (67.1 g), and R_M (18.4 g).

R_M was suspended in MeOH–H_2O (7:3) and extracted, in turn, with EtOAc and *n*-BuOH obtaining, after removal of the solvents, the residues R_{MAc} and R_{MBu}.

The R_H residue, after repeated SiO_2 flash chromatographies and preparative TLCs, gave jaceidin (6 mg; yield 0.0004%), jacein (6 mg; yield 0.0004%), 6-hydroxyluteolin-6,4′-dimethylether (3 mg; yield 0.0002%) and centaureidin (7800 mg; yield 0.51%). In a similar fashion, from the R_C residue, hispidulin (18 mg; yield 0.001%), 6-hydroxykaempferol 3,6-dimethylether (8 mg; yield 0.0005%) and β-sitosterol-3-*O*-β-D-glucoside (29 mg; yield 0.02%) were obtained.

The R_{CM} residue was submitted to Sephadex LH-20 size-exclusion chromatography with MeOH–$CHCl_3$ (9:1) as eluent and the fractions were submitted to SiO_2 column chromatographies and p-TLC, obtaining eight pure compounds: axillarin (48 mg; yield 0.02%), nepetin (20 mg; yield 0.0002%), 6-hydroxyluteolin-6,4′-dimethylether-7-*O*-β-D-glucopyranoside (335 mg; yield 0.03%), jacesiolin (13 mg; yield 0.0008%), centaurein (24 mg; yield 0.0002%), nepetin-7-*O*-β-D-glucopyranoside (455 mg; yield 0.03%), 5-caffeoylquinic acid (11 mg; yield 0.0008%), and fructopyranose (18 mg; yield 0.001%).

The R_{MAc} residue was submitted to a Sephadex LH-20 column with MeOH as eluent, obtaining 18 main fractions (A–R). From these fractions, after repeated Lobar RP-8 and RP-18 chromatography, 3-caffeoylquinic acid methyl ester (6 mg; yield 0.0004%), axillarin 7-*O*-β-D-glucopyranoside (7 mg; yield 0.0005%), isokaempferide (6 mg; yield 0.0004%), nepetin 7-sulphate (15 mg; yield 0.001%) and patuletin 7-sulphate (12 mg; yield 0.0008%) were isolated.

R_{MBu} was chromatographed over Sephadex LH-20 column with MeOH as eluent, obtaining 26 main fractions (A–Z). Fraction H gave a precipitate constituted by pure quercetin 3,3′-disulphate (12 mg; yield 0.0008%). From fractions L–M, by flash chromatography and SiO_2 p-TLC, hispidulin 7-sulphate (6 mg; yield 0.0004%) was purified. Fraction K was submitted to p-TLC obtaining pure compound **1** (18 mg; yield 0.001%).

3.4. Centradixin (*1*)

Yellowish amorphous solid; ^{1}H NMR spectral data (DMSO-d_6, 200 MHz) δ 3.73 (3H, *s*, 6-OMe), 3.78 (3H, *s*, 3-OMe), 6.90 (1H, *d*, J = 8.3 Hz, H-5′), 7.28 (1H, *s*, H-8), 7.50 (1H, *dd*, J = 8.3, 2.0 Hz, H-6′), 7.56 (1H, *d*, J = 2.0 Hz, H-2′) ; ^{1}H NMR (CD_3OD, 200 MHz) δ 3.82 (3H, *s*, 3-OMe), 3.92 (3H, *s*, 6-OMe), 6.92 (1H, *d*, J = 8.3 Hz, H-5′), 7.36 (1H, *s*, H-8), 7.59 (1H, *br d*, J = 8.3 Hz, H-6′), 7.66 (1H, *br s*, H-2′); ^{13}C NMR data see Table 1; FABMS (negative mode) *m*/*z* 448 $[M+Na-H]^-$, 425 $[M-H]^-$, 345 $[M-H-80]^-$; elemental analysis: found: C 44.60%, H 3.44%, requires: C 47.89, H 3.31.

3.5. Patuletin 7-sulphate

^{1}H NMR spectral data (DMSO-d_6, 200 MHz) δ 3.74 (3H, *s*, 6-OMe), 6.87 (1H, *d*, J = 8.3 Hz, H-5′), 7.29 (1H, *s*, H-8), 7.65 (1H, *dd*, J = 8.3, 2.0 Hz, H-6′), 7.67 (1H, *d*, J = 2.0 Hz, H-2′).

3.6. Nepetin 7-sulphate

^{1}H NMR spectral data (DMSO-d_6, 200 MHz) δ 3.73 (3H, *s*, 6-OMe), 6.75 (1H, *s*, H-3), 6.86 (1H, *d*, J = 8.8 Hz, H-5′), 7.32 (1H, *s*, H-8), 7.45 (1H, *m*, H-6′), 7.46 (1H, *br s*, H-2′).

3.7. Hispidulin 7-sulphate

^{1}H NMR spectral data (DMSO-d_6, 200 MHz) δ 3.78 (3H, *s*, 6-OMe), 6.82 (1H, *s*, H-3), 6.91 (2H, *d*, J = 8.8 Hz, H-2′ and H-6′), 7.32 (1H, *s*, H-8), 7.93 (2H, *d*, J = 8.8 Hz, H-3′ and H-5′).

References

Ahmed, A.A., Mabry, T.J., 1987. Flavonoids from *Iphiona scabra*. Phytochemistry 26, 1517–1518.

Agrawal, P.K., Takur, R.S., Bansal, M.C., 1989. Flavonoids. In: Agrawal P.K. (Ed.), Carbon-13 NMR of Flavonoids. Elsevier, Amsterdam, p. 159.

Barbera, O., Marco, J.A., Sanz, J.F., Sanchez-Parareda, J., 1986. 3-Methoxyflavones and coumarins from *Artemisia incanescens*. Phytochemistry 25, 2357–2360.

Barron, D., Ibrahim, R.K., 1987a. Quercetin and patuletin 3,3′-disulfates from *Flaveria chloraefolia*. Phytochemistry 26, 1181–1184.

Barron, D., Ibrahim, R.K., 1987b. Synthesis of flavonoids sulfates: I. Stepwise sulfation of positions 2, 7, and 4′ using *N,N*′-dicyclohexylcarbodiimide and tetrabutylammonium hydrogen sulfate. Tetrahedron 43, 5197-5202.

Barron, D., Varin, L., Ibrahim, R.K., Harborne, J.B., Williams, C.A., 1988. Sulphated flavonoids-an update. Phytochemistry 27, 2375–2395.

Berghöfer, B., Hölzl, J., 1987. Biflavonoids in *Hypericum perforatum*; part I. Isolation of I3,II8-biapigenin. Planta Med. 53, 216–218.

Bohlmann, F., Zdero, C., 1967. Über Flavone aus *Centaurea*-Arten. Tetrahedron Lett. 33, 3239–3242.

Bowie, J.H., Cameron, D.W., 1965. Colouring matters of the Aphididae. Part XXV. A comparison of aphid constituents with those of their host plants. A glyceride of sorbic acid. J. Chem. Soc 5651–5657.

Collado, I.G., Macias, F.A., Massanet, G.M., Luis, F.R., 1985. Flavonoids from *Centaurea clementei*. J. Nat. Prod 48, 819–822.

De Beck, P.O., Dijoux, M.-G., Cartier, G., Mariotte, A.-M., 1998. Quercitrin-3′-sulfate from leaves of *Leea guinensis*. Phytochemistry 47, 1171–1173.

Faulkner, I.J., Rubery, P.H., 1992. Flavonoids and flavonoid sulphates as probes of auxin-transport regulation in *Cucurbita pepo* hypocotyl segments and vesicles. Planta 186, 618–625.

Flamini, G., Antognoli, E., Morelli, I., 2001. Two new flavonoids and other compounds from the aerial parts of *Centaurea bracteata* from Italy. Phytochemistry 57, 559–564.

Habs, M., Habs, H., Berger, M.R., Schmahl, D., 1984. Negative dose-response study for carcinogenicity of orally administered rutin sulfate in Sprague-Dawley rats. Cancer Lett. 23, 103–108.

Haraguchi, H., Ohmi, I., Sakai, S., Fukuda, A., Toihara, Y., Fujimoto, T., Okamura, N., Yagi, A., 1996. Effect of *Polygonum hydropiper* sulfated flavonoids on lens aldose reductase and related enzymes. J. Nat. Prod. 59, 443–445.

Iwahashi, H., Morishita, H., Osaka, N., Kido, R., 1985. 3-*O*-Feruloyl-4-*O*-caffeoylquinic acid from coffee beans. Phytochemistry 24, 630–632.

Kaïj-a-Kamb, M., Amoros, M., Girre, L., 1992. Chimie et activités biologiques du genre *Centaurea*. Pharm. Acta Helv. 67, 178–188.

Kubo, M., Sasaki, H., Endo, T., Taguchi, H., Yoshioka, I., 1986. The constituents of *Schizonepeta tenuifolia* Briq. Structure of a new monoterpene glucoside, schizonepetoside C. Chem. Pharm. Bull. 34, 3097–3101.

Mazza, F., 2000. Itinerari alla scoperta delle erbe officinali del Monte Amiata. Stampa 2000 Ed., Abbadia S. Salvatore, Siena.

Monya, M., 1971. Caffeoylquinic derivative contents in plant species of the *Centaurea* genus. Farmacia 19, 45–50.

Nishizawa, M., Izuhara, R., Kaneko, K., Koshihara, Y., Fujimoto, Y., 1988. 5-Lipoxygenase inhibitors isolated from Gardeniae fructus. Chem. Pharm. Bull. 36, 87–95.

Pignatti, S., 1982. Flora d′Italia. Edagricole, Bologna.

Poletti, A., 1978. Fiori e Piante Medicinali. Musumeci Editore, Milano.

Redaelli, C., Formentini, L., Santaniello, E., 1980. Apigenin 7-glucoside and its 2″- and 6″-acetates from ligulate flowers of *Matricaria chamomilla*. Phytochemistry 19, 985–986.

Reher, G., Budensisky, M., 1992. Triterpenoids from plants of the Sanguisorbeae. Phytochemistry 31, 3909–3914.

Roitman, J.N., James, L.F., 1985. Chemistry of toxic range plants. Highly oxygenated flavonol methyl ethers from *Gutierrezia microcephala*. Phytochemistry 24, 835–848.

Rosler, H., Star, A.E., Mabry, T.J., 1970. New 6-methoxyflavonols from *Centaurea jacea*. Phytochemistry 10, 450–451.

Saleh, N.A.M., Bohm, B.A., Ornduff, R., 1971. Flavonoids from *Lasthenia conjugens* and *Lasthenia fremonti*. Phytochemistry 10, 611–614.

Sallusto, F., Poupot, R., Clergue, M., DePalma, R., Fournie, J.J., 2000. A flavonoid sulfate antigen activates human alphabeta CD8+ Th2 lymphocytes in pollen allergy. Eur. J. Immunol. 30, 964–968.

Seabra, R.M., Correia Alves, A., 1988. Quercetin 3-glucuronide-3′-sulphate from *Hypericum elodes*. Phytochemistry 27, 3019–3020.

Tomas-Barberan, F.A., Harborne, J.B., Self, R., 1987. Twelve 6-oxygenated flavone sulfates from *Lippia nodiflora* and *L. canescens*. Phytochemistry 26, 2281–2284.

Varin, L., Barron, D., Ibrahim, R.K., 1986. Identification and biosynthesis of glucosylated and sulphated flavonols in *Flaveria bidentis*. Z. Naturforsch. C: Biosci. 41, 813–819.

Wada, H., Fujita, M., Murakami, T., Saikai, Y., Chen, C.M., 1987. Chemical and chemotaxonomical studies of ferns. LXXIII. New flavonoids with modified B-ring from the genus *Pseudophegopteris* (Thelypteridaceae). Chem. Pharm. Bull 35, 4757–4762.

Wagner, H., Horhammer, L., Hoer, R., Murakami, T., Farkas, L., 1969. Untersuchungen über die Glykoside von *Centaurea jacea* L. Isolierung, Struktur und Synthese von 4,5,7-Trihydroxy-3′,6-dimethoxy-flavon-7-mono-b-D-glukopyranosid, einem neuen Flavonolglykosid aus den Wurzeln von *Centaurea jacea* L. Tetrahedron Lett. 39, 3411–3414.

Williams, C.A., Harborne, J.B., 1994. Flavone and flavonol glycosides. In: Harborne J.B. (Ed.), The Flavonoids: Advances in Research since 1986. Chapman and Hall, Cambridge, p. 344.

Yagi, A., Uemura, T., Okamura, N., Haraguchi, H., Imoto, T., Hashimoto, K., 1994. Antioxidative sulphated flavonoids in leaves of *Polygonum hydropiper*. Phytochemistry 35, 885–887.

PERGAMON

Phytochemistry 58 (2001) 1235–1238

PHYTOCHEMISTRY

www.elsevier.com/locate/phytochem

Ardisiaquinones from *Ardisia teysmanniana*

Lay-Kien Yang[a], Corinne Khoo-Beattie[a], Kay-Lin Goh[a], Bee-Lee Chng[a], K. Yoganathan, Yee-Hing Lai[b], Mark S. Butler[a,*]

[a]*Centre for Natural Product Research, Institute of Molecular and Cell Biology, 59A Science Park Drive, The Fleming, Singapore Science Park, 118240 Singapore*

[b]*Department of Chemistry, National University of Singapore, Kent Ridge, 119260 Singapore*

Received 22 March 2001; received in revised form 3 July 2001

Abstract

Bioassay-guided fractionation of a $CHCl_3$ extract from the leaves of *Ardisia teysmanniana* Scheff. (Myrsinaceae) has led to the isolation of three new alkyldibenzoquinone derivatives that showed inhibitory activity in an in vitro assay for UDP-MurNac synthesis. The structures of ardisiaquinone G, H and I were established using MS and NMR spectroscopic methods. © 2001 Elsevier Science Ltd. All rights reserved.

Keywords: *Ardisia teysmanniana*; Myrsinaceae; Leaves; 1,4-Benzoquinone; Ardisiaquinone

1. Introduction

The first committed step in bacterial peptidoglycan synthesis involves the conversion of UDP-N-acetylglucos amine (UDP-GlcNac) to UDP-N-acetylmuramic acid (UDP-MurNac) with the concomitant utilisation of NADPH, catalysed by the two enzymes UDP-GlcNAc transferase (MurA) and UDP-GlcNAc enolpyruvyl reductase (MurZ) (Benson et al., 1993). In the course of our search for new antimicrobials from natural resources, an enzymatic assay that coupled the reactions of the two enzymes to generate UDP-MurNac was designed to identify potential lead compounds that interfere with bacterial cell wall synthesis.

The family of Myrsinaceae consists of about 1250 plants which are classified into 37 genera (Raffauf, 1996). A $CHCl_3$ extract from the leaves of *A. teysmanniana* Scheff. (Myrsinaceae), one of 10 species of *Ardisia* found in Singapore (Keng, 1990), was found to inhibit the enzymatic assay. Bioassay-directed fractionation led to the isolation of three new alkyldibenzoquinones, ardisiaquinone G (**1**), H (**2**) and I (**3**). Ardisiaquinones A (**4**), B (**5**) and C (**6**) were first isolated from the root bark of *A. sieboldii* Miguel (Ogawa and Natori, 1968a,b; Ogawa et al., 1968) and total synthesis of ardisiaquinone A had also been reported (Fukuyama et al., 1994). In 1995, Fukuyama et al. reported the isolation of ardisiaquinone D (**7**), E (**8**) and F (**9**) from the same species and later published the total syntheses of these compounds (Fukuyama et al., 1998).

2. Results and discussion

Ardisiaquinone G (**1**) was isolated as amorphous powder. Positive ESIMS of **1** showed an $[M+H]^+$ at m/z 573 and a $[M+NH_4]^+$ ion peak at m/z 590.5. A HR–ESIMS measurement of the $[M+H]^+$ ion peak suggested a molecular formula of $C_{31}H_{40}O_{10}$. MS fragmentation at m/z 531.0 $[M-Ac]^+$ and m/z 489.5 $[M-2\times Ac]^+$ indicated the presence of two acetyl units. The ^1H NMR spectrum of **1** (Table 1) contained signals for an aliphatic chain (δ 2.38–2.44, 4 H and δ 1.20–1.50, ca. 20 H), two tertiary methyl groups (δ 1.94 and 1.96), two acetyl groups (δ 2.35 and 2.36) and two OH signals (δ 7.02 and 7.05) that disappeared upon addition of D_2O. The ^{13}C NMR spectrum revealed the presence of two methyl groups (δ 7.9 and 8.8), two acetyl groups (δ 20.3), at least 12 methylenes (δ 20–30), two carbonyl groups (δ 167.8 and 168.1) and 12 quaternary signals belonging to two benzoquinone rings. The substitution pattern of the two acetyl, two hydroxy and two methyl subunits on the benzoquinone rings was further

* Corresponding author. Tel.: +65-773-7071; fax: +65-773-7072.
E-mail address: mark@cnpr.nus.edu.sg (M.S. Butler).

0031-9422/01/$ - see front matter © 2001 Elsevier Science Ltd. All rights reserved.
PII: S0031-9422(01)00317-X

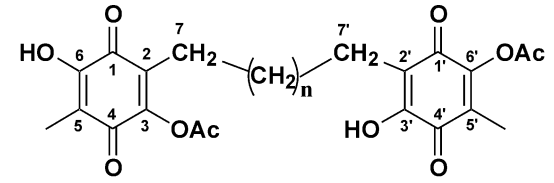

ardisiaquinone G (**1**) n = 11
ardisiaquinone H (**2**) n = 12
ardisiaquinone I (**3**) n = 13

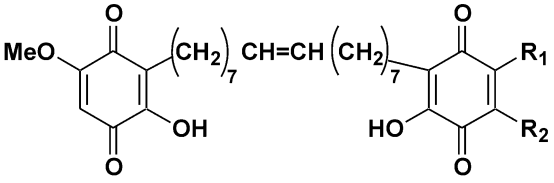

ardisiaquinone A (**4**) R_1=OMe, R_2=H
ardisiaquinone B (**5**) R_1=OH, R_2=Me
ardisiaquinone C (**6**) R_1=OAc, R_2=Me
ardisiaquinone D (**7**) R_1=OMe, R_2=OMe

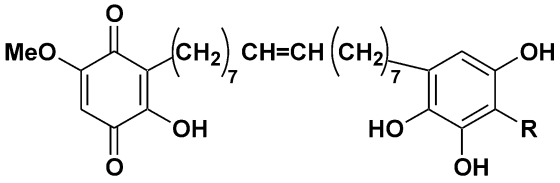

ardisiaquinone E (**8**) R = H
ardisiaquinone F (**9**) R = Me

revealed by the HMBC correlations as shown in Fig. 1. The absence of two olefinic protons at δ 5.33 and four allylic protons at δ 1.90 – 2.10 in **1** compared to other ardisiaquinones indicated that **1** contained a fully saturated aliphatic chain between the two benzoquinone rings. Further support for the structure was obtained from the MS data where the two fully substituted benzoquinone rings accounted for mass of 390, which implied that the remaining mass of 182 corresponded to 13 methylene units between the quinone moieties. The spectroscopic data of **1** were also in excellent agreement with that of the dihydro derivative of ardisiaquinone A, **10**, prepared by catalytic hydrogenation (Table 1) (Ogawa and Natori, 1968b; Ogawa et al., 1968).

The molecular formula of ardisiaquinone H (**2**) was determined to be $C_{32}H_{42}O_{10}$ on the basis of HR–ESIMS data (*m*/*z* 587.2856, calc. 587.2857). The ESIMS showed an $[M+NH_4]^+$ ion peak at *m*/*z* 604.5 and an $[M+H]^+$ at *m*/*z* 587.5, as well as two fragments at *m*/*z* 545.5 and 503.5, corresponding to a loss of one and two Ac units, respectively. The ^1H and ^{13}C NMR spectra of compound **2** matched nearly identical to that of ardisiaquinone G (**1**) (Table 1), which indicated that the extra 14 mass units were accounted for by an extra CH_2 unit in the alkyl chain.

Table 1
^1H (500 MHz) and ^{13}C NMR (125 MHz) data for compounds ardisiaquinone G (**1**), H (**2**) and I (**3**) in $CDCl_3$

Positions	**1**[a]		**2**[a]		**3**[a]	
	δ_H	δ_C	δ_H	δ_C	δ_H	δ_C
1		183.4		183.4		183.4
2		132.7		132.7		132.7
3		150.4		150.4		150.4
4		180.5		180.5		180.5
5		115.7		115.7		115.7
6		151.2		151.2		151.2
7	2.40 (*t*, 7.5)	23.4	2.40 (*t*,7.5)	23.4	2.40 (*t*,7.5)	23.4
1′		180.3		180.3		180.3
2′		120.2		120.2		120.2
3′		151.1		151.1		151.1
4′		183.7		183.7		183.7
5′		128.8		128.8		128.8
6′		150.4		150.4		150.4
7′	2.43 (*t*, 7.5)	22.9	2.43 (*t*,7.5)	22.8	2.43 (*t*, 7.5)	22.8
3-OCO		168.1		168.1		168.1
3-OCOMe	2.36 *s*	20.3	2.36 *s*	20.3	2.36 *s*	20.3
5-Me	1.94 *s*	7.9	1.94 *s*	7.9	1.95	7.9
6-OH	7.05 *s*		7.05 *s*		7.05 *s*	
3′-OH	7.02 *s*		7.02 *s*		7.02 *s*	
5-′Me	1.96 *s*	8.8	1.96	8.7	1.96 *s*	8.8
6′-OCO		167.8		167.9		167.9
6′OCOMe	2.35 *s*	20.3	2.35 *s*	20.3	2.35 *s*	20.3
$-(CH_2)_{n-}$	1.24 *m* (22 H)	28–29	1.24 *m* (24 H)	28–29	1.24 *m* (26 H)	28–29

[a] Assignments based on COSY, HMQC and HMBC.

The ESIMS of ardisiaquinone I (**3**) showed an $[M+H]^+$ ion peak at *m*/*z* 601.5 and an $[M+NH_4]^+$ ion peak at *m*/*z* 618.5 that suggested that **3** contained one extra CH_2 unit compared to **2** and two CH_2 units compared to **1**. The spectral data for **3** closely paralleled those of **1** and **2** (Table 1) which indicated that **3** contained an alkyl bridge with 15 methylene units.

When tested in the UDP-MurNac synthesis assay, ardisiaquinone G (**1**), H (**2**) and I (**3**) gave IC_{50} values of 35, 26 and 26 μM respectively. However, the same compounds failed to show any whole cell activity in the disk diffusion assay against *Staphylococcus aureus*, *S. sangui*, *Escherichia coli* and *P. aeruginosa*.

3. Experimental

3.1. General

Column chromatography was performed using Sephadex LH-20 (Pharmacia). TLC analyses was done using plates of silica gel 60 F_{254} (0.2 mm, Merck), solvent system of EtOAc–$CHCl_3$ (1:1) and visualized under UV light (254 and 366 nm). HPLC analyses and isolations were carried out on Waters LC systems, including

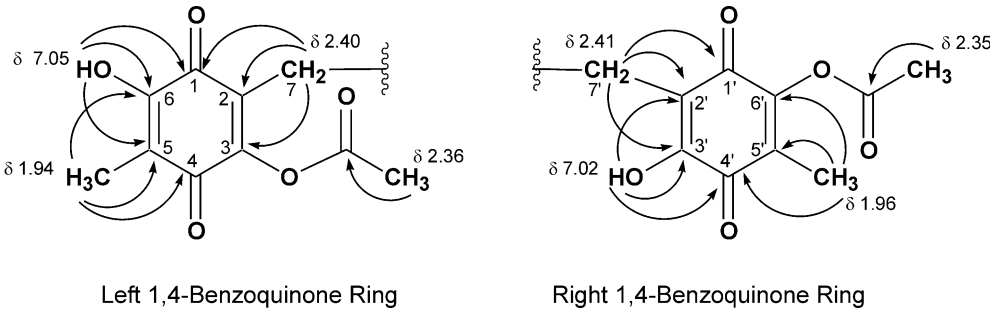

Fig. 1. HMBC correlations for the left and right 1,4-benzoquinone rings of **1**.

a 600E pump, a 490 programmable multiwavelength detector and NovaPak C_{18} column (5 μm, 40×100 mm). ^1H (500 MHz) and ^{13}C (125 MHz) NMR, ^1H–^1H COSY, HMQC and HMBC spectra were recorded on a Bruker AVANCE-500 digital NMR spectrometer, using solvent peaks as reference standard. LC–MS and MS/MS spectra were obtained on a Perkin-Elmer API 300 spectrometer operating with ESI and heated nebulizer ion sources in positive mode (CAD, 2 V; OR, +30 V; RO_3, 35 V; CEM, 3000 V), linked to a Hewlett-Packard 1100 HPLC system using a Novapak C_{18} column (3.9×50 mm). HR-MS spectra were obtained on a PerSeptive Biosystems Mariner TOF spectrometer operating with an ESI ion source in positive mode (spray tip potential, 3300 V; nozzle potential, 100 V; resolution, 5219). UV spectra were measured on an Ultraspec 2000 UV/vis spectrophotometer.

3.2. Plant material

The leaves of *A. teysmanniana* Scheff. (Myrsinaceae) were collected from Bukit Timah Nature Reserve in Singapore in October 1995. A herbarium voucher (No. 1026) was deposited in the Singapore Botanic Garden.

3.3. Extraction and separation

Dried and ground leaves (25 g) were extracted three times with $CHCl_3$ (500 ml) at room temperature with sonication for 30 min. After filtration, the $CHCl_3$ was evaporated under reduced pressure to leave an extract (2 g) that was chromatographed on Sephadex LH-20, using an EtOAc/$CHCl_3$ to MeOH/$CHCl_3$ gradient. The active fraction (0.3 g) was pooled according to TLC and separated by reversed-phase preparative HPLC using H_2O–MeCN gradient (20:80→10:90 in 15 mins, 20 ml/min) to give ardisiaquinone G (**1**) (69.4 mg, 0.3%), H (**2**) (32.7 mg, 0.1%) and I (**3**) (13.4 mg, 0.05%).

3.3.1. Ardisiaquinone G (*7*)

Yellow amorphous powder; UV (MeOH) λ_{max} nm (log ε) 209 (4.49), 295 (4.45), 535 (3.02); IR ν_{max} (KBr) 3330, 1777, 1618 cm^{-1}; (+)-ESIMS (rel. int.) *m/z*: 590.5 (35%), 573.0 (59%), 531.0 (41%), 489.5 (100%); (−)-ESIMS (rel. int.) *m/z*: 571.5 (23%), 529.5 (44%), 487.5 (100%); (+)-ESI MS/MS for *m/z* 573: 531.0, 489.0; HR–ESIMS $[M+H]^+$ 573.2700 (calc. for $C_{31}H_{41}O_{10}$ 573.2700); ^1H and ^{13}C NMR: Table 1.

3.3.2. Ardisiaquinone H (*8*)

Yellow amorphous powder; UV (MeOH) λ_{max} nm (log ε) 212 (4.53), 298 (4.38), 537 (3.38); IR ν_{max} (KBr) 3326, 1780, 1652, 1617 cm^{-1}; (+)-ESIMS (rel. int.) *m/z*: 604.5 (23%), 587.5 (39%), 545.5 (41%), 503.5 (100%); (−)-ESIMS (rel. int.) *m/z*: 585.5 (2%), 543.5 (80%), 501.5 (100%); (+)-ESI MS/MS for *m/z* 587: 545.5, 503.5; HR–ESIMS $[M+H]^+$ 587.2856 (calc. for $C_{32}H_{43}O_{10}$ 587.2857); ^1H and ^{13}C NMR: Table 1.

3.3.3. Ardisiaquinone I (*9*)

Yellow amorphous powder; UV (MeOH) λ_{max} nm (log ε) 210 (4.41), 295 (4.30), 529 (3.05); IR ν_{max} (KBr) 3327, 1771, 1643, 1617 cm^{-1}; (+)-ESIMS (rel. int.) *m/z*: 618.5 (15%), 601.5 (20%), 559.0 (31%), 517.5 (100%); (−)-ESIMS (rel. int.) *m/z*: 599.5 (9%), 557.5 (68%), 515.5 (100%); (+)-ESI MS/MS for *m/z* 601: 559.0, 517.5; HR–ESIMS $[M+H]^+$ 601.3013 (calc. for $C_{33}H_{45}O_{10}$ 601.3014)^1H and ^{13}C NMR: Table 1.

3.4. UDP-MurNac synthesis assay

Assays were performed in 96-well microtitre plates in a 100 μl reaction volume. Extracts, fractions and compounds were dissolved in 12.5% DMSO with 10 μl of solutions delivered to the wells. Typically, 40 μl of enzyme solution containing purified MurA and MurZ (260 and 425 ng/well, respectively) in 50 mM Tris–HCl (pH 8.0) and 2.5 mM DTT were added to the wells. Reaction was initiated by adding 50 μl of substrate solution containing 7.6 mM UDP-GlcNAc, 1 mM PEP, 5 mg NADPH, 40 mM KCl, 0.4 mM EDTA (pH 8.0), 100 mM Tris–HCl (pH 8.0) and 0.2 mg/ml of BSA. After 1 h incubation at 37 °C, progress of the reaction was assessed by monitoring the decrease in absorbance at 340 nm. The standard inhibitor used for the assay was the specific inhibitor of MurA, fosfomycin, which gave an average IC_{50} of 25 μM.

Acknowledgements

The authors wish to thank Mr. Haji Sidek bin Kiah and Mr. Eugene Tang for collection and identification of the plant material. We are grateful to the staff who provided the NMR spectra in the Department of Chemistry, National University of Singapore. We also express our gratitude to GlaxoSmithKline, the Economic Development Board of Singapore, the Institute of Molecular and Cell Biology, and National University of Singapore for financial support.

References

Benson, T.E., Marquardt, J.L., Marquardt, A.C., Etzkorn, F.A., Walsh, C.T., 1993. Overexpression, purification, and mechanistic study of UDP-N-acetylenolpyruvylglucosamine reductase. Biochemistry 32, 2024–2030.

Fukuyama, Y., Kiriyama, Y., Kodama, M., 1998. Naturally occurring 5-lipoxygenase inhibitors. VII. Practical synthesis of ardisiaquinones D, E and F. Chemical and Pharmaceutical Bulletin 46, 1770–1775.

Fukuyama, Y., Kiriyama, Y., Kodama, M., Iwaki, H., Hosozawa, S., Aki, S., Matsui, K., 1994. Total synthesis of ardisiaquinone A, a potent 5-lipoxygenase inhibitor, isolated from *Ardisia sieboldii*, and degree of 5-lipoxygenase inhibitory activity of its derivatives. Chemical and Pharmaceutical Bulletin 42, 2211–2213.

Fukuyama, Y., Kiriyama, Y., Kodama, M., Iwaki, H., Hosozawa, S., Aki, S., Matsui, K., 1995. Naturally occurring 5-lipoxygenase inhibitors. VI. Structures of ardisiaquinones D, E and F from *Ardisia sieboldii*. Chemical and Pharmaceutical Bulletin 43, 1391–1394.

Keng, H. 1990. The Concise Flora of Singapore. Gymnosperms and Dicotyledons. Singapore University Press, 137–138.

Ogawa, H., Natori, S., 1968a. Hydroxybenzoquinones from Myrsinaceae plants—II. Distribution among Myrsinaceae plants in Japan. Phytochemistry 7, 773–782.

Ogawa, H., Natori, S., 1968b. Hydroxybenzoquinones from Myrsinaceae plants. III. The structures of 2-hydroxy-5-methoxy-3-pentadecenylbenzoquinone and ardisiaquinones A, B and C from *Ardisia* spp. Chemical and Pharmaceutical Bulletin 16, 1709–1720.

Ogawa, H., Sakaki, S., Yoshihira, K., Natori, S., 1968. The structures of ardisiaquinones A, B and C, bis(benzoquinonyl)-olefine derivatives from *Ardisia Sieboldii* Miquel. Tetrahedron Letters 11, 1387–1392.

Raffauf, R.F., 1996. Plant Alkaloids. A Guide to Their Discovery and Distribution. Food Products Press, Binghampton, NY, 147–148.

PERGAMON

Phytochemistry 58 (2001) 1239–1244

PHYTOCHEMISTRY

www.elsevier.com/locate/phytochem

Acylated flavonol glycosides from *Eugenia jambolana* leaves

Ibrahim I. Mahmoud[a], Mohamed S.A. Marzouk[b,*], Fatma A. Moharram[a], Mohamed R. El-Gindi[a], Amel M.K. Hassan[a]

[a]*Pharmacognosy Department, Faculty of Pharmacy, Helwan University, Helwan, Cairo, Egypt*
[b]*Chemistry of Tannins and Proteins Department, National Research Centre (NRC), Tahrir St., Dokki, Cairo, Egypt*

Received 22 March 2001; received in revised form 28 July 2001

Abstract

Two acylated flavonol glycosides and 15 known polyphenols have been isolated and identified from the leaves of *Eugenca jambolana* Lam. The structures of the new compounds were identified as 3-*O*-(4″-*O*-acetyl)-α-L-rhamnopyranoside of mearnsetin (myricetin 4′-methyl ether) and myricetin 3-*O*-(4″-*O*-acetyl-2″-*O*-galloyl)-α-L-rhamnopyranoside. The complete structure elucidation of all isolated metabolites based on chemical and spectroscopic methods of analysis (UV, 1D and 2D NMR) as well as negative ESI–MS with and without CID in-source fragmentation. © 2001 Elsevier Science Ltd. All rights reserved.

Keywords: *Eugenia jambolana*; Myrtaceae; Leaves; Acylated flavonol glycosides; ID and 2D NMR; ESI–MS

1. Introduction

The genus *Eugenia* is one of 75 genera (~3000 species) belonging to the family Myrtaceae which are native in the tropics, particularly in tropical America and Australia (Hutchinson, 1960). Plants of this family are known to be rich in volatile oils which are reported for their uses in medicine. Genus *Eugenia* was reported to be used as an anti-inflammatory, analgesic, antipyretic (Karla et al., 1994a,b), antifungal (Rahhal, 1997) and peptic ulcer treatment (Tu, 1979). Fruits and seeds of *E. jambolana* used as an antidiabetic (Kelkar and Kaklij, 1997; Dhaliwal, 1999). Also anti-inflammatory compounds were characterized from *E. jambos* (Karla et al., 1996). Moreover, many *Eugenia* species were reported as very rich plants in polyphenols gallic and ellagic acid derivatives (Park et al., 1997; Son et al., 1998), tannins (Tanaka et al., 1996; Lee et al., 1997) and flavonol glycosides (Karla et al., 1994a,b; Schmeda-Hirschmann, 1995; Lee et al., 1997; Nair et al., 1999). Three flavonol glycosides were isolated from *E. jambolana* roots (Vaishnava and Gupta, 1990; Vaishnava et al., 1992). This report deals with a phytochemical study of the constitutive polyphenolic metabolites of *E. jambolana* leaves grown in Egypt.

2. Results and discussion

Using 2D-PC and different spray reagents of polyphenols, ethyl acetate extract of *E. jambolana* leaves was found to contain a complicated mixture of polyphenols, specially flavonol glycosides and some of phenolic acids together with minor ellagitannins. Fractionation of this extract on a silica gel column followed by successive separation on Sephadex LH-20 and cellulose columns afforded 17 polyphenolic metabolites. Depending on chromatographic and spectroscopic analyses, the isolated compounds were identified as gallic acid **3**, methylgallate **4**, kaempferol **5**, myricetin **6**, ellagic acid **7**, 3-*O*-methylellagic acid **8**, myricetin 3-*O*-(4″-*O*-acetyl)-α-L-rhamnopyranoside i.e (myricetrin 4″-*O*-acetate) **9**, myricetin 4′-methyl ether 3-*O*-α-L-rhamnopyranoside **10**, myricetrin **11**, chlorogenic acid **12**, quercetrin 4″-*O*-acetate **13**, quercetin 3-*O*-α-L-rhamnopyronside (quercet) **14**, kaempferol 3-*O*-β-D-glucuronopyranoside **15**, myricetin 3-*O*-β-D-glcuronopyranoside **16** and an ellagitannin, nilocitin **17**. The two new compounds were identified as mearnsetin 3-*O*-(4″-*O*-acetyl)-α-L-rhamnopyranoside **1** and myricetrin 4″-*O*-acetyl-2″-*O*-gallate **2**.

Structurally related compounds **1** and **9**–**11** were tentatively identified as myrincetin 3-*O*-glycosides according to their chromatographic properties [R_f-values, fluorescence under UV light, UV/NH_3, responses towards $FeCl_3$ and naturstoff (NA/PE) reagents] and UV spectral analyses

* Corresponding author. Tel.: +20-2-3669927.
E-mail address: msmarzouk@yahoo.co.uk (M.S.A. Marzouk).

0031-9422/01/$ - see front matter © 2001 Elsevier Science Ltd. All rights reserved.
PII: S0031-9422(01)00365-X

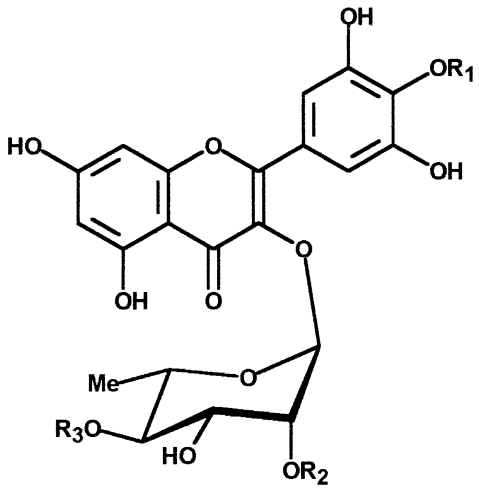

1: R_1 = Me, R_2 = H, R_3 = -$COCH_3$

2: R_1 = H, R_3 = -$COCH_3$, R_2 = 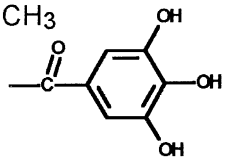

9: R_1 = R_2 = H, R_3 = -$COCH_3$

10: R_1 = Me, R_2 = R_3 = H

11: R_1 = R_2 = R_3 = H

(Table 1). UV spectra in MeOH of these compounds gave absorption maxima bands I and II at $\geqslant$350 and $\geqslant$257 nm which are characteristic for flavonols (Mabry et al., 1970). A bathochromic shift with NaOMe without decrease in intensity of band I, was diagnostic for the presence of free 4′-OH group in **9** and **11** while decrease in intensity in the case of both **1** and **10** revealed the 4′-*O*-substituted structures. The bathochromic shift in band II with NaOAc was indicative of free 7-OH groups in their structures. On the other hand, the strong bathochromic shift in band I (>60 nm) remaining after addition of HCl to $AlCl_3$ indicated the presence of free 5-OH group and suggested the absence of free 3-OH group. On account of these data, compounds **9** and **11** are expected to be myricetin 3-*O*-glycosides while **1** and **10** 4′-*O*-substituted myricetin 3-*O*-glycosides. On complete acid hydrolysis, **9** and **11** gave L-rhamnose and myricetin (CoPC), while mearnsetin (Sakushima et al., 1983) in the case of **1** and **10** (UV data) was obtained. The identity of the aglycone was more evidenced as myricetin in **9** and **11** on the basis of direct infusion −ve ESI–MS spectrometric data which showed a fragment ion peak at *m*/*z* 316, while ion peak at 331 were observed in the case of **1** and **10** indicative to myricetin 4′-methyl ether aglycone. The evidence that **10** is a methyl ether derivative of **11**, whereas **9** is its acetyl derivative was concluded from their molecular ion peaks (**11**: 463, **10**: 477, **9**: 505). Also, **1** was expected to be a methyl ether derivative of **9** due to the difference in the molecular ion peak by 14 mu (**1**: 519.3), indicative to MF of $C_{24}H_{24}O_{13}$. The complete structure elucidation was based on the comparison of ^1H and ^{13}C NMR data. The sugar moiety of all four compounds was identified as $^1C_4$-α-L-rhamnopyranoside on the basis of δ ppm and *J*-values (Table 2). The presence of an *O*-acetyl group in both **1** and **9** structures (*s*, δ 2.0 and 1.99) on C-4″ was confirmed by downfield shift of H-4′ at δ 4.69, *t* and 4.71, respectively relative to H-4″ at 3.15, *m* in free rhamnoside moiety of **10** and **11**. Presence of a singlet signal integrated to 3 protons at 6 3.74 in each of the two ^1H NMR spectra of **1** and **10**, referred to a methoxy group at 4′-position. These evidences were supported from ^{13}C NMR data (Table 3). The two carbon resonances at δ 170.0 and 21.0 were assigned to C=O and CH_3 carbons of an acetyl group in the structures of both **1** and **9**. The attachment of these groups at C-4″ was confirmed by the downfield shift of C-4″ signals (73.3 and 73.19) and upfield shift of both C-3″ and C-5″ signals (67.9, 68.03) relative to the corresponding resonances of **10** and **11** (Table 3). The presence of a methoxy group (δ 59.8 and 59.75), at 4′-position in each of **1** and **10** deduced from the downfield shifts of C-3′ and C-5′ resonances (150.8 and 150.6) comparing to

Table 1
Chromatographic properties and UV spectral data of compounds **1** and **9**–**11**

Compound	R_f values		Fluorescence[a]		Spray reagents[a]		UV data λ_{max} (nm)					
	S_1	S_2	Long UV	UV/NH_3	$FeCl_3$	NA/PE-UV	MeOH	+NaOAc	+H_3BO_3	+$AlCl_3$	+HCl	+NaOMe
1	0.84	0.40	d. pr.	Y	gr.	Org-red	218, 263, 350	225, 271, 360	227, 262, 363	232, 270, 416	223, 273, 414	222, 271, 273, 387
9	0.73	0.30	d. pr.	Y	gr.	Org.-red	220, 257, 300 *sh*, 353	245, 269, 310 *sh*, 365	243, 259, 300 *sh*,370	248, 269, 331, 427	247, 272, 327, 426	273,297sh, 395
10	0.67	0.37	d. pr.	Y	gr.	Org-red	244, 263, 350	227, 272, 358	228, 263, 353	226, 275, 338, 410	213, 273, 333, 403	219, 271, 381
11	0.53	0.25	d. pr.	Y	gr.	Org-red	241, 257, 300 *sh*, 354	244, 267, 363	243, 259, 370	248, 271, 331, 421	248, 272, 328, 426	248, 268, 346, 393

[a] d.pr. = dark purple; Y = yellow; gr. = green; org. = orange; NA/PE = Naturstoff reagent/polyethylene glycol.

Table 2
^{1}H NMR spectral data of compounds **1** and **9–11** (300 MHz, DMSO-d_6), δ ppm

H	1	9	10	11
2′/6′	6.8 *s*	6.86 *s*	6.82 *s*	6.87 *s*
8	6.38 *d* (1.8)[a]	6.36 *d* (1.9)	6.38 *d* (1.9)	6.35 *d* (1.9)
6	6.20 *d* (1.8)	6.2 *d* (1.9)	6.21 *d* (1.9)	6.18 *d* (1.9)
1″	5.18 *d* (1.7)	5.15 *d* (1.5)	5.12 *br s*	5.20 *d* (1.5)
2″	4.13 *dd* (1.7, 3.3)	4.02 *dd* (1.5, 3.3)	3.97 *dd* (1.5, 3.3)	3.96 *dd* (1.5, 3.3)
3″	3.74 hidden by OMe signal	3.75 *dd* (3.3, 9.5)	3.51 *br s*	3.6 *dd* (3.3, 9.4)
4″	4.69 *t* (9.7)	4.71 *t* (9.5)	3. 15 *m*	3.15 *t* (9.4)
5″	3.57 *m*	3.5 *m*	3.32 *m* hidden by H_2O-signal	3.46 *m*
6″	0.88 *d* (6.1)	0.72 *d* (6.1)	0.8 *d* (6.1)	0.83 *d* (6.12)
OMe	3.74 *s*		3.74 *s*	
$-\overline{CO}\underline{CH_3}$	2.0 *s*	1.99 *s*		

[a] *J*, values are given in Hz in parentheses.

Table 3
^{13}C NMR spectral data of compounds **1** and **9–11** (75 MHz, DMSO-d_6), δ ppm

C	1	9	10	11
2[a]	157.64	157.75	157.28	157.47
3	134.40	134.24	134.80	134.20
4	177.60	177.74	177.80	177.77
5	161.30	161.38	161.30	161.30
6	98.80	98.82	98.75	98.60
7	164.30	164.37	164.35	164.20
8	93.60	93.69	93.60	93.50
9[a]	156.50	156.53	156.50	156.40
10	103.99	104.12	104.18	104.01
1′[b]	124.72	119.50	124.80	119.59
2′	108.07	107.90	108.10	107.88
3′[b]	150.80	145.97	150.60	145.76
4′[b]	137.80	136.63	137.70	136.44
5′[b]	150.80	145.97	150.60	145.76
6′	108.07	107.90	108.10	107.88
1″	101.55	101.75	102.17	101.93
2″	69.90	70.02	70.03	70.00
3″[b]	67.90	68.04	70.31	70.37
4″[b]	73.19	73.30	71.13	71.26
5″[b]	67.90	68.04	70.53	70.55
6″	17.10	17.20	17.45	17.50
OMe	59.80		59.75	
$-\overline{CO}\underline{CH_3}$	170.0, 21.0	170.1, 21.07		

[a] Exchangeable carbon resonances.
[b] Carbon resonances which were affected by substitution of OMe or *O*-acetyl at C-4′ and C-4″, respectively.

those of **9** and **11** (Markham et al., 1978). The remaining carbon resonances of all structures were confirmed and completely assigned according to the ^{1}H ^{1}H– and ^{1}H ^{13}C COSY correlation spectroscopy of **9** and **11**, in addition to comparison study with the published data of related structures (Karin et al., 1989; Toshiya et al., 1991; Karla et al., 1994a,b; Hiroyuki et al., 1996). Accordingly, the structures of **9**, **10** and **11** were identified as the known compounds myricetin 3-*O*-(4″-*O*-acetyl)-α-L-$^1C_4$-rhamnopyranoside, mearnsetin 3-*O*-α-L-$^1C_4$-rhamnopyranoside and myricetin 3-*O*-α-L-$^1C_4$-rhamnopyranoside, respectively. Whereas **1** was identified as the new mearnsetin 3-*O*-(4″-*O*-acetyl)-α-L-$^1C_4$-rhamnopyranside.

Compound **2**, on the basis of chromatographic properties (R_f values, fluorescences under UV and UV/NH_3, responses towards NP/PE-UV and $FeCl_3$) was expected to be myricetin 3-*O*-glycoside. Band I (351 nm) and Band II (264 nm) in UV/MeOH spectrum together with the different bathochromic and hypsochromic shifts on addition of all diagnostic shift reagents supported the previous evidence (Mabry et al., 1970). On complete acid hydrolysis, it gave gallic acid and myricetin in the organic phase in addition to L-rhamnose in the aqueous phase (CoPC) to suggest myricetin 3-*O*-galloylrhamnoside structure. Partial hydrolysis with boiling H_2O, **2** gave **9** as an intermediate together with gallic acid indicative of a diacylated rhamnose with both gallic and acetic acids. Negative ESI–MS spectrum of **2** showed $[M–H]^-$ ion peak at *m*/*z* 657.2 as base peak corresponding to a *Mr* of 658 and MF of $C_{30}H_{26}O_{17}$. Additionally, using in-source (CID) fragmentation potential, led to observation of very significant three fragment ions at *m*/*z* 505 [M-galloyl]$^-$, 317 [myricetin-H]$^-$ and 316 [myricetin-2H]$^-$. These results suggested that the structure of **2** contains not only a galloyl moiety but also an acetyl group located on the rhamnoside moiety at C-4″. Positions of substitution of the galloyl and acetyl moieties as well as the complete structure of **2** were determined by ^{1}H and ^{13}C NMR analyses. The aglycone moiety was simply identified as myricetin through its three proton resonances of H-2′/6′, H-8 and H-6. The presence of gallic acid moiety as well as acetyl moiety was concluded through the two resonances at δ 6.96 (2H, *s*) and 2.03 (3H, *s*), assignable to H-2‴/6‴ and –CO–CH_3, respectively. Also locations of the gallic acid moiety at C-2″ and acetyl moiety at C-4″ of rhamnosyl moiety were detected through the downfield shifts of both H-2″ (5.53 ppm) and H-4″ (4.78) relative to those of corresponding resonances at δ 3.96 and 3.2 in the structure of myricetrin (**11**). The configuration and conformation of the sugar moiety were identified as

2″,4″-diacylated α-L-$^1C_4$-rhamnopyranosyl according to the δ- and J-values of all other signals of H-1″, H-3″, H-5″ and CH_3-6″. Accordingly, **2** was identified as myricetin 3-*O*-(4″-*O*-acetyl-2″-*O*-galloyl)-α-L-rhamnopyranoside. This structure was finally confirmed by the complete assignment of all C-resonances in its ^{13}C NMR spectrum by comparison with the corresponding resonances of both **11** and **9** (Table 4).

According to the downfield/upfield shift rule for the resonance of substitution position and the two adjacent carbons, acylation at C-2″ (72.5) of **2** led to downfield shift of +2.5 ppm relative to those of **11** and **9** (~70.0) together with upfield shift of both C-1″ (100.1) by −1.8 and C-3″ (67.0) by −1.0 in the case of **9** and −3.4 in the case of **11** due to the acylation also at C-4″. The acylation at C-4″ resulted in downfield shift from 71.2 (**11**) to 73.3 in **9** and 74.5 in **2**, but it led to upfield shift of C-5″ (68.5) by −2.0 relative to that of **11** (70.5). The two resonances at δ 171.26 and 22.3 were assigned to CO and CH_3 of the acetyl moiety whereas resonance at δ 166.2 was assigned to C=O of galloyl moiety. Additionally, the complete assignment of all other resonances was based on the comparison study with those of **11** and **9** as well as the published data of structurally related compounds (Hyoung et al., 1998; Yonungsoo et al., 2000). This complete assignment confirmed the configuration and conformation of the rhaninosyl moiety, as well as the complete structure of **2** as myricetin 3-*O*-(4″-*O*-acetyl-2″-*O*-galloyl)-α-L-$^1C_4$-rhamnopyranoside which was identified here as a new natural product.

This study revealed that leaves of *E. jambolana* are rich in flavonol glycosides and some of their acylated rhamnosides, which based on the myricetin or mearnsetin as aglycones in most of them. All the identified compounds were isolated for the first time from this species and both **9** and **10** were isolated in nature once before (Harborne, 1994; Ossipov et al., 1995). Also two new acylated flavonol rhamnosides were identified as two new natural products (**1** and **2**).

3. Experimental

3.1. Plant material

Leaves of *E. jambolana* Lam. were collected from the plant grown in the Zoological Garden, Giza, in July 1999. Identification of the plant was confirmed by Dr. Mohamed El-Gebaly, Lecturer of Plant Flora Taxonomy NRC, Giza, Egypt and comparison with reference herbarium specimens. Voucher specimens are kept in the herbarium, Pharmacognosy Department, Faculty of Pharmacy, Helwan University, Egypt.

Table 4
Comparison of C-resonances of rhamnoside moieties in the structures of **2**, **9** and **11**

Compound	C-1″	C-2″	C-3″	C-4″	C-5″
2	100.1	72.5	67.0	74.5	68.5
9	101.8	70.02	68.0	73.3	68.0
11	101.9	70.0	70.4	71.2	70.5

3.2. Isolation and identification

Dry powder of *E. jambolana* leaves (2 kg) was defatted with pet. ether (60–80), then extracted with hot 70% MeOH under reflux. After evaporation of the solvent, dry residue was extracted with EtOAc to give 45 g dry extract. EtOAc extract was fractionated on silica gel G column and starting the elution with pet. ether (60–80), then gradually addition of EtOAc affording collective six frs (1–6). The obtained frs were subjected separately to consecutive combination of column chromatography on microcrystalline cellulose for CC (E. Merck, Darmstadt, Germany) and sephadex LH-20 (Pharmacia, Uppsala, Sweden) with aq. EtOH and/or *n*-BuOH saturated with H_2O solvent systems to afford chromatographically pure samples of compounds **1**–**17**. All separation processes were followed up by 2D-PC and CoPC using Whatmann No. 1 paper with (S_1) *n*-BuOH–AcOH– H_2O (4:1:5, top layer) and (S_2) 15% AcOH as solvent systems. The isolated quantities were 18, 15, 20, 15, 20, 30, 12, 18, 67, 23, 53, 7, 10, 17, 21, 28 and 70 mg of compounds **1**–**17**, respectively.

3.3. UV analysis

Pure samples were measured separately as MeOH solns and with different diagnostic shift reagents (Mabry et al., 1970) on a UV IKON 940 spectrophotometer.

3.4. NMR analyses

NMR analyses were run on Brucker 300, Jeol EX-270 and 400 MHz spectrometers relative to TMS in different deuterated solvents.

3.5. Negative ESI–MS

The diluted soln of each sample, in 1:1 MeOH–H_2O was directly infused using a syringe Harvard infusion pump to a double focusing sector field mass spectrometer Finnigan MAT 95 according to the previously published conditions (Nawwar et al., 1997) as well as to LC–MS LCQ deca spectrometer (Finnigan, Bremen, Germany).

3.6. Mearnsetin 3-O-(4″-O-acetyl)-α-L-$^1C_4$-rhamnopyranoside *1*

Yellow amorphous powder; its chromatographic properties and UV spectral data (Table 1). Acid hydrolysis; a

small amount of **1** (8 mg) was hydrolysed with 2 N HCl in MeOH–H_2O (1:1), under reflux at 100 °C for 2 h to yield L-rhamnose and mearnsetin (CoPC and spray reagents). -ve ESI–MS: *m/z* 519 $[M–H]^-$, 463 [M–acetyl]$^-$, 331 [Mearnsetin–H]$^-$. ^{1}H NMR data (300 MHz, DMSO-d_6): Table 2. ^{13}C NMR (75 MHz, DMSO-d_6): Table 3.

3.7. Myricetin 3-O-(4″-O-acctyl-2″-O-galloyl)-α-L-$^1C_4$-rhamnopyranoside 2

Yellow amorphous powder; d.pr. fluorescence under UV, changed to yellow with NH_3 vapour. Org-red with NP/PE and bl-gr. with $FeCl_3$ spray reagents. R_f values: 0.64 and 0.10 in S_1 and S_2, respectively. UV spectral data λ_{max}, nm; (MeOH): 222, 264, 284, 300 (*sh*), 351; (+NaOMe): 275, 322, 395; (+NaOAc): 273, 310 (*sh*), 365; (+NaOAc/H_3BO_3): 230, 263, 369; (+$AlCl_3$): 231, 268, 331, 418; (+$AlCl_3$/HCI): 220, 270, 404. Acid hydrolysis; 7 mg of **2** were hydrolysed under the same conditions in the case of **1** to yield L-rhamnose, gallic and myricetin (CoPC and spray reagents). Partial hydrolysis; 6 mg from **2** were dissolved in H_2O and boiled under reflux for about 18 h; the reaction mix was examined by CoPC against authentic samples of gallic acid and **9**. −ve ESI–MS: *m/z* 657 $[M–H]^-$, 505 [M–gallyl]$^-$, 317 [myricetin–H]$^-$, 316 [myricetin–2H]$^-$. ^{1}H NMR data (300 MHz, DMSO-d_6): δ ppm 6.96 (2H, *s,* H-2‴/6‴), 6.9 (2H, *s,* H-2′/6′), 6.39 (1H, *d,* J=1.9 Hz, H-8), 6.21 (1H, *d,* J=1.9 Hz, H-6), 5.53 (1H, *brd,* H-2″), 5.48 (1H, *d*, J=1.5 Hz, H-1″), 4.78 (1H, *t,* J=9.8 Hz, H-4″), 4.06 (1H, *dd,* J=9.8, 3.3 Hz, H-3″), 3.4 (1H, *m* hidden by H_2O-signal, H-5″), 2.03 (3H, *s,* CO-Me) and 0.82 (3H, *d,* J=6.1 Hz, CH_3-6″). ^{13}C NMR (75 MHz, DMSO-d_6): δ ppm 178.6 (C-4), 171.3 (CO-acetyl), 166.2 (C-7‴), 165.6 (C-7), 162.6 (C-5), 159.9 (C-2), 157.8 (C-9), 147.3 (C-3‴/5‴), 146.9 (C-3′/C-5′), 139.9 (C-4‴), 138.0 (C-4′), 135.5 (C-3), 120.6 (C-1‴), 120.3 (C-1′), 110.2 (C-2‴/6‴), 109.0 (C-2′/6′), 105.36 (C-10), 100.1 (C-1″), 99.3 (C-6), 93.6 (C-8), 74.5 (C-4″), 72.5 (C-2″), 68.5 (C-5″), 67.0 (C-3″), 22.3 (Me-acetyl), 18.6 (C-6″).

Acknowledgements

We thank Professor Dr. M. Linscheid, Dr. J. Mügge and their co-workers (Institute of Chemistry, Humboldt University, Berlin, Germany) for their efforts and helpful cooperation in the MS and NMR measurements.

References

Dhaliwal, K.S., 1999. Method and composition for treatment of diabetes. Appl. 924 (512), 5.

Harborne, J.B., 1994. The Flavonoids: Advances in Research, Chapter 8, Flavone and Flavonol Glycosides. Chapman & Hall, London, UK, p. 383.

Hiroyuki, T., Soh, K., Tetsuya, S., Akiko, Y., Kohei, S., Tatsuya, T., Nobutoshi, T., 1996. Chemical evaluation of *Betula* species in Japan II. Constituents of *Betula platyphyllea* var., *japonica*. Chem. Pharm. Bull. 44, 1033–1038.

Hutchinson, J., 1960. The Families of Flowering Plants, 2nd Edition. Clarendon, Oxford, 302.

Hyoung, J.K., Eun-Rhan, W., Cha-Gyun, S., Hokoon, P., 1998. A new flavonolglycoside gallate ester from *Acer okamotoanum* and its inhibitory activity against immunodeficiency virus-1 (HIV-1) integrase. J. Nat. Prod. 61, 145–148.

Karin, C.L., Yang, S., Margaret, F.R., David, J.P., 1989. Flavonol glycosides with acetyl substitution from *Kalanchoe gracilis*. Phytochemistry 28, 2813–2818.

Karla, S., Carretero, E., Villar, A., 1994a. Anti-inflammatory activity of leaf extracts of *Eugenia jambos* in rats. J. Ethn. Pharmacology 43, 9–11.

Karla, S., Carretero, E., Villar, A., 1996. Anti-inflammatory compounds from *Eugenia jambos*. Phytother. Res. 10, S126–S127.

Karla, S., Monica, S., Emilia, C., Angel, V., 1994. Flavonoid glycosides from *Eugenia jambos*. Phytochemistry 37, 255–258.

Kelkar, S.M., Kaklij, G.S., 1997. A simple 2 step purification of antidiabetic compounds from *Eugenia jambolana* fruit pulp protolytic assistance and other properties. Phytomedicine 353–359.

Lee, M.H., Nishimto, S., Yang, L.L., Yen, K.Y., Hatano, T., Yoshida, T., Okuda, T., 1997. Two macrocyclic hydrolysable tannin dimmers from *Eugenia uniflora*. Phytochemistry 44, 1343–1349.

Mabry, T.J., Markham, K.R., Thomas, M.B., 1970. The Systematic Identification of Flavonoids. Springer, Berlin.

Markham, K.R., Ternai, B., Stanley, R., Geiger, N., 1978. Carbon-13 NMR studies of flavonoid glycosides and their acylated derivatives. Tetrahedron 34, 1389–1397.

Nair, A.G.R., Krishnam, S., Ravikrishna, C., Madhusudanan, K.P., 1999. New and rare flavonol glycosides from leaves of *Syzygium samarongense*. Fitoterapia 70, 148–151.

Nawwar, M.A., Marzouk, M.S., Nigge, W., Linscheid, M., 1997. High performance liquid chromatography/electrospray ionization mass spectrometric screening for polyphenolic compounds of *Epilobium hirsutum*—The structure of the unique ellagitannin, epilobamide-A. J. Mass Spectrom. 32, 645–654.

Ossipov, V., Nurmi, K., Loponen, J., Prokopiev, N., Haukioja, E., Pihlaja, K., 1995. HPLC isolation and identification of flavonoids from white birch *Betula pubescens* leaves. Biochem. Sys. Ecol. 23, 213.

Park, M.K., Park, J.H., Shin, Y.G., Shin, U.K., Kim, K.H., Yakhak, H., 1997. Chemical constituents of *Eugenia caryophyllata*. Pharmaceutical Society of Korea 41, 149–152.

Rahhal, M.M., 1997. Antifungal activity of some plant oils. Alexandria Sci. Exch. 18, 225–230.

Sakushima, A., Coskun, M., Hisada, S., Nishibe, S., 1983. Flavonoids from *Rhamnus pallasii*. Phytochemistry 22, 1677–1678.

Schmeda-Hirschmann, G., 1995. Flavonoids from *Calycorectes, Campomanesia, Eugenia* and *Hexachlamys* species. Fitoterapia 66, 373–374.

Son, K., Kwon, S.Y., Kim, H.P., Chang, H.W., Kang, S.S., 1998. Constituents from *Syzygium aromaticum* Merr. et Perry. Nat. Prod. Sci. 4, 263–267.

Tanaka, T., Nonaka, G.I., Nishioka, I., Kouno, I., 1996. Syzyginins A and B, two ellagitannins from *Syzygium aromaticum*. Phytochemistry 43, 1345–1348.

Toshiya, M., Akiko, J., Shigeru, K., Nobuji, N., 1991. Acetylated flavonol glycosides from *Zingiberzerumbet*. Phytochemistry 30, 2391–2392.

Tu, H., 1979. Pharmaceutical for peptic ulcer containing $FeSO_4$ and extracts of *Eugenia caryophylla* and/or liquorice extracts. Appl. 77/140 (786), 3.

Vaishnava, M.M., Gupta, K.R., 1990. Isorhamnetin 3-*O*-rutinoside from *Syzygium cumini* Lam. J. Indian Chem. Soc. 67, 785–786.

Vaishnava, M.M., Tripathy, A.K., Gupta, K.R., 1992. Flavonoid glycosides from roots of *Eugenia jambolana*. Fitoterapia 63, 259–260.

Youngsoo, K., Dae-Sig, J., Si-Hyung, P., Jieun, Y., Bo-Kyung, M., Kyung, R.M., Hyeong-Kyu, L., 2000. Flavonol glycoside gallate and ferulate esters from *Persicaria lapathifolia* as inhibitors of superoxide production in human monocytes stimulated by unopsonized zymosan. Planta Med. 66, 72–74.

PERGAMON

Phytochemistry 58 (2001) 1245–1249

PHYTOCHEMISTRY

www.elsevier.com/locate/phytochem

Xanthones from the stems of *Securidaca inappendiculata*

Xue-Dong Yang*, Li-Zhen Xu, Shi-Lin Yang

Institute of Medicinal Plant Development, Peking Union Medical College and Chinese Academy of Medical Sciences, Beijing 100094, PR China

Received 9 March 2001; received in revised form 17 July 2001

Abstract

From the stems of *Securidaca inappendiculata*, securixanthones A (1,3,7-trihydroxy-2,8-dimethoxyxanthone) and B (3,7-dimethoxy-4-hydroxyxanthone) along with ten known xanthones were isolated. Their structures were elucidated by analysis chemical and spectroscopic evidence, and the chemotaxonomic significance of these findings are also discussed. © 2001 Elsevier Science Ltd. All rights reserved.

Keywords: *Securidaca inappendiculata*; Polygalaceae; Xanthones; Securixanthone A; Securixanthone B

1. Introduction

The roots and stems of *Securidaca inappendiculata* Hassk. (Polygalaceae) are used as anti-inflammatory, anti-bacterial and anti-rheumatoid agents under the names "Chan yi teng", "Wu wei teng" or "Diu le bang" in the south of China (Jiangsu Institute of Botany, 1988). According to available literature, no phytochemical research work has been carried out on this plant. The genus *Securidaca* accumulates flavonoids (Hamburger et al., 1985; Galeffi et al., 1990), alkaloids (Costa et al., 1992; Scandola et al., 1994), saponins (Davreux and Delaude, 1971), organic acids (Mahmood et al., 1993) and sucrose derivatives (Tommasi et al., 1993).

In our search for anti-HIV active principles in *Securidaca* plants, the xanthone constituents of *S. inappendiculata* Hassk. were examined. This paper describes the structural elucidation of xanthones isolated from this plant and discusses the chemotaxonomic significance of these findings.

2. Results and discussion

The stems of *S. inappendiculata* were collected, dried, ground, and extracted with ethanol. Column chromatography combined with medium pressure liquid chromatography (MPLC) of the chloroform-soluble part yielded two new xanthones along with ten known xanthones.

Xanthone **1**, obtained as yellow needles, mp 218 °C, had a molecular formula of $C_{15}H_{12}O_7$ as established by HR–EI mass spectrometry (m/z 304.0584 $[M]^+$). The UV spectrum of **1** exhibited characteristic absorption bands of a xanthone (λ_{max}^{MeOH}, 238, 261, 312, 381 nm), and a bathochromic shift induced by addition of NaOAc suggested the presence of a free hydroxyl group at either C-6 or C-3 (Harborne, 1973). The lack of a di-ortho-hydroxyl group was evident by the absence of a shift after the addition of NaOAc and H_3BO_3. The ^1H NMR spectrum showed a chelated OH (δ 13.38), an AB system (δ 7.36 H-6 and 7.20 H-5) of two *ortho*-coupled protons ($J = 9.12$ Hz), a singlet (δ 6.37) and two methoxyl groups (δ 3.80 and 3.73). In the ^{13}C NMR spectrum, signals at δ 59.83 and δ 60.91 were indicative of two di-*ortho*-substituted methoxyl groups (Frahm and Hambloch, 1982). The positions of the substituents were confirmed unambiguously through a NOESY experiment. The NOESY spectrum of **1** (in DMSO-d_6) showed four significant cross peaks, namely) the peaks between: (1) the single aromatic proton (H-4) signal at δ 6.38 and the hydroxyl signal at δ 10.88 (OH-3); (2) the hydroxyl signal (OH-1) at δ 13.38 and the methoxyl signal at δ 3.73 (OMe-2); (3) the methoxyl signal (OMe-8) at δ 3.80 and the hydroxyl signal (OH-7) at δ 9.57 and (4) the hydroxyl signal (OH-7) at δ 9.57 and the downfield aromatic proton (H-6) at δ 7.36. This indicated that hydroxyl groups were at the C-1, C-3 and C-7 positions,

* Corresponding author. Tel.: +86-10-62899705; fax: +86-10-62896313.

E-mail address: xuedong_y@263.net (X.-D. Yang).

0031-9422/01/$ - see front matter © 2001 Elsevier Science Ltd. All rights reserved.
PII: S0031-9422(01)00356-9

and the two methoxyl groups were at the C-2 and C-8 positions. Furthermore, the presence of a 1,3-dihydroxy- 2-methoxyl moiety and a 7-hydroxy-8-methoxyl moiety in **1** was supported by analysis of the ^{13}C NMR spectrum. The C-8b, C-1, C-2, C-3, C-4 and C-4a shifts in the ^{13}C NMR spectrum of **1** were comparable to those of 1,3,6-trihydroxy-2,5-dimethoxyxanthone (**13**) (Pinto et al., 1994). The C-4b, C-5, C-6, C-7, C-8 and C-8a shifts in the ^{13}C NMR spectrum of **1** were essentially the same as those of (C-4a, C-4, C-3, C-2, C-1 and C-8b) in 2,5-dihydroxy-1-methoxyxanthone (**14**) (Minami et al., 1996). From the above data, **1** was determined to be 1,3,7-trihydroxy-2,8-dimethoxyxanthone, and was named securixanthone A.

Xanthone **2** was obtained as fine yellow needles, mp 178 °C. The molecular formula was assigned as $C_{15}H_{12}O_5$ on the basis of HR–EI mass spectrometry (*m*/*z* 272.0686 $[M]^+$). The UV spectrum (in MeOH) of **2** showed absorptions at 237, 262, 318 and 384 nm. The presence of a free hydroxyl group at either C-6 or C-3 was excluded based on the lack of any change in the UV spectrum upon addition of NaOAc. In the IR spectrum, characteristic absorptions of a xanthone were observed at 3500 and 3420 cm^{-1} (OH), 1640 cm^{-1} (conjugated carbonyl), 1620 and 1565 cm^{-1} (aromatic moieties). The ^1H NMR spectrum displayed resonances for two aromatic methoxyls (δ 3.81 and 3.86), a hydroxyl (δ 9.42), a three-proton spin system (δ 7.51, 7.40 and 7.52; $J=9.18$ and 2.98 Hz) and an AB system (δ 7.37 and 7.26) of two ortho-coupled protons ($J=9.15$ Hz). The ^{13}C NMR spectrum indicated that the aromatic methoxyl at δ 61.04 was di-*ortho*-substituted and that there were no substituted groups at either a C-1 or C-8 position according to the carbonyl carbon shift (δ 174.98) (Philip et al., 1977). Furthermore, the presence of MeO-7 rather than MeO-6 in **2** was supported by analysis of the ^{13}C NMR spectrum. The C-4b, C-5, C-6, C-7, C-8 and C-8a shifts in the ^{13}C NMR spectrum of **2** are essentially the same as those (C-4a, C-4, C-3, C-2, C-1 and C-8b) of 2-methoxyxanthone (Fernandes et al., 1998). The positions of the substituents were confirmed through a NOESY experiment. The NOESY spectrum of **2** (in DMSO-d_6) showed two significant cross peaks between the methoxyl signal (OMe-7) at δ 3.86 and the aromatic proton signals (H-8, H-6) at δ 7.52 and 7.40. Acetylation of **2** with Ac_2O in pyridine gave the acetate **2a**. In the ^1H NMR spectrum of **2a**, signals due to the protons were not shifted markedly compared to that of **2**. On the basis of this evidence, the structure of **2** was concluded to be 3,7-dimethoxy-4-hydroxyxanthone, named securixanthone B.

In addition to the two new xanthones described above, ten known xanthones, 1,6-dihydroxyxanthone (**3**) (Lin et al., 1996), 1,7-dihydroxyxanthone (**4**) (Tosa et al., 1997), 2-hydroxy-1,7-dimethoxyxanthone (**5**) (Galeffi et al., 1990), 1,7-dihydroxy-4-methoxyxanthone (**6**) (Galeffi et al., 1990), 1,7-dihydroxy-3,4-dimethoxyxanthone (**7**) (Bashir et al., 1992), 1,3,8-tri-hydroxy-2-methoxyxanthone (**8**) (Gil et al., 1990), 1,3,6-trihydroxy-2,7-dimethoxyxanthone (**9**) (Silveria et al., 1995), 1,3,7-trihydroxyxanthone (**10**) (Stout et al., 1969), 2,7-dihydroxy-1-methoxyxanthone (**11**) (Nagem et al., 1992) and 1,3,7-trihydroxy-2-methoxyxanthone (**12**) (Pinheriro et al., 1998) were isolated from the same extract. They were identified by spectral (include NOESY) and chemical data and by comparison with literature data.

2.1. Chemotaxonomic significance

The genus *Securidaca* comprises about 80 species, and are mainly distributed in the tropical regions of America. Only two species, *S. yaoshanennsis* Hao and *S. inappendiculata* Hassk, occur in China (Delectis Florae Republicae Popularis Sinicae Agendae Academiae Sinicae Edita, 1997). To our knowledge, only a few phytochemical studies of this genus have been made (Yang et al., 2000a). So, after we finished our investigation, we compared the xanthone components of this genus with those found in *Polygala* L. The two genera belong to the same tribe, Polygaleae Chodat of Polygalaceae.

More than 60 kinds of xanthones have been obtained from *Polygala* L. so far (Yang et al., 2000b). In their structures, there are three types of substituents, namely hydroxyl, methoxyl and methylenedioxyl groups and the highest number of oxygenated substituents is 6 (only 1 case). In the 13 xanthones isolated from *Securidaca* L.

Table 1
^1H NMR spectral data for compounds **1**, **2** (400 MHz, DMSO-d_6) and **1a**, **1b** (400 MHz, $CDCl_3$)[a]

H	1	1a	2	2a
1	–	–	7.37 *d* (9.2)	7.40 *d* (9.6)
2	–	–	7.26 *d* (9.2)	7.28 *d* (9.6)
3	–	–	–	–
4	6.38 s	6.87 *s*	–	
5	7.20 *d* (9.1)	7.17 *d* (9.2)	7.52 *d* (9.2)	7.42 *d* (9.1)
6	7.36 *d* (9.1)	7.35 *d* (9.2)	7.40 *dd* (9.2, 3.0)	7.31 *dd* (9.1, 3.1)
7	–	–	–	–
8	–	–	7.51 *d* (3.0)	7.68 *d* (3.1)
1-OH	13.38 *s*	–	–	–
1-OAc	–	2.53 *s*	–	–
2-OCH$_3$	3.73 *s*	3.90 *s*	–	–
3-OH	10.88 *s*	–	–	–
3-OCH$_3$	–	–	3.81 *s*	3.99 *s*
3-OAc	–	2.35 *s*	–	–
4-OH	–	–	9.42 *br. s*	
4-OAc	–	–	–	2.39 *s*
7-OH	9.57 *s*	–	3.86 *s*	–
7-OCH$_3$	–	–	–	3.91 *s*
7-OAc	–	2.39 *s*	–	–
8-OCH$_3$	3.80 *s*	3.97 *s*	–	–

[a] Assignments confirmed by NOESY; *J* (Hz) in parentheses.

[one (2-hydroxy-1,7-dimethoxyxanthone) from *S. longipedunculata* (Galeffi et al., 1990) and twelve from *S. inappendiculata* (this paper)], only have hydroxyl and methoxyl groups and the highest number of oxygenated groups are 5. In xanthones of the genus *Polygala* L., all eight possible substituted positions can be then subsituted oxygenated, but the substitution probabilities are quite different: 5 position is the least subsituted, 4 and 8 position take the second place and the 1, 2, 3 and 7 positions are most commonly. The oxygenation pattern of xanthones obtained from *Securidaca* L. has similar characteristics. The probability number of xanthones in which an oxygenated group appears at a certain position/in either *Polygala* or *Securidaca* in (Yang et al., 2000b) is illustrated in Table 3. These results strongly suggest that both genera have a chemotaxonomic relationship.

3. Experimental

3.1. General

Mps: uncorr. ^{1}H NMR: 400 MHz. ^{13}C NMR: 125 MHz (for xanthon **1** and **8**) and 100 MHz (for other xanthones), TMS as int. standard. 2D-NOE data were obtained from a NOESY experiment using the standard DISNMR software package (Bruker). IR: KBr discs. CC: silica gel and polyamide. TLC: silica gel G with visualization by UV (254 and 365 nm) and exposure to iodine vapor. TLC was used to analyze the frs. collected from CC.

3.2. Plant material

The stems of *Securidaca inappendiculata* Hassk. were collected in Yunnan province of China and identified by Professor Wen-Yan Lian (our institute) and Professor Hong Wang (Menglun Botanical Garden). Voucher specimens are deposited in the Phytochemistry Department of our institute.

3.3. Extraction and isolation

The dried and ground stems (10 kg) were extracted with 95% EtOH (30 l×3, 2 h each) under condition of reflux. The EtOH extract (750 g) was evaporated to dryness under reduced pressure then fractionated by solvent reflux in a Soxhlet apparatus (silica gel as absorbent) into $CHCl_3$, EtOAc, Me_2CO and MeOH solubles, respectively. The $CHCl_3$ soluble (10.5 g) were subjected to MPLC (silica gel, 200–300 mesh) luted with a gradient of Me_2CO in petroleum ether (95:5–50:50) to give 18 main fractions. Each fraction was purified by polyamide CC eluted with $CHCl_3$–MeOH (1:0–0:1, gradient) and Sephadex LH-20 to give xanthones **1** (8 mg) from fraction sixteen (65:35), **2** (10 mg) from fraction eight (85:15), **3** (5 mg) and **4** (13 mg) from fraction five (90:10), **5** (6 mg) from fraction ten (80:20), **6** (12 mg) and **7** (10 mg) from fraction eleven (75:25), **8** (4 mg) from fraction four (94:6), and **9** (5 mg) from fraction fourteen (70:30). The EtOAc soluble (31 g) were subjected to MPLC (silica gel, 200–300 mesh) eluted with a gradient of Me_2CO in $CHCl_3$ (100:0–40:60) to give thirty-six main fractions. Fractions 1–3 (100:0–96:4) were purified by polyamide CC eluted with $CHCl_3$–MeOH (1:0–0:1, gradient) and Sephadex LH-20 to give xanthones **10** (12 mg), **11** (20 mg) and **12** (10 mg).

3.4. 1,3,7-Trihydroxy-2,8-dimethoxyxanthone (*1*)

Fine yellow needles (from MeOH), mp 218 °C; HR–EIMS *m/z:* 304.0584, calc. for $[M]^+$, $C_{15}H_{12}O_7$: 304.0583; dark purple fluorescence under UV light (on polyamide sheet) and dark green color with $FeCl_3$; UV λ_{max}^{nm} MeOH: 238, 261, 312, 381; +NaOAc: 220, 259 sh, 315 sh, 359; +NaOAc+H_3BO_3: 222, 259 sh, 318; IR (cm^{-1}, KBr): 3400, 2940, 1650, 1610, 1580, 1479, 1400, 1300; EIMS *m/z* (rel. int.): 304 (100), 289 (52), 286 (24), 271 (20), 261 (60), 246 (30), 218 (60); ^{1}H and ^{13}C NMR spectral data: see Tables 1 and 2, respectively.

3.5. 1,3,7-Triacetoxy-2,8-dimethoxyxanthone (*1a*)

Xanthone **1** (3 mg) was treated with Ac_2O and pyridine (1:1) at room temp. overnight, dil. with H_2O and extracted with Et_2O. The dried Et_2O extract was purified by Sephadex LH-20 ($CHCl_3$: MeOH, 1:1) to give **1a** (2 mg) as white needles (from MeOH), mp 188 °C. UV λ_{max}^{nm} MeOH: 236, 277, 304, 342; +NaOAc: 212, 348; +NaOAc+H_3BO_3: 212, 348; ^{1}H NMR spectral data: see Table 1.

Table 2
^{13}C NMR spectral data for compounds **1**, **8** (125 MHz), **2**, **4**, **6**, **7**, **14** (100 MHz) and **13** (50 MHz) in DMSO-d_6

C	1	13[a]	14[b]	2	4	6	7	8
1	154.3	153.9	145.1	124.0	160.7	161.0	158.1	153.4
2	130.3	130.6	146.6	113.5	109.6	105.7	94.8	131.0
3	158.3	158.4	124.0	149.8	137.2	119.7	159.6	152.5
4	93.0	94.1	113.7	145.2	107.2	141.8	128.1	94.4
4a	151.9	152.1	149.5	146.6	155.8	149.4	148.8	159.8
4b	149.3	150.2	144.4	149.5	149.3	149.6	149.2	155.5
5	113.0	134.2	146.2	119.2	119.4	119.3	119.3	107.0
6	124.1	156.5	119.3	124.1	125.5	125.7	124.8	137.1
7	146.8	120.4	123.4	155.5	154.0	153.8	154.0	110.3
8	145.1	113.8	115.2	106.0	107.9	107.6	108.0	160.1
8a	114.3	112.5	122.6	121.9	120.4	122.0	120.1	106.6
8b	102.5	101.4	116.1	115.8	107.8	108.1	102.2	101.4
C=O	180.5	179.3	175.4	175.0	181.5	182.2	180.3	183.8
MeO	60.9	60.6	61.0	61.0	–	56.8	60.9	60.0
MeO	59.8	59.8	–	55.7	–	–	56.5	–

[a] Data from Pinto et al., 1994.
[b] Data from Minami et al., 1996.

Table 3
Probability of oxygenated groups appeared at each position of xanthone compounds

	Position	1	2	3	4	5	6	7	8
Polygala L.	Probability	64/66	45/66	57/66	13/66	2/66	20/66	46/66	9/66
	%	97	68	86	20	3	30	70	14
Securidaca L.	Probability	12/13	8/13	7/13	2/13	0/13	2/13	11/13	2/13
	%	92	62	54	15	0	15	85	15

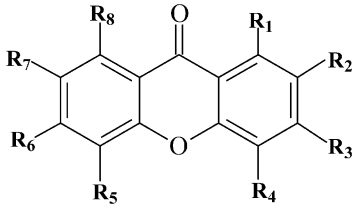

	R_1	R_2	R_3	R_4	R_5	R_6	R_7	R_8
1	HO	MeO	HO	H	H	H	HO	MeO
1a	AcO	MeO	AcO	H	H	H	AcO	MeO
2	H	H	MeO	HO	H	H	MeO	H
2a	H	H	MeO	AcO	H	H	MeO	H
3	HO	H	H	H	H	HO	H	H
4	HO	H	H	H	H	H	HO	H
5	MeO	HO	H	H	H	H	MeO	H
6	HO	H	H	MeO	H	H	HO	H
7	HO	H	MeO	MeO	H	H	HO	H
8	HO	MeO	HO	H	H	H	H	HO
9	HO	MeO	HO	H	H	HO	MeO	H
10	HO	H	HO	H	H	H	HO	H
11	MeO	HO	H	H	H	H	HO	H
12	HO	MeO	HO	H	H	H	HO	H
13	HO	MeO	HO	H	MeO	HO	H	H
14	MeO	HO	H	H	HO	H	H	H

3.6. 3,7-Dimethoxy-4-hydroxyxanthone (**2**)

Fine yellow needles (from MeOH), mp 178 °C; HR–EIMS *m/z:* 272.0686, calc. for $[M]^+$, $C_{15}H_{12}O_5$: 272.0685; bright blue fluorescence under UV light (on polyamide sheet) and green color with $FeCl_3$; UV λ_{max}^{nm} MeOH: 237, 262, 318, 384; +NaOAc: 218, 262, 318, 384; IR (cm^{-1}, KBr): 3500, 3420, 2940, 1640, 1620, 1565, 1485, 1445, 1385, 1320, 1300; EIMS *m/z* (rel. int.): 272 (60), 254 (100), 243 (15), 229 (50), 225 (30), 198 (30); ^1H and ^{13}C NMR spectral data: see Tables 1 and 2, respectively.

3.7. 3,7-Dimethoxy-4-acetoxyxanthone (**2a**)

Xanthone **2** (3 mg) was treated with Ac_2O and pyridine (1:1) at room temp. overnight, dil. with H_2O and extracted with Et_2O. The dried Et_2O extract was purified by Sephadex LH-20 ($CHCl_3$: MeOH, 1:1) to give **2a** (2.6 mg) as white needles (from MeOH), mp 164 °C; UV λ_{max}^{nm} MeOH: 241, 256, 367; +NaOAc: 212, 252, 367; ^1H NMR spectral data: see Table 1.

Acknowledgements

The authors express their gratitude to Professor Pu-Zhu Cong for his helpful suggestions for the structure elucidation by MS preparation; Professor Mu-Jian Lü and Jing-Qi Pan (Anal. Center, Chem. Dept. of Peking University) for obtaining the 400 MHz NMR and NOESY data; Professor Li-Jun Li (Institute of Materia Medica) for recording the EIMS; Mr. Jie Wang (Academy of Military Medical Sciences) for HR-MS measurements.

References

Bashir, A., Hamburger, M., Msonthi, J.D., Hostettmann, K., 1992. Isoflavones and xanthones from *Polygala virgata*. Phytochemistry 31, 309–311.

Costa, C., Bertazzo, A., Allegri, G., Curcuruto, O., Traldi, P., 1992. Indole alkaloids from the roots of an African plant *Securidaca longpedunculata*. J. Heterocyclic Chem. 29, 1641–1647.

Davreux, M., Delaude, C., 1971. Saponins of the Polygalaceae: Identification of the saponin extracted from *Securidaca welwitschii*. Bull. Soc .Roy. Sci. Liege 40, 498–501.

Delectis Florae Republicae Popularis Sinicae Agendae Academiae Sinicae Edita. 1997 Florae Republicae Popularis Sinicae, Tomus 43 (3), pp. 138–198. Science Press Beijing.

Fernandes, E.G.R., Silva, A.M.S., Cavaleiro, J.A.S., Silva, F.M., Borges, M.F.M., Pinto, M.M.M., 1998. ^{1}H and ^{13}C NMR spectroscopy of mono-, di-, tri- and tetrasubstituted xanthones. Magnetic Resonance in Chemistry 36, 305–309.

Frahm, A.W., Hambloch, H., 1982. Computer supported structure elucidation of polymethoxy- and polyacetoxyxathones. Organic Magnetic Resonance 19, 43–48.

Galeffi, C., Federici, E., Msonthi, J.D., Marini-Bettolo, G.B., Nicoletti, M., 1990. Research on African medicinal plants Part XVIII New xanthones from *Ectiadiopsis oblongifolia* and *Securidaca longipedunculata*. Fitoterapia 61, 79–81.

Gil, S., Palanca, P., Sanz, V., Tortajada, A., 1990. Synthesis of 1,2,3,8-tetraoxygenated xanthones. J. Nat. Prod. 53, 1198–1211.

Hamburger, M., Gupta, M., Hostettmann, K., 1985. Flavonol glycosides from *Securidaca diversifolia*. Phytochemistry 24, 2689–2692.

Harborne, J.B., 1973. Phytochemical Methods. Chapman & Hall, London.

Jiangsu Institute of Botany, Chinese Academy of Medical Sciences and Kunming Institute of Botany, 1988. *Xinhua Bencao Gangyao*. Vol.1. pp. 292–293. Shanghai Science and Technology Press Shanghai.

Lin, C.N., Chung, M.L., Liou, S.J., Lee, T.H., Wang, J.P., 1996. Synthesis and anti-inflammatory effects of xanthone derivatives. J. Pharm. Pharmacol. 48, 532–538.

Mahmood, N., Moore, P.S., Tommasi, N.D., Simone, F.D., Colman, S., Hay, A.J., Pizza, C., 1993. Inhibition of HIV infection by caffeoylquinic acid derivatives. Antiviral Chemistry & Chemotherapy 4, 235–240.

Minami, H., Takahashi, E., Kodama, M., Fukuyama, Y., 1996. Three xanthones from *Garcinia subelliptica*. Phytochemistry 41, 629–633.

Nagem, T.J., Da Silva, M.C., Da Silveira, J.C., 1992. Clathraxanthone, α 1,2,7-trioxygenated xanthone from *Haploclathra paniculata*. Phytochemistry 31, 2913–2914.

Philip, W.W., Sarath, P.G., Uvais, M., Sultanbawa, S., Rymantas, K., 1971. Carbon-13 NMR study of naturally occurring xanthones. Org. Magn. Reson. 9, 631–636.

Pinheiro, T.R., Filho, V.C., Santes, A.R.S., Calixto, J.B., Monache, F.D., Pizzolatti, M.G., Yunes, R.A., 1998. Three xanthones from *Polygala cyparissias*. Phytochemistry 48, 725–728.

Pinto, D.C.G., Fuzzati, N., Pazmino, X.C., Hostettmann, K., 1994. Xanthone and antifungal constituents from *Monnina obtusifolia*. Phytochemistry 37, 875–878.

Scandola, M., Games, D.E., Costa, C., Allegri, G., Bertazzo, A., 1994. Structure study of alkaloids from *Securidaca longipedunculata* roots. J. Heterocyclic Chem. 31, 219–224.

Silveria, E.R., Falcao, M.J.C., Menezes Jr., A., Kinfaron, D.G.I., Glass, T.E., 1995. Pentaoxygenated xanthones from *Bredemeyera floribunda*. Phytochemistry 39, 1433–1436.

Stout, G.H., Christensen, E.N., Balkenhol, W.J., Stevens, K.L., 1969. Xanthones of the Gentianaceae II. *Frasera albicaulis*. Tetrahedron 25, 196–1973.

Tommasi, N.D., Piacente, S., Simone, F.D., Pizza, C., 1993. New sucrose derivatives from the bark of *Securidaca longipedunculata*. J. Nat. Prod. 56, 134–137.

Tosa, H., Iinuma, M., Murakami, K.I., Ito, T., Chelladurai, V.S., 1997. Pentaoxygenated xanthones from *Bredemeyera floribunda*. Phytochemistry 45, 133–136.

Yang, X.D., Xu, L.Z., Yang, S.L., 2000a. Advances in studies on medicinal plants of *Securidaca* L. Chinese Traditional and Herbal Drugs 31, 392–393.

Yang, X.D., Xu, L.Z., Yang, S.L., 2000b. Advances in the research of chemistry and pharmacology of xanthones isolated from *Polygala* L. Natural Product Research and Development 12, 88–94.

PERGAMON

Phytochemistry 58 (2001) 1251–1256

PHYTOCHEMISTRY

www.elsevier.com/locate/phytochem

Coumaroyl flavonol glycosides from the leaves of *Ginkgo biloba*

Yuping Tang[a,b,*], Fengchang Lou[a], Jinghua Wang[a], Yanfang Li[a], Shufei Zhuang[c]

[a]*Department of Natural Medicinal Chemistry, China Pharmaceutical University, Nanjing 210038, PR China*

[b]*State Key Laboratory of Bio-organic and Natural Products Chemistry, Shanghai Institute of Organic Chemistry, Chinese Academy of Sciences, Shanghai 200032, PR China*

[c]*Shanghai Institute of Materia Medica, Chinese Academy of Sciences, Shanghai 200031, PR China*

Received 2 March 2001; received in revised form 24 May 2001

Abstract

Two coumaroyl flavonol glycosides, isorhamnetin 3-*O*-α-L-[6‴-*p*-coumaroyl-(β-D)-glucopyranosyl-(1,2)-rhamnopyranoside], and kaempferol 3-*O*-α-L-[6‴-*p*-coumaroyl-(β-D)-glucopyranosyl-(1,2)-rhamnopyranoside]-7-*O*-β-D-glucopyranoside, were isolated from the *n*-BuOH extract of *Ginkgo biloba* leaves. These two, together with six other flavonol glycosides, kaempferol 3-*O*-α-L-[6‴-*p*-coumaroyl-(β-D)-glucopyranosyl-(1,2)-rhamnopyranoside], quercetin 3-*O*-α-L-[6‴-*p*-coumaroyl-(β-D)-glucopyranosyl-(1,2)-rhamnopyranoside], quercetin 3-*O*-α-L-[6‴-*p*-coumaroyl-(β-D)-glucopyranosyl-(1,2)-rhamnopyranoside]-7-*O*-β-D-glucopyranoside, quercetin 3-*O*-β-D-glucopyranosyl-(1-2)-α-L-rhamnopyranoside, quercetin 3-*O*-β-rutinoside, and quercetin 3-*O*-β-D-glucopyranoside, showed profound antioxidant activities in DPPH and cytochrome-*c* reduction assays using the HL-60 cell culture system. © 2001 Elsevier Science Ltd. All rights reserved.

Keywords: *Ginkgo biloba* L.; Ginkgoaceae; Flavonol glycoside; Antioxidant activity

1. Introduction

Extracts from *Ginkgo biloba* L. (maidenhair tree) have been used therapeutically for centuries. Ginkgo, like ginseng, is mentioned in the traditional Chinese pharmacopoeia and the Chinese made tea from parts of the ginkgo tree for treatment of asthma and bronchitis. The *n*-BuOH extract of *G. biloba* leaves showed antioxidant activity in preliminary DPPH assays. This prompted us to search for antioxidant compounds from this plant. Bioassay-guided fractionation of the *n*-BuOH extract led to the isolation of antioxidant flavonol glycosides **1**–**13**, including two new compounds isorhamnetin 3-*O*-α-L-[6‴-*p*-coumaroyl-(β-D)-glucopyranosyl-(1,2)-rhamnopyranoside] (**1**) and kaempferol 3-*O*-α-L-[6‴-*p*-coumaroyl-(β-D)-glucopyranosyl-(1,2)-rhamnopyranoside]-7-*O*-β-D-glucopyranoside (**2**). Kaempferol 3-*O*-α-L-[6‴-*p*-coumaroyl-(β-D)-glucopyranosyl-(1,2)-rhamnopyranoside] (**3**), quercetin 3-*O*-α-L-[6‴-*p*-coumaroyl-(β-D)-glucopyranosyl-(1,2)-rhamnopyranoside] (**4**), quercetin 3-*O*-α-L-[6‴-*p*-coumaroyl-(β-D)-glucopyranosyl-(1,2)-rhamnopyranoside]-7-*O*-β-D-glucopyranoside (**5**), kaempferol 3-*O*-β-D-glucopyranosyl-(1-2)-α-L-rhamnopyranoside (**6**), isorhamnetin 3-*O*-β-D-glucopyranosyl-(1-2)-α-L-rhamnopyranoside (**7**), quercetin 3-*O*-β-D-glucopyranosyl-(1-2)-α-L-rhamnopyranoside (**8**), isorhamnetin 3-*O*-β-rutinoside (**9**), quercetin 3-*O*-*β*-rutinoside (**10**), kaempferol 3-*O*-*β*-rutinoside (**11**), quercetin 3-*O*-β-D-glucopyranoside (**12**) and kaempferol 3-*O*-β-D-glucopyranoside (**13**) were also isolated from *G. biloba* leaves.

2. Results and discussion

The *n*-BuOH extract of *G. biloba* was applied to a Si gel column using $CHCl_3$–MeOH (25:1) as eluant, followed by stepwise addition of MeOH to afford 12 fractions. Each fraction was further subjected to Si gel, and Sephadex LH-20 column chromatography, as well as reversed-phase HPLC to afford 13 flavonol glycosides **1**–**13**.

Compound **1** was obtained as a pale yellow amorphous powder. Upon acid hydrolysis of **1**, isorhamnetin, *p*-coumaric acid, glucose and rhamnose were identified

* Corresponding author at present address: State Key Laboratory of Bio-organic and Natural Products Chemistry, Shanghai Institute of Organic Chemistry, Chinese Academy of Sciences, Shanghai 200032, PR China. Tel.: +86-21-6416-3300-1599; fax: +86-21-6416-6128.

E-mail address: yptang@pub.sioc.ac.cn (Y. Tang).

0031-9422/01/$ - see front matter © 2001 Elsevier Science Ltd. All rights reserved.
PII: S0031-9422(01)00320-X

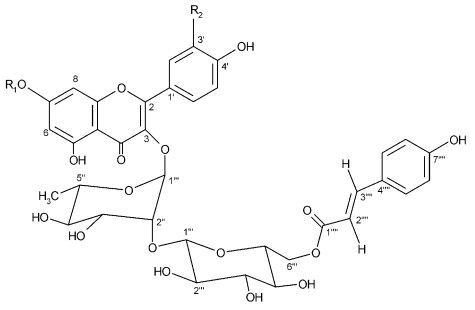

	R_1	R_2
1	H	OMe
2	glc	H
3	H	H
4	H	OH
5	glc	OH

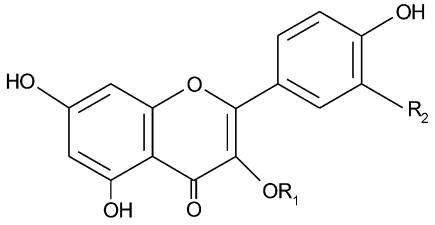

	R_1	R_2
6	-rha(2-1)-glc	H
7	-rha(2-1)-glc	OMe
8	-rha(2-1)-glc	OH
9	rutinose	OMe
10	rutinose	OH
11	rutinose	H
12	glc	OH
13	glc	H

by TLC. Isorhamnetin and *p*-coumaric acid were also identified by UV and ^{1}H NMR spectroscopy. Under UV light, compound **1** appeared as a dull brown flavonol-like fluorescent spot on silica gel and polyamide plates, indicating the substitution of the C-3 hydroxyl group. This spot changed to yellow with ammonia and to yellowish-green with Naturstoffreagenz A indicating respectively the presence of free 5- and 4′-hydroxyl groups and absence of an *ortho*-dihydroxyl group in the B-ring. The UV shift on addition of diagnostic reagents confirmed the presence of free hydroxyl groups at positions C-5, C-7 and C-4′ (Markham, 1982). Therefore, the position of the linkage between isorhamnetin and the other moiety, occurs at C-3. Its IR spectrum indicated the presence of two carbonyl groups (1656 and 1680 cm^{-1}) indicating the flavonol carbonyl and ester carbonyl groups. The positive-ion FABMS spectrum exhibited a quasi-molecular ion peak at *m*/*z* 771 $[M+H]^+$ in accordance with a *p*-coumaroyl ester of a isorhamnetin bioside. Other prominent peaks were observed at *m*/*z* 463 $[M\text{-}308+H]^+$ and *m*/*z* 317 $[aglycone+H]^+$, which showed that glucose was located between rhamnose and *p*-coumaric acid.

The ^{1}H NMR spectrum exhibited two doublets at δ 6.24 and 7.46 with large coupling constants (15.9 Hz) which identified *trans* olefinic double bond protons, and the other caused by the four aromatic ring proton signals at δ 6.72 and 7.46 (AA′BB′), which confirmed the presence of the *p*-coumaroyl subunit. The ^{1}H NMR spectrum also indicated the presence of a methoxyl signal at δ 3.84 (3H, *s*, 3′-OMe), and five aromatic proton signals at δ 6.18 (1H, *d*, H-6, $J=1.9$ Hz), 6.33 (1H, *d*, H-8, $J=1.9$ Hz), 6.90 (1H, *d*, H-5′, $J=8.4$ Hz), 7.53 (1H, *dd*, H-6′, $J=2.1$ and 8.4 Hz) and 7.86 (1H, *d*, H-2′, $J=2.1$ Hz), which confirmed the isorhamnetin 3-*O*-glycoside structure. The ^{1}H NMR spectrum also supported the presence of one rhamnose and one glucose with the rhamnose anomeric proton at δ 5.54 (H-1, brs) and the glucose H-1 at δ 4.31 (d, 7.8 Hz). The ^{1}H–^{1}H COSY and TOCSY experiments permitted the full assignment of the sugar protons (Table 1). In the ^{13}C NMR spectral data, the C-2 (rha) was shifted downfield at δ 81.7, indicating that glycosylation of the rhamnose unit by the glucopyranosyl was on in 2-hydroxyl. In the HMBC spectrum, a crosspeak between C-2 (rha) and H-1 (glc), and a crosspeak between C-2 (rha) and H-1 (rha) established the linkage point between the two sugar moieties (Table 1). In addition to this, downfield shielding of C-2 indicated that position 3 was substituted by a glycosyl moiety. This was confirmed by a crosspeak between H-1 (rha) and C-3 of the aglycone in the HMBC spectrum. The ^{13}C NMR spectrum of the sugar moiety of **1** also showed a downfield shift of C-6 glc ($\Delta+1.9$) from the chemical shift values reported for the corresponding carbon resonances of unlinked C-6 glucose such as flavonol 3-*O*-glucopyranoside (Markham et al., 1978). This shift was expected from the substituent effect of C-6 glucose acylation. This was also confirmed by a crosspeak between H-6 (glc) and C-1 (Coum) in the HMBC spectrum. Therefore, compound **1** was characterized as isorhamnetin 3-*O*-α-L-[6‴-*p*-coumaroyl-(β-D)-glucopyranosyl-(1,2)-rhamnopyranoside].

Compound **2** was a yellow amorphous powder. Upon acid hydrolysis of **2**, kaempferol, *p*-coumaric acid, glucose and rhamnose were identified by TLC. Kaempferol and *p*-coumaric acid were also identified by UV and ^{1}H NMR spectroscopy. The UV and IR spectra of **2** were similar to those of **1**. The molecular formula, $C_{42}H_{46}O_{22}$, was inferred from the $[M+H]^+$ peak at *m*/*z* 903 in the FABMS, and it was supported by ^{13}C NMR and DEPT spectroscopic analyses. The ^{1}H NMR and ^{13}C NMR spectra of **2** showed the presence of a kaempferol moiety, three sugar residues and a *p*-coumaric acid moiety. Its ^{1}H NMR, ^{13}C NMR and 2D NMR spectra showed the presence of a 3-*O*-α-L-[6‴-*p*-coumaroyl-(β-D)-glucopyranosyl-(1,2)-rhamnopyranoside] as for **1** (Table 2). A ^{13}C NMR signal at δ 162.8

Table 1
NMR spectral data for compound **1** (DMSO-d_6)

No.	^{13}C NMR		^{1}H NMR	HMBC
	δ (ppm)	mult.	δ (ppm), mult., J (Hz)	
2	156.6	*s*		H-2′,6′
3	134.4	*s*		H-1″
4	177.8	*s*		
5	161.3	*s*		H-6, 5-OH
6	98.6	*d*	6.18 (*d*, 1.9)	H-8, 5-OH, 7-OH
7	164.1	*s*		H-6,8, 7-OH
8	93.6	*d*	6.33 (*d*, 1.9)	H-6
9	156.3	*s*		H-8
10	104.0	*s*		H-6,8, 5-OH
1′	120.6	*s*		H-2′,6′
2′	113.7	*d*	7.86 (*d*, 2.1)	H-6′, 3′-OH
3′	149.1	*s*		H-2′, 3′-OH
4′	146.1	*s*		H-2′,5′,6′, 4′-OH
5′	115.5	*d*	6.90 (*d*, 8.4)	H-6′, 4′-OH
6′	122.3	*d*	7.53 (*dd*, 2.1, 8.4)	H-5′
3′-OMe	55.7	*q*	3.84 (*s*)	
5-OH			12.63 (*s*)	
7-OH			10.82 (*s*)	
4′-OH			9.74 (*s*)	
1″	100.7	*d*	5.54 (*br s*)	H-2″
2″	81.7	*d*	4.18 (*m*)	H-1″,1‴
3″	69.4	*d*	3.61 (*dd*, 3.3, 9.3)	H-2″, 3″-OH
4″	71.7	*d*	3.15 (*t*, 9.3)	H-3″,5″,6″, 4″-OH
5″	70.4	*d*	3.55 (*m*)	H-1″, 6″
6″	17.4	*q*	0.93 (*d*, 6.1)	
3″-OH			4.62 (*br d*, 9.5)	
4″-OH			4.92 (*br d*, 5.0)	
1‴	106.2	*d*	4.31 (*d*, 7.8)	H-2″,2‴
2‴	73.7	*d*	3.19 (*m*)	H-1‴,3‴, 2‴-OH
3‴	75.9	*d*	3.30 (*m*)	H-2‴, 3‴-OH
4‴	70.2	*d*	3.21 (*m*)	H-3‴,5‴, 4‴-OH
5‴	73.6	*d*	3.07 (*br t*, 6.0)	H-4‴,6‴
6‴	62.9	*t*	4.17, 4.11 (*m*)	H-5‴
2‴-OH			5.19 (*br d*, 2.6)	
3‴-OH			5.29 (*br d*, 2.4)	
4‴-OH			5.09 (*br* s)	
1⁗	166.4	*s*		H-6‴,2⁗,3⁗
2⁗	113.9	*d*	6.24 (*d*, 15.9)	H-3⁗
3⁗	145.5	*d*	7.46 (*d*, 15.9)	H-5⁗,9⁗
4⁗	125.0	*s*		H-3⁗,5⁗,9⁗
5⁗,9⁗	130.1	*d*	7.42 (*d*, 8.6)	H-3⁗,6⁗,8⁗
6⁗,8⁗	115.6	*d*	6.72 (*d*, 8.6)	H-5⁗/9⁗, 7⁗-OH
7⁗	159.7	*s*		H-5⁗,6⁗,8⁗,9⁗, 7⁗-OH
7⁗-OH			9.95 (*s*)	

was assigned to C-7, based on its long-range ^{13}C-^{1}H correlation observed in the HMBC experiment with the two ^{1}H NMR signals at δ 6.40 (H-6) and δ 6.60 (H-8). C-7 showed a three-bond correlation with an anomeric proton at δ 5.05. The 2D NMR spectra allowed the assignment of all ^{1}H and ^{13}C NMR signals of the 7-glucosyl residue, which could be identified as a glucopyranoside (Markham et al., 1982). The β-configuration of the anomeric carbon was evident from the coupling constant of H-1⁗′ (J = 7.5 Hz) observed in the ^{1}H NMR spectrum (Markham and Geiger, 1994). The structure of compound 2 is therefore kaempferol 3-*O*-α-L-[6‴-*p*-coumaroyl-(β-D)-glucopyranosyl-(1,2)-rhamnopyranoside]-7-*O*-β-D-glucopyranoside.

Compounds **3**–**8** were identified by comparing their physical and spectral data with the literature values: kaempferol 3-*O*-α-L-[6‴-*p*-coumaroyl-(β-D)-glucopyranosyl-(1,2)-rhamnopyranoside] (**3**) (Markham et al., 1992), quercetin 3-*O*-α-L-[6‴-*p*-coumaroyl-(β-D)-glucopyranosyl-(1,2)-rhamnopyranoside] (**4**) (Nasr et al., 1987; Markham et al., 1992), quercetin 3-*O*-α-L-[6‴-*p*-coumaroyl-(β-D)-glucopyranosyl-(1,2)-rhamnopyranoside]-7-*O*-β-D-glucopyranoside (**5**) (Hasler, et al. 1992), kaempferol 3-*O*-β-D-glucopyranosyl-(1-2)-α-L-rhamno-

Table 2
NMR spectral data of compound **2** (DMSO-d_6)

No.	^{13}C NMR		^{1}H NMR	HMBC
	δ (ppm)	Mult.	δ (ppm), mult., J (Hz)	
2	156.5	*s*		H-2′,6′
3	134.4	*s*		H-1″
4	177.5	*s*		
5	160.9	*s*		H-6, 5-OH
6	99.2	*d*	6.40 (*brs*)	H-8, 5-OH
7	162.8	*s*		H-6,8,1‴″
8	94.4	*d*	6.60 (*brs*)	H-6
9	155.8	*s*		H-8
10	105.6	*s*		H-6,8, 5-OH
1′	120.3	*s*		H-2′,6′
2′	130.3	*d*	7.74 (*d*, 8.6)	H-3′,6′
3′	115.3	*d*	6.91 (*d*, 8.6)	H-2′
4′	159.9	*s*		H-3′,5′, 4′-OH
5′	115.3	*d*	6.91 (*d*, 8.6)	H-6′
6′	130.3	*d*	7.74 (*d*, 8.6)	H-5′
5-OH			12.58 (*s*)	
4′-OH			10.25 (*s*)	
1″	100.6	*d*	5.57 (*br s*)	H-2″
2″	81.4	*d*	4.15 (*d*, 3.4)	H-1″,1‴
3″	70.0	*d*	3.60 (*m*)	H-2″
4″	71.5	*d*	3.13 (*m*)	H-3″,5″
5″	70.4	*d*	3.40 (*m*)	H-1″,6″
6″	17.4	*q*	0.92 (*d*, 6.2)	
1‴	106.0	*d*	4.32 (*d*, 7.8)	H-2″,2‴
2‴	73.7	*d*	3.09 (*dd*, 7.8, 8.2)	H-1‴,3‴
3‴	75.9	*d*	3.25 (*m*)	H-2‴
4‴	70.0	*d*	3.20 (*m*)	H-3‴,5‴
5‴	73.6	*d*	3.17 (*m*)	H-4‴,6‴
6‴	62.9	*t*	4.18, 4.12 (*m*)	H-5‴
1⁗	166.3	*s*		H-6‴,2⁗,3⁗
2⁗	113.9	*d*	6.22 (*d*, 15.8)	H-3⁗
3⁗	145.2	*d*	7.45 (*d*, 15.8)	H-5⁗,9⁗
4⁗	125.0	*s*		H-3⁗,5⁗,9⁗
5⁗,9⁗	130.0	*d*	7.40 (*d*, 8.6)	H-3⁗,6⁗,8⁗
6⁗,8⁗	115.6	*d*	6.70 (*d*, 8.6)	H-5⁗/9⁗, 7⁗-OH
7⁗	159.6	*s*		H-5⁗,6⁗,8⁗,9⁗, 7⁗-OH
7⁗-OH			9.94 (*s*)	
1⁗″	99.9	*d*	5.05 (*d*, 7.5)	H-2⁗″
2⁗″	73.2	*d*	3.25 (*m*)	H-1⁗″,3⁗″
3⁗″	76.4	*d*	3.25 (*m*)	H-4⁗″
4⁗″	69.8	*d*	3.15 (*m*)	H-5⁗″
5⁗″	77.1	*d*	3.45 (*m*)	H-4⁗″,6⁗″
6⁗″	60.6	*t*	3.50, 3.70 (*m*)	H-5⁗″

pyranoside (**6**) (Hasler et al., 1992), isorhamnetin 3-*O*-β-D-glucopyranosyl-(1-2)-α-L-rhamnopyranoside (**7**) (Tang et al., 2000), quercetin 3-*O*-β-D-glucopyranosyl-(1-2)-α-L-rhamnopyranoside (**8**) (Hasler et al. 1992). Compounds **9**–**13** were identified by comparison of their spectral data with those of authentic samples: isorhamnetin 3-*O*-β-rutinoside (**9**), quercetin 3-*O*-β-rutinoside (**10**), kaempferol 3-*O*-*β*-rutinoside (**11**), quercetin 3-*O*-β-D-glucopyranoside (**12**), and kaempferol 3-*O*-β-D-glucopyranoside (**13**).

For the screening and evaluation of antioxidant activity of pure compounds and/or plant extracts, DPPH and cytochrome-*c* reduction assays were adopted. Compounds **1**–**5**, **8**, **10** and **12** exhibited inhibitory activity as strong as the positive control against TPA-induced free radical formation in a HL-60 cell culture system and showed free radical scavenging activity in the DPPH assay (Table 3). Five coumaroyl flavonol glycosides (IC_{50} of **1**–**5**, 17.5, 17.9, 17.7, 13.2, 13.5 μg/ml, respectively) showed profound activity. Generally, the presence of hydroxyl substituents on the flavonoid nucleus enhanced activity, whereas substitution by methoxyl groups diminished antioxidant activity. Substitution patterns on the B-ring especially affected antioxidant potencies of the flavonoids (Arora et al., 1998). The di-OH substitution at 3′ and 4′ of the B-ring is

Table 3
Antioxidant activities of flavonol glycosides from *Ginkgo biloba* leaves

Compounds	DPPH assay (IC_{50})[a]		Cytochrome-*c* reduction assay (IC_{50})[a]	
	μg/ml	μM	μg/ml	μM
1	17.9	23.2	17.5	22.7
2	18.4	20.4	17.9	19.8
3	18.1	24.5	17.7	23.9
4	14.0	18.5	13.2	17.5
5	14.5	15.8	13.5	14.7
6	> 100		> 50	
7	> 100		> 50	
8	16.1	26.4	14.8	24.3
9	> 100		> 50	
10	16.2	26.6	14.9	24.4
11	> 100		> 50	
12	12.1	26.1	11.1	23.9
13	> 100		> 50	
Gallic acid	3.6	21.2	3.0	17.6

[a] Results are expressed as IC_{50} values (μg/ml and μM). Data for active compounds were mean of triplicates. Gallic acid used for positive control.

particularly important to the oxygen radical absorbing activity of a flavonoid (Cao et al., 1997). These trends are consistent with less active flavonoids (**6**, **7**, **9**, **11** and **13**) that possess monohydroxyl substitution in the B-ring.

3. Experimental

3.1. General experimental procedures

UV spectra were recorded in MeOH using a Perkin-Elmer Lambda 2 spectrophotometer. IR spectra were recorded in KBr using a Nicolet Impact 410 spectrometer. ^1H and ^{13}C NMR spectra were recorded on a Bruker AM-400 spectrometer. FAB-MS spectra were recorded in NAB matrix in the positive ion mode on a Finnigan MAT TSQ 7000 spectrometer. Column chromatography was performed over Si gel (200–400 mesh, Marine Chemical Factory in Qingdao, China), or Sephadex LH-20 (25–100 μm, Pharmacia).

3.2. Plant material

The leaves of *G. biloba* were collected from mature trees, growing in Nanjing, China, in November 1998, and identified by Professor Luoshan Xu in Division of Pharmacognosy and deposited in the Department of Natural Medicinal Chemistry, China Pharmaceutical University.

3.3. Extraction and isolation

The dried leaves of *G. biloba* (10.0 kg) were extracted three times with MeOH–H_2O (85:15) using an ultrasonic apparatus for 3 h. The MeOH extract (1585.6 g) was suspended in H_2O and partitioned with petroleum ether, $CHCl_3$, and *n*-BuOH, successively. The *n*-BuOH extract (520.6 g) was subjected to Si gel column chromatography eluting with $CHCl_3$–MeOH (25:1) followed by stepwise addition of MeOH to yield 12 fractions. Fraction 7 (23.2 g) was subjected to Si gel ($CHCl_3$–MeOH, 10:1), and Sephadex LH-20 (MeOH) chromatographic steps purified by HPLC (RP_{18}, 4 μm, 260 nm, MeOH-1% acetic acid, 20:80; **1**: $t_R = 30.03$ min; **2**: $t_R = 16.54$ min; **3**: $t_R = 26.03$ min; **4**: $t_R = 20.26$ min; **5**: $t_R = 13.58$ min) to give compounds **1** (8 mg), **2** (6 mg), **3** (20 mg) **4** (25 mg), and **5** (13 mg). Fraction 8 (28.6 g) was subjected to Si gel ($CHCl_3$–MeOH, 9:1), and Sephadex LH-20 (MeOH) chromatographies to give compounds **6** (22 mg), **7** (6 mg), and **8** (28 mg). Fraction 6 (36.7 g) was subjected to Si gel ($CHCl_3$-MeOH, 12:1), and Sephadex LH-20 (MeOH) chromatographies to give compounds **9** (20 mg), **10** (186 mg), and **11** (80 mg). Fraction 5 (36.7 g) was subjected to Si gel ($CHCl_3$–MeOH, 15:1), and Sephadex LH-20 (MeOH) chromatographic steps to give compounds **12** (90 mg), and **13** (76 mg).

3.4. Acidic hydrolysis of *1* and *2*

A solution of each compound (**1** and **2**) in 5 ml 6% HCl and heated for 3 h. The reaction mixture was extracted with EtOAc. The EtOAc fraction (aglycone) and the aqueous fraction (sugars) were concentrated until dryness for identification.

3.5. Identification

3.5.1. Compound *1*

Isorhamnetin 3-*O*-α-L-[6‴-*p*-coumaroyl-(β-D)-glucopyranosyl-(1,2)-rhamnopyranoside]. Pale yellow amorphous powder; UV λ_{max} (nm): MeOH: 365, 315, 265sh, 253, NaOMe: 407, 323, 270, NaOAc: 378, 330, 272, $NaOAc/H_3BO_3$: 368, 314, 267sh, 253, $AlCl_3$: 404, 313sh, 308, 283, 230, $AlCl_3$/HCl: 405, 313sh, 309, 283, 231; IR (KBr) ν_{max} 3537, 3500 (OH), 3258, 2984, 2920, 2850, 1680 (ester C=O), 1656 (α,β-unsaturated C=O), 1605, 1573, 1513, 1450, 1349, 1303, 1263, 1198, 1171, 1142, 1114, 1082, 1065, 1048, 995, 950, 820, 810, 595; ^1H NMR (400 MHz, DMSO-d_6), see Table 1; ^{13}C NMR (100 MHz, DMSO-d_6), see Table 1; FAB-MS *m*/*z* 771 $[M+H]^+$, 463 [aglycone + rha + H]$^+$, 317 [aglycone + H]$^+$.

3.5.2. Compound *2*

Kaempferol 3-*O*-α-L-[6‴-*p*-coumaroyl-(β-D)-glucopyranosyl-(1,2)-rhamnopyranoside]-7-O-β-D-glucopyranoside. Yellow amorphous powder; UV λ_{max} (nm): MeOH: 316, 268, NaOMe: 368, 278sh, NaOAc: 373, 324, 266, $NaOAc/H_3BO_3$: 321, 267, $AlCl_3$: 397, 320, 303, 277, $AlCl_3$/HCl: 396, 320, 302, 277; IR (KBr) ν_{max} 3530, 3345 (OH), 3285, 2981, 2955, 1680 (ester C=O),

1655 (α,β-unsaturated C=O), 1604, 1572, 1510, 1449, 1352, 1300, 1288, 1263, 1249, 1198, 1174, 1137, 1114, 1088, 1063, 1048, 1014, 1005, 996, 950, 820, 594; ^{1}H NMR (400 MHz, DMSO-d_6), see Table 2; ^{13}C NMR (100 MHz, DMSO-d_6), see Table 2; FABMS m/z 903 $[M+H]^+$.

3.6. Antioxidant assay

DPPH assay was performed essentially according to the modified method of Kirby and Schmidt (1997): 95 μl of 3.2×10^{-4} M of DPPH solution in absolute EtOH and 5 μl of sample solution in DMSO were mixed in a 96-well plate. The optical density was measured at 515 nm after incubation of the plate for 1 h at 37 °C. The DPPH control contained no sample but was otherwise identical. The cytochrome-*c* reduction assay was performed according to Sharma et al. (1994). HL-60 cells were maitained in RPMI 1640 medium supplemented with 5% heat-inactivated fetal calf serum, 1% penicillin-streptomycin at 37 °C in humidified atmosphere at 5% CO_2 in air. Differentiation was induced by 7-day treatment with 1.3% DMSO, and the cells were cultured in a 96-well plate (1×10^6 cells per well) in HBSS. After the addition of TPA (8 μM) to induce free radical formation, cytochrome-*c* (160 μM) and samples were added. The cells were incubated for 1 h at 37 °C, and antioxidant activity was determined by monitoring absorbance at 550 nm. The same reaction mixture, without the HL-60 cells, was used as a blank control.

Acknowledgements

This work was supported in part by the Chinese National New Drug Foundation. The authors also thank Mr. Yihua Yu (Department of Analysis, Shanghai Institute of Organic Chemistry, Chinese Academy of Science, Shanghai, China) for the NMR measurements.

References

Arora, A., Nair, M.G., Strasburg, G.M., 1998. Structure–activity relationships for antioxidant activities of a series of flavonoids in a liposomal system. Free Radical Biological Medicine 24, 1355–1363.

Cao, G., Sofic, E., Prior, R.L., 1997. Antioxidant and prooxidant behavior of flavonoids structure–activity relationships. Free Radical Biological Medicine 22, 749–760.

Hasler, A., Gross, G.A., Meier, B., Sticher, O., 1992. Complex flavonol glycosides from the leaves of *Ginkgo biloba*. Phytochemistry 31, 1391–1394.

Kirby, A.J., Schmidt, R.J., 1997. The modified method of DPPH assay for study on antioxidant activity of flavonoids. Journal of Ethnopharmacol. 56, 103–108.

Markham, K.R., 1982. Techniques of Flavonoid Identification. Academic Press, London.

Markham, K.R., Chari, V.M., Mabry, T.J. 1982. In: Harborne, J.B.and Mabry, T.J. (Eds.), The Flavonoids: Advances in Research. Chapman and Hall, London.

Markham, K.R., Geiger, H. 1994. In: Harborne, J.B. (Eds.), The Flavonoids: Advances in Research Since 1986. Chapman and Hall, London.

Markham, K.R., Geiger, H., Jaggy, H., 1992. Kaempferol-3-*O*-glucosyl(1-2)rhamnoside from *Ginkgo biloba* and reappraisal of other gluco(1-2, 1-3, and 1-4)rhamnoside structures. Phytochemistry 31, 1009–1011.

Markham, K.R., Ternai, B., Stanley, R., Geiger, H., Mabry, T.J., 1978. Carbon-13 NMR studies of flavonoids—III, naturally occurring flavonoid glycosides and acylated derivatives. Tetrahedron 34, 1389–1397.

Nasr, C., Lobstein-Guth, A., Haag-Berrurier, M., Anton, R., 1987. Quercetin coumaroyl glucorhamnoside from *Ginkgo biloba*. Phytochemistry 26, 2869–2870.

Sharma, S., Stutzman, J.D., Kelloff, G.J., Steele, V.E., 1994. Screening of potential chemopreventive agents using biochemical markers of carcinogenesis. Cancer Research 54, 5848–5855.

Tang, Y.-P., Wang, Y., Lou, F.-C., Li, Y.-F., Wang, J.-H., 2000. Flavonol glycosides from the leaves of *Ginkgo biloba*. Yaoxue Xuebao 35, 363–366.

PERGAMON

Phytochemistry 58 (2001) 1257–1262

PHYTOCHEMISTRY

www.elsevier.com/locate/phytochem

Two diacylated malvidin glycosides from *Petunia hybrida* flowers

Emmanuel Gonzalez, André Fougerousse, Raymond Brouillard*

Laboratoire de Chimie des Polyphénols, UMR 7509 du CNRS, Université Louis Pasteur, 4, rue Blaise Pascal, 67008 Strasbourg, France

Received 25 January 2001; received in revised form 5 June 2001

Abstract

Two novel diacylated and two known anthocyanins were isolated from violet flowers of *Petunia hybrida* cv Festival. The new anthocyanins are malvidin 3-*O*-(6-*O*-(4-*O*-(4-*O*-(6-*O*-feruloyl-β-D-glucopyranosyl)-*E*-*p*-coumaroyl)-α-rhamnosyl)-β-D-glucopyranoside)-5-β-D-glucopyranoside and malvidin 3-*O*-(6-*O*-(4-*O*-(4-*O*-(6-*O*-*E*-*p*-coumaroyl-β-D-glucopyranosyl)-*E*-*p*-coumaroyl)-α-rhamnosyl)-β-D-glucopyranoside)-5-β-D-glucopyranoside. The two known pigments are the 3-caffeoylglucosyl-*p*-coumaroylrutinoside-5-glucosides of malvidin and petunidin. © 2001 Elsevier Science Ltd. All rights reserved.

Keywords: *Petunia hybrida*; Solanaceae; Diacylated anthocyanins; Ferulic acid; Malvidin; ^{1}H and ^{13}C NMR spectroscopies

1. Introduction

Petunia hybrida (Solanaceae), the cultivated garden petunia, is not a true species but an artificial hybridisation between *Petunia axillaris* and *Petunia integrifolia* (Sink, 1984). Many studies concerning phytochemistry and genetic of petunia have been completed, in particular on *P. hybrida* for the establishment of the anthocyanin biosynthetic pathway (Dooner et al., 1991; Katz and Weiss, 1999; Quattrocchio et al., 1999). The inheritance of anthocyanin pigmentation is found to be controlled by multiple independent genes. At least 35 genes are known to affect flower colour in petunia (Wiering and de Vlaming, 1984). Some genes in *Petunia*, playing a role in determining pH and vacuolar pH values, are closely correlated with flower colour. In 1999, the latest reports of anthocyanin structures in that plant included the following: the 3-glucosides of the six common anthocyanidins; the 3-rutinosides of delphinidin, cyanidin, petunidin and pelargonidin; the 3-sophorosides of cyanidin and peonidin; the 3-gentiobioside and the 3,7-diglucoside of cyanidin; the 3-rutinoside-5-glucosides and the 3-(*E* or *Z*)-*p*-coumaroylrutinoside-5-glucosides of cyanidin, peonidin, petunidin, delphinidin and malvidin; the 3-caffeoylrutinoside-5-glucosides of malvidin, petunidin and peonidin; the 3-glucosyl-*p*-coumaroylrutinoside-5-glucosides of malvidin, petunidin and delphinidin; the 3-glucosyl-caffeoylrutinoside-5-glucosides of malvidin and petunidin (Wiering and de Vlaming, 1984; Griesbach et al., 1991; Ando et al., 1999; Tatsuzawa et al., 2000). Recently, six diacylated malvidin, petunidin and delphinidin derivatives have been fully characterized as the 3-caffeoylglucosyl-caffeoylrutinoside-5-glucosides of malvidin and petunidin, the 3-caffeoylglucosyl-*p*-coumaroylrutinoside-5-glucosides of malvidin, petunidin and delphinidin, and the 3-caffeoylglucosyl-*p*-coumaroylrutinoside of malvidin (Tatsuzawa et al., 1997, 1999, 2000; Fukui et al., 1998; Ando et al., 1999). In this paper, we report the isolation and the structural elucidation of two new diacylated malvidins in the violet flowers of *Petunia hybrida* cv Festival.

2. Results and discussion

Violet flower petals were extracted with methanol containing HCl (0.2%). Four major anthocyanins were isolated from the crude extract by preparative HPLC and identified as **1** (relative abundance 16%), **2** (69%), **3** (10%) and **4** (5%). The structure determination of these anthocyanins was performed by UV-visible, mass and NMR spectroscopies. **1** and **2** were identified, respectively, as petunidin 3-*O*-(6-*O*-(4-*O*-(4-*O*-(6-*O*-caffeoyl-β-D-glucopyranosyl)-E-*p*-coumaroyl)-α-rhamnosyl)-β-D-glucopyranoside)-5-*O*-β-D-glucopyranoside and malvidin 3-*O*-(6-*O*-(4-*O*-(4-*O*-(6-*O*-caffeoyl-β-D-glucopyranosyl)-E-*p*-

* Corresponding author. Tel.: +33-3-9024-1342/43; fax: +33-3-9024-1341/5001.

E-mail address: brouil@chimie.u-strasbg.fr (R. Brouillard).

0031-9422/01/$ - see front matter © 2001 Elsevier Science Ltd. All rights reserved.
PII: S0031-9422(01)00280-1

coumaroyl)-α-rhamnosyl)-β-D-glucopyranoside)-5-*O*-β-D-glucopyranoside by multiple spectral analysis (NMR, UV, MS and HPLC) but have been previously reported (Table 1) (Fukui et al., 1998; Ando et al., 1999). Two new structures, pigments **3** and **4**, were elucidated by comparison of their characteristic spectral features with those of **2**.

2.1. Pigment *3*

The UV-visible spectrum of **3** features a maximum at 543 nm and a UV-band at 285 nm. A ratio A_{440}/A_{543} of 12% indicates the presence of an anthocyanin 3,5-diglucoside and a ratio A_{UV}/A_{543} of 108% provides evidence that **3** has two acyl groups per molecule (Harborne, 1967). The FAB mass spectrum shows a molecular ion peak $[M]^+$ at 1285 *m*/*z*, corresponding to the molecular formula $C_{60}H_{69}O_{31}$ (Table 1).

Full assignment of the ^1H NMR and the ^{13}C NMR signals of **3** using H,H-COSY, H,H-ROESY, 2D-HMQC and 2D-HMBC has been carried out (Table 2). The downfield part of the ^1H NMR spectrum showed a 1H singlet at 8.92 ppm (*s*, H-4), a 2H singlet at 7.85 ppm (*s*, H-2′/H-6′) a 1H doublet at 7.02 ppm (*d*, $J=2$ Hz, H-6) and a 1H doublet at 6.98 ppm (*d*, $J=2$ Hz, H-8). An additional 6H singlet at 3.94 ppm was attributed to C-3′ and C-5′ methoxyl protons. These findings correspond to the malvidin aglycone. The observation of two sets of olefinic proton signals at 5.85 and 7.33 ppm (*d*, $J=16$ Hz) and at 6.21 and 7.48 ppm (*d*, $J=16$ Hz) indicated the presence of two cinnamic acid residues both in the *E* configuration. The first set was assigned to the *p*-coumaric acyl group. The second set was assigned, by analysis of its H,H-COSY, H,H-ROESY and HMBC spectra, to ferulic acid: a 3H singlet at 3.69 ppm was attributed to the methoxyl protons of the ferulic acyl group. These protons correlated in the H,H-ROESY spectrum with the proton H-2 of the ferulic acid moiety, and in the 2D-HMBC spectrum with the C-3 carbon of the ferulic acid moiety (Figure 1). The signal of four anomeric protons of **3**, corresponding to three glucosyl groups and one rhamnosyl group, appeared at 5.57 ppm (*d*, $J=7.7$ Hz, Glc-A), 5.21 ppm (*d*, $J=7.7$ Hz, Glc-B), 4.92 ppm (*d*, $J=7.5$ Hz, Glc-C) and 4.79 (*d*, $J=1.4$ Hz, Rha) (Table 2). The assigned glucose protons had coupling constants between 7.5 and 12.2 Hz suggesting that these glucose moieties were in the β-D-glucopyranose form. In the rhamnose moiety, the coupling constant of the anomeric proton (*d*, $J=1.4$ Hz) and the 3H doublet at 0.98 ppm (*d*, $J=6.2$ Hz, Rha–CH_3) indicated the existence of the α-rhamnopyranose form. H,H-ROESY and 2D-HMBC spectra were used to distinguish the connection sites of the cinnamic acid moieties, of the sugars and of the malvidin aglycone (Fig. 1). The signal of the anomeric proton of Glc-A correlates to the signal of the C-3 carbon, in the HMBC spectra, and to the signal of the H-4 proton in the ROESY spectrum of malvidin. The signal of the anomeric proton of Glc-B was correlated to the signal of the C-5 carbon in the HMBC spectra, and to the different signals of the protons H-6/H-8, in the ROESY spectrum of malvidin. These characteristic features revealed that malvidin 3- and 5- positions are both connected to a glucose. A cross-peak between the anomeric proton of the rhamnose at 4.79 ppm and the C-6 carbon of the Glc-A at 66.7 ppm in the HMBC spectra, revealed the linkage between these two groups. A downfield shift of proton H-4 of the rhamnose and a correlation in the HMBC spectra between this signal and the carbonyl carbon of the *p*-coumaric acid moiety revealed their connection site. A NOE effect was observed between the anomeric proton of Glc-C and the protons H-3/H-5 of the *p*-coumaric acid moiety, and a cross-peak in the HMBC spectra between this same anomeric proton and the carbon C-4 of the *p*-coumaric acid moiety, indicating that Glc-C was glycosylated on OH-4 of the *p*-coumaric acid. A downfield shift of the protons H-6 of Glc-C and a correlation in the HMBC spectra between these signals and the carbonyl carbon of the ferulic acid moiety, revealed the linkage between these two groups.

The structure of **3** was therefore determined as malvidin 3-*O*-(6-*O*-(4-*O*-(4-*O*-(6-*O*-feruloyl-β-D-glucopyranosyl)-*E*-*p*-coumaroyl)-α-rhamnosyl)-β-D-glucopyranoside)-5-*O*-β-D-glucopyranoside, which is a new anthocyanin.

Table 1
Spectral properties of anthocyanins extracted from violet petals of *Petunia hybrida* cv Festival

Anthocyanin	Spectral data in 0.1% HCl–MeOH				Rt[a] (min)	FAB–MS $[M]^+$
	λ_{max} (nm)	A_{UV}/A_{max} (%)	A_{440}/A_{max} (%)	$AlCl_3$		
1	543, 284	101	14	+	17.1	1257
2	544, 284	103	12	0	19.5	1271
3	543, 285	108	12	0	23.0	1285
4	543, 288	106	13	0	24.0	1255

[a] Column: Merck LiChrospher C_{18} (125×4 mm, 5 μm); for more details, see Experimental.

2.2. Pigment *4*

The UV-visible spectrum of **4** appeared to be very similar to that of **3**, showing a visible maximum at 543 nm and a UV band at 288 nm. A ratio A_{440}/A_{543} of 13% indicates the presence of an anthocyanin 3,5-diglycoside and the ratio A_{UV}/A_{543} of 106% provides evidence that **4** has two acyl groups per molecule. The FAB mass spectrum of **4** features a molecular ion peak $[M]^+$ at 1255 corresponding to the molecular formula $C_{59}H_{67}O_{30}$, 30 mass units lower than that of **3** (Table 1).

The different NMR spectral data of **4** are similar to those of **3**, except for the terminal moiety that was

Table 2
^{1}H and ^{13}C NMR spectral data of anthocyanins **3** and **4**

		3			**4**	
	Positions	δ ^{1}H	Signal: *J* (Hz)	δ ^{13}C	δ ^{1}H	Signal: *J* (Hz)
Malvidin						
	2			163.5		
	3			146.3		
	4	8.92	s	133.8	8.94	*s*
	5			156.5		
	6	7.02	*d*: 2	105.7	7.02	*m*
	7			169.5		
	8	6.98	*d*: 2	97.7	7.02	*m*
	9			157.3		
	10			113.0		
	1′			119.6		
	2′ and 6′	7.85	*s*	110.8	7.89	*s*
	3′ and 5′			149.8		
	4′			147.3		
	OCH3	3.94	*s*	57.4	3.93	*s*
Glucose A						
	1	5.57	*d*: 7.7	102.9	5.52	*d*: 7.7
	2	3.74	*t*: 8	75.0	3.72	*t*: 8
	3	3.64	*t*: 8	78.3	3.64	*t*: 8
	4	3.67	*t*: 8	70.5	3.72	*t*: 8
	5	3.86	*m*	77.3	3.83	*m*
	6a	4.11	*dd*: 12.2	66.7	4.10	*dd*: 12
	6b	3.84	*m*		3.86	*m*
Glucose B						
	1	5.21	*d*: 7.7	102.6	5.23	*d*: 7.7
	2	3.68	*t*: 8	75.0	3.70	*t*: 8
	3	3.60	*t*: 8	78.8	3.60	*t*: 8
	4	3.55	*t*: 8	71.2	3.55	*t*: 8
	5	3.63	*m*	78.2	3.62	*m*
	6a	3.97	*dd*: 12.2	62.3	3.95	*dd*: 12
	6b	3.78	*m*		3.85	*m*
Glucose C						
	1	4.92	*d*: 7.5	101.6	4.98	*d*: 7.6
	2	3.53	*m*	74.7	3.56	*t*: 8
	3	3.53	*m*	78.1	3.53	*m*
	4	3.40	*t*: 8.9	72.4	3.40	*t*: 8.8
	5	3.79	*t*: 8.9	75.5	3.80	*m*
	6a	4.55	*dd*: 12.2	65.0	4.55	*dd*: 11;1.8
	6b	4.38	*dd*: 12.2		4.32	*dd*: 11
Rhamnose						
	1	4.79	*d*: 1.4	102.2	4.79	*d*: 1.3
	2	3.89	*m*	72.2	3.95	*m*
	3	3.90	*m*	70.4	3.87	*m*
	4	4.89	*t*: 9.5	75.6	4.91	*t*: 9.4
	5	3.85	*m*	67.8	3.92	*m*
	6	0.98	*d*: 6.2	19.8	0.98	*d*: 6
Coumaroyl						
	1			129.7		
	2 and 6	7.23	*d*: 9	130.8	7.26	*d*: 9
	3 and 5	7.03	*d*: 9	118.3	7.02	*d*: 9
	4			160.6		
	α	5.85	*d*: 16	116.8	5.96	*d*: 16
	β	7.33	*d*: 16	145.8	7.37	*d*: 16
	C=O			168.7		

(*continued on next page*)

Table 2 (*continued*)

	3			4	
Positions	δ ^{1}H	Signal: *J* (Hz)	δ ^{13}C	δ ^{1}H	Signal: *J* (Hz)
*Feruloyl (**3**) or coumaroyl (**4**)*					
1			127.7		
2	6.89	*d*: 1.8	110.9	7.19	*d*: 8.6
3			148.8	6.64	*d*: 8.6
4			150.2		
5	6.58	*d*: 8	116.5	6.64	*d*: 8.6
6	6.78	*dd*: 8; 1.8	123.8	7.19	*d*: 8.6
α	6.21	*d*: 16	115.6	6.17	*d*: 16
β	7.48	*d*: 16	146.7	7.44	*d*: 16
C=O			168.7		
OCH3	3.69	*s*	56.5		

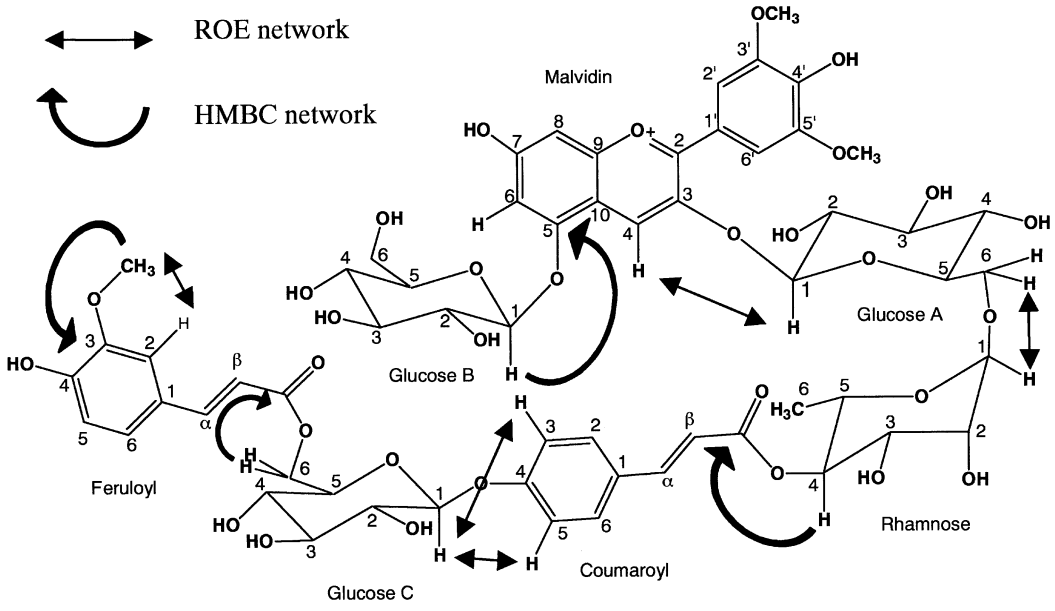

Fig. 1. Structure of **3**. Arrows feature some important ROE and HMBC networks.

demonstrated not to be a ferulic residue (Table 2). A 2H doublet at 6.64 ppm (*d*, $J = 8.6$ Hz) and a 2H doublet at 7.19 ppm (*d*, $J = 8.6$ Hz) were assigned, respectively, to the protons H-3/H-5 and H-2/H-6 of a *p*-coumaric acid moiety. The set of olefinic proton signals at 6.17 and 7.44 ppm (*d*, $J = 16$ Hz) determines the *E* configuration of the *p*-coumaric acid moiety. The connecting sites were confirmed by different NMR methods. These findings indicate that the ferulic acid moiety in **3** is replaced by the *E*-*p*-coumaric acid moiety in **4** (Fig. 2).

The structure of **4** was therefore deduced to correspond to malvidin 3-*O*-(6-*O*-(4-*O*-(4-*O*-(6-*O*-*E*-*p*-coumaroyl-β-D-glucopyranosyl)-*E*-*p*-coumaroyl)-α-rhamnosyl)-β-D-glucopyranoside)-5-*O*-β-D-glucopyranoside, which is a new anthocyanin.

The four anthocyanins extracted from petals of the violet flower of *Petunia hybrida* cv Festival are very similar and only differ by one or two atoms (Fig. 2). Two novel structures of diacylated anthocyanins, together with two already known diacylated anthocyanins, were elucidated in this work.

3. Experimental

3.1. Plant material

Plant pots of *Petunia hybrida* cv Festival were grown in window boxes on the balcony of one of the authors (E.G.). Fresh violet petals were collected during the July–September 1999 period and stored at −18 °C in a plastic bag.

3.2. Isolation

Thirty grams of violet flower petals were extracted with 200 ml of 0.2% (v/v) HCl–MeOH for 4 h at +4 °C (three times). After removal of methanol under reduced

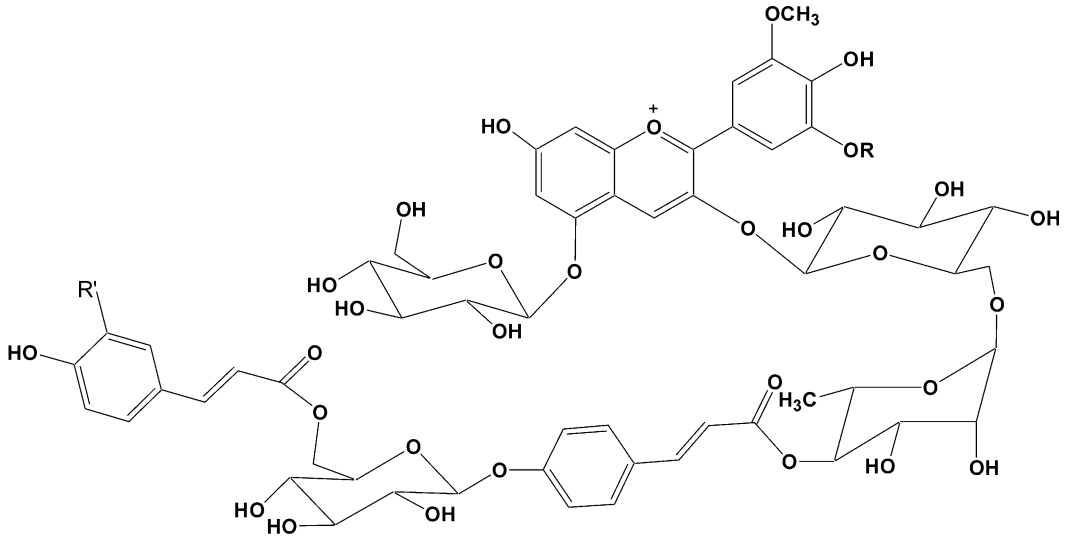

Fig. 2. Anthocyanins from violet petals of *Petunia hybrida* cv Festival. Pigments **1** R = H, R′ = OH; **2** R = CH_3, R′ = OH; **3** R = CH_3, R′ = OCH_3; **4** R = CH_3, R′ = H.

pressure, the water enriched extract was partitioned against ethyl acetate and 1.04 g of crude extract was obtained. The different pigments were purified by preparative HPLC on a Waters SymetryPrep C_{18} column (300×19 mm, 7 μm) connected to a Gilson 305/306 apparatus equipped with a UV detector monitoring at 280 nm. The solvent systems used were as follows: a linear gradient elution for 25 min from 20 to 40% solvent B (95% H_2O, 5% HCOOH) in solvent A (47.5% CH_3CN, 47.5% H_2O, 5% HCOOH). The flow rate was 10 ml/min. 125 mg of the filtered extract were dissolved in 500 μl of solvent B then were injected through a Rheodyne injector. The pigment fractions were evaporated in vacuum to dryness. **1** (6.1 mg), **2** (26.4 mg), **3** (3.8 mg) and **4** (2.0 mg) were isolated from the crude extract.

3.3. HPLC analysis

Anthocyanins were analysed by HPLC on a Merck LiChrospher C_{18} column (125×4 mm, 5 μm) connected to a LC Spectra Physics apparatus equipped with a 1040M Hewlett Packard diode array detector. Solvents and gradient elution profiles were the same as for preparative HPLC. The flow rate was 0.5 ml/min.

3.4. Spectral analysis

NMR spectra were run at 298 K on a Bruker AM-500 spectrometer at 500 and 125 MHz for ^1H and ^{13}C, respectively, in a 2.5 mm diam. tube using 10% (v/v) TFA-d/CD_3OD as solvent. Chemical shifts were reported relative to a TMS internal standard. Mass spectra were recorded in the positive mode from an AutoSpec E Micromass spectrometer using a NBA matrix.

Acknowledgements

This work is supported by a grant from the EU (BIO4 CT98).

References

Ando, T., Saito, N., Tatsuzawa, F., Kakefuda, T., Yamakage, K., Ohtani, E., Koshi-ishi, M., Matsusake, Y., Kokubun, H., Watanabe, H., Tsukamoto, T., Ueda, Y., Hashimoto, G., Marchesi, E., Asakura, K., Hara, R., Seki, H., 1999. Floral anthocyanins in wild taxa of *Petunia* (Solanaceae). Biochem. System. Ecol. 27, 623–650.

Dooner, H.K., Robbins, T.P., Jorgensen, R.A., 1991. Genetic and developmental control of anthocyanin biosynthesis. Annu. Rev. Genet. 25, 173–199.

Fukui, Y., Kusumi, T., Yoshida, K., Kondo, T., Matsuda, C., Nomoto, K., 1998. Structures of two diacylated anthocyanins from *Petunia hybrida* cv. Surfinia Violet Mini. Phytochemistry 47, 1409–1416.

Griesbach, R.J., Asen, S., Leonnarat, B.A., 1991. *Petunia hybrida* anthocyanins acylated with caffeic acid. Phytochemistry 30, 1729–1731.

Harborne, J.B., 1967. Comparative Biochemistry of the Flavonoids. Academic Press, London.

Katz, A., Weiss, D., 1999. Light regulation of anthocyanin accumulation and chalcone synthase gene expression in *Petunia* flowers. Isr. J. Plant Sci. 47, 225–229.

Quattrocchio, F., Wing, J., Van der Woude, K., Souer, E., de Wetten, N., Mol, J., Koes, R., 1999. Molecular analysis of the anthocyanin2 gene of *Petunia* and its role in the evolution of flower colour. Plant J. 11, 1433–1444.

Sink, K.C., 1984. Taxonomy. In: Sink, K.C. (Ed.), *Petunia*. Springer-Verlag, Berlin, pp. 3–9.

Tatsuzawa, F., Koshiishi, M., Ohtani, E., Ando, T., Watanabe, H., Kokubun, H., Yokoi, M., Hashimoto, G., Seki, H., Saito, N., Honda, T., 1997. Diacylated malvidin 3-rutinoside-5-glucosides from the flowers of *Petunia guarapuavensis*. Heterocycles 45, 1197–1202.

Tatsuzawa, F., Ando, T., Saito, N., Yoda, K., Kokubun, H., Watanabe, H., Hashimoto, G., Asakura, K., Hara, R., Seki, H., 1999.

Acylated malvidin 3-rutinosides in dusky violet flowers of *Petunia integrifolia* subsp. *Inflata*. Phytochemistry 52, 351–355.

Tatsuzawa, F., Ando, T., Saito, N., Kanaya, T., Kokubun, H., Tsunashima, Y., Watanabe, H., Hashimoto, G., Hara, R., Seki, H., 2000. Acylated delphinidin 3-rutinoside-5-glucosides in the flowers of *Petunia reitzii*. Phytochemistry 54, 913–917.

Wiering, H., de Vlaming, P., 1984. Inheritance and biochemistry of pigments. In: Sink, K.C. (Ed.), *Petunia*. Springer-Verlag, Berlin, pp. 49–76.

PERGAMON

Phytochemistry 58 (2001) 1263–1266

PHYTOCHEMISTRY

www.elsevier.com/locate/phytochem

An immunosuppressive tryptophan-derived alkaloid from *Lepidagathis cristata*

V. Ravikanth[a], V. L. Niranjan Reddy[a], P. Ramesh[a], T. Prabhakar Rao[a], P. V. Diwan[a], Ashok Khar[b], Y. Venkateswarlu[a,*]

[a]*Indian Institute of Chemical Technology, Hyderabad, 500 007 India*
[b]*Center for Cellular and Molecular Biology, Hyderabad, 500 007 India*

Received in revised form 3 July 2001

Abstract

An immunosuppressive, tryptophan-derived alkaloid cristatin A (**1**), and two known compounds, cycloartenol and stigmasta-5,11(12)-diene-3β-ol, were isolated from the whole plant *Lepidagathis cristata* Willd. The structures of the isolates were established by interpretation of their spectral data. © 2001 Elsevier Science Ltd. All rights reserved.

Keywords: *Lepidagathis cristata*; Acanthaceae; Cristatin A; Cycloartenol; Stigmasta 5,11(12)-dien-3β-ol; Immunosuppressive activity

1. Introduction

In the Indian system of medicine, the whole plant *Lepidagathis cristata* Willd. (Acanthaceae) is used as a remedy for skin infections and fever (Ambasta, 1992; Nadakarni and Chopra, 1996). It is a perennial, procumbent herb common in the dry places on rocks and wastelands in most districts of Andhra Pradesh, India. A literature survey has revealed that this plant afforded 6-hydroxyluteolin and 6-hydroxyluteolin-7-*O*-D apioside (Ranganathan et al., 1980). In continuation of our search for new, biologically active compounds from natural sources (Reddy et al., 1999), we have re-examined the whole plant *Lepidagathis cristata*, which afforded a new tryptophan-derived alkaloid cristatin A (**1**) and two known compounds cycloartenol (Radics et al., 1975) and Stigmasta-5,11(12)-dien-3β-ol (Alam et al., 1994). We have also examined the immunosuppressive activity of the new alkaloid **1**.

2. Results and discussion

2.1. Isolation and characterization of cristatin A (*1*)

The freshly collected, shade-dried and powdered whole plant of *L. crisata* was extracted separately with hexane and ethyl acetate. These extracts were subjected to silica gel column chromatography to afford a new tryptophan-derived alkaloid cristatin A (**1**) and two known compounds cycloartenol (Radics et al., 1975) and stigmasta-5,11(12)-dien-3β-ol (Alam et al., 1994). These two known compound structures were deduced by comparison of the obtained NMR and mass spectra with those reported in the literature.

Alkaloid **1** was obtained as a pale yellow solid, mp 260 °C, $[\alpha]_D^{25}$ +1.2° (c 0.25, $CHCl_3$) analyzing for $C_{29}H_{37}N_3O_2$ by HREIMS which indicated 13° of unsaturation. Its ^{13}C NMR spectrum (Table 1) displayed 29 carbons, of which sixteen sp^2 carbons appeared between δ 102 and 145, in addition to two amide carbonyl signals at δ 160.00 and 165.70. Thus the molecule is tricyclic.

The ^1H NMR spectrum of alkaloid **1** showed signals (Table 1) for a trisubstituted double bond proton at δ 7.18 (1H, s), two *ortho*-coupled aromatic protons at δ 7.05 (1H, d, $J=8.2$ Hz) and δ 6.98 (1H, *d*, $J=8.2$ Hz), a 1′,1′ dimethyl allyl group, two isopentenyl groups, a secondary

* Corresponding author. Tel.: +91-40-71-705-12; fax: +91-40-71-737-57/71-733-87.
E-mail address: luchem@iict.ap.nic.in (Y. Venkateswarlu).

0031-9422/01/$ - see front matter © 2001 Elsevier Science Ltd. All rights reserved.
PII: S0031-9422(01)00383-1

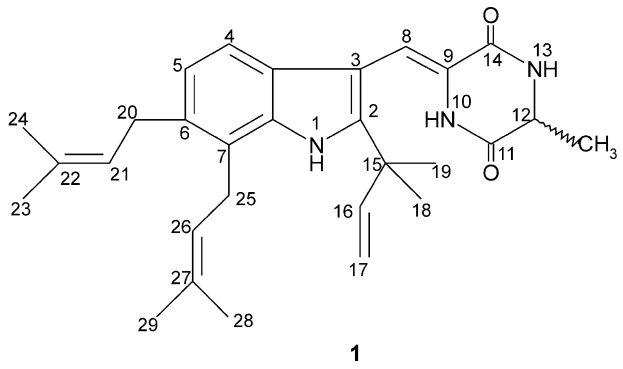

1

methyl group at δ 4.28 (1H, *q*, $J = 7.0$ Hz), and 1.59 (3H, *d*, $J = 7.0$ Hz), and three protons at δ 8.37 (1H, *s*), 7.48 (1H, *s*) and 6.88 (1H, *s*). Among these, the protons at δ 7.48 and 6.88 were exchanged with D_2O. A survey of the literature revealed that alkaloid **1** belongs to the echinulin class [*cyclo*-L-alanyl-5,7-diisopentenyl-2-(1′,1′-dimethyl allyl)-L-tryptophan] (Takamatsu, 1971) isolated from the fungus *Aspergilus echinulatus*, and to a related alkaloid tardioxopiperazine A [*cyclo*-L-alanyl-5-isopentenyl-2-(1′,1′-dimethyl allyl)-L-tryptophan] isolated from the ascomycete, *Microascus tardifaciens* (Fujimoto et al., 1999).

The structure **1** was established through the application of spectroscopic techniques, including ^1H and ^{13}C-NMR analysis. With the aid of DEPT, COSY, HMQC, HMBC, and NOE pulse sequences, the multiplicity of the proton peaks, their inter relationship and the identity of each carbon and hydrogen could be established (Fujimoto et al., 1999).

The spectral data revealed that the alkaloid **1** must have a partial structure containing a 2,3,4,5 or a 2,3,6,7-tetra substituted indole. In HMBC correlations the C-8 vinylic proton at δ 7.18 showed correlations with C-2 (142.8), C-9 (124.1), and C-14 (160.0). Thus, the signal at δ 7.18 (1H, *s*) could be due to the presence of a double bond between C-8 and C-9 carbons in alkaloid 1 as observed in dopadazine, a diketopiperazine from *Penicillium dipodomyis* and the stereochemistry at C-8, 9

Table 1
^1H and ^{13}C NMR spectral data for alkaloid **1**

Position	^1H NMR	^{13}C NMR	HMBC
NH-1	8.37 (*s*)	–	C2, C7a, C3a, C3
C2	–	142.9	
C3	–	102.9	
C3a	–	123.9	
C4	7.05 (*d*, $J = 8.2$ Hz)	123.3	C7a
C5	6.98 (*d*, $J = 8.2$ Hz)	116.7	C6, C3a, C20
C6	–	121.5	
C7	–	133.3	
C7a	–	134.6	
C8	7.18 (*s*)	112.3	C11, C14, C2, C9
C9	–	124.1	
NH-10	7.48 (*s*)	–	C11, C14, C12
C11	–	165.7	
C12	4.28 (*q*, $J = 7.0$ Hz)	51.6	C11, C14, C12-CH_3
CH_3-12	1.59 (*d*, $J = 7.0$ Hz)	20.8	C11, C12
NH-13	6.88 (*s*)	–	
C14	–	160.0	
C15	–	39.2	
C16	6.04 (*m*)	144.5	C15, C18, C19
C17	5.16 (*dd*, $J = 14.5$, 0.7, Hz)	113.0	C16, C15
	5.19 (*dd*, $J = 7.7$, 0.7 Hz)		
C18	1.60 (*s*)	27.3	C16, C2, C15
C19	1.60 (*s*)	27.3	
C21	3.43 (*d*, $J = 7.1$ Hz)	31.8	C7, C22, C6
C22	5.22 (*m*)	124.5	C20, C22, C23
C23	–	131.4	
C24	1.70 (*s*)	18.0	C22, C21
C25	1.74 (*s*)	17.9	C22, C21
C26	3.57 (*d*, $J = 7.1$ Hz)	27.2	C7a, C7, C27, C26, C6
C27	5.31 (*m*)	123.0	C25, C28, C29
C28	–	132.6	
C29	1.89 (*s*)	25.7	C27, C26

Values are recorded at 500 MHz (in $CDCl_3$ in the δ scale, with *J* values in Hz in parentheses). HMBC ($J = 7$ Hz).

indicates Z-configuration (Sorensen et al., 1999). The disposition of the two-isopentenyl groups was determined by NOED experiments. Irradiation of the C-25 methylene protons at δ 3.43 (2H, *d*, $J=7.1$ Hz) caused an enhancement of the indole NH signal at δ 8.37 (1H, *s*) and the C-26 vinylic proton at δ 5.31 (1H, *m*). Irradiation of the C-20 methylene protons at δ 3.57 (2H, *d*, $J=7.1$ Hz) caused an enhancement of the signal at δ 6.98 (1H, *d*, $J=8.2$ Hz, 5-H) and the C-21 vinylic proton at δ 5.22 (1H, *m*), indicating that the two isopentenyl groups are situated at the C-6 and C-7 positions. In the HMBC spectrum, the secondary methyl at δ 1.56 (3H, *d*, $J=7$ Hz) showed correlations with C-11 (165.7 *s*) and C-12 (51.6, *d*). The ^{1}H NMR and ^{13}C chemical shifts of the C-12 methyl of alkaloid **1** are comparable with those of reported data for echinulin isolated from an ascomycete, *Microascus tardifaciens* (Fujimoto et al., 1999) for which the stereochemistry was not assigned. From the fore-going spectral data the structure of cristatin A (**1**) was established as (*cyclo*-alanyl-6,7-disiopentenyl-2-(1′,1′-dimethylallyl-8-(*Z*)-ene-tryptophan).

2.2. Immunosuppressive activity

Fujimoto et al., recently reported that echinulin type alkaloids exhibit immunosuppressive activity (Fujimoto et al., 1999) using mouse splenic lymphocytes. The immunosuppressive activity (IC_{50}) of alkaloid **1** was assayed against Con A- (T-cells) and LPS-induced (B-cells) proliferation of mouse splenic lymphocytes, here Con A and LPS were used as controls and cyclosporin A was used as standard drug. The immunosuppressive activity of alkaloid **1** (IC_{50}) against Con A and LPS induced proliferation is higher (1 μg/ml) than the immunosuppressive activity of tardioxopiperzine A against Con A LPS induced proliferation (IC_{50} 4.5 and 0.7 μg/ml) (Fujimoto et al., 1999) and lower than that of cyclosporin A (IC_{50} 0.06 and 0.10 μg/ml). To our knowledge this is the first report of isolation of this class of alkaloid with immunosuppressive activity from plant sources.

3. Experimental

3.1. General

The ^{1}H NMR and ^{13}C NMR spectra were recorded on a Varian Unity INOVA 500 MHz spectrometer with standard pulse sequences, operating at 500 and 125 MHz, respectively and all 1D and 2D spectra (^{1}H–^{1}H COSY, NOED, HMQC and HMBC) were recorded using tetramethylsilane (TMS) as an internal standard. Chemical shifts are reported in parts per million, and coupling constants (*J*) are expressed in Hz. UV and IR spectra were recorded on Shimadzu 240 and Perkin–Elmer RXI FT-IR spectrophotometers, respectively. Mass spectra were recorded on a Finnigan-MAT 1020 instrument. Optical rotations were measured on a JASCO DIP-370 polarimeter.

3.2. Plant material

The plant material *Lepidagathis cristata* (Acanthaceae) was collected from, Bhadrachalam forest, Andhra Pradesh, India in December, 1998, and identified by Professor M. Prabhakar Rao, Department of Botany, Osmania University, Hyderabad, India. The voucher specimen (No. 002319) is kept in the herbarium of department of Botany, Osmania University.

3.3. Extraction and isolation

The shade-dried and powdered plant (750 g) *Lepidagathis cristata* was successively refluxed with hexane and ethyl acetate (3×1.5 l). The hexane extract (8 g) was subjected to silica gel chromatography eluting with hexane through hexane-ethyl acetate mixtures to ethyl acetate afforded stigmasta-5,11(12)-dien-3β-ol (100 mg). The ethyl acetate extract (17 g) was subjected to silica gel chromatography eluting with hexane through hexane-ethyl acetate mixtures to ethyl acetate to give two fractions. Fr-1 (hexane/EtOAc, 8:2) was futher CC on silica gel to afford cycloartenol (110 mg) and fr-2 (hexane/EtOAc, 6:4) was further CC on silica gel to afford alkaloid **1** (40 mg).

3.4. Cristatin A (*1*)

Obtained as a yellow solid (40 mg), mp 260 °C; $[\alpha]_D^{25}+1.2°$ (c 0.25, $CHCl_3$); UV ($CHCl_3$) λ_{max} (log ϵ) 208 (4.37), 222 (4.39), 290 (3.866), 330 (3.808); IR (KBr) ν_{max} 3367, 2967, 2926, 2361, 1685, 1636, 1438, 1380, 1326, 1039, 901, 766, 667, 492 cm^{-1}; ^{1}H and ^{13}C NMR spectral data, see Table 1; EIMS *m*/*z* (%) 459 (M^+ 66), 390 (11), 334 (8); HREIMS *m*/*z* 459.2872 [M^+] (calcd. for $C_{29}H_{37}N_3O_2$, 459.2885).

3.5. Immunosuppressive activity

Mouse splenic lymphocytes were prepared on a Ficoll–Hypaque gradient and plated in DMEM-FCS (1×10^5 cells/well). The cells were grown for 24 h with Con A (2 μg/ml) and LPS (100 ng/ml). After 24 h, the cells were treated with different concentrations of cristatin A (**1**) (0.1–5 μg/ml) and cyclosporin A (0.06–0.5 μg/ml) for 24 h. Subsequently, the cells were treated with ^{3}[H]-thymidine (10 μci/well) and incubated further for 24 h in a CO_2 incubator. The cells were harvested on GF filters, washed with 5% TCA and methanol, and counted for radioactivity.

Acknowledgements

We are thankful to Professor M. Prabhakar Rao, Department of Botany, Osmania University, Hyderabad, India, for identifying the plant; the Director, IICT and Dr. J. S. Yadav for their constant encouragement. VR and VLNR are thankful to CSIR, New Delhi and Ministry of Health, New Delhi for providing fellowships, respectively.

References

Alam, M.S., Chopra, N., Ali, M., Niwa, M., Sakae, T., 1994. Ursane and sterol derivatives from *Pleuchea lanceolata*. Phytochemistry 37 (2), 521–534.

Ambasta, S.P., 1992. In The Useful Plants of India, (pp 323). CSIR, New Delhi, India.

Fujimoto, H., Fujimaki, T., Okuyama, E., Yamazaki, M., 1999. Immunomodulatory constituents from an Ascomycete, *Microascus tardifaciens*. Chem. Pharm. Bull. 47 (10), 1426–1432.

Nadakarni, K.M., Chopra, R.N., 1996. In Indian Materia Medica, (pp 735). Popular Prakasan Pvt. Ltd., Mumbai, India.

Radics, L., Kajtar-Perdedy, M., Corsano, S., Standoli, L., 1975. Carbon-13 NMR spectra of polycyclic triterpenoids. Tetrahedron Lett. 48, 4287–4290.

Ranganathan, R.M., Nagarajan, S., Mabry, T.J., Yong-Long, L., Newman, P., 1980. 6-Hydroxy luteolin 7-O-apioside from *Lepidagathis cristata*. Phytochemistry 19, 2505–2506.

Reddy, M.V.R., Rao, M.R., Rhodes, D., Hansen, M., Rubnis, K., Bushman, F., Venkateswarlu, Y., Faulkner, D.J., 1999. Lamellarin-α 20-sulphate, an inhibitor of HIV-1 integrase active against HIV-1 virus in cell culture. J. Med. Chem. 42, 1901–1907.

Sorensen, D., Larsen, O.T., Chritophersen, C., Nielsen, H.P., Anthoni, U., 1999. Dipodazine, a diketopiperazine from *Pencillium dipodomyis*. Phytochemistry 51, 1181–1183.

Takamatsu, N., Inove, S., Kishi, Y., 1971. Synthetic study on echinulin and related compounds. Part II. A stereo-selective total synthesis of optically active echinulin. Tetrahedron Lett., 4665–4668.

PERGAMON

Phytochemistry 58 (2001) 1267–1269

PHYTOCHEMISTRY

www.elsevier.com/locate/phytochem

Alkaloids from *Cynanchum komarovii* with inhibitory activity against the tobacco mosaic virus

Tian-ying An[a], Run-qiu Huang[a], Zhao Yang[a], Dian-kun Zhang[a], Guang-ren Li[a,*], Yu-cheng Yao[b], Jun Gao[b]

[a]*Research Institute of Elemento-Organic Chemistry, Nankai University, Tianjin, 300071, People's Republic of China*
[b]*Inner Mongolia Polytechnic University, Huhehaote, Autonomous Region of Inner Mongolia, 010062, People's Republic of China*

Received 20 April 2001; received in revised form 6 August 2001

Abstract

A pyrroloisoquinoline alkaloid, 2,3-dimethoxy-6-(3-oxo-butyl)-7,9,10,11,11a,12-hexahydrobenzo[*f*]pyrrolo[*1,2-b*]isoquinoline (**1**), whose structure was determined by spectroscopic methods, was isolated from the aerial parts of *Cynanchum komarovii*, together with two known alkaloids, 7-demethoxytylophorine (**2**) and 7-demethoxytylophorine *N*-oxide (**3**). Alkaloids **2** and **3** had antiviral activities against tobacco mosaic virus. © 2001 Elsevier Science Ltd. All rights reserved.

Keywords: Pyrroloisoquinoline; Phenanthroindolizidines; Tobacco mosaic virus; *Cynanchum komarovii*; Asclepiadaceae

1. Introduction

Cynanchum komarovii Al Iljinski (Asclepiadaceae) is a wild shrub, widely distributed in the northwest part of the People's Republic of China, and is used as a Chinese herbal medicine to cure fever, diarrhea, and cholecystitis (Jiangsu New Medical College 1977). Several phenanthroindolizidine alkaloids were reported previously to occur in this species (Fang et al., 1989; Zhang et al., 1991). In the present study, an alcohol extract of *C. komarovi* was found to show moderate antiviral activity against the tobacco mosaic virus. Using a bioassay-directed fractionation approach, a new alkaloid **1** was obtained, together with two known alkaloids, 7-demethoxytylophorine **2** and 7-demethoxytylophorine *N*-oxide **3**. Alkaloid **2** was the major active substance and was more potent against TMV than **3**, whereas alkaloid **1** had no significant activity. The structures of **2** and **3** were determined by comparison with reference spectra and physical properties. (Xi et al., 1989, Zhang et al., 1991, Lavault et al.,1994). Herein we report the isolation and structure elucidation of **1**, and the activity of **1**, **2** and **3** against TMV.

2. Results and discussion

Alkaloid **1** was isolated as colorless needles from the aerial parts of *C. komarovii*. The HREIMS of **1** showed a molecular ion at *m/z* 353.1984, corresponding to the molecular formula $C_{22}H_{27}NO_3$ (calcd. as 353.1990). The presence of a naphthalene ring was suggested by the observed UV (235, 254, 315, 330 nm) (Budzikiewicz et al., 1979) and IR (1612, 1510, 1475 cm^{-1}) absorptions. A strong absorption at 1716 cm^{-1} in the IR spectrum indicated that the compound must contain a ketone carbonyl group. The ^{13}C NMR spectrum of **1** (Table 1) showed the presence of 22 carbon signals, including one carbonyl carbon (δ 208.1), three methyl carbons [of which two were oxygenated methyls (both at δ 55.8)], seven methylenes [among which two were *N*-methylenes (δ 55.0, δ 53.7)], one aliphatic methine bearing a nitrogen atom (δ 60.2), and ten aromatic carbons, including two carbons that were connected to methoxy groups (δ 149.2 and δ 149.0). The ten aromatic carbons were assigned to a naphthalene ring system. The ^1H NMR and ^1H–^1H COSY spectra of **1** showed three isolated aromatic protons at δ 7.34, δ 7.14, and δ 7.06, and three pairs of geminal protons at H_2-7 (δ 4.29 and δ 3.45), H_2-11 (δ 2.22 and δ 1.25), and H_2-12 (δ 3.30 and δ 2.86).

The ^1H NMR, ^1H–^1H COSY, ^{13}C NMR, and HMBC data of **1** (see Table 1) demonstrated the

* Corresponding author. Tel.: +86-022-23502072.
E-mail address: guangren@public.tpt.tj.cn (G. Li).

0031-9422/01/$ - see front matter © 2001 Elsevier Science Ltd. All rights reserved.
PII: S0031-9422(01)00382-X

Table 1
^{1}H NMR and ^{13}C NMR spectral data and HMBC for alkaloid **1**

Position	δ_H	δ_C	HMBC
1	7.14, *s*	102.0	3, 4a, 12a, 12b
2		149.2	
3		149.0	
4	7.06, *s*	106.6	2, 3, 4a, 5
4a		126.5	
5	7.34, *s*	124.0	4, 4a, 6a, 12b, 13
6		133.9	
6a		129.0	
7	4.29, *d*, 14.9		
	3.45, *d*, 14.9		
9	2.39, *m*	55.0	11
10	1.95, *m*	21.6	9, 11
11	1.25, *m*	31.4	9, 11a
	2.22, *m*		
11a	3.28, *m*	60.2	11
12	3.30, *m*	33.3	11, 11a, 12a,12b
	2.86, *m*		
12a		129.0	
12b		128.0	
13	2.91, *m*	26.0	5, 6, 6a, 14, 15
14	2.82, *m*	44.0	13, 15, 16
15		208.0	
16	2.15, *s*	30.1	14, 15
2-OCH_3	3.98, *s*	55.8	3
3-OCH_3	4.00, *s*	55.8	2

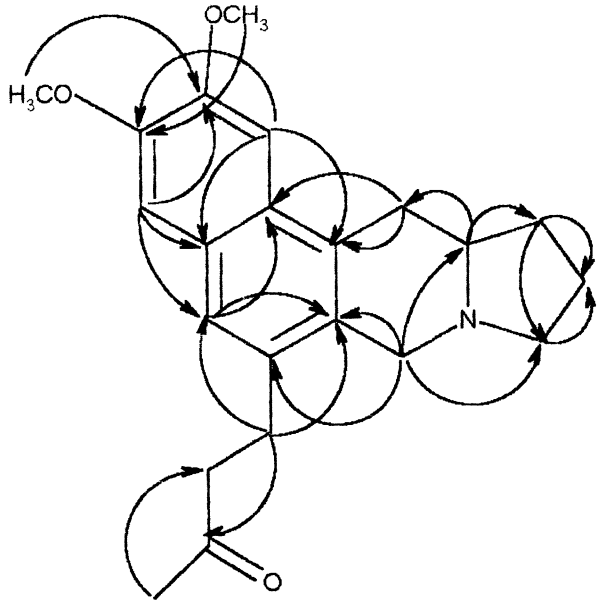

Fig. 1. Important-HMBC interactions in alkaloid **1**.

presence of a 3-oxobutyl side chain. The HMBC spectrum (Fig. 1) showed long-range correlations between H_2-7 and the carbons at δ 60.2 (C-11a), δ 55.0 (C-9), δ 133.9 (C-6), and δ 129.0 (C-6a), and correlations between H_2-12 and the carbons at δ 60.2 (C-11a), δ 31.4 (C-11), δ 129.0 (C-12a), and δ 128.0 (C-12b). In this manner, the connectivities from C-6a to C-12b could be established. The location of the 3-oxobutyl side chain at C-6 was established by analysis of the correlations between the methylene protons H_2-13 (δ 2.91) and C-5 (δ 124.0), C-6 (δ 133.9), and C-6a (δ 129.0). Accordingly, the structure of **1** was established as 2,3-dimethoxy-6-[3-oxobutyl]-7,9,10,11,11a,12- hexahydrobenzo [*f*]pyrrolo[*1,2-b*]isoquinoline. Since the NOESY spectrum did not give much information about the stereochemistry of C-11a due to overlapping of the key signal (H-11a), the stereochemistry of C-11a was not established.

Alkaloid **2** and **3** were characterized as 7-demethoxytylophorine and 7-demethoxytylophorine *N*-oxide respectively by comparing their spectral data and physical properties with that of references (Xi et al., 1989; Zhang et al., 1991; Lavault et al.,1994).

The major active alkaloid **2** exhibited 65% inhibition against the TMV at a concentration of 1.0 μg/ml. Alkaloid **3** showed 60% inhibition at 500 μg/ml and alkaloid **1** showed 15% inhibition at 500 μg/ml. A commercial antiviral agent, 2,4-dioxo-hexahydro-1,3,5-triazine, showed 50% inhibition at 500 μg/ml under the same conditions.

3. Experimental section

3.1. General experimental procedures

The melting points were determined on a Yanaco melting point apparatus and are uncorrected. Optical rotations were recorded on a Perkin-Elmer 241 MC. UV spectra were measured on a Shimadzu UV-250 spectrophotometer, and IR spectra were recorded on a Perkin-Elmer 599B spectrophotometer. NMR spectra were acquired on Bruker AC-P200, AM-400 and DRX-400 NMR spectrometers with $CDCl_3$ as solvent. Mass spectra (EIMS and HREIMS) were obtained on a MAT-7070 instrument.

3.2. Plant material

The aerial parts of *C. komarovii* were collected from the Autonomous Region of Inner Mongolia of the People's Republic of China, in August, 1996. The plant was identified by Prof. Qingru Wu (Department of Biology, Inner Mongolia Polytechnic University, Huhehaote). A voucher specimen (No: 96007) is maintained in the laboratory at the Inner Mongolia Polytechnic University.

3.3. Extraction and isolation

The air-dried aerial parts of *C. komarovii* (30 kg) were extracted with hot ethyl alcohol three times. After evaporating the alcohol in vacuo, the residue was stirred with $CHCl_3$ and extracted three times with a 5% aqueous solution of citric acid. The aqueous phase was

made alkaline (pH 9) with ammonium hydroxide (30% v/v) and extracted with $CHCl_3$. The $CHCl_3$ extract was dried (anhydr Na_2SO_4) and evaporated in vacuo to yield a crude alkaloid extract (3.5 g) which was subjected to column chromatography on Si gel eluting with various proportions of $CHCl_3$–CH_3OH–H_2O (10:1:1, 5:1:1, 5:2:1, lower layer). Each fraction was further purified sequentially using a Sephadex LH-20 column ($CHCl_3$–CH_3OH, 1:1) and a Si gel column ($CHCl_3$–CH_3OH–H_2O, lower layer). The first fraction that was eluted with $CHCl_3$–CH_3OH–H_2O (10:1:1, lower layer) afforded alkaloid **1** (11 mg) and alkaloid **2** (320 mg). Alkaloid **3** (35 mg) was obtained from the fraction that was eluted with $CHCl_3$–CH_3OH–H_2O (5:2:1, lower layer) on Si gel.

3.4. 2,3-Dimethoxy-6-(3-oxobutyl)-7,9,10,11,11a,12-hexahydrobenzo[f]pyrrolo[1,2-b]isoquinoline (*1*)

Colorless needles (0.012 g); mp 164–166 °C; $[\alpha]_D^{25}$ −71.0° (c 0.0011, $CHCl_3$); UV (CH_3OH) λ_{max} (log ϵ) 235 (3.93), 315 (3.50), 330 (3.54) nm; IR (film) ν_{max} 2961, 1716, 1612, 1510, 1476 cm^{-1}; ^1H NMR and ^{13}C NMR spectroscopic data, see Table 1; EIMS *m/z* (%) 353 $[M]^+$ (11), 295 (100), 282 (31), 247 (23); HREIMS *m/z* 353.1984 (calcd. for $C_{22}H_{27}NO_3$, 353.1990).

3.5. Antiviral activity

Activity against tobacco mosaic virus was performed by the conventional half-leaf method (Chen, 1990). A fresh leaf of *Nicotiana chinensis* Fisch. ex Lehm that had been inoculated by the juice-leaf rubbing method was cut into two halves along the main vein. Both were immersed into the solution of alkaloid **1**, **2**, and **3** (each at the concentrations of 1.0, 50, and 500 μg/ml) and distilled water for 2 s each, respectively, and then cultured at 25 °C for 72 h. Distilled water and a commercial antiviral agent, 2,4-dioxo-hexahydro-1,3,5-triazine, were used as control. The inhibition ratio was calculated by comparing the numbers of the viral inflammations on the two half leaves.

Acknowledgements

This work was supported by the Natural Science Fund of China and the State Key Laboratory of the Research Institute of Elemento-Organic Chemistry, Nankai University, Tianjin, The People's Republic of China.

References

Budzikiewicz, H., Faber, L., Herrmann, E., Perrollaz, F.F., Schlunegger, U.P., Wiegrebe, W., 1979. Vinceten, ein Benzopyrroloischinolin-Alkaloid, aus *Cynanchum vincetoxicum* (L.) Pers. (Asclepiadaceae). Liebigs Ann. Chem., 1214

Chen, N.C., 1990. Pesticide's Bioassay Technique. Press of Beijin Agriculture University, Beijing, The People's Republic of China, p. 194.

Fang, S.D., Zhang, R., Chen, Y., Xu, C.F., Lu, S.X., 1989. The chemical constituents in *Cynanchum komarovii* Al Iljinski. Acta Botanica Sinica 31, 934–958.

Jiangsu New Medical College 1977. Dictionary of Chinese Crude Drugs, Shanghai Scientific Technologic Publisher, Shanghai, p. 789.

Lavault, M., Richome, P., Bruneton, J., 1994. New phenatroindolizidine *N*-oxide alkaloids isolated from *Vincetoxicum hirudinaria*. Medic. Pharm. Acta Helv 68, 225–227.

Zhang, R., Fang, S.D., Chen, Y., Lu, S.X., 1991. The chemical constituents in *Cynanchum komarovii* Al Iljinski. Acta Botanica Sinica 33, 870–875.

PERGAMON

Phytochemistry 58 (2001) 1271–1276

PHYTOCHEMISTRY

www.elsevier.com/locate/phytochem

Cyclopeptide alkaloids from stems of *Paliurus ramossisimus*

Shoei-Sheng Lee*, Whei-Chuan Su, Karin C.S. Chen Liu

School of Pharmacy, College of Medicine, National Taiwan University, Taipei 100, Taiwan, Republic of China

Received 7 November 2000; received in revised form 30 April 2001

Abstract

Three 13-membered cyclopeptide alkaloids, paliurines G, H and I, together with six known alkaloids, nummularine H, daechuine-S3, paliurines A–C and F, were isolated from the stem of *Paliurus ramossisimus* by a combination of centrifugal partition chromatography and preparative TLC. Their structures were characterized and established on the basis of spectral analysis. A preliminary study indicated that nummularine H could shorten the methohexital induced sleeping time. © 2001 Elsevier Science Ltd. All rights reserved.

Keywords: *Paliurus ramossisimus*; Rhamnaceae; Stem; Cyclopeptide alkaloid; Paliurines G–I; Sedative effect

1. Introduction

Recently, we reported the isolation and structural characterization of seven zizyphine A-type cyclopeptide alkaloids from the root of *Paliurus ramossisimus* (Lour.) Poir (Rhamnaceae) (Lin et al., 2000), a plant growing in the wild along the west coast of Taiwan island. Six of them, i.e. paliurines A–F, were new compounds. Being interested in their potential biological activities, we need more of each as well as any other structural analogues. Thus we continued the phytochemical study of the aerial part of this plant. In the present paper we report the isolation and structural characterization of nine cyclopeptide alkaloids present in the stem of this plant. The sedative effect of some isolated compounds is also reported here.

2. Results and discussion

The ethanolic extract of the stem was processed in a manner to facilitate the separation of cyclopeptide alkaloids. After focusing on the weakly basic and less polar alkaloids by fractionation through a Si gel column, the cyclopeptide alkaloids were separated by a combination of centrifugal partition chromatography and preparative thin layer chromatography. Nine compounds were isolated and characterized. Four were found to be zizyphine A-type cyclopeptide paliurines A–C and F, having been isolated from the roots (Lin et al., 2000). The remainder (**1**–**5**) were also found to belong to the same type of 13-membered cyclopeptide alkaloids, as exemplified by their UV absorptions maxima at 265 and 317 nm (Tschesche and Kaußmann, 1975), CD spectra exhibiting two negative Cotton effects around 264 and 324 nm (Tschesche and Kaußmann, 1975), ^{1}H NMR spectra showing common signals for the 14-OMe (ca. δ 3.77), the protons H-1 (ca. δ 5.90, *d*), H-2 (ca. δ 6.93, *dd*) and H-3 (ca. δ 8.40, *d*), appearing as an AMX system (Marchand et al., 1969), and H-12 (ca. δ 6.65, *d*), H-12′ (ca. δ 6.77, *dd*) and H-13′ (ca. δ 6.86, *d*), appearing as an ABX system (Lin et al, 2000). The CD data also suggested 5*S*,8*S*,9*S* configuration for these five compounds (Schmidt et al., 1983). The coupling pattern of H-8 (ca. δ 4.39, *d*) and H-9 (ca. δ 5.40, ddd or dt) was also characteristic for a 3*S*-β-hydroxyproline unit (Tschesche and Kaußmann, 1975, Lin et al., 2000). Besides these data, the ^{1}H NMR spectra of compounds **1**–**4** had common signals at ca. δ 4.25 (*dd*, H-5), 0.86 (Me-17) and 0.95 (Me-18), assignable for a ring bond isoleucine residue (Lin et al., 2000). Their FAB mass spectra revealed two characteristic fragment ions at *m*/*z* 374 (**a**) and 216 (**b**) (Tschesche and Kaußmann, 1975). These data established compounds **1**–**4** to be zizyphine A type cyclopeptide containing isoleucine as the ring bonded amino acid. The followings describe the respective structural characterization of compounds **1**–**5**.

* Corresponding author. Tel.:/fax: +886-2-23916127.
E-mail address: shoeilee@ha.mc.ntu.edu.tw (S.-S. Lee).

0031-9422/01/$ - see front matter © 2001 Elsevier Science Ltd. All rights reserved.
PII: S0031-9422(01)00234-5

Compound **1**, an amorphous solid, had a molecular formula $C_{36}H_{49}N_5O_6$, as deduced from its FAB mass spectrum, $[M+H]^+$ at *m/z* 648, and analysis of its ^{13}C NMR spectral data. Its mass spectrum had a base peak at *m/z* 148, corresponding to the fragment ion **c** obtained from β-cleavage of the terminal *N*-monomethylated phenylalanine unit. Subtracting the ring nucleus moiety and terminal basic amino acid residue from the formula left a C_5 intermediate amino acid. Since the high resolution ^1H NMR spectrum of **1** ($CDCl_3$) (Table 1) revealed two additional methyl doublets at δ 0.83 ($J=6.7$ Hz) and 0.86 ($J=6.7$ Hz) besides those mentioned above, the intermediate amino acid was determined to be valine. Constructing these moieties together established the structure of compound **1** as shown in the figure.

Compound **2**, an amorphous solid, had a molecular formula $C_{39}H_{47}N_5O_6$, as deduced from its FAB mass spectrum, $[M+H]^+$ at *m/z* 682, and analysis of its ^{13}C NMR spectral data. Its mass spectrum had a base peak at *m/z* 134, for which fragment ion **d** was accounted. Subtracting the ring nucleus moiety and terminal basic amino acid residue, *N*-monomethylphenylalanine, from the formula left phenylalanine as an intermediate amino acid. Composing these structural moieties established **2** to be nummularine H, having been isolated from*Zizyphus nummularia* (Tschesche et al., 1977).

Compound **3**, an amorphous solid, had a molecular formula $C_{33}H_{51}N_5O_6$, as deduced from its FAB mass spectrum, $[M+H]^+$ at *m/z* 614, and analysis of its ^{13}C NMR spectral data. The high resolution ^1H NMR spectrum of **3** ($CDCl_3$) (Table 1) revealed signals for an NHMe (δ 2.34) and four additional methyl groups, including three doublets (δ 0.82, 0.91 and 0.94) and one triplet (δ 0.83), besides those mentioned above. This would suggest the intermediate and terminal amino acid residues to be isoleucine and leucine, one of which contained an

Table 1
^1H NMR spectral data (δ/ppm, *J* in Hz)[a] for compounds **1**–**5** in $CDCl_3$

Position	1	2	3	4	5
1	5.92 *d* (9.1)	5.90 *d* (9.1)	5.91 *d* (9.0)	5.91 *d* (9.0)	5.93 *d* (9.1)
2	6.93 *dd* (11.3, 9.1)	6.93 *dd* (11.3, 9.1)	6.92 *dd* (11.3, 9.0)	6.92 *dd* (11.4, 9.0)	6.92 *dd* (11.3, 9.1)
3	8.45 *d* (11.3)	8.40 *d* (11.3)	8.44 *d* (11.3)	8.44 *d* (11.3)	8.45 *d* (11.3)
5	4.26 *dd* (5.0, 4.5)	4.29 *t* (4.4)	4.25 *dd* (5.0, 4.3)	4.25 *dd* (5.1, 4.6)	4.56 *dt* (10.0, 5.0)
6	7.14 *d* (4.5)	7.27	7.20 *d* (5.0)	7.19 *d* (5.1)	7.38 *d* (5.0)
8	4.42 *d* (3.2)	4.39 *d* (3.1)	4.49 *d* (3.2)	4.47 *d* (3.2)	4.42 *d* (2.9)
9	5.52 *dt* (3.2, 7.4)	5.41 *dt* (3.1, 7.3)	5.53 *dt* (3.2, 7.2)	5.52 *dt* (3.2, 7.5)	5.41 *dt* (2.9, 7.3)
12	6.69 *d* (2.9)	6.66 *d* (2.9)	6.68 *d* (2.9)	6.68 *d* (2.9)	6.64 *d* (2.9)
12′	6.82 *dd* (9.1, 2.9)	6.77 *dd* (9.1, 2.9)	6.79 *dd* (9.0, 2.9)	6.79 *dd* (9.0, 2.9)	6.76 *dd* (9.0, 2.9)
13′	6.89 *d* (9.1)	6.86 *d* (9.1)	6.87 *d* (9.0)	6.87 *d* (9.0)	6.85 *d* (9.0)
15	2.08	2.05 *m*	2.08 *m*	2.08	3.28 *dd* (14.3, 5.0) 2.82 *dd* (14.3, 10.0)
16	1.10 and 1.35	1.12 and 1.42	1.00 and 1.35	1.09 and 1.34	7.24 *m*
17	0.86 *t* (6.9)	0.90 *t* (7.2)	0.86 *t* (7.4)	0.86 *t* (6.2)	7.24 *m*
18	0.94 *d* (6.9)	0.99 *d* (6.9)	0.95 *d* (6.8)	0.95 *d* (7.0)	7.24 *m*
19α	2.10 *m*	2.19 *m*	2.32 *m*	2.32 *m*	2.28 *m*
19β	2.60 *m*	2.41 *dddd* (13.6, 7.3, 6.5, 2.6)	2.58 *m*	2.58 *ddt* (13.2, 2.3, 6.6)	2.50 *dddd* (13.5, 7.3, 6.8, 3.2)
20α	4.28 *dt* (2.7, 8.8)	3.94 *ddd* (10.8, 8.2, 2.6)	4.34 *dt* (2.1, 9.5)	4.36 *ddd* (10.7, 8.5, 2.3)	4.05 *ddd* (10.8, 8.2, 3.0)
20β	3.55 *dt* (6.6, 10.7)	2.73 *dt* (6.5, 10.8)	3.54 *dt* (6.5, 10.7)	3.53 *dt* (6.6, 10.8)	3.40 *dt* (6.8, 10.8)
OMe	3.78 *s*	3.76 *s*	3.77 *s*	3.78 *s*	3.76 *s*
Intermediate a.a	Val	Phe	Ile	Ile	Leu
2′	4.49 *dd* (8.8, 7.7)	4.96 *dt* (6.2, 8.2)	4.59 *dd* (9.0, 7.8)	4.58 *dd* (9.0, 8.4)	4.70 *dt* (8.5, 7.0)
3′	1.93 *d* sept (8.8, 6.7)	2.94 *dd* (12.5, 6.2) 2.86 *dd* (12.5, 8.2)	1.75 *m*	1.77	1.06 *t* (7.0)
4′	0.83 *d* (6.7)		1.07and 1.44	1.06and 1.44	1.20 *m*
5′(9′)	0.86 *d* (6.7)	7.16–7.32 *m*	0.83 *t* (7.7)	0.86 *t* (6.2)	0.86 *d* (6.7)
6′(8′)		7.16–7.32 *m*	0.82 *d* (7.4)	0.82 *d*(6.8)	0.82 *d* (6.6)
7′		7.16–7.32 *m*			
2′α(N*H*)	7.26 *d* (7.7)	7.76 *d* (8.4)	7.64 *d* (9.0)	6.93 *d* (9.0)	
basic end a.a.	Phe(NMe_2)	Phe(NHMe)	Leu(NHMe)	Ile(NMe_2)	Ile(NHMe)
2″	3.29 *dd* (6.9, 6.3)	3.19 *dd* (9.1, 4.3)	2.98 *dd* (8.9, 4.8)	2.55 *d* (5.3)	2.85 *d* (4.5)
3″	3.17 *dd* (13.9, 6.9) 2.90 dd (13.0, 6.3)	3.09 *dd* (13.7, 4.1) 2.65 dd(13.7, 9.1)	1.56and 1.53	1.73	1.75 *m*
4″			1.65 *m*	1.10and 1.40	1.45 *m*
5″(9″)	7.25 *m*	7.16–7.32 *m*	0.91 *d* (6.5)	0.92 *d* (7.4)	0.91 *t* (7.2)
6″(8″)	7.25 *m*	7.16–7.32 *m*	0.94 *d* (6.3)	0.87 *d* (6.2)	0.95 *d* (7.1)
7″	7.25 *m*	7.16–7.32 *m*			
NMe	2.30 *s*	2.24 *s*	2.34 *s*	2.21 *s*	2.43 *s*

[a] Signals without multiplicity were assigned from COSY-45.

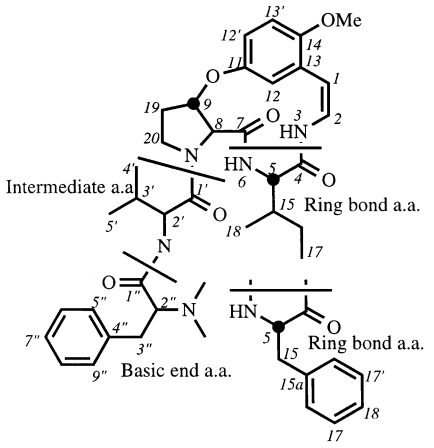

Compd	Ring bond amino acid	Intermediate amino acid	Basic end amino acid
1	Ile	Val	Phe(NMe_2)
2	Ile	Phe	Phe(NHMe)
3	Ile	Ile	Leu(NHMe)
4	Ile	Ile	Ile(NMe_2)
5	Phe	Leu	Ile(NHMe)

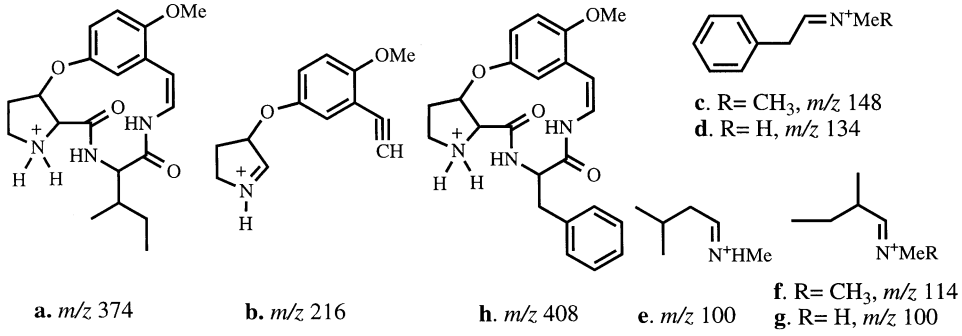

a. *m/z* 374 **b.** *m/z* 216 **h.** *m/z* 408 **e.** *m/z* 100

NHMe group. That the characteristic α-H of the terminal amino acid was located at δ 2.98 (*dd*, $J = 8.9, 4.8$ Hz) and the base peak in its mass spectrum appeared at *m/z* 100 (**e**) established *N*-monomethylleucine as the terminal amino acid residue. By elimination, the intermediate amino acid was isoleucine. Consequently, compound **3** had a structure as shown in the figure. That is **3** is mono-*N*-norpaliurine F.

Compound **4** had a molecular formula $C_{34}H_{53}N_5O_6$ as deduced from its FAB mass spectrum, $[M+H]^+$ at *m/z* 628, and analysis of its ^{13}C NMR spectral data. The high resolution ^1H NMR spectrum of **4** ($CDCl_3$) (Table 1) revealed signals of an NMe_2 (δ 2.21) and four additional methyl groups including two doublets (δ 0.82, 0.87) and two triplets (δ 0.86, 0.92) besides those signals mentioned above. This would suggest both intermediate and terminal amino acid residues to be isoleucine and *N*,*N*-dimethylisoleucine, respectively. This proposal was supported by its mass spectrum, which had a base peak at *m/z* 114, for which fragment ion **f** was accounted. These data established **4** to be daechuine-S3 (Han et al., 1989).

Compound **5** had a molecular formula $C_{36}H_{49}N_5O_6$ as deduced from its FAB mass spectrum, $[M+H]^+$ at *m/z* 648, and analysis of its ^{13}C NMR spectral data. Its ^1H NMR spectrum displayed signals for a monosubstituted phenyl group (ca. δ 7.25), four additional methyl groups including three doublets and one triplet, and an NHMe (δ 2.43). These data suggested that **5** contained three amino acid residues, i.e. Phe, Ile, and Leu. Its ^1H NMR spectrum revealed the α-H signals of these amino acid residues at δ 4.56 (*dt*), 4.70 (*dt*, $J = 8.5$, 7.0 Hz) and 2.85 (*d*). Since the latter was assignable to α-H of the terminal basic residue, this amino acid was *N*-monomethylisoleucine, as supported by its mass spectrum which had a base peak at *m/z* 100, for which fragment ion **g** was accounted. The chemical shift at δ 4.56 (*dt*, $J = 10.0$, 5.0, 5.0 Hz) was assignable to the signal of H-5, as compared to the corresponding signals of paliurines A–F (Lin et al., 2000). Upon irradiation of H-5 signals in a double resonance experiment collapsed a doublet at δ 7.38 ($J = 5.0$ Hz, H-6) to a singlet, and two double doublets at δ 3.28 ($J = 14.3$ and 5.0 Hz) and 2.82 ($J = 14.3$ and 10.0 Hz) to an AX system. This result suggested phenylalanine to be the ring bound amino acid residue. This suggestion was supported by the mass spectrum which showed a characteristic fragment ion at *m/z* 408 (**h**), accountable for the ring nucleus moiety. By elimination, the intermediate amino acid was leucine. Constructing these moieties together established the structure of **5** as shown in the figure.

The key ^1H NMR spectral data of **5** (Table 1) were assigned by three additional selected double resonance experiments, i.e. irradiation at the frequency of H-2′ (δ 4.70) and H-2 and H-20α (δ 4.05). Other proton assignments were made by analyzing their coupling patterns and comparison with the data of related cyclopeptide alkaloids such as paliurine B (Lin et al., 2000). Although **2** and **4** were known compounds, some of

their spectral data including CD, ^{13}C NMR spectral data and part of their ^{1}H NMR data remained to be assigned. Thus, following a similar approach to that of **5** allowed the assignment of the ^{1}H NMR spectral data of compounds **1**–**4** (Table 1). The ^{13}C NMR spectral data of **1**–**5** were assigned by correlation with those of paliurines A–F (Lin et al., 2000). These correlations were very consistent except the ambiguous assignment for C-15 and C-3′ in **5**. This problem was settled by using L-Leu(OMe)-L-Phe(NMe_2) as a model compound, whose ^{13}C NMR spectral data (Table 2) had been unambiguously assigned by analysis of the

Table 2
^{13}C NMR spectral data for compounds **1**–**5** and model dipeptides (δ/ppm, m[a]) in $CDCl_3$

Position	**1**	**2**	**3**	**4**	L-Ile(OMe)–L-Ile(NMe_2)	**5**	L-Leu(OMe)–L-Phe(NMe_2)
1	106.6 *d*	106.6 *d*	106.7 *d*	106.6 *d*		107.1 *d*	
2	121.5 *d*	121.6 *d*	121.7 *d*	121.7 *d*		121.5 *d*	
4	167.0 *s*	167.0 *s*	167.1 *s*	167.1 *s*		167.0 *s*	
5	60.3 *d*	60.3 *d*	60.3 *d*	60.3 *d*		56.6 *d*	
7	170.2 *s*	169.8 *s*	170.4 *s*	170.5 *s*		170.2 *s*	
8	64.4 *d*	65.0 *d*	64.9 *d*	64.8 *d*		64.6 *d*	
9	76.7 *d*	76.7 *d*	76.9 *d*	76.9 *d*		76.6 *d*	
11	151.0 *s*	151.2 *s*	151.5 *s*	151.4 *s*		151.3 *s*	
12	111.2 *d*	111.4 *d*	111.6 *d*	111.5 *d*		111.6 *d*	
12′	117.7 *d*	117.7 *d*	117.9 *d*	117.8 *d*		118.1 *d*	
13	124.2 *s*	124.8 *s*	124.9 *s*	124.8 *s*		124.6 *s*	
13′	113.8 *d*	114.2 *d*	114.4 *d*	114.3 *d*		114.3 *d*	
14	151.4 *s*	151.7 *s*	151.8 *s*	151.8 *s*		151.8 *s*	
15	35.1 *d*	35.7 *d*	35.4 *d*	35.4 *d*		36.5 *t*	
15a						136.1 *s*	
16	24.4 *t*	25.0 *t*	24.8 *t*	24.9 *t*		129.4 *d*	
17	11.7 *q*	11.8 *q*	11.6 *q*	11.9 *q*		128.8 *d*	
18	16.2 *q*	16.2 *q*	16.2 *q*	16.2 *q*		127.1 *d*	
19	32.5 *t*	32.4 *t*	32.7 *t*	32.7 *t*		32.6 *t*	
20	46.7 *t*	46.4 *t*	46.8 *t*	46.8 *t*		46.3 *t*	
Intermediate a.a	Val	Phe	Ile	Ile	L-Ile(OMe)	Leu	L-Leu(OMe)
1′	171.5 *s*	170.9 *s*	172.0 *s*	172.0 *s*	172.5 *s*	172.2 *s*	173.3 *s*
2′	54.9 *d*	51.1 *d*	53.9 *d*	53.9 *d*	56.1 *d*	48.1 *d*	50.4 *d*
3′	31.4 *d*	39.5 *t*	37.7 *d*	37.2 *d*	37.6 *d*	41.4 *t*	41.5 *t*
4′	19.1 *q*	135.6 *s*	24.7 *t*	24.8 *t*	25.2 *t*	24.8 *d*	24.8 *d*
5′(9′)	18.1 *q*	129.2 *d*	10.9 *q*	10.7 *q*	11.4 *q*	23.2 *q*	22.8 *q*
6′(8′)		128.7 *d*	15.5 *q*	15.5 *q*	15.8 *q*	21.6 *q*	21.8 *q*
7′		127.2 *d*					
basic end a.a.	Phe(NMe_2)	Phe(NHMe)	Leu(NHMe)	Ile(NMe_2)	L-Ile(NMe_2)	Ile(NHMe)	Phe(NMe_2)
1″	172.4 *s*	173.1 *s*	175.0 *s*	172.2 *s*	171.6 *s*	173.3 *s*	172.2 *s*
2″	71.0 *d*	66.0 *d*	63.9 *d*	74.7 *d*	74.6 *d*	70.1 *d*	71.0 *d*
3″	32.9 *t*	39.0 *t*	43.3 *t*	34.6 *d*	34.5 *d*	38.6 *d*	33.0 *t*
4″	139.7 *s*	137.5 *s*	25.4 *d*	27.2 *t*	27.0 *t*	25.6 *t*	139.8 *s*
5″(9″)	129.1 *d*	129.1 *d*	23.2 *q*	11.6 *q*	11.9 *q*	11.8 *q*	129.2 *d*
6″(8″)	128.3 *d*	128.7 *d*	22.1 *q*	14.9 *q*	14.6 *q*	15.9 *q*	128.3 *d*
7″	126.1 *d*	126.9 *d*					126.0 *d*
NMe	42.3 *q*	35.3 *q*	35.4 *q*	43.2 *q*	43.2 *q*	36.1 *q*	42.4 *q*
OMe	56.0 *q*	56.2 *q*	56.3 *q*	56.3 *q*	51.7 *q*	56.2 *q*	52.0 *q*

[a] Multiplicity was obtained from DEPT experiments.

Table 3
Effect of paliurines A, F and nummularine H (**2**) on methohexital induced sleeping time in mice

Sample	Sleeping time (min, mean±S.E.) (*n*)		Effect in sleeping time (%)
	Control[a]	Experiment[b]	
Paliurine A	5.95±1.72 (4)	8.30±1.50 (4)	+39.5
Paliurine F	7.67±4.06 (4)	11.17±5.06 (4)	+45.6
Nummularine H (**2**)	8.10±2.81 (7)	6.45±1.15 (7)	-20.4

[a] Control: i.p. injection of methohexital in a dose of 50 mg/kg to mice (weight, 27–33 g).
[b] Experimental group: oral administration of tested samples was given 1 h before i.p. injection of methohexital (50 mg/kg) to mice. Dose: paliurine A 14.4 mg/kg, paliurine F 10 mg/kg, and nummularine H 10 mg/kg.

COLOC spectrum (Lin et al., 2000). Since C-3 of Leu(OMe) was assigned at δ 41.5 (*t*), the corresponding C-3′ in the intermediate amino acid (Leu) in **5** was assignable at δ 41.4 (*t*). By elimination, C-15 in the ring bond amino acid (Phe) in **5** was assigned at δ 36.5 (*t*).

The stereochemistry in the ring nucleus of these compounds was deduced by the CD method as indicated above, which established both ring bond amino acids and proline to be L-form. Those of intermediate and terminal amino acids in **4** were determined by the consistency of the ^{13}C NMR spectral data of the terminal Leu(NMe_2) with the corresponding signals of a model dipeptide, L-Ile(OMe)-L-Ile(NMe_2) (Lin et al., 2000). Based on this, the terminal dipeptides in compounds **1**–**3** and **5** are assumed all L-form.

To our knowledge, compounds **1**, **3** and **5** represent the first natural occurrence of such compounds and were named paliurines G, H and I, respectively, after their plant origin.

The sedative effect of cyclopeptide alkaloids such as sanjoinine A had been reported (Han et al., 1989). In a preliminary study, we found that, in mice, nummularine H (**2**) could shorten the mexthohexital-induced sleeping time instead of prolonging as shown for the paliurines A and F (Table 3). Further studies on structure and activity relationship on such effects are needed to disclose their mechanism of action and potential use.

3. Experimental

3.1. General

Perkin Elmer 1760-X Infrared FT spectrometer (KBr); Hitachi 2000 UV (MeOH); Jasco J-710 spectropolarimeter (MeOH); Jeol JMX-HX110 Mass Spectrometer; Bruker AM-300 and AMX-400 NMR spectrometer in $CDCl_3$ (δ_H 7.24, δ_C 77.0) using Bruker standard pulse programs: in the HETCOR, HMQC, COLOC and HMBC experiments, Δ = 1 s and J = 140, 140, 8 and 8 Hz, respectively, the correlation maps consisted of 512×1 K data points per spectrum, each composed of 16–64 transients; Sanki CPC-B92-N with 6 30E cartridges (90 ml), using the upper and lower layer of the solvent system $CHCl_3$–MeOH–6% HOAc (5: 5: 3) as mobile and stationary phases, respectively, 2.0 ml/min flow rate, 700 rpm rotation speed, about 40 kg/cm^2 pressure; Si gel TLC analysis [Me_2CO–toluene–25%NH_4OH (30:70:1)].

3.2. Plant material

The stem of *Paliurus ramossisimus* for this study was collected in August 1985, along the west coast of Ho-Long village, Miao-Li county, Taiwan. A voucher specimen (no. NTUPH-19850801) has been deposited in the School of Pharmacy, National Taiwan University.

3.3. Extraction and isolation

The ground dry powders of the stem (12.00 kg) were percolated with 95%EtOH (60 l × 3). The EtOH extract was triturated with H_2O and *n*-hexane to give residue (ca 80 g) which was fractionated on a Si gel column (ca 400 g, 70–230 mesh) eluted with 5–20% MeOH in $CHCl_3$ stepwise. The components eluted with 5% MeOH elution were applied to a Si gel column (230–400 mesh, second column) eluted with $CHCl_3$ to give four fractions. Fr. 4 (0.64 g ×3) containing cyclopeptide alkaloids was fractionated via a Sanki CPC as above to give nine subfractions. Subfr. 1 (107 mg) was separated on Si gel preparative TLC plates (1 mm × 3) developed twice by toluene–Me_2CO–25%NH_4OH (70:30:1) to give **3** (21 mg, R_f 0.32). Under similar process, subfr. 4 (47.8 mg) yielded **2** (18.6 mg, R_f 0.34) and a mixture (11.7 mg) of **4** and paliurine A; subfr. 5 (22 mg) yielded paliurine F (8.6 mg, R_f 0.45), **1** (3.9 mg, R_f 0.34) and a mixture (5.6 mg) of **4** and paliurine A; subfr. 6 (105 mg) yielded paliurine F (80 mg), and **1** (16.4 mg). The mixture of **4** and paliurine A (17.3 mg) obtained above was separated on a Si gel preparative TLC (1 mm) developed five times by cyclohexane-Me_2CO (3: 1) to give **4** (6 mg) and paliurine A (7 mg), each having R_f value of 0.327 and 0.274, respectively, under the identical PTLC. Subfr. 9 (34.4 mg) was paliurine C (R_f 0.50, developed twice). Fraction 3 (0.78 g×2) from the second Si gel column was fractionated via a CPC column using similar delivery system except for the replacement of 6%HOAc by 5%HOAc to give five subfrs. These subfrs. were separated by Si gel preparative TLC using similar conditions as mentioned above to give **5** (16.9 mg, R_f 0.36) and paliurine B (20.9 mg, R_f 0.30) (from subfr. 1), **2** (32 mg), a mixture of **4** and paliurine A (31 mg) (from subfr. 3), paliurine F (42 mg) (from subfr. 4). Further separation of the mixture yielded **4** (13 mg) and paliurine A (16 mg).

3.4. Paliurine G (*1*)

Amorphous powder; $[\alpha]_D^{30}$ −335.0° (c = 0.33, MeOH). IR ν_{max} cm^{-1}: 3324, 3120, 2960, 2924, 2878, 1680, 1640, 1600 (*sh*), 1502, 1450, 1438, 1220, 1180, 1088, 1040, 796, 770, 700. UV λ_{max} nm (log ε): 262 (4.79), 316 (4.18). CD nm ($\Delta\epsilon$): 318.5 (−23.18), 263 (−44.55), 215 (−28.48). For ^1H NMR spectra: Table 1. For ^{13}C NMR spectra: Tables 2. FAB MS (positive) m/z (rel. int.): $[M+H]^+$ 648 (14), 556 (0.7), 374 (0.4, **a**), 216 (0.4, **b**), 148 (100, **c**). HREI MS m/z $[M]^+$: 647.3704. Calc. for $C_{36}H_{49}N_5O_6$: 647.3683.

3.5. Paliurine H (*3*)

Amorphous powder; $[\alpha]_D^{30}$ −412.0° (c = 0.24, MeOH). IR ν_{max} cm^{-1}: 3400, 3320, 2960, 2924, 1685, 1640, 1510,

1460, 1383, 1363, 1262, 1222, 1040, 770. UV λ_{max} nm (log ε): 264 (4.32), 317 (4.05). CD nm ($\Delta\varepsilon$): 317.5 (−17.55), 261.0 (−36.76), 214.0 (−27.23). For ^{1}H NMR spectra: Table 1. For ^{13}C NMR spectra: Tables 2. FAB MS (positive) m/z (rel. int.): $[M+H]^+$ 614 (18), 100 (100, **e**). HREI MS m/z $[M]^+$: 613.3823. Calc. for $C_{33}H_{51}N_5O_6$: 613.3839.

3.6. Paliurine I (*5*)

Amorphous powder; $[\alpha]_D^{30}$ −374.3° (c = 1.07, MeOH). IR ν_{max} cm^{-1}: 3344, 2960, 2924, 2872, 1670, 1640, 1509, 1440, 1220, 1180, 1102, 1038, 770, 699. UV λ_{max} nm (log ε): 266 (4.09), 317 (3.93). CD nm ($\Delta\varepsilon$): 318.6 (−12.48), 263 (−22.27), 216 (−14.24). For ^{1}H NMR spectra: Table 1. For ^{13}C NMR spectra: Table 2. FAB MS (positive) m/z (rel. int.): $[M+H]^+$ 648 (25), 590 (1), 521 (5), 408 (5, **h**), 100 (100, **g**). HREI MS m/z $[M]^+$: 648.3754. Calc. for $C_{36}H_{50}N_5O_6$: 648.3761.

3.7. Additional data for nummularine H (*2*)

CD nm ($\Delta\varepsilon$): 322.5 (−16.03), 313.1 (−16.03), 260.2 (−30.30), 213.3 (−14.27). For ^{1}H NMR spectra: Table 1. For ^{13}C NMR spectra: Table 2. FAB MS (positive) m/z (rel. int.): $[M+H]^+$ 682 (12), 590 (0.7), 374 (0.8, **a**), 216 (0.8, **b**), 134 (100, **d**).

3.8. Additional data for daechuine-S3 (*4*)

Amorphous powder; $[\alpha]_D^{30}$ −454.0° (c = 0.76, MeOH). CD nm ($\Delta\varepsilon$): 317.9 (−17.82), 261.2 (−35.76), 213.8 (−26.73). For ^{1}H NMR spectra: Table 1. For ^{13}C NMR spectra: Table 2. FAB MS (positive) m/z (rel. int.): $[M+H]^+$ 628 (16), 570 (1), 374 (0.5, **a**), 216 (0.5, **b**), 114 (100, **f**).

Acknowledgements

This work was supported by grants from the National Science Council, the Republic of China (NSC79-0420-B002-144 and NSC80-0420-B002-154).

References

Han, B.H., Park, M.H., Park, J.H., 1989. Chemical and pharmacological studies on sedative cyclopeptide alkaloids in some Rhamnaceae plants. Pure Appl. Chem. 61, 443–448. (and the references cited therein).

Lin, H.-y., Chen, C.H., You, B.J., Liu, K.C.S.C., Lee, S.S., 2000. Cyclopetide alkaloids from *Paliurus ramossisimus*. J. Nat. Prod. 63, 1338–1343.

Marchand, J., Pais, M., Monseur, X., Jarreau, F.X., 1969. Peptide alkaloids. VII. Lasiodine A and B, alkaloids from *Lasiodiscus marmoratus*. Tetrahedron 25, 937–954.

Schmidt, U., Lieberknecht, A., Bökens, H., Griesser, H., 1983. Total synthesis of zizyphine A. Synthesis of peptide alkaloids. 8. J. Org. Chem. 48, 2680–2685.

Tschesche, R., Elgamal, M., Eckhardt, G., 1977. Alkaloids from Rhamnaceae. XXVIII. Nummularine-G, -H and -K, new alkaloids from *Zizyphus nummularia*. Chem. Ber. 110, 2649–2655.

Tschesche, R., Kauβmann, E.U., 1975. The cyclopeptide alkaloids. In: Manske, R.H. (Ed.), The Alkaloids, Vol. 15. Academic Press, New York, pp. 165–205. (and references cited therein).

PERGAMON

Phytochemistry 58 (2001) 1277–1280

PHYTOCHEMISTRY

www.elsevier.com/locate/phytochem

Compounds from *Kadsura ananosma*

Ye-Gao Chen[a], Yu-Yuan Xie[a], Kin-Fai Cheng[b,*], Kung-Kai Cheung[b], Guo-Wei Qin[a,*]

[a]*Shanghai Institute of Materia Medica, Shanghai Institutes of Biological Sciences, Chinese Academy of Sciences, Shanghai 200031, People's Republic of China*

[b]*Department of Chemistry, The University of Hong Kong, Hong Kong, People's Republic of China*

Received in revised form 23 May 2001

Abstract

The 18-(13→12β)-*abeo*-lanostene triterpenoid acid, ananosic acid A (**1**), and the dibenzocyclooctadiene lignan, ananosin A (**2**), were isolated from the stem bark of *Kadsura ananosma*. Their structures were elucidated by extensive spectral studies and the structure of **1** was confirmed by single crystal X-ray diffraction analysis. © 2001 Elsevier Science Ltd. All rights reserved.

Keywords: *Kadsura ananosma*; Schisandraceae; Ananosic acid A; Ananosin A

1. Introduction

Plants of the Schisandraceae family are rich sources of dibenzocyclooctadiene lignans, and lanostane triterpenoid acids and lactones, which have been found to possess some beneficial pharmacological effects, including antihepatitis, antitumor, and anti-HIV activities (Liu, 1983; Liu and Li, 1995; Chen et al., 1996, 1999; Kuo et al., 1997, 1999). Previously, we have reported on the isolation and structural determination of eight lignans from *Kadsura angustifolia* (Chen et al., 1998a,b). A literature survey showed that only four sesquiterpenoids had been isolated from the plant *K. ananosma* (Zou et al., 1993). In continuing studies of Schisandraceae plants, we isolated a new 18-(13→12β)-*abeo*-lanostene triterpenoid acid, ananosic acid A (**1**), and a new dibenzocyclooctadiene lignan, ananosin A (**2**) from the stem bark of *K. ananosma*. This paper describes the isolation and structural elucidation of these two compounds.

2. Results and discussion

Repeated column chromatography of the CH_2Cl_2 extracts of the stem bark of *K. ananosma* yielded two new compounds (**1**–**2**). Ananosic acid A (**1**), colorless crystals (m.p. 164–166 °C), has the molecular formula $C_{30}H_{46}O_3$ by HREIMS. The IR spectrum displayed the absorption for an α,β-unsaturated acid (1693, 2500–3200 cm^{-1}) and hydroxyl groups (3423 cm^{-1}). The ^1H NMR spectrum revealed an angelic acid unit [δ_H 6.14 (1H, *tq*, $J=7.3$, 1.4 Hz) and 1.92 (3H, *d*, $J=1.3$ Hz)], two secondary methyl [δ_H 0.94 (3H, *d*, $J=6.8$ Hz) and 1.23 (3H, *d*, $J=7.0$ Hz)], and four tertiary methyl groups [δ_H 0.87, 0.91, 0.98, and 1.03 (each 3H, *s*)]. These features closely resembled those of lanost-24(*Z*)-en-26-oic acids isolated from Schisandraceae plants (Liu et al., 1988; Sun et al., 1996), suggesting that **1** was a lanostane triterpenoid acid. The signal at δ_H 3.54 (1H, *dd*, $J=3.7$, 2.0 Hz) indicated that a hydroxyl group was attached to C-3 with an α-orientation, the same as that of isoanwuweizic acid (**3**), which was previously isolated from *K. heteroclita* (Dai et al., 1990). The signal at δ_H 5.46 (1H, *dd*, $J=5.3$, 2.0 Hz) showed there was a tri-substituted double bond located at C-7 (8), C-9 (11), or C-5 (6). In the HMBC spectrum, the olefinic proton at δ 5.46 was correlated with the carbon resonance at δ 54.4 (C-14), suggesting that the tri-substituted double bond was at C-7 (8). Comparison of the ^1H NMR spectrum of **1** (Table 1) with that of **3** revealed that the C-13 tertiary methyl signal present in **3** (at δ_H 0.65) disappeared in **1**, instead appearing as a secondary methyl signal at δ_H 1.23 (3H, *d*, $J=7.0$ Hz), leading to the formation of a tetra-substituted double bond at C-13 (17) in **1**. In the HMBC spectrum, the ^1H signal at δ_H 0.94 (H-21) was correlated with the ^{13}C signal at δ_C 136.0 (C-17), and the ^1H signal at δ_H 1.23 (H-18) correlated with the ^{13}C sig-

* Corresponding authors. Tel.: +86-21-6431-1833, +86-21-852-2859-2682; fax: +86-21-6437-0269, +86-21-852-2858-4620.

E-mail addresses: hrscckf@hku.hk (G.-W. Qin), hrscckf@hku.hk (K.-F. Cheng).

0031-9422/01/$ - see front matter © 2001 Elsevier Science Ltd. All rights reserved.
PII: S0031-9422(01)00319-3

Table 1
NMR spectroscopic data for compound **1** in $CDCl_3$

Position	^1H	^{13}C
1	1.43 (1H, *m*), 1.62 (1H, *m*)	36.8t
2	1.89 (1H, *m*), 1.93 (1H, *m*)	27.5*t*
3	3.45 (1H, *dd*, *J* = 3.7, 2.0 Hz)	76.9*d*
4		36.9*s*
5	1.62 (1H, *m*)	36.3*d*
6	1.86 (1H, *m*), 1.95 (1H, *m*)	23.3*t*
7	5.46 (1H, *dd*, *J* = 5.3, 2.0 Hz)	117.4*d*
8		146.9*s*
9	1.64 (1H, *m*)	46.4*d*
10		34.5*s*
11	1.27 (1H, *m*), 1.64 (1H, *m*)	39.4*t*
12	2.10 (1H, *m*)	30.5*d*
13		145.8*s*
14		54.4*s*
15	1.55 (1H, *m*), 1.58 (1H, *m*)	25.1*t*
16	2.10 (1H, *m*), 2.30 (1H, *m*)	29.5*t*
17		136.0*s*
18	1.23 (3H, *d*, *J* = 7.0 Hz)	19.6*q*
19	0.87 (3H, *s*)	21.4*q*
20	2.92 (1H, *m*)	31.3*d*
21	0.94 (3H, *d*, *J* = 6.8 Hz)	20.0*q*
22	1.43 (1H, *m*), 1.62 (1H, *m*)	35.2*t*
23	2.45 (2H, *m*)	28.4*t*
24	6.14 (1H, *tq*, *J* = 7.3, 1.4 Hz)	147.2*d*
25		126.1*s*
26		173.0*s*
27	1.92 (3H, *d*, *J* = 1.3 Hz)	20.5*q*
28	1.03 (3H, *s*)	20.1*q*
29	0.98 (3H, *s*)	28.1*q*
30	0.91 (3H, *s*)	22.5*q*

nal at δ_C 145.8 (C-13), which supported the presence of a C-13(17) double bond.

An X-ray crystallographic study was performed to confirm the structure and determine the absolute configuration of **1** (Fig. 1). Thus, **1** was unambiguously elucidated as 3α-hydroxy-18(13→12β)*abeo* lanostan-7(8), 13(17), 24(*Z*)-trien-26-oic acid. The ^1H and ^{13}C NMR spectral data were fully assigned by various NMR techniques including DEPT, ^1H–^1H COSY, HSQC, and HMBC. The 18(13→12β)*abeo* lanostene triterpenoid skeleton was previously obtained by rearrangement of 3β-acetoxy-9α,11α-epoxylanostan-7-one treated with boron trifluoride-diethyl ether (Baddeley et al., 1979). To our knowledge, **1** is the first example of a 18(13→12β)*abeo* lanostene triterpenoid found in nature.

Ananosin A (**2**), colorless crystals (mp 132–134 °C), was assigned the molecular formula $C_{28}H_{34}O_9$ by HREIMS. The UV spectrum showed absorption maxima at 225 nm (log ε, 4.78) and 288 nm (log ε, 3.43), indicating that **2** was a dibenzocyclooctadiene lignan (Ikeya et al., 1979). The CD curve of **2** showed a negative Cotton effect around 241 nm and a positive one around 220 nm, suggesting that **2** possesses an *S*-biphenyl configuration (Ikeya et al., 1979). The ^1H NMR spectrum of **2** revealed signals for two aromatic protons at δ_H 6.71 and 6.34 each 1H, s), a methylenedioxy moiety [δ_H 5.98 and 5.95 (each 1H, *d*, *J* = 1.4 Hz)], and four methoxyl groups [δ_H 3.90 (6H, *s*), 3.76 and 3.64 (each 3H, *s*)] on two aromatic rings. In the cyclooctadiene ring, two secondary methyl groups at δ_H 0.95 and 1.14 (each 3H, *d*, *J* = 7.1 Hz) can be assigned to CH_3-7 and CH_3-8, respectively, suggesting no substituent at C-7 and C-8, with the two methyls in *cis*-orientation (Chen et al., 1976). The signals at δ_H 5.81 (1H, *d*, *J* = 7.0 H) and 4.66 (1H, *br s*) were assigned to two oxygen-bearing benzylic methines, indicating an ester group and a hydroxyl group substituted at C-6 and C-9, respectively, similar to the previously reported angustifolin C (**4**) (Chen et al., 1998a). In the HMBC spectrum, correlations between the aromatic proton at δ_H 6.34 (H-11) and the carbon signal at δ_C 82.2 (C-9), and the aromatic proton at δ_H 6.71 (H-4) and the carbon signal at δ_C 80.8 (C-6) supported the above assignments. IR (3473 cm^{-1}) and MS (*m*/*z* 496 [M^+-H_2O]) confirmed the presence of a hydroxyl group. The presence of a tigloyl group was deduced from the IR (1705 cm^{-1}), MS (414 [$M^+-C_4H_7COOH$], 83 [$C_4H_7CO^+$] and 55 [$C_4H_7]^+$) and ^1H NMR (Table 2) data, and further confirmed by a correlation between the proton signal at δ_H 6.21 (1H, *m*) and alkenyl methyl group at 1.67 (3H, *d*, *J* = 7.1 Hz) in the NOESY spectrum.

An aromatic proton appeared at higher field at δ_H 6.34 and the lack of correlation between this proton signal and any methoxyl signal suggested that it was adjacent to the methylenedioxy moiety (Mervic and Ghera, 1977). The correlation between the proton signal at δ_H 6.34 and benzylic methine at δ_H 4.66, and the proton signal at δ_H 6.71 and the benzylic methine at δ_H 5.81 in the NOESY spectrum, indicated that the tigloyl and hydroxyl groups were located in the 6β and 9α positions, respectively. The NOESY spectrum also showed correlations between Me-7 (δ_H 0.95) and H-4 (δ_H 6.71), and between Me-8 (δ_H 1.14) and H-9 (δ_H 4.66), suggesting that both Me-7 and Me-8 are α-oriented. On basis of the results mentioned above, the structure of ananosin A was thus determined as **2**. No coupling was showed between H-8β and H-9β, but the NOE correlation between H-4 and Me-7, H-4 and H-6α, Me-8 and H-9, and H-9 and H-11 indicated a twist-boat-chair conformation for the cyclooctadiene ring (Fig. 2).

3. Experimental

3.1. General

IR spectra were recorded as KBr pellets on a Perkin-Elmer 599B spectrophotometer. UV spectra were measured on a Shimadzu UV-3000 spectrophotometer in absolute MeOH. MS were determined on a Varian Mat-711 mass

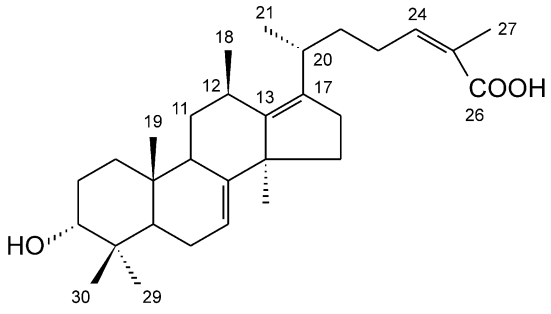

1

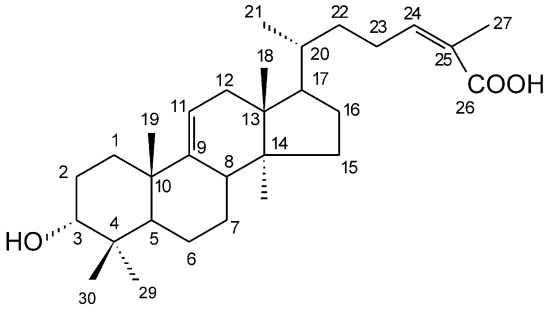

3

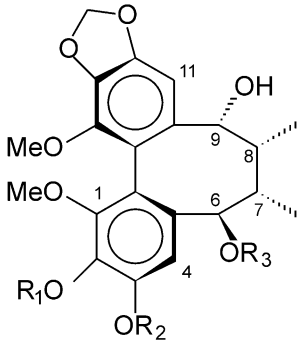

2. R_1=R_2=Me, R_3=Tig
4. R_1+R_2=CH_2, R_3=C_6H_5CO

Fig. 1. Stereoview of compound **1** from X-ray analysis.

spectrometer. NMR spectra were measured on a Brüker AM-400 spectrometer with TMS as int. standard and $CDCl_3$ as solvent. 2D-NMR spectra were performed on a Brüker DRX 500 spectrometer. Optical rotations were recorded with a JASCO Dip-181 spectropolarimeter. Silica gel (200–300 mesh) was used for column chromatography and silica gel GF_{254} for TLC (Qingdao Marine Chemical Co.)

3.2. Plant materials

The stem bark of *K. ananosma* Kerr was collected from Men-Na County of Yunnan Province, China in February 1998, and identified by Mr. Hong Wang, a botanist of Xi-Shuang-Bang-Na Botanical Garden, Chinese Academy of Sciences, where a voucher specimen (No. 9802015) is deposited.

3.3. Extraction and isolation

The dried powdered stem bark of *K. ananosma* (6.0 kg) was extracted with CH_2Cl_2 exhaustively. The CH_2Cl_2 extract was concentrated in vacuo to give a residue (500 g), which (100 g) was applied to a silica gel column, eluted with petroleum ether containing increasing amounts of Me_2CO to afford seven fractions

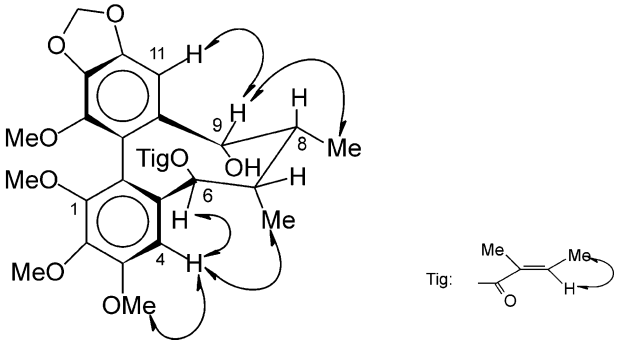

Fig. 2. NOE correlations of compound **2**.

(A–G). Fraction B was subjected to repeated column chromatography to yield ananosic acid A (**1**, 475 mg). Fraction C was treated in a similar manner as fraction B to yield ananosin A (**2**, 146 mg).

3.3.1. Ananosic acid A (*1*)

Colorless crystals, mp 132–134 °C, $[\alpha]$ −67.7° ($CHCl_3$, *c* 0.65); IR ν cm^{-1}: 3423, 2500–3200, 1693, 1620, 1458, 1380, 1250, 1238, 1070, 989. ^1H and ^{13}C NMR, see Table 1. EIMS *m*/*z* (rel. int.): 454 (4), 439 (100), 421 (10), 313 (9), 299 (2), 239 (3), 211 (2), 1171 (4), 145 (8), 105 (10). HREIMS *m*/*z*: 454.3447 [M^+], requires 454.3435.

Table 2
NMR spectrascopic data for compound **2** in $CDCl_3$

Position	^1H	^{13}C
1		152.4*s*
2		142.0*s*
3		152.6*s*
4	6.71 (1H, *s*)	110.7*d*
5		131.3*s*
6	5.81 (1H, *d*, *J* = 7.0 Hz)	80.8*d*
7	2.14 (1H, *m*)	40.0*d*
8	2.14 (1H, *m*)	40.0*d*
9	4.66 (1H, *br s*)	82.2*d*
10		141.6*s*
11	6.34 (1H, *s*)	102.0*d*
12		148.6*s*
13		135.4*s*
14		140.8*s*
15		121.8*s*
16		119.9*s*
Me-7	0.95 (1H, *d*, *J* = 7.1 Hz)	15.6*q*
Me-8	1.14 (1H, *d*, *J* = 7.1 Hz)	14.6*q*
OCH_2O	5.98 (1H, *d*, *J* = 1.4 Hz)	101.0*t*
	5.95 (1H, *d*, *J* = 1.4 Hz)	
OMe	3.64 (3H, *s*)	60.8*q*
	3.76 (3H, *s*)	59.3*q*
	3.90 (6H, *s*)	56.0*q*
		60.5*q*
Otig 1′		166.9*s*
2′		128.3*s*
3′	6.21 (1H, *m*)	137.2*d*
Me-β	1.67 (3H, *s*)	14.2*q*
Me-α	1.61 (3H, *s*)	11.7*q*

3.3.2. *Ananosin A (**2**)*

Colorless crystals, mp 132–134 °C, $[\alpha]$ −16.5° ($CHCl_3$, *c* 0.59); IR ν cm^{-1}: 3473, 1705, 1650, 1600, 1580, 1500, 1480, 1462. UV λ nm (log ε): 225 (4.78), 288 (3.43). ^1H and ^{13}C NMR, see Table 2. EIMS *m*/*z* (rel. int.): 514 (36), 496 (2), 414 (100), 383 (22), 344 (16), 223 (21), 149 (10), 83 (24), 55 (23). HREIMS *m*/*z*: 514.2200 [M^+], requires 514.2203. CD (MeOH, *c*, 0.0228) $\Delta\varepsilon_{241}$ −13.81, $\Delta\varepsilon_{220}$ +3.08.

3.3.3. *X-ray analysis of **1***

Crystal data: $C_{30}H_{46}O_3$, MW = 454.34, monoclinic, space group *C*2 (No. 5), *a* = 34.852 (3) Å, *b* = 9.412 (2) Å, *c* = 8.527 (2) Å, β = 90.11 (2)°, *V* = 2797.1 (7) $Å^3$, *Z* = 4, *D*c = 1.080 g cm^{-3}, μ (M_0-K_α) = 0.67 cm^{-1}, *F* (000) = 1000, *T* = 301 K. Crystal dimensions: 0.4×0.2×0.1 mm. The intensity was recorded with a MAR diffractometer. From a total of 11646 measurements, those 1824 reflections with $1 > 3\sigma$ (I) were retained for the analysis. The crystal structure was solved by direct methods (SIR 92[2]) and expanded by Fourier method and refinement by full-matrix least-squares using the software package TeXsan[3] on a Silicon Graphics Indy computer. The all non-H atoms were refined anisotropically. The positional parameters of the H atoms bonded to O (1) and O (3) and located in the difference Fourier synthesis were refined and 44 other H atoms at calculated positions with thermal parameters equal to 1.3 times that of the attached C atoms, were not refined.

References

Baddeley, G.V., Samaan, H.J., Simes, J.J.H., Ai, I.H., 1979. The rearrangement of 3β-acetoxy- 9,11-epoxylanostanes by boron trifluoride-diethyl ether. Journal of Chemical Society, Perkin Trans. 1, 4–14.

Chen, D.F., Zhang, S.X., Wang, H.K., Zhang, S.Y., Sun, Q.Z., Cosebtino, L.M., Lee, K.H., 1999. Novel anti-HIV lancilactone C and related triterpenes from *Kadsura lancilimba*. Journal of Natural Products 62, 94–97.

Chen, D.F., Zhang, S.X., Wang, H.K., Zhou, B.N., Wang, P., Cosentino, L.M., Lee, K.H., 1996. Two new lignans, interiotherins A and B, as anti-HIV principles from *Kadsura interior*. Journal of Natural Products 59, 1066–1068.

Chen, Y.G., Wang, P., Lin, Z.W., Sun, H.D., Qin, G.W., Xie, Y.Y., 1998a. Dibenzocyclo-octadiene lignans from *Kadsura angustifolia*. Phytochemistry 48, 1059–1062.

Chen, Y.G., Qin, G.W., Xie, Y.Y., Cheng, K.F., Lin, Z.W., Sun, H.D., Kang, Y.H., Han, B.H., 1998b. Lignans from *Kadsura angustifolia*. Journal of Asia Natural Products Research 1, 125–131.

Chen, Y.Y., Shu, Z.B., Li, L.N., 1976. Studies on fruits Schizandrae IV. Isolation and determination of the active compounds of *Schizandra chinensis* Baill. Science Sinica 19, 276–290.

Dai, P., Han, G.Q., Arison, B.H., 1990. A new triterpenoid from *Kadsura heteroclita* (Roxb) Craib. Chemical Journal of Chinese Universities 11, 423–424.

Ikeya, Y., Taguchi, H., Yosioka, I., Kobayashi, H., 1979. The constituents of *Schizandra chinensis* Baill. I. Isolation and structure determination of five new lignans, gomisins A, B, C, F and G and the absolute structure of schizandrin. Chemical and Pharmaceutical Bulletin 27, 1383–1394.

Kuo, Y.H., Kuo, L.Y., Chen, C.F., 1997. Four new C19 homolignans, schiarisanrins A, B, and D and cytotoxic schiarisanrin C, from *Schizandra arisanensis*. Journal of Organic Chemistry 62, 3242–3245.

Kuo, Y.H., Li, S.Y., Wu, M.D., Huang, R.L., Kuo, L.M., Chen, C.F., 1999. A new anti-HbeAg lignan, kadsumarin A, from *Kadsura matsudai* and *Schizandra arisanensis*. Chemical and Pharmaceutical Bulletin 47, 1047–1048.

Liu, G.T., 1983. From the study of *Schisandra chinensis* to the discovery of dimethyl biphenyl-dicarboxylate. Acta Pharmaceutical Sinica 18, 714–720.

Liu, J.S., Li, L., 1995. Kadsulignans L-N, three dibenzocyclooctadiene lignans from *Kadsura coccinea*. Phytochemistry 38, 241–246.

Liu, J.S., Huang, M.F., Tao, Y., 1988. Anwuweizoic acid and manwuweizic acid, the putative anticancer active principle of *Schisandra propinqua*. Canadian Journal of Chemistry 66, 414–416.

Mervic, M., Ghera, E., 1977. Total synthesis of (±) kadsurin. Journal of American Chemical Society 99, 7673–7678.

Sun, H.D., Qiu, S.X., Lin, L.Z., Wang, Z.Y., Lin, Z.W., Pengsuparp, T., Pezzuto, J.M., Fong, H.H.S., Cordell, G.A., Farnsworth, N.R., 1996. Nigranoic acid, a triterpenoid from *Schisandra sphaerandra* that inhibits HIV-1 reverse transcriptase. Journal of Natural Products 59, 525–527.

Zou, C., Pu, X.Y., Zhou, J., 1993. Sesquiterpenoids from *Kadsura ananosma*. Acta Botanica Yunnanica 15, 196–200.

PERGAMON

Phytochemistry 58 (2001) 1281–1287

PHYTOCHEMISTRY

www.elsevier.com/locate/phytochem

Macrolactone glycosides of three lichen acids from *Acarospora gobiensis*, a lichen of Central Asia

Tomáš Řezanka[a,*], Irina A. Guschina[b]

[a]*Institute of Microbiology, Vídeňská 1083, 14220 Prague, Czech Republic*
[b]*Institute of Ecology of the Volga River Basin of the Russian Academy of Sciences, Togliatti 445003, Russia*

Received 29 March 2001; received in revised form 13 August 2001

Abstract

The compounds isolated from the extract of Central Asian lichen (*Acarospora gobiensis* H. Magn.) comprised three new glycosides having 18-hydroxy-dihydroalloprotolichesterinic, 18-hydroxy-neodihydroprotolichesterinic and 18-hydroxy-dihydroprotolichesterinic acids as aglycones and a di- or trisaccharide moiety linked at C-18 and at the carboxylic group. These compounds, called gobienines A–C, were found to be di- or trisacharides forming a macrolactone with the aglycone. The structures were elucidated by using extensive spectroscopic analysis (1D and 2D NMR, MS, IR and ORD) and chemical and enzymatic methods. © 2001 Elsevier Science Ltd. All rights reserved.

Keywords: Macrolactone glycoside esters; Lichens of Central Asia; *Acarospora gobiensis*; Acarosporaceae; NMR; MS; IR spectra

1. Introduction

Macrolactone glycosides containing an aglycone and di- or trisaccharides are found very rarely in nature (Ikan, 1999). At present only a few examples of these unusual compounds are known to come from living organisms. The best known are compounds isolated from tropical and subtropical plants, mainly of the genus *Ipomaea* and/or family Convolvulaceae (Noda et al., 1988; Hernandez-Carlos et al., 1999; Lehmann et al., 2000). Further examples of macrocyclic lactones were isolated from a Japanese mountain shrub (*Polygala*) or roots of the genera *Sonchus*; all are glycosides that have a terpenic aglycone and two sugars (Iwagawa and Hase, 1983; Helal et al., 2000; Kobayashi et al., 2000).

Similar compounds have also been reported in *Candida bogoriensis* and *Torulopsis* (*Candida*) *bombicola* (Spencer et al., 1970). The glycolipids produced by these yeast strains contain the disaccharide sophorose (β-D-Glc-(1-2)-D-Glc) linked to a lipid moiety containing a 17-hydroxyoctadecanoic acid.

As a continuation of our search for unusual bioactive compounds from Central Asian lichens (Řezanka and Dembitsky, 1998, 1999; Řezanka and Guschina, 1999, 2000, 2001a,b), we examined the lichen *Acarospora gobiensis* H. Magn.

2. Results and discussion

Detailed investigation of fractions of oligosaccharide mixtures from *A. gobiensis* led to the isolation of three additional glycosides. These compounds were purified to homogeneity by HPLC using an amino bonded silica gel column. Structural investigation of these three new macrolactone di- and trisaccharides of lichen acids, gobienine A (**1**), gobienine B (**2**) and gobienine C (**3**) was performed by NMR and FAB–MS. Their aglycones are the following lichen acids: 18-hydroxy-dihydroalloprotolichesterinic, 18 - hydroxy - neodihydroprotolichesterinic and 18-hydroxy-dihydroprotolichesterinic acid. All were present in the relatively small amounts ($<0.01\%$ of dry mass).

Compound **1** gave either positive or negative-ion FAB–MS. The positive ion in the mass spectrum of gobienine A (**1**) was a pseudo-molecular ion at m/z 677.3751 $(M+H)^+$ which indicates the molecular formula $C_{33}H_{56}O_{14}$.

* Corresponding author. Tel.: +42-2-4752300; fax: +42-2-4752347.
E-mail address: rezanka@biomed.cas.cz (T. Řezanka).

0031-9422/01/$ - see front matter © 2001 Elsevier Science Ltd. All rights reserved.
PII: S0031-9422(01)00388-0

In addition to the common fragment peaks produced by a glycosidic cleavage of the sugar moieties in each of the oligosaccharide cores (Fig. 1), i.e. m/z 513 $(M–H-162)^-$, m/z 351 (513–162 (hexose); (aglycone))$^-$, the negative ions of compound **1** determined by FAB–MS were observed at m/z 675 $(M–H)^-$.

Treatment of **1** with esterase (EC 3.1.1.1 from porcine liver) gave compound **1a** (37.1%) together with unreacted **1**. The positive ion FAB mass spectrum of **1a** exhibited a $[M+H]^+$ ion peak at m/z 695. The negative FAB–MS of **1a** showed an $(M–H)^-$ peak at m/z 693 along with the fragment peak at m/z 369 (M–H-324 (2× hexose units))$^-$ and a peak at m/z 531 (M–H-162 (hexose unit))$^-$ in place of that detected at m/z 513 in the spectrum of **1**. The difference of 18 mass units indicated (see above) that the ester linkage of the lichen acid is placed at C-2 of second glucose (Glu″).

The use of various one- and two-dimensional NMR spectroscopic methods provided information about the interglycosidic linkage, the sequence of monosaccharide residues and the site of esterification in all these complex oligosaccharides. The ^{1}H NMR spectrum of **1a**, when compared with that of **1**, showed an upfield shift (δ 1.52 ppm) of H-2″ of the second glucose (Glc″) and a disappearance of the signal at δ 5.73 indicating a loss of lactonization. The ester linkage of the aglycone is therefore located at 2-OH of Glc″.

The acid-catalyzed hydrolysis of **1a** gave a mixture of degradation products from the aglycone and the monosaccharide. The two saccharide units were identified as D-glucose by using the acetylated-2-butyl derivatives prepared from glycosides and analyzed by gas chromatography using a capillary column (Supelco SPB-1) (Gerwig et al., 1978).

The ^{1}H NMR spectrum of **1a** showed the signal of H-18 at δ 3.76. The proton and carbon signals arising from the sugar moiety were assigned with the aid of ^{1}H–^{1}H and ^{1}H–^{13}C two-dimensional shift-correlated NMR (COSY) analyses (Tables 2 and 4).

The ^{13}C NMR spectrum of **1a** showed glycosylation shifts only at C-2′ (Δ 5.7 ppm) of the first glucose relative to those of corresponding methyl pyranoside (δ_{C-2} = 74.8) (Seo et al., 1978).

The enzymatic hydrolysis of **1a** by β-glucosidase (EC 3.2.1.21) gave **1b** (EI–MS, m/z 370 $(M)^+$). The ^{1}H NMR, ^{13}C NMR and also ORD spectra of **1b** revealed it to the 18-hydroxydihydroallo-protolichesterinic acid, previously described by Řezanka and Guschina (2001b). The coupling constants of both anomeric proton signals of the sugar moiety indicated that the mode of glycosidic linkage of the two glucopyranose units is β (Kasai et al., 1977; Tori et al., 1977). The above data indicated that **1a** is (18*R*)-18-hydroxydihydroalloprotolichesterinic acid 18-*O*-β-D-glucopyranosyl-(1″-2′)-*O*-β-D-glucopyranoside.

To complete the determination of the primary structure of compound **1**, ^{1}H and ^{13}C NMR spectra of this compound were recorded. Gobienine A (**1**) showed a well resolved ^{1}H NMR spectrum (no-overlap in the proton region between δ 3.8 and 4.4). No derivatization was needed to achieve the total structural assignment of gobienine A (**1**) which was readily made through an extensive investigation using NMR spectroscopy. A combination of ^{1}H NMR spectra with 2-D homonuclear techniques including DQF-COSY and TOCSY allowed all C-bonded protons to be sequentially assigned within

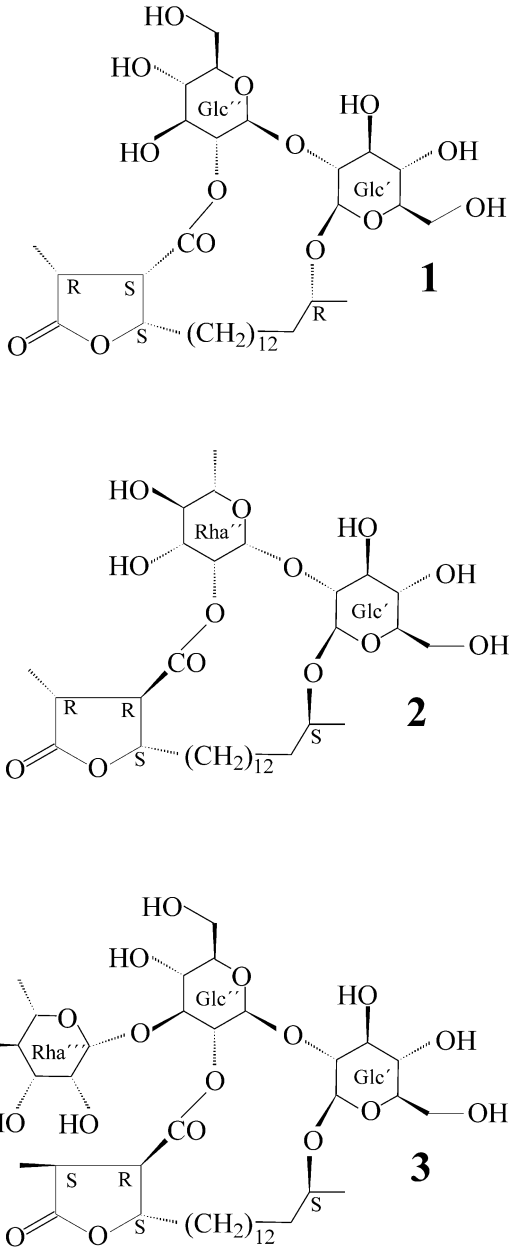

Fig. 1. The structures of gobienines A–C: (**1**) (18*R*)-18-hydroxydihydroalloprotolichesterinic acid 18-*O*-β-D-glucopyranosyl-(1″-2′)-*O*-β-D-glucopyranoside-(21,2″-lactone), (**2**) (18*S*)-hydroxyneodihydroprotolichesterinic acid 18-*O*-α-L-rhamnopyranosyl-(1″-2′)-*O*-β-D-glucopyranoside-(21,2″-lactone), (**3**) (18*S*)-hydroxydihydroprotolichesterinic acid 18-*O*-α-L-rhamnopyranosyl-(1‴-3″)-*O*-β-D-glucopyranosyl-(1″-2′)-*O*-β-D-glucopyranoside-(21,2″-lactone).

Table 1
^{1}H NMR data of **1b**–**3b**

H No.	**1b**	**2b**	**3b**
2	2.88 (1H, *dq*, $J_{2,3}=7.0$, $J_{2,20}=7.5$)	2.91 (1H, *dq*, $J_{2,3}=9.0$, $J_{2,20}=7.5$)	2.92 (1H, *dq*, $J_{2,3}=11.1$, $J_{2,20}=7.2$)
3	3.24 (1H, *dd*, $J_{3,2}=7.0$, $J_{3,4}=8.0$)	3.09 (1H, *dd*, $J_{3,2}=9.0$, $J_{3,4}=6.5$)	3.26 (1H, *dd*, $J_{3,2}=11.1$, $J_{3,4}=9.5$)
4	4.57 (1H, *ddd*, $J_{4,3}=8.0$, $J_{4,5}=8.0$ and 5.0)	4.65 (1H, *ddd*, $J_{4,3}=6.5$, $J_{4,5}=8.0$ and 4.5)	4.40 (1H, *ddd*, $J_{4,3}=9.5$, $J_{4,5}=8.0$ and 4.0)
5	1.68 (2H, *m*)	1.67 (2H, *m*)	1.70 (2H, *m*)
6–16	1.26 (22H, *m*)	1.26 (22H, *m*)	1.26 (22H, *m*)
17	1.54 (2H, *m*)	1.57 (2H, *m*)	1.56 (2H, *m*)
18	3.76 (1H, *m*)	3.80 (1H, *m*)	3.79 (1H, *m*)
19	1.16 (3H, *d*, $J=6$)	1.17 (3H, *d*, $J=6$)	1.17 (3H, *d*, $J=6$)
20	1.30 (3H, *d*, $J_{20,2}=7.5$)	1.31 (3H, *d*, $J_{20,2}=7.5$)	1.32 (3H, *d*, $J_{20,2}=7.2$)

Table 2
^{1}H NMR data of glycosides **1**–**3**

	1	**1a**	**2**	**3**
Glc 1′	5.78 (*d*, $J=7.1$)	5.64 (*d*, $J=7.6$)	5.81 (*d*, $J=7.8$)	5.65 (*d*, $J=7.7$)
2′	4.18 (*dd*, $J=7.1$, 8.1)	4.12 (*dd*, $J=7.6$, 8.1)	4.07 (*dd*, $J=7.8$, 8.0)	4.20 (*dd*, $J=8.5$, 7.7)
3′	4.26 (*dd*, $J=8.1$, 8.2)	4.18 (*dd*, $J=8.1$, 8.0)	4.12 (*dd*, $J=8.0$, 8.1)	4.10 (*dd*, $J=8.5$, 8.4)
4′	4.10 (*dd*, $J=8.2$, 8.1)	4.05 (*dd*, $J=8.0$, 8.2)	4.05 (*dd*, $J=8.1$, 8.1)	4.04 (*dd*, $J=8.4$, 8.8)
5′	3.91 (*ddd*, $J=8.1$, 6.5, 2.9)	3.90 (*ddd*, $J=8.2$, 6.1, 2.8)	3.91 (*ddd*, $J=8.1$, 6.2, 2.9)	3.94 (*ddd*, $J=8.8$, 6.2, 3.0)
6′	4.21 (*dd*, $J=11.0$, 6.5)	4.23 (*dd*, $J=10.9$, 6.1)	4.20 (*dd*, $J=10.5$, 6.2)	4.22 (*dd*, $J=10.9$, 3.0)
	4.34 (*dd*, $J=11.0$, 2.9)	4.31 (*dd*, $J=10.9$, 2.8)	4.27 (*dd*, $J=10.5$, 2.9)	4.34 (*dd*, $J=10.9$, 6.2)
Glc1″	5.61 (*d*, $J=7.5$)	5.60 (*d*, $J=7.7$)		5.68 (*d*, $J=7.3$)
2″	5.73 (*dd*, $J=7.5$, 8.0)	4.21 (*dd*, $J=7.7$, 8.0)		5.81 (*dd*, $J=7.3$, 8.0)
3″	4.23 (*dd*, $J=8.0$, 8.0)	4.25 (*dd*, $J=8.0$, 8.0)		4.16 (*dd*, $J=8.0$, 8.0)
4″	4.07 (*dd*, $J=8.0$, 8.1)	4.08 (*dd*, $J=8.0$, 8.1)		4.06 (*dd*, $J=8.0$, 8.1)
5″	3.88 (*ddd*, $J=8.1$, 6.1, 3.2)	3.92 (*dd*, $J=8.1$, 6.8, 3.2)		3.96 (*ddd*, $J=8.1$, 6.5, 3.1)
6″	4.19 (*dd*, $J=10.8$, 6.1)	4.16 (*dd*, $J=10.9$, 6.8)		4.18 (*dd*, $J=11.2$, 6.5)
6″	4.30 (*dd*, $J=10.8$, 3.2)	4.27 (*dd*, $J=10.9$, 3.2)		4.32 (*dd*, $J=11.2$, 3.1)
Rha1″			6.19 (*d*, $J=1.2$)	
2″			6.14 (*dd*, $J=1.2$, 3.7)	
3″			4.62 (*dd*, $J=9.5$, 3.7)	
4″			4.29 (*dd*, $J=9.5$, 9.7)	
5″			4.87 (*dq*, $J=9.7$, 6.6)	
6″			1.59 (*d*, $J=6.6$)	
Rha1‴				6.08 (*d*, $J=1.3$)
2‴				4.78 (*dd*, $J=1.3$, 3.9)
3‴				4.65 (*dd*, $J=9.9$, 3.9)
4‴				4.29 (*dd*, $J=9.9$, 9.5)
5‴				4.74 (*dq*, $J=9.5$, 6.8)
6‴				1.55 (*d*, $J=6.8$)

each ring system (Table 2) and all the resonances in the ^{13}C NMR spectra were assigned by using a ^{1}H-detected (^{1}H–^{13}C) one-bond correlation experiment (HMQC) (Table 4). The interglycosidic connectivities, as well as the site of lactonization, were established entirely on the basis of the observed ^{13}C–^{1}H long-range cross peaks ($^2J_{CH}$ and $^3J_{CH}$) in HMBC experiments. For example, ^{13}C–^{1}H long-range cross peaks (^3J) were observed in the spectrum of gobienine A (**1**) between C-1′ (δ 103.4) of the first glucose and H-18 of the aglycone and C-1″ of the second glucose (δ_C 103.8) and H-2′ of the first glucose (δ_H 4.18). A series of gated decoupling experiments was performed for further determination of the anomeric configuration of the glycosyl linkages, from the completely resolved multiplets for the two anomeric ^{13}C atoms of compounds **1** (Table 4), all $^1J_{CH}$ values of the glucoses were found to be <165 Hz. Such coupling constants established the mode of glycosidic linkage to be β (Collins and Ferrier, 1995) type for each of the monosaccharide units.

From the ^{1}H NMR spectra (Table 2), the esterified positions on the disaccharide cores were easily identified through strong deshielding effects relative to the non-esterified equivalents on **1a**. In this way, the primary structure of gobienine A (**1**) was established as (18*R*)-18-hydroxydihydroalloprotolichesterinic acid 18-*O*-β-D-

glucopyranosyl-(1″-2′)-*O*-β-D-glucopyranoside-(21,2″-lactone).

In **2**, both positive and negative FAB–MS were obtained (*m/z* 661.3801, $(M+H)^+$, i.e. $C_{33}H_{56}O_{13}$,). For compound **3**, the positive ion mode revealed a quasi-molecular ion peak $(M+H)^+$ at *m/z* 823.4331 indicating a molecular formula of $C_{39}H_{66}O_{18}$. The negative ion FAB–MS of compounds **2** and **3** showed the same fragmentation pathways that resulted from the cleavage of glucoside-ester bonds that yields high-mass fragment ions representing each monosaccharide and aglycone. Compounds **2** and **3** showed also the pseudomolecular peaks at *m/z* 659 $(M–H)^-$ and *m/z* 821 $(M–H)^-$, respectively. In **2** the appropriate cleavages resulted in the presence of the ions at *m/z* 497 $(M–H\text{-}162)^-$, 351 [$(M–H\text{-}162–146)^-$; (aglycone)] while **3** yielded ions at *m/z* 821 $(M–H)^-$, 675 $(M–H\text{-}146)^-$, 513 $(M–H\text{-}146–162)^-$, 351 [$(M–H\text{-}146\text{-}2\times162)^-$; (aglycone)].

The site of lactonization of **2** was placed at C-2″ of rhamnose based on the observed ^3J-coupling between the carbonyl carbon of the aglycone (δ 162.7) and its geminal proton (δ ca. 6.4) in the pyranose unit. For **3**, the position of lactonization was verified by the observed connectivities between the carbonyl group of the aglycone (δ 163.1) and H-2″ of the second glucose.

The position of lactonization was also verified by the $^3J_{CH}$ connectivities between the carbonyl group of the aglycone and proton H-2 of the monosaccharide unit in both natural disaccharides as in compound **1**.

A series of gated decoupling experiments was performed for further determination of the anomeric configuration of the glycosyl linkages and the completely resolved multiplets for the two anomeric ^{13}C atoms of compounds **2** (Table 4) showed that all $^1J_{CH}$ values of the glucoses were <165 Hz. Such coupling constants established the mode of glycosidic linkage as β of the pyranose (Collins and Ferrier, 1995) type for each of the monosaccharide units. A different diglycoside was identified as the oligosaccharide core of gobienine B (**2**) and the structure of this natural product was determined to be (18*S*)-hydroxyneodihydroprotolichesterinic acid 18-*O*-α-L-rhamnopyranosyl-(1″-2′)-*O*-β-D-glucopyranoside-(21,2″-lactone).

The ^1H and ^{13}C signals arising from the sugar moieties in the spectra of compound **3** were assigned by ^1H–^1H DQ-COSY and ^1H–^{13}C HETCOR analyses (Tables 2 and 4). The ^{13}C NMR spectrum of **3** showed the glycosylation shifts at C-3″ (Δδ 6.3) of the second glucose relative to those of corresponding methyl pyranosides (Seo et al., 1978). The selective INEPT technique (Cordell and Kinghorn, 1991), applied to gobienine C (**3**), confirmed the nature of the saccharide substitution. Thus, irradiation of the anomeric proton H-1′ of the first glucose at δ 5.65 ($^3J_{CH}=6$ Hz) selectively enhanced C-18 of the aglycone. When H-2′ of the first glucose (δ 4.20) was irradiated ($^3J_{CH}=6$ Hz), a clear enhancement of the anomeric carbon C-1″ of the second glucose resulted (δ 103.1). Irradiation of the inner glucose H-3″ at δ 4.16 ($^3J_{CH}=6$ Hz) resulted in the polarization transfer to the anomeric carbon C-1‴ (δ 102.1) of the terminal rhamnose. The application of a COLOC NMR experiment in **3** further confirmed the sequence of the sugar moiety. ^{13}C-^1H long-range cross peaks were observed and unambiguously assigned as those between C-1′ of glucose and H-18 of the aglycone and C-1‴ of the terminal rhamnose and H-3″ of inner glucose.

Table 3
^{13}C NMR data of **1b**–**3b**

C No.	1b	2b	3b
1	177.5	178.9	177.8
2	36.4	36.0	36.8
3	51.8	52.0	51.5
4	77.5	79.3	78.6
5	31.2	32.1	32.3
6	25.6	25.8	24.6
7–15		28.1–29.8	
16	25.1	25.5	24.9
17	38.1	38.5	38.6
18	68.5	68.8	68.6
19	22.8	23.4	22.9
20	12.8	13.9	14.9
21	170.1	168.7	169.5

Table 4
^{13}C NMR data of glycosides **1**–**3**

	1	1a	2	3
Glc1′	103.4	101.8	104.5	103.7
2′	80.3	80.5	80.9	80.8
3′	77.4	78.9	78.1	77.1
4′	72.1	71.2	72.0	73.0
5′	76.1	74.9	75.1	75.0
6′	63.4	64.2	64.5	64.6
6′				
Glc1″	103.8	102.8		103.1
2″	80.2	74.5		80.4
3″	78.1	78.4		86.7
4″	72.6	72.7		72.0
5″	77.9	78.1		78.3
6″	64.1	63.3		64.4
6″				
Rha1″			101.9	
2″			79.8	
3″			72.2	
4″			74.1	
5″			69.1	
6″			18.3	
Rha1‴				102.1
2‴				71.6
3‴				72.4
4‴				73.9
5‴				69.6
6‴				18.7

In compound **3**, the $^1J_{CH}$ showed the following coupling value: 163.1 Hz for the first glucose, 164.7 Hz for the second glucose and 172.5 Hz for the rhamnose. The latter value is typical for the equatorial configuration of the anomeric proton, confirming the α-L-rhamnose residue (Etse et al., 1991).

Long-range heteronuclear coupling correlations were used to determine the linkages within the trisaccharide core of gobienine C (**3**). For instance a connectivity was observed between H-2″ of the second glucose at δ 5.81 and the anomeric carbon of the first glucose at δ 103.7, and between H-3‴ of rhamnose (δ 4.65) and C-1″ of the second glucose (δ 103.1).

The signals for the sugar moiety in the ^{1}H NMR spectra of **3** and **1a** were compared in order to establish the site of lactone linkage at the oligosaccharide core. Significant downfield shifts owing to acylation were observed for the inner glucose proton H-2″ (Δ 1.60 ppm).

The above mentioned spectral evidence indicated that compound **3** is a glycoside similar to those isolated from this source, having the carbonyl group of the aglycone linked to an oligosaccharide core to form a macrocyclic lactone. Its correct structure is (18*S*)-hydroxydihydroprotolichesterinic acid 18-*O*-α-L-rhamnopyranosyl-(1‴-3″)-*O*-β-D-glucopyranosyl-(1″-2′)-*O*-β-D-glucopyranoside-(21,2″-lactone).

3. Experimental

3.1. General experimental procedures

UV spectra were measured in heptane in the range of 200–350 nm by a Cary 118 (Varian) apparatus. Optical rotatory dispersion (ORD) measurement was carried out under dry N_2 on a Jasco-500A spectropolarimeter at 24 °C. A Perkin-Elmer Model 1310 (Perkin-Elmer, Norwalk, CT, USA) IR spectrophotometer was used for scanning IR spectroscopy of acids and glycosides as neat films. NMR spectra were recorded on a Bruker AMX 500 spectrometer (Bruker Analytik, Karlsruhe, Germany) at 500.1 MHz (^{1}H), 125.7 MHz (^{13}C). High- and also low-resolution MS were recorded using a VG 7070E-HF spectrometer (70 eV). HR–FAB–MS (positive and/or negative ion mode) were obtained with a PEG-400 matrix. HPLC was carried out using Shimadzu gradient LC system (Shimadzu, Kyoto, Japan). Gas chromatographic analysis was done on a Hewlett Packard HP 5980 gas chromatograph (Hewlett Packard Ltd., Czech Republic).

3.2. Plant material

The specimen of *Acarospora gobiensis* H. Magn., (Acarosporaceae, Lecanorales, Ascolichenes) was collected in July 1996 along the shore of Lake Issyk Kul, Tian-Shan mountains. The voucher specimens are deposited in the collection of the second author (I.A. Guschina).

3.3. Extraction and isolation

The lichen specimen [100 g of air-dried lichen, see Řezanka and Guschina, (2000)] was extracted by the Blight and Dyer (1959) method and the extract was chromatographed on a column of Sephadex LH-20 eluted with EtOH–i–PrOH (fraction 1), EtOH (fraction 2) and then MeOH (fraction 3). Fraction 3 was further fractionated by HPLC on a NH_2-Bondapak (Waters Ltd., Czech Republic) column (30 cm×7.8 mm, flow rate 1.8 ml/min) with ACN–H_2O (2:5) to yield compounds **1** (2.1 mg), **2** (1.4 mg) and **3** (0.6 mg).

The identification and the D or L configuration of sugars was determined using gas chromatography according to the method of Gerwig et al. (1978), with some modifications as previously described (Řezanka and Guschina, 2000).

3.4. Acid hydrolysis of *1a*

The glycoside (~0.1 mg) was refluxed in 2 N HCl (0.5 ml) for 2 h. The degradation products of the aglycone were extracted three times with EtOAc (10 ml). After separating the organic layer, the aqueous phase was neutralized with $NaHCO_3$ and lyophilized.

3.5. Enzymatic hydrolysis

A solution of glycoside (~0.1 mg) in acetate buffer (pH 4.4, 10 ml) was treated with β-glucosidase (EC 3.2.1.21) for 48 h at 37 °C. The reaction solution was evaporated to dryness, and the residue was chromatographed on a column of silica gel (10 g), using CH_2Cl_2–MeOH–H_2O (90:10:1) to provide lichen acids for ^{1}H NMR and ORD analysis.

Glycosides (~ 0.1 mg) were suspended in $(NH_4)_2SO_4$ solution of esterase (EC 3.1.1.1, from porcine liver) at pH ~8 and incubated 15 min at 25 °C. The aglycone was extracted three times with EtOAc (10 ml). After separating the organic layer, the aqueous phase was neutralized with 0.5 N HCl and lyophilized.

3.6. (S)-MTPA and (R)-MTPA esters

Treatment of each hydroxy acid (**1b**, **2b** and **3b**) with (*R*)-(−)-MTPACl or (*S*)-(+)-MTPACl converted them into the (*S*)- and (*R*)-2-methoxy-2-trifluoromethylphenylacetic acid (MTPA) esters (**1s**, **2s**, and **3s** and **1r**, **2r** and **3r**, respectively). The values of $\Delta\delta = [\delta(S\text{-MTPA ester}) - \delta(R\text{-MTPA ester})]$ in the ^{1}H NMR spectra suggested that the absolute configuration at C-18 of compound **1** was (*R*) while that of **2** and **3** were (*S*) (Ohtani et al., 1991b). The data are shown in Table 5.

Table 5
Stereochemical analysis of compounds **1b**, **2b** and **3b** with (*R*)- and (*S*)-MTPA (Mosher) derivatives[a]

MTPA esters of compound No.	$\Delta\delta = \delta_{S\text{-ester}} - \delta_{R\text{-ester}}$ (Hz)		
	H-19	H-17	Carbinol configuration
1b	+12.8	−30.1	*R*
2b	−16.9	+26.7	*S*
3b	−15.8	+34.2	*S*

[a] The aglycones from glycosides **1**–**3** are identical from one from **1b** or **2b** or **3b**.

(*S*)-MTPA esters of free acids (**1**–**3**) (Ohtani et al., 1991a, b). To a CH_2Cl_2 solution (100 μl) of aglycone (0.3 mg), DMAP (1.0 mg), and Et_3N (2 μl) was added (*R*)-(−)-MTPACl (2.0 mg) at room temperature, and stirring was continued for 3 h. After the evaporation of the solvent, the residue was purified by Silica gel TLC (hexane–AcOEt, 2:1) to provide the (*S*)-MTPA ester as colorless oil.

(*R*)-MTPA Esters of free acids (**1**–**3**). Each aglycone (0.3 mg) was treated with (*S*)-(+)-MTPACl (2.0 mg) by the same procedure as described above to provide the (*R*)-MTPA ester as colorless oil. The data are given in Table 5.

18*R*-Hydroxydihydroalloprotolichesterinic acid **1b**, white crystals, mp 143 °C, $[\alpha]_D^{24}$ −48° (*c* 0.19, $CHCl_3$), UV λ_{max} (EtOH, nm) 218 (log ε 2.28); ORD: $[\alpha]_{222}^{24}$ nm (−790), ^{1}H NMR, ^{13}C NMR and MS spectra, see (Řezanka and Guschina, 2001b).

18*S*-Hydroxydihydroprotolichesterinic acid **2b**, white small needles, mp 105–107 °C, $[\alpha]_D^{24}$ +7.9° (*c* 0.10, $CHCl_3$), UV λ_{max} (EtOH, nm) 207 (log ε 2.74); ORD: $[\alpha]_{220}^{24}$ nm (+90), ^{1}H NMR, ^{13}C NMR and MS spectra, see (Řezanka and Guschina, 2001b).

18*S*-Hydroxyneodihydroprotolichesterinic acid **3b**, white plates, mp 127.5 °C, $[\alpha]_D^{24}$ −28.5° (*c* 0.21, $CHCl_3$), UV λ_{max} (EtOH, nm) 217 (log ε 2.42); ORD: $[\alpha]_{220}^{24}$ nm (−260), ^{1}H NMR, ^{13}C NMR and MS spectra, see (Řezanka and Guschina, 2001b).

Gobienine A, (18*R*) - 18 - hydroxydihydroalloprotolichesterinic acid 18-*O*-β-D-glucopyranosyl-(1″-2′)-*O*-β-D-glucopyranoside-(21,2″-lactone) **1**, colorless powder, mp 187 °C, $[\alpha]_D^{24}$ −61° (*c* 0.07, MeOH); UV 219 nm (log ε 3.88); IR (KBr) (cm^{-1}): 3400 (OH), 2950, 2920, 1765 (lactone), 1710 (ester); HR–FAB–MS *m*/*z* 677.3751 $(M+H)^+$, calc. for $[C_{33}H_{56}O_{14}]^+$ 677.3748; negative FAB–MS *m*/*z* 675 $(M-H)^-$, 513 (M–H-162)$^-$, 351 (M–H-162-162)$^-$; ^{1}H NMR and ^{13}C NMR spectra see Tables 1–4.

(18*R*) - 18 - Hydroxydihydroalloprotolichesterinic acid 18-*O*-β-D-glucopyranosyl-(1″-2′)-*O*-β-D-glucopyranoside **1a**, colorless powder, mp 142 °C, $[\alpha]_D^{24}$ −82° (*c* 0.12, MeOH); UV 219 nm (log ε 3.88); IR (KBr) (cm^{-1}): 3400 (OH), 2950, 2920, 1770 (lactone), 1710 (ester); positive FAB *m*/*z* 695 $(M+H)^+$, negative FAB–MS *m*/*z* 693 (M–H)$^-$, 531 (M–H-162)$^-$, 369 (M–H-162-162)$^-$.

Gobienine B, (18*S*)-hydroxyneodihydroprotolichesterinic acid 18-*O*-α-L-rhamnopyranosyl-(1″-2′)-*O*-β-D-glucopyranoside-(21,2″-lactone) **2**, colorless powder, mp 105 °C, $[\alpha]_D^{24}$ −59° (*c* 0.08, MeOH); UV 219 nm (log ε 3.88); IR (KBr) (cm^{-1}): 3400 (OH), 2950, 2920, 1765 (lactone), 1710 (ester); HR–FAB–MS *m*/*z* 661.3801 $(M+H)^+$, calc. for $[C_{33}H_{56}O_{13}]^+$ 661.3798; negative FAB–MS *m*/*z* 659 (M–H)$^-$, 497 (M–H-162)$^-$, 351 (M–H-162-146)$^-$; ^{1}H NMR and ^{13}C NMR spectra see Tables 1–4.

Gobienine C, (18*S*)-hydroxydihydroprotolichesterinic acid 18-*O*-α-L-rhamnopyranosyl-(1‴-3″)-*O*-β-D-glucopyranosyl-(1″-2′)-*O*-β-D-glucopyranoside-(21,2″-lactone) **3**, colorless powder, mp 115 °C, $[\alpha]_D^{24}$ −152° (*c* 0.05, MeOH); UV 219 nm (log ε 3.88); IR (KBr) (cm^{-1}): 3400 (OH), 2950, 2920, 1765 (lactone), 1710 (ester); HR–FAB–MS *m*/*z* 823.4331 $(M+H)^+$, calc. for $[C_{39}H_{66}O_{18}]^+$ 823.4327; negative FAB–MS *m*/*z* 821 (M–H)$^-$, 675 (M–H-146)$^-$, 513 (M–H-146-162)$^-$, 351 (M–H-146-2×162)$^-$; ^{1}H NMR and ^{13}C NMR spectra see Tables 1–4.

References

Blight, E.G., Dyer, W.J., 1959. A rapid method of total lipid extraction and purification. Can. J. Biochem. Physiol. 37, 911–917.

Collins, P., Ferrier, R., 1995. Monosaccharides. Their Chemistry and Their Roles in Natural Products. John Wiley & Sons, UK, pp. 26–32.

Cordell, G.A., Kinghorn, A.D., 1991. One-dimensional proton-carbon correlations for the structure determination of natural products. Tetrahedron 47, 3521–3534.

Etse, J.T., Gray, A.L., Lavaud, C., Massiot, G., Nuzillard, J.M., Waterman, P.G., 1991. Chemistry of the Annonaceae. 29. Structure of mezzettiaside-2, mezzettiaside-4, mezzettiaside-5, mezzettiaside-6, mezzettiaside-7, new partially esterified 1-*O*-octyl tri-rhamnosyl and tetra-rhamnosyl derivatives from *Mezzettia leptopoda*. J. Chem. Soc. Perkin Trans. I, 861–864.

Gerwig, G.J., Kamerling, J.R., Vliegenthart, J.F.G., 1978. Determination of the D and L configuration of neutral monosaccharides by high-resolution capillary GLC. Carbohydr. Res. 62, 349–357.

Helal, A.M., Nakamura, N., El-Askary, H., Hattori, M., 2000. Sesquiterpene lactone glucosides from *Sonchus asper*. Phytochemistry 53, 473–477.

Hernandez-Carlos, B., Bye, R., Pereda-Miranda, R., 1999. Orizabins V–VIII, tetrasaccharide glycolipids from the Mexican scammony root (*Ipomoea orizabensis*). J. Nat. Prod. 62, 1096–1100.

Ikan, R., 1999. Naturally Occurring Glycosides. John Wiley & Sons, New York.

Iwagawa, T., Hase, T., 1983. A bitter monoterpene diglycoside from *Viburnum urceolatum*. Phytochemistry 22, 255–256.

Kasai, R., Suzuo, M., Asakawa, Y., Tanaka, O., . Carbon-13 chemical shifts of isoprenoid-β-D-glucopyranosides and β-D-mannopyranosides. Stereochemical influences of aglycone alcohols. Tetrahedron Lett.1977 175–178.

Kobayashi, W., Miyase, T., Suzuki, S., Noguchi, N., Chen, X.M., 2000. Oligosaccharide esters from the roots of *Polygala arillata*. J. Nat. Prod. 63, 1066–1069.

Lehmann, C.W., Furstner, A., Muller, T., 2000. Macrocyclic substructure of tricolorin A—the first crystal structure of a resin glycoside. Z. Kristallographie 215, 114–117.

Noda, N., Kogetsu, H., Kawasaki, T., Miyahara, K., 1988. Scammonins I and II, the resin glycosides of radix *Scammoniae* from *Convolvulus scammonia*. Phytochemistry 29, 3565–3569.

Ohtani, I., Kusumi, T., Kashman, Y., Kakisawa, H., 1991a. High-field FT NMR application of Mosher method—the absolute-configurations of marine terpenoids. J. Am. Chem. Soc. 113, 4092–4095.

Ohtani, I., Kusumi, T., Kashman, Y., Kakisawa, H., 1991b. A new aspect of the high-field NMR application of Mosher method—the absolute-configuration of marine triterpene sipholenol A. J. Org. Chem. 56, 1296–1298.

Řezanka, T., Guschina, I.A., 2000. New glycosidic compounds of murolic, protoconstipatic and allo-murolic acids from lichens of Central Asia. Phytochemistry 54, 635–645.

Řezanka, T., Guschina, I.A., 2001a. Further new glucosides of lichen's acids from Central Asian lichens. Phytochemistry 56, 181–188.

Řezanka, T., Guschina, I.A., 2001b. Glycoside's esters from lichens of Central Asia. Phytochemistry 58, 509–516.

Řezanka, T., Dembitsky, V.M., 1998. Brominated fatty acids from lichen *Acarospora gobiensis*. Phytochemistry 50, 97–99.

Řezanka, T., Dembitsky, V.M., 1999. Novel brominated lipidic compounds from lichens of Central Asia. Phytochemistry 51, 963–968.

Řezanka, T., Guschina, I.A., 1999. Brominated depsidones from *Acarospora gobiensis*, a lichen of Central Asia. J. Nat. Prod. 62, 1675–1677.

Seo, S., Tomita, Y., Tori, K., Yoshimura, Y., 1978. Determination of the absolute configuration of a secondary hydroxy group in a chiral secondary alcohol using glycosidation shifts in carbon-13 nuclear magnetic resonance spectroscopy. J. Am. Chem. Soc. 100, 3331–3339.

Spencer, J.F.T., Gorin, P.A.J., Tulloch, A.P., 1970. Yeasts isolated from bumblebee honey from western Canada: identification with the aid of proton magnetic resonance spectra of their mannose-containing polysaccharides. Can. J. Microbiol. 16, 117–119.

Tori, K., Seo, S., Yoshimura, Y., Arita, H., Tomita, Y., 1977. Glycosidation shifts in carbon-13 NMR spectroscopy: carbon-13 signal shifts from aglycone and glucose to glucoside. Tetrahedron Lett. 179–182.

PERGAMON

Phytochemistry 58 (2001) 1289–1295

PHYTOCHEMISTRY

www.elsevier.com/locate/phytochem

Sesquiterpene coumarins from the roots of *Ferula assa-foetida*

Mohamed H. Abd El-Razek[a], Shinji Ohta[b], Ahmed A. Ahmed[c], Toshifumi Hirata[a,*]

[a]*Department of Mathematical and Life Sciences, Graduate School of Science, Hiroshima University, 1-3-1 Kagamiyama, Higashi-Hiroshima 739-8526, Japan*
[b]*Instrument Center for Chemical Analysis, Hiroshima University, 1-3-1 Kagamiyama, Higashi-Hiroshima 739-8526, Japan*
[c]*Department of Chemistry, Faculty of Science, El-Minia University, El-Minia 61519, Egypt*

Received 27 February 2001; received in revised form 13 June 2001

Abstract

From the chloroform extract of the roots of *Ferula assa-foetida*, two sesquiterpene coumarins designated assafoetidnol A and assafoetidnol B were isolated, in addition to six known compounds, gummosin, polyanthin, badrakemin, neveskone, samarcandin and galbanic acid. The structures of the sesquiterpenes new compounds were established by spectroscopic methods. © 2001 Elsevier Science Ltd. All rights reserved.

Keywords: *Ferula assa-foetida*; Umbelliferae; Resins; Sesquiterpene coumarins

1. Introduction

The genus *Ferula* presents interesting phytochemical features, such as the occurrence of sesquiterpenes (Gonzalez and Barrera, 1995; Appendino et al., 1997; Kojima et al., 1999, 2000; Chen et al., 2000; Su et al., 2000a,b) and sesquiterpene coumarins (Murray, 1989; Ahmed, 1999; Su et al., 2000a,b). *Ferula assa-foetida* grows in Kashmir, Iran and Afghanistan. It is herbaceous and perennial and grows up to 2 m high (Kapoor, 1990). One part used is an oleogum resin, obtained by incision from the roots, and this is called asa-foetida (Kapoor, 1990). The resin of *F. assa-foetida* enjoys a reputation as a folklore medicine (Boulus, 1983). In Nepal asa-foetida is considered to be a sedative, carminative, antispasmodic and a diuretic in its properties. It is also believed is have aphrodisiac properties and increases the sexual appetite (Eigner and Scholz, 1990). Indeed, asa-foetida is consumed regularly in the daily Nepali diet. It is popular household remedies and its components are used for many prescriptions in traditional healing (Eigner and Scholz, 1999). The characteristic features of this plant include the presence of glucuronic acid, galactose, arabinose and rhamnose which have been isolated from the gum (Kapoor, 1990), whereas the taste and smells are due to sulfur containing compounds. Asadisulphide (Kajimoto et al., 1989), disulfides, as well as symmetric tri- and tetrasulfides have been isolated (Rajanikanth et al., 1984). Also, umbelliferone, farnesiferol A, B and C, and ferulic acid (Caglioti et al., 1958, 1959), kamolonol (Hofer et al., 1984), assafoetidin and ferocolicin (Banerji, 1988), assacoumarin A and B (Kajimoto et al., 1989), foetidin (Buddrus et al., 1985), episamarcandin, umbelliprenin and conferol (Nassar et al., 1995), 5-hydroxyumbelliprenin, 8-hydroxyumbelliprenin and 8-acetoxyumbelliprenin (Appendino et al., 1994), and episamarcandin acetate (Nassar and Mohamed, 1998) have been isolated. Until 1994 the stereochemistry of assacoumarin B had not been elucidated, when a detailed spectroscopic investigation was carried out with the aid of 1D and 2D NMR spectroscopic techniques. This study showed that assacoumarin B has a constitution different from the originally reported and this compound was actually galbanic acid (Appendino et al., 1994), a known constituents of galbanum (Bagirov et al., 1980). We wish to report the isolation and structure elucidation of two new sesquiterpene coumarins from the resins of *Ferula assa-foetida*.

2. Results and discussion

The resins of *F. assa-foetida* were extracted with chloroform. Successive chromatographic separation led

* Corresponding author. Tel.: +81-824-247435; fax: +81-824-247435.
E-mail address: thirata@sci.hiroshima-u.ac.jp (T. Hirata).

0031-9422/01/$ - see front matter © 2001 Elsevier Science Ltd. All rights reserved.
PII: S0031-9422(01)00324-7

to the isolation of two new sesquiterpene coumarins, designated assafoetidnol A (**1**) and assafoetidnol B (**2**).

Assafoetidnol A (**1**) had a molecular formula $C_{24}H_{30}O_5$ as established by HREIMS (*m/z* 398.2106 $[M]^+$, Δ +1.3 mmu). The IR spectrum indicated the presence of hydroxyl and carbonyl groups. The structure of **1** was established from analysis of the ^1H NMR and ^{13}C NMR spectra, as shown in Table 1. Compound **1** displayed 24 carbon signals, nine being typical for an umbelliferone skeleton and the other 15 signals were ascribable to a sesquiterpene moiety. This suggested that **1** was derived from sesquiterpene and umbelliferone components. The downfield signal at δ_C 161.3 was assigned to the carbonyl carbon of the coumarin moiety. DEPT experiments classified the carbon signals to three methyls at δ_C 15.9, 31.2, and 23.2 which were attributed to C-13′, C-14′, and C-15′, respectively, three aliphatic methylenes at δ_C 27.1, 35.3 and 43.5, an olefinic carbon at δ_C 112.5 and a primary alcoholic carbon at δ_C 67.5 characteristic for C-11′, and nine methines, five of them for umbelliferone moiety at δ_C 112.8 (C-3), 143.5 (C-4), 128.7 (C-5), 113.2 (C-6) and 101.4 (C-8). Assignments of all protonated carbons were made by the analysis of the HMQC spectrum. The ^1H–^1H COSY spectrum showed that the methine proton at δ_H 1.39 (H-5′) is coupled to the downfield secondary alcoholic at δ_H 3.98 (H-6′), which in turn is coupled to the methylene protons at δ_H 2.21 (H-7′$_{ax}$) and 2.62 (H-7′$_{eq}$). The other secondary alcoholic at δ_H 3.21 (H-3′) coupled to the methylene protons at δ_H 1.66 (H-2′$_{ax}$) and 1.35 (H-2′$_{eq}$).

The location of two hydroxyl groups at C-3′ and C-6′ was proven by HMBC. The stereochemistry of **1** was deduced from the comparison of coupling constants with those of cauferin (Kuliev and Khasanov, 1978), previously isolated from *F. conocaula*. Acetylation of **1** afforded a diacetyl derivative **1a**, which showed two oxygenated carbon signals at δ_C 80.2 and 71.6, these being ascribed to the secondary alcoholic carbons. Also these facts were supported by the downfield shifts of H-3′ to δ_H 4.45 and H-6′ to δ_H 5.16. Esterfication of **1** with *p*-bromobenzoyl chloride gave assafoetidnol A di-*p*-bromobenzoate (**1b**),

Table 1
^1H and ^{13}C NMR spectral data for compounds **1** and **2** ($CDCl_3$)

	1		**2**	
	δ_H (*J* in Hz)	δ_C (multiplicity)[a]	δ_H (*J* in Hz)	δ_C (multiplicity)[a]
2		161.3 (C)		161.1 (C)
3	6.22 (9.5*d*)	112.8[b] (CH)	6.26 (9.5*d*)	113.2[c] (CH)
4	7.62 (9.5*d*)	143.5 (CH)	7.64 (9.5*d*)	143.4 (CH)
5	7.31 (8.5 *d*)	128.7 (CH)	7.37 (8.5*d*)	128.8 (CH)
6	6.79 (8.5, 2.5*dd*)	113.2[b] (CH)	6.84 (8.5, 2.5*dd*)	113.2[c] (CH)
7		161.9 (C)		161.7 (C)
8	6.77 (2.5*d*)	101.4 (CH)	6.79 (2.5*d*)	101.4 (CH)
9		155.7 (C)		155.9 (C)
10		112.5 (C)		112.7 (C)
1′	1.66 (*m*)	27.1 (CH_2)	1.73 (*m*)	30.3 (CH_2)
2′	1.66 (*m*)	35.3 (CH_2)	1.73 (*m*)	22.9(CH_2)
	1.35 (14.4, 4.9*dd*)		1.93 (*m*)	
3′	3.21 (11.3, 4.9*dd*)	78.8 (CH)	4.63 (*br s*)	79.9 (CH)
4′		39.2 (C)		37.8 (C)
5′	1.39 (10.7*d*)	51.7 (CH)	2.01 (12.0*d*)	45.3 (CH)
6′	3.98 (13.3, 10.7, 5.5*ddd*)	70.3 (CH)	3.67 (12.0, 9.5*dd*)	75.2 (CH)
7′	2.21 (13.8, 13.3*dd*)	43.5 (CH_2)	4.08 (9.5*d*)	77.3 (CH)
	2.62 (13.8, 5.5*dd*)			
8′	114.1 (C)		145.6 (C)	
9′	2.10 (6.7, 5.5*dd*)	56.0 (CH)	2.35 (6.7, 5.5*dd*)	56.9 (CH)
10′		38.3 (C)		37.3 (C)
11′	4.27 (10.1, 6.7*dd*)	67.5 (CH_2)	4.33 (10.1, 6.7*dd*)	68.2 (CH_2)
	4.05 (10.1, 5.5*dd*)		4.16 (10.1, 5.5*dd*)	
12′	4.84 (*br s*)	112.5 (CH_2)	4.97 (*brs*)	110.0 (CH_2)
	4.75 (*br s*)		5.25 (*brs*)	
13′	0.99 (*s*)	15.9 (CH_3)	1.21 (*s*)	31.1 (CH_3)
14′	1.35 (*s*)	31.2 (CH_3)	1.11 (*s*)	22.1 (CH_3)
15′	0.96 (*s*)	23.2 (CH_3)	1.06 (*s*)	23.7 (CH_3)
OAc			1.99 (*s*)	170.3 (C)
				21.1 (CH_3)

[a] Multiplicity was determined by DEPT experiments.
[b] Signals may be interchangeable.
[c] Signals may be interchangeable.

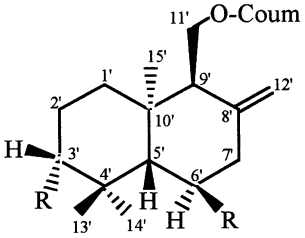

1: R=OH
1a: R=OAc
1b: R=O-*p*-BrBz

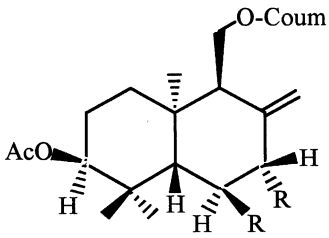

2: R=OH
2a: R=OAc
2b: R=O-*p*-BrBz

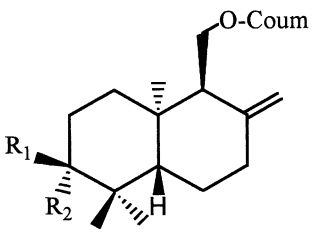

3: R_1=OH, R_2=H
4: R_1=H, R_2=OAc

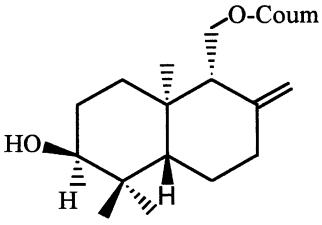

5

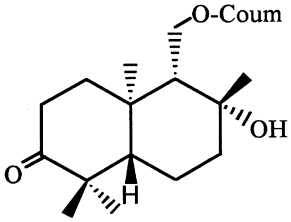

6

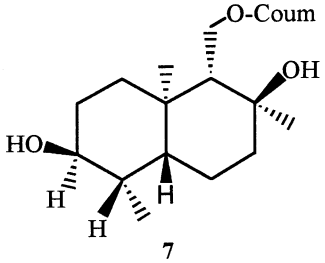

7

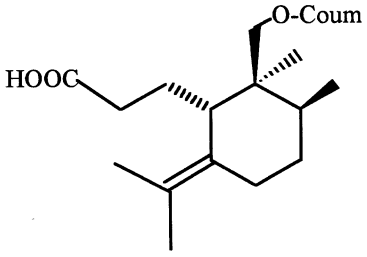

8

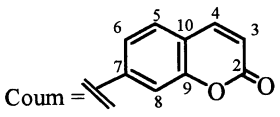

which showed a good separation of proton signals and allows a clear NOE. In NOE experiments, irradiation of H-3′ resulted in enhancements of H-13′ and H-5′ signal, as shown in Fig. 1, whereas irradiation of H-6′ resulted in enhancement of H-7′$_{eq}$, H-14′ and H-15′. Additionally, irradiation of H-9′ resulted in enhancement of Me-15′ and irradiation of Me-15′ showed a clear enhancements of H-1′$_{eq}$, H-2′$_{ax}$, H-6′ and H-9′, indicating the α-orientation of H-1′$_{eq}$, H-2′$_{ax}$, H-6′, H-9′ and Me-15′. Irradiation of H-11′ resulted in enhancements of H-1′$_{ax}$, H-5′ and H-7′$_{ax}$ signals, thereby indicating the β-orientation of H-1′$_{ax}$, H-5′, H-7′$_{ax}$ and H-11′. The NOE experiments supported the relative stereochemistry of the chiral centers. The absolute configuration of **1** was determined by the application of dibenzoate rule (Gonnella et al., 1982). The CD spectrum of the dibenzoyl derivative **1b** in MeOH exhibited a negative Cotton effect at 253 nm and a positive one at 234 nm, as shown in Fig. 2. This indicates that the absolute configuration of **1** was 3′R,6′R. Thus the complete structure of **1** was determined to be as shown in Fig. 1.

Assafoetidnol B (**2**) was estimated by the molecular formula $C_{26}H_{32}O_7$ by HRFABMS (*m*/*z* 457.2205, $[M+H]^+$, Δ −4.7 mmu). The NMR spectral data of **2** were similar to those of **1**, the main differences between both compounds being the signals assigned to the sesquiterpene unit. In the ^{1}H NMR spectrum of **2**, the presence of an additional oxygen functionality at C-7′ was determined by ^{1}H–^{1}H COSY, HMQC and HMBC. Furthermore, the downfield shift of H-3′ to δ_H 4.63 suggested that C-3′ should be acetylated. In the ^{1}H–^{1}H COSY spectrum, the H-5′ proton at δ_H 2.01 was coupled to the oxygenated methine proton at δ_H 3.67 (H-6′) which in turn was coupled to the oxygenated methine proton at δ_H 4.08 (H-7′). In the HMBC spectrum, the secondary alcoholic H-6′ (δ_H 3.67) showed HMBC correlations to C-7′ (δ_C 77.3) and C-5′ (δ_C 45.3), and the other secondary alcoholic H-7′ also showed HMBC correlations to C-6′ (δ_C 75.2), C-12′ (δ_C 110.0), and C-8′ (δ_C 145.6). Moreover, the HMBC correlations of the broad singlet at δ_H 4.63 (H-3′) with C-1′ (δ_C 30.3), C-5′ (δ_C 45.3), and the acetyl function at δ_C 170.3, proved that C-3′ should be acetylated. NOE experiments suggested the stereochemistry at C-6′ and C-7′. Irradiation of H-6′ at δ_H 3.67 resulted in enhancements of H-14′ (δ_H 1.11, 7%) and H-15′ (δ_H 1.06, 18%), whereas irradiation

of H-7′$_{ax}$ at δ_H 4.08 resulted in an enhancement H-5′$_{ax}$ (δ_H 2.01, 13%). Additionally, irradiation of H-9′$_{eq}$ at δ_H 2.35 resulted in an enhancement H-15′ (δ_H 1.06, 6%). Acetylation of **2** yielded a diacetyl derivative **2a**, which showed a downfield shift of H-6′ to δ_H 5.36 and H-7′ to δ_H 5.50 in the ^{1}H NMR spectrum. Esterification of **2** with *p*-bromobenzoyl chloride gave assafoetidnol B di-*p*-bromobenzoate (**2b**). The CD spectrum of **2b** showed a positive Cotton effect at 254 nm and a negative one at 236 nm (Fig. 3), indicating that the absolute configuration of **2** was 6′S,7′S.

Six known sesquiterpene coumarins gummosin (**3**) (Kir'yalov and Movchan, 1966; Perel'son et al., 1975), polyanthin (**4**) (Khasanov et al., 1974), badrakemin (**5**) (Kir'yalov, 1967; Perel'son et al., 1975), neveskone (**6**) (Bagirov, 1978), samarcandin (**7**) (Kir'yalov and Movchan, 1968; Nasirov et al., 1985), and galbanic acid (**8**) (Bagirov et al., 1980) were isolated and identified by the comparison of their spectral data with those published in the literature. The structures of these known compounds were also confirmed by 2D NMR (^{1}H–^{1}H COSY, HMQC and HMBC). The structure of **3** was confirmed by the X-ray crystallographic analysis, as shown in Fig. 4.

3. Experimental

3.1. Plant material

Resins of *F. assa-foetida* were obtained from a local market in Cairo in April 1999.

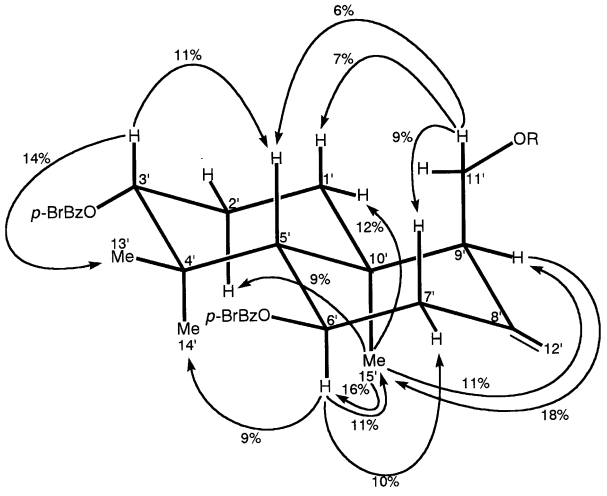

Fig. 1. Selected NOEs of **1b**.

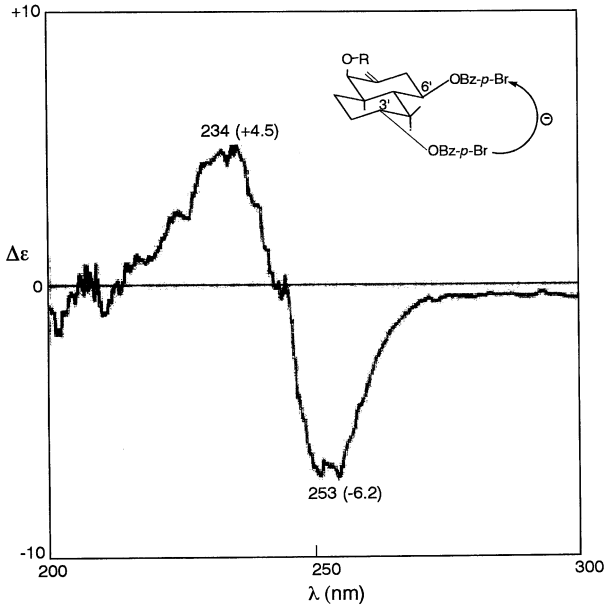

Fig. 2. CD spectrum of **1b**.

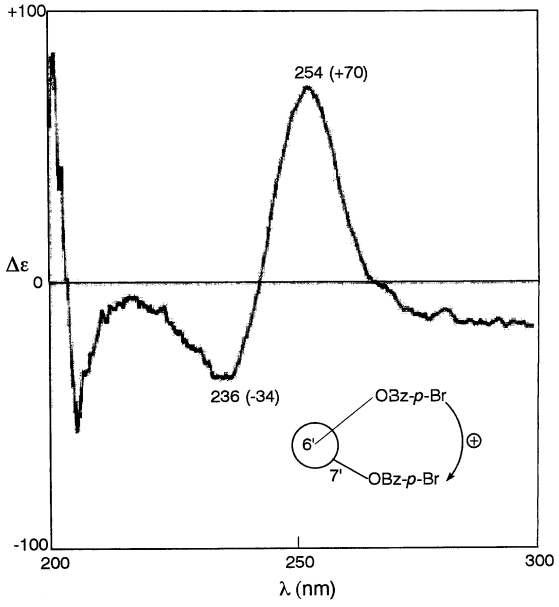

Fig. 3. CD spectrum of **2b**.

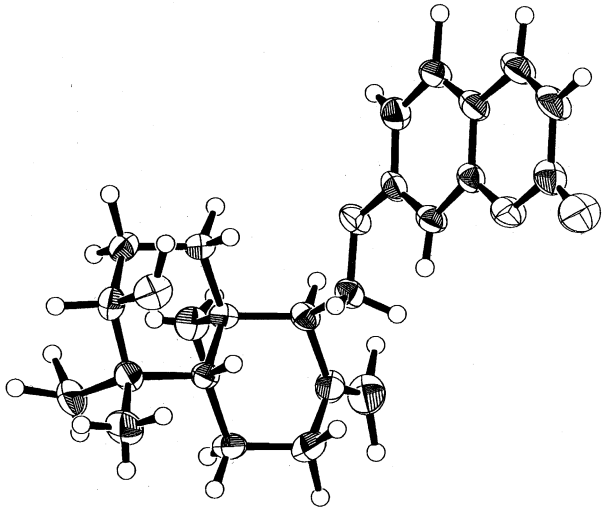

Fig. 4. ORTEP drawing of **3**.

3.2. Isolation and purification

Dried and coarsely powdered resins (250 g) were extracted with $CHCl_3$ at room temp. for 24 h. The extract (60 g) was subjected to flash chromatography over silica gel, this being eluted with hexane with an increasing amount of $CHCl_3$. Fr. A (hexane–$CHCl_3$, 1:1) was further applied to a Sephadex LH-20 column, eluted with hexane–EtOAc, 1:1 to give galbanic acid (**8**; 30 mg) and gummosin (**3**; 100 mg). Fr. B (hexane–$CHCl_3$, 1:2) was also subjected to Sephadex LH-20 chromatography (hexane–$CHCl_3$–MeOH, 5:3:0.5) to afford polyathin (**4**; 40 mg), and badrakemine (**5**; 27 mg). Fr. C ($CHCl_3$) was separated by TLC (silica gel, $CHCl_3$–MeOH, 7.0:0.5) to give neveskone (**6**; 37 mg). Fr. D ($CHCl_3$–MeOH, 85:15) was subjected to silica gel chromatography ($CHCl_3$–MeOH, 7.5:0.5), then over Sephadex LH-20 (hexane–$CHCl_3$–MeOH, 5:3:1.5) to give samarcandin (**7**; 70 mg), assafoetidnol A (**1**; 50 mg), and assfoetidnol B (**2**; 33 mg). Known compounds were identified by the comparison of their IR, MS, and ^1H NMR data with those reported in the literature.

3.3. Assafoetidnol A (*1*)

Amorphous solid; $[\alpha]_D$ −80.0° (*c* 0.2, MeOH); UV (MeOH) λ_{max} (log ε) : 322 (4.69), 258 nm (3.44); IR (film) ν_{max} 3408, 1707 cm^{-1}; HREIMS *m/z* 398.2106 $[M]^+$ (calcd. for $C_{24}H_{30}O_5$, 398.2093); EIMS *m/z* (rel. int.) 398 $[M]^+$ (3), 380 $[M–H_2O]^+$ (5), 362 $[M–2H_2O]^+$ (2), 237 [M-coumarin]$^+$ (50), 161 [M-sesquiterpene]$^+$ (100); ^1H and ^{13}C NMR spectral data see Table 1.

3.3.1. Acetylation of *1*

Compound **1** (10 mg) was refluxed in 1 ml of Ac_2O–C_5H_5N (1:1) for 2 h. The mixture was worked up by standard methods to give the diacetate **1a** (10 mg).

Colourless oil; IR (film) ν_{max} 1690, 1722 cm^{-1}; HREIMS *m/z* 482.2272 $[M]^+$ (calc. for $C_{28}H_{34}O_7$, 482.2305); EIMS *m/z* (rel. int.) 482 $[M]^+$ (4), 321 [M-coumarin]$^+$ (20), 161 [M-sesquiterpene]$^+$ (100); ^1H NMR (500 MHz, $CDCl_3$): δ 0.94 (3H, *s*, H-15′), 1.02 (3H, *s*, H-13′), 1.04 (3H, *s*, H-14′), 1.37 (1H, *dd*, *J* = 14.4, 4.9 Hz, H-2′$_{eq}$), 1.70 (3H, *m*, H-2′$_{ax}$ and H-1′), 1.79 (1H, *d*, *J* = 10.7 Hz H-5′), 1.99, 2.00 ($\underline{CH_3}CO\times2$), 2.16 (2H, *m*, H-7′$_{ax}$ and H-9′), 2.67 (1H, *dd*, *J* = 13.8, 5.5 Hz, H-7′$_{eq}$), 4.09 (1H, *dd*, *J* = 10.1, 5.5 Hz, H-11′$_a$), 4.28 (1H, *dd*, *J* = 10.1, 6.7 Hz, H-11′$_b$), 4.45 (1H, *dd*, *J* = 11.3, 4.9 Hz, H-3′), 4.81 (1H, *br s*, H-12′$_a$), 4.89 (1H, *br s*, H-12′$_b$), 5.16 (1H, *ddd*, *J* = 13.3, 10.7, 5.5 Hz, H-6′), 6.23 (1H, *d*, *J* = 9.5 Hz, H-3), 6.78 (2H, *m*, H-6 and H-8), 7.34 (1H, *d*, *J* = 8.5 Hz, H-5), 7.62 (1H, *d*, *J* = 9.5 Hz, H-4); ^{13}C NMR (125 MHz, $CDCl_3$): δ 170.9, 169.9 ($CH_3\underline{CO}$ ×2), 161.7 (C-7), 161.1 (C-2), 155.8 (C-9), 143.3 (C-8′), 142.6 (C-4), 128.8 (C-5), 113.9 (C-12′), 113.2 (C-6), 112.8 (C-3), 112.7 (C-10), 101.7 (C-8), 80.2 (C-3′), 71.6 (C-6′), 67.5 (C-11′), 55.9 (C-9′), 49.2 (C-5′), 38.7 (C-7′), 38.4 (C-4′), 37.8 (C-10′), 34.8 (C-2′), 30.5 (C-14′), 23.6 (C-1′), 23.3 (C-15′), 21.8, 21.2 ($\underline{CH_3}CO\times2$), 17.2 (C-13′).

3.3.2. p-Bromobenzoylation of *1*

To a stirred solution of **1** (8 mg) in C_5H_5N (1.5 ml) was added *p*-bromobenzoyl chloride (80 mg). After being stirred at room temp. for overnight, the mixture was worked up by standard methods to give the di-*p*-bromobenzoate **1b** (8 mg).

Colourless oil; IR (film) ν_{max} 1786, 1720, 1690, 800 cm^{-1}; CD (MeOH) see Fig. 2; HREIMS *m/z* 762.0823 $[M]^+$ (calc. for $C_{38}H_{36}O_7Br_2$, 762.0828); EIMS *m/z* (rel. int.) 762, 764, 766 $[M]^+$ (2, 4, 2), 601 [M-coumarin]$^+$ (30), 161 [M-sesquiterpene]$^+$ (100); ^1H NMR (500 MHz, $CDCl_3$): δ 1.12 (3H, *s*, H-15′), 1.14 (3H, *s*, H-13′), 1.18 (3H, *s*, H-14′), 1.50 (1H, *dd*, *J* = 14.4, 4.9 Hz, H-2′$_{eq}$), 1.90 (3H, *m*, H-2′$_{ax}$ and H-1′), 2.06 (1H, *d*, *J* = 10.7 Hz, H-5′), 2.29 (1H, *dd*, *J* = 6.7, 5.5 Hz, H-9′), 2.35 (1H, *m*, H-7′$_{ax}$), 2.81 (1H, *dd*, *J* = 13.8, 5.5 Hz, H-7′$_{eq}$), 4.19 (1H, *dd*, *J* = 10.1, 5.5 Hz, H-11′a), 4.39 (1H, *dd*, *J* = 10.1, 6.7 Hz, H-11′b), 4.76 (1H, *dd*, *J* = 11.3, 4.9 Hz, H-3′), 4.90 (1H, *br s*, H-12′$_a$), 4.94 (1H, *br s*, H-12′$_b$), 5.54 (1H, *ddd*, *J* = 13.3, 10.7, 5.5 Hz, H-6′), 6.27 (1H, *d*, *J* = 9.5 Hz, H-3), 6.85 (2H, *m*, H-6 and H-8), 7.39 (1H, *d*, *J* = 8.5 Hz, H-5), 7.55 (2H, *d*, *J* = 10 Hz, H-3″ and H-7″), 7.57 (2H, *d*, *J* = 10 Hz, H-3‴ and H-7‴), 7.68 (2H, *d*, *J* = 10 Hz, H-4″ and H-6″), 7.83 (1H, *d*, *J* = 9.5 Hz, H-4), 8.08 (2H, *d*, *J* = 10 Hz, H-4‴ and H-6‴); ^{13}C NMR (125 MHz, $CDCl_3$): δ 165.0, 164.7 (C-1″, C-1‴), 161.7 (C-7), 161.1 (C-2), 155.9 (C-9), 143.3 (C-8′), 142.4 (C-4), 132.4, 132.2, 131.9, 131.8 (C-3″, C-3‴, C-7″, C-7‴), 131.7 131.6 131.2, 131.0 (C-4″, C-4‴, C-6″, C-6‴), 130.9, 130.2 (C-2″, C-2‴), 129.6, 129.4 (C-5″, C-5‴), 128.9 (C-5), 114.2 (C-12′), 113.3 (C-6), 112.9 (C-3), 112.8 (C-10), 101.7 (C-8), 81.0 (C-3′), 72.4 (C-6′), 67.6 (C-11′), 55.9 (C-9′), 49.6 (C-5′), 38.7 (C-7′), 38.5 (C-4′), 38.3 (C-10′), 34.9 (C-2′), 31.1 (C-14′), 23.6 (C-1′), 23.4 (C-15′), 17.5 (C-13′).

3.4. Assafoetidnol B (*2*)

Amorphous solid; $[\alpha]_D$ +29.4° (*c* 0.2, MeOH); UV (MeOH) λ_{max} (log ε) :320 (4.90), 258 nm (4.20); IR (film) ν_{max} 3999, 2900, 1690 cm^{-1}; HRFABMS *m/z* 457.2205 $[M+H]^+$ (calc. for $C_{26}H_{33}O_7$, 457.2252); ^1H and ^{13}C NMR spectral data see Table 1.

3.4.1. Acetylation of *2*

As described above for **1a**, compound **2** (10 mg) was converted into the diacetate **2a** (10 mg).

Colourless oil; IR (film) ν_{max} 1690, 1720, 1733 cm^{-1}; EIMS *m/z* (rel. int.) 456 $[M]^+$ (4), 295 [M-coumarin]$^+$ (30), 161 [M-sesquiterpene]$^+$ (100); ^1H NMR (500 MHz, $CDCl_3$): δ 0.96 (3H, *s*, H-15′), 1.04 (3H, *s*, H-14′), 1.12 (3H, *s*, H-13′), 1.33 (1H, *m*, H-2′$_{eq}$), 1.71 (3H, *m*,

H-2′$_{ax}$, H-1′), 1.95 (1H, *d*, *J* = 12.0 Hz, H-5′), 1.97, 2.01, 2.10 ($\underline{CH_3}CO$ ×3), 2.28 (1H, *dd*, J = 6.7, 5.5 Hz, H-9′), 4.24 (1H, *dd*, *J* = 10.1, 5.5 Hz, H-11′$_a$), 4.39 (1H, *dd*, *J* = 10.1, 6.7 Hz, H-11′$_b$), 4.60 (1H, *br s*, H-3′), 4.96 (1H, *br s*, H-12′$_a$), 5.00 (1H, *br s*, H-12′$_b$), 5.36 (1H, *dd*, *J* = 12.0, 9.5 Hz, H-6′), 5.50 (1H, *d*, *J* = 9.5 Hz, H-7′), 6.26 (1H, *d*, *J* = 9.5 Hz, H-3), 6.83 (1H, *d*, *J* = 2.5 Hz, H-8), 6.87 (1H, *dd*, *J* = 8.5, 2.5 Hz, H-6), 7.38 (1H, *d*, *J* = 8.5 Hz, H-5), 7.64 (1H, *d*, *J* = 9.5 Hz, H-4); ^{13}C NMR (125 MHz, $CDCl_3$): δ 170.3, 170.0×2 ($CH_3\underline{CO}$× 3), 161.6 (C-7), 161.0 (C-2), 155.9 (C-9), 143.3 (C-4), 141.1 (C-8′), 129.0 (C-5), 113.4 (C-6), 113.1 (C-3), 112.8 (C-10), 111.2 (C-12′), 101.7 (C-8), 79.6 (C-3′), 75.6 (C-7′), 73.3 (C-6′), 68.5 (C-11′), 56.7 (C-9′), 44.4 (C-5′), 38.0 (C-4′), 37.0 (C-10′), 31.0 (C-13′), 30.0 (C-1′), 23.5 (C-15′), 22.5 (C-2′), 22.2 (C-14′), 21.6, 21.1, 20.6 ($\underline{CH_3}CO$×3).

3.4.2. *p*-Bromobenzoylation of **2**

As described above for **1b**, compound **2** (12 mg) was converted into the di-*p*-bromobenzoate **2b** (12 mg).

Colourless oil; IR (film) ν_{max} 1777, 1727, 1699, 799 cm^{-1}; CD (MeOH) see Fig. 3; EIMS *m*/*z* (rel. int.) 720, 722, 724 [M]$^+$ (2, 4, 2), 661 [M-coumarin]$^+$ (40), 161 [M-sesquiterpene]$^+$ (100); ^{1}H NMR (500 MHz, $CDCl_3$): δ 1.02 (3H, *s*, H-15′), 1.13 (3H, *s*, H-14′), 1.27 (3H, *s*, H-13′), 1.44 (1H, *m*, H-2′$_{eq}$), 1.80 (3H, *m*, H-2′$_{ax}$, H-1′), 2.00 (CH_3CO), 2.48 (1H, *dd*, *J* = 6.7, 5.5 Hz, H-9′), 2.61 (1H, *d*, *J* = 12.0 Hz, H-5′), 4.37 (1H, *dd*, *J* = 10.1, 5.5 Hz, H-11′$_a$), 4.47 (1H, *dd*, *J* = 10.1, 6.7 Hz, H-11′$_b$), 4.61 (1H, *br s*, H-3′), 5.02 (2H, *br s*, H-12′), 5.80 (1H, *dd*, *J* = 12.0, 9.5 Hz, H-6′), 5.87 (1H, *d*, *J* = 9.5 Hz, H-7′), 6.29 (1H, *d*, *J* = 9.5 Hz, H-3), 6.91 (2H, *m*, H-6 and H-8), 7.45 (1H, *d*, *J* = 8.5 Hz, H-5), 7.63 (4H, *m*, H-4″, H-4‴, H-6″, and H-6‴), 7.64 (1H, *d*, *J* = 9.5 Hz, H-4), 7.82 (4H, *m*, H-3″, H-3‴, H-7″, and H-7‴); ^{13}C NMR (125 MHz, $CDCl_3$): δ 170.1 ($CH_3\underline{CO}$), 165.2, 164.8 (C-1″, C-1‴), 161.5 (C-7), 161.0 (C-2), 155.7 (C-9), 143.3 (C-4), 140.9 (C-8′), 131.8×4 (C-3″, C-3‴,C-7″,C-7‴), 131.7×4 (C-4″, C-4‴, C-6″, C-6‴), 131.1×2 (C-2″, C-2‴), 128.9 (C-5), 128.5×2 (C-5″, C-5‴), 113.4 (C-6), 113.1 (C-3), 112.8 (C-10), 111.4 (C-12′), 101.7 (C-8), 79.5 (C-3′), 76.8 (C-7′), 74.0 (C-6′), 68.0 (C-11′), 56.8 (C-9′), 45.0 (C-5′), 38.3 (C-4′), 37.1 (C-10′), 31.4 (C-13′), 30.3 (C-1′), 23.6 (C-15′), 22.4 (C-2′), 22.2 (C-14′), 21.1 ($\underline{CH_3}CO$).

3.5. X-ray structure analysis of **3**

The reflection data were collected on a Mac Science DIP 2030 imaging plate area detector with monochromated Mo-K_α radiation (λ = 0.71069 Å) with ω-techniques to a maximum 2θ value of 55.7° at room temp. (22±1 °C). Of the 4605 reflections which were collected, 2625 were unique. The structure was solved by direct methods SIR 92 (Altomare et al., 1994) and expanded using Fourier techniques (Beurskens et al., 1994). The non-hydrogen atoms were refined anisotropically. Hydrogen atoms were included but not refined. The final cycle of the full-matrix least squares refinement was based on 4191 observed reflections ($I > 3.00\sigma$ (I)). The structure was finally refined to $R = 0.049$ ($R_w = 0.091$). The crystal data are: $a = 13.474$ (5) Å, $b = 7.151$ (5) Å, $c = 21.386$ (7) Å, $V = 2060.6$ (1) Å^3, space group $P2_12_12_1$, $Z = 4$, $Dc = 1.23$ g/cm^3. Atomic coordinates, bond lengths and angles, and thermal parameters have been deposited at the Cambridge Crystallographic Data Centre, UK.

References

Ahmed, A.A., 1999. Sesquiterpene coumarins and sesquiterpenes from *Ferula sinaica*. Phytochemistry 50, 109–112.

Altomare, A., Burla, M.G., Camalli, M., Cascarano, M., Giacovazzo, C., Guagliardi, A., Polidori, G., 1994. SIR 92—a program for automatic solution of crystal structures by direct methods. Journal of Applied Crystallography 27, 435.

Appendino, G., Jakupovic, J., Alloatti, S., Ballero, M., 1997. Daucane esters from *Ferula arrigonii*. Phytochemistry 45, 1639–1643.

Appendino, G., Tagliapietra, S., Nano, G.M., Jakupovic, J., 1994. Sesquiterpene coumarin ethers from Asafoetida. Phytochemistry 35, 183–186.

Bagirov, V.Yu., 1978. Coumarin from *Ferula nevskii* roots. Khimiya Prirodnykh Soedinenii 14, 652–653.

Bagirov, V.Yu., Sheichenko, V.I., Veselovskaya, N.V., Sklyar, Yu.E., Savina, A.A., Kir'yanova, I.A., 1980. Structure and stereochemistry of galbanic acid. Khimiya Prirodnykh Soedinenii 16, 620–623.

Banerji, A., Mallick, B., Chatterjee, A., Budzikiewicz, H., Breuer, M., 1988. Assafoetidin and ferocolicin, two sesquiterpenoid coumarins from *Ferula assafoetida* Regel. Tetrahedron Letters 29, 1557–1560.

Beurskens, P.T., Admiraal, G., Beurskenes, G., Bosman, W.P., de Gelder, R., Israel, R., Smits, J.M.M., 1994. The DIRDIF-94 program system, Technical Report of the Crystallography Laboratory, University of Nijmegen, The Netherlands.

Boulus, L., 1983. Medicinal Plants of North Africa. Algonae, MI,. p. 183.

Buddrus, J., Bauer, H., Abu-Mustafa, E., Khattab, A., Mishaal, S., El-Khrisy, E.A.M., Linscheid, M., 1985. Foetidin, a sesquiterpene coumarin from *Ferula assa-foetida*. Phytochemistry 24, 869–870.

Caglioti, L., Naef, H., Arigoni, D., Jeper, O., 1958. Zur kenntnis der Sesquiterpene und Azulene. Üer die Inhaltsstoffe der Asafoetida I. Farnesiferol A. Helvetica Chimica Acta 41, 2278–2287.

Caglioti, L., Naef, H., Arigoni, D., Jeper, O., 1959. Zur Kenntnis der Sesquiterpene und Azulene. Üer die Inhaltsstoffe der Asafoetida II. Farnesiferol B und C. Helvetica Chimica Acta 42, 2257–2570.

Chen, B., Teranishi, R., Kawazoe, K., Takaishi, Y., Honda, G., Itoh, M., Takeda, Y., Kodzhimatov, K.O., 2000. Sesquiterpenoids from *Ferula kuhistanica*. Phytochemistry 54, 717–754.

Eigner, D., Scholz, D., 1999. *Ferula assa-foetida* and *Curcuma longa* in traditional medical treatment and diet in Nepal. Journal of Ethnopharmacology 67, 1–6.

Eigner, D., Scholz, D., 1990. Das Zauberbchlein der Gyani Dolma. Pharmazie in userer Zeit 19, 141–152.

Gonzalez, A.G., Barrera, J.B., 1995. Chemistry and the sources of mono- and bicyclic sesquiterpenes from *Ferula* species. Progress in the Chemistry of Organic Natural Products 64, 1–92.

Gonnella, N.C., Nakanishi, K., Martin, V.S., Sharpless, K.B., 1982. General methods for determining absolute configurations of acyclic

allylic alcohols. Journal of the American Chemical Society 104, 3775–3776.

Hofer, O., Widhalm, M., Greper, H., 1994. Circular dichroism of sesquiterpene-umbelliferone ethers and structure elucidation of a new derivative isolated from the gum resin assa-foetida. Monatshefte für Chemie 115, 1207–1218.

Kajimoto, T., Yahiro, K., Nohara, T., 1989. Sesquiterpenoid and disulphide derivatives from *Ferula assa-foetida*. Phytochemistry 28, 1761–1763.

Kapoor, L.D., 1990. Handbook of Ayurvedic Medicinal Plants. CRC Press, Boca Raton, FL, p. 185.

Khasanov, T.Kh., Saidkhodzaev, A.I., Nikonov, 1974. Structure and configuration of polyanthin and polyanthinin, new coumarins of *Ferula polyantha* roots. Khimiya Prirodnykh Soedinenii 10, 517–518.

Kir'yalov, N.P., 1967. The coumarin, badrakemin from the roots of *Ferula badra-kema*. Khimiya Prirodnykh Soedinenii 3, 363–367.

Kir'yalov, N.P., Movchan, S.D., 1966. Structure of gummosin. Khimiya Prirodnykh Soedinenii 2, 383–387.

Kir'yalov, N.P., Movchan, S.D., 1968. Structure of samarcandin and samarcandone, coumarin compounds of *Ferula samarcandica*. Khimiya Prirodnykh Soedinenii 4, 73–77.

Kojima, K., Isaka, K., Ondognii, P., Zevgeegiino, O., Davgiin, K., Mizukami, H., Ogihara, Y., 1999. Sesquiterpenoid derivatives from *Ferula ferulioids* III. Chemical and Pharmaceutical Bulletin 47, 1145–1147.

Kojima, K., Isaka, K., Ondognii, P., Zevgeegiino, O., Gombosurengyin, P., Davgiin, K., Mizukami, H., Ogihara, Y., 2000. Sesquiterpenoid derivatives from *Ferula ferulioids* IV. Chemical and Pharmaceutical Bulletin 48, 353–356.

Kojima, K., Isaka, K., Purev, O., Jargalsaikhan, G., Suran, D., Mizukami, H., Ogihara, Y., 1999. Sesquiterpenoid derivatives from *Ferula ferulioids* II. Chemical and Pharmaceutical Bulletin 47, 690–691.

Kuliev, Z.A., Khasanov, T.Kh., 1978. Structure of cauferin and cauferidin. Khimiya Prirodnykh Soedinenii 14, 327–331.

Murray, R.D.H., 1989. Coumarins. Natural Product Reports 6, 591–624.

Nasirov, S.M., Saidkhodzhaev, A.I., Khasanov, T.Kh., Yagudaev, M.R., Malikov, V.M.M., 1985. Stereochemistry of terpenoid coumarins, crystal and molecular structure of samarcandin. Khimiya Prirodnykh Soedinenii 21, 184–190.

Nassar, M.I., Abu-Mustafa, E.A., Ahmed, A.A., 1995. Sesquiterpene coumarins from *Ferula assa-foetida* L. Die Pharmazie 50, 766–767.

Nassar, M.I., Mohamed, T.K., 1998. A new sesquiterpene coumarin from *Ferula assa-foetida*. Fitoterapia 69, 41–42.

Perel'son, M.E., Kir'yalov, N.P., Ban'kovskii, A.I., 1975. Configuration of Farnesiferol A, gummosin, badrakemin and coladonin. Khimiya Prirodnykh Soedinenii 11, 244–245.

Rajanikanth, R., Ravindranath, B., Shankarananrayana, M.L., 1984. Volatile polysulphides of asa-foetida. Phytochemistry 23, 899–900.

Su, B.-N., Takaishi, Y., Honda, G., Itoh, M., Takeda, Y., Kodzhimatov, O.K., Ashurmetov, O., 2000. Sesquiterpene coumarins and related derivatives from *Ferula pallida*. Journal of Natural Products 63, 436–440.

Su, B.-N., Takaishi, Y., Honda, G., Itoh, M., Takeda, Y., Kodzhimatov, O.K., Ashurmetov, O., 2000. Sesquiterpene phenylpropanoid and sesquiterpene chromone derivatives from *Ferula pallida*. Journal of Natural Products 63, 520–522.

PERGAMON

Phytochemistry 58 (2001) 1297–1303

PHYTOCHEMISTRY

www.elsevier.com/locate/phytochem

Isolation and identification of *N*-mercapto-4-formylcarbostyril, an antibiotic produced by *Pseudomonas fluorescens*

Walid Fakhouri[a,*], Frank Walker[a], Bernhard Vogler[b], Wolfgang Armbruster[c], Heinrich Buchenauer[a]

[a]*Institute of Phytomedicine, Otto-Sander-Str. 5, 70593 Stuttgart, Germany*
[b]*Institute of Chemistry, Garbenstr. 30, 70593-Stuttgart, Germany*
[c]*Institute of Food Chemistry, Garbenstr. 28, University of Hohenheim, 70593-Stuttgart, Germany*

Received 23 February 2001; received in revised form 31 July 2001

Abstract

Pseudomonas fluorescens strain G308 isolated from barley leaves produces a novel antibiotic substance that was purified by preparative TLC and HPLC and identified as *N*-mercapto-4-formylcarbostyril (Cbs) by LC/DAD, IR, LC–ES$^+$/MS, LC–ES$^-$/MS, GC–EI/MS, LC–HRES$^+$/MS, mass isotope ratios analysis, ^{1}H NMR and ^{13}C NMR analysis. The purified new antibiotic compound is effective against many phytopathogenic fungi in vitro. The compound inhibited at 25 ppm spore germination and germ tube growth of the following fungi; *Fusarium oxysporum* f. sp. *lycopersici*, *Fusarium culmorum*, *Cladosporium cucumerinum* and *Colletotrichum lagenarium*. At concentrations up to 125 ppm, the compound did not interfere with release of zoospores from sporangia and germination of encysted zoospores of *Phytophthora infestans*. © 2001 Elsevier Science Ltd. All rights reserved.

Keywords: *Pseudomonas fluorescens*; Antibiotic; Spore germination; Germ tube growth

1. Introduction

Secondary metabolites produced by microorganisms provide a rich source of novel biological active compounds. However, only a small percentage of the microorganisms has been investigated worldwide phytochemically until now. Therefore, searching for natural antimicrobial substances especially with new mode of actions is still one of the very important aspects with a big potential in the field of phytomedicine (Berdy, 1982; Hostettman and Wolfender, 1997). Fluorescent pseudomonads are among the important bioagents that have been intensively studied with regard to the production of antibiotics. An important role of antibiotics with antifungal activities in suppression of several diseases has been demonstrated, such as take-all of wheat, damping-off in cotton and black root-rot in tobacco (Howell and Stipanovic, 1980; Keel et al., 1990). Substances produced by fluorescent pseudomonads that are involved in control of diseases include for instance pyoluteorin, phenazine derivatives, hydrogen cyanide and 2,4-diacetylphloroglucinol (Howell and Stipanovic, 1980; Thomashow and Weller, 1988; Voisard et al., 1989; Keel et al., 1990). Pyrrolnitrin and oomycin A are further metabolites of fluorescent pseudomonads which are involved in biological control of damping-off in cotton and other plant pathogens (Howie and Suslow, 1991; McLoughlin et al., 1992; Burkhead et al., 1994). Pseudobactin B10, rhamnolipid, agrocin 84, 2-hexyl-5-resorcinol, 2,3-deepoxy-2,3-didehydro-rhizoxin and aeruginoic acid are also biocontrol factors produced by fluorescent pseudomonads and involved in disease suppression (Leisinger and Margraff, 1979; Kloepper et al., 1980; Kerr and Tate, 1984; Carmi and Carmeli, 1994; Wright et al., 1999; Ligon et al., 2000).

Pyrrolnitrin, produced as a secondary metabolite from *Pseudomonas pyrroconia*, represents the lead structure of the synthetically produced fungicides fenpiclonil and fludioxonil. The two synthetic derivatives have an improved photostability compared to the natural product and possess a broad disease control spectrum and low toxicity to mammals, birds and honeybees and low mobility in the soil (Nevill et al., 1988; Gehmann et al., 1990).

* Corresponding author. Tel.: +49-711-4593220; fax: +49-711-4592408.
E-mail address: fakhouri@uni-hohenheim.de (W. Fakhouri).

0031-9422/01/$ - see front matter © 2001 Elsevier Science Ltd. All rights reserved.
PII: S0031-9422(01)00344-2

The characteristics of *Pseudomonas fluorescens* strain G308, representing a potential biocontrol agent, encouraged us to examine its production of antibiotics in vitro. Thus, the aim of the present work is to isolate and identify antibiotic compounds produced by this strain.

2. Results

2.1. The biochemical and physiological characteristics of the strain G308

Pseudomonas fluorescens strain G308 biotype V isolated from the surface of barley leaves was also able to colonize tomato roots sufficiently under greenhouse conditions (data not shown). It produces beside the siderophore pyochelin, also cyanide and exoenzymes such as arginine dihydrolase, proteinase and protease.

2.2. Extraction and purification of the antibiotics

The TLC bioassay showed that the ethylacetate extract of the culture filtrate of the bacterial strain G308 in KB liquid medium exhibited two inhibition zones on the TLC when *Cladosporium cucumerinum* (3×10^7 spores/ml) and *Colletotrichum lagenarium* (2×10^6 spores/ml) were used as test organisms. The two antifungal substances had R_f values of 0.66 and 0.70. Furthermore, the purity of two compounds eluted from the silica gel was tested by HPLC-DAD (Merck-Hitachi®) with a corresponding retention times (*RT*) of 15.5 and 19.8 min, respectively. The production of the two antifungal substances by the isolate G308 in sucrose-asparagin (SuA) liquid medium was less pronounced and no antifungal compounds were detected in biomalt (BM) liquid medium.

2.3. Spectroscopic analysis and structure identification

The new antibiotic substance *N*-mercapto-4-formylcarbostyril with the R_f value of 0.70 and *RT* 19.8 min has been identified according to IR analysis, mass spectroscopy by LC–MS (ES^+/ES^-) and GC–EI/MS, high resolution mass spectroscopy (LC–$HRES^+$/MS) also ^1H, ^{13}C NMR, H–H-COSY, HSQC and HMQCSS spectra. The following data have been obtained: UV λ_{max} nm (ratio%): 222 (100%), 280 (65%) and 318 (50%); IR ν_{max} cm^{-1}: 3349, 3124, 2933, 2853, 2568, 1651, 1435, 1120, 750 and 685. The isotopic pattern of the protonated molecular ion peak in LC–$HRES^+$/MS showed the masses 206.0293 $[M+H]^+$, 207.0377 and 208.0327 with the corresponding ratios 100, 15 and 7%, respectively. LC–$HRES^+$/MS of the new compound *m/z*: $[M+H]^+$ 206.0293 ($C_{10}H_7NO_2S$, calc. mass 206.0276, mDa error 1.7). The mass fragmentation of the compound in the GC–EI/MS showed that the molecular ion peak at *m/z* 205.0 $[M]^+$ lost one carbon monoxide molecule to give peak at *m/z* 177.0 $[M–CO]^+$ and one thiol group to give peak at *m/z* 144.0 [*m/z*: 177-SH]$^+$. The ^1H NMR chemical shifts (300 MHz, $(CD_3)_2CO$) were: δ ppm 7.95 (1H, *dd*, $J=$ 8.35 and 1.16 Hz, H-7), 7.48 (1H, pseudotriplet, $J=$ 8.43, 7.14 and 1.29 Hz, H-8), 7.05 (1H, *t*, $J=$ 7.33 and 8.15 Hz, H-9), 7.12 (1H, *d*, $J=$8.36 Hz, H-10), 11.55 (1H, *br s*, H-11a, N-S-H), 8.65 (1H, *s*, H-3a), 10.1 (1H, *s*, H-13a) (Fig. 1). The ^{13}C NMR spectrum (300 MHz, $(CD_3)_2CO$) exposed: δ (multiplicity, carbon position, proton HSQC) 170.17 (*s*, C-2), 129.69 (*s*, C-3, H3a), 154.69 (*s*, C-4), 117.54 (*s*, C-5), 157.51 (*s*, C-6), 128.8 (*s*, C-7, H7a), 120.72 (*s*, C-8, H8a), 133.46 (*s*, C-9, H9a), 118.36 (*s*, C-10, H10a), 184.22 (*s*, C-13, H13a) (Fig. 2).

In addition, the new antibiotic substance after acetylation increased by 43 mass units (dalton) to be 248.0 M^+ (Fig. 3). The ^1H NMR chemical shifts (LC–NMR 500 MHz, $(CD_3)_2CO$) of the acetylated derivative compound showed all proton signals of the original antibiotic substance except the signal of the proton coupled to the nitrogen atom in the heteroaromatic ring: δ ppm 11.55 (1H, *br s*, H-11a, N-S-H), where the acetylation process at that position could be assumed (Fig. 4).

On the other hand, the antifungal substance of R_f value 0.66 and *RT* 15.5 min produced by the bacterial strain G308 was identified as pyoluteorin according to LC–ES^+/MS, isotopic pattern of the signal cluster of the mole peak, ^1H NMR and H–H-COSY spectra. Pyoluteorin is a well known antibiotic, which is produced by several *Pseudomonas fluorescens* strains (Howell and Stipanovic, 1980). The following data have been obtained: UV λ_{max} nm (ratio%): 310 (100%) and 230 (40%), GC–EI/MS *m/z* 271.0 dalton $[M]^+$, $C_{11}H_7O_3NCl_2$); isotopic patterns 271.14 (100%), 273.17 (70%) and 275.13 (10%); ^1H NMR chemical shifts (300 MHz, $(CD_3)_2CO$): δ ppm 3.8 (1H, *br s*, H-1, N-H), 6.88 (1H, *s*, H-4), 6.34 (2H, *d*, $J=$ 8.16 Hz, H-14 and H-12), 7.1 (1H, *t*, $J=$ 8.15 Hz, H-13). These data obtained were in complete agreement with the data of the standard pyoluteorin.

2.4. Antifungal bioassay in vitro

This new substance with R_f value of 0.70 and *RT* of 19.8 min showed antifungal effects in vitro against several plant pathogenic fungi. Twenty five ppm of the compound inhibited the spore germination and germ tube growth of the following fungi: *Fusarium oxysporum* f. sp. *lycopersici* (5×10^6 spores/ml), *Fusarium culmorum* (3.1×10^6 spores/ml), *Cladosporium cucumerinum* (3×10^7 spores/ml), *Colletotrichum lagenarium* (2×10^6 spores/ml).

At 100 ppm, the substance inhibited the germination of teliospores of *Ustilago maydis* und *U. nuda* (8×10^6 spores/ml). The compound did not interfere in release of zoospores from zoosporangia and germination of encysted zoospores of *Phytophthora infestans* at concentrations up to 150 ppm.

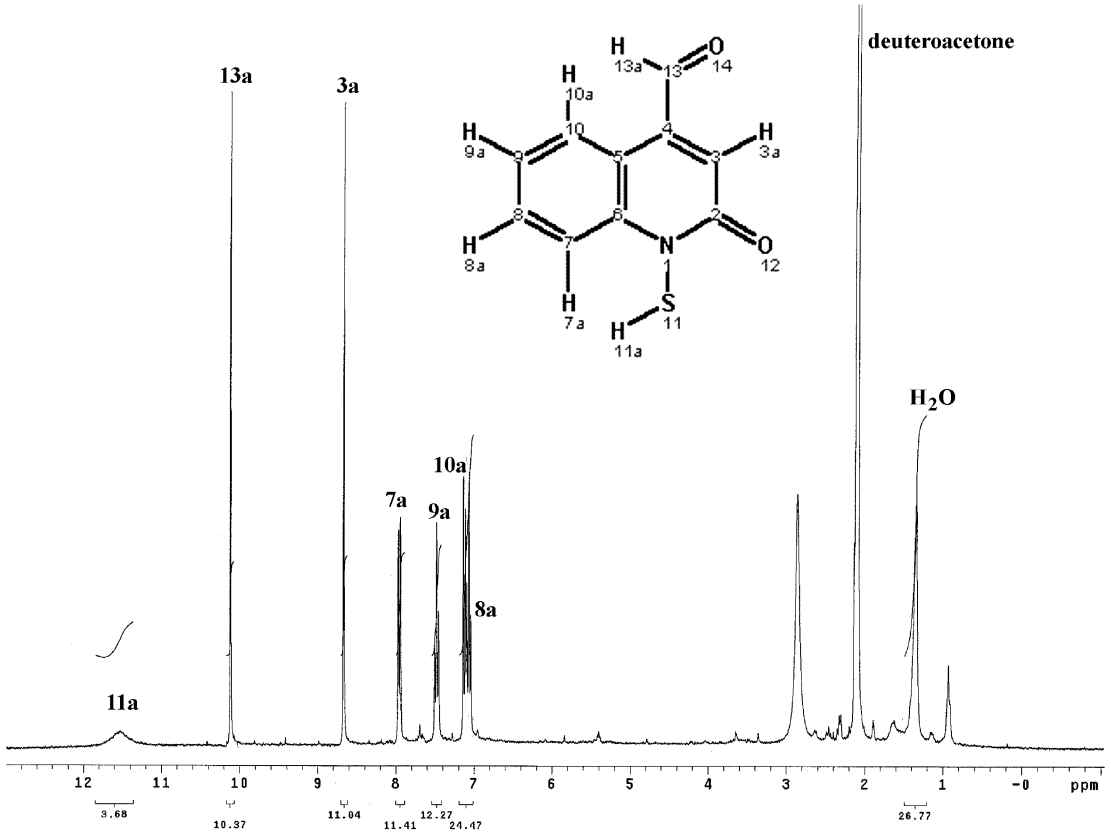

Fig. 1. ^{1}H NMR spectrum of numerated *N*-mercapto-4-formyl-carbostyril (Cbs) shows the position of proton signals and the proton integration in $[(CD_3)_2CO]$.

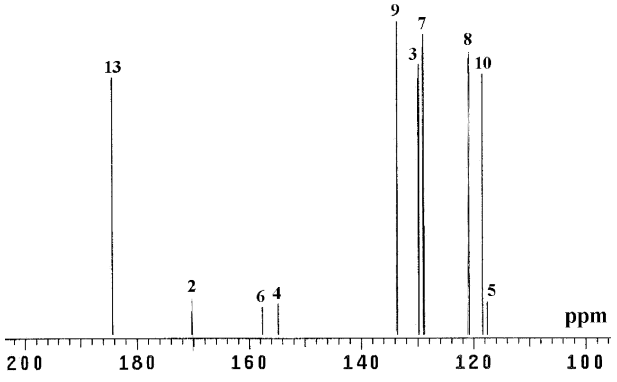

Fig. 2. ^{13}C NMR spectrum of *N*-mercapto-4-formyl-carbostyril (Cbs) shows carbon atom signals and its position.

3. Discussion

The structure of the new antibiotic compound *N*-mercapto-4-formylcarbostyril has been identified according to all data and analysis which are mentioned before. Depending on the LC/DAD absorption spectrum, the substance has three UV λ_{max} nm (ratio%): 222 (100%), 280 (65%) and 318 (50%) which could indicate the presence of the aromatic ring moiety and heteroaromatic moiety with substitution effect. The IR data showed the presence of following functional groups: carbo-amide group (3349 cm^{-1}), mercapto group (2568 cm^{-1}) and the carbonyl group (1651 cm^{-1}). The isotopic pattern of the protonated molecular ion peak at 206.0293 $[M+H]^+$ indicated the presence of one sulfur moiety. High resolution LC–ES^+/MS experiments revealed that the protonated molecular ion peak $[M+H]^+$ of the new compound is 206.0293, corresponding nearest to $C_{10}H_7NO_2S$ (calc. mass: 206.0276). GC–EI/MS spectrum confirmed that the molecular weight of the substance is 205.0 and this was proved by GC–CI^+/MS, LC–$APCI^{-1}$/MS and LC–$APCI^+$/MS in the negative and positive modes which showed a quasi-molecular ion at *m*/*z* 204.0 $[M–H^+]$ and 206 $[M+H]^+$, respectively. Furthermore, GC/MS/MS fragmentation of the new antibiotic compound revealed the presence of carbonyl group bind to the heteroaromatic ring through appearance of the corresponding molecular ion at *m*/*z*: 177.0 $[M–CO]^+$ by eliminating of the carbon monoxide group (CO) and one thiol group to give peak at *m*/*z* 144.0 [*m*/*z:* 177S-H]$^+$.

The ^{1}H and ^{13}C NMR spectra enabled us to interpret and to determine the configuration of the new antibiotic substance. The integration of the whole ^{1}H NMR signals showed the presence of 7 protons. Among these protons, 4 protons coupled to an aromatic ring, one proton coupled to the pyridine ring, one aldehyde proton and

one proton linked to S with a broad signal. The diagonal two dimensional H–H-COSY showed the coupling between the 4 aromatic protons. Integration of the whole ^{13}C NMR signals revealed the presence of 10 carbon atoms. The six signals between 120 and 160 ppm correspond to the aromatic ring, while the two signals at 170.17 and 184.22 ppm correspond to carbon coupled to the oxy and aldehyde group, respectively (Günther, 1992; Hesse et al., 1995).

The HSQC experiments showed the six proton-bearing signals in the ^{13}C NMR spectrum. Six of the seven signals in the ^{1}HNMR spectrum exhibited correlations (HMQCSS) with the carbon atoms in ^{13}C NMR spectrum. These long-range correlations (^{1}J, ^{2}J, ^{3}J and ^{4}J) allowed us to confirm the arrangement of the protons with the carbon atoms.

Furthermore, the antibiotic substance increased by 43 mass units (dalton) after acetylation by addition dryness acetic anhydride and using pyridine as a catalysator. Thus, the molecular weight of the acetylated derivative antibiotic increased to 248.0 $[M]^+$. The ^{1}H NMR spectrum of the derivative antibiotic showed the absence of the broad signal of the proton (δ ppm 11.55) link to the S atom where the acetylation happened (Fig. 4).

The nomenclature of the ground structure of our new antibiotically active carbostyril substance was already documented by Eistert et al. (1969) through synthesis of *N*-hydroxycarbostyril from expansion of *N*-hydroxyisatin. In addition, Cornforth and James (1956) proposed the biosynthesis pathway of pyo compound (pseudanes) from anthranilic acid and a β-keto acid intermediate in *Pseudomonas aeruginosa* by using the isotopes ^{14}C and ^{15}N atoms (Fig. 5). Our antibiotic compound seems to be synthesized through this pathway because it has the same ground structure with different substitution on the pyridine ring. The antifungal effect of carbostyril group as fungicide has been demonstrated in the patent of Sumitomo Chemical Company by Uematsu et al. (1979). Moreover, synthetic carbostyril derivatives were applied for patents in many pharmaceutical products with inotropic cardiotonic activity (Uchida et al., 1984; Tanaka et al., 1989).

The data of UV, LC–ES$^+$/MS ($m/z = 271.0$), isotopic pattern of the signal cluster with the distinct peak $[M–H]^+$ (270.0) indicated chlorine substituents, ^{1}H NMR and H–H-COSY spectra confirmed that the purified antibiotic compound with R_f value 0.66 and *RT* 15.5 min was indeed pyoluteorin. These data obtained are consistent with the spectra of the authentic pyoluteorin compound.

4. Experimental

4.1. Bacterial strain, characteristics and cultural media

The bacterial strain *Pseudomonas fluorescens* G308 was isolated from barley leaves (Kremer, 1994). Some of the biochemical and physiological characteristics of the strain G308 were studied according to the methods described by Mauerhofer et al. (1994), Press et al. (1997), and Voisard et al. (1989) with some modifications. For antibiotic production, three types of broth media containing different nutrient sources were used in order to encourage the production of a wide range of secondary metabolites. These media are King's B (KB),

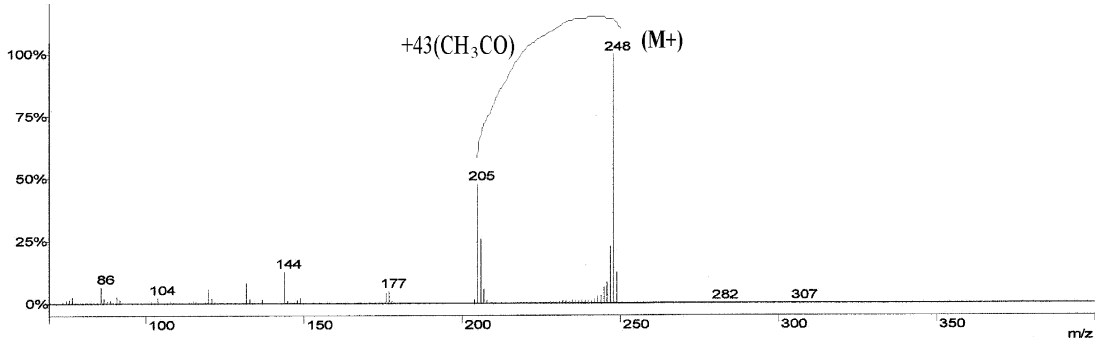

Fig. 3. EI-mass spectrum of *N*-mercapto-4-formyl-carbostyril and the acetyl-derivative of Cbs 248.0 $[M]^+$.

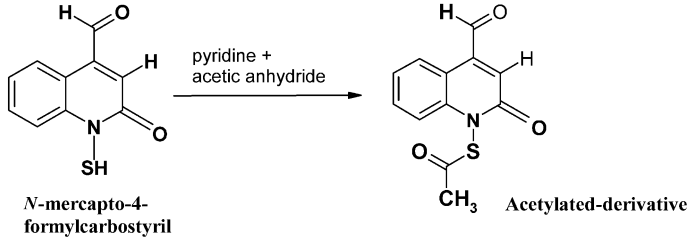

Fig. 4. The chemical structure of *N*-mercapto-4-formyl-carbostyril and its acetyl-derivative.

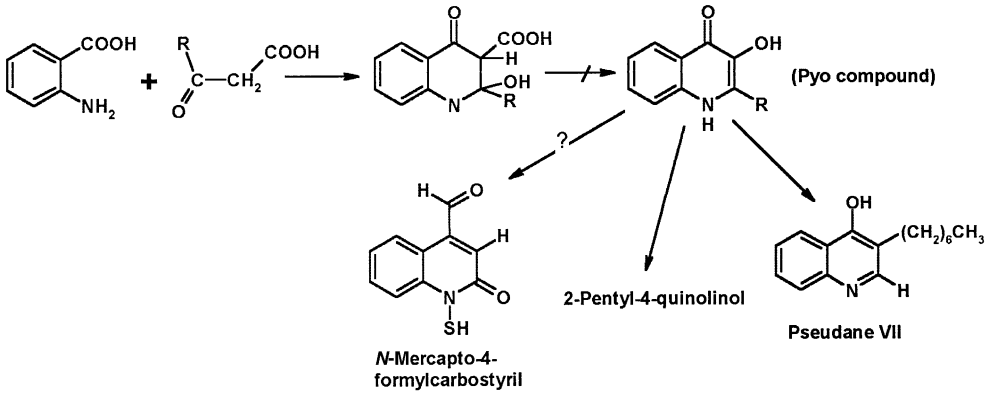

Fig. 5. Biosynthesis of pyo compound (pseudanes) from anthranilic acid and a β-keto acid intermediate as proposed by Cornforth and James (1956). Our antibiotic compound (Cbs) seems to be synthesized through this pathway.

biomalt (BM) and sucrose-asparagin (SuA) (Schaad, 1980; Shanahan et al., 1992).

4.2. Extraction and purification of the antibiotics

With regard to the antibiotic production, the isolate G308 was cultivated in 500 ml of three different media KB, BM and SuA on a shaker at 100 rpm and 28 °C for 3 days. After incubation, the pH value of the bacterial suspensions was adjusted to 2.0 with 2 N HCl. Ethylacetate (EtOAc) was added to the suspensions in a ratio of 1:1 (1/2 : 1/2 l; v/v). Then, the ethylacetate-bacterial suspensions were placed on a shaker at 200 rpm for 4 h and then centrifuged at 10,000 *g* and 4 °C for 30 min. After that, the centrifugation cups were placed in the refrigerator at −20 °C for 3 h to solidify the aqueous phase. The EtOAc phase was filtered through filter paper to remove the non dissolved compounds. The organic phase was preconcentrated in a rotary evaporator and the residue was reconstituted with 100% methanol (MeOH). Then, the volume of the methanolic extract was reduced to 1 ml by using nitrogen gas flow. Ten microliters of the MeOH extract was applied to thin layer chromatography plates (ALUGRAM-SIL-G/UV_{254}, Macherey–Nagel) and the substances in the extract developed in *tert*-butyl-methyl-ether: hexane: methanol (50: 40: 3.5; v/v/v). The antifungal properties of the bands were detected by the bioautographic method using *Cladosporium cucumerinum* (3×10^7 spores/ml) and *Colletotrichum lagenarium* (2×10^6 spores/ml) as test organisms. The procedure for locating bands and detecting zones with antibiotic activity was repeated. The bands that showed antifungal activities were scratched off from the preparative thick layer chromatography plates (Kieselgel 60 F254/Merck) and developed in *tert*-butyl-methyl-ether : hexane : methanol (50: 40: 3.5; v/v/v). The separated substances were eluted from the silica gel with acetone by using filter discs with pore diameter of 0.45 μm. The isolated substances were further purified by using preparative HPLC (a gradient pump; Kronlab HD2-200) coupled with UV/vis detector (Spectraflow 500) at wavelength of 250 nm. The MeOH extract of each sample (2 ml) was directly injected in the preparative HPLC column Kieselgel 60 (Merck 107734, 270 × 22 mm and pore diameter 0.063–0.2 mm). Separation of the compounds was done at room temperature with flow rate of 0.10 ml/min using gradient TBME : MeOH. Finally, the purity and spectrum analysis were determined by using HPLC (Merck-Hitachi®), coupled to a Waters 991 photodiode array detector (DAD) and a Merck-Hitachi (4000A) autosampler. Separation was done with a RP18 column (5 μm) at 35 °C with a flow rate of 0.5 ml/min using gradient elute phosphate buffer/ACN, maximum pressure 250 (bar) and oven temperature 25 °C.

4.3. Spectroscopy analysis and identification

4.3.1. Gradient HPLC-system with MS-detection (LC–MS)

Gradient HPLC-system series 1100 (Hewlett-Packard®) combined with an autosampler ALS G1313A, a gradient pump G1311A, a degasser G1322A were used. The mass spectrometric detector was a Micromass Platform-II (Mass Lynx® 4.0, UK) equipped with a cross flow interface. The tuning parameters for positive ion spray (ES^+) were 3.5 kV for capillary and 40 V for cone at a source temperature of 120 °C. Positive ion characterization was performed in the *m*/*e* range of 200–600 at a scan rate of 1.49 scans/s and a multiplier voltage of 650 V. Separation was carried out with a Luna® ODS column (250 × 3 mm i.d.; 5 μm, Phenomenex®) at 25 °C with a flow rate of 0.5 ml/min using H_2O/ACN in a ratio of 80:20%, maximum pressure 250 (bar) and oven temperature 25 °C. For the LC–$HRES^+$/MS analysis, the tuning parameters were 24V for cone, 23.5 LM resolution and 13.2 for HM resolution. Polyethyleneglycol 200 was used as reference substance.

4.3.2. IR, GC–EI–MS, GC–EI–MS/MS and GC–CIMS spectra

The FTIR spectra were recorded on a Nicolet Avatar 320 F.S.P. instrument (Single bounce ATR). Electron impact (EI) and chemical ionisation (CI)/mass spectra were recorded by a Varian® 3800 Gas Chromatograph coupled to an ion trap mass spectrometer operating in EI and CI modes (Varian®, Saturn 2000). An extract of the antibiotic substance in hexane was injected at a continuous flow of 1.4 ml/min on a Chrompack SIL-24 CP column. Column temperature ranged from 80 to 270 °C, while the injector and detector (trap) temperatures were 250 and 230 °C, respectively. Full-scan EI-mass spectra (m/z: 100–600) were recorded for peak identification. In addition, GC–CI/MS data were obtained using the same setup conditions of GC–EI/MS, but methanol was used as a reagent medium.

4.3.3. ^{1}H NMR and ^{13}C NMR spectra

^{1}H, ^{13}C NMR (nuclear magnetic resonance), HH-COSY (correlation spectroscopy), HSQC (hetero-single quantum correlation) and HMQCSS (hetero-multi-quantum correlation solvent substraction) spectra were recorded using Varian® (NMR-INOVA- 300 MHz and Varian® LC–NMR; stopflow INOVA-500 MHz) instruments as a gated spin echo in deuteroacetone. Shifts were reported in parts per million (ppm) downfield from TMS using the central resonance of deuteroacetone as an internal standard.

4.4. Antifungal bioassay in vitro

The antifungal activity of the purified antibiotic with the R_f value 0.7 was tested in vitro against several plant fungal pathogens. Four different concentrations of the antibiotic were used 25, 50, 100 and 150 ppm. The plant pathogens which were included in the antifungal bioassay were spore suspensions of *Fusarium oxysporum* f. sp. *lycopersici* (5×10^6 spores/ml), *Fusarium culmorum* (3.1×10^6 spores/ml), *Cladosporium cucumerinum* (3×10^7 spores/ml), *Colletotrichum lagenarium* (2×10^6 spores/ml), *Ustilago maydis* and *U. nuda* (8×10^6 spores/ml), *Phytophthora infestans* (4×10^4 sporangia/ml). The bioassay test was conducted in Eppis cups and placed in an incubator according to the optimal temperature of each fungus. Spore germination and germ tube growth were recorded 12 and 24 h after incubation by means of light microscopy. The chemically synthesized antimicrobial compound 2,4-diacetylphloroglucinol at a concentration of 25–125 ppm was included as a reference.

4.5. Acetylation of the antibiotic substance

The purified antibiotic with R_f value of 0.70 was transformed to the acetyl-derivative by addition of dry pyridine (C_5H_5N) (0.5 ml) and dry acetic anhydride (Ac_2O) (0.5 ml) to the dried antibiotic substance (2 mg) under room temperature conditions. Also, this derivatization was repeated under different temperatures ranging from 50 to 70 °C and with different time intervals (6–42 h).

Acknowledgements

The authors thank Mrs. S. Reeb and Mrs. B. Meier for the technical help and Dr. M. Mauerhofer (ETH-Zürich) for supplying the authentic pyoluteorin compound. Also, we thank so much Dr. J. Conrad, Mrs. I. Klaiber and Dr. M Lederer for the technical assistance. The financial support of the German Academic Exchange Service (DAAD, Bonn) for the first author is gratefully acknowledged.

References

Berdy, J., 1982. Recent developments of antibiotic research and classification of antibiotics according to chemical structure. In: Berdy, J. (Ed.), CRC Handbook of Antibiotic Compounds, Vol. 1. Boca Raton, pp. 309–402.

Burkhead, K.D., Schisler, D.A., Slinnger, P.J., 1994. Pyrrolnitrin production by biological control agent *Pseudomonas cepacia* B37w in culture and in colonized wounds of potatoes. Applied Environmental Microbiology 60, 2031–2039.

Carmi, R., Carmeli, S., 1994. (+)-(*S*)-Dihydroaeruginoic acid, an inhibitor of *Septoria tritici* and other phytopathogenic fungi and bacteria, produced by *Pseudomonas fluorescens*. Journal of Natural Products 57, 1200–1205.

Cornforth, J.W., James, A.T., 1956. Structure of a naturally ocurring antagonist of dihydrostreptomycin. Biochemical Journal 63, 124–130.

Eistert, B., Borggrefe, G., Selzer, H., 1969. Reaction of diazoalkanes with alpha-dicarbonyl compound and quinones. XIII. Syntheses of *N*-hyroxycarbostyrils. Justus Liebigs Annalen der Chemie 725, 3751.

Gehmann, K., Nyfeler, R., Leadbeater, A.J., Nevill, D., Sozzi, D., 1990. CGA 173506: a new phenylpyrrole fungicide for broad-spectrum disease control. Proceedings of the Brighton Crop Protection Conference-Pests and Diseases 2, 399–406.

Günther, H., 1992. NMR-Spektoskopie. Georg Thieme, Stuttgart.

Hesse, M., Meier, H., Zeeh, B., 1995. Spektroskopische Methoden in der organischen Chemie. Georg Thieme Verlag, Stuttgart.

Hostettmann, K., Wolfender, J.-L., 1997. The search for biologically active secondary metabolites. Pesticide Science 51, 471–482.

Howell, C.R., Stipanovic, R.D., 1980. Suppression of *Pythium ultimum*-induced damping-off of cotton seedlings by *Pseudomonas fluorescens* and its antibiotic pyoluteorin. Phytopathology 70, 712–715.

Howie, W.J., Suslow, T.V., 1991. Role of antibiotic biosynthesis in the inhibition of Pythium ultimum in the cotton spermosphere and rhizosphere by *Pseudomonas fluorescens*. Molecular Plant-Microbe Interactions 4, 393–399.

Keel, C., Wirthner, P.H., Oberhänsli, T.H., Voisard, C., Burger, U., Haas, D., Defago, G., 1990. Pseudomonads as antagonists of plant pathogens in the rhizosphere: role of the antibiotic 2,4-diacetylphloroglucinol in the suppression of black root rot of tobacco. Symbiosis 9, 327–341.

Kerr, A., Tate, M.E., 1984. Agrocins and the biological control of crown gall. Microbiological Science 1, 1–4.

Kloepper, J.W., Leong, J., Teintze, T., Schroth, M.N., 1980. *Pseudomonas* siderophores: a mechanism explaining disease-suppressive soils. Current Microbiology 4, 317–320.

Kremer, M., 1994. Untersuchungen zum antagonistischen Potential fluoreszierender Pseudomonaden gegenüber *Erysiphe graminis* f. sp. *hordei* und *Drechslera teres* an Gerste, Dissertation. Ulrich Grauer, Stuttgart.

Leisinger, T., Margraff, R., 1979. Secondary metabolites of the fluorescent pseudomonads. Microbiological Reviews 43, 422–442.

Ligon, J.M., Hill, D.S., Hammer, P.E., Torkewitz, N.R., Hofmann, D., Kempf, H.-J., van Pee, K.-H., 2000. Natural products with antifungal activity from *Pseudomonas* biocontrol bacteria. Pest Management Science 56, 688–695.

Mauerhofer, M., Keel, C., Haas, D., Defago, G., 1994. Pyoluteorin production by *Pseudomonas fluorescens* strain CHA0 is involved in the suppression of Pythium damping-off of cress but not of cucumber. European Journal of Plant Pathology 100, 221–232.

McLoughlin, T.J., Quinn, J.P., Betterman, A., Bookland, R., 1992. *Pseudomonas cepacia* suppression of sunflower wilt fungus and role of antifungal compounds in controlling the disease. Applied and Environmental Microbiology 58, 1760–1763.

Nevill, D., Nyfeler, R., Sozzi, D., 1988. CGA 142705, a novel fungicide for seed treatment. Proceedings of the Brighton Crop Protection Conference-Pests and Diseases 1, 65–80.

Press, C.M., Wilson, M., Tuzun, S., Kloepper, J.W., 1997. Salicylic acid produced by *Serratia macescens* 90–166 is not the primary determinant of induced systemic resistance in cucumber or tobacco. Molecular Plant–Microbe Interactions 10, 761–768.

Schaad, N.W., 1980. Laboratory Guide for Identification of Plant Pathogenic Bacteria. American Phytopathological Society, Minnesota.

Shanahan, P., O'Sullivan, D.J., Simpson, P., Glennon, J.D., O'Gara, F., 1992. Isolation of 2,4-diacetylphloroglucinol from a fluorescent pseudomonad and investigation of physiological parameters influencing its production. Applied and Environmental Microbiology 58, 353–358.

Tanaka, M., Tamada, S., Tsutsui, Y., Ei, K., Tominaga, M., Yabuchi, Y., 1989. Preparation of carbostyril derivatives as inotropic cardiotonics and their formulations. Japan Kokai Tokkoyo Koho. Patent No. JP 02229165.

Thomashow, L.S., Weller, D.M., 1988. Role of a phenazine antibiotic from *Pseudomonas fluorescens* in biological control of *Gaeumannomyces graminis* var. *tritici*. Journal of Bacteriology 170, 3499–3508.

Uchida, M., Komastu, M., Nakagawa, K., 1984. Carbostyril derivatives and pharmaceuticals containing them. Ger. Offen. Patent No. DE 3324034.

Uematsu, T., Inoue, S., Yamashita, N., 1979. Fungicidal carbostyrils for *Oryza sativa*. Japan Kokai Tokkyo Koho, Sumitomo Chemical Co. Patent No. JP 54063088.

Voisard, C., Keel, C., Haas, D., Defago, G., 1989. Cyanide production by *Pseudomonas fluorescens* helps suppress black root rot of tobacco under gnotobiotic conditions. EMBO Journal 8, 358–361.

Wright, S. A. I., Lindberg, A., Gerhardson, B., 1999. The genetic basis for the production of a fungitoxic compound by the biocontrol agent MA 342. Proceeding of 9th International Symposium of Molecular Plant-Microbe Interaction, 25–30 July.

PERGAMON

Phytochemistry 58 (2001) 1305–1309

PHYTOCHEMISTRY

www.elsevier.com/locate/phytochem

Glyceroglycolipids from *Serratula strangulata*

Jing Qiu Dai[a,*], Qi Xiu Zhu[a], Chen Yang Zhao[b], Li Yang[a], Yu Li[a]

[a]*National Laboratory of Applied Organic Chemistry, Lanzhou University, Lanzhou 730000, Gansu, People's Republic of China*
[b]*Department of Biology, Lanzhou University, Lanzhou 730000 Gansu, People's Republic of China*

Received 30 November 2000; received in revised form 17 May 2001

Abstract

The rhizomes of *Serratula strangulata* yielded three glyceroglycolipids, i.e. 1,2-di-*O*-(9*Z*,12*Z*,15*Z*-octadecatrienoyl)-3-*O*-(6-amine-6-deoxy-α-D-glucosyl)-glycerol, 1,2-di-*O*-(9*Z*,12*Z*,15*Z*-octadecatrienoyl)-3-*O*-(6-*p*-hydroxy-phenyl-propionamido-6-deoxy-α-D-glucosyl)-glycerol and 1,2-di-*O*-(9*Z*,12*Z*,15*Z*-octadecatrienoyl)-3-*O*-[α-D-glucose(1-6)-β-D-allose]-glycerol, as well as a known sesquiterpene lactone and three known phytoecdysones. Their structures were elucidated on the basis of spectral data, especially by 2D NMR spectroscopic methods and chemical conversion. These compounds exhibited significant antibacterial and antitumor activities.
© 2001 Elsevier Science Ltd. All rights reserved.

Keywords: *Serratula strangulata*; Compositae; Glyceroglycolipids; Cytotoxicity; Antimicrobial

1. Introduction

Serratula strangulata (Compositae) is a perennial herbaceous plant growing mainly in North China. Its rhizomes have been used as a traditional chinese medicine for treatment of chickenpox, toxicosis, and high cholesterol levels since ancient times (Liu, 1987). Its phytochemical or pharmacological properties have not been reported to date. In our effort to find active components from this plant, we found three new glyceroglycolipids, i.e. 1,2-di-*O*-(9*Z*,12*Z*,15*Z*-octadecatrienoyl)-3-*O*-(6-amine-6-deoxy-α-D-glucosyl)-glycerol (**1**), 1,2-di-*O*-(9*Z*,12*Z*,15*Z*-octadecatrienoyl)-3-*O*-(6-*p*-hydroxy-phenyl-propionamido-6-deoxy-α-D-glucosyl)-glycerol (**2**) and 1,2-di-*O*-(9*Z*,12*Z*,15*Z*-octadecatrienoyl)-3-*O*-[α-D-glucose(1-6)-β-D-allose]-glycerol (**3**), as well as four known compounds, centaurepensin (**4**), 20-hydroxyecdysone (**5**), 25-deoxy-11,20-dihydroxyecdysone (**6**) and 20-hydroxyecdysone-20,22-monoacetonide (**7**) from the alcohol extract of the whole plant. We report herein the isolation, structural elucidation and antibacterial and antitumor activities of the above three new glyceroglycolipids. It was found that these compounds exhibited significant antibacterial and antitumor activities, especially **2** possess strong cytotoxicity for B 16 (mouse melanoma).

2. Results and discussion

From the EtOAc- and BuOH-soluble fraction of an EtOH extract of the rhizome of *S. strangulata*, seven compounds (**1**–**7**) were purified by repeated chromatography on silica gel. Each of the isolates was subjected to detailed spectroscopic analyses in order to establish their chemical structures.

Compound **1** was isolated as a colorless gum. FAB–MS which gave a quasi-molecular ion peak at *m*/*z* 796 $(M+Na)^+$, 780 $(M+Li)^+$, as well as its elemental analysis (found: C 69.85%, H 9.70%, N 1.80%; required: C 69.86%, H 9.70%, N 1.81%) indicated that the molecular formula should be $C_{45}H_{75}NO_9$, which was proved by HR–FAB–MS (*m*/*z* 773.5422, calc. 773.5441). Its IR spectrum showed strong absorptions for hydroxyl and ester groups (3464 cm^{-1}, 1729 cm^{-1}), while the ^1H NMR spectrum exhibited two terminal methyl signals (δ 0.90, 6H, *t*), a broad methylene signal at 1.23 ppm which the integration showed 20 protons, and the signal (δ 2.30, 4H, *m*) due to two methylene protons linked to a carbonyl function. The ^1H NMR spectrum of **1** further revealed olefinic proton (δ 5.30, 12H, *m*) and methylene protons linked to double bonds (δ 1.69, 4H; δ 2.01, 4H; δ 2.75, 8H). These were consistent with the proton signals of two linolenic acid moieties (Pchelkin and Vereshchagin, 1980). In addition, coupling constant analysis of the homonuclear decoupling spectrum defined the

* Corresponding author.
E-mail address: daij1@21cn.edu.cn (J.Q. Dai).

0031-9422/01/$ - see front matter © 2001 Elsevier Science Ltd. All rights reserved.
PII: S0031-9422(01)00308-9

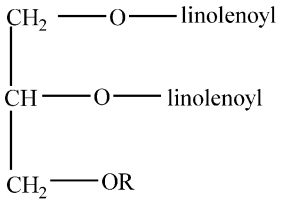

2 R =

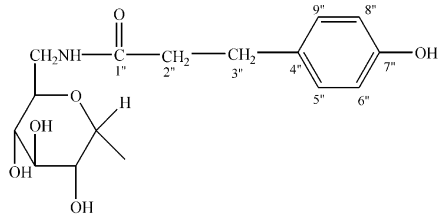

1 R =

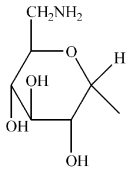

3 R =

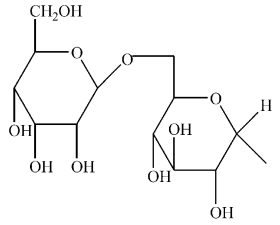

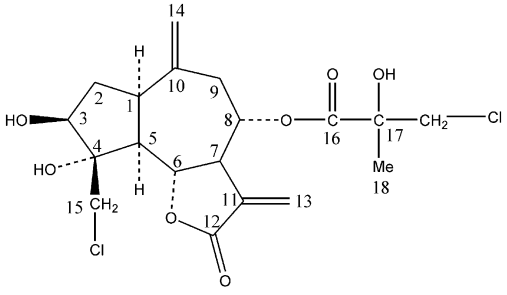

4

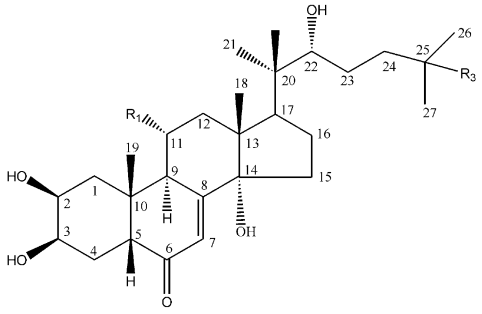

5 $R_1 = H$ $R_2 = H$ $R_3 = OH$
6 $R_1 = OH$ $R_2 = H$ $R_3 = H$

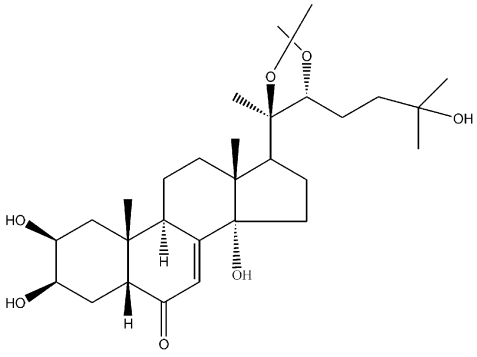

sugar component as glucose; this being consistent with the ^{13}C spectrum (Table 1). The configuration at C-1′ of the glucose was determined to be α by the coupling constant of the anomeric proton ($J = 3.5$ Hz). Treatment of **1** with NaOMe–MeOH gave mono-glucosyl-glycerol and linolenic acid. The ^{13}C NMR and DEPT spectrum of **1** confirmed the presence of linolenic acid (Frangulyan, 1987) and an α-aminoglucose moieties. Simultaneously, they also revealed three carbon signals connected to oxygen atoms: δ_C 62.62 (CH_2), 69.73 (CH) and 64.63 (CH_2), which pointed to the presence of a glyceryl moiety. The sites of attachment of the two linolenic acids and aminoglucose moiety of **1** were determined to be at C-1, C-2, C-3 respectively, by means of the HMBC, ^1H-^1HCOSY and HMQC spectrum. Because the upfield shift of C-6′ in the aminoglucose observed of ^1H NMR and ^{13}C NMR spectral analysis, the amine group should be attached to C-6′. Thus, **1** was assigned as 1,2-di-*O*-(9*Z*,12*Z*,15*Z*-octadecatrienoyl)-3-*O*-(6-amine-6-deoxy-α-D-glucosyl)-glycerol. This appears to be the first reported occurrence of glucosaminediacylglycerol in the genus *Serratula*.

Compound **2** was isolated as a colorless gum. FAB–MS showed $[M + Na]^+$ at *m*/*z* 944 and $[M + Li]^+$ at 928. Its ^1H, ^{13}C and DEPT spectrum were similar to those of **1**. In the ^1H, ^{13}C NMR spectral analyses of **2**, the extra

Table 1
^{13}C NMR data for **1**, **2** and **3** (100.62 MHz, DMSO-d_6, TMS)[a]

Carbon	1	DEPT	2	DEPT	3	DEPT
Sn-1	62.62	CH_2	62.62	CH_2	62.46	CH_2
Sn-2	69.73	CH	69.71	CH	69.65	CH
Sn-3	64.63	CH_2	64.14	CH_2	66.42	CH_2
	α-Aminoglu		α-Aminoglu		α-Glu	
1′	98.29	CH	98.31	CH	99.59	CH
2′	71.56	CH	71.61	CH	71.29	CH
3′	72.86	CH	72.92	CH	72.94	CH
4′	74.13	CH	74.16	CH	69.76	CH
5′	68.53	CH	68.53	CH	71.47	CH
6′	54.38	CH_2	54.88	CH_2	66.67	CH_2
			Amido moiety		β-Allo	
1″			172.48	C	103.20	CH
2″			40.38	CH_2	70.68	CH
3″			32.21	CH_2	70.35	CH
4″			129.54	C	66.35	CH
5″, 9″			127.68	CH	73.18	CH
6″, 8″			115.34	CH	60.63	CH_2
7″			156.17	C		

[a] Assignment from ^1H–^1H COSY, HMQC and HMBC.

signals at δ_H 7.02 (dd, $J=7.2$, 2.1 Hz), 6.69 (dd, $J=7.2$, 2.1 Hz) and δ_C 40.12 (CH_2), 32.22 (CH_2), 172.48 (ester C=O) revealed the presence of a *p*-substituted benzene ring and the partial structure –CH_2–CH_2– and carbonyl group. ^1H–^1H COSY and HMQC spectrum confirmed above assignments. According to the results of HMBC spectrum: C-1″/H-6′, H-2″, H-3″; C-4″/H-3″, H-5″ (9″); C-7″/H-6″ (8″) (Fig. 1), the structure of **2** was deduced as 1,2-di-*O*-(9*Z*,12*Z*,15*Z*-octadecatrienoyl)-3-*O*-(6-*p*-hydroxyphenyl-propionamido-6-deoxy-α-D-glucosyl)-glycerol.

Compound **3** was obtained as a colorless gum. The IR spectrum showed absorption bands due to hydroxyl and ester carbonyl at 3460, 1729 cm^{-1}. The molecular formula $C_{51}H_{84}O_{15}$ was established on the basis of the strong quasi-molecular ion peak at *m*/*z* 959 $[M+Na]^+$ and 943 $[M+Li]^+$ in the FAB–MS, together with the support of combined spectroscopic methods (^1H NMR, ^{13}C NMR and DEPT). The ^1H and ^{13}C NMR spectrum showed that **3** had the same skeleton and type as **1** and **2**. Detailed analysis of the remaining signals in the ^1H and ^{13}C NMR spectrum of **3** suggested that it possessed an allose moiety attached to the inner glucose unit. On acid hydrolysis with 2 mol/l HCl, **3** gave glucose and allose, and on acid hydrolysis with 0.5 mol/l HCl, **3** afforded only allose (identified by ^{13}C NMR and TLC), confirming the above deduction. The β-configuration of the glucosidic bond between the glucose and allose residue was determined on the basis of anomeric carbon signal at 103.2 ppm. The observation of the downfield shift of the C-6′ carbon confirmed α1-6 linkage of the two glucide units (Gong, 1983). Thus, the structure of **3** was assigned as 1,2-di-*O*-(9*Z*,12*Z*,15*Z*-octadecatrienoyl)-3-*O*-[α-D-glucose (1-6)-β-D-allose]-glycerol, which was further supported by HMBC and HMQC analysis.

During the course of the isolation of the plant extract, a sesquiterpene lactone and three phytoecdysones were also obtained in pure form. This appears to be the first reported occurrence of sesquiterpenes in the genus *Serratula*. Each of these isolates was characterized by its spectral properties and subsequently identified as centaurepensin (Harley-Mason et al., 1972), 20-hydroxyecdysone (Nishimoto et al., 1987), 25-deoxy-11,20-dihydroxyecdysone (Zhang et al., 1992) and 20-hydroxyecdysone-20, 22-monoacetonide (Zhang et al., 1992) by comparison with published spectral data and/or reference samples.

Previous studies have reported the cytotoxicity of centaurepensin against SMMC-7721 cells (Syrov et al., 1991), and interesting pharmacological effects of ecdysteroids on mammals including a stimulation of protein synthesis, and a reduction of blood glucose and cholesterol levels (Camps, 1991; Simon and Koolman, 1989). Murakami et al. (1990) also reported anti algal activity of unsaturated fatty acids. In our study, compound **1**–**3** exhibited antibacterial activity against *Bacillus. subtilis, Escherichia. coli* and *Staphylococcus. aureus*. The results were compared with chloramphenicol and are summarized in Table 2. Meanwhile, the inhibitory effects of compounds **1**–**3** on the survival of three tumor cell lines, human hepatoma cells (SMMC-7721), human uterine cervix carcinoma cells (HeLa) and mouse melanotic carcinoma cells (B16), were studied (Table 3). The survival rates of cells were determined by MTT [3-(4,5-dimethylthiazol-2-yl)-2,5-diphenyltetrazolium bromide] method. **2** exhibited the most effective antitumor activity, especially on B16, and **3** had no effect on survival of the three tested tumor cells even when its concentrations was as high as 455 μg /ml.

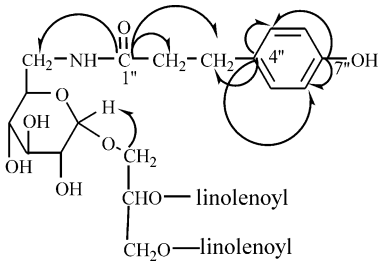

Fig. 1. The key correlations of **2** in HMBC (C⇀H).

Table 2
Antibacterial activity of compound **1**, **2**, **3**[a]

	B. subtilis	*E. coli*	*S. aureus*
Compound **1**	+	+ + +	+
Compound **2**	+ +	+ + +	+
Compound **3**	+ +	+ +	+
Chloramphenicol	+ + +	+ + +	+ + +

[a] Antimicrobial activity is defined as follows: + + + = the diameter is equal to 16–20 mm; + + = 13–15 mm; + = 10–12 mm.

Table 3
Antitumour activity of compound **1** and **2**[a]

	SMMC-7721	B16	Hela
Compound **1**	351.4±6.1	157.3±2.5	168.2±1.9
Compound **2**	151.6±6.3	70.3±2.2	121.9±3.1
Vincristine	63.2±1.8	70.7±2.8	67.2±2.2

[a] Activities are expressed as IC_{50} (50% inhibitory concentration) in μg ml^{-1}.

3. Experimental

3.1. General

FAB–MS were determined on a MS 50 (A.E.I. Brunner) and a ZAB–HS mass spectrometer. ^1H, ^{13}C and 2D NMR spectra were recorded on Bruker AM-400 MHz spectrometer using TMS as internal standard. Deuterated solvents (DMSO-d_6 for **1**–**3** and CD_3COCD_3 for **4**–**7**) were used. IR spectra were obtained as KBr pellets on Nicolet-5DX. IR spectrometer.

3.2. Plant material

The whole plants of *S. strangulata* were collected in Zhuanglang county, Gansu Province of China in August 1996 and were identified by Professor Yong-hong Zhang of Lanzhou University. A voucher specimen (No. 9602) has been deposited at the Lab. of Natural Products, Department of Chemistry, Lanzhou University, Lanzhou, PR China.

3.3. Extraction and isolation

Air-dried and powdered whole plants of *S. strangulata* (3 kg) were exhaustively extracted with 95%EtOH at room temperature. The extract was concentrated under reduced pressure. The residue (120 g) was suspended in H_2O, extracted with petroleum ether, EtOAC and BuOH, respectively. The EtOAC extract (40 g) was subjected to column chromatography on silica gel eluting with petrol and Me_2CO mixtures to afford **4** (50 mg), **5** (45 mg), **6** (28 mg), **7** (16 mg). From the BuOH extract (60 g), three glyceroglycolipids **1** (40 mg), **2** (20 mg), **3** (48 mg) were purified by silica gel chromatography using $CHCl_3$–MeOH mixtures as solvent.

3.4. 1,2-Di-O-(9Z,12Z,15Z-octadecatrienoyl)-3-O-(6-amine-6-deoxy-α-D-glucosyl)-glycerol (*1*)

Colorless gum. $[\alpha]_D^{24}$ +25.5 (*c* 3.01, MeOH), FAB–MS *m/z*: 796 $(M+Na)^+$, 780 $(M+Li)^+$; HR–FAB–MS *m/z* 773.5422, calc. for $C_{45}H_{75}NO_9$ 773.5441; Elemental analysis found: C 69.85%, H 9.70%, N 1.80%; required: C 69.86%, H 9.70%, N 1.81%. ν_{max}^{KBr} 3464∼3271, 2926, 2253, 2126, 1658, 1120, 1026, 825. ^1H NMR (DMSO-d_6) δ 0.90 (6H, *t*, *J*=7.5 Hz), 1.23 (20H, *m*), 1.69 (4H, *m*), 2.01 (4H, *m*), 2.30 (4H, *m*), 2.75 (8H, *m*), 2.54 (1H, *dd*, *J*=14.0, 7.0 Hz, H-6′ α), 2.89 (1H, *dd*, *J*=14.0, 4.2 Hz, H-6′ β), 2.90 (1H, *dd*, *J*=9.0, 9.1 Hz, H-4′), 3.17 (1H, *dd*, *J*=9.6, 3.5 Hz, H-2′), 3.34 (1H, *dd*, *J*=9.1, 9.6 Hz, H-3′), 3.44 (1H, *dd*, *J*=10.4, 4.7 Hz, *sn*-3-H_a), 3.76 (1H, *ddd*, *J*=9.0, 7.0, 4.2 Hz, H-5′), 3.87 (1H, *dd*, *J*=10.4, 5.9 Hz, *sn*-3-H_b), 4.11 (1H, *dd*, *J*=10.0, 7.4 Hz, *sn*-1-H_a), 4.32 (1H, *dd*, *J*=10.0, 2.1 Hz, *sn*-1-H_b), 4.56 (1H, *d*, *J*=3.5 Hz, H-1′), 5.11 (1H, *m*, *sn*-2-H), 5.30 (12H, *m*). For ^{13}C NMR spectral data, see Table 1.

3.5. 1,2-Di-O-(9Z,12Z,15Z-octadecatrienoyl)-3-O-(6-p-hydroxy-phenyl-propionamido-6-deoxy-α-D-glucosyl)-glycerol (*2*)

Colorless gum. $[\alpha]_D^{24}$ +25.8 (*c* 2.7, MeOH); IR ν_{max}^{KBr} cm^{-1}: 3464, 3271, 2926, 2254, 2125, 1729, 1658, 1515, 1458, 1371, 1028, 762, 627; FAB–MS *m/z*: 922 $(M+H)^+$; HR–FAB–MS *m/z* 921.5946, calc. for $C_{54}H_{83}NO_{11}$ 921.5969; ^1H NMR (DMSO-d_6) δ 0.88 (6H, *t*, *J*=7.5 Hz), 1.15 (20H, *m*), 1.47 (4H, *m*), 1.99 (4H, *m*), 1.21 (2H, *m*, H-3″), 2.22 (4H, *m*), 2.23 (2H, *m*, H-2″), 2.73 (1H, dd, *J*=14.0, 7.0 Hz, H-6′ α), 2.75 (8H, *m*), 2.90 (1H, *dd*, *J*=14.0, 4.2 Hz, H-6′ β), 2.93 (1H, *dd*, *J*=9.0, 9.1 Hz, H-4′), 3.17 (1H, *dd*, *J*=9.6, 3.5 Hz, H-2′), 3.33 (1H, *dd*, *J*=9.1, 9.6 Hz, H-3′), 3.44 (1H, *dd*, *J*=10.4, 4.7 Hz, *sn*-3-H_a), 3.77 (1H, *ddd*, *J*=9.0, 7.0, 4.2 Hz, H-5′), 3.87 (1H, *dd*, *J*=10.4, 5.9 Hz, *sn*-3-H_b), 4.11 (1H, *dd*, *J*=10.0, 7.4 Hz, *sn*-1-H_a), 4.32 (1H, *dd*, *J*=10.0, 2.1 Hz, *sn*-1-H_b), 4.56 (1H, *d*, *J*=3.5 Hz, H-1′), 5.11 (1H, *m*, *sn*-2-H), 5.30 (12H, *m*), 6.68 (2H, *dd*, J=2.1, 7.2 Hz, H-6″, 8″), 7.02 (2H, *dd*, J=2.1, 7.2 Hz, H-5″, 9″), For ^{13}C NMR spectral data, see Table 1.

3.6. 1,2-Di-O-(9Z,12Z,15Z-octadecatrienoyl)-3-O-[α-D-glucose(1-6)-β-D-allose]-glycerol (*3*)

Colorless gum. $[\alpha]_D^{24}$ +25.3 (*c* 6.01, MeOH). IR ν_{max}^{KBr} cm^{-1}: 3460, 1720, 1651; FAB–MS *m/z*: 959 $(M+Na)^+$, 937 $(M+Li)^+$. HR–FAB–MS *m/z* 936.5811, calc. for $C_{51}H_{84}O_{15}$ 936.5810. ^1H NMR (DMSO-d_6) δ 0.89 (6H, *t*, *J*=7.3 Hz), 1.20 (20H, *m*), 1.46 (4H, *m*), 1.97 (4H, *m*), 2.22 (4H, *m*), 2.72 (8H, *m*), 3.78 (1H, *dd*, *J*=11.0, 5.3 Hz, *sn*-3-H_a), 3.60 (1H, *dd*, *J*=11.0, 4.5 Hz, *sn*-3-H_b), 4.22 (1H, *dd*, *J*=12.1, 7.0 Hz, *sn*-1-H_a), 4.43 (1H, *dd*, *J*=12.1, 2.9 Hz, *sn*-1-H_b), 4.66 (1H, *dd*, J=3.5 Hz, H-1″), 5.08 (1H, *m*, *sn*-2-H), 5.26 (12H, *m*). For ^{13}C NMR spectral data, see Table 1.

3.7. Alkaline treatment of *1*

A solution of **1** (5.0 mg) in dry MeOH (1.0 ml) was treated with 5% NaOMe–MeOH (0.2 ml) at room temperature for 10 min. The reaction mixture was neutralized by using ion exchange resin (Dowex 50 W×8)

and the resin was removed by filtration. The filtrate was extracted with hexane and the hexane layer was concentrated under reduced pressure to yield methyl linolenate (3.5 mg). The methyl ester was identified by GLC comparison with authentic samples. Removal of the solvent from the MeOH layer under reduced pressure gave a residue, which was purified by SiO_2 column chromatography ($CHCl_3$–MeOH–H_2O = 6:4:1) to furnish monoglucosyl-glycerol (1.8 mg).

3.8. Acid hydrolysis of 3

A solution of **3** (15 mg) in 0.5 M HCl (5 ml) was heated at 70 °C for 3 h. After cooling, the reaction mixture was neutralized with 1% NaOH, and extracted with $CHCl_3$ (5 ml). In the aqueous layer, allose was detected with PC by direct comparison with the authentic sample of D-allose, and ^{13}C NMR of the product was consistent with those of authentic sample.

3.9. Antimicrobial assays

Three strains of bacteria, *B. subtilis*, *E. coli* and *S. aureus*, were cultured under agar. The paper-disk method (Xu and Bian, 1982) was used as an antimicrobial test, 0.1 ml of 100 μg/ml of compounds **1**, **2**, **3** or chloramphenicol (used as positive control) was added to each piece of paper. After 1 h, the disks were dried and placed on to a culture dish at 37 °C for 24 h. The antimicrobial activity was calculated by the diameter (in millimeters) of the antibacterial circle. Each test was performed in duplicate.

3.10. Cytotoxicity assays

The cytotoxicity of compounds **1–3** was tested in three cell lines: SMMC-7721 (human hepatoma), B16 (mouse melanoma) and HeLa (human carcinoma of uterine cervix). Cells were cultured at 37 °C under a humidified atmosphere of 5% CO_2 in RPMI 1640 medium supplemented with 10% fetal calf serum and dispersed in replicate 96-well plates with 1×10^4 cells/well for 24 h. Compounds **1**–**3** (10–400 μM) or vincristine (used as a positive control) were then added. After 48 h exposure to the toxins, cell viability was determined by the [3-(4,5-dimethylthiazol-2-yl)-2,5-diphenyltetrazolium bromide] (MTT) colorimetric assay (Price and McMillan, 1990) by measuring the absorbance at 595 nm with an ESILA reader. Each test was performed in triplicate.

Acknowledgements

The authors are grateful to Professor Yong-hong Zhang, Department of Chemistry, Lanzhou University, for her help in identification of plant material, and the National Laboratory of Applied Organic Chemistry and Analysis Center, Lanzhou University, PR China for measuring ^1H,^{13}C NMR spectra and FAB–MS, HR–FAB–MS, respectively. This research project was supported by the Natural Science Foundation of Gansu Province in China (ZS001-A25-001-Z).

References

Camps, F., 1991. Ecological Chemistry and Biochemistry of Plant Terpenoids. Claredon Press, Oxford, p. 331.

Frangulyan, G.A., 1987. Polyunsaturated fatty acids of the α-linolenic series from *insulin*. Chemistry of Natural Compounds 23, 168.

Gong, Y.H., 1983. ^{13}C NMR spectra of natural compounds. Chinese Journal of Magnetic Resonance 1, 113.

Harley-Mason, J., Hewson, A.T., Kennard, O., Pettersen, R.C., 1972. Isolation of centaurepensin. R. C. J. Chem. Soc. Chem. Commun., 460.

Liu, S.W., 1987. Flora Reipulicae popularis Sinicae, Vol. 78. Science Press, Beijing, p. 165.

Murakami, N., Yamada, N., Sakakibara, J., 1990. An autolytic substance in a freshwater cyanobacterium *Phormidium tenue*. Chem. Pharm. Bull. 38, 812.

Nishimoto, N., Shiobara, Y., Fujino, M., Inoue, S., Takemoto, T., De Oliveira, F., 1987. Ecdysteroids from *pfuffia iresinoides* and reassignment of some ^{13}C NMR chemical shifts. Phytochemistry 26, 2505.

Pchelkin, V.P., Vereshchagin, A.G., 1980. Qualitative composition of diacyl glycerol mixture obtained from vegetable oils. Prikl. Biokhim. Mikrobiol. 16, 423.

Price, P., McMillan, T.J., 1990. Use of tetrazolium assay in measuring the response of human tumor cells to ionising radiation. Cancer Res. 50, 1392.

Simon, P., Koolman, J., 1989. Ecdysone: From Chemistry to Mode of Action. Stuttgart Press, New York, p. 254.

Syrov, V.N., Nabiev, A.N., Khushbaktova, Z.A., Sham'yanov, I.D., Abduazimov, B.K., 1991. Hepatotropic action of sesquiterpene lactones. Khim.-Farm Zh. 25, 42.

Xu, S.Y., Bian, Q.L., 1982. Pharmacology Experimental Methods. People's Health Press, Beijing, p. 1340.

Zhang, M.L., Michael, J.S., Isaokubo, 1992. Isolation of ecdysteroids from *Vitex strickeri* using rlcc and recycling HPLC. Phytochemisty 31, 247.

PERGAMON

Phytochemistry 58 (2001) 1311–1315

PHYTOCHEMISTRY

www.elsevier.com/locate/phytochem

Oxidized heptenes from flowers of *Melodorum fruticosum*

Chaiyo Chaichantipyuth[a,*], Supachai Tiyaworanan[a], Somchai Mekaroonreung[a], Nattaya Ngamrojnavanich[b], Sophon Roengsumran[b], Songchan Puthong[c], Amorn Petsom[b,c], Tsutomu Ishikawa[d]

[a]*Department of Pharmacognosy, Faculty of Pharmaceutical Sciences, Chulalongkorn University, Bangkok 10330, Thailand*
[b]*Department of Chemistry, Faculty of Science, Chulalongkorn University, Bangkok 10330, Thailand*
[c]*Institute of Biotechnology and Genetic Engineering, Chulalongkorn University, Bangkok 10330, Thailand*
[d]*Faculty of Pharmaceutical Sciences, Chiba University, Chiba 263, Japan*

Received 12 September 2000; received in revised form 6 April 2001

Abstract

Three oxidized heptenes, 7-benzoyloxy-6-oxo-2,4*Z*-heptadiene-1,4-olide, [7-benzoyloxy-4-hydroxy-1-methoxy-2*E*,4*Z*-heptadiene-1,6-dione] and 7-benzoyloxy-6-oxo-2,4*E*-heptadiene-1,4-olide, were isolated from flowers of *Melodorum fruticosum*. Their structures were determined by spectral data analysis. The first two compounds exhibited moderate cytotoxicity against a panel of human tumor cell lines, whereas the third was inactive. © 2001 Elsevier Science Ltd. All rights reserved.

Keywords: *Melodorum fruticosum*; Annonaceae; Heptene, Cytotoxic activity

1. Introduction

In previous work on potential antitumor compounds from *Melodorum fruticosum* Lour. (Annonaceae), we isolated melodorinol (**4**) and acetylmelodorinol (**5**) as well as several open-chain analogues (Jung et al., 1990, 1991). Additional heptenes from the same plant and their cytotoxicity were also reported by another group (Tuchinda et al., 1991). In this work our continuing study on the flowers of this plant has yielded three heptenes, compounds **1**, **2** and **3**. In this paper we describe both the structural elucidation of compounds **1**–**3** as well as their cytotoxicity against a small panel of human tumor cell lines.

2. Results and discussion

Compound **1** was obtained from an EtOAc extract of the flowers of *M. fruticosum*, by precipitation, followed by re-crystallization from EtOAc. The methane CIMS of compound **1** exhibited a MH^+ at *m*/*z* 259, indicating a M^+ of *m*/*z* 258. The molecular formula, $C_{14}H_{10}O_5$, was established from the elemental analysis, CIMS, and ^1H and ^{13}C NMR spectroscopic data (Table 1). The IR spectrum showed three carbonyl absorption bands at 1790, 1731, and 1704 cm^{-1} consistent with a carbonyl ester of an α,β-unsaturated-γ-lactone ring, a carbonyl ester of benzoate, and α,β-unsaturated ketone, respectively.

The ^1H and ^{13}C NMR spectra together with 2D NMR experiments permitted the complete structure of compound **1** to be established. The ^1H NMR spectrum indicated that compound **1** possesses two methylene protons (δ 5.38), three olefinic protons (δ 5.69, 6.49, and 7.54), and five aromatic protons (δ 7.44, 7.57, and 8.09). The ^{13}C NMR spectrum revealed one methylene carbon (δ 69.3), eight sp^2 carbons (δ 107.3, 124.2, 128.4, 129.9, 133.3, and 145.0), two quaternary carbons (δ 129.3, 155.9), two carboxyl carbons (δ 165.8, 166.9) and a conjugated carbonyl carbon (δ 190.8). The presence of a benzoyl moiety was confirmed by comparison of the ^1H and ^{13}C NMR spectral data of **1** with those of melodorinol (**4**) (Jung et al., 1991). Two olefinic protons were coupled to each other with $J = 5.4$ Hz indicating that this double bond is part of the α,β-unsaturated-γ-lactone ring. The methylene carbon showed a chemical shift further downfield than typical methylene carbons, and the COLOC experiment exhibited long range coupling from the methylene protons to the carbonyl carbon of the benzoyl moiety; thus, the benzoyl moiety was determined to be part of the methylene

* Corresponding author.Tel.: +662-218-8363; fax: +662-253-0321.
E-mail address: chaiyo@chula.ac.th (C. Chaichantipyuth).

0031-9422/01/$ - see front matter © 2001 Elsevier Science Ltd. All rights reserved.
PII: S0031-9422(01)00215-1

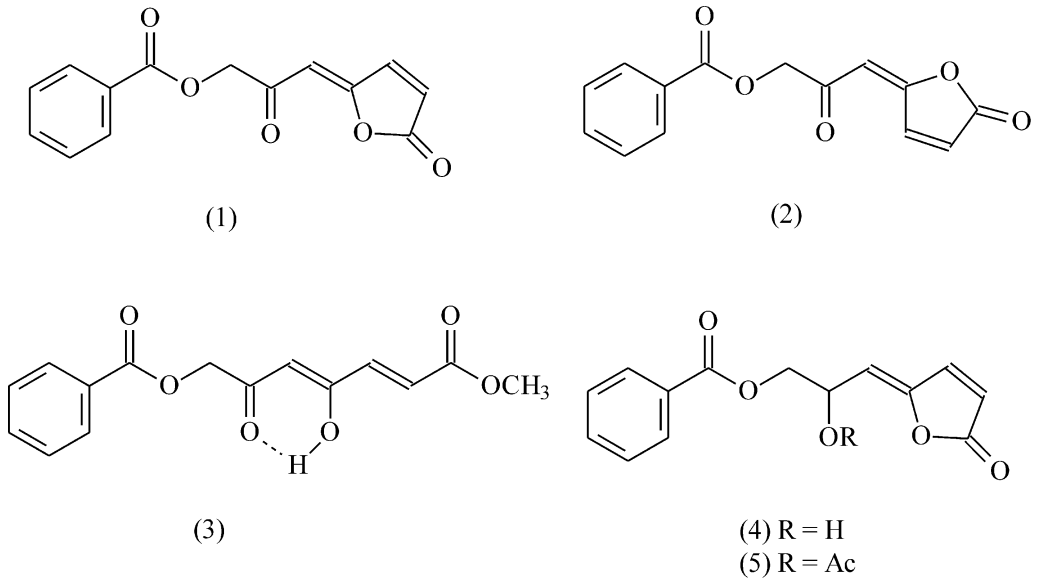

Fig. 1. Chemical structures.

Table 1
^{1}H and ^{13}C NMR spectral data (δ in ppm, J in Hz) of compounds **1**–**3**[a]

	Compound **1**		Compound **2**		Compound **3**	
Carbon	δ_C[b]	δ_H	δ_C[b]	δ_H	δ_C[b]	δ_H
C-1	166.9 *s*		167.4 *s*		165.9 *s*	
C-2	124.2 *d*	6.49 (1H, *d*, *J* = 5.7)	125.9 *d*	6.52 (1H, *d*, *J* = 5.7)	128.1 *d*	6.75 (1H, *d*, *J* = 15.6)
C-3	145.0 *d*	7.54 (1H, *d*, *J* = 5.7)	142.7 *d*	8.32 (1H, *d*, *J* = 5.7)	137.4 *d*	6.91 (1H, *d*, *J* = 15.6)
C-4	155.9 *s*		160.5 *s*		170.7 *s*	
C-5	107.3 *d*	5.69 (1H, *s*)	103.1 *d*	6.33 (1H, *br. S*)	100.2 *d*	5.86 (1H, s)
C-6	190.8 *s*		192.8 *s*		198.2 *s*	
C-7	69.3 *t*	5.38 (2H, *s*)	69.2 *t*	4.99 (2H, *s*)	66.6 *t*	4.93 (2H, s)
C-8	165.8 *s*		165.8 *s*		165.7 *s*	
C-9	129.3 *s*		128.9 *s*		128.9 *s*	
C-10/14	129.9 *d*	8.09 (2H, *d*, *J* = 7.2)	129.9 *d*	8.09 (2H, *d*, *J* = 7.2)	129.9 *d*	8.09 (2H, *d*, *J* = 7.3)
C-11/13	128.4 *d*	7.44 (2H, *dd*, *J* = 7.2, 7.2)	128.6 *d*	7.47 (1H, *dd*, *J* = 7.2,7.2)	128.6 *d*	7.47 (2H, *dd*, *J* = 7.3,7.3)
C-12	133.3 *d*	7.57 (1H, *dd*, *J* = 7.2,7.2)	133.7 *d*	7.60 (1H, *dd*, *J* = 7.2, 7.2)	133.6 *d*	7.56 (1H, *dd*, *J* = 7.3,7.3)
OCH_3		–		–	52.2 *q*	3.77 (1H, *s*)
OH		–		–	–	13.84 (1H, *br. s*)

[a] Chemical shifts are relative to the solvent signal ($CDCl_3$).
[b] Multiplicities were established from DEPT spectra (s = singlet, d = doublet, and t = triplet).

benzoyloxy moiety. One olefinic proton (δ 5.69) showed long-range coupling to the β-carbon of the α,β-unsaturated-γ-lactone ring. Thus, the presence of an sp^2 carbon at the γ-carbon of the lactone moiety was indicated. The carbonyl carbon at δ 190.8 was consistent with an α,β-unsaturated ketone. This carbon showed long-range coupling from the methylene protons, so the methylene benzoyloxy moiety and the exocyclic sp^2 carbon of the γ-lactone ring were connected via this carbonyl. However, the structure of compound **1** could be in either a cisoid or transoid configuration. Irradiation of the H-3 signal (δ 7.54) enhanced the H-5 signal (δ 5.69) (8.2%) and confirmed the cisoid configuration. Thus, compound **1** was assigned as 7-benzoyloxy-6-oxo-2,4*Z*-heptadiene-1,4-olide, a new benzoylated heptene presumably representing an oxidized form of melodorinol.

Compound **2**, $C_{14}H_{10}O_5$, was isolated as colorless bulky crystals from the 70% aqueous acetone extract of *M. fruticosum* by crystallization and then re-crystallization from EtOAc. The molecular formula was established from the elemental analysis, CIMS, and NMR data (Table 1). Using the same approach as in compound **1**, in terms of ^{1}H and ^{13}C NMR analysis including 2D NMR experiments, it was found that **2** was identical to 1 except that the chemical shifts of H-3 (δ 8.32) and C-4 (δ 160.5) were further downfield than in compound **1**, indicating that compound **2** could be in the transoid configuration. Irradiation of the H-3 signal

(δ 8.32) enhanced the H-2 signal (δ 6.51) (5.6%) but not the H-5 signal (δ 6.33). Hence, the transoid configuration was proposed; therefore compound **2** was assigned as 7-benzoyloxy-6-oxo-2,4*E*-heptadiene-1,4-olide.

Compound **3**, $C_{15}H_{14}O_6$, was isolated as a white crystalline solid from EtOAc extract by Sephadex LH-20 chromatography eluting with EtOAc followed by silica gel chromatography eluting with EtOAc in hexane and then re-crystallization from EtOAc. The EIMS of this compound exhibited MH^+ at m/z 291, indicating a M^+ of m/z 290. The molecular formula was established from the elemental analysis, EIMS, and ^1H and ^{13}C NMR data (Table 1). IR spectrum showed two strong carbonyl absorption bands at 1724 and 1587 cm^{-1} consistent with a carbonyl ester and carbonyl group with tautomeric keto-enol forms, respectively. The OH stretching appeared as a broad peak between 2800 and 3500 cm^{-1} suggesting strong hydrogen bonding nature of the hydroxyl group. The mass spectrum showed a typical benzoyl moiety at m/z 105 (base peak) and a methyl ester moiety at m/z 259 (M^+–OCH_3) and m/z 231 (M^+–$COOCH_3$). Thus, compound **3** consisted of methyl ester and tautomeric keto-enol moiety in addition to the benzoate ester as in **1** and **2**.

The ^1H NMR spectrum of **3** displayed a methoxyl proton singlet (δ 3.77), a methylene proton singlet (δ 4.93), three olefinic proton signals (δ 5.86, 6.75 and 6.92), five aromatic protons belonging to the benzoyl group (δ 7.47, 7.60 and 8.09), and the downfield signal belonging to a tautomeric proton with strong hydrogen bond (δ 13.84). The ^{13}C NMR spectrum revealed one methoxyl carbon (δ 52.2), one methylene carbon (δ 66.6), and eight sp^2 carbons (δ 100.2, 128.1, 128.6, 128.9, 129.9, 133.6, 137.4 and 165.7), two carboxyl carbons (δ 165.8, and 170.6), and one unsaturated carbonyl carbon (δ 198.2). Comparison of ^1H and ^{13}C NMR spectral data of **3** with those of melodienone and 7-hydroxy-6-hydromelodienone (Jung et al., 1990; Tuchinda et al., 1991) suggested the structure of **3** as the oxidized form of 7-hydroxy-6-hydromelodienone. Two olefinic protons at δ 6.75 and 6.91 coupled to each other with the coupling constant of 15.6 Hz indicating the *trans* configuration at C-2/C-3 of **3**. Moreover, a strong hydrogen bonding at δ 13.84 suggested the cyclic structure of the intramolecular hydrogen bonding. Therefore, compound **3** was 7-benzoyloxy-4-hydroxy-1-methoxy-2*E*,4*Z*-heptadien-1,6-dione.

In addition to **1**, **2** and **3**, the known acetylmelodorinol (**5**) (Jung et al., 1990) together with 5,7-dihydroxyflavone (Markham and Chari, 1982) and 5,7-dimethoxyflavone (Jaipetch et al., 1983) were also isolated. Their spectroscopic data were in agreement with those reported in the literature.

Compounds **1**–**3** and **5** were tested for their cytotoxicity against human tumor cell lines. Doxorubicin hydrochloride was used as a positive control. Compound **1** showed moderate activities against human breast ductol carcinoma (BT474), liver hepatocarcinoma (HEP-G2), gastric carcinoma (KATO3), and colon adenocarcinoma (SW620) with IC_{50} values of 3.0, 3.7, 3.3, and 2.6 μg/ml, respectively, but was inactive against human undifferentiated lung carcinoma (CHAGO, $IC_{50} > 10$ μg/ml) (Table 2). A similar trend was observed for compound **3** (Table 2). Compound **2** was inactive against all cell lines ($IC_{50} > 10$ μg/ml). This was perhaps due to the solubility problem of compound **2** in the test media. It was also found that compound **5** was the most active of all four heptenes tested and its cytotoxic activity was in agreement to those previously reported (Jung et al., 1990).

3. Experimental

All commercial grade solvents were distilled prior to use. Uncorr. mps were determined using a Gallenkamp melting point apparatus. UV spectra were recorded on a Shimadzu UV-160A UV/VIS spectrophotometer, whereas IR spectra were obtained on a Perkin-Elmer Spectrum 2000 FT–IR spectrophotometer. EIMS and CIMS were obtained on a Micromass Platform II mass spectrometer at 70 and 30 eV, respectively, with methane. The ^1H and ^{13}C NMR spectra were recorded at 300 and 75 MHz, respectively, on a Bruker Avance DPX-300 NMR spectrometer.

Table 2
Cytotoxicity data of compounds **1**–**3** and **5**[a]

	Cell lines[b]				
Compound	BT 474	CHAGO	HEP-G2	KATO 3	SW 620
1	3.0	> 10	3.7	3.3	2.6
2	> 10	> 10	> 10	> 10	> 10
3	5.6	> 10	5.3	3.9	4.9
5	0.2	3.1	2.1	0.4	0.3
Doxorubicin hydrochloride	0.1	2.3	0.9	1.7	1.1

[a] Results are expressed as IC_{50} values (μg/ml).

[b] BT 474, Human breast ductol carcinoma ATCC No. HTB 20; CHAGO, Human undifferentiated lung carcinoma; HEP-G2, Human liver hepatoblastoma ATCC No. HB8065; KATO 3, Human gastric carcinoma ATCC No. HTB 103; SW 620, Human colon adenocarcinoma ATCC No. CCL 227.

Microanalyses were performed on a Perkin-Elmer PE2400 Series II CHNS/O analyzer.

3.1. Plant material

Flowers of *M. fruticosum* were collected in Amphur Muang, Srisaket Province, Thailand, in March 1998. Voucher herbarium specimens (BKF No.13900) of the plant were identified and deposited at the Forest Herbarium, Royal Forest Department, Ministry of Agriculture and Cooperatives, Bangken, Bangkok, Thailand.

3.2. Extraction and isolation

The powdered, dried flowers of *M. fruticosum* (2.3 kg) were extracted successively with petroleum ether (3×3 l), EtOAc (3×3 l), and 70% aqueous acetone (3×3 l). Each extract was evaporated under reduced pressure to yield a petroleum ether (58.44 g), an EtOAc (58.04 g), and a 70% aqueous acetone extract (24.78 g), respectively. Upon standing overnight, compound **1** precipitated out from the EtOAc extract and it was re-crystallized from EtOAc to give pure colorless bulky crystals (5.89 g, 0.26%). The EtOAc mother liquor was fractionated by a Sephadex LH-20 column eluting with EtOAc to obtain 7 fractions. The fractions with similar TLC pattern were combined and subjected to Si gel column chromatography, eluting with a hexane-EtOAc gradient in a stepwise fashion. Compound **3** was obtained as a white crystalline solid (602 mg, 2.62×10^{-2}%). In addition, 5,7-dihydroxyflavone was obtained as a yellow powder (1.57 g, 0.07%) and 5,7-dimethoxyflavone was obtained as colorless crystal (31 mg, 1.3×10^{-2}%). The 70% aqueous acetone extract, after removal of solvents under reduced pressure gave 140 mg of precipitate. This precipitate was re-crystallized from EtOAc to yield colorless bulky crystals of compound **2** (60 mg, 2.6×10^{-3}%). Compound **5** (150 mg, 6.5×10^{-3}%) was isolated as colorless crystals from successive silica gel column chromatography of the petroleum ether extract.

3.3. Biological evaluation

Bioassay of cytotoxic activity against human tumor cell cultures in vitro was performed by the MTT (3-(4,5-dimethylthiazol-2-yl)-2,5-diphenyltetrazolium bromide) colorimetic method (Carmichael et al., 1987; Twentyman and Luscombe 1987).

3.4. 7-Benzoyloxy-6-oxo-2,4Z-heptadiene-1,4-olide (*1*)

Colorless bulky crystals; mp 136–138 °C; (Found C, 65.15; H, 3.87 $C_{14}H_{10}O_5$ requires: C 65.12; H, 3.90%) UV λ_{max} $CHCl_3$ nm (log ε): 283 (4.52), 243 (4.14); FTIR ν_{max}^{KBr} cm^{-1}:1790 (C=O), 1731 (C=O), 1704 (C=O), 1649 (C=C); ^1H and ^{13}C NMR: Table 1. CIMS *m/z* (rel.int.): 259 [MH^+] (0.9); EIMS *m/z* (rel. int.): 258 [M^+] (0.3), 228 (5), 136 (23), 123 (31), 105 (100), 95 (13), 77 (63), 69 (16), 51 (35).

3.5. 7-Benzoyloxy-6-oxo-2,4E-heptadiene-1,4-olide (*2*)

Colorless bulky crystals; mp 139–140 °C; (Found C, 65.11; H, 3.87 $C_{14}H_{10}O_5$ requires: C 65.12; H, 3.90%) UV λ_{max} $CHCl_3$ nm (log ε): 292 (4.17), 243 (3.89); FTIR ν_{max}^{KBr} cm^{-1} :1785 (C=O), 1731 (C=O), 1703 (C=O), 1628 (C=C); ^1H and ^{13}C NMR: Table 1. CIMS m/z (rel. int.): 287 [$M+C_2H_5^+$] (0.7) 259 [MH^+] (11); EIMS m/z (rel. int.): 258 [M^+] (0.1), 228 (3), 136 (9), 123 (20), 105 (100), 95 (8), 77 (37), 69 (9), 51 (14).

3.6. 7-Benzoyloxy-4-hydroxy-1-methoxy-2E,4Z-heptadiene-1,6-dione (*3*)

White crystalline solid; mp 116–118 °C; (Found C, 62.06; H, 4.85 $C_{15}H_{14}O_6$ requires: C 62.07; H, 4.86%) UV λ_{max} $CHCl_3$ nm (log ϵ): 317 (4.40); FTIR ν_{max}^{KBr} cm^{-1} : 3500–2700 (OH), 1724 (C=O), 1658 (C=C), 1628 (C=C), 1587 (C=O),); ^1H and ^{13}C NMR: Table 1. EIMS m/z (rel. int.): 291 [MH^+] (8), 290 [M^+] (2), 273 (3), 259 (1), 231 (30), 168 (37), 155 (64), 136 (7), 123 (52), 113 (53), 106 (14), 105 (100), 95 (20), 85 (8), 77 (82), 69 (17), 59 (15), 55 (20), 51 (59).

Acknowledgements

We thank the Graduate School and the Department of Pharmacognosy, Faculty of Pharmaceutical Sciences, Chulalongkorn University, for financial support. We are grateful to Dr. Tirayut Vilaivan, Department of Chemistry, Faculty of Science, and Dr. Khanit Suwanborirux, Department of Pharmacognosy, Faculty of Pharmaceutical Sciences, Chulalongkorn University, for helpful discussions on the NMR data.

References

Carmichael, J., DeGraff, W.G., Gazdar, A.F., Minna, J.D., Mitchell, B., 1987. Evaluation of a tetrazolium based semiautomated colorimetric assay; assessment of chemosensitivity testing. Cancer Research 47, 936.

Jaipetch, T., Reutrakul, V., Tuntiwachwuttikul, P., Santisuk, T., 1983. Flavonoids in the black rhizomes of *Boesenbergia pandurata*. Phytochemistry 22, 625.

Jung, J.H., Pummangura, S., Chaichantipyuth, C., Patarapanich, C., Fanwick, P.E., Chang, C.-J., McLaughlin, J.L., 1990. New bioactive heptenes from *Melodorum fruticosum* (Annonaceae). Tetrahedron 46, 5043.

Jung, J.H., Chang, C.-J., Smith, D.L., McLaughlin, J.L., Pummangura, S., Chaichantipyuth, C., Patarapanich, C., 1991. Additional bioactive heptenes from *Melodorum fruticosum*. Journal of Natural Products 54, 500.

Markham, K.R., Chari, V.M., 1982. Carbon-13 NMR spectroscopy of flavonoids. In: Harborne, J.B., Mabry, T.J. (Eds.), The Flavonoids: Advances in Research. Chapman and Hall, New York, pp. 19.

Tuchinda, P., Udchachon, J., Reutrakul, V., Santisuk, T., Taylor, W.C., Farnsworth, N.R., Pezzuto, J.M., Kinghorn, A.D., 1991. Bioactive butenolides from *Melodorum fruticosum*. Phytochemistry 30, 2685.

Twentyman, P.R., Luscombe, M., 1987. A study of some variables in a tetrazolium dye (MTT) based assay for cell growth and chemosensitivity. British Journal of Cancer 56, 279.

AUTHOR INDEX
VOLUME 58, NUMBER 3

Aasen, A. J., 489
Abe, T., 517
Al-Qasoumi, S. I., 475
Añón, M. C., 379
Armstrong, N. J., 451
Arruda, P., 415
Asfaw, N., 489

Beardall, J., 389
Bekkouche, K., 455
Blankenship, J. D., 395
Blunden, G., 451
Bondì, M. L., 463
Bouwmeester, H. J., 481
Bruno, M., 463
Busato, A. P., 525
Bush, L. P., 395

Callebaut, A., 493
Chaves, A. R., 379
Cherkaoui, S., 455
Christen, P., 455
Chudek, J. A., 389
Civello, P. M., 379
Clayton, M. N., 389
Cordell, G. A., 534

Daali, Y., 455
de Groot, A., 481
de Kraker, J.-W., 481
Dennis, A. L., 423

El-Olemy, M. M., 475

Fannin, F. F., 395
Franssen, M. C. R., 481

Glasl, H., 441
Gorham, J., 451
Gould, K. S., 403
Grayer, R. J., 533
Guschina, I. A., 509

Haynes, A. M., 423

Jorge, R. A., 415

Kumazawa, T., 423

Levin, R. A., 429

Markham, K. R., 403
Marshall, J. A., 423
Martínez, G. A., 379
Masuda, M., 517
McDade, L. A., 429
McInroy, S. G., 389
Menossi, M., 415
Mossa, J. S., 475
Muhammad, I., 475

Nagata, T., 493
Nes, W. D., 423

Ohba, R., 493
Ohnishi-Kameyama, M., 493
Orabi, K. Y., 475

Patel, A. V., 451
Pibiri, I., 463
Piozzi, F., 463

Raguso, R. A., 429
Raven, J. A., 389
Reicher, F., 525
Reichling, J., 534
Rosselli, S., 463
Řezanka, T., 509
Ryan, K. G., 403

Schardl, C. L., 395
Scrimgeour, C. M., 389
Shibata, T., 481
Simmonds, M. S. J., 463
Skattebøl, L., 489
Spiering, M. J., 395
Storesund, H. J., 489
Suzuki, M., 493, 517

Terahara, N., 493

Vairappan, C. S., 517
Vargas-Rechia, C. G., 525
Veuthey, J.-L., 455

Weissenberg, M., 501
Wilkes, S., 441
Wilkinson, H. H., 395